

Intended for

Dynegy Midwest Generation, LLC
10901 Baldwin Road
Baldwin, IL 62217

Date

February 18, 2025

Project No.

1940110241-005

CORRECTIVE ACTION PLAN

FLY ASH POND SYSTEM BALDWIN POWER PLANT, IEPA ID NO. W1578510001-01/02/03

**CORRECTIVE ACTION PLAN
FLY ASH POND SYSTEM BALDWIN POWER PLANT, IEPA ID
NO. W1578510001-01/02/03**

Project name **Baldwin Power Plant Fly Ash Pond System**
Project no. **1940110241-005**
Recipient **Dynegy Midwest Generation, LLC**
Document type **Corrective Action Plan**
Revision **DRAFT**
Date **February 18, 2025**
Prepared by **Christopher R. Glidden**
Checked by **J. Austin Bond, PE**
Approved by **Brian G. Hennings, PG**
Description **Corrective Action Plan for 35 I.A.C. § 845**

Ramboll
234 W. Florida Street
Fifth Floor
Milwaukee, WI 53204
USA

T 414-837-3607
F 414-837-3608
<https://ramboll.com>

Christopher Glidden
Project Engineer

J. Austin Bond, PE
Qualified Professional Engineer

Brian G. Hennings, PG
Project Officer, Hydrogeology

CONTENTS

| | | |
|-----------|---|-----------|
| 1. | Introduction | 3 |
| 1.1 | Plant and Site Information | 3 |
| 1.2 | Organization of the Corrective Action Plan | 3 |
| 1.3 | Permit Status | 3 |
| 1.4 | Closure and Source Control Status | 3 |
| 1.5 | Selected Corrective Action Remedy | 4 |
| 1.5.1 | Narrative Description of Selected Corrective Action Remedy | 4 |
| 1.5.1.1 | Narrative Discussion of Remedy Design and Function | 5 |
| 1.5.2 | Narrative Description of Proposed Remedy Operations | 6 |
| 1.5.3 | Narrative Description of Proposed Groundwater Monitoring | 6 |
| 2. | Corrective Action Overview | 8 |
| 2.1 | Corrective Measures Assessment | 8 |
| 2.2 | Analysis of Corrective Action Alternatives | 8 |
| 2.2.1 | Corrective Action Alternatives Analysis Supporting Information Report | 8 |
| 2.2.2 | Corrective Action Alternatives Analysis | 10 |
| 3. | Corrective Action Plan | 11 |
| 3.1 | General Requirements | 11 |
| 3.2 | Remedy Selection | 11 |
| 3.3 | Schedule for Implementation | 12 |
| 3.3.1 | Other Relevant Factors | 16 |
| 4. | References | 17 |

TABLES

| | |
|---------|---|
| Table 1 | Proposed Milestone Schedule for Implementing Corrective Action Remedy (Groundwater Management System) |
|---------|---|

APPENDICES

| | |
|------------|--|
| Appendix A | Corrective Action Alternatives Analysis (845.670(e)), including Corrective Measures Assessment (845.660) |
| Appendix B | Drawings and Material Specifications for Selected Remedy |

ACRONYMS AND ABBREVIATIONS

| | |
|-----------|---|
| % | percent |
| 35 I.A.C. | Title 35 of the Illinois Administrative Code |
| 40 C.F.R. | Title 40 of Code of Federal Regulations |
| amp | amperage |
| BEC | Baldwin Energy Complex |
| BPP | Baldwin Power Plant |
| bgs | below ground surface |
| CA GMP | Corrective Action Groundwater Monitoring Plan |
| CAAA | Corrective Action Alternatives Analysis |
| CAAA-SIR | Corrective Action Alternatives Analysis Supporting Information Report |
| CAP | Corrective Action Plan |
| CCR | coal combustion residuals |
| CCR Rule | 40 C.F.R. § 257 Subpart D |
| CIP | closure-in-place |
| CMA | Corrective Measures Assessment |
| COC | constituent of concern |
| CP | Construction Permit |
| CY | cubic yards |
| DMG | Dynegy Midwest Generation, LLC |
| EQ | equalization |
| FAPS | Fly Ash Pond System, also referred to as site |
| GMS | groundwater management system |
| Gradient | Gradient Corporation |
| GWE | groundwater extraction |
| GWP | groundwater polishing |
| GWPS | groundwater protection standard(s) |
| HCR | Hydrogeologic Site Characterization Report |
| HDPE | high-density polyethylene |
| HHERA | Human Health and Ecological Risk Assessment |
| ID | identification |
| IEPA | Illinois Environmental Protection Agency |
| IPCB | Illinois Pollution Control Board |
| ISGS | Illinois State Geological Survey |
| ISWS | Illinois State Water Survey |
| No. | number |
| NPDES | National Pollutant Discharge Elimination System |
| NRT | National Resource Technology, Inc. |
| OMM | operation, maintenance, and monitoring |
| PMP | potential migration pathway |
| PVC | polyvinyl chloride |
| UA | uppermost aquifer |
| UU | upper unit |
| USEPA | United States Environmental Protection Agency |
| VAC | volt alternating current |

1. INTRODUCTION

1.1 Plant and Site Information

Dynegy Midwest Generation, LLC (DMG) is the owner of the active coal-fired Baldwin Energy Complex (BEC), also referred to as the Baldwin Power Plant (BPP), in Baldwin, Randolph County, Illinois. This Corrective Action Plan (CAP) has been prepared for the Fly Ash Pond System (FAPS) at the BPP (site). Groundwater corrective action for the BPP FAPS will be performed under the requirements of Title 35 of the Illinois Administrative Code (35 I.A.C.) § 845, Standards for the Disposal of Coal Combustion Residuals in Surface Impoundments [1] and the requirements of Title 40 of the Code of Federal Regulations (40 C.F.R.) § 257, herein referred to as the Federal coal combustion residuals (CCR) Rule [2]. The FAPS is identified by Illinois Environmental Protection Agency (IEPA) identification (ID) numbers (Nos.) W1578510001-01, W1578510001-02, W1578510001-03, also referred to as Vistra Identification ID No. 605, and National Inventory of Dams No. IL50720.

1.2 Organization of the Corrective Action Plan

This CAP is organized in the following manner:

- **Section 1** includes an introduction to the FAPS, lists the status of other 35 I.A.C. § 845 permit applications submitted to IEPA, identifies the selected remedy, and provides a narrative of remedy construction;
- **Section 2** includes an overview of the corrective action process, including the results of the Corrective Measures Assessment (CMA) and Corrective Action Alternatives Analysis (CAAA);
- **Section 3** provides the CAP requirements, the selected remedy, an evaluation of effectiveness, and an implementation schedule, as required by 35 I.A.C. § 845.670; and
- **Section 4** includes reference documents used in the development of this CAP.

This CAP was prepared as an attachment to a Construction Permit (CP) application, to support obtaining a permit for Groundwater Corrective Action Construction at the FAPS, as required by 35 I.A.C. § 845.220(a) and (c).

1.3 Permit Status

The following 35 I.A.C. § 845 permit applications have been previously submitted to IEPA along with this CAP for the FAPS:

- An operating permit (OP), as required by 35 I.A.C. § 845.230, was submitted on October 25, 2021 [3].

1.4 Closure and Source Control Status

DMG completed significant source control efforts in 2020 as part of final closure of the FAPS [4]. The final closure was performed in accordance with the Closure and Post-Closure Care Plan [5] that was developed in accordance with Title 40 of the Code of Federal Regulations (40 C.F.R.) § 257 and submitted to IEPA for review. IEPA found "...that the plan...represent an appropriate means by which to close the Baldwin Fly Ash Pond System which is comprised of the East Fly Ash Pond, the Old East Fly Ash Pond and the West Fly Ash Pond" [6]. The final closure was completed in accordance with the IEPA Water Pollution Control permit 2020-EA-65016.

The FAPS closure construction included closure-in-place (CIP) of the entire FAPS. This was accomplished by removing impounded water and constructing a final cover system in accordance with 40 C.F.R. § 257.102 to minimize water infiltration into the closed FAPS and improve surface water drainage off the cover system, thus reducing generation of potentially impacted water and ultimately reducing the extent of potential CCR impacts to groundwater. The source control was predicted to lower water levels, decrease the potential transport of CCR constituents off-site and prevent groundwater protection standards (GWPS) from being exceeded in any water supply wells [7]. These completed source control activities serve as the primary groundwater corrective measure at the FAPS. The remedy presented within this Corrective Action Plan is intended to be supplementary to the primary remedy, which is the completed source control.

1.5 Selected Corrective Action Remedy

A groundwater management system (GMS), combined with the completed source control described in Section 1.4, [4] has been identified as the most appropriate remedy for the FAPS, based on the CAAA provided in **Appendix A**. Potential remedies evaluated in the CAAA included Source Control with Groundwater Polishing (GWP), Source Control with a Cutoff Wall, and Source Control with a GMS.

The CAAA, which was prepared by Gradient Corporation (Gradient), was based on a CAAA Supporting Information Report (CAAA-SIR) that was prepared by Ramboll and is attached to the CAAA. The CAAA-SIR includes the results of groundwater modeling and feasibility-level design information for each remedy.

A Groundwater Polishing Evaluation Report [8] is also attached to the CAAA. This report presents results from geochemical modeling of exceedance parameters addressed at the FAPS by the CAP. Geochemical modeling supports the assessment of GWP as a component of the proposed corrective action by evaluating the potential for chemical attenuation of constituents of concern (COC) before and after source control as a means of contextualizing the times to meet groundwater protection standards (GWPS) estimated in the flow and transport model.

1.5.1 Narrative Description of Selected Corrective Action Remedy

Corrective action consists of the completed source control (see Section 1.4) and the operation of a new GMS, which will serve to remove liquids that may accumulate from beneath the existing FAPS cover system. The GMS system will control the source to reduce to the maximum extent feasible further releases of constituents listed in 845.600 in accordance with 845.670(d)(3).

The GMS will include the construction of groundwater management extraction trenches within the footprint of the closed FAPS, which will remove liquids from the base of the CCR within the FAPS. The trenches will extend vertically through the entire observed thickness of CCR and will be terminated in the underlying native soils. Any liquids collected by the GMS will be transferred to an appropriate location for discharge in accordance with applicable permits that will be obtained after approval of the Corrective Action Plan.

The GMS will be continuously operated during the corrective action period, outside of routine shutdowns for system maintenance and/or power outages. Groundwater corrective action performance will be monitored in accordance with the Corrective Action Groundwater Monitoring

Plan (CA GMP). The system operation will cease when the FAPS monitoring well network achieves the GWPS and other considerations have been evaluated as described in the CA GMP Section 3.1.

Estimated timelines for GMS operation and times to reach the GWPS will be periodically reviewed and updated based on observed corrective action performance via an adaptive site management strategy. These periodic updated estimates will be communicated to IEPA and the public within Annual Corrective Action Monitoring Reports in accordance with the CA GMP.

Corrective action will be considered complete when a demonstration that GWPS compliance beyond the waste boundary has been achieved for at least three years after remedy operations have ceased and a corrective action completion report and certification have been submitted to IEPA in accordance with 35 I.A.C. § 845.680(e).

1.5.1.1 Narrative Discussion of Remedy Design and Function

The GMS design includes an approximately 8,700-foot collection trench alignment within the limits of the existing FAPS. Collection sumps will be installed approximately every 500 ft along the alignment. The location of the system was targeted to correspond to the portions of the FAPS where CCR is present at the lowest elevations, which generally correspond with pre-construction surface drainage features that were identified in pre-construction site drawings and available geotechnical exploration data [9]. This approach will allow the system to collect the maximum amount of liquids that may be present, thereby proactively preventing an accumulation of hydraulic head within the FAPS. Permit-level engineering drawings depicting the proposed remedy are provided in **Appendix B**, and a list of key design components includes the following:

- The trenches will be approximately 2 to 3 feet wide with a maximum depth of approximately 50 to 60 feet bgs; backfilled will consist of permeable drainage media surrounding a perforated collection pipe installed near the base of the trench.
- High-density polyethylene (HDPE) air supply and water conveyance piping will be buried within the top 3 feet of an adjacent trench during trench installation.
- Collection sumps will be spaced approximately 500 feet apart and installed down to the base of the CCR. Collection sumps will consist of a pit to collect any liquids, a pneumatic pump, and a discharge pipe that will carry any extracted liquids to a nearby compressor shed. The collection sump pits will be backfilled with gravel around slotted screens, which will house the pneumatic pump, and piezometers, which will be used to monitor the presence of liquids within the collection sumps.
- Areas of the final cover system damaged by installation of the GMS will be repaired after installation, consistent with the specifications for the completed FAPS closure.

Electrical infrastructure to support the GMS will be installed prior to delivery and placement of the GMS. Additional system infrastructure will consist of compressor sheds that will be installed approximately every 1,000 to 2,000 feet along the trench alignment. Each compressor shed is expected to contain the following equipment:

- An air compressor, air receiver tank, and a manifold consisting of control valves and pulse counters that will be used to monitor pneumatic pump air usage.
- A groundwater collection manifold consisting of control valves and flow meters to totalize any extracted liquids from each collection sump.

- An EQ tank that will temporarily store any extracted liquids.
- A transfer pump that will transfer any extracted liquids to the discharge location in accordance with applicable permits.
- Miscellaneous electrical controls to support data collection and system operation.

1.5.2 Narrative Description of Proposed Remedy Operations

Operations, maintenance, and monitoring (OMM) will be conducted on the GMS on a routine basis. OMM will consist of system-wide data collection to track water recovery and discharge rates, system-wide inspections and associated maintenance, and routine monitoring and compliance activities associated with the treatment and discharge of water via the site's NPDES permit. Waste streams associated with the GMS and its management may include:

- Accumulated sediment/solids that collect at the bottom of the EQ tanks will be intermittently removed, dried, and disposed of at a non-hazardous landfill, as needed based on accumulation rates.
- Conveyance piping will be flushed on an as-needed basis in the event organic or inorganic solids accumulation is observed on the inner wall of the conveyance pipe during routine OMM inspections.

Routine equipment maintenance will be conducted per at regular frequencies. Additionally, faulty equipment will be replaced, as needed, to keep the GMS operating in accordance with the design intent. Equipment maintenance and/or replacements may require temporary shutdown of the GMS

1.5.3 Narrative Description of Proposed Groundwater Monitoring

Corrective action groundwater monitoring will be conducted during remedy operation to evaluate the effectiveness of the corrective action remedy and whether groundwater concentrations are achieving the GWPS as predicted by the groundwater model. Groundwater data collected as part of the monitoring program will be analyzed to determine if the remedy is on track to meet GWPS and to inform adaptive management decisions if performance metrics are not achieved.

- Regular groundwater monitoring will be conducted utilizing a corrective action groundwater monitoring network designed in accordance with 35 I.A.C. § 845.680(a)(1).
- Samples will be collected for each constituent required by 35 I.A.C. § 845.600(a)(1). Samples will be collected on a quarterly basis initially and potentially reduced to a semiannual basis once five years of monitoring have occurred, in accordance with 35 I.A.C. § 845.650(b)(4). Monitoring results will be submitted to IEPA for each monitoring event, in addition to an Annual Groundwater Monitoring and Corrective Action Report, in accordance with 35 I.A.C. § 845.610(e).
- Routine maintenance of the monitoring well network will include inspecting the wells, making repairs to the wells (as needed) and rehabilitating and/or replacing wells to improve performance (as needed).

- Adaptive site management will include updates to geochemical models for each location with GWPS exceedances¹.
 - The available solid-phase data from the aquifer and these models will be used to identify potential mobilization of other COCs as groundwater returns to background conditions.
 - Groundwater monitoring results will be evaluated for consistency with modeled concentrations and documented in the monitoring reports submitted to IEPA, in accordance with 35 I.A.C. § 845.610(e).
 - If groundwater does not match expected conditions, additional methods or techniques to achieve compliance with GWPS will be evaluated and, if feasible, implemented in accordance with 35 I.A.C. § 845.680(b). These actions could include, for example, the installation of additional collection sumps to enhance liquid recovery, and the installation of additional monitoring wells to obtain groundwater data necessary to support decisions made under the adaptive management strategy.
- Corrective Action Confirmation Monitoring and Completion
 - Per 35 I.A.C. § 845.680(c), corrective action is considered complete when compliance with the GWPS has been demonstrated "at all points within the plume of contamination that lies beyond the waste boundary [...] for a period of three consecutive years". At that time, an attainment evaluation will be implemented. This will include monitoring each well for three additional years to confirm that GWPS have been achieved, in accordance 35 I.A.C. § 845.680(c).
 - It should be noted that post-closure care groundwater monitoring required for a 30-year period by 35 I.A.C. § 845.780(c) will continue to occur after corrective action groundwater monitoring is expected to be completed.
 - After completion of the corrective action confirmation monitoring period, a Corrective Action Completion Report and Certification will be prepared and submitted to IEPA, in accordance with 35 I.A.C. § 845.680(e).

¹ Throughout this document, "exceedance" or "exceedances" is intended to refer only to potential exceedances of proposed applicable background statistics or GWPSs as described in the proposed groundwater monitoring program, which was submitted to the IEPA on October 25, 2021 as part of DMG's operating permit application for the BAL FAPS. That operating permit application, including the proposed groundwater monitoring program, remains under review by the IEPA and, therefore, DMG has not identified any actual exceedances.

2. CORRECTIVE ACTION OVERVIEW

This CAP is based on the tiered assessment and analysis of alternative remedial technologies and remedies that were completed via the CMA and CAAA (**Appendix A**). The objective of these assessments was to determine the most appropriate alternative for the FAPS that, when coupled with the source control completed in the Final Closure Plan [10], would reduce the future potential footprint of COCs in groundwater and eventually attain the GWPS specified under 35 I.A.C. § 845.600.

2.1 Corrective Measures Assessment

The CMA [11] was performed for the FAPS and submitted to the IEPA on April 24, 2024, after the exceedances of the GWPS were identified. The CMA considered four corrective measures for the FAPS, including:

- Source Control with GWP;
- Source Control with GMS² (groundwater pumping wells or collection trenches);
- Source Control with Groundwater Cutoff Wall; and
- Source Control with In-Situ Treatment (permeable reactive barrier or in-situ chemical treatment).

Based on the CMA, three corrective measures, including Source Control-GWP, Source Control-GWE, and Source Control-Cutoff Wall, were identified as potentially viable for the FAPS and were included for further evaluation, design advancement, and comparative assessment within the CAAA for the FAPS. The In-Situ Treatment corrective measure was determined by the CMA to be unlikely to be effective for the FAPS and was not retained for further evaluation within the CAAA.

2.2 Analysis of Corrective Action Alternatives

2.2.1 Corrective Action Alternatives Analysis Supporting Information Report

The CAAA for the FAPS was prepared by Gradient based on the CAAA-SIR prepared by Ramboll. The CAAA-SIR, which is included as Attachment B of the CAAA provided in **Appendix A**, included additional evaluation, design advancement, and comparative assessment of the Source Control-GWP, Source Control-Deep Cutoff Wall, and Source Control-GMS corrective measures identified as potentially viable for the FAPS by the CMA. The evaluation included the completion of feasibility-level design activities for each alternative and incorporated the following tasks:

- Performing predictive groundwater modeling to evaluate the scope (*i.e.*, location and extents) of each alternative and the corresponding estimated time to achieve GWPS;
- Developing feasibility-level design drawings showing the extent in plan and elevation view of each engineered remedy;
- Estimating the time required to design, construct, and implement each remedy, in addition to ongoing operational and maintenance requirements;

² This corrective measure is referred to as groundwater extraction in the April 2024 CMA.

- Developing conceptual plans for the storage, treatment, and discharge of any liquids for applicable remedies;
- Identifying future tasks required to implement each alternative, including permitting, investigation, and design efforts; and
- Estimating relevant material quantities, labor hours, delivery miles, equipment miles, and daily commuting miles associated with constructing and operating/maintaining each remedy.

Consistent with the results of previous modeling efforts that supported the IEPA approved closure of the FAPS, the results of predictive groundwater modeling in support of the CAAA determined that the GWPS would not be attained within the 1,000 year timeline simulated. For comparative purposes, a model simulation of closure by removal (removal of all CCR from the FAPS) was also simulated and the GWPS also would not be attained within the 1,000 year timeline. This is due to the low hydraulic conductivity of the native soils (UU) and bedrock (UA); and, low groundwater flow velocities at the site. As discussed in Section 6.4 of the groundwater modeling technical memorandum, included as Appendix B of the CAAA-SIR, the following applies to these long-term model results:

- Prediction modeling of Source Control with GMS indicates significantly greater progress toward attaining the GWPS than the other alternatives or closure by removal.
- As with all models, the groundwater flow and transport model is limited by the data used for calibration, which adequately define the local groundwater flow system and the source and extent of the plume. Since data used for calibration are near the BAP and FAPS, model predictions of transport distant spatially and temporally from the calibrated conditions at the CCR units will not be as reliable as predictions closer to the CCR units and groundwater concentrations observed between 2015 and 2024.
- Simulated post-construction heads in the FAPS monitoring wells reached equilibrium at approximately 106 years following implementation of corrective action alternatives and was used as a representative simulated time period for estimating future flux reductions from the FAPS. Considering models become increasingly less reliable as the length of time increases for predictions and the model simulations indicate the groundwater flow system approaches equilibrium approximately 106 years after implementation, discussion of model results beyond 106 years should be more qualitative, such as comparison between observed future trends and predicted trends, and as a tool for comparison between model simulations.
- Following implementation of corrective action, progress toward attainment of the GWPS will be routinely monitored and updated following the adaptive site management actions provided in the Corrective Action Groundwater Monitoring Plan, Baldwin Power Plant, Fly Ash Pond System [12]. Groundwater corrective action will include monitoring and adaptive site management (**Section 1.5.3**), which includes routine review of the CSM and decision points for making updates to the CSMs and the groundwater fate and transport models as appropriate in the future.
- Corrective action alternatives were also evaluated spatially using maps of maximum simulated boron concentration and relative area in acres, including comparison of off-site simulated plume extents.

2.2.2 Corrective Action Alternatives Analysis

The CAAA (**Appendix A**) included a detailed analysis of each of the corrective action alternatives presented in the CAAA-SIR, including an evaluation of:

- Long and short-term effectiveness and protectiveness;
- Ease or difficulty of implementation;
- Degree to which community concerns are addressed; and,
- Relative amount of contamination removed from the environment.

The CAAA identified Source Control-GMS as the most appropriate corrective action for the FAPS and this remedy was selected for further design development as part of this CAP.

It should be noted that the permit-level engineering assessments, groundwater modeling, and other information contained within this CAP were developed to a higher level of design and detail than those assessments performed in the CAAA; therefore, information on items such as permitting, remedy scope, estimated time to reach GWPS, implementation schedule, etc. may differ between this CAP and the information included in the CAAA-SIR and CAAA. Information for the Source Control-GMS contained within the CAP should be considered to superseded information contained within the CAAA and CAAA-SIR.

3. CORRECTIVE ACTION PLAN

The 35 I.A.C. § 845 requirements for the CAP and corresponding demonstrations that the proposed corrective measures meet these requirements are discussed individually in this section. Many of the CAP requirements are discussed within the CMA and CAAA documents that have been prepared to support the CAP. Therefore, the demonstrations will also refer to those documents.

3.1 General Requirements

35 I.A.C. § 845.670(c): *The corrective action plan must meet the following requirements:*

- (1) Be based on the results of the corrective measures assessment conducted under 35 I.A.C. § 845.660;*
- (2) Identify a selected remedy that at a minimum, meets the standards listed in subsection (d);*
- (3) Contain the corrective action alternatives analysis specified in subsection (e); and*
- (4) Contain proposed schedules for implementation, including an analysis of the factors in subsection (f).*

This CAP is based on the results of the CMA and CAAA, which are included within **Appendix A**. The proposed schedule for implementing Source Control-GMS is provided in **Table 1**.

3.2 Remedy Selection

35 I.A.C. § 845.670(d): *The selected remedy in the corrective action plan must:*

- (1) Be protective of human health and the environment;*

No unacceptable risks to human or ecological receptors resulting from CCR exposures associated with the FAPS were identified [13]. Potential releases of CCR-derived constituents will decline over time and, consequently, potential exposures to CCR-derived constituents in the environment will also decline. The GMS is intended to reduce the accumulation of hydraulic head beneath the FAPS cover system which reduces the potential for liquids which may be from the FAPS to mix with groundwater.

- (2) Attain the groundwater protection standards specified in 35 I.A.C. § 845.600;*

Groundwater modeling used to support design of the GMS (Appendix B of the CAAA-SIR) estimates the selected remedy of source control with the GMS will attain the GWPS in greater than 100 years. This is due to the low hydraulic conductivity associated with the underlying soil and bedrock. Corrective action alternatives were also evaluated spatially using maps of maximum simulated boron concentration and relative area in acres, including, comparison of off-site simulated plume extents. Source control with GMS was the most effective remedy at reducing predicted concentrations of CCR derived constituents in groundwater and minimizing the footprint of impacted groundwater.

- (3) Control the sources of releases to reduce or eliminate, to the maximum extent feasible, further releases of constituents listed in 35 I.A.C. § 845.600 into the environment;*

Source control with GMS was selected as the most appropriate remedy for the FAPS to best minimize the expanse of the plume beyond the FAPS boundary. The FAPS was closed using a capping approach which acts as the main control mechanism to prevent further releases of CCR-derived constituents. The GMS will reduce to the maximum extent feasible further releases and minimize further off-site migration of CCR-derived constituents in groundwater until the GWPS are achieved. Adaptive site management action will be taken as described within the CA GMP if the actual remedy performance does not correspond with the expected performance described in this CAP.

(4) Remove from the environment as much of the contaminated material that was released from the CCR surface impoundment as is feasible, taking into account factors such as avoiding inappropriate disturbance of sensitive ecosystems; and

No known releases of CCR due to a structural integrity issue have occurred at the FAPS.

(5) Comply with standards for management of wastes as specified in 35 I.A.C. § 845.680(d).

The CCR managed as part of the closure will be done in accordance with all 35 I.A.C. § 845 requirements and the submitted Closure Plan [10].

3.3 Schedule for Implementation

Groundwater corrective action will begin within 90 days following approval of the Corrective Action Plan. This will include pre-construction activities, followed by corrective action construction, and then followed by corrective action operation and maintenance.

GWE is effective as an engineered control as it is intended to reduce the accumulation of hydraulic head beneath the FAPS cover system and has been demonstrated as a reliable and applicable ex-situ remedial technology by the USEPA [14]. Human and ecological receptors beyond the FAPS boundary will be protected until the GWPS are attained.

The GMS remedy was evaluated to determine if it can minimize impacts beyond the FAPS boundary and achieve GWPS at the FAPS monitoring well network. The GMS remedy improves on the time to achieve GWPS when compared to source control alone and is, therefore, in accordance with the requirements of 35 I.A.C. § 845.670.

35 I.A.C. § 845.670(f): The owner or operator must specify, as part of the corrective action plan, a schedule for implementing, of and completing, remedial activities. The schedule must require the completion of remedial activities within a reasonable time, taking into consideration the factors in this subsection (f). The owner or operator of the CCR surface impoundment must consider the following factors in determining the schedule of remedial activities:

The schedule for implementing the Source Control-GMS remedy at the FAPS is included in **Table 2**. The GMS remedy will be continuously operated during the corrective action period.

The schedule was developed considering the factors required by 35 I.A.C. § 845.670(f)(1) through (5), as summarized below.

35 I.A.C. § 845.670(f)(1): Extent and nature of contamination, as determined by the characterization required under 35 I.A.C. § 845.650(d);

The Nature and Extent Report [15], which was submitted to the IEPA in April 2024 and is included as Appendix D to the CAAA report (**Appendix A**), details exceedances of GWPS. Site investigation activities and data collected after April of 2024 have been compiled and will be provided in the same appendix to the CAAA report as an addendum to the Nature and Extent Report. Groundwater modeling and geochemical analysis were performed by Ramboll as part of the CAAA-SIR to design the remedy, and the modeling considered the nature and extent of contamination. Exceedances of the GWPS attributable to the FAPS in the UA are limited to sulfate detected in well MW-366, which is located approximately 2,000 feet upgradient of the property boundary and defined in the downgradient direction by UA wells MW-350, MW-375, and MW-391.

Exceedances of the GWPS attributable to the FAPS in the UU include boron and/or sulfate detected in wells MW-150 and MW-252. Boron and sulfate have also been observed at concentrations greater than the GWPS from individual samples collected at well MW-196, which is located approximately 200 feet south of the BPP property boundary and 75 feet south of the railroad tracks present along the southern property boundary; and MW-253R which is located on property and was installed as a replacement for well MW-253 in 2024 located approximately 300 feet south of the limits of the FAPS and 30 feet south of the railroad tracks. Sulfate concentrations of individual samples collected from the replacement well MW-253R continue to be evaluated and are further discussed in the Addendum to the Nature and Extent Report. The limits of boron and sulfate concentrations observed above the GWPS in the UU have not been detected more than 200 feet from the southern property boundary and are defined by the creek present along the southern BPP property boundary and monitoring wells including MW-195, MW-197, and MW-198 (see Figure 2.3 of the CAAA). Further discussion is provided in the Addendum to the Nature and Extent Report (in progress) provided in Appendix D of the CAAA (**Appendix A**).

35 I.A.C. § 845.670(f)(2): Reasonable probabilities of remedial technologies achieving compliance with the GWPS established by 35 I.A.C. § 845.600 and other objectives of the remedy;

Several remedies were evaluated in the CAAA and it was determined that the selected remedy (Source Control–GMS) is the most appropriate remedy to reduce, to the maximum extent feasible, further releases of constituents listed in 845.600 in accordance with 845.670(d)(3).

Groundwater modeling was performed to evaluate future groundwater quality in the vicinity of the FAPS impoundment. As noted in **Section 2.2.1**, the results of predictive groundwater modeling determined that the GWPS would not be attained for all wells within the timeline simulated for any of the groundwater corrective actions (this was also true for simulation of closure by removal). However, Source Control – GMS is the only simulated corrective action that results in continuous plume contraction 25 years following implementation.

As discussed in the CMA, source control and groundwater extraction are proven methods for addressing groundwater contamination [11].

35 I.A.C. § 845.670(f)(3): Availability of treatment or disposal capacity for CCR managed during implementation of the remedy;

The selected remedy includes CIP with a GMS. The CCR will be managed within the footprint of the existing CCR unit as discussed in the Final Closure Plan [10]. Installation of the GMS is anticipated to generate approximately 50,000 cubic yards (CY) of CCR waste, through excavation

of the extraction trenches, which must be managed and disposed of during remedy construction. The FAPS cap will be reworked to incorporate the CCR waste generated during construction of the remedy, however, multiple disposal facilities have been located in Illinois and Missouri that have capacity to receive CCR waste generated during installation of the GMS.

35 I.A.C. § 845.670(f)(4): Potential risks to human health and the environment from exposure to contamination before completion of the remedy;

A Human Health and Ecological Risk Assessment (HHERA) was completed and included as an attachment to the CAAA (**Appendix A**). The overall conclusion is that releases from the FAPS impoundment and potential groundwater contributions to surface water pose no unacceptable risks to human health or the environment. This conclusion is based on modeled and detected maximum concentrations of all COCs in surface water at the NPDES permitted discharge that were below conservative risk-based screening benchmarks. This conclusion was reached using methodology consistent with applicable USEPA risk assessment principles. The assessment relied on conservative assumptions meant to overestimate possible exposures and risks and provide an additional level of certainty in the conclusions.

35 I.A.C. § 845.670(f)(5): Resource value of the aquifer, including:

The resource value of the aquifer is discussed in the Hydrogeologic Site Characterization Report (HCR) [16], which is included as Attachment B.3 in the closure CP application. The shallow bedrock is the only water-bearing unit that is continuous across the BPP. Groundwater in the bedrock mainly occurs under semi-confined to confined conditions with the overlying unlithified unit behaving as the upper confining unit to the UA. Shallow sandstone and creviced limestone may yield small supplies in some areas, but water quality becomes poorer (i.e., highly mineralized) with increasing depth. The classification of groundwater at the Site was addressed in the Phase II investigation [7]. Field hydraulic conductivity tests performed on the Upper Groundwater Unit materials (i.e., Cahokia Formation, Equality Formation, and Vandalia Till) and Bedrock Unit materials (i.e., Mississippian and Pennsylvanian bedrock) at the Site had geometric mean hydraulic conductivities of 3.2×10^{-5} cm/s and 5.0×10^{-6} cm/s, respectively.

Geologic material with a hydraulic conductivity of less than 1×10^{-4} cm/s which does not meet the provisions of Section 620.210 (Class I), Section 620.230 (Class III), or Section 620.240 (Class IV), meets the definition of a Class II – General Resource Groundwater. Based on the detailed geologic information provided for the unlithified materials and bedrock at BPP, along with the hydrogeologic data, the groundwater in both the unlithified deposits and underlying bedrock at the Site is classified as Class II - General Resource Groundwater.

Although some thin sand seams and layers occur intermittently within the Vandalia Till in localized areas around the BPP, most groundwater supplies in upland areas are obtained from large diameter shallow bored wells. Typical water wells in the vicinity of the BPP are between 25 and 55 feet deep, 36 to 48 inches in diameter, and collect groundwater through slow percolation into the wells, which are large diameter to allow for greater water storage to compensate for the low rate of groundwater infiltration [17]. The GMS remedy will operate until the GWPS are achieved. Paragraphs (A) through (F) from 35 I.A.C. § 845.670(f)(5) are further addressed, as summarized below.

35 I.A.C. § 845.670(f)(5)(A): Current and future uses, including potential residential, agricultural, commercial industrial and ecological uses; and

Current uses and future users of the groundwater are discussed in the previous paragraph and attachments and, were considered in the CAAA as part of the HHERA, which concluded that groundwater from the FAPS impoundment and potential groundwater contributions to surface water pose no unacceptable risks to human health or the environment. No changes in future residential, commercial, or ecological use are expected. However, if future uses are modified, the potential use of the impacted groundwater is expected to be minimal because potable water service (provided by the Village) is available in the location of these properties, and the UU and UA are not capable of providing large amounts of groundwater for use in agriculture or other uses. In the absence of changes to current and future uses, there is no applicable scheduling consideration.

35 I.A.C. § 845.670(f)(5)(B): Proximity and withdrawal rate of users;

As discussed in the HHERA [13] a receptor survey was performed in 2024 and identified four wells located downgradient of the FAPS. Analytical results from additional monitoring wells installed in 2024 indicate that exceedances do not extend beyond the monitoring wells and the private wells are not currently impacted. Future exceedances are unlikely based on the predicted extent determined by the model [17]. The withdrawal rate data for these four wells is not available but in general, bored wells rely on storage to provide water during periods of high demand (<https://dph.illinois.gov/topics-services/environmental-health-protection/private-water/fact-sheets/bored-wells.html>). Based on a depth of 30 ft, a bored well may provide up to 1,000 gallons per day.

35 I.A.C. § 845.670(f)(5)(C): Groundwater quantity and quality;

Per 35 I.A.C. § 620.210, groundwater within the uppermost aquifer at the FAPS meets the definition of Class 2 – General Resource Groundwater [16]. The HHERA [13] concluded that releases from the FAPS impoundment and potential groundwater contributions to surface water pose no unacceptable risks to human health or the environment.

35 I.A.C. § 845.670(f)(5)(D): The potential impact to the subsurface ecosystem, wildlife, other natural resources, crops, vegetation, and physical structures caused by exposure to CCR constituents;

Potential receptors are discussed in HCR Sections 5.2 and 5.3. Section 3.5 of the HHERA, included as Appendix A of the CAAA and CMA/CAAA Report, discusses the ecological risk evaluation.

- Ecological receptors exposed to surface water include aquatic and marsh plants, amphibians, reptiles, and fish. The risk evaluation showed that none of the COCs in surface water exceeded protective screening benchmarks.
- Ecological receptors exposed to sediment include benthic invertebrates. The modeled sediment COCs did not exceed the conservative screening benchmarks; therefore, none of the COCs evaluated in sediment are expected to pose an unacceptable risk to ecological receptors.
- Ecological receptors were also evaluated for exposure to bioaccumulative COCs. This evaluation considered higher trophic-level wildlife with direct exposure to surface water and sediment and secondary exposure through the consumption of dietary items (e.g., plants,

invertebrates, small mammals, fish). None of the ecological COCs were identified as having potential bioaccumulative effects.

Overall, this evaluation demonstrated that none of the COCs evaluated are expected to pose an unacceptable risk to ecological receptors. In the absence of unacceptable risks to ecological receptors, there is no applicable scheduling consideration.

35 I.A.C. § 845.670(f)(5)(E): The hydrogeologic characteristic of the facility and surrounding land; and

In addition to the CCR present in the FAPS, there are two hydrostratigraphic units underlying the constructed CCR unit, described below in descending order:

- Upper unit (UU) – Predominantly clay with some silt and minor sand, silt layers, and occasional sand lenses. Includes the lithologic layers identified as the Cahokia Alluvium, Peoria Loess, Equality Formation, and Vandalia Till Member. Thin sand seams within the unit and the interface (contact) between the UU and bedrock have been identified as potential migration pathways (PMPs). No continuous sand seams were observed within or immediately adjacent to the FAPS; however, the sand seams on Site may act as a PMP due to relatively higher hydraulic conductivities.
- Uppermost aquifer (UA) (Bedrock Unit) – Pennsylvanian and Mississippian bedrock is composed of interbedded shale and limestone bedrock, which underlies and is continuous across the entire site.

The effects of these hydrostratigraphic units on schedule were considered by incorporating the geometry, hydraulic, and geochemical properties of these units into the groundwater modeling and groundwater polishing evaluation reports, attached to the CAAA-SIR and CAAA, respectively, included in **Appendix A**, which estimate the time to reach the GWPS for remedial alternatives.

The GMS remedy is intended to reduce the accumulation of hydraulic head within the CCR unit which reduces the potential for liquids that may be from the FAPS to mix with groundwater. The GMS remedy will operate until the GWPS are achieved.

35 I.A.C. § 845.670(f)(5)(F): The availability of alternative water supplies.

As discussed in subsection 35 I.A.C. § 845.670(f)(5)(B) above, there are no public water supply wells within 2,500 meters of the FAPS. There is currently no need for an alternative water supply well as there are no current unacceptable risks to human or ecological receptors at the site, and the GMS remedy will prevent off-site migration of FAPS CCR-derived constituents.

3.3.1 Other Relevant Factors

35 I.A.C. § 845.670(f)(6): Other relevant factors.

No additional factors were identified for consideration.

4. REFERENCES

- [1] "Illinois Administrative Code, Title 35, Subtitle G, Chapter I, Subchapter J, Part 845: Standards for The Disposal Of Coal Combustion Residuals In Surface Impoundments," effective April 21, 2021.
- [2] Code of Federal Regulations, "Title 40, Chapter I, Subchapter I, Part 257, Subpart D, Standards for the Disposal of Coal Combustion Residuals in Landfills and Surface Impoundments," April 17, 2015.
- [3] Burns & McDonnell, "Initial Operating Permit, Baldwin Power Plant Fly Ash System," Burns & McDonnell, Baldwin, Illinois, October 25, 2021.
- [4] Dynegy Midwest Generation, LLC, "Notification of Completion of Closure, Baldwin Energy Complex, Old East Fly Ash Pond, East Fly Ash Pond, West Ash Pond," Dynegy Midwest Generation, LLC, Baldwin, Illinois, December 17, 2020.
- [5] AECOM, "Closure and Post-Closure Care Plan for the Baldwin Fly Ash Pond System. Baldwin Energy Complex.," AECOM, Baldwin, Illinois., March 31, 2016.
- [6] Illinois Environmental Protection Agency, "Dynegy Midwest Generation, Inc. - "Baldwin Energy Complex: Baldwin Fly Ash Pond System Closure - NPDES Permit No. IL0000043."," Illinois Environmental Protection Agency, Baldwin, Illinois, August 16, 2016.
- [7] Natural Resource Technology, "Groundwater Model and Simulation of Closure Alternatives, Baldwin Ash Pond System, Baldwin Energy Complex," Natural Resource Technology, Baldwin, Illinois, June 18, 2014.
- [8] Geosyntec Consultants, Inc (Geosyntec), "Groundwater Polishing Evaluation Report Baldwin Power Plant - Fly Ash Pond System (EPA ID No. 605)," January 2025.
- [9] AECOM, "30% Design Data Report for the Dynegy Baldwin Energy Complex; West Fly Ash Pond, East Fly Ash Pond, and Old East Fly Ash Pond CCR Units," AECOM, Baldwin, Illinois, December 17, 2015.
- [10] Geosyntec Consultants, "Final Closure Plan, Baldwin Power Plant, Bottom Ash Pond (IEPA ID W1578510001-06), Baldwin Illinois," Geosyntec Consultants, Baldwin, Illinois, January 24, 2023.
- [11] Ramboll Americas Engineering Solutions, Inc., "35 I.A.C § 845 Corrective Measures Assessment, Baldwin Power Plant, Fly Ash Pond System, IEPA ID No. W1578510001-06," Ramboll Americas Engineering Solutions, Inc., Baldwin Illinois, April 24, 2024.
- [12] Ramboll Americas Engineering Solutions, "Corrective Action Groundwater Monitoring Plan, Baldwin Power Plant, Fly Ash Pond System, IEPA ID No. W1578510001-01, W1578510001-02, and W1578510001-03," Ramboll Americas Engineering Solutions, Baldwin, Illinois, February 18, 2025.
- [13] Gradient Corporation, "Human Health and Ecological Risk Assessment, Fly Ash Pond system, Baldwin Power Plant, Baldwin, Illinois," Gradient Corporation, Baldwin, Illinois, February 12, 2025.
- [14] USEPA, "Federal Remediation Technologies Roundtable, Technology Screening Matrix - Groundwater Pump and Treat," [Online]. Available: <https://www.frtr.gov/matrix/Groundwater-Pump-and-Treat/>. [Accessed 3 December 2024].

- [15] Ramboll Americas Engineering Solutions, Inc., "Nature and Extent Report, Baldwin Power Plant, Fly Ash Pond System, IEPA ID No. W1578510001-01," Ramboll Americas Engineering Solutions, Inc., Baldwin, Illinois, April 24, 2024.
- [16] Ramboll Americas Engineering Solutions, "Hydrogeological Site Characterization Report, Baldwin Power Plant, Bottom Ash Pond," Ramboll Americas Engineering Solutions, Baldwin, Illinois, October 25, 2021.
- [17] Ramboll, "Groundwater Modeling Technical Memorandum, Baldwin Power Plant, Fly Ash Pond System," Ramboll, Baldwin, Illinois, January 2024.

DRAFT

TABLES

DRAFT

Table 1. Proposed Milestone Schedule for Implementing Corrective Action Remedy (Groundwater Management System)

Corrective Action Plan

Baldwin Power Plant

Fly Ash Pond System

Baldwin, IL

| Implementation Phase | Implementation Task | Timeframe (Preliminary Estimates) |
|---|---|---|
| 1: Pre-Construction Activities | Agency Coordination, Approvals, and Permitting | 6 to 12 months |
| | Final Design and Bid Process | 24 to 36 months |
| | Timeframe to Complete Corrective Pre-Construction Activities | 30 to 48 months after CAP Approval |
| 2: Corrective Action Construction | Corrective Action Construction | 12 to 24 months |
| | Timeframe to Complete Corrective Construction | 12 to 24 months after completion of pre-construction activities |
| 3: Corrective Action O&M and Closeout | Corrective Action Monitoring (Time to Meet GWPS) | >100 years |
| | Corrective Action Confirmation Monitoring | 36 months |
| | Corrective Action Completion | 6 months |
| | Timeframe to Complete Corrective Action O&M and Closeout | >100 years after completion of construction activities |
| Total Timeline to Complete Corrective Action | | >100 years |

**APPENDIX A
CORRECTIVE ACTION ALTERNATIVES ANALYSIS
(845.670(E)), INCLUDING CORRECTIVE MEASURES
ASSESSMENT (845.660)**

Corrective Action Alternatives Analysis for the Fly Ash Pond System at the Baldwin Power Plant, Village of Baldwin, Illinois

February 14, 2025



GRADIENT

www.gradientcorp.com

One Beacon Street, 17th Floor
Boston, MA 02108
617-395-5000

Table of Contents

| | <u>Page</u> |
|--|-------------|
| Summary of Findings..... | S-1 |
| 1 Introduction | 1 |
| 1.1 Site Description and History | 1 |
| 1.1.1 Site Location and History | 1 |
| 1.1.2 CCR Impoundment..... | 1 |
| 1.1.3 Surface Water Hydrology..... | 2 |
| 1.1.4 Hydrogeology..... | 3 |
| 1.1.5 Site Vicinity | 3 |
| 1.2 Part 845 Regulatory Review and Requirements | 4 |
| 2 Corrective Action Alternatives Analysis..... | 5 |
| 2.1 Corrective Action Alternative Descriptions..... | 5 |
| 2.1.1 Alternative 1: Source Control-GWP | 6 |
| 2.1.2 Alternative 2: Source Control-Cutoff Wall | 8 |
| 2.1.3 Alternative 3: Source Control-GMS..... | 10 |
| 2.2 Long- and Short-Term Effectiveness and Protectiveness of Corrective Action Alternative (IAC Section 845.670(e)(1)) | 13 |
| 2.2.1 Magnitude of Reduction of Existing Risks/Be Protective of Human Health and the Environment (IAC Section 845.670(e)(1)(A)/IAC Section 845.670(d)(1)) | 13 |
| 2.2.2 Effectiveness of the Remedy in Controlling the Source (IAC Section 845.670(e)(2)/IAC Section 845.670(d)(3))..... | 13 |
| 2.2.3 Likelihood of Future Releases of CCR (IAC Section 845.670(e)(1)(B)) | 14 |
| 2.2.4 Type and Degree of Long-Term Management, Including Monitoring, Operation, and Maintenance (IAC Section 845.670(e)(1)(C)) | 15 |
| 2.2.5 Short-Term Risks to the Community or the Environment During Implementation of Remedy (IAC Section 845.670(e)(1)(D)) | 16 |
| 2.2.5.1 Safety Impacts | 16 |
| 2.2.5.2 Cross-Media Impacts to Air | 19 |
| 2.2.5.3 Cross-Media Impacts to Surface Water and Sediments..... | 19 |
| 2.2.5.4 Control of Exposure to Any Residual Contamination During Implementation of the Remedy..... | 20 |
| 2.2.5.5 Other Identified Impacts..... | 20 |
| 2.2.6 Time Until Groundwater Protection Standards Are Achieved/Attain the Groundwater Protection Standards Specified in Section 845.600 (IAC Section 845.670(e)(1)(E)/IAC Section 845.680(d)(2)) | 22 |

| | | |
|------------------|--|----|
| 2.2.7 | Potential for Exposure of Humans and Environmental Receptors to Remaining Wastes, Considering the Potential Threat to Human Health and the Environment Associated with Excavation, Transportation, Re-disposal, Containment, or Changes in Groundwater Flow (IAC Section 845.670(e)(1)(F)) | 23 |
| 2.2.8 | Long-Term Reliability of the Engineering and Institutional Controls (IAC Section 845.670(e)(1)(G)) | 24 |
| 2.2.9 | Potential Need for Replacement of the Remedy (IAC Section 845.670(e)(1)(H)) | 25 |
| 2.3 | The Ease or Difficulty of Implementing a Remedy (IAC Section 845.670 (e)(3)) .. | 26 |
| 2.3.1 | Degree of Difficulty Associated with Constructing the Remedy (IAC Section 845.670(e)(3)(A))..... | 26 |
| 2.3.2 | Expected Operational Reliability of the Remedy (IAC Section 845.670(e)(3)(B)) | 27 |
| 2.3.3 | Need to Coordinate with and Obtain Necessary Approvals and Permits from Other Agencies (IAC Section 845.670(e)(3)(C)) | 27 |
| 2.3.4 | Availability of Necessary Equipment and Specialists (IAC Sections 845.670(e)(3)(D) and 845.660(c)(1), "Ease of Implementation") | 28 |
| 2.3.5 | Available Capacity and Location of Needed Treatment, Storage, and Disposal Services/Comply with Standards for Management of Wastes as Specified in Section 845.680(d) (IAC Section 845.670(e)(3)(D)/IAC Section 845.670(d)(5)) | 29 |
| 2.4 | The Degree to Which Community Concerns Are Addressed by the Remedy (IAC Section 845.670(e)(4))..... | 30 |
| 2.5 | Remove From the Environment as Much of the Contaminated Material that Was Released from the CCR Surface Impoundment as Is Feasible, Taking into Account Factors such as Avoiding Inappropriate Disturbance of Sensitive Ecosystems (IAC Section 845.670(d)(4)) | 30 |
| 2.6 | Summary | 31 |
| References | | 32 |
| Appendix A | Human Health and Ecological Risk Assessment | |
| Appendix B | Corrective Action Alternatives Analysis – Supporting Information Report | |
| Appendix C | Corrective Measures Assessment | |
| Appendix D | Nature and Extent Report | |
| Appendix E | Groundwater Polishing Report | |

List of Tables

| | |
|-----------|--|
| Table S.1 | Comparison of Proposed Corrective Action Alternatives with Respect to Factors Specified in IAC Section 845.670(d) and IAC Section 845.670(e) |
| Table 2.1 | Key Parameters for the Source Control-Cutoff Wall Corrective Action Alternative |
| Table 2.2 | Key Parameters for the Source Control-GMS Corrective Action Alternative |
| Table 2.3 | Expected Number of On-Site Worker Accidents Under Each Corrective Action Alternative |
| Table 2.4 | Expected Number of Off-Site Worker Accidents Related to Off-Site Car and Truck Use Under Each Corrective Action Alternative |
| Table 2.5 | Expected Number of Community Accidents Under Each Corrective Action Alternative |
| Table 2.6 | Estimated Timeline and Implementation Schedule Under Each Corrective Action Alternative |

List of Figures

| | |
|------------|-------------------|
| Figure 1.1 | Site Location Map |
|------------|-------------------|

Abbreviations

| | |
|----------------------------|---|
| BAP | Bottom Ash Pond |
| BCU | Bedrock Confining Unit |
| BEC | Baldwin Energy Complex |
| bgs | Below Ground Surface |
| BMP | Best Management Practice |
| BPP | Baldwin Power Plant |
| BU | Bedrock Unit |
| CAA | Closure Alternatives Analysis |
| CAAA | Corrective Action Alternatives Analysis |
| CCR | Coal Combustion Residual |
| CIP | Closure-in-Place |
| CMA | Corrective Measures Assessment |
| CO | Carbon Monoxide |
| CO ₂ | Carbon Dioxide |
| CSM | Conceptual Site Model |
| CY | Cubic Yard |
| DMG | Dynegy Midwest Generation, LLC |
| FAPS | Fly Ash Pond System |
| GHG | Greenhouse Gas |
| GMP | Groundwater Monitoring Plan |
| GMS | Groundwater Management System |
| GWP | Groundwater Polishing |
| GWPS | Groundwater Protection Standard |
| IAC | Illinois Administrative Code |
| IDNR | Illinois Department of Natural Resources |
| IEPA | Illinois Environmental Protection Agency |
| MEP | Mechanical, Electrical, and Piping |
| N ₂ O | Nitrous Oxide |
| NO _x | Nitrogen Oxides |
| NPDES | National Pollutant Discharge Elimination System |
| O&M | Operations and Maintenance |
| PM | Particulate Matter |
| PMP | Potential Migration Pathway |
| QA | Quality Assurance |
| QC | Quality Control |
| SFWA | State Fish and Wildlife Area |
| SI | Surface Impound |
| Source Control-Cutoff Wall | Source Control with a Groundwater Cutoff Wall |
| Source Control-GMS | Source Control with Groundwater Management System |
| Source Control-GWP | Source Control with Groundwater Polishing |
| UA | Uppermost Aquifer |
| UGU | Upper Groundwater Unit |
| US DOT | United States Department of Transportation |

US EPA
UU
VOC

United States Environmental Protection Agency
Upper Unit
Volatile Organic Compound

DRAFT

Summary of Findings

Title 35, Part 845 of the Illinois Administrative Code (IAC) (IEPA, 2021) requires that a Corrective Action Alternatives Analysis (CAAA) be performed as part of the remedy selection, prior to undertaking any corrective actions at certain coal combustion residual (CCR)-containing impoundments, where exceedances of groundwater protection standards (GWPSs) have been identified. This report presents a CAAA for the Fly Ash Pond System (FAPS) at the Baldwin Power Plant (BPP) pursuant to the requirements under IAC Section 845.670. The goal of performing a CAAA is to holistically evaluate the potentially viable corrective actions identified in the Corrective Measures Assessment (CMA; Appendix C; Ramboll, 2024a) in order to remediate groundwater and achieve compliance with the groundwater protection standards (GWPSs) specified under IAC Section 845.600 (IEPA, 2021). This analysis assesses potentially viable corrective action alternatives based on a wide range of factors, including the efficiency, reliability, and ease of implementation of a corrective action, its potential positive and negative short- and long-term impacts on human health and the environment, and its ability to address concerns raised by the community (IEPA, 2021).

It is important to note that many CCR sites are complex groundwater environments where remedial actions would inherently take many years to complete. While no formal definition of a complex groundwater environment exists, most would agree that there are a number of common characteristics at complex groundwater sites, including the following (National Research Council, 2013):

- Highly heterogeneous subsurface environments;
- Large source zones;
- Multiple, recalcitrant constituents; and
- Long timeframes over which releases occurred.

Each of these characteristics are common at CCR sites. Surface impoundments are often tens to hundreds of acres in size and many have operated for decades, leading to large source zones and prolonged releases. Furthermore, CCR impoundments are often located in alluvial geologic settings where sands are interbedded with silts and clays. This results in a heterogeneous environment where constituent mass may persist for many years in low-permeability deposits. Finally, the constituents that are most common at CCR sites include metals and inorganics that do not naturally biodegrade. The combination of these factors results in a complex groundwater environment where remediation, even under the best of circumstances, may take many years to achieve GWPSs. It is for these reasons that the United States Environmental Protection Agency (US EPA) refused to specify what is a reasonable *versus* an unreasonable timeframe for groundwater corrective actions at CCR sites, stating that it "was truly unable to establish an outer limit on the necessary timeframes – including even a presumptive outer bound" (US EPA, 2015a, p. 21,419).

In this CAAA, all corrective actions that have been evaluated consist of source control and residual plume management. Source control is generally considered to be one of the more effective remedial action approaches. Source control involves removing the hydraulic head from an impoundment (*i.e.*, unwatering and dewatering) and preventing further downward migration of constituents. US EPA has found that "releases from surface impoundments [to groundwater] drop dramatically after closure" (US EPA, 2014, pp. 5-18 to 5-19). US EPA has also stated that source control is the most effective means of ensuring the

timely attainment of remediation objectives (US EPA, 2015b). As a result, the implementation of source control often has a substantial and immediate effect on groundwater quality improvements.

The specific source control method that is the central component of all the corrective action alternatives evaluated in this CAAA is closure-in-place (CIP). This approach was approved by IEPA in 2016 and CIP was completed in 2020 (Morris, 2020). The source control included removing water and installation of a final cover system in accordance with CFR Part 257, Subpart D to "minimize water infiltration into the closed FAPS and improve surface water drainage off the cover system, thus reducing generation of potentially impacted water and ultimately reducing the extent of CCR impacts to groundwater" (Appendix C; Ramboll, 2024a). The final cover system includes a 6-inch (in) vegetative layer and an 18-in layer of overlying barrier soil. Groundwater modeling performed in support of the Closure Plan suggested that the source control approach would provide hydraulic control of surface water run-off from the cover system and a decrease in groundwater concentrations and the off-Site transport of CCR constituents (*i.e.*, reduction in plume extent) (NRT, 2014a,b; Burns & McDonnell, 2021). Due to the reduction in the hydraulic flux out of the FAPS, the mass flux out of the FAPS would also be controlled or minimized.

Three potential corrective actions are evaluated in this CAAA: Source Control with Groundwater Polishing (Source Control-GWP), Source Control with a Groundwater Cutoff Wall (Source Control-Cutoff Wall) and Source Control with Groundwater Management System (Source Control-GMS); all alternatives consist of source control and residual plume management and all were identified as viable approaches in the CMA (Appendix C; Ramboll, 2024a). The residual plume management portions of these corrective action alternatives include groundwater polishing (GWP), a groundwater cutoff wall, and a groundwater management system (GMS).

Under the Source Control-GWP alternative, constituent concentrations in groundwater over time would be actively monitored to ensure the improvement of downgradient groundwater quality resulting from physical and geochemical attenuation mechanisms. Site-specific evaluations demonstrated that groundwater polishing is appropriate at the FAPS because Site conditions are favorable for physical and geochemical processes of inorganic contaminants *via* adsorption (Appendix E; Geosyntec Consultants, Inc., 2025). Under the Source Control-Cutoff Wall alternative, a low-permeability barrier wall would be installed within the FAPS along the southern dike extending west to the tertiary pond. The cutoff wall would be approximately 7,000 feet (ft) in length, 2 to 3 ft in width, and have a maximum depth of 85 ft below ground surface (bgs). The cutoff wall would serve as a maintenance-free physical barrier reducing the potential for CCR constituents to migrate beyond the southern property boundary. Under the Source Control-GMS alternative, a groundwater extraction system would be constructed within the interior of the FAPS to remove impacted water, reduce hydraulic head beneath the existing cover system, and prevent the migration of CCR constituents in groundwater beyond the southern property boundary. The extraction trench would extend to a depth of 50 to 60 ft bgs and be 8,700 ft long, and 2 to 3 ft wide. The trench would be backfilled with clean granular fill and capped with compacted clay to reduce surface water infiltration. The collection pipes would drain to sumps spaced throughout the trench to extract liquids. Extracted liquids would be collected and sent to an on-Site pond and discharged through either a new or existing outfall managed under the National Pollutant Discharge Elimination System (NPDES) permit for the Site. As part of each corrective action alternative, an adaptive site management plan would be implemented in order to optimize the selected remedy based on real-time data that are collected.

Table S.1 evaluates all corrective actions alternatives (Source Control-GWP, Source Control-Cutoff Wall and Source Control-GMS) with regard to each of the factors specified under IAC Section 845.670(d) and IAC Section 845.670(e) (IEPA, 2021). Based on this evaluation and the details provided in Section 2 of this report, the most appropriate corrective action for this Site is Source Control-GMS. While the time to

achieve GWPSs for all three alternatives was predicted to be in excess of 100 years¹ due to the presence of native low-permeability lithological units, groundwater modeling suggests that Source Control-GMS would be most effective at reducing plume size and minimizing the risk of CCR constituents migrating beyond the Site's southern property boundary. Thus, Source Control-GMS is the most appropriate corrective action alternative for the FAPS.

DRAFT

¹ While the model simulation period for each corrective action alternative was 1,000 years, model predictions at such lengthy future timescales are inherently uncertain.

Table S.1 Comparison of Proposed Corrective Action Alternatives with Respect to Factors Specified in IAC Section 845.670(d) and IAC Section 845.670(e)

| Evaluation Factor (Report Section; Part 845 Section) | Source Control-GWP | Source Control-Cutoff Wall | Source Control-GMS |
|---|---|--|--|
| Magnitude of Reduction of Existing Risks/Be Protective of Human Health and the Environment (Section 2.2.1; IAC Section 845.670(e)(1)(A)/ IAC Section 845.670(d)(1)) | Because current conditions do not present a risk to human health or the environment at the FAPS, there will be no unacceptable risk to human health or the environment for future conditions since the unit was closed and source control was implemented. Concentrations of CCR-related constituents will decline over time, and consequently, potential exposures to CCR-related constituents in the environment will also decline. The magnitude of the reduction of existing risks is the same for all the potential corrective action alternatives, and all three corrective action alternatives are equally protective of human health and the environment. | Because current conditions do not present a risk to human health or the environment at the FAPS, there will be no unacceptable risk to human health or the environment for future conditions since the unit was closed and source control was implemented. Concentrations of CCR-related constituents will decline over time and, consequently, potential exposures to CCR-related constituents in the environment will also decline. The magnitude of the reduction of existing risks is the same for all of the potential corrective action alternatives, and all three corrective action alternatives are equally protective of human health and the environment. | Because current conditions do not present a risk to human health or the environment at the FAPS, there will be no unacceptable risk to human health or the environment for future conditions since the unit was closed and source control was implemented. Concentrations of CCR-related constituents will decline over time and, consequently, potential exposures to CCR-related constituents in the environment will also decline. The magnitude of the reduction of existing risks is the same for all of the potential corrective action alternatives, and all three corrective action alternatives are equally protective of human health and the environment. |
| Effectiveness of the Remedy in Controlling the Source (Section 2.2.2; IAC Section 845.670(e)(2)) | | | |
| Extent to Which Containment Practices Will Reduce Further Releases/Control the Sources of Releases to Reduce or Eliminate, to the Maximum Extent Feasible (IAC Section 845.670(e)(2)(A)/ IAC Section 845.670(d)(3)) | All three alternatives include source control (which is the primary remedial measure) and residual plume management. Source control (IEPA approved CIP approach) was implemented in 2020. These source control activities would control surface water run-off on the cover system and in the surrounding area, reduce leachate concentrations, and "decrease | All three alternatives include source control (which is the primary remedial measure) and residual plume management. Source control (IEPA approved CIP approach) was implemented in 2020. These source control activities would control surface water run-off on the cover system and in the surrounding area, reduce leachate concentrations, and "decrease transport | All three alternatives include source control (which is the primary remedial measure) and residual plume management. Source control (IEPA approved CIP approach) was implemented in 2020. These source control activities would control surface water run-off on the cover system and in the surrounding area, reduce leachate concentrations, and "decrease transport |

| Evaluation Factor (Report Section; Part 845 Section) | Source Control-GWP | Source Control-Cutoff Wall | Source Control-GMS |
|---|---|--|---|
| | <p>transport [of CCR constituents] off-[S]ite both spatially and temporally" (Burns & McDonnell, 2021), controlling to the maximum extent feasible, the migration of CCR constituents in groundwater.</p> <p>Under the residual plume management for this alternative, physical and geochemical attenuation mechanisms would mitigate impacts to downgradient groundwater quality and control the residual plume (Appendix E; Geosyntec Consultants, Inc., 2025). If necessary, remedy optimizations would be implemented under the adaptive site management program.</p> | <p>[of CCR constituents] off-[S]ite both spatially and temporally" (Burns & McDonnell, 2021), controlling to the maximum extent feasible, the migration of CCR constituents in groundwater.</p> <p>Under the residual plume management for this alternative, a cutoff wall would be constructed to reduce potential CCR-constituents in groundwater from migrating off-Site. Physical and geochemical attenuation would also help control impacts to downgradient groundwater quality (Appendix E; Geosyntec Consultants, Inc., 2025). If necessary, remedy optimizations would be implemented under the adaptive site management program.</p> | <p>[of CCR constituents] off-[S]ite both spatially and temporally" (Burns & McDonnell, 2021), controlling to the maximum extent feasible, the migration of CCR constituents in groundwater.</p> <p>Under the residual plume management for this alternative, groundwater extraction trenches would remove impacted groundwater and control migration of impacted groundwater off-Site. Physical and geochemical attenuation mechanisms would also help mitigate impacts to the downgradient groundwater quality and control the residual plume (Appendix E; Geosyntec Consultants, Inc., 2025). If necessary, remedy optimizations would be implemented under the adaptive site management program.</p> |
| Extent to Which Treatment Technologies May Be Used (IAC Section 845.670(e)(2)(B)) | Source Control-GWP would rely on physical and geochemical attenuation processes. If necessary, remedy optimizations would be implemented under the adaptive site management program. | The Source Control-Cutoff Wall alternative focuses on preventing groundwater migration using an engineered physical barrier. No additional treatment technologies would be required once the cutoff wall has been constructed. The remedy also relies on physical and geochemical attenuation processes. If necessary, remedy optimizations would be implemented under the adaptive site management program. | The Source Control-GMS alternative would require utilization of an on-Site settling pond to settle solids from extracted groundwater, prior to discharge <i>via</i> an NPDES permitted outfall. Additional methods for treating extracted groundwater may be evaluated at later phases of designs. The remedy would also rely on physical and geochemical attenuation processes. If necessary, remedy optimizations would be implemented under the adaptive site management program. |

| Evaluation Factor (Report Section; Part 845 Section) | Source Control-GWP | Source Control-Cutoff Wall | Source Control-GMS |
|---|---|---|---|
| Likelihood of Future Releases of CCR (Section 2.2.3; IAC Section 845.670(e)(1)(B)) | All three corrective action alternatives include source control using CIP; the CIP source control installation was approved by IEPA and completed in 2020. A new cover system consisting of a 6-in vegetative layer and an 18-in layer of overlying barrier soil was installed over the FAPS in compliance with 40 CFR Part 257, Subpart D. Relative to pre-closure conditions, this cover system provides increased protection against berm and surface erosion, precipitation infiltration, and other adverse effects that could potentially trigger a release of CCR. There would be minimal risk of accidental CCR releases occurring post-closure under any of the alternatives. | All three corrective action alternatives include source control using CIP; the CIP source control installation was approved by IEPA and completed in 2020. A new cover system consisting of a 6-in vegetative layer and an 18-in layer of overlying barrier soil was installed over the FAPS in compliance with 40 CFR Part 257, Subpart D. Relative to pre-closure conditions, this cover system provides increased protection against berm and surface erosion, precipitation infiltration, and other adverse effects that could potentially trigger a release of CCR. There would be minimal risk of accidental CCR releases occurring post-closure under any of the alternatives. | All three corrective action alternatives include source control using CIP; the CIP source control installation was approved by IEPA and completed in 2020. A new cover system consisting of a 6-in vegetative layer and an 18-in layer of overlying barrier soil was installed over the FAPS in compliance with 40 CFR Part 257, Subpart D. Relative to pre-closure conditions, this cover system provides increased protection against berm and surface erosion, precipitation infiltration, and other adverse effects that could potentially trigger a release of CCR. There would be minimal risk of accidental CCR releases occurring post-closure under any of the alternatives. |
| Type and Degree of Long-Term Management, Including Monitoring, Operation, and Maintenance (Section 2.2.4; IAC Section 845.670(e)(1)(C)) | <p>Minimal long-term O&M efforts would be required under Source Control-GWP because it would not require the installation, operation, or maintenance of any engineered systems or structures other than maintenance of the monitoring wells. Corrective action groundwater monitoring would continue until GWPSs have been achieved.</p> <p>Post-closure care groundwater monitoring would continue for a minimum of 30 years, as required by IAC Section 845.780(c). Additionally, corrective action groundwater monitoring would continue for 3 years</p> | <p>Construction of the cutoff wall would occur in three phases. Once the cutoff wall has been installed, no O&M efforts would be required because it is a passive and below-grade structure. However, post-construction quality assurance (QA) programs may be required to validate the quality of the constructed cutoff wall. Corrective action groundwater sampling would continue until GWPSs have been achieved.</p> <p>Post-closure care groundwater monitoring will continue for a minimum of 30 years, as required by IAC Section. 845.780(c). Additionally, corrective action groundwater</p> | <p>Construction of the GMS would occur in three phases. Once the GMS has been installed, corrective action O&M would require regular inspection and maintenance of the extraction trench system, which includes maintaining pumps, conveyance lines, air compressors, <i>etc.</i>, which are essential components of the Mechanical, Electrical, and Piping (MEP) system. Routine monitoring and compliance associated with extracted groundwater discharge <i>via</i> a new or existing NPDES outfall to Kaskaskia River would also be required.</p> |

| Evaluation Factor (Report Section; Part 845 Section) | Source Control-GWP | Source Control-Cutoff Wall | Source Control-GMS |
|--|--|--|---|
| | after GWPS have been achieved. Based on the adaptive site management approach, remedy optimizations (additional methods or techniques) might be implemented to ensure achievement of the GWPSs. | monitoring would continue for 3 years after GWPS have been achieved. Based on the adaptive site management approach, remedy optimizations (additional methods or techniques) may be implemented to ensure achievement of the GWPSs. | Post-closure care groundwater monitoring will continue for a minimum of 30 years, as required by IAC Section. 845.780(c). Additionally, corrective action groundwater monitoring would continue for 3 years after GWPS have been achieved. Based on the adaptive site management approach, remedy optimizations (additional methods or techniques) may be implemented to ensure achievement of the GWPSs. |
| Short-Term Risks to the Community or the Environment During Implementation of Remedy (Section 2.2.5; IAC Section 845.670(e)(1)(D)) | | | |
| Safety Impacts | <p>Source control (IEPA approved CIP approach) was implemented in 2020. Thus, there is no further risk of accidents and injuries occurring during the implementation of the source control remedy.</p> <p>Overall, no worker accidents or injuries would be expected under the Source Control-GWP alternative because no installation, operation, and maintenance of engineered systems or structures would be required.</p> <p>Similarly, no off-Site impacts on nearby residents would be expected under the Source Control-GWP alternative.</p> | <p>Source control (IEPA approved CIP approach) was implemented in 2020. Thus, there is no further risk of accidents and injuries occurring during the implementation of the source control remedy.</p> <p>Overall, considering worker accidents occurring during residual plume management both on- and off-Site, 0.37 worker injuries and 0.015 worker fatalities would be expected under the Source Control-Cutoff Wall alternative.</p> <p>In total, an estimated 0.22 injuries and 1.7×10^{-3} fatalities would be expected to occur among community members due</p> | <p>Source control (IEPA approved CIP approach) was implemented in 2020. Thus, there is no further risk of accidents and injuries occurring during the implementation of the source control remedy.</p> <p>Overall, considering worker accidents occurring during residual plume management both on- and off-Site, 0.72 worker injuries and 0.021 worker fatalities would be expected under the Source Control-GMS alternative, which is the highest among the three alternatives.</p> |

| Evaluation Factor (Report Section; Part 845 Section) | Source Control-GWP | Source Control-Cutoff Wall | Source Control-GMS |
|--|--|--|--|
| | | to off-Site activities under the Source Control-Cutoff Wall alternative, which is higher than the injuries and fatalities expected under the Source Control-GWP alternative. | In total, an estimated 0.28 injuries and 2.2×10^{-3} fatalities would be expected to occur among community members due to off-Site activities under the Source Control-GMS alternative, which is the highest among the three alternatives. |
| Cross-Media Impacts to Air | <p>Source control (IEPA approved CIP approach) was implemented in 2020. No further air impacts associated with the implementation of the source control remedy are expected.</p> <p>Cross-media impacts to air associated with residual plume management can result from the emission of air pollutants and greenhouse gases (GHGs) from construction vehicles and equipment. These emissions are proportional to the use of construction vehicles and equipment that are required for residual plume management. Residual plume management for the Source Control-GWP alternative would be expected to have minimal air impacts, because it would not require the construction of any engineered systems or structures.</p> | <p>Source control (IEPA approved CIP approach) was implemented in 2020. No further air impacts associated with the implementation of the source control remedy are expected.</p> <p>Cross-media impacts to air associated with residual plume management can result from the emission of air pollutants and GHGs from construction vehicles and equipment. These emissions are proportional to the use of construction vehicles and equipment that are required for residual plume management. Residual plume management for the Source Control-Cutoff Wall alternative would have greater air impacts than the Source Control-GWP alternative due to the increased construction activity required for this alternative.</p> | <p>Source control (IEPA approved CIP approach) was implemented in 2020. No further air impacts associated with the implementation of the source control remedy are expected.</p> <p>Cross-media impacts to air associated with residual plume management can result from the emission of air pollutants and GHGs from construction vehicles and equipment. These emissions are proportional to the use of construction vehicles and equipment that are required for residual plume management. Residual plume management for the Source Control-GMS alternative would have greatest air impacts among all three alternatives due to the highest vehicle and equipment travel miles under this alternative.</p> |
| Cross-Media Impacts to Surface Water and Sediments | Source control was implemented in 2020; as a result, constituent mass flux from groundwater into surface water will decline over time (OBG, 2019). The source control approach included dewatering, which removed hydraulic head within the impoundment, and has | Source control was implemented in 2020; as a result, constituent mass flux from groundwater into surface water will decline over time (OBG, 2019). The source control approach included dewatering, which removed hydraulic head within the impoundment, and has | Source control was implemented in 2020; as a result, constituent mass flux from groundwater into surface water will decline over time (OBG, 2019). The source control approach included dewatering, which removed hydraulic head within the impoundment, and has |

| Evaluation Factor (Report Section; Part 845 Section) | Source Control-GWP | Source Control-Cutoff Wall | Source Control-GMS |
|---|--|---|---|
| | <p>"significantly reduced infiltration rates relative to pre-closure conditions" (Appendix C, Ramboll, 2024a). Due to the reduction in the hydraulic flux out of the FAPS, the mass flux out of the FAPS would also be controlled or minimized. Groundwater modeling performed in support of the Closure Plan suggested that the source control would control surface water run-off on the cover system, lower water levels in the FAPS, reduce groundwater concentrations, and decrease the potential off-Site transport of CCR constituents (NRT, 2014a,b; Burns & McDonnell, 2021).</p> <p>Under the Source Control-GWP alternative, minimal surface water and sediment impacts would be expected, because this alternative would not require the construction of any engineered systems or structures.</p> | <p>"significantly reduced infiltration rates relative to pre-closure conditions" (Appendix C, Ramboll, 2024a). Due to the reduction in the hydraulic flux out of the FAPS, the mass flux out of the FAPS would also be controlled or minimized. Groundwater modeling performed in support of the Closure Plan suggested that the source control would control surface water run-off on the cover system, lower water levels in the FAPS, reduce groundwater concentrations, and decrease the potential off-Site transport of CCR constituents (NRT, 2014a,b; Burns & McDonnell, 2021).</p> <p>Under residual plume management for the Source Control-Cutoff Wall alternative, surface water and sediment impacts would be higher than the Source Control-GWP alternative due to the construction of the cutoff wall. Any associated impacts would be addressed through best management practices (BMPs) in accordance with Site land disturbance permits.</p> | <p>"significantly reduced infiltration rates relative to pre-closure conditions" (Appendix C, Ramboll, 2024a). Due to the reduction in the hydraulic flux out of the FAPS, the mass flux out of the FAPS would also be controlled or minimized. Groundwater modeling performed in support of the Closure Plan suggested that the source control would control surface water run-off on the cover system, lower water levels in the FAPS, reduce groundwater concentrations, and decrease the potential off-Site transport of CCR constituents (NRT, 2014a,b; Burns & McDonnell, 2021).</p> <p>Under residual plume management for the Source Control-GMS alternative, surface water and sediment impacts would be higher than the Source Control-GWP alternative due to construction of the GMS. Any associated impacts would be addressed through BMPs in accordance with Site land disturbance permits.</p> |
| Control of Exposure to Any Residual Contamination During Implementation of the Remedy | <p>Source control (IEPA approved CIP approach) was implemented in 2020. Thus, there are no further risks of CCR exposure associated with source control implementation.</p> <p>Risks to workers arising from potential contact with residual contamination during construction activities associated</p> | <p>Source control (IEPA approved CIP approach) was implemented in 2020. Thus, there are no further risks of CCR exposure associated with source control implementation.</p> <p>Risks to workers arising from potential contact with residual contamination during construction activities associated</p> | <p>Source control (IEPA approved CIP approach) was implemented in 2020. Thus, there are no further risks of CCR exposure associated with source control implementation.</p> <p>Risks to workers arising from potential contact with residual contamination during construction activities associated</p> |

| Evaluation Factor (Report Section; Part 845 Section) | Source Control-GWP | Source Control-Cutoff Wall | Source Control-GMS |
|--|--|---|--|
| | with residual plume management would be minimal under the Source Control-GWP alternative, which would not involve exposure to soil or groundwater waste streams. | with residual plume management would be higher for the Source Control-Cutoff Wall alternative than for the Source Control-GWP alternative because the Source Control-Cutoff Wall alternative would involve excavation and disposal of excavated spoils from trenching. Any potential CCR-exposures during the Source Control-Cutoff Wall alternative would be managed through the use of rigorous safety protocols and personal protective equipment. | with residual plume management would be higher for the Source Control-GMS alternative than for the Source Control-GWP alternative, because the Source Control-GMS alternative would involve the production, management, and treatment of extracted groundwater, as well as off-Site disposal of excavated spoils generated during extraction trench. Any potential CCR-exposures during the Source Control-GMS alternative would be managed through the use of rigorous safety protocols and personal protective equipment. |
| Other Identified Impacts | <p>Source control (IEPA approved CIP approach) was implemented in 2020. Thus, there are no further impacts associated with the implementation of source control.</p> <p>The energy demands of construction equipment and vehicles associated with residual plume management would be lowest under the Source Control-GWP alternative, because this alternative would not require any significant construction or maintenance activity.</p> <p>Traffic and noise impacts associated with residual plume management are expected to be higher under the Source Control-Cutoff Wall and Source Control-GMS alternatives than the Source Control-GWP alternative, due to the construction activities that would be</p> | <p>Source control (IEPA approved CIP approach) was implemented in 2020. Thus, there are no further impacts associated with the implementation of source control.</p> <p>The energy demands of construction equipment and vehicles associated with residual plume management would be greater under the Source Control-Cutoff Wall compared to the Source Control-GWP alternative, because the Source Control-Cutoff Wall alternative would involve the construction of the barrier wall.</p> <p>Traffic and noise impacts associated with residual plume management are expected to be higher under the Source Control-Cutoff Wall alternative than the Source Control-GWP alternative due to</p> | <p>Source control (IEPA approved CIP approach) was implemented in 2020. Thus, there are no further impacts associated with the implementation of source control.</p> <p>The energy demands of construction equipment and vehicles associated with residual plume management would be greater under the Source Control-GMS compared to the Source Control-GWP alternative, because the Source Control-GMS alternative would involve construction activity and operation associated with the extraction trench and the settling pond.</p> <p>Traffic and noise impacts associated with residual plume management are expected to be higher under the Source Control-GMS alternative than the</p> |

| Evaluation Factor (Report Section; Part 845 Section) | Source Control-GWP | Source Control-Cutoff Wall | Source Control-GMS |
|--|---|--|--|
| | <p>required to construct the cutoff wall and the GMS. Traffic and noise impacts associated with residual plume management from the Source Control-GWP are expected to be minimal due to the limited amount of construction required.</p> <p>There would be no impacts to natural resources and habitat under the Source Control-GWP alternative, because no additional construction activities would be required.</p> | <p>the construction activities required to construct the barrier wall.</p> <p>Under the Source Control-Cutoff Wall alternative, some negative impacts on scenic and recreational value may occur along the Kaskaskia River, which is located approximately 0.5 mile west of the outer perimeter of the FAPS within the Kaskaskia River Watershed. A campground, the Wood Duck Marina, and the Baldwin Cemetery are in the vicinity of the Site. Given the proximity of these areas to the expected construction, it is likely that they would experience some adverse impacts such as visual disturbances, obstruction of views, and noise during the construction period. However, these impacts are expected to diminish once the construction is completed in 12 to 24 months.</p> <p>In addition, the construction of the cutoff wall under the Source Control-Cutoff Wall alternative is expected to use a significant amount of cement or bentonite, which would be introduced into the Upper Unit (UU) and Bedrock Unit (BU). Adding substantial quantities of these materials into the subsurface environment may cause alteration in groundwater pH levels and affect geochemical conditions in the subsurface.</p> | <p>Source Control-GWP alternative due to the construction activities required for the GMS.</p> <p>Under the Source Control-Cutoff Wall alternative, some negative impacts on scenic and recreational value may occur along the Kaskaskia River, which is located approximately 0.5 mile west of the outer perimeter of the FAPS within the Kaskaskia River Watershed. A campground, the Wood Duck Marina, and the Baldwin Cemetery are in the vicinity of the Site. Given the proximity of these areas to the expected construction, it is likely that they would experience some adverse impacts such as visual disturbances, obstruction of views, and noise during the construction period. However, these impacts are expected to diminish once the construction is completed in 12 to 24 months.</p> <p>The construction activities would also likely result in some short-term negative impacts to the ecosystem in the vicinity, including disturbance of habitat near the construction areas by causing alarm and escape behavior in nearby wildlife (<i>e.g.</i>, due to noise disturbances).</p> |

| Evaluation Factor (Report Section; Part 845 Section) | Source Control-GWP | Source Control-Cutoff Wall | Source Control-GMS |
|--|---|---|---|
| | | The construction activities would also likely result in some short-term negative impacts to the ecosystem in the vicinity, including disturbance of habitat near the construction areas by causing alarm and escape behavior in nearby wildlife (<i>e.g.</i> , due to noise disturbances). | |
| Time Until Groundwater Protection Standards Are Achieved/Attain the Groundwater Protection Standards Specified in Section 845.600 (Section 2.2.6; IAC Section 845.670(e)(1)(E); IAC Section 845.670(d)(2)) | <p>Groundwater modeling in support of the Closure Plan suggested that the source control would lower water levels in the FAPS, reduce leachate concentrations, and decrease the potential transport of CCR constituents off-Site (NRT, 2014a; Burns & McDonnell, 2021).</p> <p>Additional modeling was conducted for each of the corrective action alternatives to evaluate future groundwater quality in the vicinity of the FAPS as a result of residual plume management. The results of the modeling indicate that time to achieve GWPSs for all compliance wells is in excess of 100 years for all three corrective action alternatives (Appendix B; Ramboll, 2025a). This is attributed to the underlying native lithological units beneath the CCR unit, <i>i.e.</i>, the UU and BU, which consist of low-permeability soils and underlying low-permeability shale and limestone bedrock. These conditions result in extended times to</p> | <p>Groundwater modeling in support of the Closure Plan suggested that the source control would lower water levels in the FAPS, reduce leachate concentrations, and decrease the potential transport of CCR constituents off-Site (NRT, 2014a; Burns & McDonnell, 2021).</p> <p>Additional modeling was conducted for each of the corrective action alternatives to evaluate future groundwater quality in the vicinity of the FAPS as a result of residual plume management. The results of the modeling indicate that time to achieve GWPSs for all compliance wells is in excess of 100 years for all three corrective action alternatives (Appendix B; Ramboll, 2025a). This is attributed to the underlying native lithological units beneath the CCR unit, <i>i.e.</i>, the UU and BU, which consist of low-permeability soils and underlying low-permeability shale and limestone bedrock. These conditions result in extended times to attain GWPS, regardless of the remedy (Appendix B; Ramboll, 2025a).</p> | <p>Groundwater modeling in support of the Closure Plan suggested that the source control would lower water levels in the FAPS, reduce leachate concentrations, and decrease the potential transport of CCR constituents off-Site (NRT, 2014a; Burns & McDonnell, 2021).</p> <p>Additional modeling was conducted for each of the corrective action alternatives to evaluate future groundwater quality in the vicinity of the FAPS as a result of residual plume management. The results of the modeling indicate that time to achieve GWPSs for all compliance wells is in excess of 100 years all three corrective action alternatives (Appendix B; Ramboll, 2025a). This is attributed to the underlying native lithological units beneath the CCR unit, <i>i.e.</i>, the UU and BU, which consist of low-permeability soils and underlying low-permeability shale and limestone bedrock. These conditions result in extended times to attain GWPS, regardless of the remedy (Appendix B; Ramboll, 2025a).</p> |

| Evaluation Factor (Report Section; Part 845 Section) | Source Control-GWP | Source Control-Cutoff Wall | Source Control-GMS |
|--|--|--|--|
| | <p>attain GWPS, regardless of the remedy (Appendix B; Ramboll, 2025a).</p> <p>In addition, modeling indicated that the Source Control-GWP alternative would not cause the groundwater plume to contract within the model simulation period following the implementation of the corrective action alternative.</p> | <p>In addition, modeling indicated that the Source Control-Cutoff Wall alternative would not cause the groundwater plume to contract within the model simulation period following the implementation of the corrective action alternative.</p> | <p>In addition, modeling indicated that plume extents would contract over time following the implementation of Source Control-GMS alternative from 420 acres to 193 acres during the model simulation period.</p> |
| <p>Potential for Exposure of Humans and Environmental Receptors to Remaining Wastes, Considering the Potential Threat to Human Health and the Environment Associated with Excavation, Transportation, Re-disposal, Containment, or Changes in Groundwater Flow (Section 2.2.7; IAC Section 845.670(e)(1)(F))</p> | <p>Source control (IEPA approved CIP approach) was implemented in 2020. Therefore, all three corrective action alternatives are equally and fully protective with regard to exposure to residual CCR. As a result of the source control, there are no risks of CCR releases.</p> <p>The Source Control-GWP alternative would not involve exposure to the soil or groundwater waste streams and thus, there is no potential for exposure of humans and environmental receptors to wastes.</p> | <p>Source control (IEPA approved CIP approach) was implemented in 2020. Therefore, all three corrective action alternatives are equally and fully protective with regard to exposure to residual CCR. As a result of the source control, there are no risks of CCR releases.</p> <p>For construction workers, risks arising from potential contact with residual contamination during construction, operation, and maintenance activities associated with residual plume management would be higher for the Source Control-Cutoff Wall than for the Source Control-GWP alternative, because the Source Control-Cutoff Wall alternative would involve the excavation and subsequent management of Site spoils. Any potential CCR exposures occurring under the Source Control-Cutoff Wall alternative during the installation of the cutoff wall would be managed through the use of rigorous safety protocols, personal protective</p> | <p>Source control (IEPA approved CIP approach) was implemented in 2020. Therefore, all three corrective action alternatives are equally and fully protective with regard to exposure to residual CCR. As a result of the source control, there are no risks of CCR releases.</p> <p>For construction workers, risks arising from potential contact with residual contamination during construction, operation, and maintenance activities associated with residual plume management would be higher for the Source Control-GMS alternative than for the Source Control-GWP alternative because the Source Control-GMS alternative would involve the excavation and subsequent management of Site soils, as well as the production, management, and potential treatment of extracted groundwater. Any potential CCR exposures occurring under the Source Control-GMS alternative during the installation of the</p> |

| Evaluation Factor (Report Section; Part 845 Section) | Source Control-GWP | Source Control-Cutoff Wall | Source Control-GMS |
|--|--|---|--|
| | | <p>equipment, and appropriate disposal practices.</p> <p>Hydrogeological changes would be expected under the Source Control-Cutoff Wall alternative due to the installation of a low-permeability barrier wall into the UU and BU. These changes include altering flow patterns in the UU, redirecting groundwater flow around the cutoff wall, and causing changes to normal hydraulic gradients.</p> | <p>remedy would be managed through the use of rigorous safety protocols, personal protective equipment, and appropriate disposal practices.</p> <p>Some changes in groundwater flow (<i>i.e.</i>, controlled discharge into Kaskaskia River) may occur under the Source Control-GMS alternative, due to the operation of the GMS. Hydrogeological changes would also be expected under the Source Control-GMS alternative, such as lowering groundwater table in the vicinity of the extraction trench and altering flow patterns in the UU. However, changes to groundwater flow would not be expected to have an effect on the potential for the exposure of humans and environmental receptors to remaining wastes.</p> |
| <p>Long-Term Reliability of the Engineering and Institutional Controls (Section 2.2.8; IAC Section 845.670(e)(1)(G))</p> | <p>Source control (IEPA approved CIP approach) was implemented in 2020. Thus, the long-term reliability of source control would be same for all three corrective action alternatives.</p> <p>Residual plume management under the Source Control-GWP alternative would be reliable because it would rely on physical and geochemical attenuation processes and active monitoring. If necessary, remedy optimizations would be implemented under the adaptive site management program.</p> | <p>Source control (IEPA approved CIP approach) was implemented in 2020. Thus, the long-term reliability of source control would be same for all three corrective action alternatives.</p> <p>Cutoff walls are proven remedies that have been implemented at many sites. Thus, residual plume management under the Source Control-Cutoff Wall alternative would be reliable provided it is constructed in accordance with standard design specifications. The remedy consists of a passive, below-grade structure, which would not require</p> | <p>Source control (IEPA approved CIP approach) was implemented in 2020. Thus, the long-term reliability of source control would be same for all three corrective action alternatives.</p> <p>Groundwater extraction and treatment systems are proven remedies that has been implemented at many sites. Thus, residual plume management under the Source Control-GMS alternative would be expected to be reliable provided it is constructed in accordance with standard design specifications. Under this alternative, the extraction trench</p> |

| Evaluation Factor (Report Section; Part 845 Section) | Source Control-GWP | Source Control-Cutoff Wall | Source Control-GMS |
|---|--|--|---|
| | | <p>any O&M activities once it is installed. Some challenges are expected during construction, necessitating specialized equipment deployment. Quality control (QC) and quality assurance (QA) programs would be required during the construction to ensure the effectiveness of the cutoff wall. If necessary, remedy optimizations would be implemented under the adaptive site management program.</p> | <p>system would require engineering design and installation for groundwater extraction and treatment. Routine and non-routine maintenance of the system is required to ensure reliable operation of the extraction trench and pumps, as well as other MEP system components. Active groundwater monitoring would be in place, similar to those required under the Source Control-GWP alternative. If necessary, remedy optimizations would be implemented under the adaptive site management program.</p> |
| <p>Potential Need for Replacement of the Remedy (Section 2.2.9; IAC Section 845.670(e)(1)(H))</p> | <p>Replacement of the residual plume management remedy under the Source Control-GWP alternative would likely be unnecessary, because it would not require the installation, operation, and maintenance of engineered systems or structures. Adaptive site management strategies would be used to implement remedy optimizations, if necessary, to ensure that remedial goals are achieved.</p> | <p>Replacement of the residual plume management remedy under the Source Control-Cutoff Wall alternative would likely be unnecessary, because the cutoff wall is a robust, engineered, and maintenance-free subsurface structure. Adaptive site management strategies would be used to implement remedy optimizations, if necessary, to ensure that remedial goals are achieved.</p> | <p>Replacement of the residual plume management remedy under the Source Control-GMS alternative would likely be unnecessary within its standard 50-year design lifespan because the system is anticipated to be highly reliable. However, ongoing maintenance and potential replacement of system components are expected over time; these include:</p> <ul style="list-style-type: none"> ▪ Periodic maintenance, such as jetting or redevelopment of the perforated drainpipe in the extraction trench. ▪ MEP components like pumps and instrumentation would likely require servicing or replacement every 10 to 20 years, resulting in multiple replacements over the long-term operational life of the remedy. |

| Evaluation Factor (Report Section; Part 845 Section) | Source Control-GWP | Source Control-Cutoff Wall | Source Control-GMS |
|--|---|--|--|
| | | | <ul style="list-style-type: none"> ▪ Long-term degradation or fouling of the extraction trench components, including the perforated collection pipe and backfill media, may eventually necessitate replacement. Data on the performance of such systems over a timespan in excess of 100 years is limited, as these types of systems have only been in use for about 100 years. ▪ Any future replacement of the extraction trench would be evaluated through ongoing adaptive site management activities. |
| <p>Degree of Difficulty Associated with Constructing the Remedy (Section 2.3.1; IAC Section 845.670 (e)(3)(A))</p> | <p>Source control (IEPA approved CIP approach) was implemented in 2020. Thus, there would be no further construction difficulties associated with the implementation of source control.</p> <p>Residual plume management under the Source Control-GWP alternative would rely on physical and geochemical attenuation processes, and therefore would not pose any significant construction challenges.</p> | <p>Source control (IEPA approved CIP approach) was implemented in 2020. Thus, there would be no further construction difficulties associated with the implementation of Source Control.</p> <p>Residual plume management under the Source Control-Cutoff Wall alternative would rely on a barrier wall to prevent groundwater migration off-Site, as well as physical and geochemical attenuation. Some challenges may be encountered during the construction of the cutoff wall, including the following:</p> <ul style="list-style-type: none"> ▪ Implementing the remedy entails the mobilization of specialized equipment to the Site, including large cranes, clamshells, slurry cutters, and/or one-pass trenching equipment, etc. Supporting equipment such as batch | <p>Source control (IEPA approved CIP approach) was implemented in 2020. Thus, there would be no further construction difficulties associated with the implementation of Source Control.</p> <p>Residual plume management under the Source Control-GMS alternative would utilize an extraction trench and a settling pond to extract and treat contaminated groundwater to achieve reductions in contaminant plume sizes, as well as physical and geochemical attenuation. However, there may be challenges during the implementation of the GMS, including the following:</p> <ul style="list-style-type: none"> ▪ Implementing the remedy entails the mobilization of specialized equipment to the Site, including large cranes, clamshells, slurry cutters, |

| Evaluation Factor (Report Section; Part 845 Section) | Source Control-GWP | Source Control-Cutoff Wall | Source Control-GMS |
|--|--------------------|---|--|
| | | <p>plants, excavation, and grading equipment may also be used.</p> <ul style="list-style-type: none"> Although cutoff walls are commonly constructed to similar depths in comparable geologic environments, challenges during construction may still arise. These challenges may involve encountering highly permeable layers (leading to slurry loss), obstructions that necessitate specialized techniques and/or equipment for progression, or sidewall instability. The effectiveness of the cutoff wall relies on the construction techniques employed to prevent gaps, voids, or other discontinuities in the structure. Ongoing QC/QA activities are essential to prevent such defective features. Additionally, QA programs, such as coring and testing, may be necessary to validate the quality of the constructed barrier. The performance of the wall is contingent on its actual hydraulic conductivity. This necessitates ongoing monitoring and QA/QC testing for slurry mixing, placement, or soil-bentonite mixing. The goal is to ensure adherence to the designed mix and involves routine testing of samples from the wall material. | <p>and/or one-pass trenching equipment, <i>etc.</i> Supporting equipment such as batch plants, excavation, and grading equipment may also be used.</p> <ul style="list-style-type: none"> While trenches of similar depth and geology are routinely built, challenges such as encountering obstructions may necessitate specialized techniques and/or equipment. The construction may require detailed geotechnical design for the working platform. The MEP components are commonly handled by regional or local contractors and are not expected to pose construction challenges. |

| Evaluation Factor (Report Section; Part 845 Section) | Source Control-GWP | Source Control-Cutoff Wall | Source Control-GMS |
|---|---|---|---|
| Expected Operational Reliability of the Remedy (Section 2.3.2; IAC Section 845.670 (e)(3)(B)) | <p>Source control (IEPA approved CIP approach) was implemented in 2020. The operational reliability of the source control would be the same for all three corrective action alternatives.</p> <p>Residual plume management under the Source Control-GWP alternative would have high operational reliability, because this alternative would rely on natural processes and active monitoring. Adaptive site management strategies would be used to implement remedy optimizations, if necessary.</p> | <p>Source control (IEPA approved CIP approach) was implemented in 2020. The operational reliability of the source control would be the same for all three corrective action alternatives.</p> <p>Residual plume management under the Source Control-Cutoff Wall alternative would have high operational reliability because it is an established technology, as long as the cutoff wall is constructed in accordance with standard design specifications. No O&M would be required after its installation. Adaptive site management strategies would be used to implement remedy optimizations, if necessary.</p> | <p>Source control (IEPA approved CIP approach) was implemented in 2020. The operational reliability of the source control would be the same for all three corrective action alternatives.</p> <p>Residual plume management under the Source Control-GMS alternative would also have high operational reliability because it is an established technology as long as the GMS (the extraction trench and the MEP system) is constructed in accordance with standard design specifications. In addition, the remedy would require routine and non-routine maintenance of the mechanical system to ensure reliable operation.</p> <p>Adaptive site management strategies would be used to implement remedy optimizations, if necessary.</p> |
| Need to Coordinate with and Obtain Necessary Approvals and Permits from Other Agencies (Section 2.3.3; IAC Section 845.670 (e)(3)(C)) | <p>Specific permits and approvals associated with source control were the same for all corrective action alternatives and were discussed in the Closure Plan (AECOM, 2016a).</p> <p>Residual plume management under the Source Control-GWP alternative would not need additional permits from other agencies, other than the approval of the Corrective Action Plan.</p> | <p>Specific permits and approvals associated with source control were the same for all corrective action alternatives and were discussed in the Closure Plan (AECOM, 2016a).</p> <p>Residual plume management under the Source Control-Cutoff Wall alternative would require permits from the IEPA for construction of stormwater controls and BMPs. Due to modification of the FAPS embankment, an Illinois Department of Natural Resources (IDNR) Office of Water Resources, Dam Safety modification</p> | <p>Specific permits and approvals associated with source control were the same for all corrective action alternatives and were discussed in the Closure Plan (AECOM, 2016a).</p> <p>Residual plume management under the Source Control-GMS alternative would require permits from the IEPA for construction of stormwater controls, BMPs, in addition to a joint water pollution control construction and operation permit. Groundwater extracted from the extraction trench</p> |

| Evaluation Factor (Report Section; Part 845 Section) | Source Control-GWP | Source Control-Cutoff Wall | Source Control-GMS |
|---|--|--|--|
| | | <p>permit would need to be obtained. It is estimated permitting, and approval will typically take 6 to 12 months to obtain.</p> | <p>would require a modified NPDES permit. The NPDES permit would likely require renewals depending on the timeline of corrective action implementation, and typically take 18 to 24 months to obtain. Due to modification of the FAPS embankment, an IDNR Office of Water Resources, Dam Safety modification permit would need to be obtained.</p> |
| <p>Availability of Necessary Equipment and Specialists (Section 2.3.4; IAC Section 845.670 (e)(3)(D))</p> | <p>Source control (IEPA approved CIP approach) was implemented in 2020. Thus, there are no further equipment and specialist needs associated with the implementation of the source control remedy.</p> <p>Residual plume management under the Source Control-GWP alternative would require standard environmental monitoring equipment and groundwater professionals. Specialists such as geologists, hydrogeologists, statisticians (<i>i.e.</i>, statistical analysis), and geochemists would be available to collect and evaluate the data.</p> | <p>Source control (IEPA approved CIP approach) was implemented in 2020. Thus, there are no further equipment and specialist needs associated with the implementation of the source control remedy.</p> <p>Residual plume management under the Source Control-Cutoff Wall alternative would require specialists and specialty equipment for the construction of the cutoff wall.</p> <ul style="list-style-type: none"> Excavation and construction of the cutoff wall would require a specialized contractor with experience excavating similar size trenches in similar geologic environments and constructing barrier walls with similar design specifications. Specialized and often custom-built equipment including large cranes, slurry cutters, batch plants and/or one-pass construction equipment would be needed. | <p>Source control (IEPA approved CIP approach) was implemented in 2020. Thus, there are no further equipment and specialist needs associated with the implementation of the source control remedy.</p> <p>Residual plume management under the Source Control-GMS alternative would require specialists to install and manage the GMS system throughout its operational period.</p> <ul style="list-style-type: none"> Construction of the groundwater extraction system would require a specialized contractor with experience constructing similar size trenches in similar geologic environments. The contractor would probably need specialized and often custom-built equipment including one-pass construction equipment. Specialists such as design engineers, construction managers, and contractor staff with expertise in |

| Evaluation Factor (Report Section; Part 845 Section) | Source Control-GWP | Source Control-Cutoff Wall | Source Control-GMS |
|--|--------------------|---|---|
| | | <ul style="list-style-type: none"> Specialists such as design engineers, construction managers, and contractor staff with expertise in cutoff wall construction and equipment operation, would be essential. The types of equipment and specialists should have been employed for projects similar to designing and building cutoff walls. However, there may be backlogs associated with the equipment and specialists, due to the high existing demand for specialty ground improvement contractors and design specialists who are engaged with similar projects in sectors like electric utilities, dams/levees, and other areas. This alternative would also require the use of equipment and the expertise of specialists for tasks such as field data collection, groundwater sampling, groundwater sample analysis, and periodic corrective action groundwater monitoring and reporting. Similar to those in the Source Control-GWP alternative, these activities are already being conducted as part of routine groundwater monitoring in accordance with IAC Section 845.220(c)(4). | <p>trench construction and equipment operation would be essential.</p> <ul style="list-style-type: none"> The types of equipment and specialists should have been employed for projects similar to designing and installing extraction trenches. However, there may be backlogs associated with the equipment and specialists, due to the high existing demand for specialty ground improvement contractors and design specialists who are engaged with similar projects in sectors like electric utilities, dams/levees, and other areas. This alternative would necessitate the use of equipment and the expertise of specialists for tasks such as regular groundwater system O&M, field data collection, groundwater sampling, analysis, and periodic corrective action groundwater monitoring and reporting. Similar to those in the GWP alternative, some of these activities are already being conducted as part of routine groundwater monitoring in accordance with IAC Section 845.220(c)(4). |

| Evaluation Factor (Report Section; Part 845 Section) | Source Control-GWP | Source Control-Cutoff Wall | Source Control-GMS |
|---|--|--|--|
| Available Capacity and Location of Needed Treatment, Storage, and Disposal Services/Comply with Standards for Management of Wastes as Specified in Section 845.680(d) (Section 2.3.5; IAC Section 845.670 (e)(3)(D)/ IAC section 845.670(d)(5)) | No treatment, storage, or disposal services would be required for residual plume management under Source Control-GWP alternative, as GWP would not generate any significant volume of waste or wastewater. | Residual plume management for the Source Control-Cutoff Wall would generate CCR-containing spoils during the construction phase. The CCR spoils would be transported to an off-Site landfill for disposal. An evaluation would be completed to determine the best location for disposal. Excavated non-CCR spoils would be disposed at an appropriate on-Site location. No wastes would be expected to be generated during operations of the cutoff wall, and consequently, no additional treatment, storage, or disposal services would be necessary for this remedy. | Residual plume management for the Source Control-GMS alternative would generate waste during construction of the extraction trench system and management of wastewater <i>via</i> a settling pond on-Site: <ul style="list-style-type: none"> The construction of the extraction trench would generate spoils, and the waste materials consisting of predominantly CCR would be dried and disposed at an appropriate on-Site location. The extraction trench system would send extracted groundwater to an on-site settling pond, which collects solids removed during groundwater recovery <i>via</i> the pneumatic extraction pumps and transfer piping. The location of settling pond would need to be evaluated at a later phase. Discharge from the settling pond would be conveyed to an NPDES permitted outfall. Renewal of the NPDES permits may be necessary to continue operations, depending on the timeline of the corrective action implementation in relation to the remedy completion. |
| The Degree to Which Community Concerns Are Addressed by the Remedy (Section 2.4; IAC Section 845.670(e)(4)) | Some communities have expressed concerns over groundwater quality at CCR surface impoundments. The combination of source control (IEPA approved CIP approach) and residual | Some communities have expressed concerns over groundwater quality at CCR surface impoundments. The combination of source control (IEPA approved CIP approach) and residual | Some communities have expressed concerns over groundwater quality at CCR surface impoundments. The combination of source control (IEPA approved CIP approach) and residual |

| Evaluation Factor (Report Section; Part 845 Section) | Source Control-GWP | Source Control-Cutoff Wall | Source Control-GMS |
|--|---|---|---|
| | <p>plume management would cause groundwater concentrations to decline over time under all of the corrective action alternatives, as suggested by the groundwater modeling (NRT, 2014a; Burns & McDonnell, 2021), thus addressing these concerns. The CCR constituents impacts to off-Site groundwater are being monitored and will be addressed by residual plume management under the three corrective action alternatives.</p> <p>A public meeting will be held on March 20, 2025, pursuant to requirements under IAC Section 845.710(e). Questions raised by attendees will be answered at the meeting; subsequently, a written summary of all questions and responses will be made available to interested parties.</p> | <p>plume management would cause groundwater concentrations to decline over time under all of the corrective action alternatives, as suggested by the groundwater modeling (NRT, 2014a; Burns & McDonnell, 2021), thus addressing these concerns. The CCR constituents impacts to off-Site groundwater are being monitored and will be addressed by residual plume management under the three corrective action alternatives.</p> <p>A public meeting will be held on March 20, 2025, pursuant to requirements under IAC Section 845.710(e). Questions raised by attendees will be answered at the meeting; subsequently, a written summary of all questions and responses will be made available to interested parties.</p> | <p>plume management would cause groundwater concentrations to decline over time under all of the corrective action alternatives, as suggested by the groundwater modeling (NRT, 2014a; Burns & McDonnell, 2021), thus addressing these concerns. The CCR constituents impacts to off-Site groundwater are being monitored and will be addressed by residual plume management under the three corrective action alternatives.</p> <p>A public meeting will be held on March 20, 2025, pursuant to requirements under IAC Section 845.710(e). Questions raised by attendees will be answered at the meeting; subsequently, a written summary of all questions and responses will be made available to interested parties.</p> |
| <p>Remove from the Environment as Much of the Contaminated Material That Was Released from the CCR Surface Impoundment as Is Feasible, Taking into Account Factors Such as Avoiding Inappropriate Disturbance of Sensitive Ecosystems (Section 2.5; IAC Section 845.670(d)(4))</p> | <p>There have been no known releases of CCR at the FAPS. All potential corrective action alternatives include source control and residual plume management efforts. The source control was an IEPA approved CIP approach to control, minimize or eliminate, post closure infiltration of liquids into the impounded CCR.</p> <p>Additionally, residual plume management under the Source Control-GWP alternative would address impacted groundwater by relying on</p> | <p>There have been no known releases of CCR at the FAPS. All potential corrective action alternatives include source control and residual plume management efforts. The source control was an IEPA approved CIP approach to control, minimize or eliminate, post closure infiltration of liquids into the impounded CCR.</p> <p>Additionally, residual plume management under the Source Control-Cutoff Wall alternative would employ an engineered system to prevent the migration of impacted groundwater off-</p> | <p>There have been no known releases of CCR at the FAPS. All potential corrective action alternatives include source control and residual plume management efforts. The source control was an IEPA approved CIP approach to control, minimize or eliminate, post closure infiltration of liquids into the impounded CCR.</p> <p>Residual plume management under the Source Control-GMS alternative would utilize an engineered extraction system to actively remove constituent mass</p> |

| Evaluation Factor (Report Section; Part 845 Section) | Source Control-GWP | Source Control-Cutoff Wall | Source Control-GMS |
|--|--|---|--|
| | <p>natural physical and geochemical attenuation processes to reduce the residual concentrations of CCR-related constituents in groundwater. Site-specific evaluations demonstrated that conditions are favorable for the attenuation of inorganic contaminants <i>via</i> adsorption. Some desorption is predicted to occur as groundwater returns to background conditions, but the changes are expected to be minimal (Appendix E; Geosyntec Consultants, Inc., 2025).</p> <p>No ecosystems would be disturbed because no construction activities are expected under the Source Control-GWP alternative.</p> | <p>Site. Groundwater quality would also be improved as a result of physical and geochemical attenuation processes.</p> <p>The construction activities would likely result in some negative impacts to the ecosystem, including disturbance of habitat near the construction areas by causing alarm and escape behavior in nearby wildlife (<i>e.g.</i>, due to noise disturbances). Short-term impacts could also occur to sensitive aquatic and wetland species in Kaskaskia River and other wetlands and surface waters near the FAPS (see Section 1.1.3) due to sediment runoff during construction.</p> | <p>from the environment. Groundwater quality would also be improved as a result of physical and geochemical attenuation processes.</p> <p>The construction activities would likely result in some negative impacts to the ecosystem, including disturbance of habitat near the construction areas by causing alarm and escape behavior in nearby wildlife (<i>e.g.</i>, due to noise disturbances). Short-term impacts could also occur to sensitive aquatic and wetland species in Kaskaskia River and other wetlands and surface water near the FAPS (see Section 1.1.3) due to sediment runoff during construction.</p> |

Notes:

CAA = Closure Alternatives Analysis; CCR = Coal Combustion Residual; CIP = Closure-in-Place; FAPS = Fly Ash Pond System; GMS = Groundwater Management System; GWP = Groundwater Polishing; GWPS = Groundwater Protection Standard; IAC = Illinois Administrative Code; IEPA = Illinois Environmental Protection Agency; NPDES = National Pollutant Discharge Elimination System; O&M = Operations and Maintenance; Source Control-Cutoff Wall = Source Control with a Groundwater Cutoff Wall; Source Control-GMS = Source Control with Groundwater Management System; Source Control-GWP = Source Control with Groundwater Polishing.

1 Introduction

1.1 Site Description and History

1.1.1 Site Location and History

The Baldwin Power Plant (BPP) (also referred to as Baldwin Energy Complex, or BEC) is a coal-fired power generating facility owned and operated by Dynegy Midwest Generation, LLC (DMG). The facility is located approximately 1.5 miles west-northwest of the Village of Baldwin, within Randolph and St. Clair Counties, Illinois. The plant began operating its first generating unit in 1970 (Ramboll, 2024b). The BPP is currently scheduled to retire by the end of 2027.

1.1.2 CCR Impoundment

A part of its operations, BPP produces and stores coal combustion residuals (CCRs). The BPP has several surface impoundments for storage of CCR: the Bottom Ash Pond (BAP) (Vistra identification [ID] number [No.] 601, Illinois Environmental Protection Agency [IEPA] ID No. W1578510001-06), the Fly Ash Pond System (FAPS, an IEPA closed CCR Unit) (Vistra ID No. 605; IEPA ID Nos. W1578510001-01, W1578510001-02, and W1578510001-03), the Secondary Pond, Tertiary Pond, and Cooling Pond (Ramboll, 2021). The FAPS is a closed multi-unit CCR surface impound (SI) and is the subject of this report.

The FAPS (Figure 1.1) is comprised of three closed unlined SIs: the East Fly Ash Pond (76 acres), the Old East Fly Ash Pond (102 acres), and the West Fly Ash Pond (54 acres) encompassing a total surface area of 232 acres (Appendix C; Ramboll, 2024a). The FAPS external perimeter embankments were constructed in 1969 followed by embankment enhancements and expansion in 1979 and 1989, respectively. In 1995, an interior dike was constructed between East Fly Ash Pond and West Fly Ash Pond, and the dike was subsequently raised in 1999 (Ramboll, 2021). During operation, the FAPS discharged into the BAP, followed by the Secondary Pond and the Tertiary Pond, which eventually discharges *via* a National Pollutant Discharge Elimination System (NPDES)-permitted outfall to a tributary of the Kaskaskia River, located south of Baldwin Lake Cooling Pond intake structure (Ramboll, 2021). In 2016, a Closure Plan for the FAPS was developed and approved by IEPA; and closure with a final cover system was completed in November 2020 (Appendix C; Ramboll, 2024a).



Figure 1.1 Site Location Map. Adapted from Ramboll (2024b).

1.1.3 Surface Water Hydrology

The FAPS is located at the northern edge of the Baldwin Lake-Kaskaskia River Watershed (Hydrologic Unit Code 071402040908) (AECOM, 2016b). There are 28 surface water features within 1,000 meters of the Site (Ramboll, 2021). The most significant water bodies in the vicinity of the FAPS are Baldwin Lake, also known as the Baldwin Power Plant Cooling Pond, and the Kaskaskia River (Figure 1.1; Ramboll, 2024b).

The Kaskaskia River is located approximately 0.5 mile west of the outer perimeter of the FAPS within the Kaskaskia River Watershed (Google LLC, 2022; AECOM, 2016b). The segment of the Kaskaskia River adjacent to the Site (Section IL_O-97) is included on the 2022 Illinois Section 303(d) List as being impaired for aquatic life due to abnormal flow, degraded habitat, low oxygen, and sedimentation/siltation; impaired for fish consumption due to mercury and pesticides; and impaired for public and food processing water supply due to pesticides (IEPA, 2022; US EPA, 2022). The 2,018-acre Baldwin Lake, which borders the Site to the north, was constructed between 1967 and 1970. Baldwin Lake is filled by pumping water from the Kaskaskia River and is supplemented by natural precipitation. The discharge from the lake into the Kaskaskia River is regulated by a Site NPDES permit (NPDES Permit No. IL0000043) (Ramboll, 2021). As a perched lake, it is hydrologically isolated from natural surface water bodies (Ramboll, 2021).

1.1.4 Hydrogeology

The geology underlying the Site in the vicinity of the FAPS consists of unlithified materials (predominantly clay with some silt and intermittent sand seams and lenses) underlain by Pennsylvanian and Mississippian bedrock (NRT, 2016; Ramboll, 2021, 2024b). There are two distinct hydrostratigraphic units underlying the CCR at the FAPS:

- **Upper Unit (UU)²:** The UU, composed of unlithified materials, is directly beneath the FAPS. It consists of four lithologic layers – Cahokia Formation (sandy clay and clayey sand), Peoria Loess (silt and silty clay), Equality Formation (sandy clay with occasional sand seams), and Vandalia Till (clay with discontinuous sand lenses) (Ramboll, 2021a). The thickness of the UU underneath the FAPS varies between 17 ft in the eastern part of the FAPS to 56 ft in the northern and western part of the FAPS³ (Ramboll, 2024b). The unlithified materials within the UU do not represent a continuous aquifer unit (Ramboll, 2024b).
- **Bedrock Unit (BU):** The BU underlies the UU and is composed of interbedded shale and limestone bedrock, which is continuous across the entire BPP Site (Ramboll, 2021).

Thin sand lenses in the UU and the interface between the UU and the BU have both been identified as potential migration pathways (PMPs) (Ramboll, 2021a, 2024b). The BU is the uppermost aquifer (UA) (Ramboll, 2024b).

The Kaskaskia River, located to the west of FAPS, is the principal surface drainage for the region. Throughout most of the area near the FAPS, groundwater flows (both in the UU and the BU) to the west and southwest towards the bedrock valley underlying the Secondary and Tertiary Ponds (located west of FAPS) and Kaskaskia River. In the northeastern part of the FAPS, groundwater flows in a northwesterly direction and eventually discharges into the Kaskaskia River. Some groundwater in the UU may flow into the Secondary and Tertiary Ponds which drain into the Kaskaskia River. Thus, Kaskaskia River is the receiving surface water body for groundwater in the UU and the BU (Ramboll, 2021, 2024b).

1.1.5 Site Vicinity

The BPP Site is located in a predominantly agricultural area (Ramboll, 2021). It is bordered by the Kaskaskia River to the west, farmland and strip-mining areas to the north and east, and scattered residences and the Illinois Central Gulf railroad tracks to the south (Ramboll, 2024b). The village of Baldwin is approximately 1.5 miles south-southeast of the BPP.

Scenic, recreational, and historical areas near the Site include the greater Kaskaskia River State Fish and Wildlife Area (SFWA). The Kaskaskia River SFWA, which spans over 20,000 acres, is popular for fishing, boating, picnicking and wildlife viewing (IDNR, 2022). A campground is located approximately 300 ft south of the southern perimeter of the FAPS. The Wood Duck Marina is located approximately 2,000 ft west of the western perimeter of the FAPS. The Baldwin Cemetery is located approximately 2,500 ft east of the FAPS (Google LLC, 2024). Based on a review of the Illinois Department of Natural Resources (IDNR) Historic Preservation Division database and the Illinois State Archaeological Survey database, there are no historic sites located within 1,000 meters of the FAPS (Ramboll, 2021).

² The UU was referred to as the Upper Groundwater Unit (UGU) in previous reports (Ramboll, 2024b).

³ The thickness of the UU at MW-150 (to the west of the FAPS) is 13 ft (Ramboll, 2024b).

1.2 Part 845 Regulatory Review and Requirements

Title 35, Part 845 of the Illinois Administrative Code (IAC) (IEPA, 2021) requires that a Corrective Action Alternatives Analysis (CAAA) be performed as part of the remedy selection, prior to undertaking any corrective actions at certain CCR-containing impoundments where exceedances of groundwater protection standards (GWPSs) have been identified. Because exceedances⁴ of GWPSs in groundwater associated with the FAPS have been identified for boron, sulfate, and pH (Appendix D; Ramboll, 2024b), this report presents a CAAA for the FAPS pursuant to the requirements under IAC Section 845.670. The goal of a CAAA is to holistically evaluate a range of factors for the various corrective actions being considered at an impoundment, including the efficiency, reliability, and ease of implementation of the corrective action; its potential positive and negative short- and long-term impacts on human health and the environment; and its ability to address concerns raised by the community (IEPA, 2021). A CAAA is a decision-making tool that is designed to aid in the selection of a corrective action alternative.

⁴ Throughout this document, "exceedance" or "exceedances" is intended to refer only to potential exceedances of proposed applicable background statistics or Groundwater Protection Standards (GWPS) as described in the proposed groundwater monitoring program, which was submitted to IEPA on October 25, 2021 as part of Dynegy Midwest Generation's operating permit application for the FAPS (Burns & McDonnell, 2021). The operating permit application, including the proposed groundwater monitoring program, remains under review by IEPA and therefore Dynegy Midwest Generation has not identified any actual exceedances.

2 Corrective Action Alternatives Analysis

This section presents the CAAA pursuant to requirements under IAC Section 845.670 (IEPA, 2021a). The goal of a CAAA is to fully evaluate proposed viable corrective measures that were identified in the CMA. The CAAA evaluates potential corrective actions with respect to a wide range of factors, including the performance, reliability, and ease of implementation of the corrective action; its potential impacts on human health and the environment; and its ability to address concerns raised by the community (IEPA, 2021a).

Per IAC Section 845.670(d) (IEPA, 2021a), any corrective actions selected under a Corrective Action Plan must:

1. Be protective of human health and the environment;
2. Attain the groundwater protection standards specified in Section 845.600;
3. Control the sources of releases to reduce or eliminate, to the maximum extent feasible, further releases of constituents listed in Section 845.600 into the environment;
4. Remove from the environment as much of the contaminated material that was released from the CCR surface impoundment as is feasible, considering factors such as avoiding inappropriate disturbance of sensitive ecosystems; and
5. Comply with standards for management of wastes as specified in Section 845.680(d).

At the FAPS, a CAAA is required because groundwater monitoring associated with the FAPS identified exceedances of the GWPSs. Groundwater monitoring was conducted in accordance with the proposed groundwater monitoring plan (GMP) between 2015 to 2023 (Appendix D; Ramboll, 2024b). The groundwater samples collected from groundwater compliance monitoring wells were used to evaluate compliance with the groundwater quality standards listed in IAC Section 845.600(a). As of the date of this report, boron, sulfate, and pH were identified as constituents/parameters with concentrations in excess of their corresponding GWPSs (Appendix D; Ramboll, 2024b).

Three potentially viable corrective actions for the FAPS were selected in the CMA for further consideration in this CAAA. These corrective action alternatives include source control which was previously approved by IEPA. The corrective actions alternatives that are considered in this CAAA are Source Control with Groundwater Polishing (Source Control-GWP), Source Control with a Groundwater Cutoff Wall (Source Control-Cutoff Wall), Source Control with Groundwater Management System (Source Control-GMS).⁵ The corrective actions are described below in Section 2.1.

2.1 Corrective Action Alternative Descriptions

For all corrective actions evaluated in this CAAA, source control is the primary remedy. US EPA has stated that source control is the most effective means of ensuring the timely attainment of remediation objectives (US EPA, 2015b). The source control for the FAPs consisted of an IEPA approved CIP approach, which

⁵ It should be noted that the GMS system evaluated in this report is a slightly different, more robust groundwater extraction alternative compared to the system that was considered in the CMA (Ramboll, 2024a).

was completed in November 2020 and subsequently approved by IEPA in December 2020 (Morris, 2020). Specific elements of this approach included (AECOM, 2016a; Burns & McDonnell, 2021):

- Removal of water *via* pumping;
- Dewatering of CCR;
- Redistributing and reshaping existing CCR as well as contouring and grading beneath the final cover system to fill low areas;
- Construction of a final cover system consisting of a 6-in vegetative layer and an 18-in layer of overlying barrier soil, in compliance with 40 CFR Part 257, Subpart D; and
- The installation of two new detention basins and channels directing non-contact stormwater from the cover system to be collected and managed in the Secondary Pond.

The source control included removing water and installation of a final cover system in accordance with CFR Part 257, Subpart D to "minimize water infiltration into the closed FAPS and improve surface water drainage off the cover system, thus reducing generation of potentially impacted water and ultimately reducing the extent of CCR impacts to groundwater" (Appendix C; Ramboll, 2024a). Groundwater modeling performed in support of the Closure Plan suggested that the source control would provide hydraulic control of surface water on the cover system, reduce both water levels in the FAPS and groundwater contaminant concentrations, and decrease the potential for off-Site transport of CCR constituents (*i.e.*, shrink of CCR-constituent plume; NRT, 2014a,b; Burns & McDonnell, 2021). The final cover system helped establish hydrostatic equilibrium with the FAPS, and decreased off-Site migration of CCR constituents. Due to the reduction in the hydraulic flux out of the FAPS, the mass flux out of the FAPS is controlled and minimized.

In addition to source control, the corrective actions evaluated in this CAAA include residual plume management. Three potential corrective actions, identified as viable in the CMA, are evaluated in this CAAA for the FAPS:

- **Alternative 1:** Source control with Groundwater Polishing (Source Control-GWP);
- **Alternative 2:** Source control with a Groundwater Cutoff Wall (Source Control-Cutoff Wall);
- **Alternative 3:** Source control with a Groundwater Management System (Source Control-GMS).

For all three potential corrective action alternatives, adaptive site management strategies would be integrated into residual plume management. This approach ensures the timely incorporation of new Site information throughout the corrective action process in order to optimize the remediation and expedite achievement of the GWPSs. As part of the adaptive site management approach, system performance and residual plume conditions would be monitored throughout the implementation of the selected corrective action. If groundwater concentrations do not respond as expected to the corrective action, the adaptive site management approach would enable prompt adjustments, optimizations, or replacement of the remedy to ensure overall effectiveness.

2.1.1 Alternative 1: Source Control-GWP

The first corrective action alternative is Source Control-GWP. This remedy includes source control (IEPA approved CIP approach), and residual plume management based on natural physical and geochemical processes that would reduce groundwater concentrations downgradient of the FAPS. Groundwater polishing mechanisms were evaluated using geochemical speciation and reaction models. The primary

objective of the geochemical model was to support the evaluation of groundwater polishing as a potential remedy for the Site. The model focused on evaluating the dominant geochemical reactions that may occur at time scales relevant to groundwater flow, including adsorption and mineral dissolution/precipitation reactions (*i.e.*, iron and aluminum hydroxides, carbonates, and some sulfates) (Appendix E; Geosyntec Consultants, Inc., 2025). Model inputs included geochemically reactive solid mineral phases, downgradient groundwater composition, and background groundwater composition derived from site-specific data. Speciation models analyzed the distribution of chemical constituents between solid and aqueous phases, while reaction models assessed how these distributions may shift in response to changing site conditions (US EPA, 2015). Components of residual plume management for remedy alternative include:

- Groundwater concentrations would be reduced in the downgradient plume as a result of physical and geochemical attenuation processes. Site-specific evaluations have shown that groundwater polishing would reduce the groundwater concentrations and mobility of inorganic contaminants. Specifically, the results indicate that boron and sulfate attenuation *via* sorption onto mineral surfaces such as iron and aluminum oxides, would occur. Some desorption is predicted to occur as groundwater returns to background conditions, but the changes are expected to be minimal. This attenuation process would reduce the flux of CCR constituents in downgradient groundwater, and constituent concentrations should decrease (Appendix E; Geosyntec Consultants, Inc., 2025).
- Corrective action groundwater monitoring using a groundwater monitoring system designed in accordance IAC Section 845.680(c) would be performed within the plume that lies beyond the waste facility boundary.
- Adaptive site management strategies for this alternative would include geochemical modeling. Groundwater monitoring results would be evaluated and compared to the model-predicted concentrations. In situations in which observed groundwater concentrations deviate significantly from modeled conditions, alternative methods or techniques to achieve the GWPSs would be evaluated, and if viable, incorporated as per IAC Section 845.680(b).
- Confirmation groundwater sampling would be performed for 3 years after GWPS are met, in accordance with IAC Section 845.680 (c). In the event that GWPSs are not met, corrective action groundwater monitoring would continue, with potential future changes to sampling parameters and monitoring frequency. Corrective action confirmation monitoring would not be performed under such circumstances.
- Following the completion of the corrective action confirmation monitoring period, a report and certification for Corrective Action Completion would be prepared and submitted to IEPA as per IAC Section 845.680(e).

The overall corrective action implementation duration for this alternative is going to take in excess of 100 years⁶ (Appendix B; Ramboll, 2025b), including:

- Corrective action monitoring until GWPSs have been achieved;
- At least 3 years (36 months) of corrective action confirmation monitoring⁷ and
- 6 months associated with post-closure reporting.

⁶ While the model simulation period for each corrective action alternative was 1,000 years, model predictions at such lengthy future timescales are inherently uncertain.

⁷ It should be noted that post-closure care groundwater monitoring will continue for a minimum of 30 years as required by IAC Section. 845.780(c).

Although source control (*i.e.*, control-in-place [CIP]) is a primary component of the corrective action, it was completed in 2020, and therefore, the labor time, equipment usage, and mileage linked to source control are not included in this analysis. There is no labor and mileage incurred with the residual plume management under the Source Control-GWP alternative, because no construction would be required under this alternative. Mileage and labor associated with corrective action monitoring was not included in this analysis (Appendix B; Ramboll, 2025b).

2.1.2 Alternative 2: Source Control-Cutoff Wall

The second corrective action alternative is Source Control with a Groundwater Cutoff Wall. This remedy includes source control (IEPA approved CIP approach) and a cutoff wall as the residual plume management approach. The residual plume management approach would include the construction of a cutoff wall comprised of a mixture of soil and bentonite or a mixture of cement and bentonite. It would extend from the existing perimeter berm ground surface into the UU/PMP. The cutoff wall would be about 7,000 ft long, 2 to 3 ft wide, and have a maximum depth of about 85 ft below ground surface (bgs). The cutoff wall would have a low hydraulic conductivity providing a long-term, maintenance-free barrier to reduce potential impacted groundwater from migrating past the Site's southern property boundary.

Implementation of residual plume management for Source Control-Cutoff Wall is expected to include various tasks across three major phases: pre-construction activities (Phase 1), corrective action construction (Phase 2), and corrective action operations, maintenance, and closeout (Phase 3). The activities associated with each of these phases are summarized below:

- Phase 1: Pre-construction activities including obtaining permits from agencies and completing Site investigations and engineering designs.
- Phase 2: Construction of the cutoff wall and minor Site restoration of disturbed areas.
 - Mobilization of equipment and materials to the Site, and preparation for Site construction.
 - The wall would be constructed using one-pass trenching methods by excavating subgrade soils and backfilling the trench with the selected low permeability material (soil-bentonite or cement-bentonite) generated by an on-Site batch plant.
 - Excavated spoils containing CCR would be disposed of at an off-Site landfill, while construction spoils that do not contain CCR would be disposed of at an appropriate on-Site location.
 - Site restoration would be completed following the construction of the cutoff wall, including repair of the final cover system over disturbed areas and removal of construction infrastructure.
- Phase 3: Operations, Maintenance, and Closeout. Details pertaining to each of these activities are outlined below.
 - Corrective Action O&M: Because the cutoff wall is a passive, below-grade structure, no O&M would be needed following its installation.
 - Groundwater concentrations would be also reduced in the downgradient plume as a result of physical and geochemical attenuation processes.
 - Adaptive site management strategies would be employed to track remediation progress and incorporate new Site information to assure the achievement of the GWPSs. Additional investigation to update the conceptual site model (CSM), groundwater, and geochemical models may be included as part of remedy progress evaluation. If remedy progress does not

meet expectations, additional methods or techniques to achieve GWPS would be evaluated and incorporated in compliance with IAC Section 845.680 (b).

- Corrective action monitoring using a corrective action groundwater monitoring network designed in accordance with IAC Section 845.680(c) would be performed within the plume that lies beyond the waste facility boundary. If the GWPSs are met for all corrective action monitoring wells in the future, corrective action confirmation groundwater sampling would be performed for 3 years, in accordance with IAC Section 845.680 (c). If GWPSs are not met in the future, corrective action groundwater monitoring would continue, with potential future changes to sampling parameters and monitoring frequency. Corrective action confirmation monitoring would not be performed under such circumstances.
- Following the completion of the corrective action confirmation monitoring period, a report and certification for Corrective Action Completion would be prepared and submitted to IEPA as per IAC Section 845.680(e).

The overall corrective action implementation duration is going to take in excess of 100 years⁸ (Appendix B; Ramboll, 2025b), including:

- Three to four years (30 to 48 months) of pre-construction activities (Phase 1).
- One to two years (12 to 24 months) of corrective action construction (Phase 2).
- Corrective action O&M will continue until GWPS have been met, which is estimated to take in excess of 100 years⁹. Once GWPSs have been achieved, at least 3 years (36 months) of corrective action confirmation monitoring,¹⁰ and 6 months associated with post-closure reporting would be required (Appendix B; Ramboll, 2025b).

⁸ While the model simulation period for each corrective action alternative was 1,000 years, model predictions at such lengthy future timescales are inherently uncertain.

⁹ While the model simulation period for each corrective action alternative was 1,000 years, model predictions at such lengthy future timescales are inherently uncertain.

¹⁰ It should be noted that post-closure care groundwater monitoring would continue for a minimum of 30 years or until such time as GWPSs are achieved, whichever is longer, as required by IAC Section 845.780(c).

Key parameters for the Source Control-Cutoff Wall corrective action alternative are shown in Table 2.1, below.

Table 2.1 Key Parameters for the Source Control-Cutoff Wall Corrective Action Alternative^a

| Parameter^b | Value^c |
|---|--------------------------|
| Labor Hours | |
| Total On-Site Labor | 18,100 |
| Total Off-Site Labor | 0 |
| 40% Contingency | 7,260 |
| Total Labor Hours: | 25,400 |
| Vehicle and Equipment Travel Miles | |
| Vehicles On-Site | 48,700 |
| On-Site Haul Trucks (Unloaded + Loaded) | 9,060 |
| Labor Mobilization | 7,750 |
| Equipment Mobilization (Unloaded + Loaded) | 57,300 |
| Off-Site Haul Trucks (Unloaded + Loaded) | 674,000 |
| Material Deliveries (Unloaded + Loaded) | 115,000 |
| Total On-Site Vehicle and Equipment Travel Miles: | 57,800 |
| Total Off-Site Vehicle and Equipment Travel Miles: | 854,000 |
| Total Vehicle and Equipment Travel Miles: | 912,000 |

Notes:

Source Control-Cutoff Wall = Source Control with a Groundwater Cutoff Wall.

(a) Although source control (*i.e.*, control-in-place [CIP]) is a primary component of the corrective action, the source control was previously completed in 2020 and the associated labor time, equipment usage, and mileage associated with source control are not discussed in this analysis.

(b) Mileage and labor related to sampling and monitoring is not included for this analysis in any of the three alternatives.

(c) Values reported in this table were rounded to reflect 3 significant figures.

Source: Appendix B; Ramboll, 2025b.

2.1.3 Alternative 3: Source Control-GMS

The third corrective action alternative is Source Control with GMS. This remedy includes source control (IEPA approved CIP approach) and a groundwater management system as the residual plume management approach. The residual plume management would include the construction of a system to remove liquids from the interior of the FAPS. The GMS would include the construction of an extraction trench, a collection and conveyance system, and a collection pond, described below:

- The trench would be about 8,700 ft long, 2 to 3 ft wide, and extend to a depth of about 50 to 60 ft bgs with collection sumps spaced at approximately every 500 ft along the trench alignment. The trench is designed to remove liquids from low-lying areas near the base of the CCR within the interior of the FAPS.
- A mechanical, electrical and piping (MEP) system would convey extracted liquids to an on-Site settling pond. After settling, the liquids would be discharged to the Kaskaskia River to the west, either *via* an existing or a new NPDES outfall.

It should be noted that the GMS system evaluated in this report is a slightly different, more robust groundwater extraction alternative compared to the system that was considered in the CMA (Ramboll, 2024a).

The GMS would provide long-term removal of liquids from the FAPS, reducing hydraulic head beneath the existing cover system and minimizing the potential for liquids to mix with groundwater and migrate beyond the Site's southern property boundary.

Implementation of the Source Control with GMS alternative is expected to include various tasks across three major phases: pre-construction activities (Phase 1), corrective action construction (Phase 2), and corrective action operations, maintenance, and closeout (Phase 3). The activities associated with each of these phases are summarized below:

- **Phase 1:** Pre-construction activities including obtaining permits from agencies and completing Site investigations and engineering designs.
- **Phase 2:** Construction of the extraction trench system and minor Site restoration of disturbed areas.
 - Mobilization of equipment and materials to the Site, and preparation for Site construction.
 - The extraction trench would be installed utilizing specialized trenching equipment (*i.e.*, one-pass trenching methods). Collection pipes and sumps would be installed. The trench would be backfilled with granular fill and capped with low-permeability clay and topsoil.
 - Excavated soils would contain primarily CCR materials, and therefore would be dried and disposed at an appropriate on-Site location.
 - Installation of the MEP system for the conveyance of extracted groundwater. This system would include a pneumatic pump and a discharge pipe to carry extracted liquids to an equalization tank, before transferring to the settling pond.
 - The location of the settling pond would be evaluated at a later phase. Additional water treatment technologies may be considered in a subsequent design phase.
 - Site restoration would be completed following the construction of the GMS, including repair of the final cover system over disturbed areas and removal of construction infrastructure.
- **Phase 3:** Operations, Maintenance, and Closeout. Details pertaining to each of these activities are outlined below:
 - The operation of the GMS would require routine and non-routine maintenance, such as totalizer data collection, maintenance of extraction pumps and other system components, and replacement of MEP components, *etc.*
 - Routine monitoring and compliance of the Site's NPDES permit associated with the treatment and discharge of extracted fluids would be required.
 - Groundwater concentrations would also be reduced in the downgradient plume as a result of physical and geochemical attenuation processes.
 - Adaptive site management strategies would be employed to track remediation progress and incorporate new Site information to assure the achievement of the GWPSs. Additional investigation to update the conceptual site model (CSM), groundwater, and geochemical models may be included as part of remedy progress evaluation. If remedy progress does not meet expectations, additional methods or techniques to achieve GWPS would be evaluated and incorporated in compliance with IAC Section 845.680 (b).
 - Corrective action monitoring using a corrective action groundwater monitoring network designed in accordance with IAC Section 845.680(c) would be performed within the plume that lies beyond the waste facility boundary. If the GWPSs are met for all corrective action monitoring wells in the future, corrective action confirmation groundwater sampling would be

performed for 3 years, in accordance with IAC Section 845.680 (c). If GWPSs are not met in the future, corrective action groundwater monitoring would continue, with potential future changes to sampling parameters and monitoring frequency. Corrective action confirmation monitoring would not be performed under such circumstances.

- Following the completion of the corrective action confirmation monitoring period, a report and certification for Corrective Action Completion would be prepared and submitted to IEPA as per IAC Section 845.680(e).

The overall corrective action implementation duration is going to take in excess of 100 years (Appendix B; Ramboll, 2025b), including:

- Three to four years (30 to 48 months) of pre-construction activities (Phase 1).
- One to two years (12 to 24 months) of corrective action construction (Phase 2).
- Corrective action O&M is estimated to take in excess of 100 years¹¹ (*i.e.*, the time to meet GWPSs). Once GWPSs are achieved, at least 3 years (36 months) of corrective action confirmation monitoring¹² and 6 months associated with post-closure reporting would be required.

Key parameters for the Source Control-GMS alternative are shown in Table 2.2, below.

Table 2.2 Key Parameters for the Source Control-GMS Corrective Action Alternative^a

| Parameter ^b | Value ^c |
|---|--------------------|
| Labor Hours | |
| Total On-Site Labor | 45,600 |
| Total Off-Site Labor | 0 |
| 40% Contingency | 18,200 |
| Total Labor Hours: | 63,800 |
| Vehicle and Equipment Travel Miles | |
| Vehicles On-Site | 64,100 |
| On-Site Haul Trucks (Unloaded + Loaded) | 8,580 |
| Labor Mobilization | 50,800 |
| Equipment Mobilization (Unloaded + Loaded) | 66,200 |
| Off-Site Haul Trucks (Unloaded + Loaded) | 874,000 |
| Material Deliveries (Unloaded + Loaded) | 72,400 |
| Total On-Site Vehicle and Equipment Travel Miles: | 72,700 |
| Total Off-Site Vehicle and Equipment Travel Miles: | 1,060,000 |
| Total Vehicle and Equipment Travel Miles: | 1,140,000 |

Notes:

Source Control-GMS = Source Control with Groundwater Management System.

(a) Although source control (*i.e.*, control-in-place [CIP]) is a primary component of the corrective action, the source control was previously completed in 2020 and the associated labor time, equipment usage, and mileage linked to source control are not discussed in this analysis.

(b) Mileage and labor related to sampling and monitoring is not included for any of the three alternatives.

(c) Values reported in this table were rounded to reflect 3 significant figures.

Source: Appendix B; Ramboll, 2025b.

¹¹ While the model simulation period for each corrective action alternative was 1,000 years, model predictions at such lengthy future timescales are inherently uncertain.

¹² It should be noted that post-closure care groundwater monitoring would continue for a minimum of 30 years or until such time as GWPSs are achieved, whichever is longer, as required by IAC Section 845.780(c).

2.2 Long- and Short-Term Effectiveness and Protectiveness of Corrective Action Alternative (IAC Section 845.670(e)(1))

2.2.1 Magnitude of Reduction of Existing Risks/Be Protective of Human Health and the Environment (IAC Section 845.670(e)(1)(A)/IAC Section 845.670(d)(1))

There are no current unacceptable risks to human or ecological receptors at this Site associated with the FAPS (Appendix A; Gradient, 2025). Because current conditions do not present a risk to human health or the environment at the FAPS, there will be no unacceptable risk to human health or the environment for future conditions since the unit was already closed and source control was implemented. Concentrations of CCR-related constituents will decline over time and, consequently, potential exposures to CCR-related constituents in the environment will also decline. As a result of this, the magnitude of the reduction of existing risks is the same for each corrective action alternative (IAC Section 845.670(e)(1)(A)), and each corrective action alternative is equally protective of human health and the environment (IAC Section 84.670(d)(1)).

2.2.2 Effectiveness of the Remedy in Controlling the Source (IAC Section 845.670(e)(2)/IAC Section 845.670(d)(3))

Extent to Which Containment Practices Will Reduce Further Releases/Control the Sources of Releases to Reduce or Eliminate, to the Maximum Extent Feasible (IAC Section 845.670(e)(2)(A)/IAC Section 845.670(d)(3))

Source control was implemented for all three corrective action alternatives in 2020. Source control (IEPA approved CIP approach) which included dewatering of CCR and installing a final cover system. These source control activities would provide control of surface run-off on the cover system and in the surrounding area, reduce leachate concentrations, and decrease off-Site transport of CCR constituents (Burns & McDonnell, 2021). The final cover system consisting of a 6-in vegetative layer and an 18-in layer of overlying barrier soil was installed in 2020; this cover system is helping to establish hydrostatic equilibrium in the FAPS and decrease off-Site transport of CCR constituents. Due to the reduction in the hydraulic flux out of the FAPS, the mass flux out of the FAPS also is also being controlled and minimized. Therefore, all three corrective action alternatives would be equally protective with regard to source control.

The effectiveness of residual plume management for each of the corrective action alternatives is summarized below.

- Under the Source Control-GWP alternative, the attenuation of dissolved constituent concentrations remaining after source control would be achieved through natural physical and geochemical processes. Site-specific evaluations have shown that groundwater polishing would reduce the groundwater concentrations and mobility of inorganic contaminants. Specifically, the results indicate that boron and sulfate attenuation *via* sorption onto mineral surfaces such iron and aluminum oxides, would occur under current conditions (*i.e.*, post-closure). Some desorption is predicted to occur as groundwater returns to background conditions, but the changes are expected to be minimal. By monitoring groundwater concentrations and, if necessary, optimizing the remedy, the Source Control-GWP alternative would be effective at controlling residual plume areas and downgradient groundwater impacts (Appendix E; Geosyntec Consultants, Inc., 2025). In cases in which observed groundwater concentrations deviate significantly from modeled conditions, alternative methods or techniques to remove residual sources to achieve the GWPSs would be

evaluated under the adaptive site management plan, and if viable, incorporated as per IAC Section 845.680(b).

- Under the Source Control-Cutoff Wall alternative, residual plume management would be achieved by creating a physical barrier to reduce potential CCR-constituents in groundwater from migrating off the Site's southern property boundary. Physical and geochemical attenuation would also help control the residual plume and prevent downgradient migration. Cutoff walls are a frequently used corrective measure that have been determined to be an effective approach in preventing dissolved-phase groundwater plume migration at many sites. In cases in which observed groundwater concentrations deviate significantly from modeled conditions, alternative methods or techniques to achieve the GWPSs would be evaluated under the adaptive site management plan, and if viable, incorporated as per IAC Section 845.680(b).
- Under the Source Control-GMS alternative, residual plume management would be achieved by construction of a groundwater management system to remove liquids from the interior of the FAPS and reduce potential CCR-constituents in groundwater from migrating off-Site. The GMS includes an extraction trench and an MEP system. Groundwater extraction is a widely used corrective measure that has been effectively implemented at many sites to contain and capture dissolved-phase groundwater plumes. Physical and geochemical attenuation would also help control the residual plume and prevent downgradient migration. In cases in which observed groundwater concentrations deviate significantly from modeled conditions, alternative methods or techniques to achieve the GWPSs would be evaluated under the adaptive site management plan, and if viable, incorporated as per IAC Section 845.680(b).

Because all corrective action alternatives include source control, and residual plume management, all potential corrective action alternatives would be equally effective at reducing, to the maximum extent feasible, releases from both primary and residual sources (IAC Section 845.670(e)(2)(A)/IAC Section 845.670(d)(3)).

Extent to Which Treatment Technologies May Be Used (IAC Section 845.670(e)(2)(B))

Because Source Control-GWP would rely on physical and geochemical processes, no additional treatment technologies would be required under this alternative. No additional treatment technologies would be required for the Source Control-Cutoff Wall alternative once the cutoff wall has been constructed, because this approach focuses on preventing groundwater from migrating away from the FAPS using an engineered physical barrier. For the Source Control-GMS alternative, in addition to physical and geochemical, extracted liquids would be managed and treated by an on-Site settling pond, although additional methods for treating extracted groundwater may be evaluated at later phases of designs (Appendix B; Ramboll, 2025b). For all corrective action alternatives, remedy optimizations would be implemented, if necessary, under the adaptive site management program.

2.2.3 Likelihood of Future Releases of CCR (IAC Section 845.670(e)(1)(B))

All corrective action alternatives include source control using an IEPA approved CIP approach. A new cover system consisting of a 6-in vegetative layer and an 18-in layer of overlying barrier soil, was installed over the FAPS in 2020 in compliance with 40 CFR Part 257, Subpart D, and new stormwater control structures were also implemented. This cover system provides increased protection against berm and surface erosion, precipitation infiltration, and other adverse effects that could potentially trigger a release of CCR. During the construction phases of the Source Control-Cutoff Wall and Source Control-GMS alternatives, the previously installed cover system would be temporarily disturbed, while the disturbed areas would be repaired after the construction is complete. Any CCR-contact stormwater generated during this

time would be managed through a contact stormwater management system. There would be minimal risk of accidental CCR releases occurring post-closure under any of the corrective action alternatives.

2.2.4 Type and Degree of Long-Term Management, Including Monitoring, Operation, and Maintenance (IAC Section 845.670(e)(1)(C))

The type and degree of long-term residual groundwater plume management associated with each corrective action alternative is summarized below.

- Residual plume management for the Source Control-GWP alternative would not require the installation, operation, or maintenance of any engineered systems or structures, other than maintenance of the monitoring well network. The only long-term management activity required under this alternative would be corrective action groundwater monitoring and routine maintenance of the monitoring wells, which would continue for at least 3 years after GWPSs have been achieved for all wells, in accordance with IAC Section 845.680(c)(2). Post-closure care groundwater monitoring would continue for a minimum of 30 years as required by IAC Section 845.780(c). Based on the adaptive site management approach, remedy optimization (additional methods or techniques) may be implemented to ensure the achievement of the GWPSs.
- Residual plume management for the Source Control-Cutoff Wall alternative requires the installation of a physical subgrade barrier. After installation, the cutoff wall does not require maintenance. The only long-term management activity required under this alternative would be corrective action groundwater monitoring and routine maintenance of the monitoring wells, which would continue for at least 3 years after GWPSs have been achieved for all wells, in accordance with IAC Section 845.680(c)(2). Post-closure care groundwater monitoring would continue for a minimum of 30 years as required by IAC Section 845.780(c). If GWPSs are not met in the future, corrective action groundwater monitoring would continue, with potential future changes to sampling parameters and monitoring frequency. Corrective action confirmation monitoring would not be performed under such circumstances. Based on the adaptive site management approach, remedy optimization (additional methods or techniques) may be implemented to ensure the achievement of the GWPSs.
- Residual plume management for the Source Control-GMS would require multiple tasks to be completed over three phases: pre-construction activities (Phase 1), corrective action construction (Phase 2), and corrective action O&M, and closeout (Phase 3). Corrective action O&M would require regular inspection and maintenance of the mechanical system which includes maintaining pumps, conveyance lines, air compressors, *etc.*, which are important components of the MEP system. Routine monitoring and compliance associated with extracted groundwater discharge *via* a new or existing NPDES outfall to Kaskaskia River would be required. Additionally, corrective action groundwater sampling and routine maintenance of the monitoring well network would continue for at least 3 years after GWPSs have been achieved at all wells, in accordance with IAC Section 845.680(c)(2). If GWPSs are not met in the future, corrective action groundwater monitoring would continue, with potential future changes to sampling parameters and monitoring frequency. Corrective action confirmation monitoring would not be performed under such circumstances. Post-closure care groundwater monitoring would continue for a minimum of 30 years as required by IAC Section 845.780(c). Based on the adaptive site management approach, remedy optimization (additional methods or techniques) may be implemented to ensure the achievement of the GWPSs.

2.2.5 Short-Term Risks to the Community or the Environment During Implementation of Remedy (IAC Section 845.670(e)(1)(D))

2.2.5.1 Safety Impacts

Best practices would be employed during construction in order to ensure worker safety and comply with all relevant regulations, permit requirements, and safety plans. However, it is impossible to completely eliminate risks to workers during construction and/or other corrective action activities. For example, injuries and fatalities can occur due to truck accidents or equipment malfunctions. Truck accidents that occur off-Site can also result in injuries or fatalities to community members. Because the source control was implemented in 2020, there is no further risk of accidents and injuries occurring during the implementation of the corrective action alternatives. The safety impacts associated with residual plume management (*i.e.*, construction and O&M) for each corrective action alternative are described below.

- The Source Control-GWP alternative would not include installation, operation, and maintenance of engineered systems or structures, and therefore no safety impacts are expected.
- The Source Control-Cutoff Wall alternative would include the construction of a groundwater cutoff wall to prevent contaminant migration from the FAPS beyond the Site's southern property boundary. Because the cutoff wall is a passive, subsurface structure, no O&M would be needed following installation. Therefore, potential safety concerns are only associated with the construction of the cutoff wall and groundwater monitoring.
- The Source Control-GMS alternative would include the construction of an extraction trench, a MEP system, and settling pond to collect, extract, and treat CCR-impacted liquids. Potential safety concerns would be related to construction and O&M of the extraction trenches and GMS.

Worker Risks

On-Site accidents include injuries and deaths arising from the use of heavy equipment and/or earthmoving operations during Site activities. Off-Site accidents include injuries and deaths due to vehicle accidents during labor and equipment mobilization/demobilization, as well as materials/supplies hauling and deliveries.

As discussed in Section 2.1.1, there are no construction activities or operational requirements associated with residual plume management for the Source Control-GWP alternative. Ramboll estimates that residual plume management for the Source Control-Cutoff Wall corrective action alternative would require 18,100 on-Site labor hours and residual plume management for the Source Control-GMS corrective action alternative would require 45,600 on-Site labor hours (Appendix B; Ramboll, 2025b). The US Bureau of Labor Statistics (US DOL, 2020a,b) provides an estimate of the hourly fatality and injury rates for construction workers. Based on the accident rates reported by the US Bureau of Labor Statistics and the on-Site labor hours reported in Appendix B, we estimate approximately 0.19 worker injuries and 1.6×10^{-3} worker fatalities would occur on-Site under the Source Control-Cutoff Wall corrective action alternative; and approximately 0.47 worker injuries and 4.1×10^{-3} worker fatalities would occur on-Site under the Source Control-GMS corrective action alternative (Table 2.3). No worker injuries and fatalities are expected under the Source Control-GWP alternative. The number of on-Site worker accidents is therefore expected to be highest under the Source Control-GMS alternative.

Table 2.3 Expected Number of On-Site Worker Accidents Under Each Corrective Action Alternative^{a,b}

| Corrective Action Alternative | Injuries | Fatalities |
|-------------------------------|----------|----------------------|
| Source Control-GWP | 0 | 0 |
| Source Control-Cutoff Wall | 0.19 | 1.6×10^{-3} |
| Source Control-GMS | 0.47 | 4.1×10^{-3} |

Notes:

Source Control-GMS = Source Control with Groundwater Management System; Source Control-GWP = Source Control with Groundwater Polishing.

(a) Although source control (*i.e.*, closure-in-place [CIP]) is a primary component of the corrective action, source control was completed in 2020 and the worker accidents associated with source control are not included in this analysis.

(b) Worker accidents associated with groundwater sampling and monitoring are not included in this analysis for any of the alternatives.

Source: Appendix B; Ramboll, 2025b.

Off-Site, a greater number of haul truck miles, labor and equipment mobilization/demobilization miles, and material delivery miles would be required under the Source Control compared to the Source Control-GWP alternative (Tables 2.1 and 2.2). For residual plume management under the Source Control-Cutoff Wall corrective action alternative, 854,000 total off-Site vehicle and equipment travel miles would be required. For residual plume management under the Source Control-GMS corrective action alternative, 1,060,000 total off-Site vehicle and equipment travel miles would be required. In contrast, for residual plume management under the Source Control-GWP alternative, no off-Site vehicle and mileage would be required (Appendix B; Ramboll, 2025b). The United States Department of Transportation (US DOT) provides estimates of the expected number of fatalities and injuries "per vehicle mile driven" for drivers and passengers of large trucks and passenger vehicles (US DOT, 2023a224-2988). Table 2.4 shows the expected number of off-Site accidents under each corrective action alternative due to all categories of off-Site vehicle usage. For these calculations, it was assumed that labor mobilization/demobilization would rely upon passenger vehicles (cars or light trucks, including pickups, vans, and sport utility vehicles) and that hauling, equipment mobilization/demobilization, and material deliveries would rely upon large trucks. Based on US DOT's accident statistics and the mileage estimates in Appendix B, an estimated 0.18 worker injuries and 0.013 worker fatalities would be expected to occur due to off-Site activities under the Source Control-Cutoff Wall alternative; and an estimated 0.24 worker injuries and 0.016 worker fatalities would be expected to occur due to off-Site activities under the Source Control-GMS alternative. No off-Site worker accidents would be expected to occur under the Source Control-GWP alternative.

Table 2.4 Expected Number of Off-Site Worker Accidents Related to Off-Site Car and Truck Use Under Each Corrective Action Alternative^{a, b}

| Off-Site Vehicle Use Category | Source Control-GWP | | Source Control-GMS | | Source Control-Cutoff Wall | |
|---------------------------------------|--------------------|------------|----------------------|----------------------|----------------------------|----------------------|
| | Injuries | Fatalities | Injuries | Fatalities | Injuries | Fatalities |
| Hauling | 0 | 0 | 0.14 | 0.011 | 0.18 | 0.014 |
| Labor Mobilization/Demobilization | 0 | 0 | 4.6×10^{-3} | 7.4×10^{-5} | 3.0×10^{-2} | 4.8×10^{-4} |
| Equipment Mobilization/Demobilization | 0 | 0 | 1.2×10^{-2} | 9.0×10^{-4} | 1.4×10^{-2} | 1.0×10^{-3} |
| Material Deliveries | 0 | 0 | 0.024 | 1.8×10^{-3} | 1.5×10^{-2} | 1.1×10^{-3} |
| Total: | 0 | 0 | 0.18 | 0.013 | 0.24 | 0.016 |

Notes:

Source Control-GWP = Source Control with Groundwater Polishing; Source Control-GMS = Source Control with Groundwater Management System.

(a) Although source control (*i.e.*, closure-in-place [CIP]) is a primary component of the corrective action, source control was completed in 2020 and the worker accidents associated with source control are not included in this analysis.

(b) Worker accidents associated with groundwater sampling and monitoring are not included in this analysis for any of the alternatives.

Source: Appendix B; Ramboll, 2025b.

Overall, considering accidents occurring both on- and off-Site, no worker injuries and worker fatalities would be expected to occur for residual plume management under the Source Control and GWP alternative; 0.37 worker injuries and 0.015 worker fatalities would be expected to occur for residual plume management under the Source Control-Cutoff Wall alternative; and 0.72 worker injuries and 0.021 worker fatalities would be expected to occur for residual plume management under the Source Control-GMS alternative. Thus, overall risks to workers would be highest under the Source Control-GMS alternative and lowest under the Source Control-GWP alternative.

Community Risks

Vehicle accidents that occur off-Site can result in injuries or fatalities among community members as well as workers. Based on the accident statistics reported by US DOT (2023b) and the off-Site travel mileages reported in Appendix B (and summarized in Tables 2.1-2.2), off-Site vehicle accidents could result in an estimated 0.22 injuries and 1.7×10^{-3} fatalities among community members (*e.g.*, people involved in haul truck accidents that are neither haul truck drivers nor passengers, including pedestrians, drivers of other vehicles, *etc.*) for residual plume management under the Source Control-Cutoff Wall alternative (Table 2.5). For residual plume management under the Source Control-GMS alternative, off-Site vehicle accidents could result in an estimated 0.28 community injuries and 2.2×10^{-3} community fatalities. No off-Site mileage is expected under the Source Control-GWP alternative. Therefore, off-Site impacts on nearby residents, including injuries or fatalities, would be highest under the Source Control-GMS alternative, and lowest under the Source Control-GWP alternative.

Table 2.5 Expected Number of Community Accidents Under Each Corrective Action Alternative^{a, b}

| Off-Site Vehicle Use Category | Source Control-GWP | | Source Control-GMS | | Source Control-Cutoff Wall | |
|---------------------------------------|--------------------|------------|----------------------|----------------------|----------------------------|----------------------|
| | Injuries | Fatalities | Injuries | Fatalities | Injuries | Fatalities |
| Hauling | 0 | 0 | 0.18 | 1.3×10^{-3} | 0.23 | 1.7×10^{-3} |
| Labor Mobilization/Demobilization | 0 | 0 | 1.9×10^{-3} | 3.0×10^{-5} | 0.01 | 2.0×10^{-4} |
| Equipment Mobilization/Demobilization | 0 | 0 | 0.02 | 1.1×10^{-4} | 0.02 | 1.3×10^{-4} |
| Material Deliveries | 0 | 0 | 0.03 | 2.2×10^{-4} | 0.02 | 1.4×10^{-4} |
| Total: | 0 | 0 | 0.22 | 1.7×10^{-3} | 0.28 | 2.2×10^{-3} |

Notes:

Source Control-GMS = Source Control with Groundwater Management System; Source Control-GWP = Source Control Groundwater Polishing.

(a) Although source control (*i.e.*, closure-in-place [CIP]) is a primary component of the corrective action, source control was completed in 2020, and the worker accidents associated with source control are not included in this analysis

(b) Worker accidents associated with groundwater sampling and monitoring are not included in this analysis for any of the alternatives.

Source: Appendix B; Ramboll, 2025b.

2.2.5.2 Cross-Media Impacts to Air

Air pollution can occur both on-Site (*e.g.*, construction activities) and off-Site (*e.g.*, along transportation routes), potentially impacting workers as well as community members. Diesel emissions are a major source of air pollutants and greenhouse gas (GHG) emissions at construction sites. Diesel exhaust contains air pollutants, including nitrogen oxides (NO_x), particulate matter (PM), carbon monoxide (CO), and volatile organic compounds (VOCs) (Hesterberg *et al.*, 2009; Mauderly and Garshick, 2009). Construction equipment also emits GHGs, including carbon dioxide (CO₂) and possibly nitrous oxide (N₂O). The potential impact of each corrective action alternative on GHG emissions is proportional to the potential impact of each alternative on other emissions from construction vehicles and equipment. On-Site emissions would be highest for residual plume management under the Source Control-GMS alternative due to the greatest amount of on-Site vehicle travel miles required under this corrective action alternative (72,700 total on-Site travel miles under the Source Control-GMS alternative *versus* 57,800 total on-Site travel miles under the Source Control-Cutoff Wall alternative and no on-Site travel miles under the source Control-GWP alternative; Section 2.1.1; Tables 2.1-2.2). Off-Site emissions would similarly be the highest for residual plume management under the Source Control-GMS alternative, due to the greatest amount of off-Site vehicle and equipment travel miles required under this alternative (1,060,000 total off-Site travel miles under the Source Control-GMS alternative *versus* 854,000 total off-Site travel miles under the Source Control-Cutoff Wall alternative, and no off-Site travel miles Source Control-GWP alternatives; Section 2.1.1; Tables 2.1-2.2). In summary, air impacts would be highest for the Source Control-GMS alternative due to greatest vehicle travel miles, and lowest for the Source Control-GWP alternative, because no construction activities would be expected under this alternative.

2.2.5.3 Cross-Media Impacts to Surface Water and Sediments

Under all corrective action alternatives, the source control was implemented in 2020 (IEPA approved CIP approach), and as a result, constituent mass flux from groundwater into surface water will decline over time (OBG, 201922). The source control approach included dewatering, which removed the hydraulic head within the impoundment, and has "significantly reduced infiltration rates relative to pre-closure conditions" (Appendix C, Ramboll, 2024a). This further reduces the hydraulic flux through the CCR. Due to the reduction in the hydraulic flux out of the FAPS, the mass flux out of the FAPS would also be controlled and minimized. Groundwater modeling performed in support of the Closure Plan suggested that the source control would provide control on surface run-off on the cover system and reduce groundwater contaminant

concentrations, and decrease the potential transport of CCR constituents off-Site (NRT, 2014a,b; Burns & McDonnell, 2021).

Under the Source Control-GWP alternative, minimal surface water and sediment impacts would be expected, because it would not require the construction of any engineered systems or structures (other than utilizing existing monitoring wells).

Under the Source Control-Cutoff Wall and Source Control-GMS alternatives, surface water and sediment impacts associated with residual plume management would be higher than the those of Source Control-GWP alternative due to the construction activities related to each of the required engineered systems. Construction can have short-term negative impacts on surface water and sediment quality immediately adjacent to a site due to erosion and sediment runoff. Any associated impacts would be addressed through best management practices (BMPs) in accordance with Site land disturbance permits.

2.2.5.4 Control of Exposure to Any Residual Contamination During Implementation of the Remedy

Source control (IEPA approved CIP approach) was implemented in 2020. Thus, there are no further risks of CCR exposure associated with source control implementation. However, impacted soils and groundwater can be a source of CCR-related constituent exposure for workers. Risks to workers arising from potential contact with residual contamination during construction, operation, and maintenance activities associated with residual plume management would be higher for the Source Control-Cutoff Wall and Source Control-GMS alternatives than for the Source Control-GWP alternative, because the Source Control-Cutoff Wall alternative would involve excavation and disposal of excavated spoils from trenching, and the Source Control-GMS alternative would involve the production, management, and treatment of extracted water, as well as off-Site disposal of excavated spoils generated during extraction trench construction. The Source Control-GWP alternative would not involve exposure to either of the soil or groundwater waste streams associated with residual plume management. Any potential CCR-exposures during the Source Control-GMS and Source Control-Cutoff Wall alternatives would be managed through the use of rigorous safety protocols and personal protective equipment.

2.2.5.5 Other Identified Impacts

Source control (IEPA approved CIP approach) was in 2020. Thus, there are no further risks associated with source control implementation.

In addition to safety impacts, cross-media impacts, and the potential for workers to be exposed to residual contamination, construction activities and remedial operations can have significant energy demands and can cause nuisance impacts such as traffic and noise. Energy consumption at a construction site is synonymous with fossil fuel consumption, because the energy to power construction vehicles and equipment comes from the burning of fossil fuels. Fossil fuel demands considered here include the burning of diesel fuel during construction equipment and vehicle travel miles. Because GHG emission impacts and energy consumption impacts both arise from the same sources at construction sites, the trends discussed in Section 2.2.5.2 with respect to GHG emissions also apply to the evaluation of energy demands. Specifically, the energy demands of construction equipment and vehicles associated with residual plume management would be greatest under the Source Control-GMS alternative, while the energy demands under the Source Control-Cutoff Wall alternative associated with residual plume management are expected to be lower, because the latter alternative would not require any significant operational activity. The Source Control-GWP would not require construction or maintenance, so the GHG emissions are expected to be the

least as compared to the other alternatives. Energy would also be required for the operation of the extraction system under the Source Control-GMS alternative, while there is no operational energy required under the Source Control-GWP or Source Control-Cutoff Wall alternatives, because Source Control-GWP would rely on natural physical and geochemical processes, while the Source Control-Cutoff Wall would rely on the constructed barrier wall.

Similarly, traffic and noise impacts associated with the construction phase of the residual plume management are also expected to be higher under the Source Control-GMS and Source Control-Cutoff Wall alternatives than the Source Control-GWP alternative, due to the construction activities that would be required to construct the groundwater management system and Cutoff Wall. Similarly, traffic may increase temporarily around the Site under the Source Control-GMS and Source Control-Cutoff Wall alternatives due to the daily arrival and departure of the workforce, equipment mobilization/demobilization, and material deliveries. However, these impacts would be expected to largely occur at the beginning or end of each workday (for the arrival/departure of the work force), at the beginning or end of the construction period (for equipment mobilization/demobilization), and at specific times throughout the construction period (for material deliveries). Traffic and noise impacts associated with residual plume management from the Source Control-GWP alternative is expected to be minimal, because no construction activities would be expected under the Source Control-GWP alternative.

Construction activities can negatively impact natural resources and habitat near the Site, as well as scenic, and recreational value. Based on a review of the IDNR Historic Preservation Division database and the Illinois State Archaeological Survey database, there are no historic sites located within 1,000 meters of the FAPS (Ramboll, 2021). There would be no impacts associated with residual plume management under the Source Control-GWP alternative because no additional construction activities would occur. However, negative impacts on scenic and recreational value may occur along the Kaskaskia River, which is located approximately 0.5 mile west of the outer perimeter of the FAPS within the Kaskaskia River Watershed (Google LLC, 2022; AECOM, 2016b). The Kaskaskia River SFWA, which spans over 20,000 acres, is popular for fishing and wildlife viewing (IDNR, 2022). A campground is located approximately 300 ft south of the southern perimeter of the FAPS. The Wood Duck Marina is located approximately 2,000 ft west of the western perimeter of the FAPS. The Baldwin Cemetery is located approximately 2,500 ft east of the FAPS (Google LLC, 2022). Under the Source Control-Cutoff Wall and Source Control-GMS alternatives, large cranes, batch plants, and other equipment could be utilized during construction phases. Given the proximity of these areas to the expected construction, it is likely that they would experience some adverse impacts such as visual disturbance, obstruction of view, and noise during the construction period. However, these impacts are expected to diminish once the construction is completed in 12- to 24 months for the Source Control-Cutoff Wall and Source Control-GMS alternatives.

In addition, the construction of the cutoff wall under the Source Control-Cutoff Wall alternative is expected to use a significant amount of cement or bentonite, which would be introduced into the UU and BU. The process would use bentonite-based drilling mud with various additives, similar to the methods employed in well drilling but on a notably larger scale. Adding substantial quantities of these materials into the subsurface environment may cause alteration in groundwater pH levels and affect geochemical conditions in the subsurface.

The construction activities would likely to result some negative impacts to the ecosystem in the vicinity, including disturbance of habitat near the construction areas by causing alarm and escape behavior in nearby wildlife (*e.g.*, due to noise disturbances). It is also possible that limited negative short-term impacts could occur to sensitive aquatic and wetland species in Kaskaskia River and surface water ponds located within the area (see Section 1.1.3) due to sediment runoff during construction.

2.2.6 Time Until Groundwater Protection Standards Are Achieved/Attain the Groundwater Protection Standards Specified in Section 845.600 (IAC Section 845.670(e)(1)(E)/IAC Section 845.680(d)(2))

This section of the report evaluates the time required to achieve GWPSs, pursuant to requirements under IAC Section 845.670(e)(1)(E) (IEPA, 2021a) and under IAC Section 845.680(d)(2).

For most of the FAPS, groundwater flow (both in the UU and the BU) is generally to the west and southwest towards the bedrock valley underlying the Secondary and Tertiary Ponds (located west of FAPS) and the Kaskaskia River. In the northeastern part of the FAPS, groundwater flows to the northwest and eventually discharges in the Kaskaskia River. Some groundwater in the UU may flow into the Secondary and Tertiary Ponds but these units also drain to the Kaskaskia River. Thus, Kaskaskia River is the receiving surface water body for groundwater in the UU and the BU at the Site (Ramboll, 2021, 2024b).

The source control activities were completed in 2020. Groundwater modeling in support of the Closure Plan suggested that the source control would lower water levels in the FAPS, reduce groundwater contaminant concentrations, and decrease the potential off-Site transport of CCR constituents (NRT, 2014a,b; Burns & McDonnell, 2021). Additional modeling was conducted for each of the corrective action alternatives to evaluate future groundwater quality in the vicinity of the FAPS as a result of residual plume management. The results of the modeling indicate that the time to achieve GWPSs for all compliance wells is in excess of 100 years¹³ for all three corrective action alternatives¹⁴ (Appendix B; Ramboll, 2025a). This is attributed to the underlying native lithological units beneath the CCR, *i.e.*, the UU and BU, which consist of low-permeability soils and underlying low-permeability shale and limestone bedrock. These conditions result in extended times to attain GWPS, regardless of the type of evaluated remedy (Appendix B; Ramboll, 2025a). Table 2.6 summarizes and compares timeline and overall implementation schedule for both alternatives (also discussed in Section 2.1.1 to 2.1.3). The updated model results are consistent with the modeling results presented in the Closure and Post-Closure Care Plan that was prepared in 2016 in support of the Closure Plan, which was subsequently approved by IEPA (Appendix B; Ramboll, 2025b).

In addition to predicting the time to reach GWPSs in the FAPS compliance wells, spatial analyses were conducted to evaluate each alternative's effectiveness in reducing the potential future footprint of contaminants in groundwater. This approach evaluated each alternative with regard CCR constituents that may be migrating beyond the Site's southern property boundary. The results suggest that both plume footprint would not be reduced during the model simulation period for the Source Control-GWP and Source Control-Cutoff Wall alternatives; however, the plume footprint for the Source Control-GMS alternative contracted over the model simulation period from 420 acres to 193 acres (Appendix B; Ramboll, 2025a). Additionally, the model results demonstrate that the Source Control-GMS alternative would be effective at reducing the off-Site transport of CCR constituents across the southern property boundary compared to the other two alternatives (Appendix B; Ramboll, 2025a).

¹³ While the model simulation period for each corrective action alternative was 1,000 years, model predictions at such lengthy future timescales are inherently uncertain.

¹⁴ Boron was selected as a surrogate for the contaminant fate and transport simulations to evaluate the effectiveness of each of the corrective action alternative. For modeling purposes, it was assumed that boron would not significantly sorb or chemically react with aquifer solids, which is a conservative estimate for predicting contaminant transport times in the model. Geochemical modeling results indicate that chemical attenuation of boron is feasible under current site conditions (Appendix E; Geosyntec Consultants, Inc., 2025).

Table 2.6 Estimated Timeline and Implementation Schedule Under Each Corrective Action Alternative

| Implementation Phase | Implementation Task | Timeframe | | |
|--|--|--------------------|--|--|
| | | Source Control-GWP | Source Control-Cutoff Wall | Source Control-GMS |
| 1: Pre-Construction Activities | Agency Coordination, Approvals, and Permitting | NA | 6 to 12 months | 6 to 12 months |
| | Final Design and Bid Process | | 24 to 36 months | 24 to 36 months |
| | Timeframe to Complete Corrective Pre-Construction Activities | | 30 to 48 months after CAP Approval (3-4 years) | 30 to 48 months after CAP Approval (3-4 years) |
| 2: Corrective Action Construction | Corrective Action Construction | NA | 12 to 24 months | 12 to 24 months |
| | Timeframe to Complete Corrective Action Construction | | 12 to 24 months | 12 to 24 months |
| 3: Corrective Action O&M and Closeout | Corrective Action Monitoring (Time to Meet GWPS) | >100 years | >100 years | >100 years |
| | Corrective Action Confirmation Monitoring | 36 months | 36 months | 36 months |
| | Corrective Action Completion Reporting | 6 months | 6 months | 6 months |
| Total Timeline to Complete Corrective Action | | >100 years | >100 years | >100 years |

Notes:

CAP = Corrective Action Plan; NA = Non-applicable; O&M = Operations and Management; Source Control-Cutoff Wall = Source Control with a Groundwater Cutoff Wall; Source Control-GMS = Source Control with Groundwater Management System; Source Control-GWP = Source Control with Groundwater Polishing.

Source: Appendix B; Ramboll, 2025b.

2.2.7 Potential for Exposure of Humans and Environmental Receptors to Remaining Wastes, Considering the Potential Threat to Human Health and the Environment Associated with Excavation, Transportation, Re-disposal, Containment, or Changes in Groundwater Flow (IAC Section 845.670(e)(1)(F))

Section 2.2.1 describes the magnitude of reduction of existing risks under each corrective action alternative. Section 2.2.2 describes the effectiveness of the remedy in controlling the source, including the extent to which containment practices would reduce further releases. Section 2.2.3 describes the likelihood of future releases of CCR occurring under each corrective action alternative, and Section 2.2.5 describes the short-term risks to workers, the community, and the environment during implementation of the remedy, including safety impacts and control of exposure to any residual contamination. In summary, source control measures (IEPA approved CIP approach) were completed in 2020. Thus, all corrective action alternatives would essentially eliminate the potential for a sudden CCR release (e.g., due to flooding or a dike failure event) due to the absence of both free liquids and impounded water within the unit.

For construction workers, risks arising from potential contact with residual contamination during construction, operation, and maintenance activities associated with residual plume management would be higher for the Source Control-Cutoff Wall and Source Control-GMS alternatives than for the Source Control-GWP alternative, because the Source Control-Cutoff Wall and Source Control-GMS alternatives would both involve the excavation and subsequent management of Site spoils. The Source Control-GMS alternative would additionally involve the production, management, and treatment of extracted water. Any potential CCR exposures occurring under Source Control-Cutoff Wall and Source Control-GMS alternatives during groundwater extraction and treatment or soil excavation within the FAPS would be managed through the use of rigorous safety protocols, personal protective equipment, and appropriate disposal practice. The Source Control-GWP alternative would not involve exposure to either of these soil or groundwater waste streams.

Hydrogeological changes would be expected under the Source Control-Cutoff Wall alternative due to the installation of a low-permeability barrier wall that intersects with the UU and BU. These changes include altering flow patterns in the UU, redirecting groundwater flow around the cutoff wall, and causing changes to normal hydraulic gradients. Some changes in groundwater flow (*i.e.*, controlled discharge into Kaskaskia River) may occur under the Source Control-GMS alternative, due to the operation of the extraction trench. Hydrogeological changes would also be expected under the Source Control-GMS alternative, such as lowering groundwater table in the vicinity of the extraction trench and altering flow patterns in the UU. However, changes to groundwater flow would not be expected to have an effect on the potential for the exposure of humans and environmental receptors to remaining wastes.

2.2.8 Long-Term Reliability of the Engineering and Institutional Controls (IAC Section 845.670(e)(1)(G))

Source Control (IEPA approved CIP approach) was in 2020. Thus, the long-term reliability of source control would be the same for all corrective action alternatives (AECOM, 2016a). The long-term reliability of the engineering and institutional controls associated with residual plume management of each corrective alternative are summarized below.

- Residual plume management under the Source Control-GWP alternative would be reliable, because it would rely on natural physical and geochemical processes, rather than the installation, operation, and maintenance of engineered systems or structures. Under this alternative, engineering failure would not occur, and no O&M activities would be required to ensure the success of the alternative (other than those required for groundwater monitoring). Active groundwater monitoring would be in place to track the remediation progress. Should the predicted decrease in groundwater concentrations not occur, the adaptive site management approach would enable prompt adjustments or enhancements to the corrective action in accordance with IAC Section 845.680(b). This strategy would allow continuous improvement of the FAPS groundwater remediation in response to new Site information and/or the performance of the corrective action alternative.
- Cutoff walls are proven remedies that have been implemented at many sites. Thus, residual plume management under the Source Control-Cutoff Wall alternative would be reliable provided it is constructed in accordance with standard design and specifications. The remedy consists of a passive, below-grade structure, which would not require any O&M activities once it is installed. Some challenges are expected during construction, necessitating specialized equipment deployment. Quality control (QC) and quality assurance (QA) programs would be required during the construction to ensure the effectiveness of the cutoff wall. Active groundwater monitoring would be in place, similar to the monitoring required under the Source Control-GWP alternative.

- For the Source Control-GMS alternative, groundwater extraction and treatment systems are proven remedies that have been implemented at many sites. Thus, residual plume management under the Source Control-GMS alternative would be expected to be reliable provided it is constructed in accordance with standard design and specifications. Under this alternative, the extraction trench system would require engineering design and installation for groundwater extraction and treatment. Routine and non-routine maintenance of the system is required to ensure reliable operation of the extraction trench and pumps, as well as other MEP system components. Active groundwater monitoring would be in place, similar to those required under the Source Control-GWP alternative.
- For all corrective action alternatives, remedy optimizations would be implemented, if necessary, under the adaptive site management plan.

2.2.9 Potential Need for Replacement of the Remedy (IAC Section 845.670(e)(1)(H))

The potential need for the eventual replacement of the residual plume management remedy under each corrective action alternative is summarized as follows:

- Residual plume management under Source Control-GWP would rely on natural physical geochemical processes to achieve reductions in groundwater concentrations to below the GWPSs. Because no installation, operation, and maintenance of engineered systems or structures would be required, it would be unlikely that the residual plume management remedy under the Source Control-GWP alternative would need to be replaced. Adaptive site management strategies would be used to implement remedy optimizations or replacement, as necessary based on data that are collected, to ensure that remedial goals are achieved.
- Residual plume management under Source Control-Cutoff Wall would rely on a cutoff wall as a physical barrier to achieve reductions in groundwater concentrations to below GWPSs. Because the cutoff wall is a robust, engineered, and maintenance-free subsurface structure, it is unlikely that the residual plume management remedy under the Source Control-Cutoff Wall alternative would need to be replaced. Adaptive site management strategies would be used to implement remedy optimizations or replacement, as necessary based on data that are collected, to ensure that remedial goals are achieved.
- Residual plume management under Source Control-GMS would utilize an extraction trench and a settling pond to extract and treat contaminated water to achieve reductions in contaminant plume sizes, as well as physical and geochemical attenuation. The GMS system is anticipated to be highly reliable with minimal need for replacement within its standard 50-year design lifespan. However, ongoing maintenance and potential replacement of system components are expected over time, including:
 - Periodic maintenance, such as jetting or redevelopment of the perforated drainpipe in the extraction trench.
 - MEP components like pumps and other instrumentation would likely require servicing or replacement every 10 to 20 years, resulting in multiple replacements over the long-term operational life of the remedy.
 - Long-term degradation or fouling of the extraction trench components, including the perforated collection pipe and backfill media, may eventually require replacement. However, data on the performance of such systems over a timespan greater than 100 years is limited, as these types of systems have only been in use for about 100 years.
 - Any future replacement of the extraction trench would be evaluated through ongoing adaptive site management activities.

2.3 The Ease or Difficulty of Implementing a Remedy (IAC Section 845.670 (e)(3))

2.3.1 Degree of Difficulty Associated with Constructing the Remedy (IAC Section 845.670(e)(3)(A))

Source control (IEPA approved CIP approach) was implemented in 2020 (AECOM, 2016a). Thus, there would be no further construction difficulties associated with source control. The expected degree of difficulty associated with residual plume management for each of the corrective action alternatives is summarized below.

- Residual plume management under the Source Control-GWP alternative would rely on physical and geochemical attenuation processes and therefore would not pose any significant construction challenges. Therefore, there would be minimal difficulty in constructing the Source Control-GWP remedy.
- Residual plume management under the Source Control-Cutoff Wall alternative would rely on a barrier wall to prevent groundwater migration off-Site, and physical and geochemical attenuation processes to address downgradient groundwater quality impacts. Some challenges may be encountered during the construction of the cutoff wall, including the following (Appendix B; Ramboll, 2025b):
 - Implementing the remedy entails the mobilization of specialized equipment to the Site, including large cranes, clamshells, slurry cutters, and/or one-pass trenching equipment, *etc.* Supporting equipment such as batch plants, excavation, and grading equipment may also be used.
 - Although cutoff walls are commonly constructed to similar depths in comparable geologic environments, challenges during construction may still arise. These challenges may involve encountering highly permeable layers (leading to slurry loss), obstructions that necessitate specialized techniques and/or equipment for progression, or sidewall instability.
 - The effectiveness of the cutoff wall relies on the construction techniques employed to prevent gaps, voids, or other discontinuities in the structure. Ongoing QC is essential during construction as part of QA activities to prevent such defective features. Additionally, QA programs, such as coring and testing, may be necessary to validate the quality of the constructed barrier.
 - The performance of the wall is contingent on its actual hydraulic conductivity. This necessitates ongoing monitoring and QA/QC testing for slurry mixing, placement, or soil-bentonite mixing. The goal is to ensure adherence to the designed mix and involves routine testing of samples from the wall material.
- Residual plume management under the Source Control-GMS would involve utilization of an extraction trench, settling pond and conveyance system to extract and treat contaminated groundwater, in addition to physical and geochemical attenuation processes to address downgradient groundwater quality impacts. However, there may be challenges during the implementation of the GMS, including the following (Appendix B; Ramboll, 2025b):
 - Implementing the remedy entails the mobilization of specialized equipment to the Site, including large cranes, clamshells, slurry cutters, and/or one-pass trenching equipment, *etc.*

Supporting equipment such as batch plants, excavation, and grading equipment may also be used.

- While trenches of similar depth and geology are routinely built, challenges such as encountering obstructions may necessitate specialized techniques and /or equipment.
- The construction may require detailed geotechnical design for the working platform.
- The MEP components are commonly handled by regional or local contractors and are not expected to pose construction challenges.

2.3.2 Expected Operational Reliability of the Remedy (IAC Section 845.670(e)(3)(B))

Source control (IEPA approved CIP approach) was implemented in 2020 (AECOM, 2016a). Thus, the operational reliability of the remedy would be the same for all corrective action alternatives. All three corrective action alternatives would likely be highly reliable with respect to operational controls associated with residual plume management; specific details for each corrective action alternative are discussed below.

- Residual plume management under the Source Control-GWP alternative would have high operational reliability because it would rely on natural processes and active monitoring, rather than the installation, operation, and maintenance of engineered systems or structures (other than monitoring wells). Under the Source Control-GWP alternative, engineering failure would not occur, and no O&M activities would be required to ensure the success of the alternative.
- Residual plume management under the Source Control-Cutoff Wall alternative would also have high operational reliability, because it is an established remedial technology, as long as it is constructed in accordance with standard design specifications for barrier walls. The cutoff wall is a passive, continuous, and low-permeability barrier to groundwater and no O&M would be required after its installation.
- Residual plume management under the Source Control-GMS alternative would also have high operational reliability because it is an established technology as long as the GMS (*i.e.*, the extraction trench and the MEP system) is constructed in accordance with the design specifications. In addition, the remedy would require routine and non-routine maintenance of the mechanical system to ensure reliable operation.

2.3.3 Need to Coordinate with and Obtain Necessary Approvals and Permits from Other Agencies (IAC Section 845.670(e)(3)(C))

All corrective action alternatives would require regulatory approvals. Specific permits and approvals associated with source control were the same for all corrective action alternatives and were discussed in the Closure Plan (AECOM, 2016a). The specific approvals and permits associated with residual plume management for all corrective action alternatives are discussed below.

- Residual plume management under the Source Control-GWP alternative would not need additional permits from other agencies, other than the approval of the eventual Corrective Action Plan.
- Residual plume management under the Source Control-Cutoff Wall alternative would require permits from the IEPA for construction of stormwater controls and BMPs. Due to modification of the FAPS embankment, an Illinois Department of Natural Resources (IDNR) Office of Water Resources, Dam Safety modification permit would need to be obtained. It is estimated permitting, and approval will typically take 6 to 12 months to obtain (Appendix B; Ramboll, 2025b).

- Residual plume management under the Source Control-GMS alternative would require permits from the IEPA for construction of stormwater controls, BMPs, in addition to a joint water pollution control construction and operation permit. Groundwater extracted from the extraction trench would require a modified NPDES permit. The NPDES permit would likely require renewals depending on the timeline of corrective action implementation, and typically take 18 to 24 months to obtain. Due to modification of the FAPS embankment, an IDNR Office of Water Resources, Dam Safety modification permit would need to be obtained (Appendix B; Ramboll, 2025b).

2.3.4 Availability of Necessary Equipment and Specialists (IAC Sections 845.670(e)(3)(D) and 845.660(c)(1), "Ease of Implementation")

Source control (IEPA approved CIP approach) was implemented in 2020 (AECOM, 2016a). Thus, there are no further equipment and specialist needs associated with the implementation of the source control remedy. Specialized equipment and personnel are essential for field data collection and groundwater sampling for residual plume management under all potential corrective action alternatives. Additionally, the assessment of groundwater concentrations for Site constituents would necessitate laboratory equipment and specialists for all alternatives. The availability of equipment and specialists associated with residual plume management for each corrective action alternative is summarized below.

- Residual plume management under the Source Control-GWP alternative would require groundwater professionals, such as geologists, hydrogeologists, statisticians (*i.e.*, statistical analysis), and geochemists to evaluate all monitoring data, ensuring that physical and geochemical processes function as anticipated for this alternative. The equipment and specialists needed for Site groundwater monitoring and analysis are currently engaged in these tasks as part of the routine groundwater monitoring program outlined in accordance with IAC Section 845.220(c)(4).
- Residual plume management under the Source Control-Cutoff Wall alternative would require specialists and specialty equipment for the construction of the cutoff wall.
 - Excavation and construction of the cutoff wall on the Site would require a specialized contractor with experience excavating similar size trenches in similar geologic environments and constructing barrier walls with similar design specification. The contractor would probably need specialized and often custom-built equipment including large cranes, slurry cutters, batch plants and/or one-pass construction equipment.
 - Specialists involved in the design and construction of cutoff walls would be essential during both phases. This team of specialists should involve design engineers, construction managers, and contractor staff with expertise in cutoff wall construction and equipment operation.
 - The types of equipment and specialists should have been employed for projects similar to designing and building cutoff walls. However, there may be backlogs associated with the equipment and specialists, due to the high existing demand for specialty ground improvement contractors and design specialists who are engaged with similar projects in sectors like electric utilities, dams/levees, and other areas.
 - This alternative would also require the use of equipment and the expertise of specialists for tasks such as field data collection, groundwater sampling, groundwater sample analysis, and periodic corrective action groundwater monitoring and reporting. Similar to those in the Source Control-GWP alternative, these activities are already being conducted as part of routine groundwater monitoring in accordance with IAC Section 845.220(c)(4).
- Residual plume management under the Source Control-GMS alternative would require specialists to install and manage the GMS system throughout its operational period.

- Construction of the extraction system on the Site would require a specialized contractor with experience constructing similar size trenches in similar geologic environments. The contractor would probably need specialized and often custom-built equipment including one-pass construction equipment.
- Specialists involved in the design and construction of cutoff walls would be essential during both phases. This team of specialists should involve design engineers, construction managers, and contractor staff with expertise in trench construction and equipment operation. Geotechnical specialists may be required to design the working platform and monitor the FAPS embankment for any signs of distress during the one-pass trench installation.
- The types of equipment and specialists should have been employed for projects similar to designing and installing extraction trenches. However, there may be backlogs associated with the equipment and specialists, due to the high existing demand for specialty ground improvement contractors and design specialists who are engaged with similar projects in sectors like electric utilities, dams/levees, and other areas.
- This alternative would necessitate the use of equipment and the expertise of specialists for tasks such as regular groundwater system O&M, field data collection, groundwater sampling, analysis, and periodic corrective action groundwater monitoring and reporting. Similar to those in the GWP alternative, some of these activities are already being conducted as part of routine groundwater monitoring in accordance with IAC Section 845.220(c)(4).

2.3.5 Available Capacity and Location of Needed Treatment, Storage, and Disposal Services/Comply with Standards for Management of Wastes as Specified in Section 845.680(d) (IAC Section 845.670(e)(3)(D)/IAC Section 845.670(d)(5))

The available capacity and location of needed treatment, storage, and disposal services associated with residual plume management under each corrective action alternative is summarized below. All the practices employed in an alternative would comply with standards for the management of wastes as specified in IAC Section 845.670(e)(3)(D) and IAC Section 845.680(d)(5).

- Residual plume management for the Source Control-GWP remedy would not require any treatment, storage, or disposal services, because GWP is not anticipated to produce a substantial amount of waste or wastewater, aside from minor purge water volumes generated during routine groundwater sampling activities for residual plume management. This could be managed by a standard waste management contractor.
- Residual plume management for the Source Control-Cutoff Wall would generate CCR-containing spoils during the construction phase. The CCR spoils would be transported to an off-Site landfill for disposal. An evaluation would be completed to determine the best location for disposal. Excavated non-CCR spoils would be disposed of at an appropriate on-Site location. No wastes would be expected to be generated during operations of the cutoff wall, and consequently, no additional treatment, storage, or disposal services would be necessary for this remedy.
- Residual plume management for the Source Control-GMS alternative would generate waste during construction of the extraction trench system and management of wastewater through a settling pond on-Site:
 - The construction of the extraction trench would generate spoils, and the waste materials consisting of predominantly CCR would be dried and disposed at an appropriate on-Site location. An evaluation would be completed to determine the best location for disposal.

- The extraction trench system would send extracted groundwater to an on-Site settling pond, which collects solids removed during groundwater recovery *via* the pneumatic extraction pumps and transfer piping. The location of the settling pond would be evaluated at a later phase. The siting of the settling pond would need to consider limiting impacts to existing Site infrastructure, wetlands, and floodplains.
- Discharge from the settling pond would be conveyed to an NPDES permitted outfall. Renewal of the NPDES permits may be necessary to continue operations, depending on the timeline of the corrective action implementation in relation to the remedy completion.

2.4 The Degree to Which Community Concerns Are Addressed by the Remedy (IAC Section 845.670(e)(4))

Several nonprofit groups raised concerns regarding the potential impacts of the FAPS on groundwater and surface water quality including Earthjustice, the Prairie Rivers Network, and the Sierra Club (Earthjustice *et al.*, 2018; Lydersen, 2017). The combination of source control (IEPA approved CIP approach) and residual plume management would cause groundwater concentrations to decline over time under all of the corrective action alternatives (NRT, 2014a; Burns & McDonnell, 2021), thus addressing community concerns. The CCR constituents impacts to off-Site groundwater are being monitored and will be addressed by residual plume management under the three corrective action alternatives.

A public meeting will be held on March 20, 2025, pursuant to requirements under IAC Section 845.710(e). Questions raised by attendees will be answered at the meeting; subsequently, a written summary of all questions and responses will be made available to interested parties.

2.5 Remove From the Environment as Much of the Contaminated Material that Was Released from the CCR Surface Impoundment as Is Feasible, Taking into Account Factors such as Avoiding Inappropriate Disturbance of Sensitive Ecosystems (IAC Section 845.670(d)(4))

There have been no known releases of CCR at the FAPS (Ramboll, 2025c). All potential corrective action alternatives include source control (IEPA approved CIP approach). These source control activities are expected to "minimize water infiltration into the closed FAPS and improve surface water drainage off the cover system, thus reducing generation of potentially impacted water and ultimately reducing the extent of CCR impacts to groundwater" (Appendix C; Ramboll, 2024a). Groundwater modeling performed in support of the Closure Plan suggested that the source control would provide control of surface run-off on the cover system, lower water levels in the FAPS, reduce groundwater contaminant concentrations, and decrease the potential transport of CCR constituents off-Site (NRT, 2014a,b; Burns & McDonnell, 2021). Due to the reduction in the hydraulic flux out of the FAPS, the mass flux out of the FAPS would also be controlled and. Therefore, source control is preventing further releases of CCR constituents into the environment.

Moreover, residual plume management under each corrective action alternative will further result in the removal of contaminated material from the environment and/or the improvement of downgradient groundwater quality. Additional modeling was conducted for each of the corrective action alternatives to evaluate future groundwater quality in the vicinity of the FAPS as a result of residual plume management. The results predicted a reduction in size of the groundwater plume from 420 acres to 193 acres under the

Source Control-GMS alternative (Appendix B; Ramboll, 2025b). Specific considerations for residual plume management for each alternative are provided below.

- Residual plume management under the Source Control-GWP alternative would address impacted groundwater by relying on natural physical and geochemical attenuation processes to reduce the residual concentrations of CCR. Site-specific evaluations have shown that groundwater polishing would reduce the groundwater concentrations and mobility of inorganic contaminants. Specifically, the results indicate that boron and sulfate attenuation *via* sorption onto mineral surfaces such as iron and aluminum oxides, would occur under current conditions (*i.e.*, post-closure). Some desorption is predicted to occur as groundwater returns to background conditions, but the changes are expected to be minimal (Appendix E; Geosyntec Consultants, Inc., 2025). In cases in which observed groundwater concentrations deviate significantly from modeled conditions, alternative methods or techniques to remove residual sources to achieve the GWPSs would be evaluated under the adaptive site management, and if viable, incorporated as per IAC Section 845.680(b). No sensitive ecosystems would be disturbed because no construction activities would be expected under the Source Control-GWP alternative.
- Residual plume management under the Source Control-Cutoff Wall would rely on an engineered system to prevent the horizontal migration of impacted groundwater away from the FAPS. Groundwater quality would also be improved as a result of physical and geochemical attenuation processes. The construction activities would likely result in some negative impacts to the ecosystem, including disturbance of habitat near the construction areas by causing alarm and escape behavior in nearby wildlife (*e.g.*, due to noise disturbances). Short-term impacts could also occur to sensitive aquatic and wetland species in Kaskaskia River and other wetlands and surface water near the FAPS (see Section 1.1.3) due to sediment runoff during construction.
- Residual plume management under the Source Control-GMS alternative would rely on an engineered extraction system to actively remove constituent mass from the environment. Residual concentrations of CCR constituents in groundwater would also be reduced as a result of physical and geochemical attenuation processes. The construction activities would likely result in some negative impacts to the ecosystem, including disturbance of habitat near the construction areas by causing alarm and escape behavior in nearby wildlife (*e.g.*, due to noise disturbances). Short-term impacts could also occur to sensitive aquatic and wetland species in Kaskaskia River and other wetlands and surface water near the FAPS (see Section 1.1.3) due to sediment runoff during construction.

2.6 Summary

This CAAA evaluates three corrective action alternatives identified as potentially viable in the CMA with regard to each of the factors specified in IAC Section 845.670(d) and 845.670(e) (IEPA, 2021). Based on this evaluation, the most appropriate corrective action for this Site is Source Control-GMS. While the time to achieve GWPSs for all three alternatives was predicted to be in excess of 100 years due to the presence of native low-permeability lithological units, groundwater modeling suggests that Source Control-GMS would be most effective at reducing plume size and minimizing the risk of CCR constituents migrating beyond the Site's southern property boundary. Thus, Source Control-GMS is the most appropriate corrective action alternative for the FAPS.

References

AECOM. 2016a. "Closure and Post-Closure Care Plan for the Baldwin Fly Ash Pond System/at Dynegy Midwest Generation, LLC Baldwin Energy Complex, 10901 Baldwin Road, Baldwin, IL 62217 (Final)." Report to Dynegy Midwest Generation, LLC Baldwin Energy Complex, Baldwin, IL. 393p., March.

AECOM. 2016b. "Letter Report re: History of Construction, USEPA Final CCR Rule, 40 CFR § 257.73(c), Baldwin Energy Complex, Baldwin, Illinois." Report to Dynegy Midwest Generation, LLC, Baldwin, IL. 440p. October.

Burns & McDonnell. 2021. "Initial Operating Permit, Baldwin Power Plant Fly Ash System." Report to Dynegy Midwest Generation, LLC, Collinsville, IL. Submitted to Illinois Environmental Protection Agency (IEPA). 1119p., October 25.

Earthjustice; Prairie Rivers Network; Environmental Integrity Project (EIP); Sierra Club. 2018. "Cap and Run: Toxic Coal Ash Left Behind by Big Polluters Threatens Illinois Water." 45p.

Geosyntec Consultants, Inc. 2025. "Groundwater Polishing Evaluation Report, Baldwin Power Plant - Fly Ash Pond System (IEPA ID No. 605) (Draft)." Report to Dynegy Midwest Generation, LLC, Collinsville, IL. 370p., January.

Google LLC. 2022. "Google Maps." Accessed on date of map or deliverable issue at <https://www.google.com/maps>.

Google LLC. 2024. "Google Maps." Accessed on date of map or deliverable issue at <https://www.google.com/maps>.

Gradient. 2025. "Human Health and Ecological Risk Assessment, Fly Ash Pond System, Baldwin Power Plant, Baldwin, Illinois." 55p., February 12.

Hesterberg, TW; Valberg, PA; Long, CM; Bunn, WB III; Lapin, C. 2009. "Laboratory studies of diesel exhaust health effects: Implications for near-roadway exposures." EM Mag. (August):12-16. Accessed at <http://pubs.awma.org/gsearch/em/2009/8/hesterberg.pdf>.

Illinois Dept. of Natural Resources (IDNR). 2022. "About Kaskaskia River." Accessed on November 8, 2022 at <https://www2.illinois.gov/dnr/Parks/About/Pages/KaskaskiaRiver.aspx>

Illinois Environmental Protection Agency (IEPA). 2021. "Standards for the disposal of coal combustion residuals in surface impoundments." Accessed at <https://www.ilga.gov/commission/jcar/admincode/035/03500845sections.html>.

Illinois Environmental Protection Agency (IEPA). 2022. "Appendix A-1. Specific Assessment Information for Streams, 2020/2022." Bureau of Water. In Illinois Integrated Water Quality Report and Section 303(d) List, 2020/2022. 103p., May 26. Accessed at https://www2.illinois.gov/epa/topics/water-quality/watershed-management/tmdls/Documents/A1_Streams_FINAL_5-26-22.pdf

Lydersen, K. 2017. "Citizens fill void in oversight of potentially hazardous Illinois coal ash impoundments." *Energy News Network*. January 20. Accessed at <https://energynews.us/2017/01/20/citizens-fill-void-in-oversight-of-potentially-hazardous-illinois-coal-ash-impoundments/>.

Mauderly, JL; Garshick, E. 2009. "Diesel exhaust." In *Environmental Toxicants: Human Exposures and Their Health Effects (Third Edition)*. Ed.: Lippmann, M, John Wiley & Sons, Inc., Hoboken, NJ. p551-631.

Morris, P. [Dynergy Midwest Generation, LLC]. 2020. "Letter to D. LeCrone (IEPA) [re: Notification of completion of closure: Baldwin Energy Complex; Old East Fly Ash Pond, East Fly Ash Pond, and West Ash Pond]." 2p., December 17.

National Research Council (NRC). 2013. "Alternatives for Managing the Nation's Complex Contaminated Groundwater Sites." Division of Earth and Life Sciences, Water Science and Technology Board, Committee on Future Options for Management in the Nation's Subsurface Remediation Effort. National Academies Press, Washington, DC. 422p. Accessed at http://www.nap.edu/catalog.php?record_id=14668.

Natural Resource Technology, Inc. (NRT). 2014a. "Groundwater Model and Simulation of Closure Alternatives, Baldwin Ash Pond System, Baldwin Energy Complex, Baldwin, Illinois, Dynergy Midwest Generation, LLC." Report to Dynergy Operating Co., Collinsville, IL. Submitted to Illinois Environmental Protection Agency (IEPA). 49p., June 18.

Natural Resource Technology, Inc. (NRT). 2014b. "Model Report Addendum re: Prediction of Plume Stability by Groundwater Modeling, Baldwin Ash Pond System, Baldwin Energy Complex, Baldwin, Illinois." Report to Dynergy Operating Co. 23p., September 30.

Natural Resource Technology, Inc. (NRT). 2016. "Supplemental Hydrogeologic Site Characterization and Groundwater Monitoring Plan, Baldwin Fly Ash Pond System, Baldwin Energy Complex, Baldwin, Illinois." Report to Dynergy Midwest Generation, LLC, Collinsville, IL. 254p., March 31.

OBG. 2019. "Corrective Measures Assessment, Baldwin Fly Ash Pond System, Baldwin Energy Complex, 10901 Baldwin Road, Baldwin, Illinois." Part of Ramboll. Report to Dynergy Midwest Generation, LLC. 24p., September 5

Ramboll. 2021. "Hydrogeologic Site Characterization Report, Bottom Ash Pond, Baldwin Power Plant, Baldwin, Illinois (Final)." Report to Dynergy Midwest Generation, LLC. 504p., October 25.

Ramboll. 2024a. "35 I.A.C. § 845 Corrective Measures Assessment, Fly Ash Pond System, Baldwin Power Plant, Baldwin, Illinois, IEPA ID: W1578510001-01/02/03 (Draft)." Report to Dynergy Midwest Generation, LLC. 21p., April 5.

Ramboll. 2024b. "Nature and Extent Report, Baldwin Power Plant, Fly Ash Pond System, IEPA ID No. W1578510001-01, W1578510001-02, and W1578510001-03 (Final)." Report to Dynergy Midwest Generation, LLC, Baldwin, IL. 382p., April 24.

Ramboll. 2025a. "Groundwater Modeling Technical Memorandum, Baldwin Power Plant, Fly Ash Pond System, IEPA ID No. W1578510001-01/02/03 (Draft)." Report to Dynergy Midwest Generation, LLC. 44p., February 18.

Ramboll. 2025b. "Corrective Action Alternatives Analysis Supporting Information Report: Fly Ash Pond System, Baldwin Power Plant, IEPA ID NO. W1578510001-01/02/03 (Initial Draft)." Report to Dynegy Midwest Generation, LLC, Baldwin, IL. February 18.

Ramboll. 2025c. "Corrective Action Plan, Fly Ash Pond System, Baldwin Power Plant, IEPA No. W1578510001-01/02/03 (Final Draft)." Report to Dynegy Midwest Generation, LLC, Baldwin, IL. 24p., February 18.

US Dept. of Labor (US DOL). 2020a. "Fatal occupational injuries, total hours worked, and rates of fatal occupational injuries by selected worker characteristics, occupations, and industries, civilian workers, 2019." Bureau of Labor Statistics. December. Accessed at https://www.bls.gov/iif/oshwc/cfoi/cfoi_rates_2019hb.xlsx.

US Dept. of Labor (US DOL). 2020b. "Table R100. Incidence rates for nonfatal occupational injuries and illnesses involving days away from work per 10,000 full-time workers by occupation and selected events or exposures leading to injury or illness, private industry, 2019." Bureau of Labor Statistics. October. Accessed at https://www.bls.gov/iif/oshwc/osh/case/cd_r100_2019.xlsx.

US Dept. of Transportation (US DOT). 2023a. "Traffic Safety Facts 2021: A Compilation of Motor Vehicle Crash Data." National Highway Traffic Safety Administration (NHTSA), National Center for Statistics and Analysis (NCSA). DOT HS 813 527. 225p., December. Accessed at <https://crashstats.nhtsa.dot.gov/Api/Public/ViewPublication/813527>.

US Dept. of Transportation (US DOT). 2023b. "Large Truck and Bus Crash Facts 2021." Federal Motor Carrier Safety Administration, Analysis Division. FMCSA-RRA-23-002. 118p., November.

US EPA. 2014. "Human and Ecological Risk Assessment of Coal Combustion Residuals (Final)." Office of Solid Waste and Emergency Response (OSWER), Office of Resource Conservation and Recovery. Submitted to US EPA Docket. EPA-HQ-OLEM-2020-0107-0885. 1237p., December. Accessed at <http://www.regulations.gov/#!documentDetail;D=EPA-HQ-RCRA-2009-0640-11993>.

US EPA. 2015a. "Hazardous and solid waste management system; Disposal of coal combustion residuals from electric utilities (Final rule)." *Fed. Reg.* 80(74):21302-21501. 40 CFR 257, 40 CFR 261. April 17.

US EPA. 2015b. "Use of Monitored Natural Attenuation for Inorganic Contaminants in Groundwater at Superfund Sites." Office of Solid Waste and Emergency Response (OSWER). OSWER Directive 9283.1-36. 83p., August.

US EPA. 2022. "Evansville, Illinois, Watershed: Baldwin Lake-Kaskaskia River (071402040908)." Accessed at <https://mywaterway.epa.gov/community/071402040908/overview>.

Appendix A

Human Health and Ecological Risk Assessment

**Human Health and Ecological Risk Assessment
Fly Ash Pond System
Baldwin Power Plant
Baldwin, Illinois**

February 12, 2025



GRADIENT

www.gradientcorp.com

One Beacon Street, 17th Floor
Boston, MA 02108
617-395-5000

Table of Contents

| | <u>Page</u> |
|------------|---|
| 1 | Introduction 1 |
| 2 | Site Overview 3 |
| 2.1 | Site Description 3 |
| 2.2 | Geology/Hydrogeology 3 |
| 2.3 | Conceptual Site Model 4 |
| 2.4 | Groundwater Monitoring 5 |
| 2.5 | Surface Water Monitoring 9 |
| 3 | Risk Evaluation 11 |
| 3.1 | Risk Evaluation Process 11 |
| 3.2 | Human and Ecological Conceptual Exposure Models 12 |
| 3.2.1 | Human Conceptual Exposure Model 12 |
| 3.2.1.1 | Groundwater as a Drinking Water/Irrigation Source 14 |
| 3.2.1.2 | Surface Water as a Drinking Water Source 16 |
| 3.2.1.3 | Recreational Exposures 16 |
| 3.2.2 | Ecological Conceptual Exposure Model 17 |
| 3.3 | Identification of Constituents of Interest 18 |
| 3.3.1 | Human Health Constituents of Interest 18 |
| 3.3.2 | Ecological Constituents of Interest 20 |
| 3.3.3 | Surface Water and Sediment Modeling 22 |
| 3.4 | Human Health Risk Evaluation 25 |
| 3.4.1 | Residential Use of Surface Water as Drinking Water 25 |
| 3.4.2 | Recreators Exposed to Surface Water 26 |
| 3.4.3 | Recreators Exposed to Sediment 28 |
| 3.5 | Ecological Risk Evaluation 29 |
| 3.5.1 | Ecological Receptors Exposed to Surface Water 29 |
| 3.5.2 | Ecological Receptors Exposed to Sediment 30 |
| 3.5.3 | Ecological Receptors Exposed to Bioaccumulative Constituents of Interest 31 |
| 3.6 | Uncertainties and Conservatism 31 |
| 4 | Summary and Conclusions 34 |
| | References 36 |
| Appendix A | Surface Water and Sediment Modeling |
| Appendix B | Screening Benchmarks |

List of Tables

| | |
|------------|---|
| Table 2.1 | Groundwater Monitoring Wells Related to the FAPS |
| Table 2.2 | Groundwater Data Summary (2019-2024) |
| Table 2.3 | Surface Water Data Summary |
| Table 3.1 | Summary of Water Wells Within 1,000 Meters of the FAPS |
| Table 3.2 | Human Health Constituents of Interest |
| Table 3.3 | Ecological Constituents of Interest |
| Table 3.4 | Groundwater Properties Used in Modeling of the Upper Unit (UU) |
| Table 3.5 | Groundwater Properties Used in Modeling of the Uppermost Aquifer (UA or BU) |
| Table 3.6 | Surface Water Properties Used in Modeling |
| Table 3.7 | Sediment Properties Used in Modeling |
| Table 3.8 | Surface Water and Sediment Modeling Results |
| Table 3.9 | Risk Evaluation for Residents Exposed to Surface Water |
| Table 3.10 | Risk Evaluation for Recreators Exposed to Surface Water |
| Table 3.11 | Risk Evaluation for Recreators Exposed to Sediment |
| Table 3.12 | Risk Evaluation for Ecological Receptors Exposed to Surface Water |
| Table 3.13 | Risk Evaluation for Ecological Receptors Exposed to Sediment |

List of Figures

- Figure 2.1 Site Location Map
- Figure 2.2 Shallow Potentiometric Surface Map and Groundwater Flow Direction
- Figure 2.3 Monitoring Well Locations
- Figure 2.4 Surface Water Sample Location
- Figure 3.1 Overview of Risk Evaluation Methodology
- Figure 3.2 Human Conceptual Exposure Model
- Figure 3.3 Water Wells Within 1,000 Meters of the FAPS
- Figure 3.4 Kaskaskia River State Fish and Wildlife Area
- Figure 3.5 Ecological Conceptual Exposure Model

Abbreviations

| | |
|----------------|--|
| ADI | Acceptable Daily Intake |
| BAP | Bottom Ash Pond |
| BCF | Bioconcentration Factor |
| BCG | Biota Concentration Guide |
| BPP | Baldwin Power Plant |
| BU | Bedrock Unit |
| CAAA | Corrective Action Alternative Analysis |
| CCR | Coal Combustion Residuals |
| CEM | Conceptual Exposure Model |
| COI | Constituent of Interest |
| COPC | Constituent of Potential Concern |
| CSF | Cancer Slope Factor |
| CSM | Conceptual Site Model |
| CWS | Community Water Supply |
| ESV | Ecological Screening Value |
| FAPS | Fly Ash Pond System |
| GWPS | Groundwater Protection Standard |
| GWQS | Groundwater Quality Standard |
| HTC | Human Threshold Criteria |
| IAC | Illinois Administrative Code |
| ID | Identification |
| IEPA | Illinois Environmental Protection Agency |
| K _d | Equilibrium Partitioning Coefficient |
| MCL | Maximum Contaminant Level |
| NRWQC | National Recommended Water Quality Criteria |
| ORNL RAIS | Oak Ridge National Laboratory's Risk Assessment Information System |
| pCi/L | PicoCuries per Liter |
| PMP | Potential Migration Pathway |
| PRG | Preliminary Remediation Goal |
| RfD | Reference Dose |
| RME | Reasonable Maximum Exposure |
| RSL | Regional Screening Level |
| SFWA | State Fish and Wildlife Area |
| SWQS | Surface Water Quality Standard |
| UA | Uppermost Aquifer |
| UGU | Upper Groundwater Unit |
| US DOE | United States Department of Energy |
| US EPA | United States Environmental Protection Agency |
| UU | Upper Unit |

1 Introduction

Dynegy Midwest Generation, LLC operates the Baldwin Power Plant (BPP or "the Site") in Baldwin, Illinois. BPP is an electric power generating facility with coal-fired units that began operation in 1970 (Ramboll, 2021a). The BPP has several surface impoundments for storage of coal combustion residuals (CCR): the Bottom Ash Pond (BAP) (Vistra identification [ID] number [No.] 601, Illinois Environmental Protection Agency [IEPA] ID No. W1578510001-06); the Fly Ash Pond System (FAPS, an IEPA closed CCR Unit) (Vistra ID No. 605; IEPA ID Nos. W1578510001-01, W1578510001-02, and W1578510001-03); the Secondary Pond, Tertiary Pond; and Cooling Pond (Ramboll, 2021a). The FAPS, the subject of this report, includes the East Fly Ash Pond (76 acres), Old East Fly Ash Pond (102 acres), and the West Fly Ash Pond (54 acres) (NRT, 2016).

This report presents the results of an evaluation that characterizes potential risk to human and ecological receptors that may be exposed to CCR constituents in environmental media originating from the FAPS. This risk evaluation was performed to support the Corrective Action Alternative Analysis (CAAA) for the FAPS in accordance with requirements in Title 35 Part 845 of the Illinois Administrative Code (IAC) (IEPA, 2021). Human and ecological risks were evaluated for Site-specific constituents of interest (COIs). The conceptual site model (CSM) assumed that Site-related COIs in groundwater may migrate to the Kaskaskia River and affect surface water and sediment in the vicinity of the Site.

Consistent with United States Environmental Protection Agency (US EPA) guidance (US EPA, 1989), this report used a tiered approach to evaluate potential risks, which included the following steps:

1. Identify complete exposure pathways and develop a conceptual exposure model (CEM).
2. Identify Site-related COIs: Constituents detected in groundwater were considered COIs if their maximum detected concentration over the period from 2019 to 2024 exceeded a groundwater protection standard (GWPS) identified in Part 845.600 (IEPA, 2021), or a relevant surface water quality standard (SWQS) (IEPA, 2019; US EPA Region IV, 2018).
3. Perform screening-level risk analysis: Compare maximum measured or modeled COI concentrations in surface water and sediment to conservative, health-protective benchmarks in order to determine constituents of potential concern (COPCs).
4. Perform refined risk analysis: If COPCs are identified, perform a refined analysis to evaluate potential risks associated with the COPCs.
5. Formulate risk conclusions and discuss any associated uncertainties.

This assessment relies on a conservative (*i.e.*, health-protective) approach and is consistent with the risk approaches outlined in US EPA guidance. Specifically, we considered evaluation criteria detailed in IEPA guidance documents (*e.g.*, IEPA, 2013, 2019), incorporating principles and assumptions consistent with the Federal CCR Rule (US EPA, 2015a) and US EPA's "Human and Ecological Risk Assessment of Coal Combustion Residuals" (US EPA, 2014).

US EPA has established acceptable risk metrics. Risks above these US EPA-defined metrics are termed potentially "unacceptable risks." Based on the evaluation presented in this report, no unacceptable risks to human or ecological receptors resulting from CCR exposures associated with the FAPS were identified. This means that the risks from the Site are likely indistinguishable from normal background risks. Specific risk assessment results include the following:

- For groundwater used as drinking water, based on recent investigations and data collected from off-Site monitoring wells, private wells on properties south of the BPP are unlikely to be impacted by groundwater constituents associated with the BPP in excess of the GWPSs. The other private wells identified in the vicinity of the Site are upgradient or side-gradient of the BPP, and are therefore also unlikely to be impacted by groundwater constituents from the BPP. Thus, no risks were identified related to the use of groundwater.
- For surface water used as a drinking water source, all modeled COI concentrations were below the conservative risk-based screening benchmarks. Thus, no risks were identified related to the use of surface water from the Kaskaskia River adjacent to the Site.
- No unacceptable risks were identified for recreators boating in the Kaskaskia River to the west of the Site.
- No unacceptable risks were identified for recreators exposed to sediment in the Kaskaskia River to the west of the Site.
- No unacceptable risks were identified for anglers consuming locally caught fish.
- No unacceptable risks were identified for ecological receptors exposed to surface water or sediment.
- No bioaccumulative ecological risks were identified.

It should be noted that this evaluation incorporates a number of conservative assumptions that tend to overestimate exposure and risk. Moreover, while this evaluation concluded that current conditions do not present a risk to human health or the environment, it should be noted that based on the location of current off-site groundwater wells and the results of groundwater modeling (Ramboll, 2025a), future conditions are also not expected to present a risk to human health or the environment.

2 Site Overview

2.1 Site Description

The BPP is located in southwest Illinois in Randolph and St. Clair Counties. The FAPS is located "approximately one-half mile west-northwest of the Village of Baldwin" (Figure 2.1) (Ramboll, 2021a). The FAPS (Vistra ID No. 605; IEPA ID Nos. W1578510001-01, W1578510001-02, and W1578510001-03) is a Part 845 regulated CCR Unit (Ramboll, 2021a). The FAPS was approved for closure by IEPA in August 2016, with the final cover system completed in November 2020 (Ramboll, 2021a).

"The BPP property is bordered to the west by the Kaskaskia River; to the east by Baldwin Road, farmland, and strip mining areas; to the southeast by the village of Baldwin; to the south by the Illinois Central Gulf railroad tracks, scattered residences, and State Route 154; and to the north by farmland. The St. Clair/Randolph County Line crosses east-west at approximately the midpoint of Baldwin Lake (Cooling Pond)" (Figure 2.1) (Ramboll, 2021a).

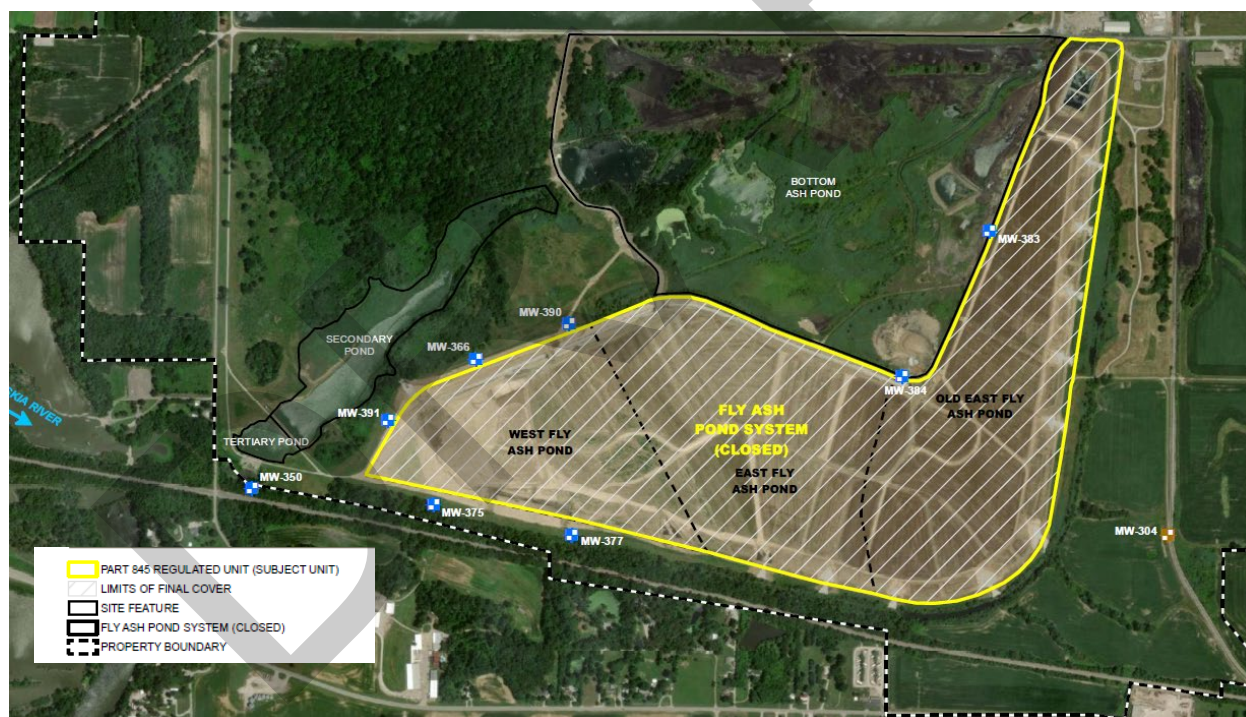


Figure 2.1 Site Location Map. Source: Ramboll (2021b).

2.2 Geology/Hydrogeology

The geology underlying the Site in the vicinity of the FAPS consists of unlithified materials (alluvium and glacial deposits) underlain by Pennsylvanian and Mississippian bedrock, which consists of shale and limestone, with lesser amount of sandstone (NRT, 2016; Ramboll, 2021a, 2024a). The unlithified materials

predominantly includes clay with some silt and intermittent sand seams and lenses. There are two distinct hydrostratigraphic units that underlie the CCR at the FAPS:

- **Upper Unit (UU)**¹: The UU, composed of unlithified materials, is directly beneath the FAPS. It consists of four lithologic layers – Cahokia Formation (sandy clay and clayey sand), Peoria Loess (silt and silty clay), Equality Formation (sandy clay with occasional sand seams), and Vandalia Till (clay with discontinuous sand lenses) (Ramboll, 2021a). The thickness of the UU underneath the FAPS varies between 17 feet in the eastern part of the FAPS to 56 feet in the northern and western part of the FAPS² (Ramboll, 2024a). The unlithified materials within the UU do not represent a continuous aquifer unit (Ramboll, 2024a).
- **Bedrock Unit (BU)**: The BU underlies the UU and is composed of interbedded shale and limestone bedrock, which is continuous across the entire BPP Site (Ramboll, 2021a). The geometric mean horizontal hydraulic conductivity for the uppermost aquifer (UA) is 5.0×10^{-6} cm/sec (Ramboll, 2021a, 2024a).

Thin sand lenses in the UU and the interface (area of contact) between the UU and the bedrock have both been identified as potential migration pathways (PMPs) (Ramboll, 2021a, 2024a). The BU is the UA (Ramboll, 2024a).

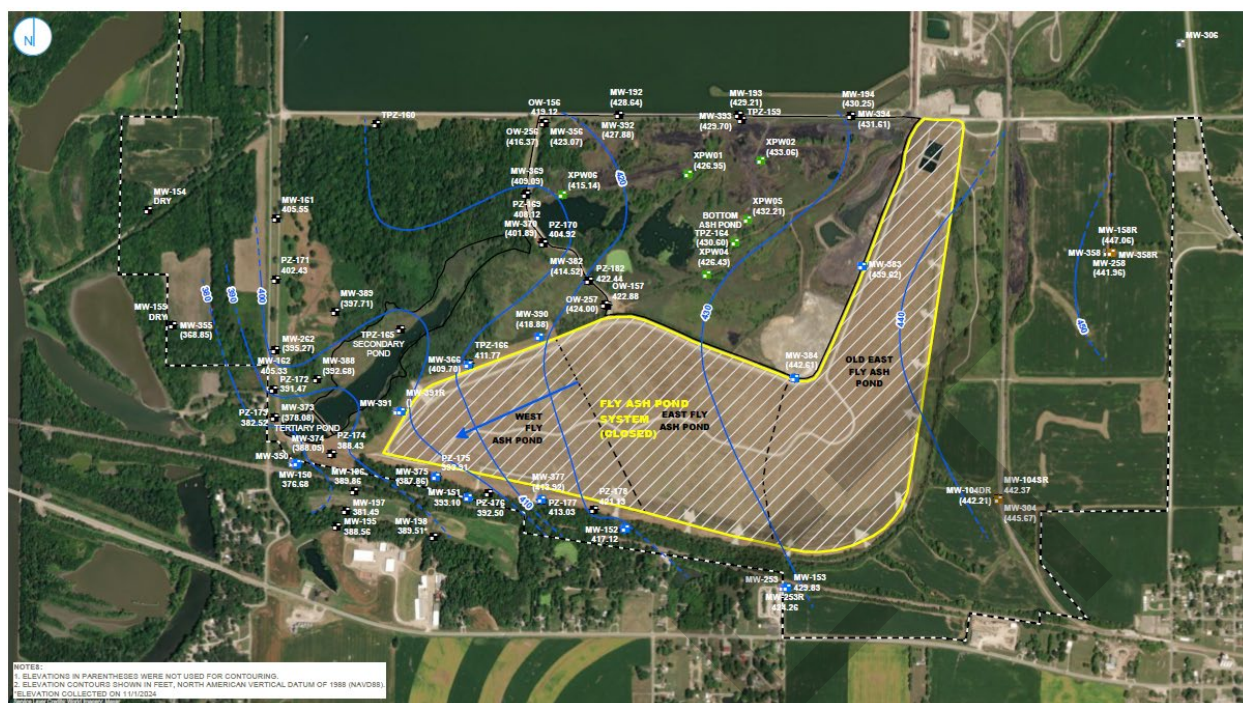
The Kaskaskia River, located to the west of FAPS, is the principal regional surface drainage. For most of the FAPS, lateral groundwater flow (both in the UU and the BU) is generally to the west and southwest toward the bedrock valley underlying the Secondary and Tertiary Ponds (located west of FAPS) and the Kaskaskia River. In the northeastern part of the FAPS, groundwater locally flows in the northwest direction but eventually flows toward the Kaskaskia River. Some groundwater in the UU may flow into the Secondary and Tertiary Ponds but subsequently drains to the Kaskaskia River. Thus, the Kaskaskia River is the receiving surface water body for groundwater in the UU and the BU (Ramboll, 2021a, 2024a).

2.3 Conceptual Site Model

A CSM describes sources of contamination, the hydrogeological units, and the physical processes that control the transport of water and solutes. In this case, the CSM describes how groundwater underlying the FAPS migrates and potentially interacts with surface water and sediment in the adjacent Kaskaskia River. The CSM was developed using site-specific hydrogeologic data (NRT, 2016; Ramboll, 2021a, 2024a), including information on groundwater flow and surface water characteristics. Groundwater (and CCR-related constituents originating from the FAPS) may migrate vertically downward through the UU into the BU (which is the UA). Groundwater flows laterally to the west and southwest through the UU and the BU and ultimately flows into the Kaskaskia River (Figure 2.2). Identified PMPs at the Site include the thin sand lenses in the UU adjacent to the FAPS, and the area of contact between the UU and the BU. Dissolved constituents in groundwater may partition between river sediments and Kaskaskia River surface water.

¹ The UU was referred to as the Upper Groundwater Unit (UGU) in previous reports (Ramboll, 2024a).

² The thickness of the UU at MW-150 (to the west of the FAPS) is 13 feet (Ramboll, 2024a).



2.4 Groundwater Monitoring

Data from the following monitoring wells were included in this risk assessment, as they are used to monitor groundwater quality downgradient and upgradient of the FAPS in both the UU and BU (Figure 2.3):

- UU or PMP: MW-150, 151, 152, 153, 195, 196, 197, 198, 252, 253/253R
- BU or UA: MW-304, 306, 350/350R, 352, 358/358R, 366, 375, 377, 383, 384, 390, 391

The well construction details are presented in Table 2.1. The analyses presented in this report rely on the available data from these wells collected between 2019 and 2024. Groundwater samples were analyzed for a suite of total metals, specified in Illinois CCR Rule Part 845.600 (IEPA, 2021),³ as well as general water quality parameters (chloride, fluoride, sulfate, and total dissolved solids). A summary of the groundwater data used in this risk evaluation is presented in Table 2.2. The use of groundwater data in this risk evaluation does not imply that detected constituents are associated with the FAPS or that they have been identified as potential groundwater exceedances.

³ Samples were analyzed for a longer list of inorganic constituents and general water quality parameters (chloride, fluoride, sulfate, and total dissolved solids), but these constituents were not evaluated in the risk evaluation.

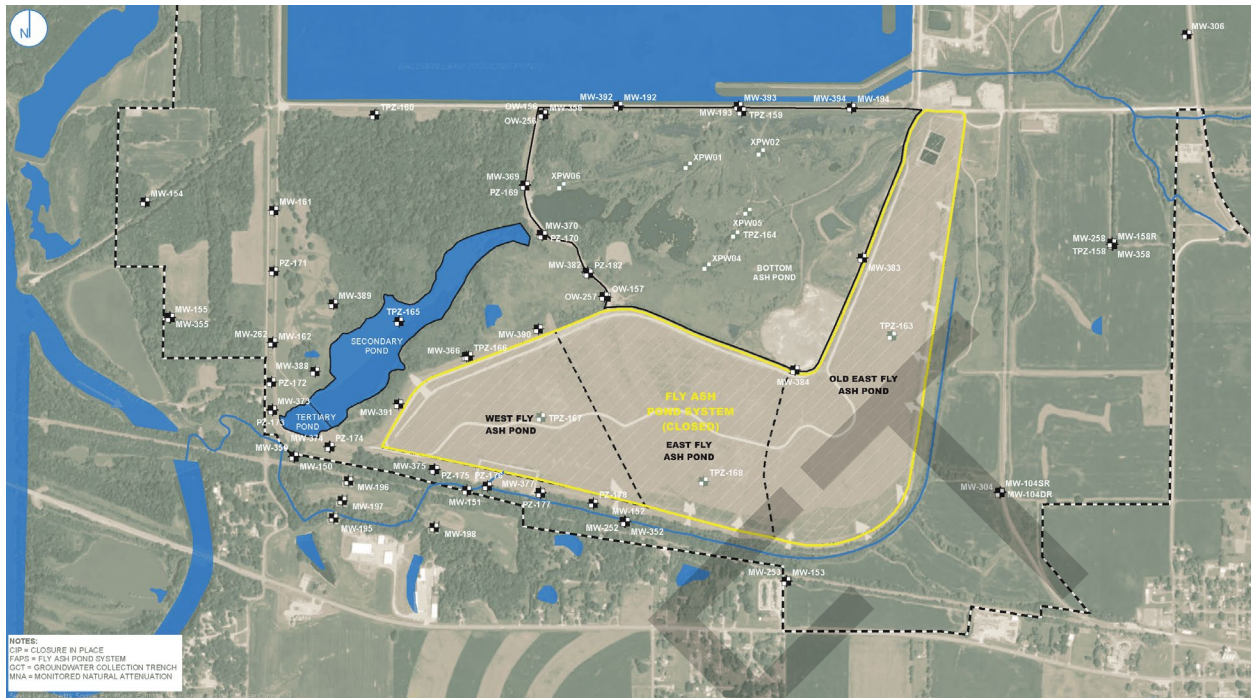


Figure 2.3 Monitoring Well Locations. Sources: Ramboll (2023, 2024b).

Table 2.1 Groundwater Monitoring Wells Related to the FAPS

| Well | Date Constructed | Screen Top Depth (ft bgs) | Screen Bottom Depth (ft bgs) | Well Depth (ft bgs) | Hydrogeologic Unit |
|-------------|------------------|---------------------------|------------------------------|---------------------|--------------------|
| MW-150 | 9/1/2010 | 15.0 | 24.7 | 25.2 | UU/PMP |
| MW-151 | 9/1/2010 | 6.1 | 15.8 | 16.3 | UU/PMP |
| MW-152 | 9/1/2010 | 7.5 | 16.7 | 17.2 | UU/PMP |
| MW-153 | 9/1/2010 | 10.4 | 20.0 | 20.5 | UU/PMP |
| MW-195 | 5/7/2024 | 38.0 | 48.0 | 48.0 | UU/PMP |
| MW-196 | 5/8/2024 | 8.0 | 18.0 | 20.0 | UU/PMP |
| MW-197 | 5/8/2024 | 7.0 | 17.0 | 20.0 | UU/PMP |
| MW-198 | 10/15/2024 | 8.0 | 18.0 | 18.0 | UU/PMP |
| MW-252 | 9/1/2010 | 44.4 | 49.0 | 49.5 | UU/PMP |
| MW-253/253R | 9/1/2010, 5/1/24 | 29.9 | 34.5 | 35.0 | UU/PMP |
| MW-304 | 10/20/2015 | 45.0 | 55.0 | 55.0 | BU/UA |
| MW-306 | 9/25/1991 | 72.7 | 87.7 | 87.7 | BU/UA |
| MW-350/350R | 9/1/2010, 5/3/24 | 41.6 | 46.2 | 46.6 | BU/UA |
| MW-352 | 9/1/2010 | 67.9 | 72.5 | 73.0 | BU/UA |
| MW-358 | 10/8/22 | 80 | 90 | 90 | BU/UA |
| MW-366 | 12/4/2015 | 42.0 | 52.0 | 52.0 | BU/UA |
| MW-375 | 11/6/2015 | 57.0 | 67.0 | 67.0 | BU/UA |
| MW-377 | 11/2/2015 | 46.0 | 56.0 | 56.0 | BU/UA |
| MW-383 | 12/21/2015 | 58.0 | 68.0 | 68.0 | BU/UA |
| MW-384 | 12/18/2015 | 60.5 | 70.5 | 70.5 | BU/UA |
| MW-390 | 3/4/2016 | 50.0 | 65.0 | 65.0 | BU/UA |
| MW-391 | 3/10/2016 | 55.0 | 70.0 | 70.0 | BU/UA |

Notes:

BU = Bedrock Unit; FAPS = Fly Ash Pond System; ft bgs = Feet Below Ground Surface; PMP = Potential Migration Pathway; UA = Uppermost Aquifer (Bedrock); UU = Upper Unit.

Wells MW-253R, MW-350R, and MW-358R are replacement wells.

Sources: Ramboll (2021a, 2024b,c).

Table 2.2 Groundwater Data Summary (2019-2024)

| Constituent | Samples with Constituent Detected | Samples Analyzed | Minimum Detected Value | Maximum Detected Value | Maximum Laboratory Detection Limit |
|--------------------------------|-----------------------------------|------------------|------------------------|------------------------|------------------------------------|
| Total Metals (mg/L) | | | | | |
| Antimony | 84 | 241 | 0.0005 | 0.005 | 0.0008 |
| Arsenic | 152 | 241 | 0.0004 | 0.0162 | 0.0087 |
| Barium | 241 | 241 | 0.0034 | 1.04 | NA |
| Beryllium | 19 | 205 | 0.0002 | 0.0018 | 0.0002 |
| Boron | 233 | 241 | 0.013 | 23 | 0.02 |
| Cadmium | 7 | 205 | 0.0002 | 0.0004 | 0.0005 |
| Chromium | 69 | 241 | 0.0007 | 0.0533 | 0.0028 |
| Cobalt | 87 | 234 | 0.0001 | 0.019 | 0.0008 |
| Lead | 49 | 227 | 0.0006 | 0.02 | 0.004 |
| Lithium | 240 | 244 | 0.0034 | 0.129 | 0.0019 |
| Mercury | 19 | 205 | 0.00006 | 0.00016 | 0.00012 |
| Molybdenum | 182 | 241 | 0.0006 | 0.142 | 0.0037 |
| Selenium | 45 | 241 | 0.0006 | 0.0062 | 0.0006 |
| Thallium | 6 | 226 | 0.001 | 0.0027 | 0.001 |
| Dissolved Metals (mg/L) | | | | | |
| Antimony | 1 | 3 | 0.0005 | 0.0005 | 0.0004 |
| Arsenic | 0 | 3 | - | - | 0.0087 |
| Barium | 3 | 3 | 0.033 | 0.093 | NA |
| Beryllium | 0 | 3 | - | - | 0.0002 |
| Boron | 216 | 234 | 0.015 | 21.8 | 0.0092 |
| Cadmium | 0 | 3 | - | - | 0.0005 |
| Chromium | 0 | 3 | - | - | 0.0028 |
| Cobalt | 0 | 3 | - | - | 0.0001 |
| Lead | 0 | 3 | - | - | 0.004 |
| Lithium | 3 | 3 | 0.0038 | 0.0945 | NA |
| Mercury | 0 | 3 | - | - | 0.00006 |
| Molybdenum | 0 | 3 | - | - | 0.0037 |
| Selenium | 1 | 3 | 0.0021 | 0.0021 | 0.0006 |
| Thallium | 0 | 3 | - | - | 0.001 |
| Radionuclides (pCi/L) | | | | | |
| Radium 226 + Radium 228 | 147 | 241 | 0.0281 | 8.54 | 2 |
| Other (mg/L or SU) | | | | | |
| pH | 386 | 386 | 6.08 | 12.4 | NA |
| Chloride | 241 | 241 | 8 | 1370 | NA |
| Fluoride | 238 | 241 | 0.11 | 4.93 | 0.2 |
| Sulfate | 235 | 241 | 5 | 1450 | 31 |
| Total Dissolved Solids | 410 | 410 | 206 | 3260 | NA |
| Other Dissolved (mg/L) | | | | | |
| Chloride | 250 | 250 | 7 | 1300 | NA |
| Fluoride | 3 | 3 | 0.43 | 1.46 | NA |
| Sulfate | 233 | 250 | 5 | 1050 | 12 |

Notes:

mg/L = Milligrams per Liter; NA = Not Available; pCi/L = PicoCuries per Liter; SU = Standard Unit.

Blank cells indicate constituent not detected.

Source: Ramboll (2025b).

2.5 Surface Water Monitoring

Two surface water samples were collected from the same location in the Kaskaskia River in November, 2016 (Hanson Professional Services Inc., 2017). The sample location is shown as the dot labeled "KRU" in Figure 2.4, and the sampling results are summarized in Table 2.3.



Figure 2.4 Surface Water Sample Location. Source: Hanson Professional Services Inc. (2017).

Table 2.3 Surface Water Data Summary

| Constituent | Samples with Constituent Detected | Samples Analyzed | Minimum Detected Value | Maximum Detected Value | Maximum Laboratory Detection Limit |
|----------------------------|-----------------------------------|------------------|------------------------|------------------------|------------------------------------|
| Total Metals (mg/L) | | | | | |
| Arsenic | 0 | 2 | - | - | 2.5E-02 |
| Barium | 2 | 2 | 7.3E-02 | 7.4E-02 | NA |
| Boron | 2 | 2 | 4.0E-02 | 4.2E-02 | NA |
| Cadmium | 0 | 2 | - | - | 2.0E-03 |
| Chromium | 0 | 2 | - | - | 5.0E-03 |
| Chromium (hexavalent) | 0 | 2 | - | - | 1.0E-02 |
| Copper | 0 | 2 | - | - | 5.0E-03 |
| Cyanide | 0 | 2 | - | - | 5.0E-03 |
| Iron | 2 | 2 | 1.2E+00 | 1.2E+00 | NA |
| Lead | 0 | 2 | - | - | 1.5E-02 |
| Manganese | 2 | 2 | 2.2E-01 | 2.3E-01 | NA |
| Mercury | 2 | 2 | 2.0E-06 | 4.0E-06 | NA |
| Nickel | 0 | 2 | - | - | 5.0E-03 |
| Phosphorus | 2 | 2 | 2.6E-01 | 2.6E-01 | NA |
| Selenium | 0 | 2 | - | - | 4.0E-02 |
| Silver | 0 | 2 | - | - | 5.0E-03 |
| Zinc | 0 | 2 | - | - | 1.0E-02 |
| Other (mg/L or SU) | | | | | |
| Chloride | 2 | 2 | 1.9E+01 | 2.1E+01 | NA |
| Fluoride | 2 | 2 | 2.1E-01 | 2.2E-01 | NA |
| pH | 2 | 2 | 8.1E+00 | 8.2E+00 | NA |
| Phenols | 0 | 2 | - | - | 5.0E-03 |
| Sulfate | 2 | 2 | 2.3E+01 | 2.3E+01 | NA |
| Total Suspended Solids | 2 | 2 | 3.5E+01 | 4.9E+01 | NA |

Notes:

mg/L = Milligrams per Liter; NA = Not Available; SU = Standard Unit.

Blank cells indicate constituent was not detected.

Source: Hanson Professional Services Inc. (2017).

3 Risk Evaluation

3.1 Risk Evaluation Process

A risk evaluation was conducted to determine whether constituents present in groundwater underlying and downgradient of the FAPS have the potential to pose adverse health effects to human and ecological receptors. The risk evaluation is consistent with the principles of risk assessment established by US EPA and has considered evaluation criteria detailed in Illinois guidance documents (e.g., IEPA, 2013, 2019).

The general risk evaluation approach is summarized in Figure 3.1 and discussed below.

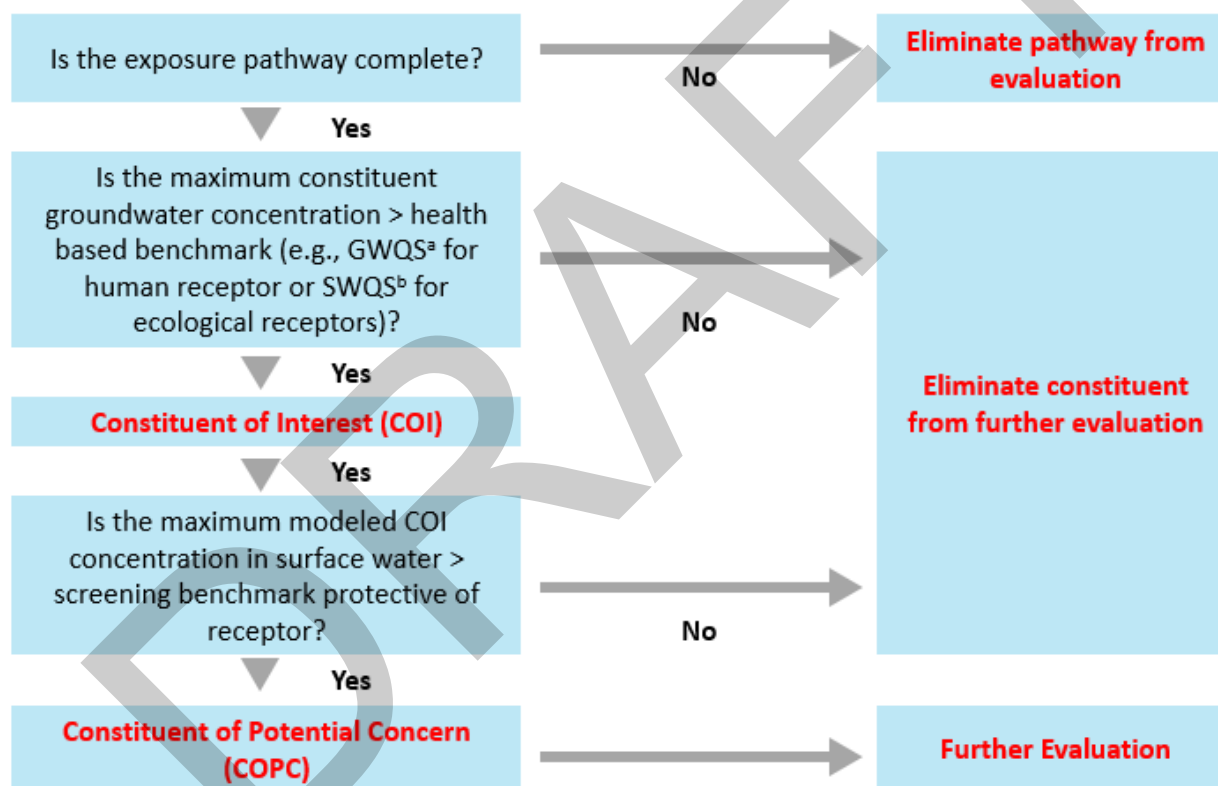


Figure 3.1 Overview of Risk Evaluation Methodology. IEPA = Illinois Environmental Protection Agency; GWQS = IEPA Groundwater Quality Standards; SWQS = IEPA Surface Water Quality Standards. (a) The IEPA Part 845 Groundwater Protection Standards (GWPS) were used to identify COIs. (b) IEPA SWQS protective of chronic exposures to aquatic organisms were used to identify ecological COIs. In the absence of an SWQS, US EPA Region IV Ecological Screening Values (ESVs) were used.

The first step in the risk evaluation was to develop the CEMs and identify complete exposure pathways. All potential receptors and exposure pathways based on groundwater use and surface water use in the vicinity of the Site were considered. Exposure pathways that are incomplete were excluded from the evaluation.

Groundwater data were used to identify COIs. COIs were identified as constituents with maximum concentrations in groundwater in excess of groundwater quality standards (GWQS)⁴ for human receptors and SWQS for ecological receptors. Based on the CSM (Section 2.2), some groundwater underlying the FAPS has the potential to interact with surface water in the Kaskaskia River. Therefore, potential FAPS-related constituents in groundwater may potentially flow toward and into surface water in the Kaskaskia River.

Surface water samples have been collected from the Kaskaskia River adjacent to the Site; however, sediment samples have not been collected from the river. Gradient modeled the potential migration of COIs from groundwater to surface water and sediment to evaluate potential risks to receptors (see Section 3.3.3).

Gradient modeled the COI concentrations in surface water and sediment based on the groundwater data from the FAPS-related wells. The measured and modeled COI concentrations in surface water and sediment were compared to conservative, generic risk-based screening benchmarks for human health and ecological receptors. These generic screening benchmarks rely on default assumptions with limited consideration of site-specific characteristics. Human health benchmarks are receptor-specific values calculated for each pathway and environmental medium that are designed to be protective of human health. Ecological benchmarks are medium-specific values designed to be protective of all potential ecological receptors exposed to surface water. Ecological and human health screening benchmarks are inherently conservative because they are intended to screen out chemicals that are of no concern with a high level of confidence. Therefore, a measured or modeled COI concentration exceeding a screening benchmark does not indicate an unacceptable risk, but only that further risk evaluation is warranted. COIs with maximum concentrations exceeding a conservative screening benchmark are identified as COPCs requiring further evaluation.

As described in more detail below, this evaluation relied on the screening assessment to demonstrate that constituents present in groundwater underlying the FAPS do not pose an unacceptable human health or ecological risk. That is, after the screening step, no COPCs were identified and further assessment was not warranted.

3.2 Human and Ecological Conceptual Exposure Models

A CEM provides an overview of the receptors and exposure pathways requiring risk evaluation. The CEM describes the source of the contamination, the mechanism that may lead to a release of contamination, the environmental media to which a receptor may be exposed, the route of exposure (exposure pathway), and the types of receptors that may be exposed to these environmental media.

3.2.1 Human Conceptual Exposure Model

The human CEM for the Site depicts the relationships between the off-Site environmental media potentially impacted by constituents in groundwater and human receptors that could be exposed to these media. Figure 3.2 presents a human CEM for the Site. It considers a human receptor who could be exposed to COIs hypothetically released from the FAPS into groundwater, surface water, sediment, and fish. The following human receptors and exposure pathways were evaluated for inclusion in the Site-specific CEM.

⁴ As discussed further in Section 3.3.2, GWQS are protective of human health and not necessarily of ecological receptors. While ecological receptors are not exposed to groundwater, groundwater can potentially enter into the adjacent surface water and impact ecological receptors. Therefore, two sets of COIs were identified: one for humans and another for ecological receptors.

- Residents – exposure to groundwater/surface water as drinking water;
- Residents – exposure to groundwater/surface water used for irrigation;
- Recreators in the river adjacent to the Site:
 - Boaters – exposure to surface water and sediment while boating;
 - Swimmers – exposure to surface water and sediment while swimming;
 - Anglers – exposure to surface water and sediment and consumption of locally caught fish.

All of these exposure pathways were considered to be complete. Section 3.2.1.1 discusses the residential drinking water and irrigation pathways. Section 3.2.1.2 provides additional description of the recreational exposures.

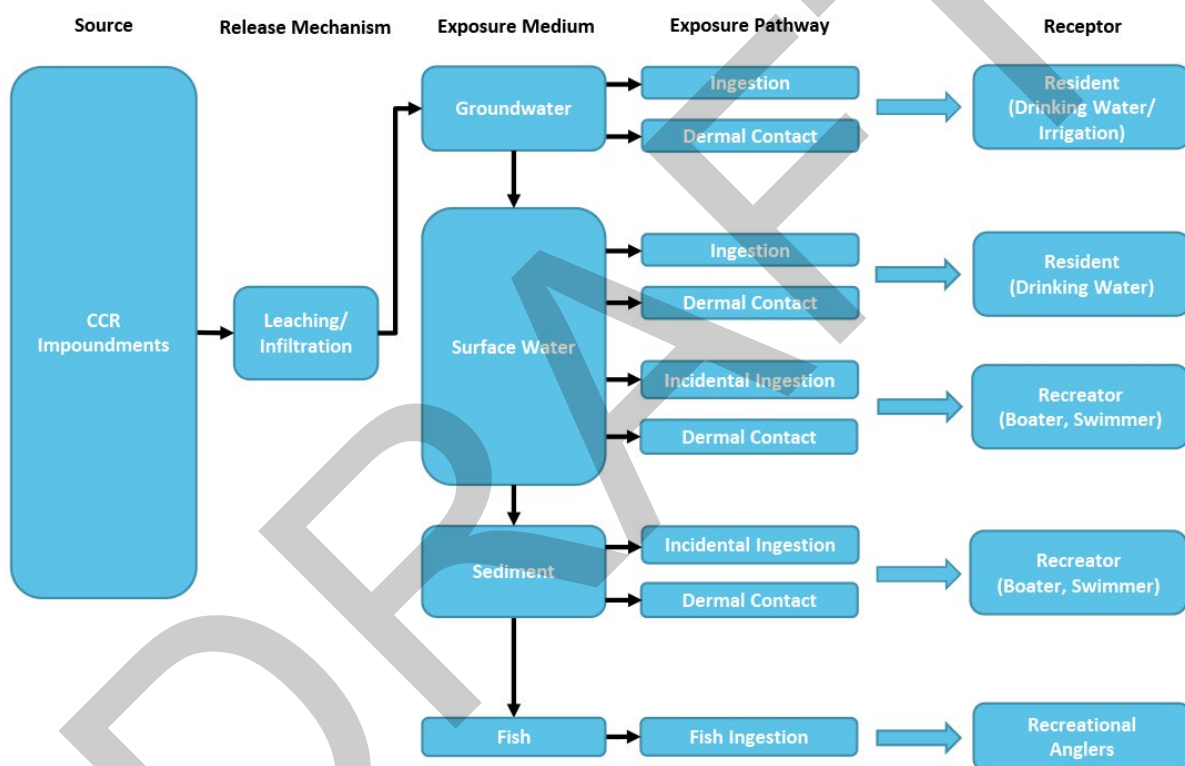


Figure 3.2 Human Conceptual Exposure Model. CCR = Coal Combustion Residuals.

3.2.1.1 Groundwater as a Drinking Water/Irrigation Source

A receptor survey was conducted in 2021 to identify potential users of groundwater in the vicinity of the FAPS (Ramboll, 2021a). Specific sources that were used in this survey include the Illinois State Geological Survey (ISGS), Illinois State Water Survey (ISWS), and the IEPA (Ramboll, 2021a). The well search was updated in 2024. A total of 19 wells were identified within 1,000 meters of the FAPS, which included 15 private water wells, and 4 monitoring wells (Table 3.1, Figure 3.3). The four monitoring wells, owned by Illinois Power, were installed in 1992 and are located north of the FAPS but within the BPP property. It should be noted that, based on their coordinates from the available databases, two of the private wells (Well 121572596900 and Well 121572592700) are located on the BPP property within the boundary of FAPS (Figure 3.3). These locations are likely incorrect and/or outdated. Because no private wells are located within the FAPS, there is no exposure to impacted groundwater at these locations.

Groundwater beneath the FAPS generally flows to the southwest towards the Kaskaskia River (Figure 2.2). One private well (121572531300) is upgradient of the FAPS and east of the BPP property boundary; it is 28 feet deep and was installed in 1984 (Figure 3.3). Since it is upgradient of the FAPS, it is not expected to be impacted by any CCR constituents in groundwater that originate from the FAPS.

Twelve (12) private wells are located south of the BPP (Figure 3.3). These wells range in depth from 24 to 72 feet and are screened in the UU and include wells that may provide water for both human and livestock uses (Table 3.1). Based on the groundwater flow direction to the southwest, seven of the private wells are side gradient of the FAPS (121570200300, 121570207100, 121570207200, 121572298400, 121572317500, 121572280600, 121572284200) and are not expected to be impacted by any CCR constituents in groundwater that originate from the FAPS. The other five private wells are on properties immediately south of the BPP (Figure 3.3). Based on an interview with the property owner, well 121572510000 was destroyed when a farmhouse was demolished. The potential groundwater impacts to the remaining four wells (1215720240900, 121572681800, A, and B) on properties south of the BPP have been investigated and are discussed below.

Four monitoring wells were installed on a property immediately to the south of the BPP in 2024 (MW-195, MW-196, MW-197, MW-198; Figure 2.3) to investigate whether the FAPS has impacted off-Site groundwater quality in this area. Wells MW-195, MW-196, and MW-197 were installed in May 2024 and MW-198 was installed in October 2024. Sampling, conducted in June, July, and October 2024, found that well MW-196 exceeded the GWPS for boron (2 mg/L) and sulfate (400 mg/L). No exceedances of the GWPSs were noted at MW-197 (sampled in June, July, and October 2024) or at MW-198 (sampled in October 2024), and as a result MW-195 was not sampled. Based on the results from MW-197 and MW-198, and the direction of groundwater flow to the southwest (Figure 2.2), private wells on properties to the south of the BPP (Figure 3.3) are unlikely to have any exceedances of the GWPSs.

Table 3.1 Summary of Water Wells Within 1,000 Meters of the FAPS

| API Number | Type | Date Drilled | Owner | Depth (ft) | Formation | Latitude | Longitude |
|--------------|---------------------|--------------|--------------------------|------------|----------------------|-----------|------------|
| 121570200300 | Water | 5/31/1961 | Baldwin City (Private) | 31 | NA | 38.183293 | -89.881861 |
| 121570207100 | Water | 12/31/1946 | Private | 72 | Shale | 38.184918 | -89.879621 |
| 121570207200 | Water | 12/31/1949 | Private | 67 | Limestone | 38.184918 | -89.879621 |
| 121570240900 | Water for livestock | 4/16/1970 | Private | 32 | Sand & gravel | 38.185276 | -89.869794 |
| 121572280600 | Water | 6/30/1974 | Private | 24 | Red sand & gravel | 38.183638 | -89.864585 |
| 121572284200 | Water | 10/1/1974 | Private | 33 | Sand & gravel | 38.183638 | -89.864585 |
| 121572298400 | Water | 5/31/1976 | Private | 35 | Sandy clay | 38.181330 | -89.869991 |
| 121572317500 | Water | 4/5/1978 | Private | NA | Sandy clay | 38.183018 | -89.865384 |
| 121572510000 | Destroyed | 3/12/1986 | Private | 37 | Sand & gravel | 38.185794 | -89.877665 |
| 121572531300 | Water | 8/23/1984 | Private | 28 | Clay & sand | 38.187248 | -89.846250 |
| 121572592700 | Water | 1992 | Private | 160 | Limestone | 38.190134 | -89.872439 |
| 121572681800 | Water | 7/10/2021 | Private | 37 | Orange sand | 38.186389 | -89.873611 |
| 121572596900 | Water | 3/19/1995 | Illinois Power (Private) | 27 | Upper unit (UU) | 38.190134 | -89.872439 |
| 121572594000 | Monitoring | 8/23/1992 | Illinois Power | 23 | Silty clay | 38.205526 | -89.857289 |
| 121572594100 | Monitoring | 8/25/1992 | Illinois Power | 18 | Brown silty clay | 38.205526 | -89.857289 |
| 121572594200 | Monitoring | 8/25/1992 | Illinois Power | 18 | Silty clay | 38.205526 | -89.857289 |
| 121572594300 | Monitoring | 8/25/1992 | Illinois Power | 18 | Silty clay, med sand | 38.205526 | -89.857289 |
| A | Water | NA | Private | 40 | NA | 38.185849 | -89.873981 |
| B | Water for livestock | 1980s | Private | NA | NA | 38.186192 | -89.870836 |

Notes:

FAPS = Fly Ash Pond System; ft = Feet; NA = Not Available.

Wells A and B are on private property to the south of the Baldwin plant, but do not have an API number (Ramboll, 2024d).

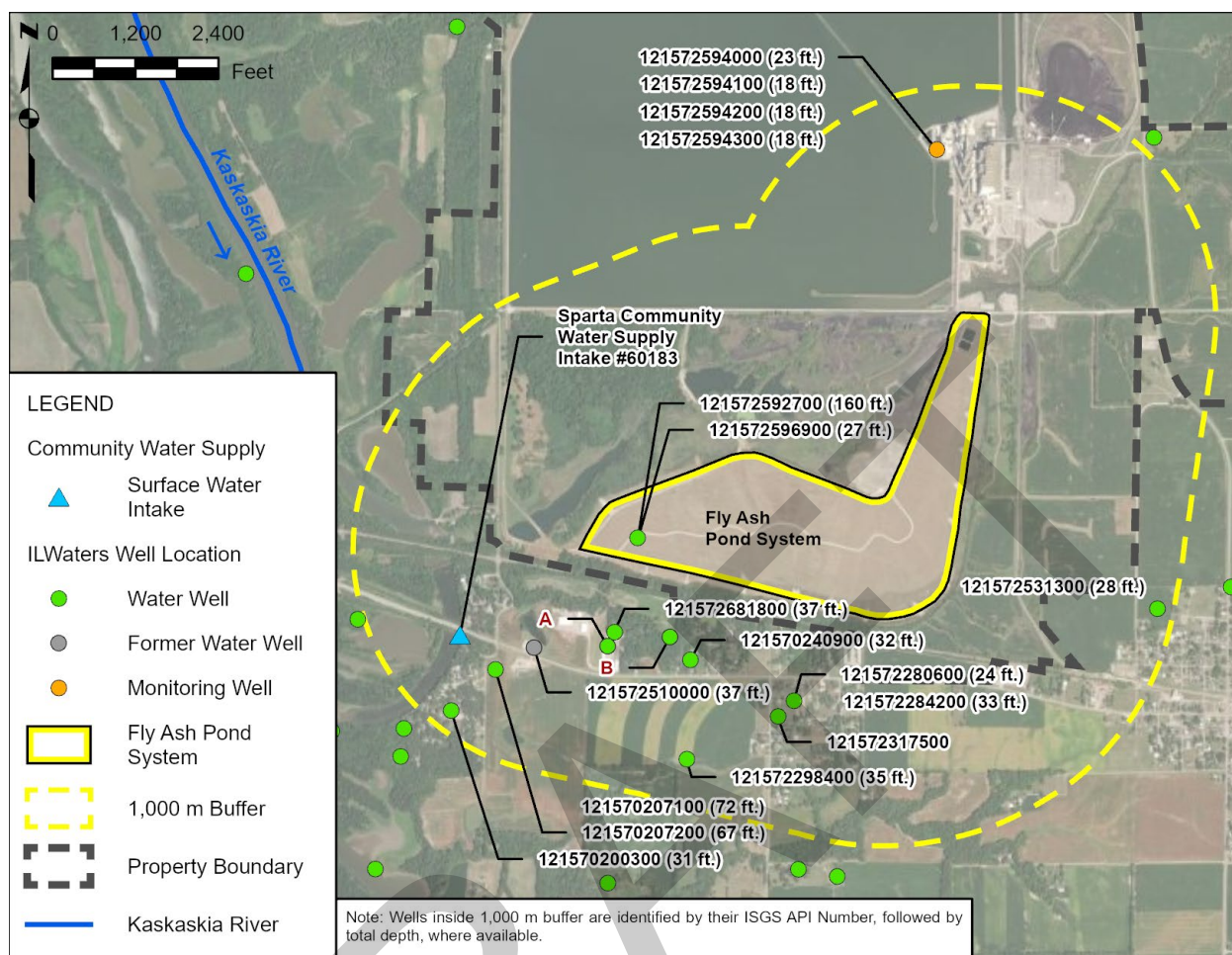


Figure 3.3 Water Wells Within 1,000 Meters of the FAPS. FAPS = Fly Ash Pond System; ISGS = Illinois State Geological Survey. Sources: Illinois State Geological Survey (2024); Ramboll (2021a); USGS (2022a); IEPA (2025).

3.2.1.2 Surface Water as a Drinking Water Source

The Sparta, Illinois, community water supply (CWS) has a surface water intake (IEPA #60183) on the Kaskaskia River 1,325 feet southwest of the BPP; the location of the intake is shown on Figure 3.3 (IEPA, 2012). Sparta CWS serves an estimated population of 6,455 people (IEPA, 2012).

3.2.1.3 Recreational Exposures

The Kaskaskia River is located to the west of the BPP. The river and its adjacent area to the west of the BPP are part of the Kaskaskia River State Fish and Wildlife Area (SFWA) (Figure 3.4) (Ramboll, 2021a). "The Illinois Department of Transportation owns the land along the river and leases most of the land to the Illinois Department of Natural Resources to manage for fish, wildlife and other recreational activities" (IDNR, 2022). The recreational uses of the SFWA include fishing, boating, hunting (IDNR, 2022). Recreational exposure to surface water and sediment may occur during activities such as boating or fishing in the river. Recreational anglers may also consume locally caught fish from the Kaskaskia River.

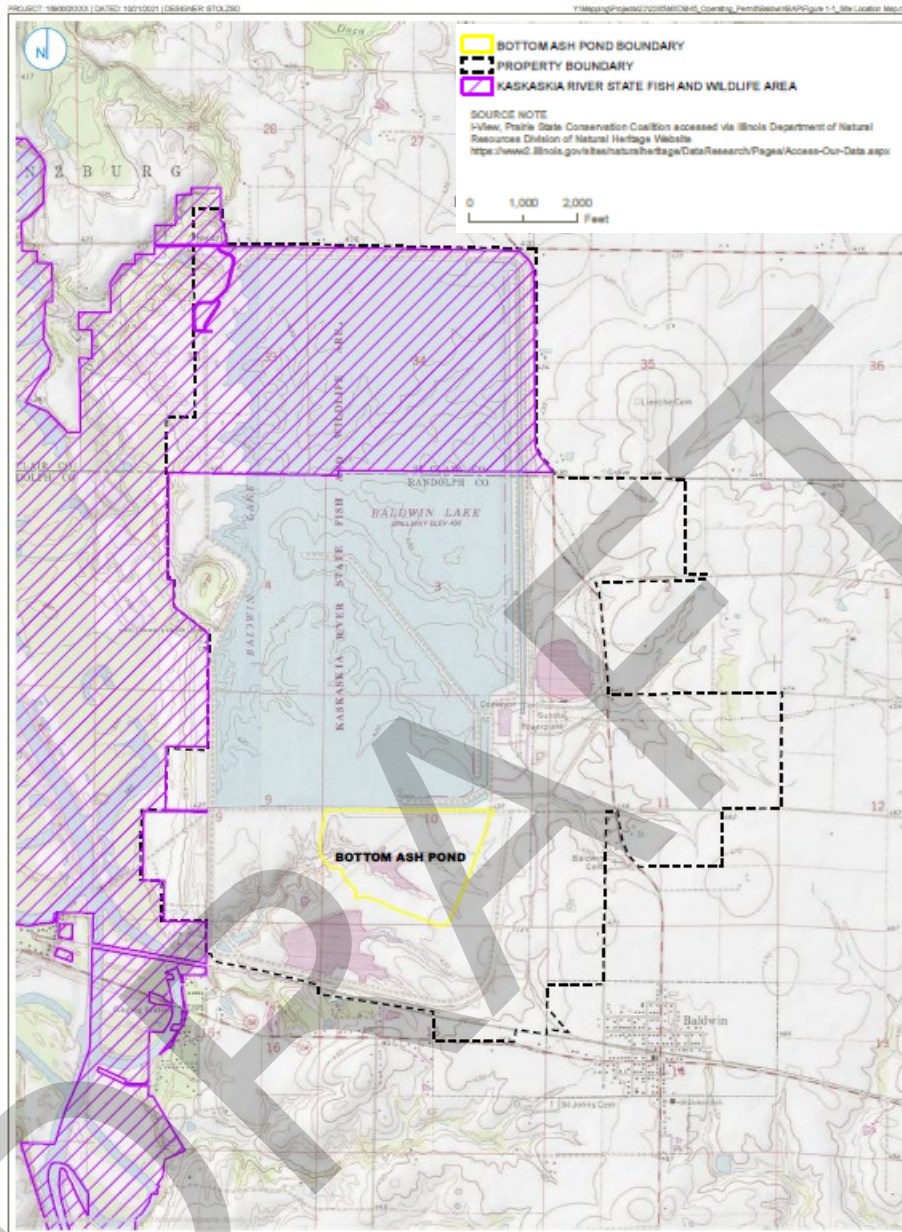


Figure 3.4 Kaskaskia River State Fish and Wildlife Area. Source: Ramboll (2021a).

3.2.2 Ecological Conceptual Exposure Model

The ecological CEM for the Site depicts the relationships between off-Site environmental media (surface water and sediment) potentially impacted by COIs in groundwater and ecological receptors that may be exposed to these media. The ecological risk evaluation considered both direct toxicity as well as secondary toxicity *via* bioaccumulation. Figure 3.5 presents the ecological CEM for the Site. The following ecological receptor groups and exposure pathways were considered:

- **Ecological Receptors Exposed to Surface Water:**
 - Aquatic plants, amphibians, reptiles, and fish.

- **Ecological Receptors Exposed to Sediment:**
 - Benthic invertebrates (*e.g.*, insects, crayfish, mussels).
- **Ecological Receptors Exposed to Bioaccumulative COIs:**
 - Higher trophic level wildlife (avian and mammalian) *via* direct exposures (surface water and sediment exposure) and secondary exposures through the consumption of prey (*e.g.*, plants, invertebrates, small mammals, fish).

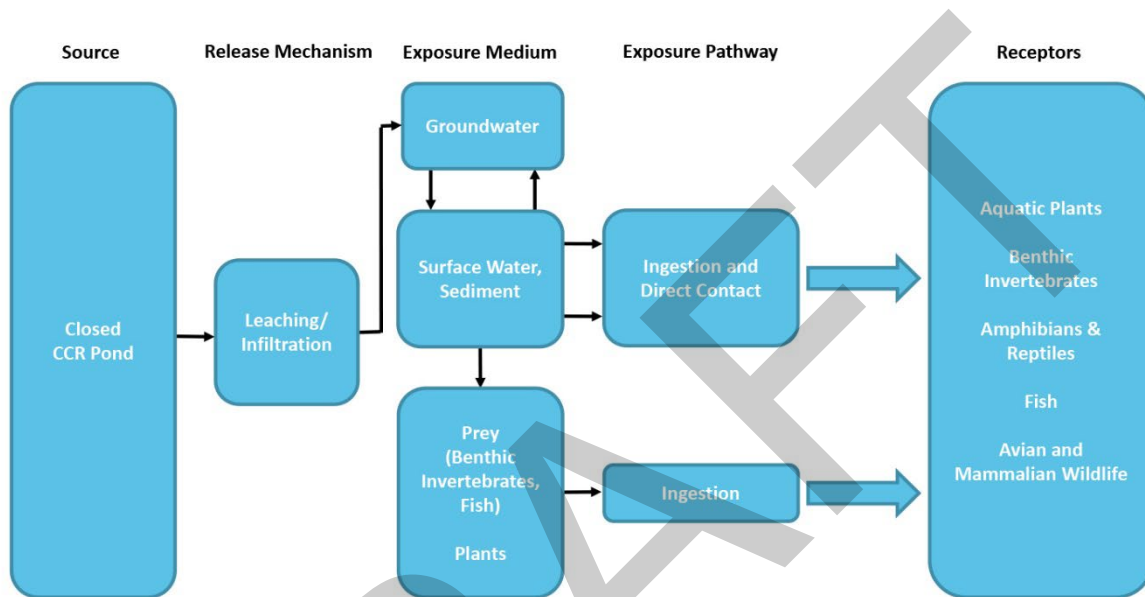


Figure 3.5 Ecological Conceptual Exposure Model. CCR = Coal Combustion Residuals.

3.3 Identification of Constituents of Interest

Risks were evaluated for COIs. A constituent was considered a COI if the maximum detected constituent concentration in groundwater exceeded a health-based benchmark. According to US EPA risk assessment guidance (US EPA, 1989), this screening step is designed to reduce the number of constituents carried through the risk evaluation that are anticipated to have a minimal contribution to the overall risk. Identified COIs are the constituents that are most likely to pose a risk concern in the surface water adjacent to the Site.

3.3.1 Human Health Constituents of Interest

For the human health risk evaluation, COIs were conservatively identified as constituents with maximum concentrations in groundwater above the GWPS listed in the Illinois CCR Rule Part 845.600 (IEPA, 2021). Gradient used the maximum detected concentrations from groundwater samples collected from all of the FAPS associated wells, regardless of hydrostratigraphic unit. The use of groundwater data in this risk evaluation does not imply that detected constituents are associated with the FAPS or that they have been identified as potential groundwater exceedances. Using this approach, the COIs that were identified for the human health risk evaluation *via* the surface water pathway include arsenic, boron, cobalt, lead, lithium, molybdenum, thallium, and radium 226 + 228 (Table 3.2).

The water quality parameters that exceeded the GWPS included pH, chloride, fluoride, sulfate, and total dissolved solids; however, these constituents were not included in the risk evaluation because the GWPS is based on aesthetic quality and there is an absence of studies regarding toxicity to human health. The US EPA secondary maximum contaminant levels (MCLs) for chloride, sulfate, and total dissolved solids are based on aesthetic quality. The secondary MCLs for chloride and sulfate (250 mg/L) are based on salty taste (US EPA, 2021). The secondary MCL for total dissolved solids (500 mg/L) is based on hardness, deposits, colored water, staining, and salty taste (US EPA, 2021). In addition, pH is a measure of the acidity of the water, and is not typically included in risk assessments. Given that these parameters are not likely to pose a human health risk concern in the event of exposure, they were not considered to be human health COIs.

Table 3.2 Human Health Constituents of Interest

| Constituent ^a | Maximum Groundwater Concentration ^b | GWPS ^c | Human Health COI ^d |
|--------------------------------|--|-------------------|-------------------------------|
| Total Metals (mg/L) | | | |
| Antimony | 5.0E-03 | 6.0E-03 | No |
| Arsenic | 1.6E-02 | 1.0E-02 | Yes |
| Barium | 1.0E+00 | 2.0E+00 | No |
| Beryllium | 1.8E-03 | 4.0E-03 | No |
| Boron | 2.3E+01 | 2.0E+00 | Yes |
| Cadmium | 4.0E-04 | 5.0E-03 | No |
| Chromium | 5.3E-02 | 1.0E-01 | No |
| Cobalt | 1.9E-02 | 6.0E-03 | Yes |
| Lead | 2.0E-02 | 7.5E-03 | Yes |
| Lithium | 1.3E-01 | 4.0E-02 | Yes |
| Mercury | 1.6E-04 | 2.0E-03 | No |
| Molybdenum | 1.4E-01 | 1.0E-01 | Yes |
| Selenium | 6.2E-03 | 5.0E-02 | No |
| Thallium | 2.7E-03 | 2.0E-03 | Yes |
| Dissolved Metals (mg/L) | | | |
| Antimony | 5.0E-04 | 6.0E-03 | No |
| Arsenic | - | 1.0E-02 | No |
| Barium | 9.3E-02 | 2.0E+00 | No |
| Beryllium | - | 4.0E-03 | No |
| Boron | 2.2E+01 | 2.0E+00 | Yes |
| Cadmium | - | 5.0E-03 | No |
| Chromium | - | 1.0E-01 | No |
| Cobalt | - | 6.0E-03 | No |
| Lead | - | 7.5E-03 | No |
| Lithium | 9.5E-02 | 4.0E-02 | Yes |
| Molybdenum | - | 1.0E-01 | No |
| Selenium | 2.1E-03 | 5.0E-02 | No |
| Thallium | - | 2.0E-03 | No |
| Radionuclides (pCi/L) | | | |
| Radium 226 + Radium 228 | 8.5E+00 | 5.0E+00 | Yes |
| Other (mg/L or SU) | | | |
| pH | 1.2E+01 | 9.0E+00 | No ^e |
| Chloride | 1.4E+03 | 2.0E+02 | No ^e |
| Fluoride | 4.9E+00 | 4.0E+00 | No ^e |

| Constituent ^a | Maximum Groundwater Concentration ^b | GWPS ^c | Human Health COI ^d |
|-------------------------------|--|-------------------|-------------------------------|
| Sulfate | 1.5E+03 | 4.0E+02 | No ^e |
| Total Dissolved Solids | 3.3E+03 | 1.2E+03 | No ^e |
| Other Dissolved (mg/L) | | | |
| Chloride | 1.3E+03 | 2.0E+02 | No ^e |
| Sulfate | 1.1E+03 | 4.0E+02 | No ^e |

Notes:

COI = Constituent of Interest; GWPS = Groundwater Protection Standard; IL = Illinois; mg/L = Milligrams per Liter; pCi/L = PicoCuries per Liter; SU = Standard Unit.

Blank cells indicate constituent was not detected.

Shaded cell indicates a compound identified as a COI.

(a) The constituents are those listed in the IL Part 845.600 GWPS (IEPA, 2021).

(b) The maximum detected groundwater concentration was used to identify COIs.

(c) The IL Part 845.600 GWPS (IEPA, 2021) were used to identify COIs.

(d) COIs are constituents for which the maximum concentration exceeds the groundwater standard.

(e) Maximum exceeds the GWPS but is not considered to be COI because the GWPS is based on aesthetic quality.

3.3.2 Ecological Constituents of Interest

The Illinois GWPS, as defined in IEPA's guidance, were developed to protect human health but not necessarily ecological receptors. While ecological receptors are not exposed to groundwater, groundwater can potentially migrate into the adjacent surface water and impact ecological receptors. Therefore, to identify ecological COIs, the maximum concentrations of constituents detected in groundwater were compared to ecological surface water benchmarks protective of aquatic life.

The surface water screening benchmarks for freshwater organisms were obtained from the following hierarchy of sources:

- IEPA (2019) SWQS. IEPA SWQS are health-protective benchmarks for aquatic life exposed to surface water on a long-term basis (*i.e.*, chronic exposure). The SWQS for several metals are hardness dependent (cadmium, chromium, copper, lead, manganese, nickel, and zinc). Screening benchmarks for these constituents were calculated assuming US EPA's default hardness of 100 mg/L (US EPA, 2022).⁵
- US EPA Region IV (2018) surface water Ecological Screening Values (ESVs) for hazardous waste sites.

Benchmarks from the United States Department of Energy's (US DOE) guidance document ("A Graded Approach for Evaluating Radiation Doses to Aquatic and Terrestrial Biota") were used for radium (US DOE, 2019). US DOE presents benchmarks for radium 226 and radium 228 (4 and 3 picoCuries per liter [pCi/L], respectively). Given that radium concentrations are expressed as total radium (radium 226+228, *i.e.*, the sum of radium 226 and radium 228), Gradient used the lower of the two benchmarks (3 pCi/L for radium 228) to evaluate total radium concentrations.

⁵ Hardness data are available from the Kaskaskia River at Roots, Illinois (USGS Site No. 595400), 16 miles downstream of the BPP. Based on 130 samples collected from April 1980 to March 1997, the average hardness at this location was 173 mg/L (USGS, 2022b). Due to the age of the samples and the distance from the site, the US EPA (2022) default hardness of 100 mg/L was used. Use of a higher hardness value would result in less stringent screening values, thus, use of the US EPA default hardness is conservative.

Consistent with the human health risk evaluation, Gradient used the maximum detected concentrations from groundwater samples collected from all of the FAPS associated wells (regardless of hydrostratigraphic unit) without considering spatial or temporal representativeness for ecological receptor exposures. The use of the maximum constituent concentrations in this evaluation is designed to conservatively identify COIs that warrant further investigation. The COIs identified for ecological receptors include boron, radium 226+228, chloride, and fluoride (Table 3.3).

Table 3.3 Ecological Constituents of Interest

| Constituent ^a | Maximum Detected Groundwater Concentration | Ecological Benchmark ^b | Basis | Ecological COI ^c |
|--------------------------------|--|-----------------------------------|------------|-----------------------------|
| Total Metals (mg/L) | | | | |
| Antimony | 5.0E-03 | 1.9E-01 | EPA R4 ESV | No |
| Arsenic | 1.6E-02 | 1.9E-01 | IEPA SWQC | No |
| Barium | 1.0E+00 | 5.0E+00 | IEPA SWQC | No |
| Beryllium | 1.8E-03 | 6.4E-02 | EPA R4 ESV | No |
| Boron | 2.3E+01 | 7.6E+00 | IEPA SWQC | Yes |
| Cadmium | 4.0E-04 | 1.1E-03 | IEPA SWQC | No |
| Chromium | 5.3E-02 | 2.1E-01 | IEPA SWQC | No |
| Cobalt | 1.9E-02 | 1.9E-02 | EPA R4 ESV | No |
| Lead | 2.0E-02 | 2.0E-02 | IEPA SWQC | No |
| Lithium | 1.3E-01 | 4.4E-01 | EPA R4 ESV | No |
| Mercury | 1.6E-04 | 1.1E-03 | IEPA SWQC | No |
| Molybdenum | 1.4E-01 | 7.2E+00 | EPA R4 ESV | No |
| Selenium | 6.2E-03 | 1.0E+00 | IEPA SWQC | No |
| Thallium | 2.7E-03 | 6.0E-03 | EPA R4 ESV | No |
| Dissolved Metals (mg/L) | | | | |
| Antimony | 5.0E-04 | 1.9E-01 | EPA R4 ESV | No |
| Arsenic | - | 1.9E-01 | IEPA SWQC | No |
| Barium | 9.3E-02 | 5.0E+00 | IEPA SWQC | No |
| Beryllium | - | 6.4E-02 | EPA R4 ESV | No |
| Boron | 2.2E+01 | 7.6E+00 | IEPA SWQC | Yes |
| Cadmium | - | 9.3E-04 | IEPA SWQC | No |
| Chromium | - | 1.8E-01 | IEPA SWQC | No |
| Cobalt | - | 1.9E-02 | EPA R4 ESV | No |
| Lead | - | 1.6E-02 | IEPA SWQC | No |
| Lithium | 9.5E-02 | 4.4E-01 | EPA R4 ESV | No |
| Molybdenum | - | 8.0E-01 | EPA R4 ESV | No |
| Selenium | 2.1E-03 | 1.0E+00 | IEPA SWQC | No |
| Thallium | - | 6.0E-03 | EPA R4 ESV | No |
| Radionuclides (pCi/L) | | | | |
| Radium 226 + Radium 228 | 8.5E+00 | 3.0E+00 | US DOE | Yes |
| Other (mg/L or SU) | | | | |
| pH | 1.2E+01 | NA | - | No |
| Chloride | 1.4E+03 | 5.0E+02 | IEPA SWQC | Yes |
| Fluoride | 4.9E+00 | 4.0E+00 | IEPA SWQC | Yes |
| Sulfate | 1.5E+03 | NA | - | No |
| Total Dissolved Solids | 3.3E+03 | NA | - | No |
| Other Dissolved (mg/L) | | | | |
| Chloride | 1.3E+03 | 5.0E+02 | IEPA SWQC | Yes |
| Sulfate | 1.1E+03 | NA | - | No |

Notes:

COI = Constituent of Interest; FAPS = Fly Ash Pond System; GWPS = Groundwater Protection Standard; IEPA SWQC = Illinois Environmental Protection Agency Surface Water Quality Criteria; IL = Illinois; mg/L = Milligrams per Liter; NA = Not Available; pCi/L = PicoCuries per Liter; US DOE = United States Department of Energy; US EPA R4 ESV = United States Environmental Protection Agency Region IV Ecological Screening Value.

Blank cells indicate constituent was not detected.

Shaded cell indicates a compound identified as a COI.

(a) The constituents are those listed in the IL Part 845.600 GWPS (IEPA, 2021) that were detected in at least one groundwater sample from the wells related to the FAPS.

(b) Ecological benchmarks are from the hierarchy of sources discussed in Section 3.3.2: IEPA SWQC (IEPA, 2019); US EPA R4 "Ecological Risk Assessment Supplemental Guidance" (US EPA Region IV, 2018); and US DOE's guidance document, "A Graded Approach for Evaluating Radiation Doses to Aquatic and Terrestrial Biota" (US DOE, 2019).

(c) Constituents with maximum detected concentrations exceeding a benchmark protective of surface water exposure are considered ecological COIs.

3.3.3 Surface Water and Sediment Modeling

Surface water sampling has been conducted in the Kaskaskia River adjacent to the Site. However, to estimate the potential contribution to surface water (and sediment) from groundwater specifically associated with the FAPS, Gradient also modeled concentrations in the Kaskaskia River surface water and sediment from groundwater flowing into the river for the detected human and ecological COIs. This is because the constituents detected in groundwater above an ecological or health-based benchmark are most likely to pose a risk concern in the adjacent surface water. Gradient modeled human health and ecological COI concentrations in the surface water and sediment using a mass balance calculation based on the surface water and groundwater mixing. The model assumes a well-mixed groundwater-surface water location.

The maximum detected concentrations in groundwater (regardless of well location) from 2019 to 2024 were conservatively used to model COI concentrations in surface water and sediment. For COIs that were measured as both total and dissolved fractions, we used the maximum of the total and dissolved COI concentrations for the modeling. For most metals, the maximum concentration was from the total fraction. Use of the total metal concentration for these COIs may overestimate surface water concentrations because dissolved concentrations, which are lower than total concentrations, represent the mobile fractions of constituents that could likely flow into and mix with surface water.

The modeling approach does not account for geochemical transformations that may occur during groundwater mixing with surface water. Gradient assumed that predicted surface water concentrations were influenced only by the physical mixing of groundwater as it enters the surface water and were not further influenced by the geochemical reactions in the water and sediment, such as precipitation. In addition, the model only predicts surface water and sediment concentrations as a result of the potential migration of COIs in FAPS-related groundwater and does not account for background concentrations in surface water or sediment.

For this evaluation, Gradient adapted a simplified and conservative form of US EPA's indirect exposure assessment methodology (US EPA, 1998) that was used in US EPA's coal combustion waste risk assessment (US EPA, 2014). The model is a mass balance calculation based on surface water and groundwater mixing and the concept that the dissolved and sorbed concentrations can be related through an equilibrium partitioning coefficient (K_d). The model assumes a well-mixed groundwater-surface water location, with partitioning among total suspended solids, dissolved water column, sediment pore water, and solid sediments.

Sorption to soil and sediment is highly dependent on the surrounding geochemical conditions. To be conservative, we ignored the natural attenuation capacity of soil and sediment and estimated the surface

water concentration based only on the physical mixing of groundwater and surface water (*i.e.*, dilution) at the point where groundwater flows into surface water.

The aquifer properties used to estimate the volume of groundwater flowing into the Kaskaskia River and surface water concentrations are presented in Table 3.4 (for the UU) and Table 3.5 (for the UA or BU). The surface water properties used in the modeling are presented in Table 3.6. The COI concentrations in sediment were modeled using the COI-specific sediment-to-water partitioning coefficients and the sediment properties presented in Table 3.7. In the absence of Site-specific information for the Kaskaskia River, Gradient used default assumptions (*e.g.*, depth of the upper benthic layer and bed sediment porosity) to model sediment concentrations. The modeled surface water and sediment concentrations are presented in Table 3.8. These modeled concentrations reflect conservative contributions from groundwater. A description of the modeling and the detailed results are presented in Appendix A.

Table 3.4 Groundwater Properties Used in Modeling of the Upper Unit (UU)

| Parameter | Value | Unit | Notes/Source |
|--|----------------------|----------------|---|
| COI Concentration | Constituent specific | mg/L | Maximum detected concentration in groundwater. |
| Cross-Sectional Area for the UU ^a | 5,944 | m ² | Estimated thickness of the UU (about 4 m) multiplied by the length of FAPS intersecting the Kaskaskia River (about 1,500 m) (Ramboll, 2024a). |
| Hydraulic Gradient | 0.016 | m/m | Average horizontal hydraulic gradient across the FAPS for the UU (Ramboll, 2021a). |
| Hydraulic Conductivity of the UU | 3.2×10^{-5} | cm/s | Geometric mean horizontal hydraulic conductivity determined for the UU wells (Ramboll, 2024a). |

Notes:

COI = Constituent of Interest; FAPS = Fly Ash Pond System; UU = Upper Unit.

(a) The cross-sectional area represents the area through which groundwater flows from the UU to the Kaskaskia River.

Table 3.5 Groundwater Properties Used in Modeling of the Uppermost Aquifer (UA or BU)

| Parameter | Value | Unit | Notes/Source |
|--|----------------------|----------------|--|
| COI Concentration | Constituent specific | mg/L | Maximum detected concentration in groundwater. |
| Cross-Sectional Area for the UA ^a | 9,144 | m ² | Estimated thickness of the bedrock aquifer (about 6 m) multiplied by the length of FAPS intersecting the Kaskaskia River (about 1,500 m) (Ramboll, 2024a). |
| Hydraulic Gradient | 0.016 | m/m | Average horizontal hydraulic gradient across the FAPS for the bedrock aquifer (Ramboll, 2021a). |
| Hydraulic Conductivity of the UA | 5.0×10^{-6} | cm/s | Geometric mean horizontal hydraulic conductivity determined for the bedrock aquifer wells (Ramboll, 2024a). |

Notes:

BU = Bedrock Unit; COI = Constituent of Interest; FAPS = Fly Ash Pond System; UA = Uppermost Aquifer.

(a) The cross-sectional area represents the area through which groundwater flows from the UA to the Kaskaskia River.

Table 3.6 Surface Water Properties Used in Modeling

| Parameter | Value | Unit | Notes/Source |
|---|----------------------|--------|---|
| Surface Water Flow Rate | 5.4×10^{11} | L/year | Representative low-flow (10 th percentile) discharge rate estimated at Kaskaskia River monitoring location USGS05595000 at New Athens, IL (2009-2022) (USGS, 2022c). |
| Total Suspended Solids (TSS) | 84.5 | mg/L | Median suspended solids concentration measured at the Kaskaskia River monitoring location USGS05595000 at New Athens, IL in 2015-2022 (USGS, 2022d). |
| Depth of the Water Column | 2.74 | m | Average water depth of the Kaskaskia River near BPP (Bist LLC, 2022). |
| Suspended Sediment to Water Partition Coefficient | Constituent specific | mg/L | Values based on US EPA (2014). |

Notes:

BPP = Baldwin Power Plant; UA = Uppermost Aquifer; US EPA = United States Environmental Protection Agency; USGS = United States Geological Survey.

Table 3.7 Sediment Properties Used in Modeling

| Parameter | Value | Unit | Notes/Source |
|---|----------------------|-------------------|---|
| Depth of Upper Benthic Layer | 0.03 | m | Default (US EPA, 2014). |
| Depth of Water Body | 2.77 | m | Depth of water column (2.74 m) in the Kaskaskia River (Bist LLC, 2022) plus depth of upper benthic layer (0.03 m) (US EPA, 2014). |
| Bed Sediment Particle Concentration | 1 | g/cm ³ | Default (US EPA, 2014). |
| Bed Sediment Porosity | 0.6 | — | Default (US EPA, 2014). |
| Total Suspended Solids (TSS) Mass per Unit Area | 0.23 | kg/m ² | Depth of water column × TSS × conversion factors (10 ⁻⁶ kg/mg and 1,000 L/m ³). |
| Sediment Mass per Unit Area | 30 | kg/m ² | Depth of upper benthic layer × bed sediment particulate concentration × conversion factors (0.001 kg/g and 10 ⁶ cm ³ /m ³). |
| Sediment to Water Partitioning Coefficients | Constituent specific | mg/L | Values based on US EPA (2014). |

Note:

US EPA = United States Environmental Protection Agency.

Table 3.8 Surface Water and Sediment Modeling Results

| COI | Maximum Measured Concentration in UU (mg/L) | Maximum Measured Concentration in UA (mg/L) | Total Water Column Concentration (mg/L) | Concentration Sorbed to Bottom Sediments (mg/kg) |
|-------------------------------|---|---|---|--|
| Arsenic | 1.62E-02 | 1.14E-02 | 3.43E-08 | 5.16E-06 |
| Boron | 2.30E+01 | 6.77E+00 | 4.48E-05 | 1.69E-04 |
| Cobalt | 1.93E-02 | 1.69E-02 | 4.23E-08 | 8.41E-06 |
| Lead | 2.00E-02 | 1.62E-02 | 4.33E-08 | 3.98E-05 |
| Lithium | 7.88E-02 | 1.29E-01 | 1.98E-07 | NA ^a |
| Molybdenum | 7.10E-03 | 1.42E-01 | 7.32E-08 | 7.41E-06 |
| Thallium | 1.50E-03 | 2.70E-03 | 3.88E-09 | 3.75E-08 |
| Radium 226 + 228 ^b | 2.92E+00 | 8.54E+00 | 8.94E-06 | 4.07E-02 |
| Chloride | 6.10E+01 | 1.37E+03 | 6.92E-04 | NA ^a |
| Fluoride | 8.50E-01 | 4.93E+00 | 3.64E-06 | 5.69E-04 |

Notes:

COI = Constituent of Interest; K_d = Equilibrium Partition Coefficient; pCi/kg = PicoCuries per Kilogram; pCi/L = PicoCuries per Liter; UA = Uppermost Aquifer; UU = Upper Unit.

(a) Lithium and chloride do not readily sorb to soil or sediment particles; a K_d value of 0 was used for the modeling.

(b) Concentration of Radium-226+228 is expressed in pCi/L for water, and pCi/kg for sediment.

3.4 Human Health Risk Evaluation

The section below presents the results of the human health risk evaluation for residential use of surface water, and recreational use (by boaters and anglers) of the Kaskaskia River adjacent to the Site. Risks were assessed using the maximum measured or modeled COIs in surface water.

3.4.1 Residential Use of Surface Water as Drinking Water

Sparta, Illinois, uses the Kaskaskia River as one source of its CWS (IL intake #60183). The maximum modeled concentrations in surface water were compared to the lower of two water quality standards (Table 3.9): the Illinois water quality standards for public water supplies (Title 35 Part 302.304 and 302.307) (IEPA, 2019), or the GWPS in Part 845.600 (IEPA, 2013). The modeled and measured surface water concentrations were well below the comparison criteria. Thus, none of the COIs evaluated would be expected to pose an unacceptable risk for the use of surface water from the Kaskaskia River as a drinking water source.

Table 3.9 Risk Evaluation for Residents Exposed to Surface Water

| COI | Maximum Surface Water Concentration (modeled) | Maximum Surface Water Concentration (measured) | Drinking Water Criterion | COPC Based on Modeled Concentrations | COPC Based on Measured Concentrations |
|----------------------|---|--|--------------------------|--------------------------------------|---------------------------------------|
| Metals (mg/L) | | | | | |
| Arsenic | 3.4E-08 | ND | 1.6E-02 | No | No |
| Boron | 4.5E-05 | 4.2E-02 | 1.0E+00 | No | No |
| Cobalt | 4.2E-08 | NT | 1.9E-02 | No | NA |
| Lead | 4.3E-08 | ND | 2.0E-02 | No | No |
| Lithium | 2.0E-07 | NT | 1.3E-01 | No | NA |
| Molybdenum | 7.3E-08 | NT | 1.4E-01 | No | NA |
| Thallium | 3.9E-09 | NT | 2.7E-03 | No | NA |

| COI | Maximum Surface Water Concentration (modeled) | Maximum Surface Water Concentration (measured) | Drinking Water Criterion | COPC Based on Modeled Concentrations | COPC Based on Measured Concentrations |
|------------------------------|---|--|--------------------------|--------------------------------------|---------------------------------------|
| Radionuclides (pCi/L) | | | | | |
| Radium 226 + 228 | 8.9E-06 | NT | 5 | No | NA |

Notes:

COI = Constituent of Interest; COPC = Constituent of Potential Concern; mg/L = Milligrams per Liter; NA = Not Applicable; ND = Not Detected; NT = Not Tested; pCi/L = PicoCuries per Liter.

3.4.2 Recreators Exposed to Surface Water

Screening Exposures: Recreators could be exposed to surface water *via* incidental ingestion and dermal contact while boating. In addition, anglers could consume fish caught in the Kaskaskia River. The maximum measured or modeled COI concentrations in surface water were used as conservative upper-end estimates of the COI concentrations to which a recreator might be exposed directly (incidental ingestion of COIs in surface water while boating) and indirectly (consumption of locally caught fish exposed to COIs in surface water).

Screening Benchmarks: Illinois surface water criteria (IEPA, 2019), known as human threshold criteria (HTC), are based on incidental exposure through contact or ingestion of small volumes of water while swimming or during other recreational activities, as well as the consumption of fish. The HTC values were calculated from the following equation (IEPA, 2019):

$$HTC = \frac{ADI}{W + (F \times BCF)}$$

where:

HTC = Human health protection criterion in milligrams per liter (mg/L)
ADI = Acceptable daily intake (mg/day)
W = Water consumption rate (L/day)
F = Fish consumption rate (kg/day)
BCF = Bioconcentration factor (L/kg tissue)

Illinois defines the acceptable daily intake (ADI) as the "maximum amount of a substance which, if ingested daily for a lifetime, results in no adverse effects to humans" (IEPA, 2019). US EPA defines its chronic reference dose (RfD) as an "estimate (with uncertainty spanning perhaps an order of magnitude) of a daily oral exposure for a chronic duration (up to a lifetime) to the human population (including sensitive subgroups) that is likely to be without an appreciable risk of deleterious effects during a lifetime" (US EPA, 2011a). Illinois lists methods to derive an ADI from the primary literature (IEPA, 2019). In accordance with Illinois guidance, Gradient derived an ADI by multiplying the MCL by the default water ingestion rate of 2 L/day (IEPA, 2019). In the absence of an MCL, Gradient applied the RfD used by US EPA to derive its Regional Screening Levels (RSLs) (US EPA, 2024a) as a conservative estimate of the ADI. The RfDs are given in mg/kg-day, while the ADIs are given in mg/day; thus, Gradient multiplied the RfD by a standard body weight of 70 kg to obtain the ADI in mg/day. The calculation of the HTC values is shown in Appendix B, Table B.1.

Gradient used bioconcentration factors (BCFs) from a hierarchy of sources. The primary BCFs were those that US EPA used to calculate the National Recommended Water Quality Criteria (NRWQC) for human health (US EPA, 2002). Other sources included BCFs used in the US EPA coal combustion ash risk assessment (US EPA, 2014) and BCFs reported by Oak Ridge National Laboratory's Risk Assessment Information System (ORNL RAIS) (ORNL, 2020).⁶ Lithium did not have a BCF value available from any authoritative source; therefore, the water quality criterion for lithium was calculated assuming a BCF of 1. This is a conservative assumption, as lithium does not readily bioaccumulate in the aquatic environment (ECHA, 2020a,b; ATSDR, 2010).

Illinois recommends a fish consumption rate of 0.020 kg/day (20 g/day) for an adult weighing 70 kg (IEPA, 2019). Illinois recommends a water consumption rate of 0.01 L/day for "incidental exposure through contact or ingestion of small volumes of water while swimming or during other recreational activities" (IEPA, 2019). Appendix B, Table B.1 presents the calculated HTC for fish and water and for fish consumption only.

The HTC for fish consumption for radium 226+228 was calculated as follows:

$$HTC = \frac{TCR}{(SF \times BAF \times F)}$$

where:

- HTC = Human health protection criterion in picoCuries per liter (pCi/L)
- TCR = Target cancer risk (1×10^{-5})
- SF = Food ingestion slope factor (risk/pCi)
- BAF = Bioaccumulation factor (L/kg tissue)
- F = Fish consumption rate (kg/day)

The food ingestion slope factor (lifetime excess total cancer risk per unit exposure, in risk/pCi) used to calculate the HTC was the highest value of those for radium 226 (Ra226), radium 228 (Ra228), and "Ra228+D" (US EPA, 2001). According to US EPA (2001), "+D" indicates that "the risks from associated short-lived radioactive decay products (*i.e.*, those decay products with radioactive half-lives less than or equal to 6 months) are also included."

Screening Risk Evaluation: The maximum modeled and measured COI concentrations in surface water were compared to the calculated Illinois HTC values (Table 3.10). All surface water concentrations were below their respective benchmarks. The HTC values are protective of recreational exposure *via* water and/or fish ingestion and do not account for dermal exposures to COIs in surface water while boating. However, given that the measured and modeled COI surface water concentrations are orders of magnitude below HTC protective of water and/or fish ingestion, dermal exposures to COIs are not expected to be a risk concern. Moreover, the dermal uptake of metals is considered to be minimal and only a small proportion of ingestion exposures. Thus, none of the COIs evaluated would be expected to pose an unacceptable risk to recreators exposed to surface water while boating and anglers consuming fish caught in the Kaskaskia River.

⁶ Although recommended by US EPA (2015b), US EPA EpiSuite 4.1 (US EPA, 2019) was not used as a source of BCFs because inorganic compounds are outside the estimation domain of the program.

Table 3.10 Risk Evaluation for Recreators Exposed to Surface Water

| COI | Maximum Surface Water Concentration | | HTC | | | COPC | |
|------------------------------|-------------------------------------|-----------------------|----------------|------------|-----------|---------------------------------|----------------------------------|
| | Modeled | Measured ^a | Water and Fish | Water Only | Fish Only | Based on Modeled Concentrations | Based on Measured Concentrations |
| Metals (mg/L) | | | | | | | |
| Arsenic | 3.4E-08 | ND | 2.2E-02 | 2.0E+00 | 2.3E-02 | No | No |
| Boron | 4.5E-05 | 4.2E-02 | 4.7E+02 | 1.4E+03 | 7.0E+02 | No | No |
| Cobalt | 4.2E-08 | NT | 3.5E-03 | 2.1E+00 | 3.5E-03 | No | NA |
| Lead | 4.3E-08 | ND | 1.5E-02 | 1.5E-02 | 1.5E-02 | No | No |
| Lithium | 2.0E-07 | NT | 4.7E+00 | 1.4E+01 | 7.0E+00 | No | NA |
| Molybdenum | 7.3E-08 | NT | 3.9E+00 | 3.5E+01 | 4.4E+00 | No | NA |
| Thallium | 3.9E-09 | NT | 1.7E-03 | 4.0E-01 | 1.7E-03 | No | NA |
| Radionuclides (pCi/L) | | | | | | | |
| Radium 226 + 228 | 8.9E-06 | NT | 1.0E+03 | 1.0E+03 | 8.7E+04 | No | NA |

Notes:

COI = Constituent of Interest; COPC = Constituent of Potential Concern; HTC = Human Threshold Criteria; mg/L = Milligrams per Liter; NA = Not Applicable; ND = Not Detected; NT = Not Tested; pCi/L = PicoCuries per Liter.

Blank cells indicate constituent was not detected.

(a) Measured concentrations are listed only for the constituents identified as COIs. Measured surface water concentrations may be different from modeled concentrations because measured data include the effects of background and other industrial sources. Modeled concentrations only represent the potential effect on surface water quality resulting from the measured groundwater concentrations.

3.4.3 Recreators Exposed to Sediment

Recreational exposure to sediment may occur during boating activity in the Kaskaskia River; exposure to sediment may occur through incidental ingestion and dermal contact.

Screening Exposures: COIs in impacted groundwater flowing into the river can sorb to sediments. In the absence of sediment data, sediment concentrations were modeled using maximum detected groundwater concentrations.

Screening Benchmarks: There are no established recreator RSLs that are protective of recreational exposures to sediment (US EPA, 2024a). Therefore, benchmarks that are protective of recreational exposures to sediment *via* incidental ingestion and dermal contact were calculated using US EPA's RSL guidance (US EPA, 2024b). These benchmarks were calculated using the recommended assumptions (*i.e.*, oral bioavailability, body weights, averaging time) and toxicity reference values (*i.e.*, RfD and cancer slope factor [CSF]). Recreators were assumed to be exposed to sediment while recreating 60 days a year (or two weekend days per week for 30 weeks a year, from April to October). The exposure duration was assumed for a child 6 years of age and an adult 20 years of age, per US EPA guidance (Stalcup, 2014). The daily recommended residential soil ingestion rates of 200 mg/day for a child and 100 mg/day for an adult are based on an all-day exposure to residential soils (Stalcup, 2014; US EPA, 2011b). Since recreational exposures to sediment are assumed to occur for less than four hours per day, one-third of the daily residential soil ingestion (67 mg/day for a child and 33 mg/day for an adult) was used as a conservative assumption. For dermal exposures, recreators were assumed to be exposed to sediment on their lower legs and feet (1,026 cm² for the child and 3,026 cm² for the adult, based on the age-weighted surface areas reported in US EPA, 2011b). While other body parts may be exposed to sediment, the contact time will likely be very short, as the sediment would wash off in the surface water. Gradient used US EPA's recommended adherence factor of 0.2 mg/cm² based on child exposure to wet soil (US EPA, 2004; Stalcup,

2014), which was used in the US EPA RSL User's Guide for a child recreator exposed to soil or sediment (US EPA, 2024b). The sediment screening benchmarks were calculated based on a target hazard quotient of 1, or a target cancer risk of 1×10^{-5} . Appendix B, Table B.2 presents the calculation of screening benchmarks protective of recreational exposures to sediment. A recreator sediment screening benchmark for radium 226+228 was based on soil Preliminary Remediation Goals (PRGs) calculated for radium 226 and radium 228 using US EPA's PRG calculator (US EPA, 2020). The lower of the two values was used as the recreator sediment screening benchmark for radium 226+228 (Appendix B, Table B.3).

Screening Risk Evaluation: The modeled sediment concentrations were well below the recreational sediment screening benchmarks (Table 3.11). Therefore, exposure to sediment is not expected to pose an unacceptable risk to recreators while boating.

Table 3.11 Risk Evaluation for Recreators Exposed to Sediment

| COI | Modeled Sediment Concentration (mg/kg) | Recreator Sediment Screening Benchmark (mg/kg) | COPC |
|-------------------------------|--|--|------|
| Metals (mg/kg) | | | |
| Arsenic | 5.2E-06 | 6.8E+01 | No |
| Boron | 1.7E-04 | 2.7E+05 | No |
| Cobalt | 8.4E-06 | 4.1E+02 | No |
| Lead | 4.0E-05 | 2.0E+02 | No |
| Lithium ^a | NA ^a | 2.7E+03 | No |
| Molybdenum | 7.4E-06 | 6.8E+03 | No |
| Thallium | 3.7E-08 | 1.4E+01 | No |
| Radionuclides (pCi/kg) | | | |
| Radium 226 + 228 | 4.1E-02 | 7.9E+03 | No |

Notes:

COI = Constituent of Interest; COPC = Constituent of Potential Concern; K_d = Equilibrium Partition Coefficient; NA = Not Applicable; pCi/kg = PicoCuries per Kilogram.

(a) Lithium does not readily sorb to soil or sediment particles; a K_d value of 0 was used for the modeling.

3.5 Ecological Risk Evaluation

Based on the ecological CEM (Figure 3.5), ecological receptors could be exposed to surface water and dietary items (*i.e.*, prey and plants) potentially impacted by identified COIs (radium 226+228 and chloride).

3.5.1 Ecological Receptors Exposed to Surface Water

Screening Exposures: The ecological evaluation considered aquatic communities in the Kaskaskia River potentially impacted by identified ecological COIs. Measured and modeled surface water concentrations were compared to risk-based ecological screening benchmarks.

Screening Benchmarks: Surface water screening benchmarks protective of aquatic life were obtained from the following hierarchy of sources:

- IEPA SWQS (IEPA, 2019), regulatory standards that are intended to protect aquatic life exposed to surface water on a long-term basis (*i.e.*, chronic exposure). For cadmium, the surface water

benchmark is hardness dependent and calculated using a default hardness of 100 mg/L (US EPA, 2022);⁷

- US EPA Region IV (2018) surface water ESVs for hazardous waste sites; and
- US DOE benchmarks from the guidance document, "A Graded Approach for Evaluating Radiation Doses to Aquatic and Terrestrial Biota" (US DOE, 2019).

Risk Evaluation: The maximum measured and modeled COI concentrations in surface water were compared to the benchmarks protective of aquatic life (Table 3.12). The measured and modeled surface water concentrations for the COIs were below their respective benchmarks. Thus, none of the COIs evaluated are expected to pose an unacceptable risk to aquatic life in the Kaskaskia River.

Table 3.12 Risk Evaluation for Ecological Receptors Exposed to Surface Water

| COI | Maximum Surface Water Concentration | | Ecological Freshwater Benchmark | Basis | COPC | |
|-----------------------|-------------------------------------|-----------------------|---------------------------------|-----------|--------------------------------|---------------------------------|
| | Modeled | Measured ^a | | | Based on Modeled Concentration | Based on Measured Concentration |
| Total Metals (mg/L) | | | | | | |
| Boron | 4.5E-05 | 4.2E-02 | 7.6E+00 | IEPA SWQC | No | No |
| Radionuclides (pCi/L) | | | | | | |
| Radium 226 + 228 | 8.9E-06 | NA | 3.0E+00 | US DOE | No | NA |
| Other (mg/L) | | | | | | |
| Chloride | 6.9E-04 | 2.1E+01 | 5.0E+02 | IEPA SWQC | No | No |
| Fluoride | 3.6E-06 | 2.2E-01 | 4.0E+00 | IEPA SWQC | No | No |

Notes:

COI = Constituent of Interest; COPC = Constituent of Potential Concern; IEPA = Illinois Environmental Protection Agency; mg/L = Milligrams per Liter; NA = Not Applicable; pCi/L = PicoCuries per Liter; SWQC = Surface Water Quality Criteria; US DOE = United States Department of Energy.

(a) COIs with no measured surface water data were listed as NA.

3.5.2 Ecological Receptors Exposed to Sediment

Screening Exposures: COIs in impacted groundwater flowing into Kaskaskia River can sorb to sediments *via* chemical partitioning. In the absence of sediment data, sediment concentrations were modeled using maximum detected groundwater concentrations. Therefore, the modeled COI sediment concentrations reflect the potential maximum Site-related sediment concentration originating from groundwater.

Screening Benchmarks: Sediment screening benchmarks were obtained from US EPA Region IV (2018). The majority of the sediment ESVs are based on threshold effect concentrations (TECs) from MacDonald *et al.* (2000), which provide consensus values that identify concentrations below which harmful effects on sediment-dwelling organisms are unlikely to be observed. In the absence of an ESV for radium 226+228, a sediment screening value of 90,000 pCi/kg was used, based on the biota concentration guide (BCG) for radium 228 (US DOE, 2019).⁸ Chloride and fluoride are not expected to sorb to sediment; therefore, risk to ecological receptors exposed to sediment was not evaluated for these constituents. The benchmarks used in this evaluation are listed in Table 3.13.

⁷ Conservatism associated with using a default hardness value are discussed in Section 3.6.

⁸ The BCG for sediment is 90 pCi/g for Ra-228 and 100 pCi/g for Ra-226; the lower of the two values was used for Ra-226+228, and converted to pCi/kg (US DOE, 2019).

Screening Risk Results: The maximum modeled COI sediment concentrations were below their respective sediment screening benchmarks (Table 3.13). The modeled sediment concentrations attributed to potential contributions from Site groundwater for all COIs were less than 1% of the sediment screening benchmark. Therefore, the modeled sediment concentrations attributed to potential contributions from Site groundwater are not expected to significantly contribute to ecological exposures in the Kaskaskia River adjacent to the Site.

Table 3.13 Risk Evaluation for Ecological Receptors Exposed to Sediment

| COI ^a | Modeled Sediment Concentration | ESV ^a | COPC | % of Benchmark |
|-------------------------------|--------------------------------|----------------------|------|----------------|
| Metals (mg/kg) | | | | |
| Boron | 1.7E-04 | 3.8E+01 ^b | No | 0.0004% |
| Radionuclides (pCi/kg) | | | | |
| Radium 226 + 228 | 4.1E-02 | 9.0E+04 ^c | No | 0.00005% |
| Other (mg/kg) | | | | |
| Chloride | NA ^d | NA | No | NA |
| Fluoride | 5.7E-04 | NA | No | NA |

Notes:

COI = Constituent of Interest; COPC = Constituent of Potential Concern; ESV = Ecological Screening Value; K_d = Equilibrium Partition Coefficient; mg/kg = Milligrams per Kilogram; NA = Not Available; NOEC = No Observable Effect Concentration; pCi/kg = PicoCuries per Kilogram; US DOE = United States Department of Energy; US EPA = United States Environmental Protection Agency.

(a) ESV from US EPA Region IV (2018).

(b) Boron NOEC of 38 mg/kg was used as a conservative benchmark for boron in the absence of an ESV (ECHA, 2019).

(c) ESV from US DOE (2019); value converted from 90 pCi/g to 90,000 pCi/kg.

(d) Chloride does not readily sorb to soil or sediment particles; a K_d value of 0 was used for the modeling.

3.5.3 Ecological Receptors Exposed to Bioaccumulative Constituents of Interest

Screening Exposures: COIs with bioaccumulative properties can impact higher trophic level wildlife exposed to these COIs *via* direct exposures (surface water and sediment exposure) and secondary exposures through the consumption of dietary items (*e.g.*, plants, invertebrates, small mammals, and fish).

Screening Benchmark: US EPA Region IV (2018) guidance and IEPA SWQS (IEPA, 2019) guidance were used to identify constituents with potential bioaccumulative effects.

Risk Evaluation: The ecological COIs (boron, radium 226+228, chloride, fluoride) were not identified as having potential bioaccumulative effects. Therefore, these COIs are not considered to pose an ecological risk *via* bioaccumulation. IEPA (2019) identifies mercury as the only metal with bioaccumulative properties, however, mercury was not considered an ecological COI.⁹

3.6 Uncertainties and Conservatism

A number of uncertainties and their potential impact on the risk evaluation are discussed below. Wherever possible, conservative assumptions were used in an effort to minimize uncertainties and overestimate rather than underestimate risks.

⁹ US EPA Region IV (2018) identifies selenium as having potential bioaccumulative effects. Although selenium was detected in groundwater, it was not considered an ecological COI.

Exposure Estimates:

- The risk evaluation included the IL Part 845.600 constituents detected in groundwater samples (above GWPS) collected from wells associated with the FAPS. However, it is possible that not all of the detected constituents are related specifically to the FAPS.
- The human health and ecological risk characterizations were based on the maximum measured or modeled COI concentrations, rather than on averages. Thus, the variability in exposure concentrations was not considered. Assuming continuous exposure to the maximum concentration overestimates human and ecological exposures, given that receptors are mobile and concentrations change over time. For example, US EPA guidance states that risks should be estimated using average exposure concentrations as represented by the 95% upper confidence limit on the mean (US EPA, 1992). Given that exposure estimates based on the maximum concentrations did not exceed risk benchmarks, Gradient has greater confidence that there is no risk concern.
- Only constituents detected in groundwater were used to identify COIs and model COI concentrations in surface water and sediment. For the constituents that were not detected in FAPS groundwater, the detection limits were below the IL Part 845.600 GWPS and thus do not require further evaluation.
- COI concentrations in surface water were modeled using the maximum detected total COI concentrations in groundwater. Modeling surface water concentrations using total metal concentrations may overestimate surface water concentrations because dissolved concentrations, which are lower than total concentrations, represent the mobile fractions of constituents that could likely flow into and mix with surface water.
- The COIs identified in this evaluation also occur naturally in the environment. Contributions to exposure from natural or other non-FAPS-related sources were not considered in the evaluation of modeled concentrations; only exposure contributions potentially attributable to Site groundwater mixing with surface water were evaluated. While not quantified, exposures from potential FAPS-related groundwater contributions are likely to represent only a small fraction of the overall human and ecological exposure to COIs that also have natural or non-FAPS-related sources.
- Screening benchmarks for human health were developed using exposure inputs based on US EPA's recommended values for reasonable maximum exposure (RME) assessments (Stalcup, 2014). RME is defined as "the highest exposure that is reasonably expected to occur at a site but that is still within the range of possible exposures" (US EPA, 2004). US EPA states the "intent of the RME is to estimate a conservative exposure case (*i.e.*, well above the average case) that is still within the range of possible exposures" (US EPA, 1989). US EPA also notes that this high-end exposure "is the highest dose estimated to be experienced by some individuals, commonly stated as approximately equal to the 90th percentile exposure category for individuals" (US EPA, 2015c). Thus, most individuals will have lower exposures than those presented in this risk assessment.

Toxicity Benchmarks:

- Screening-level ecological benchmarks were compiled from IEPA and US EPA guidance and designed to be protective of the majority of Site conditions, leaving the option for Site-specific refinement. In some cases, these benchmarks may not be representative of the Site-specific conditions or receptors found at the Site, or may not accurately reflect concentration-response relationships encountered at the Site. For example, the ecological benchmark for cadmium is hardness dependent, and Gradient relied on US EPA's default hardness of 100 mg/L. Use of a higher hardness value would increase the cadmium SWQS because benchmarks become less

stringent with higher levels of hardness. Regardless of the hardness, the maximum modeled cadmium concentration is orders of magnitude below the SWQS.

- In addition, for the ecological evaluation, Gradient conservatively assumed all constituents to be 100% bioavailable. Modeled COI concentrations in surface water are considered total COI concentrations. In addition, the measured surface water data used in this report represent total concentrations. US EPA recommends using dissolved metals as a measure of exposure to ecological receptors because it represents the bioavailable fraction of metal in water (US EPA, 1993). Therefore, the modeled surface water COI concentrations may be an overestimation of exposure concentrations to ecological receptors.
- In general, it is important to appreciate that the human health toxicity factors used in this risk evaluation are developed to account for uncertainties, such that safe exposure levels used as benchmarks are often many times lower (even orders of magnitude lower) than the levels that cause effects that have been observed in human or animal studies. For example, toxicity factors incorporate a 10-fold safety factor to protect sensitive subpopulations. This means that a risk exceedance does not necessarily equate to actual harm.

4 Summary and Conclusions

A screening-level risk evaluation was performed for Site-related constituents in groundwater at the BPP in Baldwin, Illinois. The CSM developed for the Site indicates that groundwater beneath the FAPS flows into the Kaskaskia River adjacent to the Site and may potentially impact surface water and sediment. CEMs were developed for human and ecological receptors. The complete exposure pathways for humans include recreators (boaters) in the Kaskaskia River who are exposed to surface water and sediment, and anglers who consume locally caught fish. In addition, groundwater is used for drinking water within 1,000 meters of the BPP, and surface water from the Kaskaskia River is used for a community water supply, with the closest intake 1,325 feet southwest of the BPP. The complete exposure pathways for ecological receptors include aquatic life (including aquatic and marsh plants, amphibians, reptiles, and fish) exposed to surface water; benthic invertebrates exposed to sediment; and avian and mammalian wildlife exposed to bioaccumulative COIs in surface water, sediment, and dietary items.

Groundwater data collected from 2019 to 2024 were used to estimate exposures. The available surface water data collected from the Kaskaskia River were also evaluated. For groundwater constituents retained as COIs, surface water and sediment concentrations were modeled using the maximum detected groundwater concentration. Surface water and sediment exposure estimates were screened against benchmarks protective of human health and ecological receptors for this risk evaluation.

US EPA has established acceptable risk metrics. Risks above these US EPA-defined metrics are termed potentially "unacceptable risks." Based on the evaluation presented in this report, no unacceptable risks to human or ecological receptors resulting from CCR exposures associated with the FAPS were identified. This means that the risks from the Site are likely indistinguishable from normal background risks. Specific risk assessment results include the following:

- For groundwater used as drinking water, based on recent investigations and data collected from off-Site monitoring wells, private wells on properties south of the BPP are unlikely to be impacted by groundwater constituents associated with the BPP in excess of the GWPSs. The other private wells identified in the vicinity of the Site are upgradient or side-gradient of the BPP, and are therefore also unlikely to be impacted by groundwater constituents from the BPP.
- For surface water used as a drinking water source, all modeled COI concentrations were below the conservative risk-based screening benchmarks. Therefore, none of the COIs evaluated in surface water are expected to pose an unacceptable risk for use of the Kaskaskia River as a public water supply.
- For recreators exposed to surface water, all COIs were below the conservative risk-based screening benchmarks. Therefore, none of the COIs evaluated in surface water are expected to pose an unacceptable risk to recreators in the Kaskaskia River adjacent to the Site.
- For recreators exposed to sediment *via* incidental ingestion and dermal contact, the modeled sediment concentrations were below health-protective sediment benchmarks. Therefore, the modeled sediment concentrations are not expected to pose an unacceptable risk to recreators exposed to sediment in the Kaskaskia River adjacent to the Site.
- For anglers consuming locally caught fish, the modeled concentrations of all COIs in surface water (as well as the measured data) were below conservative benchmarks protective of fish consumption.

Therefore, none of the COIs evaluated are expected to pose an unacceptable risk to recreators consuming fish caught in the Kaskaskia River.

- Ecological receptors exposed to surface water include aquatic and marsh plants, amphibians, reptiles, and fish. The risk evaluation showed that none of the modeled or measured COIs in surface water exceeded protective screening benchmarks. Ecological receptors exposed to sediment include benthic invertebrates. The modeled sediment COIs did not exceed the conservative screening benchmarks; therefore, none of the COIs evaluated in sediment are expected to pose an unacceptable risk to ecological receptors.
- Ecological receptors were also evaluated for exposure to bioaccumulative COIs. This evaluation considered higher trophic level wildlife with direct exposure to surface water and sediment and secondary exposure through the consumption of dietary items (*e.g.*, plants, invertebrates, small mammals, fish). None of the ecological COIs were identified as having potential bioaccumulative effects. Overall, this evaluation demonstrated that none of the COIs evaluated are expected to pose an unacceptable risk to ecological receptors.

It should be noted that this evaluation incorporates a number of conservative assumptions that tend to overestimate exposure and risk. The risk evaluation was based on the maximum detected COI concentration; however, US EPA guidance states that risks should be based on a representative average concentration such as the 95% upper confidence limit on the mean; thus, using the maximum concentration tends to overestimate exposure. Although the COIs identified in this evaluation also occur naturally in the environment, the contributions to exposure from natural background sources and nearby industry were not considered; thus, CCR-related exposures were likely overestimated. Exposure estimates assumed 100% metal bioavailability, which likely results in overestimates of exposure and risks. Exposure estimates were based on inputs to evaluate the "reasonable maximum exposure"; thus, most individuals will have lower exposures than those estimated in this risk assessment.

Finally, while this evaluation concluded that current conditions do not present a risk to human health or the environment, it should be noted that based on the location of current off-site groundwater wells and the results of groundwater modeling, future conditions are also not expected to present a risk to human health or the environment.

References

Agency for Toxic Substances and Disease Registry (ATSDR). 2010. "Toxicological Profile for Boron." November. Accessed at <http://www.atsdr.cdc.gov/ToxProfiles/tp26.pdf>.

Bist LLC. 2022. "Kaskaskia River bathymetry map." Accessed at <https://fishing-app.gpsnauticalcharts.com/i-boating-fishing-web-app/fishing-marine-charts-navigation.html#13.91/38.1925/-89.8696>.

European Chemicals Agency (ECHA). 2019. "Ecotoxicological information: Sediment toxicity: 001 Weight of evidence." In REACH dossier for Boron (CAS No. 7740-42-8). Accessed at <https://echa.europa.eu/registration-dossier/-/registered-dossier/14776/6/3>.

European Chemicals Agency (ECHA). 2020a. "REACH dossier for boron (CAS No. 7440428)." Accessed at <https://echa.europa.eu/registrationdossier/registereddossier/14776>.

European Chemicals Agency (ECHA). 2020b. "REACH dossier for lithium (CAS No. 7439932)." Accessed at <https://echa.europa.eu/registrationdossier/registereddossier/14178>.

Hanson Professional Services Inc. 2017. "Antidegradation Assessment for Management of Coal Combustion Residuals Impoundment Waters, Baldwin Energy Complex, Dynegy Midwest Generation, LLC, NPDES Permit No. IL0000043." Report to Dynegy Midwest Generation, LLC, Collinsville, IL. 24p., April 17.

Illinois Dept. of Natural Resources (IDNR). 2022. "Kaskaskia River." Accessed at <https://www2.illinois.gov/dnr/Parks/Pages/KaskaskiaRiver.aspx>.

Illinois Environmental Protection Agency (IEPA). 2012. "Lower Kaskaskia River Watershed TMDL Report." Bureau of Water, IEPA/BOW/12-001, 262p., February.

Illinois Environmental Protection Agency (IEPA). 2013. "Title 35: Environmental Protection, Subtitle F: Public Water Supplies, Chapter I: Pollution Control Board, Part 620: Ground Water Quality." Accessed at <https://www.ilga.gov/commission/jcar/admincode/035/035006200D04200R.html>.

Illinois Environmental Protection Agency (IEPA). 2019. "Title 35: Environmental Protection, Subtitle C: Water Pollution, Chapter I: Pollution Control Board, Part 302: Water Quality Standards." Accessed at <https://www.epa.gov/sites/default/files/2019-11/documents/ilwqs-title35-part302.pdf>

Illinois Environmental Protection Agency (IEPA). 2021. "Standards for the disposal of coal combustion residuals in surface impoundments." Accessed at <https://www.ilga.gov/commission/jcar/admincode/035/03500845sections.html>.

Illinois Environmental Protection Agency (IEPA). 2025. "Map Server (Version 10.6), GIS Layer: Community Water Supply (CWS) Surface Water Intakes." Accessed on January 28, 2025 at <https://geoservices.epa.illinois.gov/arcgis/rest/services/Water/WellsIntakes/MapServer/1>

Illinois State Geological Survey. 2024. "Illinois Water Well (ILWATER) Interactive Map." Accessed on April 5, 2024 at <https://prairie-research.maps.arcgis.com/apps/webappviewer/index.html?id=e06b64ae0c814ef3a4e43a191cb57f87>

MacDonald, DD; Ingersoll, CG; Berger, TA. 2000. "Development and evaluation of consensus-based sediment quality guidelines for freshwater ecosystems." *Arch. Environ. Contam. Toxicol.* 39:2031. doi: 10.1007/s002440010075.

Natural Resource Technology, Inc. (NRT). 2016. "Supplemental Hydrogeologic Site Characterization and Groundwater Monitoring Plan, Baldwin Fly Ash Pond System, Baldwin Energy Complex, Baldwin, Illinois." Report to Dynegy Midwest Generation, LLC (Collinsville, IL). 254p., March 31.

Oak Ridge National Laboratory (ORNL). 2020. "Risk Assessment Information System (RAIS) Toxicity Values and Physical Parameters Search." Accessed at https://rais.ornl.gov/cgi-bin/tools/TOX_search.

Ramboll. 2021a. "Hydrogeologic Site Characterization Report, Bottom Ash Pond, Baldwin Power Plant, Baldwin, Illinois (Final)." Report to Dynegy Midwest Generation, LLC. 504p., October 25.

Ramboll. 2021b. Annual Groundwater Monitoring and Corrective Action Report, Fly Ash Pond System.

Ramboll. 2023. "Groundwater Modeling Results, Baldwin Power Plant Fly Ash Pond System (Draft)." October 17.

Ramboll. 2024a. "Nature and Extent Report, Baldwin Power Plant, Fly Ash Pond System."

Ramboll. 2024b. "Shallow Unlithified Potentiometric Surface Map: 2024 Annual Groundwater Monitoring and Corrective Action Report, Fly Ash Pond System, Baldwin Power Plant, Baldwin, Illinois (Draft)." 1p., October 14.

Ramboll. 2024c. "Documentation re: Groundwater monitoring well locations." 103p.

Ramboll. 2024d. "Well Location and Exceedance Map, Baldwin Power Plant, Baldwin, Illinois." 1p., January 23.

Ramboll. 2025a. "Groundwater Modeling Technical Memorandum, Baldwin Power Plant, Fly Ash Pond System. IEPA ID No. W1578510001-01/02/03 (Draft). Report to Dynegy Midwest Generation, LLC. 44p., February 18.

Ramboll. 2025b. "Groundwater Monitoring Data, 2010-2024."

Stalcup, D. [US EPA, Office of Solid Waste and Emergency Response (OSWER)]. 2014. Memorandum to Superfund National Policy Managers, Regions 1-10 re: Human Health Evaluation Manual, Supplemental Guidance: Update of standard default exposure factors. OSWER Directive 9200.1-120, February 6. Accessed at https://www.epa.gov/sites/production/files/2015-11/documents/oswer_directive_9200.1-120_exposurefactors_corrected2.pdf.

US Dept. of Energy (US DOE). 2019. "A Graded Approach for Evaluating Radiation Doses to Aquatic and Terrestrial Biota." DOESTD11532019. Accessed at <https://www.standards.doe.gov/standards-documents/1100/1153-astd-2019>.

US EPA. 1989. "Risk Assessment Guidance for Superfund (RAGS). Volume I: Human Health Evaluation Manual (Part A) (Interim final)." Office of Emergency and Remedial Response, NTIS PB90155581, EPA540/189002, December.

US EPA. 1992. "Risk Assessment Guidance for Superfund: Supplemental Guidance to RAGS: Calculating the Concentration Term." Office of Emergency and Remedial Response, OSWER Directive 9285.708I, NTIS PB92963373, May.

US EPA. 1993. Memorandum to US EPA Directors and Regions re: Office of Water policy and technical guidance on interpretation and implementation of aquatic life metals criteria. Office of Water, EPA822F93009, October 1.

US EPA. 1998. "Methodology for assessing health risks associated with multiple pathways of exposure to combustor emissions." National Center for Environmental Assessment (NCEA), EPA 600/R98/137, December. Accessed at <https://cfpub.epa.gov/ncea/risk/hhra/recordisplay.cfm?deid=55525>.

US EPA. 2001. "Radionuclide Table: Radionuclide Carcinogenicity – Slope Factors (Federal Guidance Report No. 13 Morbidity Risk Coefficients, in Units of Picocuries)." Health Effects Assessment Summary Tables (HEAST) 72p. Accessed at https://www.epa.gov/sites/default/files/2015-02/documents/heast2_table_4-d2_0401.pdf

US EPA. 2002. "National Recommended Water Quality Criteria [NRWQC]: 2002. Human Health Criteria Calculation Matrix." Office of Water, EPA822R02012, November.

US EPA. 2004. "Risk Assessment Guidance for Superfund (RAGS). Volume I: Human Health Evaluation Manual (Part E, Supplemental Guidance for Dermal Risk Assessment) (Final)." Office of Superfund Remediation and Technology Innovation, EPA/540/R/99/005, OSWER 9285.702EP; PB99963312, July. Accessed at http://www.epa.gov/oswer/riskassessment/rags/pdf/part_e_final_revision_100307.pdf.

US EPA. 2011a. "IRIS Glossary." August 31. Accessed at https://ofmpub.epa.gov/sor_internet/registry/termreg/searchandretrieve/glossariesandkeywordlists/search.do?details=&glossaryName=IRIS%20Glossary#formTop.

US EPA. 2011b. "Exposure Factors Handbook: 2011 Edition." Office of Research and Development, National Center for Environmental Assessment (NCEA), EPA/600/R090/052F, September. Accessed at <https://www.epa.gov/expobox/aboutexposurefactorshandbook>.

US EPA. 2014. "Human and Ecological Risk Assessment of Coal Combustion Residuals (Final)." Office of Solid Waste and Emergency Response (OSWER), Office of Resource Conservation and Recovery, December. Accessed at <http://www.regulations.gov/#!documentDetail;D=EPAHQRCRA2009064011993>.

US EPA. 2015a. "Hazardous and solid waste management system; Disposal of coal combustion residuals from electric utilities (Final rule)." *Fed. Reg.* 80(74):2130221501, 40 CFR 257, 40 CFR 261, April 17.

US EPA. 2015b. "Human Health Ambient Water Quality Criteria: 2015 Update." Office of Water, EPA 820F15001, June.

US EPA. 2015c. "Conducting a Human Health Risk Assessment." October 14. Accessed at <http://www2.epa.gov/risk/conductinghumanhealthriskassessment#tab4>.

US EPA. 2019. "EPI Suite™ Estimation Program Interface." March 12. Accessed at <https://www.epa.gov/tscascreeningtools/episuitetmestimationprograminterface>.

US EPA. 2020. "Preliminary Remediation Goals for Radionuclides (PRG): PRG Calculator." Accessed at https://epaprgs.ornl.gov/cgi-bin/radionuclides/rprg_search. July 24.

US EPA. 2021. "Secondary drinking water standards: Guidance for nuisance chemicals." January 7. Accessed at <https://www.epa.gov/sdwa/secondarydrinkingwaterstandardsguidancenuisancechemicals>.

US EPA. 2022. "National Recommended Water Quality Criteria Aquatic Life Criteria Table." Accessed at <https://www.epa.gov/wqc/nationalrecommendedwaterqualitycriteriaaquaticlifecriteriatable>. January 6.

US EPA. 2024a. "Regional Screening Level (RSL) Composite Summary Table (TR=1E06, HQ=1.0)." May. Accessed at <https://semspub.epa.gov/work/HQ/404491.pdf>.

US EPA. 2024b. "Regional Screening Levels (RSLs) User's Guide." May. Accessed at <https://www.epa.gov/risk/regional-screening-levels-rsls-users-guide>.

US EPA Region IV. 2018. "Region 4 Ecological Risk Assessment Supplemental Guidance (March 2018 Update)." Superfund Division, Scientific Support Section. March. Accessed at https://www.epa.gov/sites/production/files/201803/documents/era_regional_supplemental_guidance_reportmarch2018_update.pdf.

US Geological Survey (USGS). 2022a. "USGS National Hydrography Dataset (NHD) for the State of Illinois." National Geospatial Program. March 23. Accessed on March 29, 2022 at <https://prd-tnm.s3.amazonaws.com/index.html?prefix=StagedProducts/Hydrography/NHD/State/GDB/>

US Geological Survey (USGS). 2022b. "National Water Information System Water Quality Database: Hardness Data (parameter code 900) for Site No. 05595400, Kaskaskia River at Roots, IL." Accessed at https://nwis.waterdata.usgs.gov/usa/nwis/qwdata/?site_no=05595400&agency_cd=USGS&inventory_output=0&rdb_inventory_output=file&TZoutput=0&pm_cd_compare=Greater%20than&radio_parm_cds=parm_cd_list&radio_multiple_parm_cds=00900&format=html_table&qw_attributes=0&qw_sample_wide=wide&rdb_qw_attributes=0&date_format=YYYYMMDD&rdb_compression=file&submitted_form=brief_list.

US Geological Survey (USGS). 2022c. "National Water Information System Water Quality Database: Daily mean discharge (parameter code 00060) for Site No. 05595000, Kaskaskia River at New Athens, IL." Accessed at https://nwis.waterdata.usgs.gov/nwis/dv?referred_module=sw&search_site_no=05595000&search_site_no_match_type=exact&index_pmcode_00060=1&group_key=NONE&sitefile_output_format=html_table&column_name=agency_cd&column_name=site_no&column_name=station_nm&range_selection=date_range&begin_date=18380101&end_date=2022112&format=html_table&date_format=YYYYMMDD&rdb_compression=file&list_of_search_criteria=search_site_no%20Crealttime_parameter_selection.

US Geological Survey (USGS). 2022d. "National Water Information System Water Quality Database: Suspended Sediment Data (parameter code 80154) for Site No. 05595000, Kaskaskia River at New Athens, IL." Accessed at https://nwis.waterdata.usgs.gov/usa/nwis/qwdata/?site_no=05595000&agency_cd=USGS&inventory_output=0&rdb_inventory_output=file&TZoutput=0&pm_cd_compare=Greater%20than&radio_parm_cds=parm_cd_list&radio_multiple_parm_cds=80154&format=html_table&qw_attributes=0&qw_sample_wide=wide&rdb_qw_attributes=0&date_format=YYYYMMDD&rdb_compression=file&submitted_form=brief_list.

Appendix A

Surface Water and Sediment Modeling

Gradient modeled concentrations of constituents of interest (COIs) in the Kaskaskia River surface water and sediment based on available groundwater data. First, we estimated the flow rate of COIs discharged to the Kaskaskia River *via* groundwater. Then, we adapted United States Environmental Protection Agency (US EPA) indirect exposure assessment methodology (US EPA, 1998) in order to model surface water and sediment water concentrations in the Kaskaskia River.

Model Overview

The groundwater flow to the river is represented by a one-dimensional, steady-state model. In this model, the groundwater plume migrates horizontally in the Upper Unit (UU)/Potential Migration Pathway (PMP) and the Bedrock Unit (BU)/Uppermost Aquifer (UA) prior to flowing to the Kaskaskia River. For both layers, the groundwater flow entering the river is the flow going through a cross-sectional area that has a length equal to the length of the river adjacent to the Fly Ash Pond System (FAPS) with potential coal combustion residuals (CCR)-related impacts and a height equal to each layer's estimated thickness. It was assumed that all the groundwater flowing through these two layers would ultimately discharge to the Kaskaskia River, thus the total flow into the river is the sum of the flows in the two layers. The length of the groundwater discharge zone was estimated using Google Earth Pro (Google, LLC, 2022).

The groundwater flow to the Kaskaskia River mixes with the surface water in the river. The COIs entering the river *via* groundwater can dissolve into the water column, sorb to suspended sediments, or sorb to benthic sediments. Using US EPA's indirect exposure assessment methodology (US EPA, 1998), the model evaluates the surface water and sediment COI concentrations at a location downstream of the groundwater discharge point, assuming a well-mixed water column.

Groundwater Discharge Rate

The groundwater discharge rate was evaluated using conservative assumptions. Gradient conservatively assumed that the groundwater concentrations were uniformly equal to the maximum detected concentration of each individual COI, in both the UU and the UA. Further, Gradient ignored adsorption by subsurface soil and assumed that all the groundwater flowing through UU and UA and intersecting the river bank was discharged into the river.

For each groundwater unit, the groundwater flow rate into the river was derived using Darcy's Law:

$$Q = K \times i \times A$$

where:

| | | |
|---|---|---|
| Q | = | Groundwater flow rate (m ³ /s) |
| K | = | Hydraulic conductivity (m/s) |
| i | = | Hydraulic gradient (m/m) |
| A | = | Cross-sectional area (m ²) |

For each COI, the mass discharge rate into the river was then calculated by:

$$m_c = C_c \times Q \times CF$$

where:

| | | |
|-------|---|--|
| m_c | = | Mass discharge rate of the COI (mg/year) |
| C_c | = | Maximum groundwater concentration of the COI (mg/L) |
| Q | = | Groundwater flow rate (m ³ /s) |
| CF | = | Conversion factors: 1,000 L/m ³ and 31,557,600 s/year |

The values of the aquifer parameters used for these calculations are provided in Table A.1. The calculated mass discharge rates were then used as inputs for the surface water and sediment partitioning model.

The cross-sectional area for the UU and UA were 5,943 and 12,600 m², respectively. The length of the discharge zone was estimated to be approximately 1,500 m. The height of the discharge zone was estimated to be 3.96 m for the UU and 8.40 m for the UA (Ramboll, 2021). The average horizontal hydraulic gradient was 0.013 m/m for the UU and 0.015 m/m for the UA (calculated from data in Ramboll, 2021). The average horizontal hydraulic conductivity of the UU was 0.000032 cm/sec and the UA was 0.000005 cm/sec (calculated from data in Ramboll, 2021).

Surface Water and Sediment Concentration

Groundwater discharged into the river will be diluted in the surface water flow. Constituents transported by groundwater into the surface water migrate into the water column and the bed sediments. The surface water model Gradient used to estimate the surface water and sediment concentrations is a steady-state model described in US EPA's indirect exposure assessment methodology (US EPA, 1998) and also used in US EPA's "Human and Ecological Risk Assessment of Coal Combustion Residuals," referred to herein as the CCR risk assessment (US EPA, 2014). This model describes the partitioning of constituents between surface water, suspended sediments, and benthic sediments based on equilibrium partition coefficients (K_d values). It estimates the concentrations of constituents in surface water, suspended sediments, and benthic sediments at steady-state equilibrium at a theoretical location downstream of the discharge point after complete mixing of the water column. In our analysis, we used the K_d values provided in the US EPA CCR risk assessment for all of the COIs (US EPA, 2014, Table J1). These coefficients are presented in Table A.2.

To be conservative, Gradient assumed that the constituents were not affected by dissipation or degradation once they entered the water body. The total water body concentration of the COI was calculated as follows (US EPA, 1998):

$$C_{wtot} = \frac{m_c}{V_f \times f_{water}}$$

where:

- C_{wtot} = Total water body concentration of the COI (mg/L)
- m_c = Mass discharge rate of the COI (mg/year)
- V_f = Water body annual flow (L/year)
- f_{water} = Fraction of the COI in the water column (unitless)

For the Kaskaskia River annual flow rate, Gradient conservatively used the low-flow (10th percentile) discharge rate of about 606 cubic feet per second (cfs), or 5.4×10^{11} L/year, based on the daily mean discharge rates measured at the United States Geological Survey (USGS) gauging station at New Athens, Illinois (USGS Station 05595000) between 2009 and 2022 (USGS, 2022a). The surface water parameters are presented in Table A.3.

The fraction of COIs in the water column was calculated for each COI using the sediment/water and suspended solids/water partition coefficients (US EPA, 2014). The fraction of COIs in the water column is defined as follows (US EPA, 2014):

$$f_{\text{water}} = \frac{(1 + [K_{\text{dsw}} \times \text{TSS} \times 0.000001]) \times \frac{d_w}{d_z}}{\left([1 + (K_{\text{dsw}} \times \text{TSS} \times 0.000001)] \times \frac{d_w}{d_z}\right) + ([\text{bsp} + K_{\text{dbs}} \times \text{bsc}] \times \frac{d_b}{d_z})}$$

where:

- K_{dsw} = Suspended sediment-water partition coefficient (mL/g)
- K_{dbs} = Sediment-water partition coefficient (mL/g)
- TSS = Total suspended solids in the surface water body (mg/L). Set equal to 84.5 mg/L based on the median suspended sediment concentration measured at the USGS gauging station at New Athens, Illinois (USGS Station 05595000) between 2015 and 2022 (USGS, 2022b).
- 0.000001 = Units conversion factor
- d_w = Depth of the water column (m). The depth of the water column was estimated as 2.74 m, based on bathymetry data for the Kaskaskia River near the Baldwin Power Plant (BPP) (Bist LLC, 2022).
- d_b = Depth of the upper benthic layer (m). Set equal to 0.03 m (US EPA, 2014).
- d_z = Depth of the water body (m). Calculated as $d_w + d_b$. Set equal to 2.77 m.
- bsp = Bed sediment porosity (unitless). Set equal to 0.6 (US EPA, 2014).
- bsc = Bed sediment particle concentration (g/cm^3). Set equal to $1.0 \text{ g}/\text{cm}^3$ (US EPA, 2014).

The fraction of COIs dissolved in the water column (f_d) is calculated as follows (US EPA, 2014):

$$f_d = \frac{1}{1 + K_{\text{dsw}} \times \text{TSS} \times 0.000001}$$

The values for the fraction of COI in the water column and other calculated parameters are presented in Table A.4.

The total water column concentration (C_{wcTot}) of the COIs, comprising both the dissolved and suspended sediment phases, is then calculated as follows (US EPA, 2014):

$$C_{\text{wcTot}} = C_{\text{wtot}} \times f_{\text{water}} \times \frac{d_z}{d_w}$$

Finally, the dissolved water column concentration (C_{dw}) for the COIs is calculated as follows (US EPA, 2014):

$$C_{\text{dw}} = f_d \times C_{\text{wcTot}}$$

The dissolved water column concentration (C_{dw}) was then used to calculate the concentration of COIs sorbed to suspended solids in the water column (US EPA, 1998):

$$C_{\text{sw}} = C_{\text{dw}} \times K_{\text{dsw}}$$

where:

- C_{sw} = Concentration sorbed to suspended solids (mg/kg)
- C_{dw} = Concentration dissolved in the water column (mg/L)
- K_{dsw} = Suspended solids/water partition coefficient (mL/g)

In the same way, using the total water body concentration and the fraction of COI in the benthic sediments, the model derives the total concentration in benthic sediments (US EPA, 2014):

$$C_{bstot} = f_{benth} \times C_{wtot} \times \frac{d_z}{d_b}$$

where:

- C_{bstot} = Total COI concentration in bed sediment (mg/L or g/m³)
- C_{wtot} = Total water body COI concentration (mg/L)
- f_{benth} = Fraction of COI in benthic sediments (unitless)
- d_b = Depth of the upper benthic layer (m)
- d_z = Depth of the water body (m). Calculated as $d_w + d_b$.

This value can be used to calculate dry weight sediment concentration as follows:

$$C_{seddw} = \frac{C_{bstot}}{bsc}$$

where:

- C_{seddw} = Dry weight sediment concentration (mg/kg)
- C_{bstot} = Total sediment concentration (mg/L)
- bsc = Bed sediment bulk density. Used the default value of 1 g/cm³ from US EPA (2014).

The total sediment concentration is composed of the sum of the COI concentration dissolved in the bed sediment pore water (equal to the concentration dissolved in the water column) and the COI concentration sorbed to benthic sediments (US EPA, 1998).

The COI concentration sorbed to benthic sediments was calculated as follows (US EPA, 1998):

$$C_{sb} = C_{dbs} \times K_{dbs}$$

where:

- C_{sb} = Concentration sorbed to bottom sediments (mg/kg)
- C_{dbs} = Concentration dissolved in the sediment pore water (mg/L)
- K_{dbs} = Sediments/water partition coefficient (mL/kg)

For each COI, the modeled total water column concentration, dry weight sediment concentration, and concentration sorbed to sediment are presented in Table A.5.

Table A.1 Parameters Used to Estimate Groundwater Discharge to Surface Water

| Groundwater Unit | Parameter | Name | Value | Unit |
|------------------|-----------|------------------------|----------|----------------|
| UU | A | Cross-Sectional Area | 5,940 | m ² |
| UU | i | Hydraulic Gradient | 0.013 | m/m |
| UU | K | Hydraulic Conductivity | 0.000032 | cm/s |
| UA | A | Cross-Sectional Area | 12,600 | m ² |
| UA | i | Hydraulic Gradient | 0.015 | m/m |
| UA | K | Hydraulic Conductivity | 0.000005 | cm/s |

Notes:

UA = Uppermost Aquifer or Bedrock Unit; UU = Upper Unit or PMP (Potential Migration Pathway).

Source: Hydraulic gradient and hydraulic conductivity values from Ramboll (2021).

Cross-sectional area was estimated from Ramboll (2021).

Table A.2 Partition Coefficients

| Constituent | Mean Sediment-Water Partition Coefficient (K_{dbs}) | | Mean Suspended Sediment-Water Partition Coefficient (K_{dsw}) | |
|----------------------|---|--------------|---|--------------|
| | Value (\log_{10}) (mL/g) | Value (mL/g) | Value (\log_{10}) (mL/g) | Value (mL/g) |
| Metals | | | | |
| Arsenic | 2.4 | 2.51E+02 | 3.9 | 7.94E+03 |
| Boron | 0.8 | 6.31E+00 | 3.9 | 7.94E+03 |
| Lithium ^a | – | 0 | – | 0 |
| Radionuclides | | | | |
| Radium 226+228 | – | 7.40E+03 | – | 7.40E+03 |

Notes:

Kd = Equilibrium Partition Coefficient.

Source: US EPA (2014).

(a) Lithium does not readily sorb to soils and sediments. Consequently, sediment concentrations were not modeled for this constituent (K_d was assumed to be 0).

Table A.3 Surface Water Parameters

| Parameter | Name | Value | Unit |
|-----------|--|----------------------|-------------------|
| TSS | Total Suspended Solids | 84.5 | mg/L |
| V_{fx} | Surface Water Flow Rate | 5.4×10^{11} | L/year |
| d_b | Depth of Upper Benthic Layer (default) | 0.03 | m |
| d_w | Depth of Water Column | 2.74 | m |
| d_z | Depth of Water Body | 2.77 | m |
| b_{sc} | Bed Sediment Bulk Density (default) | 1 | g/cm ³ |
| b_{sp} | Bed Sediment Porosity (default) | 0.6 | – |
| M_{TSS} | TSS Mass per Unit Area ^a | 0.23 | kg/m ² |
| M_s | Sediment Mass per Unit Area ^b | 30 | kg/m ² |

Notes:

CF = Conversion factor.

Source of default values: US EPA (2014).

(a) $M_{TSS} = TSS \times d_w \times CF1 \times CF2$.

(b) $M_s = d_b \times b_{sc} \times CF3 \times CF4$.

CF1 = 1,000 L/m³; CF2 = 1E06 kg/kg; CF3 = 1E+06 cm³/m³; CF4 = 0.001 kg/g.

Table A.4 Calculated Parameters

| COI | Fraction of COI in the Water Column (f_{water}) | Fraction of COI in the Benthic Sediments (f_{benthic}) | Fraction of COI Dissolved in the Water Column ($f_{\text{dissolved}}$) |
|----------------------|--|---|--|
| Metals | | | |
| Arsenic | 0.38 | 0.62 | 0.60 |
| Boron | 0.96 | 0.04 | 0.60 |
| Lithium | 0.99 | 0.01 | 0 |
| Radionuclides | | | |
| Radium 226+228 | 0.02 | 0.98 | 0.62 |

Note:

COI = Constituent of Interest.

Table A.5 Surface Water and Sediment Modeling Results

| COI | Groundwater Concentration (mg/L or pCi/L) | Mass Discharge Rate (mg/year or pCi/year) | Total Water Column Concentration (mg/L or pCi/L) | Concentration Sorbed to Bottom Sediments (mg/kg or pCi/kg) |
|----------------------|---|---|--|--|
| Metals | | | | |
| Arsenic | 0.014 | 1.5E+04 | 2.8E08 | 4.3E06 |
| Boron | 2.9 | 3.2E+06 | 6.0E06 | 2.3E05 |
| Lithium | 0.22 | 2.4E+05 | 4.6E07 | (a) |
| Radionuclides | | | | |
| Radium 226+228 | 4.84 | 5.3E+06 | 9.9E06 | 4.5E02 |

Notes:

COI = Constituent of Concern; mg/L = Milligrams per Liter; pCi/kg = PicoCuries per Kilogram; pCi/L = PicoCuries per Liter.

(a) Lithium does not readily sorb to soils and sediments. Consequently, sediment concentrations were not modeled for this constituent (K_d was assumed to be 0).

References

- Bist LLC. 2022. "Kaskaskia River bathymetry map." Accessed at <https://fishing-app.gpsnauticalcharts.com/i-boating-fishing-web-app/fishing-marine-charts-navigation.html#13.91/38.1925/-89.8696>.
- Google, LLC. 2022. "Google Earth Pro." Accessed at <https://www.google.com/earth/versions/#earthpro>.
- Ramboll. 2021. "Hydrogeologic Site Characterization Report, Bottom Ash Pond, Baldwin Power Plant, Baldwin, Illinois (Final)." Report to Dynegy Midwest Generation, LLC. 504p., October 25.
- US EPA. 1998. "Methodology for assessing health risks associated with multiple pathways of exposure to combustor emissions." National Center for Environmental Assessment (NCEA), EPA 600/R98/137, December. Accessed at <http://www.epa.gov/nceawww1/combust.htm>.
- US EPA. 2014. "Human and Ecological Risk Assessment of Coal Combustion Residuals (Final)." Office of Solid Waste and Emergency Response (OSWER), Office of Resource Conservation and Recovery, December. Accessed at <http://www.regulations.gov/#!documentDetail;D=EPAHQRCRA2009064011993>.
- US Geological Survey (USGS). 2022a. "National Water Information System Water Quality Database: Daily mean discharge (parameter code 00060) for Site No. 05595000, Kaskaskia River at New Athens, IL." Accessed at https://nwis.waterdata.usgs.gov/nwis/dv?referred_module=sw&search_site_no=05595000.
- US Geological Survey (USGS). 2022b. "National Water Information System Water Quality Database: Suspended Sediment Data (parameter code 80154) for Site No. 05595000, Kaskaskia River at New Athens, IL." Accessed at https://nwis.waterdata.usgs.gov/usa/nwis/qwdata/?site_no=05595000.

Appendix B

Screening Benchmarks

Table B.1 Calculated Water Quality Standards Protective of Incidental Ingestion and Fish Consumption

| Human Health COI | BCF ^a (L/kg-tissue) | Basis | MCL (mg/L) | RfD (mg/kg-day) | ADI ^b (mg/day) | Human Threshold Criteria | | |
|------------------|-----------------------------------|---------------|----------------|--------------------|--|--------------------------|-----------------------|----------------------|
| | | | | | | Water & Fish (mg/L) | Water Only (mg/L) | Fish Only (mg/L) |
| Total Metals | | | | | | | | |
| Arsenic | 44 | NRWQC (2002) | 0.010 | 0.00030 | 0.020 | 0.022 | 2.0 | 0.023 |
| Boron | 1 | (c) | NC | 0.20 | 14 | 467 | 1400 | 700 |
| Cobalt | 300 | ORNL (2020) | NC | 0.00030 | 0.021 | 0.0035 | 2.1 | 0.0035 |
| Lead | 46 | US EPA (2014) | 0.015 | NC | 0.030 | 0.015 | 0.015 | 0.015 |
| Lithium | 1 | (c) | NC | 0.002 | 0.14 | 4.7 | 14 | 7.0 |
| Molybdenum | 4 | US EPA, 2014 | NC | 0.00500 | 0.3500 | 3.9 | 35 | 4.4 |
| Thallium | 116 | NRWQC (2002) | 0.0020 | 0.000010 | 0.0040 | 0.0017 | 0.40 | 0.0017 |
| Human Health COI | BAF | | MCL (pCi/L) | ADI (pCi/day) | Food Ingestion Slope Factor ^d | Human Threshold Criteria | | |
| | SW-Fish | Basis | | | | Water & Fish (pCi/L) | Water Only (pCi/L) | Fish Only (pCi/L) |
| Radionuclides | | | | | | | | |
| Radium-226+228 | 4.0 | ORNL (2020) | 5 | 10 | 1.43E-09 | 1,000 | 1,000 | 87,413 |

Notes:

ADI = Acceptable Daily Intake; BAF = Bioaccumulation Factor; BCF = Bioconcentration Factor; COI = Constituent of Interest; HTC = Human Threshold Criteria; IEPA = Illinois Environmental Protection Agency; MCL = Maximum Contaminant Level; NC = ; NRWQC = National Recommended Water Quality Criteria; ORNL = Oak Ridge National Laboratory; RAIS = Risk Assessment Information System; RfD = Reference Dose; SW = Surface Water; US EPA = United States Environmental Protection Agency.

(a) BCFs from the following hierarchy of sources:

NRWQC (US EPA, 2002). National Recommended Water Quality Criteria: 2002. Human Health Criteria Calculation Matrix.

US EPA (2014). Human and Ecological Risk Assessment of Coal Combustion Residuals.

ORNL RAIS (ORNL, 2020). Risk Assessment Information System (RAIS) Toxicity Values and Chemical Parameters.

(b) ADI based on the MCL is calculated as the MCL (mg/L) multiplied by a water ingestion rate of 2 L/day. In the absence of an MCL, the ADI was calculated as the RfD (mg/kg-day) multiplied by the body weight (70 kg).

(c) BCF of 1 was used as a conservative assumption, due to lack of published BCF.

(d) Food ingestion slope factors for Ra-226+D and Ra-228+D were compared and the higher factor (Ra-228+D) was selected. The "+D" indicates that the risks from "associated short-lived radioactive decay products are also included" (US EPA, 2001).

Equations from IEPA (2019):

Consumption of Water and Fish

$$HTC = \frac{ADI}{W + (F \times BCF)}$$

Incidental Consumption of Water Only

$$HTC = \frac{ADI}{W}$$

Consumption of Fish Only

$$HTC = \frac{ADI}{F \times BCF}$$

Where:

| | | |
|--|-------------------|-------------|
| Human Threshold Criteria (HTC) | Chemical-specific | mg/L |
| Acceptable Daily Intake (ADI) | Chemical-specific | mg/day |
| Fish Consumption Rate (F) | 0.02 | kg/day |
| Bioconcentration Factor (BCF)/ Bioaccumulation Factor (BAF) | Chemical-specific | L/kg-tissue |
| Water Consumption Rate (W) | 0.01 | L/day |
| Body Weight | 70 | kg |
| Target Cancer Risk (TCR) | 1.0E-05 | |

$$HTC = \frac{TCR}{(SF \times BAF \times F)}$$

Table B.2 Recreator Exposure to Sediment

| COI | Relative Bioavailability B (unitless) | Dermal Absorption Fraction ABS (unitless) | Cancer | | | | Cancer SL (mg/kg) | Non-Cancer | | | | | | | | Recreator RSL Sediment (mg/kg) | Basis |
|-------------------------|---------------------------------------|---|-----------------------------|-----------------------------------|--|---|-------------------|---------------|---------------------|--|---|--|---|-----------------------|---------|--------------------------------|--------|
| | | | TRV | | Child + Adult | | | TRV | | Child | | Adult | | Child | Adult | | |
| | | | CSF (mg/kg-d) ⁻¹ | Derm. CSF (mg/kg-d) ⁻¹ | Incidental Ingestion SL _{ing} (mg/kg) | Dermal Contact SL _{derm} (mg/kg) | | RfD (mg/kg-d) | Derm. RfD (mg/kg-d) | Incidental Ingestion SL _{ing} (mg/kg) | Dermal Contact SL _{derm} (mg/kg) | Incidental Ingestion SL _{ing} (mg/kg) | Dermal Contact SL _{derm} (mg/kg) | Non-Cancer SL (mg/kg) | | | |
| | | | | | | | | | | | | | | | | | |
| Total Metals | | | | | | | | | | | | | | | | | |
| Arsenic | 1 | 3.0E-02 | 1.5E+00 | 1.5E+00 | 8.1E+01 | 4.1E+02 | 6.8E+01 | 3.0E-04 | 3.0E-04 | 4.1E+02 | 4.4E+03 | 4.4E+03 | 8.0E+03 | 3.8E+02 | 2.8E+03 | 6.8E+01 | c |
| Boron | 1 | NA | NC | NC | NC | NC | NC | 2.0E-01 | 2.0E-01 | 2.7E+05 | NA | 2.9E+06 | NA | 2.7E+05 | 2.9E+06 | 2.7E+05 | nc |
| Cobalt | 1 | NA | NC | NC | NC | NC | NC | 3.0E-04 | 3.0E-04 | 4.1E+02 | NA | 4.4E+03 | NA | 4.1E+02 | 4.4E+03 | 4.1E+02 | nc |
| Lead | 1 | NA | NC | NC | NC | NC | NC | 0.0E+00 | 0.0E+00 | 0.0E+00 | NA | 0.0E+00 | NA | NC | NC | NC | nc |
| Lithium | 1 | NA | NC | NC | NC | NC | NC | 2.0E-03 | 2.0E-03 | 2.7E+03 | NA | 2.9E+04 | NA | 2.7E+03 | 2.9E+04 | 2.7E+03 | nc |
| Molybdenum | 1 | NA | NC | NC | NC | NC | NC | 5.0E-03 | 5.0E-03 | 6.8E+03 | NA | 7.3E+04 | NA | 6.8E+03 | 7.3E+04 | 6.8E+03 | nc |
| Thallium | 1 | NA | NC | NC | NC | NC | NC | 1.0E-05 | 1.0E-05 | 1.4E+01 | NA | 1.5E+02 | NA | 1.4E+01 | 1.5E+02 | 1.4E+01 | nc |
| Dissolved Metals | | | | | | | | | | | | | | | | | |
| Boron | 1 | NA | NC | NC | NC | NC | NC | 2.0E-01 | 2.0E-01 | 2.7E+05 | NA | 2.9E+06 | NA | 2.7E+05 | 2.9E+06 | 2.7E+05 | nc |
| Lithium | 1 | NA | NC | NC | NC | NC | NC | 2.0E-03 | 2.0E-03 | 2.7E+03 | NA | 2.9E+04 | NA | 2.7E+03 | 2.9E+04 | 2.7E+03 | nc |
| Radionuclides | | | | | | | | | | | | | | | | | |
| Radium 226 + Radium 228 | 1 | NA | NC | NC | NC | NC | NC | NC | NC | NC | NC | NC | NC | NC | NC | 7.9E+03 | pCi/kg |
| Other | | | | | | | | | | | | | | | | | |
| Chloride | 1 | NA | NC | NC | NC | NC | NC | NC | NC | NC | NC | NC | NC | NC | NC | NC | nc |
| Fluoride | 1 | NA | NC | NC | NC | NC | NC | 4.0E-02 | 4.0E-02 | 5.5E+04 | NA | 5.8E+05 | NA | 5.5E+04 | 5.8E+05 | 5.5E+04 | nc |
| Sulfate | 1 | NA | NC | NC | NC | NC | NC | NC | NC | NC | NC | NC | NC | NC | NC | NC | nc |

Notes:

AL = EPA Action Level; COI = Constituent of Interest; CSF = Cancer Slope Factor; derm = Dermal Contact; ing = Ingestion; NC = No criterion available; RfD = Reference Dose; SL = Screening Level; TRV = Toxicity Reference Value. Health Benchmark defined as the lower of the Screening Levels for cancer and non-cancer. The basis of the Health Benchmark presented as c = based on cancer endpoint or nc = based on non-cancer endpoint.

Screening Benchmark =

$$\frac{1}{SL_{ing}} + \frac{1}{SL_{derm}}$$

Non-cancer SL_{ing} =

$$\frac{THQ * RfD}{Intake}$$

Cancer SL_{ing} =

$$\frac{TR}{Intake * CSF}$$

Non-cancer SL_{derm} =

$$\frac{THQ * RfD}{Intake * ABS}$$

Cancer SL_{derm} =

$$\frac{TR}{Intake * ABS * CSF}$$

$$\begin{aligned} \text{Target Cancer Risk (TR)} &= 1E-05 \\ \text{Target Hazard Quotient (THQ)} &= 1 \end{aligned}$$

Sediment – Ingestion (Chemical)

| Intake Factor (IF) = | | $\frac{IR \times EF \times ED \times CF}{BW \times AT}$ | = | 7.3E-07 Child | 6.8E-08 Adult | 6.3E-08 Child | 2.0E-08 Adult | Basis |
|----------------------|---|---|---|------------------|------------------|------------------|------------------|--|
| IR | Ingestion Rate (mg/day) | | | 67 | 33 | 67 | 33 | One-third of US EPA residential soil ingestion rate (Prof. Judgment) |
| EF | Sediment Exposure Frequency (days/year) | | | 60 | 60 | 60 | 60 | 2 days/week between April and Oct when air temp. > 70°F (Prof. Judgment) |
| ED | Exposure Duration (years) | | | 6 | 20 | 6 | 20 | Default value for Resident (US EPA, 2024b) |
| CF | Conversion Factor (kg/mg) | | | 0.000001 | 0.000001 | 0.000001 | 0.000001 | |
| BW | Body Weight (kg) | | | 15 | 80 | 15 | 80 | Default value for Resident (US EPA, 2024b) |
| AT | Averaging Time (d) | | | 2,190 | 7,300 | 25,550 | 25,550 | Default value for Resident (US EPA, 2024b) |

Sediment – Dermal Contact (Chemical)

| Intake Factor (IF) = | | SA x AF x EF x ED x CF | | = | 2.2E-06 | 1.2E-06 | 1.9E-07 | 3.6E-07 | |
|----------------------|--|------------------------|----------|---|----------|---------|----------|----------|--|
| | | BW x AT | | | Child | Adult | Child | Adult | Basis |
| SA | Surface Area Exposed to Sediment (cm²/day) | | 1,026 | | 3,026 | | 1,026 | 3,026 | Age weighted SA for lower legs and feet (US EPA, 2011b) |
| AF | Sediment Skin Adherence Factor (mg/cm²) | | 0.2 | | 0.2 | | 0.2 | 0.2 | Age weighted AF for children exposed to sediment (US EPA, 2011b) |
| EF | Sediment Exposure Frequency (days/year) | | 60 | | 60 | | 60 | 60 | 2 days/week between April and Oct when air temp. > 70°F (Prof. Judgment) |
| ED | Exposure Duration (years) | | 6 | | 20 | | 6 | 20 | Default value for Resident (US EPA, 2024b) |
| CF | Conversion Factor (kg/mg) | | 0.000001 | | 0.000001 | | 0.000001 | 0.000001 | |
| BW | Body Weight (kg) | | 15 | | 80 | | 15 | 80 | Default value for Resident (US EPA, 2024b) |
| AT | Averaging Time (d) | | 2,190 | | 7,300 | | 25,550 | 25,550 | Default value for Resident (US EPA, 2024b) |

Appendix B

Corrective Action Alternatives Analysis – Supporting Information Report

Intended for

Dynegy Midwest Generation, LLC
10901 Baldwin Road
Baldwin, IL 62217

Date

February 18, 2025

Project No.

1940110241-004

**CORRECTIVE ACTION ALTERNATIVES
ANALYSIS SUPPORTING
INFORMATION REPORT**

**FLY ASH POND SYSTEM
BALDWIN POWER PLANT
IEPA ID NO. W1578510001-01/02/03**

**CORRECTIVE ACTION ALTERNATIVES ANALYSIS
SUPPORTING INFORMATION REPORT
IEPA ID NO. W1578510001-01/02/03**

Project name **Baldwin Power Plant Fly Ash Pond System**
Project no. **1940110241-005**
Recipient **Dynegy Midwest Generation, LLC**
Document type **Corrective Action Plan**
Revision **DRAFT**
Date **February 18, 2025**
Prepared by **Christopher R. Glidden**
Checked by **J. Austin Bond, PE**
Approved by **Brian G. Hennings, PG**
Description **Corrective Action Alternatives Analysis Supporting Information Report**

Ramboll
234 W. Florida Street
Fifth Floor
Milwaukee, WI 53204
USA

T 414-837-3607
F 414-837-3608
<https://ramboll.com>

J. Austin Bond, PE
Qualified Professional Engineer

Brian G. Hennings, PG
Project Officer Hydrogeology

CONTENTS

| | | |
|-----------|--|-----------|
| 1. | Introduction and Background | 4 |
| 1.1 | Plant and Site Information | 4 |
| 1.2 | CAAA-SIR Background and Scope | 4 |
| 1.2.1 | Identified Corrective Action Alternatives | 4 |
| 1.2.2 | Scope of CAAA-SIR | 5 |
| 1.2.3 | Criterion for Estimating Remedial Alternative Effectiveness | 5 |
| 1.3 | Report Contents | 6 |
| 2. | Alternative 1 Remedy: Source Control with Groundwater Polishing | 7 |
| 2.1 | Supporting Groundwater Modeling and Time to Reach GWPS | 7 |
| 2.2 | Remedy Implementation | 7 |
| 2.2.1 | Remedy Implementation Schedule | 10 |
| 2.2.2 | Management of Extracted Groundwater | 10 |
| 2.2.3 | 35 I.A.C. § 845.670(e)(1)(H) and 35 I.A.C. § 845.670(e)(3) Information | 10 |
| 3. | Alternative 2 Remedy: Source Control with Cutoff Wall | 12 |
| 3.1 | Remedy Scoping and Groundwater Modeling Results | 12 |
| 3.2 | Remedy Implementation | 13 |
| 3.2.1 | Phase 1: Pre-Construction Activities | 13 |
| 3.2.2 | Phase 2: Corrective Action Construction | 13 |
| 3.2.3 | Phase 3: Corrective Action Operations, Maintenance, and Closeout | 14 |
| 3.2.4 | Remedy Implementation Schedule | 17 |
| 3.2.5 | Management of Extracted Groundwater | 17 |
| 3.2.6 | 35 I.A.C. § 845.670(e)(1)(H) and 35 I.A.C. § 845.670(e)(3) Information | 17 |
| 4. | Alternative 3 Remedy: Source Control with Groundwater Management System | 20 |
| 4.1 | Remedy Scoping and Groundwater Modeling Results | 20 |
| 4.2 | Remedy Implementation | 21 |
| 4.2.1 | Phase 1: Pre-Construction Activities | 21 |
| 4.2.2 | Phase 2: Corrective Action Construction | 22 |
| 4.2.3 | Phase 3: Corrective Action Operations, Maintenance, and Closeout | 24 |
| 4.2.4 | Remedy Implementation Schedule | 25 |
| 4.2.5 | Management of Extracted Liquids | 26 |
| 4.2.6 | 35 I.A.C. § 845.670(e)(1)(H) and 35 I.A.C. § 845.670(e)(3) Information | 26 |
| 5. | Material Quantity, Labor, and Mileage Estimates | 29 |
| 6. | References | 30 |

TABLES (WITHIN TEXT)

| | |
|---------|---|
| Table A | Feasibility-Level Implementation Schedule – Alternative 1 Source Control with GWP |
| Table B | Feasibility-Level Implementation Schedule – Alternative 2 Source Control with Cutoff Wall |
| Table C | Feasibility-Level Implementation Schedule – Alternative 3 Source Control with Groundwater Management System |

APPENDICES

| | |
|------------|--|
| Appendix A | Feasibility-Level Design Drawings for Alternative 2 and Alternative 3 Remedies |
| Appendix B | Groundwater Modeling Technical Memorandum |
| Appendix C | Material Quantity, Labor, and Mileage Estimates for Alternative 2 and Alternative 3 Remedies |

ACRONYMS AND ABBREVIATIONS

| | |
|-----------|---|
| 35 I.A.C. | Title 35 of the Illinois Administrative Code |
| 40 C.F.R. | Title 40 of the Code of Federal Regulations |
| bgs | below ground surface |
| BAP | Bottom Ash Pond |
| BEC | Baldwin Energy Complex |
| BMP | best management practices |
| BPP | Baldwin Power Plant |
| CAAA | Corrective Action Alternatives Analysis |
| CAAA-SIR | Corrective Action Alternatives Analysis Supporting Information Report |
| CAP | Corrective Action Plan |
| CCR | coal combustion residuals |
| CCR Rule | 40 C.F.R. § 257 Subpart D |
| cm/s | centimeters per second |
| CMA | Corrective Measures Assessment |
| COC | constituent of concern |
| CSM | conceptual site model |
| DMG | Dynegy Midwest Generation, LLC |
| EQ | equalization |
| FAPS | Fly Ash Pond System, also referred to as Site |
| GMR | Groundwater Modeling Report |
| Gradient | Gradient Corporation |
| GWPS | groundwater protection standard(s) |
| HDPE | high-density polyethylene |
| ID | identification |
| IDNR | Illinois Department of Natural Resources |
| IEPA | Illinois Environmental Protection Agency |
| Kd | soil adsorption coefficient |
| mL/g | milliliters per gram |
| PMP | potential migration pathway |
| NAVD88 | North American Vertical Datum of 1988 |
| NID | National Inventory of Dams |
| No. | number |
| NPDES | National Pollutant Discharge Elimination System |
| O&M | operations and maintenance |
| Ramboll | Ramboll Americas Engineering Solutions, Inc. |
| RS Means | RS Means Heavy Construction Cost Data |
| SI | surface impoundment |
| USEPA | United States Environmental Protection Agency |
| UU | upper unit |

1. INTRODUCTION AND BACKGROUND

1.1 Plant and Site Information

Dynegy Midwest Generation, LLC (DMG) is the owner of the active coal-fired Baldwin Energy Complex (BEC), also referred to as the Baldwin Power Plant (BPP), in Baldwin, Randolph County, Illinois. DMG intends to complete groundwater corrective action at the coal combustion residuals (CCR) surface impoundment (SI) Fly Ash Pond System (FAPS), which is comprised of the East Fly Ash Pond, the Old East Fly Ash Pond and the West Fly Ash Pond and is identified by Illinois Environmental Protection Agency (IEPA) identification (ID) numbers (Nos.) W1578510001-01, W1578510001-02, and W1578510001-03, also referred to as Vistra Identification ID No. 605, and National Inventory of Dams (NID) No. IL50720. Groundwater corrective action for the BPP FAPS will be performed under the requirements of Title 35 of the Illinois Administrative Code (35 I.A.C.) § 845, Standards for the Disposal of Coal Combustion Residuals in Surface Impoundments [1] and the requirements of Title 40 of the Code of Federal Regulations (40 C.F.R.) § 257, herein referred to as the Federal CCR Rule [2].

1.2 CAAA-SIR Background and Scope

35 I.A.C. § 845 requires a Corrective Action Alternatives Analysis (CAAA) to be completed as part of remedy selection, pursuant to the requirements of 35 I.A.C. § 845.670(e). The CAAA for the BPP FAPS was prepared by Gradient Corporation (Gradient). Ramboll Americas Engineering Solutions, Inc. (Ramboll) has prepared this Corrective Action Alternatives Analysis Supporting Information Report (CAAA-SIR) to provide information requested by Gradient to support the CAAA for the BPP FAPS.

This CAAA-SIR is a feasibility-level assessment utilized to evaluate multiple groundwater corrective action alternatives. The remedy that is ultimately selected within the CAAA, to which this CAAA-SIR is attached, was then further developed into a permit-level remedy within the Corrective Action Plan (CAP), to which the CAAA is attached. Therefore, there may be minor differences in information presented for the selected remedy between this CAAA-SIR and the CAP. Information that may be different includes, but is not limited to, groundwater quality data, groundwater modeling inputs and results, implementation schedules, time to reach GWPS, the physical dimensions and scope of the remedy, and engineering design parameters. These differences are due to further remedy refinement that is inherent with advancing the selected alternative into the permit-level remedy that is included within the CAP.

1.2.1 Identified Corrective Action Alternatives

Corrective action remedies selected for evaluation within this CAAA-SIR were identified as potentially feasible for the FAPS in the Corrective Measures Assessment (CMA), prepared by Ramboll and attached to the CAAA prepared by Gradient. The remedies identified as potentially feasible included:

- Alternative 1: Source control with groundwater polishing (GWP);
- Alternative 2: Source control with cutoff wall; and
- Alternative 3: Source control with a groundwater management system¹.

¹ This corrective measure is referred to as groundwater extraction in the April 2024 CMA.

Other remedies, including source control with in-situ chemical treatment, were determined to be infeasible for the site during the CMA process.

1.2.2 Scope of CAAA-SIR

Ramboll completed the following tasks and documented the tasks within this CAAA-SIR, for each of the corrective action alternative remedies listed in **Section 1.2.1**:

- Feasibility-level design drawings (**Appendix A**) were developed to show the approximate extents and typical sections/details of the Alternative 2 (source control with cutoff wall) and Alternative 3 (source control with a groundwater management system) remedies. Drawings were not prepared for the Alternative 1 remedy as it does not involve construction at the site.
- Narratives describing the implementation of each remedy were developed, including the pre-design, design, construction, operations, and maintenance (O&M), and closeout phases.
- Feasibility-level schedules providing the estimated time to implement the remedy were developed, including design, permitting, construction, and post-construction O&M.
- Feasibility-level plans for the management of liquids that may be within the footprint of the FAPS were developed for alternatives that include the management of extracted water.
- Information required to evaluate specific portions of 35 I.A.C. § 845.670(e) requirements were prepared, as requested by Gradient, including 35 I.A.C. § 845.670(e)(1)(H) and 35 I.A.C. § 845.670(e)(3).
- Estimates of implementation-based equipment mileage, vehicle delivery mileage, labor hour, and labor commuting mileage, were developed for each remedy alternative where physical construction and/or O&M activities are expected to occur.

All remedies presented within this CAAA-SIR were developed to integrate with the source control for the BPP FAPS that was completed in 2020 [3] in accordance with a Closure and Post-Closure Care Plan [4] that was approved by IEPA [5]. This will include maintaining the FAPS throughout the post-closure care period.

1.2.3 Criterion for Estimating Remedial Alternative Effectiveness

Groundwater modeling for each remedial alternative (included in **Appendix B**) indicates that none of the potentially feasible alternatives identified in the CMA and evaluated in this CAAA-SIR would result in GWPS being attained for all FAPS compliance monitoring wells within a 1,000-year simulation period. This is because the underlying lithological units beneath the CCR unit, identified as the upper unit (UU) and underlying bedrock uppermost aquifer (UA) in the 2024 Nature and Extent Report [6], consists of low-permeability soils and underlying low-permeability shale and limestone bedrock, resulting in extended times to attain GWPS, regardless of the type of evaluated remedy. These model results are consistent with the modeling results presented in the Closure and Post-Closure Care Plan [4] that was prepared in 2016 and subsequently approved by IEPA [5].

Therefore, in addition to evaluating which remedial alternative resulted in the shortest time to reach GWPS in the FAPS compliance wells, spatial analyses were performed to compare each remedial alternative's ability to reduce the future potential footprint of COCs in groundwater thereby minimizing the potential for COCs to migrate past the site's southern property boundary which could result in a future risk exposure pathway to off-site property owners. This analysis

utilized maps depicting the maximum plume extent of modeled boron concentration to quantify spatial distribution and area for each remedial alternative.

Results of groundwater fate and transport modeling (**Appendix B**) conservatively estimate groundwater boron concentrations at the FAPS compliance wells through the end of the 1,000-year simulation period. As noted in the groundwater technical memorandum, the model is limited by the data used for calibration, which adequately define the local groundwater flow system and the source and extent of the plume. Since data used for calibration are near the FAPS, model predictions of transport distant spatially and temporally (e.g., 1,000 years in the future) from the calibrated conditions at the CCR units will not be as reliable as predictions closer to the CCR units and concentrations observed between 2015 and 2024.

1.3 Report Contents

The following information is included within this report:

- **Section 1** includes the introduction and background;
- **Section 2** includes information for the Alternative 1 remedy: source control with GWP;
- **Section 3** includes information for the Alternative 2 remedy: source control with cutoff wall;
- **Section 4** includes information for the Alternative 3 remedy: source control with groundwater management system;
- **Section 5** includes information used to develop estimates of material quantities, labor hours, and mileage; and
- **Section 6** includes reference documents used in the development of this CAAA-SIR.

2. ALTERNATIVE 1 REMEDY: SOURCE CONTROL WITH GROUNDWATER POLISHING

The Alternative 1 remedy, source control with GWP, would include the completed source control approach which consisted of capping the waste material, after which GWP would be formally implemented. GWP is a remedial alternative that relies on natural geochemical processes and may be appropriate as recognized by the United States Environmental Protection Agency (USEPA) in a final policy directive for groundwater remediation [7].

2.1 Supporting Groundwater Modeling and Remedy Effectiveness

The COCs exceeding the GWPS at compliance groundwater monitoring wells as of the 2024 Annual Report [8] are boron and sulfate. Boron was selected for modeling the source control presented in the Closure and Post-Closure Care Plan and was identified as a surrogate for the exceedances² of sulfate. For modeling purposes, it was assumed that boron would not significantly sorb or chemically react with aquifer solids (soil adsorption coefficient [Kd] was set to 0 milliliters per gram [mL/g]) which is a conservative estimate for predicting contaminant transport times in the model. Boron transport is likely to be affected by both chemical and physical attenuation mechanisms (*i.e.*, adsorption and/or precipitation reactions as well as dilution and dispersion). Physical attenuation (dilution and dispersion) of contaminants in groundwater is simulated in the groundwater computer models. Chemical attenuation mechanisms and their effect on modeled times for exceedances to attain the GWPS are discussed in the Groundwater Polishing Evaluation Report [9].

Groundwater modeling for the Alternative 1 remedy was performed in 2014 to support the 2016 closure plan for the FAPS [4] and further refined in 2024 (**Appendix B**). The updated 2024 groundwater model estimated that the GWPS would not be attained for all FAPS compliance monitoring wells within the 1,000-year prediction model simulation period after the 2020 completion of source control implementation. Following source control and GWP in Alternative 1, the GWPS was not achieved at 16 of 23 wells evaluated following the completion of the 1,000-year model simulation. Simulated boron plume extent slowly expanded over time following implementation of Alternative 1. Based on the calculations of plume extent acreages, the area of the plume increases from 420 acres (current simulated plume area) to 561 acres (1,000-year simulated plume area) for Alternative 1. Approximately 50 acres of the 1,000-year simulated plume area occur off-site. The combined linear distance of plume simulated as intersecting the property line at the end of the 1000-year simulation was continuous and approximately 5,440 feet for Alternative 1.

2.2 Remedy Implementation

Implementation of the source control (*e.g.*, final closure of the FAPS) portion of the remedy was completed in 2020. Although a formal GWP remedy has not yet been initiated and approved by IEPA, GWP processes have been ongoing since the closure was completed. Implementation of GWP would include formalizing the GWP remedy. This would include performing corrective action

² Throughout this document, "exceedance" or "exceedances" is intended to refer only to potential exceedances of proposed applicable background statistics or GWPSs as described in the proposed groundwater monitoring program, which was submitted to the IEPA on October 25, 2021 as part of DMG's operating permit application for the BAL FAPS. That operating permit application, including the proposed groundwater monitoring program, remains under review by the IEPA and, therefore, DMG has not identified any actual exceedances.

groundwater monitoring, enacting an adaptive management strategy, and, after GWPS have been met, performing corrective action closure and completion activities. Information associated with each of these activities is described below.

- Corrective Action Groundwater Monitoring
 - Regular corrective action groundwater monitoring would be conducted utilizing a corrective action groundwater monitoring system designed in accordance with 35 I.A.C. § 845.680(c), which specifies that wells must be installed in the plume of contamination that lies beyond the waste boundary.
 - Samples would be collected for major ions for evaluating groundwater geochemistry and COCs. Samples would be collected on a quarterly basis initially and potentially reduced to a semiannual basis once five years of monitoring have occurred, in accordance with 35 I.A.C. § 845.650(b)(4).
 - Monitoring results would be submitted to IEPA for each monitoring event, in addition to an annual groundwater monitoring and corrective action report, in accordance with 35 I.A.C. § 845.610(e).
 - Routine maintenance of the monitoring well system would occur during the monitoring period. This would include inspecting the wells, making repairs to the wells (as and if needed), and rehabilitating and/or replacing wells to improve performance (as and if needed).
- Adaptive Management during Monitoring
 - The GWP analysis would include geochemical models. The available solid-phase data from the aquifer and these models would be used to identify potential mobilizations of exceedance constituents as groundwater returns to background conditions.
 - Groundwater monitoring results would be evaluated and documented in in the monitoring reports submitted to IEPA, in accordance with 35 I.A.C. § 845.610(e)
 - Remedy performance evaluation as part of adaptive site management may include additional investigation to inform updates to the CSM, groundwater, and geochemical models.
 - If remedy performance does not correspond with expectations, additional methods or techniques to achieve compliance with GWPS would be evaluated and, if feasible, implemented in accordance with 35 I.A.C. § 845.680(b).
- Corrective Action Confirmation Monitoring and Completion
 - In the event that GWPS are met in the future for all corrective action monitoring wells, corrective action confirmation groundwater monitoring would be implemented. This would include monitoring each well for three additional years to confirm that GWPS have been achieved, in accordance 35 I.A.C. § 845.680(c).
 - After completion of the corrective action confirmation monitoring period, a Corrective Action Completion Report and Certification would be prepared and submitted to IEPA, in accordance with 35 I.A.C. § 845.680(e).
 - If GWPS are not met in the future, the FAPS would remain in a perpetual state of Corrective Action Groundwater Monitoring and confirmation monitoring would not be performed.

DRAFT

2.2.1 Remedy Implementation Schedule

A feasibility-level implementation schedule for the Alternative 1 source control with GWP remedy is provided in **Table A** below.

Table A. Feasibility-Level Implementation Schedule – Alternative 1: Source Control with GWP

| Implementation Phase | Implementation Task | Timeframe* (Preliminary Estimates) |
|---|---|------------------------------------|
| Corrective Action Implementation | Corrective Action Monitoring (Time to Meet GWPS) | >100 years |
| | Corrective Action Confirmation Monitoring | 36 months |
| | Corrective Action Completion | 6 months |
| | Timeframe to Complete Corrective Action Implementation | >100 years |
| Total Timeline to Complete Corrective Action | | >100 years |

2.2.2 Management of Extracted Groundwater

No groundwater extraction would occur under this remedy.

2.2.3 35 I.A.C. § 845.670(e)(1)(H) and 35 I.A.C. § 845.670(e)(3) Information

As requested by Gradient, the following information required by 35 I.A.C. § 845.670(e)(1)(H) and 35 I.A.C. § 845.670(e)(3) has been developed for the remedy. The information was developed based on preliminary-level information contained within the CMA for the BPP FAPS and then refined based on additional feasibility-level design activities performed as part of the development of this CAAA-SIR.

- Potential Need for Replacement of the Remedy – 35 I.A.C. § 845.670(e)(1)(H)
 - No replacement of the remedy would be required for source control with GWP, as a physical remedy would not be constructed.
- Degree of Difficulty Associated with Constructing the Remedy – 35 I.A.C. § 845.670(e)(3)(A)
 - No construction would be required with the source control with GWP remedy; therefore, there is no difficulty in construction of the remedy.
- Expected Operational Reliability of the Remedy – 35 I.A.C. § 845.670(e)(3)(B)
 - A report detailing the GWP process [9] has been developed and evaluates the reliability and the potential for reversibility of the chemical attenuation mechanisms. This report is attached to the Gradient CAAA.
- Need to Coordinate with and Obtain Necessary Approvals and permits from Other Agencies – 35 I.A.C. § 845.670(e)(3)(C)
 - No permits from other agencies would be required.

- Availability of Necessary Equipment and Specialists - 35 I.A.C. § 845.670(e)(3)(D)
 - Equipment and specialists for field data collection and groundwater sampling are required for the GWP alternative. Laboratory equipment and specialists would also be required to assess groundwater concentrations of site constituents. Groundwater professionals (*i.e.*, geologists, hydrogeologists, statisticians, geochemists) would be required to perform statistical analysis and other assessments to confirm that GWP is functioning as intended and prepare corrective-action related groundwater monitoring and progress reports.
 - The equipment and specialists required for site groundwater monitoring and analysis are currently performing this work as part of the routine groundwater monitoring program in accordance with 35 I.A.C. § 845.220(c)(4). Therefore, no new equipment or specialists are required for groundwater monitoring for this alternative.
- Available Capacity and Location of Needed Treatment, Storage, and Disposal Services – 35 I.A.C. § 845.670(e)(3)(E)
 - No treatment, storage, or disposal services would be required with the source control with GWP remedy, as GWP would not generate any appreciable volume of waste or wastewater.

3. ALTERNATIVE 2 REMEDY: SOURCE CONTROL WITH CUTOFF WALL

The Alternative 2 remedy, source control with cutoff wall, would include the construction of a cutoff wall that would extend from the existing perimeter berm ground surface, which ranges from approximately 390 to 450 feet³ to an approximate elevation of 365 feet, with the wall keyed into the low-permeability bedrock underlying the UU/potential migration pathway (PMP). The total length of the cutoff wall would be approximately 7,000 feet located along the downgradient edge of the unit, and the cutoff wall would have a maximum depth of approximately 85 feet bgs. The cutoff wall would be constructed using either a mixture of soil and bentonite or cement and bentonite and would have an expected width of 2 to 3 feet. The cutoff wall would have a hydraulic conductivity value of approximately 1×10^{-7} centimeters per second (cm/s). The purpose of the cutoff wall would be to provide a long-term, maintenance-free physical barrier to reduce the potential for COCs to migrate past the site's southern property boundary to off-site property owners.

A feasibility-level drawing of the source control with cutoff wall remedy is provided as **Figure 1** in **Appendix A**.

3.1 Remedy Scoping and Groundwater Modeling Results

The location of the cutoff wall was selected by reviewing physical constraints around the FAPS where the wall could feasibly be constructed with limited impacts to other site features. The location was also selected to avoid sensitive areas such as wetlands, Waters of the United States, or floodplains, and to minimize potential impacts to the structural stability of the southern FAPS dike. This resulted in the wall being located within the FAPS, along the crest of the southern dike wall and extending west towards the tertiary pond. Since the selected location is within the current limits of the FAPS, it is not within regulatory floodplains or known wetlands, and provides a generally straight and level alignment for the wall. However, this would result in the wall impacting the final cover system of the FAPS, which would require impacted areas to be repaired after wall construction.

Construction of a cutoff wall at the downstream toe of the dike or beyond the dike would conversely require substantial modifications to the dike and may impact Waters of the United States and/or floodplains. Additionally, the proposed location allows the wall to act as a physical barrier between the FAPS and the offsite properties to the south and southwest and is generally perpendicular to existing groundwater flow patterns.

The depth of the cutoff wall was selected using iterative, three-dimensional groundwater fate and transport modeling. This included adjusting the total depth of the wall and reviewing associated times to attain GWPS and selecting a wall depth that reduced cleanup times while also improving constructability. This resulted in a wall that fully-penetrated the UU and keyed into the underlying bedrock. The thickness and hydraulic conductivity of the wall were selected based on Ramboll's design and construction experience with cutoff walls and is supported based on preliminary discussions with remedial contractors.

³ All elevations referenced in this report are in the North American Vertical Datum of 1988 (NAVD88), unless otherwise noted.

The groundwater model (**Appendix B**) estimated that the GWPS would not be attained for all FAPS compliance monitoring wells within the 1,000-year prediction model simulation period after the implementation of Alternative 2 remedy, source control with cutoff wall. Following source control and cutoff wall in Alternative 2, the GWPS was not achieved at 16 of 23 wells evaluated following the completion of the 1,000-year model simulation. Simulated boron plume extent slowly expanded over time following implementation of Alternative 2. Based on the calculations of plume extent acreages, the area of the plume increases from 420 acres (current simulated plume area) to 559 acres (1,000-year simulated plume area) for Alternative 2. Approximately 30 acres of the 1,000-year simulated plume area occur off-site. The combined linear distance of plume simulated as intersecting the property line at the end of the 1,000-year simulation was continuous and approximately 5,440 feet for Alternative 2.

3.2 Remedy Implementation

Implementation of the Alternative 2 source control with cutoff wall remedy is expected to include multiple tasks spread out over three phases, including pre-construction activities (Phase 1), corrective action construction (Phase 2), and corrective action operations, maintenance, and closeout (Phase 3). Information for each phase is described in this section.

3.2.1 Phase 1: Pre-Construction Activities

Pre-construction activities would include further pre-design investigation, obtaining permits from other agencies, completing the final design of the remedy, and selecting a remedy implementation contractor via a bidding process. Information associated with each of these activities is described below.

- Completing pre-design investigation, final design and bid activities, including:
 - Completion of final pre-design subsurface investigations, laboratory soil testing, engineering calculations, bench scale testing of proposed wall construction materials, design drawings, specifications, and a construction quality assurance plan.
 - Bidding and selection of a cutoff wall construction contractor.
- Obtaining permits from other agencies including:
 - A general stormwater permit for construction site activities through IEPA, including construction stormwater controls and other best management practices (BMPs) such as silt fences and other measures.
 - An Illinois Department of Natural Resources (IDNR) Office of Water Resources, Dam Safety modification permit would be obtained for modification of the FAPS embankment.

3.2.2 Phase 2: Corrective Action Construction

Corrective action construction would be initiated after pre-construction activities are complete. It would include mobilizing construction equipment to the site, preparing the site for construction activities, construction of the cutoff wall (which would include removal or partial replacement of existing subgrade soils with low-permeability wall materials), and performing post-construction and site restoration activities. Cutoff wall construction spoils that contain CCR materials would be containerized and disposed of at an off-site landfill. Construction spoils that do not contain CCR would be disposed of in an appropriate on-site location at the BPP.

Information associated with each of these activities is described below.

- The contractor would mobilize equipment and materials to the site, install stormwater BMPs around the construction area, construct a staging and laydown area, and construct a level working pad and/or temporary construction access roads along the cutoff wall alignment.
- Access roads would be located in areas where they minimize disturbance to the existing FAPS final cover system.
- Construction of the working platform would include removing, relocating, or modifying existing site infrastructure (*i.e.*, fencing or overhead electric piezometers, roadways, utilities) that may conflict with the construction of the cutoff wall.
- A temporary on-site batch plant and/or material handling system would be established for the purpose of generating low permeability backfill for the cutoff wall. This would include either mixing bentonite with the subgrade soils or producing a cement-bentonite slurry to place into the wall.
- The wall would likely be constructed utilizing either crane-mounted conventional construction equipment (*i.e.*, clamshell and/or slurry cutter); however, one-pass trenching/mixing or other innovative methods could be utilized if later determined to be appropriate based on site-specific subsurface conditions and constructability considerations.
- Installation of the cutoff wall would occur concurrently with the removal of some of the subsurface soils (soil-bentonite walls) or all of the subsurface soils (cement-bentonite wall).
- The wall would either be installed in a continuous unit, or if needed to support stability of the subgrade soils and sides of the wall during construction, in discontinuous panels (*i.e.*, primary panels) with secondary panels installed for connection after the primary panels have sufficiently cured/hardened.
- Excavated non-CCR soils (*e.g.*, spoils) would be disposed of on-site while excavated CCR spoils would be loaded into off-road dump trucks and transported to an approved off-site landfill for disposal that is located within Illinois or nearby in Missouri.
- Disturbed areas of the final cover system would be repaired after the wall has been installed. This would include removing the working platform, excavating disturbed final cover system soils, and recompact the final cover consistent with the original design grades and specifications for the completed final closure. This would generally involve the reuse of the current cover soils but may require the importation of additional cover soils from an on-site source.
- Site restoration would be completed following the repair of the final cover system. This would include repairing other site infrastructure that was relocated or damaged during construction and minor regrading and seeding of disturbed areas.
- Temporary BMPs would also be installed during the site restoration period, if required in accordance with site land disturbance permits. The BMPs would be removed once vegetation is established.

3.2.3 Phase 3: Corrective Action Operations, Maintenance, and Closeout

Corrective action operations, maintenance, and closure would be initiated after corrective action construction is completed. It would include performing corrective action groundwater monitoring,

and, after GWPS have been met, performing corrective action closeout and completion activities. Information associated with each of these activities is described below.

- Corrective Action O&M
 - No corrective action O&M is required following installation of the cutoff wall, as the cutoff wall would be a passive, below-grade structure, without maintenance or operational needs.
- Corrective Action Monitoring
 - Regular corrective action groundwater monitoring would be conducted using a corrective action groundwater monitoring system designed in accordance with 35 I.A.C. § 845.680(c), which specified that wells must be installed within the plume of contamination that lies beyond the waste boundary.
 - Samples would be collected for major ions for evaluating groundwater chemistry and COCs. Samples would be collected on a quarterly basis initially and potentially reduced to a semiannual basis once five years of monitoring have occurred, in accordance with 35 I.A.C. § 845.650(b)(4).
 - Monitoring results would be submitted to IEPA after each monitoring event, in addition to an annual groundwater monitoring and corrective action report, in accordance with 35 I.A.C. § 845.640(e). The annual corrective action report would include an evaluation of the actual performance of the remedy relative to the remedy's expected performance.
 - Routine maintenance of the monitoring well system would be conducted during the monitoring period. This would include inspection of the wells, making repairs to the wells (as and if needed), and rehabilitation and/or replacing the wells to improve performance (as and if needed).
 - If the remedy does not achieve its expected performance, additional methods or techniques to achieve compliance with GWPS would be evaluated and, if feasible, implemented in accordance with 35 I.A.C. § 845.680(b).
- Adaptive Management during Monitoring
 - Groundwater monitoring results would be evaluated and documented in in the monitoring reports submitted to IEPA, in accordance with 35 I.A.C. § 845.610(e).
 - Remedy progress evaluation as part of adaptive site management may include additional investigation to inform updates to the conceptual site model (CSM), groundwater, and geochemical models.
 - If remedy progress does not correspond with expectations, additional methods or techniques to achieve compliance with GWPS would be evaluated and, if feasible, implemented in accordance with 35 I.A.C. § 845.680(b).
- Corrective Action Completion
 - After completion of the corrective action confirmation monitoring period, a Corrective Action Completion Report and Certification would be prepared and submitted to IEPA, in accordance with 35 I.A.C. § 845.680(e).

- If GWPS are not met in the future, the FAPS would remain in a perpetual state of Corrective Action Groundwater Monitoring and confirmation monitoring would not be performed.

DRAFT

3.2.4 Remedy Implementation Schedule

A feasibility-level implementation schedule for the Alternative 2 source control with cutoff wall remedy is provided in **Table B** below.

Table B. Feasibility-Level Implementation Schedule – Alternative 2: Source Control with Cutoff Wall

| Implementation Phase | Implementation Task | Timeframe (Preliminary Estimates) |
|---|---|---|
| 1: Pre-Construction Activities | Agency Coordination, Approvals, and Permitting | 6 to 12 months |
| | Final Design and Bid Process | 24 to 36 months |
| | Timeframe to Complete Corrective Pre-Construction Activities | 30 to 48 months after CAP Approval |
| 2: Corrective Action Construction | Corrective Action Construction | 12 to 24 months |
| | Timeframe to Complete Corrective Action Construction | 12 to 24 months after completion of pre-construction activities |
| 3: Corrective Action O&M and Closeout | Corrective Action Monitoring (Time to Meet GWPS) | >100 years |
| | Corrective Action Confirmation Monitoring | 36 months |
| | Corrective Action Completion | 6 months |
| | Timeframe to Complete Corrective Action O&M and Closeout | >100 years after completion of construction activities |
| Total Timeline to Complete Corrective Action | | >100 years |

3.2.5 Management of Extracted Groundwater

No groundwater extraction would occur under this remedy.

3.2.6 35 I.A.C. § 845.670(e)(1)(H) and 35 I.A.C. § 845.670(e)(3) Information

As requested by Gradient, the following information required by 35 I.A.C. § 845.670(e)(1)(H) and 35 I.A.C. § 845.670(e)(3) has been developed for the remedy. The information was developed based on preliminary-level information contained within the CMA for the BPP FAPS and then refined based on additional feasibility-level design activities performed as part of the development of this CAAA-SIR.

- Potential Need for Replacement of the Remedy – 35 I.A.C. § 845.670(e)(1)(H)
 - The cutoff wall remedy is unlikely to need replacement, as the cutoff wall would be a robust, engineered, and maintenance-free subsurface structure.

- Degree of Difficulty Associated with Constructing the Remedy – 35 I.A.C. § 845.670(e)(3)(A)
 - The remedy would require mobilizing specialty equipment to the site (*i.e.*, large cranes, clamshells or slurry cutters, or one-pass trenching equipment) in addition to other supporting equipment (*i.e.*, batch plants, excavation and grading equipment).
 - While cutoff walls are routinely constructed to similar depths in similar geologic environments, they often encounter difficulties during construction. The difficulties could include encountering especially pervious layers and resulting slurry loss or encountering obstructions that require specialized techniques and/or equipment to advance past, or instability or caving in the sidewalls prior to hardening of the slurry backfill.
 - The performance of the cutoff wall would be dependent on the construction techniques employed. In order to avoid gaps, voids, or other discontinuous features or defects in the wall, continuous quality control monitoring would be required during construction.
 - The performance of the wall would also be dependent on its actual hydraulic conductivity. This would require continual monitoring, quality control testing, and quality assurance testing of slurry mixing and placement or soil-bentonite mixing in order to verify that the as-designed mix is utilized and routine testing of samples of the wall material. The wall may also require post-construction quality assurance activities (*i.e.*, coring and testing) to verify the quality of the constructed barrier.
- Expected Operational Reliability of the Remedy - 35 I.A.C. § 845.670(e)(3)(B)
 - The cutoff wall is expected to have high operational reliability if it is constructed in accordance with standard design and specifications for barrier walls. This is because the cutoff wall provides an inert, continuous, low-permeability barrier to groundwater flow.
- Need to Coordinate with and Obtain Necessary Approvals and permits from Other Agencies - 35 I.A.C. § 845.670(e)(3)(C)
 - Agency permits would need to be obtained from IEPA for construction stormwater controls and BMPs.
- Availability of Necessary Equipment and Specialists - 35 I.A.C. § 845.670(e)(3)(D)
 - Construction of the cutoff wall would require a specialized contractor experienced with constructing similar types of walls in similar geologic environments. The contractor would likely need specialized equipment, such as large cranes, clamshell buckets, slurry cutters, batch plants, or one-pass construction equipment.
 - Specialists in cutoff wall design and construction would also need to be utilized during the design and construction phase. The specialists would include design engineers, construction managers, and contractor staff experienced with cutoff wall construction and equipment operation.
 - These types of equipment and specialists have been utilized in the past for other similar types of cutoff wall design and construction projects. However, there may be shortages associated with the equipment and specialists, due to high existing backlog for specialty ground improvement contractors and design specialists who are supporting similar types of projects in the electric utility, dam/levee, and other market sectors.

- Equipment and specialists for field data collection and groundwater sampling are required for the remedy. Laboratory equipment and specialists would also be required to assess groundwater concentrations of site COCs. Groundwater professionals (*i.e.*, geologists, hydrogeologists, statisticians, geochemists) would be required to perform statistical analysis and other assessments to confirm that the remedy is functioning as intended and prepare corrective action-related groundwater monitoring and progress reports.
 - As described in **Section 2.2.3**, the equipment and specialists required for site groundwater monitoring and analysis are currently performing this work in accordance with 35 I.A.C. § 845.220(c)(4). Therefore, no new equipment or specialists are required for groundwater monitoring for this alternative.
- Available Capacity and Location of Needed Treatment, Storage, and Disposal Services – 35 I.A.C. § 845.670(e)(3)(E)
 - Wastes generated during cutoff wall construction would be limited to spoils; excavated soils would be disposed of on-site and excavated CCR would be disposed of off-site at a regional landfill. A landfill evaluation would be completed to determine the best location for disposal, taking into account several factors, including landfill capacity and hauling mileage.
 - No wastes would be generated during operation of the cutoff walls; therefore, no additional treatment, storage or disposal services would be required with the source control with cutoff wall remedy.

4. ALTERNATIVE 3 REMEDY: SOURCE CONTROL WITH GROUNDWATER MANAGEMENT SYSTEM

The Alternative 3 remedy, source control with groundwater management system, would include the construction of a system that actively controls the source of releases to reduce to the maximum extent feasible further releases of constituents. The system creates a negative gradient and removing liquids that may be or may become present within the interior of the FAPS. The groundwater management system would be comprised of the following components:

- An extraction trench which would remove liquids that may be from low-lying areas near and around the base of CCR within the interior of the FAPS.
 - The total length of the continuous trench alignment would be approximately 8,700 feet with a maximum depth of approximately 50 to 60 feet bgs.
 - The trench would be 2 to 3 feet wide and would be backfilled with highly permeable aggregate surrounding a perforated collection pipe.
 - Collection sumps would be located approximately every 500 feet along the trench alignment.
- A mechanical, electrical, and piping (MEP) system to remove extracted any liquids from the trenches and treat the liquids prior to discharge.
 - Any liquids would be pumped from each of the sumps within the extraction trenches and routed to a collection pond for settling.
 - After settling, any liquids would be discharged to either the Kaskaskia River to the west via a new or existing National Pollutant Discharge Elimination System (NPDES) outfall, and in accordance with site-specific permit requirements.

The purpose of the groundwater management system would be to provide long-term removal of liquids that may be from the FAPS. This will reduce hydraulic head beneath the existing FAPS cover system which also reduces the potential for constituents to release from the FAPS and migrate past the site's southern property boundary.

A feasibility-level drawing of the source control with groundwater management system remedy is provided as **Figure 2** in **Appendix A**.

4.1 Remedy Scoping and Groundwater Modeling Results

The location of the components which comprise the groundwater management system were selected by reviewing physical constraints within and outside of the FAPS where the system could feasibly be constructed with limited impacts to other site features. Additionally, the location of the system components was targeted to correspond to the portions of the FAPS where CCR is presumed to be present at the lowest elevations, which generally correspond with pre-construction surface drainage features. This approach would allow the system to collect the maximum amount of liquids that may be or may become present within the FAPS, thereby proactively preventing the release of constituents that may migrate past the site's southern property boundary.

The extraction trench portions of the groundwater management system would be located within the limits of the existing FAPS, as these areas correspond to the lowest elevation of CCR. Since the trenches would be completely within the limits of the FAPS, they would not be within regulatory floodplains or known wetlands, and the ground surface, which is located on top of the final cover systems, provides a generally straight and level alignment for the system. However, this would result in the system temporarily impacting the final cover system of the FAPS, which would require impacted areas to be repaired back to their current conditions after system construction.

The groundwater model (**Appendix B**) estimated that the GWPS would not be attained for all FAPS compliance monitoring wells within the 1,000-year prediction model simulation period after the implementation of Alternative 3 remedy, source control with groundwater management system. Following source control and groundwater management system in Alternative 3, the GWPS was not achieved at 4 of 23 wells evaluated following the completion of the 1,000-year model simulation. Simulated boron plume extent contracted over time following implementation of Alternative 3. Based on the calculations of plume extent acreages, the area of the plume decreases from 420 acres (current simulated plume area) to 193 acres (1,000-year simulated plume area) for Alternative 3. Approximately 20 acres of the 1,000-year simulated plume area occur off-site. The combined linear distance of plume simulated as intersecting the property line at the end of the 1,000-year simulation was approximately 2,790 feet for Alternative 3. The longest continuous linear distance of plume extent at the property line was to the southwest of the West Fly Ash Pond between monitoring well locations MW-150 and MW-151. The remaining areas that contribute to the combined linear distance of plume simulated as intersecting the property line were south of the West Fly Ash Pond and south of the East Fly Ash Pond.

4.2 Remedy Implementation

Implementation of the Alternative 3 source control with groundwater management system remedy is expected to include multiple tasks spread out over three phases, including pre-construction activities (Phase 1), corrective action construction (Phase 2), and corrective action operations, maintenance, and closeout (Phase 3). Information for each phase is described in this section.

4.2.1 Phase 1: Pre-Construction Activities

Pre-construction activities would include further pre-design investigation, obtaining permits from other agencies, completing the final design of the remedy, and selecting a remedy implementation contractor via a bidding process. Information associated with each of these activities is described below.

- Completing pre-design investigation, final design and bid activities, including:
 - Completion of final pre-design subsurface investigations, laboratory soil testing, engineering calculations, bench scale testing of proposed groundwater management system construction materials, design drawings, specifications, and a construction quality assurance plan.
 - Bidding and selection of a groundwater management system construction contractor.
- Obtaining permits from other agencies including:

- A general stormwater permit for construction site activities through IEPA, including construction stormwater controls and other BMPs such as silt fences and other measures.
- An IDNR Office of Water Resources, Dam Safety modification permit would be obtained for modification of the FAPS embankment.
- A NPDES permit would be obtained to discharge any collected liquids for the operational lifetime of the system.

4.2.2 Phase 2: Corrective Action Construction

Corrective action construction would be initiated after pre-construction activities are complete. It would include mobilizing construction equipment to the site, preparing the site for construction activities, construction of the groundwater management system, and performing post-construction and site restoration activities. Spoils generated during construction of the extraction trench components and some of the MEP components of the groundwater management system are expected to predominantly consist of CCR materials and would therefore be disposed of at an off-site landfill.

Information associated with each of these activities is described below.

- Site Preparation
 - The contractor would mobilize equipment and materials to the site, install stormwater BMPs around the construction area, construct a staging and laydown area, and construct a level working pad and/or temporary construction access roads along the alignment of the extraction trench and MEP components of the system.
 - Access roads would be located in areas where they minimize disturbance to the existing FAPS final cover system.
 - Construction of the working platform would include removing, relocating, or modifying existing site infrastructure (*i.e.*, piezometers, roadways, utilities) that may conflict with the construction of the groundwater management system.
- Extraction Trench Installation
 - The extraction trench components of the groundwater management system would likely be constructed utilizing specialized trenching equipment (*i.e.*, one-pass trenching methods) due to the relatively deep trench depths (up to approximately 60 feet). This method uses a specialized one-pass trencher to excavate subgrade soils, place collection piping and sumps, and backfill the trench with granular fill in a single operation. Other innovative methods could be utilized if later determined to be appropriate based on site-specific subsurface conditions and constructability considerations.
 - Excavated soils (*e.g.*, trench spoils) from the trenches, which would predominantly consist of CCR materials, would be placed into off-road dump trucks and relocated to another portion of the site where the material would be spread to allow the spoils to dry. The dried spoils would be loaded into off-road dump trucks and transported to an

approved off-site landfill for disposal that is located within Illinois or nearby in Missouri.

- A perforated pipe would be installed at the bottom of the extraction trenches to collect any liquids and direct them towards collection sumps. High-density polyethylene (HDPE) conveyancing piping would be installed in the top 3 feet of the trench to convey any extracted liquids to the compressor shed equalization (EQ) tanks and from the EQ tanks to a settling pond.
- The extraction trenches would be backfilled with imported clean granular material and capped with low-permeability clay and topsoil that is consistent with the design drawings and specifications for the completed final closure system. Where the trenches cross current stormwater control features, it may also be capped with an erosion resistant material such as riprap, also consistent with the design and construction specifications for the final closure system.

Collection sumps would be located every 400 to 500 feet across the length of the 8,700-foot trench alignment and would consist of a pit to hold any liquids.

- Mechanical, Electrical, and Piping Installation
 - A pneumatic pump and a discharge pipe that would carry extracted liquids to an EQ tank in the nearby compressor shed would be installed in each sump.
 - A compressor shed consisting of an air compressor, EQ tank, and transfer pump would be installed every 1,000 to 2,000 feet along the trench alignment to supply compressed air to nearby pneumatic pumps and to transfer any liquids from the EQ tank to a 4-acre settling pond.
 - Electrical power drops and a buried electrical distribution system would be installed as needed to provide power for the groundwater management and water conveyance systems.
- Discharge Management Installation
 - A settling pond has been assumed for management of liquids that may or may be associated with the FAPS. This pond would be constructed using conventional construction equipment. The settling pond would be approximately 4 acres in size and 5 feet deep. Other water treatment and management technologies may be evaluated during a later phase of design.
- Site Restoration
 - Disturbed areas of the final cover system would be repaired after the system has been installed. This would include removing any working platforms, excavating disturbed final cover system soils, and recompacting the final cover consistent with the original design grades and specifications for the completed final closure. This would generally involve the reuse of the current cover soils but may require the importation of additional cover soils from an on-site source.
 - Site restoration would be completed following the repair of the final cover system. This would include repairing site infrastructure that was relocated or

damaged during construction and minor regrading and seeding of disturbed areas.

- Temporary BMPs would also be installed during the site restoration period, if required in accordance with site land disturbance permits. The BMPs would be removed once vegetation is established.

4.2.3 Phase 3: Corrective Action Operations, Maintenance, and Closeout

Corrective action operations, maintenance, and closure would be initiated after corrective action construction is completed. It would include performing corrective action groundwater monitoring, and, after GWPS have been met, performing corrective action closeout and completion activities. Information associated with each of these activities is described below.

- Corrective Action O&M
 - Continued operation of the groundwater management system would require routine, scheduled inspections and associated maintenance including, but not limited to, totalizer data collection, and maintenance of extraction pumps as well as other system components.
 - Non-routine maintenance that may occur during extended operation of the groundwater management system may include tasks such as repair or replacement of MEP components of the system. This may include the extraction pumps, repair or replacement of a system air compressor, and flushing or jetting of water conveyance lines in the event organic or inorganic solids accumulate on the interior walls.
 - Routine monitoring and compliance activities associated with the treatment and discharge of extracted water via the site's NPDES permit and either existing or new outfall would also be completed during this phase.
- Corrective Action Monitoring
 - Regular corrective action groundwater monitoring would be conducted using a corrective action groundwater monitoring system designed in accordance with 35 I.A.C. § 845.680(c), which specified that wells must be installed within the plume of contamination that lies beyond the waste boundary.
 - Samples would be collected for COCs required by 35 I.A.C. § 845.600(a)(1). Samples will be collected on a quarterly basis initially and potentially reduced to a semiannual basis once five years of monitoring have occurred, in accordance with 35 I.A.C. § 845.650(b)(4).
 - Monitoring results will be submitted to IEPA after each monitoring event, in addition to an annual groundwater monitoring and corrective action report, in accordance with 35 I.A.C. § 845.640(e). The annual corrective action report will include an evaluation of the actual performance of the remedy relative to the remedy's expected performance.
 - Routine maintenance of the monitoring well network will be conducted during the monitoring period. This will include inspection of the wells, making repairs to the wells (as and if needed), and rehabilitation and/or replacing the wells to improve performance (as and if needed).

- If the remedy does not achieve its expected performance, additional methods or techniques to achieve compliance with GWPS would be evaluated and, if feasible, implemented in accordance with 35 I.A.C. § 845.680(b).
- Adaptive Management during Monitoring
 - Groundwater monitoring results would be evaluated and documented in in the monitoring reports submitted to IEPA, in accordance with 35 I.A.C. § 845.610(e).
 - Remedy progress evaluation as part of adaptive site management may include additional investigation to inform updates to the CSM, groundwater, and geochemical models.
 - If remedy progress does not correspond with expectations, additional methods or techniques to achieve compliance with GWPS would be evaluated and, if feasible, implemented in accordance with 35 I.A.C. § 845.680(b).
- Corrective Action Completion
 - After completion of the corrective action confirmation monitoring period, a Corrective Action Completion Report and Certification would be prepared and submitted to IEPA, in accordance with 35 I.A.C. § 845.680(e).
 - If GWPS are not met in the future, the FAPS would remain in a perpetual state of Corrective Action Groundwater Monitoring and confirmation monitoring would not be performed.

4.2.4 Remedy Implementation Schedule

A feasibility-level implementation schedule for the Alternative 3 source control with groundwater management system remedy is provided in **Table C** below.

Table C. Feasibility-Level Implementation Schedule – Alternative 3: Source Control with Groundwater Management System

| Implementation Phase | Implementation Task | Timeframe (Preliminary Estimates) |
|---|---|---|
| 1: Pre-Construction Activities | Agency Coordination, Approvals, and Permitting | 6 to 12 months |
| | Final Design and Bid Process | 24 to 36 months |
| | Timeframe to Complete Corrective Pre-Construction Activities | 30 to 48 months after CAP Approval |
| 2: Corrective Action Construction | Corrective Action Construction | 12 to 24 months |
| | Timeframe to Complete Corrective Action Construction | 12 to 24 months after completion of pre-construction activities |
| 3: Corrective Action O&M and Closeout | Corrective Action Monitoring (Time to Meet GWPS) | >100 years |
| | Corrective Action Confirmation Monitoring | 36 months |
| | Corrective Action Completion | 6 months |
| | Timeframe to Complete Corrective Action O&M and Closeout | >100 years after completion of construction activities |
| Total Timeline to Complete Corrective Action | | >100 years |

4.2.5 Management of Extracted Liquids

FAPS extracted liquids that may be present, were assumed to be managed and treated by the groundwater management system and a newly constructed settling pond to be located on-site. However, other forms of water management and/or treatment may be evaluated during future phases of design.

The settling pond would be sited to avoid conflicts with existing site infrastructure. A settling pond of approximately 4 acres in size is assumed to be sufficient to allow sediments to settle from any extracted liquids prior to discharge. Any extracted liquids would be sent to the settling pond via the pneumatic extraction pumps and transfer piping. Treated water would discharge via an existing or new NPDES outfall. Any extracted liquids would be discharged in accordance with site-specific NPDES permit requirements.

4.2.6 35 I.A.C. § 845.670(e)(1)(H) and 35 I.A.C. § 845.670(e)(3) Information

As requested by Gradient, the following information required by 35 I.A.C. § 845.670(e)(1)(H) and 35 I.A.C. § 845.670(e)(3) has been developed for the remedy. The information was developed based on preliminary-level information contained within the CMA for the BPP FAPS and then refined based on additional feasibility-level design activities performed as part of the development of this CAAA-SIR.

- Potential Need for Replacement of the Remedy – 35 I.A.C. § 845.670(e)(1)(H)
 - The groundwater management system remedy is expected to be reliable and is unlikely to need replacement over an approximately 50 year normal design life for these types of systems.
 - However, jetting or redevelopment of the perforated drainpipe within the extraction trench component may be required during the design life of the remedy.
 - The MEP components of the remedy, including the submersible sump pumps, transfer pumps, and various instrumentation and controls associated with the groundwater management system would likely need to be serviced and/or replaced over the duration of the remedy. Replacement of pumps and instrumentation and controls is likely to occur every 10 to 20 years over the duration of the remedy, resulting in multiple component replacements over the approximately 1,000-year operational life of the remedy.
 - Due to approximately 1,000-year operational life of the remedy, replacement extraction trench component of the remedy could be required due to long-term degradation and/or fouling of the perforated collection pipe and backfill granular media. Sufficient data on the performance of groundwater extraction trenches over this timeframe is not available as these types of systems have only been used for approximately 100 years or less.
 - If replacement of the extraction trench component of the remedy may be required in the future, it would be evaluated as part of ongoing adaptive site management activities.

- Degree of Difficulty Associated with Constructing the Remedy – 35 I.A.C. § 845.670(e)(3)(A)
 - The extraction trench component remedy would require mobilizing specialty equipment to the site (*i.e.*, large cranes, clamshells or slurry cutters, or potential one-pass trenching equipment) in addition to other supporting equipment (*i.e.*, excavation and grading equipment).
 - While trenches are routinely constructed to similar depths in similar geologic environments, they often encounter difficulties during construction. The difficulties could include encountering obstructions that require specialized techniques and/or equipment to advance past.
 - In addition to likely requiring a permit from the IDNR Office of Water Resources, Dam Safety section, the construction may require the detailed geotechnical design of the working platform.
 - The MEP components of the remedy are commonly constructed using regional and local contractors and are expected to have a low level of construction difficulty.
- Expected Operational Reliability of the Remedy - 35 I.A.C. § 845.670(e)(3)(B)
 - The groundwater management system is expected to have high operational reliability if constructed in accordance with the design and specifications.
 - The groundwater management system is a mechanical system that would require routine maintenance in order to reliably operate, as outlined in the Corrective Action O&M, **Section 4.2.3.**
- Need to Coordinate with and Obtain Necessary Approvals and permits from Other Agencies - 35 I.A.C. § 845.670(e)(3)(C)
 - Agency permits would need to be obtained from IEPA for construction stormwater controls and BMPs, in addition to a joint water pollution control construction and operating permit, and modifications to the site's NDPES permit or potentially a new permit. These permits typically take 18 to 24 months to obtain.
 - An IDNR Office of Water Resources, Dam Safety modification permit would be obtained for modification of the FAPS embankment.
- Availability of Necessary Equipment and Specialists - 35 I.A.C. § 845.670(e)(3)(D)
 - Construction of the groundwater management system would require a specialized contractor experienced with constructing similar types of trenches in similar geologic environments. Relatively few construction contractors with this experience, particularly using one-pass trenching equipment, are available. The contractor would likely need specialized and often custom-built one-pass construction equipment.
 - Specialists in one-pass trenching methods would also need to be utilized during the design and construction phase. The specialists would include design engineers, construction managers, and contractor staff experienced with trench construction and equipment operation.
 - Geotechnical specialists maybe needed to design the working platform and monitor the FAPS embankment for signs of distress during one-pass trench installation.

- These types of equipment and specialists have been utilized in the past for other similar types of groundwater management system designs and construction projects. However, there may be backlogs associated with the equipment and specialists, due to high existing demand for specialty ground improvement contractors and design specialists who are supporting similar types of projects in the electric utility, dam/levee, and other market sectors. These backlogs could add additional delay to the project schedule above current assumptions.
- Equipment and specialists for field data collection and groundwater sampling are required for the remedy. Laboratory equipment and specialists would also be required to assess groundwater concentrations of site COCs. Groundwater professionals (*i.e.*, geologists, hydrogeologists, statisticians, geochemists) would be required to perform statistical analysis and other assessments to confirm that the remedy is functioning as intended and prepare corrective action-related groundwater monitoring and progress reports.
 - As described in **Section 2.2.3**, the equipment and specialists required to support these activities are currently performing routine groundwater monitoring in accordance with 35 I.A.C. § 845.220(c)(4). Therefore, no new equipment or specialists are required for groundwater monitoring in this alternative.
- Available Capacity and Location of Needed Treatment, Storage, and Disposal Services - 35 I.A.C. § 845.670(e)(3)(E)
 - Wastes generated during groundwater management trench construction would be limited to trench spoils, which would predominantly consist of CCR. These spoils would be disposed of off-site at a regional landfill in Illinois or nearby in Missouri. A landfill evaluation would be completed to determine the best location for disposal taking into account several factors, including landfill capacity and hauling mileage.
 - No other wastes would be generated during operations of the groundwater management trench; therefore, no additional treatment, storage or disposal services would be required with the source control with groundwater management system remedy.

5. MATERIAL QUANTITY, LABOR, AND MILEAGE ESTIMATES

Estimates of material quantities, total labor hours, and mileage were prepared for Alternative 2 source control with cutoff wall, and Alternative 3 source control with groundwater management system to support Gradient in preparing a CAAA. Estimates were prepared for the construction and O&M of each remedy. Estimates were not prepared for Alternative 1 source control with GWP as the alternative does not require remedial construction or O&M of a physical remedy.

Both estimates were prepared utilizing the following approach:

- Major implementation (*e.g.*, construction) components and line items were identified, in accordance with the remedy implementation narratives contained within this CAAA-SIR.
- Construction quantities were estimated based on quantity estimates for volumes, areas, and units, as obtained from the feasibility-level engineering drawings and schedules included within this CAAA-SIR.
- RS Means Heavy Construction Cost Data (RS Means) [10] was utilized to estimate the crew size, equipment description, and daily output associated with each line item.
- For line items where RS Means data was not available, the crew size, equipment description, and daily output were estimated based on Ramboll's experience, information from contractors, and/or information from material suppliers.
- For the Alternative 2 source control with cutoff wall and Alternative 3 source control with groundwater management system active remedies, daily construction and O&M labor mobilization miles were estimated assuming a weekly mobilization/demobilization from St. Louis (82 miles round trip) and a local commute of 40 miles round trip per day. The number of working days and hours per week were estimated from the construction schedule developed for each remedy.
- Estimates of material delivery miles were prepared based on Ramboll's experience.

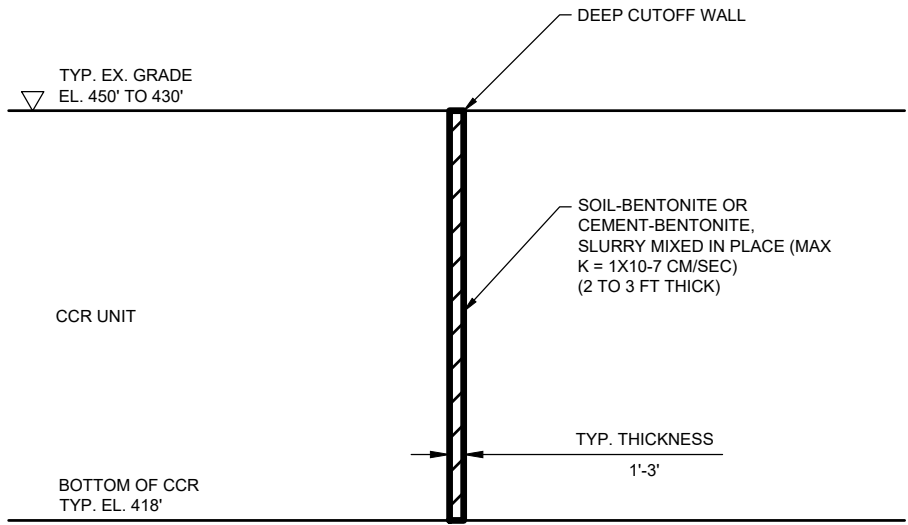
The detailed material quantity, labor, and mileage estimates are provided in **Appendix C** for each alternative.

6. REFERENCES

- [1] "35 Ill. Admn. Code Part 845, Standards for the Disposal of Coal Combustion Residuals in Surface Impoundments," Illinois Environmental Protection Agency, Springfield, IL, 2021.
- [2] Code of Federal Regulations, "Title 40, Chapter I, Subchapter I, Part 257, Subpart D, Standards for the Disposal of Coal Combustion Residuals in Landfills and Surface Impoundments," April 17, 2015.
- [3] Luminant, "Letter to Mr. Darin LeCrone, IEPA: Baldwin Energy Complex; Old East Fly Ash Pond, East Fly Ash Pond, West Ash Pond Notification of Completion of Closure," December 17, 2020.
- [4] AECOM, "Closure and Post-Closure Care Plan for the Baldwin Fly Ash Pond System. Baldwin Energy Complex.," AECOM, Baldwin, Illinois., March 31, 2016.
- [5] Illinois Environmental Protection Agency, "'Dynergy Midwest Generation, Inc. - Baldwin Energy Complex: Baldwin Fly Ash Pond System Closure - NPDES Permit No. IL0000043.'," Illinois Environmental Protection Agency, Baldwin, Illinois, August 16, 2016.
- [6] Ramboll, "Nature and Extent Report, Baldwin Power Plant, Fly Ash Pond System, IEPA No. W1578510001-01, W1578510001-02, and W1578510001-03," Ramboll, Baldwin, Illinois, April 2024.
- [7] United States Environmental Protection Agency, "Use of Monitored Natural Attenuation at Superfund, RCRA Corrective Action, and Underground Storage Tank Sites," OSWER Directive Number 9200.4-17P, April 21, 1999.
- [8] Ramboll, "2024 35 I.A.C. § 845 Annual Groundwater Monitoring and Corrective Action Report, Fly Ash Pond System, Baldwin Power Plant, IEPA ID No. W1578510001-01, W1578510001-02, and W1578510001-03," Ramboll, Baldwin, Illinois, January 2025.
- [9] Geosyntec Consultants, "Groundwater Polishing Evaluation Report, Baldwin Power Plant - Fly Ash Pond System (IEPA ID No. 605)," February 2025.
- [10] Gordian, RS Means Data version 8.7, Paducah, KY: Gordian, 2023.

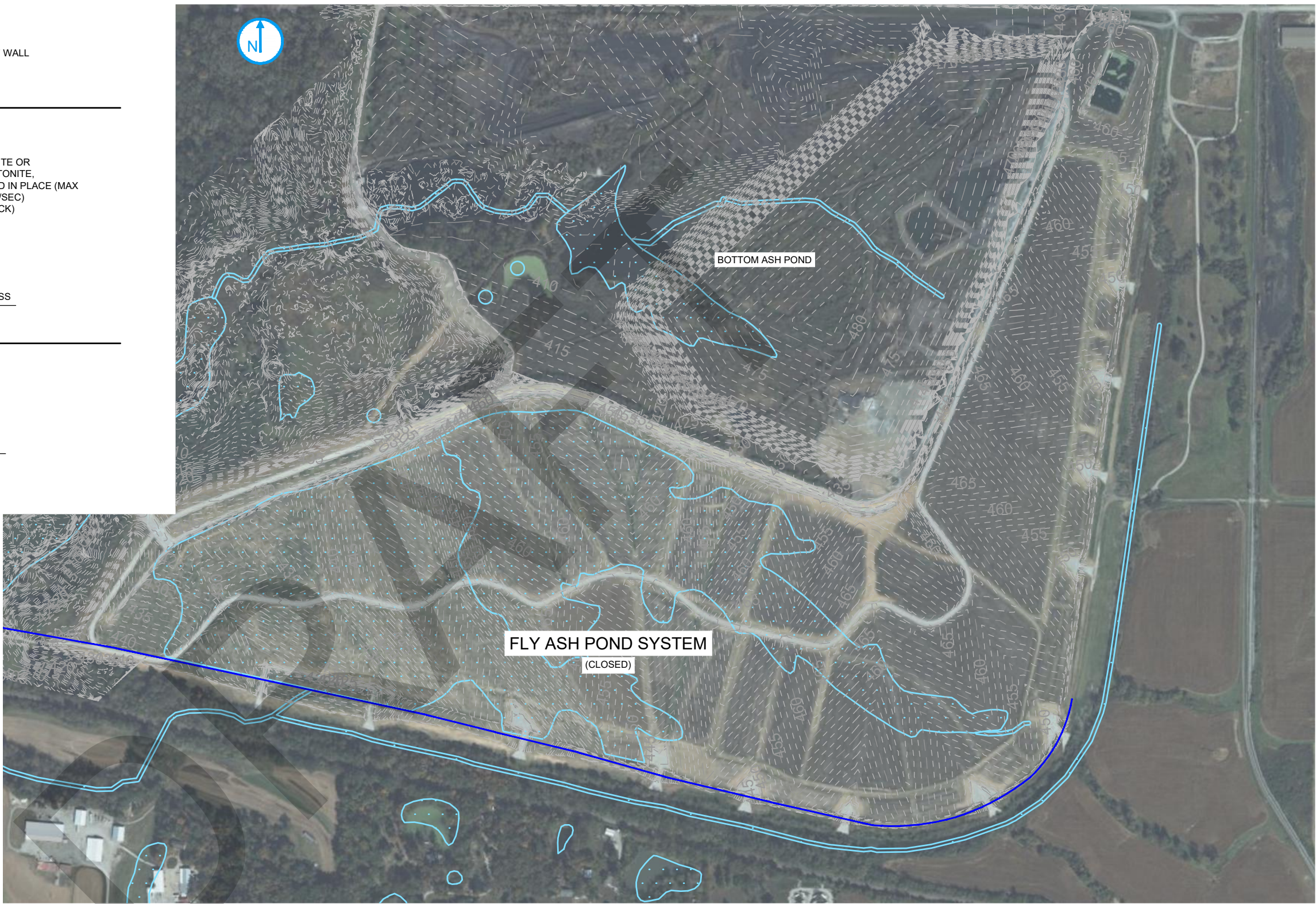
**APPENDIX A
FEASIBILITY-LEVEL DESIGN DRAWINGS FOR
ALTERNATIVE 2 AND ALTERNATIVE 3 REMEDIES**

PROJECT: DATED: 11/26/2024 DESIGNER: LEMMONB\DC\ACCDocs\ramboll gruppen astrus-1940106781-002 vistra - baldwin faps\project files\4 delivery\401 civil\CAAA-SIR\Drawings\BAL-FAP_CAAA-SIR.dwg



CUTOFF WALL DETAIL

NOT TO SCALE



SITE PLAN

- NOTE:
1. EXISTING CONTOURS REPRESENTED PER BALDWIN POWER PLANT FLY ASH POND SYSTEM PART 845 CLOSURE PLAN CONSTRUCTION DRAWINGS COMPLETED BY INGENAE, OCTOBER 2020.
 2. WETLANDS REPRESENTED AS PER ILLINOIS NATIONAL WETLANDS INVENTORY.
 3. 100-YEAR FLOODPLAIN REPRESENTED AS PER FEMA FIRM FOR THE SITE.

EXISTING

- 360 --- MAJOR CONTOUR
- - - - MINOR CONTOUR
- BODY OF WATER
- WETLANDS BOUNDARY (SEE NOTE 2)

PROPOSED

- DEEP CUTOFF WALL

ALTERNATIVE 2 REMEDY
DEEP CUTOFF WALL
FEASIBILITY-LEVEL DESIGN

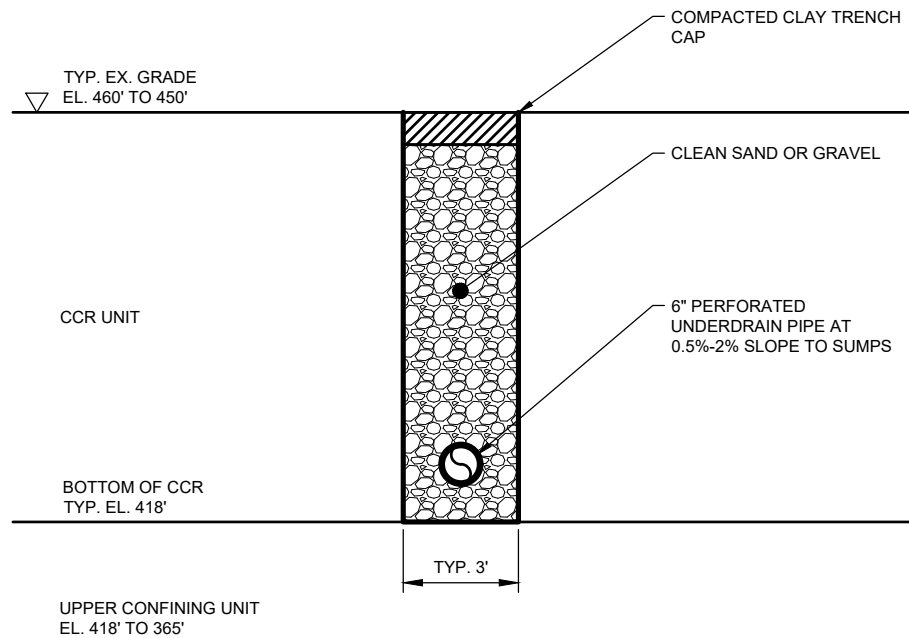
Baldwin Fly Ash Pond
Baldwin Fly Ash System Baldwin Energy Complex 10901 Baldwin Road Baldwin, IL 62217

RAMBOLL AMERICAS
ENGINEERING SOLUTIONS, INC.
A RAMBOLL COMPANY

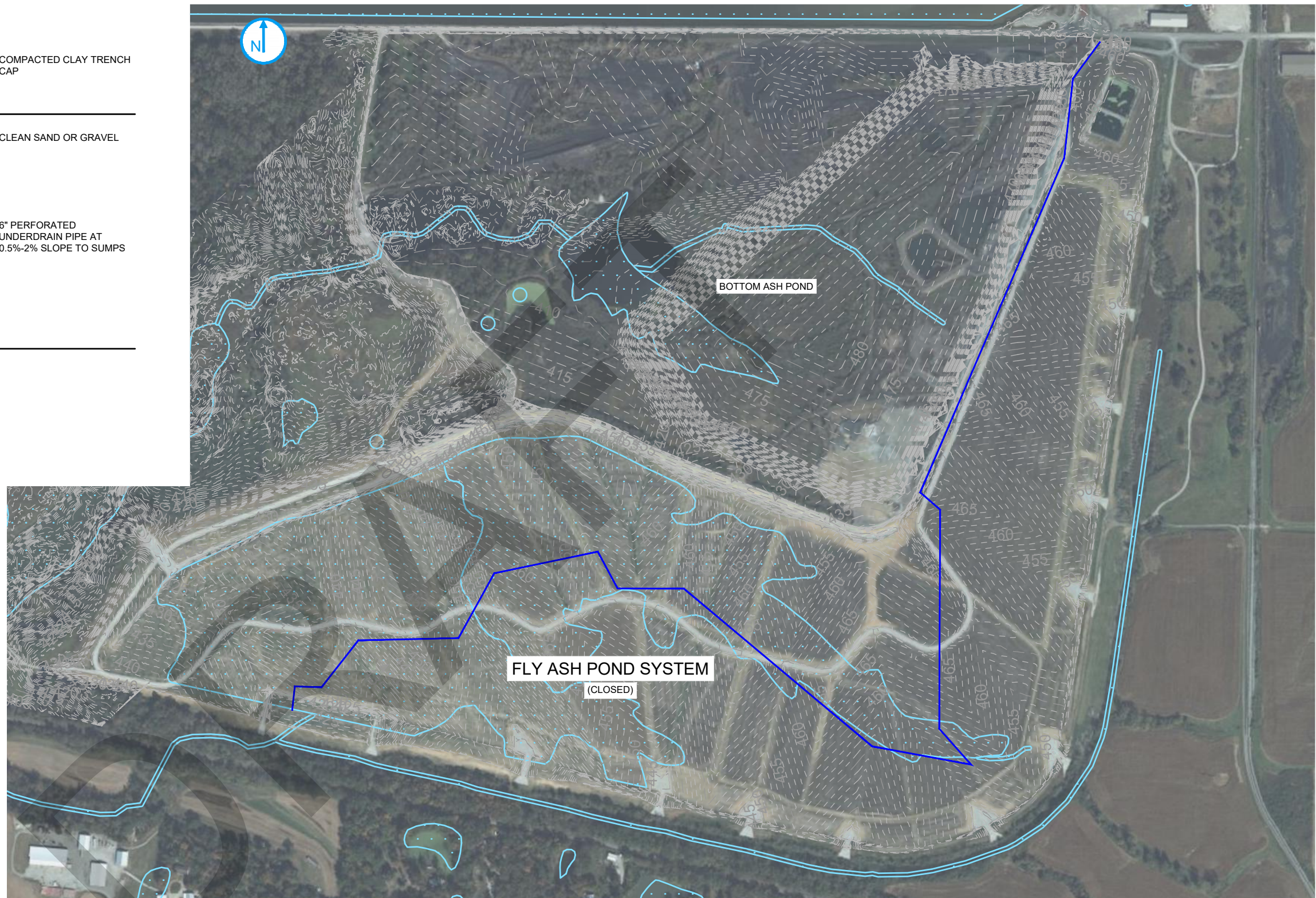


FIGURE 1

PROJECT: DATED: 11/26/2024 DESIGNER: LEMMONB\DC\ACCDocs\ramboll gruppen astrus-1940106781-002 vistra - baldwin faps\project files\4 delivery\401 civil\CAAA-SIR\Drawings\BAL-FAP_CAAA-SIR.dwg



TRENCH DETAIL
NOT TO SCALE



SITE PLAN

- NOTE:
1. EXISTING CONTOURS REPRESENTED PER BALDWIN POWER PLANT FLY ASH POND SYSTEM PART 845 CLOSURE PLAN CONSTRUCTION DRAWINGS COMPLETED BY INGENAE, OCTOBER 2020.
 2. WETLANDS REPRESENTED AS PER ILLINOIS NATIONAL WETLANDS INVENTORY.
 3. 100-YEAR FLOODPLAIN REPRESENTED AS PER FEMA FIRM FOR THE SITE.

EXISTING

- 360 --- MAJOR CONTOUR
- - - - - MINOR CONTOUR
- BODY OF WATER
- WETLANDS BOUNDARY (SEE NOTE 2)

PROPOSED

- INFILTRATION COLLECTION SYSTEM

ALTERNATIVE 3 REMEDY
INFILTRATION COLLECTION SYSTEM
FEASIBILITY-LEVEL DESIGN

Baldwin Fly Ash Pond
Baldwin Fly Ash System Baldwin Energy Complex 10901 Baldwin Road Baldwin, IL 62217

FIGURE 2

RAMBOLL AMERICAS
ENGINEERING SOLUTIONS, INC.
A RAMBOLL COMPANY



APPENDIX B
GROUNDWATER MODELING TECHNICAL MEMORANDUM

Intended for
Dynegy Midwest Generation, LLC

Date
February 18, 2025

Project No.
1940110241-005

GROUNDWATER MODELING TECHNICAL MEMORANDUM

**BALDWIN POWER PLANT, FLY ASH POND
SYSTEM**

IEPA ID NO. W1578510001-01/02/03

GROUNDWATER MODELING TECHNICAL MEMORANDUM BALDWIN POWER PLANT, FLY ASH POND SYSTEM

Project name **Baldwin Power Plant Fly Ash Pond System**
Project no. **1940110241-005**
Recipient **Dynegy Midwest Generation, LLC.**
Document type **Technical Memorandum**
Revision **DRAFT**
Date **February 18, 2025**
Prepared by **Jake J. Walczak, PG**
Checked by **J. Austin Bond, PE**
Approved by **Brian G. Hennings, PG**

Ramboll
234 W. Florida Street
Fifth Floor
Milwaukee, WI 53204
USA

T 414-837-3607
F 414-837-3608
<https://ramboll.com>

Jake J. Walczak, PG
Technical Manager

Brian G. Hennings, PG
Project Officer, Hydrogeology

| | |
|---|-----------|
| Executive Summary | 5 |
| 1. Introduction | 8 |
| 1.1 Plant and Site Information | 8 |
| 1.2 Technical Memorandum Overview | 8 |
| 1.3 Previous Groundwater Modeling Reports | 9 |
| 2. Site Background, Geology, and Hydrogeology | 11 |
| 2.1 Site Background | 11 |
| 2.2 Site Geology and Hydrogeology | 11 |
| 2.3 Groundwater Quality | 13 |
| 3. Conceptual Model | 15 |
| 3.1 Conceptual Model | 15 |
| 3.1.1 Correlation of Boron with Sulfate | 15 |
| 4. Groundwater Model Development and Calibration | 17 |
| 4.1 Model Changes for Flow and Transport Modeling Setup and Calibration | 17 |
| 4.2 HELP Model Setup and Results | 19 |
| 4.3 Steady-State Flow Model and Transport Model Calibration | 20 |
| 4.4 Calibration Flow and Transport Model Results | 20 |
| 5. Predictive Modeling | 24 |
| 5.1 Model Prediction Scenarios | 24 |
| 5.1.1 Alternative 1 – Source Control with Groundwater Polishing (GWP) | 25 |
| 5.1.2 Alternative 2 – Source Control with Cutoff Wall | 26 |
| 5.1.3 Alternative 3 – Source Control with a Groundwater Management System (GMS) | 27 |
| 5.1.4 Closure-By-Removal (CBR) Scenario | 28 |
| 6. Predictive Alternative simulation Results | 30 |
| 6.1 Prediction Scenario Results Discussion | 30 |
| 6.1.1 Comparison of Corrective Action Alternatives Against the Groundwater Protection Standard (GWPS) for Boron (2 mg/L) | 30 |
| 6.1.2 Spatial Analyses of Corrective Action Alternatives and Closure-By-Removal (CBR) Scenario | 32 |
| 6.1.2.1 Spatial Comparison of Maximum Plume Extents for Corrective Action Alternatives and Closure-By-Removal (CBR) Scenario | 32 |
| 6.1.2.2 Spatial Comparison of Off-Site Maximum Plume Extents for Corrective Action Alternatives and Closure-By-Removal (CBR) Scenario | 32 |
| 6.2 Post-Construction Flux Evaluations for Alternative 3 | 33 |
| 6.3 Assessment of Geochemical Process | 35 |
| 6.4 Discussion of Long-Term Modeling Results | 36 |
| 7. Conclusion | 38 |
| 8. References | 40 |

TABLES (IN TEXT)

Table A Progression of Simulated Timeframes to Attain GWPS in FAPS Monitoring Wells

TABLES (ATTACHED)

Table 4-1 Flow and Transport Model Calibration Targets
Table 4-2 Flow Model Input and Sensitivity Analysis Results
Table 4-3 Transport Model Input Values (Calibration)
Table 4-4 HELP Model Input and Output Values
Table 5-1 Simulated Years to Achieve GWPS for Boron (2 mg/L) at FAPS Monitoring Wells for Alternative 1
Table 5-2 Modeled Boron Plume (2 mg/L) Acreages at Select Times After Implementation
Table 5-3 Simulated Years to Achieve GWPS for Boron (2 mg/L) at FAPS Monitoring Wells for Alternative 2
Table 5-4 Simulated Years to Achieve GWPS for Boron (2 mg/L) at FAPS Monitoring Wells for Alternative 3
Table 5-5 Simulated Years to Achieve GWPS for Boron (2 mg/L) at FAPS Monitoring Wells for CBR Scenario

FIGURES (IN TEXT)

Figure A Correlation of Observed Sulfate and Boron Concentrations in Downgradient Wells

FIGURES (ATTACHED)

Figure 2-1 Site Location Map
Figure 2-2 Site Map
Figure 2-3 Monitoring Well Location Map
Figure 4-1 Observed Versus Simulated Groundwater Elevations
Figure 4-2 Observed Versus Residual Groundwater Elevations
Figure 4-3 Simulated Steady State Groundwater Level Contours from Layer 1 of the Calibrated Model
Figure 4-4 Simulated Steady State Groundwater Level Contours from Layer 2 of the Calibrated Model
Figure 4-5 Simulated Steady State Groundwater Level Contours from Layer 3 of the Calibrated Model
Figure 4-6 Simulated Steady State Groundwater Level Contours from Layer 4 of the Calibrated Model
Figure 4-7 Simulated Steady State Groundwater Level Contours from Layer 5 of the Calibrated Model
Figure 4-8 Simulated Steady State Groundwater Level Contours from Layer 6 of the Calibrated Model
Figure 4-9 Observed and Simulated Boron Concentrations (mg/L)
Figure 4-10 Layer 1 Distribution of Boron Concentrations (mg/L) in the Calibrated Model
Figure 4-11 Layer 2 Distribution of Boron Concentrations (mg/L) in the Calibrated Model
Figure 4-12 Layer 3 Distribution of Boron Concentrations (mg/L) in the Calibrated Model
Figure 4-13 Layer 4 Distribution of Boron Concentrations (mg/L) in the Calibrated Model
Figure 4-14 Layer 5 Distribution of Boron Concentrations (mg/L) in the Calibrated Model
Figure 4-15 Layer 6 Distribution of Boron Concentrations (mg/L) in the Calibrated Model
Figure 5-1 Simulated Groundwater Elevations and Boron Concentrations, 2024 and 2028
Figure 5-2 Model Predicted Boron Concentrations at FAPS Monitoring Wells for Alternative 1: Source Control with GWP
Figure 5-3 Modeled Boron Plume (2 mg/L) 25 Years After Implementation
Figure 5-4 Modeled Boron Plume (2 mg/L) 125 Years After Implementation
Figure 5-5 Modeled Boron Plume (2 mg/L) 375 Years After Implementation
Figure 5-6 Modeled Boron Plume (2 mg/L) 750 Years After Implementation

- Figure 5-7 Modeled Boron Plume (2 mg/L) 1000 Years After Implementation
- Figure 5-8 Model Predicted Boron Concentrations at FAPS Monitoring Wells for Alternative 2:
Source Control with Cutoff Wall
- Figure 5-9 Model Predicted Boron Concentrations at FAPS Monitoring Wells for Alternative 3:
Source Control with GMS
- Figure 5-10 Model Predicted Boron Concentrations at FAPS Monitoring Wells for CBR Scenario
- Figure 6-1 Reductions in Total Flux In and Out of CCR Following Implementation of Alternative 3:
Source Control with GMS
- Figure 6-2 Reductions in Total Flux In and Out of CCR 106 Years Following Implementation of
Alternative 3: Source Control with GMS
- Figure 6-3 Reductions in Total Flux In and Out of CCR Following Implementation of Alternative 3:
Source Control with GMS – Sensitivity Model
- Figure 6-4 Reductions in Total Flux In and Out of CCR 106 Years Following Implementation of
Alternative 3: Source Control with GMS – Sensitivity Model
- Figure 6-5 Simulated Groundwater Management System Liquids Removal Rates for Alternative 3:
Source Control with GMS

APPENDICES

- Appendix A Ramboll Americas Engineering Solutions, Inc. (Ramboll), 2023a. Groundwater Modeling Report Revision 1, Bottom Ash Pond. Baldwin Power Plant. Baldwin, Illinois. August 1, 2023.
- Appendix B MODFLOW, MT3DMS, HELP Model, and Flux Evaluation Data Export Files (Electronic Only)
- Appendix C HELP Model Inputs and Outputs
- Appendix D Flux Evaluation Data

ACRONYMS AND ABBREVIATIONS

| | |
|---------------|--|
| 35 I.A.C. | Title 35 of the Illinois Administrative Code |
| 40 C.F.R. | Title 40 of the Code of Federal Regulations |
| ASD | Alternative Source Demonstration |
| BAP | Bottom Ash Pond |
| bgs | below ground surface |
| BPP | Baldwin Power Plant |
| CBR | closure-by-removal |
| CCR | coal combustion residuals |
| CIP | closure-in-place |
| COC | constituent of concern |
| CSM | conceptual site model |
| DMG | Dynegy Midwest Generation, LLC |
| FAPS | Fly Ash Pond System |
| ft/day | feet per day |
| Geosyntec | Geosyntec Consultants, Inc. |
| GMR | 2023 Bottom Ash Pond Groundwater Modeling Report, Revision 1 |
| gpm | gallons per minute |
| Gradient | Gradient Corporation |
| GMS | Groundwater Management System |
| GWP | groundwater polishing |
| GWPS | groundwater protection standard(s) |
| HCR | Hydrogeologic Site Characterization Report |
| HELP | Hydrologic Evaluation of Landfill Performance |
| ID | identification |
| IEPA | Illinois Environmental Protection Agency |
| Kd | soil adsorption coefficient |
| mg/L | milligrams per liter |
| mL/g | milliliters per gram |
| NAVD88 | North American Vertical Datum of 1988 |
| NID | National Inventory of Dams |
| No. | number |
| NPDES | National Pollutant Discharge Elimination System |
| NRT | Natural Resource Technology, Inc. |
| PMP | potential migration pathway |
| Ramboll | Ramboll Americas Engineering Solutions, Inc. |
| UA | uppermost aquifer |
| USEPA | United States Environmental Protection Agency |
| USGS | United States Geological Survey |
| UU | upper unit |
| Vandalia Till | Vandalia Till Member of the Glasford Formation |

EXECUTIVE SUMMARY

Dynegy Midwest Generation, LLC (DMG) is the owner of the active coal-fired Baldwin Energy Complex, also referred to as the Baldwin Power Plant (BPP), in Baldwin, Randolph County, Illinois. DMG intends to complete groundwater corrective action at the coal combustion residuals (CCR) surface impoundment Fly Ash Pond System (FAPS), which is identified by Illinois Environmental Protection Agency (IEPA) identification (ID) numbers (Nos.) W1578510001-01, W1578510001-02, and W1578510001-03, also referred to as Vistra Identification ID No. 605, and National Inventory of Dams (NID) No. IL50721. Groundwater corrective action for the BPP FAPS will be performed under the requirements of Title 35 of the Illinois Administrative Code (35 I.A.C.) § 845, Standards for the Disposal of Coal Combustion Residuals in Surface Impoundments (IEPA, 2021) and the requirements of Title 40 of the Code of Federal Regulations (40 C.F.R.) § 257 (United States Environmental Protection Agency [USEPA], 2015). This technical memorandum is prepared to evaluate how the potential corrective action alternatives would achieve compliance with the applicable Groundwater Protection Standards (GWPS)¹; to compare changes in the magnitude and spatial distribution of boron concentrations in groundwater for each different corrective action alternative; and to describe fate and transport of contaminants in accordance with 35 I.A.C. § 845.220 (c)(2) using groundwater models.

Groundwater contaminant transport modeling was completed to demonstrate how the proposed corrective action alternatives will maintain compliance with the applicable GWPS and minimize the potential for constituents of concern (COCs) to migrate past the site's southern property boundary. Boron is commonly used as an indicator parameter for contaminant transport modeling for CCR because it is commonly present in coal ash leachate and it is mobile (*i.e.*, has low rates of sorption or degradation) in groundwater. In addition, the Corrective Measures Assessment (Ramboll Americas Engineering Solutions, Inc. [Ramboll], 2024a) identified boron as an exceedance of the GWPS at FAPS monitoring wells. Therefore, groundwater transport modeling was completed using boron.

The 2023 Bottom Ash Pond (BAP) model provided in **Appendix A**, was used as the base model to develop a groundwater flow and transport model for the FAPS at BPP. Adjustments (*e.g.*, recharge rates for the post-closure FAPS in the updated 2024 FAPS model were modified and based on updated Hydrologic Evaluation of Landfill Performance [HELP] model simulations) were made to parameter and boundary conditions to preserve model calibration (flow and transport) as documented in this technical memorandum. The objectives of the model update were to incorporate information collected since 2023 while maintaining the previous quality of calibration.

Three prediction models were developed to evaluate corrective action alternatives, consisting of source control with GWP (Alternative 1), source control with cutoff wall (Alternative 2), and source control with a Groundwater Management System ([GMS] Alternative 3). The objective of predictive modeling is to simulate changes in the magnitude and spatial distribution of boron concentrations in groundwater for each different corrective action. The results are used to

¹ Throughout this document, "exceedance" or "exceedances" is intended to refer only to potential exceedances of proposed applicable background statistics or Groundwater Protection Standards (GWPSs) as described in the proposed groundwater monitoring program, which was submitted to the IEPA on October 31, 2021 as part of DMG's operating permit application for the FAPS. That operating permit application, including the proposed groundwater monitoring program, remains under review by the IEPA and, therefore, DMG has not identified any actual exceedances.

evaluate if implementation of these actions will achieve the GWPS of 2 milligrams per liter (mg/L) for boron at 23 selected FAPS monitoring wells and to compare the differences in spatial distribution of boron within groundwater at the site. Comparison of predicted concentrations of boron in groundwater at the FAPS monitoring wells indicates the following:

- That the time to reach GWPS at the 23 FAPS monitoring wells is similar for Alternatives 1 and 2. Alternative 1 and Alternative 2 both indicate a maximum of 30% of FAPS monitoring wells (23 wells evaluated) attaining the GWPS by the end of the 1,000-year simulation.
- Alternative 3 indicates a maximum of 83% of FAPS monitoring wells (23 wells evaluated) attaining the GWPS by the end of the 1,000-year simulation, where Alternative 3 indicates significantly greater progress toward attaining the GWPS than Alternative 1 and Alternative 2 in less time (10 of the wells are below the GWPS within 25 years and stay below the GWPS for the remainder of the 1,000-year simulation).
- Because the results of the Alternative 3 simulation indicated a significant number of FAPS monitoring wells (19 of 23) attain the GWPS but did not result in all wells attaining the GWPS within the 1,000-year model, a FAPS closure-by-removal (CBR) prediction model was completed to evaluate the difference in boron concentrations simulated at 23 FAPS monitoring wells under both Alternative 3 (source control with GMS) and CBR (source removal) conditions.
- CBR results in a maximum of 57% of the monitoring wells attaining the GWPS by the end of the 1,000-year simulation, where Alternative 3 achieves greater progress toward attaining the GWPS than CBR in less time: 70% of the wells attain the GWPS within 375 years for Alternative 3; versus, a maximum of 57% of the wells attaining the GWPS at the end of the 1,000-year simulation for CBR.

Simulated concentrations of boron were also evaluated spatially using maps of maximum boron concentration at various points in time and their relative areas in acres for each model scenario. Comparison of predicted maximum boron plume extents indicates the following:

- For Alternatives 1 and 2, the boron plume extents continue to expand between 25 and 1,000 years after implementation.
- For Alternative 3, the maximum boron plume extent continually contracts from 25 to 1,000 years, where the plume is less than half the area of the calibration condition after 1,000 years, indicating the greatest reduction compared to other scenarios.
- For CBR, the maximum boron plume extent increases between 25 and 125 years, then contracts between 125 and 1,000 years.
- At the end of the 1,000-year simulation, Alternatives 1 and 2 have the largest off-site plume extents.
- Alternatives 3 and CBR have similar trends in off-site maximum plume extent, both peaking at approximately 27 acres at 750 years after implementation and then reducing to around 20 acres at 1,000 years (end of the simulations).

Evaluations of water flux through the FAPS CCR for Alternative 3 and a sensitivity model at post-closure equilibrium indicate a reduction in total flux into the unit by 60% and a reduction in total flux out of the unit by 73%. The GMS liquids removal rate is estimated to be approximately

30 gpm for the first 8 years and decreases over time to less than 10 gpm after approximately 106 years of operation when heads at FAPS monitoring wells approach post-closure equilibrium.

Results of groundwater modeling predict that more wells are likely to exceed GWPSs in the future than are currently observed in 2024. Alternative 3 results achieve greater progress toward attaining the GWPS in less time when compared to other corrective action alternatives, including the simulated CBR scenario. None of the models predict that all wells will attain the GWPS for boron within the 1,000-year timeframe, including the simulated CBR scenario. This is due to the low hydraulic conductivity of the native soils (UU) and bedrock (UA), and low groundwater flow velocities at the site. Simulated post-construction heads in the FAPS monitoring wells reach equilibrium at approximately 106 years following implementation of corrective action alternatives, which was used for estimating future flux reductions from the FAPS. Considering models become increasingly less reliable over extended timeframes, discussions of model results beyond 106 years should be qualitative and comparative. Following implementation of corrective action, progress toward attainment of the GWPS will be routinely monitored and updated per the adaptive site management actions, which involves routine review and potential updates to the CSM and groundwater fate and transport models as appropriate and as detailed in the Corrective Action Groundwater Monitoring Plan, Baldwin Power Plant, Fly Ash Pond System (Ramboll, 2025).

1. INTRODUCTION

1.1 Plant and Site Information

DMG is the owner of the active coal-fired Baldwin Energy Complex, also referred to as the Baldwin Power Plant, in Baldwin, Randolph County, Illinois. DMG intends to complete groundwater corrective action at the CCR surface impoundment FAPS, which is identified by IEPA ID Nos. W1578510001-01, W1578510001-02, and W1578510001-03, also referred to as Vistra Identification ID No. 605, and NID No. IL50721. Groundwater corrective action for the BPP FAPS will be performed under the requirements of 35 I.A.C. § 845 and the requirements of 40 C.F.R. § 257.

1.2 Technical Memorandum Overview

This technical memorandum is prepared to evaluate how the potential corrective action alternatives would achieve compliance with the applicable GWPSs; to compare changes in the magnitude and spatial distribution of boron concentrations in groundwater for each different corrective action alternative; and to describe fate and transport of contaminants in accordance with 35 I.A.C. § 845.220 (c)(2) using groundwater models. The groundwater modeling efforts consist of predictive fate and transport modeling to assess the long-term effectiveness and time for achieving GWPS as well as the spatial distribution of boron in groundwater for three corrective action alternatives:

Alternative 1. Source Control with GWP: This scenario is consistent with the closure conditions (capping of the FAPS) initially simulated in the 2014 model reports (Natural Resource Technology, Inc. [NRT], 2014b, 2014c) followed by simulations developed for the BAP closure-in-place (CIP) presented in the 2023 Bottom Ash Pond Groundwater Modeling Report Revision 1 ([GMR]; Ramboll, 2023a) which was revised to represent current conditions at the FAPS. The Alternative 1 remedy, source control with GWP, would include the completed source control approach which consisted of capping the waste material, after which GWP would be formally implemented. GWP is a remedial alternative that relies on natural geochemical processes and may be appropriate as recognized by the United States Environmental Protection Agency (USEPA) in a final policy directive for groundwater remediation (USEPA, 1999).

Alternative 2. Source Control with Cutoff Wall – assumes 7,000 feet long, 85-feet deep and 2 to 3-feet wide slurry wall. The Alternative 2 remedy, source control with cutoff wall, would include the construction of a cutoff wall that would extend from the existing perimeter berm ground surface, which ranges from approximately 390 to 450 feet² to an approximate elevation of 365 feet, with the wall keyed into the low-permeability bedrock underlying the upper unit (UU)/PMP. The total length of the cutoff wall would be approximately 7,000 feet, and the cutoff wall would have a maximum depth of approximately 85 feet below ground surface (bgs). The cutoff wall would be constructed using either a mixture of soil and bentonite or cement and bentonite and would have an expected width of 2 to 3 feet. The cutoff wall would have a hydraulic conductivity value of approximately 1×10^{-7} centimeters per second (cm/s). The purpose of the cutoff wall would be to provide a long-term, maintenance-free physical barrier to

² All elevations referenced in this report are in the North American Vertical Datum of 1988 (NAVD88), unless otherwise noted.

reduce the potential for COCs to migrate past the site's southern property boundary to off-site property owners.

Alternative 3. Source Control with a GMS – assumes an 8,700-foot long, 50 to 60 feet deep, and 2 to 3 feet wide extraction trench. The Alternative 3 remedy, source control with groundwater management system, would include the construction of a system that actively removes liquids that are present within the interior of the FAPS. The groundwater management system would be comprised of the following components:

- An extraction trench which would remove infiltrated liquids from low-lying areas near and around the base of CCR within the interior of the FAPS.
 - The total length of the continuous trench alignment would be approximately 8,700 feet with a maximum depth of approximately 50 to 60 feet bgs.
 - The trench would be 2 to 3 feet wide and would be backfilled with highly permeable aggregate surrounding a perforated collection pipe.
 - Collection sumps would be located approximately every 500 feet along the trench alignment.
- A mechanical, electrical, and piping system to remove extracted liquids from the trenches and treat the liquids prior to discharge.
 - Liquids would be pumped from each of the sumps within the extraction trenches and routed to a collection pond constructed northwest of the FAPS for settling.
 - After settling, the liquids would be discharged to either the Kaskaskia River to the west via a new or existing National Pollutant Discharge Elimination System (NPDES) outfall, and in accordance with site-specific permit requirements.

The purpose of the groundwater management system would be to provide long-term removal of liquids from the FAPS. This will reduce hydraulic head beneath the existing FAPS cover system which also reduces the potential for liquids from the FAPS to mix with groundwater and migrate past the site's southern property boundary.

In each alternative, source control is the CIP scenario that was selected as the closure alternative for the FAPS in 2016 (AECOM, 2016) and completed in 2020 (Luminant, 2020).

1.3 Previous Groundwater Modeling Reports

Groundwater models (MODFLOW, MT3DMS, and HELP) were completed in 2014 to assess the groundwater impacts associated with closure of the FAPS and predict the fate and transport of CCR leachate components, as well as estimate the time required for hydrostatic equilibrium of groundwater beneath the FAPS (NRT, 2014b; NRT, 2014c; NRT, 2016a; NRT, 2016c). Based on these assessments, a Closure and Post-Closure Care Plan (AECOM, 2016), which included a groundwater monitoring program sufficient for long-term, post-closure monitoring, was developed and approved by IEPA in a letter to the Dynegy Operating Company dated August 16, 2016. Closure activities, which included constructing a final cover system to control the potential for water infiltration into the closed CCR unit, were completed, and FAPS closure was completed November 17, 2020.

In accordance with the requirements of 35 I.A.C. § 845, Ramboll developed MODFLOW and MT3DMS groundwater flow and transport models in 2023 for the BAP, and submitted a GMR (Ramboll, 2023a). Prediction simulations were performed to evaluate the effects of closure (source control) measures (CCR consolidation and CIP closure scenario) for the BAP on the groundwater quality following initial corrective action measures, which includes removal of free liquids from the BAP. The FAPS prediction simulations presented in this technical memorandum incorporate changes in recharge rates at the BAP based on HELP-calculated average annual percolation rates resulting from consolidation and closure of the BAP as described in the GMR. The flow and transport models completed as part of the GMR for the BAP were developed independently from the 2014 FAPS flow and transport models, and included several model improvements (*e.g.*, increased number of calibration targets for flow and transport, updated calibration targets based on recent observations, refined grid and boundary conditions, increased model area, increased number of model layers [including simulated bedrock layers], refined layer bottom elevations, etc.) to significantly improve conceptual site model (CSM) representation. The BAP GMR models incorporated recent investigative data collected as part of the development of the Hydrogeologic Site Characterization Reports (HCRs), included the entirety of the FAPS extent, simulated FAPS construction based on the CSM, simulated FAPS operational history (including completion of closure in 2020), and were calibrated to flow and transport calibration targets based on data collected at FAPS groundwater monitoring system, for these reasons the FAPS models developed for this technical memorandum are based on the 2023 BAP GMR fate and transport models.

2. SITE BACKGROUND, GEOLOGY, AND HYDROGEOLOGY

2.1 Site Background

The BPP is located in Baldwin, Illinois (**Figure 2-1**). The BPP property is situated in an agricultural area. The BPP property is bordered to the west by the Kaskaskia River; to the east by Baldwin Road, farmland, and strip-mining areas; to the southeast by the Village of Baldwin; to the south by the Illinois Central Gulf railroad tracks, scattered residences, and State Route 154; and to the north by farmland (**Figure 2-2**). Additional detail on the site background is provided in the 2023 BAP GMR (Ramboll, 2023a; **Appendix A**) and is also found in the HCR for the BAP (Ramboll, 2023b), the Supplemental Hydrogeologic Site Characterization and Groundwater Monitoring Plan for the FAPS (NRT, 2016b) and the site Groundwater Quality Assessment and Phase II Hydrogeologic Investigation (NRT, 2014a).

2.2 Site Geology and Hydrogeology

A detailed summary of site conditions was provided in the revision to the Hydrogeologic Site Characterization Report (Ramboll, 2023b). The revision to the HCR includes hydrogeologic data collected after submittal of the initial HCR in 2021 (Ramboll, 2021) as part of the 2022 Hydrogeologic Site Investigation were also used to establish a CSM for the 2023 BAP GMR and is summarized herein. CCR fill material and two distinct water-bearing units have been identified in the vicinity of the BPP based on stratigraphic relationships and common hydrogeologic characteristics. The units are described as follows from the surface downward:

- **CCR:** CCR, consisting primarily of fly ash, bottom ash, and boiler slag. Also includes earthen fill deposits of predominantly clay and silt materials from on-site excavations that were used to construct berms and roads surrounding the various impoundments across the BPP. The overall (geometric mean) horizontal and vertical hydraulic conductivity for the CCR determined during the Phase II and 2022 Hydrogeologic Site Investigations are 1.5×10^{-2} centimeters per second (cm/s) and 4.1×10^{-5} cm/s, respectively. Horizontal and vertical hydraulic conductivities for this unit determined during the Phase II and 2022 Hydrogeologic Site Investigations ranged from 8.1×10^{-4} to 1.1×10^{-1} cm/s and 5.6×10^{-7} to 6.5×10^{-4} cm/s, respectively.
- **UU:** Predominantly clay with some silt and minor sand, silt layers, and occasional sand lenses. Includes the lithologic layers identified as the Cahokia Formation, Peoria Loess, Equality Formation, and Vandalia Till Member of the Glasford Formation (Vandalia Till). This unit is composed of unlithified natural geologic materials and extends from the upper saturated materials to the bedrock. As observed in the field, one or more of these four lithologic units may be present at a particular soil boring location; and, the observed lithologic unit(s) may or may not be saturated depending on location at the BPP. Given that these units are not consistently in contact with groundwater, this unit was renamed from UGU used in previous reports to UU. The term UU is synonymous with UGU used in previous documents. The overall (geometric mean) horizontal and vertical hydraulic conductivities for this unit determined during the Phase II and 2022 Hydrogeologic Site Investigations are 2.9×10^{-5} cm/s and 3.5×10^{-7} cm/s, respectively. Horizontal and vertical hydraulic conductivities for this unit determined during the Phase II and 2022 Hydrogeologic Site Investigations ranged from 3.5×10^{-7} to 6.8×10^{-4} cm/s and 6.3×10^{-9} to 4.2×10^{-4} cm/s, respectively. The overall (geometric mean) and range of horizontal hydraulic conductivities for this unit determined

during 2024 site investigation activities in support of a forthcoming Addendum to the Nature and Extent Report, Baldwin Power Plant, Fly Ash Pond System (Ramboll, 2025a) was 2.6×10^{-5} cm/s and 9.0×10^{-8} to 1.6×10^{-3} cm/s, respectively, for field hydraulic conductivity tests (slug tests) completed at monitoring wells MW-195, MW-196, MW-197, PZ-174, PZ-177. Thin sand seams and the interface (contact) between the UU and bedrock have been identified as PMPs. No continuous sand seams were observed within or immediately adjacent to the FAPS; however, the sand seams may act as a PMP due to relatively higher hydraulic conductivities (on the order of 10^{-4} cm/s) than the surrounding clays (on the order of 10^{-5} cm/s). The contacts between the unlithified material and bedrock have also been identified as PMPs where horizontal hydraulic conductivity data in BPP monitoring wells with screens and/or filter packs across or immediately above the bedrock range from 3×10^{-7} to 6×10^{-4} cm/s and have a geometric mean horizontal hydraulic conductivity of 2×10^{-5} cm/s.

- **Bedrock Unit:** This unit is composed of interbedded shale and limestone bedrock, which underlies and is continuous across the BPP and has been identified as the uppermost aquifer (UA). The horizontal hydraulic conductivity for this unit determined during the Phase II and 2022 Hydrogeologic Site Investigations ranges from 2.4×10^{-7} to 3.5×10^{-5} cm/s with a geometric mean of 1.9×10^{-6} cm/s (Ramboll, 2023b).

The extent of sand and gravel aquifers in the region are primarily found along the Kaskaskia River Valley where sand and gravel deposits are highly permeable, thick, and extensive. Outside of the Kaskaskia River Valley, the unlithified materials in upland areas are predominantly clay, which generally provide a low probability of encountering sand and gravel layers for dependable groundwater supply. Although some thin sand seams and layers occur intermittently within the Vandalia Till in localized areas around the BPP, most groundwater supplies in upland areas are obtained from large diameter shallow bored wells. Typical water wells in the vicinity of the BPP are between 25 and 55 feet deep, 36 to 48 inches in diameter, and collect groundwater through slow percolation into the wells, which are large diameter to allow for greater water storage to compensate for the low rate of groundwater infiltration (Ramboll, 2023b).

The shallow bedrock is the only water-bearing unit that is continuous across the BPP. Groundwater in the bedrock mainly occurs under semi-confined to confined conditions with the overlying unlithified unit behaving as the upper confining unit to the UA. Shallow sandstone and creviced limestone may yield small supplies in some areas, but water quality becomes poorer (*i.e.*, highly mineralized) with increasing depth.

The locations of groundwater monitoring wells are provided on **Figure 2-3**. Based on elevation measurements, lateral groundwater flow in the shallow unlithified materials and bedrock is generally to the west and southwest across the BPP (Figure 2-2 of the 2023 BAP GMR [**Appendix A**]) toward the Kaskaskia River. Groundwater flow in bedrock is toward the northwest in the east and central areas of the BAP, and southwest to northwest on the east area of the FAPS until groundwater reaches the bedrock valley feature underlying the Secondary and Tertiary Ponds west of the BAP and FAPS, at which point the flow direction veers towards this bedrock surface low. Groundwater elevations across the BPP vary seasonally, generally less than 7 feet, and range between approximately 370 and 450 feet NAVD88, although flow directions are generally consistent. Additional potentiometric surface maps are included as part of the revised HCR (Ramboll, 2023b).

In the western area of the FAPS, average horizontal hydraulic gradients in the shallow unlithified materials and bedrock were 0.015 feet per foot/feet (ft/ft) and 0.016 ft/ft, respectively, as groundwater flowed from east to west across the FAPS. Average groundwater velocities in the shallow unlithified materials and bedrock in the western area of the FAPS were 0.0082 and 0.0003 feet per day (ft/day), respectively. In general, flow velocities in the vicinity of the FAPS are consistent, varying only 0.0019 ft/day in the shallow unlithified materials and 0.0002 ft/day in the bedrock.

Groundwater in the Pennsylvanian and Mississippian-aged bedrock mainly occurs under semi-confined to confined conditions as demonstrated with vertical hydraulic gradient calculations presented in the revised HCR (Ramboll, 2023b), with the overlying unlithified unit behaving as the upper confining unit to the UA (Bedrock Unit). The relatively flat horizontal groundwater gradient beneath the BPP, and the mostly upward vertical gradients, inconsistent upward/downward vertical gradients or flowing artesian conditions observed in the UU and UA, suggests the FAPS and neighboring ponds are not areas of increased recharge or infiltration (Ramboll, 2023b). These findings are further supported by the results of the 2022 Hydrogeologic Site Investigation included as part of a revised HCR (Ramboll, 2023b).

Data collected from previous field investigations, as well as the lithologic contact and groundwater elevation data from the 2022 Hydrogeologic Site Investigation reported in the revised HCR (Ramboll, 2023b), were used to develop the groundwater model for the 2023 BAP GMR (Ramboll, 2023a; **Appendix A**). The 2023 BAP GMR MODFLOW model was used to evaluate a closure scenario at the BAP: CCR consolidation and CIP using information provided in the CCR Surface Impoundment Final Closure Plan (Geosyntec, 2022). Since the revision to the HCR and BAP GMR was completed in 2023, additional site investigation activities in support of a forthcoming Addendum to the Nature and Extent Report, Baldwin Power Plant, Fly Ash Pond System (Ramboll, 2025a) were completed and included: the installation of four off-site monitoring wells (MW-195 through MW-198); well inspection, abandonment, replacement and development of several existing monitoring wells; installation of temporary piezometers adjacent to and east of the FAPS, and in the interior of the BAP; pump testing and/or aquifer (slug) testing at select existing monitoring wells and temporary piezometers; and stream gauging at the creek south of the FAPS. Data collected prior to October 2024 were incorporated into the groundwater model used to evaluate the FAPS corrective action alternatives for this technical memorandum.

2.3 Groundwater Quality

Groundwater monitoring in accordance with the proposed Groundwater Monitoring Plan (Ramboll, 2023c) and sampling methodologies provided in the operating permit application for the FAPS began in the second quarter of 2023. In accordance with 35 I.A.C. § 845.610(b)(3)(C) and the statistical analysis plan submitted with the operating permit application (Appendix A of the Groundwater Monitoring Plan Revision 1) constituent concentrations observed at compliance monitoring wells were evaluated for compliance with the groundwater protection standards (GWPSs) described in 35 I.A.C. § 845.600 to determine exceedances of the GWPS. The following GWPS exceedances were determined in 2024³ (Ramboll, 2024c; Ramboll, 2024d; and Ramboll, 2024e):

- Boron in MW-150, and MW-391

³ GWPS exceedances determined after January 31, 2025 will be reported in the Quarter 4, 2024 Groundwater Monitoring Data and Detected Exceedances Report.

- Fluoride in MW-384
- pH (field) in MW-253 and MW-350
- Sulfate in MW-150, MW-252, MW-253R, and MW-366

An Alternative Source Demonstration (ASD) was completed on February 6, 2024 (Geosyntec, 2024) for the pH GWPS exceedance detected at MW-253 during Quarter 3, 2023. The IEPA provided written concurrence with the ASD on March 7, 2024 (IEPA, 2024). ASDs were not completed for the boron, fluoride and sulfate GWPS exceedances listed above; therefore an assessment of corrective measures (CMA) was initiated in accordance with 35 I.A.C. § 845.660(d)(3).

3. CONCEPTUAL MODEL

3.1 Conceptual Model

The HCR Revision 1 (Ramboll, 2023b), which includes data collected during the 2022 Hydrogeologic Site Investigation, is the foundation document for the site setting and CSM that describes groundwater flow at the BPP. Additional hydrogeologic data was collected after submittal of the HCR Revision 1 during the 2024 site investigation activities completed in support of a forthcoming Addendum to the Nature and Extent Report, Baldwin Power Plant, Fly Ash Pond System (Ramboll, 2025a) and supports the CSM and model development. The FAPS overlies the recharge area for the underlying geologic media (*i.e.*, low permeability clays of the UU). Groundwater enters the model domain vertically via recharge. Groundwater may also enter or exit the model through the Cooling Pond, Secondary and Tertiary Ponds, the Kaskaskia River, or the many tributary streams located within the model domain. Groundwater may also exit the model through surface water management features within the BAP. Groundwater in the un lithified materials consistently flows east to west towards the Kaskaskia River. Groundwater flow in bedrock is northwest in the east and central areas of the BAP, and southwest to northwest on the east area of the FAPS until groundwater reaches the bedrock valley feature underlying the Secondary and Tertiary Ponds west of the BAP and FAPS, at which point the flow direction veers towards this bedrock surface low at the southwestern corner of the BPP.

Groundwater contaminant transport modeling was completed to demonstrate how the proposed corrective action alternatives will attain compliance with the applicable GWPS and minimize the potential for COCs to migrate past the site's southern property boundary, which could result in a future risk exposure pathway to off-site property owners. Boron is commonly used as an indicator parameter for contaminant transport modeling for CCR because it is commonly present in coal ash leachate and it is mobile (*i.e.*, has low rates of sorption or degradation) in groundwater. Based on geochemical modeling results (Geosyntec, 2025), remobilization of attenuated boron and sulfate is unlikely to affect the time to reach the GWPS. In addition, the Corrective Measures Assessment (Ramboll, 2024a) identified boron as an exceedance of the GWPS at FAPS monitoring wells as described in **Section 2.3** of this report. Therefore, groundwater transport modeling was completed using boron. The BAP and FAPS were modeled as sources of boron within the model domain. The BAP and FAPS are constructed over low permeability clays of the UU. Mass (boron) is added to groundwater via vertical recharge through CCR, and horizontal groundwater flow through CCR where it is in contact with the water table. Boron mass flows with groundwater (on-site groundwater flow directions described above). The primary transport pathway is the UA which underlies the FAPS and is continuous across the BPP. The UU also contains PMPs in the form of thin discontinuous sand seams within the UU or at the interface (contact) between the UU and bedrock where hydraulic conductivities are relatively higher.

3.1.1 Correlation of Boron with Sulfate

Boron is considered a surrogate for other parameters that exceed the GWPS at FAPS monitoring wells that do not have approved alternative source demonstrations (*e.g.*, sulfate) because it occurs above the GWPS in the greatest number of wells and it is the constituent at the site that will likely require the longest time to achieve the groundwater protection standard. In addition, comparison of observed sulfate to boron concentrations (**Figure A** below) indicates a statistically significant correlation between these parameters in downgradient FAP monitoring wells with exceedances. The correlation coefficient (R^2) and p values (indicator of statistical significance)

are also provided on **Figure A**. Higher R^2 values (*i.e.*, closer to 1) indicate stronger correlation between parameters. A correlation is considered statistically significant when the p value is lower than 0.05. The p value is less than the target of 0.05, indicating correlations are statistically significant. The statistically significant correlation between sulfate and boron indicates boron is an appropriate surrogate for sulfate in the groundwater model, and concentrations of sulfate are expected to change consistent with model predicted boron concentrations. Accordingly, transport modeling was performed for boron as a surrogate for potential leaching of COCs attributable to the FAPS. Additional geochemical modeling and discussion of the fate of 35 I.A.C. § 845.600 parameters is provided in the Groundwater Polishing Evaluation Report, Baldwin Power Plant, Fly Ash Pond System (Geosyntec, 2025), Nature and Extent Report, Baldwin Power Plant, Fly Ash Pond System (Ramboll, 2024b) and the forthcoming Addendum to the Nature and Extent Report, Baldwin Power Plant, Fly Ash Pond System (Ramboll, 2025a) that discusses the behavior of all detected 845.600 params.

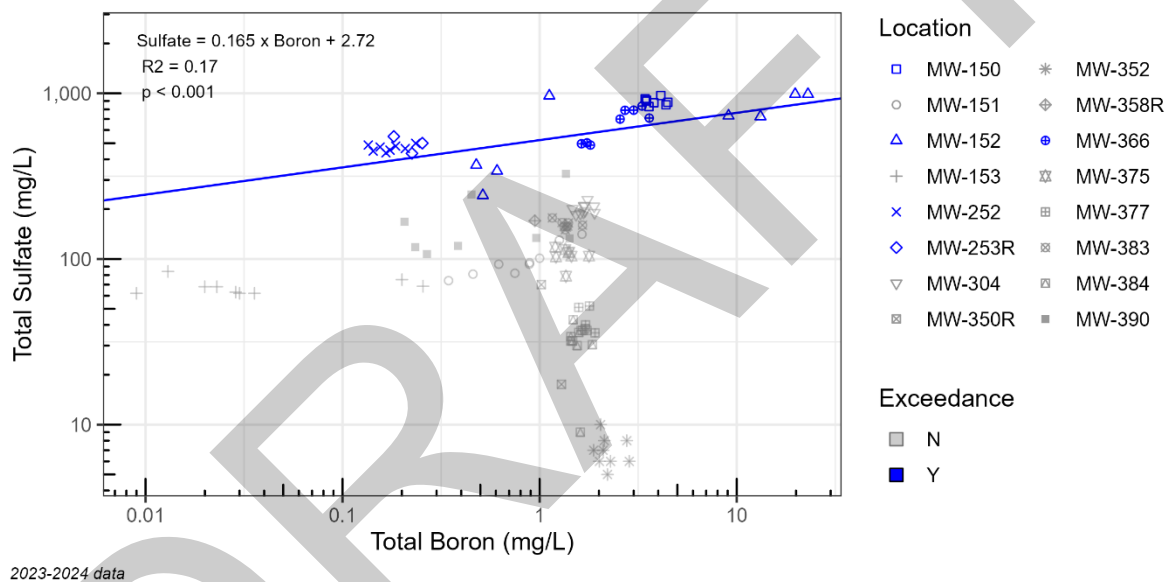


Figure A Correlation of Observed Sulfate and Boron Concentrations in Downgradient Wells (Linear regression for wells with exceedances only)

4. GROUNDWATER MODEL DEVELOPMENT AND CALIBRATION

In accordance with the requirements of 35 I.A.C. § 845, Ramboll developed MODFLOW and MT3DMS groundwater flow and transport models in 2023 for the BAP, and submitted a GMR (Ramboll, 2023a; **Appendix A**). Generally, the model boundaries, parameters, and calibration (heads, flow directions, and boron distributions) were retained for this 2024 FAPS fate and transport modeling; however, some small adjustments were made to parameter and boundary conditions to preserve model calibration (flow and transport) following updates described in **Section 2.2** (*i.e.*, the additional data collected as part of the 2024 site investigation activities in support of a forthcoming Addendum to the Nature and Extent Report, Baldwin Power Plant, Fly Ash Pond System [Ramboll, 2025a]); and head and boron concentration data collected since 2023. The objectives of the model update were to incorporate information collected since 2023 while maintaining the previous quality of calibration. Since the model update is predicated on the need to simulate additional corrective action for boron concentrations in groundwater at the site, it was important to retain to the extent practicable the previous model components and calibrations, to ensure that predicted results would be comparable to both the 2023 BAP model and the 2014 model predictions for FAPS closure.

Specifications and results of the MODFLOW/MT3DMS modeling are presented below. Electronic files containing the model inputs and outputs are provided as **Appendix B**.

4.1 Model Changes for Flow and Transport Modeling Setup and Calibration

The 2023 BAP model was used as a base model to develop a groundwater flow and transport model for the FAPS at BPP. Details of the groundwater flow model descriptions, setup (including, grid and boundary conditions, and input values and sensitivity), assumptions and limitations, and calibration results of 2023 BAP model are described in Section 5 of the GMR (Ramboll, 2023a; **Appendix A**). The following changes were made to the 2023 BAP groundwater flow and transport model in development of the 2024 FAPS groundwater flow and transport model:

- The model was updated from MODFLOW-2005 to MODFLOW-NWT. MODFLOW-NWT is a modeling program designed to solve nonlinear groundwater flow problems due to unconfined aquifer conditions and is superior in solving problems involving drying and rewetting of unconfined aquifers (Niswonger et al., 2011), which were expected for the selected corrective action alternatives. MT3DMS was retained as the transport model code.
- The FAPS model was calibrated to modified median (where anomalous groundwater elevations were first eliminated before applying the median [*e.g.*, groundwater elevations that do not represent static groundwater conditions, groundwater elevation outliers, or groundwater elevations measured in error]) groundwater elevations collected from December 2015 to July 2024. **Figure 2-3** shows the locations of groundwater monitoring wells at the BPP. Several well locations (MW-253R, MW-350R, MW-196, MW-195, MW-197) and head targets (MW-253R, MW-350R, MW-196, MW-195, MW-197, MW-373, PZ-169, PZ-170, PZ-171, PZ-172, PZ-173, PZ-174, PZ-175, PZ-176, PZ-177, PZ-178, and PZ-182) were also added to the model in the vicinity of the FAPS that were not included in the 2023 BAP model. Well locations (MW-253, MW-306, MW-350, MW-387, MW-391, and MW-307) and associated head targets (MW-253, MW-306, MW-350, and MW-307) were removed from the 2023 BAP model as the wells were abandoned and/or potentially compromised. Well MW-150 was moved from

model layer 3 to model layer 4 to improve model calibration. A summary of well locations and associated BPP groundwater flow model calibration targets is provided in **Table 4-1**.

- The FAPS model was calibrated to median groundwater total boron concentrations (except for wells where only dissolved boron data was available the median dissolved boron concentration was used as the transport model calibration target) collected from December 2015 to July 2024. **Figure 2-3** shows the locations of groundwater monitoring wells at the BPP. Several transport model concentration targets (MW-196, MW-197, MW-253R, MW-350R, OW-256, OW-257, PZ-170, PZ-174, PZ-176, PZ-178, and PZ-182) were also added to the model in the vicinity of the FAPS that were not included in the 2023 BAP model. Well transport model concentration targets (MW-203, MW-253, MW-306, MW-307, MW-350, and MW-391) were removed from the 2023 BAP model as the wells were abandoned and/or potentially compromised. A summary of well locations and associated BPP groundwater transport model calibration targets is provided in **Table 4-1**.
- The simulated river stage and associated slope of model grid cells of River boundary conditions simulating the south stream (reach 4, adjacent to the FAPS) were modified to be consistent with river elevation measurements collected during the 2024 Hydrogeologic Site Investigation and calibrate new and/or updated head calibration targets at wells along the southern property boundary. As a result of river stage elevation modification, River boundary conditions moved up or down layers to maintain river elevations above the bottom elevation of the model layer as required by the model code. River boundary conditions in layer 3 were moved to layer 4 and the original River boundary condition in layer 3 was replaced with No Flow boundary conditions to reduce model errors.
- River boundary conditions simulating the south stream (reach 4, adjacent to the FAPS) were added to model grid cells south of the West Ash Pond to simulate the potential influence of a former drainage channel identified in the area using historic pre-construction topographic maps. The addition of these River boundary conditions improved flow and transport calibration in the area south of the West Ash Pond.
- River boundary conditions simulating the Cooling Pond (reach 0) were modified to eliminate isolated areas where no River boundary conditions were present in the 2023 BAP model to reduce model errors in the FAPS model.
- River boundary conditions simulating the Kaskaskia River (reach 1) were modified by decreasing river stage and river bottom elevations to elevations that were consistent with the approximate river stage and river bottom elevations at the confluence of the simulated Kaskaskia River (reach 1) and the south stream (reach 4, adjacent to the FAPS). The revised simulated river stage for the Kaskaskia River (reach 1) continued to be within range of interpolated stage data near BPP based on New Athens, Illinois (United States Geological Survey [USGS] 5595000) and Red Bud (USGS 5595240) gaging station data as with the 2023 BAP model.
- Areas with hydraulic conductivity Zone 100 (identified in Figure 5-1 of the GMR [Ramboll, 2023a; **Appendix A**] as "Above River Boundary Condition") placed above River boundary conditions in the 2023 BAP model to improve communication between the river and the groundwater in cells above were replaced with No Flow boundary conditions in the FAPS model to reduce model errors.

- Groundwater flow model input values in the 2023 BAP model summarized in Table 5-1 of the GMR (Ramboll, 2023a) were updated as necessary to improve flow calibration in the vicinity of the FAPS. The FAPS model input values are summarized in **Table 4-2**. Sensitivity analysis of the input values was completed as part of the 2023 BAP model, the results of the sensitivity analysis is summarized in Table 5-1 of the GMR (Ramboll, 2023a; **Appendix A**).
- Groundwater transport model input values in the 2023 BAP model summarized in Table 5-2 of the GMR (Ramboll, 2023a; **Appendix A**) were updated as necessary to improve transport calibration in the vicinity of the FAPS. The FAPS model input values are summarized in **Table 4-3**. Sensitivity analysis of the input values was completed as part of the 2023 BAP model, the results of the sensitivity analysis is summarized in Table 5-3 of the GMR (Ramboll, 2023a; **Appendix A**).
- No Flow boundary conditions were added to the model in rows 1 through 11 to reduce model errors in simulated areas not relevant to flow and transport at the FAPS; and improve simulation convergence.
- Property Zone 14 (representing the spatial distribution of the PMP) including inputs for hydraulic conductivity, storage, and specific yield and porosity were modified to improve FAPS model flow and transport calibration and be consistent with data collected during the 2024 site investigation activities (e.g., field hydraulic test results, groundwater elevations, and borehole logging information).
- The model time frames were adjusted to simulate current conditions in 2024. The 2023 BAP transient transport calibration model was extended from 2022 to 2024. As in the 2023 BAP transient transport calibration model a series of two models were used in the FAPS transient transport calibration model, where transport Calibration Model 1 represented conditions before FAPS closure (1970 to 2020) and transport Calibration Model 2 represented conditions after FAPS closure in 2020.
- As described in Section 5.2.2.3 of the GMR (Ramboll, 2023a; **Appendix A**), the post-closure (after 2020) FAPS recharge rates for the Old East Ash Pond, East Fly Ash Pond, and West Fly Ash Cell (Recharge Zones 2, 3, and 4) were consistent with previous prediction modeling values used for the proposed cover system at the FAPS (NRT, 2014b, 2014c) in the 2023 BAP model. The recharge rates for the post-closure FAPS in the updated 2024 FAPS model were modified and based on updated HELP model simulations. Details of the HELP model setup and results are found in **Section 4.2** below. Like the 2023 BAP model, source concentrations are assumed to remain constant over time. Only recharge rate and Constant Head boundary conditions in the West Ash Pond (Constant Head boundary conditions used to simulate stormwater management operations in the active FAPS in Calibration Model 1 [pre-closure FAPS model] were removed in Calibration Model 2 [post-closure FAPS model]) were modified after 2020 to simulate FAPS closure.

The updated model calibration results are discussed in **Section 4.4**. The simulated groundwater elevations and boron concentrations in the transport calibration model served as the initial conditions for the prediction models described in **Section 5**.

4.2 HELP Model Setup and Results

The HELP model was developed by the USEPA. HELP is a one-dimensional hydrologic model of water movement across, into, through, and out of a landfill or soil column based on precipitation,

evapotranspiration, runoff, and the geometry and hydrogeologic properties of a layered soil and waste profile. HELP (Version 4.0; Tolaymat and Krause, 2020) was used to estimate percolation through post-closure FAPS. HELP files are included electronically (**Appendix B**), and inputs and outputs are attached to this report (**Appendix C**).

HELP input data and results are provided in **Table 4-4**. The post-closure scenario was modeled for a period of 30 years. Climatic inputs were synthetically generated using default equations developed for Belleville Scott Air Force Base, Illinois (the closest weather station included in the HELP database). Precipitation, temperature, and solar radiation was simulated based on the latitude of the FAPS. Cover system layers and CCR layer details for the post-closure FAPS included in the HELP models are based on grading plans, construction drawings, and cover system design documented in the FAPS Closure and Post-Closure Care Plan (AECOM, 2016).

HELP model results (**Table 4-4**) indicated 0.82 inches of percolation per year through the top of the FAPS cover system area. Simulation inputs and output results are presented in **Appendix C**.

4.3 Steady-State Flow Model and Transport Model Calibration

Calibration of a groundwater flow or transport model refers to the iterative process of adjusting model parameters and boundary conditions to obtain a reasonable match between observed conditions and simulation results. The primary criterion for evaluating the calibration of a groundwater flow model is the difference between observed and simulated water levels at a set of calibration targets. Calibration targets are a set of field measurements, typically groundwater elevations. For the calibration of a steady-state (time-invariant) model, the goal in selecting calibration targets is to define a set of water-level measurements that represent the average elevation of the water table or potentiometric surface at locations throughout the site. The calibration of a groundwater flow model should rely on discrete measurements of groundwater elevation to avoid the potential for interpretive bias that may result from attempting to match a contoured potentiometric surface (Konikow, 1978; Anderson and Woessner, 1992).

A model residual is defined as the calculated difference between the observed and simulated hydraulic head at a specific location (observed – simulated). Residual statistics are used to quantify and evaluate the relative fit of a model simulation to measured water level targets. The mean of model residuals is a representation of overall model bias; a value near zero is desired. The steady-state flow model and accompanying transport model were developed to represent conditions in 2024 (steady-state current conditions) and from 1970 to 2024 (transient transport modeling during operation of the impoundments and subsequent closure of the FAPS in 2020), respectively. The steady-state flow and transport model targets used in the 2023 BAP model represented conditions in 2022 and were updated for this FAPS model revision to incorporate current conditions in 2024, with the objective of a similar level of calibration (equivalent match to calibration targets) for the revised flow and transport models. Flow and transport model calibration targets and statistics are presented on **Table 4-1**. Both sets of targets were developed from data collected from December 2015 through July 2024; transport target simulated values were retrieved from the end of the model simulation (2024).

4.4 Calibration Flow and Transport Model Results

Results of the MODFLOW modeling are presented below. Electronic copies of the model files are attached to this report (**Appendix B**).

Observed and simulated heads are presented in **Figure 4-1 through Figure 4-8**. The mass balance error for the flow model was 0.00 percent and the ratio of the residual standard deviation to the range was 5.7 percent. The mass balance error for the flow model was within the target for the criteria of 1 percent and the ratio of the residual standard deviation to the range was within the target for the criteria of 10 percent. Another flow model calibration goal is that residuals are evenly distributed such that there is no bias affecting modeled flow. The observed heads are plotted versus the simulated heads and identified by layer in **Figure 4-1**. The near-linear relationship between observed and simulated values indicates that the model adequately represents the calibration dataset. The residual mean was -0.81 feet; in general, the simulated values were evenly distributed above and below the observed values. This is also illustrated for each layer in the observed versus residuals plot **Figure 4-2**. Some simulated values were overpredicted (negative values on **Figure 4-2**), where the most significant overpredicted values (exceeding 10 feet) were primarily within the UA (bedrock) of layer 6, largely at lower groundwater elevations near the Secondary and Tertiary Ponds and Kaskaskia River, near the southwest boundary of the West Ash Pond of the FAPS, or in bedrock wells screened below the decomposed bedrock. These residuals plot in the lower left quadrant of **Figure 4-2**.

The range of observed boron concentrations between December 2015 and July 2024 for the fifty-five (55) transport calibration locations are summarized in **Table 4-1**. The goals of the transport model calibration were to have predicted concentrations fall within the range of observed concentrations, and/or have predicted concentrations above and below the GWPS for boron (2 mg/L) match observed concentrations above or below the standard at each well. Eighteen (18) transport calibration locations had observed boron concentrations that ranged above and below the GWPS for boron (2 mg/L); for these locations the goal of transport model calibration was to have predicted concentrations match observed median concentrations above or below the standard at each well (for example, if the median observed concentration for a well was above the GWPS, the goal is to have predicted concentrations above the GWPS at the well). One or more of these goals were achieved at all but seven of the transport calibration location wells, specifically MW-150, MW-352, MW-356, MW-375, MW-385, OW-257, and PZ-176, where concentrations were underpredicted with the exception of MW-375, OW-257 and PZ-176 where concentrations were overpredicted (**Figure 4-9**). Calibration results are further discussed below.

- UA wells MW-352 and MW-356 were underpredicted transport calibration locations. The model simulated concentrations are below the GWPS (2 mg/L). These wells had observed boron concentrations that ranged above and below 2 mg/L with median observed concentrations only slightly above the GWPS at 2.12 and 2.02 mg/L, respectively. In other words, while the model simulated values below 2 mg/L the median observed calibration targets for these wells are very close to 2 mg/L.
- UU well MW-150 was an underpredicted transport calibration location; however, the calibrated results in this portion of the model domain are improved over the 2023 BAP model. MW-150 is located just downgradient of UU well PZ-174 which is west of the West Fly Ash Pond (Figure 2-3). Calibrated concentrations at model layer 4 monitoring wells MW-150 and PZ-174; and, model layer 3 monitoring well MW-196 were sensitive to the position of hydraulic conductivity Zone 14 (representing the PMP in model layer 3) located to the north and south of these well locations. The calibrated position of Zone 14 incorporated boring information acquired during the 2024 site investigation activities which improved the calibration for both PZ-174 and

MW-196 in this updated 2024 FAPS model. The calibration concentration for MW-150 was similar to the calibrated 2023 BAP model.

- The model under-predicts boron concentrations in UA locations MW-352, MW-356 and MW-385 where the concentrations observed (1.88 to 2.85 mg/L, 1.79 to 2.92 mg/L, and 2.45 mg/L respectively) are near the range of observed boron concentrations in upgradient bedrock wells like MW-304, where concentrations range from 1.27 to 2.16 mg/L. Since no initial concentrations were placed in the calibration model to represent the presence of boron observed in background wells, it is expected that the model may under-predict boron concentrations within the range of observed background.
- MW-385 and MW-386 are UA wells with only a single observed concentration value for calibration. MW-385 is an underpredicted UA well. MW-385 was installed in December 2015 on the former berm that was located between the active FAPS East Ash Pond and West Ash Pond. MW-385 was abandoned shortly after installation in February 2016, after collection of only one boron concentration data point. Since the data available for this well is limited, the usefulness of this location as a transport calibration point is also limited as the single data point may not be representative of current conditions. Like MW-385, MW-386 was abandoned shortly after installation, after collection of only one boron concentration data point, and was also located on the berm between the active FAPS East Ash Pond and West Ash Pond. Simulated boron concentrations at MW-386 met the calibration criteria discussed above; however, since the data available for this well is limited, like MW-385, the usefulness of this location as a transport calibration point is also limited as the single data point may not be representative of current conditions.
- UA well MW-375 was an over-predicted transport calibration location. The median target concentration is below 2 mg/L and the simulated concentration of 2.56 mg/L is greater than 2 mg/L. MW-375 had observed boron concentrations that ranged above and below 2 mg/L with a maximum concentration only slightly above the GWPS at 2.02 mg/L.
- UU well OW-257 was an over-predicted transport calibration location as it is nested with UU well OW-157 located north of the East Ash Pond of the FAPS, where the highest concentrations in the UU were observed. Simulating higher concentrations at OW-157 resulted in over-predicted transport calibration at OW-257 due to the close proximity of these two locations. It was preferred to calibrate the model to the greater of the observed boron concentrations.
- UU well PZ-176 was an over-predicted transport calibration location simulated near the limit of the simulated plume extent, where simulated concentrations in the modeled grid cell containing the well location are above the GWPS and the model grid cell immediately south of the well location are below the GWPS. Transport model calibration locations to the west (MW-151) and east (PZ-178) of PZ-176 met the calibration metrics and are below the GWPS, indicating the calibrated model accurately represents the limit of the plume extent along the southern property boundary.

The remaining 48 calibration locations had predicted concentrations that met one or more of the following goals of the transport model calibration: to have predicted concentrations fall within the range of observed concentrations; to have predicted concentrations above and below the GWPS for boron (2 mg/L) match observed concentrations observed above or below the standard at each well; and/or to have predicted concentrations above and below the GWPS for boron match observed median concentrations above or below the standard at each well. In other words, there

was a very good match between predicted and observed boron concentrations relative to wells with concentrations above and below the GWPS, for example:

- Off-site monitoring well MW-196 located southwest of the West Fly Ash Pond was calibrated to concentrations above the GWPS at the same order of magnitude as the observed concentrations above the GWPS; and, off-site monitoring well MW-197 located just downgradient of MW-196 was calibrated to concentrations below the GWPS at the same order of magnitude as the observed concentrations below the GWPS. The calibration of MW-196 and MW-197 accurately simulated the extent of the observed boron concentrations above 2 mg/L downgradient of the West Fly Ash Pond.
- UA well MW-366, located west of the FAPS, where the highest UA bedrock boron concentrations were observed, was calibrated within range of the observed values from December 2015 to July 2024. MW-366 was calibrated according to the calibration criteria described above, where observed boron concentrations at MW-366 ranged above and below the GWPS for boron (2 mg/L) with median observed concentrations below the GWPS. The calibrated value was also below the GWPS.
- UU well OW-157 located north of the East Ash Pond of the FAPS, where the highest concentrations in the UU were observed, had the highest simulated boron concentrations at BPP.

The calibration results for wells MW-196, MW-197, MW-366 and OW-157 indicate the transport calibration model was able to simulate the limits of boron above 2 mg/L along the downgradient limits of the plume and simulate the highest observed concentrations in both the UA and UU, respectively. Distribution of boron concentrations in the calibrated model are presented on **Figure 4-10 through Figure 4-15.**

5. PREDICTIVE MODELING

Prediction models were evaluated from projected remedy completion of 2028 to 1,000 years in the future (Year 3028). The objective of predictive modeling is to simulate changes in the magnitude and spatial distribution of boron concentrations in groundwater for each different corrective action. The results are used to evaluate if implementation of these actions will achieve the GWPS of 2 mg/L for boron at 23 FAPS monitoring wells and to compare the differences in spatial distribution of boron within groundwater at the site.

Twenty-three (23) downgradient FAPS monitoring wells were selected for evaluations of corrective action alternatives against the GWPS for boron (2 mg/L). Wells selected for these evaluations are as follows; MW-150, MW-151, MW-152, MW-252, MW-153, MW-253R, MW-350R, MW-352, MW-366, MW-375, MW-383, MW-384, MW-390, PZ-174, MW-196, MW-197, OW-257, MW-374, PZ-176, PZ-178, MW-377, PZ-175 and PZ-177, and referred to as FAPS monitoring wells herein. These FAPS monitoring wells were selected with an emphasis on including wells that meet at least one of the following criteria; monitoring wells downgradient of the FAPS and capable of monitoring current and future impacts associated with the FAPS, monitoring wells with a high likelihood of being included in corrective action groundwater monitoring programs for the FAPS, monitoring wells included in the current 35 I.A.C. § 845 groundwater monitoring program for the FAPS (Ramboll, 2023c), groundwater monitoring wells capable of monitoring potential impacts associated with the FAPS near the southern property boundary, and monitoring wells included as transport calibration model targets discussed in **Section 4**.

Simulated concentrations of boron were evaluated spatially using maps of combined maximum boron concentration within each layer at various points in time, and through time-series plots of boron concentrations for the FAPS monitoring wells.

5.1 Model Prediction Scenarios

The physical components of each scenario, their representation within the model, and simulation results are presented below. For all alternatives, simulation was performed by extending current conditions at the FAPS to 2028 (flow and transport calibration models). 2028 was used as the "time zero" for completion of the construction of the FAPS corrective actions for the predictive simulations of alternatives and is consistent with the model approach for the predictive simulations for the proposed CIP closure scenario at the BAP presented in the 2023 BAP GMR (Ramboll, 2023a; **Appendix A**).

The simulated BAP CIP presented in the 2023 BAP GMR includes an initial period to remove liquids from the BAP (2025 through 2027) followed by CCR removal from the western areas of the BAP, consolidation to the southeast, and eventually northeastern portions of the BAP, and construction of a cover system over the consolidated CCR. All of the following predictive simulations for the FAPS incorporated the BAP CIP model design to simulate construction and completion of consolidation and closure at the BAP as presented in the 2023 BAP GMR without changes. Discussion of corrective action performance in years assumes 2028 as the starting point for all FAPS predictive simulations of alternatives. **Figure 5-1** presents simulated boron concentrations in 2024 and 2028 (maximum concentration of boron at each location across all model layers) to illustrate the groundwater flow and transport conditions at the time of model calibration (2024, current conditions) and at the time of projected remedy completion (2028, start of prediction simulations for corrective action alternatives) for comparison.

5.1.1 Alternative 1 – Source Control with Groundwater Polishing (GWP)

The Alternative 1 remedy, source control with GWP, would include the completed source control approach which consisted of capping the waste material, after which GWP would be formally implemented. GWP is a remedial alternative that relies on natural geochemical processes and may be appropriate as recognized by the USEPA in a final policy directive for groundwater remediation (USEPA, 1999). This scenario is consistent with the closure conditions (capping of the FAPS) initially simulated in the 2014 model reports (NRT, 2014b, 2014c) and simulations developed for the closure of the bottom ash pond presented in the 2023 BAP GMR (Ramboll, 2023a; **Appendix A**) which was revised to represent current conditions at the FAPS as discussed in **Section 4**.

Simulation of GWP was performed by extending current conditions at the FAPS to 2028 during construction of the proposed closure scenario at the BAP, as described above. The current conditions were then extended for 1,000 years to complete the predictive simulation of Alternative 1. Boron concentrations at the FAPS monitoring wells are shown in **Figure 5-2**, and **Figure 5-3 to Figures 5-7** illustrate maximum boron concentrations at 25, 125, 375, 750 and 1,000 years after implementation, respectively.

Figure 5-2 presents concentrations of boron following closure at 23 of the FAPS monitoring wells for Alternative 1. The time to reach the GWPS standard for boron at these 23 FAPS monitoring well locations for Alternative 1 are also summarized in **Table 5-1**. The prediction model indicates Alternative 1 will result in boron concentrations declining below the GWPS (2 mg/L) within 260 years at 3 monitoring wells (MW-196, PZ-174 and PZ-175). Concentrations at another well (MW-197) increase after implementation for a period of time, then decrease to below the standard 311 years after implementation. These four wells are all UU monitoring wells. Three (3) monitoring wells start with and maintain levels below the GWPS for the entire 1,000-year simulation (MW-153, MW-150, and MW-253R). Following source control and GWP in Alternative 1, the GWPS was not achieved at 16 of 23 wells following the completion of the 1,000-year model simulation (**Table 5-1**).

The predicted simulations of Alternative 1 indicate the majority of downgradient wells which are initially below the GWPS are predicted to increase in concentration over time to a concentration above the GWPS within the 1,000-year simulation period. All of these wells are located in layers representing the UA with the exception of UU well PZ-178. The transport of boron in groundwater is slow due to the low permeability of the UU and UA (summarized in **Section 2.2**). Wells that have predicted increasing trends take an average of 279 years to increase to levels above the GWPS in Alternative 1. Boron concentrations in groundwater are not predicted to decrease below the GWPS at any point during the 1,000-year simulation at five (5) monitoring well locations, including wells in the UU, PMP, and UA.

Figure 5-3 to Figures 5-7 illustrate the simulated boron plume extent slowly expanding over time following implementation of Alternative 1. The calculated areas of the simulated boron plume extents are summarized in **Table 5-2** for the corrective action alternatives and includes the area of the plume extent for the calibration model (representing conditions in 2024 prior to implementation of the alternatives) for comparison. Based on the acreages included in **Table 5 2**, the area of the plume increases from 420 to 561 acres for Alternative 1.

5.1.2 Alternative 2 – Source Control with Cutoff Wall

The Alternative 2 remedy, source control with cutoff wall, would include the construction of a cutoff wall that would extend from the existing perimeter berm ground surface, which ranges from approximately 390 to 450 feet⁴ to an approximate elevation of 365 feet, with the wall keyed into the low-permeability bedrock underlying the UU/PMP. The total length of the cutoff wall would be approximately 7,000 feet, and the cutoff wall would have a maximum depth of approximately 85 feet bgs. The cutoff wall would be constructed using either a mixture of soil and bentonite or cement and bentonite and would have an expected width of 2 to 3 feet. The cutoff wall would have a hydraulic conductivity value of approximately 1×10^{-7} cm/s. The purpose of the cutoff wall would be to provide a long-term, maintenance-free physical barrier to reduce the potential for COCs to migrate past the site's southern property boundary to off-site property owners.

Model Alternative 1 was modified to include the cutoff wall located in the FAPS directly north of the southern dike wall and extending west towards the tertiary pond. The cutoff wall was simulated using the horizontal flow barrier (HFB) package in MODFLOW, with a thickness of 3 feet and a hydraulic conductivity of 1×10^{-7} cm/s. These scenarios assume no changes to the cover system installed during FAPS closure (*i.e.*, any disturbance to the existing cap on the FAPS will be remedied following cutoff wall installation). The HFB boundary conditions were placed in model layers 2 through 4 to simulate the cutoff wall extending from grade through the UU to bedrock and immediately adjacent to the FAPS along the southern boundary and extending to the tertiary pond. Simulation of the cutoff wall was performed by extending current conditions at the FAPS to 2028 during construction of the proposed CIP closure scenario at the BAP, as described in **Section 5.1**, and the cutoff wall. Following completion of construction of the cutoff wall in 2028, the Alternative 1 model was modified to simulate the cutoff wall as described above, and the simulation was run for 1,000 years to complete the predictive simulation of Alternative 2. Boron concentrations at the FAPS monitoring wells are shown in **Figure 5-8**, and **Figure 5-3 to Figures 5-7** illustrate maximum boron concentrations at 25, 125, 375, 750 and 1,000 years after implementation, respectively.

Figure 5-8 presents concentrations of boron following closure at 23 of the FAPS monitoring wells for Alternative 2. The time to reach the GWPS standard for boron at these 23 FAPS monitoring well locations for Alternative 2 are also summarized in **Table 5-3**. The prediction model indicates Alternative 2 will result in boron concentrations declining below the GWPS (2 mg/L) within 393 years at 3 monitoring wells (MW-196, PZ-174 and PZ-175). Concentrations at another well (MW-197) increase after implementation for a period of time then decrease to below the GWPS 336 years after implementation. These four wells are all UU monitoring wells. Three (3) monitoring wells start with and maintain levels below the GWPS for the entire 1,000-year simulation (MW-153, MW-150, and MW-253R). Following source control and cutoff wall in Alternative 2, the GWPS was not achieved at 16 of 23 wells following the completion of the 1,000-year model simulation (**Table 5-3**).

The predicted simulations of Alternative 2 indicate the majority of downgradient wells are initially below the GWPS but are predicted to continue to increase in concentration over time to a concentration above the GWPS within the 1,000-year simulation period. All of these wells are

⁴ All elevations referenced in this report are in the North American Vertical Datum of 1988 (NAVD88), unless otherwise noted.

located in layers representing the UA with the exception of UU well PZ-178. The transport of boron in groundwater is slow due to the low permeability UU and UA, and wells that have predicted increasing trends are taking on average 214 years to increase to levels above the GWPS in Alternative 2. Boron concentrations in groundwater are not predicted to decrease below the GWPS at any point during the 1,000-year simulation at five (5) monitoring well locations, including wells in the UU, PMP, and UA.

Figure 5-3 to Figures 5-7 illustrate the simulated boron plume extent slowly expanding over time following implementation of Alternative 2, like Alternative 1. Based on the acreages included in **Table 5-2**, the area of the plume increases from 420 to 559 acres for Alternative 2.

5.1.3 Alternative 3 – Source Control with a Groundwater Management System (GMS)

The Alternative 3 remedy, source control with groundwater management system, would include the construction of a system that actively removes liquids that are present within the interior of the FAPS. The groundwater management system would be comprised of the following components:

- An extraction trench which would remove infiltrated liquids from low-lying areas near and around the base of CCR within the interior of the FAPS.
 - The total length of the continuous trench alignment would be approximately 8,700 feet with a maximum depth of approximately 50 to 60 feet bgs.
 - The trench would be 2 to 3 feet wide and would be backfilled with highly permeable aggregate surrounding a perforated collection pipe.
 - Collection sumps would be located approximately every 500 feet along the trench alignment.
- A mechanical, electrical, and piping system to remove extracted liquids from the trenches and treat the liquids prior to discharge.
 - Liquids would be pumped from each of the sumps within the extraction trenches and routed to a collection pond constructed northwest of the FAPS for settling.
 - After settling, the liquids would be discharged to either the Kaskaskia River to the west via a new or existing NPDES outfall, and in accordance with site-specific permit requirements.

The purpose of the groundwater management system would be to provide long-term removal of liquids from the FAPS. This will reduce hydraulic head beneath the existing FAPS cover system which also reduces the potential for liquids from the FAPS to mix with groundwater and migrate past the site's southern property boundary.

Model Alternative 1 was modified to include GMS situated within the FAPS with an alignment that was configured to drain infiltrated liquids from the lowest spots within the CCR unit. Model Alternative 2 was not used because the cutoff wall is not a component of Alternative 3. In the model, the GMS was represented using the Drain package of MODFLOW, with conductance values set to 10,000 square feet per day (ft^2/d) that corresponds to hydraulic conductivity of 2.2×10^{-2} cm/sec or 62.4 ft/day to facilitate water flow. The drain stage is assumed to be 1 foot above the bottom of the CCR unit (bottom elevation of layer 1), providing sufficient space for the placement of the perforated collection pipe. The Drain boundary conditions were placed in layer 2 of the model to allow Constant Concentration boundary conditions (which represent source

concentrations in the CCR unit) to remain in layer 1 (only one boundary condition is allowed in a cell). The hydraulic conductivity of layer 1 cells above the layer 2 Drain boundary conditions was set to 3.5×10^{-3} cm/s or 10 ft/day to correspond to permeable aggregate backfill placed above the perforated collection pipes. Simulation of GMS was performed by extending current conditions at the FAPS to 2028 during construction of the proposed CIP closure scenario at the BAP, as described in **Section 5.1**, and GMS. Following completion of construction of the GMS in 2028, the Alternative 1 model was modified to simulate the GMS as described above, and the simulation was run for 1,000 years to complete the predictive simulation of Alternative 3. Boron concentrations at the FAPS monitoring wells are shown in **Figure 5-9**, and **Figure 5-3 to Figures 5-7** illustrate maximum boron concentrations at 25, 125, 375, 750 and 1,000 years after implementation, respectively.

Figure 5-9 presents concentrations of boron following closure at 23 of the FAPS monitoring wells for Alternative 3. The time to reach the GWPS standard for boron at 23 FAPS monitoring well locations for Alternative 3 are also summarized in **Table 5-4**. The prediction model indicates Alternative 3 will result in boron concentrations declining below the GWPS (2 mg/L) within 347 years at 6 monitoring wells (MW-152, PZ-177, MW-196, PZ-174, PZ-175 and PZ-176) and 770 years at another well (OW-257) where the calibrated concentration was highest among the evaluated FAPS monitoring wells. Concentrations at another three wells (MW-197, PZ-178 and MW-252) increase after implementation for a period of time then decrease to below the GWPS between 328 and 618 years after implementation. These 10 wells are UU, PMP and UA monitoring wells. Nine (9) monitoring wells start with and maintain levels below the GWPS for the entire 1,000-year simulation (including 7 wells in the UA). Following source control and GMS in Alternative 3, the GWPS was not achieved at 4 of 23 wells following the completion of the 1,000-year model simulation (**Table 5-4**).

The predicted simulations of Alternative 3 indicated three of these four downgradient wells that do not achieve GWPS within 1,000 years are initially below the GWPS but are predicted to continue to increase in concentration over time to a concentration above the GWPS within the 1,000-year simulation period. All of these wells are located in layers representing the UA. The transport of these concentrations is slow due to the low permeability UU and UA, and wells that have predicted increasing trends are taking on average 655 years to increase to levels above the GWPS in Alternative 3. One monitoring well does not show concentrations below the GWPS at any point during the 1,000-year simulation, UA monitoring well MW-375.

Figure 5-3 to Figures 5-7 illustrate the simulated boron plume extent contracting over time following implementation of Alternative 3. Based on the acreages included in **Table 5-2**, the area of the plume decreases from 420 to 193 acres for Alternative 3.

5.1.4 Closure-By-Removal (CBR) Scenario

Because the results of the Alternative 3 simulation indicated a significant number of FAPS monitoring wells (19 of 23) attain the GWPS but did not result in all wells attaining the GWPS within the 1,000-year model, a FAPS CBR prediction model was completed to evaluate the difference in boron concentrations simulated at 23 FAPS monitoring wells under both Alternative 3 (source control with GMS) and CBR (source removal) conditions. The CBR simulation is not a selected corrective action remedy and was completed only to compare and contrast the results of Alternative 3 (source control with GMS) against a scenario where the CCR within the FAPS is completely removed from the model domain (source removal).

The CBR Scenario, source removal, will include the removal of all CCR materials contained within the FAPS. The purpose of CBR is to eliminate source material and prevent future infiltration of liquids into CCR in the area of the FAPS.

Model Alternative 1 was modified to include CBR within the FAPS area. Model Alternative 2 and 3 were not used because the cutoff wall and GMS are not components of the CBR Scenario. In the model, CBR was represented by (i) applying No Flow boundary conditions in the entire FAPS footprint to simulate the absence of material in model layer 1 following CBR; (ii) setting the recharge rates within the FAPS footprint to equal ambient recharge rates; and, (iii) removing all source concentrations within the FAPS footprint following CBR (source concentrations associated with recharge zones and saturated ash cells [Constant Concentration boundary conditions]). Simulation of CBR was performed by extending current conditions at the FAPS to 2028 during construction of the proposed CIP closure scenario at the BAP, as described in **Section 5.1**, and CBR. Following completion of construction of CBR in 2028, the Alternative 1 model was modified to simulate the CBR as described above, and the simulation was run for 1,000 years to complete the predictive simulation of the CBR Scenario. For the purposes of comparison, it was assumed CBR would also be completed by 2028; however, CBR could not possibly be completed by 2028. Boron concentrations at the FAPS monitoring wells are shown in **Figure 5-10**, and **Figure 5-3 to Figures 5-7** illustrate maximum boron concentrations at 25, 125, 375, 750 and 1,000 years after implementation, respectively.

Figure 5-10 presents concentrations of boron following closure at 23 of the FAPS monitoring wells for each of the corrective action alternatives and the CBR Scenario. The time to reach the GWPS standard for boron at 23 FAPS monitoring well locations for the CBR Scenario are also summarized in **Table 5-5**. The prediction model indicates the CBR Scenario will result in boron concentrations declining below the GWPS (2 mg/L) within 168 years at 3 monitoring wells (MW-152, PZ-174, and PZ-176). Concentrations at another well (MW-252) increase after implementation for a period of time, then decrease to below the GWPS 918 years after implementation. These 4 wells are UU and UA monitoring wells. Nine (9) monitoring wells start with and maintain levels below the GWPS for the entire 1,000-year simulation (including 7 wells in the UA). Following source removal in the CBR Scenario, the GWPS was not achieved at 10 of 23 wells following the completion of the 1,000-year model simulation (**Table 5-5**).

The predicted simulations of the CBR Scenario indicated five of these ten downgradient wells are initially below the GWPS but are predicted to continue to increase in concentration over time to a concentration above the GWPS within the 1,000-year simulation period. These wells are located in layers representing the UU and UA. The transport of these concentrations is slow due to the low permeability UU and UA, and wells that have predicted increasing trends are taking on average 373 years to increase to levels above the GWPS in the CBR Scenario (two of which increase to levels above the GWPS within 30 years [UU wells MW-197 and PZ-178]). One monitoring well (MW-252) shows concentrations decreasing to concentrations below the GWPS only temporarily, between 418 and 608 years, with concentrations above the GWPS at the end of the 1,000-year simulation. Four monitoring wells in the UU, PMP, and UA (PZ-177, MW-196, PZ-175 and MW-375) do not show concentrations below the GWPS at any point during the 1,000-year simulation.

Figure 5-3 to Figures 5-7 illustrate the simulated boron plume extent contracting over time following implementation of the CBR Scenario. Based on the acreages included in **Table 5-2**, the area of the plume decreases from 420 to 387 acres for the CBR Scenario.

6. PREDICTIVE ALTERNATIVE SIMULATION RESULTS

6.1 Prediction Scenario Results Discussion

Simulations of the proposed corrective actions and the CBR Scenario were similar in that none of the three alternatives, or the CBR, demonstrated that concentrations of boron in all FAPS monitoring wells would reduce below the GWPS within the 1,000-year period. Consequently, spatial analyses were performed for each proposed corrective action and the CBR Scenario, evaluating boron concentrations at five different time intervals (25, 125, 375, 750 and 1,000 years after implementation). This comparative spatial analysis utilized maps depicting the maximum boron concentration plume extent above the GWPS for the combined simulated layers (**Figure 5-3 to Figures 5-7**), and the corresponding areas of the maximum plume extent above the GWPS for each remedial alternative. **Table 5-2** provides the quantified data for comparison of the three proposed corrective action alternatives and CBR.

6.1.1 Comparison of Corrective Action Alternatives Against the Groundwater Protection Standard (GWPS) for Boron (2 mg/L)

Comparison of predicted concentrations of boron in groundwater at the FAPS monitoring wells indicates that the time to reach GWPS at the 23 FAPS monitoring wells is similar for Alternatives 1 and 2. The 1,000-year simulations for Alternative 1 and Alternative 2 result in 7 monitoring wells attaining the GWPS (3 of which start and end below the GWPS), and 16 wells that do not attain the GWPS at the end of the simulations. **Table A** below summarizes the timeframes to attain GWPS for the FAPS monitoring wells as a percentage of the 23 FAPS monitoring wells below the GWPS for each alternative.

Table A. Progression of Simulated Timeframes to Attain GWPS in FAPS Monitoring Wells[†]

| Years [‡] After Implementation | Alternative 1: Source Control with Groundwater Polishing (GWP) | Alternative 2: Source Control with Cutoff Wall | Alternative 3: Source Control with a Groundwater Management System (GMS) | Closure-By-Removal (CBR) |
|---|--|--|--|--------------------------|
| 25 | 13% | 13% | 43% | 43% |
| 125 | 17% | 17% | 48% | 48% |
| 375 | 30% | 26% | 70% | 52% |
| 750 | 30% | 30% | 78% | 52% |
| 1,000 | 30% | 30% | 83% | 57% |

[†]: 23 wells were used to estimate time to reach GWPS in this Groundwater Modeling Technical Memorandum as described in **Section 5**.

[‡]: Years counted starting from completion of source control or source removal.

As shown in **Table A** above, Alternative 1 and Alternative 2 both indicate a maximum of 30% of FAPS monitoring wells (23 wells evaluated) attaining the GWPS by the end of the 1,000-year simulation, where Alternative 1 reaches this maximum earlier than Alternative 2. The declining and stable trends occur in Alternatives 1 and 2 as a result of reduced recharge into the FAPS following completion of the cover system. By reducing recharge, the cover system reduces percolation of solute mass from the FAPS, which decreases the boron concentration entering the

model domain. The predicted simulations of Alternatives 1 and 2 indicate the majority of downgradient wells are initially below the GWPS but are predicted to continue to increase in concentration over time to a concentration above the GWPS within the 1,000-year simulation period. The likely cause is that the cover system did not reduce heads within the FAPS enough to prevent residual groundwater boron concentrations from being pushed down into the lower hydrostratigraphic units over time. In addition, the simulated heads within the FAPS in Alternative 2 increase slightly as a result of placement of the cutoff wall along its southern boundary, which may result in an increase in the force driving impacted groundwater into the lower hydrostratigraphic units over time. The transport of boron in groundwater is slow due to the low permeability UU and UA, and wells that have predicted increasing trends are taking on average 279 and 214 years to increase to levels above the GWPS in Alternative 1 and Alternative 2, respectively. The shorter average time to increase to levels above the GWPS observed in Alternative 2 when compared to Alternative 1 is likely related to the influence of the cutoff wall on heads within the FAPS (increased heads) and subsequent increase in force driving impacted groundwater into the lower hydrostratigraphic units over time.

The 1,000-year simulation for Alternative 3 results in 19 monitoring wells that are below the GWPS (9 of which start and end below the GWPS), and 4 wells that are above the GWPS at the end of the simulation. As shown in **Table A** above, Alternative 3 indicates a maximum of 83% of FAPS monitoring wells (23 wells evaluated) attaining the GWPS by the end of the 1,000-year simulation, where Alternative 3 indicates significantly greater progress toward attaining the GWPS than Alternative 1 and Alternative 2 in less time (10 of the wells are below the GWPS within 25 years and stay below the GWPS for the remainder of the 1,000-year simulation). The declining and stable trends occur in Alternative 3 as a result of reduced recharge into the FAPS following completion of the cover system as described above for Alternative 1, as well as the significant reduction in infiltration as a result of the GMS, which further reduces mass from entering the model domain and removes existing mass from the model domain. The simulated GMS greatly reduces head within the FAPS (increasing the number of simulated dry cells) thereby reducing the force pushing impacted groundwater into deeper hydrostratigraphic units (resulting in simulated concentrations at 7 wells remaining below GWPS in the UA). Although GMS in Alternative 3 does significantly reduce the head within the FAPS there is still higher head surrounding the FAPS that can continue to drive residual boron concentrations from the UU down into the UA. The remaining head outside the area of the FAPS is likely resulting in the continued observations of boron concentrations above the GWPS in four FAPS monitoring wells in the UA following Alternative 3.

The 1,000-year simulation results for CBR indicate 13 monitoring wells will attain the GWPS (9 of which start and end below the GWPS), and 10 wells that remain above the GWPS at the end of the simulation. CBR reduces boron concentration by reducing mass from entering the model domain (reduced to zero additional mass entering the model since the source is completely removed). As shown in **Table A** above, CBR results in a maximum of 57% of FAPS monitoring wells (23 wells evaluated) attaining the GWPS by the end of the 1,000-year simulation, where Alternative 3 results achieve greater progress toward attaining the GWPS than CBR in less time (16 of the wells attain the GWPS [70%] within 375 years for Alternative 3 versus only 13 of the wells attaining the GWPS [57%] at the end of the 1,000-year simulation for CBR due to the significant reduction in infiltration, reduced head, and mass removal following implementation of Alternative 3 discussed in detail above).

6.1.2 Spatial Analyses of Corrective Action Alternatives and Closure-By-Removal (CBR) Scenario

6.1.2.1 Spatial Comparison of Maximum Plume Extents for Corrective Action Alternatives and Closure-By-Removal (CBR) Scenario

Simulated concentrations of boron were also evaluated spatially using maps of maximum boron concentration⁵ at various points in time (**Figure 5-3 to Figures 5-7**) and their relative areas in acres are provided for comparison in **Table 5-2** for each model scenario. As illustrated in **Figure 5-3 to Figures 5-7** the maximum boron plume extents continue to expand for Alternative 1 and Alternative 2 between 25 and 1,000 years after implementation of corrective action in 2028. The maximum boron plume extent for CBR increases between 25 and 125 years after 2028, then contracts between 125 and 1,000 years after implementation. Conversely, the maximum plume extent continually contracts for Alternative 3 between 25 and 1,000 years after implementation. All scenarios indicate an increase in maximum plume extent between the calibration condition and 25 years after implementation (**Table 5-2**) as the system takes a while to respond to the implemented changes.

Alternative 1 and Alternative 2 had the largest simulated maximum plume extent at the end of the 1,000-year simulation (**Table 5-2**), where both alternatives had approximately 560-acre areas with predicted groundwater concentrations above the GWPS. CBR maximum plume extent area decreased to an area of 387 acres at the end of the 1,000-year simulation, while Alternative 3 saw further reductions in maximum plume extent to an area of 193 acres at the end of the 1,000-year simulation, representing a 50% reduction in the maximum plume extent area when compared to CBR. The area of the plume 1,000 years after implementation of Alternative 3 is also less than half the area under the calibration condition, indicating a significant decrease in the size of the plume footprint overall relative to all other modeled scenarios.

6.1.2.2 Spatial Comparison of Off-Site Maximum Plume Extents for Corrective Action Alternatives and Closure-By-Removal (CBR) Scenario

Boron concentrations have been observed above the GWPS at off-site UU monitoring well MW-196 located south of the southwest limit of the West Fly Ash Pond (the off-site well closest to the property line). The limit of these observed off-site concentrations above the GWPS were defined by the observed concentrations below the GWPS at UU monitoring well MW-197 (south of MW-196). The model representing current conditions in 2024 was calibrated to the observed off-site boron concentrations, where simulated boron concentrations at MW-196 were simulated above the GWPS and boron concentrations at MW-197 were simulated below the GWPS.

Figure 5-1 illustrates the simulated boron plume extent (including simulated off-site plume extent) for the calibrated transport model representing current conditions in 2024. As a response to the observed (MW-196) and simulated future off-site concentrations of boron above the GWPS, Ramboll will conduct a receptor survey to identify off-site properties with water wells that may be susceptible to current or future groundwater impacts related to the FAPS. The Human Health and Ecological Risk Assessment for the FAPS (Gradient, 2024) currently concludes there is no unacceptable risk to human health or the environment under present or future conditions, including all future corrective action alternatives. However, should the receptor survey indicate a

⁵ The maximum extent of boron limits illustrated on the figures were created by combining the modeled boron concentration from all layers of the model into Layer 1 of the model using the "contour maximum concentrations in Layer 1" option available in the "import model results" menu of Groundwater Vistas.

risk to mitigate, the Human Health and Ecological Risk Assessment will be revised accordingly. With the implementation of the selected corrective action alternative it is anticipated that the potential releases of CCR-related constituents, as well as exposures to these constituents in the environment, will decline over time.

A spatial comparison of the simulated off-site maximum plume extents for corrective action alternative and the CBR Scenario is found below. This analysis utilized maps depicting the maximum boron concentration plume extent above the GWPS for the combined simulated layers (**Figure 5-3 to Figures 5-7**). The relative areas of the off-site maximum boron plume extents were also evaluated and compared (**Table 5-2**).

Alternative 1 and Alternative 2 had the largest simulated off-site plume extent at the end of the 1,000-year simulation, where approximately 50-acre and 30-acre areas contained concentrations above the GWPS off-site, respectively. The combined linear distance of plume simulated along the property line at the end of the 1,000-year simulation was continuous and approximately 5,440 feet for Alternative 1 and Alternative 2. Although there were increases and decreases over time between 25 and 1,000 years after implementation, the general trend was increasing off-site maximum plume extent for Alternative 1, while Alternative 2 plateaued at approximately 30 acres of area off-site at 750 years after implementation. Alternative 2 maximum plume extent off-site was likely stabilized as a result of the cutoff wall slowing or halting continued off-site plume migration.

Alternative 3 and CBR trends in off-site maximum plume extent were similar and only varied by less than two acres during all evaluated timeframes. The areas of off-site plume extent for Alternative 3 and CBR increased to a maximum of an approximately 27-acre area of off-site maximum plume extent 750 years after implementation followed by a decrease to an approximately 20-acre area of off-site plume extent at the end of the 1,000-year simulation. These results show Alternative 3 and CBR have the smallest off-site maximum plume extent when considering long-term potential off-site impacts and the difference between Alternative 3 and CBR is negligible when considering these off-site impacts. The combined linear distance of plume simulated along the property line at the end of the 1,000-year simulation was approximately 2,790 and 2,840 feet for Alternative 3 and the CBR Scenario, respectively. This difference in the combined linear distance between Alternative 3 and the CBR Scenario was negligible. Both models indicate the longest continuous linear distance of plume extent at the property line was to the southwest of the West Fly Ash Pond between monitoring well locations MW-150 and MW-151. The remaining areas that contribute to the combined linear distance of plume simulated along the property line were south of the West Fly Ash Pond and south of the East Fly Ash Pond. A longer linear section south of the West Fly Ash Pond was simulated at the property line in the CBR Scenario. No linear distance of plume was simulated along the property line at the end of the 1,000-year simulation south of the East Fly Ash Pond for the CBR Scenario, whereas a linear distance of approximately 360 feet was simulated at the property line in Alternative 3 (note this area of the Alternative 3 plume did not cross the property line).

6.2 Post-Construction Flux Evaluations for Alternative 3

Evaluations of post-construction water flux through the FAPS CCR were completed using data obtained from the Alternative 3 prediction model when simulated post-construction heads in the FAPS monitoring wells reached equilibrium at approximately 106 years following implementation. The Calibration Model 1 (pre-closure FAPS model) and post-construction Alternative 3 prediction

model simulated water flux values are summarized in **Appendix D** and discussed below. Data export files used for flux evaluations are found along with model files in **Appendix B**.

Figure 6-1 is a plot showing the changes in flux reduction (shown as negative percentage [where positive percentage represents an increase]) over time, starting from implementation of the Alternative 3 through approximately 120 years following implementation. This was determined by comparing the simulated post-construction Alternative 3 movement of water in and out of the FAPS CCR to pre-construction conditions (Calibration Model 1 [pre-closure FAPS model]). Alternative 3 was predicted to reduce total flux in of the FAPS CCR by approximately 60 percent (%) within 2 years following implementation and flux reductions remain around 60% when heads reach post-closure equilibrium. The reduction in total flux in is predicted to exceed 60% reduction for the remaining model timeframe (maximum reduction of approximately 63%). Alternative 3 was predicted to reduce total flux out of the FAPS CCR by approximately 60% when heads reach post-closure equilibrium. The reduction in total flux out is predicted to exceed approximately 60% reduction for the remaining model timeframe (maximum reduction of approximately 62%). An initial increase was predicted for total flux out of the FAPS CCR by approximately 90% within 2 years following implementation of Alternative 3, followed by reduction of total flux by approximately 10% within approximately 8 years following implementation. The cause of the simulated initial increase is discussed in the next paragraph. The groundwater flow system reached equilibrium within approximately 106 years following implementation of Alternative 3, at which time total flux in and out are predicted to reduce by approximately 60% (**Figure 6-2**).

To determine the cause of the simulated initial increase in flux-out, a sensitivity model was developed to evaluate model construction of the GMS. As described in **Section 5**, the GMS was represented using the Drain package of MODFLOW. The drain stage is assumed to be 1 foot above the bottom of the CCR unit (bottom elevation of layer 1), providing sufficient space for the placement of the perforated collection pipe. The Drain boundary conditions were placed in layer 2 of the model to allow Constant Concentration boundary conditions (which represent source concentrations in the CCR unit) to remain in layer 1 (only one boundary condition is allowed in a cell). In the sensitivity model, Drain boundary conditions representing the GMS were moved from layer 2 to layer 1. Since only one boundary condition is allowed in a cell, overlapping Constant Concentration boundary conditions in layer 1 were deleted to allow for Drain boundary condition placement in layer 1. Drain stage of layer 1 Drain boundary conditions were modified to prevent potential model errors (drain stage cannot be lower than bottom elevation of layer 1), as necessary. **Figure 6-3** is a plot showing the sensitivity model changes in flux reduction (shown as negative percentage [where positive percentage represents an increase]) over time, starting from implementation of the Alternative 3 through approximately 120 years following implementation. The flux-in and flux-out results of the sensitivity model (**Figure 6-3**) are the inverse of the original model results (**Figure 6-1**).

The difference in flux in and out between the initial model and the sensitivity model can be attributed to the position of the Drain boundary conditions relative to the movement of water in and out of the FAPS CCR, where the initial model has Drain boundary conditions along the base of ash surface and outside of the FAPS CCR (layer 2) and the sensitivity model has Drain boundary conditions along the base of ash surface and inside of the FAPS CCR (layer 1). As Drain boundary conditions remove water from the FAPS CCR as a function of the GMS, water is prevented from moving into the FAPS CCR from layer 2 Drain boundary conditions below the

FAPS CCR in the initial model, while water is prevented from moving out of the FAPS CCR from layer 1 Drain boundary conditions within the unit in the sensitivity model. In other words, as a function of the position of the Drain boundary conditions in the model construction more water is allowed to move out of the FAPS CCR in the initial model, while more water is allowed to move into the FAPS CCR in the sensitivity model. Both models indicate a significant reduction in flux in and out of the FAPS CCR when compared to the Calibration Model 1 (pre-closure FAPS model).

When simulated post construction heads reach equilibrium in the sensitivity model the reduction in total flux in is predicted to be approximately 42% and total flux out was predicted to be reduced by approximately 73% (**Figure 6-4**). The reduction in total flux in is predicted to be approximately 50% and the reduction in total flux out is predicted to exceed 70% for the remaining model timeframe.

The groundwater flow system reaches equilibrium within approximately 106 years following implementation of the Alternative 3, at which time total flux in and out are predicted to reduce by approximately 60% for the initial model and flux in and out are predicted to reduce by approximately 42 and 73%, respectively, for the sensitivity model (**Figures 6-2 and 6-4**). Since the GMS will be removing water from the FAPS the original simulation results are more representative of the anticipated reduction in flux in (60%); and, the sensitivity simulation results are more representative of the anticipated reduction in flux out (73% reduction) that would be expected following implementation.

Based on the initial and sensitivity models, flux in and out are predicted to reduce by approximately 60% and 73%, respectively, after approximately 106 years following implementation of the Alternative 3 when heads reach post-closure equilibrium at the FAPS monitoring wells. Total flux in includes flux through the CCR (25 gpm) and the modeled Constant Head boundary conditions (3 gpm) used to simulate surface water management within the active FAPS, with no surface water management within the closed FAPS. Prior to construction of Alternative 3 (*i.e.*, Calibration Model 1 [pre-closure FAPS model]) the total groundwater flux into the CCR is the same as total flux out at approximately 28 gpm (**Appendix D**). When the groundwater system reaches post-closure equilibrium approximately 106 years following implementation of Alternative 3, the groundwater flux into and out of the CCR is also similar at approximately 11 and 8 gpm, respectively.

Simulation of Alternative 3 remedy assumed operation of the GMS. The simulated rate of liquids removal by the GMS versus time data from the flow prediction model (MODFLOW-NWT model) for Alternative 3 remedy was plotted in **Figure 6-5**. As shown in the figure, the liquids removal rate is higher at the beginning of the operation (*e.g.*, greater than 30 gpm for the first 8 years of the operation) due to higher initial groundwater elevations at the start of liquids removal. As simulated, groundwater level near the GMS decrease as operation of the GMS continues, as does the simulated rate of liquids removal. The rate of liquids removal decreases to less than 10 gpm after approximately 106 years of operation when heads at FAPS monitoring wells approach post-closure equilibrium. The minimum rate of liquids removal is predicted to be approximately 6.4 gpm at the end of the simulation.

6.3 Assessment of Geochemical Process

This groundwater flow and transport model estimates the time for boron to reach the GWPS under different potential corrective actions based on physical components of GWP. As described

in the GMR for the 2023 BAP model, it was assumed that boron would not significantly sorb or chemically react with aquifer solids (soil adsorption coefficient [Kd] was set to 0 milliliters per gram [mL/g]), which is a conservative estimate for estimating contaminant transport times.

The results of the groundwater polishing evaluation (Geosyntec, 2025), which applied geochemical modeling, indicate that chemical attenuation of boron and sulfate is feasible under current conditions through sorption to iron and aluminum oxide solids. Barite precipitation is also predicted to contribute to the chemical attenuation of sulfate. Though a small amount of desorption of boron and sulfate is predicted with background groundwater interaction, the impact of the desorption to aqueous boron and sulfate concentrations is negated by interaction with background groundwater that contains lower concentrations of both parameters. Aqueous boron and sulfate concentrations should decrease below the GWPS at all wells in the compliance monitoring system post-source control. Based on modeling results, remobilization of attenuated boron and sulfate is unlikely to affect the time to reach the GWPS.

6.4 Discussion of Long-Term Modeling Results

Potential GWPS exceedances of boron, fluoride, and sulfate have been determined at five individual active⁶ monitoring locations as of 2024 (**Section 2.3**). Results of groundwater modeling predict that more wells are likely to exceed GWPSs in the future. The modeling results presented in **Figures 5-2, 5-8, 5-9, and 5-10** illustrate predicted boron concentrations over time with the following observations:

- Alternative 3 indicates significantly greater progress toward attaining the GWPS than Alternative 1 and Alternative 2 in less time.
 - 10 of the wells are below the GWPS within 25 years and will stay below the GWPS for the remainder of the 1,000-year simulation.
- Alternative 3 results also achieve greater progress toward attaining the GWPS than CBR in less time.
 - 16 of the wells attain the GWPS within 375 years for Alternative 3 versus 13 of the wells attaining the GWPS at the end of the 1,000-year simulation for CBR.
- None of the models predict that all wells will attain the GWPS for boron within the 1,000-year timeframe, including the simulated CBR scenario.
 - This is due to the low hydraulic conductivity of the native soils (UU) and bedrock (UA); and, low groundwater flow velocities at the site.

As with all models, this groundwater flow and transport model is limited by the data used for calibration, which adequately define the local groundwater flow system and the source and extent of the plume. Since data used for calibration are near the BAP and FAPS, model predictions of transport distant spatially and temporally from the calibrated conditions at the CCR units will not be as reliable as predictions closer to the CCR units and groundwater concentrations observed between 2015 and 2024. Groundwater corrective action will include monitoring and adaptive site management which includes routine review of the CSM and decision points for making updates to the CSMs and the groundwater fate and transport models as appropriate in the future.

⁶ MW-391 was abandoned on October 9, 2024

Simulated post-construction heads in the FAPS monitoring wells reached equilibrium at approximately 106 years following implementation of corrective action alternatives and was used as a representative simulated time period for estimating future flux reductions from the FAPS (**Section 6.2**). Considering that: (1) models become increasingly less reliable as the length of time increases for predictions and (2) the model simulations indicate the groundwater flow system approaches equilibrium approximately 106 years after implementation; discussion of model results beyond 106 years should be more qualitative such as comparison between observed future trends and predicted trends, and as a tool for comparison between model simulations. Following implementation of corrective action, progress toward attainment of the GWPS will be routinely monitored and updated following the adaptive site management actions provided in the Corrective Action Groundwater Monitoring Plan, Baldwin Power Plant, Fly Ash Pond System (Ramboll, 2025b).

7. CONCLUSION

Existing site-specific three-dimensional groundwater flow (MODFLOW) and transport models (MT3DMS) were revised and employed to evaluate how the potential corrective action alternatives would achieve compliance with the applicable GWPS; to compare changes in the magnitude and spatial distribution of boron concentrations in groundwater for each different corrective action alternative; and to describe fate and transport of contaminants in accordance with 35 I.A.C. § 845.220 (c)(2) using groundwater models. Boron was selected for simulation of groundwater quality changes resulting from the FAPS and was shown to be an acceptable surrogate for modeling groundwater quality changes in other site COCs (sulfate). It was assumed that boron would not significantly sorb or chemically react with aquifer solids (K_d was set to 0 mL/g) which is a conservative estimate for predicting contaminant transport times in the model. Based on an assessment of geochemical processes at the site, remobilization of attenuated boron and sulfate is unlikely to affect the estimated times to reach the GWPS.

Three prediction models were developed to evaluate corrective action alternatives, consisting of source control with GWP (Alternative 1), cutoff wall (Alternative 2), and a groundwater management system (Alternative 3). The objective of predictive modeling is to simulate changes in the magnitude and spatial distribution of boron concentrations in groundwater for each different corrective action. The results are used to evaluate if implementation of these actions will achieve the GWPS of 2 mg/L for boron at 23 FAPS monitoring wells and to compare the differences in spatial distribution of boron within groundwater at the site.

Comparison of predicted concentrations of boron in groundwater at the FAPS monitoring wells indicates that the time to reach GWPS at the 23 FAPS monitoring wells is similar for Alternatives 1 and 2. Alternative 1 and Alternative 2 both indicate a maximum of 30% of FAPS monitoring wells (23 wells evaluated) attaining the GWPS by the end of the 1,000-year simulation. Alternative 3 indicates a maximum of 83% of FAPS monitoring wells (23 wells evaluated) attaining the GWPS by the end of the 1,000-year simulation, where Alternative 3 indicates significantly greater progress toward attaining the GWPS than Alternative 1 and Alternative 2 in less time (10 of the wells are below the GWPS within 25 years and stay below the GWPS for the remainder of the 1,000-year simulation).

Because the results of the Alternative 3 simulation did not result in all wells attaining the GWPS within the 1,000-year model, a FAPS CBR prediction model was completed to evaluate the difference in boron concentrations simulated at the 23 FAPS monitoring wells under both Alternative 3 (source control with GMS) and CBR (source removal) conditions. CBR results in a maximum of 57% of the monitoring wells attaining the GWPS by the end of the 1,000-year simulation, where Alternative 3 achieves greater progress toward attaining the GWPS than CBR in less time: 70% of the wells attain the GWPS within 375 years for Alternative 3; versus, a maximum of 57% of the wells attaining the GWPS at the end of the 1,000-year simulation for CBR.

Simulated concentrations of boron were also evaluated spatially using maps of maximum boron concentration at various points in time and their relative areas in acres for each model scenario. The maximum boron plume extents continue to expand for Alternative 1 and Alternative 2 between 25 and 1,000 years after implementation of corrective action in 2028. The maximum boron plume extent for CBR increases between 25 and 125 years after 2028, then contracts between 125 and 1,000 years after implementation. The maximum plume extent continually

contracts for Alternative 3 between 25 and 1,000 years after implementation. The area of the plume 1,000 years after implementation of Alternative 3 is also less than half the area under the calibration condition, indicating a significant improvement in the reduction of the plume footprint overall and the greatest reduction in plume footprint when compared to other scenarios.

Alternative 3 and CBR trends in off-site maximum plume extent were similar and only varied by less than two acres during all evaluated timeframes. The areas of off-site plume extent for Alternative 3 and CBR increased to a maximum of an approximately 27-acre area of off-site maximum plume extent 750 years after implementation followed by a decrease to an approximately 20-acre area of off-site plume extent at the end of the 1,000-year simulation.

Evaluations of water flux through the FAPS CCR for Alternative 3 and a sensitivity model at post-closure equilibrium indicate a reduction in total flux into the unit by 60% and a reduction in total flux out of the unit by 73%. The GMS liquids removal rate is estimated to be approximately 30 gpm for the first 8 years and decreases over time to less than 10 gpm after approximately 106 years of operation when heads at FAPS monitoring wells approach post-closure equilibrium.

Results of all groundwater modeling scenarios predict that more wells are likely to exceed GWPSs in the future than are currently observed in 2024. Alternative 3 results achieve greater progress toward attaining the GWPS in less time when compared to other corrective action alternatives, including the simulated CBR scenario. None of the models predict that all wells will attain the GWPS for boron within the 1,000-year timeframe, including the simulated CBR scenario. This is due to the low hydraulic conductivity of the native soils (UU) and bedrock (UA), and low groundwater flow velocities at the site. Simulated post-construction heads in the FAPS monitoring wells reach equilibrium at approximately 106 years following implementation of corrective action alternatives, which was used for estimating future flux reductions from the FAPS. Considering models become increasingly less reliable over extended timeframes, discussions of model results beyond 106 years should be qualitative and comparative. Following implementation of corrective action, progress toward attainment of the GWPS will be routinely monitored and updated per the adaptive site management actions, which involves routine review and potential updates to the CSM and groundwater fate and transport models as appropriate and is detailed in the Corrective Action Groundwater Monitoring Plan, Baldwin Power Plant, Fly Ash Pond System (Ramboll, 2025).

8. REFERENCES

- AECOM, 2016. Closure and Post-Closure Care Plan for the Baldwin Fly Ash Pond System at Dynegy Midwest Generation, LLC Baldwin Energy Complex, Baldwin, Illinois. March.
- Anderson, Mary P., and Woessner, William W., 1992. Applied groundwater modeling: simulation of flow and advective transport, Academic Press, Inc., San Diego, CA.
- Geosyntec Consultants, Inc. (Geosyntec), 2022. CCR Surface Impoundment Final Closure Plan, Baldwin Power Plant, Bottom Ash Pond, Baldwin, Illinois. December 12.
- Geosyntec Consultants, Inc. (Geosyntec), 2024. Alternative Source Demonstration Baldwin Power Plant Fly Ash Pond System (Unit ID #605), IEPA ID: WI578510001-01, -02, -03, 35 I.A.C. 850.650. February 6, 2024.
- Geosyntec Consultants, Inc. (Geosyntec), 2025. Groundwater Polishing Evaluation Report, Baldwin Power Plant, Fly Ash Pond System, Baldwin, Illinois. February 2025.
- Gradient Corporation (Gradient), 2024. Human Health and Ecological Risk Assessment, Fly Ash Pond System, Baldwin Power Plant, Baldwin Illinois. September 4, 2024.
- Illinois Environmental Protection Agency (IEPA), 2016. Dynegy Midwest Generation, Inc. – Baldwin Energy Complex: Baldwin Fly Ash Pond System Closure – NPDES Permit No. IL000043, letter from William Buscher (IEPA) to Rick Diericx (Dynegy Operating Company). August 16.
- Illinois Environmental Protection Agency (IEPA), 2021. Illinois Administrative Code, Title 35, Subtitle G, Chapter I, Subchapter J, Part 845: Standards for The Disposal Of Coal Combustion Residuals In Surface Impoundments, effective April 21, 2021.
- Illinois Environmental Protection Agency, "Re: Baldwin Power Plant Fly Ash Pond System," March 7, 2024.
- Konikow, L., 1978. Calibration of Groundwater Models, in Proceedings of the Specialty Conferences on Verification of Mathematical and Physical Models in Hydraulic Engineering. College Park, Maryland, August 9-11, 1978.
- Luminant, 2020. Letter to Mr. Darin LeCrone, IEPA: Baldwin Energy Complex; Old East Fly Ash Pond, East Fly Ash Pond, West Ash Pond Notification of Completion of Closure, December 17, 2020.
- Natural Resource Technology, Inc. (NRT), 2014a. Groundwater Quality Assessment and Phase II Hydrogeologic Investigation, Baldwin Ash Pond System. June 11.
- Natural Resource Technology, Inc. (NRT), 2014b. Groundwater Model and Simulation of Closure Alternatives, Baldwin Ash Pond System. June 18.
- Natural Resource Technology, Inc. (NRT), 2014c. Groundwater Model and Simulation of Closure Alternatives, Model Report Addendum Baldwin Ash Pond System. September 30.
- Natural Resource Technology, Inc. (NRT), 2016a. Hydrostatic Modeling Report, Baldwin Fly Ash Pond System Baldwin Energy Complex, Baldwin, Illinois. March 31.

Natural Resource Technology, Inc. (NRT), 2016b. Supplemental Hydrogeologic Site Characterization and Groundwater Monitoring Plan, Baldwin Fly Ash Pond System, Baldwin, Illinois. Prepared for Dynegy Midwest Generation, LLC by Natural Resource Technology, Inc. March 31.

Natural Resource Technology, Inc. (NRT), 2016c. Technical Memorandum: Baldwin Energy Complex Ash Pond Closure and Post-Closure Plan – Response to Illinois EPA Comments. August 8.

Niswonger, R.G., Panday, Sorab, and Ibaraki, Motomu, 2011. MODFLOW-NWT, A Newton formulation for MODFLOW-2005: U.S. Geological Survey Techniques and Methods 6–A37, 44 p.

Ramboll Americas Engineering Solutions, Inc. (Ramboll), 2021. Hydrogeologic Site Characterization Report. Bottom Ash Pond, Baldwin Power Plant, Baldwin, Illinois. October 25.

Ramboll Americas Engineering Solutions, Inc. (Ramboll), 2023a. Groundwater Modeling Report Revision 1, Bottom Ash Pond. Baldwin Power Plant. Baldwin, Illinois. August 1, 2023.

Ramboll Americas Engineering Solutions, Inc. (Ramboll), 2023b. Hydrogeologic Site Characterization Report Revision 1. Bottom Ash Pond, Baldwin Power Plant, Baldwin, Illinois. August 1.

Ramboll Americas Engineering Solutions, Inc. (Ramboll), 2023c. Groundwater Monitoring Plan Revision 1. Fly Ash Pond System, Baldwin Power Plant, Baldwin, Illinois. August 25.

Ramboll Americas Engineering Solutions, Inc. (Ramboll), 2024a. 35 I.A.C. § 845 Corrective Measures Assessment, Fly Ash Pond System, Baldwin Power Plant, Baldwin, Illinois. April 2024.

Ramboll Americas Engineering Solutions, Inc. (Ramboll), 2024b. Nature and Extent Report, Baldwin Power Plant, Fly Ash Pond System, IEPA No. W1578510001-01, W1578510001-02, and W1578510001-03, Baldwin, Illinois, April 2024

Ramboll Americas Engineering Solutions, Inc. (Ramboll), 2024c. Groundwater Monitoring Data and Detected Exceedances, Quarter 1 2024, Fly Ash Pond System, Baldwin Energy Complex, Baldwin, Illinois. May 10, 2024.

Ramboll Americas Engineering Solutions, Inc. (Ramboll), 2024d. Groundwater Monitoring Data and Detected Exceedances, Quarter 2 2024, Fly Ash Pond System, Baldwin Energy Complex, Baldwin, Illinois. July 19, 2024.

Ramboll Americas Engineering Solutions, Inc. (Ramboll), 2024e. Groundwater Monitoring Data and Detected Exceedances, Quarter 3 2024, Fly Ash Pond System, Baldwin Energy Complex, Baldwin, Illinois. October 25, 2024.

Ramboll Americas Engineering Solutions, Inc. (Ramboll), 2025a. Addendum to the Nature and Extent Report, Baldwin Power Plant, Fly Ash Pond System, IEPA No. W1578510001-01, W1578510001-02, and W1578510001-03, Baldwin, Illinois, 2025, *In Development*.

Ramboll Americas Engineering Solutions, Inc. (Ramboll), 2025b. Corrective Action Groundwater Monitoring Plan, Baldwin Power Plant, Fly Ash Pond System, IEPA No. W1578510001-01, W1578510001-02, and W1578510001-03, Baldwin, Illinois, 2025, *In Development*.

United States Environmental Protection Agency (USEPA), 1999. Use of Monitored Natural Attenuation at Superfund, RCRA Corrective Action, and Underground Storage Tank Sites, OSWER Directive Number 9200.4-17P, April 21, 1999.

United States Environmental Protection Agency (USEPA), 2015. Code of Federal Regulations, Title 40, Chapter I, Subchapter I, Part 257, Subpart D, Standards for the Disposal of Coal Combustion Residuals in Landfills and Surface Impoundments, April 17, 2015.

DRAFT

TABLES

DRAFT

TABLE 4-1. FLOW AND TRANSPORT MODEL CALIBRATION TARGETS

GROUNDWATER MODELING TECHNICAL MEMORANDUM
BALDWIN POWER PLANT
FLY ASH POND SYSTEM
BALDWIN, IL

| Well ID | Monitored Hydrogeologic Unit | Modeled Target Location (Layer Number) | Flow Model Target Groundwater Elevation (Modified Median Value December 2015 to July 2024 [feet NAVD88] ¹) | Transport Model Target Total Boron Concentrations December 2015 to July 2024 (mg/L) | | |
|----------|------------------------------|--|--|---|---------------------|--------------------|
| | | | | Minimum | Median | Maximum |
| MW-104DR | UU | 3 | 445.15 | 0.016 ⁴ | 0.02 ⁴ | 0.177 ⁴ |
| MW-104SR | UU | 2 | 445.22 | 0.05 ⁴ | 0.1425 ⁴ | 0.243 ⁴ |
| MW-116 | UU | 4 | 448.77 | 0.023 | 0.024 | 0.025 |
| MW-126 | UU | 2 | 459.46 | 0.0092 | 0.0106 | 0.012 |
| MW-150 | UU | 4 | 377.38 | 3.43 | 3.59 | 4.38 |
| MW-151 | UU | 5 | 394.38 | 0.345 | 0.818 | 1.26 |
| MW-152 | UU | 3 | 419.44 | 0.477 | 1.12 | 19.8 |
| MW-153 | UU | 2 | 431.88 | 0.009 | 0.02585 | 0.2 |
| MW-154 | UU | 5 | 376.93 | 0.016 ⁴ | 0.02 ⁴ | 0.056 ⁴ |
| MW-155 | UU | 3 | 373.98 | 0.0092 ⁴ | 0.02 ⁴ | 0.2 ⁴ |
| MW-158R | UU | 2 | 448.47 | 0.0254 | 0.061 | 0.0666 |
| MW-192 | UU | 2 | 428.74 | 0.01 | 0.0376 | 0.0686 |
| MW-193 | UU | 3 | 429.07 | 0.01 | 0.0496 | 0.0645 |
| MW-194 | UU | 3 | 431.03 | 0.01 | 0.021 | 0.2 |
| MW-204 | UA | 6 | 443.27 | 0.754 | 1.02 | 1.35 |
| MW-252 | UU | 5 | 422.56 | 0.135 | 0.166 | 0.235 |
| MW-253R | UU | 5 | 427.46 ³ | 0.182 | 0.182 | 0.182 |
| MW-258 | UA | 5 | 441.95 | 1.03 | 1.225 | 1.35 |
| MW-304 | UA | 6 | 445.66 | 1.27 | 1.68 | 2.16 |
| MW-350R | UA | 6 | 370.32 ³ | 1.02 | 1.02 | 1.02 |
| MW-352 | UA | 6 | 423.42 ² | 1.88 | 2.115 | 2.85 |
| MW-355 | UA | 6 | 370.34 | 0.0092 ⁴ | 0.024 ⁴ | 0.577 ⁴ |
| MW-356 | UA | 6 | 424.92 ² | 1.79 | 2.02 | 2.92 |
| MW-358 | UA | 6 | No Target | 0.142 | 1.38 | 1.67 |
| MW-366 | UA | 6 | 410.45 | 1.19 | 1.67 | 3.6 |
| MW-369 | UA | 6 | 413.31 ² | 0.232 | 0.918 | 2.4 |
| MW-370 | UA | 6 | 402.59 | 1.56 | 1.825 | 2.67 |
| MW-374 | UA | 6 | 388.64 | No Target | | |
| MW-375 | UA | 6 | 391.22 | 0.979 | 1.375 | 2.06 |
| MW-377 | UA | 6 | 416.38 | 1.54 | 1.725 | 2.01 |
| MW-382 | UA | 5 | 414.93 | 1.59 | 1.75 | 2.57 |
| MW-383 | UA | 6 | 440.48 | 1.16 | 1.395 | 2.05 |
| MW-384 | UA | 6 | 444.34 | 1.26 | 1.48 | 2.26 |
| MW-385 | UA | 6 | No Target | 2.45 | 2.45 | 2.45 |
| MW-386 | UA | 6 | No Target | 1.34 | 1.34 | 1.34 |
| MW-388 | UA | 6 | 393.27 | No Target | | |
| MW-389 | UA | 6 | 399.29 | No Target | | |
| MW-390 | UA | 6 | 419.17 | 0.175 | 0.4985 | 2.3 |
| MW-392 | UA | 6 | 428.4 | 1.57 | 1.86 | 2.7 |
| MW-393 | UA | 6 | 429.51 | 1.53 | 1.74 | 2.76 |
| MW-394 | UA | 6 | 431.78 | 1.39 | 1.8 | 2.89 |
| OW-156 | UU | 2 | 420.78 | 0.02 | 0.024 | 0.03 |
| OW-157 | UU | 2 | 426.41 | 44.6 | 45.2 | 45.3 |
| OW-256 | UU | 3 | No Target | 0.156 | 0.192 | 0.267 |
| OW-257 | UU | 5 | No Target | 0.463 | 0.509 | 0.693 |
| TPZ-164 | CCR | 1 | 431.14 | 0.922 | 1.34 | 2.04 |
| XPW01 | CCR | 1 | 427.54 | 0.563 | 0.93 | 1.03 |
| XPW02 | CCR | 1 | 433.52 | 0.87 | 1.18 | 1.52 |
| XPW04 | CCR | 1 | 426.78 | 0.835 | 1.15 | 1.38 |
| XPW05 | CCR | 1 | 432.52 | 0.828 | 1.02 | 1.57 |
| XPW06 | CCR | 1 | 415.17 | 1.55 | 2.8 | 4.64 |
| MW-196 | UU | 3 | 388.73 ³ | 3 | 3.925 | 4.85 |
| MW-195 | UU | 3 | 388.61 ³ | No Target | | |
| MW-197 | UU | 3 | 385.02 ³ | 0.0254 | 0.0309 | 0.0364 |
| MW-373 | UA | 6 | 377.36 | No Target | | |
| PZ-169 | UU | 3 | 409.56 | No Target | | |
| PZ-170 | UU | 5 | 405.93 | 0.255 | 0.286 | 0.426 |
| PZ-171 | UU | 3 | 403.5 | No Target | | |
| PZ-172 | UU | 4 | 391.78 | No Target | | |
| PZ-173 | UU | 4 | 383.16 | No Target | | |
| PZ-174 | UU | 4 | 389.04 | 4.03 | 4.03 | 4.03 |
| PZ-175 | UU | 4 | 394.97 | No Target | | |
| PZ-176 | UU | 5 | 394.52 | 1.21 | 1.21 | 1.21 |
| PZ-177 | UU | 3 | 413.89 | No Target | | |
| PZ-178 | UU | 4 | 422.12 | 0.663 | 0.663 | 0.663 |
| PZ-182 | UU | 3 | 413.43 | 0.396 | 0.484 | 0.684 |

[O: EGP 1/3/23, C: JJW 1/4/23, U: JJW 5/2/23, C: EGP 5/16/23, U:JJW 1/17/25, C: EGP 1/30/25]

TABLE 4-1. FLOW AND TRANSPORT MODEL CALIBRATION TARGETS

GROUNDWATER MODELING TECHNICAL MEMORANDUM
BALDWIN POWER PLANT
FLY ASH POND SYSTEM
BALDWIN, IL

Notes:

¹ Target groundwater elevations represent modified median groundwater elevations from December 2015 to July 2024. Anomalous groundwater elevations (e.g., groundwater elevations that do not represent static groundwater conditions, groundwater elevation outliers, or groundwater elevations measured in error) monitored between December 2015 and July 2024 were removed from the median groundwater elevation calculations used as flow calibration targets.

² Target groundwater elevation used 2022 target from 2023 Bottom Ash Pond Groundwater Modeling Report.

³ Target groundwater elevation used single value due to limited data (typically most recent measurement) for wells constructed or reoccupied in 2024.

⁴ Target boron concentration used dissolved boron data from March 2015 to July 2024.

ID = identification

mg/L = milligrams per liter

NAVD88 = North American Vertical Datum of 1988

Hydrogeologic Unit:

CCR = coal combustion residuals

UA = uppermost aquifer

UU = upper unit

DRAFT

TABLE 4-2. FLOW MODEL INPUT AND SENSITIVITY ANALYSIS RESULTS
GROUNDWATER MODELING TECHNICAL MEMORANDUM
BALDWIN POWER PLANT
FLY ASH POND SYSTEM
BALDWIN, IL

| Zone | Zone Description | Materials | ft/d | cm/s | Kh/Kv | Value Source | Sensitivity ¹ |
|-----------------------------------|--------------------------------|------------|-------------------|----------|-------|--|--------------------------|
| Horizontal Hydraulic Conductivity | | | Calibration Model | | | | |
| 1 | UU | silty clay | 0.085 | 3.00E-05 | NA | Calibrated - Near Geomean Hydraulic Conductivity Field Test Results for Wells Screened in the Upper Unit (Ramboll, 2023b) | Moderate |
| 2 | Old East Fly Ash Pond | CCR | 0.5 | 1.76E-04 | NA | Calibrated - Near Geomean of Vertical Hydraulic Conductivity Laboratory Test Results from FAPS Wells (Ramboll, 2023b) | Negligible |
| 3 | East Fly Ash Pond | CCR | 0.5 | 1.76E-04 | NA | Calibrated - Near Geomean of Vertical Hydraulic Conductivity Laboratory Test Results from FAPS Wells (Ramboll, 2023b) | Low |
| 4 | West Fly Ash Pond | CCR | 0.5 | 1.76E-04 | NA | Calibrated - Near Geomean of Vertical Hydraulic Conductivity Laboratory Test Results from FAPS Wells (Ramboll, 2023b) | Low |
| 7 | Bottom Ash Pond | CCR | 1.5 | 5.29E-04 | NA | Calibrated - Near Minimum Hydraulic Conductivity Field Test Results for Wells Screened in BAP (Ramboll, 2023b) | Moderate |
| 8 | UA (Decomposed Bedrock) | bedrock | 0.05 | 1.76E-05 | NA | Calibrated - Within Range of Hydraulic Conductivity Field Test Results for Wells Screened in Bedrock (Ramboll, 2023b) | Low |
| 9 | UA | bedrock | 0.05 | 1.76E-05 | NA | Calibrated - Within Range of Hydraulic Conductivity Field Test Results for Wells Screened in Bedrock (Ramboll, 2023b) | High |
| 10 | UU (Top of Vandalia) | silty clay | 0.085 | 3.00E-05 | NA | Calibrated - Near Geomean Hydraulic Conductivity Field Test Results for Wells Screened in the Upper Unit (Ramboll, 2023b) | Low |
| 12 | River Alluvium | silty clay | 0.1 | 3.53E-05 | NA | Calibrated | Low |
| 14 | PMP | sand seams | 2.0 | 7.06E-04 | NA | Calibrated - Near Geomean Hydraulic Conductivity Field Test Results for Wells Screened Across Upper Unit Sands (Ramboll, 2023b; Ramboll, 2025) | Moderate |
| 16 | Fill at BAP & FAPS Boundary | fill | 0.5 | 1.76E-04 | NA | Calibrated | Negligible |
| 100 | Above River Boundary Condition | NA | 500 | 1.76E-01 | NA | Calibrated - Conductivity Value to Allow Groundwater Flow to River Boundary Conditions | Negligible |
| Vertical Hydraulic Conductivity | | | Calibration Model | | | | |
| 1 | UU | silty clay | 0.0085 | 3.00E-06 | 10 | Calibrated - Within Range of Upper Unit Vertical Hydraulic Conductivity Laboratory Test Results (Ramboll, 2023b) | Moderate |
| 2 | Old East Fly Ash Pond | CCR | 0.5 | 1.76E-04 | 1 | Calibrated - Near Geomean of Vertical Hydraulic Conductivity Laboratory Test Results from FAPS Wells (Ramboll, 2023b) | Negligible |
| 3 | East Fly Ash Pond | CCR | 0.5 | 1.76E-04 | 1 | Calibrated - Near Geomean of Vertical Hydraulic Conductivity Laboratory Test Results from FAPS Wells (Ramboll, 2023b) | Negligible |
| 4 | West Fly Ash Pond | CCR | 0.5 | 1.76E-04 | 1 | Calibrated - Near Geomean of Vertical Hydraulic Conductivity Laboratory Test Results from FAPS Wells (Ramboll, 2023b) | Negligible |
| 7 | Bottom Ash Pond | CCR | 1.5 | 5.29E-04 | 1 | Calibrated - Near BAP Well TPZ-164 Vertical Hydraulic Conductivity Laboratory Test Results (Ramboll, 2023b) | Negligible |
| 8 | UA (Decomposed Bedrock) | bedrock | 0.01 | 3.53E-06 | 5 | Calibrated | Low |

TABLE 4-2. FLOW MODEL INPUT AND SENSITIVITY ANALYSIS RESULTS
GROUNDWATER MODELING TECHNICAL MEMORANDUM
BALDWIN POWER PLANT
FLY ASH POND SYSTEM
BALDWIN, IL

| Zone | Zone Description | Materials | ft/d | cm/s | Kh/Kv | Value Source | Sensitivity ¹ |
|---------------------------------|--------------------------------|------------|--|----------|-------|--|--------------------------|
| Vertical Hydraulic Conductivity | | | Calibration Model | | | | |
| 9 | UA | bedrock | 0.005 | 1.76E-06 | 10 | Calibrated | Moderate |
| 10 | UU (Top of Vandalia) | silty clay | 0.0085 | 3.00E-06 | 10 | Calibrated - Within Range of Upper Unit Vertical Hydraulic Conductivity Laboratory Test Results (Ramboll, 2023b) | Low |
| 12 | River Alluvium | silty clay | 0.1 | 3.53E-05 | 1 | Calibrated | Negligible |
| 14 | PMP | sand seams | 2.0 | 7.06E-04 | 1 | Calibrated - Near Geomean Hydraulic Conductivity Field Test Results for Wells Screened Across Upper Unit Sands (Ramboll, 2023b; Ramboll, 2025) | Negligible |
| 16 | Fill at BAP & FAPS Boundary | fill | 0.5 | 1.76E-04 | NA | Calibrated | Negligible |
| 100 | Above River Boundary Condition | NA | 500 | 1.76E-01 | 1 | Calibrated - Conductivity Value to Allow Groundwater Flow to River Boundary Conditions | Negligible |
| Zone | Zone Description | Materials | ft/d | in/year | Kh/Kv | Value Source | Sensitivity ¹ |
| Recharge | | | Calibration Model | | | | |
| 1 | Silty Clay | silty clay | 1.00E-05 | 0.04 | NA | Calibrated | Low |
| 2 | Old East Fly Ash Pond | CCR | 1.87E-04 | 0.82 | NA | HELP model output for cover system simulation based on design documented in the FAPS Closure and Post-Closure Care Plan (AECOM, 2016) | Low |
| 3 | East Fly Ash Pond | CCR | 1.87E-04 | 0.82 | NA | HELP model output for cover system simulation based on design documented in the FAPS Closure and Post-Closure Care Plan (AECOM, 2016) | Low |
| 4 | West Fly Ash Pond | CCR | 1.87E-04 | 0.82 | NA | HELP model output for cover system simulation based on design documented in the FAPS Closure and Post-Closure Care Plan (AECOM, 2016) | Low |
| 5 | Secondary Pond | silty clay | 1.00E-05 | 0.04 | NA | Calibrated | Negligible |
| 6 | Tertiary Pond | silty clay | 1.00E-05 | 0.04 | NA | Calibrated | Negligible |
| 7 | Bottom Ash Pond | CCR | 1.80E-04 | 0.79 | NA | Calibrated | Low |
| Storage | | | Not used in steady-state calibration model | | | | |
| 1 | UU | silty clay | | | | | |
| 2 | Old East Fly Ash Pond | CCR | | | | | |
| 3 | East Fly Ash Pond | CCR | | | | | |
| 4 | West Fly Ash Pond | CCR | | | | | |
| 7 | Bottom Ash Pond | CCR | | | | | |
| 8 | UA (Decomposed Bedrock) | bedrock | | | | | |
| 9 | UA | bedrock | | | | | |
| 10 | UU (Top of Vandalia) | silty clay | | | | | |
| 12 | River Alluvium | silty clay | | | | | |
| 14 | PMP | sand seams | | | | | |
| 16 | Fill at BAP & FAPS Boundary | fill | | | | | |
| 100 | Above River Boundary Condition | NA | | | | | |

TABLE 4-2. FLOW MODEL INPUT AND SENSITIVITY ANALYSIS RESULTS
GROUNDWATER MODELING TECHNICAL MEMORANDUM
BALDWIN POWER PLANT
FLY ASH POND SYSTEM
BALDWIN, IL

| River Parameters | | | | | | | |
|------------------|--|--------------------------|-----------------|-------------------------------------|-------------------------------------|---|-------------|
| | Relative Location | Stage of River (feet) | Sensitivity | River Bottom Elevation (feet) | Hydraulic Conductivity (ft/d) | Average River Conductance (ft ² /d) | Sensitivity |
| Reach 0 | Cooling Pond | 429 | Moderate | 410 | 3.80 | 3.80E+04 | Negligible |
| Reach 1 | Kaskaskia River | 368 | High | 363 | 5.17 | 5.17E+04 | Negligible |
| Reach 2 | South Stream (Southern Limit of Model Domain) | 456.03-370.27 | Negligible | 452.03-365.81 | 2.08 | 2.08E+04 | Negligible |
| Reach 3 | South Stream (Between Reach 2 and Reach 4) | 449.98-370.17 | Moderate | 447.98-368.17 | 2.05 | 2.05E+04 | Negligible |
| Reach 4 | South Stream (Adjacent to FAPS) | 440-368 | Moderately High | 438-366 | 0.36 | 3.60E+03 | Negligible |
| Reach 5 | Northwest Stream (West of Cooling Pond) | 410.66-370.38 | Negligible | 408.66-368.38 | 3.89 | 3.89E+04 | Negligible |
| Reach 7 | Northeast Stream (East of Cooling Pond) | 454.75-427.06 | High | 452.75-425.06 | 2.60 | 2.60E+04 | Negligible |
| Reach 8 | Secondary and Tertiary Pond | 396 | Low | 394.87-376.17 | 0.26 | 2.60E+03 | Negligible |

TABLE 4-2. FLOW MODEL INPUT AND SENSITIVITY ANALYSIS RESULTS
GROUNDWATER MODELING TECHNICAL MEMORANDUM
BALDWIN POWER PLANT
FLY ASH POND SYSTEM
BALDWIN, IL

| River Parameters | | | | | | | |
|--------------------------|---------------------------|---|-------------|------------|------------|------------|----|
| Value Source | NA | Calibrated - Cooling Pond Stage (Reach 0) Approximates Elevation at which Pond is Maintained; Kaskasia River Stage (Reach 1) at Baldwin Power Plant Based on Interpolated Stage Data Provided at New Athens, Illinois (USGS 5595000) and Red Bud (USGS 5595240); River Stage at Reaches 2 through 7 Approximate Topography; River Stage at Reach 8 Based on Historic Groundwater Elevation within Secondary and Tertiary Ponds at TPZ-165 | NA | Calibrated | Calibrated | Calibrated | NA |
| Constant Head Parameters | | | | | | | |
| | Relative Location | Head at Boundary (feet) | Sensitivity | | | | |
| Reach 0 | BAP Constant Head West | 415 | Negligible | | | | |
| Reach 1 | BAP Constant Head Central | 425 | Negligible | | | | |
| Value Source | NA | Calibrated - Head at Boundary Based on Estimated Water Surface Elevation within BAP | NA | | | | |

[O: EGP 1/21/25; C: JJW 1/22/25]

Notes:

¹ Sensitivity Explanation (sensitivity analysis was completed as part of the 2023 BAP Model [Ramboll, 2023a])

Negligible - SSR changed by less than 1%

Low - SSR change between 1% and 10%

Moderate - SSR change between 10% and 50%

Moderately High - SSR change between 50% and 100%

High - SSR change greater than 100%

SSR = sum of squared residuals

- - - = not tested

BAP = bottom ash pond

FAPS = fly ash pond system

cm/s = centimeters per second

ft/d = feet per day

ft²/day = feet squared per day

in/yr = inches per year

Kh/Kv = anisotropy ratio

NA = not applicable

Hydrogeologic Unit:

CCR = coal combustion residuals

PMP = potential migration pathway

UA = uppermost aquifer

UU = upper unit

References:

AECOM, 2016. Closure and Post-Closure Care Plan for the Baldwin Fly Ash Pond System at Dynegy Midwest Generation, LLC Baldwin Energy Complex, Baldwin, Illinois. March.

Ramboll Americas Engineering Solutions, Inc. (Ramboll), 2023a. Groundwater Modeling Report Revision 1, Bottom Ash Pond. Baldwin Power Plant. Baldwin, Illinois. August 1, 2023.

Ramboll Americas Engineering Solutions, Inc. (Ramboll), 2023b. Hydrogeologic Site Characterization Report Revision 1. Bottom Ash Pond, Baldwin Power Plant, Baldwin, Illinois. August 1.

Ramboll Americas Engineering Solutions, Inc. (Ramboll), 2025. Addendum to the Nature and Extent Report, Baldwin Power Plant, Fly Ash Pond System, IEPA No. W1578510001-01, W1578510001-02, and W1578510001-03, Baldwin, Illinois, 2025

Natural Resource Technology, Inc. (NRT), 2014b. Groundwater Model and Simulation of Closure Alternatives, Baldwin Ash Pond System. June 18.

Natural Resource Technology, Inc. (NRT), 2014c. Groundwater Model and Simulation of Closure Alternatives, Model Report Addendum Baldwin Ash Pond System. September 30.

TABLE 4-3. TRANSPORT MODEL INPUT VALUES (CALIBRATION)

GROUNDWATER MODELING TECHNICAL MEMORANDUM
BALDWIN POWER PLANT
FLY ASH POND SYSTEM
BALDWIN, IL

| Zone or Reach | Hydrostratigraphic Unit | Materials | Calibration Model | | | | | | Value Source | Sensitivity |
|---|---------------------------------|-----------|--|--|----------------------------------|--|--|--|--------------|-------------|
| | | | Calibration Model 1 Dates: 1970-2020 Recharge (ft/d) | Calibration Model 2 Dates: 2021-2024 Recharge (ft/d) | Boron Concentration (mg/L) | Calibration Model 1 Dates: 1970-2020 Constant Head (feet) | Calibration Model 2 Dates: 2021-2024 Constant Head (feet) | | | |
| Initial Concentration | | | | | | | | | | |
| Entire Domain | NA | NA | NA | NA | 0 | NA | NA | NA | - - - | |
| Source Concentration (recharge) | | | | | | | | | | |
| Zone 2 | Old East Fly Ash Pond | CCR | 4.00E-04 | 1.87E-04 | 38 | NA | NA | HELP model output for cover system simulation based on design documented in the FAPS Closure and Post-Closure Care Plan (AECOM, 2016a) | - - - | |
| Zone 3 | East Fly Ash Pond | CCR | 8.00E-04 | 1.87E-04 | 79 | NA | NA | HELP model output for cover system simulation based on design documented in the FAPS Closure and Post-Closure Care Plan (AECOM, 2016a) | - - - | |
| Zone 4 | West Fly Ash Pond | CCR | 6.00E-04 | 1.87E-04 | 47 | NA | NA | HELP model output for cover system simulation based on design documented in the FAPS Closure and Post-Closure Care Plan (AECOM, 2016a) | - - - | |
| Zone 7 | Bottom Ash Pond (West) | CCR | 1.80E-04 | 1.80E-04 | 4 | NA | NA | calibrated | - - - | |
| Zone 8 | Bottom Ash Pond (East) | CCR | 1.80E-04 | 1.80E-04 | 1.5 | NA | NA | calibrated | - - - | |
| Source Concentration (constant concentration cells) and Stormwater Management (constant head cells) | | | | | | | | | | |
| Reach 2 | Old East Fly Ash Pond | CCR | NA | NA | 38 | NA | NA | calibrated | - - - | |
| Reach 3 | East Fly Ash Pond | CCR | NA | NA | 79 | NA | NA | calibrated | - - - | |
| Reach 4 | West Fly Ash Pond Constant Head | CCR | NA | NA | 47 | 424.3 | NA | calibrated - head at boundary consistent with stormwater management practices within the active FAPS (AECOM, 2016b) | - - - | |
| Reach 14 | West Fly Ash Pond (Berm) | CCR | NA | NA | 47 | NA | NA | calibrated | - - - | |
| Reach 0 | BAP Constant Head West | CCR | NA | NA | 4 | 415 | 415 | calibrated - head at boundary based on estimated water surface elevation within BAP | - - - | |
| Reach 1 | BAP Constand Head Central | CCR | NA | NA | 4 | 425 | 425 | calibrated - head at boundary based on estimated water surface elevation within BAP | - - - | |
| Reach 7 | Bottom Ash Pond (West) | CCR | NA | NA | 4 | NA | NA | calibrated | - - - | |
| Reach 8 | Bottom Ash Pond (East) | CCR | NA | NA | 1.5 | NA | NA | calibrated | - - - | |

TABLE 4-3. TRANSPORT MODEL INPUT VALUES (CALIBRATION)

GROUNDWATER MODELING TECHNICAL MEMORANDUM
BALDWIN POWER PLANT
FLY ASH POND SYSTEM
BALDWIN, IL

| Storage, Specific Yield and Effective Porosity | | | | | | | |
|--|--------------------------------|------------|---------|----------------|--------------------|---|---------------------------------|
| Zone | Hydrostratigraphic Unit | Materials | Storage | Specific Yield | Effective Porosity | Value Source | Sensitivity |
| 1 | UU | silty clay | 0.003 | 0.15 | 0.15 | Storage Estimated from Literature (Fetter, 1988); Specific Yield Set Equal to Effective Porosity; Calibrated - Effective Porosity Estimated from Literature (Fetter, 1988; Morris and Johnson, 1967; Heath, 1983; Walton, 1988) | see Table 5-3 of Ramboll, 2023a |
| 2 | Old East Fly Ash Pond | CCR | 0.003 | 0.2 | 0.2 | Storage Estimated from Literature (Fetter, 1988); Specific Yield Set Equal to Effective Porosity; Calibrated - Effective Porosity Estimated from Literature (Fetter, 1988; Morris and Johnson, 1967; Heath, 1983; Walton, 1988) | see Table 5-3 of Ramboll, 2023a |
| 3 | East Fly Ash Pond | CCR | 0.003 | 0.2 | 0.2 | Storage Estimated from Literature (Fetter, 1988); Specific Yield Set Equal to Effective Porosity; Calibrated - Effective Porosity Estimated from Literature (Fetter, 1988; Morris and Johnson, 1967; Heath, 1983; Walton, 1988) | see Table 5-3 of Ramboll, 2023a |
| 4 | West Fly Ash Pond | CCR | 0.003 | 0.2 | 0.2 | Storage Estimated from Literature (Fetter, 1988); Specific Yield Set Equal to Effective Porosity; Calibrated - Effective Porosity Estimated from Literature (Fetter, 1988; Morris and Johnson, 1967; Heath, 1983; Walton, 1988) | see Table 5-3 of Ramboll, 2023a |
| 7 | Bottom Ash Pond | CCR | 0.003 | 0.25 | 0.25 | Storage Estimated from Literature (Fetter, 1988); Specific Yield Set Equal to Effective Porosity; Calibrated - Effective Porosity Estimated from Literature (Fetter, 1988; Morris and Johnson, 1967; Heath, 1983; Walton, 1988) | see Table 5-3 of Ramboll, 2023a |
| 8 | UA (Decomposed Bedrock) | bedrock | 0.003 | 0.15 | 0.15 | Storage Estimated from Literature (Fetter, 1988); Specific Yield Set Equal to Effective Porosity; Calibrated - Effective Porosity Estimated from Literature (Fetter, 1988; Morris and Johnson, 1967; Heath, 1983; Walton, 1988) | see Table 5-3 of Ramboll, 2023a |
| 9 | UA | bedrock | 0.003 | 0.3 | 0.3 | Storage Estimated from Literature (Fetter, 1988); Specific Yield Set Equal to Effective Porosity; Calibrated - Effective Porosity Estimated from Literature (Fetter, 1988; Morris and Johnson, 1967; Heath, 1983; Walton, 1988) | see Table 5-3 of Ramboll, 2023a |
| 10 | UU (Top of Vandalia) | silty clay | 0.003 | 0.15 | 0.15 | Storage Estimated from Literature (Fetter, 1988); Specific Yield Set Equal to Effective Porosity; Calibrated - Effective Porosity Estimated from Literature (Fetter, 1988; Morris and Johnson, 1967; Heath, 1983; Walton, 1988) | see Table 5-3 of Ramboll, 2023a |
| 12 | River Alluvium | silty clay | 0.003 | 0.15 | 0.15 | Storage Estimated from Literature (Fetter, 1988); Specific Yield Set Equal to Effective Porosity; Calibrated - Effective Porosity Estimated from Literature (Fetter, 1988; Morris and Johnson, 1967; Heath, 1983; Walton, 1988) | see Table 5-3 of Ramboll, 2023a |
| 14 | PMP | sand seams | 0.003 | 0.25 | 0.25 | Storage Estimated from Literature (Fetter, 1988); Specific Yield Set Equal to Effective Porosity; Calibrated - Effective Porosity Estimated from Literature (Fetter, 1988; Morris and Johnson, 1967; Heath, 1983; Walton, 1988) | see Table 5-3 of Ramboll, 2023a |
| 16 | Fill at BAP & FAPS Boundary | fill | 0.003 | 0.2 | 0.2 | Storage Estimated from Literature (Fetter, 1988); Specific Yield Set Equal to Effective Porosity; Calibrated - Effective Porosity Estimated from Literature (Fetter, 1988; Morris and Johnson, 1967; Heath, 1983; Walton, 1988) | see Table 5-3 of Ramboll, 2023a |
| 100 | Above River Boundary Condition | NA | 0.003 | 0.5 | 0.5 | Storage Estimated from Literature (Fetter, 1988); Specific Yield Set Equal to Effective Porosity; Calibrated - Effective Porosity Estimated from Literature (Fetter, 1988; Morris and Johnson, 1967; Heath, 1983; Walton, 1988) | see Table 5-3 of Ramboll, 2023a |

TABLE 4-3. TRANSPORT MODEL INPUT VALUES (CALIBRATION)

GROUNDWATER MODELING TECHNICAL MEMORANDUM
BALDWIN POWER PLANT
FLY ASH POND SYSTEM
BALDWIN, IL

| Dispersivity | | | | | | |
|-------------------|-------------------------|-----------|---------------------|-------------------|-----------------|-------------|
| Applicable Region | Hydrostratigraphic Unit | Materials | Longitudinal (feet) | Transverse (feet) | Vertical (feet) | Sensitivity |
| Entire Domain | NA | NA | 5 | 0.5 | 0.05 | - - - |

[O: EGP 1/21/25, C: JJW 1/22/25]

Notes:

¹ The concentrations from the end of the calibrated transport model were imported as initial concentrations for the prediction model runs.

² Sensitivity Explanation (sensitivity analysis was completed as part of the 2023 BAP Model [Ramboll, 2023a])

- - - = not tested
ft/d = feet per day
mg/L = milligrams per liter
NA = not applicable

Hydrogeologic Unit:

CCR = coal combustion residuals
PMP = potential migration pathway
UA = uppermost aquifer
UU = upper unit

References:

AECOM, 2016a. Closure and Post-Closure Care Plan for the Baldwin Fly Ash Pond System at Dynegy Midwest Generation, LLC Baldwin Energy Complex, Baldwin, Illinois. March.
AECOM, 2016b. RE: History of Construction, USEPA Final Rule, 40 C.F.R. § 257.73 (c), Baldwin Energy Complex, Baldwin, Illinois. October.
Fetter, C.W., 1988, Applied Hydrogeology, Merrill Publishing Company, Columbus, Ohio.
Morris, D.A and A.I. Johnson, 1967. Summary of hydrologic and physical properties of rock and soil materials as analyzed by the Hydrologic Laboratory of the U.S. Geological Survey. U.S. Geological Survey Water-Supply Paper 1839-D, 42p.
Heath, R.C., 1983. Basic ground-water hydrology, U.S. Geological Survey Water-Supply Paper 2220, 86p.
Walton, W.C., 1988. Practical Aspects of Groundwater Modeling. National Water Well Association, Worthington, Ohio.
Natural Resource Technology, Inc. (NRT), 2014b. Groundwater Model and Simulation of Closure Alternatives, Baldwin Ash Pond System. June 18.
Natural Resource Technology, Inc. (NRT), 2014c. Groundwater Model and Simulation of Closure Alternatives, Model Report Addendum Baldwin Ash Pond System. September 30.
Ramboll Americas Engineering Solutions, Inc. (Ramboll), 2023a. Groundwater Modeling Report Revision 1, Bottom Ash Pond. Baldwin Power Plant. Baldwin, Illinois. August 1, 2023.
Ramboll Americas Engineering Solutions, Inc. (Ramboll), 2023b. Hydrogeologic Site Characterization Report Revision 1. Bottom Ash Pond, Baldwin Power Plant, Baldwin, Illinois. August 1.

TABLE 4-4. HELP MODEL INPUT AND OUTPUT VALUES

GROUNDWATER MODELING TECHNICAL MEMORANDUM

BALDWIN POWER PLANT

FLY ASH POND SYSTEM

BALDWIN, IL

| Closure Scenario Number (Drainage Length) | FAPS CIP - Current Conditions | Notes |
|--|---|---|
| Input Parameter | | |
| Climate-General | | |
| City | Baldwin, IL | Nearby city to the Site within HELP database |
| Latitude | 38.18 | Site latitude |
| Evaporative Zone Depth | 6 | Estimated based on geographic location (Illinois) and uppermost soil type (Tolaymat, T. and Krause, M 2020) |
| Maximum Leaf Area Index | 4.5 | Maximum for geographic location (Illinois) (Tolaymat, T. and Krause, M, 2020) |
| Growing Season Period, Average Wind Speed, and Quarterly Relative Humidity | Belleville Scott Air Force Base, IL | Nearby city to the FAPS within HELP database |
| Number of Years for Synthetic Data Generation | 30 | |
| Temperature, Evapotranspiration, and Precipitation | Precipitation, temperature, and solar radiation was simulated based on HELP V4 weather simulation for: Lat/Long: 38.18/ -89.85 | |
| Soils-General | | |
| % where runoff possible | 100 | |
| Area (acres) | 232 | |
| Specify Initial Moisture Content | No | |
| Surface Water/Snow | Model Calculated | |

TABLE 4-4. HELP MODEL INPUT AND OUTPUT VALUES

GROUNDWATER MODELING TECHNICAL MEMORANDUM

BALDWIN POWER PLANT

FLY ASH POND SYSTEM

BALDWIN, IL

| Closure Scenario Number (Drainage Length) | FAPS CIP - Current Conditions | Notes |
|--|---|--|
| Soils-Layers | | |
| 1 | Vegetative Soil Layer (HELP Final Cover Soil [topmost layer]) | Layers details for CIP areas based on grading plans, construction drawings, and cover system design for Baldwin FAPS |
| 2 | Protective Soil Layer (HELP Vertical Percolation Layer) | |
| 3 | Unsaturated CCR Material (HELP Waste) | |
| Soil Parameters--Layer 1 | | |
| Type | 1 | Vertical Percolation Layer (Cover Soil) |
| Thickness (in) | 6 | design thickness |
| Texture | 9 | Defaults used |
| Description | Silt Loam | |
| Saturated Hydraulic Conductivity (cm/s) | 1.90E-04 | Default used for CIP area |
| Soil Parameters--Layer 2 | | |
| Type | 3 | Barrier Soil Liner; Geosynthetic Drainage Net |
| Thickness (in) | 18 | Custom used from watershed geo |
| Texture | 43 | Defaults used |
| Description | Barrier Soil | |
| Saturated Hydraulic Conductivity (cm/s) | 1.00E-07 | Custom used from watershed geo |
| Soil Parameters--Layer 3 | | |
| Type | 1 | Waste; Geomembrane Liner |
| Thickness (in) | 306.6 | design thickness |
| Texture | 83 | Defaults used |

TABLE 4-4. HELP MODEL INPUT AND OUTPUT VALUES

GROUNDWATER MODELING TECHNICAL MEMORANDUM

BALDWIN POWER PLANT

FLY ASH POND SYSTEM

BALDWIN, IL

| Closure Scenario Number (Drainage Length) | FAPS CIP - Current Conditions | Notes |
|--|---------------------------------------|---|
| Description | Unsaturated CCR Material (HELP Waste) | |
| Saturated Hydraulic Conductivity (cm/s) | 1.00E-04 | Customs used from Construction Completion and Construction Quality Assurance Report for Final Closure and watershed geo |
| Soils--Runoff | | |
| Runoff Curve Number | 80 | HELP-computed curve number |
| Slope | 1.60% | Estimated from construction design drawings |
| Length (ft) | 1290 | estimated maximum flow path |
| Vegetation | fair | fair indicating fair stand of grass on surface |
| Execution Parameters | | |
| Years | 30 | |
| Report Daily | No | |
| Report Monthly | No | |
| Report Annual | Yes | |
| Output Parameter | | |
| Unsaturated Percolation Rate (in/yr) | 0.82 | |

[OB: EGP 1/21/25; CB: JJW 1/22/25]

Notes:

% = percent

cm/s = centimeters per second

ft = feet

HELP = Hydrologic Evaluation of Landfill Performance

in = inches

in/yr = inches per year

References:

Tolaymat, T. and Krause, M, 2020. Hydrologic Evaluation of Landfill Performance: HELP 4.0 User Manual . United States Environmental Protection Agency, Washington, DC, EPA/600/B 20/219.

TABLE 5-1. SIMULATED YEARS TO ACHIEVE GWPS FOR BORON (2 MG/L) AT FAPS MONITORING WELLS FOR ALTERNATIVE 1

GROUNDWATER MODELING TECHNICAL MEMORANDUM

BALDWIN POWER PLANT

FLY ASH POND SYSTEM

BALDWIN, IL

| Alternative 1: Source Control with Groundwater Polishing (GWP) | | | | | | | |
|---|----------------------|-------------------------|-------------|---|---|---|---|
| Well | Modeled Layer | HSU | Area | Simulated Year Below GWPS (2 mg/L Boron) | Simulated Year Above GWPS (2 mg/L Boron) | Simulated Year Below GWPS (2 mg/L Boron) | Final Simulated Year Below GWPS (2 mg/L Boron) |
| MW-153 | 2 | UU | East | 0 | -- | -- | 0 |
| MW-152 | 3 | UU | South | NA | -- | -- | NA |
| PZ-177 | 3 | PMP | South | NA | -- | -- | NA |
| MW-196 | 3 | UU | South | 260 | -- | -- | 260 |
| MW-197 | 3 | UU | South | 0 | 30 | 311 | 311 |
| MW-150 | 4 | UU | South | 0 | -- | -- | 0 |
| PZ-174 | 4 | UU | South | 74 | -- | -- | 74 |
| PZ-175 | 4 | UU | South | 215 | -- | -- | 215 |
| PZ-178 | 4 | UU | South | 0 | 4 | NA | NA |
| MW-253R | 5 | UA (Decomposed Bedrock) | East | 0 | -- | -- | 0 |
| OW-257 | 5 | UA (Decomposed Bedrock) | North | NA | -- | -- | NA |
| MW-151 | 5 | UA (Decomposed Bedrock) | South | 0 | 346 | NA | NA |
| MW-252 | 5 | UA (Decomposed Bedrock) | South | 0 | 24 | NA | NA |
| PZ-176 | 5 | UA (Decomposed Bedrock) | South | NA | -- | -- | NA |
| MW-383 | 6 | UA | North | 0 | 283 | NA | NA |
| MW-384 | 6 | UA | North | 0 | 178 | NA | NA |
| MW-350R | 6 | UA | South | 0 | 826 | NA | NA |
| MW-352 | 6 | UA | South | 0 | 426 | NA | NA |
| MW-374 | 6 | UA | South | 0 | 159 | NA | NA |
| MW-375 | 6 | UA | South | NA | -- | -- | NA |
| MW-377 | 6 | UA | South | 0 | 392 | NA | NA |
| MW-366 | 6 | UA | West | 0 | 101 | NA | NA |
| MW-390 | 6 | UA | West | 0 | 328 | NA | NA |

[OB: JJW 1/21/25; C: EGP 1/30/25]

TABLE 5-1. SIMULATED YEARS TO ACHIEVE GWPS FOR BORON (2 MG/L) AT FAPS MONITORING WELLS FOR ALTERNATIVE 1

GROUNDWATER MODELING TECHNICAL MEMORANDUM

BALDWIN POWER PLANT

FLY ASH POND SYSTEM

BALDWIN, IL

Notes:

Value of "0" indicates concentration at or below GWPS at start of prediction simulation

Bold values indicate concentration at or below GWPS at end of prediction simulation

GWP = Groundwater Polishing

GWPS = Groundwater Protection Standard

HSU = hydrostratigraphic unit

mg/L = milligrams per liter

NA = not applicable, concentration does not achieve GWPS

Hydrogeologic Unit:

PMP = potential migration pathway

UA = uppermost aquifer

UU = upper unit

TABLE 5-2. MODELED BORON PLUME (2 MG/L) ACREAGES AT SELECT TIMES AFTER IMPLEMENTATION

GROUNDWATER MODELING TECHNICAL MEMORANDUM

BALDWIN POWER PLANT

FLY ASH POND SYSTEM

BALDWIN, IL

| Modeled Scenario | Years After Implementation | Modeled Boron Plume (2 mg/L) Acres | Off-Site Area of Modeled Boron Plume (2 mg/L) Acres |
|--|----------------------------|------------------------------------|---|
| Current Conditions (Calibration Model 2) | 0 | 420.25 | 9.59 |
| Alternative 1: Source Control with Groundwater Polishing (GWP) | 25 | 469.78 | 11.34 |
| | 125 | 491.53 | 15.68 |
| | 375 | 512.21 | 13.83 |
| | 750 | 542.48 | 34.37 |
| | 1000 | 560.51 | 49.32 |
| Alternative 2: Source Control with Cutoff Wall | 25 | 468.22 | 11.20 |
| | 125 | 489.24 | 15.21 |
| | 375 | 511.67 | 14.45 |
| | 750 | 543.05 | 31.91 |
| | 1000 | 558.85 | 31.91 |
| Alternative 3: Source Control with Groundwater Management System (GMS) | 25 | 465.20 | 11.26 |
| | 125 | 435.11 | 15.86 |
| | 375 | 323.07 | 17.30 |
| | 750 | 234.62 | 26.11 |
| | 1000 | 192.66 | 19.41 |
| Closure By Removal (CBR) | 25 | 465.43 | 11.24 |
| | 125 | 474.32 | 15.49 |
| | 375 | 455.02 | 19.06 |
| | 750 | 419.40 | 26.64 |
| | 1000 | 387.02 | 18.35 |

[OB: JJW 1/21/25; CB: EGP 1/30/25]

Notes:

CBR = closure-by-removal

GMS = Groundwater Management System

GWP = Groundwater Polishing

GWPS = Groundwater Protection Standard

mg/L = milligrams per liter

TABLE 5-3. SIMULATED YEARS TO ACHIEVE GWPS FOR BORON (2 MG/L) AT FAPS MONITORING WELLS FOR ALTERNATIVE 2

GROUNDWATER MODELING TECHNICAL MEMORANDUM

BALDWIN POWER PLANT

FLY ASH POND SYSTEM

BALDWIN, IL

| Alternative 2: Source Control with Cutoff Wall | | | | | | | |
|--|---------------|-------------------------|-------|--|--|--|--|
| Well | Modeled Layer | HSU | Area | Simulated Year Below GWPS (2 mg/L Boron) | Simulated Year Above GWPS (2 mg/L Boron) | Simulated Year Below GWPS (2 mg/L Boron) | Final Simulated Year Below GWPS (2 mg/L Boron) |
| MW-153 | 2 | UU | East | 0 | -- | -- | 0 |
| MW-152 | 3 | UU | South | NA | -- | -- | NA |
| PZ-177 | 3 | PMP | South | NA | -- | -- | NA |
| MW-196 | 3 | UU | South | 296 | -- | -- | 296 |
| MW-197 | 3 | UU | South | 0 | 30 | 336 | 336 |
| MW-150 | 4 | UU | South | 0 | -- | -- | 0 |
| PZ-174 | 4 | UU | South | 80 | -- | -- | 80 |
| PZ-175 | 4 | UU | South | 393 | -- | -- | 393 |
| PZ-178 | 4 | UU | South | 0 | 18 | NA | NA |
| MW-253R | 5 | UA (Decomposed Bedrock) | East | 0 | -- | -- | 0 |
| OW-257 | 5 | UA (Decomposed Bedrock) | North | NA | -- | -- | NA |
| MW-151 | 5 | UA (Decomposed Bedrock) | South | 0 | 284 | NA | NA |
| MW-252 | 5 | UA (Decomposed Bedrock) | South | 0 | 46 | NA | NA |
| PZ-176 | 5 | UA (Decomposed Bedrock) | South | NA | -- | -- | NA |
| MW-383 | 6 | UA | North | 0 | 282 | NA | NA |
| MW-384 | 6 | UA | North | 0 | 173 | NA | NA |
| MW-350R | 6 | UA | South | 0 | 520 | NA | NA |
| MW-352 | 6 | UA | South | 0 | 261 | NA | NA |
| MW-374 | 6 | UA | South | 0 | 158 | NA | NA |
| MW-375 | 6 | UA | South | NA | -- | -- | NA |
| MW-377 | 6 | UA | South | 0 | 216 | NA | NA |
| MW-366 | 6 | UA | West | 0 | 94 | NA | NA |
| MW-390 | 6 | UA | West | 0 | 298 | NA | NA |

[OB: JJW 1/21/25; C: EGP 1/30/25]

TABLE 5-3. SIMULATED YEARS TO ACHIEVE GWPS FOR BORON (2 MG/L) AT FAPS MONITORING WELLS FOR ALTERNATIVE 2

GROUNDWATER MODELING TECHNICAL MEMORANDUM

BALDWIN POWER PLANT

FLY ASH POND SYSTEM

BALDWIN, IL

Notes:

Value of "0" indicates concentration at or below GWPS at start of prediction simulation

Bold values indicate concentration at or below GWPS at end of prediction simulation

GWPS = Groundwater Protection Standard

HSU = hydrostratigraphic unit

mg/L = milligrams per liter

NA = not applicable, concentration does not achieve GWPS

Hydrogeologic Unit:

PMP = potential migration pathway

UA = uppermost aquifer

UU = upper unit

DRAFT

TABLE 5-4. SIMULATED YEARS TO ACHIEVE GWPS FOR BORON (2 MG/L) AT FAPS MONITORING WELLS FOR ALTERNATIVE 3

GROUNDWATER MODELING TECHNICAL MEMORANDUM

BALDWIN POWER PLANT

FLY ASH POND SYSTEM

BALDWIN, IL

| Alternative 3: Source Control with Groundwater Management System (GMS) | | | | | | | |
|---|----------------------|-------------------------|-------------|---|---|---|---|
| Well | Modeled Layer | HSU | Area | Simulated Year Below GWPS (2 mg/L Boron) | Simulated Year Above GWPS (2 mg/L Boron) | Simulated Year Below GWPS (2 mg/L Boron) | Final Simulated Year Below GWPS (2 mg/L Boron) |
| MW-153 | 2 | UU | East | 0 | -- | -- | 0 |
| MW-152 | 3 | UU | South | 216 | -- | -- | 216 |
| PZ-177 | 3 | PMP | South | 347 | -- | -- | 347 |
| MW-196 | 3 | UU | South | 266 | -- | -- | 266 |
| MW-197 | 3 | UU | South | 0 | 30 | 328 | 328 |
| MW-150 | 4 | UU | South | 0 | -- | -- | 0 |
| PZ-174 | 4 | UU | South | 72 | -- | -- | 72 |
| PZ-175 | 4 | UU | South | 182 | -- | -- | 182 |
| PZ-178 | 4 | UU | South | 0 | 4 | 468 | 468 |
| MW-253R | 5 | UA (Decomposed Bedrock) | East | 0 | -- | -- | 0 |
| OW-257 | 5 | UA (Decomposed Bedrock) | North | 770 | -- | -- | 770 |
| MW-151 | 5 | UA (Decomposed Bedrock) | South | 0 | -- | -- | 0 |
| MW-252 | 5 | UA (Decomposed Bedrock) | South | 0 | 26 | 618 | 618 |
| PZ-176 | 5 | UA (Decomposed Bedrock) | South | 16 | -- | -- | 16 |
| MW-383 | 6 | UA | North | 0 | -- | -- | 0 |
| MW-384 | 6 | UA | North | 0 | -- | -- | 0 |
| MW-350R | 6 | UA | South | 0 | -- | -- | 0 |
| MW-352 | 6 | UA | South | 0 | 815 | NA | NA |
| MW-374 | 6 | UA | South | 0 | 170 | NA | NA |
| MW-375 | 6 | UA | South | NA | -- | -- | NA |
| MW-377 | 6 | UA | South | 0 | -- | -- | 0 |
| MW-366 | 6 | UA | West | 0 | -- | -- | 0 |
| MW-390 | 6 | UA | West | 0 | 980 | NA | NA |

[OB: JJW 1/21/25; C: EGP 1/30/25]

TABLE 5-4. SIMULATED YEARS TO ACHIEVE GWPS FOR BORON (2 MG/L) AT FAPS MONITORING WELLS FOR ALTERNATIVE 3

GROUNDWATER MODELING TECHNICAL MEMORANDUM

BALDWIN POWER PLANT

FLY ASH POND SYSTEM

BALDWIN, IL

Notes:

Value of "0" indicates concentration at or below GWPS at start of prediction simulation

Bold values indicate concentration at or below GWPS at end of prediction simulation

GMS = Groundwater Management System

GWPS = Groundwater Protection Standard

HSU = hydrostratigraphic unit

mg/L = milligrams per liter

NA = not applicable, concentration does not achieve GWPS

Hydrogeologic Unit:

PMP = potential migration pathway

UA = uppermost aquifer

UU = upper unit

TABLE 5-5. SIMULATED YEARS TO ACHIEVE GWPS FOR BORON (2 MG/L) AT FAPS MONITORING WELLS FOR CBR SCENARIO

GROUNDWATER MODELING TECHNICAL MEMORANDUM

BALDWIN POWER PLANT

FLY ASH POND SYSTEM

BALDWIN, IL

| Closure By Removal (CBR) | | | | | | | |
|--------------------------|---------------|-------------------------|-------|--|--|--|--|
| Well | Modeled Layer | HSU | Area | Simulated Year Below GWPS (2 mg/L Boron) | Simulated Year Above GWPS (2 mg/L Boron) | Simulated Year Below GWPS (2 mg/L Boron) | Final Simulated Year Below GWPS (2 mg/L Boron) |
| MW-153 | 2 | UU | East | 0 | -- | -- | 0 |
| MW-152 | 3 | UU | South | 168 | -- | -- | 168 |
| PZ-177 | 3 | PMP | South | NA | -- | -- | NA |
| MW-196 | 3 | UU | South | NA | -- | -- | NA |
| MW-197 | 3 | UU | South | 0 | 30 | NA | NA |
| MW-150 | 4 | UU | South | 0 | -- | -- | 0 |
| PZ-174 | 4 | UU | South | 66 | -- | -- | 66 |
| PZ-175 | 4 | UU | South | NA | -- | -- | NA |
| PZ-178 | 4 | UU | South | 0 | 8 | NA | NA |
| MW-253R | 5 | UA (Decomposed Bedrock) | East | 0 | -- | -- | 0 |
| OW-257 | 5 | UA (Decomposed Bedrock) | North | 418 | 608 | NA | NA |
| MW-151 | 5 | UA (Decomposed Bedrock) | South | 0 | -- | -- | 0 |
| MW-252 | 5 | UA (Decomposed Bedrock) | South | 0 | 276 | 918 | 918 |
| PZ-176 | 5 | UA (Decomposed Bedrock) | South | 22 | -- | -- | 22 |
| MW-383 | 6 | UA | North | 0 | -- | -- | 0 |
| MW-384 | 6 | UA | North | 0 | -- | -- | 0 |
| MW-350R | 6 | UA | South | 0 | 732 | NA | NA |
| MW-352 | 6 | UA | South | 0 | 910 | NA | NA |
| MW-374 | 6 | UA | South | 0 | 185 | NA | NA |
| MW-375 | 6 | UA | South | NA | -- | -- | NA |
| MW-377 | 6 | UA | South | 0 | -- | -- | 0 |
| MW-366 | 6 | UA | West | 0 | -- | -- | 0 |
| MW-390 | 6 | UA | West | 0 | -- | -- | 0 |

[OB: JJW 1/21/25; C: EGP 1/30/25]

TABLE 5-5. SIMULATED YEARS TO ACHIEVE GWPS FOR BORON (2 MG/L) AT FAPS MONITORING WELLS FOR CBR SCENARIO

GROUNDWATER MODELING TECHNICAL MEMORANDUM

BALDWIN POWER PLANT

FLY ASH POND SYSTEM

BALDWIN, IL

Notes:

Value of "0" indicates concentration at or below GWPS at start of prediction simulation

Bold values indicate concentration at or below GWPS at end of prediction simulation

CBR = closure-by-removal

GWPS = Groundwater Protection Standard

HSU = hydrostratigraphic unit

mg/L = milligrams per liter

NA = not applicable, concentration does not achieve GWPS

Hydrogeologic Unit:

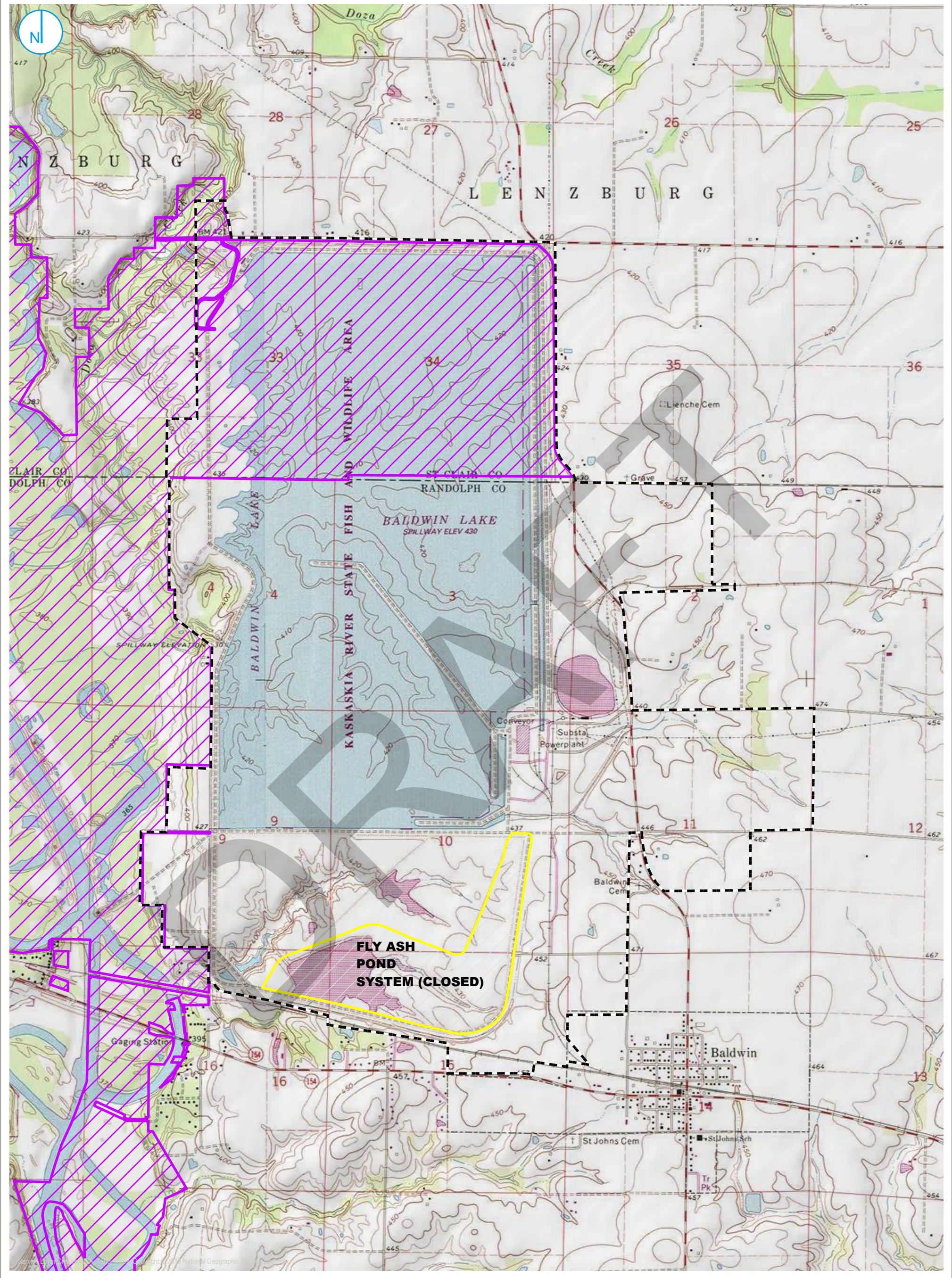
PMP = potential migration pathway

UA = uppermost aquifer

UU = upper unit

FIGURES

DRAFT



- REGULATED UNIT (SUBJECT UNIT)
- PROPERTY BOUNDARY
- KASKASKIA RIVER STATE FISH AND WILDLIFE AREA

SOURCE NOTE
I-View, Prairie State Conservation Coalition accessed via Illinois Department of Natural Resources Division of Natural Heritage Website
<https://www2.illinois.gov/sites/naturalheritage/DataResearch/Pages/Access-Our-Data.aspx>

0 1,000 2,000
Feet

SITE LOCATION MAP

FIGURE 2-1

PROJECT: 169000XXXX | DATED: 1/17/2025 | DESIGNER: GALARINIC
Y:\Mapping\Projects\22\2285\MXDCAAA_SIR\Baldwin\FAP\Modelling\TechMemo.aprx\Figure 2-2, Site Map



- REGULATED UNIT (SUBJECT UNIT)
- SITE FEATURE
- CAPPED AREA
- PROPERTY BOUNDARY

0 400 800 Feet

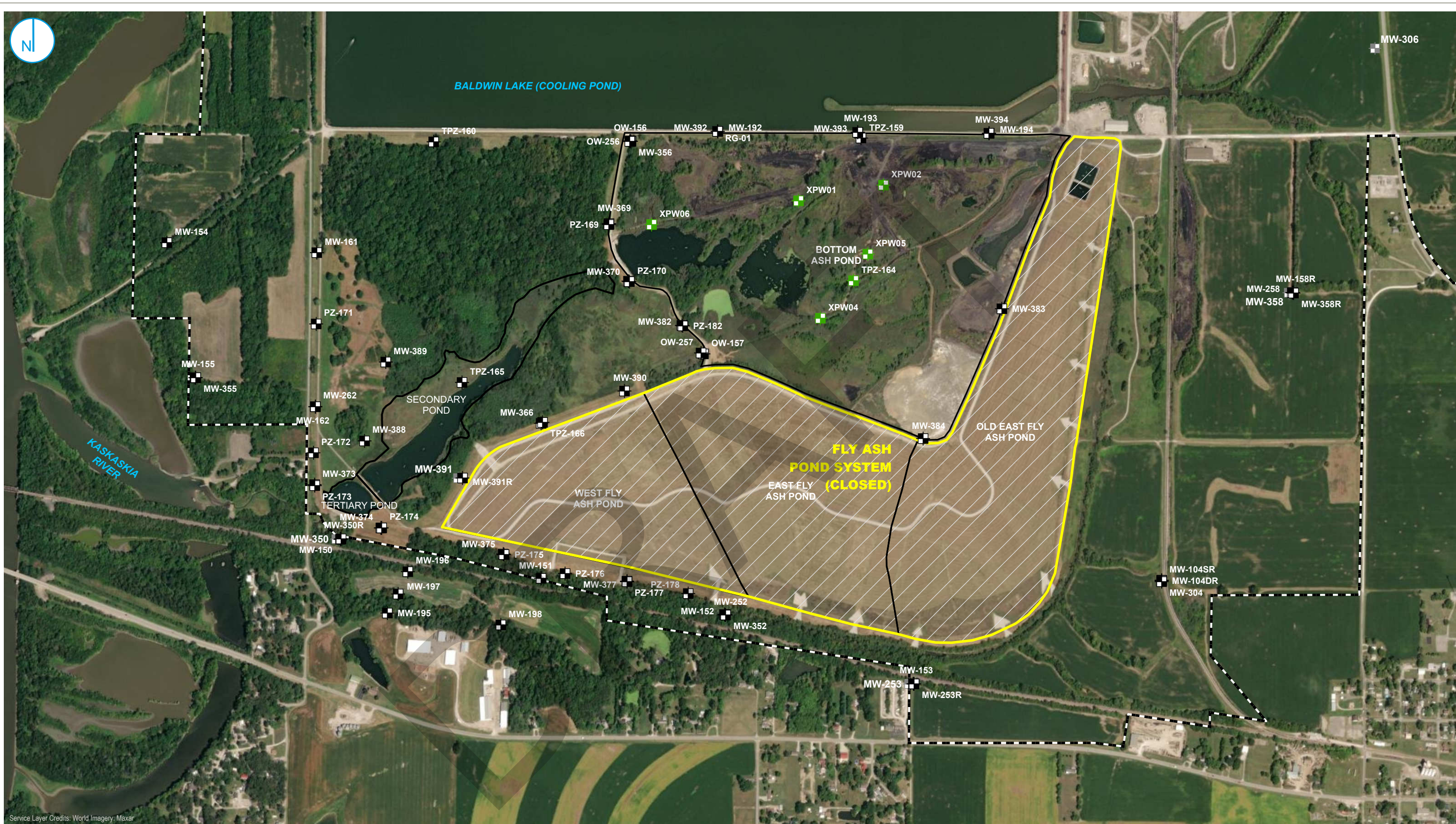
SITE MAP

GROUNDWATER MODELING TECHNICAL MEMORANDUM
FLY ASH POND SYSTEM
BALDWIN POWER PLANT
BALDWIN, ILLINOIS

FIGURE 2-2

RAMBOLL AMERICAS
ENGINEERING SOLUTIONS, INC.





- MONITORING WELL
- POREWATER WELL
- RAIN GAGE
- MONITORING WELL CLOSED IN 2024
- REGULATED UNIT (SUBJECT UNIT)
- SITE FEATURE
- CAPPED AREA
- PROPERTY BOUNDARY



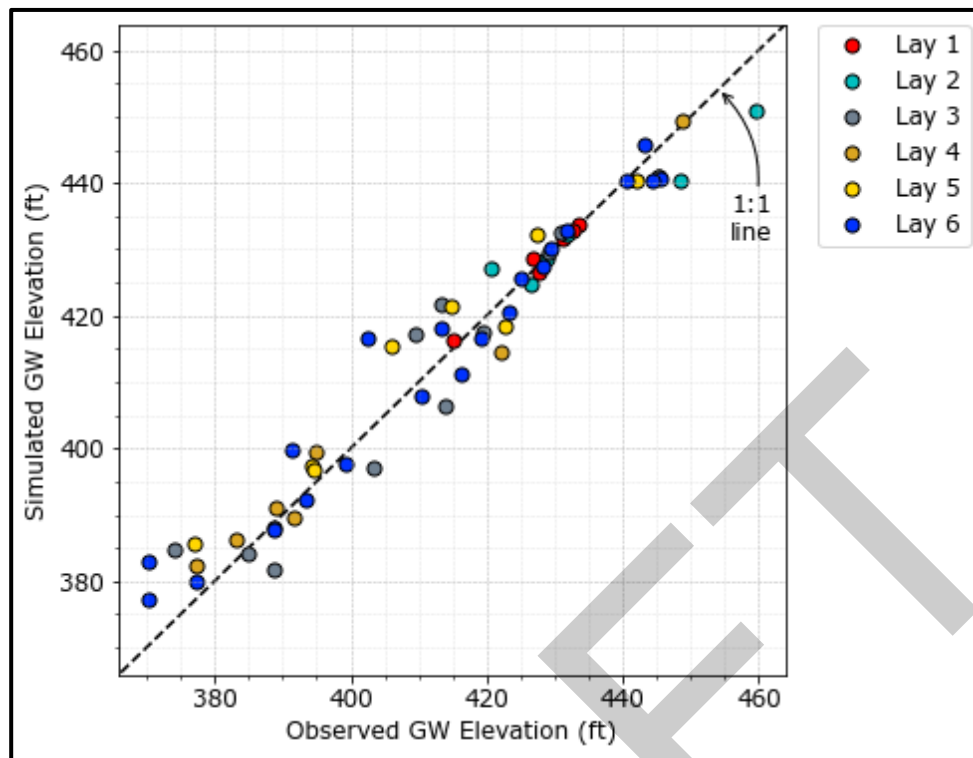
MONITORING WELL LOCATION MAP

GROUNDWATER MODELING TECHNICAL MEMORANDUM
FLY ASH POND SYSTEM
BALDWIN POWER PLANT
BALDWIN, ILLINOIS

FIGURE 2-3

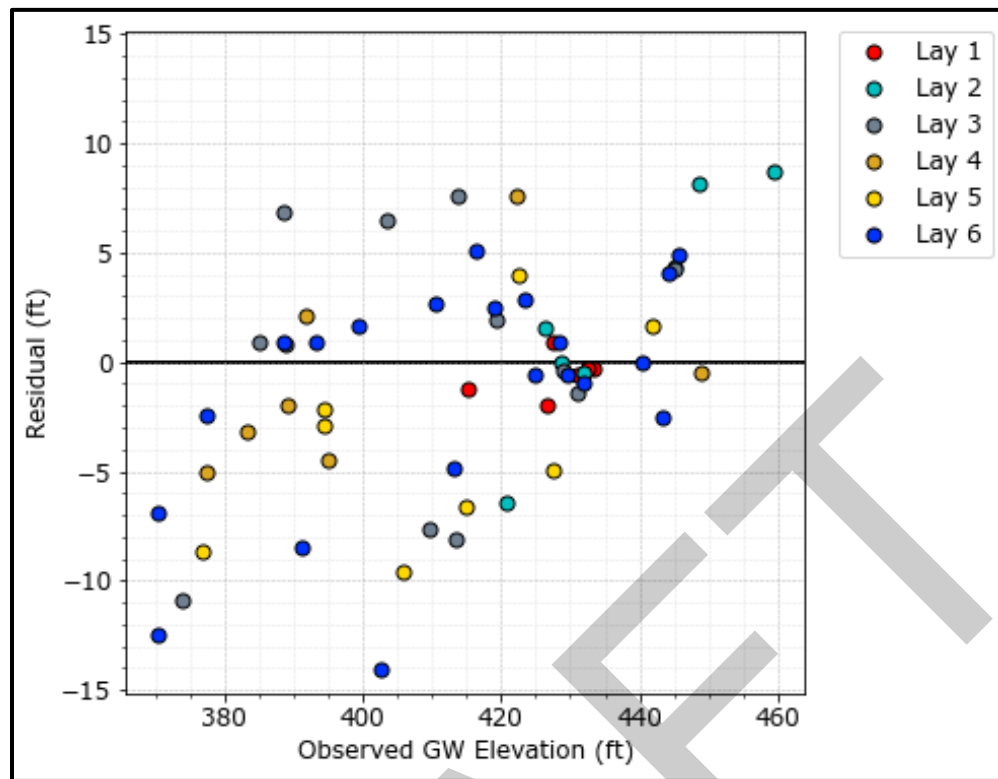
RAMBOLL AMERICAS
ENGINEERING SOLUTIONS, INC.





OBSERVED VERSUS SIMULATED GROUNDWATER ELEVATIONS

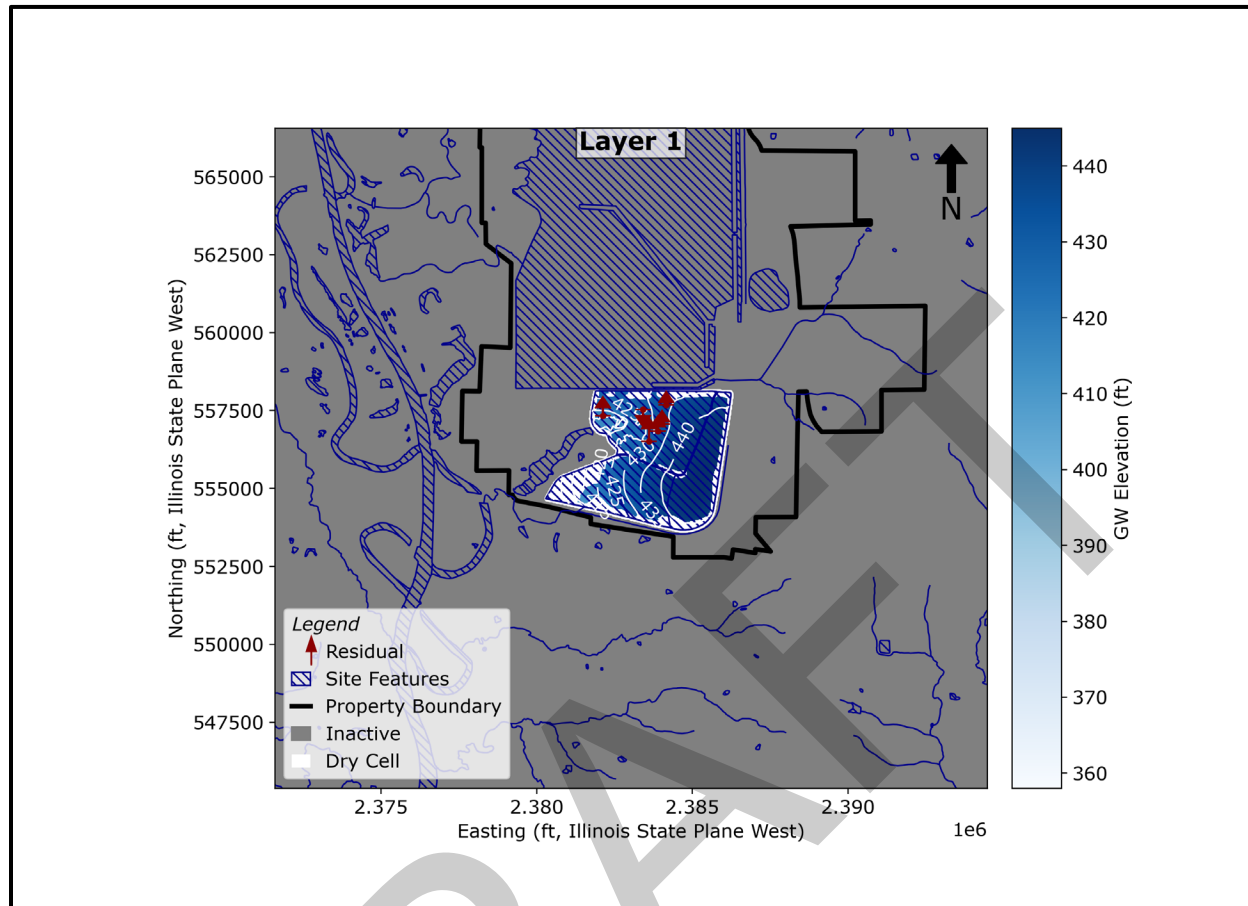
GROUNDWATER MODELING TECHNICAL MEMORANDUM
FLY ASH POND SYSTEM
BALDWIN POWER PLANT
BALDWIN, ILLINOIS



OBSERVED VERSUS RESIDUAL GROUNDWATER ELEVATIONS

GROUNDWATER MODELING TECHNICAL MEMORANDUM
 FLY ASH POND SYSTEM
 BALDWIN POWER PLANT
 BALDWIN, ILLINOIS

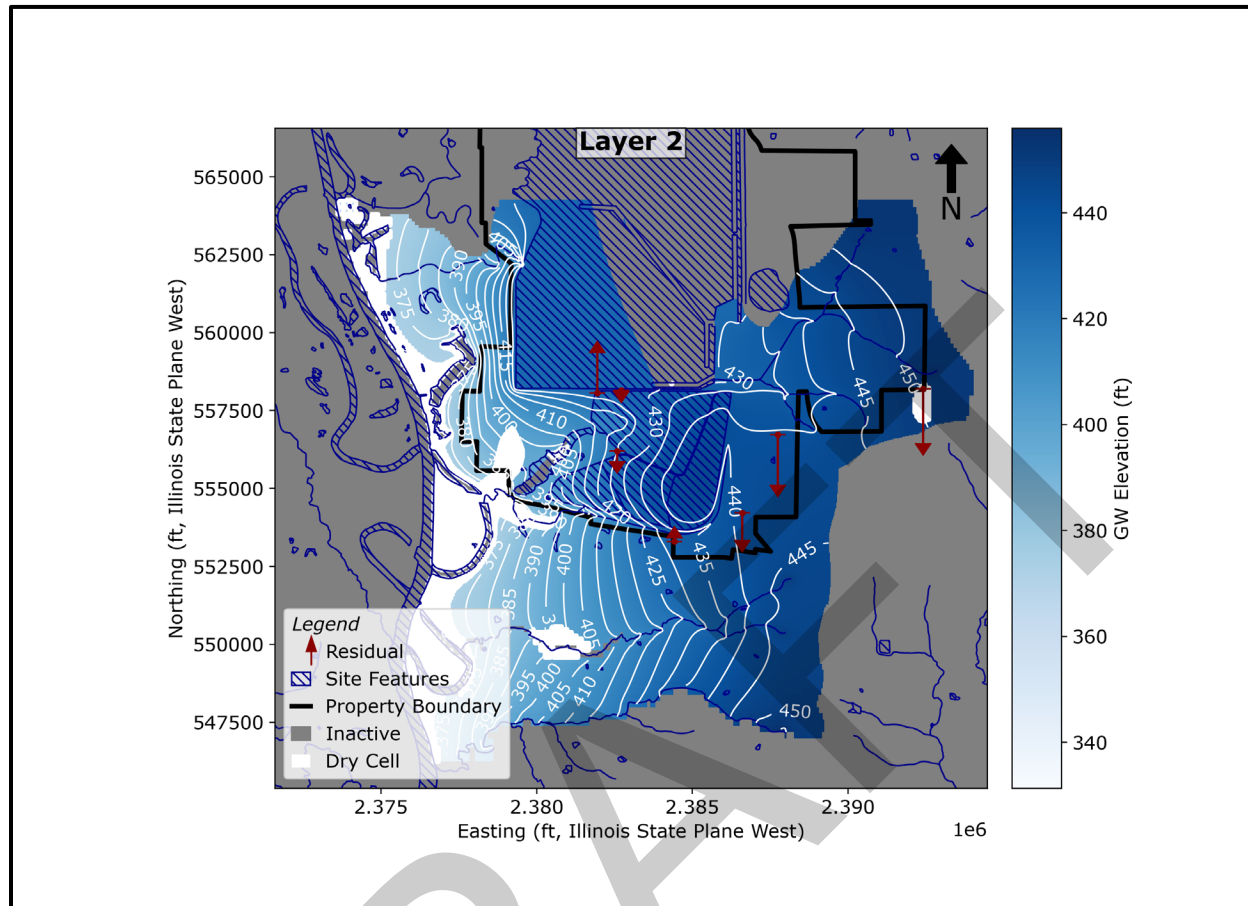




SIMULATED STEADY STATE GROUNDWATER LEVEL CONTOURS FROM LAYER 1 OF THE
CALIBRATED MODEL

GROUNDWATER MODELING TECHNICAL MEMORANDUM
FLY ASH POND SYSTEM
BALDWIN POWER PLANT
BALDWIN, ILLINOIS

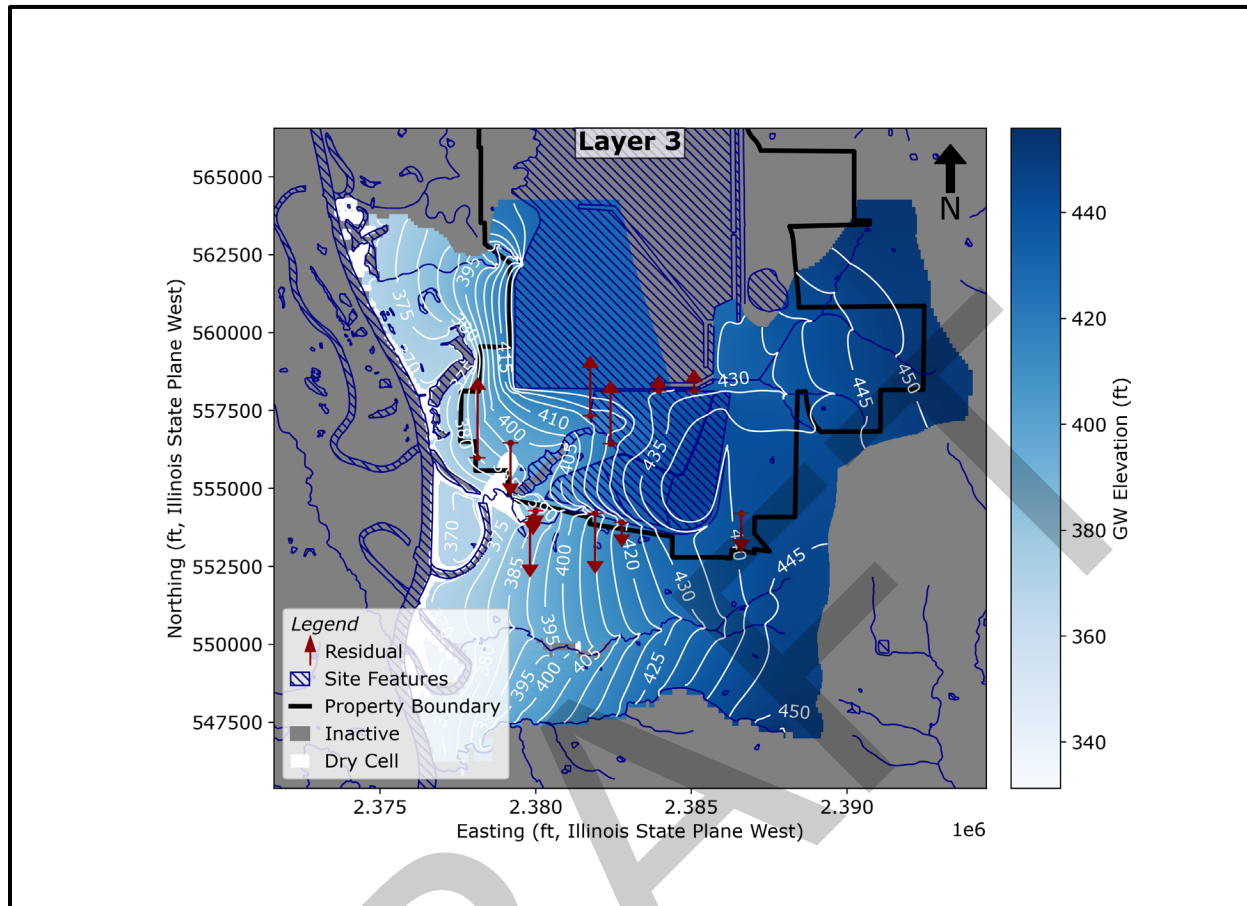
RAMBOLL



SIMULATED STEADY STATE GROUNDWATER LEVEL CONTOURS FROM LAYER 2 OF THE CALIBRATED MODEL

GROUNDWATER MODELING TECHNICAL MEMORANDUM
 FLY ASH POND SYSTEM
 BALDWIN POWER PLANT
 BALDWIN, ILLINOIS

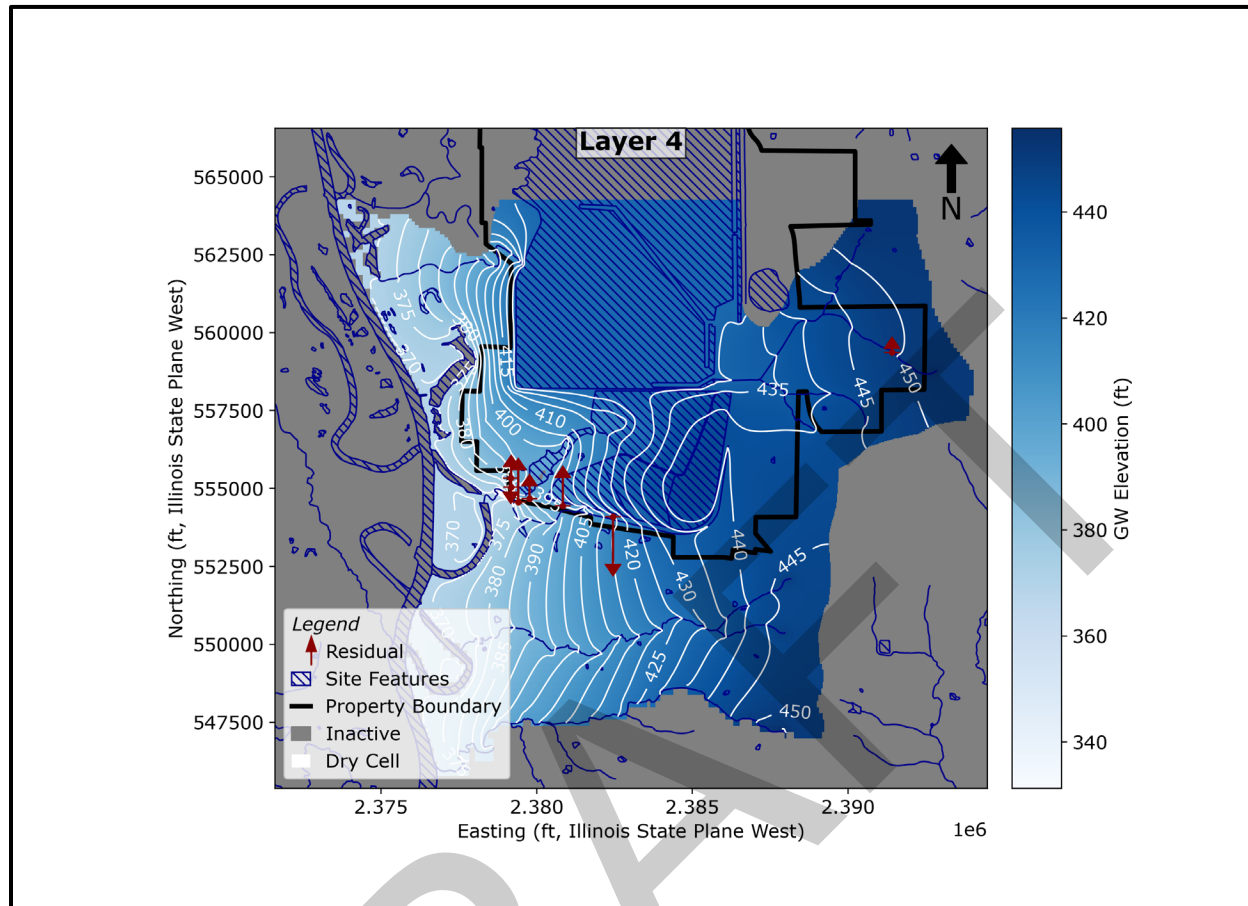
RAMBOLL



SIMULATED STEADY STATE GROUNDWATER LEVEL CONTOURS FROM LAYER 3 OF THE CALIBRATED MODEL

GROUNDWATER MODELING TECHNICAL MEMORANDUM
 FLY ASH POND SYSTEM
 BALDWIN POWER PLANT
 BALDWIN, ILLINOIS

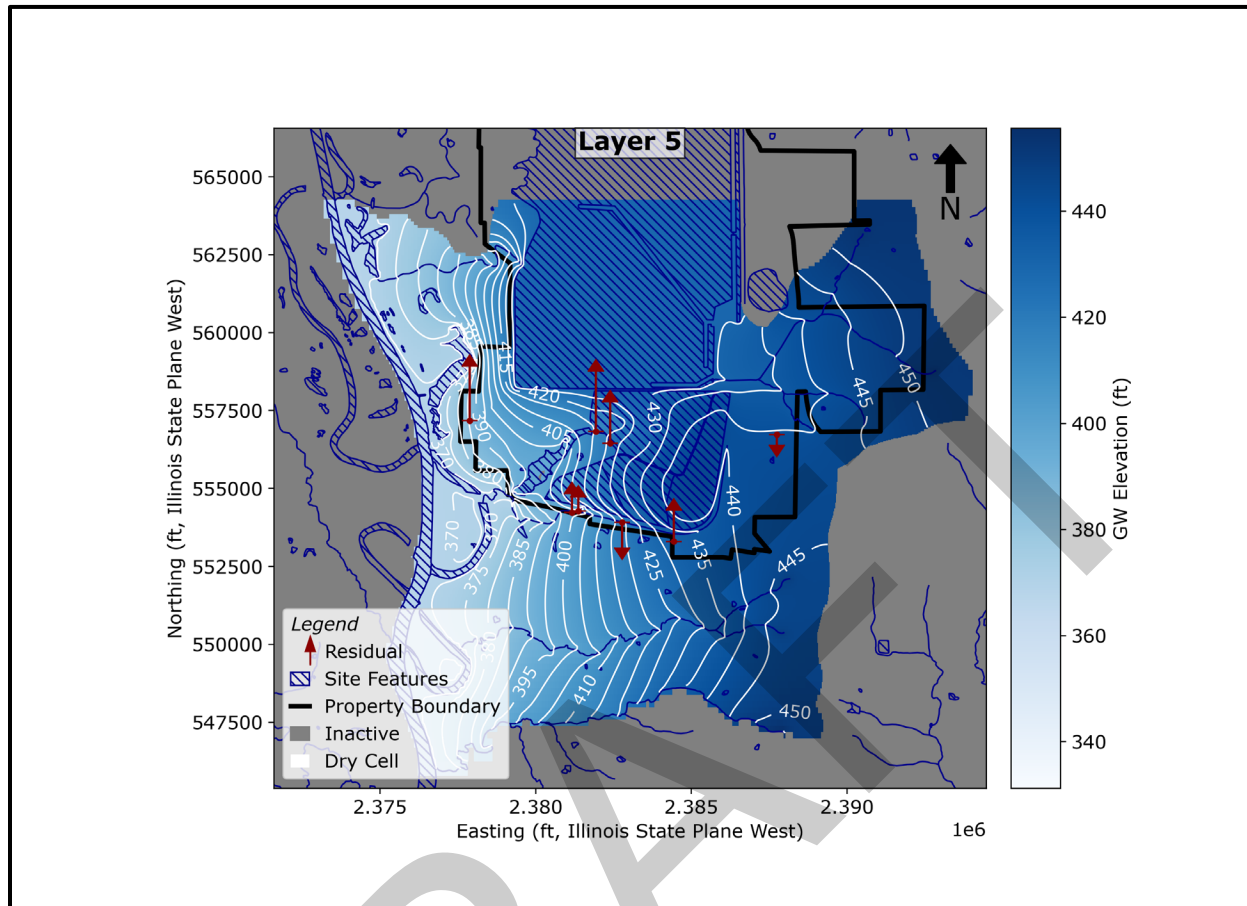
RAMBOLL



SIMULATED STEADY STATE GROUNDWATER LEVEL CONTOURS FROM LAYER 4 OF THE CALIBRATED MODEL

GROUNDWATER MODELING TECHNICAL MEMORANDUM
 FLY ASH POND SYSTEM
 BALDWIN POWER PLANT
 BALDWIN, ILLINOIS

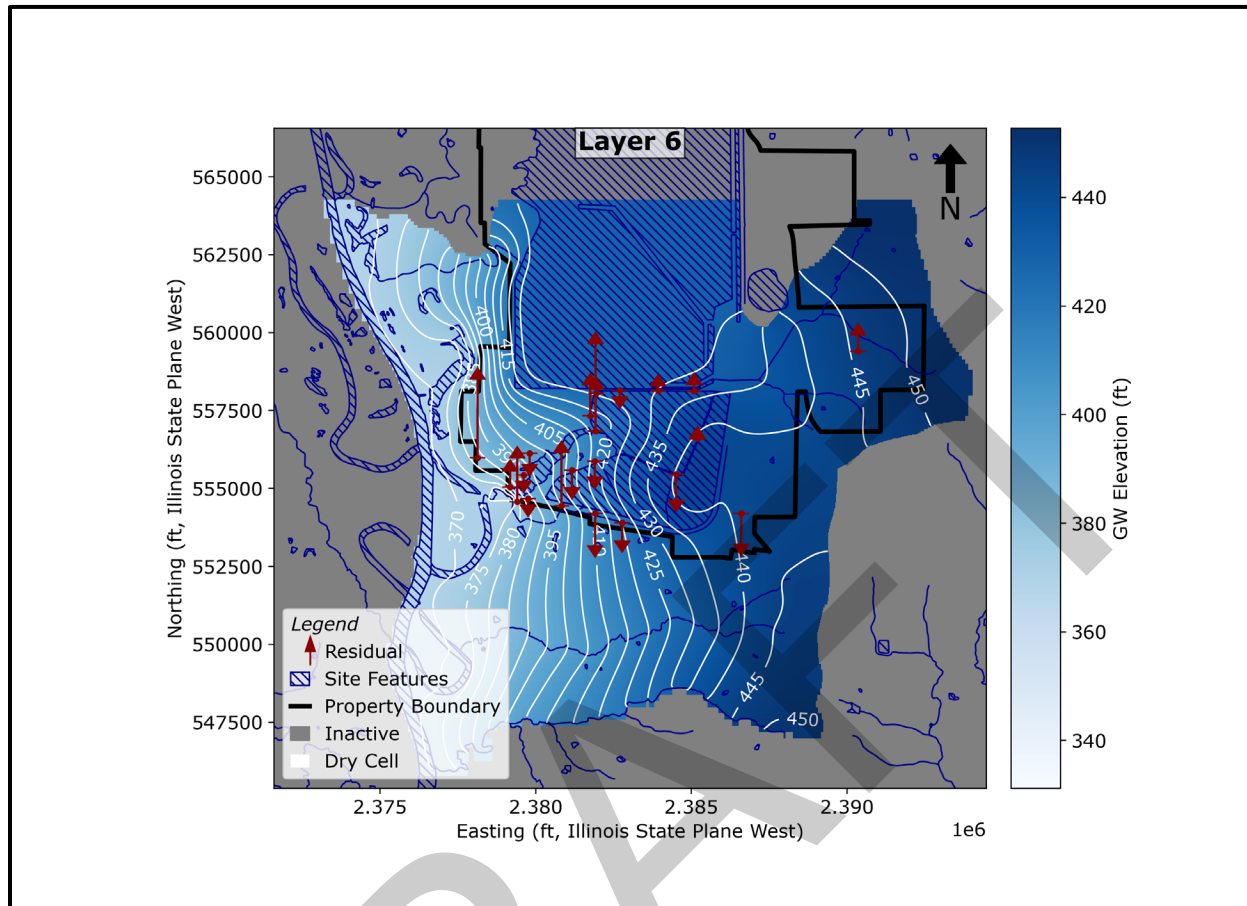
RAMBOLL



SIMULATED STEADY STATE GROUNDWATER LEVEL CONTOURS FROM LAYER 5 OF THE CALIBRATED MODEL

GROUNDWATER MODELING TECHNICAL MEMORANDUM
 FLY ASH POND SYSTEM
 BALDWIN POWER PLANT
 BALDWIN, ILLINOIS

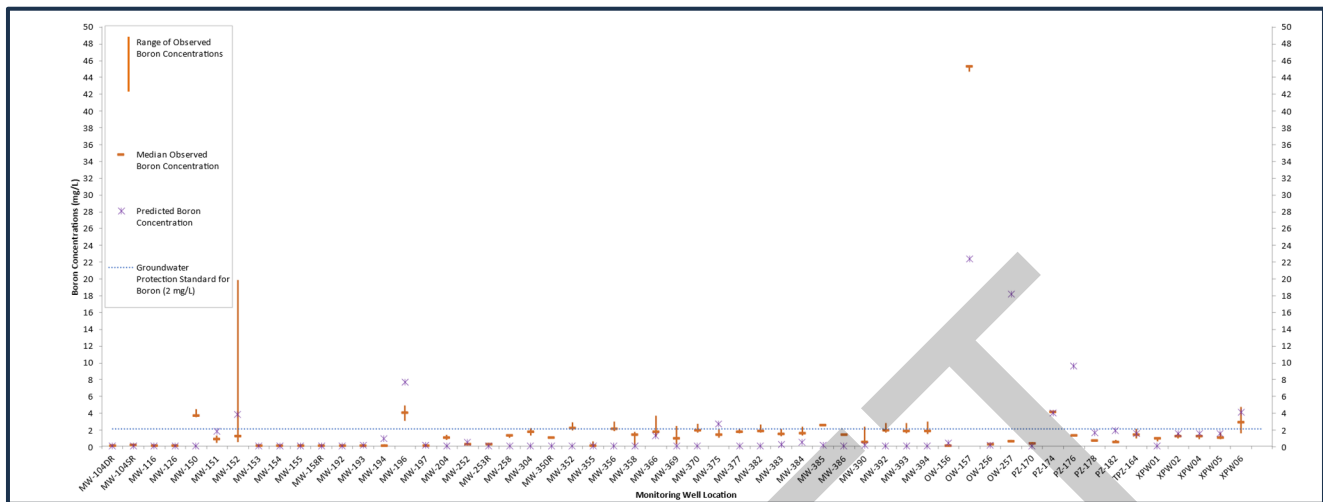
RAMBOLL



SIMULATED STEADY STATE GROUNDWATER LEVEL CONTOURS FROM LAYER 6 OF THE CALIBRATED MODEL

GROUNDWATER MODELING TECHNICAL MEMORANDUM
 FLY ASH POND SYSTEM
 BALDWIN POWER PLANT
 BALDWIN, ILLINOIS

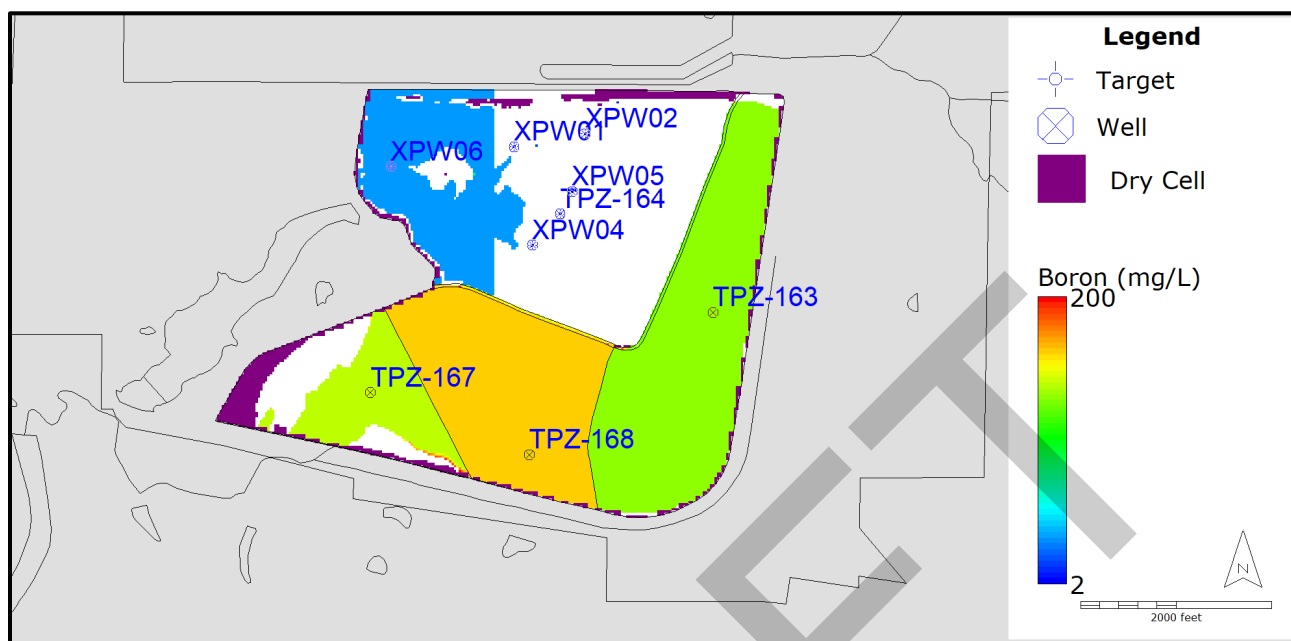
RAMBOLL



OBSERVED AND SIMULATED BORON CONCENTRATIONS (mg/L)

GROUNDWATER MODELING TECHNICAL MEMORANDUM
FLY ASH POND SYSTEM
BALDWIN POWER PLANT
BALDWIN, ILLINOIS

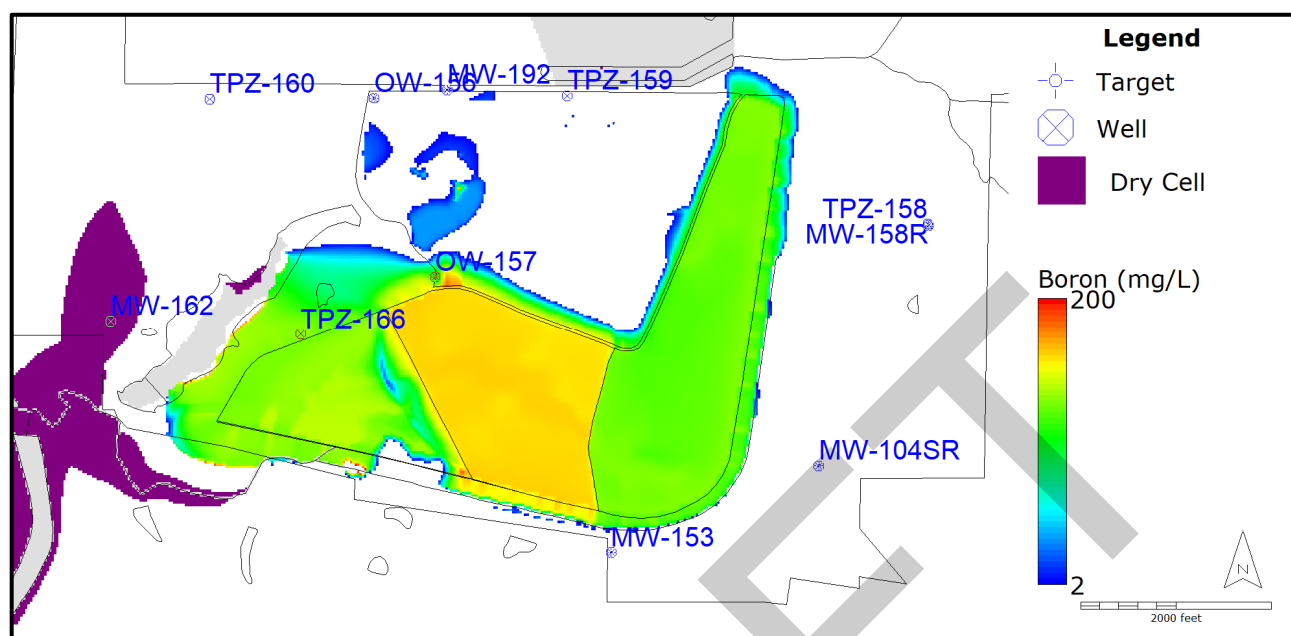




LAYER 1 DISTRIBUTION OF BORON CONCENTRATIONS (mg/L) IN THE CALIBRATED MODEL

GROUNDWATER MODELING TECHNICAL MEMORANDUM
 FLY ASH POND SYSTEM
 BALDWIN POWER PLANT
 BALDWIN, ILLINOIS

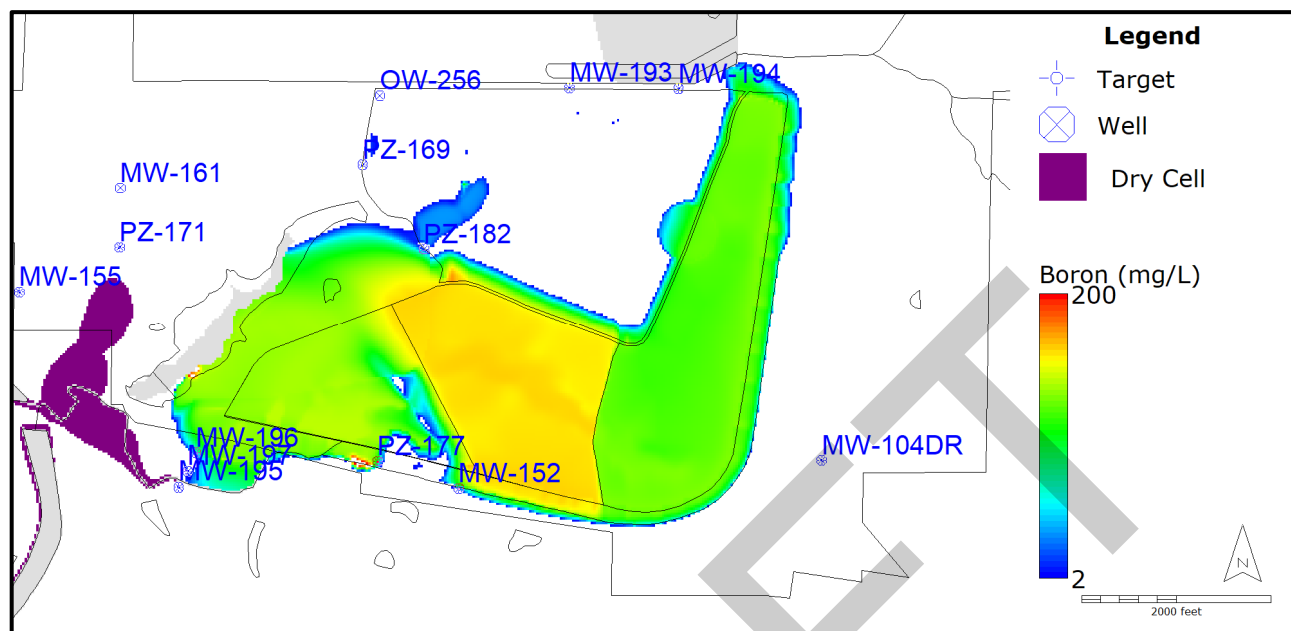
RAMBOLL



LAYER 2 DISTRIBUTION OF BORON CONCENTRATIONS (mg/L) IN THE CALIBRATED MODEL

GROUNDWATER MODELING TECHNICAL MEMORANDUM
 FLY ASH POND SYSTEM
 BALDWIN POWER PLANT
 BALDWIN, ILLINOIS

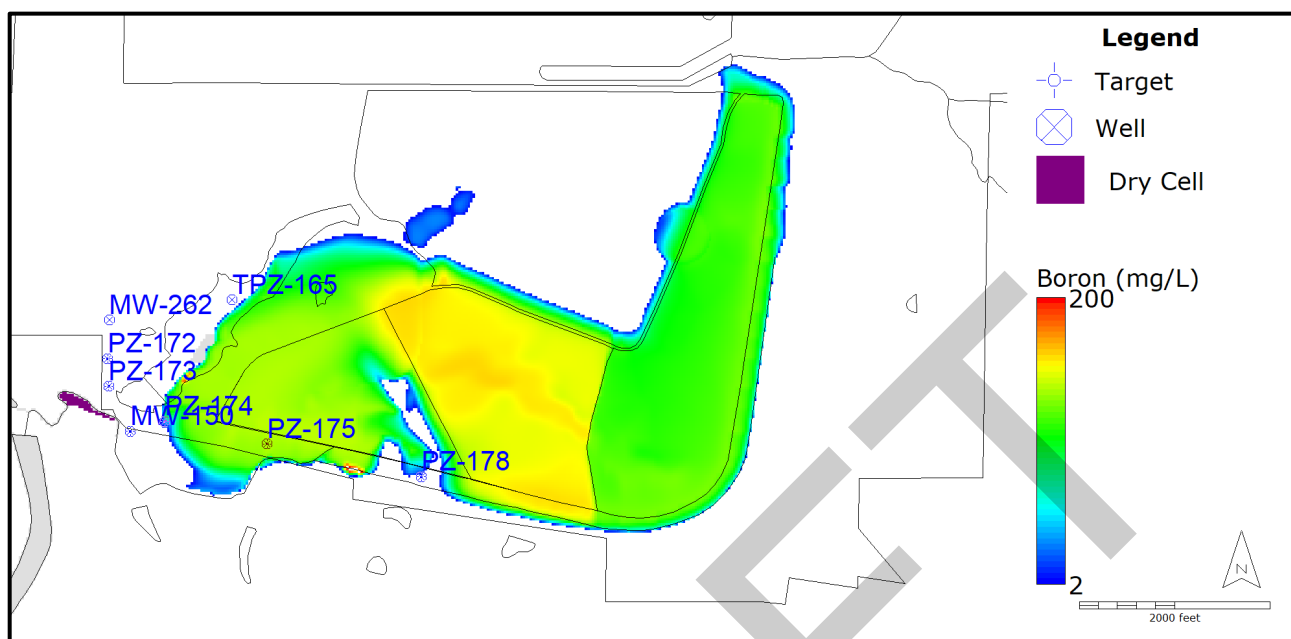
RAMBOLL



LAYER 3 DISTRIBUTION OF BORON CONCENTRATIONS (mg/L) IN THE CALIBRATED MODEL

GROUNDWATER MODELING TECHNICAL MEMORANDUM
 FLY ASH POND SYSTEM
 BALDWIN POWER PLANT
 BALDWIN, ILLINOIS

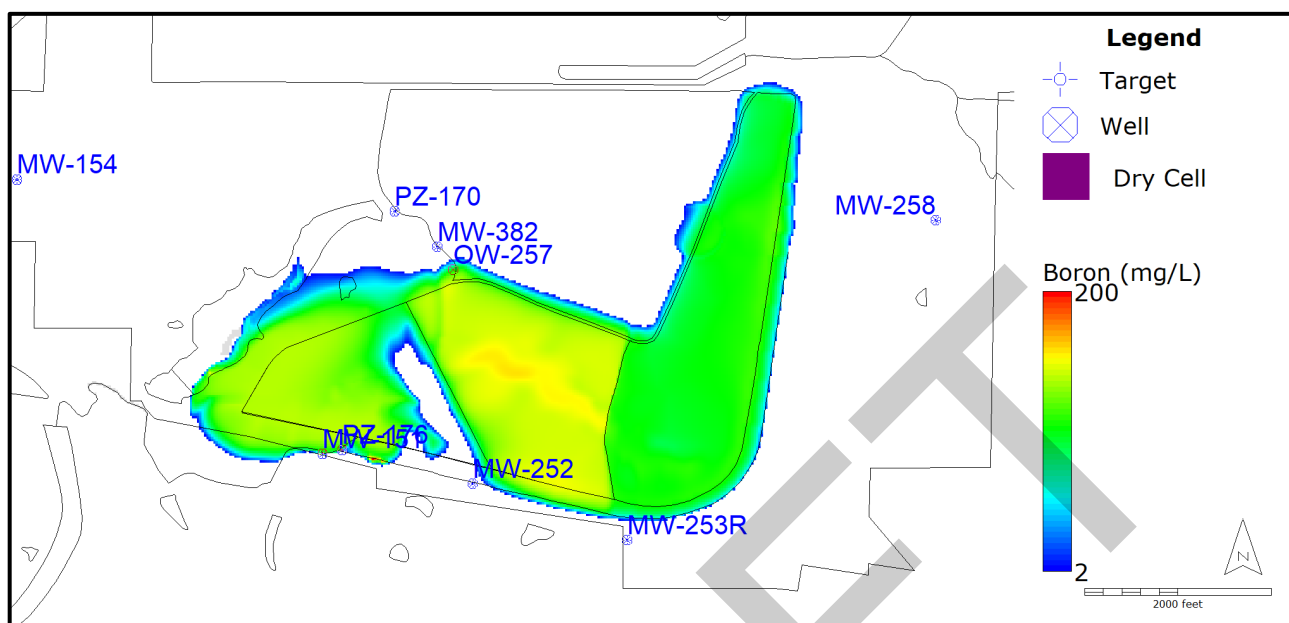
RAMBOLL



LAYER 4 DISTRIBUTION OF BORON CONCENTRATIONS (mg/L) IN THE CALIBRATED MODEL

GROUNDWATER MODELING TECHNICAL MEMORANDUM
 FLY ASH POND SYSTEM
 BALDWIN POWER PLANT
 BALDWIN, ILLINOIS

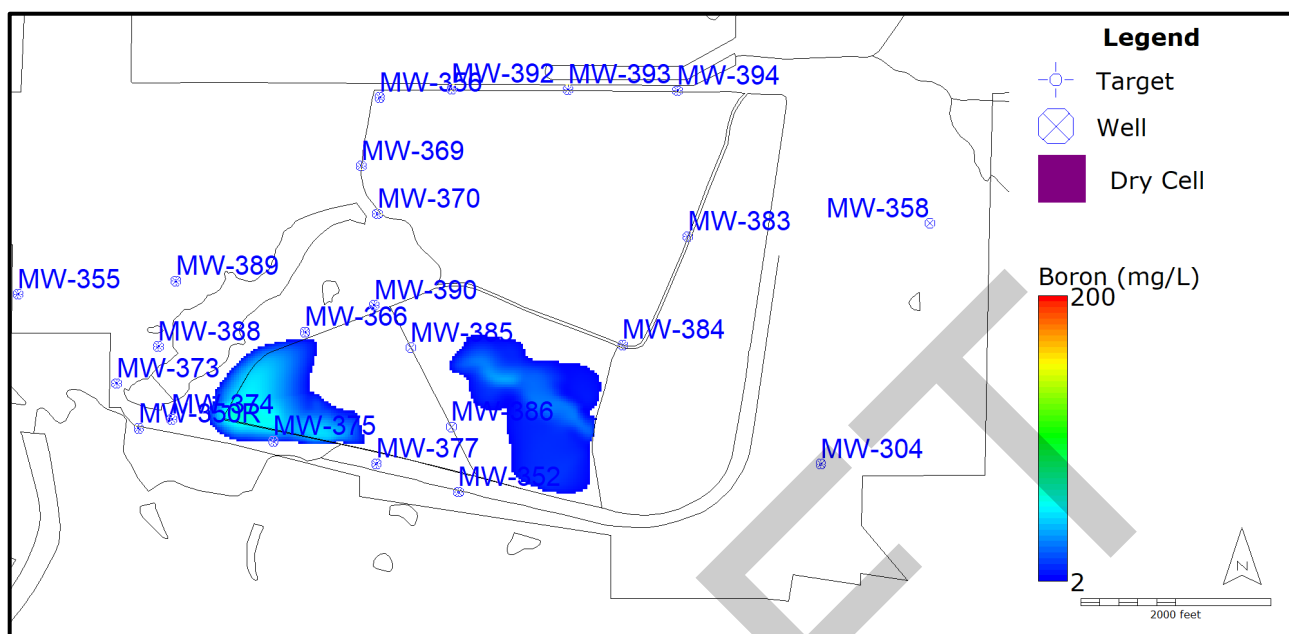
RAMBOLL



LAYER 5 DISTRIBUTION OF BORON CONCENTRATIONS (mg/L) IN THE CALIBRATED MODEL

GROUNDWATER MODELING TECHNICAL MEMORANDUM
 FLY ASH POND SYSTEM
 BALDWIN POWER PLANT
 BALDWIN, ILLINOIS

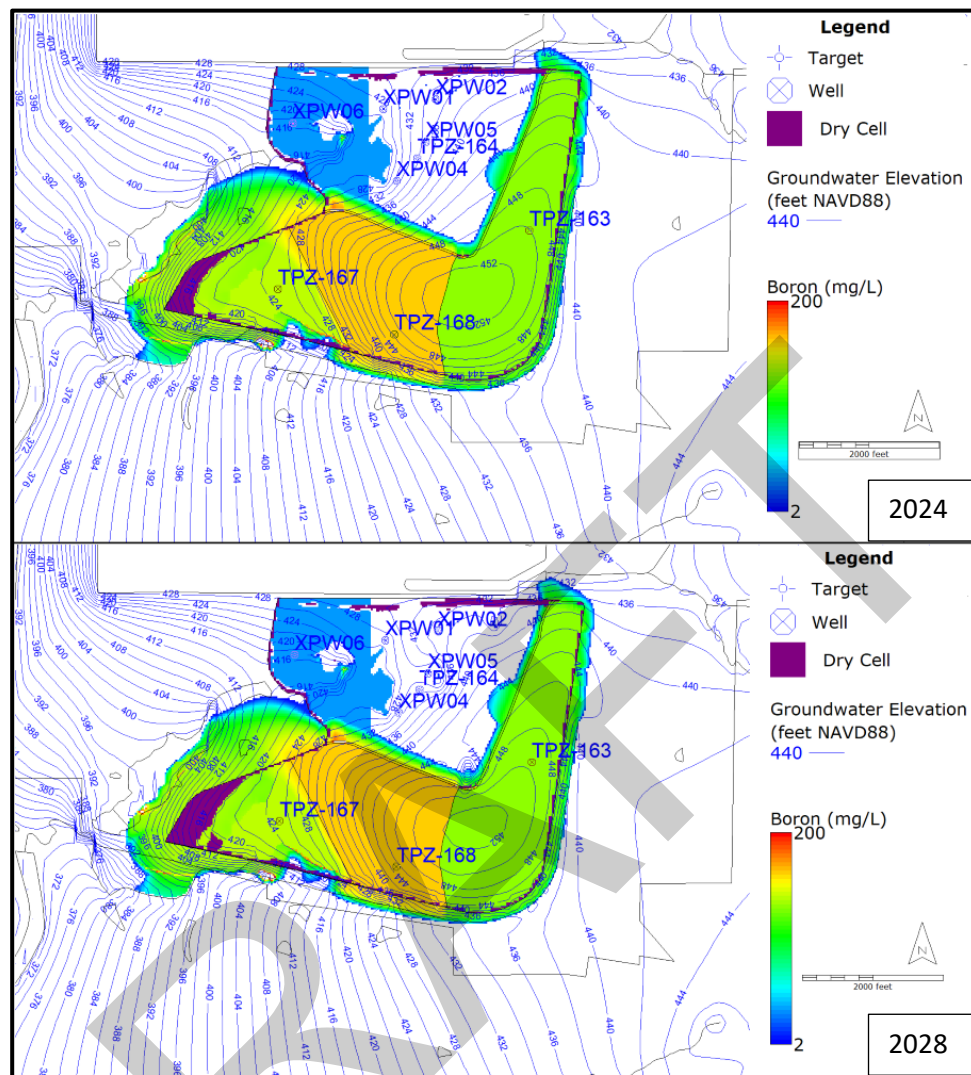
RAMBOLL



LAYER 6 DISTRIBUTION OF BORON CONCENTRATIONS (mg/L) IN THE CALIBRATED MODEL

GROUNDWATER MODELING TECHNICAL MEMORANDUM
 FLY ASH POND SYSTEM
 BALDWIN POWER PLANT
 BALDWIN, ILLINOIS

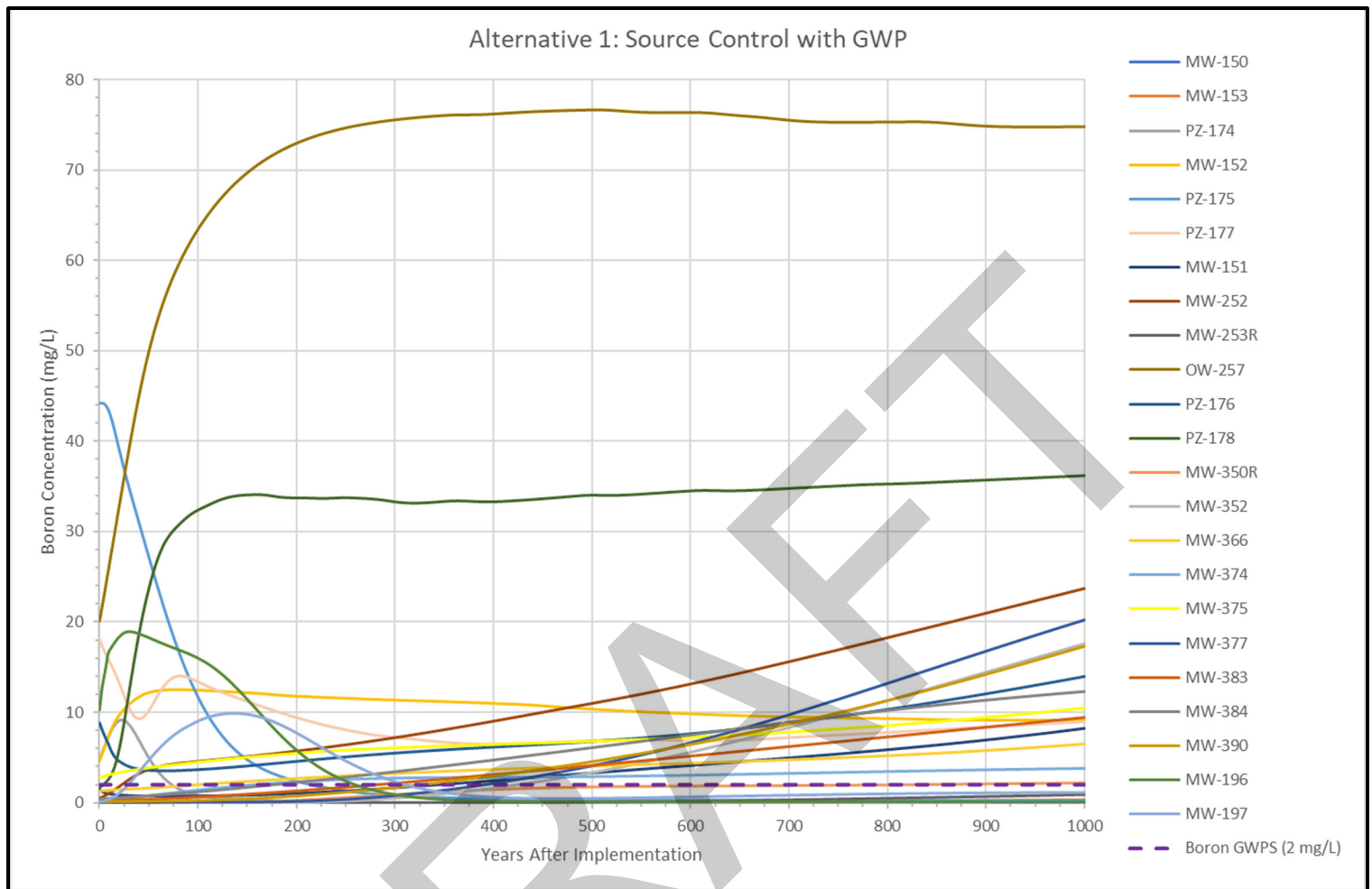
RAMBOLL



SIMULATED GROUNDWATER ELEVATIONS AND BORON CONCENTRATIONS, 2024 AND 2028

GROUNDWATER MODELING TECHNICAL MEMORANDUM
FLY ASH POND SYSTEM
BALDWIN POWER PLANT
BALDWIN, ILLINOIS

RAMBOLL

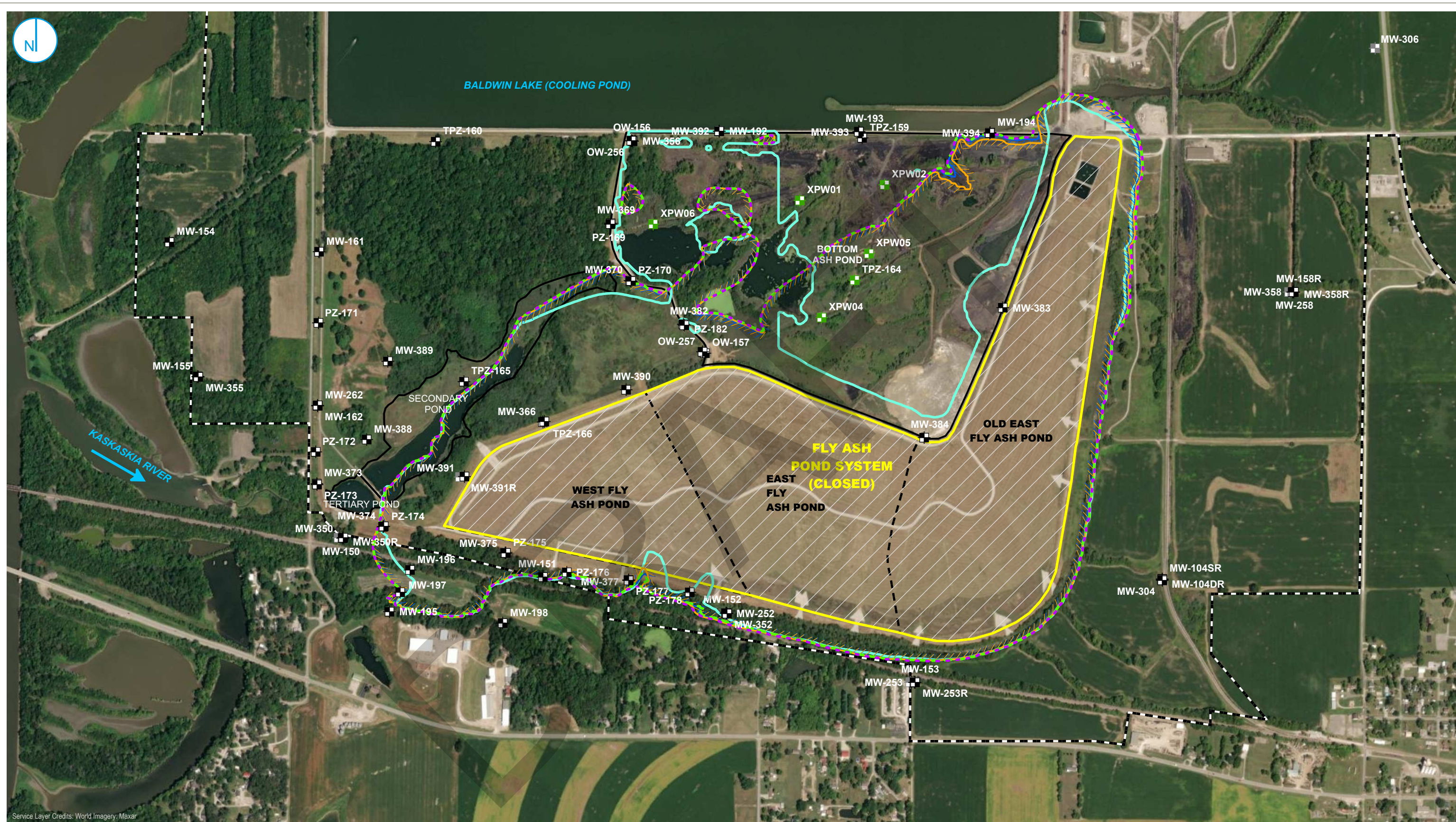


MODEL PREDICTED BORON CONCENTRATIONS AT FAPS MONITORING WELLS FOR
ALTERNATIVE 1: SOURCE CONTROL WITH GWP

GROUNDWATER MODELING TECHNICAL MEMORANDUM
FLY ASH POND SYSTEM
BALDWIN POWER PLANT
BALDWIN, ILLINOIS

RAMBOLL

PROJECT: 169000XXXXX | DATED: 2/3/2025 | DESIGNER: GALARNMC
Y:\Mapping\Projects\22\2265\MXD\CAAA_SIR\Baldwin\FPS\Modeling\Tech Memo.aprx | Figure 5-3: Boron Plume 25 Years



- MONITORING WELL
- POREWATER WELL
- CLOSED MONITORING WELL
- REGULATED UNIT (SUBJECT UNIT)
- SITE FEATURE
- CAPPED AREA
- PROPERTY BOUNDARY
- ALTERNATIVE 1. SOURCE CONTROL WITH GROUNDWATER POLISHING (GWP)
- ALTERNATIVE 2. SOURCE CONTROL WITH CUTOFF WALL
- ALTERNATIVE 3. SOURCE CONTROL WITH GROUNDWATER MANAGEMENT SYSTEM (GMS)
- CLOSURE BY REMOVAL (CBR)
- CALIBRATION MODEL PLUME EXTENT

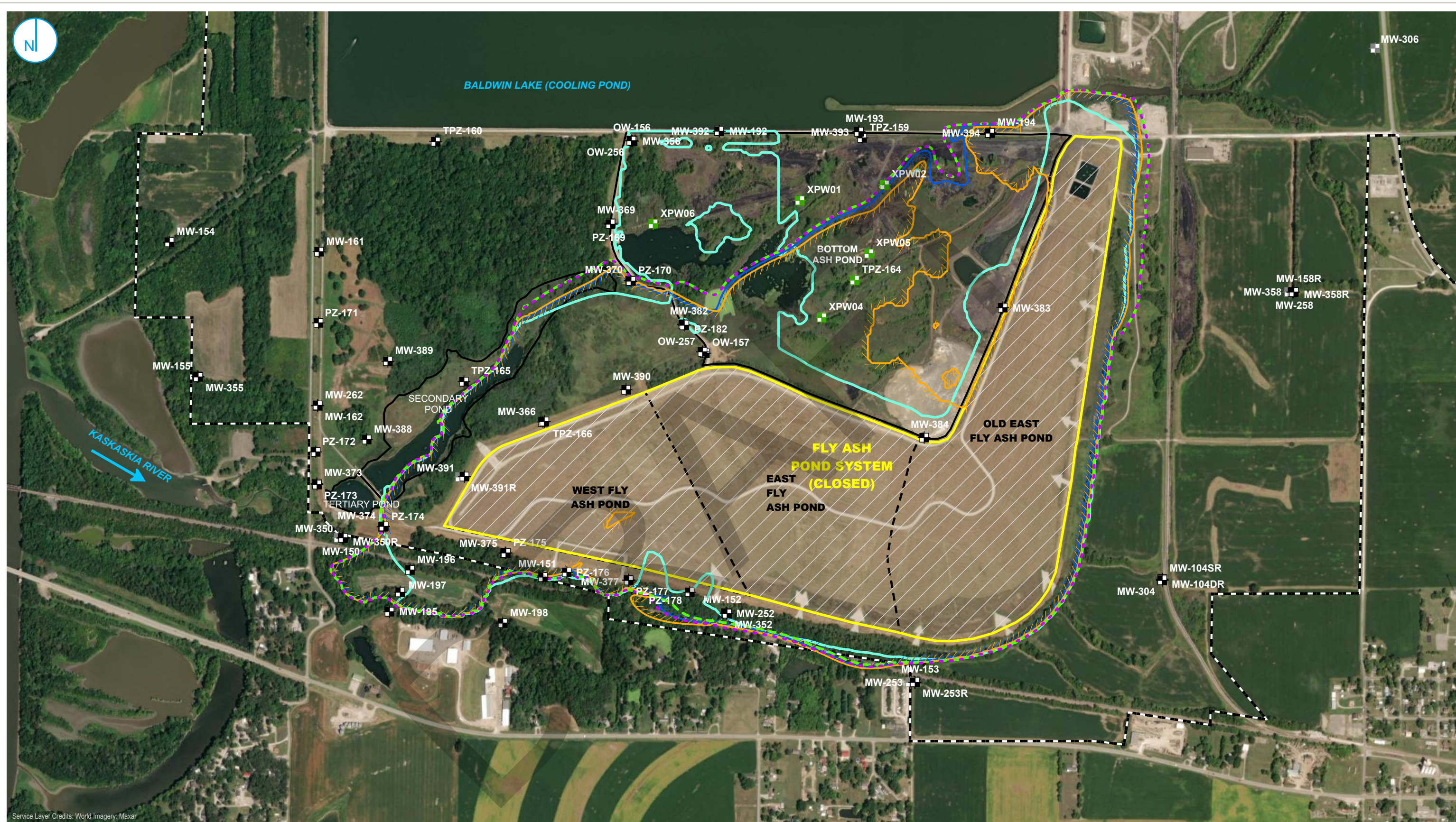
MODELED BORON PLUME (2 MG/L) 25 YEARS AFTER IMPLEMENTATION

GROUNDWATER MODELING TECHNICAL MEMORANDUM
FLY ASH POND SYSTEM
BALDWIN POWER PLANT
BALDWIN, ILLINOIS

FIGURE 5-3

RAMBOLL AMERICAS
ENGINEERING SOLUTIONS, INC.





- MONITORING WELL
- POREWATER WELL
- CLOSED MONITORING WELL

- REGULATED UNIT (SUBJECT UNIT)
- SITE FEATURE
- CAPPED AREA
- PROPERTY BOUNDARY

- ALTERNATIVE 1. SOURCE CONTROL WITH GROUNDWATER POLISHING (GWP)
- ALTERNATIVE 2. SOURCE CONTROL WITH CUTOFF WALL
- ALTERNATIVE 3. SOURCE CONTROL WITH GROUNDWATER MANAGEMENT SYSTEM (GMS)
- CLOSURE BY REMOVAL (CBR)
- CALIBRATION MODEL PLUME EXTENT

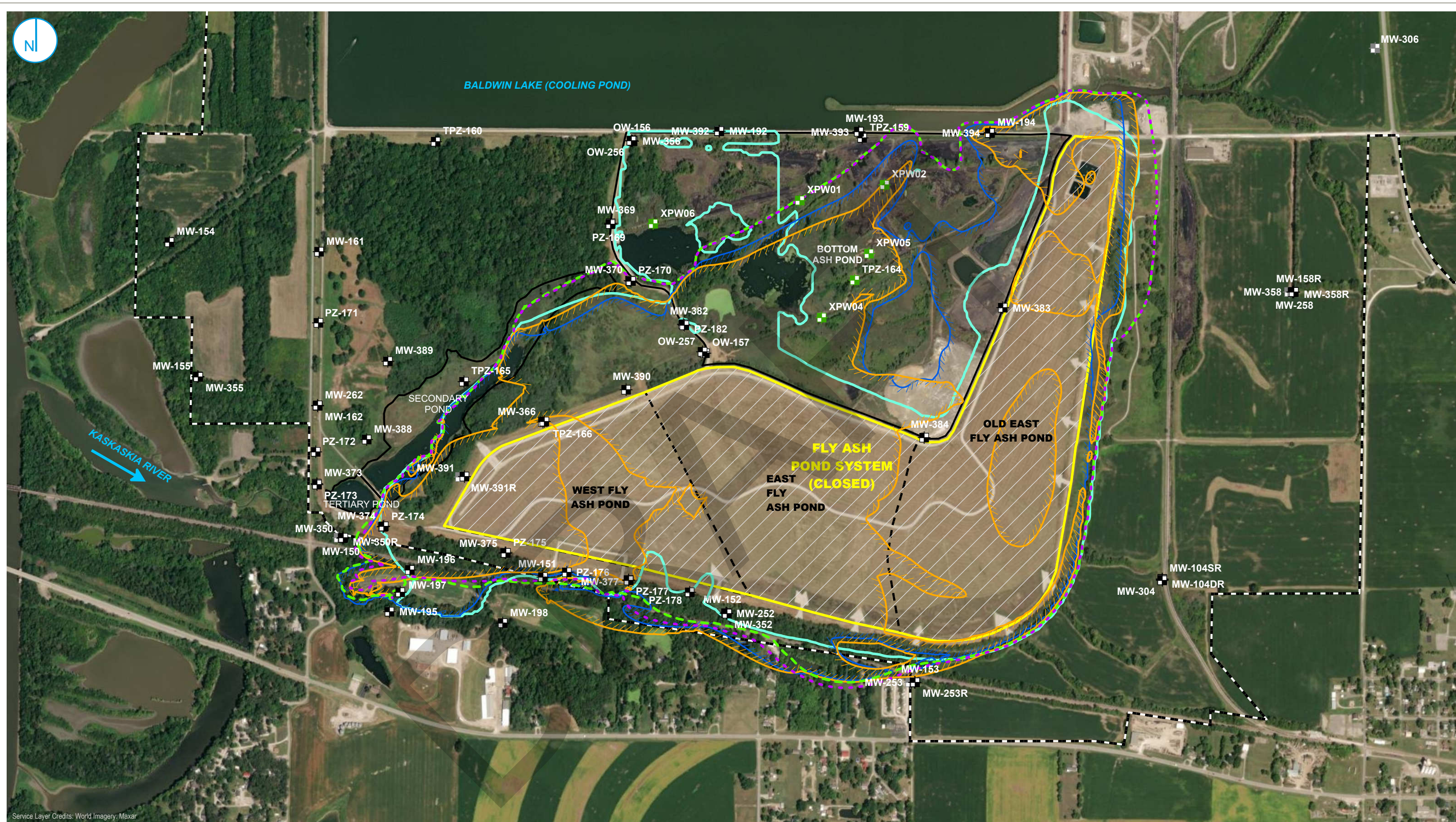
MODELED BORON PLUME (2 MG/L) 125 YEARS AFTER IMPLEMENTATION

GROUNDWATER MODELING TECHNICAL MEMORANDUM
FLY ASH POND SYSTEM
BALDWIN POWER PLANT
BALDWIN, ILLINOIS

FIGURE 5-4

RAMBOLL AMERICAS
ENGINEERING SOLUTIONS, INC.





- | | | |
|------------------------|-------------------------------|--|
| MONITORING WELL | REGULATED UNIT (SUBJECT UNIT) | ALTERNATIVE 1. SOURCE CONTROL WITH GROUNDWATER POLISHING (GWP) |
| POREWATER WELL | SITE FEATURE | ALTERNATIVE 2. SOURCE CONTROL WITH CUTOFF WALL |
| CLOSED MONITORING WELL | CAPPED AREA | ALTERNATIVE 3. SOURCE CONTROL WITH GROUNDWATER MANAGEMENT SYSTEM (GMS) |
| | PROPERTY BOUNDARY | CLOSURE BY REMOVAL (CBR) |
| | | CALIBRATION MODEL PLUME EXTENT |

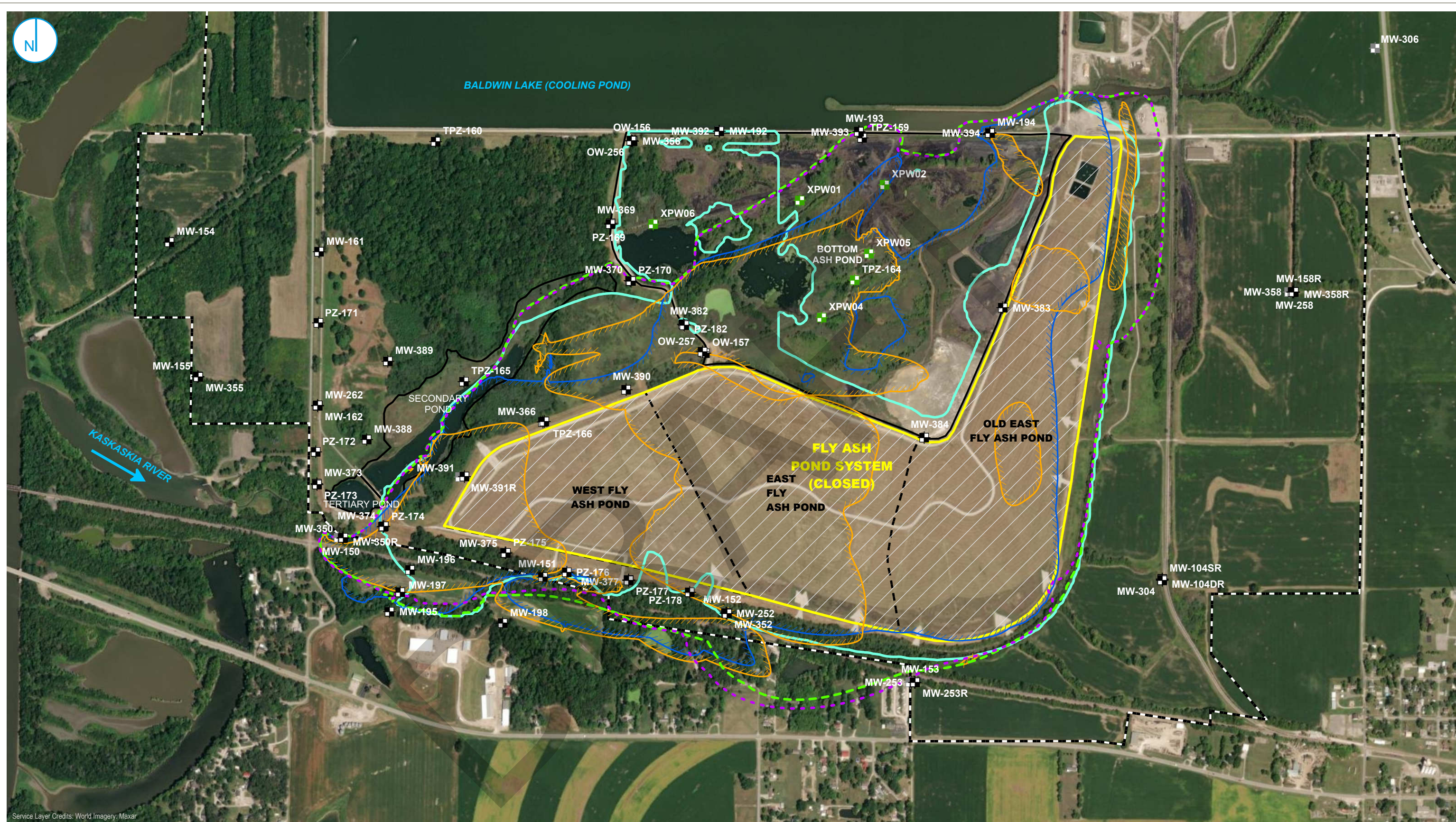
MODELED BORON PLUME (2 MG/L) 375 YEARS AFTER IMPLEMENTATION

GROUNDWATER MODELING TECHNICAL MEMORANDUM
FLY ASH POND SYSTEM
BALDWIN POWER PLANT
BALDWIN, ILLINOIS

FIGURE 5-5

RAMBOLL AMERICAS
ENGINEERING SOLUTIONS, INC.





- MONITORING WELL
- POREWATER WELL
- CLOSED MONITORING WELL

- REGULATED UNIT (SUBJECT UNIT)
- SITE FEATURE
- CAPPED AREA
- PROPERTY BOUNDARY

- ALTERNATIVE 1. SOURCE CONTROL WITH GROUNDWATER POLISHING (GWP)
- ALTERNATIVE 2. SOURCE CONTROL WITH CUTOFF WALL
- ALTERNATIVE 3. SOURCE CONTROL WITH GROUNDWATER MANAGEMENT SYSTEM (GMS)
- CLOSURE BY REMOVAL (CBR)
- CALIBRATION MODEL PLUME EXTENT



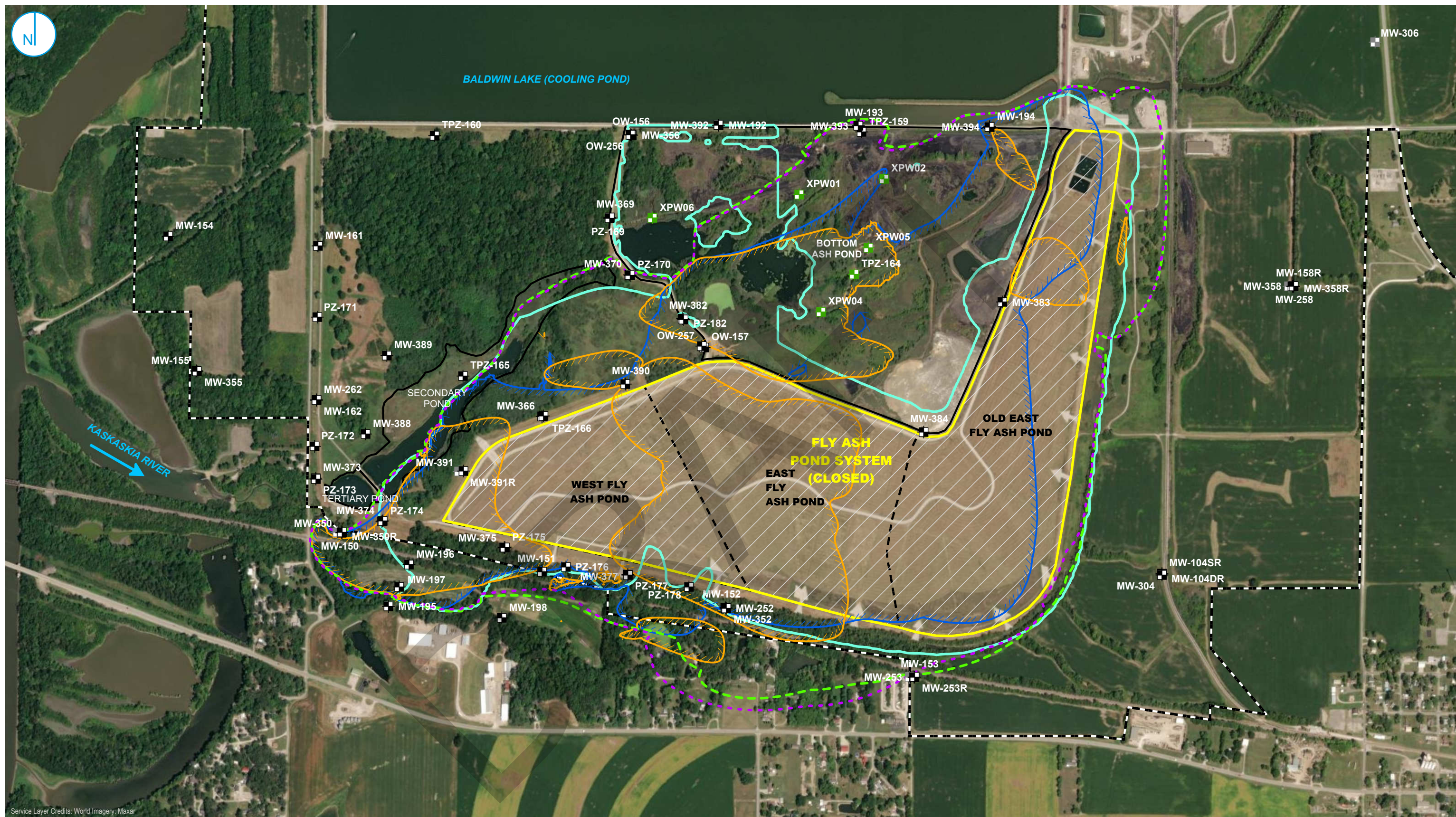
MODELED BORON PLUME (2 MG/L) 750 YEARS AFTER IMPLEMENTATION

GROUNDWATER MODELING TECHNICAL MEMORANDUM
FLY ASH POND SYSTEM
BALDWIN POWER PLANT
BALDWIN, ILLINOIS

FIGURE 5-6

RAMBOLL AMERICAS
ENGINEERING SOLUTIONS, INC.





- MONITORING WELL
- POREWATER WELL
- CLOSED MONITORING WELL

- REGULATED UNIT (SUBJECT UNIT)
- SITE FEATURE
- CAPPED AREA
- PROPERTY BOUNDARY

- ALTERNATIVE 1. SOURCE CONTROL WITH GROUNDWATER POLISHING (GWP)
- ALTERNATIVE 2. SOURCE CONTROL WITH CUTOFF WALL
- ALTERNATIVE 3. SOURCE CONTROL WITH GROUNDWATER MANAGEMENT SYSTEM (GMS)
- CLOSURE BY REMOVAL (CBR)
- CALIBRATION MODEL PLUME EXTENT

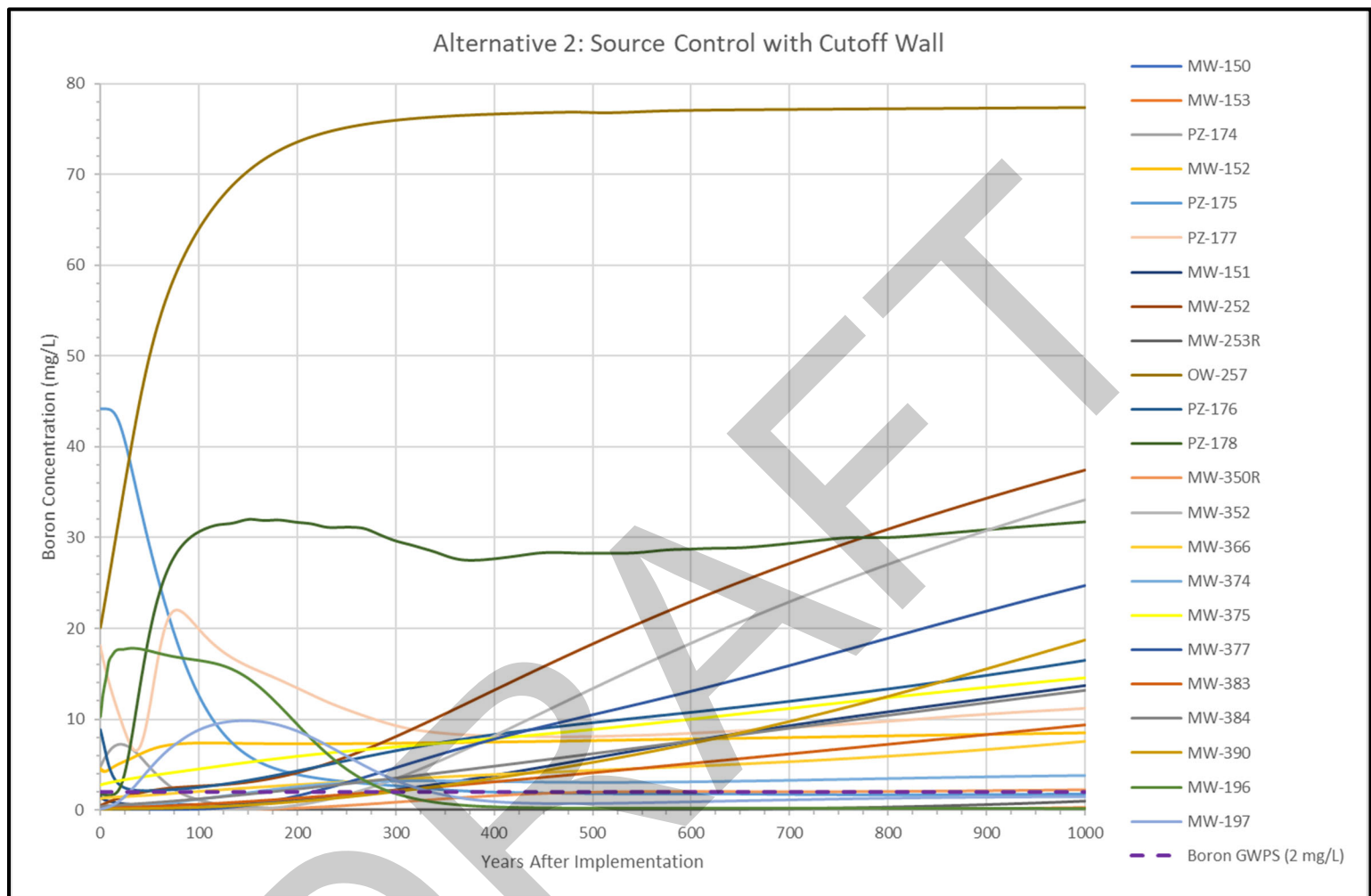
MODELED BORON PLUME (2 MG/L) 1000 YEARS AFTER IMPLEMENTATION

GROUNDWATER MODELING TECHNICAL MEMORANDUM
FLY ASH POND SYSTEM
BALDWIN POWER PLANT
BALDWIN, ILLINOIS

FIGURE 5-7

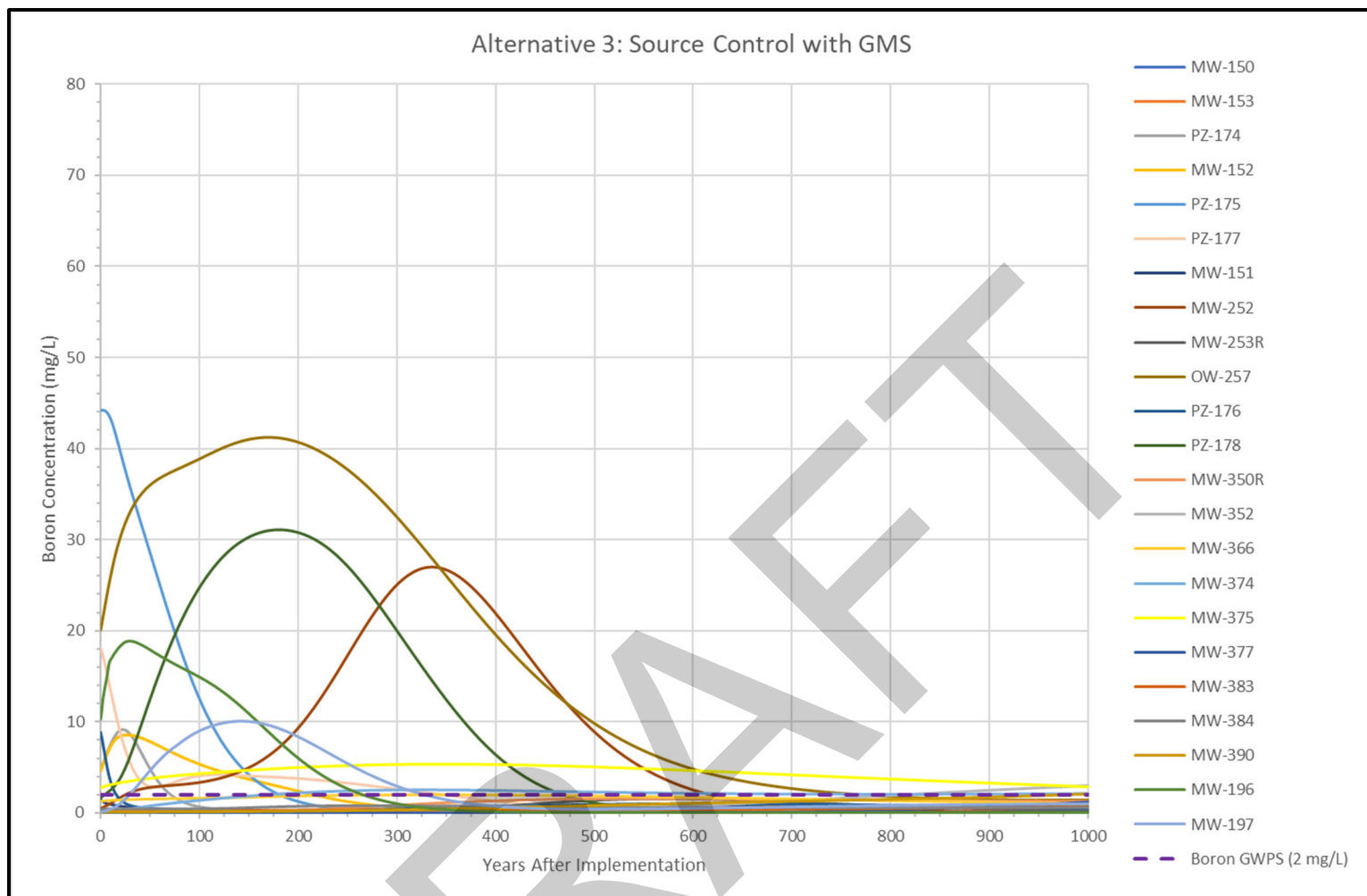
RAMBOLL AMERICAS
ENGINEERING SOLUTIONS, INC.





MODEL PREDICTED BORON CONCENTRATIONS AT FAPS MONITORING WELLS FOR
ALTERNATIVE 2: SOURCE CONTROL WITH CUTOFF WALL

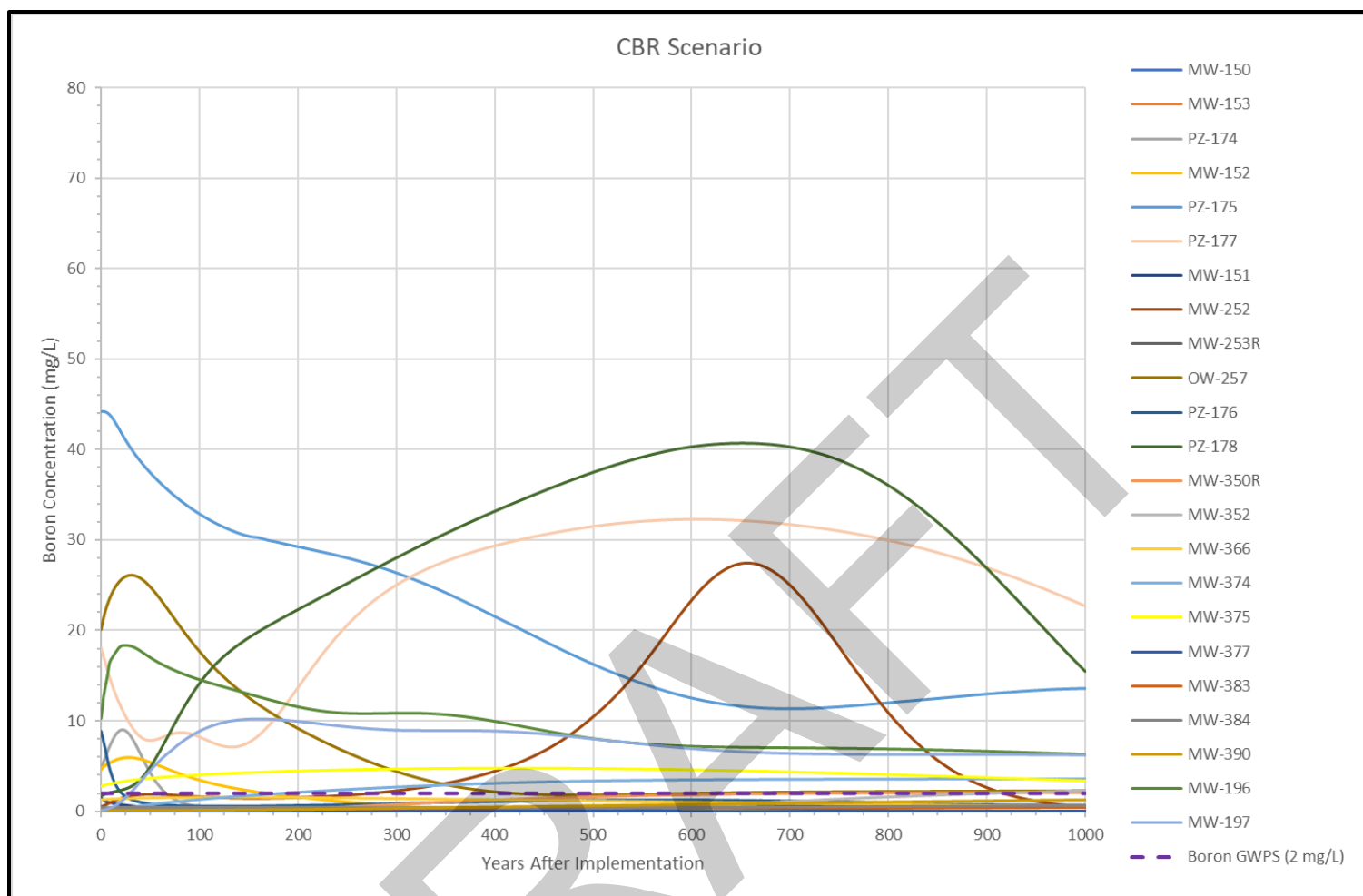
GROUNDWATER MODELING TECHNICAL MEMORANDUM
FLY ASH POND SYSTEM
BALDWIN POWER PLANT
BALDWIN, ILLINOIS



MODEL PREDICTED BORON CONCENTRATIONS AT FAPS MONITORING WELLS FOR
ALTERNATIVE 3: SOURCE CONTROL WITH GMS

GROUNDWATER MODELING TECHNICAL MEMORANDUM
FLY ASH POND SYSTEM
BALDWIN POWER PLANT
BALDWIN, ILLINOIS

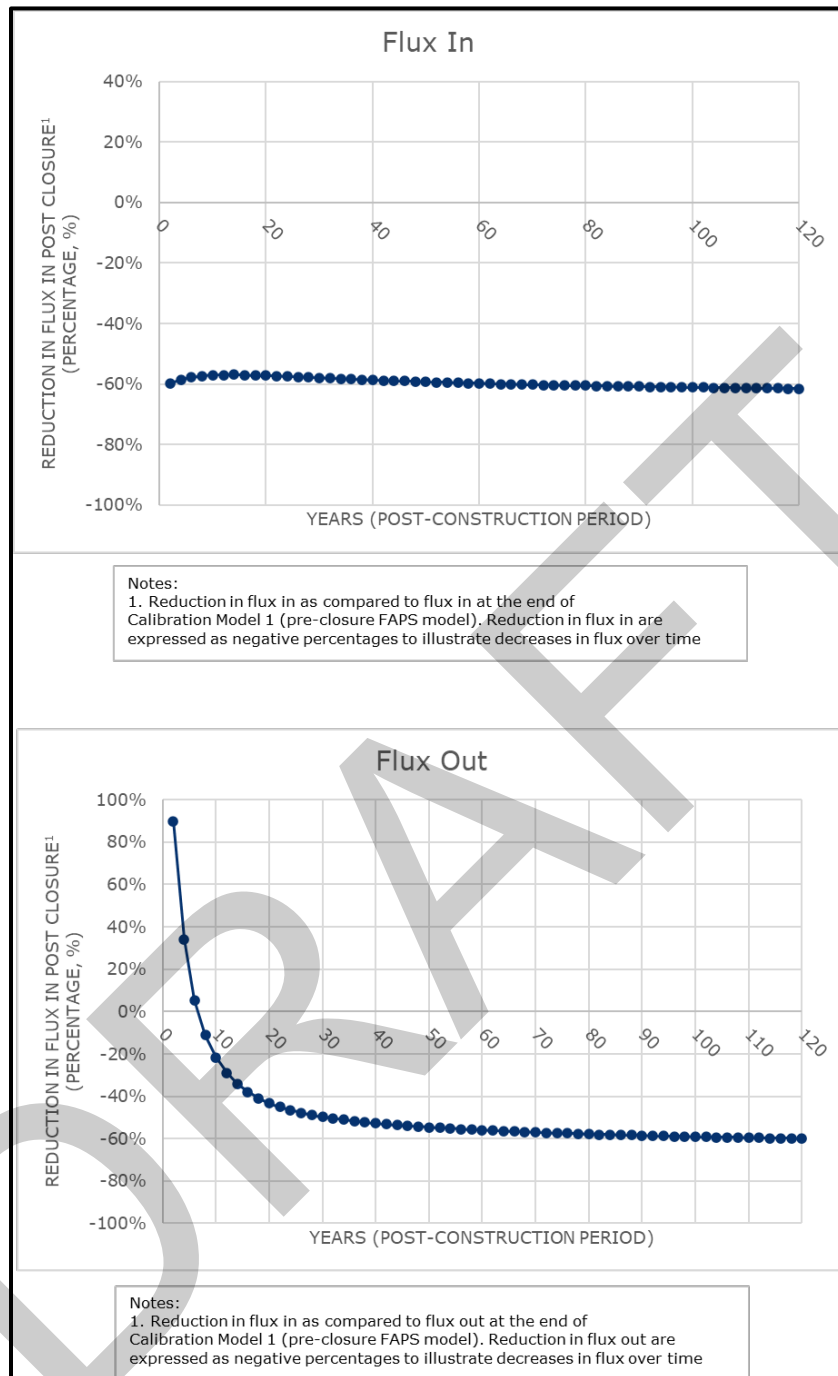
RAMBOLL



MODEL PREDICTED BORON CONCENTRATIONS AT FAPS MONITORING WELLS FOR CBR
SCENARIO

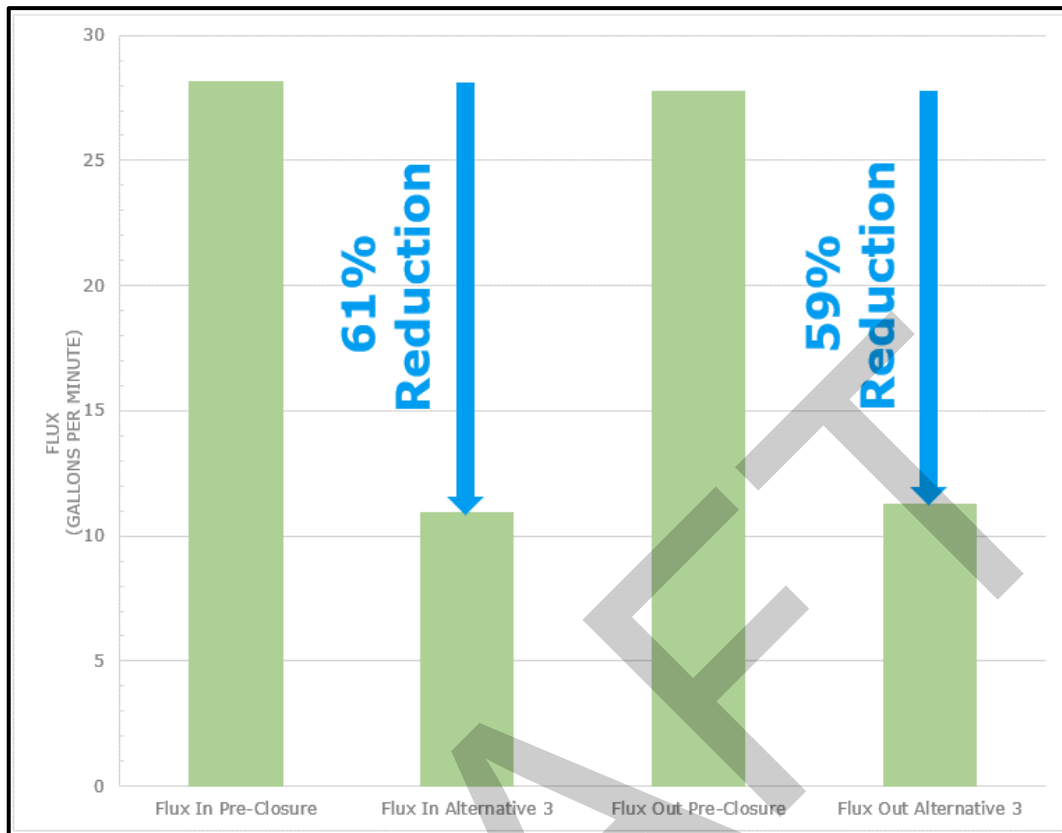
GROUNDWATER MODELING TECHNICAL MEMORANDUM
FLY ASH POND SYSTEM
BALDWIN POWER PLANT
BALDWIN, ILLINOIS

RAMBOLL



REDUCTIONS IN TOTAL FLUX IN AND OUT OF CCR FOLLOWING IMPLEMENTATION OF ALTERNATIVE 3: SOURCE CONTROL WITH GMS

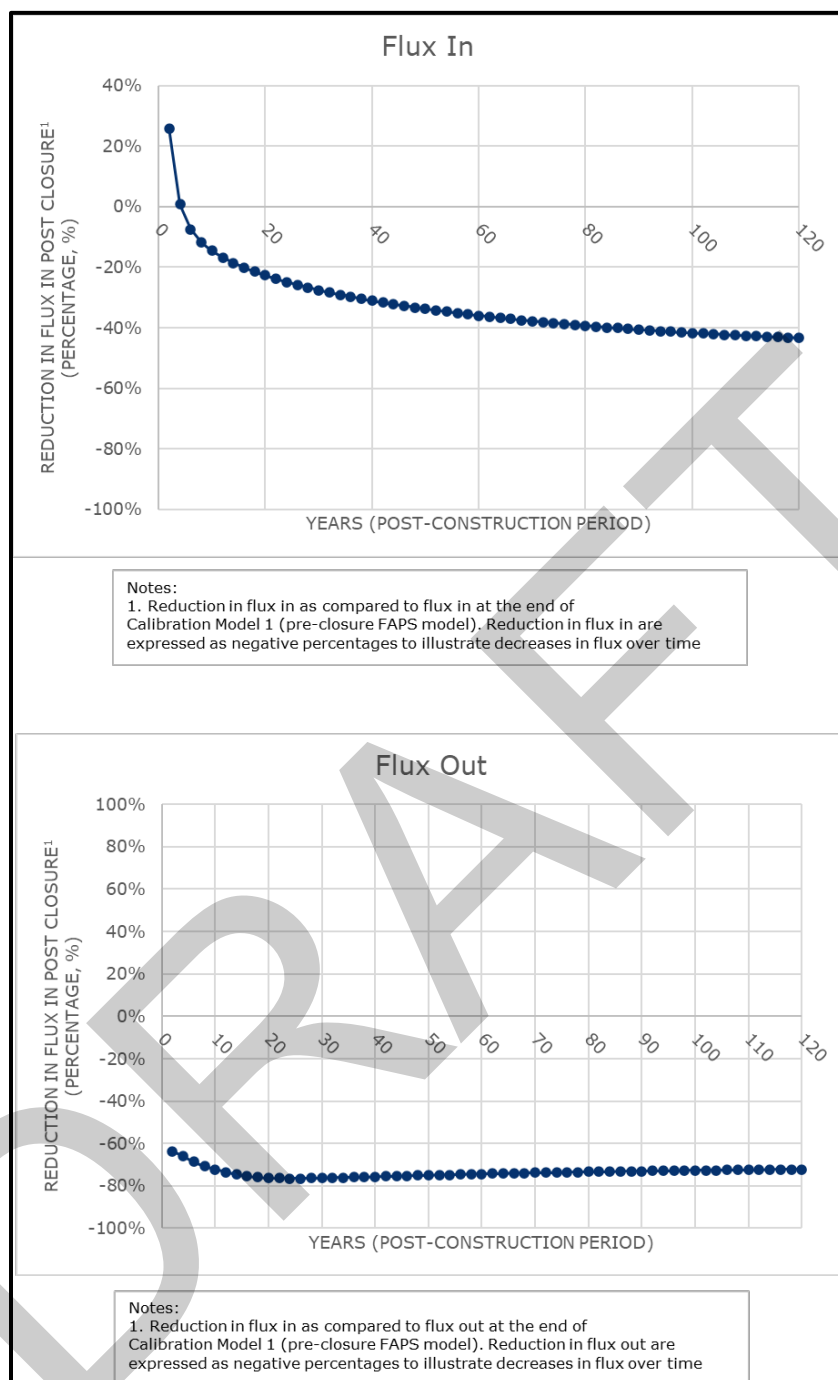
GROUNDWATER MODELING TECHNICAL MEMORANDUM
FLY ASH POND SYSTEM
BALDWIN POWER PLANT
BALDWIN, ILLINOIS



REDUCTIONS IN TOTAL FLUX IN AND OUT OF CCR 106 YEARS FOLLOWING
IMPLEMENTATION OF ALTERNATIVE 3: SOURCE CONTROL WITH GMS

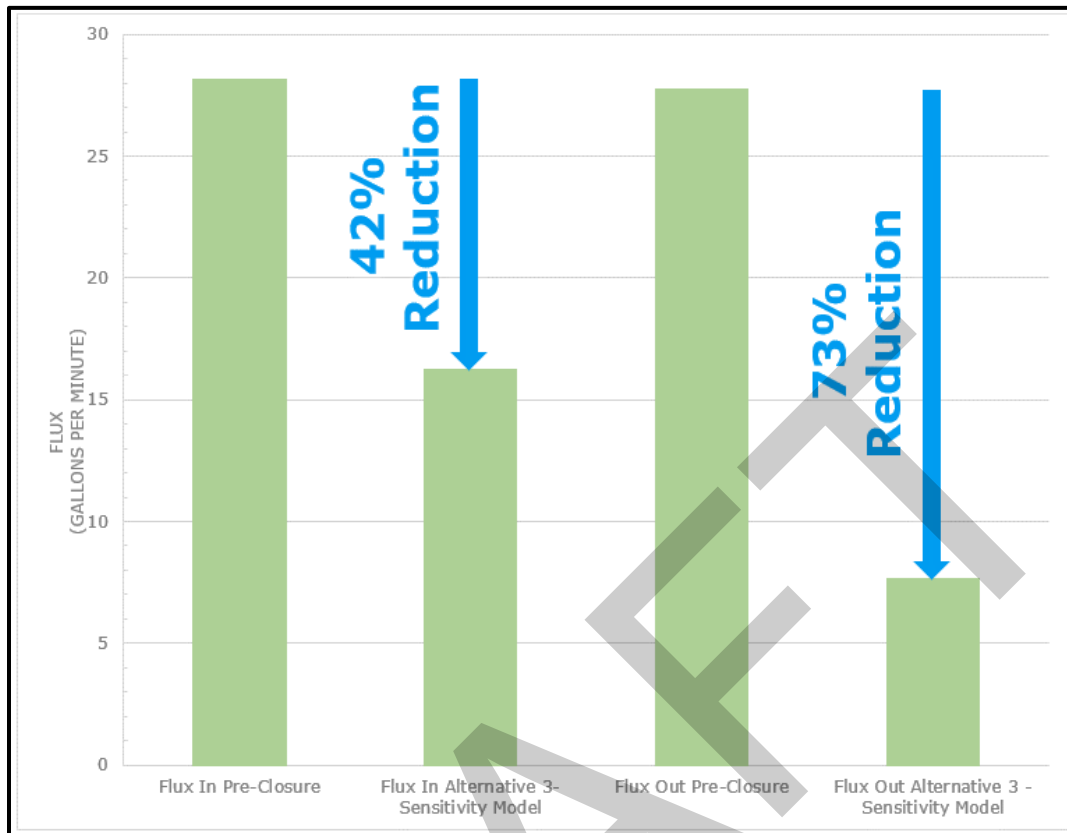
GROUNDWATER MODELING TECHNICAL MEMORANDUM
FLY ASH POND SYSTEM
BALDWIN POWER PLANT
BALDWIN, ILLINOIS

RAMBOLL



**REDUCTIONS IN TOTAL FLUX IN AND OUT OF CCR FOLLOWING IMPLEMENTATION OF
ALTERNATIVE 3: SOURCE CONTROL WITH GMS – SENSITIVITY MODEL**

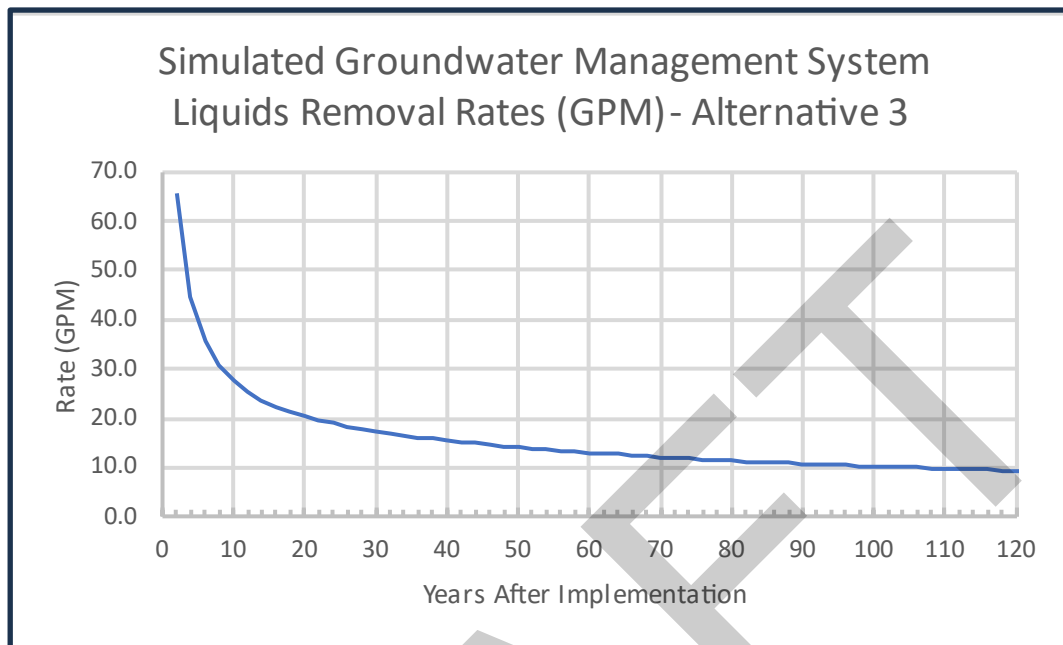
GROUNDWATER MODELING TECHNICAL MEMORANDUM
 FLY ASH POND SYSTEM
 BALDWIN POWER PLANT
 BALDWIN, ILLINOIS



REDUCTIONS IN TOTAL FLUX IN AND OUT OF CCR 106 YEARS FOLLOWING
IMPLEMENTATION OF ALTERNATIVE 3: SOURCE CONTROL WITH GMS –
SENSITIVITY MODEL

GROUNDWATER MODELING TECHNICAL MEMORANDUM
FLY ASH POND SYSTEM
BALDWIN POWER PLANT

RAMBOLL



SIMULATED GROUNDWATER MANAGEMENT SYSTEM LIQUIDS REMOVAL RATES FOR
ALTERNATIVE 3: SOURCE CONTROL WITH GMS

GROUNDWATER MODELING TECHNICAL MEMORANDUM
FLY ASH POND SYSTEM
BALDWIN POWER PLANT
BALDWIN, ILLINOIS

RAMBOLL

APPENDIX A
RAMBOLL AMERICAS ENGINEERING SOLUTIONS, INC.
(RAMBOLL), 2023A. GROUNDWATER MODELING REPORT
REVISION 1, BOTTOM ASH POND. BALDWIN POWER
PLANT. BALDWIN , ILLINOIS. AUGUST 1, 2023.

Intended for
Dynegy Midwest Generation, LLC

Date
August 1, 2023

Project No.
1940102653

GROUNDWATER MODELING REPORT REVISION 1


**BOTTOM ASH POND
BALDWIN POWER PLANT
BALDWIN, ILLINOIS**

GROUNDWATER MODELING REPORT REVISION 1 BALDWIN POWER PLANT BOTTOM ASH POND

Project Name **Baldwin Power Plant Bottom Ash Pond**
Project No. **1940102653**
Recipient **Dynegy Midwest Generation, LLC**
Document Type **Groundwater Modeling Report**
Revision **Revision 1**
Date **August 1, 2023**

Ramboll
234 W. Florida Street
Fifth Floor
Milwaukee, WI 53204
USA

T 414-837-3607
F 414-837-3608
<https://ramboll.com>



Jake J. Walczak, PG
Senior Hydrogeologist



Brian G. Hennings, PG
Senior Managing Hydrogeologist

CONTENTS

| | |
|---|-----------|
| Executive Summary | 6 |
| 1. Introduction | 9 |
| 1.1 Overview | 9 |
| 1.2 Site Location and Background | 9 |
| 1.3 Site History and Unit Description | 9 |
| 2. Site Geology and Hydrogeology | 11 |
| 3. Groundwater Quality | 15 |
| 4. Groundwater Model | 18 |
| 4.1 Overview | 18 |
| 4.2 Conceptual Site Model | 18 |
| 4.3 Model Approach | 19 |
| 5. Model Setup and Calibration | 20 |
| 5.1 Model Descriptions | 20 |
| 5.2 Flow and Transport Model Setup | 21 |
| 5.2.1 Grid and Boundary Conditions | 21 |
| 5.2.2 Flow Model Input Values and Sensitivity | 21 |
| 5.2.2.1 Model Layers | 22 |
| 5.2.2.2 Hydraulic Conductivity | 22 |
| 5.2.2.3 Recharge | 23 |
| 5.2.2.4 Storage and Specific Yield | 23 |
| 5.2.2.5 River Parameters | 24 |
| 5.2.2.6 Constant Head Boundary Parameters | 24 |
| 5.2.3 Transport Model Input Values and Sensitivity | 25 |
| 5.2.3.1 Initial Concentrations | 25 |
| 5.2.3.2 Source Concentrations | 25 |
| 5.2.3.3 Effective Porosity | 26 |
| 5.2.3.4 Storage and Specific Yield Sensitivity | 26 |
| 5.2.3.5 Dispersivity | 26 |
| 5.2.3.6 Retardation | 27 |
| 5.3 Flow and Transport Model Assumptions and Limitations | 27 |
| 5.4 Calibration Flow and Transport Model Results | 28 |
| 6. Simulation of CIP Closure Scenario | 31 |
| 6.1 Overview and Prediction Model Development | 31 |
| 6.2 HELP Model Setup and Results | 32 |
| 6.3 Simulation of CIP Closure Scenario | 32 |
| 6.3.1 CIP Closure Scenario Groundwater Flow System and Predicted Boron Concentrations | 33 |
| 7. Conclusions | 36 |
| 8. References | 38 |

TABLES (IN TEXT)

| | |
|---------|-------------------------|
| Table A | History of Construction |
|---------|-------------------------|

TABLES (ATTACHED)

| | |
|-----------|--|
| Table 2-1 | Monitoring Well Locations and Construction Details |
| Table 2-2 | Flow and Transport Model Calibration Targets |
| Table 5-1 | Flow Model Input and Sensitivity Analysis Results |
| Table 5-2 | Transport Model Input Values (Calibration) |
| Table 5-3 | Transport Model Input Values (Sensitivity) |
| Table 6-1 | HELP Model Input and Output Values |
| Table 6-2 | Prediction Model Input Values |

FIGURES (ATTACHED)

| | |
|-------------|---|
| Figure 1-1 | Site Location Map |
| Figure 1-2 | Site Map |
| Figure 2-1 | Monitoring Well Location Map |
| Figure 2-2 | Bedrock Potentiometric Surface Map November 14, 2022 |
| Figure 4-1 | Closure Scenario Calibration and Prediction Model Timeline |
| Figure 5-1 | Model Area Map |
| Figure 5-2 | Boundary Conditions for Layer 1 of the Calibrated Numerical Model |
| Figure 5-3 | Boundary Conditions for Layer 2 of the Calibrated Numerical Model |
| Figure 5-4 | Boundary Conditions for Layer 3 of the Calibrated Numerical Model |
| Figure 5-5 | Boundary Conditions for Layer 4 of the Calibrated Numerical Model |
| Figure 5-6 | Boundary Conditions for Layer 5 of the Calibrated Numerical Model |
| Figure 5-7 | Boundary Conditions for Layer 6 of the Calibrated Numerical Model |
| Figure 5-8 | Bottom Elevation of Model Layer 1 |
| Figure 5-9 | Bottom Elevation of Model Layer 2 |
| Figure 5-10 | Bottom Elevation of Model Layer 3 |
| Figure 5-11 | Bottom Elevation of Model Layer 4 |
| Figure 5-12 | Bottom Elevation of Model Layer 5 |
| Figure 5-13 | Bottom Elevation of Model Layer 6 |
| Figure 5-14 | Spatial Distribution of Hydraulic Conductivity Zones for Layer 1 in the Numerical Model |
| Figure 5-15 | Spatial Distribution of Hydraulic Conductivity Zones for Layer 2 in the Numerical Model |
| Figure 5-16 | Spatial Distribution of Hydraulic Conductivity Zones for Layer 3 in the Numerical Model |
| Figure 5-17 | Spatial Distribution of Hydraulic Conductivity Zones for Layer 4 in the Numerical Model |
| Figure 5-18 | Spatial Distribution of Hydraulic Conductivity Zones for Layer 5 in the Numerical Model |
| Figure 5-19 | Spatial Distribution of Hydraulic Conductivity Zones for Layer 6 in the Numerical Model |
| Figure 5-20 | Model Recharge Distribution (Steady State Calibration Model) |
| Figure 5-21 | Observed Versus Simulated Steady State Groundwater Levels from the Calibration Model |
| Figure 5-22 | Simulated Groundwater Level Residuals from the Calibrated Model |
| Figure 5-23 | Simulated Steady State Groundwater Level Contours from Layer 1 of the Calibrated Model |
| Figure 5-24 | Simulated Steady State Groundwater Level Contours from Layer 2 of the Calibrated Model |
| Figure 5-25 | Simulated Steady State Groundwater Level Contours from Layer 3 of the Calibrated Model |
| Figure 5-26 | Simulated Steady State Groundwater Level Contours from Layer 4 of the Calibrated Model |
| Figure 5-27 | Simulated Steady State Groundwater Level Contours from Layer 5 of the Calibrated Model |
| Figure 5-28 | Simulated Steady State Groundwater Level Contours from Layer 6 of the Calibrated Model |
| Figure 5-29 | Observed and Simulated Boron Concentrations (mg/L) |
| Figure 5-30 | Layer 1 Distribution of Boron Concentrations (mg/L) in the Calibrated Model (CCR) |

| | |
|-------------|--|
| Figure 5-31 | Layer 2 Distribution of Boron Concentrations (mg/L) in the Calibrated Model (UU [Upper Silty Clay]) |
| Figure 5-32 | Layer 3 Distribution of Boron Concentrations (mg/L) in the Calibrated Model (UU [PMP/Top of Vandalia]) |
| Figure 5-33 | Layer 4 Distribution of Boron Concentrations (mg/L) in the Calibrated Model (UU [Lower Silty Clay]) |
| Figure 5-34 | Layer 5 Distribution of Boron Concentrations (mg/L) in the Calibrated Model (UA [Decomposed Bedrock]) |
| Figure 5-35 | Layer 6 Distribution of Boron Concentrations (mg/L) in the Calibrated Model (UA) |
| Figure 6-1 | Recharge and Stormwater Management Modifications for Closure in Place |
| Figure 6-2 | Reductions in Total Flux in and Out of CCR Following Implementation of the CIP Closure Scenario |
| Figure 6-3 | Reductions in Total Flux in and Out of CCR 93 Years Following Implementation of the CIP Closure Scenario |
| Figure 6-4 | CIP - Model Predicted Boron Concentration |
| Figure 6-5 | CIP - Model Predicted Maximum Boron Plume in All Layers Approximately 93 Years After Implementation |
| Figure 6-6 | CIP and CBR - Model Predicted Boron Concentration at Proposed BAP Compliance Monitoring Wells PZ-182, OW-257, and MW-382 |

APPENDICES

| | |
|------------|---|
| Appendix A | History of Potential Exceedances Revision 1 (Ramboll, 2023c) |
| Appendix B | 40 C.F.R. § 257.95(g)(3)(ii): Alternate Source Demonstration, Baldwin Power Plant, Bottom Ash Pond, CCR Unit 601 (Ramboll, 2023a) |
| Appendix C | MODFLOW, HELP Model, and Flux Evaluation Data Export Files (Electronic Only) |
| Appendix D | HELP Model Output Files |
| Appendix E | Flux Evaluation Data |

ACRONYMS AND ABBREVIATIONS

| | |
|--------------|--|
| § | Section |
| 35 I.A.C. | Title 35 of the Illinois Administrative Code |
| 40 C.F.R. | Title 40 of the Code of Federal Regulations |
| ASD | Alternate Source Demonstration |
| BAP | Bottom Ash Pond |
| BPP | Baldwin Power Plant |
| CCR | coal combustion residuals |
| CIP | closure in place |
| cm/s | centimeters per second |
| Cooling Pond | Baldwin Lake |
| CSM | conceptual site model |
| DMG | Dynegy Midwest Generation, LLC |
| FAPS | Fly Ash Pond System |
| ft/day | feet/foot per day |
| ft/ft | feet per foot/feet |
| Geosyntec | Geosyntec Consultants, Inc. |
| GMP | Groundwater Monitoring Plan |
| GMR | Groundwater Modeling Report |
| gpm | gallons per minute |
| GWPS | Groundwater Protection Standard |
| HCR | Hydrogeologic Site Characterization Report |
| HELP | Hydrologic Evaluation of Landfill Performance |
| HUC | Hydrologic Unit Code |
| ID | Identification |
| IEPA | Illinois Environmental Protection Agency |
| Kd | distribution coefficient |
| Kh/Kv | vertical anisotropy |
| mg/L | milligrams per liter |
| mL/g | milliliters per gram |
| NAVD88 | North American Vertical Datum of 1988 |
| NGVD29 | National Geodetic Vertical Datum of 1929 |
| NID | National Inventory of Dams |
| No. | number |
| NPDES | National Pollutant Discharge Elimination System |
| NRT | Natural Resource Technology, Inc. |
| Phase II | Groundwater Quality Assessment and Phase II Hydrogeologic Investigation |
| PMP | potential migration pathway |
| Ramboll | Ramboll Americas Engineering Solutions, Inc. |
| SI | surface impoundment |
| Site | combined area including the BAP, FAPS, Secondary Pond, Tertiary Pond, and Cooling Pond |
| SDA | spray dry absorption |
| SSR | sum of squared residuals |

| | |
|----------------|---|
| S _y | specific yield |
| TDS | Total Dissolved Solids |
| TVD | total-variation-diminishing |
| UA | uppermost aquifer |
| UGU | Upper Groundwater Unit |
| USEPA | United States Environmental Protection Agency |
| USGS | United States Geological Survey |
| UU | Upper Unit |

DRAFT

EXECUTIVE SUMMARY

Ramboll Americas Engineering Solutions, Inc. (Ramboll) has prepared this Groundwater Modeling Report (GMR) on behalf of the Baldwin Power Plant (BPP), operated by Dynegy Midwest Generation, LLC (DMG), in accordance with requirements of Title 35 of the Illinois Administrative Code (35 I.A.C.) Section (§) 845: Standards for the Disposal of Coal Combustion Residuals in Surface Impoundments. This document presents the results of predictive groundwater modeling simulations for the proposed closure scenario for the Bottom Ash Pond (BAP). The BAP (coal combustion residuals [CCR] unit Identification [ID] number [No.] 601, Illinois Environmental Protection Agency [IEPA] ID No. W1578510001-06, and National Inventory of Dams [NID] No. IL50721) is the only active CCR unit present on the BPP property. The Fly Ash Pond System (FAPS) is a closed CCR unit on the BPP property (CCR unit ID 605; IEPA ID Nos. W1578510001-01, W1578510001-02, and W1578510001-03; and NID No. IL50721).

The BPP is located in Baldwin, Illinois (**Figure 1-1**). The BPP property is situated in an agricultural area. The BPP property is bordered to the west by the Kaskaskia River; to the east by Baldwin Road, farmland, and strip-mining areas; to the southeast by the Village of Baldwin; to the south by the Illinois Central Gulf railroad tracks, scattered residences, and State Route 154; and to the north by farmland (**Figure 1-2**).

A detailed summary of site conditions was provided in the revision to the Hydrogeologic Site Characterization Report (HCR; Ramboll, 2023d). The revision to the HCR includes hydrogeologic data collected after submittal of the initial HCR in 2021 (Ramboll, 2021c) as part of the 2022 Hydrogeologic Site Investigation were also used to establish a conceptual site model (CSM) for this GMR and is summarized herein. Three distinct water-bearing units have been identified in the vicinity of the BAP based on stratigraphic relationships and common hydrogeologic characteristics. The units are described as follows from the surface downward:

- **CCR:** CCR, consisting primarily of fly ash, bottom ash, and boiler slag. Also includes earthen fill deposits of predominantly clay and silt materials from on-site excavations that were used to construct berms and roads surrounding the various impoundments across the Site.
- **Upper Unit (UU):** Predominantly clay with some silt and minor sand, silt layers, and occasional sand lenses. Includes the lithologic layers identified as the Cahokia Formation, Peoria Loess, Equality Formation, and Vandalia Till. This unit is composed of unlithified natural geologic materials and extends from the upper saturated materials to the bedrock. Thin sand seams and the interface (contact) between the UU and bedrock have been identified as potential migration pathways (PMPs). No continuous sand seams were observed within or immediately adjacent to the BAP; however, the sand seams may act as a PMP due to relatively higher hydraulic conductivities. The acronym UU and the materials it contains is synonymous with Upper Groundwater Unit (UGU) used in previous documents.
- **Bedrock Unit:** This unit is considered the uppermost aquifer (UA). Pennsylvanian and Mississippian-aged bedrock is composed of interbedded shale and limestone bedrock, which underlies and is continuous across the entire Site.

The extent of sand and gravel aquifers in the region are primarily found along the Kaskaskia River Valley where sand and gravel deposits are highly permeable, thick, and extensive. Outside of the Kaskaskia River Valley, the unlithified materials in upland areas are predominantly clay, which generally provide a low probability of encountering sand and gravel layers for dependable groundwater supply. Although some thin sand seams and layers occur intermittently within the

Vandalia Till in localized areas around the BPP, most groundwater supplies in upland areas are obtained from large diameter shallow bored wells. Typical water wells in the vicinity of the BPP are between 25 and 55 feet deep, 36 to 48 inches in diameter, and collect groundwater through slow percolation into the wells, which are large diameter to allow for greater water storage to compensate for the low rate of groundwater infiltration (Ramboll, 2023d).

The shallow bedrock is the only water-bearing unit that is continuous across the Site. Groundwater in the bedrock mainly occurs under semi-confined to confined conditions with the overlying unlithified unit behaving as the upper confining unit to the UA. Shallow sandstone and creviced limestone may yield small supplies in some areas, but water quality becomes poorer (*i.e.*, highly mineralized) with increasing depth.

Data collected from previous field investigations, as well as the lithologic contact and groundwater elevation data from the 2022 Hydrogeologic Site Investigation reported in the revised HCR (Ramboll, 2023d), were used to develop a groundwater model for the BAP. The MODFLOW model was used to evaluate a closure scenario: CCR consolidation and closure in place (CIP) using information provided in the CCR Surface Impoundment Final Closure Plan (Geosyntec Consultants, Inc. [Geosyntec], 2022a).

The CIP closure scenario was predicted to reduce total flux in and out of the BAP CCR by greater than 90 percent within 30 days following implementation of the CIP closure scenario. This was determined by comparing the post-construction movement of water in and out of the consolidated BAP CCR to pre-construction conditions. The reduction in total flux in and out of the consolidated BAP CCR is predicted to exceed 90 percent reduction for the remaining model timeframe. In general, the greatest predicted reduction in heads among the proposed BAP compliance monitoring wells takes place within approximately 93 years following implementation of the CIP closure scenario, at which time total flux in and out are predicted to reduce by 95 and 93 percent respectively. Due to the low hydraulic conductivity of the UU and UA materials, heads are not predicted to stabilize at all proposed BAP compliance monitoring wells until approximately 482 years following implementation of the CIP closure scenario, at which time total flux in and out are predicted to reduce by approximately 96 percent.

A monitoring well network was included in a proposed BAP Groundwater Monitoring Plan (GMP) (Ramboll 2021a) to satisfy requirements of 35 I.A.C. § 845 and was submitted as part of the operating permit application for the BAP in 2021. Additional wells completed in 2022 are included in a revision to the proposed GMP (Ramboll, 2023b) that will be included as part of the final construction permit application for submittal to IEPA no later than August 1, 2023. A review and summary of data collected from 2015 through May 2023 are included in the revised HCR (Ramboll, 2023d).

Quarterly monitoring under 35 I.A.C. § 845.650(b) will commence no later than the second quarter of 2023. As such, comparisons of groundwater contaminant concentrations to the Groundwater Protection Standard (GWPS) in this report are considered potential exceedances. Potential exceedances of the GWPS are presented in the attached revision to the History of Potential Exceedances (**Appendix A**, Ramboll, 2023c) and discussed in **Section 3** of this report. Based on statistical analysis, evaluation of subsequent potential exceedances of the GWPS, and intention to pursue Alternate Source Demonstrations (ASDs), it has been determined there are no potential exceedances of applicable groundwater standards attributable to the BAP.

Groundwater contaminant transport modeling was completed to demonstrate how the proposed CIP closure plan will maintain compliance with the applicable GWPS. Boron is commonly used as

an indicator parameter for contaminant transport modeling for CCR because it is commonly present in coal ash leachate and it is mobile (*i.e.*, has low rates of sorption or degradation) in groundwater. The revised History of Potential Exceedances did not identify boron as a potential exceedance of the GWPS; however, boron has been detected in BAP porewater and groundwater; therefore, groundwater transport modeling was completed using boron.

The model domain for evaluating boron transport following closure of the BAP includes the closed FAPS which is present along the eastern and southern boundaries of the BAP. The FAPS completed IEPA approved closure activities in November of 2020, and it is another potential source of boron within the model domain. The closure plan for the FAPS also included groundwater modeling of boron transport. Boron transport within the current BAP model was compared to the results from the previous FAPS closure plan modeling and found that simulated flow and transport associated with the FAPS are consistent between the two models. As described in this report, proposed BAP compliance wells PZ-182, OW-257, and MW-382 are located in the direction of groundwater flow from the north central area of the FAPS between the FAPS (East Fly Ash Pond) and the surface water drainage feature near the west end of the BAP. Because these wells are downgradient of the FAPS which is an alternate source of boron, and groundwater quality at these wells is not attributable to the BAP, these wells were not included in the evaluation of BAP compliance with the GWPS following implementation of the CIP scenario.

Additionally, a BAP closure by removal (CBR) closure scenario prediction model was completed to evaluate the difference in post-construction boron concentrations simulated at PZ-182, OW-257, and MW-382 under both CIP and CBR conditions. Concentrations are predicted to increase above the GWPS for boron (2 milligrams per liter [mg/L]) following implementation of both BAP CIP and CBR closure scenarios in these three wells. Maximum concentrations within the modeling timeframes at these wells are predicted to be on the same order of magnitude for both BAP CIP and CBR closure scenarios. Since concentrations at proposed BAP compliance monitoring wells PZ-182, OW-257, and MW-382 increase to concentrations above the GWPS following implementation of the CBR closure scenario, after BAP source concentrations have been removed, the source for predicted post-construction concentrations within the model domain can only be attributable to the closed FAPS. These results support the conclusion that wells PZ-182, OW-257, and MW-382 should not be included in the evaluation of BAP compliance with the GWPS following implementation of the CIP scenario.

Results of groundwater fate and transport modeling conservatively estimate that groundwater boron concentrations at the proposed BAP compliance wells that are not influenced by the FAPS will remain below the GWPS following implementation of the CIP scenario at the BAP.

1. INTRODUCTION

1.1 Overview

In accordance with requirements of 35 I.A.C. § 845, Ramboll has prepared this GMR on behalf of the BPP, operated by DMG. This report applies specifically to the CCR unit referred to as the BAP (**Figure 1-1**). The BAP is a 177-acre unlined CCR surface impoundment (SI) used to manage CCR and non-CCR waste streams at the BPP. This GMR presents and evaluates the results of predictive groundwater modeling simulations for a proposed CIP closure scenario which includes: CCR removal from the western areas of the BAP, consolidation to the southeast, and eventually northeastern portions of the BAP, and construction of a cover system over the remaining CCR following initial corrective action measures (removal of free liquids from the BAP).

1.2 Site Location and Background

The BPP is located in southwest Illinois in Randolph and St. Clair Counties. The Randolph County portion of the BPP is located within Sections 2, 3, 4, 9, 10, 11, 14, 15, and 16 of Township 4 South and Range 7 West. The St. Clair County portion of the property is located within Sections 33, 34, and 35 of Township 3 South and Range 7 West. The BAP is approximately one-half mile west-northwest of the Village of Baldwin (**Figure 1-1**).

The BPP property is bordered to the west by the Kaskaskia River; to the east by Baldwin Road, farmland, and strip-mining areas; to the southeast by the Village of Baldwin; to the south by the Illinois Central Gulf railroad tracks, scattered residences, and State Route 154; and to the north by farmland. The St. Clair/Randolph County Line crosses east-west at approximately the midpoint of Baldwin Lake (*i.e.*, Cooling Pond). **Figure 1-1** shows the location of the BPP; **Figure 1-2** is a site map showing the location of the BAP (a 35 I.A.C. § 845 regulated CCR unit and the subject of this GMR), FAPS (an IEPA closed CCR unit), Secondary Pond, Tertiary Pond, and Cooling Pond. The combined area including the BAP, FAPS, Secondary Pond, Tertiary Pond, and Cooling Pond will hereinafter be referred to as the Site.

1.3 Site History and Unit Description

The BPP is a coal-fired electrical generating plant that began operation of its first unit in 1970; two additional generating units were put into service in 1973 and 1975. The plant initially burned bituminous coal from Illinois and switched to subbituminous coal in 1999. Total plant generating capacity is approximately 1,892 megawatts.

The BAP is classified as an existing, unlined CCR SI and covers an area of approximately 177 acres in the southern portion of the BPP property (**Figure 1-2**). The BAP is surrounded by a perimeter road and is bounded to the north by the Cooling Pond, and to the east and south by the closed FAPS CCR Multi-Unit. The BAP is also bounded to the west by the easternmost wooded area that surrounds the Secondary and Tertiary Ponds. The BAP is being used to store and dispose of sluiced bottom ash, some of which is mined for beneficial use, to temporarily store spray dry absorption (SDA) waste, and to clarify plant process water, including other non-CCR station process wastewaters, prior to discharge in accordance with the BPP's National Pollutant Discharge Elimination System (NPDES) permit (AECOM, 2016b; IEPA, 2016).

The FAPS at the BPP is a closed CCR Multi-Unit consisting of three unlined SIs: Old East Fly Ash Pond (IEPA Unit ID W1578510001-01), the East Fly Ash Pond (IEPA Unit ID W1578510001-02), and West Fly Ash Pond (IEPA Unit ID W1578510001-03), with a combined surface area of

approximately 232 acres (**Figure 1-2**). During operation, the FAPS discharged water to the BAP. The receiving water bodies for the BAP were the Secondary Pond, and in turn the Tertiary Pond, which ultimately discharges towards a tributary of the Kaskaskia River, south of the Cooling Pond intake structure. A Groundwater Quality Assessment and Phase II Hydrogeologic Investigation (Phase II; Natural Resource Technology, Inc. [NRT], 2014a) was followed by a Supplemental Hydrogeologic Site Characterization and Groundwater Monitoring Plan dated March 31, 2016 (NRT, 2016a) with revised pages included in the response to IEPA July 13, 2016 comments in the technical memorandum dated August 8, 2016 (NRT, 2016b) to define the hydrogeology and to assess the groundwater impacts related to the FAPS. Groundwater models were also completed to assess the groundwater impacts associated with closure of the FAPS and predict the fate and transport of CCR leachate components, as well as estimate the time required for hydrostatic equilibrium of groundwater beneath the FAPS (NRT, 2014b; NRT, 2014c; NRT, 2016c). Based on these assessments, a Closure and Post-Closure Care Plan (AECOM, 2016a), which included a groundwater monitoring program sufficient for long-term, post-closure monitoring, was developed and approved by IEPA in a letter to the Dynegy Operating Company dated August 16, 2016. Closure activities, which included constructing a final cover system to control the potential for water infiltration into the closed CCR unit, were completed, and FAPS closure was completed November 17, 2020. The approximate dates of construction of each successive stage of the BAP and FAPS are summarized in **Table A** below (AECOM, 2016b).

Table A. History of Construction

| Date | Event |
|------|---|
| 1969 | Construction of Old East Fly Ash Pond, East Fly Ash Pond, and West Fly Ash Pond external perimeter embankment |
| 1979 | Construction of East Fly Ash Pond and West Fly Ash Pond northern embankment |
| 1989 | Raise inboard perimeter of the entire East Fly Ash Pond and West Fly Ash Pond |
| 1995 | Construction of interior dike between the East Fly Ash Pond and West Fly Ash Pond |
| 1999 | Raise of interior dike between the East Fly Ash Pond and West Fly Ash Pond; replacement of outlet pipe from the West Fly Ash Pond to the Secondary Pond |
| 2012 | Modification of BAP embankment (original construction date unknown) |
| 2016 | Closure Plan completed for the FAPS and approved by IEPA |
| 2020 | FAPS closure activities, including construction of a final cover system, and FAPS closure completed |

2. SITE GEOLOGY AND HYDROGEOLOGY

BAP hydrogeologic data presented in the initial HCR (Ramboll, 2021c) and BAP hydrogeologic data collected after submittal of the initial HCR in 2021 as part of the 2022 Hydrogeologic Site Investigation and included in the revision to the HCR (Ramboll, 2023d) were used to establish a CSM for this GMR and is summarized below. Refer to the revision to the HCR (Ramboll, 2023d) for more details of regional and local site characteristics. BAP hydrogeologic data collected as part of the 2022 Hydrogeologic Site Investigation are presented in a revised HCR (Ramboll, 2023d) to be included in a construction permit application for submittal to IEPA no later than August 1, 2023. Surface elevations range from approximately 415 feet North American Vertical Datum of 1988 (NAVD88) in the east side of the BAP to 450 feet NAVD88 in the west side of the BAP. Topographic maps drawn prior to construction indicate the areas of the BAP were generally between 400 and 430 feet National Geodetic Vertical Datum of 1929 (NGVD29), which included a drainage feature near the west end of the BAP (Figure 2-2 of the revised HCR). Topography in the vicinity of the Site (**Figure 1-1**) ranges from approximately 370 feet NAVD88 along the Kaskaskia River southwest of the Site to 450 feet NAVD88 towards the south and east. The principal surface drainage for the region is the Kaskaskia River.

There are five principal types of unlithified materials above the bedrock in the vicinity of the BAP, these include the following in descending order:

- Fill, predominantly coal ash (fly ash, bottom ash, and slag) within the CCR units, but also including general fill within constructed levees around the Cooling Pond, constructed berms around the Site, and constructed railroad embankments south of the Site;
- Alluvial clay, sandy clay, and clayey sand of the Cahokia Formation (ranging in thickness at the BAP from 13 to 27 feet);
- Silt and silty clay of the Peoria Loess (ranging in thickness at the BAP from 2 to 23 feet);
- Clay and sandy clay of the Equality Formation (ranging in thickness at the BAP from 8 to 37 feet), with occasional sand seams and lenses; and
- Clay and sandy clay diamictos of the Vandalia Till (ranging in thickness at the BAP from 11 to 37 feet) with intermittent and discontinuous sand lenses.

Depth to bedrock ranges from approximately 28.4 feet towards the west end of the BAP (MW-370) to approximately 57 feet immediately north of the BAP (MW-393).

Three distinct water-bearing units have been identified in the vicinity of the BAP based on stratigraphic relationships and common hydrogeologic characteristics. The units are described as follows from the surface downward:

- **CCR:** CCR, consisting primarily of fly ash, bottom ash, and boiler slag. Also includes earthen fill deposits of predominantly clay and silt materials from on-site excavations that were used to construct berms and roads surrounding the various impoundments across the Site. The overall (geometric mean) horizontal and vertical hydraulic conductivity for the CCR determined during the Phase II and 2022 Hydrogeologic Site Investigations are 1.5×10^{-2} centimeters per second (cm/s) and 4.1×10^{-5} cm/s, respectively. Horizontal and vertical hydraulic conductivities for this unit determined during the Phase II and 2022 Hydrogeologic

Site Investigations ranged from 8.1×10^{-4} to 1.1×10^{-1} cm/s and 5.6×10^{-7} to 6.5×10^{-4} cm/s, respectively.

- **UU:** Predominantly clay with some silt and minor sand, silt layers, and occasional sand lenses. Includes the lithologic layers identified as the Cahokia Formation, Peoria Loess, Equality Formation, and Vandalia Till. This unit is composed of unlithified natural geologic materials and extends from the upper saturated materials to the bedrock. As observed in the field, one or more of these four lithologic units may be present at a particular soil boring location; and, the observed lithologic unit(s) may or may not be saturated depending on location at the Site. Given that these units are not consistently in contact with groundwater, this unit was renamed from UGU used in previous reports to UU. The term UU is synonymous with UGU used in previous documents. The overall (geometric mean) horizontal and vertical hydraulic conductivities for this unit determined during the Phase II and 2022 Hydrogeologic Site Investigations are 2.9×10^{-5} cm/s and 3.5×10^{-7} cm/s, respectively. Horizontal and vertical hydraulic conductivities for this unit determined during the Phase II and 2022 Hydrogeologic Site Investigations ranged from 3.5×10^{-7} to 6.8×10^{-4} cm/s and 6.3×10^{-9} to 4.2×10^{-4} cm/s, respectively. Thin sand seams and the interface (contact) between the UU and bedrock have been identified as PMPs. No continuous sand seams were observed within or immediately adjacent to the BAP; however, the sand seams may act as a PMP due to relatively higher hydraulic conductivities (on the order of 10^{-4} cm/s) than the surrounding clays (on the order of 10^{-5} cm/s). The contacts between the unlithified material and bedrock have also been identified as PMPs where horizontal hydraulic conductivity data in Site monitoring wells with screens and/or filter packs across or immediately above the bedrock range from 3×10^{-7} to 6×10^{-4} cm/s and have a geometric mean horizontal hydraulic conductivity of 2×10^{-5} cm/s.
- **Bedrock Unit:** This unit is composed of interbedded shale and limestone bedrock, which underlies and is continuous across the entire Site and has been identified as the UA. The horizontal hydraulic conductivity for this unit determined during the Phase II and 2022 Hydrogeologic Site Investigations ranges from 2.4×10^{-7} to 3.5×10^{-5} cm/s with a geometric mean of 1.9×10^{-6} cm/s (Ramboll, 2023d).

In general, the UU consists of low permeability clays and silts. Within the UU, only thin and intermittent sand lenses are present within predominantly clay deposits; thus, the unlithified materials do not represent a continuous aquifer unit. Thin, non-continuous sandy deposits (*i.e.*, PMPs) that exist across the Site do not appear to extend to the FAPS and BAP as evidenced by soil borings adjacent to the CCR units in which no sand was observed.

The extent of sand and gravel aquifers in the region are primarily found along the Kaskaskia River Valley where sand and gravel deposits are highly permeable, thick, and extensive. Outside of the Kaskaskia River Valley, the unlithified materials in upland areas are predominantly clay, which generally provide a low probability of encountering sand and gravel layers for dependable groundwater supply. Although some thin sand seams and layers occur intermittently within the Vandalia Till in localized areas around the BPP, most groundwater supplies in upland areas are obtained from large diameter shallow bored wells. Typical water wells in the vicinity of the BPP are between 25 and 55 feet deep, 36 to 48 inches in diameter, and collect groundwater through slow percolation into the wells, which are large diameter to allow for greater water storage to compensate for the low rate of groundwater infiltration (Ramboll, 2023d).

The underlying bedrock at the Site is Pennsylvanian and Mississippian bedrock, mainly limestone and shale. A bedrock low is present at the southwest corner of the Site and extends

northeastward. The Tertiary Pond in the southwest corner of the Site corresponds to the lowest observed bedrock surface elevation (372.6 feet NAVD88). Higher bedrock elevations are present east of the BPP and FAPS as observed at MW-358 (428.6 feet NAVD88). The bedrock in the vicinity of the BAP yields small amounts of water from interconnected pores, cracks, fractures, crevices, joints, and bedding planes. The shallow bedrock is the only water-bearing unit that is continuous across the Site. Shallow sandstone and creviced limestone may yield small supplies in some areas, but water quality becomes poorer (*i.e.*, highly mineralized) with increasing depth. The Pennsylvanian and Mississippian rocks generally have low porosities and permeabilities, are not a reliable source of groundwater, and the quality varies considerably (Pryor, 1956). Limestones intercepted at the Site are generally light to dark gray, fine-grained, thin bedded, banded, argillaceous, and competent except where weathered. Weathering of the limestone produces a calcareous clay. Limestone layers are often interbedded with thin shale layers and are sometimes fossiliferous or sandy. The shale layers are generally weathered, competent, silty, slightly micaceous, fissile, and dark gray. Where highly weathered shale (*i.e.*, decomposed bedrock) was encountered, the shale was non-fissile and resembled an unlithified stiff clay with medium to high plasticity.

The locations of groundwater monitoring wells are provided on **Figure 2-1**. Based on elevation measurements, lateral groundwater flow in the shallow unlithified materials and bedrock is generally to the west and southwest across the Site (**Figure 2-2**) toward the Kaskaskia River. Groundwater flow in bedrock is toward the northwest in the east and central areas of the BAP, and southwest to northwest on the east area of the FAPS until groundwater reaches the bedrock valley feature underlying the Secondary and Tertiary Ponds west of the BAP and FAPS, at which point the flow direction veers towards this bedrock surface low. Groundwater elevations across the Site vary seasonally, generally less than 7 feet, and range between approximately 370 and 450 feet NAVD88, although flow directions are generally consistent. Additional potentiometric surface maps are located in Figures 3-2 to 3-5 and Appendix E of the revised HCR (Ramboll, 2023d).

In the western area of the FAPS, average horizontal hydraulic gradients in the shallow unlithified materials and bedrock were 0.015 feet per foot/feet (ft/ft) and 0.016 ft/ft, respectively, as groundwater flowed from east to west across the FAPS. Average groundwater velocities in the shallow unlithified materials and bedrock in the western area of the FAPS were 0.0082 and 0.0003 feet per day (ft/day), respectively. In general, flow velocities in the vicinity of the FAPS are consistent, varying only 0.0019 ft/day in the shallow unlithified materials and 0.0002 ft/day in the bedrock.

Between monitoring wells in the northeastern portion of the BAP, average horizontal hydraulic gradients in the shallow unlithified materials and bedrock were 0.004 and 0.003 ft/ft, respectively, as groundwater flowed southeast to northwest across the BAP. Average groundwater velocities in the shallow unlithified materials and bedrock in the northeast portion of the BAP were 0.0023 and 0.0001 ft/day, respectively. Between monitoring wells in the western portion of the BAP average horizontal hydraulic gradients in the shallow unlithified materials and bedrock were 0.011 and 0.017 ft/ft, respectively, as groundwater flowed northeast to southwest across the BAP. Average groundwater velocities in the west area of the BAP in shallow unlithified materials and bedrock were 0.0058 and 0.0003 ft/day, respectively. In general, flow velocities are consistent, varying only 0.001 ft/day in shallow unlithified materials and 0.0001 ft/day in bedrock in the vicinity of the BAP.

Groundwater in the Pennsylvanian and Mississippian-aged bedrock mainly occurs under semi confined to confined conditions as demonstrated with vertical hydraulic gradient calculations presented in the revised HCR (Ramboll, 2023d), with the overlying unlithified unit behaving as the upper confining unit to the UA (Bedrock Unit). The relatively flat horizontal groundwater gradient beneath the Site, and the mostly upward vertical gradients, inconsistent upward/downward vertical gradients or flowing artesian conditions observed in the UU and UA, suggests the BAP and neighboring ponds are not areas of increased recharge or infiltration (Ramboll, 2023d).

In 2022, additional wells were installed as part of the 2022 Hydrogeologic Site Investigation, after the initial HCR was completed (Ramboll, 2021c), for further hydrogeologic investigation and water quality evaluation. The results of the 2022 Hydrogeologic Site Investigation and water quality evaluation are included in a revised HCR (Ramboll, 2023d). A summary of monitoring well locations and construction details for wells used in this GMR are included in **Table 2-1** and the locations are depicted on **Figure 2-1**. Groundwater elevation readings and lithologic contact information from the wells completed in 2022 have been incorporated into this GMR. Groundwater elevation data from 48 of the 78 total monitoring wells included in **Table 2-1** and depicted on **Figure 2-1**, were utilized as groundwater model flow calibration targets as summarized in **Table 2-2** and described in **Sections 5.2 and 5.2.2**. Boron concentration data from 50 of the 78 total monitoring wells included in **Table 2-1** and depicted on **Figure 2-1**, were utilized as transport model calibration targets as summarized in **Table 2-2** and described in **Sections 5.2 and 5.2.3**. Complete documentation of the 2022 Hydrogeologic Site Investigation activities at the BAP including boring logs, monitoring well and piezometer construction forms, and summary tables of testing results (e.g., groundwater analytical results, horizontal and vertical gradient calculations, and single well aquifer test results), are provided in a revised HCR (Ramboll, 2023d).

3. GROUNDWATER QUALITY

The classification of groundwater at the Site was addressed in the Phase II investigation (NRT, 2014a). Field hydraulic conductivity tests performed on the UU materials (*i.e.*, Cahokia Formation, Equality Formation, and Vandalia Till) and Bedrock Unit materials (*i.e.*, Mississippian and Pennsylvanian bedrock) as part of the Phase II and 2022 Hydrogeologic Site Investigations had geometric mean hydraulic conductivities of 2.9×10^{-5} cm/s and 1.9×10^{-6} cm/s, respectively.

Geologic material with a hydraulic conductivity of less than 1×10^{-4} cm/s which does not meet the provisions of 35 I.A.C. § 620.210 (Class I), 35 I.A.C. § 620.230 (Class III), or 35 I.A.C. § 620.240 (Class IV), meets the definition of a Class II – General Resource Groundwater (35 I.A.C. § 620.220). Based on the detailed geologic information provided for the unlithified materials and bedrock at BPP, along with the hydrogeologic data, the groundwater in both the unlithified deposits and underlying bedrock at the Site is classified as Class II - General Resource Groundwater.

Bedrock was intercepted at 42 borings/well locations installed during the Phase II Investigation, the investigation for Supplemental Hydrogeologic Site Characterization and Groundwater Monitoring Plan, and the 2022 Hydrogeologic Site Investigation (Ramboll, 2023d). The UA at the Site is the shallow Pennsylvanian and Mississippian-aged bedrock that immediately underlies the unlithified deposits. The shallow bedrock yields water through interconnected secondary porosity features (*e.g.*, cracks, fractures, crevices, joints, bedding planes, and other secondary openings). The shallow bedrock is the only water-bearing unit that is continuous across the Site. Groundwater in the Pennsylvanian and Mississippian-aged bedrock mainly occurs under semi-confined to confined conditions with the overlying unlithified unit behaving as the upper confining unit to the UA. Off-site, immediately upgradient and downgradient of the BPP property boundaries, both the shallow glacial deposits and the shallow bedrock have served as a source of water supply (see water well survey in Section 5.1 of the revised HCR; Ramboll, 2023d). The shallow unlithified deposits off-site have yielded water through intermittent, discontinuous sand lenses and, in the bedrock, through fractured sandstone and limestone. However, within the boundaries of the Site, only thin and intermittent sand lenses are present within predominantly clay deposits; thus, the unlithified materials do not represent a continuous aquifer unit. Based on the above, the Bedrock Unit is the only viable aquifer in the vicinity of the Site and was designated as the UA in the Supplemental Hydrogeologic Site Characterization and Groundwater Monitoring Plan (NRT, 2016b), consistent with the United States Environmental Protection Agency (USEPA) definition in Title 40 of the Code of Federal Regulations (40 C.F.R.) § 257.53.

Water quality in the UA (*i.e.*, Pennsylvanian and Mississippian-aged bedrock) decreases with increasing depth as water becomes increasingly mineralized. Further, the ability of the unit to store and transmit water is dependent on the density of bedrock features that contribute to secondary porosities and whether those features are interconnected enough to yield water. Therefore, the lower limit of the UA is the depth at which either the groundwater is mineralized to a point that it is no longer a useable water source, or the secondary porosities do not yield a sufficient volume of groundwater to produce a useable water supply.

A monitoring well network was included in a proposed BAP GMP (Ramboll 2021a) to satisfy requirements of 35 I.A.C. § 845 and was submitted as part of the operating permit application for the BAP in 2021. Additional wells completed in 2022 are included in a revision to the

proposed GMP (Ramboll, 2023b) that will be included as part of the construction permit application for submittal to IEPA no later than August 1, 2023. A review and summary of data collected from 2015 through May 2023 are included in the revised HCR (Ramboll, 2023d). Groundwater data collected from the 40 C.F.R. § 257 network monitoring wells and proposed 35 I.A.C. § 845 monitoring wells between 2015 and 2023 were evaluated with respect to standards included in 35 I.A.C. § 845.600(a)(1) in the revised HPE (**Appendix A**, Ramboll, 2023c). This data set was selected because it includes parameters (total metals) consistent with the parameter list in 35 I.A.C. § 845.600(a)(1). Based on this data set, there were no consistent and/or significant concentrations of antimony, barium, boron, cadmium, calcium, mercury, molybdenum, pH, selenium, sulfate, and total dissolved solids (TDS) greater than the GWPSs. A summary of groundwater statistical analysis is provided in the revised HPE (Ramboll, 2023c). The Determination of Potential Exceedances (Table 1 of **Appendix A**) and Summary of Potential Exceedances (Table 2 of **Appendix A**) indicate the parameter well pairs listed below were detected at concentrations greater than the applicable 35 I.A.C. § 845.600(a)(1) standards and are considered potential exceedances:

- Arsenic at well OW-257
- Beryllium at well OW-257
- Chromium at well OW-257
- Chloride at well MW-370
- Cobalt at well OW-257
- Fluoride at well MW-393
- Lead at well OW-257
- Lithium at well OW-257
- Radium 226 and 228 combined at well OW-257
- Thallium at well OW-257

An ASD (**Appendix B**) was prepared by Ramboll (2023a) to further evaluate previously identified potential GWPS exceedances at UU compliance well MW-370. The results of the evaluation demonstrated that the potential GWPS exceedance of lithium in well MW-370 was not related to the BAP based on several lines of evidence presented in the ASD. Additional data is being collected to support multiple lines of evidence demonstrating the CCR unit is also not the source of observed detections of lithium at OW-257. Since an ASD is being pursued, and potential GWPS exceedances for lithium are not related to the BAP, lithium will not be discussed further in this GMR.

ASDs will be pursued for potential exceedances of chloride and fluoride at wells MW-370 and MW-393, respectively. ASDs will also be pursued for potential exceedances at proposed UU compliance well OW-257. Additional data is being collected to support multiple lines of evidence demonstrating the CCR unit is not the source of observed detections. Since ASDs are being pursued, arsenic, beryllium, chromium, chloride, cobalt, fluoride, lead, lithium, radium 226 and 228 combined, and thallium will not be discussed further in this GMR.

Quarterly monitoring under 35 I.A.C. § 845.650(b) will commence no later than the second quarter of 2023. As such, comparisons of groundwater contaminant concentrations to the GWPS

in this report are considered potential exceedances. Potential exceedances of the GWPS are presented in the attached revision to the History of Potential Exceedances (**Appendix A**). Based on statistical analysis, evaluation of subsequent potential exceedances of the GWPS, and intention to pursue ASDs, it has been determined there are no potential exceedances of applicable groundwater standards attributable to the BAP.

DRAFT

4. GROUNDWATER MODEL

4.1 Overview

Data collected from previous field investigations, as well as the lithologic contact, groundwater elevation, and boron concentration data from 2022 Hydrogeologic Site Investigation and subsequent groundwater sampling events included in the revised HCR (Ramboll, 2023d), were used to develop a groundwater flow and transport model for the BAP. The MODFLOW (flow) and MT3DMS (transport) models were used to evaluate one closure scenario: CCR consolidation and CIP using information provided in the CCR Surface Impoundment Final Closure Plan (Geosyntec, 2022a). The results of the MODFLOW and MT3DMS modeling of the CIP closure scenario are summarized in this GMR. Associated model files are included as **Appendix C**. Contaminant transport modeling was completed in 2023 following the collection of additional groundwater samples from the monitoring wells installed in 2022. Transport modeling results are provided in this revised GMR and will be included in a construction permit application for submittal to IEPA no later than August 1, 2023.

4.2 Conceptual Site Model

The revised HCR (Ramboll, 2023d) is the foundation document for the site setting and CSM that describes groundwater flow at the Site. Additional hydrogeologic data was collected after submittal of the initial in 2021 HCR (Ramboll, 2021c) during the 2022 Hydrogeologic Site Investigation and included in this GMR to support the CSM and develop the model. The BAP overlies the recharge area for the underlying geologic media (*i.e.*, low permeability clays of the UU). Groundwater enters the model domain vertically via recharge. Groundwater may also enter or exit the model through the Cooling Pond, Secondary and Tertiary Ponds, the Kaskaskia River, or the many tributary streams located within the model domain. Groundwater may also exit the model through surface water management features within the BAP. Groundwater in the un lithified materials consistently flows east to west towards the Kaskaskia River. Groundwater flow in bedrock is northwest in the east and central areas of the BAP, and southwest to northwest on the east area of the FAPS until groundwater reaches the bedrock valley feature underlying the Secondary and Tertiary Ponds west of the BAP and FAPS, at which point the flow direction veers towards this bedrock surface low at the southwestern corner of the Site.

Groundwater contaminant transport modeling was completed to demonstrate how the proposed CIP closure scenario will maintain compliance with the applicable GWPS. Boron is commonly used as an indicator parameter for contaminant transport modeling for CCR because it is commonly present in coal ash leachate and it is mobile (*i.e.*, has low rates of sorption or degradation) in groundwater. The revision to the History of Potential Exceedances (**Appendix A**, Ramboll, 2023c) did not identify boron as a potential exceedance of the GWPS; however, boron has been detected in BAP porewater and groundwater. Therefore, groundwater transport modeling was completed using boron. The BAP and FAPS were modeled as sources of boron within the model domain. The BAP and FAPS are constructed over low permeability clays of the UU. Mass (boron) is added to groundwater via vertical recharge through CCR, and horizontal groundwater flow through CCR where it is in contact with the water table. Boron mass flows with groundwater (onsite groundwater flow directions described above). The primary transport pathway is the UA which underlies the BAP and is continuous across the entire Site. The UU also contains PMPs in the form of thin discontinuous sand seams within the UU or at the interface (contact) between the UU and bedrock where hydraulic conductivities are relatively higher.

4.3 Model Approach

A three-dimensional groundwater flow and transport model was calibrated to represent the conceptual flow system described above. Initial steady state flow modeling was performed to represent current Site conditions in 2022 following closure of the FAPS in 2020. This flow model was calibrated to match median groundwater elevations for recent groundwater elevation data. The calibrated steady state flow model was used to develop a calibrated transient flow and transport model to match recent boron concentrations observed at each monitoring well. The calibrated model was then used to evaluate the effectiveness of the CIP closure scenario. The start of the transient flow and transport model was initiated in 1970 (model year 0) when the BPP began operation and the BAP and FAPS were active (initial conditions model) through 2020 (51 model years) when closure at the FAPS was complete. Three models were included for the closure prediction simulation. The first model simulated an extended period of current conditions, 2021 to 2024 (4 model years). The second model simulated a period for the removal of free liquids, 2025 to 2027 (3 model years). The third model simulated the final closure conditions, 2028 to 3027 (1,000 model years). The prediction modeling timeline for the CIP closure scenario is illustrated in **Figure 4-1**.

Three model codes were used to simulate groundwater flow and contaminant transport:

- Groundwater flow was modeled in three dimensions using MODFLOW 2005
- Contaminant transport was modeled in three dimensions using MT3DMS
- Percolation (recharge) after consolidation of CCR and cover system construction was modeled using the results of the Hydrologic Evaluation of Landfill Performance (HELP) model.

5. MODEL SETUP AND CALIBRATION

5.1 Model Descriptions

For the construction and calibration of the numerical groundwater flow model for the Site, Ramboll selected the model code MODFLOW, a publicly available groundwater flow simulation program developed by the United States Geological Survey (USGS) (McDonald and Harbaugh, 1988). MODFLOW is thoroughly documented, widely used by consultants, government agencies and researchers, and is consistently accepted in regulatory and litigation proceedings. MODFLOW uses a finite difference approximation to solve a three-dimensional head distribution in a transient, multi-layer, heterogeneous, anisotropic, variable-gradient, variable-thickness, confined or unconfined flow system—given user-supplied inputs of hydraulic conductivity, aquifer/layer thickness, recharge, wells, and boundary conditions. The program also calculates water balance at wells, rivers, and drains.

Major assumptions of the MODFLOW code are: (i) groundwater flow is governed by Darcy's law; (ii) the formation behaves as a continuous porous medium; (iii) flow is not affected by chemical, temperature, or density gradients; and (iv) hydraulic properties are constant within a grid cell. Other assumptions concerning the finite difference equation can be found in McDonald and Harbaugh (1988). MODFLOW 2005 was used for these simulations with Groundwater Vistas 8 software for model pre- and post- processing tasks (Environmental Simulations, Inc., 2018).

MT3DMS (Zheng and Wang, 1998) is an update of MT3D. It calculates concentration distribution for a single dissolved solute as a function of time and space. Concentration is distributed over a three-dimensional, non-uniform, transient flow field. Solute mass may be input at discrete points (wells, drains, river nodes, constant head cells), or distributed evenly or unevenly over the land surface (recharge).

MT3DMS accounts for advection, dispersion, diffusion, first-order decay, and sorption. Sorption can be calculated using linear, Freundlich, or Langmuir isotherms. First-order decay terms may be differentiated for the adsorbed and dissolved phases.

The program uses the standard finite difference method, the particle-tracking-based Eulerian-Lagrangian methods, and the higher-order finite-volume total-variation-diminishing (TVD) method for the solution schemes. The finite difference solution has numerical dispersion for low-dispersivity transport scenarios but conserves good mass balance. The particle-tracking method avoids numerical dispersion but was not accurate in conserving mass. The TVD solution is not subject to significant numerical distribution and adequately conserves mass, but is numerically intensive, particularly for long-term models such as developed for the BAP. The finite difference solution was used for this simulation.

Major assumptions of MT3DMS are: (i) changes in the concentration field do not affect the flow field; (ii) changes in the concentration of one solute do not affect the concentration of another solute; (iii) chemical and hydraulic properties are constant within a grid cell; and (iv) sorption is instantaneous and fully reversible, while decay is not reversible.

The HELP model was developed by the USEPA. HELP is a one-dimensional hydrologic model of water movement across, into, through, and out of a landfill or soil column based on precipitation, evapotranspiration, runoff, and the geometry and hydrogeologic properties of a layered soil and

waste profile. For this modeling, results of the HELP model, HELP Version 4.0 (Tolaymat and Krause, 2020), were used to estimate the hydraulic conditions beneath consolidation areas.

5.2 Flow and Transport Model Setup

The modeled area was approximately 11,125 feet (445 rows) by 16,375 feet (655 columns) with the BAP located in the east-central portion of the model. The western edge of the model is bounded by the Kaskaskia River. The north, east, and south edges of the model were selected to maintain sufficient distance from the BAP to reduce boundary interference with model calculations, while not extending too far past the extent of available calibration data. The model area is displayed in **Figure 5-1**.

The MODFLOW model was calibrated to median groundwater elevation collected from December 2015 to June 2022. The flow model calibration targets are presented in **Table 2-2**. MT3DMS was run on the calibrated flow model and model-simulated concentrations were calibrated to the range of observed boron concentration values at the monitoring wells from December 2015 to December 2022 presented in **Table 2-2**. Multiple iterations of MODFLOW and MT3DMS calibration were performed to achieve an acceptable match to observed flow and transport data. For the BAP, the calibrated flow and transport models were used in predictive modeling to evaluate the CIP closure scenario by consolidating CCR and using HELP modeled recharge values to simulate changes proposed in the closure scenario.

5.2.1 Grid and Boundary Conditions

A six-layer, 445 x 655 node grid was established with 25-foot grid spacing in the vicinity of the BAP and BPP property. The grid increases gradually to a maximum 450-foot row spacing and 225-foot column spacing near the edges of the model. The model grid and boundary conditions are illustrated in **Figures 5-2 through 5-7**. All edges of the model are no-flow (*i.e.*, Neumann) boundaries in all layers of the model with the exceptions of the western edge in layer 4, where a river (mixed) boundary was placed to simulate the mean flow conditions of the Kaskaskia River, and vary between no-flow (*i.e.*, Neumann) and river (*i.e.*, mixed) boundaries on the northern edge in layers 2 through 4, where a river (*i.e.*, mixed) boundary was placed to simulate the Cooling Pond, and the southern edge in layers 2 through 4, where river (*i.e.*, mixed) boundary was placed to simulate the southernmost tributary. The limits of the model domain approximate the limits of the Kaskaskia River subwatershed (Hydrologic Unit Code [HUC] boundary) in which the BPP and BAP reside. The top of the model was a time-dependent specified flux (*i.e.*, Neumann) boundary, with specified flux rates equal to the recharge rate. Surface water features within the active BAP were simulated in the model as constant head boundaries.

5.2.2 Flow Model Input Values and Sensitivity

Flow model input values and sensitivity analysis results are presented in **Table 5-1** and described below.

The modeled well location layers and flow model calibration targets (*i.e.*, median groundwater elevations from December 2015 to June 2022 [or November 2022 groundwater elevations for wells constructed or reoccupied in 2022] and target well locations) are summarized in **Table 2-2**. Anomalous groundwater elevations (*e.g.*, groundwater elevations that do not represent static groundwater conditions, groundwater elevation outliers, or groundwater elevations measured in error) monitored between December 2015 and June 2022 were removed from the median groundwater elevation calculations used as flow calibration targets. UU wells MW-151, MW-154,

MW-252, and MW-253 are screened just above or at the interface between the UU and decomposed bedrock of the UA and may be hydraulically connected to multiple hydrostratigraphic units (*i.e.*, multiple modeled layers). In the flow calibration model, flow calibration targets for UU wells MW-151, MW-154, MW-252, and MW-253 were placed in the decomposed bedrock model layer, which exhibited heads more representative of the groundwater observations in these wells.

Sensitivity analysis was conducted by changing input values and observing changes in the sum of squared residuals (SSR). Horizontal conductivity, vertical conductivity, and river conductance terms were all varied between one-tenth and ten times calibrated values. Recharge terms were varied between one-half and two times calibrated values. River stage for river reach 0 (*i.e.*, Cooling Pond) and river reach 1 (*i.e.*, Kaskaskia River) were varied between 98.5 and 101.5 percent of calibrated values. River stage for river reaches 2 through 8 and constant head reaches 0 and 1 were varied between 99.5 and 100.5 percent of calibrated values. When the calibrated model was tested, SSR was 1,210.53. Sensitivity test results were categorized into negligible, low, moderate, moderately high, and high sensitivity based on the change in SSR as summarized in the notes in **Table 5-1**.

5.2.2.1 Model Layers

All available boring log data included in the revised HCR (Ramboll, 2023d) and lithologic contacts from the 2022 Hydrogeologic Site Investigation activities were used to develop surfaces utilizing Surfer® software for each of the three distinct water-bearing units described in **Section 2**. Layer 1 (**Figure 5-8**) modeled only CCR material within the limits of the BAP and FAPS; no flow cells were used outside the limits of the CCR units. The approximate base of ash surface in the BAP was provided by Geosyntec, which was developed using historic pre-construction topographic maps and incorporated base of ash data collected by Ramboll from borings within the BAP completed in 2022. The approximate base of ash surface in the FAPS was developed using historic pre-construction topographic maps. The modeled UU was split into three modeled layers, where model layer 2 (**Figure 5-9**) represented the upper silty clay of the UU, model layer 3 (**Figure 5-10**) represented a discontinuous transmissive zone within the UU (this unit is considered a PMP) or represented the approximate top of Vandalia Till/lower silty clay of UU in absence of a transmissive zone, and model layer 4 (**Figure 5-11**) represented the lower silty clay of the UU. Model layer 5 (**Figure 5-12**) represented the decomposed bedrock of the UA near the contact between the UU and UA. Model layer 6 (**Figure 5-13**) represented the deeper more competent bedrock of the UA. The bottom elevation of the UA (*i.e.*, bedrock) in layer 6 was flat lying and assumed to be an elevation of 200 feet NAVD88. The resulting surfaces were imported as layers into the model to represent the distribution and change in thickness of each water-bearing unit across the model domain.

5.2.2.2 Hydraulic Conductivity

Hydraulic conductivity values and sensitivity results are summarized in **Table 5-1**. When available, these values were derived from field or laboratory measured values reported in the revised HCR (Ramboll, 2023d) and collected during the 2022 Hydrogeologic Site Investigation, to be representative of site-specific conditions. The sources of the hydraulic conductivity values are summarized in **Table 5-1**. Conductivity zones that did not have representative site data were determined through model calibration. No horizontal anisotropy was assumed. Vertical anisotropy (presented as K_h/K_v in **Table 5-1**) was applied to conductivity zones to simulate preferential flow in the horizontal direction in the UU and UA.

The spatial distribution of the hydraulic conductivity zones in each layer (**Figures 5-14 through 5-19**) simulates the distribution of hydraulic conductivity as reported in the revised HCR (Ramboll, 2023d) and determined from hydrogeologic data collected during the 2022 Hydrogeologic Site Investigation. All hydraulic conductivity zones were laterally continuous within the model with the exception of the CCR hydraulic conductivity zones Old East Fly Ash Pond, East Fly Ash Pond, West Fly Ash Cell, and BAP (zones 2, 3, 4, and 7); the fill at the BAP and FAPS boundary (zone 16), the river alluvium hydraulic conductivity zone (zone 12); and the PMP hydraulic conductivity zone (zone 14). The limits of the ash fill were determined from data presented in the revised HCR (Ramboll, 2023d) and determined from hydrogeologic data collected during the 2022 Hydrogeologic Site Investigation. The ash fill extent was propagated through all related ash fill property zones (*i.e.*, recharge, storage, specific yield [S_y], and effective porosity). Conductivity zone 100 (identified on figures as "Above River BC") was placed above river cells to improve communication between the river and the groundwater in layers above the layer in which the river boundary condition was placed.

The model had a high sensitivity to changes in horizontal conductivity in zone 9 (*i.e.*, UA), and a moderate sensitivity in zone 1 (*i.e.*, UU), zone 7 (*i.e.*, BAP), and zone 14 (*i.e.*, PMP); the model had a low or negligible sensitivity to changes in horizontal conductivity in the remaining hydraulic conductivity zones. The model had a moderate sensitivity to changes in vertical conductivity in zone 1 (*i.e.*, UU) and zone 9 (*i.e.*, UA), while the model exhibited a negligible sensitivity in the remaining hydraulic conductivity zones.

5.2.2.3 Recharge

Recharge rates (**Table 5-1**) were determined through calibration of the model to median groundwater elevation collected from December 2015 to June 2022, as presented in **Table 2-2**. The spatial distribution of recharge zones was based on the location and type of material present at land surface (**Figure 5-20**). Seven different zones were created to simulate recharge in the model area. A single silty clay zone (zone 1) was used to simulate ambient recharge over the upper silty clay of the UU outside the limits of the CCR units. Zones 5 and 6 were used to simulate recharge over the upper silty clay of the UU in the area of the Secondary Pond and Tertiary Pond, respectively. The recharge occurring through the ash fill placed in the FAPS and BAP was split into four different values, where recharge was varied based upon the historical use of each ash fill area and the response of flow calibration target heads. Post-closure FAPS recharge rates for the Old East Ash Pond, East Fly Ash Pond, and West Fly Ash Cell (zones 2, 3, and 4) were consistent with previous prediction modeling values used for the proposed cover system at the FAPS (NRT, 2014b). The BAP was simulated with a single zone (zone 7) which also had the greatest recharge value within the model domain.

The model had low sensitivity to changes in recharge in all zones, with the exception of zones 5 (Secondary Pond) and 6 (Tertiary Pond), where sensitivity was negligible.

5.2.2.4 Storage and Specific Yield

The calibration model did not use these terms because it was run at steady state. For the transport model, which was run in transient, no field data defining these terms were available so published values were used consistent with Fetter (1988). S_y was set to equal effective porosity values described in **Section 5.2.3.3**. The spatial distribution of the storage and S_y zones were consistent with those of the hydraulic conductivity zones. The sensitivity of these parameters was tested by evaluating their effect on the transport model as described in **Section 5.2.3.4**.

5.2.2.5 River Parameters

River reaches are illustrated in **Figure 5-1**. The Kaskaskia River was simulated using head-dependent flux nodes in modeled river reach 1 that required inputs for river stage, width, bed thickness, and bed hydraulic conductivity (**Table 5-1**). River width, bed thickness, and bed hydraulic conductivity parameters were used to calculate a conductance term for the boundary node. This conductance term was determined by adjusting hydraulic conductivity during model calibration. The calibrated hydraulic conductivity value was set at 5.17 ft/day. The length of the modeled river extends from the northernmost extent of the model domain to the southernmost extent of the model domain using river reach 1. The modeled river stage in the calibration model was based on available Kaskaskia River stage data at Red Bud, Illinois (USGS 05595240) and at New Athens, Illinois (USGS 05595000) gaging stations in 2021 and 2022. No slope was applied to the upstream and downstream modeled river stage as calculated gradients between the two gaging stations were determined to be negligible across the length of the model domain. The river boundary was placed in layer 4 corresponding with simulated river elevation (**Figure 5-5**).

The Cooling Pond was simulated using head-dependent flux nodes in modeled river reach 0 (**Table 5-1**). The conductance term was determined by adjusting hydraulic conductivity during model calibration. The calibrated hydraulic conductivity value was set at 3.8 ft/day. The river stage in the calibration model approximated the elevation at which the Cooling Pond is maintained (Ramboll, 2023d). The river boundary was placed in layers 2 through 4 corresponding with simulated river elevation (**Figures 5-3 through 5-5**).

The Secondary and Tertiary ponds were simulated using head-dependent flux nodes in modeled river reach 8 (**Table 5-1**). The conductance term was determined by adjusting hydraulic conductivity during model calibration. The calibrated hydraulic conductivity value was set at 0.26 ft/day. The river stage in the calibration model approximated historic groundwater elevations measured in monitoring well TPZ-165 placed within the limits of the Secondary Pond (**Figure 2-1**) (NRT, 2014a). The bottom of the river boundary was estimated using historic topographic maps and placed in layers 2 through 6 corresponding with simulated river elevation (**Figures 5-3 through 5-7**).

The remaining tributaries were simulated using head-dependent flux nodes in modeled river reaches 2 through 5 and reach 7 (**Table 5-1**). The conductance terms were determined by adjusting hydraulic conductivity during model calibration. Calibrated hydraulic conductivity values by tributary river reach are shown in **Table 5-1**. The river stage in the calibration model approximated local topography for each reach. The river boundaries were placed in layers 2 through 5 corresponding with simulated river elevation (**Figures 5-3 through 5-6**).

The model had moderate and high sensitivity to changes in river stage at reach 0 (Cooling Pond) and reach 1 (Kaskaskia River), respectively. The model had high sensitivity at reach 7 (northeast stream [east of Cooling Pond]) and moderate to moderately high sensitivity at reach 3 (south stream [between reach 2 and reach 4]) and reach 4 (south stream [adjacent to FAPS]) (**Table 5-1**). The remaining river reaches had low to negligible sensitivity to changes in river stage. The model had negligible sensitivity to changes in river conductance.

5.2.2.6 Constant Head Boundary Parameters

Surface water features within the active BAP were simulated in the model as constant head boundaries. The constant head boundaries required inputs for head at the boundaries (elevation).

These constant head boundary features act as discharge features within the BAP, which is consistent with stormwater management practices within the active BAP (AECOM, 2016b). The head at the boundaries for reaches 0 and 1 estimated water surface elevation within the BAP. The constant head boundaries were placed in layer 1 within the BAP (**Figure 5-2**).

The model had negligible sensitivity to changes in head in reach 0 (BAP constant head west) and reach 1 (BAP constant head central).

5.2.3 Transport Model Input Values and Sensitivity

MT3DMS input values are listed in **Table 5-2** and described below. Sensitivity of the transport model is summarized in **Table 5-3**.

Groundwater transport was calibrated to groundwater boron concentration ranges at each well as measured from the monitoring wells between December 2015 and December 2022. The transport model calibration targets are summarized in **Table 2-2**.

Sensitivity analysis was conducted by changing input values and observing percent change in boron concentration at each well from the calibrated model boron concentration. Effective porosity was varied by decreasing and increasing calibrated model values by 0.05. Storage values were multiplied and divided by a factor of 10, and S_y by a factor of 2. High S_y sensitivity was not analyzed for zone 100 (identified on figures as "Above River BC") since the calibration value was already near upper limits of acceptable values for S_y (0.5).

5.2.3.1 Initial Concentrations

No initial concentrations were placed in the calibration model. The flow model was run as transient, and concentration was added to the model through recharge and constant concentration cells starting at the same time as the flow simulation. Two models (Calibration Model 1 and Calibration Model 2) run in series were used to calibrate concentrations to current observations and simulate changes in CCR unit operations at the Site from construction (1970) to present day (2022 [*i.e.*, current conditions]). The first model (Calibration Model 1) started at the time of BAP and FAPS construction (1970) and ended in 2020 (51-year calibration model period) when the FAPS was closed. The second model (Calibration Model 2) started in 2021 and ended in 2022 (2-year calibration model period) following the FAPS closure and included reduced recharge in the FAPS consistent with estimated closed FAPS recharge values in the 2014 FAPS groundwater modeling report (NRT, 2014b; NRT, 2014c), and removal of constant head cells in the West Ash Pond that were used to simulate stormwater management operations in the active FAPS in Calibration Model 1 to simulate the reduced activity in this area of the pond. The transport model timeline is illustrated in **Figure 4-1**.

5.2.3.2 Source Concentrations

Five concentration sources in the form of vertical percolation (recharge zones) through CCR were simulated in layer 1 for calibration (**Figure 5-20 and Table 5-2**) (recharge zones in order of greatest to least simulated recharge): (i) percolation through CCR in the active BAP (zone 7, BAP [West]; zone 8, BAP [East]), and (ii) percolation through CCR in the FAPS (zone 2, Old East Fly Ash Pond; zone 3, East Fly Ash Pond; zone 4, West Fly Ash Pond) active 1970 to 2020 (Calibration Model 1) and closed 2020 to 2022 (Calibration Model 2). All five sources were simulated by assigning concentration to the recharge input. Recharge rates in the active BAP were consistent across zone 7 (BAP [West]) and zone 8 (BAP [East]) which approximately bisect

the active BAP; however, concentrations applied to recharge zones 7 and 8 were 4 and 1.5 mg/L, respectively, to reflect concentrations of boron observed at CCR porewater wells in each side of the active BAP.

The CCR sources were also simulated with constant concentration cells placed in layer 1 to simulate saturated ash conditions (see constant concentration cell reaches described in **Table 5-2**). From the model perspective, this means that when the simulated water level is above the base of these cells, water that passes through the cell will take on the assigned concentration. The spatial distributions of source concentrations applied to constant concentration cell reaches (saturated ash cells) are consistent with the spatial distributions of concentrations applied to the recharge zones. All source concentrations were calibrated in the transport model to the boron concentration data collected from December 2015 to December 2022.

Because these are the sources of concentration in the model, the model will be highly sensitive to changes in the input values. For that reason, sensitivity testing was not completed for the source values.

5.2.3.3 Effective Porosity

Effective porosity for each modeled zone were derived from an average between estimated values of 0.20 for silt material, 0.267 for gravel, 0.07 for clay, and 0.28 for sand (Fetter, 1988; Morris and Johnson, 1967; Heath, 1983), for each material modeled then adjusted during model calibration and presented in **Table 5-2**. The spatial distribution of the effective porosity zones was consistent with those of the hydraulic conductivity zones.

Sensitivity testing was completed on all wells and the results are provided in **Table 5-3**. Monitoring locations where the calibrated and tested concentrations were below 0.1 mg/L boron are not included in the following discussion of model sensitivity to boron transport. The model had a negligible to moderately high sensitivity to decreases in porosity values, with exception of MW-382 where sensitivity was high. The model had a negligible to moderate sensitivity to increases in porosity values, with exception of three monitoring locations where sensitivity was moderately high (*i.e.*, MW-382, MW-385, and MW-390).

5.2.3.4 Storage and Specific Yield Sensitivity

Sensitivity testing was completed on all wells and the results are provided in **Table 5-3**. Monitoring locations where the calibrated and tested concentrations were below 0.1 mg/L boron are not included in the following discussion of model sensitivity to boron transport. The transport model had a negligible to moderate sensitivity to decreases in storage and S_y , with exception of seven monitoring locations where sensitivity was moderately high (*i.e.*, MW-151, MW-366, MW-375, MW-382, MW-384, MW-385, and MW-390). The transport model had a negligible to moderately high sensitivity to increases in storage and S_y , with exception of three monitoring locations where sensitivity was high (*i.e.*, MW-382, MW-385, and MW-390).

5.2.3.5 Dispersivity

Physical attenuation (dilution and dispersion) of contaminants is simulated in MT3DMS. Dispersion in porous media refers to the spreading of contaminants over a greater region than would be predicted solely from the average groundwater velocity vectors (Anderson, 1979; Anderson, 1984). Dispersion is caused by both mechanical dispersion, a result of deviations of actual velocity at a microscale from the average groundwater velocity, and molecular diffusion

driven by concentration gradients. Molecular diffusion is generally secondary and negligible compared to the effects of mechanical dispersion and only becomes important when groundwater velocity is very low [immobile water]. The sum of mechanical dispersion and molecular diffusion is termed hydrodynamic dispersion, or simply dispersion (Zheng and Wang, 1998).

Dispersivity values were applied to the entire model domain and determined during calibration. Longitudinal dispersivity was set at 5 feet. The transverse and vertical dispersivity were set at 1/10 and 1/100 of longitudinal dispersivity. These input values were determined during model calibration. With travel distances of less than 100 feet for groundwater from the source to the majority of the monitoring points, the model is not expected to be sensitive to dispersivity inputs and the sensitivity of the model to dispersivity was not tested.

5.2.3.6 Retardation

It was assumed that boron would not significantly sorb or chemically react with aquifer solids (distribution coefficient [Kd] was set to 0 milliliters per gram [mL/g]) which is a conservative estimate for estimating contaminant transport times. Boron transport is likely to be affected by both chemical and physical attenuation mechanisms (*i.e.*, adsorption and/or precipitation reactions as well as dilution and dispersion). Further assessment of these processes and how they affect boron transport at the Site will be completed as part of future remedy selection evaluations. For the purposes of this GMR, and as mentioned at the beginning of this section, no retardation was applied to boron transport in the model (*i.e.*, Kd was set to 0).

5.3 Flow and Transport Model Assumptions and Limitations

Simplifying assumptions were made while developing this model:

- Following closure of the FAPS in 2020, the groundwater flow system can be simulated as steady state for calibration to current conditions.
- Natural recharge is constant over the long term.
- Fluctuations in river stage do not affect groundwater flow over the long term.
- Hydraulic conductivity is consistent within each material (hydraulic conductivity zone) modeled.
- The approximate base of ash surface in the BAP was provided by Geosyntec, which was developed using historic pre-construction topographic maps and incorporated base of ash data collected by Ramboll from borings within the BAP completed in 2022. The approximate base of ash surface in the FAPS was developed using historic pre-construction topographic maps.
- Constant head cells were used to simulate surface water management features during operation of the CCR units.
- Recharge rates were modified, and constant head cells were removed after 2020 in the area of the FAPS to simulate closure.
- Source concentrations are assumed to remain constant over time. Only recharge rate was modified after 2020 to simulate FAPS closure.
- Boron is not adsorbed and does not decay; mixing and dispersion are the only attenuation mechanisms.

The model is limited by the data used for calibration, which adequately define the local groundwater flow system and the source and extent of the plume. Since data used for calibration are near the BAP and FAPS, model predictions of transport distant spatially and temporally from the calibrated conditions at the CCR units will not be as reliable as predictions closer to the CCR units and concentrations observed between 2015 and 2022.

5.4 Calibration Flow and Transport Model Results

Results of the MODFLOW modeling are presented below. Electronic copies of the model files are attached to this report (**Appendix C**).

Observed and simulated heads are presented in **Figure 5-21 through Figure 5-28**. The mass balance error for the flow model was 0.02 percent and the ratio of the residual standard deviation to the range was 5.4 percent. The mass balance error for the flow model was within the target for the criteria of 1 percent and the ratio of the residual standard deviation to the range was within the target for the criteria of 10 percent. Another flow model calibration goal is that residuals are evenly distributed such that there is no bias affecting modeled flow. The observed heads are plotted versus the simulated heads and identified by layer in **Figure 5-21**. The near-linear relationship between observed and simulated values indicates that the model adequately represents the calibration dataset. The residual mean was -1.33 feet; in general, the simulated values were evenly distributed above and below the observed values. This is also illustrated by layer in the observed versus residuals plot **Figure 5-22**. Some simulated values were overpredicted (negative values on **Figure 5-22**), where the most significant overpredicted values (exceeding 10 feet) were primarily within the UA (bedrock) of layer 6, largely at lower groundwater elevations near the Secondary and Tertiary Ponds, near the southwest boundary of the West Ash Pond of the FAPS, or in bedrock wells screened below the decomposed bedrock. These residuals plot in the lower left quadrant of **Figure 5-22**.

The range of observed boron concentrations between December 2015 and December 2022 for the fifty (50) transport calibration locations are summarized in **Table 2-2**. The goals of the transport model calibration were to have predicted concentrations fall within the range of observed concentrations, and/or have predicted concentrations above and below the GWPS for boron (2 mg/L) match observed concentrations above or below the standard at each well. Twenty (20) transport calibration locations had observed boron concentrations that ranged above and below the GWPS for boron (2 mg/L); for these locations the goal of transport model calibration was to have predicted concentrations above and below the GWPS for boron match observed median concentrations above or below the standard at each well (for example, if the median observed concentration for a well was above the GWPS, the goal is to have predicted concentrations above the GWPS at the well). One or more of these goals were achieved at all but five of the transport calibration location wells, specifically MW-150, MW-151, MW-356, MW-385, and MW-394, where concentrations were underpredicted with the exception of MW-151, where concentrations were overpredicted (**Figure 5-29**). Deviations from the observed boron concentrations are discussed below.

- MW-150, MW-356, and MW-394 were underpredicted transport calibration locations and had observed boron concentrations that ranged above and below the GWPS for boron (2 mg/L) with median observed concentrations only slightly above the GWPS for boron at 2.12, 2.01, and 2.02 mg/L, respectively.

- UU well MW-150 is nested with MW-350 at the southwest corner of the Site near the Tertiary Pond. The MW-150/MW-350 well nest was observed to have generally downward vertical gradients in the revised HCR (Ramboll, 2023d); however, other nested wells near the Secondary and Tertiary ponds indicate the presence of upward gradients between the UA and UU. The model calibration resulted in upward vertical gradients in these areas including the MW-150/MW-350 wells nest. The modeled gradients at this well nest likely inhibit the downward migration of simulated boron concentrations to MW-150. Nested well MW-350 has low observed boron concentrations and met the model calibration criteria discussed above.
- In general, the model under-predicts boron concentrations in bedrock locations like MW-356 and MW-394 where the range of concentrations observed (1.79 to 2.92 mg/L and 1.87 to 2.23 mg/L, respectively) are near the range of observed boron concentrations in upgradient bedrock wells like MW-304, where concentrations range from 1.27 to 2.16 mg/L. Since no initial concentrations were placed in the calibration model to represent the presence of boron observed in background wells, it is expected that the model may under-predict boron concentrations within the range of observed background.
- MW-385 is an under-predicted bedrock well identified as a UA well in the revised HCR (Ramboll, 2023d). MW-385 was installed in December 2015 on the former berm that was located between the active FAPS East Ash Pond and West Ash Pond. MW-385 was abandoned shortly after installation in February 2016, after collection of only one boron concentration data point. Since the data available for this well is limited, the usefulness of this location as a transport calibration point is also limited as the single data point may not be representative of current conditions. Like MW-385, MW-386 was abandoned shortly after installation, after collection of only one boron concentration data point, and was also located on the berm between the active FAPS East Ash Pond and West Ash Pond. Simulated boron concentrations at MW-386 met the calibration criteria discussed above; however, since the data available for this well is limited, like MW-385, the usefulness of this location as a transport calibration point is also limited as the single data point may not be representative of current conditions.
- MW-151 is identified as a UU well in the revised HCR (Ramboll, 2023d). MW-151 was constructed with a filter pack that extends from the UU into the weathered bedrock. This well was modeled in layer 5 which represents the decomposed bedrock rather than UU layers 2 through 4. Boron concentrations are over-predicted by the model at this location which may be associated with the well being screened across multiple model layers.

The remaining calibration locations had predicted concentrations that met one or more of the following goals of the transport model calibration: to have predicted concentrations fall within the range of observed concentrations; to have predicted concentrations above and below the GWPS for boron (2 mg/L) match observed concentrations observed above or below the standard at each well; and/or to have predicted concentrations above and below the GWPS for boron match observed median concentrations above or below the standard at each well. In other words, there was a very good match between predicted and observed boron concentrations relative to wells with concentrations above and below the GWPS. For example, UA well MW-391, located west of the FAPS, where the highest UA bedrock boron concentrations were observed, was calibrated near the median concentration of the observed values from December 2015 to December 2022. Similarly, UU well OW-157 located north of the East Ash Pond of the FAPS, where the highest concentrations in the UU were observed, had the highest predicted boron concentrations on Site. The calibration result for wells MW-391 and OW-157 indicate the transport calibration model was able to simulate the highest observed concentrations in both the UA and UU, respectively. The

simulated boron concentrations at porewater wells within the BAP also approximated the median of the observed boron concentrations, with the exception of XPW01 which was simulated as dry, indicating the simulated BAP boron source concentrations were representative. The distribution of boron concentrations in the calibrated model are presented on **Figure 5-30 through Figure 5-35**.

DRAFT

6. SIMULATION OF CIP CLOSURE SCENARIO

6.1 Overview and Prediction Model Development

Prediction simulations were performed to evaluate the effects of closure (source control) measures (CCR consolidation and CIP closure scenario) for the BAP on the groundwater quality following initial corrective action measures, which includes removal of free liquids from the BAP. As discussed in **Section 5.2.3.5**, physical attenuation (dilution and dispersion) of contaminants in groundwater is simulated in MT3DMS, which captures the physical process of natural attenuation as part of corrective actions for the closure scenario simulated. No retardation was applied to boron transport in the model (*i.e.*, K_d was set to 0) as discussed in **Section 5.2.3.6**. The following methods were used to develop the prediction models and simulate the CIP closure scenario:

- Extend the modeled existing conditions (calibration conditions) approximately 2 years prior to applying initial corrective action measures to allow time for IEPA coordination, approvals, and permitting; as well as the final design and bid process according to the schedule in the CCR Surface Impoundment Final Closure Plan (Geosyntec, 2022a).
- Define CCR removal and consolidation areas based on designs provided in the CCR Surface Impoundment Final Closure Plan (Geosyntec, 2022a).
- Apply several constant head cell areas to the BAP for the dewatering period (approximately 3 years) to remove free liquids within the BAP (initial corrective action measures).
- Apply drains (drain input parameters approximated designs provided in the CCR Surface Impoundment Final Closure Plan [Geosyntec, 2022a]) to simulate storm water management within CCR removal areas following closure.
- Apply no flow cells and remove recharge in the CCR removal areas to simulate the absence of material in model layer 1 following consolidation and cover system construction.
- Remove source concentrations within the CCR removal areas (source concentrations associated with recharge zones and saturated ash cells [constant concentration cells]).
- Apply reduced recharge in the consolidated CIP areas to simulate the effects of the cover system on the groundwater flow system (HELP calculated percolation rates were developed based on cover system construction materials and designs provided in the CCR Surface Impoundment Final Closure Plan (Geosyntec, 2022a).

HELP modeling input and output values are summarized in **Table 6-1** and described in detail below. Prediction simulations were performed to evaluate changes in the groundwater flow system from the CIP closure scenario. The following simplifying assumptions were made during the simulations:

- In the CIP closure scenario, HELP-calculated average annual percolation rates were developed from a 30-year HELP model run. This 30-year HELP-calculated percolation rate remained constant over duration of the closure scenario prediction model run following closure.
- Changes in recharge resulting from dewatering, CCR removal, consolidation, construction of the cover system, and final grading (recharge rates are based on HELP-calculated average annual percolation rates) have an instantaneous effect on recharge and percolation through surface materials.

- The geocomposite drainage layer and geomembrane liner placed over the ash consolidation area were assumed to have good field placement and assumed to have the same slope as the final grade of the overlying cover materials based on the design drawings provided in the CCR Surface Impoundment Final Closure Plan (Geosyntec, 2022a).
- CCR removal areas were assumed to have the same topography as the former approximated base of ash surface in the BAP.

6.2 HELP Model Setup and Results

HELP (Version 4.0; Tolaymat and Krause, 2020) was used to estimate percolation through the top and slopes of the BAP CIP Consolidation area. HELP files are included electronically (**Appendix C**), and outputs are attached to this report (**Appendix D**).

HELP input data and results are provided in **Table 6-1**. All scenarios were modeled for a period of 30 years. Climatic inputs were synthetically generated using default equations developed for Belleville Scott Air Force Base, Illinois (the closest weather station included in the HELP database). Precipitation, temperature, and solar radiation was simulated based on the latitude of the BAP. Thickness and type of the geosynthetic drainage layer, geotextile protective cushion layer, geomembrane liner, soil backfill, and soil runoff input parameters were developed for the ash consolidation scenario using data provided the CCR Surface Impoundment Final Closure Plan (Geosyntec, 2022a).

HELP model results (**Table 6-1**) indicated 0.000239 inches of percolation per year through the top of the BAP CIP consolidation and cover system area, and 0.000007 inches of percolation per year through the slopes of the BAP consolidation and cover system areas. The differences in HELP model runs for each area included the type of lateral drainage layer or cushion, soil runoff slope, and the soil runoff slope length; all other HELP model input parameters were the same for each simulated area. Two additional HELP model simulations were completed to support the *Proposed Alternative Final Protective Layer Equivalency Demonstration* (Geosyntec, 2022b) which is an appendix to the Construction Permit Application to which this report is also attached. Results of these two additional HELP simulations were not incorporated in the MODFLOW simulations for closure. Simulation inputs and output results are presented in **Appendix D**.

6.3 Simulation of CIP Closure Scenario

The calibrated model was used to evaluate the effectiveness of the CIP closure scenario by defining CCR removal and consolidation areas, reducing head to simulate a dewatering period (approximately 3 years), removing source concentrations within the removal areas, applying drains to simulate storm water management within CCR removal areas following closure, applying no flow cells and removing recharge in the CCR removal areas to simulate the absence of material in model layer 1 following closure, and applying reduced recharge in the consolidation and CIP areas to simulate the effects of the cover system on transport.

As discussed in the model approach **Section 4.3** and illustrated on **Figure 4-1**, the start of the transient flow and transport model was initiated in 1970 (model year 0), when the BPP began operation and the BAP and FAPS were active (initial conditions model), through 2020 (51 model years) when closure at the FAPS was complete. Three models were included for the closure prediction simulation. The first model simulated an extended period of current conditions, 2021 to 2024 (4 model years). The second model simulated a period for the removal of free liquids, 2025

to 2027 (3 model years). The third model simulated the final closure conditions, 2028 to 3027 (1,000 model years). The prediction model input values are summarized in **Table 6-2**.

6.3.1 CIP Closure Scenario Groundwater Flow System and Predicted Boron Concentrations

The design for CIP includes an initial 3-year dewatering period to remove free liquids followed by CCR removal from the western areas of the BAP, consolidation to the southeast, and eventually northeastern portions of the BAP, and construction of a cover system over the remaining CCR (**Figure 6-1**).

Post-construction heads decrease at monitoring wells surrounding the CCR removal and consolidated CIP areas of the BAP following dewatering and implementation of CIP. In general, the greatest predicted reduction in heads among the proposed BAP compliance monitoring wells (MW-192, MW-193, MW-356, MW-369, MW-370, MW-382, MW-392, MW393, MW-394, OW-256, OW-257, PZ-170, and PZ-182) takes place within approximately 93 years following implementation of the CIP closure scenario. The heads at these wells continue to decrease until they are predicted to stabilize (approximate hydraulic steady state); however, due to the low hydraulic conductivity of the UU and UA materials, heads are not predicted to stabilize at all proposed BAP compliance monitoring wells until approximately 482 years following implementation of the CIP closure scenario. Groundwater flow directions are predicted to remain consistent with current flow directions.

Evaluations of post-construction water flux through the consolidated and covered BAP CCR were completed using data obtained from the CIP closure scenario prediction model when simulated post-construction heads in the proposed BAP compliance monitoring wells reached their most significant reduction in heads at approximately 93 years following implementation of the CIP closure scenario. The pre-construction (calibration model) and post-construction CIP closure scenario prediction model simulated water flux values are summarized in **Appendix E** and discussed below. Data export files used for flux evaluations are found along with model files in **Appendix C**.

Figure 6-2 is a plot showing the changes in flux reduction (shown as negative percentage) over time, starting from implementation of the CIP closure scenario through approximately 100 years following implementation. The CIP closure scenario was predicted to reduce total flux in and out of the BAP CCR by greater than 90 percent within 30 days following implementation of the CIP closure scenario. This was determined by comparing the post-construction movement of water in and out of the consolidated BAP CCR to pre-construction conditions. The reduction in total flux in and out of the consolidated BAP CCR is predicted to exceed 90 percent reduction for the remaining model timeframe. In general, the greatest predicted reduction in heads among the proposed BAP compliance monitoring wells takes place within approximately 93 years following implementation of the CIP closure scenario, at which time total flux in and out are predicted to reduce by 95 and 93 percent, respectively (**Figure 6-3**). Flux in and out are predicted to reduce by approximately 96 percent after approximately 482 years following implementation of the CIP closure scenario when heads are predicted to stabilize at the BAP compliance wells. Prior to construction (*i.e.*, current existing conditions) the total groundwater flux into the CCR is 10.90 gallons per minute (gpm) versus a total flux out of 10.77 gpm (**Appendix E**). Total flux out includes flux through the CCR (3.39 gpm) and the modeled constant head cells (7.38 gpm) used to simulate surface water management within the active BAP. Approximately 93 years following

implementation of the CIP closure scenario, the groundwater flux into and out of the CCR is equal at approximately 0.56 and 0.70 gpm, respectively, with no surface water management within the CIP area.

An evaluation of simulated boron plumes greater than the GWPS (2 mg/L for boron) in both pre-construction calibration models and post-construction prediction models indicated several proposed BAP compliance monitoring wells (PZ-182, OW-257, MW-382) to be potentially influenced by boron concentrations associated with the closed FAPS. The model domain for evaluating boron transport following closure of the BAP includes the closed FAPS, which is present along the eastern and southern boundaries of the BAP. The FAPS completed IEPA approved closure activities in November of 2020, and it is another potential source of boron within the model domain. The closure plan for the FAPS also included groundwater modeling of boron transport. The evaluation included a review of maximum plume extents associated with the FAPS presented in the 2014 FAPS groundwater modeling reports (NRT, 2014b; NRT, 2014c) (completed as part of the FAPS Closure Plan Report [AECOM, 2016a]), as well as a review of simulated groundwater flow directions and simulated boron concentrations in both the BAP pre-construction calibration and BAP post-construction prediction models. Groundwater elevations and boron concentrations at FAPS closure monitoring wells were calibrated during development of the current BAP flow and transport model and the simulation period was extended to 1,000 years to verify consistent results with the 2014 FAPS groundwater modeling reports. Changes in FAPS operations were incorporated into the current BAP modeling (utilizing similar changes in recharge used to simulate closure in the previous 2014 model). Boron transport within the current BAP model was compared to the results from the previous FAPS closure plan modeling and found that simulated flow and transport associated with the FAPS are consistent between the two models. Proposed BAP compliance wells PZ-182, OW-257, and MW-382 are located in the direction of groundwater flow from the north central area of the FAPS between the FAPS (East Ash Pond) and the surface water drainage feature near the west end of the BAP. Because these wells are downgradient of the FAPS, which is an alternate source of boron, these wells were not included in the evaluation of BAP compliance with the GWPS following implementation of the CIP closure scenario.

Simulated boron concentrations at the remaining proposed BAP compliance monitoring wells (PZ-170, OW-256, MW-192, MW-193, MW-370, MW-369, MW-392, MW-393, and MW-394) were below the GWPS (2 mg/L for boron) during the pre-construction period (calibration model), and prediction modeling results indicated these proposed BAP compliance monitoring wells would continue to remain below the GWPS for the post-construction modeling timeframe following dewatering and consolidation (**Figure 6-4**). The maximum extent of the plume above the GWPS for boron (2 mg/L) at 93 years following implementation of the CIP closure scenario, when simulated post-construction heads in the proposed BAP compliance monitoring wells reached their most significant reduction in heads, is illustrated in **Figure 6-5**, where boron exceedances are within the footprint of the former BAP except where source concentrations are potentially associated with the closed FAPS.

Additionally, a BAP CBR closure scenario prediction model was completed to evaluate the difference in post-construction boron concentrations simulated at PZ-182, OW-257, and MW-382 under both CIP and CBR conditions. The CBR closure scenario was simulated by: (i) extending the initial 3-year dewatering period to remove free liquids used in the CIP prediction model to an initial 9-year dewatering period, as the CBR construction timeframe is longer than CIP (see

information provided in the CCR Surface Impoundment Final Closure Plan [Geosyntec, 2022a] which is an appendix to the Construction Permit Application to which this report is also attached); (ii) applying no flow cells and removing recharge in the entire BAP footprint to simulate the absence of material in model layer 1 following CBR; and, (iii) removing all source concentrations within the BAP footprint following CBR (source concentrations associated with recharge zones and saturated ash cells [constant concentration cells]). A timeseries plot of predicted boron concentrations following implementation of the BAP CIP and CBR closure scenarios at proposed BAP compliance monitoring wells PZ-182, OW-257, and MW-382 is provided in **Figure 6-6**. As illustrated in **Figure 6-6**, concentrations are predicted to increase above the GWPS for boron (2 mg/L) following implementation of both BAP CIP and CBR closure scenarios in these three wells. Maximum concentrations within the modeling timeframes at these wells are predicted to be on the same order of magnitude for both BAP CIP and CBR closure scenarios.

The differences in predicted concentrations between CIP and CBR illustrated on **Figure 6-6** are likely due to slightly lower heads simulated at PZ-182, OW-257, and MW-382 in the CBR scenario, which increases the hydraulic gradient beneath the BAP which drives more rapid predicted arrival of boron in these wells from the FAPS. Since concentrations at proposed BAP compliance monitoring wells PZ-182, OW-257, and MW-382 increase to concentrations above the GWPS following implementation of the CBR closure scenario when BAP source concentrations have been removed, the source for predicted post-construction concentrations within the model domain must be the closed FAPS. These results support the conclusion that wells PZ-182, OW-257, and MW-382 should not be included in the evaluation of BAP compliance with the GWPS following implementation of the CIP closure scenario.

Although predicted boron concentrations at proposed BAP compliance wells PZ-182 and MW-382 are influenced by the FAPS, simulated boron concentrations at these wells started below the GWPS during the pre-construction period (calibration model) and an initial decrease in predicted concentrations was observed immediately following implementation of the BAP CIP closure scenario (**Figure 6-4**). The initial decrease in predicted boron concentrations is followed by a predicted increase in concentrations at approximately 14 and 80 years in wells PZ-182 and MW-382, respectively, following implementation of the CIP closure scenario as simulated concentrations associated with the FAPS begin to influence predicted boron concentrations in wells further along the flow path between the FAPS (East Ash Pond) and the drainage feature near the west end of the BAP.

Results of groundwater fate and transport modeling conservatively estimate that groundwater boron concentrations at the proposed BAP compliance wells that are not influenced by the FAPS will remain below the GWPS following implementation of the CIP closure scenario at the BAP. The model is limited by the data used for calibration, which adequately define the local groundwater flow system and the source and extent of the plume. Since data used for calibration are near the BAP and FAPS, model predictions of transport distant spatially and temporally from the calibrated conditions at the CCR units will not be as reliable as predictions closer to the CCR units and concentrations observed between 2015 and 2022.

7. CONCLUSIONS

This GMR has been prepared to evaluate the groundwater flow system and transport of boron concentrations at the BAP and how the proposed CIP closure scenario will reduce total flux in and out of the CCR and maintain compliance with the GWPS for boron (2 mg/L) in the post-construction BAP. Groundwater elevation data collected from sampling events from December 2015 to June 2022 (or November 2022 groundwater elevations for wells constructed or reoccupied in 2022) and boron concentration data collected from sampling events from December 2015 to December 2022 were used to develop a groundwater flow and transport model for the BPP BAP and surrounding area. The MODFLOW and MT3DMS models were then used to evaluate the CIP closure scenario which includes: CCR removal from the western areas of the BAP, consolidation to the southeast, and eventually northeastern portions of the BAP, and construction of a cover system over the remaining CCR following initial corrective action measures (removal of free liquids from the BAP) using information provided in the CCR Surface Impoundment Final Closure Plan (Geosyntec, 2022a).

The CIP closure scenario was predicted to reduce total flux in and out of the BAP CCR by greater than 90 percent within 30 days following implementation of the CIP closure scenario. This was determined by comparing the post-construction movement of water in and out of the consolidated BAP CCR to pre-construction conditions. The reduction in total flux in and out of the consolidated BAP CCR is predicted to exceed 90 percent reduction for the remaining model timeframe. In general, the greatest predicted reduction in heads among the proposed BAP compliance monitoring wells takes place within approximately 93 years following implementation of the CIP closure scenario, at which time total flux in and out are predicted to reduce by 95 and 93 percent, respectively. Due to the low hydraulic conductivity of the UU and UA materials, heads are not predicted to stabilize at all proposed BAP compliance monitoring wells until approximately 482 years following implementation of the CIP closure scenario, at which time total flux in and out are predicted to reduce by approximately 96 percent.

The model domain for evaluating boron transport following closure of the BAP includes the closed FAPS which is present along the eastern and southern boundaries of the BAP. The FAPS completed IEPA approved closure activities in November of 2020, and it is another potential source of boron within the model domain. The closure plan for the FAPS also included groundwater modeling of boron transport. Boron transport within the current BAP model was compared to the results from the previous FAPS closure plan modeling and found that simulated flow and transport associated with the FAPS are consistent between the two models. As described in this report, proposed BAP compliance wells PZ-182, OW-257, and MW-382 are located in the direction of groundwater flow from the north central area of the FAPS between the FAPS (East Ash Pond) and the surface water drainage feature near the west end of the BAP. Because these wells are downgradient of the FAPS which is an alternate source of boron, and groundwater quality at these wells is not attributable to the BAP, these wells were not included in the evaluation of BAP compliance with the GWPS following implementation of the CIP closure scenario.

Additionally, a BAP CBR closure scenario prediction model was completed to evaluate the difference in post-construction boron concentrations simulated at PZ-182, OW-257, and MW-382 under both CIP and CBR conditions. Concentrations are predicted to increase above the GWPS for boron (2 mg/L) following implementation of both BAP CIP and CBR closure scenarios in these

three wells. Maximum concentrations within the modeling timeframes at these wells are predicted to be on the same order of magnitude for both BAP CIP and CBR closure scenarios. Since concentrations at proposed BAP compliance monitoring wells PZ-182, OW-257, and MW-382 increase to concentrations above the GWPS following implementation of the CBR closure scenario, after BAP source concentrations have been removed, the source for predicted post-construction concentrations within the model domain can only be attributable to the closed FAPS. These results support the conclusion that wells PZ-182, OW-257, and MW-382 should not be included in the evaluation of BAP compliance with the GWPS following implementation of the CIP closure scenario.

Results of groundwater fate and transport modeling conservatively estimate that groundwater boron concentrations at the proposed BAP compliance wells that are not influenced by the FAPS will remain below the GWPS following implementation of the CIP closure scenario at the BAP.

8. REFERENCES

- AECOM, 2016a. Closure and Post-Closure Care Plan for the Baldwin Fly Ash Pond System at Dynegy Midwest Generation, LLC Baldwin Energy Complex, Baldwin, Illinois. March.
- AECOM, 2016b. RE: History of Construction, USEPA Final Rule, 40 C.F.R. § 257.73 (c), Baldwin Energy Complex, Baldwin, Illinois. October.
- Anderson, M.P., 1979. *Using models to simulate the movement of contaminants through groundwater flow systems*. CRC Critical Rev. Environ. Control., 9(2), p. 97-156.
- Anderson, M.P., 1984. *Movement of contaminants in groundwater: groundwater transport -- advection and dispersion*. Groundwater Contamination. National Academy Press, Washington, D.C. p. 37-45.
- Environmental Simulations, Inc., 2018. Groundwater Vistas 8 Software.
- Fetter, C.W., 1988. Applied Hydrogeology. Merrill Publishing Company, Columbus, Ohio.
- Geosyntec Consultants, Inc. (Geosyntec), 2022a. CCR Surface Impoundment Final Closure Plan, Baldwin Power Plant, Bottom Ash Pond, Baldwin, Illinois. December 12.
- Geosyntec Consultants, Inc. (Geosyntec), 2022b. Construction Permit Application, Baldwin Power Plant, Bottom Ash Pond, Baldwin, Illinois. November 14.
- Heath, R.C., 1983. Basic Groundwater Hydrology, U.S. Geological Survey Water-Supply Paper 2220, 86p.
- Illinois Environmental Protection Agency (IEPA), 2016. Dynegy Midwest Generation, Inc. – Baldwin Energy Complex: Baldwin Fly Ash Pond System Closure – NPDES Permit No. IL000043, letter from William Buscher (IEPA) to Rick Diericx (Dynegy Operating Company). August 16.
- McDonald, M.G., and A.W. Harbaugh, 1988. A Modular Three-Dimensional Finite-Difference Ground-Water Flow Model: Techniques of Water-Resources Investigations, Techniques of Water-Resources of the United States Geological Survey. Book 6, Chapter A1.
- Morris, D.A and A.I. Johnson, 1967. Summary of hydrologic and physical properties of rock and soil materials as analyzed by the Hydrologic Laboratory of the U.S. Geological Survey. U.S. Geological Survey Water-Supply Paper 1839-D, 42p.
- Natural Resource Technology, Inc. (NRT), 2014a. Groundwater Quality Assessment and Phase II Hydrogeologic Investigation, Baldwin Ash Pond System. June 11.
- Natural Resource Technology, Inc. (NRT), 2014b. Groundwater Model and Simulation of Closure Alternatives, Baldwin Ash Pond System. June 18.
- Natural Resource Technology, Inc. (NRT), 2014c. Groundwater Model and Simulation of Closure Alternatives, Model Report Addendum Baldwin Ash Pond System. September 30.
- Natural Resource Technology, Inc. (NRT), 2016a. Supplemental Hydrogeologic Site Characterization and Groundwater Monitoring Plan, Baldwin Fly Ash Pond System, Baldwin,

Illinois. Prepared for Dynegy Midwest Generation, LLC by Natural Resource Technology, Inc. March 31.

Natural Resource Technology, Inc. (NRT), 2016b. Technical Memorandum: Baldwin Energy Complex Ash Pond Closure and Post-Closure Plan – Response to Illinois EPA Comments. August 8.

Natural Resource Technology, Inc. (NRT), 2016c. Hydrostatic Modeling Report, Baldwin Fly Ash Pond System Baldwin Energy Complex, Baldwin, Illinois. March 31.

Pryor, Wayne A., 1956. Groundwater Geology in Southern Illinois: A Preliminary Geologic Report.

Ramboll Americas Engineering Solutions, Inc. (Ramboll), 2021a. Groundwater Monitoring Plan. Bottom Ash Pond, Baldwin Power Plant, Baldwin, Illinois. October 25.

Ramboll Americas Engineering Solutions, Inc. (Ramboll), 2021b. History of Potential Exceedances. Bottom Ash Pond, Baldwin Power Plant, Baldwin, Illinois. October 17.

Ramboll Americas Engineering Solutions, Inc. (Ramboll), 2021c. Hydrogeologic Site Characterization Report. Bottom Ash Pond, Baldwin Power Plant, Baldwin, Illinois. October 25.

Ramboll Americas Engineering Solutions, Inc. (Ramboll), 2023a. Alternate Source Demonstration. Baldwin Power Plant, Bottom Ash Pond, CCR Unit 601. April 30.

Ramboll Americas Engineering Solutions, Inc. (Ramboll), 2023b. Groundwater Monitoring Plan Revision 1. Bottom Ash Pond, Baldwin Power Plant, Baldwin, Illinois. August 1.

Ramboll Americas Engineering Solutions, Inc. (Ramboll), 2023c. History of Potential Exceedances Revision 1. Bottom Ash Pond, Baldwin Power Plant, Baldwin, Illinois. August 1.

Ramboll Americas Engineering Solutions, Inc. (Ramboll), 2023d. Hydrogeologic Site Characterization Report Revision 1. Bottom Ash Pond, Baldwin Power Plant, Baldwin, Illinois. August 1.

Tolaymat, T. and Krause, M, 2020. Hydrologic Evaluation of Landfill Performance: HELP 4.0 User Manual. United States Environmental Protection Agency, Washington, DC, EPA/600/B 20/219.

Zheng, Z., and P.P. Wang, 1998. *MT3DMS, a Modular Three-Dimensional Multispecies Transport Model*. Model documentation and user's guide prepared by the University of Alabama Hydrogeology Group for the United States Army Corps of Engineers (USACE).

TABLES

DRAFT

TABLE 2-1. MONITORING WELL LOCATIONS AND CONSTRUCTION DETAILS
GROUNDWATER MODELING REPORT
BALDWIN POWER PLANT
BOTTOM ASH POND
BALDWIN, ILLINOIS

| Well Number | HSU | Date Constructed | Top of PVC Elevation (ft) | Measuring Point Elevation (ft) | Measuring Point Description | Ground Elevation (ft) | Screen Top Depth (ft BGS) | Screen Bottom Depth (ft BGS) | Screen Top Elevation (ft) | Screen Bottom Elevation (ft) | Well Depth (ft BGS) | Bottom of Boring Elevation (ft) | Screen Length (ft) | Screen Diameter (inches) | Latitude (Decimal Degrees) | Longitude (Decimal Degrees) |
|-------------|-----|------------------|---------------------------|--------------------------------|-----------------------------|-----------------------|---------------------------|------------------------------|---------------------------|------------------------------|---------------------|---------------------------------|--------------------|--------------------------|----------------------------|-----------------------------|
| MW-104SR | UU | 2011-08-01 | 455.54 | 455.54 | Top of PVC | 452.52 | 4.80 | 14.80 | 447.80 | 437.70 | 15.00 | 437.50 | 10 | 2 | 38.188355 | -89.853434 |
| MW-104DR | UU | 2011-08-01 | 455.62 | 455.62 | Top of PVC | 452.62 | 23.20 | 28.20 | 429.40 | 424.40 | 28.50 | 417.60 | 5.1 | 2 | 38.188344 | -89.853434 |
| MW-116 | UU | 1991-09-30 | 457.97 | 547.97 | Top of PVC | 454.90 | 15.00 | 25.00 | 439.90 | 429.90 | 25.00 | 429.90 | 10 | 2 | -- | -- |
| MW-126 | UU | 2009-06-19 | 469.84 | 469.84 | Top of PVC | 466.84 | 9.95 | 19.31 | 456.89 | 447.53 | 19.31 | 446.87 | 9.36 | 2 | -- | -- |
| MW-150 | UU | 2010-09-01 | 396.54 | 396.54 | Top of PVC | 393.84 | 15.00 | 24.70 | 378.80 | 369.20 | 25.20 | 368.70 | 9.6 | 2 | 38.189401 | -89.878468 |
| MW-151 | UU | 2010-09-01 | 399.96 | 399.96 | Top of PVC | 397.22 | 6.10 | 15.80 | 391.10 | 381.40 | 16.30 | 380.90 | 9.6 | 2 | 38.188449 | -89.872354 |
| MW-152 | UU | 2010-09-01 | 424.99 | 424.99 | Top of PVC | 422.18 | 7.50 | 16.70 | 414.70 | 405.50 | 17.20 | 405.00 | 9.3 | 2 | 38.187569 | -89.866764 |
| MW-153 | UU | 2010-09-01 | 445.67 | 445.67 | Top of PVC | 442.77 | 10.40 | 20.00 | 432.40 | 422.80 | 20.50 | 422.30 | 9.6 | 2 | 38.185884 | -89.86101 |
| MW-154 | UU | 2010-09-01 | 387.76 | 387.76 | Top of PVC | 384.99 | 7.50 | 12.20 | 377.50 | 372.80 | 12.70 | 372.30 | 4.6 | 2 | 38.196555 | -89.883732 |
| MW-155 | UU | 2010-09-01 | 393.55 | 393.55 | Top of PVC | 390.62 | 10.30 | 19.90 | 380.30 | 370.70 | 20.50 | 370.20 | 9.6 | 2 | 38.193312 | -89.882878 |
| MW-158R | UU | 2022-10-08 | 456.24 | 456.24 | Top of PVC | 453.56 | 8.00 | 18.00 | 445.56 | 435.56 | 18.00 | 435.56 | 10 | 2 | 38.195275 | -89.849411 |
| MW-161 | UU | 2013-08-01 | 431.27 | 431.27 | Top of PVC | 428.74 | 23.30 | 32.80 | 405.40 | 396.00 | 33.40 | 384.00 | 9.5 | 2 | 38.19631 | -89.879159 |
| MW-162 | UU | 2013-08-01 | 433.20 | 433.20 | Top of PVC | 430.83 | 15.90 | 25.30 | 415.00 | 405.50 | 25.90 | 404.90 | 9.5 | 2 | 38.192595 | -89.879221 |
| MW-192 | UU | 2022-09-27 | 436.94 | 436.94 | Top of PVC | 434.04 | 20.00 | 30.00 | 414.04 | 404.04 | 30.00 | 400.04 | 10 | 2 | 38.199203 | -89.866927 |
| MW-193 | UU | 2022-10-04 | 438.06 | 438.06 | Top of PVC | 434.51 | 22.00 | 32.00 | 412.51 | 402.51 | 32.00 | 402.51 | 10 | 2 | 38.199173 | -89.862658 |
| MW-194 | UU | 2022-10-05 | 438.20 | 438.20 | Top of PVC | 435.43 | 18.00 | 28.00 | 407.43 | 397.43 | 28.00 | 405.43 | 10 | 2 | 38.199138 | -89.858653 |
| MW-203 | UA | -- | 457.53 | 457.53 | Top of PVC | 455.66 | 67.00 | 77.00 | 388.66 | 378.66 | 78.00 | 377.67 | 10 | 2 | -- | -- |
| MW-204 | UA | 1991-09-30 | 456.02 | 456.02 | Top of PVC | 453.30 | 68.00 | 78.00 | 385.30 | 375.30 | 79.00 | 79.00 | 10 | 2 | -- | -- |
| MW-252 | UU | 2010-09-01 | 425.07 | 425.07 | Top of PVC | 422.27 | 44.40 | 49.00 | 377.90 | 373.20 | 49.50 | 372.70 | 4.6 | 2 | 38.187563 | -89.866745 |
| MW-253 | UU | 2010-09-01 | 445.84 | 445.84 | Top of PVC | 442.70 | 29.90 | 34.50 | 412.80 | 408.20 | 35.00 | 407.70 | 4.6 | 2 | 38.185885 | -89.861026 |
| MW-258 | UA | 2022-10-07 | 456.12 | 456.12 | Top of PVC | 453.50 | 40.00 | 50.00 | 413.59 | 403.59 | 50.00 | 390.50 | 10 | 2 | 38.195276 | -89.849429 |
| MW-262 | UU | 2013-08-01 | 433.21 | 433.21 | Top of PVC | 430.86 | 42.10 | 46.60 | 388.70 | 384.20 | 47.20 | 379.90 | 4.5 | 2 | 38.192605 | -89.87922 |
| MW-304 | UA | 2015-10-20 | 455.49 | 455.49 | Top of PVC | 453.03 | 45.00 | 55.00 | 408.00 | 398.00 | 55.00 | 317.60 | 10 | 2 | 38.188332 | -89.853441 |

TABLE 2-1. MONITORING WELL LOCATIONS AND CONSTRUCTION DETAILS
GROUNDWATER MODELING REPORT
BALDWIN POWER PLANT
BOTTOM ASH POND
BALDWIN, ILLINOIS

| Well Number | HSU | Date Constructed | Top of PVC Elevation (ft) | Measuring Point Elevation (ft) | Measuring Point Description | Ground Elevation (ft) | Screen Top Depth (ft BGS) | Screen Bottom Depth (ft BGS) | Screen Top Elevation (ft) | Screen Bottom Elevation (ft) | Well Depth (ft BGS) | Bottom of Boring Elevation (ft) | Screen Length (ft) | Screen Diameter (inches) | Latitude (Decimal Degrees) | Longitude (Decimal Degrees) |
|-------------|-----|------------------|---------------------------|--------------------------------|-----------------------------|-----------------------|---------------------------|------------------------------|---------------------------|------------------------------|---------------------|---------------------------------|--------------------|--------------------------|----------------------------|-----------------------------|
| MW-306 | UA | 1991-09-25 | 453.17 | 453.17 | Top of PVC | 450.91 | 72.70 | 87.70 | 378.20 | 363.20 | 87.70 | 361.20 | 15 | 2 | 38.20114 | -89.846756 |
| MW-307 | UA | 1991-09-16 | 436.66 | 436.66 | Top of PVC | 434.00 | 57.00 | 72.00 | 377.00 | 362.00 | 74.00 | 333.00 | 15 | 2 | -- | -- |
| MW-350 | UA | 2010-09-01 | 396.80 | 396.80 | Top of PVC | 394.11 | 41.60 | 46.20 | 352.50 | 347.90 | 46.60 | 347.40 | 4.6 | 2 | 38.189416 | -89.878477 |
| MW-352 | UA | 2010-09-01 | 425.04 | 425.04 | Top of PVC | 422.36 | 67.90 | 72.50 | 354.50 | 349.80 | 73.00 | 348.60 | 4.6 | 2 | 38.187554 | -89.866729 |
| MW-355 | UA | 2010-09-01 | 393.69 | 393.69 | Top of PVC | 390.82 | 27.40 | 32.00 | 363.40 | 358.80 | 32.50 | 358.20 | 4.6 | 2 | 38.193305 | -89.882865 |
| MW-356 | UA | 2015-10-01 | 427.60 | 427.60 | Top of PVC | 425.18 | 56.00 | 66.00 | 369.20 | 359.20 | 66.00 | 290.20 | 10 | 2 | 38.198963 | -89.869578 |
| MW-358 | UA | 2022-10-08 | 455.73 | 455.73 | Top of PVC | 453.59 | 80.00 | 90.00 | 373.73 | 363.73 | 90.00 | 363.59 | 10 | 2 | 38.195275 | -89.849417 |
| MW-366 | UA | 2015-12-04 | 425.08 | 425.08 | Top of PVC | 422.54 | 42.00 | 52.00 | 380.50 | 370.50 | 52.00 | 368.20 | 10 | 2 | 38.192191 | -89.872345 |
| MW-369 | UA | 2015-11-19 | 422.71 | 422.71 | Top of PVC | 420.49 | 56.00 | 66.00 | 364.50 | 354.50 | 66.00 | 349.80 | 10 | 2 | 38.196986 | -89.870258 |
| MW-370 | UA | 2015-11-25 | 420.85 | 420.85 | Top of PVC | 418.67 | 53.00 | 63.00 | 365.70 | 355.70 | 63.00 | 352.70 | 10 | 2 | 38.195603 | -89.869669 |
| MW-373 | UA | 2015-10-28 | 391.32 | 391.32 | Top of PVC | 388.80 | 20.00 | 30.00 | 368.80 | 358.80 | 30.00 | 293.70 | 10 | 2 | 38.190726 | -89.879258 |
| MW-374 | UA | 2015-11-10 | 400.91 | 400.91 | Top of PVC | 398.41 | 30.00 | 40.00 | 368.40 | 358.40 | 40.00 | 356.10 | 10 | 2 | 38.189682 | -89.877242 |
| MW-375 | UA | 2015-11-06 | 423.05 | 423.05 | Top of PVC | 420.50 | 57.00 | 67.00 | 363.50 | 353.50 | 67.00 | 335.80 | 10 | 2 | 38.189045 | -89.873514 |
| MW-377 | UA | 2015-11-02 | 421.36 | 421.36 | Top of PVC | 418.75 | 46.00 | 56.00 | 372.80 | 362.80 | 56.00 | 360.50 | 10 | 2 | 38.188386 | -89.869742 |
| MW-382 | UA | 2015-11-23 | 431.19 | 431.19 | Top of PVC | 428.67 | 56.00 | 66.00 | 372.70 | 362.70 | 66.00 | 358.10 | 10 | 2 | 38.19454 | -89.868044 |
| MW-383 | UA | 2015-12-21 | 459.49 | 459.49 | Top of PVC | 457.18 | 58.00 | 68.00 | 399.20 | 389.20 | 68.00 | 384.20 | 10 | 2 | 38.194913 | -89.858286 |
| MW-384 | UA | 2015-12-18 | 458.95 | 458.95 | Top of PVC | 456.70 | 60.50 | 70.50 | 396.20 | 386.20 | 70.50 | 362.60 | 10 | 2 | 38.191789 | -89.860699 |
| MW-385 | UA | 2015-12-16 | 454.56 | 454.56 | Top of PVC | 454.82 | 80.00 | 90.00 | 374.80 | 364.80 | 90.00 | 361.80 | 10 | 2 | 38.191729 | -89.86847 |
| MW-386 | UA | 2015-12-11 | 454.17 | 454.17 | Top of PVC | 454.67 | 76.00 | 86.00 | 378.70 | 368.70 | 86.00 | 365.70 | 10 | 2 | 38.189441 | -89.866991 |
| MW-387 | UA | 2015-11-18 | 426.63 | 426.63 | Top of PVC | 424.01 | 48.00 | 58.00 | 376.00 | 366.00 | 58.00 | 362.70 | 10 | 2 | 38.190905 | -89.874773 |
| MW-388 | UA | 2015-12-12 | 408.92 | 408.92 | Top of PVC | 406.28 | 33.00 | 43.00 | 373.30 | 363.30 | 43.00 | 361.10 | 10 | 2 | 38.191785 | -89.87773 |
| MW-389 | UA | 2015-12-01 | 419.90 | 419.90 | Top of PVC | 417.30 | 42.00 | 52.00 | 375.30 | 365.30 | 52.00 | 361.60 | 10 | 2 | 38.193679 | -89.877076 |
| MW-390 | UA | 2016-03-04 | 428.06 | 428.06 | Top of PVC | 425.98 | 50.00 | 65.00 | 376.00 | 361.00 | 65.00 | 358.00 | 15 | 2 | 38.192956 | -89.869793 |
| MW-391 | UA | 2016-03-10 | 426.63 | 426.63 | Top of PVC | 424.24 | 55.00 | 70.00 | 369.20 | 354.20 | 70.00 | 349.80 | 15 | 2 | 38.190869 | -89.874759 |

TABLE 2-1. MONITORING WELL LOCATIONS AND CONSTRUCTION DETAILS
GROUNDWATER MODELING REPORT
BALDWIN POWER PLANT
BOTTOM ASH POND
BALDWIN, ILLINOIS

| Well Number | HSU | Date Constructed | Top of PVC Elevation (ft) | Measuring Point Elevation (ft) | Measuring Point Description | Ground Elevation (ft) | Screen Top Depth (ft BGS) | Screen Bottom Depth (ft BGS) | Screen Top Elevation (ft) | Screen Bottom Elevation (ft) | Well Depth (ft BGS) | Bottom of Boring Elevation (ft) | Screen Length (ft) | Screen Diameter (inches) | Latitude (Decimal Degrees) | Longitude (Decimal Degrees) |
|-------------|-----|------------------|---------------------------|--------------------------------|-----------------------------|-----------------------|---------------------------|------------------------------|---------------------------|------------------------------|---------------------|---------------------------------|--------------------|--------------------------|----------------------------|-----------------------------|
| MW-392 | UA | 2022-09-26 | 437.02 | 437.02 | Top of PVC | 434.07 | 74.00 | 84.00 | 360.07 | 350.07 | 84.00 | 350.07 | 10 | 2 | 38.199203 | -89.866934 |
| MW-393 | UA | 2022-10-04 | 437.86 | 437.86 | Top of PVC | 434.59 | 75.00 | 85.00 | 359.59 | 349.59 | 85.00 | 349.59 | 10 | 2 | 38.199174 | -89.862666 |
| MW-394 | UA | 2022-10-05 | 438.29 | 438.29 | Top of PVC | 435.51 | 73.00 | 83.00 | 362.51 | 352.51 | 83.00 | 350.51 | 10 | 2 | 38.199136 | -89.85866 |
| OW-156 | UU | 2010-09-01 | 427.87 | 427.87 | Top of PVC | 425.14 | 7.90 | 17.20 | 417.30 | 407.90 | 17.70 | 407.40 | 9.3 | 2 | 38.198969 | -89.869592 |
| OW-157 | UU | 2010-09-01 | 432.64 | 432.64 | Top of PVC | 429.90 | 7.80 | 17.10 | 422.10 | 412.80 | 17.60 | 412.30 | 9.3 | 2 | 38.19384 | -89.867384 |
| OW-256 | UU | 2013-08-01 | 427.70 | 427.70 | Top of PVC | 425.20 | 28.00 | 32.50 | 397.20 | 392.70 | 33.10 | 389.20 | 4.5 | 2 | 38.198966 | -89.86961 |
| OW-257 | UU | 2013-08-01 | 431.02 | 431.02 | Top of PVC | 428.17 | 34.00 | 38.50 | 394.20 | 389.70 | 39.10 | 388.60 | 4.5 | 2 | 38.193865 | -89.867456 |
| PZ-169 | UU | 2015-07-28 | 422.60 | 422.60 | Top of PVC | 420.01 | 31.50 | 41.50 | 388.50 | 378.50 | 41.50 | 378.00 | 10 | 2 | 38.196962 | -89.870253 |
| PZ-170 | UU | 2015-07-29 | 421.43 | 421.43 | Top of PVC | 418.58 | 21.10 | 31.10 | 397.50 | 387.50 | 31.10 | 387.50 | 10 | 2 | 38.195585 | -89.869632 |
| PZ-171 | UU | 2015-07-31 | 434.15 | 434.15 | Top of PVC | 431.54 | 28.00 | 38.00 | 403.50 | 393.50 | 38.00 | 393.50 | 10 | 2 | 38.194595 | -89.879189 |
| PZ-172 | UU | 2015-08-03 | 412.95 | 412.95 | Top of PVC | 410.22 | 16.00 | 26.00 | 394.20 | 384.20 | 26.00 | 384.00 | 10 | 2 | 38.191491 | -89.879283 |
| PZ-173 | UU | 2015-08-03 | 391.46 | 391.46 | Top of PVC | 388.43 | 3.50 | 13.50 | 384.90 | 374.90 | 13.50 | 374.30 | 10 | 2 | 38.1907 | -89.879247 |
| PZ-174 | UU | 2015-08-04 | 401.92 | 401.92 | Top of PVC | 398.97 | 14.50 | 24.50 | 384.50 | 374.50 | 24.50 | 374.30 | 10 | 2 | 38.189682 | -89.877209 |
| PZ-175 | UU | 2015-08-07 | 423.01 | 423.01 | Top of PVC | 419.87 | 40.00 | 50.00 | 379.90 | 369.90 | 50.00 | 369.70 | 10 | 2 | 38.189032 | -89.873481 |
| PZ-176 | UU | 2015-08-06 | 406.44 | 406.44 | Top of PVC | 403.46 | 18.10 | 28.10 | 385.40 | 375.40 | 28.60 | 374.90 | 10 | 2 | 38.188565 | -89.871623 |
| PZ-177 | UU | 2015-08-06 | 420.90 | 420.90 | Top of PVC | 417.93 | 20.50 | 30.50 | 397.40 | 387.40 | 30.50 | 387.20 | 10 | 2 | 38.188361 | -89.869736 |
| PZ-178 | UU | 2015-08-05 | 431.26 | 431.26 | Top of PVC | 428.45 | 33.00 | 43.00 | 395.50 | 385.50 | 43.00 | 385.00 | 10 | 2 | 38.188076 | -89.867868 |
| PZ-182 | UU | 2015-07-30 | 431.61 | 431.61 | Top of PVC | 428.47 | 24.00 | 34.00 | 404.50 | 394.50 | 34.00 | 394.50 | 10 | 2 | 38.194512 | -89.86801 |
| TPZ-158 | UU | 2013-08-01 | 456.26 | 456.26 | Top of PVC | 453.26 | 9.20 | 18.30 | 444.00 | 435.00 | 18.90 | 434.30 | 9.1 | 1.3 | 38.195308 | -89.849428 |
| TPZ-159 | UU | 2013-08-01 | 447.64 | 447.64 | Top of PVC | 444.69 | 20.00 | 29.00 | 424.70 | 415.70 | 29.60 | 394.70 | 9.1 | 1.3 | 38.199022 | -89.862558 |
| TPZ-160 | UU | 2013-08-01 | 431.49 | 431.49 | Top of PVC | 428.59 | 9.80 | 18.80 | 418.80 | 409.80 | 19.40 | 393.60 | 9.1 | 1.3 | 38.19896 | -89.875586 |
| TPZ-163 | CCR | 2013-08-01 | 458.41 | 458.41 | Top of PVC | 455.51 | 8.60 | 18.10 | 446.90 | 437.40 | 18.70 | 410.50 | 9.5 | 2 | 38.19274 | -89.857249 |
| TPZ-164 | CCR | 2013-08-01 | 435.10 | 435.10 | Top of PVC | 432.50 | 5.20 | 9.70 | 427.30 | 422.80 | 10.30 | 422.20 | 4.5 | 2 | 38.195586 | -89.862797 |
| TPZ-165 | UU | 2013-08-01 | 398.85 | 398.85 | Top of PVC | 396.10 | 7.80 | 16.80 | 388.30 | 379.30 | 17.40 | 378.70 | 9.1 | 1.3 | 38.193174 | -89.874746 |

TABLE 2-1. MONITORING WELL LOCATIONS AND CONSTRUCTION DETAILS
GROUNDWATER MODELING REPORT
BALDWIN POWER PLANT
BOTTOM ASH POND
BALDWIN, ILLINOIS

| Well Number | HSU | Date Constructed | Top of PVC Elevation (ft) | Measuring Point Elevation (ft) | Measuring Point Description | Ground Elevation (ft) | Screen Top Depth (ft BGS) | Screen Bottom Depth (ft BGS) | Screen Top Elevation (ft) | Screen Bottom Elevation (ft) | Well Depth (ft BGS) | Bottom of Boring Elevation (ft) | Screen Length (ft) | Screen Diameter (inches) | Latitude (Decimal Degrees) | Longitude (Decimal Degrees) |
|-------------|-----|------------------|---------------------------|--------------------------------|-----------------------------|-----------------------|---------------------------|------------------------------|---------------------------|------------------------------|---------------------|---------------------------------|--------------------|--------------------------|----------------------------|-----------------------------|
| TPZ-166 | UU | 2013-08-01 | 425.18 | 425.18 | Top of PVC | 422.33 | 15.30 | 24.70 | 407.10 | 397.60 | 25.30 | 396.80 | 9.5 | 2 | 38.1922 | -89.872297 |
| TPZ-167 | CCR | 2013-08-01 | 441.38 | 441.38 | Top of PVC | 438.63 | 21.40 | 30.90 | 417.20 | 407.70 | 31.50 | 389.90 | 9.5 | 2 | 38.190478 | -89.869723 |
| TPZ-168 | CCR | 2013-08-01 | 457.53 | 457.53 | Top of PVC | 454.93 | 15.80 | 25.30 | 439.20 | 429.70 | 25.80 | 384.90 | 9.5 | 2 | 38.188681 | -89.863954 |
| XPW01 | CCR | 2022-09-23 | 437.66 | 437.66 | Top of PVC | 435.12 | 7.00 | 12.00 | 428.12 | 423.12 | 12.00 | 421.12 | 5 | 2 | 38.197522 | -89.864474 |
| XPW02 | CCR | 2022-09-24 | 437.92 | 437.92 | Top of PVC | 434.86 | 6.00 | 11.00 | 428.86 | 423.86 | 11.00 | 420.86 | 5 | 2 | 38.197894 | -89.86188 |
| XPW04 | CCR | 2022-09-24 | 434.58 | 434.58 | Top of PVC | 430.59 | 6.50 | 16.50 | 424.09 | 414.09 | 16.50 | 410.59 | 10 | 2 | 38.194698 | -89.863819 |
| XPW05 | CCR | 2022-09-24 | 437.27 | 437.27 | Top of PVC | 434.12 | 18.00 | 28.00 | 416.12 | 406.12 | 28.00 | 404.12 | 10 | 2 | 38.196233 | -89.862366 |
| XPW06 | CCR | 2022-09-22 | 417.72 | 417.72 | Top of PVC | 418.06 | 5.00 | 10.00 | 412.99 | 407.99 | 10.00 | 402.06 | 5 | 2 | 38.196967 | -89.868954 |

Notes:
All elevation data are presented relative to the North American Vertical Datum 1988 (NAVD88), GEOID 12A
-- = data not available
BGS = below ground surface
CCR = coal combustion residuals
ft = foot or feet
HSU = Hydrostratigraphic Unit
PVC = polyvinyl chloride
UA = uppermost aquifer
UU = upper unit

generated 01/09/2023, 11:09:49 AM CST

TABLE 2-2. FLOW AND TRANSPORT MODEL CALIBRATION TARGETS

GROUNDWATER MODELING REPORT

BALDWIN POWER PLANT

BOTTOM ASH POND

BALDWIN, IL

| Well ID | Monitored Hydrogeologic Unit | Modeled Target Location (Layer Number) | Flow Model Target Groundwater Elevation (Modified Median Value December 2015 to June 2022 [feet NAVD88] ¹) | Transport Model Target Total Boron Concentrations December 2015 to December 2022 (mg/L) | | |
|----------|------------------------------|--|--|---|---------------------|--------------------|
| | | | | Minimum | Median | Maximum |
| MW-104DR | UU | 3 | 445.01 | 0.0191 | 0.02 | 0.05 |
| MW-104SR | UU | 2 | 446.42 | 0.04 | 0.128 | 0.237 |
| MW-116 | UU | 4 | 449.61 ² | 0.023 | 0.024 | 0.025 |
| MW-126 | UU | 2 | 459.57 ² | 0.0092 | 0.0106 | 0.012 |
| MW-150 | UU | 3 | 377.70 | 0.31 ³ | 2.12 ³ | 4.29 ³ |
| MW-151 | UU | 5 | 395.62 | 0.217 ³ | 0.267 ³ | 0.507 ³ |
| MW-152 | UU | 3 | 419.87 | 0.015 ³ | 9.92 ³ | 29 ³ |
| MW-153 | UU | 2 | 432.69 | 0.009 ³ | 0.02 ³ | 21.5 ³ |
| MW-154 | UU | 5 | 379.61 | 0.018 ³ | 0.02 ³ | 0.056 ³ |
| MW-155 | UU | 3 | 373.98 | 0.0114 ³ | 0.02 ³ | 0.05 ³ |
| MW-158R | UU | 2 | 442.63 ² | 0.0254 | 0.0347 | 0.061 |
| MW-192 | UU | 2 | 428.57 ² | 0.0525 | 0.0537 | 0.0686 |
| MW-193 | UU | 3 | 429.02 ² | 0.0473 | 0.059 | 0.0645 |
| MW-194 | UU | 3 | 431.32 ² | 0.019 | 0.022 | 0.023 |
| MW-203 | UA | 6 | No Target | 0.907 | 0.907 | 0.907 |
| MW-204 | UA | 6 | 442.82 ² | 1.02 | 1.03 | 1.35 |
| MW-252 | UU | 5 | 424.93 | 0.12 ³ | 0.144 ³ | 1.47 ³ |
| MW-253 | UU | 5 | 434.66 | 0.0333 ³ | 0.0604 ³ | 0.24 ³ |
| MW-258 | UA | 5 | 441.95 ² | 1.03 | 1.27 | 1.35 |
| MW-304 | UA | 6 | 445.93 | 1.27 | 1.685 | 2.16 |
| MW-306 | UA | 6 | 435.63 | 0.025 | 0.2 | 0.634 |
| MW-307 | UA | 6 | 431.10 ² | 1.2 | 1.47 | 1.63 |
| MW-350 | UA | 6 | 374.27 | 0.541 | 0.652 | 0.9 |
| MW-352 | UA | 6 | 423.42 | 0.76 ³ | 1.82 ³ | 2.09 ³ |
| MW-355 | UA | 6 | 370.39 | 0.02 ³ | 0.024 ³ | 0.05 ³ |
| MW-356 | UA | 6 | 424.92 | 1.79 | 2.01 | 2.92 |
| MW-358 | UA | 6 | No Target | 1.1 | 1.25 | 1.67 |
| MW-366 | UA | 6 | 409.99 | 1.19 | 1.66 | 2.7 |
| MW-369 | UA | 6 | 413.31 | 0.592 | 1.55 | 2.4 |
| MW-370 | UA | 6 | 402.35 | 1.56 | 1.82 | 2.67 |
| MW-374 | UA | 6 | 388.62 | No Target | | |
| MW-375 | UA | 6 | 392.00 | 0.979 | 1.37 | 2.06 |
| MW-377 | UA | 6 | 416.56 | 1.54 | 1.74 | 2.01 |
| MW-382 | UA | 5 | 414.96 | 1.6 | 1.75 | 2.57 |
| MW-383 | UA | 6 | 441.03 | 1.26 | 1.42 | 2.05 |
| MW-384 | UA | 6 | 445.34 | 1.26 | 1.48 | 2.26 |
| MW-385 | UA | 6 | No Target | 2.45 | 2.45 | 2.45 |
| MW-386 | UA | 6 | No Target | 1.34 | 1.34 | 1.34 |
| MW-388 | UA | 6 | 393.34 | No Target | | |
| MW-389 | UA | 6 | 400.58 | No Target | | |
| MW-390 | UA | 6 | 423.44 | 0.175 | 0.546 | 2.3 |
| MW-391 | UA | 6 | No Target | 1.3 | 3.25 | 8.91 |
| MW-392 | UA | 6 | 428.08 ² | 1.57 | 1.72 | 2.33 |
| MW-393 | UA | 6 | 429.29 ² | 1.53 | 1.83 | 2.04 |
| MW-394 | UA | 6 | 432.69 ² | 1.87 | 2.02 | 2.23 |
| OW-156 | UU | 2 | 421.74 | 0.02 ³ | 0.024 ³ | 0.03 ³ |
| OW-157 | UU | 2 | 426.61 | 44.6 ³ | 45.2 ³ | 45.3 ³ |
| TPZ-164 | CCR | 1 | 431.14 | 1.09 | 1.47 | 2.04 |
| XPW01 | CCR | 1 | 426.15 ² | 0.93 | 0.942 | 1.03 |
| XPW02 | CCR | 1 | 433.52 ² | 1.18 | 1.2 | 1.52 |
| XPW04 | CCR | 1 | 426.56 ² | 1.15 | 1.28 | 1.38 |
| XPW05 | CCR | 1 | 432.43 ² | 1.02 | 1.16 | 1.25 |
| XPW06 | CCR | 1 | 415.07 ² | 2.29 | 3.86 | 4.64 |

[O: EGP 1/3/23, C: JJW 1/4/23, U: JJW 5/2/23, C: EGP 5/16/23]

Notes:

¹ Target groundwater elevations represent modified median groundwater elevations from December 2015 to June 2022. Anomalous groundwater elevations (e.g., groundwater elevations that do not represent static groundwater conditions, groundwater elevation outliers, or groundwater elevations measured in error) monitored between December 2015 and June 2022 were removed from the median groundwater elevation calculations used as flow calibration targets.

² Target groundwater elevation used most recent measurement (November 2022) for wells constructed or reoccupied in 2022

³ Target boron concentration used dissolved boron data from November 2010 to December 2022

ID = identification

mg/L = milligrams per liter

NAVD88 = North American Vertical Datum of 1988

Hydrogeologic Unit:

CCR = coal combustion residuals

UA = uppermost aquifer

UU = upper unit

TABLE 5-1. FLOW MODEL INPUT AND SENSITIVITY ANALYSIS RESULTS

GROUNDWATER MODELING REPORT

BALDWIN POWER PLANT

BOTTOM ASH POND

BALDWIN, ILLINOIS

| Zone | Zone Description | Materials | ft/d | cm/s | Kh/Kv | Value Source | Sensitivity ¹ |
|-----------------------------------|--------------------------------|------------|-------------------|----------|-------|---|--------------------------|
| Horizontal Hydraulic Conductivity | | | Calibration Model | | | | |
| 1 | UU | silty clay | 0.07 | 2.47E-05 | NA | Calibrated - Near Geomean Hydraulic Conductivity Field Test Results for Wells Screened in the Upper Unit (Ramboll, 2023d) | Moderate |
| 2 | Old East Fly Ash Pond | CCR | 0.5 | 1.76E-04 | NA | Calibrated - Near Geomean of Vertical Hydraulic Conductivity Laboratory Test Results from FAPS Wells (Ramboll, 2023d) | Negligible |
| 3 | East Fly Ash Pond | CCR | 0.5 | 1.76E-04 | NA | Calibrated - Near Geomean of Vertical Hydraulic Conductivity Laboratory Test Results from FAPS Wells (Ramboll, 2023d) | Low |
| 4 | West Fly Ash Pond | CCR | 0.5 | 1.76E-04 | NA | Calibrated - Near Geomean of Vertical Hydraulic Conductivity Laboratory Test Results from FAPS Wells (Ramboll, 2023d) | Low |
| 7 | Bottom Ash Pond | CCR | 1.5 | 5.29E-04 | NA | Calibrated - Near Minimum Hydraulic Conductivity Field Test Results for Wells Screened in BAP (Ramboll, 2023d) | Moderate |
| 8 | UA (Decomposed Bedrock) | bedrock | 0.05 | 1.76E-05 | NA | Calibrated - Within Range of Hydraulic Conductivity Field Test Results for Wells Screened in Bedrock (Ramboll, 2023d) | Low |
| 9 | UA | bedrock | 0.05 | 1.76E-05 | NA | Calibrated - Within Range of Hydraulic Conductivity Field Test Results for Wells Screened in Bedrock (Ramboll, 2023d) | High |
| 10 | UU (Top of Vandalia) | silty clay | 0.07 | 2.47E-05 | NA | Calibrated - Near Geomean Hydraulic Conductivity Field Test Results for Wells Screened in the Upper Unit (Ramboll, 2023d) | Low |
| 12 | River Alluvium | silty clay | 0.6 | 2.12E-04 | NA | Calibrated | Low |
| 14 | PMP | sand seams | 0.3 | 1.06E-04 | NA | Calibrated - Near Geomean Hydraulic Conductivity Field Test Results for Wells Screened Across Upper Unit Sands (Ramboll, 2023d) | Moderate |
| 16 | Fill at BAP & FAPS Boundary | fill | 0.5 | 1.76E-04 | NA | Calibrated | Negligible |
| 100 | Above River Boundary Condition | NA | 500 | 1.76E-01 | NA | Calibrated - Conductivity Value to Allow Groundwater Flow to River Boundary Conditions | Negligible |
| Vertical Hydraulic Conductivity | | | Calibration Model | | | | |
| 1 | UU | silty clay | 0.007 | 2.47E-06 | 10 | Calibrated - Within Range of Upper Unit Vertical Hydraulic Conductivity Laboratory Test Results (Ramboll, 2023d) | Moderate |
| 2 | Old East Fly Ash Pond | CCR | 0.5 | 1.76E-04 | 1 | Calibrated - Near Geomean of Vertical Hydraulic Conductivity Laboratory Test Results from FAPS Wells (Ramboll, 2023d) | Negligible |
| 3 | East Fly Ash Pond | CCR | 0.5 | 1.76E-04 | 1 | Calibrated - Near Geomean of Vertical Hydraulic Conductivity Laboratory Test Results from FAPS Wells (Ramboll, 2023d) | Negligible |
| 4 | West Fly Ash Pond | CCR | 0.5 | 1.76E-04 | 1 | Calibrated - Near Geomean of Vertical Hydraulic Conductivity Laboratory Test Results from FAPS Wells (Ramboll, 2023d) | Negligible |
| 7 | Bottom Ash Pond | CCR | 1.5 | 5.29E-04 | 1 | Calibrated - Near BAP Well TPZ-164 Vertical Hydraulic Conductivity Laboratory Test Results (Ramboll, 2023d) | Negligible |
| 8 | UA (Decomposed Bedrock) | bedrock | 0.01 | 3.53E-06 | 5 | Calibrated | Low |

TABLE 5-1. FLOW MODEL INPUT AND SENSITIVITY ANALYSIS RESULTS
GROUNDWATER MODELING REPORT
BALDWIN POWER PLANT
BOTTOM ASH POND
BALDWIN, ILLINOIS

| Zone | Zone Description | Materials | ft/d | cm/s | Kh/Kv | Value Source | Sensitivity ¹ |
|---------------------------------|--------------------------------|------------|--|----------|-------|---|--------------------------|
| Vertical Hydraulic Conductivity | | | Calibration Model | | | | |
| 9 | UA | bedrock | 0.005 | 1.76E-06 | 10 | Calibrated | Moderate |
| 10 | UU (Top of Vandalia) | silty clay | 0.007 | 2.47E-06 | 10 | Calibrated - Within Range of Upper Unit Vertical Hydraulic Conductivity Laboratory Test Results (Ramboll, 2023d) | Low |
| 12 | River Alluvium | silty clay | 0.6 | 2.12E-04 | 1 | Calibrated | Negligible |
| 14 | PMP | sand seams | 0.3 | 1.06E-04 | 1 | Calibrated - Near Geomean Hydraulic Conductivity Field Test Results for Wells Screened Across Upper Unit Sands (Ramboll, 2023d) | Negligible |
| 16 | Fill at BAP & FAPS Boundary | fill | 0.5 | 1.76E-04 | NA | Calibrated | Negligible |
| 100 | Above River Boundary Condition | NA | 500 | 1.76E-01 | 1 | Calibrated - Conductivity Value to Allow Groundwater Flow to River Boundary Conditions | Negligible |
| Recharge | | | Calibration Model | | | | |
| 1 | Silty Clay | silty clay | 1.00E-05 | 0.04 | NA | Calibrated | Low |
| 2 | Old East Fly Ash Pond | CCR | 6.80E-05 | 0.30 | NA | calibrated - 2021-2022 recharge at FAPS consistent with estimated closed FAPS recharge values in 2014 FAPS groundwater modeling report (NRT, 2014b; NRT, 2014c) | Low |
| 3 | East Fly Ash Pond | CCR | 6.80E-05 | 0.30 | NA | calibrated - 2021-2022 recharge at FAPS consistent with estimated closed FAPS recharge values in 2014 FAPS groundwater modeling report (NRT, 2014b; NRT, 2014c) | Low |
| 4 | West Fly Ash Pond | CCR | 6.80E-05 | 0.30 | NA | calibrated - 2021-2022 recharge at FAPS consistent with estimated closed FAPS recharge values in 2014 FAPS groundwater modeling report (NRT, 2014b; NRT, 2014c) | Low |
| 5 | Secondary Pond | silty clay | 1.00E-05 | 0.04 | NA | Calibrated | Negligible |
| 6 | Tertiary Pond | silty clay | 1.00E-05 | 0.04 | NA | Calibrated | Negligible |
| 7 | Bottom Ash Pond | CCR | 1.80E-04 | 0.79 | NA | Calibrated | Low |
| Storage | | | | | | | |
| 1 | UU | silty clay | Not used in steady-state calibration model | | | | |
| 2 | Old East Fly Ash Pond | CCR | | | | | |
| 3 | East Fly Ash Pond | CCR | | | | | |
| 4 | West Fly Ash Pond | CCR | | | | | |
| 7 | Bottom Ash Pond | CCR | | | | | |
| 8 | UA (Decomposed Bedrock) | bedrock | | | | | |
| 9 | UA | bedrock | | | | | |
| 10 | UU (Top of Vandalia) | silty clay | | | | | |
| 12 | River Alluvium | silty clay | | | | | |
| 14 | PMP | sand seams | | | | | |
| 16 | Fill at BAP & FAPS Boundary | fill | | | | | |
| 100 | Above River Boundary Condition | NA | | | | | |

TABLE 5-1. FLOW MODEL INPUT AND SENSITIVITY ANALYSIS RESULTS
GROUNDWATER MODELING REPORT
BALDWIN POWER PLANT
BOTTOM ASH POND
BALDWIN, ILLINOIS

| River Parameters | | | | | | | |
|------------------|--|-----------------------|-----------------|-------------------------------|-------------------------------|--|-------------|
| | Relative Location | Stage of River (feet) | Sensitivity | River Bottom Elevation (feet) | Hydraulic Conductivity (ft/d) | Average River Conductance (ft ² /d) | Sensitivity |
| Reach 0 | Cooling Pond | 429 | Moderate | 410 | 3.80 | 3.80E+04 | Negligible |
| Reach 1 | Kaskaskia River | 370 | High | 365 | 5.17 | 5.17E+04 | Negligible |
| Reach 2 | South Stream (Southern Limit of Model Domain) | 456.03-370 | Negligible | 452.03-365.54 | 2.08 | 2.08E+04 | Negligible |
| Reach 3 | South Stream (Between Reach 2 and Reach 4) | 449.98-370.06 | Moderate | 447.98-368.06 | 2.05 | 2.05E+04 | Negligible |
| Reach 4 | South Stream (Adjacent to FAPS) | 445-368 | Moderately High | 443-366 | 0.36 | 3.60E+03 | Negligible |
| Reach 5 | Northwest Stream (West of Cooling Pond) | 410.66-370 | Negligible | 408.66-368 | 3.89 | 3.89E+04 | Negligible |
| Reach 7 | Northeast Stream (East of Cooling Pond) | 454.75-427 | High | 452.75-425 | 2.60 | 2.60E+04 | Negligible |
| Reach 8 | Secondary and Tertiary Pond | 396 | Low | 394.99-376.17 | 0.26 | 2.60E+03 | Negligible |

TABLE 5-1. FLOW MODEL INPUT AND SENSITIVITY ANALYSIS RESULTS

GROUNDWATER MODELING REPORT

BALDWIN POWER PLANT

BOTTOM ASH POND

BALDWIN, ILLINOIS

| River Parameters | | | | | | | |
|--------------------------|---------------------------|---|-------------|------------|------------|------------|----|
| Value Source | NA | Calibrated - Cooling Pond Stage (Reach 0) Approximates Elevation at which Pond is Maintained; Kaskasia River Stage (Reach 1) at Baldwin Power Plant Based on Interpolated Stage Data Provided at New Athens, Illinois (USGS 5595000) and Red Bud (USGS 5595240); River Stage at Reaches 2 through 7 Approximate Topography; River Stage at Reach 8 Based on Historic Groundwater Elevation within Secondary and Tertiary Ponds at TPZ-165 | NA | Calibrated | Calibrated | Calibrated | NA |
| Constant Head Parameters | | | | | | | |
| | Relative Location | Head at Boundary (feet) | Sensitivity | | | | |
| Reach 0 | BAP Constant Head West | 415 | Negligible | | | | |
| Reach 1 | BAP Constand Head Central | 425 | Negligible | | | | |
| Value Source | NA | Calibrated - Head at Boundary Based on Estimated Water Surface Elevation within BAP | NA | | | | |

[O: JJW 2/17/2023 ; C: EGP 5/18/23]

Notes:

¹ Sensitivity Explanation:

Negligible - SSR changed by less than 1%

Low - SSR change between 1% and 10%

Moderate - SSR change between 10% and 50%

Moderately High - SSR change between 50% and 100%

High - SSR change greater than 100%

SSR = sum of squared residuals

- - - = not tested

BAP = bottom ash pond

FAPS = fly ash pond system

cm/s = centimeters per second

ft/d = feet per day

ft²/day = feet squared per day

in/yr = inches per year

Kh/Kv = anisotropy ratio

NA = not applicable

Hydrogeologic Unit:

CCR = coal combustion residuals

PMP = potential migration pathway

UA = uppermost aquifer

UU = upper unit

References:

Ramboll Americas Engineering Solutions, Inc. (Ramboll), 2023d. Hydrogeologic Site Characterization Report Revision 1. Bottom Ash Pond, Baldwin Power Plant, Baldwin, Illinois. August 1.

Natural Resource Technology, Inc. (NRT), 2014b. Groundwater Model and Simulation of Closure Alternatives, Baldwin Ash Pond System. June 18.

Natural Resource Technology, Inc. (NRT), 2014c. Groundwater Model and Simulation of Closure Alternatives, Model Report Addendum Baldwin Ash Pond System. September 30.

TABLE 5-2. TRANSPORT MODEL INPUT VALUES (CALIBRATION)
GROUNDWATER MODELING REPORT
BALDWIN POWER PLANT
BOTTOM ASH POND
BALDWIN, ILLINOIS

| | Hydrostratigraphic Unit | Materials | Calibration Model | | | | | | Value Source | Sensitivity |
|---|---------------------------------|-----------|--|--|----------------------------------|--|--|---|--------------|-------------|
| | | | Calibration Model 1 Dates: 1970-2020 Recharge (ft/d) | Calibration Model 2 Dates: 2021-2022 Recharge (ft/d) | Boron Concentration (mg/L) | Calibration Model 1 Dates: 1970-2020 Constant Head (feet) | Calibration Model 2 Dates: 2021-2022 Constant Head (feet) | | | |
| Initial Concentration | | | | | | | | | | |
| Entire Domain | NA | NA | NA | NA | 0 | NA | NA | NA | - - - | |
| Source Concentration (recharge) | | | | | | | | | | |
| Zone 2 | Old East Fly Ash Pond | CCR | 4.00E-04 | 6.80E-05 | 38 | NA | NA | calibrated - 2021-2022 recharge at FAPS consistent with estimated closed FAPS recharge values in 2014 FAPS groundwater modeling report (NRT, 2014b; NRT, 2014c) | - - - | |
| Zone 3 | East Fly Ash Pond | CCR | 8.00E-04 | 6.80E-05 | 79 | NA | NA | calibrated - 2021-2022 recharge at FAPS consistent with estimated closed FAPS recharge values in 2014 FAPS groundwater modeling report (NRT, 2014b; NRT, 2014c) | - - - | |
| Zone 4 | West Fly Ash Pond | CCR | 6.00E-04 | 6.80E-05 | 47 | NA | NA | calibrated - 2021-2022 recharge at FAPS consistent with estimated closed FAPS recharge values in 2014 FAPS groundwater modeling report (NRT, 2014b; NRT, 2014c) | - - - | |
| Zone 7 | Bottom Ash Pond (West) | CCR | 1.80E-04 | 1.80E-04 | 4 | NA | NA | calibrated | - - - | |
| Zone 8 | Bottom Ash Pond (East) | CCR | 1.80E-04 | 1.80E-04 | 1.5 | NA | NA | calibrated | - - - | |
| Source Concentration (constant concentration cells) and Stormwater Management (constant head cells) | | | | | | | | | | |
| Reach 2 | Old East Fly Ash Pond | CCR | NA | NA | 38 | NA | NA | calibrated | - - - | |
| Reach 3 | East Fly Ash Pond | CCR | NA | NA | 79 | NA | NA | calibrated | - - - | |
| Reach 4 | West Fly Ash Pond Constant Head | CCR | NA | NA | 47 | 424.3 | NA | calibrated - head at boundary consistent with stormwater management practices within the active FAPS (AECOM, 2016b) | - - - | |
| Reach 14 | West Fly Ash Pond (Berm) | CCR | NA | NA | 47 | NA | NA | calibrated | - - - | |
| Reach 0 | BAP Constant Head West | CCR | NA | NA | 4 | 415 | 415 | calibrated - head at boundary based on estimated water surface elevation within BAP | - - - | |
| Reach 1 | BAP Constand Head Central | CCR | NA | NA | 4 | 425 | 425 | calibrated - head at boundary based on estimated water surface elevation within BAP | - - - | |
| Reach 7 | Bottom Ash Pond (West) | CCR | NA | NA | 4 | NA | NA | calibrated | - - - | |
| Reach 8 | Bottom Ash Pond (East) | CCR | NA | NA | 1.5 | NA | NA | calibrated | - - - | |

TABLE 5-2. TRANSPORT MODEL INPUT VALUES (CALIBRATION)

GROUNDWATER MODELING REPORT

BALDWIN POWER PLANT

BOTTOM ASH POND

BALDWIN, ILLINOIS

| Storage, Specific Yield and Effective Porosity | | | | | | | |
|--|--------------------------------|------------|---------|----------------|--------------------|---|---------------|
| Zone | Hydrostratigraphic Unit | Materials | Storage | Specific Yield | Effective Porosity | Value Source | Sensitivity |
| 1 | UU | silty clay | 0.003 | 0.15 | 0.15 | Storage Estimated from Literature (Fetter, 1988); Specific Yield Set Equal to Effective Porosity; Calibrated - Effective Porosity Estimated from Literature (Fetter, 1988; Morris and Johnson, 1967; Heath, 1983; Walton, 1988) | see Table 5-3 |
| 2 | Old East Fly Ash Pond | CCR | 0.003 | 0.2 | 0.2 | Storage Estimated from Literature (Fetter, 1988); Specific Yield Set Equal to Effective Porosity; Calibrated - Effective Porosity Estimated from Literature (Fetter, 1988; Morris and Johnson, 1967; Heath, 1983; Walton, 1988) | see Table 5-3 |
| 3 | East Fly Ash Pond | CCR | 0.003 | 0.2 | 0.2 | Storage Estimated from Literature (Fetter, 1988); Specific Yield Set Equal to Effective Porosity; Calibrated - Effective Porosity Estimated from Literature (Fetter, 1988; Morris and Johnson, 1967; Heath, 1983; Walton, 1988) | see Table 5-3 |
| 4 | West Fly Ash Pond | CCR | 0.003 | 0.2 | 0.2 | Storage Estimated from Literature (Fetter, 1988); Specific Yield Set Equal to Effective Porosity; Calibrated - Effective Porosity Estimated from Literature (Fetter, 1988; Morris and Johnson, 1967; Heath, 1983; Walton, 1988) | see Table 5-3 |
| 7 | Bottom Ash Pond | CCR | 0.003 | 0.25 | 0.25 | Storage Estimated from Literature (Fetter, 1988); Specific Yield Set Equal to Effective Porosity; Calibrated - Effective Porosity Estimated from Literature (Fetter, 1988; Morris and Johnson, 1967; Heath, 1983; Walton, 1988) | see Table 5-3 |
| 8 | UA (Decomposed Bedrock) | bedrock | 0.003 | 0.15 | 0.15 | Storage Estimated from Literature (Fetter, 1988); Specific Yield Set Equal to Effective Porosity; Calibrated - Effective Porosity Estimated from Literature (Fetter, 1988; Morris and Johnson, 1967; Heath, 1983; Walton, 1988) | see Table 5-3 |
| 9 | UA | bedrock | 0.003 | 0.3 | 0.3 | Storage Estimated from Literature (Fetter, 1988); Specific Yield Set Equal to Effective Porosity; Calibrated - Effective Porosity Estimated from Literature (Fetter, 1988; Morris and Johnson, 1967; Heath, 1983; Walton, 1988) | see Table 5-3 |
| 10 | UU (Top of Vandalia) | silty clay | 0.003 | 0.15 | 0.15 | Storage Estimated from Literature (Fetter, 1988); Specific Yield Set Equal to Effective Porosity; Calibrated - Effective Porosity Estimated from Literature (Fetter, 1988; Morris and Johnson, 1967; Heath, 1983; Walton, 1988) | see Table 5-3 |
| 12 | River Alluvium | silty clay | 0.003 | 0.15 | 0.15 | Storage Estimated from Literature (Fetter, 1988); Specific Yield Set Equal to Effective Porosity; Calibrated - Effective Porosity Estimated from Literature (Fetter, 1988; Morris and Johnson, 1967; Heath, 1983; Walton, 1988) | see Table 5-3 |
| 14 | PMP | sand seams | 0.003 | 0.25 | 0.25 | Storage Estimated from Literature (Fetter, 1988); Specific Yield Set Equal to Effective Porosity; Calibrated - Effective Porosity Estimated from Literature (Fetter, 1988; Morris and Johnson, 1967; Heath, 1983; Walton, 1988) | see Table 5-3 |
| 16 | Fill at BAP & FAPS Boundary | fill | 0.003 | 0.2 | 0.2 | Storage Estimated from Literature (Fetter, 1988); Specific Yield Set Equal to Effective Porosity; Calibrated - Effective Porosity Estimated from Literature (Fetter, 1988; Morris and Johnson, 1967; Heath, 1983; Walton, 1988) | see Table 5-3 |
| 100 | Above River Boundary Condition | NA | 0.003 | 0.5 | 0.5 | Storage Estimated from Literature (Fetter, 1988); Specific Yield Set Equal to Effective Porosity; Calibrated - Effective Porosity Estimated from Literature (Fetter, 1988; Morris and Johnson, 1967; Heath, 1983; Walton, 1988) | see Table 5-3 |

TABLE 5-2. TRANSPORT MODEL INPUT VALUES (CALIBRATION)

GROUNDWATER MODELING REPORT
BALDWIN POWER PLANT
BOTTOM ASH POND
BALDWIN, ILLINOIS

| Dispersivity | | | | | | |
|-------------------|-------------------------|-----------|---------------------|-------------------|-----------------|-------------|
| Applicable Region | Hydrostratigraphic Unit | Materials | Longitudinal (feet) | Transverse (feet) | Vertical (feet) | Sensitivity |
| Entire Domain | NA | NA | 5 | 0.5 | 0.05 | - - - |

[O: JJW 5/5/2023, C: EGP 5/22/23]

Notes:

¹ The concentrations from the end of the calibrated transport model were imported as initial concentrations for the prediction model runs.
- - - = not tested
ft/d = feet per day
mg/L = milligrams per liter
NA = not applicable

Hydrogeologic Unit:
CCR = coal combustion residuals
PMP = potential migration pathway
UA = uppermost aquifer
UU = upper unit

References:

AECOM, 2016b. RE: History of Construction, USEPA Final Rule, 40 C.F.R. § 257.73 (c), Baldwin Energy Complex, Baldwin, Illinois. October.
Fetter, C.W., 1988, Applied Hydrogeology, Merrill Publishing Company, Columbus, Ohio.
Morris, D.A and A.I. Johnson, 1967. Summary of hydrologic and physical properties of rock and soil materials as analyzed by the Hydrologic Laboratory of the U.S. Geological Survey. U.S. Geological Survey Water-Supply Paper 1839-D, 42p.
Heath, R.C., 1983. Basic ground-water hydrology, U.S. Geological Survey Water-Supply Paper 2220, 86p.
Walton, W.C., 1988. Practical Aspects of Groundwater Modeling. National Water Well Association, Worthington, Ohio.
Natural Resource Technology, Inc. (NRT), 2014b. Groundwater Model and Simulation of Closure Alternatives, Baldwin Ash Pond System. June 18.
Natural Resource Technology, Inc. (NRT), 2014c. Groundwater Model and Simulation of Closure Alternatives, Model Report Addendum Baldwin Ash Pond System. September 30.

TABLE 5-3. TRANSPORT MODEL INPUT VALUES (SENSITIVITY)
GROUNDWATER MODELING REPORT
BALDWIN POWER PLANT
BOTTOM ASH POND
BALDWIN, ILLINOIS

| Well ID | Calibration Concentration (mg/L) | Storage and Specific Yield | | | | Effective Porosity | | | |
|---------|--|--|--------------------------|--|--------------------------|--|--------------------------|--|--------------------------|
| | | File Name | | File Name | | File Name | | File Name | |
| | | BAL_Conc_324_T_A_s_sy_low.gwv BAL_Conc_324_T_B_2_s_sy_low.gwv | | BAL_Conc_324_T_A_s_sy_high.gwv BAL_Conc_324_T_B_2_s_sy_high.gwv | | BAL_Conc_324_T_A_por_low.gwv BAL_Conc_324_T_B_2_por_low.gwv | | BAL_Conc_324_T_A_por_high.gwv BAL_Conc_324_T_B_2_por_high.gwv | |
| | | Concentration (mg/L) | Sensitivity ¹ | Concentration (mg/L) | Sensitivity ¹ | Concentration (mg/L) | Sensitivity ¹ | Concentration (mg/L) | Sensitivity ¹ |
| MW-116 | 0.0 | 0.0 | negligible | 0.0 | negligible | 0.0 | negligible | 0.0 | negligible |
| MW-126 | 0.0 | 0.0 | negligible | 0.0 | negligible | 0.0 | negligible | 0.0 | negligible |
| MW-158R | 0.0 | 0.0 | negligible | 0.0 | negligible | 0.0 | negligible | 0.0 | negligible |
| MW-192 | 2.3E-02 | 2.2E-02 | low | 2.3E-02 | low | 2.5E-02 | moderate | 2.0E-02 | moderate |
| MW-193 | 0.2 | 0.3 | moderate | 0.2 | low | 0.3 | moderate | 0.2 | moderate |
| MW-194 | 1.3 | 1.2 | low | 1.3 | negligible | 1.4 | low | 1.2 | low |
| MW-203 | 0.0 | 0.0 | negligible | 0.0 | negligible | 0.0 | negligible | 0.0 | negligible |
| MW-204 | 0.0 | 0.0 | negligible | 0.0 | negligible | 0.0 | negligible | 0.0 | negligible |
| MW-258 | 0.0 | 0.0 | negligible | 0.0 | negligible | 0.0 | negligible | 0.0 | negligible |
| MW-304 | 0.0 | 0.0 | negligible | 0.0 | negligible | 0.0 | negligible | 0.0 | negligible |
| MW-306 | 0.0 | 0.0 | negligible | 0.0 | negligible | 0.0 | negligible | 0.0 | negligible |
| MW-307 | 0.0 | 0.0 | negligible | 0.0 | negligible | 0.0 | negligible | 0.0 | negligible |
| MW-350 | 0.0 | 0.0 | negligible | 0.0 | negligible | 0.0 | negligible | 0.0 | negligible |
| MW-356 | 5.0E-06 | 3.0E-06 | moderate | 6.0E-06 | moderate | 9.0E-06 | moderately high | 3.0E-06 | moderate |
| MW-358 | 0.0 | 0.0 | negligible | 0.0 | negligible | 0.0 | negligible | 0.0 | negligible |
| MW-366 | 1.5 | 0.6 | moderately high | 2.4 | moderately high | 2.0 | moderate | 1.1 | moderate |
| MW-369 | 0.0 | 0.0 | negligible | 0.0 | negligible | 0.0 | negligible | 0.0 | negligible |
| MW-370 | 0.0 | 0.0 | negligible | 0.0 | negligible | 0.0 | negligible | 0.0 | negligible |
| MW-375 | 1.3 | 0.5 | moderately high | 1.9 | moderate | 1.8 | moderate | 0.9 | moderate |
| MW-377 | 4.9E-03 | 0.0 | high | 3.0E-02 | high | 1.2E-02 | high | 1.4E-03 | moderately high |
| MW-382 | 0.3 | 4.44E-03 | moderately high | 1.5 | high | 0.7 | high | 0.2 | moderately high |
| MW-383 | 4.6E-02 | 1.2E-02 | moderately high | 4.2E-02 | low | 9.0E-02 | moderately high | 2.4E-02 | moderate |
| MW-384 | 0.2 | 0.1 | moderately high | 0.1 | moderately high | 0.3 | moderately high | 0.1 | moderate |
| MW-385 | 0.2 | 2.62E-03 | moderately high | 0.7 | high | 0.3 | moderately high | 0.1 | moderately high |
| MW-386 | 4.0E-02 | 0.0 | high | 1.3E-01 | high | 9.1E-02 | high | 1.5E-02 | moderately high |
| MW-390 | 0.2 | 4.48E-03 | moderately high | 0.5 | high | 0.3 | moderately high | 0.1 | moderately high |
| MW-391 | 3.5 | 2.7 | moderate | 3.8 | low | 4.1 | moderate | 2.9 | moderate |
| MW-392 | 0.0 | 0.0 | negligible | 0.0 | negligible | 0.0 | negligible | 0.0 | negligible |
| MW-393 | 0.0 | 0.0 | negligible | 0.0 | negligible | 0.0 | negligible | 0.0 | negligible |
| MW-394 | 0.0 | 0.0 | negligible | 0.0 | negligible | 0.0 | negligible | 0.0 | negligible |
| TPZ-164 | 1.5 | 1.5 | negligible | 1.5 | negligible | 1.5 | negligible | 1.5 | negligible |
| XPW01 | 0.0 | 0.0 | negligible | 0.0 | negligible | 0.0 | negligible | 0.0 | negligible |
| XPW02 | 1.5 | 1.5 | negligible | 1.5 | negligible | 1.5 | negligible | 1.5 | negligible |
| XPW04 | 1.5 | 1.5 | negligible | 1.5 | negligible | 1.5 | negligible | 1.5 | negligible |
| XPW05 | 1.5 | 1.5 | negligible | 1.5 | negligible | 1.5 | negligible | 1.5 | negligible |
| XPW06 | 4.0 | 4.0 | negligible | 4.0 | negligible | 4.0 | negligible | 4.0 | negligible |

TABLE 5-3. TRANSPORT MODEL INPUT VALUES (SENSITIVITY)
GROUNDWATER MODELING REPORT
BALDWIN POWER PLANT
BOTTOM ASH POND
BALDWIN, ILLINOIS

| Well ID | Calibration Concentration (mg/L) | Storage and Specific Yield | | | | Effective Porosity | | | |
|----------|--|--|--------------------------|--|--------------------------|--|--------------------------|--|--------------------------|
| | | File Name | | File Name | | File Name | | File Name | |
| | | BAL_Conc_324_T_A_s_sy_low.gwv BAL_Conc_324_T_B_2_s_sy_low.gwv | | BAL_Conc_324_T_A_s_sy_high.gwv BAL_Conc_324_T_B_2_s_sy_high.gwv | | BAL_Conc_324_T_A_por_low.gwv BAL_Conc_324_T_B_2_por_low.gwv | | BAL_Conc_324_T_A_por_high.gwv BAL_Conc_324_T_B_2_por_high.gwv | |
| | | Concentration (mg/L) | Sensitivity ¹ | Concentration (mg/L) | Sensitivity ¹ | Concentration (mg/L) | Sensitivity ¹ | Concentration (mg/L) | Sensitivity ¹ |
| MW-104SR | 0.0 | 0.0 | negligible | 0.0 | negligible | 0.0 | negligible | 0.0 | negligible |
| MW-104DR | 0.0 | 0.0 | negligible | 0.0 | negligible | 0.0 | negligible | 0.0 | negligible |
| MW-150 | 0.0 | 0.0 | negligible | 0.0 | negligible | 0.0 | negligible | 0.0 | negligible |
| MW-151 | 6.1 | 2.8 | moderately high | 10.3 | moderately high | 9.7 | moderately high | 3.1 | moderate |
| MW-152 | 2.5 | 2.9 | moderate | 1.1 | moderately high | 3.7 | moderate | 1.6 | moderate |
| MW-153 | 9.0E-06 | 0.0 | high | 3.0E-06 | moderately high | 1.0E-04 | high | 1.0E-06 | moderately high |
| MW-154 | 0.0 | 0.0 | negligible | 0.0 | negligible | 0.0 | negligible | 0.0 | negligible |
| MW-155 | 0.0 | 0.0 | negligible | 0.0 | negligible | 0.0 | negligible | 0.0 | negligible |
| MW-252 | 0.0 | 0.0 | negligible | 0.0 | negligible | 0.0 | negligible | 0.0 | negligible |
| MW-253 | 0.0 | 0.0 | negligible | 0.0 | negligible | 6.00E-06 | negligible | 0.0 | negligible |
| MW-352 | 1.0E-06 | 2.1E-05 | high | 0.0 | high | 0.0 | high | 1.0E-06 | negligible |
| MW-355 | 0.0 | 0.0 | negligible | 0.0 | negligible | 0.0 | negligible | 0.0 | negligible |
| OW-156 | 0.7 | 0.7 | negligible | 0.7 | low | 0.7 | low | 0.6 | low |
| OW-157 | 14.8 | 19.4 | moderate | 7.3 | moderately high | 20.0 | moderate | 11.3 | moderate |
| | | S*0.1 Sy*0.5 | | S*10 Sy*2 ² | | Porosity-0.05 | | Porosity+0.05 | |

[O: JJW 5/22/23; C: EGP 5/23/23]

Notes:

- ¹ Sensitivity Explanation:
Negligible = concentration changed by less than 1%
Low = concentration change between 1% and 10%
Moderate = concentration change between 10% and 50%
Moderately High = concentration change between 50% and 100%
High = concentration change greater than 100%
- ID = identification
mg/L = milligrams per liter
S = storativity
Sy = specific yield
- ² High specific yield sensitivity not analyzed for zone 100 (Above River Boundary Conditions) since the calibration value was already near upper limits of acceptable values for specific yield

TABLE 6-1. HELP MODEL INPUT AND OUTPUT VALUES

GROUNDWATER MODELING REPORT

BALDWIN POWER PLANT

BOTTOM ASH POND

BALDWIN, ILLINOIS

| Closure Scenario Number (Drainage Length) | BAP CIP - Consolidation Area (Top) | BAP CIP - Consolidation Area (Slopes) | Notes |
|--|---|---|---|
| Input Parameter | | | |
| Climate-General | | | |
| City | Baldwin, IL | Baldwin, IL | Nearby city to the Site within HELP database |
| Latitude | 38.18 | 38.18 | Site latitude |
| Evaporative Zone Depth | 18 | 18 | Estimated based on geographic location (Illinois) and uppermost soil type (Tolaymat, T. and Krause, M 2020) |
| Maximum Leaf Area Index | 4.5 | 4.5 | Maximum for geographic location (Illinois) (Tolaymat, T. and Krause, M, 2020) |
| Growing Season Period, Average Wind Speed, and Quarterly Relative Humidity | Belleville Scott Air Force Base, IL | Belleville Scott Air Force Base, IL | Nearby city to the Baldwin Ash Pond within HELP database |
| Number of Years for Synthetic Data Generation | 30 | 30 | |
| Temperature, Evapotranspiration, and Precipitation | Precipitation, temperature, and solar radiation was simulated based on HELP V4 weather simulation for: Lat/Long: 38.18/ -89.85 | Precipitation, temperature, and solar radiation was simulated based on HELP V4 weather simulation for: Lat/Long: 38.18/ -89.85 | |
| Soils-General | | | |
| % where runoff possible | 100 | 100 | |
| Area (acres) | 53.73 | 21.39 | CIP - Consolidation and Cover System Area based on construction drawing for Baldwin Ash Pond |
| Specify Initial Moisture Content | No | No | |
| Surface Water/Snow | Model Calculated | Model Calculated | |
| Soils-Layers | | | |
| 1 | Vegetative Soil Layer (HELP Final Cover Soil [topmost layer]) | Vegetative Soil Layer (HELP Final Cover Soil [topmost layer]) | Layers details for CIP areas based on grading plans, construction drawings, and cover system design for Baldwin BAP |
| 2 | Protective Soil Layer (HELP Vertical Percolation Layer) | Protective Soil Layer (HELP Vertical Percolation Layer) | |
| 3 | Geotextile Protective Layer (Custom) | Geocomposite Drainage Layer (HELP Geosynthetic Drainage Net) | |
| 4 | Geomembrane Liner | Geomembrane Liner | |
| 5 | Unsaturated CCR Material (HELP Waste) | Unsaturated CCR Material (HELP Waste) | |
| Soil Parameters--Layer 1 | | | |
| Type | 1 | 1 | Vertical Percolation Layer (Cover Soil) |
| Thickness (in) | 6 | 6 | Layer 1 thickness is the average thickness of unsaturated backfill material |
| Texture | 26 | 26 | Default used for CIP Consolidation area |
| Description | Silty Clay Loam (Moderate) | Silty Clay Loam (Moderate) | |
| Saturated Hydraulic Conductivity (cm/s) | 1.90E-06 | 1.90E-06 | Default used for CIP Consolidation area |
| Soil Parameters--Layer 2 | | | |
| Type | 1 | 1 | Vertical Percolation Layer (BAP) |
| Thickness (in) | 18 | 18 | design thickness |

TABLE 6-1. HELP MODEL INPUT AND OUTPUT VALUES

GROUNDWATER MODELING REPORT

BALDWIN POWER PLANT

BOTTOM ASH POND

BALDWIN, ILLINOIS

| Closure Scenario Number (Drainage Length) | BAP CIP - Consolidation Area (Top) | BAP CIP - Consolidation Area (Slopes) | Notes |
|--|---------------------------------------|---------------------------------------|--|
| Texture | 28 | 28 | Defaults used |
| Description | Silty Clay (Moderate) | Silty Clay (Moderate) | |
| Saturated Hydraulic Conductivity (cm/s) | 1.20E-06 | 1.20E-06 | Defaults used |
| Soil Parameters--Layer 3 | | | |
| Type | 2 | 2 | Lateral Drainage Layer |
| Thickness (in) | 0.175 | 0.2 | design thickness |
| Texture | 43 | 20 | Custom used for the top area of the CIP and a Default used for the slopes |
| Description | 16 oz Nonwoven Geotextile | Geosynthetic Drainage Net | |
| Saturated Hydraulic Conductivity (cm/s) | 3.00E-01 | 1.00E+01 | Custom used for the top area of the CIP and a Defaults used for the slopes |
| Soil Parameters--Layer 4 | | | |
| Type | 4 | 4 | Flexible Membrane Liner |
| Thickness (in) | 0.04 | 0.04 | design thickness |
| Texture | 36 | 36 | Defaults used |
| Description | LDPE Membrane | LDPE Membrane | |
| Saturated Hydraulic Conductivity (cm/s) | 4.00E -13 | 4.00E -13 | Defaults used |
| Soil Parameters--Layer 5 | | | |
| Type | 1 | 1 | Vertical Percolation Layer (Waste) |
| Thickness (in) | 545.28 | 231.72 | design thickness |
| Texture | 83 | 83 | Custom used for CCR material |
| Description | Unsaturated CCR Material (HELP Waste) | Unsaturated CCR Material (HELP Waste) | |
| Saturated Hydraulic Conductivity (cm/s) | 5.29E-04 | 5.29E-04 | Custom used for CCR material from HCR average |
| Soils--Runoff | | | |
| Runoff Curve Number | 89.8 | 91.1 | HELP-computed curve number |
| Slope | 2.00% | 25.00% | Estimated from construction design drawings |
| Length (ft) | 600 | 150 | estimated maximum flow path |
| Vegetation | fair | fair | fair indicating fair stand of grass on surface of soil backfill |
| Execution Parameters | | | |
| Years | 30 | 30 | |
| Report Daily | No | No | |
| Report Monthly | No | No | |
| Report Annual | Yes | Yes | |
| Output Parameter | | | |
| Unsaturated Percolation Rate (in/yr) | 0.000239 | 0.000007 | |

Notes:

% = percent

ft = feet

HELP = Hydrologic Evaluation of Landfill Performance

References:

Tolaymat, T. and Krause, M, 2020. Hydrologic Evaluation of Landfill Performance: HELP 4.0 User Manual . United States Environmental Protection Agency, Washington, DC, EPA/600/B 20/219.

Ramboll Americas Engineering Solutions, Inc. (Ramboll), 2021. Hydrogeologic Site Characterization Report. Newton Primary Ash Pond. Newton Power Plant. Newton, Illinois.

in = inches

in/yr = inches per year

Lat = latitude

Long = longitude

CBR = Closure By Removal

CIP = Closure In Place

HCR = Hydrogeologic Characterization Report

[O: EGP 12/15/22, C: LCA 12/16/22]

TABLE 6-2. PREDICTION MODEL INPUT VALUES
GROUNDWATER MODELING REPORT
BALDWIN POWER PLANT
BOTTOM ASH POND
BALDWIN, ILLINOIS

| Scenario: CIP (CCR removal from the western areas of the Bottom Ash Pond, consolidation to the eastern areas of the Bottom Ash Pond, and construction of a cover system over the remaining CCR) | | | | | | | | | | |
|---|-------------|--------------------------------------|---------------|-------------------------------------|-------------------|------------------|---|--------------|----------------------|-------------------------------|
| Prediction Model | Model Years | Zone Description | Recharge Zone | Boron Recharge Concentration (mg/L) | Recharge (ft/day) | Recharge (in/yr) | Source Concentration (constant concentration cells) and Stormwater Management (constant head cells) Description | Reach Number | Constant Head (feet) | Constant Concentration (mg/L) |
| Initial Conditions | 51 | Old East Fly Ash Pond | 2 | 38 | 4.00E-04 | 1.75 | Old East Fly Ash Pond | 2 | -- | 38 |
| Initial Conditions | 51 | East Fly Ash Pond | 3 | 79 | 8.00E-04 | 3.50 | East Fly Ash Pond | 3 | -- | 79 |
| Initial Conditions | 51 | West Fly Ash Cell | 4 | 47 | 6.00E-04 | 2.63 | -- | -- | -- | -- |
| Initial Conditions | 51 | -- | -- | -- | -- | -- | West Fly Ash Pond Constant Head | 4 | 424.3 | 47 |
| Initial Conditions | 51 | -- | -- | -- | -- | -- | West Fly Ash Pond (Berm) | 14 | -- | 47 |
| Initial Conditions | 51 | -- | -- | -- | -- | -- | BAP Constant Head West | 0 | 415.0 | 4 |
| Initial Conditions | 51 | -- | -- | -- | -- | -- | BAP Constand Head Central | 1 | 425.0 | 4 |
| Initial Conditions | 51 | Bottom Ash Pond (West) | 7 | 4 | 1.80E-04 | 0.79 | Bottom Ash Pond (West) | 7 | -- | 4 |
| Initial Conditions | 51 | Bottom Ash Pond (East) | 8 | 1.5 | 1.80E-04 | 0.79 | Bottom Ash Pond (East) | 8 | -- | 1.5 |
| Exisiting Conditions | 4 | Old East Fly Ash Pond (Post-Closure) | 2 | 38 | 6.80E-05 | 0.30 | Old East Fly Ash Pond | 2 | -- | 38 |
| Exisiting Conditions | 4 | East Fly Ash Pond (Post-Closure) | 3 | 79 | 6.80E-05 | 0.30 | East Fly Ash Pond | 3 | -- | 79 |
| Exisiting Conditions | 4 | West Fly Ash Cell (Post-Closure) | 4 | 47 | 6.80E-05 | 0.30 | -- | -- | -- | -- |
| Exisiting Conditions | 4 | -- | -- | -- | -- | -- | West Fly Ash Pond Constant Head | 4 | -- | 47 |
| Exisiting Conditions | 4 | -- | -- | -- | -- | -- | West Fly Ash Pond (Berm) | 14 | -- | 47 |
| Exisiting Conditions | 4 | -- | -- | -- | -- | -- | BAP Constant Head West | 0 | 415.0 | 4 |
| Exisiting Conditions | 4 | -- | -- | -- | -- | -- | BAP Constand Head Central | 1 | 425.0 | 4 |
| Exisiting Conditions | 4 | Bottom Ash Pond (West) | 7 | 4 | 1.80E-04 | 0.79 | Bottom Ash Pond (West) | 7 | -- | 4 |
| Exisiting Conditions | 4 | Bottom Ash Pond (East) | 8 | 1.5 | 1.80E-04 | 0.79 | Bottom Ash Pond (East) | 8 | -- | 1.5 |
| Dewatering | 3 | Old East Fly Ash Pond (Post-Closure) | 2 | 38 | 6.80E-05 | 0.30 | Old East Fly Ash Pond | 2 | -- | 38 |
| Dewatering | 3 | East Fly Ash Pond (Post-Closure) | 3 | 79 | 6.80E-05 | 0.30 | East Fly Ash Pond | 3 | -- | 79 |
| Dewatering | 3 | West Fly Ash Cell (Post-Closure) | 4 | 47 | 6.80E-05 | 0.30 | -- | -- | -- | -- |
| Dewatering | 3 | -- | -- | -- | -- | -- | West Fly Ash Pond Constant Head | 4 | -- | 47 |
| Dewatering | 3 | -- | -- | -- | -- | -- | West Fly Ash Pond (Berm) | 14 | -- | 47 |
| Dewatering | 3 | -- | -- | -- | -- | -- | BAP Constant Head West | 0 | 415.0 | 4 |
| Dewatering | 3 | -- | -- | -- | -- | -- | BAP Constand Head Central | 1 | 425.0 | 4 |
| Dewatering | 3 | Bottom Ash Pond (West) | 7 | 4 | 1.80E-04 | 0.79 | Bottom Ash Pond (West) | 7 | -- | 4 |
| Dewatering | 3 | Bottom Ash Pond (East) | 8 | 1.5 | 1.80E-04 | 0.79 | Bottom Ash Pond (East) | 8 | -- | 1.5 |
| Dewatering | 3 | -- | -- | -- | -- | -- | CIP Area Dewater Constant Head (Northeast) | 26 | 433 | 1.5 |
| Dewatering | 3 | -- | -- | -- | -- | -- | CIP Area Dewater Constant Head (West Central) | 23 | 420 | 1.5 |
| Dewatering | 3 | -- | -- | -- | -- | -- | CIP Area Dewater Constant Head (Southeast) | 24 | 433 | 1.5 |
| CIP | 1000 | Old East Fly Ash Pond (Post-Closure) | 2 | 38 | 6.80E-05 | 0.30 | Old East Fly Ash Pond | 2 | -- | 38 |
| CIP | 1000 | East Fly Ash Pond (Post-Closure) | 3 | 79 | 6.80E-05 | 0.30 | East Fly Ash Pond | 3 | -- | 79 |
| CIP | 1000 | West Fly Ash Cell (Post-Closure) | 4 | 47 | 6.80E-05 | 0.30 | -- | -- | -- | -- |

TABLE 6-2. PREDICTION MODEL INPUT VALUES

GROUNDWATER MODELING REPORT

BALDWIN POWER PLANT

BOTTOM ASH POND

BALDWIN, ILLINOIS

| Scenario: CIP (CCR removal from the western areas of the Bottom Ash Pond, consolidation to the eastern areas of the Bottom Ash Pond, and construction of a cover system over the remaining CCR) | | | | | | | | | | |
|---|-----------------------------|---|-----------------------------|--|--|------------------|---|--------------|--|-------------------------------|
| Prediction Model | Model Years | Zone Description | Recharge Zone | Boron Recharge Concentration (mg/L) | Recharge (ft/day) | Recharge (in/yr) | Source Concentration (constant concentration cells) and Stormwater Management (constant head cells) Description | Reach Number | Constant Head (feet) | Constant Concentration (mg/L) |
| CIP | 1000 | -- | -- | -- | -- | -- | West Fly Ash Pond Constant Head | 4 | -- | 47 |
| CIP | 1000 | -- | -- | -- | -- | -- | West Fly Ash Pond (Berm) | 14 | -- | 47 |
| CIP | 1000 | -- | -- | -- | -- | -- | BAP Constant Head West | 0 | 415.0 | 4 |
| CIP | 1000 | -- | -- | -- | -- | -- | BAP Constand Head Central | 1 | 425.0 | 4 |
| CIP | 1000 | Removal Area - Bottom Ash Pond (Post-Closure) | 7 | -- | 0 | 0 | -- | -- | -- | -- |
| CIP | 1000 | CIP Top - Bottom Ash Pond (Post-Closure) | 8 | 4 | 5.46E-08 | 2.39E-04 | | | -- | -- |
| CIP | 1000 | CIP Slopes - Bottom Ash Pond (Post-Closure) | 9 | 4 | 1.60E-09 | 7.01E-06 | | | -- | -- |
| CIP | 1000 | -- | -- | -- | -- | -- | CIP Area - Bottom Ash Pond (Post-Closure) | 20 | -- | 4 |
| Prediction Model | Construction Period (years) | Zone Description | Hydraulic Conductivity Zone | Horizontal Hydraulic Conductivity (ft/d) | Horizontal Hydraulic Conductivity (cm/s) | | Vertical Hydraulic Conductivity (ft/d) | | Vertical Hydraulic Conductivity (cm/s) | |
| Initial Conditions | 51 | Bottom Ash Pond | 7 | 1.5 | 5.29E-04 | | 1.5 | | 5.29E-04 | |
| Exisiting Conditions | 4 | Bottom Ash Pond | 7 | 1.5 | 5.29E-04 | | 1.5 | | 5.29E-04 | |
| Dewatering | 3 | Bottom Ash Pond | 7 | 1.5 | 5.29E-04 | | 1.5 | | 5.29E-04 | |
| CIP | 1000 | CIP Top - Bottom Ash Pond (Post-Closure) | 18 | 1.5 | 5.29E-04 | | 1.5 | | 5.29E-04 | |
| CIP | 1000 | CIP Slopes - Bottom Ash Pond (Post-Closure) | 19 | 1.5 | 5.29E-04 | | 1.5 | | 5.29E-04 | |
| Prediction Model | Construction Period (years) | Drain Reach | Relative Location | Stage of Drain (feet) | Thickness of Drain Bed (feet) | | Hydraulic Conductivity (ft/d) | | Drain Conductance (ft ² /d) | |
| CIP | 1000 | 10 | BAP Drain West | 410 | 1 | | 6.00 | | 6.00E+04 | |

[O: JJW 1/6/23; EGP 5/22/23]

Notes:

-- = boundary condition or property zone not included in prediction model

CCR = coal combustion residuals

CIP = Closure In Place

ft²/day = feet squared per day

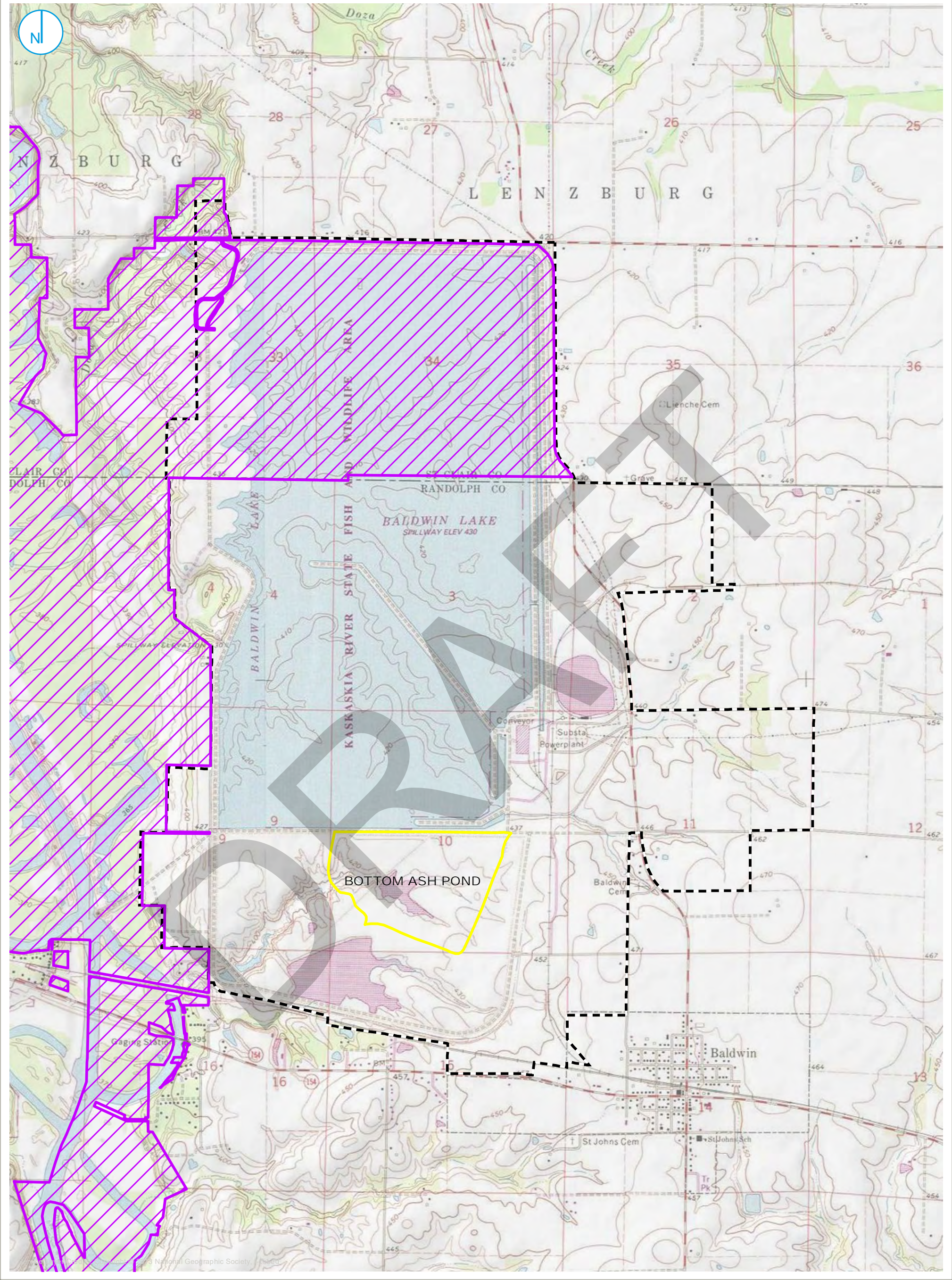
ft/day = feet per day

in/yr = inches per year

cm/s = centimeters per second

FIGURES

DRAFT



- BOTTOM ASH POND BOUNDARY
- PROPERTY BOUNDARY
- KASKASKIA RIVER STATE FISH AND WILDLIFE AREA

SOURCE NOTE
I-View, Prairie State Conservation Coalition accessed via Illinois Department of Natural Resources Division of Natural Heritage Website
<https://www2.illinois.gov/sites/naturalheritage/DataResearch/Pages/Access-Our-Data.aspx>

SITE LOCATION MAP

FIGURE 1-1





- 35 I.A.C. § 845 REGULATED UNIT (SUBJECT UNIT)
- LIMITS OF FINAL COVER
- SITE FEATURE
- FLY ASH POND SYSTEM (CLOSED)
- PROPERTY BOUNDARY

0 400 800
Feet

SITE MAP

GROUNDWATER MODELING REPORT
BOTTOM ASH POND
BALDWIN POWER PLANT
BALDWIN, ILLINOIS

FIGURE 1-2

RAMBOLL AMERICAS
ENGINEERING SOLUTIONS, INC.



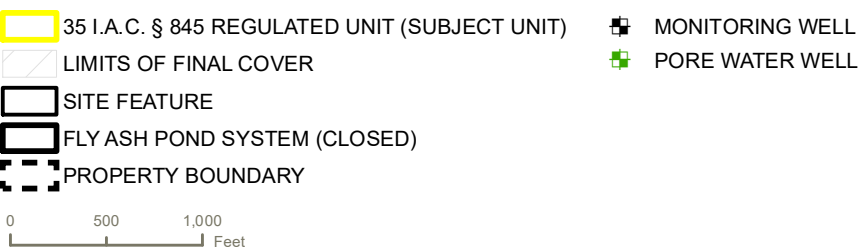
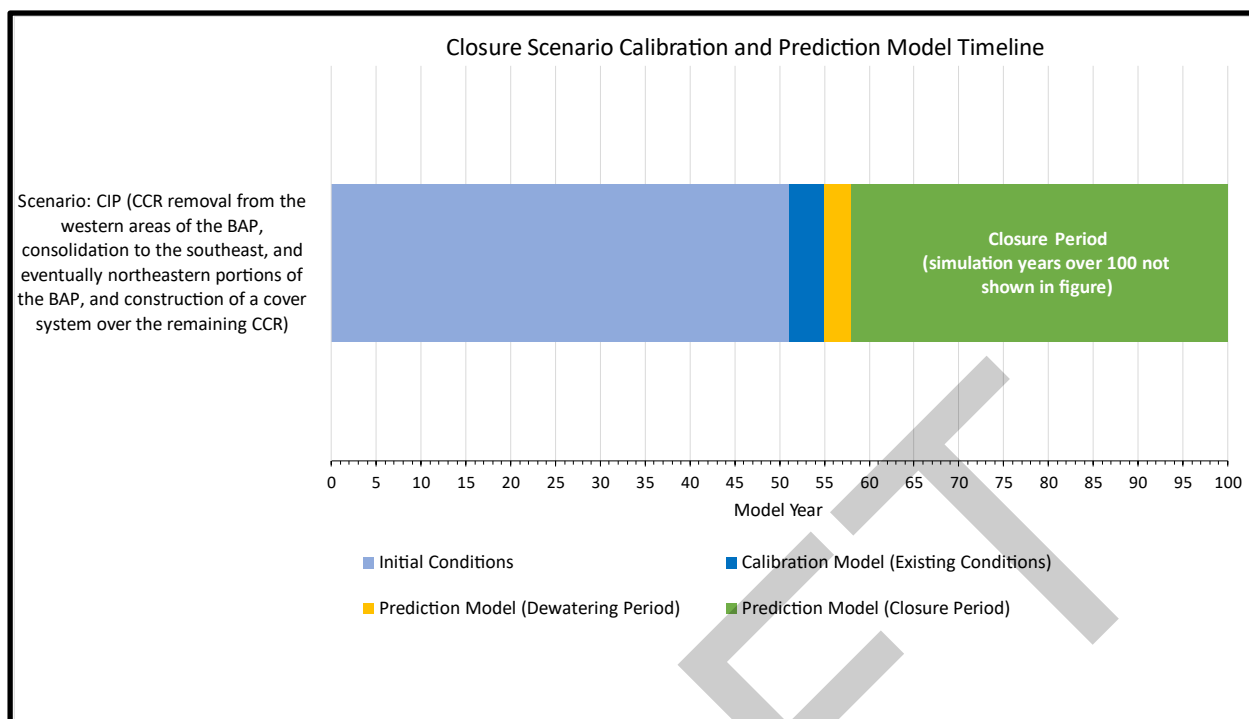


FIGURE 2-1

RAMBOLL AMERICAS
ENGINEERING SOLUTIONS, INC.





CLOSURE SCENARIO CALIBRATION AND PREDICTION MODEL TIMELINE

GROUNDWATER MODELING REPORT
 BOTTOM ASH POND
 BALDWIN POWER PLANT
 BALDWIN, ILLINOIS

RAMBOLL



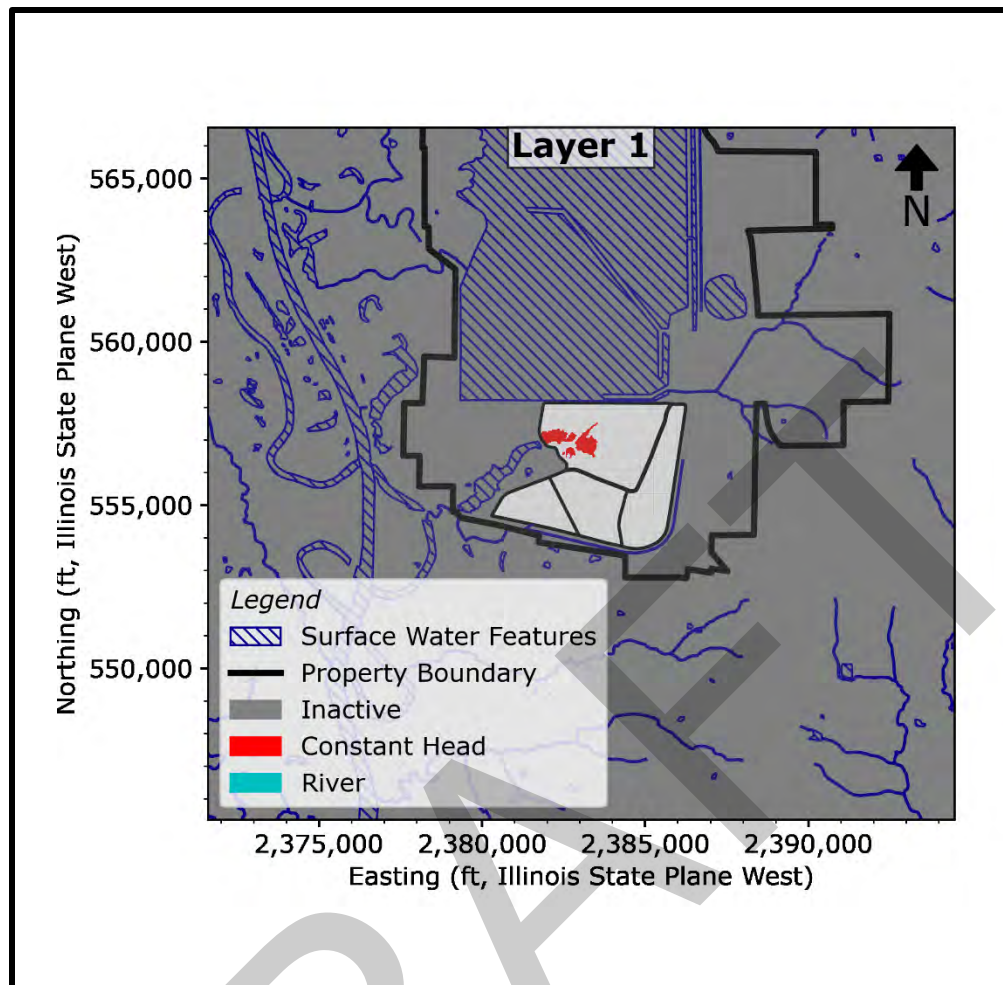
Service Layer Credits: Source: Esri, Maxar, Earthstar Geographics, and the GIS User Community

- 35 I.A.C. § 845 REGULATED UNIT (SUBJECT UNIT)
- MODEL DOMAIN
- FLY ASH POND SYSTEM (CLOSED)
- NO FLOW AREA
- LIMITS OF FINAL COVER
- RIVER
- WATERBODY
- SITE FEATURE

MODEL AREA MAP

FIGURE 5-1

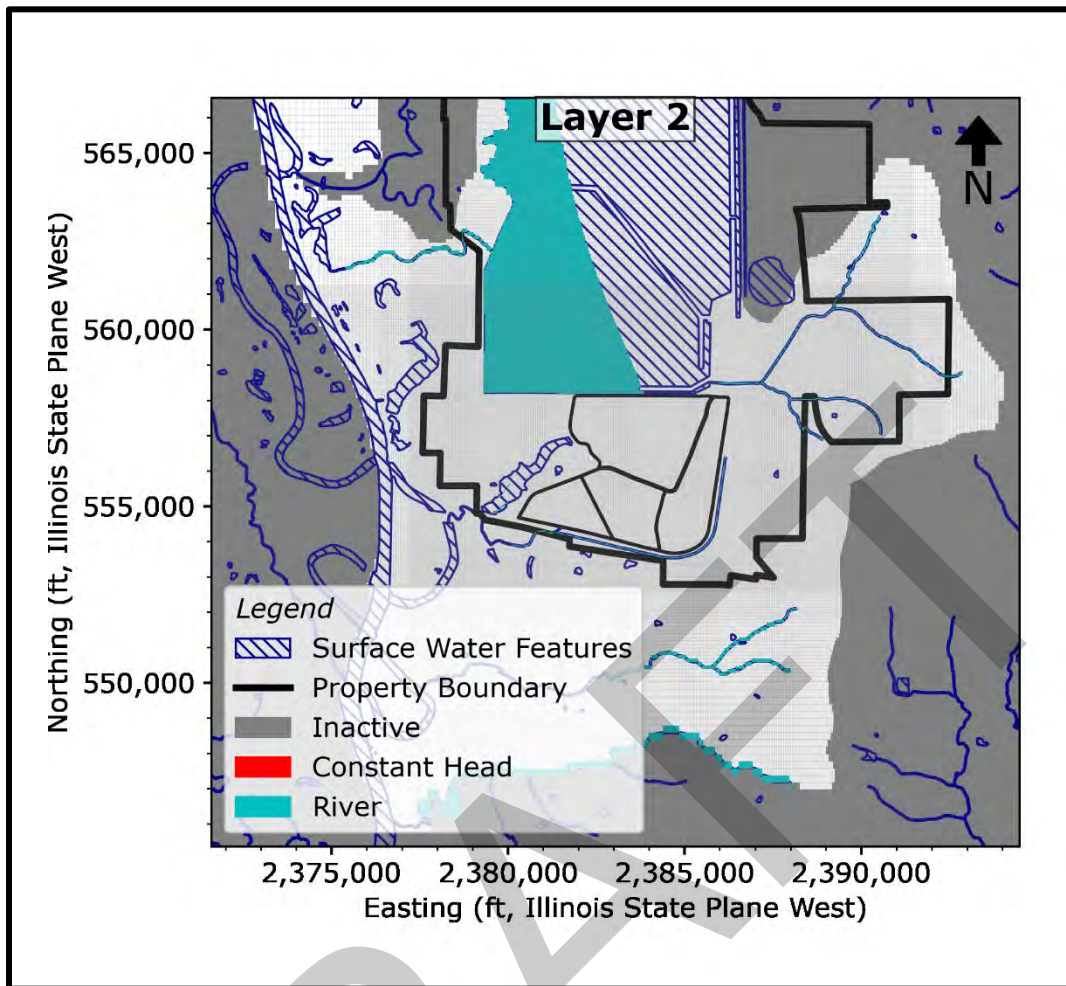




BOUNDARY CONDITIONS FOR LAYER 1 OF THE CALIBRATED NUMERICAL MODEL

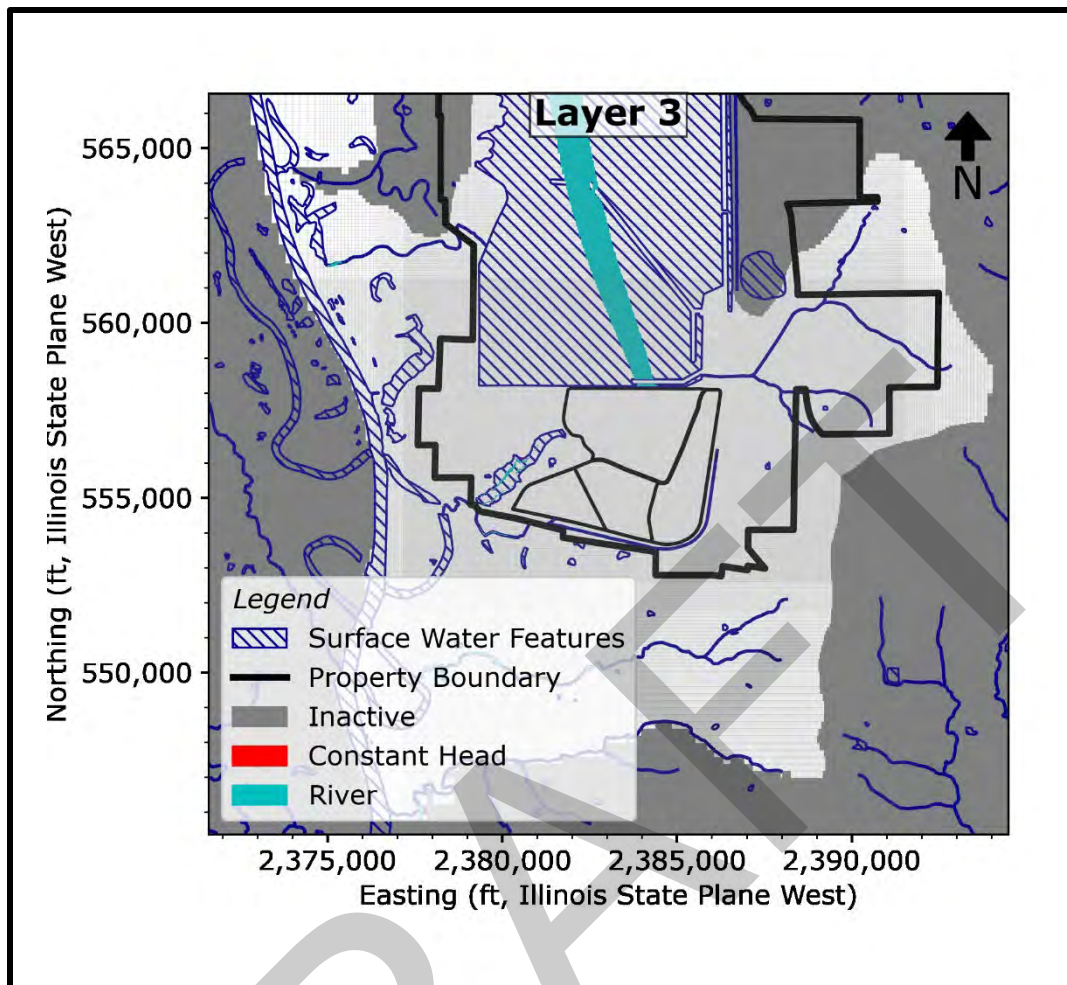
GROUNDWATER MODELING REPORT
 BOTTOM ASH POND
 BALDWIN POWER PLANT
 BALDWIN, ILLINOIS

RAMBOLL



BOUNDARY CONDITIONS FOR LAYER 2 OF THE CALIBRATED NUMERICAL MODEL

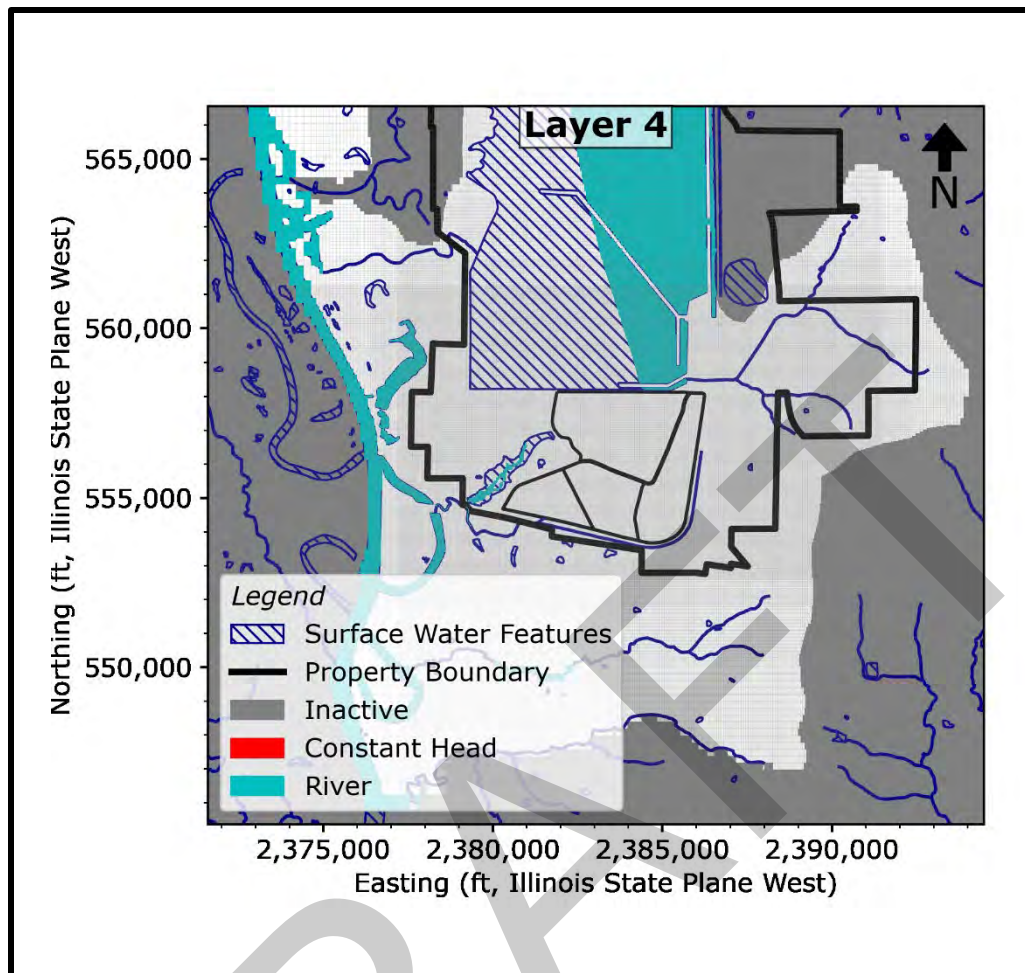
GROUNDWATER MODELING REPORT
 BOTTOM ASH POND
 BALDWIN POWER PLANT
 BALDWIN, ILLINOIS



BOUNDARY CONDITIONS FOR LAYER 3 OF THE CALIBRATED NUMERICAL MODEL

GROUNDWATER MODELING REPORT
 BOTTOM ASH POND
 BALDWIN POWER PLANT
 BALDWIN, ILLINOIS

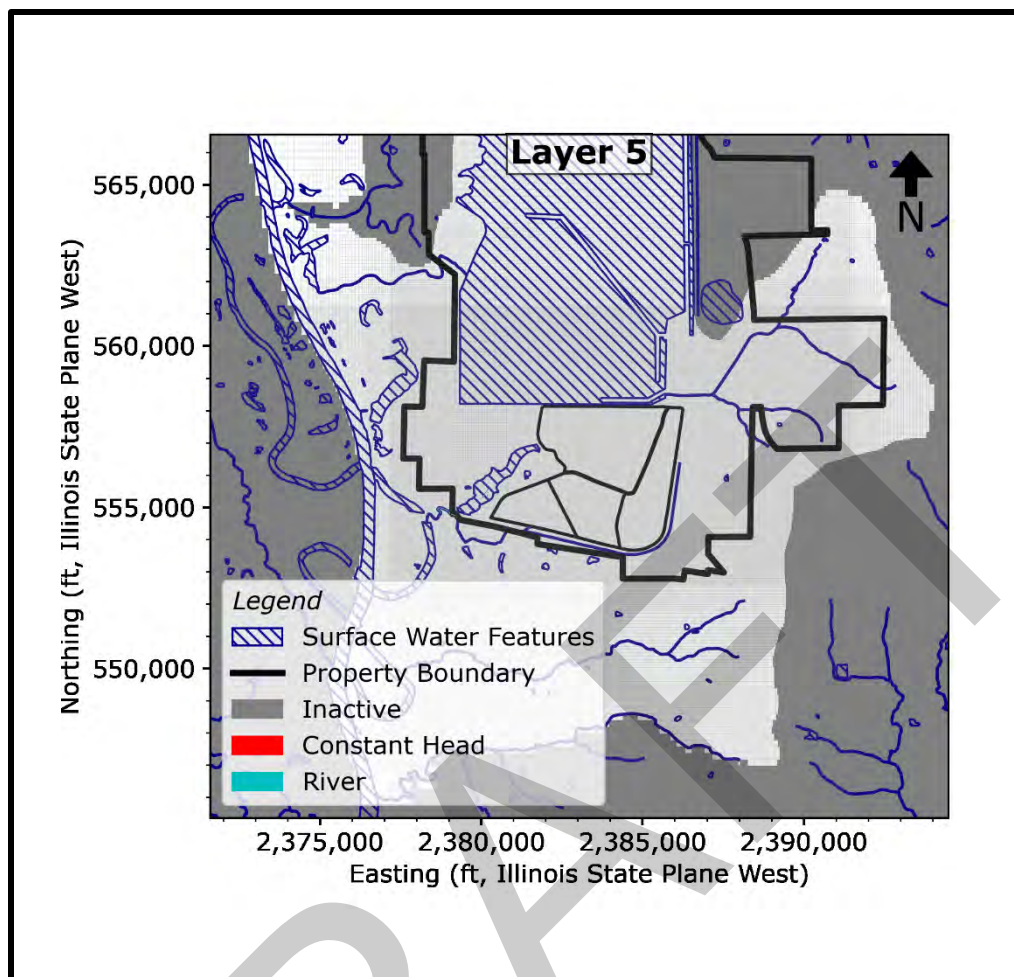
RAMBOLL



BOUNDARY CONDITIONS FOR LAYER 4 OF THE CALIBRATED NUMERICAL MODEL

GROUNDWATER MODELING REPORT
 BOTTOM ASH POND
 BALDWIN POWER PLANT
 BALDWIN, ILLINOIS

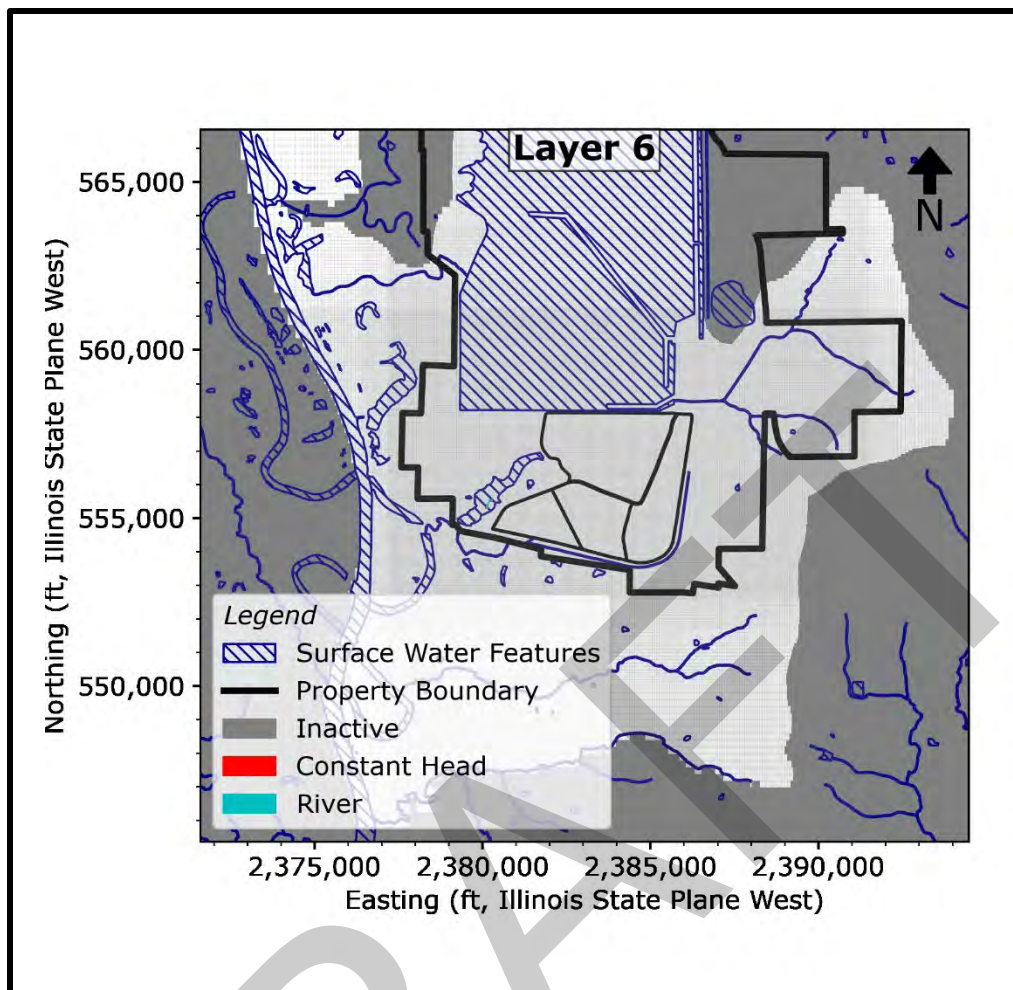
RAMBOLL



BOUNDARY CONDITIONS FOR LAYER 5 OF THE CALIBRATED NUMERICAL MODEL

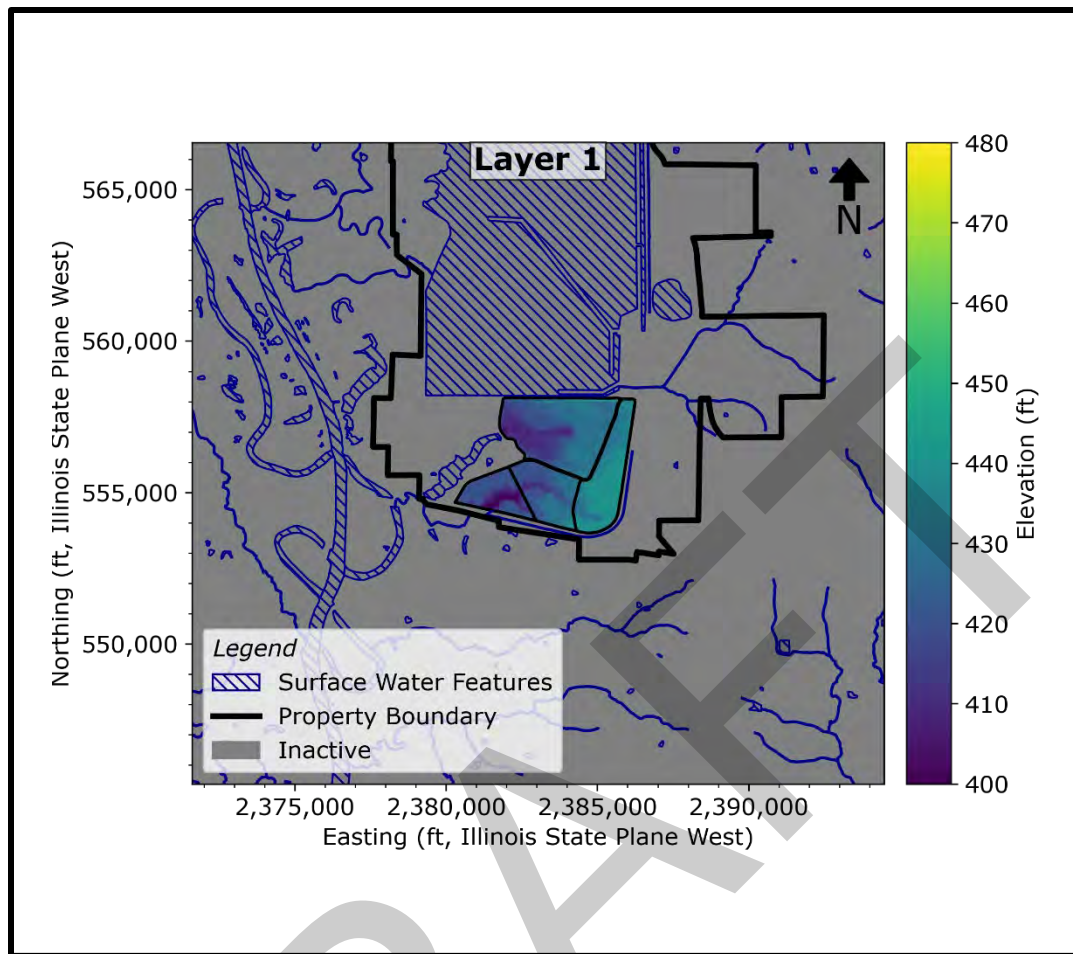
GROUNDWATER MODELING REPORT
 BOTTOM ASH POND
 BALDWIN POWER PLANT
 BALDWIN, ILLINOIS

RAMBOLL



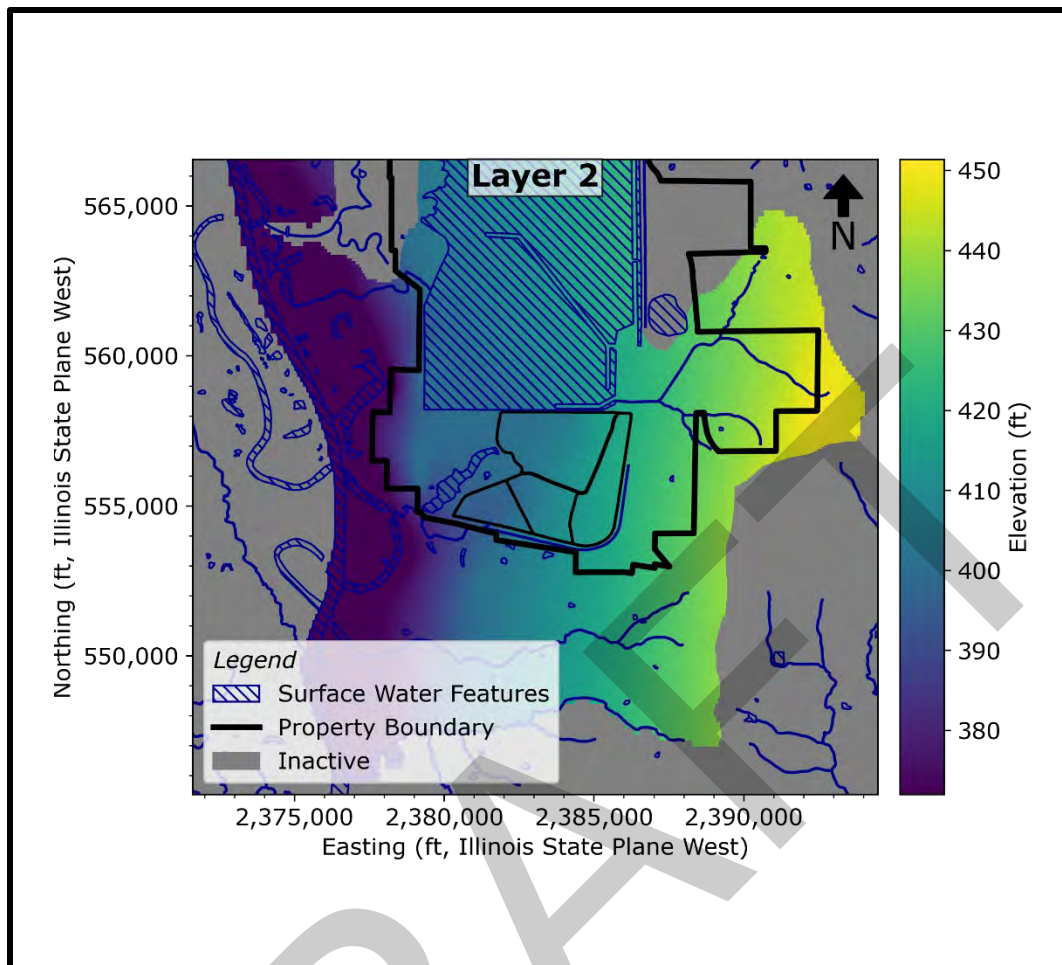
BOUNDARY CONDITIONS FOR LAYER 6 OF THE CALIBRATED NUMERICAL MODEL

GROUNDWATER MODELING REPORT
 BOTTOM ASH POND
 BALDWIN POWER PLANT
 BALDWIN, ILLINOIS



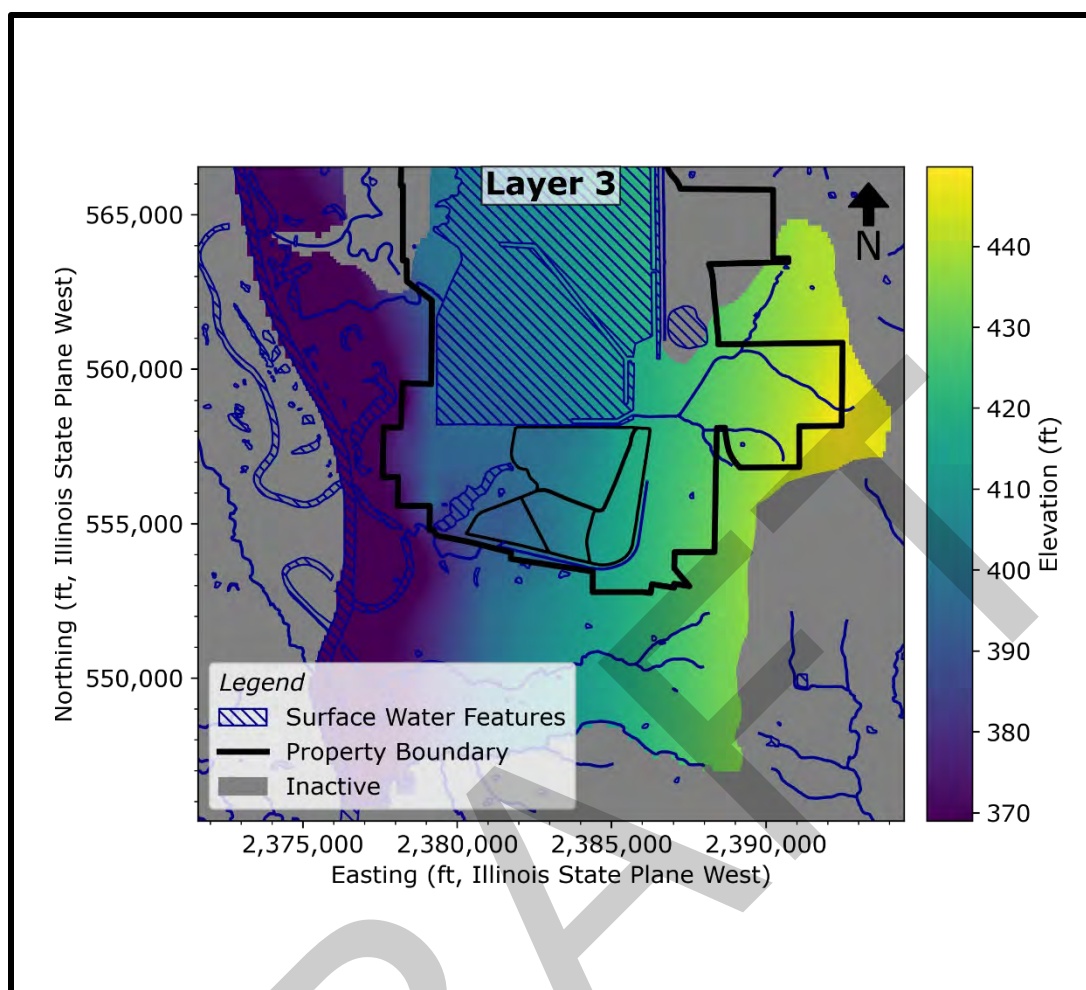
BOTTOM ELEVATION OF MODEL LAYER 1

GROUNDWATER MODELING REPORT
 BOTTOM ASH POND
 BALDWIN POWER PLANT
 BALDWIN, ILLINOIS



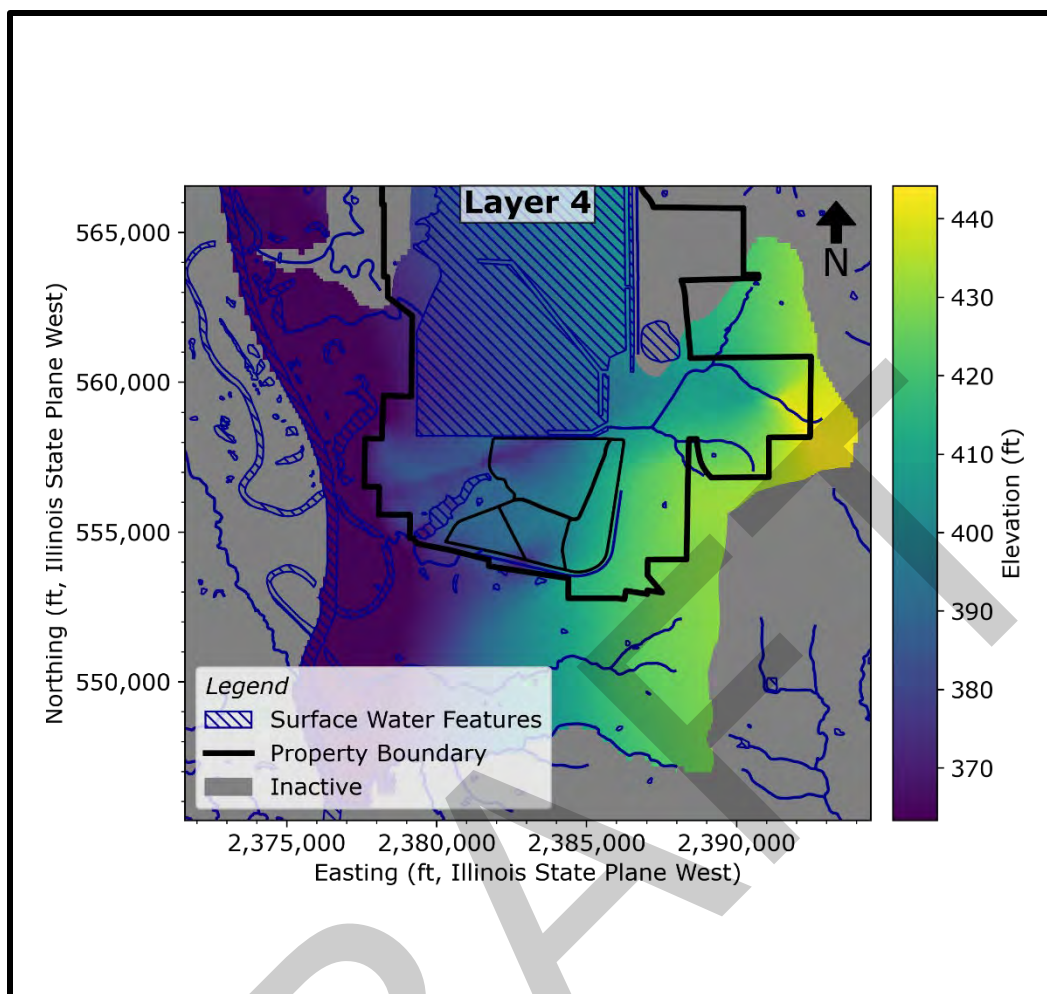
BOTTOM ELEVATION OF MODEL LAYER 2

GROUNDWATER MODELING REPORT
 BOTTOM ASH POND
 BALDWIN POWER PLANT
 BALDWIN, ILLINOIS



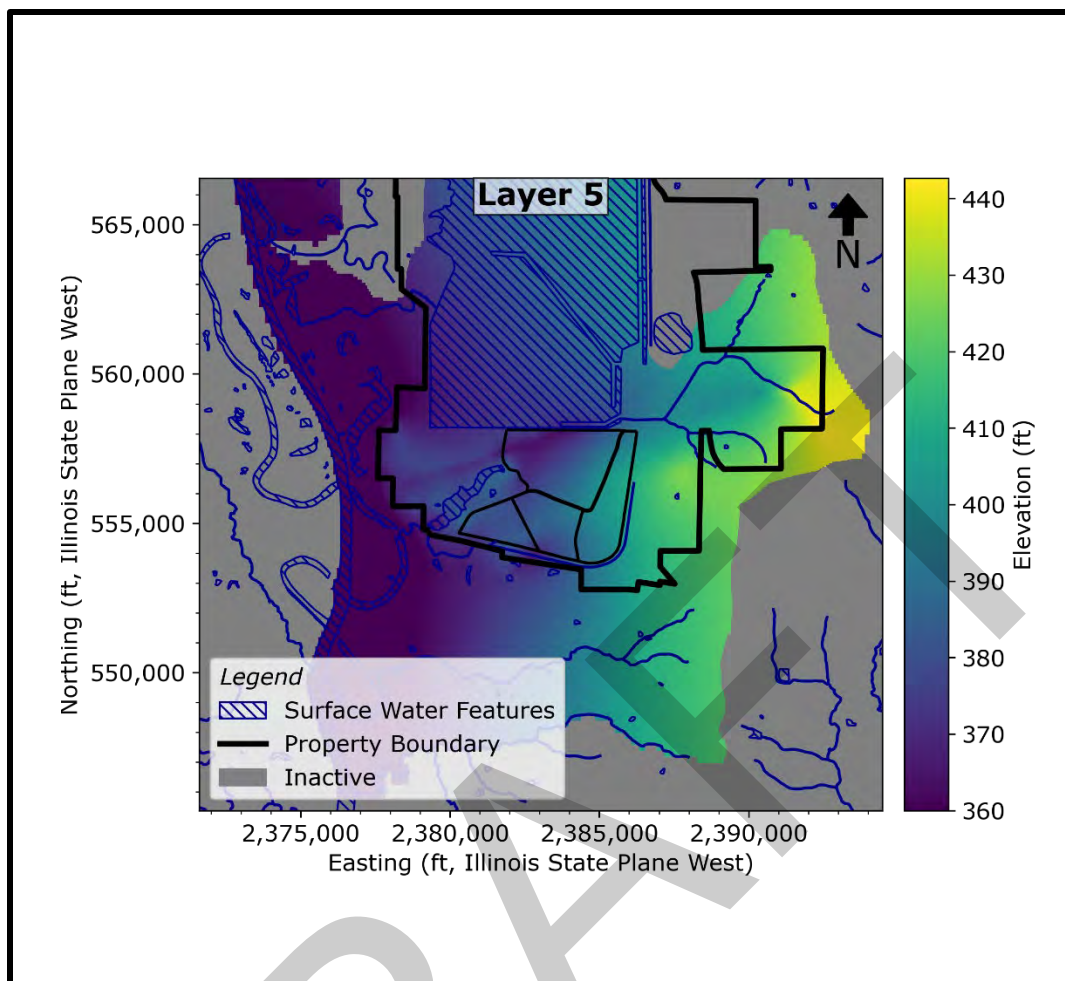
BOTTOM ELEVATION OF MODEL LAYER 3

GROUNDWATER MODELING REPORT
BOTTOM ASH POND
BALDWIN POWER PLANT
BALDWIN, ILLINOIS



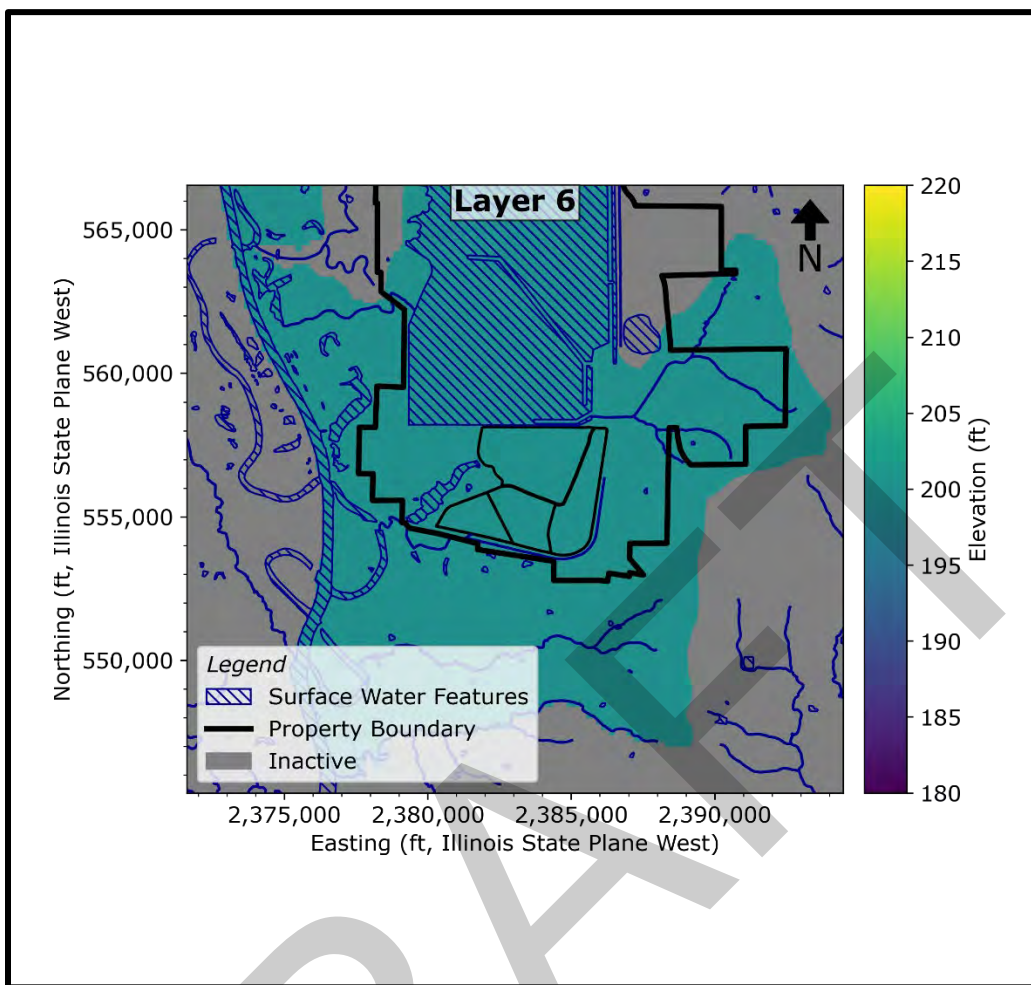
BOTTOM ELEVATION OF MODEL LAYER 4

GROUNDWATER MODELING REPORT
BOTTOM ASH POND
BALDWIN POWER PLANT
BALDWIN, ILLINOIS



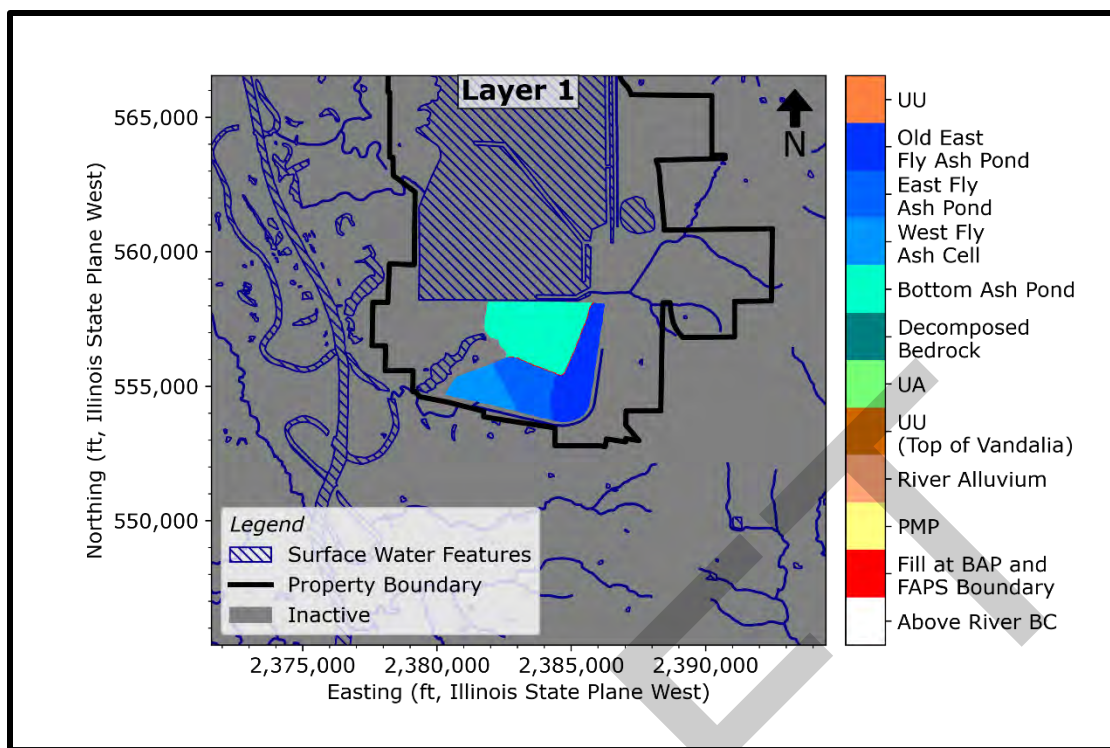
BOTTOM ELEVATION OF MODEL LAYER 5

GROUNDWATER MODELING REPORT
 BOTTOM ASH POND
 BALDWIN POWER PLANT
 BALDWIN, ILLINOIS



BOTTOM ELEVATION OF MODEL LAYER 6

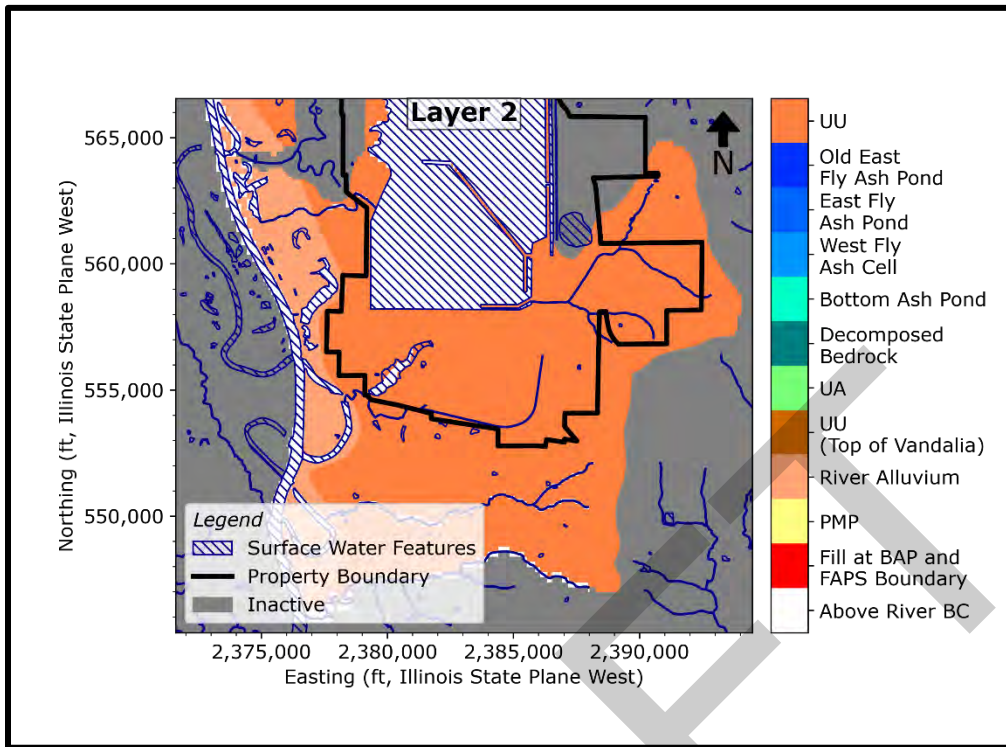
GROUNDWATER MODELING REPORT
 BOTTOM ASH POND
 BALDWIN POWER PLANT
 BALDWIN, ILLINOIS



SPATIAL DISTRIBUTION OF HYDRAULIC CONDUCTIVITY ZONES FOR LAYER 1 IN THE NUMERICAL MODEL

GROUNDWATER MODELING REPORT
 BOTTOM ASH POND
 BALDWIN POWER PLANT
 BALDWIN, ILLINOIS

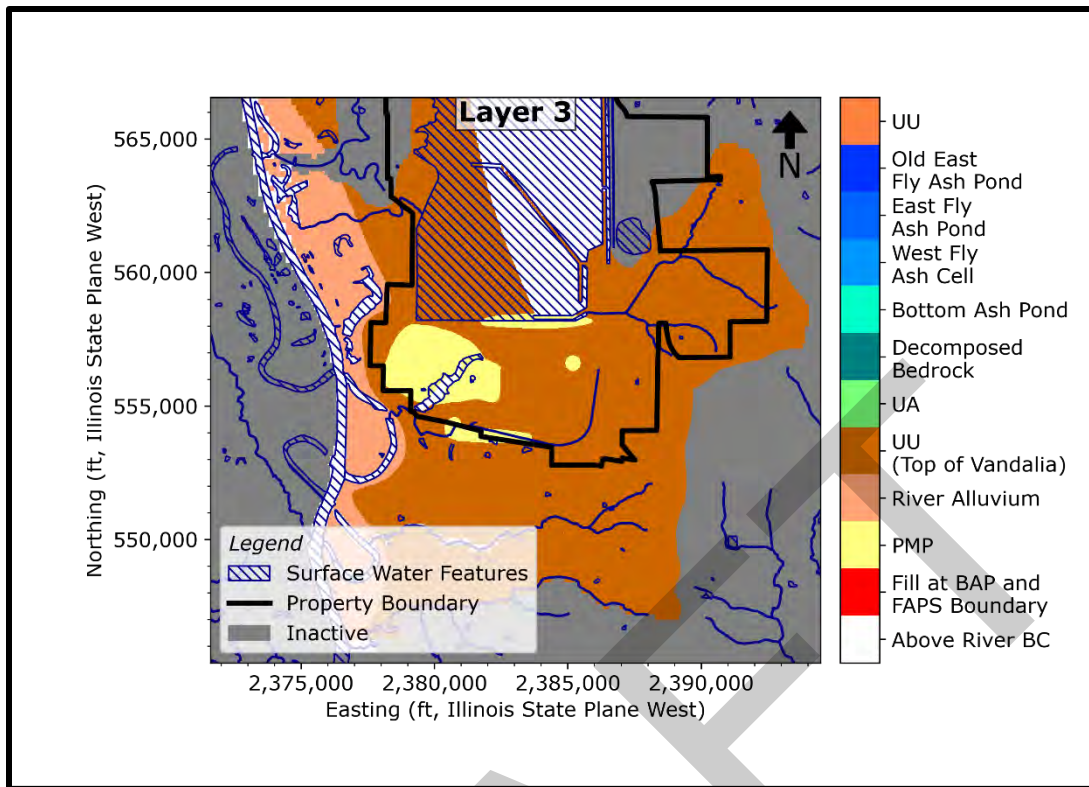
RAMBOLL



SPATIAL DISTRIBUTION OF HYDRAULIC CONDUCTIVITY ZONES FOR LAYER 2 IN THE NUMERICAL MODEL

GROUNDWATER MODELING REPORT
 BOTTOM ASH POND
 BALDWIN POWER PLANT
 BALDWIN, ILLINOIS

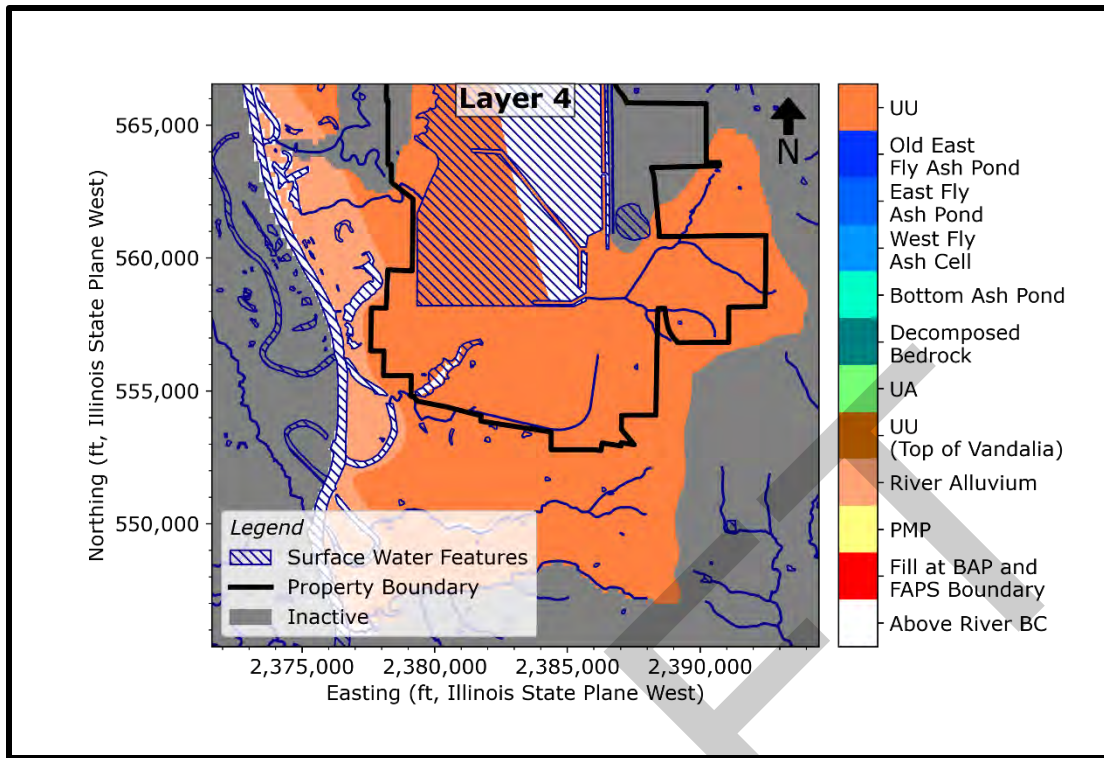
RAMBOLL



SPATIAL DISTRIBUTION OF HYDRAULIC CONDUCTIVITY ZONES FOR LAYER 3 IN THE NUMERICAL MODEL

GROUNDWATER MODELING REPORT
 BOTTOM ASH POND
 BALDWIN POWER PLANT
 BALDWIN, ILLINOIS

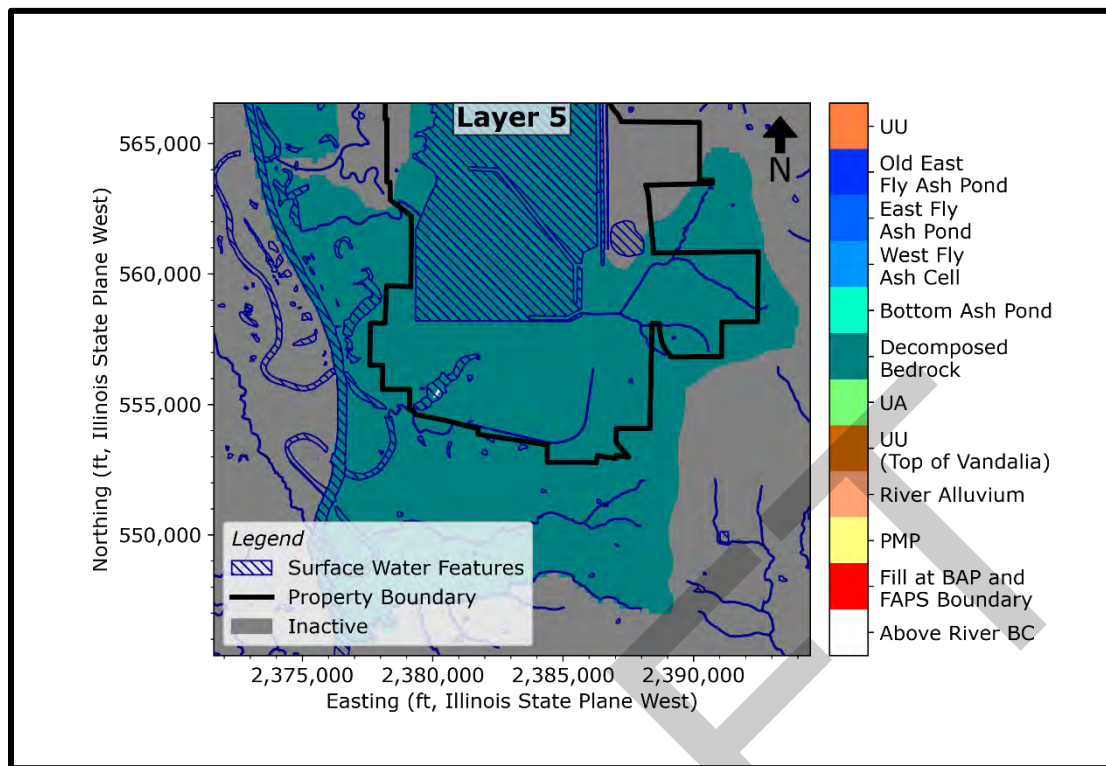
RAMBOLL



SPATIAL DISTRIBUTION OF HYDRAULIC CONDUCTIVITY ZONES FOR LAYER 4 IN THE NUMERICAL MODEL

GROUNDWATER MODELING REPORT
 BOTTOM ASH POND
 BALDWIN POWER PLANT
 BALDWIN, ILLINOIS

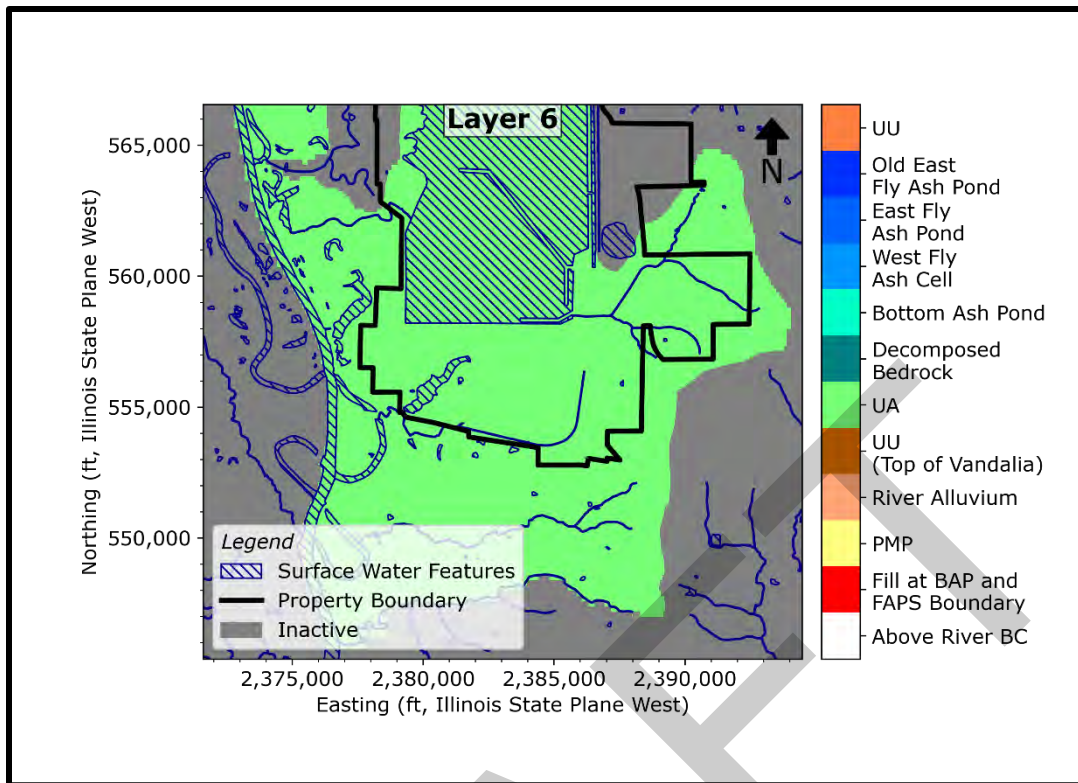
RAMBOLL



SPATIAL DISTRIBUTION OF HYDRAULIC CONDUCTIVITY ZONES FOR LAYER 5 IN THE NUMERICAL MODEL

GROUNDWATER MODELING REPORT
 BOTTOM ASH POND
 BALDWIN POWER PLANT
 BALDWIN, ILLINOIS

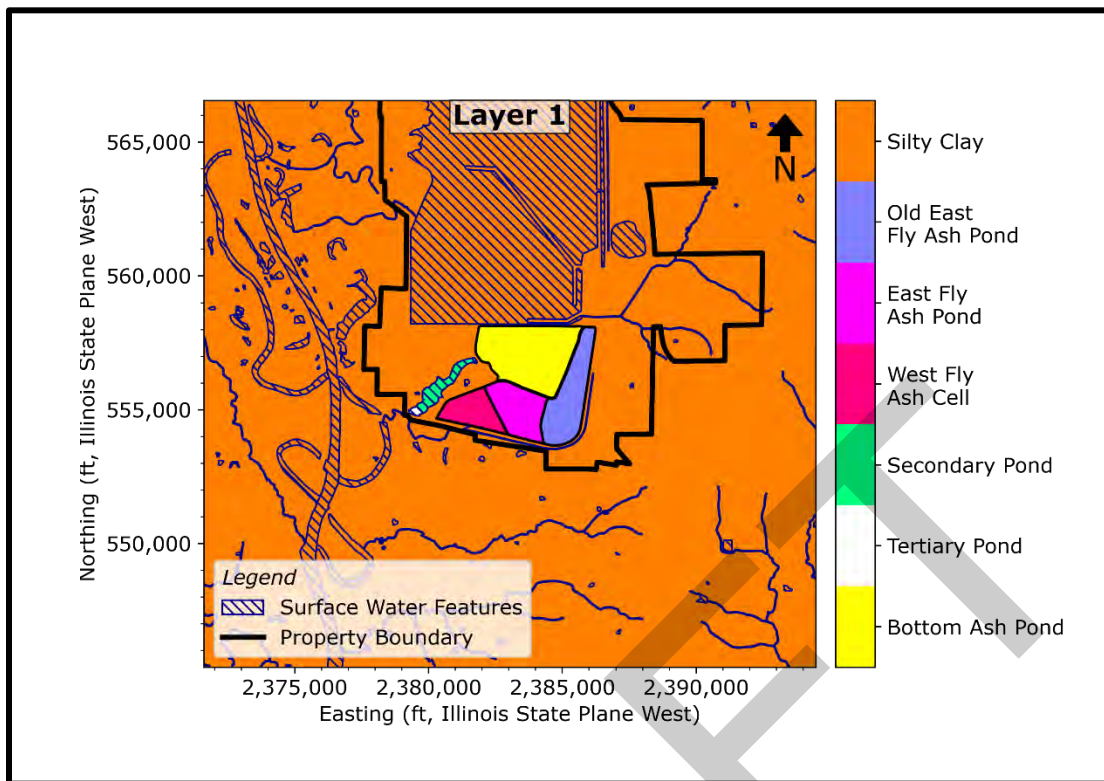
RAMBOLL



SPATIAL DISTRIBUTION OF HYDRAULIC CONDUCTIVITY ZONES FOR LAYER 6 IN THE NUMERICAL MODEL

GROUNDWATER MODELING REPORT
 BOTTOM ASH POND
 BALDWIN POWER PLANT
 BALDWIN, ILLINOIS

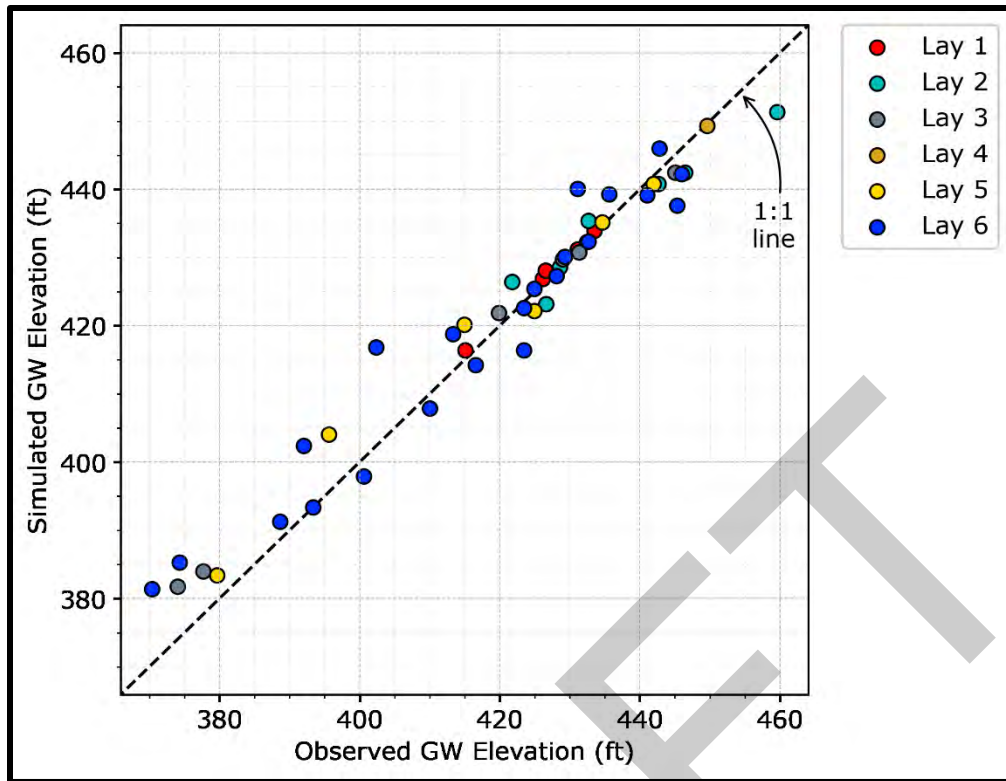
RAMBOLL



MODEL RECHARGE DISTRIBUTION (STEADY STATE CALIBRATION MODEL)

GROUNDWATER MODELING REPORT
BOTTOM ASH POND
BALDWIN POWER PLANT
BALDWIN, ILLINOIS

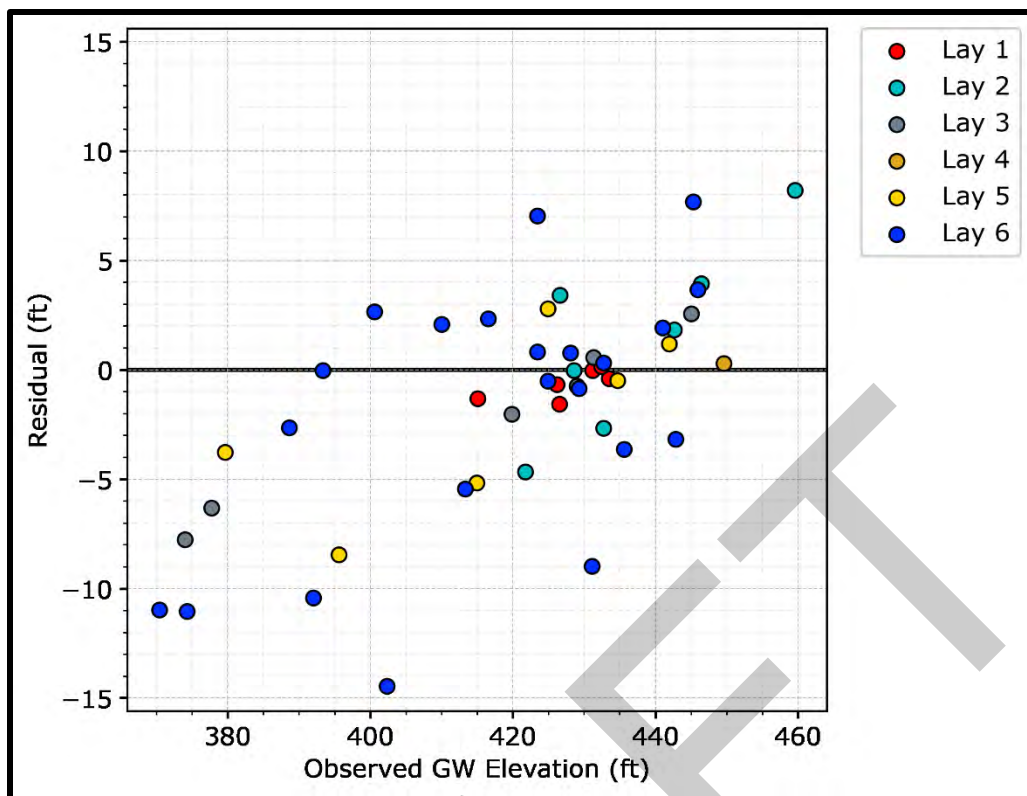
RAMBOLL



OBSERVED VERSUS SIMULATED STEADY STATE GROUNDWATER LEVELS FROM THE CALIBRATION MODEL

GROUNDWATER MODELING REPORT
 BOTTOM ASH POND
 BALDWIN POWER PLANT
 BALDWIN, ILLINOIS

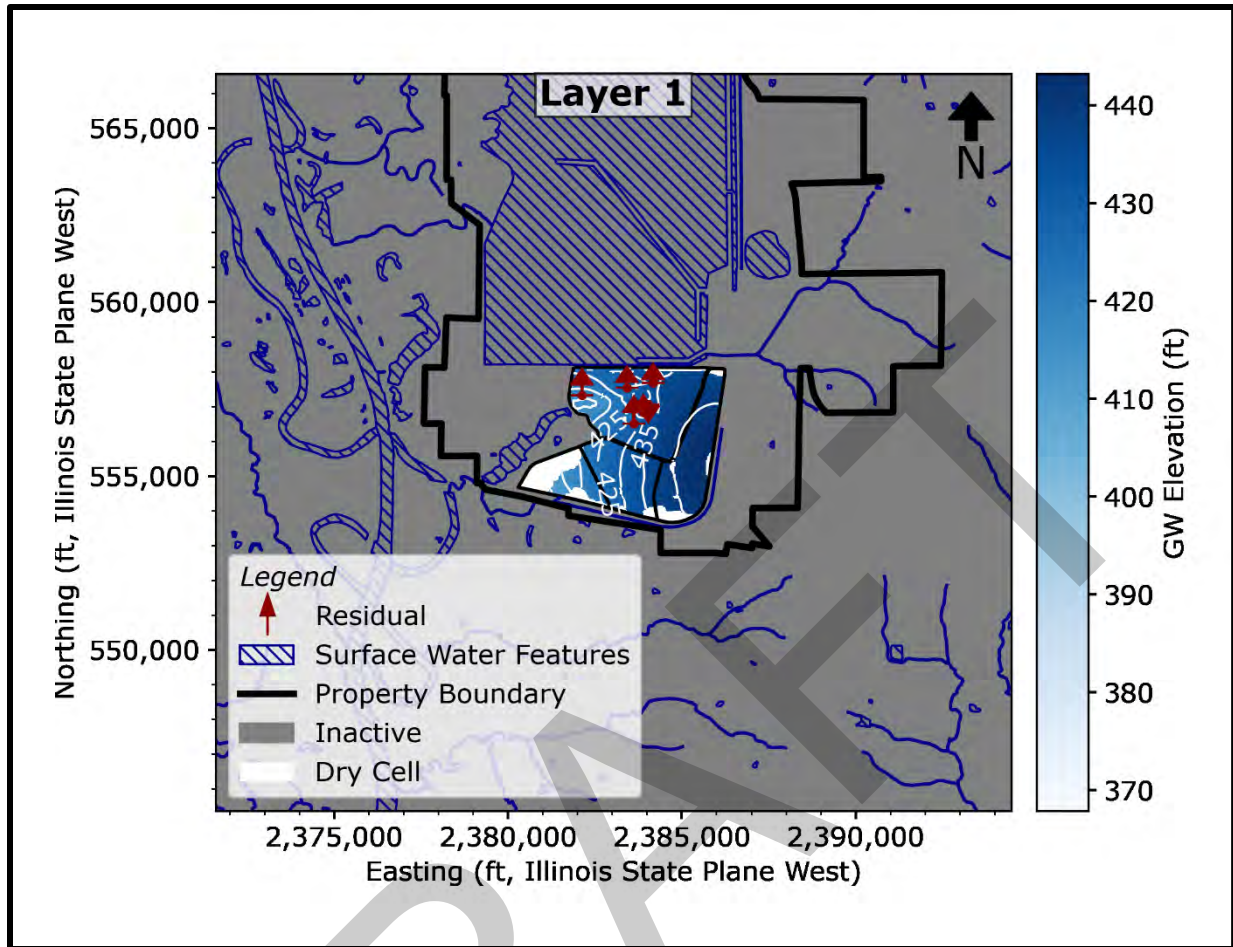




SIMULATED GROUNDWATER LEVEL RESIDUALS FROM THE CALIBRATED MODEL

GROUNDWATER MODELING REPORT
BOTTOM ASH POND
BALDWIN POWER PLANT
BALDWIN, ILLINOIS

RAMBOLL

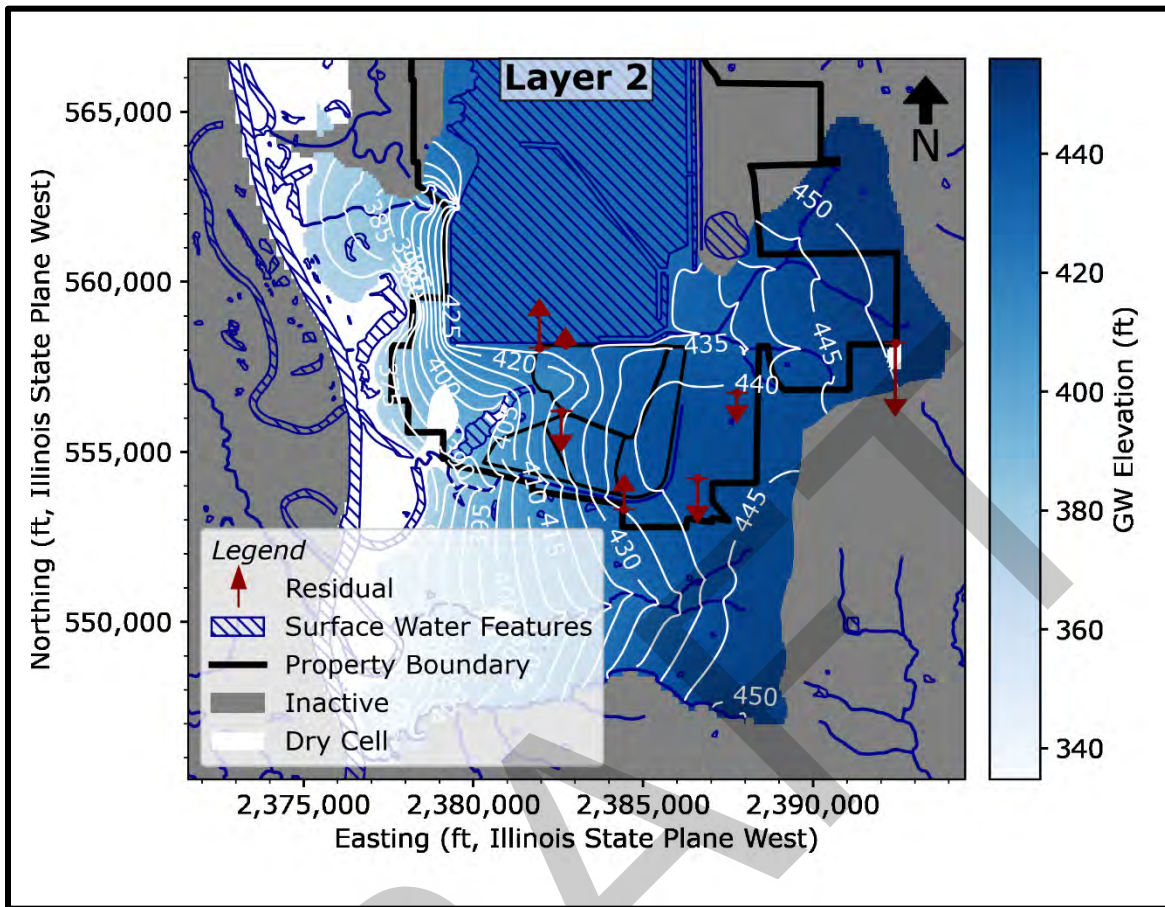


NOTE: RED DOTS INDICATE WELLS AND ARROW DIRECTION INDICATES BIAS IN SIMULATED GROUNDWATER LEVEL (NORTH ARROW = OVERESTIMATION, SOUTH ARROW = UNDERESTIMATION)

SIMULATED STEADY STATE GROUNDWATER LEVEL CONTOURS FROM LAYER 1 OF THE CALIBRATED MODEL

GROUNDWATER MODELING REPORT
 BOTTOM ASH POND
 BALDWIN POWER PLANT
 BALDWIN, ILLINOIS

RAMBOLL

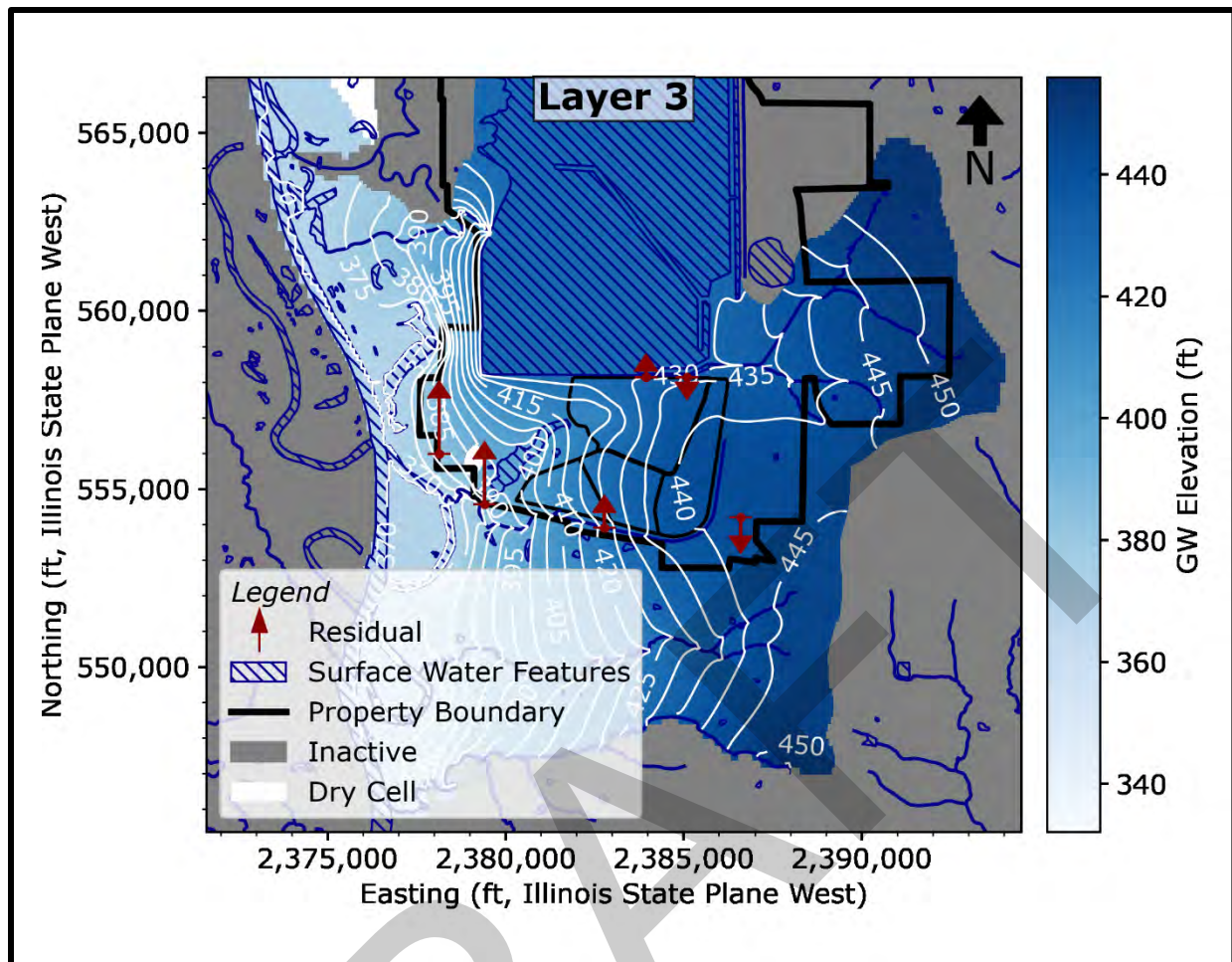


NOTE: RED DOTS INDICATE WELLS AND ARROW DIRECTION INDICATES BIAS IN SIMULATED GROUNDWATER LEVEL (NORTH ARROW = OVERESTIMATION, SOUTH ARROW = UNDERESTIMATION)

SIMULATED STEADY STATE GROUNDWATER LEVEL CONTOURS FROM LAYER 2 OF THE CALIBRATED MODEL

GROUNDWATER MODELING REPORT
 BOTTOM ASH POND
 BALDWIN POWER PLANT
 BALDWIN, ILLINOIS

RAMBOLL

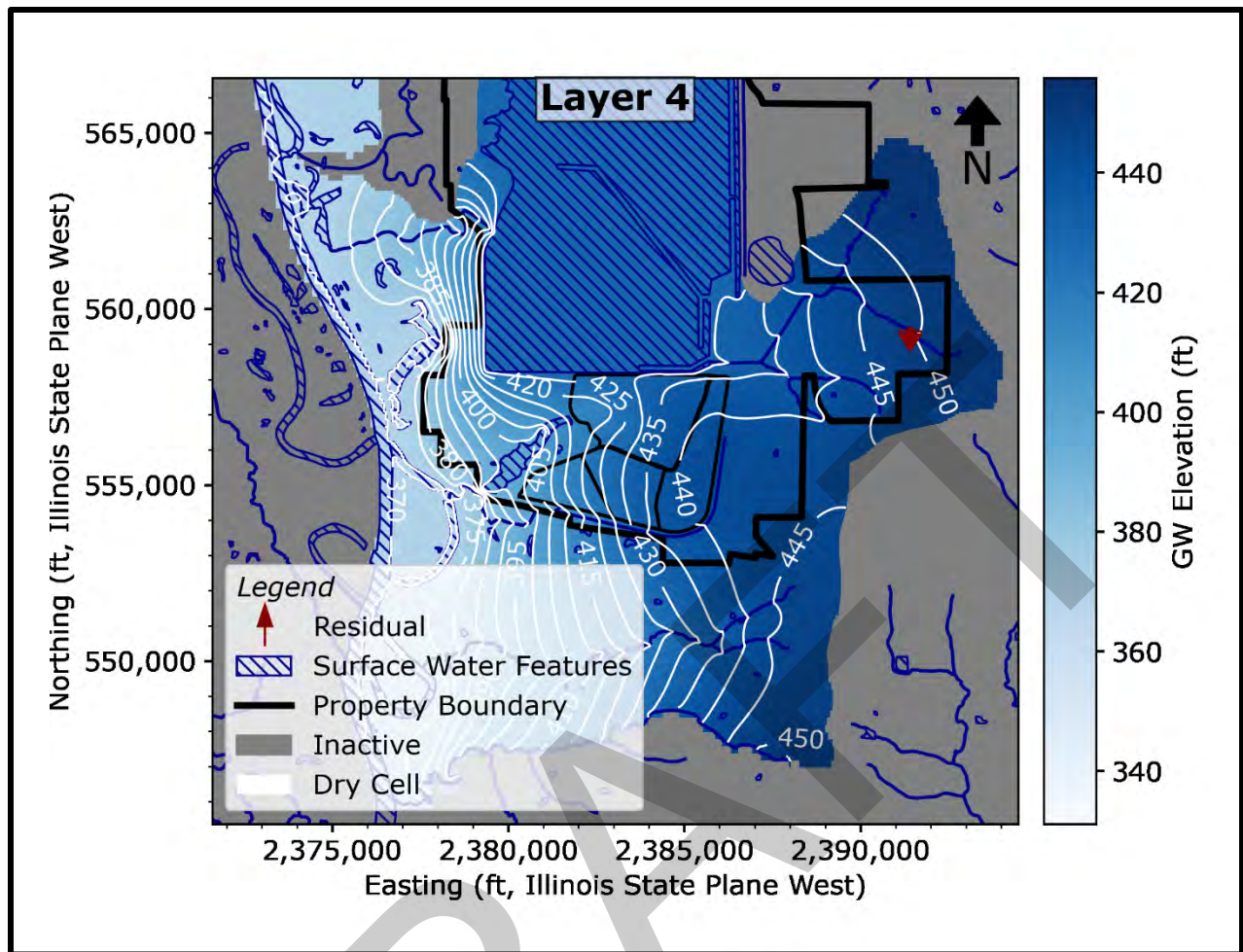


NOTE: RED DOTS INDICATE WELLS AND ARROW DIRECTION INDICATES BIAS IN SIMULATED GROUNDWATER LEVEL (NORTH ARROW = OVERESTIMATION, SOUTH ARROW = UNDERESTIMATION)

SIMULATED STEADY STATE GROUNDWATER LEVEL CONTOURS FROM LAYER 3 OF THE CALIBRATED MODEL

GROUNDWATER MODELING REPORT
 BOTTOM ASH POND
 BALDWIN POWER PLANT
 BALDWIN, ILLINOIS

RAMBOLL

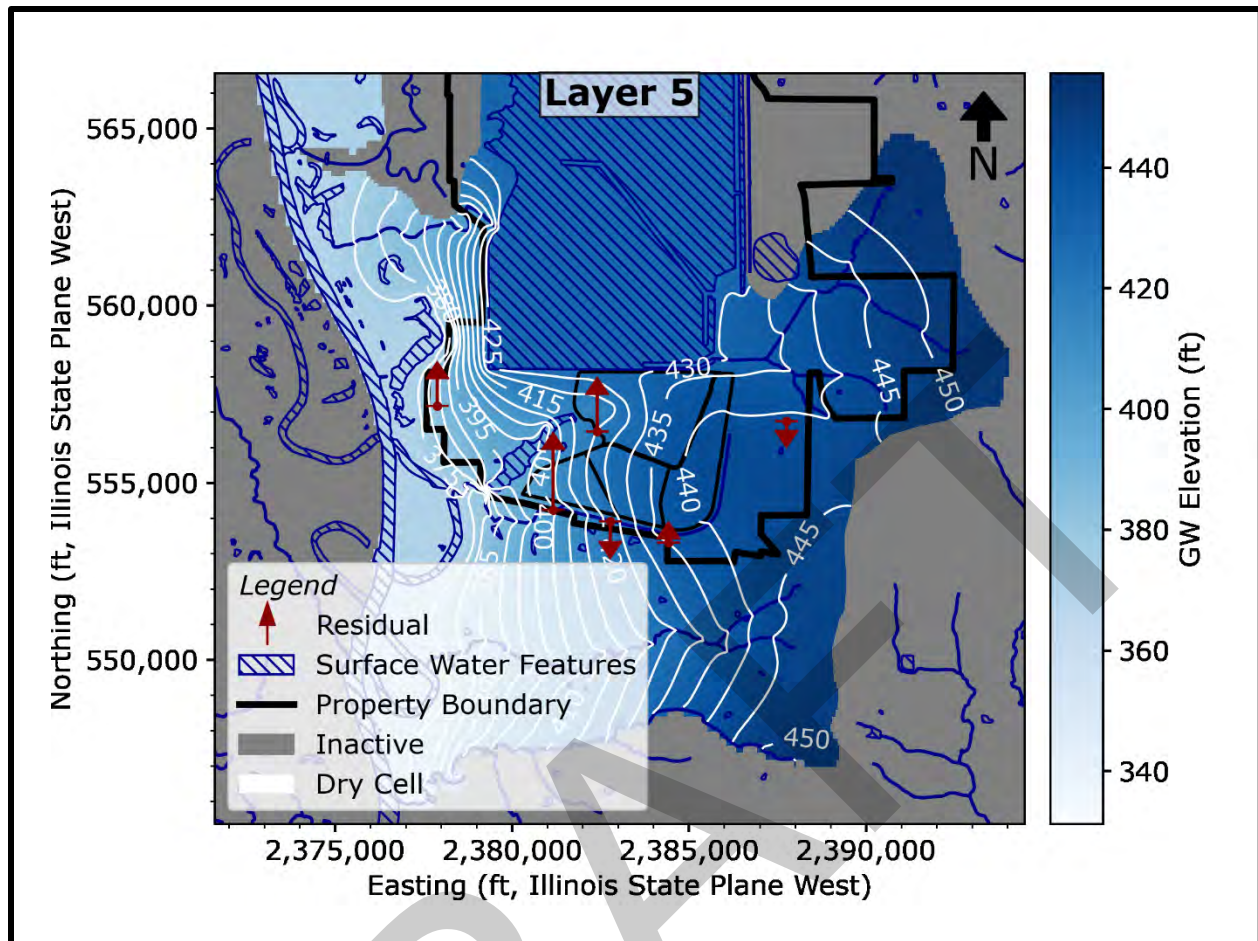


NOTE: RED DOTS INDICATE WELLS AND ARROW DIRECTION INDICATES BIAS IN SIMULATED GROUNDWATER LEVEL (NORTH ARROW = OVERESTIMATION, SOUTH ARROW = UNDERESTIMATION)

SIMULATED STEADY STATE GROUNDWATER LEVEL CONTOURS FROM LAYER 4 OF THE CALIBRATED MODEL

GROUNDWATER MODELING REPORT
 BOTTOM ASH POND
 BALDWIN POWER PLANT
 BALDWIN, ILLINOIS

RAMBOLL

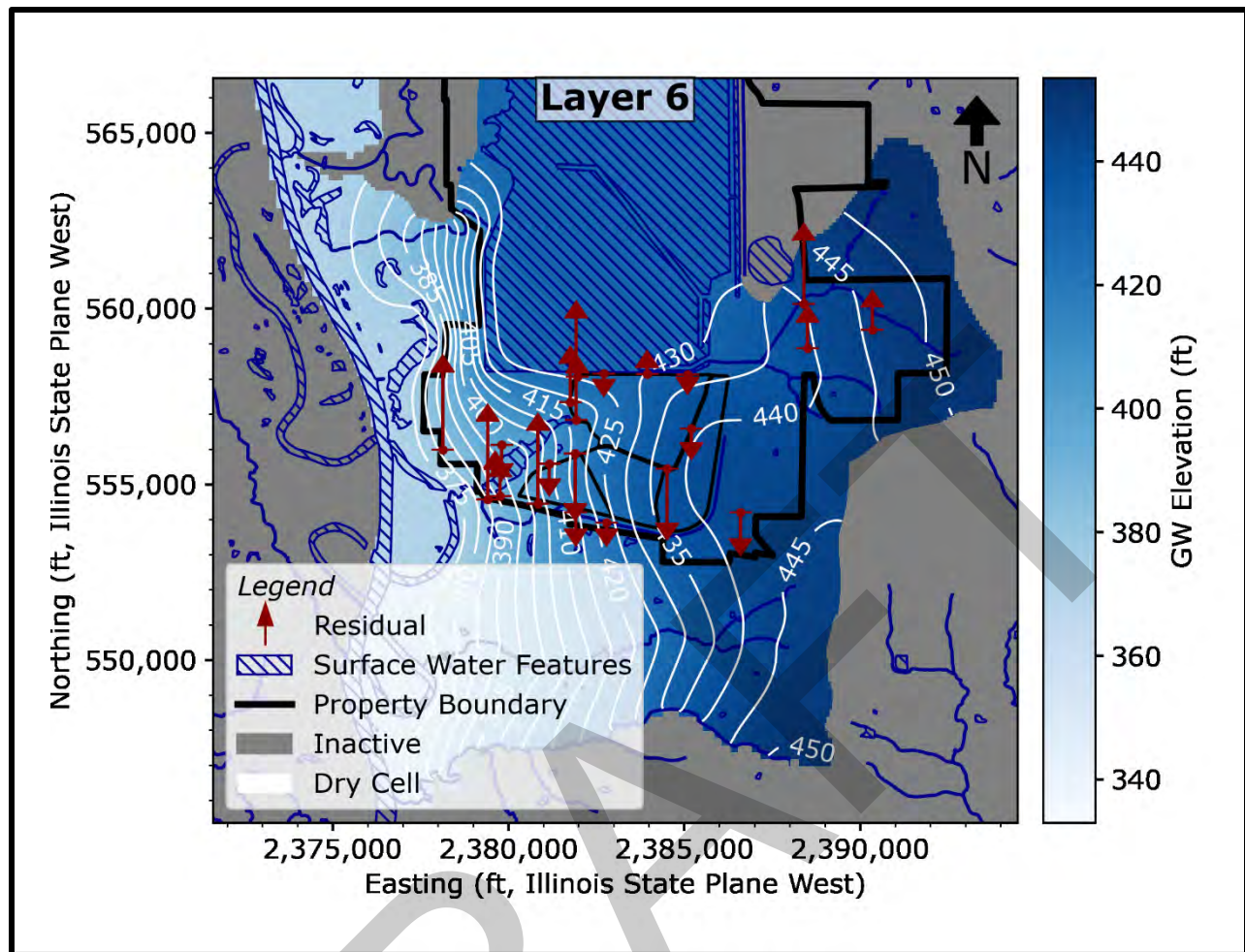


NOTE: RED DOTS INDICATE WELLS AND ARROW DIRECTION INDICATES BIAS IN SIMULATED GROUNDWATER LEVEL (NORTH ARROW = OVERESTIMATION, SOUTH ARROW = UNDERESTIMATION)

SIMULATED STEADY STATE GROUNDWATER LEVEL CONTOURS FROM LAYER 5 OF THE CALIBRATED MODEL

GROUNDWATER MODELING REPORT
 BOTTOM ASH POND
 BALDWIN POWER PLANT
 BALDWIN, ILLINOIS

RAMBOLL

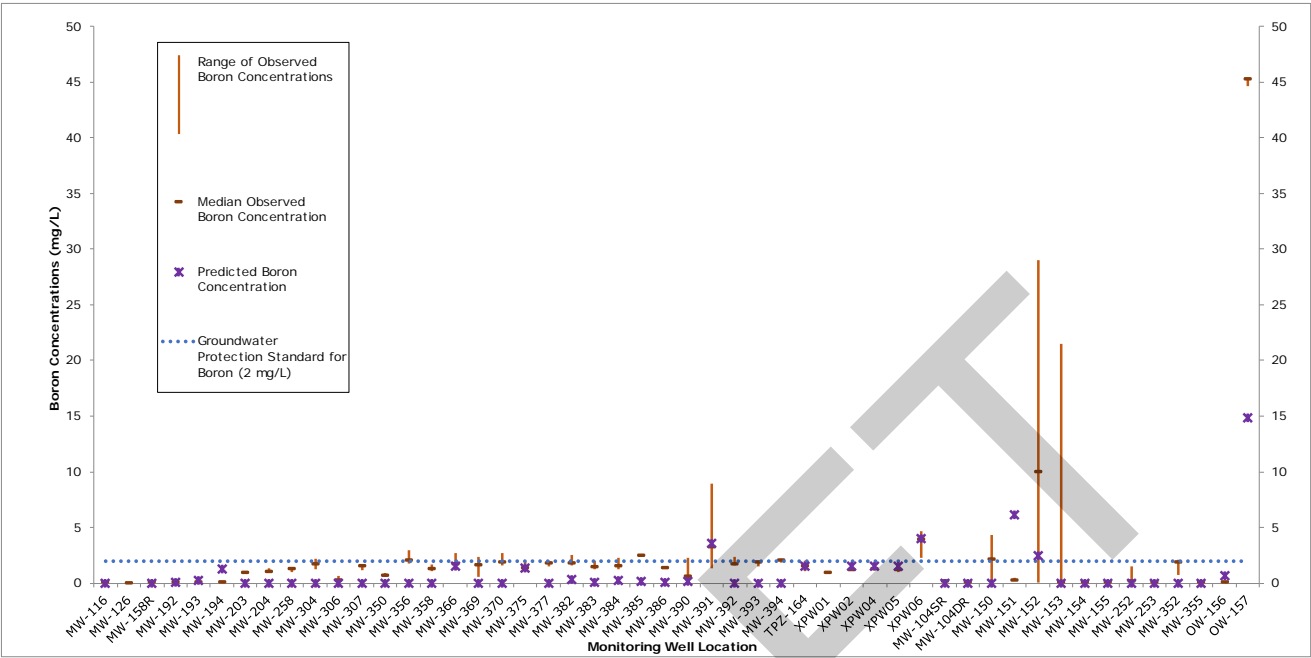


NOTE: RED DOTS INDICATE WELLS AND ARROW DIRECTION INDICATES BIAS IN SIMULATED GROUNDWATER LEVEL (NORTH ARROW = OVERESTIMATION, SOUTH ARROW = UNDERESTIMATION)

SIMULATED STEADY STATE GROUNDWATER LEVEL CONTOURS FROM LAYER 6 OF THE CALIBRATED MODEL

GROUNDWATER MODELING REPORT
 BOTTOM ASH POND
 BALDWIN POWER PLANT
 BALDWIN, ILLINOIS

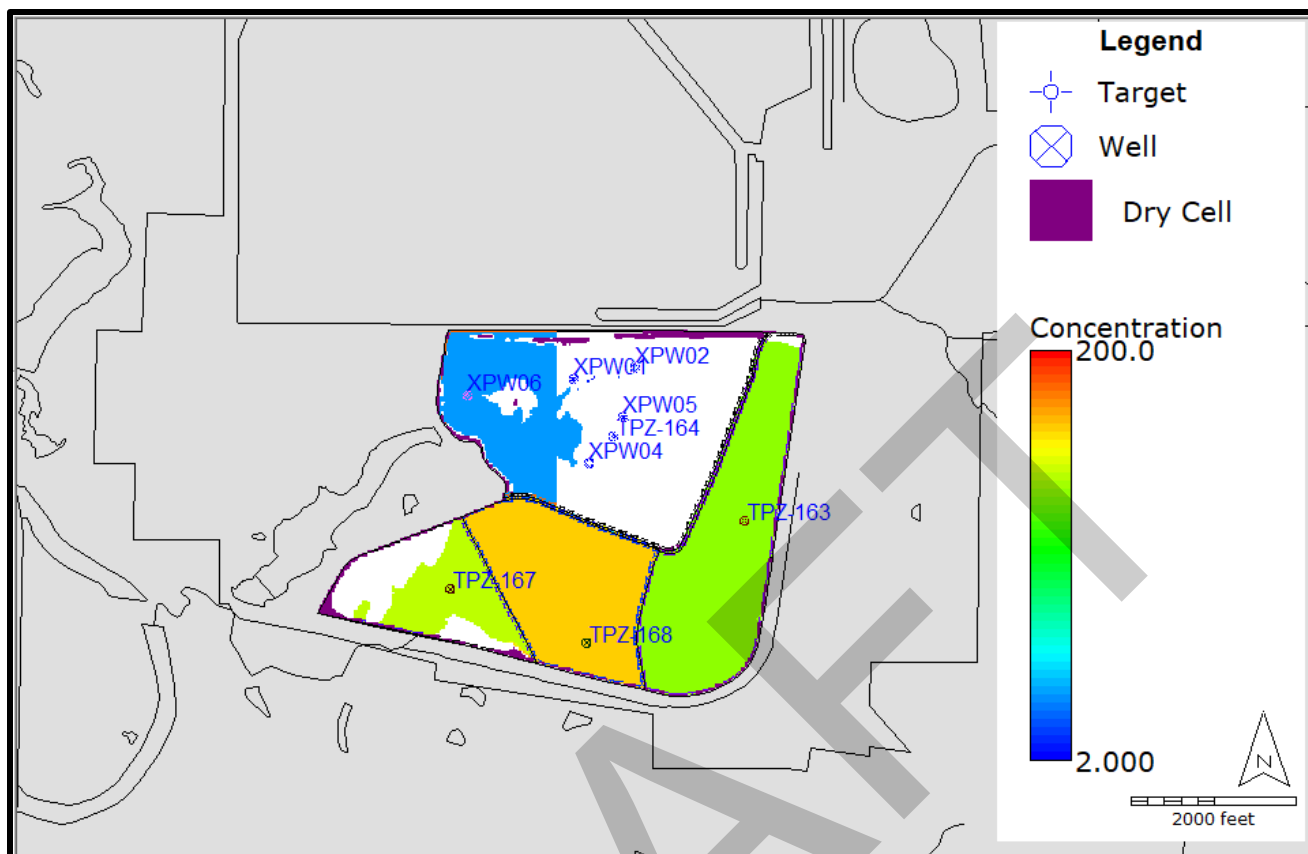
RAMBOLL



OBSERVED AND SIMULATED BORON CONCENTRATIONS (mg/L)

GROUNDWATER MODELING REPORT
BOTTOM ASH POND
BALDWIN POWER PLANT
BALDWIN, ILLINOIS

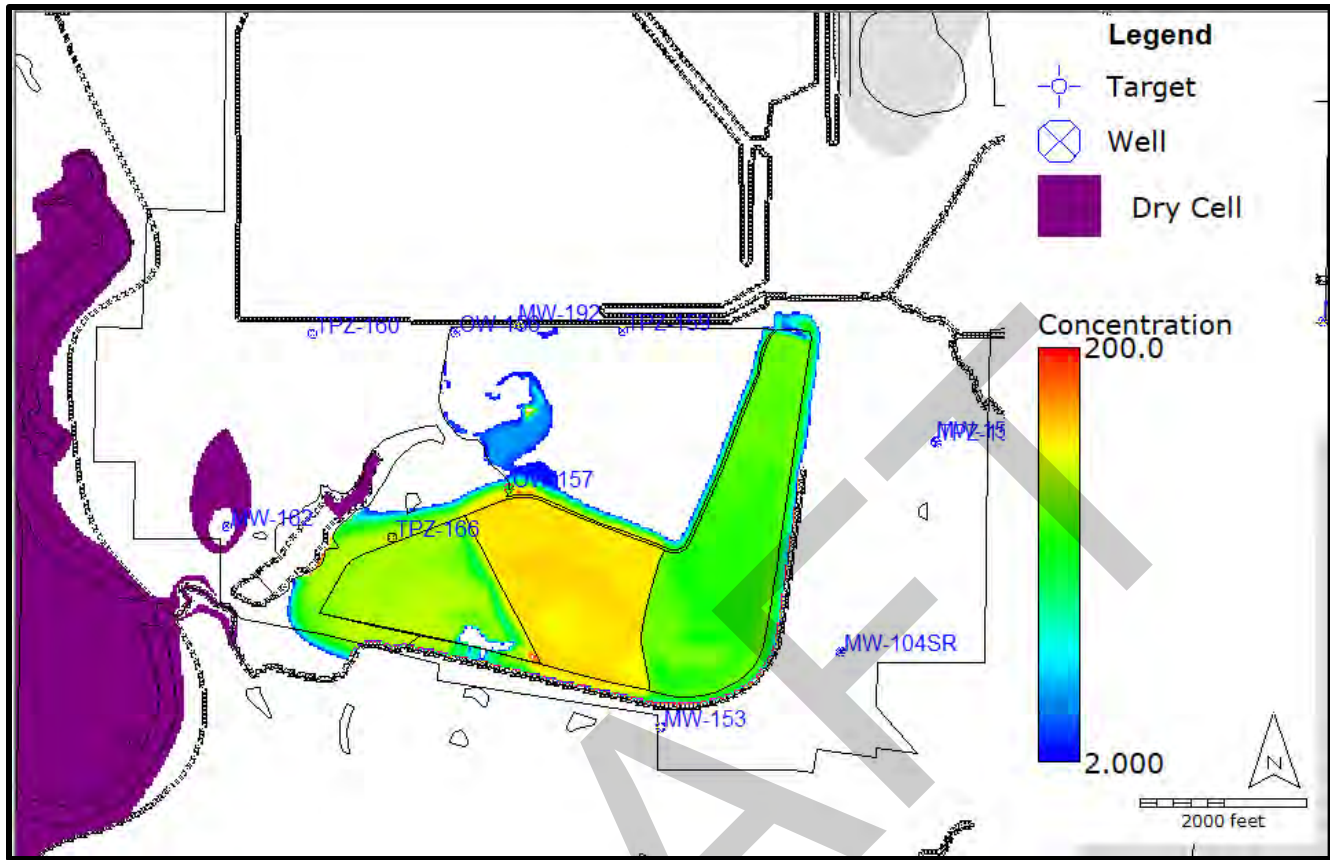




LAYER 1 DISTRIBUTION OF BORON CONCENTRATIONS (mg/L) IN THE CALIBRATED MODEL (CCR)

GROUNDWATER MODELING REPORT
 BOTTOM ASH POND
 BALDWIN POWER PLANT
 BALDWIN, ILLINOIS

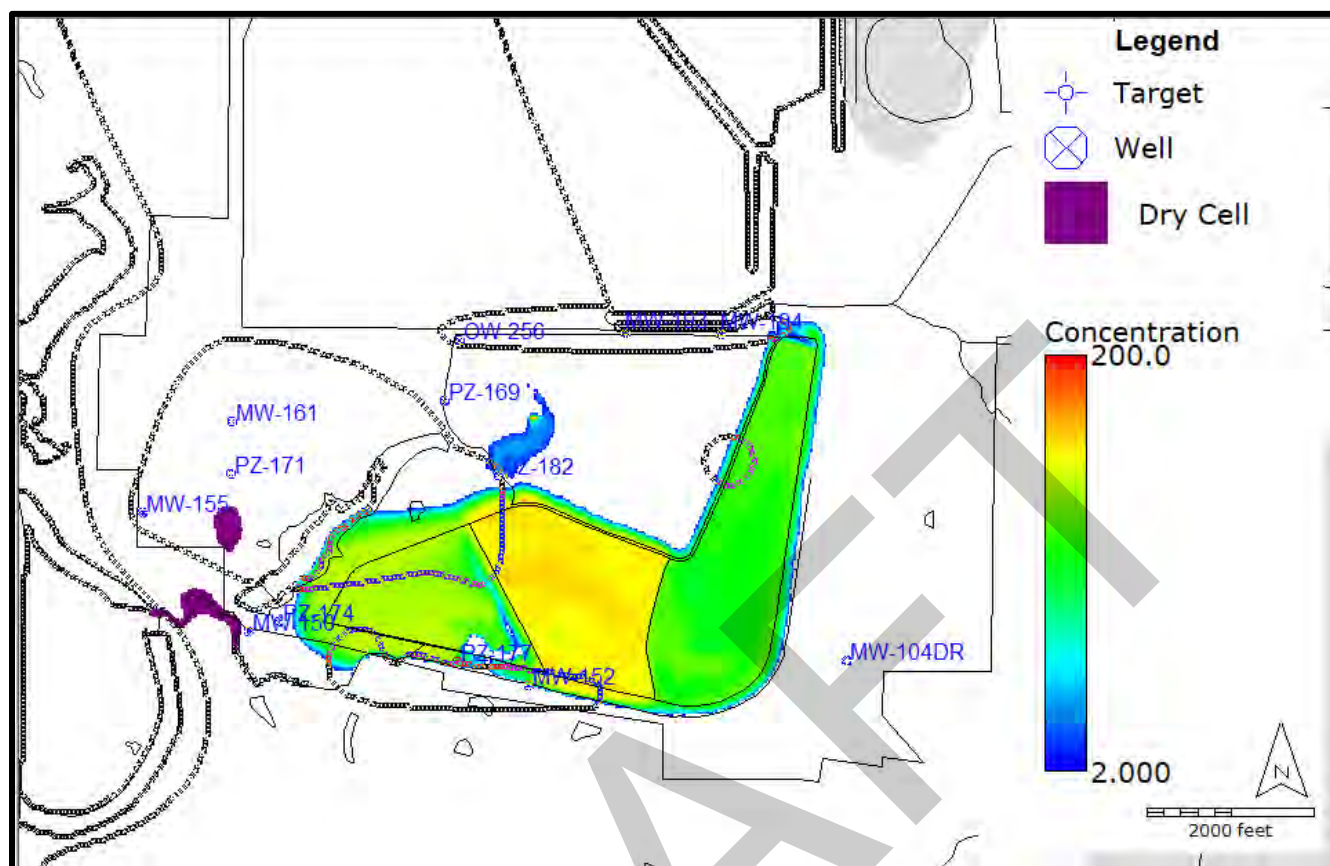
RAMBOLL



LAYER 2 DISTRIBUTION OF BORON CONCENTRATIONS (mg/L) IN THE CALIBRATED MODEL
(UU [UPPER SILTY CLAY])

GROUNDWATER MODELING REPORT
BOTTOM ASH POND
BALDWIN POWER PLANT
BALDWIN, ILLINOIS

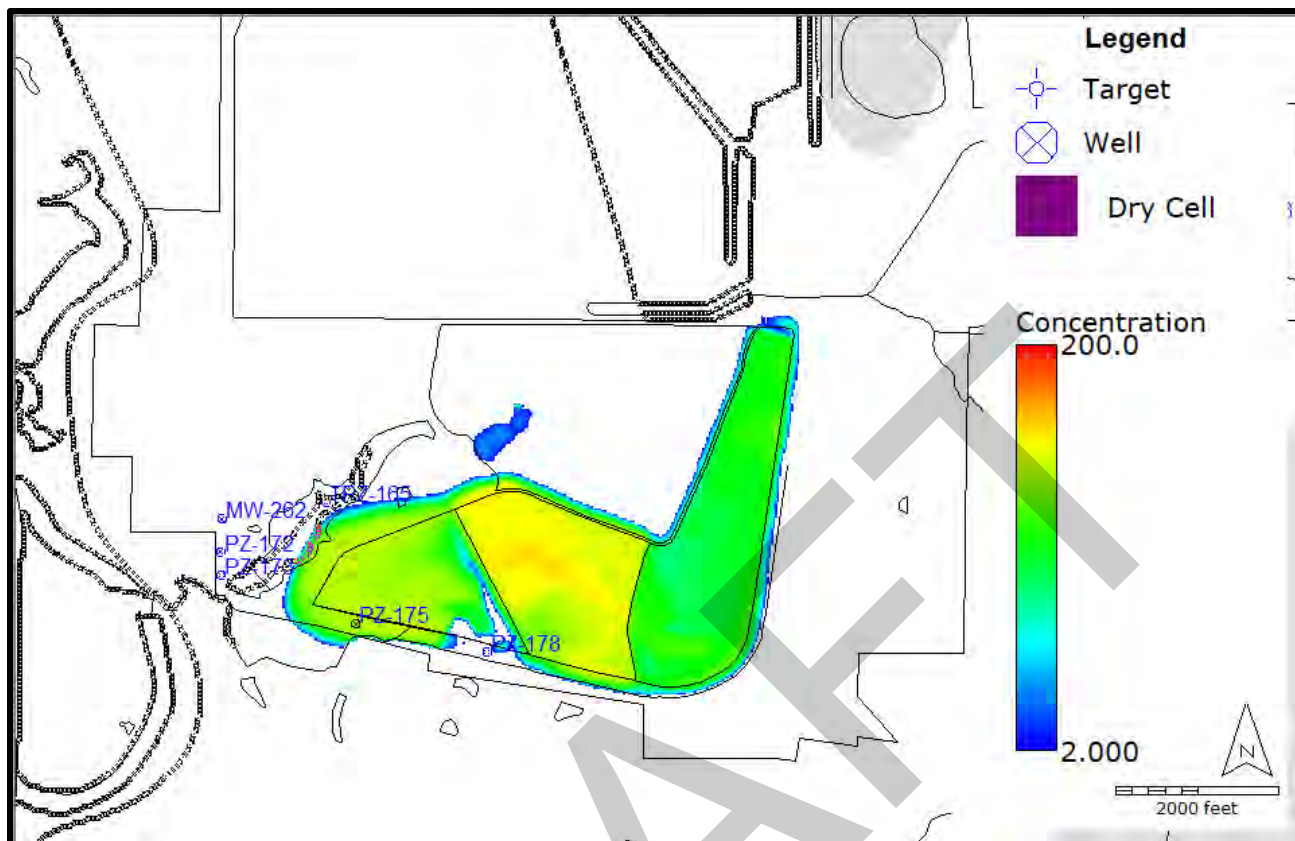
RAMBOLL



LAYER 3 DISTRIBUTION OF BORON CONCENTRATIONS (mg/L) IN THE CALIBRATED MODEL
(UU [PMP/TOP OF VANDALIA])

GROUNDWATER MODELING REPORT
BOTTOM ASH POND
BALDWIN POWER PLANT
BALDWIN, ILLINOIS

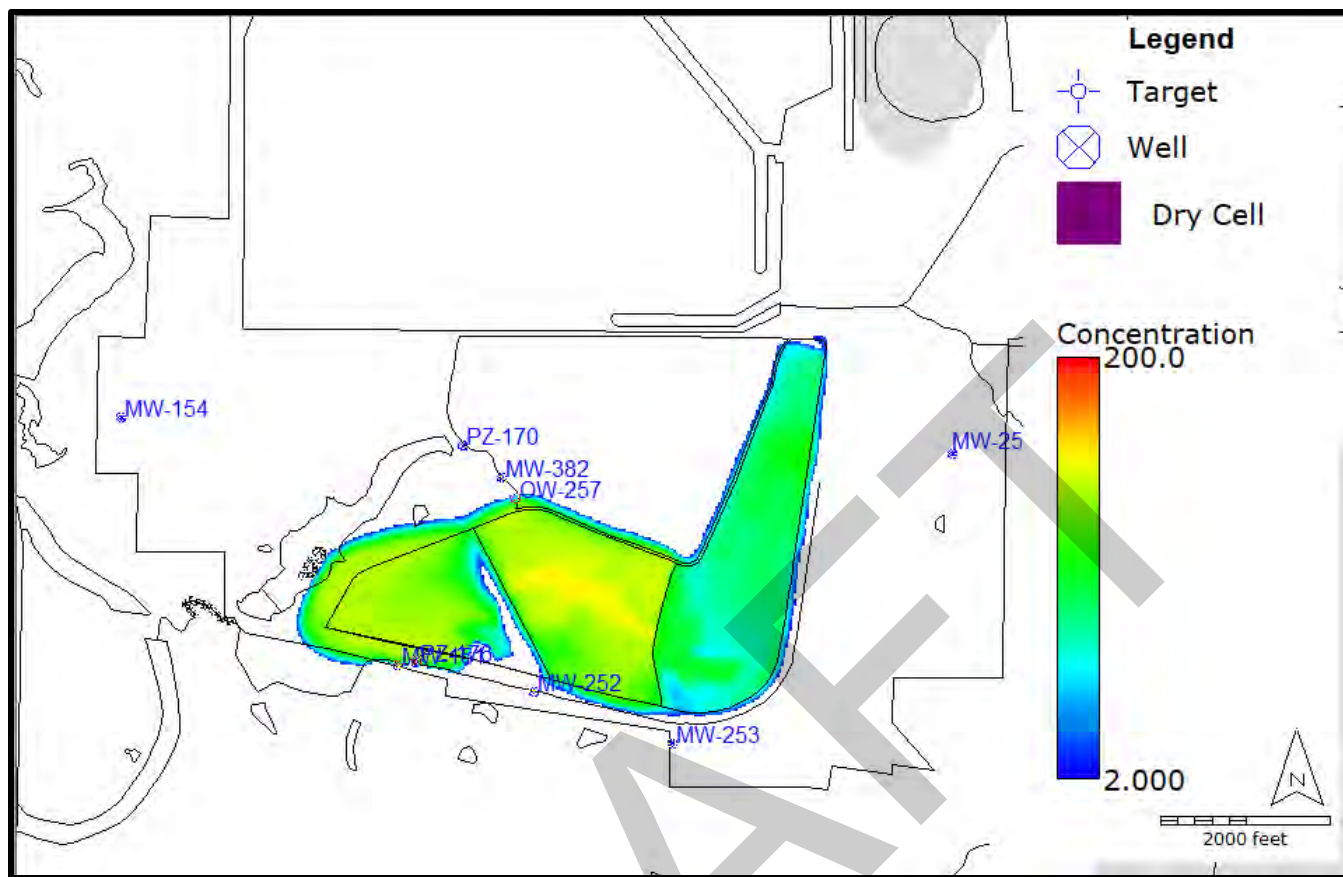
RAMBOLL



LAYER 4 DISTRIBUTION OF BORON CONCENTRATIONS (mg/L) IN THE CALIBRATED MODEL
(UU [LOWER SILTY CLAY])

GROUNDWATER MODELING REPORT
BOTTOM ASH POND
BALDWIN POWER PLANT
BALDWIN, ILLINOIS

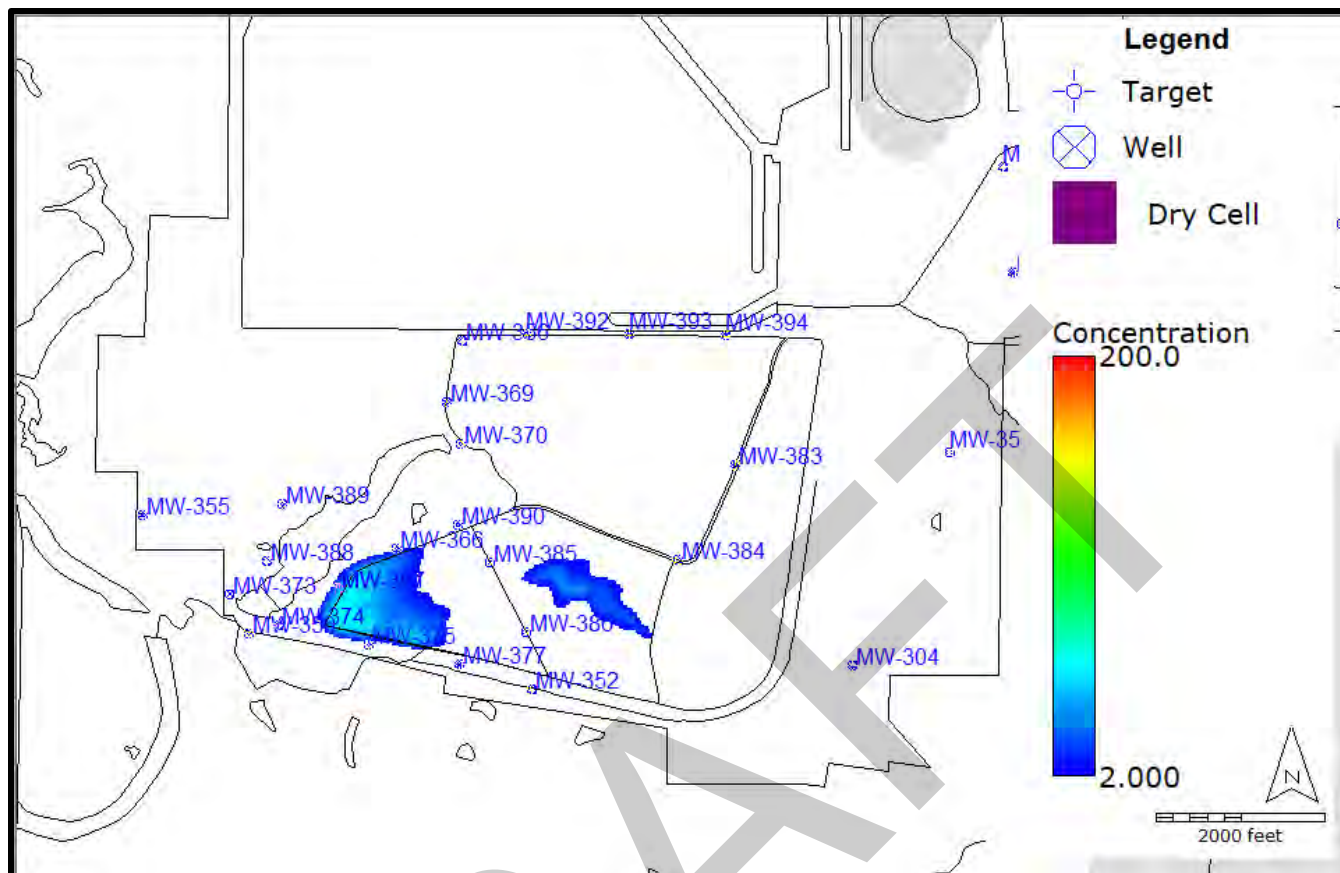
RAMBOLL



LAYER 5 DISTRIBUTION OF BORON CONCENTRATIONS (mg/L) IN THE CALIBRATED MODEL
(UA [DECOMPOSED BEDROCK])

GROUNDWATER MODELING REPORT
BOTTOM ASH POND
BALDWIN POWER PLANT
BALDWIN, ILLINOIS

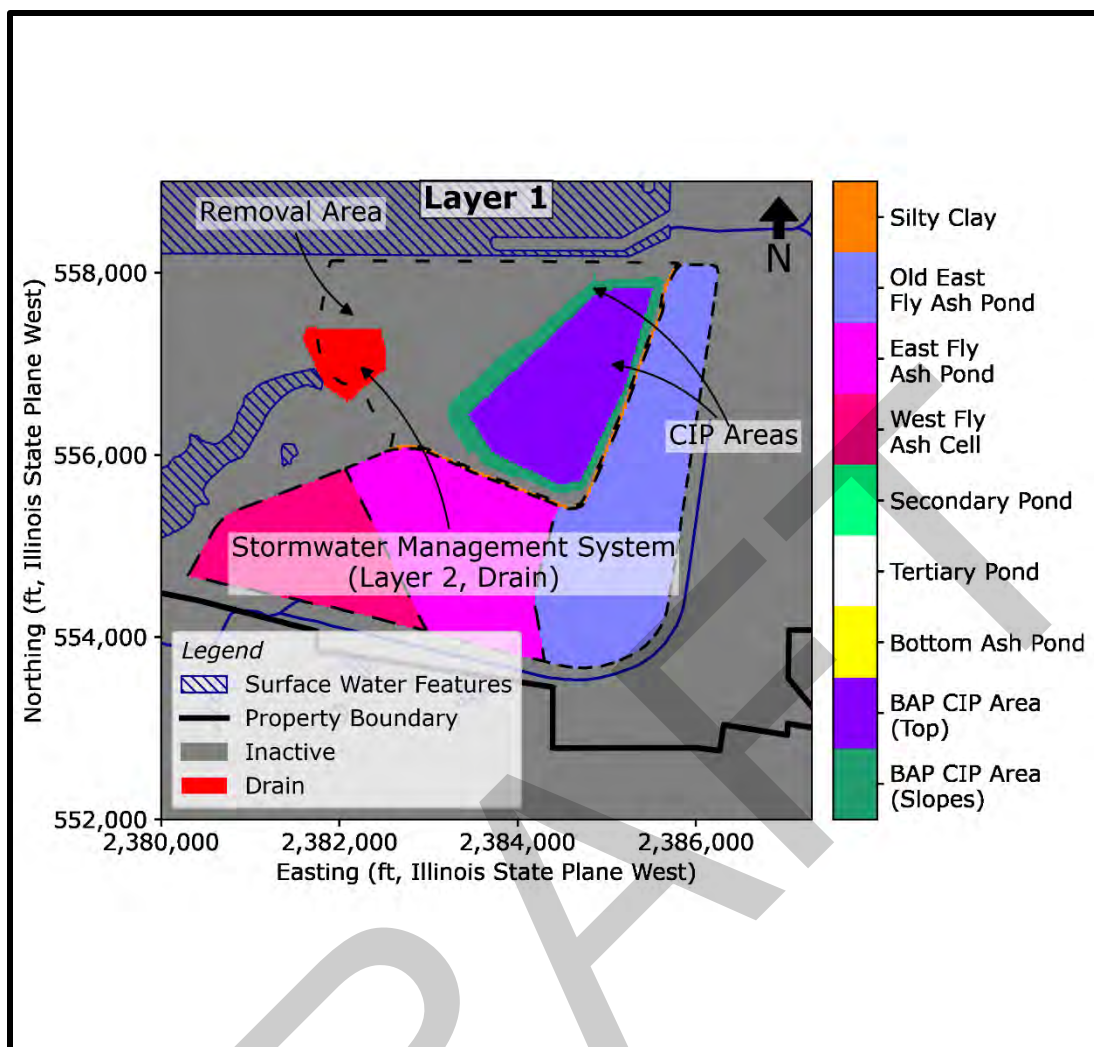
RAMBOLL



LAYER 6 DISTRIBUTION OF BORON CONCENTRATIONS (mg/L) IN THE CALIBRATED MODEL (UA)

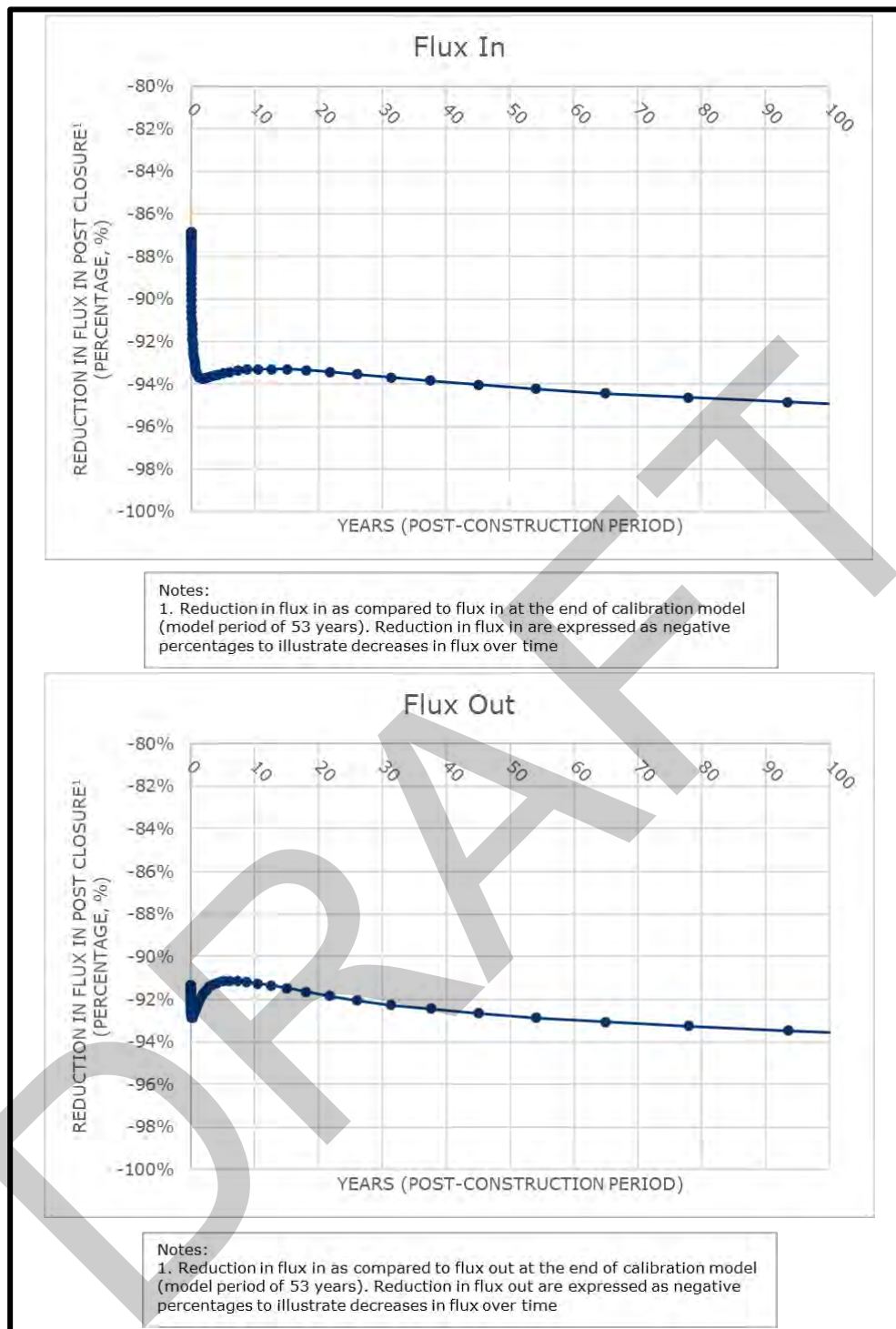
GROUNDWATER MODELING REPORT
 BOTTOM ASH POND
 BALDWIN POWER PLANT
 BALDWIN, ILLINOIS

RAMBOLL



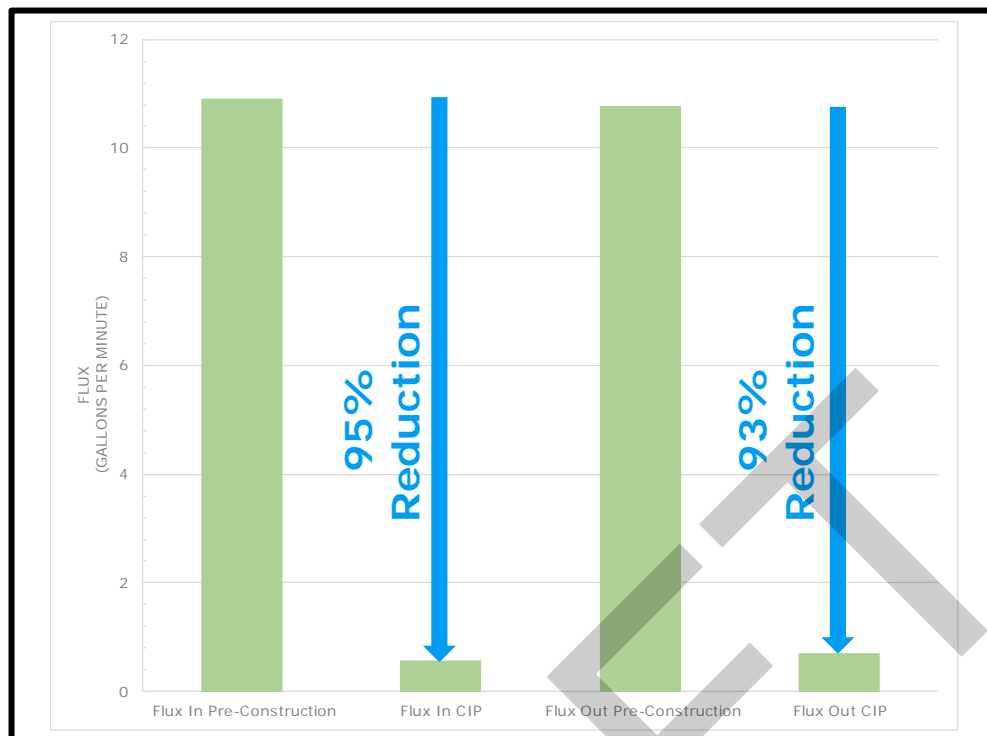
RECHARGE AND STORMWATER MANAGEMENT MODIFICATIONS FOR CLOSURE IN PLACE

GROUNDWATER MODELING REPORT
 BOTTOM ASH POND
 BALDWIN POWER PLANT
 BALDWIN, ILLINOIS



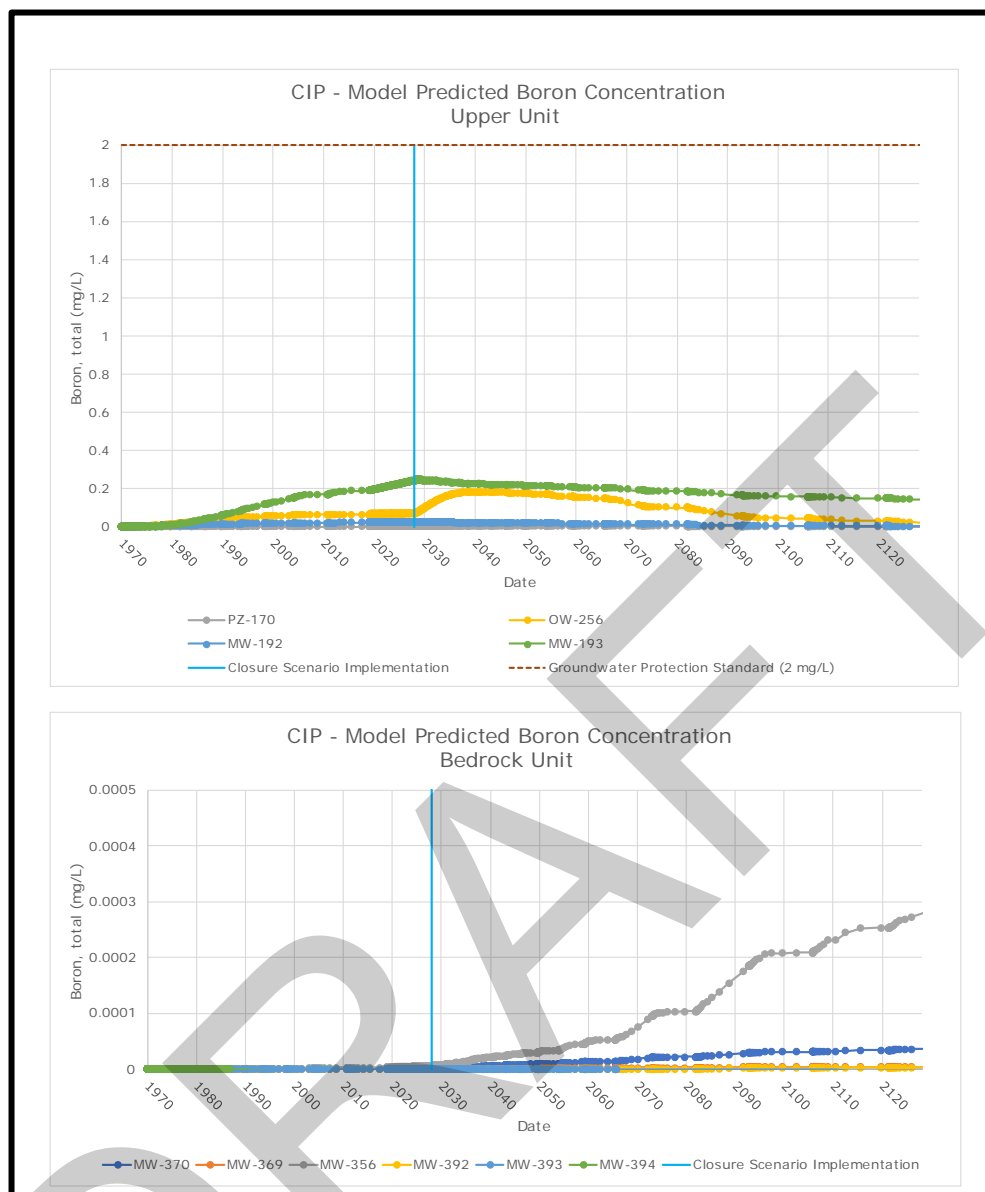
REDUCTIONS IN TOTAL FLUX IN AND OUT OF CCR FOLLOWING IMPLEMENTATION OF THE CIP CLOSURE SCENARIO

GROUNDWATER MODELING REPORT
BOTTOM ASH POND
BALDWIN POWER PLANT
BALDWIN, ILLINOIS



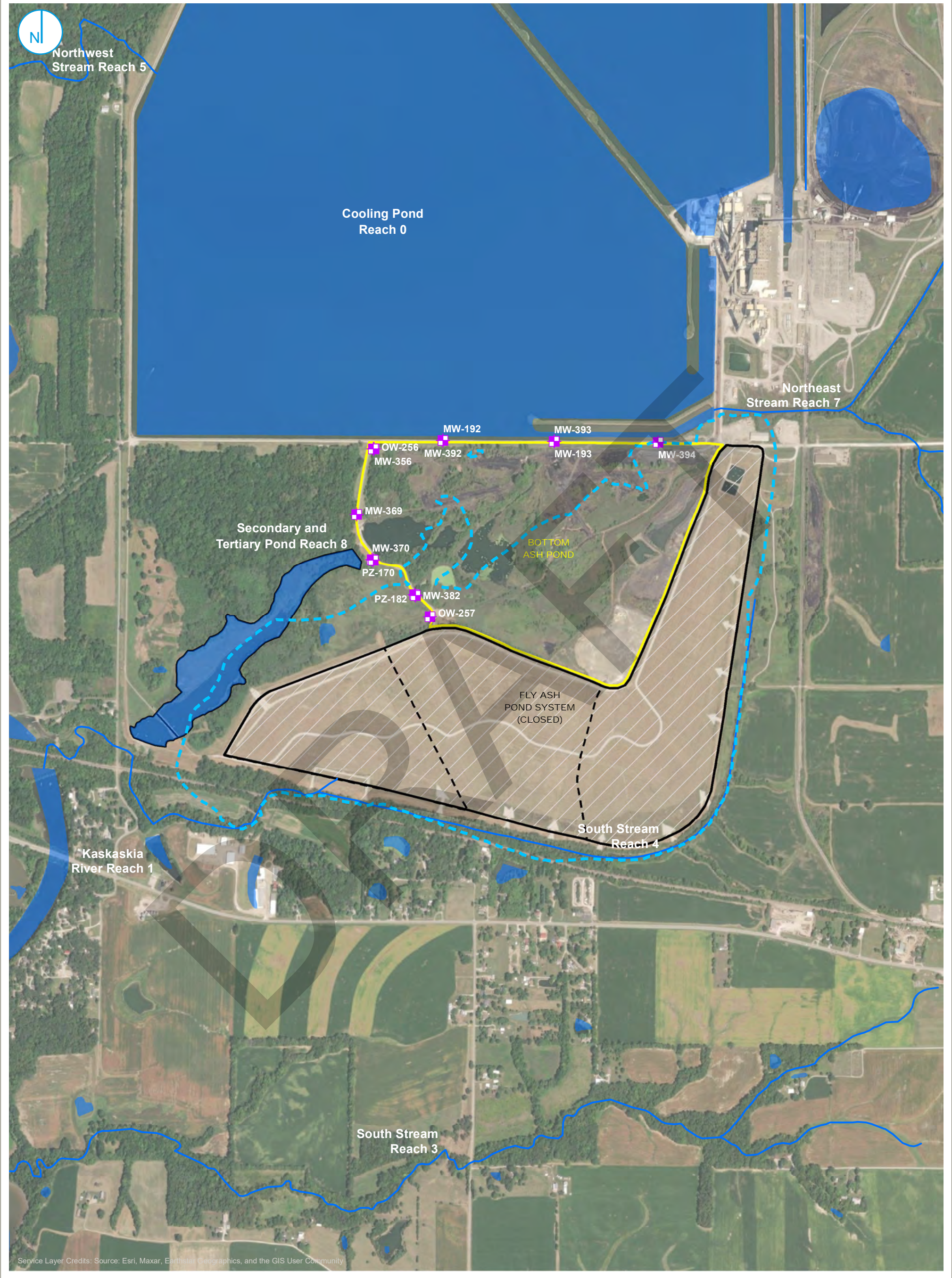
REDUCTIONS IN TOTAL FLUX IN AND OUT OF CCR 93 YEARS FOLLOWING IMPLEMENTATION OF THE CIP CLOSURE SCENARIO

GROUNDWATER MODELING REPORT
BOTTOM ASH POND
BALDWIN POWER PLANT
BALDWIN, ILLINOIS



CIP - MODEL PREDICTED BORON CONCENTRATION

GROUNDWATER MODELING REPORT
 BOTTOM ASH POND
 BALDWIN POWER PLANT
 BALDWIN, ILLINOIS



- 35 I.A.C. § 845 REGULATED UNIT (SUBJECT UNIT)
- FLY ASH POND SYSTEM
- LIMITS OF FINAL COVER
- SITE FEATURE
- RIVER
- WATERBODY

- MAXIMUM EXTENT OF THE BORON PLUME ABOVE THE STANDARD
- GWPS FOR BORON (2 mg/L) AT 93 YEARS FOLLOWING IMPLEMENTATION OF THE CIP CLOSURE SCENARIO
- PROPOSED BAP COMPLIANCE WELLS

CIP - MODEL PREDICTED MAXIMUM BORON PLUME IN ALL LAYERS APPROXIMATELY 93 YEARS AFTER IMPLEMENTATION

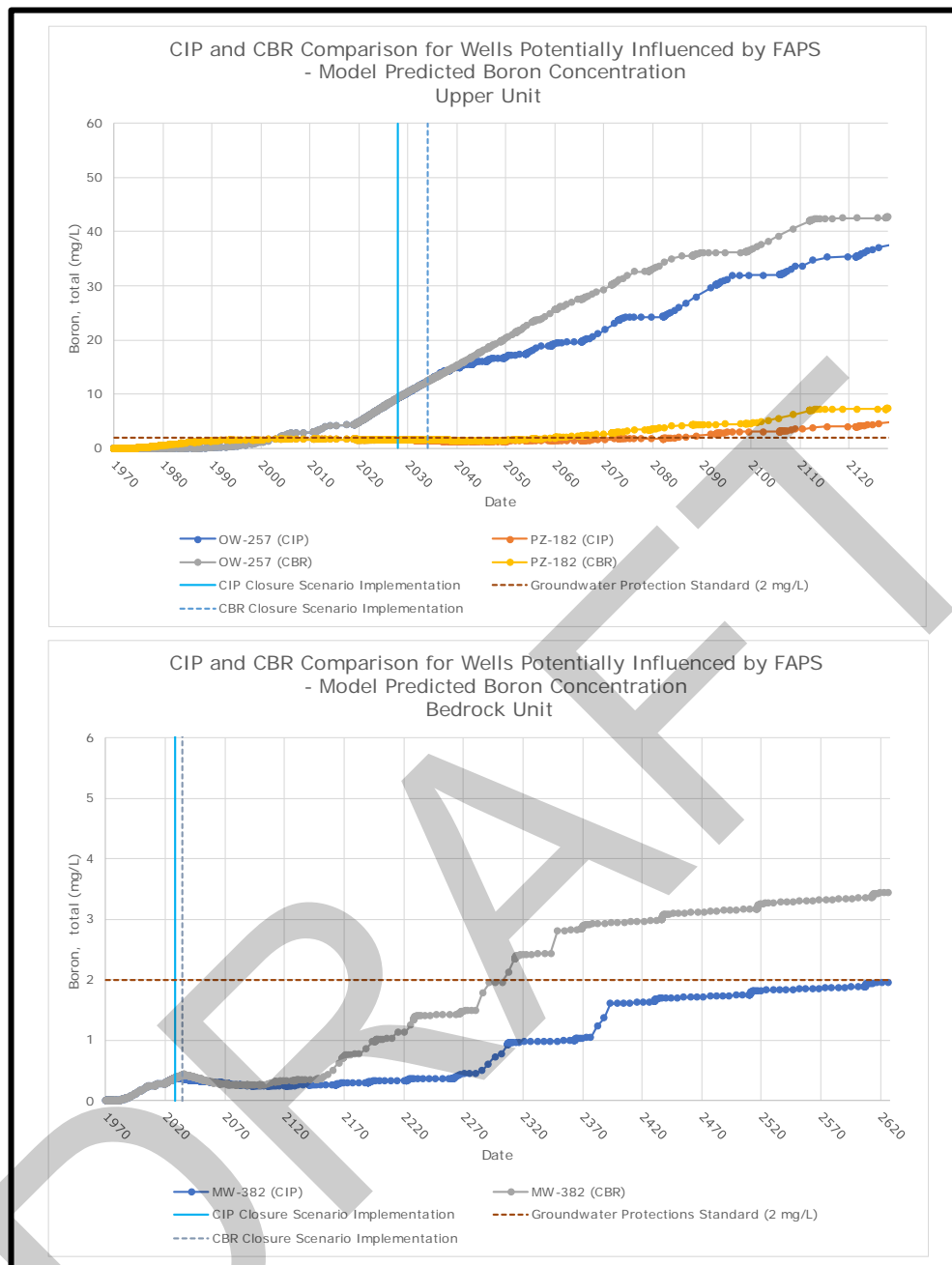
GROUNDWATER MODELING REPORT
BOTTOM ASH POND
BALDWIN POWER PLANT
BALDWIN, ILLINOIS

FIGURE 6-5

RAMBOLL AMERICAS
ENGINEERING SOLUTIONS, INC.



0 500 1,000 Feet



CIP AND CBR - MODEL PREDICTED BORON CONCENTRATION AT PROPOSED BAP COMPLIANCE MONITORING WELLS PZ-182, OW-257, AND MW-382

GROUNDWATER MODELING REPORT
 BOTTOM ASH POND
 BALDWIN POWER PLANT
 BALDWIN, ILLINOIS

APPENDICES

DRAFT

**APPENDIX A
HISTORY OF POTENTIAL EXCEEDANCES
REVISION 1 (RAMBOLL, 2023c)**

DRAFT

HISTORY OF POTENTIAL EXCEEDANCES REVISION 1 BOTTOM ASH POND BALDWIN POWER PLANT BALDWIN, ILLINOIS

This revision of the History of Potential Exceedances, and any corrective action taken to remediate groundwater, is provided to meet the requirements of Title 35 of the Illinois Administrative Code (35 I.A.C.) § 845.230(d)(2)(M) for the Baldwin Power Plant Bottom Ash Pond (BAP), Illinois Environmental Protection Agency (IEPA) ID No. W1578510001-06.

Note

Groundwater concentrations from 2015 to 2023 presented in the revised Hydrogeologic Site Characterization Report Revision 1 (HCR) Table 4-1, and evaluated and summarized in the following tables, are considered potential exceedances. DMG entered into a compliance commitment agreement (CCA) with IEPA on December 28, 2022. Groundwater monitoring in accordance with the CCA will follow the proposed groundwater monitoring plan and sampling methodologies provided in the operating permit application for the BAP and is scheduled to commence no later than the second quarter of 2023. After the BAP has been issued an approved operating permit, groundwater monitoring shall be conducted in accordance with that operating permit.

Alternate sources for potential exceedances as allowed by 35 I.A.C. § 845.650(e) have not yet been evaluated. These will be evaluated and presented in future submittals to IEPA as appropriate.

Table 1 summarizes how the potential exceedances were determined. Table 2 is a summary of all potential exceedances.

Background Concentrations

Background monitoring wells used to calculate background concentrations at the BAP include MW-304, MW-306, and MW-358.

For all monitoring wells presented in Tables 1 and 2, background concentrations calculated from sampling events in 2022 to 2023 were compared to the standards identified in 35 I.A.C. § 845.600(a)(1). For constituents with calculated background concentrations in greater than the standards in 35 I.A.C. § 845.600(a)(1), those calculated background concentrations were used as GWPSs for comparing to statistical calculation results for each well to determine potential exceedances. Statistical result calculations consider concentrations from all sampling events in 2015 through May of 2023.

Corrective Action

No corrective actions have been taken to remediate the groundwater.

TABLE 1. DETERMINATION OF POTENTIAL EXCEEDANCES
HISTORY OF POTENTIAL EXCEEDANCES
BALDWIN POWER PLANT
BOTTOM ASH POND
BALDWIN, ILLINOIS

| Sample Location | HSU | Program | Constituent | Result Unit | Sample Date Range | Statistical Calculation | Statistical Result | GWPS | Background | Part 845 Standard | GWPS Source |
|-----------------|-----|---------|--------------------------------|-------------|-------------------------|-------------------------|--------------------|--------|------------|-------------------|---------------------|
| MW-192 | UU | 845 | Antimony, total | mg/L | 10/27/2022 - 05/16/2023 | CI around median | 0.00100 | 0.006 | 0.0023 | 0.006 | Standard |
| MW-192 | UU | 845 | Arsenic, total | mg/L | 10/27/2022 - 05/16/2023 | CI around geomean | 0.00146 | 0.010 | 0.010 | 0.01 | Background |
| MW-192 | UU | 845 | Barium, total | mg/L | 10/27/2022 - 05/16/2023 | CI around mean | 0.0825 | 2.0 | 0.26 | 2 | Standard |
| MW-192 | UU | 845 | Beryllium, total | mg/L | 10/27/2022 - 05/16/2023 | All ND - Last | 0.0005 | 0.004 | 0.0005 | 0.004 | Standard |
| MW-192 | UU | 845 | Boron, total | mg/L | 10/27/2022 - 05/16/2023 | CI around mean | 0.0241 | 2.2 | 2.2 | 2 | Background |
| MW-192 | UU | 845 | Cadmium, total | mg/L | 10/27/2022 - 05/16/2023 | All ND - Last | 0.002 | 0.005 | 0.002 | 0.005 | Standard |
| MW-192 | UU | 845 | Chloride, total | mg/L | 10/27/2022 - 05/16/2023 | CB around linear reg | 18.9 | 1370 | 1370 | 200 | Background |
| MW-192 | UU | 845 | Chromium, total | mg/L | 10/27/2022 - 05/16/2023 | All ND - Last | 0.005 | 0.10 | 0.013 | 0.1 | Standard |
| MW-192 | UU | 845 | Cobalt, total | mg/L | 10/27/2022 - 05/16/2023 | CI around mean | 0.000910 | 0.006 | 0.0022 | 0.006 | Standard |
| MW-192 | UU | 845 | Fluoride, total | mg/L | 10/27/2022 - 05/16/2023 | CI around mean | 0.403 | 4.0 | 3.8 | 4 | Standard |
| MW-192 | UU | 845 | Lead, total | mg/L | 10/27/2022 - 05/16/2023 | CI around median | 0.00100 | 0.0075 | 0.0022 | 0.0075 | Standard |
| MW-192 | UU | 845 | Lithium, total | mg/L | 10/27/2022 - 05/16/2023 | CI around mean | 0.00725 | 0.14 | 0.14 | 0.04 | Background |
| MW-192 | UU | 845 | Mercury, total | mg/L | 10/27/2022 - 05/16/2023 | All ND - Last | 0.0002 | 0.002 | 0.0002 | 0.002 | Standard |
| MW-192 | UU | 845 | Molybdenum, total | mg/L | 10/27/2022 - 05/16/2023 | CI around mean | 0.00248 | 0.10 | 0.078 | 0.1 | Standard |
| MW-192 | UU | 845 | pH (field) | SU | 10/27/2022 - 05/16/2023 | CI around median | 6.5/7.0 | 6.5/11 | 7.5/11.1 | 6.5/9 | Standard/Background |
| MW-192 | UU | 845 | Radium 226 + Radium 228, total | pCi/L | 10/27/2022 - 05/16/2023 | CI around mean | 0.244 | 5.0 | 3.8 | 5 | Standard |
| MW-192 | UU | 845 | Selenium, total | mg/L | 10/27/2022 - 05/16/2023 | All ND - Last | 0.001 | 0.050 | 0.0032 | 0.05 | Standard |
| MW-192 | UU | 845 | Sulfate, total | mg/L | 10/27/2022 - 05/16/2023 | CB around linear reg | 11.0 | 762 | 762 | 400 | Background |
| MW-192 | UU | 845 | Thallium, total | mg/L | 10/27/2022 - 05/16/2023 | All ND - Last | 0.002 | 0.002 | 0.002 | 0.002 | Standard |
| MW-192 | UU | 845 | Total Dissolved Solids | mg/L | 10/27/2022 - 05/16/2023 | CI around mean | 432 | 3260 | 3260 | 1200 | Background |
| MW-193 | UU | 845 | Antimony, total | mg/L | 10/27/2022 - 05/15/2023 | All ND - Last | 0.001 | 0.006 | 0.0023 | 0.006 | Standard |
| MW-193 | UU | 845 | Arsenic, total | mg/L | 10/27/2022 - 05/15/2023 | CI around mean | 0.00124 | 0.010 | 0.010 | 0.01 | Background |
| MW-193 | UU | 845 | Barium, total | mg/L | 10/27/2022 - 05/15/2023 | CI around mean | 0.0703 | 2.0 | 0.26 | 2 | Standard |
| MW-193 | UU | 845 | Beryllium, total | mg/L | 10/27/2022 - 05/15/2023 | All ND - Last | 0.0005 | 0.004 | 0.0005 | 0.004 | Standard |
| MW-193 | UU | 845 | Boron, total | mg/L | 10/27/2022 - 05/15/2023 | CI around mean | 0.0287 | 2.2 | 2.2 | 2 | Background |
| MW-193 | UU | 845 | Cadmium, total | mg/L | 10/27/2022 - 05/15/2023 | All ND - Last | 0.002 | 0.005 | 0.002 | 0.005 | Standard |
| MW-193 | UU | 845 | Chloride, total | mg/L | 10/27/2022 - 05/15/2023 | CI around mean | 34.8 | 1370 | 1370 | 200 | Background |

TABLE 1. DETERMINATION OF POTENTIAL EXCEEDANCES
HISTORY OF POTENTIAL EXCEEDANCES
BALDWIN POWER PLANT
BOTTOM ASH POND
BALDWIN, ILLINOIS

| Sample Location | HSU | Program | Constituent | Result Unit | Sample Date Range | Statistical Calculation | Statistical Result | GWPS | Background | Part 845 Standard | GWPS Source |
|-----------------|-----|---------|--------------------------------|-------------|-------------------------|-------------------------|--------------------|--------|------------|-------------------|---------------------|
| MW-193 | UU | 845 | Chromium, total | mg/L | 10/27/2022 - 05/15/2023 | CI around median | 0.00150 | 0.10 | 0.013 | 0.1 | Standard |
| MW-193 | UU | 845 | Cobalt, total | mg/L | 10/27/2022 - 05/15/2023 | Most recent sample | 0.00100 | 0.006 | 0.0022 | 0.006 | Standard |
| MW-193 | UU | 845 | Fluoride, total | mg/L | 10/27/2022 - 05/15/2023 | CB around linear reg | 0.191 | 4.0 | 3.8 | 4 | Standard |
| MW-193 | UU | 845 | Lead, total | mg/L | 10/27/2022 - 05/15/2023 | All ND - Last | 0.008 | 0.0075 | 0.0022 | 0.0075 | Standard |
| MW-193 | UU | 845 | Lithium, total | mg/L | 10/27/2022 - 05/15/2023 | CI around mean | 0.00474 | 0.14 | 0.14 | 0.04 | Background |
| MW-193 | UU | 845 | Mercury, total | mg/L | 10/27/2022 - 05/15/2023 | All ND - Last | 0.0002 | 0.002 | 0.0002 | 0.002 | Standard |
| MW-193 | UU | 845 | Molybdenum, total | mg/L | 10/27/2022 - 05/15/2023 | CI around median | 0.00150 | 0.10 | 0.078 | 0.1 | Standard |
| MW-193 | UU | 845 | pH (field) | SU | 10/27/2022 - 05/15/2023 | CI around mean | 6.7/7.2 | 6.5/11 | 7.5/11.1 | 6.5/9 | Standard/Background |
| MW-193 | UU | 845 | Radium 226 + Radium 228, total | pCi/L | 10/27/2022 - 05/15/2023 | CI around mean | 0.376 | 5.0 | 3.8 | 5 | Standard |
| MW-193 | UU | 845 | Selenium, total | mg/L | 10/27/2022 - 05/15/2023 | All ND - Last | 0.001 | 0.050 | 0.0032 | 0.05 | Standard |
| MW-193 | UU | 845 | Sulfate, total | mg/L | 10/27/2022 - 05/15/2023 | CI around mean | 152 | 762 | 762 | 400 | Background |
| MW-193 | UU | 845 | Thallium, total | mg/L | 10/27/2022 - 05/15/2023 | All ND - Last | 0.002 | 0.002 | 0.002 | 0.002 | Standard |
| MW-193 | UU | 845 | Total Dissolved Solids | mg/L | 10/27/2022 - 05/15/2023 | CI around mean | 523 | 3260 | 3260 | 1200 | Background |
| MW-194 | UU | 845 | Antimony, total | mg/L | 10/27/2022 - 05/15/2023 | CI around median | 0.00100 | 0.006 | 0.0023 | 0.006 | Standard |
| MW-194 | UU | 845 | Arsenic, total | mg/L | 10/27/2022 - 05/15/2023 | CB around linear reg | -0.000853 | 0.010 | 0.010 | 0.01 | Background |
| MW-194 | UU | 845 | Barium, total | mg/L | 10/27/2022 - 05/15/2023 | CI around mean | 0.0844 | 2.0 | 0.26 | 2 | Standard |
| MW-194 | UU | 845 | Beryllium, total | mg/L | 10/27/2022 - 05/15/2023 | All ND - Last | 0.0005 | 0.004 | 0.0005 | 0.004 | Standard |
| MW-194 | UU | 845 | Boron, total | mg/L | 10/27/2022 - 05/15/2023 | CI around median | 0.0200 | 2.2 | 2.2 | 2 | Background |
| MW-194 | UU | 845 | Cadmium, total | mg/L | 10/27/2022 - 05/15/2023 | All ND - Last | 0.002 | 0.005 | 0.002 | 0.005 | Standard |
| MW-194 | UU | 845 | Chloride, total | mg/L | 10/27/2022 - 05/15/2023 | CI around mean | 28.0 | 1370 | 1370 | 200 | Background |
| MW-194 | UU | 845 | Chromium, total | mg/L | 10/27/2022 - 05/15/2023 | CI around median | 0.00150 | 0.10 | 0.013 | 0.1 | Standard |
| MW-194 | UU | 845 | Cobalt, total | mg/L | 10/27/2022 - 05/15/2023 | CI around mean | 0.000487 | 0.006 | 0.0022 | 0.006 | Standard |
| MW-194 | UU | 845 | Fluoride, total | mg/L | 10/27/2022 - 05/15/2023 | CI around mean | 0.272 | 4.0 | 3.8 | 4 | Standard |
| MW-194 | UU | 845 | Lead, total | mg/L | 10/27/2022 - 05/15/2023 | CI around median | 0.00100 | 0.0075 | 0.0022 | 0.0075 | Standard |
| MW-194 | UU | 845 | Lithium, total | mg/L | 10/27/2022 - 05/15/2023 | CI around mean | 0.00580 | 0.14 | 0.14 | 0.04 | Background |
| MW-194 | UU | 845 | Mercury, total | mg/L | 10/27/2022 - 05/15/2023 | All ND - Last | 0.0002 | 0.002 | 0.0002 | 0.002 | Standard |
| MW-194 | UU | 845 | Molybdenum, total | mg/L | 10/27/2022 - 05/15/2023 | CI around mean | 0.00200 | 0.10 | 0.078 | 0.1 | Standard |

TABLE 1. DETERMINATION OF POTENTIAL EXCEEDANCES
HISTORY OF POTENTIAL EXCEEDANCES
BALDWIN POWER PLANT
BOTTOM ASH POND
BALDWIN, ILLINOIS

| Sample Location | HSU | Program | Constituent | Result Unit | Sample Date Range | Statistical Calculation | Statistical Result | GWPS | Background | Part 845 Standard | GWPS Source |
|-----------------|-----|---------|--------------------------------|-------------|-------------------------|-------------------------|--------------------|--------|------------|-------------------|---------------------|
| MW-194 | UU | 845 | pH (field) | SU | 10/27/2022 - 05/15/2023 | CB around linear reg | 6.3/6.9 | 6.5/11 | 7.5/11.1 | 6.5/9 | Standard/Background |
| MW-194 | UU | 845 | Radium 226 + Radium 228, total | pCi/L | 10/27/2022 - 05/15/2023 | CI around mean | 0.160 | 5.0 | 3.8 | 5 | Standard |
| MW-194 | UU | 845 | Selenium, total | mg/L | 10/27/2022 - 05/15/2023 | All ND - Last | 0.001 | 0.050 | 0.0032 | 0.05 | Standard |
| MW-194 | UU | 845 | Sulfate, total | mg/L | 10/27/2022 - 05/15/2023 | CB around linear reg | 80.9 | 762 | 762 | 400 | Background |
| MW-194 | UU | 845 | Thallium, total | mg/L | 10/27/2022 - 05/15/2023 | All ND - Last | 0.002 | 0.002 | 0.002 | 0.002 | Standard |
| MW-194 | UU | 845 | Total Dissolved Solids | mg/L | 10/27/2022 - 05/15/2023 | CI around mean | 440 | 3260 | 3260 | 1200 | Background |
| MW-356 | UA | 257 | Antimony, total | mg/L | 12/29/2015 - 05/16/2023 | CI around median | 0.00100 | 0.006 | 0.0023 | 0.006 | Standard |
| MW-356 | UA | 257 | Arsenic, total | mg/L | 12/29/2015 - 05/16/2023 | CI around median | 0.00100 | 0.010 | 0.010 | 0.01 | Background |
| MW-356 | UA | 257 | Barium, total | mg/L | 12/29/2015 - 05/16/2023 | CI around median | 0.0297 | 2.0 | 0.26 | 2 | Standard |
| MW-356 | UA | 257 | Beryllium, total | mg/L | 12/29/2015 - 05/16/2023 | All ND - Last | 0.0005 | 0.004 | 0.0005 | 0.004 | Standard |
| MW-356 | UA | 257 | Boron, total | mg/L | 12/29/2015 - 05/16/2023 | CI around median | 1.94 | 2.2 | 2.2 | 2 | Background |
| MW-356 | UA | 257 | Cadmium, total | mg/L | 12/29/2015 - 05/16/2023 | All ND - Last | 0.002 | 0.005 | 0.002 | 0.005 | Standard |
| MW-356 | UA | 257 | Chloride, total | mg/L | 12/29/2015 - 05/16/2023 | CB around linear reg | 28.6 | 1370 | 1370 | 200 | Background |
| MW-356 | UA | 257 | Chromium, total | mg/L | 12/29/2015 - 05/16/2023 | All ND - Last | 0.005 | 0.10 | 0.013 | 0.1 | Standard |
| MW-356 | UA | 257 | Cobalt, total | mg/L | 12/29/2015 - 05/16/2023 | All ND - Last | 0.001 | 0.006 | 0.0022 | 0.006 | Standard |
| MW-356 | UA | 257 | Fluoride, total | mg/L | 12/29/2015 - 05/16/2023 | CI around mean | 1.92 | 4.0 | 3.8 | 4 | Standard |
| MW-356 | UA | 257 | Fluoride, total | mg/L | 12/29/2015 - 05/16/2023 | CI around mean | 1.92 | 4.0 | 3.8 | 4 | Standard |
| MW-356 | UA | 257 | Lead, total | mg/L | 12/29/2015 - 05/16/2023 | CI around median | 0.00100 | 0.0075 | 0.0022 | 0.0075 | Standard |
| MW-356 | UA | 257 | Lithium, total | mg/L | 12/29/2015 - 05/16/2023 | CB around linear reg | 0.0551 | 0.14 | 0.14 | 0.04 | Background |
| MW-356 | UA | 257 | Mercury, total | mg/L | 12/29/2015 - 05/16/2023 | All ND - Last | 0.0002 | 0.002 | 0.0002 | 0.002 | Standard |
| MW-356 | UA | 257 | Molybdenum, total | mg/L | 12/29/2015 - 05/16/2023 | CI around median | 0.00150 | 0.10 | 0.078 | 0.1 | Standard |
| MW-356 | UA | 257 | pH (field) | SU | 12/29/2015 - 05/16/2023 | CI around median | 7.7/7.8 | 6.5/11 | 7.5/11.1 | 6.5/9 | Standard/Background |
| MW-356 | UA | 257 | Radium 226 + Radium 228, total | pCi/L | 12/29/2015 - 05/16/2023 | CI around median | 0.100 | 5.0 | 3.8 | 5 | Standard |
| MW-356 | UA | 257 | Selenium, total | mg/L | 12/29/2015 - 05/16/2023 | All ND - Last | 0.001 | 0.050 | 0.0032 | 0.05 | Standard |
| MW-356 | UA | 257 | Sulfate, total | mg/L | 12/29/2015 - 05/16/2023 | CI around mean | 44.4 | 758 | 758 | 400 | Background |
| MW-356 | UA | 257 | Thallium, total | mg/L | 12/29/2015 - 05/16/2023 | All ND - Last | 0.002 | 0.002 | 0.002 | 0.002 | Standard |
| MW-356 | UA | 257 | Total Dissolved Solids | mg/L | 12/29/2015 - 05/16/2023 | CI around mean | 663 | 3260 | 3260 | 1200 | Background |

TABLE 1. DETERMINATION OF POTENTIAL EXCEEDANCES
HISTORY OF POTENTIAL EXCEEDANCES
BALDWIN POWER PLANT
BOTTOM ASH POND
BALDWIN, ILLINOIS

| Sample Location | HSU | Program | Constituent | Result Unit | Sample Date Range | Statistical Calculation | Statistical Result | GWPS | Background | Part 845 Standard | GWPS Source |
|-----------------|-----|---------|--------------------------------|-------------|-------------------------|-------------------------|--------------------|--------|------------|-------------------|---------------------|
| MW-369 | UA | 257 | Antimony, total | mg/L | 12/29/2015 - 05/16/2023 | CB around T-S line | -0.00196 | 0.006 | 0.0023 | 0.006 | Standard |
| MW-369 | UA | 257 | Arsenic, total | mg/L | 12/29/2015 - 05/16/2023 | CI around geomean | 0.00151 | 0.010 | 0.010 | 0.01 | Background |
| MW-369 | UA | 257 | Barium, total | mg/L | 12/29/2015 - 05/16/2023 | CB around T-S line | 0.0730 | 2.0 | 0.26 | 2 | Standard |
| MW-369 | UA | 257 | Beryllium, total | mg/L | 12/29/2015 - 05/16/2023 | All ND - Last | 0.0005 | 0.004 | 0.0005 | 0.004 | Standard |
| MW-369 | UA | 257 | Boron, total | mg/L | 12/29/2015 - 05/16/2023 | CB around linear reg | -0.171 | 2.2 | 2.2 | 2 | Background |
| MW-369 | UA | 257 | Cadmium, total | mg/L | 12/29/2015 - 05/16/2023 | All ND - Last | 0.002 | 0.005 | 0.002 | 0.005 | Standard |
| MW-369 | UA | 257 | Chloride, total | mg/L | 12/29/2015 - 05/16/2023 | CI around geomean | 84.1 | 1370 | 1370 | 200 | Background |
| MW-369 | UA | 257 | Chromium, total | mg/L | 12/29/2015 - 05/16/2023 | CB around T-S line | 0.00145 | 0.10 | 0.013 | 0.1 | Standard |
| MW-369 | UA | 257 | Cobalt, total | mg/L | 12/29/2015 - 05/16/2023 | CI around median | 0.00100 | 0.006 | 0.0022 | 0.006 | Standard |
| MW-369 | UA | 257 | Fluoride, total | mg/L | 12/29/2015 - 05/16/2023 | CB around T-S line | -0.139 | 4.0 | 3.8 | 4 | Standard |
| MW-369 | UA | 257 | Fluoride, total | mg/L | 12/29/2015 - 05/16/2023 | CB around T-S line | -0.139 | 4.0 | 3.8 | 4 | Standard |
| MW-369 | UA | 257 | Lead, total | mg/L | 12/29/2015 - 05/16/2023 | CI around median | 0.00100 | 0.0075 | 0.0022 | 0.0075 | Standard |
| MW-369 | UA | 257 | Lithium, total | mg/L | 12/29/2015 - 05/16/2023 | CI around mean | 0.0212 | 0.14 | 0.14 | 0.04 | Background |
| MW-369 | UA | 257 | Mercury, total | mg/L | 12/29/2015 - 05/16/2023 | All ND - Last | 0.0002 | 0.002 | 0.0002 | 0.002 | Standard |
| MW-369 | UA | 257 | Molybdenum, total | mg/L | 12/29/2015 - 05/16/2023 | CB around T-S line | -0.00666 | 0.10 | 0.078 | 0.1 | Standard |
| MW-369 | UA | 257 | pH (field) | SU | 12/29/2015 - 05/16/2023 | CB around linear reg | 6.5/8.1 | 6.5/11 | 7.5/11.1 | 6.5/9 | Standard/Background |
| MW-369 | UA | 257 | Radium 226 + Radium 228, total | pCi/L | 12/29/2015 - 05/16/2023 | CI around mean | 0.376 | 5.0 | 3.8 | 5 | Standard |
| MW-369 | UA | 257 | Selenium, total | mg/L | 12/29/2015 - 05/16/2023 | CB around T-S line | -0.0273 | 0.050 | 0.0032 | 0.05 | Standard |
| MW-369 | UA | 257 | Sulfate, total | mg/L | 12/29/2015 - 05/16/2023 | CB around T-S line | -73.6 | 758 | 758 | 400 | Background |
| MW-369 | UA | 257 | Thallium, total | mg/L | 12/29/2015 - 05/16/2023 | All ND - Last | 0.002 | 0.002 | 0.002 | 0.002 | Standard |
| MW-369 | UA | 257 | Total Dissolved Solids | mg/L | 12/29/2015 - 05/16/2023 | CI around median | 726 | 3260 | 3260 | 1200 | Background |
| MW-370 | UA | 257 | Antimony, total | mg/L | 12/29/2015 - 05/16/2023 | CB around T-S line | -0.000389 | 0.006 | 0.0023 | 0.006 | Standard |
| MW-370 | UA | 257 | Arsenic, total | mg/L | 12/29/2015 - 05/16/2023 | CB around T-S line | 0.000139 | 0.010 | 0.010 | 0.01 | Background |
| MW-370 | UA | 257 | Barium, total | mg/L | 12/29/2015 - 05/16/2023 | CB around T-S line | 0.0241 | 2.0 | 0.26 | 2 | Standard |
| MW-370 | UA | 257 | Beryllium, total | mg/L | 12/29/2015 - 05/16/2023 | All ND - Last | 0.0005 | 0.004 | 0.0005 | 0.004 | Standard |
| MW-370 | UA | 257 | Boron, total | mg/L | 12/29/2015 - 05/16/2023 | CI around median | 1.79 | 2.2 | 2.2 | 2 | Background |
| MW-370 | UA | 257 | Cadmium, total | mg/L | 12/29/2015 - 05/16/2023 | All ND - Last | 0.002 | 0.005 | 0.002 | 0.005 | Standard |

TABLE 1. DETERMINATION OF POTENTIAL EXCEEDANCES
HISTORY OF POTENTIAL EXCEEDANCES
BALDWIN POWER PLANT
BOTTOM ASH POND
BALDWIN, ILLINOIS

| Sample Location | HSU | Program | Constituent | Result Unit | Sample Date Range | Statistical Calculation | Statistical Result | GWPS | Background | Part 845 Standard | GWPS Source |
|-----------------|-----|---------|--------------------------------|-------------|-------------------------|-------------------------|--------------------|--------|------------|-------------------|---------------------|
| MW-370 | UA | 257 | Chloride, total | mg/L | 12/29/2015 - 05/16/2023 | CB around linear reg | 1380 | 1370 | 1370 | 200 | Background |
| MW-370 | UA | 257 | Chromium, total | mg/L | 12/29/2015 - 05/16/2023 | CB around T-S line | 0.00142 | 0.10 | 0.013 | 0.1 | Standard |
| MW-370 | UA | 257 | Cobalt, total | mg/L | 12/29/2015 - 05/16/2023 | CI around median | 0.00100 | 0.006 | 0.0022 | 0.006 | Standard |
| MW-370 | UA | 257 | Fluoride, total | mg/L | 12/29/2015 - 05/16/2023 | CB around linear reg | 3.02 | 4.0 | 3.8 | 4 | Standard |
| MW-370 | UA | 257 | Fluoride, total | mg/L | 12/29/2015 - 05/16/2023 | CB around linear reg | 3.02 | 4.0 | 3.8 | 4 | Standard |
| MW-370 | UA | 257 | Lead, total | mg/L | 12/29/2015 - 05/16/2023 | All ND - Last | 0.008 | 0.0075 | 0.0022 | 0.0075 | Standard |
| MW-370 | UA | 257 | Lithium, total | mg/L | 12/29/2015 - 05/16/2023 | CI around mean | 0.130 | 0.14 | 0.14 | 0.04 | Background |
| MW-370 | UA | 257 | Mercury, total | mg/L | 12/29/2015 - 05/16/2023 | All ND - Last | 0.0002 | 0.002 | 0.0002 | 0.002 | Standard |
| MW-370 | UA | 257 | Molybdenum, total | mg/L | 12/29/2015 - 05/16/2023 | CB around linear reg | 0.00644 | 0.10 | 0.078 | 0.1 | Standard |
| MW-370 | UA | 257 | pH (field) | SU | 12/29/2015 - 05/16/2023 | CB around linear reg | 7.3/7.6 | 6.5/11 | 7.5/11.1 | 6.5/9 | Standard/Background |
| MW-370 | UA | 257 | Radium 226 + Radium 228, total | pCi/L | 12/29/2015 - 05/16/2023 | CI around geomean | 0.517 | 5.0 | 3.8 | 5 | Standard |
| MW-370 | UA | 257 | Selenium, total | mg/L | 12/29/2015 - 05/16/2023 | Most recent sample | 0.00100 | 0.050 | 0.0032 | 0.05 | Standard |
| MW-370 | UA | 257 | Sulfate, total | mg/L | 12/29/2015 - 05/16/2023 | CI around mean | 248 | 758 | 758 | 400 | Background |
| MW-370 | UA | 257 | Thallium, total | mg/L | 12/29/2015 - 05/16/2023 | All ND - Last | 0.002 | 0.002 | 0.002 | 0.002 | Standard |
| MW-370 | UA | 257 | Total Dissolved Solids | mg/L | 12/29/2015 - 05/16/2023 | CB around linear reg | 2940 | 3260 | 3260 | 1200 | Background |
| MW-382 | UA | 257 | Antimony, total | mg/L | 12/29/2015 - 05/16/2023 | All ND - Last | 0.001 | 0.006 | 0.0023 | 0.006 | Standard |
| MW-382 | UA | 257 | Arsenic, total | mg/L | 12/29/2015 - 05/16/2023 | CI around median | 0.00110 | 0.010 | 0.010 | 0.01 | Background |
| MW-382 | UA | 257 | Barium, total | mg/L | 12/29/2015 - 05/16/2023 | CI around mean | 0.0172 | 2.0 | 0.26 | 2 | Standard |
| MW-382 | UA | 257 | Beryllium, total | mg/L | 12/29/2015 - 05/16/2023 | CI around median | 0.00100 | 0.004 | 0.0005 | 0.004 | Standard |
| MW-382 | UA | 257 | Boron, total | mg/L | 12/29/2015 - 05/16/2023 | CI around median | 1.72 | 2.2 | 2.2 | 2 | Background |
| MW-382 | UA | 257 | Cadmium, total | mg/L | 12/29/2015 - 05/16/2023 | All ND - Last | 0.002 | 0.005 | 0.002 | 0.005 | Standard |
| MW-382 | UA | 257 | Chloride, total | mg/L | 12/29/2015 - 05/16/2023 | CI around mean | 34.9 | 1370 | 1370 | 200 | Background |
| MW-382 | UA | 257 | Chromium, total | mg/L | 12/29/2015 - 05/16/2023 | CB around linear reg | 0.00577 | 0.10 | 0.013 | 0.1 | Standard |
| MW-382 | UA | 257 | Cobalt, total | mg/L | 12/29/2015 - 05/16/2023 | CB around T-S line | 0.00100 | 0.006 | 0.0022 | 0.006 | Standard |
| MW-382 | UA | 257 | Fluoride, total | mg/L | 12/29/2015 - 05/16/2023 | CI around geomean | 2.80 | 4.0 | 3.8 | 4 | Standard |
| MW-382 | UA | 257 | Fluoride, total | mg/L | 12/29/2015 - 05/16/2023 | CI around geomean | 2.80 | 4.0 | 3.8 | 4 | Standard |
| MW-382 | UA | 257 | Lead, total | mg/L | 12/29/2015 - 05/16/2023 | CB around T-S line | 0.00100 | 0.0075 | 0.0022 | 0.0075 | Standard |

TABLE 1. DETERMINATION OF POTENTIAL EXCEEDANCES
HISTORY OF POTENTIAL EXCEEDANCES
BALDWIN POWER PLANT
BOTTOM ASH POND
BALDWIN, ILLINOIS

| Sample Location | HSU | Program | Constituent | Result Unit | Sample Date Range | Statistical Calculation | Statistical Result | GWPS | Background | Part 845 Standard | GWPS Source |
|-----------------|-----|---------|--------------------------------|-------------|-------------------------|-------------------------|--------------------|--------|------------|-------------------|---------------------|
| MW-382 | UA | 257 | Lithium, total | mg/L | 12/29/2015 - 05/16/2023 | CI around mean | 0.0580 | 0.14 | 0.14 | 0.04 | Background |
| MW-382 | UA | 257 | Mercury, total | mg/L | 12/29/2015 - 05/16/2023 | All ND - Last | 0.0002 | 0.002 | 0.0002 | 0.002 | Standard |
| MW-382 | UA | 257 | Molybdenum, total | mg/L | 12/29/2015 - 05/16/2023 | CB around T-S line | 0.00222 | 0.10 | 0.078 | 0.1 | Standard |
| MW-382 | UA | 257 | pH (field) | SU | 12/29/2015 - 05/16/2023 | CI around mean | 7.7/7.9 | 6.5/11 | 7.5/11.1 | 6.5/9 | Standard/Background |
| MW-382 | UA | 257 | Radium 226 + Radium 228, total | pCi/L | 12/29/2015 - 05/16/2023 | CI around geomean | 0.289 | 5.0 | 3.8 | 5 | Standard |
| MW-382 | UA | 257 | Selenium, total | mg/L | 12/29/2015 - 05/16/2023 | All ND - Last | 0.001 | 0.050 | 0.0032 | 0.05 | Standard |
| MW-382 | UA | 257 | Sulfate, total | mg/L | 12/29/2015 - 05/16/2023 | CB around linear reg | 354 | 758 | 758 | 400 | Background |
| MW-382 | UA | 257 | Thallium, total | mg/L | 12/29/2015 - 05/16/2023 | All ND - Last | 0.002 | 0.002 | 0.002 | 0.002 | Standard |
| MW-382 | UA | 257 | Total Dissolved Solids | mg/L | 12/29/2015 - 05/16/2023 | CB around linear reg | 1060 | 3260 | 3260 | 1200 | Background |
| MW-392 | UA | 845 | Antimony, total | mg/L | 10/27/2022 - 05/16/2023 | CI around median | 0.00100 | 0.006 | 0.0023 | 0.006 | Standard |
| MW-392 | UA | 845 | Arsenic, total | mg/L | 10/27/2022 - 05/16/2023 | CI around geomean | 0.000901 | 0.010 | 0.010 | 0.01 | Background |
| MW-392 | UA | 845 | Barium, total | mg/L | 10/27/2022 - 05/16/2023 | CI around mean | 0.0345 | 2.0 | 0.26 | 2 | Standard |
| MW-392 | UA | 845 | Beryllium, total | mg/L | 10/27/2022 - 05/16/2023 | All ND - Last | 0.0005 | 0.004 | 0.0005 | 0.004 | Standard |
| MW-392 | UA | 845 | Boron, total | mg/L | 10/27/2022 - 05/16/2023 | CI around mean | 1.58 | 2.2 | 2.2 | 2 | Background |
| MW-392 | UA | 845 | Cadmium, total | mg/L | 10/27/2022 - 05/16/2023 | All ND - Last | 0.002 | 0.005 | 0.002 | 0.005 | Standard |
| MW-392 | UA | 845 | Chloride, total | mg/L | 10/27/2022 - 05/16/2023 | CI around median | 334 | 1370 | 1370 | 200 | Background |
| MW-392 | UA | 845 | Chromium, total | mg/L | 10/27/2022 - 05/16/2023 | CI around median | 0.00150 | 0.10 | 0.013 | 0.1 | Standard |
| MW-392 | UA | 845 | Cobalt, total | mg/L | 10/27/2022 - 05/16/2023 | CI around median | 0.00100 | 0.006 | 0.0022 | 0.006 | Standard |
| MW-392 | UA | 845 | Fluoride, total | mg/L | 10/27/2022 - 05/16/2023 | CB around linear reg | 3.63 | 4.0 | 3.8 | 4 | Standard |
| MW-392 | UA | 845 | Lead, total | mg/L | 10/27/2022 - 05/16/2023 | CI around median | 0.00100 | 0.0075 | 0.0022 | 0.0075 | Standard |
| MW-392 | UA | 845 | Lithium, total | mg/L | 10/27/2022 - 05/16/2023 | CI around mean | 0.0497 | 0.14 | 0.14 | 0.04 | Background |
| MW-392 | UA | 845 | Mercury, total | mg/L | 10/27/2022 - 05/16/2023 | All ND - Last | 0.0002 | 0.002 | 0.0002 | 0.002 | Standard |
| MW-392 | UA | 845 | Molybdenum, total | mg/L | 10/27/2022 - 05/16/2023 | CI around median | 0.00150 | 0.10 | 0.078 | 0.1 | Standard |
| MW-392 | UA | 845 | pH (field) | SU | 10/27/2022 - 05/16/2023 | CI around mean | 7.3/7.9 | 6.5/11 | 7.5/11.1 | 6.5/9 | Standard/Background |
| MW-392 | UA | 845 | Radium 226 + Radium 228, total | pCi/L | 10/27/2022 - 05/16/2023 | CI around mean | 0.237 | 5.0 | 3.8 | 5 | Standard |
| MW-392 | UA | 845 | Selenium, total | mg/L | 10/27/2022 - 05/16/2023 | All ND - Last | 0.001 | 0.050 | 0.0032 | 0.05 | Standard |
| MW-392 | UA | 845 | Sulfate, total | mg/L | 10/27/2022 - 05/16/2023 | CI around geomean | 45.9 | 762 | 762 | 400 | Background |

TABLE 1. DETERMINATION OF POTENTIAL EXCEEDANCES
HISTORY OF POTENTIAL EXCEEDANCES
BALDWIN POWER PLANT
BOTTOM ASH POND
BALDWIN, ILLINOIS

| Sample Location | HSU | Program | Constituent | Result Unit | Sample Date Range | Statistical Calculation | Statistical Result | GWPS | Background | Part 845 Standard | GWPS Source |
|-----------------|-----|---------|--------------------------------|-------------|-------------------------|-------------------------|--------------------|--------|------------|-------------------|---------------------|
| MW-392 | UA | 845 | Thallium, total | mg/L | 10/27/2022 - 05/16/2023 | All ND - Last | 0.002 | 0.002 | 0.002 | 0.002 | Standard |
| MW-392 | UA | 845 | Total Dissolved Solids | mg/L | 10/27/2022 - 05/16/2023 | CI around mean | 1410 | 3260 | 3260 | 1200 | Background |
| MW-393 | UA | 845 | Antimony, total | mg/L | 10/27/2022 - 05/15/2023 | CI around median | 0.00100 | 0.006 | 0.0023 | 0.006 | Standard |
| MW-393 | UA | 845 | Arsenic, total | mg/L | 10/27/2022 - 05/15/2023 | CI around median | 0.00100 | 0.010 | 0.010 | 0.01 | Background |
| MW-393 | UA | 845 | Barium, total | mg/L | 10/27/2022 - 05/15/2023 | CI around geomean | 0.0224 | 2.0 | 0.26 | 2 | Standard |
| MW-393 | UA | 845 | Beryllium, total | mg/L | 10/27/2022 - 05/15/2023 | All ND - Last | 0.0005 | 0.004 | 0.0005 | 0.004 | Standard |
| MW-393 | UA | 845 | Boron, total | mg/L | 10/27/2022 - 05/15/2023 | CI around mean | 1.47 | 2.2 | 2.2 | 2 | Background |
| MW-393 | UA | 845 | Cadmium, total | mg/L | 10/27/2022 - 05/15/2023 | All ND - Last | 0.002 | 0.005 | 0.002 | 0.005 | Standard |
| MW-393 | UA | 845 | Chloride, total | mg/L | 10/27/2022 - 05/15/2023 | CB around linear reg | 617 | 1370 | 1370 | 200 | Background |
| MW-393 | UA | 845 | Chromium, total | mg/L | 10/27/2022 - 05/15/2023 | CI around median | 0.00150 | 0.10 | 0.013 | 0.1 | Standard |
| MW-393 | UA | 845 | Cobalt, total | mg/L | 10/27/2022 - 05/15/2023 | CI around median | 0.00100 | 0.006 | 0.0022 | 0.006 | Standard |
| MW-393 | UA | 845 | Fluoride, total | mg/L | 10/27/2022 - 05/15/2023 | CB around linear reg | 7.49 | 4.0 | 3.8 | 4 | Standard |
| MW-393 | UA | 845 | Lead, total | mg/L | 10/27/2022 - 05/15/2023 | All ND - Last | 0.008 | 0.0075 | 0.0022 | 0.0075 | Standard |
| MW-393 | UA | 845 | Lithium, total | mg/L | 10/27/2022 - 05/15/2023 | CI around mean | 0.0519 | 0.14 | 0.14 | 0.04 | Background |
| MW-393 | UA | 845 | Mercury, total | mg/L | 10/27/2022 - 05/15/2023 | All ND - Last | 0.0002 | 0.002 | 0.0002 | 0.002 | Standard |
| MW-393 | UA | 845 | Molybdenum, total | mg/L | 10/27/2022 - 05/15/2023 | CI around mean | -0.000199 | 0.10 | 0.078 | 0.1 | Standard |
| MW-393 | UA | 845 | pH (field) | SU | 10/27/2022 - 05/15/2023 | CI around mean | 7.7/8.4 | 6.5/11 | 7.5/11.1 | 6.5/9 | Standard/Background |
| MW-393 | UA | 845 | Radium 226 + Radium 228, total | pCi/L | 10/27/2022 - 05/15/2023 | CI around mean | 0.0868 | 5.0 | 3.8 | 5 | Standard |
| MW-393 | UA | 845 | Selenium, total | mg/L | 10/27/2022 - 05/15/2023 | All ND - Last | 0.001 | 0.050 | 0.0032 | 0.05 | Standard |
| MW-393 | UA | 845 | Sulfate, total | mg/L | 10/27/2022 - 05/15/2023 | CB around linear reg | 104 | 762 | 762 | 400 | Background |
| MW-393 | UA | 845 | Thallium, total | mg/L | 10/27/2022 - 05/15/2023 | All ND - Last | 0.002 | 0.002 | 0.002 | 0.002 | Standard |
| MW-393 | UA | 845 | Total Dissolved Solids | mg/L | 10/27/2022 - 05/15/2023 | CI around median | 826 | 3260 | 3260 | 1200 | Background |
| MW-394 | UA | 845 | Antimony, total | mg/L | 10/27/2022 - 05/15/2023 | CI around mean | 0.000850 | 0.006 | 0.0023 | 0.006 | Standard |
| MW-394 | UA | 845 | Arsenic, total | mg/L | 10/27/2022 - 05/15/2023 | CI around median | 0.00100 | 0.010 | 0.010 | 0.01 | Background |
| MW-394 | UA | 845 | Barium, total | mg/L | 10/27/2022 - 05/15/2023 | CI around mean | 0.0258 | 2.0 | 0.26 | 2 | Standard |
| MW-394 | UA | 845 | Beryllium, total | mg/L | 10/27/2022 - 05/15/2023 | All ND - Last | 0.0005 | 0.004 | 0.0005 | 0.004 | Standard |
| MW-394 | UA | 845 | Boron, total | mg/L | 10/27/2022 - 05/15/2023 | CI around mean | 1.53 | 2.2 | 2.2 | 2 | Background |

TABLE 1. DETERMINATION OF POTENTIAL EXCEEDANCES
HISTORY OF POTENTIAL EXCEEDANCES
BALDWIN POWER PLANT
BOTTOM ASH POND
BALDWIN, ILLINOIS

| Sample Location | HSU | Program | Constituent | Result Unit | Sample Date Range | Statistical Calculation | Statistical Result | GWPS | Background | Part 845 Standard | GWPS Source |
|-----------------|-----|---------|--------------------------------|-------------|-------------------------|-------------------------|--------------------|--------|------------|-------------------|---------------------|
| MW-394 | UA | 845 | Cadmium, total | mg/L | 10/27/2022 - 05/15/2023 | All ND - Last | 0.002 | 0.005 | 0.002 | 0.005 | Standard |
| MW-394 | UA | 845 | Chloride, total | mg/L | 10/27/2022 - 05/15/2023 | CI around mean | 490 | 1370 | 1370 | 200 | Background |
| MW-394 | UA | 845 | Chromium, total | mg/L | 10/27/2022 - 05/15/2023 | CI around mean | -0.00000691 | 0.10 | 0.013 | 0.1 | Standard |
| MW-394 | UA | 845 | Cobalt, total | mg/L | 10/27/2022 - 05/15/2023 | CI around median | 0.00100 | 0.006 | 0.0022 | 0.006 | Standard |
| MW-394 | UA | 845 | Fluoride, total | mg/L | 10/27/2022 - 05/15/2023 | CI around mean | 3.25 | 4.0 | 3.8 | 4 | Standard |
| MW-394 | UA | 845 | Lead, total | mg/L | 10/27/2022 - 05/15/2023 | CI around median | 0.00100 | 0.0075 | 0.0022 | 0.0075 | Standard |
| MW-394 | UA | 845 | Lithium, total | mg/L | 10/27/2022 - 05/15/2023 | CI around mean | 0.0438 | 0.14 | 0.14 | 0.04 | Background |
| MW-394 | UA | 845 | Mercury, total | mg/L | 10/27/2022 - 05/15/2023 | All ND - Last | 0.0002 | 0.002 | 0.0002 | 0.002 | Standard |
| MW-394 | UA | 845 | Molybdenum, total | mg/L | 10/27/2022 - 05/15/2023 | CI around mean | 0.00443 | 0.10 | 0.078 | 0.1 | Standard |
| MW-394 | UA | 845 | pH (field) | SU | 10/27/2022 - 05/15/2023 | CI around mean | 7.6/8.1 | 6.5/11 | 7.5/11.1 | 6.5/9 | Standard/Background |
| MW-394 | UA | 845 | Radium 226 + Radium 228, total | pCi/L | 10/27/2022 - 05/15/2023 | CI around mean | 0.301 | 5.0 | 3.8 | 5 | Standard |
| MW-394 | UA | 845 | Selenium, total | mg/L | 10/27/2022 - 05/15/2023 | Most recent sample | 0.00100 | 0.050 | 0.0032 | 0.05 | Standard |
| MW-394 | UA | 845 | Sulfate, total | mg/L | 10/27/2022 - 05/15/2023 | CB around linear reg | 77.3 | 762 | 762 | 400 | Background |
| MW-394 | UA | 845 | Thallium, total | mg/L | 10/27/2022 - 05/15/2023 | All ND - Last | 0.002 | 0.002 | 0.002 | 0.002 | Standard |
| MW-394 | UA | 845 | Total Dissolved Solids | mg/L | 10/27/2022 - 05/15/2023 | CI around mean | 1770 | 3260 | 3260 | 1200 | Background |
| OW-256 | UU | 257 | Antimony, total | mg/L | 03/14/2023 - 05/17/2023 | Most recent sample | 0.001 | 0.006 | 0.0023 | 0.006 | Standard |
| OW-256 | UU | 257 | Arsenic, total | mg/L | 03/14/2023 - 05/17/2023 | Most recent sample | 0.0100 | 0.010 | 0.010 | 0.01 | Background |
| OW-256 | UU | 257 | Barium, total | mg/L | 03/14/2023 - 05/17/2023 | Most recent sample | 0.102 | 2.0 | 0.26 | 2 | Standard |
| OW-256 | UU | 257 | Beryllium, total | mg/L | 03/14/2023 - 05/17/2023 | Most recent sample | 0.0005 | 0.004 | 0.0005 | 0.004 | Standard |
| OW-256 | UU | 257 | Boron, total | mg/L | 03/14/2023 - 05/17/2023 | Most recent sample | 0.187 | 2.2 | 2.2 | 2 | Background |
| OW-256 | UU | 257 | Cadmium, total | mg/L | 03/14/2023 - 05/17/2023 | Most recent sample | 0.002 | 0.005 | 0.002 | 0.005 | Standard |
| OW-256 | UU | 257 | Chloride, total | mg/L | 03/14/2023 - 05/17/2023 | Most recent sample | 54.0 | 1370 | 1370 | 200 | Background |
| OW-256 | UU | 257 | Chromium, total | mg/L | 03/14/2023 - 05/17/2023 | Most recent sample | 0.005 | 0.10 | 0.013 | 0.1 | Standard |
| OW-256 | UU | 257 | Cobalt, total | mg/L | 03/14/2023 - 05/17/2023 | Most recent sample | 0.00150 | 0.006 | 0.0022 | 0.006 | Standard |
| OW-256 | UU | 257 | Fluoride, total | mg/L | 03/14/2023 - 05/17/2023 | Most recent sample | 0.250 | 4.0 | 3.8 | 4 | Standard |
| OW-256 | UU | 257 | Fluoride, total | mg/L | 03/14/2023 - 05/17/2023 | Most recent sample | 0.250 | 4.0 | 3.8 | 4 | Standard |
| OW-256 | UU | 257 | Lead, total | mg/L | 03/14/2023 - 05/17/2023 | Most recent sample | 0.008 | 0.0075 | 0.0022 | 0.0075 | Standard |

TABLE 1. DETERMINATION OF POTENTIAL EXCEEDANCES
HISTORY OF POTENTIAL EXCEEDANCES
BALDWIN POWER PLANT
BOTTOM ASH POND
BALDWIN, ILLINOIS

| Sample Location | HSU | Program | Constituent | Result Unit | Sample Date Range | Statistical Calculation | Statistical Result | GWPS | Background | Part 845 Standard | GWPS Source |
|-----------------|-----|---------|--------------------------------|-------------|-------------------------|-------------------------|--------------------|--------|------------|-------------------|---------------------|
| OW-256 | UU | 257 | Lithium, total | mg/L | 03/14/2023 - 05/17/2023 | Most recent sample | 0.00500 | 0.14 | 0.14 | 0.04 | Background |
| OW-256 | UU | 257 | Mercury, total | mg/L | 03/14/2023 - 05/17/2023 | Most recent sample | 0.0002 | 0.002 | 0.0002 | 0.002 | Standard |
| OW-256 | UU | 257 | Molybdenum, total | mg/L | 03/14/2023 - 05/17/2023 | Most recent sample | 0.01 | 0.10 | 0.078 | 0.1 | Standard |
| OW-256 | UU | 257 | pH (field) | SU | 03/14/2023 - 05/17/2023 | Most recent sample | 6.7/6.7 | 6.5/11 | 7.5/11.1 | 6.5/9 | Standard/Background |
| OW-256 | UU | 257 | Radium 226 + Radium 228, total | pCi/L | 03/14/2023 - 05/17/2023 | Most recent sample | 0.717 | 5.0 | 3.8 | 5 | Standard |
| OW-256 | UU | 257 | Selenium, total | mg/L | 03/14/2023 - 05/17/2023 | Most recent sample | 0.001 | 0.050 | 0.0032 | 0.05 | Standard |
| OW-256 | UU | 257 | Sulfate, total | mg/L | 03/14/2023 - 05/17/2023 | Most recent sample | 64.0 | 758 | 758 | 400 | Background |
| OW-256 | UU | 257 | Thallium, total | mg/L | 03/14/2023 - 05/17/2023 | Most recent sample | 0.002 | 0.002 | 0.002 | 0.002 | Standard |
| OW-256 | UU | 257 | Total Dissolved Solids | mg/L | 03/14/2023 - 05/17/2023 | Most recent sample | 514 | 3260 | 3260 | 1200 | Background |
| OW-257 | UU | 257 | Antimony, total | mg/L | 03/14/2023 - 05/17/2023 | Most recent sample | 0.00500 | 0.006 | 0.0023 | 0.006 | Standard |
| OW-257 | UU | 257 | Arsenic, total | mg/L | 03/14/2023 - 05/17/2023 | Most recent sample | 0.103 | 0.010 | 0.010 | 0.01 | Background |
| OW-257 | UU | 257 | Barium, total | mg/L | 03/14/2023 - 05/17/2023 | Most recent sample | 0.975 | 2.0 | 0.26 | 2 | Standard |
| OW-257 | UU | 257 | Beryllium, total | mg/L | 03/14/2023 - 05/17/2023 | Most recent sample | 0.00970 | 0.004 | 0.0005 | 0.004 | Standard |
| OW-257 | UU | 257 | Boron, total | mg/L | 03/14/2023 - 05/17/2023 | Most recent sample | 0.490 | 2.2 | 2.2 | 2 | Background |
| OW-257 | UU | 257 | Cadmium, total | mg/L | 03/14/2023 - 05/17/2023 | Most recent sample | 0.00450 | 0.005 | 0.002 | 0.005 | Standard |
| OW-257 | UU | 257 | Chloride, total | mg/L | 03/14/2023 - 05/17/2023 | Most recent sample | 7.00 | 1370 | 1370 | 200 | Background |
| OW-257 | UU | 257 | Chromium, total | mg/L | 03/14/2023 - 05/17/2023 | Most recent sample | 0.214 | 0.10 | 0.013 | 0.1 | Standard |
| OW-257 | UU | 257 | Cobalt, total | mg/L | 03/14/2023 - 05/17/2023 | Most recent sample | 0.203 | 0.006 | 0.0022 | 0.006 | Standard |
| OW-257 | UU | 257 | Fluoride, total | mg/L | 03/14/2023 - 05/17/2023 | Most recent sample | 0.370 | 4.0 | 3.8 | 4 | Standard |
| OW-257 | UU | 257 | Fluoride, total | mg/L | 03/14/2023 - 05/17/2023 | Most recent sample | 0.370 | 4.0 | 3.8 | 4 | Standard |
| OW-257 | UU | 257 | Lead, total | mg/L | 03/14/2023 - 05/17/2023 | Most recent sample | 0.214 | 0.0075 | 0.0022 | 0.0075 | Standard |
| OW-257 | UU | 257 | Lithium, total | mg/L | 03/14/2023 - 05/17/2023 | Most recent sample | 0.207 | 0.14 | 0.14 | 0.04 | Background |
| OW-257 | UU | 257 | Mercury, total | mg/L | 03/14/2023 - 05/17/2023 | Most recent sample | 0.0002 | 0.002 | 0.0002 | 0.002 | Standard |
| OW-257 | UU | 257 | Molybdenum, total | mg/L | 03/14/2023 - 05/17/2023 | Most recent sample | 0.0100 | 0.10 | 0.078 | 0.1 | Standard |
| OW-257 | UU | 257 | pH (field) | SU | 03/14/2023 - 05/17/2023 | Most recent sample | 6.8/6.8 | 6.5/11 | 7.5/11.1 | 6.5/9 | Standard/Background |
| OW-257 | UU | 257 | Radium 226 + Radium 228, total | pCi/L | 03/14/2023 - 05/17/2023 | Most recent sample | 25.3 | 5.0 | 3.8 | 5 | Standard |
| OW-257 | UU | 257 | Selenium, total | mg/L | 03/14/2023 - 05/17/2023 | Most recent sample | 0.001 | 0.050 | 0.0032 | 0.05 | Standard |

TABLE 1. DETERMINATION OF POTENTIAL EXCEEDANCES
HISTORY OF POTENTIAL EXCEEDANCES
BALDWIN POWER PLANT
BOTTOM ASH POND
BALDWIN, ILLINOIS

| Sample Location | HSU | Program | Constituent | Result Unit | Sample Date Range | Statistical Calculation | Statistical Result | GWPS | Background | Part 845 Standard | GWPS Source |
|-----------------|-----|---------|--------------------------------|-------------|-------------------------|-------------------------|--------------------|--------|------------|-------------------|---------------------|
| OW-257 | UU | 257 | Sulfate, total | mg/L | 03/14/2023 - 05/17/2023 | Most recent sample | 118 | 758 | 758 | 400 | Background |
| OW-257 | UU | 257 | Thallium, total | mg/L | 03/14/2023 - 05/17/2023 | Most recent sample | 0.01 | 0.002 | 0.002 | 0.002 | Standard |
| OW-257 | UU | 257 | Total Dissolved Solids | mg/L | 03/14/2023 - 05/17/2023 | Most recent sample | 1270 | 3260 | 3260 | 1200 | Background |
| PZ-170 | UU | 257 | Antimony, total | mg/L | 03/14/2023 - 05/17/2023 | Most recent sample | 0.00100 | 0.006 | 0.0023 | 0.006 | Standard |
| PZ-170 | UU | 257 | Arsenic, total | mg/L | 03/14/2023 - 05/17/2023 | Most recent sample | 0.01 | 0.010 | 0.010 | 0.01 | Background |
| PZ-170 | UU | 257 | Barium, total | mg/L | 03/14/2023 - 05/17/2023 | Most recent sample | 0.0975 | 2.0 | 0.26 | 2 | Standard |
| PZ-170 | UU | 257 | Beryllium, total | mg/L | 03/14/2023 - 05/17/2023 | Most recent sample | 0.0005 | 0.004 | 0.0005 | 0.004 | Standard |
| PZ-170 | UU | 257 | Boron, total | mg/L | 03/14/2023 - 05/17/2023 | Most recent sample | 0.267 | 2.2 | 2.2 | 2 | Background |
| PZ-170 | UU | 257 | Cadmium, total | mg/L | 03/14/2023 - 05/17/2023 | Most recent sample | 0.002 | 0.005 | 0.002 | 0.005 | Standard |
| PZ-170 | UU | 257 | Chloride, total | mg/L | 03/14/2023 - 05/17/2023 | Most recent sample | 35.0 | 1370 | 1370 | 200 | Background |
| PZ-170 | UU | 257 | Chromium, total | mg/L | 03/14/2023 - 05/17/2023 | Most recent sample | 0.00500 | 0.10 | 0.013 | 0.1 | Standard |
| PZ-170 | UU | 257 | Cobalt, total | mg/L | 03/14/2023 - 05/17/2023 | Most recent sample | 0.00460 | 0.006 | 0.0022 | 0.006 | Standard |
| PZ-170 | UU | 257 | Fluoride, total | mg/L | 03/14/2023 - 05/17/2023 | Most recent sample | 0.180 | 4.0 | 3.8 | 4 | Standard |
| PZ-170 | UU | 257 | Fluoride, total | mg/L | 03/14/2023 - 05/17/2023 | Most recent sample | 0.180 | 4.0 | 3.8 | 4 | Standard |
| PZ-170 | UU | 257 | Lead, total | mg/L | 03/14/2023 - 05/17/2023 | Most recent sample | 0.008 | 0.0075 | 0.0022 | 0.0075 | Standard |
| PZ-170 | UU | 257 | Lithium, total | mg/L | 03/14/2023 - 05/17/2023 | Most recent sample | 0.0291 | 0.14 | 0.14 | 0.04 | Background |
| PZ-170 | UU | 257 | Mercury, total | mg/L | 03/14/2023 - 05/17/2023 | Most recent sample | 0.0002 | 0.002 | 0.0002 | 0.002 | Standard |
| PZ-170 | UU | 257 | Molybdenum, total | mg/L | 03/14/2023 - 05/17/2023 | Most recent sample | 0.01 | 0.10 | 0.078 | 0.1 | Standard |
| PZ-170 | UU | 257 | pH (field) | SU | 03/14/2023 - 05/17/2023 | Most recent sample | 6.5/6.5 | 6.5/11 | 7.5/11.1 | 6.5/9 | Standard/Background |
| PZ-170 | UU | 257 | Radium 226 + Radium 228, total | pCi/L | 03/14/2023 - 05/17/2023 | Most recent sample | 0.181 | 5.0 | 3.8 | 5 | Standard |
| PZ-170 | UU | 257 | Selenium, total | mg/L | 03/14/2023 - 05/17/2023 | Most recent sample | 0.001 | 0.050 | 0.0032 | 0.05 | Standard |
| PZ-170 | UU | 257 | Sulfate, total | mg/L | 03/14/2023 - 05/17/2023 | Most recent sample | 170 | 758 | 758 | 400 | Background |
| PZ-170 | UU | 257 | Thallium, total | mg/L | 03/14/2023 - 05/17/2023 | Most recent sample | 0.002 | 0.002 | 0.002 | 0.002 | Standard |
| PZ-170 | UU | 257 | Total Dissolved Solids | mg/L | 03/14/2023 - 05/17/2023 | Most recent sample | 730 | 3260 | 3260 | 1200 | Background |
| PZ-182 | UU | 257 | Antimony, total | mg/L | 03/14/2023 - 05/17/2023 | Most recent sample | 0.001 | 0.006 | 0.0023 | 0.006 | Standard |
| PZ-182 | UU | 257 | Arsenic, total | mg/L | 03/14/2023 - 05/17/2023 | Most recent sample | 0.0100 | 0.010 | 0.010 | 0.01 | Background |
| PZ-182 | UU | 257 | Barium, total | mg/L | 03/14/2023 - 05/17/2023 | Most recent sample | 0.0692 | 2.0 | 0.26 | 2 | Standard |

TABLE 1. DETERMINATION OF POTENTIAL EXCEEDANCES
HISTORY OF POTENTIAL EXCEEDANCES
BALDWIN POWER PLANT
BOTTOM ASH POND
BALDWIN, ILLINOIS

| Sample Location | HSU | Program | Constituent | Result Unit | Sample Date Range | Statistical Calculation | Statistical Result | GWPS | Background | Part 845 Standard | GWPS Source |
|-----------------|-----|---------|--------------------------------|-------------|-------------------------|-------------------------|--------------------|--------|------------|-------------------|---------------------|
| PZ-182 | UU | 257 | Beryllium, total | mg/L | 03/14/2023 - 05/17/2023 | Most recent sample | 0.0005 | 0.004 | 0.0005 | 0.004 | Standard |
| PZ-182 | UU | 257 | Boron, total | mg/L | 03/14/2023 - 05/17/2023 | Most recent sample | 0.484 | 2.2 | 2.2 | 2 | Background |
| PZ-182 | UU | 257 | Cadmium, total | mg/L | 03/14/2023 - 05/17/2023 | Most recent sample | 0.002 | 0.005 | 0.002 | 0.005 | Standard |
| PZ-182 | UU | 257 | Chloride, total | mg/L | 03/14/2023 - 05/17/2023 | Most recent sample | 88.0 | 1370 | 1370 | 200 | Background |
| PZ-182 | UU | 257 | Chromium, total | mg/L | 03/14/2023 - 05/17/2023 | Most recent sample | 0.005 | 0.10 | 0.013 | 0.1 | Standard |
| PZ-182 | UU | 257 | Cobalt, total | mg/L | 03/14/2023 - 05/17/2023 | Most recent sample | 0.00100 | 0.006 | 0.0022 | 0.006 | Standard |
| PZ-182 | UU | 257 | Fluoride, total | mg/L | 03/14/2023 - 05/17/2023 | Most recent sample | 0.190 | 4.0 | 3.8 | 4 | Standard |
| PZ-182 | UU | 257 | Fluoride, total | mg/L | 03/14/2023 - 05/17/2023 | Most recent sample | 0.190 | 4.0 | 3.8 | 4 | Standard |
| PZ-182 | UU | 257 | Lead, total | mg/L | 03/14/2023 - 05/17/2023 | Most recent sample | 0.00750 | 0.0075 | 0.0022 | 0.0075 | Standard |
| PZ-182 | UU | 257 | Lithium, total | mg/L | 03/14/2023 - 05/17/2023 | Most recent sample | 0.00690 | 0.14 | 0.14 | 0.04 | Background |
| PZ-182 | UU | 257 | Mercury, total | mg/L | 03/14/2023 - 05/17/2023 | Most recent sample | 0.0002 | 0.002 | 0.0002 | 0.002 | Standard |
| PZ-182 | UU | 257 | Molybdenum, total | mg/L | 03/14/2023 - 05/17/2023 | Most recent sample | 0.01 | 0.10 | 0.078 | 0.1 | Standard |
| PZ-182 | UU | 257 | pH (field) | SU | 03/14/2023 - 05/17/2023 | Most recent sample | 6.6/6.6 | 6.5/11 | 7.5/11.1 | 6.5/9 | Standard/Background |
| PZ-182 | UU | 257 | Radium 226 + Radium 228, total | pCi/L | 03/14/2023 - 05/17/2023 | Most recent sample | 0.925 | 5.0 | 3.8 | 5 | Standard |
| PZ-182 | UU | 257 | Selenium, total | mg/L | 03/14/2023 - 05/17/2023 | Most recent sample | 0.001 | 0.050 | 0.0032 | 0.05 | Standard |
| PZ-182 | UU | 257 | Sulfate, total | mg/L | 03/14/2023 - 05/17/2023 | Most recent sample | 254 | 758 | 758 | 400 | Background |
| PZ-182 | UU | 257 | Thallium, total | mg/L | 03/14/2023 - 05/17/2023 | Most recent sample | 0.002 | 0.002 | 0.002 | 0.002 | Standard |
| PZ-182 | UU | 257 | Total Dissolved Solids | mg/L | 03/14/2023 - 05/17/2023 | Most recent sample | 1120 | 3260 | 3260 | 1200 | Background |

TABLE 1. DETERMINATION OF POTENTIAL EXCEEDANCES
HISTORY OF POTENTIAL EXCEEDANCES
BALDWIN POWER PLANT
BOTTOM ASH POND
BALDWIN, ILLINOIS

Notes:

Potential exceedance of GWPS

HSU = hydrostratigraphic unit:
 UA = Uppermost Aquifer
 UU = Upper Unit
Program = regulatory program data were collected under:
 257 = 40 C.F.R. Part 257 Subpart D (Standards for the Disposal of Coal Combustion Residuals in Landfills and Surface Impoundments)
 845 = 35 I.A.C. Part 845 (Sampling events completed to assess well locations for inclusion in the Part 845 monitoring well network)
mg/L = milligrams per liter
pCi/L = picocuries per liter
SU = standard units
Sample Count = number of samples from Sampled Date Range used to calculate the Statistical Result
Statistical Calculation = method used to calculate the statistical result:
Statistical Result = calculated in accordance with Statistical Analysis Plan using constituent concentrations observed at monitoring well during all sampling events within the specified date range
For pH, the values presented are the lower / upper limits
GWPS = Groundwater Protection Standard
GWPS Source:
 Standard = standard specified in 35 I.A.C. § 845.600(a)(1)
 Background = background concentration (see cover page for additional information)

TABLE 2. SUMMARY OF POTENTIAL EXCEEDANCES
HISTORY OF POTENTIAL EXCEEDANCES
BALDWIN POWER PLANT
BOTTOM ASH POND
BALDWIN, ILLINOIS

| Sample Location | HSU | Program | Constituent | Result Unit | Sample Date Range | Statistical Calculation | Statistical Result | GWPS | Background | Part 845 Standard | GWPS Source |
|-----------------|-----|---------|--------------------------------|-------------|-------------------------|-------------------------|--------------------|--------|------------|-------------------|-------------|
| MW-370 | UA | 257 | Chloride, total | mg/L | 12/29/2015 - 05/16/2023 | CB around linear reg | 1380 | 1370 | 1370 | 200 | Background |
| MW-393 | UA | 845 | Fluoride, total | mg/L | 10/27/2022 - 05/15/2023 | CB around linear reg | 7.49 | 4.0 | 3.8 | 4 | Standard |
| OW-257 | UU | 257 | Arsenic, total | mg/L | 03/14/2023 - 05/17/2023 | Most recent sample | 0.103 | 0.010 | 0.010 | 0.01 | Background |
| OW-257 | UU | 257 | Beryllium, total | mg/L | 03/14/2023 - 05/17/2023 | Most recent sample | 0.00970 | 0.004 | 0.0005 | 0.004 | Standard |
| OW-257 | UU | 257 | Chromium, total | mg/L | 03/14/2023 - 05/17/2023 | Most recent sample | 0.214 | 0.10 | 0.013 | 0.1 | Standard |
| OW-257 | UU | 257 | Cobalt, total | mg/L | 03/14/2023 - 05/17/2023 | Most recent sample | 0.203 | 0.006 | 0.0022 | 0.006 | Standard |
| OW-257 | UU | 257 | Lead, total | mg/L | 03/14/2023 - 05/17/2023 | Most recent sample | 0.214 | 0.0075 | 0.0022 | 0.0075 | Standard |
| OW-257 | UU | 257 | Lithium, total | mg/L | 03/14/2023 - 05/17/2023 | Most recent sample | 0.207 | 0.14 | 0.14 | 0.04 | Background |
| OW-257 | UU | 257 | Radium 226 + Radium 228, total | pCi/L | 03/14/2023 - 05/17/2023 | Most recent sample | 25.3 | 5.0 | 3.8 | 5 | Standard |
| OW-257 | UU | 257 | Thallium, total | mg/L | 03/14/2023 - 05/17/2023 | Most recent sample | 0.01 | 0.002 | 0.002 | 0.002 | Standard |

Notes:
HSU = hydrostratigraphic unit:
 UA = Uppermost Aquifer
 UU = Upper Unit
Program = regulatory program data were collected under:
 257 = 40 C.F.R. Part 257 Subpart D (Standards for the Disposal of Coal Combustion Residuals in Landfills and Surface Impoundments)
 845 = 35 I.A.C. Part 845 (Sampling events completed to assess well locations for inclusion in the Part 845 monitoring well network)
mg/L = milligrams per liter
pCi/L = picocuries per liter
SU = standard units
Sample Count = number of samples from Sampled Date Range used to calculate the Statistical Result
Statistical Calculation = method used to calculate the statistical result:
Statistical Result = calculated in accordance with Statistical Analysis Plan using constituent concentrations observed at monitoring well during all sampling events within the specified date range
For pH, the values presented are the lower / upper limits
GWPS = Groundwater Protection Standard
GWPS Source:
 Standard = standard specified in 35 I.A.C. § 845.600(a)(1)
 Background = background concentration (see cover page for additional information)

**APPENDIX B
ALTERNATE SOURCE DEMONSTRATION
BALDWIN POWER PLANT, BOTTOM ASH POND,
CCR UNIT 601 (RAMBOLL, 2023a)**

DRAFT

Intended for
Dynegy Midwest Generation, LLC

Date
April 30, 2023

Project No.
1940102203-001

40 C.F.R. § 257.95(g)(3)(ii):
ALTERNATE SOURCE DEMONSTRATION
BALDWIN POWER PLANT
BOTTOM ASH POND
CCR UNIT 601

CERTIFICATIONS

I, Brian G. Hennings, a professional geologist in good standing in the State of Illinois, certify that the information in this report is accurate as of the date of my signature below. The content of this report is not to be used other than for its intended purpose and meaning, or for extrapolations beyond the interpretations contained herein.



Brian G. Hennings
Professional Geologist
196.001482
Illinois
Ramboll Americas Engineering Solutions, Inc.
Date: April 30, 2023



I, Anne Frances Ackerman, a qualified professional engineer in good standing in the State of Illinois, certify that the information in this report is accurate as of the date of my signature below. The content of this report is not to be used other than for its intended purpose and meaning, or for extrapolations beyond the interpretations contained herein.



Anne Frances Ackerman
Qualified Professional Engineer
062-060586
Illinois
Ramboll Americas Engineering Solutions, Inc.
Date: April 30, 2023



CONTENTS

| | | |
|-----------|---|-----------|
| 1. | Introduction | 3 |
| 2. | Background | 4 |
| 2.1 | Site Location and Description | 4 |
| 2.2 | Groundwater Monitoring | 4 |
| 2.3 | Site Hydrogeology and Stratigraphy | 4 |
| 3. | Alternate Source Demonstration: Lines of Evidence | 6 |
| 3.1 | LOE #1: The lithium concentration in the BAP porewater is lower than the concentrations observed in compliance monitoring well location MW-370. | 6 |
| 3.2 | LOE #2: Compliance monitoring well MW-370 has a similar ionic composition to upgradient monitoring well MW-358. | 7 |
| 3.3 | LOE #3: An aquifer solids evaluation identified naturally occurring lithium associated with the shale bedrock as a source of lithium in the Uppermost Aquifer | 8 |
| 4. | Conclusions | 10 |
| 5. | References | 11 |

TABLES (IN TEXT)

| | |
|---------|---|
| Table A | Summary Statistics for Lithium in MW-370 and BAP Porewater (December 2015 to March 2023). |
|---------|---|

FIGURES (IN TEXT)

| | |
|----------|--|
| Figure A | Stiff Diagram Showing Ionic Composition of Samples of BAP Background (Brown), Compliance Groundwater (Blue), and upgradient groundwater (Tan). |
|----------|--|

FIGURES (ATTACHED)

| | |
|----------|--|
| Figure 1 | Sampling Location Map |
| Figure 2 | Potentiometric Surface Map – December 12, 2022 |
| Figure 3 | Cross Section Location Map |
| Figure 4 | Cross Section A-A' |

APPENDICES

| | |
|------------|---|
| Appendix A | Technical Memorandum – Evaluation of Lithium Sources within Aquifer Solids, Baldwin Power Station – Bottom Ash Pond (Geosyntec Consultants, Inc., 2023) |
|------------|---|

ACRONYMS AND ABBREVIATIONS

| | |
|-----------|--|
| 40 C.F.R. | Title 40 of the Code of Federal Regulations |
| 35 I.A.C. | Title 35 of the Illinois Administrative Code |
| A5D | Assessment Monitoring Sampling Event A5D |
| ASD | Alternate Source Demonstration |
| BAP | Bottom Ash Pond |
| bgs | below ground surface |
| BPP | Baldwin Power Plant |
| CCR | coal combustion residuals |
| cm/s | centimeters per second |
| FAPS | Fly Ash Pond System |
| GWPS | groundwater protection standard |
| IEPA | Illinois Environmental Protection Agency |
| LOE(s) | line(s) of evidence |
| mg/L | milligrams per liter |
| NAVD88 | North American Vertical Datum of 1988 |
| NRT | Natural Resource Technology, Inc. |
| NRT/OBG | Natural Resource Technology, an OBG Company |
| PMP | potential migration pathways |
| Ramboll | Ramboll Americas Engineering Solutions, Inc. |
| SEP | Sequential extraction procedure |
| SSI | statistically significant increase |
| SSL | statistically significant level |
| XRD | X-ray diffraction |

1. INTRODUCTION

Title 40 of the Code of Federal Regulations (40 C.F.R.) § 257.95(g)(3)(ii) allows the owner or operator of a coal combustion residuals (CCR) unit 90 days from the date of determination of statistically significant levels (SSLs) over groundwater protection standards (GWPS) of groundwater constituents listed in Appendix IV of 40 C.F.R. § 257 to complete a written demonstration that a source other than the CCR unit being monitored caused the SSL(s) (Alternate Source Demonstration [ASD]), or that the SSL(s) resulted from error in sampling, analysis, statistical evaluation, or natural variation in groundwater quality.

This ASD has been prepared on behalf of Dynegy Midwest Generation, LLC, by Ramboll Americas Engineering Solutions, Inc. (Ramboll), to provide pertinent information pursuant to 40 C.F.R. § 257.95(g)(3)(ii) for the Baldwin Power Plant (BPP) Bottom Ash Pond (BAP) located near Baldwin, Illinois.

The most recent Assessment Monitoring sampling event (A5D) was completed on September 30, 2022, and analytical data was received on November 15, 2022. Additional background and compliance monitoring wells were installed around the BAP in September and October of 2022. Following the well installations, eight monthly rounds of groundwater sampling were initiated per 35 I.A.C. § 845. Analytical data from all monitoring events, from December 2015 through A5D, were evaluated in accordance with the Statistical Analysis Plan (Natural Resource Technology, an OBG Company [NRT/OBG], 2017a) to determine any statistically significant increases (SSIs) of Appendix III parameters over background concentrations or SSLs of Appendix IV parameters over GWPSs. That evaluation identified one SSL at a compliance monitoring well as follows:

- Lithium at well MW-370

Pursuant to 40 C.F.R. § 257.95(g)(3)(ii), the lines of evidence (LOEs) presented in **Section 3** demonstrate that sources other than the BAP were the cause of the lithium SSL listed above. This ASD was completed by April 30, 2023, within 90 days of determination of the SSLs (January 30, 2023), as required by 40 C.F.R. § 257.95(g)(3)(ii).

2. BACKGROUND

2.1 Site Location and Description

The BPP is located in southwest Illinois in Randolph and St. Clair Counties. The Randolph County portion of the BPP is located within Sections 2, 3, 4, 9, 10, 11, 14, 15, and 16 of Township 4 South and Range 7 West. The St. Clair County portion of the property is located within Sections 33, 34, and 35 of Township 3 South and Range 7 West. The BAP is approximately one-half mile west-northwest of the Village of Baldwin.

The BPP property is bordered to the west by the Kaskaskia River; to the east by Baldwin Road, farmland, and strip-mining areas; to the southeast by the Village of Baldwin; to the south by the Illinois Central Gulf railroad tracks, scattered residences, and State Route 154; and to the north by farmland. The St. Clair/Randolph County Line crosses east-west at approximately the midpoint of Baldwin Lake (Cooling Pond). **Figure 1** shows the location of the BAP, as well as the Fly Ash Pond System (FAPS), Secondary Pond, Tertiary Pond, and Baldwin Lake (Cooling Pond). The BAP is adjacent to the FAPS, which was approved for closure by Illinois Environmental Protection Agency (IEPA) on August 16, 2016.

2.2 Groundwater Monitoring

The BAP groundwater monitoring system for compliance with 40 C.F.R. § 257 consists of two background monitoring wells (MW-304 and MW-306) and four compliance monitoring wells (MW-356, MW-369, MW-370, and MW-382). A map showing the groundwater monitoring system, including the CCR unit and all background and compliance monitoring wells, is presented in **Figure 1**. **Figure 1** also shows porewater location TPZ-164, as well as the monitoring wells that were installed in 2022. New monitoring well MW-358 was installed in 2022 upgradient of the BAP and compliance monitoring well MW-370 (compliance monitoring well with identified lithium SSL) with a well screen (363.7 to 373.7 feet North American Vertical Datum of 1988 [NAVD88]) that overlaps with MW-370 well screen elevations (355.6 to 365.6 feet NAVD88).

Groundwater samples are collected and analyzed in accordance with the Sampling and Analysis Plan prepared for the BAP (NRT/OBG, 2017b). Statistical evaluation of analytical data is performed in accordance with the Statistical Analysis Plan (NRT/OBG, 2017a).

2.3 Site Hydrogeology and Stratigraphy

Three hydrostratigraphic units are present at the Site, including CCR, an upper unit, and a bedrock unit. These units are described in detail in the Supplemental Hydrogeologic Site Characterization and Groundwater Monitoring Plan (Natural Resources Technology, Inc. [NRT], 2016) and the Hydrogeologic Site Characterization Report (Ramboll, 2021); and are summarized below.

- **CCR:** CCR, consisting primarily of fly ash, bottom ash, and boiler slag. Also includes earthen fill deposits of predominantly clay and silt materials from on-site excavations that were used to construct berms and roads surrounding the various impoundments across the Site. The 2022 Site Investigation observed up to 28.2 feet of bottom ash towards the center of the BAP (XPW05).
- **Upper Unit:** Predominantly clay with some silt and minor sand, silt layers, and occasional sand lenses. Includes the lithologic layers identified as the Cahokia Alluvium, Peoria Loess,

Equality Formation, and Vandalia Till Member. This unit is composed of unlithified natural geologic materials and extends from the water table to the bedrock. Thin sand seams and the interface (contact) between the Upper Unit and bedrock have been identified as potential migration pathways (PMPs). No continuous sand seams were observed in the Upper Unit within or immediately adjacent to the BAP; however, the sand seams may act as a PMP due to relatively higher hydraulic conductivities (on the order of 10^{-4} centimeters per second [cm/s]) than the surrounding clays (on the order of 10^{-5} cm/s).

- **Bedrock Unit:** Shallow bedrock beneath the BAP yields small amounts of water from interconnected pores, cracks, fractures, crevices, joints, and bedding planes and is the only water-bearing unit that is continuous across the Site; this unit is considered the Uppermost Aquifer (UA) and is composed of Pennsylvanian and Mississippian-aged interbedded shale and limestone bedrock having a regional strike that is generally north to northeast with a dip of 2 to 3 degrees to the east into the Illinois Basin (Breeden et. al, 2018; Bristol and Howard, 1971). The surface elevation varies across the site, generally sloping downward from east to west, and the unlithified Upper Unit thins from east to west. The top of bedrock depth ranges between 12.5 feet below ground surface (bgs) near the Kaskaskia River and 70 feet bgs within the East Fly Ash Pond (part of the FAPS). Limestone layers intercepted at the Site are generally light to dark gray, fine-grained, thin bedded, banded, argillaceous, and competent except where weathered. Weathering of the limestone produces a calcareous clay. The limestone layers are interbedded with thin shale layers and are sometimes fossiliferous or sandy. The shale layers are generally weathered, competent, silty, slightly micaceous, fissile, and dark gray. Where highly weathered shale (*i.e.*, decomposed bedrock) was encountered, the shale was non-fissile and resembled an unlithified stiff clay with medium to high plasticity. Bedrock in the vicinity of

Water quality in the Uppermost Aquifer (*i.e.*, Pennsylvanian and Mississippian-aged bedrock) degrades with increasing depth as water becomes increasingly mineralized. Therefore, water quality at monitoring wells with screens placed in deeper bedrock layers (*e.g.*, MW-358 and MW-370) would be expected to demonstrate more influence from the naturally increased mineralization than wells screened shallower in the bedrock. Groundwater flow in bedrock is toward the northwest in the east and central areas of the BAP, and southwest in the east area of the FAPS. The Secondary and Tertiary ponds were created in a former drainage channel and bedrock groundwater flows toward these ponds as illustrated in **Figure 2**. Groundwater elevations vary seasonally, generally less than 7 feet, although flow directions are generally consistent. Groundwater elevations across the Site range between approximately 370 and 450 feet NAVD88.

3. ALTERNATE SOURCE DEMONSTRATION: LINES OF EVIDENCE

This ASD is based on the following LOEs:

1. The lithium concentration in the BAP porewater is lower than the concentrations observed in compliance monitoring well location MW-370.
2. Compliance monitoring well MW-370 has a similar ionic composition to upgradient monitoring well MW-358.
3. An aquifer solids evaluation identified naturally occurring lithium associated with the shale bedrock as a source for lithium in the Uppermost Aquifer.

These LOEs are described and supported in greater detail below. Monitoring wells and the BAP porewater sample locations are shown in **Figure 1**.

3.1 LOE #1: The lithium concentration in the BAP porewater is lower than the concentrations observed in compliance monitoring well location MW-370.

Table A below provides summary statistics for lithium in background wells, MW-370 and BAP porewater collected from TPZ-164, and the five new porewater wells installed in 2022.

Table A. Summary Statistics for Lithium in MW-370 and BAP Porewater (December 2015 to March 2023).

| Sample Location | Lithium (milligrams per liter [mg/L]) | | |
|-------------------------------------|---------------------------------------|---------|--------|
| | Minimum | Maximum | Median |
| Background Groundwater ¹ | 0.010 | 0.096 | 0.055 |
| Exceedance Groundwater (MW-370) | 0.098 | 0.22 | 0.14 |
| BAP Porewater ² | <0.005 | 0.035 | 0.013 |

Notes:

¹Background groundwater was collected at monitoring wells MW-304 and MW-306.

²BAP porewater was collected at TPZ-164 (September 2018 through November 2022), XPW01, XPW02, XPW04, XPW05, and XPW06 (October 2022 through January 2023).

The following observations can be made from **Table A** above:

- Concentrations of lithium in background wells ranged from 0.010 to 0.096 mg/L, with a median concentration of 0.055 mg/L.
- Concentrations of lithium in downgradient compliance monitoring well MW-370 ranged from 0.098 to 0.22 mg/L, with a median concentration of 0.14 mg/L.
- Concentrations of lithium in BAP porewater ranged from non-detect (<0.005 mg/L) to 0.035 mg/L, with a median concentration of 0.013 mg/L.
- The median lithium concentration observed in porewater is an order of magnitude lower than the median lithium concentrations observed in compliance monitoring well MW-370.
- The highest observed lithium concentration in porewater is approximately six times lower than the maximum concentration observed in compliance monitoring well MW-370.

If the BAP was the source of lithium in downgradient groundwater, BAP porewater concentrations of lithium would be expected to be higher than the groundwater concentrations. The median lithium concentration observed in porewater is below the median lithium concentrations observed in both background and compliance groundwater monitoring wells, indicating that lithium concentrations are not related to the BAP.

3.2 LOE #2: Compliance monitoring well MW-370 has a similar ionic composition to upgradient monitoring well MW-358.

Stiff diagrams graphically represent ionic composition of aqueous solutions. **Figure A** on the following page shows a series of Stiff diagrams that display the ionic compositions of groundwater from background monitoring wells (brown); compliance monitoring wells (blue); and upgradient monitoring well MW-358 (tan). Polygons with similar shapes on Stiff diagrams indicate solutions with similar ionic compositions, whereas polygons with different shapes indicate solutions with dissimilar ionic compositions. The larger the area of the polygon, the greater the concentration of the various ions. A Stiff diagram was included in **Figure A** for one out-of-network, upgradient, monitoring well, MW-358, due to similarities with MW-370 with respect to ionic composition, well screen elevation, and the composition of the bedrock material.

Compliance monitoring well MW-370 has chloride as the dominant anion and a substantially higher proportion of Na+K, similar to upgradient well MW-358. Upgradient monitoring well MW-358 is screened in a similar shaley bedrock material and at a similar elevation to MW-370 (**Figures 3 and 4**). The similarity in ionic composition in compliance well MW-370 and upgradient well MW-358 suggests that groundwater at these locations and depths is from a similar lithologic material that has undergone a similar amount of naturally occurring dissolution, and supports the conclusion that natural variability of groundwater in the Uppermost Aquifer is responsible for the lithium SSL at MW-370.

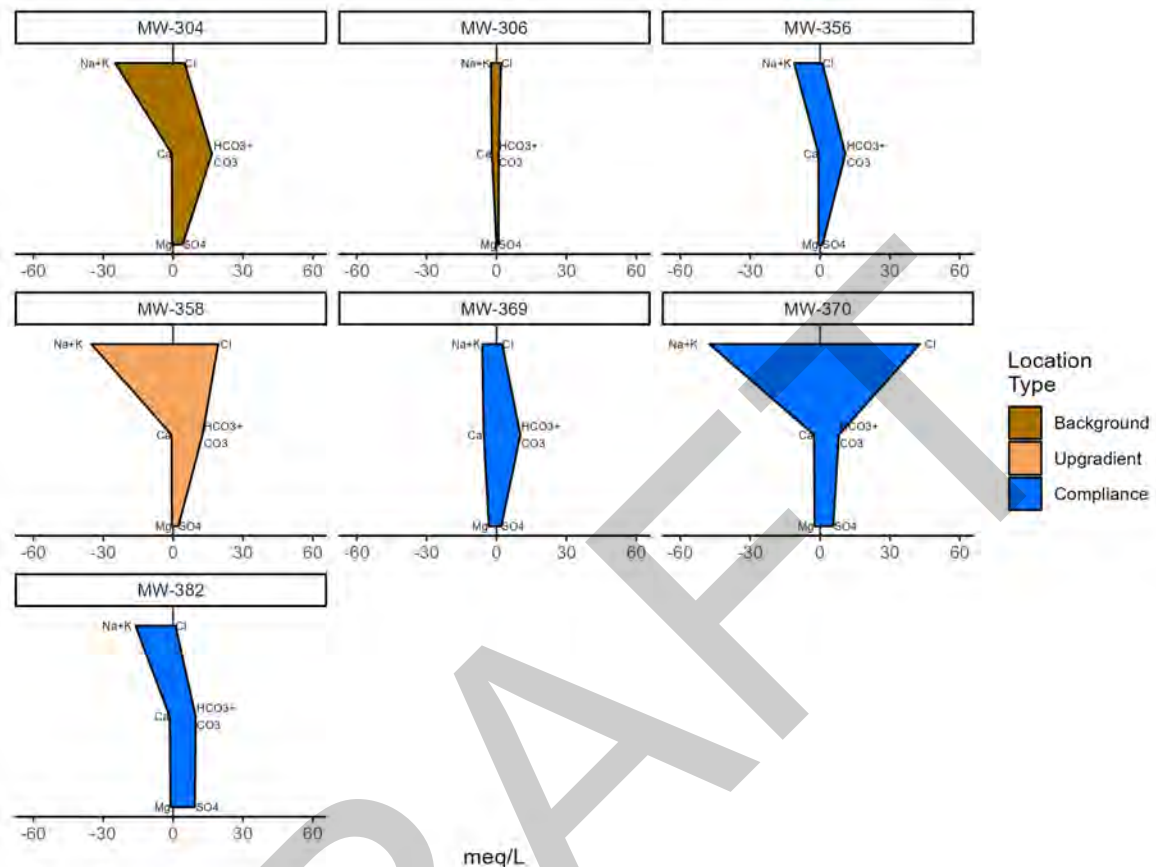


Figure A. Stiff Diagram Showing Ionic Composition of Samples of BAP Background (Brown), Compliance Groundwater (Blue), and Upgradient Groundwater (Tan).

3.3 LOE #3: An aquifer solids evaluation identified naturally occurring lithium associated with the shale bedrock as a source of lithium in the Uppermost Aquifer

Solid phase analyses were completed on samples collected from the Site to support the conclusion that lithium concentrations in groundwater at MW-370 are associated with naturally occurring lithium in the Uppermost Aquifer materials (limestone and shale bedrock formation). A review of the geochemical and site conditions was completed by Geosyntec Consultants, Inc. and is included as **Appendix A**. The following conclusions were made based on the results of the aquifer solids evaluation:

- Lithium host-minerals occur in the UA throughout the Site and constitute natural sources of lithium in BAP soils.
- Lithium is present in both upgradient and downgradient shale samples at the Site, with the largest concentrations observed in upgradient solids samples.
- Natural lithium occurrence in aquifer material from the Site is associated with multiple phases and therefore interacts with groundwater through different mechanisms at different locations and depths.

- Naturally occurring lithium associated with the shale bedrock comprising the UA at the Site was identified as a source of lithium in Site groundwater.

DRAFT

4. CONCLUSIONS

Based on the following three LOEs, it has been demonstrated that the lithium SSL at MW-370 is not due to the BAP:

1. The lithium concentration in the BAP porewater is lower than the concentrations observed in compliance monitoring well location MW-370.
2. Compliance monitoring well MW-370 has a similar ionic composition to upgradient monitoring well MW-358.
3. An aquifer solids evaluation identified naturally occurring lithium associated with the shale bedrock as a source for lithium in the Uppermost Aquifer.

This information serves as the written ASD prepared in accordance with 40 C.F.R. § 257.95(g)(3)(ii) that the SSL observed during the ASD sampling event was not due to the BAP. Therefore, a corrective measures assessment is not required, and the BAP will remain in assessment monitoring. Additional data is being collected to identify the source of the SSLs.

5. REFERENCES

Breeden, J.R., J.A. Devera, W.J. Nelson, and F.B. Denny, 2018. Bedrock Geology of Baldwin Quadrangle, Randolph and St. Clair Counties, Illinois: Illinois State Geological Survey, USGS-STATEMAP contract report, 2 sheets, 1:24,000.

Bristol, H.M., and Howard, R.H., 1971. Paleogeologic map of the Sub- Pennsylvanian Chesterian (Upper Mississippian) surface in the Illinois Basin: Illinois State Geological Survey, Circular 458, plate 1.

Geosyntec Consultants, Inc., 2023. Technical Memorandum – Evaluation of Lithium Sources within Aquifer Solids, Baldwin Power Station – Bottom Ash Pond, April 24, 2023.

Natural Resource Technology, Inc. (NRT), 2016. *Supplemental Hydrogeologic Site Characterization and Groundwater Monitoring Plan. Baldwin Fly Ash Pond System. Baldwin Energy Complex, Baldwin, IL.*

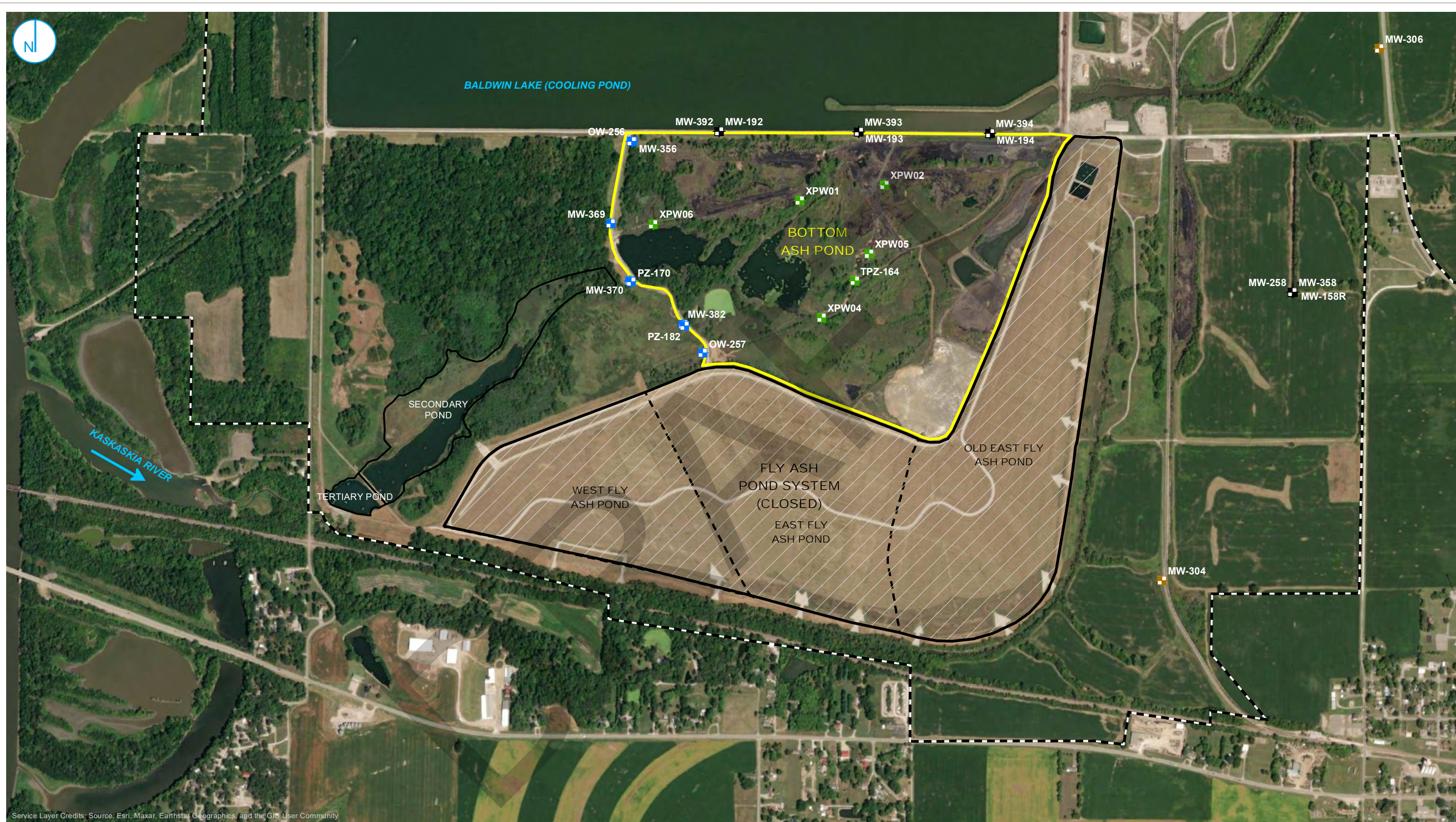
Natural Resource Technology, an OBG Company (NRT/OBG), 2017a. *Statistical Analysis Plan, Baldwin Energy Complex, Havana Power Station, Hennepin Power Station, Wood River Power Station, Dynegy Midwest Generation, LLC.* October 17, 2017.

Natural Resource Technology, an OBG Company (NRT/OBG), 2017b. *Sampling and Analysis Plan, Final, Baldwin Bottom Ash Pond, Baldwin Energy Complex, Baldwin, Illinois, Project No. 2285.* October 17, 2017.

Ramboll Americas Engineering Solutions, Inc. (Ramboll), 2021. *Hydrogeologic Site Characterization Report. Baldwin Bottom Ash Pond. Baldwin Power Plant. Baldwin, Illinois.*

FIGURES

DRAFT



Service Layer Credits: Source: Esri, Maxar, Earthstar Geographics, and the GIS User Community

- | | |
|-----------------|-------------------------------|
| BACKGROUND WELL | REGULATED UNIT (SUBJECT UNIT) |
| COMPLIANCE WELL | FLY ASH POND SYSTEM (CLOSED) |
| MONITORING WELL | SITE FEATURE |
| PORE WATER WELL | CAPPED AREA |
| | PROPERTY BOUNDARY |

0 400 800 Feet

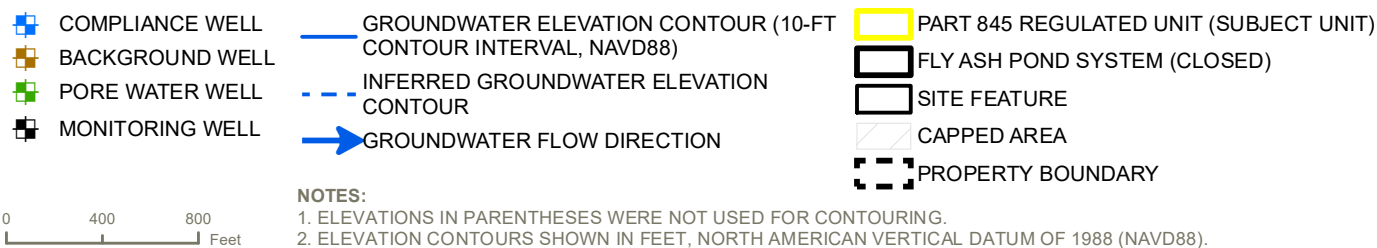
SAMPLING LOCATION MAP

ALTERNATE SOURCE DEMONSTRATION
BOTTOM ASH POND
BALDWIN POWER PLANT
BALDWIN, ILLINOIS

FIGURE 1

RAMBOLL AMERICAS
ENGINEERING SOLUTIONS, INC.

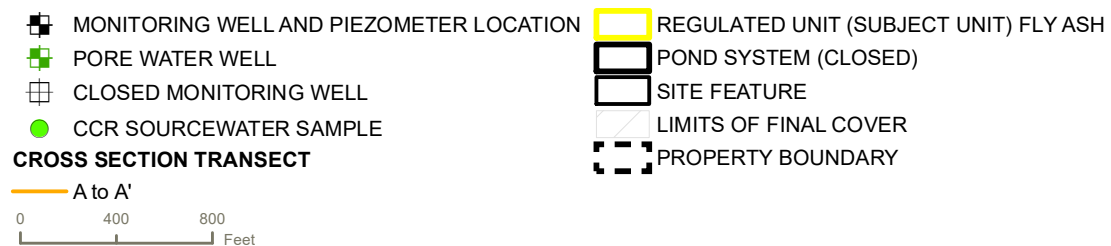
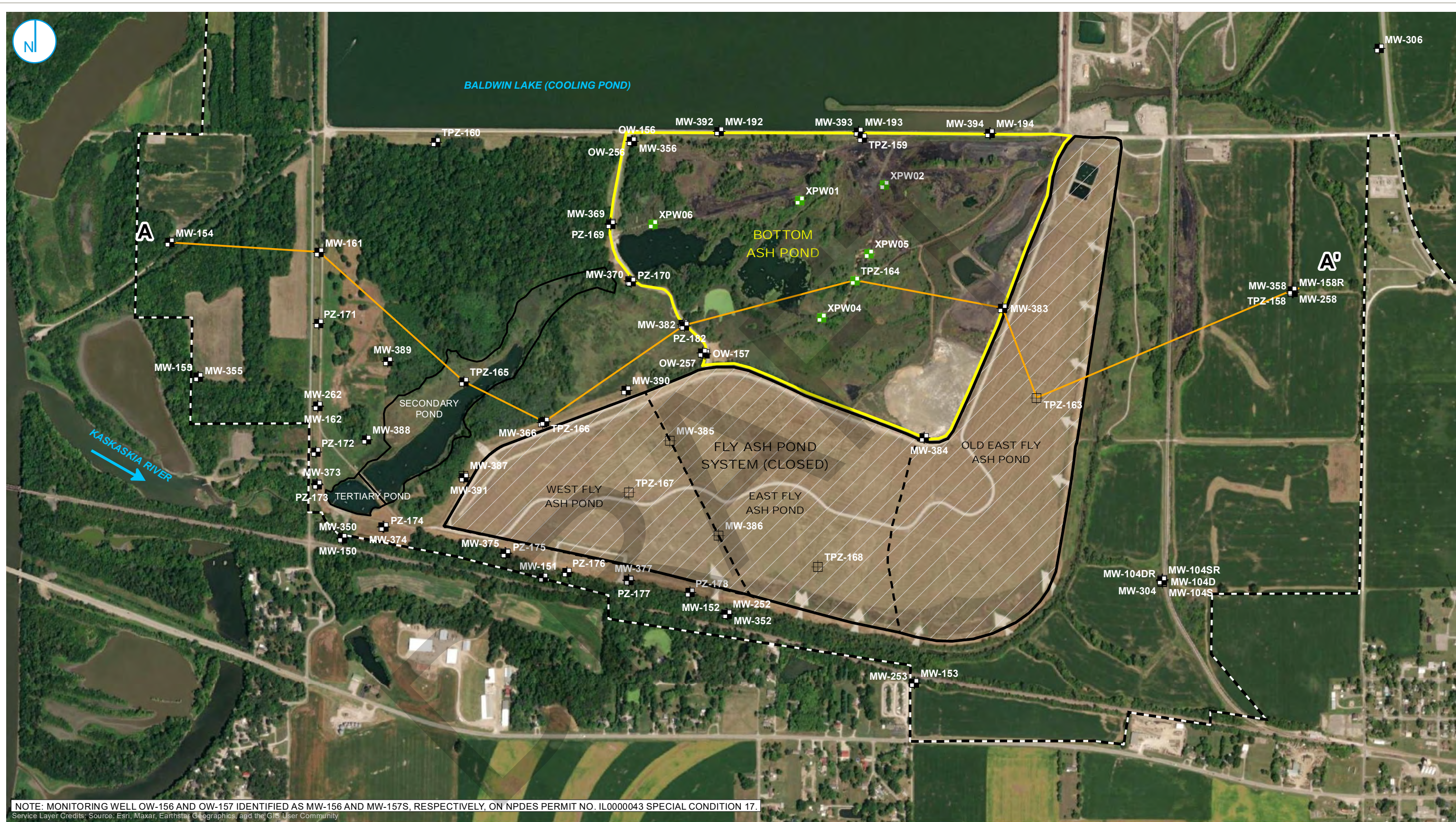




ALTERNATE SOURCE DEMONSTRATION
BOTTOM ASH POND
BALDWIN POWER PLANT
BALDWIN, ILLINOIS



PROJECT: 169000XXXX | DATED: 4/24/2023 | DESIGNER: GALARNMC
Y:\Mapping\Projects\22\2285\MXD\Alt_Sources\DemBaldwin_Alt_Sources\Figure 3_Cross Section Locations.mxd



CROSS SECTION LOCATION MAP

ALTERNATE SOURCE DEMONSTRATION
BOTTOM ASH POND
BALDWIN POWER PLANT
BALDWIN, ILLINOIS

FIGURE 3

RAMBOLL AMERICAS
ENGINEERING SOLUTIONS, INC.

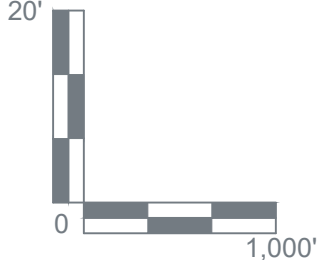
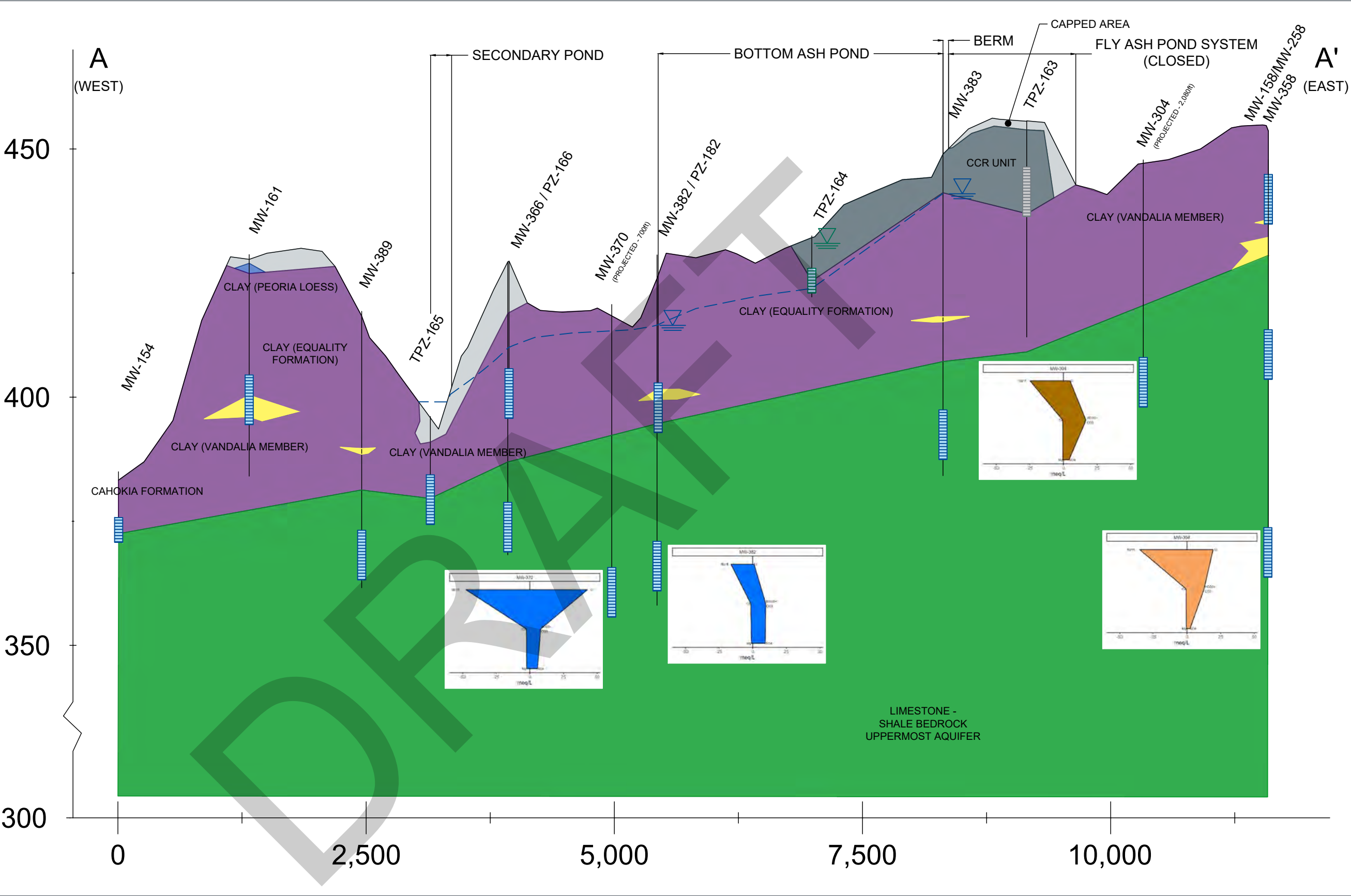


- NOTES**
- 1. This profile was developed by interpolation between widely spaced boreholes. Only at the borehole location should it be considered as an approximately accurate representation and then only to the degree implied by the notes on the borehole logs.
 - 2. Scale is approximate.
 - 3. Vertical scale is exaggerated 50X.
 - 4. Groundwater elevations measured on December 12, 2022.

STIFF DIAGRAM LOCATION TYPE:

- BACKGROUND
- UPGRADIENT
- COMPLIANCE

- LEGEND**
- COAL COMBUSTION RESIDUALS (CCR)
 - FILL
 - CLAY (CL/CH)
 - SILT (ML)
 - SAND (SP/SM/SW)
 - BEDROCK / WEATHERED BEDROCK (INTERBEDDED SHALE, LIMESTONE, SANDSTONE, V. LITTLE SS)
 - WELL SCREEN INTERVAL
 - UPPERMOST AQUIFER POTENTIOMETRIC SURFACE
 - UPPERMOST AQUIFER GROUNDWATER ELEVATION
 - POREWATER ELEVATION
 - OTHER GROUNDWATER / SURFACE WATER ELEVATION(S)



CROSS SECTION A-A'

**ALTERNATE SOURCE DEMONSTRATION
BOTTOM ASH POND**

BALDWIN POWER PLANT
BALDWIN, ILLINOIS

FIGURE 4

RAMBOLL AMERICAS
ENGINEERING SOLUTIONS, INC.

RAMBOLL

APPENDICES

DRAFT

**APPENDIX A
TECHNICAL MEMORANDUM - EVALUATION OF LITHIUM
SOURCES WITHIN AQUIFER SOLIDS, BALDWIN POWER
STATION - BOTTOM ASH POND (GEOSYNTEC
CONSULTANTS, INC., 2023)**

TECHNICAL MEMORANDUM

Date: April 24, 2023

To: Brian Voelker - Vistra

Copies to: Stu Cravens and Phil Morris - Vistra

From: Allison Kreinberg and Ryan Fimmen, Ph.D. - Geosyntec Consultants

Subject: Evaluation of Lithium Sources within Aquifer Solids
Baldwin Power Station – Bottom Ash Pond

Geosyntec Consultants, Inc. (Geosyntec) has completed a review of geochemical and site conditions at the Baldwin Power Plant Bottom Ash Pond (BAP; the Site) to evaluate the influence of the bedrock lithology on groundwater composition at downgradient monitoring well MW-370.

Alternate source demonstrations (ASDs) prepared by Ramboll Americas Engineering Solutions, Inc. (Ramboll) concluded that sources other than the BAP were the cause of statistically significant levels (SSL) of lithium at MW-370. This technical review has identified naturally occurring lithium associated with the shale bedrock as a source of elevated lithium in Site groundwater.

SITE CONDITIONS

The groundwater monitoring network for the BAP consists of four downgradient compliance wells (MW-356, MW-369, MW-370, and MW-382) and two upgradient background wells (MW-304 and MW-306). These monitoring locations are shown in the map provided as **Attachment 1**. Site geology consists of glacial drift deposits comprised of clastic material overlying Pennsylvanian and Mississippian-age bedrock (Ramboll, 2021). The geologic units comprising subsurface lithologies at the Site are listed in descending order:

- Equality Formation: predominantly clay and sandy clay, with intermittent sand lenses and some secondary carbonate concretions
- Pearl Formation: predominantly fine-medium grained sand with intermittent gravel
- Vandalia Till: clay and sandy clay diamicton with intermittent silt, sand, and gravel lenses
- Bedrock: Mississippian-age limestone and shale which underlies unconsolidated material beneath the western portion of the Site, and Pennsylvanian-age limestone and shale which underlies unconsolidated material beneath the eastern portion of the Site. The gradual

change from Mississippian bedrock to Pennsylvanian bedrock is believed to occur approximately beneath the central portion of the Site (Willman et al., 1967).

Limestone bedrock at the Site is generally thinly bedded, argillaceous, and competent, with localized areas of increased weathering (Ramboll, 2021). The result of this limestone weathering is a calcareous clay lithology. Layers of limestone bedrock are interbedded with thin shale layers which are sometimes calcareous and sometimes siliciclastic. The shale layers are generally more weathered than the limestone bedrock but are generally still competent. Locations of highly weathered, non-fissile, clay-like shale with medium to high plasticity have been observed.

The Uppermost Aquifer (UA) in the vicinity of the BAP is the shallow limestone/shale bedrock. Although sand lenses are present within the unconsolidated material overlying bedrock, these lenses have not been found to be laterally continuous. Groundwater in the vicinity of the BAP flows through bedrock from east to west primarily through secondary porosity features, predominantly joints and fractures, which are present at variable frequencies within the UA.

Geologic cross-sections of the lithology underlying the BAP are provided as **Attachment 2**. The fracture network within the deeper portions of the UA bedrock is overlain by unconsolidated, predominantly low permeability clay with some silt, resulting in confined to semi-confined groundwater conditions with mostly upward vertical gradients and or flowing artesian conditions observed in the unconsolidated and UA bedrock units across the Site. The observed upward vertical gradients (upwelling) result in deeper groundwater characteristic of older lithologies mixing with shallow formation water in the UA. The flat horizontal groundwater gradient beneath the Site and the mostly upward vertical gradients also suggests the BAP is not an area of significantly increased recharge or infiltration to the UA. Groundwater quality in the UA has observed to decrease with increasing depths as confined formation water is increasingly mineralized (Ramboll, 2021).

GROUNDWATER CONDITIONS

The observed lithium SSL was identified by comparing the reported groundwater concentrations at downgradient monitoring well MW-370 to the site-specific groundwater protection standard (GWPS). The site-specific GWPS for lithium was established at 0.0958 mg/L, as the Site background concentrations were greater than the health-based level of 0.040 mg/L established in 40 CFR § 257.95(h)(2). Groundwater samples collected from recently installed upgradient monitoring well MW-358, which is screened in the Mississippian-age limestone and shale bedrock strata, contained lithium concentrations ranging from 0.0592 to 0.0957 mg/L. These upgradient concentrations, as well as previously observed results from background well MW-304, are elevated with respect to the health-based GWPS. This observation indicates that lithium is present at concentrations across the Site which suggest that a naturally occurring geogenic source of lithium to groundwater is present in these strata.

AQUIFER SOLIDS EVALUATION

Geosyntec reviewed the results of analyses completed on solid phase samples collected from the Site to support the conclusion that the lithium concentrations in groundwater at MW-370 in excess of the site-specific GWPS are associated with the limestone and shale bedrock formation.

Samples were collected from soil borings advanced in September and October 2022 at one location upgradient of the BAP (MW-358) and three locations downgradient of the BAP (MW-392, MW-393, and MW-394). These boring logs, plus the boring log for monitoring well MW-370, are provided as **Attachment 3**. Additional information regarding monitoring well construction and lithology depths of these locations and MW-370 is provided in **Table 1**. Three samples each were collected from various depth intervals/lithologies at MW-358 and MW-392, and one sample each was collected from the unconsolidated overburden at MW-393 and MW-394¹. The samples were submitted for analysis of mineralogy via X-ray diffraction (XRD), total lithium, and lithium distribution within the aquifer solids using sequential extraction procedure (SEP). SEP uses progressively stronger reagents to solubilize metals from increasingly recalcitrant phases. Although these procedures do not identify the specific metal phases in a soil/aquifer matrix, they do provide a means to evaluate association of constituents with different classes of solids (Tessier et al, 1979).

Results for total and SEP analyses of lithium in these samples are presented in **Table 2** and the analytical laboratory reports are provided as **Attachment 4**. As a first step to evaluate data quality in an SEP analysis, the sum of individual extraction steps from the SEP was compared to the total lithium concentration. The sum of the SEP procedure is not expected to be exactly equal to the total metals analysis but should generally be consistent with the total metals analysis. As can be seen in **Table 2**, the total lithium concentrations ranged from 6.0 micrograms per gram of material ($\mu\text{g/g}$) to 20 $\mu\text{g/g}$ in the shale samples. The summed concentrations of lithium from the SEP analyses ranged from 7 to 73 $\mu\text{g/g}$. The results were generally consistent between the total metals analyses and the summed SEP steps, indicating good metals recovery and data quality. One notable exception is the sample collected from 86-88 feet (ft.) below ground surface (bgs) at upgradient location MW-358, which had a total lithium concentration of 20.0 $\mu\text{g/g}$ and a summed SEP total of 73 $\mu\text{g/g}$. While a difference was observed, both results indicate lithium is present within shale materials upgradient of the Site.

These results indicate that lithium is present in both upgradient and downgradient shale samples at the Site, with the largest concentrations observed in upgradient samples. Most lithium in these samples was found to be associated with the residual metals fraction, which is typically considered to be immobile and not readily soluble. The abundance of lithium within the residual fraction

¹ Select samples, including those collected from MW-393 and MW-394, are excluded from subsequent results tables and discussion to emphasize findings associated with the bedrock lithologies.

indicates association with inseparable primary mineral phases such as clay minerals (Tessier et al., 1979). Lithium was also found to be associated with iron/manganese oxides in multiple samples (maximum of 25% associated with iron/manganese oxides in the sample collected from the 47-49 ft. bgs samples from MW-358), and a small component of lithium was found to be associated with organic material in the 86-88 ft. bgs sample collected from MW-358. These results indicate that natural lithium occurrence in aquifer material from the Site is associated with multiple phases and therefore interacts with groundwater through different mechanisms at different locations and depths.

Clay minerals are known to be common geosorbents for naturally occurring lithium (Starkey, 1982). Lithium is known to leach from lithium-hosting igneous rocks and micas through weathering processes. Mineral alteration reactions occurring in micas may result in lithium-rich micas transforming directly to illitic clays, and then to mixed-layer and smectite clays. The lithium within these primary minerals either becomes incorporated directly into the crystal structures of these clay minerals or is transported in solution and later concentrated in brines through evaporation (Ronov et al., 1970). Lithium-enriched brines constitute a common source of lithium in clay minerals, as eroded fine-grained materials deposited in these brines are capable of housing aqueous lithium within vacant sites in octahedral layers comprising their crystal structures (Schultz, 1969). SEP results from **Table 2** support the conclusion that naturally occurring lithium is observed in soils around the BAP, and that the majority of this lithium is associated with the residual solids fraction which consists of primary minerals. Field lithologic descriptions of samples indicate that nearly all of the samples collected and analyzed consist of clay or shale, both of which are comprised primarily of mica and clay minerals which are known to be hosts of natural lithium. Based on SEP results and lithologic observations, the data suggests that lithium in BAP soils is naturally occurring and primarily associated with micas and clays, with a smaller component associated with leachable oxides and organic material.

Mineralogical analyses were completed using X-ray diffraction (XRD) to evaluate whole rock mineralogy and evaluate the abundance of clays and micas within the aquifer solids. Whole rock mineralogy results are provided in **Table 3**. Sample mineralogy consists predominantly of quartz, mica (muscovite), feldspars (albite and microcline), and clay minerals (chlorite, kaolinite) (**Table 3**). Of these minerals, muscovite and clays are known hosts of natural lithium within their crystal structures (Zawidzki, 1976; Starkey, 1982). The combined abundances of muscovite or clay minerals account for between 30 to 49% of samples within the bedrock shale samples, with an average value of 43%. As indicated on **Table 3**, these minerals are present at sizeable abundances both upgradient and downgradient of the BAP, indicating that these lithium-host minerals occur in the UA throughout the Site and constitute natural sources of lithium.

MW-370 is screened from 53-63 ft. bgs within an interval of shaley limestone, with additional shale and clay directly overlying this material, as indicated by the boring log included in **Attachment 3**. It is likely that lithium-hosting micas and clay minerals are present within the

screened interval of this monitoring well, the leachable component of which may act as a geogenic source of lithium in groundwater. Additionally, groundwater downgradient of the BAP may be mixing with deeper groundwater in contact with lithium-bearing micas and clay minerals within the deep shale lithologies observed upgradient of the Site due to the observed upward vertical gradient within the bedrock unit.

CONCLUSION

Naturally occurring lithium associated with the shale bedrock comprising the UA at the Site was identified as a source for lithium in Site groundwater. Solid phase samples collected from upgradient and downgradient locations around the BAP contained variable lithium, with the highest total lithium concentration observed in the background deep shale sample. SEP analyses of the solid phase samples determined that the majority of lithium in the solid phase is associated with the residual metals fraction. The residual metals fraction corresponds to primary minerals such as micas and clay minerals, which are known to host natural lithium in their crystal structures, either as a result of mineral formation (micas) or depositional/alteration processes (clays). XRD confirmed the presence of micas and clay minerals in the aquifer solids at an average of 43% of the bedrock total mineralogy, suggesting an abundance of common lithium-hosting minerals which may release lithium to groundwater. This solid phase assessment supports the determination that MW-370 groundwater geochemistry appears to be related to shaley aquifer solid material.

REFERENCES

- Ramboll. 2019. Alternative Source Demonstration. Baldwin Bottom Ash Pond. April.
- Ramboll. 2022. Annual Groundwater Monitoring and Corrective Action Report. Baldwin Bottom Ash Pond. January
- Ramboll. 2021. Hydrogeologic Site Characterization Report. Baldwin Bottom Ash Pond. October.
- Ronov, A.B., Migdisov, A.A., Voskresenskaya, N.T., and Korzine, G.A. 1970. Geochemistry of lithium in the sedimentary cycle. *Geochemistry International*. v. 7, p. 75-102.
- Schultz, L.G. 1969. Lithium and potassium absorption, dehydroxylation temperature, and structural water content of aluminous smectites. *Clays and Clay Minerals*. v. 17, no. 3, p. 115-150.
- Starkey, H.C. 1982. The role of clays in fixing lithium. United States Geological Survey. Bulletin 1278-F.
- Tessier, A., Campbell, P.G.C., and Bisson, M. 1979. Sequential extraction procedure for the speciation of particulate trace metals. *Analytical Chemistry*. v. 5, no.7, p. 844-851.
- Willman, H.B., and others. 1967. Geologic Map of Illinois. Illinois State Geologic Survey. Champaign, Illinois.
- Zawidzki, Pawel. 1976. Lithium distribution in micas and its bearing on the lithium geochemistry of granitoids. *Polska Akademia Nauk, Archiwum Mineralogiczne*. v. 32, p. 95-152.

DRAFT

TABLES

**Table 1 - Relevant Monitoring Well Information
Baldwin Power Plant**

Geosyntec Consultants, Inc.

| Monitoring Well | Well Classification | Screened Interval | Depth of Well | Geologic Material Within Screened Interval | Interval of Observed Alluvial Clay | Interval of Observed Bedrock |
|-----------------|---------------------|-------------------|---------------|--|------------------------------------|------------------------------|
| MW-370 | Downgradient | 53-63 | 66 | Shaley limestone, Limestone | 0-28.5 | 28.5-66 |
| MW-358 | Upgradient | 80-90 | 90 | Limestone, Shale | 4-21 | 21-90 |
| MW-392 | Downgradient | 74-84 | 84 | Shale, Limestone | 1-33 | 52-84 |
| MW-393 | Downgradient | 75-85 | 85 | Shale | 1-27, 31-40 | 57-85 |
| MW-394 | Downgradient | 73-83 | 85 | Shale, Limestone | 3-20, 22-37 | 37-85 |

Notes:

Depths provided in units of feet below ground surface

Observed clay and bedrock intervals are based on the boring logs provided in Attachment 3.

**Table 2 - Lithium SEP Results Summary
Baldwin Power Plant**

Geosyntec Consultants, Inc.

| Well ID | MW-358 | | MW-358 | | MW-392 | | MW-392 | |
|---------------------------------------|---------------|------------|-------------------|------------|---------------|------------|----------------------------------|------------|
| Depth (ft) | (47-49) | | (86-88) | | (66-68) | | (80-82) | |
| Location | Upgradient | | Upgradient | | Downgradient | | Downgradient | |
| Boring Log Description | Shallow Shale | | Deeper Shale Body | | Shale | | Shale transitioning to limestone | |
| Total Lithium | 6.0 | | 20.0 | | 15.0 | | 8.0 | |
| SEP Results | | | | | | | | |
| | Concentration | % of Total | Concentration | % of Total | Concentration | % of Total | Concentration | % of Total |
| Water Soluble Fraction | <2 | -- | <2 | -- | <2 | -- | <2 | -- |
| Exchangeable Metals Fraction | <2 | -- | <2 | -- | <2 | -- | <2 | -- |
| Metals Bound to Carbonates Fraction | <2 | -- | <2 | -- | <2 | -- | <2 | -- |
| Metals Bound to Fe/Mn Oxides Fraction | 3.0 | 25% | 5.0 | 7% | 2.0 | 10% | <2 | -- |
| Bound to Organic Material Fraction | <2 | -- | 3.0 | 4% | <2 | -- | <2 | -- |
| Residual Metals Fraction | 9.0 | 75% | 65.0 | 89% | 19.0 | 90% | 7.0 | 100% |
| SEP Total | 12.0 | 100% | 73.0 | 100% | 21.0 | 100% | 7.0 | 100% |

Notes:

SEP - sequential extraction procedure

All results shown in microgram of lithium per gram of soil (µg/g).

Total lithium was analyzed using aqua regia digest, ICP-MS

Non-detect values are shown as less than the detection limit.

The lithium fraction associated with each SEP phase is shown.

% of total lithium is calculated from the sum of the SEP fractions.

**Table 3 - Summary of Rietveld Quantitative Analysis
X-Ray Diffraction Results
Baldwin Power Plant**

Geosyntec Consultants, Inc.

| Well ID | | | MW-358 | MW-358 | MW-392 | MW-392 |
|-------------------------|--|--------------|---------------|-------------------|--------------|----------------------------------|
| Depth (ft bgs) | | | (47-49) | (86-88) | (66-68) | (80-82) |
| Location | | | Upgradient | Upgradient | Downgradient | Downgradient |
| Boring Log Description | | | Shallow Shale | Deeper Shale Body | Shale | Shale transitioning to limestone |
| Mineral/Compound | Formula | Mineral Type | (wt %) | (wt %) | (wt %) | (wt %) |
| Quartz | SiO ₂ | Silicate | 33.0 | 34.9 | 27.2 | 29.1 |
| Muscovite | KAl ₂ (AlSi ₃ O ₁₀)(OH) ₂ | Mica | 37.6 | 30.5 | 29.7 | 14.5 |
| Albite | NaAlSi ₃ O ₈ | Feldspar | 8.2 | 3.4 | 4.5 | 1.0 |
| Microcline | KAlSi ₃ O ₈ | Feldspar | 9.4 | 8.1 | 6.9 | 2.9 |
| Chlorite | (Fe,(Mg,Mn) ₅ ,Al)(Si ₃ Al)O ₁₀ (OH) ₈ | Clay | - | - | 16.3 | 6.8 |
| Diaspore | aAlO.OH | Oxyhydroxide | - | - | - | - |
| Pyrite | FeS ₂ | Sulfide | 1.0 | 0.8 | - | 1.2 |
| Kaolinite | Al ₂ Si ₂ O ₅ (OH) ₄ | Clay | 9.0 | 18.4 | - | 8.2 |
| Calcite | CaCO ₃ | Carbonate | 1.8 | 1.7 | 14.8 | 31.5 |
| Anatase | TiO ₂ | Oxide | - | 2.1 | 0.7 | 0.4 |
| Leucite | KAlSi ₂ O ₆ | Zeolite | - | - | - | 2.4 |
| Siderite | FeCO ₃ | Carbonate | - | - | - | 1.9 |
| Dolomite | CaMg(CO ₃) ₂ | Carbonate | - | - | - | - |
| Gypsum | CaSO ₄ ·2H ₂ O | Sulfate | - | - | - | - |
| Diopside | CaMgSi ₂ O ₆ | Pyroxene | - | - | - | - |
| Clay Minerals Total | | | 9 | 18 | 16 | 15 |
| Clays + Muscovite Total | | | 47 | 49 | 46 | 30 |

Notes

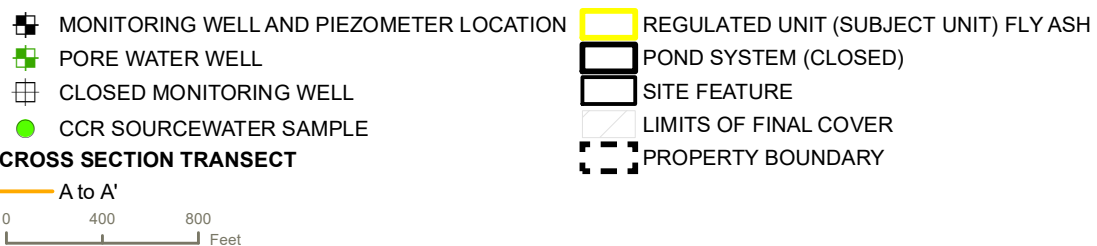
Zero values indicate that the mineral was included in the refinement, but the calculated concentration is below a measurable value.

Dashes indicate that the mineral was not identified by the analyst and not included in the refinement calculation for the sample

The weight percent quantities indicated have been normalized to a sum of 100%. The quantity of amorphous material has not been determined.

Sample depths are shown in feet below ground surface (ft bgs).

ATTACHMENT 1
Cross Section Location Map



ALTERNATE SOURCE DEMONSTRATION
BOTTOM ASH POND
BALDWIN POWER PLANT
BALDWIN, ILLINOIS



ATTACHMENT 2
Cross Section A-A'

C:\Users\Engelhsa\OneDrive - Ramboll\Projects\Visitra\EVS\Baldwin\Working Files\CAD\Baldwin Cross Sections.dwg

PROJECT: 1940100806 DATED: 4/24/2023 2:04 PM DESIGNER: ENGELHSA

- NOTES**
- 1. This profile was developed by interpolation between widely spaced boreholes. Only at the borehole location should it be considered as an approximately accurate representation and then only to the degree implied by the notes on the borehole logs.
 - 2. Scale is approximate.
 - 3. Vertical scale is exaggerated 50X.
 - 4. Groundwater elevations measured on December 12, 2022.

STIFF DIAGRAM LOCATION TYPE:

- BACKGROUND
- UPGRADIENT
- COMPLIANCE

- LEGEND**
- COAL COMBUSTION RESIDUALS (CCR)
 - FILL
 - CLAY (CL/CH)
 - SILT (ML)
 - SAND (SP/SM/SW)
 - BEDROCK / WEATHERED BEDROCK (INTERBEDDED SHALE, LIMESTONE, SANDSTONE, V. LITTLE SS)
 - WELL SCREEN INTERVAL
 - UPPERMOST AQUIFER POTENTIOMETRIC SURFACE
 - UPPERMOST AQUIFER GROUNDWATER ELEVATION
 - POREWATER ELEVATION
 - OTHER GROUNDWATER / SURFACE WATER ELEVATION(S)

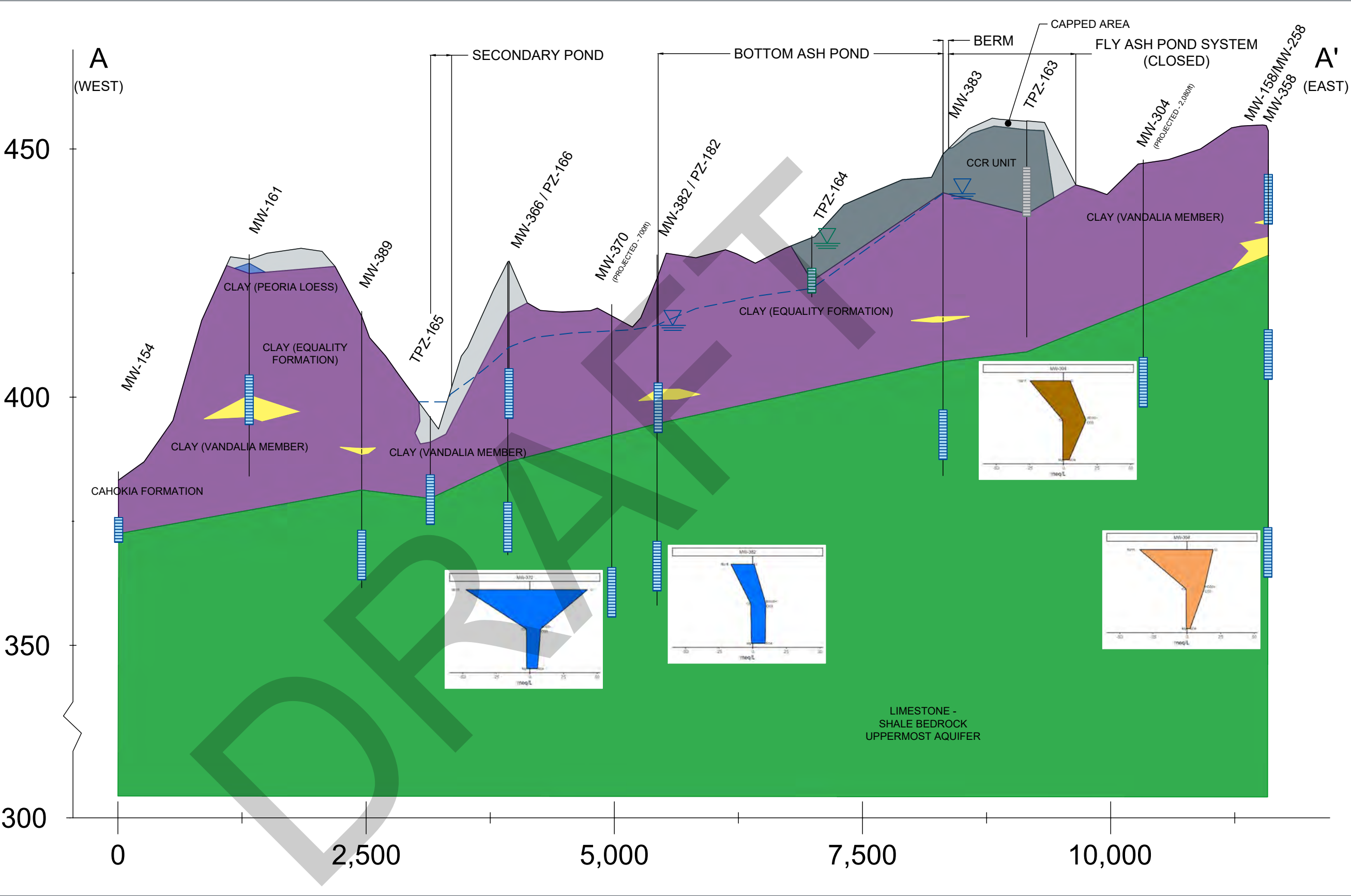
















FIGURE 4

RAMBOLL AMERICAS
ENGINEERING SOLUTIONS, INC.

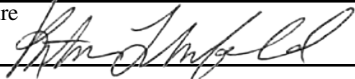


ATTACHMENT 3
Boring Logs

| | | | | | |
|--|--|--|--|--|--|
| Facility/Project Name Baldwin Energy Complex | | License/Permit/Monitoring Number | | Boring Number MW-370 | |
| Boring Drilled By: Name of crew chief (first, last) and Firm Mark Baetje Bulldog Drilling | | Date Drilling Started 11/20/2015 | | Date Drilling Completed 11/24/2015 | |
| Common Well Name MW-370 | | Final Static Water Level Feet (NAVD88) | | Surface Elevation 418.67 Feet (NAVD88) | |
| | | | | Borehole Diameter 8.3 inches | |
| Local Grid Origin <input type="checkbox"/> (estimated: <input type="checkbox"/>) or Boring Location <input checked="" type="checkbox"/> | | Lat <u>38° 11' 44.1702"</u> | | Local Grid Location | |
| State Plane 556,826.50 N, 2,381,936.14 E <input checked="" type="checkbox"/> E/W | | Long <u>-89° 52' 10.8084"</u> | | <input type="checkbox"/> N <input type="checkbox"/> E <input type="checkbox"/> S <input type="checkbox"/> W | |
| 1/4 of <u> </u> 1/4 of Section <u> </u> , T <u> </u> N, R <u> </u> | | | | Feet <u> </u> Feet <u> </u> | |
| Facility ID | | County Randolph | | State Illinois | |
| | | | | Civil Town/City/ or Village Baldwin | |

| Sample | | Blow Counts | Depth In Feet | Soil/Rock Description And Geologic Origin For Each Major Unit | U S C S | Graphic Log | Well Diagram | Soil Properties | | | | | RQD/ Comments |
|--------------------|---------------------------------|-------------|---------------|---|---------|---|---|-------------------------------|---------------------|-----------------|---------------------|-------|---|
| Number and Type | Length Att. & Recovered (in) | | | | | | | Compressive Strength (tsf) | Moisture Content | Liquid Limit | Plasticity Index | P 200 | |
| | | | 1 | 0 - 2' SILTY CLAY CL/ML. | CL/ML |  |  | | | | | | 0-28' Blind Drilled. See log PZ-170 for soil description. |
| | | | 2 | 2 - 4' Shelby Tube Sample. | | | | | | | | | |
| | | | 3 | | | | | | | | | | |
| | | | 4 | 4 - 8' SILTY CLAY CL/ML. | |  |  | | | | | | |
| | | | 5 | | | | | | | | | | |
| | | | 6 | | CL/ML |  |  | | | | | | |
| | | | 7 | | | | | | | | | | |
| | | | 8 | 8 - 10' SILTY CLAY to LEAN CLAY : CL/ML. | |  |  | | | | | | |
| | | | 9 | | CL/ML |  |  | | | | | | |
| | | | 10 | 10 - 12' LEAN CLAY : CL. | |  |  | | | | | | |
| | | | 11 | | CL |  |  | | | | | | |
| | | | 12 | | | | | | | | | | |

I hereby certify that the information on this form is true and correct to the best of my knowledge.

| | | |
|--|--|--|
| Signature  | Firm Natural Resource Technology 234 W. Florida St., Fifth Floor, Milwaukee, WI 53204 | Tel: (414) 837-3607 Fax: (414) 837-3608 |
|--|--|--|

Boring Number **MW-370**

Page 2 of 4

| Sample | | Blow Counts | Depth In Feet | Soil/Rock Description And Geologic Origin For Each Major Unit | U S C S | Graphic Log | Well Diagram | Soil Properties | | | | | RQD/ Comments |
|-----------------|------------------------------|-------------|---------------|--|---------|-------------|--------------|----------------------------|------------------|--------------|------------------|-------|------------------|
| Number and Type | Length Att. & Recovered (in) | | | | | | | Compressive Strength (tsf) | Moisture Content | Liquid Limit | Plasticity Index | P 200 | |
| | | | | 12 - 14' Shelby Tube Sample. | | | | | | | | | |
| | | | 13 | | | | | | | | | | |
| | | | 14 | 14 - 24' SILTY CLAY CL/ML. | | | | | | | | | |
| | | | 15 | | | | | | | | | | |
| | | | 16 | | | | | | | | | | |
| | | | 17 | | | | | | | | | | |
| | | | 18 | | | | | | | | | | |
| | | | 19 | | | | | | | | | | |
| | | | 20 | | | | | | | | | | |
| | | | 21 | | | | | | | | | | |
| | | | 22 | | | | | | | | | | |
| | | | 23 | | | | | | | | | | |
| | | | 24 | 24 - 26' Shelby Tube Sample. | | | | | | | | | |
| | | | 25 | | | | | | | | | | |
| | | | 26 | 26 - 28' SILTY CLAY CL/ML. | | | | | | | | | |
| | | | 27 | | | | | | | | | | |
| | | | 28 | 28 - 28.4' LEAN CLAY : CL, yellowish brown (10YR 5/4), trace angular limestone gravel, soft, medium plasticity, moist. | | | | | | | | | |
| | | | 29 | 28.4 - 28.9' SHALE : BDX (SH), gray, highly decomposed, very weak. | | | | | | | | | |
| | | | 30 | 28.9 - 38.1' SHALEY LIMESTONE : BDX (LS/SH), light gray to gray, intensely fractured (extremely narrow to moderately narrow apertures), medium to thickly bedded, microcrystalline, moderately decomposed, very strong. | | | | | | | | | |
| | | | 31 | | | | | | | | | | |
| | | | 32 | | | | | | | | | | |

1

SS

1

CORE

10

10

60

18.5

23

50/4"

Core 1,
RQD=51%

1 SS 10
1 CORE 60
18.5

23
50/4"

Core 1,
RQD=51%



Page 3 of 4

| Sample | | Blow Counts | Depth In Feet | Soil/Rock Description And Geologic Origin For Each Major Unit | U S C S | Graphic Log | Well Diagram | Soil Properties | | | | | RQD/ Comments |
|-----------------|------------------------------|-------------|--|--|-------------|-------------|--------------|----------------------------|------------------|--------------|------------------|--------------------|------------------|
| Number and Type | Length Att. & Recovered (in) | | | | | | | Compressive Strength (tsf) | Moisture Content | Liquid Limit | Plasticity Index | P 200 | |
| 2 CORE | 51.5 12 | | 33 | 28.9 - 38.1' SHALEY LIMESTONE: BDX (LS/SH), light gray to gray, intensely fractured (extremely narrow to moderately narrow apertures), medium to thickly bedded, microcrystalline, moderately decomposed, very strong. <i>(continued)</i> | BDX (LS/SH) | | | | | | | Core 2, RQD=0% | |
| | | 34 | 33.9' - 38.1' gray, greenish gray in fractures, trace fossils, moderately to highly decomposed, slightly to moderately disintegrated, clay in shoe with a hard, reddish brown inclusion. | | | | | | | | | | |
| | | 35 | | | | | | | | | | | |
| | | 36 | 36' - 37.9' vertical fracture. | | | | | | | | | | |
| 3 CORE | 24 25 | | 38 | 38.1 - 44' SHALE: BDX (SH), bluish gray, intensely fractured (extremely narrow to narrow apertures), highly decomposed, weak. | | | | | | | | Core 3, RQD=40% | |
| | | 39 | | | | | | | | | | | |
| 4 CORE | 24 11 | | 40 | | BDX (SH) | | | | | | | Core 4, RQD=0% | |
| | | 41 | 40.6' - 40.8 shaley limestone layer, light gray to gray, microcrystalline, moderately decomposed, very strong. | | | | | | | | | | |
| 5 CORE | 36 32 | | 42 | 41.1' - 43.2 gray, moderately to highly decomposed. | | | | | | | | Core 5, RQD=78% | |
| | | 43 | | | | | | | | | | | |
| 6 CORE | 12 28 | | 44 | 44 - 45.7' SHALEY LIMESTONE: BDX (LS/SH), light gray to gray, intensely fractured (extremely narrow to narrow apertures), thin to medium bedded, microcrystalline, slightly decomposed, clay cement in apertures, very strong. | BDX (LS/SH) | | | | | | | Core 6, RQD=29% | |
| | | 45 | 45' shale layer, bluish gray, moderately fractured (extremely narrow to narrow apertures), highly decomposed, weak. | | | | | | | | | | |
| 7 CORE | 45 27 | | 46 | 45.7 - 52.2' SHALE: BDX (SH), bluish gray, moderately fractured (tight to narrow), highly decomposed, weak. | | | | | | | | Core 7, RQD=65% | |
| | | 47 | | | | | | | | | | | |
| 8 CORE | 24 30 | | 48 | | BDX (SH) | | | | | | | Core 8, RQD=78% | |
| | | 49 | | | | | | | | | | | |
| | | 50 | | | | | | | | | | | |
| | | 51 | | | | | | | | | | | |
| 9 CORE | 24 24 | | 52 | | | | | | | | | Core 9, RQD=0% | |
| | | | | | | | | | | | | | |




Page 4 of 4

| Sample | | Blow Counts | Depth In Feet | Soil/Rock Description And Geologic Origin For Each Major Unit | U S C S | Graphic Log | Well Diagram | Soil Properties | | | | | RQD/ Comments |
|-----------------|------------------------------|-------------|---------------|--|---------|-------------|--------------|----------------------------|------------------|--------------|------------------|--|------------------|
| Number and Type | Length Att. & Recovered (in) | | | | | | | Compressive Strength (tsf) | Moisture Content | Liquid Limit | Plasticity Index | P 200 | |
| 10 CORE | 24 36 | | 53 | 52' clay cement. | | | | | | | | Core 10, RQD=0% | |
| | | | 54 | 52.2 - 61.7' SHALEY LIMESTONE: BDX (LS/SH), light gray to gray, intensely fractured (very narrow to narrow), thin to medium bedded, microcrystalline, slightly decomposed, cemented clay in apertures, very strong. | | | | | | | | | |
| 11 CORE | 24 30 | | 55 | 52.7' - 53' clayey sand in aperture. | | | | | | | | Core 11, RQD=18% | |
| | | | 56 | 53' - 53.1 shale bed, bluish gray, fossiliferous, moderately fractured (very narrow to narrow), highly decomposed, weak. | | | | | | | | | |
| 12 CORE | 30 27 | | 57 | 53.1' white to bluish gray, gray in the fractures (extremely narrow to moderately narrow apertures), thinly to medium bedded, slightly to moderately disintegrated. | | | | | | | | Core 12, RQD=39% | |
| | | | 58 | 55.7' moderately disintegrated. | | | | | | | | | |
| 13 CORE | 36 53 | | 59 | 58.1' highly decomposed. | | | | | | | | Core 13, RQD=89% | |
| | | | 60 | | | | | | | | | | |
| | | | 61 | | | | | | | | | Bedrock corehole reamed 6" in diameter to 66' for well installation. | |
| | | | 62 | 61.7 - 65.3' LIMESTONE: BDX (LS). | | | | | | | | | |
| | | | 63 | | | | | | | | | | |
| | | | 64 | | | | | | | | | | |
| | | | 65 | 65.3 - 66' Overdrilled for Well Installation. | | | | | | | | | |
| | | | 66 | 66' End of Boring. | | | | | | | | | |

| | | | | | |
|--|--|--|--|--|--|
| Facility/Project Name Baldwin Power Plant | | License/Permit/Monitoring Number | | Boring Number MW358 | |
| Boring Drilled By: Name of crew chief (first, last) and Firm Blake Weller Cascade Drilling | | Date Drilling Started 10/5/2022 | | Date Drilling Completed 10/8/2022 | |
| Common Well Name MW358 | | Final Static Water Level Feet (NAVD88) | | Surface Elevation 453.59 Feet (NAVD88) | |
| | | | | Borehole Diameter 6.0 inches | |
| Local Grid Origin <input type="checkbox"/> (estimated: <input type="checkbox"/>) or Boring Location <input checked="" type="checkbox"/> | | Lat <u>38° 11' 42.9882"</u> | | Local Grid Location | |
| State Plane <u>556,726.26 N, 2,387,756.63 E</u> <input checked="" type="checkbox"/> E/W | | Long <u>-89° 50' 57.9018"</u> | | <input type="checkbox"/> N <input type="checkbox"/> E <input type="checkbox"/> S <input type="checkbox"/> W | |
| 1/4 of <u>1/4</u> of Section <u>T</u> , <u>N</u> , <u>R</u> | | Facility ID | | County Randolph | |
| | | State IL | | Civil Town/City/ or Village Baldwin | |

| Sample | | Blow Counts | Depth In Feet | Soil/Rock Description And Geologic Origin For Each Major Unit | U S C S | Graphic Log | Well Diagram | PID 10.6 eV Lamp | Soil Properties | | | | | RQD/ Comments |
|--------------------|---------------------------------|-------------|---------------|--|----------|----------------|-----------------|------------------|-------------------------------|---------------------|-----------------|---------------------|-------|--|
| Number and Type | Length Att. & Recovered (in) | | | | | | | | Compressive Strength (tsf) | Moisture Content | Liquid Limit | Plasticity Index | P 200 | |
| 1 CS | 180 97 | | | 0 - 3.8' SILT : ML, very dark grayish brown (10YR 3/2), organic material (0-10%), moist to wet. | | | | | | | | | | CS= Core Sample |
| | | | 1 | | | | | | | | | | | Measured Rock Quality Designation (RQD) was modified due to drilling methods, modified RQD equals the sum of recovered core sections greater than 4 inches in length divided by total core recovery. |
| | | | 2 | 2.1' dry. | ML | | | | | | | | | |
| | | | 3 | | | | | | | | | | | |
| | | | 4 | 3.8 - 8.9' CLAYEY SILT : ML/CL, light gray (10YR 7/2), very dark grayish brown (10YR 3/2) and yellowish brown (10YR 5/8) mottling (20-30%), dry. | | | | | | | | | | |
| | | | 5 | | | | | | | | | | | |
| | | | 6 | | ML/CL | | | | | | | | | |
| | | | 7 | | | | | | | | | | | |
| | | | 8 | | | | | | | | | | | |
| | | | 9 | 8.9 - 13' SILTY CLAY WITH SAND : (CL/ML)S, grayish brown (10YR 5/2), strong brown (7.5YR 5/6) and very dark brown (10YR 2/2) mottling (20-30%), organic material (0-10%), low toughness, low to medium plasticity, stiff. | | | | | | | | | | |
| | | | 10 | | (CL/ML)S | | | | | | | | | |
| | | | 11 | | | | | | | | | | | |
| | | | 12 | | | | | | | | | | | |

I hereby certify that the information on this form is true and correct to the best of my knowledge.

| | | |
|---|---|--|
| Signature  | Firm Ramboll 234 W Florida Street, 5th Floor, Milwaukee, WI 53204 | Tel: (414)837-3607 Fax: (414)837-3608 |
|---|---|--|

Boring Number MW358

Page 2 of 5

| Sample | | Blow Counts | Depth In Feet | Soil/Rock Description And Geologic Origin For Each Major Unit | U S C S | Graphic Log | Well Diagram | PID 10.6 eV Lamp | Soil Properties | | | | | | RQD/ Comments |
|-----------------|------------------------------|-------------|---------------|---|----------|-------------|--------------|------------------|----------------------------|------------------|--------------|------------------|-------|--|--|
| Number and Type | Length Att. & Recovered (in) | | | | | | | | Compressive Strength (tsf) | Moisture Content | Liquid Limit | Plasticity Index | P 200 | | |
| 2 CS | 60 60 | | 13 | 13 - 17.8' SILTY CLAY : CL/ML, grayish brown (10YR 5/2), strong brown (7.5YR 5/6) and very dark brown (10YR 2/2) mottling (20-30%), low toughness, medium to high plasticity, stiff to very stiff. | (CL/ML)S | | | | | | | | | | |
| | | | 14 | | CL/ML | | | | | | | | | | |
| | | | 15 | 16.1' mottling discontinues. | | | | | | | | | | | |
| | | | 16 | | | | | | | | | | | | |
| | | | 17 | 17.8 - 21' SILTY CLAY WITH SAND : (CL/ML)S, brown (10YR 5/3), strong brown (7.5YR 5/6) and gray (10YR 6/1) mottling (20-30%), gravel (5-15%), no dilatancy, high toughness, low to medium plasticity, hard, moist. | (CL/ML)S | | | | | | | | | | |
| | | | 18 | | | | | | | | | | | | |
| 3 CS | 48 36 | | 19 | 21 - 26.5' SHALE : BDX (SH), dark gray (GLEYS 1 4/N), weathered, thin bedding, moderately fractured. | | | | | | | | | | | |
| | | | 20 | | | | | | | | | | | | |
| | | | 21 | 24' -25.2' wet. | BDX (SH) | | | | | | | | | | RUN #4: Modified RQD = (21/32) = 66% |
| 4 CORE | 36 32 | | 22 | | | | | | | | | | | | |
| | | | 23 | 26.5 - 27.5' LIMESTONE : BDX (LS), dark gray (5Y 4/1), shaley, fossiliferous, very strong. | BDX (LS) | | | | | | | | | | RUN #5: Modified RQD = (0/29) = 0% |
| | | | 24 | | | | | | | | | | | | |
| 5 CORE | 36 29 | | 25 | 27.5 - 31.3' SHALE : BDX (SH), grayish black (N2), weathered, highly decomposed to residual soil, wet to moist. | | | | | | | | | | | |
| | | | 26 | | | | | | | | | | | | |
| | | | 27 | 29.3' thinly bedded, moderately decomposed. | BDX (SH) | | | | | | | | | | |
| | | | 28 | | | | | | | | | | | | |
| | | | 29 | 30' slightly decomposed to competent, moderately fractured. | | | | | | | | | | | |
| | | | 30 | | | | | | | | | | | | |
| 6 CORE | 72 60 | | 31 | 31.3 - 32' COAL : COAL, black (N1). | COAL | | | | | | | | | | RUN #6: Modified RQD = (45/60) = 75% |
| | | | 32 | | | | | | | | | | | | |

RUN #4:
Modified
RQD =
(21/32) =
66%


RUN #5:
Modified
RQD =
(0/29) = 0%

RUN #6:
Modified
RQD =
(45/60) =
75%

| | | | | | |
|--|--|---|--|--|--|
| Facility/Project Name Baldwin Power Plant | | License/Permit/Monitoring Number | | Boring Number MW392 | |
| Boring Drilled By: Name of crew chief (first, last) and Firm Blake Weller Cascade Drilling | | Date Drilling Started 9/9/2022 | | Date Drilling Completed 9/26/2022 | |
| Common Well Name MW392 | | Final Static Water Level Feet (NAVD88) | | Surface Elevation 434.07 Feet (NAVD88) | |
| | | | | Borehole Diameter 6.0 inches | |
| Local Grid Origin <input type="checkbox"/> (estimated: <input type="checkbox"/>) or Boring Location <input checked="" type="checkbox"/> | | Lat <u>38° 11' 57.132"</u> | | Local Grid Location | |
| State Plane 558,140.20 N, 2,382,717.92 E <input checked="" type="checkbox"/> E/W | | Long <u>-89° 52' 0.9632"</u> | | <input type="checkbox"/> N <input type="checkbox"/> E <input type="checkbox"/> S <input type="checkbox"/> W | |
| 1/4 of <u> </u> 1/4 of Section <u> </u> , T <u> </u> N, R <u> </u> | | Facility ID | | County Randolph | |
| | | State IL | | Civil Town/City/ or Village Baldwin | |

| Sample | | Blow Counts | Depth In Feet | Soil/Rock Description And Geologic Origin For Each Major Unit | U S C S | Graphic Log | Well Diagram | PID 10.6 eV Lamp | Soil Properties | | | | | RQD/ Comments |
|-----------------|------------------------------|-------------|---------------|--|-----------------|-------------|--------------|------------------|----------------------------|------------------|--------------|------------------|--|------------------|
| Number and Type | Length Att. & Recovered (in) | | | | | | | | Compressive Strength (tsf) | Moisture Content | Liquid Limit | Plasticity Index | P 200 | |
| 1 CS | 120 46 | | 1 | 0 - 1.2' FILL, WELL-GRADED GRAVEL WITH CLAY: GW-GC, pinkish gray (7.5YR 6/2), angular, moist. | (FILL) GW-GC | | | | | | | | CS= Core Sample | |
| | | | 2 | 1.2 - 16' FILL, LEAN CLAY: CL, light brown (7.5YR 6/4), sand (0-5%), no dilatancy, low to medium plasticity, moist. | (FILL) CL | | | | | | | | Measured Rock Quality Designation (RQD) was modified due to drilling methods, modified RQD equals the sum of recovered core sections greater than 4 inches in length divided by total core recovery. | |
| 2 CS | 120 62 | | 10 | | | | | | | | | | | |
| | | | 11 | | | | | | | | | | | |
| | | | 12 | | | | | | | | | | | |

I hereby certify that the information on this form is true and correct to the best of my knowledge.

| | | |
|---|---|--|
| Signature  | Firm Ramboll 234 W Florida Street, 5th Floor, Milwaukee, WI 53204 | Tel: (414)837-3607 Fax: (414)837-3608 |
|---|---|--|

RUN #10:
Modified
RQD =
(28/48) =
58%


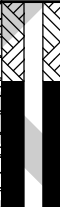




| | | | | | |
|--|--|---|--|--|--|
| Facility/Project Name Baldwin Power Plant | | License/Permit/Monitoring Number | | Boring Number MW393 | |
| Boring Drilled By: Name of crew chief (first, last) and Firm Blake Weller Cascade Drilling | | Date Drilling Started 9/9/2022 | | Date Drilling Completed 10/4/2022 | |
| Common Well Name MW393 | | Final Static Water Level Feet (NAVD88) | | Surface Elevation 434.59 Feet (NAVD88) | |
| | | | | Borehole Diameter 6.0 inches | |
| Local Grid Origin <input type="checkbox"/> (estimated: <input type="checkbox"/>) or Boring Location <input checked="" type="checkbox"/> | | Lat <u>38° 11' 57.027"</u> | | Local Grid Location | |
| State Plane 558,133.57 N, 2,383,944.49 E <input checked="" type="checkbox"/> E/W | | Long <u>-89° 51' 45.5976"</u> | | <input type="checkbox"/> N <input type="checkbox"/> E <input type="checkbox"/> S <input type="checkbox"/> W | |
| 1/4 of <u> </u> 1/4 of Section <u> </u> , T <u> </u> N, R <u> </u> | | Facility ID | | County Randolph | |
| | | State IL | | Civil Town/City/ or Village Baldwin | |

| Sample | | | Blow Counts | Depth In Feet | Soil/Rock Description And Geologic Origin For Each Major Unit | U S C S | Graphic Log | Well Diagram | PID 10.6 eV Lamp | Soil Properties | | | | | RQD/ Comments |
|--------------------|---------------------------------|-------------------------------|-------------|--|---|---------|----------------|-----------------|------------------|---------------------|-----------------|---------------------|-------|--|--|
| Number and Type | Length Att. & Recovered (in) | Compressive Strength (tsf) | | | | | | | | Moisture Content | Liquid Limit | Plasticity Index | P 200 | | |
| 1 CS | 120 86 | | | 0 - 1' FILL, WELL-GRADED GRAVEL: GW, pinkish gray (7.5YR 6/2), angular, moist. | (FILL) GW | | | | | | | | | | CS= Core Sample |
| | | | 1 | 1 - 20' FILL, LEAN CLAY: CL, brown (7.5YR 6/4), sand (0-5%), no dilatancy, low to medium plasticity, moist. | (FILL) CL | | | | | | | | | | Measured Rock Quality Designation (RQD) was modified due to drilling methods, modified RQD equals the sum of recovered core sections greater than 4 inches in length divided by total core recovery. |
| | | | 2 | | | | | | | | | | | | |
| | | | 3 | | | | | | | | | | | | |
| | | | 4 | | | | | | | | | | | | |
| | | | 5 | | | | | | | | | | | | |
| | | | 6 | | | | | | | | | | | | |
| | | | 7 | | | | | | | | | | | | |
| | | | 8 | | | | | | | | | | | | |
| | | | 9 | | | | | | | | | | | | |
| | | | 10 | 10' sand (0-5%), iron concretions (0-5%). | | | | | | | | | | | |
| 2 CS | 120 120 | | | | | | | | | | | | | | |
| | | | | | | | | | | | | | | | |
| | | | | | | | | | | | | | | | |
| | | | | | | | | | | | | | | | |
| | | | | | | | | | | | | | | | |
| | | | | | | | | | | | | | | | |
| | | | | | | | | | | | | | | | |
| | | | | | | | | | | | | | | | |
| | | | | | | | | | | | | | | | |
| | | | | | | | | | | | | | | | |
| | | | | | | | | | | | | | | | |
| | | | | | | | | | | | | | | | |
| | | | | | | | | | | | | | | | |
| | | | | | | | | | | | | | | | |
| | | | | | | | | | | | | | | | |
| | | | | | | | | | | | | | | | |
| | | | | | | | | | | | | | | | |
| | | | | | | | | | | | | | | | |
| | | | | | | | | | | | | | | | |
| | | | | | | | | | | | | | | | |
| | | | | | | | | | | | | | | | |
| | | | | | | | | | | | | | | | |
| | | | | | | | | | | | | | | | |
| | | | | | | | | | | | | | | | |
| | | | | | | | | | | | | | | | |
| | | | | | | | | | | | | | | | |
| | | | | | | | | | | | | | | | |
| | | | | | | | | | | | | | | | |
| | | | | | | | | | | | | | | | |
| | | | | | | | | | | | | | | | |
| | | | | | | | | | | | | | | | |
| | | | | | | | | | | | | | | | |
| | | | | | | | | | | | | | | | |
| | | | | | | | | | | | | | | | |
| | | | | | | | | | | | | | | | |
| | | | | | | | | | | | | | | | |
| | | | | | | | | | | | | | | | |
| | | | | | | | | | | | | | | | |
| | | | | | | | | | | | | | | | |
| | | | | | | | | | | | | | | | |
| | | | | | | | | | | | | | | | |
| | | | | | | | | | | | | | | | |
| | | | | | | | | | | | | | | | |
| | | | | | | | | | | | | | | | |
| | | | | | | | | | | | | | | | |
| | | | | | | | | | | | | | | | |
| | | | | | | | | | | | | | | | |
| | | | | | | | | | | | | | | | |
| | | | | | | | | | | | | | | | |
| | | | | | | | | | | | | | | | |
| | | | | | | | | | | | | | | | |
| | | | | | | | | | | | | | | | |
| | | | | | | | | | | | | | | | |
| | | | | | | | | | | | | | | | |
| | | | | | | | | | | | | | | | |
| | | | | | | | | | | | | | | | |
| | | | | | | | | | | | | | | | |
| | | | | | | | | | | | | | | | |
| | | | | | | | | | | | | | | | |
| | | | | | | | | | | | | | | | |
| | | | | | | | | | | | | | | | |
| | | | | | | | | | | | | | | | |
| | | | | | | | | | | | | | | | |
| | | | | | | | | | | | | | | | |
| | | | | | | | | | | | | | | | |
| | | | | | | | | | | | | | | | |
| | | | | | | | | | | | | | | | |
| | | | | | | | | | | | | | | | |
| | | | | | | | | | | | | | | | |
| | | | | | | | | | | | | | | | |
| | | | | | | | | | | | | | | | |
| | | | | | | | | | | | | | | | |
| | | | | | | | | | | | | | | | |

I hereby certify that the information on this form is true and correct to the best of my knowledge.

| | | |
|-----------|---|--|
| Signature | Firm Ramboll 234 W Florida Street, 5th Floor, Milwaukee, WI 53204 | Tel: (414)837-3607 Fax: (414)837-3608 |
|-----------|---|--|

| | | | | | |
|--|--|---|--|--|--|
| Facility/Project Name Baldwin Power Plant | | License/Permit/Monitoring Number | | Boring Number MW394 | |
| Boring Drilled By: Name of crew chief (first, last) and Firm Blake Weller Cascade Drilling | | Date Drilling Started 9/25/2022 | | Date Drilling Completed 10/5/2022 | |
| Common Well Name MW394 | | Final Static Water Level Feet (NAVD88) | | Surface Elevation 435.51 Feet (NAVD88) | |
| | | | | Borehole Diameter 6.0 inches | |
| Local Grid Origin <input type="checkbox"/> (estimated: <input type="checkbox"/>) or Boring Location <input checked="" type="checkbox"/> | | Lat <u>38° 11' 56.8911"</u> | | Local Grid Location | |
| State Plane 558,123.63 N, 2,385,095.76 E <input checked="" type="checkbox"/> E/W | | Long <u>-89° 51' 31.1756"</u> | | <input type="checkbox"/> N <input type="checkbox"/> E <input type="checkbox"/> S <input type="checkbox"/> W | |
| 1/4 of <u> </u> 1/4 of Section <u> </u> , T <u> </u> N, R <u> </u> | | Facility ID | | County Randolph | |
| | | State IL | | Civil Town/City/ or Village Baldwin | |

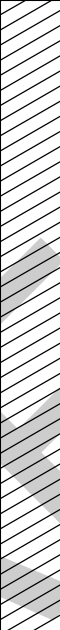













| Sample | | Blow Counts | Depth In Feet | Soil/Rock Description And Geologic Origin For Each Major Unit | U S C S | Graphic Log | Well Diagram | PID 10.6 eV Lamp | Soil Properties | | | | | RQD/ Comments |
|-----------------|------------------------------|-------------|---------------|---|-----------------|--|---|------------------|----------------------------|------------------|--------------|------------------|--|------------------|
| Number and Type | Length Att. & Recovered (in) | | | | | | | | Compressive Strength (tsf) | Moisture Content | Liquid Limit | Plasticity Index | P 200 | |
| 1 CS | 72 67 | | 1 | 0 - 2.6' FILL, WELL-GRADED GRAVEL WITH CLAY: GW-GC, brown (10YR 4/3), angular, moist. | (FILL) GW-GC |  |  | | | | | | CS= Core Sample | |
| | | | 2 | | | | | | | | | | Measured Rock Quality Designation (RQD) was modified due to drilling methods, modified RQD equals the sum of recovered core sections greater than 4 inches in length divided by total core recovery. | |
| | | | 3 | 2.6 - 20' LEAN CLAY: CL, brown (10YR 5/3), reddish brown bottling (20%), sand (0-5%), low to medium plasticity, very stiff to hard, moist. | |  |  | | 4 | | | | | |
| | | | 4 | | | | | | | | | | | |
| | | | 5 | | | | | | 4 | | | | | |
| | | | 6 | | | | | | | | | | | |
| 2 CS | 120 120 | | 7 | | CL |  |  | | 2.5 | | | | | |
| | | | 8 | | | | | | 3.5 | | | | | |
| | | | 9 | | | | | | 2 | | | | | |
| | | | 10 | 9.2' brown (7.5YR 5/3), medium to high plasticity. | | | | | 2 | | | | | |
| | | | 11 | | | | | | 3 | | | | | |
| | | | 12 | | | | | | 2.25 | | | | | |

I hereby certify that the information on this form is true and correct to the best of my knowledge.

| | | |
|---|---|--|
| Signature  | Firm Ramboll 234 W Florida Street, 5th Floor, Milwaukee, WI 53204 | Tel: (414)837-3607 Fax: (414)837-3608 |
|---|---|--|

Boring Number MW394

Page 2 of 5

| Sample | | Blow Counts | Depth In Feet | Soil/Rock Description And Geologic Origin For Each Major Unit | USCS | Graphic Log | Well Diagram | PID 10.6 eV Lamp | Soil Properties | | | | | RQD/ Comments |
|-----------------|------------------------------|-------------|--|---|------|--|---|---|----------------------------|---|---|---|---|------------------|
| Number and Type | Length Att. & Recovered (in) | | | | | | | | Compressive Strength (tsf) | Moisture Content | Liquid Limit | Plasticity Index | P 200 | |
| 3 CS | 120 120 | | 13 | 2.6 - 20' LEAN CLAY: CL, brown (10YR 5/3), reddish brown bottling (20%), sand (0-5%), low to medium plasticity, very stiff to hard, moist. (continued) | CL |  |  |  | 2.25 |  |  |  |  | |
| | | 14 | 14' low to medium plasticity. | 2.5 | | | | | | | | | | |
| | | 15 | | | | | | | | | | | | |
| | | 16 | | | | | | | | | | | | |
| | | 17 | 16.5' increasing sand and gravel content, gray (GLEY 1 5/1) iron concretions (50%). | | | | | | | | | | | |
| | | 18 | | | | | | | | | | | | |
| | | 19 | | | | | | | | | | | | |
| | | 20 | | | | | | | | | | | | |
| | | 21 | | | | | | | | | | | | |
| | | 22 | | | | | | | | | | | | |
| 4 CS | 120 112 | | 20 | 20 - 22.1' SILTY SAND: SM, yellowish brown (10YR 5/6), fine sand, clay (0-5%), moist. | SM |  |  |  | |  |  |  |  | |
| | | 21 | | | | | | | | | | | | |
| | | 22 | | | | | | | | | | | | |
| | | 23 | 22.1 - 36.8' LEAN CLAY: CL, dark yellowish brown (10YR 4/4), greenish gray (GLEY 1 5/10Y) and yellowish brown (10YR 5/6) mottling, sand (0-5%), medium to high plasticity, hard, moist. | 4.5 | | | | | | | | | | |
| | | 24 | 4.5 | | | | | | | | | | | |
| | | 25 | | | | | | | | | | | | |
| | | 26 | 4.5 | | | | | | | | | | | |
| | | 27 | 4.5 | | | | | | | | | | | |
| | | 28 | 4.5 | | | | | | | | | | | |
| | | 29 | 4.5 | | | | | | | | | | | |
| | 30 | 4.5 | | | | | | | | | | | | |
| | 31 | 4.5 | | | | | | | | | | | | |
| | 32 | 4.5 | | | | | | | | | | | | |

ATTACHMENT 4
Analytical Laboratory Reports

**SGS Canada Inc.**

P.O. Box 4300 - 185 Concession St.
Lakefield - Ontario - KOL 2H0
Phone: 705-652-2000 FAX: 705-652-6365

28-February-2023

Ramboll Americas Engineering Solutions, Inc.

Attn : Evvan Plank

P.O# Box 4873
Syracuse, New York
13221-7873, USA

Phone: 315-463-7554
Fax:

Date Rec. : 24 November 2022
LR Report: CA19218-NOV22
Reference: Baldwin Power Plant Drilling

Copy: #1

CERTIFICATE OF ANALYSIS

Final Report

| Analysis | 1: Analysis Start Date | 2: Analysis Start Time Completed | 3: Analysis DateCompleted | 4: Analysis Time | 5: MW-358 (13-15) | 6: MW-358 (47-49) | 7: MW-358 (86-88) | 8: MW-392 (80-82) |
|--------------------|------------------------------|--|---------------------------------|------------------------|----------------------|----------------------|----------------------|----------------------|
| Sample Date & Time | | | | | 05-Oct-22 14:05 | 06-Oct-22 15:00 | 08-Oct-22 18:00 | 26-Sep-22 16:00 |
| Ag [µg/g] | 19-Jan-23 | 23:42 | 31-Jan-23 | 09:43 | < 0.05 | < 0.05 | < 0.05 | < 0.05 |
| Al [µg/g] | 19-Jan-23 | 23:42 | 31-Jan-23 | 09:43 | 30 | 540 | 380 | 18 |
| As [µg/g] | 19-Jan-23 | 23:42 | 31-Jan-23 | 09:43 | < 0.5 | < 0.5 | < 0.5 | < 0.5 |
| Ba [µg/g] | 19-Jan-23 | 23:42 | 31-Jan-23 | 09:43 | 0.4 | 11 | 4.2 | < 0.1 |
| Be [µg/g] | 19-Jan-23 | 23:42 | 31-Jan-23 | 09:43 | < 0.02 | 0.06 | 0.05 | < 0.02 |
| B [µg/g] | 19-Jan-23 | 23:42 | 31-Jan-23 | 09:43 | < 1 | 8 | 10 | 3 |
| Bi [µg/g] | 19-Jan-23 | 23:42 | 31-Jan-23 | 09:43 | < 0.09 | < 0.09 | < 0.09 | < 0.09 |
| Ca [µg/g] | 19-Jan-23 | 23:42 | 31-Jan-23 | 09:43 | 21 | 300 | 140 | 75 |
| Cd [µg/g] | 19-Jan-23 | 23:42 | 31-Jan-23 | 09:43 | < 0.05 | < 0.05 | < 0.05 | < 0.05 |
| Co [µg/g] | 19-Jan-23 | 23:42 | 31-Jan-23 | 09:43 | < 0.01 | 0.04 | 0.86 | 0.02 |
| Cr [µg/g] | 19-Jan-23 | 23:42 | 31-Jan-23 | 09:43 | < 0.5 | < 0.5 | < 0.5 | < 0.5 |
| Cu [µg/g] | 19-Jan-23 | 23:42 | 31-Jan-23 | 09:43 | < 0.1 | < 0.1 | 0.1 | < 0.1 |
| Fe [µg/g] | 19-Jan-23 | 23:42 | 31-Jan-23 | 09:43 | 17 | 240 | 190 | < 1 |
| K [µg/g] | 19-Jan-23 | 23:42 | 31-Jan-23 | 09:43 | 7 | 250 | 190 | 41 |
| Li [µg/g] | 19-Jan-23 | 23:42 | 31-Jan-23 | 09:43 | < 2 | < 2 | < 2 | < 2 |
| Mg [µg/g] | 19-Jan-23 | 23:42 | 31-Jan-23 | 09:43 | 9 | 210 | 150 | 19 |
| Mn [µg/g] | 19-Jan-23 | 23:42 | 31-Jan-23 | 09:43 | < 0.5 | 0.6 | 0.9 | < 0.5 |
| Mo [µg/g] | 19-Jan-23 | 23:42 | 31-Jan-23 | 09:43 | < 0.1 | < 0.1 | < 0.1 | < 0.1 |
| Na [µg/g] | 19-Jan-23 | 23:42 | 31-Jan-23 | 09:43 | 65 | 1800 | 1600 | 850 |
| Ni [µg/g] | 19-Jan-23 | 23:42 | 31-Jan-23 | 09:43 | < 0.5 | < 0.5 | 1.2 | < 0.5 |
| P [µg/g] | 19-Jan-23 | 23:42 | 31-Jan-23 | 09:43 | < 3 | 6 | < 3 | < 3 |
| Pb [µg/g] | 19-Jan-23 | 23:42 | 31-Jan-23 | 09:43 | < 0.1 | < 0.1 | 0.2 | < 0.1 |
| Si [µg/g] | 19-Jan-23 | 23:42 | 31-Jan-23 | 09:43 | 100 | 950 | 750 | 59 |
| Sb [µg/g] | 19-Jan-23 | 23:42 | 31-Jan-23 | 09:43 | < 0.8 | < 0.8 | < 0.8 | < 0.8 |
| Se [µg/g] | 19-Jan-23 | 23:42 | 31-Jan-23 | 09:43 | < 0.7 | < 0.7 | < 0.7 | < 0.7 |
| Sr [µg/g] | 19-Jan-23 | 23:42 | 31-Jan-23 | 09:43 | 0.1 | 13 | 5.9 | 1.4 |
| Sn [µg/g] | 19-Jan-23 | 23:42 | 31-Jan-23 | 09:43 | < 0.5 | < 0.5 | < 0.5 | < 0.5 |
| Ti [µg/g] | 19-Jan-23 | 23:42 | 31-Jan-23 | 09:43 | 1.1 | 0.6 | 0.5 | 0.6 |
| Tl [µg/g] | 19-Jan-23 | 23:42 | 31-Jan-23 | 09:43 | < 0.02 | < 0.02 | < 0.02 | < 0.02 |
| U [µg/g] | 19-Jan-23 | 23:42 | 31-Jan-23 | 09:43 | < 0.002 | 0.006 | 0.029 | < 0.002 |
| V [µg/g] | 19-Jan-23 | 23:42 | 31-Jan-23 | 09:43 | < 3 | < 3 | < 3 | < 3 |
| Zn [µg/g] | 19-Jan-23 | 23:42 | 31-Jan-23 | 09:43 | < 0.7 | < 0.7 | < 0.7 | < 0.7 |

SGS Canada Inc.

P.O. Box 4300 - 185 Concession St.

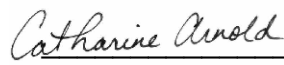
Lakefield - Ontario - KOL 2H0

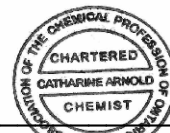
Phone: 705-652-2000 FAX: 705-652-6365

LR Report : CA19218-NOV22

| Analysis | 9: MW-392 (32-33.5) | 10: MW-393 (24-25.5) | 11: MW-394 (20.5-22) | 12: MW-392 (66-68) |
|--------------------|------------------------|-------------------------|-------------------------|-----------------------|
| Sample Date & Time | 27-Sep-22 09:00 | 04-Oct-22 16:00 | 25-Sep-22 16:00 | 26-Sep-22 12:00 |
| Ag [µg/g] | < 0.05 | < 0.05 | < 0.05 | < 0.05 |
| Al [µg/g] | 33 | 26 | 24 | 59 |
| As [µg/g] | < 0.5 | < 0.5 | < 0.5 | < 0.5 |
| Ba [µg/g] | 0.5 | 0.3 | 0.3 | 0.3 |
| Be [µg/g] | < 0.02 | < 0.02 | < 0.02 | < 0.02 |
| B [µg/g] | < 1 | < 1 | < 1 | 5 |
| Bi [µg/g] | < 0.09 | < 0.09 | < 0.09 | < 0.09 |
| Ca [µg/g] | 130 | 28 | 25 | 89 |
| Cd [µg/g] | < 0.05 | < 0.05 | < 0.05 | < 0.05 |
| Co [µg/g] | 0.02 | < 0.01 | 0.01 | 0.02 |
| Cr [µg/g] | < 0.5 | < 0.5 | < 0.5 | < 0.5 |
| Cu [µg/g] | < 0.1 | < 0.1 | < 0.1 | < 0.1 |
| Fe [µg/g] | 27 | 14 | 20 | 28 |
| K [µg/g] | 16 | 9 | 12 | 92 |
| Li [µg/g] | < 2 | < 2 | < 2 | < 2 |
| Mg [µg/g] | 40 | 12 | 12 | 44 |
| Mn [µg/g] | 1.4 | 0.7 | 0.6 | < 0.5 |
| Mo [µg/g] | < 0.1 | < 0.1 | < 0.1 | < 0.1 |
| Na [µg/g] | 44 | 49 | 43 | 720 |
| Ni [µg/g] | < 0.5 | < 0.5 | < 0.5 | < 0.5 |
| P [µg/g] | < 3 | < 3 | < 3 | < 3 |
| Pb [µg/g] | < 0.1 | < 0.1 | < 0.1 | < 0.1 |
| Si [µg/g] | 100 | 80 | 91 | 140 |
| Sb [µg/g] | < 0.8 | < 0.8 | < 0.8 | < 0.8 |
| Se [µg/g] | < 0.7 | < 0.7 | < 0.7 | < 0.7 |
| Sr [µg/g] | 0.3 | < 0.1 | < 0.1 | 1.8 |
| Sn [µg/g] | < 0.5 | < 0.5 | < 0.5 | < 0.5 |
| Ti [µg/g] | 0.6 | 0.6 | 0.9 | 0.5 |
| Tl [µg/g] | < 0.02 | < 0.02 | < 0.02 | < 0.02 |
| U [µg/g] | < 0.002 | < 0.002 | < 0.002 | < 0.002 |
| V [µg/g] | < 3 | < 3 | < 3 | < 3 |
| Zn [µg/g] | < 0.7 | < 0.7 | < 0.7 | < 0.7 |

Water Soluble Fraction


Catharine Arnold, B.Sc., C.Chem
Project Specialist,
Environment, Health & Safety



**SGS Canada Inc.**

P.O. Box 4300 - 185 Concession St.
Lakefield - Ontario - K0L 2H0
Phone: 705-652-2000 FAX: 705-652-6365

Tessier Leach Fraction 2 - Exchangeable Metals

28-February-2023

Ramboll Americas Engineering Solutions, Inc.

Attn : Evvan Plank

P.O# Box 4873
Syracuse, New York
13221-7873, USA

Phone: 315-463-7554
Fax:

Date Rec. : 24 November 2022
LR Report: CA19219-NOV22
Reference: Baldwin Power Plant Drilling

Copy: #1

CERTIFICATE OF ANALYSIS

Final Report

| Analysis | 1: Analysis Start Date | 2: Analysis Start Time Completed | 3: Analysis DateCompleted | 4: Analysis Time | 5: MW-358 (13-15) | 6: MW-358 (47-49) | 7: MW-358 (86-88) | 8: MW-392 (80-82) |
|--------------------|------------------------------|--|---------------------------------|------------------------|----------------------|----------------------|----------------------|----------------------|
| Sample Date & Time | | | | | 05-Oct-22 14:05 | 06-Oct-22 15:00 | 08-Oct-22 18:00 | 26-Sep-22 16:00 |
| Ag [µg/g] | 19-Jan-23 | 23:42 | 31-Jan-23 | 09:43 | < 0.05 | < 0.05 | < 0.05 | < 0.05 |
| Al [µg/g] | 19-Jan-23 | 23:42 | 31-Jan-23 | 09:43 | 9 | 17 | 8 | 9 |
| As [µg/g] | 19-Jan-23 | 23:42 | 31-Jan-23 | 09:43 | < 0.5 | < 0.5 | < 0.5 | < 0.5 |
| Ba [µg/g] | 19-Jan-23 | 23:42 | 31-Jan-23 | 09:43 | 48 | 55 | 15 | 3.0 |
| Be [µg/g] | 19-Jan-23 | 23:42 | 31-Jan-23 | 09:43 | < 0.02 | < 0.02 | < 0.02 | < 0.02 |
| B [µg/g] | 19-Jan-23 | 23:42 | 31-Jan-23 | 09:43 | < 1 | < 1 | 1 | < 1 |
| Bi [µg/g] | 19-Jan-23 | 23:42 | 31-Jan-23 | 09:43 | < 0.09 | < 0.09 | < 0.09 | < 0.09 |
| Ca [µg/g] | 19-Jan-23 | 23:42 | 31-Jan-23 | 09:43 | 2000 | 2500 | 1300 | 3500 |
| Cd [µg/g] | 19-Jan-23 | 23:42 | 31-Jan-23 | 09:43 | < 0.05 | < 0.05 | < 0.05 | < 0.05 |
| Co [µg/g] | 19-Jan-23 | 23:42 | 31-Jan-23 | 09:43 | < 0.01 | < 0.01 | 0.58 | 0.24 |
| Cr [µg/g] | 19-Jan-23 | 23:42 | 31-Jan-23 | 09:43 | < 0.5 | < 0.5 | < 0.5 | < 0.5 |
| Cu [µg/g] | 19-Jan-23 | 23:42 | 31-Jan-23 | 09:43 | < 0.1 | < 0.1 | < 0.1 | < 0.1 |
| Fe [µg/g] | 19-Jan-23 | 23:42 | 31-Jan-23 | 09:43 | 2 | 21 | < 1 | 12 |
| K [µg/g] | 19-Jan-23 | 23:42 | 31-Jan-23 | 09:43 | 37 | 430 | 300 | 160 |
| Li [µg/g] | 19-Jan-23 | 23:42 | 31-Jan-23 | 09:43 | < 2 | < 2 | < 2 | < 2 |
| Mn [µg/g] | 19-Jan-23 | 23:42 | 31-Jan-23 | 09:44 | 6.5 | 0.7 | 1.8 | 3.6 |
| Mo [µg/g] | 19-Jan-23 | 23:42 | 31-Jan-23 | 09:44 | < 0.1 | < 0.1 | < 0.1 | < 0.1 |
| Na [µg/g] | 19-Jan-23 | 23:42 | 31-Jan-23 | 09:44 | 45 | 3200 | 2600 | 420 |
| Ni [µg/g] | 19-Jan-23 | 23:42 | 31-Jan-23 | 09:44 | < 0.5 | < 0.5 | < 0.5 | 0.7 |
| Pb [µg/g] | 19-Jan-23 | 23:42 | 31-Jan-23 | 09:44 | < 0.1 | < 0.1 | < 0.1 | < 0.1 |
| P [µg/g] | 19-Jan-23 | 23:42 | 31-Jan-23 | 09:44 | < 3 | 4 | < 3 | 43 |
| Sb [µg/g] | 19-Jan-23 | 23:42 | 31-Jan-23 | 09:44 | < 0.8 | < 0.8 | < 0.8 | < 0.8 |
| Se [µg/g] | 19-Jan-23 | 23:42 | 31-Jan-23 | 09:44 | < 0.7 | < 0.7 | < 0.7 | < 0.7 |
| Sn [µg/g] | 19-Jan-23 | 23:42 | 31-Jan-23 | 09:44 | < 0.5 | < 0.5 | < 0.5 | < 0.5 |
| Sr [µg/g] | 19-Jan-23 | 23:42 | 31-Jan-23 | 09:44 | 11 | 100 | 52 | 76 |
| Ti [µg/g] | 19-Jan-23 | 23:42 | 31-Jan-23 | 09:44 | 0.9 | 0.3 | 0.2 | 0.1 |
| Tl [µg/g] | 19-Jan-23 | 23:42 | 31-Jan-23 | 09:44 | < 0.02 | < 0.02 | < 0.02 | < 0.02 |
| U [µg/g] | 19-Jan-23 | 23:42 | 31-Jan-23 | 09:44 | < 0.002 | 0.009 | 0.006 | 0.043 |
| V [µg/g] | 19-Jan-23 | 23:42 | 31-Jan-23 | 09:44 | < 3 | < 3 | < 3 | < 3 |
| Zn [µg/g] | 19-Jan-23 | 23:42 | 31-Jan-23 | 09:44 | < 0.7 | < 0.7 | < 0.7 | < 0.7 |

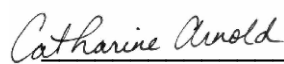
SGS Canada Inc.

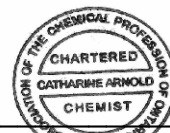
P.O. Box 4300 - 185 Concession St.
Lakefield - Ontario - K0L 2H0
Phone: 705-652-2000 FAX: 705-652-6365

LR Report : CA19219-NOV22

| Analysis | 9: MW-392 (32-33.5) | 10: MW-393 (24-25.5) | 11: MW-394 (20.5-22) | 12: MW-392 (66-68) |
|--------------------|------------------------|-------------------------|-------------------------|-----------------------|
| Sample Date & Time | 27-Sep-22 09:00 | 04-Oct-22 16:00 | 25-Sep-22 16:00 | 26-Sep-22 12:00 |
| Ag [µg/g] | < 0.05 | < 0.05 | < 0.05 | < 0.05 |
| Al [µg/g] | 10 | 12 | 12 | 10 |
| As [µg/g] | < 0.5 | < 0.5 | < 0.5 | < 0.5 |
| Ba [µg/g] | 16 | 16 | 10 | 4.3 |
| Be [µg/g] | < 0.02 | < 0.02 | < 0.02 | < 0.02 |
| B [µg/g] | < 1 | < 1 | < 1 | 2 |
| Bi [µg/g] | < 0.09 | < 0.09 | < 0.09 | < 0.09 |
| Ca [µg/g] | 2500 | 1400 | 2100 | 3700 |
| Cd [µg/g] | < 0.05 | < 0.05 | < 0.05 | < 0.05 |
| Co [µg/g] | 0.02 | < 0.01 | < 0.01 | 0.02 |
| Cr [µg/g] | < 0.5 | < 0.5 | < 0.5 | < 0.5 |
| Cu [µg/g] | < 0.1 | < 0.1 | < 0.1 | < 0.1 |
| Fe [µg/g] | 8 | 9 | 8 | 10 |
| K [µg/g] | 44 | 35 | 60 | 360 |
| Li [µg/g] | < 2 | < 2 | < 2 | < 2 |
| Mn [µg/g] | 3.5 | 1.7 | 3.2 | 2.5 |
| Mo [µg/g] | < 0.1 | < 0.1 | < 0.1 | < 0.1 |
| Na [µg/g] | 17 | 22 | 30 | 480 |
| Ni [µg/g] | < 0.5 | < 0.5 | < 0.5 | < 0.5 |
| Pb [µg/g] | < 0.1 | < 0.1 | < 0.1 | < 0.1 |
| P [µg/g] | < 3 | < 3 | 4 | < 3 |
| Sb [µg/g] | < 0.8 | < 0.8 | < 0.8 | < 0.8 |
| Se [µg/g] | < 0.7 | < 0.7 | < 0.7 | < 0.7 |
| Sn [µg/g] | < 0.5 | < 0.5 | < 0.5 | < 0.5 |
| Sr [µg/g] | 6.5 | 4.3 | 7.4 | 75 |
| Ti [µg/g] | 0.1 | 0.6 | 0.3 | < 0.1 |
| Tl [µg/g] | < 0.02 | < 0.02 | < 0.02 | < 0.02 |
| U [µg/g] | < 0.002 | < 0.002 | < 0.002 | 0.004 |
| V [µg/g] | < 3 | < 3 | < 3 | < 3 |
| Zn [µg/g] | < 0.7 | < 0.7 | < 0.7 | < 0.7 |

Fraction 2 Exchangeable Metals


Catharine Arnold, B.Sc., C.Chem
Project Specialist,
Environment, Health & Safety



**SGS Canada Inc.**

P.O. Box 4300 - 185 Concession St.
Lakefield - Ontario - KOL 2H0
Phone: 705-652-2000 FAX: 705-652-6365

Tessier Leach Fraction 3 - Metals Bound to Carbonates

28-February-2023

Ramboll Americas Engineering Solutions, Inc.

Attn : Evvan Plank

P.O# Box 4873
Syracuse, New York
13221-7873, USA

Phone: 315-463-7554
Fax:

Date Rec. : 24 November 2022
LR Report: CA19220-NOV22
Reference: Ramboll Power Plant Drilling

Copy: #1

CERTIFICATE OF ANALYSIS

Final Report

| Analysis | 1: Analysis Start Date | 2: Analysis Start Time Completed | 3: Analysis DateCompleted | 4: Analysis Time | 5: MW-358 (13-15) | 6: MW-358 (47-49) | 7: MW-358 (86-88) | 8: MW-392 (80-82) |
|--------------------|------------------------------|--|---------------------------------|------------------------|----------------------|----------------------|----------------------|----------------------|
| Sample Date & Time | | | | | 05-Oct-22 14:05 | 06-Oct-22 15:00 | 08-Oct-22 18:00 | 26-Sep-22 16:00 |
| Ag [µg/g] | 19-Jan-23 | 23:42 | 31-Jan-23 | 09:45 | < 0.05 | < 0.05 | < 0.05 | < 0.05 |
| Al [µg/g] | 19-Jan-23 | 23:42 | 31-Jan-23 | 09:45 | 30 | 55 | 56 | 25 |
| As [µg/g] | 19-Jan-23 | 23:42 | 31-Jan-23 | 09:45 | < 0.5 | < 0.5 | < 0.5 | < 0.5 |
| Ba [µg/g] | 19-Jan-23 | 23:42 | 31-Jan-23 | 09:45 | 25 | 23 | 6.9 | 2.8 |
| Be [µg/g] | 19-Jan-23 | 23:42 | 31-Jan-23 | 09:45 | 0.09 | 0.10 | 0.07 | 0.03 |
| B [µg/g] | 19-Jan-23 | 23:42 | 31-Jan-23 | 09:45 | < 1 | 2 | 3 | 4 |
| Bi [µg/g] | 19-Jan-23 | 23:42 | 31-Jan-23 | 09:45 | < 0.09 | < 0.09 | < 0.09 | < 0.09 |
| Ca [µg/g] | 19-Jan-23 | 23:42 | 31-Jan-23 | 09:45 | 110 | 1300 | 770 | 52000 |
| Cd [µg/g] | 19-Jan-23 | 23:42 | 31-Jan-23 | 09:45 | < 0.05 | < 0.05 | < 0.05 | < 0.05 |
| Co [µg/g] | 19-Jan-23 | 23:42 | 31-Jan-23 | 09:45 | 0.04 | 0.02 | 2.3 | 1.0 |
| Cr [µg/g] | 19-Jan-23 | 23:42 | 31-Jan-23 | 09:45 | < 0.5 | < 0.5 | < 0.5 | < 0.5 |
| Cu [µg/g] | 19-Jan-23 | 23:42 | 31-Jan-23 | 09:45 | 0.6 | 0.2 | 0.6 | 0.2 |
| Fe [µg/g] | 19-Jan-23 | 23:42 | 31-Jan-23 | 09:45 | 40 | 45 | 42 | 25 |
| K [µg/g] | 19-Jan-23 | 23:42 | 31-Jan-23 | 09:45 | 15 | 180 | 120 | 90 |
| Li [µg/g] | 19-Jan-23 | 23:42 | 31-Jan-23 | 09:45 | < 2 | < 2 | < 2 | < 2 |
| Mn [µg/g] | 19-Jan-23 | 23:42 | 31-Jan-23 | 09:45 | 13 | 7.0 | 4.3 | 77 |
| Mo [µg/g] | 19-Jan-23 | 23:42 | 31-Jan-23 | 09:45 | < 0.1 | < 0.1 | < 0.1 | < 0.1 |
| Ni [µg/g] | 19-Jan-23 | 23:42 | 31-Jan-23 | 09:46 | < 0.5 | < 0.5 | 1.9 | 2.7 |
| Pb [µg/g] | 19-Jan-23 | 23:42 | 31-Jan-23 | 09:46 | 0.2 | 0.1 | 0.9 | 1.9 |
| P [µg/g] | 19-Jan-23 | 23:42 | 31-Jan-23 | 09:46 | < 3 | 13 | < 3 | 100 |
| Sb [µg/g] | 19-Jan-23 | 23:42 | 31-Jan-23 | 09:46 | < 0.8 | < 0.8 | < 0.8 | < 0.8 |
| Se [µg/g] | 19-Jan-23 | 23:42 | 31-Jan-23 | 09:46 | < 0.7 | < 0.7 | < 0.7 | < 0.7 |
| Si [µg/g] | 19-Jan-23 | 23:42 | 31-Jan-23 | 09:46 | 96 | 160 | 150 | 33 |
| Sn [µg/g] | 19-Jan-23 | 23:42 | 31-Jan-23 | 09:46 | < 0.5 | < 0.5 | < 0.5 | < 0.5 |
| Sr [µg/g] | 19-Jan-23 | 23:42 | 31-Jan-23 | 09:46 | 0.5 | 10 | 7.3 | 99 |
| Ti [µg/g] | 19-Jan-23 | 23:42 | 31-Jan-23 | 09:46 | 0.8 | 0.6 | 0.5 | 1.0 |
| Tl [µg/g] | 19-Jan-23 | 23:42 | 31-Jan-23 | 09:46 | < 0.02 | < 0.02 | < 0.02 | < 0.02 |
| U [µg/g] | 19-Jan-23 | 23:42 | 31-Jan-23 | 09:46 | 0.19 | 0.094 | 0.13 | 0.31 |
| V [µg/g] | 19-Jan-23 | 23:42 | 31-Jan-23 | 09:46 | < 3 | < 3 | < 3 | < 3 |
| Zn [µg/g] | 19-Jan-23 | 23:42 | 31-Jan-23 | 09:46 | < 0.7 | < 0.7 | < 0.7 | 3.7 |

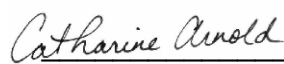
SGS Canada Inc.

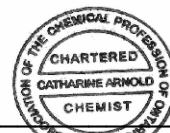
P.O. Box 4300 - 185 Concession St.
Lakefield - Ontario - KOL 2H0
Phone: 705-652-2000 FAX: 705-652-6365

LR Report : CA19220-NOV22

| Analysis | 9: MW-392 (32-33.5) | 10: MW-393 (24-25.5) | 11: MW-394 (20.5-22) | 12: MW-392 (66-68) |
|--------------------|------------------------|-------------------------|-------------------------|-----------------------|
| Sample Date & Time | 27-Sep-22 09:00 | 04-Oct-22 16:00 | 25-Sep-22 16:00 | 26-Sep-22 12:00 |
| Ag [µg/g] | < 0.05 | < 0.05 | < 0.05 | < 0.05 |
| Al [µg/g] | 30 | 28 | 23 | 28 |
| As [µg/g] | < 0.5 | < 0.5 | < 0.5 | < 0.5 |
| Ba [µg/g] | 19 | 15 | 12 | 5.0 |
| Be [µg/g] | 0.06 | 0.04 | 0.04 | 0.07 |
| B [µg/g] | < 1 | < 1 | < 1 | 3 |
| Bi [µg/g] | < 0.09 | < 0.09 | < 0.09 | < 0.09 |
| Ca [µg/g] | 1500 | 56 | 140 | 35000 |
| Cd [µg/g] | < 0.05 | < 0.05 | < 0.05 | < 0.05 |
| Co [µg/g] | 0.05 | 0.02 | 0.03 | 0.27 |
| Cr [µg/g] | < 0.5 | < 0.5 | < 0.5 | < 0.5 |
| Cu [µg/g] | 0.8 | 0.2 | 0.2 | 0.6 |
| Fe [µg/g] | 9 | 14 | 10 | 300 |
| K [µg/g] | 16 | 10 | 15 | 130 |
| Li [µg/g] | < 2 | < 2 | < 2 | < 2 |
| Mn [µg/g] | 20 | 4.4 | 7.0 | 144 |
| Mo [µg/g] | < 0.1 | < 0.1 | < 0.1 | < 0.1 |
| Ni [µg/g] | < 0.5 | < 0.5 | < 0.5 | < 0.5 |
| Pb [µg/g] | 0.2 | 0.1 | 0.1 | 0.4 |
| P [µg/g] | < 3 | < 3 | 4 | < 3 |
| Sb [µg/g] | < 0.8 | < 0.8 | < 0.8 | < 0.8 |
| Se [µg/g] | < 0.7 | < 0.7 | < 0.7 | < 0.7 |
| Si [µg/g] | 130 | 90 | 99 | 96 |
| Sn [µg/g] | < 0.5 | < 0.5 | < 0.5 | < 0.5 |
| Sr [µg/g] | 1.5 | 0.3 | 0.8 | 59 |
| Ti [µg/g] | 0.1 | 1.9 | 0.6 | < 0.1 |
| Tl [µg/g] | < 0.02 | < 0.02 | < 0.02 | < 0.02 |
| U [µg/g] | 0.12 | 0.14 | 0.17 | 0.100 |
| V [µg/g] | < 3 | < 3 | < 3 | < 3 |
| Zn [µg/g] | < 0.7 | < 0.7 | < 0.7 | 1.0 |

Fraction 3 Metals Bound to Carbonates


Catharine Arnold, B.Sc., C.Chem
Project Specialist,
Environment, Health & Safety



SGS Canada Inc.

P.O. Box 4300 - 185 Concession St.
Lakefield - Ontario - K0L 2H0
Phone: 705-652-2000 FAX: 705-652-6365

28-February-2023

Ramboll Americas Engineering Solutions, Inc.

Attn : Evvan Plank

P.O# Box 4873
Syracuse, New York
13221-7873, USA

Phone: 315-463-7554
Fax:

Date Rec. : 24 November 2022
LR Report: CA19221-NOV22
Reference: Baldwin Power Plant Drilling

Copy: #1

CERTIFICATE OF ANALYSIS

Final Report

| Analysis | 3: Analysis Completed Date | 4: Analysis Completed Time | 5: MW-358 (13-15) | 6: MW-358 (47-49) | 7: MW-358 (86-88) | 8: MW-392 (80-82) | 9: MW-392 (32-33.5) |
|--------------------|----------------------------------|----------------------------------|----------------------|----------------------|----------------------|----------------------|------------------------|
| Sample Date & Time | | | 05-Oct-22 14:05 | 06-Oct-22 15:00 | 08-Oct-22 18:00 | 26-Sep-22 16:00 | 27-Sep-22 09:00 |
| Ag [µg/g] | 31-Jan-23 | 09:47 | < 0.01 | < 0.01 | < 0.01 | < 0.01 | 0.01 |
| Al [µg/g] | 31-Jan-23 | 09:47 | 290 | 310 | 340 | 220 | 220 |
| As [µg/g] | 31-Jan-23 | 09:47 | < 0.5 | < 0.5 | < 0.5 | 1.3 | < 0.5 |
| Ba [µg/g] | 31-Jan-23 | 09:47 | 16 | 6.4 | 1.6 | 4.1 | 56 |
| Be [µg/g] | 31-Jan-23 | 09:47 | 0.26 | 0.16 | 0.15 | 0.15 | 0.21 |
| B [µg/g] | 31-Jan-23 | 09:47 | < 1 | 5 | 6 | 6 | < 1 |
| Bi [µg/g] | 31-Jan-23 | 09:47 | < 0.09 | < 0.09 | < 0.09 | 0.14 | < 0.09 |
| Ca [µg/g] | 31-Jan-23 | 09:47 | 71 | 320 | 250 | 130000 | 2300 |
| Cd [µg/g] | 31-Jan-23 | 09:47 | < 0.05 | < 0.05 | < 0.05 | 0.13 | 0.18 |
| Co [µg/g] | 31-Jan-23 | 09:47 | 3.8 | 0.33 | 3.0 | 2.3 | 5.1 |
| Cr [µg/g] | 31-Jan-23 | 09:47 | 2.3 | 1.2 | 1.3 | 1.0 | 0.9 |
| Cu [µg/g] | 31-Jan-23 | 09:47 | 1.6 | 0.4 | 0.7 | 0.1 | 2.9 |
| Fe [µg/g] | 31-Jan-23 | 09:47 | 1600 | 1600 | 1200 | 1800 | 1100 |
| K [µg/g] | 31-Jan-23 | 09:47 | 16 | 140 | 110 | 43 | 19 |
| Li [µg/g] | 31-Jan-23 | 09:47 | < 2 | 3 | 5 | < 2 | < 2 |
| Mn [µg/g] | 31-Jan-23 | 09:47 | 240 | 3.1 | 2.9 | 190 | 500 |
| Mo [µg/g] | 31-Jan-23 | 09:47 | < 0.1 | < 0.1 | < 0.1 | < 0.1 | < 0.1 |
| Ni [µg/g] | 31-Jan-23 | 09:47 | 3.1 | 2.7 | 4.5 | 6.5 | 3.1 |
| Pb [µg/g] | 31-Jan-23 | 09:47 | 3.3 | 0.2 | 1.2 | 8.4 | 3.7 |
| P [µg/g] | 31-Jan-23 | 09:47 | 19 | 110 | 77 | 400 | 31 |
| Sb [µg/g] | 31-Jan-23 | 09:47 | < 0.8 | < 0.8 | < 0.8 | < 0.8 | < 0.8 |
| Se [µg/g] | 31-Jan-23 | 09:47 | < 0.7 | < 0.7 | < 0.7 | < 0.7 | < 0.7 |
| Si [µg/g] | 31-Jan-23 | 09:47 | 920 | 910 | 710 | 270 | 600 |
| Sn [µg/g] | 31-Jan-23 | 09:47 | < 0.5 | < 0.5 | < 0.5 | < 0.5 | < 0.5 |
| Sr [µg/g] | 31-Jan-23 | 09:47 | 0.4 | 3.1 | 2.8 | 237 | 1.7 |
| Ti [µg/g] | 31-Jan-23 | 09:47 | 0.4 | 0.1 | 0.3 | < 0.1 | < 0.1 |
| Tl [µg/g] | 31-Jan-23 | 09:47 | < 0.02 | < 0.02 | < 0.02 | < 0.02 | < 0.02 |
| U [µg/g] | 31-Jan-23 | 09:47 | 0.26 | 0.068 | 0.17 | 0.62 | 0.15 |
| V [µg/g] | 31-Jan-23 | 09:47 | 5 | < 3 | < 3 | < 3 | 3 |
| Zn [µg/g] | 31-Jan-23 | 09:47 | 2.9 | 1.9 | 1.9 | 13 | 3.8 |

SGS Canada Inc.

P.O. Box 4300 - 185 Concession St.


Lakefield - Ontario - KOL 2H0

Phone: 705-652-2000 FAX: 705-652-6365

LR Report : CA19221-NOV22

| Analysis | 10: MW-393 (24-25.5) | 11: MW-394 (20.5-22) | 12: MW-392 (66-68) |
|--------------------|-------------------------|-------------------------|-----------------------|
| Sample Date & Time | 04-Oct-22 16:00 | 25-Sep-22 16:00 | 26-Sep-22 12:00 |
| Ag [µg/g] | < 0.01 | 0.02 | < 0.01 |
| Al [µg/g] | 290 | 270 | 490 |
| As [µg/g] | < 0.5 | < 0.5 | < 0.5 |
| Ba [µg/g] | 45 | 35 | 1.5 |
| Be [µg/g] | 0.16 | 0.18 | 0.18 |
| B [µg/g] | < 1 | < 1 | 4 |
| Bi [µg/g] | < 0.09 | < 0.09 | 0.14 |
| Ca [µg/g] | 100 | 350 | 7600 |
| Cd [µg/g] | 0.06 | 0.14 | < 0.05 |
| Co [µg/g] | 4.3 | 3.5 | 0.62 |
| Cr [µg/g] | 1.2 | 1.2 | 2.0 |
| Cu [µg/g] | 1.5 | 2.0 | 0.9 |
| Fe [µg/g] | 1500 | 1200 | 2700 |
| K [µg/g] | 15 | 22 | 120 |
| Li [µg/g] | < 2 | < 2 | 2 |
| Mn [µg/g] | 380 | 260 | 63 |
| Mo [µg/g] | < 0.1 | < 0.1 | < 0.1 |
| Ni [µg/g] | 3.2 | 3.7 | 2.5 |
| Pb [µg/g] | 3.5 | 2.1 | 0.9 |
| P [µg/g] | 17 | 91 | 110 |
| Sb [µg/g] | < 0.8 | < 0.8 | < 0.8 |
| Se [µg/g] | < 0.7 | < 0.7 | < 0.7 |
| Si [µg/g] | 660 | 850 | 650 |
| Sn [µg/g] | < 0.5 | < 0.5 | < 0.5 |
| Sr [µg/g] | 0.5 | 1.3 | 26 |
| Ti [µg/g] | 0.3 | 0.2 | 0.2 |
| Tl [µg/g] | < 0.02 | < 0.02 | < 0.02 |
| U [µg/g] | 0.12 | 0.18 | 0.082 |
| V [µg/g] | < 3 | 5 | < 3 |
| Zn [µg/g] | 4.3 | 7.8 | 2.8 |

Fraction 4 Metals Bound to Fe and Mn Oxides

Catharine Arnold

Catharine Arnold, B.Sc., C.Chem
Project Specialist,
Environment, Health & Safety



SGS Canada Inc.

P.O. Box 4300 - 185 Concession St.
Lakefield - Ontario - K0L 2H0
Phone: 705-652-2000 FAX: 705-652-6365

28-February-2023

Ramboll Americas Engineering Solutions, Inc.

Attn : Evvan Plank

P.O# Box 4873
Syracuse, New York
13221-7873, USA

Date Rec. : 24 November 2022
LR Report: CA19222-NOV22
Reference: Baldwin Power plant Drilling

Copy: #1

Phone: 315-463-7554
Fax:

CERTIFICATE OF ANALYSIS

Final Report

| Analysis | 3: Analysis Completed Date | 4: Analysis Completed Time | 5: MW-358 (13-15) | 6: MW-358 (47-49) | 7: MW-358 (86-88) | 8: MW-392 (80-82) | 9: MW-392 (32-33.5) |
|--------------------|----------------------------------|----------------------------------|----------------------|----------------------|----------------------|----------------------|------------------------|
| Sample Date & Time | | | 05-Oct-22 14:05 | 06-Oct-22 15:00 | 08-Oct-22 18:00 | 26-Sep-22 16:00 | 27-Sep-22 09:00 |
| Ag [µg/g] | 31-Jan-23 | 09:48 | 0.14 | 0.15 | 0.08 | 0.07 | 0.06 |
| Al [µg/g] | 31-Jan-23 | 09:48 | 980 | 1300 | 1100 | 130 | 610 |
| As [µg/g] | 31-Jan-23 | 09:48 | < 0.5 | < 0.5 | < 0.5 | < 0.5 | < 0.5 |
| Ba [µg/g] | 31-Jan-23 | 09:48 | 15 | 11 | 1.8 | 3.6 | 36 |
| Be [µg/g] | 31-Jan-23 | 09:48 | 0.13 | 0.32 | 0.16 | 0.07 | 0.12 |
| B [µg/g] | 31-Jan-23 | 09:48 | < 1 | 2 | 2 | 2 | < 1 |
| Bi [µg/g] | 31-Jan-23 | 09:48 | < 0.09 | < 0.09 | < 0.09 | < 0.09 | < 0.09 |
| Ca [µg/g] | 31-Jan-23 | 09:48 | 160 | 490 | 220 | 8600 | 840 |
| Cd [µg/g] | 31-Jan-23 | 09:48 | < 0.05 | < 0.05 | < 0.05 | 0.20 | < 0.05 |
| Co [µg/g] | 31-Jan-23 | 09:48 | 1.4 | 0.45 | 9.7 | 3.3 | 1.3 |
| Cr [µg/g] | 31-Jan-23 | 09:48 | 2.1 | 1.0 | 1.2 | < 0.5 | 1.6 |
| Cu [µg/g] | 31-Jan-23 | 09:48 | 0.5 | 1.0 | 1.8 | 1.9 | 0.4 |
| Fe [µg/g] | 31-Jan-23 | 09:48 | 150 | 610 | 1800 | 220 | 83 |
| K [µg/g] | 31-Jan-23 | 09:48 | 15 | 104 | 79 | 25 | 15 |
| Li [µg/g] | 31-Jan-23 | 09:48 | < 2 | < 2 | 3 | < 2 | < 2 |
| Mg [µg/g] | 31-Jan-23 | 09:48 | 170 | 1100 | 870 | 200 | 500 |
| Mn [µg/g] | 31-Jan-23 | 09:48 | 85 | 3.6 | 15 | 16 | 92 |
| Mo [µg/g] | 31-Jan-23 | 09:48 | < 0.1 | < 0.1 | < 0.1 | 0.2 | 0.4 |
| Na [µg/g] | 31-Jan-23 | 09:48 | 110 | 180 | 150 | 90 | 75 |
| Ni [µg/g] | 31-Jan-23 | 09:48 | 1.9 | 4.3 | 13 | 15 | 2.1 |
| Pb [µg/g] | 31-Jan-23 | 09:48 | 1.6 | 0.1 | 1.6 | 3.8 | 1.3 |
| P [µg/g] | 31-Jan-23 | 09:48 | < 3 | < 3 | < 3 | 290 | 5 |
| Sb [µg/g] | 31-Jan-23 | 09:48 | < 0.8 | < 0.8 | < 0.8 | < 0.8 | < 0.8 |
| Se [µg/g] | 31-Jan-23 | 09:48 | < 0.7 | < 0.7 | < 0.7 | < 0.7 | < 0.7 |
| Si [µg/g] | 31-Jan-23 | 09:48 | 590 | 480 | 420 | 130 | 530 |
| Sn [µg/g] | 31-Jan-23 | 09:48 | < 0.5 | < 0.5 | < 0.5 | < 0.5 | < 0.5 |
| Sr [µg/g] | 31-Jan-23 | 09:48 | 0.5 | 5.1 | 2.8 | 48 | 0.9 |
| Ti [µg/g] | 31-Jan-23 | 09:48 | 0.7 | < 0.1 | < 0.1 | < 0.1 | 2.9 |
| Tl [µg/g] | 31-Jan-23 | 09:48 | < 0.02 | < 0.02 | 0.02 | 0.05 | < 0.02 |
| U [µg/g] | 31-Jan-23 | 09:48 | 0.17 | 0.13 | 0.19 | 0.25 | 0.060 |
| V [µg/g] | 31-Jan-23 | 09:48 | < 3 | < 3 | < 3 | < 3 | 3 |
| Zn [µg/g] | 31-Jan-23 | 09:48 | 1.4 | < 0.7 | 1.8 | 41 | 1.7 |

SGS Canada Inc.

P.O. Box 4300 - 185 Concession St.

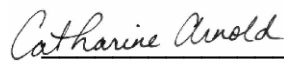
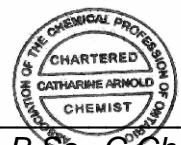
Lakefield - Ontario - KOL 2H0

Phone: 705-652-2000 FAX: 705-652-6365

LR Report : CA19222-NOV22

| Analysis | 10: MW-393 (24-25.5) | 11: MW-394 (20.5-22) | 12: MW-392 (66-68) |
|--------------------|-------------------------|-------------------------|-----------------------|
| Sample Date & Time | 04-Oct-22 16:00 | 25-Sep-22 16:00 | 26-Sep-22 12:00 |
| Ag [µg/g] | < 0.05 | < 0.05 | < 0.05 |
| Al [µg/g] | 660 | 870 | 820 |
| As [µg/g] | < 0.5 | < 0.5 | < 0.5 |
| Ba [µg/g] | 33 | 45 | 1.5 |
| Be [µg/g] | 0.08 | 0.15 | 0.18 |
| B [µg/g] | < 1 | < 1 | 2 |
| Bi [µg/g] | < 0.09 | < 0.09 | < 0.09 |
| Ca [µg/g] | 88 | 300 | 2400 |
| Cd [µg/g] | < 0.05 | < 0.05 | < 0.05 |
| Co [µg/g] | 1.2 | 2.3 | 0.68 |
| Cr [µg/g] | 1.2 | 1.5 | 1.1 |
| Cu [µg/g] | 0.3 | 0.8 | 1.4 |
| Fe [µg/g] | 93 | 120 | 680 |
| K [µg/g] | 14 | 21 | 70 |
| Li [µg/g] | < 2 | < 2 | < 2 |
| Mg [µg/g] | 150 | 280 | 730 |
| Mn [µg/g] | 100 | 164 | 15 |
| Mo [µg/g] | 0.1 | 0.3 | < 0.1 |
| Na [µg/g] | 48 | 170 | 95 |
| Ni [µg/g] | 1.6 | 3.5 | 2.9 |
| Pb [µg/g] | 1.7 | 1.3 | 0.9 |
| P [µg/g] | 4 | 8 | < 3 |
| Sb [µg/g] | < 0.8 | < 0.8 | < 0.8 |
| Se [µg/g] | < 0.7 | < 0.7 | < 0.7 |
| Si [µg/g] | 470 | 650 | 470 |
| Sn [µg/g] | < 0.5 | < 0.5 | < 0.5 |
| Sr [µg/g] | 0.3 | 1.2 | 9.8 |
| Ti [µg/g] | 2.1 | 2.5 | < 0.1 |
| Tl [µg/g] | < 0.02 | < 0.02 | < 0.02 |
| U [µg/g] | 0.065 | 0.16 | 0.080 |
| V [µg/g] | < 3 | 4 | < 3 |
| Zn [µg/g] | 1.6 | 4.0 | 0.9 |

Fraction 5 Bound to Organic Material



Catharine Arnold, B.Sc., C.Chem
Project Specialist,
Environment, Health & Safety

SGS Canada Inc.

P.O. Box 4300 - 185 Concession St.
Lakefield - Ontario - KOL 2H0
Phone: 705-652-2000 FAX: 705-652-6365

28-February-2023

Ramboll Americas Engineering Solutions, Inc.

Attn : Evvan Plank

P.O# Box 4873
Syracuse, New York
13221-7873, USA

Date Rec. : 24 November 2022
LR Report: CA19223-NOV22
Reference: Baldwin Power Plant Drilling

Copy: #1

Phone: 315-463-7554
Fax:

CERTIFICATE OF ANALYSIS

Final Report

| Analysis | 3: Analysis Completed Date | 4: Analysis Completed Time | 5: MW-358 (13-15) | 6: MW-358 (47-49) | 7: MW-358 (86-88) | 8: MW-392 (80-82) | 9: MW-392 (32-33.5) |
|--------------------|----------------------------------|----------------------------------|----------------------|----------------------|----------------------|----------------------|------------------------|
| Sample Date & Time | | | 05-Oct-22 14:05 | 06-Oct-22 15:00 | 08-Oct-22 18:00 | 26-Sep-22 16:00 | 27-Sep-22 09:00 |
| Ag [µg/g] | 31-Jan-23 | 09:48 | 0.09 | < 0.05 | < 0.05 | < 0.05 | 0.07 |
| Al [µg/g] | 31-Jan-23 | 09:48 | 44000 | 63000 | 71000 | 27000 | 45000 |
| As [µg/g] | 31-Jan-23 | 09:48 | 5.8 | 2.3 | 9.8 | 10 | 8.6 |
| Ba [µg/g] | 31-Jan-23 | 09:48 | 390 | 150 | 140 | 56 | 320 |
| Be [µg/g] | 31-Jan-23 | 09:48 | 0.65 | 1.4 | 1.5 | 0.68 | 0.87 |
| B [µg/g] | 31-Jan-23 | 09:48 | 13 | 60 | 62 | 26 | 21 |
| Bi [µg/g] | 31-Jan-23 | 09:48 | 0.25 | 0.26 | 0.18 | 0.14 | 0.25 |
| Ca [µg/g] | 31-Jan-23 | 09:48 | 2500 | 150 | 120 | 20000 | 1400 |
| Cd [µg/g] | 31-Jan-23 | 09:48 | 0.06 | < 0.05 | < 0.05 | 0.11 | 0.08 |
| Co [µg/g] | 31-Jan-23 | 09:48 | 3.3 | 7.2 | 6.4 | 2.0 | 6.4 |
| Cr [µg/g] | 31-Jan-23 | 09:48 | 34 | 69 | 75 | 37 | 40 |
| Cu [µg/g] | 31-Jan-23 | 09:48 | 10 | 9.9 | 5.7 | 7.2 | 15 |
| Fe [µg/g] | 31-Jan-23 | 09:48 | 22000 | 42000 | 22000 | 14000 | 28000 |
| K [µg/g] | 31-Jan-23 | 09:48 | 11000 | 18000 | 16000 | 5100 | 13000 |
| Li [µg/g] | 31-Jan-23 | 09:48 | 18 | 9 | 65 | 7 | 20 |
| Mg [µg/g] | 31-Jan-23 | 09:48 | 2700 | 7800 | 7600 | 4100 | 3300 |
| Mn [µg/g] | 31-Jan-23 | 09:48 | 110 | 70 | 51 | 50 | 130 |
| Mo [µg/g] | 31-Jan-23 | 09:48 | 0.9 | 0.3 | 0.1 | 0.1 | 0.9 |
| Na [µg/g] | 31-Jan-23 | 09:48 | 6700 | 560 | 830 | 550 | 5200 |
| Ni [µg/g] | 31-Jan-23 | 09:48 | 14 | 32 | 29 | 13 | 21 |
| Pb [µg/g] | 31-Jan-23 | 09:48 | 10 | 8.0 | 7.0 | 17 | 12 |
| P [µg/g] | 31-Jan-23 | 09:48 | 260 | 240 | 160 | 7200 | 300 |
| Sb [µg/g] | 31-Jan-23 | 09:48 | < 0.8 | < 0.8 | < 0.8 | < 0.8 | < 0.8 |
| Se [µg/g] | 31-Jan-23 | 09:48 | < 0.7 | < 0.7 | < 0.7 | < 0.7 | < 0.7 |
| Si [µg/g] | 31-Jan-23 | 09:48 | 160000 | 66000 | 51000 | 73000 | 65000 |
| Sn [µg/g] | 31-Jan-23 | 09:48 | 5.4 | 5.8 | 5.8 | 4.9 | 5.2 |
| Sr [µg/g] | 31-Jan-23 | 09:48 | 89 | 30 | 25 | 130 | 79 |
| Ti [µg/g] | 31-Jan-23 | 09:48 | 2400 | 670 | 570 | 520 | 980 |
| Tl [µg/g] | 31-Jan-23 | 09:48 | 0.47 | 0.42 | 0.42 | 0.17 | 0.51 |
| U [µg/g] | 31-Jan-23 | 09:48 | 1.3 | 0.30 | 0.99 | 2.7 | 1.1 |
| V [µg/g] | 31-Jan-23 | 09:48 | 54 | 73 | 86 | 95 | 57 |
| Zn [µg/g] | 31-Jan-23 | 09:48 | 37 | 47 | 32 | 43 | 53 |

SGS Canada Inc.

P.O. Box 4300 - 185 Concession St.

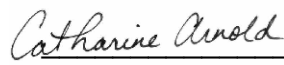
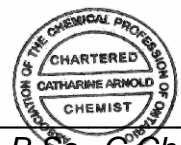
Lakefield - Ontario - KOL 2H0

Phone: 705-652-2000 FAX: 705-652-6365

LR Report : CA19223-NOV22

| Analysis | 10: MW-393 (24-25.5) | 11: MW-394 (20.5-22) | 12: MW-392 (66-68) |
|--------------------|-------------------------|-------------------------|-----------------------|
| Sample Date & Time | 04-Oct-22 16:00 | 25-Sep-22 16:00 | 26-Sep-22 12:00 |
| Ag [µg/g] | < 0.05 | < 0.05 | < 0.05 |
| Al [µg/g] | 33000 | 45000 | 59000 |
| As [µg/g] | 10 | 9.8 | 0.9 |
| Ba [µg/g] | 300 | 410 | 93 |
| Be [µg/g] | 0.56 | 0.83 | 1.2 |
| B [µg/g] | 15 | 16 | 53 |
| Bi [µg/g] | 0.18 | 0.27 | 0.20 |
| Ca [µg/g] | 1700 | 3000 | 170 |
| Cd [µg/g] | < 0.05 | 0.11 | < 0.05 |
| Co [µg/g] | 3.2 | 5.0 | 6.4 |
| Cr [µg/g] | 24 | 35 | 71 |
| Cu [µg/g] | 9.9 | 13 | 12 |
| Fe [µg/g] | 19000 | 27000 | 43000 |
| K [µg/g] | 12000 | 14000 | 17000 |
| Li [µg/g] | 13 | 16 | 19 |
| Mg [µg/g] | 2200 | 3400 | 9500 |
| Mn [µg/g] | 80 | 140 | 47 |
| Mo [µg/g] | 0.7 | 2.7 | 0.2 |
| Na [µg/g] | 5100 | 7700 | 490 |
| Ni [µg/g] | 13 | 18 | 31 |
| Pb [µg/g] | 9.1 | 13 | 4.1 |
| P [µg/g] | 230 | 460 | 170 |
| Sb [µg/g] | < 0.8 | < 0.8 | < 0.8 |
| Se [µg/g] | < 0.7 | < 0.7 | < 0.7 |
| Si [µg/g] | 61000 | 43000 | 62000 |
| Sn [µg/g] | 4.6 | 5.2 | 5.6 |
| Sr [µg/g] | 70 | 110 | 22 |
| Ti [µg/g] | 780 | 1100 | 560 |
| Tl [µg/g] | 0.35 | 0.50 | 0.36 |
| U [µg/g] | 0.61 | 1.1 | 0.097 |
| V [µg/g] | 35 | 57 | 70 |
| Zn [µg/g] | 37 | 54 | 48 |

Fraction 6 Residual metals



Catharine Arnold, B.Sc., C.Chem
Project Specialist,
Environment, Health & Safety

SGS Canada Inc.

P.O. Box 4300 - 185 Concession St.
Lakefield - Ontario - K0L 2H0
Phone: 705-652-2000 FAX: 705-652-6365

28-February-2023

Ramboll Americas Engineering Solutions, Inc.

Attn : Evvan Plank

P.O# Box 4873
Syracuse, New York
13221-7873, USA

Phone: 315-463-7554
Fax:

Date Rec. : 24 November 2022
LR Report: CA19224-NOV22
Reference: Baldwon Power Plant Drilling

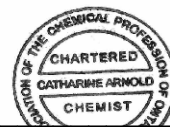
Copy: #1

CERTIFICATE OF ANALYSIS

Final Report

| Analysis | 1: Analysis Start Date | 2: Analysis Start Time Completed | 3: Analysis DateCompleted | 4: Analysis Time | 6: MW-358 (47-49) | 7: MW-358 (86-88) | 8: MW-392 (80-82) | 12: MW-392 (66-68) |
|--------------------|------------------------------|--|---------------------------------|------------------------|----------------------|----------------------|----------------------|-----------------------|
| Sample Date & Time | | | | | 06-Oct-22 15:00 | 08-Oct-22 18:00 | 26-Sep-22 16:00 | 26-Sep-22 12:00 |
| Hg MS [ug/g] | 09-Dec-22 | 16:29 | 12-Dec-22 | 15:05 | < 0.05 | < 0.05 | < 0.05 | < 0.05 |
| As [ug/g] | 09-Dec-22 | 16:29 | 12-Dec-22 | 15:05 | 2.1 | 11 | 17 | 1.0 |
| B [ug/g] | 09-Dec-22 | 16:29 | 12-Dec-22 | 15:05 | 11 | 16 | 16 | 13 |
| Ba [ug/g] | 09-Dec-22 | 16:29 | 12-Dec-22 | 15:05 | 140 | 45 | 40 | 21 |
| Be [ug/g] | 09-Dec-22 | 16:29 | 12-Dec-22 | 15:05 | 0.85 | 0.67 | 0.85 | 0.70 |
| Cd [ug/g] | 09-Dec-22 | 16:29 | 12-Dec-22 | 15:05 | < 0.02 | < 0.02 | 0.36 | 0.09 |
| Co [ug/g] | 09-Dec-22 | 16:29 | 12-Dec-22 | 15:05 | 4.4 | 23 | 12 | 6.2 |
| Cr [ug/g] | 09-Dec-22 | 16:29 | 12-Dec-22 | 15:05 | 9.5 | 12 | 17 | 16 |
| Li [ug/g] | 09-Dec-22 | 16:29 | 12-Dec-22 | 15:05 | 6 | 20 | 8 | 15 |
| Mo [ug/g] | 09-Dec-22 | 16:29 | 12-Dec-22 | 15:05 | 0.3 | 0.3 | 0.3 | 0.3 |
| Pb [ug/g] | 09-Dec-22 | 16:29 | 12-Dec-22 | 15:05 | 5.7 | 9.6 | 17 | 4.9 |
| Se [ug/g] | 09-Dec-22 | 16:29 | 12-Dec-22 | 15:05 | < 0.7 | < 0.7 | 1.4 | < 0.7 |
| Tl [ug/g] | 09-Dec-22 | 16:29 | 12-Dec-22 | 15:05 | 0.05 | 0.06 | 0.04 | 0.03 |

Catharine Arnold, B.Sc., C.Chem
Project Specialist,
Environment, Health & Safety





SGS Canada Inc.

P.O. Box 4300 - 185 Concession St.

Lakefield - Ontario - KOL 2H0

Phone: 705-652-2000 FAX: 705-652-6365

LR Report : CA19224-NOV22

DRAFT



Quantitative X-Ray Diffraction by Rietveld Refinement

Report Prepared for: Environmental Services

Project Number/ LIMS No. Custom XRD/MI4508-DEC22

Sample Receipt: December 7, 2022

Sample Analysis: December 15, 2022

Reporting Date: December 21, 2022

Instrument: BRUKER AXS D8 Advance Diffractometer

Test Conditions: Co radiation, 35 kV, 40 mA; Detector: LYNXEYE
Regular Scanning: Step: 0.02°, Step time: 0.75s, 2θ range: 6-80°

Interpretations : PDF2/PDF4 powder diffraction databases issued by the International Center for Diffraction Data (ICDD). DiffracPlus Eva and Topas software.

Detection Limit: 0.5-2%. Strongly dependent on crystallinity.

Contents:

- 1) Method Summary
- 2) Quantitative XRD Results
- 3) XRD Pattern(s)

Kim Gibbs, H.B.Sc., P.Geo.
Senior Mineralogist

Huyun Zhou, Ph.D., P.Geo.
Senior Mineralogist

ACCREDITATION: SGS Natural Resources Lakefield is accredited to the requirements of ISO/IEC 17025 for specific tests as listed on our scope of accreditation, including geochemical, mineralogical and trade mineral tests. To view a list of the accredited methods, please visit the following website and search SGS Canada Inc. - Minerals: <https://www.scc.ca/en/search/palcan>.



Method Summary

The Rietveld Method of Mineral Identification by XRD (ME-LR-MIN-MET-MN-D05) method used by SGS Natural Resources is accredited to the requirements of ISO/IEC 17025.

Mineral Identification and Interpretation:

Mineral identification and interpretation involves matching the diffraction pattern of an unknown material to patterns of single-phase reference materials. The reference patterns are compiled by the Joint Committee on Powder Diffraction Standards - International Center for Diffraction Data (JCPDS-ICDD) database and released on software as Powder Diffraction Files (PDF).

Interpretations do not reflect the presence of non-crystalline and/or amorphous compounds, except when internal standards have been added by request. Mineral proportions may be strongly influenced by crystallinity, crystal structure and preferred orientations. Mineral or compound identification and quantitative analysis results should be accompanied by supporting chemical assay data or other additional tests.

Quantitative Rietveld Analysis:

Quantitative Rietveld Analysis is performed by using Topas 4.2 (Bruker AXS), a graphics based profile analysis program built around a non-linear least squares fitting system, to determine the amount of different phases present in a multicomponent sample. Whole pattern analyses are predicated by the fact that the X-ray diffraction pattern is a total sum of both instrumental and specimen factors. Unlike other peak intensity-based methods, the Rietveld method uses a least squares approach to refine a theoretical line profile until it matches the obtained experimental patterns.

Rietveld refinement is completed with a set of minerals specifically identified for the sample. Zero values indicate that the mineral was included in the refinement calculations, but the calculated concentration was less than 0.05wt%. Minerals not identified by the analyst are not included in refinement calculations for specific samples and are indicated with a dash.

DISCLAIMER: This document is issued by the Company under its General Conditions of Service accessible at <http://www.sgs.com/en/Terms-and-Conditions.aspx>. Attention is drawn to the limitation of liability, indemnification and jurisdiction issues defined therein. Any holder of this document is advised that information contained hereon reflects the Company's findings at the time of its intervention only and within the limits of Client's instructions, if any. The Company's sole responsibility is to its Client and this document does not exonerate parties to a transaction from exercising all their rights and obligations under the transaction documents. Any unauthorized alteration, forgery or falsification of the content or appearance of this document is unlawful and offenders may be prosecuted to the fullest extent of the law.

WARNING: The sample(s) to which the findings recorded herein (the "Findings") relate was(were) drawn and / or provided by the Client or by a third party acting at the Client's direction. The Findings constitute no warranty of the sample's representativeness of any goods and strictly relate to the sample(s). The Company accepts no liability with regard to the origin or source from which the sample(s) is/are said to be extracted.

Summary of Rietveld Quantitative Analysis X-Ray Diffraction Results

| Mineral/Compound | MW-358 (13-15) DEC4508-01 (wt %) | MW-358 (47-49) DEC4508-02 (wt %) | MW-358 (86-88) DEC4508-03 (wt %) | MW-392 (80-82) DEC4508-04 (wt %) |
|------------------|--|--|--|--|
| Quartz | 58.9 | 33.0 | 34.9 | 29.1 |
| Muscovite | 11.2 | 37.6 | 30.5 | 14.5 |
| Albite | 13.3 | 8.2 | 3.4 | 1.0 |
| Microcline | 5.3 | 9.4 | 8.1 | 2.9 |
| Chlorite | 10.8 | - | - | 6.8 |
| Diaspore | 0.5 | - | - | - |
| Pyrite | - | 1.0 | 0.8 | 1.2 |
| Kaolinite | - | 9.0 | 18.4 | 8.2 |
| Calcite | - | 1.8 | 1.7 | 31.5 |
| Anatase | - | - | 2.1 | 0.4 |
| Leucite | - | - | - | 2.4 |
| Siderite | - | - | - | 1.9 |
| Dolomite | - | - | - | - |
| Gypsum | - | - | - | - |
| Diopside | - | - | - | - |
| TOTAL | 100 | 100 | 100 | 100 |

Zero values indicate that the mineral was included in the refinement, but the calculated concentration is below a measurable value.

Dashes indicate that the mineral was not identified by the analyst and not included in the refinement calculation for the sample.

The weight percent quantities indicated have been normalized to a sum of 100%. The quantity of amorphous material has not been determined.

| Mineral/Compound | Formula |
|------------------|--|
| Quartz | SiO ₂ |
| Muscovite | KAl ₂ (AlSi ₃ O ₁₀)(OH) ₂ |
| Albite | NaAlSi ₃ O ₈ |
| Microcline | KAlSi ₃ O ₈ |
| Chlorite | (Fe,(Mg,Mn) ₅ ,Al)(Si ₃ Al)O ₁₀ (OH) ₈ |
| Diaspore | αAlO.OH |
| Pyrite | FeS ₂ |
| Kaolinite | Al ₂ Si ₂ O ₅ (OH) ₄ |
| Calcite | CaCO ₃ |
| Anatase | TiO ₂ |
| Leucite | KAlSi ₂ O ₆ |
| Siderite | FeCO ₃ |
| Dolomite | CaMg(CO ₃) ₂ |
| Gypsum | CaSO ₄ ·2H ₂ O |
| Diopside | CaMgSi ₂ O ₆ |

Summary of Rietveld Quantitative Analysis X-Ray Diffraction Results

| Mineral/Compound | MW-392 (32-33.5) DEC4508-05 (wt %) | MW-393 (24-25.5) DEC4508-06 (wt %) | MW-394 (20.5-22) DEC4508-07 (wt %) | MW-392 (66-68) DEC4508-08 (wt %) |
|------------------|--|--|--|--|
| Quartz | 53.5 | 68.2 | 54.9 | 27.2 |
| Muscovite | 13.1 | 13.0 | 11.7 | 29.7 |
| Albite | 8.5 | 7.4 | 13.1 | 4.5 |
| Microcline | 6.8 | 9.5 | 6.7 | 6.9 |
| Chlorite | 7.0 | - | 7.0 | 16.3 |
| Diaspore | - | - | - | - |
| Pyrite | - | 0.3 | 0.3 | - |
| Kaolinite | 7.5 | - | 5.0 | - |
| Calcite | - | - | - | 14.8 |
| Anatase | - | - | - | 0.7 |
| Leucite | - | - | - | - |
| Siderite | - | - | - | - |
| Dolomite | 1.2 | - | - | - |
| Gypsum | 0.4 | - | - | - |
| Diopside | 1.7 | 1.6 | 1.4 | - |
| TOTAL | 100 | 100 | 100 | 100 |

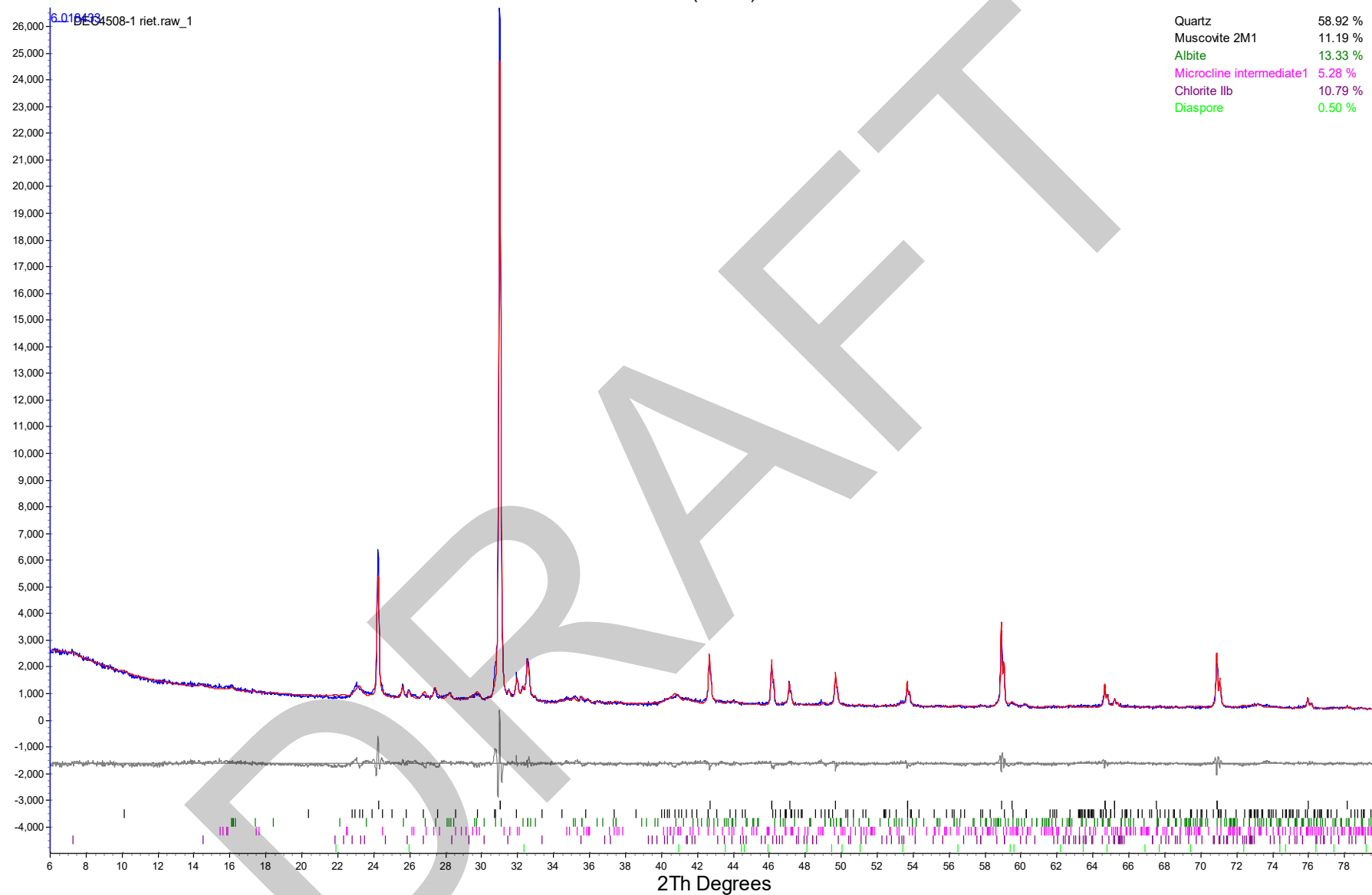
Zero values indicate that the mineral was included in the refinement, but the calculated concentration is below a measurable value.

Dashes indicate that the mineral was not identified by the analyst and not included in the refinement calculation for the sample.

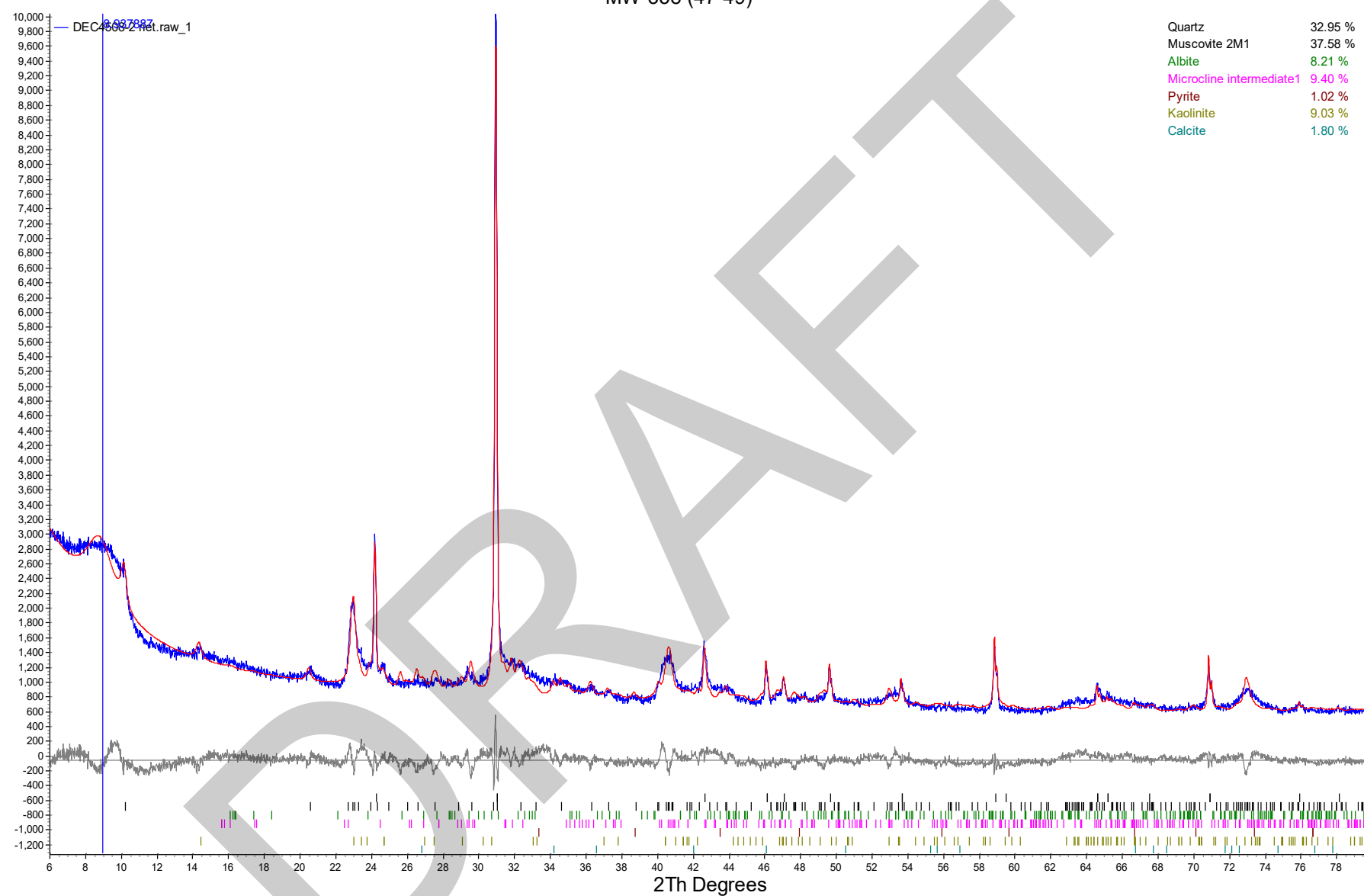
The weight percent quantities indicated have been normalized to a sum of 100%. The quantity of amorphous material has not been determined.

| Mineral/Compound | Formula |
|------------------|--|
| Quartz | SiO ₂ |
| Muscovite | KAl ₂ (AlSi ₃ O ₁₀)(OH) ₂ |
| Albite | NaAlSi ₃ O ₈ |
| Microcline | KAlSi ₃ O ₈ |
| Chlorite | (Fe,(Mg,Mn) ₅ ,Al)(Si ₃ Al)O ₁₀ (OH) ₈ |
| Diaspore | αAlO.OH |
| Pyrite | FeS ₂ |
| Kaolinite | Al ₂ Si ₂ O ₅ (OH) ₄ |
| Calcite | CaCO ₃ |
| Anatase | TiO ₂ |
| Leucite | KAlSi ₂ O ₆ |
| Siderite | FeCO ₃ |
| Dolomite | CaMg(CO ₃) ₂ |
| Gypsum | CaSO ₄ ·2H ₂ O |
| Diopside | CaMgSi ₂ O ₆ |

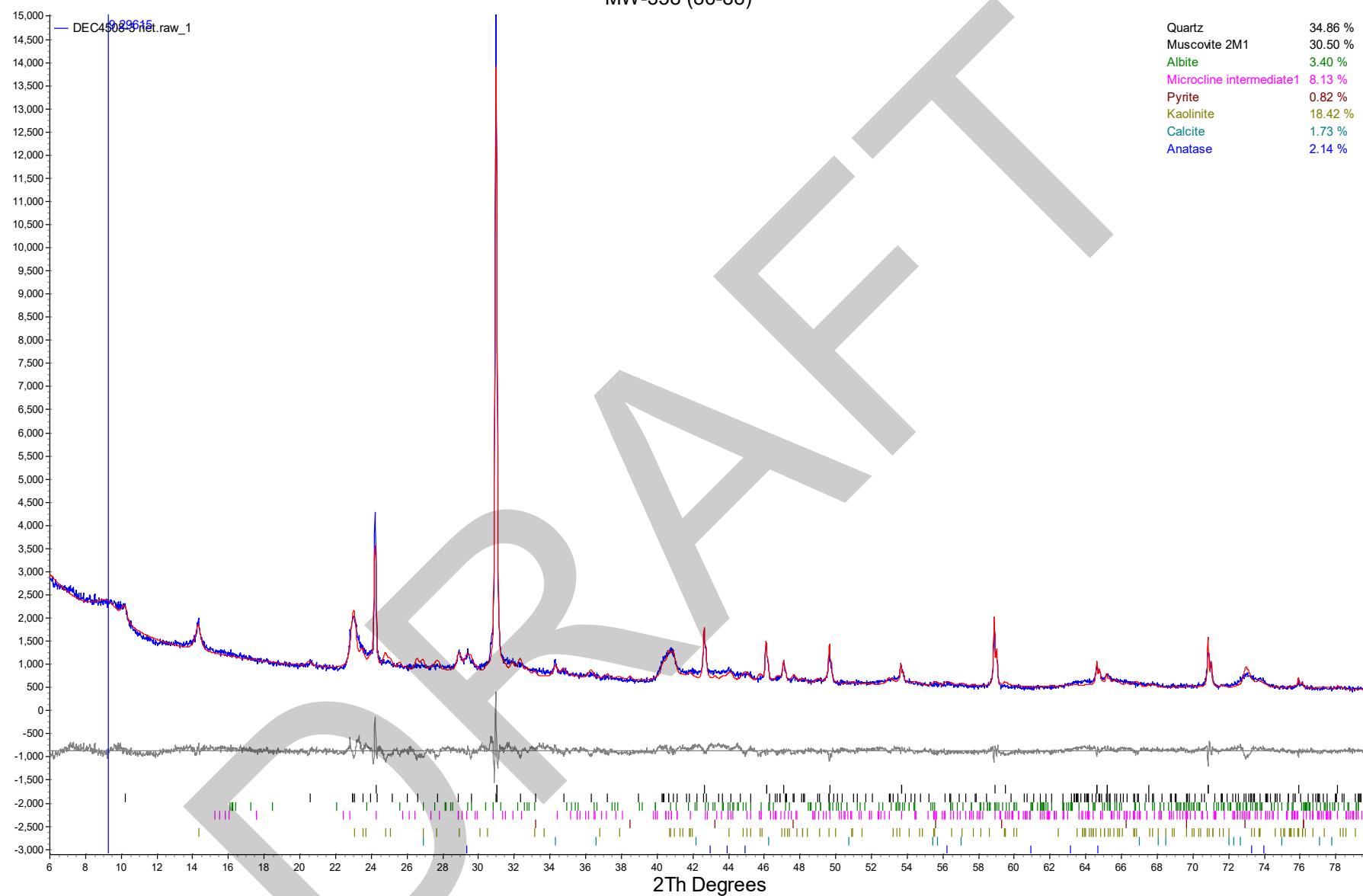
MW-358 (13-15)



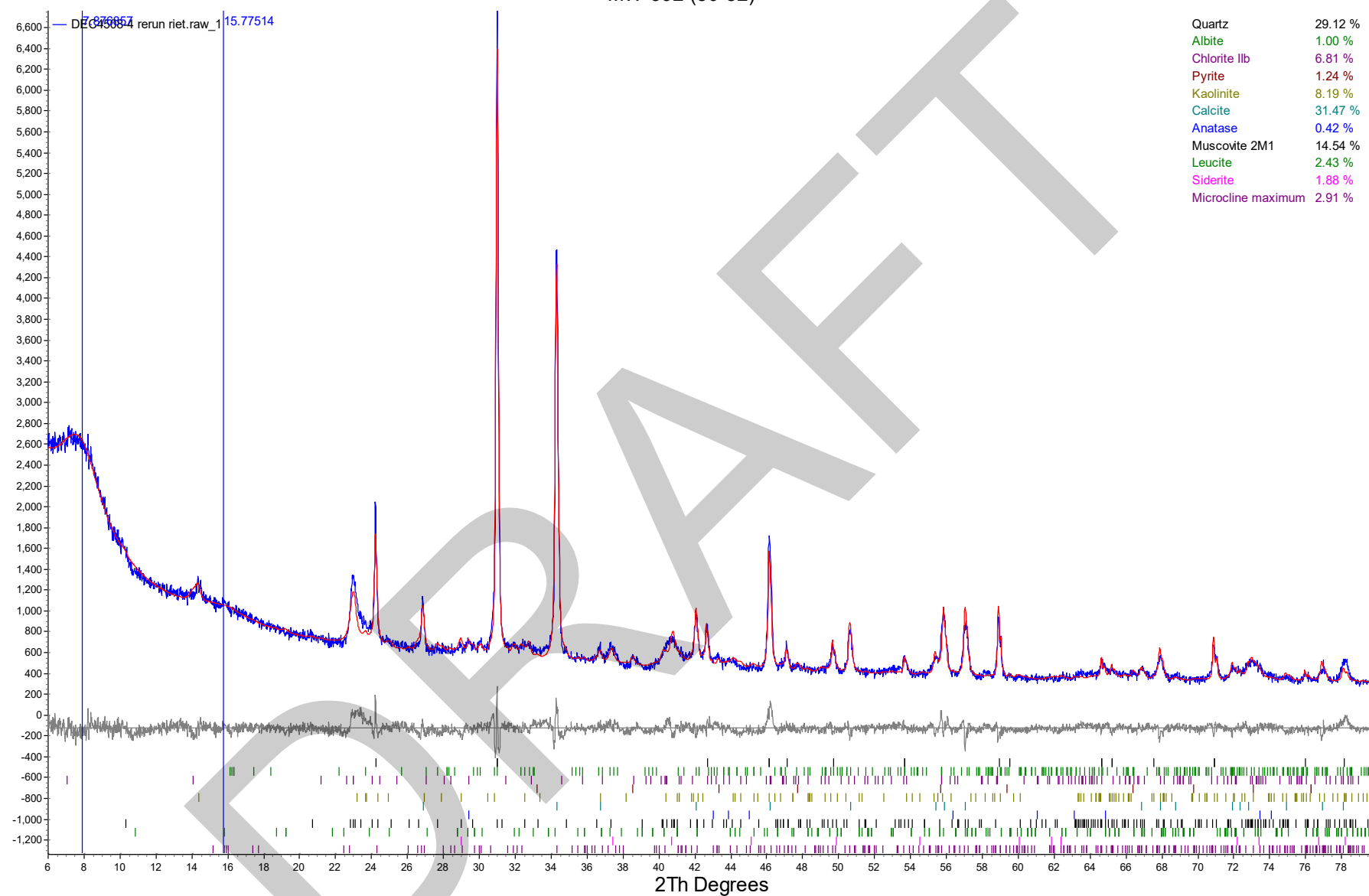
MW-358 (47-49)



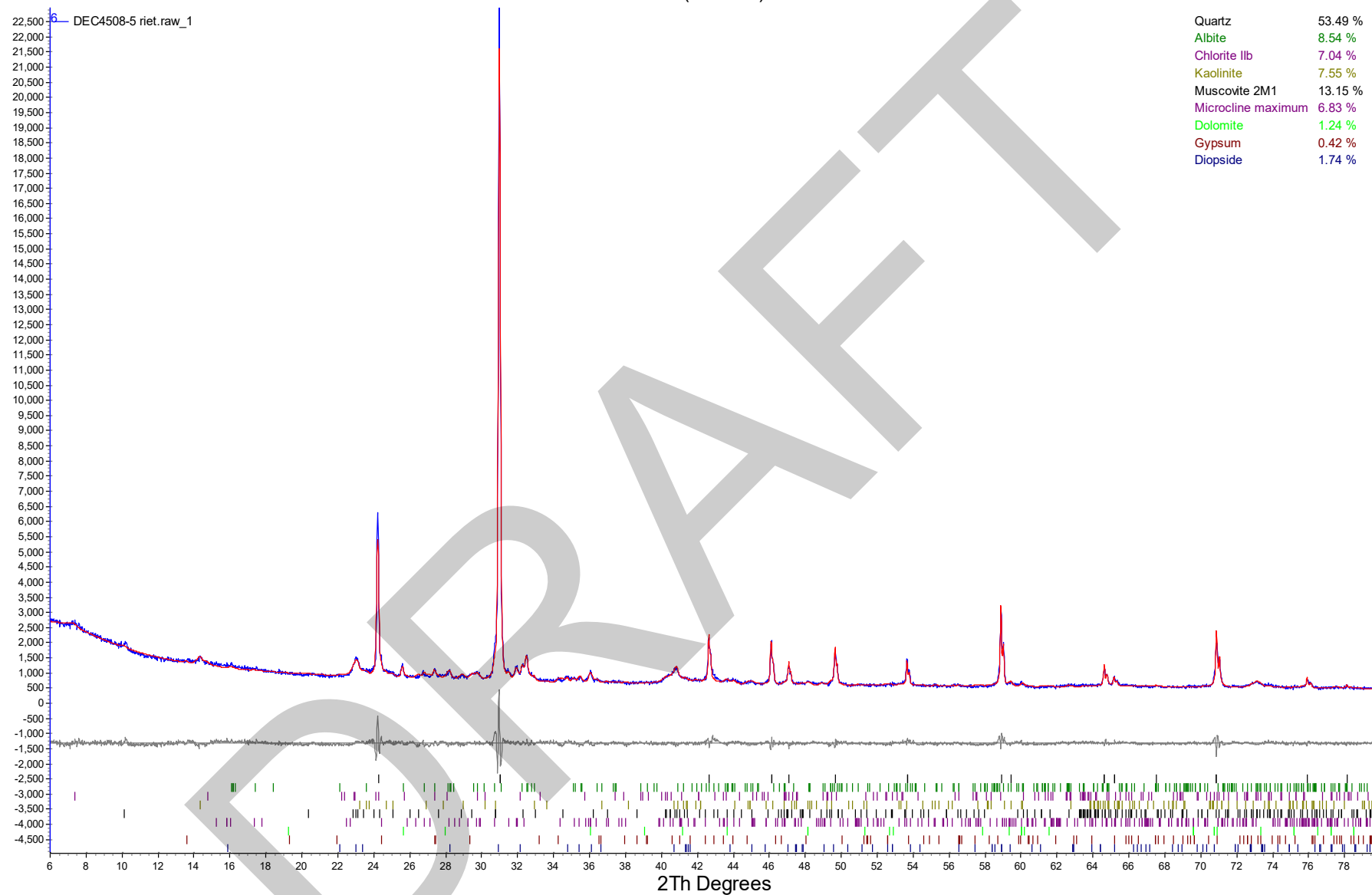
MW-358 (86-88)



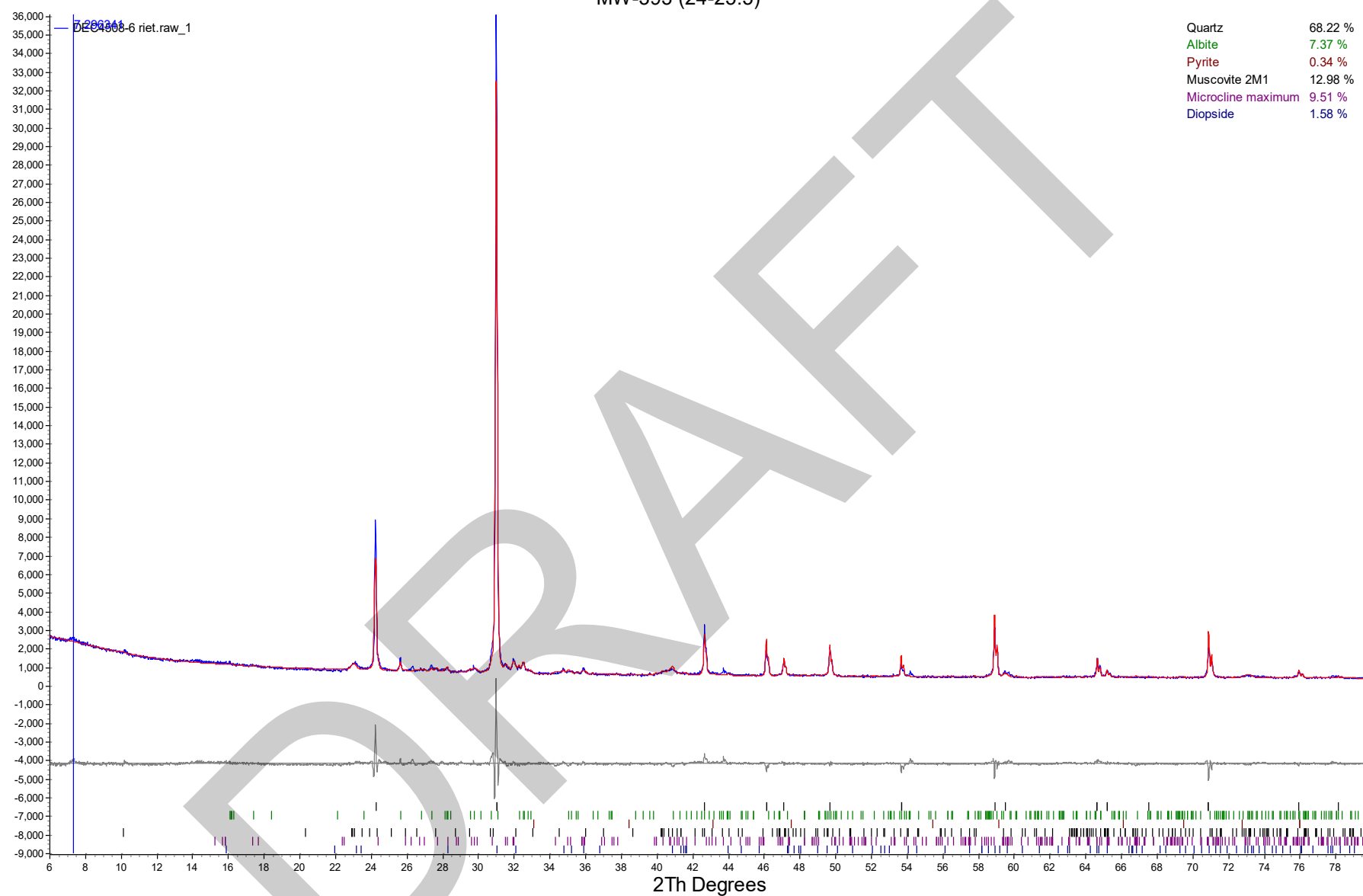
MW-392 (80-82)



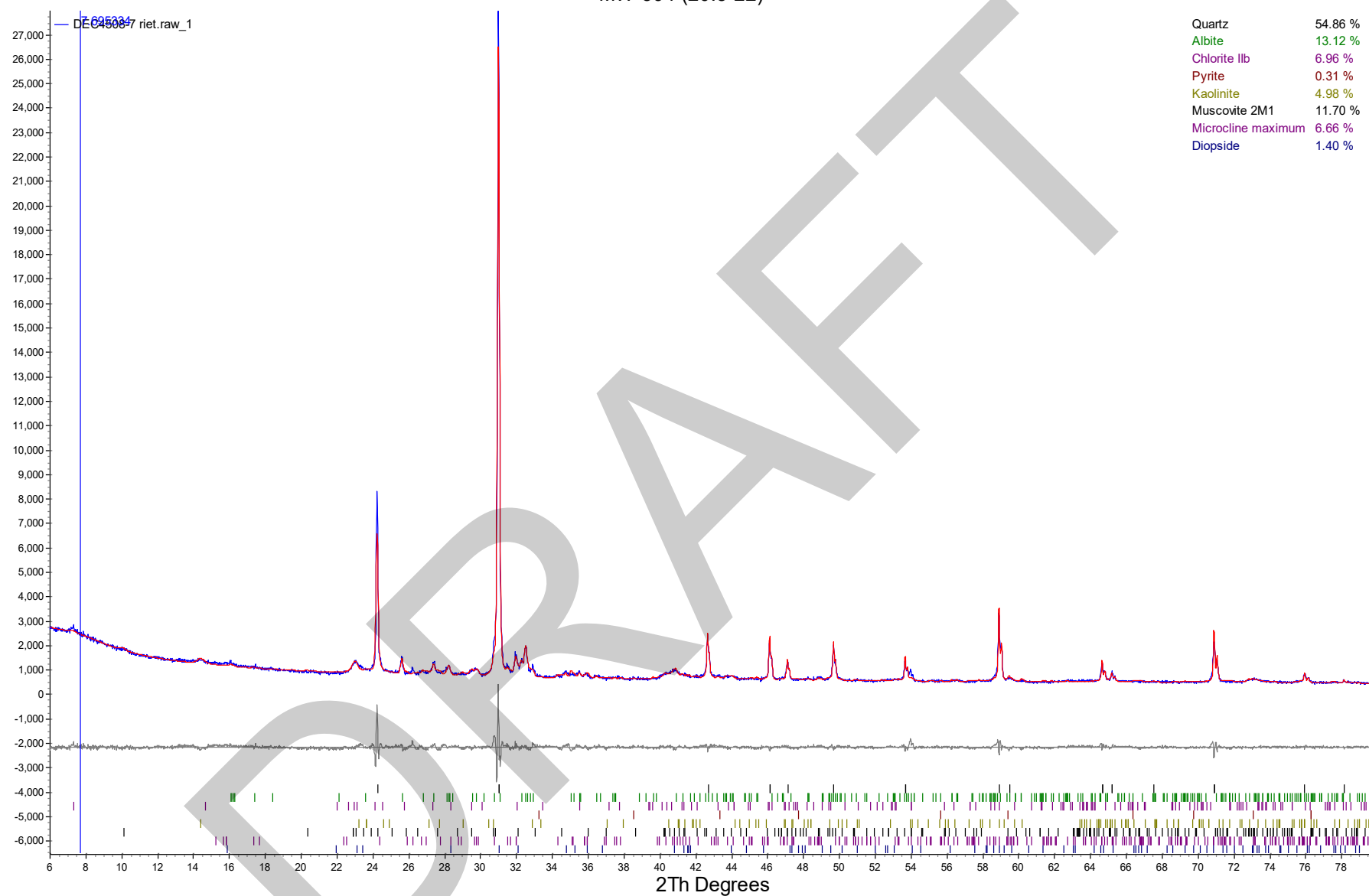
MW-392 (32-33.5)



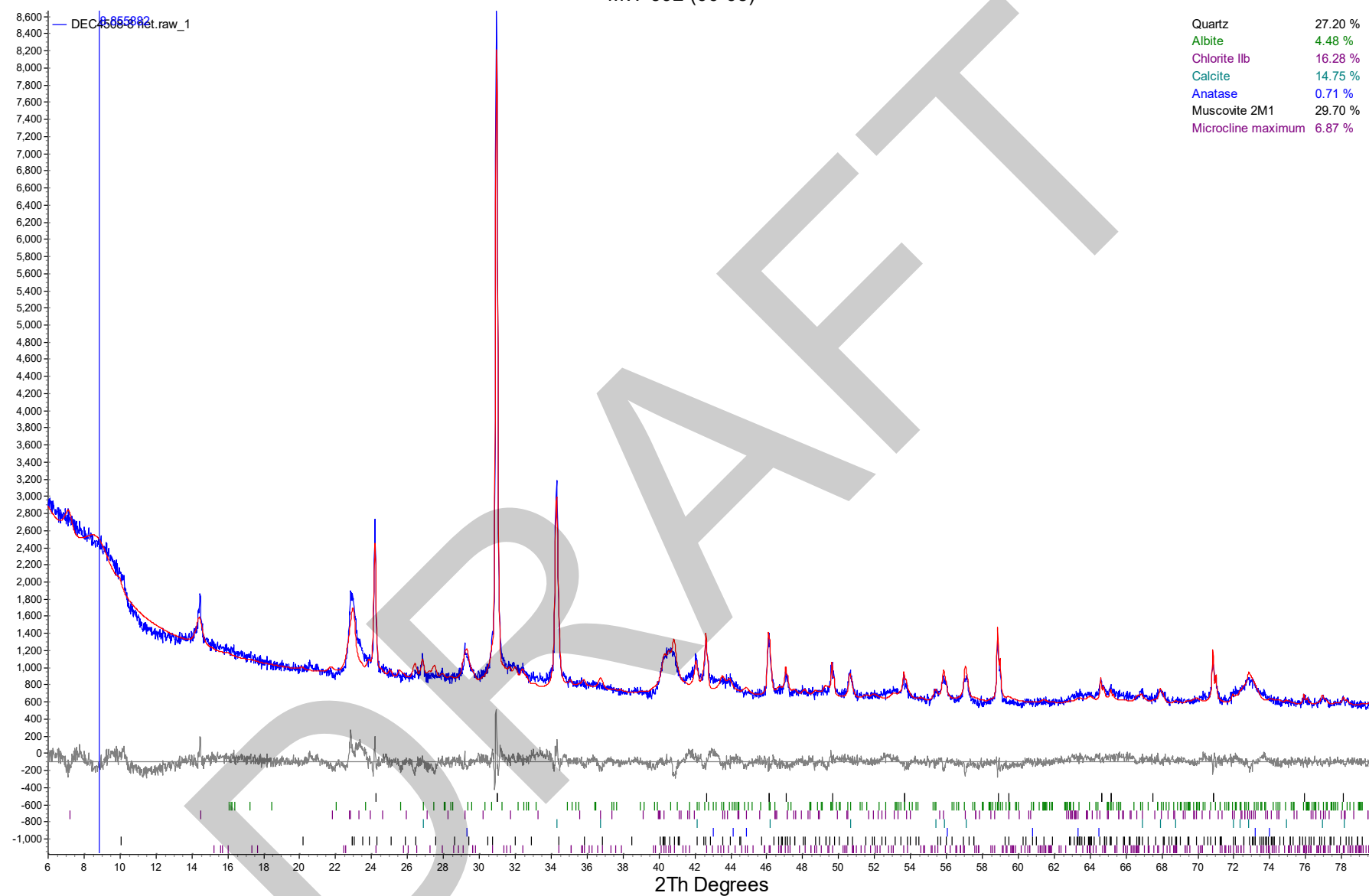
MW-393 (24-25.5)



MW-394 (20.5-22)



MW-392 (66-68)



APPENDIX C
MODFLOW, HELP MODEL, AND FLUX EVALUATION
DATA EXPORT FILES (ELECTRONIC ONLY)

APPENDIX D

HELP MODEL OUTPUT FILES

DRAFT

HYDROLOGIC EVALUATION OF LANDFILL PERFORMANCE
HELP MODEL VERSION 4.0 BETA (2018)
DEVELOPED BY USEPA NATIONAL RISK MANAGEMENT RESEARCH LABORATORY

Title: BAL BAP CIP Cons Slopes **Simulated On:** 1/6/2023 7:23

Layer 1

Type 1 - Vertical Percolation Layer (Cover Soil)
SiCL - Silty Clay Loam (Moderate)
Material Texture Number 26

| | | |
|----------------------------------|---|-----------------|
| Thickness | = | 6 inches |
| Porosity | = | 0.445 vol/vol |
| Field Capacity | = | 0.393 vol/vol |
| Wilting Point | = | 0.277 vol/vol |
| Initial Soil Water Content | = | 0.3673 vol/vol |
| Effective Sat. Hyd. Conductivity | = | 1.90E-06 cm/sec |

Layer 2

Type 1 - Vertical Percolation Layer
SiC - Silty Clay (Moderate)
Material Texture Number 28

| | | |
|----------------------------------|---|-----------------|
| Thickness | = | 18 inches |
| Porosity | = | 0.452 vol/vol |
| Field Capacity | = | 0.411 vol/vol |
| Wilting Point | = | 0.311 vol/vol |
| Initial Soil Water Content | = | 0.3948 vol/vol |
| Effective Sat. Hyd. Conductivity | = | 1.20E-06 cm/sec |

Layer 3

Type 2 - Lateral Drainage Layer
Drainage Net (0.5 cm)
Material Texture Number 20

| | | |
|----------------------------------|---|-----------------|
| Thickness | = | 0.2 inches |
| Porosity | = | 0.85 vol/vol |
| Field Capacity | = | 0.01 vol/vol |
| Wilting Point | = | 0.005 vol/vol |
| Initial Soil Water Content | = | 0.01 vol/vol |
| Effective Sat. Hyd. Conductivity | = | 1.00E+01 cm/sec |
| Slope | = | 25 % |
| Drainage Length | = | 150 ft |

Layer 4

Type 4 - Flexible Membrane Liner

LDPE Membrane

Material Texture Number 36

| | | |
|----------------------------------|---|-----------------|
| Thickness | = | 0.04 inches |
| Effective Sat. Hyd. Conductivity | = | 4.00E-13 cm/sec |
| FML Pinhole Density | = | 1 Holes/Acre |
| FML Installation Defects | = | 1 Holes/Acre |
| FML Placement Quality | = | 3 Good |

Layer 5

Type 1 - Vertical Percolation Layer (Waste)

Electric Plant Coal Bottom Ash

Material Texture Number 83

| | | |
|----------------------------------|---|-----------------|
| Thickness | = | 231.72 inches |
| Porosity | = | 0.578 vol/vol |
| Field Capacity | = | 0.076 vol/vol |
| Wilting Point | = | 0.025 vol/vol |
| Initial Soil Water Content | = | 0.076 vol/vol |
| Effective Sat. Hyd. Conductivity | = | 5.29E-04 cm/sec |

Note: Initial moisture content of the layers and snow water were computed as nearly steady-state values by HELP.

General Design and Evaporative Zone Data

| | | |
|--------------------------------------|---|---------------|
| SCS Runoff Curve Number | = | 91.1 |
| Fraction of Area Allowing Runoff | = | 100 % |
| Area projected on a horizontal plane | = | 21.39 acres |
| Evaporative Zone Depth | = | 18 inches |
| Initial Water in Evaporative Zone | = | 6.845 inches |
| Upper Limit of Evaporative Storage | = | 8.094 inches |
| Lower Limit of Evaporative Storage | = | 5.394 inches |
| Initial Snow Water | = | 0 inches |
| Initial Water in Layer Materials | = | 26.923 inches |
| Total Initial Water | = | 26.923 inches |
| Total Subsurface Inflow | = | 0 inches/year |

Note: SCS Runoff Curve Number was calculated by HELP.

Evapotranspiration and Weather Data

| | | |
|---------------------------------------|---|---------------|
| Station Latitude | = | 38.18 Degrees |
| Maximum Leaf Area Index | = | 4.5 |
| Start of Growing Season (Julian Date) | = | 104 days |

| | | |
|---------------------------------------|---|----------|
| End of Growing Season (Julian Date) | = | 285 days |
| Average Wind Speed | = | 8 mph |
| Average 1st Quarter Relative Humidity | = | 72 % |
| Average 2nd Quarter Relative Humidity | = | 64 % |
| Average 3rd Quarter Relative Humidity | = | 71 % |
| Average 4th Quarter Relative Humidity | = | 72 % |

Note: Evapotranspiration data was obtained for Baldwin, Illinois

Normal Mean Monthly Precipitation (inches)

| <u>Jan/Jul</u> | <u>Feb/Aug</u> | <u>Mar/Sep</u> | <u>Apr/Oct</u> | <u>May/Nov</u> | <u>Jun/Dec</u> |
|----------------|----------------|----------------|----------------|----------------|----------------|
| 2.421014 | 2.032335 | 4.330912 | 4.401604 | 4.511846 | 4.068128 |
| 4.023992 | 2.88724 | 2.952714 | 2.941943 | 4.289265 | 2.800511 |

Note: Precipitation was simulated based on HELP V4 weather simulation for:
Lat/Long: 38.18/-89.85

Normal Mean Monthly Temperature (Degrees Fahrenheit)

| <u>Jan/Jul</u> | <u>Feb/Aug</u> | <u>Mar/Sep</u> | <u>Apr/Oct</u> | <u>May/Nov</u> | <u>Jun/Dec</u> |
|----------------|----------------|----------------|----------------|----------------|----------------|
| 35 | 44.8 | 49.4 | 61.2 | 72.7 | 82.1 |
| 84.9 | 81.7 | 72.6 | 59.4 | 50.1 | 43.9 |

Note: Temperature was simulated based on HELP V4 weather simulation for:
Lat/Long: 38.18/-89.85
Solar radiation was simulated based on HELP V4 weather simulation for:
Lat/Long: 38.18/-89.85

Average Annual Totals Summary

Title: BAL BAP CIP Cons Slopes

Simulated on: 1/6/2023 7:24

| | Average Annual Totals for Years 1 - 30* | | | |
|---|---|------------|--------------|-----------|
| | (inches) | [std dev] | (cubic feet) | (percent) |
| Precipitation | 41.66 | [4.8] | 3,234,836.6 | 100.00 |
| Runoff | 16.562 | [3.613] | 1,285,952.1 | 39.75 |
| Evapotranspiration | 24.541 | [2.705] | 1,905,475.7 | 58.90 |
| Subprofile1 | | | | |
| Lateral drainage collected from Layer 3 | 0.5339 | [0.485] | 41,451.4 | 1.28 |
| Percolation/leakage through Layer 4 | 0.000007 | [0.000006] | 0.5720 | 0.00 |
| Average Head on Top of Layer 4 | 0.0002 | [0.0002] | --- | --- |
| Subprofile2 | | | | |
| Percolation/leakage through Layer 5 | 0.000007 | [0.000007] | 0.5716 | 0.00 |
| Water storage | | | | |
| Change in water storage | 0.0252 | [0.7492] | 1,956.9 | 0.06 |

* Note: Average inches are converted to volume based on the user-specified area.

HYDROLOGIC EVALUATION OF LANDFILL PERFORMANCE
HELP MODEL VERSION 4.0 BETA (2018)
DEVELOPED BY USEPA NATIONAL RISK MANAGEMENT RESEARCH LABORATORY

Title: BAL BAP CIP Cons Top **Simulated On:** 1/6/2023 7:18

Layer 1

Type 1 - Vertical Percolation Layer (Cover Soil)
SiCL - Silty Clay Loam (Moderate)
Material Texture Number 26

| | | |
|----------------------------------|---|-----------------|
| Thickness | = | 6 inches |
| Porosity | = | 0.445 vol/vol |
| Field Capacity | = | 0.393 vol/vol |
| Wilting Point | = | 0.277 vol/vol |
| Initial Soil Water Content | = | 0.3673 vol/vol |
| Effective Sat. Hyd. Conductivity | = | 1.90E-06 cm/sec |

Layer 2

Type 1 - Vertical Percolation Layer
SiC - Silty Clay (Moderate)
Material Texture Number 28

| | | |
|----------------------------------|---|-----------------|
| Thickness | = | 18 inches |
| Porosity | = | 0.452 vol/vol |
| Field Capacity | = | 0.411 vol/vol |
| Wilting Point | = | 0.311 vol/vol |
| Initial Soil Water Content | = | 0.3951 vol/vol |
| Effective Sat. Hyd. Conductivity | = | 1.20E-06 cm/sec |

Layer 3

Type 2 - Lateral Drainage Layer
16 oz Nonwoven Geotextile
Material Texture Number 43

| | | |
|----------------------------------|---|-----------------|
| Thickness | = | 0.11 inches |
| Porosity | = | 0.85 vol/vol |
| Field Capacity | = | 0.01 vol/vol |
| Wilting Point | = | 0.005 vol/vol |
| Initial Soil Water Content | = | 0.01 vol/vol |
| Effective Sat. Hyd. Conductivity | = | 3.00E-01 cm/sec |
| Slope | = | 2 % |
| Drainage Length | = | 600 ft |

Layer 4

Type 4 - Flexible Membrane Liner

LDPE Membrane

Material Texture Number 36

| | | |
|----------------------------------|---|-----------------|
| Thickness | = | 0.04 inches |
| Effective Sat. Hyd. Conductivity | = | 4.00E-13 cm/sec |
| FML Pinhole Density | = | 1 Holes/Acre |
| FML Installation Defects | = | 1 Holes/Acre |
| FML Placement Quality | = | 3 Good |

Layer 5

Type 1 - Vertical Percolation Layer (Waste)

Electric Plant Coal Bottom Ash

Material Texture Number 83

| | | |
|----------------------------------|---|-----------------|
| Thickness | = | 545.28 inches |
| Porosity | = | 0.578 vol/vol |
| Field Capacity | = | 0.076 vol/vol |
| Wilting Point | = | 0.025 vol/vol |
| Initial Soil Water Content | = | 0.076 vol/vol |
| Effective Sat. Hyd. Conductivity | = | 5.29E-04 cm/sec |

Note: Initial moisture content of the layers and snow water were computed as nearly steady-state values by HELP.

General Design and Evaporative Zone Data

| | | |
|--------------------------------------|---|---------------|
| SCS Runoff Curve Number | = | 89.8 |
| Fraction of Area Allowing Runoff | = | 100 % |
| Area projected on a horizontal plane | = | 53.73 acres |
| Evaporative Zone Depth | = | 18 inches |
| Initial Water in Evaporative Zone | = | 6.849 inches |
| Upper Limit of Evaporative Storage | = | 8.094 inches |
| Lower Limit of Evaporative Storage | = | 5.394 inches |
| Initial Snow Water | = | 0 inches |
| Initial Water in Layer Materials | = | 50.759 inches |
| Total Initial Water | = | 50.759 inches |
| Total Subsurface Inflow | = | 0 inches/year |

Note: SCS Runoff Curve Number was calculated by HELP.

Evapotranspiration and Weather Data

| | | |
|---------------------------------------|---|---------------|
| Station Latitude | = | 38.18 Degrees |
| Maximum Leaf Area Index | = | 4.5 |
| Start of Growing Season (Julian Date) | = | 104 days |

| | | |
|---------------------------------------|---|----------|
| End of Growing Season (Julian Date) | = | 285 days |
| Average Wind Speed | = | 8 mph |
| Average 1st Quarter Relative Humidity | = | 72 % |
| Average 2nd Quarter Relative Humidity | = | 64 % |
| Average 3rd Quarter Relative Humidity | = | 71 % |
| Average 4th Quarter Relative Humidity | = | 72 % |

Note: Evapotranspiration data was obtained for Baldwin, Illinois

Normal Mean Monthly Precipitation (inches)

| <u>Jan/Jul</u> | <u>Feb/Aug</u> | <u>Mar/Sep</u> | <u>Apr/Oct</u> | <u>May/Nov</u> | <u>Jun/Dec</u> |
|----------------|----------------|----------------|----------------|----------------|----------------|
| 2.421014 | 2.032335 | 4.330912 | 4.401604 | 4.511846 | 4.068128 |
| 4.023992 | 2.88724 | 2.952714 | 2.941943 | 4.289265 | 2.800511 |

Note: Precipitation was simulated based on HELP V4 weather simulation for:
Lat/Long: 38.18/-89.85

Normal Mean Monthly Temperature (Degrees Fahrenheit)

| <u>Jan/Jul</u> | <u>Feb/Aug</u> | <u>Mar/Sep</u> | <u>Apr/Oct</u> | <u>May/Nov</u> | <u>Jun/Dec</u> |
|----------------|----------------|----------------|----------------|----------------|----------------|
| 35 | 44.8 | 49.4 | 61.2 | 72.7 | 82.1 |
| 84.9 | 81.7 | 72.6 | 59.4 | 50.1 | 43.9 |

Note: Temperature was simulated based on HELP V4 weather simulation for:
Lat/Long: 38.18/-89.85
Solar radiation was simulated based on HELP V4 weather simulation for:
Lat/Long: 38.18/-89.85

Average Annual Totals Summary

Title: BAL BAP CIP Cons Top
Simulated on: 1/6/2023 7:19

| | Average Annual Totals for Years 1 - 30* | | | |
|---|---|------------|--------------|-----------|
| | (inches) | [std dev] | (cubic feet) | (percent) |
| Precipitation | 41.66 | [4.8] | 8,125,655.5 | 100.00 |
| Runoff | 16.544 | [3.658] | 3,226,692.1 | 39.71 |
| Evapotranspiration | 24.605 | [2.679] | 4,798,963.4 | 59.06 |
| Subprofile1 | | | | |
| Lateral drainage collected from Layer 3 | 0.4260 | [0.3581] | 83,079.3 | 1.02 |
| Percolation/leakage through Layer 4 | 0.061216 | [0.074113] | 11,939.6 | 0.15 |
| Average Head on Top of Layer 4 | 0.7474 | [0.9614] | --- | --- |
| Subprofile2 | | | | |
| Percolation/leakage through Layer 5 | 0.000239 | [0.000259] | 46.6 | 0.00 |
| Water storage | | | | |
| Change in water storage | 0.0865 | [0.7368] | 16,874.2 | 0.21 |

* Note: Average inches are converted to volume based on the user-specified area.

APPENDIX E
FLUX EVALUATION DATA

DRAFT

APPENDIX E. FLUX EVALUATION DATA

GROUNDWATER MODELING REPORT

BALDWIN POWER PLANT

BOTTOM ASH POND

BALDWIN, ILLINOIS

| Calibration Model | | | | | |
|---|--|---|---|-------------------------|---|
| Model | Years (Model Period) | HSU | Total Flux In ¹ (ft ³ /d) | Total Flux In (gpm) | |
| Calibration Model | 53 | CCR | 2098.27 | 10.90 | |
| Model | Years (Model Period) | HSU | Total Flux Out ¹ (ft ³ /d) | Total Flux Out (gpm) | |
| Calibration Model | 53 | CCR | -652.13 | -3.39 | |
| Model | Model Period | Boundary Condition | Total Flux Out ¹ (ft ³ /d) | Total Flux Out (gpm) | |
| Calibration Model | 53 | Constant Head (Stormwater Management within Active BAP) | -1420.44 | -7.38 | |
| Scenario: CIP (CCR removal from the western areas of the BAP, consolidation to the southeast, and eventually northeastern portions of the BAP, and construction of a cover system over the remaining CCR) | | | | | |
| Prediction Model | Years (Post- Construction Period) | HSU | Total Flux In ¹ (ft ³ /d) | Total Flux In (gpm) | Reduction in Flux In Post Closure ² (Percentage, %) |
| CIP | 93 | CCR | 108.27 | 0.56 | 95% |
| Prediction Model | Years (Post- Construction Period) | HSU | Total Flux Out ¹ (ft ³ /d) | Total Flux Out (gpm) | Reduction in Flux Out Post Closure ² (Percentage, %) |
| CIP | 93 | CCR | -135.25 | -0.70 | 93% |

[O: JJW 1/5/23; C: EGP 1/6/23; C: BGH 1/19/23; U: JJW 5/17/23 C: EGP 5/23/23]

Notes:

1. Reduction in flux as compared to flux at the end of calibration model (model period of 53 years) including flux through constant head boundary conditions in the calibration model when applicable (flux out).

2. Total flux in and out source data provided in flux calculation data files included in Appendix C.

BAP = Bottom Ash Pond

CCR = coal combustion residuals

CIP = closure in place

HSU = Hydrostratigraphic Unit

% = percentage

ft³/d = cubic feet per day

gpm = gallons per minute

**APPENDIX B
MODFLOW, MT3DMS, HELP MODEL, AND FLUX EVALUATION
DATA EXPORT FILES
(ELECTRONIC ONLY)**

APPENDIX C
HELP MODEL INPUTS AND OUTPUTS

DRAFT

HYDROLOGIC EVALUATION OF LANDFILL PERFORMANCE
HELP MODEL VERSION 4.0 BETA (2018)
DEVELOPED BY USEPA NATIONAL RISK MANAGEMENT RESEARCH LABORATORY

Title: BAL FAPS - As-Is - K3 **Simulated On:** 6/5/2024 12:20

Layer 1

Type 1 - Vertical Percolation Layer (Cover Soil)

SiL - Silty Loam

Material Texture Number 9

| | | |
|----------------------------------|---|-----------------|
| Thickness | = | 6 inches |
| Porosity | = | 0.501 vol/vol |
| Field Capacity | = | 0.284 vol/vol |
| Wilting Point | = | 0.135 vol/vol |
| Initial Soil Water Content | = | 0.501 vol/vol |
| Effective Sat. Hyd. Conductivity | = | 1.90E-04 cm/sec |

Layer 2

Type 3 - Barrier Soil Liner

Silty Clay

Material Texture Number 43

| | | |
|----------------------------------|---|-----------------|
| Thickness | = | 18 inches |
| Porosity | = | 0.427 vol/vol |
| Field Capacity | = | 0.418 vol/vol |
| Wilting Point | = | 0.367 vol/vol |
| Initial Soil Water Content | = | 0.427 vol/vol |
| Effective Sat. Hyd. Conductivity | = | 1.00E-07 cm/sec |

Layer 3

Type 1 - Vertical Percolation Layer (Waste)

Unsaturated CCR Material (HELP Waste)

Material Texture Number 83

| | | |
|----------------------------------|---|-----------------|
| Thickness | = | 306.6 inches |
| Porosity | = | 0.541 vol/vol |
| Field Capacity | = | 0.187 vol/vol |
| Wilting Point | = | 0.047 vol/vol |
| Initial Soil Water Content | = | 0.1888 vol/vol |
| Effective Sat. Hyd. Conductivity | = | 1.00E-04 cm/sec |

Note: Initial moisture content of the layers and snow water were computed as nearly steady-state values by HELP.

General Design and Evaporative Zone Data

| | | |
|--------------------------------------|---|----------------|
| SCS Runoff Curve Number | = | 80 |
| Fraction of Area Allowing Runoff | = | 100 % |
| Area projected on a horizontal plane | = | 232 acres |
| Evaporative Zone Depth | = | 6 inches |
| Initial Water in Evaporative Zone | = | 3.006 inches |
| Upper Limit of Evaporative Storage | = | 3.006 inches |
| Lower Limit of Evaporative Storage | = | 0.81 inches |
| Initial Snow Water | = | 0.21492 inches |
| Initial Water in Layer Materials | = | 68.58 inches |
| Total Initial Water | = | 68.795 inches |
| Total Subsurface Inflow | = | 0 inches/year |

Note: SCS Runoff Curve Number was calculated by HELP.

Evapotranspiration and Weather Data

| | | |
|---------------------------------------|---|---------------|
| Station Latitude | = | 38.18 Degrees |
| Maximum Leaf Area Index | = | 4.5 |
| Start of Growing Season (Julian Date) | = | 97 days |
| End of Growing Season (Julian Date) | = | 300 days |
| Average Wind Speed | = | 8 mph |
| Average 1st Quarter Relative Humidity | = | 72 % |
| Average 2nd Quarter Relative Humidity | = | 64 % |
| Average 3rd Quarter Relative Humidity | = | 71 % |
| Average 4th Quarter Relative Humidity | = | 72 % |

Note: Evapotranspiration data was obtained for ,

Normal Mean Monthly Precipitation (inches)

| <u>Jan/Jul</u> | <u>Feb/Aug</u> | <u>Mar/Sep</u> | <u>Apr/Oct</u> | <u>May/Nov</u> | <u>Jun/Dec</u> |
|----------------|----------------|----------------|----------------|----------------|----------------|
| 2.360428 | 2.90231 | 3.416467 | 4.240202 | 4.279031 | 4.261632 |
| 4.118166 | 2.73529 | 2.651068 | 3.526861 | 4.231645 | 3.374315 |

Note: Precipitation was simulated based on HELP V4 weather simulation for:
Lat/Long: 38.18/-89.85

Normal Mean Monthly Temperature (Degrees Fahrenheit)

| <u>Jan/Jul</u> | <u>Feb/Aug</u> | <u>Mar/Sep</u> | <u>Apr/Oct</u> | <u>May/Nov</u> | <u>Jun/Dec</u> |
|----------------|----------------|----------------|----------------|----------------|----------------|
| 35 | 37.6 | 48 | 58.5 | 73.8 | 82.1 |
| 84.5 | 83.4 | 74.7 | 61.4 | 51.2 | 40.3 |

Note: Temperature was simulated based on HELP V4 weather simulation for:
 Lat/Long: 38.18/-89.85
 Solar radiation was simulated based on HELP V4 weather simulation for:
 Lat/Long: 38.18/-89.85

DRAFT

Average Annual Totals Summary

Title: BAL FAPS - As-Is - K3
Simulated on: 6/5/2024 12:23

| | Average Annual Totals for Years 1 - 30* | | | |
|-------------------------------------|---|------------|--------------|-----------|
| | (inches) | [std dev] | (cubic feet) | (percent) |
| Precipitation | 42.10 | [5.94] | 35,452,759.3 | 100.00 |
| Runoff | 10.656 | [4.485] | 8,973,742.1 | 25.31 |
| Evapotranspiration | 30.469 | [4.137] | 25,659,382.5 | 72.38 |
| Subprofile1 | | | | |
| Percolation/leakage through Layer 2 | 0.983323 | [0.103717] | 828,115.5 | 2.34 |
| Average Head on Top of Layer 2 | 2.1299 | [0.3463] | --- | --- |
| Subprofile2 | | | | |
| Percolation/leakage through Layer 3 | 0.816873 | [0.220265] | 687,937.5 | 1.94 |
| Water storage | | | | |
| Change in water storage | 0.1564 | [0.9348] | 131,697.2 | 0.37 |

* Note: Average inches are converted to volume based on the user-specified area.

APPENDIX D
FLUX EVALUATION DATA

DRAFT

APPENDIX D. FLUX EVALUATION DATA

GROUNDWATER MODELING TECHNICAL MEMORANDUM
BALDWIN POWER PLANT
FLY ASH POND SYSTEM
BALDWIN, ILLINOIS

| Calibration Model 1 (pre-closure FAPS model) | | | | | |
|--|---|---|--|---|---|
| Model | Modeled Year | HSU | Total Flux In¹ (ft³/d) | Total Flux In (gpm) | |
| Calibration Model | 2020 | CCR | 4836.47 | 25.12 | |
| Model | Modeled Year | Boundary Condition | Total Flux In¹ (ft³/d) | Total Flux In (gpm) | |
| Calibration Model | 2020 | Constant Head (Stormwater Management within Active FAPS) | 577.57 | 3.00 | |
| Model | Modeled Year | HSU | Total Flux Out^{1,3} (ft³/d) | Total Flux Out³ (gpm) | |
| Calibration Model | 2020 | CCR | -5342.95 | -27.76 | |
| Alternative 3 – Source Control with a Groundwater Management System (GMS) | | | | | |
| Prediction Model | Years (Post-Construction Period) | HSU | Total Flux In¹ (ft³/d) | Total Flux In (gpm) | Reduction in Flux In Post Closure² (Percentage, %) |
| Alternative 3 | 106 | CCR | 2098.87 | 10.90 | 61% |
| Prediction Model | Years (Post-Construction Period) | HSU | Total Flux Out^{1,3} (ft³/d) | Total Flux Out³ (gpm) | Reduction in Flux Out Post Closure² (Percentage, %) |
| Alternative 3 | 106 | CCR | -2171.46 | -11.28 | 59% |
| Prediction Model | Years (Post-Construction Period) | HSU | Total Flux In¹ (ft³/d) | Total Flux In (gpm) | Reduction in Flux In Post Closure² (Percentage, %) |
| Alternative 3 - Sensitivity Model | 106 | CCR | 3125.70 | 16.24 | 42% |
| Prediction Model | Years (Post-Construction Period) | HSU | Total Flux Out^{1,3} (ft³/d) | Total Flux Out³ (gpm) | Reduction in Flux Out Post Closure² (Percentage, %) |
| Alternative 3 - Sensitivity Model | 106 | CCR | -1468.16 | -7.63 | 73% |

[O: JJW 1/14/25 C: KLT 1/31/2025]

Notes:

1. Total flux in and out source data provided in flux calculation data files included in Appendix B.
 2. Reduction in flux as compared to flux at the end of Calibration Model 1 (model period of 51 years) including flux through constant head boundary conditions in the calibration model when applicable (flux in).
 3. Flux out expressed as negative values.
- % = percentage
FAPS = Fly Ash Pond System
CCR = coal combustion residuals
ft³/d = cubic feet per day
gpm = gallons per minute
GMS = groundwater management system
HSU = Hydrostratigraphic Unit

**APPENDIX C
MATERIAL QUANTITY, LABOR, AND MILEAGE
ESTIMATES FOR ALTERNATIVE 2 AND ALTERNATIVE 3
REMEDIES**

**DYNEGY MIDWEST GENERATION, LLC. - BALDWIN POWER PLANT
CORRECTIVE ACTION ALTERNATIVES ANALYSIS SUPPORTING INFORMATION REPORT (CAAA-SIR)
ALTERNATIVE 2 - SOURCE CONTROL WITH CUTOFF WALL (CW)¹**

| ITEM NO. | ENGINEERING, PRE-CONSTRUCTION, AND CONSTRUCTION SUPPORT TASKS | Units | Quantity | Crew | Daily Output | Labor Hours | Equipment Hours | Notes |
|---|--|-------------|----------|--------|--------------|--------------|-----------------|---|
| 1 | Pre-Design Investigation, Final Cutoff Wall Design and Bid Support | LS | 1 | - | - | - | - | Assumed based on Ramboll previous project experience. |
| 2 | Engineering Support and CQA During Construction | LS | 1 | Eng | - | 2,865 | 1,146 | Assumed based on Ramboll previous project experience. |
| ENGINEERING, PRE-CONSTRUCTION, AND CONSTRUCTION SUPPORT TASKS ESTIMATED SUBTOTAL | | | | | | 2,865 | 1,146 | |
| ITEM NO. | SITE PREPARATION | Units | Quantity | Crew | Daily Output | Labor Hours | Equipment Hours | Notes |
| 3 | Mobilization and De-Mobilization | LS | 1 | - | - | - | - | Mobilization/demobilization estimated based on previous Ramboll experience. |
| | General Construction Mobilization and De-Mobilization | LS | 1 | - | - | - | - | Assumed based on Ramboll previous project experience. |
| | Trenching Equipment Mobilization, Assembly, and De-Mobilization | LS | 1 | - | - | - | - | One-pass technology specific equipment mobilization derived from ROM cost provided by specialty contractor. |
| 4 | Staging/Laydown Area Preparation | - | - | - | - | 1,235 | 382 | Assumes 3-acre staging areas will be needed for construction of the cutoff wall. |
| | Staging Area Grading | EA | 1.0 | B11L | 1.8 | 8.9 | 4.4 | 312213200200: Rough grade open sites 10,000-20,000 S.F., grader. This total includes working pad only. |
| | Subgrade Stabilization Nonwoven Geotextile | SY | 14,520 | 2 Clab | 2500 | 93 | 0.0 | 313219161550: Geosynthetic soil stabilization, geotextile fabric, non-woven, 120 lb tensile strength includes scarifying and compaction; assume we need for 3-acre staging/laydown area. This total includes working pad only. |
| | Install Crushed Gravel Road (18" Thick) - Staging Area | SY | 14,520 | B14 | 615 | 1,133 | 378 | 015523500100: Temporary, roads, gravel fill, 18" gravel depth (scaled), excluding surfacing. Assumes 3-acre staging/laydown area. This total includes working pad only. |
| 5 | Preparation Work Pad and Temporary Roads | - | - | - | - | 4,177 | 1,323 | Assumes the general work area associated with the cutoff wall will have temporary access roads installed in order to make way for construction equipment needed for the install. |
| | Access Roads and Work Pad Grading | EA | 21 | B11L | 1.8 | 189 | 94 | 312213200200: Rough grade open sites 10,000-20,000 S.F., grader, work pad area, access road. Assumes grading will be needed for the 7,000-ft by 50-ft cutoff wall alignment and 1,500-ft by 50-ft access road. |
| | Subgrade Stabilization Nonwoven Geotextile | SY | 47,222 | 2 Clab | 2500 | 302 | 0.0 | 313219161550: Geosynthetic soil stabilization, geotextile fabric, non-woven, 120 lb tensile strength includes scarifying and compaction; for the 7,000-ft by 50-ft cutoff wall alignment and 1,500-ft by 50-ft access road. |
| | Install Crushed Gravel Road (18" Thick) - Temporary Roads | SY | 47,222 | B14 | 615 | 3,686 | 1,229 | 015523500100: Temporary, roads, gravel fill, 18" gravel depth (scaled), excluding surfacing. Spanning the 7,000-ft by 50-ft cutoff wall alignment and 1,500-ft by 50-ft access road. |
| 6 | Construction Soil Erosion & Sediment Controls | - | - | - | - | 1,380 | 460 | Assumes soil erosion and sediment controls will be implemented only during the cutoff wall construction. |
| | Silt Fence | LF | 36,892 | B62 | 650 | 1,362 | 454 | 312514161000: Synthetic erosion control, silt fence, install and remove, 3' high. Assumes silt fence is installed down both sides of the cutoff wall alignment, both sides of the access road, and around 3-acre staging/laydown area (approx. 1500 LF perimeter). Assumes the silt fence will get replaced once during construction. |
| | Sediment Log, Filter Sock | LF | 738 | A2 | 1000 | 18 | 5.9 | 312514160705: Sediment Log, Filter Sock, 9." Assume filter socks are needed along perimeter of cutoff wall, access road and staging/laydown area at an occurrence of 1 every 50 feet. Assumes the sediment log, filter sock will get replaced once during construction. |
| 7 | Construction Facilities | MO - in use | - | - | - | - | - | Includes monthly rentals associated with one (1) office trailer, three (3) storage trailers, and four (4) portable toilets. |
| | Office Trailer | MO - in use | 24 | - | - | - | - | 015213200350: Office trailer, furnished, no hookups, 32' x 8', rent per month. Assume quantity of one (1). |
| | Storage Trailers | MO - in use | 72 | - | - | - | - | 015213201350: Storage boxes, 40' x 8', rent per month. Assume quantity of three (3). |
| | Portable Toilet | MO - in use | 96 | - | - | - | - | 015433406410: Rent toilet, portable chemical. Assume quantity of four (4). |
| 8 | Geotechnical Monitoring | LS | - | GM | - | 600 | 0.0 | Assumes installation of inclinometers, survey prisms, and settlement monitoring devices along the southern trench where the dike will be modified for work pad installation. Assumes a 4-person crew installs the monitoring system over a period of 3 weeks. Based on Ramboll experience. |
| SITE PREPARATION ESTIMATED SUBTOTAL | | | | | | 7,392 | 2,165 | |

| ITEM NO. | CUTOFF WALL CONSTRUCTION | Units | Quantity | Crew | Daily Output | Labor Hours | Equipment Hours | Notes |
|---|--|-------------------|----------|------|--------------|--------------------------|------------------------------|---|
| 9 | Installation of Cutoff Wall | LF | 7,000 | B12H | 80 | 1,400 | 700 | Information provided by subsurface contractor. Spoils to be disposed of in offsite landfill. Assumes 7,000-foot wall alignment. Crew code selected to mimic the proposed crew provided by specialty contractor. |
| 10 | Spoils Management and Disposal | CY - in place | 70,000 | - | - | 6,372 | 9,526 | Hauling and management of trench excavation spoils to the AP for placement beneath the final cover system. |
| | Excavation and Loading of Material | CY - as excavated | 77,000 | B14B | 5000 | 185 | 123 | 312316435320: Excavating, large volume projects; excavation with truck loading; excavator, 6 C.Y. bucket, 100% fill factor (assume 10% fluff factor from ground to excavated). |
| | Pushing Materials to Excavator | CY - as excavated | 77,000 | B10B | 1000 | 924 | 616 | 312323170020: Spread dumped material, no compaction, by dozer. Dozer support for excavation. Daily output edited to match excavation based on experience. |
| | Hauling and Dumping Onsite of Material for Moisture Conditioning | CY - as excavated | 77,000 | B34G | 850 | 725 | 725 | 312323206170: Hauling; no loading equipment, including hauling, waiting, loading/dumping; 34 C.Y. off-road, 15 min wait/ld/uld., 15 MPH, cycle 2 mile. |
| | Spreading/Drying Moisture Conditioning | CY - as excavated | 38,500 | B10B | 1000 | 462 | 308 | 312323170020: Spread dumped material, no compaction, by dozer. Daily output edited to match excavation based on experience. |
| | Dust Control Moisture Conditioning Prior to Loading | CY - as excavated | 21,000 | B45 | 1888 | 178 | 178 | 312323239000: Water, 3000 gal. truck, 3 mile haul. Assume 30% of volume will need to be wetted. |
| | Loading of Material | CY - as excavated | 77,000 | B14B | 5605 | 165 | 110 | 312316434420: Excavating, large volume projects; restricted loading trucks; loader, 6 C.Y. bucket, 95% fill factor (assume 10% fluff factor from ground to excavated). |
| | Hauling Material to Landfill | CY - as excavated | 77,000 | B34C | 165 | 3,733 | 7,467 | 312323203080: Hauling; no loading equipment, including hauling, waiting, loading/dumping; 16.5 C.Y. truck off-road, 15 min wait/ld/uld., 40 MPH, cycle 20 miles |
| | Landfill Tipping | TON | 88,358 | - | - | - | - | Information gathered from four local landfills with an average unit weight of 85 pcf. Assumes material is classified as non-hazardous waste. |
| CUTOFF WALL CONSTRUCTION | | | | | | 7,772 | 10,226 | |
| ITEM NO. | SITE RESTORATION | Units | Quantity | Crew | Daily Output | Labor Hours | Equipment Hours | Notes |
| 11 | Site Restoration | - | - | - | - | 115 | 115 | Assumes restoration of grade surface following cutoff wall installation. |
| | Lime | MSF | 556 | B66 | 700 | 6.4 | 6.4 | 329113234250: Soil preparation, structural soil mixing, spread soil conditioners, ground limestone, 1#/S.Y., tractor spreader. Unit multiplied by 1.1 to account for soils possibly being void of nutrients. |
| | Fertilizer | MSF | 556 | B66 | 700 | 6.4 | 6.4 | 329113234150: Soil preparation, structural soil mixing, spread soil conditioners, fertilizer, 0.2#/S.Y., tractor spreader. Unit multiplied by 1.1 to account for soils possibly being void of nutrients. |
| | Grassland Mix | MSF | 556 | B66 | 52 | 85 | 85 | 329219142300: Seeding athletic fields, seeding fescue, tall, 5.5 lb. per M.S.F., tractor spreader. Quantity all disturbed areas minus wetland area, pollinator area, and 15-acre pond in consolidated area. |
| | Mulch | MSF | 556 | B65 | 530 | 17 | 17 | 329113160350: Mulching, Hay, 1" deep, power mulcher, large. |
| SITE RESTORATION ESTIMATED SUBTOTAL | | | | | | 115 | 115 | |
| TOTAL CONSTRUCTION ESTIMATED SUBTOTAL | | | | | | 15,278 | 12,507 | |
| | | | | | | Total Labor Hours | Total Equipment Hours | |
| ENGINEERING AND CONSTRUCTION SUBTOTAL | | | | | | 18,100 | 13,700 | |
| CORRECTIVE ACTION OPERATION AND MAINTENANCE SUBTOTAL | | | | | | - | - | |
| ALTERNATIVE 2 SUBTOTAL | | | | | | 18,100 | 13,700 | |

NOTES:

- Alternative 2: Source Control with cut off wall estimated to take approximately 1,000 years to achieve groundwater protection standards (GWPS-35 I.A.C Section 845.600) at all perimeter wells associated with the Fly Ash Pond System (FAPS). For the purpose of this assessment, a total duration of 30 years is used.
- RS Means refers to the 2024 Quarter 4 online edition of RS Means Commercial New Construction.
- See crew tab (Alt 2-Crew) for assumptions regarding crew size, total labor hours and required construction equipment, as needed, for each task.
- See mileage tab (Alt 2-Mileage) for assumptions regarding total mileage for tasks outlined in this alternative.

ACRONYMS:
 CW = Cutoff Wall
 CY = Cubic Yard
 EA = Each
 FAPS = Fly Ash Pond System
 GWPS = Groundwater Protection Standards
 LB = Pounds
 LF = Linear Foot
 LS = Lump Sum
 MO = Month
 MSF = Square Feet Divided by 1000
 O&M = Operation and Maintenance
 PCF = Pounds per Cubic Foot
 SY = Square Yards



CREW CODES
DYNEGY MIDWEST GENERATION, LLC. - BALDWIN POWER PLANT
CORRECTIVE ACTION ALTERNATIVES ANALYSIS SUPPORTING INFORMATION REPORT (CAAA-SIR)
ALTERNATIVE 2 - SOURCE CONTROL WITH CUTOFF WALL (CW)

| | | | | | | | Project Total | |
|------------------------|-----------|---|-------------------|--|-----------------------|-----------|--------------------|------------------------------|
| Item No. | Crew Code | Labor | Daily Labor Hours | Equipment | Daily Equipment Hours | Crew Size | Onsite Labor Hours | Onsite Heavy Equipment Hours |
| Construction | | | | | | | | |
| 4,5,7 | 2 Clab | Laborer x2 | 16 | None | 0 | 2 | 395 | 0 |
| 6 | A2 | Laborer x2 Truck Driver x1 | 24 | Flatbed Truck, Gas, 1.5 ton | 8 | 3 | 18 | 6 |
| 10 | B10B | Operator x1 Laborer x0.5 | 12 | Dozer, 200 H.P. | 8 | 1.5 | 1,386 | 924 |
| 4,5 | B11L | Operator (med) x 1 Laborer x 1 | 16 | Grader, 30,000lb | 8 | 2 | 198 | 99 |
| 9 | B12H | Laborer x1 Operator x1 | 16 | 1 Crawler Crane, 25 Ton 1 Clamshell Bucket, 1 C.Y. | 8 | 2 | 1,400 | 700 |
| 4,5,7 | B14 | Labor Foreman x 1 Operator (light) x1 Laborer x 4 | 48 | Backhoe Loader, 48 H.P. | 16 | 6 | 4,819 | 1,606 |
| 10 | B14B | Operator x1 Laborer x0.5 | 12 | Hyd. Excavator, 6 C.Y. | 8 | 1.5 | 350 | 233 |
| 10 | B34C | Truck Driver (heavy) x 1 | 8 | Tractor Truck, 380 H.P. x 1 Dump Trailer, 16.5 C.Y. x 1 | 16 | 1 | 3,733 | 7,467 |
| 10 | B34G | Truck Driver x1 | 8 | Dump Truck, Off Hwy., 50 ton | 8 | 1 | 725 | 725 |
| 10 | B45 | Operator (medium) x 1 Truck Driver (heavy) x 1 | 16 | 3000 Gallon Tanker x 1 Truck Tractor, 380 H.P. x 1 | 16 | 1 | 178 | 178 |
| 6 | B62 | Laborer x2 Operator x 1 | 24 | Loader, Skid Steer, 30 H.P. | 8 | 3 | 1,362 | 454 |
| 11 | B65 | Laborer x1 Truck Driver (light) x1 | 16 | 1 Power Mulcher (large) 1 Flatbed Truck, Gas, 1.5 ton | 16 | 2 | 17 | 17 |
| 11 | B66 | Operator (light) x1 | 8 | 1 Loader-Backhoe, 40 H.P. | 8 | 1 | 98 | 98 |
| 2 | Eng | Engineering Staff x1.2 | 10 | Side by Side x1 | 4 | 1.2 | 2,865 | 1,146 |
| 8 | GM | Operator x1 Engineering Staff x3 | 32 | Service Vehicle | 0 | 1.2 | 600 | 0 |
| Construction Subtotals | | | | | | | 18,100 | 13,700 |
| Totals | | | | | | | 18,100 | 13,700 |

Note: Blue shaded crew codes were created by Ramboll based on experience (not pulled from RS Means).



CONSTRUCTION MILEAGE AND LABOR ESTIMATES
DYNEGY MIDWEST GENERATION, LLC. - BALDWIN POWER PLANT
CORRECTIVE ACTION ALTERNATIVES ANALYSIS SUPPORTING INFORMATION REPORT (CAAA-SIR)
ALTERNATIVE 2 - SOURCE CONTROL WITH CUTOFF WALL (CW)

| Item | Quantity | Assumptions |
|---|----------|--|
| Labor Total Hours | 18,144 | Per projected construction total (does not include contingency) |
| Duration of Onsite Construction Days | 287 | Total calendar days |
| Average Daily Crew Size | 11.3 | Assumes multiple crew sizes and a 10 hour work day Assumes 1 Ramboll personnel daily for construction oversight |
| Daily Labor Mobilization Miles | 7,749 | Includes mob/demob from STL (82 miles round trip) and local daily commute mileage (40 miles per day) |
| Vehicle Miles Onsite | 48,713 | 1 mile per day round trip from gate to parking 5 miles per day for onsite miles 9 miles per day local trips (Vil. of Baldwin) No contingency included |
| Equipment Mobilization Miles - Unloaded | 28,655 | Average of 500 miles round trip for equipment hauling Average 1 load of equipment per working week |
| Equipment Mobilization Miles - Loaded | 28,655 | Average of 500 miles round trip for equipment hauling Average 1 load of equipment per working week |
| Onsite Haul Truck Miles - Unloaded | 4,529 | 34 CY Off Road Dump Truck 2 miles round trip per load |
| Onsite Haul Truck Miles - Loaded | 4,529 | 34 CY Off Road Dump Truck 2 miles round trip per load |
| Offsite Haul Truck Miles - Unloaded | 337,097 | Assumes 16 CY loads of material are delivered to the site from a regional supplier located within 50 miles of the site |
| Offsite Haul Truck Miles - Loaded | 337,097 | Assumes truck is returning to the regional supplier located within 50 miles of the site |
| Material Delivery Miles - Unloaded | 57,310 | Misc. construction materials (cement, bales, etc) Assumes 200 mile round trip on a daily basis |
| Material Delivery Miles - Loaded | 57,310 | Misc. construction materials (cement, bales, etc) Assumes 200 mile round trip on a daily basis |

O&M Mileage and Labor Estimates

| Item | Quantity | Assumptions |
|---|----------|------------------|
| Labor Total Hours | 0 | No O&M for Alt 2 |
| Duration of Onsite O&M Days | 0 | - |
| Average Daily Crew Size | 0 | - |
| Daily Labor Mobilization Miles | 0 | - |
| Vehicles Miles Onsite | 0 | - |
| Equipment Mobilization Miles - Unloaded | 0 | - |
| Equipment Mobilization Miles - Loaded | 0 | - |
| Onsite Haul Truck Miles - Unloaded | 0 | - |
| Onsite Haul Truck Miles - Loaded | 0 | - |
| Offsite Haul Truck Miles - Unloaded | 0 | - |
| Offsite Haul Truck Miles - Loaded | 0 | - |
| Material Delivery Miles - Unloaded | 0 | - |
| Material Delivery Miles - Loaded | 0 | - |

ACRONYMS:

O&M = Operation and Maintenance

**DYNEGY MIDWEST GENERATION, LLC. - BALDWIN POWER PLANT
CORRECTIVE ACTION ALTERNATIVES ANALYSIS SUPPORTING INFORMATION REPORT (CAAA-SIR)
ALTERNATIVE 3 - SOURCE CONTROL WITH GROUNDWATER MANAGEMENT SYSTEM (GMS)¹**

| ITEM NO. | ENGINEERING, PRE-CONSTRUCTION, AND CONSTRUCTION SUPPORT TASKS | Units | Quantity | Crew | Daily Output | Labor Hours | Equipment Hours | Notes |
|---|---|-------------|----------|--------|--------------|--------------|-----------------|---|
| 1 | Pre-Design Investigation, Final Groundwater Extraction Trench Design, and Bid Support | LS | 1 | - | - | 0 | 0 | Assumed based on Ramboll previous project experience. |
| 2 | Engineering Support and CQA During Construction | LS | 1 | Eng | - | 1,810 | 724 | Assumed based on Ramboll previous project experience. |
| ENGINEERING, PRE-CONSTRUCTION, AND CONSTRUCTION SUPPORT ESTIMATED SUBTOTAL | | | | | | 1,810 | 720 | |
| ITEM NO. | SITE PREPARATION | Units | Quantity | Crew | Daily Output | Labor Hours | Equipment Hours | Notes |
| 3 | Mobilization and De-Mobilization | LS | - | - | - | - | - | Assumed based on Ramboll previous project experience. |
| | General Construction Mobilization and De-Mobilization | LS | 1 | - | - | - | - | Assumed based on Ramboll previous project experience. |
| | Trenching Equipment Mobilization, Assembly, and De-Mobilization | LS | 1 | - | - | - | - | One-pass technology specific equipment mobilization derived from ROM cost provided by specialty contractor. |
| 4 | Staging Area and Settling Pond Area Preparation | - | - | - | - | 1,362 | 257 | Assumes construction of a 3-acre staging area and 4-acre settling pond. Once prepared, surface grading and stabilization will be completed in this 7-acre area. |
| | Staging Area and Pond Base Grading | EA | 15 | B11L | 1.8 | 136 | 68 | 312213200200: Rough grade open sites 10,000-20,000 S.F., grader. Assumes grading will be needed for the 4-acre settling pond, and 3-acre staging/laydown area. |
| | Subsurface Stabilization Nonwoven Geotextile - Staging Area | SY | 14,520 | 2 Clab | 2500 | 93 | 0.0 | 313219161550: Geosynthetic soil stabilization, geotextile fabric, non-woven, 120 lb tensile strength includes scarifying and compaction. Assumes 3 acre staging area will need geosynthetic. |
| | Install Crushed Gravel Road (18" Thick) - Staging Area | SY | 14,520 | B14 | 615 | 1,133 | 189 | 015523500100: Temporary, roads, gravel fill, 18" gravel depth (scaled), excluding surfacing. Assumes 3 acre staging area will include a gravel base. |
| 5 | Access Road and Work Pad Preparation | - | - | - | - | 4,275 | 725 | Assumes construction of a 8,200-ft long and 50-ft wide work pad along the groundwater management system trench alignment and a 500-ft long and 50-ft wide access road leading to the fly ash pond. Once prepared, surface grading and stabilization will be completed in this 3-acre area. |
| | Access Roads and Work Pad Grading | EA | 22 | B11L | 1.8 | 193 | 97 | 312213200200: Rough grade open sites 10,000-20,000 S.F., grader., work pad area, access road. Assumes grading of 50-ft wide work pad along the (8,200 ft) alignment and (500 ft) access road. |
| | Subsurface Stabilization Nonwoven Geotextile | SY | 48,333 | 2 Clab | 2500 | 309 | - | 313219161550: Geosynthetic soil stabilization, geotextile fabric, non-woven, 120 lb tensile strength includes scarifying and compaction; grading along the (8,200 ft) alignment and (500 ft) access road. |
| | Install Crushed Gravel Trench Work Pad (18" Thick) | SY | 48,333 | B14 | 615 | 3,772 | 629 | 015523500100: Temporary, roads, gravel fill, 18" gravel depth (scaled), excluding surfacing. Assumes grading along the (8,200 ft) alignment and (500 ft) access road. |
| 6 | Construction Soil Erosion & Sediment Controls | - | - | - | - | 1,541 | 514 | Assumes construction of a 50-ft wide work pad/access road for the full length of the groundwater management system collection trench and other earthwork areas. Once prepared, surface grading and stabilization will be completed along the trench work pad/access road. |
| | Silt Fence | LF | 41,200 | B62 | 650 | 1,521 | 507 | 312514161000: Synthetic erosion control, silt fence, install and remove, 3' high. Assumes silt fence is installed on both sides of the filtrate collection trench alignments (8,200 ft), on both sides of the access road (500 ft). around the perimeter of the 3 - acre staging area [1,500 ft], and around the perimeter of the 4-acre settling pond [1,700 ft]. Assumes the silt fence will get replaced once during construction. |
| | Sediment Log, Filter Sock | LF | 824 | A2 | 1000 | 20 | 6.6 | 312514160705: Sediment Log, Filter Sock, 9". Assume sediment log is needed along both sides of alignment of extraction trench (8,200 LF long), staging area, and settling pond perimeter (1,670 LF). Assume one filter sock is needed for every 50 ft of silt fence. Assumes the sediment log, filter sock will get replaced once during construction. |
| 7 | Construction Facilities | - | - | - | - | - | - | Includes monthly rentals associated with one (1) office trailer, two (2) storage trailers, and four (4) portable toilets for one year of construction activities. |
| | Office Trailer | MO - in use | 24 | - | - | - | - | 015213200350: Office trailer, furnished, no hookups, 32' x 8', rent per month. Assume quantity of one (1). |
| | Storage Trailers | MO - in use | 48 | - | - | - | - | 015213201350: Storage boxes, 40' x 8', rent per month. Unit rate doubled to assume quantity of two (2) boxes onsite. |
| | Portable Toilet | MO - in use | 96 | - | - | - | - | 015433406410: Rent toilet, portable chemical. Unit rate multiplied by 4 to assume quantity of four (4) units onsite. |
| SITE PREPARATION ESTIMATED SUBTOTAL | | | | | | 7,178 | 1,496 | |

| ITEM NO. | Groundwater Management System Construction | Units | Quantity | Crew | Daily Output | Labor Hours | Equipment Hours | Notes |
|---|--|-------------------|----------|--------|--------------|-------------|-----------------|---|
| 8 | Installation of Groundwater Management System Trench (one pass) | LF | 8,200 | B12H | 80 | 1,640 | 1,640 | Installation of groundwater management system trench using one-pass technology performed by a specialty contractor. Information provided by specialty contractor. Assumes one trench totaling 8,200 ft in length with an approximate depth of 50 ft (depth varies). Crew code selected to mimic the proposed crew provided by specialty contractor. |
| 9 | Trench Spoils Excavation and Disposal | CY - in place | 45,556 | - | - | 4,147 | 3,770 | Hauling and management of trench excavation spoils to the AP for placement beneath the final cover system. |
| | Excavation and Loading of Material | CY - as excavated | 50,111 | B14B | 5000 | 120 | 80 | 312316435320: Excavating, large volume projects; excavation with truck loading; excavator, 6 C.Y. bucket, 100% fill factor (assume 10% fluff factor from ground to excavated). |
| | Pushing Materials to Excavator | CY - as excavated | 50,111 | B10B | 1000 | 601 | 401 | 312323170020: Spread dumped material, no compaction, by dozer. Dozer support for excavation. Daily output edited to match excavation based on experience. |
| | Hauling and Dumping Onsite of Material for Moisture Conditioning | CY - as excavated | 50,111 | B34G | 850 | 472 | 472 | 312323206170: Hauling; no loading equipment, including hauling, waiting, loading/dumping; 34 C.Y. off-road, 15 min wait/ld/uld., 15 MPH, cycle 2 mile. |
| | Spreading/Drying Moisture Conditioning | CY - as excavated | 25,056 | B10B | 1000 | 301 | 200 | 312323170020: Spread dumped material, no compaction, by dozer. Daily output edited to match excavation based on experience. |
| | Dust Control Moisture Conditioning Prior to Loading | CY - as excavated | 13,667 | B45 | 1888 | 116 | 116 | 312323239000: Water, 3000 gal. truck, 3 mile haul. Assume 30% of volume will need to be wetted. |
| | Loading of Material | CY - as excavated | 50,111 | B14B | 5605 | 107 | 72 | 312316434420: Excavating, large volume projects; restricted loading trucks; loader, 6 C.Y. bucket, 95% fill factor (assume 10% fluff factor from ground to excavated). |
| | Hauling Material Offsite | CY - as excavated | 50,111 | B34C | 165 | 2,430 | 2,430 | 312323203080: Hauling; no loading equipment, including hauling, waiting, loading/dumping; 16.5 C.Y. truck off-road, 15 min wait/ld/uld., 40 MPH, cycle 20 miles. |
| | Landfill Tipping | CY - as excavated | 50,111 | - | - | - | - | Assumed landfill tipping. |
| 10 | Groundwater Management System Mechanical Installation | - | - | - | - | 1,160 | 195 | Installation of a system to pump and convey extracted groundwater from the trenches to the new settling pond and associated discharge. |
| | Install Sump Pumps | EA | 18 | Q1 | 1.8 | 162 | 0.0 | 221429132010: Wet-pit-mounted, vertical sump pump, single stage, 25 GPM, 1 HP, 1-1/2" discharge. Assumes one pump per 450 ft of groundwater management system trench. |
| | Install Equalization Tank | EA | 8 | B6 | 1.0 | 192 | 64 | Lump sum for installation of equalization tank at each trench and associated site preparation and instrumentation. Assumes 2 days for installation. |
| | Install Transfer Pumps and Controllers | EA | 8 | R30 | 1.0 | 208 | 0.0 | Lump sum for installation of transfer pump and pump controller at each extraction trench to convey water from settling pond to discharge outfall based on Ramboll project experience. Assumes inclusion of housing structure and 2 days for installation. |
| | Excavate Utility Trench for Lines for Component Electric Hookup | LF | 7,200 | B54 | 860 | 67 | 67 | 312316142750: Utility trench excavating, chain trencher, 40 HP operator riding, 12" wide trench and backfill, 18" deep. Trench installed from power drop/compressor shed to groundwater management trench to supply compressed air and power to sump pits. |
| | Install Mechanical Elements and Piping | EA | 8 | R30 | - | 390 | 0.0 | Assumes lump sum for furnishing all mechanical elements (air compressors, sump pumps, transfer pumps) and associated HDPE housing piping for distribution of power and housing of mechanical elements throughout the groundwater management system trench system. Assumes approximately 15 days of work. |
| | Excavate Utility Trench for Conveyance to Settling Pond | LF | 1,000 | B54 | 860 | 9.3 | 9.3 | 312316142750: Utility trench excavating, chain trencher, 40 HP operator riding, 12" wide trench and backfill, 18" deep. Utility trench installed from groundwater extraction trench to convey extracted water to the settling pond. |
| | Install 8" HDPE Conveyance Pipe to Settling Pond | LF | 1,000 | B22A | 320 | 125 | 50 | 331413350300: Water supply distribution piping, piping HDPE, butt fusion joints, 40' lengths, 8" diameter, SDR 21. Includes labor, materials, and machine for installation and welding of HDPE pipe for conveying extracted water from trenches to settling pond. |
| | Backfill Utility Trench with Granular Trench Backfill | CY - as excavated | 56 | B10R | 100 | 6.7 | 4.4 | 312316133060: Backfill trench, F.E. loader, wheel mtd., 1 C.Y. bucket, 200' haul. Backfill with granular trench backfill. Quantity based on trench dimensions 12" wide, 18" deep, 1,000 ft long. |
| 11 | Electrical Installation | - | - | - | - | 1,073 | 432 | Electrical Installation activities include 15 kV distribution, local transformers at each compressor shed supplying 480/277VAC power on the secondary side of the transformer. |
| | Installing Medium Voltage along Trench Alignment | LF | 7,200 | R15 | 1,850 | 187 | 62 | 2650513166450: Medium-cable single cable, copper XLP shielding, 15 kV, 250 kcmil, direct curial, excludes splicing & terminations. Labor and equipment hours were estimated assuming that four (4) 250 kcmil cables will be needed to supply three phase power to the compressor sheds. |
| | Pad Mounted Transformer Installation | EA | 8 | R3 | 0.65 | 246 | 49 | 261219100100: Transformer, oil filled, 5 kV or 15 kV, with taps, 277/480VAC secondary, 3 phase, 150 kVA pad mounted. Assumes a 15 kV pad mounted transformer will be placed at each compressor shed to supply power to shed components. |
| | Compressor Shed Electrical and Controls | EA | 8 | 2 Elec | 0.2 | 640 | 320 | Assumes 2 electricians will install all electrical distribution equipment to compressor shed components and each shed will take 1-week of labor to complete. |
| 12 | Construction of Compressor & Mechanical Sheds | - | - | - | - | 540 | 180 | Lump sum based on Ramboll experience for construction of housing unit for air compressor sheds. |
| | Construct Compressor Shed | EA | 8 | B6 | - | 540 | 180 | Assumes pre-fabricated mechanical instrumentation shelter, installed primarily by hand with light equipment assistance. Hours are based on Ramboll experience. Sheds will be fitted with hydraulic transfer equipment (air compressor and transfer pump) and will be located along the trench alignment. |
| 13 | Installation of Settling Pond | - | - | - | - | 5,326 | 2,721 | Quantity based on 4-acre pond, 5 feet deep. Assume all excavated material is reused for berm construction. |
| | Excavation of Settling Pond | BCY | 32,267 | B12C | 1320 | 391 | 196 | 312316420260: Excavating, bulk bank measure, hydraulic, crawler mtd., 2 C.Y. cap (165 CY/hr). 15% addition included for loading of material onto trucks. Assumes size of settling pond to be 4 acres and 5 feet deep. |
| | Loading of Material | CY - as excavated | 35,493 | B14B | 5605 | 76 | 51 | 312316434420: Excavating, large volume projects; restricted loading trucks; loader, 6 C.Y. bucket, 95% fill factor (assume 10% fluff factor from ground to excavated). |
| | Hauling Material Offsite | CY - as excavated | 35,493 | B34C | 165 | 1,721 | 1,721 | 312323203080: Hauling; no loading equipment, including hauling, waiting, loading/dumping; 16.5 C.Y. truck off-road, 15 min wait/ld/uld., 40 MPH, cycle 20 miles. |
| | Landfill Tipping | CY - as excavated | 35,493 | - | - | - | - | Assumed landfill tipping generated used IEPA landfill tipping table. Assumes material is classified as non-hazardous waste. |
| | Subsurface Stabilization Nonwoven Geotextile | SY | 19,360 | 2 Clab | 2500 | 124 | 0.0 | 313219161550: Geosynthetic soil stabilization, geotextile fabric, non-woven, 120 lb tensile strength includes scarifying and compaction. Assumes 4 acre settling pond. |
| | Settling Pond Liner | SF | 174,240 | B63B | 1850 | 3,014 | 753 | 310519531100: Reservoir liners, membrane lining, 40 mil, LLDPE. Assumes 4 acre ft print. |
| GROUNDWATER MANAGEMENT SYSTEM TRENCH CONSTRUCTION | | | | | - | 13,885 | 8,937 | |

| ITEM NO. | SITE RESTORATION | Units | Quantity | Crew | Daily Output | Labor Hours | Equipment Hours | Notes |
|--|---|-------------------|----------|------|--------------|-------------------|-----------------------|--|
| 14 | Site Restoration | - | - | - | - | 136 | 135 | Assumes restoration of grade surface following groundwater management system trench installation activities. |
| | Lime | MSF | 650 | B66 | 700 | 8.0 | 7.4 | 329113234250: Soil preparation, structural soil mixing, spread soil conditioners, ground limestone, 1#/S.Y., tractor spreader. Unit multiplied by 1.1 to account for soils possibly being void of nutrients. Quantity assumes areas include staging area, temporary roads, as well as areas adjacent to sediment pond. |
| | Fertilizer | MSF | 650 | B66 | 700 | 8.0 | 7.4 | 329113234150: Soil preparation, structural soil, mixing, spread soil conditioners, fertilizer, 0.2#/S.Y., tractor spreader. Unit multiplied by 1.1 to account for soils possibly being void of nutrients. Quantity assumes areas include staging area, temporary roads, as well as areas adjacent to sediment pond. |
| | Grassland Mix | MSF | 650 | B66 | 52 | 100 | 100 | 329219142300: Seeding athletic fields, seeding fescue, tall, 5.5 lb. per M.S.F., tractor spreader. Quantity assumes areas include staging area, temporary roads, as well as areas adjacent to sediment pond. |
| | Mulch | MSF | 650 | B65 | 530 | 20 | 20 | 329113160350: Mulching, Hay, 1" deep, power mulcher, large. Quantity assumes areas include staging area, temporary roads, as well as areas adjacent to sediment pond. |
| 15 | Final Cover Restoration | - | - | - | - | 3,350 | 3,242 | Assumes restoration of 18" thick X 50' wide clay cap footprint following groundwater management system trench installation activities. |
| | Clay | CY | 22,778 | B13D | 376 | 969 | 969 | Imported clay for south area ramp. Assumes 8000 CY. Based on Ramboll experience. Assumes 18" cap and 50' wide restoration. |
| | Haul Material to Site | CY - as excavated | 22,778 | B34C | 99 | 1,841 | 1,841 | 312323203104: Cycle hauling(wait, load, travel, unload or dump & return) time per cycle, excavated or borrow, loose cubic yards, 15 min load/wait/unload, 16.5 C.Y. truck, cycle 50 miles, 45 mph, excludes loading equipment. |
| | Hauling Stockpiled Clay | CY - as excavated | 22,778 | B34G | 850 | 214.4 | 214.4 | 312323206170: Hauling; no loading equipment, including hauling, waiting, loading/dumping; 34 C.Y. off-road, 15 min wait/ld./uld., 15 MPH, cycle 2 mile. |
| | Spread Lifts for Clay | CY - as excavated | 22,778 | B10B | 1000 | 273 | 182.2 | 312323170020: Spread dumped material, no compaction, by dozer. Daily output edited to match excavation based on experience. |
| | Compaction of Clay | CY - in place | 22,778 | B10Y | 5200 | 52.6 | 35.0 | 312323235060: Compaction; Riding, vibrating roller, 12" lifts, 2 passes. RS Means Crew is B10Y. RS Means unit rate halved for 24" lifts. |
| SITE RESTORATION ESTIMATED SUBTOTAL | | | | | - | 3,486 | 3,376 | |
| TOTAL CONSTRUCTION ESTIMATED SUBTOTAL | | | | | - | 26,400 | 14,500 | |
| ITEM NO. | CORRECTIVE ACTION OPERATION AND MAINTENANCE | Units | Quantity | Crew | Daily Output | Labor Hours | Equipment Hours | Notes |
| 16 | Groundwater Extraction Trench Operation & Maintenance | - | - | - | - | 9,600 | 0.0 | Assumes routine monitoring, maintenance, and electrical service charges for the duration of system operation. |
| | Field Maintenance | Days | 480 | TM | - | 9,600 | 0.0 | Assumes quarterly maintenance on pneumatic pumps and air compressors over 30 years of operation. Each quarterly maintenance event assumes 2 staff for 4 days to check, clean, and service all mechanical parts. |
| | Electrical Distribution and Service Charges | MO | 360 | - | - | - | - | Monthly electrical distribution and usage for operating the extraction and transfer pumps. |
| 17 | Non-routine System O&M | - | - | - | - | 9,600 | 3,000 | Assumes non-routine tasks including flushing of groundwater conveyance lines and periodic site visits (e.g., alarm responses or equipment troubleshooting). |
| | Groundwater Conveyance Line Flushing - Vacuum Truck | LF | 492,000 | VT | - | 6,000 | 3,000 | 330130116140: Pipe, internal cleaning and inspection, cleaning, power rodder with header & cutts, 4"-12" diameter. Assumes one 5-day cleaning event of 8,200 LF of 8" HDPE pipe twice per year for a total of 30 years. |
| | Non-Routine Site Visits/Alarm Responses | LS | 360 | OM | - | 3,600 | 0.0 | Assumes 12 non-routine site visits per year over 30 years of operation. Each non-routine event assumes 2 staff for 1 day. |
| 18 | Engineering Oversight/Support | LS | 30 | - | - | - | - | Assumes office-based engineering support over 30 years of operation. |
| CORRECTIVE ACTION OPERATION AND MAINTENANCE SUBTOTAL | | | | - | - | 19,200 | 3,000 | |
| | | | | | | Total Labor Hours | Total Equipment Hours | |
| ENGINEERING AND CONSTRUCTION SUBTOTAL | | | | | - | - | 26,400 | 14,500 |
| CORRECTIVE ACTION OPERATION AND MAINTENANCE SUBTOTAL | | | | | - | - | 19,200 | 3,000 |
| SUBTOTAL | | | | | | | 45,600 | 17,500 |

NOTES:

- Alternative 3: Groundwater Management System is estimated to take approximately 1,000+ years to achieve groundwater protection standards (GWPS-35 I.A.C Section 845.600) at all perimeter wells associated with the Fly Ash Pond System (FAPS). For the purpose of this assessment, a total duration of 30 years is used.
- RS Means refers to the 2024 Quarter 4 online edition of RS Means Commercial New Construction.
- See crew tab (Alt 3 - Crews) for assumptions regarding crew size, total labor hours and required construction equipment, as needed, for each task.
- See mileage tab (Alt 3 - Mileage and Labor) for assumptions regarding total mileage for tasks outlined in this alternative.

ACRONYMS:

CY = Cubic Yard
Bank: Material in natural compacted state
EA = Each
FAPS = Fly Ash Pond System
GMS = Groundwater Management System
GWPS = Groundwater Protection Standards
LB = Pound
LF = Linear Foot
LS = Lump Sum
MO = Month
MSF = square feet divided by 1000
O&M = Operation and Maintenance
SF = Square Feet
SY = Square Yard

CREW CODES
DYNEGY MIDWEST GENERATION, LLC. - BALDWIN POWER PLANT
CORRECTIVE ACTION ALTERNATIVES ANALYSIS SUPPORTING INFORMATION REPORT (CAAA-SIR)
ALTERNATIVE 3 - SOURCE CONTROL WITH GROUNDWATER MANAGEMENT SYSTEM

| Item No. | Crew Code | Labor | Daily Labor Hours | Equipment | Daily Equipment Hours | Onsite Labor Hours | Onsite Heavy Equipment Hours |
|---|-----------|--|-------------------|--|-----------------------|--------------------|------------------------------|
| Construction | | | | | | | |
| 4,5,13 | 2 Clab | Laborer x 2 | 16 | None | 0 | 526 | 0 |
| 11 | 2 Elec | Electrician x 2 | 16 | Crew Truck x 1 | 8 | 640 | 320 |
| 6 | A2 | Laborer x 2 Truck Driver (light) x 1 | 24 | Flatbed Truck, Gas, 1.5 ton | 8 | 20 | 7 |
| 10,12 | B6 | Laborer x 2 Operator (light) x 1 | 24 | Backhoe Loader, 48 H.P. | 8 | 732 | 244 |
| 9,15 | B10B | Operator (med) x1 Laborer x0.5 | 12 | Dozer, 200 H.P. | 8 | 1,175 | 784 |
| 10 | B10R | Operator (med) x 1 Laborer x 0.5 | 12 | Frontend loader, W.M., 1 C.Y. | 8 | 7 | 4 |
| 15 | B10Y | Operator (med) x1 Laborer x0.5 | 12 | 1 Vibr. Roller, Towed, 12 ton | 8 | 53 | 35 |
| 4,5 | B11L | Operator (med) x 1 Laborer x 1 | 16 | Grader, 30,000lb | 8 | 329 | 164 |
| 13 | B12C | Operator (med) x 1 Laborer x 1 | 16 | Hydraulic excavator, 2 C.Y. | 8 | 391 | 196 |
| 8 | B12H | Operator (crane) x 1 Laborer x 1 | 16 | Crawler Crane, 25-ton, x 1 Clamshell Bucket, 1 C.Y. x 1 | 16 | 1,640 | 1,640 |
| 15 | B13D | Operator (crane) x 1 Laborer x 1 | 16 | Hydraulic excavator, 1 C.Y. Trench Box | 16 | 969 | 969 |
| 4,5 | B14 | Labor Foreman x 1 Operator (light) x1 Laborer x 4 | 48 | Backhoe Loader, 48 H.P. | 8 | 4,906 | 818 |
| 9,13 | B14B | Operator (crane) x 1 Laborer x 0.5 | 12 | Hydraulic excavator, 6. C.Y. | 8 | 304 | 202 |
| 10 | B22A | Labor Foreman x 1 Skilled Worker x 1 Laborer x 2 Operator (crane) x 1 | 40 | S.P. Crane, 4x4, 5 ton Butt Fusion Machine, 4-12" diam. | 16 | 125 | 50 |
| 9,13,15 | B34C | Truck Driver x 1 | 8 | Truck Tractor, 6x4, 380 H.P. Dump Trailer, 16.5 C.Y. | 8 | 5,991 | 5,991 |
| 9,15 | B34G | Truck Driver x 1 | 8 | Dump Truck, Off Hwy., 50 ton | 8 | 686 | 686 |
| 9 | B45 | Operator (medium) x 1 Truck Driver (heavy) x 1 | 16 | 3000 Gallon Tanker x 1 Truck Tractor, 380 H.P. x 1 | 16 | 116 | 116 |
| 10 | B54 | Operator (light) x 1 | 8 | Trencher, Chain, 40 H.P. | 8 | 76 | 76 |
| 6 | B62 | Laborer x 2 Operator (light) x 1 | 24 | Loader, Skid Steer, 30 H.P. | 8 | 1,521 | 507 |
| 13 | B63B | Labor Foreman x 1 Laborer x 2 Operator (light) x 1 | 32 | Loader, Skid Steer, 78 H.P. | 8 | 3,014 | 753 |
| 14 | B65 | Laborer x1 Truck Driver (light) x 1 | 16 | Power Mulcher (large) Flatbed Truck, Gas, 1.5 ton | 16 | 20 | 20 |
| 14 | B66 | Operator (light) x 1 | 8 | Loader-Backhoe, 40 H.P. | 8 | 116 | 115 |
| 10 | Q1 | Plumber x1 Plumber Apprentice x1 | 16 | None | 0 | 162 | 0 |
| 11 | R3 | Electrician Foreman x1 Electrician x1 Electrician Operators x0.5 | 20 | S.P. Crane 4x4 | 4 | 246 | 49 |
| 11 | R15 | Electrician Foreman x1 Electrician x4 Electrician Operators x1 | 48 | Crew Truck x2 | 16 | 187 | 62 |
| 10 | R30 | Electrician Foreman x 0.25 Electrician x 1 Laborer (Semi-Skilled) x 2 | 26 | None | 0 | 598 | 0 |
| 2 | Eng | Engineering Staff x 1.2 | 10 | Side by Side x1 | 4 | 1,810 | 724 |
| Construction Subtotals | | | | | | 26,400 | 14,500 |
| Corrective Action Operation & Maintenance | | | | | | | |
| 17 | OM | Laborer x 1 | 10 | Service Truck x1 | 0 | 3,600 | 0 |
| 16 | TM | Maintenance Crew x 2 | 20 | Service Truck x2 Hand Tools | 0 | 9,600 | 0 |
| 17 | VT | Laborer x 1 Operator x 1 | 20 | Vacuum Truck with Flushing Capabilities | 10 | 6,000 | 3,000 |
| O&M Subtotals | | | | | | 19,200 | 3,000 |
| Totals | | | | | | 45,600 | 17,500 |

Note: Blue shaded crew codes were created by Ramboll based on experience (not pulled from RS Means).

ACRONYMS:

O&M = Operation and Maintenance

CONSTRUCTION MILEAGE AND LABOR ESTIMATES
DYNEGY MIDWEST GENERATION, LLC. - BALDWIN POWER PLANT
CORRECTIVE ACTION ALTERNATIVES ANALYSIS SUPPORTING INFORMATION REPORT (CAAA-SIR)
ALTERNATIVE 3 - SOURCE CONTROL WITH GROUNDWATER MANAGEMENT SYSTEM

| Item | Quantity | Assumptions |
|---|----------|--|
| Labor Total Hours | 26,400 | Per projected construction total (does not include contingency or O&M labor hours) |
| Duration of Onsite Construction Days | 181 | Total calendar days |
| Average Daily Crew Size | 13 | Assumes multiple crew sizes and a 10 hour work day Assumes 1 Ramboll personnel daily for construction oversight |
| Daily Labor Mobilization Miles | 10,132 | Includes mob/demob from STL (82 miles round trip) and local daily commute mileage (40 miles per day) |
| Vehicles Miles Onsite | 35,296 | 1 mile per day round trip from gate to parking 5 miles per day for onsite miles 9 miles per day local trips (Vil. of Baldwin) No contingency included |
| Equipment Mobilization Miles - Unloaded | 18,100 | Average of 500 miles one-way trip for equipment hauling Average 1 load of equipment per working week for a 5 day work week. |
| Equipment Mobilization Miles - Loaded | 18,100 | Average of 500 miles one-way trip for equipment hauling Average 1 load of equipment per working week for a 5 day work week. |
| Onsite Haul Truck Miles - Unloaded | 4,288 | 34 CY Off Road Dump Truck 2 miles per trip per load |
| Onsite Haul Truck Miles - Loaded | 4,288 | 34 CY Off Road Dump Truck 2 miles per trip per load |
| Offsite Haul Truck Miles - Unloaded | 436,903 | 16 CY loads of material are delivered to the site from a regional supplier located within 50 miles of the site. Assumes truck is returning to the origin location. |
| Offsite Haul Truck Miles - Loaded | 436,903 | 16 CY loads of material are delivered to the site from a regional supplier located within 50 miles of the site. Assumes truck is returning to the origin location. |
| Material Delivery Miles - Unloaded | 36,201 | Misc. construction materials (erosion controls, piping, geotextile) Assumes 200 mile round trip on a daily basis |
| Material Delivery Miles - Loaded | 36,201 | Misc. construction materials (erosion controls, piping, geotextile) Assumes 200 mile round trip on a daily basis |

O&M Mileage and Labor Estimates

| Item | Quantity | Assumptions |
|---|----------|--|
| Labor Total Hours | 19,200 | Per projected O&M total in cost estimate (does not include contingency) |
| Duration of Onsite O&M Days | 960 | Total days |
| Average Daily Crew Size | 2 | Assumes multiple crew sizes and a 10 hour work day |
| Daily Labor Mobilization Miles | 40,649 | Includes mob/demob from STL (82 miles round trip) and local daily commute mileage (40 miles per day) |
| Vehicles Miles Onsite | 28,800 | 1 mile per day round trip from gate to parking 5 miles per day for onsite miles 9 miles per day local trips (Vil. of Baldwin) No contingency included |
| Equipment Mobilization Miles - Unloaded | 15,000 | Average of 500 miles one-way trip for equipment hauling Average 1 load of equipment per year |
| Equipment Mobilization Miles - Loaded | 15,000 | Average of 170 miles one-way trip for equipment hauling Average 1 load of equipment per year |
| Onsite Haul Truck Miles - Unloaded | 0 | No material hauling onsite will occur under this alternative |
| Onsite Haul Truck Miles - Loaded | 0 | No material hauling onsite will occur under this alternative |
| Offsite Haul Truck Miles - Unloaded | 0 | No material hauling offsite will occur under this alternative |
| Offsite Haul Truck Miles - Loaded | 0 | No material hauling offsite will occur under this alternative |
| Material Delivery Miles - Unloaded | 0 | No materials will be delivered during O&M |
| Material Delivery Miles - Loaded | 0 | No materials will be delivered during O&M |

ACRONYMS:

O&M = Operation and Maintenance

Appendix C

Corrective Measures Assessment

Intended for
Dynegy Midwest Generation, LLC

Date
April 24, 2024

Project No.
1940103584-001

35 I.A.C. § 845 CORRECTIVE MEASURES ASSESSMENT

FLY ASH POND SYSTEM

BALDWIN POWER PLANT

BALDWIN, ILLINOIS

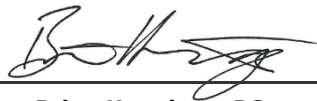
IEPA ID: W1578510001-01/02/03

35 I.A.C. § 845 CORRECTIVE MEASURES ASSESSMENT BALDWIN POWER PLANT FLY ASH POND SYSTEM

Project name **Baldwin Power Plant Fly Ash Pond System**
Project no. **1940103584-001**
Recipient **Dynegy Midwest Generation, LLC**
Document type **35 I.A.C. § 845 Corrective Measures Assessment**
Revision **FINAL**
Date **April 24, 2024**
Prepared by **Frances Ackerman, RG, PE**
Checked by **Lucas P. Carr, PE**
Approved by **Brian G. Hennings, PG**



Frances Ackerman, RG, PE
Senior Managing Engineer



Brian Hennings, PG
Project Officer, Hydrogeology

CONTENTS

| | | |
|-----------|---|-----------|
| 1. | Introduction | 1 |
| 1.1 | Source Control and Residual Plume Management | 1 |
| 1.2 | Adaptive Site Management | 1 |
| 2. | Site Information | 3 |
| 2.1 | Conceptual Site Model | 3 |
| 2.2 | Groundwater Quality | 4 |
| 3. | Corrective Measures Assessment Methodology | 5 |
| 4. | Description of Potential Corrective Measure Technologies | 6 |
| 4.1 | Source Control with Groundwater Polishing | 6 |
| 4.2 | Source Control with Groundwater Extraction | 7 |
| 4.3 | Source Control with a Cutoff Wall | 8 |
| 4.4 | Source Control with In-Situ Chemical Treatment | 8 |
| 5. | Assessment of Corrective Measure Technologies | 10 |
| 5.1 | Requirements | 10 |
| 5.2 | Groundwater Corrective Technology Assessment | 10 |
| 5.2.1 | Source Control with Groundwater Polishing | 10 |
| 5.2.2 | Source Control with Groundwater Extraction | 11 |
| 5.2.3 | Source Control with Groundwater Cutoff Wall | 12 |
| 5.2.4 | Source Control with In-Situ Chemical Treatment | 13 |
| 5.3 | Technologies Advanced to CAAA | 14 |
| 6. | References | 15 |

TABLES

| | |
|-----------|---|
| Table 5-1 | 35 I.A.C. § 845 Corrective Measures Assessment Matrix |
|-----------|---|

FIGURES

| | |
|------------|--|
| Figure 2-1 | Site Location Map |
| Figure 2-2 | Site Map |
| Figure 2-3 | Uppermost Aquifer Potentiometric Surface Map - May 15-17, 2023 |
| Figure 2-4 | Monitoring Well Location Map |

ACRONYMS AND ABBREVIATIONS

| | |
|-----------|---|
| 35 I.A.C. | Title 35 of the Illinois Administrative Code |
| 40 C.F.R. | Title 40 of the Code of Federal Regulations |
| ASD | Alternative Source Demonstration |
| BPP | Baldwin Power Plant |
| BAP | Bottom Ash Pond |
| CAAA | Corrective Action Alternatives Analysis |
| CAP | Corrective Action Plan |
| CCR | coal combustion residuals |
| CIP | closure-in-place |
| CMA | assessment of groundwater corrective measures |
| cm/s | centimeters per second |
| CSM | conceptual site model |
| DMG | Dynegy Midwest Generation, LLC |
| E001 | Event 1; quarter 2, 2023 |
| E002 | Event 2; quarter 3, 2023 |
| E003 | Event 3; quarter 4, 2023 |
| EPRI | Electric Power Research Institute |
| FAPS | Fly Ash Pond System |
| GMP | groundwater monitoring plan |
| GWPS | groundwater protection standard(s) |
| HCR | Hydrogeologic Site Characterization Report |
| ID | identification |
| IDNR | Illinois Department of Natural Resources |
| IEPA | Illinois Environmental Protection Agency |
| ITRC | National Research Council, Interstate Technology & Regulatory Council |
| IX | Ion Exchange |
| NID | National Inventory of Dams |
| No. | number |
| NPDES | National Pollutant Discharge Elimination System |
| NRT | Natural Resource Technology |
| NRT/OBG | Natural Resource Technology, an OBG Company |
| PMP | Potential Migration Pathway |
| PRB | permeable reactive barrier |
| Ramboll | Ramboll Americas Engineering Solutions, Inc. |
| SI | surface impoundment |
| UA | uppermost aquifer |
| UU | Upper Unit |
| USEPA | United States Environmental Protection Agency |
| ZVI | zero-valent iron |

1. INTRODUCTION

Ramboll Americas Engineering Solutions, Inc. (Ramboll) has developed this assessment of groundwater corrective measures (CMA) on behalf of the Baldwin Power Plant (BPP), owned by Dynegy Midwest Generation, LLC (DMG), to assist in the compliance with the requirements of Title 35 of the Illinois Administrative Code (35 I.A.C.) § 845. This assessment applies specifically to the coal combustion residuals (CCR) surface impoundment (SI) referred to as the Fly Ash Pond System (FAPS), also referred to as Vistra Identification (ID) Number (No.) 605, Illinois Environmental Protection Agency (IEPA) ID Nos. W1578510001-01, W1578510001-02, and W1578510001-03, and National Inventory of Dams (NID) No. IL50721. This report addresses content requirements specific to 35 I.A.C. § 845.660 (Assessment of Corrective Measures) for exceedances of boron and sulfate at the FAPS.

1.1 Source Control and Residual Plume Management

DMG completed significant source control and residual plume management efforts in 2020 as part of final closure of the FAPS (DMG, 2020). The final closure was performed in accordance with the Closure and Post-Closure Care Plan (AECOM, 2016) that was developed in accordance with Title 40 of the Code of Federal Regulations (40 C.F.R.) § 257 and submitted to IEPA for review. IEPA found *"...that the plan...represent an appropriate means by which to close the Baldwin Fly Ash Pond System which is comprised of the East Fly Ash Pond, the Old East Fly Ash Pond and the West Fly Ash Pond"* (IEPA, 2016). The final closure was addressed in accordance with the IEPA Water Pollution Control permit 2020-EA-65016.

The FAPS closure construction included closure-in-place (CIP) of the entire FAPS. This was accomplished by removing impounded water and constructing a final cover system in accordance with 40 C.F.R. § 257.102 to minimize water infiltration into the closed FAPS and improve surface water drainage off the cover system, thus reducing generation of potentially impacted water and ultimately reducing the extent of CCR impacts to groundwater. The source control was predicted to lower water levels, decrease the potential transport of CCR constituents off-site and prevent groundwater protection standards (GWPS) from being exceeded in any water supply wells (Natural Resource Technology [NRT], 2014a). These source control activities will serve as the primary groundwater corrective measure at the FAPS. The potentially feasible corrective measures presented herein are intended to be supplementary to the primary source control and are intended to serve as management measures to address any residual plume that may remain after completion of source control.

1.2 Adaptive Site Management

Adaptive site management strategies will be employed as an integral part of ongoing corrective action at the FAPS. The adaptive site management approach will allow timely incorporation of new site information over the closure and post-closure life cycle of the FAPS to ensure the achievement of the GWPS. The adaptive site management approach is proposed to expedite progress toward meeting the GWPS while acknowledging uncertainties, such as the persistence of current groundwater flow directions and flux quantities and potential related changes in geochemical conditions. A structured decision-making process and explicitly planned iterations between the implemented corrective measures and monitoring results will ensure that active remediation is occurring. System performance and the condition of the residual plume will be monitored as the corrective measure(s) selected through the 35 I.A.C. § 845.710 Corrective

Action Plan (CAP) process are implemented to supplement the source control measures described above. If the groundwater concentrations do not decrease consistent with modeling predictions, the adaptive site management approach will facilitate timely modifications or enhancements to the corrective measure(s), as needed, in accordance with 35 I.A.C. § 845.680(b). This approach will be employed to provide continuous improvement to the FAPS groundwater remediation in response to new site information and/or the performance of the selected corrective measure(s).

The planned adaptive site management strategies are generally consistent with National Research Council, Interstate Technology & Regulatory Council (ITRC) and United States Environmental Protection Agency (USEPA) methodologies developed to address sites with long remediation times and high levels of uncertainty regarding the remedial actions necessary to achieve final and protective remediation goals (USEPA, 2022). The elements of the proposed adaptive site management strategy at the FAPS will be responsive to the changing conditions associated with pond closure and performance of the selected corrective measure(s) and will include the following:

1. Implementing the groundwater corrective measure(s) selected as part of the CAP for the current conditions at the FAPS. The selected corrective measures may include a combination of the technologies presented in this CMA.
2. Establishing both the absolute remedial objective and functional (interim) goals to monitor progress toward the remedial objective. Achieving the GWPS for 35 I.A.C. § 845.600 constituents at the downgradient waste boundary is the remedial objective for the FAPS. Specific functional goals will be developed as part of the CAP process. The functional goals will be measurable thresholds for future action and may include short-term or technology-specific objectives and triggers. Functional goals may vary for different locations, CCR constituents or other site-specific considerations (ITRC, 2017) and will serve as benchmarks for comparison to ongoing groundwater monitoring at the FAPS.
3. Ongoing groundwater monitoring at the FAPS will continue throughout the implementation of source control and residual plume management activities. Post-closure monitoring will continue for a period of at least 30 years, in accordance with 35 I.A.C. § 845.780. A comprehensive groundwater monitoring plan (GMP) will be developed as part of the CAP process in accordance with 35 I.A.C. § 845.670 and 35 I.A.C. § 845.220(c)(4). The GMP will include the functional goals and proposed action levels.
4. Groundwater monitoring information will be used to guide decisions regarding whether progress toward the remedial goal is advancing as expected and/or whether additional actions may be needed to achieve the remedial objective, in conjunction with IEPA, as required by 35 I.A.C. § 845.680(b).

2. SITE INFORMATION

The BPP is located in southwest Illinois in Randolph and St. Clair Counties. The FAPS is approximately one-half mile west-northwest of the Village of Baldwin (**Figure 2-1**). The FAPS is a closed CCR SI consisting of three closed, unlined CCR sub-units identified as follows: Old East Fly Ash Pond (IEPA Unit ID W1578510001-01), the East Fly Ash Pond (IEPA Unit ID W1578510001-02), and West Fly Ash Pond (IEPA Unit ID W1578510001-03). The three sub-units comprise the FAPS and are surrounded by a continuous earthen embankment. Prior to closure, the sub-units were divided utilizing internal splitter dikes to support plant operations. The combined surface area of the FAPS is approximately 232 acres (**Figure 2-2**).

A Closure and Post-Closure Care Plan (AECOM, 2016), which included a groundwater monitoring program sufficient for long-term, post-closure monitoring, was developed and approved by IEPA in a letter to DMG dated August 16, 2016 (IEPA, 2016). Closure activities, which included constructing a final cover system to control the potential for water infiltration into the closed CCR unit, were completed by November 17, 2020 (IEPA, 2016).

2.1 Conceptual Site Model

Significant site investigation has been completed at the BPP to characterize the geology, hydrogeology, and groundwater quality. Based on the extensive investigation and monitoring, the FAPS has been well characterized, as detailed in the Hydrogeologic Site Characterization Report (HCR; Ramboll, 2021) and HCR Revision 1 (Ramboll, 2023a), prepared to comply with the requirements specified in 35 I.A.C. § 845.620. The HCR and revised HCR expand upon the Hydrogeologic Monitoring Plan (Natural Resource Technology, an OBG Company [NRT/OBG], 2017). The conceptual site model (CSM) is presented below.

The following two distinct hydrostratigraphic units have been identified beneath the FAPS, based on stratigraphic relationships and common hydrogeologic characteristics:

- **Upper Unit (UU)/Potential Migration Pathway (PMP):** Predominantly clay with some silt and minor sand, silt layers, and occasional sand lenses. This unit is composed of unlithified natural geologic materials and extends from the upper saturated materials to the bedrock. Thin sand seams and the interface (*i.e.*, contact) between the UU and bedrock have been identified as PMPs. No continuous sand seams were observed within or immediately adjacent to the FAPS; however, the sand seams may act as a PMP due to relatively higher hydraulic conductivities.
- **Bedrock Unit:** This unit is considered the uppermost aquifer (UA) and is composed of interbedded shale and limestone bedrock, which underlies and is continuous across the entire Site.

Lateral groundwater flow in the shallow unlithified materials and bedrock is generally to the west and southwest across the Site toward the Kaskaskia River. Groundwater flow in bedrock is toward the northwest in the east and central areas of the FAPS, and southwest to northwest on the east area of the FAPS. Once groundwater reaches the bedrock valley feature underlying the Secondary and Tertiary Ponds (non-CCR units), located west of the Bottom Ash Pond (BAP) and FAPS, the flow direction veers towards this bedrock surface low. Groundwater elevations and contours for the May 15-17, 2023 monitoring event (Event 1 [E001]) are presented in

Figure 2-3.

2.2 Groundwater Quality

Groundwater monitoring in accordance with the proposed GMP and sampling methodologies provided in the operating permit application for the FAPS began in the second quarter of 2023. The 35 I.A.C. § 845 groundwater monitoring system is displayed on **Figure 2-4** and consists of two background monitoring wells screened in the bedrock (*i.e.*, UA), nine compliance wells installed in the bedrock (*i.e.*, UA), and six compliance wells installed within the un lithified UU/PMP. The groundwater samples collected from the 17 wells are used to monitor and evaluate groundwater quality and demonstrate compliance with the groundwater quality standards listed in 35 I.A.C. § 845.600(a). The monitoring wells yield groundwater samples that represent the quality of downgradient groundwater at the CCR boundary (as required in 35 I.A.C. § 845.630(a)(2)).

The E001 sampling event was completed on May 23, 2023. In accordance with 35 I.A.C. § 845.610(b)(3)(C), statistically derived values were compared with the GWPSs summarized in 35 I.A.C. § 845.600 to determine exceedances of the GWPS (Ramboll, 2023b). The statistical determination identified the following GWPS exceedances at compliance groundwater monitoring wells:

- Boron at PMP well MW-150 and UA well MW-391;
- Sulfate at PMP well MW-150;

Subsequent compliance sampling events for Quarter 3 and Quarter 4 2023 (Event 2 [E002] and Event 3 [E003]) were completed in August and November 2023 and groundwater samples were evaluated for exceedances of the GWPS as described in 35 I.A.C. § 845.600 (Ramboll, 2023c; Ramboll, 2024). Additional exceedances were identified during the E002 and E003 monitoring events:

- Boron at PMP well MW-152
- pH at PMP well MW-253

An alternative source determination (ASD), as allowed by 35 I.A.C. § 845.650(e), was completed for the pH exceedance at well MW-253 (Geosyntec Consultants, Inc., 2024) and received concurrence in a letter from the IEPA dated March 7, 2024 (IEPA, 2024). Therefore, this CMA will address identified GWPS exceedances, exclusive of pH exceedance at MW-253, in accordance with 35 I.A.C. § 845.660.

3. CORRECTIVE MEASURES ASSESSMENT METHODOLOGY

This section describes the CMA methodology initiated in response to the identification of exceedances of the GWPSs for 35 I.A.C. § 845.600 constituents at the downgradient waste boundary of the FAPS during the E001 groundwater monitoring event (Ramboll, 2023b). The CMA was initiated on November 26, 2023, within 90 days after the detection of boron and sulfate exceedance(s) of GWPS. Under 35 I.A.C. § 845, owners and operators of existing CCR SIs must initiate the CMA in accordance with 35 I.A.C. § 845.660 if one or more constituents are detected, and confirmed by an immediate resample, to be in exceedance of a GWPS in 35 I.A.C. § 845.600, and the owner or operator has not demonstrated that: a source other than the CCR SI caused the exceedance, or that the exceedance of the GWPS resulted from error in sampling, analysis, statistical evaluation, natural variation in groundwater quality or a change in the potentiometric surface and groundwater flow direction (*i.e.*, ASD).

The CMA is the first step in developing a long-term CAP to address the GWPS exceedances at CCR SIs. The process provides a systematic, rational method for evaluating potential corrective measures by first identifying potentially viable technologies and assessing them using qualitative information to eliminate from consideration infeasible or otherwise unacceptable remedial technologies (*i.e.*, the 35 I.A.C. § 845.660 CMA). The remaining technologies will be evaluated individually, or assembled into combined alternatives, and further evaluated under the 35 I.A.C. § 845.670 CAP process.

This CMA identified applicable corrective measure technologies and evaluated them for viability, given the site-specific conditions and considerations at the FAPS, by addressing the following 35 I.A.C. § 845.660 evaluation criteria:

- Performance, reliability, ease of implementation and potential impacts of appropriate potential remedies, including safety impacts, cross-media impacts, and control of exposure to any residual contamination;
- Time required to begin and complete the CAP; and
- Institutional requirements, such as State or local permit requirements or other environmental or public health requirements, that may substantially affect implementation of the CAP.

The evaluation included qualitative and/or semi-quantitative screening of the potential corrective measures (technologies) relative to their general performance, reliability, and ease of implementation characteristics and their potential impacts, timeframes, and institutional requirements to assess the viability of each technology to address the GWPS exceedances at the FAPS. This approach provided a reasoned set of corrective measures that could be used, either individually or in combination, to supplement the completed source control measures described in **Section 1.1**. This set of corrective measures will be further evaluated through the CAP process.

4. DESCRIPTION OF POTENTIAL CORRECTIVE MEASURE TECHNOLOGIES

The potential groundwater corrective measures summarized below are applicable to the FAPS and were included in the CMA development and analysis. Site-specific considerations provided in **Section 2** were used to evaluate potential groundwater corrective measures. Each of the corrective measures evaluated may be capable of satisfying the requirements and objectives, listed in **Section 3**, to varying degrees of effectiveness. The corrective measure review process was intended to yield a set of applicable corrective measures that could be used to supplement the primary corrective action, namely the completed source control activities described in **Section 1.1** (CIP with final cover system). The completed source control has significantly reduced infiltration rates relative to pre-closure conditions. Ongoing monitoring will be an integral part of all corrective measures to verify and document the remedial process. The corrective measures ultimately advanced to the Corrective Action Alternatives Analysis (CAAA) and selected in the CAP will be used to enhance the effectiveness of the completed source control and may be used independently or combined into specific remedial alternatives to leverage the advantages of multiple corrective measures to attain GWPSs.

Source control measures were completed in 2020 at the FAPS, as described in **Section 1.1**; all of the evaluated corrective measure technologies are proposed to be supplemental and complementary to source control activities. The following potential corrective measures, commonly used to mitigate groundwater impacts, were considered as a part of the CMA process:

- Source Control with Groundwater Polishing;
- Source Control with Groundwater Extraction (groundwater pumping wells or collection trenches);
- Source Control with a Cutoff Wall; and
- Source Control with In-Situ Treatment (Permeable Reactive Barrier [PRB] or In-Situ Chemical Treatment).

4.1 Source Control with Groundwater Polishing

Both federal and state regulators have long recognized that natural geochemical processes can be an acceptable component of a remedial action when it can achieve remedial action objectives in a reasonable timeframe. In 1999, USEPA published a final policy directive for groundwater remediation and described the process as follows:

- *"The reliance on natural attenuation processes (within the context of a carefully controlled and monitored site cleanup approach) to achieve site-specific remediation objectives within a time frame that is reasonable compared to that offered by other more active methods. The 'natural attenuation processes' that are at work in such a remediation approach include a variety of physical, chemical, or biological processes that, under favorable conditions, act without human intervention to reduce the mass, toxicity, mobility, volume, or concentration of contaminants in soil or groundwater. These in-situ processes include biodegradation; dispersion; dilution; sorption; volatilization; radioactive decay; and chemical or biological stabilization, transformation, or destruction of contaminants."* (USEPA, 1999).

The USEPA has stated that source control is the most effective means of ensuring the timely attainment of remediation objectives (USEPA, 1999). Natural geochemical processes may be appropriate as a “finishing step” after effective source control implementation (*i.e.*, groundwater polishing), to reduce the residual mass remaining in the groundwater after closure, if there are no risks to receptors and/or the contaminant plume is not expanding. Thus, groundwater polishing would be used in conjunction with the significant planned source control effort at the site, which consisted of a hybrid consolidate-and-cap approach with a final cover system described in **Section 1.1**.

In 2015, USEPA addressed remediation of inorganic compounds in groundwater and noted that the use of natural geochemical processes to address inorganic contaminants: (1) is not intended to constitute a treatment process for inorganic contaminants; (2) when appropriately implemented, can help to restore an aquifer to beneficial uses by immobilizing contaminants onto aquifer solids and providing the primary means for attenuation of contaminants in groundwater; and (3) is not intended to be a “do nothing” response (USEPA, 2015). Rather, documenting the applicability of natural geochemical processes for groundwater remediation should be thoroughly and adequately supported with site-specific characterization data and analysis (USEPA, 1999; USEPA, 2007; USEPA, 2015).

Both physical and chemical processes can contribute to the reduction in mass, toxicity, mobility, volume, or concentration of contaminants in groundwater. Physical processes applicable to CCR include dilution, dispersion, and flushing. Chemical processes applicable to CCR constituents in groundwater include precipitation and coprecipitation (*e.g.*, incorporation into sulfide minerals), sorption (*e.g.*, to iron, manganese, aluminum; to other metal oxides or oxyhydroxides; or to sulfide minerals or organic matter), and ion exchange.

All inorganic compounds are subject to physical processes, and under typical environmental conditions the physical mechanisms most often exert the dominant control on the CCR constituents of interest, such as sulfate and chloride, and lithium to a more variable degree. Chemical mechanisms are also likely to be active, though not often dominant, such as adsorption, ion exchange, and organic complexation. In combination with source control, these natural controls can provide an effective means to polish residual loading and achieve the GWPS in a reasonable timeframe. Additional data collection and analysis may be required to support the USEPA’s evaluation framework (USEPA, 2015) and obtain regulatory approval.

4.2 Source Control with Groundwater Extraction

Groundwater extraction is one of the most widely used groundwater corrective technologies and has a long history of performance. This corrective measure includes installation of one or more groundwater pumping wells or an extraction trench to control and extract impacted groundwater. Groundwater extraction captures and contains impacted groundwater and can limit plume expansion and/or off-site migration. Construction of a groundwater extraction system typically includes, but is not limited to, the following primary components:

- Designing and constructing a groundwater extraction system consisting of one or more extraction wells or trenches and operating at a rate to allow capture of CCR impacted groundwater within the UA and or the UD/PMP.
- Management of extracted groundwater, which may include modification to the existing National Pollutant Discharge Elimination System (NPDES) permit.

- Ongoing inspection and maintenance of the groundwater extraction system.

Remediation of inorganics by groundwater extraction can be effective, but systems do not always perform as expected. A combination of factors, including geologic heterogeneities, difficulty in flushing low-permeability zones, and rates of contaminant desorption from aquifer solids can limit effectiveness. Groundwater extraction systems require ongoing operation and maintenance to address issues such as iron bacteria and well fouling and to ensure optimal performance. The extracted groundwater must be managed, either by ex-situ treatment or disposal.

Groundwater extraction may reduce the timeframe to achieve GWPS and contain the groundwater constituents that exceed the GWPS. Extraction could be accomplished using a groundwater pumping well system or an extraction trench.

4.3 Source Control with a Cutoff Wall

Since the late 1970s and early 1980s, vertical cutoff walls have been used to control and/or isolate impacted groundwater. Low-permeability cutoff walls can be used to prevent horizontal off-site migration of potentially impacted groundwater. Cutoff walls act as barriers to lateral transport of impacted groundwater and can isolate soils that have been impacted by CCR to prevent mixing with unimpacted groundwater. Cutoff walls are often used in conjunction with an interior pumping system to establish an inward gradient within the cutoff wall. The gradient imparted by the pumping system maintains an inward flow through the wall, keeping it from acting as a groundwater dam and controlling potential end-around or breakout flow of contaminated groundwater. Constructing the cutoff wall such that it intersects a low-permeability material at its base, referred to as "keying", greatly increases its effectiveness.

A commonly used cutoff wall construction technology is the slurry trench method, which consists of excavating a trench and backfilling it with a soil-bentonite mixture, often created with the excavated soils, or, for deeper walls, a cement-bentonite mixture that is produced at an onsite batch plant. The trench is temporarily supported with bentonite slurry pumped into the trench during excavation (D'Appolonia and Ryan, 1979). Cutoff wall excavation uses conventional hydraulic excavators, hydraulic excavators equipped with specialized booms to extend their reach (*i.e.*, long-stick excavators), clamshells, or more specialized equipment such as hydromills or secant-pile drill rigs, depending upon trench depth, material excavated, and type of material that the wall is keyed into.

Cutoff walls are a widely accepted technology for containing impacted groundwater. Combining groundwater polishing with a limited cutoff wall and groundwater extraction in specific areas may provide advantages over independent use of these potential corrective technologies. Cutoff walls can be used in combination with groundwater extraction or as part of a PRB system (as the "funnel" in a funnel-and-gate system; **Section 3.4**).

4.4 Source Control with In-Situ Chemical Treatment

The use of in-situ treatment, either by injection or PRBs, is a widely used technology for treating impacted groundwater. However, in-situ treatment techniques for boron and sulfate are not well established; therefore, performance is unknown.

Chemical treatment could consist of injection of reactive materials into the subsurface to treat contaminants at specific, targeted locations. Alternatively, treatment could be accomplished via PRB, where subsurface barriers (*i.e.*, cutoff walls) are placed at locations designed to direct the

contaminant plume along a flow path through the reactive media. In either system, the contaminants are transformed or otherwise rendered into environmentally acceptable forms to attain remediation concentration goals downgradient of the barrier (Electric Power Research Institute [EPRI], 2006).

As groundwater passes through the PRB under natural gradients, dissolved constituents in the groundwater react with the reactive media and are transformed or immobilized. A variety of media have been used or proposed for use in PRBs. Zero-valent iron (ZVI) has been shown to effectively immobilize some CCR constituents, including arsenic, chromium, cobalt, molybdenum, selenium, and sulfate. Use of a combination media consisting of ZVI and a boron-selective ion exchange resin to treat boron has been documented in a pilot-scale test (EPRI, 2006).

System configurations include continuous PRBs, in which the reactive media extends across the entire path of the contaminant plume; and funnel-and-gate systems, where low-permeability barriers are installed to control groundwater flow through a permeable gate containing the reactive media. Continuous PRBs intersect the entire contaminant plume and do not materially impact the groundwater flow system. Design may or may not include keying the PRB into a low-permeability unit at depth. Funnel-and-gate systems utilize a system of barriers to groundwater flow (funnels) to direct the contaminant plume through the reactive gate. The barriers, typically some form of cutoff wall, are keyed into a low-permeability unit at depth to prevent short circuiting of the plume. Funnel-and-gate design must consider the residence time to allow chemical reactions to occur. Directing the contaminant plume through the reactive gate can significantly increase the flow velocity, thus reducing residence time.

Design of in-situ treatment systems requires rigorous site investigation to characterize the site hydrogeology and to delineate the contaminant plume. A thorough understanding of the geochemical and redox characteristics of the plume is critical to assess the feasibility of the process and select appropriate reactive media. Laboratory studies, including batch studies and column studies using samples of site groundwater, are needed to determine the effectiveness of the selected reactive media at the site (EPRI, 2006). The main considerations in selecting reactive media are as follows (Gavaskar et al., 1998 as cited by EPRI, 2006):

- **Reactivity** - The media should be of adequate reactivity to immobilize a contaminant within the residence time of the design.
- **Hydraulic performance** - The media should provide adequate flow through the PRB, meaning a greater particle size than the surrounding aquifer materials. Alternatively, gravel beds have been emplaced in front of barriers to direct flow through the barrier.
- **Stability** - The media should remain reactive for an amount of time that makes its use economically advantageous over other technologies.
- **Environmentally compatible by-products** - Any by-products of media reaction should be environmentally acceptable. For example, iron released by zero-valent iron corrosion should not occur at levels exceeding regulatory acceptance levels.

Availability and price: The media should be easy to obtain in large quantities at a price that does not negate the economic feasibility of using a PRB.

5. ASSESSMENT OF CORRECTIVE MEASURE TECHNOLOGIES

This CMA was initiated to address exceedances of the 35 I.A.C. § 845.600 GWPS at the downgradient waste boundary of the FAPS (**Section 2.2**).

5.1 Requirements

The potential groundwater corrective technologies described in the previous section were evaluated relative to the requirements presented in **Section 1.1** and reiterated below:

- Performance, reliability, ease of implementation and potential impacts of appropriate potential remedies, including safety impacts, cross-media impacts, and control of exposure to any residual contamination;
- Time required to begin and complete the CAP; and
- Institutional requirements, such as State or local permit requirement or other environmental or public health requirements that may substantially affect implementation of the CAP.

Table 5-1 presents the qualitative CMA evaluation of each corrective technology relative to these requirements, as well as their ability to address boron and sulfate GWPS exceedances. The following sections provide a summary of these evaluations and a discussion of the potential groundwater corrective measure technologies that may be viable, either independently or in combination, to address GWPS exceedances. This section also provides a summary of corrective measure technologies that have been retained and advanced for evaluation as part of the CAAA process for selecting the final remedy for the FAPS per 35 I.A.C. § 845.670.

5.2 Groundwater Corrective Technology Assessment

Source control, consisting of CIP and capping with a final cover system, is the primary groundwater corrective measure for the FAPS and was completed in 2020. Each of the potential groundwater corrective measure technologies would supplement the positive impact of prior closure activities. The following sections evaluate groundwater corrective measure technologies that, when combined with the completed source control, may be viable to address the boron and sulfate GWPS exceedances. Technologies that are not viable for addressing exceedances of GWPS at the FAPS will be eliminated from further evaluation and viable technologies will be advanced for further evaluation as part of the CAAA process per 35 I.A.C. § 845.600.

5.2.1 Source Control with Groundwater Polishing

Completed source control corrective measures (**Section 1.1**) have reduced the mass loading to the groundwater system. Performance of groundwater polishing, which may be currently ongoing at the site, may be limited in the low permeability UU. The time estimated for plume contraction at the FAPS is relatively long, based on previous groundwater modeling (NRT, 2014a; NRT, 2014b). Groundwater polishing may not significantly reduce the time required to attain the GWPS in either the UA or the overlying UU/PMP due to the low permeability of both these hydrostratigraphic units.

Groundwater polishing by natural geochemical processes is a widely accepted component of groundwater remediation and is routinely approved by the USEPA when paired with source

control. The performance of groundwater polishing as a groundwater corrective measure varies based on site-specific conditions and additional data collection may be needed to support the design and achieve regulatory approval. The low permeability of the UU and bedrock UA suggests performance by physical processes may be limited in addressing the boron in the UA. The chemical processes in the fine-grained UU require further evaluation.

Naturally occurring geochemical processes are currently ongoing at the post-closure FAPS and will continue to affect post-closure groundwater constituent concentrations. Ongoing monitoring of groundwater conditions is needed to better understand the mechanisms and efficacy of the groundwater polishing process and to confirm the effectiveness over time. Thus, additional groundwater sample collection and analyses would be required to characterize potential mechanisms, as discussed above, and to provide long term monitoring of the remedial progress. Enhancements to the groundwater monitoring system may be required to ensure that groundwater polishing is occurring as predicted, consistent with the adaptive site management approach. The reliability of groundwater polishing as a groundwater corrective measure is high because operation and maintenance requirements are limited. However, the reliability can also vary based on site-specific hydrogeologic and geochemical conditions.

Following characterization and approval of the CAP, monitoring of the groundwater polishing processes and comparison to functional goals established to monitor progress toward the remedial objective could begin as quickly as within a few months of CAP approval.

No potential safety impacts or exposure to human health or environmental receptors are expected to result from implementing the groundwater polishing processes. Timeframes to achieve GWPS are dependent on site-specific conditions, which require detailed technical analysis which are ongoing and will be evaluated in connection with the CAAA. Selecting groundwater polishing as a corrective measure for the FAPS will require CAP permit by the IEPA.

Monitoring the groundwater polishing to track progress toward achievement of the GWPS, in conjunction with source control at the FAPS, would require long-term maintenance and monitoring of the groundwater monitoring system to confirm source control and verify the effectiveness in reducing groundwater concentrations to levels below the GWPS. Monitoring activities could be initiated immediately after approval of the CAP permit.

Groundwater polishing processes will continue to occur naturally at the FAPS. It may be a viable corrective measure for the boron and sulfate exceedances at the FAPS. Therefore, it is being advanced to the CAAA for further evaluation.

5.2.2 Source Control with Groundwater Extraction

Source control will reduce the mass loading to the groundwater system and implementing a groundwater extraction system may reduce the time required to attain the GWPS in the UA and reduce the potential for off-site migration. However, the groundwater impacts already present in the low permeability UU may limit the reduction in time to attain the GWPS that can be achieved by a groundwater extraction system. A groundwater collection trench may be feasible to mitigate potential plume migration to the south and west.

Groundwater extraction is a widely accepted corrective measure with a long track record of performance and reliability. It is routinely approved by the IEPA. For a corrective measure using groundwater extraction to effectively control off-site flow and/or to remove potentially

contaminated groundwater, horizontal and vertical capture zone(s) must be created. However, the low permeability UU and UA may restrict the ability to pump at rates high enough to establish the required capture zone(s) or would require a high density of wells. Alternatively, a groundwater collection trench could be utilized. Other means to enhance the effects of groundwater extraction could also be used, such as maintaining lower water levels in the downgradient Tertiary and Secondary Ponds, thereby increasing hydraulic gradients, and potentially accelerating the time to attain GWPS. However, performance of groundwater extraction in the UA may not address CCR constituents in the UU due to the UU's low permeability.

Implementation of a groundwater extraction system presents design challenges due to the hydraulic conditions of the UU and the UA and the plume configuration. Extracted groundwater would need to be managed, which may include modification of the existing NPDES permit and treatment prior to discharge, if necessary. Specialized treatment equipment may be required, and ongoing operations and maintenance activities would be necessary.

There could be some impacts associated with constructing and operating a groundwater extraction system, including some limited exposure to extracted groundwater. Additional data collection and analyses would be required to design an extraction system. Construction could be completed within 1 to 3 years. Time of implementation is approximately 3 to 4 years after approval of the CAP permit, including characterization, design, permitting, and construction. Timeframes to achieve GWPS are dependent on site-specific conditions. An extraction system may reduce the post-closure time to attain GWPS in the UA. However, accelerated attainment of the GWPS is expected to be limited in the UU. The model-predicted times to achieve the GWPS in the UU, potentially hundreds of years, may result in a correspondingly long operations and maintenance program for any groundwater extraction system.

Implementing a groundwater extraction system at the FAPS would require IEPA approval of the CAP permit, and discharge of extracted groundwater would require a modification to the NPDES permit. Depending upon the location of the extraction system, an Illinois Department of Natural Resources (IDNR) dam safety modification permit may also be required to construct the system.

The viability of groundwater extraction in combination with other corrective measure(s) will be further evaluated as part of the CAAA, potentially using groundwater fate and transport modeling. Therefore, the groundwater extraction is being advanced to the CAAA for further evaluation.

5.2.3 Source Control with Groundwater Cutoff Wall

Source control will reduce the mass loading to the groundwater system and implementing additional groundwater corrective measures may reduce the time required to attain the GWPS in the UA. However, the groundwater impacts already present in the low permeability UU may limit the reduction in time to attain the GWPS. Groundwater cutoff walls are a widely accepted corrective measure used to control and/or isolate impacted groundwater and are routinely approved by the IEPA. Cutoff walls have a long history of reliable performance as hydraulic barriers, provided they are properly designed and constructed. However, if not coupled with a groundwater extraction system, a cutoff wall will provide directional groundwater control only and may result in redistribution of contaminants and potentially GWPS exceedances at new locations.

The effectiveness of a cutoff wall as a hydraulic barrier relies on the contrast between the hydraulic conductivity of the native geologic materials (*i.e.*, the UU and/or UA) and the cutoff wall. The most effective barriers have hydraulic conductivity values that are several orders of magnitude lower than the geologic materials they are in contact with. The effectiveness of a cutoff wall, typically designed with hydraulic conductivity of 1×10^{-7} centimeters per second (cm/s), constructed in the low permeability UU and/or UA, would be limited. Construction of a cutoff wall extending into the bedrock UA would likely require specialized equipment and may prove difficult, potentially requiring several years of continuous construction.

Cutoff walls are designed to act as hydraulic barriers; as a result, cutoff walls inherently alter the existing groundwater flow system. Changes to the existing groundwater flow system may need to be controlled to maximize the effectiveness of the remedy by, for example, combining a cutoff wall with groundwater extraction to control build-up of hydraulic head upgradient and around the cutoff walls. Additional data collection and analyses would be required to design a cutoff wall. Construction of only the cutoff wall could be completed within 2 to 3 years. Constructing a cutoff wall at the FAPS would require IEPA approval of the CAP permit and, depending on the location, an IDNR dam safety modification permit may be required.

To attain GWPS, cutoff walls require a separate groundwater corrective measure to operate in concert with the cutoff wall(s). A cutoff wall at the FAPS alone would not be a viable corrective measure for the boron and sulfate exceedances. Cutoff walls are commonly coupled with groundwater polishing and/or groundwater extraction, possibly with treatment of extracted groundwater, to attain GWPS. Use of a cutoff wall coupled with groundwater extraction/treatment to supplement the ongoing groundwater polishing may provide improvement over source control in accelerating the time to attain GWPS. Time of implementation for the cutoff wall, hydraulic head control (*i.e.*, groundwater extraction), and any necessary treatment is approximately 5 to 8 years, including characterization, design, permitting, and construction. The viability of a cutoff wall in combination of other corrective measure(s) will be further evaluated as part of the CAAA, potentially using groundwater fate and transport modeling. Therefore, the cutoff wall is being advanced to the CAAA for further evaluation.

5.2.4 Source Control with In-Situ Chemical Treatment

Source control will reduce the mass loading to the groundwater system and implementing additional groundwater corrective measures may reduce the time required to attain the GWPS in the UA. Use of in-situ treatment, either through targeted injection of reactive media or in PRB systems, to transform contaminants into environmentally acceptable forms to attain the GWPS was considered.

In-situ treatment using ion exchange to address boron and sulfate exceedances in groundwater is not an established or widely accepted groundwater corrective measure; therefore, its performance and reliability are unknown. Regulatory acceptance of this innovative approach to achieving the GWPS is uncertain.

In-situ treatment presents design and construction challenges, including targeted reactive media delivery via injection to the UU and/or UA. Construction of a PRB system would have the same limitations as a cutoff wall due to the similarity between the low hydraulic conductivity of the PRB and the UU. Injection or a PRB may not be feasible in the bedrock UA. Depending upon the

location of the PRB system, construction may affect the FAPS embankment and/or final cover system and periodic change-outs of ion exchange (IX) resin media may be required.

Additional data collection and analyses would be required to design an in-situ treatment system and bench scale and/or pilot scale testing may be required to demonstrate performance and reliability. Time of implementation is approximately 4 to 6 years after approval of the CAP permit, including characterization, design, permitting, and construction. Timeframes to achieve GWPS are dependent on demonstrations of performance and reliability along with regulatory acceptance. It is not known whether in-situ treatment would reduce the time to attain GWPS in the UA relative to the expected long post-closure timeframe predicted by the groundwater modeling.

Due to the uncertain performance, reliability and potential for regulatory hurdles, in-situ chemical treatment is not a viable corrective measure for the boron and sulfate exceedances at the FAPS and is not being advanced to the CAAA for further evaluation.

5.3 Technologies Advanced to CAAA

Based on the evaluations presented above, the following potential corrective technologies are being advanced to the CAAA for more detailed evaluations, individually or in combination, and cost estimation:

- Source control with groundwater polishing;
- Source control with groundwater extraction; and
- Source control with a groundwater cutoff wall.

6. REFERENCES

- AECOM, 2016. *Closure and Post-Closure Care Plan for the Baldwin Fly Ash Pond System. Baldwin Energy Complex. Baldwin, Illinois.* March 31, 2016.
- D'Appolonia, D.J., and Ryan, C.R., 1979. *Soil-Bentonite Slurry Trench Cut-Off Walls*, Geotechnical Exhibition and Technical Conference, Chicago, Illinois.
- Dynegy Midwest Generation (DMG), 2020. *Baldwin Energy Complex; Old East Fly Ash Pond, East Fly Ash Pond, West Ash Pond Notification of Completion of Closure.* December 17, 2020.
- Electric Power Research Institute (EPRI), 2006. *Groundwater Remediation of Inorganic Constituents at Coal Combustion Project Management Sites, Technical Report #1012584*, October 2006.
- Gavaskar, A.R., N Gupta, B.M. Sass, R.J. Janosy and D. O'Sullivan, 1998. *Permeable Reactive Barriers for Groundwater Remediation: Design, Construction and Monitoring.* Battelle Press.
- Geosyntec Consultants, Inc., 2024. *Alternative Source Demonstration Baldwin Power Plant Fly Ash Pond System (Unit ID #605), IEPA ID: WI578510001-01, -02, -03, 35 IAC 850.650.* February 6, 2024.
- Illinois Environmental Protection Agency, 2016. "Dynegy Midwest Generation, Inc. - Baldwin Energy Complex: Baldwin Fly Ash Pond System Closure - NDPEs Permit No. IL0000043." August 16, 2016.
- Illinois Environmental Protection Agency, "Re: Baldwin Power Plant Fly Ash Pond System," March 7, 2024.
- Interstate Technology & Regulatory Council (ITRC), 2017. *Remediation Management of Complex Sites.* RMCS-1. Washington, D.C.: Interstate Technology & Regulatory Council, Remediation Management of Complex Sites Team. <https://rmcs-1.itrcweb.org>.
- Natural Resource Technology, 2014a. *Groundwater Model and Simulation of Closure Alternatives, Baldwin Ash Pond System, Baldwin Energy Complex, Baldwin Illinois.* June 18, 2014.
- Natural Resource Technology, 2014b. *Prediction of Plume Stability by Groundwater Modeling, Baldwin Ash Pond System, Baldwin Energy Complex, Baldwin Illinois.* September 30, 2014.
- Natural Resource Technology, an OBG Company (NRT/OBG), 2017. *Hydrogeologic Monitoring Plan, Baldwin Bottom Ash Pond, CCR Unit ID 601, Baldwin Fly Ash Pond System – CCR Multi-Unit ID 605, Baldwin Energy Complex, Baldwin, Illinois.* October 17, 2017.
- Ramboll Americas Engineering Solutions, Inc. (Ramboll), 2021. *Hydrogeologic Site Characterization Report, Bottom Ash Pond, Baldwin Power Plant, Baldwin, Illinois.* October 25, 2021.
- Ramboll Americas Engineering Solutions, Inc. (Ramboll), 2023a. *Hydrogeologic Site Characterization Report Revision 1. Bottom Ash Pond. Baldwin Power Plant. Baldwin, Illinois.* August 1, 2023.

Ramboll Americas Engineering Solutions, Inc. (Ramboll), 2023b. *Groundwater Monitoring Data and Detected Exceedances, Quarter 2 2023, Fly Ash Pond System, Baldwin Energy Complex, Baldwin, Illinois*. August 22, 2023.

Ramboll Americas Engineering Solutions, Inc. (Ramboll), 2023c. *35 I.A.C. § 845.610(B)(3)(D) Groundwater Monitoring Data and Detected Exceedances – Quarter 3, 2023. Fly Ash Pond System, Baldwin Power Plant, Baldwin, Illinois*. Ramboll Americas Engineering Solutions, Inc. December.

Ramboll Americas Engineering Solutions, Inc. (Ramboll), 2024. *35 I.A.C. § 845.610(B)(3)(D) Groundwater Monitoring Data and Detected Exceedances – Quarter 4, 2023. Fly Ash Pond System, Baldwin Power Plant, Baldwin, Illinois*. Ramboll Americas Engineering Solutions, Inc. February 9, 2024.

United States Environmental Protection Agency (USEPA), 1999. *Use of Monitored Natural Attenuation at Superfund, RCRA Corrective Action, and Underground Storage Tank Sites. Directive No. 9200.U-17P*. Washington, D.C.: EPA, Office of Solid Waste and Emergency Response.

United States Environmental Protection Agency (USEPA), 2007. *Monitored Natural Attenuation of Inorganic Contaminants in Ground Water, Volume 1 – Technical Basis for Assessment. EPA/600/R-07/139*. National Risk Management Research Laboratory, Office of Research and Development, U.S. Environmental Protection Agency, Cincinnati, Ohio. October 2007.

United States Environmental Protection Agency (USEPA), 2015. *Use of Monitored Natural Attenuation for Inorganic Contaminants in Groundwater at Superfund Sites. Directive No. 9283.1-36*. U.S. Environmental Protection Agency, Office of Solid Waste and Emergency Response. August 2015.

United States Environmental Protection Agency (USEPA), 2022. *Adaptive Site Management – A Framework for Implementing Adaptive Management at Contaminated Sediment Superfund Sites. Directive No. 9200.1-166*. U.S. Environmental Protection Agency. June 2022.

TABLES

DRAFT

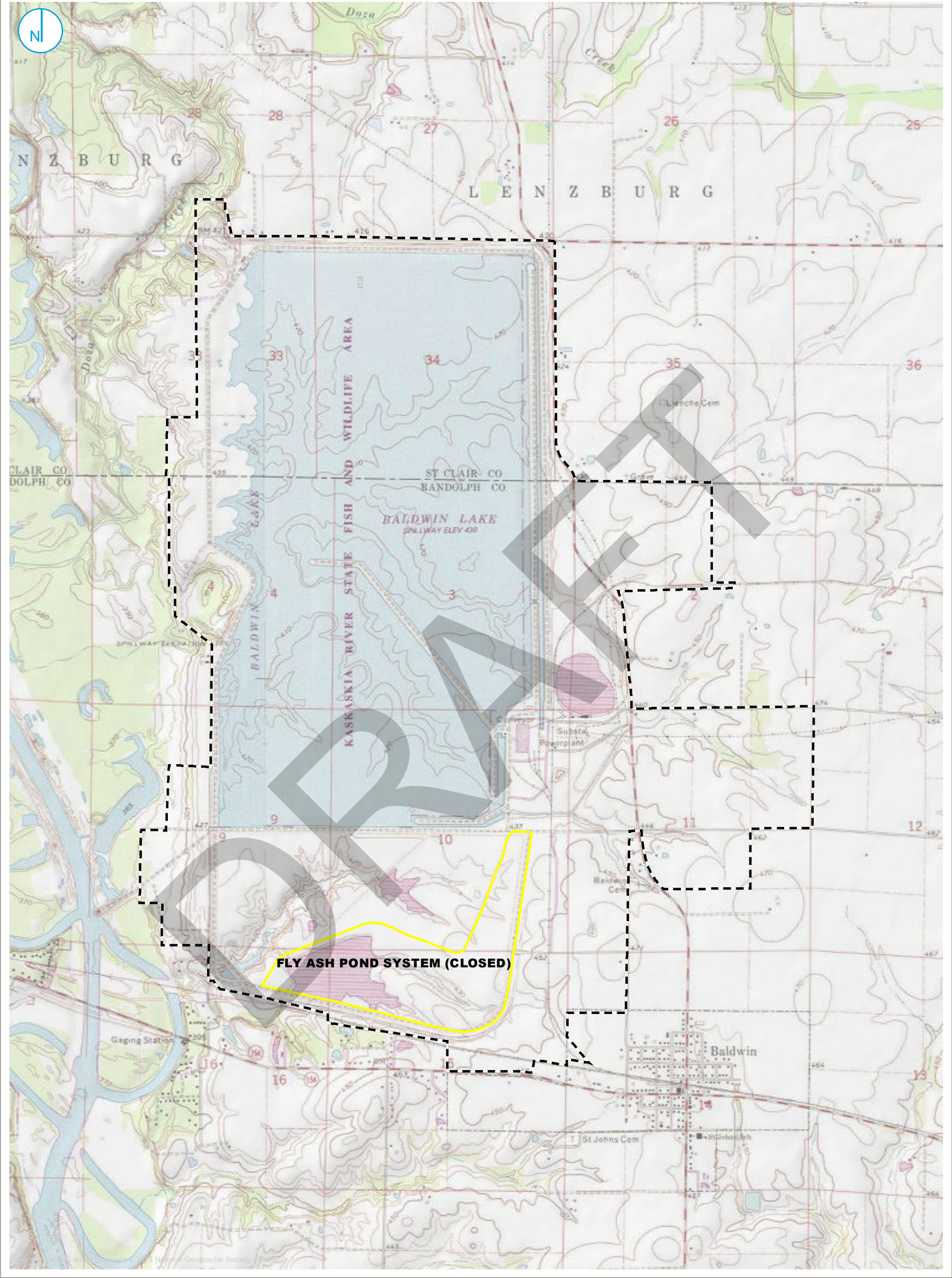
TABLE 5-1.
35 I.A.C. PART 845 CORRECTIVE MEASURES ASSESSMENT MATRIX
FLY ASH POND SYSTEM
BALDWIN POWER PLANT
BALDWIN, ILLINOIS

| Remedy | Evaluation Factors | | | | | | |
|--|--|--|--|---|---|--|---|
| | Performance | Reliability | Ease of Implementation | Potential Impacts of Remedy (safety impacts, cross-media impacts, control of exposure to any residual contamination) | Time Required to Begin and Implement Remedy ¹ | Time to Attain Groundwater Protection Standards | Institutional Requirements (state/local permit requirements, environmental/public health requirements that affect implementation of remedy) |
| Source Control with Groundwater Polishing | Performs best paired with source control, which was completed at the site using a clay cap in 2020. Sequential extraction data will be obtained as part of the ongoing evaluation. Limited potential for physical processes in the low permeability uppermost aquifer (UA). | Ongoing analysis will evaluate whether the geochemical mechanisms have low reversibility, the aquifer has sufficient capacity, and the hydrogeology is favorable for physical processes. | Evaluation is underway and is expected to be completed in 2024. Long-term monitoring would be required. Implementing would not require extensive specialized equipment or contractors. | None identified. | Approximately 90 days after Corrective Action Plan (CAP) permit approval. | Dependent on site-specific conditions including source decay rate. Attainment of groundwater protection standards (GWPS) will be limited by the low permeability UU and bedrock UA. Hence timeframes for groundwater polishing and other measures may be similar. | Illinois Environmental Protection Agency (IEPA) approval of the CAP is required. |
| Source Control with Groundwater Extraction | Widely accepted, routinely approved; variable performance based on site-specific conditions. May be limited by low permeability upper unit (UU) and bedrock UA. A groundwater collection trench may be feasible to mitigate plume migration near the southern site boundary. | Reliable if properly designed, constructed, and maintained. Groundwater treatment prior to discharge can be considered if indicated by performance monitoring. | Specialized contractors may be necessary for construction of the groundwater extraction system. Design challenges due to hydraulic conditions of UU and bedrock UA and the plume configuration. Extracted groundwater would require management. Groundwater treatment, if needed, may require specialized equipment/contractors. | Alters groundwater flow system. Potential for some limited exposure to extracted groundwater. Groundwater extraction may induce settlement, which could cause structural impacts to the embankments, existing final cover system, and/or adjacent structures. | Design, permitting and construction is expected to take 3 to 4 years after CAP permit approval. | Dependent on site-specific conditions. Attainment of GWPS will be limited by the low permeability UU and bedrock UA. | IEPA approval of the CAP is required. Extracted groundwater discharge may require a National Pollution Discharge Elimination System (NPDES) permit modification. A Illinois Department of Natural Resources (IDNR) dam safety modification permit might also be required, depending on location of wells and settlement potential. Cutoff wall may also require an evaluation and/or permitting of wetlands and/or Waters of the US impacts, if determined to be necessary. |
| Source Control with Groundwater Cutoff Wall | Widely accepted, routinely approved, good performance if properly designed and constructed, however may not be feasible for the UU and bedrock UA. | Reliable for groundwater flow directional control if properly designed and constructed. | Widely used, established technology. If feasible to construct a cutoff wall in the bedrock of the UA, construction would likely require specialized equipment and delay implementation (compared to groundwater extraction only). | Alters groundwater flow system but does not provide any treatment. Can result in unintended consequences resulting from redirecting contaminants to areas where they are not currently present. May cause structural impacts to the embankment or existing final cover system, depending on the location of the wall. | Design, permitting and construction are expected to take 5 to 8 years after CAP permit approval. | Provides groundwater directional control only. Combination with another groundwater corrective measure, such as groundwater extraction or a permeable reactive barrier, would reduce time to achieve and maintain GWPS. | IEPA approval of the CAP is required. An IDNR dam safety permit may also be required depending on the location of the cutoff wall. Cutoff wall may also require an evaluation and/or permitting of wetlands and/or Waters of the US impacts, if determined to be necessary. |
| Source Control with In-Situ Treatment (Permeable Reactive Barrier or In-situ Chemical Treatment) | In-Situ treatment using ion exchange (IX) resins not well established for boron or sulfate, therefore performance is unknown. | Variable reliability based on site-specific physical and geochemical conditions. May not be feasible in bedrock UA. Unknown reliability for boron and sulfate. | Design challenges associated with groundwater hydraulics. May not be feasible in bedrock UA. Could require periodic change-outs of IX resin media. | Alters groundwater flow system. PRB may cause structural impacts to the embankment dike or existing final cover system, depending on the location of the barrier. | May require bench scale and/or pilot scale testing as part of design. Design, permitting and construction are expected to take 7 to 8 years after CAP approval. | There is uncertainty regarding whether a permeable reactive barrier would reduce sulfate and boron concentrations to achieve the GWPS. Dependent on conditions specific to the reactive media used and the site. Treatment technology not well understood. GWPS attainment will be limited by low permeability bedrock UA. | IEPA approval of the CAP permit is required. IEPA approval of this innovative and relatively unproven solution may be challenging. A IDNR dam safety permit modification may also be required, depending on the location of the permeable reaction barrier (PRB). PRB may also require an evaluation and/or permitting of wetlands and/or waters of the US impacts, if determined to be necessary. |

Notes: ¹ Time required to begin and implement remedy includes design, permitting and construction.

FIGURES

DRAFT



REGULATED UNIT (SUBJECT UNIT)

PROPERTY BOUNDARY

SITE LOCATION MAP

FIGURE 2-1

0 1,000 2,000 Feet



- | | |
|---------------------------------------|-----------------------|
| REGULATED UNIT (SUBJECT UNIT) FLY ASH | SITE FEATURE |
| POND SYSTEM (CLOSED) | LIMITS OF FINAL COVER |
| | PROPERTY BOUNDARY |

0 400 800 Feet

SITE MAP

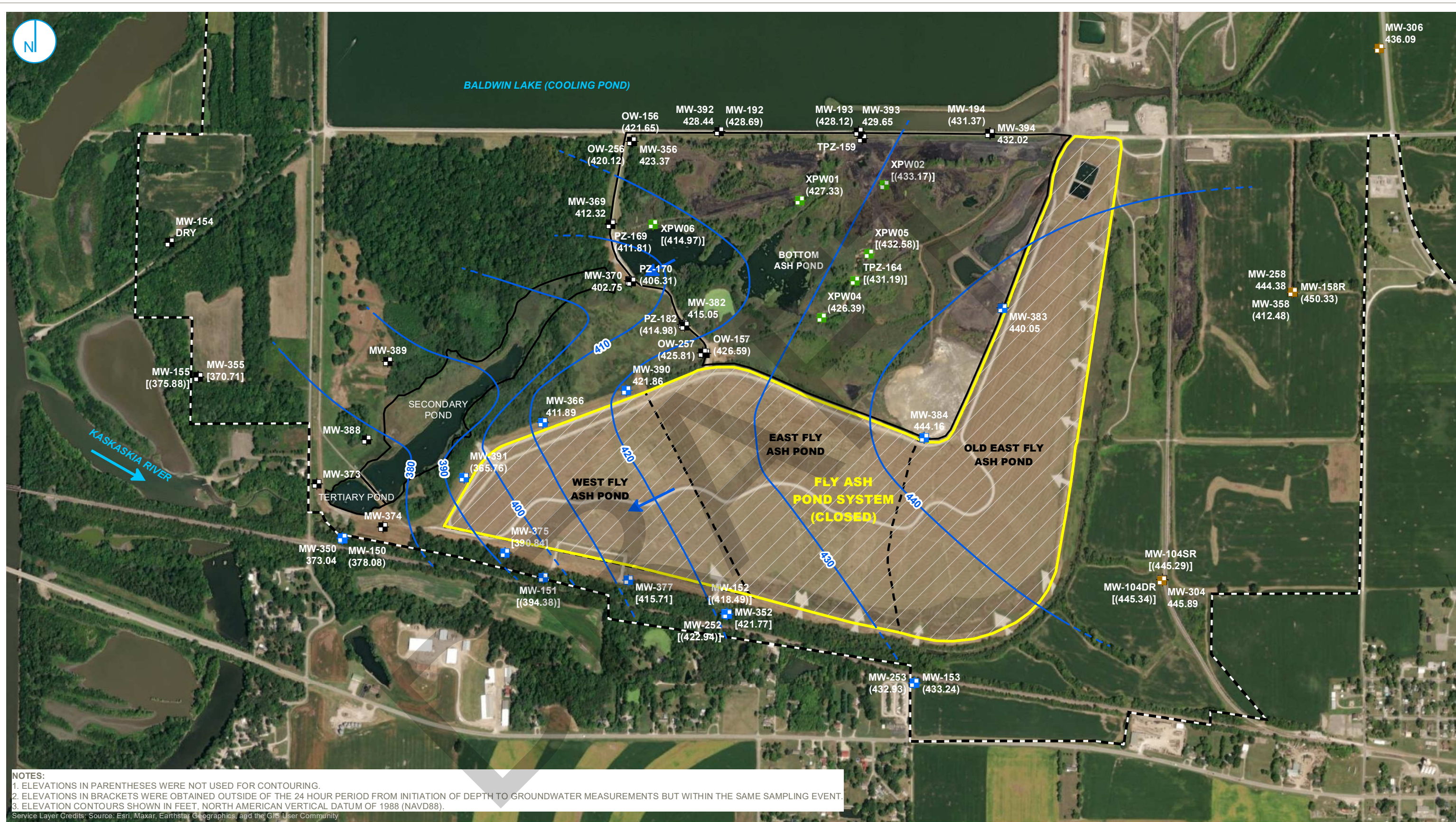
FIGURE 2-2

35 I.A.C. § 845 CORRECTIVE MEASURES ASSESSMENT
FLY ASH POND SYSTEM
BALDWIN POWER PLANT
BALDWIN, ILLINOIS

RAMBOLL AMERICAS
ENGINEERING SOLUTIONS, INC.



PROJECT: 169000XXXX | DATED: 10/31/2023 | DESIGNER: GALARNMC
Y:\Mapping\Projects\22\2285\MXD\GW_Contours\Round_2023\Baldwin\FAPS_605\FAPS Pot Surface 20230516.mxd



NOTES:
1. ELEVATIONS IN PARENTHESES WERE NOT USED FOR CONTOURING.
2. ELEVATIONS IN BRACKETS WERE OBTAINED OUTSIDE OF THE 24 HOUR PERIOD FROM INITIATION OF DEPTH TO GROUNDWATER MEASUREMENTS BUT WITHIN THE SAME SAMPLING EVENT.
3. ELEVATION CONTOURS SHOWN IN FEET, NORTH AMERICAN VERTICAL DATUM OF 1988 (NAVD88).
Service Layer Credits: Source: Esri, Maxar, Earthstar Geographics, and the GIS User Community

- | | | |
|------------------------------|--|---------------------------------|
| ■ COMPLIANCE MONITORING WELL | — GROUNDWATER ELEVATION CONTOUR (10-FT CONTOUR INTERVAL, NAVD88) | ■ REGULATED UNIT (SUBJECT UNIT) |
| ■ BACKGROUND MONITORING WELL | - - - INFERRED GROUNDWATER ELEVATION CONTOUR | ■ SITE FEATURE |
| ■ MONITORING WELL | → GROUNDWATER FLOW DIRECTION | ■ CAPPED AREA |
| ■ PORE WATER WELL | | ■ PROPERTY BOUNDARY |

POTENTIOMETRIC SURFACE MAP MAY 15-17, 2023

2023 ANNUAL GROUNDWATER MONITORING AND CORRECTIVE ACTION REPORT

FLY ASH POND SYSTEM
BALDWIN POWER PLANT
BALDWIN, ILLINOIS

FIGURE 2-3

RAMBOLL AMERICAS
ENGINEERING SOLUTIONS, INC.



PROJECT: 169000XXXX | DATED: 7/31/2023 | DESIGNER: GALARNMC
Y:\Mapping\Projects\22\2285\MXD\B45_Operating_Permit\Baldwin\FAPS\GMP\Figure 2-2_BAL_FAPS Expanded Monitoring Well Network.mxd



- BACKGROUND MONITORING WELL
- COMPLIANCE MONITORING WELL
- REGULATED UNIT (SUBJECT UNIT) SITE
- FEATURE
- CAPPED AREA
- PROPERTY BOUNDARY

0 400 800 Feet

MONITORING WELL LOCATION MAP

35 I.A.C. § 845 CORRECTIVE MEASURES ASSESSMENT
FLY ASH POND SYSTEM
BALDWIN POWER PLANT
BALDWIN, ILLINOIS

FIGURE 2-4

RAMBOLL AMERICAS
ENGINEERING SOLUTIONS, INC.



Appendix D

Nature and Extent Report

Intended for

Dynegy Midwest Generation, LLC
10901 Baldwin Road
Baldwin, IL 62217

Date

April 24, 2024

Project No.

1940103584-001

NATURE AND EXTENT REPORT

BALDWIN POWER PLANT, FLY ASH POND SYSTEM, IEPA ID NO. W1578510001-01, W1578510001-02, AND W1578510001-03

**NATURE AND EXTENT REPORT
BALDWIN POWER PLANT, FLY ASH POND SYSTEM, IEPA
ID NO. W1578510001-01, W1578510001-02, AND
W1578510001-03**

Project name **Baldwin Power Plant Fly Ash Pond System**
Project no. **1940103584-001**
Recipient **Dynegy Midwest Generation, LLC**
Document type **Nature and Extent Report**
Revision **FINAL**
Date **April 24, 2024**
Prepared by **Nathaniel Keller and Alison O'Connor**
Checked by **Melanie Conklin**
Approved by **Brian G. Hennings, PG**

Ramboll
234 W. Florida Street
Fifth Floor
Milwaukee, WI 53204
USA

T 414-837-3607
F 414-837-3608
<https://ramboll.com>



Alison O'Connor, PhD
Geochemist



Nathaniel R. Keller
Senior Technical Manager, Hydrogeology



Brian G. Hennings, PG
Project Officer, Hydrogeology

CONTENTS

| | |
|---|-----------|
| EXECUTIVE SUMMARY | 4 |
| 1. Introduction | 6 |
| 2. Background | 7 |
| 2.1 Site Location and Description | 7 |
| 2.2 Description of CCR SI | 7 |
| 2.3 Geology and Hydrogeology | 7 |
| 2.3.1 Hydrostratigraphic Units | 8 |
| 2.3.2 Uppermost Aquifer | 8 |
| 2.3.3 Potential Migration Pathways | 9 |
| 2.3.4 Regional Bedrock Geology | 9 |
| 2.3.5 Water Table Elevation and Groundwater Flow Direction | 9 |
| 2.3.5.1 Vertical Hydraulic Gradients | 10 |
| 2.3.5.2 Impact of Surface Water Bodies on Groundwater Flow | 11 |
| 2.3.6 Hydraulic Conductivities | 11 |
| 2.3.6.1 Field Hydraulic Conductivities | 11 |
| 2.3.6.2 Laboratory Hydraulic Conductivities | 11 |
| 2.4 Groundwater Monitoring | 12 |
| 2.5 Hydrogeologic Conceptual Site Model | 12 |
| 3. Occurrence and Distribution of Groundwater Exceedances (Extent) | 14 |
| 3.1 Additional Investigation to Define Nature and Extent | 14 |
| 3.2 Extents in the Upper Unit (PMP) | 15 |
| 3.2.1 Boron | 15 |
| 3.2.2 Sulfate | 16 |
| 3.3 Extent in Uppermost Aquifer (Bedrock Unit) | 16 |
| 3.3.1 Boron | 16 |
| 4. Geochemical Conceptual Site Model (Nature) | 17 |
| 5. Combined Geochemical and Hydrogeologic Conceptual Site Models | 18 |
| 5.1 Boron Conceptual Site Model | 18 |
| 5.2 Sulfate Conceptual Site Model | 18 |
| 6. Conclusions and Future Activities | 19 |
| 7. References | 20 |

TABLES (ATTACHED)

| | |
|-----------|--|
| Table 2-1 | Summary of Groundwater Elevations |
| Table 2-2 | Field Horizontal Hydraulic Conductivities |
| Table 2-3 | Laboratory Vertical Hydraulic Conductivities |
| Table 3-1 | Monitoring Well Construction Details |
| Table 3-2 | Exceedance Parameter Statistical Results |
| Table 3-3 | Summary of Groundwater Data |

FIGURES (ATTACHED)

| | |
|------------|-------------------|
| Figure 2-1 | Site Location Map |
| Figure 2-2 | Site Map |

| | |
|------------|---|
| Figure 2-3 | Base of CCR |
| Figure 2-4 | Sand Seam Observations, Thickness and Elevations |
| Figure 2-5 | Top of Uppermost Aquifer |
| Figure 2-6 | Shallow Unlithified Potentiometric Surface Map, May 2023 (E001) |
| Figure 2-7 | Uppermost Aquifer Potentiometric Surface Map, May 2023 (E001) |
| Figure 2-8 | Monitoring Well Location Map |
| Figure 3-1 | GWPS Exceedance Map Upper Unit |
| Figure 3-2 | Groundwater Elevations and Boron Concentrations in MW-152 |
| Figure 3-3 | GWPS Exceedance Map Uppermost Aquifer |

APPENDICES

| | |
|------------|---|
| Appendix A | Geologic Cross-Sections |
| Appendix B | Select Hydrographs |
| Appendix C | Vertical Hydraulic Gradients |
| Appendix D | Off-Site Groundwater Quality Results (Kelron, 2012) |
| Appendix E | Geochemical Conceptual Site Model |

ACRONYMS AND ABBREVIATIONS

| | |
|--------------|--|
| 35 I.A.C. | Title 35 of the Illinois Administrative Code |
| ASD | Alternative Source Demonstration |
| BPP | Baldwin Power Plant |
| CCR | coal combustion residuals |
| Closure Plan | Closure and Post-Closure Care Plan for the Baldwin Fly Ash Pond System |
| CMA | Corrective Measures Assessment |
| cm/s | centimeters per second |
| CSM | conceptual site model |
| E001 | Event 1 |
| E002 | Event 2 |
| E003 | Event 3 |
| FAPS | Fly Ash Pond System |
| GCSM | geochemical conceptual site model |
| GWPS | groundwater protection standard |
| IEPA | Illinois Environmental Protection Agency |
| LCL | lower confidence limit |
| mg/L | milligrams per liter |
| NAVD88 | North American Vertical Datum 1988 |
| PMP | potential migration pathway |
| SI | surface impoundment |
| UA | uppermost aquifer |
| UU | Upper Unit |
| USEPA | United States Environmental Protection Agency |
| USGS | United States Geological Survey |

EXECUTIVE SUMMARY

Groundwater samples collected at the Baldwin Power Plant (BPP) Fly Ash Pond System (FAPS) during May 2023 for the Quarter 2, 2023 compliance sampling event (Event 1 [E001]) were evaluated for exceedances of the groundwater protection standards (GWPS) described in Title 35 of the Illinois Administrative Code (35 I.A.C.) § 845.600. Exceedances were identified in the following hydrostratigraphic units and wells:

- Detected Upper Unit (UU) and Potential Migration Pathway (PMP) Exceedances:
 - Boron and sulfate at MW-150
- Detected Uppermost Aquifer (UA) (Bedrock Unit) Exceedances:
 - Boron at MW-391

As a result of the identified E001 exceedances, a Corrective Measures Assessment (CMA) was initiated on November 26, 2023 in accordance with 35 I.A.C. § 845.660 and was submitted April 24, 2024 [1]. The subsequent compliance sampling events for the Quarter 3 and Quarter 4 2023 sampling events (Event 2 [E002] and Event 3 [E003]) were completed in August and November 2023 and groundwater samples were evaluated for exceedances of the GWPS as described in 35 I.A.C. § 845.600. In addition to the exceedances listed above, the following exceedances were identified in the following hydrostratigraphic units and wells during the E002 Event:

- Detected UU and PMP Exceedances:
 - Boron at MW-152
 - pH at MW-253

Exceedances identified during the E003 event were consistent with those listed above.

An alternative source demonstration (ASD) was completed for the pH exceedance at well MW-253 and received concurrence in a letter from the Illinois Environmental Protection Agency (IEPA) dated March 7, 2024 [2]. Therefore, the pH exceedance at well MW-253 was not incorporated into the CMA per 35 I.A.C. § 845.650(e)(3). The remaining E002 exceedance (boron at MW-152) was evaluated with respect to the groundwater model, feasible alternatives, and remedy extents and was determined to not substantially affect the findings and conclusions of the previously initiated CMA evaluations and has therefore been incorporated into the CMA and this report.

As required by 35 I.A.C. § 845.650(d)(1) this report characterizes the nature and extent of boron and sulfate to support a complete and accurate assessment of the corrective measures. The report also evaluates relevant site conditions to determine how they may affect the corrective measures ultimately selected for the FAPS and documents the additional measures taken in accordance with 35 I.A.C. § 845.650(d).

Boron was detected above the GWPS within two hydrostratigraphic units: the shallow UU and in the deeper UA. The lateral and downgradient extent of boron in the UU is being further evaluated but is adequately defined by sampling of historical piezometers as well as results from the Kaskaskia River [3]. The vertical migration of boron concentrations above the GWPS in the UU is limited by low hydraulic conductivity clay and silt of the UU and the underlying shale bedrock. Samples from deeper nested monitoring wells, which have reported no exceedances following comparison of the lower confidence limits (LCLs) to the GWPSs described in 35 I.A.C. § 845.600

provide evidence that boron impacts are not migrating downward. The lateral and downgradient extent of boron in the UA is limited by the Secondary Pond directly adjacent to MW-391 to the west and along with groundwater quality data from monitoring wells in the UA that did not report exceedances following comparison of LCLs to the GWPSs described in 35 I.A.C. § 845.600. Samples collected from the Secondary and Tertiary Ponds, as well as the Kaskaskia River indicate all boron concentrations in surface water are below 1.2 milligrams per liter (mg/L) [3].

Sulfate was detected above the GWPS within the UU at a single location. The lateral and downgradient extent of sulfate in the UU is being further evaluated but is adequately defined by sampling of historical piezometers as well as results from the Kaskaskia River [3]. The vertical migration of sulfate in the UU is limited by low hydraulic conductivities of the UU and underlying shale bedrock and supported by the results of nested monitoring well MW-350 which has reported no exceedances following comparison to the GWPSs described in 35 I.A.C. § 845.600. Samples collected from the Secondary and Tertiary Ponds as well as the Kaskaskia River indicate all sulfate concentrations in surface water are below 200 mg/L [3].

1. INTRODUCTION

35 I.A.C. § 845.650(d)(1) requires the owner or operator of a coal combustion residuals (CCR) surface impoundment (SI) to characterize the nature and extent of a release and relevant site conditions that may affect the remedy ultimately selected for a CCR SI if any constituent regulated under 35 I.A.C. § 845 is found to exceed the GWPS. This report documents the nature and extent of constituents detected above the GWPS that are attributable to the BPP FAPS.

The groundwater data and analysis in this report includes results from historical sampling (initiated in 2015) through E003, which was completed on November 3, 2023. Results of events E001, E002, and E003 were submitted and placed in the facility's operating record within 60 days of receiving final laboratory analytical data [4, 5, 6] as required by 35 I.A.C. § 845.800(d)(15). The statistical determination presented in the report identified the following exceedances of the GWPS at compliance groundwater wells in the following hydrostratigraphic units:

- Detected UU and PMP Exceedances:
 - Boron at MW-150 and MW-152
 - pH at MW-253
 - Sulfate at MW-150
- Detected UA (Bedrock Unit) Exceedances:
 - Boron at MW-391

An ASD, as allowed by 35 I.A.C. § 845.650(e), was completed for the pH exceedance at UA monitoring well MW-253 [2] and received concurrence in a letter from the IEPA dated March 7, 2024 [7].

This Nature and Extent Report discusses in detail the extent of the boron and sulfate exceedances as well as a geochemical conceptual site model (GCSM) describing the nature of these exceedances.

2. BACKGROUND

2.1 Site Location and Description

The BPP is located in southwest Illinois in Randolph and St. Clair Counties. The Randolph County portion of the BPP is located within Sections 2, 3, 4, 9, 10, 11, 14, 15, and 16 of Township 4 South and Range 7 West. The St. Clair County portion of the property is located within Sections 33, 34, and 35 of Township 3 South and Range 7 West. The FAPS is approximately one-half mile west-northwest of the Village of Baldwin (**Figure 2-1**).

The BPP property is bordered to the west by the Kaskaskia River; to the east by Baldwin Road, farmland, and strip-mining areas; to the southeast by the village of Baldwin; to the south by the Illinois Central Gulf railroad tracks, scattered residences, and State Route 154; and to the north by farmland. The St. Clair/Randolph County Line crosses east-west at approximately the midpoint of Baldwin Lake (*i.e.*, Cooling Pond). **Figure 2-1** shows the location of the BPP; **Figure 2-2** is a site map showing the location of the FAPS, Bottom Ash Pond (BAP), Secondary Pond, Tertiary Pond, and Cooling Pond. The combined area, including the BAP, FAPS, Secondary Pond, and Tertiary Pond, will hereinafter be referred to as the Site.

2.2 Description of CCR SI

The BPP began operation in 1970 and initially burned bituminous coal from Illinois, switching to subbituminous coal in 1999. The FAPS is a closed Multi-Unit CCR SI consisting of three unlined SIs: Old East Fly Ash Pond (IEPA Unit ID W1578510001-01), East Fly Ash Pond (IEPA Unit ID W1578510001-02), and West Fly Ash Pond (IEPA Unit ID W1578510001-03), with a combined surface area of approximately 263 acres. The external perimeter of the three subunits within the FAPS was originally constructed in 1969. The Old East Fly Ash Pond and East Fly Ash Pond were used to store and dispose of fly ash from the BPP, while the West Fly Ash Pond was used to store and dispose of dry-stacked fly ash and to clarify CCR contact stormwater [8].

AECOM submitted the Closure and Post-Closure Care Plan for the Baldwin Fly Ash Pond System (Closure Plan) dated March 2016 to the IEPA, and it was approved on August 16, 2016 [9]. The Closure Plan included the Groundwater Monitoring Plan [10] which defined groundwater monitoring for the FAPS following approval of the Closure Plan. Dewatering of the FAPS was initiated in 2018 and closure of the FAPS was completed on November 17, 2020, as documented in the Notification of Completion of Closure [11].

The CCR unit consists primarily of fly ash, bottom ash, and boiler slag and may be present from the pre-closure surface (ranging from approximately 418 to 466 feet¹) to a minimum elevation of approximately 401 feet along a historic drainage feature that runs approximately through the center of the FAPS (**Figure 2-3**). The unit is encompassed by earthen fill deposits of predominantly clay and silt materials from on-site excavations that were used to construct berms and roads surrounding the various impoundments across the Site.

2.3 Geology and Hydrogeology

The information used to describe the hydrogeology is based on the local geology obtained from published sources, hydrogeologic investigation data, and boring data collected from Site

¹ All elevations in this report are referenced to North American Vertical Datum of 1988 (NAVD88) unless otherwise noted.

investigations conducted from 2010 to 2023 [12, 10, 13]. Note that information collected from the adjacent BAP is incorporated into this document where appropriate because it is representative of the Site conditions.

2.3.1 Hydrostratigraphic Units

In addition to CCR, materials at the BPP have been categorized into two hydrostratigraphic units at the FAPS based on stratigraphic relationships, geologic composition, and common hydrogeologic properties. The units, listed from surface downward, are summarized as follows:

- **UU:** Predominantly clay with some silt and minor sand, silt layers, and occasional sand lenses. Includes the lithologic layers identified as the Cahokia Alluvium, Peoria Loess, Equality Formation, and Vandalia Till Member. This unit is composed of unlithified natural geologic materials present above the top of bedrock, ranging in thickness at the Site between 17 and 56 feet. Thin sand seams within the unit and the interface (contact) between the UU and bedrock have been identified as potential migration pathways. No continuous sand seams were observed within or immediately adjacent to the FAPS; however, the sand seams on Site may act as a PMP due to relatively higher hydraulic conductivities. The acronym UU and the materials it contains is synonymous with Upper Groundwater Unit used in previous documents.
- **Bedrock Unit:** This unit is considered the UA. Pennsylvanian and Mississippian-aged bedrock is composed of interbedded shale and limestone bedrock, which underlies and is continuous across the entire Site (**Appendix A**). Review of regional literature [14] indicates that three formations are present at the bedrock surface onsite including (from youngest [eastern portions of site] to oldest [western portion of the site]): Menard Formation; Waltersburg, Vienna, and Tar Springs Formation; and Glen Dean and Hardinsburg Formation. In many of the boring logs from the Site [12], the bedrock is described as highly weathered.

2.3.2 Uppermost Aquifer

Off-site, immediately upgradient and downgradient of the BPP property boundaries, both the shallow glacial deposits and the shallow bedrock have served as a source of water supply [12]. The shallow unlithified deposits off-Site have yielded water through intermittent, discontinuous sand lenses and, in the bedrock, through fractured sandstone and limestone. In general, within the boundaries of the Site, the UU (shallow unlithified deposits) consists of low permeability clays and silts. Within the UU, only thin and intermittent sand lenses are present within predominantly clay deposits; thus, the unlithified materials do not represent a continuous aquifer unit (**Figure 2-4**). Thin, non-continuous sandy deposits (*i.e.*, PMPs) that exist across the Site do not appear to extend to the FAPS as evidenced by soil borings adjacent to the CCR unit in which no sand was observed.

Based on the above, the Bedrock Unit is the only viable aquifer in the vicinity of the Site and was designated as the UA in the Supplemental Hydrogeologic Site Characterization and Groundwater Monitoring Plan [10], consistent with the USEPA definition in Title 40 of the Code of Federal Regulations § 257.53 [15].

The UA at the Site is the shallow Pennsylvanian and Mississippian -aged bedrock that immediately underlies the unlithified deposits. The top of the UA (bedrock surface) is provided in **Figure 2-5**. Based on the geologic information, the top of the aquifer is highest in elevation near the eastern portion of the Old East Fly Ash Pond, with an elevation of approximately 415 feet,

and slopes downward to the west and south to approximately 380 feet near MW-352 and MW-375. The shallow bedrock yields water through interconnected secondary porosity features (e.g., cracks, fractures, crevices, joints, bedding planes, and other secondary openings). The shallow bedrock is the only water-bearing unit that is continuous across the Site. Groundwater in the Pennsylvanian and Mississippian-aged bedrock mainly occurs under semi-confined to confined conditions, with the overlying unlithified unit behaving as the upper confining unit to the UA.

Water quality in the UA (i.e., Pennsylvanian and Mississippian-aged bedrock) decreases with increasing depth as water becomes increasingly mineralized [16]. Further, the ability of the unit to store and transmit water is dependent on the density of bedrock features that contribute to secondary porosities and whether those features are interconnected enough to yield water. Therefore, the lower limit of the UA is the depth at which either the groundwater is mineralized to a point that it is no longer a useable water source, or the secondary porosities do not yield a sufficient volume of groundwater to produce a useable water supply.

2.3.3 Potential Migration Pathways

Thin, non-continuous sandy deposits (i.e., PMPs) appear disseminated across the Site and range from a single locally continuous unsaturated sand seam up to 7.9 feet in thickness to isolated, discontinuous thin seams of 0.2 to 1 feet in thickness. Two overlapping sand seams that appear to be continuous between adjacent borings occur to the west of the Secondary Pond (**Figure 2-4**) and are vertically separated by at least 6 feet of clay. The shallower sand seam, at elevations between 395 to 403 feet NAVD88, is not saturated. In addition to these sand seams identified adjacent to the BAP, the contacts between the unlithified material and bedrock have been identified as a PMP, where horizontal hydraulic conductivity data in Site monitoring wells with screens and/or filter packs across or immediately above the bedrock are higher than the surrounding clays [12].

2.3.4 Regional Bedrock Geology

Bedrock within the vicinity of the BPP varies depending on proximity relative to the Kaskaskia River [17, 18, 19]. Underlying the BPP Site and Cooling Pond and the Kaskaskia River Bottomlands are Pennsylvanian and Mississippian bedrock, which primarily consists of limestone and shale with some sandstone. Bedrock generally occurs within 50 feet of the ground surface; with the uppermost Mississippian bedrock being the Menard Formation (up to 60 feet thick), Tar Springs, Vienna, and Waltersburg units (up to approximately 90 feet thick) and Glen Dean and Hardinsburg Formation which is up to 100 feet thick. These formations consist of variable amounts of shale, mudstone, limestone, and siltstone with minor amounts of sandstone; the Glen Dean and Hardinsburg Formations predominate under the eastern portion of the Site and Cooling Pond, and the Waltersburg, Vienna, and Tar Springs Formations are located under the eastern half of the FAPS and background locations. Areas to the east of the Site are immediately underlain by the Carbondale Formation, which pinches out towards the west.

2.3.5 Water Table Elevation and Groundwater Flow Direction

Historically elevated heads within the pond resulted in migration of impacted water into the UU and UA. Following closure, heads within the pond were predicted to decline over a period of approximately 2-4 years until they reach equilibrium [20].

As indicated in **Section 2.3.2**, the groundwater in the UA is separated from overlying CCR material by the UU, consisting of low permeability material ranging in thickness from 17 feet east

of the FAPS to 56 feet north and west of the FAPS. Groundwater flow in the UU is generally to the west and southwest across the Site, towards the Kaskaskia River (*i.e.*, regional receiving body) (**Figure 2-6**). Similar to groundwater flow in the shallow unlithified materials, flow direction in the bedrock is generally to the west and southwest across the Site (**Figure 2-7**). In the east and central areas of the BAP, groundwater flow in the bedrock is northwest, and in the east area of the FAPS, flow is both southwest to northwest. As groundwater approaches the bedrock valley feature underlying the Secondary and Tertiary Ponds west of the BAP and FAPS, the flow direction veers toward this bedrock surface low. Groundwater elevations exhibit seasonal variation, generally less than 7 feet per year and maintains generally consistent flow directions. Following the initiation of closure and dewatering, groundwater elevations in monitoring wells along the northwest side of the FAPS (MW-366 and MW-390) began to exhibit seasonal variability, while MW-391 had a significant increase in 2017-2018 during closure dewatering activities before returning to historical levels (**Appendix B**). These wells generally occur along a small bedrock peninsula, where bedrock slopes downward, both to the north and south of these locations. South of the FAPS, groundwater elevations in bedrock monitoring wells (MW-350, MW-352, MW-375, and MW-377) exhibit less seasonal variability and have generally declined following closure (**Appendix B**).

Spatially across the FAPS, groundwater elevations range from 370 feet in the southwestern portion of the Site to 450 feet in the eastern portion of the Site (**Table 2-1**). The piezometric head at locations MW-252 and MW-352 are generally above ground surface throughout the year, and MW-152 tends to be above ground surface during the spring.

2.3.5.1 Vertical Hydraulic Gradients

Vertical hydraulic gradients were calculated based on available groundwater elevation data during the March 2016 to August 2023 monitoring period at nested well pairs both within the unlithified deposits (shallow and deep) and between the unlithified deposits and bedrock. Vertical gradients within the UU vary from strong upward gradients (indicating confining and even artesian conditions) to semi-confined conditions with both upward and downward gradients. Vertical gradients between the bedrock and the UU also vary in direction and strength. Results of the vertical hydraulic gradient observations across the Site are included in **Appendix C** and presented below:

- UU (*i.e.*, PMP) to UA:
 - Gradients calculated between MW-104DR (PMP) and MW-304 (UA) were seasonally variable, consistently upward during winter events and consistently downward across summer events.
 - Gradients calculated between MW-158R (PMP) and MW-258 (UA) were consistently downward across monitored events.
 - Gradients calculated between MW-252 (PMP) and MW-352 (UA) were consistently downwards across monitored events.
 - Gradients calculated between MW-150 (PMP) and MW-350 (UA) were consistently downwards across monitored events.
 - Gradients calculated between MW-155 (PMP) and MW-355 (UA) were mostly downward, with some observations of upward gradients.

- Gradients calculated between PZ-182 (PMP) and MW-382 (UA) were slightly downward across most monitored events, with some observations of upward gradients.

2.3.5.2 Impact of Surface Water Bodies on Groundwater Flow

Baldwin Lake (Cooling Pond) is the largest water body in the vicinity of the BPP. The surface water elevation of Baldwin Lake is maintained at approximately 429 to 430 feet. Potentiometric surface elevations of downgradient/side-gradient wells near Baldwin Lake range from 422 to 430 feet. Groundwater flow in the UA generally flows perpendicular to and away from Baldwin Lake across the BAP and FAPS. The Secondary Pond and Tertiary Pond do not appear to be altering groundwater flow direction in the UU or UA. The primary influence of groundwater flow direction in the UU and UA is flow toward the Kaskaskia River, topographic lows, and localized bedrock topographic lows associated with former drainage features.

2.3.6 Hydraulic Conductivities

2.3.6.1 Field Hydraulic Conductivities

Field hydraulic conductivity tests were conducted at the FAPS by Natural Resource Technology during 2014 investigation activities [21]. The results are summarized in **Table 2-2**, and discussed below:

- **CCR:** No field hydraulic conductivity tests were performed within the CCR.
- **UU:** Field hydraulic conductivity tests conducted in wells screened within the UU (MW-104DR, MW-151, MW-152, MW-156, MW-157, MW-161, TPZ-166, MW-252, MW-253, OW-256, OW-257, and MW-262) ranged from 3.5×10^{-7} to 6.8×10^{-4} centimeters per second (cm/s), with a geometric mean of 3.2×10^{-5} cm/s.
- **UA:** Results of field hydraulic conductivity tests conducted in wells screened within the UA (MW-350, MW-352, and MW-355) ranged from 1.7×10^{-6} to 3.5×10^{-5} cm/s, with a geometric mean of 5.0×10^{-6} cm/s.

2.3.6.2 Laboratory Hydraulic Conductivities

Falling head permeability tests (ASTM D5084 Method F) were performed in the laboratory on samples collected during the 2014 investigations [21]. The results are summarized in **Table 2-3** and discussed below.

- **CCR:** Four samples were collected from CCR borings TPZ-163, TPZ-164, TPZ-167, and TPZ-168. Samples were collected in CCR materials at 1.5 to 3.5, 3.0 to 5.0, 29.0 to 30.0, and 3.0 to 5.0 feet below ground surface (bgs), respectively. Laboratory falling head permeability test results for the four CCR samples indicated a geometric mean vertical hydraulic conductivity of 1.6×10^{-4} cm/s with a range of 9.7×10^{-6} to 6.5×10^{-4} cm/s.
- **UU:** Laboratory falling head permeability results of two samples collected from the Cahokia Formation indicated a geometric mean vertical hydraulic conductivity of 1.6×10^{-6} cm/s and ranged from 7.8×10^{-6} to 3.4×10^{-7} cm/s. One sample was collected from the Equality Formation at boring location TPZ-164. Laboratory falling head permeability test results for this sample of the Equality Formation indicated a vertical hydraulic conductivity of 1.3×10^{-6} cm/s. Laboratory falling head permeability results of five samples collected from the Vandalia till indicated a geometric mean vertical hydraulic conductivity of 6.1×10^{-7} cm/s with a range from 6.3×10^{-9} to 4.2×10^{-4} cm/s.

- **Bedrock:** No laboratory hydraulic conductivity tests were performed on bedrock samples.

2.4 Groundwater Monitoring

The proposed monitoring system for the FAPS at the time the exceedances were reported is shown on **Figure 2-8** and consists of three background monitoring wells (MW-304, MW-306, and MW-358) installed in bedrock, nine compliance wells (MW-350, MW-352, MW-366, MW-375, MW-377, MW-383, MW-384, MW-390, and MW-391) installed in bedrock, and six compliance wells (MW-150, MW-151, MW-152, MW-153, MW-252, and MW-253) installed within the unlithified materials, considered to be the PMP.

2.5 Hydrogeologic Conceptual Site Model

The Hydrogeologic Site Characterization Report [22] and information provided above forms the foundation of the FAPS hydrogeological setting. The FAPS overlies a potential recharge area for the underlying transmissive geologic media, which are composed of unlithified deposits (*i.e.*, low permeability clays of the UU and PMP). Recharge migrates downward, into and through the UU and PMP into the UA. Groundwater may also enter the system through the Cooling Pond, Secondary and Tertiary Ponds, the Kaskaskia River, or the many tributary streams located near the FAPS.

Groundwater in the unlithified areas consistently flows east to west towards the Kaskaskia River, with localized variations towards surficial drainage. Groundwater flow in bedrock is northwest in the east and central areas of the BAP, and southwest to northwest on the east area of the FAPS until groundwater reaches the bedrock valley feature underlying the Secondary and Tertiary Ponds west of the BAP and FAPS, at which point the flow direction veers towards this bedrock surface low at the southwestern corner of the Site.

The geologic conceptual model for the Site used for the groundwater modeling [23] consists of the following layers:

- CCR – consisting of primarily fly ash, bottom ash, and boiler slag, within the limits of the BAP and FAPS.
- UU:
 - Upper silty clay - composed of the Cahokia Formation, Peoria Loess, and Equality Formation.
 - PMP – Thin, non-continuous sandy deposits disseminated across the Site.
 - Lower silty clay – Vandalia Till
- Decomposed Bedrock – decomposed interbedded shale and limestone bedrock of the UA at the contact between the Vandalia Till and deep bedrock.
- Deep Bedrock – Deep competent bedrock of the UA yielding small amounts of water from interconnected pores, cracks, fractures, crevices, joints, and bedding planes.

The United States Geological Survey (USGS) National Map places the BPP within the lower Kaskaskia watershed subbasin (Hydrologic Unit Code 07140204) [24]. The FAPS hydrogeologic conceptual site model (CSM) extent is bounded by a hydrological catchment (watershed) divide to the west based on watershed data from USGS. Kaskaskia River is the receiving body of water for surface water.

Precipitation infiltrates and recharges the groundwater table throughout the Site and upgradient. Groundwater in the UU migrates downward into the clay and discontinuous sands of the Cahokia Formation, Peoria Loess, and Equality Formation. Where these sands are present, they are considered a PMP for groundwater adjacent to the FAPS and localized lateral migration of groundwater may occur. The weathered bedrock of the UA is separated from the PMP sands and the base of CCR in the FAPS by the laterally continuous low permeability UU (Vandalia Till). The bedrock in the vicinity of the FAPS yields small amounts of water from interconnected pores, cracks, fractures, crevices, joints, and bedding planes. The shallow bedrock is the only water-bearing unit that is continuous across the Site. Shallow sandstone and creviced limestone may yield small supplies in some areas, but water quality becomes poorer (*i.e.*, highly mineralized) with increasing depth.

Based on the geology and hydrogeology, monitoring wells at the FAPS can be separated into four distinct groupings which exhibit similar geologic and hydraulic characteristics. Monitoring well groupings are summarized as follows:

- UU/PMP wells: shallow wells (less than 40 feet bgs) screened in low to moderate permeability materials (generally $\leq 10^{-5}$ cm/s) downgradient of the FAPS including MW-150, MW-151, MW-152, MW-153, MW-252, MW-253. Based on the water levels measured within the FAPS, UU/PMP wells are downgradient of the FAPS.
- Eastern UA wells: wells located on the eastern half of the FAPS (including background wells MW-304, MW-306, and MW-358; and northern downgradient wells MW-383, and MW-384) where the top of the UA is slightly shallower (approximately 30 to 50 feet bgs). Groundwater flow directions indicate these wells are currently upgradient of the former drainage feature that was present prior to construction of the FAPS. Groundwater elevations in MW-383 and 384 exhibit limited seasonal variability and have generally declined following dewatering and closure.
- Northwest UA wells: wells located along the northwest side of the FAPS (MW-366, MW-390, and MW-391) where the top of the UA is slightly deeper (approximately 40 to 60 feet bgs), but the bedrock surface resembles a peninsula, with the surface sloping down both north towards the secondary pond and south towards the former drainage feature. Groundwater flow directions indicate these wells are at a position where flow begins to converge toward the bedrock low, and represents groundwater from the western portion of the FAPS. Groundwater elevations at MW-366 and MW-391 begin to show seasonal variability following initiation of dewatering and closure in 2017-2018. Elevations at MW-391 spiked significantly between 2017 and 2018 to levels consistent with the UU/PMP wells, suggesting that a connection between these units may have been present or created during construction dewatering and management of water.
- Southern UA wells: wells located along the southern boundary and also southwest of the FAPS (MW-350, MW-352, MW-374, MW-375, and MW-377) where the top of the UA is slightly deeper (approximately 40 to 60 feet bgs), and the wells are in a location where the bedrock surface is sloping to the south. Groundwater elevations measured in these wells show little seasonal variability and overall have declined slightly since dewatering and closure was initiated in 2017-2018.

3. OCCURRENCE AND DISTRIBUTION OF GROUNDWATER EXCEEDANCES (EXTENT)

As described in Section 1, exceedances from sample events E001, E002, and E003, performed at the FAPS, and for which an ASD was not completed, include the following parameters and wells by hydrostratigraphic unit:

- Detected UU/PMP Exceedances:
 - Boron at MW-150, and MW-152
 - Sulfate at MW-150
- Detected UA (Bedrock Unit) Exceedances:
 - Boron at MW-391

The extents of exceedances discussed below were defined using existing monitoring wells, including wells present onsite (**Table 3-1**) that may not be included in the 35 I.A.C. § 845 monitoring program.

3.1 Additional Investigation to Define Nature and Extent

Solid phase data were evaluated to assess potential geological sources of exceedance parameters and to inform the GCSM (discussed further in **Section 4**). Solid phase data were not collected from the CCR source material prior to completion of closure of the unit in 2020. Four borings were advanced in 2022 and 2023 at the FAPS and solid samples were collected from both the UA and the UU adjacent to paired monitoring wells MW-150 and MW-350 and solid samples were collected from the UA adjacent to three monitoring wells (MW-352, MW-366, and MW-391). Borings were also advanced adjacent to four additional locations at the BPP BAP, with solids collected from the UU and UA at three locations (MW-358, MW-392, and MW-393) and solids collected from the UU at MW-394. These solids were characterized using a variety of analytical techniques including the following:

- Loss on Ignition;
- Total Organic Carbon Analysis;
- Cation Exchange Capacity Analysis;
- EPA 6010A for Total Metals (35 I.A.C. § 845.600 parameters plus aluminum, bismuth, copper, iron, magnesium, manganese, nickel, potassium, silver, strontium, tin, titanium, uranium, vanadium, yttrium, and zinc and boron via Bulk Characterization);
- EPA 6010B for 6-step sequential extraction (boron and iron; on only MW-358, MW-392, MW393, and MW-394));
- Bulk Mineralogy by Rietvelt X-ray diffraction analysis; and,
- Bulk Elemental Composition by X-ray fluorescence analysis.

Historically, an offsite investigation was completed to evaluate the potential migration of boron and sulfate to the south and southwest of the FAPS ([25], **Appendix D**). The investigation included the installation of eight temporary piezometers to evaluate concentrations of boron, sulfate, and total dissolved solids downgradient of UU wells MW-150 and MW-152.

3.2 Extents in the Upper Unit (PMP)

Exceedances are identified quarterly following comparison to the GWPSs described in 35 I.A.C. § 845.600. The LCLs vary as the dataset is updated to include additional quarterly events (**Table 3-2**). The discussion below includes ranges of concentrations measured in wells with exceedances, because there is no single value for statistical evaluations.

3.2.1 Boron

Boron concentrations in monitoring wells MW-150 and MW-152 resulted in identified exceedances of the GWPS (2.16 mg/L, **Figure 3-1**). The concentrations and extent of boron exceedances at the FAPS are summarized as follows:

- MW-150 – Exceedances were reported in all three compliance sampling events with concentrations ranging from 2.87 to 4.37 mg/L. The primary source and lateral and downgradient extent of boron concentrations in proximity to MW-150 is currently being evaluated. In March 2012, dissolved concentrations of boron and sulfate in temporary piezometer BPZ7 were reported at 0.252 mg/L and 215 mg/L, respectively (**Appendix D**). Concentrations of boron and sulfate in MW-150 during the same timeframe were 0.56 mg/L and 584 mg/L, respectively. The extent is ultimately limited by an oxbow of the Kaskaskia River approximately 900 feet to the west/southwest of MW-150 in connection with the Kaskaskia River. Samples collected within the river [3] indicate boron concentrations are less than 0.05 mg/L.

Vertically, the extent of boron is limited by low hydraulic conductivity of the UU with a range of 6.3×10^{-9} to 4.2×10^{-4} cm/s (**Section 2.3.6**). The concentration of boron at MW-150 is also defined vertically by MW-350, a deeper well nested with MW-150 and screened in the UA. At MW-350 the maximum measured concentration of boron was 0.585 mg/L, which was measured during E002.

- MW-152 – Concentrations resulting in a GWPS exceedance determination were only measured in MW-152 during compliance sampling event E002, with a reported result for boron of 9.09 mg/L (**Table 3-2²**). The concentrations of boron at this location are highly variable and have been attributed to seasonal groundwater elevations (**Figure 3-2**). Concentrations are lowest in the spring when groundwater elevations are higher, and higher in the fall when groundwater elevations are low. The downgradient extent is bounded to the west by monitoring well MW-151, with a maximum concentration of 0.89 mg/L during E003 (**Table 3-3**). In March 2012, concentrations of dissolved boron southwest (BPZ4) and southeast (BPZ1) of MW-152 were 0.0435 mg/L and 0.0096 mg/L, respectively (**Appendix D**). The concentration of dissolved boron at MW-152 during the same time frame was approximately 18 mg/L. The observed reduction in concentrations at MW-152 indicates that higher concentrations are not expected off-Site.

Vertically, the extent of boron is limited by low hydraulic conductivity of the UU with a range 6.3×10^{-9} to 4.2×10^{-4} cm/s (Section 2.3.6). MW-152 is also defined vertically by monitoring wells MW-252 and MW-352, deeper wells nested with MW-152 and screened below MW-152 in the UU and UA, respectively. MW-252 and MW-352 concentrations were not identified as exceedances following comparison to the GWPSs described in 35 I.A.C. § 845.600.

² The negative LCL calculated for boron at MW-152 at E003 represents the confidence interval around the mean. When the standard deviation (i.e., variability) of data is high, the calculated lower confidence level may be less than 0.

3.2.2 Sulfate

Sulfate concentrations in monitoring well MW-150 resulted in identified exceedances of the GWPS (762 mg/L). The concentrations and extent of the sulfate exceedance at the FAPS are summarized as follows (**Figure 3-1**):

- MW-150 – Exceedances were reported in compliance sampling events E001 and E002. The primary source, transport mechanism, and lateral and downgradient distribution of sulfate concentrations in proximity to MW-150 are currently being evaluated. Concentrations of dissolved sulfate in MW-150 have increased from 584 mg/L to 1,050 mg/L between 2012 and 2023. In BPZ7 in 2012, the concentration of sulfate was 215 mg/L (**Appendix D**). The downgradient extent is ultimately limited by an oxbow of the Kaskaskia River, approximately 900 feet to the west/southwest of MW-150.

Vertically, the extent of sulfate is limited by low hydraulic conductivity of the UU, with a range 6.3×10^{-9} to 4.2×10^{-4} cm/s (Section 2.3.6). Concentrations of sulfate in MW-150 is also defined vertically by MW-350, a deeper well nested with MW-150 screened in the UA. The maximum concentration of sulfate detected in MW-350 was 102 mg/L (**Table 3-3**), which was detected during E002.

3.3 Extent in Uppermost Aquifer (Bedrock Unit)

Exceedances are identified quarterly following comparison to the GWPSs described in 35 I.A.C. § 845.600. The LCLs vary as the dataset is updated to include additional quarterly events (**Table 3-2**). The discussion below includes ranges of concentrations measured in wells with exceedances, because there is no single value for LCLs.

3.3.1 Boron

Concentrations of boron resulted in exceedances of the GWPS (2.16 mg/L) at UA well MW-391 (**Figure 3-3**). Concentrations and the extent of boron at this location is summarized as follows:

- MW-391 - Exceedances were determined in all three compliance sampling events. The lateral and downgradient extent of boron concentrations in proximity to MW-391 are limited by the Secondary and Tertiary Ponds immediately adjacent to the monitoring well to the west. Downgradient extent is additionally bound by MW-350 with a maximum measured concentration of 0.585 mg/L boron detected during E002.

Vertically, the extent of the boron impacts are limited by the low permeability shale bedrock which decreases with depth as the secondary porosities do not yield a sufficient volume of groundwater to produce a useable water supply. In addition, water quality decreases with increasing depth as water becomes increasingly mineralized [16].

4. GEOCHEMICAL CONCEPTUAL SITE MODEL (NATURE)

A GCSM was developed to describe the conditions of the groundwater in the vicinity of the BPP FAPS in support of the CMA and is summarized here (full analysis presented in **Appendix E**). The GCSM describes the geochemical processes that contribute to the mobilization, distribution, and attenuation of chemicals in the environment. As discussed in previous sections, the exceedances observed at the FAPS include boron and sulfate.

The GCSM includes two hydrostratigraphic units: the shallow UU PMP and the deeper UA. The primary source of boron and sulfate to groundwaters of the UA and UU PMP within the monitoring system is the FAPS CCR source water. CCR source water samples, collected from the porewater monitoring wells screened within the CCR materials at the FAP, and the FAP relationship to hydrogeological patterns at the Site, are the primary factors defining the distribution of boron and sulfate concentrations at the Site. Boron was identified within UA solids at concentrations that suggest that aquifer solids could provide an additional potential natural geogenic source of boron to groundwater, and groundwater from background wells consistently exhibited boron concentrations consistent with a natural geogenic source. The observation of pyrite within solids of shale portions of the UA could provide an additional source of sulfate to groundwater via pyrite oxidation, as pyrite is not expected to be a stable mineral phase under observed groundwater redox conditions and sulfate concentrations at background wells are indicative of a potential additional natural source.

Boron and sulfate in the groundwater system may be attenuated via surface complexation reactions within portions of the UU PMP and the UA. Conditions within groundwater from both the UA and UU PMP are typically predicted to favor amorphous iron oxide stability at most locations, and the presence of iron oxides in some Site solids supporting the occurrence of this mechanism. Limited variability in pH or redox conditions is observed between upgradient background and downgradient locations. Boron may be further attenuated via interactions with clay minerals, which are observed in solids across both the UU and UA. The observation of gypsum, although limited to the shale bedrock portions of the UA, indicates that precipitation of gypsum may be another potential attenuation mechanism for sulfate at locations near the FAPS.

5. COMBINED GEOCHEMICAL AND HYDROGEOLOGIC CONCEPTUAL SITE MODELS

5.1 Boron Conceptual Site Model

The CSM describing current conditions at the FAPS combining the hydrogeologic and geochemical CSMs for boron is as follows. Water that may come into contact with CCR in the FAPS becomes porewater within the unlined CCR unit. Porewater (i.e., CCR source water) containing elevated concentrations of boron mixes with groundwater underlying and adjacent to the UU. Groundwater within the UU/PMP in the vicinity of the FAPS travels horizontally outward from the FAPS, migrating toward the Secondary Pond or the drainage ditch to the south, but ultimately toward the Kaskaskia River. Groundwater may also migrate vertically into the clay of the UU that separates the UU from the UA. If groundwater reaches the UA, it migrates slowly in the formation due to the low permeability of the shale bedrock. Boron concentrations are attenuated physically through dilution and dispersion; and may be chemically attenuated via surface complexation to iron oxides and clay minerals, which are observed in solids within both the UU and UA.

The distribution of boron exceedances is being further refined but the extent is currently defined by a combination of wells in the UU and UA with concentrations below the GWPS and ultimately by the concentrations observed in surface water [3]. The presence or absence of exceedances can be attributed to variability in the geology and porewater concentrations, changes in groundwater elevations and flow directions, and the extent of water migration between the UU and UA.

5.2 Sulfate Conceptual Site Model

The CSM describing current conditions at the FAPS combining the hydrogeologic and geochemical CSMs for sulfate is as follows. Water that may come into contact with CCR in the FAPS becomes porewater within the unlined CCR unit. Porewater containing elevated concentrations of sulfate mixes with groundwater underlying and adjacent to the UU. Groundwater within the UU/PMP in the vicinity of the FAPS travels horizontally outward from the FAPS, migrating toward the Secondary Pond or the drainage ditch to the south, but ultimately toward the Kaskaskia River. Groundwater may also migrate vertically into the clay of the UU that separates the UU from the UA. If it reaches the UA, it migrates slowly in the formation due to the low permeability of the shale bedrock. Sulfate concentrations are attenuated physically through dilution and dispersion and may be geochemically attenuated via surface complexation to iron oxides within portions of the UU PMP and the UA. The observation of gypsum, although limited to the shale bedrock portions of the UA, indicates that precipitation of gypsum may be another potential attenuation mechanism for sulfate at locations near the FAPS.

The limit of sulfate exceedances is being further evaluated but is currently defined by a combination of wells in the UU and UA with concentrations below the GWPS and ultimately by the concentrations observed in surface water [3]. The presence or absence of exceedances can be attributed to variability in the geology and CCR source water (porewater) concentrations, changes in groundwater elevations and flow directions, and the extent of water migration between the UU and UA.

6. CONCLUSIONS AND FUTURE ACTIVITIES

In accordance with 35 I.A.C. § 845.650(d)(1), the nature and extent of GWPS exceedances of boron and sulfate have been described in sufficient detail to support a complete and accurate assessment of the corrective measures necessary to effectively clean up all releases from the FAPS.

As discussed in Sections 3.3.1 and 3.3.2, additional refinement of the distribution of boron and sulfate near MW-150 and boron near MW-152 is ongoing in UU wells. Additional investigation is planned to further evaluate the boron exceedance in MW-391 as well as understand the mechanisms that potentially influence groundwater elevations and boron concentrations. Activities include:

- Evaluation of MW-391 to determine if the well has been compromised and identify potential mechanisms causing the rapid water elevation shifts during dewatering and closure.
- Sampling of additional piezometers in the UU near MW-150 and MW-152.
- Survey and water elevation monitoring of the drainage ditch near MW-152 to further evaluate how the ditch may interact with shallow groundwater.
- Pending access agreement with adjacent property owner, installation of additional wells south of the western limit of the FAPS to evaluate potential migration of boron and sulfate in the UU near MW-150.

Findings from sampling of these additional wells and other activities will be incorporated into the final Corrective Action Plan Permit application, which will be submitted in 2025.

Boron was selected for modeling source control presented in the Final Closure Plan and is considered a surrogate for sulfate. For modeling purposes, it was assumed that boron would not significantly sorb or chemically react with aquifer solids (soil adsorption coefficient was set to 0 milliliters per gram) which is a conservative estimate for predicting contaminant transport times in the model. Additional geochemical modeling will be completed to evaluate how sorption to solid phases may affect sulfate mobility and therefore the time to reach the GWPS for this parameter.

7. REFERENCES

- [1] Ramboll Americas Engineering Solutions, Inc. (Ramboll), "35 I.A.C. § 845 Corrective Measures Assessment, Fly Ash Pond System, Baldwin Power Plant, Baldwin, Illinois, IEPA IF: W1578510001-01/02/03," April 24, 2024.
- [2] Geosyntec Consultants, Inc., "Alternative Source Demonstration, Baldwin Power Plant Fly Ash Pond System (Unit ID #605), IEPA ID: W1578510001-01, -02, -03, 35 I.A.C. 845.600," February 6, 2024.
- [3] Hanson Professional Services Inc, "Antidegradation Assessment for Management of Coal Combustion Residuals Impoundment Waters Baldwin Energy Complex, Dynegy Midwest Generation, LLC," 2017.
- [4] Ramboll Americas Engineering Solutions, Inc., "35 I.A.C. § 845.610(B)(3)(D) Groundwater Monitoring Data and Detected Exceedances, 2023 Quarter 2, Fly Ash Pond System, Baldwin Power Plant, Baldwin, Illinois," August 28, 2023.
- [5] Ramboll Americas Engineering Solutions, Inc., "35 I.A.C. § 845.610(B)(3)(D) Groundwater Monitoring Data and Detected Exceedances, 2023 Quarter 3, Fly Ash Pond System, Baldwin Power Plant, Baldwin, Illinois," December 10, 2023.
- [6] Ramboll Americas Engineering Solutions, Inc., "35 I.A.C. § 845.610(B)(3)(D) Groundwater Monitoring Data and Detected Exceedances, 2023 Quarter 3, Fly Ash Pond System, Baldwin Power Plant, Baldwin, Illinois," March 16, 2024.
- [7] Illinois Environmental Protection Agency, "Re: Baldwin Power Plant Fly Ash Pond System," March 7, 2024.
- [8] AECOM, "RE: History of Construction, USEPA Final Rule, 40 C.F.R. § 257.73(c), Baldwin Energy Complex, Baldwin, Illinois," October, 2016.
- [9] AECOM, "Closure and Post-Closure Care Plan for the Baldwin Fly Ash Pond System. Baldwin Energy Complex. Baldwin, Illinois," March 31, 2016.
- [10] Natural Resource Technology, Inc., "Supplemental Hydrogeologic Site Characterization and Groundwater Monitoring Plan. Baldwin Fly Ash Pond System. Baldwin Energy Complex, Baldwin, IL," March 31, 2016.
- [11] Luminant, "Baldwin Energy Complex; Old East Fly Ash Pond, East Fly Ash Pond, West Ash Pond, Notification of Completion of Closure," December 17, 2020.
- [12] Ramboll Americas Engineering Solutions, Inc., "Hydrogeologic Site Characterization Report, Revision 1. Bottom Ash Pond, Baldwin Power Plant, Baldwin, Illinois. Dynegy Midwest Generation, LLC," August 1, 2023.
- [13] Ramboll Americas Engineering Solutions, Inc., "Hydrogeologic Site Characterization Report. Baldwin Bottom Ash Pond. Baldwin Power Plant. Baldwin, Illinois," October 25, 2021.
- [14] I. S. G. Survey, "Bedrock Geology of Baldwin Quadrangle, Randolph and St. Clair Counties, Illinois," 2018.
- [15] United States Environmental Protection Agency, "Code of Federal Regulations, Title 40, Chapter I, Subchapter I, Part 257, Subpart D, Standards for the Disposal of Coal Combustion Residuals in Landfills and Surface Impoundments, effective April 17, 2015. Accessed from URL <https://www.ecfr.gov/current/ti>," April 17, 2015.

- [16] W. A. Pryor, "Groundwater Geology in Southern Illinois: A Preliminary Geologic Report. Illinois State Geological Survey, Circular 212.," Urbana, Illinois, 1956.
- [17] R. C. Berg and J. P. and Kempton, "Stack-Unit Mapping of Geologic Materials in Illinois to a Depth of 15 Meters. Illinois State Geological Survey, Circular 542.," Champaign, Illinois, 1988.
- [18] J. A. Devera, "Geology of Red Bud Quadrangle, Randolph, Monroe and St. Clair Counties, Illinois. Illinois State Geological Survey, Illinois Preliminary Geologic Map, IPGM Red Bud-G, 1:24,000," 2004.
- [19] D. A. a. N. D. W. Grimley, "Surficial Geology of Red Bud Quadrangle, Randolph, Monroe and St. Clair Counties, Illinois. Illinois State Geological Survey, Illinois Geologic Quadrangle Map, IGQ Red Bud-SG," 2010.
- [20] Natural Resource Technology, Inc., "Hydrostatic Modeling Report, Baldwin Fly Ash Pond System, Baldwin Energy Complex, Baldwin, Illinois.," March 24, 2016.
- [21] Natural Resource Technology, "Groundwater Quality Assessment and Phase II Hydrogeologic Assessment. Baldwin Ash Pond System. Baldwin Energy Complex. Baldwin, Illinois. Dynegy Midwest Generation, LLC.," June 11, 2014.
- [22] Ramboll Americas Engineering Solutions, Inc., "Hydrogeologic Site Characterization Report. Newton Power Plant, Primary Ash Pond, Newton, Illinois. Illinois Power Generating Company.," October 25, 2021.
- [23] Ramboll Americas Engineering Solutions, Inc., "Groundwater Monitoring Report, Baldwin Power Plant, Bottom Ash Pond, Baldwin, Illinois. Dynegy Midwest Generation, LLC.," August 1, 2023.
- [24] U. S. G. Survey, USGS Water Resources Links for 07140204 - Lower Kaskaskia, U.S. Geological Survey, 2019.
- [25] KELRON Environmental, "Off-Site Groundwater Quality Results, Baldwin Energy Complex, Baldwin, Illinois," April 16, 2012.

TABLES

DRAFT

Table 2-1. Summary of Groundwater Elevations
Nature and Extent Report
Baldwin Power Plant
Fly Ash Pond System
Baldwin, Illinois

| DATE | 1/10/2023 | 2/20/2023 | 3/13/2023 - 3/15/2023 | 4/16/2023 | 5/16/2023 | 5/17/2023 - 5/19/2023 | 5/22/2023 - 5/23/2023 | 6/16/2023 - 6/22/2023 | 7/10/2023 | 7/16/2023 | 8/2/2023 - 8/3/2023 | 8/7/2023 | 9/30/2023 | 10/30/2023 | 11/6/2023 - 11/7/2023 | 12/13/2023 |
|----------|-----------|-----------|-----------------------|-----------|-----------|-----------------------|-----------------------|-----------------------|-----------|-----------|---------------------|----------|-----------|------------|-----------------------|------------|
| LOCATION | | | | | | | | | | | | | | | | |
| MW-104DR | 446.91 | -- | 447.67 | -- | -- | -- | 445.34 | -- | -- | -- | 441.67 | -- | -- | 438.82 | 438.71 | -- |
| MW-104SR | 446.74 | -- | 447.62 | -- | -- | -- | 445.29 | -- | -- | -- | 441.64 | -- | -- | -- | 438.59 | -- |
| MW-150 | -- | -- | 378.83 | 379.52 | 378.08 | 377.87 | -- | 376.63 | -- | 375.98 | 375.89 | -- | -- | 375.92 | 376.01 | 376.34 |
| MW-151 | -- | -- | 395.30 | -- | -- | 394.38 | -- | -- | 394.18 | -- | 391.89 | -- | -- | 392.38 | 392.49 | 392.51 |
| MW-152 | -- | -- | 419.44 | -- | -- | 418.49 | -- | -- | -- | -- | 416.80 | -- | 416.92 | 416.80 | 417.05 | 417.13 |
| MW-153 | -- | -- | 434.85 | 435.60 | 433.24 | -- | 432.81 | 430.17 | 429.17 | 429.09 | 429.48 | -- | 428.56 | 427.83 | 427.74 | 427.69 |
| MW-154 | -- | -- | -- | -- | -- | -- | -- | -- | -- | -- | -- | -- | -- | -- | 372.70 | -- |
| MW-155 | -- | -- | 376.21 | -- | -- | -- | 375.88 | -- | -- | -- | -- | 373.60 | -- | -- | 371.64 | -- |
| MW-252 | -- | -- | 420.39 | 423.30 | -- | 422.94 | -- | -- | -- | -- | 422.26 | -- | -- | 421.77 | 421.61 | 421.68 |
| MW-253 | -- | -- | 433.51 | 435.50 | 432.93 | -- | 432.24 | -- | -- | -- | 429.69 | -- | -- | 428.77 | 423.19 | 428.37 |
| MW-304 | 445.57 | 445.84 | 445.97 | 445.91 | 445.89 | -- | 445.96 | 445.66 | -- | 445.5 | 445.65 | -- | 445.18 | 445.24 | 445.00 | 445.15 |
| MW-306 | 435.31 | 435.97 | 436.07 | 436.19 | 436.09 | -- | 436.06 | 435.75 | -- | 435.61 | 435.68 | -- | -- | 433.21 | 435.14 | 435.04 |
| MW-350 | -- | -- | 372.71 | 373.27 | 373.04 | 373.06 | -- | 373.06 | -- | 372.83 | 372.91 | -- | 372.69 | 372.47 | 368.02 | 371.87 |
| MW-352 | -- | -- | 424.39 | -- | -- | 421.77 | -- | -- | 419.72 | -- | 411.55 | -- | -- | 418.76 | 407.37 | 414.59 |
| MW-355 | -- | -- | 371.11 | -- | -- | -- | 370.71 | -- | -- | -- | -- | 368.43 | -- | 363.75 | 368.78 | -- |
| MW-358 | 386.37 | 442.61 | 442.83 | 399.36 | 412.48 | 412.81 | -- | 413.89 | -- | 421.07 | 424.63 | -- | 422.57 | 427.56 | 420.88 | 415.65 |
| MW-366 | -- | -- | 410.28 | -- | 411.89 | -- | -- | -- | -- | -- | 406.82 | -- | -- | 406.07 | 405.83 | -- |
| MW-375 | -- | -- | 391.25 | -- | -- | 390.84 | -- | -- | -- | -- | 389.49 | -- | -- | 387.81 | 385.64 | 387.37 |
| MW-377 | -- | -- | 415.80 | -- | -- | -- | 415.71 | -- | -- | -- | 415.19 | -- | -- | 414.52 | 414.30 | 414.30 |
| MW-383 | 440.48 | -- | 441.17 | 439.08 | 440.05 | -- | 440.33 | 436.30 | -- | 439.05 | 439.57 | -- | 439.08 | 439.37 | 433.41 | 438.70 |
| MW-384 | 444.14 | -- | 444.80 | 444.34 | 444.16 | -- | 444.26 | 443.77 | -- | 443.79 | 443.85 | -- | -- | 443.25 | 452.76 | 442.75 |
| MW-390 | 420.46 | -- | 422.75 | -- | -- | 421.86 | -- | -- | -- | -- | 419.17 | -- | -- | 418.03 | 418.26 | 418.06 |
| MW-391 | -- | -- | 367.93 | 365.58 | 365.76 | 365.89 | -- | 360.73 | -- | 360.94 | 361.21 | -- | 360.35 | 358.63 | 355.48 | 355.81 |
| OW-156 | 421.25 | -- | 424.14 | -- | 421.65 | -- | -- | -- | -- | -- | -- | -- | -- | 417.67 | 418.21 | -- |
| OW-157 | 426.92 | -- | 427.48 | -- | 426.59 | -- | -- | -- | -- | -- | -- | -- | -- | 423.12 | 423.80 | -- |

Notes:
-- = Not Measured
All groundwater elevation data are presented relative to the North American Vertical Datum 1988 (NAVD88).

Table 2-2. Field Horizontal Hydraulic Conductivities

Nature and Extent Report

Baldwin Power Plant

Fly Ash Pond System

Baldwin, Illinois

| Monitoring Well Number | Depth Interval Tested (feet) | Analysis Method | Lithologic Layer | Primary Lithologies within Screened Well Interval | Horizontal Hydraulic Conductivity (cm/s) |
|--|------------------------------|-------------------------|--|--|--|
| Upper Unit | | | | | |
| MW-104DR | 23.2 - 28.2 | Bouwer-Rice | Vandalia Till Member | Sand (fine-medium), Sandy Clay, and Silty Clay | 6.8E-04 |
| MW-151 | 6.1 - 15.8 | Bouwer-Rice | Cahokia Formation | Sandy Clay, Silty Clay, and Clay | 1.1E-05 |
| MW-152 | 7.5 - 16.7 | Bouwer-Rice | Equality Formation | Clay, Sand, and Sandy Clay | 7.0E-05 |
| MW-161 | 23.3 - 32.8 | Bouwer-Rice | Equality Formation | Silty Clay, Sand with Silt | 8.1E-05 |
| MW-252 | 44.4 - 49.0 | Bouwer-Rice | Vandalia Till Member | Clay | 1.9E-06 |
| MW-253 | 29.9 - 34.5 | Bouwer-Rice | Vandalia Till Member | Clay, shaley | 3.5E-07 |
| MW-262 | 42.1 - 46.6 | Bouwer-Rice | Vandalia Till Member | Sand with Silt, Sandy Silt, Silty Clay, and Sand (fine-coarse) | 6.0E-04 |
| OW-156 | 7.9 - 17.2 | Bouwer-Rice | Equality Formation | Clay and Silty Clay | 4.3E-05 |
| OW-157 | 7.8 - 17.1 | Bouwer-Rice | Equality Formation | Clay with Silt, Clay with Sand, and Clay | 1.3E-04 |
| OW-256 | 28.0 - 32.5 | Bouwer-Rice | Vandalia Till Member | Silty Clay, Sand (fine-medium) | 2.2E-04 |
| OW-257 | 34.0 - 38.5 | Bouwer-Rice / KGS Model | Vandalia Till Member | Silty Clay, Shale and Clay | 3.3E-06 |
| TPZ-166 | 15.3 - 24.7 | Bouwer-Rice | Vandalia Till Member | Silty Clay | 1.9E-05 |
| Geometric Mean Hydraulic Conductivity | | | | | 3.2E-05 |
| Uppermost Aquifer | | | | | |
| MW-350 | 41.6 - 46.2 | Bouwer-Rice | Mississippian Bedrock | Limestone, massive, hard to very hard; RQD = 96% (Excellent) | 2.1E-06 |
| MW-352 | 67.9 - 72.5 | Bouwer-Rice | Pennsylvanian or Mississippian Bedrock | Limestone, medium hard to hard; RQD = 57% (Fair) | 1.7E-06 |
| MW-355 | 27.4 - 32.0 | Bouwer-Rice | Mississippian Bedrock | Limestone, medium soft, fossiliferous; RQD = 57% (Fair) | 3.5E-05 |
| Geometric Mean Hydraulic Conductivity | | | | | 5.0E-06 |

[O: JJW 4/12/21, U: CJC 4/15/24, C: EGP 4/15/24]

Notes:

cm/s = centimeters per second

Reference:

Bouwer-Rice = Bouwer and Rice Analytical Method for Unconfined Aquifers, 1976. (note: also used for Confined Aquifers)

KGS Model = KGS overdamped slug test analysis model (Hyder et al., 1994)

Data source was the Groundwater Quality Assessment and Phase II Hydrogeologic Investigation (NRT, 2014)

Table 2-3. Laboratory Vertical Hydraulic Conductivities

Nature and Extent Report

Baldwin Power Plant

Fly Ash Pond System

Baldwin, Illinois

| Monitoring Well Number | Depth Interval Tested (feet) | Analysis Method | Lithologic Layer | Primary Lithologies within Sample Interval | Horizontal Hydraulic Conductivity (cm/s) |
|--------------------------|------------------------------|-----------------------------|---------------------------------------|---|--|
| Fill Unit (CCR) | | | | | |
| TPZ-163 | 1.5 - 3.5 | Geotechnology (2013) | Ash Pond System: Fly Ash / Bottom Ash | Ash (USCS classification: Silty Sand, fine grained) | 2.5E-04 |
| TPZ-164 | 3.0 - 5.0 | Geotechnology (2013) | Ash Pond System: Bottom Ash | Ash (USCS classification: Sandy Silt, fine grained sand) | 6.5E-04 |
| TPZ-167 | 29.0 - 30.0 | Geotechnology (2013) | Ash Pond System: Fly Ash | Ash (USCS classification: Silt) | 9.7E-06 |
| TPZ-168 | 3.0 - 5.0 | Geotechnology (2013) | Ash Pond System: Fly Ash | Ash (USCS classification: Sandy Silt, fine-medium grained sand) | 4.2E-04 |
| | | | | Geometric Mean Hydraulic Conductivity | 1.6E-04 |
| Upper Unit | | | | | |
| MW-154 | 8.0 - 9.2 | Shively Geotechnical (2010) | Cahokia Formation | Sandy Clay with Gravel | 7.8E-06 |
| MW-252 | 44.0 - 46.0 | Shively Geotechnical (2010) | Vandalia Member | Clay | 6.3E-09 |
| MW-262 | 33.5 - 35.5 | Geotechnology (2013) | Vandalia Member | Clay | 9.9E-09 |
| Uppermost Aquifer | | | | | |
| MW-350 | 18.0 - 20.0 | Shively Geotechnical (2010) | Cahokia Formation | Clay | 3.4E-07 |
| TPZ-163 | 28.0 - 30.0 | Geotechnology (2013) | Vandalia Member | Clay, trace fine sand | 4.2E-04 |
| TPZ-164 | 10.0 - 12.0 | Geotechnology (2013) | Equality Formation | Clay | 1.3E-06 |
| TPZ-165 | 8.0 - 10.0 | Geotechnology (2013) | Vandalia Member | Clay, trace sand | 5.3E-06 |
| TPZ-167 | 32.0 - 34.0 | Geotechnology (2013) | Vandalia Member | Clay with sand | 6.2E-07 |
| | | | | Geometric Mean Hydraulic Conductivity | 8.6E-07 |

[O: JJW 4/12/21, U: CJC 4/15/24, C: EGP 4/15/24]

Notes:

cm/s = centimeters per second

Reference:

Shively Geotechnical (2010): see Appendix C of Baldwin Bottom Ash Pond System Hydrogeologic Characterization Report, Revision 1 (Ramboll, 2023)

Geotechnology (2013): see Appendix C of Baldwin Bottom Ash Pond System Hydrogeologic Characterization Report, Revision 1 (Ramboll, 2023)

Data source was the Groundwater Quality Assessment and Phase II Hydrogeologic Investigation (NRT, 2014)

Table 3-1. Monitoring Well Construction Details

Nature and Extent Report
Baldwin Power Plant
Fly Ash Pond System
Baldwin, Illinois

| Location | HSU | Date Constructed | Top of PVC Elevation (ft) | Measuring Point Elevation (ft) | Measuring Point Description | Ground Elevation (ft) | Screen Top Depth (ft bgs) | Screen Bottom Depth (ft bgs) | Screen Top Elevation (ft) | Screen Bottom Elevation (ft) | Well Depth (ft bgs) | Bottom of Boring Elevation (ft) | Screen Length (ft) | Screen Diameter (inches) | Latitude (Decimal Degrees) | Longitude (Decimal Degrees) |
|----------|-----|------------------|---------------------------|--------------------------------|-----------------------------|-----------------------|---------------------------|------------------------------|---------------------------|------------------------------|---------------------|---------------------------------|--------------------|--------------------------|----------------------------|-----------------------------|
| MW-150 | PMP | 2010-09-01 | 396.5 | 396.7 | Top of PVC | 393.8 | 15 | 24.7 | 378.8 | 369.2 | 25.2 | 368.7 | 9.6 | 2 | 38.189401 | -89.878468 |
| MW-151 | PMP | 2010-09-01 | 400.0 | 400.1 | Top of PVC | 397.2 | 6.1 | 15.8 | 391.1 | 381.4 | 16.3 | 380.9 | 9.6 | 2 | 38.188449 | -89.872354 |
| MW-152 | PMP | 2010-09-01 | 425.0 | 425.2 | Top of PVC | 422.2 | 7.5 | 16.7 | 414.7 | 405.5 | 17.2 | 405.0 | 9.3 | 2 | 38.187569 | -89.866764 |
| MW-153 | PMP | 2010-09-01 | 445.7 | 445.8 | Top of PVC | 442.8 | 10.4 | 20 | 432.4 | 422.8 | 20.5 | 422.3 | 9.6 | 2 | 38.185884 | -89.86101 |
| MW-252 | PMP | 2010-09-01 | 425.1 | 425.2 | Top of PVC | 422.3 | 44.4 | 49 | 377.9 | 373.2 | 49.5 | 372.7 | 4.6 | 2 | 38.187563 | -89.866745 |
| MW-253 | PMP | 2010-09-01 | 445.8 | 446.0 | Top of PVC | 442.7 | 29.9 | 34.5 | 412.8 | 408.2 | 35 | 407.7 | 4.6 | 2 | 38.185885 | -89.861026 |
| MW-304 | UA | 2015-10-20 | 455.5 | 455.4 | Top of PVC | 453.0 | 45 | 55 | 408.0 | 398.0 | 55 | 317.6 | 10 | 2 | 38.188332 | -89.853441 |
| MW-350 | UA | 2010-09-01 | 396.8 | 397.0 | Top of PVC | 394.1 | 41.6 | 46.2 | 352.5 | 347.9 | 46.6 | 347.4 | 4.6 | 2 | 38.189416 | -89.878477 |
| MW-352 | UA | 2010-09-01 | 425.0 | 425.2 | Top of PVC | 422.4 | 67.9 | 72.5 | 354.5 | 349.8 | 73 | 348.6 | 4.6 | 2 | 38.187554 | -89.866729 |
| MW-358 | UA | 2022-10-08 | 455.7 | 455.9 | Top of PVC | 453.6 | 80 | 90 | 373.7 | 363.7 | 90 | 363.6 | 10 | 2 | 38.195275 | -89.849417 |
| MW-366 | UA | 2015-12-04 | 425.1 | 425.2 | Top of PVC | 422.5 | 42 | 52 | 380.5 | 370.5 | 52 | 368.2 | 10 | 2 | 38.192191 | -89.872345 |
| MW-375 | UA | 2015-11-06 | 423.1 | 423.2 | Top of PVC | 420.5 | 57 | 67 | 363.5 | 353.5 | 67 | 335.8 | 10 | 2 | 38.189045 | -89.873514 |
| MW-377 | UA | 2015-11-02 | 421.4 | 421.5 | Top of PVC | 418.8 | 46 | 56 | 372.8 | 362.8 | 56 | 360.5 | 10 | 2 | 38.188386 | -89.869742 |
| MW-383 | UA | 2015-12-21 | 459.5 | 459.7 | Top of PVC | 457.2 | 58 | 68 | 399.2 | 389.2 | 68 | 384.2 | 10 | 2 | 38.194913 | -89.858286 |
| MW-384 | UA | 2015-12-18 | 458.9 | 459.1 | Top of PVC | 456.7 | 60.5 | 70.5 | 396.2 | 386.2 | 70.5 | 362.6 | 10 | 2 | 38.191789 | -89.860699 |
| MW-390 | UA | 2016-03-04 | 428.1 | 427.8 | Top of PVC | 426.0 | 50 | 65 | 376.0 | 361.0 | 65 | 358.0 | 15 | 2 | 38.192956 | -89.869793 |
| MW-391 | UA | 2016-03-10 | 426.6 | 426.8 | Top of PVC | 424.2 | 55 | 70 | 369.2 | 354.2 | 70 | 349.8 | 15 | 2 | 38.190869 | -89.874759 |

Notes:

All elevation data are presented relative to the North American Vertical Datum 1988 (NAVD88), GEOID 12A
bgs = below ground surface
ft = foot or feet
HSU = Hydrostratigraphic Unit
UA = Uppermost Aquifer
PMP = Potential Migration Pathway
PVC = polyvinyl chloride

Table 3-2. Exceedance Parameter Statistical Results

Nature and Extent Report

Baldwin Power Plant

Fly Ash Pond System

Baldwin, Illinois

| Location | Parameter | Unit | Groundwater Protection Standard | 2023 Q2 LCL | 2023 Q3 LCL | 2023 Q4 LCL |
|----------|----------------|------|---------------------------------|-------------|-------------|-------------|
| MW-150 | Boron, total | mg/L | 2.16 | 4.12 | 4.38 | 2.87 |
| MW-152 | Boron, total | mg/L | 2.16 | 0.515 | 9.09 | -13.3 |
| MW-391 | Boron, total | mg/L | 2.16 | 2.42 | 2.41 | 2.50 |
| MW-150 | Sulfate, total | mg/L | 762 | 970 | 852 | 749 |
| MW-253 | pH (field) | SU | 6.5/11.1 | | 11.3/11.8 | 11.2/11.7 |

Notes:

LCL = Lower Confidence Level

mg/L = milligrams per liter

SU = standard unit

Table 3-3. Summary of Groundwater Data
Nature and Extent Report
Baldwin Power Plant
Fly Ash Pond System
Baldwin, Illinois

| HSU | Location | Well Type | Parameter | Unit | Sample Count | Non-Detect Results | Percent Non-Detect Results | First Sample | Last Sample | Minimum | Median | Mean | Maximum |
|-----|----------|-----------|----------------|------|--------------|--------------------|----------------------------|--------------|-------------|---------|--------|-------|---------|
| PMP | MW-150 | C | Boron, total | mg/L | 4 | 0 | 0 | 2023/03/15 | 2023/11/03 | 3.43 | 3.9 | 3.9 | 4.38 |
| PMP | MW-150 | C | Sulfate, total | mg/L | 4 | 0 | 0 | 2023/03/15 | 2023/11/03 | 832 | 890 | 900 | 970 |
| PMP | MW-150 | C | pH (field) | SU | 36 | 0 | 0 | 2015/03/25 | 2023/11/03 | 6.7 | 7.2 | 7.1 | 7.5 |
| PMP | MW-151 | C | Boron, total | mg/L | 5 | 0 | 0 | 2023/03/15 | 2023/10/31 | 0.345 | 0.75 | 0.67 | 0.889 |
| PMP | MW-151 | C | Sulfate, total | mg/L | 5 | 0 | 0 | 2023/03/15 | 2023/10/31 | 74.0 | 82 | 85 | 95.0 |
| PMP | MW-151 | C | pH (field) | SU | 29 | 0 | 0 | 2017/03/16 | 2023/10/31 | 6.7 | 6.9 | 6.9 | 7.2 |
| PMP | MW-152 | C | Boron, total | mg/L | 4 | 0 | 0 | 2023/03/15 | 2023/10/31 | 0.477 | 4.8 | 7.5 | 19.8 |
| PMP | MW-152 | C | Sulfate, total | mg/L | 4 | 0 | 0 | 2023/03/15 | 2023/10/31 | 242 | 550 | 580 | 988 |
| PMP | MW-152 | C | pH (field) | SU | 36 | 0 | 0 | 2015/03/25 | 2023/10/31 | 6.6 | 6.9 | 6.9 | 7.5 |
| PMP | MW-153 | C | Boron, total | mg/L | 5 | 4 | 80 | 2023/03/15 | 2023/11/03 | <0.009 | 0.030 | 0.059 | <0.013 |
| PMP | MW-153 | C | Sulfate, total | mg/L | 5 | 0 | 0 | 2023/03/15 | 2023/11/03 | 62.0 | 68.0 | 66 | 75.0 |
| PMP | MW-153 | C | pH (field) | SU | 37 | 0 | 0 | 2015/03/25 | 2023/11/03 | 6.1 | 7.1 | 7.1 | 7.4 |
| PMP | MW-252 | C | Boron, total | mg/L | 4 | 0 | 0 | 2023/03/15 | 2023/10/31 | 0.143 | 0.16 | 0.16 | 0.174 |
| PMP | MW-252 | C | Sulfate, total | mg/L | 4 | 0 | 0 | 2023/03/15 | 2023/10/31 | 437 | 450 | 450 | 474 |
| PMP | MW-252 | C | pH (field) | SU | 36 | 0 | 0 | 2015/03/25 | 2023/10/31 | 6.6 | 6.8 | 6.9 | 7.6 |
| PMP | MW-253 | C | Boron, total | mg/L | 3 | 1 | 33 | 2023/03/15 | 2023/11/03 | <0.02 | 0.070 | 0.055 | 0.0853 |
| PMP | MW-253 | C | Sulfate, total | mg/L | 3 | 0 | 0 | 2023/03/15 | 2023/11/03 | 140 | 150 | 160 | 174 |
| PMP | MW-253 | C | pH (field) | SU | 35 | 0 | 0 | 2015/03/25 | 2023/11/03 | 9.8 | 12 | 11 | 12.4 |
| UA | MW-304 | B | Boron, total | mg/L | 29 | 0 | 0 | 2015/12/29 | 2023/11/01 | 1.27 | 1.7 | 1.7 | 2.16 |
| UA | MW-304 | B | Sulfate, total | mg/L | 29 | 0 | 0 | 2015/12/29 | 2023/11/01 | 157 | 190 | 190 | 231 |
| UA | MW-304 | B | pH (field) | SU | 40 | 0 | 0 | 2015/12/29 | 2023/11/01 | 7.4 | 7.9 | 7.9 | 8.2 |
| UA | MW-358 | B | Boron, total | mg/L | 10 | 0 | 0 | 2022/10/27 | 2023/11/01 | 1.10 | 1.4 | 1.4 | 1.67 |
| UA | MW-358 | B | Sulfate, total | mg/L | 10 | 2 | 20 | 2022/10/27 | 2023/11/01 | 8.00 | 24 | 40 | 108 |
| UA | MW-358 | B | pH (field) | SU | 10 | 0 | 0 | 2022/10/27 | 2023/11/01 | 7.6 | 7.9 | 7.9 | 8.4 |
| UA | MW-350 | C | Boron, total | mg/L | 10 | 0 | 0 | 2020/03/26 | 2023/11/03 | 0.538 | 0.62 | 0.63 | 0.900 |
| UA | MW-350 | C | Sulfate, total | mg/L | 10 | 0 | 0 | 2020/03/26 | 2023/11/03 | 52.0 | 92 | 87 | 113 |
| UA | MW-350 | C | pH (field) | SU | 38 | 0 | 0 | 2015/03/25 | 2023/11/03 | 8.0 | 12 | 11 | 12.8 |
| UA | MW-352 | C | Boron, total | mg/L | 5 | 0 | 0 | 2023/03/15 | 2023/10/31 | 1.88 | 2.1 | 2.2 | 2.77 |
| UA | MW-352 | C | Sulfate, total | mg/L | 5 | 1 | 20 | 2023/03/15 | 2023/10/31 | 6.00 | 7.0 | 7.6 | <6 |
| UA | MW-352 | C | pH (field) | SU | 37 | 0 | 0 | 2015/03/25 | 2023/10/31 | 6.7 | 7.6 | 7.7 | 9.0 |
| UA | MW-366 | C | Boron, total | mg/L | 23 | 0 | 0 | 2016/01/20 | 2023/11/02 | 1.19 | 1.7 | 1.7 | 2.70 |
| UA | MW-366 | C | Sulfate, total | mg/L | 23 | 0 | 0 | 2016/01/20 | 2023/11/02 | 33.0 | 430 | 340 | 700 |
| UA | MW-366 | C | pH (field) | SU | 23 | 0 | 0 | 2016/01/20 | 2023/11/02 | 6.7 | 7.0 | 7.0 | 7.5 |
| UA | MW-375 | C | Boron, total | mg/L | 23 | 0 | 0 | 2016/01/20 | 2023/11/03 | 0.979 | 1.4 | 1.4 | 2.06 |
| UA | MW-375 | C | Sulfate, total | mg/L | 23 | 0 | 0 | 2016/01/20 | 2023/11/03 | 83.0 | 120 | 140 | 243 |
| UA | MW-375 | C | pH (field) | SU | 23 | 0 | 0 | 2016/01/20 | 2023/11/03 | 7.0 | 7.8 | 7.7 | 7.9 |

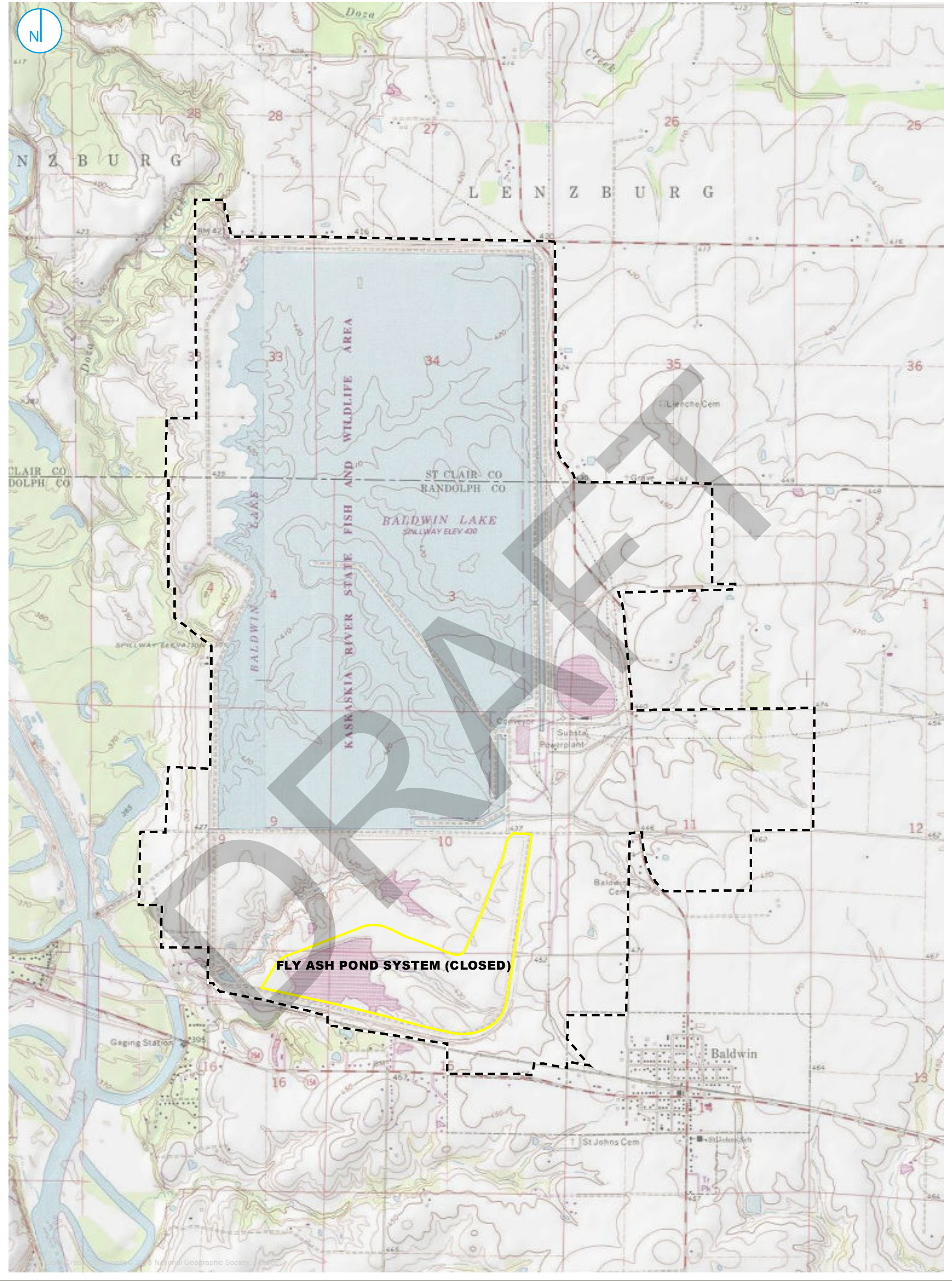
Table 3-3. Summary of Groundwater Data
Nature and Extent Report
Baldwin Power Plant
Fly Ash Pond System
Baldwin, Illinois

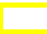
| HSU | Location | Well Type | Parameter | Unit | Sample Count | Non-Detect Results | Percent Non-Detect Results | First Sample | Last Sample | Minimum | Median | Mean | Maximum |
|-----|----------|-----------|----------------|------|--------------|--------------------|----------------------------|--------------|-------------|---------|--------|------|---------|
| UA | MW-377 | C | Boron, total | mg/L | 23 | 0 | 0 | 2016/01/19 | 2023/11/03 | 1.54 | 1.7 | 1.7 | 2.01 |
| UA | MW-377 | C | Sulfate, total | mg/L | 23 | 0 | 0 | 2016/01/19 | 2023/11/03 | 37.0 | 39 | 40 | 51.0 |
| UA | MW-377 | C | pH (field) | SU | 23 | 0 | 0 | 2016/01/19 | 2023/11/03 | 6.9 | 7.2 | 7.2 | 7.7 |
| UA | MW-383 | C | Boron, total | mg/L | 23 | 0 | 0 | 2016/01/21 | 2023/11/01 | 1.16 | 1.4 | 1.4 | 2.05 |
| UA | MW-383 | C | Sulfate, total | mg/L | 23 | 0 | 0 | 2016/01/21 | 2023/11/01 | 150 | 180 | 180 | 212 |
| UA | MW-383 | C | pH (field) | SU | 23 | 0 | 0 | 2016/01/21 | 2023/11/01 | 7.3 | 7.6 | 7.6 | 7.8 |
| UA | MW-384 | C | Boron, total | mg/L | 23 | 0 | 0 | 2016/01/21 | 2023/11/01 | 1.26 | 1.5 | 1.5 | 2.26 |
| UA | MW-384 | C | Sulfate, total | mg/L | 23 | 0 | 0 | 2016/01/21 | 2023/11/01 | 30.0 | 100 | 94 | 178 |
| UA | MW-384 | C | pH (field) | SU | 23 | 0 | 0 | 2016/01/21 | 2023/11/01 | 7.2 | 8.0 | 7.9 | 8.1 |
| UA | MW-390 | C | Boron, total | mg/L | 23 | 0 | 0 | 2016/03/22 | 2023/11/02 | 0.175 | 0.55 | 0.86 | 2.30 |
| UA | MW-390 | C | Sulfate, total | mg/L | 23 | 0 | 0 | 2016/03/22 | 2023/11/02 | 102 | 150 | 160 | 234 |
| UA | MW-390 | C | pH (field) | SU | 23 | 0 | 0 | 2016/03/22 | 2023/11/02 | 6.8 | 7.2 | 7.2 | 7.8 |
| UA | MW-391 | C | Boron, total | mg/L | 17 | 0 | 0 | 2016/12/22 | 2023/11/03 | 1.30 | 3.2 | 4.0 | 8.91 |
| UA | MW-391 | C | Sulfate, total | mg/L | 17 | 0 | 0 | 2016/12/22 | 2023/11/03 | 426 | 760 | 910 | 1,760 |
| UA | MW-391 | C | pH (field) | SU | 18 | 0 | 0 | 2016/12/22 | 2023/11/03 | 7.3 | 7.7 | 7.7 | 8.2 |


Notes:
B = Background
C = Compliance
HSU = Hydrostratigraphic Unit
mg/L = milligrams per liter
PMP = Potential Migration Pathway
SU = standard unit
UA = Uppermost Aquifer

FIGURES

DRAFT



 FLY ASH POND SYSTEM

 PROPERTY BOUNDARY

SITE LOCATION MAP

FIGURE 2-1

0 1,000 2,000
Feet



REGULATED UNIT (SUBJECT UNIT) FLY ASH
POND SYSTEM (CLOSED)

SITE FEATURE
LIMITS OF FINAL COVER
PROPERTY BOUNDARY

0 400 800 Feet

SITE MAP

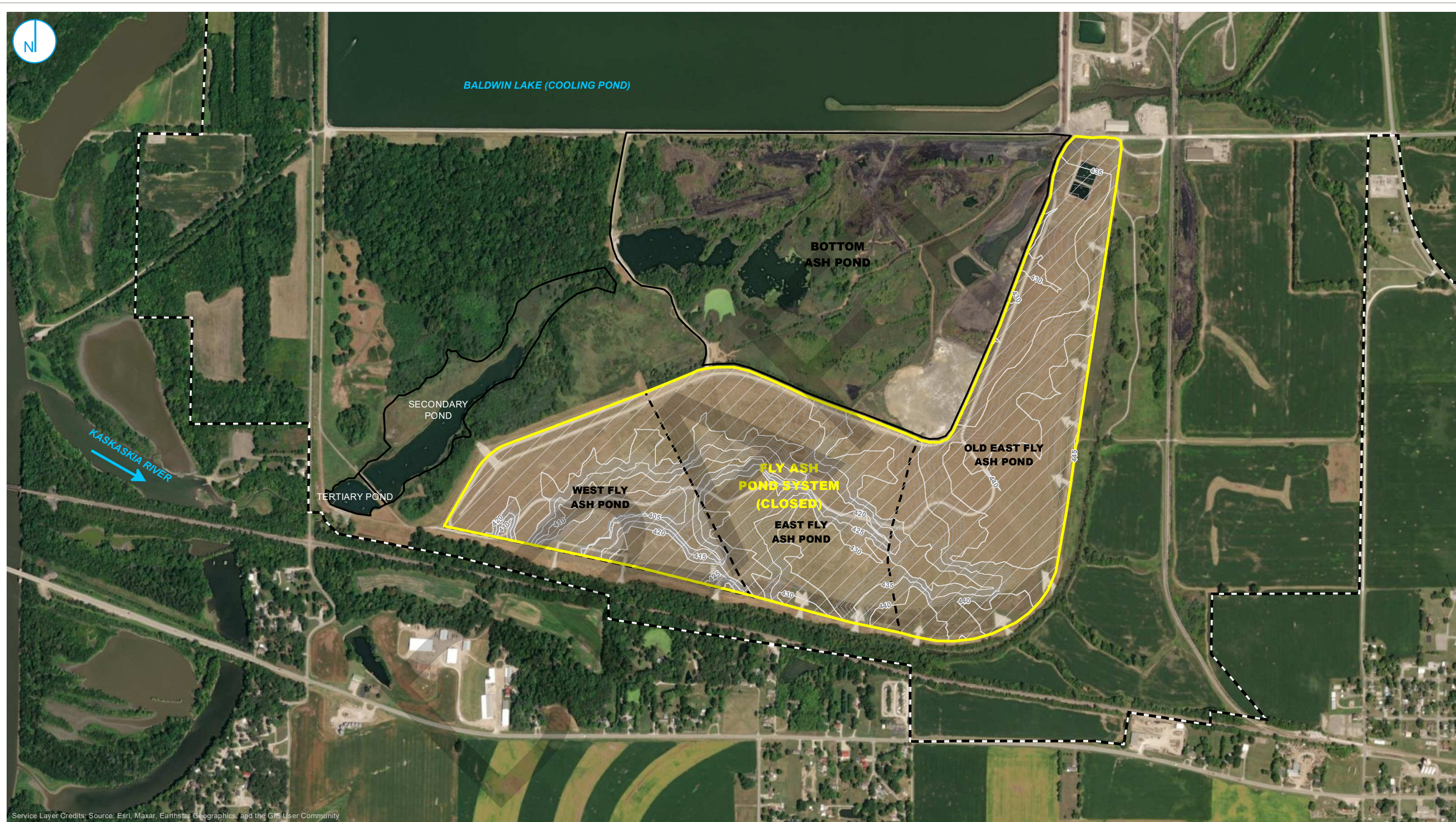
NATURE AND EXTENT REPORT
FLY ASH POND SYSTEM
BALDWIN POWER PLANT
BALDWIN, ILLINOIS

FIGURE 2-2

RAMBOLL AMERICAS
ENGINEERING SOLUTIONS, INC.

RAMBOLL

PROJECT: 169000XXXX | DATED: 4/11/2024 | DESIGNER: galammc
Y:\Mapping\Projects\222285\MXD\Nature_and_Extent\Report\Figure 1_BAL_FAPS_BOA.mxd



- 5FT TOPOGRAPHIC CONTOUR
- 1FT TOPOGRAPHIC CONTOUR
- REGULATED UNIT (SUBJECT UNIT)
- SITE FEATURE
- CAPPED AREA
- PROPERTY BOUNDARY

0 400 800 Feet

BASE OF CCR

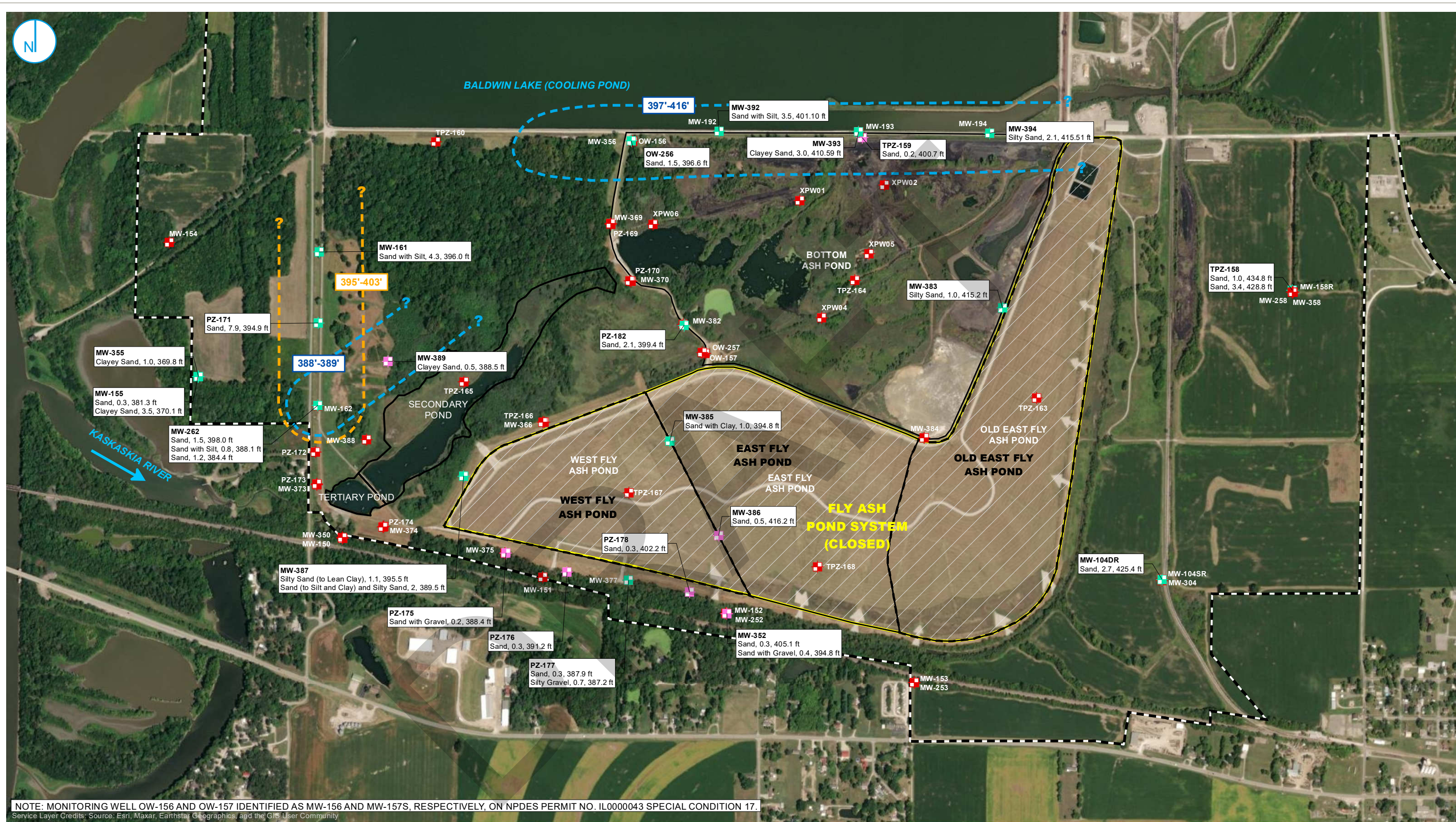
NATURE AND EXTENT REPORT
FLY ASH POND SYSTEM
BALDWIN POWER PLANT
BALDWIN, ILLINOIS

FIGURE 2-3

RAMBOLL AMERICAS
ENGINEERING SOLUTIONS, INC.

RAMBOLL

PROJECT: 169000XXXX | DATED: 4/17/2024 | DESIGNER: galammc
Y:\Mapping\Projects\222285\MXD\Nature_and_Extent_Report\Figure 2-4_Sand Seam Observations Thickness and Elevations.mxd



- | | | |
|---|---|-------------------------------|
| BORING LOCATION WITH OBSERVED SAND SEAM > 0.5 FT | AREAS OF POTENTIALLY INTERCONNECTED SAND SEAMS AND SEAM ELEVATION INTERVAL - - - - - UNSATURATED SAND SEAM - - - - - SATURATED SAND SEAM | REGULATED UNIT (SUBJECT UNIT) |
| BORING LOCATION WITH OBSERVED SAND SEAM <= 0.5 FT | | SITE FEATURE |
| BORING LOCATION WITH NO OBSERVED SAND SEAM | | LIMITS OF FINAL COVER |
| | | PROPERTY BOUNDARY |

BORING/WELL NUMBER
SEAM DESCRIPTION, SEAM THICKNESS (FT), SEAM BASE ELEVATION

0 400 800
Feet

SAND SEAM OBSERVATIONS, THICKNESS AND ELEVATIONS

NATURE AND EXTENT REPORT
FLY ASH POND SYSTEM
BALDWIN POWER PLANT
BALDWIN, ILLINOIS

FIGURE 2-4

RAMBOLL AMERICAS
ENGINEERING SOLUTIONS, INC.



PROJECT: 169000XXXX | DATED: 4/11/2024 | DESIGNER: galammc
Y:\Mapping\Projects\222285\MXD\Nature_and_Extent\BAL\Nature_and_Extent\Figure 2-6_Bedrock Topography.mxd



- | | | |
|--------------------------|--|---------------------------------|
| ■ MONITORING WELL | — BEDROCK ELEVATION CONTOUR | ■ REGULATED UNIT (SUBJECT UNIT) |
| ■ PORE WATER WELL | - - - INFERRED BEDROCK ELEVATION CONTOUR | ■ SITE FEATURE |
| ■ CLOSED MONITORING WELL | | ■ LIMITS OF FINAL COVER |
| ■ CLOSED PORE WATER WELL | | ■ PROPERTY BOUNDARY |
| ● AECOM BORING LOCATION | | |

0 400 800 Feet

TOP OF UPPERMOST AQUIFER

NATURE AND EXTENT REPORT
FLY ASH POND SYSTEM
BALDWIN POWER PLANT
BALDWIN, ILLINOIS

FIGURE 2-5

RAMBOLL AMERICAS
ENGINEERING SOLUTIONS, INC.



PROJECT: 169000XXXX | DATED: 12/21/2023 | DESIGNER: GALARMIC
Y:\Mapping\Projects\22\2285\MXD\GWL_Contours\Round_2023\Baldwin\FAPS_605\FAPS Unlith Pot Surface 20230516.mxd



- COMPLIANCE MONITORING WELL
- BACKGROUND MONITORING WELL
- MONITORING WELL
- PORE WATER WELL
- GROUNDWATER ELEVATION CONTOUR (10-FT CONTOUR INTERVAL, NAVD88)
- INFERRED GROUNDWATER ELEVATION CONTOUR
- GROUNDWATER FLOW DIRECTION
- REGULATED UNIT (SUBJECT UNIT)
- SITE FEATURE
- CAPPED
- PROPERTY BOUNDARY

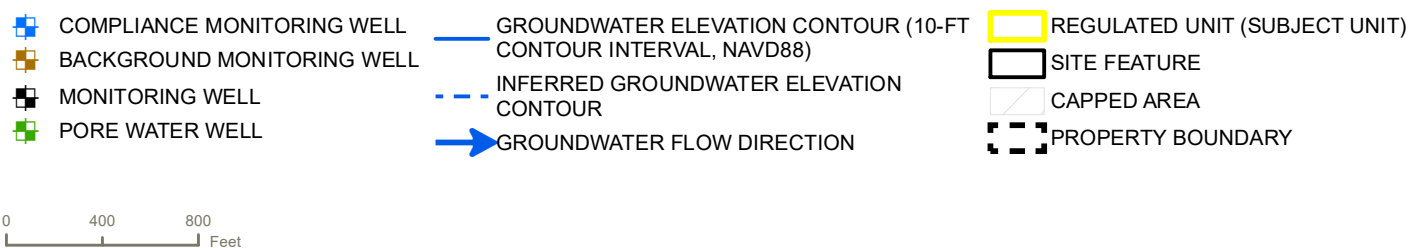
SHALLOW UNLITHIFIED POTENTIOMETRIC SURFACE MAP, MAY 2023 (E001)

NATURE AND EXTENT REPORT
FLY ASH POND SYSTEM
BALDWIN POWER PLANT
BALDWIN, ILLINOIS

FIGURE 2-6

RAMBOLL AMERICAS
ENGINEERING SOLUTIONS, INC.

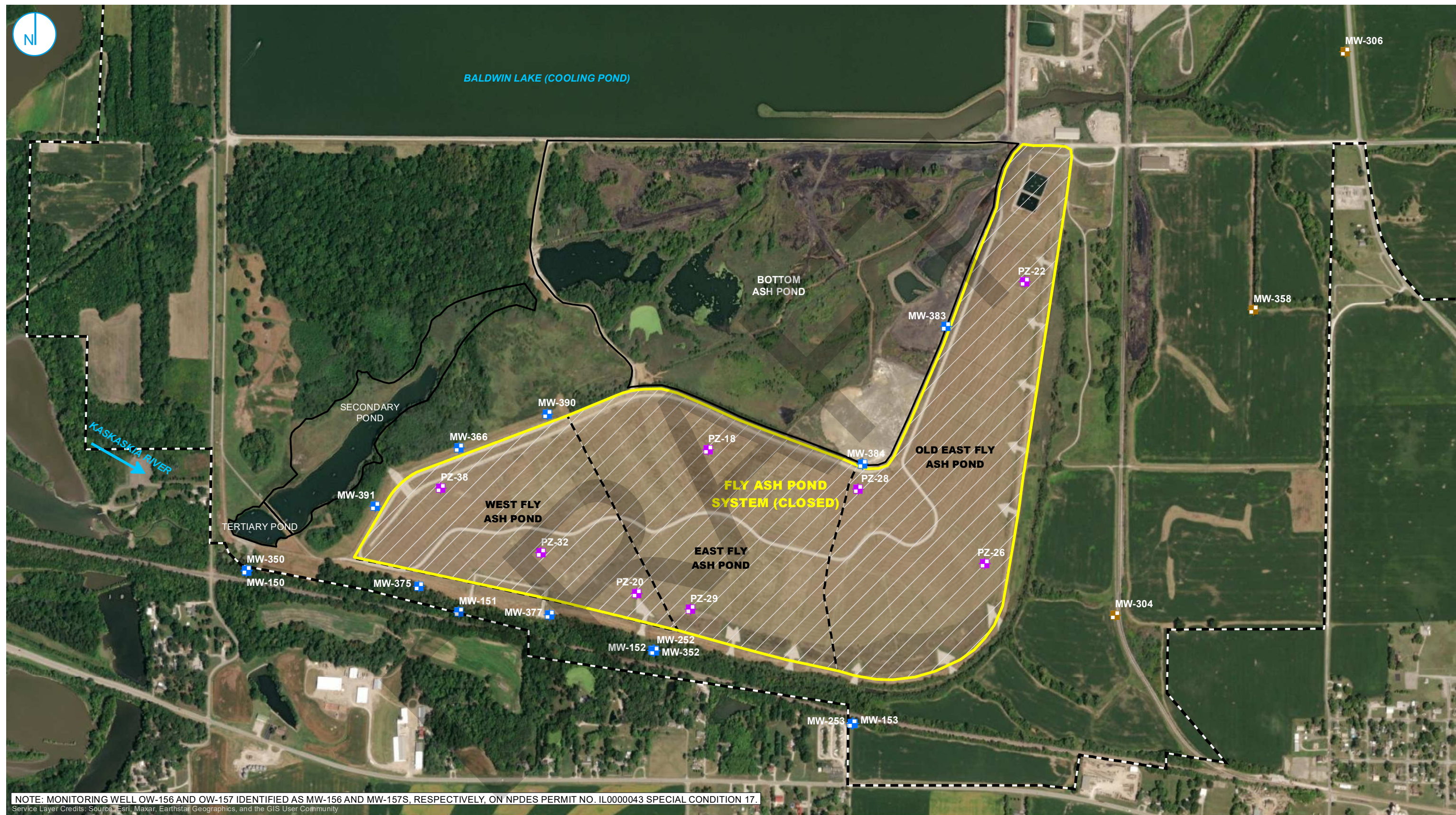




NATURE AND EXTENT REPORT
FLY ASH POND SYSTEM
BALDWIN POWER PLANT
BALDWIN, ILLINOIS

RAMBOLL AMERICAS
ENGINEERING SOLUTIONS, INC.

PROJECT: 169000XXXX | DATED: 4/17/2024 | DESIGNER: galammc
Y:\Mapping\Projects\22\2285\MXD\Nature_and_Extent\BALINature_and_Extent_Report\Figure 2-8_Monitoring Well Location Network.mxd



- COMPLIANCE MONITORING WELL
- BACKGROUND MONITORING WELL
- SUPPLEMENTAL PIEZOMETER
- REGULATED UNIT (SUBJECT UNIT)
- FLY ASH POND SYSTEM (CLOSED)
- SITE FEATURE
- LIMITS OF FINAL COVER
- PROPERTY BOUNDARY

0 400 800 Feet

MONITORING WELL LOCATION MAP

NATURE AND EXTENT REPORT
FLY ASH POND SYSTEM
BALDWIN POWER PLANT
BALDWIN, ILLINOIS

FIGURE 2-8

RAMBOLL AMERICAS
ENGINEERING SOLUTIONS, INC.

RAMBOLL

PROJECT: 169000XXXX | DATED: 4/15/2024 | DESIGNER: galarmmc
Y:\Mapping\Projects\22\2285\MXD\Nature_and_Extent\BAL\Nature_and_Extent_Report\Figure 3-2_BAL 605 GWPS UU.mxd



- | | |
|--------------------------------------|---------------------------------|
| ● TOTAL BORON EXCEEDANCE | ■ REGULATED UNIT (SUBJECT UNIT) |
| ● TOTAL SULFATE EXCEEDANCE | ■ SITE FEATURE |
| ● COMPLIANCE WELL WITHOUT EXCEEDANCE | ■ CAPPED AREA |
| | ■ PROPERTY BOUNDARY |



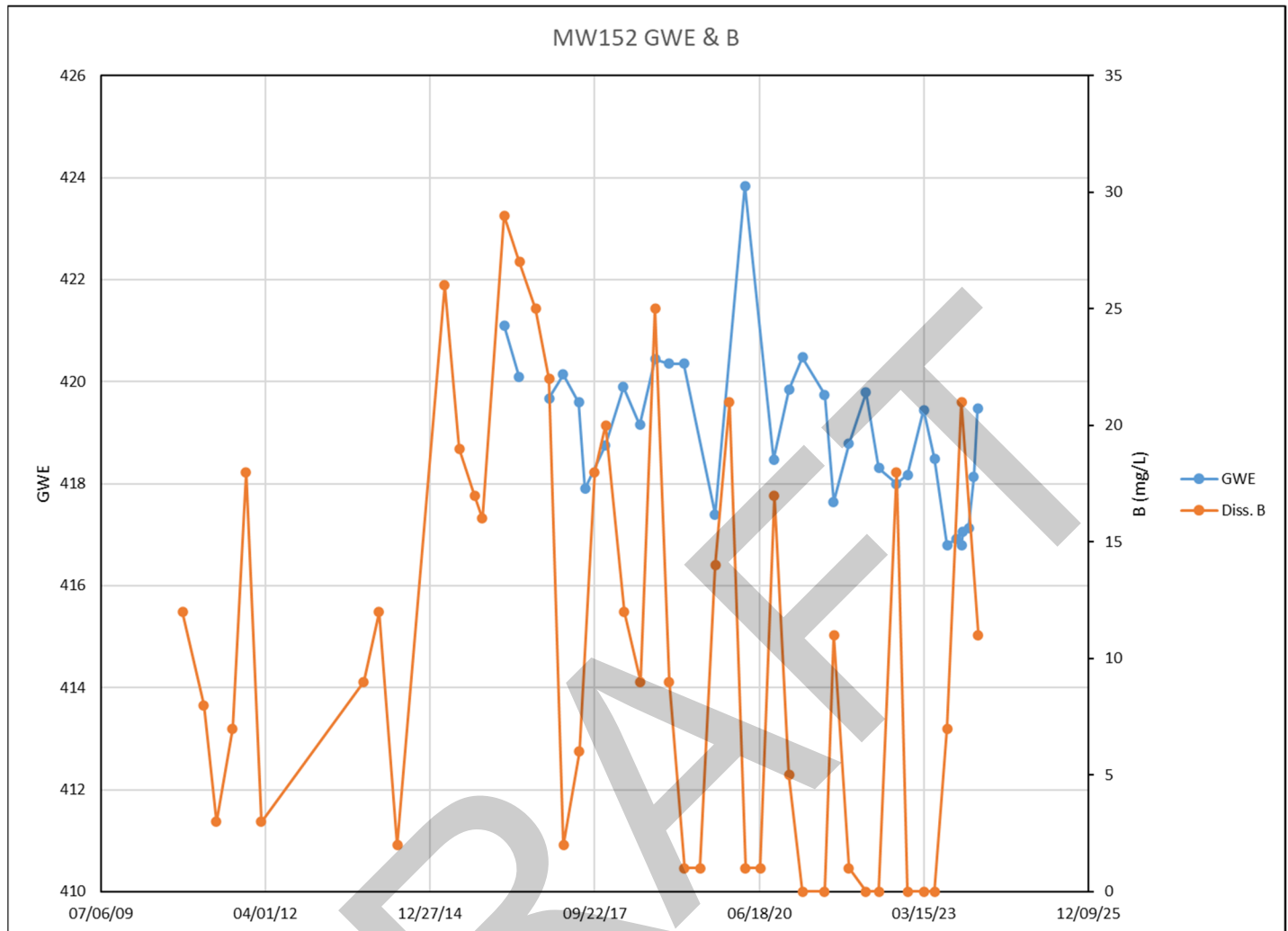
GWPS EXCEEDANCE MAP UPPER UNIT

NATURE AND EXTENT REPORT
FLY ASH POND SYSTEM
BALDWIN POWER PLANT
BALDWIN, ILLINOIS

FIGURE 3-1

RAMBOLL AMERICAS
ENGINEERING SOLUTIONS, INC.





PROJECT: 169000XXXX | DATED: 4/15/2024 | DESIGNER: galarmmc
Y:\Mapping\Projects\2212285\MXD\Nature_and_Extent\BAL\Nature_and_Extent_Report\Figure 3-1_BAL 605 GWPS UA.mxd



- TOTAL BORON EXCEEDANCE
- COMPLIANCE WELL WITHOUT EXCEEDANCE
- REGULATED UNIT (SUBJECT UNIT)
- SITE FEATURE
- CAPPED AREA
- PROPERTY BOUNDARY

GWPS EXCEEDANCE MAP UPPERMOST AQUIFER

NATURE AND EXTENT REPORT
FLY ASH POND SYSTEM
BALDWIN POWER PLANT
BALDWIN, ILLINOIS

FIGURE 3-3

RAMBOLL AMERICAS
ENGINEERING SOLUTIONS, INC.



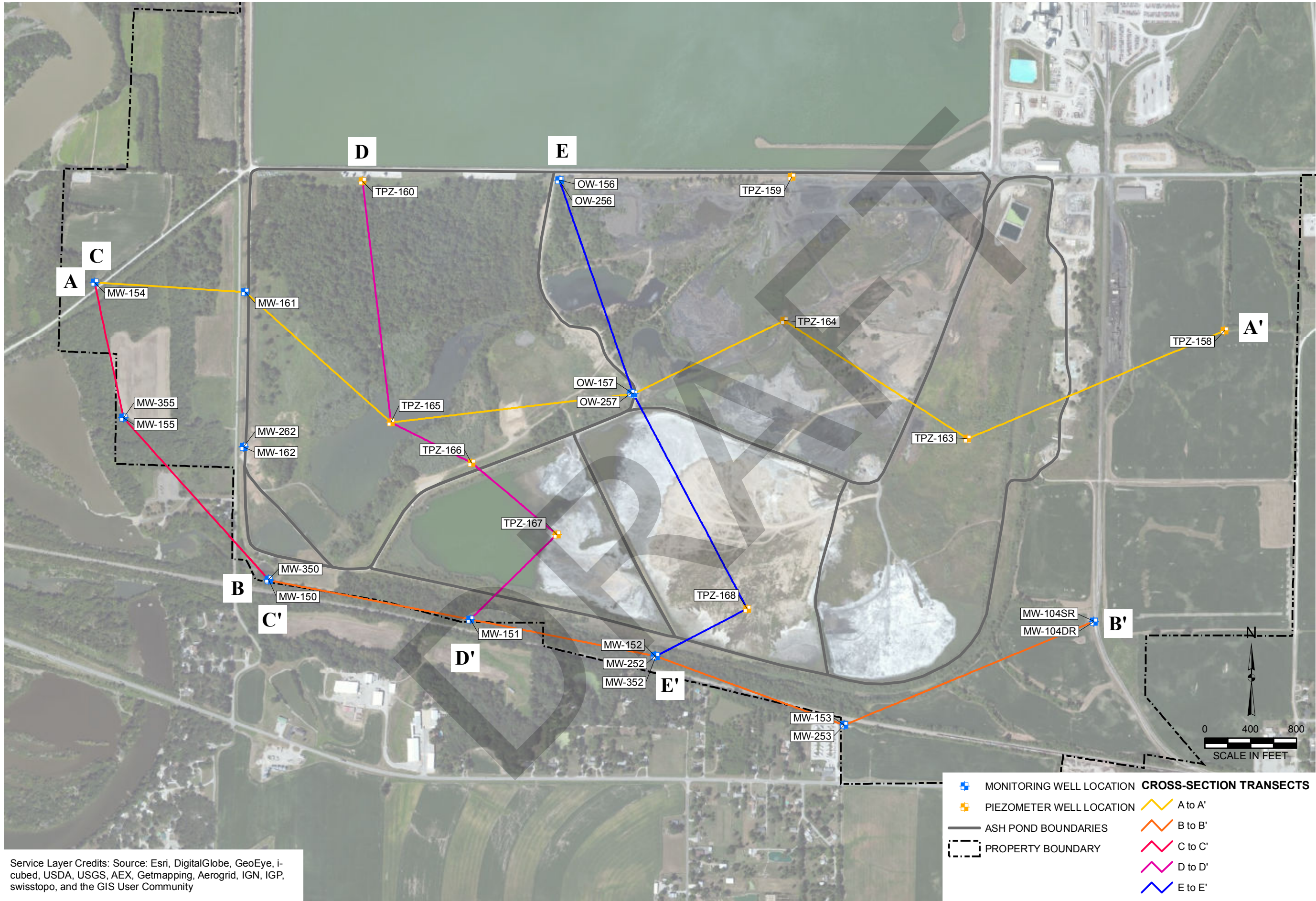
APPENDICES

DRAFT

APPENDIX A
Geologic Cross-Sections

DRAFT

Y:\Mapping\Projects\212189\MXD\HydroGeo_Rpt\Figure 7_Cross Section Location Map.mxd Author: tushman Date/Time: 6/10/2014, 9:16:53 AM



DRAWN BY/DATE:
TDC 4/30/14
REVIEWED BY/DATE:
SJC 4/27/14
APPROVED BY/DATE:
SJC 6/9/14

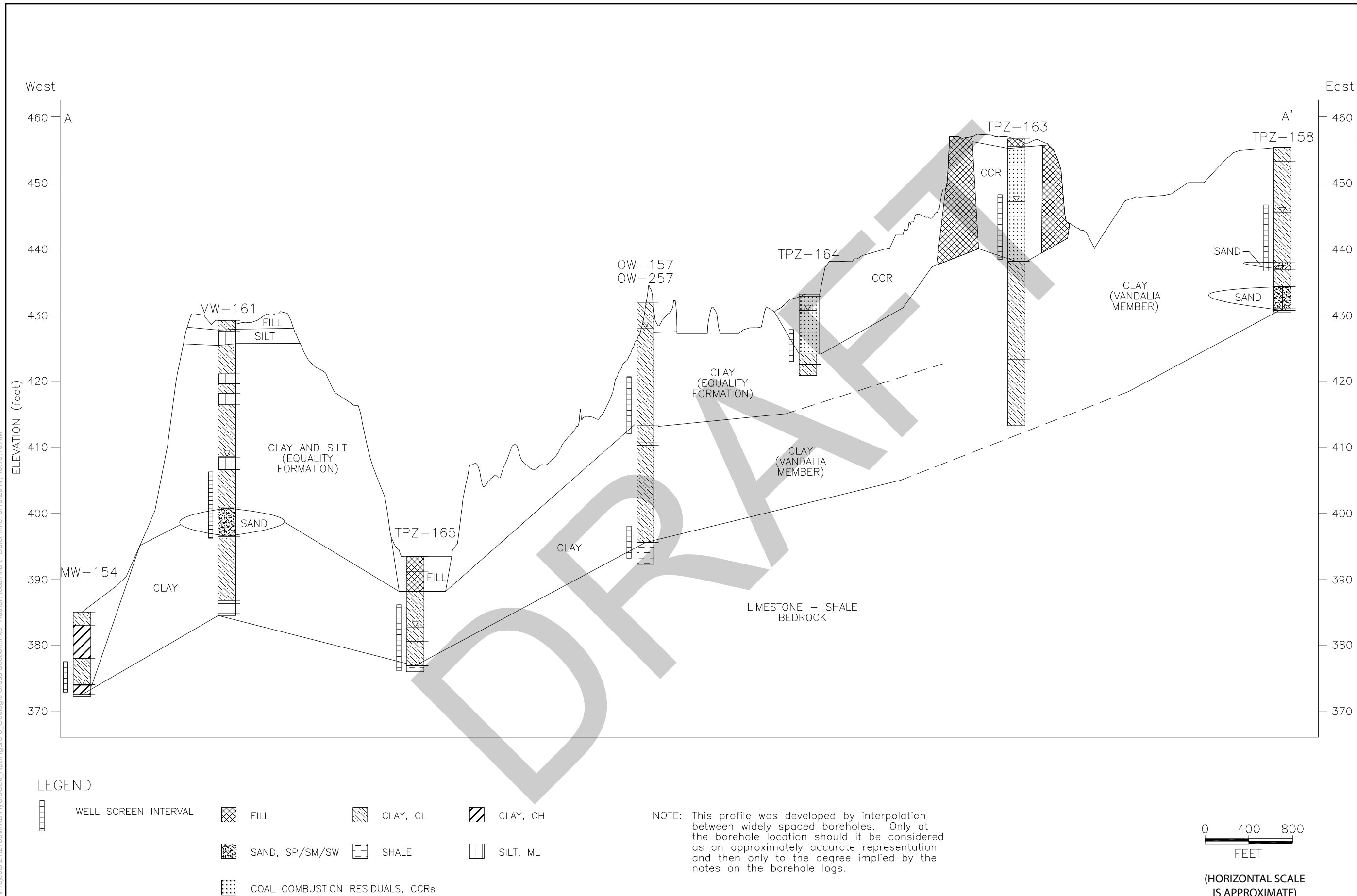
CROSS SECTION LOCATION MAP
GROUNDWATER QUALITY ASSESSMENT AND PHASE II HYDROGEOLOGIC INVESTIGATION
BALDWIN ASH POND SYSTEM, BALDWIN ENERGY COMPLEX
10901 BALDWIN ROAD BALDWIN, ILLINOIS 62217

PROJECT NO: 2189

FIGURE NO: 7



Y:\Mapping\Projects\212189\WDXD\HydroGeo_Rpt\Figure 8_Geologic Cross Section.mxd Author: tushman Date/Time: 5/16/2014 10:18:13 AM



DRAWN BY/DATE:
TDC 5/15/14
REVIEWED BY/DATE:
SJC 5/16/14
APPROVED BY/DATE:
SJC 6/9/14

GEOLOGIC CROSS SECTION A-A'

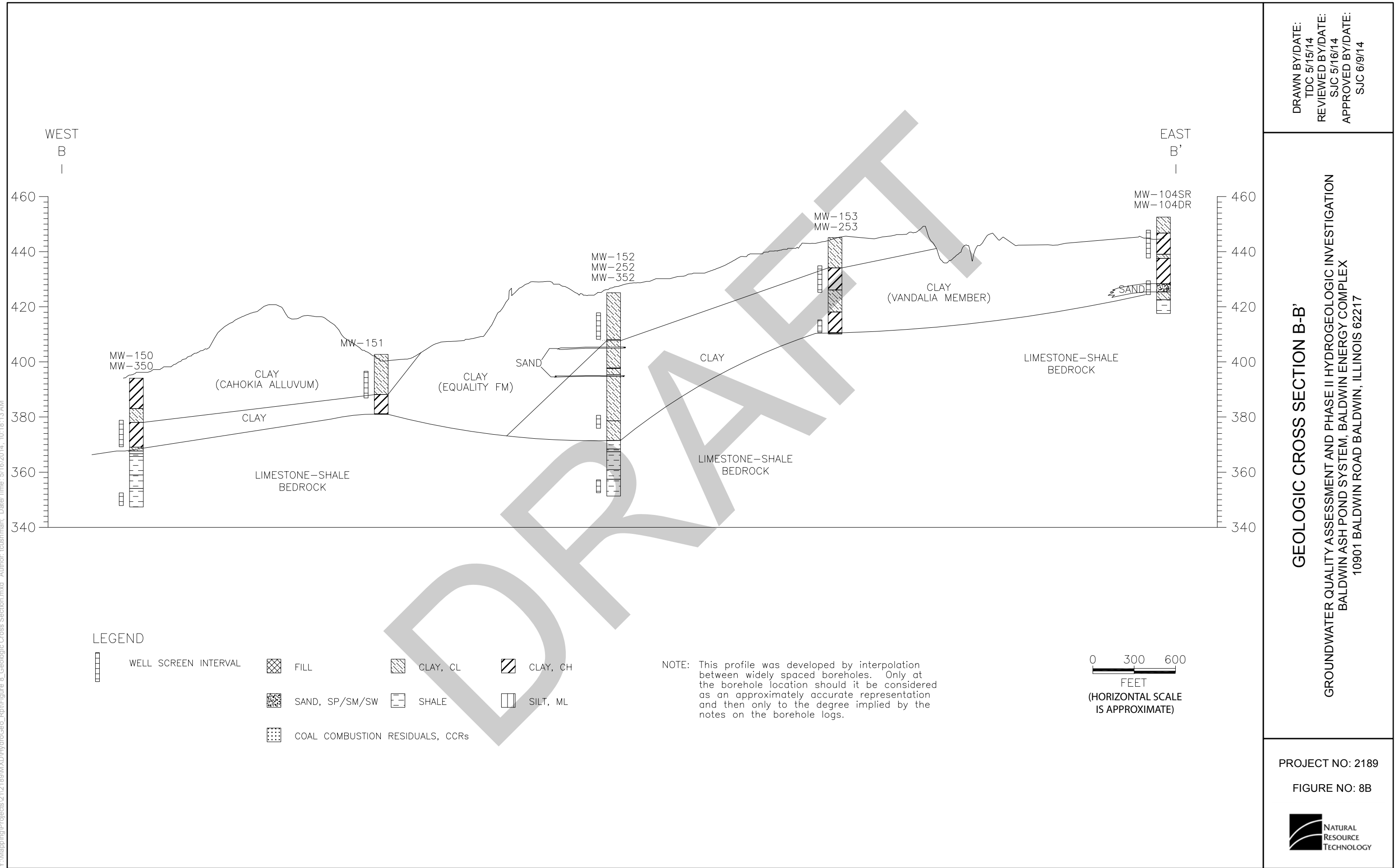
GROUNDWATER QUALITY ASSESSMENT AND PHASE II HYDROGEOLOGIC INVESTIGATION
BALDWIN ASH POND SYSTEM, BALDWIN ENERGY COMPLEX
10901 BALDWIN ROAD BALDWIN, ILLINOIS 62217

PROJECT NO: 2189

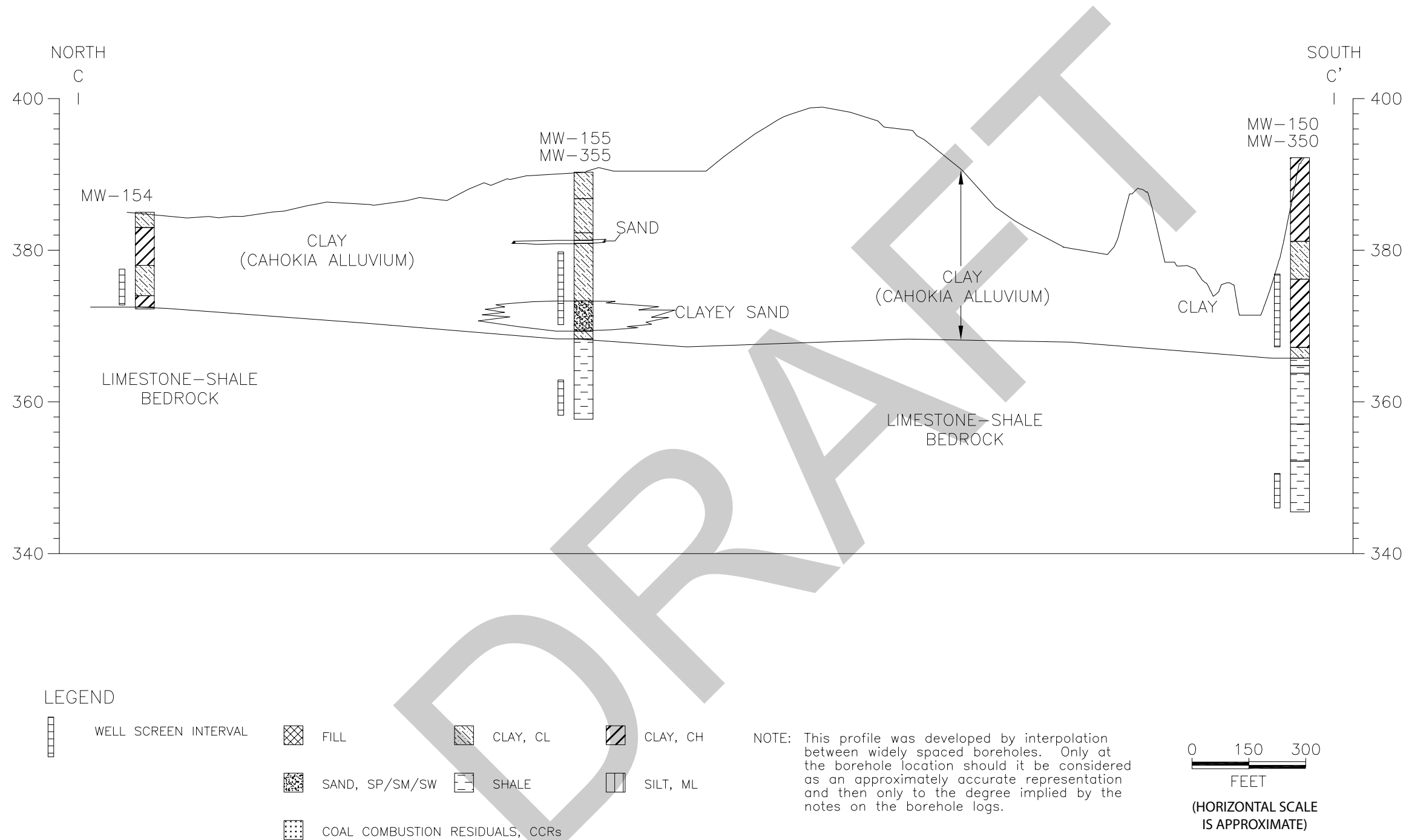
FIGURE NO: 8A



Y:\Mapping\Projects\212189\MXD\HydroGeo_Rpt\Figure 8_Geologic Cross Section.mxd Author: tushman Date/Time: 5/16/2014, 10:18:13 AM



Y:\Mapping\Projects\212189\MXD\HydroGeo_Rpt\Figure 8_Geologic Cross Section.mxd Author: tushman Date/Time: 5/16/2014, 10:18:13 AM



DRAWN BY/DATE:
TDC 5/15/14
REVIEWED BY/DATE:
SJC 5/16/14
APPROVED BY/DATE:
SJC 6/9/14

GEOLOGIC CROSS SECTION C-C'

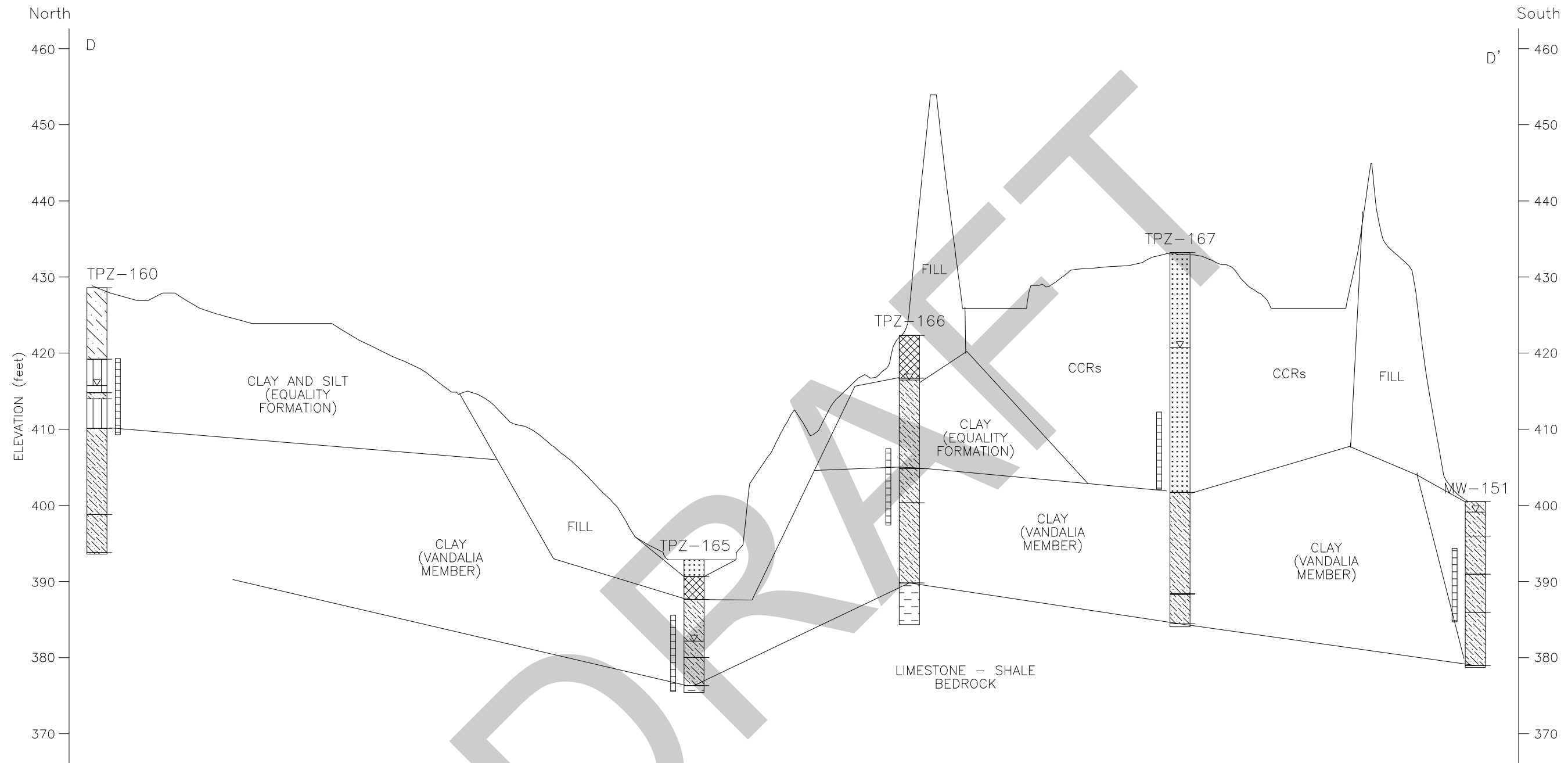
GROUNDWATER QUALITY ASSESSMENT AND PHASE II HYDROGEOLOGIC INVESTIGATION
BALDWIN ASH POND SYSTEM, BALDWIN ENERGY COMPLEX
10901 BALDWIN ROAD BALDWIN, ILLINOIS 62217

PROJECT NO: 2189

FIGURE NO: 8C



Y:\Mapping\Projects\212189\WDXD\HydroGeo_Rpt\Figure 8_Geologic Cross Section.mxd Author: tushman Date/Time: 5/16/2014 10:18:13 AM



LEGEND

| | | | | | | | |
|--|---------------------------------|--|-------|--|----------|--|----------|
| | WELL SCREEN INTERVAL | | FILL | | CLAY, CL | | CLAY, CH |
| | SAND, SP/SM/SW | | SHALE | | SILT, ML | | |
| | COAL COMBUSTION RESIDUALS, CCRs | | | | | | |

NOTE: This profile was developed by interpolation between widely spaced boreholes. Only at the borehole location should it be considered as an approximately accurate representation and then only to the degree implied by the notes on the borehole logs.

0 200 400
FEET
(HORIZONTAL SCALE IS APPROXIMATE)

DRAWN BY/DATE:
TDC 5/15/14
REVIEWED BY/DATE:
SJC 5/16/14
APPROVED BY/DATE:
SJC 6/9/14

GEOLOGIC CROSS SECTION D-D'

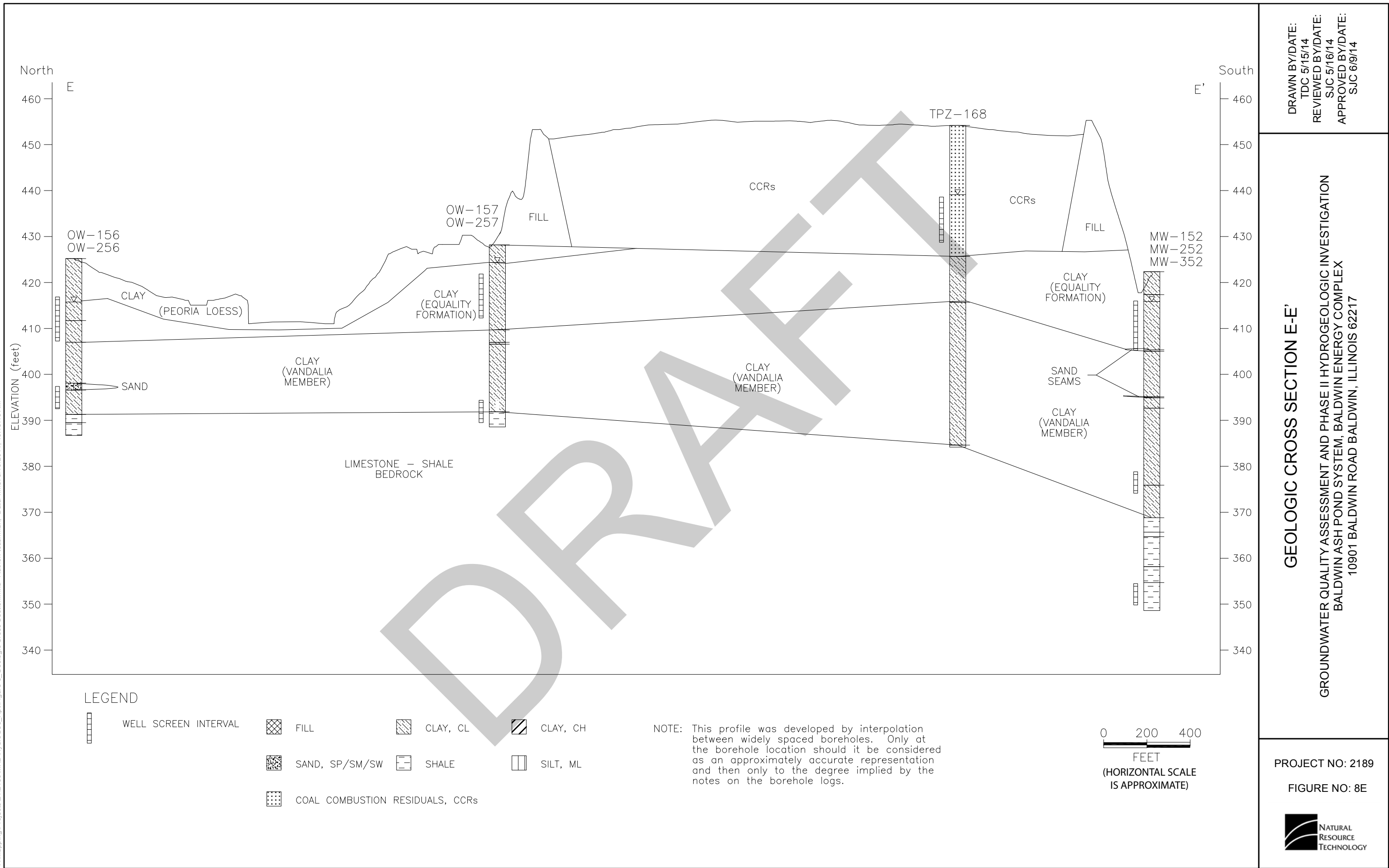
GROUNDWATER QUALITY ASSESSMENT AND PHASE II HYDROGEOLOGIC INVESTIGATION
BALDWIN ASH POND SYSTEM, BALDWIN ENERGY COMPLEX
10901 BALDWIN ROAD BALDWIN, ILLINOIS 62217

PROJECT NO: 2189

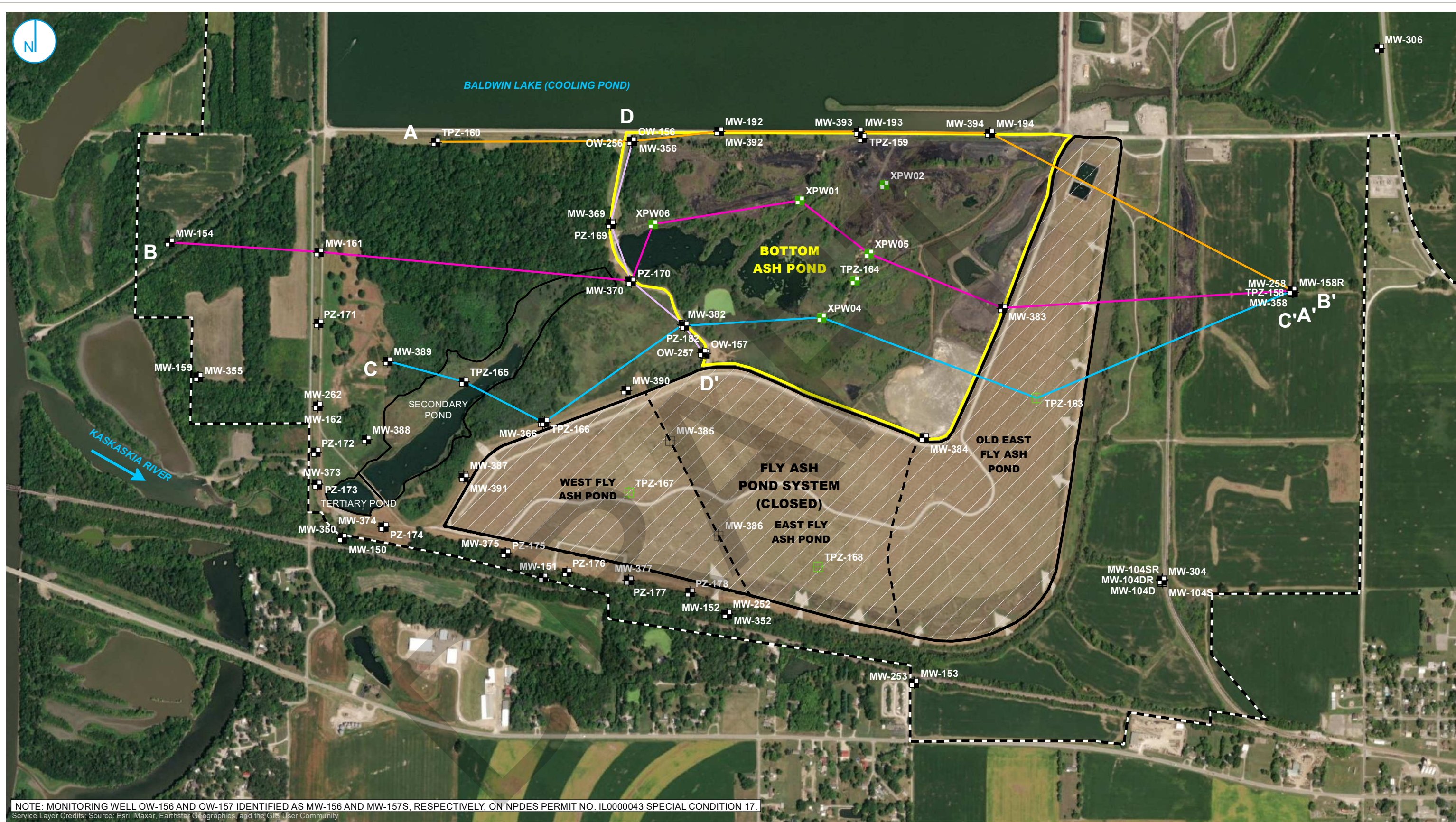
FIGURE NO: 8D



Y:\Mapping\Projects\212189\MXD\HydroGeo_Rpt\Figure 8_Geologic Cross Section.mxd Author: tcushman Date/Time: 5/16/2014, 10:18:13 AM



PROJECT: 169000XXXX | DATED: 5/9/2023 | DESIGNER: GALARNMC
Y:\Mapping\Projects\22\2285\MXD\845_Operating_Permit\Baldwin\BAP\2023_Update\Figure 2-6_Cross Section Locations.mxd



NOTE: MONITORING WELL OW-156 AND OW-157 IDENTIFIED AS MW-156 AND MW-157S, RESPECTIVELY, ON NPDES PERMIT NO. IL0000043 SPECIAL CONDITION 17.
Service Layer Credits: Source: Esri, Maxar, Earthstar Geographics, and the GIS User Community

- | | | |
|---|-------------------------------|-------------------------------|
| MONITORING WELL AND PIEZOMETER LOCATION | CROSS SECTION TRANSECT | REGULATED UNIT (SUBJECT UNIT) |
| PORE WATER WELL | A to A' | FLY ASH POND SYSTEM (CLOSED) |
| CLOSED MONITORING WELL | B to B' | SITE FEATURE |
| CLOSED PORE WATER WELL | C to C' | LIMITS OF FINAL COVER |
| | D to D' | PROPERTY BOUNDARY |



CROSS SECTION LOCATION MAP

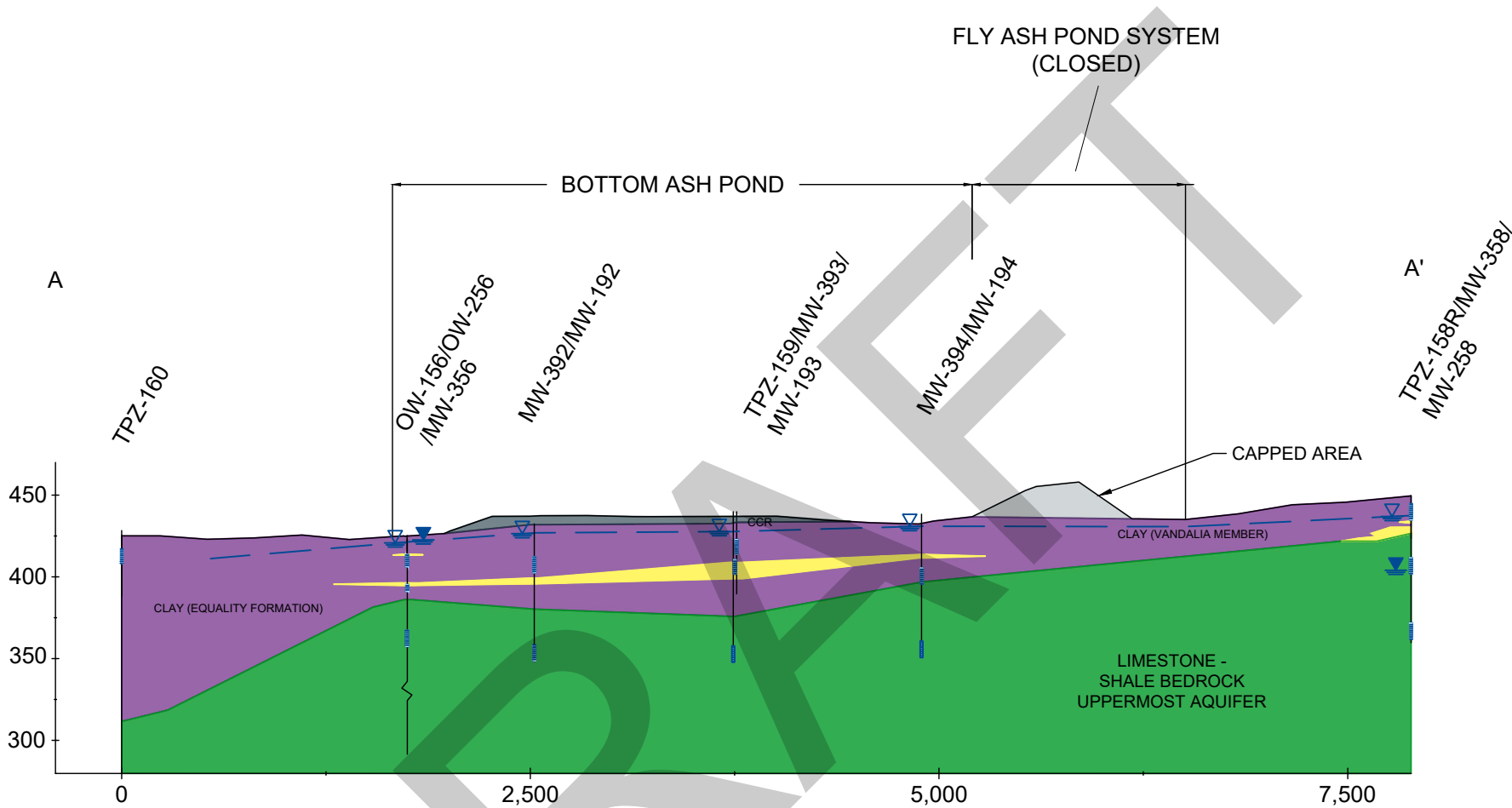
HYDROGEOLOGIC SITE
CHARACTERIZATION REPORT REVISION 1
BOTTOM ASH POND
BALDWIN POWER PLANT
BALDWIN, ILLINOIS

FIGURE 2-6

RAMBOLL AMERICAS
ENGINEERING SOLUTIONS, INC.

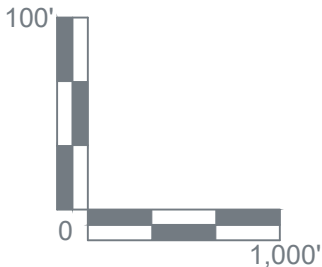


- NOTES**
1. This profile was developed by interpolation between widely spaced boreholes. Only at the borehole location should it be considered as an approximately accurate representation and then only to the degree implied by the notes on the borehole logs.
 2. Scale is approximate.
 3. Vertical scale is exaggerated 10X.
 4. Groundwater elevations measured on March 15, 2023.



- LEGEND**
- COAL COMBUSTION RESIDUALS (CCR)
 - FILL
 - CLAY
 - SILT
 - SAND
 - BEDROCK / WEATHERED BEDROCK (INTERBEDDED SHALE, LIMESTONE)

- WELL SCREEN INTERVAL
- UPPERMOST AQUIFER POTENTIOMETRIC SURFACE
- UPPERMOST AQUIFER GROUNDWATER ELEVATION
- OTHER GROUNDWATER / SURFACE WATER ELEVATION(S)



**CROSS SECTIONS
A-A'**

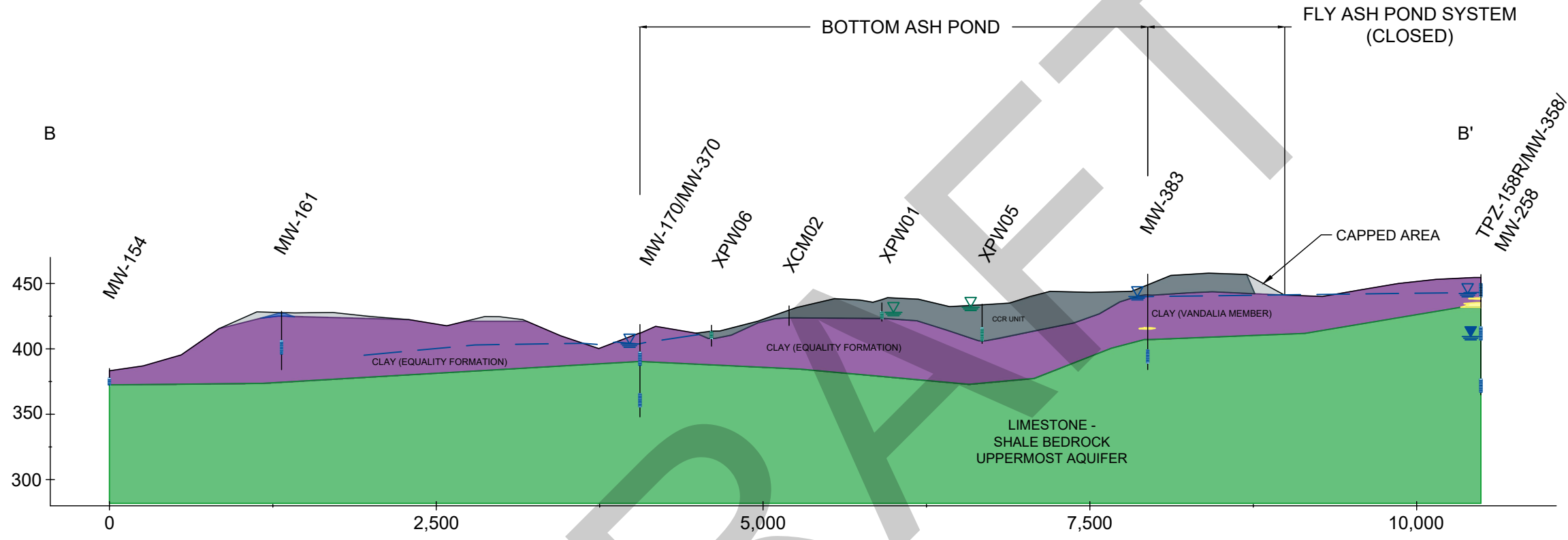
**HYDROGEOLOGIC SITE
CHARACTERIZATION REPORT REVISION 1
BOTTOM ASH POND**

BALDWIN POWER PLANT
BALDWIN, ILLINOIS

FIGURE 2-7

RAMBOLL AMERICAS
ENGINEERING SOLUTIONS, INC.



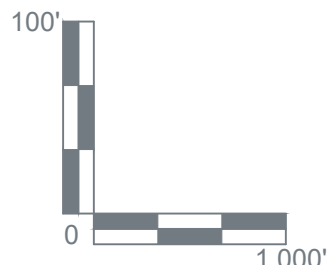


- NOTES**
- 1. These profiles were developed by interpolation between widely spaced boreholes. Only at the borehole location should it be considered as an approximately accurate representation and then only to the degree implied by the notes on the borehole logs.
 - 2. Scale is approximate.
 - 3. Vertical scale is exaggerated 10X.
 - 4. Groundwater elevations measured on March 15, 2023.

LEGEND

| | |
|--|---|
| | COAL COMBUSTION RESIDUALS (CCR) |
| | FILL |
| | CLAY |
| | SILT |
| | SAND |
| | BEDROCK / WEATHERED BEDROCK (INTERBEDDED SHALE, LIMESTONE) |

| | |
|--|--|
| | WELL SCREEN INTERVAL |
| | UPPERMOST AQUIFER POTENTIOMETRIC SURFACE |
| | UPPERMOST AQUIFER GROUNDWATER ELEVATION |
| | POREWATER ELEVATION |
| | OTHER GROUNDWATER / SURFACE WATER ELEVATION(S) |



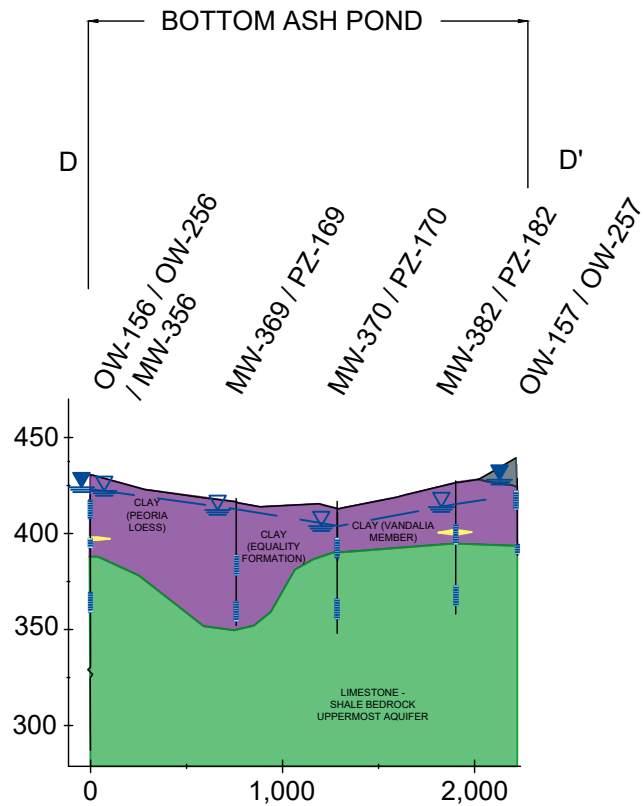
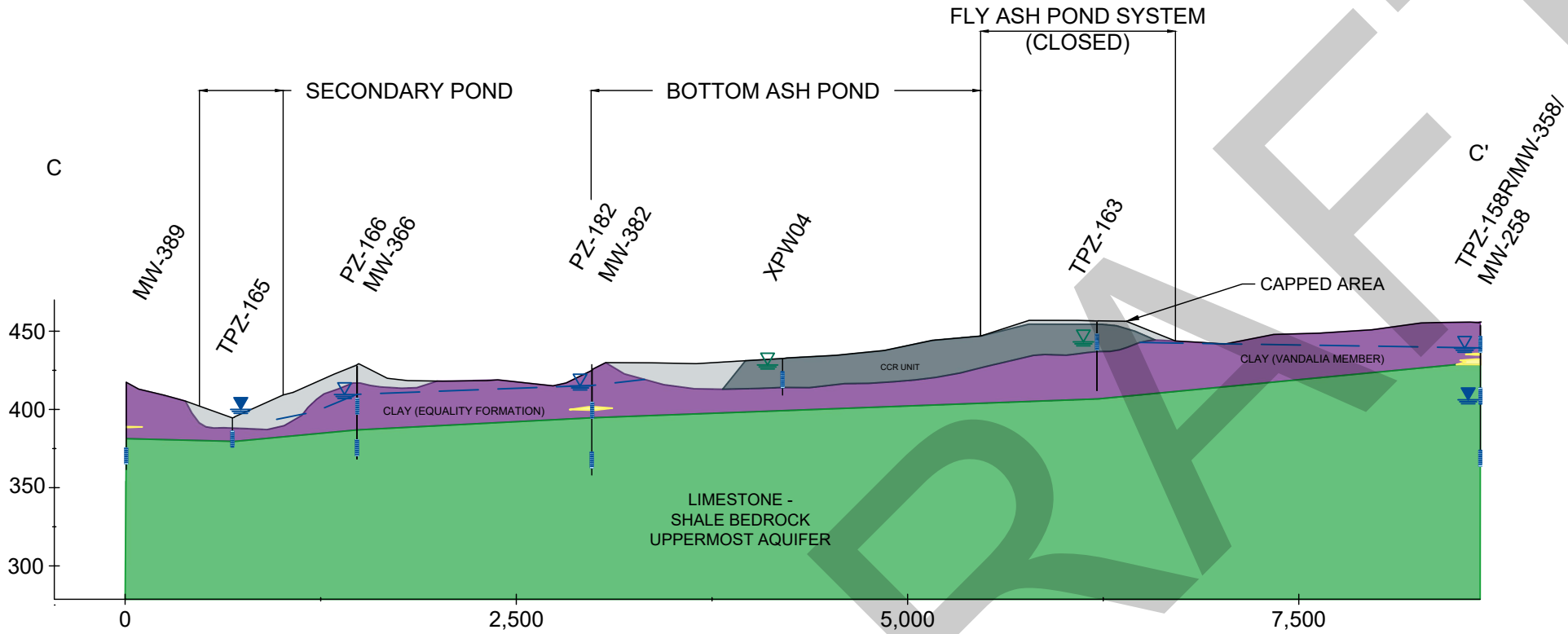
**CROSS SECTIONS
B-B'**

**HYDROGEOLOGIC SITE
CHARACTERIZATION REPORT REVISION 1
BOTTOM ASH POND**

BALDWIN POWER PLANT
BALDWIN, ILLINOIS

C:\Users\Engelhsa\OneDrive - Ramboll\Projects\Vistra\Modeling & Calcs\BAL\CAD\2023_CrossSections\Baldwin_Cross Sections.dwg
PROJECT: 1940100806 DATED: 6/26/2023 11:34 PM DESIGNER: ENGELHSA

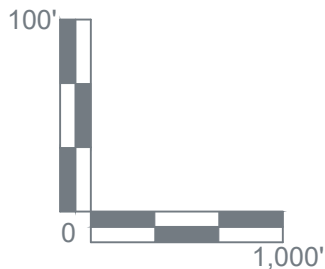
- NOTES**
1. This profile was developed by interpolation between widely spaced boreholes. Only at the borehole location should it be considered as an approximately accurate representation and then only to the degree implied by the notes on the borehole logs.
 2. Scale is approximate.
 3. Vertical scale is exaggerated 10X.
 4. Groundwater elevations measured on March 15, 2023.



LEGEND

- COAL COMBUSTION RESIDUALS (CCR)
- FILL
- CLAY
- SILT
- SAND
- BEDROCK / WEATHERED BEDROCK
(INTERBEDDED SHALE, LIMESTONE)

- WELL SCREEN INTERVAL
- UPPERMOST AQUIFER POTENTIOMETRIC SURFACE
- UPPERMOST AQUIFER GROUNDWATER ELEVATION
- POREWATER ELEVATION
- OTHER GROUNDWATER / SURFACE WATER ELEVATION(S)



**CROSS SECTIONS
C-C' AND D-D'**

**HYDROGEOLOGIC SITE
CHARACTERIZATION REPORT REVISION 1
BOTTOM ASH POND**

BALDWIN POWER PLANT
BALDWIN, ILLINOIS

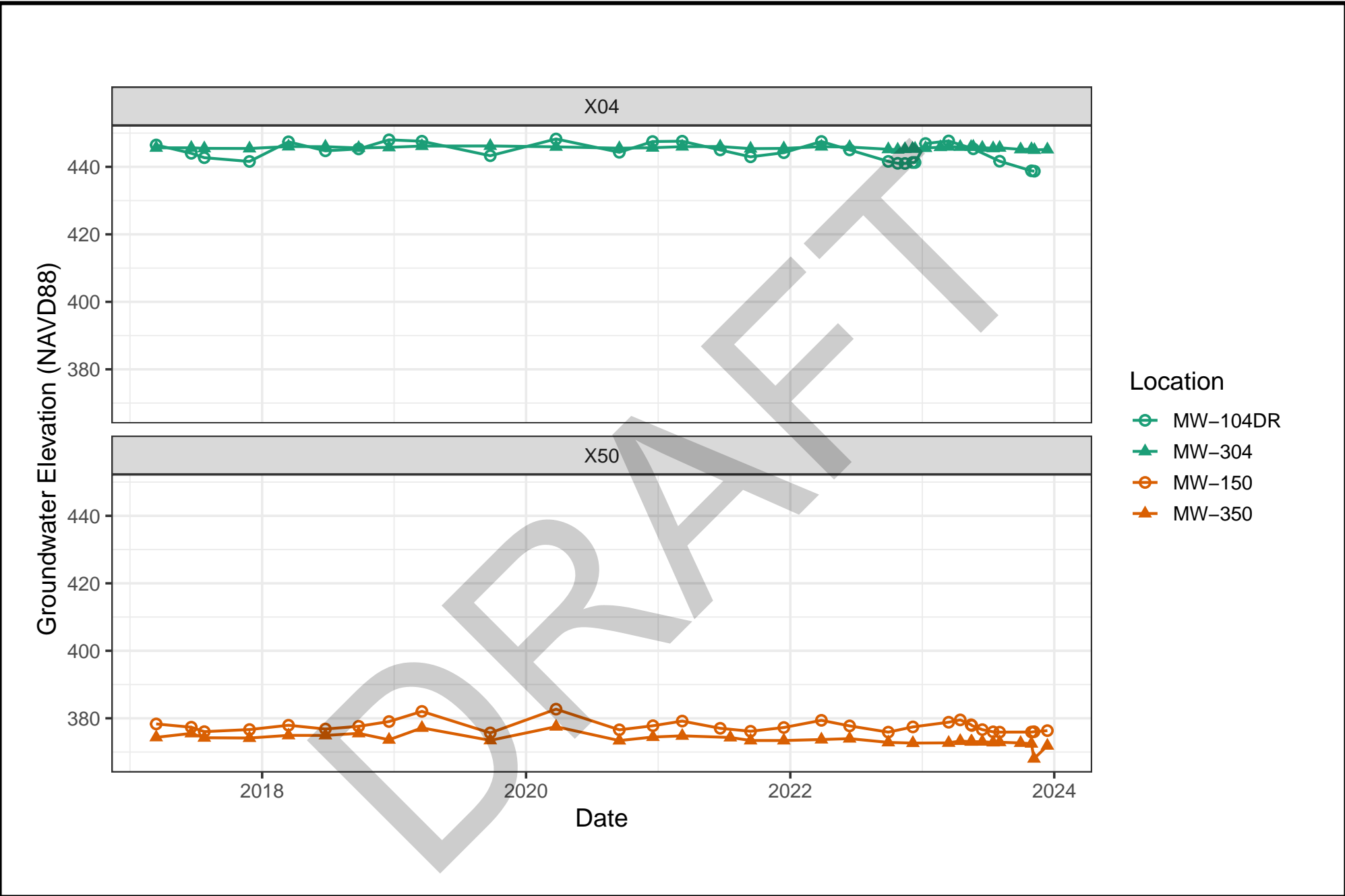
FIGURE 2-9

RAMBOLL AMERICAS
ENGINEERING SOLUTIONS, INC.

RAMBOLL

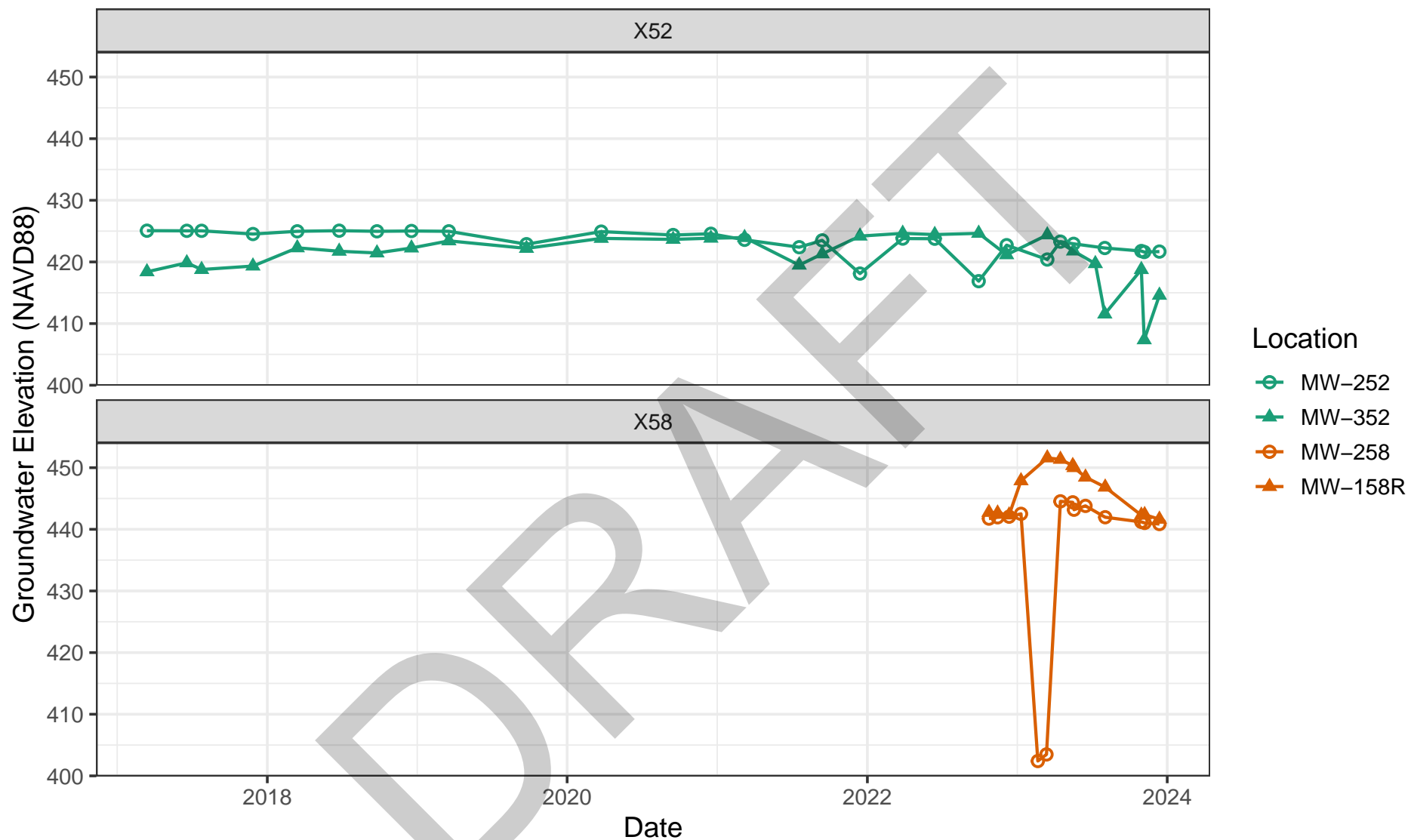
APPENDIX B
Select Hydrographs

DRAFT



Hydrographs

Nature and Extent Report
Baldwin Fly Ash Pond System
Baldwin, IL



Hydrographs

Nature and Extent Report
Baldwin Fly Ash Pond System
Baldwin, IL

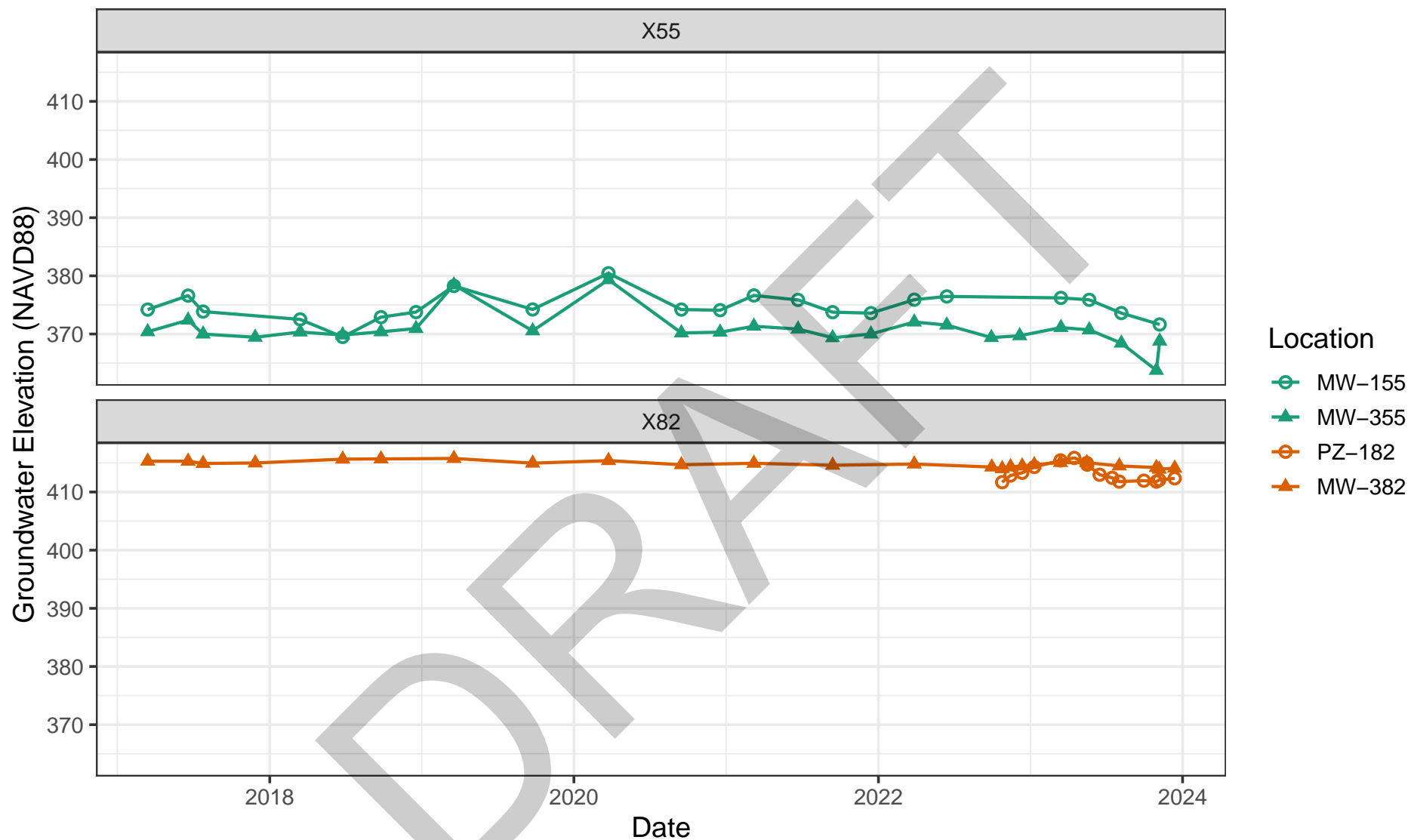
Drafter: AOC

Date: 2024-04-17

Contract Number: 1940103584

Figure

2



Hydrographs

Nature and Extent Report
Baldwin Fly Ash Pond System
Baldwin, IL

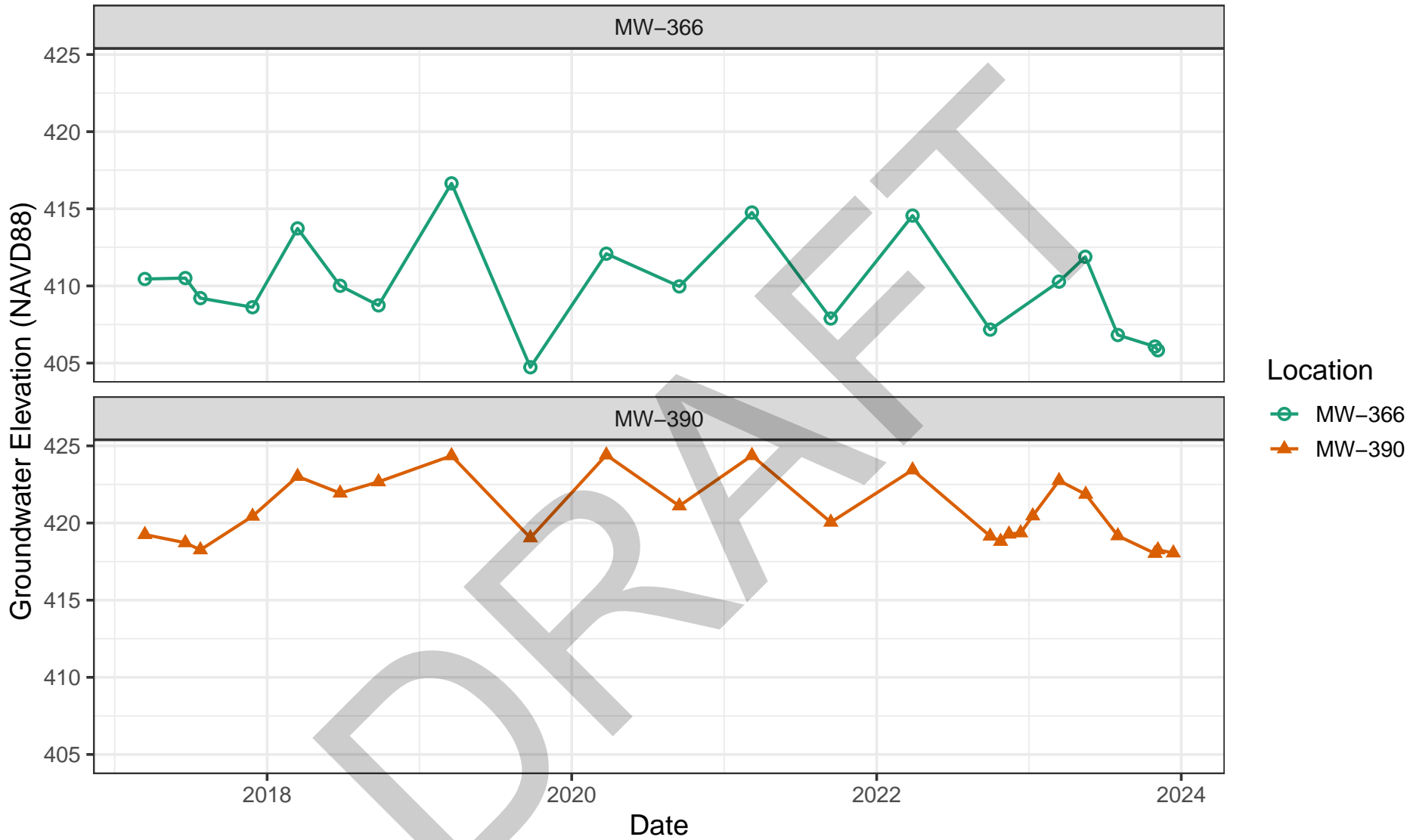
Drafter: AOC

Date: 2024-04-17

Contract Number: 1940103584

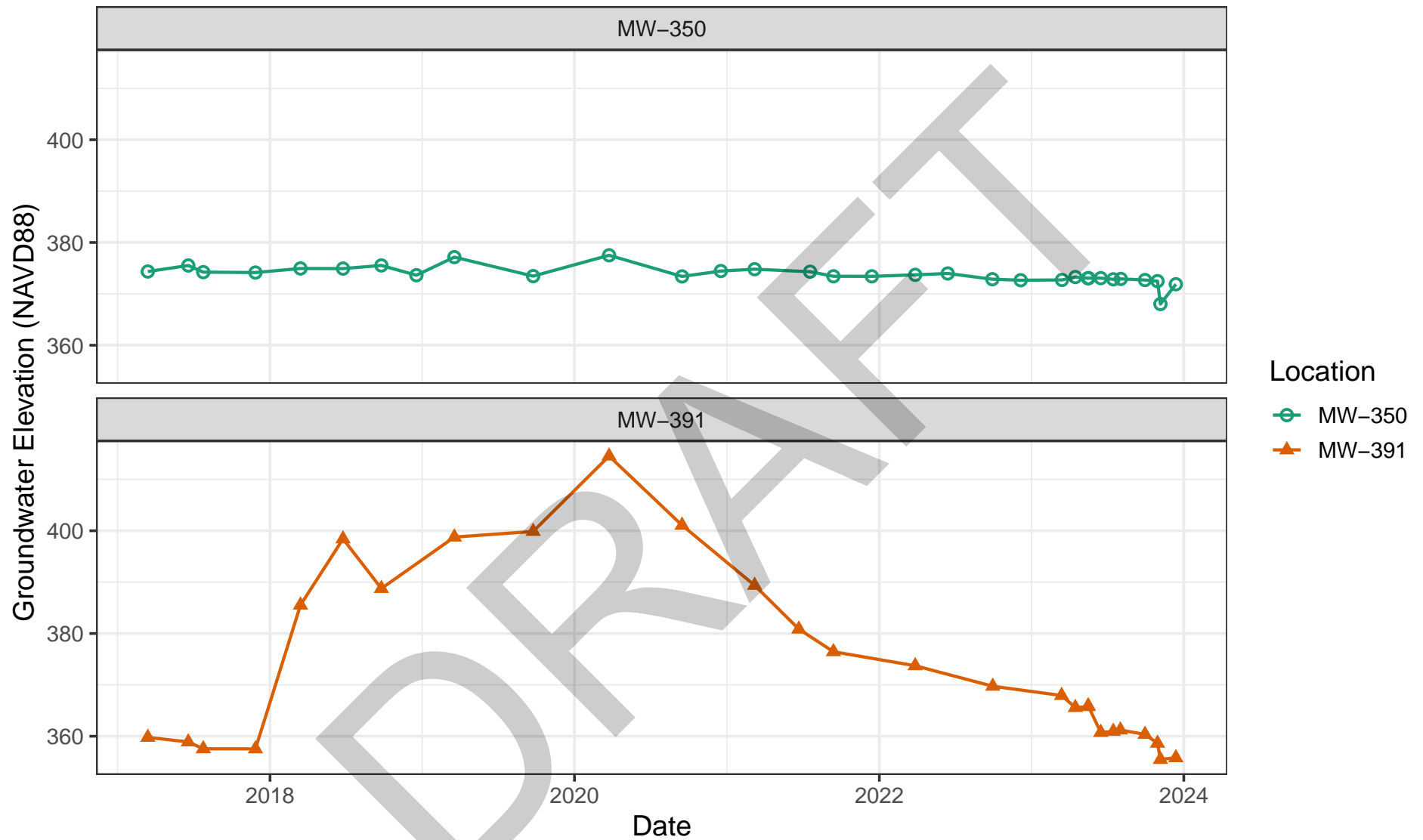
Figure

3



Hydrographs

Nature and Extent Report
Baldwin Fly Ash Pond System
Baldwin, IL



Hydrographs

Nature and Extent Report
Baldwin Fly Ash Pond System
Baldwin, IL

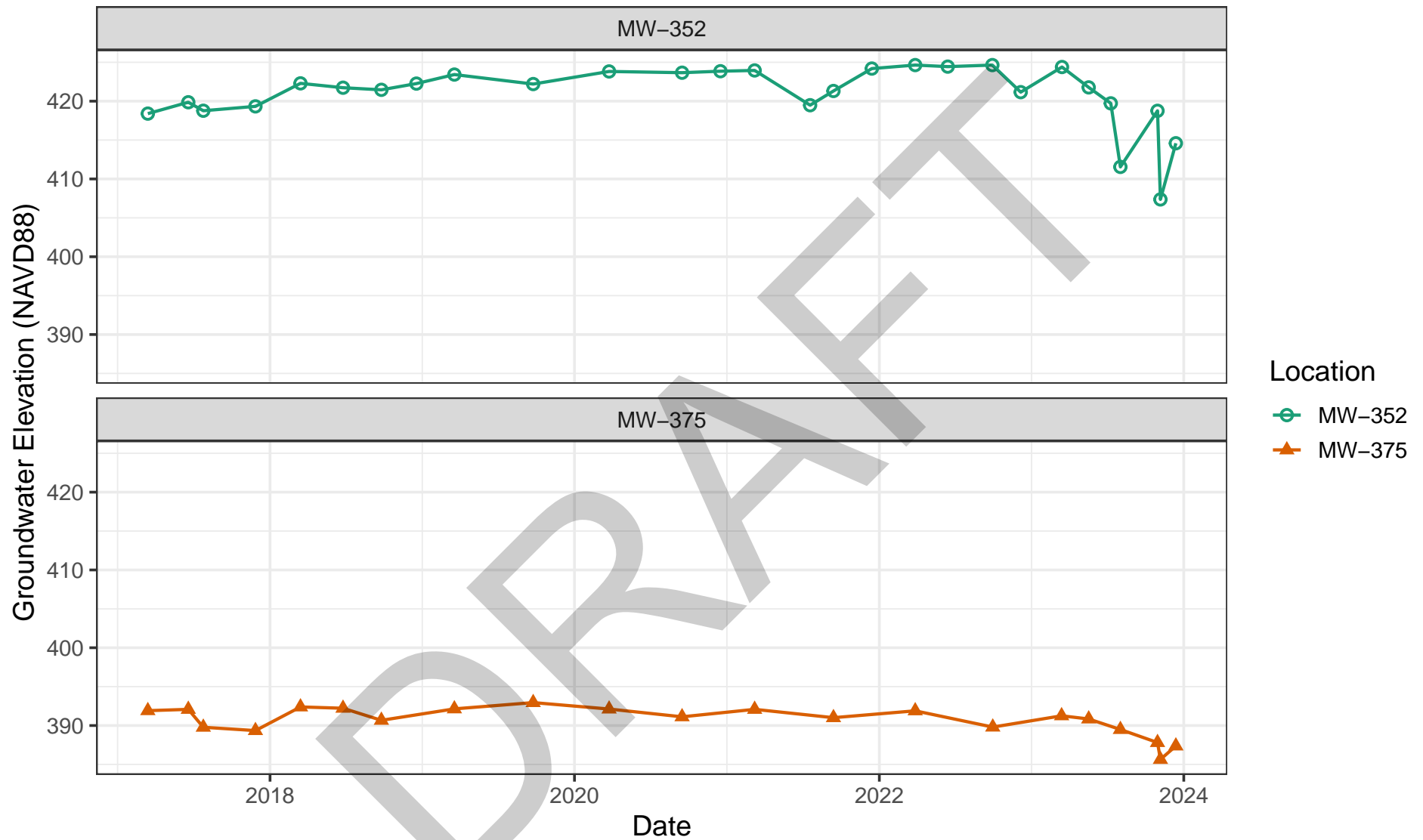
Drafter: AOC

Date: 2024-04-17

Contract Number: 1940103584

Figure

5



Hydrographs

Nature and Extent Report
Baldwin Fly Ash Pond System
Baldwin, IL

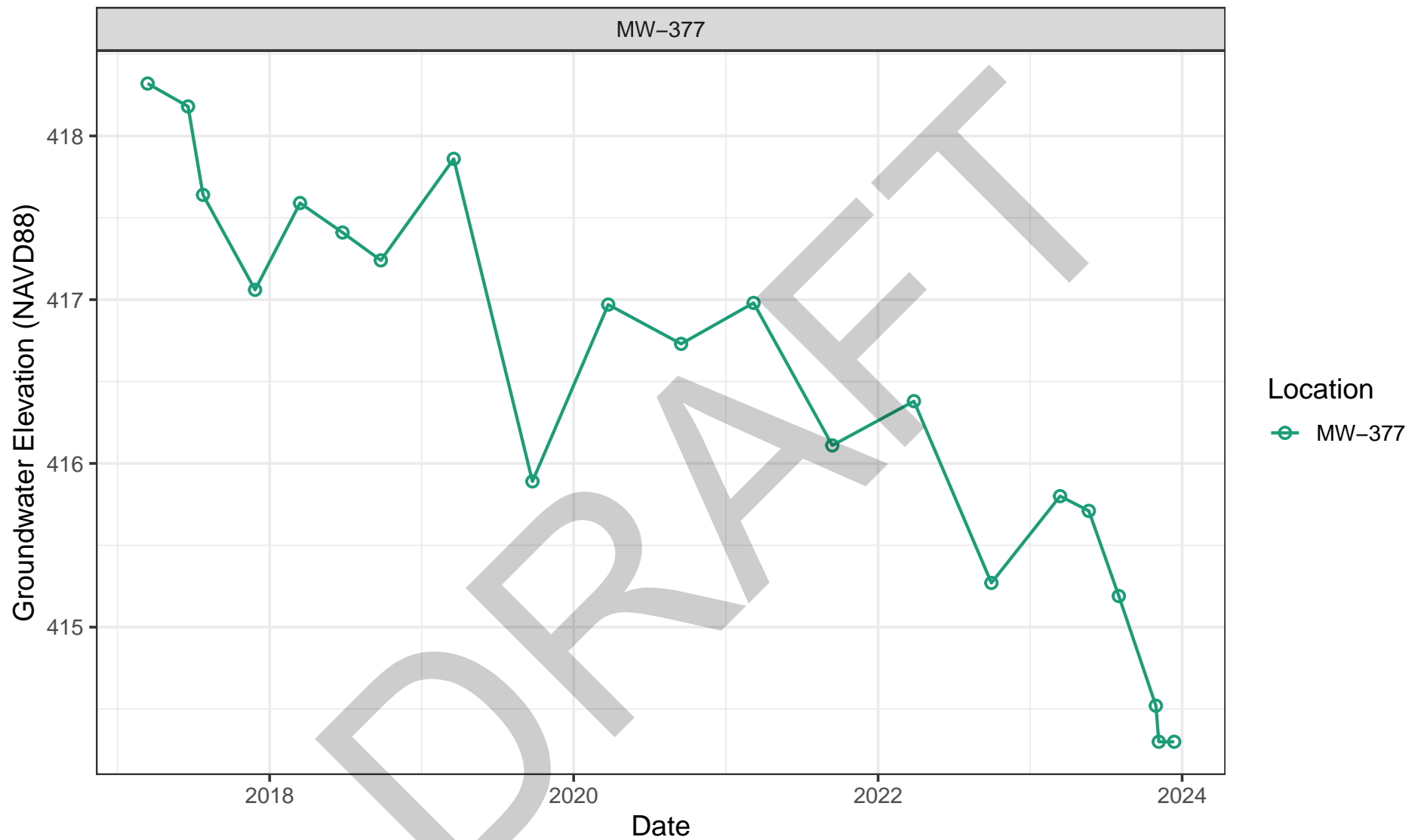
Drafter: AOC

Date: 2024-04-17

Contract Number: 1940103584

Figure

6



Hydrographs

Nature and Extent Report
Baldwin Fly Ash Pond System
Baldwin, IL

Drafter: AOC

Date: 2024-04-17

Contract Number: 1940103584

Figure

7

APPENDIX C
Vertical Hydraulic Gradients

DRAFT

APPENDIX C. VERTICAL HYDRAULIC GRADIENTS

NATURE AND EXTENT REPORT

BALDWIN POWER PLANT

FLY ASH POND SYSTEM

BALDWIN, ILLINOIS

| Date | MW-104SR Groundwater Elevation (ft NAVD88) | MW-104DR Groundwater Elevation (ft NAVD88) | Head Change (ft) | Distance Change ¹ (ft) | Vertical Hydraulic Gradient ² (dh/dl) | |
|-------------------------------------|---|---|------------------------|---|--|------|
| | UU (Vandalia) | UU (Vandalia) | | | | |
| 3/21/2016 | 447.33 | 447.39 | -0.06 | 20.41 | -0.003 | up |
| 6/21/2016 | 445.22 | 445.27 | -0.05 | 18.30 | -0.003 | up |
| 9/19/2016 | 447.05 | 447.12 | -0.07 | 20.13 | -0.003 | up |
| 12/21/2016 | 444.45 | 444.52 | -0.07 | 17.53 | -0.004 | up |
| 3/14/2017 | 446.42 | 446.48 | -0.06 | 19.50 | -0.003 | up |
| 6/19/2017 | 443.95 | 444.02 | -0.07 | 17.03 | -0.004 | up |
| 7/25/2017 | 442.66 | 442.72 | -0.06 | 15.74 | -0.004 | up |
| 11/27/2017 | 441.54 | 441.60 | -0.06 | 14.62 | -0.004 | up |
| 3/15/2018 | 447.34 | 447.42 | -0.08 | 20.42 | -0.004 | up |
| 6/25/2018 | 444.68 | 444.75 | -0.07 | 17.76 | -0.004 | up |
| 9/25/2018 | 445.24 | 445.31 | -0.07 | 18.32 | -0.004 | up |
| 12/18/2018 | 447.91 | 448.01 | -0.10 | 15.83 | -0.006 | up |
| 3/19/2019 | 447.54 | 447.59 | -0.05 | 20.62 | -0.002 | up |
| 9/24/2019 | 443.29 | 443.30 | -0.01 | 16.37 | -0.001 | flat |
| 3/24/2020 | 448.20 | 448.26 | -0.06 | 15.83 | -0.004 | up |
| 9/15/2020 | 444.29 | 444.32 | -0.03 | 17.37 | -0.002 | up |
| 12/16/2020 | 447.46 | 447.50 | -0.04 | 20.54 | -0.002 | up |
| 3/8/2021 | 447.54 | 447.60 | -0.06 | 20.62 | -0.003 | up |
| 6/21/2021 | 445.24 | 445.01 | 0.23 | 18.32 | 0.013 | down |
| 9/14/2021 | 442.91 | 442.97 | -0.06 | 15.99 | -0.004 | up |
| 12/14/2021 | 444.15 | 444.20 | -0.05 | 17.23 | -0.003 | up |
| 3/28/2022 | 447.51 | 447.52 | -0.01 | 20.59 | 0.000 | flat |
| 6/14/2022 | 444.99 | 445.02 | -0.03 | 18.07 | -0.002 | up |
| 9/29/2022 | 444.09 | 441.62 | 2.47 | 17.17 | 0.144 | down |
| 12/5/2022 | 441.24 | 441.30 | -0.06 | 14.32 | -0.004 | up |
| Middle of screen elevation MW-104SR | | | | | 442.8 | |
| Middle of screen elevation MW-104DR | | | | | 426.9 | |
| Top of screen elevation MW-104SR | | | | | 447.8 | |
| Top of screen elevation MW-104DR | | | | | 429.4 | |

APPENDIX C. VERTICAL HYDRAULIC GRADIENTS

NATURE AND EXTENT REPORT

BALDWIN POWER PLANT

FLY ASH POND SYSTEM

BALDWIN, ILLINOIS

| Date | MW-104DR Groundwater Elevation (ft NAVD88) | MW-304 Groundwater Elevation (ft NAVD88) | Head Change (ft) | Distance Change ¹ (ft) | Vertical Hydraulic Gradient ² (dh/dl) | |
|-------------------------------------|---|---|------------------------|---|--|------|
| | UU (Vandalia) | BU | | | | |
| 3/21/2016 | 447.39 | 445.08 | 2.31 | 23.89 | 0.097 | down |
| 6/21/2016 | 445.27 | 445.08 | 0.19 | 23.89 | 0.008 | down |
| 9/19/2016 | 447.12 | 444.97 | 2.15 | 23.89 | 0.090 | down |
| 12/21/2016 | 444.52 | 444.97 | -0.45 | 23.89 | -0.019 | up |
| 3/14/2017 | 446.48 | 445.64 | 0.84 | 23.89 | 0.035 | down |
| 6/19/2017 | 444.02 | 445.64 | -1.62 | 23.89 | -0.068 | up |
| 7/25/2017 | 442.72 | 445.48 | -2.76 | 23.89 | -0.116 | up |
| 11/27/2017 | 441.60 | 445.44 | -3.84 | 23.89 | -0.161 | up |
| 3/15/2018 | 447.42 | 446.02 | 1.40 | 23.89 | 0.059 | down |
| 6/25/2018 | 444.75 | 445.98 | -1.23 | 23.89 | -0.051 | up |
| 9/25/2018 | 445.31 | 445.60 | -0.29 | 23.89 | -0.012 | up |
| 12/18/2018 | 448.01 | 445.78 | 2.23 | 23.89 | 0.093 | down |
| 3/19/2019 | 447.59 | 446.16 | 1.43 | 23.89 | 0.060 | down |
| 9/24/2019 | 443.30 | 446.19 | -2.89 | 23.89 | -0.121 | up |
| 3/24/2020 | 448.26 | 445.93 | 2.33 | 23.89 | 0.098 | down |
| 9/15/2020 | 444.32 | 445.52 | -1.20 | 23.89 | -0.050 | up |
| 12/16/2020 | 447.50 | 445.67 | 1.83 | 23.89 | 0.077 | down |
| 3/8/2021 | 447.60 | 445.99 | 1.61 | 23.89 | 0.067 | down |
| 6/21/2021 | 445.01 | 446.02 | -1.01 | 23.89 | -0.042 | up |
| 9/14/2021 | 442.97 | 445.40 | -2.43 | 23.89 | -0.102 | up |
| 12/14/2021 | 444.20 | 445.47 | -1.27 | 23.89 | -0.053 | up |
| 3/28/2022 | 447.52 | 445.99 | 1.53 | 23.89 | 0.064 | down |
| 6/14/2022 | 445.02 | 445.86 | -0.84 | 23.89 | -0.035 | up |
| 9/29/2022 | 441.62 | 434.04 | 7.58 | 23.89 | 0.317 | down |
| 12/5/2022 | 441.30 | 445.35 | -4.05 | 23.89 | -0.170 | up |
| Middle of screen elevation MW-104DR | | | | | 426.9 | |
| Middle of screen elevation MW-304 | | | | | 403.0 | |
| Top of screen elevation MW-104DR | | | | | 429.4 | |
| Top of screen elevation MW-304 | | | | | 408.0 | |

APPENDIX C. VERTICAL HYDRAULIC GRADIENTS

NATURE AND EXTENT REPORT

BALDWIN POWER PLANT

FLY ASH POND SYSTEM

BALDWIN, ILLINOIS

| Date | MW-153 Groundwater Elevation (ft NAVD88) | MW-253 Groundwater Elevation (ft NAVD88) | Head Change (ft) | Distance Change ¹ (ft) | Vertical Hydraulic Gradient ² (dh/dl) | |
|-----------------------------------|---|---|------------------------|---|--|------|
| | UU (Vandalia) | UU (Vandalia) | | | | |
| 3/21/2016 | 435.58 | 435.89 | -0.31 | 17.07 | -0.018 | up |
| 6/21/2016 | 432.92 | 434.66 | -1.74 | 17.07 | -0.102 | up |
| 9/19/2016 | 436.69 | 435.27 | 1.42 | 17.07 | 0.083 | down |
| 12/21/2016 | 432.55 | 434.51 | -1.96 | 17.07 | -0.115 | up |
| 3/14/2017 | 434.19 | 435.09 | -0.90 | 17.07 | -0.053 | up |
| 6/22/2017 | 431.88 | 432.76 | -0.88 | 21.35 | -0.041 | up |
| 7/25/2017 | 430.10 | 432.76 | -2.66 | 19.57 | -0.136 | up |
| 11/27/2017 | 430.37 | 431.33 | -0.96 | 19.84 | -0.048 | up |
| 3/15/2018 | 434.62 | 434.74 | -0.12 | 17.07 | -0.007 | up |
| 6/25/2018 | 432.15 | 432.89 | -0.74 | 21.62 | -0.034 | up |
| 9/25/2018 | 432.69 | 433.73 | -1.04 | 17.07 | -0.061 | up |
| 12/18/2018 | 437.62 | 436.55 | 1.07 | 17.07 | 0.063 | down |
| 3/19/2019 | 439.02 | 437.82 | 1.20 | 17.07 | 0.070 | down |
| 9/24/2019 | 429.90 | 431.38 | -1.48 | 19.37 | -0.076 | up |
| 3/24/2020 | 439.75 | 438.73 | 1.02 | 17.07 | 0.060 | down |
| 9/15/2020 | 431.37 | 431.93 | -0.56 | 20.84 | -0.027 | up |
| 12/17/2020 | 434.36 | 433.57 | 0.79 | 17.07 | 0.046 | down |
| 3/8/2021 | 436.65 | 435.69 | 0.96 | 17.07 | 0.056 | down |
| 6/22/2021 | 432.07 | 432.56 | -0.49 | 21.54 | -0.023 | up |
| 9/16/2021 | 430.47 | 431.19 | -0.72 | 19.94 | -0.036 | up |
| 12/15/2021 | 431.60 | 431.62 | -0.02 | 21.07 | -0.001 | flat |
| 3/29/2022 | 436.77 | 435.11 | 1.66 | 17.07 | 0.097 | down |
| 6/15/2022 | 432.49 | 432.86 | -0.37 | 17.07 | -0.022 | up |
| 9/29/2022 | 428.82 | 429.86 | -1.04 | 18.29 | -0.057 | up |
| 12/6/2022 | 429.67 | 430.09 | -0.42 | 19.14 | -0.022 | up |
| Middle of screen elevation MW-153 | | | | | 427.6 | |
| Middle of screen elevation MW-253 | | | | | 410.5 | |
| Top of screen elevation MW-153 | | | | | 432.4 | |
| Top of screen elevation MW-253 | | | | | 412.8 | |

APPENDIX C. VERTICAL HYDRAULIC GRADIENTS

NATURE AND EXTENT REPORT

BALDWIN POWER PLANT

FLY ASH POND SYSTEM

BALDWIN, ILLINOIS

| Date | MW-152 Groundwater Elevation (ft NAVD88) | MW-252 Groundwater Elevation (ft NAVD88) | Head Change (ft) | Distance Change ¹ (ft) | Vertical Hydraulic Gradient ² (dh/dl) | |
|-----------------------------------|---|---|------------------------|---|--|------|
| | UU (Equality) | UU (Vandalia) | | | | |
| 3/21/2016 | 421.10 | 424.93 | -3.83 | 34.54 | -0.111 | up |
| 6/21/2016 | 420.09 | 424.57 | -4.48 | 34.54 | -0.130 | up |
| 12/21/2016 | 419.67 | 425.06 | -5.39 | 34.54 | -0.156 | up |
| 3/14/2017 | 420.14 | 425.07 | -4.93 | 34.54 | -0.143 | up |
| 6/19/2017 | 419.59 | 425.05 | -5.46 | 34.54 | -0.158 | up |
| 7/25/2017 | 417.90 | 425.05 | -7.15 | 34.54 | -0.207 | up |
| 11/27/2017 | 418.76 | 424.53 | -5.77 | 34.54 | -0.167 | up |
| 3/15/2018 | 419.89 | 424.97 | -5.08 | 34.54 | -0.147 | up |
| 6/25/2018 | 419.15 | 425.07 | -5.92 | 34.54 | -0.171 | up |
| 9/25/2018 | 420.44 | 424.97 | -4.53 | 34.54 | -0.131 | up |
| 12/18/2018 | 420.35 | 425.02 | -4.67 | 34.54 | -0.135 | up |
| 3/19/2019 | 420.35 | 424.97 | -4.62 | 34.54 | -0.134 | up |
| 9/24/2019 | 417.40 | 422.88 | -5.48 | 34.54 | -0.159 | up |
| 3/24/2020 | 423.84 | 424.92 | -1.08 | 34.54 | -0.031 | up |
| 9/15/2020 | 418.47 | 424.37 | -5.90 | 34.54 | -0.171 | up |
| 12/16/2020 | 419.84 | 424.57 | -4.73 | 34.54 | -0.137 | up |
| 3/8/2021 | 420.48 | 423.59 | -3.11 | 34.54 | -0.090 | up |
| 7/19/2021 | 419.74 | 422.39 | -2.65 | 34.54 | -0.077 | up |
| 9/14/2021 | 417.26 | 423.50 | -6.24 | 34.54 | -0.181 | up |
| 12/14/2021 | 418.78 | 418.11 | 0.67 | 34.54 | 0.019 | down |
| 3/28/2022 | 419.79 | 423.79 | -4.00 | 34.54 | -0.116 | up |
| 6/14/2022 | 418.31 | 423.77 | -5.46 | 34.54 | -0.158 | up |
| 9/29/2022 | 418.00 | 416.88 | 1.12 | 34.54 | 0.032 | down |
| 12/6/2022 | 418.17 | 422.72 | -4.55 | 34.54 | -0.132 | up |
| Middle of screen elevation MW-152 | | | | | 410.1 | |
| Middle of screen elevation MW-252 | | | | | 375.6 | |
| Top of screen elevation MW-152 | | | | | 414.7 | |
| Top of screen elevation MW-252 | | | | | 377.9 | |

APPENDIX C. VERTICAL HYDRAULIC GRADIENTS

NATURE AND EXTENT REPORT

BALDWIN POWER PLANT

FLY ASH POND SYSTEM

BALDWIN, ILLINOIS

| Date | MW-252 Groundwater Elevation (ft NAVD88) | MW-352 Groundwater Elevation (ft NAVD88) | Head Change (ft) | Distance Change ¹ (ft) | Vertical Hydraulic Gradient ² (dh/dl) | |
|-----------------------------------|---|---|------------------------|---|--|------|
| | UU (Vandalia) | BU | | | | |
| 3/21/2016 | 424.93 | 423.88 | 1.05 | 23.41 | 0.045 | down |
| 6/21/2016 | 424.57 | 424.34 | 0.23 | 23.41 | 0.010 | down |
| 12/21/2016 | 425.06 | 422.54 | 2.52 | 23.41 | 0.108 | down |
| 3/14/2017 | 425.07 | 418.40 | 6.67 | 23.41 | 0.285 | down |
| 6/19/2017 | 425.05 | 419.86 | 5.19 | 23.41 | 0.222 | down |
| 7/25/2017 | 425.05 | 418.77 | 6.28 | 23.41 | 0.268 | down |
| 11/27/2017 | 424.53 | 419.33 | 5.20 | 23.41 | 0.222 | down |
| 3/15/2018 | 424.97 | 422.29 | 2.68 | 23.41 | 0.114 | down |
| 6/25/2018 | 425.07 | 421.73 | 3.34 | 23.41 | 0.143 | down |
| 9/25/2018 | 424.97 | 421.46 | 3.51 | 23.41 | 0.150 | down |
| 12/18/2018 | 425.02 | 422.26 | 2.76 | 23.41 | 0.118 | down |
| 3/19/2019 | 424.97 | 423.42 | 1.55 | 23.41 | 0.066 | down |
| 9/24/2019 | 422.88 | 422.20 | 0.68 | 23.41 | 0.029 | down |
| 3/24/2020 | 424.92 | 423.82 | 1.10 | 23.41 | 0.047 | down |
| 9/15/2020 | 424.37 | 423.66 | 0.71 | 23.41 | 0.030 | down |
| 12/16/2020 | 424.57 | 423.85 | 0.72 | 23.41 | 0.031 | down |
| 3/8/2021 | 423.59 | 423.95 | -0.36 | 23.41 | -0.015 | up |
| 7/19/2021 | 423.95 | 423.50 | 0.45 | 23.41 | 0.019 | down |
| 9/14/2021 | 419.48 | 418.11 | 1.37 | 23.41 | 0.059 | down |
| 12/14/2021 | 421.31 | 423.79 | -2.48 | 23.41 | -0.106 | up |
| 3/28/2022 | 424.19 | 423.77 | 0.42 | 23.41 | 0.018 | down |
| 6/14/2022 | 424.64 | 416.88 | 7.76 | 23.41 | 0.331 | down |
| 9/29/2022 | 424.44 | 422.72 | 1.72 | 23.41 | 0.073 | down |
| 12/6/2022 | 425.00 | 421.16 | 3.84 | 23.41 | 0.164 | down |
| Middle of screen elevation MW-252 | | | | | 375.6 | |
| Middle of screen elevation MW-352 | | | | | 352.2 | |
| Top of screen elevation MW-252 | | | | | 377.9 | |
| Top of screen elevation MW-352 | | | | | 354.5 | |

APPENDIX C. VERTICAL HYDRAULIC GRADIENTS

NATURE AND EXTENT REPORT

BALDWIN POWER PLANT

FLY ASH POND SYSTEM

BALDWIN, ILLINOIS

| Date | MW-150 Groundwater Elevation (ft NAVD88) | MW-350 Groundwater Elevation (ft NAVD88) | Head Change (ft) | Distance Change ¹ (ft) | Vertical Hydraulic Gradient ² (dh/dl) | |
|-----------------------------------|---|---|------------------------|---|--|------|
| | UU (Cahokia) | BU | | | | |
| 3/21/2016 | 379.22 | 374.57 | 4.65 | 23.79 | 0.195 | down |
| 6/21/2016 | 377.59 | 375.26 | 2.33 | 27.38 | 0.085 | down |
| 12/21/2016 | 377.70 | 374.66 | 3.04 | 27.49 | 0.111 | down |
| 3/14/2017 | 378.32 | 374.35 | 3.97 | 28.11 | 0.141 | down |
| 6/19/2017 | 377.35 | 375.52 | 1.83 | 27.14 | 0.067 | down |
| 7/25/2017 | 376.04 | 374.23 | 1.81 | 25.83 | 0.070 | down |
| 11/27/2017 | 376.66 | 374.15 | 2.51 | 26.45 | 0.095 | down |
| 3/15/2018 | 377.93 | 374.94 | 2.99 | 27.72 | 0.108 | down |
| 6/25/2018 | 376.82 | 374.92 | 1.90 | 26.61 | 0.071 | down |
| 9/25/2018 | 377.62 | 375.53 | 2.09 | 27.41 | 0.076 | down |
| 12/18/2018 | 379.03 | 373.63 | 5.40 | 23.79 | 0.227 | down |
| 3/19/2019 | 382.04 | 377.15 | 4.89 | 23.79 | 0.206 | down |
| 9/24/2019 | 375.67 | 373.45 | 2.22 | 25.46 | 0.087 | down |
| 3/24/2020 | 382.70 | 377.51 | 5.19 | 23.79 | 0.218 | down |
| 9/15/2020 | 376.58 | 373.39 | 3.19 | 26.37 | 0.121 | down |
| 12/17/2020 | 377.79 | 374.44 | 3.35 | 27.58 | 0.121 | down |
| 3/8/2021 | 379.17 | 374.80 | 4.37 | 23.79 | 0.184 | down |
| 6/21/2021 | 377.03 | -- | -- | -- | -- | -- |
| 9/14/2021 | 376.15 | 373.42 | 2.73 | 25.94 | 0.105 | down |
| 12/14/2021 | 377.26 | 373.11 | 4.15 | 27.05 | 0.153 | down |
| 3/28/2022 | 379.39 | 373.70 | 5.69 | 23.79 | 0.239 | down |
| 6/14/2022 | 377.74 | -- | -- | -- | -- | -- |
| 9/29/2022 | 375.89 | 372.85 | 3.04 | 25.68 | 0.118 | down |
| 12/6/2022 | 377.44 | 372.65 | 4.79 | 27.23 | 0.176 | down |
| Middle of screen elevation MW-150 | | | | | 374.0 | |
| Middle of screen elevation MW-350 | | | | | 350.2 | |
| Top of screen elevation MW-150 | | | | | 378.8 | |
| Top of screen elevation MW-350 | | | | | 352.5 | |

APPENDIX C. VERTICAL HYDRAULIC GRADIENTS

NATURE AND EXTENT REPORT

BALDWIN POWER PLANT

FLY ASH POND SYSTEM

BALDWIN, ILLINOIS

| Date | MW-155 Groundwater Elevation (ft NAVD88) | MW-355 Groundwater Elevation (ft NAVD88) | Head Change (ft) | Distance Change ¹ (ft) | Vertical Hydraulic Gradient ² (dh/dl) | |
|-----------------------------------|---|---|------------------------|---|--|------|
| | UU (Cahokia) | BU | | | | |
| 3/21/2016 | 376.85 | 373.83 | 3.02 | 15.74 | 0.192 | down |
| 6/21/2016 | 375.80 | 371.14 | 4.66 | 14.69 | 0.317 | down |
| 9/19/2016 | 373.85 | 372.22 | 1.63 | 12.74 | 0.128 | down |
| 12/21/2016 | 373.39 | 370.23 | 3.16 | 12.28 | 0.257 | down |
| 3/14/2017 | 374.20 | 370.39 | 3.81 | 13.09 | 0.291 | down |
| 6/19/2017 | 376.60 | 372.39 | 4.21 | 15.49 | 0.272 | down |
| 7/25/2017 | 373.86 | 369.99 | 3.87 | 12.75 | 0.304 | down |
| 3/15/2018 | 372.51 | 370.34 | 2.17 | 11.40 | 0.190 | down |
| 6/25/2018 | 369.49 | 369.82 | -0.33 | 8.38 | -0.039 | up |
| 9/25/2018 | 372.90 | 370.38 | 2.52 | 11.79 | 0.214 | down |
| 12/18/2018 | 373.77 | 370.94 | 2.83 | 12.66 | 0.224 | down |
| 3/19/2019 | 378.26 | 378.44 | -0.18 | 17.15 | -0.010 | up |
| 9/24/2019 | 374.22 | 370.54 | 3.68 | 13.11 | 0.281 | down |
| 3/24/2020 | 380.45 | 379.34 | 1.11 | 14.39 | 0.077 | down |
| 9/15/2020 | 374.20 | 370.19 | 4.01 | 13.09 | 0.306 | down |
| 12/17/2020 | 374.10 | 370.31 | 3.79 | 12.99 | 0.292 | down |
| 3/8/2021 | 376.63 | 371.34 | 5.29 | 15.52 | 0.341 | down |
| 6/22/2021 | 375.86 | 370.85 | 5.01 | 14.75 | 0.340 | down |
| 9/16/2021 | 373.76 | 369.36 | 4.40 | 12.65 | 0.348 | down |
| 12/14/2021 | 373.59 | 370.00 | 3.59 | 12.48 | 0.288 | down |
| 3/29/2022 | 375.90 | 372.06 | 3.84 | 14.79 | 0.260 | down |
| 6/15/2022 | 376.46 | 371.54 | 4.92 | 15.35 | 0.321 | down |
| Middle of screen elevation MW-155 | | | | | 375.5 | |
| Middle of screen elevation MW-355 | | | | | 361.1 | |
| Top of screen elevation MW-155 | | | | | 380.3 | |
| Top of screen elevation MW-355 | | | | | 363.4 | |

APPENDIX C. VERTICAL HYDRAULIC GRADIENTS

NATURE AND EXTENT REPORT

BALDWIN POWER PLANT

FLY ASH POND SYSTEM

BALDWIN, ILLINOIS

| Date | OW-156 Groundwater Elevation (ft NAVD88) | MW-356 Groundwater Elevation (ft NAVD88) | Head Change (ft) | Distance Change ¹ (ft) | Vertical Hydraulic Gradient ² (dh/dl) | |
|-----------------------------------|---|---|------------------------|---|--|------|
| | UU (Equality) | BU | | | | |
| 3/21/2016 | 420.78 | 424.77 | -3.99 | 48.42 | -0.082 | up |
| 6/21/2016 | 421.10 | 424.89 | -3.79 | 48.42 | -0.078 | up |
| 9/19/2016 | 423.33 | 425.03 | -1.70 | 48.42 | -0.035 | up |
| 12/21/2016 | 422.10 | 424.82 | -2.72 | 48.42 | -0.056 | up |
| 3/14/2017 | 423.45 | 425.06 | -1.61 | 48.42 | -0.033 | up |
| 6/19/2017 | 423.70 | 425.20 | -1.50 | 48.42 | -0.031 | up |
| 7/25/2017 | 419.17 | 425.05 | -5.88 | 48.42 | -0.121 | up |
| 11/27/2017 | 419.82 | 424.88 | -5.06 | 48.42 | -0.105 | up |
| 6/25/2018 | 420.06 | 425.06 | -5.00 | 48.42 | -0.103 | up |
| 9/25/2018 | 421.74 | 425.03 | -3.29 | 48.42 | -0.068 | up |
| 3/19/2019 | 424.35 | 424.95 | -0.60 | 48.42 | -0.012 | up |
| 9/24/2019 | 418.48 | 424.58 | -6.10 | 48.42 | -0.126 | up |
| 3/24/2020 | 424.87 | 424.37 | 0.50 | 48.42 | 0.010 | down |
| 9/15/2020 | 419.68 | 423.98 | -4.30 | 48.42 | -0.089 | up |
| 12/17/2020 | 422.85 | -- | -- | -- | -- | -- |
| 3/8/2021 | 424.22 | 423.66 | 0.56 | 48.42 | 0.012 | down |
| 6/22/2021 | 420.04 | -- | -- | -- | -- | -- |
| 9/15/2021 | 418.49 | 423.61 | -5.12 | 48.42 | -0.106 | up |
| 3/29/2022 | 424.27 | 423.40 | 0.87 | 48.42 | 0.018 | down |
| 9/30/2022 | 420.85 | 423.28 | -2.43 | 48.42 | -0.050 | up |
| Middle of screen elevation OW-156 | | | | | 412.6 | |
| Middle of screen elevation MW-356 | | | | | 364.2 | |
| Top of screen elevation OW-156 | | | | | 380.3 | |
| Top of screen elevation MW-356 | | | | | 363.4 | |

APPENDIX C. VERTICAL HYDRAULIC GRADIENTS

NATURE AND EXTENT REPORT

BALDWIN POWER PLANT

FLY ASH POND SYSTEM

BALDWIN, ILLINOIS

| Date | MW-158R Groundwater Elevation (ft NAVD88) | MW-258 Groundwater Elevation (ft NAVD88) | Head Change (ft) | Distance Change ¹ (ft) | Vertical Hydraulic Gradient ² (dh/dl) | |
|------------------------------------|--|---|------------------------|---|--|------|
| | UU (Equality) | BU | | | | |
| 10/27/2022 | 442.74 | 441.74 | 1.00 | 34.15 | 0.029 | down |
| 11/17/2022 | 442.63 | 441.95 | 0.68 | 34.04 | 0.020 | down |
| 12/13/2022 | 442.32 | 442.05 | 0.27 | 33.73 | 0.008 | down |
| 1/11/2023 | 447.87 | 442.52 | 5.35 | 31.97 | 0.167 | down |
| 2/20/2023 | -- | 442.92 | -- | 31.97 | -- | -- |
| Middle of screen elevation MW-158R | | | | | 440.6 | |
| Middle of screen elevation MW-258 | | | | | 408.6 | |
| Top of screen elevation MW-158R | | | | | 445.6 | |
| Top of screen elevation MW-258 | | | | | 413.6 | |

| Date | PZ-170 Groundwater Elevation (ft NAVD88) | MW-370 Groundwater Elevation (ft NAVD88) | Head Change (ft) | Distance Change ¹ (ft) | Vertical Hydraulic Gradient ² (dh/dl) | |
|-----------------------------------|---|---|------------------------|---|--|------|
| | UU (Equality) | BU | | | | |
| 10/27/2022 | 404.21 | 401.72 | 2.49 | 31.80 | 0.078 | down |
| 11/16/2022 | 404.41 | 401.78 | 2.63 | 31.80 | 0.083 | down |
| 12/13/2022 | 404.82 | 402.17 | 2.65 | 31.80 | 0.083 | down |
| 1/12/2023 | 406.02 | 402.60 | 3.42 | 31.80 | 0.108 | down |
| 2/20/2023 | -- | 402.75 | -- | 31.80 | -- | -- |
| Middle of screen elevation PZ-170 | | | | | 392.5 | |
| Middle of screen elevation MW-370 | | | | | 360.7 | |
| Top of screen elevation PZ-170 | | | | | 397.5 | |
| Top of screen elevation MW-370 | | | | | 365.7 | |

| Date | PZ-182 Groundwater Elevation (ft NAVD88) | MW-382 Groundwater Elevation (ft NAVD88) | Head Change (ft) | Distance Change ¹ (ft) | Vertical Hydraulic Gradient ² (dh/dl) | |
|-----------------------------------|---|---|------------------------|---|--|------|
| | UU (Equality) | BU | | | | |
| 10/25/2022 | 411.69 | 414.01 | -2.32 | -31.80 | 0.073 | down |
| 11/14/2022 | 412.84 | 414.34 | -1.50 | -31.80 | 0.047 | down |
| 12/12/2022 | 413.31 | 414.47 | -1.16 | -31.80 | 0.036 | down |
| 1/10/2023 | 414.31 | 414.69 | -0.38 | -31.80 | 0.012 | down |
| 3/14/2023 | 415.44 | 415.07 | 0.37 | -31.80 | -0.012 | up |
| Middle of screen elevation PZ-182 | | | | | 367.7 | |
| Middle of screen elevation MW-382 | | | | | 399.5 | |
| Top of screen elevation PZ-182 | | | | | 372.7 | |
| Top of screen elevation MW-382 | | | | | 404.5 | |

APPENDIX C. VERTICAL HYDRAULIC GRADIENTS

NATURE AND EXTENT REPORT

BALDWIN POWER PLANT

FLY ASH POND SYSTEM

BALDWIN, ILLINOIS

| Date | MW-192 Groundwater Elevation (ft NAVD88) | MW-392 Groundwater Elevation (ft NAVD88) | Head Change (ft) | Distance Change ¹ (ft) | Vertical Hydraulic Gradient ² (dh/dl) | |
|-----------------------------------|---|---|------------------------|---|--|------|
| | UU (Equality) | BU | | | | |
| 10/27/2022 | 428.41 | 427.68 | 0.73 | 53.97 | 0.014 | down |
| 11/16/2022 | 428.57 | 428.08 | 0.49 | 53.97 | 0.009 | down |
| 12/13/2022 | 428.61 | 428.41 | 0.20 | 53.97 | 0.004 | down |
| 1/12/2023 | 428.91 | 428.61 | 0.30 | 53.97 | 0.006 | down |
| 2/20/2023 | 428.94 | 428.97 | -0.03 | 53.97 | -0.001 | flat |
| Middle of screen elevation MW-192 | | | | | 409.0 | |
| Middle of screen elevation MW-392 | | | | | 355.1 | |
| Top of screen elevation MW-192 | | | | | 414.0 | |
| Top of screen elevation MW-392 | | | | | 360.1 | |

| Date | MW-193 Groundwater Elevation (ft NAVD88) | MW-393 Groundwater Elevation (ft NAVD88) | Head Change (ft) | Distance Change ¹ (ft) | Vertical Hydraulic Gradient ² (dh/dl) | |
|-----------------------------------|---|---|------------------------|---|--|------|
| | UU (Equality) | BU | | | | |
| 10/27/2022 | 428.95 | 427.06 | 1.89 | 52.93 | 0.036 | down |
| 11/16/2022 | 429.02 | 429.29 | -0.27 | 52.93 | -0.005 | up |
| 12/13/2022 | 429.07 | 429.52 | -0.45 | 52.93 | -0.009 | up |
| 1/12/2023 | 429.30 | 429.51 | -0.21 | 52.93 | -0.004 | up |
| 2/20/2023 | 431.24 | 429.35 | 1.89 | 52.93 | 0.036 | down |
| Middle of screen elevation MW-193 | | | | | 407.5 | |
| Middle of screen elevation MW-393 | | | | | 354.6 | |
| Top of screen elevation MW-193 | | | | | 412.5 | |
| Top of screen elevation MW-393 | | | | | 359.6 | |

APPENDIX C. VERTICAL HYDRAULIC GRADIENTS

NATURE AND EXTENT REPORT

BALDWIN POWER PLANT

FLY ASH POND SYSTEM

BALDWIN, ILLINOIS

| Date | MW-194 Groundwater Elevation (ft NAVD88) | MW-394 Groundwater Elevation (ft NAVD88) | Head Change (ft) | Distance Change ¹ (ft) | Vertical Hydraulic Gradient ² (dh/dl) | |
|------------|---|---|-----------------------------------|---|--|----|
| | UU (Equality) | BU | | | | |
| 10/27/2022 | 430.43 | 431.52 | -1.09 | 44.72 | -0.024 | up |
| 11/16/2022 | 431.32 | 432.69 | -1.37 | 44.72 | -0.031 | up |
| 12/13/2022 | 431.39 | 433.18 | -1.79 | 44.72 | -0.040 | up |
| 1/12/2023 | 431.60 | 432.99 | -1.39 | 44.72 | -0.031 | up |
| 2/20/2023 | 431.69 | 432.91 | -1.22 | 44.72 | -0.027 | up |
| | | | Middle of screen elevation MW-194 | | 407.2 | |
| | | | Middle of screen elevation MW-394 | | 362.5 | |
| | | | Middle of screen elevation MW-194 | | 402.4 | |
| | | | Middle of screen elevation MW-394 | | 357.5 | |

[O: EGP 4/27/23, C: SSW 5/2/23]

Notes:

¹ Distance change was calculated using the midpoint of the piezometer screen and water table surface. If the water table surface was above the top of the monitoring well screen, then distance change was calculated using the midpoint of both screens.

² Vertical gradients between ± 0.0015 are considered flat, and typically have less than 0.02 foot difference in groundwater elevation between wells.

BU = bedrock unit

dh = head change

dl = distance change

ft = foot/feet

NAVD88 = North American Vertical Datum of 1988

PMP = potential migration pathway

UU = upper unit

APPENDIX D
Off-Site Groundwater Quality Results (Kelron, 2012)



April 16, 2012

Rick Diericx, Senior Director
Environmental Compliance Group
Dynergy Operating Company
604 Pierce Blvd
O'Fallon, IL 62269

Dear Mr. Diericx:

**Subject: Off-Site Groundwater Quality Results
Baldwin Energy Complex, Baldwin, Illinois**

This groundwater report has been prepared by Kelron Environmental (Kelron) on behalf of Dynergy Operating Company to present the results of an off-site groundwater quality investigation near the Baldwin Energy Complex's (BEC's) ash pond system, which is owned and operated by Dynergy Midwest Generation, LLC. The purpose of the investigation was to assess shallow off-site groundwater quality for the presence of inorganic parameters related to coal combustion residuals (CCRs).

METHODS OF INVESTIGATION

This investigation was targeted specifically to assess groundwater quality off-site to the south and southwest of the BEC's ash pond system. A total of eight shallow temporary piezometers were installed – six to the south of existing on-site monitoring well MW-152 and two to the west and southwest of on-site monitoring well MW-150. The temporary piezometers were installed on March 5 and 6, 2012 using an AMS PowerProbe 9500-VTR rig using direct push methods for both soil sampling and temporary piezometer installation. All drilling and well installations were performed by Terra Drill, Inc. of Dupon, Illinois under the direct supervision of Kelron. Each direct-push probe hole was continuously sampled to determine the geology and into each a 1-inch diameter pre-packed screened piezometer was installed and completed with a flushmount well vault. The pre-pack well screens consisted of 5-foot lengths of Schedule 40 polyvinyl chloride (PVC) with 0.010-inch slots and a pre-pack of ultrafine (120 mesh) silica sand with two layers of nylon mesh. Total open area of each well screen was approximately 2 percent. The boring and temporary piezometer logs are provided in Attachment 3. Well construction details are summarized on Table 1 (Attachment 1).

Following completion of all eight piezometers they were located in the field with a handheld GPS system and surveyed for elevation to an accuracy of 0.01 foot relative to the nearest benchmarks at the BEC. Due to the very low permeability of the predominantly clay materials within which most of the piezometers were installed, groundwater samples were not collected from the eight wells until static groundwater levels were reached. All wells were sampled on March 15, 2012 using a peristaltic pump with ¼-inch inner-diameter low density polyethylene (LDPE) tubing. During pumping of each well the groundwater was monitored for the field parameters of temperature, specific conductance, pH, and groundwater depth, with all data recorded on field data sheets (Attachment 4). A field duplicate (sample identification BPZ93) was collected from temporary piezometer BPZ3 for quality assurance/quality control purposes. Groundwater samples were collected in laboratory prepared bottles with the appropriate preservatives, placed in an iced cooler, and delivered to Teklab, Inc. in Collinsville, Illinois for analysis of total boron, total sulfate,

and total dissolved solids (TDS). The laboratory analytical report and chain of custody are provided in Attachment 5.

PIEZOMETER LOCATIONS AND GROUNDWATER LEVELS

The off-site temporary piezometer locations are shown on Figure 1 (Attachment 2) relative to the approximate property boundary of the BEC. Two north-south lines of temporary piezometers were installed along Magnolia Drive (BPZ1, BPZ2, BPZ3) to the east, and Ruby Lane (BPZ4, BPZ5, BPZ6) to the west, of on-site monitoring well nest MW-152, MW-252, and MW-352. Two temporary piezometers were installed along Conservation Road to the southwest (BPZ7) and northwest (BPZ8) of on-site monitoring well nest MW-150 and MW-350. An elevation cross-section of the eight temporary piezometers (Figure 2 [Attachment 2]) shows that ground surface elevation decreases significantly from south to north towards the BEC property along both Magnolia Drive and Ruby Lane. In order to intercept groundwater the piezometer screens were installed to successively greater depths from south to north towards the BEC.

Groundwater levels were measured on three occasions (Table 2 [Attachment 1]): following completion of the eight temporary piezometers (March 6, 2012); approximately 24 hours after installation (March 7, 2012); and prior to sampling on March 15, 2012. Upon initial completion five of the eight piezometers were dry, with no groundwater in the wells. One day after completion there was still one dry piezometer (BPZ5), four with very deep and non-static water levels (i.e., groundwater levels still recovering), and three with static water levels. Nine days after installation the groundwater levels in all eight temporary piezometers had reached static levels, at which time they were all measured for groundwater elevation prior to collection of groundwater samples.

The shallow groundwater elevation map shown on Figure 3 (Attachment 2) was prepared utilizing groundwater levels measured at both the BEC ash pond system network of monitoring wells and the eight off-site temporary piezometers. Groundwater elevations at temporary piezometers BPZ1 through BPZ6 decrease from south to north and from east to west, with the shallow groundwater flow direction towards the west and northwest. Groundwater flow in the vicinity of the south-central property boundary of the BEC converges towards a perennial earthen drainage channel that is present north of the railroad tracks and south of the ash pond system. The drainage channel and low lying area south of the ash ponds and adjacent to the railroad tracks acts as a groundwater capture zone for topographically higher areas to the north (i.e., ash ponds) and south of the railroad tracks.

Groundwater flow in the vicinity of off-site temporary piezometers BPZ7 and BPZ8 is towards the west and southwest.

GROUNDWATER QUALITY RESULTS

Table 3 (Attachment 1) summarizes the groundwater quality data for the eight temporary piezometers for the March 15, 2012 sampling event. The concentrations for the field measured parameter of pH and the laboratory analyzed parameters of total sulfate, total boron, and total dissolved solids are provided on the table and compared to the State of Illinois groundwater quality standards for Class I potable resource groundwater (IAC 35 Part 620 Section 410). The Class I standards were exceeded in groundwater at two temporary piezometers. Piezometer BPZ4 exceeded the sulfate standard with a concentration of 817 milligrams per Liter (mg/L) versus the Class I standard of 400 mg/L, and the TDS standard with a concentration of 1,640 mg/L versus the Class I standard of 1,200 mg/L. Piezometer BPZ7 exceeded the TDS standard with a concentration of 1,220 mg/L. No other parameters at any other piezometers exceeded Class I standards.

With the exception of piezometer BPZ4, all other samples collected from the piezometers along Magnolia Drive and Ruby Lane were below the total sulfate and TDS standards. Total boron concentrations, the primary indicator of the presence of CCR leachate, were below the Class I standard in the samples collected from all six piezometers along Magnolia Drive and Ruby Lane and were similar to what has been analyzed at groundwater monitoring wells MW-104S and MW-104D, which are upgradient to the BEC ash pond system. Groundwater elevations in the area along the BEC south property line and railroad tracks reflect the ground surface topography, with the dominant groundwater flow direction being from both the north and the south towards the earthen east-west drainage channel between the railroad tracks and ash ponds. Groundwater flow within the low-lying area south of the ash ponds and adjacent to the railroad tracks is toward the west-northwest, with the low topographic area along the drainage channel acting as a groundwater capture zone. Piezometer BPZ4 is topographically the lowest of all the piezometers as it is nearest to this drainage channel. The other five piezometers are at higher topographic elevations and upgradient from the railroad tracks and drainage channel. No potable or non-potable water wells have been documented in the area south of the BEC ash pond system.

The other location with a Class I groundwater exceedance was at temporary piezometer BPZ7, which had a TDS concentration (1,220 mg/L) slightly greater than the groundwater standard (1,200 mg/L). All other parameter concentrations in the groundwater at this location and BPZ8 were less than Class I standards. The geology in the vicinity of these piezometers is characterized by low permeability clay and shale-limestone bedrock within 25 feet of ground surface. No potable or non-potable water wells have been documented in this area southwest of the BEC ash pond system.

Should you have any questions about the material presented in this summary letter, please contact us at your convenience.

Sincerely,



Stuart J. Cravens, ILPG / CGWP
Senior Hydrogeologist

- Attachments:
1. Tables
 2. Figures
 3. Boring and Temporary Piezometer Logs
 4. Water Sample Field Data Sheets
 5. Laboratory Analytical Report and Chain of Custody

ATTACHMENT 1

Table 1. Temporary Piezometer Construction Details

Table 2. Groundwater Levels and Elevations: March 2012

Table 3. Groundwater Quality Data – March 15, 2012 Sampling Event

Table 1. Temporary Piezometer Construction Details
Off-Site Groundwater Quality Investigation - Baldwin Ash Pond System
Baldwin Energy Complex; Baldwin, IL

| Temporary Piezometer Number | Installation Date | Driller | Piezometer Top Elevation | Ground Elevation | Screen Top Depth (BGS) | Screen Bottom Depth (BGS) | Screen Top Elevation | Screen Bottom Elevation | Screen Length | Probehole Depth from Ground Surface | Bottom of Probehole Elevation | Piezometer Depth from Ground Surface | Piezometer Depth from Top of Casing |
|-----------------------------------|----------------------|-------------|--------------------------------|---------------------|---------------------------------|------------------------------------|----------------------------|-------------------------------|------------------|--|-------------------------------------|---|---|
| BPZ1 | 03/06/12 | Terra Drill | 434.53 | 434.77 | 12.88 | 17.88 | 421.89 | 416.89 | 5.00 | 20.0 | 414.8 | 17.98 | 17.74 |
| BPZ2 | 03/06/12 | Terra Drill | 439.84 | 440.10 | 9.41 | 14.41 | 430.69 | 425.69 | 5.00 | 15.0 | 425.1 | 14.51 | 14.25 |
| BPZ3 | 03/06/12 | Terra Drill | 450.39 | 450.58 | 14.77 | 19.77 | 435.81 | 430.81 | 5.00 | 20.0 | 430.6 | 19.87 | 19.68 |
| BPZ4 | 03/06/12 | Terra Drill | 429.01 | 429.32 | 18.08 | 23.08 | 411.24 | 406.24 | 5.00 | 30.0 | 399.3 | 23.18 | 22.87 |
| BPZ5 | 03/06/12 | Terra Drill | 432.49 | 432.65 | 14.61 | 19.61 | 418.04 | 413.04 | 5.00 | 20.0 | 412.7 | 19.71 | 19.55 |
| BPZ6 | 03/06/12 | Terra Drill | 437.48 | 437.73 | 14.47 | 19.47 | 423.26 | 418.26 | 5.00 | 20.0 | 417.7 | 19.57 | 19.32 |
| BPZ7 | 03/05/12 | Terra Drill | 397.39 | 397.70 | 17.53 | 22.53 | 380.17 | 375.17 | 5.00 | 25.0 | 372.7 | 22.63 | 22.32 |
| BPZ8 | 03/05/12 | Terra Drill | 393.06 | 393.51 | 10.67 | 15.67 | 382.84 | 377.84 | 5.00 | 18.0 | 375.5 | 15.77 | 15.32 |

Notes:

All depth and elevation measurements are in feet.

All elevations as measured on 03/09/12.

All piezometers constructed with Schedule 40 PVC, 1-inch diameter, 10-slot screens with pre-pack of ultrafine (120 mesh) silica sand with 2 layers of nylon mesh; open area = 2%.

Table 2. Groundwater Levels and Elevations: March 2012
Off-Site Groundwater Quality Investigation - Baldwin Ash Pond System
Baldwin Energy Complex, Baldwin, Illinois

| Temporary Piezometer Number | Ground Surface Elevation (feet NGVD) | Measuring Point Elevation (feet NGVD) | Piezometer Depth from Top of Casing (feet) | Groundwater Depth (feet below MP) | | | Groundwater Elevation (feet NGVD) | | |
|-----------------------------------|---|--|---|-----------------------------------|--------------------------------|--------------------------------|-----------------------------------|--------------------------------|--------------------------------|
| | | | | 1 03/06/12 15:10 - 15:40 | 2 03/07/12 14:50 - 16:02 | 3 03/15/12 09:00 - 12:00 | 1 03/06/12 15:10 - 15:40 | 2 03/07/12 14:50 - 16:02 | 3 03/15/12 09:00 - 12:00 |
| BPZ1 | 434.77 | 434.53 | 17.74 | Dry | 14.66 ns | 6.62 | - - | - - | 427.91 |
| BPZ2 | 440.10 | 439.84 | 14.25 | 3.40 | 1.37 | 1.21 | 436.44 | 438.47 | 438.63 |
| BPZ3 | 450.58 | 450.39 | 19.68 | 4.45 | 1.76 | 1.65 | 445.94 | 448.63 | 448.74 |
| BPZ4 | 429.32 | 429.01 | 22.87 | Dry | 21.79 ns | 17.59 | - - | - - | 411.42 |
| BPZ5 | 432.65 | 432.49 | 19.55 | Dry | Dry | 14.67 | - - | - - | 417.82 |
| BPZ6 | 437.73 | 437.48 | 19.32 | Dry | 17.51 ns | 11.47 | - - | - - | 426.01 |
| BPZ7 | 397.70 | 397.39 | 22.32 | Dry | 22.19 ns | 19.03 | - - | - - | 378.36 |
| BPZ8 | 393.51 | 393.06 | 15.32 | 2.90 | 3.00 | 3.04 | 390.16 | 390.06 | 390.02 |

Notes:

All depth and elevation measurements are in feet.

- - No groundwater elevation provided for non-static groundwater level.

MP Measuring Point (top of well casing).

NGVD Vertical elevation relative to the National Geodetic Vertical Datum.

ns Non-static water level.

**Table 3. Groundwater Quality Data - March 15, 2012 Sampling Event
Off-Site Groundwater Quality Investigation - Baldwin Ash Pond System
Baldwin Energy Complex; Baldwin, Illinois**

| Parameter, Unit | Class I Groundwater Standard ¹ | Temporary Piezometer Number | | | | | | | |
|------------------------------|---|-----------------------------|-------|-------|--------|--------|-------|-------|--------|
| | | BPZ1 | BPZ2 | BPZ3 | BPZ4 | BPZ5 | BPZ6 | BPZ7 | BPZ8 |
| Field Parameters | | | | | | | | | |
| pH (standard units) | 6.5 / 9.0* | 7.48 | 7.21 | 6.96 | 7.14 | 7.39 | 7.30 | 6.85 | 7.55 |
| General Chemistry Parameters | | | | | | | | | |
| Total Sulfate (mg/L) | 400 | 119 | 92 | 85 | 817 | 27 | 70 | 215 | 76 |
| Total Dissolved Solids, mg/L | 1,200 | 502 | 676 | 500 | 1,640 | 394 | 664 | 1,220 | 434 |
| Metals | | | | | | | | | |
| Total Boron (mg/l) | 2.0 | 0.0096 | 0.012 | 0.011 | 0.0435 | 0.0314 | 0.010 | 0.252 | 0.0354 |

Notes:

¹ Groundwater quality standards for Class I: Potable Resource Groundwater (IAC 35 Part 620 Section 410).

* Lower and Upper limits for pH is the Class I groundwater quality standard of 6.5 and 9.0 Standard Units.

< = Below method reporting limit.

mg/L = milligrams per Liter.

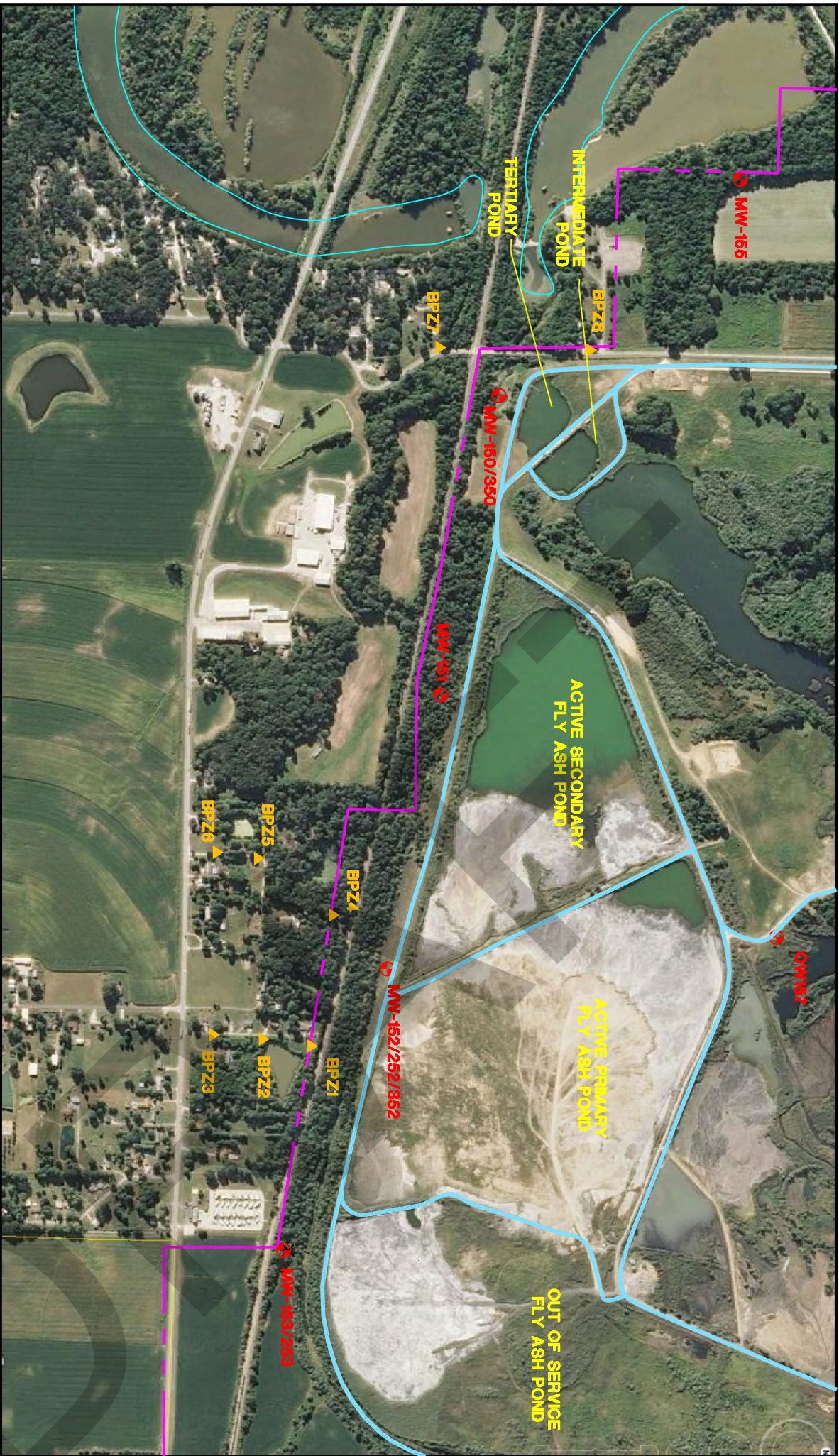
Exceeds Class I Groundwater Quality Standard.

ATTACHMENT 2

Figure 1. Temporary Off-Site Piezometer Locations

Figure 2. Temporary Piezometer Screen Elevations

**Figure 3. Baldwin Ash Pond System Shallow Groundwater Elevation
Map: March 6 – 15, 2012**



LEGEND

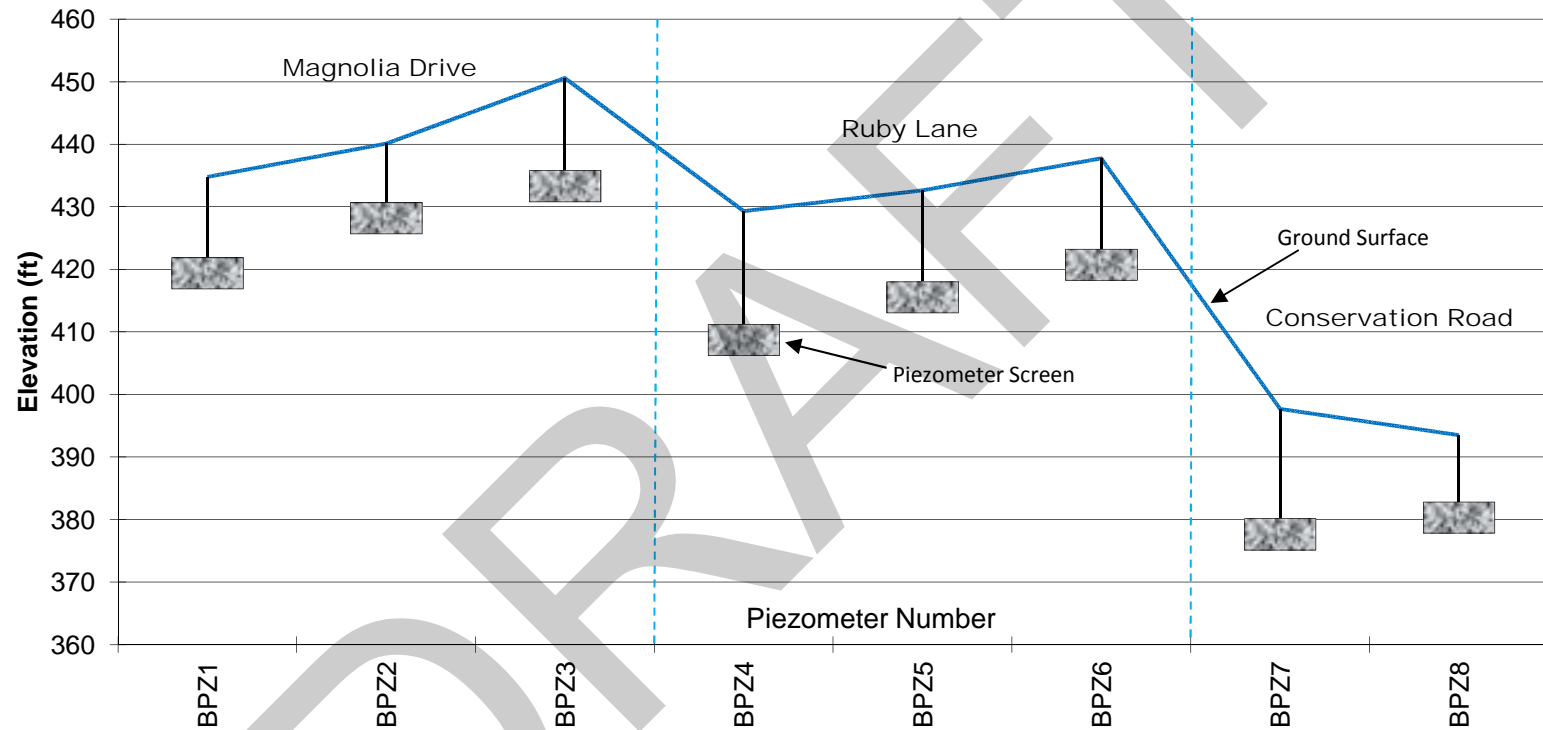
- Monitoring well location and number
- Temporary piezometer location and number
- Ash pond
- Approximate property boundary, Baldwin Energy Complex, Baldwin, Illinois

TITLE:
TEMPORARY OFF-SITE PIEZOMETER LOCATIONS
BALDWIN ASH POND SYSTEM
BALDWIN, ILLINOIS

| | | | | | |
|-------|---------|-------|----|---------------------------------|-------------------|
| DWN: | TMM | DES: | SC | PROJECT NO: | 62410020011 |
| CHKD: | | APPD: | | DYNEGY MIDWEST GENERATION, LLC. | BALDWIN, ILLINOIS |
| DATE: | 3/22/12 | REV: | 0 | FIGURE 1 | |



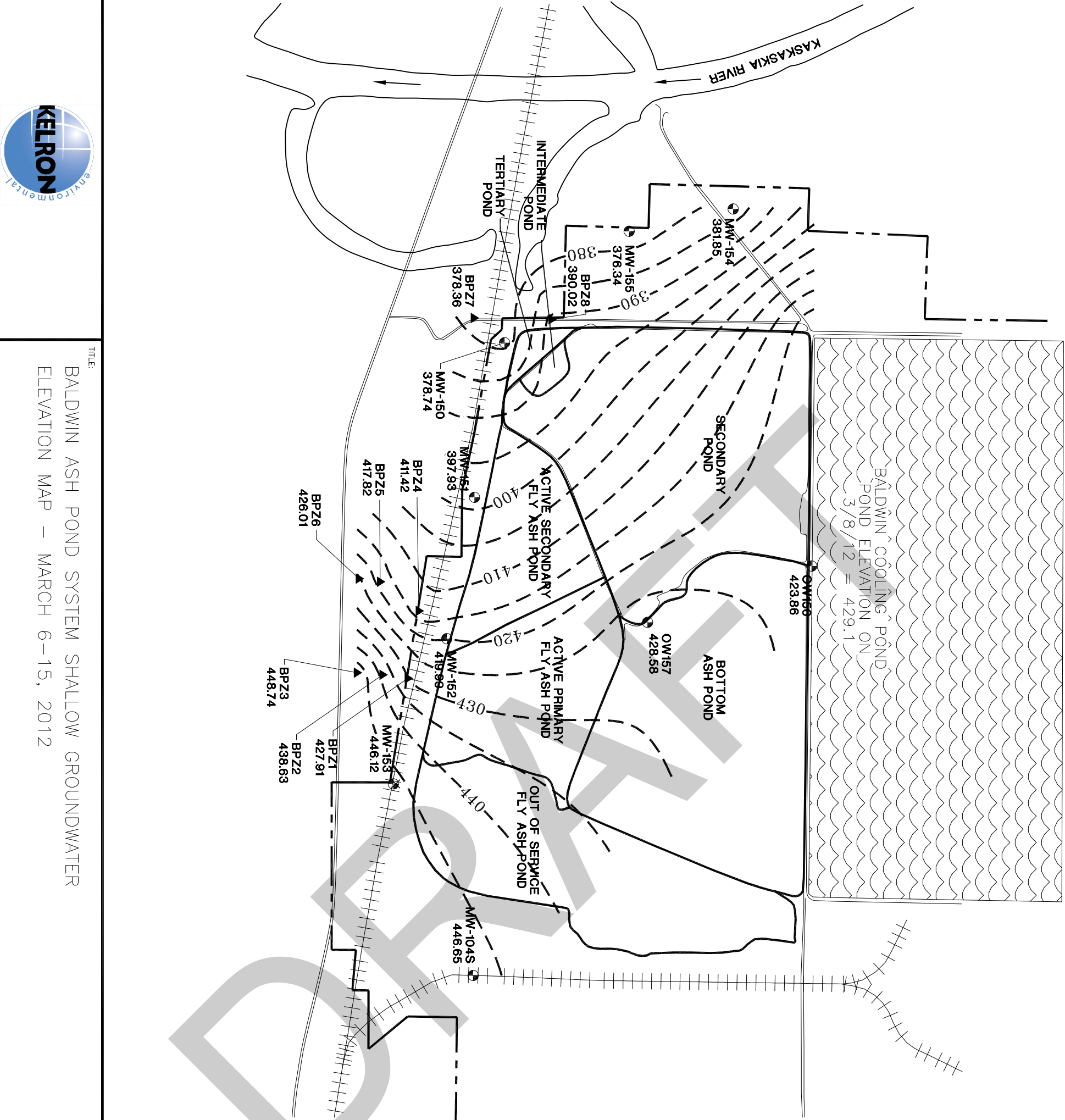
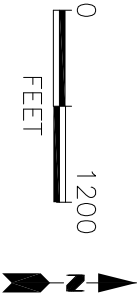
Figure 2. Temporary Piezometer Screen Elevations
Off-Site Groundwater Quality Investigation - Baldwin Ash Pond System
Baldwin Energy Complex; Baldwin, Illinois
Dynegy Midwest Generation, LLC





TITLE:
BALDWIN ASH POND SYSTEM SHALLOW GROUNDWATER
ELEVATION MAP – MARCH 6–15, 2012

| | | | | |
|-------|---------|-------|----|---------------------------------|
| DWN: | TMM | DES: | SC | PROJECT NO: 62410020011 |
| CHKD: | | APPD: | | DYNEGY MIDWEST GENERATION, LLC. |
| DATE: | 3/22/12 | REV: | 0 | BALDWIN, ILLINOIS |



LEGEND

- MW-111 MONITORING WELL LOCATION AND NUMBER
- ▲ BPZ1 TEMPORARY PIEZOMETER LOCATION AND NUMBER
- - - - - POTENTIOMETRIC SURFACE CONTOUR (FEET)
- APPROXIMATE PROPERTY BOUNDARY, BALDWIN ENERGY COMPLEX, BALDWIN, ILLINOIS

NOTES: 1. Elevations are in feet with respect to Mean Sea Level.
2. Elevation contours are based on interpolation between widely spaced well locations. Only at the well is the elevation actually known.

BALDWIN COOLING POND
POND ELEVATION ON
3/8/12 = 429.1

ATTACHMENT 3

Boring and Temporary Piezometer Logs

DRAFT

**KELRON
ENVIRONMENTAL
INCORPORATED**

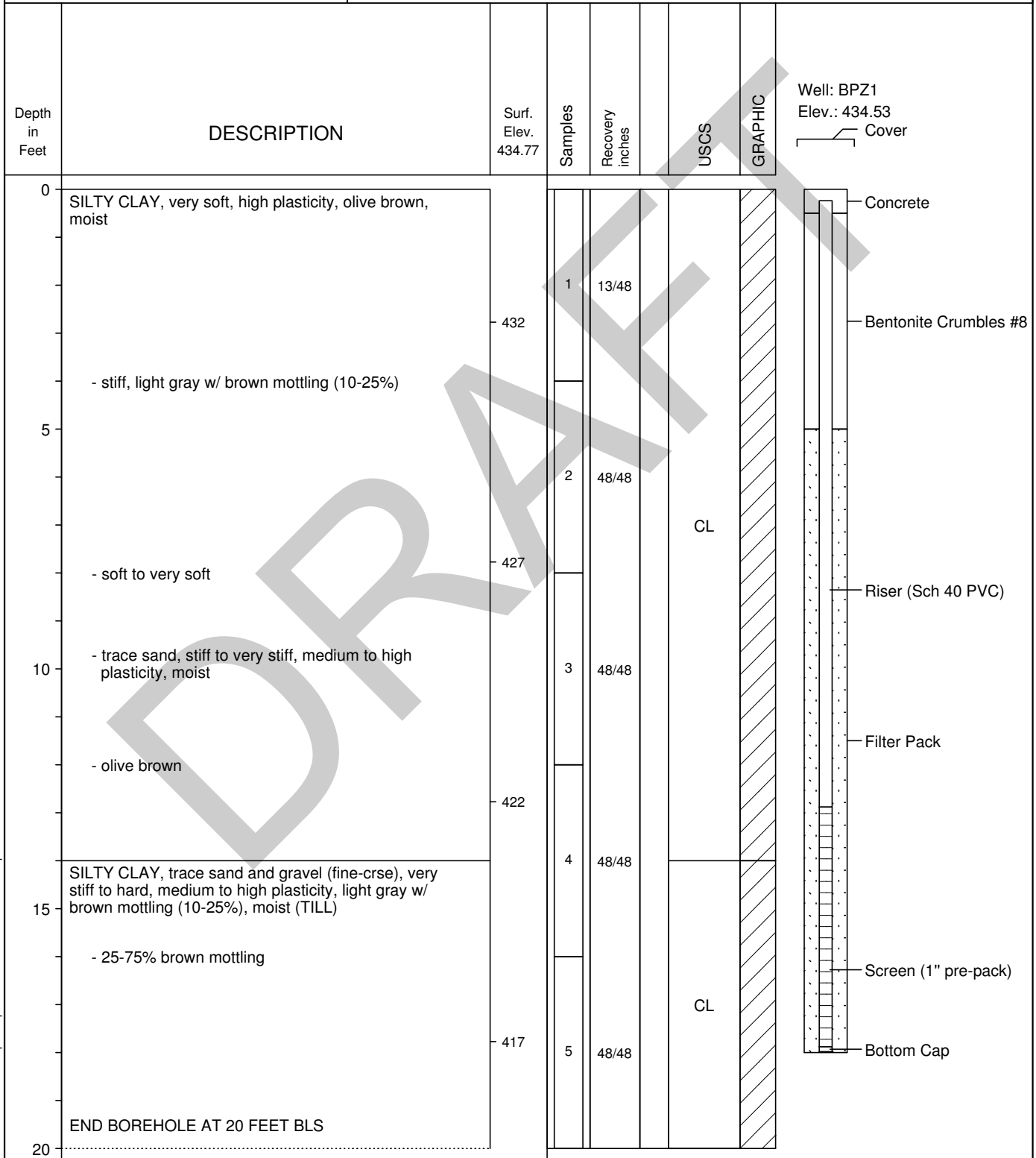
LOG OF BORING BPZ1

(Page 1 of 1)

Off-Site Groundwater Quality Investigation
BaldwinAsh Pond System
Baldwin Energy Complex, Baldwin, IL
Dynegy Midwest Generation, LLC

Date Completed : 03/06/2012
Hole Diameter : 2.75"
Drilling Method : AMS PowerProbe 9500-VTR
Sampling Method : MacroCore (1.25" ID)
Drilling Company : Terra Drill

Driller : Jim Dittmaier
Geologist : S. Cravens (Kelron Env)
Land Surface Elevation: 434.77
Top of Casing Elevation 434.53
X,Y Coordinates :



**KELRON
ENVIRONMENTAL
INCORPORATED**

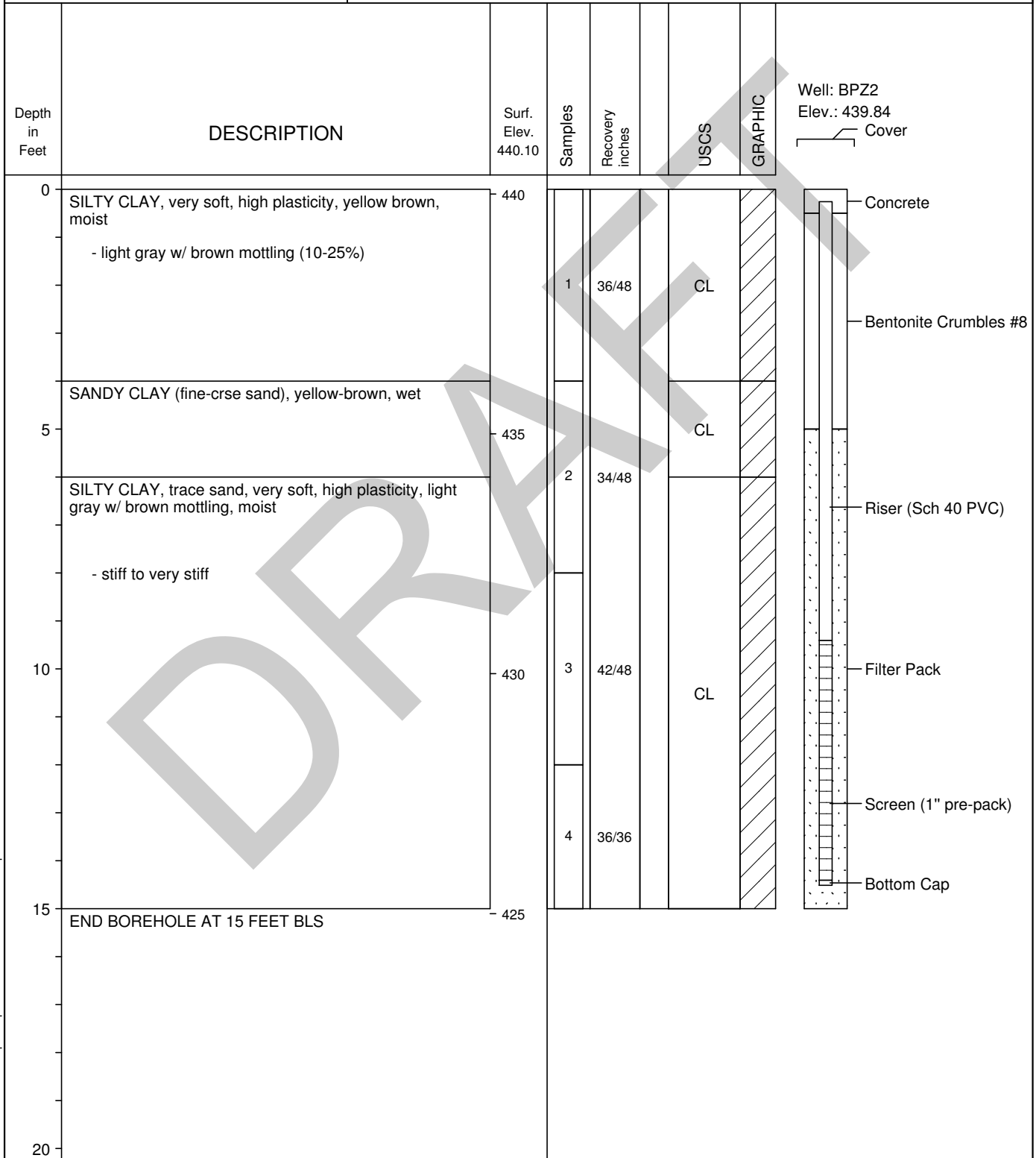
LOG OF BORING BPZ2

(Page 1 of 1)

Off-Site Groundwater Quality Investigation
BaldwinAsh Pond System
Baldwin Energy Complex, Baldwin, IL
Dynegy Midwest Generation, LLC

Date Completed : 03/06/2012
Hole Diameter : 2.75"
Drilling Method : AMS PowerProbe 9500-VTR
Sampling Method : MacroCore (1.25" ID)
Drilling Company : Terra Drill

Driller : Jim Dittmaier
Geologist : S. Cravens (Kelron Env)
Land Surface Elevation: 440.10
Top of Casing Elevation 439.84
X,Y Coordinates :



**KELRON
ENVIRONMENTAL
INCORPORATED**

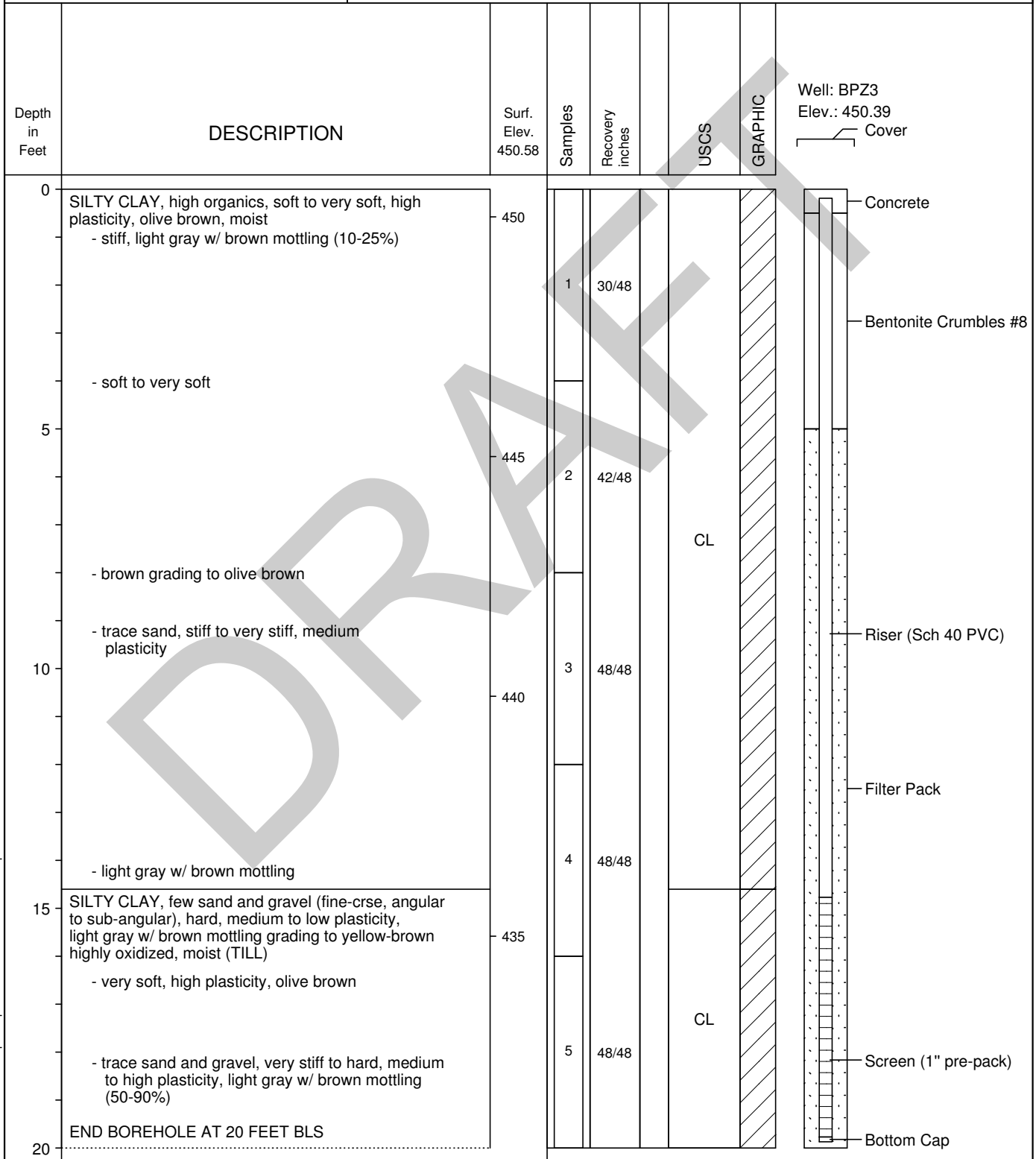
LOG OF BORING BPZ3

(Page 1 of 1)

Off-Site Groundwater Quality Investigation
BaldwinAsh Pond System
Baldwin Energy Complex, Baldwin, IL
Dynegy Midwest Generation, LLC

Date Completed : 03/06/2012
Hole Diameter : 2.75"
Drilling Method : AMS PowerProbe 9500-VTR
Sampling Method : MacroCore (1.25" ID)
Drilling Company : Terra Drill

Driller : Jim Dittmaier
Geologist : S. Cravens (Kelron Env)
Land Surface Elevation: 450.58
Top of Casing Elevation 450.39
X,Y Coordinates :



**KELRON
ENVIRONMENTAL
INCORPORATED**

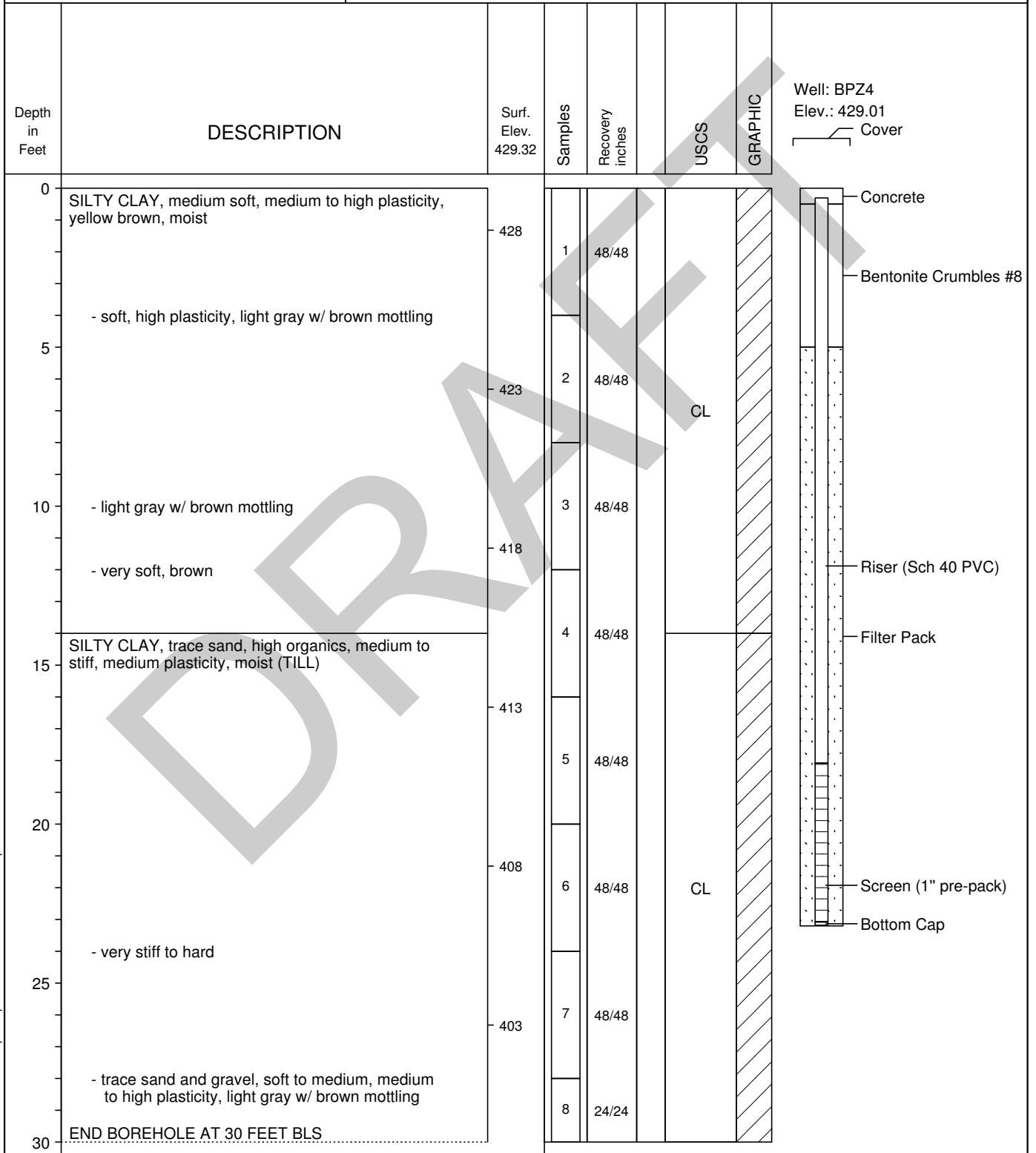
LOG OF BORING BPZ4

(Page 1 of 1)

Off-Site Groundwater Quality Investigation
BaldwinAsh Pond System
Baldwin Energy Complex, Baldwin, IL
Dynegy Midwest Generation, LLC

Date Completed : 03/06/2012
Hole Diameter : 2.75"
Drilling Method : AMS PowerProbe 9500-VTR
Sampling Method : MacroCore (1.25" ID)
Drilling Company : Terra Drill

Driller : Jim Dittmaier
Geologist : S. Cravens (Kelron Env)
Land Surface Elevation: 429.32
Top of Casing Elevation 429.01
X,Y Coordinates :



**KELRON
ENVIRONMENTAL
INCORPORATED**

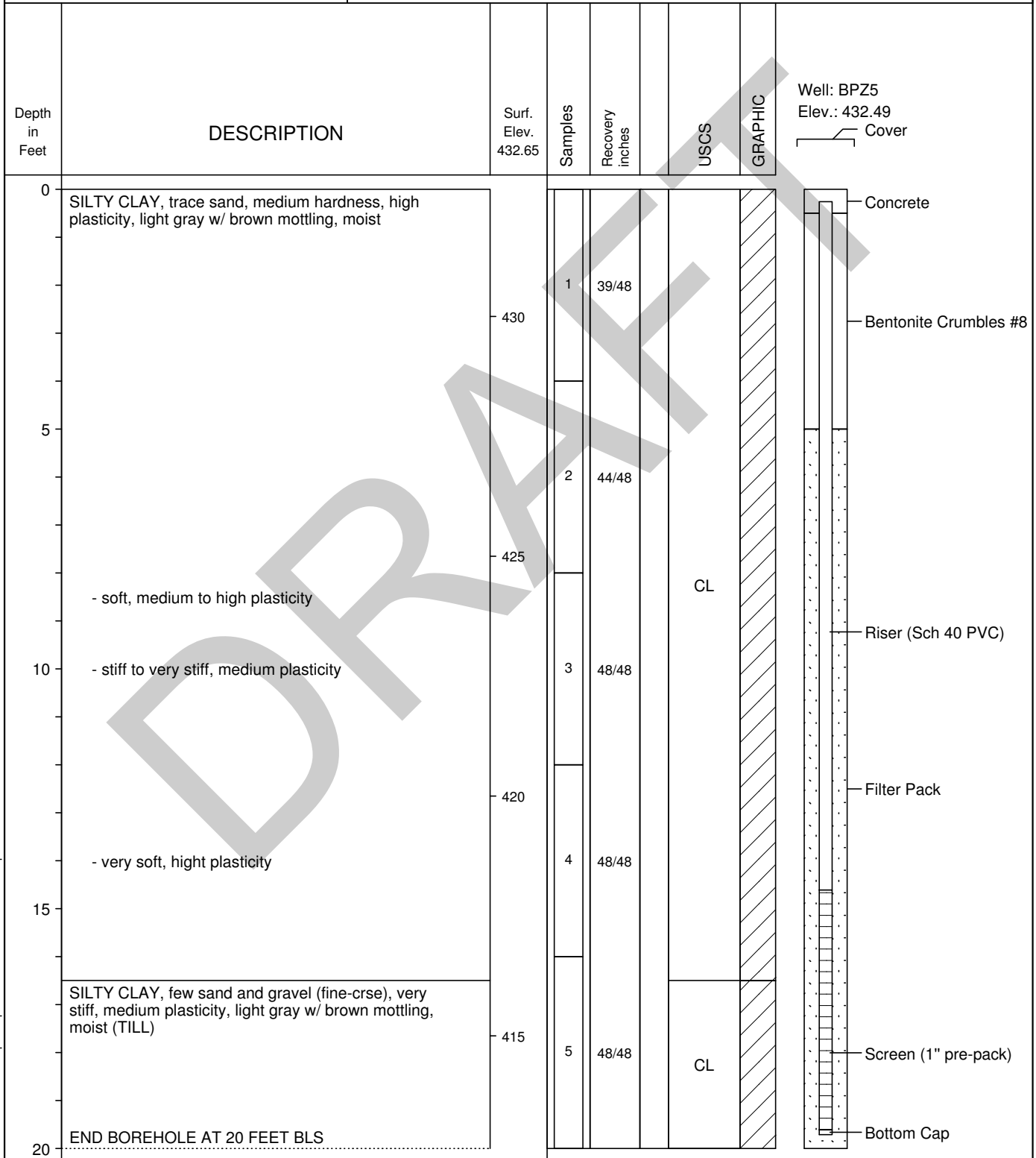
LOG OF BORING BPZ5

(Page 1 of 1)

Off-Site Groundwater Quality Investigation
BaldwinAsh Pond System
Baldwin Energy Complex, Baldwin, IL
Dynegy Midwest Generation, LLC

Date Completed : 03/06/2012
Hole Diameter : 2.75"
Drilling Method : AMS PowerProbe 9500-VTR
Sampling Method : MacroCore (1.25" ID)
Drilling Company : Terra Drill

Driller : Jim Dittmaier
Geologist : S. Cravens (Kelron Env)
Land Surface Elevation: 432.65
Top of Casing Elevation 432.49
X,Y Coordinates :



**KELRON
ENVIRONMENTAL
INCORPORATED**

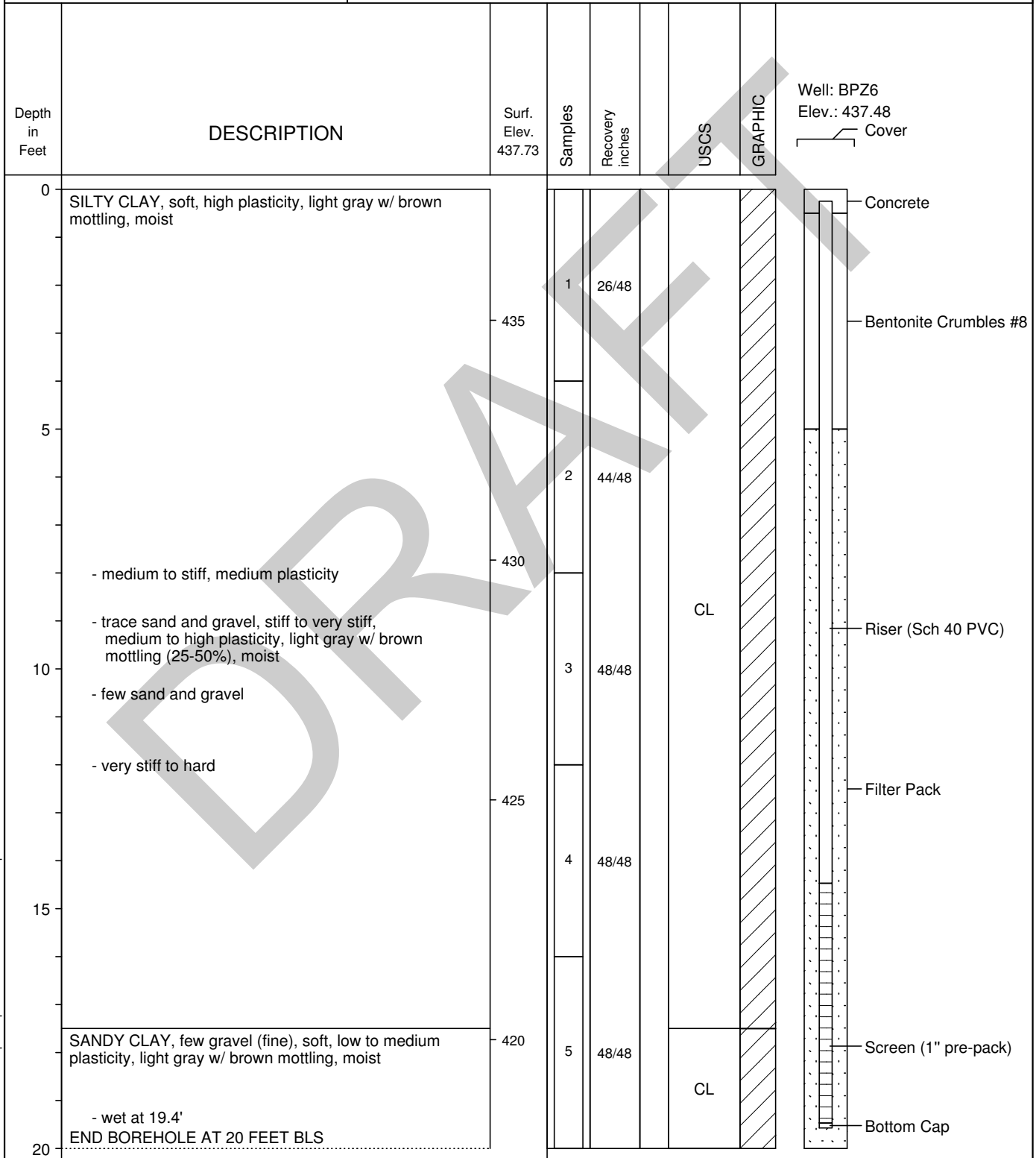
LOG OF BORING BPZ6

(Page 1 of 1)

Off-Site Groundwater Quality Investigation
BaldwinAsh Pond System
Baldwin Energy Complex, Baldwin, IL
Dynegy Midwest Generation, LLC

Date Completed : 03/06/2012
Hole Diameter : 2.75"
Drilling Method : AMS PowerProbe 9500-VTR
Sampling Method : MacroCore (1.25" ID)
Drilling Company : Terra Drill

Driller : Jim Dittmaier
Geologist : S. Cravens (Kelron Env)
Land Surface Elevation: 437.73
Top of Casing Elevation 437.48
X,Y Coordinates :



**KELRON
ENVIRONMENTAL
INCORPORATED**

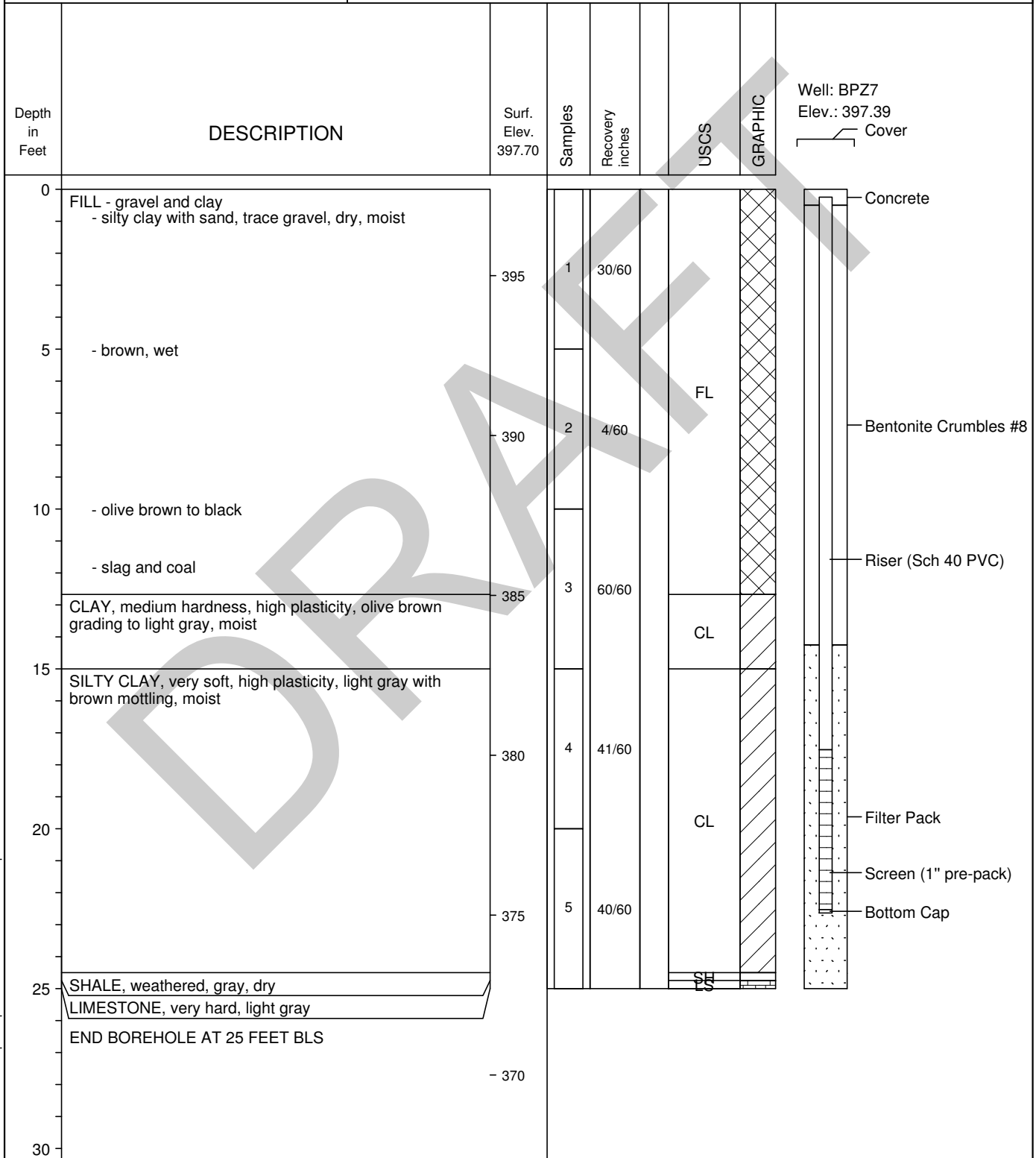
LOG OF BORING BPZ7

(Page 1 of 1)

Off-Site Groundwater Quality Investigation
BaldwinAsh Pond System
Baldwin Energy Complex, Baldwin, IL
Dynegy Midwest Generation, LLC

Date Completed : 03/05/2012
Hole Diameter : 2.75"
Drilling Method : AMS PowerProbe 9500-VTR
Sampling Method : MacroCore (1.25" ID)
Drilling Company : Terra Drill

Driller : Jim Dittmaier
Geologist : S. Cravens (Kelron Env)
Land Surface Elevation: 397.70
Top of Casing Elevation 397.39
X,Y Coordinates :



**KELRON
ENVIRONMENTAL
INCORPORATED**

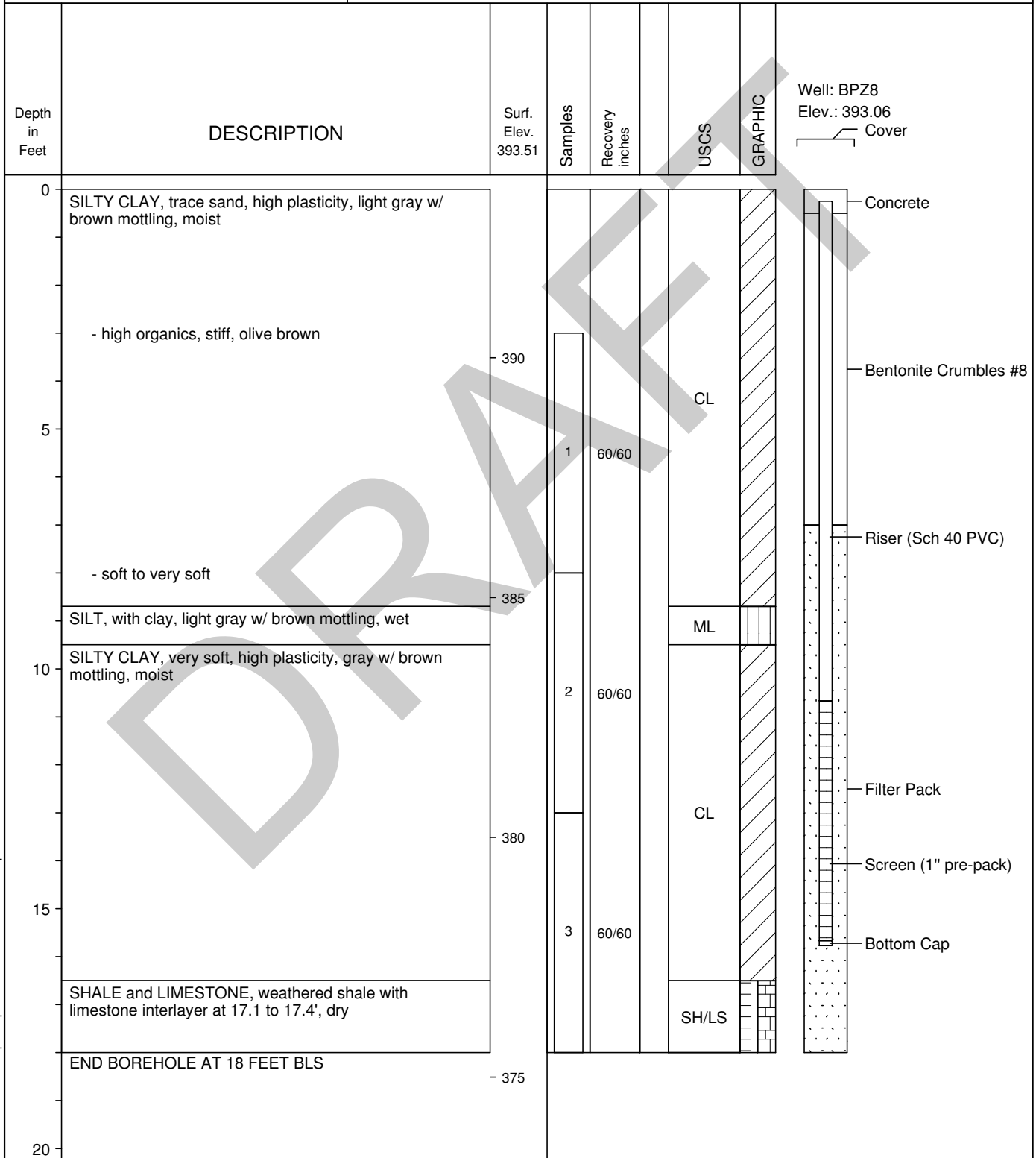
LOG OF BORING BPZ8

(Page 1 of 1)

Off-Site Groundwater Quality Investigation
BaldwinAsh Pond System
Baldwin Energy Complex, Baldwin, IL
Dynegy Midwest Generation, LLC

Date Completed : 03/05/2012
Hole Diameter : 2.75"
Drilling Method : AMS PowerProbe 9500-VTR
Sampling Method : MacroCore (1.25" ID)
Drilling Company : Terra Drill

Driller : Jim Dittmaier
Geologist : S. Cravens (Kelron Env)
Land Surface Elevation: 393.51
Top of Casing Elevation 393.06
X,Y Coordinates :



ATTACHMENT 4

Water Sample Field Data Sheets

DRAFT

Location No. BP21**WATER SAMPLING DATA**Sample Type: ☒ Groundwater ☐ Surface Water ☐ Other _____ Date 3/15/12Project Name BEC Off-Site Groundwater Investigation Project No. 47602Project Manager Stuart Cravens Phase Task No. _____Site Address ☐ Ruby Lane ☒ Magnolia Drive ☐ Conservation Road Baldwin, Illinois**Sampling Specifications**

Requested Sampling

Depth Interval (feet) _____

Requested Wait Following

Development/Purging (hours) _____

Initial Measurements

Time Elapsed From Final Development/Purging (hours) _____

Initial Water Depth (feet) 6.62 m @ 1000

Nonaqueous Liquids Present (Describe) _____

Water Quality/Water Collection

Spec Cond. = Specific Conductivity

| Date | Time | Sampler Initials | Water Quality Readings | | | | Water Collection Data | | | | | Notes (Explain in Comments Below) |
|---------|------|------------------|------------------------|------|--|-----------------------------|--------------------------------|------------------------------|------------------------------|------|------------------------------|--------------------------------------|
| | | | Temp. (°C) | pH | | Spec Cond. (µmhos/cm) | Volume Removed (gallons) | Removal Rate (gal/min) | Pump Intake Depth (ft) | Bail | Final Water Depth (ft) | |
| 3-15-12 | 1804 | SJC | 18.2 | 7.66 | | 899 | 0.18 | | 17.6' | | - | Clear |
| " | 1808 | SJC | 18.0 | 7.63 | | 891 | 0.20 | | ↓ | | - | SAA |
| " | 1818 | SJC | 15.2 | 7.48 | | 611 | 0.50 | | ↓ | | 13.5' | SAA |
| | | | | | | | | | | | | |
| | | | | | | | | | | | | |

Container Type: G = Clear Glass; A = Amber Glass; P = Plastic; V = VOA Vial (Glass); O = Other (Specify)

Sample ContainersPreservatives: H = HCl; N = HNO₃; S = H₂SO₄; A = NaOH; O = Other (Specify); — = None

| Analytical Parameter List | Container | | | Field Filtered | | Preserved | Cooled During Collection | | Comments |
|---------------------------|-----------|------|-------------|----------------|----|-----------|--------------------------|----|--------------------|
| | Number | Type | Volume (mL) | Yes | No | | Yes | No | |
| SD4/TDS | 1 | 500P | 500 | | X | — | X | | Sample BP21 @ 1818 |
| BUNA | 1 | 250P | 250 | | X | N | X | | |
| | | | | | | | | | |
| | | | | | | | | | |
| | | | | | | | | | |
| | | | | | | | | | |
| | | | | | | | | | |
| | | | | | | | | | |
| | | | | | | | | | |
| | | | | | | | | | |

Filter Type _____ Chain-of-Custody Form Number _____

Comments well depth = 17.74' mSignature [Signature] Date 3/15/12 Reviewer _____ Date _____

Location No. BP22**WATER SAMPLING DATA**Sample Type: ☒ Groundwater ☐ Surface Water ☐ Other _____ Date 3/5/12Project Name BEC Off-Site Groundwater InvestigationProject No. 47602Project Manager Stuart Cravens

Phase Task No. _____

Site Address ☐ Ruby Lane ☒ Magnolia Drive ☐ Conservation Road Baldwin, Illinois**Sampling Specifications****Initial Measurements**

Requested Sampling

Time Elapsed From Final Development/Purging (hours) _____

Depth Interval (feet) _____

Requested Wait Following

Initial Water Depth (feet) 10.21' mp @ 0935

Development/Purging (hours) _____

Nonaqueous Liquids Present (Describe) _____

Water Quality/Water Collection

Spec Cond. = Specific Conductivity

| Date | Time | Sampler Initials | Water Quality Readings | | | | Water Collection Data | | | | | Notes (Explain in Comments Below) |
|--------|------|------------------|------------------------|------|--|-----------------------------|--------------------------------|------------------------------|------------------------------|------|------------------------------|--------------------------------------|
| | | | Temp. (°C) | pH | | Spec Cond. (µmhos/cm) | Volume Removed (gallons) | Removal Rate (gal/min) | Pump Intake Depth (ft) | Bail | Final Water Depth (ft) | |
| 3/5/12 | 0934 | SO2 | 13.5 | 7.42 | | — | 0.10 | | 13.75' | | | Clear |
| 11 | 0942 | SO2 | 13.0 | 7.32 | | 1,120 | 0.25 | | ↓ | | | lt. brown |
| 11 | 0944 | SO2 | 13.3 | 7.21 | | 1,117 | 0.40 | | ↓ | | 11.77 | SAA |
| | | | | | | | | | | | | |
| | | | | | | | | | | | | |

Container Type: G = Clear Glass; A = Amber Glass; P = Plastic; V = VOA Vial (Glass); O = Other (Specify)

Sample ContainersPreservatives: H = HCl; N = HNO₃; S = H₂SO₄; A = NaOH; O = Other (Specify); — = None

| Analytical Parameter List | Container | | | Field Filtered | | Preserved | Cooled During Collection | | Comments |
|---------------------------|-----------|------|-------------|----------------|----|-----------|--------------------------|----|--------------------|
| | Number | Type | Volume (mL) | Yes | No | | Yes | No | |
| SD4/TDS | 1 | SDP | P | | X | — | X | | Sample BP22 @ 0944 |
| Boron | 1 | SDP | P | | X | N | X | | |
| | | | | | | | | | |
| | | | | | | | | | |
| | | | | | | | | | |
| | | | | | | | | | |
| | | | | | | | | | |
| | | | | | | | | | |
| | | | | | | | | | |

Filter Type _____

Chain-of-Custody Form Number _____

Comments well depth = 14.25' mpSignature A. H. L.Date 3/5/12

Reviewer _____

Date _____

Location No. BPZ3**WATER SAMPLING DATA**Sample Type: ☒ Groundwater ☐ Surface Water ☐ Other _____ Date 3-15-12Project Name BEC Off-Site Groundwater InvestigationProject No. 47602Project Manager Stuart Cravens

Phase Task No. _____

Site Address ☐ Ruby Lane ☒ Magnolia Drive ☐ Conservation Road Baldwin, Illinois**Sampling Specifications**

Requested Sampling

Depth Interval (feet) _____

Requested Wait Following

Development/Purging (hours) _____

Initial Measurements

Time Elapsed From Final Development/Purging (hours) _____

Initial Water Depth (feet) 165' mp @ 0910

Nonaqueous Liquids Present (Describe) _____

Water Quality/Water Collection

Spec Cond. = Specific Conductivity

| Water Quality/Water Collection | | | | | | | | | | | | Notes (Explain in Comments Below) |
|--------------------------------|------|------------------|------------------------|------|--|-----------------------|--------------------------|------------------------|------------------------|------|------------------------|--------------------------------------|
| Date | Time | Sampler Initials | Water Quality Readings | | | | Water Collection Data | | | | | |
| | | | Temp. (°C) | pH | | Spec Cond. (µmhos/cm) | Volume Removed (gallons) | Removal Rate (gal/min) | Pump Intake Depth (ft) | Bail | Final Water Depth (ft) | |
| 3-15-12 | 0900 | SJC | - | - | | - | 0 | | 19.5 | | | |
| " | 0903 | SJC | 18.2 | 7.16 | | 898 | 0.25 | | ↓ | | | clear |
| " | 0910 | SJC | 17.9 | 6.96 | | 1,080 | 0.50 | | ↓ | | 11.07 | clear |
| | | | | | | | | | | | | |
| | | | | | | | | | | | | |

Container Type: G = Clear Glass; A = Amber Glass; P = Plastic; V = VOA Vial (Glass); O = Other (Specify)

Sample ContainersPreservatives: H = HCl; N = HNO₃; S = H₂SO₄; A = NaOH; O = Other (Specify); — = None

| Analytical Parameter List | Container | | | Field Filtered | | Preserved | Cooled During Collection | | Comments |
|---------------------------|-----------|------|-------------|----------------|----|-----------|--------------------------|----|----------------------|
| | Number | Type | Volume (mL) | Yes | No | | Yes | No | |
| SO ₄ /TDS | 1 | HOPE | 500 | | X | — | X | | Sample BPZ3 @ 0918 |
| Boron | 1 | HOPE | 250 | | X | N | X | | Sample BP2 93 @ 0920 |
| SO ₄ /TDS | 1 | P | 500 | X | | — | X | | |
| Boron | 1 | P | 250 | X | | N | X | | |
| | | | | | | | | | |
| | | | | | | | | | |
| | | | | | | | | | |
| | | | | | | | | | |
| | | | | | | | | | |
| | | | | | | | | | |

Filter Type _____

Chain-of-Custody Form Number _____

Comments weather - cldy, ~ 68°F, wind < 5 mph
well depth = 19.68' mpSignature [Signature]Date 3/15/12

Reviewer _____

Date _____

Location No. BP24**WATER SAMPLING DATA**Sample Type: ☒ Groundwater ☐ Surface Water ☐ Other _____ Date 3/15/12Project Name BEC Off-Site Groundwater InvestigationProject No. 47602Project Manager Stuart Cravens

Phase Task No. _____

Site Address ☒ Ruby Lane ☐ Magnolia Drive ☐ Conservation Road Baldwin, Illinois**Sampling Specifications****Initial Measurements**

Requested Sampling

Depth Interval (feet) _____

Time Elapsed From Final Development/Purging (hours) _____

Requested Wait Following

Development/Purging (hours) _____

Initial Water Depth (feet) 17.59' m @ 11:03

Nonaqueous Liquids Present (Describe) _____

Water Quality/Water Collection

Spec Cond. = Specific Conductivity

| Date | Time | Sampler Initials | Water Quality Readings | | | | Water Collection Data | | | | | Notes (Explain in Comments Below) |
|---------|-------|------------------|------------------------|------|--|-----------------------------|--------------------------------|------------------------------|------------------------------|------|------------------------------|--------------------------------------|
| | | | Temp. (°C) | pH | | Spec Cond. (µmhos/cm) | Volume Removed (gallons) | Removal Rate (gal/min) | Pump Intake Depth (ft) | Bail | Final Water Depth (ft) | |
| 3/15/12 | 11:08 | SC | 17.1 | 7.41 | | 2,165 | 0.1 | | 22.7' | | | Clear |
| 11 | 11:10 | SC | 17.4 | 7.38 | | 2,160 | 0.25 | | 11 | | | Clear |
| 11 | 11:12 | SC | 17.4 | 7.44 | | 3,082 | — | | 11 | | 20.79 | Clear |
| | | | | | | | | | | | | |
| | | | | | | | | | | | | |

Container Type: G = Clear Glass; A = Amber Glass; P = Plastic; V = VOA Vial (Glass); O = Other (Specify)

Sample ContainersPreservatives: H = HCl; N = HNO₃; S = H₂SO₄; A = NaOH; O = Other (Specify); — = None

| Analytical Parameter List | Container | | | Field Filtered | | Preserved | Cooled During Collection | | Comments |
|---------------------------|-----------|------|-------------|----------------|----|-----------|--------------------------|----|------------------------|
| | Number | Type | Volume (mL) | Yes | No | | Yes | No | |
| SO ₄ /TDS | 1 | P | 500 | | X | — | X | | Sample BP24 @ 11:10 |
| BOD ₅ | 1 | P | 250 | | X | N | X | | |
| | | | | | | | | | |
| | | | | | | | | | |
| | | | | | | | | | |
| | | | | | | | | | |
| | | | | | | | | | |
| | | | | | | | | | |
| | | | | | | | | | |

Filter Type _____ Chain-of-Custody Form Number _____

Comments Cloudy, Rain/Thunder, ~70°F, wind S-10S, well depth = 22.87' m

Signature _____

Date 3/15/12

Reviewer _____

Date _____

Location No. BP25**WATER SAMPLING DATA**Sample Type: ☒ Groundwater ☐ Surface Water ☐ Other _____ Date 3-15-12Project Name BEC Off-Site Groundwater Investigation Project No. 47602Project Manager Stuart Cravens Phase Task No. _____Site Address ☒ Ruby Lane ☐ Magnolia Drive ☐ Conservation Road Baldwin, Illinois**Sampling Specifications**

Requested Sampling

Depth Interval (feet) _____

Requested Wait Following

Development/Purging (hours) _____

Initial Measurements

Time Elapsed From Final Development/Purging (hours) _____

Initial Water Depth (feet) 14.67' mp @ 1042

Nonaqueous Liquids Present (Describe) _____

Water Quality/Water Collection

Spec Cond. = Specific Conductivity

| Date | Time | Sampler Initials | Water Quality Readings | | | | Water Collection Data | | | | | Notes (Explain in Comments Below) |
|---------|------|------------------|------------------------|------|--|--------------------------|-----------------------------|---------------------------|---------------------------|------|---------------------------|--------------------------------------|
| | | | Temp. (°C) | pH | | Spec Cond. (µmhos/cm) | Volume Removed (gallons) | Removal Rate (gal/min) | Pump Intake Depth (ft) | Bail | Final Water Depth (ft) | |
| 3-15-12 | 1044 | SCZ | 17.2 | 7.54 | | 802 | 2.10 | | 19.0' | | — | clear |
| 3-15-12 | 1048 | SCZ | 16.9 | 7.39 | | 567 | 0.25 | | 4 | | 18.25 | clear |
| | | | | | | | | | | | | |
| | | | | | | | | | | | | |
| | | | | | | | | | | | | |

Container Type: G = Clear Glass; A = Amber Glass; P = Plastic; V = VOA Vial (Glass); O = Other (Specify)

Sample ContainersPreservatives: H = HCl; N = HNO₃; S = H₂SO₄; A = NaOH; O = Other (Specify); — = None

| Analytical Parameter List | Container | | | Field Filtered | | Preserved | Cooled During Collection | | Comments |
|---------------------------|-----------|------|-------------|----------------|----|-----------|--------------------------|----|-----------------------|
| | Number | Type | Volume (mL) | Yes | No | | Yes | No | |
| SO ₄ /TDS | 1 | P | 500 | | X | — | X | | Sample BP25 @ 1048 |
| BODH | 1 | P | 250 | | X | — | X | | |
| | | | | | | | | | |
| | | | | | | | | | |
| | | | | | | | | | |
| | | | | | | | | | |
| | | | | | | | | | |
| | | | | | | | | | |
| | | | | | | | | | |
| | | | | | | | | | |

Filter Type _____ Chain-of-Custody Form Number _____

Comments clay, rain/thunder, 70°F, wind S-10S, well depth = 14.55' mpSignature [Signature] Date 3/15/12 Reviewer _____ Date _____

Location No. BP26**WATER SAMPLING DATA**Sample Type: ☒ Groundwater ☐ Surface Water ☐ Other _____ Date 3-15-12Project Name BEC Off-Site Groundwater InvestigationProject No. 47602Project Manager Stuart Cravens

Phase Task No. _____

Site Address ☒ Ruby Lane ☐ Magnolia Drive ☐ Conservation Road Baldwin, Illinois**Sampling Specifications**

Requested Sampling

Depth Interval (feet) _____

Requested Wait Following

Development/Purging (hours) _____

Initial Measurements

Time Elapsed From Final Development/Purging (hours) _____

Initial Water Depth (feet) 11.47 @ 1022

Nonaqueous Liquids Present (Describe) _____

Water Quality/Water Collection

Spec Cond. = Specific Conductivity

| Date | Time | Sampler Initials | Water Quality Readings | | | | Water Collection Data | | | | | Notes (Explain in Comments Below) |
|---------|------|------------------|------------------------|------|--|-----------------------------|--------------------------------|------------------------------|------------------------------|------|------------------------------|--------------------------------------|
| | | | Temp. (°C) | pH | | Spec Cond. (µmhos/cm) | Volume Removed (gallons) | Removal Rate (gal/min) | Pump Intake Depth (ft) | Bail | Final Water Depth (ft) | |
| 3-15-12 | 1026 | SVZ | 17.2 | 7.60 | | 1,099 | 0.25 | | 14.8 | | | clear |
| " | 1031 | SVZ | 15.4 | 7.30 | | 1,053 | 0.40 | | " | | 18.25 | clay |
| | | | | | | | | | | | | |
| | | | | | | | | | | | | |
| | | | | | | | | | | | | |

Container Type: G = Clear Glass; A = Amber Glass; P = Plastic; V = VOA Vial (Glass); O = Other (Specify)

Sample ContainersPreservatives: H = HCl; N = HNO₃; S = H₂SO₄; A = NaOH; O = Other (Specify); — = None

| Analytical Parameter List | Container | | | Field Filtered | | Preserved | Cooled During Collection | | Comments |
|---------------------------|-----------|------|-------------|----------------|----|-----------|--------------------------|----|--------------------|
| | Number | Type | Volume (mL) | Yes | No | | Yes | No | |
| SO ₄ /PDS | 1 | P | 500 | | X | — | X | | Sample BP26 @ 1032 |
| Boron | 1 | P | 250 | | X | N | X | | |
| | | | | | | | | | |
| | | | | | | | | | |
| | | | | | | | | | |
| | | | | | | | | | |
| | | | | | | | | | |
| | | | | | | | | | |
| | | | | | | | | | |

Filter Type _____

Chain-of-Custody Form Number _____

Comments Drizzle, ~72°F, SE ~ S by wind, well depth = 19.32' mpSignature [Signature]Date 3/15/12

Reviewer _____ Date _____

Location No. BP27**WATER SAMPLING DATA**Sample Type: ☒ Groundwater ☐ Surface Water ☐ Other _____ Date 3-15-12Project Name BEC Off-Site Groundwater InvestigationProject No. 47602Project Manager Stuart Cravens

Phase Task No. _____

Site Address ☐ Ruby Lane ☐ Magnolia Drive ☒ Conservation Road Baldwin, Illinois**Sampling Specifications**

Requested Sampling

Depth Interval (feet) _____

Requested Wait Following

Development/Purging (hours) _____

Initial Measurements

Time Elapsed From Final Development/Purging (hours) _____

Initial Water Depth (feet) 19.03' @ 1149

Nonaqueous Liquids Present (Describe) _____

Water Quality/Water Collection

Spec Cond. = Specific Conductivity

| Date | Time | Sampler Initials | Water Quality Readings | | | | Water Collection Data | | | | | Notes (Explain in Comments Below) |
|---------|------|------------------|------------------------|------|--|-----------------------------|--------------------------------|------------------------------|------------------------------|------|------------------------------|--------------------------------------|
| | | | Temp. (°C) | pH | | Spec Cond. (µmhos/cm) | Volume Removed (L or mL) | Removal Rate (gal/min) | Pump Intake Depth (ft) | Bail | Final Water Depth (ft) | |
| 3/15/12 | 1153 | STC | 18.0 | 7.01 | | 1,749 | 100mL | | 22.0 | | | Clear |
| " | 1155 | STC | 17.7 | 6.85 | | 1,721 | 200mL | | 11 | | 21.53 | Clear |
| | | | | | | | | | | | | |
| | | | | | | | | | | | | |
| | | | | | | | | | | | | |

Container Type: G = Clear Glass; A = Amber Glass; P = Plastic; V = VOA Vial (Glass); O = Other (Specify)

Sample ContainersPreservatives: H = HCl; N = HNO₃; S = H₂SO₄; A = NaOH; O = Other (Specify); — = None

| Analytical Parameter List | Container | | | Field Filtered | | Preserved | Cooled During Collection | | Comments |
|---------------------------|-----------|------|-------------|----------------|----|-----------|--------------------------|----|-----------------------|
| | Number | Type | Volume (mL) | Yes | No | | Yes | No | |
| SD4/TDS | 1 | P | 500 | | X | — | X | | Sample BP27 @ 1155 |
| BODN | 1 | P | 250 | | X | N | X | | |
| | | | | | | | | | |
| | | | | | | | | | |
| | | | | | | | | | |
| | | | | | | | | | |
| | | | | | | | | | |
| | | | | | | | | | |
| | | | | | | | | | |
| | | | | | | | | | |

Filter Type _____

Chain-of-Custody Form Number _____

Comments Cldy, 78°F, mid < 5m SW, well depth = 22.32' mp.Signature STCDate 3/15/12

Reviewer _____

Date _____

Location No. BP28**WATER SAMPLING DATA**Sample Type: ☒ Groundwater ☐ Surface Water ☐ Other _____ Date 3-15-12Project Name BEC Off-Site Groundwater InvestigationProject No. 47602Project Manager Stuart Cravens

Phase Task No. _____

Site Address ☐ Ruby Lane ☐ Magnolia Drive ☒ Conservation Road Baldwin, Illinois**Sampling Specifications**

Requested Sampling

Depth Interval (feet) _____

Requested Wait Following

Development/Purging (hours) _____

Initial Measurements

Time Elapsed From Final Development/Purging (hours) _____

Initial Water Depth (feet) 3.04' @ 1131

Nonaqueous Liquids Present (Describe) _____

Water Quality/Water Collection

Spec Cond. = Specific Conductivity

| Date | Time | Sampler Initials | Water Quality Readings | | | | Water Collection Data | | | | | Notes (Explain in Comments Below) |
|---------|------|------------------|------------------------|------|--|-----------------------------|--------------------------------|------------------------------|------------------------------|------|------------------------------|--------------------------------------|
| | | | Temp. (°C) | pH | | Spec Cond. (µmhos/cm) | Volume Removed (gallons) | Removal Rate (gal/min) | Pump Intake Depth (ft) | Bail | Final Water Depth (ft) | |
| 3/15/12 | 1135 | STC | 17.2 | 7.64 | | 705 | 0.25 | | 15.0' | | - | clear |
| " | 1137 | STC | 15.1 | 7.55 | | 694 | 0.50 | | " | | 13.76 | cldy |
| | | | | | | | | | | | | |
| | | | | | | | | | | | | |
| | | | | | | | | | | | | |

Container Type: G = Clear Glass; A = Amber Glass; P = Plastic; V = VOA Vial (Glass); O = Other (Specify)

Sample ContainersPreservatives: H = HCl; N = HNO₃; S = H₂SO₄; A = NaOH; O = Other (Specify); — = None

| Analytical Parameter List | Container | | | Field Filtered | | Preserved | Cooled During Collection | | Comments |
|---------------------------|-----------|------|-------------|----------------|----|-----------|--------------------------|----|-----------------------|
| | Number | Type | Volume (mL) | Yes | No | | Yes | No | |
| SDH/TDS | 1 | P | 500 | | X | — | X | | Sample BP28 @ 1138 |
| Boron | 1 | P | 250 | | X | N | X | | |
| | | | | | | | | | |
| | | | | | | | | | |
| | | | | | | | | | |
| | | | | | | | | | |
| | | | | | | | | | |
| | | | | | | | | | |
| | | | | | | | | | |
| | | | | | | | | | |

Filter Type _____ Chain-of-Custody Form Number _____

Comments cldy, 73°F, wind vs mph SW. well depth = 15.32' apSignature [Signature] Date 3/15/12 Reviewer _____ Date _____

ATTACHMENT 5

Laboratory Analytical Report and Chain of Custody

DRAFT

March 23, 2012

Stu Cravens
Kelron Environmental
1213 Dorchester
Champaign, IL 61821
TEL: (217) 390-1503
FAX: (217) 355-1385



RE: BEC Offsite/47602

WorkOrder: 12030744

Dear Stu Cravens:

TEKLAB, INC received 9 samples on 3/15/2012 2:41:00 PM for the analysis presented in the following report.

Samples are analyzed on an as received basis unless otherwise requested and documented. The sample results contained in this report relate only to the requested analytes of interest as directed on the chain of custody. NELAP accredited fields of testing are indicated by the letters NELAP under the Certification column. All tests are performed in the Collinsville, IL laboratory unless otherwise noted in the Case Narrative.

All quality control criteria applicable to the test methods employed for this project have been satisfactorily met and are in accordance with NELAP except where noted. The following report shall not be reproduced, except in full, without the written approval of Teklab, Inc.

If you have any questions regarding these tests results, please feel free to call.

Sincerely,



Elizabeth A. Hurley
Project Manager
(618)344-1004 ex 33
ehurley@teklabinc.com

Client: Kelron Environmental

Work Order: 12030744

Client Project: BEC Offsite/47602

Report Date: 23-Mar-12

Abbr Definition

| | |
|-------|--|
| CCV | Continuing calibration verification is a check of a standard to determine the state of calibration of an instrument between recalibration. |
| DF | Dilution factor is the dilution performed during analysis only and does not take into account any dilutions made during sample preparation. The reported result is final and includes all dilutions factors. |
| DNI | Did not ignite |
| DUP | Laboratory duplicate is an aliquot of a sample taken from the same container under laboratory conditions for independent processing and analysis independently of the original aliquot. |
| ICV | Initial calibration verification is a check of a standard to determine the state of calibration of an instrument before sample analysis is initiated. |
| IDPH | IL Dept. of Public Health |
| LCS | Laboratory control sample, spiked with verified known amounts of analytes, is analyzed exactly like a sample to establish intra-laboratory or analyst specific precision and bias or to assess the performance of all or a portion of the measurement system. The acceptable recovery range is in the QC Package (provided upon request). |
| LCS D | Laboratory control sample duplicate is a replicate laboratory control sample that is prepared and analyzed in order to determine the precision of the approved test method. The acceptable recovery range is listed in the QC Package (provided upon request). |
| MB | Method blank is a sample of a matrix similar to the batch of associated sample (when available) that is free from the analytes of interest and is processed simultaneously with and under the same conditions as samples through all steps of the analytical procedures, and in which no target analytes or interferences should present at concentrations that impact the analytical results for sample analyses. |
| MDL | Method detection limit means the minimum concentration of a substance that can be measured and reported with 99% confidence that the analyte concentration is greater than zero and is determined from analysis of a sample in a given matrix type containing the analyte. |
| MS | Matrix spike is an aliquot of matrix fortified (spiked) with known quantities of specific analytes that is subjected to the entire analytical procedures in order to determine the effect of the matrix on an approved test method's recovery system. The acceptable recovery range is listed in the QC Package (provided upon request). |
| MSD | Matrix spike duplicate means a replicate matrix spike that is prepared and analyzed in order to determine the precision of the approved test method. The acceptable recovery range is listed in the QC Package (provided upon request). |
| MW | Molecular weight |
| ND | Not Detected at the Reporting Limit |
| NELAP | NELAP Accredited |
| PQL | Practical quantitation limit means the lowest level that can be reliably achieved within specified limits of precision and accuracy during routine laboratory operation conditions. The acceptable recovery range is listed in the QC Package (provided upon request). |
| RL | The reporting limit the lowest level that the data is displayed in the final report. The reporting limit may vary according to customer request or sample dilution. The reporting limit may not be less than the MDL. |
| RPD | Relative percent difference is a calculated difference between two recoveries (ie. MS/MSD). The acceptable recovery limit is listed in the QC Package (provided upon request). |
| SPK | The spike is a known mass of target analyte added to a blank sample or sub-sample; used to determine recovery deficiency or for other quality control purposes. |
| Surr | Surrogates are compounds which are similar to the analytes of interest in chemical composition and behavior in the analytical process, but which are not normally found in environmental samples. |
| TNTC | Too numerous to count (> 200 CFU) |

Qualifiers

| | |
|--|--|
| # - Unknown hydrocarbon | B - Analyte detected in associated Method Blank |
| E - Value above quantitation range | H - Holding times exceeded |
| J - Analyte detected below quantitation limits | M - Manual Integration used to determine area response |
| ND - Not Detected at the Reporting Limit | R - RPD outside accepted recovery limits |
| S - Spike Recovery outside recovery limits | X - Value exceeds Maximum Contaminant Level |

Client: Kelron Environmental**Work Order:** 12030744**Client Project:** BEC Offsite/47602**Report Date:** 23-Mar-12**Cooler Receipt Temp:** 5.8 °C

Locations and Accreditations

Collinsville

Address 5445 Horseshoe Lake Road
Collinsville, IL 62234-7425

Phone (618) 344-1004

Fax (618) 344-1005

Email jhriley@teklabinc.com

Springfield

Address 3920 Pintail Dr
Springfield, IL 62711-9415

Phone (217) 698-1004

Fax (217) 698-1005

Email kmccclain@teklabinc.com

Kansas City

Address 8421 Nieman Road
Lenexa, KS 66214

Phone (913) 541-1998

Fax (913) 541-1998

Email dthompson@teklabinc.com

| State | Dept | Cert # | NELAP | Exp Date | Lab |
|-----------|------|---------|-------|-----------|--------------|
| Illinois | IEPA | 100226 | NELAP | 1/31/2013 | Collinsville |
| Kansas | KDHE | E-10374 | NELAP | 1/31/2013 | Collinsville |
| Louisiana | LDEQ | 166493 | NELAP | 6/30/2012 | Collinsville |
| Louisiana | LDEQ | 166578 | NELAP | 6/30/2012 | Springfield |
| Arkansas | ADEQ | 88-0966 | | 3/14/2012 | Collinsville |
| Illinois | IDPH | 17584 | | 4/30/2012 | Collinsville |
| Kentucky | UST | 0073 | | 5/26/2012 | Collinsville |
| Missouri | MDNR | 00930 | | 4/13/2013 | Collinsville |
| Oklahoma | ODEQ | 9978 | | 8/31/2012 | Collinsville |

Client: Kelron Environmental

Work Order: 12030744

Client Project: BEC Offsite/47602

Report Date: 23-Mar-12

Lab ID: 12030744-001

Client Sample ID: BPZ3

Matrix: AQUEOUS

Collection Date: 03/15/2012 9:18

| Analyses | Certification | RL | Qual | Result | Units | DF | Date Analyzed | Batch |
|---|---------------|--------|------|--------------|-------|----|------------------|---------|
| STANDARD METHODS 18TH ED. 2540 C (TOTAL) | | | | | | | | |
| Total Dissolved Solids | NELAP | 20 | | 500 | mg/L | 1 | 03/16/2012 10:29 | R161252 |
| SW-846 9036 (TOTAL) | | | | | | | | |
| Sulfate | NELAP | 75 | | 85 | mg/L | 1 | 03/19/2012 12:17 | R161318 |
| SW-846 3005A, 6010B, METALS BY ICP (TOTAL) | | | | | | | | |
| Boron | NELAP | 0.0200 | J | 0.011 | mg/L | 1 | 03/19/2012 17:13 | 76111 |

DRAFT

Client: Kelron Environmental

Work Order: 12030744

Client Project: BEC Offsite/47602

Report Date: 23-Mar-12

Lab ID: 12030744-002

Client Sample ID: BPZ93

Matrix: AQUEOUS

Collection Date: 03/15/2012 9:20

| Analyses | Certification | RL | Qual | Result | Units | DF | Date Analyzed | Batch |
|---|---------------|--------|------|--------------|-------|----|------------------|---------|
| STANDARD METHODS 18TH ED. 2540 C (TOTAL) | | | | | | | | |
| Total Dissolved Solids | NELAP | 20 | | 500 | mg/L | 1 | 03/16/2012 10:29 | R161252 |
| SW-846 9036 (TOTAL) | | | | | | | | |
| Sulfate | NELAP | 75 | | 87 | mg/L | 1 | 03/19/2012 12:19 | R161318 |
| SW-846 3005A, 6010B, METALS BY ICP (TOTAL) | | | | | | | | |
| Boron | NELAP | 0.0200 | J | 0.016 | mg/L | 1 | 03/19/2012 17:30 | 76111 |

DRAFT

Client: Kelron Environmental

Work Order: 12030744

Client Project: BEC Offsite/47602

Report Date: 23-Mar-12

Lab ID: 12030744-003

Client Sample ID: BPZ2

Matrix: AQUEOUS

Collection Date: 03/15/2012 9:44

| Analyses | Certification | RL | Qual | Result | Units | DF | Date Analyzed | Batch |
|---|---------------|--------|------|--------------|-------|----|------------------|---------|
| STANDARD METHODS 18TH ED. 2540 C (TOTAL) | | | | | | | | |
| Total Dissolved Solids | NELAP | 20 | | 676 | mg/L | 1 | 03/16/2012 10:30 | R161252 |
| SW-846 9036 (TOTAL) | | | | | | | | |
| Sulfate | NELAP | 75 | | 92 | mg/L | 1 | 03/19/2012 12:25 | R161318 |
| SW-846 3005A, 6010B, METALS BY ICP (TOTAL) | | | | | | | | |
| Boron | NELAP | 0.0200 | J | 0.012 | mg/L | 1 | 03/19/2012 17:35 | 76111 |

DRAFT

Client: Kelron Environmental**Work Order:** 12030744**Client Project:** BEC Offsite/47602**Report Date:** 23-Mar-12**Lab ID:** 12030744-004**Client Sample ID:** BPZ1**Matrix:** AQUEOUS**Collection Date:** 03/15/2012 10:10

| Analyses | Certification | RL | Qual | Result | Units | DF | Date Analyzed | Batch |
|---|---------------|--------|------|---------------|-------|----|------------------|---------|
| STANDARD METHODS 18TH ED. 2540 C (TOTAL) | | | | | | | | |
| Total Dissolved Solids | NELAP | 20 | | 502 | mg/L | 1 | 03/16/2012 10:30 | R161252 |
| SW-846 9036 (TOTAL) | | | | | | | | |
| Sulfate | NELAP | 75 | | 119 | mg/L | 1 | 03/19/2012 12:27 | R161318 |
| SW-846 3005A, 6010B, METALS BY ICP (TOTAL) | | | | | | | | |
| Boron | NELAP | 0.0200 | J | 0.0096 | mg/L | 1 | 03/19/2012 17:41 | 76111 |

Client: Kelron Environmental

Work Order: 12030744

Client Project: BEC Offsite/47602

Report Date: 23-Mar-12

Lab ID: 12030744-005

Client Sample ID: BPZ6

Matrix: AQUEOUS

Collection Date: 03/15/2012 10:32

| Analyses | Certification | RL | Qual | Result | Units | DF | Date Analyzed | Batch |
|---|---------------|--------|------|--------------|-------|----|------------------|---------|
| STANDARD METHODS 18TH ED. 2540 C (TOTAL) | | | | | | | | |
| Total Dissolved Solids | NELAP | 20 | | 664 | mg/L | 1 | 03/16/2012 10:31 | R161252 |
| SW-846 9036 (TOTAL) | | | | | | | | |
| Sulfate | NELAP | 75 | J | 70 | mg/L | 1 | 03/19/2012 12:30 | R161318 |
| SW-846 3005A, 6010B, METALS BY ICP (TOTAL) | | | | | | | | |
| Boron | NELAP | 0.0200 | J | 0.010 | mg/L | 1 | 03/19/2012 17:46 | 76111 |

DRAFT

Client: Kelron Environmental**Work Order:** 12030744**Client Project:** BEC Offsite/47602**Report Date:** 23-Mar-12**Lab ID:** 12030744-006**Client Sample ID:** BPZ5**Matrix:** AQUEOUS**Collection Date:** 03/15/2012 10:48

| Analyses | Certification | RL | Qual | Result | Units | DF | Date Analyzed | Batch |
|---|---------------|--------|------|---------------|-------|----|------------------|---------|
| STANDARD METHODS 18TH ED. 2540 C (TOTAL) | | | | | | | | |
| Total Dissolved Solids | NELAP | 20 | | 394 | mg/L | 1 | 03/16/2012 10:32 | R161252 |
| SW-846 9036 (TOTAL) | | | | | | | | |
| Sulfate | NELAP | 20 | | 27 | mg/L | 2 | 03/22/2012 16:31 | R161459 |
| SW-846 3005A, 6010B, METALS BY ICP (TOTAL) | | | | | | | | |
| Boron | NELAP | 0.0200 | | 0.0314 | mg/L | 1 | 03/19/2012 17:52 | 76111 |

Client: Kelron Environmental

Work Order: 12030744

Client Project: BEC Offsite/47602

Report Date: 23-Mar-12

Lab ID: 12030744-007

Client Sample ID: BPZ4

Matrix: AQUEOUS

Collection Date: 03/15/2012 11:10

| Analyses | Certification | RL | Qual | Result | Units | DF | Date Analyzed | Batch |
|---|---------------|--------|------|---------------|-------|----|------------------|---------|
| STANDARD METHODS 18TH ED. 2540 C (TOTAL) | | | | | | | | |
| Total Dissolved Solids | NELAP | 20 | | 1640 | mg/L | 1 | 03/16/2012 10:33 | R161252 |
| SW-846 9036 (TOTAL) | | | | | | | | |
| Sulfate | NELAP | 750 | | 817 | mg/L | 10 | 03/19/2012 13:23 | R161318 |
| SW-846 3005A, 6010B, METALS BY ICP (TOTAL) | | | | | | | | |
| Boron | NELAP | 0.0200 | | 0.0435 | mg/L | 1 | 03/19/2012 18:08 | 76111 |

DRAFT

Client: Kelron Environmental

Work Order: 12030744

Client Project: BEC Offsite/47602

Report Date: 23-Mar-12

Lab ID: 12030744-008

Client Sample ID: BPZ8

Matrix: AQUEOUS

Collection Date: 03/15/2012 11:38

| Analyses | Certification | RL | Qual | Result | Units | DF | Date Analyzed | Batch |
|---|---------------|--------|------|---------------|-------|----|------------------|---------|
| STANDARD METHODS 18TH ED. 2540 C (TOTAL) | | | | | | | | |
| Total Dissolved Solids | NELAP | 20 | | 434 | mg/L | 1 | 03/16/2012 10:39 | R161252 |
| SW-846 9036 (TOTAL) | | | | | | | | |
| Sulfate | NELAP | 75 | | 76 | mg/L | 1 | 03/19/2012 12:41 | R161318 |
| SW-846 3005A, 6010B, METALS BY ICP (TOTAL) | | | | | | | | |
| Boron | NELAP | 0.0200 | | 0.0354 | mg/L | 1 | 03/19/2012 18:13 | 76111 |

DRAFT

Client: Kelron Environmental

Work Order: 12030744

Client Project: BEC Offsite/47602

Report Date: 23-Mar-12

Lab ID: 12030744-009

Client Sample ID: BPZ7

Matrix: AQUEOUS

Collection Date: 03/15/2012 11:55

| Analyses | Certification | RL | Qual | Result | Units | DF | Date Analyzed | Batch |
|---|---------------|--------|------|--------------|-------|----|------------------|---------|
| STANDARD METHODS 18TH ED. 2540 C (TOTAL) | | | | | | | | |
| Total Dissolved Solids | NELAP | 20 | | 1220 | mg/L | 1 | 03/16/2012 10:40 | R161252 |
| SW-846 9036 (TOTAL) | | | | | | | | |
| Sulfate | NELAP | 75 | | 215 | mg/L | 1 | 03/19/2012 12:46 | R161318 |
| SW-846 3005A, 6010B, METALS BY ICP (TOTAL) | | | | | | | | |
| Boron | NELAP | 0.0200 | | 0.252 | mg/L | 1 | 03/19/2012 18:19 | 76111 |

DRAFT

Client: Kelron Environmental

Work Order: 12030744

Client Project: BEC Offsite/47602

Report Date: 23-Mar-12

Carrier: Employee

Received By: HLR

Completed by:

On:

15-Mar-12

Timothy W. Mathis

Reviewed by:

On:

15-Mar-12

Michael L. Austin

Pages to follow: Chain of custody

1

Extra pages included

0

Shipping container/cooler in good condition?

Yes ☒

No ☐

Not Present ☐

Temp °C 5.8

Type of thermal preservation?

None ☐

Ice ☒

Blue Ice ☐

Dry Ice ☐

Chain of custody present?

Yes ☒

No ☐

Chain of custody signed when relinquished and received?

Yes ☒

No ☐

Chain of custody agrees with sample labels?

Yes ☒

No ☐

Samples in proper container/bottle?

Yes ☒

No ☐

Sample containers intact?

Yes ☒

No ☐

Sufficient sample volume for indicated test?

Yes ☒

No ☐

All samples received within holding time?

Yes ☒

No ☐

Reported field parameters measured:

Field ☐

Lab ☐

NA ☒

Container/Temp Blank temperature in compliance?

Yes ☒

No ☐

When thermal preservation is required, samples are compliant with a temperature between 0.1°C - 6.0°C, or when samples are received on ice the same day as collected.

Water – at least one vial per sample has zero headspace?

Yes ☐

No ☐

No VOA vials ☒

Water - TOX containers have zero headspace?

Yes ☐

No ☐

No TOX containers ☒

Water - pH acceptable upon receipt?

Yes ☒

No ☐

Any No responses must be detailed below or on the COC.

CHAIN OF CUSTODY

pg. 1 of 1 Work Order # 2117
12030744

TEKLAB, INC. 5445 Horseshoe Lake Road ~ Collinsville, IL 62234 ~ Phone: (618) 344-1004 ~ Fax: (618) 344-1005

Client: Stuart Cravens
Address: Kelton Environmental, 1213 Dorchester Dr
City / State / Zip: Champaign, IL 61821-7031
Contact: Cravens Phone: 217-390-1503
E-Mail: kelton1@comcast.net Fax: -

Samples on: ☒ Ice ☐ Blue Ice ☐ No Ice 5.8 °C
Preserved in: ☐ Lab ☒ Field FOR LAB USE ONLY
Lab Notes: TM 315.12
Comments:

- Are these samples known to be involved in litigation? If yes, a surcharge will apply. ☐ Yes ☐ No
- Are these samples known to be hazardous? ☐ Yes ☐ No
- Are there any required reporting limits to be met on the requested analysis? If yes, please provide limits in comment section. ☐ Yes ☐ No

| Project Name / Number | | Sample Collector's Name | | | | | | | |
|--|-----------------------|--------------------------|------------------|------|--------------------------------|-----|------|--------------------|-------|
| BEC OFFSITE / 47602 | | S. Cravens | | | | | | | |
| Results Requested <input checked="" type="checkbox"/> Standard <input type="checkbox"/> 1-2 Day (100% Surcharge) <input type="checkbox"/> Other <input type="checkbox"/> 3 Day (50% Surcharge) | Billing Instructions | # and Type of Containers | | | | | | | |
| | ke l m n / Cravens | UNPRES | HNO ₃ | NaOH | H ₂ SO ₄ | HCL | MeOH | NaHSO ₄ | Other |
| Lab Use Only | Sample Identification | Date/Time Sampled | | | | | | | |
| 0000774 | BPZ 3 | 3-15-12/0918 | 1 | 1 | | | | | |
| 002 | BPZ 93 | 0920 | 1 | 1 | | | | | |
| 003 | BPZ 2 | 0944 | 1 | 1 | | | | | |
| 004 | BPZ 1 | 1010 | 1 | 1 | | | | | |
| 005 | BPZ 6 | 1032 | 1 | 1 | | | | | |
| 006 | BPZ 5 | 1048 | 1 | 1 | | | | | |
| 007 | BPZ 4 | 1110 | 1 | 1 | | | | | |
| 008 | BPZ 8 | 1138 | 1 | 1 | | | | | |
| 009 | BPZ 7 | 3-15-12/1155 | 1 | 1 | | | | | |

| INDICATE ANALYSIS REQUESTED | | | | | | | | | |
|-----------------------------|--|--|--|--|--|--|--|--|--|
| | | | | | | | | | |
| | | | | | | | | | |
| | | | | | | | | | |
| | | | | | | | | | |
| | | | | | | | | | |
| | | | | | | | | | |
| | | | | | | | | | |
| | | | | | | | | | |
| | | | | | | | | | |
| | | | | | | | | | |
| | | | | | | | | | |
| | | | | | | | | | |
| | | | | | | | | | |
| | | | | | | | | | |
| | | | | | | | | | |
| | | | | | | | | | |
| | | | | | | | | | |
| | | | | | | | | | |
| | | | | | | | | | |
| | | | | | | | | | |
| | | | | | | | | | |
| | | | | | | | | | |
| | | | | | | | | | |
| | | | | | | | | | |
| | | | | | | | | | |
| | | | | | | | | | |
| | | | | | | | | | |
| | | | | | | | | | |
| | | | | | | | | | |
| | | | | | | | | | |
| | | | | | | | | | |
| | | | | | | | | | |
| | | | | | | | | | |
| | | | | | | | | | |
| | | | | | | | | | |
| | | | | | | | | | |
| | | | | | | | | | |
| | | | | | | | | | |
| | | | | | | | | | |
| | | | | | | | | | |
| | | | | | | | | | |
| | | | | | | | | | |
| | | | | | | | | | |
| | | | | | | | | | |
| | | | | | | | | | |
| | | | | | | | | | |
| | | | | | | | | | |
| | | | | | | | | | |
| | | | | | | | | | |
| | | | | | | | | | |
| | | | | | | | | | |
| | | | | | | | | | |
| | | | | | | | | | |
| | | | | | | | | | |
| | | | | | | | | | |
| | | | | | | | | | |
| | | | | | | | | | |
| | | | | | | | | | |
| | | | | | | | | | |
| | | | | | | | | | |
| | | | | | | | | | |
| | | | | | | | | | |
| | | | | | | | | | |
| | | | | | | | | | |
| | | | | | | | | | |
| | | | | | | | | | |
| | | | | | | | | | |
| | | | | | | | | | |
| | | | | | | | | | |
| | | | | | | | | | |
| | | | | | | | | | |
| | | | | | | | | | |
| | | | | | | | | | |
| | | | | | | | | | |
| | | | | | | | | | |
| | | | | | | | | | |
| | | | | | | | | | |
| | | | | | | | | | |
| | | | | | | | | | |
| | | | | | | | | | |
| | | | | | | | | | |
| | | | | | | | | | |
| | | | | | | | | | |
| | | | | | | | | | |
| | | | | | | | | | |
| | | | | | | | | | |
| | | | | | | | | | |
| | | | | | | | | | |
| | | | | | | | | | |
| | | | | | | | | | |
| | | | | | | | | | |
| | | | | | | | | | |
| | | | | | | | | | |
| | | | | | | | | | |
| | | | | | | | | | |
| | | | | | | | | | |
| | | | | | | | | | |
| | | | | | | | | | |
| | | | | | | | | | |
| | | | | | | | | | |
| | | | | | | | | | |
| | | | | | | | | | |
| | | | | | | | | | |
| | | | | | | | | | |
| | | | | | | | | | |
| | | | | | | | | | |
| | | | | | | | | | |

| Relinquished By | | Date / Time | |
|--------------------|--|-----------------------|--|
| <u>[Signature]</u> | | <u>3-15-12 / 1441</u> | |
| Received By | | Date / Time | |
| <u>[Signature]</u> | | <u>3/15/12 1441</u> | |

The individual signing this agreement on behalf of client acknowledges that he/she has read and understands the terms and conditions of this agreement, on the reverse side, and that he/she has the authority to sign on behalf of client.

WHITE & YELLOW - LAB PINK - SAMPLER'S COPY

APPENDIX E
Geochemical Conceptual Site Model

DRAFT



engineers | scientists | innovators

Geochemical Conceptual Site Model

Baldwin Power Plant – Fly Ash Pond System

(CCR Unit #605)

Prepared for

Dynegy Midwest Generation, LLC
1500 Eastport Plaza Drive
Collinsville, Illinois 62234

Prepared by

Geosyntec Consultants, Inc.
134 N. LaSalle Street, Suite 300
Chicago, Illinois 60602

Project Number: GLP8068

April 2024

TABLE OF CONTENTS

| | |
|--|----|
| 1. EXECUTIVE SUMMARY | 1 |
| 2. INTRODUCTION | 2 |
| 3. SITE BACKGROUND | 3 |
| 3.1 Site Overview | 3 |
| 3.2 Groundwater Monitoring Network | 3 |
| 4. GEOCHEMICAL SITE CONDITIONS | 5 |
| 4.1 Constituent Transport and Fate | 5 |
| 4.2 Site Solids Characterization | 5 |
| 4.2.1 Loss on Ignition, Total Organic Carbon, and Cation Exchange Capacity | 6 |
| 4.2.2 Total Metals and Boron via Bulk Characterization | 7 |
| 4.2.3 Sequential Extraction Procedure Analysis of Metals and Boron | 8 |
| 4.2.4 Mineralogical Analysis | 8 |
| 4.3 Aqueous Geochemistry | 9 |
| 4.3.1 Redox/pH Summary | 10 |
| 4.3.2 Exceedance Parameters | 11 |
| 4.3.3 Pourbaix Diagrams | 13 |
| 4.3.4 Total and Dissolved Iron and Manganese Concentrations | 14 |
| 4.3.5 Major Ion Distribution and Groundwater Signatures | 14 |
| 5. GEOCHEMICAL CONCEPTUAL SITE MODEL | 16 |
| 5.1 Source and Mobilization Mechanisms | 16 |
| 5.2 Potential and Observed Attenuation Mechanisms | 16 |
| 6. REFERENCES | 18 |

LIST OF FIGURES

| | |
|------------|---|
| Figure 1a | pH Time Series – Uppermost Aquifer |
| Figure 1b | pH Time Series – Potential Migration Pathway |
| Figure 2a | ORP Time Series - Uppermost Aquifer |
| Figure 2b | ORP Time Series - Potential Migration Pathway |
| Figure 3a | Boron Concentration Time Series - Uppermost Aquifer |
| Figure 3b | Dissolved Boron Concentration Time Series - Uppermost Aquifer |
| Figure 4a | Sulfate Concentration Time Series - Uppermost Aquifer |
| Figure 4b | Dissolved Sulfate Concentration Time Series - Uppermost Aquifer |
| Figure 5a | Groundwater Elevation Time Series – Uppermost Aquifer |
| Figure 5b | Groundwater Elevation Time Series – Potential Migration Pathway |
| Figure 6a | Boron Concentration Time Series – Potential Migration Pathway |
| Figure 6b | Dissolved Boron Concentration Time Series - – Potential Migration Pathway |
| Figure 7a | Sulfate Concentration Time Series Potential Migration Pathway |
| Figure 7b | Dissolved Sulfate Concentration Time Series – Potential Migration Pathway |
| Figure 8a | Iron Pourbaix Diagram, Ferrihydrite – Uppermost Aquifer |
| Figure 8b | Iron Pourbaix Diagram, Magnetite – Uppermost Aquifer |
| Figure 8c | Iron Pourbaix Diagram; Hematite – Uppermost Aquifer |
| Figure 8d | Iron Pourbaix Diagram, Ferrihydrite– Potential Migration Pathway |
| Figure 8e | Iron Pourbaix Diagram, Magnetite – Potential Migration Pathway |
| Figure 9a | Manganese Pourbaix Diagram – Uppermost Aquifer |
| Figure 9b | Manganese Pourbaix Diagram – Potential Migration Pathway |
| Figure 10a | Piper Diagram – Uppermost Aquifer |
| Figure 10b | Piper Diagram – Potential Migration Pathway |

LIST OF TABLES

| | |
|----------|--|
| Table 1 | CEC and LOI of Site Solids |
| Table 2 | Bulk Characterization of Site Solids |
| Table 3 | XRF Analysis of Site Solids |
| Table 4 | Boron and Iron Characterization of SEP Fraction of Site Solids |
| Table 5a | XRD Analysis of PMP Solids |
| Table 5b | XRD Analysis of UA Solids |
| Table 6 | FAPS Porewater Chemistry |
| Table 7 | Eh-pH Diagram Inputs |
| Table 8 | Total and Dissolved Aqueous Iron and Manganese Results |

LIST OF ATTACHMENTS

| | |
|---------------|--|
| Attachment A: | Site Layout Figure |
| Attachment B: | Proposed Part 845 Groundwater Monitoring Network |
| Attachment C: | Monitoring Well Construction Details |
| Attachment D: | Boring Logs |
| Attachment E: | Site Solids Bulk Characterization & Total Metals Analytical Data |
| Attachment F: | X-Ray Fluorescence Analytical Data |
| Attachment G: | Sequential Extraction Procedure Analytical Data |
| Attachment H: | X-Ray Diffraction Analytical Data |
| Attachment I: | Aqueous Phase Data Summary |

ACRONYMS AND ABBREVIATIONS

| | |
|-----------|---|
| BAP | Bottom Ash Pond |
| BPP | Baldwin Power Plant |
| bgs | below ground surface |
| CEC | cation exchange capacity |
| CCR | coal combustion residuals |
| cm/s | centimeters per second |
| COCs | constituents of concern |
| FAPS | Fly Ash Pond System |
| HSU | hydrostratigraphic unit |
| GCSM | geochemical conceptual site model |
| GWPS | groundwater protection standards |
| I.A.C. | Illinois Administrative Code |
| IEPA | Illinois Environmental Protection Agency |
| LOI | loss on ignition |
| meq/100 g | milliequivalents per 100 grams |
| mg/kg | milligrams per kilogram |
| mg/L | milligrams per liter |
| N&E | nature and extent |
| ORP | oxidation-reduction potential |
| PMP | potential migration pathway |
| SEP | sequential extraction procedure |
| SU | standard units |
| UA | uppermost aquifer |
| USEPA | United States Environmental Protection Agency |
| UU | upper unit |
| XRD | X-Ray diffraction |
| XRF | X-Ray fluorescence |

1. EXECUTIVE SUMMARY

This report documents the development of a geochemical conceptual site model (GCSM) to describe subsurface conditions at the Baldwin Power Plant (BPP) Fly Ash Pond System (FAPS) coal combustion residuals (CCR) unit (Unit #605). A GCSM describes the geochemical processes that contribute to the mobilization, distribution, and attenuation of chemicals in the environment. The GCSM was prepared in support of an evaluation of the nature and extent (N&E) of exceedances of constituents of concern (COCs) above the groundwater protection standards (GWPS) at the FAPS.

The exceedances observed at the FAPS were boron and sulfate. Constituents of concern (COC) exceedances are present in two hydrostratigraphic units at the site: the upper unit (UU) potential migration pathway (PMP), comprised predominantly of clay with silt and minor sand, silt layers, and occasional sand lenses, and the uppermost aquifer (UA), comprised of Pennsylvanian and Mississippian-aged interbedded shale and limestone bedrock.

The primary source of boron and sulfate to groundwaters of the UA and UU PMP within the monitoring network is the FAPS coal combustion residual porewater (i.e., CCR source water), based on COC concentrations within the source and relationships to hydrogeological patterns at the site. Boron was identified within UA solids at concentrations that suggest that aquifer solids could provide an additional potential natural geogenic source of boron to groundwater, and groundwater from background wells consistently exhibited boron concentrations consistent with a natural geogenic source. The observation of pyrite within solids of shale portions of the UA could provide an additional source of sulfate to groundwater via pyrite oxidation, as pyrite is not expected to be a stable mineral phase under observed groundwater redox conditions and sulfate concentrations at background wells are indicative of a potential additional natural source.

Boron and sulfate in the groundwater system may be attenuated via surface complexation reactions within portions of the UU PMP and the UA. Conditions within groundwater from both the UA and UU PMP are typically predicted to favor amorphous iron oxide stability at most locations, and the presence of iron oxides in some site solids supporting the occurrence of this mechanism. Limited variability in pH or redox conditions is observed between upgradient background and downgradient locations. Boron may be further attenuated via interactions with clay minerals, which are observed in solids across both the UU and UA. The observation of gypsum, although limited to the shale bedrock portions of the UA, indicates that precipitation of gypsum may be another potential attenuation mechanism for sulfate at locations near the FAPS.

2. INTRODUCTION

This report documents the development of a geochemical conceptual site model (GCSM) to describe subsurface conditions at the Baldwin Power Plant (BPP) Fly Ash Pond System (FAPS) coal combustion residuals (CCR) unit (Unit #605). A GCSM describes the geochemical processes that contribute to the mobilization, distribution, and attenuation of chemicals in the environment. The GCSM was prepared in support of an evaluation of the nature and extent (N&E) of exceedances of constituents of concern (COCs) above the groundwater protection standards (GWPS) at the FAPS. The document has been prepared as an appendix to the BPP FAPS N&E Report prepared by Ramboll Americas Engineering Solutions, Inc. (Ramboll). Parameters with exceedances above the GWPS at the Baldwin FAPS for the second, third, and fourth quarters of 2023 (Q2 2023, Q3, 2023, and Q4 2023) sampling events completed under Illinois Administrative Code (I.A.C.) Title 35 § 845.630 are boron and sulfate. Exceedances of boron were observed at compliance monitoring wells MW-150, MW-152, and MW-391 and an exceedance of sulfate was observed at MW-150. The boron and sulfate exceedances are present in the upper unit (UU) potential migration pathway (PMP) at MW-150 and for boron at MW-152. The boron exceedance at MW-391 is present within the uppermost aquifer (UA).

An exceedance of pH was observed at compliance monitoring well MW-252 during the Q3 2023 sampling event. However, an alternative source demonstration (ASD), as allowed by I.A.C. 845.650(e), was completed for the pH exceedance (Geosyntec 2024). The pH ASD was accepted by IEPA on March 7, 2024 (IEPA 2024); therefore, pH is not included as a COC in this GCSM.

3. SITE BACKGROUND

3.1 Site Overview

An overview of site characteristics and hydrogeology is presented in the BPP FAPS N&E Report. A site layout figure is provided in Attachment A.¹ Briefly, the Baldwin FAPS impoundment is located to the south of the Bottom Ash Pond (BAP) CCR unit (Unit # 601). The BPP property is bordered by Baldwin Road to the east; the village of Baldwin to the southeast; Illinois Central Gulf railroad tracks, State Road 154, and scattered residences to the south; the Kaskaskia River to the west; and farmland to the north. The FAPS was closed in-place in 2020 in accordance with the closure plan approved by the Illinois Environmental Protection Agency (IEPA) on August 16, 2016 (IEPA 2016). Prior to closure, the FAPS comprised the West Fly Ash Pond, East Fly Ash Pond, and Old East Fly Ash Pond.

A Supplemental Hydrogeologic Site Characterization and Groundwater Monitoring Plan (Natural Resource Technology, Inc. [NRT] 2016) and the Hydrogeologic Site Characterization Report (Ramboll 2021) have previously described the hydrostratigraphic units (HSUs) present in the vicinity of the BPP FAPS, which consist of the UU and a Bedrock Unit. The UU is predominantly clay with silt and minor sand, silt layers, and occasional sand lenses. The UU includes lithologies identified as the Cahokia Formation, Peoria Loess, Equality Formation, and Vandalia Till. Thin sand seams present at the contact between the UU and Bedrock Unit have been identified as potential migration pathways (PMPs) due to higher hydraulic conductivities in comparison to those in the surrounding clays (e.g., 10^{-4} centimeters per second [cm/s] in sands compared with 10^{-5} cm/s in clays) (Ramboll 2023a). Continuous sand seams have not been observed in the UU. Due to the predominance of clay and only thin and intermittent sand lenses, this unit is not considered a continuous aquifer unit within the site boundary (NRT 2016; Ramboll 2021).

Pennsylvanian and Mississippian-aged interbedded shale and limestone bedrock, which comprise the Bedrock Unit, continuously underlies the BPP and is considered the uppermost aquifer (UA) at the site. The top of the Bedrock Unit ranges from 12.5 feet below ground surface (bgs) near the Kaskaskia River to 70 feet bgs under the footprint of the former East Fly Ash Pond (part of the FAPS). The Bedrock Unit is the UA.

3.2 Groundwater Monitoring Network

A groundwater monitoring network was proposed in accordance with I.A.C. Title 35 Section 845.630 to monitor groundwater quality which passes the waste boundary as part of the Operating Permit application to IEPA for the FAPS (Ramboll 2023b). Monitoring well locations at the BPP, including those not included in the proposed groundwater monitoring network, are shown in Attachment B. Well construction information is provided in Attachment C.²

¹ This figure is also provided as Figure 2-1 of the BPP FAPS N&E Report.

² This table is also provided as Table 3-1 of the BPP FAPS N&E Report.

Groundwater flow in the UA is southwest to northwest in the east area of the FAPS until groundwater reaches the bedrock valley feature underlying the Secondary and Tertiary Ponds west of the FAPS, at which point the flow direction becomes southwest following this low bedrock surface. Groundwater flow directions are generally consistent across seasons. A detailed discussion of the hydrogeology of the Site is presented in Section 2 of the BPP FAPS N&E Report.

DRAFT

4. GEOCHEMICAL SITE CONDITIONS

4.1 Constituent Transport and Fate

Boron is primarily present in groundwater as boric acid (H_3BO_3) or borate ($\text{B}[\text{OH}]^{4-}$) (Bolan et al. 2023). The speciation of boron depends on pH: at pH below 9.2 standard units (SU), H_3BO_3 is the dominant species (NCBI 2024a). Boron is not subject to oxidation/reduction reactions (Lemarchand et al. 2015; Bolan et al. 2023). Boron primarily sorbs to positively charged sites on solid metal oxide phases, including iron and aluminum oxides (Goldberg and Glaubig 1985; Bolan et al. 2023). Boron sorbs most extensively to amorphous metal oxides between pH 7 SU and 8 SU (Goldberg and Glaubig, 1985). Boron can also sorb to organic surfaces such as humic acids or coal under favorable conditions, most extensively between pH 8 and 10 SU (LeMarchand et al. 2015). Clay minerals have been correlated with boron sorption in soils (Goldberg, 1997), with this sorption mechanism presenting an additional potential attenuation mechanism for boron under favorable geochemical conditions.

Sulfate is the primary form of oxidized sulfur ($\text{S}(\text{VI})$) in the environment and is a divalent oxyanion at pH values greater than 2 SU (Stumm and Morgan 1996). Sulfate in groundwater may sorb onto positively charged sites on solid metal oxide phases, most commonly iron and manganese oxides (Brown et al. 1999). The extent and strength of sulfate sorption to metal oxide surfaces depends on pH, ionic strength, and oxide surface area available for sorption. Sulfate can also form insoluble complexes such as barite (BaSO_4) (NCBI 2024b). Sulfate in groundwater may be reduced to elemental sulfur ($\text{S}(0)$) or sulfide ($\text{S}(-\text{II})$) under sufficiently reducing conditions, a process governed by local microbial communities (Stumm and Morgan 1996). Generally, reduced sulfur is less mobile in groundwater than sulfate. Reduced sulfur readily precipitates as metal sulfides and sorbs to solid phases such as iron and manganese oxides (Stumm and Morgan 1996).

4.2 Site Solids Characterization

Solid phase data were not collected from the CCR source material prior to completion of unit closure in 2020.

Solids from across the Site were characterized to determine the type and abundance of minerals present in the UU and the UA, their geochemical properties, and their effect on the geochemistry of the groundwater system. Solids were characterized using a variety of analytical techniques, the results of which are presented in Tables 1 through 5. Solids were collected from four locations adjacent to existing wells in the FAPS monitoring network as follows:

- MW-150/MW-350, a co-located well pair located downgradient and west of the FAPS. Solids were collected from two intervals within the UU that represent the PMP and two intervals to represent predominantly shale and limestone lithologies within the UA. Exceedances of boron and sulfate in groundwater were identified at MW-150 during the Q2 2023 statistical evaluation.

- MW-352, located downgradient and south of the FAPS. Solids were collected from two intervals that represent both predominantly shale and limestone lithologies within the UA. Samples were not collected from intervals representative of UU for the paired location MW-152, because the boron exceedance at MW-152 was first identified in the Q3 2023 statistical evaluation.
- MW-366, located downgradient of the FAPS and northwest of the former West Fly Ash Pond, with solids collected from the UA shale.
- MW-391, located downgradient and west of the FAPS, with solids collected from three intervals that represent predominantly shale, weathered shale, and limestone lithologies within the UA. An exceedance of boron was identified at MW-391 during the Q2 2023 statistical evaluation.

The monitoring well locations are shown on Attachment 2. Boring logs for these locations are provided in Attachment D.

Samples from four additional locations across the site were analyzed as part of investigations at the BPP BAP but the materials are representative of conditions within the same HSUs beneath the FAPS as these HSUs are observed continuously across the Site. These solids were collected from multiple intervals adjacent to existing wells, specifically:

- MW-358, located upgradient and east of the FAPS and representative of background conditions for both the FAPS and BAP. Solids were collected within three intervals – one from the UU which represents the PMP and two from shale of the UA ;
- MW-392, located sidegradient and north of the BAP, with solids collected from three intervals – one within clay/sand of the UU and two within the UA shale;
- MW-393, located sidegradient and north of the BAP, with solids collected from two intervals – one within clay/sand of the UU and one within the UA shale;
- MW-394, located sidegradient and north of the BAP, with solids collected from sand within the UU.

Boring logs for these locations are also provided in Attachment D.

4.2.1 Loss on Ignition, Total Organic Carbon, and Cation Exchange Capacity

Loss on ignition (LOI) represents the combustible portions of a solid material and is often used as an approximation of organic matter in a sample. This can also be estimated via measurement of total organic carbon (TOC). The cation exchange capacity (CEC) of a solid represents the total negative surface charge of that material, which is related to the material's surface potential to sorb cations. Amorphous iron hydroxides, organic matter, and clays all tend to possess high negative surface charges and therefore tend to contribute to higher CEC values. The CEC and LOI values

for solids are presented in Table 1 and laboratory analytical results are provided in Attachment E. CEC and LOI values are both consistently high in the vicinity of the FAPS (CEC: 12.94 – 173.79 milliequivalents per 100 g of sample [meq/100 g]; LOI: 8.4 – 40.5 percent by dry weight [% wt]), indicating that the solids have significant organic matter present, likely associated with the shale lithologies. Where measured, the TOC content for shale varied between 0.16 – 1.4 % wt (Table 1). Solids at MW-150 exhibited the lowest CEC and LOI values in the vicinity of the FAPS, consistent with the sandy clay substrate of the UU PMP. All other samples in the vicinity of the FAPS were collected from the UA solids. Samples collected from lithologies identified as predominantly limestone exhibit the highest CEC and LOI values (CEC: 164.7 – 173.79 meq/100g; LOI: 37.1 – 40.5% wt) analyzed at the site, which suggests significant contribution of organic matter from the observed interbedded thin shale layers within the limestone bedrock. UU PMP solids collected near the BAP exhibited similarly low LOI values, while shales collected at MW-392 displayed lower CEC values than those observed near the FAPS, which may be related to variable degrees of weathering within the HSUs.

4.2.2 Total Metals and Boron via Bulk Characterization

Total metals were analyzed to determine the major and trace metal content of the solids. Total iron concentrations in UA solids sampled from across the Site range from 5,300 milligrams per kilogram [mg/kg] to 23,000 mg/kg and total iron is observed to be elevated within the UU PMP solids (19,000 and 38,000 mg/kg) relative to UA solids (Table 2; Attachment E). UA samples from limestone lithologies have lower iron concentrations (5,300 mg/kg to 5,600 mg/kg) than shale samples (11,000 mg/kg to 23,000 mg/kg). The abundance of iron within the bulk solids matrix of both the UA and UU PMP indicates that iron-bearing minerals are likely present within the system. Total manganese concentrations are relatively low in UA solids (190 mg/kg to 1,200 mg/kg), and higher in UU solids (770 and 830 mg/kg) (Table 2; Attachment E). Total aluminum concentrations were lowest in limestone lithologies of the UA (4,800 to 5,900 mg/kg), and relatively higher in both shale lithologies of the UA (16,000 to 81,000 mg/kg) and the UU PMP (42,000 to 66,000 mg/kg) (Table 2; Attachment E). Boron concentrations within solids were analyzed in the vicinity of the BAP, with concentrations in the UA ranging from 11 to 16 mg/kg. Sulfate concentrations within UA solids, as measured in leachate after HCl digestion of solids for samples from MW-358 and MW-392, ranged between 50 to 620 mg/kg (Table 2, Attachment E).

X-Ray fluorescence (XRF) was conducted for identification of the bulk elemental composition of solids (Table 3; Attachment F). Solids from the UU PMP are predominantly composed of silicon (52.3 to 79.7 wt %) and aluminum (8.1 to 11.7 wt %) consistent with the sand and clay lithologies described for the UU. UA solids are predominantly composed of aluminum (1.0 to 19.2 wt %), silicon (6.7 to 59.6 wt %), and calcium (0.5 to 49.4 wt %), consistent with the shale and limestone expected within the bedrock locations. Iron is observed within all solid phase samples, ranging from 0.7 to 7.7 wt %. Manganese was observed in all UU solids and 12 out of 14 UA solids. Manganese was observed at low abundances in both the UU and UA, ranging from 0.02 to 0.18 wt %.

4.2.3 Sequential Extraction Procedure Analysis of Metals and Boron

Samples of composited material from select BAP-associated boring locations were submitted to SGS Canada (Lakefield, ON) for sequential extraction procedure (SEP). SEPs are chemical extractions used to dissolve metals from specific solid-associated phases. SEPs use progressively stronger reagents to solubilize metals from increasingly recalcitrant phases. Although these procedures do not identify the discrete solid phases in a soil/aquifer matrix, they do provide a means to evaluate the class of solids and relative stability in relation to general solubility, changes in oxidation/reduction (redox) potential, and pH fluctuations (Tessier et al. 1979, Kuo et al. 1983, Sposito et al. 1984, Hickey and Kittrick 1984, Gruebel et al. 1988). Therefore, SEP data are useful to infer the mechanism and potential reversibility of attenuation processes. The results of the 6-step extraction procedure and analysis are provided in Table 4 and Attachment G.

Boron was detected in the residual metals fraction of all samples (13 to 62 mg/kg, comprising 63 to 100% of the extracted boron), which may be associated with the presence of micas and clays within both the UA and UU. All UA solids also had detectable amounts of boron in the water soluble, carbonate-bound, iron or manganese oxide bound, and organic material bound fractions at relatively low proportions of the total boron (typically <10% in a given fraction). The observation of detectable concentrations of boron in relatively mobile fractions (e.g. water soluble and carbonate-bound) at the MW-358 background location is consistent with a potential native geogenic source of boron within the UA at the site.

The vast majority of iron within solids from both the UA (>87%) and UU PMP (>92%) is bound within the residual metals fraction, consistent across both background and compliance locations (Table 4). Iron was also identified in the fraction typically associated with iron or manganese oxides, with proportions ranging from 3.8 to 7.3% in UU PMP solids and 3.6 to 11.2% of total iron within UA solids. UA solids collected within shale lithologies also displayed iron associated with the organic material bound fraction (1.4 to 7.1%), consistent with the increased sorptive capacity associated with the organic matter content whose presence is indicated by the high LOI values of these solids.

4.2.4 Mineralogical Analysis

X-Ray diffraction (XRD) with Rietveld refinement was conducted for identification of minerals in solid samples. XRD is an analytical technique that provides information about the identity of the crystalline material within a sample but does not provide information about non-crystalline or amorphous phases. XRD results are normalized to 100% of the total weight, meaning that material not characterized by XRD is ignored in the percent calculation. Solids from the UU PMP (MW-150, MW-358, MW-392, MW-393, and MW-394) were predominantly composed of quartz, ranging from 32.4 to 64.1% of the minerals present (Table 5a; Attachment H). Muscovite (2.0 to 9.1%), feldspar minerals including albite (6.4 to 12.8%) and microcline (6.5 to 10.1%), and a variety of clays (10.4 to 15.9% total) were observed as additional primary crystalline mineral phases. These results are consistent with the field observations documented in the boring logs

provided in Attachment D. Low abundances of magnetite (detected to 0.9%) were observed, but otherwise crystalline forms of iron oxides were not observed in UU PMP solids. Combined with XRF data observations of iron abundances between 2.8 to 5.0 wt % in solids across the UU PMP and limited observations of other iron-bearing crystalline minerals (e.g. ankerite), these results provide evidence that the majority of iron within UU PMP solids is present as non-crystalline or amorphous phases. Diaspore, an aluminum oxide, was detected at low abundances (0.2 to 0.5%) within UU PMP solids, including at background well MW-358.

Solids from shale-dominated portions of the UA (MW-350, MW-352, MW-358, MW-366, MW-391, and MW-392) exhibited mixed mineral compositions, with significant proportions of clay minerals (3.4 to 41.2%), quartz (11.2 to 30.7%), muscovite (4.3 to 19.7%) and calcite (0.5 to 74.9%). Solids from limestone dominated portions of the UA (MW-350 and MW-391) were predominantly calcite (80.5 to 90.2 %) and quartz (5.2 to 10.7%), with low proportions of clays (1.6 to 3.5%) (Table 5b; Attachment H). These results are consistent with the field observations documented in the boring logs provided in Attachment D. Gypsum was observed at low abundance (1.92 wt %) in the shale bedrock at MW-350, which suggests that precipitation of sulfate is possible under some aquifer conditions. Iron oxides, including magnetite (0.2 to 1.4%) and hematite (0.2 – 0.4%) were observed in low abundances in the shale portions of the UA. No crystalline iron oxides were observed in the limestone dominated portions of the UA. Both ankerite (0.2 to 10.0%) and pyrite (0.1 to 1.6%) are observed in solids across the UA, suggesting that a significant portion of the total iron within UA solids could be associated with minerals other than crystalline iron oxides, consistent with observation of iron abundances between 0.7 to 7.7 wt % for UA XRF results. Rhodochrosite was observed at low abundance (0.7%) at MW-350 within a shale-dominated depth interval. Crystalline manganese-bearing mineral phases were not identified in other solid samples, consistent with the low elemental abundances of manganese observed in the XRF results for UA samples. While diaspore was detected at one location in the UA, MW-392, crystalline aluminum-oxide mineral phases do not appear to be widely distributed.

Kaolinite, montmorillonite, and illite have been correlated with boron retention in soils (Goldberg 1997). Of those three clay types, illite exhibits the greatest rate of boron adsorption, and was observed in each solid sample from both the UA and UU at abundances ranging from 0.6 to 15.0%. Montmorillonite and kaolinite were also present in the majority of solids (0.2 to 14.0% and 0.5 to 15.0%, respectively). The abundance of clay minerals within solids presents an additional potential attenuation mechanism for boron within the UA and UU.

4.3 Aqueous Geochemistry

FAPS porewater (i.e., CCR source water) and groundwater from wells across the UA and UU were analyzed for a range of geochemical parameters and presented in Figures 1a through 10b. FAPS porewater was collected and analyzed during two periods – prior to unit closure (September 2013 to June 2014) from three locations and a one-time collection of porewater from sumps during

closure activities in May 2020.³ The United States Environmental Protection Agency (USEPA) considers the use of porewater data as the most appropriate approach to estimate constituent fluxes to groundwater from CCR surface impoundments. As per USEPA, “this is because porewater better represents the leachate seeping from the bottom of the impoundment than impoundment water samples” (USEPA 2015). For clarity in interpretation, the figures present data from the UA and UU well locations separately. UA well locations are shown with circular symbology on the figures, whereas UU locations are shown as triangles. The groundwater data used in the site evaluation is summarized in Attachment I.

An ASD, submitted on 8 February 2024 and accepted by IEPA on 7 March 2024, indicated that groundwater data from MW-253 was impacted by well construction issues, resulting in anomalously high pH values (~10-12 SU) (Geosyntec 2024). A review of groundwater data at the site found that background well MW-306 and downgradient compliance well MW-350 also appear to be impacted by well construction issues based on their anomalously high pH values. Because these infrastructure issues are anticipated to potentially impact groundwater geochemistry, these three wells (MW-253, MW-306, MW-350) have been excluded from the following discussion, tables, and figures.

4.3.1 Redox/pH Summary

The oxidation-reduction (redox) potential (ORP) and pH in aqueous systems are major controls on the speciation of redox-active chemicals such as iron, manganese, and sulfate.

Within the FAPS prior to closure, CCR porewater exhibited a wide range of pH values, from 7.7 to 11.9 SU (Table 6). In wells across the groundwater monitoring network, pH values appear to be stable and circumneutral (Figures 1a & 1b for the UA and UU PMP, respectively). UA groundwater pH values largely range between 7 to 8 SU, consistent with the high buffering capacity expected from the limestone lithologies of the bedrock. Background wells MW-304 and MW-358 range between pH 7.5 to 8.4 SU, similar to observations at downgradient compliance wells MW-375, MW-384, and MW-391 and above the range observed at downgradient compliance wells MW-366, MW-377, and MW-390, which exhibit pH values between 6.75 and 7.25 SU. UU well groundwater pH varies between 6.5 to 7.5 (Figure 1b), consistent with the lower buffering capacity expected with the sandy clay substrate of the UU PMP as compared to the shale and limestone lithologies of the UA.

Groundwater within the UA background well locations upgradient of the FAPS (MW-304 and MW-358) exhibits a range of redox conditions, with fluctuations between reducing and oxidizing conditions observed (Figure 2a). These fluctuating conditions within unaffected portions of UA groundwater do not appear to follow a seasonal pattern and have occurred at MW-304 for the entirety of the monitoring record (Figure 2a). Groundwater at all compliance wells downgradient of the FAPS within the UA follow a similar pattern, with fluctuations between reducing and

³ FAPS porewater data are excluded from the time series graphs and provided in Table 6 due to the limited number of available data points and relevant constituents.

oxidizing conditions occurring frequently. Observation of this pattern across the UA monitoring network indicates that redox fluctuations are driven by HSU characteristics and are not reflective of FAPS porewater influences. Groundwater within the UU typically exhibits consistently oxidizing conditions, except for MW-150 which exhibits more variable redox conditions which may be related to the location of MW-150 downgradient of the Secondary and Tertiary Ponds. (Figure 2b).

4.3.2 Exceedance Parameters

4.3.2.1 FAPS Porewater

Prior to unit closure, FAPS porewater (i.e., CCR source water) exhibited total boron concentrations from 0.663 to 102 milligrams per liter (mg/L) and total sulfate concentrations that ranged from 750 to 2,630 mg/L, consistent with leachate from CCR units (Table 6) (EPRI 2017). Dissolved boron concentrations (ranging from 36.3 to 94.7 mg/L) and dissolved sulfate concentrations (495 to 2,820 mg/L) were similarly elevated where analyzed, indicating a majority of boron and sulfate within the porewater are in the dissolved fraction. Results for both total and dissolved boron are notably higher than concentrations reported in groundwater (Sections 4.3.2.2 and 4.3.2.3). Concentrations of both boron and sulfate were consistently lower at TPZ-163 (located within the Old East Fly Ash Pond portion of the FAPS); these lower concentrations may be related to an early cessation of material deposition within this portion of the FAPS. Porewater collected from sumps during closure exhibited similarly elevated total sulfate and boron concentrations (1,080 to 1,840 mg/L and 10.6 to 60.3 mg/L, respectively), except at Sump 13 (84 mg/L and 0.66 mg/L, respectively), suggesting potential dilution from unaffected waters during closure activities at this location.

4.3.2.2 UA

UA background wells MW-304 and MW-358 exhibited a range of boron concentrations in groundwater, with MW-304 exhibiting boron concentrations at or below the GWPS of 2.16 mg/L (1.27 to 2.16 mg/L), and MW-358 consistently below the GWPS (1.1 to 1.67 mg/L) (Figure 3a). Total boron concentrations in the UA remained generally stable through time across the site, with notable exceptions at MW-391, MW-390, and MW-366 as discussed below. Where analyzed, dissolved boron concentrations trends within the UA mirrored total boron concentration trends (Figure 3b).

Total sulfate concentration trends within UA background wells (MW-304 and MW-358) were consistent with those observed for boron concentrations, with MW-304 exhibiting relatively elevated concentrations (157 to 231 mg/L) and MW-358 exhibiting consistently lower concentrations (8 to 108 mg/L) (Figure 4a). Patterns of total sulfate concentrations in downgradient UA are generally consistent with those observed for total boron (Figure 4a). Where analyzed, dissolved sulfate concentrations within downgradient UA well locations were stable through time and relatively low, typically less than 250 mg/L (Figure 4b).

MW-391 exhibits a sharp increase in total boron (1.88 to 8.91 mg/L) and total sulfate (758 to 1,760 mg/L) concentrations between 2017 and 2018 sampling events. This is likely a result of water diversion activities completed as a part of dewatering within the FAPS during closure, as the increase in total boron and sulfate concentrations was concurrent with a change in groundwater elevation of nearly 40 feet at MW-391 (Figure 5a). The highest groundwater elevation at MW-391 (414.54 ft above mean sea level on 24 March 2020) is consistent with groundwater elevations recorded in the PMP (Figure 5b) and may have resulted in temporary connectivity with the UU PMP HSU.

Total sulfate concentrations in groundwater at MW-366 increased sharply (64 to 526 mg/L) over the same period as sulfate in MW-391 but did not show a similar change in total boron concentrations (1.66 to 1.53 mg/L). In contrast, MW-390 groundwater boron (1.3 to 0.21 mg/L) concentrations fell over the same period and remain low through recent sampling efforts, with sulfate concentrations remaining largely stable (233 to 141 mg/L). Neither MW-366 nor MW-390 exhibit changes in groundwater elevations concurrent with changes in sulfate and/or boron concentrations, but the location of all three of these monitoring locations on the northwest edge of the West Fly Ash Pond suggests that the geochemical changes observed are caused by a similar hydrologic driver.

4.3.2.3 *UU PMP*

Total boron data is limited to a few recent sampling events for UU PMP groundwater wells, but concentrations appear to be stable through time and well below the GWPS, except for at MW-150 where concentrations are above the GWPS (3.43 to 4.12 mg/L) (Figure 6a). Dissolved boron concentrations are also above the GWPS at MW-150 (Figure 6b), with observations of dissolved boron appearing to increase gradually over time. Dissolved boron concentrations are more than 50% of total boron concentrations at MW-150, such that dissolved boron is the predominant form of boron observed at this location. The gradual increase in dissolved boron concentrations in groundwater at MW-150 is being further evaluated to identify the primary source and transport mechanism but may be related to the low hydraulic conductivity in the UU PMP (Section 2.3.6 of the BPP FAPS N&E Report). Both total and dissolved sulfate concentrations within the UU PMP mirror patterns observed for boron (Figures 7a & 7b).

MW-152 currently exhibits a strong seasonal pattern with regard to dissolved boron and dissolved sulfate concentrations, with both analytes spiking well above the GWPS during September sampling efforts, then returning to much lower concentrations (below the GWPS for both boron and sulfate) by sampling during the following March. This pattern is observable in data from 2016 through the most recent sampling efforts. While statistically significant levels of sulfate have not been identified at MW-152 to date, a boron exceedance was noted during the Q3 2023 statistical evaluation. The observed pattern in concentrations correlates with groundwater elevations as discussed in Section 3.2.1 of the BPP N&E Report. A similar seasonal pattern is not observed at MW-352, the associated well within the UA.

4.3.3 Pourbaix Diagrams

Eh-pH (Pourbaix) diagrams can be used to illustrate the predicted stability of specific phases at thermodynamic equilibrium under the conditions observed for a groundwater sample. Select crystalline mineral species were suppressed to be representative of anticipated groundwater conditions (e.g. mineral formation not anticipated to be kinetically favored), except when identified in XRD data from solids in the site.

Using conditions observed at well MW-391 on 17 May 2023 to represent groundwater within the UA (Table 7), amorphous iron oxyhydroxides (represented by ferrihydrite) are predicted to be stable under groundwater conditions at some locations, while at other locations solid phase iron minerals are not expected to be stable (Figure 8a).⁴ Conditions at MW-391, which had a boron exceedance, are favorable for ferrihydrite stability. Background well MW-304 exhibits conditions predicted to be stable for amorphous ferrihydrite formation for all recent monitoring events, while conditions at background well MW-358 indicate that groundwater at this well is experiencing dynamic equilibrium conditions in which chemical reactions between dissolved iron and amorphous iron oxyhydroxides can occur. This appears to be driven by the variable redox conditions observed across the UA (Section 4.3.1). Solids collected from background location MW-358 exhibited low abundances of magnetite (Table 5b), and when magnetite is not suppressed as a possible mineral species during modeling, magnetite is predicted to be stable at all locations across the UA (Figure 8b). Similarly, when hematite is not suppressed as a possible mineral phase during modeling, hematite is predicted to be stable across the UA (Figure 8c), consistent with the observation of low abundances of hematite in a subset of UA solids (Table 5b). Taken together, these modeling results suggest that iron oxides, whether amorphous or crystalline, are likely to be present in the UA under most aquifer conditions and may serve as reactive surfaces for potential attenuation. Neither ankerite nor pyrite, which were identified via XRD, are expected to be thermodynamically stable within the UA based upon the observed redox conditions (Figures 8a-8c), suggesting that dissolution of these minerals could provide a source of iron for formation of amorphous iron oxide coatings.

Similar aquifer conditions are predicted at locations within the UU PMP, modeled using groundwater conditions from MW-150 sampled on 18 May 2023 (Table 7; Figure 8d). As observed for the UA, ferrihydrite stability is variable, with stability predicted under HSU conditions at some locations (MW-151, MW-152, and MW-153), while at others amorphous iron minerals are not expected to be stable (MW-150 and MW-252). While variable boron and sulfate concentrations were observed at UU PMP well MW-152, these changes are not correlated to ferrihydrite stability at MW-152. Crystalline magnetite is expected to be stable at all PMP locations (Figure 8e), which is consistent with the low abundances of magnetite detected via XRD in solids near MW-150 (Table 5a). Ankerite is not expected to be thermodynamically stable within the UU PMP based upon the observed redox conditions; dissolution of ankerite could provide a source of iron for

⁴ Field ORP measurements were converted to Eh by adding +200 millivolts to correct for the Ag/AgCl electrode.

formation of amorphous iron oxide coatings. Taken together, these modeling results suggest that iron oxides, whether amorphous or crystalline (e.g. magnetite), are present in the PMP under most groundwater conditions.

A review of Eh-pH conditions for manganese found that solid phase manganese minerals, including manganese oxides, are not predicted to be stable under conditions within either the UU PMP or UA across the site (Figures 9a and 9b, respectively).

4.3.4 Total and Dissolved Iron and Manganese Concentrations

The distribution of iron and manganese between total and dissolved phases can provide insights on site redox conditions and constituent behavior. A comparison of the total and dissolved iron and manganese data for the Q2 through Q4 2023 events is provided in Table 8. Total iron was detected at all locations analyzed during this time period, with reported values ranging from 0.014 mg/L at UA background well MW-304 to 25.2 mg/L at downgradient UU PMP well MW-151. UU PMP groundwaters exhibit greater total iron concentrations than UA wells, consistent with the greater concentrations of solid phase iron observed at these locations (Table 2). Background well MW-304 groundwater has consistently low total and dissolved iron, while background well MW-358 groundwater has some of the highest total iron concentrations observed for UA groundwaters (0.685 and 0.908 mg/L), with turbidity values similar at the two locations. This is consistent with the relatively high abundance of total iron in the solids at MW-358 (Table 3) and the greater relative stability of ferrihydrite at MW-358 (Figure 8a). Dissolved iron was detected at 8 of 15 locations analyzed, with reported values ranging from 0.024 mg/L to 0.619 mg/L. Where dissolved iron was detected, the dissolved concentration was typically less than 50% of the total iron value, providing evidence that iron is largely associated with particulates suspended in groundwater. This was not observed at MW-352, with dissolved iron a greater proportion of total iron at these locations, consistent with geochemical conditions which periodically favor dissolution of iron oxides (Figure 8a).

Total manganese was detected at all locations analyzed, with reported values ranging from 0.0028 mg/L at UU PMP well MW-150 to 1.68 mg/L at downgradient UA well MW-366 (Table 8). Dissolved manganese values ranged from 0.0013 mg/L at UA downgradient well MW-375 to 0.681 mg/L at downgradient UA well MW-390. At locations where dissolved manganese was detected, dissolved concentrations as percentage of total concentration varied widely across both the UU PMP (2 to 91 %) and UA (2 to greater than 100%). This is consistent with the predicted mobilization of manganese to the aqueous phase based on the Pourbaix diagrams (Figures 9a and 9b), and the lack of observed crystalline manganese-bearing minerals (like rhodochrosite) across most of the site (Tables 5a & 5b).

4.3.5 Major Ion Distribution and Groundwater Signatures

Piper diagrams were constructed using data from both HSUs to visualize major ion distributions in groundwater. Piper diagrams are a common tool for assessing geochemical similarities or differences in terms of the major ion distributions between aqueous samples. FAPS porewaters

exhibit major anion compositions that are sulfate-dominated (greater than 80%) and major cation compositions that are dominated by monovalent cations (sodium and potassium; Figures 10a & 10b). UA groundwaters exhibit a wider range of geochemical compositions than UU PMP waters, with many locations clustering near background wells MW-304 and MW-358 (Figure 10a). These wells are characterized by a major cation composition that is dominated by sodium and potassium, with relatively even proportions of major anions. MW-352, MW-366, MW-377 and MW-390 do not appear similar to this cluster of UA groundwaters, as they have greater contributions from divalent cations (magnesium and calcium). These wells do not have an identifiable shared hydrologic or geochemical characteristic that would alter the geochemical composition of the groundwater at these locations; they are dispersed across the Site, are screened within both shale and limestone lithologies, and do not exhibit redox conditions different from other locations within the UA.

UU PMP groundwaters exhibit relatively consistent major cation distributions with relatively even proportions of magnesium and calcium, and relatively lower proportions of sodium and potassium (Figure 10b). UU PMP groundwaters consistently have low contributions of chloride, but major anion compositions range from alkalinity-dominated (MW-151) to sulfate-dominated (MW-150), similar to FAPS porewater. The distribution of anions at MW-152 has variable contributions of sulfate and alkalinity, consistent with the observed seasonal variability in sulfate concentrations at this monitoring location (Figure 7b).

5. GEOCHEMICAL CONCEPTUAL SITE MODEL

5.1 Source and Mobilization Mechanisms

Boron is naturally abundant in coals and is concentrated within CCR, primarily as polyborate (B_2O_3) surface coatings on particles (EPRI 1998). Boron was identified in the CCR porewater at concentrations up to 102 mg/L. The likely primary source of boron to the UA and UU PMP is the FAPS CCR porewater based on boron concentrations within the source and relationships to hydrogeological patterns at the site (i.e., correlated increases between boron and groundwater elevation at MW-391). Boron was identified within UA solids at concentrations that suggest that aquifer solids could provide a secondary additional potential natural geogenic source of boron to groundwater, and groundwater from background wells consistently exhibited boron concentrations consistent with a natural geogenic source.

Reduced sulfur species (e.g. pyrite) can be naturally abundant in coals; after coal fly ash production, sulfate is the dominant sulfur species associated with fly ash. Sulfate is concentrated on the surface of fly ash particles and the majority of sulfate mineral phases are soluble under environmental conditions, such that sulfate associated with fly ash is leachable (Izquierdo and Querol 2012). The likely primary source of sulfate to the UA and UU is the FAPS CCR porewater. Sulfate was identified in the CCR porewater at concentrations up to 2,820 mg/L. Sulfate was identified within UA solids at background well locations at concentrations that indicate a potential natural source of sulfate to groundwater, although this sulfate was not observed in crystalline mineral phases at these locations. The observation of pyrite within solids of shale portions of the UA could provide a secondary additional source of sulfate to groundwater via pyrite oxidation, as pyrite is not expected to be a stable mineral phase under observed redox conditions (Figures 8a to 8c).

5.2 Potential and Observed Attenuation Mechanisms

Boron exceedances were identified in both the UA and PMP hydrologic units at the Site. Boron is anticipated to largely be present as the neutral $B(OH)_3$ boric acid species as groundwater pH values are below the pK_a for boric acid (9.2) in both HSUs. Conditions within groundwater from both the UA and UU PMP are typically predicted to favor amorphous ferrihydrite (iron oxide) stability at most locations, and the presence of iron oxides in some solids (Tables 5a & 5b) suggests a portion of the boron in the groundwater system may be attenuated via surface complexation reactions within portions of the UU PMP and the UA. Given the low abundance of total manganese in the solids (Table 1) and the predicted instability of solid manganese phases (Figures 5a and 5b), manganese oxides are not expected to be an important source of adsorption sites. Boron is also known to be attenuated via interactions with clay minerals (Goldberg 1997); the XRD results identified the presence of a number of clay minerals across both the UU and UA (Tables 5a & 5b). Observations of boron associated with the organic matter bound fraction in the SEP analysis (Table 4), as well as the high organic matter content inferred from LOI values indicates that organic matter could be an additional geosorbent for boron within both UU PMP and UA solids (Lemarchand et

al., 2015). Together, these factors suggest that chemical attenuation of boron via interactions with aquifer solid phases such as metal oxides or organic surfaces is possible at locations downgradient of the FAPS.

Sulfate exceedances are currently limited to MW-150, which is screened within the UU PMP. Sulfate is typically considered to be a conservative species within groundwater at circumneutral pH conditions, although precipitation of sulfate-containing mineral phases (e.g., gypsum) and sorption onto positively charged mineral surfaces are both potential attenuation mechanisms. Sulfate attenuation is expected to occur largely as the result of sorption onto iron oxides and oxyhydroxides associated with solids. Both SEP and XRD analyses (Tables 3, 5a, & 5b) support the presence of both crystalline and amorphous iron oxide phases across the Site in both the UU PMP and UA. While modeling of redox conditions within groundwater from MW-150 is not predicted to favor iron oxide stability, at most locations in both the UA and UU PMP redox conditions are typically predicted to favor iron oxide stability, including at background wells MW-304 and MW-358. The observation of gypsum, although limited to downgradient MW-350 in the shale bedrock portions of the UA, indicates that precipitation of gypsum may be another potential attenuation mechanism at locations near the FAPS.

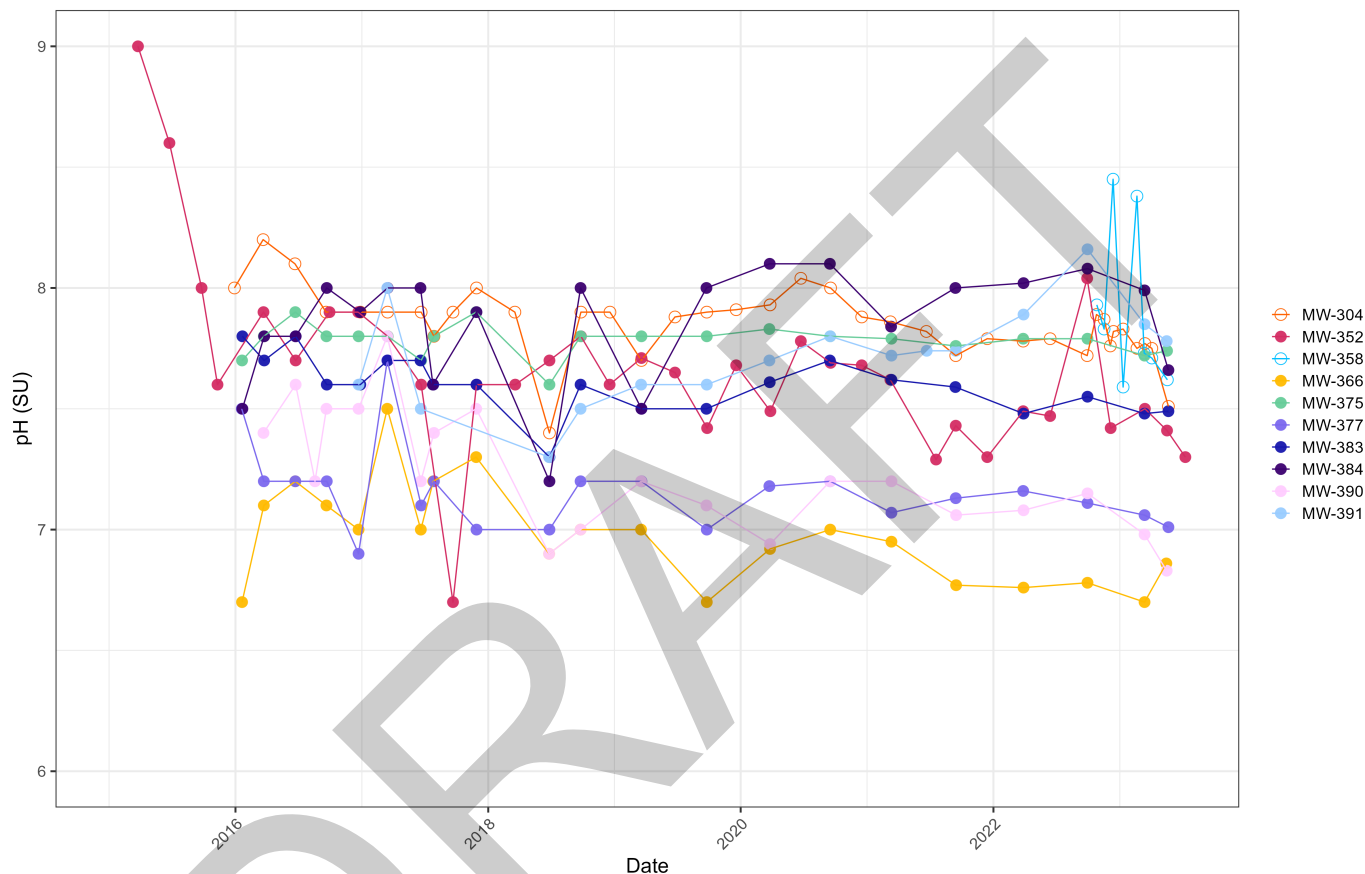
6. REFERENCES

- Bolan, S., Wijesekara, H., Amarasiri, D., Zhang, T., Ragályi, P., Brdar-Jokanović, M., Rékási, M., Lin, J., Padhye, L., Zhao, H., Wang, L., Rinklebe, J., Wang, H., Siddique, K., Kirkham, M., Bolan, N. 2023. "Boron contamination and its risk management in terrestrial and aquatic environmental settings". *Science of the Total Environment*. 164744
- Brown, G E J, V Henrich, W Casey, D Clark, C Eggleston, A Felmy, D W Goodman, M Gratzel, G Maciel, M I McCarthy, K H Nealson, D Sverjensky, M Toney, J M Zachara. 1999. "Metal Oxide Surfaces and Their Interactions with Aqueous Solutions and Microbial Organisms". *Chemical Reviews*, 99, p. 77-174.
- Buszka, P M, J Fitzpatrick, L R Watson, and R T Kay. 2004. "Evaluation of Ground-Water and Boron Sources by Use of Boron Stable-Isotope Ratios, Tritium, and Selected Water-Chemistry Constituents near Beverly Shores, Northwestern Indiana." USGS Scientific Investigations Report Series 2007-5166.
- Electric Power Research Institute (EPRI). 2017. "Application of Isotopic Methods to Coal Combustion Residual Groundwater Quality Investigations". Report 3002010911.
- EPRI. 1998. "Leaching of Inorganic Constituents from Coal Combustion By-Products Under Field and Laboratory Conditions, Volume 1." Final Report TR-111773-V1.
- IEPA. 2016. "Dynergy Midwest Generation, Inc. – Baldwin Energy Complex: Baldwin Fly Ash Pond System Closure – NPDES Permit No. IL000043." Letter from William Buscher (Illinois Environmental Protection Agency) to Rick Diericx (Dynergy Operating Company). August 16.
- IEPA. 2024. "Baldwin Power Plan Fly Ash Pond System; W1578510001-01, -02, -03, Alternative Source Demonstration (ASD) Submittal." Letter from Darin LeCrone (Illinois Environmental Protection Agency) to Phil Morris (Illinois Power Generating Company). March 7.
- Maria Izquierdo, Xavier Querol. 2012. Leaching behaviour of elements from coal combustion fly ash: An overview. *International Journal of Coal Geology*, 194, 54-66.
- Lemarchand, D, A D Jacobson, D Cividini, and F Chabaux. 2015. "The major ion, $^{87}\text{Sr}/^{86}\text{Sr}$, and d^{11}B geochemistry of groundwater in the Wyodak-Anderson coal bed aquifer (Powder River Basin, Wyoming, USA)". *Comptes Rendus Geoscience*, 347, 348-357.
- Geosyntec Consultants, Inc. (Geosyntec). 2024. "Alternative Source Demonstration. Baldwin Power Plant Fly Ash Pond System (Unit ID #605), IEPA ID: W1578510001-01, -02, -03, 35 IAC 845.650." February.
- Goldberg, S. 1997. "Reactions of Boron with Soils". *Plant and Soil*, 193, 35-48.

- Goldberg, S. and Glaubig, R.A. 1985. Boron Adsorption on Aluminum and Iron Oxide Minerals. *Soil Science Society of America Journal*, 49: 1374-1379.
- Gruebel, K A, J A Davies, and J O Leckie. 1988. “The Feasibility of Using Sequential Extraction Techniques for Arsenic and Selenium in Soils and Sediments”. *Soil Sci. Soc. Am. J.* 52, 390-397.
- Hickey, M G and J A Kittrick. 1984. “Chemical Partitioning of Cadmium, Copper, Nickel, and Zinc in Soils and Sediments Containing High Levels of Heavy Metals”. *J. Environ. Qual.* 13, 372-376.
- Kuo, S, P E Heilman, and A S Baker. 1983. “Distribution and Forms of Copper, Zinc, Cadmium, Iron, and Manganese in Soils Near a Copper Smelter”. *Soil Sci.* 135, 101-109.
- National Center for Biotechnology Information (NCBI). 2024a. PubChem Compound Summary for CID 7628, Boric Acid. <https://pubchem.ncbi.nlm.nih.gov/compound/Boric-Acid>. Accessed Feb. 6, 2024.
- National Center for Biotechnology Information (NCBI). 2024b. PubChem Compound Summary for CID 24414, Barium Sulfate. <https://pubchem.ncbi.nlm.nih.gov/compound/Barium-Sulfate>. Accessed Feb. 6, 2024.
- Natural Resource Technology (NRT). 2016. *Supplemental Hydrogeologic Site Characterization and Groundwater Monitoring Plan. Baldwin Fly Ash Pond System. Baldwin Energy Complex, Baldwin, IL.*
- Ramboll Americas Engineering Solutions, Inc. (Ramboll). 2021. “*Hydrogeologic Site Characterization Report. Baldwin Bottom Ash Pond. Baldwin Power Plant. Baldwin, Illinois.* October.
- Ramboll. 2023a. 35 I.A.C. § 845.610(B)(3)(D) *Groundwater Monitoring Data and Detected Exceedances – 2023 Quarter 2. Bottom Ash Pond, Baldwin Power Plant, Baldwin, Illinois.* Ramboll Americas Engineering Solutions, Inc. August.
- Ramboll. 2023b. “*Groundwater Monitoring Plan, Revision 1. Fly Ash Pond System.*” Baldwin Power Plant. Baldwin, Illinois. August.
- Stumm, W., J J Morgan. 1996. *Aquatic Chemistry: Chemical Equilibria and Rates in Natural Waters*, 3rd ed., Wiley-Interscience.
- Sposito, G, C S LeVesque, J P LeClaire, and N Senesi. 1984. “Methodologies to Predict the Mobility and Availability of Hazardous Metals in Sludge-Amended Soils. California Water Resource Center”. University of California, Davis, CA.
- Tessier A., P.G.C. Campbell, and M. Bisson, 1979. “Sequential Extraction Procedures for the Speciation of Particulate Trace Metals”. *Anal. Chem.* 51(7), 844-851.
- USEPA. 2015. Federal Register, Vol. 80, No. 74, Rules and Regulations, April 17, 2015.

FIGURES

pH across UA Monitoring Network



Notes:
 SU: Standard Units
 Background wells shown with open symbols.

pH Time Series – Uppermost Aquifer
 Baldwin Power Plant – Fly Ash Pond System

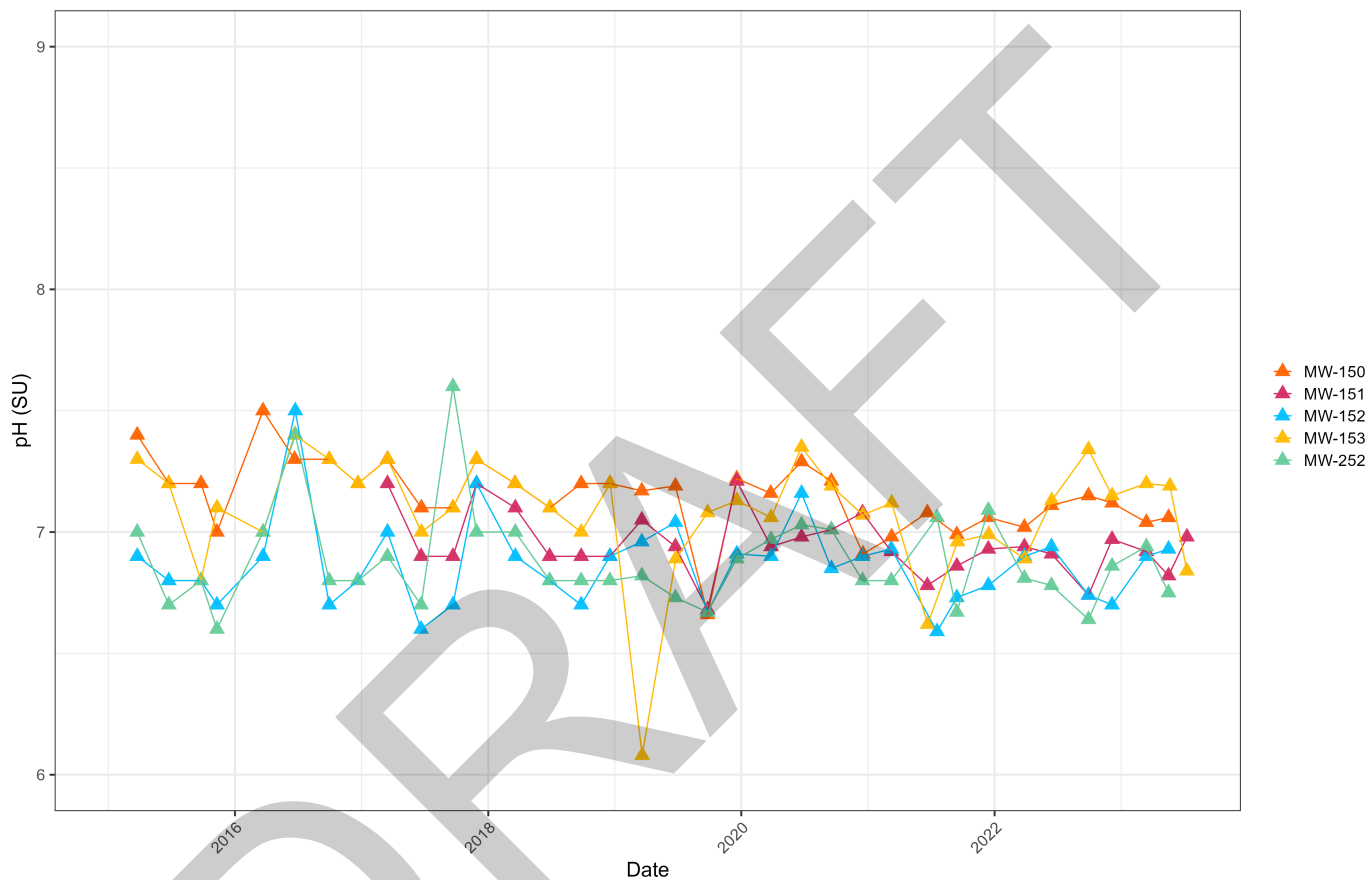
Geosyntec
 consultants

Figure
1a

Columbus, Ohio

February 2024

pH across PMP Monitoring Network



Notes:
SU: Standard Units

pH Time Series – Potential Migration Pathway
Baldwin Power Plant – Fly Ash Pond System

Geosyntec
consultants

Columbus, Ohio

February 2024

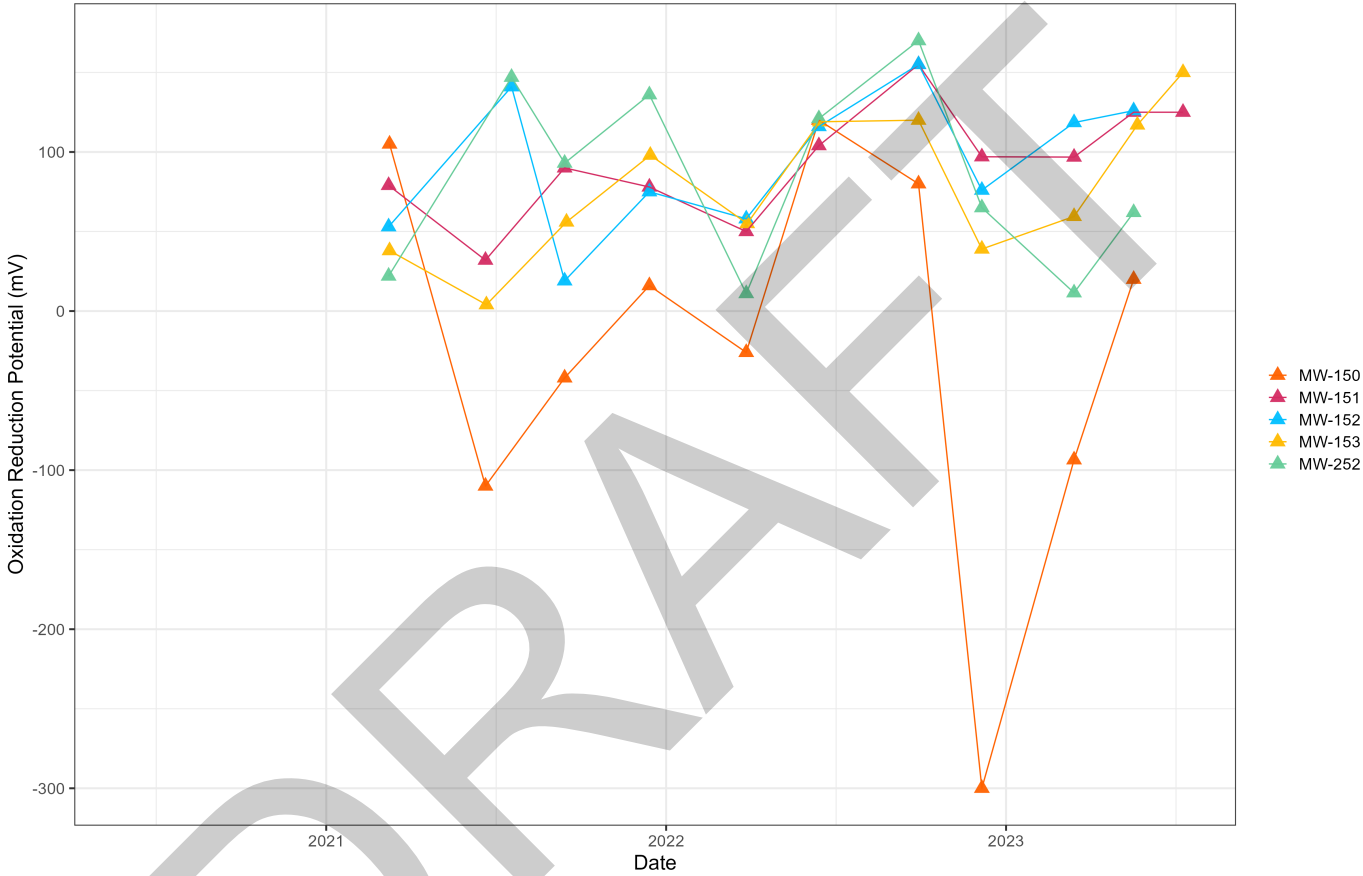
Figure
1b

ORP across UA Monitoring Network



| | | |
|--|--|----------------------|
| <p>Notes: mV: millivolts Background wells shown with open symbols.</p> | <p>ORP Time Series – Uppermost Aquifer Baldwin Power Plant – Fly Ash Pond System</p> | |
| | <p>Geosyntec consultants</p> | <p>Figure 2a</p> |
| | <p>Columbus, Ohio</p> | <p>February 2024</p> |

ORP across PMP Monitoring Network



Notes:
mV: millivolts

ORP Time Series – Potential Migration Pathway
Baldwin Power Plant – Fly Ash Pond System

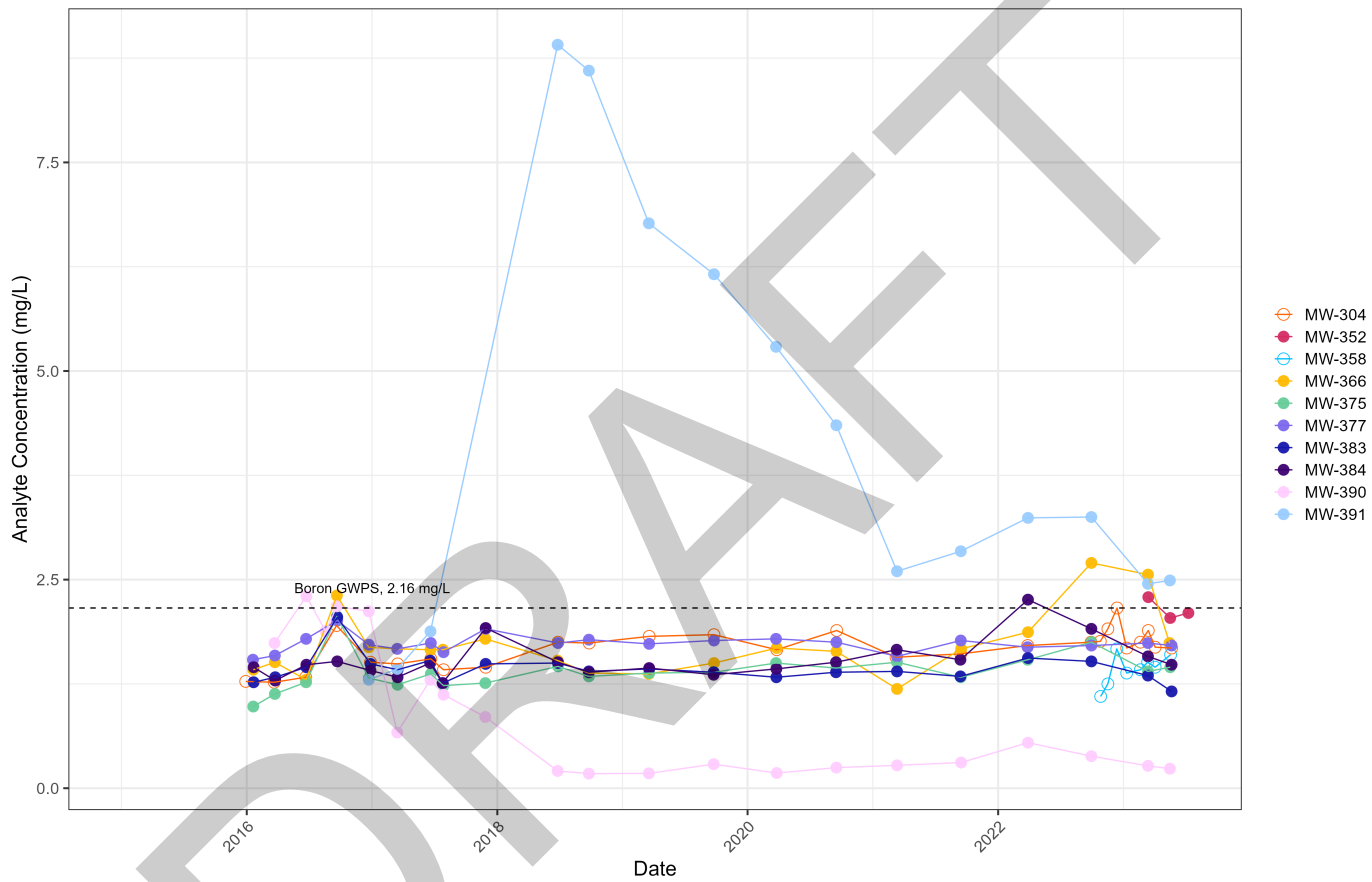
Geosyntec
consultants

Figure
2b

Columbus, Ohio

February 2024

Total Boron across UA Monitoring Network



Notes:
mg/L: milligrams per liter
GWPS: Groundwater Protection Standard
Background wells shown with open symbols.

Boron Concentration Time Series – Uppermost Aquifer
Baldwin Power Plant – Fly Ash Pond System

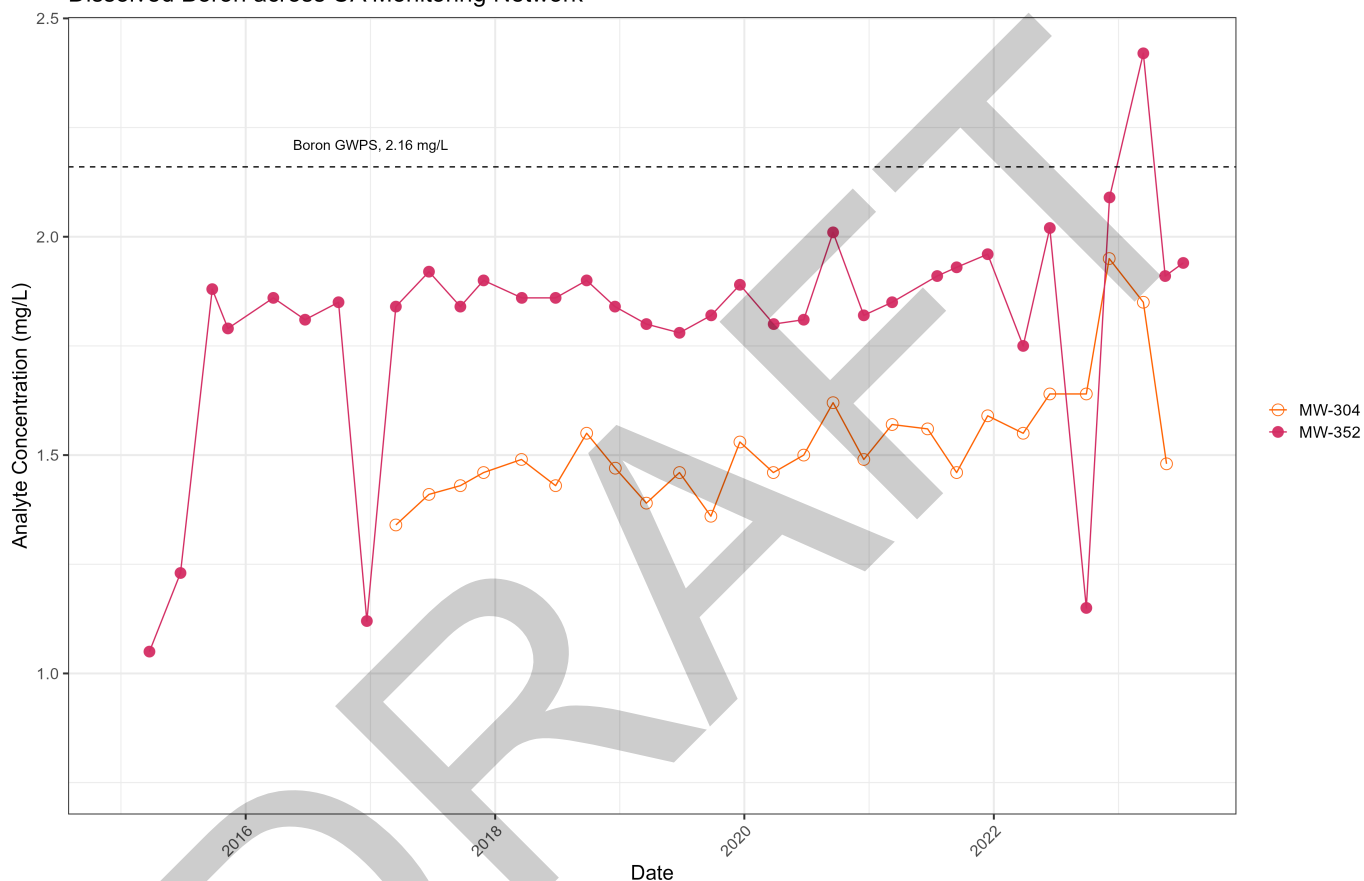


Figure
3a

Columbus, Ohio

February 2024

Dissolved Boron across UA Monitoring Network



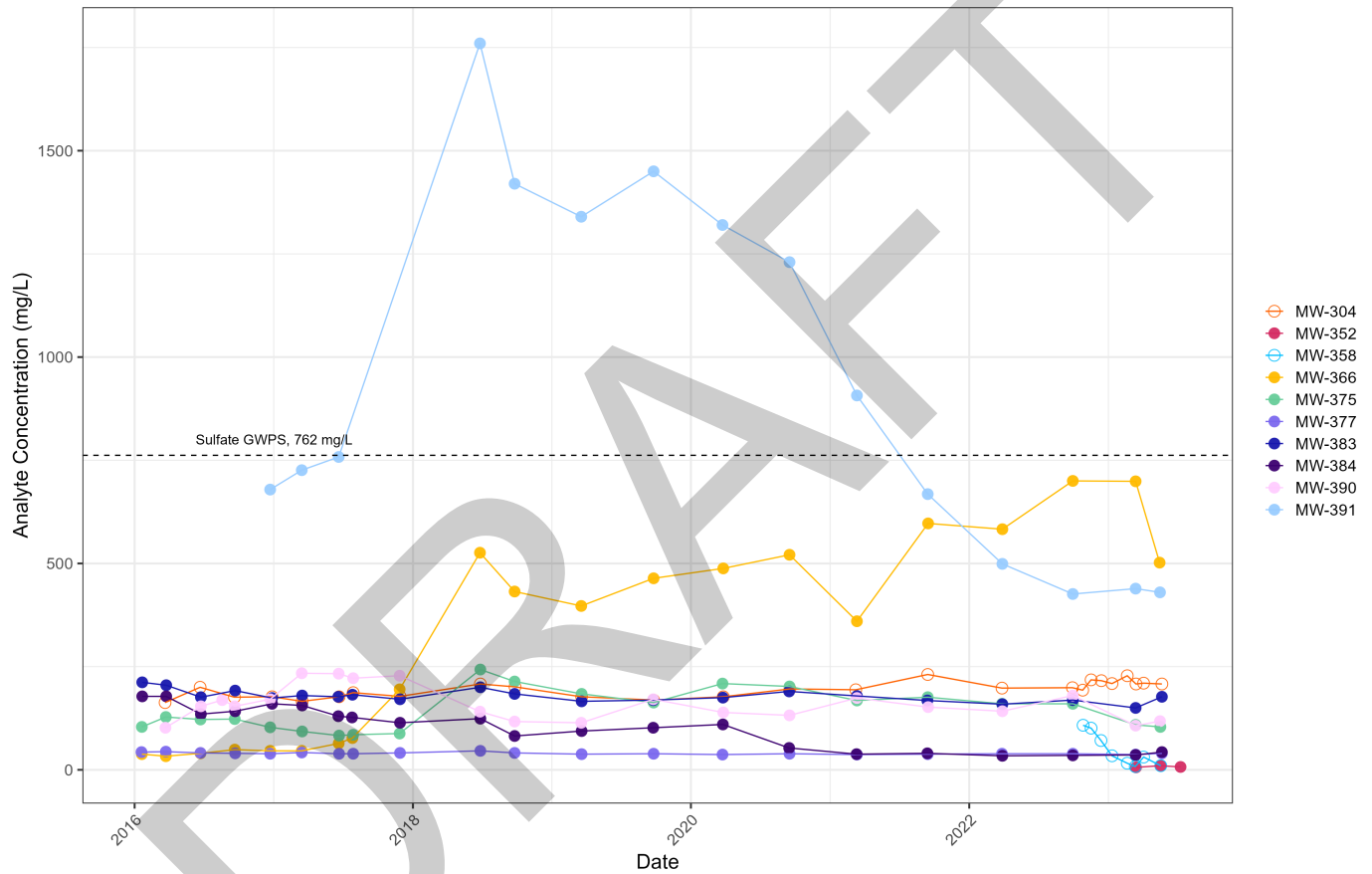
Notes:
 mg/L: milligrams per liter
 GWPS: Groundwater Protection Standard
 Background wells shown with open symbols.

Dissolved Boron Concentration Time Series – Uppermost Aquifer
 Baldwin Power Plant – Fly Ash Pond System



Figure
3b

Total Sulfate across UA Monitoring Network



Notes:
 mg/L: milligrams per liter
 GWPS: Groundwater Protection Standard
 Background wells shown with open symbols.

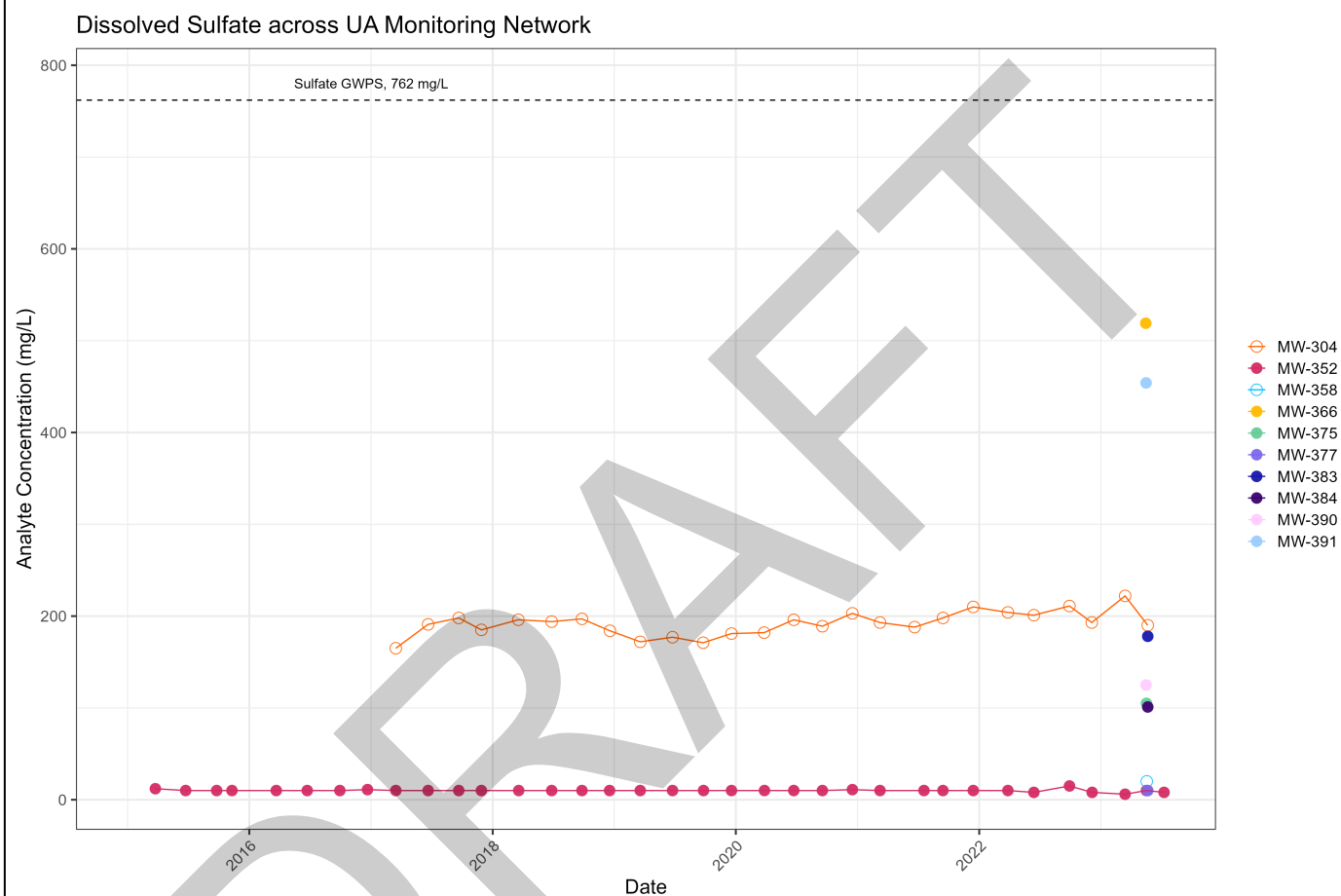
Sulfate Concentration Time Series – Uppermost Aquifer
 Baldwin Power Plant – Fly Ash Pond System

Geosyntec
 consultants

Figure
4a

Columbus, Ohio

February 2024



Notes:
 mg/L: milligrams per liter
 GWPS: Groundwater Protection Standard
 Background wells shown with open symbols.

Dissolved Sulfate Concentration Time Series – Uppermost Aquifer
 Baldwin Power Plant – Fly Ash Pond System

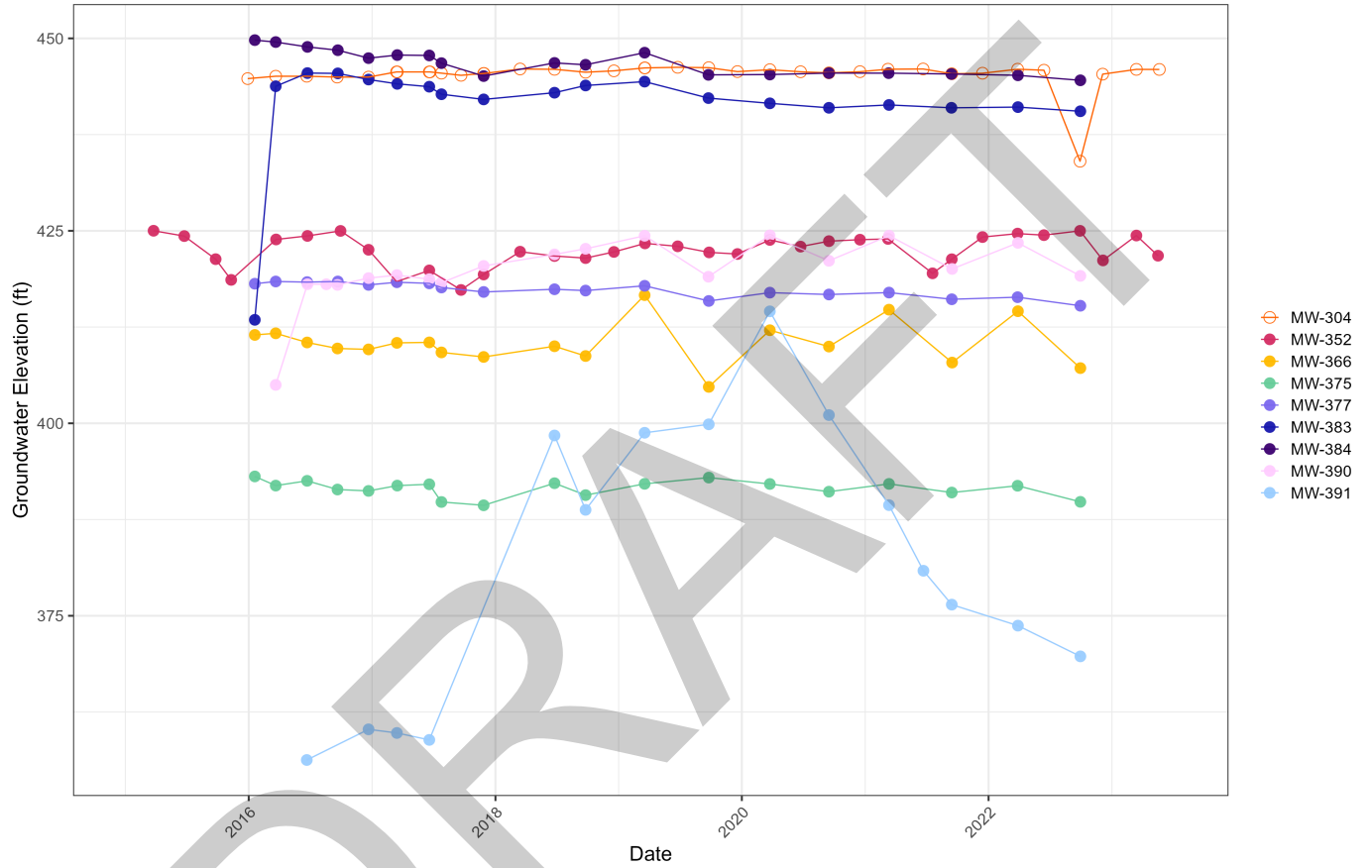
Geosyntec
 consultants

Columbus, Ohio

February 2024

Figure
4b

Groundwater Elevation across UA Monitoring Network



Notes:
ft: feet
Background wells shown with open symbols.

Groundwater Elevation Time Series – Uppermost Aquifer
Baldwin Power Plant – Fly Ash Pond System

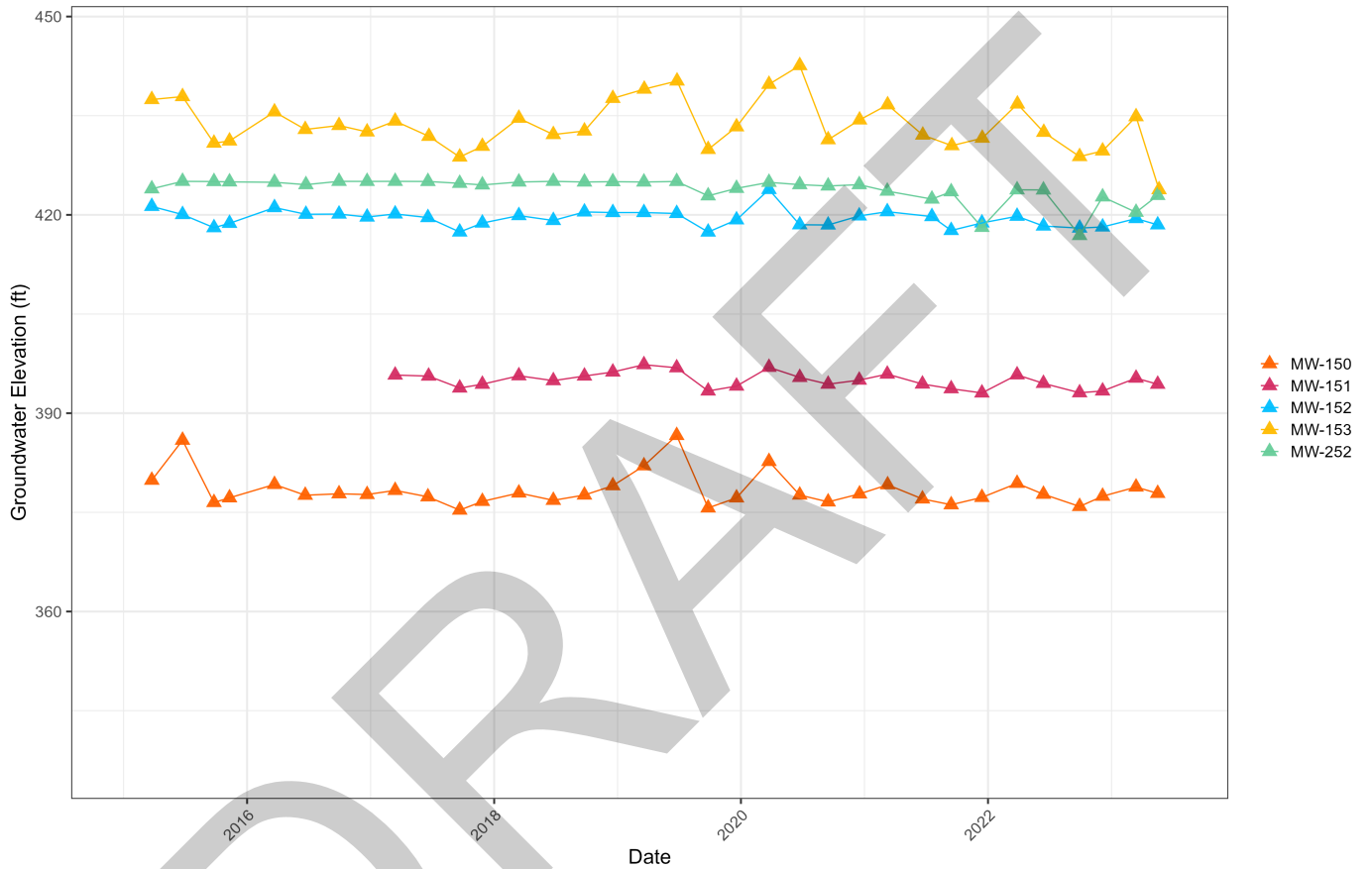
Geosyntec
consultants

Figure
5a

Columbus, Ohio

February 2024

Groundwater Elevation across PMP Monitoring Network



Notes:
ft: feet

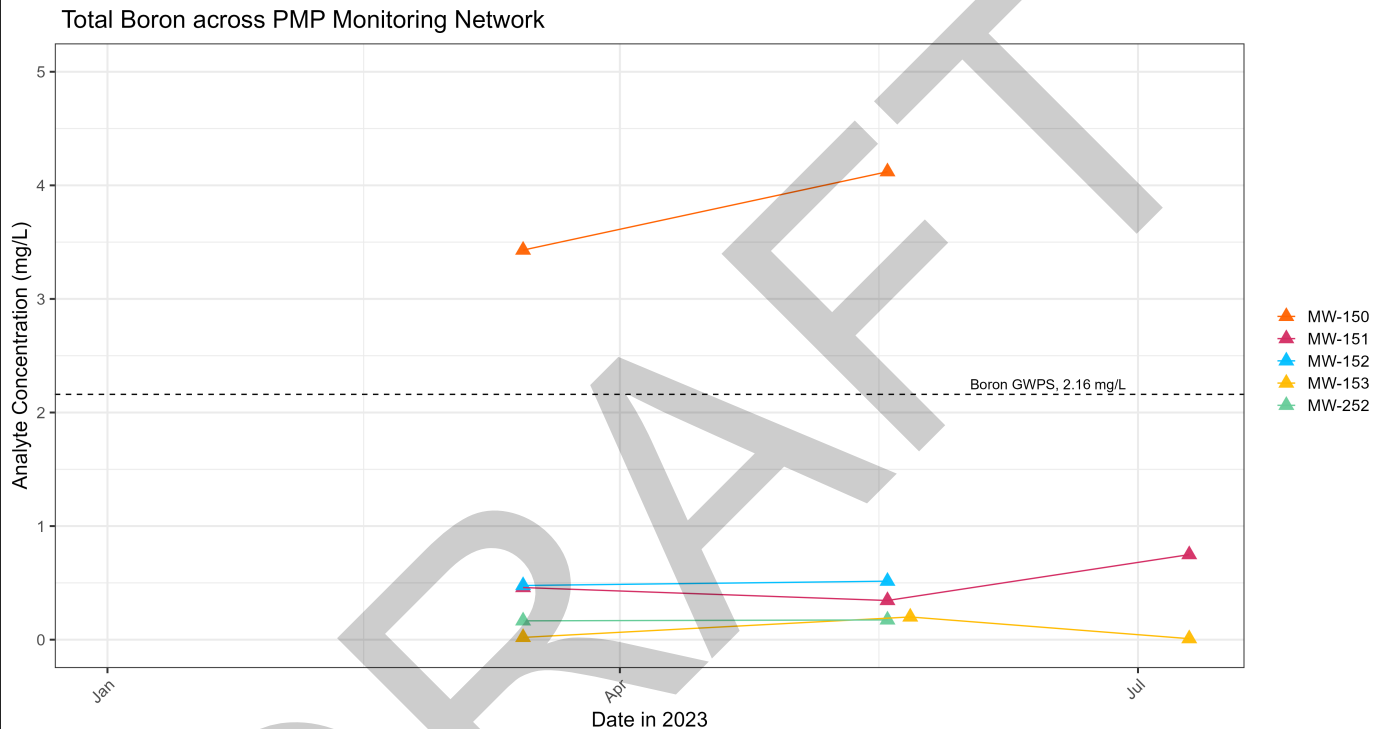
Groundwater Elevation Time Series – Potential Migration Pathway
Baldwin Power Plant – Fly Ash Pond System

Geosyntec
consultants

Columbus, Ohio

February 2024

Figure
5b



Notes:
 mg/L: milligrams per liter
 GWPS: Groundwater Protection Standard

Boron Concentration Time Series – Potential Migration Pathway
 Baldwin Power Plant – Fly Ash Pond System

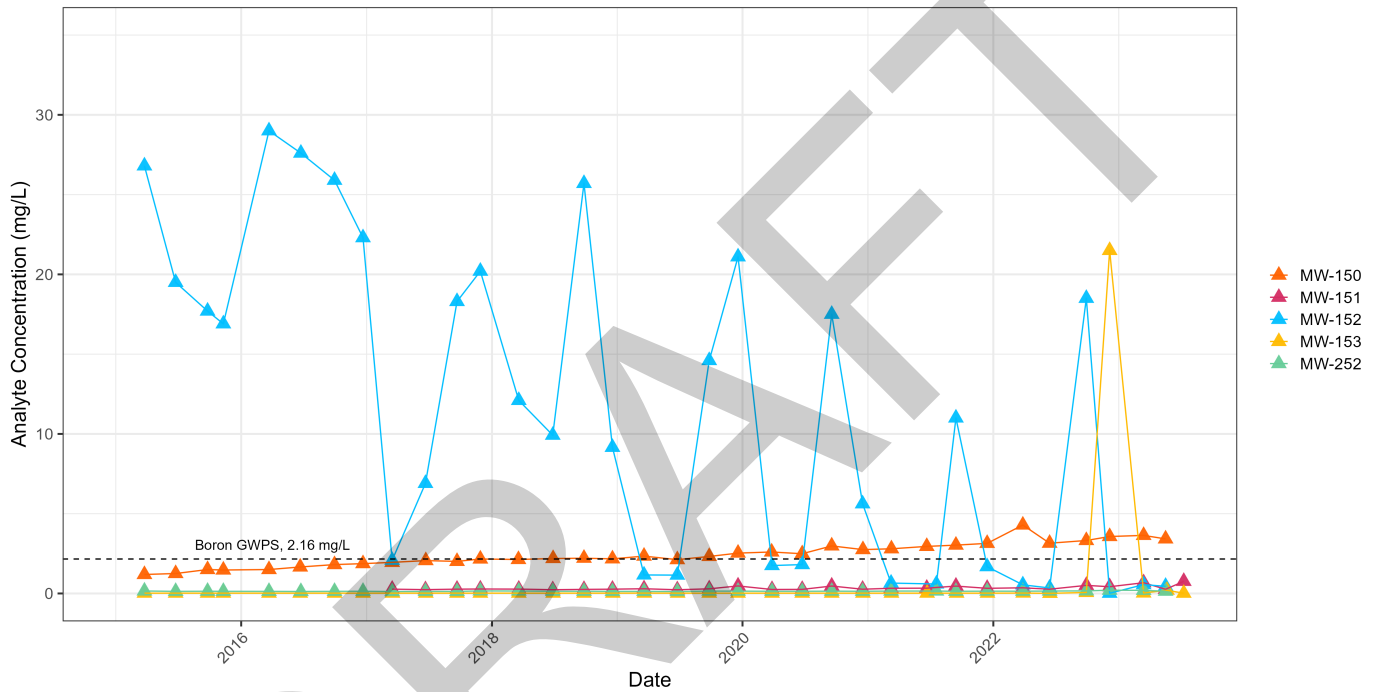
Geosyntec
 consultants

Columbus, Ohio

February 2024

Figure
6a

Dissolved Boron across PMP Monitoring Network



Notes:
 mg/L: milligrams per liter
 GWPS: Groundwater Protection Standard

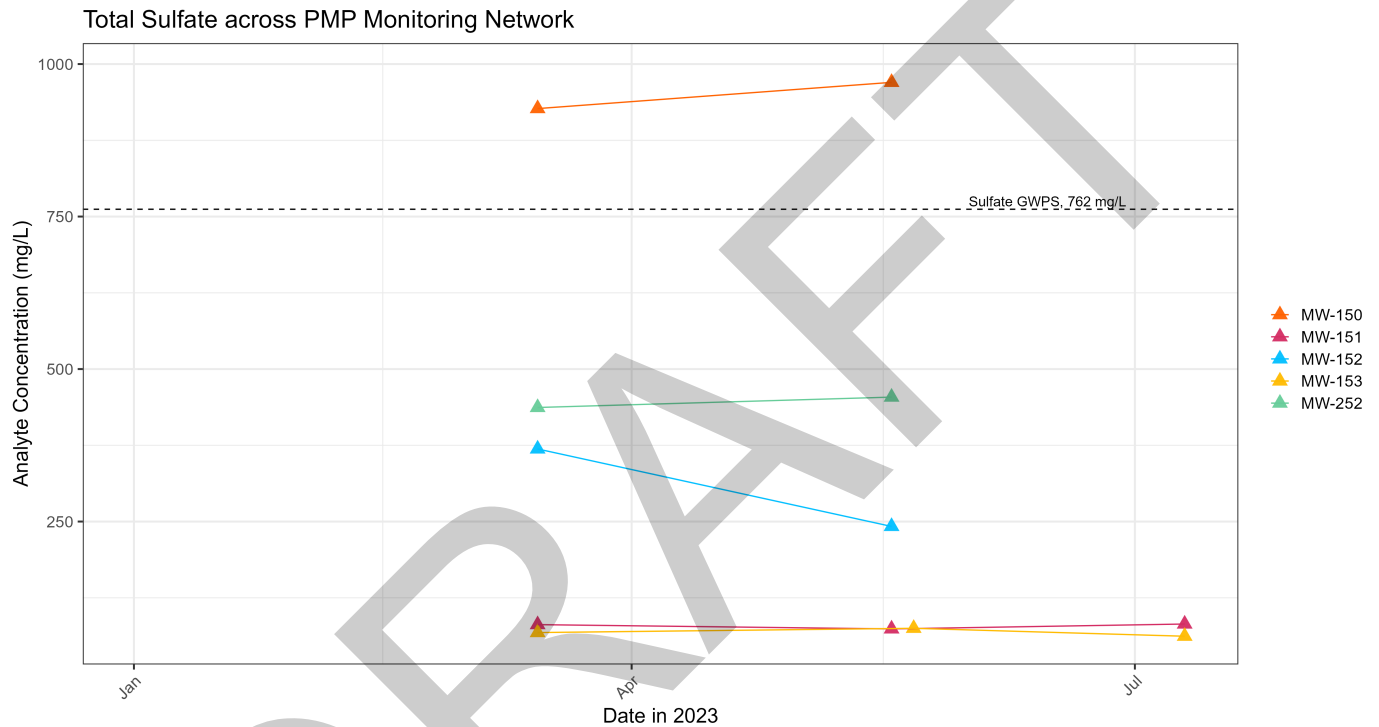
Dissolved Boron Concentration Time Series – Potential Migration Pathway
 Baldwin Power Plant – Fly Ash Pond System

Geosyntec
 consultants

Columbus, Ohio

February 2024

Figure
6b



Notes:
 mg/L: milligrams per liter
 GWPS: Groundwater Protection Standard

Sulfate Concentration Time Series – Potential Migration Pathway
 Baldwin Power Plant – Fly Ash Pond System

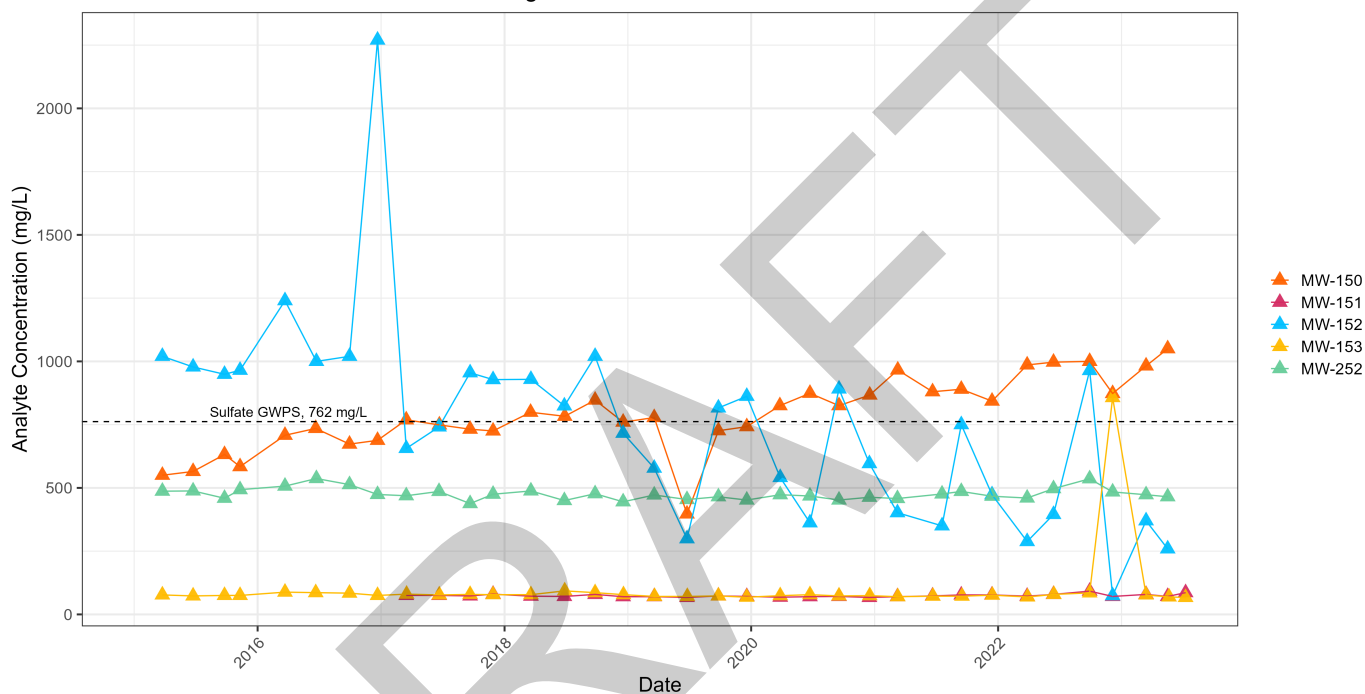
Geosyntec
 consultants

Columbus, Ohio

February 2024

Figure
7a

Dissolved Sulfate across PMP Monitoring Network



Notes:
mg/L: milligrams per liter
GWPS: Groundwater Protection Standard

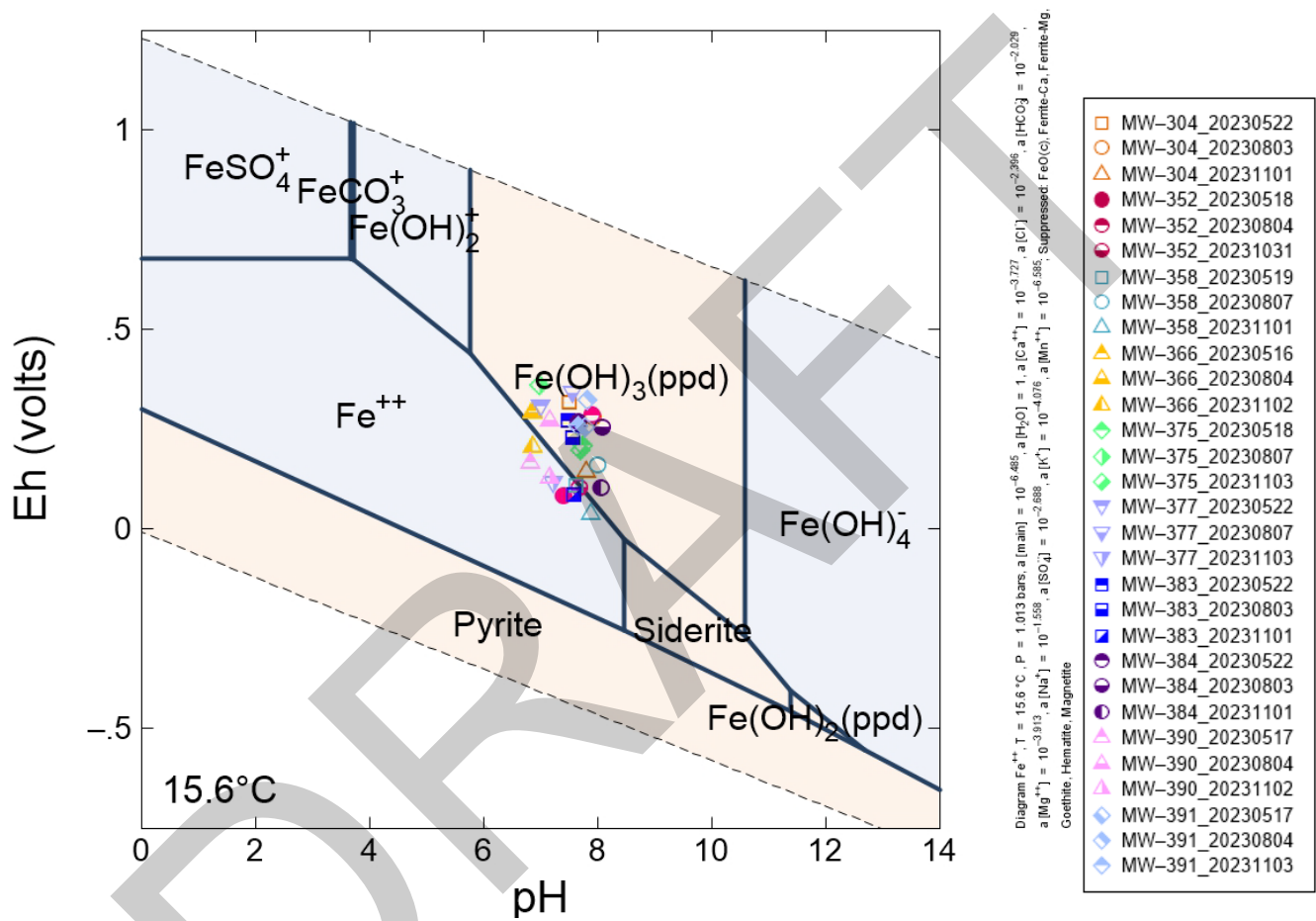
Dissolved Sulfate Concentration Time Series – Potential Migration Pathway
Baldwin Power Plant – Fly Ash Pond System

Geosyntec
consultants

Figure
7b

Columbus, Ohio

February 2024



Notes:

1. Diagram was generated using conditions observed at well MW-391 on 5/17/23.
2. The three most recent available pH and ORP data points for each location are displayed.
3. Hematite, ferrite-Ca, ferrite-Mg, goethite, crystalline iron oxide, and magnetite were suppressed during model generation.

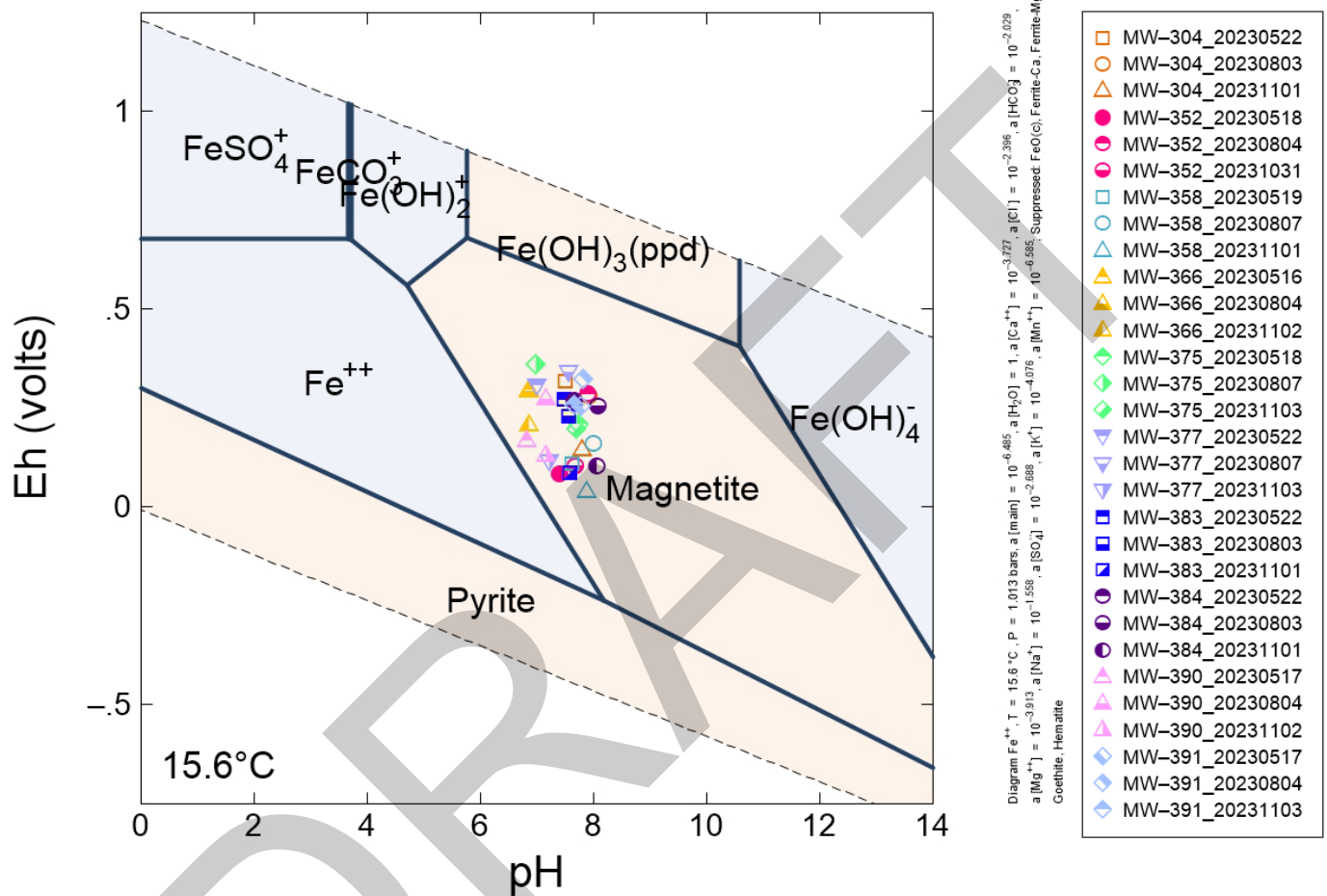
**Iron Pourbaix Diagram, Ferrihydrite – Uppermost Aquifer
Baldwin Power Plant – Fly Ash Pond System**

Geosyntec
consultants

Figure
8a

Columbus, Ohio

February 2024



Notes:

- Diagram was generated using conditions observed at well MW-391 on 5/17/23.
- The three most recent available pH and ORP data points for each location are displayed.
- Ferrite-Ca, ferrite-Mg, goethite, crystalline iron oxide, and hematite were suppressed during model generation.

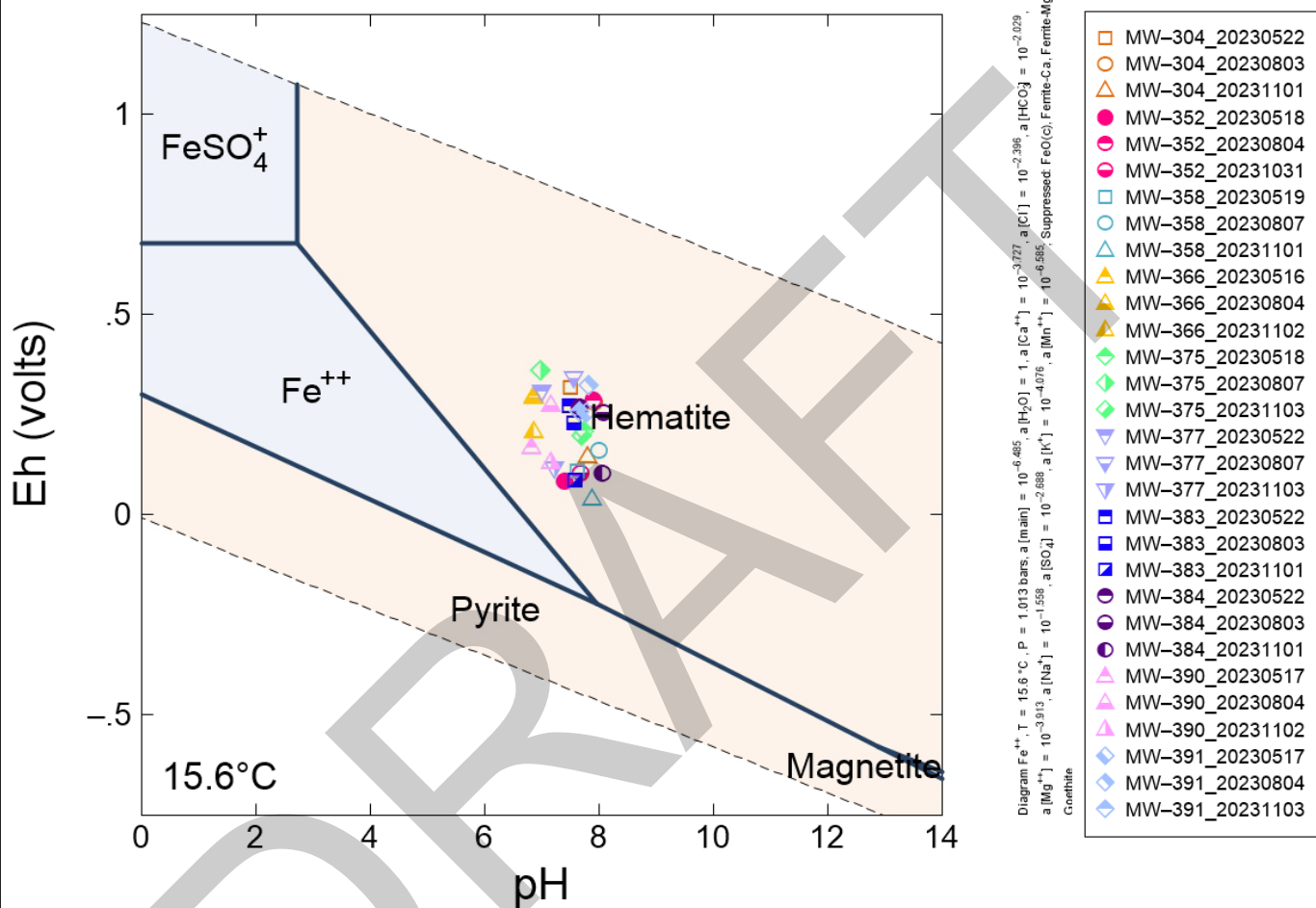
Iron Pourbaix Diagram, Magnetite – Uppermost Aquifer Baldwin Power Plant – Fly Ash Pond System

Geosyntec
consultants

Figure
8b

Columbus, Ohio

February 2024



Notes:

- Diagram was generated using conditions observed at well MW-391 on 5/17/23.
- The three most recent available pH and ORP data points for each location are displayed.
- Ferrite-Ca, ferrite-Mg, goethite, and crystalline iron oxide were suppressed during model generation.

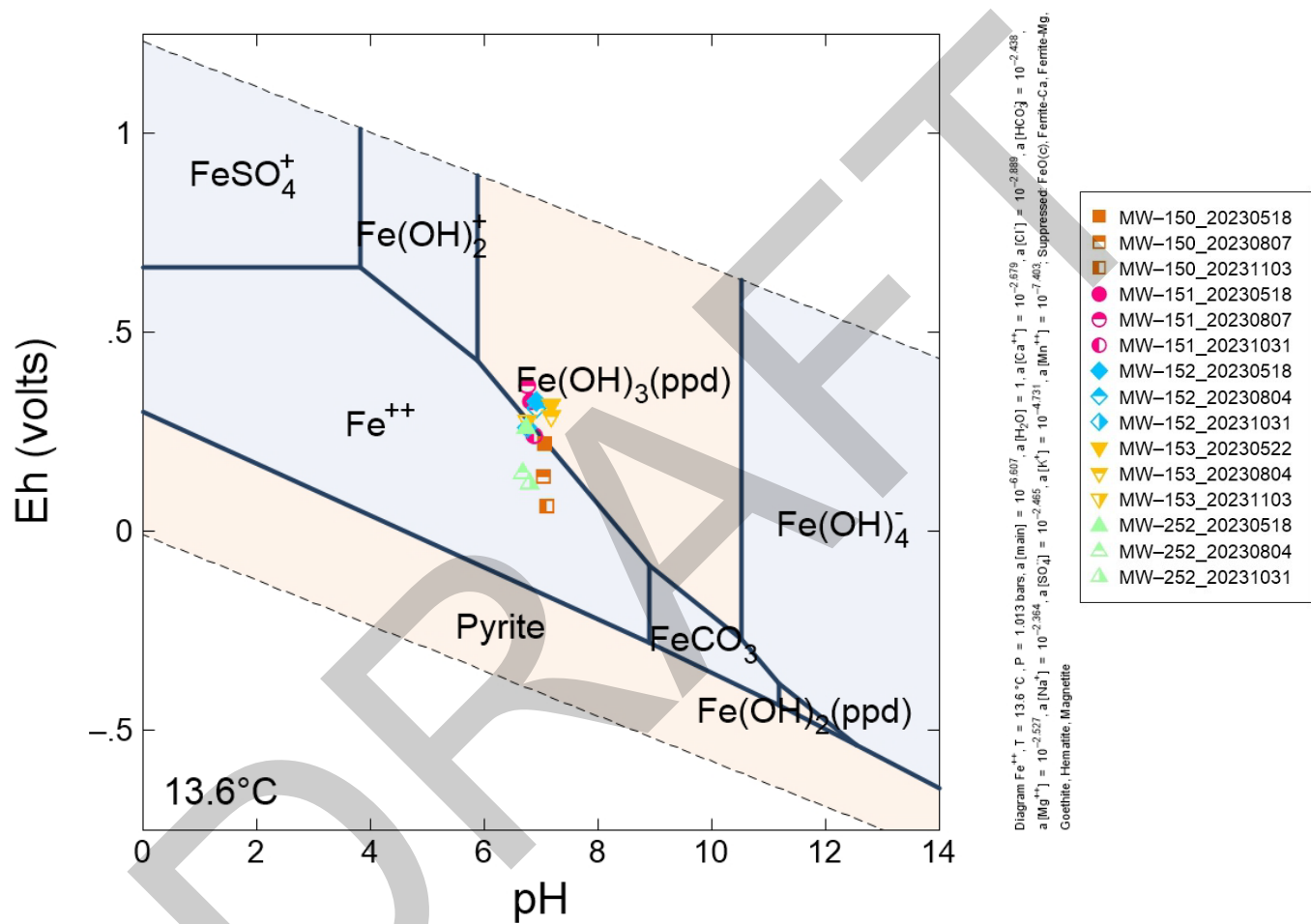
Iron Pourbaix Diagram, Hematite – Uppermost Aquifer
 Baldwin Power Plant – Fly Ash Pond System

Geosyntec
 consultants

Figure
8c

Columbus, Ohio

February 2024



Notes:

1. Diagram was generated using conditions observed at well MW-150 on 5/18/23.
2. The three most recent available pH and ORP data points for each location are displayed.
3. Hematite, ferrite-Ca, ferrite-Mg, goethite, crystalline iron oxide, and magnetite were suppressed during model generation.

Iron Pourbaix Diagram, Ferrihydrite – Potential Migration Pathway

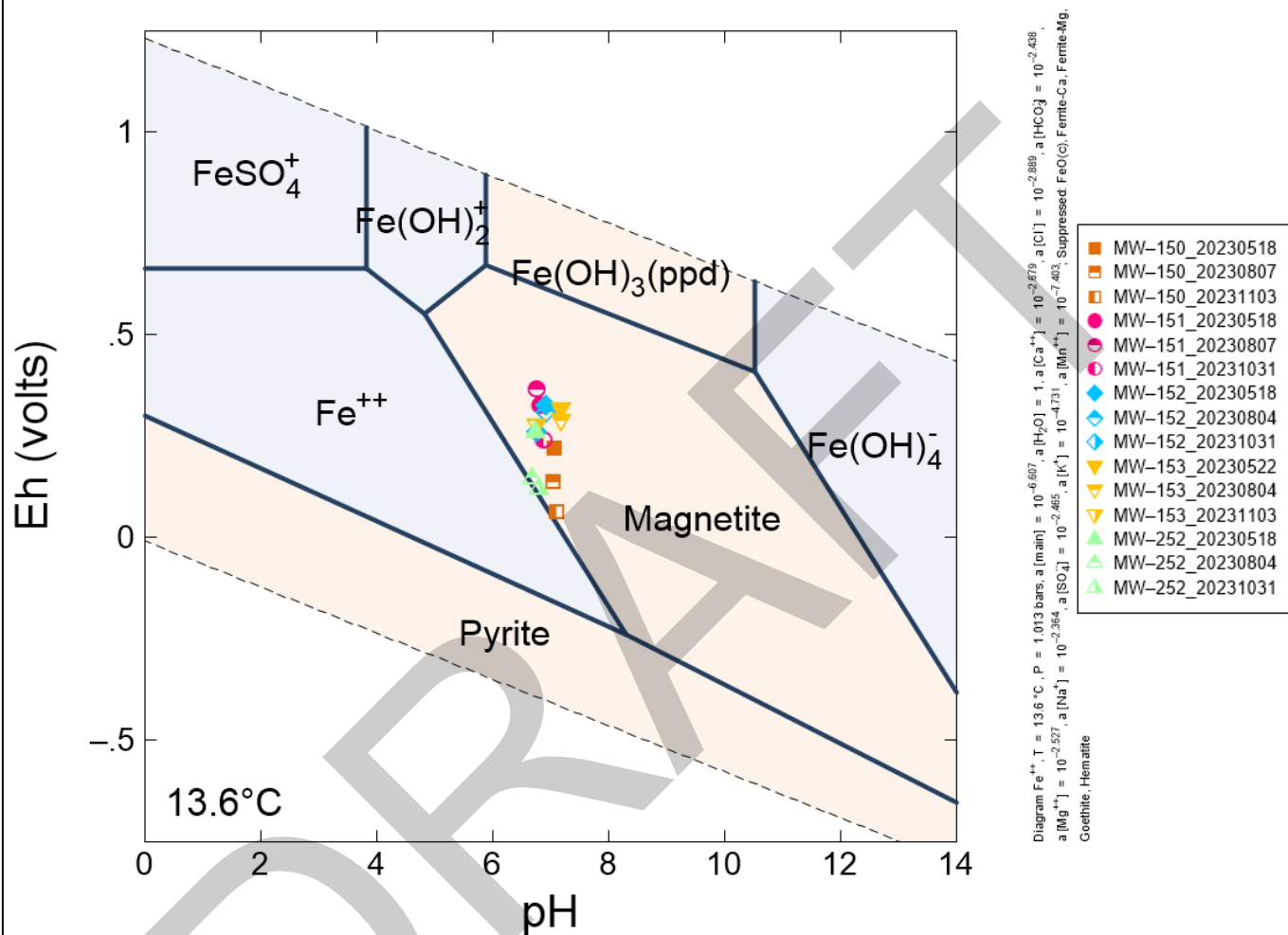
Baldwin Power Plant – Fly Ash Pond System

Geosyntec
consultants

Figure
8d

Columbus, Ohio

February 2024



Notes:

- Diagram was generated using conditions observed at well MW-150 on 5/18/23.
- The three most recent available pH and ORP data points for each location are displayed.
- Hematite, ferrite-Ca, ferrite-Mg, goethite, and crystalline iron oxide were suppressed during model generation.

Iron Pourbaix Diagram, Magnetite – Potential Migration Pathway

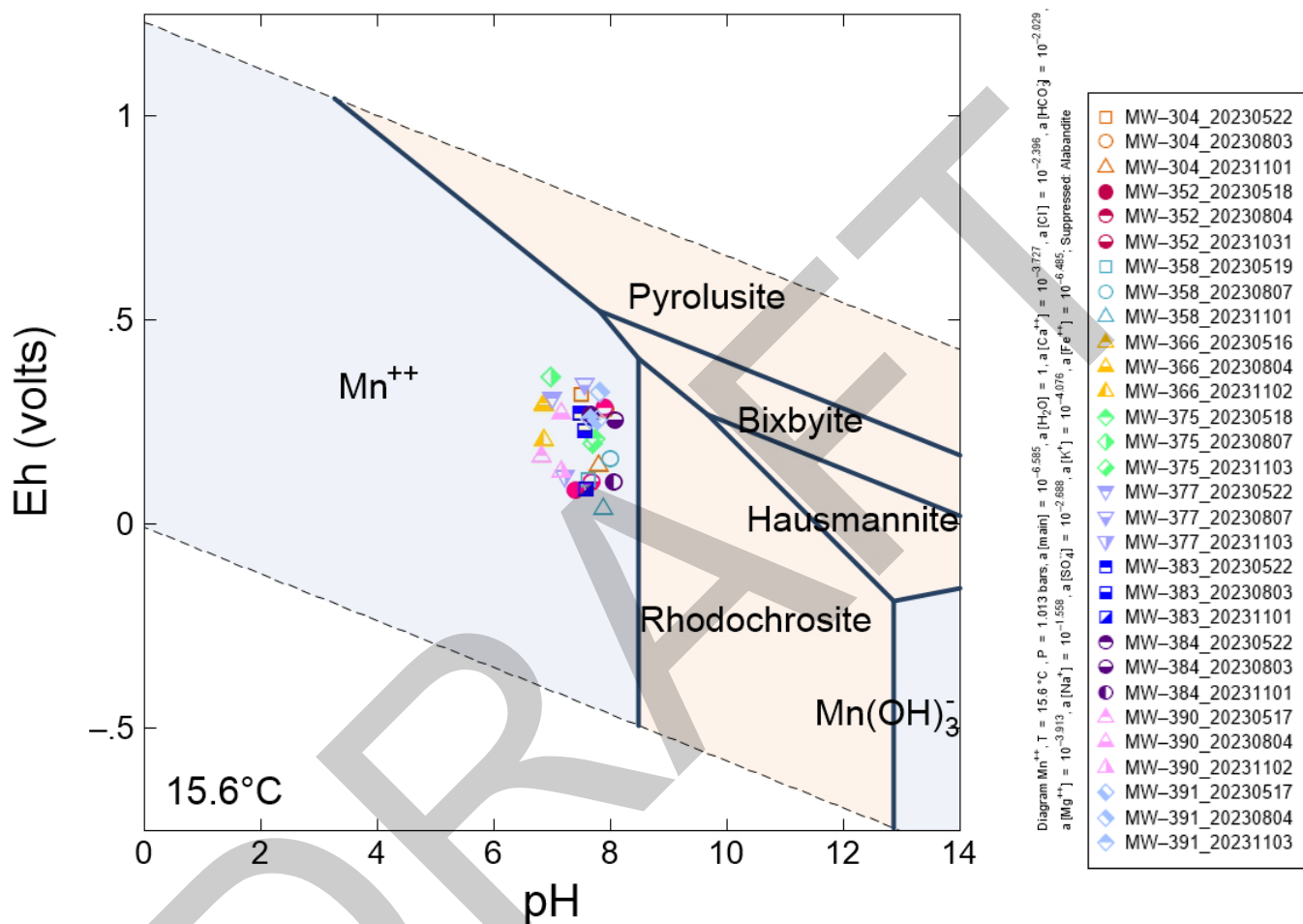
Baldwin Power Plant – Fly Ash Pond System

Geosyntec
consultants

Figure
8e

Columbus, Ohio

February 2024



Notes:

- Diagram was generated using conditions observed at well MW-391 on 5/17/23.
- The three most recent available pH and ORP data points for each location are displayed.
- Alabandite was suppressed during model generation.

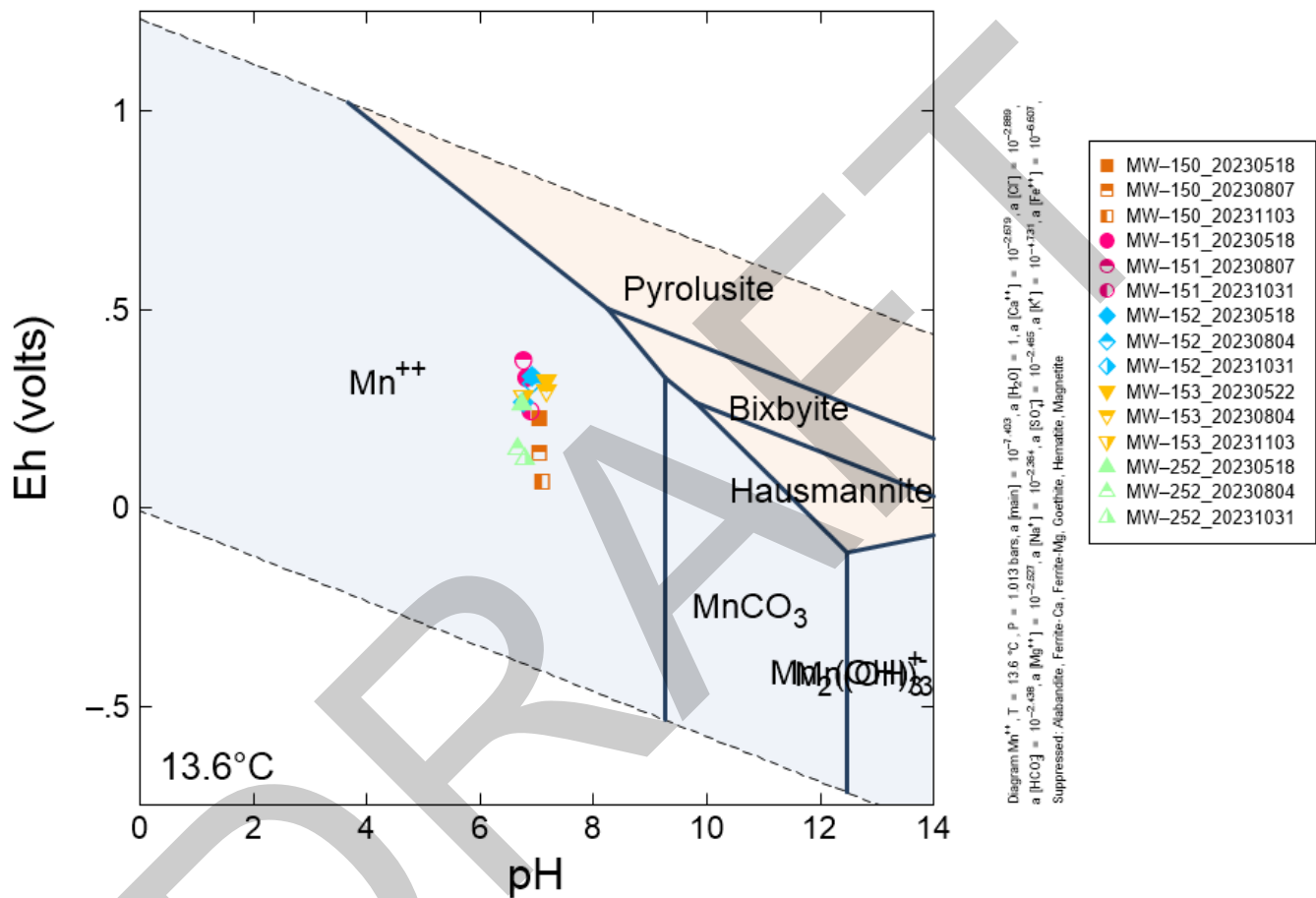
**Manganese Pourbaix Diagram – Uppermost Aquifer
Baldwin Power Plant – Fly Ash Pond System**

Geosyntec
consultants

**Figure
9a**

Columbus, Ohio

February 2024



Notes:

- Diagram was generated using conditions observed at well MW-150 on 5/18/23.
- The three most recent available pH and ORP data points for each location are displayed.
- Alabandite was suppressed during model generation.

Manganese Pourbaix Diagram– Potential Migration Pathway

Baldwin Power Plant – Fly Ash Pond System

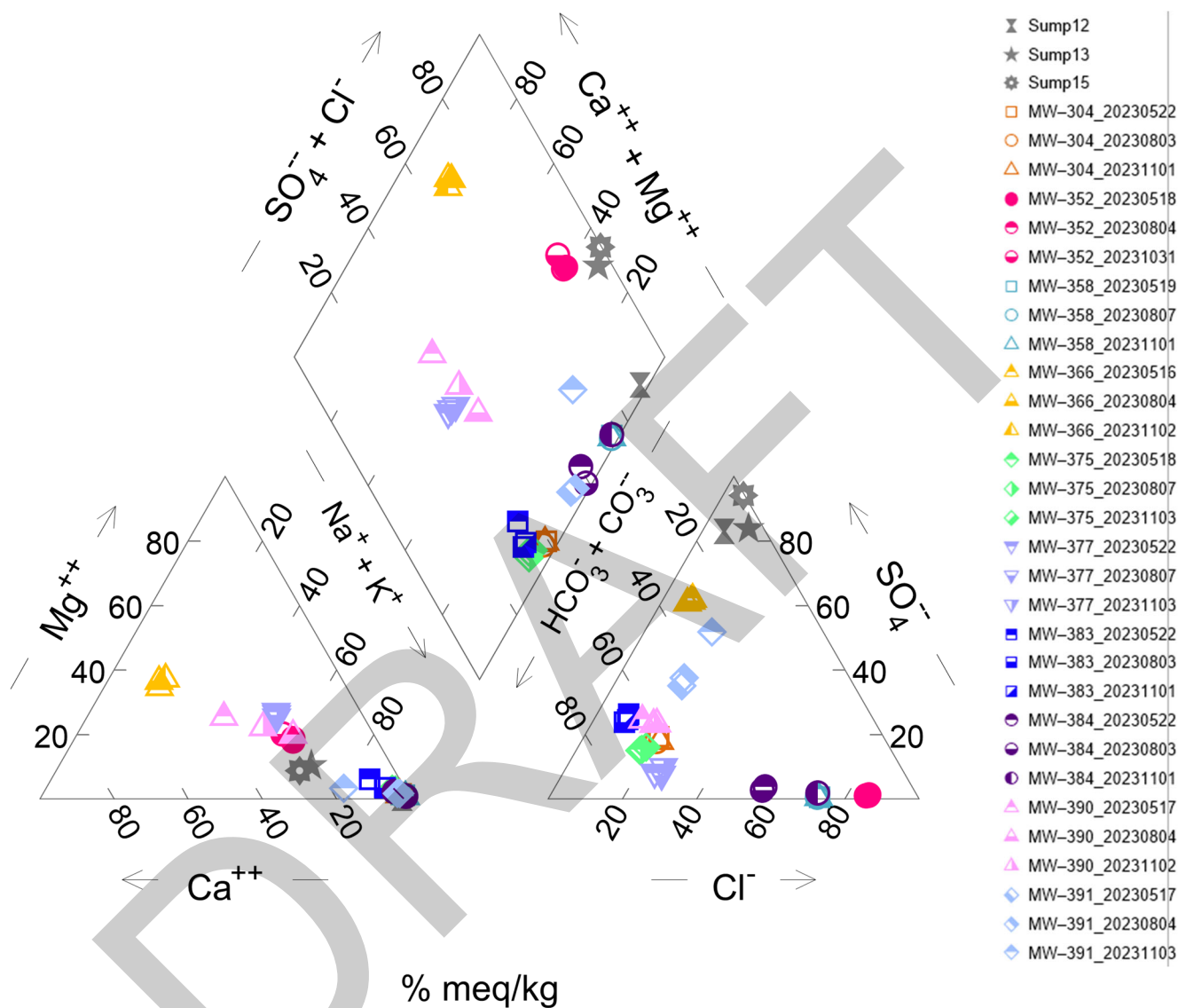
Geosyntec
consultants

Columbus, Ohio

February 2024

Figure

9b



Notes:

- The three most recent available data points for each location are displayed.
 - FAPS porewater locations Sump12, Sump13, and Sump 15 are shown with gray coloring and solid symbology
- % meq/kg: percent milliequivalents per kilogram

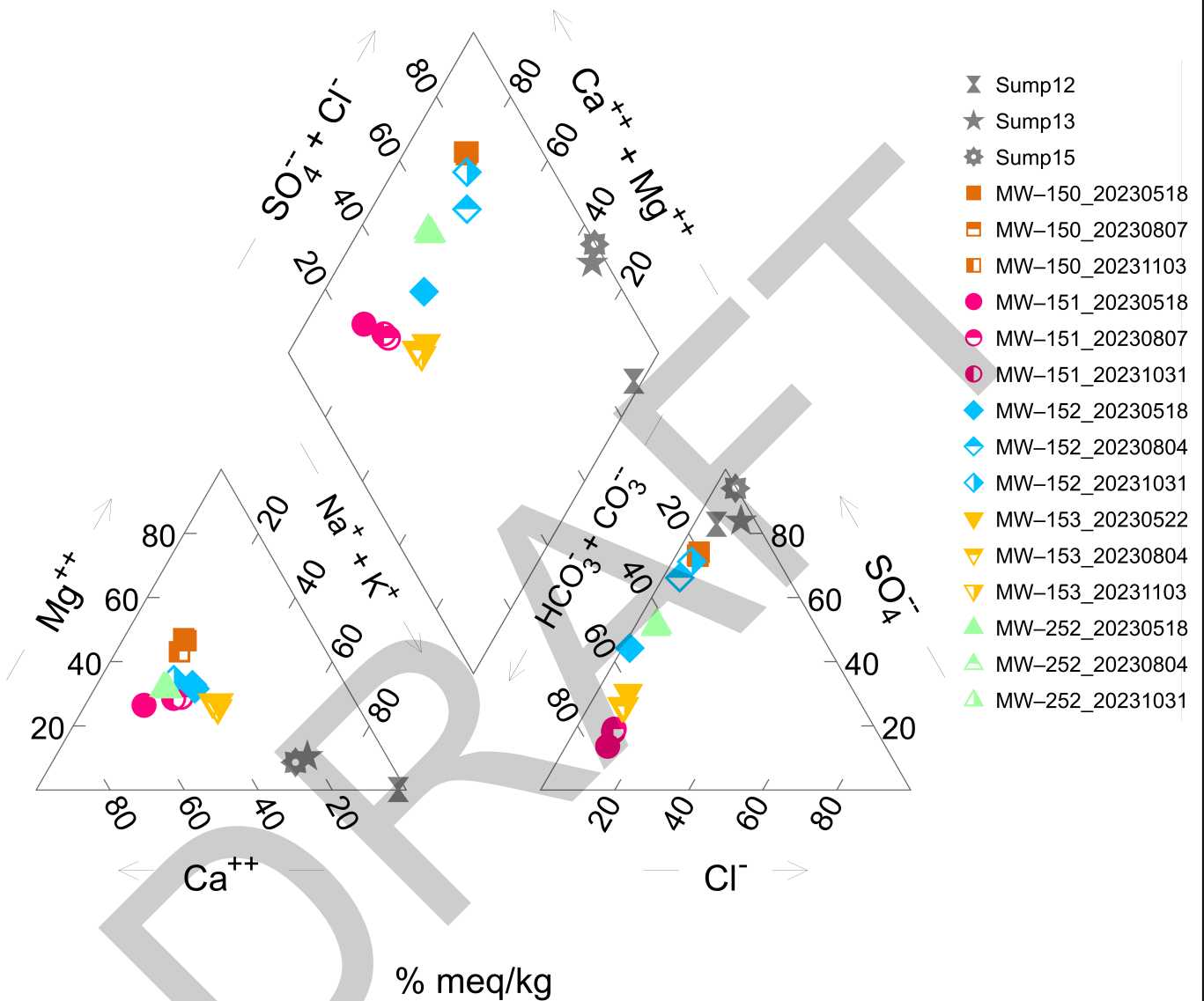
Piper Diagram – UA Wells
Baldwin Power Plant – Fly Ash Pond System

Geosyntec
consultants

Figure
10a

Columbus, Ohio

February 2024



Notes:

1. The three most recent available data points for each location are displayed.
 2. FAPS porewater locations Sump12, Sump13, and Sump 15 are shown with gray coloring and solid symbology.
- % meq/kg: percent milliequivalents per kilogram

Piper Diagram – Potential Migration Pathway
Baldwin Power Plant – Fly Ash Pond System

Geosyntec
consultants

Columbus, Ohio

February 2024

Figure
10b

DRAFT

TABLES

**Table 1. CEC and LOI of Site Solids
Geochemical Conceptual Site Model
Baldwin Power Plant - Fly Ash Pond System**

Geosyntec Consultants, Inc.

| Well ID | MW-150 | MW-150 | MW-350 | MW-350 | MW-350 | MW-352 | MW-352 | MW-366 | MW-391 | REP MW-391 |
|------------------------------|-----------------|-----------------|-----------------|-----------------|-----------------|-----------------|-----------------|-----------------|-----------------|-----------------|
| Depth (ft bgs) | (15-20) | (20-25) | (35-40) | (42-46) | (42-46) | (50-60) | (60-70) | (40-52) | (50-51) | (50-51) |
| Well Characterization | FAPS Compliance | FAPS Compliance | FAPS Compliance | FAPS Compliance | FAPS Compliance | FAPS Compliance | FAPS Compliance | FAPS Compliance | FAPS Compliance | FAPS Compliance |
| Sampled Aquifer Unit | PMP | PMP | UA | UA | UA | UA | UA | UA | UA | UA |
| Field Boring Log Description | Sandy clay | Sandy clay | Shale | Limestone | Limestone | Shale | Shale | Shale | Weathered shale | Weathered shale |
| CEC (meq/100 g solid) | 12.94 | 18.94 | 67.49 | 173.79 | 173.68 | 134.55 | 146.45 | 71.09 | 53.7 | - |
| LOI (%) | 8.45 | 15.5 | 24.2 | 37.1 | 37.4 | 30.7 | 31.5 | 19.8 | 20.3 | 19.9 |
| TOC (%) | - | - | - | - | - | - | - | - | - | - |

| Well ID | MW-391 | MW-391 | MW-358 | MW-358 | MW-358 | MW-392 | MW-392 | MW-393 | MW-394 | MW-392 |
|------------------------------|-----------------|-----------------|------------|---------------|-------------------|----------------------------------|-----------------------------------|----------------|----------------|----------------|
| Depth (ft bgs) | (55-72) | (51-44) | (13-15) | (47-49) | (86-88) | (80-82) | (32-33.5) | (24-25.5) | (20.5-22) | (66-68) |
| Well Characterization | FAPS Compliance | FAPS Compliance | Background | Background | Background | BAP Compliance | BAP Compliance | BAP Compliance | BAP Compliance | BAP Compliance |
| Sampled Aquifer Unit | UA | UA | PMP | UA | UA | UA | PMP | PMP | PMP | UA |
| Field Boring Log Description | Limestone | Shale | Silty clay | Shallow shale | Deeper shale body | Shale transitioning to limestone | Clay with increasing sand content | Clayey sand | Silty sand | Shale |
| CEC (meq/100 g solid) | 164.7 | 149.37 | - | 43.59 | 24.23 | 38.72 | - | - | - | 38.34 |
| LOI (%) | 40.5 | 33.2 | 5.47 | 9.79 | 9.74 | 21.6 | 6.15 | 3.82 | 5.09 | 13.8 |
| TOC (%) | - | - | - | 0.16 | 0.47 | 1.4 | - | - | - | 0.18 |

Notes

Sample depth is shown in feet below ground surface (ft bgs)

Dashes indicate sample was not analyzed for analyte

BAP: Bottom Ash Pond

CEC: cation exchange capacity

FAPS: Fly Ash Pond System

meq/100 g solid: milliequivalents per 100 grams solids

LOI: loss on ignition

PMP: potential migration pathway

TOC: total organic carbon

UA: uppermost aquifer

Table 2. Bulk Characterization of Site Solids
Geochemical Conceptual Site Model
Baldwin Power Plant - Fly Ash Pond System

| Well ID | MW-150 | MW-150 | MW-350 | MW-350 | MW-350 | MW-352 | MW-352 | MW-366 | MW-391 | MW-391 | MW-391 | MW-358 | MW-358 | MW-392 | MW-392 |
|------------------------------|-----------------|-----------------|-----------------|-----------------|-----------------|-----------------|-----------------|-----------------|-----------------|-----------------|-----------------|---------------|-------------------|----------------------------------|----------------|
| Depth (ft bgs) | (15-20) | (20-25) | (35-40) | (42-46) | (42-46) | (50-60) | (60-70) | (40-52) | (50-51) | (51-55) | (55-72) | (47-49) | (86-88) | (80-82) | (66-68) |
| Well Characterization | FAPS Compliance | FAPS Compliance | FAPS Compliance | FAPS Compliance | FAPS Compliance | FAPS Compliance | FAPS Compliance | FAPS Compliance | FAPS Compliance | FAPS Compliance | FAPS Compliance | Background | Background | BAP Compliance | BAP Compliance |
| Sampled Aquifer Unit | PMP | PMP | UA | UA | UA | UA | UA | UA | UA | UA | UA | UA | UA | UA | UA |
| Field Boring Log Description | Sandy clay | Sandy clay | Shale | Limestone | Limestone | Shale | Shale | Shale | Weathered shale | Shale | Limestone | Shallow shale | Deeper shale body | Shale transitioning to limestone | Shale |
| Analyte | (mg/kg) | (mg/kg) | (mg/kg) | (mg/kg) | (mg/kg) | (mg/kg) | (mg/kg) | (mg/kg) | (mg/kg) | (mg/kg) | (mg/kg) | (mg/kg) | (mg/kg) | (mg/kg) | (mg/kg) |
| Aluminum | 42000 | 66000 | 56000 | 5900 | 5900 | 36000 | 16000 | 81000 | 61000 | 21000 | 4800 | - | - | - | - |
| Antimony | < 0.8 | < 0.8 | < 0.8 | < 0.8 | < 0.8 | < 0.8 | < 0.8 | < 0.8 | < 0.8 | < 0.8 | < 0.8 | - | - | - | - |
| Arsenic | 4.3 | 11.0 | 6.1 | 1.9 | 1.6 | 5.3 | 7.5 | 4.9 | 8.8 | 4.0 | 3.2 | 2.1 | 11.0 | 17.0 | 1.0 |
| Barium | 500.0 | 560.0 | 150.0 | 59.0 | 46.0 | 73.0 | 45.0 | 180.0 | 160.0 | 64.0 | 19.0 | 140 | 45 | 40 | 21 |
| Beryllium | 1.1 | 1.9 | 1.6 | 0.2 | 0.3 | 1.0 | 0.5 | 2.3 | 2.1 | 0.6 | 0.2 | 0.9 | 0.7 | 0.9 | 0.7 |
| Bismuth | 0.1 | 0.2 | 0.2 | < 0.09 | < 0.09 | 0.1 | < 0.09 | 0.3 | 0.2 | < 0.09 | < 0.09 | - | - | - | - |
| Boron | - | - | - | - | - | - | - | - | - | - | - | 11 | 16 | 16 | 13 |
| Cadmium | 0.2 | 0.3 | 0.3 | 0.3 | 0.4 | 0.1 | 0.9 | 0.6 | 0.1 | 0.2 | 0.7 | < 0.02 | < 0.02 | 0.4 | 0.1 |
| Calcium | 32000 | 57000 | 120000 | 320000 | 340000 | 190000 | 220000 | 95000 | 92000 | 260000 | 340000 | - | - | - | - |
| Chromium | 47.0 | 74.0 | 70.0 | 13.0 | 14.0 | 46.0 | 42.0 | 110.0 | 78.0 | 30.0 | 11.0 | 9.5 | 12 | 17 | 16.0 |
| Cobalt | 7.7 | 13.0 | 8.6 | 1.3 | 1.3 | 4.2 | 2.5 | 6.2 | 9.9 | 4.6 | 1.6 | 4.4 | 23 | 12 | 6.2 |
| Copper | 11.0 | 25.0 | 8.9 | 2.9 | 2.2 | 4.2 | 3.9 | 10.0 | 13.0 | 3.6 | 1.7 | - | - | - | - |
| Iron | 19000 | 38000 | 22000 | 5500 | 5300 | 16000 | 11000 | 23000 | 23000 | 12000 | 5600 | - | - | - | - |
| Lead | 13.0 | 17.0 | 10.0 | 3.0 | 3.0 | 6.0 | 5.0 | 17.0 | 20.0 | 7.0 | 4.0 | 5.7 | 9.6 | 17.0 | 4.9 |
| Lithium | 19.0 | 44.0 | 31.0 | 4.8 | 4.7 | 14.0 | 16.0 | 37.0 | 16.0 | 7.4 | 3.6 | 6.0 | 20.0 | 8.0 | 15.0 |
| Magnesium | 15000 | 21000 | 22000 | 4600 | 4600 | 16000 | 24000 | 12000 | 10000 | 5700 | 4500 | - | - | - | - |
| Manganese | 770 | 830 | 190 | 270 | 270 | 330 | 200 | 220 | 370 | 1200 | 590 | - | - | - | - |
| Mercury | - | - | - | - | - | - | - | - | - | - | - | < 0.05 | < 0.05 | < 0.05 | < 0.05 |
| Molybdenum | 1.2 | 1.7 | 0.8 | 0.6 | 0.5 | 0.5 | 2.2 | 0.7 | 0.5 | 0.3 | 1.0 | 0.3 | 0.3 | 0.3 | 0.3 |
| Nickel | 20.0 | 38.0 | 32.0 | 4.9 | 4.7 | 17.0 | 16.0 | 26.0 | 36.0 | 19.0 | 8.0 | - | - | - | - |
| Potassium | 17000 | 22000 | 13000 | 2100 | 1900 | 7900 | 3900 | 21000 | 18000 | 4700 | 1200 | - | - | - | - |
| Selenium | 0.2 | 0.6 | 0.9 | 0.2 | 0.2 | 0.4 | 0.8 | 2.7 | 1.6 | 0.3 | 0.5 | < 0.7 | < 0.7 | 1.4 | < 0.7 |
| Silver | < 0.5 | < 0.5 | < 0.5 | < 0.5 | < 0.5 | < 0.5 | < 0.5 | < 0.5 | < 0.5 | < 0.5 | < 0.5 | - | - | - | - |
| Strontium | 150 | 170 | 390 | 470 | 510 | 360 | 460 | 320 | 230 | 410 | 530 | - | - | - | - |
| Sulfate | - | - | - | - | - | - | - | - | - | - | - | 50 | 620 | 280 | 100 |
| Thallium | 0.4 | 0.6 | 0.4 | 0.1 | 0.1 | 0.2 | 0.2 | 0.5 | 0.4 | 0.1 | 0.0 | 0.1 | 0.1 | 0.0 | 0.0 |
| Tin | < 6 | 6.5 | 6.9 | < 6 | < 6 | 6.2 | < 6 | 7.5 | 6.8 | < 6 | < 6 | - | - | - | - |
| Titanium | 1900 | 3000 | 2300 | 310 | 310 | 1400 | 760 | 3500 | 2500 | 910 | 210 | - | - | - | - |
| Uranium | 1.7 | 2.5 | 3.2 | 1.1 | 1.0 | 1.9 | 2.4 | 3.7 | 2.9 | 1.2 | 2.1 | - | - | - | - |
| Vanadium | 57 | 110 | 70 | 14.0 | 14 | 45 | 29 | 150 | 68 | 28 | 9.4 | - | - | - | - |
| Yttrium | 13 | 20 | 14 | 8.8 | 8.7 | 8.9 | 9.3 | 19 | 32 | 11 | 7.6 | - | - | - | - |
| Zinc | 43 | 87 | 74 | 36 | 42 | 30 | 83 | 68 | 49 | 34 | 87 | - | - | - | - |

Notes:
Sample depth is shown in feet below ground surface (ft bgs)
Dashes indicate analyte was not reported by lab for sample
Non-detect values are shown as less than the reporting limit
BAP: Bottom Ash Pond
FAPS: Fly Ash Pond System
mg/kg: milligrams per kilogram
PMP: potential migration pathway
UA: uppermost aquifer

Table 3. XRF Analysis of Site Solids
Geochemical Conceptual Site Model
Baldwin Power Plant - Fly Ash Pond System

| Well ID | MW-150 | MW-150 | MW-350 | MW-350 | MW-350 | MW-352 | MW-352 | MW-366 | MW-391 | MW-391 | MW-391 | REP MW-391 |
|------------------------------------|------------|------------|---------|-----------|-----------|---------|---------|---------|-----------------|---------|-----------|-----------------|
| Depth (ft bgs) | (15-20) | (20-25) | (35-40) | (42-46) | (42-46) | (50-60) | (60-70) | (40-52) | (50-51) | (44-51) | (55-72) | (50-51) |
| Well | FAPS | FAPS | FAPS | FAPS | FAPS | FAPS | FAPS | FAPS | FAPS | FAPS | FAPS | FAPS |
| Sampled Aquifer Unit | PMP | PMP | UA | UA | UA | UA | UA | UA | UA | UA | UA | UA |
| Field Boring Log Description | Sandy clay | Sandy clay | Shale | Limestone | Limestone | Shale | Shale | Shale | Weathered shale | Shale | Limestone | Weathered shale |
| Analyte | (wt %) | (wt %) | (wt %) | (wt %) | (wt %) | (wt %) | (wt %) | (wt %) | (wt %) | (wt %) | (wt %) | (wt %) |
| Al ₂ O ₃ | 8.09 | 11.67 | 10.58 | 1.20 | 1.15 | 7.21 | 3.37 | 14.89 | 12.44 | 4.29 | 1.02 | 12.50 |
| CaO | 4.75 | 7.90 | 17.23 | 45.90 | 46.26 | 29.29 | 32.08 | 13.30 | 14.05 | 37.45 | 49.44 | 14.14 |
| Cr ₂ O ₃ | 0.01 | 0.01 | <0.01 | <0.01 | <0.01 | <0.01 | <0.01 | 0.01 | 0.01 | <0.01 | <0.01 | <0.01 |
| Fe ₂ O ₃ | 2.75 | 5.03 | 3.18 | 0.77 | 0.70 | 2.30 | 1.57 | 3.17 | 3.44 | 1.70 | 0.83 | 3.46 |
| K ₂ O | 2.01 | 2.47 | 1.52 | 0.24 | 0.22 | 0.99 | 0.49 | 2.35 | 2.29 | 0.60 | 0.16 | 2.30 |
| MgO | 2.53 | 3.41 | 3.80 | 0.80 | 0.77 | 2.91 | 4.21 | 2.01 | 1.84 | 1.05 | 0.80 | 1.85 |
| MnO/Mn ₃ O ₄ | 0.12 | 0.11 | 0.02 | 0.03 | 0.03 | 0.05 | 0.03 | 0.03 | 0.06 | 0.18 | 0.09 | 0.05 |
| Na ₂ O | 1.09 | 0.73 | 0.19 | 0.12 | 0.09 | 0.15 | 0.20 | 0.68 | 0.19 | 0.07 | 0.04 | 0.19 |
| P ₂ O ₅ | 0.10 | 0.13 | 0.10 | 0.06 | 0.05 | 0.05 | 0.09 | 0.22 | 0.52 | 0.11 | 0.12 | 0.48 |
| SiO ₂ | 69.69 | 52.27 | 37.06 | 13.62 | 13.06 | 26.00 | 25.84 | 41.40 | 44.24 | 21.26 | 6.70 | 44.33 |
| TiO ₂ | 0.46 | 0.57 | 0.42 | 0.05 | 0.05 | 0.26 | 0.14 | 0.58 | 0.54 | 0.17 | 0.04 | 0.53 |
| V ₂ O ₅ | 0.01 | 0.02 | 0.01 | <0.01 | <0.01 | <0.01 | <0.01 | 0.03 | 0.02 | <0.01 | <0.01 | 0.01 |

| Well ID | MW-358 | MW-358 | MW-358 | MW-392 | MW-392 | MW-393 | MW-394 | MW-392 |
|------------------------------------|------------|---------------|-------------------|----------------------------------|-----------------------------------|----------------|----------------|----------------|
| Depth (ft bgs) | (13-15) | (47-49) | (86-88) | (80-82) | (32-33.5) | (24-25.5) | (20.5-22) | (66-68) |
| Well Characterization | Background | Background | Background | BAP Compliance | BAP Compliance | BAP Compliance | BAP Compliance | BAP Compliance |
| Sampled Aquifer | PMP | UA | UA | UA | PMP | PMP | PMP | UA |
| Field Boring Log Description | Silty clay | Shallow shale | Deeper shale body | Shale transitioning to limestone | Clay with increasing sand content | Clayey sand | Silty sand | Shale |
| Analyte | (wt %) | (wt %) | (wt %) | (wt %) | (wt %) | (wt %) | (wt %) | (wt %) |
| Al ₂ O ₃ | 10.60 | 17.20 | 19.20 | 8.17 | 10.70 | 8.70 | 11.00 | 15.30 |
| CaO | 0.73 | 0.57 | 0.50 | 25.40 | 1.35 | 0.55 | 0.92 | 6.38 |
| Cr ₂ O ₃ | < 0.01 | 0.01 | 0.01 | < 0.01 | < 0.01 | < 0.01 | < 0.01 | < 0.01 |
| Fe ₂ O ₃ | 3.72 | 7.01 | 4.34 | 2.76 | 4.54 | 3.27 | 4.46 | 7.66 |
| K ₂ O | 1.87 | 3.38 | 2.79 | 1.02 | 2.00 | 2.16 | 2.14 | 2.87 |
| MgO | 0.67 | 1.99 | 1.90 | 1.58 | 1.20 | 0.55 | 0.85 | 2.46 |
| MnO/Mn ₃ O ₄ | 0.07 | < 0.01 | < 0.01 | 0.04 | 0.11 | 0.09 | 0.09 | 0.03 |
| Na ₂ O | 1.04 | 0.83 | 0.77 | 0.40 | 0.87 | 0.94 | 1.27 | 0.29 |
| P ₂ O ₅ | 0.08 | 0.10 | 0.10 | 3.84 | 0.10 | 0.08 | 0.17 | 0.08 |
| SiO ₂ | 75.20 | 58.30 | 59.60 | 33.60 | 72.30 | 79.70 | 73.00 | 50.70 |
| TiO ₂ | 0.73 | 0.72 | 0.82 | 0.29 | 0.67 | 0.50 | 0.75 | 0.58 |
| V ₂ O ₅ | 0.02 | 0.02 | 0.02 | 0.02 | 0.01 | < 0.01 | 0.01 | 0.02 |

Notes

Sample depth is shown in feet below ground surface (ft bgs).

Non-detect values are shown as less than the reporting limit.

Results are not normalized to 100%, with some portion of sample mass uncharacterized.

Analytes are presented as the respective oxide species of the element of interest, consistent with the sample processing prior to analysis.

Mn reported as MnO for Bottom Ash Pond (BAP) Compliance and Background samples and Mn₃O₄ for Fly Ash Pond System (FAPS) Compliance samples.

PMP: potential migration pathway

UA: uppermost aquifer

wt %: percentage by weight

Table 4. Boron and Iron Characterization of SEP Fraction of Site Solids
Geochemical Conceptual Site Model
Baldwin Power Plant - Fly Ash Pond System

| Well ID | | | MW-358 | | MW-358 | | MW-358 | | MW-392 | | MW-392 | | MW-393 | | MW-394 | | MW-392 | |
|------------------------------|---|---|------------|------------|---------------|------------|-------------------|------------|----------------------------------|------------|-----------------------------------|------------|----------------|------------|----------------|------------|----------------|------------|
| Depth (ft bgs) | | | (13-15) | | (47-49) | | (86-88) | | (80-82) | | (32-33.5) | | (24-25.5) | | (20.5-22) | | (66-68) | |
| Well Characterization | | | Background | | Background | | Background | | BAP Compliance | | BAP Compliance | | BAP Compliance | | BAP Compliance | | BAP Compliance | |
| Sampled Aquifer Unit | | | PMP | | UA | | UA | | UA | | PMP | | PMP | | PMP | | UA | |
| Field Boring Log Description | | | Silty clay | | Shallow shale | | Deeper shale body | | Shale transitioning to limestone | | Clay with increasing sand content | | Clayey sand | | Silty sand | | Shale | |
| Fraction | Reagent | Boron SEP | µg/g | % of Total | µg/g | % of Total | µg/g | % of Total | µg/g | % of Total | µg/g | % of Total | µg/g | % of Total | µg/g | % of Total | µg/g | % of Total |
| 1 | Deionized Water | Water Soluble Fraction | < 1 | - | 8 | 10.4 | 10 | 11.9 | 3 | 7.3 | < 1 | - | < 1 | - | < 1 | - | 5 | 7.2 |
| 2 | MgCl ₂ | Exchangeable Metals Fraction | < 1 | - | < 1 | - | 1 | 1.2 | < 1 | - | < 1 | - | < 1 | - | < 1 | - | 2 | 2.9 |
| 3 | Sodium acetate, acetic acid | Metals Bound to Carbonates Fraction | < 1 | - | 2 | 2.6 | 3 | 3.6 | 4 | 9.8 | < 1 | - | < 1 | - | < 1 | - | 3 | 4.3 |
| 4 | Hydroxylamine HCl and acetic acid | Metals Bound to Fe and Mn Oxides Fraction | < 1 | - | 5 | 6.5 | 6 | 7.1 | 6 | 14.6 | < 1 | - | < 1 | - | < 1 | - | 4 | 5.8 |
| 5 | HNO ₃ , H ₂ O ₂ , and ammonium acetate | Bound to Organic Material Fraction | < 1 | - | 2 | 2.6 | 2 | 2.4 | 2 | 4.9 | < 1 | - | < 1 | - | < 1 | - | 2 | 2.9 |
| 6 | HNO ₃ , HCl, and HF | Residual Metals Fraction | 13 | 100 | 60 | 77.9 | 62 | 73.8 | 26 | 63.4 | 21 | 100 | 15 | 100 | 16 | 100 | 53 | 76.8 |
| SEP Total | | | 13 | - | 77 | - | 84 | - | 41 | - | 21 | - | 15 | - | 16 | - | 69 | - |
| | | | | | | | | | | | | | | | | | | |
| Fraction | Reagent | Iron SEP | µg/g | % of Total | µg/g | % of Total | µg/g | % of Total | µg/g | % of Total | µg/g | % of Total | µg/g | % of Total | µg/g | % of Total | µg/g | % of Total |
| 1 | Deionized Water | Water Soluble Fraction | 17 | 0.1 | 240 | 0.5 | 190 | 0.8 | < 1 | - | 27 | 0.09 | 14 | 0.07 | 20 | 0.07 | 28 | 0.06 |
| 2 | MgCl ₂ | Exchangeable Metals Fraction | 2 | 0.01 | 21 | 0.05 | < 1 | - | 12 | 0.1 | 8 | 0.03 | 9 | 0.04 | 8 | 0.03 | 10 | 0.02 |
| 3 | Sodium acetate, acetic acid | Metals Bound to Carbonates Fraction | 40 | 0.2 | 45 | 0.1 | 42 | 0.2 | 25 | 0.2 | 9 | 0.03 | 14 | 0.07 | 10 | 0.04 | 300 | 0.6 |
| 4 | Hydroxylamine HCl and acetic acid | Metals Bound to Fe and Mn Oxides Fraction | 1600 | 6.7 | 1600 | 3.6 | 1200 | 4.8 | 1800 | 11.2 | 1100 | 3.8 | 1500 | 7.3 | 1200 | 4.2 | 2700 | 5.8 |
| 5 | HNO ₃ , H ₂ O ₂ , and ammonium acetate | Bound to Organic Material Fraction | 150 | 0.6 | 610 | 1.4 | 1800 | 7.1 | 220 | 1.4 | 83 | 0.3 | 93 | 0.5 | 120 | 0.4 | 680 | 1.5 |
| 6 | HNO ₃ , HCl, and HF | Residual Metals Fraction | 22000 | 92.4 | 42000 | 94.3 | 22000 | 87.2 | 14000 | 87.2 | 28000 | 95.8 | 19000 | 92.1 | 27000 | 95.2 | 43000 | 92.0 |
| SEP Total | | | 23809 | - | 44516 | - | 25232 | - | 16057 | - | 29227 | - | 20630 | - | 28358 | - | 46718 | - |

Notes
Sample depth is shown in feet below ground surface (ft bgs).
Non-detect values are shown as less than the reporting limit.
µg/g: micrograms per gram
BAP: Bottom Ash Pond
PMP: potential migration pathway
UA: uppermost aquifer

Table 5a. XRD Analysis of PMP Solids
Geochemical Conceptual Site Model
Baldwin Power Plant - Fly Ash Pond System

Geosyntec Consultants, Inc.

| Well ID | | | MW-150 | MW-150 | MW-358 | MW-392 | MW-393 | MW-394 |
|------------------------------|--|----------------|-----------------|-----------------|------------|-----------------------------------|----------------|----------------|
| Depth (ft bgs) | | | (15-20) | (20-25) | (13-15) | (32-33.5) | (24-25.5) | (20.5-22) |
| Well Characterization | | | FAPS Compliance | FAPS Compliance | Background | BAP Compliance | BAP Compliance | BAP Compliance |
| Sampled Aquifer Unit | | | PMP | PMP | PMP | PMP | PMP | PMP |
| Field Boring Log Description | | | Sandy clay | Sandy clay | Silty clay | Clay with increasing sand content | Clayey sand | Silty sand |
| Mineral/Compound | Formula | Mineral Type | (wt %) | (wt %) | (wt %) | (wt %) | (wt %) | (wt %) |
| Quartz | SiO ₂ | Silicate | 53.5 | 32.4 | 52.7 | 52.1 | 64.1 | 55.4 |
| Albite | NaAlSi ₃ O ₈ | Feldspar | 11.3 | 9.0 | 12.3 | 9.1 | 6.4 | 12.8 |
| Microcline | KAlSi ₃ O ₈ | Feldspar | 8.0 | 9.7 | 7.3 | 6.5 | 10.1 | 7.3 |
| Dolomite | CaMg(CO ₃) ₂ | Carbonate | 9.4 | 11.2 | - | - | - | - |
| Calcite | CaCO ₃ | Carbonate | 2.9 | 9.5 | - | 0.0 | 0.0 | 0.2 |
| Ankerite | CaFe(CO ₃) ₂ | Carbonate | - | - | - | 1.4 | 0.9 | 0.5 |
| Actinolite | Ca ₂ (Mg,Fe)Si ₈ O ₂₂ (OH) ₂ | Amphibole | 2.0 | 0.5 | - | - | - | - |
| Magnetite | Fe ₃ O ₄ | Oxide | 0.3 | 0.5 | 0.9 | 0.1 | 0.0 | 0.1 |
| Hematite | Fe ₂ O ₃ | Oxide | - | - | - | - | - | - |
| Anatase | TiO ₂ | Oxide | - | - | 0.2 | 0.6 | 0.3 | 0.3 |
| Diaspore | aAlO.OH | Oxide | - | - | 0.3 | - | 0.2 | 0.5 |
| Fluorapatite | Ca ₅ (PO ₄) ₃ F | Phosphate | - | - | - | 0.3 | - | 0.2 |
| Muscovite | KAl ₂ (AlSi ₃ O ₁₀)(OH) ₂ | Mica | 2.0 | 9.1 | 7.7 | 9.0 | 5.5 | 7.6 |
| Clay Minerals | | | | | | | | |
| Chlorite | (Fe,(Mg,Mn) ₅ ,Al)(Si ₃ Al)O ₁₀ (OH) ₈ | Sheet silicate | - | 0.7 | - | - | - | - |
| Chlorite IIb | (Fe,(Mg,Mn) ₅ ,Al)(Si ₃ Al)O ₁₀ (OH) ₈ | Sheet silicate | - | - | 2.6 | 5.8 | 1.2 | 3.1 |
| Montmorillonite | (Na,Ca) _{0.3} (Al,Mg) ₂ Si ₄ O ₁₀ (OH) ₂ ·10H ₂ O | Clay | 5.5 | 9.0 | - | - | - | - |
| Montmorillonite-12A | (Na,Ca) _{0.3} (Al,Mg) ₂ Si ₄ O ₁₀ (OH) ₂ ·10H ₂ O | Clay | - | - | 4.9 | - | - | - |
| Montmorillonite-14A | (Na,Ca) _{0.3} (Al,Mg) ₂ Si ₄ O ₁₀ (OH) ₂ ·10H ₂ O | Clay | - | - | - | 3.3 | 3.5 | 3.6 |
| Illite | (K,H ₃ O)(Al,Mg,Fe) ₂ (Si,Al) ₄ O ₁₀ [(OH) ₂ ·(H ₂ O)] | Clay | 4.0 | 6.8 | 5.0 | 0.7 | 1.0 | 0.6 |
| Illite-Montmorillonite - 11A | KAl ₄ (Si,Al) ₈ O ₁₀ (OH) ₄ ·4H ₂ O | Clay | - | - | - | 2.7 | 2.1 | 3.0 |
| Kaolinite | Al ₂ Si ₂ O ₅ (OH) ₄ | Clay | 1.0 | 1.5 | 5.3 | 6.8 | 3.2 | 4.2 |
| Nontronite | Fe ₂ (Al,Si) ₄ O ₁₀ (OH) ₂ Na _{0.3} (H ₂ O) ₄ | Clay | - | - | 0.6 | 1.6 | 1.4 | 0.5 |
| Clay Minerals Total | | | 10.4 | 17.3 | 15.9 | 15.0 | 11.1 | 12.0 |
| Clays + Muscovite Total | | | 12.4 | 27.1 | 26.2 | 29.8 | 17.9 | 22.6 |

Notes

Dashes indicate mineral was not identified by lab

Sample depth is shown in feet below ground surface (ft bgs).

The weight percent quantities indicated have been normalized to a sum of 100% using only minerals included in the refinement.

BAP: Bottom Ash Pond

FAPS: Fly Ash Pond System

ft bgs: feet below ground surface

PMP: potential migration pathway

wt %: percentage by weight

Table 5b. XRD Analysis of UA Solids
Geochemical Conceptual Site Model
Baldwin Power Plant - Fly Ash Pond System

| Well ID | | | MW-350 | MW-350 | MW-350 | MW-352 | MW-352 | MW-366 | MW-391 | MW-391 | MW-391 | MW-358 | MW-358 | MW-392 | MW-392 |
|------------------------------|--|----------------|-----------------|-----------------|-----------------|-----------------|-----------------|-----------------|-----------------|-----------------|-----------------|---------------|-------------------|----------------------------------|----------------|
| Depth (ft bgs) | | | (35-40) | (42-46) | (42-46) | (50-60) | (60-70) | (40-52) | (50-51) | (51-55) | (55-72) | (47-49) | (86-88) | (80-82) | (66-68) |
| Well Characterization | | | FAPS Compliance | FAPS Compliance | FAPS Compliance | FAPS Compliance | FAPS Compliance | FAPS Compliance | FAPS Compliance | FAPS Compliance | FAPS Compliance | Background | Background | BAP Compliance | BAP Compliance |
| Sampled Aquifer Unit | | | UA | UA | UA | UA | UA | UA | UA | UA | UA | UA | UA | UA | UA |
| Field Boring Log Description | | | Shale | Limestone | Limestone | Shale | Shale | Shale | Weathered shale | Shale | Limestone | Shallow shale | Deeper shale body | Shale transitioning to limestone | Shale |
| Mineral/Compound | Formula | Mineral Type | (wt %) | (wt %) | (wt %) | (wt %) | (wt %) | (wt %) | (wt %) | (wt %) | (wt %) | (wt %) | (wt %) | (wt %) | (wt %) |
| Quartz | SiO ₂ | Silicate | 17.7 | 10.4 | 10.7 | 11.2 | 19.4 | 14.2 | 24.2 | 13.1 | 5.2 | 29.2 | 30.7 | 29.8 | 22.7 |
| Dolomite | CaMg(CO ₃) ₂ | Carbonate | 4.4 | 0.8 | 0.4 | 3.5 | 6.2 | 0.3 | - | - | - | - | - | - | - |
| Calcite | CaCO ₃ | Carbonate | 27.2 | 80.5 | 84.6 | 57.2 | 49.5 | 33.9 | 35.5 | 74.9 | 90.2 | 0.5 | 1.0 | 28.1 | 14.9 |
| Ankerite | CaFe(CO ₃) ₂ | Carbonate | 7.3 | 0.4 | 0.2 | 4.7 | 10.0 | 1.6 | - | 0.0 | 0.4 | - | - | - | 0.8 |
| Rhodochrosite | MnCO ₃ | Carbonate | 0.7 | - | - | - | - | - | - | - | - | - | - | - | - |
| Albite | NaAlSi ₃ O ₈ | Feldspar | 2.5 | 0.4 | 0.6 | 0.2 | 0.2 | 1.8 | 2.2 | 0.4 | 0.0 | 0.4 | 2.5 | 0.6 | 0.6 |
| Microcline | KAlSi ₃ O ₈ | Feldspar | 4.6 | 2.1 | 0.5 | 2.1 | 1.3 | 5.3 | 3.2 | 1.9 | 0.3 | 8.6 | 5.9 | 1.0 | 5.1 |
| Gypsum | CaSO ₄ ·2H ₂ O | Sulfate | 1.9 | - | - | - | - | - | - | - | - | - | - | - | - |
| Pyrite | FeS ₂ | Sulfide | 1.6 | - | - | 0.6 | 0.8 | 1.3 | 0.2 | 0.1 | 0.3 | - | - | - | - |
| Actinolite | Ca ₂ (Mg,Fe) ₅ Si ₈ O ₂₂ (OH) ₂ | Amphibole | 1.3 | - | - | - | - | - | - | - | - | - | - | - | - |
| Magnetite | Fe ₃ O ₄ | Oxide | 0.8 | - | - | 0.2 | - | - | 0.7 | 0.4 | - | 0.5 | 0.3 | 1.4 | 0.1 |
| Hematite | Fe ₂ O ₃ | Oxide | 0.4 | - | - | 0.2 | 0.4 | - | - | - | - | - | - | - | - |
| Anatase | TiO ₂ | Oxide | 0.6 | - | - | - | - | 0.6 | 0.5 | 0.5 | - | 0.8 | 1.8 | 0.8 | 1.0 |
| Diaspore | aAlO.OH | Oxide | - | - | - | - | - | - | - | - | - | - | - | - | 2.8 |
| Fluorapatite | Ca ₅ (PO ₄) ₃ F | Phosphate | - | - | - | - | - | - | - | - | - | - | - | 2.7 | 0.2 |
| Muscovite | KAl ₂ (AlSi ₃ O ₁₀)(OH) ₂ | Mica | 11.8 | 1.9 | 1.4 | 6.4 | 4.3 | 12.9 | 17.6 | 5.3 | 2.0 | 18.8 | 19.7 | 13.1 | 15.9 |
| Clay Minerals | | | | | | | | | | | | | | | |
| Montmorillonite | (Na,Ca) _{0.3} (Al,Mg) ₂ Si ₄ O ₁₀ (OH) ₂ ·10H ₂ O | Clay | 10.5 | 2.1 | 0.2 | 7.8 | 2.6 | 14.0 | - | 2.2 | 0.9 | - | - | - | - |
| Montmorillonite-12A | (Na,Ca) _{0.3} (Al,Mg) ₂ Si ₄ O ₁₀ (OH) ₂ ·10H ₂ O | Clay | - | - | - | - | - | - | - | - | - | 6.8 | 4.8 | - | 5.8 |
| Montmorillonite-14A | (Na,Ca) _{0.3} (Al,Mg) ₂ Si ₄ O ₁₀ (OH) ₂ ·10H ₂ O | Clay | - | - | - | - | - | - | - | - | - | - | - | 3.5 | - |
| Illite | (K,H ₃ O)(Al,Mg,Fe) ₂ (Si,Al) ₄ O ₁₀ [(OH) ₂ ,(H ₂ O)] | Clay | 3.2 | 0.9 | 0.6 | 3.2 | 2.6 | 6.1 | 7.9 | 1.2 | 0.9 | 15.0 | 9.2 | 4.1 | 10.4 |
| Illite-Montmorillonite - 11A | KAl ₄ (Si,Al) ₈ O ₁₀ (OH) ₄ ·4H ₂ O | Clay | - | - | - | - | - | - | - | - | - | 8.8 | 2.7 | 3.6 | 7.1 |
| Illite-Montmorillonite | KAl ₄ (Si,Al) ₈ O ₂₀ (OH) ₄ ·8H ₂ O | Clay | - | - | - | - | - | - | 8.0 | - | - | - | - | - | - |
| Kaolinite | Al ₂ Si ₂ O ₅ (OH) ₄ | Clay | 3.2 | 0.5 | 0.6 | 2.4 | 0.8 | 4.2 | - | - | - | 4.8 | 15.0 | 5.5 | 3.6 |
| Nontronite | Fe ₂ (Al,Si) ₄ O ₁₀ (OH) ₂ Na _{0.3} (H ₂ O) ₄ | Clay | - | - | - | - | - | - | - | - | - | 4.6 | 4.3 | 4.2 | 3.3 |
| Chlorite | (Fe,(Mg,Mn) ₅ ,Al)(Si ₃ Al)O ₁₀ (OH) ₈ | Sheet silicate | 0.2 | 0.0 | 0.2 | 0.2 | 1.8 | 3.7 | - | - | - | - | - | - | - |
| Chlorite IIb | (Fe,(Mg,Mn) ₅ ,Al)(Si ₃ Al)O ₁₀ (OH) ₈ | Sheet silicate | - | - | - | - | - | - | - | - | - | 1.3 | 2.0 | 1.6 | 6.1 |
| Clay Minerals Total | | | 17.1 | 3.5 | 1.6 | 13.6 | 7.8 | 28.0 | 15.9 | 3.4 | 1.8 | 41.2 | 38.1 | 22.5 | 36.1 |
| Clays + Muscovite Total | | | 28.9 | 5.5 | 3.0 | 20.0 | 12.2 | 40.9 | 33.5 | 8.7 | 3.8 | 60.0 | 57.8 | 35.6 | 19.6 |

Notes
Dashes indicate mineral was not identified by lab
Sample depth is shown in feet below ground surface (ft bgs).
The weight percent quantities indicated have been normalized to a sum of 100% using only minerals included in the refinement.
BAP: Bottom Ash Pond
FAPS: Fly Ash Pond System
ft bgs: feet below ground surface
UA: uppermost aquifer
wt %: percentage by weight

Table 6. FAPS Porewater Chemistry
Geochemical Conceptual Site Model
Baldwin Power Plant - Fly Ash Pond System

| Location Name | Sample Date | pH (SU) | Total Sulfate (mg/L) | Dissolved Sulfate (mg/L) | Total Boron (mg/L) | Dissolved Boron (mg/L) | Total Iron (mg/L) | Dissolved Iron (mg/L) | Total Manganese (mg/L) | Dissolved Manganese (mg/L) |
|---------------|-------------|------------|-------------------------|-----------------------------|-----------------------|---------------------------|----------------------|--------------------------|---------------------------|-------------------------------|
| TPZ-163 | 2013/09/17 | 9.7 | 750 | - | 39.7 | - | 7.86 | - | 0.13 | - |
| | 2013/11/20 | 8.8 | - | 626 | - | 37.2 | - | < 0.02 | - | < 0.005 |
| | 2014/02/18 | 7.6 | - | 610 | - | 37.8 | - | < 0.02 | - | < 0.005 |
| | 2014/06/12 | 9.5 | - | 495 | - | 36.3 | - | < 0.02 | - | < 0.005 |
| TPZ-167 | 2013/09/17 | 9.9 | 1740 | - | 64.4 | - | 0.57 | - | 0.01 | - |
| | 2013/11/20 | 8.2 | - | 1850 | - | 53 | - | < 0.02 | - | < 0.005 |
| | 2014/02/18 | 7.7 | - | 1840 | - | 54.5 | - | < 0.02 | - | < 0.005 |
| | 2014/06/11 | 10 | - | 1650 | - | 60 | - | < 0.02 | - | < 0.005 |
| TPZ-168 | 2013/09/17 | 10.8 | 2630 | - | 102 | - | 90.6 | - | 1.58 | - |
| | 2013/11/20 | 9.2 | - | 2760 | - | 87.2 | - | < 0.02 | - | < 0.005 |
| | 2014/02/18 | 8.1 | - | 2820 | - | 78.8 | - | 0.06 | - | < 0.005 |
| | 2014/06/11 | 11.9 | - | 2240 | - | 94.7 | - | 0.055 | - | < 0.005 |
| Sump 12 | 2020/05/15 | 11.8 | 1840 | - | 60.3 | - | 0.96 | < 0.025 | 0.0104 | < 0.002 |
| Sump 13 | 2020/05/15 | 9.0 | 84 | - | 0.663 | - | 10.9 | < 0.025 | 0.054 | < 0.002 |
| Sump 15 | 2020/05/15 | 8.2 | 1080 | - | 10.6 | - | 0.5 | < 0.025 | 1.82 | 1.7 |

Notes
SU: standard units
mg/L: milligrams per liter
- : Analyte not included in analyses for sampling date

Table 7. Eh-pH Diagram Inputs
Geochemical Conceptual Site Model
Baldwin Power Plant - Fly Ash Pond System

Geosyntec Consultants, Inc.

| Well ID | | MW-391 | MW-150 |
|------------------------|------|-----------|-----------|
| Sample Date | | 5/17/2023 | 5/18/2023 |
| Aquifer Unit | | UA | PMP |
| Input Parameter | Unit | | |
| Temperature | °C | 15.6 | 13.6 |
| pH | SU | 7.78 | 7.06 |
| Calcium | mg/L | 18.7 | 223 |
| Chloride | mg/L | 170 | 56 |
| Bicarbonate Alkalinity | mg/L | 728 | 336 |
| Magnesium | mg/L | 6.6 | 173 |
| Sodium | mg/L | 767 | 121 |
| Potassium | mg/L | 3.96 | 0.893 |
| Sulfate | mg/L | 430 | 970 |
| Total Manganese | mg/L | 0.0348 | 0.0055 |
| Total Iron | mg/L | 1.88 | 0.038 |

Notes

°C - degrees Celsius

mg/L - milligrams per liter

PMP - potential migration pathway

SU - standard units

UA - uppermost aquifer

Table 8. Total and Dissolved Aqueous Iron and Manganese Results**Geochemical Conceptual Site Model****Baldwin Power Plant - Fly Ash Pond System***Geosyntec Consultants, Inc.*

| Well ID | Sampled Aquifer Unit | Date | Dissolved Iron | Total Iron | Dissolved Manganese | Total Manganese |
|---------|----------------------|------------|----------------|------------|---------------------|-----------------|
| | | | (mg/L) | (mg/L) | (mg/L) | (mg/L) |
| MW-150 | PMP | 5/18/2023 | <0.02 | 0.038 | 0.0038 | 0.0055 |
| | | 8/7/2023 | 0.0666 | 0.166 | 0.0025 | 0.0028 |
| | | 11/3/2023 | 0.0728 | 0.157 | 0.0025 | 0.0088 |
| MW-151 | PMP | 5/18/2023 | <0.02 | 25.2 | 0.0151 | 0.805 |
| | | 8/7/2023 | <0.0115 | 4.81 | 0.0177 | 0.118 |
| | | 10/31/2023 | 0.013 | 5.55 | 0.0133 | 0.237 |
| MW-152 | PMP | 5/18/2023 | <0.02 | 1.35 | 0.0073 | 0.0506 |
| | | 8/4/2023 | <0.025 | 3.04 | 0.0176 | 0.114 |
| | | 10/31/2023 | <0.0115 | 7.75 | 0.0244 | 0.247 |
| MW-153 | PMP | 5/22/2023 | <0.02 | 10.6 | <0.0025 | 0.089 |
| | | 8/4/2023 | <0.0115 | 0.089 | 0.0041 | 0.0068 |
| | | 11/3/2023 | <0.0115 | 0.243 | 0.0032 | 0.0114 |
| MW-252 | PMP | 5/18/2023 | 0.0499 | 1.28 | 0.396 | 0.502 |
| | | 8/4/2023 | 0.562 | 3.08 | 0.293 | 0.323 |
| | | 10/31/2023 | 0.619 | 1.99 | 0.303 | 0.351 |
| MW-304 | UA | 5/22/2023 | <0.02 | <0.02 | <0.0025 | <0.0025 |
| | | 8/3/2023 | <0.0115 | 0.014 | 0.0014 | 0.0032 |
| | | 11/1/2023 | <0.0115 | <0.0115 | 0.002 | 0.0044 |
| MW-352 | UA | 5/18/2023 | 0.164 | 0.356 | 0.0152 | 0.0179 |
| | | 8/4/2023 | 0.482 | 0.307 | 0.0334 | 0.0112 |
| | | 10/31/2023 | 0.392 | 0.459 | 0.0423 | 0.0162 |
| MW-358 | UA | 5/19/2023 | 0.242 | 0.685 | 0.182 | 0.225 |
| | | 8/7/2023 | 0.221 | 0.908 | 0.16 | 0.227 |
| MW-366 | UA | 5/16/2023 | <0.02 | 0.0649 | 0.0281 | 1.68 |
| | | 8/4/2023 | <0.025 | 0.023 | 0.0169 | 0.267 |
| MW-375 | UA | 5/18/2023 | <0.02 | 0.0854 | <0.0025 | 0.0098 |
| | | 8/7/2023 | <0.0115 | 0.1 | 0.0013 | 0.0158 |
| MW-377 | UA | 5/22/2023 | 0.024 | 0.07 | 0.011 | 0.016 |
| | | 8/7/2023 | <0.025 | 0.0371 | 0.0072 | 0.0125 |
| MW-383 | UA | 5/22/2023 | <0.02 | 0.0901 | 0.0269 | 0.0564 |
| | | 8/3/2023 | 0.359 | 0.0471 | 0.0382 | 0.0333 |
| MW-384 | UA | 5/22/2023 | <0.02 | 0.824 | 0.0031 | 0.0088 |
| | | 8/3/2023 | 0.0115 | 0.117 | 0.0066 | 0.018 |
| MW-390 | UA | 5/17/2023 | <0.02 | 0.126 | 0.364 | 0.709 |
| | | 8/4/2023 | <0.025 | 0.0631 | 0.681 | 0.088 |
| MW-391 | UA | 5/17/2023 | <0.02 | 1.88 | 0.007 | 0.0348 |
| | | 8/4/2023 | <0.023 | 0.219 | 0.0115 | 0.0102 |

Notes

Non-detect values are shown as less than the reporting limit.

mg/L: milligrams per liter

PMP: potential migration pathway

UA: uppermost aquifer

Attachment A
Site Layout Figure



REGULATED UNIT (SUBJECT UNIT) FLY ASH
POND SYSTEM (CLOSED)

SITE FEATURE
LIMITS OF FINAL COVER
PROPERTY BOUNDARY

0 400 800 Feet

SITE MAP

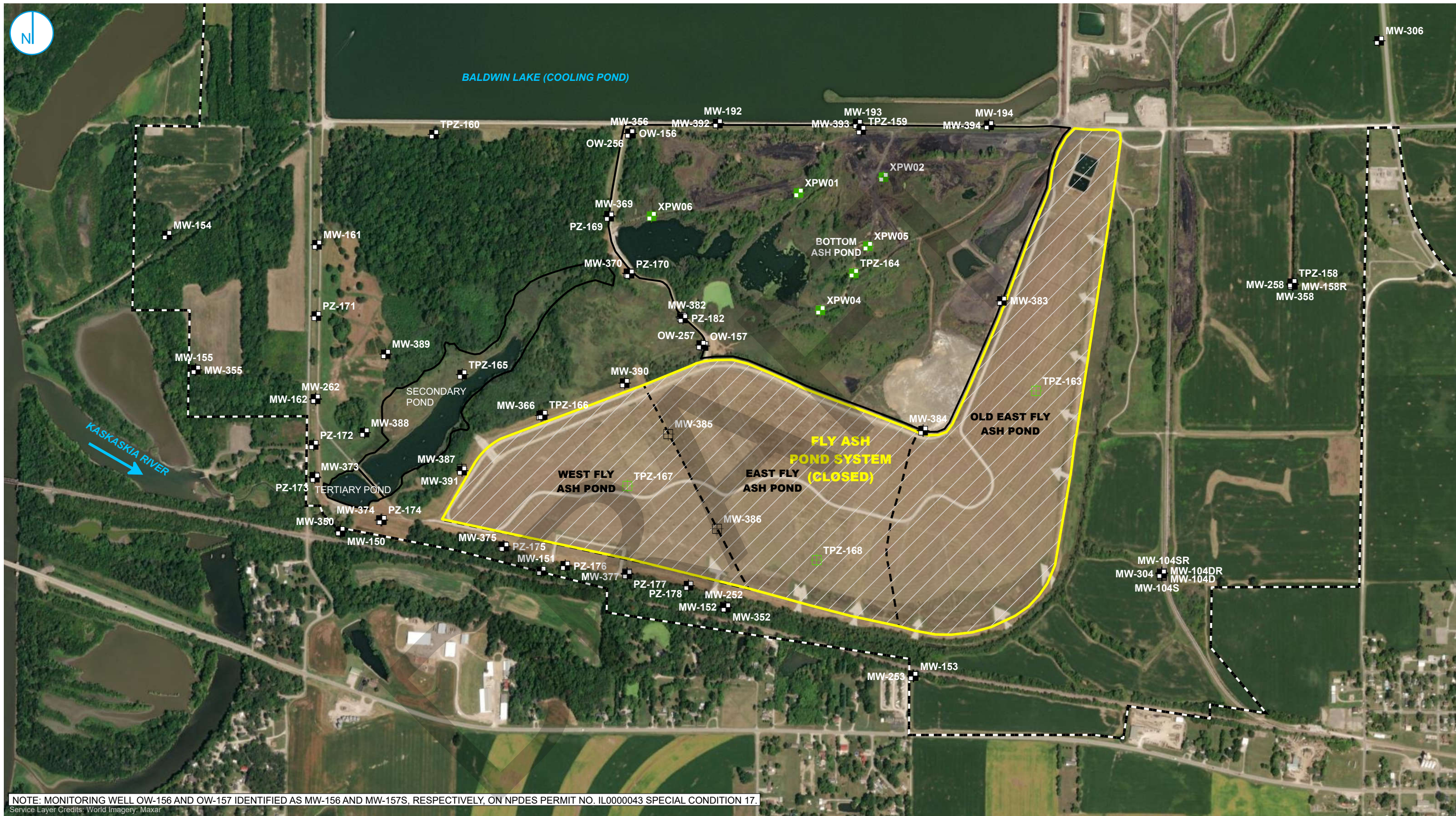
35 I.A.C. § 845 GROUNDWATER MONITORING PLAN REVISION 1
FLY ASH POND SYSTEM
BALDWIN POWER PLANT
BALDWIN, ILLINOIS

FIGURE 1-2

RAMBOLL AMERICAS
ENGINEERING SOLUTIONS, INC.

RAMBOLL

Attachment B
**Proposed Part 845 Groundwater Monitoring
Network**



- | | |
|---|---------------------------------|
| ■ MONITORING WELL AND PIEZOMETER LOCATION | ■ REGULATED UNIT (SUBJECT UNIT) |
| ■ PORE WATER WELL | ■ SITE FEATURE |
| ■ CLOSED MONITORING WELL | ■ CAPPED AREA |
| ■ CLOSED PORE WATER WELL | ■ PROPERTY BOUNDARY |

0 400 800
Feet

MONITORING WELL LOCATION MAP

35 I.A.C. § 845 GROUNDWATER MONITORING PLAN REVISION 1
FLY ASH POND SYSTEM
BALDWIN POWER PLANT
BALDWIN, ILLINOIS

FIGURE 2-1

RAMBOLL AMERICAS
ENGINEERING SOLUTIONS, INC.



Attachment C
Monitoring Well Construction Information

Attachment C. Monitoring Well Construction Details

Geochemical Conceptual Site Model
Baldwin Fly Ash Pond System
Baldwin Power Plant
Baldwin, IL

| Location | HSU | Date Constructed | Top of PVC Elevation (ft) | Measuring Point Elevation (ft) | Measuring Point Description | Ground Elevation (ft) | Screen Top Depth (ft bgs) | Screen Bottom Depth (ft bgs) | Screen Top Elevation (ft) | Screen Bottom Elevation (ft) | Well Depth (ft bgs) | Bottom of Boring Elevation (ft) | Screen Length (ft) | Screen Diameter (inches) | Latitude (Decimal Degrees) | Longitude (Decimal Degrees) |
|----------|-----|------------------|---------------------------|--------------------------------|-----------------------------|-----------------------|---------------------------|------------------------------|---------------------------|------------------------------|---------------------|---------------------------------|--------------------|--------------------------|----------------------------|-----------------------------|
| MW-150 | PMP | 2010-09-01 | 396.5 | 396.7 | Top of PVC | 393.8 | 15 | 24.7 | 378.8 | 369.2 | 25.2 | 368.7 | 9.6 | 2 | 38.189401 | -89.878468 |
| MW-151 | PMP | 2010-09-01 | 400.0 | 400.1 | Top of PVC | 397.2 | 6.1 | 15.8 | 391.1 | 381.4 | 16.3 | 380.9 | 9.6 | 2 | 38.188449 | -89.872354 |
| MW-152 | PMP | 2010-09-01 | 425.0 | 425.2 | Top of PVC | 422.2 | 7.5 | 16.7 | 414.7 | 405.5 | 17.2 | 405.0 | 9.3 | 2 | 38.187569 | -89.866764 |
| MW-153 | PMP | 2010-09-01 | 445.7 | 445.8 | Top of PVC | 442.8 | 10.4 | 20 | 432.4 | 422.8 | 20.5 | 422.3 | 9.6 | 2 | 38.185884 | -89.86101 |
| MW-252 | PMP | 2010-09-01 | 425.1 | 425.2 | Top of PVC | 422.3 | 44.4 | 49 | 377.9 | 373.2 | 49.5 | 372.7 | 4.6 | 2 | 38.187563 | -89.866745 |
| MW-253 | PMP | 2010-09-01 | 445.8 | 446.0 | Top of PVC | 442.7 | 29.9 | 34.5 | 412.8 | 408.2 | 35 | 407.7 | 4.6 | 2 | 38.185885 | -89.861026 |
| MW-304 | UA | 2015-10-20 | 455.5 | 455.4 | Top of PVC | 453.0 | 45 | 55 | 408.0 | 398.0 | 55 | 317.6 | 10 | 2 | 38.188332 | -89.853441 |
| MW-350 | UA | 2010-09-01 | 396.8 | 397.0 | Top of PVC | 394.1 | 41.6 | 46.2 | 352.5 | 347.9 | 46.6 | 347.4 | 4.6 | 2 | 38.189416 | -89.878477 |
| MW-352 | UA | 2010-09-01 | 425.0 | 425.2 | Top of PVC | 422.4 | 67.9 | 72.5 | 354.5 | 349.8 | 73 | 348.6 | 4.6 | 2 | 38.187554 | -89.866729 |
| MW-358 | UA | 2022-10-08 | 455.7 | 455.9 | Top of PVC | 453.6 | 80 | 90 | 373.7 | 363.7 | 90 | 363.6 | 10 | 2 | 38.195275 | -89.849417 |
| MW-366 | UA | 2015-12-04 | 425.1 | 425.2 | Top of PVC | 422.5 | 42 | 52 | 380.5 | 370.5 | 52 | 368.2 | 10 | 2 | 38.192191 | -89.872345 |
| MW-375 | UA | 2015-11-06 | 423.1 | 423.2 | Top of PVC | 420.5 | 57 | 67 | 363.5 | 353.5 | 67 | 335.8 | 10 | 2 | 38.189045 | -89.873514 |
| MW-377 | UA | 2015-11-02 | 421.4 | 421.5 | Top of PVC | 418.8 | 46 | 56 | 372.8 | 362.8 | 56 | 360.5 | 10 | 2 | 38.188386 | -89.869742 |
| MW-383 | UA | 2015-12-21 | 459.5 | 459.7 | Top of PVC | 457.2 | 58 | 68 | 399.2 | 389.2 | 68 | 384.2 | 10 | 2 | 38.194913 | -89.858286 |
| MW-384 | UA | 2015-12-18 | 458.9 | 459.1 | Top of PVC | 456.7 | 60.5 | 70.5 | 396.2 | 386.2 | 70.5 | 362.6 | 10 | 2 | 38.191789 | -89.860699 |
| MW-390 | UA | 2016-03-04 | 428.1 | 427.8 | Top of PVC | 426.0 | 50 | 65 | 376.0 | 361.0 | 65 | 358.0 | 15 | 2 | 38.192956 | -89.869793 |
| MW-391 | UA | 2016-03-10 | 426.6 | 426.8 | Top of PVC | 424.2 | 55 | 70 | 369.2 | 354.2 | 70 | 349.8 | 15 | 2 | 38.190869 | -89.874759 |

Notes:
All elevation data are presented relative to the North American Vertical Datum 1988 (NAVD88), GEOID 12A
bgs = below ground surface
ft = foot or feet
HSU = Hydrostratigraphic Unit
UA = Uppermost Aquifer
PMP = Potential Migration Pathway
PVC = polyvinyl chloride

Attachment D
Boring Logs

**KELRON
ENVIRONMENTAL
INCORPORATED**

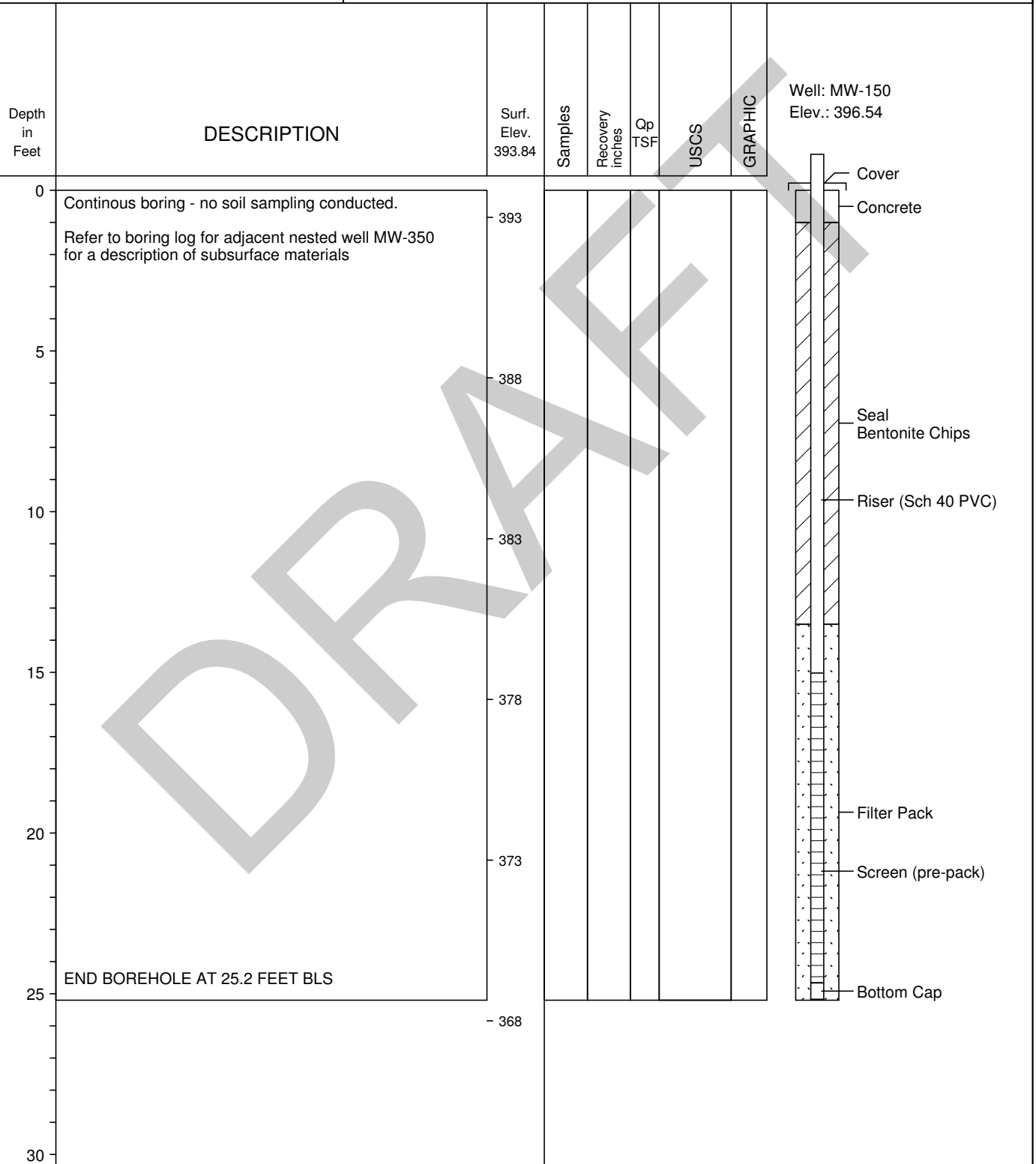
LOG OF BORING MW-150

(Page 1 of 1)

Ash Pond System Monitoring Well Network
Baldwin Energy Complex
Dynegy Midwest Generation, Inc.
Location: Twp 04S, Rng 07W, 16 SE, NW, NE

Date Completed : 09/08/2010
Hole Diameter : 8 1/2"OD; 4 1/4" ID
Drilling Method : Hollow-Stem (CME-550)
Sampling Method : MacroCore (60")
Drilling Company : Terra Drill, Inc.

Driller : Matt Cooper
Geologist : Brendon Wilder (PSC)
Land Surface Elevation: 393.84
Top of Casing Elevation 396.54
X,Y Coordinates : 2379413, 554563



**KELRON
ENVIRONMENTAL
INCORPORATED**

LOG OF BORING MW-350

(Page 1 of 2)

Ash Pond System Monitoring Well Network
Baldwin Energy Complex
Dynegy Midwest Generation, Inc.
Location: Twp 04S, Rng 07W, 16 SE, NW, NE

Date Completed : 09/07/2010
Hole Diameter : 8 1/2" OD / 4 1/4" ID: 3 7/8" rock
Drilling Method : Hollow-Stem/Rotary (CME-550)
Sampling Method : MacroCore (60")/NX Core
Drilling Company : PSC
Driller : Matt Cooper
Geologist : Brendon Wilder (PSC)
Land Surface Elevation: 394.11
Top of Casing Elevation 396.80
X,Y Coordinates : 2379410, 554568

| Depth in Feet | DESCRIPTION | Surf. Elev. 394.11 | Samples | Recovery inches | Qp TSF | USCS | GRAPHIC | |
|---------------------|---|--------------------------|---------|--------------------|-----------|-------|---------|-------------------------------|
| 0 | CLAY, very stiff to hard, brown, grayish-brown (10YR 5/2) mottled yellowish brown (10YR 5/8), dry | 394 | 1 | 19/54 | 4.5 | | | Well: MW-350 Elev.: 396.80 |
| | | | 2 | | 2.25 | | | Cover |
| | | | 3 | | | | | Concrete |
| 5 | - grain size analysis @ 5 - 6 ft: 2.3% sand, 42.4% silt, 55.3% clay | 389 | 4 | 47/60 | 4.5 | CH | | |
| | | | 5 | | 3.5 | | | |
| | | | 6 | | 3.25 | | | |
| | | | 7 | | 4.0 | | | |
| 10 | | 384 | 8 | 60/60 | 2.75 | | | |
| | CLAY, brown to olive brown, moist | | 9 | | 2.75 | | | |
| | - grain size analysis @ 11 - 12 ft: 8.4% sand, 39.3% silt, 52.3% clay | | 10 | | 2.75 | | | |
| | | | 11 | | 1.75 | CL/CH | | Grout Bentonite Slurry |
| | | | 12 | | 2.0 | | | Riser (Sch 40 PVC) |
| 15 | | 379 | | | | | | |
| | CLAY, soft, high plasticity, dark yellow brown, moist; 1-2" sand seams at 17' and 19' | | 13 | 45/60 | | | | |
| | - grain size analysis @ 18 - 20 ft: 1.8% sand, 21.9% silt, 76.3% clay | | | | | | | |
| | - very stiff to hard, high plasticity | | | | | CH | | |
| 20 | | 374 | 14 | 60/60 | | | | |
| | | | 15 | 23/23 | | | | |
| 25 | | | | | | | | |

**KELRON
ENVIRONMENTAL
INCORPORATED**

LOG OF BORING MW-350

(Page 2 of 2)

Ash Pond System Monitoring Well Network
Baldwin Energy Complex
Dynegy Midwest Generation, Inc.
Location: Twp 04S, Rng 07W, 16 SE, NW, NE

Date Completed : 09/07/2010
Hole Diameter : 8 1/2" OD / 4 1/4" ID: 3 7/8" rock
Drilling Method : Hollow-Stem/Rotary (CME-550)
Sampling Method : MacroCore (60")/NX Core
Drilling Company : PSC
Driller : Matt Cooper
Geologist : Brendon Wilder (PSC)
Land Surface Elevation: 394.11
Top of Casing Elevation 396.80
X,Y Coordinates : 2379410, 554568

| Depth in Feet | DESCRIPTION | Surf. Elev. 394.11 | Samples | Recovery inches | Qp TSF | USCS | GRAPHIC | |
|---------------------|---|--------------------------|---------|--------------------|-----------|-------|---------|------------------------|
| 25 | - Auger refusal at 26.4 feet bgs | 369 | 15 | 23/23 | | CL | | Grout Bentonite Slurry |
| | LIMESTONE and SHALE, interbedded, banded, solid, very soft, light to dark gray; slightly weathered | | | | | LS/SH | | |
| | LIMESTONE, banded, medium bedded, solid, hard, medium gray; unweathered | | | | | LS | | |
| 30 | LIMESTONE and SHALE, interbedded; limestone is banded, medium bedded, hard, medium gray; shale is very soft to medium soft, dark gray | 364 | | | | | | |
| | Borehole diameter from 26.4 to 46.7 feet bgs = 3 7/8" | | 16 | 116/120 | | LS/SH | | Seal Bentonite Chips |
| | RQD for 26.4 - 36.4' = 72% (Fair) Recovery = 116/120" | | | | | | | |
| 35 | SHALE, banded, medium bedded, solid, soft to medium soft, dark gray | 359 | | | | SH | | Riser (Sch 40 PVC) |
| 40 | LIMESTONE, banded, massive, solid, hard to very hard, light to medium gray | 354 | 17 | 118/120 | | LS | | Filter Pack |
| 45 | RQD for 36.4 - 46.4' = 96% (Excellent) Recovery = 118/120" | 349 | | | | | | Screen (pre-pack) |
| | END BOREHOLE AT 46.7 FEET BLS | | | | | | | Bottom Cap |
| 50 | | | | | | | | |

**KELRON
ENVIRONMENTAL
INCORPORATED**

LOG OF BORING MW-350

(Page 1 of 2)

Ash Pond System Monitoring Well Network
Baldwin Energy Complex
Dynegy Midwest Generation, Inc.
Location: Twp 04S, Rng 07W, 16 SE, NW, NE

Date Completed : 09/07/2010
Hole Diameter : 8 1/2" OD / 4 1/4" ID: 3 7/8" rock
Drilling Method : Hollow-Stem/Rotary (CME-550)
Sampling Method : MacroCore (60")/NX Core
Drilling Company : PSC
Driller : Matt Cooper
Geologist : Brendon Wilder (PSC)
Land Surface Elevation: 394.11
Top of Casing Elevation 396.80
X,Y Coordinates : 2379410, 554568

| Depth in Feet | DESCRIPTION | Surf. Elev. 394.11 | Samples | Recovery inches | Qp TSF | USCS | GRAPHIC | |
|---------------------|---|--------------------------|---------|--------------------|-----------|-------|---------|-------------------------------|
| 0 | CLAY, very stiff to hard, brown, grayish-brown (10YR 5/2) mottled yellowish brown (10YR 5/8), dry | 394 | 1 | 19/54 | 4.5 | | | Well: MW-350 Elev.: 396.80 |
| | | | 2 | | 2.25 | | | Cover |
| | | | 3 | | | | | Concrete |
| 5 | - grain size analysis @ 5 - 6 ft: 2.3% sand, 42.4% silt, 55.3% clay | 389 | 4 | 47/60 | 4.5 | CH | | |
| | | | 5 | | 3.5 | | | |
| | | | 6 | | 3.25 | | | |
| | | | 7 | | 4.0 | | | |
| 10 | | 384 | 8 | 60/60 | 2.75 | | | |
| | CLAY, brown to olive brown, moist | | 9 | | 2.75 | | | |
| | - grain size analysis @ 11 - 12 ft: 8.4% sand, 39.3% silt, 52.3% clay | | 10 | | 2.75 | | | |
| | | | 11 | | 1.75 | CL/CH | | Grout Bentonite Slurry |
| | | | 12 | | 2.0 | | | Riser (Sch 40 PVC) |
| 15 | | 379 | | | | | | |
| | CLAY, soft, high plasticity, dark yellow brown, moist; 1-2" sand seams at 17' and 19' | | 13 | 45/60 | | | | |
| | - grain size analysis @ 18 - 20 ft: 1.8% sand, 21.9% silt, 76.3% clay | | | | | | | |
| | - very stiff to hard, high plasticity | | | | | | | |
| 20 | | 374 | 14 | 60/60 | | CH | | |
| | | | | | | | | |
| 25 | | | 15 | 23/23 | | | | |

**KELRON
ENVIRONMENTAL
INCORPORATED**

LOG OF BORING MW-350

(Page 2 of 2)

Ash Pond System Monitoring Well Network
Baldwin Energy Complex
Dynegy Midwest Generation, Inc.
Location: Twp 04S, Rng 07W, 16 SE, NW, NE

Date Completed : 09/07/2010
Hole Diameter : 8 1/2"OD / 4 1/4" ID: 3 7/8" rock
Drilling Method : Hollow-Stem/Rotary (CME-550)
Sampling Method : MacroCore (60")/NX Core
Drilling Company : PSC
Driller : Matt Cooper
Geologist : Brendon Wilder (PSC)
Land Surface Elevation: 394.11
Top of Casing Elevation 396.80
X,Y Coordinates : 2379410, 554568

| Depth in Feet | DESCRIPTION | Surf. Elev. 394.11 | Samples | Recovery inches | Qp TSF | USCS | GRAPHIC | |
|---------------------|---|--------------------------|---------|--------------------|-----------|-------|---------|------------------------|
| 25 | - Auger refusal at 26.4 feet bgs | 369 | 15 | 23/23 | | CL | | Grout Bentonite Slurry |
| | LIMESTONE and SHALE, interbedded, banded, solid, very soft, light to dark gray; slightly weathered | | | | | LS/SH | | |
| | LIMESTONE, banded, medium bedded, solid, hard, medium gray; unweathered | | | | | LS | | |
| 30 | LIMESTONE and SHALE, interbedded; limestone is banded, medium bedded, hard, medium gray; shale is very soft to medium soft, dark gray | 364 | | | | | | |
| | Borehole diameter from 26.4 to 46.7 feet bgs = 3 7/8" | | 16 | 116/120 | | LS/SH | | Seal Bentonite Chips |
| | RQD for 26.4 - 36.4' = 72% (Fair) Recovery = 116/120" | | | | | | | |
| 35 | SHALE, banded, medium bedded, solid, soft to medium soft, dark gray | 359 | | | | | | Riser (Sch 40 PVC) |
| | | | | | | SH | | |
| 40 | LIMESTONE, banded, massive, solid, hard to very hard, light to medium gray | 354 | 17 | 118/120 | | LS | | Filter Pack |
| | | | | | | | | |
| 45 | RQD for 36.4 - 46.4' = 96% (Excellent) Recovery = 118/120" | 349 | | | | | | Screen (pre-pack) |
| | END BOREHOLE AT 46.7 FEET BLS | | | | | | | Bottom Cap |
| 50 | | | | | | | | |

**KELRON
ENVIRONMENTAL
INCORPORATED**

LOG OF BORING MW-352

(Page 1 of 3)

Ash Pond System Monitoring Well Network
Baldwin Energy Complex
Dynegy Midwest Generation, Inc.
Location: Twp 04S, Rng 07W, 16 SE, NE, NE

Date Completed : 09/16/2010
Hole Diameter : 8 1/2" OD / 4 1/4" ID: 3 7/8" rock
Drilling Method : Hollow-Stem/Rotary (CME-550)
Sampling Method : MacroCore (60")/NX Core
Drilling Company : PSC
Driller : Matt Cooper
Geologist : Brendon Wilder (PSC)
Land Surface Elevation: 422.36
Top of Casing Elevation 425.04
X,Y Coordinates : 2382789, 553901

| Depth in Feet | DESCRIPTION | Surf. Elev. 422.36 | Samples | Recovery inches | Qp TSF | USCS | GRAPHIC | |
|---------------------|---|--------------------------|---------|--------------------|-----------|------|---------|-------------------------------|
| 0 | SILTY CLAY, very stiff to hard, yellow brown (10YR 5/6), dry | 422 | 1 | 46/48 | 4.5+ | CL | | Well: MW-352 Elev.: 425.04 |
| | | | 2 | 60/60 | 3.5 | | | Cover |
| 5 | CLAY, trace sand and fine gravel, very stiff, high plasticity, few black organic material | 417 | 3 | | 4.0 | | | Concrete |
| | | | 4 | | 2.75 | | | |
| | | | 5 | | 3.0 | | | |
| 10 | - medium hard | 412 | 6 | 60/60 | 2.75 | CL | | |
| | - soft | | 7 | | 2.0 | | | |
| | | | 8 | | 1.0 | | | |
| | | | 9 | | 1.25 | | | Grout Bentonite Slurry |
| 15 | - medium hard | 407 | 10 | 60/60 | 1.5 | | | Riser (Sch 40 PVC) |
| | | | 11 | | 2.5 | | | |
| | SAND, poorly graded, loose, wet (4-inch thick) | | 12 | | 2.75 | SP | | |
| | SANDY CLAY, trace fine gravel, yellow brown to olive brown (2.5Y 5/3) | | 13 | | 3.5 | | | |
| 20 | | 402 | 14 | 60/60 | 4.5+ | CL | | |
| | | | 15 | | 2.5 | | | |
| | | | 16 | | 2.5 | | | |
| | | | 17 | | 2.75 | | | |
| 25 | | | 18 | 48/60 | 2.5 | | | |

**KELRON
ENVIRONMENTAL
INCORPORATED**

LOG OF BORING MW-352

(Page 2 of 3)

Ash Pond System Monitoring Well Network
Baldwin Energy Complex
Dynegy Midwest Generation, Inc.
Location: Twp 04S, Rng 07W, 16 SE, NE, NE

Date Completed : 09/16/2010
Hole Diameter : 8 1/2" OD / 4 1/4" ID: 3 7/8" rock
Drilling Method : Hollow-Stem/Rotary (CME-550)
Sampling Method : MacroCore (60")/NX Core
Drilling Company : PSC
Driller : Matt Cooper
Geologist : Brendon Wilder (PSC)
Land Surface Elevation: 422.36
Top of Casing Elevation 425.04
X,Y Coordinates : 2382789, 553901

| Depth in Feet | DESCRIPTION | Surf. Elev. 422.36 | Samples | Recovery inches | Qp TSF | USCS | GRAPHIC | |
|---------------------|---|--------------------------|---------|--------------------|-----------|-------|---------|---------------------------|
| 25 | - grain size analysis @ 26.5 - 27.5 ft: 33.7% sand, 27.1% silt, 39.2% clay SAND with few gravel, yellow brown CLAY, some sand and fine gravel, hard to very hard, high plasticity, dark yellow brown (10YR 4/6) | 397 | 18 | 48/60 | 2.5 | CL | | |
| | | | | | | SP | | |
| | | | 19 | 60/60 | 3.0 | CL | | |
| 30 | CLAY, lean to fat | 392 | 20 | | 3.0 | | | |
| | - grain size analysis @ 32 - 33 ft: 13.2% sand, 43.9% silt, 42.8% clay | | 21 | | 3.5 | | | |
| | | | 22 | | 3.0 | | | |
| 35 | - medium hard, high plasticity, gray brown to light olive brown (2.5Y 5/2-5/3) - trace silt, dark yellow brown (10YR 4/4) | 387 | 23 | 48/60 | 1.5 | | | |
| | | | 24 | | 1.5 | | | |
| | | | 25 | | 1.75 | | | |
| | | | 26 | | 1.5 | CL/CH | | |
| 40 | | 382 | 27 | 54/60 | 1.75 | | | Grout Bentonite Slurry |
| | | | 28 | | 2.0 | | | |
| | | | 29 | | 2.5 | | | |
| | | | 30 | | 2.5 | | | |
| 45 | CLAY, medium hard, low plasticity, olive brown (2.5Y 5/4) | 377 | 31 | 57/60 | 2.0 | | | Riser (Sch 40 PVC) |
| | | | 32 | | 1.75 | | | |
| | | | 33 | | 1.75 | | | |
| | | | 34 | | 2.5 | | | |
| | | | 35 | | 1.75 | CL | | |
| 50 | | | 36 | 3/3 | | | | |

**KELRON
ENVIRONMENTAL
INCORPORATED**

LOG OF BORING MW-352

(Page 3 of 3)

Ash Pond System Monitoring Well Network
Baldwin Energy Complex
Dynegy Midwest Generation, Inc.
Location: Twp 04S, Rng 07W, 16 SE, NE, NE

Date Completed : 09/16/2010
Hole Diameter : 8 1/2" OD / 4 1/4" ID: 3 7/8" rock
Drilling Method : Hollow-Stem/Rotary (CME-550)
Sampling Method : MacroCore (60")/NX Core
Drilling Company : PSC
Driller : Matt Cooper
Geologist : Brendon Wilder (PSC)
Land Surface Elevation: 422.36
Top of Casing Elevation 425.04
X,Y Coordinates : 2382789, 553901

| Depth in Feet | DESCRIPTION | Surf. Elev. 422.36 | Samples | Recovery inches | Qp TSF | USCS | GRAPHIC | |
|---------------------|---|--------------------------|---------|--------------------|-----------|------|---------|--|
| 50 | | 372 | | | | CL | | |
| | - Auger refusal at 53.7 feet bgs | | | | | | | |
| 55 | LIMESTONE, weathered, thinly laminated, medium hard to hard, gray | 367 | 37 | 5/5 | | LS | | |
| | | | 38 | 8/27 | | | | |
| | SHALE, clayey, gray | | | | | SH | | |
| | LIMESTONE, occasional shale partings | | 39 | 19/60 | | | | |
| 60 | | 362 | | | | LS | | |
| | - laminated, fossiliferous, medium gray | | | | | | | |
| | | | 40 | 54/60 | | | | |
| 65 | SHALE, soft, dark gray | 357 | | | | SH | | |
| | | | | | | | | |
| | LIMESTONE, medium hard to hard, light gray | | 41 | 59/60 | | | | |
| 70 | Borehole diameter from 53.7 to 73.8 feet bgs = 3 7/8" | 352 | | | | LS | | |
| | RQD for 53.8 - 73.8' = 57% (Fair) Recovery = 173/240" | | 42 | 33/34 | | | | |
| | END BOREHOLE AT 73.8 FEET BLS | | | | | | | |
| 75 | | | | | | | | |

Well: MW-352
Elev.: 425.04

Grout
Bentonite Slurry

Riser (Sch 40 PVC)

Seal
Bentonite Chips

Filter Pack

Screen (pre-pack)

Bottom Cap

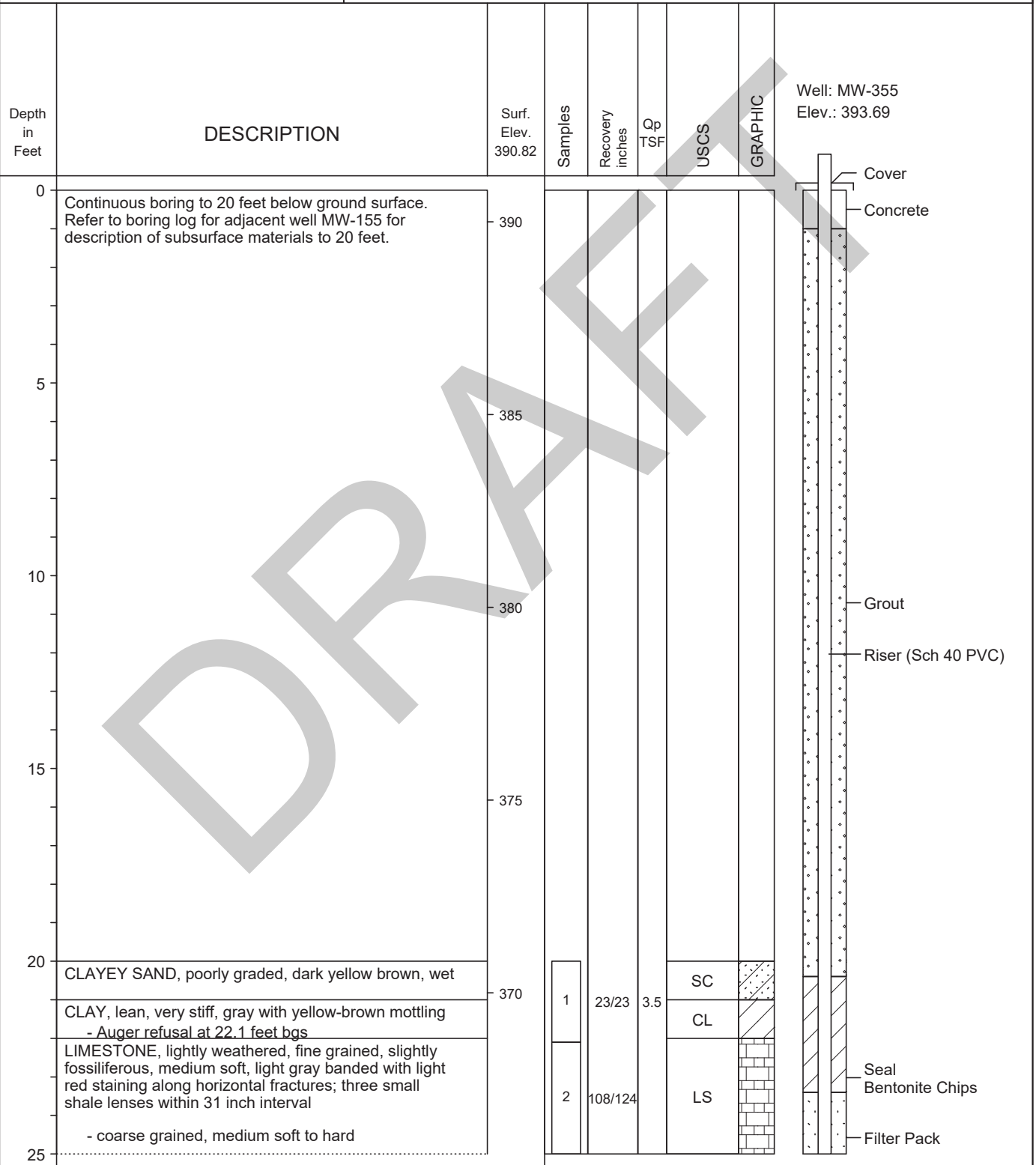
**KELRON
ENVIRONMENTAL
INCORPORATED**

LOG OF BORING MW-355

(Page 1 of 2)

Ash Pond System Monitoring Well Network
Baldwin Energy Complex
Dynegy Midwest Generation, Inc.
Location: Twp 04S, Rng 07W, 09 SW, SE, SW

Date Completed : 09/14/2010
Hole Diameter : 8 1/2" OD / 4 1/4" ID; 3 7/8" rock
Drilling Method : Hollow-Stem/Rotary (CME-550)
Sampling Method : MacroCore (60")/NX Core
Drilling Company : Terra Drill, Inc.
Driller : Matt Cooper
Geologist : Brendon Wilder (PSC)
Land Surface Elevation: 390.82
Top of Casing Elevation 393.69
X,Y Coordinates : 2378145, 555980



| | | | | | |
|--|--|---|--|--|--|
| Facility/Project Name Baldwin Energy Complex | | License/Permit/Monitoring Number | | Boring Number MW-366 | |
| Boring Drilled By: Name of crew chief (first, last) and Firm Jim Dittmaier Bulldog Drilling | | Date Drilling Started 12/3/2015 | | Date Drilling Completed 12/4/2015 | |
| Common Well Name MW-366 | | Final Static Water Level Feet (NAVD88) | | Surface Elevation 422.54 Feet (NAVD88) | |
| | | | | Borehole Diameter 8.3 inches | |
| Local Grid Origin <input type="checkbox"/> (estimated: <input type="checkbox"/>) or Boring Location <input checked="" type="checkbox"/> | | Lat <u>38° 11' 31.8876"</u> | | Local Grid Location | |
| State Plane 555,581.80 N, 2,381,171.15 E <input checked="" type="checkbox"/> E/W | | Long <u>-89° 52' 20.4414"</u> | | <input type="checkbox"/> N <input type="checkbox"/> E <input type="checkbox"/> S <input type="checkbox"/> W | |
| 1/4 of <u> </u> 1/4 of Section <u> </u> , T <u> </u> N, R <u> </u> | | | | Feet <u> </u> Feet <u> </u> | |

| | | | |
|-------------|---------------------------|--------------------------|---|
| Facility ID | County Randolph | State Illinois | Civil Town/City/ or Village Baldwin |
|-------------|---------------------------|--------------------------|---|



| Sample | | Blow Counts | Depth In Feet | Soil/Rock Description And Geologic Origin For Each Major Unit | U S C S | Graphic Log | Well Diagram | Soil Properties | | | | | RQD/ Comments |
|--------------------|---------------------------------|-------------|----------------------------------|---|-----------------|----------------|-----------------|-------------------------------|---------------------|-----------------|---------------------|-------|--|
| Number and Type | Length Att. & Recovered (in) | | | | | | | Compressive Strength (tsf) | Moisture Content | Liquid Limit | Plasticity Index | P 200 | |
| | | | 0 - 5.6' FILL, SILTY CLAY CL/ML. | | (FILL) CL/ML | | | | | | | | 0-33' Blind Drilled. See logs TPZ-166 and B-13-4 for soil description. |
| | | | 5.6 - 33' SILTY CLAY CL/ML. | | CL/ML | | | | | | | | |
| | | | | | | | | | | | | | |
| | | | | | | | | | | | | | |
| | | | | | | | | | | | | | |
| | | | | | | | | | | | | | |
| | | | | | | | | | | | | | |
| | | | | | | | | | | | | | |
| | | | | | | | | | | | | | |
| | | | | | | | | | | | | | |
| | | | | | | | | | | | | | |
| | | | | | | | | | | | | | |
| | | | | | | | | | | | | | |
| | | | | | | | | | | | | | |
| | | | | | | | | | | | | | |
| | | | | | | | | | | | | | |
| | | | | | | | | | | | | | |
| | | | | | | | | | | | | | |
| | | | | | | | | | | | | | |
| | | | | | | | | | | | | | |
| | | | | | | | | | | | | | |
| | | | | | | | | | | | | | |
| | | | | | | | | | | | | | |
| | | | | | | | | | | | | | |
| | | | | | | | | | | | | | |
| | | | | | | | | | | | | | |
| | | | | | | | | | | | | | |
| | | | | | | | | | | | | | |
| | | | | | | | | | | | | | |
| | | | | | | | | | | | | | |
| | | | | | | | | | | | | | |
| | | | | | | | | | | | | | |
| | | | | | | | | | | | | | |
| | | | | | | | | | | | | | |
| | | | | | | | | | | | | | |
| | | | | | | | | | | | | | |
| | | | | | | | | | | | | | |
| | | | | | | | | | | | | | |
| | | | | | | | | | | | | | |
| | | | | | | | | | | | | | |
| | | | | | | | | | | | | | |
| | | | | | | | | | | | | | |
| | | | | | | | | | | | | | |
| | | | | | | | | | | | | | |
| | | | | | | | | | | | | | |
| | | | | | | | | | | | | | |
| | | | | | | | | | | | | | |
| | | | | | | | | | | | | | |
| | | | | | | | | | | | | | |
| | | | | | | | | | | | | | |
| | | | | | | | | | | | | | |
| | | | | | | | | | | | | | |
| | | | | | | | | | | | | | |
| | | | | | | | | | | | | | |
| | | | | | | | | | | | | | |
| | | | | | | | | | | | | | |
| | | | | | | | | | | | | | |
| | | | | | | | | | | | | | |
| | | | | | | | | | | | | | |
| | | | | | | | | | | | | | |
| | | | | | | | | | | | | | |
| | | | | | | | | | | | | | |
| | | | | | | | | | | | | | |
| | | | | | | | | | | | | | |
| | | | | | | | | | | | | | |
| | | | | | | | | | | | | | |
| | | | | | | | | | | | | | |
| | | | | | | | | | | | | | |
| | | | | | | | | | | | | | |
| | | | | | | | | | | | | | |
| | | | | | | | | | | | | | |
| | | | | | | | | | | | | | |
| | | | | | | | | | | | | | |
| | | | | | | | | | | | | | |
| | | | | | | | | | | | | | |
| | | | | | | | | | | | | | |
| | | | | | | | | | | | | | |
| | | | | | | | | | | | | | |
| | | | | | | | | | | | | | |
| | | | | | | | | | | | | | |
| | | | | | | | | | | | | | |
| | | | | | | | | | | | | | |
| | | | | | | | | | | | | | |
| | | | | | | | | | | | | | |
| | | | | | | | | | | | | | |
| | | | | | | | | | | | | | |
| | | | | | | | | | | | | | |
| | | | | | | | | | | | | | |
| | | | | | | | | | | | | | |
| | | | | | | | | | | | | | |
| | | | | | | | | | | | | | |
| | | | | | | | | | | | | | |
| | | | | | | | | | | | | | |

I hereby certify that the information on this form is true and correct to the best of my knowledge.

| | | |
|--|--|--|
| Signature  | Firm Natural Resource Technology 234 W. Florida St., Fifth Floor, Milwaukee, WI 53204 | Tel: (414) 837-3607 Fax: (414) 837-3608 |
|--|--|--|



Page 2 of 4

| Sample | | Blow Counts | Depth In Feet | Soil/Rock Description And Geologic Origin For Each Major Unit | U S C S | Graphic Log | Well Diagram | | Soil Properties | | | | | RQD/ Comments |
|--------------------|---------------------------------|-------------|---------------|---|---------|--|--|--|-------------------------------|---------------------|-----------------|---------------------|-------|------------------|
| Number and Type | Length Att. & Recovered (in) | | | | | | | | Compressive Strength (tsf) | Moisture Content | Liquid Limit | Plasticity Index | P 200 | |
| | | | 13 | 5.6 - 33' SILTY CLAY CL/ML. <i>(continued)</i> | |  |  | | | | | | | |
| | | | 14 | | | | | | | | | | | |
| | | | 15 | | | | | | | | | | | |
| | | | 16 | | | | | | | | | | | |
| | | | 17 | | | | | | | | | | | |
| | | | 18 | | | | | | | | | | | |
| | | | 19 | | | | | | | | | | | |
| | | | 20 | | | | | | | | | | | |
| | | | 21 | | | | | | | | | | | |
| | | | 22 | | | | | | | | | | | |
| | | | 23 | | | | | | | | | | | |
| | | | 24 | | | | | | | | | | | |
| | | | 25 | | | | | | | | | | | |
| | | | 26 | | | | | | | | | | | |
| | | | 27 | | | | | | | | | | | |
| | | | 28 | | | | | | | | | | | |
| | | | 29 | | | | | | | | | | | |
| | | | 30 | | | | | | | | | | | |
| | | | 31 | | | | | | | | | | | |
| | | | 32 | | | | | | | | | | | |





Page 3 of 4

[illegible]




Page 4 of 4

| Sample | | Blow Counts | Depth In Feet | Soil/Rock Description And Geologic Origin For Each Major Unit | U S C S | Graphic Log | Well Diagram | Soil Properties | | | | | | RQD/ Comments | |
|--------------------|---------------------------------|-------------|---------------|---|----------------|--|---|-------------------------------|---------------------|-----------------|---------------------|-------|--|------------------|--|
| Number and Type | Length Att. & Recovered (in) | | | | | | | Compressive Strength (tsf) | Moisture Content | Liquid Limit | Plasticity Index | P 200 | | | |
| | | | 53 | 49.8 - 54.3' SHALEY LIMESTONE: BDX (LS/SH), fossiliferous, slightly fractured. <i>(continued)</i> | BDX (LS/SH) |  |  | | | | | | | | Bedrock corehole reamed 6" in diameter to 54' for well installation. |
| | | | 54 | 52.8' - 53.1 shale bed. 53.1' fossiliferous. | | | | | | | | | | | |
| | | | | 54.3' End of Boring. | | | | | | | | | | | |

| | | | | | |
|--|--|--|--|--|--|
| Facility/Project Name Baldwin Power Plant | | License/Permit/Monitoring Number | | Boring Number MW358 | |
| Boring Drilled By: Name of crew chief (first, last) and Firm Blake Weller Cascade Drilling | | Date Drilling Started 10/5/2022 | | Date Drilling Completed 10/8/2022 | |
| Common Well Name MW358 | | Final Static Water Level Feet (NAVD88) | | Surface Elevation 453.59 Feet (NAVD88) | |
| | | | | Borehole Diameter 6.0 inches | |
| Local Grid Origin <input type="checkbox"/> (estimated: <input type="checkbox"/>) or Boring Location <input checked="" type="checkbox"/> | | Lat <u>38° 11' 42.9882"</u> | | Local Grid Location | |
| State Plane <u>556,726.26 N, 2,387,756.63 E</u> <input checked="" type="checkbox"/> E/W | | Long <u>-89° 50' 57.9018"</u> | | <input type="checkbox"/> N <input type="checkbox"/> E <input type="checkbox"/> S <input type="checkbox"/> W | |
| 1/4 of <u>1/4</u> of Section <u>T</u> , <u>N</u> , <u>R</u> | | Feet | | Feet | |
| Facility ID | | County Randolph | | State IL | |
| | | | | Civil Town/City/ or Village Baldwin | |

| Sample | | Blow Counts | Depth In Feet | Soil/Rock Description And Geologic Origin For Each Major Unit | USCS | Graphic Log | Well Diagram | PID 10.6 eV Lamp | Soil Properties | | | | | RQD/ Comments |
|-----------------|------------------------------|-------------|---|--|---|-------------|--------------|------------------|----------------------------|------------------|--------------|------------------|-------|---|
| Number and Type | Length Att. & Recovered (in) | | | | | | | | Compressive Strength (tsf) | Moisture Content | Liquid Limit | Plasticity Index | P 200 | |
| 1 CS | 180 97 | | 1 2 3 4 5 6 7 8 9 10 11 12 | 0 - 3.8' SILT : ML, very dark grayish brown (10YR 3/2), organic material (0-10%), moist to wet. 2.1' dry. 3.8 - 8.9' CLAYEY SILT : ML/CL, light gray (10YR 7/2), very dark grayish brown (10YR 3/2) and yellowish brown (10YR 5/8) mottling (20-30%), dry. 8.9 - 13' SILTY CLAY WITH SAND : (CL/ML)S, grayish brown (10YR 5/2), strong brown (7.5YR 5/6) and very dark brown (10YR 2/2) mottling (20-30%), organic material (0-10%), low toughness, low to medium plasticity, stiff. | ML ML/CL (CL/ML)S | | | | | | | | | CS= Core Sample Measured Rock Quality Designation (RQD) was modified due to drilling methods, modified RQD equals the sum of recovered core sections greater than 4 inches in length divided by total core recovery. |

I hereby certify that the information on this form is true and correct to the best of my knowledge.

| | | |
|--|---|--|
| Signature  | Firm Ramboll 234 W Florida Street, 5th Floor, Milwaukee, WI 53204 | Tel: (414)837-3607 Fax: (414)837-3608 |
|--|---|--|

Boring Number MW358

Page 2 of 5

| Sample | | Blow Counts | Depth In Feet | Soil/Rock Description And Geologic Origin For Each Major Unit | USCS | Graphic Log | Well Diagram | PID 10.6 eV Lamp | Soil Properties | | | | | RQD/ Comments | |
|-----------------|------------------------------|-------------|---------------|---|----------|-------------|--------------|------------------|----------------------------|------------------|--------------|------------------|-------|------------------|---|
| Number and Type | Length Att. & Recovered (in) | | | | | | | | Compressive Strength (tsf) | Moisture Content | Liquid Limit | Plasticity Index | P 200 | | |
| 2 CS | 60 60 | | 13 | 13 - 17.8' SILTY CLAY : CL/ML, grayish brown (10YR 5/2), strong brown (7.5YR 5/6) and very dark brown (10YR 2/2) mottling (20-30%), low toughness, medium to high plasticity, stiff to very stiff. | (CL/ML)S | | | | | | | | | | |
| | | | 14 | | | | | | | | | | | | |
| 3 CS | 48 36 | | 15 | 16.1' mottling discontinues. | CL/ML | | | | | | | | | | |
| | | | 16 | | | | | | | | | | | | |
| 4 CORE | 36 32 | | 17 | 17.8 - 21' SILTY CLAY WITH SAND : (CL/ML)S, brown (10YR 5/3), strong brown (7.5YR 5/6) and gray (10YR 6/1) mottling (20-30%), gravel (5-15%), no dilatancy, high toughness, low to medium plasticity, hard, moist. | (CL/ML)S | | | | | | | | | | |
| | | | 18 | | | | | | | | | | | | |
| 5 CORE | 36 29 | | 19 | 21 - 26.5' SHALE : BDX (SH), dark gray (GLEY 1 4/N), weathered, thin bedding, moderately fractured. | BDX (SH) | | | | | | | | | | RUN #4: Modified RQD = (21/32) = 66% |
| | | | 20 | | | | | | | | | | | | |
| 6 CORE | 72 60 | | 21 | 24' -25.2' wet. | BDX (SH) | | | | | | | | | | |
| | | | 22 | | | | | | | | | | | | |
| | | | 23 | 26.5 - 27.5' LIMESTONE : BDX (LS), dark gray (5Y 4/1), shaley, fossiliferous, very strong. | BDX (LS) | | | | | | | | | | |
| | | | 24 | | | | | | | | | | | | |
| | | | 25 | 27.5 - 31.3' SHALE : BDX (SH), grayish black (N2), weathered, highly decomposed to residual soil, wet to moist. | BDX (SH) | | | | | | | | | | RUN #5: Modified RQD = (0/29) = 0% |
| | | | 26 | | | | | | | | | | | | |
| | | | 27 | 29.3' thinly bedded, moderately decomposed. | BDX (SH) | | | | | | | | | | |
| | | | 28 | | | | | | | | | | | | |
| | | | 29 | 30' slightly decomposed to competent, moderately fractured. | BDX (SH) | | | | | | | | | | |
| | | | 30 | | | | | | | | | | | | |
| | | | 31 | 31.3 - 32' COAL : COAL, black (N1). | COAL | | | | | | | | | | RUN #6: Modified RQD = (45/60) = 75% |
| | | | 32 | | | | | | | | | | | | |

RUN #4:
Modified
RQD =
(21/32) =
66%

RUN #5:
Modified
RQD =
(0/29) = 0%

RUN #6:
Modified
RQD =
(45/60) =
75%

Page 5 of 5

| Sample | | Blow Counts | Depth In Feet | Soil/Rock Description And Geologic Origin For Each Major Unit | U S C S | Graphic Log | Well Diagram | PID 10.6 eV Lamp | Soil Properties | | | | | RQD/ Comments |
|-----------------|------------------------------|-------------|--|---|----------|-------------|--------------|------------------|----------------------------|------------------|--------------|------------------|--|---|
| Number and Type | Length Att. & Recovered (in) | | | | | | | | Compressive Strength (tsf) | Moisture Content | Liquid Limit | Plasticity Index | P 200 | |
| 15 CORE | 60 56 | | 73 | 64 - 75.3' SHALE: BDX (SH), medium dark gray (N4) to medium gray (N5), strong, thinly bedded to laminated, moderately fractured. <i>(continued)</i> | BDX (SH) | | | | | | | | | RUN #15: Modified RQD = Not Recorded |
| | | | 74 | | | | | | | | | | | |
| | | | 75 | 75.3 - 77.1' LIMESTONE: BDX (LS), gray (5Y 6/1), fossiliferous, very strong. | BDX (LS) | | | | | | | | | |
| | | | 76 | | | | | | | | | | | |
| | | 77 | 77.1 - 78.2' SHALE: BDX (SH), medium dark gray (N4), weathered, weak to moderate strength, moderately decomposed. | BDX (SH) | | | | | | | | | | |
| | | 78 | | | | | | | | | | | | |
| | | | 79 | 78.2 - 84.8' LIMESTONE: BDX (LS), medium dark gray (N4) to medium gray (N5), shaley, fossiliferous, very strong, moderately fractured, laminations (0-5%). | BDX (LS) | | | | | | | | RUN #16: Modified RQD = (23/51) = 45% | |
| 16 CORE | 60 51 | | 80 | | | | | | | | | | | |
| | | | 81 | | | | | | | | | | | |
| | | | 82 | | | | | | | | | | | |
| | | | 83 | 84.8 - 90' SHALE: BDX (SH), dark gray (N3), weathered, weak to moderate strength, moderately decomposed, moderately fractured, thin bedding. | BDX (SH) | | | | | | | | RUN #17: Modified RQD = (28/60) = 47% | |
| 17 CORE | 60 60 | | 84 | | | | | | | | | | | |
| | | | 85 | | | | | | | | | | | |
| | | | 86 | | | | | | | | | | | |
| | | | 87 | 90' End of Boring. | | | | | | | | | | |
| | | 88 | | | | | | | | | | | | |
| | | 89 | | | | | | | | | | | | |
| | | 90 | | | | | | | | | | | | |



SOIL BORING LOG INFORMATION

Page 1 of 5

| | | | | | |
|--|--|---|--|---|--|
| Facility/Project Name Baldwin Energy Complex | | License/Permit/Monitoring Number | | Boring Number MW-391 | |
| Boring Drilled By: Name of crew chief (first, last) and Firm Jim Dittmaier Bulldog Drilling | | Date Drilling Started 3/7/2016 | | Date Drilling Completed 3/10/2016 | |
| Common Well Name MW-391 | | Final Static Water Level Feet (NAVD88) | | Surface Elevation 424.24 Feet (NAVD88) | |
| | | | | Borehole Diameter 8.3 inches | |
| Local Grid Origin <input type="checkbox"/> (estimated: <input type="checkbox"/>) or Boring Location <input checked="" type="checkbox"/> | | Lat 38° 11' 27.1285 " | | Local Grid Location | |
| State Plane 555,100.63 N, 2,380,477.06 E <input checked="" type="checkbox"/> E/W | | Long -89° 52' 29.1339 " | | <input type="checkbox"/> N <input type="checkbox"/> E | |
| 1/4 of T 1/4 of Section N, R | | | | <input type="checkbox"/> S <input type="checkbox"/> W | |

| | | | |
|-------------|---------------------------|--------------------------|---|
| Facility ID | County Randolph | State Illinois | Civil Town/City/ or Village Baldwin |
|-------------|---------------------------|--------------------------|---|

| Sample | | Blow Counts | Depth In Feet | Soil/Rock Description And Geologic Origin For Each Major Unit | USCS | Graphic Log | Well Diagram | Soil Properties | | | | | RQD/ Comments |
|--------------------|---------------------------------|-------------|--|---|------|----------------|-----------------|-------------------------------|---------------------|-----------------|---------------------|-------|------------------|
| Number and Type | Length Att. & Recovered (in) | | | | | | | Compressive Strength (tsf) | Moisture Content | Liquid Limit | Plasticity Index | P 200 | |
| | | | 0 1 2 3 4 5 6 7 8 9 10 11 12 | 0 - 4' SILTY CLAY CL/ML. < | | | | | | | | | |









I hereby certify that the information on this form is true and correct to the best of my knowledge.

| | | |
|---------------|--|--|
| Signature | Firm Natural Resource Technology 234 W. Florida St., Fifth Floor, Milwaukee, WI 53204 | Tel: (414) 837-3607 Fax: (414) 837-3608 |
|---------------|--|--|

Template: ILLINOIS BORING LOG - Project: BALDWIN GINT.GPJ



Page 2 of 5

| Sample | | Blow Counts | Depth In Feet | Soil/Rock Description And Geologic Origin For Each Major Unit | U S C S | Graphic Log | Well Diagram | | Soil Properties | | | | | RQD/ Comments |
|--------------------|---------------------------------|-------------|---------------|---|---------|---|--|--|-------------------------------|---------------------|-----------------|---------------------|-------|------------------|
| Number and Type | Length Att. & Recovered (in) | | | | | | | | Compressive Strength (tsf) | Moisture Content | Liquid Limit | Plasticity Index | P 200 | |
| | | | 13 | 12 - 24' SILTY CLAY CL/ML. | |  |  | | | | | | | |
| | | | 14 | | | | | | | | | | | |
| | | | 15 | | | | | | | | | | | |
| | | | 16 | | | | | | | | | | | |
| | | | 17 | | | | | | | | | | | |
| | | | 18 | | | | | | | | | | | |
| | | | 19 | | | | | | | | | | | |
| | | | 20 | | | | | | | | | | | |
| | | | 21 | 24 - 27.4' LEAN CLAY: CL. | |  |  | | | | | | | |
| | | | 22 | | | | | | | | | | | |
| | | | 23 | | | | | | | | | | | |
| | | | 24 | | | | | | | | | | | |
| | | | 25 | 27.4 - 28.5' SILTY SAND: SM. | |  |  | | | | | | | |
| | | | 26 | | | | | | | | | | | |
| | | | 27 | 28.5 - 32.5' SILTY CLAY CL/ML. | |  |  | | | | | | | |
| | | | 28 | | | | | | | | | | | |
| | | | 29 | | | | | | | | | | | |
| | | | 30 | | | | | | | | | | | |
| | | | 31 | | | | | | | | | | | |
| | | | 32 | | | | | | | | | | | |



Page 3 of 5

[illegible]

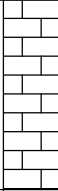



Page 4 of 5

| Sample | | | Blow Counts | Depth In Feet | Soil/Rock Description And Geologic Origin For Each Major Unit | U S C S | Graphic Log | Well Diagram | Soil Properties | | | | | RQD/ Comments | |
|--------------------|---------------------------------|-------------------------------|-------------|---------------|---|----------------|-------------|--------------|---------------------|-----------------|---------------------|-------|--|------------------|--------------------------|
| Number and Type | Length Att. & Recovered (in) | Compressive Strength (tsf) | | | | | | | Moisture Content | Liquid Limit | Plasticity Index | P 200 | | | |
| | | | | 53 | 49.7 - 60' SHALEY LIMESTONE: BDX (LS/SH), light gray, medium to thinly bedded, moderately to highly decomposed, moderately fractured (tight to narrow apertures). <i>(continued)</i> | | | | | | | | | | |
| 5 CS | 60 58.5 | | | 54 | | | | | | | | | | | |
| | | | | 55 | 54.7' light gray, moderately decomposed, moderately fractured, decomposition and fracture density decrease with depth. | | | | | | | | | | Core 5, RQD = 96% |
| | | | | 56 | | BDX (LS/SH) | | | | | | | | | |
| | | | | 57 | | | | | | | | | | | |
| | | | | 58 | | | | | | | | | | | |
| | | | | 59 | | | | | | | | | | | |
| 6 CS | 60 52.5 | | | 60 | 60 - 74.4' LIMESTONE: BDX (LS), white, massive, slightly fractured (extremely narrow to very narrow apertures). | | | | | | | | | | Core 6, RQD =99% |
| | | | | 61 | | | | | | | | | | | |
| | | | | 62 | | | | | | | | | | | |
| | | | | 63 | | | | | | | | | | | |
| | | | | 64 | | | | | | | | | | | |
| 7 CS | 60 63.25 | | | 65 | 64.4' slightly fractured (very narrow aperture). | | | | | | | | | | Core 7, RQD = 100% |
| | | | | 66 | | BDX (LS) | | | | | | | | | |
| | | | | 67 | | | | | | | | | | | |
| | | | | 68 | | | | | | | | | | | |
| | | | | 69 | | | | | | | | | | | |
| 8 CS | 60 55 | | | 70 | 69.8' unfractured. | | | | | | | | | | Core 8, RQD = 100% |
| | | | | 71 | | | | | | | | | | | |
| | | | | 72 | | | | | | | | | | | |

Boring Number **MW-391**


Page 5 of 5

| Sample | | Blow Counts | Depth In Feet | Soil/Rock Description And Geologic Origin For Each Major Unit | U S C S | Graphic Log | Well Diagram | | Soil Properties | | | | | RQD/ Comments |
|--------------------|---------------------------------|-------------|---------------|---|----------|--|---|--|-------------------------------|---------------------|-----------------|---------------------|-------|---|
| Number and Type | Length Att. & Recovered (in) | | | | | | | | Compressive Strength (tsf) | Moisture Content | Liquid Limit | Plasticity Index | P 200 | |
| | | | 73 | 60 - 74.4' LIMESTONE: BDX (LS), white, massive, slightly fractured (extremely narrow to very narrow apertures). <i>(continued)</i> | BDX (LS) |  |  | | | | | | | Bedrock corehole reamed to 6" in diameter to 72' bgs for well installation. |
| | | | 74 | | | | | | | | | | | |
| | | | | 74.4' End of Boring. | | | | | | | | | | |

| | | | | | |
|--|--|--|--|--|--|
| Facility/Project Name Baldwin Power Plant | | License/Permit/Monitoring Number | | Boring Number MW392 | |
| Boring Drilled By: Name of crew chief (first, last) and Firm Blake Weller Cascade Drilling | | Date Drilling Started 9/9/2022 | | Date Drilling Completed 9/26/2022 | |
| Common Well Name MW392 | | Final Static Water Level Feet (NAVD88) | | Surface Elevation 434.07 Feet (NAVD88) | |
| | | | | Borehole Diameter 6.0 inches | |
| Local Grid Origin <input type="checkbox"/> (estimated: <input type="checkbox"/>) or Boring Location <input checked="" type="checkbox"/> | | Lat 38° 11' 57.132" | | Local Grid Location | |
| State Plane 558,140.20 N, 2,382,717.92 E <input checked="" type="checkbox"/> E/W | | Long -89° 52' 0.9632" | | <input type="checkbox"/> N <input type="checkbox"/> E <input type="checkbox"/> S <input type="checkbox"/> W | |
| 1/4 of T N, R | | 1/4 of Section | | Feet Feet | |
| Facility ID | | County Randolph | | State IL | |
| | | | | Civil Town/City/ or Village Baldwin | |

| Sample | | | Blow Counts | Depth In Feet | Soil/Rock Description And Geologic Origin For Each Major Unit | U S C S | Graphic Log | Well Diagram | PID 10.6 eV Lamp | Soil Properties | | | | | | RQD/ Comments |
|--------------------|---------------------------------|-------------------------------|-------------|--|---|---------|----------------|-----------------|------------------|---------------------|-----------------|---------------------|-------|--|--|------------------|
| Number and Type | Length Att. & Recovered (in) | Compressive Strength (tsf) | | | | | | | | Moisture Content | Liquid Limit | Plasticity Index | P 200 | | | |
| 1 CS | 120 46 | | | 0 - 1.2' FILL, WELL-GRADED GRAVEL WITH CLAY: GW-GC, pinkish gray (7.5YR 6/2), angular, moist. | (FILL) GW-GC | | | | | | | | | | CS= Core Sample | |
| | | | | 1.2 - 16' FILL, LEAN CLAY: CL, light brown (7.5YR 6/4), sand (0-5%), no dilatancy, low to medium plasticity, moist. | (FILL) CL | | | | | | | | | | Measured Rock Quality Designation (RQD) was modified due to drilling methods, modified RQD equals the sum of recovered core sections greater than 4 inches in length divided by total core recovery. | |
| 2 CS | 120 62 | | | | | | | | | | | | | | | |

I hereby certify that the information on this form is true and correct to the best of my knowledge.

| | | |
|--|---|--|
| Signature  | Firm Ramboll 234 W Florida Street, 5th Floor, Milwaukee, WI 53204 | Tel: (414)837-3607 Fax: (414)837-3608 |
|--|---|--|

| | | | | | |
|--|--|--|--|--|--|
| Facility/Project Name Baldwin Power Plant | | License/Permit/Monitoring Number | | Boring Number MW393 | |
| Boring Drilled By: Name of crew chief (first, last) and Firm Blake Weller Cascade Drilling | | Date Drilling Started 9/9/2022 | | Date Drilling Completed 10/4/2022 | |
| Common Well Name MW393 | | Final Static Water Level Feet (NAVD88) | | Surface Elevation 434.59 Feet (NAVD88) | |
| | | | | Borehole Diameter 6.0 inches | |
| Local Grid Origin <input type="checkbox"/> (estimated: <input type="checkbox"/>) or Boring Location <input checked="" type="checkbox"/> | | Lat <u>38° 11' 57.027"</u> | | Local Grid Location | |
| State Plane 558,133.57 N, 2,383,944.49 E <input checked="" type="checkbox"/> E/W | | Long <u>-89° 51' 45.5976"</u> | | <input type="checkbox"/> N <input type="checkbox"/> E <input type="checkbox"/> S <input type="checkbox"/> W | |
| 1/4 of <u> </u> 1/4 of Section <u> </u> , T <u> </u> N, R <u> </u> | | Facility ID | | County Randolph | |
| | | State IL | | Civil Town/City/ or Village Baldwin | |

| Sample | | | Blow Counts | Depth In Feet | Soil/Rock Description And Geologic Origin For Each Major Unit | U S C S | Graphic Log | Well Diagram | PID 10.6 eV Lamp | Soil Properties | | | | | RQD/ Comments |
|--------------------|---------------------------------|-------------------------------|-------------|--|---|---------|----------------|-----------------|------------------|---------------------|-----------------|---------------------|-------|--|--|
| Number and Type | Length Att. & Recovered (in) | Compressive Strength (tsf) | | | | | | | | Moisture Content | Liquid Limit | Plasticity Index | P 200 | | |
| 1 CS | 120 86 | | | 0 - 1' FILL, WELL-GRADED GRAVEL: GW, pinkish gray (7.5YR 6/2), angular, moist. | (FILL) GW | | | | | | | | | | CS= Core Sample |
| | | | | 1 - 20' FILL, LEAN CLAY: CL, brown (7.5YR 6/4), sand (0-5%), no dilatancy, low to medium plasticity, moist. | | | | | | | | | | | Measured Rock Quality Designation (RQD) was modified due to drilling methods, modified RQD equals the sum of recovered core sections greater than 4 inches in length divided by total core recovery. |
| | | | | | (FILL) CL | | | | | | | | | | |
| 2 CS | 120 120 | | | 10' sand (0-5%), iron concretions (0-5%). | | | | | | | | | | | |

I hereby certify that the information on this form is true and correct to the best of my knowledge.





| | | |
|--|---|--|
| Signature  | Firm Ramboll 234 W Florida Street, 5th Floor, Milwaukee, WI 53204 | Tel: (414)837-3607 Fax: (414)837-3608 |
|--|---|--|

Boring Number MW393

Page 4 of 5

| Sample | | Blow Counts | Depth In Feet | Soil/Rock Description And Geologic Origin For Each Major Unit | USCS | Graphic Log | Well Diagram | PID 10.6 eV Lamp | Soil Properties | | | | | RQD/ Comments |
|-----------------|------------------------------|-------------|---|---|------|-------------|--------------|------------------|----------------------------|------------------|--------------|--|-------|--|
| Number and Type | Length Att. & Recovered (in) | | | | | | | | Compressive Strength (tsf) | Moisture Content | Liquid Limit | Plasticity Index | P 200 | |
| 7 CORE | 120 60 | | 53 | 50 - 55' SILT: ML, dark gray (7.5YR 4/1), sand (0-5%), very stiff to hard, dry. <i>(continued)</i> | ML | | | | | | | | | RUN #7: Modified RQD = (31/60) = 52% |
| | | 54 | | | | | | | | | | | | |
| | | 55 | 55 - 57' CLAYEY SILT: ML/CL, gray (10YR 6/1), sand (0-5%), gravel (0-5%), medium plasticity, moist. | ML/CL | | | | | | | | | | |
| | | 56 | | | | | | | | | | | | |
| | | 57 | 57 - 60' LIMESTONE: BDX (LS), gray (10YR 6/1), rock flour and angular chips (<2"). | BDX (LS) | | | | | | | | | | |
| | | 58 | | | | | | | | | | | | |
| | | 59 | | | | | | | | | | | | |
| | | 60 | 60 - 70' SHALE: BDX (SH), medium gray (N5), weathered, very weak, residual soil, soft, slightly fractured. | BDX (SH) | | | | | | | | | | |
| | | 61 | | | | | | | | | | | | |
| | | 62 | | | | | | | | | | | | |
| 63 | | | | | | | | | | | | | | |
| 64 | | | | | | | | | | | | | | |
| 65 | | | | | | | | | | | | | | |
| 66 | | | | | | | | | | | | | | |
| 67 | | | | | | | | | | | | | | |
| 68 | | | | | | | | | | | | | | |
| 69 | | | | | | | | | | | | | | |
| 8 CORE | 42 40 | 70 | 70 - 73.5' LIMESTONE: BDX (LS), medium dark gray (N4), weathered, shaley, thinly bedded, moderately fractured. | BDX (LS) | | | | | | | | RUN #8: Modified RQD = (32/40) = 80% | | |
| | | 71 | | | | | | | | | | | | |
| | | 72 | | | | | | | | | | | | |

| | | | | | |
|--|--|---|--|--|--|
| Facility/Project Name Baldwin Power Plant | | License/Permit/Monitoring Number | | Boring Number MW394 | |
| Boring Drilled By: Name of crew chief (first, last) and Firm Blake Weller Cascade Drilling | | Date Drilling Started 9/25/2022 | | Date Drilling Completed 10/5/2022 | |
| Common Well Name MW394 | | Final Static Water Level Feet (NAVD88) | | Surface Elevation 435.51 Feet (NAVD88) | |
| | | | | Borehole Diameter 6.0 inches | |
| Local Grid Origin <input type="checkbox"/> (estimated: <input type="checkbox"/>) or Boring Location <input checked="" type="checkbox"/> | | Lat <u>38° 11' 56.8911"</u> | | Local Grid Location | |
| State Plane 558,123.63 N, 2,385,095.76 E <input checked="" type="checkbox"/> E/W | | Long <u>-89° 51' 31.1756"</u> | | <input type="checkbox"/> N <input type="checkbox"/> E <input type="checkbox"/> S <input type="checkbox"/> W | |
| 1/4 of <u> </u> 1/4 of Section <u> </u> , T <u> </u> N, R <u> </u> | | Facility ID | | County Randolph | |
| | | State IL | | Civil Town/City/ or Village Baldwin | |

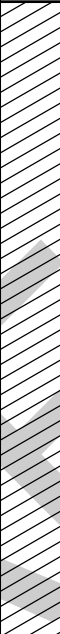






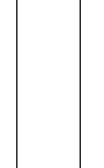
| Sample | | Blow Counts | Depth In Feet | Soil/Rock Description And Geologic Origin For Each Major Unit | U S C S | Graphic Log | Well Diagram | PID 10.6 eV Lamp | Soil Properties | | | | | | RQD/ Comments |
|--------------------|---------------------------------|-------------|---------------|---|-----------------|--|---|------------------|-------------------------------|---------------------|-----------------|---------------------|-------|--|------------------|
| Number and Type | Length Att. & Recovered (in) | | | | | | | | Compressive Strength (tsf) | Moisture Content | Liquid Limit | Plasticity Index | P 200 | | |
| 1 CS | 72 67 | | 1 | 0 - 2.6' FILL, WELL-GRADED GRAVEL WITH CLAY: GW-GC, brown (10YR 4/3), angular, moist. | (FILL) GW-GC |  |  | | | | | | | CS= Core Sample | |
| | | | 2 | | | | | | | | | | | Measured Rock Quality Designation (RQD) was modified due to drilling methods, modified RQD equals the sum of recovered core sections greater than 4 inches in length divided by total core recovery. | |
| | | | 3 | 2.6 - 20' LEAN CLAY: CL, brown (10YR 5/3), reddish brown bottling (20%), sand (0-5%), low to medium plasticity, very stiff to hard, moist. | |  |  | | 4 | | | | | | |
| | | | 4 | | | | | | | | | | | | |
| | | | 5 | | | | | | 4 | | | | | | |
| | | | 6 | | | | | | | | | | | | |
| 2 CS | 120 120 | | 7 | | CL | | | | 2.5 | | | | | | |
| | | | 8 | | | | | | 3.5 | | | | | | |
| | | | 9 | | | | | | 2 | | | | | | |
| | | | 10 | 9.2' brown (7.5YR 5/3), medium to high plasticity. | | | | | 2 | | | | | | |
| | | | 11 | | | | | | 3 | | | | | | |
| | | | 12 | | | | | | 2.25 | | | | | | |

I hereby certify that the information on this form is true and correct to the best of my knowledge.

| | | |
|---|---|--|
| Signature  | Firm Ramboll 234 W Florida Street, 5th Floor, Milwaukee, WI 53204 | Tel: (414)837-3607 Fax: (414)837-3608 |
|---|---|--|




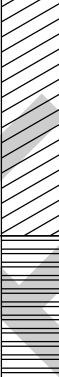


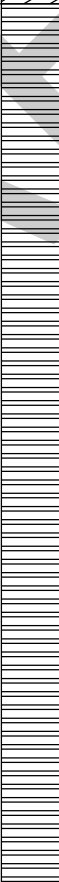


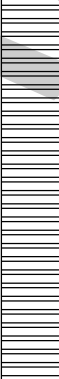








Boring Number MW394

Page 2 of 5

| Sample | | Blow Counts | Depth In Feet | Soil/Rock Description And Geologic Origin For Each Major Unit | USCS | Graphic Log | Well Diagram | PID 10.6 eV Lamp | Soil Properties | | | | | RQD/ Comments |
|-----------------|------------------------------|-------------|---|---|------|--|---|---|----------------------------|---|--------------|------------------|-------|------------------|
| Number and Type | Length Att. & Recovered (in) | | | | | | | | Compressive Strength (tsf) | Moisture Content | Liquid Limit | Plasticity Index | P 200 | |
| 3 CS | 120 120 | | 13 | 2.6 - 20' LEAN CLAY: CL, brown (10YR 5/3), reddish brown bottling (20%), sand (0-5%), low to medium plasticity, very stiff to hard, moist. (continued) | CL |  |  |  | 2.25 |  | | | | |
| | | 14 | 14' low to medium plasticity. | 2.5 | | | | | | | | | | |
| | | 15 | | | | | | | | | | | | |
| | | 16 | | | | | | | | | | | | |
| | | 17 | 16.5' increasing sand and gravel content, gray (GLEYS 1 5/1) iron concretions (50%). | | | | | | | | | | | |
| | | 18 | | | | | | | | | | | | |
| | | 19 | | | | | | | | | | | | |
| | | 20 | | | | | | | | | | | | |
| | | 21 | | | | | | | | | | | | |
| | | 22 | | | | | | | | | | | | |
| 4 CS | 120 112 | | 20 | 20 - 22.1' SILTY SAND: SM, yellowish brown (10YR 5/6), fine sand, clay (0-5%), moist. | SM |  |  |  | |  | | | | |
| | | 21 | | | | | | | | | | | | |
| | | 22 | | | | | | | | | | | | |
| | | 23 | 22.1 - 36.8' LEAN CLAY: CL, dark yellowish brown (10YR 4/4), greenish gray (GLEYS 1 5/10Y) and yellowish brown (10YR 5/6) mottling, sand (0-5%), medium to high plasticity, hard, moist. | 4.5 | | | | | | | | | | |
| | | 24 | 4.5 | | | | | | | | | | | |
| | | 25 | | | | | | | | | | | | |
| | | 26 | 4.5 | | | | | | | | | | | |
| | | 27 | 4.5 | | | | | | | | | | | |
| | | 28 | 4.5 | | | | | | | | | | | |
| | | 29 | 4.5 | | | | | | | | | | | |
| | | 30 | 4.5 | | | | | | | | | | | |
| | | 31 | 4.5 | | | | | | | | | | | |
| 32 | 4.5 | | | | | | | | | | | | | |

Boring Number MW394

Page 3 of 5

| Sample | | Blow Counts | Depth In Feet | Soil/Rock Description And Geologic Origin For Each Major Unit | USCS | Graphic Log | Well Diagram | PID 10.6 eV Lamp | Soil Properties | | | | | RQD/ Comments | | |
|-----------------|------------------------------|-------------|--|---|--|---|---|--|---|--|---|---|-------|------------------|--|--|
| Number and Type | Length Att. & Recovered (in) | | | | | | | | Compressive Strength (tsf) | Moisture Content | Liquid Limit | Plasticity Index | P 200 | | | |
| 5 CS | 120 113 | | 33 | 22.1 - 36.8' LEAN CLAY: CL, dark yellowish brown (10YR 4/4), greenish gray (GLE Y 1 5/10Y) and yellowish brown (10YR 5/6) mottling, sand (0-5%), medium to high plasticity, hard, moist. (continued) | CL |  |  |  | 3.75 | | | | | | | |
| | | 4.25 | | | | | | | | | | | | | | |
| | | 4.5 | | | | | | | | | | | | | | |
| | | | | 34 | 34.4' olive yellow (5Y 6/6), low to medium plasticity. | CL |  |  |  | | | | | | | |
| | | 35 | | | | | | | | | | | | | | |
| 36 | | | | | | | | | | | | | | | | |
| 6 CS | 96 96 | | 37 | 36.8 - 48' Weathered SHALE Bedrock: BDX (SH), pale olive (5Y 6/3), weathered, argillaceous, fissile, moist. | BDX (SH) |  |  |  | | | | | | | | |
| | | 38 | | | | | | | | | | | | | | |
| | | 39 | | | | | | | | | | | | | | |
| | | 40 | 40' olive gray (5Y 5/2). | | | | | | BDX (SH) |  |  |  | | | | |
| | | 41 | | | | | | | | | | | | | | |
| | | 42 | | | | | | | | | | | | | | |
| | | 43 | | | | | | | | | | | | | | |
| | | 44 | | | | | | | | | | | | | | |
| | | 45 | | | | | | | | | | | | | | |
| | | 46 | | | | | | | | | | | | | | |
| | | 47 | | | | | | | | | | | | | | |
| | | 48 | 48 - 58' LIMESTONE: to SHALE: BDX (LS), olive gray (5Y 4/2), interbedded limestone and shale, fissile. | BDX (LS) |  |  |  | | | | | | | | | |
| | | 49 | | | | | | | | | | | | | | |
| | | 50 | | | | | | 50' - 50.2' limestone, very strong. | BDX (LS) |  |  |  | | | | |
| | | 51 | | | | | | | | | | | | | | |
| | | 52 | | | | | | | | | | | | | | |

Attachment E
Site Solids Bulk Characterization & Total Metals
Analytical Data

**SGS Canada Inc.**

P.O. Box 4300 - 185 Concession St.
Lakefield - Ontario - K0L 2H0
Phone: 705-652-2000 FAX: 705-652-6365

Trace Metals - Strong Acid Digest, ICP-MS

Project : PO# GLP8064

26-September-2023

Geosyntec Consultant

Attn : Allison Kreinberg/Brian Aces

2100 Commonwealth Boulevard, Suit 100
Ann Arbor, Michigan
48108, USA

Date Rec. : 31 July 2023
LR Report: CA19071-JUL23
Reference: Baldwin - PO# GLP8064

Copy: #1

Phone: 734-794-1545
Fax:

CERTIFICATE OF ANALYSIS

Final Report

| Analysis | 1: Analysis Start Date | 2: Analysis Start Time | 3: Analysis Completed Date | 4: Analysis Completed Time | 5: BAL-1-15-20-20230 620 | 6: BAL-1-20-25-20230 620 | 7: BAL-1-35-40-20230 620 |
|--------------------|------------------------------|------------------------------|-------------------------------------|-------------------------------------|--------------------------------|--------------------------------|--------------------------------|
| Sample Date & Time | | | | | 20-Jun-23 11:00 | 20-Jun-23 11:15 | 20-Jun-23 12:30 |
| Ag [µg/g] | 23-Sep-23 | 02:32 | 25-Sep-23 | 17:30 | < 0.5 | < 0.5 | < 0.5 |
| Al [µg/g] | 23-Sep-23 | 02:32 | 25-Sep-23 | 17:30 | 42000 | 66000 | 56000 |
| As [µg/g] | 23-Sep-23 | 02:32 | 25-Sep-23 | 17:30 | 4.3 | 11 | 6.1 |
| Ba [µg/g] | 23-Sep-23 | 02:32 | 25-Sep-23 | 17:30 | 500 | 560 | 150 |
| Be [µg/g] | 23-Sep-23 | 02:32 | 25-Sep-23 | 17:30 | 1.1 | 1.9 | 1.6 |
| Bi [µg/g] | 23-Sep-23 | 02:32 | 25-Sep-23 | 17:30 | 0.13 | 0.23 | 0.15 |
| Ca [µg/g] | 23-Sep-23 | 02:32 | 25-Sep-23 | 17:30 | 32000 | 57000 | 120000 |
| Cd [µg/g] | 23-Sep-23 | 02:32 | 25-Sep-23 | 17:30 | 0.23 | 0.30 | 0.34 |
| Co [µg/g] | 23-Sep-23 | 02:32 | 25-Sep-23 | 17:30 | 7.7 | 13 | 8.6 |
| Cr [µg/g] | 23-Sep-23 | 02:32 | 25-Sep-23 | 17:30 | 47 | 74 | 70 |
| Cu [µg/g] | 23-Sep-23 | 02:32 | 25-Sep-23 | 17:30 | 11 | 25 | 8.9 |
| Fe [µg/g] | 23-Sep-23 | 02:32 | 25-Sep-23 | 17:30 | 19000 | 38000 | 22000 |
| K [µg/g] | 23-Sep-23 | 02:32 | 25-Sep-23 | 17:30 | 17000 | 22000 | 13000 |
| Li [µg/g] | 23-Sep-23 | 02:32 | 25-Sep-23 | 17:30 | 19 | 44 | 31 |
| Mg [µg/g] | 23-Sep-23 | 02:32 | 25-Sep-23 | 17:30 | 15000 | 21000 | 22000 |
| Mn [µg/g] | 23-Sep-23 | 02:32 | 25-Sep-23 | 17:30 | 770 | 830 | 190 |
| Mo [µg/g] | 23-Sep-23 | 02:32 | 25-Sep-23 | 17:30 | 1.2 | 1.7 | 0.8 |
| Ni [µg/g] | 23-Sep-23 | 02:32 | 25-Sep-23 | 17:30 | 20 | 38 | 32 |
| Pb [µg/g] | 23-Sep-23 | 02:32 | 25-Sep-23 | 17:30 | 13 | 17 | 10 |
| Sb [µg/g] | 23-Sep-23 | 02:32 | 25-Sep-23 | 17:30 | < 0.8 | < 0.8 | < 0.8 |
| Se [µg/g] | 23-Sep-23 | 02:32 | 25-Sep-23 | 17:30 | 0.2 | 0.6 | 0.9 |
| Sn [µg/g] | 23-Sep-23 | 02:32 | 25-Sep-23 | 17:30 | < 6 | 6.5 | 6.9 |
| Sr [µg/g] | 23-Sep-23 | 02:32 | 25-Sep-23 | 17:30 | 150 | 170 | 390 |
| Ti [µg/g] | 23-Sep-23 | 02:32 | 25-Sep-23 | 17:30 | 1900 | 3000 | 2300 |
| Tl [µg/g] | 23-Sep-23 | 02:32 | 25-Sep-23 | 17:30 | 0.42 | 0.61 | 0.39 |
| U [µg/g] | 23-Sep-23 | 02:32 | 25-Sep-23 | 17:30 | 1.7 | 2.5 | 3.2 |
| V [µg/g] | 23-Sep-23 | 02:32 | 25-Sep-23 | 17:30 | 57 | 110 | 70 |
| Y [µg/g] | 23-Sep-23 | 02:32 | 25-Sep-23 | 17:30 | 13 | 20 | 14 |
| Zn [µg/g] | 23-Sep-23 | 02:32 | 25-Sep-23 | 17:30 | 43 | 87 | 74 |

SGS Canada Inc.

P.O. Box 4300 - 185 Concession St.
Lakefield - Ontario - KOL 2H0
Phone: 705-652-2000 FAX: 705-652-6365

Project : PO# GLP8064

LR Report : CA19071-JUL23

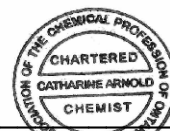
| Analysis | 8: BAL-1-42-46-20230 620 | 9: BAL-1-42-46-2-2023 0620 | 10: BAL-2-50-60-20230 621 | 11: BAL-2-60-70-20230 621 | 12: BAL-3-40-52-20230 621 | 13: BAL-4-50-51-20230 622 |
|--------------------|--------------------------------|----------------------------------|---------------------------------|---------------------------------|---------------------------------|---------------------------------|
| Sample Date & Time | 20-Jun-23 13:00 | 20-Jun-23 13:30 | 21-Jun-23 09:00 | 21-Jun-23 09:30 | 21-Jun-23 14:00 | 21-Jun-23 16:40 |
| Ag [µg/g] | < 0.5 | < 0.5 | < 0.5 | < 0.5 | < 0.5 | < 0.5 |
| Al [µg/g] | 5900 | 5900 | 36000 | 16000 | 81000 | 61000 |
| As [µg/g] | 1.9 | 1.6 | 5.3 | 7.5 | 4.9 | 8.8 |
| Ba [µg/g] | 59 | 46 | 73 | 45 | 180 | 160 |
| Be [µg/g] | 0.24 | 0.25 | 1.0 | 0.48 | 2.3 | 2.1 |
| Bi [µg/g] | < 0.09 | < 0.09 | 0.10 | < 0.09 | 0.26 | 0.20 |
| Ca [µg/g] | 320000 | 340000 | 190000 | 220000 | 95000 | 92000 |
| Cd [µg/g] | 0.32 | 0.38 | 0.13 | 0.88 | 0.60 | 0.14 |
| Co [µg/g] | 1.3 | 1.3 | 4.2 | 2.5 | 6.2 | 9.9 |
| Cr [µg/g] | 13 | 14 | 46 | 42 | 110 | 78 |
| Cu [µg/g] | 2.9 | 2.2 | 4.2 | 3.9 | 10 | 13 |
| Fe [µg/g] | 5500 | 5300 | 16000 | 11000 | 23000 | 23000 |
| K [µg/g] | 2100 | 1900 | 7900 | 3900 | 21000 | 18000 |
| Li [µg/g] | 4.8 | 4.7 | 14 | 16 | 37 | 16 |
| Mg [µg/g] | 4600 | 4600 | 16000 | 24000 | 12000 | 10000 |
| Mn [µg/g] | 270 | 270 | 330 | 200 | 220 | 370 |
| Mo [µg/g] | 0.6 | 0.5 | 0.5 | 2.2 | 0.7 | 0.5 |
| Ni [µg/g] | 4.9 | 4.7 | 17 | 16 | 26 | 36 |
| Pb [µg/g] | 3 | 3 | 6 | 5 | 17 | 20 |
| Sb [µg/g] | < 0.8 | < 0.8 | < 0.8 | < 0.8 | < 0.8 | < 0.8 |
| Se [µg/g] | 0.2 | 0.2 | 0.4 | 0.8 | 2.7 | 1.6 |
| Sn [µg/g] | < 6 | < 6 | 6.2 | < 6 | 7.5 | 6.8 |
| Sr [µg/g] | 470 | 510 | 360 | 460 | 320 | 230 |
| Ti [µg/g] | 310 | 310 | 1400 | 760 | 3500 | 2500 |
| Tl [µg/g] | 0.06 | 0.06 | 0.21 | 0.19 | 0.50 | 0.44 |
| U [µg/g] | 1.1 | 1.0 | 1.9 | 2.4 | 3.7 | 2.9 |
| V [µg/g] | 14 | 14 | 45 | 29 | 150 | 68 |
| Y [µg/g] | 8.8 | 8.7 | 8.9 | 9.3 | 19 | 32 |
| Zn [µg/g] | 36 | 42 | 30 | 83 | 68 | 49 |

| Analysis | 14: BAL-4-51-55-20230 622 | 15: BAL-4-55-72-20230 622 |
|--------------------|---------------------------------|---------------------------------|
| Sample Date & Time | 22-Jun-23 08:40 | 22-Jun-23 10:10 |
| Ag [µg/g] | < 0.5 | < 0.5 |
| Al [µg/g] | 21000 | 4800 |
| As [µg/g] | 4.0 | 3.2 |
| Ba [µg/g] | 64 | 19 |
| Be [µg/g] | 0.63 | 0.24 |
| Bi [µg/g] | < 0.09 | < 0.09 |
| Ca [µg/g] | 260000 | 340000 |
| Cd [µg/g] | 0.21 | 0.68 |
| Co [µg/g] | 4.6 | 1.6 |

| Analysis | 14: | 15: |
|-----------|-------------------|-------------------|
| | BAL-4-51-55-20230 | BAL-4-55-72-20230 |
| | 622 | 622 |
| Cr [µg/g] | 30 | 11 |
| Cu [µg/g] | 3.6 | 1.7 |
| Fe [µg/g] | 12000 | 5600 |
| K [µg/g] | 4700 | 1200 |
| Li [µg/g] | 7.4 | 3.6 |
| Mg [µg/g] | 5700 | 4500 |
| Mn [µg/g] | 1200 | 590 |
| Mo [µg/g] | 0.3 | 1.0 |
| Ni [µg/g] | 19 | 8.0 |
| Pb [µg/g] | 7 | 4 |
| Sb [µg/g] | < 0.8 | < 0.8 |
| Se [µg/g] | 0.3 | 0.5 |
| Sn [µg/g] | < 6 | < 6 |
| Sr [µg/g] | 410 | 530 |
| Ti [µg/g] | 910 | 210 |
| Tl [µg/g] | 0.13 | 0.04 |
| U [µg/g] | 1.2 | 2.1 |
| V [µg/g] | 28 | 9.4 |
| Y [µg/g] | 11 | 7.6 |
| Zn [µg/g] | 34 | 87 |

Catharine Arnold

Catharine Arnold, B.Sc., C.Chem
Project Specialist,
Environment, Health & Safety



SGS Canada Inc.

P.O. Box 4300 - 185 Concession St.
Lakefield - Ontario - K0L 2H0
Phone: 705-652-2000 FAX: 705-652-6365

28-February-2023

Ramboll Americas Engineering Solutions, Inc.

Attn : Evvan Plank

P.O# Box 4873
Syracuse, New York
13221-7873, USA

Phone: 315-463-7554
Fax:

Date Rec. : 24 November 2022
LR Report: CA19224-NOV22
Reference: Baldwon Power Plant Drilling

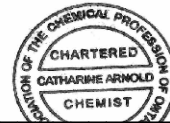
Copy: #1

CERTIFICATE OF ANALYSIS

Final Report

| Analysis | 1: Analysis Start Date | 2: Analysis Start Time Completed | 3: Analysis DateCompleted | 4: Analysis Time | 6: MW-358 (47-49) | 7: MW-358 (86-88) | 8: MW-392 (80-82) | 12: MW-392 (66-68) |
|--------------------|------------------------------|--|---------------------------------|------------------------|----------------------|----------------------|----------------------|-----------------------|
| Sample Date & Time | | | | | 06-Oct-22 15:00 | 08-Oct-22 18:00 | 26-Sep-22 16:00 | 26-Sep-22 12:00 |
| Hg MS [ug/g] | 09-Dec-22 | 16:29 | 12-Dec-22 | 15:05 | < 0.05 | < 0.05 | < 0.05 | < 0.05 |
| As [ug/g] | 09-Dec-22 | 16:29 | 12-Dec-22 | 15:05 | 2.1 | 11 | 17 | 1.0 |
| B [ug/g] | 09-Dec-22 | 16:29 | 12-Dec-22 | 15:05 | 11 | 16 | 16 | 13 |
| Ba [ug/g] | 09-Dec-22 | 16:29 | 12-Dec-22 | 15:05 | 140 | 45 | 40 | 21 |
| Be [ug/g] | 09-Dec-22 | 16:29 | 12-Dec-22 | 15:05 | 0.85 | 0.67 | 0.85 | 0.70 |
| Cd [ug/g] | 09-Dec-22 | 16:29 | 12-Dec-22 | 15:05 | < 0.02 | < 0.02 | 0.36 | 0.09 |
| Co [ug/g] | 09-Dec-22 | 16:29 | 12-Dec-22 | 15:05 | 4.4 | 23 | 12 | 6.2 |
| Cr [ug/g] | 09-Dec-22 | 16:29 | 12-Dec-22 | 15:05 | 9.5 | 12 | 17 | 16 |
| Li [ug/g] | 09-Dec-22 | 16:29 | 12-Dec-22 | 15:05 | 6 | 20 | 8 | 15 |
| Mo [ug/g] | 09-Dec-22 | 16:29 | 12-Dec-22 | 15:05 | 0.3 | 0.3 | 0.3 | 0.3 |
| Pb [ug/g] | 09-Dec-22 | 16:29 | 12-Dec-22 | 15:05 | 5.7 | 9.6 | 17 | 4.9 |
| Se [ug/g] | 09-Dec-22 | 16:29 | 12-Dec-22 | 15:05 | < 0.7 | < 0.7 | 1.4 | < 0.7 |
| Tl [ug/g] | 09-Dec-22 | 16:29 | 12-Dec-22 | 15:05 | 0.05 | 0.06 | 0.04 | 0.03 |

Catharine Arnold, B.Sc., C.Chem
Project Specialist,
Environment, Health & Safety



SGS Canada Inc.

P.O. Box 4300 - 185 Concession St.

Lakefield - Ontario - K0L 2H0

Phone: 705-652-2000 FAX: 705-652-6365

LR Report : CA19224-NOV22

DRAFT

SGS Canada Inc.

P.O. Box 4300 - 185 Concession St.
Lakefield - Ontario - K0L 2H0
Phone: 705-652-2000 FAX: 705-652-6365

28-February-2023

Ramboll Americas Engineering Solutions, Inc.

Attn : Evvan Plank

P.O# Box 4873
Syracuse, New York
13221-7873, USA

Phone: 315-463-7554
Fax:

Date Rec. : 24 November 2022
LR Report: CA19226-NOV22
Reference: Baldwin Power Plant Drilling

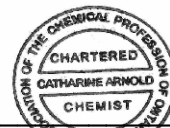
Copy: #1

CERTIFICATE OF ANALYSIS

Final Report

| Analysis | 1: Analysis Start Date | 2: Analysis Start Time Completed | 3: Analysis DateCompleted | 4: Analysis Time | 6: MW-358 (47-49) | 7: MW-358 (86-88) | 8: MW-392 (80-82) | 12: MW-392 (66-68) |
|-------------------------------------|------------------------------|--|---------------------------------|------------------------|----------------------|----------------------|----------------------|-----------------------|
| Sample Date & Time | | | | | 06-Oct-22 15:00 | 08-Oct-22 18:00 | 26-Sep-22 16:00 | 26-Sep-22 12:00 |
| Cl [$\mu\text{g/g}$] | 15-Dec-22 | 20:55 | --- | --- | 22 | 70 | 34 | 45 |
| SO ₄ [$\mu\text{g/g}$] | 15-Dec-22 | 20:55 | 29-Dec-22 | 13:45 | 50 | 620 | 280 | 100 |
| F [%] | 08-Dec-22 | 18:18 | 12-Dec-22 | 08:47 | 0.091 | 0.091 | 0.42 | 0.095 |
| TKN [as N %] | 30-Nov-22 | 09:28 | 02-Dec-22 | 11:00 | 0.06 | 0.05 | < 0.01 | 0.05 |
| Ra226 [Bq/g] | 12-Dec-22 | 08:48 | 12-Dec-22 | 14:33 | 0.07 | < 0.01 | 0.09 | < 0.01 |

Catharine Arnold
Catharine Arnold, B.Sc., C.Chem
Project Specialist,
Environment, Health & Safety





SGS Canada Inc.

P.O. Box 4300 - 185 Concession St.

Lakefield - Ontario - KOL 2H0

Phone: 705-652-2000 FAX: 705-652-6365

LR Report : CA19226-NOV22

DRAFT

Attachment F
X-Ray Fluorescence Analytical Data



ANALYSIS REPORT BBM23-31379

To F400101 SGS CANADA INC
LISA THOMPSON
185 Concession Street
Lakefield K0L 2H0
ON
CANADA

| | | | |
|-------------------|-------------------------|------------------|---------------------------|
| Order Number | PO# | Date Received | 23-Aug-2023 |
| Submission Number | CA19072-JUL23 / 11 Pulp | Date Analysed | 30-Aug-2023 - 06-Sep-2023 |
| Number of Samples | 11 | Date Completed | 09-Sep-2023 |
| | | SGS Order Number | BBM23-31379 |

Methods Summary

| Number of Sample | Method Code | Description |
|------------------|-------------|---|
| 11 | G_PHY01V | Loss on ignition (LOI), Furnace, variable wt, variable temp |
| 11 | GO_XRF72 | Borate Fusion, XRF, Ore Grade |

Comments

Preparation of samples was performed at the SGS Lakefield site.

Analysis of samples was performed at the SGS Burnaby site.

Authorised Signatory


John Chiang
Laboratory Operations Manager



This document is issued by the Company under its General Conditions of Service accessible at <https://www.sgs.com/en/Terms-and-Conditions.aspx>. Attention is drawn to the limitation of liability, indemnification and jurisdiction issues defined therein. Any holder of this document is advised that information contained hereon reflects the Company's findings at the time of its intervention only and within the limits of Client's instructions, if any. The Company's sole responsibility is to its Client and this document does not exonerate parties to a transaction from exercising all their rights and obligations under the transaction documents. Any unauthorized alteration, forgery or falsification of the content or appearance of this document is unlawful and offenders may be prosecuted to the fullest extent of the law.

WARNING: The sample(s) to which the findings recorded herein (the "Findings") relate was(were) drawn and / or provided by the Client or by a third party acting at the Client's direction. The Findings constitute no warranty of the sample's representativeness of any goods and strictly relate to the sample(s). The Company accepts no liability with regard to the origin or source from which the sample(s) is/are said to be extracted. The findings report on the samples provided by the client and are not intended for commercial or contractual settlement purposes.

- not analysed | -- element not determined | I.S. insufficient sample | L.N.R. listed not received

13-Sep-2023 11:22PM BBM_U0046912617

Page 1 of 4

MIN-M_COA_ROW-Last Modified Date: 05-Nov-2019



Order Number
Submission Number
Number of Samples

PO#
CA19072-JUL23 / 11 Pulp
11

ANALYSIS REPORT BBM23-31379

| Element Method Lower Limit Upper Limit Unit | LOI G_PHY01V -10 100 % | @Al2O3 GO_XRF72 0.01 100 % | @CaO GO_XRF72 0.01 60 % | @Cr2O3 GO_XRF72 0.01 5 % | @Fe2O3 GO_XRF72 0.01 100 % | @K2O GO_XRF72 0.01 70 % |
|---|------------------------------------|--|-------------------------------------|--------------------------------------|--|-------------------------------------|
| BAL-1-15-20-20230620 | 8.44916 | 8.09 | 4.75 | 0.01 | 2.75 | 2.01 |
| BAL-1-20-25-20230620 | 15.4785 | 11.67 | 7.90 | 0.01 | 5.03 | 2.47 |
| BAL-1-35-40-20230620 | 24.1700 | 10.58 | 17.23 | <0.01 | 3.18 | 1.52 |
| BAL-1-42-46-20230620 | 37.0600 | 1.20 | 45.90 | <0.01 | 0.77 | 0.24 |
| BAL-1-42-46-2-20230620 | 37.3963 | 1.15 | 46.26 | <0.01 | 0.70 | 0.22 |
| BAL-2-50-60-20230621 | 30.7069 | 7.21 | 29.29 | <0.01 | 2.30 | 0.99 |
| BAL-2-60-70-20230621 | 31.5237 | 3.37 | 32.08 | <0.01 | 1.57 | 0.49 |
| BAL-3-40-52-20230621 | 19.8000 | 14.89 | 13.30 | 0.01 | 3.17 | 2.35 |
| BAL-4-50-51-20230622 | 20.3420 | 12.44 | 14.05 | 0.01 | 3.44 | 2.29 |
| BAL-4-51-44-20230622 | 33.2034 | 4.29 | 37.45 | <0.01 | 1.70 | 0.60 |
| BAL-4-55-72-20230622 | 40.5259 | 1.02 | 49.44 | <0.01 | 0.83 | 0.16 |
| *Std OREAS 70b | 6.78796 | - | - | - | - | - |
| *Rep BAL-4-50-51-20230622 | 19.8760 | - | - | - | - | - |
| *Std OREAS 70b | - | 7.12 | 4.28 | 0.18 | 7.95 | 0.71 |
| *Rep BAL-4-50-51-20230622 | - | 12.50 | 14.14 | <0.01 | 3.46 | 2.30 |
| *Blk BLANK | - | <0.01 | <0.01 | <0.01 | <0.01 | <0.01 |
| *Std OREAS 751 | - | 15.87 | 1.04 | <0.01 | 2.40 | 2.89 |

| Element Method Lower Limit Upper Limit Unit | @MgO GO_XRF72 0.01 100 % | Mn3O4 GO_XRF72 0.01 100 % | @Na2O GO_XRF72 0.01 60 % | @P2O5 GO_XRF72 0.01 55 % | @SiO2 GO_XRF72 0.01 100 % | @TiO2 GO_XRF72 0.01 100 % |
|---|--------------------------------------|---------------------------------------|--------------------------------------|--------------------------------------|---------------------------------------|---------------------------------------|
| BAL-1-15-20-20230620 | 2.53 | 0.12 | 1.09 | 0.10 | 69.69 | 0.46 |
| BAL-1-20-25-20230620 | 3.41 | 0.11 | 0.73 | 0.13 | 52.27 | 0.57 |

- not analysed | -- element not determined | I.S. insufficient sample | L.N.R. listed not received



Order Number
Submission Number
Number of Samples

PO#
CA19072-JUL23 / 11 Pulp
11

ANALYSIS REPORT BBM23-31379

| Element Method Lower Limit Upper Limit Unit | @MgO GO_XRF72 0.01 100 % | Mn3O4 GO_XRF72 0.01 100 % | @Na2O GO_XRF72 0.01 60 % | @P2O5 GO_XRF72 0.01 55 % | @SiO2 GO_XRF72 0.01 100 % | @TiO2 GO_XRF72 0.01 100 % |
|---|--------------------------------------|---------------------------------------|--------------------------------------|--------------------------------------|---------------------------------------|---------------------------------------|
| BAL-1-35-40-20230620 | 3.80 | 0.02 | 0.19 | 0.10 | 37.06 | 0.42 |
| BAL-1-42-46-20230620 | 0.80 | 0.03 | 0.12 | 0.06 | 13.62 | 0.05 |
| BAL-1-42-46-2-20230620 | 0.77 | 0.03 | 0.09 | 0.05 | 13.06 | 0.05 |
| BAL-2-50-60-20230621 | 2.91 | 0.05 | 0.15 | 0.05 | 26.00 | 0.26 |
| BAL-2-60-70-20230621 | 4.21 | 0.03 | 0.20 | 0.09 | 25.84 | 0.14 |
| BAL-3-40-52-20230621 | 2.01 | 0.03 | 0.68 | 0.22 | 41.40 | 0.58 |
| BAL-4-50-51-20230622 | 1.84 | 0.06 | 0.19 | 0.52 | 44.24 | 0.54 |
| BAL-4-51-44-20230622 | 1.05 | 0.18 | 0.07 | 0.11 | 21.26 | 0.17 |
| BAL-4-55-72-20230622 | 0.80 | 0.09 | 0.04 | 0.12 | 6.70 | 0.04 |
| *Std OREAS 70b | 22.38 | 0.16 | 1.04 | 0.05 | 48.48 | 0.30 |
| *Rep BAL-4-50-51-20230622 | 1.85 | 0.05 | 0.19 | 0.48 | 44.33 | 0.53 |
| *Blk BLANK | <0.01 | <0.01 | 0.01 | <0.01 | <0.01 | <0.01 |
| *Std OREAS 751 | 0.50 | 0.10 | 3.40 | 0.27 | 71.34 | 0.24 |

| Element Method Lower Limit Upper Limit Unit | @V2O5 GO_XRF72 0.01 10 % | Sum GO_XRF72 0.01 100 % |
|---|--------------------------------------|-------------------------------------|
| BAL-1-15-20-20230620 | 0.01 | 91.71 |
| BAL-1-20-25-20230620 | 0.02 | 84.43 |
| BAL-1-35-40-20230620 | 0.01 | 75.12 |
| BAL-1-42-46-20230620 | <0.01 | 63.09 |
| BAL-1-42-46-2-20230620 | <0.01 | 62.68 |

- not analysed | -- element not determined | I.S. insufficient sample | L.N.R. listed not received



Order Number PO#
Submission Number CA19072-JUL23 / 11 Pulp
Number of Samples 11

ANALYSIS REPORT BBM23-31379

| Element Method | @V2O5 GO_XRF72 | Sum GO_XRF72 |
|-------------------------------|-------------------|-----------------|
| Lower Limit | 0.01 | 0.01 |
| Upper Limit | 10 | 100 |
| Unit | % | % |
| BAL-2-50-60- 20230621 | <0.01 | 69.93 |
| BAL-2-60-70- 20230621 | <0.01 | 69.01 |
| BAL-3-40-52- 20230621 | 0.03 | 79.23 |
| BAL-4-50-51- 20230622 | 0.02 | 79.70 |
| BAL-4-51-44- 20230622 | <0.01 | 67.05 |
| BAL-4-55-72- 20230622 | <0.01 | 59.71 |
| *Std OREAS 70b | 0.01 | 93.40 |
| *Rep BAL-4-50-51- 20230622 | 0.01 | 79.95 |
| *Blk BLANK | <0.01 | 0.03 |
| *Std OREAS 751 | <0.01 | 98.27 |

SGS Canada Minerals Burnaby conforms to the requirements of ISO/IEC17025 for specific tests as listed on their scope of accreditation found at <https://www.scc.ca/en/search/laboratories/sgs>
Tests and Elements marked with an "@" symbol in the report denote ISO/IEC17025 accreditation.

- not analysed | -- element not determined | I.S. insufficient sample | L.N.R. listed not received

**SGS Canada Inc.**

P.O. Box 4300 - 185 Concession St.
 Lakefield - Ontario - K0L 2H0
 Phone: 705-652-2000 FAX: 705-652-6365

28-February-2023

Ramboll Americas Engineering Solutions, Inc.

Attn : Evvan Plank

P.O# Box 4873
 Syracuse, New York
 13221-7873, USA

Phone: 315-463-7554
 Fax:

Date Rec. : 24 November 2022
LR Report: CA19227-NOV22
Reference: Baldwin Power Plant Drilling

Copy: #1

CERTIFICATE OF ANALYSIS

Final Report

| Analysis | 1: Analysis Start Date | 2: Analysis Start Time | 3: Analysis Completed Date | 4: Analysis Completed Time | 5: MW-358 (13-15) | 6: MW-358 (47-49) | 7: MW-358 (86-88) |
|------------------------------------|------------------------------|------------------------------|----------------------------------|----------------------------------|----------------------|----------------------|----------------------|
| Sample Date & Time | | | | | 05-Oct-22 14:05 | 06-Oct-22 15:00 | 08-Oct-22 18:00 |
| SiO ₂ [%] | 06-Dec-22 | 16:18 | 12-Dec-22 | 09:35 | 75.2 | 58.3 | 59.6 |
| Al ₂ O ₃ [%] | 06-Dec-22 | 16:18 | 12-Dec-22 | 09:35 | 10.6 | 17.2 | 19.2 |
| Fe ₂ O ₃ [%] | 06-Dec-22 | 16:18 | 12-Dec-22 | 09:35 | 3.72 | 7.01 | 4.34 |
| MgO [%] | 06-Dec-22 | 16:18 | 12-Dec-22 | 09:35 | 0.67 | 1.99 | 1.90 |
| CaO [%] | 06-Dec-22 | 16:18 | 12-Dec-22 | 09:35 | 0.73 | 0.57 | 0.50 |
| Na ₂ O [%] | 06-Dec-22 | 16:18 | 12-Dec-22 | 09:35 | 1.04 | 0.83 | 0.77 |
| K ₂ O [%] | 06-Dec-22 | 16:18 | 12-Dec-22 | 09:35 | 1.87 | 3.38 | 2.79 |
| TiO ₂ [%] | 06-Dec-22 | 16:18 | 12-Dec-22 | 09:35 | 0.73 | 0.72 | 0.82 |
| P ₂ O ₅ [%] | 06-Dec-22 | 16:18 | 12-Dec-22 | 09:35 | 0.08 | 0.10 | 0.10 |
| MnO [%] | 06-Dec-22 | 16:18 | 12-Dec-22 | 09:35 | 0.07 | < 0.01 | < 0.01 |
| Cr ₂ O ₃ [%] | 06-Dec-22 | 16:18 | 12-Dec-22 | 09:35 | < 0.01 | 0.01 | 0.01 |
| V ₂ O ₅ [%] | 06-Dec-22 | 16:18 | 12-Dec-22 | 09:35 | 0.02 | 0.02 | 0.02 |
| LOI [%] | 06-Dec-22 | 16:18 | 12-Dec-22 | 09:35 | 5.47 | 9.79 | 9.74 |
| Sum [%] | 06-Dec-22 | 16:18 | 12-Dec-22 | 09:35 | 100.3 | 99.9 | 99.8 |

| Analysis | 8: MW-392 (80-82) | 9: MW-392 (32-33.5) | 10: MW-393 (24-25.5) | 11: MW-394 (20.5-22) | 12: MW-392 (66-68) |
|------------------------------------|----------------------|------------------------|-------------------------|-------------------------|-----------------------|
| Sample Date & Time | 26-Sep-22 16:00 | 27-Sep-22 09:00 | 04-Oct-22 16:00 | 25-Sep-22 16:00 | 26-Sep-22 12:00 |
| SiO ₂ [%] | 33.6 | 72.3 | 79.7 | 73.0 | 50.7 |
| Al ₂ O ₃ [%] | 8.17 | 10.7 | 8.70 | 11.0 | 15.3 |
| Fe ₂ O ₃ [%] | 2.76 | 4.54 | 3.27 | 4.46 | 7.66 |
| MgO [%] | 1.58 | 1.20 | 0.55 | 0.85 | 2.46 |
| CaO [%] | 25.4 | 1.35 | 0.55 | 0.92 | 6.38 |
| Na ₂ O [%] | 0.40 | 0.87 | 0.94 | 1.27 | 0.29 |
| K ₂ O [%] | 1.02 | 2.00 | 2.16 | 2.14 | 2.87 |
| TiO ₂ [%] | 0.29 | 0.67 | 0.50 | 0.75 | 0.58 |
| P ₂ O ₅ [%] | 3.84 | 0.10 | 0.08 | 0.17 | 0.08 |

SGS Canada Inc.

P.O. Box 4300 - 185 Concession St.
Lakefield - Ontario - KOL 2H0
Phone: 705-652-2000 FAX: 705-652-6365

LR Report : CA19227-NOV22

| Analysis | 8: MW-392 (80-82) | 9: MW-392 (32-33.5) | 10: MW-393 (24-25.5) | 11: MW-394 (20.5-22) | 12: MW-392 (66-68) |
|-----------|----------------------|------------------------|-------------------------|-------------------------|-----------------------|
| MnO [%] | 0.04 | 0.11 | 0.09 | 0.09 | 0.03 |
| Cr2O3 [%] | < 0.01 | < 0.01 | < 0.01 | < 0.01 | < 0.01 |
| V2O5 [%] | 0.02 | 0.01 | < 0.01 | 0.01 | 0.02 |
| LOI [%] | 21.6 | 6.15 | 3.82 | 5.09 | 13.8 |
| Sum [%] | 98.8 | 100.0 | 100.3 | 99.8 | 100.1 |

Catharine Arnold
Catharine Arnold, B.Sc., C.Chem
Project Specialist,
Environment, Health & Safety



DRAFT



SGS Canada Inc.

P.O. Box 4300 - 185 Concession St.

Lakefield - Ontario - KOL 2H0

Phone: 705-652-2000 FAX: 705-652-6365

LR Report : CA19227-NOV22

DRAFT

Attachment G
Sequential Extraction Procedure Analytical Data

**SGS Canada Inc.**

P.O. Box 4300 - 185 Concession St.
Lakefield - Ontario - KOL 2H0
Phone: 705-652-2000 FAX: 705-652-6365

28-February-2023

Ramboll Americas Engineering Solutions, Inc.

Attn : Evvan Plank

P.O# Box 4873
Syracuse, New York
13221-7873, USA

Phone: 315-463-7554
Fax:

Date Rec. : 24 November 2022
LR Report: CA19218-NOV22
Reference: Baldwin Power Plant Drilling

Copy: #1

CERTIFICATE OF ANALYSIS

Final Report

| Analysis | 1: Analysis Start Date | 2: Analysis Start Time Completed | 3: Analysis DateCompleted | 4: Analysis Time | 5: MW-358 (13-15) | 6: MW-358 (47-49) | 7: MW-358 (86-88) | 8: MW-392 (80-82) |
|--------------------|------------------------------|--|---------------------------------|------------------------|----------------------|----------------------|----------------------|----------------------|
| Sample Date & Time | | | | | 05-Oct-22 14:05 | 06-Oct-22 15:00 | 08-Oct-22 18:00 | 26-Sep-22 16:00 |
| Ag [µg/g] | 19-Jan-23 | 23:42 | 31-Jan-23 | 09:43 | < 0.05 | < 0.05 | < 0.05 | < 0.05 |
| Al [µg/g] | 19-Jan-23 | 23:42 | 31-Jan-23 | 09:43 | 30 | 540 | 380 | 18 |
| As [µg/g] | 19-Jan-23 | 23:42 | 31-Jan-23 | 09:43 | < 0.5 | < 0.5 | < 0.5 | < 0.5 |
| Ba [µg/g] | 19-Jan-23 | 23:42 | 31-Jan-23 | 09:43 | 0.4 | 11 | 4.2 | < 0.1 |
| Be [µg/g] | 19-Jan-23 | 23:42 | 31-Jan-23 | 09:43 | < 0.02 | 0.06 | 0.05 | < 0.02 |
| B [µg/g] | 19-Jan-23 | 23:42 | 31-Jan-23 | 09:43 | < 1 | 8 | 10 | 3 |
| Bi [µg/g] | 19-Jan-23 | 23:42 | 31-Jan-23 | 09:43 | < 0.09 | < 0.09 | < 0.09 | < 0.09 |
| Ca [µg/g] | 19-Jan-23 | 23:42 | 31-Jan-23 | 09:43 | 21 | 300 | 140 | 75 |
| Cd [µg/g] | 19-Jan-23 | 23:42 | 31-Jan-23 | 09:43 | < 0.05 | < 0.05 | < 0.05 | < 0.05 |
| Co [µg/g] | 19-Jan-23 | 23:42 | 31-Jan-23 | 09:43 | < 0.01 | 0.04 | 0.86 | 0.02 |
| Cr [µg/g] | 19-Jan-23 | 23:42 | 31-Jan-23 | 09:43 | < 0.5 | < 0.5 | < 0.5 | < 0.5 |
| Cu [µg/g] | 19-Jan-23 | 23:42 | 31-Jan-23 | 09:43 | < 0.1 | < 0.1 | 0.1 | < 0.1 |
| Fe [µg/g] | 19-Jan-23 | 23:42 | 31-Jan-23 | 09:43 | 17 | 240 | 190 | < 1 |
| K [µg/g] | 19-Jan-23 | 23:42 | 31-Jan-23 | 09:43 | 7 | 250 | 190 | 41 |
| Li [µg/g] | 19-Jan-23 | 23:42 | 31-Jan-23 | 09:43 | < 2 | < 2 | < 2 | < 2 |
| Mg [µg/g] | 19-Jan-23 | 23:42 | 31-Jan-23 | 09:43 | 9 | 210 | 150 | 19 |
| Mn [µg/g] | 19-Jan-23 | 23:42 | 31-Jan-23 | 09:43 | < 0.5 | 0.6 | 0.9 | < 0.5 |
| Mo [µg/g] | 19-Jan-23 | 23:42 | 31-Jan-23 | 09:43 | < 0.1 | < 0.1 | < 0.1 | < 0.1 |
| Na [µg/g] | 19-Jan-23 | 23:42 | 31-Jan-23 | 09:43 | 65 | 1800 | 1600 | 850 |
| Ni [µg/g] | 19-Jan-23 | 23:42 | 31-Jan-23 | 09:43 | < 0.5 | < 0.5 | 1.2 | < 0.5 |
| P [µg/g] | 19-Jan-23 | 23:42 | 31-Jan-23 | 09:43 | < 3 | 6 | < 3 | < 3 |
| Pb [µg/g] | 19-Jan-23 | 23:42 | 31-Jan-23 | 09:43 | < 0.1 | < 0.1 | 0.2 | < 0.1 |
| Si [µg/g] | 19-Jan-23 | 23:42 | 31-Jan-23 | 09:43 | 100 | 950 | 750 | 59 |
| Sb [µg/g] | 19-Jan-23 | 23:42 | 31-Jan-23 | 09:43 | < 0.8 | < 0.8 | < 0.8 | < 0.8 |
| Se [µg/g] | 19-Jan-23 | 23:42 | 31-Jan-23 | 09:43 | < 0.7 | < 0.7 | < 0.7 | < 0.7 |
| Sr [µg/g] | 19-Jan-23 | 23:42 | 31-Jan-23 | 09:43 | 0.1 | 13 | 5.9 | 1.4 |
| Sn [µg/g] | 19-Jan-23 | 23:42 | 31-Jan-23 | 09:43 | < 0.5 | < 0.5 | < 0.5 | < 0.5 |
| Ti [µg/g] | 19-Jan-23 | 23:42 | 31-Jan-23 | 09:43 | 1.1 | 0.6 | 0.5 | 0.6 |
| Tl [µg/g] | 19-Jan-23 | 23:42 | 31-Jan-23 | 09:43 | < 0.02 | < 0.02 | < 0.02 | < 0.02 |
| U [µg/g] | 19-Jan-23 | 23:42 | 31-Jan-23 | 09:43 | < 0.002 | 0.006 | 0.029 | < 0.002 |
| V [µg/g] | 19-Jan-23 | 23:42 | 31-Jan-23 | 09:43 | < 3 | < 3 | < 3 | < 3 |
| Zn [µg/g] | 19-Jan-23 | 23:42 | 31-Jan-23 | 09:43 | < 0.7 | < 0.7 | < 0.7 | < 0.7 |

SGS Canada Inc.

P.O. Box 4300 - 185 Concession St.

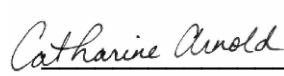
Lakefield - Ontario - K0L 2H0

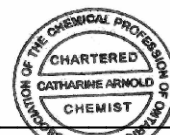
Phone: 705-652-2000 FAX: 705-652-6365

LR Report : CA19218-NOV22

| Analysis | 9: MW-392 (32-33.5) | 10: MW-393 (24-25.5) | 11: MW-394 (20.5-22) | 12: MW-392 (66-68) |
|--------------------|------------------------|-------------------------|-------------------------|-----------------------|
| Sample Date & Time | 27-Sep-22 09:00 | 04-Oct-22 16:00 | 25-Sep-22 16:00 | 26-Sep-22 12:00 |
| Ag [µg/g] | < 0.05 | < 0.05 | < 0.05 | < 0.05 |
| Al [µg/g] | 33 | 26 | 24 | 59 |
| As [µg/g] | < 0.5 | < 0.5 | < 0.5 | < 0.5 |
| Ba [µg/g] | 0.5 | 0.3 | 0.3 | 0.3 |
| Be [µg/g] | < 0.02 | < 0.02 | < 0.02 | < 0.02 |
| B [µg/g] | < 1 | < 1 | < 1 | 5 |
| Bi [µg/g] | < 0.09 | < 0.09 | < 0.09 | < 0.09 |
| Ca [µg/g] | 130 | 28 | 25 | 89 |
| Cd [µg/g] | < 0.05 | < 0.05 | < 0.05 | < 0.05 |
| Co [µg/g] | 0.02 | < 0.01 | 0.01 | 0.02 |
| Cr [µg/g] | < 0.5 | < 0.5 | < 0.5 | < 0.5 |
| Cu [µg/g] | < 0.1 | < 0.1 | < 0.1 | < 0.1 |
| Fe [µg/g] | 27 | 14 | 20 | 28 |
| K [µg/g] | 16 | 9 | 12 | 92 |
| Li [µg/g] | < 2 | < 2 | < 2 | < 2 |
| Mg [µg/g] | 40 | 12 | 12 | 44 |
| Mn [µg/g] | 1.4 | 0.7 | 0.6 | < 0.5 |
| Mo [µg/g] | < 0.1 | < 0.1 | < 0.1 | < 0.1 |
| Na [µg/g] | 44 | 49 | 43 | 720 |
| Ni [µg/g] | < 0.5 | < 0.5 | < 0.5 | < 0.5 |
| P [µg/g] | < 3 | < 3 | < 3 | < 3 |
| Pb [µg/g] | < 0.1 | < 0.1 | < 0.1 | < 0.1 |
| Si [µg/g] | 100 | 80 | 91 | 140 |
| Sb [µg/g] | < 0.8 | < 0.8 | < 0.8 | < 0.8 |
| Se [µg/g] | < 0.7 | < 0.7 | < 0.7 | < 0.7 |
| Sr [µg/g] | 0.3 | < 0.1 | < 0.1 | 1.8 |
| Sn [µg/g] | < 0.5 | < 0.5 | < 0.5 | < 0.5 |
| Ti [µg/g] | 0.6 | 0.6 | 0.9 | 0.5 |
| Tl [µg/g] | < 0.02 | < 0.02 | < 0.02 | < 0.02 |
| U [µg/g] | < 0.002 | < 0.002 | < 0.002 | < 0.002 |
| V [µg/g] | < 3 | < 3 | < 3 | < 3 |
| Zn [µg/g] | < 0.7 | < 0.7 | < 0.7 | < 0.7 |

Water Soluble Fraction


Catharine Arnold, B.Sc., C.Chem
Project Specialist,
Environment, Health & Safety



**SGS Canada Inc.**

P.O. Box 4300 - 185 Concession St.
Lakefield - Ontario - K0L 2H0
Phone: 705-652-2000 FAX: 705-652-6365

Tessier Leach Fraction 2 - Exchangeable Metals

28-February-2023

Ramboll Americas Engineering Solutions, Inc.

Attn : Evvan Plank

P.O# Box 4873
Syracuse, New York
13221-7873, USA

Phone: 315-463-7554
Fax:

Date Rec. : 24 November 2022
LR Report: CA19219-NOV22
Reference: Baldwin Power Plant Drilling

Copy: #1

CERTIFICATE OF ANALYSIS

Final Report

| Analysis | 1: Analysis Start Date | 2: Analysis Start Time Completed | 3: Analysis DateCompleted | 4: Analysis Time | 5: MW-358 (13-15) | 6: MW-358 (47-49) | 7: MW-358 (86-88) | 8: MW-392 (80-82) |
|--------------------|------------------------------|--|---------------------------------|------------------------|----------------------|----------------------|----------------------|----------------------|
| Sample Date & Time | | | | | 05-Oct-22 14:05 | 06-Oct-22 15:00 | 08-Oct-22 18:00 | 26-Sep-22 16:00 |
| Ag [µg/g] | 19-Jan-23 | 23:42 | 31-Jan-23 | 09:43 | < 0.05 | < 0.05 | < 0.05 | < 0.05 |
| Al [µg/g] | 19-Jan-23 | 23:42 | 31-Jan-23 | 09:43 | 9 | 17 | 8 | 9 |
| As [µg/g] | 19-Jan-23 | 23:42 | 31-Jan-23 | 09:43 | < 0.5 | < 0.5 | < 0.5 | < 0.5 |
| Ba [µg/g] | 19-Jan-23 | 23:42 | 31-Jan-23 | 09:43 | 48 | 55 | 15 | 3.0 |
| Be [µg/g] | 19-Jan-23 | 23:42 | 31-Jan-23 | 09:43 | < 0.02 | < 0.02 | < 0.02 | < 0.02 |
| B [µg/g] | 19-Jan-23 | 23:42 | 31-Jan-23 | 09:43 | < 1 | < 1 | 1 | < 1 |
| Bi [µg/g] | 19-Jan-23 | 23:42 | 31-Jan-23 | 09:43 | < 0.09 | < 0.09 | < 0.09 | < 0.09 |
| Ca [µg/g] | 19-Jan-23 | 23:42 | 31-Jan-23 | 09:43 | 2000 | 2500 | 1300 | 3500 |
| Cd [µg/g] | 19-Jan-23 | 23:42 | 31-Jan-23 | 09:43 | < 0.05 | < 0.05 | < 0.05 | < 0.05 |
| Co [µg/g] | 19-Jan-23 | 23:42 | 31-Jan-23 | 09:43 | < 0.01 | < 0.01 | 0.58 | 0.24 |
| Cr [µg/g] | 19-Jan-23 | 23:42 | 31-Jan-23 | 09:43 | < 0.5 | < 0.5 | < 0.5 | < 0.5 |
| Cu [µg/g] | 19-Jan-23 | 23:42 | 31-Jan-23 | 09:43 | < 0.1 | < 0.1 | < 0.1 | < 0.1 |
| Fe [µg/g] | 19-Jan-23 | 23:42 | 31-Jan-23 | 09:43 | 2 | 21 | < 1 | 12 |
| K [µg/g] | 19-Jan-23 | 23:42 | 31-Jan-23 | 09:43 | 37 | 430 | 300 | 160 |
| Li [µg/g] | 19-Jan-23 | 23:42 | 31-Jan-23 | 09:43 | < 2 | < 2 | < 2 | < 2 |
| Mn [µg/g] | 19-Jan-23 | 23:42 | 31-Jan-23 | 09:44 | 6.5 | 0.7 | 1.8 | 3.6 |
| Mo [µg/g] | 19-Jan-23 | 23:42 | 31-Jan-23 | 09:44 | < 0.1 | < 0.1 | < 0.1 | < 0.1 |
| Na [µg/g] | 19-Jan-23 | 23:42 | 31-Jan-23 | 09:44 | 45 | 3200 | 2600 | 420 |
| Ni [µg/g] | 19-Jan-23 | 23:42 | 31-Jan-23 | 09:44 | < 0.5 | < 0.5 | < 0.5 | 0.7 |
| Pb [µg/g] | 19-Jan-23 | 23:42 | 31-Jan-23 | 09:44 | < 0.1 | < 0.1 | < 0.1 | < 0.1 |
| P [µg/g] | 19-Jan-23 | 23:42 | 31-Jan-23 | 09:44 | < 3 | 4 | < 3 | 43 |
| Sb [µg/g] | 19-Jan-23 | 23:42 | 31-Jan-23 | 09:44 | < 0.8 | < 0.8 | < 0.8 | < 0.8 |
| Se [µg/g] | 19-Jan-23 | 23:42 | 31-Jan-23 | 09:44 | < 0.7 | < 0.7 | < 0.7 | < 0.7 |
| Sn [µg/g] | 19-Jan-23 | 23:42 | 31-Jan-23 | 09:44 | < 0.5 | < 0.5 | < 0.5 | < 0.5 |
| Sr [µg/g] | 19-Jan-23 | 23:42 | 31-Jan-23 | 09:44 | 11 | 100 | 52 | 76 |
| Ti [µg/g] | 19-Jan-23 | 23:42 | 31-Jan-23 | 09:44 | 0.9 | 0.3 | 0.2 | 0.1 |
| Tl [µg/g] | 19-Jan-23 | 23:42 | 31-Jan-23 | 09:44 | < 0.02 | < 0.02 | < 0.02 | < 0.02 |
| U [µg/g] | 19-Jan-23 | 23:42 | 31-Jan-23 | 09:44 | < 0.002 | 0.009 | 0.006 | 0.043 |
| V [µg/g] | 19-Jan-23 | 23:42 | 31-Jan-23 | 09:44 | < 3 | < 3 | < 3 | < 3 |
| Zn [µg/g] | 19-Jan-23 | 23:42 | 31-Jan-23 | 09:44 | < 0.7 | < 0.7 | < 0.7 | < 0.7 |

SGS Canada Inc.

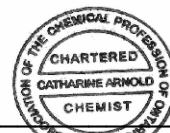
P.O. Box 4300 - 185 Concession St.
Lakefield - Ontario - KOL 2H0
Phone: 705-652-2000 FAX: 705-652-6365

LR Report : CA19219-NOV22

| Analysis | 9: MW-392 (32-33.5) | 10: MW-393 (24-25.5) | 11: MW-394 (20.5-22) | 12: MW-392 (66-68) |
|--------------------|------------------------|-------------------------|-------------------------|-----------------------|
| Sample Date & Time | 27-Sep-22 09:00 | 04-Oct-22 16:00 | 25-Sep-22 16:00 | 26-Sep-22 12:00 |
| Ag [µg/g] | < 0.05 | < 0.05 | < 0.05 | < 0.05 |
| Al [µg/g] | 10 | 12 | 12 | 10 |
| As [µg/g] | < 0.5 | < 0.5 | < 0.5 | < 0.5 |
| Ba [µg/g] | 16 | 16 | 10 | 4.3 |
| Be [µg/g] | < 0.02 | < 0.02 | < 0.02 | < 0.02 |
| B [µg/g] | < 1 | < 1 | < 1 | 2 |
| Bi [µg/g] | < 0.09 | < 0.09 | < 0.09 | < 0.09 |
| Ca [µg/g] | 2500 | 1400 | 2100 | 3700 |
| Cd [µg/g] | < 0.05 | < 0.05 | < 0.05 | < 0.05 |
| Co [µg/g] | 0.02 | < 0.01 | < 0.01 | 0.02 |
| Cr [µg/g] | < 0.5 | < 0.5 | < 0.5 | < 0.5 |
| Cu [µg/g] | < 0.1 | < 0.1 | < 0.1 | < 0.1 |
| Fe [µg/g] | 8 | 9 | 8 | 10 |
| K [µg/g] | 44 | 35 | 60 | 360 |
| Li [µg/g] | < 2 | < 2 | < 2 | < 2 |
| Mn [µg/g] | 3.5 | 1.7 | 3.2 | 2.5 |
| Mo [µg/g] | < 0.1 | < 0.1 | < 0.1 | < 0.1 |
| Na [µg/g] | 17 | 22 | 30 | 480 |
| Ni [µg/g] | < 0.5 | < 0.5 | < 0.5 | < 0.5 |
| Pb [µg/g] | < 0.1 | < 0.1 | < 0.1 | < 0.1 |
| P [µg/g] | < 3 | < 3 | 4 | < 3 |
| Sb [µg/g] | < 0.8 | < 0.8 | < 0.8 | < 0.8 |
| Se [µg/g] | < 0.7 | < 0.7 | < 0.7 | < 0.7 |
| Sn [µg/g] | < 0.5 | < 0.5 | < 0.5 | < 0.5 |
| Sr [µg/g] | 6.5 | 4.3 | 7.4 | 75 |
| Ti [µg/g] | 0.1 | 0.6 | 0.3 | < 0.1 |
| Tl [µg/g] | < 0.02 | < 0.02 | < 0.02 | < 0.02 |
| U [µg/g] | < 0.002 | < 0.002 | < 0.002 | 0.004 |
| V [µg/g] | < 3 | < 3 | < 3 | < 3 |
| Zn [µg/g] | < 0.7 | < 0.7 | < 0.7 | < 0.7 |

Fraction 2 Exchangeable Metals

Catharine Arnold
Catharine Arnold, B.Sc., C.Chem
Project Specialist,
Environment, Health & Safety



**SGS Canada Inc.**

P.O. Box 4300 - 185 Concession St.
Lakefield - Ontario - K0L 2H0
Phone: 705-652-2000 FAX: 705-652-6365

28-February-2023

Ramboll Americas Engineering Solutions, Inc.

Attn : Evvan Plank

P.O# Box 4873
Syracuse, New York
13221-7873, USA

Phone: 315-463-7554
Fax:

Date Rec. : 24 November 2022
LR Report: CA19220-NOV22
Reference: Ramboll Power Plant Drilling

Copy: #1

CERTIFICATE OF ANALYSIS

Final Report

| Analysis | 1: Analysis Start Date | 2: Analysis Start Time Completed | 3: Analysis DateCompleted | 4: Analysis Time | 5: MW-358 (13-15) | 6: MW-358 (47-49) | 7: MW-358 (86-88) | 8: MW-392 (80-82) |
|--------------------|------------------------------|--|---------------------------------|------------------------|----------------------|----------------------|----------------------|----------------------|
| Sample Date & Time | | | | | 05-Oct-22 14:05 | 06-Oct-22 15:00 | 08-Oct-22 18:00 | 26-Sep-22 16:00 |
| Ag [µg/g] | 19-Jan-23 | 23:42 | 31-Jan-23 | 09:45 | < 0.05 | < 0.05 | < 0.05 | < 0.05 |
| Al [µg/g] | 19-Jan-23 | 23:42 | 31-Jan-23 | 09:45 | 30 | 55 | 56 | 25 |
| As [µg/g] | 19-Jan-23 | 23:42 | 31-Jan-23 | 09:45 | < 0.5 | < 0.5 | < 0.5 | < 0.5 |
| Ba [µg/g] | 19-Jan-23 | 23:42 | 31-Jan-23 | 09:45 | 25 | 23 | 6.9 | 2.8 |
| Be [µg/g] | 19-Jan-23 | 23:42 | 31-Jan-23 | 09:45 | 0.09 | 0.10 | 0.07 | 0.03 |
| B [µg/g] | 19-Jan-23 | 23:42 | 31-Jan-23 | 09:45 | < 1 | 2 | 3 | 4 |
| Bi [µg/g] | 19-Jan-23 | 23:42 | 31-Jan-23 | 09:45 | < 0.09 | < 0.09 | < 0.09 | < 0.09 |
| Ca [µg/g] | 19-Jan-23 | 23:42 | 31-Jan-23 | 09:45 | 110 | 1300 | 770 | 52000 |
| Cd [µg/g] | 19-Jan-23 | 23:42 | 31-Jan-23 | 09:45 | < 0.05 | < 0.05 | < 0.05 | < 0.05 |
| Co [µg/g] | 19-Jan-23 | 23:42 | 31-Jan-23 | 09:45 | 0.04 | 0.02 | 2.3 | 1.0 |
| Cr [µg/g] | 19-Jan-23 | 23:42 | 31-Jan-23 | 09:45 | < 0.5 | < 0.5 | < 0.5 | < 0.5 |
| Cu [µg/g] | 19-Jan-23 | 23:42 | 31-Jan-23 | 09:45 | 0.6 | 0.2 | 0.6 | 0.2 |
| Fe [µg/g] | 19-Jan-23 | 23:42 | 31-Jan-23 | 09:45 | 40 | 45 | 42 | 25 |
| K [µg/g] | 19-Jan-23 | 23:42 | 31-Jan-23 | 09:45 | 15 | 180 | 120 | 90 |
| Li [µg/g] | 19-Jan-23 | 23:42 | 31-Jan-23 | 09:45 | < 2 | < 2 | < 2 | < 2 |
| Mn [µg/g] | 19-Jan-23 | 23:42 | 31-Jan-23 | 09:45 | 13 | 7.0 | 4.3 | 77 |
| Mo [µg/g] | 19-Jan-23 | 23:42 | 31-Jan-23 | 09:45 | < 0.1 | < 0.1 | < 0.1 | < 0.1 |
| Ni [µg/g] | 19-Jan-23 | 23:42 | 31-Jan-23 | 09:46 | < 0.5 | < 0.5 | 1.9 | 2.7 |
| Pb [µg/g] | 19-Jan-23 | 23:42 | 31-Jan-23 | 09:46 | 0.2 | 0.1 | 0.9 | 1.9 |
| P [µg/g] | 19-Jan-23 | 23:42 | 31-Jan-23 | 09:46 | < 3 | 13 | < 3 | 100 |
| Sb [µg/g] | 19-Jan-23 | 23:42 | 31-Jan-23 | 09:46 | < 0.8 | < 0.8 | < 0.8 | < 0.8 |
| Se [µg/g] | 19-Jan-23 | 23:42 | 31-Jan-23 | 09:46 | < 0.7 | < 0.7 | < 0.7 | < 0.7 |
| Si [µg/g] | 19-Jan-23 | 23:42 | 31-Jan-23 | 09:46 | 96 | 160 | 150 | 33 |
| Sn [µg/g] | 19-Jan-23 | 23:42 | 31-Jan-23 | 09:46 | < 0.5 | < 0.5 | < 0.5 | < 0.5 |
| Sr [µg/g] | 19-Jan-23 | 23:42 | 31-Jan-23 | 09:46 | 0.5 | 10 | 7.3 | 99 |
| Ti [µg/g] | 19-Jan-23 | 23:42 | 31-Jan-23 | 09:46 | 0.8 | 0.6 | 0.5 | 1.0 |
| Tl [µg/g] | 19-Jan-23 | 23:42 | 31-Jan-23 | 09:46 | < 0.02 | < 0.02 | < 0.02 | < 0.02 |
| U [µg/g] | 19-Jan-23 | 23:42 | 31-Jan-23 | 09:46 | 0.19 | 0.094 | 0.13 | 0.31 |
| V [µg/g] | 19-Jan-23 | 23:42 | 31-Jan-23 | 09:46 | < 3 | < 3 | < 3 | < 3 |
| Zn [µg/g] | 19-Jan-23 | 23:42 | 31-Jan-23 | 09:46 | < 0.7 | < 0.7 | < 0.7 | 3.7 |

SGS Canada Inc.

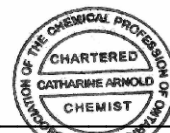
P.O. Box 4300 - 185 Concession St.
Lakefield - Ontario - KOL 2H0
Phone: 705-652-2000 FAX: 705-652-6365

LR Report : CA19220-NOV22

| Analysis | 9: MW-392 (32-33.5) | 10: MW-393 (24-25.5) | 11: MW-394 (20.5-22) | 12: MW-392 (66-68) |
|--------------------|------------------------|-------------------------|-------------------------|-----------------------|
| Sample Date & Time | 27-Sep-22 09:00 | 04-Oct-22 16:00 | 25-Sep-22 16:00 | 26-Sep-22 12:00 |
| Ag [µg/g] | < 0.05 | < 0.05 | < 0.05 | < 0.05 |
| Al [µg/g] | 30 | 28 | 23 | 28 |
| As [µg/g] | < 0.5 | < 0.5 | < 0.5 | < 0.5 |
| Ba [µg/g] | 19 | 15 | 12 | 5.0 |
| Be [µg/g] | 0.06 | 0.04 | 0.04 | 0.07 |
| B [µg/g] | < 1 | < 1 | < 1 | 3 |
| Bi [µg/g] | < 0.09 | < 0.09 | < 0.09 | < 0.09 |
| Ca [µg/g] | 1500 | 56 | 140 | 35000 |
| Cd [µg/g] | < 0.05 | < 0.05 | < 0.05 | < 0.05 |
| Co [µg/g] | 0.05 | 0.02 | 0.03 | 0.27 |
| Cr [µg/g] | < 0.5 | < 0.5 | < 0.5 | < 0.5 |
| Cu [µg/g] | 0.8 | 0.2 | 0.2 | 0.6 |
| Fe [µg/g] | 9 | 14 | 10 | 300 |
| K [µg/g] | 16 | 10 | 15 | 130 |
| Li [µg/g] | < 2 | < 2 | < 2 | < 2 |
| Mn [µg/g] | 20 | 4.4 | 7.0 | 144 |
| Mo [µg/g] | < 0.1 | < 0.1 | < 0.1 | < 0.1 |
| Ni [µg/g] | < 0.5 | < 0.5 | < 0.5 | < 0.5 |
| Pb [µg/g] | 0.2 | 0.1 | 0.1 | 0.4 |
| P [µg/g] | < 3 | < 3 | 4 | < 3 |
| Sb [µg/g] | < 0.8 | < 0.8 | < 0.8 | < 0.8 |
| Se [µg/g] | < 0.7 | < 0.7 | < 0.7 | < 0.7 |
| Si [µg/g] | 130 | 90 | 99 | 96 |
| Sn [µg/g] | < 0.5 | < 0.5 | < 0.5 | < 0.5 |
| Sr [µg/g] | 1.5 | 0.3 | 0.8 | 59 |
| Ti [µg/g] | 0.1 | 1.9 | 0.6 | < 0.1 |
| Tl [µg/g] | < 0.02 | < 0.02 | < 0.02 | < 0.02 |
| U [µg/g] | 0.12 | 0.14 | 0.17 | 0.100 |
| V [µg/g] | < 3 | < 3 | < 3 | < 3 |
| Zn [µg/g] | < 0.7 | < 0.7 | < 0.7 | 1.0 |

Fraction 3 Metals Bound to Carbonates

Catharine Arnold
Catharine Arnold, B.Sc., C.Chem
Project Specialist,
Environment, Health & Safety



SGS Canada Inc.

P.O. Box 4300 - 185 Concession St.
Lakefield - Ontario - K0L 2H0
Phone: 705-652-2000 FAX: 705-652-6365

28-February-2023

Ramboll Americas Engineering Solutions, Inc.

Attn : Evvan Plank

P.O# Box 4873
Syracuse, New York
13221-7873, USA

Phone: 315-463-7554
Fax:

Date Rec. : 24 November 2022
LR Report: CA19221-NOV22
Reference: Baldwin Power Plant Drilling

Copy: #1

CERTIFICATE OF ANALYSIS

Final Report

| Analysis | 3: Analysis Completed Date | 4: Analysis Completed Time | 5: MW-358 (13-15) | 6: MW-358 (47-49) | 7: MW-358 (86-88) | 8: MW-392 (80-82) | 9: MW-392 (32-33.5) |
|--------------------|----------------------------------|----------------------------------|----------------------|----------------------|----------------------|----------------------|------------------------|
| Sample Date & Time | | | 05-Oct-22 14:05 | 06-Oct-22 15:00 | 08-Oct-22 18:00 | 26-Sep-22 16:00 | 27-Sep-22 09:00 |
| Ag [µg/g] | 31-Jan-23 | 09:47 | < 0.01 | < 0.01 | < 0.01 | < 0.01 | 0.01 |
| Al [µg/g] | 31-Jan-23 | 09:47 | 290 | 310 | 340 | 220 | 220 |
| As [µg/g] | 31-Jan-23 | 09:47 | < 0.5 | < 0.5 | < 0.5 | 1.3 | < 0.5 |
| Ba [µg/g] | 31-Jan-23 | 09:47 | 16 | 6.4 | 1.6 | 4.1 | 56 |
| Be [µg/g] | 31-Jan-23 | 09:47 | 0.26 | 0.16 | 0.15 | 0.15 | 0.21 |
| B [µg/g] | 31-Jan-23 | 09:47 | < 1 | 5 | 6 | 6 | < 1 |
| Bi [µg/g] | 31-Jan-23 | 09:47 | < 0.09 | < 0.09 | < 0.09 | 0.14 | < 0.09 |
| Ca [µg/g] | 31-Jan-23 | 09:47 | 71 | 320 | 250 | 130000 | 2300 |
| Cd [µg/g] | 31-Jan-23 | 09:47 | < 0.05 | < 0.05 | < 0.05 | 0.13 | 0.18 |
| Co [µg/g] | 31-Jan-23 | 09:47 | 3.8 | 0.33 | 3.0 | 2.3 | 5.1 |
| Cr [µg/g] | 31-Jan-23 | 09:47 | 2.3 | 1.2 | 1.3 | 1.0 | 0.9 |
| Cu [µg/g] | 31-Jan-23 | 09:47 | 1.6 | 0.4 | 0.7 | 0.1 | 2.9 |
| Fe [µg/g] | 31-Jan-23 | 09:47 | 1600 | 1600 | 1200 | 1800 | 1100 |
| K [µg/g] | 31-Jan-23 | 09:47 | 16 | 140 | 110 | 43 | 19 |
| Li [µg/g] | 31-Jan-23 | 09:47 | < 2 | 3 | 5 | < 2 | < 2 |
| Mn [µg/g] | 31-Jan-23 | 09:47 | 240 | 3.1 | 2.9 | 190 | 500 |
| Mo [µg/g] | 31-Jan-23 | 09:47 | < 0.1 | < 0.1 | < 0.1 | < 0.1 | < 0.1 |
| Ni [µg/g] | 31-Jan-23 | 09:47 | 3.1 | 2.7 | 4.5 | 6.5 | 3.1 |
| Pb [µg/g] | 31-Jan-23 | 09:47 | 3.3 | 0.2 | 1.2 | 8.4 | 3.7 |
| P [µg/g] | 31-Jan-23 | 09:47 | 19 | 110 | 77 | 400 | 31 |
| Sb [µg/g] | 31-Jan-23 | 09:47 | < 0.8 | < 0.8 | < 0.8 | < 0.8 | < 0.8 |
| Se [µg/g] | 31-Jan-23 | 09:47 | < 0.7 | < 0.7 | < 0.7 | < 0.7 | < 0.7 |
| Si [µg/g] | 31-Jan-23 | 09:47 | 920 | 910 | 710 | 270 | 600 |
| Sn [µg/g] | 31-Jan-23 | 09:47 | < 0.5 | < 0.5 | < 0.5 | < 0.5 | < 0.5 |
| Sr [µg/g] | 31-Jan-23 | 09:47 | 0.4 | 3.1 | 2.8 | 237 | 1.7 |
| Ti [µg/g] | 31-Jan-23 | 09:47 | 0.4 | 0.1 | 0.3 | < 0.1 | < 0.1 |
| Tl [µg/g] | 31-Jan-23 | 09:47 | < 0.02 | < 0.02 | < 0.02 | < 0.02 | < 0.02 |
| U [µg/g] | 31-Jan-23 | 09:47 | 0.26 | 0.068 | 0.17 | 0.62 | 0.15 |
| V [µg/g] | 31-Jan-23 | 09:47 | 5 | < 3 | < 3 | < 3 | 3 |
| Zn [µg/g] | 31-Jan-23 | 09:47 | 2.9 | 1.9 | 1.9 | 13 | 3.8 |

SGS Canada Inc.

P.O. Box 4300 - 185 Concession St.

Lakefield - Ontario - KOL 2H0

Phone: 705-652-2000 FAX: 705-652-6365

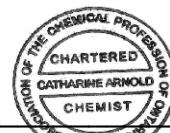
LR Report : CA19221-NOV22

| Analysis | 10: MW-393 (24-25.5) | 11: MW-394 (20.5-22) | 12: MW-392 (66-68) |
|--------------------|-------------------------|-------------------------|-----------------------|
| Sample Date & Time | 04-Oct-22 16:00 | 25-Sep-22 16:00 | 26-Sep-22 12:00 |
| Ag [µg/g] | < 0.01 | 0.02 | < 0.01 |
| Al [µg/g] | 290 | 270 | 490 |
| As [µg/g] | < 0.5 | < 0.5 | < 0.5 |
| Ba [µg/g] | 45 | 35 | 1.5 |
| Be [µg/g] | 0.16 | 0.18 | 0.18 |
| B [µg/g] | < 1 | < 1 | 4 |
| Bi [µg/g] | < 0.09 | < 0.09 | 0.14 |
| Ca [µg/g] | 100 | 350 | 7600 |
| Cd [µg/g] | 0.06 | 0.14 | < 0.05 |
| Co [µg/g] | 4.3 | 3.5 | 0.62 |
| Cr [µg/g] | 1.2 | 1.2 | 2.0 |
| Cu [µg/g] | 1.5 | 2.0 | 0.9 |
| Fe [µg/g] | 1500 | 1200 | 2700 |
| K [µg/g] | 15 | 22 | 120 |
| Li [µg/g] | < 2 | < 2 | 2 |
| Mn [µg/g] | 380 | 260 | 63 |
| Mo [µg/g] | < 0.1 | < 0.1 | < 0.1 |
| Ni [µg/g] | 3.2 | 3.7 | 2.5 |
| Pb [µg/g] | 3.5 | 2.1 | 0.9 |
| P [µg/g] | 17 | 91 | 110 |
| Sb [µg/g] | < 0.8 | < 0.8 | < 0.8 |
| Se [µg/g] | < 0.7 | < 0.7 | < 0.7 |
| Si [µg/g] | 660 | 850 | 650 |
| Sn [µg/g] | < 0.5 | < 0.5 | < 0.5 |
| Sr [µg/g] | 0.5 | 1.3 | 26 |
| Ti [µg/g] | 0.3 | 0.2 | 0.2 |
| Tl [µg/g] | < 0.02 | < 0.02 | < 0.02 |
| U [µg/g] | 0.12 | 0.18 | 0.082 |
| V [µg/g] | < 3 | 5 | < 3 |
| Zn [µg/g] | 4.3 | 7.8 | 2.8 |

Fraction 4 Metals Bound to Fe and Mn Oxides

Catharine Arnold

Catharine Arnold, B.Sc., C.Chem
Project Specialist,
Environment, Health & Safety



SGS Canada Inc.

P.O. Box 4300 - 185 Concession St.
Lakefield - Ontario - KOL 2H0
Phone: 705-652-2000 FAX: 705-652-6365

28-February-2023

Ramboll Americas Engineering Solutions, Inc.

Attn : Evvan Plank

P.O# Box 4873
Syracuse, New York
13221-7873, USA

Date Rec. : 24 November 2022
LR Report: CA19222-NOV22
Reference: Baldwin Power plant Drilling

Copy: #1

Phone: 315-463-7554
Fax:

CERTIFICATE OF ANALYSIS

Final Report

| Analysis | 3: Analysis Completed Date | 4: Analysis Completed Time | 5: MW-358 (13-15) | 6: MW-358 (47-49) | 7: MW-358 (86-88) | 8: MW-392 (80-82) | 9: MW-392 (32-33.5) |
|--------------------|----------------------------------|----------------------------------|----------------------|----------------------|----------------------|----------------------|------------------------|
| Sample Date & Time | | | 05-Oct-22 14:05 | 06-Oct-22 15:00 | 08-Oct-22 18:00 | 26-Sep-22 16:00 | 27-Sep-22 09:00 |
| Ag [µg/g] | 31-Jan-23 | 09:48 | 0.14 | 0.15 | 0.08 | 0.07 | 0.06 |
| Al [µg/g] | 31-Jan-23 | 09:48 | 980 | 1300 | 1100 | 130 | 610 |
| As [µg/g] | 31-Jan-23 | 09:48 | < 0.5 | < 0.5 | < 0.5 | < 0.5 | < 0.5 |
| Ba [µg/g] | 31-Jan-23 | 09:48 | 15 | 11 | 1.8 | 3.6 | 36 |
| Be [µg/g] | 31-Jan-23 | 09:48 | 0.13 | 0.32 | 0.16 | 0.07 | 0.12 |
| B [µg/g] | 31-Jan-23 | 09:48 | < 1 | 2 | 2 | 2 | < 1 |
| Bi [µg/g] | 31-Jan-23 | 09:48 | < 0.09 | < 0.09 | < 0.09 | < 0.09 | < 0.09 |
| Ca [µg/g] | 31-Jan-23 | 09:48 | 160 | 490 | 220 | 8600 | 840 |
| Cd [µg/g] | 31-Jan-23 | 09:48 | < 0.05 | < 0.05 | < 0.05 | 0.20 | < 0.05 |
| Co [µg/g] | 31-Jan-23 | 09:48 | 1.4 | 0.45 | 9.7 | 3.3 | 1.3 |
| Cr [µg/g] | 31-Jan-23 | 09:48 | 2.1 | 1.0 | 1.2 | < 0.5 | 1.6 |
| Cu [µg/g] | 31-Jan-23 | 09:48 | 0.5 | 1.0 | 1.8 | 1.9 | 0.4 |
| Fe [µg/g] | 31-Jan-23 | 09:48 | 150 | 610 | 1800 | 220 | 83 |
| K [µg/g] | 31-Jan-23 | 09:48 | 15 | 104 | 79 | 25 | 15 |
| Li [µg/g] | 31-Jan-23 | 09:48 | < 2 | < 2 | 3 | < 2 | < 2 |
| Mg [µg/g] | 31-Jan-23 | 09:48 | 170 | 1100 | 870 | 200 | 500 |
| Mn [µg/g] | 31-Jan-23 | 09:48 | 85 | 3.6 | 15 | 16 | 92 |
| Mo [µg/g] | 31-Jan-23 | 09:48 | < 0.1 | < 0.1 | < 0.1 | 0.2 | 0.4 |
| Na [µg/g] | 31-Jan-23 | 09:48 | 110 | 180 | 150 | 90 | 75 |
| Ni [µg/g] | 31-Jan-23 | 09:48 | 1.9 | 4.3 | 13 | 15 | 2.1 |
| Pb [µg/g] | 31-Jan-23 | 09:48 | 1.6 | 0.1 | 1.6 | 3.8 | 1.3 |
| P [µg/g] | 31-Jan-23 | 09:48 | < 3 | < 3 | < 3 | 290 | 5 |
| Sb [µg/g] | 31-Jan-23 | 09:48 | < 0.8 | < 0.8 | < 0.8 | < 0.8 | < 0.8 |
| Se [µg/g] | 31-Jan-23 | 09:48 | < 0.7 | < 0.7 | < 0.7 | < 0.7 | < 0.7 |
| Si [µg/g] | 31-Jan-23 | 09:48 | 590 | 480 | 420 | 130 | 530 |
| Sn [µg/g] | 31-Jan-23 | 09:48 | < 0.5 | < 0.5 | < 0.5 | < 0.5 | < 0.5 |
| Sr [µg/g] | 31-Jan-23 | 09:48 | 0.5 | 5.1 | 2.8 | 48 | 0.9 |
| Ti [µg/g] | 31-Jan-23 | 09:48 | 0.7 | < 0.1 | < 0.1 | < 0.1 | 2.9 |
| Tl [µg/g] | 31-Jan-23 | 09:48 | < 0.02 | < 0.02 | 0.02 | 0.05 | < 0.02 |
| U [µg/g] | 31-Jan-23 | 09:48 | 0.17 | 0.13 | 0.19 | 0.25 | 0.060 |
| V [µg/g] | 31-Jan-23 | 09:48 | < 3 | < 3 | < 3 | < 3 | 3 |
| Zn [µg/g] | 31-Jan-23 | 09:48 | 1.4 | < 0.7 | 1.8 | 41 | 1.7 |

SGS Canada Inc.

P.O. Box 4300 - 185 Concession St.

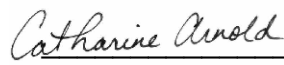
Lakefield - Ontario - KOL 2H0

Phone: 705-652-2000 FAX: 705-652-6365

LR Report : CA19222-NOV22

| Analysis | 10: MW-393 (24-25.5) | 11: MW-394 (20.5-22) | 12: MW-392 (66-68) |
|--------------------|-------------------------|-------------------------|-----------------------|
| Sample Date & Time | 04-Oct-22 16:00 | 25-Sep-22 16:00 | 26-Sep-22 12:00 |
| Ag [µg/g] | < 0.05 | < 0.05 | < 0.05 |
| Al [µg/g] | 660 | 870 | 820 |
| As [µg/g] | < 0.5 | < 0.5 | < 0.5 |
| Ba [µg/g] | 33 | 45 | 1.5 |
| Be [µg/g] | 0.08 | 0.15 | 0.18 |
| B [µg/g] | < 1 | < 1 | 2 |
| Bi [µg/g] | < 0.09 | < 0.09 | < 0.09 |
| Ca [µg/g] | 88 | 300 | 2400 |
| Cd [µg/g] | < 0.05 | < 0.05 | < 0.05 |
| Co [µg/g] | 1.2 | 2.3 | 0.68 |
| Cr [µg/g] | 1.2 | 1.5 | 1.1 |
| Cu [µg/g] | 0.3 | 0.8 | 1.4 |
| Fe [µg/g] | 93 | 120 | 680 |
| K [µg/g] | 14 | 21 | 70 |
| Li [µg/g] | < 2 | < 2 | < 2 |
| Mg [µg/g] | 150 | 280 | 730 |
| Mn [µg/g] | 100 | 164 | 15 |
| Mo [µg/g] | 0.1 | 0.3 | < 0.1 |
| Na [µg/g] | 48 | 170 | 95 |
| Ni [µg/g] | 1.6 | 3.5 | 2.9 |
| Pb [µg/g] | 1.7 | 1.3 | 0.9 |
| P [µg/g] | 4 | 8 | < 3 |
| Sb [µg/g] | < 0.8 | < 0.8 | < 0.8 |
| Se [µg/g] | < 0.7 | < 0.7 | < 0.7 |
| Si [µg/g] | 470 | 650 | 470 |
| Sn [µg/g] | < 0.5 | < 0.5 | < 0.5 |
| Sr [µg/g] | 0.3 | 1.2 | 9.8 |
| Ti [µg/g] | 2.1 | 2.5 | < 0.1 |
| Tl [µg/g] | < 0.02 | < 0.02 | < 0.02 |
| U [µg/g] | 0.065 | 0.16 | 0.080 |
| V [µg/g] | < 3 | 4 | < 3 |
| Zn [µg/g] | 1.6 | 4.0 | 0.9 |

Fraction 5 Bound to Organic Material

Catharine Arnold

Catharine Arnold, B.Sc., C.Chem
Project Specialist,
Environment, Health & Safety

SGS Canada Inc.

P.O. Box 4300 - 185 Concession St.
Lakefield - Ontario - KOL 2H0
Phone: 705-652-2000 FAX: 705-652-6365

28-February-2023

Ramboll Americas Engineering Solutions, Inc.

Attn : Evvan Plank

P.O# Box 4873
Syracuse, New York
13221-7873, USA

Date Rec. : 24 November 2022
LR Report: CA19223-NOV22
Reference: Baldwin Power Plant Drilling

Copy: #1

Phone: 315-463-7554
Fax:

CERTIFICATE OF ANALYSIS

Final Report

| Analysis | 3: Analysis Completed Date | 4: Analysis Completed Time | 5: MW-358 (13-15) | 6: MW-358 (47-49) | 7: MW-358 (86-88) | 8: MW-392 (80-82) | 9: MW-392 (32-33.5) |
|--------------------|----------------------------------|----------------------------------|----------------------|----------------------|----------------------|----------------------|------------------------|
| Sample Date & Time | | | 05-Oct-22 14:05 | 06-Oct-22 15:00 | 08-Oct-22 18:00 | 26-Sep-22 16:00 | 27-Sep-22 09:00 |
| Ag [µg/g] | 31-Jan-23 | 09:48 | 0.09 | < 0.05 | < 0.05 | < 0.05 | 0.07 |
| Al [µg/g] | 31-Jan-23 | 09:48 | 44000 | 63000 | 71000 | 27000 | 45000 |
| As [µg/g] | 31-Jan-23 | 09:48 | 5.8 | 2.3 | 9.8 | 10 | 8.6 |
| Ba [µg/g] | 31-Jan-23 | 09:48 | 390 | 150 | 140 | 56 | 320 |
| Be [µg/g] | 31-Jan-23 | 09:48 | 0.65 | 1.4 | 1.5 | 0.68 | 0.87 |
| B [µg/g] | 31-Jan-23 | 09:48 | 13 | 60 | 62 | 26 | 21 |
| Bi [µg/g] | 31-Jan-23 | 09:48 | 0.25 | 0.26 | 0.18 | 0.14 | 0.25 |
| Ca [µg/g] | 31-Jan-23 | 09:48 | 2500 | 150 | 120 | 20000 | 1400 |
| Cd [µg/g] | 31-Jan-23 | 09:48 | 0.06 | < 0.05 | < 0.05 | 0.11 | 0.08 |
| Co [µg/g] | 31-Jan-23 | 09:48 | 3.3 | 7.2 | 6.4 | 2.0 | 6.4 |
| Cr [µg/g] | 31-Jan-23 | 09:48 | 34 | 69 | 75 | 37 | 40 |
| Cu [µg/g] | 31-Jan-23 | 09:48 | 10 | 9.9 | 5.7 | 7.2 | 15 |
| Fe [µg/g] | 31-Jan-23 | 09:48 | 22000 | 42000 | 22000 | 14000 | 28000 |
| K [µg/g] | 31-Jan-23 | 09:48 | 11000 | 18000 | 16000 | 5100 | 13000 |
| Li [µg/g] | 31-Jan-23 | 09:48 | 18 | 9 | 65 | 7 | 20 |
| Mg [µg/g] | 31-Jan-23 | 09:48 | 2700 | 7800 | 7600 | 4100 | 3300 |
| Mn [µg/g] | 31-Jan-23 | 09:48 | 110 | 70 | 51 | 50 | 130 |
| Mo [µg/g] | 31-Jan-23 | 09:48 | 0.9 | 0.3 | 0.1 | 0.1 | 0.9 |
| Na [µg/g] | 31-Jan-23 | 09:48 | 6700 | 560 | 830 | 550 | 5200 |
| Ni [µg/g] | 31-Jan-23 | 09:48 | 14 | 32 | 29 | 13 | 21 |
| Pb [µg/g] | 31-Jan-23 | 09:48 | 10 | 8.0 | 7.0 | 17 | 12 |
| P [µg/g] | 31-Jan-23 | 09:48 | 260 | 240 | 160 | 7200 | 300 |
| Sb [µg/g] | 31-Jan-23 | 09:48 | < 0.8 | < 0.8 | < 0.8 | < 0.8 | < 0.8 |
| Se [µg/g] | 31-Jan-23 | 09:48 | < 0.7 | < 0.7 | < 0.7 | < 0.7 | < 0.7 |
| Si [µg/g] | 31-Jan-23 | 09:48 | 160000 | 66000 | 51000 | 73000 | 65000 |
| Sn [µg/g] | 31-Jan-23 | 09:48 | 5.4 | 5.8 | 5.8 | 4.9 | 5.2 |
| Sr [µg/g] | 31-Jan-23 | 09:48 | 89 | 30 | 25 | 130 | 79 |
| Ti [µg/g] | 31-Jan-23 | 09:48 | 2400 | 670 | 570 | 520 | 980 |
| Tl [µg/g] | 31-Jan-23 | 09:48 | 0.47 | 0.42 | 0.42 | 0.17 | 0.51 |
| U [µg/g] | 31-Jan-23 | 09:48 | 1.3 | 0.30 | 0.99 | 2.7 | 1.1 |
| V [µg/g] | 31-Jan-23 | 09:48 | 54 | 73 | 86 | 95 | 57 |
| Zn [µg/g] | 31-Jan-23 | 09:48 | 37 | 47 | 32 | 43 | 53 |

SGS Canada Inc.

P.O. Box 4300 - 185 Concession St.

Lakefield - Ontario - KOL 2H0

Phone: 705-652-2000 FAX: 705-652-6365

LR Report : CA19223-NOV22

| Analysis | 10: MW-393 (24-25.5) | 11: MW-394 (20.5-22) | 12: MW-392 (66-68) |
|--------------------|-------------------------|-------------------------|-----------------------|
| Sample Date & Time | 04-Oct-22 16:00 | 25-Sep-22 16:00 | 26-Sep-22 12:00 |
| Ag [µg/g] | < 0.05 | < 0.05 | < 0.05 |
| Al [µg/g] | 33000 | 45000 | 59000 |
| As [µg/g] | 10 | 9.8 | 0.9 |
| Ba [µg/g] | 300 | 410 | 93 |
| Be [µg/g] | 0.56 | 0.83 | 1.2 |
| B [µg/g] | 15 | 16 | 53 |
| Bi [µg/g] | 0.18 | 0.27 | 0.20 |
| Ca [µg/g] | 1700 | 3000 | 170 |
| Cd [µg/g] | < 0.05 | 0.11 | < 0.05 |
| Co [µg/g] | 3.2 | 5.0 | 6.4 |
| Cr [µg/g] | 24 | 35 | 71 |
| Cu [µg/g] | 9.9 | 13 | 12 |
| Fe [µg/g] | 19000 | 27000 | 43000 |
| K [µg/g] | 12000 | 14000 | 17000 |
| Li [µg/g] | 13 | 16 | 19 |
| Mg [µg/g] | 2200 | 3400 | 9500 |
| Mn [µg/g] | 80 | 140 | 47 |
| Mo [µg/g] | 0.7 | 2.7 | 0.2 |
| Na [µg/g] | 5100 | 7700 | 490 |
| Ni [µg/g] | 13 | 18 | 31 |
| Pb [µg/g] | 9.1 | 13 | 4.1 |
| P [µg/g] | 230 | 460 | 170 |
| Sb [µg/g] | < 0.8 | < 0.8 | < 0.8 |
| Se [µg/g] | < 0.7 | < 0.7 | < 0.7 |
| Si [µg/g] | 61000 | 43000 | 62000 |
| Sn [µg/g] | 4.6 | 5.2 | 5.6 |
| Sr [µg/g] | 70 | 110 | 22 |
| Ti [µg/g] | 780 | 1100 | 560 |
| Tl [µg/g] | 0.35 | 0.50 | 0.36 |
| U [µg/g] | 0.61 | 1.1 | 0.097 |
| V [µg/g] | 35 | 57 | 70 |
| Zn [µg/g] | 37 | 54 | 48 |

Fraction 6 Residual metals

Catharine Arnold
Catharine Arnold, B.Sc., C.Chem
Project Specialist,
Environment, Health & Safety



SGS Canada Inc.

P.O. Box 4300 - 185 Concession St.
Lakefield - Ontario - K0L 2H0
Phone: 705-652-2000 FAX: 705-652-6365

28-February-2023

Ramboll Americas Engineering Solutions, Inc.

Attn : Evvan Plank

P.O# Box 4873
Syracuse, New York
13221-7873, USA

Phone: 315-463-7554
Fax:

Date Rec. : 24 November 2022
LR Report: CA19224-NOV22
Reference: Baldwon Power Plant Drilling

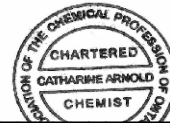
Copy: #1

CERTIFICATE OF ANALYSIS

Final Report

| Analysis | 1: Analysis Start Date | 2: Analysis Start Time Completed | 3: Analysis DateCompleted | 4: Analysis Time | 6: MW-358 (47-49) | 7: MW-358 (86-88) | 8: MW-392 (80-82) | 12: MW-392 (66-68) |
|--------------------|------------------------------|--|---------------------------------|------------------------|----------------------|----------------------|----------------------|-----------------------|
| Sample Date & Time | | | | | 06-Oct-22 15:00 | 08-Oct-22 18:00 | 26-Sep-22 16:00 | 26-Sep-22 12:00 |
| Hg MS [ug/g] | 09-Dec-22 | 16:29 | 12-Dec-22 | 15:05 | < 0.05 | < 0.05 | < 0.05 | < 0.05 |
| As [ug/g] | 09-Dec-22 | 16:29 | 12-Dec-22 | 15:05 | 2.1 | 11 | 17 | 1.0 |
| B [ug/g] | 09-Dec-22 | 16:29 | 12-Dec-22 | 15:05 | 11 | 16 | 16 | 13 |
| Ba [ug/g] | 09-Dec-22 | 16:29 | 12-Dec-22 | 15:05 | 140 | 45 | 40 | 21 |
| Be [ug/g] | 09-Dec-22 | 16:29 | 12-Dec-22 | 15:05 | 0.85 | 0.67 | 0.85 | 0.70 |
| Cd [ug/g] | 09-Dec-22 | 16:29 | 12-Dec-22 | 15:05 | < 0.02 | < 0.02 | 0.36 | 0.09 |
| Co [ug/g] | 09-Dec-22 | 16:29 | 12-Dec-22 | 15:05 | 4.4 | 23 | 12 | 6.2 |
| Cr [ug/g] | 09-Dec-22 | 16:29 | 12-Dec-22 | 15:05 | 9.5 | 12 | 17 | 16 |
| Li [ug/g] | 09-Dec-22 | 16:29 | 12-Dec-22 | 15:05 | 6 | 20 | 8 | 15 |
| Mo [ug/g] | 09-Dec-22 | 16:29 | 12-Dec-22 | 15:05 | 0.3 | 0.3 | 0.3 | 0.3 |
| Pb [ug/g] | 09-Dec-22 | 16:29 | 12-Dec-22 | 15:05 | 5.7 | 9.6 | 17 | 4.9 |
| Se [ug/g] | 09-Dec-22 | 16:29 | 12-Dec-22 | 15:05 | < 0.7 | < 0.7 | 1.4 | < 0.7 |
| Tl [ug/g] | 09-Dec-22 | 16:29 | 12-Dec-22 | 15:05 | 0.05 | 0.06 | 0.04 | 0.03 |

Catharine Arnold, B.Sc., C.Chem
Project Specialist,
Environment, Health & Safety



SGS Canada Inc.

P.O. Box 4300 - 185 Concession St.

Lakefield - Ontario - K0L 2H0

Phone: 705-652-2000 FAX: 705-652-6365

LR Report : CA19224-NOV22

DRAFT

Attachment H
X-Ray Diffraction Analytical Data

Quantitative X-Ray Diffraction by Rietveld Refinement

Report Prepared for: Environmental Services

Project Number/ LIMS No. Custom XRD/MI4527-AUG23

Sample Receipt: August 10, 2023

Sample Analysis: August 25, 2023

Reporting Date: September 15, 2023

Instrument: BRUKER AXS D8 Advance Diffractometer

Test Conditions: Co radiation, 35 kV, 40 mA; Detector: LYNXEYE
Regular Scanning: Step: 0.02°, Step time: 0.75s, 2θ range: 6-80°
Clay Section Scanning: Step: 0.01°, Step time: 0.2s, 2θ range: 3-40°

Interpretations: PDF2/PDF4 powder diffraction databases issued by the International Center for Diffraction Data (ICDD). DiffracPlus Eva and Topas software.

Detection Limit: 0.5-2%. Strongly dependent on crystallinity.

Contents:
1) Method Summary
2) Quantitative XRD Results
3) XRD Pattern(s)



Kim Gibbs, H.B.Sc., P.Geo.
Senior Mineralogist



Huiyun Zhou, Ph.D., P.Geo.
Senior Mineralogist

ACCREDITATION: SGS Natural Resources Lakefield is accredited to the requirements of ISO/IEC 17025 for specific tests as listed on our scope of accreditation, including geochemical, mineralogical and trade mineral tests. To view a list of the accredited methods, please visit the following website and search SGS Canada Inc. - Minerals: <https://www.scc.ca/en/search/palcan>.



Method Summary

The Rietveld Method of Mineral Identification by XRD (ME-LR-MIN-MET-MN-D05) method used by SGS Natural Resources is accredited to the requirements of ISO/IEC 17025.

Mineral Identification and Interpretation:

Mineral identification and interpretation involves matching the diffraction pattern of an unknown material to patterns of single-phase reference materials. The reference patterns are compiled by the Joint Committee on Powder Diffraction Standards - International Center for Diffraction Data (JCPDS-ICDD) database and released on software as Powder Diffraction Files (PDF).

Interpretations do not reflect the presence of non-crystalline and/or amorphous compounds, except when internal standards have been added by request. Mineral proportions may be strongly influenced by crystallinity, crystal structure and preferred orientations. Mineral or compound identification and quantitative analysis results should be accompanied by supporting chemical assay data or other additional tests.

Clay Mineral Separation and Identification:

Clay minerals are typically fine-grained ($<2\ \mu\text{m}$) phyllosilicates in sedimentary rock. Due to the poor crystallinity and fine size of clay minerals, separation of the clay fraction from bulk samples by centrifuge is required. A slide of the oriented clay fraction is prepared and scanned followed by a series of procedures (the addition of ethylene glycol and high temperature heating). Clay minerals are identified by their individual diffraction patterns and changes in their diffraction pattern after different treatments. Clay speciation and mineral identification of the bulk sample are performed using DIFFRACplus EVA (Bruker AXS).

Quantitative Rietveld Analysis:

Quantitative Rietveld Analysis is performed by using Topas 4.2 (Bruker AXS), a graphics based profile analysis program built around a non-linear least squares fitting system, to determine the amount of different phases present in a multicomponent sample. Whole pattern analyses are predicated by the fact that the X-ray diffraction pattern is a total sum of both instrumental and specimen factors. Unlike other peak intensity-based methods, the Rietveld method uses a least squares approach to refine a theoretical line profile until it matches the obtained experimental patterns.

Rietveld refinement is completed with a set of minerals specifically identified for the sample. Zero values indicate that the mineral was included in the refinement calculations, but the calculated concentration was less than 0.05wt%. Minerals not identified by the analyst are not included in refinement calculations for specific samples and are indicated with a dash.

DISCLAIMER: This document is issued by the Company under its General Conditions of Service accessible at <http://www.sgs.com/en/Terms-and-Conditions.aspx>. Attention is drawn to the limitation of liability, indemnification and jurisdiction issues defined therein. Any holder of this document is advised that information contained hereon reflects the Company's findings at the time of its intervention only and within the limits of Client's instructions, if any. The Company's sole responsibility is to its Client and this document does not exonerate parties to a transaction from exercising all their rights and obligations under the transaction documents. Any unauthorized alteration, forgery or falsification of the content or appearance of this document is unlawful and offenders may be prosecuted to the fullest extent of the law.

WARNING: The sample(s) to which the findings recorded herein (the "Findings") relate was(were) drawn and / or provided by the Client or by a third party acting at the Client's direction. The Findings constitute no warranty of the sample's representativeness of any goods and strictly relate to the sample(s). The Company accepts no liability with regard to the origin or source from which the sample(s) is/are said to be extracted.

Summary of Rietveld Quantitative Analysis X-Ray Diffraction Results

| Mineral/Compound | BAL-1-15-20- 20230620 AUG4527-01 (wt %) | BAL-1-20-25- 20230620 AUG4527-02 (wt %) | BAL-1-35-40- 20230620 AUG4527-03 (wt %) | BAL-1-42-46- 20230620 AUG4527-04 (wt %) | BAL-1-42-46-2- 20230620 AUG4527-05 (wt %) | BAL-2-50-60- 20230621 AUG4527-06 (wt %) |
|------------------------|--|--|--|--|--|--|
| Quartz | 53.5 | 32.4 | 17.7 | 10.4 | 10.7 | 11.2 |
| Actinolite | 2.0 | 0.5 | 1.3 | - | - | - |
| Albite | 11.3 | 9.0 | 2.5 | 0.4 | 0.6 | 0.2 |
| Microcline | 8.0 | 9.7 | 4.6 | 2.1 | 0.5 | 2.1 |
| Dolomite | 9.4 | 11.2 | 4.4 | 0.8 | 0.4 | 3.5 |
| Calcite | 2.9 | 9.5 | 27.2 | 80.5 | 84.6 | 57.2 |
| Magnetite | 0.3 | 0.5 | 0.8 | - | - | 0.2 |
| Muscovite | 2.0 | 9.1 | 11.8 | 1.9 | 1.4 | 6.4 |
| Chlorite | - | 0.7 | 0.2 | 0.0 | 0.2 | 0.2 |
| Pyrite | - | - | 1.6 | - | - | 0.6 |
| Ankerite | - | - | 7.3 | 0.4 | 0.2 | 4.7 |
| Gypsum | - | - | 1.9 | - | - | - |
| Hematite | - | - | 0.4 | - | - | 0.2 |
| Anatase | - | - | 0.6 | - | - | - |
| Rhodochrosite | - | - | 0.7 | - | - | - |
| Clay | | | | | | |
| Montmorillonite | 5.5 | 9.0 | 10.5 | 2.1 | 0.2 | 7.8 |
| Illite | 4.0 | 6.8 | 3.2 | 0.9 | 0.6 | 3.2 |
| Kaolinite | 1.0 | 1.5 | 3.2 | 0.5 | 0.6 | 2.4 |
| Illite-Montmorillonite | - | - | - | - | - | - |
| TOTAL | 100 | 100 | 100 | 100 | 100 | 100 |

Zero values indicate that the mineral was included in the refinement, but the calculated concentration is below a measurable value.

Dashes indicate that the mineral was not identified by the analyst and not included in the refinement calculation for the sample.

The weight percent quantities indicated have been normalized to a sum of 100%. The quantity of amorphous material has not been determined.

| Mineral/Compound | Formula |
|------------------------|--|
| Quartz | SiO ₂ |
| Actinolite | Ca ₂ (Mg,Fe) ₅ Si ₈ O ₂₂ (OH) ₂ |
| Albite | NaAlSi ₃ O ₈ |
| Microcline | KAlSi ₃ O ₈ |
| Dolomite | CaMg(CO ₃) ₂ |
| Calcite | CaCO ₃ |
| Magnetite | Fe ₃ O ₄ |
| Muscovite | KAl ₂ (AlSi ₃ O ₁₀)(OH) ₂ |
| Chlorite | (Fe,(Mg,Mn) ₅ ,Al)(Si ₃ Al)O ₁₀ (OH) ₈ |
| Pyrite | FeS ₂ |
| Ankerite | CaFe(CO ₃) ₂ |
| Gypsum | CaSO ₄ ·2H ₂ O |
| Hematite | Fe ₂ O ₃ |
| Anatase | TiO ₂ |
| Rhodochrosite | MnCO ₃ |
| Montmorillonite | (Na,Ca) _{0.3} (Al,Mg) ₂ Si ₄ O ₁₀ (OH) ₂ ·10H ₂ O |
| Illite | (K,H ₃ O)(Al,Mg,Fe) ₂ (Si,Al) ₄ O ₁₀ [(OH) ₂ ,(H ₂ O)] |
| Kaolinite | Al ₂ Si ₂ O ₅ (OH) ₄ |
| Illite-Montmorillonite | KAl ₄ (Si,Al) ₈ O ₂₀ (OH) ₄ ·8H ₂ O |

Summary of Rietveld Quantitative Analysis X-Ray Diffraction Results

| Mineral/Compound | BAL-2-60-70- 20230621 AUG4527-07 (wt %) | BAL-3-40-52- 20230621 AUG4527-08 (wt %) | BAL-4-50-51- 20230622 AUG4527-09 (wt %) | BAL-4-51-55- 20230622 AUG4527-10 (wt %) | BAL-4-55-72- 20230622 AUG4527-11 (wt %) |
|------------------------|--|--|--|--|--|
| Quartz | 19.4 | 14.2 | 24.2 | 13.1 | 5.2 |
| Actinolite | - | - | - | - | - |
| Albite | 0.2 | 1.8 | 2.2 | 0.4 | 0.0 |
| Microcline | 1.3 | 5.3 | 3.2 | 1.9 | 0.3 |
| Dolomite | 6.2 | 0.3 | - | - | - |
| Calcite | 49.5 | 33.9 | 35.5 | 74.9 | 90.2 |
| Magnetite | - | - | 0.7 | 0.4 | - |
| Muscovite | 4.3 | 12.9 | 17.6 | 5.3 | 2.0 |
| Chlorite | 1.8 | 3.7 | - | - | - |
| Pyrite | 0.8 | 1.3 | 0.2 | 0.1 | 0.3 |
| Ankerite | 10.0 | 1.6 | - | 0.0 | 0.4 |
| Gypsum | - | - | - | - | - |
| Hematite | 0.4 | - | - | - | - |
| Anatase | - | 0.6 | 0.5 | 0.5 | - |
| Rhodochrosite | - | - | - | - | - |
| Clay | | | | | |
| Montmorillonite | 2.6 | 14.0 | - | 2.2 | 0.9 |
| Illite | 2.6 | 6.1 | 7.9 | 1.2 | 0.9 |
| Kaolinite | 0.8 | 4.2 | - | - | - |
| Illite-Montmorillonite | - | - | 8.0 | - | - |
| TOTAL | 100 | 100 | 100 | 100 | 100 |

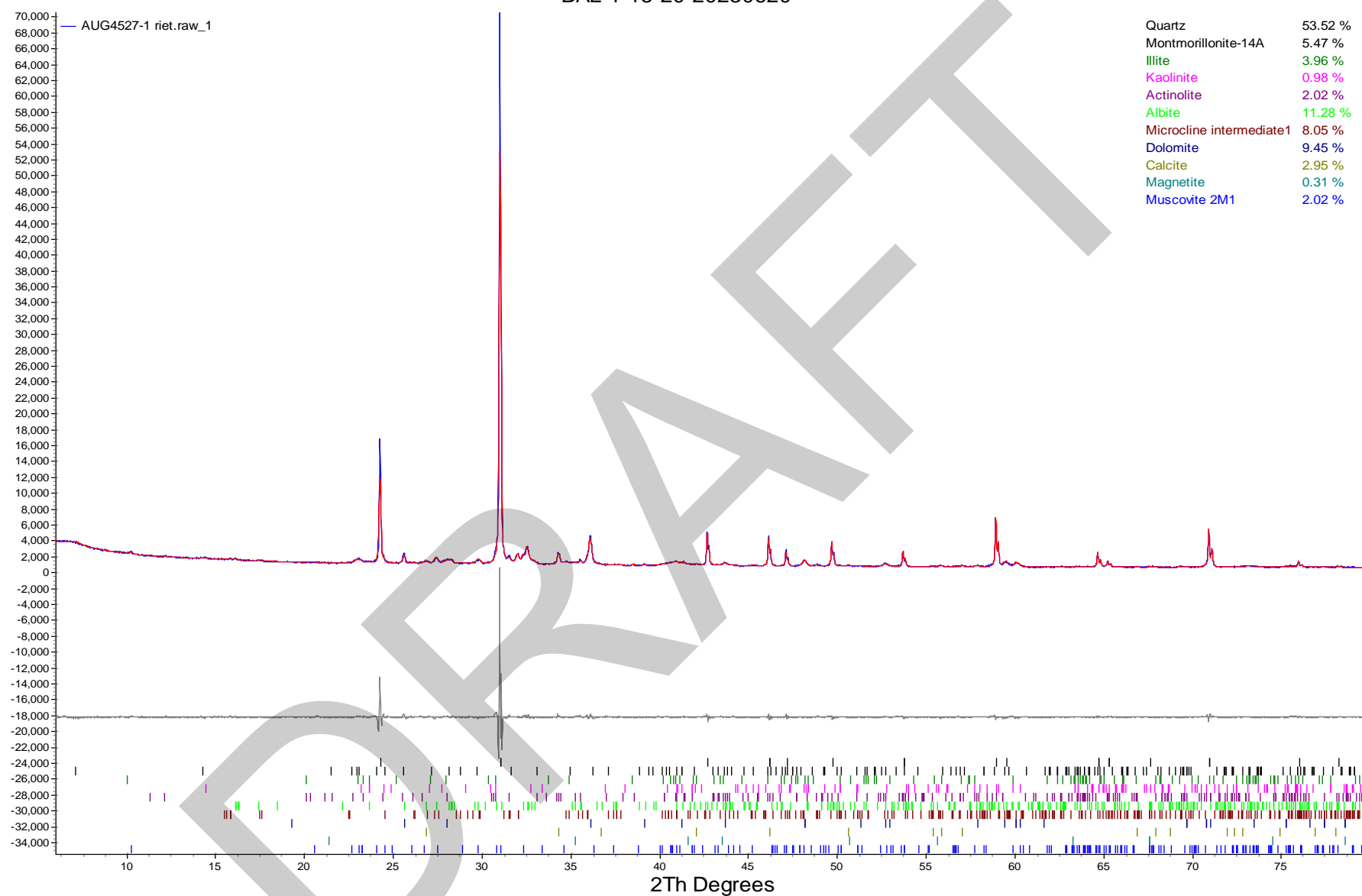
Zero values indicate that the mineral was included in the refinement, but the calculated concentration is below a measurable value.

Dashes indicate that the mineral was not identified by the analyst and not included in the refinement calculation for the sample.

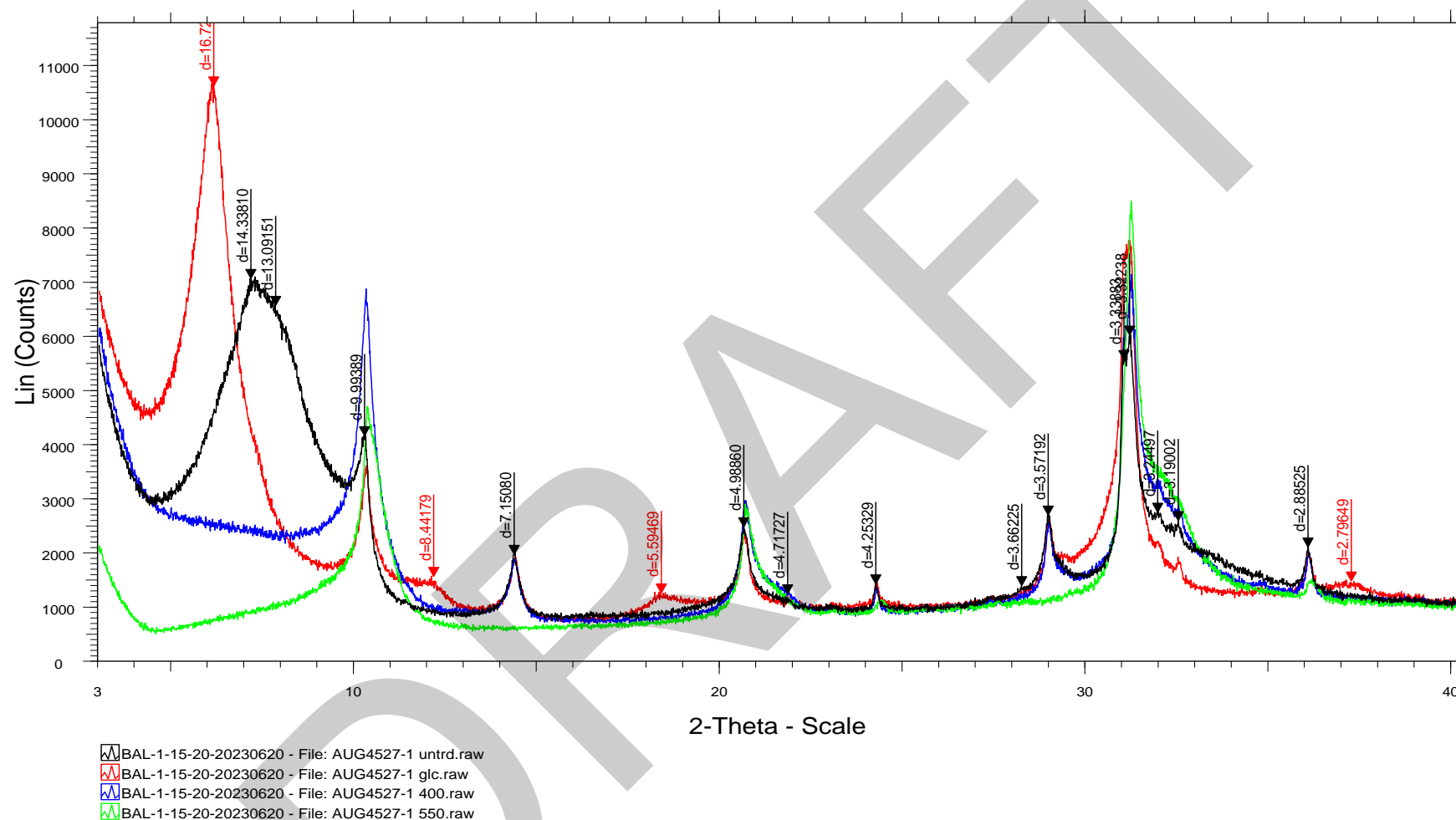
The weight percent quantities indicated have been normalized to a sum of 100%. The quantity of amorphous material has not been determined.

| Mineral/Compound | Formula |
|------------------------|--|
| Quartz | SiO ₂ |
| Actinolite | Ca ₂ (Mg,Fe) ₅ Si ₈ O ₂₂ (OH) ₂ |
| Albite | NaAlSi ₃ O ₈ |
| Microcline | KAlSi ₃ O ₈ |
| Dolomite | CaMg(CO ₃) ₂ |
| Calcite | CaCO ₃ |
| Magnetite | Fe ₃ O ₄ |
| Muscovite | KAl ₂ (AlSi ₃ O ₁₀)(OH) ₂ |
| Chlorite | (Fe,(Mg,Mn) ₅ ,Al)(Si ₃ Al)O ₁₀ (OH) ₈ |
| Pyrite | FeS ₂ |
| Ankerite | CaFe(CO ₃) ₂ |
| Gypsum | CaSO ₄ ·2H ₂ O |
| Hematite | Fe ₂ O ₃ |
| Anatase | TiO ₂ |
| Rhodochrosite | MnCO ₃ |
| Montmorillonite | (Na,Ca) _{0.3} (Al,Mg) ₂ Si ₄ O ₁₀ (OH) ₂ ·10H ₂ O |
| Illite | (K,H ₃ O)(Al,Mg,Fe) ₂ (Si,Al) ₄ O ₁₀ [(OH) ₂ ,(H ₂ O)] |
| Kaolinite | Al ₂ Si ₂ O ₅ (OH) ₄ |
| Illite-Montmorillonite | KAl ₄ (Si,Al) ₈ O ₂₀ (OH) ₄ ·8H ₂ O |

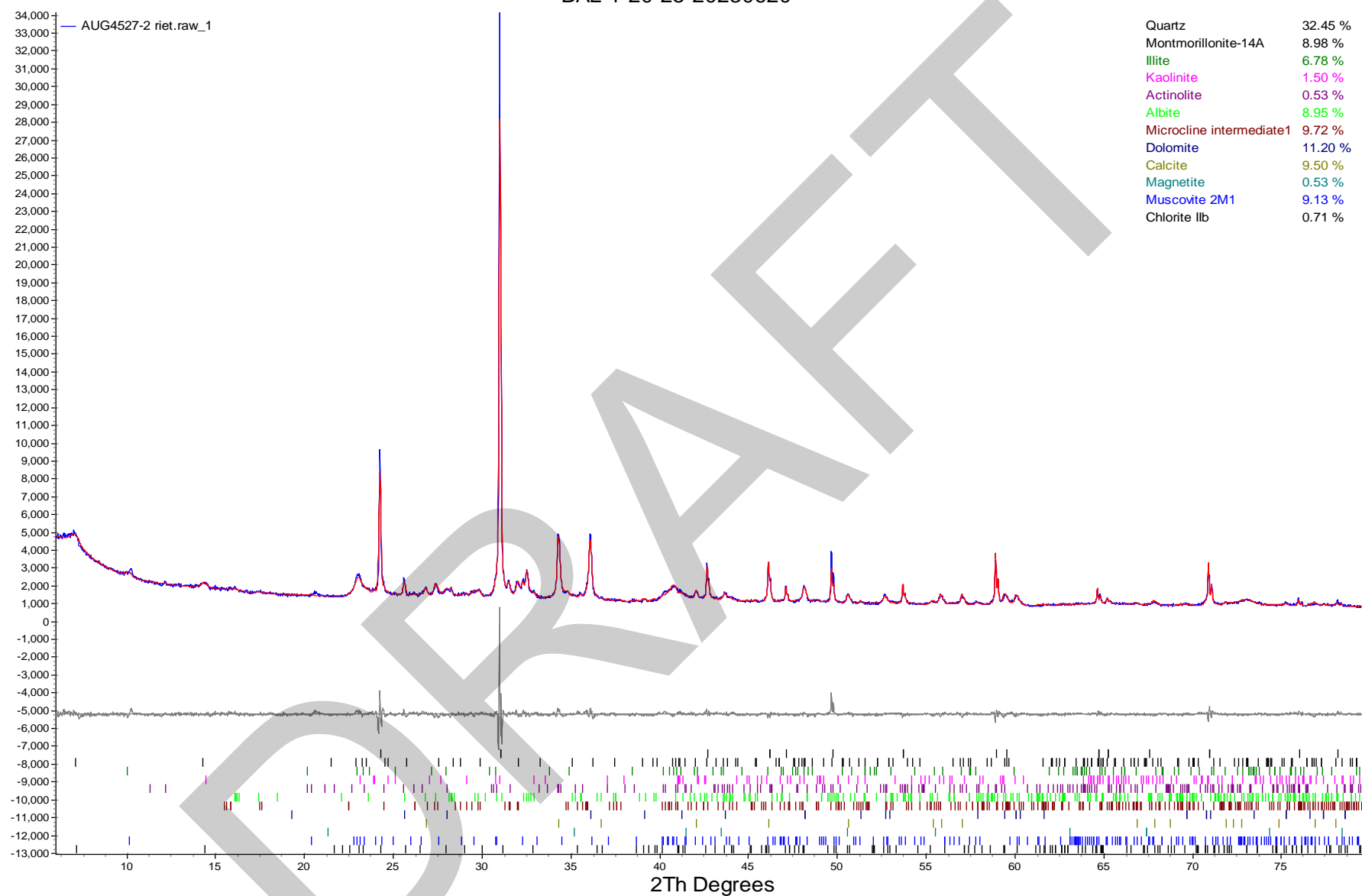
BAL-1-15-20-20230620



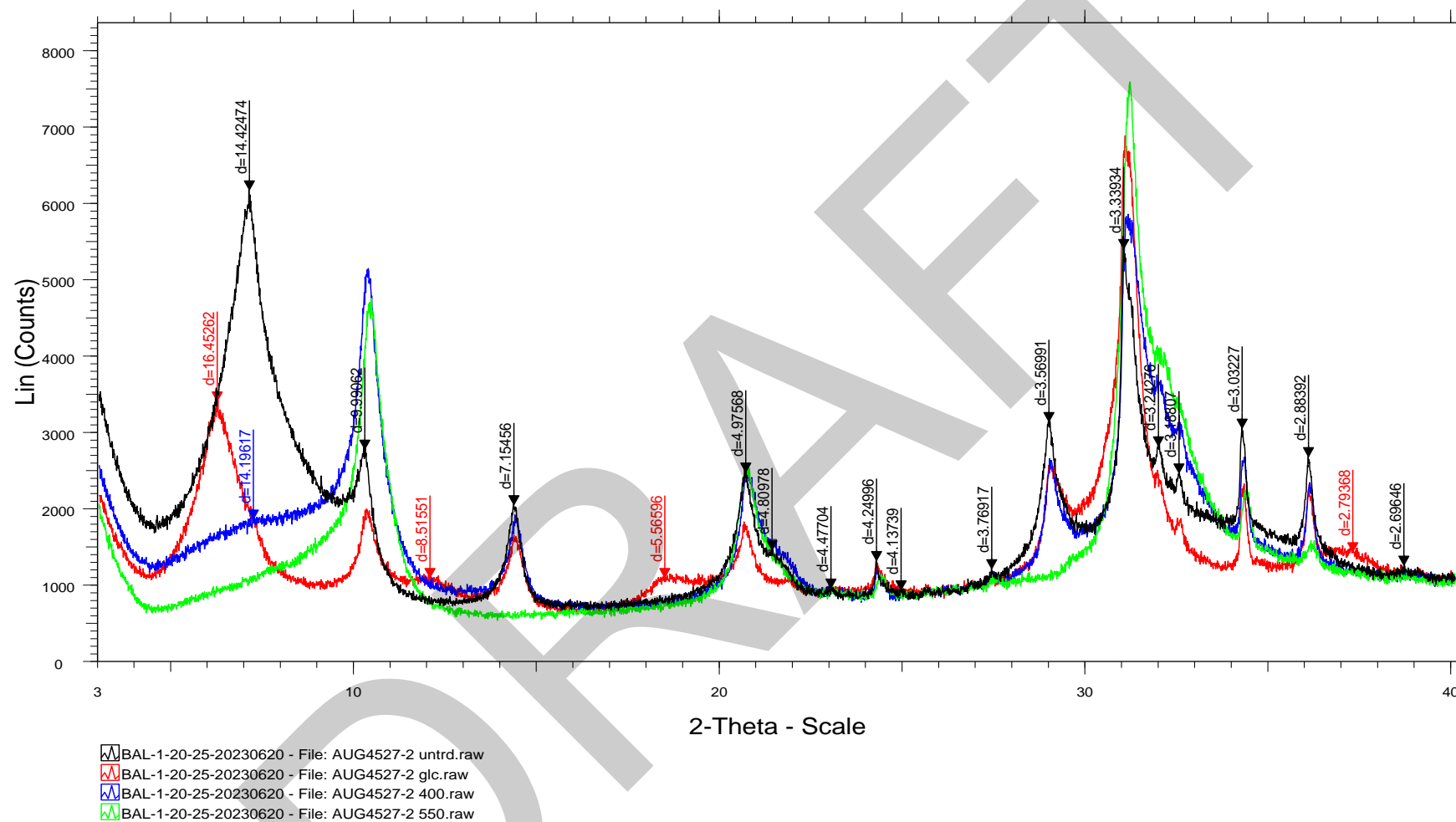
BAL-1-15-20-20230620



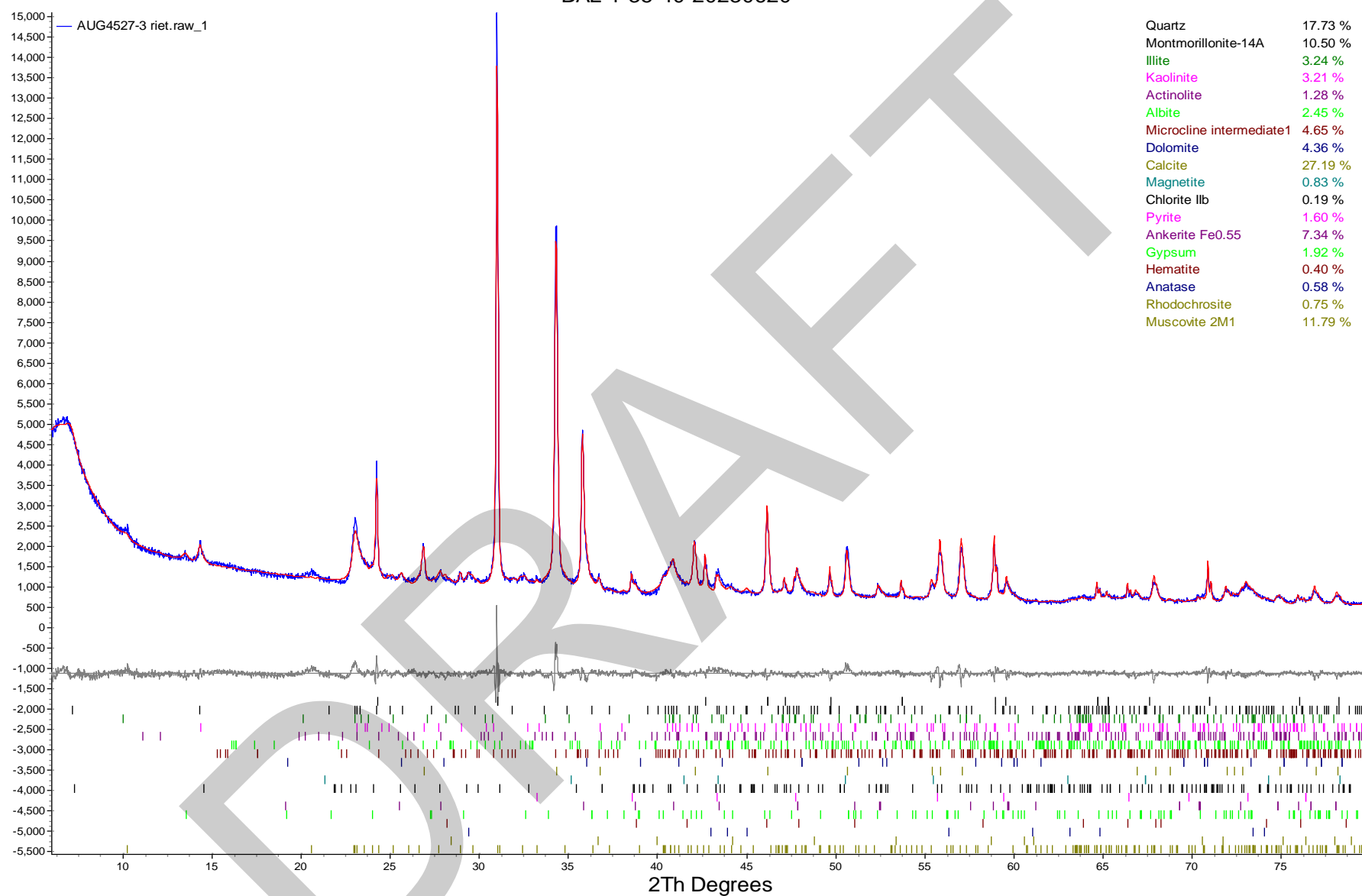
BAL-1-20-25-20230620



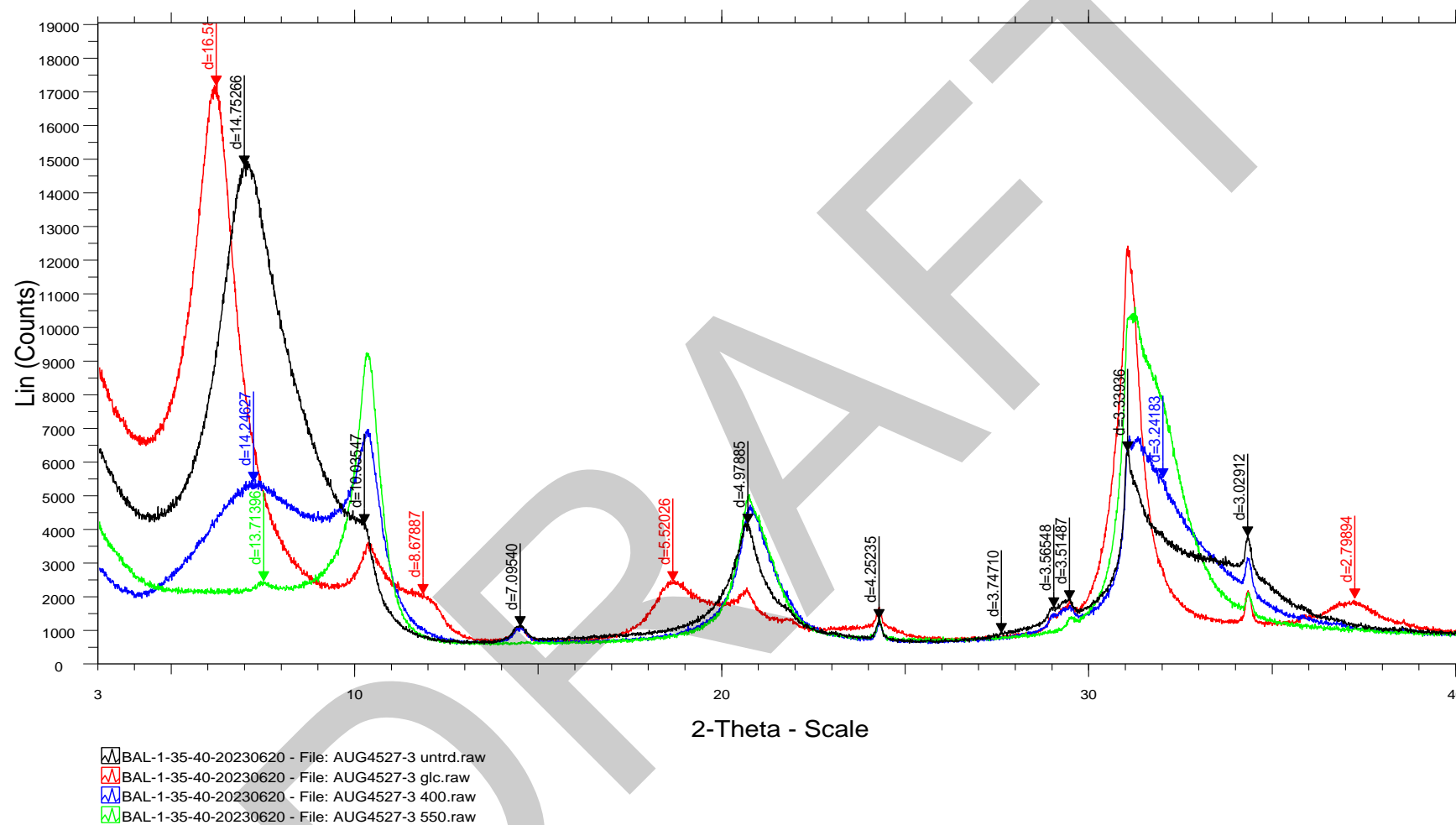
BAL-1-20-25-20230620

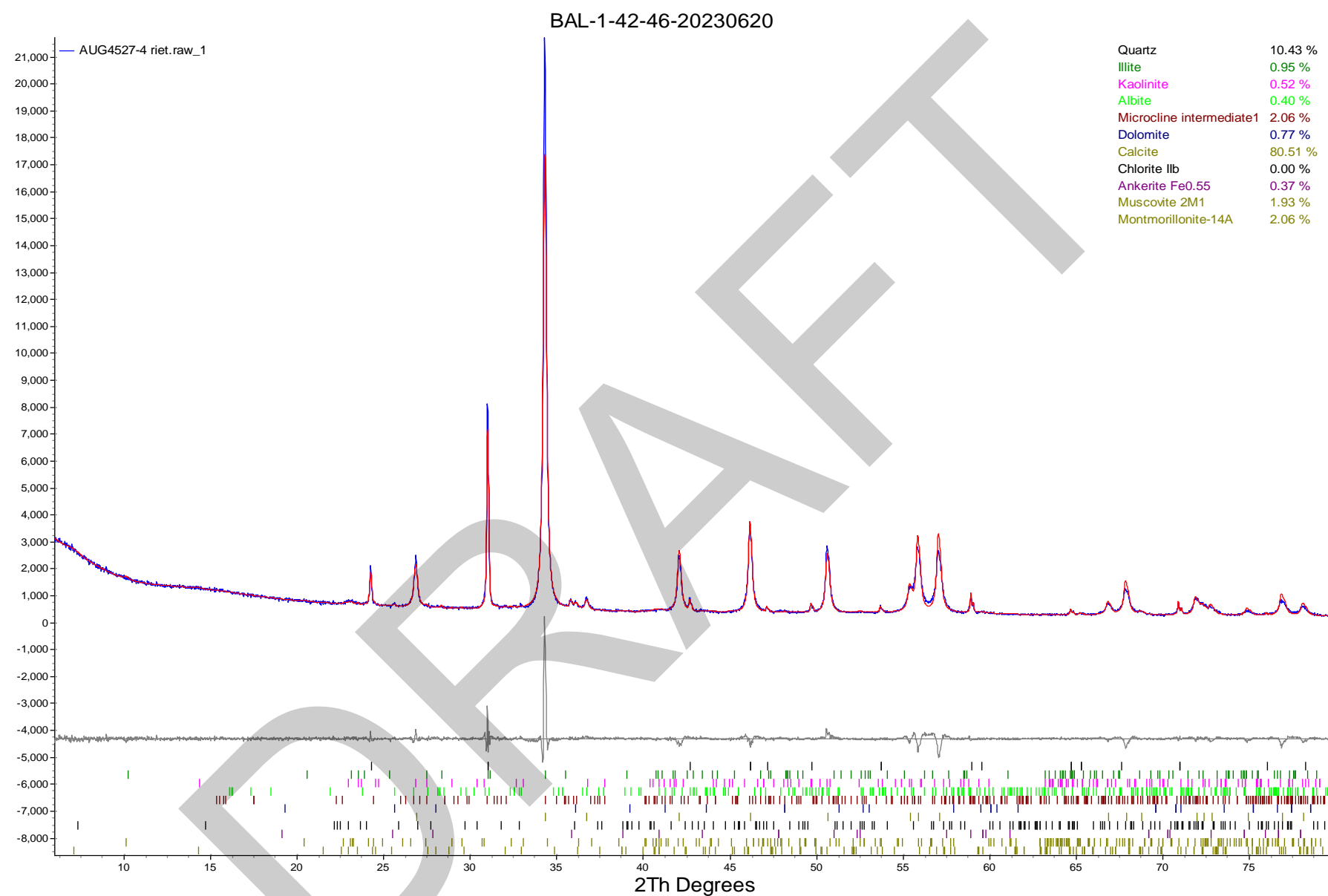


BAL-1-35-40-20230620

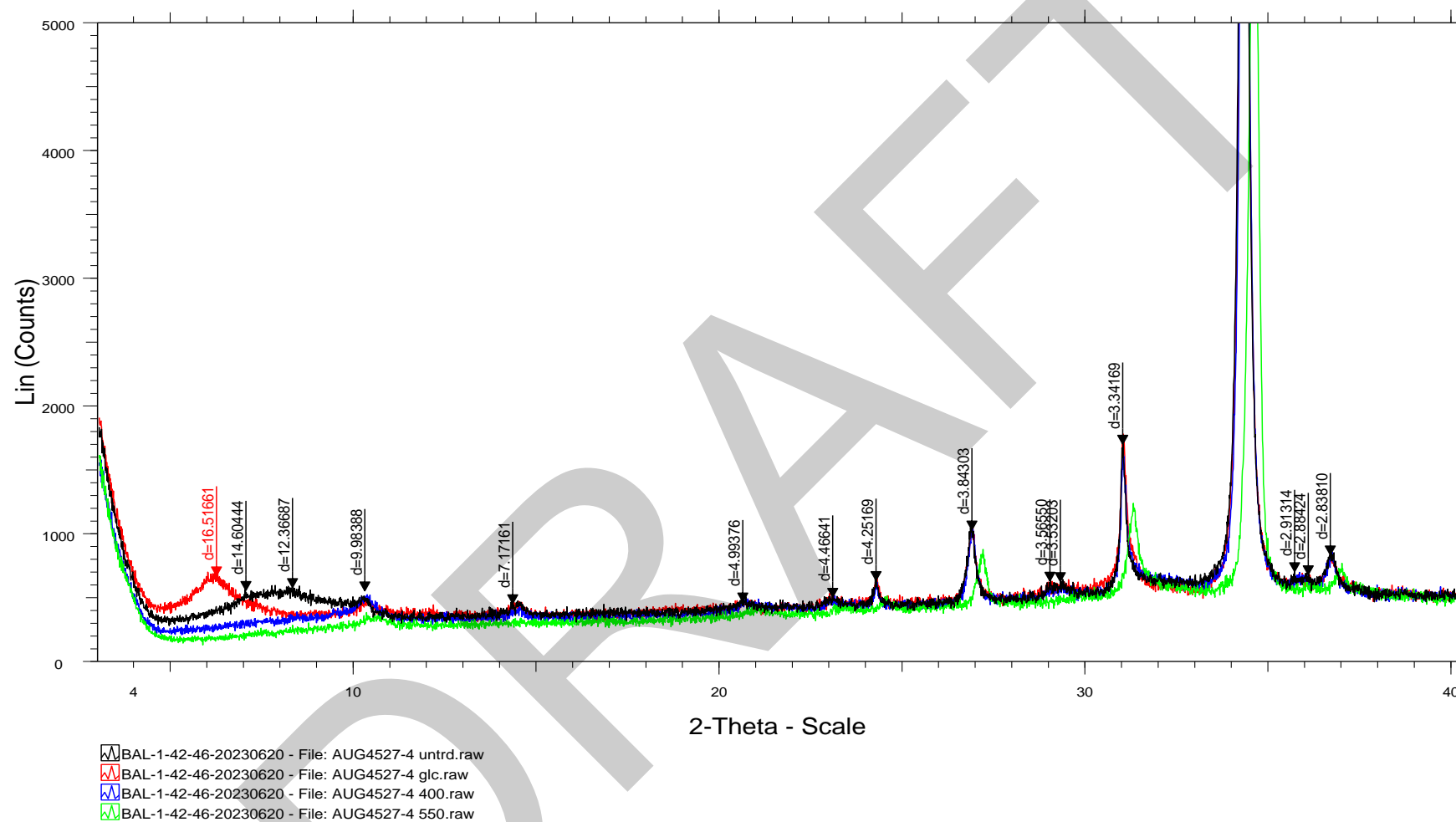


BAL-1-35-40-20230620

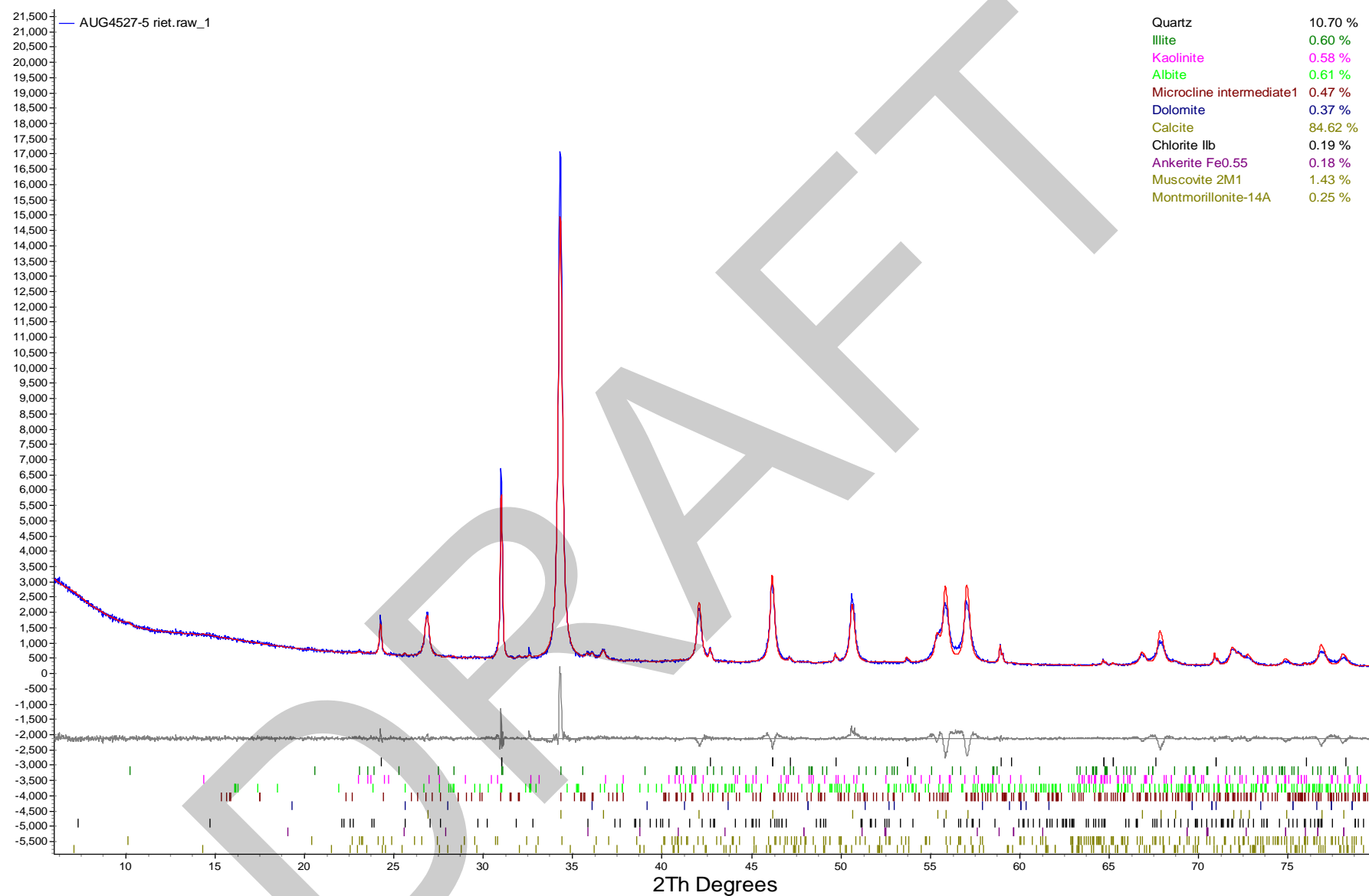




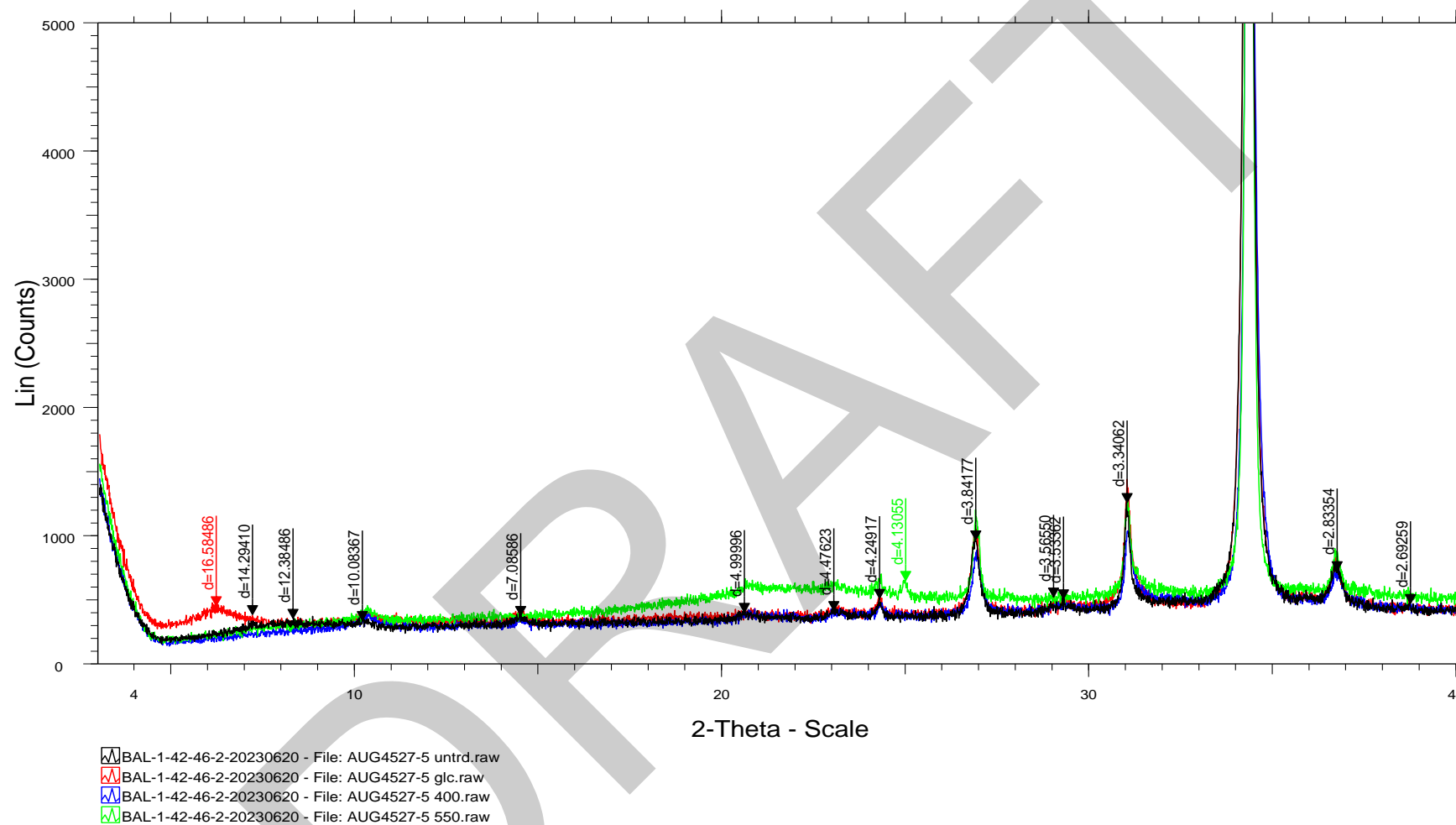
BAL-1-42-46-20230620



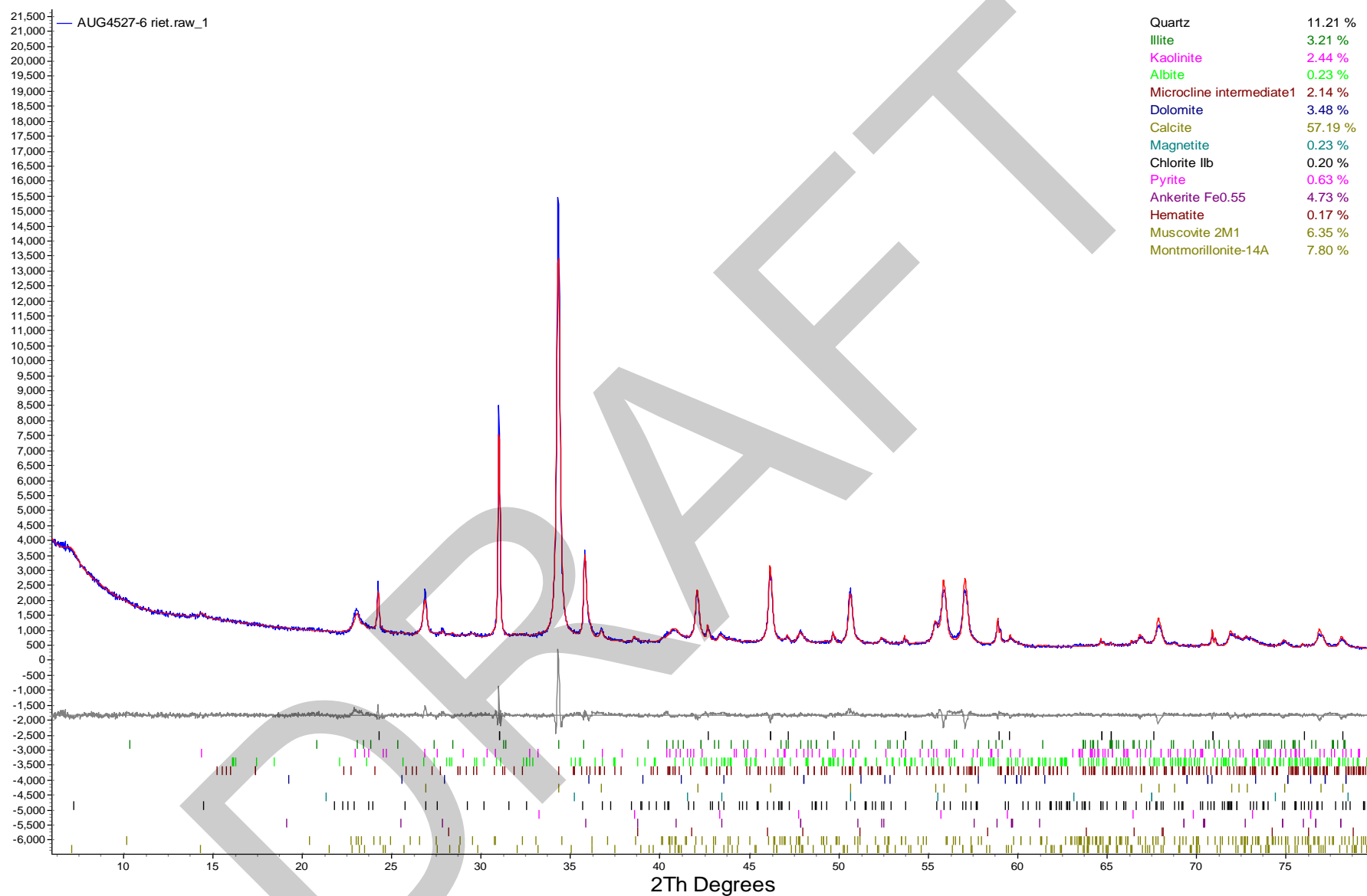
BAL-1-42-46-2-20230620



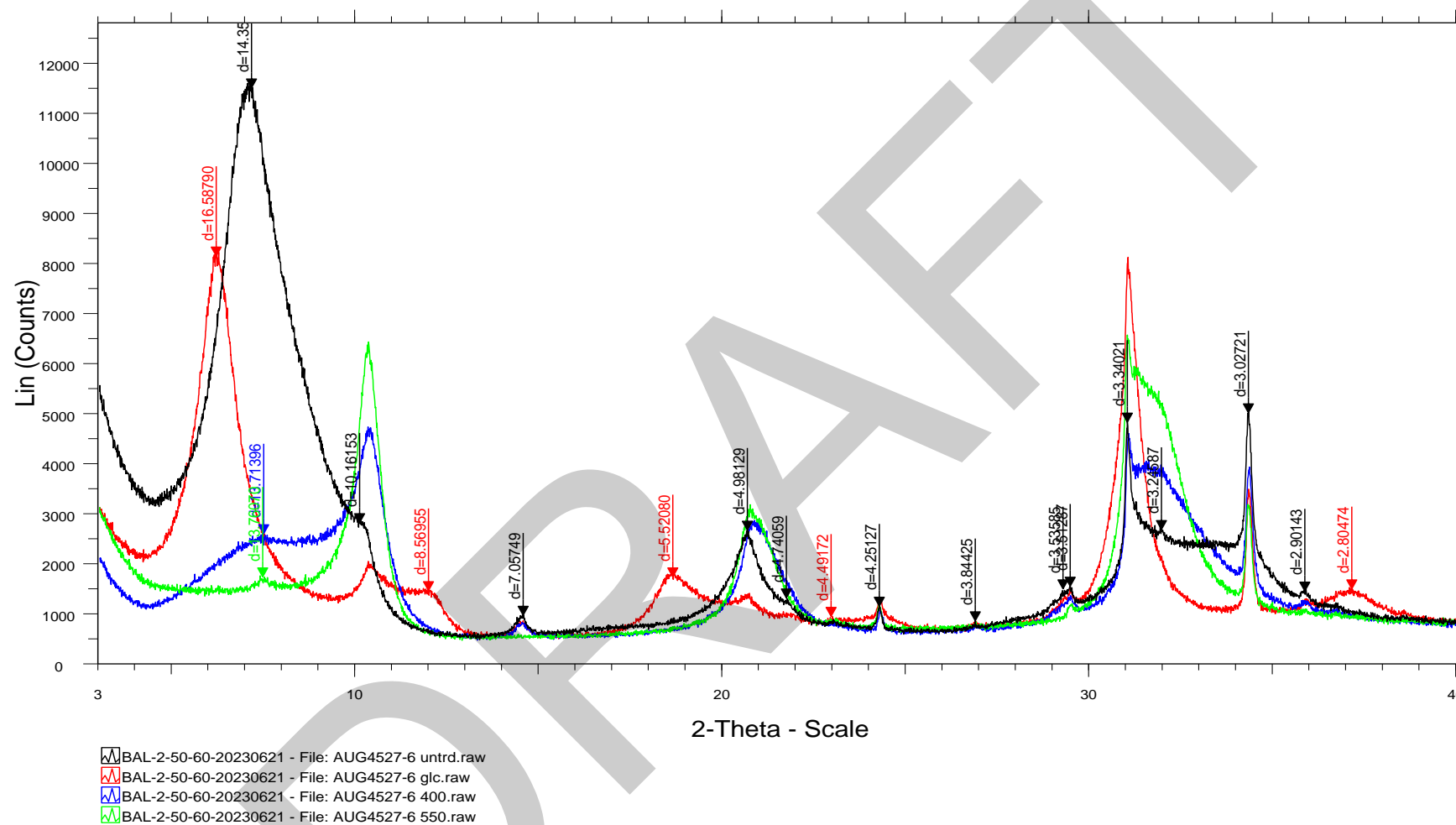
BAL-1-42-46-2-20230620

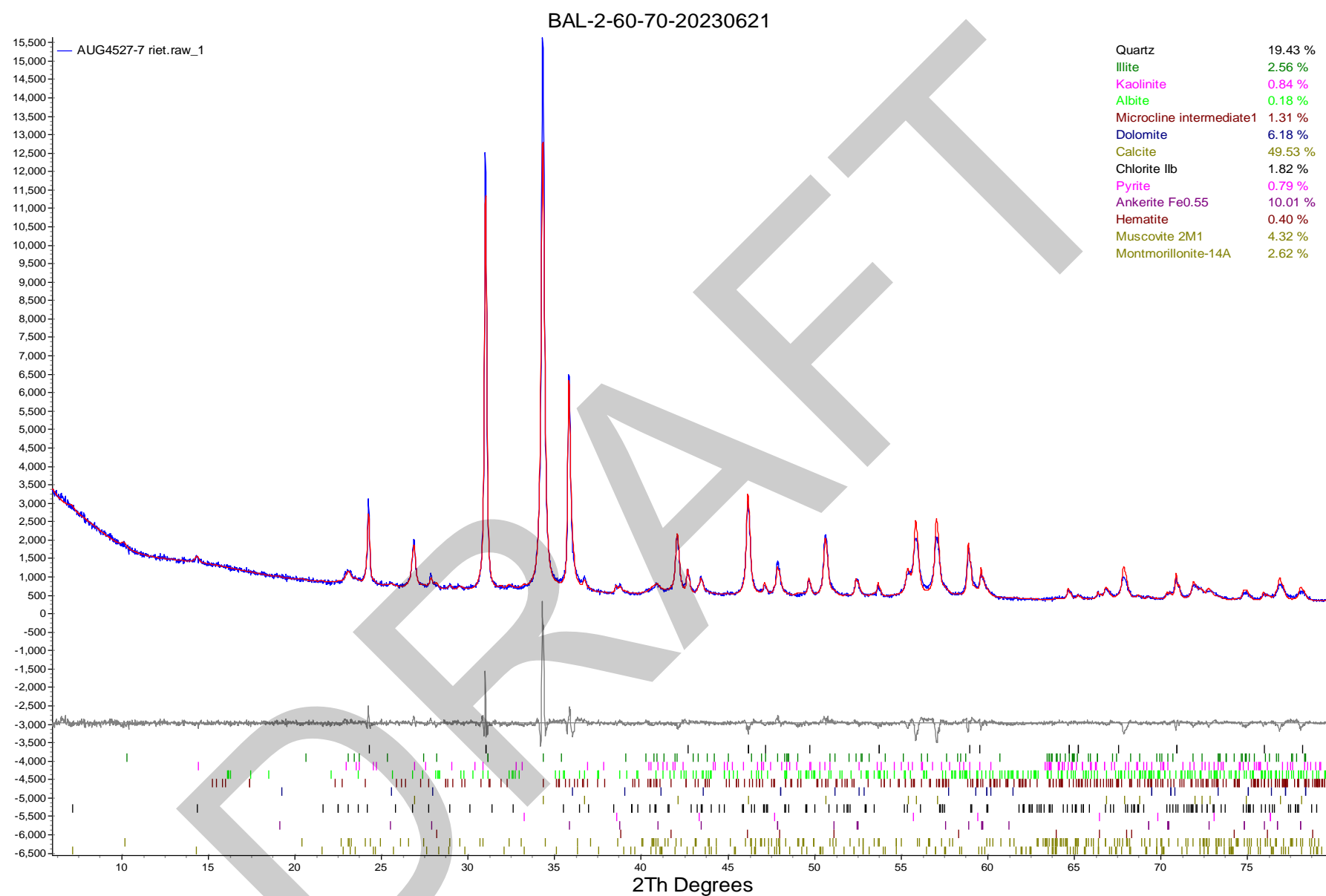


BAL-2-50-60-20230620

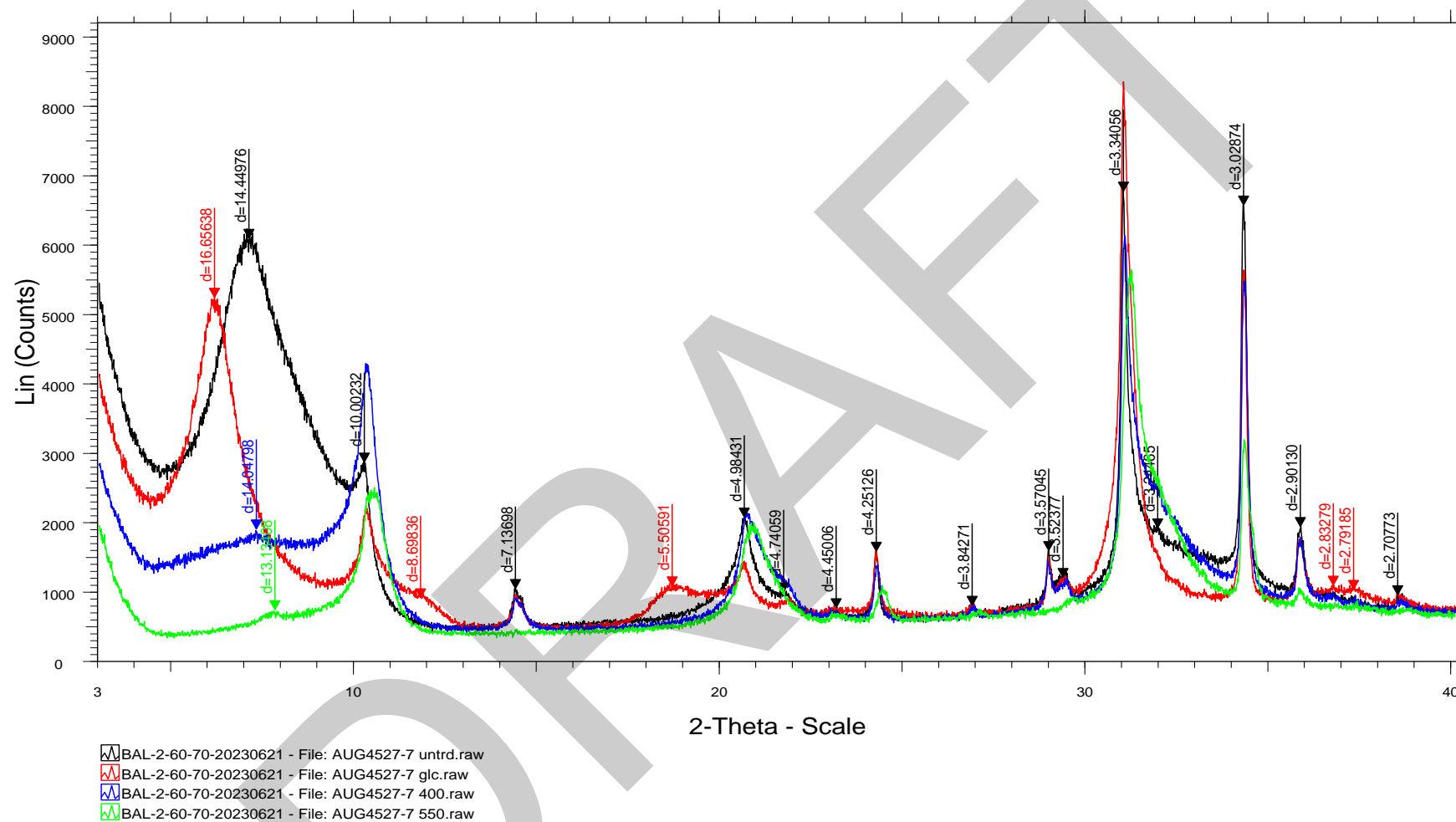


BAL-2-50-60-20230621

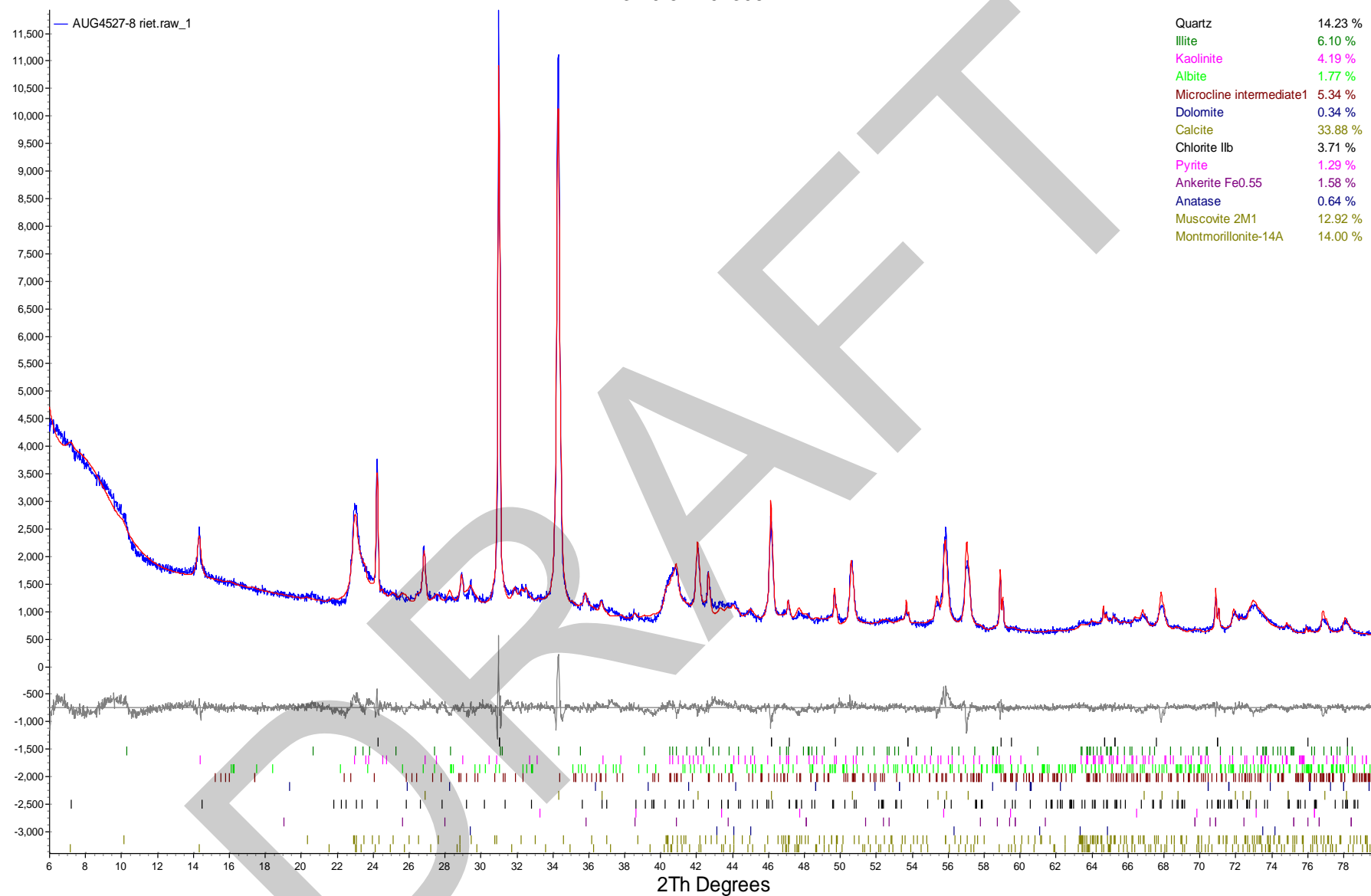




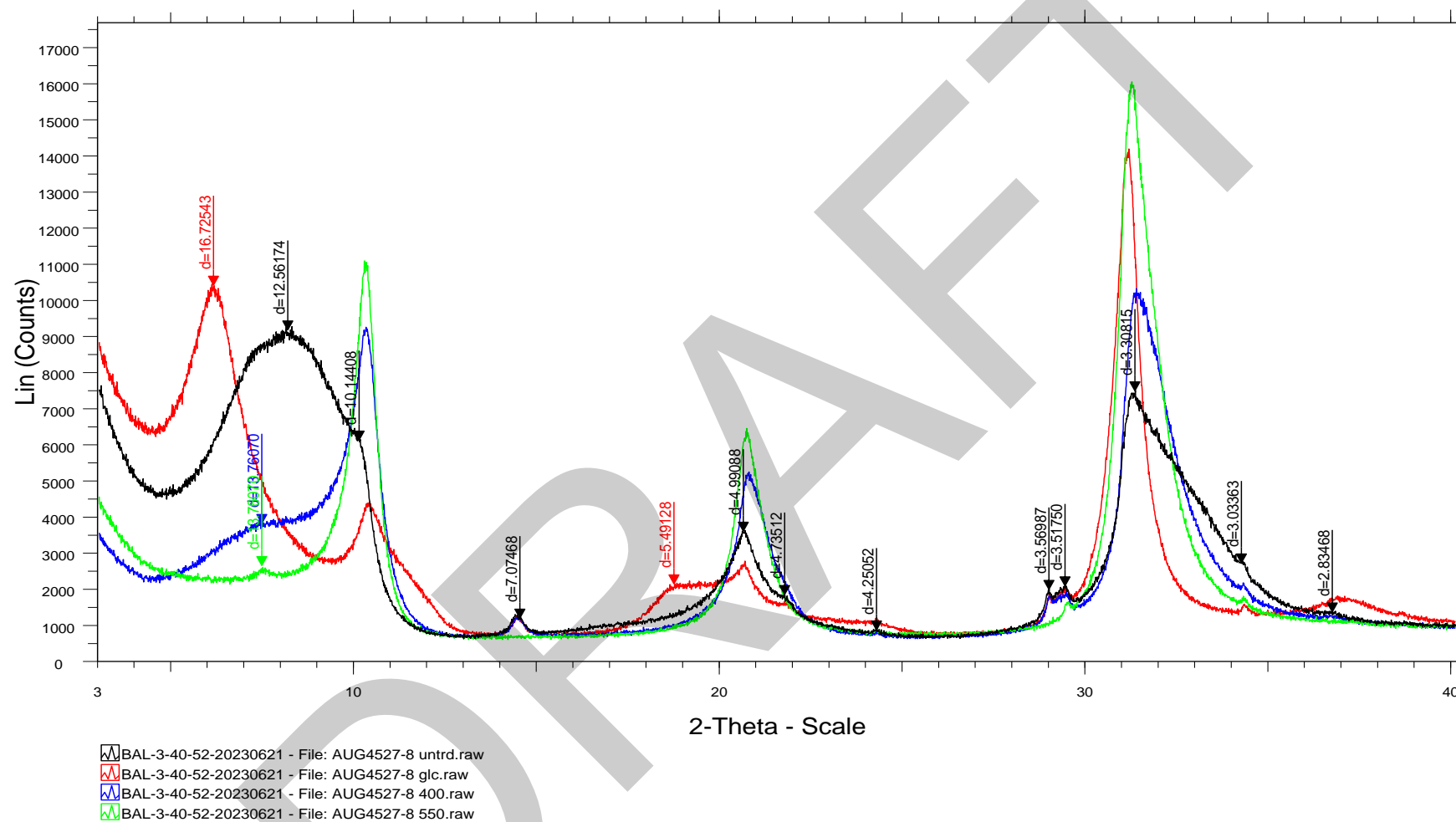
BAL-2-60-70-20230621



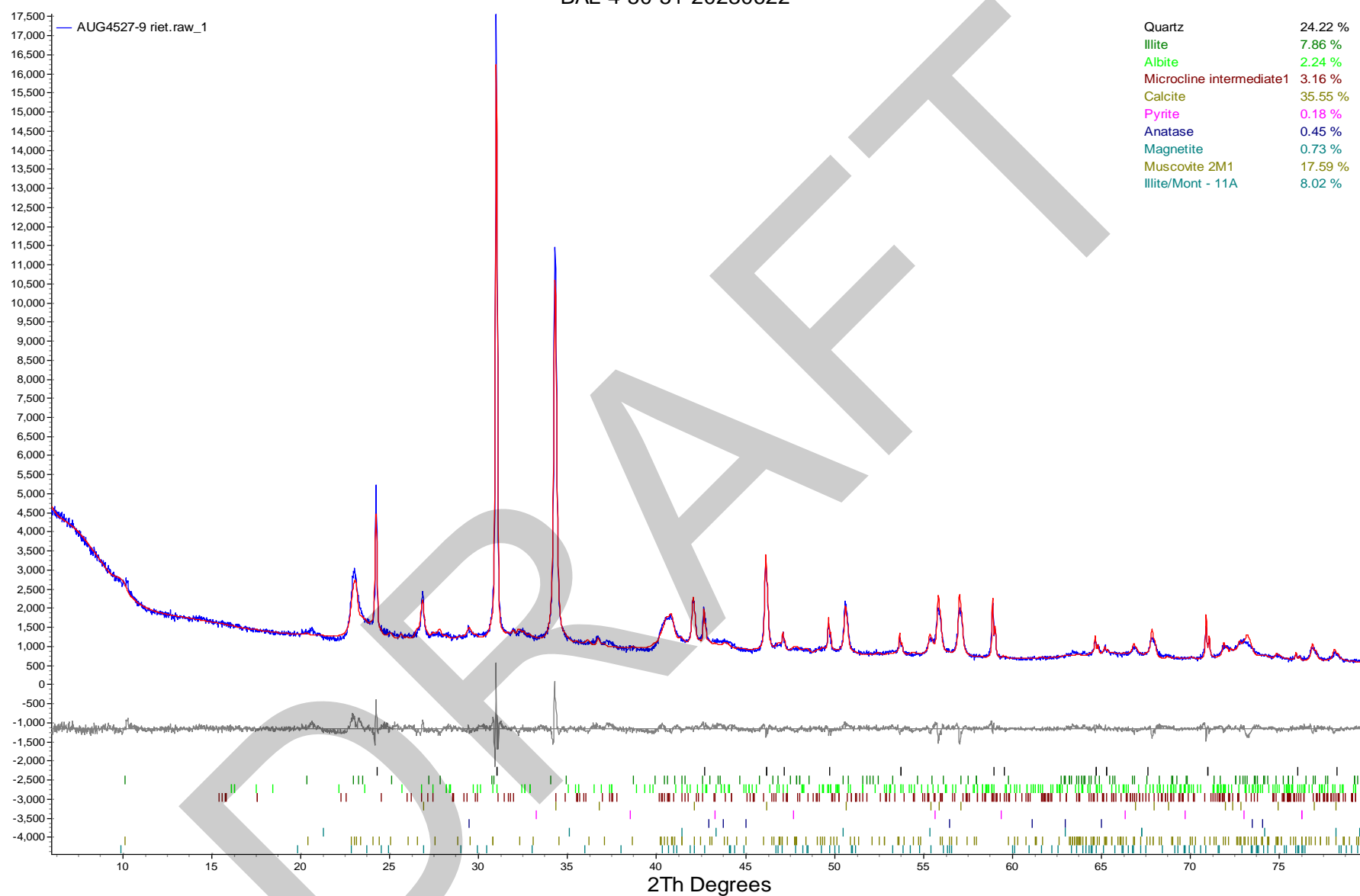
BAL-3-40-52-20230621



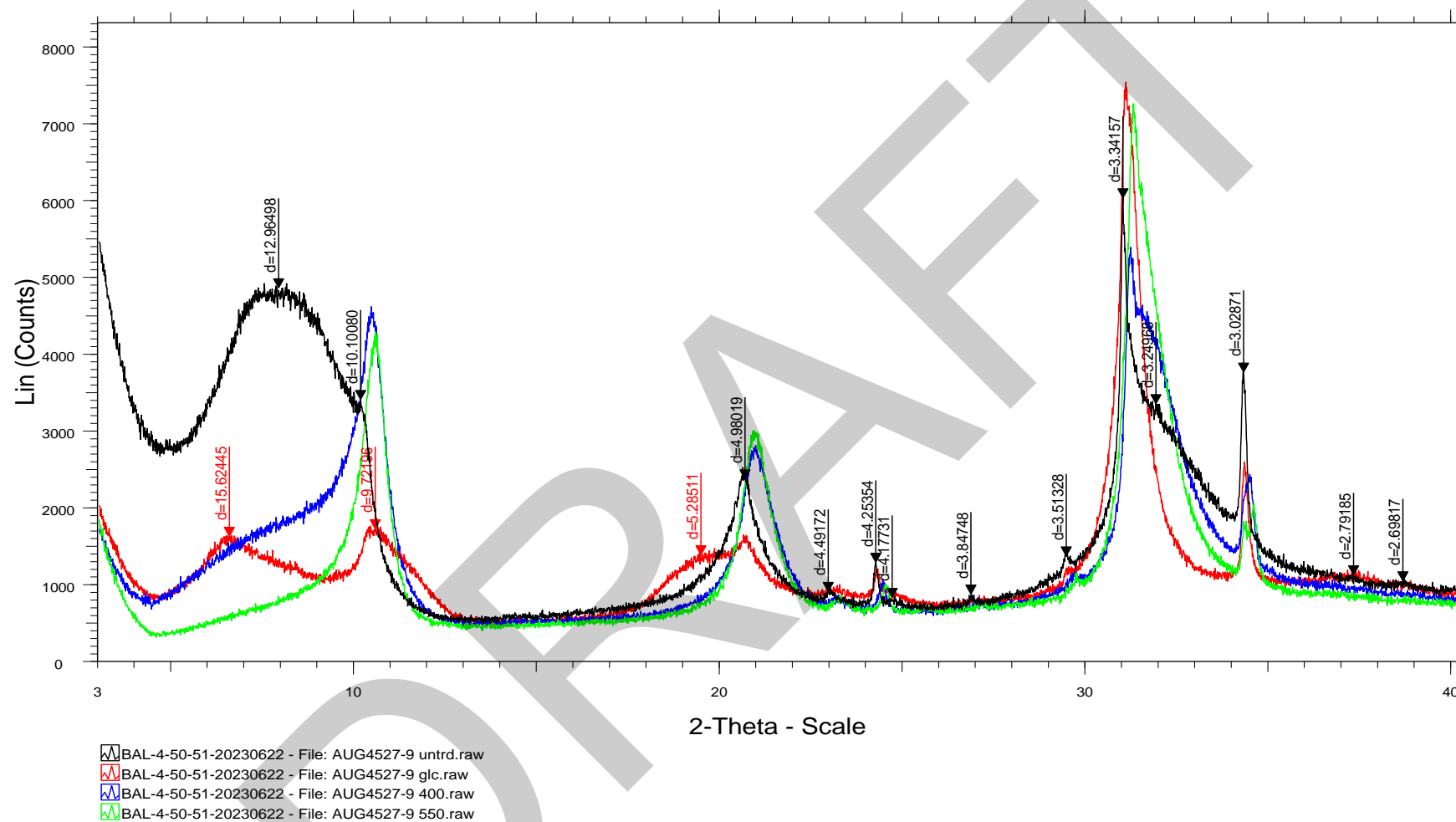
BAL-3-40-52-20230621

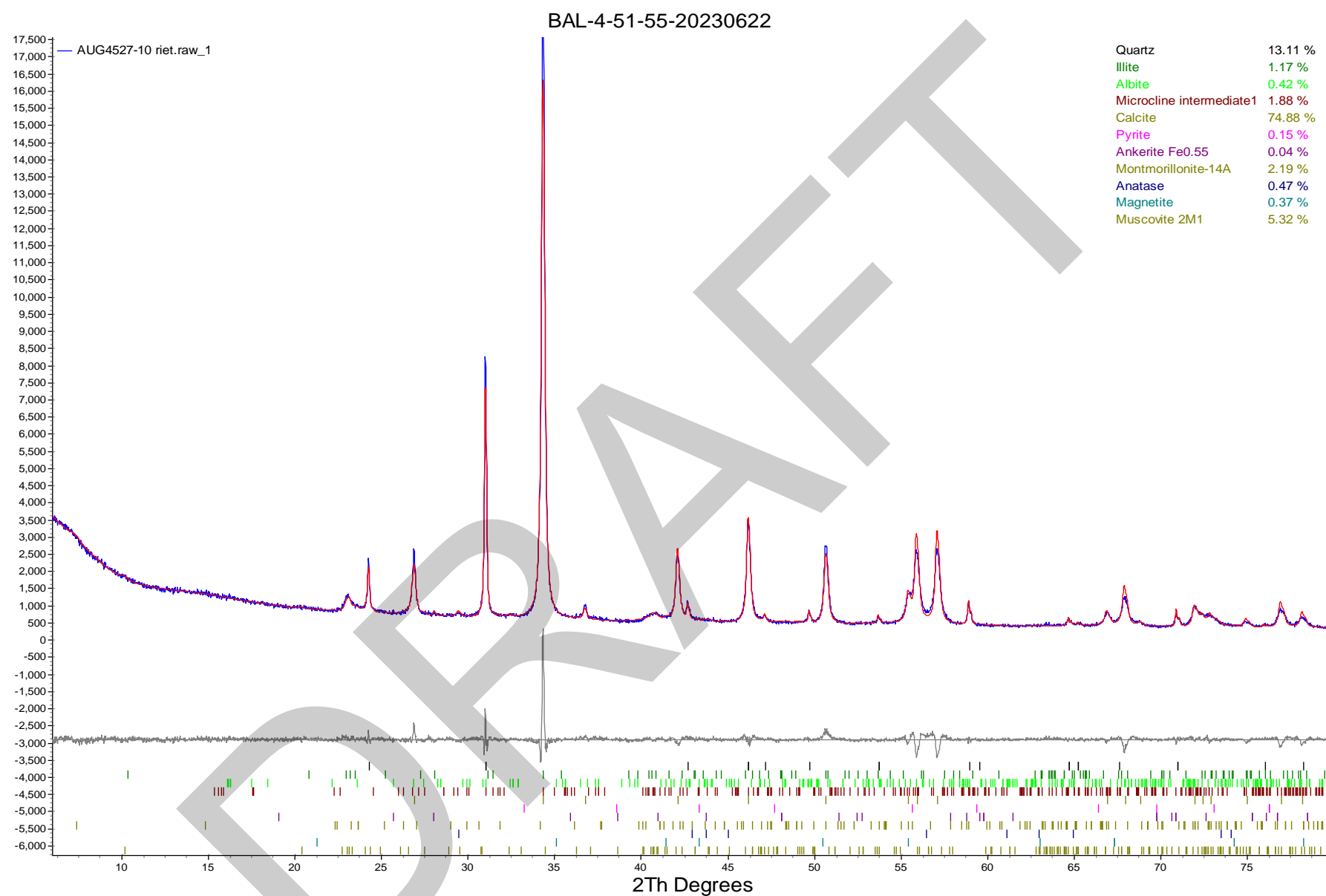


BAL-4-50-51-20230622

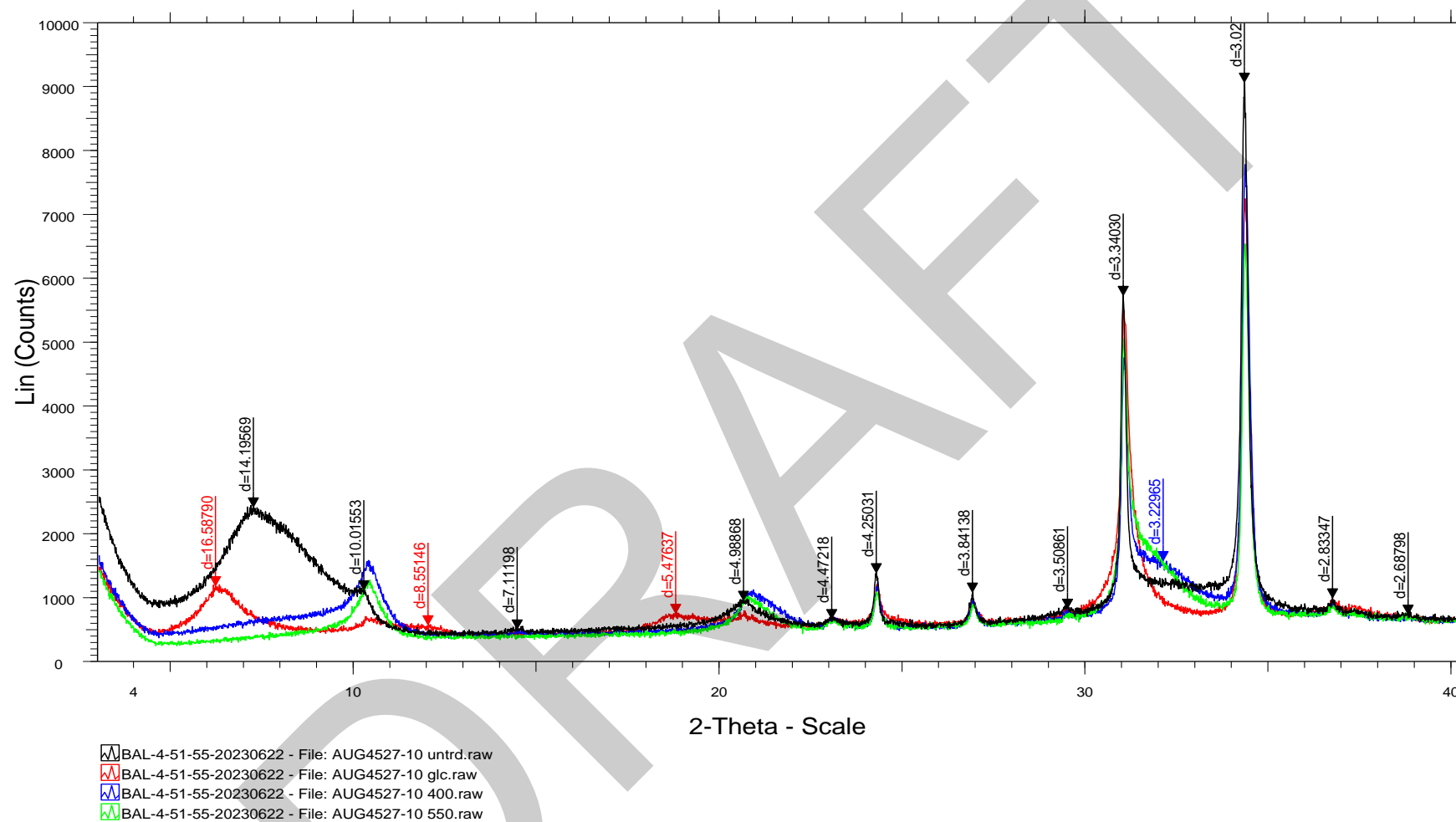


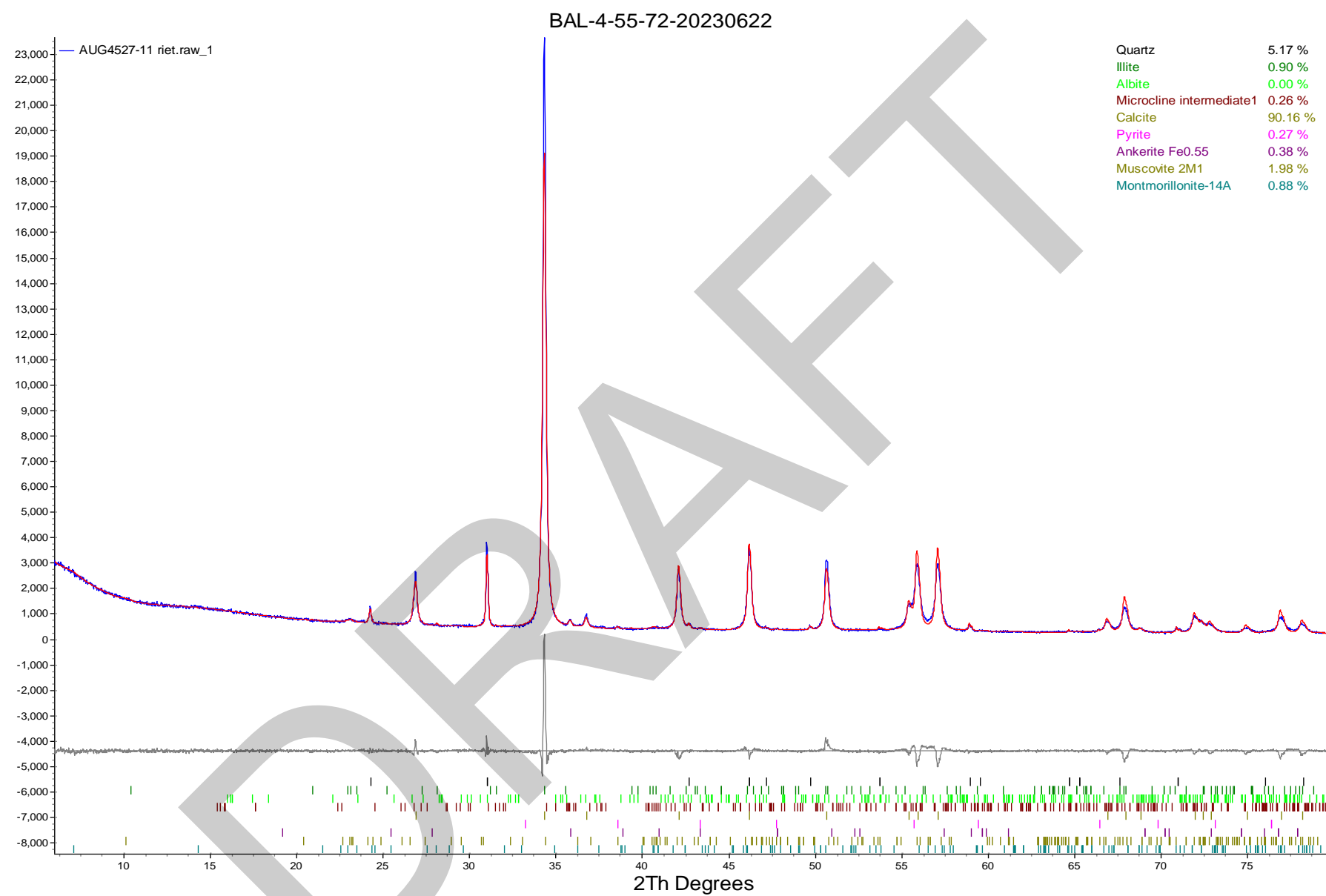
BAL-4-50-51-20230622



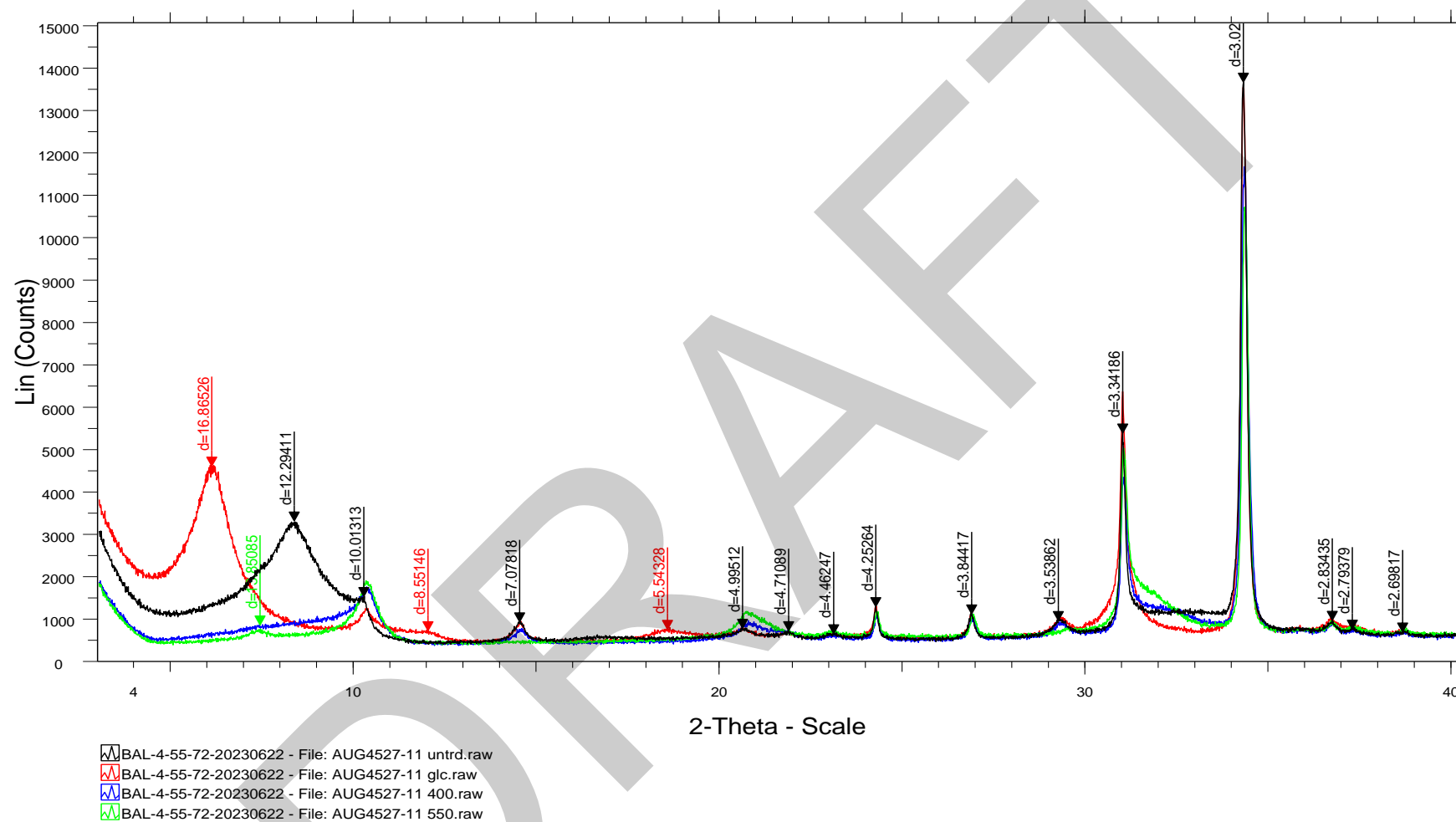


BAL-4-51-55-20230622





BAL-4-55-72-20230622





Quantitative X-Ray Diffraction by Rietveld Refinement

Report Prepared for: Environmental Services
Project Number/ LIMS No. Custom XRD/MI4508-DEC22
Sample Receipt: December 7, 2022
Sample Analysis: December 15, 2022
Reporting Date: April 24, 2023

Instrument: BRUKER AXS D8 Advance Diffractometer
Test Conditions (Bulk): Co radiation, 35 kV, 40 mA; Detector: LYNXEYE
Regular Scanning: Step: 0.02°, Step time: 0.75s, 2θ range: 6-80°
Test Conditions (Clay): Co radiation, 35 kV, 40 mA; Detector: LYNXEYE
Regular Scanning: Step: 0.02°, Step time: 1s, 2θ range: 3-80°
Clay Section Scanning: Step: 0.01°, Step time: 0.2s, 2θ range: 3-40°
Interpretations: PDF2/PDF4 powder diffraction databases issued by the International Center for Diffraction Data (ICDD). DiffracPlus Eva and Topas software.
Detection Limit: 0.5-2%. Strongly dependent on crystallinity.

Contents:
1) Method Summary
2) Quantitative XRD Results
3) XRD Pattern(s)

Kim Gibbs, H.B.Sc., P.Geo.
Senior Mineralogist

Huyun Zhou, Ph.D., P.Geo.
Senior Mineralogist

ACCREDITATION: SGS Natural Resources Lakefield is accredited to the requirements of ISO/IEC 17025 for specific tests as listed on our scope of accreditation, including geochemical, mineralogical and trade mineral tests. To view a list of the accredited methods, please visit the following website and search SGS Canada Inc. - Minerals: <https://www.scc.ca/en/search/palcan>.

Method Summary

The Rietveld Method of Mineral Identification by XRD (ME-LR-MIN-MET-MN-D05) method used by SGS Natural Resources is accredited to the requirements of ISO/IEC 17025.

Mineral Identification and Interpretation:

Mineral identification and interpretation involves matching the diffraction pattern of an unknown material to patterns of single-phase reference materials. The reference patterns are compiled by the Joint Committee on Powder Diffraction Standards - International Center for Diffraction Data (JCPDS-ICDD) database and released on software as Powder Diffraction Files (PDF).

Interpretations do not reflect the presence of non-crystalline and/or amorphous compounds, except when internal standards have been added by request. Mineral proportions may be strongly influenced by crystallinity, crystal structure and preferred orientations. Mineral or compound identification and quantitative analysis results should be accompanied by supporting chemical assay data or other additional tests.

Clay Mineral Separation and Identification:

Clay minerals are typically fine-grained ($<2\ \mu\text{m}$) phyllosilicates in sedimentary rock. Due to the poor crystallinity and fine size of clay minerals, separation of the clay fraction from bulk samples by centrifuge is required. A slide of the oriented clay fraction is prepared and scanned followed by a series of procedures (the addition of ethylene glycol and high temperature heating). Clay minerals are identified by their individual diffraction patterns and changes in their diffraction pattern after different treatments. Clay speciation and mineral identification of the bulk sample are performed using DIFFRACplus EVA (Bruker AXS).

Quantitative Rietveld Analysis:

Quantitative Rietveld Analysis is performed by using Topas 4.2 (Bruker AXS), a graphics based profile analysis program built around a non-linear least squares fitting system, to determine the amount of different phases present in a multicomponent sample. Whole pattern analyses are predicated by the fact that the X-ray diffraction pattern is a total sum of both instrumental and specimen factors. Unlike other peak intensity-based methods, the Rietveld method uses a least squares approach to refine a theoretical line profile until it matches the obtained experimental patterns.

Rietveld refinement is completed with a set of minerals specifically identified for the sample. Zero values indicate that the mineral was included in the refinement calculations, but the calculated concentration was less than 0.05wt%. Minerals not identified by the analyst are not included in refinement calculations for specific samples and are indicated with a dash.

DISCLAIMER: This document is issued by the Company under its General Conditions of Service accessible at <http://www.sgs.com/en/Terms-and-Conditions.aspx>. Attention is drawn to the limitation of liability, indemnification and jurisdiction issues defined therein. Any holder of this document is advised that information contained hereon reflects the Company's findings at the time of its intervention only and within the limits of Client's instructions, if any. The Company's sole responsibility is to its Client and this document does not exonerate parties to a transaction from exercising all their rights and obligations under the transaction documents. Any unauthorized alteration, forgery or falsification of the content or appearance of this document is unlawful and offenders may be prosecuted to the fullest extent of the law.

WARNING: The sample(s) to which the findings recorded herein (the "Findings") relate was(were) drawn and / or provided by the Client or by a third party acting at the Client's direction. The Findings constitute no warranty of the sample's representativeness of any goods and strictly relate to the sample(s). The Company accepts no liability with regard to the origin or source from which the sample(s) is/are said to be extracted.

Summary of Rietveld Quantitative Analysis X-Ray Diffraction Results

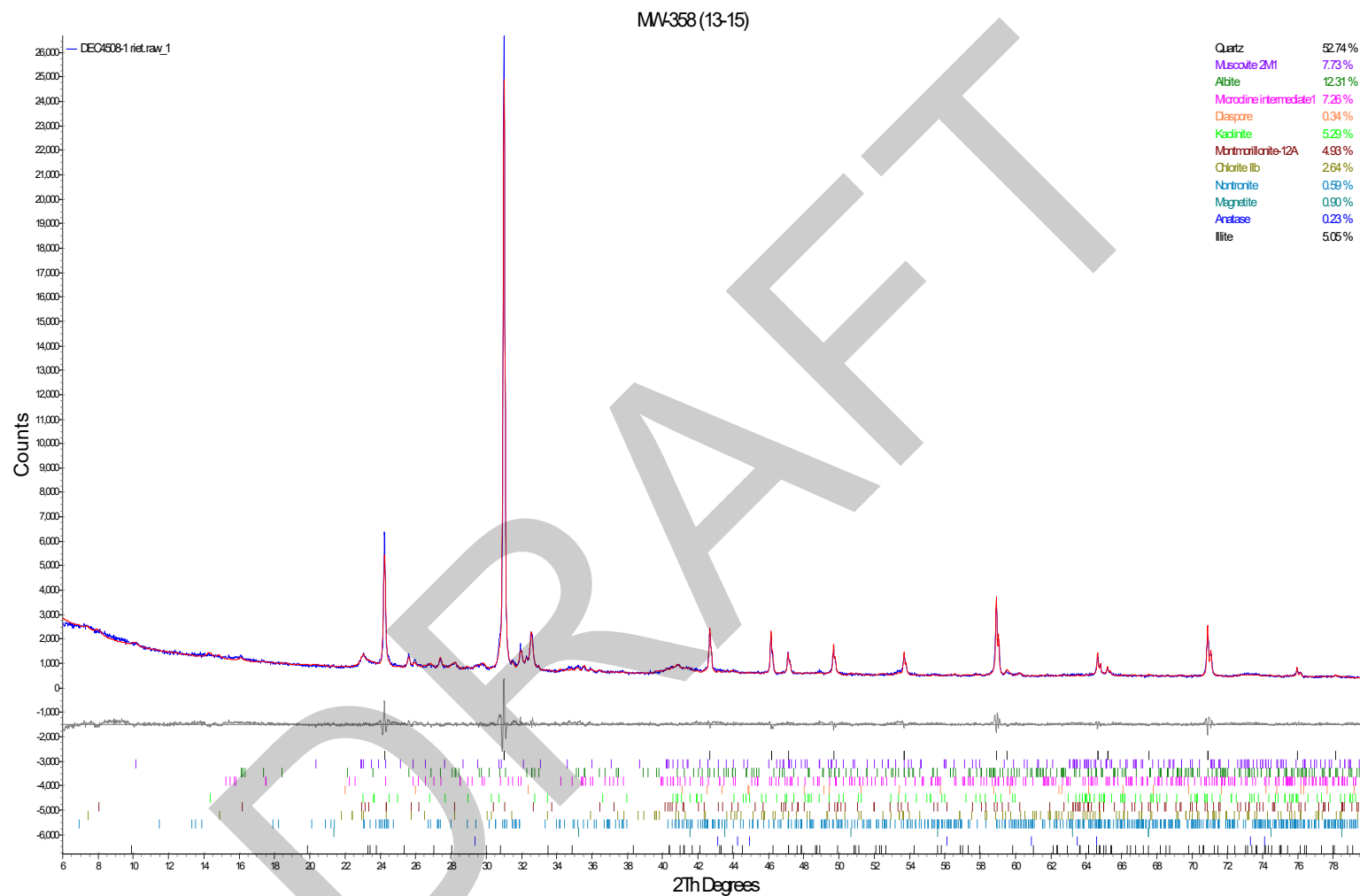
| Mineral/Compound | MW-358 (13-15) DEC4508-1 (wt %) | MW-358 (47-49) DEC4508-2 (wt %) | MW-358 (86-88) DEC4508-3 (wt %) | MW-392 (80-82) DEC4508-4 (wt %) | MW-392 (32-33.5) DEC4508-5 (wt %) | MW-393 (24-25.5) DEC4508-6 (wt %) | MW-394 (20.5-22) DEC4508-7 (wt %) | MW-392 (66-68) DEC4508-8 (wt %) |
|---------------------|---------------------------------------|---------------------------------------|---------------------------------------|---------------------------------------|---|---|---|---------------------------------------|
| Quartz | 52.7 | 29.2 | 30.7 | 29.8 | 52.1 | 64.1 | 55.4 | 22.7 |
| Muscovite | 7.7 | 18.8 | 19.7 | 13.1 | 9.0 | 5.5 | 7.6 | 15.9 |
| Albite | 12.3 | 0.4 | 2.5 | 0.6 | 9.1 | 6.4 | 12.8 | 0.6 |
| Microcline | 7.3 | 8.6 | 5.9 | 1.0 | 6.5 | 10.1 | 7.3 | 5.1 |
| Diaspore | 0.3 | - | - | - | - | 0.2 | 0.5 | 2.8 |
| Magnetite | 0.9 | 0.5 | 0.3 | 1.4 | 0.1 | 0.0 | 0.1 | 0.1 |
| Anatase | 0.2 | 0.8 | 1.8 | 0.8 | 0.6 | 0.3 | 0.3 | 1.0 |
| Calcite | - | 0.5 | 1.0 | 28.1 | 0.0 | 0.0 | 0.2 | 14.9 |
| Fluorapatite | - | - | - | 2.7 | 0.3 | - | 0.2 | 0.2 |
| Ankerite | - | - | - | - | 1.4 | 0.9 | 0.5 | 0.8 |
| Clay | | | | | | | | |
| Kaolinite | 5.3 | 4.8 | 15.0 | 5.5 | 6.8 | 3.2 | 4.2 | 3.6 |
| Montmorillonite-12A | 4.9 | 6.8 | 4.8 | - | - | - | - | 5.8 |
| Montmorillonite-14A | - | - | - | 3.5 | 3.3 | 3.5 | 3.6 | - |
| Nontronite | 0.6 | 4.6 | 4.3 | 4.2 | 1.6 | 1.4 | 0.5 | 3.3 |
| Illite/Mont - 11A | - | 8.8 | 2.7 | 3.6 | 2.7 | 2.1 | 3.0 | 7.1 |
| Illite | 5.0 | 15.0 | 9.2 | 4.1 | 0.7 | 1.0 | 0.6 | 10.4 |
| Chlorite IIb | 2.6 | 1.3 | 2.0 | 1.6 | 5.8 | 1.2 | 3.1 | 6.1 |
| TOTAL | 100 | 100 | 100 | 100 | 100 | 100 | 100 | 100 |

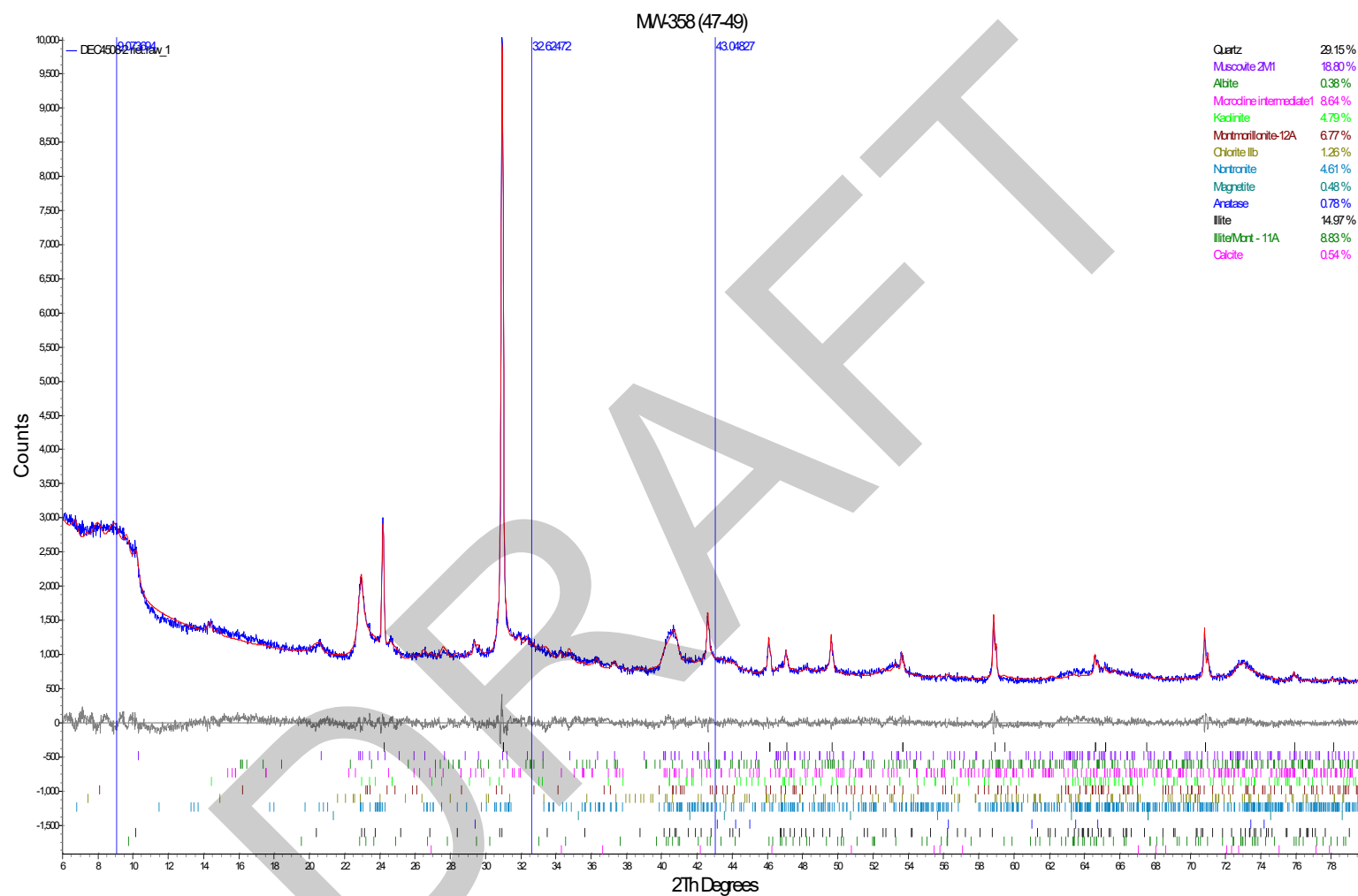
Zero values indicate that the mineral was included in the refinement, but the calculated concentration is below a measurable value.

Dashes indicate that the mineral was not identified by the analyst and not included in the refinement calculation for the sample.

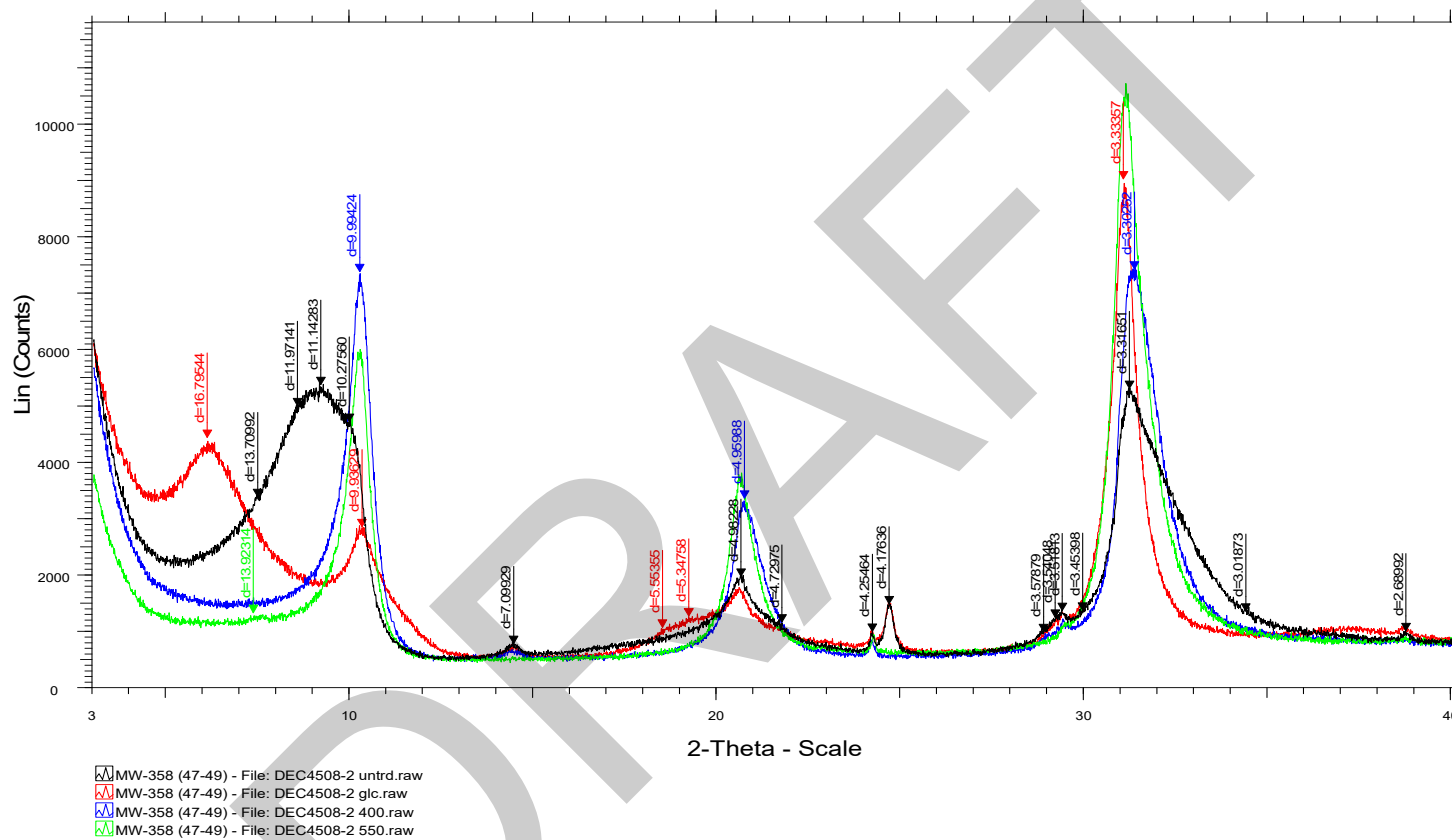
The weight percent quantities indicated have been normalized to a sum of 100%. The quantity of amorphous material has not been determined.

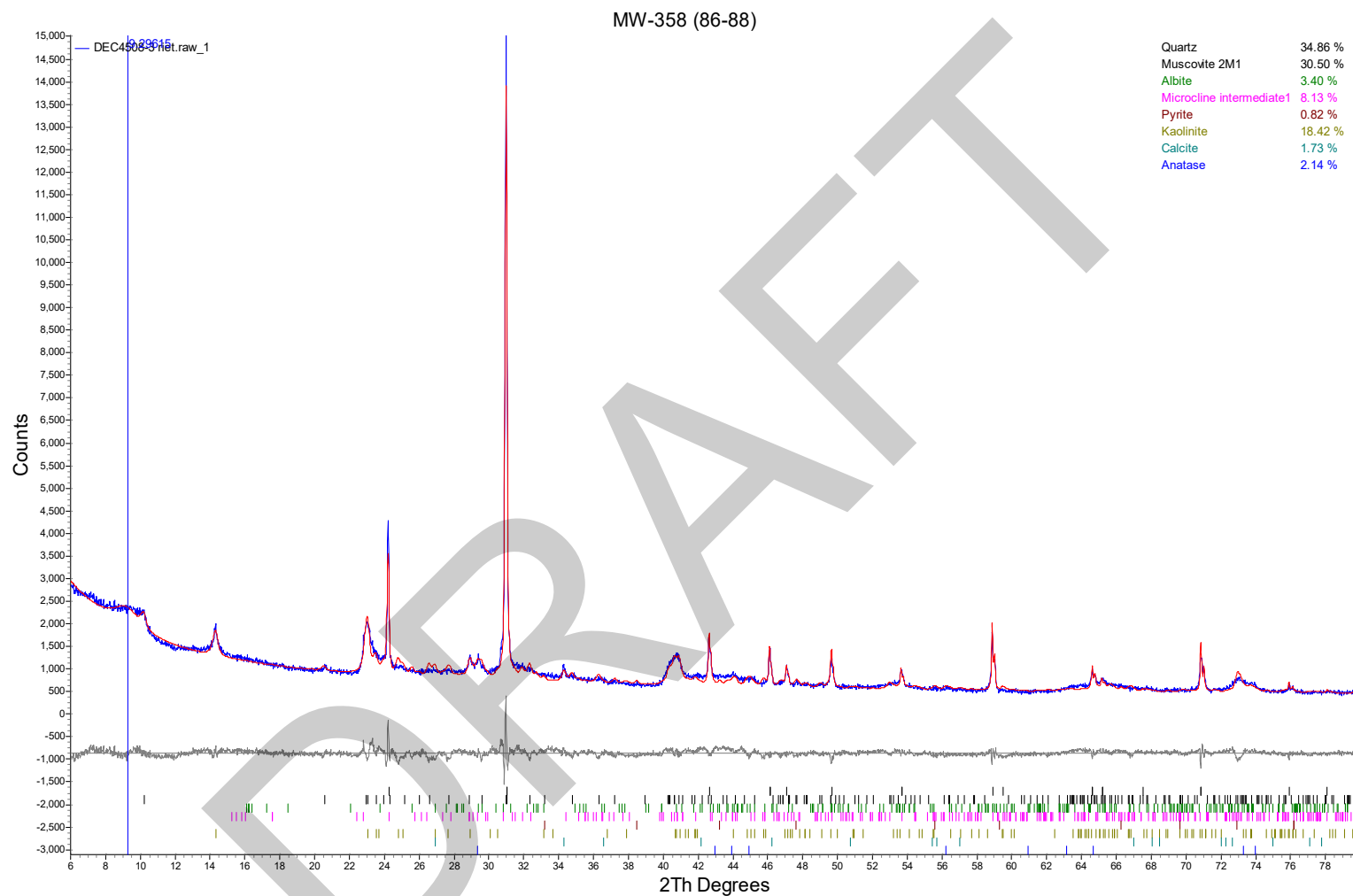
| Mineral/Compound | Formula |
|------------------|--|
| Quartz | SiO ₂ |
| Muscovite | KAl ₂ (AlSi ₃ O ₁₀)(OH) ₂ |
| Albite | NaAlSi ₃ O ₈ |
| Microcline | KAlSi ₃ O ₈ |
| Diaspore | α-Al ₂ O ₃ |
| Magnetite | Fe ₃ O ₄ |
| Anatase | TiO ₂ |
| Calcite | CaCO ₃ |
| Fluorapatite | Ca ₅ (PO ₄) ₃ F |
| Ankerite | CaFe(CO ₃) ₂ |
| Kaolinite | Al ₂ Si ₂ O ₅ (OH) ₄ |
| Montmorillonite | (Na,Ca) _{0.3} (Al,Mg) ₂ Si ₄ O ₁₀ (OH) ₂ ·10H ₂ O |
| Nontronite | Fe ₂ (Al,Si) ₄ O ₁₀ (OH) ₂ Na _{0.3} (H ₂ O) ₄ |
| Illite/Mont | KAl ₄ (Si,Al) ₈ O ₁₀ (OH) ₄ ·4H ₂ O |
| Illite | (K,H ₃ O)(Al,Mg,Fe) ₂ (Si,Al) ₄ O ₁₀ [(OH) ₂ ·(H ₂ O)] |
| Chlorite | (Fe,(Mg,Mn) ₅ ,Al)(Si ₃ Al)O ₁₀ (OH) ₈ |



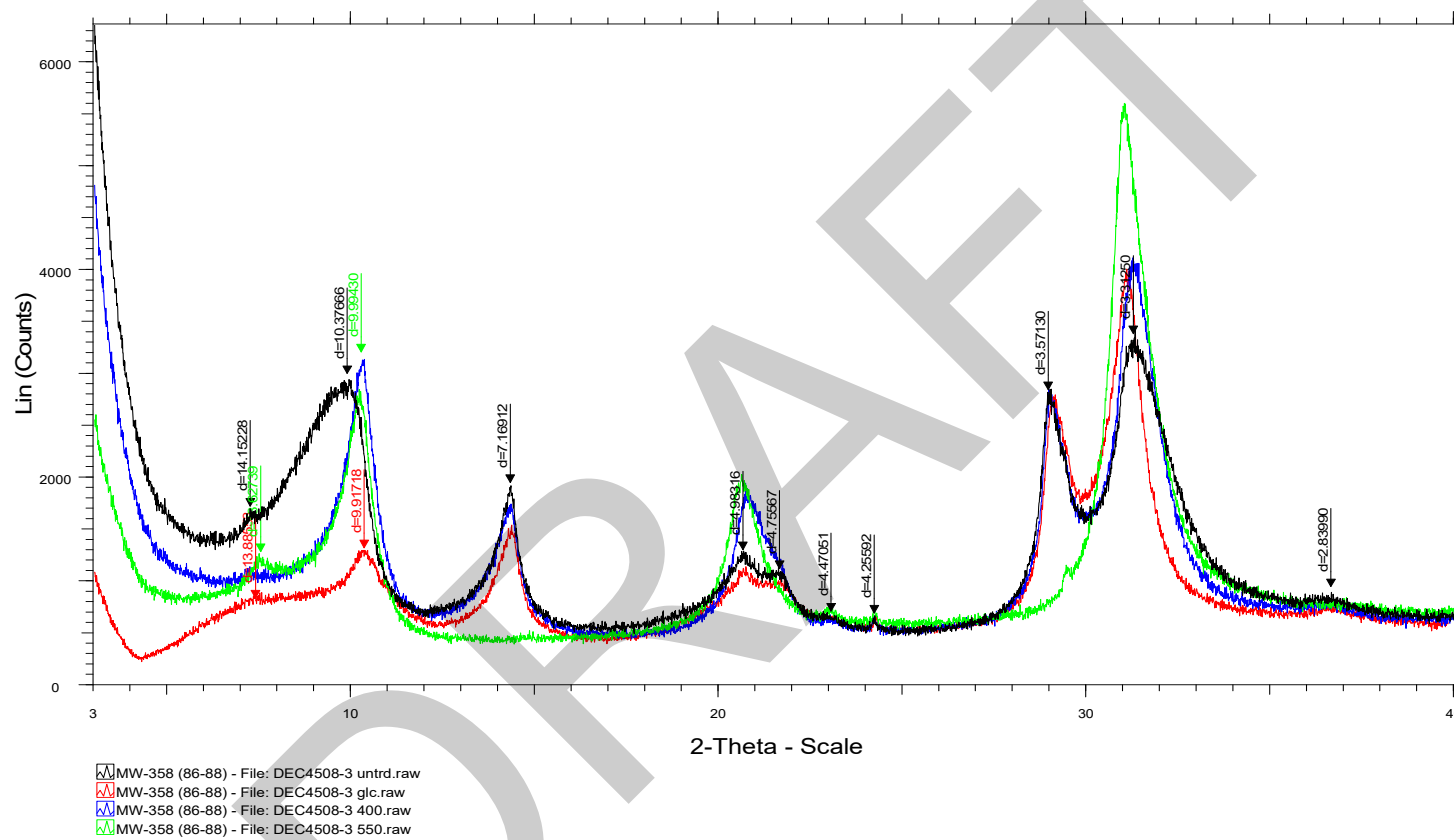


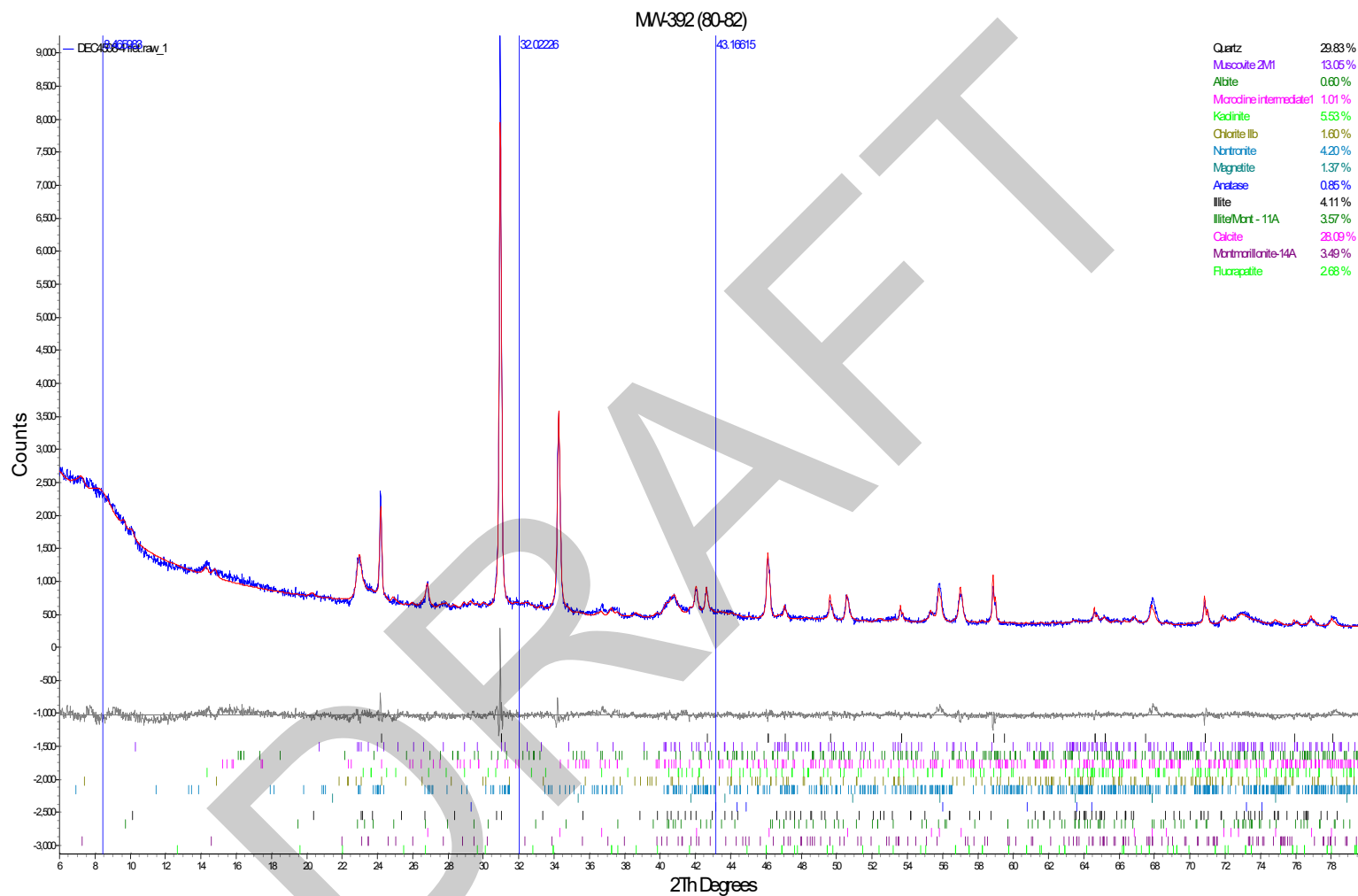
MW-358 (47-49)



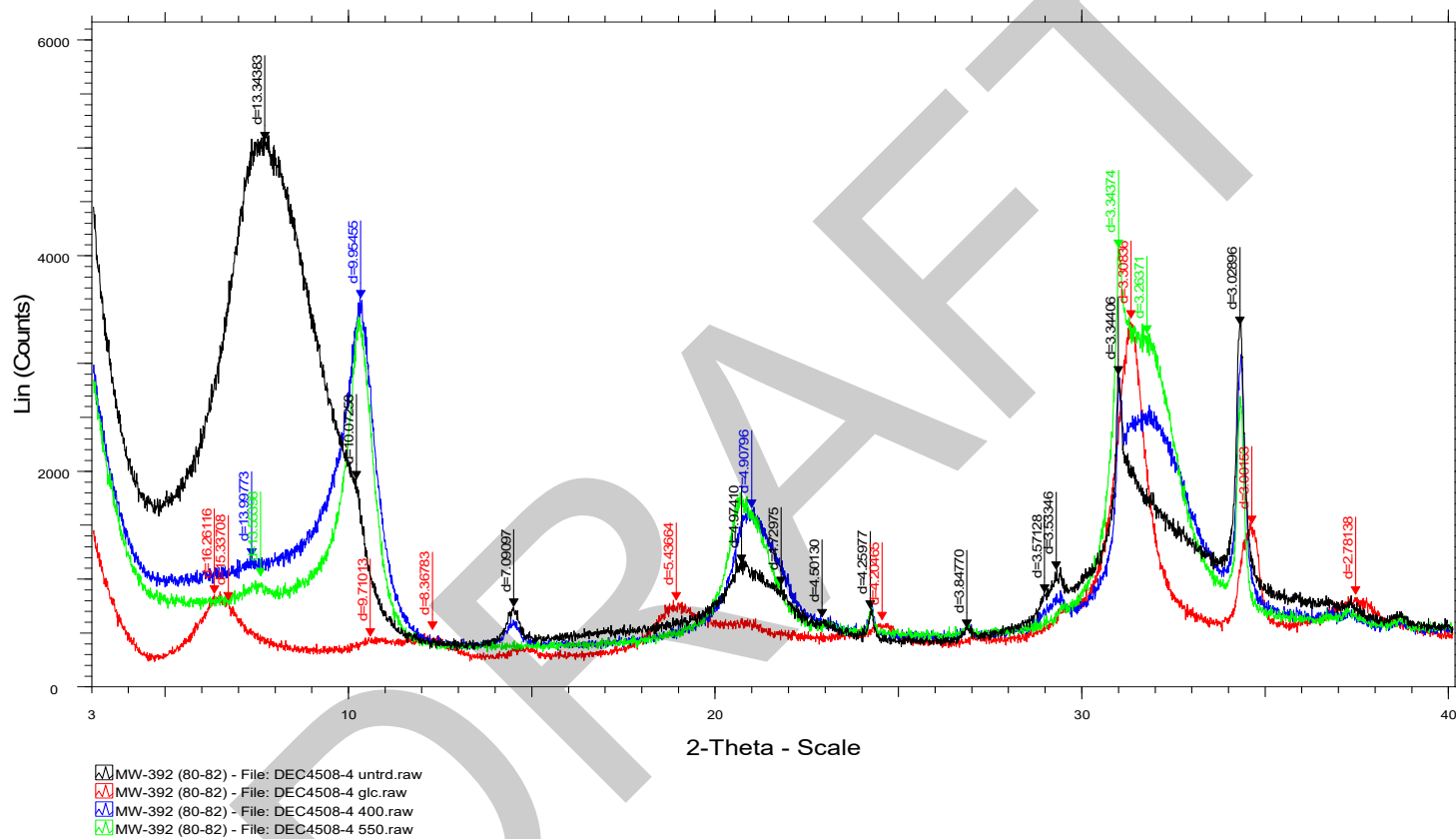


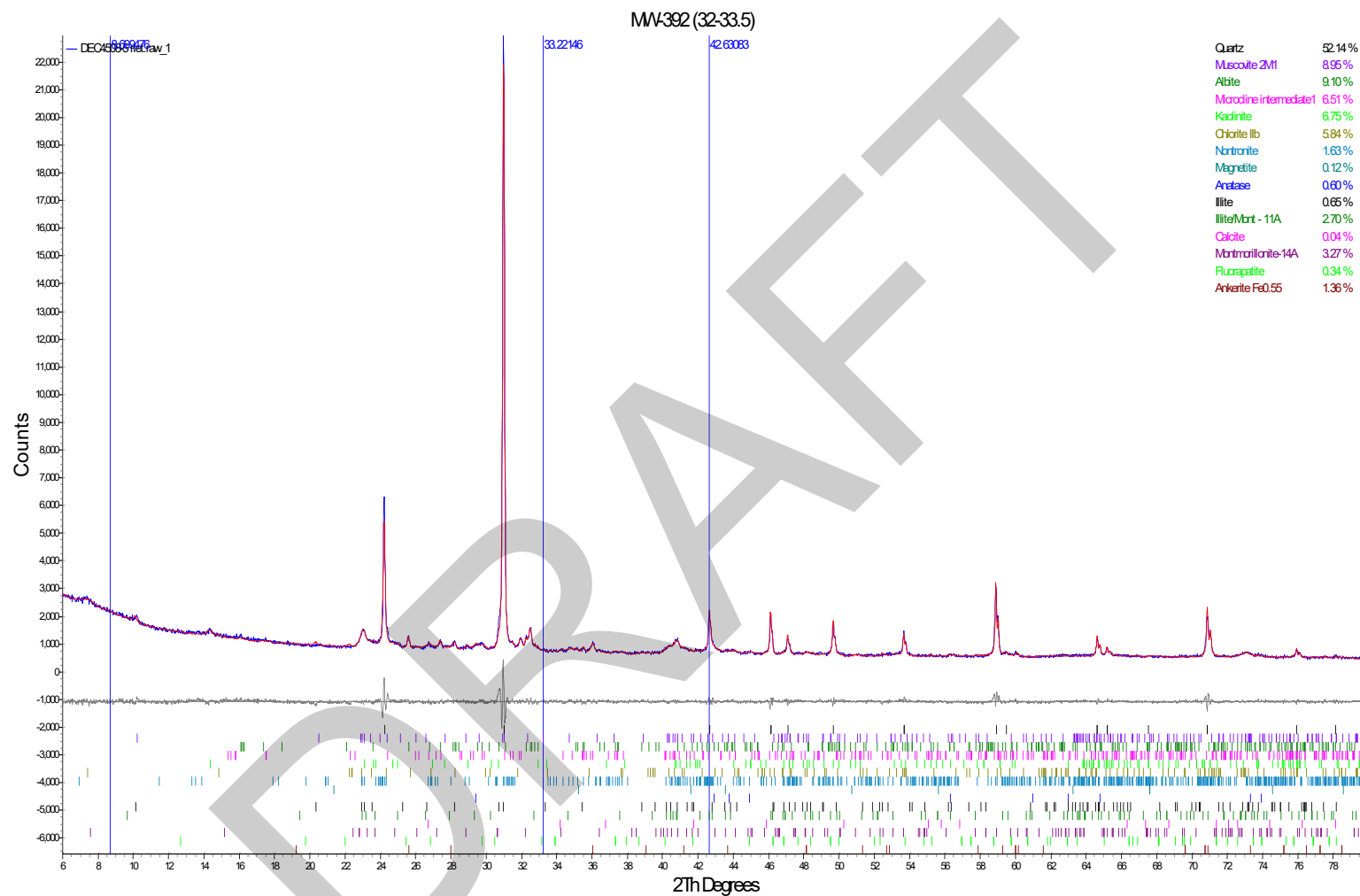
MW-358 (86-88)



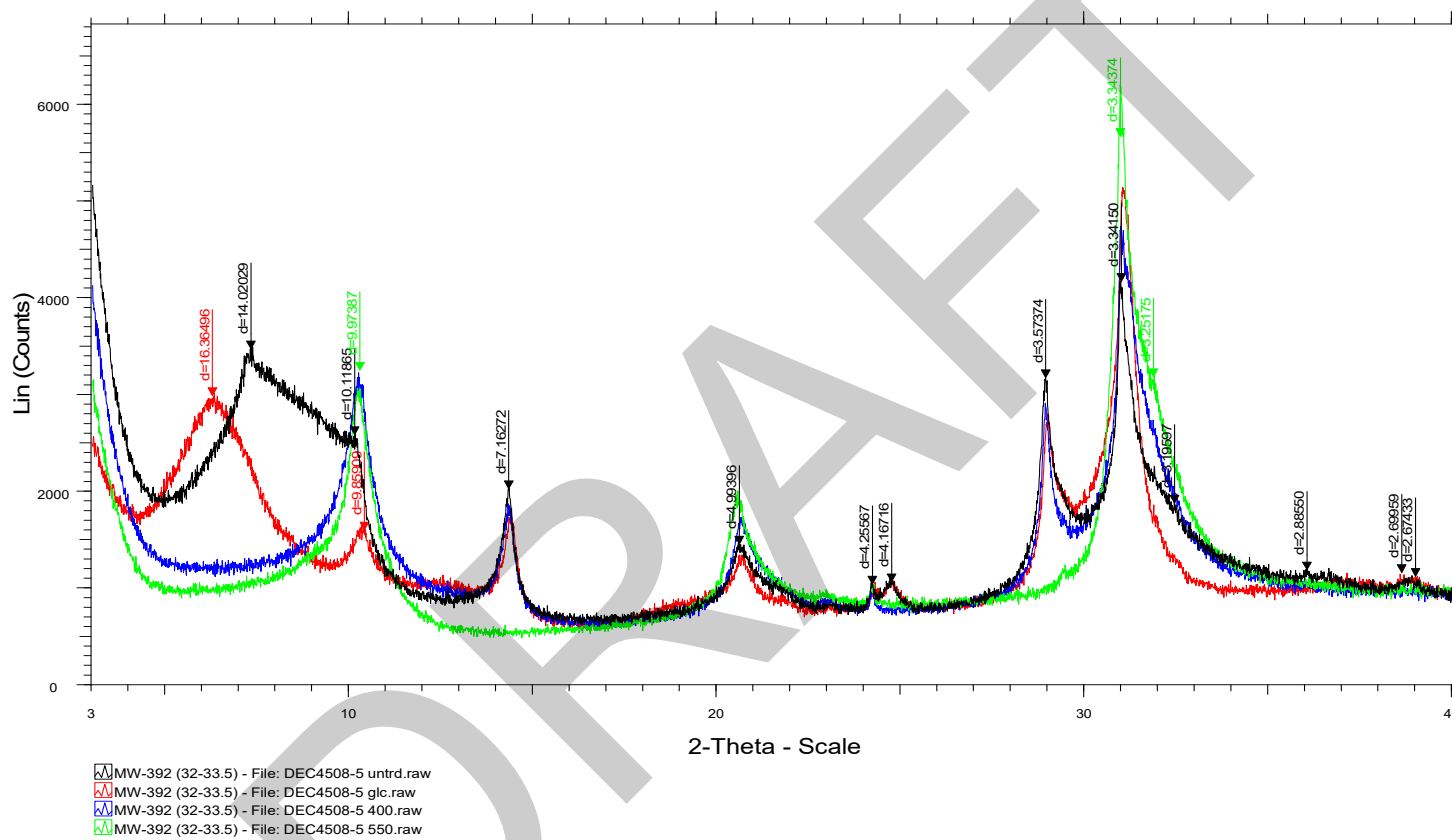


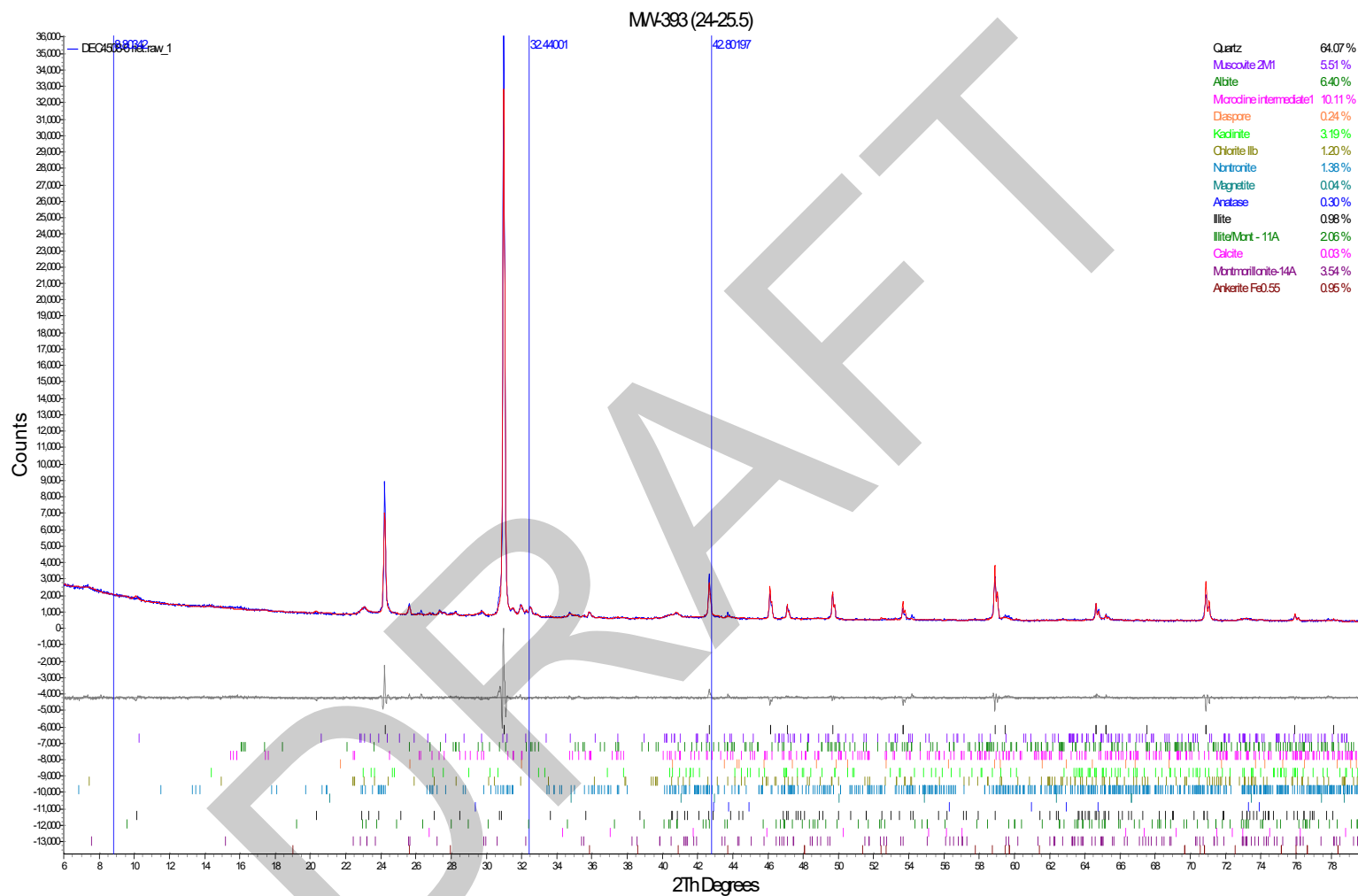
MW-392 (80-82)

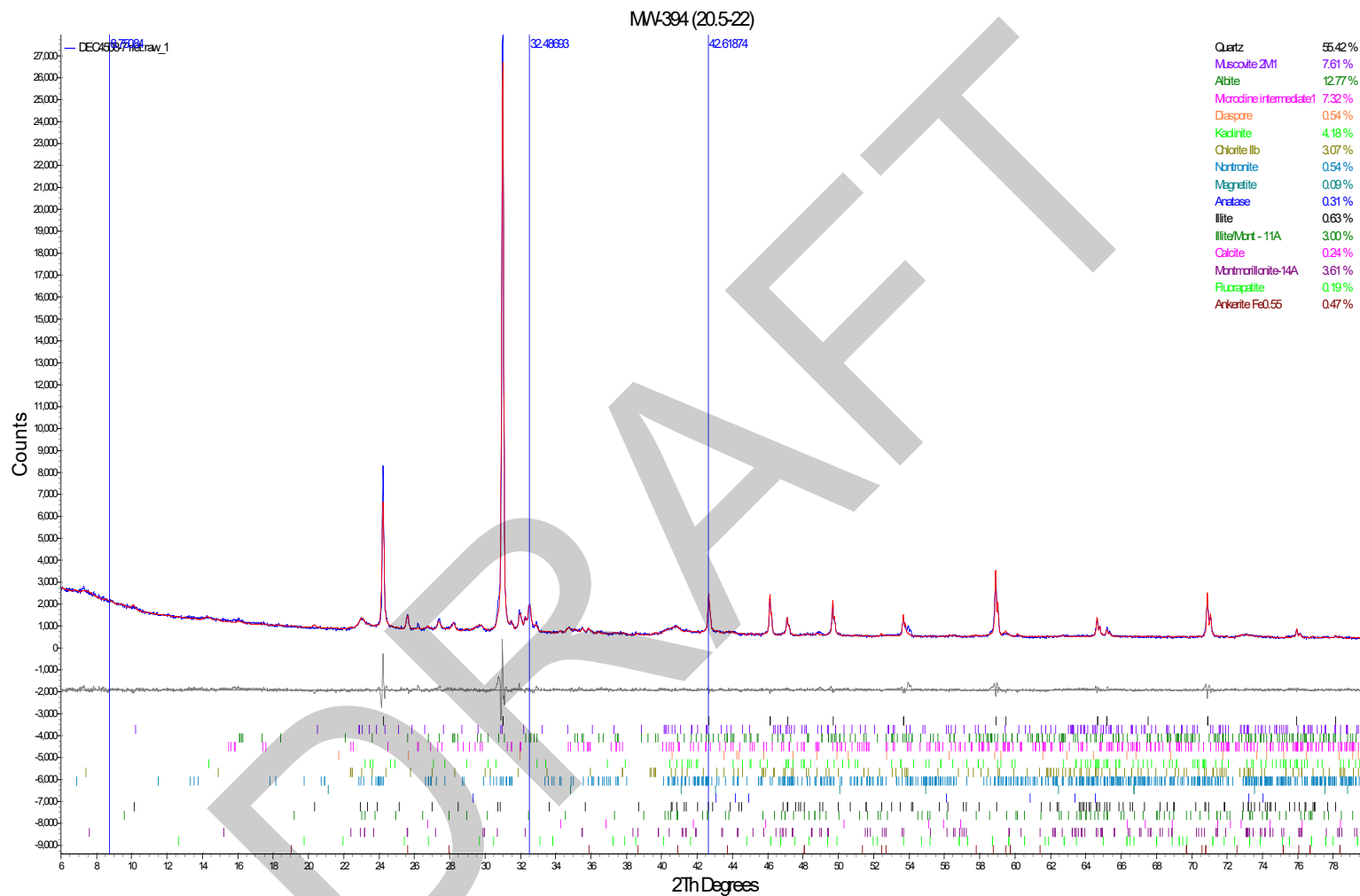


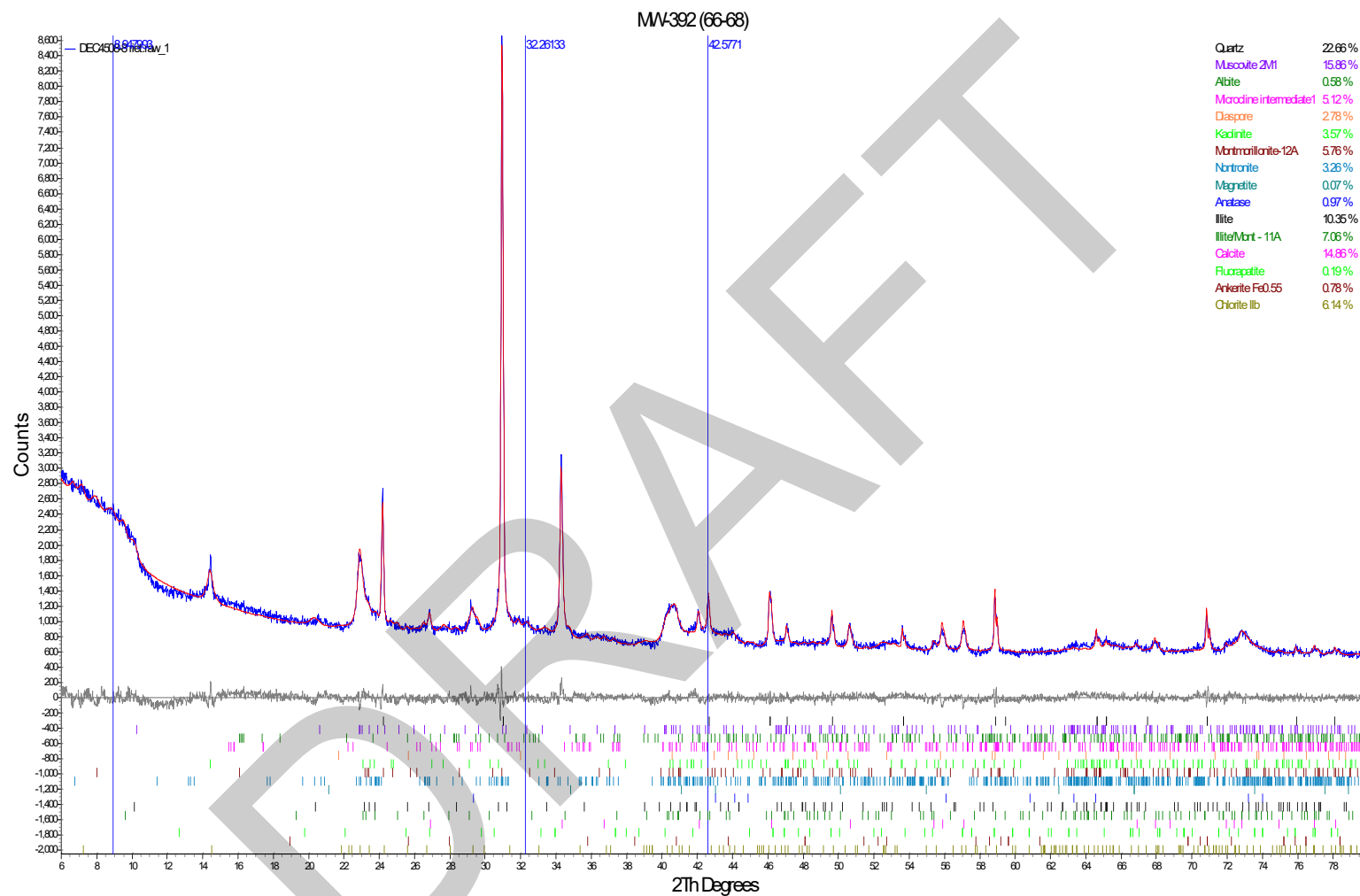


MW-392 (32-33.5)

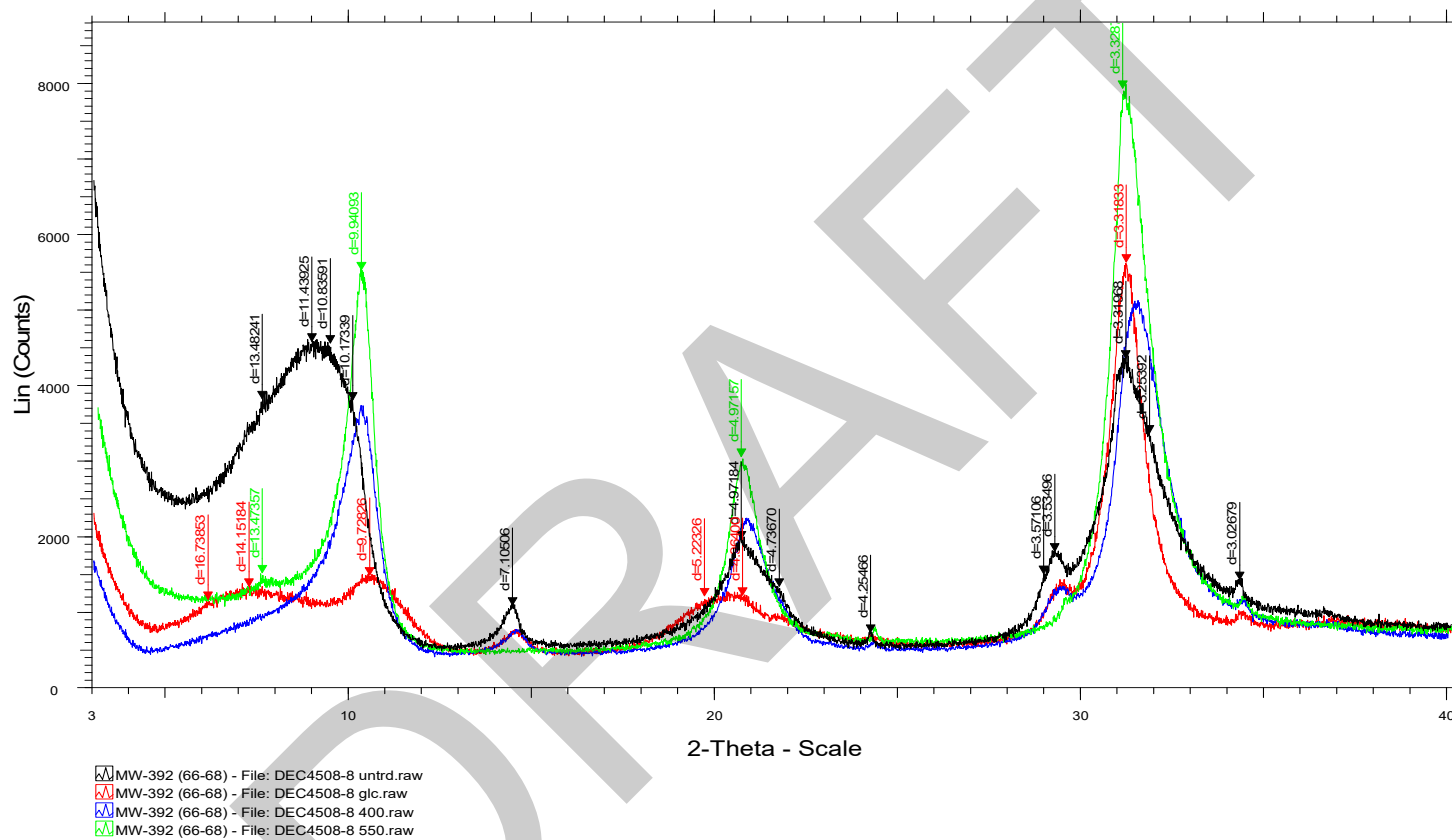








MW-392 (66-68)



Attachment I
Aqueous Phase Data Summary

Attachment I. Site Groundwater Data

Geochemical Conceptual Site Model

Baldwin Fly Ash Pond System

Baldwin Power Plant

Baldwin, IL

| HSU | Location | Well Type | Date | Parameter | Unit | Result |
|-----|----------|-----------|------------|-------------------------------|------|--------|
| PMP | MW-150 | C | 2013/09/16 | pH (field) | SU | 7.6 |
| PMP | MW-150 | C | 2013/11/20 | pH (field) | SU | 7.1 |
| PMP | MW-150 | C | 2014/02/19 | pH (field) | SU | 7.0 |
| PMP | MW-150 | C | 2014/06/11 | pH (field) | SU | 7.3 |
| PMP | MW-150 | C | 2015/03/25 | pH (field) | SU | 7.4 |
| PMP | MW-150 | C | 2015/06/24 | pH (field) | SU | 7.2 |
| PMP | MW-150 | C | 2015/09/25 | pH (field) | SU | 7.2 |
| PMP | MW-150 | C | 2015/11/10 | pH (field) | SU | 7.0 |
| PMP | MW-150 | C | 2016/03/22 | pH (field) | SU | 7.5 |
| PMP | MW-150 | C | 2016/06/21 | pH (field) | SU | 7.3 |
| PMP | MW-150 | C | 2016/09/29 | pH (field) | SU | 7.3 |
| PMP | MW-150 | C | 2016/12/21 | pH (field) | SU | 7.2 |
| PMP | MW-150 | C | 2017/03/16 | pH (field) | SU | 7.3 |
| PMP | MW-150 | C | 2017/06/22 | pH (field) | SU | 7.1 |
| PMP | MW-150 | C | 2017/09/21 | pH (field) | SU | 7.1 |
| PMP | MW-150 | C | 2017/11/28 | pH (field) | SU | 7.3 |
| PMP | MW-150 | C | 2018/03/19 | pH (field) | SU | 7.2 |
| PMP | MW-150 | C | 2018/06/28 | pH (field) | SU | 7.1 |
| PMP | MW-150 | C | 2018/09/26 | pH (field) | SU | 7.2 |
| PMP | MW-150 | C | 2018/12/18 | pH (field) | SU | 7.2 |
| PMP | MW-150 | C | 2019/03/20 | pH (field) | SU | 7.2 |
| PMP | MW-150 | C | 2019/06/25 | pH (field) | SU | 7.2 |
| PMP | MW-150 | C | 2019/09/26 | pH (field) | SU | 6.7 |
| PMP | MW-150 | C | 2019/12/19 | pH (field) | SU | 7.2 |
| PMP | MW-150 | C | 2020/03/26 | pH (field) | SU | 7.2 |
| PMP | MW-150 | C | 2020/06/23 | pH (field) | SU | 7.3 |
| PMP | MW-150 | C | 2020/09/17 | pH (field) | SU | 7.2 |
| PMP | MW-150 | C | 2020/12/17 | pH (field) | SU | 6.9 |
| PMP | MW-150 | C | 2021/03/10 | pH (field) | SU | 7.0 |
| PMP | MW-150 | C | 2021/06/21 | pH (field) | SU | 7.1 |
| PMP | MW-150 | C | 2021/09/14 | pH (field) | SU | 7.0 |
| PMP | MW-150 | C | 2021/12/14 | pH (field) | SU | 7.1 |
| PMP | MW-150 | C | 2022/03/28 | pH (field) | SU | 7.0 |
| PMP | MW-150 | C | 2022/06/14 | pH (field) | SU | 7.1 |
| PMP | MW-150 | C | 2022/09/29 | pH (field) | SU | 7.2 |
| PMP | MW-150 | C | 2022/12/06 | pH (field) | SU | 7.1 |
| PMP | MW-150 | C | 2023/03/15 | pH (field) | SU | 7.0 |
| PMP | MW-150 | C | 2023/05/18 | pH (field) | SU | 7.1 |
| PMP | MW-150 | C | 2023/08/07 | pH (field) | SU | 7.0 |
| PMP | MW-150 | C | 2023/11/03 | pH (field) | SU | 7.1 |
| PMP | MW-150 | C | 2021/03/10 | Oxidation Reduction Potential | mV | 105 |
| PMP | MW-150 | C | 2021/06/21 | Oxidation Reduction Potential | mV | -110 |
| PMP | MW-150 | C | 2021/09/14 | Oxidation Reduction Potential | mV | -42.0 |
| PMP | MW-150 | C | 2021/12/14 | Oxidation Reduction Potential | mV | 16.0 |
| PMP | MW-150 | C | 2022/03/28 | Oxidation Reduction Potential | mV | -26.0 |
| PMP | MW-150 | C | 2022/06/14 | Oxidation Reduction Potential | mV | 120 |
| PMP | MW-150 | C | 2022/09/29 | Oxidation Reduction Potential | mV | 80.0 |
| PMP | MW-150 | C | 2022/12/06 | Oxidation Reduction Potential | mV | <-300 |
| PMP | MW-150 | C | 2023/03/15 | Oxidation Reduction Potential | mV | -93.5 |
| PMP | MW-150 | C | 2023/05/18 | Oxidation Reduction Potential | mV | 20.0 |
| PMP | MW-150 | C | 2023/08/07 | Oxidation Reduction Potential | mV | -65.0 |
| PMP | MW-150 | C | 2023/11/03 | Oxidation Reduction Potential | mV | -139 |
| PMP | MW-150 | C | 2021/03/10 | Eh | V | 0.30 |
| PMP | MW-150 | C | 2021/06/21 | Eh | V | 0.087 |
| PMP | MW-150 | C | 2021/09/14 | Eh | V | 0.15 |

Attachment I. Site Groundwater Data

Geochemical Conceptual Site Model

Baldwin Fly Ash Pond System

Baldwin Power Plant

Baldwin, IL

| | | | | | | |
|-----|--------|---|------------|-------------------------|------------|--------|
| PMP | MW-150 | C | 2021/12/14 | Eh | V | 0.21 |
| PMP | MW-150 | C | 2022/03/28 | Eh | V | 0.17 |
| PMP | MW-150 | C | 2022/06/14 | Eh | V | 0.32 |
| PMP | MW-150 | C | 2022/09/29 | Eh | V | 0.28 |
| PMP | MW-150 | C | 2022/12/06 | Eh | V | -0.10 |
| PMP | MW-150 | C | 2023/03/15 | Eh | V | 0.10 |
| PMP | MW-150 | C | 2023/05/18 | Eh | V | 0.22 |
| PMP | MW-150 | C | 2023/08/07 | Eh | V | 0.13 |
| PMP | MW-150 | C | 2023/11/03 | Eh | V | 0.057 |
| PMP | MW-150 | C | 2023/03/15 | Alkalinity, bicarbonate | mg/L CaCO3 | 358 |
| PMP | MW-150 | C | 2023/05/18 | Alkalinity, bicarbonate | mg/L CaCO3 | 336 |
| PMP | MW-150 | C | 2023/08/07 | Alkalinity, bicarbonate | mg/L CaCO3 | 314 |
| PMP | MW-150 | C | 2023/11/03 | Alkalinity, bicarbonate | mg/L CaCO3 | 304 |
| PMP | MW-150 | C | 2023/03/15 | Barium, total | mg/L | 0.0156 |
| PMP | MW-150 | C | 2023/05/18 | Barium, total | mg/L | 0.0170 |
| PMP | MW-150 | C | 2023/08/07 | Barium, total | mg/L | 0.0194 |
| PMP | MW-150 | C | 2023/11/03 | Barium, total | mg/L | 0.0162 |
| PMP | MW-150 | C | 2013/09/16 | Boron, total | mg/L | 0.680 |
| PMP | MW-150 | C | 2023/03/15 | Boron, total | mg/L | 3.43 |
| PMP | MW-150 | C | 2023/05/18 | Boron, total | mg/L | 4.12 |
| PMP | MW-150 | C | 2023/08/07 | Boron, total | mg/L | 4.38 |
| PMP | MW-150 | C | 2023/11/03 | Boron, total | mg/L | 3.59 |
| PMP | MW-150 | C | 2023/03/15 | Calcium, total | mg/L | 188 |
| PMP | MW-150 | C | 2023/05/18 | Calcium, total | mg/L | 223 |
| PMP | MW-150 | C | 2023/08/07 | Calcium, total | mg/L | 186 |
| PMP | MW-150 | C | 2023/11/03 | Calcium, total | mg/L | 206 |
| PMP | MW-150 | C | 2013/09/16 | Chloride, total | mg/L | 54.0 |
| PMP | MW-150 | C | 2023/03/15 | Chloride, total | mg/L | 56.0 |
| PMP | MW-150 | C | 2023/05/18 | Chloride, total | mg/L | 56.0 |
| PMP | MW-150 | C | 2023/08/07 | Chloride, total | mg/L | 53.0 |
| PMP | MW-150 | C | 2023/11/03 | Chloride, total | mg/L | 49.0 |
| PMP | MW-150 | C | 2013/11/20 | Iron, dissolved | mg/L | 0.0700 |
| PMP | MW-150 | C | 2014/02/19 | Iron, dissolved | mg/L | <0.007 |
| PMP | MW-150 | C | 2014/06/11 | Iron, dissolved | mg/L | <0.007 |
| PMP | MW-150 | C | 2015/03/25 | Iron, dissolved | mg/L | <0.007 |
| PMP | MW-150 | C | 2015/06/24 | Iron, dissolved | mg/L | 0.0350 |
| PMP | MW-150 | C | 2015/09/25 | Iron, dissolved | mg/L | 0.127 |
| PMP | MW-150 | C | 2015/11/10 | Iron, dissolved | mg/L | 0.0388 |
| PMP | MW-150 | C | 2016/03/22 | Iron, dissolved | mg/L | 0.0247 |
| PMP | MW-150 | C | 2016/06/21 | Iron, dissolved | mg/L | 0.0276 |
| PMP | MW-150 | C | 2016/09/29 | Iron, dissolved | mg/L | <0.007 |
| PMP | MW-150 | C | 2016/12/21 | Iron, dissolved | mg/L | <0.007 |
| PMP | MW-150 | C | 2017/03/16 | Iron, dissolved | mg/L | <0.007 |
| PMP | MW-150 | C | 2017/06/22 | Iron, dissolved | mg/L | <0.007 |
| PMP | MW-150 | C | 2017/09/21 | Iron, dissolved | mg/L | <0.007 |
| PMP | MW-150 | C | 2017/11/28 | Iron, dissolved | mg/L | <0.007 |
| PMP | MW-150 | C | 2018/03/19 | Iron, dissolved | mg/L | <0.007 |
| PMP | MW-150 | C | 2018/06/28 | Iron, dissolved | mg/L | <0.02 |
| PMP | MW-150 | C | 2018/09/26 | Iron, dissolved | mg/L | <0.02 |
| PMP | MW-150 | C | 2018/12/18 | Iron, dissolved | mg/L | <0.02 |
| PMP | MW-150 | C | 2019/03/20 | Iron, dissolved | mg/L | <0.02 |
| PMP | MW-150 | C | 2019/06/25 | Iron, dissolved | mg/L | <0.02 |
| PMP | MW-150 | C | 2019/09/26 | Iron, dissolved | mg/L | <0.02 |
| PMP | MW-150 | C | 2019/12/19 | Iron, dissolved | mg/L | <0.02 |
| PMP | MW-150 | C | 2020/03/26 | Iron, dissolved | mg/L | <0.02 |
| PMP | MW-150 | C | 2020/06/23 | Iron, dissolved | mg/L | <0.02 |
| PMP | MW-150 | C | 2020/09/17 | Iron, dissolved | mg/L | 0.106 |

Attachment I. Site Groundwater Data

Geochemical Conceptual Site Model

Baldwin Fly Ash Pond System

Baldwin Power Plant

Baldwin, IL

| | | | | | | |
|-----|--------|---|------------|----------------------|------|---------|
| PMP | MW-150 | C | 2020/12/17 | Iron, dissolved | mg/L | <0.02 |
| PMP | MW-150 | C | 2021/03/10 | Iron, dissolved | mg/L | <0.04 |
| PMP | MW-150 | C | 2021/06/21 | Iron, dissolved | mg/L | <0.04 |
| PMP | MW-150 | C | 2021/09/14 | Iron, dissolved | mg/L | <0.02 |
| PMP | MW-150 | C | 2021/12/14 | Iron, dissolved | mg/L | <0.02 |
| PMP | MW-150 | C | 2022/03/28 | Iron, dissolved | mg/L | <0.015 |
| PMP | MW-150 | C | 2022/06/14 | Iron, dissolved | mg/L | <0.02 |
| PMP | MW-150 | C | 2022/09/29 | Iron, dissolved | mg/L | <0.0115 |
| PMP | MW-150 | C | 2022/12/06 | Iron, dissolved | mg/L | <0.0115 |
| PMP | MW-150 | C | 2023/03/15 | Iron, dissolved | mg/L | 0.0140 |
| PMP | MW-150 | C | 2023/05/18 | Iron, dissolved | mg/L | <0.02 |
| PMP | MW-150 | C | 2023/08/07 | Iron, dissolved | mg/L | 0.0666 |
| PMP | MW-150 | C | 2023/11/03 | Iron, dissolved | mg/L | 0.0728 |
| PMP | MW-150 | C | 2023/03/15 | Magnesium, total | mg/L | 175 |
| PMP | MW-150 | C | 2023/05/18 | Magnesium, total | mg/L | 173 |
| PMP | MW-150 | C | 2023/08/07 | Magnesium, total | mg/L | 145 |
| PMP | MW-150 | C | 2023/11/03 | Magnesium, total | mg/L | 135 |
| PMP | MW-150 | C | 2013/11/20 | Manganese, dissolved | mg/L | 0.0300 |
| PMP | MW-150 | C | 2014/02/19 | Manganese, dissolved | mg/L | <0.0016 |
| PMP | MW-150 | C | 2014/06/11 | Manganese, dissolved | mg/L | 0.00600 |
| PMP | MW-150 | C | 2015/03/25 | Manganese, dissolved | mg/L | 0.0240 |
| PMP | MW-150 | C | 2015/06/24 | Manganese, dissolved | mg/L | 0.00300 |
| PMP | MW-150 | C | 2015/09/25 | Manganese, dissolved | mg/L | 0.0125 |
| PMP | MW-150 | C | 2015/11/10 | Manganese, dissolved | mg/L | 0.00480 |
| PMP | MW-150 | C | 2016/03/22 | Manganese, dissolved | mg/L | <0.0005 |
| PMP | MW-150 | C | 2016/06/21 | Manganese, dissolved | mg/L | <0.0005 |
| PMP | MW-150 | C | 2016/09/29 | Manganese, dissolved | mg/L | <0.0005 |
| PMP | MW-150 | C | 2016/12/21 | Manganese, dissolved | mg/L | <0.0005 |
| PMP | MW-150 | C | 2017/03/16 | Manganese, dissolved | mg/L | <0.0005 |
| PMP | MW-150 | C | 2017/06/22 | Manganese, dissolved | mg/L | <0.0005 |
| PMP | MW-150 | C | 2017/09/21 | Manganese, dissolved | mg/L | <0.0005 |
| PMP | MW-150 | C | 2017/11/28 | Manganese, dissolved | mg/L | <0.0005 |
| PMP | MW-150 | C | 2018/03/19 | Manganese, dissolved | mg/L | <0.0005 |
| PMP | MW-150 | C | 2018/06/28 | Manganese, dissolved | mg/L | <0.0025 |
| PMP | MW-150 | C | 2018/09/26 | Manganese, dissolved | mg/L | <0.0025 |
| PMP | MW-150 | C | 2018/12/18 | Manganese, dissolved | mg/L | <0.0025 |
| PMP | MW-150 | C | 2019/03/20 | Manganese, dissolved | mg/L | <0.0025 |
| PMP | MW-150 | C | 2019/06/25 | Manganese, dissolved | mg/L | <0.0025 |
| PMP | MW-150 | C | 2019/09/26 | Manganese, dissolved | mg/L | <0.0025 |
| PMP | MW-150 | C | 2019/12/19 | Manganese, dissolved | mg/L | <0.0025 |
| PMP | MW-150 | C | 2020/03/26 | Manganese, dissolved | mg/L | <0.0025 |
| PMP | MW-150 | C | 2020/06/23 | Manganese, dissolved | mg/L | <0.0025 |
| PMP | MW-150 | C | 2020/09/17 | Manganese, dissolved | mg/L | <0.0025 |
| PMP | MW-150 | C | 2020/12/17 | Manganese, dissolved | mg/L | <0.0025 |
| PMP | MW-150 | C | 2021/03/10 | Manganese, dissolved | mg/L | <0.0025 |
| PMP | MW-150 | C | 2021/06/21 | Manganese, dissolved | mg/L | <0.0025 |
| PMP | MW-150 | C | 2021/09/14 | Manganese, dissolved | mg/L | <0.0025 |
| PMP | MW-150 | C | 2021/12/14 | Manganese, dissolved | mg/L | <0.0025 |
| PMP | MW-150 | C | 2022/03/28 | Manganese, dissolved | mg/L | <0.0008 |
| PMP | MW-150 | C | 2022/06/14 | Manganese, dissolved | mg/L | <0.0025 |
| PMP | MW-150 | C | 2022/09/29 | Manganese, dissolved | mg/L | 0.00160 |
| PMP | MW-150 | C | 2022/12/06 | Manganese, dissolved | mg/L | 0.00180 |
| PMP | MW-150 | C | 2023/03/15 | Manganese, dissolved | mg/L | <0.0008 |
| PMP | MW-150 | C | 2023/05/18 | Manganese, dissolved | mg/L | 0.00380 |
| PMP | MW-150 | C | 2023/08/07 | Manganese, dissolved | mg/L | 0.00250 |
| PMP | MW-150 | C | 2023/11/03 | Manganese, dissolved | mg/L | 0.00250 |
| PMP | MW-150 | C | 2023/05/18 | Phosphate, dissolved | mg/L | 0.0980 |

Attachment I. Site Groundwater Data

Geochemical Conceptual Site Model

Baldwin Fly Ash Pond System

Baldwin Power Plant

Baldwin, IL

| | | | | | | |
|-----|--------|---|------------|------------------------|-----------|--------|
| PMP | MW-150 | C | 2023/08/07 | Phosphate, dissolved | mg/L | 0.0710 |
| PMP | MW-150 | C | 2023/03/15 | Potassium, total | mg/L | 0.731 |
| PMP | MW-150 | C | 2023/05/18 | Potassium, total | mg/L | 0.893 |
| PMP | MW-150 | C | 2023/08/07 | Potassium, total | mg/L | 0.864 |
| PMP | MW-150 | C | 2023/11/03 | Potassium, total | mg/L | 0.806 |
| PMP | MW-150 | C | 2023/05/18 | Silicon, dissolved | mg/L | 10.3 |
| PMP | MW-150 | C | 2023/08/07 | Silicon, dissolved | mg/L | 9.45 |
| PMP | MW-150 | C | 2023/03/15 | Sodium, total | mg/L | 125 |
| PMP | MW-150 | C | 2023/05/18 | Sodium, total | mg/L | 121 |
| PMP | MW-150 | C | 2023/08/07 | Sodium, total | mg/L | 94.8 |
| PMP | MW-150 | C | 2023/11/03 | Sodium, total | mg/L | 102 |
| PMP | MW-150 | C | 2013/09/16 | Sulfate, total | mg/L | 570 |
| PMP | MW-150 | C | 2023/03/15 | Sulfate, total | mg/L | 927 |
| PMP | MW-150 | C | 2023/05/18 | Sulfate, total | mg/L | 970 |
| PMP | MW-150 | C | 2023/08/07 | Sulfate, total | mg/L | 852 |
| PMP | MW-150 | C | 2023/11/03 | Sulfate, total | mg/L | 832 |
| PMP | MW-150 | C | 2013/09/16 | Temperature (Celsius) | degrees C | 14.8 |
| PMP | MW-150 | C | 2013/11/20 | Temperature (Celsius) | degrees C | 13.3 |
| PMP | MW-150 | C | 2014/02/19 | Temperature (Celsius) | degrees C | 12.7 |
| PMP | MW-150 | C | 2014/06/11 | Temperature (Celsius) | degrees C | 13.0 |
| PMP | MW-150 | C | 2015/03/25 | Temperature (Celsius) | degrees C | 13.7 |
| PMP | MW-150 | C | 2015/06/24 | Temperature (Celsius) | degrees C | 13.5 |
| PMP | MW-150 | C | 2015/09/25 | Temperature (Celsius) | degrees C | 14.0 |
| PMP | MW-150 | C | 2015/11/10 | Temperature (Celsius) | degrees C | 13.5 |
| PMP | MW-150 | C | 2016/03/22 | Temperature (Celsius) | degrees C | 14.5 |
| PMP | MW-150 | C | 2016/06/21 | Temperature (Celsius) | degrees C | 14.3 |
| PMP | MW-150 | C | 2016/09/29 | Temperature (Celsius) | degrees C | 14.0 |
| PMP | MW-150 | C | 2016/12/21 | Temperature (Celsius) | degrees C | 13.8 |
| PMP | MW-150 | C | 2017/03/16 | Temperature (Celsius) | degrees C | 13.6 |
| PMP | MW-150 | C | 2017/06/22 | Temperature (Celsius) | degrees C | 14.4 |
| PMP | MW-150 | C | 2017/09/21 | Temperature (Celsius) | degrees C | 15.0 |
| PMP | MW-150 | C | 2017/11/28 | Temperature (Celsius) | degrees C | 14.9 |
| PMP | MW-150 | C | 2018/03/19 | Temperature (Celsius) | degrees C | 14.9 |
| PMP | MW-150 | C | 2018/06/28 | Temperature (Celsius) | degrees C | 14.4 |
| PMP | MW-150 | C | 2018/09/26 | Temperature (Celsius) | degrees C | 14.4 |
| PMP | MW-150 | C | 2018/12/18 | Temperature (Celsius) | degrees C | 14.1 |
| PMP | MW-150 | C | 2019/03/20 | Temperature (Celsius) | degrees C | 13.0 |
| PMP | MW-150 | C | 2019/06/25 | Temperature (Celsius) | degrees C | 13.5 |
| PMP | MW-150 | C | 2019/09/26 | Temperature (Celsius) | degrees C | 13.8 |
| PMP | MW-150 | C | 2019/12/19 | Temperature (Celsius) | degrees C | 13.9 |
| PMP | MW-150 | C | 2020/03/26 | Temperature (Celsius) | degrees C | 13.4 |
| PMP | MW-150 | C | 2020/06/23 | Temperature (Celsius) | degrees C | 13.3 |
| PMP | MW-150 | C | 2020/09/17 | Temperature (Celsius) | degrees C | 13.8 |
| PMP | MW-150 | C | 2020/12/17 | Temperature (Celsius) | degrees C | 12.3 |
| PMP | MW-150 | C | 2021/03/10 | Temperature (Celsius) | degrees C | 13.6 |
| PMP | MW-150 | C | 2021/06/21 | Temperature (Celsius) | degrees C | 13.2 |
| PMP | MW-150 | C | 2021/09/14 | Temperature (Celsius) | degrees C | 13.9 |
| PMP | MW-150 | C | 2021/12/14 | Temperature (Celsius) | degrees C | 14.3 |
| PMP | MW-150 | C | 2022/03/28 | Temperature (Celsius) | degrees C | 13.2 |
| PMP | MW-150 | C | 2022/06/14 | Temperature (Celsius) | degrees C | 14.3 |
| PMP | MW-150 | C | 2022/09/29 | Temperature (Celsius) | degrees C | 13.8 |
| PMP | MW-150 | C | 2022/12/06 | Temperature (Celsius) | degrees C | 13.6 |
| PMP | MW-150 | C | 2023/03/15 | Temperature (Celsius) | degrees C | 13.4 |
| PMP | MW-150 | C | 2023/05/18 | Temperature (Celsius) | degrees C | 13.6 |
| PMP | MW-150 | C | 2023/08/07 | Temperature (Celsius) | degrees C | 14.0 |
| PMP | MW-150 | C | 2023/11/03 | Temperature (Celsius) | degrees C | 13.6 |
| PMP | MW-150 | C | 2013/09/16 | Total Dissolved Solids | mg/L | 1,090 |

Attachment I. Site Groundwater Data

Geochemical Conceptual Site Model

Baldwin Fly Ash Pond System

Baldwin Power Plant

Baldwin, IL

| | | | | | | |
|-----|--------|---|------------|------------------------|------|-------|
| PMP | MW-150 | C | 2013/11/20 | Total Dissolved Solids | mg/L | 1,090 |
| PMP | MW-150 | C | 2014/02/19 | Total Dissolved Solids | mg/L | 1,200 |
| PMP | MW-150 | C | 2014/06/11 | Total Dissolved Solids | mg/L | 1,300 |
| PMP | MW-150 | C | 2015/03/25 | Total Dissolved Solids | mg/L | 1,270 |
| PMP | MW-150 | C | 2015/06/24 | Total Dissolved Solids | mg/L | 1,340 |
| PMP | MW-150 | C | 2015/09/25 | Total Dissolved Solids | mg/L | 1,210 |
| PMP | MW-150 | C | 2015/11/10 | Total Dissolved Solids | mg/L | 1,180 |
| PMP | MW-150 | C | 2016/03/22 | Total Dissolved Solids | mg/L | 1,410 |
| PMP | MW-150 | C | 2016/06/21 | Total Dissolved Solids | mg/L | 1,440 |
| PMP | MW-150 | C | 2016/09/29 | Total Dissolved Solids | mg/L | 1,470 |
| PMP | MW-150 | C | 2016/12/21 | Total Dissolved Solids | mg/L | 1,440 |
| PMP | MW-150 | C | 2017/03/16 | Total Dissolved Solids | mg/L | 1,570 |
| PMP | MW-150 | C | 2017/06/22 | Total Dissolved Solids | mg/L | 1,520 |
| PMP | MW-150 | C | 2017/09/21 | Total Dissolved Solids | mg/L | 1,390 |
| PMP | MW-150 | C | 2017/11/28 | Total Dissolved Solids | mg/L | 1,500 |
| PMP | MW-150 | C | 2018/03/19 | Total Dissolved Solids | mg/L | 1,540 |
| PMP | MW-150 | C | 2018/06/28 | Total Dissolved Solids | mg/L | 1,530 |
| PMP | MW-150 | C | 2018/09/26 | Total Dissolved Solids | mg/L | 1,550 |
| PMP | MW-150 | C | 2018/12/18 | Total Dissolved Solids | mg/L | 1,620 |
| PMP | MW-150 | C | 2019/03/20 | Total Dissolved Solids | mg/L | 1,520 |
| PMP | MW-150 | C | 2019/06/25 | Total Dissolved Solids | mg/L | 1,700 |
| PMP | MW-150 | C | 2019/09/26 | Total Dissolved Solids | mg/L | 1,490 |
| PMP | MW-150 | C | 2019/12/19 | Total Dissolved Solids | mg/L | 1,540 |
| PMP | MW-150 | C | 2020/03/26 | Total Dissolved Solids | mg/L | 1,580 |
| PMP | MW-150 | C | 2020/06/23 | Total Dissolved Solids | mg/L | 1,640 |
| PMP | MW-150 | C | 2020/09/17 | Total Dissolved Solids | mg/L | 1,590 |
| PMP | MW-150 | C | 2020/12/17 | Total Dissolved Solids | mg/L | 1,590 |
| PMP | MW-150 | C | 2021/03/10 | Total Dissolved Solids | mg/L | 1,730 |
| PMP | MW-150 | C | 2021/06/21 | Total Dissolved Solids | mg/L | 1,660 |
| PMP | MW-150 | C | 2021/09/14 | Total Dissolved Solids | mg/L | 1,550 |
| PMP | MW-150 | C | 2021/12/14 | Total Dissolved Solids | mg/L | 1,560 |
| PMP | MW-150 | C | 2022/03/28 | Total Dissolved Solids | mg/L | 1,770 |
| PMP | MW-150 | C | 2022/06/14 | Total Dissolved Solids | mg/L | 1,790 |
| PMP | MW-150 | C | 2022/09/29 | Total Dissolved Solids | mg/L | 1,680 |
| PMP | MW-150 | C | 2022/12/06 | Total Dissolved Solids | mg/L | 1,640 |
| PMP | MW-150 | C | 2023/03/15 | Total Dissolved Solids | mg/L | 1,770 |
| PMP | MW-150 | C | 2023/05/18 | Total Dissolved Solids | mg/L | 1,790 |
| PMP | MW-150 | C | 2023/08/07 | Total Dissolved Solids | mg/L | 1,670 |
| PMP | MW-150 | C | 2023/11/03 | Total Dissolved Solids | mg/L | 1,620 |
| PMP | MW-151 | C | 2013/09/16 | pH (field) | SU | 7.2 |
| PMP | MW-151 | C | 2013/11/20 | pH (field) | SU | 7.1 |
| PMP | MW-151 | C | 2014/02/19 | pH (field) | SU | 7.1 |
| PMP | MW-151 | C | 2014/06/12 | pH (field) | SU | 6.3 |
| PMP | MW-151 | C | 2017/03/16 | pH (field) | SU | 7.2 |
| PMP | MW-151 | C | 2017/06/21 | pH (field) | SU | 6.9 |
| PMP | MW-151 | C | 2017/09/21 | pH (field) | SU | 6.9 |
| PMP | MW-151 | C | 2017/11/28 | pH (field) | SU | 7.2 |
| PMP | MW-151 | C | 2018/03/20 | pH (field) | SU | 7.1 |
| PMP | MW-151 | C | 2018/06/27 | pH (field) | SU | 6.9 |
| PMP | MW-151 | C | 2018/09/26 | pH (field) | SU | 6.9 |
| PMP | MW-151 | C | 2018/12/18 | pH (field) | SU | 6.9 |
| PMP | MW-151 | C | 2019/03/20 | pH (field) | SU | 7.0 |
| PMP | MW-151 | C | 2019/06/25 | pH (field) | SU | 6.9 |
| PMP | MW-151 | C | 2019/09/26 | pH (field) | SU | 6.7 |
| PMP | MW-151 | C | 2019/12/19 | pH (field) | SU | 7.2 |
| PMP | MW-151 | C | 2020/03/27 | pH (field) | SU | 6.9 |
| PMP | MW-151 | C | 2020/06/23 | pH (field) | SU | 7.0 |

Attachment I. Site Groundwater Data

Geochemical Conceptual Site Model

Baldwin Fly Ash Pond System

Baldwin Power Plant

Baldwin, IL

| | | | | | | |
|-----|--------|---|------------|-------------------------------|------------|--------|
| PMP | MW-151 | C | 2020/09/17 | pH (field) | SU | 7.0 |
| PMP | MW-151 | C | 2020/12/16 | pH (field) | SU | 7.1 |
| PMP | MW-151 | C | 2021/03/09 | pH (field) | SU | 6.9 |
| PMP | MW-151 | C | 2021/06/21 | pH (field) | SU | 6.8 |
| PMP | MW-151 | C | 2021/09/14 | pH (field) | SU | 6.9 |
| PMP | MW-151 | C | 2021/12/14 | pH (field) | SU | 6.9 |
| PMP | MW-151 | C | 2022/03/28 | pH (field) | SU | 6.9 |
| PMP | MW-151 | C | 2022/06/14 | pH (field) | SU | 6.9 |
| PMP | MW-151 | C | 2022/09/29 | pH (field) | SU | 6.7 |
| PMP | MW-151 | C | 2022/12/06 | pH (field) | SU | 7.0 |
| PMP | MW-151 | C | 2023/03/15 | pH (field) | SU | 6.9 |
| PMP | MW-151 | C | 2023/05/18 | pH (field) | SU | 6.8 |
| PMP | MW-151 | C | 2023/07/10 | pH (field) | SU | 7.0 |
| PMP | MW-151 | C | 2023/08/07 | pH (field) | SU | 6.8 |
| PMP | MW-151 | C | 2023/10/31 | pH (field) | SU | 6.9 |
| PMP | MW-151 | C | 2021/03/09 | Oxidation Reduction Potential | mV | 79.0 |
| PMP | MW-151 | C | 2021/06/21 | Oxidation Reduction Potential | mV | 32.0 |
| PMP | MW-151 | C | 2021/09/14 | Oxidation Reduction Potential | mV | 90.0 |
| PMP | MW-151 | C | 2021/12/14 | Oxidation Reduction Potential | mV | 78.0 |
| PMP | MW-151 | C | 2022/03/28 | Oxidation Reduction Potential | mV | 50.0 |
| PMP | MW-151 | C | 2022/06/14 | Oxidation Reduction Potential | mV | 104 |
| PMP | MW-151 | C | 2022/09/29 | Oxidation Reduction Potential | mV | 155 |
| PMP | MW-151 | C | 2022/12/06 | Oxidation Reduction Potential | mV | 97.0 |
| PMP | MW-151 | C | 2023/03/15 | Oxidation Reduction Potential | mV | 96.8 |
| PMP | MW-151 | C | 2023/05/18 | Oxidation Reduction Potential | mV | 125 |
| PMP | MW-151 | C | 2023/07/10 | Oxidation Reduction Potential | mV | 125 |
| PMP | MW-151 | C | 2023/08/07 | Oxidation Reduction Potential | mV | 166 |
| PMP | MW-151 | C | 2023/10/31 | Oxidation Reduction Potential | mV | 40.0 |
| PMP | MW-151 | C | 2021/03/09 | Eh | V | 0.28 |
| PMP | MW-151 | C | 2021/06/21 | Eh | V | 0.23 |
| PMP | MW-151 | C | 2021/09/14 | Eh | V | 0.28 |
| PMP | MW-151 | C | 2021/12/14 | Eh | V | 0.27 |
| PMP | MW-151 | C | 2022/03/28 | Eh | V | 0.25 |
| PMP | MW-151 | C | 2022/06/14 | Eh | V | 0.30 |
| PMP | MW-151 | C | 2022/09/29 | Eh | V | 0.35 |
| PMP | MW-151 | C | 2022/12/06 | Eh | V | 0.29 |
| PMP | MW-151 | C | 2023/03/15 | Eh | V | 0.29 |
| PMP | MW-151 | C | 2023/05/18 | Eh | V | 0.32 |
| PMP | MW-151 | C | 2023/07/10 | Eh | V | 0.32 |
| PMP | MW-151 | C | 2023/08/07 | Eh | V | 0.36 |
| PMP | MW-151 | C | 2023/10/31 | Eh | V | 0.23 |
| PMP | MW-151 | C | 2023/03/15 | Alkalinity, bicarbonate | mg/L CaCO3 | 436 |
| PMP | MW-151 | C | 2023/05/18 | Alkalinity, bicarbonate | mg/L CaCO3 | 523 |
| PMP | MW-151 | C | 2023/08/07 | Alkalinity, bicarbonate | mg/L CaCO3 | 443 |
| PMP | MW-151 | C | 2023/10/31 | Alkalinity, bicarbonate | mg/L CaCO3 | 474 |
| PMP | MW-151 | C | 2023/03/15 | Barium, total | mg/L | 0.0599 |
| PMP | MW-151 | C | 2023/05/18 | Barium, total | mg/L | 0.138 |
| PMP | MW-151 | C | 2023/07/10 | Barium, total | mg/L | 0.0550 |
| PMP | MW-151 | C | 2023/08/07 | Barium, total | mg/L | 0.0666 |
| PMP | MW-151 | C | 2023/10/31 | Barium, total | mg/L | 0.0759 |
| PMP | MW-151 | C | 2013/09/16 | Boron, total | mg/L | 0.240 |
| PMP | MW-151 | C | 2023/03/15 | Boron, total | mg/L | 0.459 |
| PMP | MW-151 | C | 2023/05/18 | Boron, total | mg/L | 0.345 |
| PMP | MW-151 | C | 2023/07/10 | Boron, total | mg/L | 0.749 |
| PMP | MW-151 | C | 2023/08/07 | Boron, total | mg/L | 0.887 |
| PMP | MW-151 | C | 2023/10/31 | Boron, total | mg/L | 0.889 |
| PMP | MW-151 | C | 2023/03/15 | Calcium, total | mg/L | 113 |

Attachment I. Site Groundwater Data

Geochemical Conceptual Site Model

Baldwin Fly Ash Pond System

Baldwin Power Plant

Baldwin, IL

| | | | | | | |
|-----|--------|---|------------|----------------------|------|---------|
| PMP | MW-151 | C | 2023/05/18 | Calcium, total | mg/L | 187 |
| PMP | MW-151 | C | 2023/07/10 | Calcium, total | mg/L | 116 |
| PMP | MW-151 | C | 2023/08/07 | Calcium, total | mg/L | 108 |
| PMP | MW-151 | C | 2023/10/31 | Calcium, total | mg/L | 123 |
| PMP | MW-151 | C | 2013/09/16 | Chloride, total | mg/L | 36.0 |
| PMP | MW-151 | C | 2023/03/15 | Chloride, total | mg/L | 37.0 |
| PMP | MW-151 | C | 2023/05/18 | Chloride, total | mg/L | 46.0 |
| PMP | MW-151 | C | 2023/07/10 | Chloride, total | mg/L | 38.0 |
| PMP | MW-151 | C | 2023/08/07 | Chloride, total | mg/L | 38.0 |
| PMP | MW-151 | C | 2023/10/31 | Chloride, total | mg/L | 41.0 |
| PMP | MW-151 | C | 2013/11/20 | Iron, dissolved | mg/L | <0.007 |
| PMP | MW-151 | C | 2014/02/19 | Iron, dissolved | mg/L | <0.007 |
| PMP | MW-151 | C | 2014/06/12 | Iron, dissolved | mg/L | <0.007 |
| PMP | MW-151 | C | 2017/03/16 | Iron, dissolved | mg/L | <0.007 |
| PMP | MW-151 | C | 2017/06/21 | Iron, dissolved | mg/L | <0.007 |
| PMP | MW-151 | C | 2017/09/21 | Iron, dissolved | mg/L | <0.007 |
| PMP | MW-151 | C | 2017/11/28 | Iron, dissolved | mg/L | <0.007 |
| PMP | MW-151 | C | 2018/03/20 | Iron, dissolved | mg/L | <0.007 |
| PMP | MW-151 | C | 2018/06/27 | Iron, dissolved | mg/L | <0.02 |
| PMP | MW-151 | C | 2018/09/26 | Iron, dissolved | mg/L | <0.02 |
| PMP | MW-151 | C | 2018/12/18 | Iron, dissolved | mg/L | <0.02 |
| PMP | MW-151 | C | 2019/03/20 | Iron, dissolved | mg/L | <0.02 |
| PMP | MW-151 | C | 2019/06/25 | Iron, dissolved | mg/L | <0.02 |
| PMP | MW-151 | C | 2019/09/26 | Iron, dissolved | mg/L | <0.02 |
| PMP | MW-151 | C | 2019/12/19 | Iron, dissolved | mg/L | <0.02 |
| PMP | MW-151 | C | 2020/03/27 | Iron, dissolved | mg/L | <0.02 |
| PMP | MW-151 | C | 2020/06/23 | Iron, dissolved | mg/L | <0.02 |
| PMP | MW-151 | C | 2020/09/17 | Iron, dissolved | mg/L | <0.02 |
| PMP | MW-151 | C | 2020/12/16 | Iron, dissolved | mg/L | <0.02 |
| PMP | MW-151 | C | 2021/03/09 | Iron, dissolved | mg/L | <0.02 |
| PMP | MW-151 | C | 2021/06/21 | Iron, dissolved | mg/L | <0.02 |
| PMP | MW-151 | C | 2021/09/14 | Iron, dissolved | mg/L | <0.02 |
| PMP | MW-151 | C | 2021/12/14 | Iron, dissolved | mg/L | <0.02 |
| PMP | MW-151 | C | 2022/03/28 | Iron, dissolved | mg/L | <0.015 |
| PMP | MW-151 | C | 2022/06/14 | Iron, dissolved | mg/L | <0.02 |
| PMP | MW-151 | C | 2022/09/29 | Iron, dissolved | mg/L | <0.0115 |
| PMP | MW-151 | C | 2022/12/06 | Iron, dissolved | mg/L | <0.0115 |
| PMP | MW-151 | C | 2023/03/15 | Iron, dissolved | mg/L | <0.0115 |
| PMP | MW-151 | C | 2023/05/18 | Iron, dissolved | mg/L | <0.02 |
| PMP | MW-151 | C | 2023/08/07 | Iron, dissolved | mg/L | <0.0115 |
| PMP | MW-151 | C | 2023/10/31 | Iron, dissolved | mg/L | 0.0130 |
| PMP | MW-151 | C | 2023/03/15 | Magnesium, total | mg/L | 41.7 |
| PMP | MW-151 | C | 2023/05/18 | Magnesium, total | mg/L | 51.7 |
| PMP | MW-151 | C | 2023/08/07 | Magnesium, total | mg/L | 40.5 |
| PMP | MW-151 | C | 2023/10/31 | Magnesium, total | mg/L | 43.6 |
| PMP | MW-151 | C | 2013/11/20 | Manganese, dissolved | mg/L | <0.0016 |
| PMP | MW-151 | C | 2014/02/19 | Manganese, dissolved | mg/L | <0.0016 |
| PMP | MW-151 | C | 2014/06/12 | Manganese, dissolved | mg/L | 0.00500 |
| PMP | MW-151 | C | 2017/03/16 | Manganese, dissolved | mg/L | 0.0100 |
| PMP | MW-151 | C | 2017/06/21 | Manganese, dissolved | mg/L | 0.00320 |
| PMP | MW-151 | C | 2017/09/21 | Manganese, dissolved | mg/L | 0.00300 |
| PMP | MW-151 | C | 2017/11/28 | Manganese, dissolved | mg/L | 0.00630 |
| PMP | MW-151 | C | 2018/03/20 | Manganese, dissolved | mg/L | 0.00320 |
| PMP | MW-151 | C | 2018/06/27 | Manganese, dissolved | mg/L | <0.0025 |
| PMP | MW-151 | C | 2018/09/26 | Manganese, dissolved | mg/L | 0.0689 |
| PMP | MW-151 | C | 2018/12/18 | Manganese, dissolved | mg/L | <0.0025 |
| PMP | MW-151 | C | 2019/03/20 | Manganese, dissolved | mg/L | <0.0025 |

Attachment I. Site Groundwater Data

Geochemical Conceptual Site Model

Baldwin Fly Ash Pond System

Baldwin Power Plant

Baldwin, IL

| | | | | | | |
|-----|--------|---|------------|-----------------------|-----------|---------|
| PMP | MW-151 | C | 2019/06/25 | Manganese, dissolved | mg/L | <0.0025 |
| PMP | MW-151 | C | 2019/09/26 | Manganese, dissolved | mg/L | 0.00900 |
| PMP | MW-151 | C | 2019/12/19 | Manganese, dissolved | mg/L | <0.0025 |
| PMP | MW-151 | C | 2020/03/27 | Manganese, dissolved | mg/L | <0.0025 |
| PMP | MW-151 | C | 2020/06/23 | Manganese, dissolved | mg/L | <0.0025 |
| PMP | MW-151 | C | 2020/09/17 | Manganese, dissolved | mg/L | 0.00880 |
| PMP | MW-151 | C | 2020/12/16 | Manganese, dissolved | mg/L | <0.0025 |
| PMP | MW-151 | C | 2021/03/09 | Manganese, dissolved | mg/L | <0.0025 |
| PMP | MW-151 | C | 2021/06/21 | Manganese, dissolved | mg/L | <0.0025 |
| PMP | MW-151 | C | 2021/09/14 | Manganese, dissolved | mg/L | 0.00810 |
| PMP | MW-151 | C | 2021/12/14 | Manganese, dissolved | mg/L | 0.00910 |
| PMP | MW-151 | C | 2022/03/28 | Manganese, dissolved | mg/L | 0.00320 |
| PMP | MW-151 | C | 2022/06/14 | Manganese, dissolved | mg/L | 0.00470 |
| PMP | MW-151 | C | 2022/09/29 | Manganese, dissolved | mg/L | 0.00320 |
| PMP | MW-151 | C | 2022/12/06 | Manganese, dissolved | mg/L | 0.00370 |
| PMP | MW-151 | C | 2023/03/15 | Manganese, dissolved | mg/L | 0.00350 |
| PMP | MW-151 | C | 2023/05/18 | Manganese, dissolved | mg/L | 0.0151 |
| PMP | MW-151 | C | 2023/08/07 | Manganese, dissolved | mg/L | 0.0177 |
| PMP | MW-151 | C | 2023/10/31 | Manganese, dissolved | mg/L | 0.0133 |
| PMP | MW-151 | C | 2023/05/18 | Phosphate, dissolved | mg/L | <0.005 |
| PMP | MW-151 | C | 2023/08/07 | Phosphate, dissolved | mg/L | <0.005 |
| PMP | MW-151 | C | 2023/03/15 | Potassium, total | mg/L | 1.68 |
| PMP | MW-151 | C | 2023/05/18 | Potassium, total | mg/L | 5.43 |
| PMP | MW-151 | C | 2023/08/07 | Potassium, total | mg/L | 2.37 |
| PMP | MW-151 | C | 2023/10/31 | Potassium, total | mg/L | 2.64 |
| PMP | MW-151 | C | 2023/05/18 | Silicon, dissolved | mg/L | 5.37 |
| PMP | MW-151 | C | 2023/08/07 | Silicon, dissolved | mg/L | 5.38 |
| PMP | MW-151 | C | 2023/03/15 | Sodium, total | mg/L | 48.2 |
| PMP | MW-151 | C | 2023/05/18 | Sodium, total | mg/L | 56.3 |
| PMP | MW-151 | C | 2023/08/07 | Sodium, total | mg/L | 64.6 |
| PMP | MW-151 | C | 2023/10/31 | Sodium, total | mg/L | 64.9 |
| PMP | MW-151 | C | 2013/09/16 | Sulfate, total | mg/L | 90.0 |
| PMP | MW-151 | C | 2023/03/15 | Sulfate, total | mg/L | 81.0 |
| PMP | MW-151 | C | 2023/05/18 | Sulfate, total | mg/L | 74.0 |
| PMP | MW-151 | C | 2023/07/10 | Sulfate, total | mg/L | 82.0 |
| PMP | MW-151 | C | 2023/08/07 | Sulfate, total | mg/L | 93.0 |
| PMP | MW-151 | C | 2023/10/31 | Sulfate, total | mg/L | 95.0 |
| PMP | MW-151 | C | 2013/09/16 | Temperature (Celsius) | degrees C | 17.3 |
| PMP | MW-151 | C | 2013/11/20 | Temperature (Celsius) | degrees C | 14.2 |
| PMP | MW-151 | C | 2014/02/19 | Temperature (Celsius) | degrees C | 8.50 |
| PMP | MW-151 | C | 2014/06/12 | Temperature (Celsius) | degrees C | 13.8 |
| PMP | MW-151 | C | 2017/03/16 | Temperature (Celsius) | degrees C | 10.8 |
| PMP | MW-151 | C | 2017/06/21 | Temperature (Celsius) | degrees C | 15.1 |
| PMP | MW-151 | C | 2017/09/21 | Temperature (Celsius) | degrees C | 18.1 |
| PMP | MW-151 | C | 2017/11/28 | Temperature (Celsius) | degrees C | 16.3 |
| PMP | MW-151 | C | 2018/03/20 | Temperature (Celsius) | degrees C | 10.8 |
| PMP | MW-151 | C | 2018/06/27 | Temperature (Celsius) | degrees C | 14.6 |
| PMP | MW-151 | C | 2018/09/26 | Temperature (Celsius) | degrees C | 18.3 |
| PMP | MW-151 | C | 2018/12/18 | Temperature (Celsius) | degrees C | 13.1 |
| PMP | MW-151 | C | 2019/03/20 | Temperature (Celsius) | degrees C | 9.30 |
| PMP | MW-151 | C | 2019/06/25 | Temperature (Celsius) | degrees C | 14.2 |
| PMP | MW-151 | C | 2019/09/26 | Temperature (Celsius) | degrees C | 17.0 |
| PMP | MW-151 | C | 2019/12/19 | Temperature (Celsius) | degrees C | 12.8 |
| PMP | MW-151 | C | 2020/06/23 | Temperature (Celsius) | degrees C | 14.0 |
| PMP | MW-151 | C | 2020/09/17 | Temperature (Celsius) | degrees C | 17.3 |
| PMP | MW-151 | C | 2020/12/16 | Temperature (Celsius) | degrees C | 13.1 |
| PMP | MW-151 | C | 2021/03/09 | Temperature (Celsius) | degrees C | 10.9 |

Attachment I. Site Groundwater Data

Geochemical Conceptual Site Model

Baldwin Fly Ash Pond System

Baldwin Power Plant

Baldwin, IL

| | | | | | | |
|-----|--------|---|------------|------------------------|-----------|------|
| PMP | MW-151 | C | 2021/06/21 | Temperature (Celsius) | degrees C | 14.3 |
| PMP | MW-151 | C | 2021/09/14 | Temperature (Celsius) | degrees C | 18.7 |
| PMP | MW-151 | C | 2021/12/14 | Temperature (Celsius) | degrees C | 15.2 |
| PMP | MW-151 | C | 2022/03/28 | Temperature (Celsius) | degrees C | 10.4 |
| PMP | MW-151 | C | 2022/06/14 | Temperature (Celsius) | degrees C | 19.9 |
| PMP | MW-151 | C | 2022/09/29 | Temperature (Celsius) | degrees C | 16.9 |
| PMP | MW-151 | C | 2022/12/06 | Temperature (Celsius) | degrees C | 13.9 |
| PMP | MW-151 | C | 2023/03/15 | Temperature (Celsius) | degrees C | 11.6 |
| PMP | MW-151 | C | 2023/05/18 | Temperature (Celsius) | degrees C | 12.6 |
| PMP | MW-151 | C | 2023/07/10 | Temperature (Celsius) | degrees C | 15.2 |
| PMP | MW-151 | C | 2023/08/07 | Temperature (Celsius) | degrees C | 16.3 |
| PMP | MW-151 | C | 2023/10/31 | Temperature (Celsius) | degrees C | 16.4 |
| PMP | MW-151 | C | 2013/09/16 | Total Dissolved Solids | mg/L | 526 |
| PMP | MW-151 | C | 2013/11/20 | Total Dissolved Solids | mg/L | 542 |
| PMP | MW-151 | C | 2014/02/19 | Total Dissolved Solids | mg/L | 538 |
| PMP | MW-151 | C | 2014/06/12 | Total Dissolved Solids | mg/L | 562 |
| PMP | MW-151 | C | 2017/03/16 | Total Dissolved Solids | mg/L | 514 |
| PMP | MW-151 | C | 2017/06/21 | Total Dissolved Solids | mg/L | 536 |
| PMP | MW-151 | C | 2017/09/21 | Total Dissolved Solids | mg/L | 514 |
| PMP | MW-151 | C | 2017/11/28 | Total Dissolved Solids | mg/L | 590 |
| PMP | MW-151 | C | 2018/03/20 | Total Dissolved Solids | mg/L | 542 |
| PMP | MW-151 | C | 2018/06/27 | Total Dissolved Solids | mg/L | 568 |
| PMP | MW-151 | C | 2018/09/26 | Total Dissolved Solids | mg/L | 588 |
| PMP | MW-151 | C | 2018/12/18 | Total Dissolved Solids | mg/L | 550 |
| PMP | MW-151 | C | 2019/03/20 | Total Dissolved Solids | mg/L | 550 |
| PMP | MW-151 | C | 2019/06/25 | Total Dissolved Solids | mg/L | 525 |
| PMP | MW-151 | C | 2019/09/26 | Total Dissolved Solids | mg/L | 584 |
| PMP | MW-151 | C | 2019/12/19 | Total Dissolved Solids | mg/L | 604 |
| PMP | MW-151 | C | 2020/03/27 | Total Dissolved Solids | mg/L | 556 |
| PMP | MW-151 | C | 2020/06/23 | Total Dissolved Solids | mg/L | 496 |
| PMP | MW-151 | C | 2020/09/17 | Total Dissolved Solids | mg/L | 556 |
| PMP | MW-151 | C | 2020/12/16 | Total Dissolved Solids | mg/L | 552 |
| PMP | MW-151 | C | 2021/03/09 | Total Dissolved Solids | mg/L | 542 |
| PMP | MW-151 | C | 2021/06/21 | Total Dissolved Solids | mg/L | 566 |
| PMP | MW-151 | C | 2021/09/14 | Total Dissolved Solids | mg/L | 518 |
| PMP | MW-151 | C | 2021/12/14 | Total Dissolved Solids | mg/L | 520 |
| PMP | MW-151 | C | 2022/03/28 | Total Dissolved Solids | mg/L | 558 |
| PMP | MW-151 | C | 2022/06/14 | Total Dissolved Solids | mg/L | 544 |
| PMP | MW-151 | C | 2022/09/29 | Total Dissolved Solids | mg/L | 586 |
| PMP | MW-151 | C | 2022/12/06 | Total Dissolved Solids | mg/L | 560 |
| PMP | MW-151 | C | 2023/03/15 | Total Dissolved Solids | mg/L | 586 |
| PMP | MW-151 | C | 2023/05/18 | Total Dissolved Solids | mg/L | 545 |
| PMP | MW-151 | C | 2023/07/10 | Total Dissolved Solids | mg/L | 602 |
| PMP | MW-151 | C | 2023/08/07 | Total Dissolved Solids | mg/L | 595 |
| PMP | MW-151 | C | 2023/10/31 | Total Dissolved Solids | mg/L | 600 |
| PMP | MW-152 | C | 2013/09/16 | pH (field) | SU | 7.0 |
| PMP | MW-152 | C | 2013/11/20 | pH (field) | SU | 7.2 |
| PMP | MW-152 | C | 2014/02/19 | pH (field) | SU | 6.4 |
| PMP | MW-152 | C | 2014/06/12 | pH (field) | SU | 6.5 |
| PMP | MW-152 | C | 2015/03/25 | pH (field) | SU | 6.9 |
| PMP | MW-152 | C | 2015/06/24 | pH (field) | SU | 6.8 |
| PMP | MW-152 | C | 2015/09/25 | pH (field) | SU | 6.8 |
| PMP | MW-152 | C | 2015/11/10 | pH (field) | SU | 6.7 |
| PMP | MW-152 | C | 2016/03/22 | pH (field) | SU | 6.9 |
| PMP | MW-152 | C | 2016/06/23 | pH (field) | SU | 7.5 |
| PMP | MW-152 | C | 2016/09/29 | pH (field) | SU | 6.7 |
| PMP | MW-152 | C | 2016/12/21 | pH (field) | SU | 6.8 |

Attachment I. Site Groundwater Data

Geochemical Conceptual Site Model

Baldwin Fly Ash Pond System

Baldwin Power Plant

Baldwin, IL

| | | | | | | |
|-----|--------|---|------------|-------------------------------|------------|--------|
| PMP | MW-152 | C | 2017/03/16 | pH (field) | SU | 7.0 |
| PMP | MW-152 | C | 2017/06/21 | pH (field) | SU | 6.6 |
| PMP | MW-152 | C | 2017/09/21 | pH (field) | SU | 6.7 |
| PMP | MW-152 | C | 2017/11/28 | pH (field) | SU | 7.2 |
| PMP | MW-152 | C | 2018/03/20 | pH (field) | SU | 6.9 |
| PMP | MW-152 | C | 2018/06/27 | pH (field) | SU | 6.8 |
| PMP | MW-152 | C | 2018/09/26 | pH (field) | SU | 6.7 |
| PMP | MW-152 | C | 2018/12/18 | pH (field) | SU | 6.9 |
| PMP | MW-152 | C | 2019/03/20 | pH (field) | SU | 7.0 |
| PMP | MW-152 | C | 2019/06/25 | pH (field) | SU | 7.0 |
| PMP | MW-152 | C | 2019/09/26 | pH (field) | SU | 6.7 |
| PMP | MW-152 | C | 2019/12/19 | pH (field) | SU | 6.9 |
| PMP | MW-152 | C | 2020/03/27 | pH (field) | SU | 6.9 |
| PMP | MW-152 | C | 2020/06/23 | pH (field) | SU | 7.2 |
| PMP | MW-152 | C | 2020/09/17 | pH (field) | SU | 6.8 |
| PMP | MW-152 | C | 2020/12/16 | pH (field) | SU | 6.9 |
| PMP | MW-152 | C | 2021/03/09 | pH (field) | SU | 6.9 |
| PMP | MW-152 | C | 2021/07/19 | pH (field) | SU | 6.6 |
| PMP | MW-152 | C | 2021/09/14 | pH (field) | SU | 6.7 |
| PMP | MW-152 | C | 2021/12/14 | pH (field) | SU | 6.8 |
| PMP | MW-152 | C | 2022/03/28 | pH (field) | SU | 6.9 |
| PMP | MW-152 | C | 2022/06/14 | pH (field) | SU | 6.9 |
| PMP | MW-152 | C | 2022/09/29 | pH (field) | SU | 6.7 |
| PMP | MW-152 | C | 2022/12/06 | pH (field) | SU | 6.7 |
| PMP | MW-152 | C | 2023/03/15 | pH (field) | SU | 6.9 |
| PMP | MW-152 | C | 2023/05/18 | pH (field) | SU | 6.9 |
| PMP | MW-152 | C | 2023/08/04 | pH (field) | SU | 6.9 |
| PMP | MW-152 | C | 2023/10/31 | pH (field) | SU | 6.8 |
| PMP | MW-152 | C | 2021/03/09 | Oxidation Reduction Potential | mV | 53.0 |
| PMP | MW-152 | C | 2021/07/19 | Oxidation Reduction Potential | mV | 141 |
| PMP | MW-152 | C | 2021/09/14 | Oxidation Reduction Potential | mV | 19.0 |
| PMP | MW-152 | C | 2021/12/14 | Oxidation Reduction Potential | mV | 75.0 |
| PMP | MW-152 | C | 2022/03/28 | Oxidation Reduction Potential | mV | 58.0 |
| PMP | MW-152 | C | 2022/06/14 | Oxidation Reduction Potential | mV | 116 |
| PMP | MW-152 | C | 2022/09/29 | Oxidation Reduction Potential | mV | 155 |
| PMP | MW-152 | C | 2022/12/06 | Oxidation Reduction Potential | mV | 76.0 |
| PMP | MW-152 | C | 2023/03/15 | Oxidation Reduction Potential | mV | 118 |
| PMP | MW-152 | C | 2023/05/18 | Oxidation Reduction Potential | mV | 126 |
| PMP | MW-152 | C | 2023/08/04 | Oxidation Reduction Potential | mV | 108 |
| PMP | MW-152 | C | 2023/10/31 | Oxidation Reduction Potential | mV | 60.0 |
| PMP | MW-152 | C | 2021/03/09 | Eh | V | 0.25 |
| PMP | MW-152 | C | 2021/07/19 | Eh | V | 0.34 |
| PMP | MW-152 | C | 2021/09/14 | Eh | V | 0.21 |
| PMP | MW-152 | C | 2021/12/14 | Eh | V | 0.27 |
| PMP | MW-152 | C | 2022/03/28 | Eh | V | 0.26 |
| PMP | MW-152 | C | 2022/06/14 | Eh | V | 0.31 |
| PMP | MW-152 | C | 2022/09/29 | Eh | V | 0.35 |
| PMP | MW-152 | C | 2022/12/06 | Eh | V | 0.27 |
| PMP | MW-152 | C | 2023/03/15 | Eh | V | 0.32 |
| PMP | MW-152 | C | 2023/05/18 | Eh | V | 0.32 |
| PMP | MW-152 | C | 2023/08/04 | Eh | V | 0.30 |
| PMP | MW-152 | C | 2023/10/31 | Eh | V | 0.26 |
| PMP | MW-152 | C | 2023/03/15 | Alkalinity, bicarbonate | mg/L CaCO3 | 408 |
| PMP | MW-152 | C | 2023/05/18 | Alkalinity, bicarbonate | mg/L CaCO3 | 375 |
| PMP | MW-152 | C | 2023/08/04 | Alkalinity, bicarbonate | mg/L CaCO3 | 414 |
| PMP | MW-152 | C | 2023/10/31 | Alkalinity, bicarbonate | mg/L CaCO3 | 417 |
| PMP | MW-152 | C | 2023/03/15 | Barium, total | mg/L | 0.0112 |

Attachment I. Site Groundwater Data

Geochemical Conceptual Site Model

Baldwin Fly Ash Pond System

Baldwin Power Plant

Baldwin, IL

| | | | | | | |
|-----|--------|---|------------|------------------|------|---------|
| PMP | MW-152 | C | 2023/05/18 | Barium, total | mg/L | 0.0167 |
| PMP | MW-152 | C | 2023/08/04 | Barium, total | mg/L | 0.0330 |
| PMP | MW-152 | C | 2023/10/31 | Barium, total | mg/L | 0.0454 |
| PMP | MW-152 | C | 2013/09/16 | Boron, total | mg/L | 9.09 |
| PMP | MW-152 | C | 2023/03/15 | Boron, total | mg/L | 0.477 |
| PMP | MW-152 | C | 2023/05/18 | Boron, total | mg/L | 0.515 |
| PMP | MW-152 | C | 2023/08/04 | Boron, total | mg/L | 9.09 |
| PMP | MW-152 | C | 2023/10/31 | Boron, total | mg/L | 19.8 |
| PMP | MW-152 | C | 2023/03/15 | Calcium, total | mg/L | 125 |
| PMP | MW-152 | C | 2023/05/18 | Calcium, total | mg/L | 116 |
| PMP | MW-152 | C | 2023/08/04 | Calcium, total | mg/L | 209 |
| PMP | MW-152 | C | 2023/10/31 | Calcium, total | mg/L | 268 |
| PMP | MW-152 | C | 2013/09/16 | Chloride, total | mg/L | 49.0 |
| PMP | MW-152 | C | 2023/03/15 | Chloride, total | mg/L | 10.0 |
| PMP | MW-152 | C | 2023/05/18 | Chloride, total | mg/L | 8.00 |
| PMP | MW-152 | C | 2023/08/04 | Chloride, total | mg/L | 37.0 |
| PMP | MW-152 | C | 2023/10/31 | Chloride, total | mg/L | 54.0 |
| PMP | MW-152 | C | 2013/11/20 | Iron, dissolved | mg/L | 0.0700 |
| PMP | MW-152 | C | 2014/02/19 | Iron, dissolved | mg/L | 0.0500 |
| PMP | MW-152 | C | 2014/06/12 | Iron, dissolved | mg/L | 0.456 |
| PMP | MW-152 | C | 2015/03/25 | Iron, dissolved | mg/L | 0.0440 |
| PMP | MW-152 | C | 2015/06/24 | Iron, dissolved | mg/L | 0.118 |
| PMP | MW-152 | C | 2015/09/25 | Iron, dissolved | mg/L | 0.0333 |
| PMP | MW-152 | C | 2015/11/10 | Iron, dissolved | mg/L | 0.0759 |
| PMP | MW-152 | C | 2016/03/22 | Iron, dissolved | mg/L | <0.007 |
| PMP | MW-152 | C | 2016/06/23 | Iron, dissolved | mg/L | 0.0346 |
| PMP | MW-152 | C | 2016/09/29 | Iron, dissolved | mg/L | <0.007 |
| PMP | MW-152 | C | 2016/12/21 | Iron, dissolved | mg/L | <0.007 |
| PMP | MW-152 | C | 2017/03/16 | Iron, dissolved | mg/L | <0.007 |
| PMP | MW-152 | C | 2017/06/21 | Iron, dissolved | mg/L | <0.007 |
| PMP | MW-152 | C | 2017/09/21 | Iron, dissolved | mg/L | 0.190 |
| PMP | MW-152 | C | 2017/11/28 | Iron, dissolved | mg/L | 0.280 |
| PMP | MW-152 | C | 2018/03/20 | Iron, dissolved | mg/L | <0.007 |
| PMP | MW-152 | C | 2018/06/27 | Iron, dissolved | mg/L | <0.02 |
| PMP | MW-152 | C | 2018/09/26 | Iron, dissolved | mg/L | <0.02 |
| PMP | MW-152 | C | 2018/12/18 | Iron, dissolved | mg/L | <0.02 |
| PMP | MW-152 | C | 2019/03/20 | Iron, dissolved | mg/L | <0.02 |
| PMP | MW-152 | C | 2019/06/25 | Iron, dissolved | mg/L | <0.02 |
| PMP | MW-152 | C | 2019/09/26 | Iron, dissolved | mg/L | 0.0456 |
| PMP | MW-152 | C | 2019/12/19 | Iron, dissolved | mg/L | <0.02 |
| PMP | MW-152 | C | 2020/03/27 | Iron, dissolved | mg/L | <0.02 |
| PMP | MW-152 | C | 2020/06/23 | Iron, dissolved | mg/L | <0.02 |
| PMP | MW-152 | C | 2020/09/17 | Iron, dissolved | mg/L | <0.02 |
| PMP | MW-152 | C | 2020/12/16 | Iron, dissolved | mg/L | <0.02 |
| PMP | MW-152 | C | 2021/03/09 | Iron, dissolved | mg/L | <0.02 |
| PMP | MW-152 | C | 2021/07/19 | Iron, dissolved | mg/L | <0.02 |
| PMP | MW-152 | C | 2021/09/14 | Iron, dissolved | mg/L | <0.02 |
| PMP | MW-152 | C | 2021/12/14 | Iron, dissolved | mg/L | <0.02 |
| PMP | MW-152 | C | 2022/03/28 | Iron, dissolved | mg/L | <0.015 |
| PMP | MW-152 | C | 2022/06/14 | Iron, dissolved | mg/L | <0.02 |
| PMP | MW-152 | C | 2022/09/29 | Iron, dissolved | mg/L | <0.0115 |
| PMP | MW-152 | C | 2022/12/06 | Iron, dissolved | mg/L | 0.253 |
| PMP | MW-152 | C | 2023/03/15 | Iron, dissolved | mg/L | <0.0115 |
| PMP | MW-152 | C | 2023/05/18 | Iron, dissolved | mg/L | <0.02 |
| PMP | MW-152 | C | 2023/08/04 | Iron, dissolved | mg/L | <0.012 |
| PMP | MW-152 | C | 2023/10/31 | Iron, dissolved | mg/L | <0.0115 |
| PMP | MW-152 | C | 2023/03/15 | Magnesium, total | mg/L | 59.2 |

Attachment I. Site Groundwater Data

Geochemical Conceptual Site Model

Baldwin Fly Ash Pond System

Baldwin Power Plant

Baldwin, IL

| | | | | | | |
|-----|--------|---|------------|----------------------|------|---------|
| PMP | MW-152 | C | 2023/05/18 | Magnesium, total | mg/L | 53.5 |
| PMP | MW-152 | C | 2023/08/04 | Magnesium, total | mg/L | 100 |
| PMP | MW-152 | C | 2023/10/31 | Magnesium, total | mg/L | 122 |
| PMP | MW-152 | C | 2013/11/20 | Manganese, dissolved | mg/L | 0.00500 |
| PMP | MW-152 | C | 2014/02/19 | Manganese, dissolved | mg/L | <0.0016 |
| PMP | MW-152 | C | 2014/06/12 | Manganese, dissolved | mg/L | 0.102 |
| PMP | MW-152 | C | 2015/03/25 | Manganese, dissolved | mg/L | 0.0100 |
| PMP | MW-152 | C | 2015/06/24 | Manganese, dissolved | mg/L | 0.0910 |
| PMP | MW-152 | C | 2015/09/25 | Manganese, dissolved | mg/L | 0.0192 |
| PMP | MW-152 | C | 2015/11/10 | Manganese, dissolved | mg/L | 0.0398 |
| PMP | MW-152 | C | 2016/03/22 | Manganese, dissolved | mg/L | 0.0180 |
| PMP | MW-152 | C | 2016/06/23 | Manganese, dissolved | mg/L | 0.134 |
| PMP | MW-152 | C | 2016/09/29 | Manganese, dissolved | mg/L | 0.0311 |
| PMP | MW-152 | C | 2016/12/21 | Manganese, dissolved | mg/L | 0.0199 |
| PMP | MW-152 | C | 2017/03/16 | Manganese, dissolved | mg/L | 0.00810 |
| PMP | MW-152 | C | 2017/06/21 | Manganese, dissolved | mg/L | 0.0100 |
| PMP | MW-152 | C | 2017/09/21 | Manganese, dissolved | mg/L | 0.0100 |
| PMP | MW-152 | C | 2017/11/28 | Manganese, dissolved | mg/L | 0.0200 |
| PMP | MW-152 | C | 2018/03/20 | Manganese, dissolved | mg/L | 0.00670 |
| PMP | MW-152 | C | 2018/06/27 | Manganese, dissolved | mg/L | <0.0025 |
| PMP | MW-152 | C | 2018/09/26 | Manganese, dissolved | mg/L | 0.0173 |
| PMP | MW-152 | C | 2018/12/18 | Manganese, dissolved | mg/L | 0.0105 |
| PMP | MW-152 | C | 2019/03/20 | Manganese, dissolved | mg/L | <0.0025 |
| PMP | MW-152 | C | 2019/06/25 | Manganese, dissolved | mg/L | <0.0025 |
| PMP | MW-152 | C | 2019/09/26 | Manganese, dissolved | mg/L | 0.0374 |
| PMP | MW-152 | C | 2019/12/19 | Manganese, dissolved | mg/L | <0.005 |
| PMP | MW-152 | C | 2020/03/27 | Manganese, dissolved | mg/L | 0.00730 |
| PMP | MW-152 | C | 2020/06/23 | Manganese, dissolved | mg/L | <0.0025 |
| PMP | MW-152 | C | 2020/09/17 | Manganese, dissolved | mg/L | 0.0163 |
| PMP | MW-152 | C | 2020/12/16 | Manganese, dissolved | mg/L | 0.0123 |
| PMP | MW-152 | C | 2021/03/09 | Manganese, dissolved | mg/L | <0.0025 |
| PMP | MW-152 | C | 2021/07/19 | Manganese, dissolved | mg/L | <0.0025 |
| PMP | MW-152 | C | 2021/09/14 | Manganese, dissolved | mg/L | 0.0183 |
| PMP | MW-152 | C | 2021/12/14 | Manganese, dissolved | mg/L | 0.00850 |
| PMP | MW-152 | C | 2022/03/28 | Manganese, dissolved | mg/L | 0.00620 |
| PMP | MW-152 | C | 2022/06/14 | Manganese, dissolved | mg/L | 0.00610 |
| PMP | MW-152 | C | 2022/09/29 | Manganese, dissolved | mg/L | 0.0153 |
| PMP | MW-152 | C | 2022/12/06 | Manganese, dissolved | mg/L | 0.0209 |
| PMP | MW-152 | C | 2023/03/15 | Manganese, dissolved | mg/L | 0.00310 |
| PMP | MW-152 | C | 2023/05/18 | Manganese, dissolved | mg/L | 0.00730 |
| PMP | MW-152 | C | 2023/08/04 | Manganese, dissolved | mg/L | 0.0176 |
| PMP | MW-152 | C | 2023/10/31 | Manganese, dissolved | mg/L | 0.0244 |
| PMP | MW-152 | C | 2023/05/18 | Phosphate, dissolved | mg/L | 0.0150 |
| PMP | MW-152 | C | 2023/08/04 | Phosphate, dissolved | mg/L | 0.0400 |
| PMP | MW-152 | C | 2023/03/15 | Potassium, total | mg/L | 0.515 |
| PMP | MW-152 | C | 2023/05/18 | Potassium, total | mg/L | 0.717 |
| PMP | MW-152 | C | 2023/08/04 | Potassium, total | mg/L | 1.34 |
| PMP | MW-152 | C | 2023/10/31 | Potassium, total | mg/L | 1.86 |
| PMP | MW-152 | C | 2023/05/18 | Silicon, dissolved | mg/L | 8.72 |
| PMP | MW-152 | C | 2023/08/04 | Silicon, dissolved | mg/L | 9.62 |
| PMP | MW-152 | C | 2023/03/15 | Sodium, total | mg/L | 107 |
| PMP | MW-152 | C | 2023/05/18 | Sodium, total | mg/L | 86.9 |
| PMP | MW-152 | C | 2023/08/04 | Sodium, total | mg/L | 149 |
| PMP | MW-152 | C | 2023/10/31 | Sodium, total | mg/L | 134 |
| PMP | MW-152 | C | 2013/09/16 | Sulfate, total | mg/L | 873 |
| PMP | MW-152 | C | 2023/03/15 | Sulfate, total | mg/L | 369 |
| PMP | MW-152 | C | 2023/05/18 | Sulfate, total | mg/L | 242 |

Attachment I. Site Groundwater Data

Geochemical Conceptual Site Model

Baldwin Fly Ash Pond System

Baldwin Power Plant

Baldwin, IL

| | | | | | | |
|-----|--------|---|------------|------------------------|-----------|-------|
| PMP | MW-152 | C | 2023/08/04 | Sulfate, total | mg/L | 732 |
| PMP | MW-152 | C | 2023/10/31 | Sulfate, total | mg/L | 988 |
| PMP | MW-152 | C | 2013/09/16 | Temperature (Celsius) | degrees C | 16.2 |
| PMP | MW-152 | C | 2013/11/20 | Temperature (Celsius) | degrees C | 13.7 |
| PMP | MW-152 | C | 2014/02/19 | Temperature (Celsius) | degrees C | 9.50 |
| PMP | MW-152 | C | 2014/06/12 | Temperature (Celsius) | degrees C | 12.9 |
| PMP | MW-152 | C | 2015/03/25 | Temperature (Celsius) | degrees C | 10.0 |
| PMP | MW-152 | C | 2015/06/24 | Temperature (Celsius) | degrees C | 14.0 |
| PMP | MW-152 | C | 2015/09/25 | Temperature (Celsius) | degrees C | 16.3 |
| PMP | MW-152 | C | 2015/11/10 | Temperature (Celsius) | degrees C | 15.2 |
| PMP | MW-152 | C | 2016/03/22 | Temperature (Celsius) | degrees C | 12.2 |
| PMP | MW-152 | C | 2016/06/23 | Temperature (Celsius) | degrees C | 15.1 |
| PMP | MW-152 | C | 2016/09/29 | Temperature (Celsius) | degrees C | 16.4 |
| PMP | MW-152 | C | 2016/12/21 | Temperature (Celsius) | degrees C | 13.9 |
| PMP | MW-152 | C | 2017/03/16 | Temperature (Celsius) | degrees C | 11.5 |
| PMP | MW-152 | C | 2017/06/21 | Temperature (Celsius) | degrees C | 14.3 |
| PMP | MW-152 | C | 2017/09/21 | Temperature (Celsius) | degrees C | 16.8 |
| PMP | MW-152 | C | 2017/11/28 | Temperature (Celsius) | degrees C | 16 |
| PMP | MW-152 | C | 2018/03/20 | Temperature (Celsius) | degrees C | 12.1 |
| PMP | MW-152 | C | 2018/06/27 | Temperature (Celsius) | degrees C | 14.6 |
| PMP | MW-152 | C | 2018/09/26 | Temperature (Celsius) | degrees C | 16.4 |
| PMP | MW-152 | C | 2018/12/18 | Temperature (Celsius) | degrees C | 13.7 |
| PMP | MW-152 | C | 2019/03/20 | Temperature (Celsius) | degrees C | 10.7 |
| PMP | MW-152 | C | 2019/06/25 | Temperature (Celsius) | degrees C | 13.7 |
| PMP | MW-152 | C | 2019/09/26 | Temperature (Celsius) | degrees C | 15.7 |
| PMP | MW-152 | C | 2019/12/19 | Temperature (Celsius) | degrees C | 13.6 |
| PMP | MW-152 | C | 2020/03/27 | Temperature (Celsius) | degrees C | 12.0 |
| PMP | MW-152 | C | 2020/06/23 | Temperature (Celsius) | degrees C | 13.3 |
| PMP | MW-152 | C | 2020/09/17 | Temperature (Celsius) | degrees C | 15.6 |
| PMP | MW-152 | C | 2020/12/16 | Temperature (Celsius) | degrees C | 13.6 |
| PMP | MW-152 | C | 2021/03/09 | Temperature (Celsius) | degrees C | 11.5 |
| PMP | MW-152 | C | 2021/07/19 | Temperature (Celsius) | degrees C | 13.8 |
| PMP | MW-152 | C | 2021/09/14 | Temperature (Celsius) | degrees C | 15.8 |
| PMP | MW-152 | C | 2021/12/14 | Temperature (Celsius) | degrees C | 14.6 |
| PMP | MW-152 | C | 2022/03/28 | Temperature (Celsius) | degrees C | 11.4 |
| PMP | MW-152 | C | 2022/06/14 | Temperature (Celsius) | degrees C | 14.2 |
| PMP | MW-152 | C | 2022/09/29 | Temperature (Celsius) | degrees C | 16.9 |
| PMP | MW-152 | C | 2022/12/06 | Temperature (Celsius) | degrees C | 14.1 |
| PMP | MW-152 | C | 2023/03/15 | Temperature (Celsius) | degrees C | 11.8 |
| PMP | MW-152 | C | 2023/05/18 | Temperature (Celsius) | degrees C | 12.7 |
| PMP | MW-152 | C | 2023/08/04 | Temperature (Celsius) | degrees C | 15.1 |
| PMP | MW-152 | C | 2023/10/31 | Temperature (Celsius) | degrees C | 14.3 |
| PMP | MW-152 | C | 2013/09/16 | Total Dissolved Solids | mg/L | 1,620 |
| PMP | MW-152 | C | 2013/11/20 | Total Dissolved Solids | mg/L | 1,720 |
| PMP | MW-152 | C | 2014/02/19 | Total Dissolved Solids | mg/L | 1,770 |
| PMP | MW-152 | C | 2014/06/12 | Total Dissolved Solids | mg/L | 1,530 |
| PMP | MW-152 | C | 2015/03/25 | Total Dissolved Solids | mg/L | 2,150 |
| PMP | MW-152 | C | 2015/06/24 | Total Dissolved Solids | mg/L | 2,150 |
| PMP | MW-152 | C | 2015/09/25 | Total Dissolved Solids | mg/L | 1,920 |
| PMP | MW-152 | C | 2015/11/10 | Total Dissolved Solids | mg/L | 1,920 |
| PMP | MW-152 | C | 2016/03/22 | Total Dissolved Solids | mg/L | 2,150 |
| PMP | MW-152 | C | 2016/06/23 | Total Dissolved Solids | mg/L | 2,260 |
| PMP | MW-152 | C | 2016/09/29 | Total Dissolved Solids | mg/L | 2,240 |
| PMP | MW-152 | C | 2016/12/21 | Total Dissolved Solids | mg/L | 1,870 |
| PMP | MW-152 | C | 2017/03/16 | Total Dissolved Solids | mg/L | 1,480 |
| PMP | MW-152 | C | 2017/06/21 | Total Dissolved Solids | mg/L | 1,610 |
| PMP | MW-152 | C | 2017/09/21 | Total Dissolved Solids | mg/L | 1,940 |

Attachment I. Site Groundwater Data

Geochemical Conceptual Site Model

Baldwin Fly Ash Pond System

Baldwin Power Plant

Baldwin, IL

| | | | | | | |
|-----|--------|---|------------|------------------------|------|-------|
| PMP | MW-152 | C | 2017/11/28 | Total Dissolved Solids | mg/L | 2,010 |
| PMP | MW-152 | C | 2018/03/20 | Total Dissolved Solids | mg/L | 1,770 |
| PMP | MW-152 | C | 2018/06/27 | Total Dissolved Solids | mg/L | 1,760 |
| PMP | MW-152 | C | 2018/09/26 | Total Dissolved Solids | mg/L | 2,170 |
| PMP | MW-152 | C | 2018/12/18 | Total Dissolved Solids | mg/L | 1,550 |
| PMP | MW-152 | C | 2019/03/20 | Total Dissolved Solids | mg/L | 1,340 |
| PMP | MW-152 | C | 2019/06/25 | Total Dissolved Solids | mg/L | 894 |
| PMP | MW-152 | C | 2019/09/26 | Total Dissolved Solids | mg/L | 1,790 |
| PMP | MW-152 | C | 2019/12/19 | Total Dissolved Solids | mg/L | 1,880 |
| PMP | MW-152 | C | 2020/03/27 | Total Dissolved Solids | mg/L | 1,250 |
| PMP | MW-152 | C | 2020/06/23 | Total Dissolved Solids | mg/L | 900 |
| PMP | MW-152 | C | 2020/09/17 | Total Dissolved Solids | mg/L | 1,850 |
| PMP | MW-152 | C | 2020/12/16 | Total Dissolved Solids | mg/L | 1,340 |
| PMP | MW-152 | C | 2021/03/09 | Total Dissolved Solids | mg/L | 948 |
| PMP | MW-152 | C | 2021/07/19 | Total Dissolved Solids | mg/L | 868 |
| PMP | MW-152 | C | 2021/09/14 | Total Dissolved Solids | mg/L | 1,300 |
| PMP | MW-152 | C | 2021/12/14 | Total Dissolved Solids | mg/L | 1,100 |
| PMP | MW-152 | C | 2022/03/28 | Total Dissolved Solids | mg/L | 786 |
| PMP | MW-152 | C | 2022/06/14 | Total Dissolved Solids | mg/L | 880 |
| PMP | MW-152 | C | 2022/09/29 | Total Dissolved Solids | mg/L | 1,780 |
| PMP | MW-152 | C | 2022/12/06 | Total Dissolved Solids | mg/L | 368 |
| PMP | MW-152 | C | 2023/03/15 | Total Dissolved Solids | mg/L | 904 |
| PMP | MW-152 | C | 2023/05/18 | Total Dissolved Solids | mg/L | 706 |
| PMP | MW-152 | C | 2023/08/04 | Total Dissolved Solids | mg/L | 1,510 |
| PMP | MW-152 | C | 2023/10/31 | Total Dissolved Solids | mg/L | 1,790 |
| PMP | MW-153 | C | 2013/09/17 | pH (field) | SU | 7.3 |
| PMP | MW-153 | C | 2013/11/21 | pH (field) | SU | 6.6 |
| PMP | MW-153 | C | 2014/02/19 | pH (field) | SU | 7.2 |
| PMP | MW-153 | C | 2014/06/11 | pH (field) | SU | 7.1 |
| PMP | MW-153 | C | 2015/03/25 | pH (field) | SU | 7.3 |
| PMP | MW-153 | C | 2015/06/24 | pH (field) | SU | 7.2 |
| PMP | MW-153 | C | 2015/09/25 | pH (field) | SU | 6.8 |
| PMP | MW-153 | C | 2015/11/10 | pH (field) | SU | 7.1 |
| PMP | MW-153 | C | 2016/03/22 | pH (field) | SU | 7.0 |
| PMP | MW-153 | C | 2016/06/21 | pH (field) | SU | 7.4 |
| PMP | MW-153 | C | 2016/09/29 | pH (field) | SU | 7.3 |
| PMP | MW-153 | C | 2016/12/21 | pH (field) | SU | 7.2 |
| PMP | MW-153 | C | 2017/03/17 | pH (field) | SU | 7.3 |
| PMP | MW-153 | C | 2017/06/22 | pH (field) | SU | 7.0 |
| PMP | MW-153 | C | 2017/09/21 | pH (field) | SU | 7.1 |
| PMP | MW-153 | C | 2017/11/28 | pH (field) | SU | 7.3 |
| PMP | MW-153 | C | 2018/03/20 | pH (field) | SU | 7.2 |
| PMP | MW-153 | C | 2018/06/28 | pH (field) | SU | 7.1 |
| PMP | MW-153 | C | 2018/09/26 | pH (field) | SU | 7.0 |
| PMP | MW-153 | C | 2018/12/19 | pH (field) | SU | 7.2 |
| PMP | MW-153 | C | 2019/03/21 | pH (field) | SU | 6.1 |
| PMP | MW-153 | C | 2019/06/26 | pH (field) | SU | 6.9 |
| PMP | MW-153 | C | 2019/09/26 | pH (field) | SU | 7.1 |
| PMP | MW-153 | C | 2019/12/19 | pH (field) | SU | 7.1 |
| PMP | MW-153 | C | 2020/03/27 | pH (field) | SU | 7.1 |
| PMP | MW-153 | C | 2020/06/23 | pH (field) | SU | 7.3 |
| PMP | MW-153 | C | 2020/09/17 | pH (field) | SU | 7.2 |
| PMP | MW-153 | C | 2020/12/17 | pH (field) | SU | 7.1 |
| PMP | MW-153 | C | 2021/03/10 | pH (field) | SU | 7.1 |
| PMP | MW-153 | C | 2021/06/22 | pH (field) | SU | 6.6 |
| PMP | MW-153 | C | 2021/09/16 | pH (field) | SU | 7.0 |
| PMP | MW-153 | C | 2021/12/15 | pH (field) | SU | 7.0 |

Attachment I. Site Groundwater Data

Geochemical Conceptual Site Model

Baldwin Fly Ash Pond System

Baldwin Power Plant

Baldwin, IL

| | | | | | | |
|-----|--------|---|------------|-------------------------------|------------|---------|
| PMP | MW-153 | C | 2022/03/29 | pH (field) | SU | 6.9 |
| PMP | MW-153 | C | 2022/06/15 | pH (field) | SU | 7.1 |
| PMP | MW-153 | C | 2022/09/29 | pH (field) | SU | 7.3 |
| PMP | MW-153 | C | 2022/12/06 | pH (field) | SU | 7.2 |
| PMP | MW-153 | C | 2023/03/15 | pH (field) | SU | 7.2 |
| PMP | MW-153 | C | 2023/05/22 | pH (field) | SU | 7.2 |
| PMP | MW-153 | C | 2023/07/10 | pH (field) | SU | 6.8 |
| PMP | MW-153 | C | 2023/08/04 | pH (field) | SU | 7.2 |
| PMP | MW-153 | C | 2023/11/03 | pH (field) | SU | 6.8 |
| PMP | MW-153 | C | 2021/03/10 | Oxidation Reduction Potential | mV | 38.0 |
| PMP | MW-153 | C | 2021/06/22 | Oxidation Reduction Potential | mV | 4.00 |
| PMP | MW-153 | C | 2021/09/16 | Oxidation Reduction Potential | mV | 56.0 |
| PMP | MW-153 | C | 2021/12/15 | Oxidation Reduction Potential | mV | 98.0 |
| PMP | MW-153 | C | 2022/03/29 | Oxidation Reduction Potential | mV | 55.0 |
| PMP | MW-153 | C | 2022/06/15 | Oxidation Reduction Potential | mV | 119 |
| PMP | MW-153 | C | 2022/09/29 | Oxidation Reduction Potential | mV | 120 |
| PMP | MW-153 | C | 2022/12/06 | Oxidation Reduction Potential | mV | 39.0 |
| PMP | MW-153 | C | 2023/03/15 | Oxidation Reduction Potential | mV | 59.5 |
| PMP | MW-153 | C | 2023/05/22 | Oxidation Reduction Potential | mV | 117 |
| PMP | MW-153 | C | 2023/07/10 | Oxidation Reduction Potential | mV | 150 |
| PMP | MW-153 | C | 2023/08/04 | Oxidation Reduction Potential | mV | 89.0 |
| PMP | MW-153 | C | 2023/11/03 | Oxidation Reduction Potential | mV | 77.0 |
| PMP | MW-153 | C | 2021/03/10 | Eh | V | 0.23 |
| PMP | MW-153 | C | 2021/06/22 | Eh | V | 0.20 |
| PMP | MW-153 | C | 2021/09/16 | Eh | V | 0.25 |
| PMP | MW-153 | C | 2021/12/15 | Eh | V | 0.29 |
| PMP | MW-153 | C | 2022/03/29 | Eh | V | 0.25 |
| PMP | MW-153 | C | 2022/06/15 | Eh | V | 0.31 |
| PMP | MW-153 | C | 2022/09/29 | Eh | V | 0.32 |
| PMP | MW-153 | C | 2022/12/06 | Eh | V | 0.23 |
| PMP | MW-153 | C | 2023/03/15 | Eh | V | 0.26 |
| PMP | MW-153 | C | 2023/05/22 | Eh | V | 0.31 |
| PMP | MW-153 | C | 2023/07/10 | Eh | V | 0.35 |
| PMP | MW-153 | C | 2023/08/04 | Eh | V | 0.28 |
| PMP | MW-153 | C | 2023/11/03 | Eh | V | 0.27 |
| PMP | MW-153 | C | 2023/03/15 | Alkalinity, bicarbonate | mg/L CaCO3 | 197 |
| PMP | MW-153 | C | 2023/05/22 | Alkalinity, bicarbonate | mg/L CaCO3 | 195 |
| PMP | MW-153 | C | 2023/08/04 | Alkalinity, bicarbonate | mg/L CaCO3 | 198 |
| PMP | MW-153 | C | 2023/11/03 | Alkalinity, bicarbonate | mg/L CaCO3 | 196 |
| PMP | MW-153 | C | 2023/03/15 | Barium, total | mg/L | 0.0366 |
| PMP | MW-153 | C | 2023/05/22 | Barium, total | mg/L | 0.0867 |
| PMP | MW-153 | C | 2023/07/10 | Barium, total | mg/L | 0.0365 |
| PMP | MW-153 | C | 2023/08/04 | Barium, total | mg/L | 0.0357 |
| PMP | MW-153 | C | 2023/11/03 | Barium, total | mg/L | 0.0335 |
| PMP | MW-153 | C | 2013/09/17 | Boron, total | mg/L | 0.0200 |
| PMP | MW-153 | C | 2023/03/15 | Boron, total | mg/L | <0.02 |
| PMP | MW-153 | C | 2023/05/22 | Boron, total | mg/L | <0.013 |
| PMP | MW-153 | C | 2023/07/10 | Boron, total | mg/L | <0.009 |
| PMP | MW-153 | C | 2023/08/04 | Boron, total | mg/L | 0.0357 |
| PMP | MW-153 | C | 2023/11/03 | Boron, total | mg/L | <0.0092 |
| PMP | MW-153 | C | 2023/03/15 | Calcium, total | mg/L | 50.9 |
| PMP | MW-153 | C | 2023/05/22 | Calcium, total | mg/L | 50.6 |
| PMP | MW-153 | C | 2023/07/10 | Calcium, total | mg/L | 48.8 |
| PMP | MW-153 | C | 2023/08/04 | Calcium, total | mg/L | 52.8 |
| PMP | MW-153 | C | 2023/11/03 | Calcium, total | mg/L | 52.3 |
| PMP | MW-153 | C | 2013/09/17 | Chloride, total | mg/L | 23.0 |
| PMP | MW-153 | C | 2023/03/15 | Chloride, total | mg/L | 17.0 |

Attachment I. Site Groundwater Data

Geochemical Conceptual Site Model

Baldwin Fly Ash Pond System

Baldwin Power Plant

Baldwin, IL

| | | | | | | |
|-----|--------|---|------------|----------------------|------|---------|
| PMP | MW-153 | C | 2023/05/22 | Chloride, total | mg/L | 16.0 |
| PMP | MW-153 | C | 2023/07/10 | Chloride, total | mg/L | 15.0 |
| PMP | MW-153 | C | 2023/08/04 | Chloride, total | mg/L | 16.0 |
| PMP | MW-153 | C | 2023/11/03 | Chloride, total | mg/L | 17.0 |
| PMP | MW-153 | C | 2013/11/21 | Iron, dissolved | mg/L | <0.007 |
| PMP | MW-153 | C | 2014/02/19 | Iron, dissolved | mg/L | <0.007 |
| PMP | MW-153 | C | 2014/06/11 | Iron, dissolved | mg/L | <0.007 |
| PMP | MW-153 | C | 2015/03/25 | Iron, dissolved | mg/L | <0.007 |
| PMP | MW-153 | C | 2015/06/24 | Iron, dissolved | mg/L | <0.007 |
| PMP | MW-153 | C | 2015/09/25 | Iron, dissolved | mg/L | <0.007 |
| PMP | MW-153 | C | 2015/11/10 | Iron, dissolved | mg/L | <0.007 |
| PMP | MW-153 | C | 2016/03/22 | Iron, dissolved | mg/L | <0.007 |
| PMP | MW-153 | C | 2016/06/21 | Iron, dissolved | mg/L | <0.007 |
| PMP | MW-153 | C | 2016/09/29 | Iron, dissolved | mg/L | <0.007 |
| PMP | MW-153 | C | 2016/12/21 | Iron, dissolved | mg/L | <0.007 |
| PMP | MW-153 | C | 2017/03/17 | Iron, dissolved | mg/L | 0.0200 |
| PMP | MW-153 | C | 2017/06/22 | Iron, dissolved | mg/L | <0.007 |
| PMP | MW-153 | C | 2017/09/21 | Iron, dissolved | mg/L | <0.007 |
| PMP | MW-153 | C | 2017/11/28 | Iron, dissolved | mg/L | <0.007 |
| PMP | MW-153 | C | 2018/03/20 | Iron, dissolved | mg/L | <0.007 |
| PMP | MW-153 | C | 2018/06/28 | Iron, dissolved | mg/L | <0.02 |
| PMP | MW-153 | C | 2018/09/26 | Iron, dissolved | mg/L | <0.02 |
| PMP | MW-153 | C | 2018/12/19 | Iron, dissolved | mg/L | <0.02 |
| PMP | MW-153 | C | 2019/03/21 | Iron, dissolved | mg/L | <0.02 |
| PMP | MW-153 | C | 2019/06/26 | Iron, dissolved | mg/L | <0.02 |
| PMP | MW-153 | C | 2019/09/26 | Iron, dissolved | mg/L | <0.02 |
| PMP | MW-153 | C | 2019/12/19 | Iron, dissolved | mg/L | <0.02 |
| PMP | MW-153 | C | 2020/03/27 | Iron, dissolved | mg/L | <0.02 |
| PMP | MW-153 | C | 2020/06/23 | Iron, dissolved | mg/L | <0.02 |
| PMP | MW-153 | C | 2020/09/17 | Iron, dissolved | mg/L | <0.02 |
| PMP | MW-153 | C | 2020/12/17 | Iron, dissolved | mg/L | <0.02 |
| PMP | MW-153 | C | 2021/03/10 | Iron, dissolved | mg/L | <0.02 |
| PMP | MW-153 | C | 2021/06/22 | Iron, dissolved | mg/L | <0.02 |
| PMP | MW-153 | C | 2021/09/16 | Iron, dissolved | mg/L | <0.02 |
| PMP | MW-153 | C | 2021/12/15 | Iron, dissolved | mg/L | 0.0739 |
| PMP | MW-153 | C | 2022/03/29 | Iron, dissolved | mg/L | 0.0489 |
| PMP | MW-153 | C | 2022/06/15 | Iron, dissolved | mg/L | <0.02 |
| PMP | MW-153 | C | 2022/09/29 | Iron, dissolved | mg/L | 0.0274 |
| PMP | MW-153 | C | 2022/12/06 | Iron, dissolved | mg/L | <0.0115 |
| PMP | MW-153 | C | 2023/03/15 | Iron, dissolved | mg/L | <0.0115 |
| PMP | MW-153 | C | 2023/05/22 | Iron, dissolved | mg/L | <0.02 |
| PMP | MW-153 | C | 2023/08/04 | Iron, dissolved | mg/L | <0.0115 |
| PMP | MW-153 | C | 2023/11/03 | Iron, dissolved | mg/L | <0.0115 |
| PMP | MW-153 | C | 2023/03/15 | Magnesium, total | mg/L | 21.4 |
| PMP | MW-153 | C | 2023/05/22 | Magnesium, total | mg/L | 22.4 |
| PMP | MW-153 | C | 2023/08/04 | Magnesium, total | mg/L | 22.3 |
| PMP | MW-153 | C | 2023/11/03 | Magnesium, total | mg/L | 20.8 |
| PMP | MW-153 | C | 2013/11/21 | Manganese, dissolved | mg/L | 0.0300 |
| PMP | MW-153 | C | 2014/02/19 | Manganese, dissolved | mg/L | <0.0016 |
| PMP | MW-153 | C | 2014/06/11 | Manganese, dissolved | mg/L | 0.00900 |
| PMP | MW-153 | C | 2015/03/25 | Manganese, dissolved | mg/L | 0.0160 |
| PMP | MW-153 | C | 2015/06/24 | Manganese, dissolved | mg/L | 0.00900 |
| PMP | MW-153 | C | 2015/09/25 | Manganese, dissolved | mg/L | 0.00840 |
| PMP | MW-153 | C | 2015/11/10 | Manganese, dissolved | mg/L | 0.00870 |
| PMP | MW-153 | C | 2016/03/22 | Manganese, dissolved | mg/L | 0.00690 |
| PMP | MW-153 | C | 2016/06/21 | Manganese, dissolved | mg/L | 0.00800 |
| PMP | MW-153 | C | 2016/09/29 | Manganese, dissolved | mg/L | 0.0193 |

Attachment I. Site Groundwater Data

Geochemical Conceptual Site Model

Baldwin Fly Ash Pond System

Baldwin Power Plant

Baldwin, IL

| | | | | | | |
|-----|--------|---|------------|-----------------------|-----------|---------|
| PMP | MW-153 | C | 2016/12/21 | Manganese, dissolved | mg/L | 0.0257 |
| PMP | MW-153 | C | 2017/03/17 | Manganese, dissolved | mg/L | 0.0100 |
| PMP | MW-153 | C | 2017/06/22 | Manganese, dissolved | mg/L | 0.0100 |
| PMP | MW-153 | C | 2017/09/21 | Manganese, dissolved | mg/L | 0.00730 |
| PMP | MW-153 | C | 2017/11/28 | Manganese, dissolved | mg/L | 0.00890 |
| PMP | MW-153 | C | 2018/03/20 | Manganese, dissolved | mg/L | 0.0147 |
| PMP | MW-153 | C | 2018/06/28 | Manganese, dissolved | mg/L | 0.0116 |
| PMP | MW-153 | C | 2018/09/26 | Manganese, dissolved | mg/L | 0.0114 |
| PMP | MW-153 | C | 2018/12/19 | Manganese, dissolved | mg/L | 0.0120 |
| PMP | MW-153 | C | 2019/03/21 | Manganese, dissolved | mg/L | 0.00890 |
| PMP | MW-153 | C | 2019/06/26 | Manganese, dissolved | mg/L | 0.00830 |
| PMP | MW-153 | C | 2019/09/26 | Manganese, dissolved | mg/L | 0.00800 |
| PMP | MW-153 | C | 2019/12/19 | Manganese, dissolved | mg/L | <0.0025 |
| PMP | MW-153 | C | 2020/03/27 | Manganese, dissolved | mg/L | 0.00820 |
| PMP | MW-153 | C | 2020/06/23 | Manganese, dissolved | mg/L | <0.0025 |
| PMP | MW-153 | C | 2020/09/17 | Manganese, dissolved | mg/L | <0.0025 |
| PMP | MW-153 | C | 2020/12/17 | Manganese, dissolved | mg/L | 0.00920 |
| PMP | MW-153 | C | 2021/03/10 | Manganese, dissolved | mg/L | <0.0025 |
| PMP | MW-153 | C | 2021/06/22 | Manganese, dissolved | mg/L | <0.0025 |
| PMP | MW-153 | C | 2021/09/16 | Manganese, dissolved | mg/L | 0.00700 |
| PMP | MW-153 | C | 2021/12/15 | Manganese, dissolved | mg/L | 0.0193 |
| PMP | MW-153 | C | 2022/03/29 | Manganese, dissolved | mg/L | 0.0106 |
| PMP | MW-153 | C | 2022/06/15 | Manganese, dissolved | mg/L | 0.00500 |
| PMP | MW-153 | C | 2022/09/29 | Manganese, dissolved | mg/L | 0.00550 |
| PMP | MW-153 | C | 2022/12/06 | Manganese, dissolved | mg/L | 0.00620 |
| PMP | MW-153 | C | 2023/03/15 | Manganese, dissolved | mg/L | 0.00400 |
| PMP | MW-153 | C | 2023/05/22 | Manganese, dissolved | mg/L | <0.0025 |
| PMP | MW-153 | C | 2023/08/04 | Manganese, dissolved | mg/L | 0.00410 |
| PMP | MW-153 | C | 2023/11/03 | Manganese, dissolved | mg/L | 0.00320 |
| PMP | MW-153 | C | 2023/05/22 | Phosphate, dissolved | mg/L | <0.005 |
| PMP | MW-153 | C | 2023/08/04 | Phosphate, dissolved | mg/L | 0.0370 |
| PMP | MW-153 | C | 2023/03/15 | Potassium, total | mg/L | 0.200 |
| PMP | MW-153 | C | 2023/05/22 | Potassium, total | mg/L | 1.11 |
| PMP | MW-153 | C | 2023/08/04 | Potassium, total | mg/L | 0.230 |
| PMP | MW-153 | C | 2023/11/03 | Potassium, total | mg/L | 0.0990 |
| PMP | MW-153 | C | 2023/05/22 | Silicon, dissolved | mg/L | 10.2 |
| PMP | MW-153 | C | 2023/08/04 | Silicon, dissolved | mg/L | 9.47 |
| PMP | MW-153 | C | 2023/03/15 | Sodium, total | mg/L | 48.4 |
| PMP | MW-153 | C | 2023/05/22 | Sodium, total | mg/L | 55.4 |
| PMP | MW-153 | C | 2023/08/04 | Sodium, total | mg/L | 53.3 |
| PMP | MW-153 | C | 2023/11/03 | Sodium, total | mg/L | 57.0 |
| PMP | MW-153 | C | 2013/09/17 | Sulfate, total | mg/L | 75.0 |
| PMP | MW-153 | C | 2023/03/15 | Sulfate, total | mg/L | 68.0 |
| PMP | MW-153 | C | 2023/05/22 | Sulfate, total | mg/L | 75.0 |
| PMP | MW-153 | C | 2023/07/10 | Sulfate, total | mg/L | 62.0 |
| PMP | MW-153 | C | 2023/08/04 | Sulfate, total | mg/L | 62.0 |
| PMP | MW-153 | C | 2023/11/03 | Sulfate, total | mg/L | 62.0 |
| PMP | MW-153 | C | 2013/09/17 | Temperature (Celsius) | degrees C | 15.5 |
| PMP | MW-153 | C | 2013/11/21 | Temperature (Celsius) | degrees C | 14.1 |
| PMP | MW-153 | C | 2014/02/19 | Temperature (Celsius) | degrees C | 13.7 |
| PMP | MW-153 | C | 2014/06/11 | Temperature (Celsius) | degrees C | 13.2 |
| PMP | MW-153 | C | 2015/03/25 | Temperature (Celsius) | degrees C | 12.9 |
| PMP | MW-153 | C | 2015/06/24 | Temperature (Celsius) | degrees C | 14.3 |
| PMP | MW-153 | C | 2015/09/25 | Temperature (Celsius) | degrees C | 15.2 |
| PMP | MW-153 | C | 2015/11/10 | Temperature (Celsius) | degrees C | 15.5 |
| PMP | MW-153 | C | 2016/03/22 | Temperature (Celsius) | degrees C | 12.6 |
| PMP | MW-153 | C | 2016/06/21 | Temperature (Celsius) | degrees C | 14.5 |

Attachment I. Site Groundwater Data

Geochemical Conceptual Site Model

Baldwin Fly Ash Pond System

Baldwin Power Plant

Baldwin, IL

| | | | | | | |
|-----|--------|---|------------|------------------------|-----------|------|
| PMP | MW-153 | C | 2016/09/29 | Temperature (Celsius) | degrees C | 15.4 |
| PMP | MW-153 | C | 2016/12/21 | Temperature (Celsius) | degrees C | 15.1 |
| PMP | MW-153 | C | 2017/03/17 | Temperature (Celsius) | degrees C | 13.6 |
| PMP | MW-153 | C | 2017/06/22 | Temperature (Celsius) | degrees C | 15.0 |
| PMP | MW-153 | C | 2017/09/21 | Temperature (Celsius) | degrees C | 16.5 |
| PMP | MW-153 | C | 2017/11/28 | Temperature (Celsius) | degrees C | 16.2 |
| PMP | MW-153 | C | 2018/03/20 | Temperature (Celsius) | degrees C | 14.1 |
| PMP | MW-153 | C | 2018/06/28 | Temperature (Celsius) | degrees C | 14.1 |
| PMP | MW-153 | C | 2018/09/26 | Temperature (Celsius) | degrees C | 16.4 |
| PMP | MW-153 | C | 2018/12/19 | Temperature (Celsius) | degrees C | 14.8 |
| PMP | MW-153 | C | 2019/03/21 | Temperature (Celsius) | degrees C | 12.1 |
| PMP | MW-153 | C | 2019/06/26 | Temperature (Celsius) | degrees C | 13.9 |
| PMP | MW-153 | C | 2019/09/26 | Temperature (Celsius) | degrees C | 15.3 |
| PMP | MW-153 | C | 2019/12/19 | Temperature (Celsius) | degrees C | 13.9 |
| PMP | MW-153 | C | 2020/03/27 | Temperature (Celsius) | degrees C | 13.3 |
| PMP | MW-153 | C | 2020/06/23 | Temperature (Celsius) | degrees C | 13.9 |
| PMP | MW-153 | C | 2020/09/17 | Temperature (Celsius) | degrees C | 15.6 |
| PMP | MW-153 | C | 2020/12/17 | Temperature (Celsius) | degrees C | 14.8 |
| PMP | MW-153 | C | 2021/03/10 | Temperature (Celsius) | degrees C | 13.4 |
| PMP | MW-153 | C | 2021/06/22 | Temperature (Celsius) | degrees C | 13.7 |
| PMP | MW-153 | C | 2021/09/16 | Temperature (Celsius) | degrees C | 15.4 |
| PMP | MW-153 | C | 2021/12/15 | Temperature (Celsius) | degrees C | 15.4 |
| PMP | MW-153 | C | 2022/03/29 | Temperature (Celsius) | degrees C | 13.3 |
| PMP | MW-153 | C | 2022/06/15 | Temperature (Celsius) | degrees C | 14.6 |
| PMP | MW-153 | C | 2022/09/29 | Temperature (Celsius) | degrees C | 15.6 |
| PMP | MW-153 | C | 2022/12/06 | Temperature (Celsius) | degrees C | 14.7 |
| PMP | MW-153 | C | 2023/03/15 | Temperature (Celsius) | degrees C | 13.3 |
| PMP | MW-153 | C | 2023/05/22 | Temperature (Celsius) | degrees C | 13.5 |
| PMP | MW-153 | C | 2023/07/10 | Temperature (Celsius) | degrees C | 15.6 |
| PMP | MW-153 | C | 2023/08/04 | Temperature (Celsius) | degrees C | 14.9 |
| PMP | MW-153 | C | 2023/11/03 | Temperature (Celsius) | degrees C | 15.5 |
| PMP | MW-153 | C | 2013/09/17 | Total Dissolved Solids | mg/L | 448 |
| PMP | MW-153 | C | 2013/11/21 | Total Dissolved Solids | mg/L | 384 |
| PMP | MW-153 | C | 2014/02/19 | Total Dissolved Solids | mg/L | 402 |
| PMP | MW-153 | C | 2014/06/11 | Total Dissolved Solids | mg/L | 426 |
| PMP | MW-153 | C | 2015/03/25 | Total Dissolved Solids | mg/L | 354 |
| PMP | MW-153 | C | 2015/06/24 | Total Dissolved Solids | mg/L | 442 |
| PMP | MW-153 | C | 2015/09/25 | Total Dissolved Solids | mg/L | 354 |
| PMP | MW-153 | C | 2015/11/10 | Total Dissolved Solids | mg/L | 360 |
| PMP | MW-153 | C | 2016/03/22 | Total Dissolved Solids | mg/L | 364 |
| PMP | MW-153 | C | 2016/06/21 | Total Dissolved Solids | mg/L | 398 |
| PMP | MW-153 | C | 2016/09/29 | Total Dissolved Solids | mg/L | 408 |
| PMP | MW-153 | C | 2016/12/21 | Total Dissolved Solids | mg/L | 390 |
| PMP | MW-153 | C | 2017/03/17 | Total Dissolved Solids | mg/L | 342 |
| PMP | MW-153 | C | 2017/06/22 | Total Dissolved Solids | mg/L | 404 |
| PMP | MW-153 | C | 2017/09/21 | Total Dissolved Solids | mg/L | 336 |
| PMP | MW-153 | C | 2017/11/28 | Total Dissolved Solids | mg/L | 428 |
| PMP | MW-153 | C | 2018/03/20 | Total Dissolved Solids | mg/L | 394 |
| PMP | MW-153 | C | 2018/06/28 | Total Dissolved Solids | mg/L | 414 |
| PMP | MW-153 | C | 2018/09/26 | Total Dissolved Solids | mg/L | 406 |
| PMP | MW-153 | C | 2018/12/19 | Total Dissolved Solids | mg/L | 408 |
| PMP | MW-153 | C | 2019/03/21 | Total Dissolved Solids | mg/L | 392 |
| PMP | MW-153 | C | 2019/06/26 | Total Dissolved Solids | mg/L | 404 |
| PMP | MW-153 | C | 2019/09/26 | Total Dissolved Solids | mg/L | 370 |
| PMP | MW-153 | C | 2019/12/19 | Total Dissolved Solids | mg/L | 402 |
| PMP | MW-153 | C | 2020/03/27 | Total Dissolved Solids | mg/L | 364 |
| PMP | MW-153 | C | 2020/06/23 | Total Dissolved Solids | mg/L | 362 |

Attachment I. Site Groundwater Data

Geochemical Conceptual Site Model

Baldwin Fly Ash Pond System

Baldwin Power Plant

Baldwin, IL

| | | | | | | |
|-----|--------|---|------------|-------------------------------|------|-------|
| PMP | MW-153 | C | 2020/09/17 | Total Dissolved Solids | mg/L | 334 |
| PMP | MW-153 | C | 2020/12/17 | Total Dissolved Solids | mg/L | 368 |
| PMP | MW-153 | C | 2021/03/10 | Total Dissolved Solids | mg/L | 390 |
| PMP | MW-153 | C | 2021/06/22 | Total Dissolved Solids | mg/L | 362 |
| PMP | MW-153 | C | 2021/09/16 | Total Dissolved Solids | mg/L | 370 |
| PMP | MW-153 | C | 2021/12/15 | Total Dissolved Solids | mg/L | 396 |
| PMP | MW-153 | C | 2022/03/29 | Total Dissolved Solids | mg/L | 378 |
| PMP | MW-153 | C | 2022/06/15 | Total Dissolved Solids | mg/L | 338 |
| PMP | MW-153 | C | 2022/09/29 | Total Dissolved Solids | mg/L | 374 |
| PMP | MW-153 | C | 2022/12/06 | Total Dissolved Solids | mg/L | 1,940 |
| PMP | MW-153 | C | 2023/03/15 | Total Dissolved Solids | mg/L | 358 |
| PMP | MW-153 | C | 2023/05/22 | Total Dissolved Solids | mg/L | 350 |
| PMP | MW-153 | C | 2023/07/10 | Total Dissolved Solids | mg/L | 378 |
| PMP | MW-153 | C | 2023/08/04 | Total Dissolved Solids | mg/L | 396 |
| PMP | MW-153 | C | 2023/11/03 | Total Dissolved Solids | mg/L | 384 |
| PMP | MW-252 | C | 2013/09/16 | pH (field) | SU | 7.0 |
| PMP | MW-252 | C | 2013/11/20 | pH (field) | SU | 7.1 |
| PMP | MW-252 | C | 2014/02/19 | pH (field) | SU | 8.1 |
| PMP | MW-252 | C | 2014/06/12 | pH (field) | SU | 6.4 |
| PMP | MW-252 | C | 2015/03/25 | pH (field) | SU | 7.0 |
| PMP | MW-252 | C | 2015/06/24 | pH (field) | SU | 6.7 |
| PMP | MW-252 | C | 2015/09/25 | pH (field) | SU | 6.8 |
| PMP | MW-252 | C | 2015/11/10 | pH (field) | SU | 6.6 |
| PMP | MW-252 | C | 2016/03/22 | pH (field) | SU | 7.0 |
| PMP | MW-252 | C | 2016/06/23 | pH (field) | SU | 7.4 |
| PMP | MW-252 | C | 2016/09/29 | pH (field) | SU | 6.8 |
| PMP | MW-252 | C | 2016/12/21 | pH (field) | SU | 6.8 |
| PMP | MW-252 | C | 2017/03/16 | pH (field) | SU | 6.9 |
| PMP | MW-252 | C | 2017/06/21 | pH (field) | SU | 6.7 |
| PMP | MW-252 | C | 2017/09/21 | pH (field) | SU | 7.6 |
| PMP | MW-252 | C | 2017/11/28 | pH (field) | SU | 7.0 |
| PMP | MW-252 | C | 2018/03/20 | pH (field) | SU | 7.0 |
| PMP | MW-252 | C | 2018/06/27 | pH (field) | SU | 6.8 |
| PMP | MW-252 | C | 2018/09/26 | pH (field) | SU | 6.8 |
| PMP | MW-252 | C | 2018/12/18 | pH (field) | SU | 6.8 |
| PMP | MW-252 | C | 2019/03/20 | pH (field) | SU | 6.8 |
| PMP | MW-252 | C | 2019/06/25 | pH (field) | SU | 6.7 |
| PMP | MW-252 | C | 2019/09/26 | pH (field) | SU | 6.7 |
| PMP | MW-252 | C | 2019/12/19 | pH (field) | SU | 6.9 |
| PMP | MW-252 | C | 2020/03/27 | pH (field) | SU | 7.0 |
| PMP | MW-252 | C | 2020/06/23 | pH (field) | SU | 7.0 |
| PMP | MW-252 | C | 2020/09/17 | pH (field) | SU | 7.0 |
| PMP | MW-252 | C | 2020/12/16 | pH (field) | SU | 6.8 |
| PMP | MW-252 | C | 2021/03/09 | pH (field) | SU | 6.8 |
| PMP | MW-252 | C | 2021/07/19 | pH (field) | SU | 7.1 |
| PMP | MW-252 | C | 2021/09/14 | pH (field) | SU | 6.7 |
| PMP | MW-252 | C | 2021/12/14 | pH (field) | SU | 7.1 |
| PMP | MW-252 | C | 2022/03/28 | pH (field) | SU | 6.8 |
| PMP | MW-252 | C | 2022/06/14 | pH (field) | SU | 6.8 |
| PMP | MW-252 | C | 2022/09/29 | pH (field) | SU | 6.6 |
| PMP | MW-252 | C | 2022/12/06 | pH (field) | SU | 6.9 |
| PMP | MW-252 | C | 2023/03/15 | pH (field) | SU | 6.9 |
| PMP | MW-252 | C | 2023/05/18 | pH (field) | SU | 6.8 |
| PMP | MW-252 | C | 2023/08/04 | pH (field) | SU | 6.7 |
| PMP | MW-252 | C | 2023/10/31 | pH (field) | SU | 6.8 |
| PMP | MW-252 | C | 2021/03/09 | Oxidation Reduction Potential | mV | 22.0 |
| PMP | MW-252 | C | 2021/07/19 | Oxidation Reduction Potential | mV | 147 |

Attachment I. Site Groundwater Data

Geochemical Conceptual Site Model

Baldwin Fly Ash Pond System

Baldwin Power Plant

Baldwin, IL

| | | | | | | |
|-----|--------|---|------------|-------------------------------|------------|--------|
| PMP | MW-252 | C | 2021/09/14 | Oxidation Reduction Potential | mV | 93.0 |
| PMP | MW-252 | C | 2021/12/14 | Oxidation Reduction Potential | mV | 136 |
| PMP | MW-252 | C | 2022/03/28 | Oxidation Reduction Potential | mV | 11.0 |
| PMP | MW-252 | C | 2022/06/14 | Oxidation Reduction Potential | mV | 121 |
| PMP | MW-252 | C | 2022/09/29 | Oxidation Reduction Potential | mV | 170 |
| PMP | MW-252 | C | 2022/12/06 | Oxidation Reduction Potential | mV | 65.0 |
| PMP | MW-252 | C | 2023/03/15 | Oxidation Reduction Potential | mV | 11.5 |
| PMP | MW-252 | C | 2023/05/18 | Oxidation Reduction Potential | mV | 62.0 |
| PMP | MW-252 | C | 2023/08/04 | Oxidation Reduction Potential | mV | -51.0 |
| PMP | MW-252 | C | 2023/10/31 | Oxidation Reduction Potential | mV | -77.0 |
| PMP | MW-252 | C | 2021/03/09 | Eh | V | 0.22 |
| PMP | MW-252 | C | 2021/07/19 | Eh | V | 0.34 |
| PMP | MW-252 | C | 2021/09/14 | Eh | V | 0.29 |
| PMP | MW-252 | C | 2021/12/14 | Eh | V | 0.33 |
| PMP | MW-252 | C | 2022/03/28 | Eh | V | 0.21 |
| PMP | MW-252 | C | 2022/06/14 | Eh | V | 0.31 |
| PMP | MW-252 | C | 2022/09/29 | Eh | V | 0.37 |
| PMP | MW-252 | C | 2022/12/06 | Eh | V | 0.26 |
| PMP | MW-252 | C | 2023/03/15 | Eh | V | 0.21 |
| PMP | MW-252 | C | 2023/05/18 | Eh | V | 0.26 |
| PMP | MW-252 | C | 2023/08/04 | Eh | V | 0.14 |
| PMP | MW-252 | C | 2023/10/31 | Eh | V | 0.12 |
| PMP | MW-252 | C | 2023/03/15 | Alkalinity, bicarbonate | mg/L CaCO3 | 486 |
| PMP | MW-252 | C | 2023/05/18 | Alkalinity, bicarbonate | mg/L CaCO3 | 479 |
| PMP | MW-252 | C | 2023/08/04 | Alkalinity, bicarbonate | mg/L CaCO3 | 486 |
| PMP | MW-252 | C | 2023/10/31 | Alkalinity, bicarbonate | mg/L CaCO3 | 503 |
| PMP | MW-252 | C | 2023/03/15 | Barium, total | mg/L | 0.0290 |
| PMP | MW-252 | C | 2023/05/18 | Barium, total | mg/L | 0.0377 |
| PMP | MW-252 | C | 2023/08/04 | Barium, total | mg/L | 0.0359 |
| PMP | MW-252 | C | 2023/10/31 | Barium, total | mg/L | 0.0315 |
| PMP | MW-252 | C | 2013/09/16 | Boron, total | mg/L | 0.240 |
| PMP | MW-252 | C | 2023/03/15 | Boron, total | mg/L | 0.166 |
| PMP | MW-252 | C | 2023/05/18 | Boron, total | mg/L | 0.174 |
| PMP | MW-252 | C | 2023/08/04 | Boron, total | mg/L | 0.143 |
| PMP | MW-252 | C | 2023/10/31 | Boron, total | mg/L | 0.155 |
| PMP | MW-252 | C | 2023/03/15 | Calcium, total | mg/L | 191 |
| PMP | MW-252 | C | 2023/05/18 | Calcium, total | mg/L | 224 |
| PMP | MW-252 | C | 2023/08/04 | Calcium, total | mg/L | 210 |
| PMP | MW-252 | C | 2023/10/31 | Calcium, total | mg/L | 209 |
| PMP | MW-252 | C | 2013/09/16 | Chloride, total | mg/L | 39.0 |
| PMP | MW-252 | C | 2023/03/15 | Chloride, total | mg/L | 37.0 |
| PMP | MW-252 | C | 2023/05/18 | Chloride, total | mg/L | 38.0 |
| PMP | MW-252 | C | 2023/08/04 | Chloride, total | mg/L | 37.0 |
| PMP | MW-252 | C | 2023/10/31 | Chloride, total | mg/L | 37.0 |
| PMP | MW-252 | C | 2013/11/20 | Iron, dissolved | mg/L | 0.0700 |
| PMP | MW-252 | C | 2014/02/19 | Iron, dissolved | mg/L | <0.007 |
| PMP | MW-252 | C | 2014/06/12 | Iron, dissolved | mg/L | <0.007 |
| PMP | MW-252 | C | 2015/03/25 | Iron, dissolved | mg/L | <0.007 |
| PMP | MW-252 | C | 2015/06/24 | Iron, dissolved | mg/L | 0.100 |
| PMP | MW-252 | C | 2015/09/25 | Iron, dissolved | mg/L | <0.007 |
| PMP | MW-252 | C | 2015/11/10 | Iron, dissolved | mg/L | 0.0221 |
| PMP | MW-252 | C | 2016/03/22 | Iron, dissolved | mg/L | 0.130 |
| PMP | MW-252 | C | 2016/06/23 | Iron, dissolved | mg/L | 0.245 |
| PMP | MW-252 | C | 2016/09/29 | Iron, dissolved | mg/L | 0.0243 |
| PMP | MW-252 | C | 2016/12/21 | Iron, dissolved | mg/L | <0.007 |
| PMP | MW-252 | C | 2017/03/16 | Iron, dissolved | mg/L | <0.007 |
| PMP | MW-252 | C | 2017/06/21 | Iron, dissolved | mg/L | <0.007 |

Attachment I. Site Groundwater Data

Geochemical Conceptual Site Model

Baldwin Fly Ash Pond System

Baldwin Power Plant

Baldwin, IL

| | | | | | | |
|-----|--------|---|------------|----------------------|------|---------|
| PMP | MW-252 | C | 2017/09/21 | Iron, dissolved | mg/L | 0.0800 |
| PMP | MW-252 | C | 2017/11/28 | Iron, dissolved | mg/L | 0.110 |
| PMP | MW-252 | C | 2018/03/20 | Iron, dissolved | mg/L | 0.108 |
| PMP | MW-252 | C | 2018/06/27 | Iron, dissolved | mg/L | <0.02 |
| PMP | MW-252 | C | 2018/09/26 | Iron, dissolved | mg/L | <0.02 |
| PMP | MW-252 | C | 2018/12/18 | Iron, dissolved | mg/L | 0.186 |
| PMP | MW-252 | C | 2019/03/20 | Iron, dissolved | mg/L | <0.02 |
| PMP | MW-252 | C | 2019/06/25 | Iron, dissolved | mg/L | <0.02 |
| PMP | MW-252 | C | 2019/09/26 | Iron, dissolved | mg/L | <0.02 |
| PMP | MW-252 | C | 2019/12/19 | Iron, dissolved | mg/L | <0.02 |
| PMP | MW-252 | C | 2020/03/27 | Iron, dissolved | mg/L | <0.02 |
| PMP | MW-252 | C | 2020/06/23 | Iron, dissolved | mg/L | <0.02 |
| PMP | MW-252 | C | 2020/09/17 | Iron, dissolved | mg/L | 0.0641 |
| PMP | MW-252 | C | 2020/12/16 | Iron, dissolved | mg/L | <0.02 |
| PMP | MW-252 | C | 2021/03/09 | Iron, dissolved | mg/L | 0.127 |
| PMP | MW-252 | C | 2021/07/19 | Iron, dissolved | mg/L | <0.02 |
| PMP | MW-252 | C | 2021/09/14 | Iron, dissolved | mg/L | <0.02 |
| PMP | MW-252 | C | 2021/12/14 | Iron, dissolved | mg/L | <0.02 |
| PMP | MW-252 | C | 2022/03/28 | Iron, dissolved | mg/L | <0.015 |
| PMP | MW-252 | C | 2022/06/14 | Iron, dissolved | mg/L | <0.02 |
| PMP | MW-252 | C | 2022/09/29 | Iron, dissolved | mg/L | 0.177 |
| PMP | MW-252 | C | 2022/12/06 | Iron, dissolved | mg/L | 0.0794 |
| PMP | MW-252 | C | 2023/03/15 | Iron, dissolved | mg/L | 1.37 |
| PMP | MW-252 | C | 2023/05/18 | Iron, dissolved | mg/L | 0.0499 |
| PMP | MW-252 | C | 2023/08/04 | Iron, dissolved | mg/L | 0.562 |
| PMP | MW-252 | C | 2023/10/31 | Iron, dissolved | mg/L | 0.619 |
| PMP | MW-252 | C | 2023/03/15 | Magnesium, total | mg/L | 77.4 |
| PMP | MW-252 | C | 2023/05/18 | Magnesium, total | mg/L | 87.6 |
| PMP | MW-252 | C | 2023/08/04 | Magnesium, total | mg/L | 82.5 |
| PMP | MW-252 | C | 2023/10/31 | Magnesium, total | mg/L | 81.5 |
| PMP | MW-252 | C | 2013/11/20 | Manganese, dissolved | mg/L | 0.110 |
| PMP | MW-252 | C | 2014/02/19 | Manganese, dissolved | mg/L | 0.0100 |
| PMP | MW-252 | C | 2014/06/12 | Manganese, dissolved | mg/L | 0.0570 |
| PMP | MW-252 | C | 2015/03/25 | Manganese, dissolved | mg/L | 0.0530 |
| PMP | MW-252 | C | 2015/06/24 | Manganese, dissolved | mg/L | 0.198 |
| PMP | MW-252 | C | 2015/09/25 | Manganese, dissolved | mg/L | 0.582 |
| PMP | MW-252 | C | 2015/11/10 | Manganese, dissolved | mg/L | 0.152 |
| PMP | MW-252 | C | 2016/03/22 | Manganese, dissolved | mg/L | 0.249 |
| PMP | MW-252 | C | 2016/06/23 | Manganese, dissolved | mg/L | 0.248 |
| PMP | MW-252 | C | 2016/09/29 | Manganese, dissolved | mg/L | 0.126 |
| PMP | MW-252 | C | 2016/12/21 | Manganese, dissolved | mg/L | 0.0827 |
| PMP | MW-252 | C | 2017/03/16 | Manganese, dissolved | mg/L | 0.0800 |
| PMP | MW-252 | C | 2017/06/21 | Manganese, dissolved | mg/L | 0.140 |
| PMP | MW-252 | C | 2017/09/21 | Manganese, dissolved | mg/L | 0.160 |
| PMP | MW-252 | C | 2017/11/28 | Manganese, dissolved | mg/L | 0.180 |
| PMP | MW-252 | C | 2018/03/20 | Manganese, dissolved | mg/L | 0.179 |
| PMP | MW-252 | C | 2018/06/27 | Manganese, dissolved | mg/L | 0.171 |
| PMP | MW-252 | C | 2018/09/26 | Manganese, dissolved | mg/L | 0.300 |
| PMP | MW-252 | C | 2018/12/18 | Manganese, dissolved | mg/L | 0.128 |
| PMP | MW-252 | C | 2019/03/20 | Manganese, dissolved | mg/L | 0.00730 |
| PMP | MW-252 | C | 2019/06/25 | Manganese, dissolved | mg/L | 0.0851 |
| PMP | MW-252 | C | 2019/09/26 | Manganese, dissolved | mg/L | 0.0696 |
| PMP | MW-252 | C | 2019/12/19 | Manganese, dissolved | mg/L | 0.0938 |
| PMP | MW-252 | C | 2020/03/27 | Manganese, dissolved | mg/L | 0.0258 |
| PMP | MW-252 | C | 2020/06/23 | Manganese, dissolved | mg/L | <0.0025 |
| PMP | MW-252 | C | 2020/09/17 | Manganese, dissolved | mg/L | 0.0975 |
| PMP | MW-252 | C | 2020/12/16 | Manganese, dissolved | mg/L | 0.0785 |

Attachment I. Site Groundwater Data

Geochemical Conceptual Site Model

Baldwin Fly Ash Pond System

Baldwin Power Plant

Baldwin, IL

| | | | | | | |
|-----|--------|---|------------|-----------------------|-----------|---------|
| PMP | MW-252 | C | 2021/03/09 | Manganese, dissolved | mg/L | 0.129 |
| PMP | MW-252 | C | 2021/07/19 | Manganese, dissolved | mg/L | 0.0459 |
| PMP | MW-252 | C | 2021/09/14 | Manganese, dissolved | mg/L | 0.0708 |
| PMP | MW-252 | C | 2021/12/14 | Manganese, dissolved | mg/L | 0.135 |
| PMP | MW-252 | C | 2022/03/28 | Manganese, dissolved | mg/L | 0.0929 |
| PMP | MW-252 | C | 2022/06/14 | Manganese, dissolved | mg/L | 0.00460 |
| PMP | MW-252 | C | 2022/09/29 | Manganese, dissolved | mg/L | 0.172 |
| PMP | MW-252 | C | 2022/12/06 | Manganese, dissolved | mg/L | 0.121 |
| PMP | MW-252 | C | 2023/03/15 | Manganese, dissolved | mg/L | 0.221 |
| PMP | MW-252 | C | 2023/05/18 | Manganese, dissolved | mg/L | 0.396 |
| PMP | MW-252 | C | 2023/08/04 | Manganese, dissolved | mg/L | 0.293 |
| PMP | MW-252 | C | 2023/10/31 | Manganese, dissolved | mg/L | 0.303 |
| PMP | MW-252 | C | 2023/05/18 | Phosphate, dissolved | mg/L | 0.212 |
| PMP | MW-252 | C | 2023/08/04 | Phosphate, dissolved | mg/L | 0.0740 |
| PMP | MW-252 | C | 2023/03/15 | Potassium, total | mg/L | 1.38 |
| PMP | MW-252 | C | 2023/05/18 | Potassium, total | mg/L | 1.68 |
| PMP | MW-252 | C | 2023/08/04 | Potassium, total | mg/L | 1.89 |
| PMP | MW-252 | C | 2023/10/31 | Potassium, total | mg/L | 1.48 |
| PMP | MW-252 | C | 2023/05/18 | Silicon, dissolved | mg/L | 7.03 |
| PMP | MW-252 | C | 2023/08/04 | Silicon, dissolved | mg/L | 6.74 |
| PMP | MW-252 | C | 2023/03/15 | Sodium, total | mg/L | 81.7 |
| PMP | MW-252 | C | 2023/05/18 | Sodium, total | mg/L | 104 |
| PMP | MW-252 | C | 2023/08/04 | Sodium, total | mg/L | 94.9 |
| PMP | MW-252 | C | 2023/10/31 | Sodium, total | mg/L | 89.2 |
| PMP | MW-252 | C | 2013/09/16 | Sulfate, total | mg/L | 500 |
| PMP | MW-252 | C | 2023/03/15 | Sulfate, total | mg/L | 437 |
| PMP | MW-252 | C | 2023/05/18 | Sulfate, total | mg/L | 454 |
| PMP | MW-252 | C | 2023/08/04 | Sulfate, total | mg/L | 448 |
| PMP | MW-252 | C | 2023/10/31 | Sulfate, total | mg/L | 474 |
| PMP | MW-252 | C | 2013/09/16 | Temperature (Celsius) | degrees C | 14.1 |
| PMP | MW-252 | C | 2013/11/20 | Temperature (Celsius) | degrees C | 13.8 |
| PMP | MW-252 | C | 2014/02/19 | Temperature (Celsius) | degrees C | 10.9 |
| PMP | MW-252 | C | 2014/06/12 | Temperature (Celsius) | degrees C | 14.3 |
| PMP | MW-252 | C | 2015/03/25 | Temperature (Celsius) | degrees C | 12.8 |
| PMP | MW-252 | C | 2015/06/24 | Temperature (Celsius) | degrees C | 13.7 |
| PMP | MW-252 | C | 2015/09/25 | Temperature (Celsius) | degrees C | 14.5 |
| PMP | MW-252 | C | 2015/11/10 | Temperature (Celsius) | degrees C | 13.7 |
| PMP | MW-252 | C | 2016/03/22 | Temperature (Celsius) | degrees C | 15 |
| PMP | MW-252 | C | 2016/06/23 | Temperature (Celsius) | degrees C | 14.4 |
| PMP | MW-252 | C | 2016/09/29 | Temperature (Celsius) | degrees C | 14.8 |
| PMP | MW-252 | C | 2016/12/21 | Temperature (Celsius) | degrees C | 13.5 |
| PMP | MW-252 | C | 2017/03/16 | Temperature (Celsius) | degrees C | 12.0 |
| PMP | MW-252 | C | 2017/06/21 | Temperature (Celsius) | degrees C | 14.0 |
| PMP | MW-252 | C | 2017/09/21 | Temperature (Celsius) | degrees C | 15.4 |
| PMP | MW-252 | C | 2017/11/28 | Temperature (Celsius) | degrees C | 14.2 |
| PMP | MW-252 | C | 2018/03/20 | Temperature (Celsius) | degrees C | 13.8 |
| PMP | MW-252 | C | 2018/06/27 | Temperature (Celsius) | degrees C | 14.9 |
| PMP | MW-252 | C | 2018/09/26 | Temperature (Celsius) | degrees C | 14.2 |
| PMP | MW-252 | C | 2018/12/18 | Temperature (Celsius) | degrees C | 13.6 |
| PMP | MW-252 | C | 2019/03/20 | Temperature (Celsius) | degrees C | 13.3 |
| PMP | MW-252 | C | 2019/06/25 | Temperature (Celsius) | degrees C | 14.8 |
| PMP | MW-252 | C | 2019/09/26 | Temperature (Celsius) | degrees C | 14.0 |
| PMP | MW-252 | C | 2019/12/19 | Temperature (Celsius) | degrees C | 13.5 |
| PMP | MW-252 | C | 2020/03/27 | Temperature (Celsius) | degrees C | 14.1 |
| PMP | MW-252 | C | 2020/06/23 | Temperature (Celsius) | degrees C | 13.6 |
| PMP | MW-252 | C | 2020/09/17 | Temperature (Celsius) | degrees C | 14.1 |
| PMP | MW-252 | C | 2020/12/16 | Temperature (Celsius) | degrees C | 13.5 |

Attachment I. Site Groundwater Data

Geochemical Conceptual Site Model

Baldwin Fly Ash Pond System

Baldwin Power Plant

Baldwin, IL

| | | | | | | |
|-----|--------|---|------------|------------------------|-----------|-------|
| PMP | MW-252 | C | 2021/03/09 | Temperature (Celsius) | degrees C | 13.0 |
| PMP | MW-252 | C | 2021/07/19 | Temperature (Celsius) | degrees C | 17.3 |
| PMP | MW-252 | C | 2021/09/14 | Temperature (Celsius) | degrees C | 16.8 |
| PMP | MW-252 | C | 2021/12/14 | Temperature (Celsius) | degrees C | 12.8 |
| PMP | MW-252 | C | 2022/03/28 | Temperature (Celsius) | degrees C | 13.7 |
| PMP | MW-252 | C | 2022/06/14 | Temperature (Celsius) | degrees C | 17.2 |
| PMP | MW-252 | C | 2022/09/29 | Temperature (Celsius) | degrees C | 15.4 |
| PMP | MW-252 | C | 2022/12/06 | Temperature (Celsius) | degrees C | 13.7 |
| PMP | MW-252 | C | 2023/03/15 | Temperature (Celsius) | degrees C | 13.3 |
| PMP | MW-252 | C | 2023/05/18 | Temperature (Celsius) | degrees C | 14.3 |
| PMP | MW-252 | C | 2023/08/04 | Temperature (Celsius) | degrees C | 18.9 |
| PMP | MW-252 | C | 2023/10/31 | Temperature (Celsius) | degrees C | 13.5 |
| PMP | MW-252 | C | 2013/09/16 | Total Dissolved Solids | mg/L | 1,260 |
| PMP | MW-252 | C | 2013/11/20 | Total Dissolved Solids | mg/L | 1,250 |
| PMP | MW-252 | C | 2014/02/19 | Total Dissolved Solids | mg/L | 1,310 |
| PMP | MW-252 | C | 2014/06/12 | Total Dissolved Solids | mg/L | 1,390 |
| PMP | MW-252 | C | 2015/03/25 | Total Dissolved Solids | mg/L | 1,270 |
| PMP | MW-252 | C | 2015/06/24 | Total Dissolved Solids | mg/L | 1,320 |
| PMP | MW-252 | C | 2015/09/25 | Total Dissolved Solids | mg/L | 1,250 |
| PMP | MW-252 | C | 2015/11/10 | Total Dissolved Solids | mg/L | 1,250 |
| PMP | MW-252 | C | 2016/03/22 | Total Dissolved Solids | mg/L | 1,300 |
| PMP | MW-252 | C | 2016/06/23 | Total Dissolved Solids | mg/L | 1,270 |
| PMP | MW-252 | C | 2016/09/29 | Total Dissolved Solids | mg/L | 1,280 |
| PMP | MW-252 | C | 2016/12/21 | Total Dissolved Solids | mg/L | 1,310 |
| PMP | MW-252 | C | 2017/03/16 | Total Dissolved Solids | mg/L | 1,270 |
| PMP | MW-252 | C | 2017/06/21 | Total Dissolved Solids | mg/L | 1,320 |
| PMP | MW-252 | C | 2017/09/21 | Total Dissolved Solids | mg/L | 1,230 |
| PMP | MW-252 | C | 2017/11/28 | Total Dissolved Solids | mg/L | 1,290 |
| PMP | MW-252 | C | 2018/03/20 | Total Dissolved Solids | mg/L | 1,260 |
| PMP | MW-252 | C | 2018/06/27 | Total Dissolved Solids | mg/L | 1,290 |
| PMP | MW-252 | C | 2018/09/26 | Total Dissolved Solids | mg/L | 1,280 |
| PMP | MW-252 | C | 2018/12/18 | Total Dissolved Solids | mg/L | 1,270 |
| PMP | MW-252 | C | 2019/03/20 | Total Dissolved Solids | mg/L | 1,300 |
| PMP | MW-252 | C | 2019/06/25 | Total Dissolved Solids | mg/L | 1,330 |
| PMP | MW-252 | C | 2019/09/26 | Total Dissolved Solids | mg/L | 1,250 |
| PMP | MW-252 | C | 2019/12/19 | Total Dissolved Solids | mg/L | 1,230 |
| PMP | MW-252 | C | 2020/03/27 | Total Dissolved Solids | mg/L | 1,240 |
| PMP | MW-252 | C | 2020/06/23 | Total Dissolved Solids | mg/L | 1,200 |
| PMP | MW-252 | C | 2020/09/17 | Total Dissolved Solids | mg/L | 1,200 |
| PMP | MW-252 | C | 2020/12/16 | Total Dissolved Solids | mg/L | 1,200 |
| PMP | MW-252 | C | 2021/03/09 | Total Dissolved Solids | mg/L | 1,190 |
| PMP | MW-252 | C | 2021/07/19 | Total Dissolved Solids | mg/L | 1,140 |
| PMP | MW-252 | C | 2021/09/14 | Total Dissolved Solids | mg/L | 1,160 |
| PMP | MW-252 | C | 2021/12/14 | Total Dissolved Solids | mg/L | 1,130 |
| PMP | MW-252 | C | 2022/03/28 | Total Dissolved Solids | mg/L | 1,180 |
| PMP | MW-252 | C | 2022/06/14 | Total Dissolved Solids | mg/L | 1,200 |
| PMP | MW-252 | C | 2022/09/29 | Total Dissolved Solids | mg/L | 1,080 |
| PMP | MW-252 | C | 2022/12/06 | Total Dissolved Solids | mg/L | 1,230 |
| PMP | MW-252 | C | 2023/03/15 | Total Dissolved Solids | mg/L | 1,130 |
| PMP | MW-252 | C | 2023/05/18 | Total Dissolved Solids | mg/L | 1,200 |
| PMP | MW-252 | C | 2023/08/04 | Total Dissolved Solids | mg/L | 1,260 |
| PMP | MW-252 | C | 2023/10/31 | Total Dissolved Solids | mg/L | 1,220 |
| PMP | MW-253 | C | 2013/09/17 | pH (field) | SU | 10.6 |
| PMP | MW-253 | C | 2013/11/21 | pH (field) | SU | 8.6 |
| PMP | MW-253 | C | 2014/02/19 | pH (field) | SU | 7.9 |
| PMP | MW-253 | C | 2014/06/11 | pH (field) | SU | 11.4 |
| PMP | MW-253 | C | 2015/03/25 | pH (field) | SU | 12.4 |

Attachment I. Site Groundwater Data

Geochemical Conceptual Site Model

Baldwin Fly Ash Pond System

Baldwin Power Plant

Baldwin, IL

| | | | | | | |
|-----|--------|---|------------|-------------------------------|------------|-------|
| PMP | MW-253 | C | 2015/06/24 | pH (field) | SU | 12.4 |
| PMP | MW-253 | C | 2015/09/25 | pH (field) | SU | 11.1 |
| PMP | MW-253 | C | 2015/11/10 | pH (field) | SU | 10.1 |
| PMP | MW-253 | C | 2016/03/22 | pH (field) | SU | 11.8 |
| PMP | MW-253 | C | 2016/06/21 | pH (field) | SU | 11.9 |
| PMP | MW-253 | C | 2016/09/29 | pH (field) | SU | 11.7 |
| PMP | MW-253 | C | 2016/12/21 | pH (field) | SU | 11.0 |
| PMP | MW-253 | C | 2017/03/17 | pH (field) | SU | 10.6 |
| PMP | MW-253 | C | 2017/06/22 | pH (field) | SU | 11.7 |
| PMP | MW-253 | C | 2017/09/21 | pH (field) | SU | 9.8 |
| PMP | MW-253 | C | 2017/11/28 | pH (field) | SU | 10.3 |
| PMP | MW-253 | C | 2018/03/20 | pH (field) | SU | 11.9 |
| PMP | MW-253 | C | 2018/06/28 | pH (field) | SU | 11.8 |
| PMP | MW-253 | C | 2018/09/26 | pH (field) | SU | 11.8 |
| PMP | MW-253 | C | 2018/12/19 | pH (field) | SU | 11.8 |
| PMP | MW-253 | C | 2019/03/21 | pH (field) | SU | 12.2 |
| PMP | MW-253 | C | 2019/06/26 | pH (field) | SU | 12.0 |
| PMP | MW-253 | C | 2019/09/26 | pH (field) | SU | 11.3 |
| PMP | MW-253 | C | 2019/12/19 | pH (field) | SU | 11.0 |
| PMP | MW-253 | C | 2020/03/27 | pH (field) | SU | 12.1 |
| PMP | MW-253 | C | 2020/06/23 | pH (field) | SU | 12.4 |
| PMP | MW-253 | C | 2020/09/17 | pH (field) | SU | 11.6 |
| PMP | MW-253 | C | 2020/12/17 | pH (field) | SU | 12.0 |
| PMP | MW-253 | C | 2021/03/10 | pH (field) | SU | 11.8 |
| PMP | MW-253 | C | 2021/06/22 | pH (field) | SU | 11.7 |
| PMP | MW-253 | C | 2021/09/16 | pH (field) | SU | 11.3 |
| PMP | MW-253 | C | 2021/12/15 | pH (field) | SU | 11.2 |
| PMP | MW-253 | C | 2022/03/29 | pH (field) | SU | 11.6 |
| PMP | MW-253 | C | 2022/06/15 | pH (field) | SU | 11.6 |
| PMP | MW-253 | C | 2022/09/29 | pH (field) | SU | 11.4 |
| PMP | MW-253 | C | 2022/12/06 | pH (field) | SU | 10.7 |
| PMP | MW-253 | C | 2023/03/15 | pH (field) | SU | 11.8 |
| PMP | MW-253 | C | 2023/08/04 | pH (field) | SU | 11.3 |
| PMP | MW-253 | C | 2023/11/03 | pH (field) | SU | 10.8 |
| PMP | MW-253 | C | 2021/03/10 | Oxidation Reduction Potential | mV | -179 |
| PMP | MW-253 | C | 2021/06/22 | Oxidation Reduction Potential | mV | <-300 |
| PMP | MW-253 | C | 2021/09/16 | Oxidation Reduction Potential | mV | -72.0 |
| PMP | MW-253 | C | 2021/12/15 | Oxidation Reduction Potential | mV | -8.00 |
| PMP | MW-253 | C | 2022/03/29 | Oxidation Reduction Potential | mV | -180 |
| PMP | MW-253 | C | 2022/06/15 | Oxidation Reduction Potential | mV | -35.0 |
| PMP | MW-253 | C | 2022/09/29 | Oxidation Reduction Potential | mV | -2.00 |
| PMP | MW-253 | C | 2022/12/06 | Oxidation Reduction Potential | mV | <-300 |
| PMP | MW-253 | C | 2023/03/15 | Oxidation Reduction Potential | mV | -114 |
| PMP | MW-253 | C | 2023/08/04 | Oxidation Reduction Potential | mV | 68.0 |
| PMP | MW-253 | C | 2023/11/03 | Oxidation Reduction Potential | mV | -35.0 |
| PMP | MW-253 | C | 2021/03/10 | Eh | V | 0.017 |
| PMP | MW-253 | C | 2021/06/22 | Eh | V | -0.11 |
| PMP | MW-253 | C | 2021/09/16 | Eh | V | 0.12 |
| PMP | MW-253 | C | 2021/12/15 | Eh | V | 0.19 |
| PMP | MW-253 | C | 2022/03/29 | Eh | V | 0.016 |
| PMP | MW-253 | C | 2022/06/15 | Eh | V | 0.16 |
| PMP | MW-253 | C | 2022/09/29 | Eh | V | 0.19 |
| PMP | MW-253 | C | 2022/12/06 | Eh | V | -0.10 |
| PMP | MW-253 | C | 2023/03/15 | Eh | V | 0.082 |
| PMP | MW-253 | C | 2023/08/04 | Eh | V | 0.26 |
| PMP | MW-253 | C | 2023/11/03 | Eh | V | 0.16 |
| PMP | MW-253 | C | 2023/03/15 | Alkalinity, carbonate | mg/L CaCO3 | 57.0 |

Attachment I. Site Groundwater Data

Geochemical Conceptual Site Model

Baldwin Fly Ash Pond System

Baldwin Power Plant

Baldwin, IL

| | | | | | | |
|-----|--------|---|------------|-----------------------|------------|---------|
| PMP | MW-253 | C | 2023/08/04 | Alkalinity, carbonate | mg/L CaCO3 | 29.0 |
| PMP | MW-253 | C | 2023/11/03 | Alkalinity, carbonate | mg/L CaCO3 | 14.0 |
| PMP | MW-253 | C | 2023/03/15 | Barium, total | mg/L | 0.112 |
| PMP | MW-253 | C | 2023/08/04 | Barium, total | mg/L | 0.0562 |
| PMP | MW-253 | C | 2023/11/03 | Barium, total | mg/L | 0.157 |
| PMP | MW-253 | C | 2013/09/17 | Boron, total | mg/L | 0.0600 |
| PMP | MW-253 | C | 2023/03/15 | Boron, total | mg/L | <0.02 |
| PMP | MW-253 | C | 2023/08/04 | Boron, total | mg/L | 0.0698 |
| PMP | MW-253 | C | 2023/11/03 | Boron, total | mg/L | 0.0853 |
| PMP | MW-253 | C | 2023/03/15 | Calcium, total | mg/L | 202 |
| PMP | MW-253 | C | 2023/08/04 | Calcium, total | mg/L | 75.0 |
| PMP | MW-253 | C | 2023/11/03 | Calcium, total | mg/L | 70.8 |
| PMP | MW-253 | C | 2013/09/17 | Chloride, total | mg/L | 15.0 |
| PMP | MW-253 | C | 2023/03/15 | Chloride, total | mg/L | 21.0 |
| PMP | MW-253 | C | 2023/08/04 | Chloride, total | mg/L | 21.0 |
| PMP | MW-253 | C | 2023/11/03 | Chloride, total | mg/L | 22.0 |
| PMP | MW-253 | C | 2013/11/21 | Iron, dissolved | mg/L | <0.007 |
| PMP | MW-253 | C | 2014/02/19 | Iron, dissolved | mg/L | <0.007 |
| PMP | MW-253 | C | 2014/06/11 | Iron, dissolved | mg/L | <0.007 |
| PMP | MW-253 | C | 2015/03/25 | Iron, dissolved | mg/L | <0.007 |
| PMP | MW-253 | C | 2015/06/24 | Iron, dissolved | mg/L | <0.007 |
| PMP | MW-253 | C | 2015/09/25 | Iron, dissolved | mg/L | <0.007 |
| PMP | MW-253 | C | 2015/11/10 | Iron, dissolved | mg/L | <0.007 |
| PMP | MW-253 | C | 2016/03/22 | Iron, dissolved | mg/L | <0.007 |
| PMP | MW-253 | C | 2016/06/21 | Iron, dissolved | mg/L | <0.007 |
| PMP | MW-253 | C | 2016/09/29 | Iron, dissolved | mg/L | <0.007 |
| PMP | MW-253 | C | 2016/12/21 | Iron, dissolved | mg/L | <0.007 |
| PMP | MW-253 | C | 2017/03/17 | Iron, dissolved | mg/L | <0.007 |
| PMP | MW-253 | C | 2017/06/22 | Iron, dissolved | mg/L | <0.007 |
| PMP | MW-253 | C | 2017/09/21 | Iron, dissolved | mg/L | <0.007 |
| PMP | MW-253 | C | 2017/11/28 | Iron, dissolved | mg/L | <0.007 |
| PMP | MW-253 | C | 2018/03/20 | Iron, dissolved | mg/L | <0.007 |
| PMP | MW-253 | C | 2018/06/28 | Iron, dissolved | mg/L | <0.02 |
| PMP | MW-253 | C | 2018/09/26 | Iron, dissolved | mg/L | <0.02 |
| PMP | MW-253 | C | 2018/12/19 | Iron, dissolved | mg/L | <0.02 |
| PMP | MW-253 | C | 2019/03/21 | Iron, dissolved | mg/L | <0.02 |
| PMP | MW-253 | C | 2019/06/26 | Iron, dissolved | mg/L | <0.02 |
| PMP | MW-253 | C | 2019/09/26 | Iron, dissolved | mg/L | <0.02 |
| PMP | MW-253 | C | 2019/12/19 | Iron, dissolved | mg/L | <0.02 |
| PMP | MW-253 | C | 2020/03/27 | Iron, dissolved | mg/L | <0.02 |
| PMP | MW-253 | C | 2020/06/23 | Iron, dissolved | mg/L | <0.02 |
| PMP | MW-253 | C | 2020/09/17 | Iron, dissolved | mg/L | <0.02 |
| PMP | MW-253 | C | 2020/12/17 | Iron, dissolved | mg/L | <0.02 |
| PMP | MW-253 | C | 2021/03/10 | Iron, dissolved | mg/L | <0.02 |
| PMP | MW-253 | C | 2021/06/22 | Iron, dissolved | mg/L | <0.02 |
| PMP | MW-253 | C | 2021/09/16 | Iron, dissolved | mg/L | <0.02 |
| PMP | MW-253 | C | 2021/12/15 | Iron, dissolved | mg/L | <0.02 |
| PMP | MW-253 | C | 2022/03/29 | Iron, dissolved | mg/L | <0.015 |
| PMP | MW-253 | C | 2022/06/15 | Iron, dissolved | mg/L | <0.02 |
| PMP | MW-253 | C | 2022/09/29 | Iron, dissolved | mg/L | <0.0115 |
| PMP | MW-253 | C | 2022/12/06 | Iron, dissolved | mg/L | <0.0115 |
| PMP | MW-253 | C | 2023/03/15 | Iron, dissolved | mg/L | <0.0115 |
| PMP | MW-253 | C | 2023/08/04 | Iron, dissolved | mg/L | <0.0115 |
| PMP | MW-253 | C | 2023/11/03 | Iron, dissolved | mg/L | <0.0115 |
| PMP | MW-253 | C | 2023/03/15 | Magnesium, total | mg/L | 0.301 |
| PMP | MW-253 | C | 2023/08/04 | Magnesium, total | mg/L | 2.29 |
| PMP | MW-253 | C | 2023/11/03 | Magnesium, total | mg/L | 2.82 |

Attachment I. Site Groundwater Data

Geochemical Conceptual Site Model

Baldwin Fly Ash Pond System

Baldwin Power Plant

Baldwin, IL

| | | | | | | |
|-----|--------|---|------------|-----------------------|-----------|----------|
| PMP | MW-253 | C | 2013/11/21 | Manganese, dissolved | mg/L | <0.0016 |
| PMP | MW-253 | C | 2014/02/19 | Manganese, dissolved | mg/L | <0.0016 |
| PMP | MW-253 | C | 2014/06/11 | Manganese, dissolved | mg/L | <0.0016 |
| PMP | MW-253 | C | 2015/03/25 | Manganese, dissolved | mg/L | <0.0005 |
| PMP | MW-253 | C | 2015/06/24 | Manganese, dissolved | mg/L | <0.0005 |
| PMP | MW-253 | C | 2015/09/25 | Manganese, dissolved | mg/L | <0.0005 |
| PMP | MW-253 | C | 2015/11/10 | Manganese, dissolved | mg/L | <0.0005 |
| PMP | MW-253 | C | 2016/03/22 | Manganese, dissolved | mg/L | <0.0005 |
| PMP | MW-253 | C | 2016/06/21 | Manganese, dissolved | mg/L | <0.0005 |
| PMP | MW-253 | C | 2016/09/29 | Manganese, dissolved | mg/L | <0.0005 |
| PMP | MW-253 | C | 2016/12/21 | Manganese, dissolved | mg/L | <0.0005 |
| PMP | MW-253 | C | 2017/03/17 | Manganese, dissolved | mg/L | <0.0005 |
| PMP | MW-253 | C | 2017/06/22 | Manganese, dissolved | mg/L | <0.0005 |
| PMP | MW-253 | C | 2017/09/21 | Manganese, dissolved | mg/L | <0.0005 |
| PMP | MW-253 | C | 2017/11/28 | Manganese, dissolved | mg/L | <0.0005 |
| PMP | MW-253 | C | 2018/03/20 | Manganese, dissolved | mg/L | <0.0005 |
| PMP | MW-253 | C | 2018/06/28 | Manganese, dissolved | mg/L | <0.0025 |
| PMP | MW-253 | C | 2018/09/26 | Manganese, dissolved | mg/L | <0.0025 |
| PMP | MW-253 | C | 2018/12/19 | Manganese, dissolved | mg/L | <0.0025 |
| PMP | MW-253 | C | 2019/03/21 | Manganese, dissolved | mg/L | <0.0025 |
| PMP | MW-253 | C | 2019/06/26 | Manganese, dissolved | mg/L | <0.0025 |
| PMP | MW-253 | C | 2019/09/26 | Manganese, dissolved | mg/L | <0.0025 |
| PMP | MW-253 | C | 2019/12/19 | Manganese, dissolved | mg/L | <0.0025 |
| PMP | MW-253 | C | 2020/03/27 | Manganese, dissolved | mg/L | <0.0025 |
| PMP | MW-253 | C | 2020/06/23 | Manganese, dissolved | mg/L | <0.0025 |
| PMP | MW-253 | C | 2020/09/17 | Manganese, dissolved | mg/L | <0.0025 |
| PMP | MW-253 | C | 2020/12/17 | Manganese, dissolved | mg/L | <0.0025 |
| PMP | MW-253 | C | 2021/03/10 | Manganese, dissolved | mg/L | <0.0025 |
| PMP | MW-253 | C | 2021/06/22 | Manganese, dissolved | mg/L | <0.0025 |
| PMP | MW-253 | C | 2021/09/16 | Manganese, dissolved | mg/L | <0.0025 |
| PMP | MW-253 | C | 2021/12/15 | Manganese, dissolved | mg/L | <0.0025 |
| PMP | MW-253 | C | 2022/03/29 | Manganese, dissolved | mg/L | <0.0008 |
| PMP | MW-253 | C | 2022/06/15 | Manganese, dissolved | mg/L | <0.0025 |
| PMP | MW-253 | C | 2022/09/29 | Manganese, dissolved | mg/L | <0.0008 |
| PMP | MW-253 | C | 2022/12/06 | Manganese, dissolved | mg/L | 0.000900 |
| PMP | MW-253 | C | 2023/03/15 | Manganese, dissolved | mg/L | <0.0008 |
| PMP | MW-253 | C | 2023/08/04 | Manganese, dissolved | mg/L | <0.0008 |
| PMP | MW-253 | C | 2023/11/03 | Manganese, dissolved | mg/L | <0.0008 |
| PMP | MW-253 | C | 2023/08/04 | Phosphate, dissolved | mg/L | 0.0250 |
| PMP | MW-253 | C | 2023/03/15 | Potassium, total | mg/L | 1.89 |
| PMP | MW-253 | C | 2023/08/04 | Potassium, total | mg/L | 1.46 |
| PMP | MW-253 | C | 2023/11/03 | Potassium, total | mg/L | 1.31 |
| PMP | MW-253 | C | 2023/08/04 | Silicon, dissolved | mg/L | 1.21 |
| PMP | MW-253 | C | 2023/03/15 | Sodium, total | mg/L | 38.3 |
| PMP | MW-253 | C | 2023/08/04 | Sodium, total | mg/L | 40.7 |
| PMP | MW-253 | C | 2023/11/03 | Sodium, total | mg/L | 39.2 |
| PMP | MW-253 | C | 2013/09/17 | Sulfate, total | mg/L | 349 |
| PMP | MW-253 | C | 2023/03/15 | Sulfate, total | mg/L | 140 |
| PMP | MW-253 | C | 2023/08/04 | Sulfate, total | mg/L | 154 |
| PMP | MW-253 | C | 2023/11/03 | Sulfate, total | mg/L | 174 |
| PMP | MW-253 | C | 2013/09/17 | Temperature (Celsius) | degrees C | 15.6 |
| PMP | MW-253 | C | 2013/11/21 | Temperature (Celsius) | degrees C | 13.9 |
| PMP | MW-253 | C | 2014/02/19 | Temperature (Celsius) | degrees C | 14.4 |
| PMP | MW-253 | C | 2014/06/11 | Temperature (Celsius) | degrees C | 14.1 |
| PMP | MW-253 | C | 2015/03/25 | Temperature (Celsius) | degrees C | 14.1 |
| PMP | MW-253 | C | 2015/06/24 | Temperature (Celsius) | degrees C | 14.8 |
| PMP | MW-253 | C | 2015/09/25 | Temperature (Celsius) | degrees C | 14.6 |

Attachment I. Site Groundwater Data

Geochemical Conceptual Site Model

Baldwin Fly Ash Pond System

Baldwin Power Plant

Baldwin, IL

| | | | | | | |
|-----|--------|---|------------|------------------------|-----------|------|
| PMP | MW-253 | C | 2015/11/10 | Temperature (Celsius) | degrees C | 14.8 |
| PMP | MW-253 | C | 2016/03/22 | Temperature (Celsius) | degrees C | 13.3 |
| PMP | MW-253 | C | 2016/06/21 | Temperature (Celsius) | degrees C | 14.8 |
| PMP | MW-253 | C | 2016/09/29 | Temperature (Celsius) | degrees C | 14.9 |
| PMP | MW-253 | C | 2016/12/21 | Temperature (Celsius) | degrees C | 14.0 |
| PMP | MW-253 | C | 2017/03/17 | Temperature (Celsius) | degrees C | 14.3 |
| PMP | MW-253 | C | 2017/06/22 | Temperature (Celsius) | degrees C | 15.5 |
| PMP | MW-253 | C | 2017/09/21 | Temperature (Celsius) | degrees C | 15.5 |
| PMP | MW-253 | C | 2017/11/28 | Temperature (Celsius) | degrees C | 15.4 |
| PMP | MW-253 | C | 2018/03/20 | Temperature (Celsius) | degrees C | 14.9 |
| PMP | MW-253 | C | 2018/06/28 | Temperature (Celsius) | degrees C | 15.1 |
| PMP | MW-253 | C | 2018/09/26 | Temperature (Celsius) | degrees C | 15.5 |
| PMP | MW-253 | C | 2018/12/19 | Temperature (Celsius) | degrees C | 14.3 |
| PMP | MW-253 | C | 2019/03/21 | Temperature (Celsius) | degrees C | 12.4 |
| PMP | MW-253 | C | 2019/06/26 | Temperature (Celsius) | degrees C | 15.9 |
| PMP | MW-253 | C | 2019/09/26 | Temperature (Celsius) | degrees C | 14.8 |
| PMP | MW-253 | C | 2019/12/19 | Temperature (Celsius) | degrees C | 13.4 |
| PMP | MW-253 | C | 2020/03/27 | Temperature (Celsius) | degrees C | 14.3 |
| PMP | MW-253 | C | 2020/06/23 | Temperature (Celsius) | degrees C | 14.4 |
| PMP | MW-253 | C | 2020/09/17 | Temperature (Celsius) | degrees C | 14.9 |
| PMP | MW-253 | C | 2020/12/17 | Temperature (Celsius) | degrees C | 14.1 |
| PMP | MW-253 | C | 2021/03/10 | Temperature (Celsius) | degrees C | 13.8 |
| PMP | MW-253 | C | 2021/06/22 | Temperature (Celsius) | degrees C | 17.6 |
| PMP | MW-253 | C | 2021/09/16 | Temperature (Celsius) | degrees C | 15.7 |
| PMP | MW-253 | C | 2021/12/15 | Temperature (Celsius) | degrees C | 14.9 |
| PMP | MW-253 | C | 2022/03/29 | Temperature (Celsius) | degrees C | 14.3 |
| PMP | MW-253 | C | 2022/06/15 | Temperature (Celsius) | degrees C | 16.8 |
| PMP | MW-253 | C | 2022/09/29 | Temperature (Celsius) | degrees C | 14.5 |
| PMP | MW-253 | C | 2022/12/06 | Temperature (Celsius) | degrees C | 13.7 |
| PMP | MW-253 | C | 2023/03/15 | Temperature (Celsius) | degrees C | 14.1 |
| PMP | MW-253 | C | 2023/08/04 | Temperature (Celsius) | degrees C | 15.0 |
| PMP | MW-253 | C | 2023/11/03 | Temperature (Celsius) | degrees C | 15.9 |
| PMP | MW-253 | C | 2013/09/17 | Total Dissolved Solids | mg/L | 546 |
| PMP | MW-253 | C | 2013/11/21 | Total Dissolved Solids | mg/L | 602 |
| PMP | MW-253 | C | 2014/02/19 | Total Dissolved Solids | mg/L | 564 |
| PMP | MW-253 | C | 2014/06/11 | Total Dissolved Solids | mg/L | 668 |
| PMP | MW-253 | C | 2015/03/25 | Total Dissolved Solids | mg/L | 820 |
| PMP | MW-253 | C | 2015/06/24 | Total Dissolved Solids | mg/L | 928 |
| PMP | MW-253 | C | 2015/09/25 | Total Dissolved Solids | mg/L | 346 |
| PMP | MW-253 | C | 2015/11/10 | Total Dissolved Solids | mg/L | 300 |
| PMP | MW-253 | C | 2016/03/22 | Total Dissolved Solids | mg/L | 546 |
| PMP | MW-253 | C | 2016/06/21 | Total Dissolved Solids | mg/L | 568 |
| PMP | MW-253 | C | 2016/09/29 | Total Dissolved Solids | mg/L | 446 |
| PMP | MW-253 | C | 2016/12/21 | Total Dissolved Solids | mg/L | 414 |
| PMP | MW-253 | C | 2017/03/17 | Total Dissolved Solids | mg/L | 352 |
| PMP | MW-253 | C | 2017/06/22 | Total Dissolved Solids | mg/L | 555 |
| PMP | MW-253 | C | 2017/09/21 | Total Dissolved Solids | mg/L | 436 |
| PMP | MW-253 | C | 2017/11/28 | Total Dissolved Solids | mg/L | 496 |
| PMP | MW-253 | C | 2018/03/20 | Total Dissolved Solids | mg/L | 668 |
| PMP | MW-253 | C | 2018/06/28 | Total Dissolved Solids | mg/L | 570 |
| PMP | MW-253 | C | 2018/09/26 | Total Dissolved Solids | mg/L | 560 |
| PMP | MW-253 | C | 2018/12/19 | Total Dissolved Solids | mg/L | 645 |
| PMP | MW-253 | C | 2019/03/21 | Total Dissolved Solids | mg/L | 910 |
| PMP | MW-253 | C | 2019/06/26 | Total Dissolved Solids | mg/L | 685 |
| PMP | MW-253 | C | 2019/09/26 | Total Dissolved Solids | mg/L | 320 |
| PMP | MW-253 | C | 2019/12/19 | Total Dissolved Solids | mg/L | 370 |
| PMP | MW-253 | C | 2020/03/27 | Total Dissolved Solids | mg/L | 894 |

Attachment I. Site Groundwater Data

Geochemical Conceptual Site Model

Baldwin Fly Ash Pond System

Baldwin Power Plant

Baldwin, IL

| | | | | | | |
|-----|--------|---|------------|-------------------------------|------|-------|
| PMP | MW-253 | C | 2020/06/23 | Total Dissolved Solids | mg/L | 518 |
| PMP | MW-253 | C | 2020/09/17 | Total Dissolved Solids | mg/L | 376 |
| PMP | MW-253 | C | 2020/12/17 | Total Dissolved Solids | mg/L | 530 |
| PMP | MW-253 | C | 2021/03/10 | Total Dissolved Solids | mg/L | 758 |
| PMP | MW-253 | C | 2021/06/22 | Total Dissolved Solids | mg/L | 500 |
| PMP | MW-253 | C | 2021/09/16 | Total Dissolved Solids | mg/L | 360 |
| PMP | MW-253 | C | 2021/12/15 | Total Dissolved Solids | mg/L | 378 |
| PMP | MW-253 | C | 2022/03/29 | Total Dissolved Solids | mg/L | 720 |
| PMP | MW-253 | C | 2022/06/15 | Total Dissolved Solids | mg/L | 530 |
| PMP | MW-253 | C | 2022/09/29 | Total Dissolved Solids | mg/L | 332 |
| PMP | MW-253 | C | 2022/12/06 | Total Dissolved Solids | mg/L | 320 |
| PMP | MW-253 | C | 2023/03/15 | Total Dissolved Solids | mg/L | 540 |
| PMP | MW-253 | C | 2023/08/04 | Total Dissolved Solids | mg/L | 328 |
| PMP | MW-253 | C | 2023/11/03 | Total Dissolved Solids | mg/L | 316 |
| UA | MW-304 | B | 2015/12/29 | pH (field) | SU | 8.0 |
| UA | MW-304 | B | 2016/03/21 | pH (field) | SU | 8.2 |
| UA | MW-304 | B | 2016/06/21 | pH (field) | SU | 8.1 |
| UA | MW-304 | B | 2016/09/19 | pH (field) | SU | 7.9 |
| UA | MW-304 | B | 2016/12/27 | pH (field) | SU | 7.9 |
| UA | MW-304 | B | 2017/03/16 | pH (field) | SU | 7.9 |
| UA | MW-304 | B | 2017/06/21 | pH (field) | SU | 7.9 |
| UA | MW-304 | B | 2017/07/28 | pH (field) | SU | 7.8 |
| UA | MW-304 | B | 2017/09/21 | pH (field) | SU | 7.9 |
| UA | MW-304 | B | 2017/11/28 | pH (field) | SU | 8.0 |
| UA | MW-304 | B | 2018/03/19 | pH (field) | SU | 7.9 |
| UA | MW-304 | B | 2018/06/27 | pH (field) | SU | 7.4 |
| UA | MW-304 | B | 2018/09/26 | pH (field) | SU | 7.9 |
| UA | MW-304 | B | 2018/12/19 | pH (field) | SU | 7.9 |
| UA | MW-304 | B | 2019/03/20 | pH (field) | SU | 7.7 |
| UA | MW-304 | B | 2019/06/25 | pH (field) | SU | 7.9 |
| UA | MW-304 | B | 2019/09/25 | pH (field) | SU | 7.9 |
| UA | MW-304 | B | 2019/12/19 | pH (field) | SU | 7.9 |
| UA | MW-304 | B | 2020/03/26 | pH (field) | SU | 7.9 |
| UA | MW-304 | B | 2020/06/23 | pH (field) | SU | 8.0 |
| UA | MW-304 | B | 2020/09/17 | pH (field) | SU | 8.0 |
| UA | MW-304 | B | 2020/12/16 | pH (field) | SU | 7.9 |
| UA | MW-304 | B | 2021/03/09 | pH (field) | SU | 7.9 |
| UA | MW-304 | B | 2021/06/21 | pH (field) | SU | 7.8 |
| UA | MW-304 | B | 2021/09/14 | pH (field) | SU | 7.7 |
| UA | MW-304 | B | 2021/12/14 | pH (field) | SU | 7.8 |
| UA | MW-304 | B | 2022/03/28 | pH (field) | SU | 7.8 |
| UA | MW-304 | B | 2022/06/14 | pH (field) | SU | 7.8 |
| UA | MW-304 | B | 2022/09/29 | pH (field) | SU | 7.7 |
| UA | MW-304 | B | 2022/10/26 | pH (field) | SU | 7.9 |
| UA | MW-304 | B | 2022/11/17 | pH (field) | SU | 7.9 |
| UA | MW-304 | B | 2022/12/05 | pH (field) | SU | 7.8 |
| UA | MW-304 | B | 2022/12/14 | pH (field) | SU | 7.8 |
| UA | MW-304 | B | 2023/01/11 | pH (field) | SU | 7.8 |
| UA | MW-304 | B | 2023/02/20 | pH (field) | SU | 7.8 |
| UA | MW-304 | B | 2023/03/15 | pH (field) | SU | 7.8 |
| UA | MW-304 | B | 2023/04/04 | pH (field) | SU | 7.8 |
| UA | MW-304 | B | 2023/05/22 | pH (field) | SU | 7.5 |
| UA | MW-304 | B | 2023/08/03 | pH (field) | SU | 7.9 |
| UA | MW-304 | B | 2023/11/01 | pH (field) | SU | 7.8 |
| UA | MW-304 | B | 2015/12/29 | Oxidation Reduction Potential | mV | 214 |
| UA | MW-304 | B | 2016/03/21 | Oxidation Reduction Potential | mV | 47.0 |
| UA | MW-304 | B | 2016/06/21 | Oxidation Reduction Potential | mV | -15.0 |

Attachment I. Site Groundwater Data

Geochemical Conceptual Site Model

Baldwin Fly Ash Pond System

Baldwin Power Plant

Baldwin, IL

| | | | | | | |
|----|--------|---|------------|-------------------------------|----|-------|
| UA | MW-304 | B | 2016/09/19 | Oxidation Reduction Potential | mV | -64.0 |
| UA | MW-304 | B | 2016/12/27 | Oxidation Reduction Potential | mV | -51.0 |
| UA | MW-304 | B | 2017/03/16 | Oxidation Reduction Potential | mV | -39.0 |
| UA | MW-304 | B | 2017/06/21 | Oxidation Reduction Potential | mV | -65.0 |
| UA | MW-304 | B | 2017/07/28 | Oxidation Reduction Potential | mV | -67.0 |
| UA | MW-304 | B | 2017/11/28 | Oxidation Reduction Potential | mV | 47.0 |
| UA | MW-304 | B | 2018/06/27 | Oxidation Reduction Potential | mV | 57.0 |
| UA | MW-304 | B | 2018/09/26 | Oxidation Reduction Potential | mV | -165 |
| UA | MW-304 | B | 2019/03/20 | Oxidation Reduction Potential | mV | <-300 |
| UA | MW-304 | B | 2019/09/25 | Oxidation Reduction Potential | mV | -15.0 |
| UA | MW-304 | B | 2020/03/26 | Oxidation Reduction Potential | mV | -14.0 |
| UA | MW-304 | B | 2020/09/17 | Oxidation Reduction Potential | mV | -48.0 |
| UA | MW-304 | B | 2021/03/09 | Oxidation Reduction Potential | mV | -6.00 |
| UA | MW-304 | B | 2021/06/21 | Oxidation Reduction Potential | mV | -78.0 |
| UA | MW-304 | B | 2021/09/14 | Oxidation Reduction Potential | mV | -24.0 |
| UA | MW-304 | B | 2021/12/14 | Oxidation Reduction Potential | mV | 56.0 |
| UA | MW-304 | B | 2022/03/28 | Oxidation Reduction Potential | mV | -21.0 |
| UA | MW-304 | B | 2022/06/14 | Oxidation Reduction Potential | mV | 105 |
| UA | MW-304 | B | 2022/09/29 | Oxidation Reduction Potential | mV | 86.0 |
| UA | MW-304 | B | 2022/10/26 | Oxidation Reduction Potential | mV | 30.9 |
| UA | MW-304 | B | 2022/11/17 | Oxidation Reduction Potential | mV | 160 |
| UA | MW-304 | B | 2022/12/05 | Oxidation Reduction Potential | mV | 48.0 |
| UA | MW-304 | B | 2022/12/14 | Oxidation Reduction Potential | mV | 191 |
| UA | MW-304 | B | 2023/01/11 | Oxidation Reduction Potential | mV | 52.0 |
| UA | MW-304 | B | 2023/02/20 | Oxidation Reduction Potential | mV | 53.2 |
| UA | MW-304 | B | 2023/03/15 | Oxidation Reduction Potential | mV | 31.9 |
| UA | MW-304 | B | 2023/04/04 | Oxidation Reduction Potential | mV | -95.0 |
| UA | MW-304 | B | 2023/05/22 | Oxidation Reduction Potential | mV | 116 |
| UA | MW-304 | B | 2023/08/03 | Oxidation Reduction Potential | mV | 78.0 |
| UA | MW-304 | B | 2023/11/01 | Oxidation Reduction Potential | mV | -56.0 |
| UA | MW-304 | B | 2015/12/29 | Eh | V | 0.41 |
| UA | MW-304 | B | 2016/03/21 | Eh | V | 0.24 |
| UA | MW-304 | B | 2016/06/21 | Eh | V | 0.18 |
| UA | MW-304 | B | 2016/09/19 | Eh | V | 0.12 |
| UA | MW-304 | B | 2016/12/27 | Eh | V | 0.15 |
| UA | MW-304 | B | 2017/03/16 | Eh | V | 0.16 |
| UA | MW-304 | B | 2017/06/21 | Eh | V | 0.12 |
| UA | MW-304 | B | 2017/07/28 | Eh | V | 0.13 |
| UA | MW-304 | B | 2017/11/28 | Eh | V | 0.24 |
| UA | MW-304 | B | 2018/06/27 | Eh | V | 0.25 |
| UA | MW-304 | B | 2018/09/26 | Eh | V | 0.027 |
| UA | MW-304 | B | 2019/03/20 | Eh | V | -0.10 |
| UA | MW-304 | B | 2019/09/25 | Eh | V | 0.18 |
| UA | MW-304 | B | 2020/03/26 | Eh | V | 0.18 |
| UA | MW-304 | B | 2020/09/17 | Eh | V | 0.15 |
| UA | MW-304 | B | 2021/03/09 | Eh | V | 0.19 |
| UA | MW-304 | B | 2021/06/21 | Eh | V | 0.12 |
| UA | MW-304 | B | 2021/09/14 | Eh | V | 0.17 |
| UA | MW-304 | B | 2021/12/14 | Eh | V | 0.25 |
| UA | MW-304 | B | 2022/03/28 | Eh | V | 0.18 |
| UA | MW-304 | B | 2022/06/14 | Eh | V | 0.30 |
| UA | MW-304 | B | 2022/09/29 | Eh | V | 0.28 |
| UA | MW-304 | B | 2022/10/26 | Eh | V | 0.23 |
| UA | MW-304 | B | 2022/11/17 | Eh | V | 0.36 |
| UA | MW-304 | B | 2022/12/05 | Eh | V | 0.24 |
| UA | MW-304 | B | 2022/12/14 | Eh | V | 0.39 |
| UA | MW-304 | B | 2023/01/11 | Eh | V | 0.25 |

Attachment I. Site Groundwater Data

Geochemical Conceptual Site Model

Baldwin Fly Ash Pond System

Baldwin Power Plant

Baldwin, IL

| | | | | | | |
|----|--------|---|------------|-------------------------|------------|--------|
| UA | MW-304 | B | 2023/02/20 | Eh | V | 0.25 |
| UA | MW-304 | B | 2023/03/15 | Eh | V | 0.23 |
| UA | MW-304 | B | 2023/04/04 | Eh | V | 0.100 |
| UA | MW-304 | B | 2023/05/22 | Eh | V | 0.31 |
| UA | MW-304 | B | 2023/08/03 | Eh | V | 0.27 |
| UA | MW-304 | B | 2023/11/01 | Eh | V | 0.14 |
| UA | MW-304 | B | 2017/07/28 | Alkalinity, bicarbonate | mg/L CaCO3 | 800 |
| UA | MW-304 | B | 2020/03/26 | Alkalinity, bicarbonate | mg/L CaCO3 | 802 |
| UA | MW-304 | B | 2020/09/17 | Alkalinity, bicarbonate | mg/L CaCO3 | 836 |
| UA | MW-304 | B | 2021/03/09 | Alkalinity, bicarbonate | mg/L CaCO3 | 784 |
| UA | MW-304 | B | 2021/09/14 | Alkalinity, bicarbonate | mg/L CaCO3 | 784 |
| UA | MW-304 | B | 2022/03/28 | Alkalinity, bicarbonate | mg/L CaCO3 | 843 |
| UA | MW-304 | B | 2022/09/29 | Alkalinity, bicarbonate | mg/L CaCO3 | 826 |
| UA | MW-304 | B | 2022/10/26 | Alkalinity, bicarbonate | mg/L CaCO3 | 801 |
| UA | MW-304 | B | 2022/11/17 | Alkalinity, bicarbonate | mg/L CaCO3 | 818 |
| UA | MW-304 | B | 2022/12/14 | Alkalinity, bicarbonate | mg/L CaCO3 | 833 |
| UA | MW-304 | B | 2023/01/11 | Alkalinity, bicarbonate | mg/L CaCO3 | 844 |
| UA | MW-304 | B | 2023/02/20 | Alkalinity, bicarbonate | mg/L CaCO3 | 854 |
| UA | MW-304 | B | 2023/03/15 | Alkalinity, bicarbonate | mg/L CaCO3 | 814 |
| UA | MW-304 | B | 2023/04/04 | Alkalinity, bicarbonate | mg/L CaCO3 | 853 |
| UA | MW-304 | B | 2023/05/22 | Alkalinity, bicarbonate | mg/L CaCO3 | 836 |
| UA | MW-304 | B | 2023/08/03 | Alkalinity, bicarbonate | mg/L CaCO3 | 838 |
| UA | MW-304 | B | 2023/11/01 | Alkalinity, bicarbonate | mg/L CaCO3 | 823 |
| UA | MW-304 | B | 2022/09/29 | Alkalinity, carbonate | mg/L CaCO3 | 10.0 |
| UA | MW-304 | B | 2022/10/26 | Alkalinity, carbonate | mg/L CaCO3 | 24.0 |
| UA | MW-304 | B | 2023/11/01 | Alkalinity, carbonate | mg/L CaCO3 | 32.0 |
| UA | MW-304 | B | 2015/12/29 | Barium, total | mg/L | 0.0191 |
| UA | MW-304 | B | 2016/03/21 | Barium, total | mg/L | 0.0195 |
| UA | MW-304 | B | 2016/06/21 | Barium, total | mg/L | 0.0199 |
| UA | MW-304 | B | 2016/09/19 | Barium, total | mg/L | 0.0238 |
| UA | MW-304 | B | 2016/12/27 | Barium, total | mg/L | 0.0199 |
| UA | MW-304 | B | 2017/03/16 | Barium, total | mg/L | 0.0171 |
| UA | MW-304 | B | 2017/06/21 | Barium, total | mg/L | 0.0206 |
| UA | MW-304 | B | 2017/07/28 | Barium, total | mg/L | 0.0193 |
| UA | MW-304 | B | 2018/06/27 | Barium, total | mg/L | 0.0210 |
| UA | MW-304 | B | 2018/09/26 | Barium, total | mg/L | 0.0229 |
| UA | MW-304 | B | 2019/03/20 | Barium, total | mg/L | 0.0214 |
| UA | MW-304 | B | 2019/09/25 | Barium, total | mg/L | 0.0211 |
| UA | MW-304 | B | 2020/03/26 | Barium, total | mg/L | 0.0212 |
| UA | MW-304 | B | 2020/09/17 | Barium, total | mg/L | 0.0192 |
| UA | MW-304 | B | 2021/03/09 | Barium, total | mg/L | 0.0200 |
| UA | MW-304 | B | 2021/09/14 | Barium, total | mg/L | 0.0189 |
| UA | MW-304 | B | 2022/03/28 | Barium, total | mg/L | 0.0194 |
| UA | MW-304 | B | 2022/09/29 | Barium, total | mg/L | 0.0183 |
| UA | MW-304 | B | 2022/10/26 | Barium, total | mg/L | 0.0186 |
| UA | MW-304 | B | 2022/11/17 | Barium, total | mg/L | 0.0209 |
| UA | MW-304 | B | 2022/12/14 | Barium, total | mg/L | 0.0191 |
| UA | MW-304 | B | 2023/01/11 | Barium, total | mg/L | 0.0173 |
| UA | MW-304 | B | 2023/02/20 | Barium, total | mg/L | 0.0216 |
| UA | MW-304 | B | 2023/03/15 | Barium, total | mg/L | 0.0206 |
| UA | MW-304 | B | 2023/04/04 | Barium, total | mg/L | 0.0324 |
| UA | MW-304 | B | 2023/05/22 | Barium, total | mg/L | 0.0199 |
| UA | MW-304 | B | 2023/08/03 | Barium, total | mg/L | 0.0201 |
| UA | MW-304 | B | 2023/11/01 | Barium, total | mg/L | 0.0199 |
| UA | MW-304 | B | 2015/12/29 | Boron, total | mg/L | 1.28 |
| UA | MW-304 | B | 2016/03/21 | Boron, total | mg/L | 1.27 |
| UA | MW-304 | B | 2016/06/21 | Boron, total | mg/L | 1.33 |

Attachment I. Site Groundwater Data

Geochemical Conceptual Site Model

Baldwin Fly Ash Pond System

Baldwin Power Plant

Baldwin, IL

| | | | | | | |
|----|--------|---|------------|-----------------|------|------|
| UA | MW-304 | B | 2016/09/19 | Boron, total | mg/L | 1.95 |
| UA | MW-304 | B | 2016/12/27 | Boron, total | mg/L | 1.51 |
| UA | MW-304 | B | 2017/03/16 | Boron, total | mg/L | 1.49 |
| UA | MW-304 | B | 2017/06/21 | Boron, total | mg/L | 1.55 |
| UA | MW-304 | B | 2017/07/28 | Boron, total | mg/L | 1.42 |
| UA | MW-304 | B | 2017/11/28 | Boron, total | mg/L | 1.45 |
| UA | MW-304 | B | 2018/06/27 | Boron, total | mg/L | 1.75 |
| UA | MW-304 | B | 2018/09/26 | Boron, total | mg/L | 1.74 |
| UA | MW-304 | B | 2019/03/20 | Boron, total | mg/L | 1.82 |
| UA | MW-304 | B | 2019/09/25 | Boron, total | mg/L | 1.84 |
| UA | MW-304 | B | 2020/03/26 | Boron, total | mg/L | 1.66 |
| UA | MW-304 | B | 2020/09/17 | Boron, total | mg/L | 1.89 |
| UA | MW-304 | B | 2021/03/09 | Boron, total | mg/L | 1.57 |
| UA | MW-304 | B | 2021/09/14 | Boron, total | mg/L | 1.61 |
| UA | MW-304 | B | 2022/03/28 | Boron, total | mg/L | 1.71 |
| UA | MW-304 | B | 2022/09/29 | Boron, total | mg/L | 1.75 |
| UA | MW-304 | B | 2022/10/26 | Boron, total | mg/L | 1.76 |
| UA | MW-304 | B | 2022/11/17 | Boron, total | mg/L | 1.91 |
| UA | MW-304 | B | 2022/12/14 | Boron, total | mg/L | 2.16 |
| UA | MW-304 | B | 2023/01/11 | Boron, total | mg/L | 1.68 |
| UA | MW-304 | B | 2023/02/20 | Boron, total | mg/L | 1.75 |
| UA | MW-304 | B | 2023/03/15 | Boron, total | mg/L | 1.89 |
| UA | MW-304 | B | 2023/04/04 | Boron, total | mg/L | 1.69 |
| UA | MW-304 | B | 2023/05/22 | Boron, total | mg/L | 1.68 |
| UA | MW-304 | B | 2023/08/03 | Boron, total | mg/L | 1.61 |
| UA | MW-304 | B | 2023/11/01 | Boron, total | mg/L | 1.67 |
| UA | MW-304 | B | 2015/12/29 | Calcium, total | mg/L | 9.64 |
| UA | MW-304 | B | 2016/03/21 | Calcium, total | mg/L | 9.86 |
| UA | MW-304 | B | 2016/06/21 | Calcium, total | mg/L | 14.3 |
| UA | MW-304 | B | 2016/09/19 | Calcium, total | mg/L | 16.5 |
| UA | MW-304 | B | 2016/12/27 | Calcium, total | mg/L | 15.4 |
| UA | MW-304 | B | 2017/03/16 | Calcium, total | mg/L | 6.91 |
| UA | MW-304 | B | 2017/06/21 | Calcium, total | mg/L | 17.8 |
| UA | MW-304 | B | 2017/07/28 | Calcium, total | mg/L | 13.2 |
| UA | MW-304 | B | 2017/11/28 | Calcium, total | mg/L | 11.4 |
| UA | MW-304 | B | 2018/06/27 | Calcium, total | mg/L | 12.9 |
| UA | MW-304 | B | 2018/09/26 | Calcium, total | mg/L | 13.1 |
| UA | MW-304 | B | 2019/03/20 | Calcium, total | mg/L | 13.7 |
| UA | MW-304 | B | 2019/09/25 | Calcium, total | mg/L | 18.4 |
| UA | MW-304 | B | 2020/03/26 | Calcium, total | mg/L | 17.2 |
| UA | MW-304 | B | 2020/09/17 | Calcium, total | mg/L | 15.3 |
| UA | MW-304 | B | 2021/03/09 | Calcium, total | mg/L | 12.7 |
| UA | MW-304 | B | 2021/09/14 | Calcium, total | mg/L | 13.3 |
| UA | MW-304 | B | 2022/03/28 | Calcium, total | mg/L | 14.5 |
| UA | MW-304 | B | 2022/09/29 | Calcium, total | mg/L | 10.2 |
| UA | MW-304 | B | 2022/10/26 | Calcium, total | mg/L | 10.8 |
| UA | MW-304 | B | 2022/11/17 | Calcium, total | mg/L | 9.48 |
| UA | MW-304 | B | 2022/12/14 | Calcium, total | mg/L | 10.0 |
| UA | MW-304 | B | 2023/01/11 | Calcium, total | mg/L | 8.50 |
| UA | MW-304 | B | 2023/02/20 | Calcium, total | mg/L | 10.7 |
| UA | MW-304 | B | 2023/03/15 | Calcium, total | mg/L | 10.6 |
| UA | MW-304 | B | 2023/04/04 | Calcium, total | mg/L | 8.91 |
| UA | MW-304 | B | 2023/05/22 | Calcium, total | mg/L | 9.63 |
| UA | MW-304 | B | 2023/08/03 | Calcium, total | mg/L | 11.4 |
| UA | MW-304 | B | 2023/11/01 | Calcium, total | mg/L | 12.0 |
| UA | MW-304 | B | 2015/12/29 | Chloride, total | mg/L | 124 |
| UA | MW-304 | B | 2016/03/21 | Chloride, total | mg/L | 131 |

Attachment I. Site Groundwater Data

Geochemical Conceptual Site Model

Baldwin Fly Ash Pond System

Baldwin Power Plant

Baldwin, IL

| | | | | | | |
|----|--------|---|------------|------------------|------|---------|
| UA | MW-304 | B | 2016/06/21 | Chloride, total | mg/L | 140 |
| UA | MW-304 | B | 2016/09/19 | Chloride, total | mg/L | 138 |
| UA | MW-304 | B | 2016/12/27 | Chloride, total | mg/L | 141 |
| UA | MW-304 | B | 2017/03/16 | Chloride, total | mg/L | 144 |
| UA | MW-304 | B | 2017/06/21 | Chloride, total | mg/L | 152 |
| UA | MW-304 | B | 2017/07/28 | Chloride, total | mg/L | 155 |
| UA | MW-304 | B | 2017/11/28 | Chloride, total | mg/L | 138 |
| UA | MW-304 | B | 2018/06/27 | Chloride, total | mg/L | 151 |
| UA | MW-304 | B | 2018/09/26 | Chloride, total | mg/L | 151 |
| UA | MW-304 | B | 2019/03/20 | Chloride, total | mg/L | 148 |
| UA | MW-304 | B | 2019/09/25 | Chloride, total | mg/L | 152 |
| UA | MW-304 | B | 2020/03/26 | Chloride, total | mg/L | 153 |
| UA | MW-304 | B | 2020/09/17 | Chloride, total | mg/L | 161 |
| UA | MW-304 | B | 2021/03/09 | Chloride, total | mg/L | 159 |
| UA | MW-304 | B | 2021/09/14 | Chloride, total | mg/L | 168 |
| UA | MW-304 | B | 2022/03/28 | Chloride, total | mg/L | 161 |
| UA | MW-304 | B | 2022/09/29 | Chloride, total | mg/L | 174 |
| UA | MW-304 | B | 2022/10/26 | Chloride, total | mg/L | 175 |
| UA | MW-304 | B | 2022/11/17 | Chloride, total | mg/L | 175 |
| UA | MW-304 | B | 2022/12/14 | Chloride, total | mg/L | 181 |
| UA | MW-304 | B | 2023/01/11 | Chloride, total | mg/L | 185 |
| UA | MW-304 | B | 2023/02/20 | Chloride, total | mg/L | 186 |
| UA | MW-304 | B | 2023/03/15 | Chloride, total | mg/L | 173 |
| UA | MW-304 | B | 2023/04/04 | Chloride, total | mg/L | 168 |
| UA | MW-304 | B | 2023/05/22 | Chloride, total | mg/L | 162 |
| UA | MW-304 | B | 2023/08/03 | Chloride, total | mg/L | 160 |
| UA | MW-304 | B | 2023/11/01 | Chloride, total | mg/L | 166 |
| UA | MW-304 | B | 2017/03/16 | Iron, dissolved | mg/L | <0.007 |
| UA | MW-304 | B | 2017/06/21 | Iron, dissolved | mg/L | <0.007 |
| UA | MW-304 | B | 2017/09/21 | Iron, dissolved | mg/L | <0.007 |
| UA | MW-304 | B | 2017/11/28 | Iron, dissolved | mg/L | <0.007 |
| UA | MW-304 | B | 2018/03/19 | Iron, dissolved | mg/L | <0.007 |
| UA | MW-304 | B | 2018/06/27 | Iron, dissolved | mg/L | <0.02 |
| UA | MW-304 | B | 2018/09/26 | Iron, dissolved | mg/L | <0.02 |
| UA | MW-304 | B | 2018/12/19 | Iron, dissolved | mg/L | <0.02 |
| UA | MW-304 | B | 2019/03/20 | Iron, dissolved | mg/L | <0.02 |
| UA | MW-304 | B | 2019/06/25 | Iron, dissolved | mg/L | <0.02 |
| UA | MW-304 | B | 2019/09/25 | Iron, dissolved | mg/L | <0.02 |
| UA | MW-304 | B | 2019/12/19 | Iron, dissolved | mg/L | <0.02 |
| UA | MW-304 | B | 2020/03/26 | Iron, dissolved | mg/L | <0.02 |
| UA | MW-304 | B | 2020/06/23 | Iron, dissolved | mg/L | <0.02 |
| UA | MW-304 | B | 2020/09/17 | Iron, dissolved | mg/L | <0.02 |
| UA | MW-304 | B | 2020/12/16 | Iron, dissolved | mg/L | <0.02 |
| UA | MW-304 | B | 2021/03/09 | Iron, dissolved | mg/L | <0.02 |
| UA | MW-304 | B | 2021/06/21 | Iron, dissolved | mg/L | <0.02 |
| UA | MW-304 | B | 2021/09/14 | Iron, dissolved | mg/L | <0.02 |
| UA | MW-304 | B | 2021/12/14 | Iron, dissolved | mg/L | <0.02 |
| UA | MW-304 | B | 2022/03/28 | Iron, dissolved | mg/L | <0.0115 |
| UA | MW-304 | B | 2022/06/14 | Iron, dissolved | mg/L | <0.02 |
| UA | MW-304 | B | 2022/09/29 | Iron, dissolved | mg/L | <0.0115 |
| UA | MW-304 | B | 2022/12/05 | Iron, dissolved | mg/L | <0.0115 |
| UA | MW-304 | B | 2023/03/15 | Iron, dissolved | mg/L | <0.0115 |
| UA | MW-304 | B | 2023/05/22 | Iron, dissolved | mg/L | <0.02 |
| UA | MW-304 | B | 2023/08/03 | Iron, dissolved | mg/L | <0.0115 |
| UA | MW-304 | B | 2023/11/01 | Iron, dissolved | mg/L | <0.0115 |
| UA | MW-304 | B | 2017/07/28 | Magnesium, total | mg/L | 5.33 |
| UA | MW-304 | B | 2020/03/26 | Magnesium, total | mg/L | 7.14 |

Attachment I. Site Groundwater Data

Geochemical Conceptual Site Model

Baldwin Fly Ash Pond System

Baldwin Power Plant

Baldwin, IL

| | | | | | | |
|----|--------|---|------------|----------------------|------|---------|
| UA | MW-304 | B | 2020/09/17 | Magnesium, total | mg/L | 6.18 |
| UA | MW-304 | B | 2021/03/09 | Magnesium, total | mg/L | 5.62 |
| UA | MW-304 | B | 2021/09/14 | Magnesium, total | mg/L | 5.79 |
| UA | MW-304 | B | 2022/03/28 | Magnesium, total | mg/L | 6.11 |
| UA | MW-304 | B | 2022/09/29 | Magnesium, total | mg/L | 4.42 |
| UA | MW-304 | B | 2022/10/26 | Magnesium, total | mg/L | 4.74 |
| UA | MW-304 | B | 2022/11/17 | Magnesium, total | mg/L | 4.29 |
| UA | MW-304 | B | 2022/12/14 | Magnesium, total | mg/L | 4.23 |
| UA | MW-304 | B | 2023/01/11 | Magnesium, total | mg/L | 3.84 |
| UA | MW-304 | B | 2023/02/20 | Magnesium, total | mg/L | 4.39 |
| UA | MW-304 | B | 2023/03/15 | Magnesium, total | mg/L | 4.47 |
| UA | MW-304 | B | 2023/04/04 | Magnesium, total | mg/L | 3.90 |
| UA | MW-304 | B | 2023/05/22 | Magnesium, total | mg/L | 4.36 |
| UA | MW-304 | B | 2023/08/03 | Magnesium, total | mg/L | 4.76 |
| UA | MW-304 | B | 2023/11/01 | Magnesium, total | mg/L | 5.02 |
| UA | MW-304 | B | 2017/03/16 | Manganese, dissolved | mg/L | <0.0005 |
| UA | MW-304 | B | 2017/06/21 | Manganese, dissolved | mg/L | <0.0005 |
| UA | MW-304 | B | 2017/09/21 | Manganese, dissolved | mg/L | <0.0005 |
| UA | MW-304 | B | 2017/11/28 | Manganese, dissolved | mg/L | <0.0005 |
| UA | MW-304 | B | 2018/03/19 | Manganese, dissolved | mg/L | <0.0005 |
| UA | MW-304 | B | 2018/06/27 | Manganese, dissolved | mg/L | <0.0025 |
| UA | MW-304 | B | 2018/09/26 | Manganese, dissolved | mg/L | <0.0025 |
| UA | MW-304 | B | 2018/12/19 | Manganese, dissolved | mg/L | <0.0025 |
| UA | MW-304 | B | 2019/03/20 | Manganese, dissolved | mg/L | <0.0025 |
| UA | MW-304 | B | 2019/06/25 | Manganese, dissolved | mg/L | <0.0025 |
| UA | MW-304 | B | 2019/09/25 | Manganese, dissolved | mg/L | <0.0025 |
| UA | MW-304 | B | 2019/12/19 | Manganese, dissolved | mg/L | <0.0025 |
| UA | MW-304 | B | 2020/03/26 | Manganese, dissolved | mg/L | <0.0025 |
| UA | MW-304 | B | 2020/06/23 | Manganese, dissolved | mg/L | <0.0025 |
| UA | MW-304 | B | 2020/09/17 | Manganese, dissolved | mg/L | <0.0025 |
| UA | MW-304 | B | 2020/12/16 | Manganese, dissolved | mg/L | <0.0025 |
| UA | MW-304 | B | 2021/03/09 | Manganese, dissolved | mg/L | <0.0025 |
| UA | MW-304 | B | 2021/06/21 | Manganese, dissolved | mg/L | <0.0025 |
| UA | MW-304 | B | 2021/09/14 | Manganese, dissolved | mg/L | <0.0025 |
| UA | MW-304 | B | 2021/12/14 | Manganese, dissolved | mg/L | <0.0025 |
| UA | MW-304 | B | 2022/03/28 | Manganese, dissolved | mg/L | 0.00290 |
| UA | MW-304 | B | 2022/06/14 | Manganese, dissolved | mg/L | <0.0025 |
| UA | MW-304 | B | 2022/09/29 | Manganese, dissolved | mg/L | 0.00130 |
| UA | MW-304 | B | 2022/12/05 | Manganese, dissolved | mg/L | 0.00230 |
| UA | MW-304 | B | 2023/03/15 | Manganese, dissolved | mg/L | 0.00140 |
| UA | MW-304 | B | 2023/05/22 | Manganese, dissolved | mg/L | <0.0025 |
| UA | MW-304 | B | 2023/08/03 | Manganese, dissolved | mg/L | 0.00140 |
| UA | MW-304 | B | 2023/11/01 | Manganese, dissolved | mg/L | 0.00200 |
| UA | MW-304 | B | 2023/05/22 | Phosphate, dissolved | mg/L | 0.0520 |
| UA | MW-304 | B | 2023/08/03 | Phosphate, dissolved | mg/L | 0.0310 |
| UA | MW-304 | B | 2017/07/28 | Potassium, total | mg/L | 2.18 |
| UA | MW-304 | B | 2020/03/26 | Potassium, total | mg/L | 2.36 |
| UA | MW-304 | B | 2020/09/17 | Potassium, total | mg/L | 2.48 |
| UA | MW-304 | B | 2021/03/09 | Potassium, total | mg/L | 2.12 |
| UA | MW-304 | B | 2021/09/14 | Potassium, total | mg/L | 2.36 |
| UA | MW-304 | B | 2022/03/28 | Potassium, total | mg/L | 2.34 |
| UA | MW-304 | B | 2022/09/29 | Potassium, total | mg/L | 2.20 |
| UA | MW-304 | B | 2022/10/26 | Potassium, total | mg/L | 2.15 |
| UA | MW-304 | B | 2022/11/17 | Potassium, total | mg/L | 1.98 |
| UA | MW-304 | B | 2022/12/14 | Potassium, total | mg/L | 2.05 |
| UA | MW-304 | B | 2023/01/11 | Potassium, total | mg/L | 2.08 |
| UA | MW-304 | B | 2023/02/20 | Potassium, total | mg/L | 2.33 |

Attachment I. Site Groundwater Data

Geochemical Conceptual Site Model

Baldwin Fly Ash Pond System

Baldwin Power Plant

Baldwin, IL

| | | | | | | |
|----|--------|---|------------|-----------------------|-----------|------|
| UA | MW-304 | B | 2023/03/15 | Potassium, total | mg/L | 2.10 |
| UA | MW-304 | B | 2023/04/04 | Potassium, total | mg/L | 2.40 |
| UA | MW-304 | B | 2023/05/22 | Potassium, total | mg/L | 2.41 |
| UA | MW-304 | B | 2023/08/03 | Potassium, total | mg/L | 2.31 |
| UA | MW-304 | B | 2023/11/01 | Potassium, total | mg/L | 2.26 |
| UA | MW-304 | B | 2023/05/22 | Silicon, dissolved | mg/L | 3.85 |
| UA | MW-304 | B | 2023/08/03 | Silicon, dissolved | mg/L | 3.55 |
| UA | MW-304 | B | 2017/07/28 | Sodium, total | mg/L | 516 |
| UA | MW-304 | B | 2020/03/26 | Sodium, total | mg/L | 556 |
| UA | MW-304 | B | 2020/09/17 | Sodium, total | mg/L | 631 |
| UA | MW-304 | B | 2021/03/09 | Sodium, total | mg/L | 570 |
| UA | MW-304 | B | 2021/09/14 | Sodium, total | mg/L | 565 |
| UA | MW-304 | B | 2022/03/28 | Sodium, total | mg/L | 555 |
| UA | MW-304 | B | 2022/09/29 | Sodium, total | mg/L | 570 |
| UA | MW-304 | B | 2022/10/26 | Sodium, total | mg/L | 587 |
| UA | MW-304 | B | 2022/11/17 | Sodium, total | mg/L | 564 |
| UA | MW-304 | B | 2022/12/14 | Sodium, total | mg/L | 604 |
| UA | MW-304 | B | 2023/01/11 | Sodium, total | mg/L | 626 |
| UA | MW-304 | B | 2023/02/20 | Sodium, total | mg/L | 617 |
| UA | MW-304 | B | 2023/03/15 | Sodium, total | mg/L | 569 |
| UA | MW-304 | B | 2023/04/04 | Sodium, total | mg/L | 642 |
| UA | MW-304 | B | 2023/05/22 | Sodium, total | mg/L | 582 |
| UA | MW-304 | B | 2023/08/03 | Sodium, total | mg/L | 617 |
| UA | MW-304 | B | 2023/11/01 | Sodium, total | mg/L | 629 |
| UA | MW-304 | B | 2015/12/29 | Sulfate, total | mg/L | 157 |
| UA | MW-304 | B | 2016/03/21 | Sulfate, total | mg/L | 163 |
| UA | MW-304 | B | 2016/06/21 | Sulfate, total | mg/L | 200 |
| UA | MW-304 | B | 2016/09/19 | Sulfate, total | mg/L | 176 |
| UA | MW-304 | B | 2016/12/27 | Sulfate, total | mg/L | 177 |
| UA | MW-304 | B | 2017/03/16 | Sulfate, total | mg/L | 166 |
| UA | MW-304 | B | 2017/06/21 | Sulfate, total | mg/L | 177 |
| UA | MW-304 | B | 2017/07/28 | Sulfate, total | mg/L | 187 |
| UA | MW-304 | B | 2017/11/28 | Sulfate, total | mg/L | 178 |
| UA | MW-304 | B | 2018/06/27 | Sulfate, total | mg/L | 208 |
| UA | MW-304 | B | 2018/09/26 | Sulfate, total | mg/L | 201 |
| UA | MW-304 | B | 2019/03/20 | Sulfate, total | mg/L | 177 |
| UA | MW-304 | B | 2019/09/25 | Sulfate, total | mg/L | 169 |
| UA | MW-304 | B | 2020/03/26 | Sulfate, total | mg/L | 177 |
| UA | MW-304 | B | 2020/09/17 | Sulfate, total | mg/L | 196 |
| UA | MW-304 | B | 2021/03/09 | Sulfate, total | mg/L | 194 |
| UA | MW-304 | B | 2021/09/14 | Sulfate, total | mg/L | 231 |
| UA | MW-304 | B | 2022/03/28 | Sulfate, total | mg/L | 198 |
| UA | MW-304 | B | 2022/09/29 | Sulfate, total | mg/L | 199 |
| UA | MW-304 | B | 2022/10/26 | Sulfate, total | mg/L | 193 |
| UA | MW-304 | B | 2022/11/17 | Sulfate, total | mg/L | 218 |
| UA | MW-304 | B | 2022/12/14 | Sulfate, total | mg/L | 216 |
| UA | MW-304 | B | 2023/01/11 | Sulfate, total | mg/L | 209 |
| UA | MW-304 | B | 2023/02/20 | Sulfate, total | mg/L | 228 |
| UA | MW-304 | B | 2023/03/15 | Sulfate, total | mg/L | 208 |
| UA | MW-304 | B | 2023/04/04 | Sulfate, total | mg/L | 210 |
| UA | MW-304 | B | 2023/05/22 | Sulfate, total | mg/L | 208 |
| UA | MW-304 | B | 2023/08/03 | Sulfate, total | mg/L | 188 |
| UA | MW-304 | B | 2023/11/01 | Sulfate, total | mg/L | 191 |
| UA | MW-304 | B | 2015/12/29 | Temperature (Celsius) | degrees C | 14.8 |
| UA | MW-304 | B | 2016/03/21 | Temperature (Celsius) | degrees C | 15.6 |
| UA | MW-304 | B | 2016/06/21 | Temperature (Celsius) | degrees C | 17.9 |
| UA | MW-304 | B | 2016/09/19 | Temperature (Celsius) | degrees C | 25.2 |

Attachment I. Site Groundwater Data

Geochemical Conceptual Site Model

Baldwin Fly Ash Pond System

Baldwin Power Plant

Baldwin, IL

| | | | | | | |
|----|--------|---|------------|------------------------|-----------|-------|
| UA | MW-304 | B | 2016/12/27 | Temperature (Celsius) | degrees C | 13.4 |
| UA | MW-304 | B | 2017/03/16 | Temperature (Celsius) | degrees C | 12.5 |
| UA | MW-304 | B | 2017/06/21 | Temperature (Celsius) | degrees C | 23.9 |
| UA | MW-304 | B | 2017/07/28 | Temperature (Celsius) | degrees C | 19.7 |
| UA | MW-304 | B | 2017/09/21 | Temperature (Celsius) | degrees C | 16.8 |
| UA | MW-304 | B | 2017/11/28 | Temperature (Celsius) | degrees C | 15.9 |
| UA | MW-304 | B | 2018/03/19 | Temperature (Celsius) | degrees C | 14.6 |
| UA | MW-304 | B | 2018/06/27 | Temperature (Celsius) | degrees C | 20.5 |
| UA | MW-304 | B | 2018/09/26 | Temperature (Celsius) | degrees C | 20.3 |
| UA | MW-304 | B | 2018/12/19 | Temperature (Celsius) | degrees C | 14.4 |
| UA | MW-304 | B | 2019/03/20 | Temperature (Celsius) | degrees C | 13.4 |
| UA | MW-304 | B | 2019/06/25 | Temperature (Celsius) | degrees C | 16.5 |
| UA | MW-304 | B | 2019/09/25 | Temperature (Celsius) | degrees C | 17.6 |
| UA | MW-304 | B | 2019/12/19 | Temperature (Celsius) | degrees C | 13.6 |
| UA | MW-304 | B | 2020/03/26 | Temperature (Celsius) | degrees C | 14.0 |
| UA | MW-304 | B | 2020/06/23 | Temperature (Celsius) | degrees C | 15.5 |
| UA | MW-304 | B | 2020/09/17 | Temperature (Celsius) | degrees C | 16.5 |
| UA | MW-304 | B | 2020/12/16 | Temperature (Celsius) | degrees C | 13.9 |
| UA | MW-304 | B | 2021/03/09 | Temperature (Celsius) | degrees C | 15.2 |
| UA | MW-304 | B | 2021/06/21 | Temperature (Celsius) | degrees C | 16.2 |
| UA | MW-304 | B | 2021/09/14 | Temperature (Celsius) | degrees C | 17.2 |
| UA | MW-304 | B | 2021/12/14 | Temperature (Celsius) | degrees C | 15.0 |
| UA | MW-304 | B | 2022/03/28 | Temperature (Celsius) | degrees C | 13.4 |
| UA | MW-304 | B | 2022/06/14 | Temperature (Celsius) | degrees C | 18.3 |
| UA | MW-304 | B | 2022/09/29 | Temperature (Celsius) | degrees C | 16.5 |
| UA | MW-304 | B | 2022/10/26 | Temperature (Celsius) | degrees C | 16.8 |
| UA | MW-304 | B | 2022/11/17 | Temperature (Celsius) | degrees C | 15.4 |
| UA | MW-304 | B | 2022/12/05 | Temperature (Celsius) | degrees C | 14.5 |
| UA | MW-304 | B | 2022/12/14 | Temperature (Celsius) | degrees C | 15.4 |
| UA | MW-304 | B | 2023/01/11 | Temperature (Celsius) | degrees C | 15.5 |
| UA | MW-304 | B | 2023/02/20 | Temperature (Celsius) | degrees C | 14.4 |
| UA | MW-304 | B | 2023/03/15 | Temperature (Celsius) | degrees C | 13.2 |
| UA | MW-304 | B | 2023/04/04 | Temperature (Celsius) | degrees C | 15.8 |
| UA | MW-304 | B | 2023/05/22 | Temperature (Celsius) | degrees C | 15.2 |
| UA | MW-304 | B | 2023/08/03 | Temperature (Celsius) | degrees C | 16.2 |
| UA | MW-304 | B | 2023/11/01 | Temperature (Celsius) | degrees C | 15.3 |
| UA | MW-304 | B | 2015/12/29 | Total Dissolved Solids | mg/L | 1,090 |
| UA | MW-304 | B | 2016/03/21 | Total Dissolved Solids | mg/L | 1,200 |
| UA | MW-304 | B | 2016/06/21 | Total Dissolved Solids | mg/L | 1,220 |
| UA | MW-304 | B | 2016/09/19 | Total Dissolved Solids | mg/L | 1,220 |
| UA | MW-304 | B | 2016/12/27 | Total Dissolved Solids | mg/L | 1,230 |
| UA | MW-304 | B | 2017/03/16 | Total Dissolved Solids | mg/L | 1,280 |
| UA | MW-304 | B | 2017/06/21 | Total Dissolved Solids | mg/L | 1,360 |
| UA | MW-304 | B | 2017/07/28 | Total Dissolved Solids | mg/L | 1,330 |
| UA | MW-304 | B | 2017/09/21 | Total Dissolved Solids | mg/L | 1,350 |
| UA | MW-304 | B | 2017/11/28 | Total Dissolved Solids | mg/L | 1,330 |
| UA | MW-304 | B | 2018/03/19 | Total Dissolved Solids | mg/L | 1,360 |
| UA | MW-304 | B | 2018/06/27 | Total Dissolved Solids | mg/L | 1,360 |
| UA | MW-304 | B | 2018/09/26 | Total Dissolved Solids | mg/L | 1,420 |
| UA | MW-304 | B | 2018/12/19 | Total Dissolved Solids | mg/L | 1,440 |
| UA | MW-304 | B | 2019/03/20 | Total Dissolved Solids | mg/L | 1,390 |
| UA | MW-304 | B | 2019/06/25 | Total Dissolved Solids | mg/L | 1,420 |
| UA | MW-304 | B | 2019/09/25 | Total Dissolved Solids | mg/L | 1,350 |
| UA | MW-304 | B | 2019/12/19 | Total Dissolved Solids | mg/L | 1,450 |
| UA | MW-304 | B | 2020/03/26 | Total Dissolved Solids | mg/L | 1,320 |
| UA | MW-304 | B | 2020/06/23 | Total Dissolved Solids | mg/L | 1,410 |
| UA | MW-304 | B | 2020/09/17 | Total Dissolved Solids | mg/L | 1,320 |

Attachment I. Site Groundwater Data

Geochemical Conceptual Site Model

Baldwin Fly Ash Pond System

Baldwin Power Plant

Baldwin, IL

| | | | | | | |
|----|--------|---|------------|-------------------------------|------------|--------|
| UA | MW-304 | B | 2020/12/16 | Total Dissolved Solids | mg/L | 1,440 |
| UA | MW-304 | B | 2021/03/09 | Total Dissolved Solids | mg/L | 1,350 |
| UA | MW-304 | B | 2021/06/21 | Total Dissolved Solids | mg/L | 1,440 |
| UA | MW-304 | B | 2021/09/14 | Total Dissolved Solids | mg/L | 1,290 |
| UA | MW-304 | B | 2021/12/14 | Total Dissolved Solids | mg/L | 1,400 |
| UA | MW-304 | B | 2022/03/28 | Total Dissolved Solids | mg/L | 1,410 |
| UA | MW-304 | B | 2022/06/14 | Total Dissolved Solids | mg/L | 1,430 |
| UA | MW-304 | B | 2022/09/29 | Total Dissolved Solids | mg/L | 1,470 |
| UA | MW-304 | B | 2022/10/26 | Total Dissolved Solids | mg/L | 1,450 |
| UA | MW-304 | B | 2022/11/17 | Total Dissolved Solids | mg/L | 1,490 |
| UA | MW-304 | B | 2022/12/05 | Total Dissolved Solids | mg/L | 1,480 |
| UA | MW-304 | B | 2022/12/14 | Total Dissolved Solids | mg/L | 1,300 |
| UA | MW-304 | B | 2023/01/11 | Total Dissolved Solids | mg/L | 1,450 |
| UA | MW-304 | B | 2023/02/20 | Total Dissolved Solids | mg/L | 1,470 |
| UA | MW-304 | B | 2023/03/15 | Total Dissolved Solids | mg/L | 1,230 |
| UA | MW-304 | B | 2023/04/04 | Total Dissolved Solids | mg/L | 1,460 |
| UA | MW-304 | B | 2023/05/22 | Total Dissolved Solids | mg/L | 1,420 |
| UA | MW-304 | B | 2023/08/03 | Total Dissolved Solids | mg/L | 1,380 |
| UA | MW-304 | B | 2023/11/01 | Total Dissolved Solids | mg/L | 1,470 |
| UA | MW-358 | B | 2022/10/27 | pH (field) | SU | 7.9 |
| UA | MW-358 | B | 2022/11/17 | pH (field) | SU | 7.8 |
| UA | MW-358 | B | 2022/12/13 | pH (field) | SU | 8.4 |
| UA | MW-358 | B | 2023/01/11 | pH (field) | SU | 7.6 |
| UA | MW-358 | B | 2023/02/20 | pH (field) | SU | 8.4 |
| UA | MW-358 | B | 2023/03/13 | pH (field) | SU | 7.7 |
| UA | MW-358 | B | 2023/04/04 | pH (field) | SU | 7.7 |
| UA | MW-358 | B | 2023/05/19 | pH (field) | SU | 7.6 |
| UA | MW-358 | B | 2023/08/07 | pH (field) | SU | 8.0 |
| UA | MW-358 | B | 2023/11/01 | pH (field) | SU | 7.9 |
| UA | MW-358 | B | 2022/10/27 | Oxidation Reduction Potential | mV | -167 |
| UA | MW-358 | B | 2022/11/17 | Oxidation Reduction Potential | mV | 200 |
| UA | MW-358 | B | 2022/12/13 | Oxidation Reduction Potential | mV | -266 |
| UA | MW-358 | B | 2023/01/11 | Oxidation Reduction Potential | mV | 180 |
| UA | MW-358 | B | 2023/02/20 | Oxidation Reduction Potential | mV | -132 |
| UA | MW-358 | B | 2023/03/13 | Oxidation Reduction Potential | mV | -188 |
| UA | MW-358 | B | 2023/04/04 | Oxidation Reduction Potential | mV | -207 |
| UA | MW-358 | B | 2023/05/19 | Oxidation Reduction Potential | mV | -91.0 |
| UA | MW-358 | B | 2023/08/07 | Oxidation Reduction Potential | mV | -42.0 |
| UA | MW-358 | B | 2023/11/01 | Oxidation Reduction Potential | mV | -162 |
| UA | MW-358 | B | 2022/10/27 | Eh | V | 0.029 |
| UA | MW-358 | B | 2022/11/17 | Eh | V | 0.40 |
| UA | MW-358 | B | 2022/12/13 | Eh | V | -0.068 |
| UA | MW-358 | B | 2023/01/11 | Eh | V | 0.38 |
| UA | MW-358 | B | 2023/02/20 | Eh | V | 0.064 |
| UA | MW-358 | B | 2023/03/13 | Eh | V | 0.0094 |
| UA | MW-358 | B | 2023/04/04 | Eh | V | -0.013 |
| UA | MW-358 | B | 2023/05/19 | Eh | V | 0.10 |
| UA | MW-358 | B | 2023/08/07 | Eh | V | 0.15 |
| UA | MW-358 | B | 2023/11/01 | Eh | V | 0.034 |
| UA | MW-358 | B | 2022/10/27 | Alkalinity, bicarbonate | mg/L CaCO3 | 601 |
| UA | MW-358 | B | 2022/11/17 | Alkalinity, bicarbonate | mg/L CaCO3 | 758 |
| UA | MW-358 | B | 2022/12/13 | Alkalinity, bicarbonate | mg/L CaCO3 | 859 |
| UA | MW-358 | B | 2023/01/11 | Alkalinity, bicarbonate | mg/L CaCO3 | 841 |
| UA | MW-358 | B | 2023/02/20 | Alkalinity, bicarbonate | mg/L CaCO3 | 847 |
| UA | MW-358 | B | 2023/03/13 | Alkalinity, bicarbonate | mg/L CaCO3 | 856 |
| UA | MW-358 | B | 2023/04/04 | Alkalinity, bicarbonate | mg/L CaCO3 | 851 |
| UA | MW-358 | B | 2023/05/19 | Alkalinity, bicarbonate | mg/L CaCO3 | 817 |

Attachment I. Site Groundwater Data

Geochemical Conceptual Site Model

Baldwin Fly Ash Pond System

Baldwin Power Plant

Baldwin, IL

| | | | | | | |
|----|--------|---|------------|-------------------------|------------|--------|
| UA | MW-358 | B | 2023/08/07 | Alkalinity, bicarbonate | mg/L CaCO3 | 833 |
| UA | MW-358 | B | 2023/11/01 | Alkalinity, bicarbonate | mg/L CaCO3 | 829 |
| UA | MW-358 | B | 2022/10/27 | Alkalinity, carbonate | mg/L CaCO3 | 32.0 |
| UA | MW-358 | B | 2023/05/19 | Alkalinity, carbonate | mg/L CaCO3 | 18.0 |
| UA | MW-358 | B | 2023/08/07 | Alkalinity, carbonate | mg/L CaCO3 | 10.0 |
| UA | MW-358 | B | 2023/11/01 | Alkalinity, carbonate | mg/L CaCO3 | 11.0 |
| UA | MW-358 | B | 2022/10/27 | Barium, total | mg/L | 0.0933 |
| UA | MW-358 | B | 2022/11/17 | Barium, total | mg/L | 0.172 |
| UA | MW-358 | B | 2022/12/13 | Barium, total | mg/L | 0.168 |
| UA | MW-358 | B | 2023/01/11 | Barium, total | mg/L | 0.165 |
| UA | MW-358 | B | 2023/02/20 | Barium, total | mg/L | 0.201 |
| UA | MW-358 | B | 2023/03/13 | Barium, total | mg/L | 0.166 |
| UA | MW-358 | B | 2023/04/04 | Barium, total | mg/L | 0.261 |
| UA | MW-358 | B | 2023/05/19 | Barium, total | mg/L | 0.192 |
| UA | MW-358 | B | 2023/08/07 | Barium, total | mg/L | 0.235 |
| UA | MW-358 | B | 2023/11/01 | Barium, total | mg/L | 0.162 |
| UA | MW-358 | B | 2022/10/27 | Boron, total | mg/L | 1.10 |
| UA | MW-358 | B | 2022/11/17 | Boron, total | mg/L | 1.25 |
| UA | MW-358 | B | 2022/12/13 | Boron, total | mg/L | 1.67 |
| UA | MW-358 | B | 2023/01/11 | Boron, total | mg/L | 1.38 |
| UA | MW-358 | B | 2023/02/20 | Boron, total | mg/L | 1.42 |
| UA | MW-358 | B | 2023/03/13 | Boron, total | mg/L | 1.51 |
| UA | MW-358 | B | 2023/04/04 | Boron, total | mg/L | 1.45 |
| UA | MW-358 | B | 2023/05/19 | Boron, total | mg/L | 1.60 |
| UA | MW-358 | B | 2023/08/07 | Boron, total | mg/L | 1.60 |
| UA | MW-358 | B | 2023/11/01 | Boron, total | mg/L | 1.38 |
| UA | MW-358 | B | 2022/10/27 | Calcium, total | mg/L | 12.8 |
| UA | MW-358 | B | 2022/11/17 | Calcium, total | mg/L | 15.8 |
| UA | MW-358 | B | 2022/12/13 | Calcium, total | mg/L | 18.6 |
| UA | MW-358 | B | 2023/01/11 | Calcium, total | mg/L | 14.0 |
| UA | MW-358 | B | 2023/02/20 | Calcium, total | mg/L | 13.2 |
| UA | MW-358 | B | 2023/03/13 | Calcium, total | mg/L | 10.9 |
| UA | MW-358 | B | 2023/04/04 | Calcium, total | mg/L | 11.4 |
| UA | MW-358 | B | 2023/05/19 | Calcium, total | mg/L | 12.5 |
| UA | MW-358 | B | 2023/08/07 | Calcium, total | mg/L | 9.87 |
| UA | MW-358 | B | 2023/11/01 | Calcium, total | mg/L | 11.3 |
| UA | MW-358 | B | 2022/10/27 | Chloride, total | mg/L | 688 |
| UA | MW-358 | B | 2022/11/17 | Chloride, total | mg/L | 992 |
| UA | MW-358 | B | 2022/12/13 | Chloride, total | mg/L | 1,120 |
| UA | MW-358 | B | 2023/01/11 | Chloride, total | mg/L | 1,200 |
| UA | MW-358 | B | 2023/02/20 | Chloride, total | mg/L | 1,330 |
| UA | MW-358 | B | 2023/03/13 | Chloride, total | mg/L | 1,340 |
| UA | MW-358 | B | 2023/04/04 | Chloride, total | mg/L | 1,370 |
| UA | MW-358 | B | 2023/05/19 | Chloride, total | mg/L | 1,300 |
| UA | MW-358 | B | 2023/08/07 | Chloride, total | mg/L | 1,290 |
| UA | MW-358 | B | 2023/11/01 | Chloride, total | mg/L | 1,310 |
| UA | MW-358 | B | 2023/05/19 | Iron, dissolved | mg/L | 0.242 |
| UA | MW-358 | B | 2023/08/07 | Iron, dissolved | mg/L | 0.221 |
| UA | MW-358 | B | 2022/10/27 | Magnesium, total | mg/L | 5.66 |
| UA | MW-358 | B | 2022/11/17 | Magnesium, total | mg/L | 7.53 |
| UA | MW-358 | B | 2022/12/13 | Magnesium, total | mg/L | 8.62 |
| UA | MW-358 | B | 2023/01/11 | Magnesium, total | mg/L | 6.96 |
| UA | MW-358 | B | 2023/02/20 | Magnesium, total | mg/L | 6.40 |
| UA | MW-358 | B | 2023/03/13 | Magnesium, total | mg/L | 5.64 |
| UA | MW-358 | B | 2023/04/04 | Magnesium, total | mg/L | 5.89 |
| UA | MW-358 | B | 2023/05/19 | Magnesium, total | mg/L | 6.07 |
| UA | MW-358 | B | 2023/08/07 | Magnesium, total | mg/L | 5.06 |

Attachment I. Site Groundwater Data

Geochemical Conceptual Site Model

Baldwin Fly Ash Pond System

Baldwin Power Plant

Baldwin, IL

| | | | | | | |
|----|--------|---|------------|------------------------|-----------|-------|
| UA | MW-358 | B | 2023/11/01 | Magnesium, total | mg/L | 5.80 |
| UA | MW-358 | B | 2023/05/19 | Manganese, dissolved | mg/L | 0.182 |
| UA | MW-358 | B | 2023/08/07 | Manganese, dissolved | mg/L | 0.160 |
| UA | MW-358 | B | 2023/05/19 | Phosphate, dissolved | mg/L | 0.390 |
| UA | MW-358 | B | 2023/08/07 | Phosphate, dissolved | mg/L | 0.252 |
| UA | MW-358 | B | 2022/10/27 | Potassium, total | mg/L | 8.56 |
| UA | MW-358 | B | 2022/11/17 | Potassium, total | mg/L | 7.33 |
| UA | MW-358 | B | 2022/12/13 | Potassium, total | mg/L | 6.51 |
| UA | MW-358 | B | 2023/01/11 | Potassium, total | mg/L | 5.58 |
| UA | MW-358 | B | 2023/02/20 | Potassium, total | mg/L | 5.25 |
| UA | MW-358 | B | 2023/03/13 | Potassium, total | mg/L | 4.05 |
| UA | MW-358 | B | 2023/04/04 | Potassium, total | mg/L | 5.19 |
| UA | MW-358 | B | 2023/05/19 | Potassium, total | mg/L | 4.48 |
| UA | MW-358 | B | 2023/08/07 | Potassium, total | mg/L | 4.20 |
| UA | MW-358 | B | 2023/11/01 | Potassium, total | mg/L | 3.90 |
| UA | MW-358 | B | 2023/05/19 | Silicon, dissolved | mg/L | 3.54 |
| UA | MW-358 | B | 2023/08/07 | Silicon, dissolved | mg/L | 3.56 |
| UA | MW-358 | B | 2022/10/27 | Sodium, total | mg/L | 802 |
| UA | MW-358 | B | 2022/11/17 | Sodium, total | mg/L | 991 |
| UA | MW-358 | B | 2022/12/13 | Sodium, total | mg/L | 1,100 |
| UA | MW-358 | B | 2023/01/11 | Sodium, total | mg/L | 1,250 |
| UA | MW-358 | B | 2023/02/20 | Sodium, total | mg/L | 1,390 |
| UA | MW-358 | B | 2023/03/13 | Sodium, total | mg/L | 1,190 |
| UA | MW-358 | B | 2023/04/04 | Sodium, total | mg/L | 1,330 |
| UA | MW-358 | B | 2023/05/19 | Sodium, total | mg/L | 1,260 |
| UA | MW-358 | B | 2023/08/07 | Sodium, total | mg/L | 1,260 |
| UA | MW-358 | B | 2023/11/01 | Sodium, total | mg/L | 1,320 |
| UA | MW-358 | B | 2022/10/27 | Sulfate, total | mg/L | 108 |
| UA | MW-358 | B | 2022/11/17 | Sulfate, total | mg/L | 101 |
| UA | MW-358 | B | 2022/12/13 | Sulfate, total | mg/L | 71.0 |
| UA | MW-358 | B | 2023/01/11 | Sulfate, total | mg/L | 34.0 |
| UA | MW-358 | B | 2023/02/20 | Sulfate, total | mg/L | 16.0 |
| UA | MW-358 | B | 2023/03/13 | Sulfate, total | mg/L | 8.00 |
| UA | MW-358 | B | 2023/04/04 | Sulfate, total | mg/L | <31 |
| UA | MW-358 | B | 2023/05/19 | Sulfate, total | mg/L | <12 |
| UA | MW-358 | B | 2023/08/07 | Sulfate, total | mg/L | 9.00 |
| UA | MW-358 | B | 2023/11/01 | Sulfate, total | mg/L | 11.0 |
| UA | MW-358 | B | 2022/10/27 | Temperature (Celsius) | degrees C | 14.5 |
| UA | MW-358 | B | 2022/11/17 | Temperature (Celsius) | degrees C | 13.3 |
| UA | MW-358 | B | 2022/12/13 | Temperature (Celsius) | degrees C | 11.6 |
| UA | MW-358 | B | 2023/01/11 | Temperature (Celsius) | degrees C | 14.9 |
| UA | MW-358 | B | 2023/02/20 | Temperature (Celsius) | degrees C | 14.0 |
| UA | MW-358 | B | 2023/03/13 | Temperature (Celsius) | degrees C | 12.2 |
| UA | MW-358 | B | 2023/04/04 | Temperature (Celsius) | degrees C | 16.7 |
| UA | MW-358 | B | 2023/05/19 | Temperature (Celsius) | degrees C | 18.2 |
| UA | MW-358 | B | 2023/08/07 | Temperature (Celsius) | degrees C | 16.1 |
| UA | MW-358 | B | 2023/11/01 | Temperature (Celsius) | degrees C | 14.6 |
| UA | MW-358 | B | 2022/10/27 | Total Dissolved Solids | mg/L | 1,990 |
| UA | MW-358 | B | 2022/11/17 | Total Dissolved Solids | mg/L | 2,620 |
| UA | MW-358 | B | 2022/12/13 | Total Dissolved Solids | mg/L | 3,260 |
| UA | MW-358 | B | 2023/01/11 | Total Dissolved Solids | mg/L | 2,690 |
| UA | MW-358 | B | 2023/02/20 | Total Dissolved Solids | mg/L | 3,080 |
| UA | MW-358 | B | 2023/03/13 | Total Dissolved Solids | mg/L | 2,880 |
| UA | MW-358 | B | 2023/04/04 | Total Dissolved Solids | mg/L | 2,990 |
| UA | MW-358 | B | 2023/05/19 | Total Dissolved Solids | mg/L | 3,040 |
| UA | MW-358 | B | 2023/08/07 | Total Dissolved Solids | mg/L | 3,160 |
| UA | MW-358 | B | 2023/11/01 | Total Dissolved Solids | mg/L | 3,140 |

Attachment I. Site Groundwater Data

Geochemical Conceptual Site Model

Baldwin Fly Ash Pond System

Baldwin Power Plant

Baldwin, IL

| | | | | | | |
|----|--------|---|------------|-------------------------------|----|--------|
| UA | MW-350 | C | 2013/09/16 | pH (field) | SU | 12.3 |
| UA | MW-350 | C | 2013/11/20 | pH (field) | SU | 11.8 |
| UA | MW-350 | C | 2014/02/19 | pH (field) | SU | 8.1 |
| UA | MW-350 | C | 2014/06/11 | pH (field) | SU | 12.4 |
| UA | MW-350 | C | 2015/03/25 | pH (field) | SU | 12.8 |
| UA | MW-350 | C | 2015/06/24 | pH (field) | SU | 12.5 |
| UA | MW-350 | C | 2015/09/25 | pH (field) | SU | 12.6 |
| UA | MW-350 | C | 2015/11/10 | pH (field) | SU | 12.2 |
| UA | MW-350 | C | 2016/03/22 | pH (field) | SU | 12.6 |
| UA | MW-350 | C | 2016/06/21 | pH (field) | SU | 12.2 |
| UA | MW-350 | C | 2016/09/29 | pH (field) | SU | 12.1 |
| UA | MW-350 | C | 2016/12/21 | pH (field) | SU | 11.9 |
| UA | MW-350 | C | 2017/03/16 | pH (field) | SU | 12.2 |
| UA | MW-350 | C | 2017/06/22 | pH (field) | SU | 11.7 |
| UA | MW-350 | C | 2017/09/21 | pH (field) | SU | 11.4 |
| UA | MW-350 | C | 2017/11/28 | pH (field) | SU | 11.7 |
| UA | MW-350 | C | 2018/03/19 | pH (field) | SU | 11.4 |
| UA | MW-350 | C | 2018/06/28 | pH (field) | SU | 11.2 |
| UA | MW-350 | C | 2018/09/26 | pH (field) | SU | 11.6 |
| UA | MW-350 | C | 2018/12/18 | pH (field) | SU | 11.7 |
| UA | MW-350 | C | 2019/03/20 | pH (field) | SU | 11.9 |
| UA | MW-350 | C | 2019/06/25 | pH (field) | SU | 11.9 |
| UA | MW-350 | C | 2019/09/26 | pH (field) | SU | 11.0 |
| UA | MW-350 | C | 2019/12/19 | pH (field) | SU | 10.9 |
| UA | MW-350 | C | 2020/03/26 | pH (field) | SU | 11.7 |
| UA | MW-350 | C | 2020/06/23 | pH (field) | SU | 11.4 |
| UA | MW-350 | C | 2020/09/16 | pH (field) | SU | 11.0 |
| UA | MW-350 | C | 2020/09/17 | pH (field) | SU | 10.7 |
| UA | MW-350 | C | 2020/12/17 | pH (field) | SU | 11.1 |
| UA | MW-350 | C | 2021/03/10 | pH (field) | SU | 11.0 |
| UA | MW-350 | C | 2021/07/19 | pH (field) | SU | 8.4 |
| UA | MW-350 | C | 2021/09/14 | pH (field) | SU | 8.0 |
| UA | MW-350 | C | 2021/12/14 | pH (field) | SU | 10.1 |
| UA | MW-350 | C | 2022/03/28 | pH (field) | SU | 11.6 |
| UA | MW-350 | C | 2022/06/14 | pH (field) | SU | 11.4 |
| UA | MW-350 | C | 2022/09/29 | pH (field) | SU | 11.6 |
| UA | MW-350 | C | 2022/12/06 | pH (field) | SU | 11.3 |
| UA | MW-350 | C | 2023/03/15 | pH (field) | SU | 11.5 |
| UA | MW-350 | C | 2023/05/18 | pH (field) | SU | 11.4 |
| UA | MW-350 | C | 2023/08/07 | pH (field) | SU | 11.5 |
| UA | MW-350 | C | 2023/11/03 | pH (field) | SU | 8.4 |
| UA | MW-350 | C | 2020/03/26 | Oxidation Reduction Potential | mV | -299 |
| UA | MW-350 | C | 2020/09/16 | Oxidation Reduction Potential | mV | -270 |
| UA | MW-350 | C | 2021/03/10 | Oxidation Reduction Potential | mV | <-300 |
| UA | MW-350 | C | 2021/07/19 | Oxidation Reduction Potential | mV | -250 |
| UA | MW-350 | C | 2021/09/14 | Oxidation Reduction Potential | mV | -253 |
| UA | MW-350 | C | 2021/12/14 | Oxidation Reduction Potential | mV | -204 |
| UA | MW-350 | C | 2022/03/28 | Oxidation Reduction Potential | mV | -254 |
| UA | MW-350 | C | 2022/06/14 | Oxidation Reduction Potential | mV | -7.00 |
| UA | MW-350 | C | 2022/09/29 | Oxidation Reduction Potential | mV | -21.0 |
| UA | MW-350 | C | 2022/12/06 | Oxidation Reduction Potential | mV | <-300 |
| UA | MW-350 | C | 2023/03/15 | Oxidation Reduction Potential | mV | -147 |
| UA | MW-350 | C | 2023/05/18 | Oxidation Reduction Potential | mV | -123 |
| UA | MW-350 | C | 2023/08/07 | Oxidation Reduction Potential | mV | -7.00 |
| UA | MW-350 | C | 2023/11/03 | Oxidation Reduction Potential | mV | -242 |
| UA | MW-350 | C | 2020/03/26 | Eh | V | -0.10 |
| UA | MW-350 | C | 2020/09/16 | Eh | V | -0.074 |

Attachment I. Site Groundwater Data

Geochemical Conceptual Site Model

Baldwin Fly Ash Pond System

Baldwin Power Plant

Baldwin, IL

| | | | | | | |
|----|--------|---|------------|-------------------------|------------|---------|
| UA | MW-350 | C | 2021/03/10 | Eh | V | -0.10 |
| UA | MW-350 | C | 2021/07/19 | Eh | V | -0.056 |
| UA | MW-350 | C | 2021/09/14 | Eh | V | -0.059 |
| UA | MW-350 | C | 2021/12/14 | Eh | V | -0.0086 |
| UA | MW-350 | C | 2022/03/28 | Eh | V | -0.057 |
| UA | MW-350 | C | 2022/06/14 | Eh | V | 0.19 |
| UA | MW-350 | C | 2022/09/29 | Eh | V | 0.18 |
| UA | MW-350 | C | 2022/12/06 | Eh | V | -0.10 |
| UA | MW-350 | C | 2023/03/15 | Eh | V | 0.050 |
| UA | MW-350 | C | 2023/05/18 | Eh | V | 0.073 |
| UA | MW-350 | C | 2023/08/07 | Eh | V | 0.19 |
| UA | MW-350 | C | 2023/11/03 | Eh | V | -0.046 |
| UA | MW-350 | C | 2021/09/14 | Alkalinity, bicarbonate | mg/L CaCO3 | 231 |
| UA | MW-350 | C | 2020/03/26 | Alkalinity, carbonate | mg/L CaCO3 | 62.0 |
| UA | MW-350 | C | 2020/09/16 | Alkalinity, carbonate | mg/L CaCO3 | 68.0 |
| UA | MW-350 | C | 2021/03/10 | Alkalinity, carbonate | mg/L CaCO3 | 78.0 |
| UA | MW-350 | C | 2022/03/28 | Alkalinity, carbonate | mg/L CaCO3 | 54.0 |
| UA | MW-350 | C | 2022/09/29 | Alkalinity, carbonate | mg/L CaCO3 | 56.0 |
| UA | MW-350 | C | 2023/03/15 | Alkalinity, carbonate | mg/L CaCO3 | 26.0 |
| UA | MW-350 | C | 2023/05/18 | Alkalinity, carbonate | mg/L CaCO3 | 55.0 |
| UA | MW-350 | C | 2023/08/07 | Alkalinity, carbonate | mg/L CaCO3 | 49.0 |
| UA | MW-350 | C | 2023/11/03 | Alkalinity, carbonate | mg/L CaCO3 | 92.0 |
| UA | MW-350 | C | 2020/03/26 | Barium, total | mg/L | 0.244 |
| UA | MW-350 | C | 2020/09/16 | Barium, total | mg/L | 0.165 |
| UA | MW-350 | C | 2021/03/10 | Barium, total | mg/L | 0.169 |
| UA | MW-350 | C | 2021/09/14 | Barium, total | mg/L | 0.179 |
| UA | MW-350 | C | 2022/03/28 | Barium, total | mg/L | 0.329 |
| UA | MW-350 | C | 2022/09/29 | Barium, total | mg/L | 0.296 |
| UA | MW-350 | C | 2023/03/15 | Barium, total | mg/L | 0.304 |
| UA | MW-350 | C | 2023/05/18 | Barium, total | mg/L | 0.327 |
| UA | MW-350 | C | 2023/08/07 | Barium, total | mg/L | 0.267 |
| UA | MW-350 | C | 2023/11/03 | Barium, total | mg/L | 0.201 |
| UA | MW-350 | C | 2013/09/16 | Boron, total | mg/L | 0.0200 |
| UA | MW-350 | C | 2020/03/26 | Boron, total | mg/L | 0.635 |
| UA | MW-350 | C | 2020/09/16 | Boron, total | mg/L | 0.541 |
| UA | MW-350 | C | 2021/03/10 | Boron, total | mg/L | 0.682 |
| UA | MW-350 | C | 2021/09/14 | Boron, total | mg/L | 0.622 |
| UA | MW-350 | C | 2022/03/28 | Boron, total | mg/L | 0.900 |
| UA | MW-350 | C | 2022/09/29 | Boron, total | mg/L | 0.669 |
| UA | MW-350 | C | 2023/03/15 | Boron, total | mg/L | 0.613 |
| UA | MW-350 | C | 2023/05/18 | Boron, total | mg/L | 0.560 |
| UA | MW-350 | C | 2023/08/07 | Boron, total | mg/L | 0.585 |
| UA | MW-350 | C | 2023/11/03 | Boron, total | mg/L | 0.538 |
| UA | MW-350 | C | 2020/03/26 | Calcium, total | mg/L | 52.9 |
| UA | MW-350 | C | 2020/09/16 | Calcium, total | mg/L | 16.6 |
| UA | MW-350 | C | 2021/03/10 | Calcium, total | mg/L | 20.9 |
| UA | MW-350 | C | 2021/09/14 | Calcium, total | mg/L | 25.1 |
| UA | MW-350 | C | 2022/03/28 | Calcium, total | mg/L | 124 |
| UA | MW-350 | C | 2022/09/29 | Calcium, total | mg/L | 72.0 |
| UA | MW-350 | C | 2023/03/15 | Calcium, total | mg/L | 81.0 |
| UA | MW-350 | C | 2023/05/18 | Calcium, total | mg/L | 84.0 |
| UA | MW-350 | C | 2023/08/07 | Calcium, total | mg/L | 39.6 |
| UA | MW-350 | C | 2023/11/03 | Calcium, total | mg/L | 49.0 |
| UA | MW-350 | C | 2013/09/16 | Chloride, total | mg/L | 33.0 |
| UA | MW-350 | C | 2020/03/26 | Chloride, total | mg/L | 52.0 |
| UA | MW-350 | C | 2020/09/16 | Chloride, total | mg/L | 48.0 |
| UA | MW-350 | C | 2021/03/10 | Chloride, total | mg/L | 43.0 |

Attachment I. Site Groundwater Data

Geochemical Conceptual Site Model

Baldwin Fly Ash Pond System

Baldwin Power Plant

Baldwin, IL

| | | | | | | |
|----|--------|---|------------|----------------------|------|---------|
| UA | MW-350 | C | 2021/09/14 | Chloride, total | mg/L | 29.0 |
| UA | MW-350 | C | 2022/03/28 | Chloride, total | mg/L | 58.0 |
| UA | MW-350 | C | 2022/09/29 | Chloride, total | mg/L | 65.0 |
| UA | MW-350 | C | 2023/03/15 | Chloride, total | mg/L | 58.0 |
| UA | MW-350 | C | 2023/05/18 | Chloride, total | mg/L | 50.0 |
| UA | MW-350 | C | 2023/08/07 | Chloride, total | mg/L | 54.0 |
| UA | MW-350 | C | 2023/11/03 | Chloride, total | mg/L | 47.0 |
| UA | MW-350 | C | 2013/11/20 | Iron, dissolved | mg/L | <0.007 |
| UA | MW-350 | C | 2014/02/19 | Iron, dissolved | mg/L | <0.007 |
| UA | MW-350 | C | 2014/06/11 | Iron, dissolved | mg/L | <0.007 |
| UA | MW-350 | C | 2015/03/25 | Iron, dissolved | mg/L | <0.007 |
| UA | MW-350 | C | 2015/06/24 | Iron, dissolved | mg/L | <0.007 |
| UA | MW-350 | C | 2015/09/25 | Iron, dissolved | mg/L | <0.007 |
| UA | MW-350 | C | 2015/11/10 | Iron, dissolved | mg/L | <0.007 |
| UA | MW-350 | C | 2016/03/22 | Iron, dissolved | mg/L | <0.007 |
| UA | MW-350 | C | 2016/06/21 | Iron, dissolved | mg/L | <0.007 |
| UA | MW-350 | C | 2016/09/29 | Iron, dissolved | mg/L | <0.007 |
| UA | MW-350 | C | 2016/12/21 | Iron, dissolved | mg/L | <0.007 |
| UA | MW-350 | C | 2017/03/16 | Iron, dissolved | mg/L | <0.007 |
| UA | MW-350 | C | 2017/06/22 | Iron, dissolved | mg/L | <0.007 |
| UA | MW-350 | C | 2017/09/21 | Iron, dissolved | mg/L | <0.007 |
| UA | MW-350 | C | 2017/11/28 | Iron, dissolved | mg/L | <0.007 |
| UA | MW-350 | C | 2018/03/19 | Iron, dissolved | mg/L | <0.007 |
| UA | MW-350 | C | 2018/06/28 | Iron, dissolved | mg/L | <0.02 |
| UA | MW-350 | C | 2018/09/26 | Iron, dissolved | mg/L | <0.02 |
| UA | MW-350 | C | 2018/12/18 | Iron, dissolved | mg/L | <0.02 |
| UA | MW-350 | C | 2019/03/20 | Iron, dissolved | mg/L | <0.02 |
| UA | MW-350 | C | 2019/06/25 | Iron, dissolved | mg/L | <0.02 |
| UA | MW-350 | C | 2019/09/26 | Iron, dissolved | mg/L | <0.02 |
| UA | MW-350 | C | 2019/12/19 | Iron, dissolved | mg/L | <0.02 |
| UA | MW-350 | C | 2020/03/26 | Iron, dissolved | mg/L | <0.02 |
| UA | MW-350 | C | 2020/06/23 | Iron, dissolved | mg/L | <0.02 |
| UA | MW-350 | C | 2020/09/17 | Iron, dissolved | mg/L | <0.02 |
| UA | MW-350 | C | 2020/12/17 | Iron, dissolved | mg/L | <0.02 |
| UA | MW-350 | C | 2021/03/10 | Iron, dissolved | mg/L | <0.02 |
| UA | MW-350 | C | 2021/07/19 | Iron, dissolved | mg/L | <0.02 |
| UA | MW-350 | C | 2021/09/14 | Iron, dissolved | mg/L | <0.02 |
| UA | MW-350 | C | 2021/12/14 | Iron, dissolved | mg/L | <0.02 |
| UA | MW-350 | C | 2022/03/28 | Iron, dissolved | mg/L | <0.015 |
| UA | MW-350 | C | 2022/06/14 | Iron, dissolved | mg/L | <0.02 |
| UA | MW-350 | C | 2022/09/29 | Iron, dissolved | mg/L | <0.0115 |
| UA | MW-350 | C | 2022/12/06 | Iron, dissolved | mg/L | <0.0115 |
| UA | MW-350 | C | 2023/03/15 | Iron, dissolved | mg/L | <0.0115 |
| UA | MW-350 | C | 2023/05/18 | Iron, dissolved | mg/L | <0.02 |
| UA | MW-350 | C | 2023/08/07 | Iron, dissolved | mg/L | <0.0115 |
| UA | MW-350 | C | 2023/11/03 | Iron, dissolved | mg/L | <0.0115 |
| UA | MW-350 | C | 2020/03/26 | Magnesium, total | mg/L | 0.113 |
| UA | MW-350 | C | 2020/09/16 | Magnesium, total | mg/L | 0.262 |
| UA | MW-350 | C | 2021/03/10 | Magnesium, total | mg/L | 1.43 |
| UA | MW-350 | C | 2021/09/14 | Magnesium, total | mg/L | 4.38 |
| UA | MW-350 | C | 2022/03/28 | Magnesium, total | mg/L | 0.0837 |
| UA | MW-350 | C | 2022/09/29 | Magnesium, total | mg/L | 0.350 |
| UA | MW-350 | C | 2023/03/15 | Magnesium, total | mg/L | 0.172 |
| UA | MW-350 | C | 2023/05/18 | Magnesium, total | mg/L | 0.646 |
| UA | MW-350 | C | 2023/08/07 | Magnesium, total | mg/L | 0.784 |
| UA | MW-350 | C | 2023/11/03 | Magnesium, total | mg/L | 5.33 |
| UA | MW-350 | C | 2013/11/20 | Manganese, dissolved | mg/L | <0.0016 |

Attachment I. Site Groundwater Data

Geochemical Conceptual Site Model

Baldwin Fly Ash Pond System

Baldwin Power Plant

Baldwin, IL

| | | | | | | |
|----|--------|---|------------|----------------------|------|---------|
| UA | MW-350 | C | 2014/02/19 | Manganese, dissolved | mg/L | <0.0016 |
| UA | MW-350 | C | 2014/06/11 | Manganese, dissolved | mg/L | <0.0016 |
| UA | MW-350 | C | 2015/03/25 | Manganese, dissolved | mg/L | <0.0005 |
| UA | MW-350 | C | 2015/06/24 | Manganese, dissolved | mg/L | <0.0005 |
| UA | MW-350 | C | 2015/09/25 | Manganese, dissolved | mg/L | <0.0005 |
| UA | MW-350 | C | 2015/11/10 | Manganese, dissolved | mg/L | <0.0005 |
| UA | MW-350 | C | 2016/03/22 | Manganese, dissolved | mg/L | <0.0005 |
| UA | MW-350 | C | 2016/06/21 | Manganese, dissolved | mg/L | <0.0005 |
| UA | MW-350 | C | 2016/09/29 | Manganese, dissolved | mg/L | <0.0005 |
| UA | MW-350 | C | 2016/12/21 | Manganese, dissolved | mg/L | <0.0005 |
| UA | MW-350 | C | 2017/03/16 | Manganese, dissolved | mg/L | <0.0005 |
| UA | MW-350 | C | 2017/06/22 | Manganese, dissolved | mg/L | <0.0005 |
| UA | MW-350 | C | 2017/09/21 | Manganese, dissolved | mg/L | <0.0005 |
| UA | MW-350 | C | 2017/11/28 | Manganese, dissolved | mg/L | <0.0005 |
| UA | MW-350 | C | 2018/03/19 | Manganese, dissolved | mg/L | <0.0005 |
| UA | MW-350 | C | 2018/06/28 | Manganese, dissolved | mg/L | <0.0025 |
| UA | MW-350 | C | 2018/09/26 | Manganese, dissolved | mg/L | <0.0025 |
| UA | MW-350 | C | 2018/12/18 | Manganese, dissolved | mg/L | <0.0025 |
| UA | MW-350 | C | 2019/03/20 | Manganese, dissolved | mg/L | <0.0025 |
| UA | MW-350 | C | 2019/06/25 | Manganese, dissolved | mg/L | <0.0025 |
| UA | MW-350 | C | 2019/09/26 | Manganese, dissolved | mg/L | <0.0025 |
| UA | MW-350 | C | 2019/12/19 | Manganese, dissolved | mg/L | <0.0025 |
| UA | MW-350 | C | 2020/03/26 | Manganese, dissolved | mg/L | <0.0025 |
| UA | MW-350 | C | 2020/06/23 | Manganese, dissolved | mg/L | <0.0025 |
| UA | MW-350 | C | 2020/09/17 | Manganese, dissolved | mg/L | <0.0025 |
| UA | MW-350 | C | 2020/12/17 | Manganese, dissolved | mg/L | <0.0025 |
| UA | MW-350 | C | 2021/03/10 | Manganese, dissolved | mg/L | <0.0025 |
| UA | MW-350 | C | 2021/07/19 | Manganese, dissolved | mg/L | <0.0025 |
| UA | MW-350 | C | 2021/09/14 | Manganese, dissolved | mg/L | <0.0025 |
| UA | MW-350 | C | 2021/12/14 | Manganese, dissolved | mg/L | <0.0025 |
| UA | MW-350 | C | 2022/03/28 | Manganese, dissolved | mg/L | <0.0008 |
| UA | MW-350 | C | 2022/06/14 | Manganese, dissolved | mg/L | <0.0025 |
| UA | MW-350 | C | 2022/09/29 | Manganese, dissolved | mg/L | <0.0008 |
| UA | MW-350 | C | 2022/12/06 | Manganese, dissolved | mg/L | <0.0008 |
| UA | MW-350 | C | 2023/03/15 | Manganese, dissolved | mg/L | <0.0008 |
| UA | MW-350 | C | 2023/05/18 | Manganese, dissolved | mg/L | <0.0025 |
| UA | MW-350 | C | 2023/08/07 | Manganese, dissolved | mg/L | <0.0008 |
| UA | MW-350 | C | 2023/11/03 | Manganese, dissolved | mg/L | <0.0008 |
| UA | MW-350 | C | 2023/05/18 | Phosphate, dissolved | mg/L | <0.005 |
| UA | MW-350 | C | 2023/08/07 | Phosphate, dissolved | mg/L | <0.005 |
| UA | MW-350 | C | 2020/03/26 | Potassium, total | mg/L | 4.27 |
| UA | MW-350 | C | 2020/09/16 | Potassium, total | mg/L | 5.66 |
| UA | MW-350 | C | 2021/03/10 | Potassium, total | mg/L | 4.69 |
| UA | MW-350 | C | 2021/09/14 | Potassium, total | mg/L | 5.52 |
| UA | MW-350 | C | 2022/03/28 | Potassium, total | mg/L | 5.10 |
| UA | MW-350 | C | 2022/09/29 | Potassium, total | mg/L | 5.00 |
| UA | MW-350 | C | 2023/03/15 | Potassium, total | mg/L | 4.12 |
| UA | MW-350 | C | 2023/05/18 | Potassium, total | mg/L | 5.01 |
| UA | MW-350 | C | 2023/08/07 | Potassium, total | mg/L | 4.46 |
| UA | MW-350 | C | 2023/11/03 | Potassium, total | mg/L | 4.81 |
| UA | MW-350 | C | 2023/05/18 | Silicon, dissolved | mg/L | 5.18 |
| UA | MW-350 | C | 2023/08/07 | Silicon, dissolved | mg/L | 2.25 |
| UA | MW-350 | C | 2020/03/26 | Sodium, total | mg/L | 73.0 |
| UA | MW-350 | C | 2020/09/16 | Sodium, total | mg/L | 76.4 |
| UA | MW-350 | C | 2021/03/10 | Sodium, total | mg/L | 77.6 |
| UA | MW-350 | C | 2021/09/14 | Sodium, total | mg/L | 74.3 |
| UA | MW-350 | C | 2022/03/28 | Sodium, total | mg/L | 67.9 |

Attachment I. Site Groundwater Data

Geochemical Conceptual Site Model

Baldwin Fly Ash Pond System

Baldwin Power Plant

Baldwin, IL

| | | | | | | |
|----|--------|---|------------|-----------------------|-----------|------|
| UA | MW-350 | C | 2022/09/29 | Sodium, total | mg/L | 70.2 |
| UA | MW-350 | C | 2023/03/15 | Sodium, total | mg/L | 68.6 |
| UA | MW-350 | C | 2023/05/18 | Sodium, total | mg/L | 91.2 |
| UA | MW-350 | C | 2023/08/07 | Sodium, total | mg/L | 71.7 |
| UA | MW-350 | C | 2023/11/03 | Sodium, total | mg/L | 85.1 |
| UA | MW-350 | C | 2013/09/16 | Sulfate, total | mg/L | <5 |
| UA | MW-350 | C | 2020/03/26 | Sulfate, total | mg/L | 71.0 |
| UA | MW-350 | C | 2020/09/16 | Sulfate, total | mg/L | 74.0 |
| UA | MW-350 | C | 2021/03/10 | Sulfate, total | mg/L | 52.0 |
| UA | MW-350 | C | 2021/09/14 | Sulfate, total | mg/L | 99.0 |
| UA | MW-350 | C | 2022/03/28 | Sulfate, total | mg/L | 74.0 |
| UA | MW-350 | C | 2022/09/29 | Sulfate, total | mg/L | 113 |
| UA | MW-350 | C | 2023/03/15 | Sulfate, total | mg/L | 88.0 |
| UA | MW-350 | C | 2023/05/18 | Sulfate, total | mg/L | 97.0 |
| UA | MW-350 | C | 2023/08/07 | Sulfate, total | mg/L | 102 |
| UA | MW-350 | C | 2023/11/03 | Sulfate, total | mg/L | 100 |
| UA | MW-350 | C | 2013/09/16 | Temperature (Celsius) | degrees C | 14.6 |
| UA | MW-350 | C | 2013/11/20 | Temperature (Celsius) | degrees C | 13.5 |
| UA | MW-350 | C | 2014/02/19 | Temperature (Celsius) | degrees C | 13.3 |
| UA | MW-350 | C | 2014/06/11 | Temperature (Celsius) | degrees C | 14.3 |
| UA | MW-350 | C | 2015/03/25 | Temperature (Celsius) | degrees C | 14.4 |
| UA | MW-350 | C | 2015/06/24 | Temperature (Celsius) | degrees C | 14.4 |
| UA | MW-350 | C | 2015/09/25 | Temperature (Celsius) | degrees C | 13.8 |
| UA | MW-350 | C | 2015/11/10 | Temperature (Celsius) | degrees C | 13.5 |
| UA | MW-350 | C | 2016/03/22 | Temperature (Celsius) | degrees C | 14.4 |
| UA | MW-350 | C | 2016/06/21 | Temperature (Celsius) | degrees C | 14.3 |
| UA | MW-350 | C | 2016/09/29 | Temperature (Celsius) | degrees C | 13.8 |
| UA | MW-350 | C | 2016/12/21 | Temperature (Celsius) | degrees C | 13.3 |
| UA | MW-350 | C | 2017/03/16 | Temperature (Celsius) | degrees C | 13.8 |
| UA | MW-350 | C | 2017/06/22 | Temperature (Celsius) | degrees C | 14.5 |
| UA | MW-350 | C | 2017/09/21 | Temperature (Celsius) | degrees C | 14.6 |
| UA | MW-350 | C | 2017/11/28 | Temperature (Celsius) | degrees C | 14.6 |
| UA | MW-350 | C | 2018/03/19 | Temperature (Celsius) | degrees C | 14.7 |
| UA | MW-350 | C | 2018/06/28 | Temperature (Celsius) | degrees C | 15.2 |
| UA | MW-350 | C | 2018/09/26 | Temperature (Celsius) | degrees C | 14.2 |
| UA | MW-350 | C | 2018/12/18 | Temperature (Celsius) | degrees C | 13.7 |
| UA | MW-350 | C | 2019/03/20 | Temperature (Celsius) | degrees C | 13.5 |
| UA | MW-350 | C | 2019/06/25 | Temperature (Celsius) | degrees C | 14.4 |
| UA | MW-350 | C | 2019/09/26 | Temperature (Celsius) | degrees C | 13.9 |
| UA | MW-350 | C | 2019/12/19 | Temperature (Celsius) | degrees C | 13.4 |
| UA | MW-350 | C | 2020/03/26 | Temperature (Celsius) | degrees C | 14.2 |
| UA | MW-350 | C | 2020/06/23 | Temperature (Celsius) | degrees C | 14.6 |
| UA | MW-350 | C | 2020/09/16 | Temperature (Celsius) | degrees C | 14.7 |
| UA | MW-350 | C | 2020/09/17 | Temperature (Celsius) | degrees C | 15.1 |
| UA | MW-350 | C | 2020/12/17 | Temperature (Celsius) | degrees C | 13.1 |
| UA | MW-350 | C | 2021/03/10 | Temperature (Celsius) | degrees C | 13.9 |
| UA | MW-350 | C | 2021/07/19 | Temperature (Celsius) | degrees C | 16.8 |
| UA | MW-350 | C | 2021/09/14 | Temperature (Celsius) | degrees C | 16.8 |
| UA | MW-350 | C | 2021/12/14 | Temperature (Celsius) | degrees C | 15.2 |
| UA | MW-350 | C | 2022/03/28 | Temperature (Celsius) | degrees C | 13.5 |
| UA | MW-350 | C | 2022/06/14 | Temperature (Celsius) | degrees C | 17.3 |
| UA | MW-350 | C | 2022/09/29 | Temperature (Celsius) | degrees C | 13.8 |
| UA | MW-350 | C | 2022/12/06 | Temperature (Celsius) | degrees C | 13.2 |
| UA | MW-350 | C | 2023/03/15 | Temperature (Celsius) | degrees C | 13.7 |
| UA | MW-350 | C | 2023/05/18 | Temperature (Celsius) | degrees C | 14.1 |
| UA | MW-350 | C | 2023/08/07 | Temperature (Celsius) | degrees C | 13.9 |
| UA | MW-350 | C | 2023/11/03 | Temperature (Celsius) | degrees C | 13.7 |

Attachment I. Site Groundwater Data

Geochemical Conceptual Site Model

Baldwin Fly Ash Pond System

Baldwin Power Plant

Baldwin, IL

| | | | | | | |
|----|--------|---|------------|------------------------|------|-------|
| UA | MW-350 | C | 2013/09/16 | Total Dissolved Solids | mg/L | 1,640 |
| UA | MW-350 | C | 2013/11/20 | Total Dissolved Solids | mg/L | 1,370 |
| UA | MW-350 | C | 2014/02/19 | Total Dissolved Solids | mg/L | 1,420 |
| UA | MW-350 | C | 2014/06/11 | Total Dissolved Solids | mg/L | 1,580 |
| UA | MW-350 | C | 2015/03/25 | Total Dissolved Solids | mg/L | 1,430 |
| UA | MW-350 | C | 2015/06/24 | Total Dissolved Solids | mg/L | 1,430 |
| UA | MW-350 | C | 2015/09/25 | Total Dissolved Solids | mg/L | 1,140 |
| UA | MW-350 | C | 2015/11/10 | Total Dissolved Solids | mg/L | 690 |
| UA | MW-350 | C | 2016/03/22 | Total Dissolved Solids | mg/L | 712 |
| UA | MW-350 | C | 2016/06/21 | Total Dissolved Solids | mg/L | 906 |
| UA | MW-350 | C | 2016/09/29 | Total Dissolved Solids | mg/L | 600 |
| UA | MW-350 | C | 2016/12/21 | Total Dissolved Solids | mg/L | 536 |
| UA | MW-350 | C | 2017/03/16 | Total Dissolved Solids | mg/L | 624 |
| UA | MW-350 | C | 2017/06/22 | Total Dissolved Solids | mg/L | 475 |
| UA | MW-350 | C | 2017/09/21 | Total Dissolved Solids | mg/L | 246 |
| UA | MW-350 | C | 2017/11/28 | Total Dissolved Solids | mg/L | 454 |
| UA | MW-350 | C | 2018/03/19 | Total Dissolved Solids | mg/L | 376 |
| UA | MW-350 | C | 2018/06/28 | Total Dissolved Solids | mg/L | 346 |
| UA | MW-350 | C | 2018/09/26 | Total Dissolved Solids | mg/L | 385 |
| UA | MW-350 | C | 2018/12/18 | Total Dissolved Solids | mg/L | 425 |
| UA | MW-350 | C | 2019/03/20 | Total Dissolved Solids | mg/L | 578 |
| UA | MW-350 | C | 2019/06/25 | Total Dissolved Solids | mg/L | 485 |
| UA | MW-350 | C | 2019/09/26 | Total Dissolved Solids | mg/L | 368 |
| UA | MW-350 | C | 2019/12/19 | Total Dissolved Solids | mg/L | 324 |
| UA | MW-350 | C | 2020/03/26 | Total Dissolved Solids | mg/L | 344 |
| UA | MW-350 | C | 2020/06/23 | Total Dissolved Solids | mg/L | 258 |
| UA | MW-350 | C | 2020/09/16 | Total Dissolved Solids | mg/L | 230 |
| UA | MW-350 | C | 2020/09/17 | Total Dissolved Solids | mg/L | 226 |
| UA | MW-350 | C | 2020/12/17 | Total Dissolved Solids | mg/L | 260 |
| UA | MW-350 | C | 2021/03/10 | Total Dissolved Solids | mg/L | 272 |
| UA | MW-350 | C | 2021/07/19 | Total Dissolved Solids | mg/L | 362 |
| UA | MW-350 | C | 2021/09/14 | Total Dissolved Solids | mg/L | 402 |
| UA | MW-350 | C | 2021/12/14 | Total Dissolved Solids | mg/L | 248 |
| UA | MW-350 | C | 2022/03/28 | Total Dissolved Solids | mg/L | 494 |
| UA | MW-350 | C | 2022/06/14 | Total Dissolved Solids | mg/L | 350 |
| UA | MW-350 | C | 2022/09/29 | Total Dissolved Solids | mg/L | 382 |
| UA | MW-350 | C | 2022/12/06 | Total Dissolved Solids | mg/L | 372 |
| UA | MW-350 | C | 2023/03/15 | Total Dissolved Solids | mg/L | 414 |
| UA | MW-350 | C | 2023/05/18 | Total Dissolved Solids | mg/L | 420 |
| UA | MW-350 | C | 2023/08/07 | Total Dissolved Solids | mg/L | 328 |
| UA | MW-350 | C | 2023/11/03 | Total Dissolved Solids | mg/L | 306 |
| UA | MW-352 | C | 2013/09/16 | pH (field) | SU | 9.4 |
| UA | MW-352 | C | 2013/11/20 | pH (field) | SU | 7.3 |
| UA | MW-352 | C | 2014/02/19 | pH (field) | SU | 6.5 |
| UA | MW-352 | C | 2014/06/12 | pH (field) | SU | 8.9 |
| UA | MW-352 | C | 2015/03/25 | pH (field) | SU | 9.0 |
| UA | MW-352 | C | 2015/06/24 | pH (field) | SU | 8.6 |
| UA | MW-352 | C | 2015/09/25 | pH (field) | SU | 8.0 |
| UA | MW-352 | C | 2015/11/10 | pH (field) | SU | 7.6 |
| UA | MW-352 | C | 2016/03/22 | pH (field) | SU | 7.9 |
| UA | MW-352 | C | 2016/06/23 | pH (field) | SU | 7.7 |
| UA | MW-352 | C | 2016/09/29 | pH (field) | SU | 7.9 |
| UA | MW-352 | C | 2016/12/21 | pH (field) | SU | 7.9 |
| UA | MW-352 | C | 2017/03/16 | pH (field) | SU | 7.8 |
| UA | MW-352 | C | 2017/06/21 | pH (field) | SU | 7.6 |
| UA | MW-352 | C | 2017/09/21 | pH (field) | SU | 6.7 |
| UA | MW-352 | C | 2017/11/28 | pH (field) | SU | 7.6 |

Attachment I. Site Groundwater Data

Geochemical Conceptual Site Model

Baldwin Fly Ash Pond System

Baldwin Power Plant

Baldwin, IL

| | | | | | | |
|----|--------|---|------------|-------------------------------|------------|--------|
| UA | MW-352 | C | 2018/03/20 | pH (field) | SU | 7.6 |
| UA | MW-352 | C | 2018/06/27 | pH (field) | SU | 7.7 |
| UA | MW-352 | C | 2018/09/26 | pH (field) | SU | 7.8 |
| UA | MW-352 | C | 2018/12/18 | pH (field) | SU | 7.6 |
| UA | MW-352 | C | 2019/03/20 | pH (field) | SU | 7.7 |
| UA | MW-352 | C | 2019/06/25 | pH (field) | SU | 7.7 |
| UA | MW-352 | C | 2019/09/26 | pH (field) | SU | 7.4 |
| UA | MW-352 | C | 2019/12/19 | pH (field) | SU | 7.7 |
| UA | MW-352 | C | 2020/03/27 | pH (field) | SU | 7.5 |
| UA | MW-352 | C | 2020/06/23 | pH (field) | SU | 7.8 |
| UA | MW-352 | C | 2020/09/17 | pH (field) | SU | 7.7 |
| UA | MW-352 | C | 2020/12/16 | pH (field) | SU | 7.7 |
| UA | MW-352 | C | 2021/03/09 | pH (field) | SU | 7.6 |
| UA | MW-352 | C | 2021/07/19 | pH (field) | SU | 7.3 |
| UA | MW-352 | C | 2021/09/14 | pH (field) | SU | 7.4 |
| UA | MW-352 | C | 2021/12/14 | pH (field) | SU | 7.3 |
| UA | MW-352 | C | 2022/03/28 | pH (field) | SU | 7.5 |
| UA | MW-352 | C | 2022/06/14 | pH (field) | SU | 7.5 |
| UA | MW-352 | C | 2022/09/29 | pH (field) | SU | 8.0 |
| UA | MW-352 | C | 2022/12/06 | pH (field) | SU | 7.4 |
| UA | MW-352 | C | 2023/03/15 | pH (field) | SU | 7.5 |
| UA | MW-352 | C | 2023/05/18 | pH (field) | SU | 7.4 |
| UA | MW-352 | C | 2023/07/10 | pH (field) | SU | 7.3 |
| UA | MW-352 | C | 2023/08/04 | pH (field) | SU | 7.9 |
| UA | MW-352 | C | 2023/10/31 | pH (field) | SU | 7.7 |
| UA | MW-352 | C | 2021/03/09 | Oxidation Reduction Potential | mV | -140 |
| UA | MW-352 | C | 2021/07/19 | Oxidation Reduction Potential | mV | 34.0 |
| UA | MW-352 | C | 2021/09/14 | Oxidation Reduction Potential | mV | -123 |
| UA | MW-352 | C | 2021/12/14 | Oxidation Reduction Potential | mV | -28.0 |
| UA | MW-352 | C | 2022/03/28 | Oxidation Reduction Potential | mV | -144 |
| UA | MW-352 | C | 2022/06/14 | Oxidation Reduction Potential | mV | 90.0 |
| UA | MW-352 | C | 2022/09/29 | Oxidation Reduction Potential | mV | 133 |
| UA | MW-352 | C | 2022/12/06 | Oxidation Reduction Potential | mV | <-300 |
| UA | MW-352 | C | 2023/03/15 | Oxidation Reduction Potential | mV | -162 |
| UA | MW-352 | C | 2023/05/18 | Oxidation Reduction Potential | mV | -119 |
| UA | MW-352 | C | 2023/07/10 | Oxidation Reduction Potential | mV | 65.0 |
| UA | MW-352 | C | 2023/08/04 | Oxidation Reduction Potential | mV | 85.0 |
| UA | MW-352 | C | 2023/10/31 | Oxidation Reduction Potential | mV | -98.0 |
| UA | MW-352 | C | 2021/03/09 | Eh | V | 0.057 |
| UA | MW-352 | C | 2021/07/19 | Eh | V | 0.23 |
| UA | MW-352 | C | 2021/09/14 | Eh | V | 0.069 |
| UA | MW-352 | C | 2021/12/14 | Eh | V | 0.17 |
| UA | MW-352 | C | 2022/03/28 | Eh | V | 0.054 |
| UA | MW-352 | C | 2022/06/14 | Eh | V | 0.28 |
| UA | MW-352 | C | 2022/09/29 | Eh | V | 0.33 |
| UA | MW-352 | C | 2022/12/06 | Eh | V | -0.10 |
| UA | MW-352 | C | 2023/03/15 | Eh | V | 0.035 |
| UA | MW-352 | C | 2023/05/18 | Eh | V | 0.077 |
| UA | MW-352 | C | 2023/07/10 | Eh | V | 0.26 |
| UA | MW-352 | C | 2023/08/04 | Eh | V | 0.28 |
| UA | MW-352 | C | 2023/10/31 | Eh | V | 0.098 |
| UA | MW-352 | C | 2023/03/15 | Alkalinity, bicarbonate | mg/L CaCO3 | 143 |
| UA | MW-352 | C | 2023/05/18 | Alkalinity, bicarbonate | mg/L CaCO3 | 147 |
| UA | MW-352 | C | 2023/08/04 | Alkalinity, bicarbonate | mg/L CaCO3 | 147 |
| UA | MW-352 | C | 2023/10/31 | Alkalinity, bicarbonate | mg/L CaCO3 | 149 |
| UA | MW-352 | C | 2023/03/15 | Barium, total | mg/L | 0.0867 |
| UA | MW-352 | C | 2023/05/18 | Barium, total | mg/L | 0.0891 |

Attachment I. Site Groundwater Data

Geochemical Conceptual Site Model

Baldwin Fly Ash Pond System

Baldwin Power Plant

Baldwin, IL

| | | | | | | |
|----|--------|---|------------|-----------------|------|--------|
| UA | MW-352 | C | 2023/07/10 | Barium, total | mg/L | 0.0898 |
| UA | MW-352 | C | 2023/08/04 | Barium, total | mg/L | 0.0856 |
| UA | MW-352 | C | 2023/10/31 | Barium, total | mg/L | 0.122 |
| UA | MW-352 | C | 2013/09/16 | Boron, total | mg/L | 1.42 |
| UA | MW-352 | C | 2023/03/15 | Boron, total | mg/L | 2.29 |
| UA | MW-352 | C | 2023/05/18 | Boron, total | mg/L | 2.04 |
| UA | MW-352 | C | 2023/07/10 | Boron, total | mg/L | 2.10 |
| UA | MW-352 | C | 2023/08/04 | Boron, total | mg/L | 1.88 |
| UA | MW-352 | C | 2023/10/31 | Boron, total | mg/L | 2.77 |
| UA | MW-352 | C | 2023/03/15 | Calcium, total | mg/L | 97.8 |
| UA | MW-352 | C | 2023/05/18 | Calcium, total | mg/L | 88.3 |
| UA | MW-352 | C | 2023/07/10 | Calcium, total | mg/L | 105 |
| UA | MW-352 | C | 2023/08/04 | Calcium, total | mg/L | 87.0 |
| UA | MW-352 | C | 2023/10/31 | Calcium, total | mg/L | 93.3 |
| UA | MW-352 | C | 2013/09/16 | Chloride, total | mg/L | 580 |
| UA | MW-352 | C | 2023/03/15 | Chloride, total | mg/L | 576 |
| UA | MW-352 | C | 2023/05/18 | Chloride, total | mg/L | 569 |
| UA | MW-352 | C | 2023/07/10 | Chloride, total | mg/L | 582 |
| UA | MW-352 | C | 2023/08/04 | Chloride, total | mg/L | 529 |
| UA | MW-352 | C | 2023/10/31 | Chloride, total | mg/L | 567 |
| UA | MW-352 | C | 2013/11/20 | Iron, dissolved | mg/L | <0.007 |
| UA | MW-352 | C | 2014/02/19 | Iron, dissolved | mg/L | <0.007 |
| UA | MW-352 | C | 2014/06/12 | Iron, dissolved | mg/L | <0.007 |
| UA | MW-352 | C | 2015/03/25 | Iron, dissolved | mg/L | <0.007 |
| UA | MW-352 | C | 2015/06/24 | Iron, dissolved | mg/L | <0.007 |
| UA | MW-352 | C | 2015/09/25 | Iron, dissolved | mg/L | <0.007 |
| UA | MW-352 | C | 2015/11/10 | Iron, dissolved | mg/L | <0.007 |
| UA | MW-352 | C | 2016/03/22 | Iron, dissolved | mg/L | 0.0220 |
| UA | MW-352 | C | 2016/06/23 | Iron, dissolved | mg/L | 0.0285 |
| UA | MW-352 | C | 2016/09/29 | Iron, dissolved | mg/L | 0.0224 |
| UA | MW-352 | C | 2016/12/21 | Iron, dissolved | mg/L | <0.007 |
| UA | MW-352 | C | 2017/03/16 | Iron, dissolved | mg/L | 0.0500 |
| UA | MW-352 | C | 2017/06/21 | Iron, dissolved | mg/L | 0.120 |
| UA | MW-352 | C | 2017/09/21 | Iron, dissolved | mg/L | 0.140 |
| UA | MW-352 | C | 2017/11/28 | Iron, dissolved | mg/L | 0.120 |
| UA | MW-352 | C | 2018/03/20 | Iron, dissolved | mg/L | 0.109 |
| UA | MW-352 | C | 2018/06/27 | Iron, dissolved | mg/L | 0.125 |
| UA | MW-352 | C | 2018/09/26 | Iron, dissolved | mg/L | 0.151 |
| UA | MW-352 | C | 2018/12/18 | Iron, dissolved | mg/L | 0.159 |
| UA | MW-352 | C | 2019/03/20 | Iron, dissolved | mg/L | 0.0824 |
| UA | MW-352 | C | 2019/06/25 | Iron, dissolved | mg/L | 0.125 |
| UA | MW-352 | C | 2019/09/26 | Iron, dissolved | mg/L | 0.145 |
| UA | MW-352 | C | 2019/12/19 | Iron, dissolved | mg/L | 0.190 |
| UA | MW-352 | C | 2020/03/27 | Iron, dissolved | mg/L | 0.144 |
| UA | MW-352 | C | 2020/06/23 | Iron, dissolved | mg/L | 0.323 |
| UA | MW-352 | C | 2020/09/17 | Iron, dissolved | mg/L | 0.472 |
| UA | MW-352 | C | 2020/12/16 | Iron, dissolved | mg/L | 0.374 |
| UA | MW-352 | C | 2021/03/09 | Iron, dissolved | mg/L | 0.184 |
| UA | MW-352 | C | 2021/07/19 | Iron, dissolved | mg/L | 0.262 |
| UA | MW-352 | C | 2021/09/14 | Iron, dissolved | mg/L | 0.220 |
| UA | MW-352 | C | 2021/12/14 | Iron, dissolved | mg/L | 0.263 |
| UA | MW-352 | C | 2022/03/28 | Iron, dissolved | mg/L | 0.222 |
| UA | MW-352 | C | 2022/06/14 | Iron, dissolved | mg/L | 0.224 |
| UA | MW-352 | C | 2022/09/29 | Iron, dissolved | mg/L | 0.0318 |
| UA | MW-352 | C | 2022/12/06 | Iron, dissolved | mg/L | 0.373 |
| UA | MW-352 | C | 2023/03/15 | Iron, dissolved | mg/L | 0.194 |
| UA | MW-352 | C | 2023/05/18 | Iron, dissolved | mg/L | 0.164 |

Attachment I. Site Groundwater Data

Geochemical Conceptual Site Model

Baldwin Fly Ash Pond System

Baldwin Power Plant

Baldwin, IL

| | | | | | | |
|----|--------|---|------------|----------------------|------|---------|
| UA | MW-352 | C | 2023/08/04 | Iron, dissolved | mg/L | 0.482 |
| UA | MW-352 | C | 2023/10/31 | Iron, dissolved | mg/L | 0.392 |
| UA | MW-352 | C | 2023/03/15 | Magnesium, total | mg/L | 47.7 |
| UA | MW-352 | C | 2023/05/18 | Magnesium, total | mg/L | 41.7 |
| UA | MW-352 | C | 2023/08/04 | Magnesium, total | mg/L | 43.9 |
| UA | MW-352 | C | 2023/10/31 | Magnesium, total | mg/L | 46.4 |
| UA | MW-352 | C | 2013/11/20 | Manganese, dissolved | mg/L | <0.0016 |
| UA | MW-352 | C | 2014/02/19 | Manganese, dissolved | mg/L | <0.0016 |
| UA | MW-352 | C | 2014/06/12 | Manganese, dissolved | mg/L | <0.0016 |
| UA | MW-352 | C | 2015/03/25 | Manganese, dissolved | mg/L | <0.0005 |
| UA | MW-352 | C | 2015/06/24 | Manganese, dissolved | mg/L | <0.0005 |
| UA | MW-352 | C | 2015/09/25 | Manganese, dissolved | mg/L | 0.00660 |
| UA | MW-352 | C | 2015/11/10 | Manganese, dissolved | mg/L | 0.00530 |
| UA | MW-352 | C | 2016/03/22 | Manganese, dissolved | mg/L | 0.00560 |
| UA | MW-352 | C | 2016/06/23 | Manganese, dissolved | mg/L | 0.00560 |
| UA | MW-352 | C | 2016/09/29 | Manganese, dissolved | mg/L | 0.00540 |
| UA | MW-352 | C | 2016/12/21 | Manganese, dissolved | mg/L | 0.00390 |
| UA | MW-352 | C | 2017/03/16 | Manganese, dissolved | mg/L | 0.00560 |
| UA | MW-352 | C | 2017/06/21 | Manganese, dissolved | mg/L | 0.00770 |
| UA | MW-352 | C | 2017/09/21 | Manganese, dissolved | mg/L | 0.00580 |
| UA | MW-352 | C | 2017/11/28 | Manganese, dissolved | mg/L | 0.00600 |
| UA | MW-352 | C | 2018/03/20 | Manganese, dissolved | mg/L | 0.00590 |
| UA | MW-352 | C | 2018/06/27 | Manganese, dissolved | mg/L | <0.0025 |
| UA | MW-352 | C | 2018/09/26 | Manganese, dissolved | mg/L | <0.0025 |
| UA | MW-352 | C | 2018/12/18 | Manganese, dissolved | mg/L | <0.0025 |
| UA | MW-352 | C | 2019/03/20 | Manganese, dissolved | mg/L | <0.0025 |
| UA | MW-352 | C | 2019/06/25 | Manganese, dissolved | mg/L | <0.0025 |
| UA | MW-352 | C | 2019/09/26 | Manganese, dissolved | mg/L | <0.0025 |
| UA | MW-352 | C | 2019/12/19 | Manganese, dissolved | mg/L | <0.0025 |
| UA | MW-352 | C | 2020/03/27 | Manganese, dissolved | mg/L | <0.0025 |
| UA | MW-352 | C | 2020/06/23 | Manganese, dissolved | mg/L | 0.0312 |
| UA | MW-352 | C | 2020/09/17 | Manganese, dissolved | mg/L | 0.0210 |
| UA | MW-352 | C | 2020/12/16 | Manganese, dissolved | mg/L | 0.0107 |
| UA | MW-352 | C | 2021/03/09 | Manganese, dissolved | mg/L | 0.0113 |
| UA | MW-352 | C | 2021/07/19 | Manganese, dissolved | mg/L | 0.00860 |
| UA | MW-352 | C | 2021/09/14 | Manganese, dissolved | mg/L | 0.0161 |
| UA | MW-352 | C | 2021/12/14 | Manganese, dissolved | mg/L | 0.0109 |
| UA | MW-352 | C | 2022/03/28 | Manganese, dissolved | mg/L | 0.00870 |
| UA | MW-352 | C | 2022/06/14 | Manganese, dissolved | mg/L | 0.0103 |
| UA | MW-352 | C | 2022/09/29 | Manganese, dissolved | mg/L | 0.00400 |
| UA | MW-352 | C | 2022/12/06 | Manganese, dissolved | mg/L | 0.00870 |
| UA | MW-352 | C | 2023/03/15 | Manganese, dissolved | mg/L | 0.0111 |
| UA | MW-352 | C | 2023/05/18 | Manganese, dissolved | mg/L | 0.0152 |
| UA | MW-352 | C | 2023/08/04 | Manganese, dissolved | mg/L | 0.0334 |
| UA | MW-352 | C | 2023/10/31 | Manganese, dissolved | mg/L | 0.0423 |
| UA | MW-352 | C | 2023/05/18 | Phosphate, dissolved | mg/L | 0.221 |
| UA | MW-352 | C | 2023/08/04 | Phosphate, dissolved | mg/L | 0.0740 |
| UA | MW-352 | C | 2023/03/15 | Potassium, total | mg/L | 3.61 |
| UA | MW-352 | C | 2023/05/18 | Potassium, total | mg/L | 3.77 |
| UA | MW-352 | C | 2023/08/04 | Potassium, total | mg/L | 3.83 |
| UA | MW-352 | C | 2023/10/31 | Potassium, total | mg/L | 3.78 |
| UA | MW-352 | C | 2023/05/18 | Silicon, dissolved | mg/L | 7.14 |
| UA | MW-352 | C | 2023/08/04 | Silicon, dissolved | mg/L | 6.33 |
| UA | MW-352 | C | 2023/03/15 | Sodium, total | mg/L | 234 |
| UA | MW-352 | C | 2023/05/18 | Sodium, total | mg/L | 263 |
| UA | MW-352 | C | 2023/08/04 | Sodium, total | mg/L | 262 |
| UA | MW-352 | C | 2023/10/31 | Sodium, total | mg/L | 241 |

Attachment I. Site Groundwater Data

Geochemical Conceptual Site Model

Baldwin Fly Ash Pond System

Baldwin Power Plant

Baldwin, IL

| | | | | | | |
|----|--------|---|------------|------------------------|-----------|-------|
| UA | MW-352 | C | 2013/09/16 | Sulfate, total | mg/L | <5 |
| UA | MW-352 | C | 2023/03/15 | Sulfate, total | mg/L | 6.00 |
| UA | MW-352 | C | 2023/05/18 | Sulfate, total | mg/L | <6 |
| UA | MW-352 | C | 2023/07/10 | Sulfate, total | mg/L | 7.00 |
| UA | MW-352 | C | 2023/08/04 | Sulfate, total | mg/L | 7.00 |
| UA | MW-352 | C | 2023/10/31 | Sulfate, total | mg/L | 8.00 |
| UA | MW-352 | C | 2013/09/16 | Temperature (Celsius) | degrees C | 14.6 |
| UA | MW-352 | C | 2013/11/20 | Temperature (Celsius) | degrees C | 13.3 |
| UA | MW-352 | C | 2014/02/19 | Temperature (Celsius) | degrees C | 11.5 |
| UA | MW-352 | C | 2014/06/12 | Temperature (Celsius) | degrees C | 14.3 |
| UA | MW-352 | C | 2015/03/25 | Temperature (Celsius) | degrees C | 13.3 |
| UA | MW-352 | C | 2015/06/24 | Temperature (Celsius) | degrees C | 14.6 |
| UA | MW-352 | C | 2015/09/25 | Temperature (Celsius) | degrees C | 15.3 |
| UA | MW-352 | C | 2015/11/10 | Temperature (Celsius) | degrees C | 13.8 |
| UA | MW-352 | C | 2016/03/22 | Temperature (Celsius) | degrees C | 14.4 |
| UA | MW-352 | C | 2016/06/23 | Temperature (Celsius) | degrees C | 16.6 |
| UA | MW-352 | C | 2016/09/29 | Temperature (Celsius) | degrees C | 14.5 |
| UA | MW-352 | C | 2016/12/21 | Temperature (Celsius) | degrees C | 13.2 |
| UA | MW-352 | C | 2017/03/16 | Temperature (Celsius) | degrees C | 13.2 |
| UA | MW-352 | C | 2017/06/21 | Temperature (Celsius) | degrees C | 15.6 |
| UA | MW-352 | C | 2017/09/21 | Temperature (Celsius) | degrees C | 14.3 |
| UA | MW-352 | C | 2017/11/28 | Temperature (Celsius) | degrees C | 14.8 |
| UA | MW-352 | C | 2018/03/20 | Temperature (Celsius) | degrees C | 12.9 |
| UA | MW-352 | C | 2018/06/27 | Temperature (Celsius) | degrees C | 14.9 |
| UA | MW-352 | C | 2018/09/26 | Temperature (Celsius) | degrees C | 15.4 |
| UA | MW-352 | C | 2018/12/18 | Temperature (Celsius) | degrees C | 13.0 |
| UA | MW-352 | C | 2019/03/20 | Temperature (Celsius) | degrees C | 12.5 |
| UA | MW-352 | C | 2019/06/25 | Temperature (Celsius) | degrees C | 14.6 |
| UA | MW-352 | C | 2019/09/26 | Temperature (Celsius) | degrees C | 15.1 |
| UA | MW-352 | C | 2019/12/19 | Temperature (Celsius) | degrees C | 13.1 |
| UA | MW-352 | C | 2020/03/27 | Temperature (Celsius) | degrees C | 13.8 |
| UA | MW-352 | C | 2020/06/23 | Temperature (Celsius) | degrees C | 14.6 |
| UA | MW-352 | C | 2020/09/17 | Temperature (Celsius) | degrees C | 15.4 |
| UA | MW-352 | C | 2020/12/16 | Temperature (Celsius) | degrees C | 12.2 |
| UA | MW-352 | C | 2021/03/09 | Temperature (Celsius) | degrees C | 13.4 |
| UA | MW-352 | C | 2021/07/19 | Temperature (Celsius) | degrees C | 16.8 |
| UA | MW-352 | C | 2021/09/14 | Temperature (Celsius) | degrees C | 19.9 |
| UA | MW-352 | C | 2021/12/14 | Temperature (Celsius) | degrees C | 13.4 |
| UA | MW-352 | C | 2022/03/28 | Temperature (Celsius) | degrees C | 11.9 |
| UA | MW-352 | C | 2022/06/14 | Temperature (Celsius) | degrees C | 19.0 |
| UA | MW-352 | C | 2022/09/29 | Temperature (Celsius) | degrees C | 16.8 |
| UA | MW-352 | C | 2022/12/06 | Temperature (Celsius) | degrees C | 12.8 |
| UA | MW-352 | C | 2023/03/15 | Temperature (Celsius) | degrees C | 13.1 |
| UA | MW-352 | C | 2023/05/18 | Temperature (Celsius) | degrees C | 14.8 |
| UA | MW-352 | C | 2023/07/10 | Temperature (Celsius) | degrees C | 19.5 |
| UA | MW-352 | C | 2023/08/04 | Temperature (Celsius) | degrees C | 16.4 |
| UA | MW-352 | C | 2023/10/31 | Temperature (Celsius) | degrees C | 14.1 |
| UA | MW-352 | C | 2013/09/16 | Total Dissolved Solids | mg/L | 1,130 |
| UA | MW-352 | C | 2013/11/20 | Total Dissolved Solids | mg/L | 996 |
| UA | MW-352 | C | 2014/02/19 | Total Dissolved Solids | mg/L | 768 |
| UA | MW-352 | C | 2014/06/12 | Total Dissolved Solids | mg/L | 1,090 |
| UA | MW-352 | C | 2015/03/25 | Total Dissolved Solids | mg/L | 874 |
| UA | MW-352 | C | 2015/06/24 | Total Dissolved Solids | mg/L | 1,100 |
| UA | MW-352 | C | 2015/09/25 | Total Dissolved Solids | mg/L | 1,210 |
| UA | MW-352 | C | 2015/11/10 | Total Dissolved Solids | mg/L | 1,100 |
| UA | MW-352 | C | 2016/03/22 | Total Dissolved Solids | mg/L | 1,130 |
| UA | MW-352 | C | 2016/06/23 | Total Dissolved Solids | mg/L | 1,200 |

Attachment I. Site Groundwater Data

Geochemical Conceptual Site Model

Baldwin Fly Ash Pond System

Baldwin Power Plant

Baldwin, IL

| | | | | | | |
|----|--------|---|------------|-------------------------------|------|-------|
| UA | MW-352 | C | 2016/09/29 | Total Dissolved Solids | mg/L | 744 |
| UA | MW-352 | C | 2016/12/21 | Total Dissolved Solids | mg/L | 850 |
| UA | MW-352 | C | 2017/03/16 | Total Dissolved Solids | mg/L | 1,120 |
| UA | MW-352 | C | 2017/06/21 | Total Dissolved Solids | mg/L | 1,210 |
| UA | MW-352 | C | 2017/09/21 | Total Dissolved Solids | mg/L | 1,090 |
| UA | MW-352 | C | 2017/11/28 | Total Dissolved Solids | mg/L | 1,220 |
| UA | MW-352 | C | 2018/03/20 | Total Dissolved Solids | mg/L | 1,100 |
| UA | MW-352 | C | 2018/06/27 | Total Dissolved Solids | mg/L | 1,210 |
| UA | MW-352 | C | 2018/09/26 | Total Dissolved Solids | mg/L | 1,360 |
| UA | MW-352 | C | 2018/12/18 | Total Dissolved Solids | mg/L | 1,120 |
| UA | MW-352 | C | 2019/03/20 | Total Dissolved Solids | mg/L | 1,150 |
| UA | MW-352 | C | 2019/06/25 | Total Dissolved Solids | mg/L | 1,240 |
| UA | MW-352 | C | 2019/09/26 | Total Dissolved Solids | mg/L | 1,320 |
| UA | MW-352 | C | 2019/12/19 | Total Dissolved Solids | mg/L | 1,180 |
| UA | MW-352 | C | 2020/03/27 | Total Dissolved Solids | mg/L | 1,130 |
| UA | MW-352 | C | 2020/06/23 | Total Dissolved Solids | mg/L | 1,290 |
| UA | MW-352 | C | 2020/09/17 | Total Dissolved Solids | mg/L | 1,230 |
| UA | MW-352 | C | 2020/12/16 | Total Dissolved Solids | mg/L | 1,160 |
| UA | MW-352 | C | 2021/03/09 | Total Dissolved Solids | mg/L | 1,210 |
| UA | MW-352 | C | 2021/07/19 | Total Dissolved Solids | mg/L | 1,280 |
| UA | MW-352 | C | 2021/09/14 | Total Dissolved Solids | mg/L | 1,140 |
| UA | MW-352 | C | 2021/12/14 | Total Dissolved Solids | mg/L | 1,100 |
| UA | MW-352 | C | 2022/03/28 | Total Dissolved Solids | mg/L | 1,090 |
| UA | MW-352 | C | 2022/06/14 | Total Dissolved Solids | mg/L | 1,220 |
| UA | MW-352 | C | 2022/09/29 | Total Dissolved Solids | mg/L | 978 |
| UA | MW-352 | C | 2022/12/06 | Total Dissolved Solids | mg/L | 1,160 |
| UA | MW-352 | C | 2023/03/15 | Total Dissolved Solids | mg/L | 1,080 |
| UA | MW-352 | C | 2023/05/18 | Total Dissolved Solids | mg/L | 1,270 |
| UA | MW-352 | C | 2023/07/10 | Total Dissolved Solids | mg/L | 1,330 |
| UA | MW-352 | C | 2023/08/04 | Total Dissolved Solids | mg/L | 1,280 |
| UA | MW-352 | C | 2023/10/31 | Total Dissolved Solids | mg/L | 1,170 |
| UA | MW-366 | C | 2016/01/20 | pH (field) | SU | 6.7 |
| UA | MW-366 | C | 2016/03/23 | pH (field) | SU | 7.1 |
| UA | MW-366 | C | 2016/06/22 | pH (field) | SU | 7.2 |
| UA | MW-366 | C | 2016/09/20 | pH (field) | SU | 7.1 |
| UA | MW-366 | C | 2016/12/22 | pH (field) | SU | 7.0 |
| UA | MW-366 | C | 2017/03/15 | pH (field) | SU | 7.5 |
| UA | MW-366 | C | 2017/06/20 | pH (field) | SU | 7.0 |
| UA | MW-366 | C | 2017/07/26 | pH (field) | SU | 7.2 |
| UA | MW-366 | C | 2017/11/27 | pH (field) | SU | 7.3 |
| UA | MW-366 | C | 2018/06/26 | pH (field) | SU | 6.9 |
| UA | MW-366 | C | 2018/09/25 | pH (field) | SU | 7.0 |
| UA | MW-366 | C | 2019/03/19 | pH (field) | SU | 7.0 |
| UA | MW-366 | C | 2019/09/25 | pH (field) | SU | 6.7 |
| UA | MW-366 | C | 2020/03/26 | pH (field) | SU | 6.9 |
| UA | MW-366 | C | 2020/09/16 | pH (field) | SU | 7.0 |
| UA | MW-366 | C | 2021/03/12 | pH (field) | SU | 7.0 |
| UA | MW-366 | C | 2021/09/15 | pH (field) | SU | 6.8 |
| UA | MW-366 | C | 2022/03/29 | pH (field) | SU | 6.8 |
| UA | MW-366 | C | 2022/09/30 | pH (field) | SU | 6.8 |
| UA | MW-366 | C | 2023/03/14 | pH (field) | SU | 6.7 |
| UA | MW-366 | C | 2023/05/16 | pH (field) | SU | 6.9 |
| UA | MW-366 | C | 2023/08/04 | pH (field) | SU | 6.9 |
| UA | MW-366 | C | 2023/11/02 | pH (field) | SU | 6.9 |
| UA | MW-366 | C | 2016/01/20 | Oxidation Reduction Potential | mV | 81.0 |
| UA | MW-366 | C | 2016/03/23 | Oxidation Reduction Potential | mV | 63.0 |
| UA | MW-366 | C | 2016/06/22 | Oxidation Reduction Potential | mV | -17.0 |

Attachment I. Site Groundwater Data

Geochemical Conceptual Site Model

Baldwin Fly Ash Pond System

Baldwin Power Plant

Baldwin, IL

| | | | | | | |
|----|--------|---|------------|-------------------------------|------------|--------|
| UA | MW-366 | C | 2016/09/20 | Oxidation Reduction Potential | mV | -46.0 |
| UA | MW-366 | C | 2016/12/22 | Oxidation Reduction Potential | mV | -2.00 |
| UA | MW-366 | C | 2017/03/15 | Oxidation Reduction Potential | mV | 3.00 |
| UA | MW-366 | C | 2017/06/20 | Oxidation Reduction Potential | mV | 48.0 |
| UA | MW-366 | C | 2017/07/26 | Oxidation Reduction Potential | mV | 111 |
| UA | MW-366 | C | 2017/11/27 | Oxidation Reduction Potential | mV | 139 |
| UA | MW-366 | C | 2018/06/26 | Oxidation Reduction Potential | mV | 25.0 |
| UA | MW-366 | C | 2018/09/25 | Oxidation Reduction Potential | mV | 45.0 |
| UA | MW-366 | C | 2019/03/19 | Oxidation Reduction Potential | mV | -60.0 |
| UA | MW-366 | C | 2019/09/25 | Oxidation Reduction Potential | mV | -106 |
| UA | MW-366 | C | 2020/03/26 | Oxidation Reduction Potential | mV | 60.0 |
| UA | MW-366 | C | 2020/09/16 | Oxidation Reduction Potential | mV | -66.0 |
| UA | MW-366 | C | 2021/03/12 | Oxidation Reduction Potential | mV | -18.0 |
| UA | MW-366 | C | 2021/09/15 | Oxidation Reduction Potential | mV | -17.0 |
| UA | MW-366 | C | 2022/03/29 | Oxidation Reduction Potential | mV | -17.0 |
| UA | MW-366 | C | 2022/09/30 | Oxidation Reduction Potential | mV | 138 |
| UA | MW-366 | C | 2023/03/14 | Oxidation Reduction Potential | mV | 5.90 |
| UA | MW-366 | C | 2023/05/16 | Oxidation Reduction Potential | mV | 95.0 |
| UA | MW-366 | C | 2023/08/04 | Oxidation Reduction Potential | mV | 92.0 |
| UA | MW-366 | C | 2023/11/02 | Oxidation Reduction Potential | mV | 9.00 |
| UA | MW-366 | C | 2016/01/20 | Eh | V | 0.28 |
| UA | MW-366 | C | 2016/03/23 | Eh | V | 0.26 |
| UA | MW-366 | C | 2016/06/22 | Eh | V | 0.17 |
| UA | MW-366 | C | 2016/09/20 | Eh | V | 0.15 |
| UA | MW-366 | C | 2016/12/22 | Eh | V | 0.19 |
| UA | MW-366 | C | 2017/03/15 | Eh | V | 0.20 |
| UA | MW-366 | C | 2017/06/20 | Eh | V | 0.24 |
| UA | MW-366 | C | 2017/07/26 | Eh | V | 0.30 |
| UA | MW-366 | C | 2017/11/27 | Eh | V | 0.33 |
| UA | MW-366 | C | 2018/06/26 | Eh | V | 0.22 |
| UA | MW-366 | C | 2018/09/25 | Eh | V | 0.24 |
| UA | MW-366 | C | 2019/03/19 | Eh | V | 0.14 |
| UA | MW-366 | C | 2019/09/25 | Eh | V | 0.088 |
| UA | MW-366 | C | 2020/03/26 | Eh | V | 0.26 |
| UA | MW-366 | C | 2020/09/16 | Eh | V | 0.13 |
| UA | MW-366 | C | 2021/03/12 | Eh | V | 0.18 |
| UA | MW-366 | C | 2021/09/15 | Eh | V | 0.18 |
| UA | MW-366 | C | 2022/03/29 | Eh | V | 0.18 |
| UA | MW-366 | C | 2022/09/30 | Eh | V | 0.33 |
| UA | MW-366 | C | 2023/03/14 | Eh | V | 0.20 |
| UA | MW-366 | C | 2023/05/16 | Eh | V | 0.29 |
| UA | MW-366 | C | 2023/08/04 | Eh | V | 0.29 |
| UA | MW-366 | C | 2023/11/02 | Eh | V | 0.20 |
| UA | MW-366 | C | 2017/07/26 | Alkalinity, bicarbonate | mg/L CaCO3 | 412 |
| UA | MW-366 | C | 2020/03/26 | Alkalinity, bicarbonate | mg/L CaCO3 | 314 |
| UA | MW-366 | C | 2020/09/16 | Alkalinity, bicarbonate | mg/L CaCO3 | 324 |
| UA | MW-366 | C | 2021/03/12 | Alkalinity, bicarbonate | mg/L CaCO3 | 280 |
| UA | MW-366 | C | 2021/09/15 | Alkalinity, bicarbonate | mg/L CaCO3 | 313 |
| UA | MW-366 | C | 2022/03/29 | Alkalinity, bicarbonate | mg/L CaCO3 | 340 |
| UA | MW-366 | C | 2022/09/30 | Alkalinity, bicarbonate | mg/L CaCO3 | 321 |
| UA | MW-366 | C | 2023/03/14 | Alkalinity, bicarbonate | mg/L CaCO3 | 350 |
| UA | MW-366 | C | 2023/05/16 | Alkalinity, bicarbonate | mg/L CaCO3 | 308 |
| UA | MW-366 | C | 2023/08/04 | Alkalinity, bicarbonate | mg/L CaCO3 | 315 |
| UA | MW-366 | C | 2023/11/02 | Alkalinity, bicarbonate | mg/L CaCO3 | 326 |
| UA | MW-366 | C | 2016/01/20 | Barium, total | mg/L | 0.0793 |
| UA | MW-366 | C | 2016/03/23 | Barium, total | mg/L | 0.0827 |
| UA | MW-366 | C | 2016/06/22 | Barium, total | mg/L | 0.0817 |

Attachment I. Site Groundwater Data

Geochemical Conceptual Site Model

Baldwin Fly Ash Pond System

Baldwin Power Plant

Baldwin, IL

| | | | | | | |
|----|--------|---|------------|----------------|------|--------|
| UA | MW-366 | C | 2016/09/20 | Barium, total | mg/L | 0.110 |
| UA | MW-366 | C | 2016/12/22 | Barium, total | mg/L | 0.0762 |
| UA | MW-366 | C | 2017/03/15 | Barium, total | mg/L | 0.0764 |
| UA | MW-366 | C | 2017/06/20 | Barium, total | mg/L | 0.0770 |
| UA | MW-366 | C | 2017/07/26 | Barium, total | mg/L | 0.0696 |
| UA | MW-366 | C | 2018/06/26 | Barium, total | mg/L | 0.0441 |
| UA | MW-366 | C | 2018/09/25 | Barium, total | mg/L | 0.0623 |
| UA | MW-366 | C | 2019/03/19 | Barium, total | mg/L | 0.0348 |
| UA | MW-366 | C | 2019/09/25 | Barium, total | mg/L | 0.0617 |
| UA | MW-366 | C | 2020/03/26 | Barium, total | mg/L | 0.0322 |
| UA | MW-366 | C | 2020/09/16 | Barium, total | mg/L | 0.0391 |
| UA | MW-366 | C | 2021/03/12 | Barium, total | mg/L | 0.0424 |
| UA | MW-366 | C | 2021/09/15 | Barium, total | mg/L | 0.0507 |
| UA | MW-366 | C | 2022/03/29 | Barium, total | mg/L | 0.0753 |
| UA | MW-366 | C | 2022/09/30 | Barium, total | mg/L | 0.0607 |
| UA | MW-366 | C | 2023/03/14 | Barium, total | mg/L | 0.0565 |
| UA | MW-366 | C | 2023/05/16 | Barium, total | mg/L | 0.0305 |
| UA | MW-366 | C | 2023/08/04 | Barium, total | mg/L | 0.0348 |
| UA | MW-366 | C | 2023/11/02 | Barium, total | mg/L | 0.0547 |
| UA | MW-366 | C | 2016/01/20 | Boron, total | mg/L | 1.42 |
| UA | MW-366 | C | 2016/03/23 | Boron, total | mg/L | 1.51 |
| UA | MW-366 | C | 2016/06/22 | Boron, total | mg/L | 1.30 |
| UA | MW-366 | C | 2016/09/20 | Boron, total | mg/L | 2.31 |
| UA | MW-366 | C | 2016/12/22 | Boron, total | mg/L | 1.69 |
| UA | MW-366 | C | 2017/03/15 | Boron, total | mg/L | 1.67 |
| UA | MW-366 | C | 2017/06/20 | Boron, total | mg/L | 1.66 |
| UA | MW-366 | C | 2017/07/26 | Boron, total | mg/L | 1.66 |
| UA | MW-366 | C | 2017/11/27 | Boron, total | mg/L | 1.79 |
| UA | MW-366 | C | 2018/06/26 | Boron, total | mg/L | 1.53 |
| UA | MW-366 | C | 2018/09/25 | Boron, total | mg/L | 1.38 |
| UA | MW-366 | C | 2019/03/19 | Boron, total | mg/L | 1.37 |
| UA | MW-366 | C | 2019/09/25 | Boron, total | mg/L | 1.50 |
| UA | MW-366 | C | 2020/03/26 | Boron, total | mg/L | 1.68 |
| UA | MW-366 | C | 2020/09/16 | Boron, total | mg/L | 1.64 |
| UA | MW-366 | C | 2021/03/12 | Boron, total | mg/L | 1.19 |
| UA | MW-366 | C | 2021/09/15 | Boron, total | mg/L | 1.67 |
| UA | MW-366 | C | 2022/03/29 | Boron, total | mg/L | 1.87 |
| UA | MW-366 | C | 2022/09/30 | Boron, total | mg/L | 2.70 |
| UA | MW-366 | C | 2023/03/14 | Boron, total | mg/L | 2.56 |
| UA | MW-366 | C | 2023/05/16 | Boron, total | mg/L | 1.74 |
| UA | MW-366 | C | 2023/08/04 | Boron, total | mg/L | 1.63 |
| UA | MW-366 | C | 2023/11/02 | Boron, total | mg/L | 1.81 |
| UA | MW-366 | C | 2016/01/20 | Calcium, total | mg/L | 74.5 |
| UA | MW-366 | C | 2016/03/23 | Calcium, total | mg/L | 72.9 |
| UA | MW-366 | C | 2016/06/22 | Calcium, total | mg/L | 70.4 |
| UA | MW-366 | C | 2016/09/20 | Calcium, total | mg/L | 103 |
| UA | MW-366 | C | 2016/12/22 | Calcium, total | mg/L | 67.7 |
| UA | MW-366 | C | 2017/03/15 | Calcium, total | mg/L | 74.4 |
| UA | MW-366 | C | 2017/06/20 | Calcium, total | mg/L | 70.1 |
| UA | MW-366 | C | 2017/07/26 | Calcium, total | mg/L | 73.0 |
| UA | MW-366 | C | 2017/11/27 | Calcium, total | mg/L | 108 |
| UA | MW-366 | C | 2018/06/26 | Calcium, total | mg/L | 141 |
| UA | MW-366 | C | 2018/09/25 | Calcium, total | mg/L | 127 |
| UA | MW-366 | C | 2019/03/19 | Calcium, total | mg/L | 146 |
| UA | MW-366 | C | 2019/09/25 | Calcium, total | mg/L | 166 |
| UA | MW-366 | C | 2020/03/26 | Calcium, total | mg/L | 168 |
| UA | MW-366 | C | 2020/09/16 | Calcium, total | mg/L | 175 |

Attachment I. Site Groundwater Data

Geochemical Conceptual Site Model

Baldwin Fly Ash Pond System

Baldwin Power Plant

Baldwin, IL

| | | | | | | |
|----|--------|---|------------|----------------------|------|--------|
| UA | MW-366 | C | 2021/03/12 | Calcium, total | mg/L | 163 |
| UA | MW-366 | C | 2021/09/15 | Calcium, total | mg/L | 181 |
| UA | MW-366 | C | 2022/03/29 | Calcium, total | mg/L | 186 |
| UA | MW-366 | C | 2022/09/30 | Calcium, total | mg/L | 227 |
| UA | MW-366 | C | 2023/03/14 | Calcium, total | mg/L | 244 |
| UA | MW-366 | C | 2023/05/16 | Calcium, total | mg/L | 187 |
| UA | MW-366 | C | 2023/08/04 | Calcium, total | mg/L | 184 |
| UA | MW-366 | C | 2023/11/02 | Calcium, total | mg/L | 177 |
| UA | MW-366 | C | 2016/01/20 | Chloride, total | mg/L | 9.00 |
| UA | MW-366 | C | 2016/03/23 | Chloride, total | mg/L | 8.00 |
| UA | MW-366 | C | 2016/06/22 | Chloride, total | mg/L | 12.0 |
| UA | MW-366 | C | 2016/09/20 | Chloride, total | mg/L | 17.0 |
| UA | MW-366 | C | 2016/12/22 | Chloride, total | mg/L | 14.0 |
| UA | MW-366 | C | 2017/03/15 | Chloride, total | mg/L | 14.0 |
| UA | MW-366 | C | 2017/06/20 | Chloride, total | mg/L | 16.0 |
| UA | MW-366 | C | 2017/07/26 | Chloride, total | mg/L | 18.0 |
| UA | MW-366 | C | 2017/11/27 | Chloride, total | mg/L | 31.0 |
| UA | MW-366 | C | 2018/06/26 | Chloride, total | mg/L | 50.0 |
| UA | MW-366 | C | 2018/09/25 | Chloride, total | mg/L | 47.0 |
| UA | MW-366 | C | 2019/03/19 | Chloride, total | mg/L | 43.0 |
| UA | MW-366 | C | 2019/09/25 | Chloride, total | mg/L | 47.0 |
| UA | MW-366 | C | 2020/03/26 | Chloride, total | mg/L | 47.0 |
| UA | MW-366 | C | 2020/09/16 | Chloride, total | mg/L | 53.0 |
| UA | MW-366 | C | 2021/03/12 | Chloride, total | mg/L | 39.0 |
| UA | MW-366 | C | 2021/09/15 | Chloride, total | mg/L | 47.0 |
| UA | MW-366 | C | 2022/03/29 | Chloride, total | mg/L | 46.0 |
| UA | MW-366 | C | 2022/09/30 | Chloride, total | mg/L | 56.0 |
| UA | MW-366 | C | 2023/03/14 | Chloride, total | mg/L | 55.0 |
| UA | MW-366 | C | 2023/05/16 | Chloride, total | mg/L | 48.0 |
| UA | MW-366 | C | 2023/08/04 | Chloride, total | mg/L | 47.0 |
| UA | MW-366 | C | 2023/11/02 | Chloride, total | mg/L | 42.0 |
| UA | MW-366 | C | 2023/05/16 | Iron, dissolved | mg/L | <0.02 |
| UA | MW-366 | C | 2023/08/04 | Iron, dissolved | mg/L | <0.012 |
| UA | MW-366 | C | 2017/07/26 | Magnesium, total | mg/L | 44.6 |
| UA | MW-366 | C | 2020/03/26 | Magnesium, total | mg/L | 73.2 |
| UA | MW-366 | C | 2020/09/16 | Magnesium, total | mg/L | 87.7 |
| UA | MW-366 | C | 2021/03/12 | Magnesium, total | mg/L | 66.8 |
| UA | MW-366 | C | 2021/09/15 | Magnesium, total | mg/L | 81.6 |
| UA | MW-366 | C | 2022/03/29 | Magnesium, total | mg/L | 105 |
| UA | MW-366 | C | 2022/09/30 | Magnesium, total | mg/L | 98.4 |
| UA | MW-366 | C | 2023/03/14 | Magnesium, total | mg/L | 110 |
| UA | MW-366 | C | 2023/05/16 | Magnesium, total | mg/L | 78.2 |
| UA | MW-366 | C | 2023/08/04 | Magnesium, total | mg/L | 82.3 |
| UA | MW-366 | C | 2023/11/02 | Magnesium, total | mg/L | 84.3 |
| UA | MW-366 | C | 2023/05/16 | Manganese, dissolved | mg/L | 0.0281 |
| UA | MW-366 | C | 2023/08/04 | Manganese, dissolved | mg/L | 0.0169 |
| UA | MW-366 | C | 2023/05/16 | Phosphate, dissolved | mg/L | 0.0150 |
| UA | MW-366 | C | 2023/08/04 | Phosphate, dissolved | mg/L | 0.0340 |
| UA | MW-366 | C | 2017/07/26 | Potassium, total | mg/L | 3.85 |
| UA | MW-366 | C | 2020/03/26 | Potassium, total | mg/L | 5.15 |
| UA | MW-366 | C | 2020/09/16 | Potassium, total | mg/L | 5.45 |
| UA | MW-366 | C | 2021/03/12 | Potassium, total | mg/L | 3.91 |
| UA | MW-366 | C | 2021/09/15 | Potassium, total | mg/L | 4.39 |
| UA | MW-366 | C | 2022/03/29 | Potassium, total | mg/L | 5.35 |
| UA | MW-366 | C | 2022/09/30 | Potassium, total | mg/L | 4.65 |
| UA | MW-366 | C | 2023/03/14 | Potassium, total | mg/L | 4.44 |
| UA | MW-366 | C | 2023/05/16 | Potassium, total | mg/L | 4.05 |

Attachment I. Site Groundwater Data

Geochemical Conceptual Site Model

Baldwin Fly Ash Pond System

Baldwin Power Plant

Baldwin, IL

| | | | | | | |
|----|--------|---|------------|-----------------------|-----------|------|
| UA | MW-366 | C | 2023/08/04 | Potassium, total | mg/L | 4.05 |
| UA | MW-366 | C | 2023/11/02 | Potassium, total | mg/L | 4.39 |
| UA | MW-366 | C | 2023/05/16 | Silicon, dissolved | mg/L | 8.80 |
| UA | MW-366 | C | 2023/08/04 | Silicon, dissolved | mg/L | 7.81 |
| UA | MW-366 | C | 2017/07/26 | Sodium, total | mg/L | 57.5 |
| UA | MW-366 | C | 2020/03/26 | Sodium, total | mg/L | 74.3 |
| UA | MW-366 | C | 2020/09/16 | Sodium, total | mg/L | 81.8 |
| UA | MW-366 | C | 2021/03/12 | Sodium, total | mg/L | 59.5 |
| UA | MW-366 | C | 2021/09/15 | Sodium, total | mg/L | 63.3 |
| UA | MW-366 | C | 2022/03/29 | Sodium, total | mg/L | 76.8 |
| UA | MW-366 | C | 2022/09/30 | Sodium, total | mg/L | 68.2 |
| UA | MW-366 | C | 2023/03/14 | Sodium, total | mg/L | 70.0 |
| UA | MW-366 | C | 2023/05/16 | Sodium, total | mg/L | 61.6 |
| UA | MW-366 | C | 2023/08/04 | Sodium, total | mg/L | 56.9 |
| UA | MW-366 | C | 2023/11/02 | Sodium, total | mg/L | 63.4 |
| UA | MW-366 | C | 2016/01/20 | Sulfate, total | mg/L | 38.0 |
| UA | MW-366 | C | 2016/03/23 | Sulfate, total | mg/L | 33.0 |
| UA | MW-366 | C | 2016/06/22 | Sulfate, total | mg/L | 40.0 |
| UA | MW-366 | C | 2016/09/20 | Sulfate, total | mg/L | 49.0 |
| UA | MW-366 | C | 2016/12/22 | Sulfate, total | mg/L | 46.0 |
| UA | MW-366 | C | 2017/03/15 | Sulfate, total | mg/L | 46.0 |
| UA | MW-366 | C | 2017/06/20 | Sulfate, total | mg/L | 64.0 |
| UA | MW-366 | C | 2017/07/26 | Sulfate, total | mg/L | 77.0 |
| UA | MW-366 | C | 2017/11/27 | Sulfate, total | mg/L | 195 |
| UA | MW-366 | C | 2018/06/26 | Sulfate, total | mg/L | 526 |
| UA | MW-366 | C | 2018/09/25 | Sulfate, total | mg/L | 432 |
| UA | MW-366 | C | 2019/03/19 | Sulfate, total | mg/L | 397 |
| UA | MW-366 | C | 2019/09/25 | Sulfate, total | mg/L | 464 |
| UA | MW-366 | C | 2020/03/26 | Sulfate, total | mg/L | 488 |
| UA | MW-366 | C | 2020/09/16 | Sulfate, total | mg/L | 521 |
| UA | MW-366 | C | 2021/03/12 | Sulfate, total | mg/L | 360 |
| UA | MW-366 | C | 2021/09/15 | Sulfate, total | mg/L | 597 |
| UA | MW-366 | C | 2022/03/29 | Sulfate, total | mg/L | 583 |
| UA | MW-366 | C | 2022/09/30 | Sulfate, total | mg/L | 700 |
| UA | MW-366 | C | 2023/03/14 | Sulfate, total | mg/L | 699 |
| UA | MW-366 | C | 2023/05/16 | Sulfate, total | mg/L | 502 |
| UA | MW-366 | C | 2023/08/04 | Sulfate, total | mg/L | 496 |
| UA | MW-366 | C | 2023/11/02 | Sulfate, total | mg/L | 487 |
| UA | MW-366 | C | 2016/01/20 | Temperature (Celsius) | degrees C | 10.2 |
| UA | MW-366 | C | 2016/03/23 | Temperature (Celsius) | degrees C | 14.7 |
| UA | MW-366 | C | 2016/06/22 | Temperature (Celsius) | degrees C | 22.9 |
| UA | MW-366 | C | 2016/09/20 | Temperature (Celsius) | degrees C | 21.1 |
| UA | MW-366 | C | 2016/12/22 | Temperature (Celsius) | degrees C | 14.0 |
| UA | MW-366 | C | 2017/03/15 | Temperature (Celsius) | degrees C | 12.6 |
| UA | MW-366 | C | 2017/06/20 | Temperature (Celsius) | degrees C | 19.4 |
| UA | MW-366 | C | 2017/07/26 | Temperature (Celsius) | degrees C | 23.6 |
| UA | MW-366 | C | 2017/11/27 | Temperature (Celsius) | degrees C | 17.6 |
| UA | MW-366 | C | 2018/06/26 | Temperature (Celsius) | degrees C | 20.6 |
| UA | MW-366 | C | 2018/09/25 | Temperature (Celsius) | degrees C | 16.4 |
| UA | MW-366 | C | 2019/03/19 | Temperature (Celsius) | degrees C | 14.8 |
| UA | MW-366 | C | 2019/09/25 | Temperature (Celsius) | degrees C | 16.5 |
| UA | MW-366 | C | 2020/03/26 | Temperature (Celsius) | degrees C | 14.1 |
| UA | MW-366 | C | 2020/09/16 | Temperature (Celsius) | degrees C | 15.4 |
| UA | MW-366 | C | 2021/03/12 | Temperature (Celsius) | degrees C | 13.4 |
| UA | MW-366 | C | 2021/09/15 | Temperature (Celsius) | degrees C | 16.6 |
| UA | MW-366 | C | 2022/03/29 | Temperature (Celsius) | degrees C | 13.0 |
| UA | MW-366 | C | 2022/09/30 | Temperature (Celsius) | degrees C | 16.6 |

Attachment I. Site Groundwater Data

Geochemical Conceptual Site Model

Baldwin Fly Ash Pond System

Baldwin Power Plant

Baldwin, IL

| | | | | | | |
|----|--------|---|------------|-------------------------------|-----------|-------|
| UA | MW-366 | C | 2023/03/14 | Temperature (Celsius) | degrees C | 13.5 |
| UA | MW-366 | C | 2023/05/16 | Temperature (Celsius) | degrees C | 14.5 |
| UA | MW-366 | C | 2023/08/04 | Temperature (Celsius) | degrees C | 15.4 |
| UA | MW-366 | C | 2023/11/02 | Temperature (Celsius) | degrees C | 15.7 |
| UA | MW-366 | C | 2016/01/20 | Total Dissolved Solids | mg/L | 416 |
| UA | MW-366 | C | 2016/03/23 | Total Dissolved Solids | mg/L | 450 |
| UA | MW-366 | C | 2016/06/22 | Total Dissolved Solids | mg/L | 434 |
| UA | MW-366 | C | 2016/09/20 | Total Dissolved Solids | mg/L | 398 |
| UA | MW-366 | C | 2016/12/22 | Total Dissolved Solids | mg/L | 430 |
| UA | MW-366 | C | 2017/03/15 | Total Dissolved Solids | mg/L | 478 |
| UA | MW-366 | C | 2017/06/20 | Total Dissolved Solids | mg/L | 474 |
| UA | MW-366 | C | 2017/07/26 | Total Dissolved Solids | mg/L | 474 |
| UA | MW-366 | C | 2017/11/27 | Total Dissolved Solids | mg/L | 740 |
| UA | MW-366 | C | 2018/06/26 | Total Dissolved Solids | mg/L | 1,060 |
| UA | MW-366 | C | 2018/09/25 | Total Dissolved Solids | mg/L | 1,050 |
| UA | MW-366 | C | 2019/03/19 | Total Dissolved Solids | mg/L | 1,030 |
| UA | MW-366 | C | 2019/09/25 | Total Dissolved Solids | mg/L | 1,130 |
| UA | MW-366 | C | 2020/03/26 | Total Dissolved Solids | mg/L | 1,090 |
| UA | MW-366 | C | 2020/09/16 | Total Dissolved Solids | mg/L | 1,100 |
| UA | MW-366 | C | 2021/03/12 | Total Dissolved Solids | mg/L | 876 |
| UA | MW-366 | C | 2021/09/15 | Total Dissolved Solids | mg/L | 1,140 |
| UA | MW-366 | C | 2022/03/29 | Total Dissolved Solids | mg/L | 1,230 |
| UA | MW-366 | C | 2022/09/30 | Total Dissolved Solids | mg/L | 1,350 |
| UA | MW-366 | C | 2023/03/14 | Total Dissolved Solids | mg/L | 1,490 |
| UA | MW-366 | C | 2023/05/16 | Total Dissolved Solids | mg/L | 1,160 |
| UA | MW-366 | C | 2023/08/04 | Total Dissolved Solids | mg/L | 1,190 |
| UA | MW-366 | C | 2023/11/02 | Total Dissolved Solids | mg/L | 1,370 |
| UA | MW-375 | C | 2016/01/20 | pH (field) | SU | 7.7 |
| UA | MW-375 | C | 2016/03/23 | pH (field) | SU | 7.8 |
| UA | MW-375 | C | 2016/06/22 | pH (field) | SU | 7.9 |
| UA | MW-375 | C | 2016/09/20 | pH (field) | SU | 7.8 |
| UA | MW-375 | C | 2016/12/22 | pH (field) | SU | 7.8 |
| UA | MW-375 | C | 2017/03/16 | pH (field) | SU | 7.8 |
| UA | MW-375 | C | 2017/06/21 | pH (field) | SU | 7.7 |
| UA | MW-375 | C | 2017/07/28 | pH (field) | SU | 7.8 |
| UA | MW-375 | C | 2017/11/27 | pH (field) | SU | 7.9 |
| UA | MW-375 | C | 2018/06/27 | pH (field) | SU | 7.6 |
| UA | MW-375 | C | 2018/09/25 | pH (field) | SU | 7.8 |
| UA | MW-375 | C | 2019/03/20 | pH (field) | SU | 7.8 |
| UA | MW-375 | C | 2019/09/25 | pH (field) | SU | 7.8 |
| UA | MW-375 | C | 2020/03/24 | pH (field) | SU | 7.8 |
| UA | MW-375 | C | 2020/09/16 | pH (field) | SU | 7.8 |
| UA | MW-375 | C | 2021/03/12 | pH (field) | SU | 7.8 |
| UA | MW-375 | C | 2021/09/14 | pH (field) | SU | 7.8 |
| UA | MW-375 | C | 2022/03/28 | pH (field) | SU | 7.8 |
| UA | MW-375 | C | 2022/09/30 | pH (field) | SU | 7.8 |
| UA | MW-375 | C | 2023/03/14 | pH (field) | SU | 7.7 |
| UA | MW-375 | C | 2023/05/18 | pH (field) | SU | 7.7 |
| UA | MW-375 | C | 2023/08/07 | pH (field) | SU | 7.0 |
| UA | MW-375 | C | 2023/11/03 | pH (field) | SU | 7.7 |
| UA | MW-375 | C | 2016/01/20 | Oxidation Reduction Potential | mV | 24.0 |
| UA | MW-375 | C | 2016/03/23 | Oxidation Reduction Potential | mV | 32.0 |
| UA | MW-375 | C | 2016/06/22 | Oxidation Reduction Potential | mV | 17.0 |
| UA | MW-375 | C | 2016/09/20 | Oxidation Reduction Potential | mV | -15.0 |
| UA | MW-375 | C | 2016/12/22 | Oxidation Reduction Potential | mV | -27.0 |
| UA | MW-375 | C | 2017/03/16 | Oxidation Reduction Potential | mV | 71.0 |
| UA | MW-375 | C | 2017/06/21 | Oxidation Reduction Potential | mV | 18.0 |

Attachment I. Site Groundwater Data

Geochemical Conceptual Site Model

Baldwin Fly Ash Pond System

Baldwin Power Plant

Baldwin, IL

| | | | | | | |
|----|--------|---|------------|-------------------------------|------------|--------|
| UA | MW-375 | C | 2017/07/28 | Oxidation Reduction Potential | mV | 47.0 |
| UA | MW-375 | C | 2017/11/27 | Oxidation Reduction Potential | mV | 79.0 |
| UA | MW-375 | C | 2018/06/27 | Oxidation Reduction Potential | mV | 149 |
| UA | MW-375 | C | 2018/09/25 | Oxidation Reduction Potential | mV | 131 |
| UA | MW-375 | C | 2019/03/20 | Oxidation Reduction Potential | mV | -12.0 |
| UA | MW-375 | C | 2019/09/25 | Oxidation Reduction Potential | mV | 24.0 |
| UA | MW-375 | C | 2020/03/24 | Oxidation Reduction Potential | mV | 13.0 |
| UA | MW-375 | C | 2020/09/16 | Oxidation Reduction Potential | mV | -97.0 |
| UA | MW-375 | C | 2021/03/12 | Oxidation Reduction Potential | mV | -2.00 |
| UA | MW-375 | C | 2021/09/14 | Oxidation Reduction Potential | mV | -106 |
| UA | MW-375 | C | 2022/03/28 | Oxidation Reduction Potential | mV | -63.0 |
| UA | MW-375 | C | 2022/09/30 | Oxidation Reduction Potential | mV | 61.0 |
| UA | MW-375 | C | 2023/03/14 | Oxidation Reduction Potential | mV | -68.3 |
| UA | MW-375 | C | 2023/05/18 | Oxidation Reduction Potential | mV | 7.00 |
| UA | MW-375 | C | 2023/08/07 | Oxidation Reduction Potential | mV | 160 |
| UA | MW-375 | C | 2023/11/03 | Oxidation Reduction Potential | mV | -3.00 |
| UA | MW-375 | C | 2016/01/20 | Eh | V | 0.22 |
| UA | MW-375 | C | 2016/03/23 | Eh | V | 0.23 |
| UA | MW-375 | C | 2016/06/22 | Eh | V | 0.21 |
| UA | MW-375 | C | 2016/09/20 | Eh | V | 0.17 |
| UA | MW-375 | C | 2016/12/22 | Eh | V | 0.17 |
| UA | MW-375 | C | 2017/03/16 | Eh | V | 0.27 |
| UA | MW-375 | C | 2017/06/21 | Eh | V | 0.21 |
| UA | MW-375 | C | 2017/07/28 | Eh | V | 0.24 |
| UA | MW-375 | C | 2017/11/27 | Eh | V | 0.27 |
| UA | MW-375 | C | 2018/06/27 | Eh | V | 0.34 |
| UA | MW-375 | C | 2018/09/25 | Eh | V | 0.32 |
| UA | MW-375 | C | 2019/03/20 | Eh | V | 0.18 |
| UA | MW-375 | C | 2019/09/25 | Eh | V | 0.22 |
| UA | MW-375 | C | 2020/03/24 | Eh | V | 0.21 |
| UA | MW-375 | C | 2020/09/16 | Eh | V | 0.098 |
| UA | MW-375 | C | 2021/03/12 | Eh | V | 0.19 |
| UA | MW-375 | C | 2021/09/14 | Eh | V | 0.089 |
| UA | MW-375 | C | 2022/03/28 | Eh | V | 0.13 |
| UA | MW-375 | C | 2022/09/30 | Eh | V | 0.26 |
| UA | MW-375 | C | 2023/03/14 | Eh | V | 0.13 |
| UA | MW-375 | C | 2023/05/18 | Eh | V | 0.20 |
| UA | MW-375 | C | 2023/08/07 | Eh | V | 0.35 |
| UA | MW-375 | C | 2023/11/03 | Eh | V | 0.19 |
| UA | MW-375 | C | 2017/07/28 | Alkalinity, bicarbonate | mg/L CaCO3 | 620 |
| UA | MW-375 | C | 2020/03/24 | Alkalinity, bicarbonate | mg/L CaCO3 | 572 |
| UA | MW-375 | C | 2020/09/16 | Alkalinity, bicarbonate | mg/L CaCO3 | 586 |
| UA | MW-375 | C | 2021/03/12 | Alkalinity, bicarbonate | mg/L CaCO3 | 580 |
| UA | MW-375 | C | 2021/09/14 | Alkalinity, bicarbonate | mg/L CaCO3 | 585 |
| UA | MW-375 | C | 2022/03/28 | Alkalinity, bicarbonate | mg/L CaCO3 | 591 |
| UA | MW-375 | C | 2022/09/30 | Alkalinity, bicarbonate | mg/L CaCO3 | 593 |
| UA | MW-375 | C | 2023/03/14 | Alkalinity, bicarbonate | mg/L CaCO3 | 594 |
| UA | MW-375 | C | 2023/05/18 | Alkalinity, bicarbonate | mg/L CaCO3 | 585 |
| UA | MW-375 | C | 2023/08/07 | Alkalinity, bicarbonate | mg/L CaCO3 | 605 |
| UA | MW-375 | C | 2023/11/03 | Alkalinity, bicarbonate | mg/L CaCO3 | 598 |
| UA | MW-375 | C | 2022/09/30 | Alkalinity, carbonate | mg/L CaCO3 | 6.00 |
| UA | MW-375 | C | 2023/11/03 | Alkalinity, carbonate | mg/L CaCO3 | 12.0 |
| UA | MW-375 | C | 2016/01/20 | Barium, total | mg/L | 0.0303 |
| UA | MW-375 | C | 2016/03/23 | Barium, total | mg/L | 0.0264 |
| UA | MW-375 | C | 2016/06/22 | Barium, total | mg/L | 0.0247 |
| UA | MW-375 | C | 2016/09/20 | Barium, total | mg/L | 0.0375 |
| UA | MW-375 | C | 2016/12/22 | Barium, total | mg/L | 0.0239 |

Attachment I. Site Groundwater Data

Geochemical Conceptual Site Model

Baldwin Fly Ash Pond System

Baldwin Power Plant

Baldwin, IL

| | | | | | | |
|----|--------|---|------------|----------------|------|--------|
| UA | MW-375 | C | 2017/03/16 | Barium, total | mg/L | 0.0237 |
| UA | MW-375 | C | 2017/06/21 | Barium, total | mg/L | 0.0250 |
| UA | MW-375 | C | 2017/07/28 | Barium, total | mg/L | 0.0243 |
| UA | MW-375 | C | 2018/06/27 | Barium, total | mg/L | 0.0297 |
| UA | MW-375 | C | 2018/09/25 | Barium, total | mg/L | 0.0263 |
| UA | MW-375 | C | 2019/03/20 | Barium, total | mg/L | 0.0271 |
| UA | MW-375 | C | 2019/09/25 | Barium, total | mg/L | 0.0263 |
| UA | MW-375 | C | 2020/03/24 | Barium, total | mg/L | 0.0259 |
| UA | MW-375 | C | 2020/09/16 | Barium, total | mg/L | 0.0238 |
| UA | MW-375 | C | 2021/03/12 | Barium, total | mg/L | 0.0245 |
| UA | MW-375 | C | 2021/09/14 | Barium, total | mg/L | 0.0230 |
| UA | MW-375 | C | 2022/03/28 | Barium, total | mg/L | 0.0226 |
| UA | MW-375 | C | 2022/09/30 | Barium, total | mg/L | 0.0312 |
| UA | MW-375 | C | 2023/03/14 | Barium, total | mg/L | 0.0244 |
| UA | MW-375 | C | 2023/05/18 | Barium, total | mg/L | 0.0290 |
| UA | MW-375 | C | 2023/08/07 | Barium, total | mg/L | 0.0338 |
| UA | MW-375 | C | 2023/11/03 | Barium, total | mg/L | 0.0211 |
| UA | MW-375 | C | 2016/01/20 | Boron, total | mg/L | 0.979 |
| UA | MW-375 | C | 2016/03/23 | Boron, total | mg/L | 1.13 |
| UA | MW-375 | C | 2016/06/22 | Boron, total | mg/L | 1.27 |
| UA | MW-375 | C | 2016/09/20 | Boron, total | mg/L | 2.06 |
| UA | MW-375 | C | 2016/12/22 | Boron, total | mg/L | 1.32 |
| UA | MW-375 | C | 2017/03/16 | Boron, total | mg/L | 1.24 |
| UA | MW-375 | C | 2017/06/21 | Boron, total | mg/L | 1.37 |
| UA | MW-375 | C | 2017/07/28 | Boron, total | mg/L | 1.23 |
| UA | MW-375 | C | 2017/11/27 | Boron, total | mg/L | 1.26 |
| UA | MW-375 | C | 2018/06/27 | Boron, total | mg/L | 1.46 |
| UA | MW-375 | C | 2018/09/25 | Boron, total | mg/L | 1.34 |
| UA | MW-375 | C | 2019/03/20 | Boron, total | mg/L | 1.38 |
| UA | MW-375 | C | 2019/09/25 | Boron, total | mg/L | 1.39 |
| UA | MW-375 | C | 2020/03/24 | Boron, total | mg/L | 1.50 |
| UA | MW-375 | C | 2020/09/16 | Boron, total | mg/L | 1.44 |
| UA | MW-375 | C | 2021/03/12 | Boron, total | mg/L | 1.51 |
| UA | MW-375 | C | 2021/09/14 | Boron, total | mg/L | 1.33 |
| UA | MW-375 | C | 2022/03/28 | Boron, total | mg/L | 1.54 |
| UA | MW-375 | C | 2022/09/30 | Boron, total | mg/L | 1.75 |
| UA | MW-375 | C | 2023/03/14 | Boron, total | mg/L | 1.40 |
| UA | MW-375 | C | 2023/05/18 | Boron, total | mg/L | 1.45 |
| UA | MW-375 | C | 2023/08/07 | Boron, total | mg/L | 1.78 |
| UA | MW-375 | C | 2023/11/03 | Boron, total | mg/L | 1.35 |
| UA | MW-375 | C | 2016/01/20 | Calcium, total | mg/L | 14.9 |
| UA | MW-375 | C | 2016/03/23 | Calcium, total | mg/L | 12.1 |
| UA | MW-375 | C | 2016/06/22 | Calcium, total | mg/L | 11.2 |
| UA | MW-375 | C | 2016/09/20 | Calcium, total | mg/L | 18.1 |
| UA | MW-375 | C | 2016/12/22 | Calcium, total | mg/L | 9.63 |
| UA | MW-375 | C | 2017/03/16 | Calcium, total | mg/L | 9.96 |
| UA | MW-375 | C | 2017/06/21 | Calcium, total | mg/L | 8.82 |
| UA | MW-375 | C | 2017/07/28 | Calcium, total | mg/L | 8.97 |
| UA | MW-375 | C | 2017/11/27 | Calcium, total | mg/L | 10.6 |
| UA | MW-375 | C | 2018/06/27 | Calcium, total | mg/L | 24.0 |
| UA | MW-375 | C | 2018/09/25 | Calcium, total | mg/L | 19.7 |
| UA | MW-375 | C | 2019/03/20 | Calcium, total | mg/L | 21.0 |
| UA | MW-375 | C | 2019/09/25 | Calcium, total | mg/L | 20.7 |
| UA | MW-375 | C | 2020/03/24 | Calcium, total | mg/L | 24.7 |
| UA | MW-375 | C | 2020/09/16 | Calcium, total | mg/L | 13.8 |
| UA | MW-375 | C | 2021/03/12 | Calcium, total | mg/L | 14.6 |
| UA | MW-375 | C | 2021/09/14 | Calcium, total | mg/L | 11.8 |

Attachment I. Site Groundwater Data

Geochemical Conceptual Site Model

Baldwin Fly Ash Pond System

Baldwin Power Plant

Baldwin, IL

| | | | | | | |
|----|--------|---|------------|----------------------|------|---------|
| UA | MW-375 | C | 2022/03/28 | Calcium, total | mg/L | 11.0 |
| UA | MW-375 | C | 2022/09/30 | Calcium, total | mg/L | 12.7 |
| UA | MW-375 | C | 2023/03/14 | Calcium, total | mg/L | 11.2 |
| UA | MW-375 | C | 2023/05/18 | Calcium, total | mg/L | 13.7 |
| UA | MW-375 | C | 2023/08/07 | Calcium, total | mg/L | 9.80 |
| UA | MW-375 | C | 2023/11/03 | Calcium, total | mg/L | 10.7 |
| UA | MW-375 | C | 2016/01/20 | Chloride, total | mg/L | 77.0 |
| UA | MW-375 | C | 2016/03/23 | Chloride, total | mg/L | 77.0 |
| UA | MW-375 | C | 2016/06/22 | Chloride, total | mg/L | 90.0 |
| UA | MW-375 | C | 2016/09/20 | Chloride, total | mg/L | 96.0 |
| UA | MW-375 | C | 2016/12/22 | Chloride, total | mg/L | 98.0 |
| UA | MW-375 | C | 2017/03/16 | Chloride, total | mg/L | 93.0 |
| UA | MW-375 | C | 2017/06/21 | Chloride, total | mg/L | 91.0 |
| UA | MW-375 | C | 2017/07/28 | Chloride, total | mg/L | 96.0 |
| UA | MW-375 | C | 2017/11/27 | Chloride, total | mg/L | 90.0 |
| UA | MW-375 | C | 2018/06/27 | Chloride, total | mg/L | 103 |
| UA | MW-375 | C | 2018/09/25 | Chloride, total | mg/L | 107 |
| UA | MW-375 | C | 2019/03/20 | Chloride, total | mg/L | 95.0 |
| UA | MW-375 | C | 2019/09/25 | Chloride, total | mg/L | 97.0 |
| UA | MW-375 | C | 2020/03/24 | Chloride, total | mg/L | 105 |
| UA | MW-375 | C | 2020/09/16 | Chloride, total | mg/L | 111 |
| UA | MW-375 | C | 2021/03/12 | Chloride, total | mg/L | 104 |
| UA | MW-375 | C | 2021/09/14 | Chloride, total | mg/L | 114 |
| UA | MW-375 | C | 2022/03/28 | Chloride, total | mg/L | 106 |
| UA | MW-375 | C | 2022/09/30 | Chloride, total | mg/L | 118 |
| UA | MW-375 | C | 2023/03/14 | Chloride, total | mg/L | 92.0 |
| UA | MW-375 | C | 2023/05/18 | Chloride, total | mg/L | 90.0 |
| UA | MW-375 | C | 2023/08/07 | Chloride, total | mg/L | 90.0 |
| UA | MW-375 | C | 2023/11/03 | Chloride, total | mg/L | 98.0 |
| UA | MW-375 | C | 2023/05/18 | Iron, dissolved | mg/L | <0.02 |
| UA | MW-375 | C | 2023/08/07 | Iron, dissolved | mg/L | <0.0115 |
| UA | MW-375 | C | 2017/07/28 | Magnesium, total | mg/L | 5.14 |
| UA | MW-375 | C | 2020/03/24 | Magnesium, total | mg/L | 11.8 |
| UA | MW-375 | C | 2020/09/16 | Magnesium, total | mg/L | 7.97 |
| UA | MW-375 | C | 2021/03/12 | Magnesium, total | mg/L | 5.98 |
| UA | MW-375 | C | 2021/09/14 | Magnesium, total | mg/L | 6.09 |
| UA | MW-375 | C | 2022/03/28 | Magnesium, total | mg/L | 6.41 |
| UA | MW-375 | C | 2022/09/30 | Magnesium, total | mg/L | 6.49 |
| UA | MW-375 | C | 2023/03/14 | Magnesium, total | mg/L | 6.09 |
| UA | MW-375 | C | 2023/05/18 | Magnesium, total | mg/L | 6.92 |
| UA | MW-375 | C | 2023/08/07 | Magnesium, total | mg/L | 5.52 |
| UA | MW-375 | C | 2023/11/03 | Magnesium, total | mg/L | 5.96 |
| UA | MW-375 | C | 2023/05/18 | Manganese, dissolved | mg/L | <0.0025 |
| UA | MW-375 | C | 2023/08/07 | Manganese, dissolved | mg/L | 0.00130 |
| UA | MW-375 | C | 2023/05/18 | Phosphate, dissolved | mg/L | 0.0310 |
| UA | MW-375 | C | 2023/08/07 | Phosphate, dissolved | mg/L | 0.0400 |
| UA | MW-375 | C | 2017/07/28 | Potassium, total | mg/L | 2.36 |
| UA | MW-375 | C | 2020/03/24 | Potassium, total | mg/L | 3.26 |
| UA | MW-375 | C | 2020/09/16 | Potassium, total | mg/L | 3.08 |
| UA | MW-375 | C | 2021/03/12 | Potassium, total | mg/L | 2.42 |
| UA | MW-375 | C | 2021/09/14 | Potassium, total | mg/L | 2.57 |
| UA | MW-375 | C | 2022/03/28 | Potassium, total | mg/L | 2.78 |
| UA | MW-375 | C | 2022/09/30 | Potassium, total | mg/L | 2.84 |
| UA | MW-375 | C | 2023/03/14 | Potassium, total | mg/L | 2.43 |
| UA | MW-375 | C | 2023/05/18 | Potassium, total | mg/L | 2.95 |
| UA | MW-375 | C | 2023/08/07 | Potassium, total | mg/L | 2.74 |
| UA | MW-375 | C | 2023/11/03 | Potassium, total | mg/L | 2.73 |

Attachment I. Site Groundwater Data

Geochemical Conceptual Site Model

Baldwin Fly Ash Pond System

Baldwin Power Plant

Baldwin, IL

| | | | | | | |
|----|--------|---|------------|-----------------------|-----------|------|
| UA | MW-375 | C | 2023/05/18 | Silicon, dissolved | mg/L | 3.56 |
| UA | MW-375 | C | 2023/08/07 | Silicon, dissolved | mg/L | 3.46 |
| UA | MW-375 | C | 2017/07/28 | Sodium, total | mg/L | 352 |
| UA | MW-375 | C | 2020/03/24 | Sodium, total | mg/L | 388 |
| UA | MW-375 | C | 2020/09/16 | Sodium, total | mg/L | 440 |
| UA | MW-375 | C | 2021/03/12 | Sodium, total | mg/L | 333 |
| UA | MW-375 | C | 2021/09/14 | Sodium, total | mg/L | 330 |
| UA | MW-375 | C | 2022/03/28 | Sodium, total | mg/L | 388 |
| UA | MW-375 | C | 2022/09/30 | Sodium, total | mg/L | 354 |
| UA | MW-375 | C | 2023/03/14 | Sodium, total | mg/L | 369 |
| UA | MW-375 | C | 2023/05/18 | Sodium, total | mg/L | 419 |
| UA | MW-375 | C | 2023/08/07 | Sodium, total | mg/L | 383 |
| UA | MW-375 | C | 2023/11/03 | Sodium, total | mg/L | 415 |
| UA | MW-375 | C | 2016/01/20 | Sulfate, total | mg/L | 104 |
| UA | MW-375 | C | 2016/03/23 | Sulfate, total | mg/L | 128 |
| UA | MW-375 | C | 2016/06/22 | Sulfate, total | mg/L | 122 |
| UA | MW-375 | C | 2016/09/20 | Sulfate, total | mg/L | 123 |
| UA | MW-375 | C | 2016/12/22 | Sulfate, total | mg/L | 103 |
| UA | MW-375 | C | 2017/03/16 | Sulfate, total | mg/L | 93.0 |
| UA | MW-375 | C | 2017/06/21 | Sulfate, total | mg/L | 83.0 |
| UA | MW-375 | C | 2017/07/28 | Sulfate, total | mg/L | 85.0 |
| UA | MW-375 | C | 2017/11/27 | Sulfate, total | mg/L | 88.0 |
| UA | MW-375 | C | 2018/06/27 | Sulfate, total | mg/L | 243 |
| UA | MW-375 | C | 2018/09/25 | Sulfate, total | mg/L | 214 |
| UA | MW-375 | C | 2019/03/20 | Sulfate, total | mg/L | 184 |
| UA | MW-375 | C | 2019/09/25 | Sulfate, total | mg/L | 163 |
| UA | MW-375 | C | 2020/03/24 | Sulfate, total | mg/L | 209 |
| UA | MW-375 | C | 2020/09/16 | Sulfate, total | mg/L | 202 |
| UA | MW-375 | C | 2021/03/12 | Sulfate, total | mg/L | 168 |
| UA | MW-375 | C | 2021/09/14 | Sulfate, total | mg/L | 176 |
| UA | MW-375 | C | 2022/03/28 | Sulfate, total | mg/L | 160 |
| UA | MW-375 | C | 2022/09/30 | Sulfate, total | mg/L | 160 |
| UA | MW-375 | C | 2023/03/14 | Sulfate, total | mg/L | 109 |
| UA | MW-375 | C | 2023/05/18 | Sulfate, total | mg/L | 104 |
| UA | MW-375 | C | 2023/08/07 | Sulfate, total | mg/L | 104 |
| UA | MW-375 | C | 2023/11/03 | Sulfate, total | mg/L | 114 |
| UA | MW-375 | C | 2016/01/20 | Temperature (Celsius) | degrees C | 10.4 |
| UA | MW-375 | C | 2016/03/23 | Temperature (Celsius) | degrees C | 14.3 |
| UA | MW-375 | C | 2016/06/22 | Temperature (Celsius) | degrees C | 24.7 |
| UA | MW-375 | C | 2016/09/20 | Temperature (Celsius) | degrees C | 26.9 |
| UA | MW-375 | C | 2016/12/22 | Temperature (Celsius) | degrees C | 11.6 |
| UA | MW-375 | C | 2017/03/16 | Temperature (Celsius) | degrees C | 12.5 |
| UA | MW-375 | C | 2017/06/21 | Temperature (Celsius) | degrees C | 18.1 |
| UA | MW-375 | C | 2017/07/28 | Temperature (Celsius) | degrees C | 19.8 |
| UA | MW-375 | C | 2017/11/27 | Temperature (Celsius) | degrees C | 14.9 |
| UA | MW-375 | C | 2018/06/27 | Temperature (Celsius) | degrees C | 19.0 |
| UA | MW-375 | C | 2018/09/25 | Temperature (Celsius) | degrees C | 20.7 |
| UA | MW-375 | C | 2019/03/20 | Temperature (Celsius) | degrees C | 13.3 |
| UA | MW-375 | C | 2019/09/25 | Temperature (Celsius) | degrees C | 15.6 |
| UA | MW-375 | C | 2020/03/24 | Temperature (Celsius) | degrees C | 13.0 |
| UA | MW-375 | C | 2020/09/16 | Temperature (Celsius) | degrees C | 15.0 |
| UA | MW-375 | C | 2021/03/12 | Temperature (Celsius) | degrees C | 13.2 |
| UA | MW-375 | C | 2021/09/14 | Temperature (Celsius) | degrees C | 16.2 |
| UA | MW-375 | C | 2022/03/28 | Temperature (Celsius) | degrees C | 13.5 |
| UA | MW-375 | C | 2022/09/30 | Temperature (Celsius) | degrees C | 14.8 |
| UA | MW-375 | C | 2023/03/14 | Temperature (Celsius) | degrees C | 12.6 |
| UA | MW-375 | C | 2023/05/18 | Temperature (Celsius) | degrees C | 15.0 |

Attachment I. Site Groundwater Data

Geochemical Conceptual Site Model

Baldwin Fly Ash Pond System

Baldwin Power Plant

Baldwin, IL

| | | | | | | |
|----|--------|---|------------|-------------------------------|-----------|-------|
| UA | MW-375 | C | 2023/08/07 | Temperature (Celsius) | degrees C | 15.8 |
| UA | MW-375 | C | 2023/11/03 | Temperature (Celsius) | degrees C | 14.2 |
| UA | MW-375 | C | 2016/01/20 | Total Dissolved Solids | mg/L | 472 |
| UA | MW-375 | C | 2016/03/23 | Total Dissolved Solids | mg/L | 904 |
| UA | MW-375 | C | 2016/06/22 | Total Dissolved Solids | mg/L | 934 |
| UA | MW-375 | C | 2016/09/20 | Total Dissolved Solids | mg/L | 902 |
| UA | MW-375 | C | 2016/12/22 | Total Dissolved Solids | mg/L | 876 |
| UA | MW-375 | C | 2017/03/16 | Total Dissolved Solids | mg/L | 904 |
| UA | MW-375 | C | 2017/06/21 | Total Dissolved Solids | mg/L | 916 |
| UA | MW-375 | C | 2017/07/28 | Total Dissolved Solids | mg/L | 882 |
| UA | MW-375 | C | 2017/11/27 | Total Dissolved Solids | mg/L | 928 |
| UA | MW-375 | C | 2018/06/27 | Total Dissolved Solids | mg/L | 1,110 |
| UA | MW-375 | C | 2018/09/25 | Total Dissolved Solids | mg/L | 1,100 |
| UA | MW-375 | C | 2019/03/20 | Total Dissolved Solids | mg/L | 1,040 |
| UA | MW-375 | C | 2019/09/25 | Total Dissolved Solids | mg/L | 1,010 |
| UA | MW-375 | C | 2020/03/24 | Total Dissolved Solids | mg/L | 1,000 |
| UA | MW-375 | C | 2020/09/16 | Total Dissolved Solids | mg/L | 1,010 |
| UA | MW-375 | C | 2021/03/12 | Total Dissolved Solids | mg/L | 1,010 |
| UA | MW-375 | C | 2021/09/14 | Total Dissolved Solids | mg/L | 976 |
| UA | MW-375 | C | 2022/03/28 | Total Dissolved Solids | mg/L | 1,020 |
| UA | MW-375 | C | 2022/09/30 | Total Dissolved Solids | mg/L | 1,030 |
| UA | MW-375 | C | 2023/03/14 | Total Dissolved Solids | mg/L | 940 |
| UA | MW-375 | C | 2023/05/18 | Total Dissolved Solids | mg/L | 950 |
| UA | MW-375 | C | 2023/08/07 | Total Dissolved Solids | mg/L | 926 |
| UA | MW-375 | C | 2023/11/03 | Total Dissolved Solids | mg/L | 968 |
| UA | MW-377 | C | 2016/01/19 | pH (field) | SU | 7.5 |
| UA | MW-377 | C | 2016/03/23 | pH (field) | SU | 7.2 |
| UA | MW-377 | C | 2016/06/22 | pH (field) | SU | 7.2 |
| UA | MW-377 | C | 2016/09/21 | pH (field) | SU | 7.2 |
| UA | MW-377 | C | 2016/12/22 | pH (field) | SU | 6.9 |
| UA | MW-377 | C | 2017/03/15 | pH (field) | SU | 7.7 |
| UA | MW-377 | C | 2017/06/21 | pH (field) | SU | 7.1 |
| UA | MW-377 | C | 2017/07/28 | pH (field) | SU | 7.2 |
| UA | MW-377 | C | 2017/11/28 | pH (field) | SU | 7.0 |
| UA | MW-377 | C | 2018/06/27 | pH (field) | SU | 7.0 |
| UA | MW-377 | C | 2018/09/25 | pH (field) | SU | 7.2 |
| UA | MW-377 | C | 2019/03/20 | pH (field) | SU | 7.2 |
| UA | MW-377 | C | 2019/09/25 | pH (field) | SU | 7.0 |
| UA | MW-377 | C | 2020/03/24 | pH (field) | SU | 7.2 |
| UA | MW-377 | C | 2020/09/16 | pH (field) | SU | 7.2 |
| UA | MW-377 | C | 2021/03/12 | pH (field) | SU | 7.1 |
| UA | MW-377 | C | 2021/09/14 | pH (field) | SU | 7.1 |
| UA | MW-377 | C | 2022/03/28 | pH (field) | SU | 7.2 |
| UA | MW-377 | C | 2022/09/30 | pH (field) | SU | 7.1 |
| UA | MW-377 | C | 2023/03/14 | pH (field) | SU | 7.1 |
| UA | MW-377 | C | 2023/05/22 | pH (field) | SU | 7.0 |
| UA | MW-377 | C | 2023/08/07 | pH (field) | SU | 7.6 |
| UA | MW-377 | C | 2023/11/03 | pH (field) | SU | 7.2 |
| UA | MW-377 | C | 2016/01/19 | Oxidation Reduction Potential | mV | 47.0 |
| UA | MW-377 | C | 2016/03/23 | Oxidation Reduction Potential | mV | -17.0 |
| UA | MW-377 | C | 2016/06/22 | Oxidation Reduction Potential | mV | -54.0 |
| UA | MW-377 | C | 2016/09/21 | Oxidation Reduction Potential | mV | -59.0 |
| UA | MW-377 | C | 2016/12/22 | Oxidation Reduction Potential | mV | -14.0 |
| UA | MW-377 | C | 2017/03/15 | Oxidation Reduction Potential | mV | -22.0 |
| UA | MW-377 | C | 2017/06/21 | Oxidation Reduction Potential | mV | -24.0 |
| UA | MW-377 | C | 2017/07/28 | Oxidation Reduction Potential | mV | -19.0 |
| UA | MW-377 | C | 2017/11/28 | Oxidation Reduction Potential | mV | 157 |

Attachment I. Site Groundwater Data

Geochemical Conceptual Site Model

Baldwin Fly Ash Pond System

Baldwin Power Plant

Baldwin, IL

| | | | | | | |
|----|--------|---|------------|-------------------------------|------------|--------|
| UA | MW-377 | C | 2018/06/27 | Oxidation Reduction Potential | mV | 89.0 |
| UA | MW-377 | C | 2018/09/25 | Oxidation Reduction Potential | mV | -20.0 |
| UA | MW-377 | C | 2019/03/20 | Oxidation Reduction Potential | mV | -37.0 |
| UA | MW-377 | C | 2019/09/25 | Oxidation Reduction Potential | mV | -2.00 |
| UA | MW-377 | C | 2020/03/24 | Oxidation Reduction Potential | mV | 35.0 |
| UA | MW-377 | C | 2020/09/16 | Oxidation Reduction Potential | mV | -21.0 |
| UA | MW-377 | C | 2021/03/12 | Oxidation Reduction Potential | mV | 44.0 |
| UA | MW-377 | C | 2021/09/14 | Oxidation Reduction Potential | mV | -2.00 |
| UA | MW-377 | C | 2022/03/28 | Oxidation Reduction Potential | mV | -17.0 |
| UA | MW-377 | C | 2022/09/30 | Oxidation Reduction Potential | mV | 106 |
| UA | MW-377 | C | 2023/03/14 | Oxidation Reduction Potential | mV | -27.7 |
| UA | MW-377 | C | 2023/05/22 | Oxidation Reduction Potential | mV | 108 |
| UA | MW-377 | C | 2023/08/07 | Oxidation Reduction Potential | mV | 142 |
| UA | MW-377 | C | 2023/11/03 | Oxidation Reduction Potential | mV | -84.0 |
| UA | MW-377 | C | 2016/01/19 | Eh | V | 0.25 |
| UA | MW-377 | C | 2016/03/23 | Eh | V | 0.18 |
| UA | MW-377 | C | 2016/06/22 | Eh | V | 0.14 |
| UA | MW-377 | C | 2016/09/21 | Eh | V | 0.13 |
| UA | MW-377 | C | 2016/12/22 | Eh | V | 0.18 |
| UA | MW-377 | C | 2017/03/15 | Eh | V | 0.17 |
| UA | MW-377 | C | 2017/06/21 | Eh | V | 0.16 |
| UA | MW-377 | C | 2017/07/28 | Eh | V | 0.17 |
| UA | MW-377 | C | 2017/11/28 | Eh | V | 0.35 |
| UA | MW-377 | C | 2018/06/27 | Eh | V | 0.28 |
| UA | MW-377 | C | 2018/09/25 | Eh | V | 0.17 |
| UA | MW-377 | C | 2019/03/20 | Eh | V | 0.16 |
| UA | MW-377 | C | 2019/09/25 | Eh | V | 0.19 |
| UA | MW-377 | C | 2020/03/24 | Eh | V | 0.23 |
| UA | MW-377 | C | 2020/09/16 | Eh | V | 0.17 |
| UA | MW-377 | C | 2021/03/12 | Eh | V | 0.24 |
| UA | MW-377 | C | 2021/09/14 | Eh | V | 0.19 |
| UA | MW-377 | C | 2022/03/28 | Eh | V | 0.18 |
| UA | MW-377 | C | 2022/09/30 | Eh | V | 0.30 |
| UA | MW-377 | C | 2023/03/14 | Eh | V | 0.17 |
| UA | MW-377 | C | 2023/05/22 | Eh | V | 0.30 |
| UA | MW-377 | C | 2023/08/07 | Eh | V | 0.34 |
| UA | MW-377 | C | 2023/11/03 | Eh | V | 0.11 |
| UA | MW-377 | C | 2017/07/28 | Alkalinity, bicarbonate | mg/L CaCO3 | 440 |
| UA | MW-377 | C | 2020/03/24 | Alkalinity, bicarbonate | mg/L CaCO3 | 442 |
| UA | MW-377 | C | 2020/09/16 | Alkalinity, bicarbonate | mg/L CaCO3 | 436 |
| UA | MW-377 | C | 2021/03/12 | Alkalinity, bicarbonate | mg/L CaCO3 | 436 |
| UA | MW-377 | C | 2021/09/14 | Alkalinity, bicarbonate | mg/L CaCO3 | 437 |
| UA | MW-377 | C | 2022/03/28 | Alkalinity, bicarbonate | mg/L CaCO3 | 420 |
| UA | MW-377 | C | 2022/09/30 | Alkalinity, bicarbonate | mg/L CaCO3 | 416 |
| UA | MW-377 | C | 2023/03/14 | Alkalinity, bicarbonate | mg/L CaCO3 | 422 |
| UA | MW-377 | C | 2023/05/22 | Alkalinity, bicarbonate | mg/L CaCO3 | 434 |
| UA | MW-377 | C | 2023/08/07 | Alkalinity, bicarbonate | mg/L CaCO3 | 427 |
| UA | MW-377 | C | 2023/11/03 | Alkalinity, bicarbonate | mg/L CaCO3 | 432 |
| UA | MW-377 | C | 2016/01/19 | Barium, total | mg/L | 0.0580 |
| UA | MW-377 | C | 2016/03/23 | Barium, total | mg/L | 0.0637 |
| UA | MW-377 | C | 2016/06/22 | Barium, total | mg/L | 0.0663 |
| UA | MW-377 | C | 2016/09/21 | Barium, total | mg/L | 0.0755 |
| UA | MW-377 | C | 2016/12/22 | Barium, total | mg/L | 0.0625 |
| UA | MW-377 | C | 2017/03/15 | Barium, total | mg/L | 0.0646 |
| UA | MW-377 | C | 2017/06/21 | Barium, total | mg/L | 0.0602 |
| UA | MW-377 | C | 2017/07/28 | Barium, total | mg/L | 0.0631 |
| UA | MW-377 | C | 2018/06/27 | Barium, total | mg/L | 0.0643 |

Attachment I. Site Groundwater Data

Geochemical Conceptual Site Model

Baldwin Fly Ash Pond System

Baldwin Power Plant

Baldwin, IL

| | | | | | | |
|----|--------|---|------------|----------------|------|--------|
| UA | MW-377 | C | 2018/09/25 | Barium, total | mg/L | 0.0608 |
| UA | MW-377 | C | 2019/03/20 | Barium, total | mg/L | 0.0672 |
| UA | MW-377 | C | 2019/09/25 | Barium, total | mg/L | 0.0630 |
| UA | MW-377 | C | 2020/03/24 | Barium, total | mg/L | 0.0625 |
| UA | MW-377 | C | 2020/09/16 | Barium, total | mg/L | 0.0599 |
| UA | MW-377 | C | 2021/03/12 | Barium, total | mg/L | 0.0609 |
| UA | MW-377 | C | 2021/09/14 | Barium, total | mg/L | 0.0630 |
| UA | MW-377 | C | 2022/03/28 | Barium, total | mg/L | 0.0554 |
| UA | MW-377 | C | 2022/09/30 | Barium, total | mg/L | 0.0589 |
| UA | MW-377 | C | 2023/03/14 | Barium, total | mg/L | 0.0631 |
| UA | MW-377 | C | 2023/05/22 | Barium, total | mg/L | 0.0603 |
| UA | MW-377 | C | 2023/08/07 | Barium, total | mg/L | 0.0636 |
| UA | MW-377 | C | 2023/11/03 | Barium, total | mg/L | 0.0555 |
| UA | MW-377 | C | 2016/01/19 | Boron, total | mg/L | 1.54 |
| UA | MW-377 | C | 2016/03/23 | Boron, total | mg/L | 1.59 |
| UA | MW-377 | C | 2016/06/22 | Boron, total | mg/L | 1.79 |
| UA | MW-377 | C | 2016/09/21 | Boron, total | mg/L | 2.01 |
| UA | MW-377 | C | 2016/12/22 | Boron, total | mg/L | 1.72 |
| UA | MW-377 | C | 2017/03/15 | Boron, total | mg/L | 1.67 |
| UA | MW-377 | C | 2017/06/21 | Boron, total | mg/L | 1.74 |
| UA | MW-377 | C | 2017/07/28 | Boron, total | mg/L | 1.63 |
| UA | MW-377 | C | 2017/11/28 | Boron, total | mg/L | 1.91 |
| UA | MW-377 | C | 2018/06/27 | Boron, total | mg/L | 1.74 |
| UA | MW-377 | C | 2018/09/25 | Boron, total | mg/L | 1.78 |
| UA | MW-377 | C | 2019/03/20 | Boron, total | mg/L | 1.73 |
| UA | MW-377 | C | 2019/09/25 | Boron, total | mg/L | 1.77 |
| UA | MW-377 | C | 2020/03/24 | Boron, total | mg/L | 1.79 |
| UA | MW-377 | C | 2020/09/16 | Boron, total | mg/L | 1.75 |
| UA | MW-377 | C | 2021/03/12 | Boron, total | mg/L | 1.58 |
| UA | MW-377 | C | 2021/09/14 | Boron, total | mg/L | 1.77 |
| UA | MW-377 | C | 2022/03/28 | Boron, total | mg/L | 1.69 |
| UA | MW-377 | C | 2022/09/30 | Boron, total | mg/L | 1.71 |
| UA | MW-377 | C | 2023/03/14 | Boron, total | mg/L | 1.74 |
| UA | MW-377 | C | 2023/05/22 | Boron, total | mg/L | 1.71 |
| UA | MW-377 | C | 2023/08/07 | Boron, total | mg/L | 1.65 |
| UA | MW-377 | C | 2023/11/03 | Boron, total | mg/L | 1.58 |
| UA | MW-377 | C | 2016/01/19 | Calcium, total | mg/L | 54.3 |
| UA | MW-377 | C | 2016/03/23 | Calcium, total | mg/L | 55.1 |
| UA | MW-377 | C | 2016/06/22 | Calcium, total | mg/L | 61.0 |
| UA | MW-377 | C | 2016/09/21 | Calcium, total | mg/L | 69.5 |
| UA | MW-377 | C | 2016/12/22 | Calcium, total | mg/L | 55.4 |
| UA | MW-377 | C | 2017/03/15 | Calcium, total | mg/L | 60.9 |
| UA | MW-377 | C | 2017/06/21 | Calcium, total | mg/L | 53.4 |
| UA | MW-377 | C | 2017/07/28 | Calcium, total | mg/L | 57.4 |
| UA | MW-377 | C | 2017/11/28 | Calcium, total | mg/L | 63.2 |
| UA | MW-377 | C | 2018/06/27 | Calcium, total | mg/L | 54.1 |
| UA | MW-377 | C | 2018/09/25 | Calcium, total | mg/L | 55.9 |
| UA | MW-377 | C | 2019/03/20 | Calcium, total | mg/L | 68.1 |
| UA | MW-377 | C | 2019/09/25 | Calcium, total | mg/L | 57.8 |
| UA | MW-377 | C | 2020/03/24 | Calcium, total | mg/L | 54.0 |
| UA | MW-377 | C | 2020/09/16 | Calcium, total | mg/L | 56.2 |
| UA | MW-377 | C | 2021/03/12 | Calcium, total | mg/L | 54.7 |
| UA | MW-377 | C | 2021/09/14 | Calcium, total | mg/L | 55.2 |
| UA | MW-377 | C | 2022/03/28 | Calcium, total | mg/L | 56.0 |
| UA | MW-377 | C | 2022/09/30 | Calcium, total | mg/L | 57.3 |
| UA | MW-377 | C | 2023/03/14 | Calcium, total | mg/L | 55.1 |
| UA | MW-377 | C | 2023/05/22 | Calcium, total | mg/L | 53.2 |

Attachment I. Site Groundwater Data

Geochemical Conceptual Site Model

Baldwin Fly Ash Pond System

Baldwin Power Plant

Baldwin, IL

| | | | | | | |
|----|--------|---|------------|----------------------|------|---------|
| UA | MW-377 | C | 2023/08/07 | Calcium, total | mg/L | 52.8 |
| UA | MW-377 | C | 2023/11/03 | Calcium, total | mg/L | 60.2 |
| UA | MW-377 | C | 2016/01/19 | Chloride, total | mg/L | 82.0 |
| UA | MW-377 | C | 2016/03/23 | Chloride, total | mg/L | 79.0 |
| UA | MW-377 | C | 2016/06/22 | Chloride, total | mg/L | 86.0 |
| UA | MW-377 | C | 2016/09/21 | Chloride, total | mg/L | 98.0 |
| UA | MW-377 | C | 2016/12/22 | Chloride, total | mg/L | 95.0 |
| UA | MW-377 | C | 2017/03/15 | Chloride, total | mg/L | 90.0 |
| UA | MW-377 | C | 2017/06/21 | Chloride, total | mg/L | 94.0 |
| UA | MW-377 | C | 2017/07/28 | Chloride, total | mg/L | 93.0 |
| UA | MW-377 | C | 2017/11/28 | Chloride, total | mg/L | 90.0 |
| UA | MW-377 | C | 2018/06/27 | Chloride, total | mg/L | 93.0 |
| UA | MW-377 | C | 2018/09/25 | Chloride, total | mg/L | 96.0 |
| UA | MW-377 | C | 2019/03/20 | Chloride, total | mg/L | 90.0 |
| UA | MW-377 | C | 2019/09/25 | Chloride, total | mg/L | 93.0 |
| UA | MW-377 | C | 2020/03/24 | Chloride, total | mg/L | 99.0 |
| UA | MW-377 | C | 2020/09/16 | Chloride, total | mg/L | 97.0 |
| UA | MW-377 | C | 2021/03/12 | Chloride, total | mg/L | 94.0 |
| UA | MW-377 | C | 2021/09/14 | Chloride, total | mg/L | 100 |
| UA | MW-377 | C | 2022/03/28 | Chloride, total | mg/L | 92.0 |
| UA | MW-377 | C | 2022/09/30 | Chloride, total | mg/L | 99.0 |
| UA | MW-377 | C | 2023/03/14 | Chloride, total | mg/L | 90.0 |
| UA | MW-377 | C | 2023/05/22 | Chloride, total | mg/L | 93.0 |
| UA | MW-377 | C | 2023/08/07 | Chloride, total | mg/L | 102 |
| UA | MW-377 | C | 2023/11/03 | Chloride, total | mg/L | 103 |
| UA | MW-377 | C | 2023/05/22 | Iron, dissolved | mg/L | 0.0240 |
| UA | MW-377 | C | 2023/08/07 | Iron, dissolved | mg/L | <0.012 |
| UA | MW-377 | C | 2017/07/28 | Magnesium, total | mg/L | 38.9 |
| UA | MW-377 | C | 2020/03/24 | Magnesium, total | mg/L | 39.2 |
| UA | MW-377 | C | 2020/09/16 | Magnesium, total | mg/L | 43.6 |
| UA | MW-377 | C | 2021/03/12 | Magnesium, total | mg/L | 39.8 |
| UA | MW-377 | C | 2021/09/14 | Magnesium, total | mg/L | 37.2 |
| UA | MW-377 | C | 2022/03/28 | Magnesium, total | mg/L | 38.9 |
| UA | MW-377 | C | 2022/09/30 | Magnesium, total | mg/L | 37.9 |
| UA | MW-377 | C | 2023/03/14 | Magnesium, total | mg/L | 36.9 |
| UA | MW-377 | C | 2023/05/22 | Magnesium, total | mg/L | 37.8 |
| UA | MW-377 | C | 2023/08/07 | Magnesium, total | mg/L | 35.9 |
| UA | MW-377 | C | 2023/11/03 | Magnesium, total | mg/L | 38.4 |
| UA | MW-377 | C | 2023/05/22 | Manganese, dissolved | mg/L | 0.0110 |
| UA | MW-377 | C | 2023/08/07 | Manganese, dissolved | mg/L | 0.00720 |
| UA | MW-377 | C | 2023/05/22 | Phosphate, dissolved | mg/L | <0.005 |
| UA | MW-377 | C | 2023/08/07 | Phosphate, dissolved | mg/L | <0.005 |
| UA | MW-377 | C | 2017/07/28 | Potassium, total | mg/L | 3.48 |
| UA | MW-377 | C | 2020/03/24 | Potassium, total | mg/L | 3.44 |
| UA | MW-377 | C | 2020/09/16 | Potassium, total | mg/L | 3.94 |
| UA | MW-377 | C | 2021/03/12 | Potassium, total | mg/L | 3.29 |
| UA | MW-377 | C | 2021/09/14 | Potassium, total | mg/L | 3.28 |
| UA | MW-377 | C | 2022/03/28 | Potassium, total | mg/L | 3.77 |
| UA | MW-377 | C | 2022/09/30 | Potassium, total | mg/L | 3.47 |
| UA | MW-377 | C | 2023/03/14 | Potassium, total | mg/L | 3.07 |
| UA | MW-377 | C | 2023/05/22 | Potassium, total | mg/L | 3.56 |
| UA | MW-377 | C | 2023/08/07 | Potassium, total | mg/L | 3.44 |
| UA | MW-377 | C | 2023/11/03 | Potassium, total | mg/L | 3.49 |
| UA | MW-377 | C | 2023/05/22 | Silicon, dissolved | mg/L | 4.43 |
| UA | MW-377 | C | 2023/08/07 | Silicon, dissolved | mg/L | 4.11 |
| UA | MW-377 | C | 2017/07/28 | Sodium, total | mg/L | 129 |
| UA | MW-377 | C | 2020/03/24 | Sodium, total | mg/L | 135 |

Attachment I. Site Groundwater Data

Geochemical Conceptual Site Model

Baldwin Fly Ash Pond System

Baldwin Power Plant

Baldwin, IL

| | | | | | | |
|----|--------|---|------------|------------------------|-----------|------|
| UA | MW-377 | C | 2020/09/16 | Sodium, total | mg/L | 155 |
| UA | MW-377 | C | 2021/03/12 | Sodium, total | mg/L | 137 |
| UA | MW-377 | C | 2021/09/14 | Sodium, total | mg/L | 123 |
| UA | MW-377 | C | 2022/03/28 | Sodium, total | mg/L | 144 |
| UA | MW-377 | C | 2022/09/30 | Sodium, total | mg/L | 130 |
| UA | MW-377 | C | 2023/03/14 | Sodium, total | mg/L | 135 |
| UA | MW-377 | C | 2023/05/22 | Sodium, total | mg/L | 133 |
| UA | MW-377 | C | 2023/08/07 | Sodium, total | mg/L | 131 |
| UA | MW-377 | C | 2023/11/03 | Sodium, total | mg/L | 148 |
| UA | MW-377 | C | 2016/01/19 | Sulfate, total | mg/L | 43.0 |
| UA | MW-377 | C | 2016/03/23 | Sulfate, total | mg/L | 44.0 |
| UA | MW-377 | C | 2016/06/22 | Sulfate, total | mg/L | 41.0 |
| UA | MW-377 | C | 2016/09/21 | Sulfate, total | mg/L | 40.0 |
| UA | MW-377 | C | 2016/12/22 | Sulfate, total | mg/L | 39.0 |
| UA | MW-377 | C | 2017/03/15 | Sulfate, total | mg/L | 42.0 |
| UA | MW-377 | C | 2017/06/21 | Sulfate, total | mg/L | 39.0 |
| UA | MW-377 | C | 2017/07/28 | Sulfate, total | mg/L | 39.0 |
| UA | MW-377 | C | 2017/11/28 | Sulfate, total | mg/L | 41.0 |
| UA | MW-377 | C | 2018/06/27 | Sulfate, total | mg/L | 46.0 |
| UA | MW-377 | C | 2018/09/25 | Sulfate, total | mg/L | 41.0 |
| UA | MW-377 | C | 2019/03/20 | Sulfate, total | mg/L | 38.0 |
| UA | MW-377 | C | 2019/09/25 | Sulfate, total | mg/L | 39.0 |
| UA | MW-377 | C | 2020/03/24 | Sulfate, total | mg/L | 37.0 |
| UA | MW-377 | C | 2020/09/16 | Sulfate, total | mg/L | 39.0 |
| UA | MW-377 | C | 2021/03/12 | Sulfate, total | mg/L | 37.0 |
| UA | MW-377 | C | 2021/09/14 | Sulfate, total | mg/L | 38.0 |
| UA | MW-377 | C | 2022/03/28 | Sulfate, total | mg/L | 39.0 |
| UA | MW-377 | C | 2022/09/30 | Sulfate, total | mg/L | 39.0 |
| UA | MW-377 | C | 2023/03/14 | Sulfate, total | mg/L | 37.0 |
| UA | MW-377 | C | 2023/05/22 | Sulfate, total | mg/L | 40.0 |
| UA | MW-377 | C | 2023/08/07 | Sulfate, total | mg/L | 37.0 |
| UA | MW-377 | C | 2023/11/03 | Sulfate, total | mg/L | 51.0 |
| UA | MW-377 | C | 2016/01/19 | Temperature (Celsius) | degrees C | 10.9 |
| UA | MW-377 | C | 2016/03/23 | Temperature (Celsius) | degrees C | 13.8 |
| UA | MW-377 | C | 2016/06/22 | Temperature (Celsius) | degrees C | 24.0 |
| UA | MW-377 | C | 2016/09/21 | Temperature (Celsius) | degrees C | 21.7 |
| UA | MW-377 | C | 2016/12/22 | Temperature (Celsius) | degrees C | 13.6 |
| UA | MW-377 | C | 2017/03/15 | Temperature (Celsius) | degrees C | 14.0 |
| UA | MW-377 | C | 2017/06/21 | Temperature (Celsius) | degrees C | 25.9 |
| UA | MW-377 | C | 2017/07/28 | Temperature (Celsius) | degrees C | 19.1 |
| UA | MW-377 | C | 2017/11/28 | Temperature (Celsius) | degrees C | 15.0 |
| UA | MW-377 | C | 2018/06/27 | Temperature (Celsius) | degrees C | 22.2 |
| UA | MW-377 | C | 2018/09/25 | Temperature (Celsius) | degrees C | 24.7 |
| UA | MW-377 | C | 2019/03/20 | Temperature (Celsius) | degrees C | 12.7 |
| UA | MW-377 | C | 2019/09/25 | Temperature (Celsius) | degrees C | 18.4 |
| UA | MW-377 | C | 2020/03/24 | Temperature (Celsius) | degrees C | 12.8 |
| UA | MW-377 | C | 2020/09/16 | Temperature (Celsius) | degrees C | 16.1 |
| UA | MW-377 | C | 2021/03/12 | Temperature (Celsius) | degrees C | 12.6 |
| UA | MW-377 | C | 2021/09/14 | Temperature (Celsius) | degrees C | 21.3 |
| UA | MW-377 | C | 2022/03/28 | Temperature (Celsius) | degrees C | 13.3 |
| UA | MW-377 | C | 2022/09/30 | Temperature (Celsius) | degrees C | 17.3 |
| UA | MW-377 | C | 2023/03/14 | Temperature (Celsius) | degrees C | 13.8 |
| UA | MW-377 | C | 2023/05/22 | Temperature (Celsius) | degrees C | 15.2 |
| UA | MW-377 | C | 2023/08/07 | Temperature (Celsius) | degrees C | 15.4 |
| UA | MW-377 | C | 2023/11/03 | Temperature (Celsius) | degrees C | 16.6 |
| UA | MW-377 | C | 2016/01/19 | Total Dissolved Solids | mg/L | 552 |
| UA | MW-377 | C | 2016/03/23 | Total Dissolved Solids | mg/L | 606 |

Attachment I. Site Groundwater Data

Geochemical Conceptual Site Model

Baldwin Fly Ash Pond System

Baldwin Power Plant

Baldwin, IL

| | | | | | | |
|----|--------|---|------------|-------------------------------|------|-------|
| UA | MW-377 | C | 2016/06/22 | Total Dissolved Solids | mg/L | 628 |
| UA | MW-377 | C | 2016/09/21 | Total Dissolved Solids | mg/L | 592 |
| UA | MW-377 | C | 2016/12/22 | Total Dissolved Solids | mg/L | 606 |
| UA | MW-377 | C | 2017/03/15 | Total Dissolved Solids | mg/L | 628 |
| UA | MW-377 | C | 2017/06/21 | Total Dissolved Solids | mg/L | 614 |
| UA | MW-377 | C | 2017/07/28 | Total Dissolved Solids | mg/L | 590 |
| UA | MW-377 | C | 2017/11/28 | Total Dissolved Solids | mg/L | 652 |
| UA | MW-377 | C | 2018/06/27 | Total Dissolved Solids | mg/L | 614 |
| UA | MW-377 | C | 2018/09/25 | Total Dissolved Solids | mg/L | 646 |
| UA | MW-377 | C | 2019/03/20 | Total Dissolved Solids | mg/L | 614 |
| UA | MW-377 | C | 2019/09/25 | Total Dissolved Solids | mg/L | 626 |
| UA | MW-377 | C | 2020/03/24 | Total Dissolved Solids | mg/L | 580 |
| UA | MW-377 | C | 2020/09/16 | Total Dissolved Solids | mg/L | 580 |
| UA | MW-377 | C | 2021/03/12 | Total Dissolved Solids | mg/L | 606 |
| UA | MW-377 | C | 2021/09/14 | Total Dissolved Solids | mg/L | 580 |
| UA | MW-377 | C | 2022/03/28 | Total Dissolved Solids | mg/L | 642 |
| UA | MW-377 | C | 2022/09/30 | Total Dissolved Solids | mg/L | 622 |
| UA | MW-377 | C | 2023/03/14 | Total Dissolved Solids | mg/L | 612 |
| UA | MW-377 | C | 2023/05/22 | Total Dissolved Solids | mg/L | 608 |
| UA | MW-377 | C | 2023/08/07 | Total Dissolved Solids | mg/L | 646 |
| UA | MW-377 | C | 2023/11/03 | Total Dissolved Solids | mg/L | 628 |
| UA | MW-383 | C | 2016/01/21 | pH (field) | SU | 7.8 |
| UA | MW-383 | C | 2016/03/24 | pH (field) | SU | 7.7 |
| UA | MW-383 | C | 2016/06/23 | pH (field) | SU | 7.8 |
| UA | MW-383 | C | 2016/09/21 | pH (field) | SU | 7.6 |
| UA | MW-383 | C | 2016/12/27 | pH (field) | SU | 7.6 |
| UA | MW-383 | C | 2017/03/16 | pH (field) | SU | 7.7 |
| UA | MW-383 | C | 2017/06/19 | pH (field) | SU | 7.7 |
| UA | MW-383 | C | 2017/07/26 | pH (field) | SU | 7.6 |
| UA | MW-383 | C | 2017/11/28 | pH (field) | SU | 7.6 |
| UA | MW-383 | C | 2018/06/27 | pH (field) | SU | 7.3 |
| UA | MW-383 | C | 2018/09/25 | pH (field) | SU | 7.6 |
| UA | MW-383 | C | 2019/03/20 | pH (field) | SU | 7.5 |
| UA | MW-383 | C | 2019/09/24 | pH (field) | SU | 7.5 |
| UA | MW-383 | C | 2020/03/25 | pH (field) | SU | 7.6 |
| UA | MW-383 | C | 2020/09/15 | pH (field) | SU | 7.7 |
| UA | MW-383 | C | 2021/03/12 | pH (field) | SU | 7.6 |
| UA | MW-383 | C | 2021/09/13 | pH (field) | SU | 7.6 |
| UA | MW-383 | C | 2022/03/29 | pH (field) | SU | 7.5 |
| UA | MW-383 | C | 2022/09/30 | pH (field) | SU | 7.6 |
| UA | MW-383 | C | 2023/03/14 | pH (field) | SU | 7.5 |
| UA | MW-383 | C | 2023/05/22 | pH (field) | SU | 7.5 |
| UA | MW-383 | C | 2023/08/03 | pH (field) | SU | 7.6 |
| UA | MW-383 | C | 2023/11/01 | pH (field) | SU | 7.6 |
| UA | MW-383 | C | 2016/01/21 | Oxidation Reduction Potential | mV | 89.0 |
| UA | MW-383 | C | 2016/03/24 | Oxidation Reduction Potential | mV | 46.0 |
| UA | MW-383 | C | 2016/06/23 | Oxidation Reduction Potential | mV | -52.0 |
| UA | MW-383 | C | 2016/09/21 | Oxidation Reduction Potential | mV | -46.0 |
| UA | MW-383 | C | 2016/12/27 | Oxidation Reduction Potential | mV | -27.0 |
| UA | MW-383 | C | 2017/03/16 | Oxidation Reduction Potential | mV | -2.00 |
| UA | MW-383 | C | 2017/06/19 | Oxidation Reduction Potential | mV | -35.0 |
| UA | MW-383 | C | 2017/07/26 | Oxidation Reduction Potential | mV | 56.0 |
| UA | MW-383 | C | 2017/11/28 | Oxidation Reduction Potential | mV | 25.0 |
| UA | MW-383 | C | 2018/06/27 | Oxidation Reduction Potential | mV | 12.0 |
| UA | MW-383 | C | 2018/09/25 | Oxidation Reduction Potential | mV | -10.0 |
| UA | MW-383 | C | 2019/03/20 | Oxidation Reduction Potential | mV | -84.0 |
| UA | MW-383 | C | 2019/09/24 | Oxidation Reduction Potential | mV | -51.0 |

Attachment I. Site Groundwater Data

Geochemical Conceptual Site Model

Baldwin Fly Ash Pond System

Baldwin Power Plant

Baldwin, IL

| | | | | | | |
|----|--------|---|------------|-------------------------------|------------|--------|
| UA | MW-383 | C | 2020/03/25 | Oxidation Reduction Potential | mV | -10.0 |
| UA | MW-383 | C | 2020/09/15 | Oxidation Reduction Potential | mV | -32.0 |
| UA | MW-383 | C | 2021/03/12 | Oxidation Reduction Potential | mV | -73.0 |
| UA | MW-383 | C | 2021/09/13 | Oxidation Reduction Potential | mV | -5.00 |
| UA | MW-383 | C | 2022/03/29 | Oxidation Reduction Potential | mV | -70.0 |
| UA | MW-383 | C | 2022/09/30 | Oxidation Reduction Potential | mV | 100 |
| UA | MW-383 | C | 2023/03/14 | Oxidation Reduction Potential | mV | -44.0 |
| UA | MW-383 | C | 2023/05/22 | Oxidation Reduction Potential | mV | 70.0 |
| UA | MW-383 | C | 2023/08/03 | Oxidation Reduction Potential | mV | 29.0 |
| UA | MW-383 | C | 2023/11/01 | Oxidation Reduction Potential | mV | -114 |
| UA | MW-383 | C | 2016/01/21 | Eh | V | 0.28 |
| UA | MW-383 | C | 2016/03/24 | Eh | V | 0.24 |
| UA | MW-383 | C | 2016/06/23 | Eh | V | 0.13 |
| UA | MW-383 | C | 2016/09/21 | Eh | V | 0.14 |
| UA | MW-383 | C | 2016/12/27 | Eh | V | 0.17 |
| UA | MW-383 | C | 2017/03/16 | Eh | V | 0.19 |
| UA | MW-383 | C | 2017/06/19 | Eh | V | 0.15 |
| UA | MW-383 | C | 2017/07/26 | Eh | V | 0.25 |
| UA | MW-383 | C | 2017/11/28 | Eh | V | 0.22 |
| UA | MW-383 | C | 2018/06/27 | Eh | V | 0.20 |
| UA | MW-383 | C | 2018/09/25 | Eh | V | 0.18 |
| UA | MW-383 | C | 2019/03/20 | Eh | V | 0.11 |
| UA | MW-383 | C | 2019/09/24 | Eh | V | 0.14 |
| UA | MW-383 | C | 2020/03/25 | Eh | V | 0.18 |
| UA | MW-383 | C | 2020/09/15 | Eh | V | 0.16 |
| UA | MW-383 | C | 2021/03/12 | Eh | V | 0.12 |
| UA | MW-383 | C | 2021/09/13 | Eh | V | 0.19 |
| UA | MW-383 | C | 2022/03/29 | Eh | V | 0.12 |
| UA | MW-383 | C | 2022/09/30 | Eh | V | 0.29 |
| UA | MW-383 | C | 2023/03/14 | Eh | V | 0.15 |
| UA | MW-383 | C | 2023/05/22 | Eh | V | 0.26 |
| UA | MW-383 | C | 2023/08/03 | Eh | V | 0.22 |
| UA | MW-383 | C | 2023/11/01 | Eh | V | 0.080 |
| UA | MW-383 | C | 2017/07/26 | Alkalinity, bicarbonate | mg/L CaCO3 | 556 |
| UA | MW-383 | C | 2020/03/25 | Alkalinity, bicarbonate | mg/L CaCO3 | 592 |
| UA | MW-383 | C | 2020/09/15 | Alkalinity, bicarbonate | mg/L CaCO3 | 590 |
| UA | MW-383 | C | 2021/03/12 | Alkalinity, bicarbonate | mg/L CaCO3 | 553 |
| UA | MW-383 | C | 2021/09/13 | Alkalinity, bicarbonate | mg/L CaCO3 | 581 |
| UA | MW-383 | C | 2022/03/29 | Alkalinity, bicarbonate | mg/L CaCO3 | 575 |
| UA | MW-383 | C | 2022/09/30 | Alkalinity, bicarbonate | mg/L CaCO3 | 585 |
| UA | MW-383 | C | 2023/03/14 | Alkalinity, bicarbonate | mg/L CaCO3 | 569 |
| UA | MW-383 | C | 2023/05/22 | Alkalinity, bicarbonate | mg/L CaCO3 | 561 |
| UA | MW-383 | C | 2023/08/03 | Alkalinity, bicarbonate | mg/L CaCO3 | 571 |
| UA | MW-383 | C | 2023/11/01 | Alkalinity, bicarbonate | mg/L CaCO3 | 569 |
| UA | MW-383 | C | 2023/11/01 | Alkalinity, carbonate | mg/L CaCO3 | 9.00 |
| UA | MW-383 | C | 2016/01/21 | Barium, total | mg/L | 0.0339 |
| UA | MW-383 | C | 2016/03/24 | Barium, total | mg/L | 0.0320 |
| UA | MW-383 | C | 2016/06/23 | Barium, total | mg/L | 0.0307 |
| UA | MW-383 | C | 2016/09/21 | Barium, total | mg/L | 0.0360 |
| UA | MW-383 | C | 2016/12/27 | Barium, total | mg/L | 0.0310 |
| UA | MW-383 | C | 2017/03/16 | Barium, total | mg/L | 0.0324 |
| UA | MW-383 | C | 2017/06/19 | Barium, total | mg/L | 0.0361 |
| UA | MW-383 | C | 2017/07/26 | Barium, total | mg/L | 0.0346 |
| UA | MW-383 | C | 2018/06/27 | Barium, total | mg/L | 0.0398 |
| UA | MW-383 | C | 2018/09/25 | Barium, total | mg/L | 0.0363 |
| UA | MW-383 | C | 2019/03/20 | Barium, total | mg/L | 0.0414 |
| UA | MW-383 | C | 2019/09/24 | Barium, total | mg/L | 0.0410 |

Attachment I. Site Groundwater Data

Geochemical Conceptual Site Model

Baldwin Fly Ash Pond System

Baldwin Power Plant

Baldwin, IL

| | | | | | | |
|----|--------|---|------------|-----------------|------|--------|
| UA | MW-383 | C | 2020/03/25 | Barium, total | mg/L | 0.0421 |
| UA | MW-383 | C | 2020/09/15 | Barium, total | mg/L | 0.0449 |
| UA | MW-383 | C | 2021/03/12 | Barium, total | mg/L | 0.0406 |
| UA | MW-383 | C | 2021/09/13 | Barium, total | mg/L | 0.0443 |
| UA | MW-383 | C | 2022/03/29 | Barium, total | mg/L | 0.0617 |
| UA | MW-383 | C | 2022/09/30 | Barium, total | mg/L | 0.0481 |
| UA | MW-383 | C | 2023/03/14 | Barium, total | mg/L | 0.0446 |
| UA | MW-383 | C | 2023/05/22 | Barium, total | mg/L | 0.0442 |
| UA | MW-383 | C | 2023/08/03 | Barium, total | mg/L | 0.0427 |
| UA | MW-383 | C | 2023/11/01 | Barium, total | mg/L | 0.0479 |
| UA | MW-383 | C | 2016/01/21 | Boron, total | mg/L | 1.27 |
| UA | MW-383 | C | 2016/03/24 | Boron, total | mg/L | 1.33 |
| UA | MW-383 | C | 2016/06/23 | Boron, total | mg/L | 1.45 |
| UA | MW-383 | C | 2016/09/21 | Boron, total | mg/L | 2.05 |
| UA | MW-383 | C | 2016/12/27 | Boron, total | mg/L | 1.49 |
| UA | MW-383 | C | 2017/03/16 | Boron, total | mg/L | 1.42 |
| UA | MW-383 | C | 2017/06/19 | Boron, total | mg/L | 1.53 |
| UA | MW-383 | C | 2017/07/26 | Boron, total | mg/L | 1.26 |
| UA | MW-383 | C | 2017/11/28 | Boron, total | mg/L | 1.49 |
| UA | MW-383 | C | 2018/06/27 | Boron, total | mg/L | 1.50 |
| UA | MW-383 | C | 2018/09/25 | Boron, total | mg/L | 1.40 |
| UA | MW-383 | C | 2019/03/20 | Boron, total | mg/L | 1.43 |
| UA | MW-383 | C | 2019/09/24 | Boron, total | mg/L | 1.39 |
| UA | MW-383 | C | 2020/03/25 | Boron, total | mg/L | 1.33 |
| UA | MW-383 | C | 2020/09/15 | Boron, total | mg/L | 1.39 |
| UA | MW-383 | C | 2021/03/12 | Boron, total | mg/L | 1.40 |
| UA | MW-383 | C | 2021/09/13 | Boron, total | mg/L | 1.34 |
| UA | MW-383 | C | 2022/03/29 | Boron, total | mg/L | 1.56 |
| UA | MW-383 | C | 2022/09/30 | Boron, total | mg/L | 1.52 |
| UA | MW-383 | C | 2023/03/14 | Boron, total | mg/L | 1.35 |
| UA | MW-383 | C | 2023/05/22 | Boron, total | mg/L | 1.16 |
| UA | MW-383 | C | 2023/08/03 | Boron, total | mg/L | 1.33 |
| UA | MW-383 | C | 2023/11/01 | Boron, total | mg/L | 1.40 |
| UA | MW-383 | C | 2016/01/21 | Calcium, total | mg/L | 16.2 |
| UA | MW-383 | C | 2016/03/24 | Calcium, total | mg/L | 15.7 |
| UA | MW-383 | C | 2016/06/23 | Calcium, total | mg/L | 14.9 |
| UA | MW-383 | C | 2016/09/21 | Calcium, total | mg/L | 20.2 |
| UA | MW-383 | C | 2016/12/27 | Calcium, total | mg/L | 14.9 |
| UA | MW-383 | C | 2017/03/16 | Calcium, total | mg/L | 16.2 |
| UA | MW-383 | C | 2017/06/19 | Calcium, total | mg/L | 16.1 |
| UA | MW-383 | C | 2017/07/26 | Calcium, total | mg/L | 16.1 |
| UA | MW-383 | C | 2017/11/28 | Calcium, total | mg/L | 18.4 |
| UA | MW-383 | C | 2018/06/27 | Calcium, total | mg/L | 17.0 |
| UA | MW-383 | C | 2018/09/25 | Calcium, total | mg/L | 16.8 |
| UA | MW-383 | C | 2019/03/20 | Calcium, total | mg/L | 18.4 |
| UA | MW-383 | C | 2019/09/24 | Calcium, total | mg/L | 19.2 |
| UA | MW-383 | C | 2020/03/25 | Calcium, total | mg/L | 18.2 |
| UA | MW-383 | C | 2020/09/15 | Calcium, total | mg/L | 18.3 |
| UA | MW-383 | C | 2021/03/12 | Calcium, total | mg/L | 17.2 |
| UA | MW-383 | C | 2021/09/13 | Calcium, total | mg/L | 17.1 |
| UA | MW-383 | C | 2022/03/29 | Calcium, total | mg/L | 17.9 |
| UA | MW-383 | C | 2022/09/30 | Calcium, total | mg/L | 19.4 |
| UA | MW-383 | C | 2023/03/14 | Calcium, total | mg/L | 18.2 |
| UA | MW-383 | C | 2023/05/22 | Calcium, total | mg/L | 23.8 |
| UA | MW-383 | C | 2023/08/03 | Calcium, total | mg/L | 17.3 |
| UA | MW-383 | C | 2023/11/01 | Calcium, total | mg/L | 18.8 |
| UA | MW-383 | C | 2016/01/21 | Chloride, total | mg/L | 41.0 |

Attachment I. Site Groundwater Data

Geochemical Conceptual Site Model

Baldwin Fly Ash Pond System

Baldwin Power Plant

Baldwin, IL

| | | | | | | |
|----|--------|---|------------|----------------------|------|--------|
| UA | MW-383 | C | 2016/03/24 | Chloride, total | mg/L | 39.0 |
| UA | MW-383 | C | 2016/06/23 | Chloride, total | mg/L | 39.0 |
| UA | MW-383 | C | 2016/09/21 | Chloride, total | mg/L | 40.0 |
| UA | MW-383 | C | 2016/12/27 | Chloride, total | mg/L | 41.0 |
| UA | MW-383 | C | 2017/03/16 | Chloride, total | mg/L | 40.0 |
| UA | MW-383 | C | 2017/06/19 | Chloride, total | mg/L | 40.0 |
| UA | MW-383 | C | 2017/07/26 | Chloride, total | mg/L | 40.0 |
| UA | MW-383 | C | 2017/11/28 | Chloride, total | mg/L | 39.0 |
| UA | MW-383 | C | 2018/06/27 | Chloride, total | mg/L | 39.0 |
| UA | MW-383 | C | 2018/09/25 | Chloride, total | mg/L | 40.0 |
| UA | MW-383 | C | 2019/03/20 | Chloride, total | mg/L | 39.0 |
| UA | MW-383 | C | 2019/09/24 | Chloride, total | mg/L | 41.0 |
| UA | MW-383 | C | 2020/03/25 | Chloride, total | mg/L | 40.0 |
| UA | MW-383 | C | 2020/09/15 | Chloride, total | mg/L | 45.0 |
| UA | MW-383 | C | 2021/03/12 | Chloride, total | mg/L | 42.0 |
| UA | MW-383 | C | 2021/09/13 | Chloride, total | mg/L | 45.0 |
| UA | MW-383 | C | 2022/03/29 | Chloride, total | mg/L | 50.0 |
| UA | MW-383 | C | 2022/09/30 | Chloride, total | mg/L | 42.0 |
| UA | MW-383 | C | 2023/03/14 | Chloride, total | mg/L | 40.0 |
| UA | MW-383 | C | 2023/05/22 | Chloride, total | mg/L | 43.0 |
| UA | MW-383 | C | 2023/08/03 | Chloride, total | mg/L | 43.0 |
| UA | MW-383 | C | 2023/11/01 | Chloride, total | mg/L | 46.0 |
| UA | MW-383 | C | 2023/05/22 | Iron, dissolved | mg/L | <0.02 |
| UA | MW-383 | C | 2023/08/03 | Iron, dissolved | mg/L | 0.359 |
| UA | MW-383 | C | 2017/07/26 | Magnesium, total | mg/L | 6.23 |
| UA | MW-383 | C | 2020/03/25 | Magnesium, total | mg/L | 7.38 |
| UA | MW-383 | C | 2020/09/15 | Magnesium, total | mg/L | 7.96 |
| UA | MW-383 | C | 2021/03/12 | Magnesium, total | mg/L | 7.36 |
| UA | MW-383 | C | 2021/09/13 | Magnesium, total | mg/L | 6.52 |
| UA | MW-383 | C | 2022/03/29 | Magnesium, total | mg/L | 6.68 |
| UA | MW-383 | C | 2022/09/30 | Magnesium, total | mg/L | 7.71 |
| UA | MW-383 | C | 2023/03/14 | Magnesium, total | mg/L | 7.12 |
| UA | MW-383 | C | 2023/05/22 | Magnesium, total | mg/L | 10.5 |
| UA | MW-383 | C | 2023/08/03 | Magnesium, total | mg/L | 6.72 |
| UA | MW-383 | C | 2023/11/01 | Magnesium, total | mg/L | 7.00 |
| UA | MW-383 | C | 2023/05/22 | Manganese, dissolved | mg/L | 0.0269 |
| UA | MW-383 | C | 2023/08/03 | Manganese, dissolved | mg/L | 0.0382 |
| UA | MW-383 | C | 2023/05/22 | Phosphate, dissolved | mg/L | <0.005 |
| UA | MW-383 | C | 2023/08/03 | Phosphate, dissolved | mg/L | 0.0150 |
| UA | MW-383 | C | 2017/07/26 | Potassium, total | mg/L | 1.92 |
| UA | MW-383 | C | 2020/03/25 | Potassium, total | mg/L | 2.10 |
| UA | MW-383 | C | 2020/09/15 | Potassium, total | mg/L | 2.40 |
| UA | MW-383 | C | 2021/03/12 | Potassium, total | mg/L | 2.03 |
| UA | MW-383 | C | 2021/09/13 | Potassium, total | mg/L | 1.95 |
| UA | MW-383 | C | 2022/03/29 | Potassium, total | mg/L | 2.15 |
| UA | MW-383 | C | 2022/09/30 | Potassium, total | mg/L | 2.14 |
| UA | MW-383 | C | 2023/03/14 | Potassium, total | mg/L | 1.96 |
| UA | MW-383 | C | 2023/05/22 | Potassium, total | mg/L | 2.17 |
| UA | MW-383 | C | 2023/08/03 | Potassium, total | mg/L | 2.18 |
| UA | MW-383 | C | 2023/11/01 | Potassium, total | mg/L | 2.14 |
| UA | MW-383 | C | 2023/05/22 | Silicon, dissolved | mg/L | 5.64 |
| UA | MW-383 | C | 2023/08/03 | Silicon, dissolved | mg/L | 5.11 |
| UA | MW-383 | C | 2017/07/26 | Sodium, total | mg/L | 320 |
| UA | MW-383 | C | 2020/03/25 | Sodium, total | mg/L | 346 |
| UA | MW-383 | C | 2020/09/15 | Sodium, total | mg/L | 386 |
| UA | MW-383 | C | 2021/03/12 | Sodium, total | mg/L | 349 |
| UA | MW-383 | C | 2021/09/13 | Sodium, total | mg/L | 302 |

Attachment I. Site Groundwater Data

Geochemical Conceptual Site Model

Baldwin Fly Ash Pond System

Baldwin Power Plant

Baldwin, IL

| | | | | | | |
|----|--------|---|------------|------------------------|-----------|------|
| UA | MW-383 | C | 2022/03/29 | Sodium, total | mg/L | 350 |
| UA | MW-383 | C | 2022/09/30 | Sodium, total | mg/L | 314 |
| UA | MW-383 | C | 2023/03/14 | Sodium, total | mg/L | 315 |
| UA | MW-383 | C | 2023/05/22 | Sodium, total | mg/L | 290 |
| UA | MW-383 | C | 2023/08/03 | Sodium, total | mg/L | 349 |
| UA | MW-383 | C | 2023/11/01 | Sodium, total | mg/L | 374 |
| UA | MW-383 | C | 2016/01/21 | Sulfate, total | mg/L | 212 |
| UA | MW-383 | C | 2016/03/24 | Sulfate, total | mg/L | 205 |
| UA | MW-383 | C | 2016/06/23 | Sulfate, total | mg/L | 176 |
| UA | MW-383 | C | 2016/09/21 | Sulfate, total | mg/L | 192 |
| UA | MW-383 | C | 2016/12/27 | Sulfate, total | mg/L | 174 |
| UA | MW-383 | C | 2017/03/16 | Sulfate, total | mg/L | 180 |
| UA | MW-383 | C | 2017/06/19 | Sulfate, total | mg/L | 177 |
| UA | MW-383 | C | 2017/07/26 | Sulfate, total | mg/L | 182 |
| UA | MW-383 | C | 2017/11/28 | Sulfate, total | mg/L | 171 |
| UA | MW-383 | C | 2018/06/27 | Sulfate, total | mg/L | 200 |
| UA | MW-383 | C | 2018/09/25 | Sulfate, total | mg/L | 184 |
| UA | MW-383 | C | 2019/03/20 | Sulfate, total | mg/L | 166 |
| UA | MW-383 | C | 2019/09/24 | Sulfate, total | mg/L | 169 |
| UA | MW-383 | C | 2020/03/25 | Sulfate, total | mg/L | 175 |
| UA | MW-383 | C | 2020/09/15 | Sulfate, total | mg/L | 190 |
| UA | MW-383 | C | 2021/03/12 | Sulfate, total | mg/L | 179 |
| UA | MW-383 | C | 2021/09/13 | Sulfate, total | mg/L | 168 |
| UA | MW-383 | C | 2022/03/29 | Sulfate, total | mg/L | 159 |
| UA | MW-383 | C | 2022/09/30 | Sulfate, total | mg/L | 169 |
| UA | MW-383 | C | 2023/03/14 | Sulfate, total | mg/L | 150 |
| UA | MW-383 | C | 2023/05/22 | Sulfate, total | mg/L | 177 |
| UA | MW-383 | C | 2023/08/03 | Sulfate, total | mg/L | 157 |
| UA | MW-383 | C | 2023/11/01 | Sulfate, total | mg/L | 165 |
| UA | MW-383 | C | 2016/01/21 | Temperature (Celsius) | degrees C | 15.2 |
| UA | MW-383 | C | 2016/03/24 | Temperature (Celsius) | degrees C | 16.1 |
| UA | MW-383 | C | 2016/06/23 | Temperature (Celsius) | degrees C | 27.4 |
| UA | MW-383 | C | 2016/09/21 | Temperature (Celsius) | degrees C | 22.7 |
| UA | MW-383 | C | 2016/12/27 | Temperature (Celsius) | degrees C | 14.7 |
| UA | MW-383 | C | 2017/03/16 | Temperature (Celsius) | degrees C | 16.9 |
| UA | MW-383 | C | 2017/06/19 | Temperature (Celsius) | degrees C | 24.0 |
| UA | MW-383 | C | 2017/07/26 | Temperature (Celsius) | degrees C | 21.7 |
| UA | MW-383 | C | 2017/11/28 | Temperature (Celsius) | degrees C | 18.6 |
| UA | MW-383 | C | 2018/06/27 | Temperature (Celsius) | degrees C | 23.2 |
| UA | MW-383 | C | 2018/09/25 | Temperature (Celsius) | degrees C | 20.4 |
| UA | MW-383 | C | 2019/03/20 | Temperature (Celsius) | degrees C | 16.6 |
| UA | MW-383 | C | 2019/09/24 | Temperature (Celsius) | degrees C | 19.7 |
| UA | MW-383 | C | 2020/03/25 | Temperature (Celsius) | degrees C | 17.8 |
| UA | MW-383 | C | 2020/09/15 | Temperature (Celsius) | degrees C | 18.7 |
| UA | MW-383 | C | 2021/03/12 | Temperature (Celsius) | degrees C | 17.3 |
| UA | MW-383 | C | 2021/09/13 | Temperature (Celsius) | degrees C | 22.3 |
| UA | MW-383 | C | 2022/03/29 | Temperature (Celsius) | degrees C | 17.9 |
| UA | MW-383 | C | 2022/09/30 | Temperature (Celsius) | degrees C | 18.2 |
| UA | MW-383 | C | 2023/03/14 | Temperature (Celsius) | degrees C | 17.2 |
| UA | MW-383 | C | 2023/05/22 | Temperature (Celsius) | degrees C | 18.4 |
| UA | MW-383 | C | 2023/08/03 | Temperature (Celsius) | degrees C | 19.1 |
| UA | MW-383 | C | 2023/11/01 | Temperature (Celsius) | degrees C | 17.5 |
| UA | MW-383 | C | 2016/01/21 | Total Dissolved Solids | mg/L | 800 |
| UA | MW-383 | C | 2016/03/24 | Total Dissolved Solids | mg/L | 828 |
| UA | MW-383 | C | 2016/06/23 | Total Dissolved Solids | mg/L | 916 |
| UA | MW-383 | C | 2016/09/21 | Total Dissolved Solids | mg/L | 840 |
| UA | MW-383 | C | 2016/12/27 | Total Dissolved Solids | mg/L | 910 |

Attachment I. Site Groundwater Data

Geochemical Conceptual Site Model

Baldwin Fly Ash Pond System

Baldwin Power Plant

Baldwin, IL

| | | | | | | |
|----|--------|---|------------|-------------------------------|------|-------|
| UA | MW-383 | C | 2017/03/16 | Total Dissolved Solids | mg/L | 890 |
| UA | MW-383 | C | 2017/06/19 | Total Dissolved Solids | mg/L | 912 |
| UA | MW-383 | C | 2017/07/26 | Total Dissolved Solids | mg/L | 890 |
| UA | MW-383 | C | 2017/11/28 | Total Dissolved Solids | mg/L | 962 |
| UA | MW-383 | C | 2018/06/27 | Total Dissolved Solids | mg/L | 926 |
| UA | MW-383 | C | 2018/09/25 | Total Dissolved Solids | mg/L | 940 |
| UA | MW-383 | C | 2019/03/20 | Total Dissolved Solids | mg/L | 920 |
| UA | MW-383 | C | 2019/09/24 | Total Dissolved Solids | mg/L | 922 |
| UA | MW-383 | C | 2020/03/25 | Total Dissolved Solids | mg/L | 874 |
| UA | MW-383 | C | 2020/09/15 | Total Dissolved Solids | mg/L | 884 |
| UA | MW-383 | C | 2021/03/12 | Total Dissolved Solids | mg/L | 960 |
| UA | MW-383 | C | 2021/09/13 | Total Dissolved Solids | mg/L | 864 |
| UA | MW-383 | C | 2022/03/29 | Total Dissolved Solids | mg/L | 896 |
| UA | MW-383 | C | 2022/09/30 | Total Dissolved Solids | mg/L | 906 |
| UA | MW-383 | C | 2023/03/14 | Total Dissolved Solids | mg/L | 890 |
| UA | MW-383 | C | 2023/05/22 | Total Dissolved Solids | mg/L | 872 |
| UA | MW-383 | C | 2023/08/03 | Total Dissolved Solids | mg/L | 882 |
| UA | MW-383 | C | 2023/11/01 | Total Dissolved Solids | mg/L | 934 |
| UA | MW-384 | C | 2016/01/21 | pH (field) | SU | 7.5 |
| UA | MW-384 | C | 2016/03/24 | pH (field) | SU | 7.8 |
| UA | MW-384 | C | 2016/06/23 | pH (field) | SU | 7.8 |
| UA | MW-384 | C | 2016/09/21 | pH (field) | SU | 8.0 |
| UA | MW-384 | C | 2016/12/27 | pH (field) | SU | 7.9 |
| UA | MW-384 | C | 2017/03/16 | pH (field) | SU | 8.0 |
| UA | MW-384 | C | 2017/06/19 | pH (field) | SU | 8.0 |
| UA | MW-384 | C | 2017/07/25 | pH (field) | SU | 7.6 |
| UA | MW-384 | C | 2017/11/28 | pH (field) | SU | 7.9 |
| UA | MW-384 | C | 2018/06/27 | pH (field) | SU | 7.2 |
| UA | MW-384 | C | 2018/09/25 | pH (field) | SU | 8.0 |
| UA | MW-384 | C | 2019/03/20 | pH (field) | SU | 7.5 |
| UA | MW-384 | C | 2019/09/24 | pH (field) | SU | 8.0 |
| UA | MW-384 | C | 2020/03/25 | pH (field) | SU | 8.1 |
| UA | MW-384 | C | 2020/09/15 | pH (field) | SU | 8.1 |
| UA | MW-384 | C | 2021/03/11 | pH (field) | SU | 7.8 |
| UA | MW-384 | C | 2021/09/13 | pH (field) | SU | 8.0 |
| UA | MW-384 | C | 2022/03/29 | pH (field) | SU | 8.0 |
| UA | MW-384 | C | 2022/09/30 | pH (field) | SU | 8.1 |
| UA | MW-384 | C | 2023/03/14 | pH (field) | SU | 8.0 |
| UA | MW-384 | C | 2023/05/22 | pH (field) | SU | 7.7 |
| UA | MW-384 | C | 2023/08/03 | pH (field) | SU | 8.1 |
| UA | MW-384 | C | 2023/11/01 | pH (field) | SU | 8.1 |
| UA | MW-384 | C | 2016/01/21 | Oxidation Reduction Potential | mV | 68.0 |
| UA | MW-384 | C | 2016/03/24 | Oxidation Reduction Potential | mV | 102 |
| UA | MW-384 | C | 2016/06/23 | Oxidation Reduction Potential | mV | -23.0 |
| UA | MW-384 | C | 2016/09/21 | Oxidation Reduction Potential | mV | -78.0 |
| UA | MW-384 | C | 2016/12/27 | Oxidation Reduction Potential | mV | -61.0 |
| UA | MW-384 | C | 2017/03/16 | Oxidation Reduction Potential | mV | -33.0 |
| UA | MW-384 | C | 2017/06/19 | Oxidation Reduction Potential | mV | -191 |
| UA | MW-384 | C | 2017/07/25 | Oxidation Reduction Potential | mV | -91.0 |
| UA | MW-384 | C | 2017/11/28 | Oxidation Reduction Potential | mV | -25.0 |
| UA | MW-384 | C | 2018/06/27 | Oxidation Reduction Potential | mV | -40.0 |
| UA | MW-384 | C | 2018/09/25 | Oxidation Reduction Potential | mV | -250 |
| UA | MW-384 | C | 2019/03/20 | Oxidation Reduction Potential | mV | -123 |
| UA | MW-384 | C | 2019/09/24 | Oxidation Reduction Potential | mV | -157 |
| UA | MW-384 | C | 2020/03/25 | Oxidation Reduction Potential | mV | -104 |
| UA | MW-384 | C | 2020/09/15 | Oxidation Reduction Potential | mV | -95.0 |
| UA | MW-384 | C | 2021/03/11 | Oxidation Reduction Potential | mV | 2.00 |

Attachment I. Site Groundwater Data

Geochemical Conceptual Site Model

Baldwin Fly Ash Pond System

Baldwin Power Plant

Baldwin, IL

| | | | | | | |
|----|--------|---|------------|-------------------------------|------------|---------|
| UA | MW-384 | C | 2021/09/13 | Oxidation Reduction Potential | mV | -93.0 |
| UA | MW-384 | C | 2022/03/29 | Oxidation Reduction Potential | mV | -136 |
| UA | MW-384 | C | 2022/09/30 | Oxidation Reduction Potential | mV | 65.0 |
| UA | MW-384 | C | 2023/03/14 | Oxidation Reduction Potential | mV | -112 |
| UA | MW-384 | C | 2023/05/22 | Oxidation Reduction Potential | mV | 69.0 |
| UA | MW-384 | C | 2023/08/03 | Oxidation Reduction Potential | mV | 54.0 |
| UA | MW-384 | C | 2023/11/01 | Oxidation Reduction Potential | mV | -99.0 |
| UA | MW-384 | C | 2016/01/21 | Eh | V | 0.27 |
| UA | MW-384 | C | 2016/03/24 | Eh | V | 0.30 |
| UA | MW-384 | C | 2016/06/23 | Eh | V | 0.17 |
| UA | MW-384 | C | 2016/09/21 | Eh | V | 0.11 |
| UA | MW-384 | C | 2016/12/27 | Eh | V | 0.14 |
| UA | MW-384 | C | 2017/03/16 | Eh | V | 0.16 |
| UA | MW-384 | C | 2017/06/19 | Eh | V | -0.0013 |
| UA | MW-384 | C | 2017/07/25 | Eh | V | 0.096 |
| UA | MW-384 | C | 2017/11/28 | Eh | V | 0.17 |
| UA | MW-384 | C | 2018/06/27 | Eh | V | 0.15 |
| UA | MW-384 | C | 2018/09/25 | Eh | V | -0.057 |
| UA | MW-384 | C | 2019/03/20 | Eh | V | 0.073 |
| UA | MW-384 | C | 2019/09/24 | Eh | V | 0.036 |
| UA | MW-384 | C | 2020/03/25 | Eh | V | 0.091 |
| UA | MW-384 | C | 2020/09/15 | Eh | V | 0.099 |
| UA | MW-384 | C | 2021/03/11 | Eh | V | 0.20 |
| UA | MW-384 | C | 2021/09/13 | Eh | V | 0.099 |
| UA | MW-384 | C | 2022/03/29 | Eh | V | 0.058 |
| UA | MW-384 | C | 2022/09/30 | Eh | V | 0.26 |
| UA | MW-384 | C | 2023/03/14 | Eh | V | 0.083 |
| UA | MW-384 | C | 2023/05/22 | Eh | V | 0.26 |
| UA | MW-384 | C | 2023/08/03 | Eh | V | 0.25 |
| UA | MW-384 | C | 2023/11/01 | Eh | V | 0.096 |
| UA | MW-384 | C | 2017/07/25 | Alkalinity, bicarbonate | mg/L CaCO3 | 632 |
| UA | MW-384 | C | 2020/03/25 | Alkalinity, bicarbonate | mg/L CaCO3 | 638 |
| UA | MW-384 | C | 2020/09/15 | Alkalinity, bicarbonate | mg/L CaCO3 | 674 |
| UA | MW-384 | C | 2021/03/11 | Alkalinity, bicarbonate | mg/L CaCO3 | 608 |
| UA | MW-384 | C | 2021/09/13 | Alkalinity, bicarbonate | mg/L CaCO3 | 632 |
| UA | MW-384 | C | 2022/03/29 | Alkalinity, bicarbonate | mg/L CaCO3 | 605 |
| UA | MW-384 | C | 2022/09/30 | Alkalinity, bicarbonate | mg/L CaCO3 | 617 |
| UA | MW-384 | C | 2023/03/14 | Alkalinity, bicarbonate | mg/L CaCO3 | 586 |
| UA | MW-384 | C | 2023/05/22 | Alkalinity, bicarbonate | mg/L CaCO3 | 594 |
| UA | MW-384 | C | 2023/08/03 | Alkalinity, bicarbonate | mg/L CaCO3 | 634 |
| UA | MW-384 | C | 2023/11/01 | Alkalinity, bicarbonate | mg/L CaCO3 | 619 |
| UA | MW-384 | C | 2021/03/11 | Alkalinity, carbonate | mg/L CaCO3 | 26.0 |
| UA | MW-384 | C | 2022/03/29 | Alkalinity, carbonate | mg/L CaCO3 | 23.0 |
| UA | MW-384 | C | 2022/09/30 | Alkalinity, carbonate | mg/L CaCO3 | 14.0 |
| UA | MW-384 | C | 2023/05/22 | Alkalinity, carbonate | mg/L CaCO3 | 11.0 |
| UA | MW-384 | C | 2023/08/03 | Alkalinity, carbonate | mg/L CaCO3 | 16.0 |
| UA | MW-384 | C | 2023/11/01 | Alkalinity, carbonate | mg/L CaCO3 | 30.0 |
| UA | MW-384 | C | 2016/01/21 | Barium, total | mg/L | 0.0221 |
| UA | MW-384 | C | 2016/03/24 | Barium, total | mg/L | 0.0245 |
| UA | MW-384 | C | 2016/06/23 | Barium, total | mg/L | 0.0282 |
| UA | MW-384 | C | 2016/09/21 | Barium, total | mg/L | 0.0258 |
| UA | MW-384 | C | 2016/12/27 | Barium, total | mg/L | 0.0275 |
| UA | MW-384 | C | 2017/03/16 | Barium, total | mg/L | 0.0283 |
| UA | MW-384 | C | 2017/06/19 | Barium, total | mg/L | 0.0277 |
| UA | MW-384 | C | 2017/07/25 | Barium, total | mg/L | 0.0264 |
| UA | MW-384 | C | 2018/06/27 | Barium, total | mg/L | 0.0332 |
| UA | MW-384 | C | 2018/09/25 | Barium, total | mg/L | 0.0285 |

Attachment I. Site Groundwater Data

Geochemical Conceptual Site Model

Baldwin Fly Ash Pond System

Baldwin Power Plant

Baldwin, IL

| | | | | | | |
|----|--------|---|------------|----------------|------|--------|
| UA | MW-384 | C | 2019/03/20 | Barium, total | mg/L | 0.0336 |
| UA | MW-384 | C | 2019/09/24 | Barium, total | mg/L | 0.0305 |
| UA | MW-384 | C | 2020/03/25 | Barium, total | mg/L | 0.0322 |
| UA | MW-384 | C | 2020/09/15 | Barium, total | mg/L | 0.0394 |
| UA | MW-384 | C | 2021/03/11 | Barium, total | mg/L | 0.0430 |
| UA | MW-384 | C | 2021/09/13 | Barium, total | mg/L | 0.0521 |
| UA | MW-384 | C | 2022/03/29 | Barium, total | mg/L | 0.0285 |
| UA | MW-384 | C | 2022/09/30 | Barium, total | mg/L | 0.0666 |
| UA | MW-384 | C | 2023/03/14 | Barium, total | mg/L | 0.0530 |
| UA | MW-384 | C | 2023/05/22 | Barium, total | mg/L | 0.0513 |
| UA | MW-384 | C | 2023/08/03 | Barium, total | mg/L | 0.0287 |
| UA | MW-384 | C | 2023/11/01 | Barium, total | mg/L | 0.0324 |
| UA | MW-384 | C | 2016/01/21 | Boron, total | mg/L | 1.45 |
| UA | MW-384 | C | 2016/03/24 | Boron, total | mg/L | 1.29 |
| UA | MW-384 | C | 2016/06/23 | Boron, total | mg/L | 1.48 |
| UA | MW-384 | C | 2016/09/21 | Boron, total | mg/L | 1.52 |
| UA | MW-384 | C | 2016/12/27 | Boron, total | mg/L | 1.41 |
| UA | MW-384 | C | 2017/03/16 | Boron, total | mg/L | 1.33 |
| UA | MW-384 | C | 2017/06/19 | Boron, total | mg/L | 1.50 |
| UA | MW-384 | C | 2017/07/25 | Boron, total | mg/L | 1.26 |
| UA | MW-384 | C | 2017/11/28 | Boron, total | mg/L | 1.92 |
| UA | MW-384 | C | 2018/06/27 | Boron, total | mg/L | 1.51 |
| UA | MW-384 | C | 2018/09/25 | Boron, total | mg/L | 1.39 |
| UA | MW-384 | C | 2019/03/20 | Boron, total | mg/L | 1.44 |
| UA | MW-384 | C | 2019/09/24 | Boron, total | mg/L | 1.36 |
| UA | MW-384 | C | 2020/03/25 | Boron, total | mg/L | 1.43 |
| UA | MW-384 | C | 2020/09/15 | Boron, total | mg/L | 1.51 |
| UA | MW-384 | C | 2021/03/11 | Boron, total | mg/L | 1.66 |
| UA | MW-384 | C | 2021/09/13 | Boron, total | mg/L | 1.54 |
| UA | MW-384 | C | 2022/03/29 | Boron, total | mg/L | 2.26 |
| UA | MW-384 | C | 2022/09/30 | Boron, total | mg/L | 1.91 |
| UA | MW-384 | C | 2023/03/14 | Boron, total | mg/L | 1.58 |
| UA | MW-384 | C | 2023/05/22 | Boron, total | mg/L | 1.48 |
| UA | MW-384 | C | 2023/08/03 | Boron, total | mg/L | 1.47 |
| UA | MW-384 | C | 2023/11/01 | Boron, total | mg/L | 1.55 |
| UA | MW-384 | C | 2016/01/21 | Calcium, total | mg/L | 22.6 |
| UA | MW-384 | C | 2016/03/24 | Calcium, total | mg/L | 22.5 |
| UA | MW-384 | C | 2016/06/23 | Calcium, total | mg/L | 23.2 |
| UA | MW-384 | C | 2016/09/21 | Calcium, total | mg/L | 22.3 |
| UA | MW-384 | C | 2016/12/27 | Calcium, total | mg/L | 19.8 |
| UA | MW-384 | C | 2017/03/16 | Calcium, total | mg/L | 20.5 |
| UA | MW-384 | C | 2017/06/19 | Calcium, total | mg/L | 19.5 |
| UA | MW-384 | C | 2017/07/25 | Calcium, total | mg/L | 19.3 |
| UA | MW-384 | C | 2017/11/28 | Calcium, total | mg/L | 20.7 |
| UA | MW-384 | C | 2018/06/27 | Calcium, total | mg/L | 21.4 |
| UA | MW-384 | C | 2018/09/25 | Calcium, total | mg/L | 19.8 |
| UA | MW-384 | C | 2019/03/20 | Calcium, total | mg/L | 21.5 |
| UA | MW-384 | C | 2019/09/24 | Calcium, total | mg/L | 19.8 |
| UA | MW-384 | C | 2020/03/25 | Calcium, total | mg/L | 19.4 |
| UA | MW-384 | C | 2020/09/15 | Calcium, total | mg/L | 18.4 |
| UA | MW-384 | C | 2021/03/11 | Calcium, total | mg/L | 17.6 |
| UA | MW-384 | C | 2021/09/13 | Calcium, total | mg/L | 20.0 |
| UA | MW-384 | C | 2022/03/29 | Calcium, total | mg/L | 6.83 |
| UA | MW-384 | C | 2022/09/30 | Calcium, total | mg/L | 19.4 |
| UA | MW-384 | C | 2023/03/14 | Calcium, total | mg/L | 18.2 |
| UA | MW-384 | C | 2023/05/22 | Calcium, total | mg/L | 17.4 |
| UA | MW-384 | C | 2023/08/03 | Calcium, total | mg/L | 5.32 |

Attachment I. Site Groundwater Data

Geochemical Conceptual Site Model

Baldwin Fly Ash Pond System

Baldwin Power Plant

Baldwin, IL

| | | | | | | |
|----|--------|---|------------|----------------------|------|---------|
| UA | MW-384 | C | 2023/11/01 | Calcium, total | mg/L | 8.11 |
| UA | MW-384 | C | 2016/01/21 | Chloride, total | mg/L | 138 |
| UA | MW-384 | C | 2016/03/24 | Chloride, total | mg/L | 109 |
| UA | MW-384 | C | 2016/06/23 | Chloride, total | mg/L | 141 |
| UA | MW-384 | C | 2016/09/21 | Chloride, total | mg/L | 158 |
| UA | MW-384 | C | 2016/12/27 | Chloride, total | mg/L | 187 |
| UA | MW-384 | C | 2017/03/16 | Chloride, total | mg/L | 206 |
| UA | MW-384 | C | 2017/06/19 | Chloride, total | mg/L | 170 |
| UA | MW-384 | C | 2017/07/25 | Chloride, total | mg/L | 179 |
| UA | MW-384 | C | 2017/11/28 | Chloride, total | mg/L | 234 |
| UA | MW-384 | C | 2018/06/27 | Chloride, total | mg/L | 248 |
| UA | MW-384 | C | 2018/09/25 | Chloride, total | mg/L | 396 |
| UA | MW-384 | C | 2019/03/20 | Chloride, total | mg/L | 216 |
| UA | MW-384 | C | 2019/09/24 | Chloride, total | mg/L | 197 |
| UA | MW-384 | C | 2020/03/25 | Chloride, total | mg/L | 229 |
| UA | MW-384 | C | 2020/09/15 | Chloride, total | mg/L | 493 |
| UA | MW-384 | C | 2021/03/11 | Chloride, total | mg/L | 488 |
| UA | MW-384 | C | 2021/09/13 | Chloride, total | mg/L | 501 |
| UA | MW-384 | C | 2022/03/29 | Chloride, total | mg/L | 466 |
| UA | MW-384 | C | 2022/09/30 | Chloride, total | mg/L | 531 |
| UA | MW-384 | C | 2023/03/14 | Chloride, total | mg/L | 474 |
| UA | MW-384 | C | 2023/05/22 | Chloride, total | mg/L | 492 |
| UA | MW-384 | C | 2023/08/03 | Chloride, total | mg/L | 508 |
| UA | MW-384 | C | 2023/11/01 | Chloride, total | mg/L | 978 |
| UA | MW-384 | C | 2023/05/22 | Iron, dissolved | mg/L | <0.02 |
| UA | MW-384 | C | 2023/08/03 | Iron, dissolved | mg/L | <0.0115 |
| UA | MW-384 | C | 2017/07/25 | Magnesium, total | mg/L | 7.24 |
| UA | MW-384 | C | 2020/03/25 | Magnesium, total | mg/L | 7.96 |
| UA | MW-384 | C | 2020/09/15 | Magnesium, total | mg/L | 7.91 |
| UA | MW-384 | C | 2021/03/11 | Magnesium, total | mg/L | 7.25 |
| UA | MW-384 | C | 2021/09/13 | Magnesium, total | mg/L | 7.86 |
| UA | MW-384 | C | 2022/03/29 | Magnesium, total | mg/L | 2.79 |
| UA | MW-384 | C | 2022/09/30 | Magnesium, total | mg/L | 7.59 |
| UA | MW-384 | C | 2023/03/14 | Magnesium, total | mg/L | 7.23 |
| UA | MW-384 | C | 2023/05/22 | Magnesium, total | mg/L | 7.00 |
| UA | MW-384 | C | 2023/08/03 | Magnesium, total | mg/L | 2.37 |
| UA | MW-384 | C | 2023/11/01 | Magnesium, total | mg/L | 3.41 |
| UA | MW-384 | C | 2023/05/22 | Manganese, dissolved | mg/L | 0.00310 |
| UA | MW-384 | C | 2023/08/03 | Manganese, dissolved | mg/L | 0.00660 |
| UA | MW-384 | C | 2023/05/22 | Phosphate, dissolved | mg/L | 0.0280 |
| UA | MW-384 | C | 2023/08/03 | Phosphate, dissolved | mg/L | 0.0460 |
| UA | MW-384 | C | 2017/07/25 | Potassium, total | mg/L | 1.92 |
| UA | MW-384 | C | 2020/03/25 | Potassium, total | mg/L | 2.11 |
| UA | MW-384 | C | 2020/09/15 | Potassium, total | mg/L | 2.66 |
| UA | MW-384 | C | 2021/03/11 | Potassium, total | mg/L | 2.10 |
| UA | MW-384 | C | 2021/09/13 | Potassium, total | mg/L | 2.47 |
| UA | MW-384 | C | 2022/03/29 | Potassium, total | mg/L | 2.03 |
| UA | MW-384 | C | 2022/09/30 | Potassium, total | mg/L | 2.64 |
| UA | MW-384 | C | 2023/03/14 | Potassium, total | mg/L | 2.15 |
| UA | MW-384 | C | 2023/05/22 | Potassium, total | mg/L | 2.65 |
| UA | MW-384 | C | 2023/08/03 | Potassium, total | mg/L | 1.90 |
| UA | MW-384 | C | 2023/11/01 | Potassium, total | mg/L | 2.04 |
| UA | MW-384 | C | 2023/05/22 | Silicon, dissolved | mg/L | 4.23 |
| UA | MW-384 | C | 2023/08/03 | Silicon, dissolved | mg/L | 3.85 |
| UA | MW-384 | C | 2017/07/25 | Sodium, total | mg/L | 396 |
| UA | MW-384 | C | 2020/03/25 | Sodium, total | mg/L | 474 |
| UA | MW-384 | C | 2020/09/15 | Sodium, total | mg/L | 668 |

Attachment I. Site Groundwater Data

Geochemical Conceptual Site Model

Baldwin Fly Ash Pond System

Baldwin Power Plant

Baldwin, IL

| | | | | | | |
|----|--------|---|------------|------------------------|-----------|-------|
| UA | MW-384 | C | 2021/03/11 | Sodium, total | mg/L | 610 |
| UA | MW-384 | C | 2021/09/13 | Sodium, total | mg/L | 553 |
| UA | MW-384 | C | 2022/03/29 | Sodium, total | mg/L | 677 |
| UA | MW-384 | C | 2022/09/30 | Sodium, total | mg/L | 577 |
| UA | MW-384 | C | 2023/03/14 | Sodium, total | mg/L | 577 |
| UA | MW-384 | C | 2023/05/22 | Sodium, total | mg/L | 575 |
| UA | MW-384 | C | 2023/08/03 | Sodium, total | mg/L | 695 |
| UA | MW-384 | C | 2023/11/01 | Sodium, total | mg/L | 709 |
| UA | MW-384 | C | 2016/01/21 | Sulfate, total | mg/L | 178 |
| UA | MW-384 | C | 2016/03/24 | Sulfate, total | mg/L | 178 |
| UA | MW-384 | C | 2016/06/23 | Sulfate, total | mg/L | 135 |
| UA | MW-384 | C | 2016/09/21 | Sulfate, total | mg/L | 142 |
| UA | MW-384 | C | 2016/12/27 | Sulfate, total | mg/L | 160 |
| UA | MW-384 | C | 2017/03/16 | Sulfate, total | mg/L | 156 |
| UA | MW-384 | C | 2017/06/19 | Sulfate, total | mg/L | 130 |
| UA | MW-384 | C | 2017/07/25 | Sulfate, total | mg/L | 127 |
| UA | MW-384 | C | 2017/11/28 | Sulfate, total | mg/L | 114 |
| UA | MW-384 | C | 2018/06/27 | Sulfate, total | mg/L | 124 |
| UA | MW-384 | C | 2018/09/25 | Sulfate, total | mg/L | 82.0 |
| UA | MW-384 | C | 2019/03/20 | Sulfate, total | mg/L | 94.0 |
| UA | MW-384 | C | 2019/09/24 | Sulfate, total | mg/L | 102 |
| UA | MW-384 | C | 2020/03/25 | Sulfate, total | mg/L | 110 |
| UA | MW-384 | C | 2020/09/15 | Sulfate, total | mg/L | 53.0 |
| UA | MW-384 | C | 2021/03/11 | Sulfate, total | mg/L | 38.0 |
| UA | MW-384 | C | 2021/09/13 | Sulfate, total | mg/L | 40.0 |
| UA | MW-384 | C | 2022/03/29 | Sulfate, total | mg/L | 34.0 |
| UA | MW-384 | C | 2022/09/30 | Sulfate, total | mg/L | 35.0 |
| UA | MW-384 | C | 2023/03/14 | Sulfate, total | mg/L | 36.0 |
| UA | MW-384 | C | 2023/05/22 | Sulfate, total | mg/L | 43.0 |
| UA | MW-384 | C | 2023/08/03 | Sulfate, total | mg/L | 32.0 |
| UA | MW-384 | C | 2023/11/01 | Sulfate, total | mg/L | 30.0 |
| UA | MW-384 | C | 2016/01/21 | Temperature (Celsius) | degrees C | 12.6 |
| UA | MW-384 | C | 2016/03/24 | Temperature (Celsius) | degrees C | 14.6 |
| UA | MW-384 | C | 2016/06/23 | Temperature (Celsius) | degrees C | 22.4 |
| UA | MW-384 | C | 2016/09/21 | Temperature (Celsius) | degrees C | 24.4 |
| UA | MW-384 | C | 2016/12/27 | Temperature (Celsius) | degrees C | 13.7 |
| UA | MW-384 | C | 2017/03/16 | Temperature (Celsius) | degrees C | 13.6 |
| UA | MW-384 | C | 2017/06/19 | Temperature (Celsius) | degrees C | 23.4 |
| UA | MW-384 | C | 2017/07/25 | Temperature (Celsius) | degrees C | 26.6 |
| UA | MW-384 | C | 2017/11/28 | Temperature (Celsius) | degrees C | 16.4 |
| UA | MW-384 | C | 2018/06/27 | Temperature (Celsius) | degrees C | 19.8 |
| UA | MW-384 | C | 2018/09/25 | Temperature (Celsius) | degrees C | 19.1 |
| UA | MW-384 | C | 2019/03/20 | Temperature (Celsius) | degrees C | 14.9 |
| UA | MW-384 | C | 2019/09/24 | Temperature (Celsius) | degrees C | 18.5 |
| UA | MW-384 | C | 2020/03/25 | Temperature (Celsius) | degrees C | 16.4 |
| UA | MW-384 | C | 2020/09/15 | Temperature (Celsius) | degrees C | 17.6 |
| UA | MW-384 | C | 2021/03/11 | Temperature (Celsius) | degrees C | 15.4 |
| UA | MW-384 | C | 2021/09/13 | Temperature (Celsius) | degrees C | 20.7 |
| UA | MW-384 | C | 2022/03/29 | Temperature (Celsius) | degrees C | 16.7 |
| UA | MW-384 | C | 2022/09/30 | Temperature (Celsius) | degrees C | 17.0 |
| UA | MW-384 | C | 2023/03/14 | Temperature (Celsius) | degrees C | 15.7 |
| UA | MW-384 | C | 2023/05/22 | Temperature (Celsius) | degrees C | 17.0 |
| UA | MW-384 | C | 2023/08/03 | Temperature (Celsius) | degrees C | 17.5 |
| UA | MW-384 | C | 2023/11/01 | Temperature (Celsius) | degrees C | 16.3 |
| UA | MW-384 | C | 2016/01/21 | Total Dissolved Solids | mg/L | 992 |
| UA | MW-384 | C | 2016/03/24 | Total Dissolved Solids | mg/L | 1,080 |
| UA | MW-384 | C | 2016/06/23 | Total Dissolved Solids | mg/L | 1,110 |

Attachment I. Site Groundwater Data

Geochemical Conceptual Site Model

Baldwin Fly Ash Pond System

Baldwin Power Plant

Baldwin, IL

| | | | | | | |
|----|--------|---|------------|-------------------------------|------|-------|
| UA | MW-384 | C | 2016/09/21 | Total Dissolved Solids | mg/L | 1,080 |
| UA | MW-384 | C | 2016/12/27 | Total Dissolved Solids | mg/L | 1,220 |
| UA | MW-384 | C | 2017/03/16 | Total Dissolved Solids | mg/L | 1,230 |
| UA | MW-384 | C | 2017/06/19 | Total Dissolved Solids | mg/L | 1,120 |
| UA | MW-384 | C | 2017/07/25 | Total Dissolved Solids | mg/L | 1,090 |
| UA | MW-384 | C | 2017/11/28 | Total Dissolved Solids | mg/L | 1,230 |
| UA | MW-384 | C | 2018/06/27 | Total Dissolved Solids | mg/L | 1,200 |
| UA | MW-384 | C | 2018/09/25 | Total Dissolved Solids | mg/L | 1,510 |
| UA | MW-384 | C | 2019/03/20 | Total Dissolved Solids | mg/L | 1,180 |
| UA | MW-384 | C | 2019/09/24 | Total Dissolved Solids | mg/L | 1,120 |
| UA | MW-384 | C | 2020/03/25 | Total Dissolved Solids | mg/L | 1,150 |
| UA | MW-384 | C | 2020/09/15 | Total Dissolved Solids | mg/L | 1,520 |
| UA | MW-384 | C | 2021/03/11 | Total Dissolved Solids | mg/L | 1,540 |
| UA | MW-384 | C | 2021/09/13 | Total Dissolved Solids | mg/L | 1,440 |
| UA | MW-384 | C | 2022/03/29 | Total Dissolved Solids | mg/L | 1,520 |
| UA | MW-384 | C | 2022/09/30 | Total Dissolved Solids | mg/L | 1,600 |
| UA | MW-384 | C | 2023/03/14 | Total Dissolved Solids | mg/L | 1,500 |
| UA | MW-384 | C | 2023/05/22 | Total Dissolved Solids | mg/L | 1,480 |
| UA | MW-384 | C | 2023/08/03 | Total Dissolved Solids | mg/L | 1,570 |
| UA | MW-384 | C | 2023/11/01 | Total Dissolved Solids | mg/L | 1,540 |
| UA | MW-390 | C | 2016/03/22 | pH (field) | SU | 7.4 |
| UA | MW-390 | C | 2016/06/23 | pH (field) | SU | 7.6 |
| UA | MW-390 | C | 2016/08/18 | pH (field) | SU | 7.2 |
| UA | MW-390 | C | 2016/09/20 | pH (field) | SU | 7.5 |
| UA | MW-390 | C | 2016/12/22 | pH (field) | SU | 7.5 |
| UA | MW-390 | C | 2017/03/15 | pH (field) | SU | 7.8 |
| UA | MW-390 | C | 2017/06/20 | pH (field) | SU | 7.2 |
| UA | MW-390 | C | 2017/07/28 | pH (field) | SU | 7.4 |
| UA | MW-390 | C | 2017/11/27 | pH (field) | SU | 7.5 |
| UA | MW-390 | C | 2018/06/26 | pH (field) | SU | 6.9 |
| UA | MW-390 | C | 2018/09/25 | pH (field) | SU | 7.0 |
| UA | MW-390 | C | 2019/03/19 | pH (field) | SU | 7.2 |
| UA | MW-390 | C | 2019/09/24 | pH (field) | SU | 7.1 |
| UA | MW-390 | C | 2020/03/26 | pH (field) | SU | 6.9 |
| UA | MW-390 | C | 2020/09/16 | pH (field) | SU | 7.2 |
| UA | MW-390 | C | 2021/03/12 | pH (field) | SU | 7.2 |
| UA | MW-390 | C | 2021/09/15 | pH (field) | SU | 7.1 |
| UA | MW-390 | C | 2022/03/29 | pH (field) | SU | 7.1 |
| UA | MW-390 | C | 2022/09/30 | pH (field) | SU | 7.2 |
| UA | MW-390 | C | 2023/03/14 | pH (field) | SU | 7.0 |
| UA | MW-390 | C | 2023/05/17 | pH (field) | SU | 6.8 |
| UA | MW-390 | C | 2023/08/04 | pH (field) | SU | 7.2 |
| UA | MW-390 | C | 2023/11/02 | pH (field) | SU | 7.2 |
| UA | MW-390 | C | 2016/03/22 | Oxidation Reduction Potential | mV | 132 |
| UA | MW-390 | C | 2016/06/23 | Oxidation Reduction Potential | mV | 7.00 |
| UA | MW-390 | C | 2016/08/18 | Oxidation Reduction Potential | mV | -19.0 |
| UA | MW-390 | C | 2016/09/20 | Oxidation Reduction Potential | mV | -28.0 |
| UA | MW-390 | C | 2016/12/22 | Oxidation Reduction Potential | mV | -16.0 |
| UA | MW-390 | C | 2017/03/15 | Oxidation Reduction Potential | mV | -66.0 |
| UA | MW-390 | C | 2017/06/20 | Oxidation Reduction Potential | mV | -124 |
| UA | MW-390 | C | 2017/07/28 | Oxidation Reduction Potential | mV | -92.0 |
| UA | MW-390 | C | 2017/11/27 | Oxidation Reduction Potential | mV | 204 |
| UA | MW-390 | C | 2018/06/26 | Oxidation Reduction Potential | mV | -18.0 |
| UA | MW-390 | C | 2018/09/25 | Oxidation Reduction Potential | mV | -162 |
| UA | MW-390 | C | 2019/03/19 | Oxidation Reduction Potential | mV | -128 |
| UA | MW-390 | C | 2019/09/24 | Oxidation Reduction Potential | mV | -133 |
| UA | MW-390 | C | 2020/03/26 | Oxidation Reduction Potential | mV | -14.0 |

Attachment I. Site Groundwater Data

Geochemical Conceptual Site Model

Baldwin Fly Ash Pond System

Baldwin Power Plant

Baldwin, IL

| | | | | | | |
|----|--------|---|------------|-------------------------------|------------|--------|
| UA | MW-390 | C | 2020/09/16 | Oxidation Reduction Potential | mV | -105 |
| UA | MW-390 | C | 2021/03/12 | Oxidation Reduction Potential | mV | -65.0 |
| UA | MW-390 | C | 2021/09/15 | Oxidation Reduction Potential | mV | -98.0 |
| UA | MW-390 | C | 2022/03/29 | Oxidation Reduction Potential | mV | -106 |
| UA | MW-390 | C | 2022/09/30 | Oxidation Reduction Potential | mV | 55.0 |
| UA | MW-390 | C | 2023/03/14 | Oxidation Reduction Potential | mV | -70.2 |
| UA | MW-390 | C | 2023/05/17 | Oxidation Reduction Potential | mV | -32.0 |
| UA | MW-390 | C | 2023/08/04 | Oxidation Reduction Potential | mV | 73.0 |
| UA | MW-390 | C | 2023/11/02 | Oxidation Reduction Potential | mV | -70.0 |
| UA | MW-390 | C | 2016/03/22 | Eh | V | 0.33 |
| UA | MW-390 | C | 2016/06/23 | Eh | V | 0.20 |
| UA | MW-390 | C | 2016/08/18 | Eh | V | 0.17 |
| UA | MW-390 | C | 2016/09/20 | Eh | V | 0.16 |
| UA | MW-390 | C | 2016/12/22 | Eh | V | 0.18 |
| UA | MW-390 | C | 2017/03/15 | Eh | V | 0.13 |
| UA | MW-390 | C | 2017/06/20 | Eh | V | 0.065 |
| UA | MW-390 | C | 2017/07/28 | Eh | V | 0.10 |
| UA | MW-390 | C | 2017/11/27 | Eh | V | 0.40 |
| UA | MW-390 | C | 2018/06/26 | Eh | V | 0.17 |
| UA | MW-390 | C | 2018/09/25 | Eh | V | 0.030 |
| UA | MW-390 | C | 2019/03/19 | Eh | V | 0.068 |
| UA | MW-390 | C | 2019/09/24 | Eh | V | 0.061 |
| UA | MW-390 | C | 2020/03/26 | Eh | V | 0.18 |
| UA | MW-390 | C | 2020/09/16 | Eh | V | 0.090 |
| UA | MW-390 | C | 2021/03/12 | Eh | V | 0.13 |
| UA | MW-390 | C | 2021/09/15 | Eh | V | 0.095 |
| UA | MW-390 | C | 2022/03/29 | Eh | V | 0.091 |
| UA | MW-390 | C | 2022/09/30 | Eh | V | 0.25 |
| UA | MW-390 | C | 2023/03/14 | Eh | V | 0.13 |
| UA | MW-390 | C | 2023/05/17 | Eh | V | 0.16 |
| UA | MW-390 | C | 2023/08/04 | Eh | V | 0.27 |
| UA | MW-390 | C | 2023/11/02 | Eh | V | 0.12 |
| UA | MW-390 | C | 2017/07/28 | Alkalinity, bicarbonate | mg/L CaCO3 | 392 |
| UA | MW-390 | C | 2020/03/26 | Alkalinity, bicarbonate | mg/L CaCO3 | 376 |
| UA | MW-390 | C | 2020/09/16 | Alkalinity, bicarbonate | mg/L CaCO3 | 408 |
| UA | MW-390 | C | 2021/03/12 | Alkalinity, bicarbonate | mg/L CaCO3 | 422 |
| UA | MW-390 | C | 2021/09/15 | Alkalinity, bicarbonate | mg/L CaCO3 | 416 |
| UA | MW-390 | C | 2022/03/29 | Alkalinity, bicarbonate | mg/L CaCO3 | 413 |
| UA | MW-390 | C | 2022/09/30 | Alkalinity, bicarbonate | mg/L CaCO3 | 435 |
| UA | MW-390 | C | 2023/03/14 | Alkalinity, bicarbonate | mg/L CaCO3 | 374 |
| UA | MW-390 | C | 2023/05/17 | Alkalinity, bicarbonate | mg/L CaCO3 | 382 |
| UA | MW-390 | C | 2023/08/04 | Alkalinity, bicarbonate | mg/L CaCO3 | 426 |
| UA | MW-390 | C | 2023/11/02 | Alkalinity, bicarbonate | mg/L CaCO3 | 440 |
| UA | MW-390 | C | 2016/03/22 | Barium, total | mg/L | 0.0330 |
| UA | MW-390 | C | 2016/06/23 | Barium, total | mg/L | 0.0299 |
| UA | MW-390 | C | 2016/08/18 | Barium, total | mg/L | 0.0289 |
| UA | MW-390 | C | 2016/09/20 | Barium, total | mg/L | 0.0258 |
| UA | MW-390 | C | 2016/12/22 | Barium, total | mg/L | 0.0228 |
| UA | MW-390 | C | 2017/03/15 | Barium, total | mg/L | 0.0520 |
| UA | MW-390 | C | 2017/06/20 | Barium, total | mg/L | 0.0400 |
| UA | MW-390 | C | 2017/07/28 | Barium, total | mg/L | 0.0385 |
| UA | MW-390 | C | 2018/06/26 | Barium, total | mg/L | 0.0806 |
| UA | MW-390 | C | 2018/09/25 | Barium, total | mg/L | 0.101 |
| UA | MW-390 | C | 2019/03/19 | Barium, total | mg/L | 0.0962 |
| UA | MW-390 | C | 2019/09/24 | Barium, total | mg/L | 0.0830 |
| UA | MW-390 | C | 2020/03/26 | Barium, total | mg/L | 0.0895 |
| UA | MW-390 | C | 2020/09/16 | Barium, total | mg/L | 0.0785 |

Attachment I. Site Groundwater Data

Geochemical Conceptual Site Model

Baldwin Fly Ash Pond System

Baldwin Power Plant

Baldwin, IL

| | | | | | | |
|----|--------|---|------------|-----------------|------|--------|
| UA | MW-390 | C | 2021/03/12 | Barium, total | mg/L | 0.0838 |
| UA | MW-390 | C | 2021/09/15 | Barium, total | mg/L | 0.0695 |
| UA | MW-390 | C | 2022/03/29 | Barium, total | mg/L | 0.0552 |
| UA | MW-390 | C | 2022/09/30 | Barium, total | mg/L | 0.105 |
| UA | MW-390 | C | 2023/03/14 | Barium, total | mg/L | 0.0674 |
| UA | MW-390 | C | 2023/05/17 | Barium, total | mg/L | 0.0886 |
| UA | MW-390 | C | 2023/08/04 | Barium, total | mg/L | 0.0225 |
| UA | MW-390 | C | 2023/11/02 | Barium, total | mg/L | 0.0442 |
| UA | MW-390 | C | 2016/03/22 | Boron, total | mg/L | 1.74 |
| UA | MW-390 | C | 2016/06/23 | Boron, total | mg/L | 2.30 |
| UA | MW-390 | C | 2016/08/18 | Boron, total | mg/L | 1.88 |
| UA | MW-390 | C | 2016/09/20 | Boron, total | mg/L | 2.18 |
| UA | MW-390 | C | 2016/12/22 | Boron, total | mg/L | 2.12 |
| UA | MW-390 | C | 2017/03/15 | Boron, total | mg/L | 0.668 |
| UA | MW-390 | C | 2017/06/20 | Boron, total | mg/L | 1.30 |
| UA | MW-390 | C | 2017/07/28 | Boron, total | mg/L | 1.12 |
| UA | MW-390 | C | 2017/11/27 | Boron, total | mg/L | 0.854 |
| UA | MW-390 | C | 2018/06/26 | Boron, total | mg/L | 0.207 |
| UA | MW-390 | C | 2018/09/25 | Boron, total | mg/L | 0.175 |
| UA | MW-390 | C | 2019/03/19 | Boron, total | mg/L | 0.178 |
| UA | MW-390 | C | 2019/09/24 | Boron, total | mg/L | 0.288 |
| UA | MW-390 | C | 2020/03/26 | Boron, total | mg/L | 0.182 |
| UA | MW-390 | C | 2020/09/16 | Boron, total | mg/L | 0.247 |
| UA | MW-390 | C | 2021/03/12 | Boron, total | mg/L | 0.274 |
| UA | MW-390 | C | 2021/09/15 | Boron, total | mg/L | 0.308 |
| UA | MW-390 | C | 2022/03/29 | Boron, total | mg/L | 0.546 |
| UA | MW-390 | C | 2022/09/30 | Boron, total | mg/L | 0.384 |
| UA | MW-390 | C | 2023/03/14 | Boron, total | mg/L | 0.268 |
| UA | MW-390 | C | 2023/05/17 | Boron, total | mg/L | 0.234 |
| UA | MW-390 | C | 2023/08/04 | Boron, total | mg/L | 1.42 |
| UA | MW-390 | C | 2023/11/02 | Boron, total | mg/L | 0.962 |
| UA | MW-390 | C | 2016/03/22 | Calcium, total | mg/L | 55.0 |
| UA | MW-390 | C | 2016/06/23 | Calcium, total | mg/L | 53.6 |
| UA | MW-390 | C | 2016/08/18 | Calcium, total | mg/L | 53.1 |
| UA | MW-390 | C | 2016/09/20 | Calcium, total | mg/L | 52.8 |
| UA | MW-390 | C | 2016/12/22 | Calcium, total | mg/L | 49.6 |
| UA | MW-390 | C | 2017/03/15 | Calcium, total | mg/L | 53.0 |
| UA | MW-390 | C | 2017/06/20 | Calcium, total | mg/L | 57.4 |
| UA | MW-390 | C | 2017/07/28 | Calcium, total | mg/L | 58.6 |
| UA | MW-390 | C | 2017/11/27 | Calcium, total | mg/L | 69.7 |
| UA | MW-390 | C | 2018/06/26 | Calcium, total | mg/L | 68.4 |
| UA | MW-390 | C | 2018/09/25 | Calcium, total | mg/L | 90.4 |
| UA | MW-390 | C | 2019/03/19 | Calcium, total | mg/L | 89.2 |
| UA | MW-390 | C | 2019/09/24 | Calcium, total | mg/L | 90.9 |
| UA | MW-390 | C | 2020/03/26 | Calcium, total | mg/L | 96.7 |
| UA | MW-390 | C | 2020/09/16 | Calcium, total | mg/L | 91.8 |
| UA | MW-390 | C | 2021/03/12 | Calcium, total | mg/L | 92.2 |
| UA | MW-390 | C | 2021/09/15 | Calcium, total | mg/L | 90.2 |
| UA | MW-390 | C | 2022/03/29 | Calcium, total | mg/L | 88.1 |
| UA | MW-390 | C | 2022/09/30 | Calcium, total | mg/L | 100 |
| UA | MW-390 | C | 2023/03/14 | Calcium, total | mg/L | 82.6 |
| UA | MW-390 | C | 2023/05/17 | Calcium, total | mg/L | 96.0 |
| UA | MW-390 | C | 2023/08/04 | Calcium, total | mg/L | 58.4 |
| UA | MW-390 | C | 2023/11/02 | Calcium, total | mg/L | 74.0 |
| UA | MW-390 | C | 2016/03/22 | Chloride, total | mg/L | 24.0 |
| UA | MW-390 | C | 2016/06/23 | Chloride, total | mg/L | 36.0 |
| UA | MW-390 | C | 2016/08/18 | Chloride, total | mg/L | 77.0 |

Attachment I. Site Groundwater Data

Geochemical Conceptual Site Model

Baldwin Fly Ash Pond System

Baldwin Power Plant

Baldwin, IL

| | | | | | | |
|----|--------|---|------------|----------------------|------|--------|
| UA | MW-390 | C | 2016/09/20 | Chloride, total | mg/L | 61.0 |
| UA | MW-390 | C | 2016/12/22 | Chloride, total | mg/L | 74.0 |
| UA | MW-390 | C | 2017/03/15 | Chloride, total | mg/L | 125 |
| UA | MW-390 | C | 2017/06/20 | Chloride, total | mg/L | 127 |
| UA | MW-390 | C | 2017/07/28 | Chloride, total | mg/L | 123 |
| UA | MW-390 | C | 2017/11/27 | Chloride, total | mg/L | 112 |
| UA | MW-390 | C | 2018/06/26 | Chloride, total | mg/L | 64.0 |
| UA | MW-390 | C | 2018/09/25 | Chloride, total | mg/L | 69.0 |
| UA | MW-390 | C | 2019/03/19 | Chloride, total | mg/L | 67.0 |
| UA | MW-390 | C | 2019/09/24 | Chloride, total | mg/L | 116 |
| UA | MW-390 | C | 2020/03/26 | Chloride, total | mg/L | 87.0 |
| UA | MW-390 | C | 2020/09/16 | Chloride, total | mg/L | 71.0 |
| UA | MW-390 | C | 2021/03/12 | Chloride, total | mg/L | 106 |
| UA | MW-390 | C | 2021/09/15 | Chloride, total | mg/L | 62.0 |
| UA | MW-390 | C | 2022/03/29 | Chloride, total | mg/L | 80.0 |
| UA | MW-390 | C | 2022/09/30 | Chloride, total | mg/L | 115 |
| UA | MW-390 | C | 2023/03/14 | Chloride, total | mg/L | 54.0 |
| UA | MW-390 | C | 2023/05/17 | Chloride, total | mg/L | 47.0 |
| UA | MW-390 | C | 2023/08/04 | Chloride, total | mg/L | 74.0 |
| UA | MW-390 | C | 2023/11/02 | Chloride, total | mg/L | 72.0 |
| UA | MW-390 | C | 2023/05/17 | Iron, dissolved | mg/L | <0.02 |
| UA | MW-390 | C | 2023/08/04 | Iron, dissolved | mg/L | <0.012 |
| UA | MW-390 | C | 2017/07/28 | Magnesium, total | mg/L | 29.8 |
| UA | MW-390 | C | 2020/03/26 | Magnesium, total | mg/L | 42.2 |
| UA | MW-390 | C | 2020/09/16 | Magnesium, total | mg/L | 42.6 |
| UA | MW-390 | C | 2021/03/12 | Magnesium, total | mg/L | 40.4 |
| UA | MW-390 | C | 2021/09/15 | Magnesium, total | mg/L | 38.6 |
| UA | MW-390 | C | 2022/03/29 | Magnesium, total | mg/L | 39.9 |
| UA | MW-390 | C | 2022/09/30 | Magnesium, total | mg/L | 42.4 |
| UA | MW-390 | C | 2023/03/14 | Magnesium, total | mg/L | 34.6 |
| UA | MW-390 | C | 2023/05/17 | Magnesium, total | mg/L | 39.4 |
| UA | MW-390 | C | 2023/08/04 | Magnesium, total | mg/L | 32.2 |
| UA | MW-390 | C | 2023/11/02 | Magnesium, total | mg/L | 34.8 |
| UA | MW-390 | C | 2023/05/17 | Manganese, dissolved | mg/L | 0.364 |
| UA | MW-390 | C | 2023/08/04 | Manganese, dissolved | mg/L | 0.681 |
| UA | MW-390 | C | 2023/05/17 | Phosphate, dissolved | mg/L | 0.0860 |
| UA | MW-390 | C | 2023/08/04 | Phosphate, dissolved | mg/L | 0.0180 |
| UA | MW-390 | C | 2017/07/28 | Potassium, total | mg/L | 5.62 |
| UA | MW-390 | C | 2020/03/26 | Potassium, total | mg/L | 4.17 |
| UA | MW-390 | C | 2020/09/16 | Potassium, total | mg/L | 3.88 |
| UA | MW-390 | C | 2021/03/12 | Potassium, total | mg/L | 3.42 |
| UA | MW-390 | C | 2021/09/15 | Potassium, total | mg/L | 3.26 |
| UA | MW-390 | C | 2022/03/29 | Potassium, total | mg/L | 4.05 |
| UA | MW-390 | C | 2022/09/30 | Potassium, total | mg/L | 4.14 |
| UA | MW-390 | C | 2023/03/14 | Potassium, total | mg/L | 3.08 |
| UA | MW-390 | C | 2023/05/17 | Potassium, total | mg/L | 3.78 |
| UA | MW-390 | C | 2023/08/04 | Potassium, total | mg/L | 3.70 |
| UA | MW-390 | C | 2023/11/02 | Potassium, total | mg/L | 3.99 |
| UA | MW-390 | C | 2023/05/17 | Silicon, dissolved | mg/L | 7.77 |
| UA | MW-390 | C | 2023/08/04 | Silicon, dissolved | mg/L | 7.23 |
| UA | MW-390 | C | 2017/07/28 | Sodium, total | mg/L | 225 |
| UA | MW-390 | C | 2020/03/26 | Sodium, total | mg/L | 98.7 |
| UA | MW-390 | C | 2020/09/16 | Sodium, total | mg/L | 84.2 |
| UA | MW-390 | C | 2021/03/12 | Sodium, total | mg/L | 107 |
| UA | MW-390 | C | 2021/09/15 | Sodium, total | mg/L | 68.4 |
| UA | MW-390 | C | 2022/03/29 | Sodium, total | mg/L | 122 |
| UA | MW-390 | C | 2022/09/30 | Sodium, total | mg/L | 113 |

Attachment I. Site Groundwater Data

Geochemical Conceptual Site Model

Baldwin Fly Ash Pond System

Baldwin Power Plant

Baldwin, IL

| | | | | | | |
|----|--------|---|------------|------------------------|-----------|------|
| UA | MW-390 | C | 2023/03/14 | Sodium, total | mg/L | 75.5 |
| UA | MW-390 | C | 2023/05/17 | Sodium, total | mg/L | 106 |
| UA | MW-390 | C | 2023/08/04 | Sodium, total | mg/L | 178 |
| UA | MW-390 | C | 2023/11/02 | Sodium, total | mg/L | 143 |
| UA | MW-390 | C | 2016/03/22 | Sulfate, total | mg/L | 102 |
| UA | MW-390 | C | 2016/06/23 | Sulfate, total | mg/L | 154 |
| UA | MW-390 | C | 2016/08/18 | Sulfate, total | mg/L | 169 |
| UA | MW-390 | C | 2016/09/20 | Sulfate, total | mg/L | 154 |
| UA | MW-390 | C | 2016/12/22 | Sulfate, total | mg/L | 171 |
| UA | MW-390 | C | 2017/03/15 | Sulfate, total | mg/L | 234 |
| UA | MW-390 | C | 2017/06/20 | Sulfate, total | mg/L | 233 |
| UA | MW-390 | C | 2017/07/28 | Sulfate, total | mg/L | 222 |
| UA | MW-390 | C | 2017/11/27 | Sulfate, total | mg/L | 228 |
| UA | MW-390 | C | 2018/06/26 | Sulfate, total | mg/L | 141 |
| UA | MW-390 | C | 2018/09/25 | Sulfate, total | mg/L | 117 |
| UA | MW-390 | C | 2019/03/19 | Sulfate, total | mg/L | 114 |
| UA | MW-390 | C | 2019/09/24 | Sulfate, total | mg/L | 171 |
| UA | MW-390 | C | 2020/03/26 | Sulfate, total | mg/L | 139 |
| UA | MW-390 | C | 2020/09/16 | Sulfate, total | mg/L | 132 |
| UA | MW-390 | C | 2021/03/12 | Sulfate, total | mg/L | 174 |
| UA | MW-390 | C | 2021/09/15 | Sulfate, total | mg/L | 152 |
| UA | MW-390 | C | 2022/03/29 | Sulfate, total | mg/L | 142 |
| UA | MW-390 | C | 2022/09/30 | Sulfate, total | mg/L | 180 |
| UA | MW-390 | C | 2023/03/14 | Sulfate, total | mg/L | 107 |
| UA | MW-390 | C | 2023/05/17 | Sulfate, total | mg/L | 118 |
| UA | MW-390 | C | 2023/08/04 | Sulfate, total | mg/L | 133 |
| UA | MW-390 | C | 2023/11/02 | Sulfate, total | mg/L | 134 |
| UA | MW-390 | C | 2016/03/22 | Temperature (Celsius) | degrees C | 15.2 |
| UA | MW-390 | C | 2016/06/23 | Temperature (Celsius) | degrees C | 22.3 |
| UA | MW-390 | C | 2016/08/18 | Temperature (Celsius) | degrees C | 20.5 |
| UA | MW-390 | C | 2016/09/20 | Temperature (Celsius) | degrees C | 22.0 |
| UA | MW-390 | C | 2016/12/22 | Temperature (Celsius) | degrees C | 13.2 |
| UA | MW-390 | C | 2017/03/15 | Temperature (Celsius) | degrees C | 12.4 |
| UA | MW-390 | C | 2017/06/20 | Temperature (Celsius) | degrees C | 23.8 |
| UA | MW-390 | C | 2017/07/28 | Temperature (Celsius) | degrees C | 18.5 |
| UA | MW-390 | C | 2017/11/27 | Temperature (Celsius) | degrees C | 16.4 |
| UA | MW-390 | C | 2018/06/26 | Temperature (Celsius) | degrees C | 20.7 |
| UA | MW-390 | C | 2018/09/25 | Temperature (Celsius) | degrees C | 19.5 |
| UA | MW-390 | C | 2019/03/19 | Temperature (Celsius) | degrees C | 14.4 |
| UA | MW-390 | C | 2019/09/24 | Temperature (Celsius) | degrees C | 17.2 |
| UA | MW-390 | C | 2020/03/26 | Temperature (Celsius) | degrees C | 13.8 |
| UA | MW-390 | C | 2020/09/16 | Temperature (Celsius) | degrees C | 16.4 |
| UA | MW-390 | C | 2021/03/12 | Temperature (Celsius) | degrees C | 13.0 |
| UA | MW-390 | C | 2021/09/15 | Temperature (Celsius) | degrees C | 18.4 |
| UA | MW-390 | C | 2022/03/29 | Temperature (Celsius) | degrees C | 12.8 |
| UA | MW-390 | C | 2022/09/30 | Temperature (Celsius) | degrees C | 17.0 |
| UA | MW-390 | C | 2023/03/14 | Temperature (Celsius) | degrees C | 13.4 |
| UA | MW-390 | C | 2023/05/17 | Temperature (Celsius) | degrees C | 15.4 |
| UA | MW-390 | C | 2023/08/04 | Temperature (Celsius) | degrees C | 17.3 |
| UA | MW-390 | C | 2023/11/02 | Temperature (Celsius) | degrees C | 16.6 |
| UA | MW-390 | C | 2016/03/22 | Total Dissolved Solids | mg/L | 590 |
| UA | MW-390 | C | 2016/06/23 | Total Dissolved Solids | mg/L | 722 |
| UA | MW-390 | C | 2016/08/18 | Total Dissolved Solids | mg/L | 778 |
| UA | MW-390 | C | 2016/09/20 | Total Dissolved Solids | mg/L | 704 |
| UA | MW-390 | C | 2016/12/22 | Total Dissolved Solids | mg/L | 780 |
| UA | MW-390 | C | 2017/03/15 | Total Dissolved Solids | mg/L | 898 |
| UA | MW-390 | C | 2017/06/20 | Total Dissolved Solids | mg/L | 894 |

Attachment I. Site Groundwater Data

Geochemical Conceptual Site Model

Baldwin Fly Ash Pond System

Baldwin Power Plant

Baldwin, IL

| | | | | | | |
|----|--------|---|------------|-------------------------------|------|-------|
| UA | MW-390 | C | 2017/07/28 | Total Dissolved Solids | mg/L | 842 |
| UA | MW-390 | C | 2017/11/27 | Total Dissolved Solids | mg/L | 898 |
| UA | MW-390 | C | 2018/06/26 | Total Dissolved Solids | mg/L | 636 |
| UA | MW-390 | C | 2018/09/25 | Total Dissolved Solids | mg/L | 660 |
| UA | MW-390 | C | 2019/03/19 | Total Dissolved Solids | mg/L | 646 |
| UA | MW-390 | C | 2019/09/24 | Total Dissolved Solids | mg/L | 800 |
| UA | MW-390 | C | 2020/03/26 | Total Dissolved Solids | mg/L | 654 |
| UA | MW-390 | C | 2020/09/16 | Total Dissolved Solids | mg/L | 644 |
| UA | MW-390 | C | 2021/03/12 | Total Dissolved Solids | mg/L | 852 |
| UA | MW-390 | C | 2021/09/15 | Total Dissolved Solids | mg/L | 682 |
| UA | MW-390 | C | 2022/03/29 | Total Dissolved Solids | mg/L | 742 |
| UA | MW-390 | C | 2022/09/30 | Total Dissolved Solids | mg/L | 826 |
| UA | MW-390 | C | 2023/03/14 | Total Dissolved Solids | mg/L | 544 |
| UA | MW-390 | C | 2023/05/17 | Total Dissolved Solids | mg/L | 642 |
| UA | MW-390 | C | 2023/08/04 | Total Dissolved Solids | mg/L | 740 |
| UA | MW-390 | C | 2023/11/02 | Total Dissolved Solids | mg/L | 750 |
| UA | MW-391 | C | 2016/12/22 | pH (field) | SU | 7.6 |
| UA | MW-391 | C | 2017/03/15 | pH (field) | SU | 8.0 |
| UA | MW-391 | C | 2017/06/20 | pH (field) | SU | 7.5 |
| UA | MW-391 | C | 2018/06/26 | pH (field) | SU | 7.3 |
| UA | MW-391 | C | 2018/09/25 | pH (field) | SU | 7.5 |
| UA | MW-391 | C | 2019/03/19 | pH (field) | SU | 7.6 |
| UA | MW-391 | C | 2019/09/25 | pH (field) | SU | 7.6 |
| UA | MW-391 | C | 2020/03/24 | pH (field) | SU | 7.7 |
| UA | MW-391 | C | 2020/09/16 | pH (field) | SU | 7.8 |
| UA | MW-391 | C | 2021/03/12 | pH (field) | SU | 7.7 |
| UA | MW-391 | C | 2021/06/22 | pH (field) | SU | 7.7 |
| UA | MW-391 | C | 2021/09/14 | pH (field) | SU | 7.7 |
| UA | MW-391 | C | 2022/03/29 | pH (field) | SU | 7.9 |
| UA | MW-391 | C | 2022/09/30 | pH (field) | SU | 8.2 |
| UA | MW-391 | C | 2023/03/14 | pH (field) | SU | 7.8 |
| UA | MW-391 | C | 2023/05/17 | pH (field) | SU | 7.8 |
| UA | MW-391 | C | 2023/08/04 | pH (field) | SU | 7.8 |
| UA | MW-391 | C | 2023/11/03 | pH (field) | SU | 7.7 |
| UA | MW-391 | C | 2016/12/22 | Oxidation Reduction Potential | mV | 1.00 |
| UA | MW-391 | C | 2017/03/15 | Oxidation Reduction Potential | mV | 14.0 |
| UA | MW-391 | C | 2017/06/20 | Oxidation Reduction Potential | mV | 116 |
| UA | MW-391 | C | 2018/06/26 | Oxidation Reduction Potential | mV | 101 |
| UA | MW-391 | C | 2018/09/25 | Oxidation Reduction Potential | mV | 140 |
| UA | MW-391 | C | 2019/03/19 | Oxidation Reduction Potential | mV | 63.0 |
| UA | MW-391 | C | 2019/09/25 | Oxidation Reduction Potential | mV | 56.0 |
| UA | MW-391 | C | 2020/03/24 | Oxidation Reduction Potential | mV | 73.0 |
| UA | MW-391 | C | 2020/09/16 | Oxidation Reduction Potential | mV | 22.0 |
| UA | MW-391 | C | 2021/03/12 | Oxidation Reduction Potential | mV | 7.00 |
| UA | MW-391 | C | 2021/06/22 | Oxidation Reduction Potential | mV | 31.0 |
| UA | MW-391 | C | 2021/09/14 | Oxidation Reduction Potential | mV | -4.00 |
| UA | MW-391 | C | 2022/03/29 | Oxidation Reduction Potential | mV | -6.00 |
| UA | MW-391 | C | 2022/09/30 | Oxidation Reduction Potential | mV | 110 |
| UA | MW-391 | C | 2023/03/14 | Oxidation Reduction Potential | mV | -6.10 |
| UA | MW-391 | C | 2023/05/17 | Oxidation Reduction Potential | mV | 53.0 |
| UA | MW-391 | C | 2023/08/04 | Oxidation Reduction Potential | mV | 122 |
| UA | MW-391 | C | 2023/11/03 | Oxidation Reduction Potential | mV | 55.0 |
| UA | MW-391 | C | 2016/12/22 | Eh | V | 0.20 |
| UA | MW-391 | C | 2017/03/15 | Eh | V | 0.21 |
| UA | MW-391 | C | 2017/06/20 | Eh | V | 0.31 |
| UA | MW-391 | C | 2018/06/26 | Eh | V | 0.29 |
| UA | MW-391 | C | 2018/09/25 | Eh | V | 0.33 |

Attachment I. Site Groundwater Data

Geochemical Conceptual Site Model

Baldwin Fly Ash Pond System

Baldwin Power Plant

Baldwin, IL

| | | | | | | |
|----|--------|---|------------|-------------------------|------------|--------|
| UA | MW-391 | C | 2019/03/19 | Eh | V | 0.26 |
| UA | MW-391 | C | 2019/09/25 | Eh | V | 0.25 |
| UA | MW-391 | C | 2020/03/24 | Eh | V | 0.27 |
| UA | MW-391 | C | 2020/09/16 | Eh | V | 0.22 |
| UA | MW-391 | C | 2021/03/12 | Eh | V | 0.20 |
| UA | MW-391 | C | 2021/06/22 | Eh | V | 0.23 |
| UA | MW-391 | C | 2021/09/14 | Eh | V | 0.19 |
| UA | MW-391 | C | 2022/03/29 | Eh | V | 0.19 |
| UA | MW-391 | C | 2022/09/30 | Eh | V | 0.31 |
| UA | MW-391 | C | 2023/03/14 | Eh | V | 0.19 |
| UA | MW-391 | C | 2023/05/17 | Eh | V | 0.25 |
| UA | MW-391 | C | 2023/08/04 | Eh | V | 0.32 |
| UA | MW-391 | C | 2023/11/03 | Eh | V | 0.25 |
| UA | MW-391 | C | 2020/03/24 | Alkalinity, bicarbonate | mg/L CaCO3 | 590 |
| UA | MW-391 | C | 2020/09/16 | Alkalinity, bicarbonate | mg/L CaCO3 | 588 |
| UA | MW-391 | C | 2021/03/12 | Alkalinity, bicarbonate | mg/L CaCO3 | 566 |
| UA | MW-391 | C | 2021/09/14 | Alkalinity, bicarbonate | mg/L CaCO3 | 560 |
| UA | MW-391 | C | 2022/03/29 | Alkalinity, bicarbonate | mg/L CaCO3 | 540 |
| UA | MW-391 | C | 2022/09/30 | Alkalinity, bicarbonate | mg/L CaCO3 | 632 |
| UA | MW-391 | C | 2023/03/14 | Alkalinity, bicarbonate | mg/L CaCO3 | 734 |
| UA | MW-391 | C | 2023/05/17 | Alkalinity, bicarbonate | mg/L CaCO3 | 728 |
| UA | MW-391 | C | 2023/08/04 | Alkalinity, bicarbonate | mg/L CaCO3 | 743 |
| UA | MW-391 | C | 2023/11/03 | Alkalinity, bicarbonate | mg/L CaCO3 | 643 |
| UA | MW-391 | C | 2022/03/29 | Alkalinity, carbonate | mg/L CaCO3 | 22.0 |
| UA | MW-391 | C | 2022/09/30 | Alkalinity, carbonate | mg/L CaCO3 | 24.0 |
| UA | MW-391 | C | 2023/05/17 | Alkalinity, carbonate | mg/L CaCO3 | 6.00 |
| UA | MW-391 | C | 2023/11/03 | Alkalinity, carbonate | mg/L CaCO3 | 17.0 |
| UA | MW-391 | C | 2016/12/22 | Barium, total | mg/L | 0.0293 |
| UA | MW-391 | C | 2017/03/15 | Barium, total | mg/L | 0.0332 |
| UA | MW-391 | C | 2017/06/20 | Barium, total | mg/L | 0.0350 |
| UA | MW-391 | C | 2018/06/26 | Barium, total | mg/L | 0.0475 |
| UA | MW-391 | C | 2018/09/25 | Barium, total | mg/L | 0.0450 |
| UA | MW-391 | C | 2019/03/19 | Barium, total | mg/L | 0.0366 |
| UA | MW-391 | C | 2019/09/25 | Barium, total | mg/L | 0.0330 |
| UA | MW-391 | C | 2020/03/24 | Barium, total | mg/L | 0.0297 |
| UA | MW-391 | C | 2020/09/16 | Barium, total | mg/L | 0.0256 |
| UA | MW-391 | C | 2021/03/12 | Barium, total | mg/L | 0.0161 |
| UA | MW-391 | C | 2021/09/14 | Barium, total | mg/L | 0.0165 |
| UA | MW-391 | C | 2022/03/29 | Barium, total | mg/L | 0.0135 |
| UA | MW-391 | C | 2022/09/30 | Barium, total | mg/L | 0.0222 |
| UA | MW-391 | C | 2023/03/14 | Barium, total | mg/L | 0.0209 |
| UA | MW-391 | C | 2023/05/17 | Barium, total | mg/L | 0.0287 |
| UA | MW-391 | C | 2023/08/04 | Barium, total | mg/L | 0.0234 |
| UA | MW-391 | C | 2023/11/03 | Barium, total | mg/L | 0.124 |
| UA | MW-391 | C | 2016/12/22 | Boron, total | mg/L | 1.30 |
| UA | MW-391 | C | 2017/03/15 | Boron, total | mg/L | 1.43 |
| UA | MW-391 | C | 2017/06/20 | Boron, total | mg/L | 1.88 |
| UA | MW-391 | C | 2018/06/26 | Boron, total | mg/L | 8.91 |
| UA | MW-391 | C | 2018/09/25 | Boron, total | mg/L | 8.60 |
| UA | MW-391 | C | 2019/03/19 | Boron, total | mg/L | 6.77 |
| UA | MW-391 | C | 2019/09/25 | Boron, total | mg/L | 6.16 |
| UA | MW-391 | C | 2020/03/24 | Boron, total | mg/L | 5.29 |
| UA | MW-391 | C | 2020/09/16 | Boron, total | mg/L | 4.35 |
| UA | MW-391 | C | 2021/03/12 | Boron, total | mg/L | 2.60 |
| UA | MW-391 | C | 2021/09/14 | Boron, total | mg/L | 2.84 |
| UA | MW-391 | C | 2022/03/29 | Boron, total | mg/L | 3.24 |
| UA | MW-391 | C | 2022/09/30 | Boron, total | mg/L | 3.25 |

Attachment I. Site Groundwater Data

Geochemical Conceptual Site Model

Baldwin Fly Ash Pond System

Baldwin Power Plant

Baldwin, IL

| | | | | | | |
|----|--------|---|------------|----------------------|------|---------|
| UA | MW-391 | C | 2023/03/14 | Boron, total | mg/L | 2.45 |
| UA | MW-391 | C | 2023/05/17 | Boron, total | mg/L | 2.49 |
| UA | MW-391 | C | 2023/08/04 | Boron, total | mg/L | 2.38 |
| UA | MW-391 | C | 2023/11/03 | Boron, total | mg/L | 3.75 |
| UA | MW-391 | C | 2016/12/22 | Calcium, total | mg/L | 22.4 |
| UA | MW-391 | C | 2017/03/15 | Calcium, total | mg/L | 24.5 |
| UA | MW-391 | C | 2017/06/20 | Calcium, total | mg/L | 23.6 |
| UA | MW-391 | C | 2018/06/26 | Calcium, total | mg/L | 78.9 |
| UA | MW-391 | C | 2018/09/25 | Calcium, total | mg/L | 64.6 |
| UA | MW-391 | C | 2019/03/19 | Calcium, total | mg/L | 44.7 |
| UA | MW-391 | C | 2019/09/25 | Calcium, total | mg/L | 35.5 |
| UA | MW-391 | C | 2020/03/24 | Calcium, total | mg/L | 21.4 |
| UA | MW-391 | C | 2020/09/16 | Calcium, total | mg/L | 24.7 |
| UA | MW-391 | C | 2021/03/12 | Calcium, total | mg/L | 7.06 |
| UA | MW-391 | C | 2021/09/14 | Calcium, total | mg/L | 8.95 |
| UA | MW-391 | C | 2022/03/29 | Calcium, total | mg/L | 6.63 |
| UA | MW-391 | C | 2022/09/30 | Calcium, total | mg/L | 8.06 |
| UA | MW-391 | C | 2023/03/14 | Calcium, total | mg/L | 11.3 |
| UA | MW-391 | C | 2023/05/17 | Calcium, total | mg/L | 18.7 |
| UA | MW-391 | C | 2023/08/04 | Calcium, total | mg/L | 15.0 |
| UA | MW-391 | C | 2023/11/03 | Calcium, total | mg/L | 183 |
| UA | MW-391 | C | 2016/12/22 | Chloride, total | mg/L | 258 |
| UA | MW-391 | C | 2017/03/15 | Chloride, total | mg/L | 274 |
| UA | MW-391 | C | 2017/06/20 | Chloride, total | mg/L | 300 |
| UA | MW-391 | C | 2018/06/26 | Chloride, total | mg/L | 168 |
| UA | MW-391 | C | 2018/09/25 | Chloride, total | mg/L | 181 |
| UA | MW-391 | C | 2019/03/19 | Chloride, total | mg/L | 182 |
| UA | MW-391 | C | 2019/09/25 | Chloride, total | mg/L | 194 |
| UA | MW-391 | C | 2020/03/24 | Chloride, total | mg/L | 206 |
| UA | MW-391 | C | 2020/09/16 | Chloride, total | mg/L | 186 |
| UA | MW-391 | C | 2021/03/12 | Chloride, total | mg/L | 147 |
| UA | MW-391 | C | 2021/09/14 | Chloride, total | mg/L | 116 |
| UA | MW-391 | C | 2022/03/29 | Chloride, total | mg/L | 110 |
| UA | MW-391 | C | 2022/09/30 | Chloride, total | mg/L | 147 |
| UA | MW-391 | C | 2023/03/14 | Chloride, total | mg/L | 161 |
| UA | MW-391 | C | 2023/05/17 | Chloride, total | mg/L | 170 |
| UA | MW-391 | C | 2023/08/04 | Chloride, total | mg/L | 174 |
| UA | MW-391 | C | 2023/11/03 | Chloride, total | mg/L | 228 |
| UA | MW-391 | C | 2023/05/17 | Iron, dissolved | mg/L | <0.02 |
| UA | MW-391 | C | 2023/08/04 | Iron, dissolved | mg/L | <0.023 |
| UA | MW-391 | C | 2020/03/24 | Magnesium, total | mg/L | 13.6 |
| UA | MW-391 | C | 2020/09/16 | Magnesium, total | mg/L | 14.0 |
| UA | MW-391 | C | 2021/03/12 | Magnesium, total | mg/L | 3.92 |
| UA | MW-391 | C | 2021/09/14 | Magnesium, total | mg/L | 4.55 |
| UA | MW-391 | C | 2022/03/29 | Magnesium, total | mg/L | 3.58 |
| UA | MW-391 | C | 2022/09/30 | Magnesium, total | mg/L | 3.88 |
| UA | MW-391 | C | 2023/03/14 | Magnesium, total | mg/L | 5.01 |
| UA | MW-391 | C | 2023/05/17 | Magnesium, total | mg/L | 6.60 |
| UA | MW-391 | C | 2023/08/04 | Magnesium, total | mg/L | 6.64 |
| UA | MW-391 | C | 2023/11/03 | Magnesium, total | mg/L | 21.9 |
| UA | MW-391 | C | 2023/05/17 | Manganese, dissolved | mg/L | 0.00700 |
| UA | MW-391 | C | 2023/08/04 | Manganese, dissolved | mg/L | 0.0115 |
| UA | MW-391 | C | 2023/05/17 | Phosphate, dissolved | mg/L | 0.0250 |
| UA | MW-391 | C | 2023/08/04 | Phosphate, dissolved | mg/L | 0.0520 |
| UA | MW-391 | C | 2020/03/24 | Potassium, total | mg/L | 4.75 |
| UA | MW-391 | C | 2020/09/16 | Potassium, total | mg/L | 5.50 |
| UA | MW-391 | C | 2021/03/12 | Potassium, total | mg/L | 2.39 |

Attachment I. Site Groundwater Data

Geochemical Conceptual Site Model

Baldwin Fly Ash Pond System

Baldwin Power Plant

Baldwin, IL

| | | | | | | |
|----|--------|---|------------|------------------------|-----------|-------|
| UA | MW-391 | C | 2021/09/14 | Potassium, total | mg/L | 2.70 |
| UA | MW-391 | C | 2022/03/29 | Potassium, total | mg/L | 2.60 |
| UA | MW-391 | C | 2022/09/30 | Potassium, total | mg/L | 2.99 |
| UA | MW-391 | C | 2023/03/14 | Potassium, total | mg/L | 3.06 |
| UA | MW-391 | C | 2023/05/17 | Potassium, total | mg/L | 3.96 |
| UA | MW-391 | C | 2023/08/04 | Potassium, total | mg/L | 3.66 |
| UA | MW-391 | C | 2023/11/03 | Potassium, total | mg/L | 6.70 |
| UA | MW-391 | C | 2023/05/17 | Silicon, dissolved | mg/L | 3.27 |
| UA | MW-391 | C | 2023/08/04 | Silicon, dissolved | mg/L | 3.28 |
| UA | MW-391 | C | 2020/03/24 | Sodium, total | mg/L | 1,040 |
| UA | MW-391 | C | 2020/09/16 | Sodium, total | mg/L | 972 |
| UA | MW-391 | C | 2021/03/12 | Sodium, total | mg/L | 541 |
| UA | MW-391 | C | 2021/09/14 | Sodium, total | mg/L | 527 |
| UA | MW-391 | C | 2022/03/29 | Sodium, total | mg/L | 554 |
| UA | MW-391 | C | 2022/09/30 | Sodium, total | mg/L | 607 |
| UA | MW-391 | C | 2023/03/14 | Sodium, total | mg/L | 663 |
| UA | MW-391 | C | 2023/05/17 | Sodium, total | mg/L | 767 |
| UA | MW-391 | C | 2023/08/04 | Sodium, total | mg/L | 791 |
| UA | MW-391 | C | 2023/11/03 | Sodium, total | mg/L | 1,030 |
| UA | MW-391 | C | 2016/12/22 | Sulfate, total | mg/L | 679 |
| UA | MW-391 | C | 2017/03/15 | Sulfate, total | mg/L | 726 |
| UA | MW-391 | C | 2017/06/20 | Sulfate, total | mg/L | 758 |
| UA | MW-391 | C | 2018/06/26 | Sulfate, total | mg/L | 1,760 |
| UA | MW-391 | C | 2018/09/25 | Sulfate, total | mg/L | 1,420 |
| UA | MW-391 | C | 2019/03/19 | Sulfate, total | mg/L | 1,340 |
| UA | MW-391 | C | 2019/09/25 | Sulfate, total | mg/L | 1,450 |
| UA | MW-391 | C | 2020/03/24 | Sulfate, total | mg/L | 1,320 |
| UA | MW-391 | C | 2020/09/16 | Sulfate, total | mg/L | 1,230 |
| UA | MW-391 | C | 2021/03/12 | Sulfate, total | mg/L | 907 |
| UA | MW-391 | C | 2021/09/14 | Sulfate, total | mg/L | 668 |
| UA | MW-391 | C | 2022/03/29 | Sulfate, total | mg/L | 499 |
| UA | MW-391 | C | 2022/09/30 | Sulfate, total | mg/L | 426 |
| UA | MW-391 | C | 2023/03/14 | Sulfate, total | mg/L | 439 |
| UA | MW-391 | C | 2023/05/17 | Sulfate, total | mg/L | 430 |
| UA | MW-391 | C | 2023/08/04 | Sulfate, total | mg/L | 489 |
| UA | MW-391 | C | 2023/11/03 | Sulfate, total | mg/L | 870 |
| UA | MW-391 | C | 2016/12/22 | Temperature (Celsius) | degrees C | 14.5 |
| UA | MW-391 | C | 2017/03/15 | Temperature (Celsius) | degrees C | 13.9 |
| UA | MW-391 | C | 2017/06/20 | Temperature (Celsius) | degrees C | 23.2 |
| UA | MW-391 | C | 2018/06/26 | Temperature (Celsius) | degrees C | 18.2 |
| UA | MW-391 | C | 2018/09/25 | Temperature (Celsius) | degrees C | 17.9 |
| UA | MW-391 | C | 2019/03/19 | Temperature (Celsius) | degrees C | 14.8 |
| UA | MW-391 | C | 2019/09/25 | Temperature (Celsius) | degrees C | 17.8 |
| UA | MW-391 | C | 2020/03/24 | Temperature (Celsius) | degrees C | 12.9 |
| UA | MW-391 | C | 2020/09/16 | Temperature (Celsius) | degrees C | 15.6 |
| UA | MW-391 | C | 2021/03/12 | Temperature (Celsius) | degrees C | 14.3 |
| UA | MW-391 | C | 2021/06/22 | Temperature (Celsius) | degrees C | 15.8 |
| UA | MW-391 | C | 2021/09/14 | Temperature (Celsius) | degrees C | 20.4 |
| UA | MW-391 | C | 2022/03/29 | Temperature (Celsius) | degrees C | 14.0 |
| UA | MW-391 | C | 2022/09/30 | Temperature (Celsius) | degrees C | 15.6 |
| UA | MW-391 | C | 2023/03/14 | Temperature (Celsius) | degrees C | 14.4 |
| UA | MW-391 | C | 2023/05/17 | Temperature (Celsius) | degrees C | 15.6 |
| UA | MW-391 | C | 2023/08/04 | Temperature (Celsius) | degrees C | 16.4 |
| UA | MW-391 | C | 2023/11/03 | Temperature (Celsius) | degrees C | 15.1 |
| UA | MW-391 | C | 2016/12/22 | Total Dissolved Solids | mg/L | 1,980 |
| UA | MW-391 | C | 2017/03/15 | Total Dissolved Solids | mg/L | 2,260 |
| UA | MW-391 | C | 2017/06/20 | Total Dissolved Solids | mg/L | 2,460 |

Attachment I. Site Groundwater Data

Geochemical Conceptual Site Model

Baldwin Fly Ash Pond System

Baldwin Power Plant

Baldwin, IL

| | | | | | | |
|----|--------|---|------------|------------------------|------|-------|
| UA | MW-391 | C | 2018/06/26 | Total Dissolved Solids | mg/L | 3,030 |
| UA | MW-391 | C | 2018/09/25 | Total Dissolved Solids | mg/L | 3,090 |
| UA | MW-391 | C | 2019/03/19 | Total Dissolved Solids | mg/L | 3,110 |
| UA | MW-391 | C | 2019/09/25 | Total Dissolved Solids | mg/L | 2,980 |
| UA | MW-391 | C | 2020/03/24 | Total Dissolved Solids | mg/L | 2,870 |
| UA | MW-391 | C | 2020/09/16 | Total Dissolved Solids | mg/L | 2,630 |
| UA | MW-391 | C | 2021/03/12 | Total Dissolved Solids | mg/L | 2,180 |
| UA | MW-391 | C | 2021/09/14 | Total Dissolved Solids | mg/L | 1,620 |
| UA | MW-391 | C | 2022/03/29 | Total Dissolved Solids | mg/L | 1,510 |
| UA | MW-391 | C | 2022/09/30 | Total Dissolved Solids | mg/L | 1,660 |
| UA | MW-391 | C | 2023/03/14 | Total Dissolved Solids | mg/L | 1,860 |
| UA | MW-391 | C | 2023/05/17 | Total Dissolved Solids | mg/L | 1,970 |
| UA | MW-391 | C | 2023/08/04 | Total Dissolved Solids | mg/L | 2,090 |
| UA | MW-391 | C | 2023/11/03 | Total Dissolved Solids | mg/L | 2,590 |

Notes:

< = results is less than detection limit

B = Background

C = Compliance

HSU = Hydrostratigraphic Unit

PMP = Potential Migration Pathway

UA = Uppermost Aquifer

mg/L = milligrams per liter

SU = standard units

V = volts

ADDENDUM TO NATURE AND EXTENT REPORT

(IN DEVELOPMENT)

Appendix E

Groundwater Polishing Report

Groundwater Polishing Evaluation Report

Baldwin Power Plant – Fly Ash Pond System

(IEPA ID No. 605)

Prepared for

Dynegy Midwest Generation, LLC

1500 Eastport Plaza Drive
Collinsville, Illinois 62234

Prepared by

Geosyntec Consultants, Inc.
500 W. Wilson Bridge Road, Suite 250
Worthington, Ohio 43085

Project Number: GLP8068

February 18, 2025

TABLE OF CONTENTS

| | |
|--|----|
| EXECUTIVE SUMMARY | 1 |
| 1. INTRODUCTION | 2 |
| 2. SITE BACKGROUND | 4 |
| 2.1 Site Overview | 4 |
| 2.2 Identified Exceedances of the GWPS | 5 |
| 2.3 Geochemical Conceptual Site Model | 5 |
| 3. GROUNDWATER POLISHING REMEDY EVALUATION | 7 |
| 3.1 Methods | 7 |
| 3.1.1 Model Set-Up | 8 |
| 3.1.2 Solid Phase Inputs | 8 |
| 3.1.3 Aqueous Phase Inputs | 9 |
| 3.2 Results and Discussion | 9 |
| 3.2.1 Model Results | 9 |
| 3.2.2 Speciation Modeling | 12 |
| 3.2.3 Reaction Modeling | 13 |
| 4. CONCLUSIONS | 14 |
| 5. REFERENCES | 15 |

LIST OF TABLES

| | |
|---------|---|
| Table 1 | Summary of Geochemical Model Inputs |
| Table 2 | Geochemical Modeling Response of Sorbing Phases |

LIST OF INTERNAL FIGURES

| | |
|----------|--------------------------------|
| Figure 1 | Percentage of Sorbed Boron |
| Figure 2 | Modeled Boron Behavior |
| Figure 3 | Percentage of Sorbed Sulfate |
| Figure 4 | Modeled Sulfate Behavior |
| Figure 5 | Modeled Sorbing Phase Behavior |

LIST OF ATTACHMENTS

| | |
|--------------|--|
| Attachment A | Potentiometric Surface Maps - August 2-3, 2023 |
| Attachment B | PHREEQC Input File and Thermodynamic Database |
| Attachment C | Details of Geochemical Model Parameterization |
| Attachment D | Complete Geochemical Modeling Outputs |

DRAFT

ACRONYMS AND ABBREVIATIONS

| | |
|----------|---|
| 35 I.A.C | Title 35 of the Illinois Administrative Code |
| CAAA | Corrective Actions Alternative Analysis |
| CCR | Coal combustion residuals |
| COC | Constituent of concern |
| FAPS | Fly Ash Pond System |
| GCSM | Geochemical conceptual site model |
| GWPS | Groundwater protection standard |
| IEPA | Illinois Environmental Protection Agency |
| mg/kg | milligrams per kilogram |
| PMP | Potential migration pathway |
| redox | oxidation-reduction |
| SEP | Sequential extraction procedure |
| UA | Uppermost aquifer |
| USEPA | United States Environmental Protection Agency |
| UU | Upper unit |
| wt % | percent by weight |
| XRD | X-ray diffraction |

EXECUTIVE SUMMARY

This document has been prepared as an attachment to the Corrective Actions Alternative Analysis (CAAA) prepared by Gradient for the Baldwin Power Plant Fly Ash Pond System (FAPS). The constituents of concern (COCs) addressed in the CAAA and in this document are boron and sulfate, which have been identified as having exceedances of the site-specific groundwater protection standards (GWPS). Natural geochemical processes may be appropriate as a “polishing step” for residual plume management after effective source control implementation if there are no risks to receptors and/or the contaminant plume is not expanding (United States Environmental Protection Agency [USEPA] 1999; USEPA 2015). Source control is a major component of every corrective action considered in the CAAA, and there are no risks to human health or the environment at Baldwin FAPS.

Natural groundwater polishing processes, which include both physical and chemical mechanisms, reduce the concentration of COCs in the groundwater. After source control is implemented, a geochemical trailing gradient may form in the subsurface as conditions undergo a return to background water quality which could affect chemical groundwater polishing mechanisms (Savannah River National Laboratory, 2011). This report supports groundwater polishing as a component of the proposed corrective action by evaluating the contribution of chemical mechanisms to groundwater polishing under current conditions and after source control implementation. The groundwater flow and transport model estimated the time to reach the GWPS based on hydraulic properties of the aquifer. The results of this groundwater polishing evaluation contextualize these estimates by evaluating the potential for attenuation of COCs and for previously attenuated COCs to be mobilized to groundwater as groundwater quality returns to background conditions.

Groundwater polishing mechanisms were assessed using speciation and reaction geochemical models: speciation models assess the distribution of constituents between solid and aqueous phases, and reaction models evaluate how that distribution may change with changing site conditions (USEPA 2015). Inputs to the model include geochemically reactive solid mineral phases, compliance well groundwater composition, and background groundwater composition based on site-specific data.

The results of the groundwater polishing evaluation indicate that chemical attenuation of boron and sulfate is feasible under current conditions through sorption to iron and aluminum oxide solids. Barite precipitation is also predicted to contribute to the chemical attenuation of sulfate. Though a small amount of desorption of boron and sulfate is predicted with background groundwater interaction, the impact of the desorption to aqueous boron and sulfate concentrations is negated by interaction with background groundwater that contains lower concentrations of both parameters. Aqueous boron and sulfate concentrations are expected to decrease below the GWPS at all wells in the compliance network post-source control and corrective action. Based on modeling results, remobilization of attenuated boron and sulfate is unlikely to affect the time to reach the GWPS. These results will inform corrective action groundwater monitoring and adaptive site management, critical components every corrective action considered in the CAAA.

1. INTRODUCTION

This document has been prepared as an attachment to the Corrective Actions Alternatives Analysis (CAAA) prepared by Gradient for the Baldwin Power Plant Fly Ash Pond System (FAPS). The purpose of the CAAA is to holistically evaluate potentially viable corrective actions to remediate groundwater and achieve compliance with GWPS for all monitored parameters under Title 35 of the Illinois Administrative Code (35 I.A.C.) § 845.600. The constituents of concern (COCs) addressed in the CAAA and in this document are boron and sulfate, which have been identified as having exceedances¹ of the site-specific groundwater protection standards (GWPS). In the CAAA, all corrective actions considered consist of source control and residual plume management. Natural geochemical processes may be appropriate as a “polishing step” for residual plume management after effective source control implementation, if there are no risks to receptors and/or the contaminant plume is not expanding (United States Environmental Protection Agency [USEPA] 1999; USEPA 2015). Source control is a major component of every corrective action considered in the CAAA, and there are no risks to human health or the environment at Baldwin FAPS.²

Groundwater polishing processes include both physical and chemical mechanisms within the subsurface which reduce the concentration of COCs in the groundwater. Physical components of groundwater polishing, including advection, dilution, and dispersion, are assessed by groundwater flow and transport modeling (Groundwater Modeling Technical Memorandum³). Chemical mechanisms of groundwater polishing include sorption and mineral precipitation. After source control is implemented, a geochemical trailing gradient may form in the subsurface as conditions undergo a return to background water quality which could affect chemical groundwater polishing mechanisms (Savannah River National Laboratory [SRNL], 2011). The chemical mechanisms of groundwater polishing at Baldwin FAPS are evaluated herein using a geochemical modeling-based approach informed by site-specific data. This report uses geochemical modeling to evaluate the influence of chemical mechanisms to groundwater polishing under current conditions and after source control implementation.

The groundwater flow and transport model (Groundwater Modeling Technical Memorandum⁴) estimated the time for boron (as a conservative surrogate) to reach the GWPSs under different potential corrective actions based on physical components of groundwater polishing and did not incorporate any potential chemical controls on chemical distribution. This geochemical modeling

¹ Throughout this document, “exceedance” or “exceedances” is intended to refer only to potential exceedances of proposed applicable background statistics or groundwater protection standards (GWPSs) as described in the proposed groundwater monitoring program which was submitted to the IEPA on October 25, 2021 as part of Dynegy Midwest Generation, LLC’s operating permit application for the FAPS. That operating permit application, including the proposed groundwater monitoring program, remains under review by the IEPA and therefore Dynegy Midwest Generation, LLC has not identified any actual exceedances.

² The Human Health and Ecological Risk Assessment serves as Appendix A of the CAAA to which this report is attached.

³ The Groundwater Modeling Technical Memorandum serves as Appendix B.1 of the Corrective Action Supporting Information Report; the Corrective Action Supporting Information Report serves as Appendix B of the CAAA to which this report is attached.

⁴ Ibid.

effort supports the assessment of groundwater polishing as a component of the proposed corrective action by evaluating the potential for chemical attenuation of COCs before and after source control as a means of contextualizing the times estimated in the flow and transport model. This analysis also provides an initial foundation for understanding groundwater chemistry to inform adaptive site management as a key component of the Corrective Action Groundwater Monitoring Plan⁵.

DRAFT

⁵ The Corrective Action Groundwater Monitoring Plan serves as Appendix B.1 to the Construction Permit Application.

2. SITE BACKGROUND

2.1 Site Overview

A thorough overview of general site characteristics is presented in Section 1 of the CAAA to which this document is attached and summarized here. The Baldwin Power Plant is owned by Dynegy Midwest Generation, LLC. The facility is bordered by the village of Baldwin, Illinois to the southeast; Baldwin Road, farmland, and strip-mining areas to the east; Illinois Central Gulf railroad tracks, State Road 154, and scattered residences to the south; the Kaskaskia River to the west; and farmland to the north. The Baldwin FAPS impoundment is located to the south of the Bottom Ash Pond coal combustion residuals (CCR) unit. The FAPS comprised the West Fly Ash Pond, East Fly Ash Pond, and Old East Fly Ash Pond and has been closed in-place since 2020.

A groundwater monitoring network was proposed in the Operating Permit Application (Burns and McDonnell, 2021)⁶ in accordance with 35 I.A.C. § 845.630 to monitor groundwater quality which passes the waste boundary as part of the Operating Permit Application to Illinois Environmental Protection Agency (IEPA) for the FAPS unit. The proposed groundwater monitoring network is shown in **Attachment A**. The monitoring network consists of 15 compliance monitoring wells (MW-150, MW-151, MW-152, MW-153, MW-252, MW-253R, MW-350R, MW-352, MW-366, MW-375, MW-377, MW-383, MW-384, MW-390, and MW-391R) and two background wells (MW-304 and MW-358R).

The geology underlying the Site in the vicinity of the FAPS consists of two distinct hydrostratigraphic units (Natural Resource Technology, Inc., 2016):

- **Upper Unit (UU):** The UU underlies the FAPS and consists predominately of clay with silt and minor sand, silt layers, and occasional sand lenses. The UU includes lithologies identified as the Cahokia Formation, Peoria Loess, Equality Formation, and Vandalia Till. Thin sand seams present at the contact between the UU and the Bedrock Unit have been identified as a potential migration pathways (PMP). Due to the presence of clay and only thin and intermittent sand lenses in the UU, this unit is not considered a continuous aquifer unit.
- **Bedrock Unit (UA):** The bedrock unit underlies the UU and is comprised of Pennsylvanian and Mississippian-aged interbedded shale and limestone bedrock. The bedrock unit is considered the uppermost aquifer (UA).

Groundwater in the UU generally flows west and southwest towards the Kaskaskia River. Groundwater within the UA flows southwest to northwest in the eastern section of the FAPS until it reaches a bedrock valley feature to the west of the FAPS at which point the flow direction becomes southwest and follows the bedrock surface. Vertical groundwater migration between the

⁶ Illinois Environmental Protection Agency approved the following changes to the proposed network due to evidence of bentonite grout contamination: abandonment of background well MW-306 and replacement of compliance wells MW-253 and MW-350. IEPA was notified on August 16 and September 16, 2024, that MW-391 and MW-358 (respectively) no longer provided representative samples of the uppermost aquifer and would be replaced.

UU PMP and UA varies seasonally and spatially across the site. Vertical migration is generally downward from the UU PMP to the UA, though upward migration has been observed during winter sampling events. A map showing representative UA groundwater flow direction at the site is shown in **Attachment A**.

2.2 Identified Exceedances of the GWPS

The following GWPS exceedances at compliance groundwater monitoring wells likely attributable to the Baldwin FAPS were observed from 2023 Q2 through Q1 2024 (Ramboll 2024):

- Boron – Observed at monitoring wells MW-150 and MW-152.
- Sulfate – Observed at monitoring wells MW-150, MW-152, and MW-366.

The data set for geochemical modeling was finalized after the 2024 Q1 sampling event. Groundwater at these compliance wells is representative of groundwater conditions downgradient of the unit, and samples may be referred to as downgradient groundwater.

GWPS exceedances in the FAPS network occur within the UU PMP (MW-150, MW-152, and MW-252) and UA (MW-366). All wells containing boron or sulfate exceedances are located generally south-southwest of the FAPS unit. Boron and sulfate concentrations at MW-152 exhibit a strong seasonal pattern, with concentrations of both analytes increasing in the fall and decreasing in the spring.

Modeling parameters with observed exceedances is appropriate to the scope of the CAAA. Additionally, the selected remedy will meet the performance standards of 35 I.A.C. § 845.670(d) and the Corrective Action Plan will be submitted to the Agency on or before April 24, 2025. Once implemented and completed, the selected remedy will prevent further releases and minimize the footprint of impacted groundwater until the GWPS are achieved.

2.3 Geochemical Conceptual Site Model

A Geochemical Conceptual Site Model (GCSM)⁷ was developed for Baldwin FAPS to describe the geochemical processes that contribute to mobilization and attenuation of constituents in the environment under current conditions, including evaluating whether chemical interactions of COCs with aquifer solids contribute to attenuation of aqueous concentrations at compliance monitoring wells (Geosyntec 2024). This discussion relies on lab reports and raw data previously presented in the Nature and Extent Report submitted to IEPA on April 24, 2024 (Ramboll 2024) in accordance with 35 I.A.C. § 845.650(d)(1) and provided again in as Appendix D of the CAAA to which this report is attached.

The primary source of boron and sulfate to groundwater in the UU PMP and UA within the monitoring network is the FAPS CCR porewater. This finding is based on COC concentrations

⁷ The GCSM is a component of the Nature and Extent Report previously submitted to IEPA (Ramboll 2023) and provided with relevant updates as Appendix D of the CAAA to which this report is attached.

within the source and relationships to hydrogeological patterns at the site. Limited variability in pH or redox conditions is observed between upgradient background and downgradient locations.

The observation of pyrite within shaley portions of the UA could provide an additional source of geogenic sulfate to groundwater via pyrite oxidation. Pyrite is not expected to be a stable mineral phase under observed groundwater oxidation-reduction (redox) conditions and sulfate concentrations at background wells are indicative of a potential additional natural source.

Boron and sulfate in the groundwater system may be attenuated via surface complexation reactions with iron and aluminum oxides within portions of the UU PMP and the UA. Conditions within groundwater from both the UU PMP and UA are typically predicted to favor amorphous iron oxide stability at most locations, and the presence of iron-bearing minerals in some site solids supports the occurrence of this mechanism. Crystalline iron oxides (magnetite and hematite) were observed in low abundance (0.2 to 1.4 percent by weight [wt %]) in the UU PMP and UA in X-ray diffraction (XRD) analyses, though given the abundance of iron observed in X-ray fluorescence analysis (0.7 to 7.7 wt %), the majority of iron minerals are expected to exist in non-crystalline or amorphous phases.

Boron may be further attenuated via interactions with clay minerals (e.g., kaolinite), which were observed at notable abundances (1.6 to 41.2 wt %) in solids across both the UU and UA. The observation of gypsum, although limited to the shale bedrock portions of the UA, indicates that precipitation of gypsum may be another potential attenuation mechanism for sulfate at locations near the FAPS and may also act as a geogenic source of sulfate in the event of gypsum dissolution.

The GCSM findings suggest the potential for chemical attenuation of boron and sulfate based on detected abundances of iron oxides, clay minerals, and gypsum, and groundwater redox conditions which are favorable for the stability of these potential sorbing surfaces.

3. GROUNDWATER POLISHING REMEDY EVALUATION

This groundwater polishing evaluation uses geochemical modeling to evaluate chemical attenuation of COCs under current conditions and to predict changes in attenuation at exceedance locations following source control and corrective action to further assess if chemical mechanisms of groundwater polishing will contribute to the remedy achieving the GWPS in a reasonable amount of time. Speciation and reaction models are geochemical models that can be used to evaluate the potential for chemical attenuation in groundwater. Speciation models assess the distribution of constituents between solid and aqueous phases, and reaction models evaluate how that distribution may change with changing site conditions (USEPA 2015). The results of geochemical modeling provide insight into groundwater polishing mechanisms and additional context for the time estimated to reach the GWPS determined by the groundwater flow and transport model⁸, which is based on hydraulic properties of the aquifer and does not take into account chemical interactions of boron within the hydrologic unit.

3.1 Methods

Geochemical modeling was done in PHREEQC Version 3 (USGS 2021) using a modified MINETQ v4 thermodynamic database (as described in relevant sections below). The geochemical modeling of groundwater polishing under current conditions and conditions after source control is completed includes speciation and reaction modeling (USEPA 2015):

1. Speciation: To understand groundwater polishing mechanisms under current conditions, a solid phase representative of site conditions is equilibrated with current downgradient groundwater. The results of speciation modeling represent the association of COCs with the solid phase under current conditions through mechanisms such as sorption or precipitation.
2. Reaction: In the reaction modeling, the solid phase generated during the speciation modeling phase is reacted iteratively with background groundwater. These results represent the geochemical conditions expected after the source is controlled during which a trailing geochemical gradient may be created (SRNL 2011). The reactions with background groundwater assess the potential for a trailing geochemical gradient to drive changes in groundwater chemistry. Persistence of elevated groundwater COC concentrations over several reaction iterations suggests a trailing geochemical gradient may affect the time to reach the GWPS.

The equilibrium thermodynamic modeling approach used herein allows that the solid and aqueous phases reach equilibrium during each step. The primary goal of this model is to inform the assessment of groundwater polishing as an appropriate remedy for the site by evaluating dominant geochemical reactions that may occur at time scales relevant to groundwater flow, including adsorption and certain mineral dissolution/precipitation (i.e., iron and aluminum (hydr)oxides,

⁸ The Groundwater Modeling Technical Memorandum serves as Appendix B.1 of the Corrective Action Supporting Information Report; the Corrective Action Supporting Information Report serves as Appendix B of the CAAA to which this report is attached.

carbonates, and some sulfates) as identified in the GCSM⁹. The model therefore includes those parameters that are expected to contribute to those reactions (as discussed below) and does not include every constituent of the solid phase and groundwater in order to capture “the salient aspects of the system’s behavior without introducing unnecessary complexity” (USEPA 2015). This model is therefore a semi-quantitative estimation of chemical behavior in the subsurface rather than a prediction of groundwater quality, consistent with USEPA guidance that geochemical modeling “is often most helpful for identifying relative changes in contaminant speciation and distribution” (USEPA 2015).

3.1.1 Model Set-Up

Inputs to the model include solid phase composition, downgradient groundwater composition for wells with exceedances of boron or sulfate, and background groundwater composition. The PHREEQC input file and modified MINTEQ v4 database are provided in **Attachment B**. The data included for model parameterization is summarized in **Table 1** and discussed in greater detail in **Attachment C**. All data used in the model and discussed below are provided in the Nature and Extent Report¹⁰.

3.1.2 Solid Phase Inputs

Iron hydroxide (ferrihydrite [$\text{Fe}(\text{OH})_3$]) and aluminum hydroxide (gibbsite [$\text{Al}(\text{OH})_3$]) are widespread in the environment and known to act as sorbing phases for many groundwater constituents, including boron and sulfate (Dzombak and Morel 1990; Karamalidis and Dzombak 2010). Model input concentrations for ferrihydrite and gibbsite are ideally derived from sequential extraction procedure (SEP) analyses of iron and aluminum, respectively. Because SEP analyses for aluminum were not completed for Baldwin FAPS samples, and SEP analyses for iron did not include evaluation of the critical amorphous component for Baldwin FAPS samples, model input concentrations for ferrihydrite for Baldwin FAPS were derived using site-specific total metals and an SEP dataset compiled from analogous geological systems as described in greater detail in **Attachment C**. Gibbsite input concentrations for Baldwin FAPS were taken directly from the analogous compiled SEP dataset.

Metal oxide concentrations representing the 25th percentile, median, and 75th percentile of the observed data were used to test the sensitivity of the model to the amount of sorbing phases present. Both ferrihydrite and gibbsite were allowed to dissolve or precipitate in the reaction phase of the model.

Calcite and dolomite were included as mineral phases in the model because carbonate mineral formation and dissolution are often major controls on groundwater pH (Stumm and Morgan 1996; Stackelberg et al. 2020). Calcite and dolomite are present in site aquifer solids, and model input

⁹ The GCSM is a component of the Nature and Extent Report previously submitted to IEPA (Ramboll 2024) and is provided with relevant updates as Appendix D of the CAAA to which this report is attached.

¹⁰ The Nature and Extent Report was previously submitted to IEPA (Ramboll 2024) and is provided with relevant updates as Appendix D of the CAAA to which this report is attached. The Nature and Extent report contains laboratory reports and tabulated results from solid phase analysis and tabulated results from groundwater analyses. Laboratory reports for groundwater data are provided quarterly to IEPA and posted to the facility’s operating record in accordance with 35 I.A.C. § 845.800(d)(15).

concentration were based on site-specific XRD results. Both calcite and dolomite were allowed to dissolve or precipitate in the reaction phase of the model.

Barite (BaSO_4) and gypsum (CaSO_4) are minerals that contain sulfate and have the potential to form under ambient environmental conditions in a timeframe consistent with the remedial effort. These minerals therefore may affect sulfate attenuation. Neither mineral phase was observed in mineralogical results for wells containing GWPS exceedances of COCs; therefore, both were made available to precipitate from the aqueous solution but did not have initial concentrations provided.

3.1.3 Aqueous Phase Inputs

In addition to the COCs, the following parameters are included to capture the expected attenuation and mobilization mechanisms (see **Section 2.3**):

- Temperature, pH and p_e ¹¹.
- Major ions: Alkalinity, chloride, fluoride, calcium, magnesium, potassium, and sodium.
- Oxyanions: Silicon and phosphate.
- Redox-active metals: Aluminum, iron, and manganese.
- Remaining constituents regulated under 35 I.A.C. § 845.600¹².

This full suite of geochemical parameters for this model was measured in Quarter 2 and Quarter 3, 2023, and Quarter 4, 2024 for wells MW-304, MW-150 and MW-152; Quarter 1 and Quarter 4, 2024 for wells MW-252 and MW-366; and Quarter 4, 2024, for well MW-358R. For wells with more than one data point available, the medians of the results at each well were used in the model to represent average groundwater interacting with the solid phase. For downgradient wells with exceedances of the COCs (**Section 2.2**), the median for each parameter was calculated for each location individually. For background wells, a single median for each parameter was calculated using data from all both background locations (see **Section 2.1**).

3.2 Results and Discussion

3.2.1 Model Results

Geochemical modeling results are shown on **Figures 1 through 5** below. Current geochemical conditions are represented in model output figures as ‘Speciation Model’ and subsequent reaction calculation results are represented with ‘First Reaction’ and ‘Second Reaction’. Full modeling results are provided in **Attachment D**.

¹¹ See **Attachment C** for details.

¹² Mercury, thallium, total dissolved solids, and radium were not included in the model. Mercury reactions within the environment are highly complex and would require a separate modeling effort, and the high frequency of non-detect concentrations in the groundwater indicate it would not contribute to model outcomes. Thallium forms a non-reactive monovalent cation and is rarely detected in the groundwater and is therefore not expected to contribute to model outcomes. Total dissolved solids are not a chemical parameter, but rather the result of other chemical abundances taken together. Radium is not included in most thermodynamic databases.

Figure 1: Percentage of Sorbed Boron

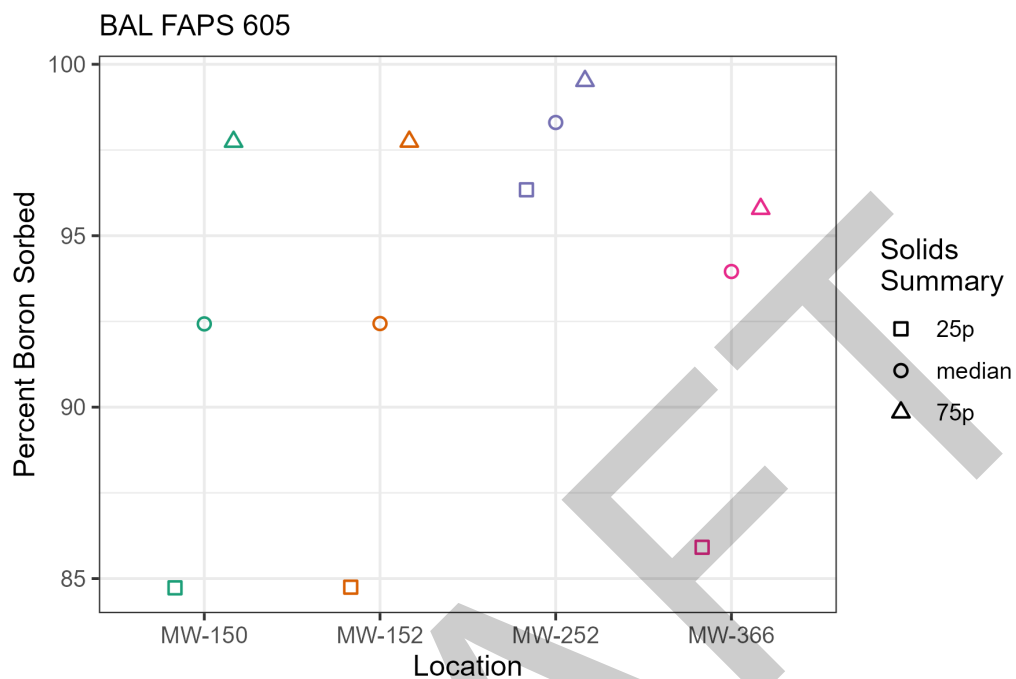


Figure 2: Modeled Boron Behavior

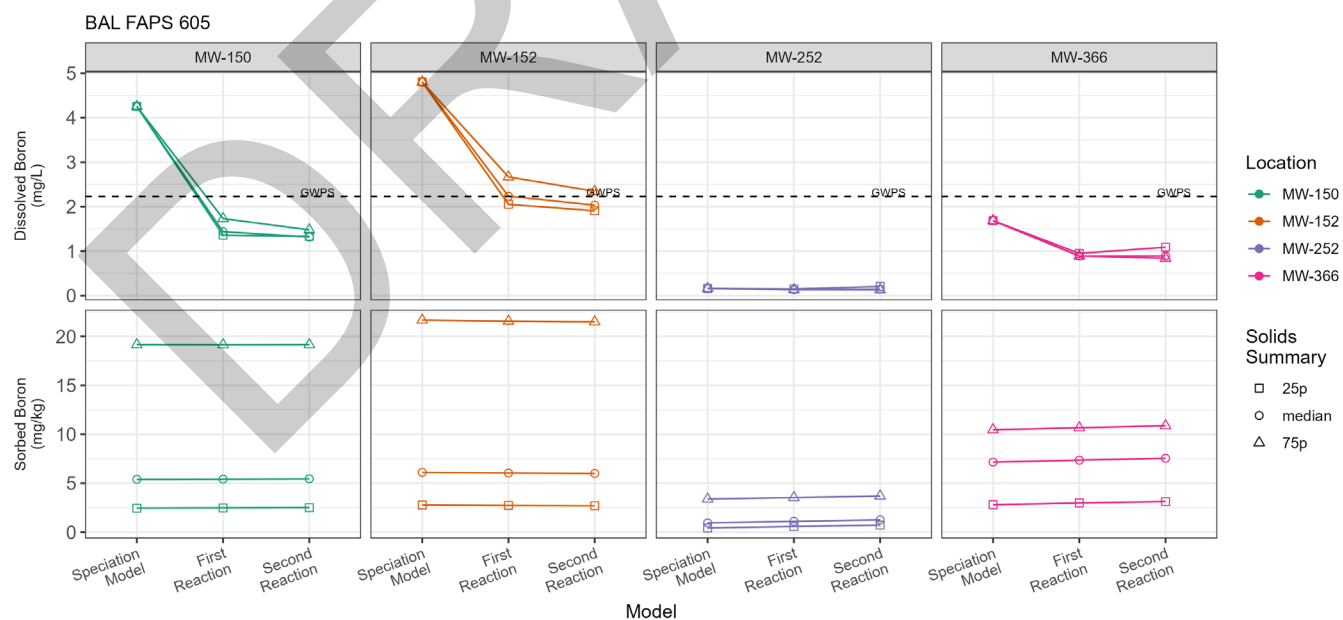


Figure 3: Percentage of Sorbed Sulfate

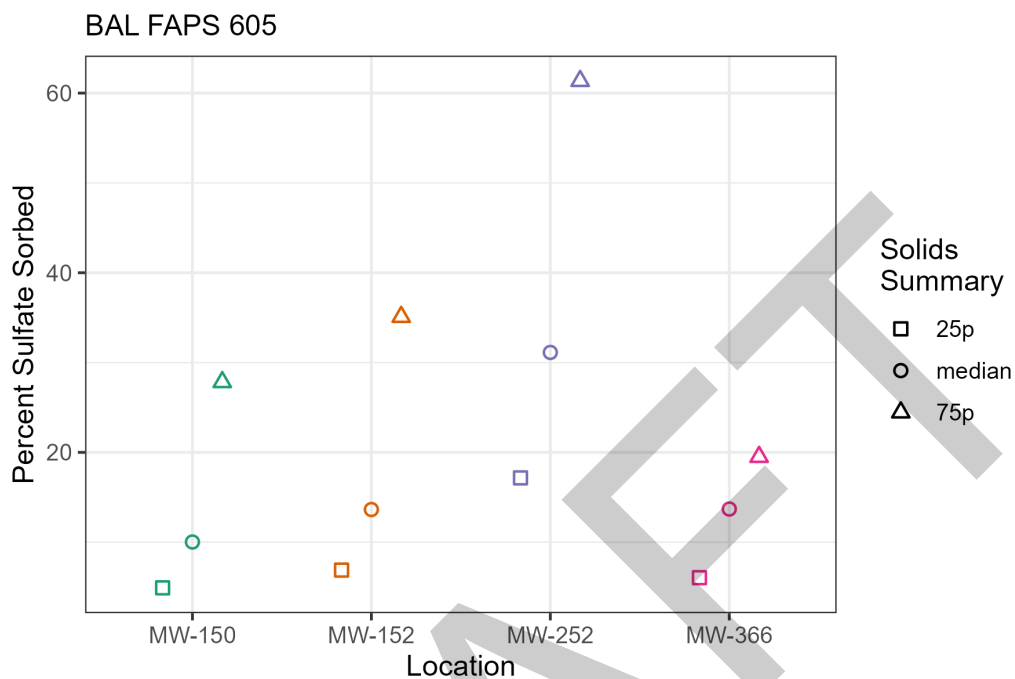


Figure 4: Modeled Sulfate Behavior

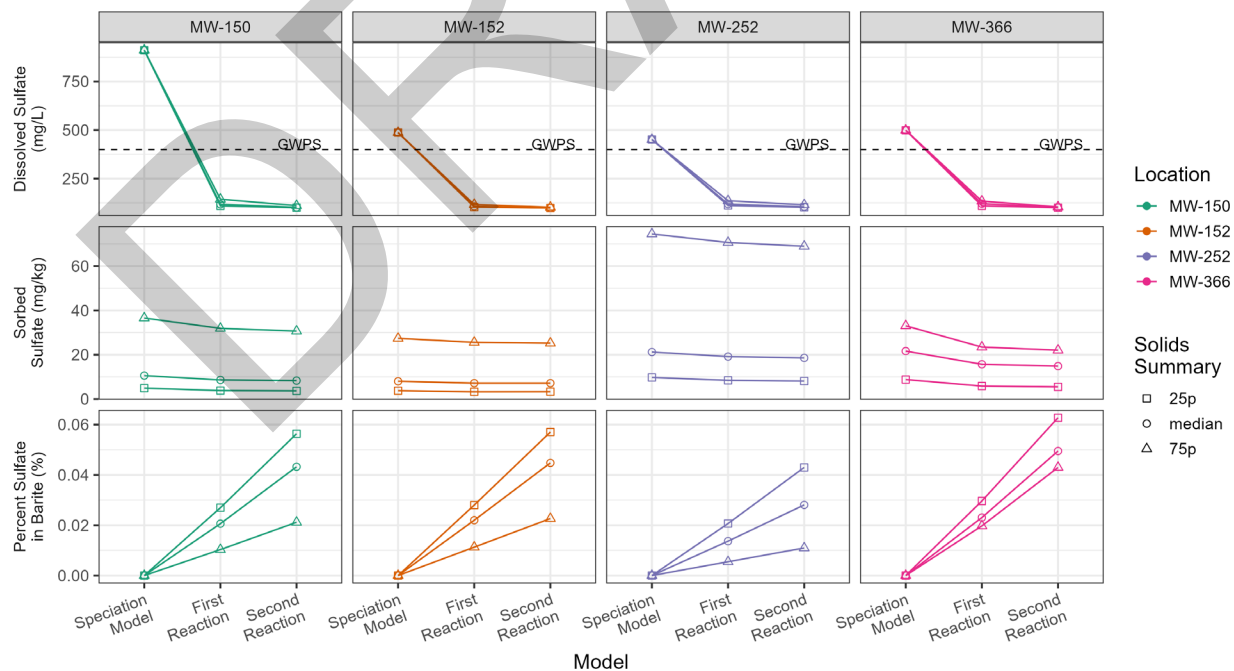
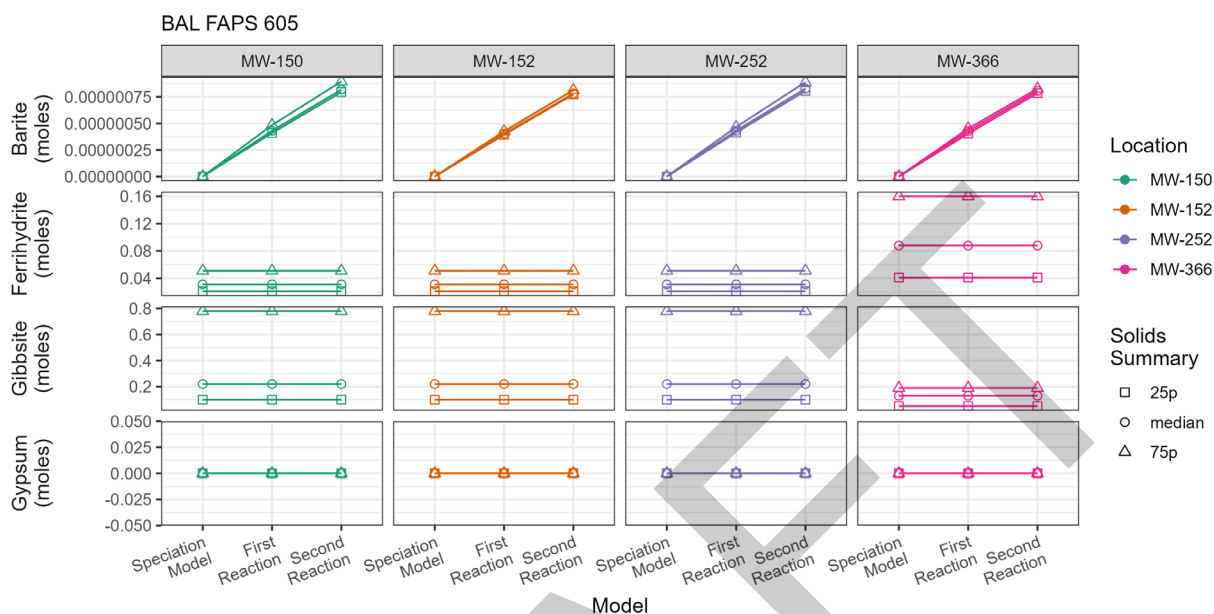


Figure 5: Modeled Sorbing Phase Behavior



3.2.2 Speciation Modeling

Results of the speciation modeling support the determination of the GCSM that chemical attenuation of boron and sulfate is likely. Speciation calculations indicate that at wells with boron exceedances (i.e., MW-150 and MW-152) between 84 and 96% of boron present in (modeled) downgradient compliance well groundwater will sorb to mineral surfaces (**Figure 1**), with most of the predicted sorption associated with the aluminum oxide (gibbsite) phase (**Attachment D**). Sensitivity assessments demonstrate the influence of variable sorbing mineral mass inputs on boron sorption, with the 25th percentile and 75th percentile values for mineral mass accounting for differences of up to 12% of aqueous boron sorbed under current conditions. These predicted percentages of aqueous boron sorbed correspond to sorbed boron masses ranging from approximately 2.5 to 22 milligrams of boron per kilogram of solid (mg/kg) (**Figure 2**). Model results using the median solid-phase inputs yield total sorbed boron masses of approximately 6 mg/kg for all wells with boron exceedances. These results suggest that boron sorption under current geochemical conditions is thermodynamically favorable, although the absolute amount of sorbed boron is somewhat sensitive to the amount of sorbent.

Speciation calculations for sulfate indicate that at wells with sulfate exceedances (i.e., MW-150, MW-152, and MW-366) between 5 and 35% of sulfate present in (modeled) downgradient compliance well groundwater will sorb to mineral surfaces (**Figure 3**). These predicted percentages of aqueous sulfate sorbed correspond to sorbed sulfate masses ranging from approximately 4 to 38 mg/kg (**Figure 4**). Sensitivity assessments demonstrate the influence of variable sorbing mineral mass inputs on sulfate sorption, with the 25th percentile and 75th percentile values for mineral mass accounting for differences of up to 36% of aqueous sulfate sorbed under current conditions. Model results using the median solid-phase inputs yield total sorbed sulfate masses of approximately 10 to 21 mg/kg. Similar results are observed at MW-252, which does not

currently have a sulfate exceedance. These results suggest that sulfate sorption is likely under current geochemical conditions, although the absolute amount of sorbed sulfate is sensitive to the amount of sorbent.

3.2.3 Reaction Modeling

Results of reaction modeling conducted to simulate conditions following source control demonstrate that aqueous boron and sulfate concentrations decrease with background groundwater interaction (**Figure 2, Figure 4**). Little boron desorption is predicted at wells with boron exceedances (MW-150 and MW-152) through two reaction cycles. The impact of this minor desorption on aqueous boron concentrations is negated by the background groundwater which contains less aqueous boron. Well MW-150 is predicted to achieve the boron GWPS after the first reaction and well MW-152 is predicted to achieve the boron GWPS after the second reaction for the median and 25th percentile model scenarios. The decreasing trend of aqueous boron concentrations with iterative reactions at MW-152 indicates that aqueous boron at this location will decrease below the GWPS even at the 75% of sorbent solid mass input given additional reaction time.

Aqueous sulfate concentrations are predicted to decrease at all wells with each iterative reaction (**Figure 4**). Some degree (< 10 mg/kg) of sulfate desorption is predicted with background groundwater interaction, depending on the model scenario. However, the impact of this desorption on aqueous sulfate concentrations is negated because the background groundwater contains less aqueous sulfate. Barite precipitation is predicted in all post-source control scenarios, which provides an additional attenuation mechanism for aqueous sulfate. All modeled wells are predicted to achieve the sulfate GWPS following the first reaction.

Boron and sulfate are predicted to sorb to ferrihydrite and gibbsite. Both minerals are predicted to be stable and exhibit minor (less than 0.01%, **Table 2**) predicted dissolution under post-source control conditions (**Figure 5**). Barite is predicted to precipitate under post-source control conditions in all model scenarios. The predicted stability of sorbing mineral phases and precipitation of barite under post-source control conditions demonstrates the continued feasibility of boron and sulfate chemical attenuation mechanisms in the FAPS.

These results suggest that chemical attenuation of boron and sulfate should remain sustainable following source control efforts. The primary chemical attenuation mechanism for boron is anticipated to be sorption to iron and aluminum oxide mineral phases which are predicted to be stable in post-source control conditions. Chemical attenuation mechanisms for sulfate are expected to include sorption to iron and aluminum oxide minerals and precipitation of barite. Results suggest that the flow and transport model conclusions are approximately correct for boron and sulfate, and that the time to reach the respective GWPS is not anticipated to be affected by desorption of COCs from the solid phase.

4. CONCLUSIONS

This report evaluated the contribution of chemical mechanisms to groundwater polishing via geochemical modeling. The results of the groundwater polishing evaluation also contextualize estimates of the modeled time to reach the GWPS by evaluating potential changes in COC attenuation as groundwater quality returns to background conditions.

Geochemical modeling of current FAPS chemical conditions demonstrates chemical attenuation of boron and sulfate via sorption to aquifer solids, particularly iron and aluminum oxides and (applicable to sulfate only) precipitation of barite. Modeling of anticipated post-source control conditions predicts some desorption of boron and sulfate from solids. However, desorption will be offset by interaction with background groundwater containing low aqueous COC concentrations, resulting in net aqueous boron and sulfate concentration decreases at wells with exceedances. Barite precipitation is predicted under post-source control conditions which will provide an additional attenuation mechanism for sulfate. Modeling also predicts that iron and aluminum oxide sorbing minerals phases will remain stable in post-source control conditions, and as a result this chemical attenuation mechanism will remain viable.

Results of the geochemical modeling suggest that the time to reach the boron and sulfate GWPS determined by the groundwater flow and transport model is not anticipated to be impacted by desorption from aquifer solids under post-source control conditions. The results will inform corrective action groundwater monitoring and adaptive site management, critical components of every corrective action considered in the CAAA.

5. REFERENCES

- Burns and McDonnell. 2021. Initial Operating Permit, Baldwin Power Plant Fly Ash System, October 25.
- Dzombak D.A. and Morel F.M.M. 1990. Surface Complexation Modeling: Hydrous Ferric Oxide. John Wiley & Sons, New York.
- Geosyntec. 2024. Geochemical Conceptual Site Model – Baldwin Power Plant, Fly Ash Pond System (CCR Unit #605). April.
- Karamalidis A.K. and Dzombak D.A. 2010. Surface Complexation Modeling: Gibbsite. John Wiley & Sons, New York.
- Natural Resource Technology, Inc. 2016. Supplemental Hydrogeologic Site Characterization and Groundwater Monitoring Plan, Baldwin Fly Ash Pond System, Baldwin Energy Complex. March.
- Ramboll. 2024. Nature and Extent Report – Baldwin Power Plant, Fly Ash Pond System, IEPA ID No. W1578510001-01, W1578510001-02, and W1578510001-03. April.
- Savannah River National Laboratory. 2011. The Scenarios Approach to Attenuation-Based Remedies for Inorganic and Radionuclide Contaminants. SRNL-STI-2011-00459. August.
- Stackelberg P.E., Belitz K., Brown C.J., Erickson M.L., Elliot S.M., Kauffman L.J., Ransom K.M., and Reddy J.E. 2020. Machine Learning Predictions of pH in the Glacial Aquifer System, Northern USA. Groundwater, 59(3):352-368. <https://doi.org/10.1111/gwat.13063>
- Stumm W. and Morgan J.J. 1996. Aquatic Chemistry: Chemical Equilibria and Rates in Natural Waters. Third edition. John Wiley & Sons, New York.
- USEPA. 1999. Use of Monitored Natural Attenuation at Superfund, RCRA Corrective Action, and Underground Storage Tank Sites. Office of Solid Waste and Emergency Response. Directive 9200.4-17P. April.
- USEPA. 2015. Use of Monitored Natural Attenuation for Inorganic Contaminants in Groundwater at Superfund Sites. Office of Solid Waste and Emergency Response. Directive 9283.1-36. August.
- United States Geological Survey (USGS). 2021. PHREEQC Version 3. December. <https://www.usgs.gov/software/phreeqc-version-3>

DRAFT

TABLES

Table 1. Summary of Geochemical Model Inputs
Groundwater Polishing Evaluation Report
Baldwin Power Plant - Fly Ash Pond System

Geosyntec Consultants, Inc.

| Model Component | Parameters | Data source(s) |
|---|--|---|
| Solid Phase | Iron (hydr)oxides, aluminum (hydr)oxides | Site-specific total metals and X-ray diffraction results from solid samples which were refined using representative results from sequential extraction data |
| | Calcite and dolomite | X-ray diffraction results |
| Downgradient groundwater (COC exceedance locations) | Boron, sulfate, iron, manganese, major ions ¹ , 845 constituents ¹ | Median concentrations per well from data collected in Q2 and Q3 2023 |
| Background groundwater | | Median concentrations from all network background wells using data collected in Q2 and Q3 2023 |

¹See Section 3.1.1.2 for details.

**Table 2. Geochemical Modeling Response of Sorbing Phases
Groundwater Polishing Evaluation Report
Baldwin Power Plant - Fly Ash Pond System**

| Parameter | Hydrostratigraphic Unit | Location | Summary Type | First Reaction Change | | Second Reaction Change | |
|--------------|-------------------------|----------|--------------|-----------------------|-------|------------------------|-------|
| | | | | mg/kg | % | mg/kg | % |
| Ferrihydrite | PMP | MW-150 | 25p | 0.022 | <0.01 | 0.022 | <0.01 |
| | | | median | 0.022 | <0.01 | 0.022 | <0.01 |
| | | | 75p | 0.022 | <0.01 | 0.022 | <0.01 |
| | | MW-152 | 25p | 0.022 | <0.01 | 0.022 | <0.01 |
| | | | median | 0.022 | <0.01 | 0.022 | <0.01 |
| | | | 75p | 0.022 | <0.01 | 0.022 | <0.01 |
| | | MW-252 | 25p | 0.022 | <0.01 | 0.022 | <0.01 |
| | | | median | 0.022 | <0.01 | 0.022 | <0.01 |
| | | | 75p | 0.022 | <0.01 | 0.022 | <0.01 |
| | UA | MW-366 | 25p | 0.058 | <0.01 | 0.058 | <0.01 |
| | | | median | 0.058 | <0.01 | 0.058 | <0.01 |
| | | | 75p | 0.058 | <0.01 | 0.058 | <0.01 |
| Gibbsite | PMP | MW-150 | 25p | 0.007 | <0.01 | 0.007 | <0.01 |
| | | | median | 0.007 | <0.01 | 0.007 | <0.01 |
| | | | 75p | 0.007 | <0.01 | 0.007 | <0.01 |
| | | MW-152 | 25p | 0.007 | <0.01 | 0.007 | <0.01 |
| | | | median | 0.007 | <0.01 | 0.007 | <0.01 |
| | | | 75p | 0.007 | <0.01 | 0.007 | <0.01 |
| | | MW-252 | 25p | 0.007 | <0.01 | 0.007 | <0.01 |
| | | | median | 0.007 | <0.01 | 0.007 | <0.01 |
| | | | 75p | 0.007 | <0.01 | 0.007 | <0.01 |
| | UA | MW-366 | 25p | 0.019 | <0.01 | 0.019 | <0.01 |
| | | | median | 0.020 | <0.01 | 0.019 | <0.01 |
| | | | 75p | 0.020 | <0.01 | 0.019 | <0.01 |
| Barite | PMP | MW-150 | 25p | 0.010 | NA | 0.009 | 93.97 |
| | | | median | 0.010 | NA | 0.009 | 90.10 |
| | | | 75p | 0.012 | NA | 0.010 | 84.69 |
| | | MW-152 | 25p | 0.010 | NA | 0.009 | 96.53 |
| | | | median | 0.010 | NA | 0.009 | 94.33 |
| | | | 75p | 0.010 | NA | 0.009 | 91.09 |
| | | MW-252 | 25p | 0.010 | NA | 0.010 | 94.57 |
| | | | median | 0.010 | NA | 0.010 | 92.09 |
| | | | 75p | 0.011 | NA | 0.010 | 90.77 |
| | UA | MW-366 | 25p | 0.026 | NA | 0.024 | 94.32 |
| | | | median | 0.027 | NA | 0.024 | 88.48 |
| | | | 75p | 0.029 | NA | 0.024 | 82.94 |

Notes:

% = percent

25p = 25th percentile

75p = 75th percentile

mg/kg = milligram/kilogram

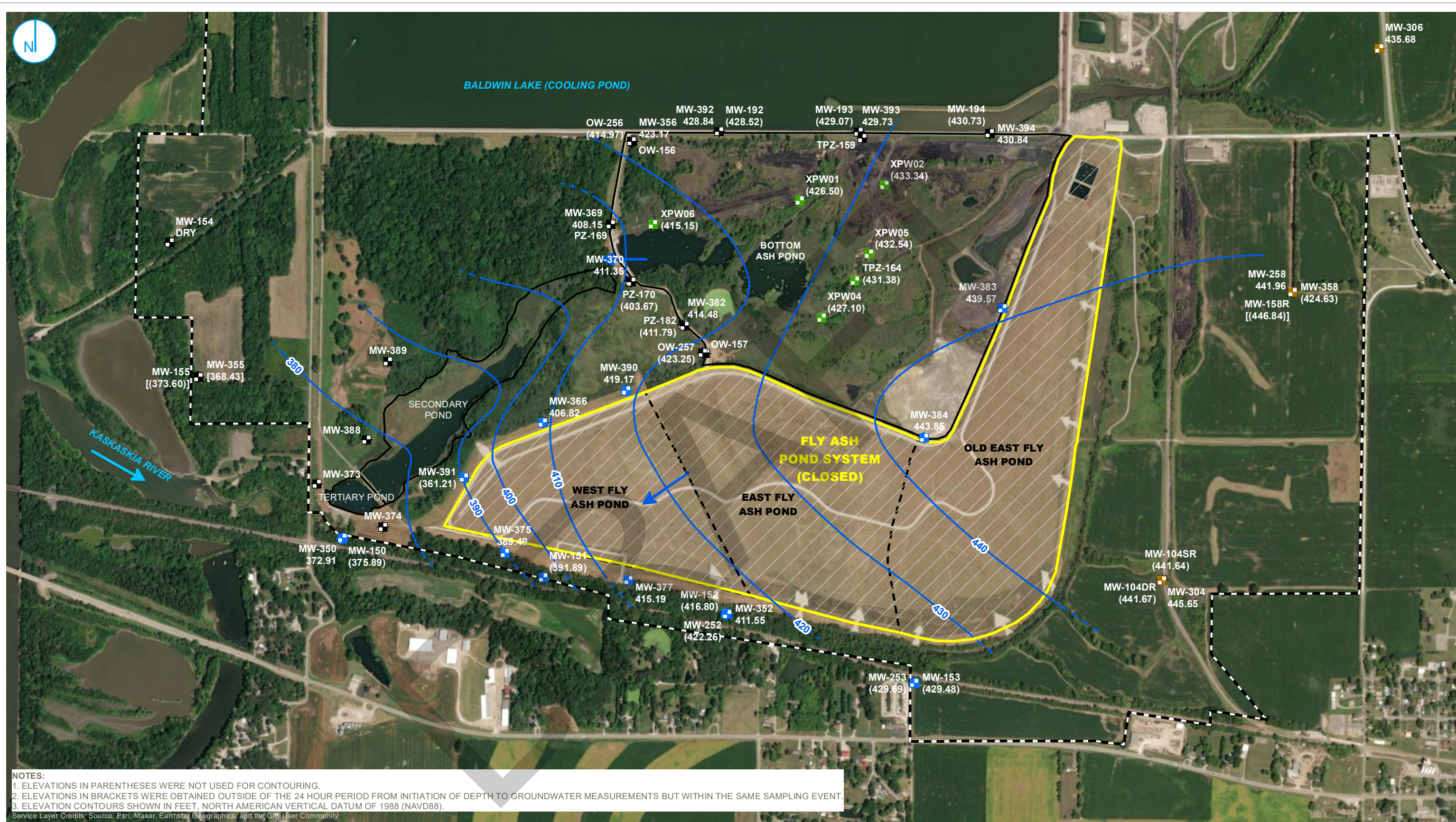
UA = Uppermost Aquifer

PMP = Potential migration pathways

NA = not applicable

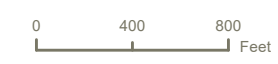
ATTACHMENT A
Potentiometric Surface Maps – August 2-3, 2023

PROJECT: 169000XXXX | DATED: 12/19/2023 | DESIGNER: GALARNMC
Y:\Mapping\Projects\22\2285\MXD\GW_Contours\Round_2023\Baldwin\FAPS_605\FAPS Pot Surface 20230802.mxd



NOTES:
1. ELEVATIONS IN PARENTHESES WERE NOT USED FOR CONTOURING.
2. ELEVATIONS IN BRACKETS WERE OBTAINED OUTSIDE OF THE 24 HOUR PERIOD FROM INITIATION OF DEPTH TO GROUNDWATER MEASUREMENTS BUT WITHIN THE SAME SAMPLING EVENT.
3. ELEVATION CONTOURS SHOWN IN FEET, NORTH AMERICAN VERTICAL DATUM OF 1988 (NAVD88).
Service Layer Credits: Source: Esri, Maxar, Earthstar Geographics, and the GIS User Community

- | | | |
|----------------------------|--|-------------------------------|
| COMPLIANCE MONITORING WELL | GROUNDWATER ELEVATION CONTOUR (10-FT CONTOUR INTERVAL, NAVD88) | REGULATED UNIT (SUBJECT UNIT) |
| BACKGROUND MONITORING WELL | INFERRED GROUNDWATER ELEVATION CONTOUR | SITE FEATURE |
| PORE WATER WELL | GROUNDWATER FLOW DIRECTION | CAPPED |
| MONITORING WELL | | PROPERTY BOUNDARY |



POTENTIOMETRIC SURFACE MAP AUGUST 2-3, 2023

2023 ANNUAL GROUNDWATER MONITORING AND CORRECTIVE ACTION REPORT
FLY ASH POND SYSTEM
BALDWIN POWER PLANT
BALDWIN, ILLINOIS

RAMBOLL AMERICAS
ENGINEERING SOLUTIONS, INC.



PROJECT: 169000XXX | DATED: 12/21/2023 | DESIGNER: GALARMIC
Y:\Mapping\Projects\22\2285\MXD\GWL_Contours\Round_2023\Baldwin\FAPS_605\FAPS Unlith Pot Surface 20230802.mxd



NOTES:
1. ELEVATIONS IN PARENTHESES WERE NOT USED FOR CONTOURING.
2. ELEVATION CONTOURS SHOWN IN FEET, NORTH AMERICAN VERTICAL DATUM OF 1988 (NAVD88).
Service Layer Credits: Source: Esri, Maxar, Earthstar Geographics, and the GIS User Community

- | | | |
|------------------------------|--|---------------------------------|
| ■ COMPLIANCE MONITORING WELL | — GROUNDWATER ELEVATION CONTOUR (10-FT CONTOUR INTERVAL, NAVD88) | ■ REGULATED UNIT (SUBJECT UNIT) |
| ■ BACKGROUND MONITORING WELL | - - - INFERRED GROUNDWATER ELEVATION CONTOUR | ■ SITE FEATURE |
| ■ MONITORING WELL | → GROUNDWATER FLOW DIRECTION | ■ CAPPED |
| ■ PORE WATER WELL | | ■ PROPERTY BOUNDARY |



SHALLOW UNLITHIFIED POTENTIOMETRIC SURFACE MAP AUGUST 2-3, 2023

2023 ANNUAL GROUNDWATER MONITORING AND CORRECTIVE ACTION REPORT
FLY ASH POND SYSTEM
BALDWIN POWER PLANT
BALDWIN, ILLINOIS

RAMBOLL AMERICAS
ENGINEERING SOLUTIONS, INC.



ATTACHMENT B
**PHREEQC Input Files and Thermodynamic
Database**

25th Percentile Metal Oxides/No Charge Balance

SELECTED_OUTPUT 1

-file BAL_845_605_25p_cb-false_out.csv

-charge_balance true

-percent_error true

-totals S(6) B Li As C(4) Cl F Ca Mg Na K Ba Si P Mn Fe Al Sb Be Cd Cr Co Pb Mo Se Hfo_s
Hfo_w Hao_

-molalities Hfo_wOH Hfo_wOH2+ Hfo_wOHSO4-2 Hfo_wSO4- Hfo_wOSi(OH)3

Hfo_wOSiO(OH)2- Hfo_wHCO3 Hfo_wCO3- Hfo_wPO4-2

Hfo_wHPO4- Hfo_wH2PO4 Hfo_sCO3- Hfo_sHCO3

Hfo_sHPO4- Hfo_sH2BO3 Hfo_sH2PO4 Hfo_sOSi(OH)3

Hfo_sOSiO(OH)2- Hfo_sOHSO4-2 Hfo_sSO4-

Hao_SO4- Hao_OHSO4-2 Hao_H2BO3 Hao_H3BO4-

-equilibrium_phases Ferrihydrite Gibbsite Barite Calcite Dolomite(ordered) Gypsum

-saturation_indices Ferrihydrite Gibbsite Barite Calcite Dolomite(ordered) Gypsum

SOLUTION 1 #MW-150 (C - PMP)

redox pe

units mg/l

density 1

pH 7.055

pe 3.36

temp 13.8

S(6) 911 as SO4

B 4.25

Li 0.0504

As 0.002425

C(4) 194.5 as CO3

Cl 54.5

F 0.725

Ca 204.5

Mg 159

Na 107.9

K 0.8785

Ba 0.0182

Si 9.875

P 0.0275

Mn 0.00315

Fe 0.0383

Al 0.017625

Sb 0.0002

Be 0.0001

Cd 0.000175

Cr 0.00105

Co 0.00005

Pb 0.00115

Mo 0.001675

Se 0.0011

end

SOLUTION 2 #MW-152 (C - PMP)

redox pe

units mg/l

density 1

pH 6.93
pe 5.81
temp 13.9
S(6) 487 as SO4
B 4.8025
Li 0.006325
As 0.002675
C(4) 236.5 as CO3
Cl 22.5
F 0.35
Ca 162.5
Mg 76.75
Na 117.95
K 1.0285
Ba 0.02485
Si 9.17
P 0.009
Mn 0.01245
Fe 0.008
Al 0.010175
Sb 0.0002
Be 0.00025
Cd 0.000175
Cr 0.00255
Co 0.00095
Pb 0.002
Mo 0.001325
Se 0.00045
end

SOLUTION 3 #MW-252 (C - PMP)

redox pe
units mg/l
density 1
pH 6.715
pe 3.79
temp 16.6
S(6) 451 as SO4
B 0.1585
Li 0.01265
As 0.002725
C(4) 289 as CO3
Cl 37.5
F 0.23
Ca 217
Mg 85.05
Na 99.45
K 1.785
Ba 0.0368
Si 6.885
P 0.0465
Mn 0.3445
Fe 0.30595
Al 0.0063

Sb 0.0024
Be 0.0001
Cd 0.000175
Cr 0.00315
Co 0.00205
Pb 0.0019
Mo 0.001325
Se 0.0003
end

SOLUTION 4 #MW-366 (C - UA)

redox pe
units mg/l
density 1
pH 6.865
pe 5.365
temp 14.95
S(6) 499 as SO4
B 1.685
Li 0.006225
As 0.002375
C(4) 187 as CO3
Cl 47.5
F 0.375
Ca 185.5
Mg 80.25
Na 59.25
K 4.05
Ba 0.03265
Si 8.305
P 0.008
Mn 0.0225
Fe 0.008
Al 0.0063
Sb 0.0004
Be 0.0001
Cd 0.000175
Cr 0.000875
Co 0.0017
Pb 0.00115
Mo 0.00305
Se 0.0003
end

EQUILIBRIUM_PHASES 1 #MW-150 (C - PMP) - 25p

Barite 0 0
Gypsum 0 0
Gibbsite 0 0.1
Ferrihydrite 0 0.021
Calcite 0 0.1
Dolomite(ordered) 0 0

SURFACE 1

Hfo_wOH Ferrihydrite equilibrium_phase 0.2 53400
Hfo_sOH Ferrihydrite equilibrium_phase 0.005 53400
Hao_OH Gibbsite equilibrium_phase 0.033 2496

-equil 1
save surface 1
end

EQUILIBRIUM_PHASES 2 #MW-152 (C - PMP) - 25p
Barite 0 0
Gypsum 0 0
Gibbsite 0 0.1
Ferrihydrite 0 0.021
Calcite 0 0.1
Dolomite(ordered) 0 0

SURFACE 2
Hfo_wOH Ferrihydrite equilibrium_phase 0.2 53400
Hfo_sOH Ferrihydrite equilibrium_phase 0.005 53400
Hao_OH Gibbsite equilibrium_phase 0.033 2496
-equil 2
save surface 2
end

EQUILIBRIUM_PHASES 3 #MW-252 (C - PMP) - 25p
Barite 0 0
Gypsum 0 0
Gibbsite 0 0.1
Ferrihydrite 0 0.021
Calcite 0 0.1
Dolomite(ordered) 0 0

SURFACE 3
Hfo_wOH Ferrihydrite equilibrium_phase 0.2 53400
Hfo_sOH Ferrihydrite equilibrium_phase 0.005 53400
Hao_OH Gibbsite equilibrium_phase 0.033 2496
-equil 3
save surface 3
end

EQUILIBRIUM_PHASES 4 #MW-366 (C - UA) - 25p
Barite 0 0
Gypsum 0 0
Gibbsite 0 0.051
Ferrihydrite 0 0.041
Calcite 0 10
Dolomite(ordered) 0 0

SURFACE 4
Hfo_wOH Ferrihydrite equilibrium_phase 0.2 53400
Hfo_sOH Ferrihydrite equilibrium_phase 0.005 53400
Hao_OH Gibbsite equilibrium_phase 0.033 2496
-equil 4
save surface 4
end

SOLUTION 5 #average background
redox pe
units mg/l
density 1
pH 7.77
pe 4.015

temp 16.15
S(6) 98.5
B 1.605
Li 0.07785
As 0.004075
C(4) 501.5
Cl 726 charge
F 2.515
Ca 10.635
Mg 4.91
Na 938.5
K 3.305
Ba 0.10605
Si 3.555
P 0.0495
Mn 0.0807
Fe 0.1155
Al 0.0268
Sb 0.0002
Be 0.0001
Cd 0.000175
Cr 0.0012
Co 0.00005
Pb 0.00115
Mo 0.007875
Se 0.0003

SAVE solution 5

end

#FIRST REACTION

#MW-150 (C - PMP) - First Reaction

USE SOLUTION 5

USE EQUILIBRIUM_PHASES 1

USE SURFACE 1

SAVE equilibrium_phases 1

SAVE surface 1

end

#MW-150 (C - PMP) - Second Reaction

USE SOLUTION 5

USE EQUILIBRIUM_PHASES 1

USE SURFACE 1

SAVE equilibrium_phases 1

SAVE surface 1

end

#MW-152 (C - PMP) - First Reaction

USE SOLUTION 5

USE EQUILIBRIUM_PHASES 2

USE SURFACE 2

SAVE equilibrium_phases 2

SAVE surface 2

end

#MW-152 (C - PMP) - Second Reaction

USE SOLUTION 5
USE EQUILIBRIUM_PHASES 2
USE SURFACE 2
SAVE equilibrium_phases 2
SAVE surface 2
end

#MW-252 (C - PMP) - First Reaction
USE SOLUTION 5
USE EQUILIBRIUM_PHASES 3
USE SURFACE 3
SAVE equilibrium_phases 3
SAVE surface 3
end

#MW-252 (C - PMP) - Second Reaction
USE SOLUTION 5
USE EQUILIBRIUM_PHASES 3
USE SURFACE 3
SAVE equilibrium_phases 3
SAVE surface 3
end

#MW-366 (C - UA) - First Reaction
USE SOLUTION 5
USE EQUILIBRIUM_PHASES 4
USE SURFACE 4
SAVE equilibrium_phases 4
SAVE surface 4
end

#MW-366 (C - UA) - Second Reaction
USE SOLUTION 5
USE EQUILIBRIUM_PHASES 4
USE SURFACE 4
SAVE equilibrium_phases 4
SAVE surface 4
end

25th Percentile Metal Oxides/Charge Balance on Chloride

SELECTED_OUTPUT 1

-file BAL_845_605_25p_cb-true_out.csv

-charge_balance true

-percent_error true

-totals S(6) B Li As C(4) Cl F Ca Mg Na K Ba Si P Mn Fe Al Sb Be Cd Cr Co Pb Mo Se Hfo_s
Hfo_w Hao_

-molalities Hfo_wOH Hfo_wOH2+ Hfo_wOHSO4-2 Hfo_wSO4- Hfo_wOSi(OH)3

Hfo_wOSiO(OH)2- Hfo_wHCO3 Hfo_wCO3- Hfo_wPO4-2

Hfo_wHPO4- Hfo_wH2PO4 Hfo_sCO3- Hfo_sHCO3

Hfo_sHPO4- Hfo_sH2BO3 Hfo_sH2PO4 Hfo_sOSi(OH)3

Hfo_sOSiO(OH)2- Hfo_sOHSO4-2 Hfo_sSO4-

Hao_SO4- Hao_OHSO4-2 Hao_H2BO3 Hao_H3BO4-

-equilibrium_phases Ferrihydrite Gibbsite Barite Calcite Dolomite(ordered) Gypsum

-saturation_indices Ferrihydrite Gibbsite Barite Calcite Dolomite(ordered) Gypsum

SOLUTION 1 #MW-150 (C - PMP)

redox pe

units mg/l

density 1

pH 7.055

pe 3.36

temp 13.8

S(6) 911 as SO4

B 4.25

Li 0.0504

As 0.002425

C(4) 194.5 as CO3

Cl 54.5 charge

F 0.725

Ca 204.5

Mg 159

Na 107.9

K 0.8785

Ba 0.0182

Si 9.875

P 0.0275

Mn 0.00315

Fe 0.0383

Al 0.017625

Sb 0.0002

Be 0.0001

Cd 0.000175

Cr 0.00105

Co 0.00005

Pb 0.00115

Mo 0.001675

Se 0.0011

end

SOLUTION 2 #MW-152 (C - PMP)

redox pe

units mg/l

density 1

pH 6.93
pe 5.81
temp 13.9
S(6) 487 as SO4
B 4.8025
Li 0.006325
As 0.002675
C(4) 236.5 as CO3
Cl 22.5 charge
F 0.35
Ca 162.5
Mg 76.75
Na 117.95
K 1.0285
Ba 0.02485
Si 9.17
P 0.009
Mn 0.01245
Fe 0.008
Al 0.010175
Sb 0.0002
Be 0.00025
Cd 0.000175
Cr 0.00255
Co 0.00095
Pb 0.002
Mo 0.001325
Se 0.00045
end

SOLUTION 3 #MW-252 (C - PMP)

redox pe
units mg/l
density 1
pH 6.715
pe 3.79
temp 16.6
S(6) 451 as SO4
B 0.1585
Li 0.01265
As 0.002725
C(4) 289 as CO3
Cl 37.5 charge
F 0.23
Ca 217
Mg 85.05
Na 99.45
K 1.785
Ba 0.0368
Si 6.885
P 0.0465
Mn 0.3445
Fe 0.30595
Al 0.0063

Sb 0.0024
Be 0.0001
Cd 0.000175
Cr 0.00315
Co 0.00205
Pb 0.0019
Mo 0.001325
Se 0.0003
end

SOLUTION 4 #MW-366 (C - UA)

redox pe
units mg/l
density 1
pH 6.865
pe 5.365
temp 14.95
S(6) 499 as SO4
B 1.685
Li 0.006225
As 0.002375
C(4) 187 as CO3
Cl 47.5 charge
F 0.375
Ca 185.5
Mg 80.25
Na 59.25
K 4.05
Ba 0.03265
Si 8.305
P 0.008
Mn 0.0225
Fe 0.008
Al 0.0063
Sb 0.0004
Be 0.0001
Cd 0.000175
Cr 0.000875
Co 0.0017
Pb 0.00115
Mo 0.00305
Se 0.0003
end

EQUILIBRIUM_PHASES 1 #MW-150 (C - PMP) - 25p

Barite 0 0
Gypsum 0 0
Gibbsite 0 0.1
Ferrihydrite 0 0.021
Calcite 0 0.1
Dolomite(ordered) 0 0

SURFACE 1

Hfo_wOH Ferrihydrite equilibrium_phase 0.2 53400
Hfo_sOH Ferrihydrite equilibrium_phase 0.005 53400
Hao_OH Gibbsite equilibrium_phase 0.033 2496

-equil 1
save surface 1
end

EQUILIBRIUM_PHASES 2 #MW-152 (C - PMP) - 25p
Barite 0 0
Gypsum 0 0
Gibbsite 0 0.1
Ferrihydrite 0 0.021
Calcite 0 0.1
Dolomite(ordered) 0 0

SURFACE 2
Hfo_wOH Ferrihydrite equilibrium_phase 0.2 53400
Hfo_sOH Ferrihydrite equilibrium_phase 0.005 53400
Hao_OH Gibbsite equilibrium_phase 0.033 2496
-equil 2
save surface 2
end

EQUILIBRIUM_PHASES 3 #MW-252 (C - PMP) - 25p
Barite 0 0
Gypsum 0 0
Gibbsite 0 0.1
Ferrihydrite 0 0.021
Calcite 0 0.1
Dolomite(ordered) 0 0

SURFACE 3
Hfo_wOH Ferrihydrite equilibrium_phase 0.2 53400
Hfo_sOH Ferrihydrite equilibrium_phase 0.005 53400
Hao_OH Gibbsite equilibrium_phase 0.033 2496
-equil 3
save surface 3
end

EQUILIBRIUM_PHASES 4 #MW-366 (C - UA) - 25p
Barite 0 0
Gypsum 0 0
Gibbsite 0 0.051
Ferrihydrite 0 0.041
Calcite 0 10
Dolomite(ordered) 0 0

SURFACE 4
Hfo_wOH Ferrihydrite equilibrium_phase 0.2 53400
Hfo_sOH Ferrihydrite equilibrium_phase 0.005 53400
Hao_OH Gibbsite equilibrium_phase 0.033 2496
-equil 4
save surface 4
end

SOLUTION 5 #average background
redox pe
units mg/l
density 1
pH 7.77
pe 4.015

temp 16.15
S(6) 98.5
B 1.605
Li 0.07785
As 0.004075
C(4) 501.5
Cl 726 charge
F 2.515
Ca 10.635
Mg 4.91
Na 938.5
K 3.305
Ba 0.10605
Si 3.555
P 0.0495
Mn 0.0807
Fe 0.1155
Al 0.0268
Sb 0.0002
Be 0.0001
Cd 0.000175
Cr 0.0012
Co 0.00005
Pb 0.00115
Mo 0.007875
Se 0.0003

SAVE solution 5

end

#FIRST REACTION

#MW-150 (C - PMP) - First Reaction

USE SOLUTION 5

USE EQUILIBRIUM_PHASES 1

USE SURFACE 1

SAVE equilibrium_phases 1

SAVE surface 1

end

#MW-150 (C - PMP) - Second Reaction

USE SOLUTION 5

USE EQUILIBRIUM_PHASES 1

USE SURFACE 1

SAVE equilibrium_phases 1

SAVE surface 1

end

#MW-152 (C - PMP) - First Reaction

USE SOLUTION 5

USE EQUILIBRIUM_PHASES 2

USE SURFACE 2

SAVE equilibrium_phases 2

SAVE surface 2

end

#MW-152 (C - PMP) - Second Reaction

USE SOLUTION 5
USE EQUILIBRIUM_PHASES 2
USE SURFACE 2
SAVE equilibrium_phases 2
SAVE surface 2
end

#MW-252 (C - PMP) - First Reaction
USE SOLUTION 5
USE EQUILIBRIUM_PHASES 3
USE SURFACE 3
SAVE equilibrium_phases 3
SAVE surface 3
end

#MW-252 (C - PMP) - Second Reaction
USE SOLUTION 5
USE EQUILIBRIUM_PHASES 3
USE SURFACE 3
SAVE equilibrium_phases 3
SAVE surface 3
end

#MW-366 (C - UA) - First Reaction
USE SOLUTION 5
USE EQUILIBRIUM_PHASES 4
USE SURFACE 4
SAVE equilibrium_phases 4
SAVE surface 4
end

#MW-366 (C - UA) - Second Reaction
USE SOLUTION 5
USE EQUILIBRIUM_PHASES 4
USE SURFACE 4
SAVE equilibrium_phases 4
SAVE surface 4
end

75th Percentile Metal Oxides/No Charge Balance

SELECTED_OUTPUT 1

-file BAL_845_605_75p_cb-false_out.csv

-charge_balance true

-percent_error true

-totals S(6) B Li As C(4) Cl F Ca Mg Na K Ba Si P Mn Fe Al Sb Be Cd Cr Co Pb Mo Se Hfo_s
Hfo_w Hao_

-molalities Hfo_wOH Hfo_wOH2+ Hfo_wOHSO4-2 Hfo_wSO4- Hfo_wOSi(OH)3

Hfo_wOSiO(OH)2- Hfo_wHCO3 Hfo_wCO3- Hfo_wPO4-2

Hfo_wHPO4- Hfo_wH2PO4 Hfo_sCO3- Hfo_sHCO3

Hfo_sHPO4- Hfo_sH2BO3 Hfo_sH2PO4 Hfo_sOSi(OH)3

Hfo_sOSiO(OH)2- Hfo_sOHSO4-2 Hfo_sSO4-

Hao_SO4- Hao_OHSO4-2 Hao_H2BO3 Hao_H3BO4-

-equilibrium_phases Ferrihydrite Gibbsite Barite Calcite Dolomite(ordered) Gypsum

-saturation_indices Ferrihydrite Gibbsite Barite Calcite Dolomite(ordered) Gypsum

SOLUTION 1 #MW-150 (C - PMP)

redox pe

units mg/l

density 1

pH 7.055

pe 3.36

temp 13.8

S(6) 911 as SO4

B 4.25

Li 0.0504

As 0.002425

C(4) 194.5 as CO3

Cl 54.5

F 0.725

Ca 204.5

Mg 159

Na 107.9

K 0.8785

Ba 0.0182

Si 9.875

P 0.0275

Mn 0.00315

Fe 0.0383

Al 0.017625

Sb 0.0002

Be 0.0001

Cd 0.000175

Cr 0.00105

Co 0.00005

Pb 0.00115

Mo 0.001675

Se 0.0011

end

SOLUTION 2 #MW-152 (C - PMP)

redox pe

units mg/l

density 1

pH 6.93
pe 5.81
temp 13.9
S(6) 487 as SO4
B 4.8025
Li 0.006325
As 0.002675
C(4) 236.5 as CO3
Cl 22.5
F 0.35
Ca 162.5
Mg 76.75
Na 117.95
K 1.0285
Ba 0.02485
Si 9.17
P 0.009
Mn 0.01245
Fe 0.008
Al 0.010175
Sb 0.0002
Be 0.00025
Cd 0.000175
Cr 0.00255
Co 0.00095
Pb 0.002
Mo 0.001325
Se 0.00045
end

SOLUTION 3 #MW-252 (C - PMP)

redox pe
units mg/l
density 1
pH 6.715
pe 3.79
temp 16.6
S(6) 451 as SO4
B 0.1585
Li 0.01265
As 0.002725
C(4) 289 as CO3
Cl 37.5
F 0.23
Ca 217
Mg 85.05
Na 99.45
K 1.785
Ba 0.0368
Si 6.885
P 0.0465
Mn 0.3445
Fe 0.30595
Al 0.0063

Sb 0.0024
Be 0.0001
Cd 0.000175
Cr 0.00315
Co 0.00205
Pb 0.0019
Mo 0.001325
Se 0.0003
end

SOLUTION 4 #MW-366 (C - UA)

redox pe
units mg/l
density 1
pH 6.865
pe 5.365
temp 14.95
S(6) 499 as SO4
B 1.685
Li 0.006225
As 0.002375
C(4) 187 as CO3
Cl 47.5
F 0.375
Ca 185.5
Mg 80.25
Na 59.25
K 4.05
Ba 0.03265
Si 8.305
P 0.008
Mn 0.0225
Fe 0.008
Al 0.0063
Sb 0.0004
Be 0.0001
Cd 0.000175
Cr 0.000875
Co 0.0017
Pb 0.00115
Mo 0.00305
Se 0.0003
end

EQUILIBRIUM_PHASES 1 #MW-150 (C - PMP) - 75p

Barite 0 0
Gypsum 0 0
Gibbsite 0 0.78
Ferrihydrite 0 0.051
Calcite 0 0.1
Dolomite(ordered) 0 0

SURFACE 1

Hfo_wOH Ferrihydrite equilibrium_phase 0.2 53400
Hfo_sOH Ferrihydrite equilibrium_phase 0.005 53400
Hao_OH Gibbsite equilibrium_phase 0.033 2496

-equil 1
save surface 1
end

EQUILIBRIUM_PHASES 2 #MW-152 (C - PMP) - 75p
Barite 0 0
Gypsum 0 0
Gibbsite 0 0.78
Ferrihydrite 0 0.051
Calcite 0 0.1
Dolomite(ordered) 0 0

SURFACE 2
Hfo_wOH Ferrihydrite equilibrium_phase 0.2 53400
Hfo_sOH Ferrihydrite equilibrium_phase 0.005 53400
Hao_OH Gibbsite equilibrium_phase 0.033 2496
-equil 2
save surface 2
end

EQUILIBRIUM_PHASES 3 #MW-252 (C - PMP) - 75p
Barite 0 0
Gypsum 0 0
Gibbsite 0 0.78
Ferrihydrite 0 0.051
Calcite 0 0.1
Dolomite(ordered) 0 0

SURFACE 3
Hfo_wOH Ferrihydrite equilibrium_phase 0.2 53400
Hfo_sOH Ferrihydrite equilibrium_phase 0.005 53400
Hao_OH Gibbsite equilibrium_phase 0.033 2496
-equil 3
save surface 3
end

EQUILIBRIUM_PHASES 4 #MW-366 (C - UA) - 75p
Barite 0 0
Gypsum 0 0
Gibbsite 0 0.19
Ferrihydrite 0 0.16
Calcite 0 10
Dolomite(ordered) 0 0

SURFACE 4
Hfo_wOH Ferrihydrite equilibrium_phase 0.2 53400
Hfo_sOH Ferrihydrite equilibrium_phase 0.005 53400
Hao_OH Gibbsite equilibrium_phase 0.033 2496
-equil 4
save surface 4
end

SOLUTION 5 #average background
redox pe
units mg/l
density 1
pH 7.77
pe 4.015

temp 16.15
S(6) 98.5
B 1.605
Li 0.07785
As 0.004075
C(4) 501.5
Cl 726 charge
F 2.515
Ca 10.635
Mg 4.91
Na 938.5
K 3.305
Ba 0.10605
Si 3.555
P 0.0495
Mn 0.0807
Fe 0.1155
Al 0.0268
Sb 0.0002
Be 0.0001
Cd 0.000175
Cr 0.0012
Co 0.00005
Pb 0.00115
Mo 0.007875
Se 0.0003

SAVE solution 5

end

#FIRST REACTION

#MW-150 (C - PMP) - First Reaction

USE SOLUTION 5

USE EQUILIBRIUM_PHASES 1

USE SURFACE 1

SAVE equilibrium_phases 1

SAVE surface 1

end

#MW-150 (C - PMP) - Second Reaction

USE SOLUTION 5

USE EQUILIBRIUM_PHASES 1

USE SURFACE 1

SAVE equilibrium_phases 1

SAVE surface 1

end

#MW-152 (C - PMP) - First Reaction

USE SOLUTION 5

USE EQUILIBRIUM_PHASES 2

USE SURFACE 2

SAVE equilibrium_phases 2

SAVE surface 2

end

#MW-152 (C - PMP) - Second Reaction

USE SOLUTION 5
USE EQUILIBRIUM_PHASES 2
USE SURFACE 2
SAVE equilibrium_phases 2
SAVE surface 2
end

#MW-252 (C - PMP) - First Reaction
USE SOLUTION 5
USE EQUILIBRIUM_PHASES 3
USE SURFACE 3
SAVE equilibrium_phases 3
SAVE surface 3
end

#MW-252 (C - PMP) - Second Reaction
USE SOLUTION 5
USE EQUILIBRIUM_PHASES 3
USE SURFACE 3
SAVE equilibrium_phases 3
SAVE surface 3
end

#MW-366 (C - UA) - First Reaction
USE SOLUTION 5
USE EQUILIBRIUM_PHASES 4
USE SURFACE 4
SAVE equilibrium_phases 4
SAVE surface 4
end

#MW-366 (C - UA) - Second Reaction
USE SOLUTION 5
USE EQUILIBRIUM_PHASES 4
USE SURFACE 4
SAVE equilibrium_phases 4
SAVE surface 4
end

75th Percentile Metal Oxides/Charge Balance on Chloride

SELECTED_OUTPUT 1

-file BAL_845_605_75p_cb-true_out.csv

-charge_balance true

-percent_error true

-totals S(6) B Li As C(4) Cl F Ca Mg Na K Ba Si P Mn Fe Al Sb Be Cd Cr Co Pb Mo Se Hfo_s
Hfo_w Hao_

-molalities Hfo_wOH Hfo_wOH2+ Hfo_wOHSO4-2 Hfo_wSO4- Hfo_wOSi(OH)3

Hfo_wOSiO(OH)2- Hfo_wHCO3 Hfo_wCO3- Hfo_wPO4-2

Hfo_wHPO4- Hfo_wH2PO4 Hfo_sCO3- Hfo_sHCO3

Hfo_sHPO4- Hfo_sH2BO3 Hfo_sH2PO4 Hfo_sOSi(OH)3

Hfo_sOSiO(OH)2- Hfo_sOHSO4-2 Hfo_sSO4-

Hao_SO4- Hao_OHSO4-2 Hao_H2BO3 Hao_H3BO4-

-equilibrium_phases Ferrihydrite Gibbsite Barite Calcite Dolomite(ordered) Gypsum

-saturation_indices Ferrihydrite Gibbsite Barite Calcite Dolomite(ordered) Gypsum

SOLUTION 1 #MW-150 (C - PMP)

redox pe

units mg/l

density 1

pH 7.055

pe 3.36

temp 13.8

S(6) 911 as SO4

B 4.25

Li 0.0504

As 0.002425

C(4) 194.5 as CO3

Cl 54.5 charge

F 0.725

Ca 204.5

Mg 159

Na 107.9

K 0.8785

Ba 0.0182

Si 9.875

P 0.0275

Mn 0.00315

Fe 0.0383

Al 0.017625

Sb 0.0002

Be 0.0001

Cd 0.000175

Cr 0.00105

Co 0.00005

Pb 0.00115

Mo 0.001675

Se 0.0011

end

SOLUTION 2 #MW-152 (C - PMP)

redox pe

units mg/l

density 1

pH 6.93
pe 5.81
temp 13.9
S(6) 487 as SO4
B 4.8025
Li 0.006325
As 0.002675
C(4) 236.5 as CO3
Cl 22.5 charge
F 0.35
Ca 162.5
Mg 76.75
Na 117.95
K 1.0285
Ba 0.02485
Si 9.17
P 0.009
Mn 0.01245
Fe 0.008
Al 0.010175
Sb 0.0002
Be 0.00025
Cd 0.000175
Cr 0.00255
Co 0.00095
Pb 0.002
Mo 0.001325
Se 0.00045
end

SOLUTION 3 #MW-252 (C - PMP)

redox pe
units mg/l
density 1
pH 6.715
pe 3.79
temp 16.6
S(6) 451 as SO4
B 0.1585
Li 0.01265
As 0.002725
C(4) 289 as CO3
Cl 37.5 charge
F 0.23
Ca 217
Mg 85.05
Na 99.45
K 1.785
Ba 0.0368
Si 6.885
P 0.0465
Mn 0.3445
Fe 0.30595
Al 0.0063

Sb 0.0024
Be 0.0001
Cd 0.000175
Cr 0.00315
Co 0.00205
Pb 0.0019
Mo 0.001325
Se 0.0003
end

SOLUTION 4 #MW-366 (C - UA)

redox pe
units mg/l
density 1
pH 6.865
pe 5.365
temp 14.95
S(6) 499 as SO4
B 1.685
Li 0.006225
As 0.002375
C(4) 187 as CO3
Cl 47.5 charge
F 0.375
Ca 185.5
Mg 80.25
Na 59.25
K 4.05
Ba 0.03265
Si 8.305
P 0.008
Mn 0.0225
Fe 0.008
Al 0.0063
Sb 0.0004
Be 0.0001
Cd 0.000175
Cr 0.000875
Co 0.0017
Pb 0.00115
Mo 0.00305
Se 0.0003
end

EQUILIBRIUM_PHASES 1 #MW-150 (C - PMP) - 75p

Barite 0 0
Gypsum 0 0
Gibbsite 0 0.78
Ferrihydrite 0 0.051
Calcite 0 0.1
Dolomite(ordered) 0 0

SURFACE 1

Hfo_wOH Ferrihydrite equilibrium_phase 0.2 53400
Hfo_sOH Ferrihydrite equilibrium_phase 0.005 53400
Hao_OH Gibbsite equilibrium_phase 0.033 2496

-equil 1
save surface 1
end

EQUILIBRIUM_PHASES 2 #MW-152 (C - PMP) - 75p
Barite 0 0
Gypsum 0 0
Gibbsite 0 0.78
Ferrihydrite 0 0.051
Calcite 0 0.1
Dolomite(ordered) 0 0

SURFACE 2
Hfo_wOH Ferrihydrite equilibrium_phase 0.2 53400
Hfo_sOH Ferrihydrite equilibrium_phase 0.005 53400
Hao_OH Gibbsite equilibrium_phase 0.033 2496
-equil 2
save surface 2
end

EQUILIBRIUM_PHASES 3 #MW-252 (C - PMP) - 75p
Barite 0 0
Gypsum 0 0
Gibbsite 0 0.78
Ferrihydrite 0 0.051
Calcite 0 0.1
Dolomite(ordered) 0 0

SURFACE 3
Hfo_wOH Ferrihydrite equilibrium_phase 0.2 53400
Hfo_sOH Ferrihydrite equilibrium_phase 0.005 53400
Hao_OH Gibbsite equilibrium_phase 0.033 2496
-equil 3
save surface 3
end

EQUILIBRIUM_PHASES 4 #MW-366 (C - UA) - 75p
Barite 0 0
Gypsum 0 0
Gibbsite 0 0.19
Ferrihydrite 0 0.16
Calcite 0 10
Dolomite(ordered) 0 0

SURFACE 4
Hfo_wOH Ferrihydrite equilibrium_phase 0.2 53400
Hfo_sOH Ferrihydrite equilibrium_phase 0.005 53400
Hao_OH Gibbsite equilibrium_phase 0.033 2496
-equil 4
save surface 4
end

SOLUTION 5 #average background
redox pe
units mg/l
density 1
pH 7.77
pe 4.015

temp 16.15
S(6) 98.5
B 1.605
Li 0.07785
As 0.004075
C(4) 501.5
Cl 726 charge
F 2.515
Ca 10.635
Mg 4.91
Na 938.5
K 3.305
Ba 0.10605
Si 3.555
P 0.0495
Mn 0.0807
Fe 0.1155
Al 0.0268
Sb 0.0002
Be 0.0001
Cd 0.000175
Cr 0.0012
Co 0.00005
Pb 0.00115
Mo 0.007875
Se 0.0003

SAVE solution 5

end

#FIRST REACTION

#MW-150 (C - PMP) - First Reaction

USE SOLUTION 5

USE EQUILIBRIUM_PHASES 1

USE SURFACE 1

SAVE equilibrium_phases 1

SAVE surface 1

end

#MW-150 (C - PMP) - Second Reaction

USE SOLUTION 5

USE EQUILIBRIUM_PHASES 1

USE SURFACE 1

SAVE equilibrium_phases 1

SAVE surface 1

end

#MW-152 (C - PMP) - First Reaction

USE SOLUTION 5

USE EQUILIBRIUM_PHASES 2

USE SURFACE 2

SAVE equilibrium_phases 2

SAVE surface 2

end

#MW-152 (C - PMP) - Second Reaction

USE SOLUTION 5
USE EQUILIBRIUM_PHASES 2
USE SURFACE 2
SAVE equilibrium_phases 2
SAVE surface 2
end

#MW-252 (C - PMP) - First Reaction
USE SOLUTION 5
USE EQUILIBRIUM_PHASES 3
USE SURFACE 3
SAVE equilibrium_phases 3
SAVE surface 3
end

#MW-252 (C - PMP) - Second Reaction
USE SOLUTION 5
USE EQUILIBRIUM_PHASES 3
USE SURFACE 3
SAVE equilibrium_phases 3
SAVE surface 3
end

#MW-366 (C - UA) - First Reaction
USE SOLUTION 5
USE EQUILIBRIUM_PHASES 4
USE SURFACE 4
SAVE equilibrium_phases 4
SAVE surface 4
end

#MW-366 (C - UA) - Second Reaction
USE SOLUTION 5
USE EQUILIBRIUM_PHASES 4
USE SURFACE 4
SAVE equilibrium_phases 4
SAVE surface 4
end

Median Metal Oxides/No Charge Balance

SELECTED_OUTPUT 1

-file BAL_845_605_median_cb-false_out.csv

-charge_balance true

-percent_error true

-totals S(6) B Li As C(4) Cl F Ca Mg Na K Ba Si P Mn Fe Al Sb Be Cd Cr Co Pb Mo Se Hfo_s
Hfo_w Hao_

-molalities Hfo_wOH Hfo_wOH2+ Hfo_wOHSO4-2 Hfo_wSO4- Hfo_wOSi(OH)3

Hfo_wOSiO(OH)2- Hfo_wHCO3 Hfo_wCO3- Hfo_wPO4-2

Hfo_wHPO4- Hfo_wH2PO4 Hfo_sCO3- Hfo_sHCO3

Hfo_sHPO4- Hfo_sH2BO3 Hfo_sH2PO4 Hfo_sOSi(OH)3

Hfo_sOSiO(OH)2- Hfo_sOHSO4-2 Hfo_sSO4-

Hao_SO4- Hao_OHSO4-2 Hao_H2BO3 Hao_H3BO4-

-equilibrium_phases Ferrihydrite Gibbsite Barite Calcite Dolomite(ordered) Gypsum

-saturation_indices Ferrihydrite Gibbsite Barite Calcite Dolomite(ordered) Gypsum

SOLUTION 1 #MW-150 (C - PMP)

redox pe

units mg/l

density 1

pH 7.055

pe 3.36

temp 13.8

S(6) 911 as SO4

B 4.25

Li 0.0504

As 0.002425

C(4) 194.5 as CO3

Cl 54.5

F 0.725

Ca 204.5

Mg 159

Na 107.9

K 0.8785

Ba 0.0182

Si 9.875

P 0.0275

Mn 0.00315

Fe 0.0383

Al 0.017625

Sb 0.0002

Be 0.0001

Cd 0.000175

Cr 0.00105

Co 0.00005

Pb 0.00115

Mo 0.001675

Se 0.0011

end

SOLUTION 2 #MW-152 (C - PMP)

redox pe

units mg/l

density 1

pH 6.93
pe 5.81
temp 13.9
S(6) 487 as SO4
B 4.8025
Li 0.006325
As 0.002675
C(4) 236.5 as CO3
Cl 22.5
F 0.35
Ca 162.5
Mg 76.75
Na 117.95
K 1.0285
Ba 0.02485
Si 9.17
P 0.009
Mn 0.01245
Fe 0.008
Al 0.010175
Sb 0.0002
Be 0.00025
Cd 0.000175
Cr 0.00255
Co 0.00095
Pb 0.002
Mo 0.001325
Se 0.00045
end

SOLUTION 3 #MW-252 (C - PMP)

redox pe
units mg/l
density 1
pH 6.715
pe 3.79
temp 16.6
S(6) 451 as SO4
B 0.1585
Li 0.01265
As 0.002725
C(4) 289 as CO3
Cl 37.5
F 0.23
Ca 217
Mg 85.05
Na 99.45
K 1.785
Ba 0.0368
Si 6.885
P 0.0465
Mn 0.3445
Fe 0.30595
Al 0.0063

Sb 0.0024
Be 0.0001
Cd 0.000175
Cr 0.00315
Co 0.00205
Pb 0.0019
Mo 0.001325
Se 0.0003
end

SOLUTION 4 #MW-366 (C - UA)

redox pe
units mg/l
density 1
pH 6.865
pe 5.365
temp 14.95
S(6) 499 as SO4
B 1.685
Li 0.006225
As 0.002375
C(4) 187 as CO3
Cl 47.5
F 0.375
Ca 185.5
Mg 80.25
Na 59.25
K 4.05
Ba 0.03265
Si 8.305
P 0.008
Mn 0.0225
Fe 0.008
Al 0.0063
Sb 0.0004
Be 0.0001
Cd 0.000175
Cr 0.000875
Co 0.0017
Pb 0.00115
Mo 0.00305
Se 0.0003
end

EQUILIBRIUM_PHASES 1 #MW-150 (C - PMP) - median

Barite 0 0
Gypsum 0 0
Gibbsite 0 0.22
Ferrihydrite 0 0.031
Calcite 0 0.1
Dolomite(ordered) 0 0

SURFACE 1

Hfo_wOH Ferrihydrite equilibrium_phase 0.2 53400
Hfo_sOH Ferrihydrite equilibrium_phase 0.005 53400
Hao_OH Gibbsite equilibrium_phase 0.033 2496

-equil 1
save surface 1
end

EQUILIBRIUM_PHASES 2 #MW-152 (C - PMP) - median
Barite 0 0
Gypsum 0 0
Gibbsite 0 0.22
Ferrihydrite 0 0.031
Calcite 0 0.1
Dolomite(ordered) 0 0

SURFACE 2
Hfo_wOH Ferrihydrite equilibrium_phase 0.2 53400
Hfo_sOH Ferrihydrite equilibrium_phase 0.005 53400
Hao_OH Gibbsite equilibrium_phase 0.033 2496
-equil 2
save surface 2
end

EQUILIBRIUM_PHASES 3 #MW-252 (C - PMP) - median
Barite 0 0
Gypsum 0 0
Gibbsite 0 0.22
Ferrihydrite 0 0.031
Calcite 0 0.1
Dolomite(ordered) 0 0

SURFACE 3
Hfo_wOH Ferrihydrite equilibrium_phase 0.2 53400
Hfo_sOH Ferrihydrite equilibrium_phase 0.005 53400
Hao_OH Gibbsite equilibrium_phase 0.033 2496
-equil 3
save surface 3
end

EQUILIBRIUM_PHASES 4 #MW-366 (C - UA) - median
Barite 0 0
Gypsum 0 0
Gibbsite 0 0.13
Ferrihydrite 0 0.088
Calcite 0 10
Dolomite(ordered) 0 0

SURFACE 4
Hfo_wOH Ferrihydrite equilibrium_phase 0.2 53400
Hfo_sOH Ferrihydrite equilibrium_phase 0.005 53400
Hao_OH Gibbsite equilibrium_phase 0.033 2496
-equil 4
save surface 4
end

SOLUTION 5 #average background
redox pe
units mg/l
density 1
pH 7.77
pe 4.015

temp 16.15
S(6) 98.5
B 1.605
Li 0.07785
As 0.004075
C(4) 501.5
Cl 726 charge
F 2.515
Ca 10.635
Mg 4.91
Na 938.5
K 3.305
Ba 0.10605
Si 3.555
P 0.0495
Mn 0.0807
Fe 0.1155
Al 0.0268
Sb 0.0002
Be 0.0001
Cd 0.000175
Cr 0.0012
Co 0.00005
Pb 0.00115
Mo 0.007875
Se 0.0003

SAVE solution 5

end

#FIRST REACTION

#MW-150 (C - PMP) - First Reaction

USE SOLUTION 5

USE EQUILIBRIUM_PHASES 1

USE SURFACE 1

SAVE equilibrium_phases 1

SAVE surface 1

end

#MW-150 (C - PMP) - Second Reaction

USE SOLUTION 5

USE EQUILIBRIUM_PHASES 1

USE SURFACE 1

SAVE equilibrium_phases 1

SAVE surface 1

end

#MW-152 (C - PMP) - First Reaction

USE SOLUTION 5

USE EQUILIBRIUM_PHASES 2

USE SURFACE 2

SAVE equilibrium_phases 2

SAVE surface 2

end

#MW-152 (C - PMP) - Second Reaction

USE SOLUTION 5
USE EQUILIBRIUM_PHASES 2
USE SURFACE 2
SAVE equilibrium_phases 2
SAVE surface 2
end

#MW-252 (C - PMP) - First Reaction
USE SOLUTION 5
USE EQUILIBRIUM_PHASES 3
USE SURFACE 3
SAVE equilibrium_phases 3
SAVE surface 3
end

#MW-252 (C - PMP) - Second Reaction
USE SOLUTION 5
USE EQUILIBRIUM_PHASES 3
USE SURFACE 3
SAVE equilibrium_phases 3
SAVE surface 3
end

#MW-366 (C - UA) - First Reaction
USE SOLUTION 5
USE EQUILIBRIUM_PHASES 4
USE SURFACE 4
SAVE equilibrium_phases 4
SAVE surface 4
end

#MW-366 (C - UA) - Second Reaction
USE SOLUTION 5
USE EQUILIBRIUM_PHASES 4
USE SURFACE 4
SAVE equilibrium_phases 4
SAVE surface 4
end

Median Metal Oxides/Charge Balance on Chloride

SELECTED_OUTPUT 1

-file BAL_845_605_median_cb-true_out.csv

-charge_balance true

-percent_error true

-totals S(6) B Li As C(4) Cl F Ca Mg Na K Ba Si P Mn Fe Al Sb Be Cd Cr Co Pb Mo Se Hfo_s
Hfo_w Hao_

-molalities Hfo_wOH Hfo_wOH2+ Hfo_wOHSO4-2 Hfo_wSO4- Hfo_wOSi(OH)3

Hfo_wOSiO(OH)2- Hfo_wHCO3 Hfo_wCO3- Hfo_wPO4-2

Hfo_wHPO4- Hfo_wH2PO4 Hfo_sCO3- Hfo_sHCO3

Hfo_sHPO4- Hfo_sH2BO3 Hfo_sH2PO4 Hfo_sOSi(OH)3

Hfo_sOSiO(OH)2- Hfo_sOHSO4-2 Hfo_sSO4-

Hao_SO4- Hao_OHSO4-2 Hao_H2BO3 Hao_H3BO4-

-equilibrium_phases Ferrihydrite Gibbsite Barite Calcite Dolomite(ordered) Gypsum

-saturation_indices Ferrihydrite Gibbsite Barite Calcite Dolomite(ordered) Gypsum

SOLUTION 1 #MW-150 (C - PMP)

redox pe

units mg/l

density 1

pH 7.055

pe 3.36

temp 13.8

S(6) 911 as SO4

B 4.25

Li 0.0504

As 0.002425

C(4) 194.5 as CO3

Cl 54.5 charge

F 0.725

Ca 204.5

Mg 159

Na 107.9

K 0.8785

Ba 0.0182

Si 9.875

P 0.0275

Mn 0.00315

Fe 0.0383

Al 0.017625

Sb 0.0002

Be 0.0001

Cd 0.000175

Cr 0.00105

Co 0.00005

Pb 0.00115

Mo 0.001675

Se 0.0011

end

SOLUTION 2 #MW-152 (C - PMP)

redox pe

units mg/l

density 1

pH 6.93
pe 5.81
temp 13.9
S(6) 487 as SO4
B 4.8025
Li 0.006325
As 0.002675
C(4) 236.5 as CO3
Cl 22.5 charge
F 0.35
Ca 162.5
Mg 76.75
Na 117.95
K 1.0285
Ba 0.02485
Si 9.17
P 0.009
Mn 0.01245
Fe 0.008
Al 0.010175
Sb 0.0002
Be 0.00025
Cd 0.000175
Cr 0.00255
Co 0.00095
Pb 0.002
Mo 0.001325
Se 0.00045
end

SOLUTION 3 #MW-252 (C - PMP)

redox pe
units mg/l
density 1
pH 6.715
pe 3.79
temp 16.6
S(6) 451 as SO4
B 0.1585
Li 0.01265
As 0.002725
C(4) 289 as CO3
Cl 37.5 charge
F 0.23
Ca 217
Mg 85.05
Na 99.45
K 1.785
Ba 0.0368
Si 6.885
P 0.0465
Mn 0.3445
Fe 0.30595
Al 0.0063

Sb 0.0024
Be 0.0001
Cd 0.000175
Cr 0.00315
Co 0.00205
Pb 0.0019
Mo 0.001325
Se 0.0003
end

SOLUTION 4 #MW-366 (C - UA)

redox pe
units mg/l
density 1
pH 6.865
pe 5.365
temp 14.95
S(6) 499 as SO4
B 1.685
Li 0.006225
As 0.002375
C(4) 187 as CO3
Cl 47.5 charge
F 0.375
Ca 185.5
Mg 80.25
Na 59.25
K 4.05
Ba 0.03265
Si 8.305
P 0.008
Mn 0.0225
Fe 0.008
Al 0.0063
Sb 0.0004
Be 0.0001
Cd 0.000175
Cr 0.000875
Co 0.0017
Pb 0.00115
Mo 0.00305
Se 0.0003
end

EQUILIBRIUM_PHASES 1 #MW-150 (C - PMP) - median

Barite 0 0
Gypsum 0 0
Gibbsite 0 0.22
Ferrihydrite 0 0.031
Calcite 0 0.1
Dolomite(ordered) 0 0

SURFACE 1

Hfo_wOH Ferrihydrite equilibrium_phase 0.2 53400
Hfo_sOH Ferrihydrite equilibrium_phase 0.005 53400
Hao_OH Gibbsite equilibrium_phase 0.033 2496

-equil 1
save surface 1
end

EQUILIBRIUM_PHASES 2 #MW-152 (C - PMP) - median
Barite 0 0
Gypsum 0 0
Gibbsite 0 0.22
Ferrihydrite 0 0.031
Calcite 0 0.1
Dolomite(ordered) 0 0

SURFACE 2
Hfo_wOH Ferrihydrite equilibrium_phase 0.2 53400
Hfo_sOH Ferrihydrite equilibrium_phase 0.005 53400
Hao_OH Gibbsite equilibrium_phase 0.033 2496
-equil 2
save surface 2
end

EQUILIBRIUM_PHASES 3 #MW-252 (C - PMP) - median
Barite 0 0
Gypsum 0 0
Gibbsite 0 0.22
Ferrihydrite 0 0.031
Calcite 0 0.1
Dolomite(ordered) 0 0

SURFACE 3
Hfo_wOH Ferrihydrite equilibrium_phase 0.2 53400
Hfo_sOH Ferrihydrite equilibrium_phase 0.005 53400
Hao_OH Gibbsite equilibrium_phase 0.033 2496
-equil 3
save surface 3
end

EQUILIBRIUM_PHASES 4 #MW-366 (C - UA) - median
Barite 0 0
Gypsum 0 0
Gibbsite 0 0.13
Ferrihydrite 0 0.088
Calcite 0 10
Dolomite(ordered) 0 0

SURFACE 4
Hfo_wOH Ferrihydrite equilibrium_phase 0.2 53400
Hfo_sOH Ferrihydrite equilibrium_phase 0.005 53400
Hao_OH Gibbsite equilibrium_phase 0.033 2496
-equil 4
save surface 4
end

SOLUTION 5 #average background
redox pe
units mg/l
density 1
pH 7.77
pe 4.015

temp 16.15
S(6) 98.5
B 1.605
Li 0.07785
As 0.004075
C(4) 501.5
Cl 726 charge
F 2.515
Ca 10.635
Mg 4.91
Na 938.5
K 3.305
Ba 0.10605
Si 3.555
P 0.0495
Mn 0.0807
Fe 0.1155
Al 0.0268
Sb 0.0002
Be 0.0001
Cd 0.000175
Cr 0.0012
Co 0.00005
Pb 0.00115
Mo 0.007875
Se 0.0003

SAVE solution 5

end

#FIRST REACTION

#MW-150 (C - PMP) - First Reaction

USE SOLUTION 5

USE EQUILIBRIUM_PHASES 1

USE SURFACE 1

SAVE equilibrium_phases 1

SAVE surface 1

end

#MW-150 (C - PMP) - Second Reaction

USE SOLUTION 5

USE EQUILIBRIUM_PHASES 1

USE SURFACE 1

SAVE equilibrium_phases 1

SAVE surface 1

end

#MW-152 (C - PMP) - First Reaction

USE SOLUTION 5

USE EQUILIBRIUM_PHASES 2

USE SURFACE 2

SAVE equilibrium_phases 2

SAVE surface 2

end

#MW-152 (C - PMP) - Second Reaction

USE SOLUTION 5
USE EQUILIBRIUM_PHASES 2
USE SURFACE 2
SAVE equilibrium_phases 2
SAVE surface 2
end

#MW-252 (C - PMP) - First Reaction
USE SOLUTION 5
USE EQUILIBRIUM_PHASES 3
USE SURFACE 3
SAVE equilibrium_phases 3
SAVE surface 3
end

#MW-252 (C - PMP) - Second Reaction
USE SOLUTION 5
USE EQUILIBRIUM_PHASES 3
USE SURFACE 3
SAVE equilibrium_phases 3
SAVE surface 3
end

#MW-366 (C - UA) - First Reaction
USE SOLUTION 5
USE EQUILIBRIUM_PHASES 4
USE SURFACE 4
SAVE equilibrium_phases 4
SAVE surface 4
end

#MW-366 (C - UA) - Second Reaction
USE SOLUTION 5
USE EQUILIBRIUM_PHASES 4
USE SURFACE 4
SAVE equilibrium_phases 4
SAVE surface 4
end

Database

#\$Id: minteq.v4.dat 12387 2017-02-09 16:41:47Z dlpark \$

SOLUTION_MASTER_SPECIES

Alkalinity CO3-2 2.0 HCO3 61.0173

E e- 0 0 0

O H2O 0 0 16.00

O(-2) H2O 0 0

O(0) O2 0 0

Ag Ag+ 0.0 Ag 107.868

Al Al+3 0.0 Al 26.9815

As H3AsO4 -1.0 As 74.9216

As(3) H3AsO3 0.0 As

As(5) H3AsO4 -1.0 As

B H3BO3 0.0 B 10.81

Ba Ba+2 0.0 Ba 137.33

Be Be+2 0.0 Be 9.0122

Br Br- 0.0 Br 79.904

C CO3-2 2.0 CO3 12.0111

C(4) CO3-2 2.0 CO3 12.0111

Cyanide Cyanide- 1.0 Cyanide 26.0177

Dom_a Dom_a 0.0 C 12.0111

Dom_b Dom_b 0.0 C 12.0111

Dom_c Dom_c 0.0 C 12.0111

Ca Ca+2 0.0 Ca 40.078

Cd Cd+2 0.0 Cd 112.41

Cl Cl- 0.0 Cl 35.453

Co Co+3 -1.0 Co 58.9332

Co(2) Co+2 0.0 Co

Co(3) Co+3 -1.0 Co

Cr CrO4-2 1.0 Cr 51.996

Cr(2) Cr+2 0.0 Cr

Cr(3) Cr(OH)2+ 0.0 Cr

Cr(6) CrO4-2 1.0 Cr

Cu Cu+2 0.0 Cu 63.546

Cu(1) Cu+ 0.0 Cu

Cu(2) Cu+2 0.0 Cu

F F- 0.0 F 18.9984

Fe Fe+3 -2.0 Fe 55.847

Fe(2) Fe+2 0.0 Fe

Fe(3) Fe+3 -2.0 Fe

H H+ -1.0 H 1.0079

H(0) H2 0 H

H(1) H+ -1.0 H

Hg Hg(OH)2 0.0 Hg 200.59

Hg(0) Hg 0.0 Hg

Hg(1) Hg2+2 0.0 Hg

Hg(2) Hg(OH)2 0.0 Hg

I I- 0.0 I 126.904

K K+ 0.0 K 39.0983

Li Li+ 0.0 Li 6.941

Mg Mg+2 0.0 Mg 24.305

Mn Mn+3 0.0 Mn 54.938

Mn(2) Mn+2 0.0 Mn
Mn(3) Mn+3 0.0 Mn
Mn(6) MnO4-2 0.0 Mn
Mn(7) MnO4- 0.0 Mn
Mo MoO4-2 0.0 Mo 95.94
N NO3- 0.0 N 14.0067
N(-3) NH4+ 0.0 N
N(3) NO2- 0.0 N
N(5) NO3- 0.0 N
Na Na+ 0.0 Na 22.9898
Ni Ni+2 0.0 Ni 58.69
P PO4-3 2.0 P 30.9738
Pb Pb+2 0.0 Pb 207.2
S SO4-2 0.0 SO4 32.066
S(-2) HS- 1.0 S
#S(0) S 0.0 S
S(6) SO4-2 0.0 SO4
Sb Sb(OH)6- 0.0 Sb 121.75
Sb(3) Sb(OH)3 0.0 Sb
Sb(5) Sb(OH)6- 0.0 Sb
Se SeO4-2 0.0 Se 78.96
Se(-2) HSe- 0.0 Se
Se(4) HSeO3- 0.0 Se
Se(6) SeO4-2 0.0 Se
Si H4SiO4 0.0 SiO2 28.0843
Sn Sn(OH)6-2 0.0 Sn 118.71
Sn(2) Sn(OH)2 0.0 Sn
Sn(4) Sn(OH)6-2 0.0 Sn
Sr Sr+2 0.0 Sr 87.62
Ti Ti(OH)3 0.0 Ti 204.383
Ti(1) Ti+ 0.0 Ti
Ti(3) Ti(OH)3 0.0 Ti
U UO2+2 0.0 U 238.029
U(3) U+3 0.0 U
U(4) U+4 -4.0 U
U(5) UO2+ 0.0 U
U(6) UO2+2 0.0 U
V VO2+ -2.0 V 50.94
V(2) V+2 0.0 V
V(3) V+3 -3.0 V
V(4) VO+2 0.0 V
V(5) VO2+ -2.0 V
Zn Zn+2 0.0 Zn 65.39
Benzoate Benzoate- 0.0 121.116 121.116
Phenylacetate Phenylacetate- 0.0 135.142 135.142
Isophthalate Isophthalate-2 0.0 164.117 164.117
Diethylamine Diethylamine 1.0 73.138 73.138
Butylamine Butylamine 1.0 73.138 73.138
Methylamine Methylamine 1.0 31.057 31.057
Dimethylamine Dimethylamine 1.0 45.084 45.084
Hexylamine Hexylamine 1.0 101.192 101.192
Ethylenediamine Ethylenediamine 2.0 60.099 60.099
Propylamine Propylamine 1.0 59.111 59.111
Isopropylamine Isopropylamine 1.0 59.111 59.111

Trimethylamine Trimethylamine 1.0 59.111 59.111
 Citrate Citrate-3 2.0 189.102 189.102
 Nta Nta-3 1.0 188.117 188.117
 Edta Edta-4 2.0 288.214 288.214
 Propionate Propionate- 1.0 73.072 73.072
 Butyrate Butyrate- 1.0 87.098 87.098
 Isobutyrate Isobutyrate- 1.0 87.098 87.098
 Two_picoline Two_picoline 1.0 93.128 93.128
 Three_picoline Three_picoline 1.0 93.128 93.128
 Four_picoline Four_picoline 1.0 93.128 93.128
 Formate Formate- 0.0 45.018 45.018
 Isovalerate Isovalerate- 1.0 101.125 101.125
 Valerate Valerate- 1.0 101.125 101.125
 Acetate Acetate- 1.0 59.045 59.045
 Tartarate Tartarate-2 0.0 148.072 148.072
 Glycine Glycine- 1.0 74.059 74.059
 Salicylate Salicylate-2 1.0 136.107 136.107
 Glutamate Glutamate-2 1.0 145.115 145.115
 Phthalate Phthalate-2 1.0 164.117 164.117
 SOLUTION_SPECIES
 e- = e-
 log_k 0
 H2O = H2O
 log_k 0
 Ag+ = Ag+
 log_k 0
 Al+3 = Al+3
 log_k 0
 H3AsO4 = H3AsO4
 log_k 0
 H3BO3 = H3BO3
 log_k 0
 Ba+2 = Ba+2
 log_k 0
 Be+2 = Be+2
 log_k 0
 Br- = Br-
 log_k 0
 CO3-2 = CO3-2
 log_k 0
 Cyanide- = Cyanide-
 log_k 0
 Dom_a = Dom_a
 log_k 0
 Dom_b = Dom_b
 log_k 0
 Dom_c = Dom_c
 log_k 0
 Ca+2 = Ca+2
 log_k 0
 Cd+2 = Cd+2
 log_k 0
 Cl- = Cl-
 log_k 0

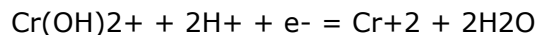
Co+3 = Co+3
log_k 0
CrO4-2 = CrO4-2
log_k 0
Cu+2 = Cu+2
log_k 0
F- = F-
log_k 0
Fe+3 = Fe+3
log_k 0
H+ = H+
log_k 0
Hg(OH)2 = Hg(OH)2
log_k 0
I- = I-
log_k 0
K+ = K+
log_k 0
Li+ = Li+
log_k 0
Mg+2 = Mg+2
log_k 0
Mn+3 = Mn+3
log_k 0
MoO4-2 = MoO4-2
log_k 0
NO3- = NO3-
log_k 0
Na+ = Na+
log_k 0
Ni+2 = Ni+2
log_k 0
PO4-3 = PO4-3
log_k 0
Pb+2 = Pb+2
log_k 0
SO4-2 = SO4-2
log_k 0
Sb(OH)6- = Sb(OH)6-
log_k 0
SeO4-2 = SeO4-2
log_k 0
H4SiO4 = H4SiO4
log_k 0
Sn(OH)6-2 = Sn(OH)6-2
log_k 0
Sr+2 = Sr+2
log_k 0
Ti(OH)3 = Ti(OH)3
log_k 0
UO2+2 = UO2+2
log_k 0
VO2+ = VO2+
log_k 0

Benzoate- = Benzoate-
log_k 0
Phenylacetate- = Phenylacetate-
log_k 0
Isophthalate-2 = Isophthalate-2
log_k 0
Zn+2 = Zn+2
log_k 0
Diethylamine = Diethylamine
log_k 0
Butylamine = Butylamine
log_k 0
Methylamine = Methylamine
log_k 0
Dimethylamine = Dimethylamine
log_k 0
Hexylamine = Hexylamine
log_k 0
Ethylenediamine = Ethylenediamine
log_k 0
Propylamine = Propylamine
log_k 0
Isopropylamine = Isopropylamine
log_k 0
Trimethylamine = Trimethylamine
log_k 0
Citrate-3 = Citrate-3
log_k 0
Nta-3 = Nta-3
log_k 0
Edta-4 = Edta-4
log_k 0
Propionate- = Propionate-
log_k 0
Butyrate- = Butyrate-
log_k 0
Isobutyrate- = Isobutyrate-
log_k 0
Two_picoline = Two_picoline
log_k 0
Three_picoline = Three_picoline
log_k 0
Four_picoline = Four_picoline
log_k 0
Formate- = Formate-
log_k 0
Isovalerate- = Isovalerate-
log_k 0
Valerate- = Valerate-
log_k 0
Acetate- = Acetate-
log_k 0
Tartarate-2 = Tartarate-2
log_k 0

Glycine- = Glycine-
 log_k 0
 Salicylate-2 = Salicylate-2
 log_k 0
 Glutamate-2 = Glutamate-2
 log_k 0
 Phthalate-2 = Phthalate-2
 log_k 0
 SOLUTION_SPECIES
 $\text{Fe}^{+3} + \text{e}^- = \text{Fe}^{+2}$
 log_k 13.032
 delta_h -42.7 kJ
 -gamma 0 0
 # Id: 2802810
 # log K source: Bard85
 # Delta H source: Bard85
 #T and ionic strength:
 $\text{H}_3\text{AsO}_4 + 2\text{e}^- + 2\text{H}^+ = \text{H}_3\text{AsO}_3 + \text{H}_2\text{O}$
 log_k 18.898
 delta_h -125.6 kJ
 -gamma 0 0
 # Id: 600610
 # log K source: Bard85
 # Delta H source: MTQ3.11
 #T and ionic strength:
 $\text{Sb}(\text{OH})_6^- + 2\text{e}^- + 3\text{H}^+ = \text{Sb}(\text{OH})_3 + 3\text{H}_2\text{O}$
 log_k 24.31
 delta_h 0 kJ
 -gamma 0 0
 # Id: 7407410
 # log K source: Bard85
 # Delta H source: MTQ3.11
 #T and ionic strength:
 $\text{UO}_2^{+2} + 3\text{e}^- + 4\text{H}^+ = \text{U}^{+3} + 2\text{H}_2\text{O}$
 log_k 0.42
 delta_h -42 kJ
 -gamma 0 0
 # Id: 8908930
 # log K source: MTQ3.11
 # Delta H source: MTQ3.11
 #T and ionic strength:
 $\text{UO}_2^{+2} + 2\text{e}^- + 4\text{H}^+ = \text{U}^{+4} + 2\text{H}_2\text{O}$
 log_k 9.216
 delta_h -144.1 kJ
 -gamma 0 0
 # Id: 8918930
 # log K source: MTQ3.11
 # Delta H source: MTQ3.11
 #T and ionic strength:
 $\text{UO}_2^{+2} + \text{e}^- = \text{UO}_2^+$
 log_k 2.785
 delta_h -13.8 kJ
 -gamma 0 0
 # Id: 8928930

log K source: MTQ3.11
 # Delta H source: MTQ3.11
 #T and ionic strength:
 $\text{e}^- + \text{Mn}^{+3} = \text{Mn}^{+2}$
 log_k 25.35
 delta_h -107.8 kJ
 -gamma 0 0
 # Id: 4704710
 # log K source: Bard85
 # Delta H source: MTQ3.11
 #T and ionic strength:
 $\text{Co}^{+3} + \text{e}^- = \text{Co}^{+2}$
 log_k 32.4
 delta_h 0 kJ
 -gamma 0 0
 # Id: 2002010
 # log K source: Bard85
 # Delta H source: MTQ3.11
 #T and ionic strength:
 $\text{Cu}^{+2} + \text{e}^- = \text{Cu}^{+}$
 log_k 2.69
 delta_h 6.9 kJ
 -gamma 0 0
 # Id: 2302310
 # log K source: Bard85
 # Delta H source: MTQ3.11
 #T and ionic strength:
 $\text{V}^{+3} + \text{e}^- = \text{V}^{+2}$
 log_k -4.31
 delta_h 0 kJ
 -gamma 0 0
 # Id: 9009010
 # log K source: Bard85
 # Delta H source: MTQ3.11
 #T and ionic strength:
 $\text{VO}^{+2} + \text{e}^- + 2\text{H}^+ = \text{V}^{+3} + \text{H}_2\text{O}$
 log_k 5.696
 delta_h 0 kJ
 -gamma 0 0
 # Id: 9019020
 # log K source: Bard85
 # Delta H source: MTQ3.11
 #T and ionic strength:
 $\text{VO}_2^+ + \text{e}^- + 2\text{H}^+ = \text{VO}^{+2} + \text{H}_2\text{O}$
 log_k 16.903
 delta_h -122.7 kJ
 -gamma 0 0
 # Id: 9029030
 # log K source: Bard85
 # Delta H source: MTQ3.11
 #T and ionic strength:
 $\text{SO}_4^{-2} + 9\text{H}^+ + 8\text{e}^- = \text{HS}^- + 4\text{H}_2\text{O}$
 log_k 33.66
 delta_h -60.14 kJ

-gamma 0 0
 # Id: 7307320
 # log K source: MTQ3.11
 # Delta H source: MTQ3.11
 #T and ionic strength:
 $\text{Sn(OH)}_6^{2-} + 2e^- + 4\text{H}^+ = \text{Sn(OH)}_2 + 4\text{H}_2\text{O}$
 log_k 19.2
 delta_h 0 kJ
 -gamma 0 0
 # Id: 7907910
 # log K source: Bard85
 # Delta H source: MTQ3.11
 #T and ionic strength:
 $\text{Tl(OH)}_3 + 2e^- + 3\text{H}^+ = \text{Tl}^+ + 3\text{H}_2\text{O}$
 log_k 45.55
 delta_h 0 kJ
 -gamma 0 0
 # Id: 8708710
 # log K source: Bard85
 # Delta H source: MTQ3.11
 #T and ionic strength:
 $\text{HSeO}_3^- + 6e^- + 6\text{H}^+ = \text{HSe}^- + 3\text{H}_2\text{O}$
 log_k 44.86
 delta_h 0 kJ
 -gamma 0 0
 # Id: 7607610
 # log K source: Bard85
 # Delta H source: MTQ3.11
 #T and ionic strength:
 $\text{SeO}_4^{2-} + 2e^- + 3\text{H}^+ = \text{HSeO}_3^- + \text{H}_2\text{O}$
 log_k 36.308
 delta_h -201.2 kJ
 -gamma 0 0
 # Id: 7617620
 # log K source: Bard85
 # Delta H source: MTQ3.11
 #T and ionic strength:
 $0.5\text{Hg}_2^{2+} + e^- = \text{Hg}$
 log_k 6.5667
 delta_h -45.735 kJ
 -gamma 0 0
 # Id: 3600000
 # log K source: NIST2.1.1
 # Delta H source: NIST2.1.1
 #T and ionic strength:
 $2\text{Hg(OH)}_2 + 4\text{H}^+ + 2e^- = \text{Hg}_2^{2+} + 4\text{H}_2\text{O}$
 log_k 43.185
 delta_h -63.59 kJ
 -gamma 0 0
 # Id: 3603610
 # log K source: Bard85
 # Delta H source: MTQ3.11
 #T and ionic strength:



log_k 2.947

delta_h 6.36 kJ

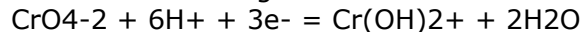
-gamma 0 0

Id: 2102110

log K source: MTQ3.11

Delta H source: MTQ3.11

#T and ionic strength:



log_k 67.376

delta_h -103 kJ

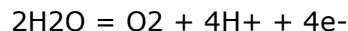
-gamma 0 0

Id: 2112120

log K source: MTQ3.11

Delta H source: MTQ3.11

#T and ionic strength:



Adjusted for equation to aqueous species

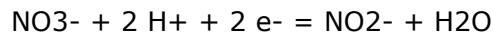
log_k -85.9951

-analytic 38.0229 7.99407E-03 -2.7655e+004 -1.4506e+001 199838.45



log_k -3.15

delta_h -1.759 kcal



log_k 28.570

delta_h -43.760 kcal

-gamma 3.0000 0.0000



log_k 119.077

delta_h -187.055 kcal

-gamma 2.5000 0.0000



log_k -127.794

delta_h 822.67 kJ

-gamma 3 0

Id: 4700020

log K source: NIST2.1.1

Delta H source: NIST2.1.1

#T and ionic strength:



log_k -118.422

delta_h 711.07 kJ

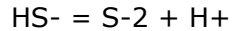
-gamma 5 0

Id: 4700021

log K source: NIST2.1.1

Delta H source: NIST2.1.1

#T and ionic strength:



log_k -17.3

delta_h 49.4 kJ

-gamma 5 0

Id: 3307301

log K source: LMa1987
 # Delta H source: NIST2.1.1
 #T and ionic strength: 0.00 25.0
 $\text{HSe}^- = \text{Se}^{2-} + \text{H}^+$
 log_k -15
 delta_h 48.116 kJ
 -gamma 0 0
 # Id: 3307601
 # log K source: SCD3.02 (1968 DKa)
 # Delta H source: MTQ3.11
 #T and ionic strength: 0.00 25.0
 $\text{Ti}(\text{OH})_3 + 3\text{H}^+ = \text{Ti}^{3+} + 3\text{H}_2\text{O}$
 log_k 3.291
 delta_h 0 kJ
 -gamma 0 0
 # Id: 8713300
 # log K source: NIST46.3
 # Delta H source: MTQ3.11
 #T and ionic strength: 0.00 25.0
 $0.5\text{Hg}_2^{2+} + \text{e}^- = \text{Hg}$
 log_k 6.5667
 delta_h -45.735 kJ
 -gamma 0 0
 # Id: 3600000
 # log K source: NIST2.1.1
 # Delta H source: NIST2.1.1
 #T and ionic strength:
 $\text{Hg}(\text{OH})_2 + 2\text{H}^+ = \text{Hg}^{2+} + 2\text{H}_2\text{O}$
 log_k 6.194
 delta_h -39.72 kJ
 -gamma 0 0
 # Id: 3613300
 # log K source: NIST46.3
 # Delta H source: NIST46.3
 #T and ionic strength: 0.00 25.0
 $\text{Cr}(\text{OH})_2^{2+} + 2\text{H}^+ = \text{Cr}^{3+} + 2\text{H}_2\text{O}$
 log_k 9.5688
 delta_h -129.62 kJ
 -gamma 0 0
 # Id: 2113300
 # log K source: NIST46.3
 # Delta H source: NIST46.3
 #T and ionic strength: 0.10 20.0
 $\text{H}_2\text{O} = \text{OH}^- + \text{H}^+$
 log_k -13.997
 delta_h 55.81 kJ
 -gamma 3.5 0
 # Id: 3300020
 # log K source: NIST46.4
 # Delta H source: NIST46.4
 #T and ionic strength: 0.00 25.0
 $\text{Sn}(\text{OH})_2 + 2\text{H}^+ = \text{Sn}^{2+} + 2\text{H}_2\text{O}$
 log_k 7.094
 delta_h 0 kJ

-gamma 0 0
 # Id: 7903301
 # log K source: NIST46.4
 # Delta H source: MTQ3.11
 #T and ionic strength: 0.00 25.0
 $\text{Sn(OH)}_2 + \text{H}^+ = \text{SnOH}^+ + \text{H}_2\text{O}$
 log_k 3.697
 delta_h 0 kJ
 -gamma 0 0
 # Id: 7903302
 # log K source: NIST46.4
 # Delta H source: MTQ3.11
 #T and ionic strength: 0.00 25.0
 $\text{Sn(OH)}_2 + \text{H}_2\text{O} = \text{Sn(OH)}_3^- + \text{H}^+$
 log_k -9.497
 delta_h 0 kJ
 -gamma 0 0
 # Id: 7903303
 # log K source: NIST46.4
 # Delta H source: MTQ3.11
 #T and ionic strength: 0.00 25.0
 $2\text{Sn(OH)}_2 + 2\text{H}^+ = \text{Sn}_2(\text{OH})_2^{2+} + 2\text{H}_2\text{O}$
 log_k 9.394
 delta_h 0 kJ
 -gamma 0 0
 # Id: 7903304
 # log K source: NIST46.4
 # Delta H source: MTQ3.11
 #T and ionic strength: 0.00 25.0
 $3\text{Sn(OH)}_2 + 2\text{H}^+ = \text{Sn}_3(\text{OH})_4^{2+} + 2\text{H}_2\text{O}$
 log_k 14.394
 delta_h 0 kJ
 -gamma 0 0
 # Id: 7903305
 # log K source: NIST46.4
 # Delta H source: MTQ3.11
 #T and ionic strength: 0.00 25.0
 $\text{Sn(OH)}_2 = \text{HSnO}_2^- + \text{H}^+$
 log_k -8.9347
 delta_h 0 kJ
 -gamma 0 0
 # Id: 7903306
 # log K source: Bard85
 # Delta H source: MTQ3.11
 #T and ionic strength:
 $\text{Sn(OH)}_6^{2-} + 6\text{H}^+ = \text{Sn}^{4+} + 6\text{H}_2\text{O}$
 log_k 21.2194
 delta_h 0 kJ
 -gamma 0 0
 # Id: 7913301
 # log K source: Bard85
 # Delta H source: MTQ3.11
 #T and ionic strength:
 $\text{Sn(OH)}_6^{2-} = \text{SnO}_3^{2-} + 3\text{H}_2\text{O}$

log_k -2.2099
 delta_h 0 kJ
 -gamma 0 0
 # Id: 7913302
 # log K source: Bard85
 # Delta H source: MTQ3.11
 #T and ionic strength:
 $\text{Pb}^{+2} + \text{H}_2\text{O} = \text{PbOH}^+ + \text{H}^+$
 log_k -7.597
 delta_h 0 kJ
 -gamma 0 0
 # Id: 6003300
 # log K source: NIST46.3
 # Delta H source: MTQ3.11
 #T and ionic strength: 0.00 25.0
 $\text{Pb}^{+2} + 2\text{H}_2\text{O} = \text{Pb(OH)}_2 + 2\text{H}^+$
 log_k -17.094
 delta_h 0 kJ
 -gamma 0 0
 # Id: 6003301
 # log K source: NIST46.3
 # Delta H source: MTQ3.11
 #T and ionic strength: 0.00 25.0
 $\text{Pb}^{+2} + 3\text{H}_2\text{O} = \text{Pb(OH)}_3^- + 3\text{H}^+$
 log_k -28.091
 delta_h 0 kJ
 -gamma 0 0
 # Id: 6003302
 # log K source: NIST46.3
 # Delta H source: MTQ3.11
 #T and ionic strength: 0.00 25.0
 $2\text{Pb}^{+2} + \text{H}_2\text{O} = \text{Pb}_2\text{OH}^{+3} + \text{H}^+$
 log_k -6.397
 delta_h 0 kJ
 -gamma 0 0
 # Id: 6003303
 # log K source: NIST46.3
 # Delta H source: MTQ3.11
 #T and ionic strength: 0.00 25.0
 $3\text{Pb}^{+2} + 4\text{H}_2\text{O} = \text{Pb}_3(\text{OH})_4^{+2} + 4\text{H}^+$
 log_k -23.888
 delta_h 115.24 kJ
 -gamma 0 0
 # Id: 6003304
 # log K source: NIST46.3
 # Delta H source: NIST46.3
 #T and ionic strength: 0.00 25.0
 $\text{Pb}^{+2} + 4\text{H}_2\text{O} = \text{Pb(OH)}_4^{-2} + 4\text{H}^+$
 log_k -39.699
 delta_h 0 kJ
 -gamma 0 0
 # Id: 6003305
 # log K source: MTQ3.11
 # Delta H source: MTQ3.11

#T and ionic strength:
 $4\text{Pb}^{+2} + 4\text{H}_2\text{O} = \text{Pb}_4(\text{OH})_4^{+4} + 4\text{H}^+$
 log_k -19.988
 delta_h 88.24 kJ
 -gamma 0 0
 # Id: 6003306
 # log K source: NIST46.4
 # Delta H source: NIST46.4
 #T and ionic strength: 0.00 25.0
 $\text{H}_3\text{BO}_3 + \text{F}^- = \text{BF}(\text{OH})_3^-$
 log_k -0.399
 delta_h 7.7404 kJ
 -gamma 2.5 0
 # Id: 902700
 # log K source: MTQ3.11
 # Delta H source: MTQ3.11
 #T and ionic strength:
 $\text{H}_3\text{BO}_3 + 2\text{F}^- + \text{H}^+ = \text{BF}_2(\text{OH})_2^- + \text{H}_2\text{O}$
 log_k 7.63
 delta_h 6.8408 kJ
 -gamma 2.5 0
 # Id: 902701
 # log K source: MTQ3.11
 # Delta H source: MTQ3.11
 #T and ionic strength:
 $\text{H}_3\text{BO}_3 + 3\text{F}^- + 2\text{H}^+ = \text{BF}_3\text{OH}^- + 2\text{H}_2\text{O}$
 log_k 13.22
 delta_h -20.4897 kJ
 -gamma 2.5 0
 # Id: 902702
 # log K source: NIST2.1.1
 # Delta H source: NIST2.1.1
 #T and ionic strength:
 $\text{Al}^{+3} + \text{H}_2\text{O} = \text{AlOH}^{+2} + \text{H}^+$
 log_k -4.997
 delta_h 47.81 kJ
 -gamma 5.4 0
 # Id: 303300
 # log K source: NIST46.3
 # Delta H source: NIST46.3
 #T and ionic strength: 0.00 25.0
 $\text{Al}^{+3} + 2\text{H}_2\text{O} = \text{Al}(\text{OH})_2^{+} + 2\text{H}^+$
 log_k -10.094
 delta_h 0 kJ
 -gamma 5.4 0
 # Id: 303301
 # log K source: NIST46.3
 # Delta H source: MTQ3.11
 #T and ionic strength: 0.00 25.0
 $\text{Al}^{+3} + 3\text{H}_2\text{O} = \text{Al}(\text{OH})_3 + 3\text{H}^+$
 log_k -16.791
 delta_h 0 kJ
 -gamma 0 0
 # Id: 303303

log K source: NIST46.3
 # Delta H source: MTQ3.11
 #T and ionic strength: 0.00 25.0
 $\text{Al}^{3+} + 4\text{H}_2\text{O} = \text{Al}(\text{OH})_4^- + 4\text{H}^+$
 log_k -22.688
 delta_h 173.24 kJ
 -gamma 4.5 0
 # Id: 303302
 # log K source: NIST46.3
 # Delta H source: NIST46.3
 #T and ionic strength: 0.00 25.0
 $\text{Ti}^+ + \text{H}_2\text{O} = \text{TiOH} + \text{H}^+$
 log_k -13.207
 delta_h 56.81 kJ
 -gamma 0 0
 # Id: 8703300
 # log K source: NIST46.3
 # Delta H source: NIST46.3
 #T and ionic strength: 0.00 25.0
 $\text{Ti}(\text{OH})_3 + 2\text{H}^+ = \text{TiOH}_2^+ + 2\text{H}_2\text{O}$
 log_k 2.694
 delta_h 0 kJ
 -gamma 0 0
 # Id: 8713301
 # log K source: NIST46.3
 # Delta H source: NIST46.3
 #T and ionic strength: 0.00 25.0
 $\text{Ti}(\text{OH})_3 + \text{H}^+ = \text{Ti}(\text{OH})_2^+ + \text{H}_2\text{O}$
 log_k 1.897
 delta_h 0 kJ
 -gamma 0 0
 # Id: 8713302
 # log K source: NIST46.3
 # Delta H source: MTQ3.11
 #T and ionic strength: 0.00 25.0
 $\text{Ti}(\text{OH})_3 + \text{H}_2\text{O} = \text{Ti}(\text{OH})_4^- + \text{H}^+$
 log_k -11.697
 delta_h 0 kJ
 -gamma 0 0
 # Id: 8713303
 # log K source: NIST46.3
 # Delta H source: MTQ3.11
 #T and ionic strength: 0.00 25.0
 $\text{Zn}^{2+} + \text{H}_2\text{O} = \text{ZnOH}^+ + \text{H}^+$
 log_k -8.997
 delta_h 55.81 kJ
 -gamma 0 0
 # Id: 9503300
 # log K source: NIST46.3
 # Delta H source: NIST46.3
 #T and ionic strength: 0.00 25.0
 $\text{Zn}^{2+} + 2\text{H}_2\text{O} = \text{Zn}(\text{OH})_2 + 2\text{H}^+$
 log_k -17.794
 delta_h 0 kJ

-gamma 0 0
 # Id: 9503301
 # log K source: NIST46.3
 # Delta H source: MTQ3.11
 #T and ionic strength: 0.00 25.0
 $\text{Zn}^{+2} + 3\text{H}_2\text{O} = \text{Zn}(\text{OH})_3^- + 3\text{H}^+$
 log_k -28.091
 delta_h 0 kJ
 -gamma 0 0
 # Id: 9503302
 # log K source: NIST46.3
 # Delta H source: MTQ3.11
 #T and ionic strength: 0.00 25.0
 $\text{Zn}^{+2} + 4\text{H}_2\text{O} = \text{Zn}(\text{OH})_4^{2-} + 4\text{H}^+$
 log_k -40.488
 delta_h 0 kJ
 -gamma 0 0
 # Id: 9503303
 # log K source: NIST46.3
 # Delta H source: MTQ3.11
 #T and ionic strength: 0.00 25.0
 $\text{Cd}^{+2} + \text{H}_2\text{O} = \text{CdOH}^+ + \text{H}^+$
 log_k -10.097
 delta_h 54.81 kJ
 -gamma 0 0
 # Id: 1603300
 # log K source: NIST46.3
 # Delta H source: NIST46.3
 #T and ionic strength: 0.00 25.0
 $\text{Cd}^{+2} + 2\text{H}_2\text{O} = \text{Cd}(\text{OH})_2 + 2\text{H}^+$
 log_k -20.294
 delta_h 0 kJ
 -gamma 0 0
 # Id: 1603301
 # log K source: NIST46.3
 # Delta H source: MTQ3.11
 #T and ionic strength: 0.00 25.0
 $\text{Cd}^{+2} + 3\text{H}_2\text{O} = \text{Cd}(\text{OH})_3^- + 3\text{H}^+$
 log_k -32.505
 delta_h 0 kJ
 -gamma 0 0
 # Id: 1603302
 # log K source: NIST46.3
 # Delta H source: MTQ3.11
 #T and ionic strength: 3.00 25.0
 $\text{Cd}^{+2} + 4\text{H}_2\text{O} = \text{Cd}(\text{OH})_4^{2-} + 4\text{H}^+$
 log_k -47.288
 delta_h 0 kJ
 -gamma 0 0
 # Id: 1603303
 # log K source: NIST46.3
 # Delta H source: MTQ3.11
 #T and ionic strength: 0.00 25.0
 $2\text{Cd}^{+2} + \text{H}_2\text{O} = \text{Cd}_2\text{OH}^{+3} + \text{H}^+$

log_k -9.397
delta_h 45.81 kJ
-gamma 0 0
Id: 1603304
log K source: NIST46.3
Delta H source: NIST46.3
#T and ionic strength: 0.00 25.0
 $\text{Hg}(\text{OH})_2 + \text{H}^+ = \text{HgOH}^+ + \text{H}_2\text{O}$
log_k 2.797
delta_h -18.91 kJ
-gamma 0 0
Id: 3613302
log K source: NIST46.3
Delta H source: NIST46.3
#T and ionic strength: 0.00 25.0
 $\text{Hg}(\text{OH})_2 + \text{H}_2\text{O} = \text{Hg}(\text{OH})_3^- + \text{H}^+$
log_k -14.897
delta_h 0 kJ
-gamma 0 0
Id: 3613303
log K source: NIST46.3
Delta H source: MTQ3.11
#T and ionic strength: 0.00 25.0
 $\text{Cu}^{+2} + \text{H}_2\text{O} = \text{CuOH}^+ + \text{H}^+$
log_k -7.497
delta_h 35.81 kJ
-gamma 4 0
Id: 2313300
log K source: NIST46.3
Delta H source: NIST46.3
#T and ionic strength: 0.00 25.0
 $\text{Cu}^{+2} + 2\text{H}_2\text{O} = \text{Cu}(\text{OH})_2 + 2\text{H}^+$
log_k -16.194
delta_h 0 kJ
-gamma 0 0
Id: 2313301
log K source: NIST46.3
Delta H source: MTQ3.11
#T and ionic strength: 0.00 25.0
 $\text{Cu}^{+2} + 3\text{H}_2\text{O} = \text{Cu}(\text{OH})_3^- + 3\text{H}^+$
log_k -26.879
delta_h 0 kJ
-gamma 0 0
Id: 2313302
log K source: NIST46.3
Delta H source: MTQ3.11
#T and ionic strength: 1.00 25.0
 $\text{Cu}^{+2} + 4\text{H}_2\text{O} = \text{Cu}(\text{OH})_4^{-2} + 4\text{H}^+$
log_k -39.98
delta_h 0 kJ
-gamma 0 0
Id: 2313303
log K source: NIST46.3
Delta H source: MTQ3.11

#T and ionic strength: 1.00 25.0
 $2\text{Cu}^{+2} + 2\text{H}_2\text{O} = \text{Cu}_2(\text{OH})_2^{+2} + 2\text{H}^{+}$
 log_k -10.594
 delta_h 76.62 kJ
 -gamma 0 0
 # Id: 2313304
 # log K source: NIST46.3
 # Delta H source: NIST46.3
 #T and ionic strength: 0.00 25.0
 $\text{Ag}^{+} + \text{H}_2\text{O} = \text{AgOH} + \text{H}^{+}$
 log_k -11.997
 delta_h 0 kJ
 -gamma 0 0
 # Id: 203300
 # log K source: NIST46.3
 # Delta H source: MTQ3.11
 #T and ionic strength: 0.00 25.0
 $\text{Ag}^{+} + 2\text{H}_2\text{O} = \text{Ag}(\text{OH})_2^{-} + 2\text{H}^{+}$
 log_k -24.004
 delta_h 0 kJ
 -gamma 0 0
 # Id: 203301
 # log K source: NIST46.3
 # Delta H source: MTQ3.11
 #T and ionic strength: 0.00 25.0
 $\text{Ni}^{+2} + \text{H}_2\text{O} = \text{NiOH}^{+} + \text{H}^{+}$
 log_k -9.897
 delta_h 51.81 kJ
 -gamma 0 0
 # Id: 5403300
 # log K source: NIST46.3
 # Delta H source: NIST46.3
 #T and ionic strength: 0.00 25.0
 $\text{Ni}^{+2} + 2\text{H}_2\text{O} = \text{Ni}(\text{OH})_2 + 2\text{H}^{+}$
 log_k -18.994
 delta_h 0 kJ
 -gamma 0 0
 # Id: 5403301
 # log K source: NIST46.3
 # Delta H source: MTQ3.11
 #T and ionic strength: 0.00 25.0
 $\text{Ni}^{+2} + 3\text{H}_2\text{O} = \text{Ni}(\text{OH})_3^{-} + 3\text{H}^{+}$
 log_k -29.991
 delta_h 0 kJ
 -gamma 0 0
 # Id: 5403302
 # log K source: NIST46.3
 # Delta H source: MTQ3.11
 #T and ionic strength: 0.00 25.0
 $\text{Co}^{+2} + \text{H}_2\text{O} = \text{CoOH}^{+} + \text{H}^{+}$
 log_k -9.697
 delta_h 0 kJ
 -gamma 0 0
 # Id: 2003300

log K source: NIST46.4
 # Delta H source: MTQ3.11
 #T and ionic strength: 0.00 25.0
 $\text{Co}^{+2} + 2\text{H}_2\text{O} = \text{Co}(\text{OH})_2 + 2\text{H}^+$
 log_k -18.794
 delta_h 0 kJ
 -gamma 0 0
 # Id: 2003301
 # log K source: NIST46.4
 # Delta H source: MTQ3.11
 #T and ionic strength: 0.00 25.0
 $\text{Co}^{+2} + 3\text{H}_2\text{O} = \text{Co}(\text{OH})_3^- + 3\text{H}^+$
 log_k -31.491
 delta_h 0 kJ
 -gamma 0 0
 # Id: 2003302
 # log K source: NIST46.4
 # Delta H source: MTQ3.11
 #T and ionic strength: 0.00 25.0
 $\text{Co}^{+2} + 4\text{H}_2\text{O} = \text{Co}(\text{OH})_4^{-2} + 4\text{H}^+$
 log_k -46.288
 delta_h 0 kJ
 -gamma 0 0
 # Id: 2003303
 # log K source: NIST46.4
 # Delta H source: MTQ3.11
 #T and ionic strength: 0.00 25.0
 $2\text{Co}^{+2} + \text{H}_2\text{O} = \text{Co}_2\text{OH}^{+3} + \text{H}^+$
 log_k -10.997
 delta_h 0 kJ
 -gamma 0 0
 # Id: 2003304
 # log K source: NIST46.4
 # Delta H source: MTQ3.11
 #T and ionic strength: 0.00 25.0
 $4\text{Co}^{+2} + 4\text{H}_2\text{O} = \text{Co}_4(\text{OH})_4^{+4} + 4\text{H}^+$
 log_k -30.488
 delta_h 0 kJ
 -gamma 0 0
 # Id: 2003306
 # log K source: NIST46.4
 # Delta H source: MTQ3.11
 #T and ionic strength: 0.00 25.0
 $\text{Co}^{+2} + 2\text{H}_2\text{O} = \text{CoOOH}^- + 3\text{H}^+$
 log_k -32.0915
 delta_h 260.454 kJ
 -gamma 0 0
 # Id: 2003305
 # log K source: NIST2.1.1
 # Delta H source: MTQ3.11
 #T and ionic strength:
 $\text{Co}^{+3} + \text{H}_2\text{O} = \text{CoOH}^{+2} + \text{H}^+$
 log_k -1.291
 delta_h 0 kJ

-gamma 0 0
Id: 2013300
log K source: NIST46.4
Delta H source: MTQ3.11
#T and ionic strength: 3.00 25.0
 $\text{Fe}^{+2} + \text{H}_2\text{O} = \text{FeOH}^+ + \text{H}^+$
log_k -9.397
delta_h 55.81 kJ
-gamma 5 0
Id: 2803300
log K source: NIST46.3
Delta H source: NIST46.3
#T and ionic strength: 0.00 25.0
 $\text{Fe}^{+2} + 2\text{H}_2\text{O} = \text{Fe}(\text{OH})_2 + 2\text{H}^+$
log_k -20.494
delta_h 119.62 kJ
-gamma 0 0
Id: 2803302
log K source: NIST46.3
Delta H source: NIST46.3
#T and ionic strength: 0.00 25.0
 $\text{Fe}^{+2} + 3\text{H}_2\text{O} = \text{Fe}(\text{OH})_3^- + 3\text{H}^+$
log_k -28.991
delta_h 126.43 kJ
-gamma 5 0
Id: 2803301
log K source: NIST46.3
Delta H source: NIST46.3
#T and ionic strength: 0.00 25.0
 $\text{Fe}^{+3} + \text{H}_2\text{O} = \text{FeOH}^{+2} + \text{H}^+$
log_k -2.187
delta_h 41.81 kJ
-gamma 5 0
Id: 2813300
log K source: NIST46.3
Delta H source: NIST46.3
#T and ionic strength: 0.00 25.0
 $\text{Fe}^{+3} + 2\text{H}_2\text{O} = \text{Fe}(\text{OH})_2^+ + 2\text{H}^+$
log_k -4.594
delta_h 0 kJ
-gamma 5.4 0
Id: 2813301
log K source: NIST46.3
Delta H source: MTQ3.11
#T and ionic strength: 0.00 25.0
 $\text{Fe}^{+3} + 3\text{H}_2\text{O} = \text{Fe}(\text{OH})_3 + 3\text{H}^+$
log_k -12.56
delta_h 103.8 kJ
-gamma 0 0
Id: 2813302
log K source: Nord90
Delta H source: Nord90
#T and ionic strength: 0.00 25.0
 $\text{Fe}^{+3} + 4\text{H}_2\text{O} = \text{Fe}(\text{OH})_4^- + 4\text{H}^+$

log_k -21.588
 delta_h 0 kJ
 -gamma 5.4 0
 # Id: 2813303
 # log K source: NIST46.3
 # Delta H source: MTQ3.11
 #T and ionic strength: 0.00 25.0
 $2\text{Fe}^{+3} + 2\text{H}_2\text{O} = \text{Fe}_2(\text{OH})_2^{+4} + 2\text{H}^+$
 log_k -2.854
 delta_h 57.62 kJ
 -gamma 0 0
 # Id: 2813304
 # log K source: NIST46.3
 # Delta H source: NIST46.3
 #T and ionic strength: 0.00 25.0
 $3\text{Fe}^{+3} + 4\text{H}_2\text{O} = \text{Fe}_3(\text{OH})_4^{+5} + 4\text{H}^+$
 log_k -6.288
 delta_h 65.24 kJ
 -gamma 0 0
 # Id: 2813305
 # log K source: NIST46.3
 # Delta H source: NIST46.3
 #T and ionic strength: 0.00 25.0
 $\text{Mn}^{+2} + \text{H}_2\text{O} = \text{MnOH}^+ + \text{H}^+$
 log_k -10.597
 delta_h 55.81 kJ
 -gamma 5 0
 # Id: 4703300
 # log K source: NIST46.3
 # Delta H source: NIST46.3
 #T and ionic strength: 0.00 25.0
 $\text{Mn}^{+2} + 3\text{H}_2\text{O} = \text{Mn}(\text{OH})_3^- + 3\text{H}^+$
 log_k -34.8
 delta_h 0 kJ
 -gamma 5 0
 # Id: 4703301
 # log K source: MTQ3.11
 # Delta H source: MTQ3.11
 #T and ionic strength:
 $\text{Mn}^{+2} + 4\text{H}_2\text{O} = \text{Mn}(\text{OH})_4^{-2} + 4\text{H}^+$
 log_k -48.288
 delta_h 0 kJ
 -gamma 5 0
 # Id: 4703302
 # log K source: NIST46.4
 # Delta H source: MTQ3.11
 #T and ionic strength: 0.00 25.0
 $\text{Mn}^{+2} + 4\text{H}_2\text{O} = \text{MnO}_4^- + 8\text{H}^+ + 5\text{e}^-$
 log_k -127.794
 delta_h 822.67 kJ
 -gamma 3 0
 # Id: 4700020
 # log K source: NIST2.1.1
 # Delta H source: NIST2.1.1

#T and ionic strength:
 $\text{Mn}^{2+} + 4\text{H}_2\text{O} = \text{MnO}_4^{2-} + 8\text{H}^+ + 4\text{e}^-$
 log_k -118.422
 delta_h 711.07 kJ
 -gamma 5 0
 # Id: 4700021
 # log K source: NIST2.1.1
 # Delta H source: NIST2.1.1
 #T and ionic strength:
 $\text{Cr}(\text{OH})_2^{2+} + \text{H}^+ = \text{Cr}(\text{OH})_3 + \text{H}_2\text{O}$
 log_k 5.9118
 delta_h -77.91 kJ
 -gamma 0 0
 # Id: 2113301
 # log K source: NIST46.3
 # Delta H source: NIST46.3
 #T and ionic strength: 0.00 25.0
 $\text{Cr}(\text{OH})_2^{2+} + \text{H}_2\text{O} = \text{Cr}(\text{OH})_3 + \text{H}^+$
 log_k -8.4222
 delta_h 0 kJ
 -gamma 0 0
 # Id: 2113302
 # log K source: SCD3.02 (1983 RCa)
 # Delta H source: MTQ3.11
 #T and ionic strength: 0.00 25.0
 $\text{Cr}(\text{OH})_2^{2+} + 2\text{H}_2\text{O} = \text{Cr}(\text{OH})_4^- + 2\text{H}^+$
 log_k -17.8192
 delta_h 0 kJ
 -gamma 0 0
 # Id: 2113303
 # log K source: SCD3.02 (1983 RCa)
 # Delta H source: MTQ3.11
 #T and ionic strength: 0.00 25.0
 $\text{Cr}(\text{OH})_2^{2+} = \text{CrO}_2^- + 2\text{H}^+$
 log_k -17.7456
 delta_h 0 kJ
 -gamma 0 0
 # Id: 2113304
 # log K source: MTQ3.11
 # Delta H source: MTQ3.11
 #T and ionic strength:
 $\text{V}^{2+} + \text{H}_2\text{O} = \text{VOH}^+ + \text{H}^+$
 log_k -6.487
 delta_h 59.81 kJ
 -gamma 0 0
 # Id: 9003300
 # log K source: NIST46.3
 # Delta H source: NIST46.3
 #T and ionic strength: 0.00 25.0
 $\text{V}^{3+} + \text{H}_2\text{O} = \text{VOH}^{2+} + \text{H}^+$
 log_k -2.297
 delta_h 43.81 kJ
 -gamma 0 0
 # Id: 9013300

log K source: NIST46.3
 # Delta H source: NIST46.3
 #T and ionic strength: 0.00 25.0
 $V^{+3} + 2H_2O = V(OH)_2^{+} + 2H^{+}$
 log_k -6.274
 delta_h 0 kJ
 -gamma 0 0
 # Id: 9013301
 # log K source: NIST46.3
 # Delta H source: MTQ3.11
 #T and ionic strength: 1.00 20.0
 $V^{+3} + 3H_2O = V(OH)_3^{+} + 3H^{+}$
 log_k -3.0843
 delta_h 0 kJ
 -gamma 0 0
 # Id: 9013302
 # log K source: SCD3.02 (1978 TKa)
 # Delta H source: MTQ3.11
 #T and ionic strength: 0.10 20.0
 $2V^{+3} + 2H_2O = V_2(OH)_2^{+4} + 2H^{+}$
 log_k -3.794
 delta_h 0 kJ
 -gamma 0 0
 # Id: 9013304
 # log K source: NIST46.3
 # Delta H source: MTQ3.11
 #T and ionic strength: 0.00 25.0
 $2V^{+3} + 3H_2O = V_2(OH)_3^{+3} + 3H^{+}$
 log_k -10.1191
 delta_h 0 kJ
 -gamma 0 0
 # Id: 9013303
 # log K source: NIST46.3
 # Delta H source: MTQ3.11
 #T and ionic strength: 3.00 25.0
 $VO^{+2} + 2H_2O = V(OH)_3^{+} + H^{+}$
 log_k -5.697
 delta_h 0 kJ
 -gamma 0 0
 # Id: 9023300
 # log K source: NIST46.4
 # Delta H source: MTQ3.11
 #T and ionic strength: 0.00 25.0
 $2VO^{+2} + 2H_2O = H_2V_2O_4^{+2} + 2H^{+}$
 log_k -6.694
 delta_h 53.62 kJ
 -gamma 0 0
 # Id: 9023301
 # log K source: NIST46.4
 # Delta H source: NIST46.4
 #T and ionic strength: 0.00 25.0
 $U^{+4} + H_2O = UOH^{+3} + H^{+}$
 log_k -0.597
 delta_h 47.81 kJ

-gamma 0 0
 # Id: 8913300
 # log K source: NIST46.3
 # Delta H source: NIST46.3
 #T and ionic strength: 0.00 25.0
 $U+4 + 2H_2O = U(OH)_2+2 + 2H+$
 log_k -2.27
 delta_h 74.1823 kJ
 -gamma 0 0
 # Id: 8913301
 # log K source: MTQ3.11
 # Delta H source: MTQ3.11
 #T and ionic strength:
 $U+4 + 3H_2O = U(OH)_3+ + 3H+$
 log_k -4.935
 delta_h 94.7467 kJ
 -gamma 0 0
 # Id: 8913302
 # log K source: MTQ3.11
 # Delta H source: MTQ3.11
 #T and ionic strength:
 $U+4 + 4H_2O = U(OH)_4 + 4H+$
 log_k -8.498
 delta_h 103.596 kJ
 -gamma 0 0
 # Id: 8913303
 # log K source: MTQ3.11
 # Delta H source: MTQ3.11
 #T and ionic strength:
 $U+4 + 5H_2O = U(OH)_5- + 5H+$
 log_k -13.12
 delta_h 115.374 kJ
 -gamma 0 0
 # Id: 8913304
 # log K source: MTQ3.11
 # Delta H source: MTQ3.11
 #T and ionic strength:
 $6U+4 + 15H_2O = U_6(OH)_{15+9} + 15H+$
 log_k -17.155
 delta_h 0 kJ
 -gamma 0 0
 # Id: 8913305
 # log K source: NIST46.3
 # Delta H source: MTQ3.11
 #T and ionic strength: 0.00 25.0
 $UO_2+2 + H_2O = UO_2OH+ + H+$
 log_k -5.897
 delta_h 47.81 kJ
 -gamma 0 0
 # Id: 8933300
 # log K source: NIST46.3
 # Delta H source: NIST46.3
 #T and ionic strength: 0.00 25.0
 $2UO_2+2 + 2H_2O = (UO_2)_2(OH)_2+2 + 2H+$

log_k -5.574
 delta_h 41.82 kJ
 -gamma 0 0
 # Id: 8933301
 # log K source: NIST46.3
 # Delta H source: NIST46.3
 #T and ionic strength: 0.00 25.0
 $3\text{UO}_2^{2+} + 5\text{H}_2\text{O} = (\text{UO}_2)_3(\text{OH})_5^{5+} + 5\text{H}^+$
 log_k -15.585
 delta_h 108.05 kJ
 -gamma 0 0
 # Id: 8933302
 # log K source: NIST46.3
 # Delta H source: NIST46.3
 #T and ionic strength: 0.00 25.0
 $\text{Be}^{2+} + \text{H}_2\text{O} = \text{BeOH}^+ + \text{H}^+$
 log_k -5.397
 delta_h 0 kJ
 -gamma 6.5 0
 # Id: 1103301
 # log K source: NIST46.4
 # Delta H source: MTQ3.11
 #T and ionic strength: 0.00 25.0
 $\text{Be}^{2+} + 2\text{H}_2\text{O} = \text{Be}(\text{OH})_2 + 2\text{H}^+$
 log_k -13.594
 delta_h 0 kJ
 -gamma 6.5 0
 # Id: 1103302
 # log K source: NIST46.4
 # Delta H source: MTQ3.11
 #T and ionic strength: 0.00 25.0
 $\text{Be}^{2+} + 3\text{H}_2\text{O} = \text{Be}(\text{OH})_3^- + 3\text{H}^+$
 log_k -23.191
 delta_h 0 kJ
 -gamma 6.5 0
 # Id: 1103303
 # log K source: NIST46.4
 # Delta H source: MTQ3.11
 #T and ionic strength: 0.00 25.0
 $\text{Be}^{2+} + 4\text{H}_2\text{O} = \text{Be}(\text{OH})_4^{2-} + 4\text{H}^+$
 log_k -37.388
 delta_h 0 kJ
 -gamma 6.5 0
 # Id: 1103304
 # log K source: NIST46.4
 # Delta H source: MTQ3.11
 #T and ionic strength: 0.00 25.0
 $2\text{Be}^{2+} + \text{H}_2\text{O} = \text{Be}_2\text{OH}^{3+} + \text{H}^+$
 log_k -3.177
 delta_h 0 kJ
 -gamma 6.5 0
 # Id: 1103305
 # log K source: NIST46.4
 # Delta H source: MTQ3.11

#T and ionic strength: 0.10 25.0
 $3\text{Be}^{+2} + 3\text{H}_2\text{O} = \text{Be}_3(\text{OH})_3^{+3} + 3\text{H}^+$
 log_k -8.8076
 delta_h 0 kJ
 -gamma 6.5 0
 # Id: 1103306
 # log K source: NIST46.4
 # Delta H source: MTQ3.11
 #T and ionic strength: 0.10 25.0
 $\text{Mg}^{+2} + \text{H}_2\text{O} = \text{MgOH}^+ + \text{H}^+$
 log_k -11.397
 delta_h 67.81 kJ
 -gamma 6.5 0
 # Id: 4603300
 # log K source: NIST46.3
 # Delta H source: NIST46.3
 #T and ionic strength: 0.00 25.0
 $\text{Ca}^{+2} + \text{H}_2\text{O} = \text{CaOH}^+ + \text{H}^+$
 log_k -12.697
 delta_h 64.11 kJ
 -gamma 6 0
 # Id: 1503300
 # log K source: NIST46.3
 # Delta H source: NIST46.3
 #T and ionic strength: 0.00 25.0
 $\text{Sr}^{+2} + \text{H}_2\text{O} = \text{SrOH}^+ + \text{H}^+$
 log_k -13.177
 delta_h 60.81 kJ
 -gamma 5 0
 # Id: 8003300
 # log K source: NIST46.3
 # Delta H source: NIST46.3
 #T and ionic strength: 0.00 25.0
 $\text{Ba}^{+2} + \text{H}_2\text{O} = \text{BaOH}^+ + \text{H}^+$
 log_k -13.357
 delta_h 60.81 kJ
 -gamma 5 0
 # Id: 1003300
 # log K source: NIST46.3
 # Delta H source: NIST46.3
 #T and ionic strength: 0.00 25.0
 $\text{H}^+ + \text{F}^- = \text{HF}$
 log_k 3.17
 delta_h 13.3 kJ
 -gamma 0 0
 # Id: 3302700
 # log K source: NIST46.3
 # Delta H source: NIST46.3
 #T and ionic strength: 0.00 25.0
 $\text{H}^+ + 2\text{F}^- = \text{HF}_2^-$
 log_k 3.75
 delta_h 17.4 kJ
 -gamma 3.5 0
 # Id: 3302701

log K source: NIST46.3
 # Delta H source: NIST46.3
 #T and ionic strength: 0.00 25.0
 $2F^- + 2H^+ = H_2F_2$
 log_k 6.768
 delta_h 0 kJ
 -gamma 0 0
 # Id: 3302702
 # log K source: MTQ3.11
 # Delta H source: MTQ3.11
 #T and ionic strength:
 $Sb(OH)_3 + F^- + H^+ = SbOF + 2H_2O$
 log_k 6.1864
 delta_h 0 kJ
 -gamma 0 0
 # Id: 7402700
 # log K source: PNL89
 # Delta H source: PNL89
 #T and ionic strength:
 $Sb(OH)_3 + F^- + H^+ = Sb(OH)_2F + H_2O$
 log_k 6.1937
 delta_h 0 kJ
 -gamma 0 0
 # Id: 7402702
 # log K source: PNL89
 # Delta H source: PNL89
 #T and ionic strength:
 $H_4SiO_4 + 4H^+ + 6F^- = SiF_6^{2-} + 4H_2O$
 log_k 30.18
 delta_h -68 kJ
 -gamma 5 0
 # Id: 7702700
 # log K source: Nord90
 # Delta H source: Nord90
 #T and ionic strength: 0.00 25.0
 $Sn(OH)_2 + 2H^+ + F^- = SnF^+ + 2H_2O$
 log_k 11.582
 delta_h 0 kJ
 -gamma 0 0
 # Id: 7902701
 # log K source: NIST46.4
 # Delta H source: MTQ3.11
 #T and ionic strength: 1.00 25.0
 $Sn(OH)_2 + 2H^+ + 2F^- = SnF_2 + 2H_2O$
 log_k 14.386
 delta_h 0 kJ
 -gamma 0 0
 # Id: 7902702
 # log K source: NIST46.4
 # Delta H source: MTQ3.11
 #T and ionic strength: 1.00 25.0
 $Sn(OH)_2 + 2H^+ + 3F^- = SnF_3^- + 2H_2O$
 log_k 17.206
 delta_h 0 kJ

-gamma 0 0
 # Id: 7902703
 # log K source: NIST46.4
 # Delta H source: MTQ3.11
 #T and ionic strength: 1.00 25.0
 $\text{Sn(OH)}_6^{2-} + 6\text{H}^+ + 6\text{F}^- = \text{SnF}_6^{2-} + 6\text{H}_2\text{O}$
 log_k 33.5844
 delta_h 0 kJ
 -gamma 0 0
 # Id: 7912701
 # log K source: Bard85
 # Delta H source: MTQ3.11
 #T and ionic strength:
 $\text{Pb}^{2+} + \text{F}^- = \text{PbF}^+$
 log_k 1.848
 delta_h 0 kJ
 -gamma 0 0
 # Id: 6002700
 # log K source: NIST46.3
 # Delta H source: MTQ3.11
 #T and ionic strength: 1.00 25.0
 $\text{Pb}^{2+} + 2\text{F}^- = \text{PbF}_2$
 log_k 3.142
 delta_h 0 kJ
 -gamma 0 0
 # Id: 6002701
 # log K source: NIST46.3
 # Delta H source: MTQ3.11
 #T and ionic strength: 1.00 25.0
 $\text{Pb}^{2+} + 3\text{F}^- = \text{PbF}_3^-$
 log_k 3.42
 delta_h 0 kJ
 -gamma 0 0
 # Id: 6002702
 # log K source: SCD3.02 (1956 TKa)
 # Delta H source: MTQ3.11
 #T and ionic strength: 0.00 25.0
 $\text{Pb}^{2+} + 4\text{F}^- = \text{PbF}_4^{2-}$
 log_k 3.1
 delta_h 0 kJ
 -gamma 0 0
 # Id: 6002703
 # log K source: SCD3.02 (1956 TKa)
 # Delta H source: MTQ3.11
 #T and ionic strength: 0.00 25.0
 $\text{H}_3\text{BO}_3 + 3\text{H}^+ + 4\text{F}^- = \text{BF}_4^- + 3\text{H}_2\text{O}$
 log_k 19.912
 delta_h -18.67 kJ
 -gamma 2.5 0
 # Id: 902703
 # log K source: NIST46.3
 # Delta H source: NIST2.1.1
 #T and ionic strength: 1.00 25.0
 $\text{Al}^{3+} + \text{F}^- = \text{AlF}^{2+}$

log_k 7
delta_h 4.6 kJ
-gamma 5.4 0
Id: 302700
log K source: NIST46.3
Delta H source: NIST46.3
#T and ionic strength: 0.00 25.0
 $\text{Al}^{+3} + 2\text{F}^- = \text{AlF}_2^+$
log_k 12.6
delta_h 8.3 kJ
-gamma 5.4 0
Id: 302701
log K source: NIST46.3
Delta H source: NIST46.3
#T and ionic strength: 0.00 25.0
 $\text{Al}^{+3} + 3\text{F}^- = \text{AlF}_3$
log_k 16.7
delta_h 8.7 kJ
-gamma 0 0
Id: 302702
log K source: NIST46.3
Delta H source: NIST46.3
#T and ionic strength: 0.00 25.0
 $\text{Al}^{+3} + 4\text{F}^- = \text{AlF}_4^-$
log_k 19.4
delta_h 8.7 kJ
-gamma 4.5 0
Id: 302703
log K source: NIST46.3
Delta H source: NIST46.3
#T and ionic strength: 0.00 25.0
 $\text{Tl}^+ + \text{F}^- = \text{TlF}$
log_k 0.1
delta_h 0 kJ
-gamma 0 0
Id: 8702700
log K source: NIST46.3
Delta H source: MTQ3.11
#T and ionic strength: 0.00 25.0
 $\text{Zn}^{+2} + \text{F}^- = \text{ZnF}^+$
log_k 1.3
delta_h 11 kJ
-gamma 0 0
Id: 9502700
log K source: NIST46.3
Delta H source: NIST46.3
#T and ionic strength: 0.00 25.0
 $\text{Cd}^{+2} + \text{F}^- = \text{CdF}^+$
log_k 1.2
delta_h 5 kJ
-gamma 0 0
Id: 1602700
log K source: NIST46.3
Delta H source: NIST46.3

#T and ionic strength: 0.00 25.0
 $\text{Cd}^{+2} + 2\text{F}^- = \text{CdF}_2$
log_k 1.5
delta_h 0 kJ
-gamma 0 0
Id: 1602701
log K source: MTQ3.11
Delta H source: MTQ3.11
#T and ionic strength:
 $\text{Hg}(\text{OH})_2 + 2\text{H}^+ + \text{F}^- = \text{HgF}^+ + 2\text{H}_2\text{O}$
log_k 7.763
delta_h -35.72 kJ
-gamma 0 0
Id: 3612701
log K source: NIST46.3
Delta H source: NIST46.3
#T and ionic strength: 0.50 25.0
 $\text{Cu}^{+2} + \text{F}^- = \text{CuF}^+$
log_k 1.8
delta_h 13 kJ
-gamma 0 0
Id: 2312700
log K source: NIST46.3
Delta H source: NIST46.3
#T and ionic strength: 0.00 25.0
 $\text{Ag}^+ + \text{F}^- = \text{AgF}$
log_k 0.4
delta_h 12 kJ
-gamma 0 0
Id: 202700
log K source: NIST46.3
Delta H source: NIST46.3
#T and ionic strength: 0.00 25.0
 $\text{Ni}^{+2} + \text{F}^- = \text{NiF}^+$
log_k 1.4
delta_h 7.1 kJ
-gamma 0 0
Id: 5402700
log K source: NIST46.3
Delta H source: NIST46.3
#T and ionic strength: 0.00 25.0
 $\text{Co}^{+2} + \text{F}^- = \text{CoF}^+$
log_k 1.5
delta_h 9.2 kJ
-gamma 0 0
Id: 2002700
log K source: NIST46.4
Delta H source: NIST46.4
#T and ionic strength: 0.00 25.0
 $\text{Fe}^{+3} + \text{F}^- = \text{FeF}^{+2}$
log_k 6.04
delta_h 10 kJ
-gamma 5 0
Id: 2812700

log K source: NIST46.3
Delta H source: NIST46.3
#T and ionic strength: 0.00 25.0
 $\text{Fe}^{+3} + 2\text{F}^- = \text{FeF}_2^+$
log_k 10.4675
delta_h 17 kJ
-gamma 5 0
Id: 2812701
log K source: NIST46.3
Delta H source: NIST46.3
#T and ionic strength: 0.50 25.0
 $\text{Fe}^{+3} + 3\text{F}^- = \text{FeF}_3$
log_k 13.617
delta_h 29 kJ
-gamma 0 0
Id: 2812702
log K source: NIST46.3
Delta H source: NIST46.3
#T and ionic strength: 0.50 25.0
 $\text{Mn}^{+2} + \text{F}^- = \text{MnF}^+$
log_k 1.6
delta_h 11 kJ
-gamma 5 0
Id: 4702700
log K source: NIST46.3
Delta H source: NIST46.3
#T and ionic strength: 0.00 25.0
 $\text{Cr}(\text{OH})_2^+ + 2\text{H}^+ + \text{F}^- = \text{CrF}^{+2} + 2\text{H}_2\text{O}$
log_k 14.7688
delta_h -70.2452 kJ
-gamma 0 0
Id: 2112700
log K source: NIST46.3
Delta H source: MTQ3.11
#T and ionic strength: 0.00 25.0
 $\text{VO}^{+2} + \text{F}^- = \text{VOF}^+$
log_k 3.778
delta_h 7.9 kJ
-gamma 0 0
Id: 9022700
log K source: NIST46.3
Delta H source: NIST46.3
#T and ionic strength: 1.00 25.0
 $\text{VO}^{+2} + 2\text{F}^- = \text{VOF}_2$
log_k 6.352
delta_h 14 kJ
-gamma 0 0
Id: 9022701
log K source: NIST46.3
Delta H source: NIST46.3
#T and ionic strength: 1.00 25.0
 $\text{VO}^{+2} + 3\text{F}^- = \text{VOF}_3^-$
log_k 7.902
delta_h 20 kJ

-gamma 0 0
Id: 9022702
log K source: NIST46.3
Delta H source: NIST46.3
#T and ionic strength: 1.00 25.0
 $\text{VO}^{2+} + 4\text{F}^- = \text{VOF}_4^{2-}$
log_k 8.508
delta_h 26 kJ
-gamma 0 0
Id: 9022703
log K source: NIST46.3
Delta H source: NIST46.3
#T and ionic strength: 1.00 25.0
 $\text{VO}_2^{+} + \text{F}^- = \text{VO}_2\text{F}$
log_k 3.244
delta_h 0 kJ
-gamma 0 0
Id: 9032700
log K source: NIST46.3
Delta H source: MTQ3.11
#T and ionic strength: 1.00 25.0
 $\text{VO}_2^{+} + 2\text{F}^- = \text{VO}_2\text{F}_2^{-}$
log_k 5.804
delta_h 0 kJ
-gamma 0 0
Id: 9032701
log K source: NIST46.3
Delta H source: MTQ3.11
#T and ionic strength: 1.00 20.0
 $\text{VO}_2^{+} + 3\text{F}^- = \text{VO}_2\text{F}_3^{2-}$
log_k 6.9
delta_h 0 kJ
-gamma 0 0
Id: 9032702
log K source: NIST46.3
Delta H source: MTQ3.11
#T and ionic strength: 1.00 20.0
 $\text{VO}_2^{+} + 4\text{F}^- = \text{VO}_2\text{F}_4^{3-}$
log_k 6.592
delta_h 0 kJ
-gamma 0 0
Id: 9032703
log K source: NIST46.3
Delta H source: MTQ3.11
#T and ionic strength: 1.00 20.0
 $\text{U}^{4+} + \text{F}^- = \text{UF}^{3+}$
log_k 9.3
delta_h 21.1292 kJ
-gamma 0 0
Id: 8912700
log K source: NIST46.3
Delta H source: MTQ3.11
#T and ionic strength: 0.00 25.0
 $\text{U}^{4+} + 2\text{F}^- = \text{UF}_2^{2+}$

log_k 16.4
delta_h 30.1248 kJ
-gamma 0 0
Id: 8912701
log K source: NIST46.3
Delta H source: MTQ3.11
#T and ionic strength: 0.00 25.0
 $\text{U}^{+4} + 3\text{F}^{-} = \text{UF}_3^{+}$
log_k 21.6
delta_h 29.9156 kJ
-gamma 0 0
Id: 8912702
log K source: NIST46.3
Delta H source: MTQ3.11
#T and ionic strength: 0.00 25.0
 $\text{U}^{+4} + 4\text{F}^{-} = \text{UF}_4$
log_k 23.64
delta_h 19.2464 kJ
-gamma 0 0
Id: 8912703
log K source: MTQ3.11
Delta H source: MTQ3.11
#T and ionic strength:
 $\text{U}^{+4} + 5\text{F}^{-} = \text{UF}_5^{-}$
log_k 25.238
delta_h 20.2924 kJ
-gamma 0 0
Id: 8912704
log K source: MTQ3.11
Delta H source: MTQ3.11
#T and ionic strength:
 $\text{U}^{+4} + 6\text{F}^{-} = \text{UF}_6^{-2}$
log_k 27.718
delta_h 13.8072 kJ
-gamma 0 0
Id: 8912705
log K source: MTQ3.11
Delta H source: MTQ3.11
#T and ionic strength:
 $\text{UO}_2^{+2} + \text{F}^{-} = \text{UO}_2\text{F}^{+}$
log_k 5.14
delta_h 1 kJ
-gamma 0 0
Id: 8932700
log K source: NIST46.3
Delta H source: NIST46.3
#T and ionic strength: 0.00 25.0
 $\text{UO}_2^{+2} + 2\text{F}^{-} = \text{UO}_2\text{F}_2$
log_k 8.6
delta_h 2 kJ
-gamma 0 0
Id: 8932701
log K source: NIST46.3
Delta H source: NIST46.3

#T and ionic strength: 0.00 25.0
 $\text{UO}_2^{2+} + 3\text{F}^- = \text{UO}_2\text{F}_3^-$
log_k 11
delta_h 2 kJ
-gamma 0 0
Id: 8932702
log K source: NIST46.3
Delta H source: NIST46.3
#T and ionic strength: 0.00 25.0
 $\text{UO}_2^{2+} + 4\text{F}^- = \text{UO}_2\text{F}_4^{2-}$
log_k 11.9
delta_h 0.4 kJ
-gamma 0 0
Id: 8932703
log K source: NIST46.3
Delta H source: NIST46.3
#T and ionic strength: 0.00 25.0
 $\text{Be}^{2+} + \text{F}^- = \text{BeF}^+$
log_k 5.249
delta_h 0 kJ
-gamma 0 0
Id: 1102701
log K source: NIST46.4
Delta H source: NIST46.4
#T and ionic strength: 0.50 25.0
 $\text{Be}^{2+} + 2\text{F}^- = \text{BeF}_2$
log_k 9.1285
delta_h -4 kJ
-gamma 0 0
Id: 1102702
log K source: NIST46.4
Delta H source: NIST46.4
#T and ionic strength: 0.50 25.0
 $\text{Be}^{2+} + 3\text{F}^- = \text{BeF}_3^-$
log_k 11.9085
delta_h -8 kJ
-gamma 0 0
Id: 1102703
log K source: NIST46.4
Delta H source: NIST46.4
#T and ionic strength: 0.50 25.0
 $\text{Mg}^{2+} + \text{F}^- = \text{MgF}^+$
log_k 2.05
delta_h 13 kJ
-gamma 4.5 0
Id: 4602700
log K source: NIST46.3
Delta H source: NIST46.3
#T and ionic strength: 0.00 25.0
 $\text{Ca}^{2+} + \text{F}^- = \text{CaF}^+$
log_k 1.038
delta_h 14 kJ
-gamma 5 0
Id: 1502700

log K source: NIST46.3
 # Delta H source: NIST46.3
 #T and ionic strength: 1.00 25.0
 $\text{Sr}^{+2} + \text{F}^{-} = \text{SrF}^{+}$
 log_k 0.548
 delta_h 16 kJ
 -gamma 0 0
 # Id: 8002701
 # log K source: NIST46.4
 # Delta H source: NIST46.4
 #T and ionic strength: 1.00 25.0
 $\text{Na}^{+} + \text{F}^{-} = \text{NaF}$
 log_k -0.2
 delta_h 12 kJ
 -gamma 0 0
 # Id: 5002700
 # log K source: NIST46.3
 # Delta H source: NIST46.3
 #T and ionic strength: 0.00 25.0
 $\text{Sn}(\text{OH})_2 + 2\text{H}^{+} + \text{Cl}^{-} = \text{SnCl}^{+} + 2\text{H}_2\text{O}$
 log_k 8.734
 delta_h 0 kJ
 -gamma 0 0
 # Id: 7901801
 # log K source: NIST46.4
 # Delta H source: NIST46.4
 #T and ionic strength: 0.00 25.0
 $\text{Sn}(\text{OH})_2 + 2\text{H}^{+} + 2\text{Cl}^{-} = \text{SnCl}_2 + 2\text{H}_2\text{O}$
 log_k 9.524
 delta_h 0 kJ
 -gamma 0 0
 # Id: 7901802
 # log K source: NIST46.4
 # Delta H source: NIST46.4
 #T and ionic strength: 0.00 25.0
 $\text{Sn}(\text{OH})_2 + 2\text{H}^{+} + 3\text{Cl}^{-} = \text{SnCl}_3^{-} + 2\text{H}_2\text{O}$
 log_k 8.3505
 delta_h 0 kJ
 -gamma 0 0
 # Id: 7901803
 # log K source: NIST46.4
 # Delta H source: NIST46.4
 #T and ionic strength: 2.00 25.0
 $\text{Pb}^{+2} + \text{Cl}^{-} = \text{PbCl}^{+}$
 log_k 1.55
 delta_h 8.7 kJ
 -gamma 0 0
 # Id: 6001800
 # log K source: NIST46.3
 # Delta H source: NIST46.3
 #T and ionic strength: 0.00 25.0
 $\text{Pb}^{+2} + 2\text{Cl}^{-} = \text{PbCl}_2$
 log_k 2.2
 delta_h 12 kJ

-gamma 0 0
Id: 6001801
log K source: NIST46.3
Delta H source: NIST46.3
#T and ionic strength: 0.00 25.0
 $\text{Pb}^{+2} + 3\text{Cl}^- = \text{PbCl}_3^-$
log_k 1.8
delta_h 4 kJ
-gamma 0 0
Id: 6001802
log K source: NIST46.3
Delta H source: NIST46.3
#T and ionic strength: 0.00 25.0
 $\text{Pb}^{+2} + 4\text{Cl}^- = \text{PbCl}_4^{-2}$
log_k 1.46
delta_h 14.7695 kJ
-gamma 0 0
Id: 6001803
log K source: SCD3.02 (1984 SEa)
Delta H source: MTQ3.11
#T and ionic strength: 0.00 25.0
 $\text{Ti}^+ + \text{Cl}^- = \text{TiCl}$
log_k 0.51
delta_h -6.2 kJ
-gamma 0 0
Id: 8701800
log K source: NIST46.3
Delta H source: NIST46.3
#T and ionic strength: 0.00 25.0
 $\text{Ti}^+ + 2\text{Cl}^- = \text{TiCl}_2^-$
log_k 0.28
delta_h 0 kJ
-gamma 0 0
Id: 8701801
log K source: SCD3.02 (1992 RAb)
Delta H source: MTQ3.11
#T and ionic strength: 0.00 25.0
 $\text{Ti}(\text{OH})_3 + 3\text{H}^+ + \text{Cl}^- = \text{TiCl}^{+2} + 3\text{H}_2\text{O}$
log_k 11.011
delta_h 0 kJ
-gamma 0 0
Id: 8711800
log K source: NIST46.3
Delta H source: NIST46.3
#T and ionic strength: 0.00 25.0
 $\text{Ti}(\text{OH})_3 + 3\text{H}^+ + 2\text{Cl}^- = \text{TiCl}_2^+ + 3\text{H}_2\text{O}$
log_k 16.771
delta_h 0 kJ
-gamma 0 0
Id: 8711801
log K source: NIST46.3
Delta H source: NIST46.3
#T and ionic strength: 0.00 25.0
 $\text{Ti}(\text{OH})_3 + 3\text{H}^+ + 3\text{Cl}^- = \text{TiCl}_3 + 3\text{H}_2\text{O}$

log_k 19.791
 delta_h 0 kJ
 -gamma 0 0
 # Id: 8711802
 # log K source: NIST46.3
 # Delta H source: NIST46.3
 #T and ionic strength: 0.00 25.0
 $\text{Ti}(\text{OH})_3 + 3\text{H}^+ + 4\text{Cl}^- = \text{TiCl}_4^- + 3\text{H}_2\text{O}$
 log_k 21.591
 delta_h 0 kJ
 -gamma 0 0
 # Id: 8711803
 # log K source: NIST46.3
 # Delta H source: NIST46.3
 #T and ionic strength: 0.00 25.0
 $\text{Ti}(\text{OH})_3 + \text{Cl}^- + 2\text{H}^+ = \text{TiOHCl}^+ + 2\text{H}_2\text{O}$
 log_k 10.629
 delta_h 0 kJ
 -gamma 0 0
 # Id: 8711804
 # log K source: MTQ3.11
 # Delta H source: MTQ3.11
 #T and ionic strength:
 $\text{Zn}^{+2} + \text{Cl}^- = \text{ZnCl}^+$
 log_k 0.4
 delta_h 5.4 kJ
 -gamma 4 0
 # Id: 9501800
 # log K source: NIST46.3
 # Delta H source: NIST46.3
 #T and ionic strength: 0.00 25.0
 $\text{Zn}^{+2} + 2\text{Cl}^- = \text{ZnCl}_2$
 log_k 0.6
 delta_h 37 kJ
 -gamma 0 0
 # Id: 9501801
 # log K source: NIST46.3
 # Delta H source: NIST46.3
 #T and ionic strength: 0.00 25.0
 $\text{Zn}^{+2} + 3\text{Cl}^- = \text{ZnCl}_3^-$
 log_k 0.5
 delta_h 39.999 kJ
 -gamma 4 0
 # Id: 9501802
 # log K source: MTQ3.11
 # Delta H source: MTQ3.11
 #T and ionic strength:
 $\text{Zn}^{+2} + 4\text{Cl}^- = \text{ZnCl}_4^{2-}$
 log_k 0.199
 delta_h 45.8566 kJ
 -gamma 5 0
 # Id: 9501803
 # log K source: MTQ3.11
 # Delta H source: MTQ3.11

#T and ionic strength:
 $\text{Zn}^{+2} + \text{H}_2\text{O} + \text{Cl}^- = \text{ZnOHCl} + \text{H}^+$
 log_k -7.48
 delta_h 0 kJ
 -gamma 0 0
 # Id: 9501804
 # log K source: MTQ3.11
 # Delta H source: MTQ3.11
 #T and ionic strength:
 $\text{Cd}^{+2} + \text{Cl}^- = \text{CdCl}^+$
 log_k 1.98
 delta_h 1 kJ
 -gamma 0 0
 # Id: 1601800
 # log K source: NIST46.3
 # Delta H source: NIST46.3
 #T and ionic strength: 0.00 25.0
 $\text{Cd}^{+2} + 2\text{Cl}^- = \text{CdCl}_2$
 log_k 2.6
 delta_h 3 kJ
 -gamma 0 0
 # Id: 1601801
 # log K source: NIST46.3
 # Delta H source: NIST46.3
 #T and ionic strength: 0.00 25.0
 $\text{Cd}^{+2} + 3\text{Cl}^- = \text{CdCl}_3^-$
 log_k 2.4
 delta_h 10 kJ
 -gamma 0 0
 # Id: 1601802
 # log K source: NIST46.3
 # Delta H source: NIST46.3
 #T and ionic strength: 0.00 25.0
 $\text{Cd}^{+2} + \text{H}_2\text{O} + \text{Cl}^- = \text{CdOHCl} + \text{H}^+$
 log_k -7.404
 delta_h 18.2213 kJ
 -gamma 0 0
 # Id: 1601803
 # log K source: MTQ3.11
 # Delta H source: MTQ3.11
 #T and ionic strength:
 $\text{Hg}(\text{OH})_2 + 2\text{H}^+ + \text{Cl}^- = \text{HgCl}^+ + 2\text{H}_2\text{O}$
 log_k 13.494
 delta_h -62.72 kJ
 -gamma 0 0
 # Id: 3611800
 # log K source: NIST46.3
 # Delta H source: NIST46.3
 #T and ionic strength: 0.00 25.0
 $\text{Hg}(\text{OH})_2 + 2\text{H}^+ + 2\text{Cl}^- = \text{HgCl}_2 + 2\text{H}_2\text{O}$
 log_k 20.194
 delta_h -92.42 kJ
 -gamma 0 0
 # Id: 3611801

log K source: NIST46.3
 # Delta H source: NIST46.3
 #T and ionic strength: 0.00 25.0
 $\text{Hg(OH)}_2 + 2\text{H}^+ + 3\text{Cl}^- = \text{HgCl}_3^- + 2\text{H}_2\text{O}$
 log_k 21.194
 delta_h -94.02 kJ
 -gamma 0 0
 # Id: 3611802
 # log K source: NIST46.3
 # Delta H source: NIST46.3
 #T and ionic strength: 0.00 25.0
 $\text{Hg(OH)}_2 + 2\text{H}^+ + 4\text{Cl}^- = \text{HgCl}_4^{2-} + 2\text{H}_2\text{O}$
 log_k 21.794
 delta_h -100.72 kJ
 -gamma 0 0
 # Id: 3611803
 # log K source: NIST46.3
 # Delta H source: NIST46.3
 #T and ionic strength: 0.00 25.0
 $\text{Hg(OH)}_2 + \text{Cl}^- + \text{I}^- + 2\text{H}^+ = \text{HgClI} + 2\text{H}_2\text{O}$
 log_k 25.532
 delta_h -135.3 kJ
 -gamma 0 0
 # Id: 3611804
 # log K source: NIST2.1.1
 # Delta H source: NIST2.1.1
 #T and ionic strength:
 $\text{Hg(OH)}_2 + \text{H}^+ + \text{Cl}^- = \text{HgClOH} + \text{H}_2\text{O}$
 log_k 10.444
 delta_h -42.72 kJ
 -gamma 0 0
 # Id: 3611805
 # log K source: NIST46.3
 # Delta H source: NIST46.3
 #T and ionic strength: 1.00 25.0
 $\text{Cu}^{+2} + \text{Cl}^- = \text{CuCl}^+$
 log_k 0.2
 delta_h 8.3 kJ
 -gamma 4 0
 # Id: 2311800
 # log K source: NIST46.3
 # Delta H source: NIST46.3
 #T and ionic strength: 0.00 25.0
 $\text{Cu}^{+2} + 2\text{Cl}^- = \text{CuCl}_2$
 log_k -0.26
 delta_h 44.183 kJ
 -gamma 0 0
 # Id: 2311801
 # log K source: SCD3.02 (1989 IPa)
 # Delta H source: MTQ3.11
 #T and ionic strength: 0.00 25.0
 $\text{Cu}^{+2} + 3\text{Cl}^- = \text{CuCl}_3^-$
 log_k -2.29
 delta_h 57.279 kJ

-gamma 4 0
Id: 2311802
log K source: MTQ3.11
Delta H source: MTQ3.11
#T and ionic strength:
 $\text{Cu}^{+2} + 4\text{Cl}^- = \text{CuCl}_4^{2-}$
log_k -4.59
delta_h 32.5515 kJ
-gamma 5 0
Id: 2311803
log K source: MTQ3.11
Delta H source: MTQ3.11
#T and ionic strength:
 $\text{Cu}^+ + 2\text{Cl}^- = \text{CuCl}_2^-$
log_k 5.42
delta_h -1.7573 kJ
-gamma 4 0
Id: 2301800
log K source: NIST46.3
Delta H source: MTQ3.11
#T and ionic strength: 0.00 25.0
 $\text{Cu}^+ + 3\text{Cl}^- = \text{CuCl}_3^{2-}$
log_k 4.75
delta_h 1.0878 kJ
-gamma 5 0
Id: 2301801
log K source: NIST46.3
Delta H source: MTQ3.11
#T and ionic strength: 0.00 25.0
 $\text{Cu}^+ + \text{Cl}^- = \text{CuCl}$
log_k 3.1
delta_h 0 kJ
-gamma 0 0
Id: 2301802
log K source: NIST46.4
Delta H source: MTQ3.11
#T and ionic strength: 0.00 25.0
 $\text{Ag}^+ + \text{Cl}^- = \text{AgCl}$
log_k 3.31
delta_h -12 kJ
-gamma 0 0
Id: 201800
log K source: NIST46.3
Delta H source: NIST46.3
#T and ionic strength: 0.00 25.0
 $\text{Ag}^+ + 2\text{Cl}^- = \text{AgCl}_2^-$
log_k 5.25
delta_h -16 kJ
-gamma 0 0
Id: 201801
log K source: NIST46.3
Delta H source: NIST46.3
#T and ionic strength: 0.00 25.0
 $\text{Ag}^+ + 3\text{Cl}^- = \text{AgCl}_3^{2-}$

log_k 5.2
delta_h 0 kJ
-gamma 0 0
Id: 201802
log K source: NIST46.3
Delta H source: MTQ3.11
#T and ionic strength: 0.00 25.0
 $\text{Ag}^+ + 4\text{Cl}^- = \text{AgCl}_4^{3-}$
log_k 5.51
delta_h 0 kJ
-gamma 0 0
Id: 201803
log K source: MTQ3.11
Delta H source: MTQ3.11
#T and ionic strength:
 $\text{Ni}^{+2} + \text{Cl}^- = \text{NiCl}^+$
log_k 0.408
delta_h 2 kJ
-gamma 0 0
Id: 5401800
log K source: NIST46.3
Delta H source: NIST46.3
#T and ionic strength: 1.00 25.0
 $\text{Ni}^{+2} + 2\text{Cl}^- = \text{NiCl}_2$
log_k -1.89
delta_h 0 kJ
-gamma 0 0
Id: 5401801
log K source: SCD3.02 (1989 IPa)
Delta H source: MTQ3.11
#T and ionic strength: 0.00 25.0
 $\text{Co}^{+2} + \text{Cl}^- = \text{CoCl}^+$
log_k 0.539
delta_h 2 kJ
-gamma 0 0
Id: 2001800
log K source: NIST46.4
Delta H source: NIST46.4
#T and ionic strength: 0.50 25.0
 $\text{Co}^{+3} + \text{Cl}^- = \text{CoCl}^{+2}$
log_k 2.3085
delta_h 16 kJ
-gamma 0 0
Id: 2011800
log K source: NIST46.4
Delta H source: NIST46.4
#T and ionic strength: 0.50 25.0
 $\text{Fe}^{+3} + \text{Cl}^- = \text{FeCl}^{+2}$
log_k 1.48
delta_h 23 kJ
-gamma 5 0
Id: 2811800
log K source: NIST46.3
Delta H source: NIST46.3

#T and ionic strength: 0.00 25.0
 $\text{Fe}^{+3} + 2\text{Cl}^- = \text{FeCl}_2^+$
log_k 2.13
delta_h 0 kJ
-gamma 5 0
Id: 2811801
log K source: NIST46.3
Delta H source: MTQ3.11
#T and ionic strength: 0.00 25.0
 $\text{Fe}^{+3} + 3\text{Cl}^- = \text{FeCl}_3$
log_k 1.13
delta_h 0 kJ
-gamma 0 0
Id: 2811802
log K source: Nord90
Delta H source: MTQ3.11
#T and ionic strength: 0.00 25.0
 $\text{Mn}^{+2} + \text{Cl}^- = \text{MnCl}^+$
log_k 0.1
delta_h 0 kJ
-gamma 5 0
Id: 4701800
log K source: NIST46.3
Delta H source: MTQ3.11
#T and ionic strength: 0.00 20.0
 $\text{Mn}^{+2} + 2\text{Cl}^- = \text{MnCl}_2$
log_k 0.25
delta_h 0 kJ
-gamma 0 0
Id: 4701801
log K source: Nord90
Delta H source: MTQ3.11
#T and ionic strength: 0.00 25.0
 $\text{Mn}^{+2} + 3\text{Cl}^- = \text{MnCl}_3^-$
log_k -0.31
delta_h 0 kJ
-gamma 5 0
Id: 4701802
log K source: Nord90
Delta H source: MTQ3.11
#T and ionic strength: 0.00 25.0
 $\text{Cr}(\text{OH})_2^+ + 2\text{H}^+ + \text{Cl}^- = \text{CrCl}_2^+ + 2\text{H}_2\text{O}$
log_k 9.6808
delta_h -103.62 kJ
-gamma 0 0
Id: 2111800
log K source: NIST46.3
Delta H source: NIST46.3
#T and ionic strength: 1.00 25.0
 $\text{Cr}(\text{OH})_2^+ + 2\text{Cl}^- + 2\text{H}^+ = \text{CrCl}_2^+ + 2\text{H}_2\text{O}$
log_k 8.658
delta_h -39.2208 kJ
-gamma 0 0
Id: 2111801

log K source: MTQ3.11
 # Delta H source: MTQ3.11
 #T and ionic strength:
 $\text{Cr(OH)}_2^{2+} + 2\text{Cl}^- + \text{H}^+ = \text{CrOHCl}_2 + \text{H}_2\text{O}$
 log_k 2.9627
 delta_h 0 kJ
 -gamma 0 0
 # Id: 2111802
 # log K source: MTQ3.11
 # Delta H source: MTQ3.11
 #T and ionic strength:
 $\text{VO}^{2+} + \text{Cl}^- = \text{VOCl}^+$
 log_k 0.448
 delta_h 0 kJ
 -gamma 0 0
 # Id: 9021800
 # log K source: NIST46.3
 # Delta H source: MTQ3.11
 #T and ionic strength: 1.00 20.0
 $\text{U}^{4+} + \text{Cl}^- = \text{UCl}^{3+}$
 log_k 1.7
 delta_h -20 kJ
 -gamma 0 0
 # Id: 8911800
 # log K source: NIST46.3
 # Delta H source: NIST46.3
 #T and ionic strength: 0.00 25.0
 $\text{UO}_2^{2+} + \text{Cl}^- = \text{UO}_2\text{Cl}^+$
 log_k 0.21
 delta_h 16 kJ
 -gamma 0 0
 # Id: 8931800
 # log K source: NIST46.3
 # Delta H source: NIST46.3
 #T and ionic strength: 0.00 25.0
 $\text{Be}^{2+} + \text{Cl}^- = \text{BeCl}^+$
 log_k 0.2009
 delta_h 0 kJ
 -gamma 5 0
 # Id: 1101801
 # log K source: NIST46.4
 # Delta H source: MTQ3.11
 #T and ionic strength: 0.70 20.0
 $\text{Sn(OH)}_2 + 2\text{H}^+ + \text{Br}^- = \text{SnBr}^+ + 2\text{H}_2\text{O}$
 log_k 8.254
 delta_h 0 kJ
 -gamma 0 0
 # Id: 7901301
 # log K source: NIST46.4
 # Delta H source: NIST46.4
 #T and ionic strength: 0.00 25.0
 $\text{Sn(OH)}_2 + 2\text{H}^+ + 2\text{Br}^- = \text{SnBr}_2 + 2\text{H}_2\text{O}$
 log_k 8.794
 delta_h 0 kJ

-gamma 0 0
 # Id: 7901302
 # log K source: NIST46.4
 # Delta H source: NIST46.4
 #T and ionic strength: 0.00 25.0
 $\text{Sn(OH)}_2 + 2\text{H}^+ + 3\text{Br}^- = \text{SnBr}_3^- + 2\text{H}_2\text{O}$
 log_k 7.48
 delta_h 0 kJ
 -gamma 0 0
 # Id: 7901303
 # log K source: NIST46.4
 # Delta H source: NIST46.4
 #T and ionic strength: 3.00 25.0
 $\text{Pb}^{+2} + \text{Br}^- = \text{PbBr}^+$
 log_k 1.7
 delta_h 8 kJ
 -gamma 0 0
 # Id: 6001300
 # log K source: NIST46.3
 # Delta H source: NIST46.3
 #T and ionic strength: 0.00 25.0
 $\text{Pb}^{+2} + 2\text{Br}^- = \text{PbBr}_2$
 log_k 2.6
 delta_h -4 kJ
 -gamma 0 0
 # Id: 6001301
 # log K source: NIST46.3
 # Delta H source: NIST46.3
 #T and ionic strength: 0.00 25.0
 $\text{Ti}^+ + \text{Br}^- = \text{TiBr}$
 log_k 0.91
 delta_h -12 kJ
 -gamma 0 0
 # Id: 8701300
 # log K source: NIST46.3
 # Delta H source: NIST46.3
 #T and ionic strength: 0.00 25.0
 $\text{Ti}^+ + 2\text{Br}^- = \text{TiBr}_2^-$
 log_k -0.384
 delta_h 12.36 kJ
 -gamma 0 0
 # Id: 8701301
 # log K source: NIST46.3
 # Delta H source: NIST2.1.1
 #T and ionic strength: 4.00 25.0
 $\text{Ti}^+ + \text{Br}^- + \text{Cl}^- = \text{TiBrCl}^-$
 log_k 0.8165
 delta_h 0 kJ
 -gamma 0 0
 # Id: 8701302
 # log K source: MTQ3.11
 # Delta H source: MTQ3.11
 #T and ionic strength:
 $\text{Ti}^+ + \text{I}^- + \text{Br}^- = \text{TiIBr}^-$

log_k 2.185
delta_h 0 kJ
-gamma 0 0
Id: 8703802
log K source: MTQ3.11
Delta H source: MTQ3.11
#T and ionic strength:
 $\text{Ti}(\text{OH})_3 + 3\text{H}^+ + \text{Br}^- = \text{TIBr}^{2+} + 3\text{H}_2\text{O}$
log_k 12.803
delta_h 0 kJ
-gamma 0 0
Id: 8711300
log K source: NIST46.3
Delta H source: MTQ3.11
#T and ionic strength: 1.00 25.0
 $\text{Ti}(\text{OH})_3 + 3\text{H}^+ + 2\text{Br}^- = \text{TIBr}_2^+ + 3\text{H}_2\text{O}$
log_k 20.711
delta_h 0 kJ
-gamma 0 0
Id: 8711301
log K source: NIST46.3
Delta H source: MTQ3.11
#T and ionic strength: 1.00 25.0
 $\text{Ti}(\text{OH})_3 + 3\text{Br}^- + 3\text{H}^+ = \text{TIBr}_3 + 3\text{H}_2\text{O}$
log_k 27.0244
delta_h 0 kJ
-gamma 0 0
Id: 8711302
log K source: MTQ3.11
Delta H source: MTQ3.11
#T and ionic strength:
 $\text{Ti}(\text{OH})_3 + 4\text{Br}^- + 3\text{H}^+ = \text{TIBr}_4^- + 3\text{H}_2\text{O}$
log_k 31.1533
delta_h 0 kJ
-gamma 0 0
Id: 8711303
log K source: MTQ3.11
Delta H source: MTQ3.11
#T and ionic strength:
 $\text{Zn}^{2+} + \text{Br}^- = \text{ZnBr}^+$
log_k -0.07
delta_h 1 kJ
-gamma 0 0
Id: 9501300
log K source: NIST46.3
Delta H source: NIST46.3
#T and ionic strength: 0.00 25.0
 $\text{Zn}^{2+} + 2\text{Br}^- = \text{ZnBr}_2$
log_k -0.98
delta_h 0 kJ
-gamma 0 0
Id: 9501301
log K source: MTQ3.11
Delta H source: MTQ3.11

#T and ionic strength:
 $\text{Cd}^{+2} + \text{Br}^- = \text{CdBr}^+$
 log_k 2.15
 delta_h -3 kJ
 -gamma 0 0
 # Id: 1601300
 # log K source: NIST46.3
 # Delta H source: NIST46.3
 #T and ionic strength: 0.00 25.0
 $\text{Cd}^{+2} + 2\text{Br}^- = \text{CdBr}_2$
 log_k 3
 delta_h -3 kJ
 -gamma 0 0
 # Id: 1601301
 # log K source: NIST46.3
 # Delta H source: NIST46.3
 #T and ionic strength: 0.00 25.0
 $\text{Hg}(\text{OH})_2 + 2\text{H}^+ + \text{Br}^- = \text{HgBr}^+ + 2\text{H}_2\text{O}$
 log_k 15.803
 delta_h -81.92 kJ
 -gamma 0 0
 # Id: 3611301
 # log K source: NIST46.3
 # Delta H source: NIST46.3
 #T and ionic strength: 0.50 25.0
 $\text{Hg}(\text{OH})_2 + 2\text{H}^+ + 2\text{Br}^- = \text{HgBr}_2 + 2\text{H}_2\text{O}$
 log_k 24.2725
 delta_h -127.12 kJ
 -gamma 0 0
 # Id: 3611302
 # log K source: NIST46.3
 # Delta H source: NIST46.3
 #T and ionic strength: 0.50 25.0
 $\text{Hg}(\text{OH})_2 + 2\text{H}^+ + 3\text{Br}^- = \text{HgBr}_3^- + 2\text{H}_2\text{O}$
 log_k 26.7025
 delta_h -138.82 kJ
 -gamma 0 0
 # Id: 3611303
 # log K source: NIST46.3
 # Delta H source: NIST46.3
 #T and ionic strength: 0.50 25.0
 $\text{Hg}(\text{OH})_2 + 2\text{H}^+ + 4\text{Br}^- = \text{HgBr}_4^{-2} + 2\text{H}_2\text{O}$
 log_k 27.933
 delta_h -153.72 kJ
 -gamma 0 0
 # Id: 3611304
 # log K source: NIST46.3
 # Delta H source: NIST46.3
 #T and ionic strength: 0.50 25.0
 $\text{Hg}(\text{OH})_2 + \text{Br}^- + \text{Cl}^- + 2\text{H}^+ = \text{HgBrCl} + 2\text{H}_2\text{O}$
 log_k 22.1811
 delta_h -113.77 kJ
 -gamma 0 0
 # Id: 3611305

log K source: NIST2.1.1
 # Delta H source: NIST2.1.1
 #T and ionic strength:
 $\text{Hg}(\text{OH})_2 + \text{Br}^- + \text{I}^- + 2\text{H}^+ = \text{HgBrI} + 2\text{H}_2\text{O}$
 log_k 27.3133
 delta_h -151.27 kJ
 -gamma 0 0
 # Id: 3611306
 # log K source: NIST2.1.1
 # Delta H source: NIST2.1.1
 #T and ionic strength:
 $\text{Hg}(\text{OH})_2 + \text{Br}^- + 3\text{I}^- + 2\text{H}^+ = \text{HgBrI}_3 - 2 + 2\text{H}_2\text{O}$
 log_k 34.2135
 delta_h 0 kJ
 -gamma 0 0
 # Id: 3611307
 # log K source: MTQ3.11
 # Delta H source: MTQ3.11
 #T and ionic strength:
 $\text{Hg}(\text{OH})_2 + 2\text{Br}^- + 2\text{I}^- + 2\text{H}^+ = \text{HgBr}_2\text{I}_2 - 2 + 2\text{H}_2\text{O}$
 log_k 32.3994
 delta_h 0 kJ
 -gamma 0 0
 # Id: 3611308
 # log K source: MTQ3.11
 # Delta H source: MTQ3.11
 #T and ionic strength:
 $\text{Hg}(\text{OH})_2 + 3\text{Br}^- + \text{I}^- + 2\text{H}^+ = \text{HgBr}_3\text{I} - 2 + 2\text{H}_2\text{O}$
 log_k 30.1528
 delta_h 0 kJ
 -gamma 0 0
 # Id: 3611309
 # log K source: MTQ3.11
 # Delta H source: MTQ3.11
 #T and ionic strength:
 $\text{Hg}(\text{OH})_2 + \text{H}^+ + \text{Br}^- = \text{HgBrOH} + \text{H}_2\text{O}$
 log_k 12.433
 delta_h 0 kJ
 -gamma 0 0
 # Id: 3613301
 # log K source: NIST46.3
 # Delta H source: MTQ3.11
 #T and ionic strength: 0.50 25.0
 $\text{Ag}^+ + \text{Br}^- = \text{AgBr}$
 log_k 4.6
 delta_h 0 kJ
 -gamma 0 0
 # Id: 201300
 # log K source: NIST46.3
 # Delta H source: MTQ3.11
 #T and ionic strength: 0.00 25.0
 $\text{Ag}^+ + 2\text{Br}^- = \text{AgBr}_2^-$
 log_k 7.5
 delta_h 0 kJ

-gamma 0 0
Id: 201301
log K source: NIST46.3
Delta H source: MTQ3.11
#T and ionic strength: 0.00 25.0
 $\text{Ag}^+ + 3\text{Br}^- = \text{AgBr}_3^{2-}$
log_k 8.1
delta_h 0 kJ
-gamma 0 0
Id: 201302
log K source: NIST46.3
Delta H source: MTQ3.11
#T and ionic strength: 0.00 25.0
 $\text{Ni}^{+2} + \text{Br}^- = \text{NiBr}^+$
log_k 0.5
delta_h 0 kJ
-gamma 0 0
Id: 5401300
log K source: MTQ3.11
Delta H source: MTQ3.11
#T and ionic strength:
 $\text{Cr}(\text{OH})_2^{2+} + \text{Br}^- + 2\text{H}^+ = \text{CrBr}^{+2} + 2\text{H}_2\text{O}$
log_k 7.5519
delta_h -46.9068 kJ
-gamma 0 0
Id: 2111300
log K source: MTQ3.11
Delta H source: MTQ3.11
#T and ionic strength:
 $\text{Be}^{+2} + \text{Br}^- = \text{BeBr}^+$
log_k 0.1009
delta_h 0 kJ
-gamma 5 0
Id: 1101301
log K source: NIST46.4
Delta H source: MTQ3.11
#T and ionic strength: 0.70 20.0
 $\text{Pb}^{+2} + \text{I}^- = \text{PbI}^+$
log_k 2
delta_h 0 kJ
-gamma 0 0
Id: 6003800
log K source: NIST46.3
Delta H source: MTQ3.11
#T and ionic strength: 0.00 25.0
 $\text{Pb}^{+2} + 2\text{I}^- = \text{PbI}_2$
log_k 3.2
delta_h 0 kJ
-gamma 0 0
Id: 6003801
log K source: NIST46.3
Delta H source: MTQ3.11
#T and ionic strength: 0.00 25.0
 $\text{Tl}^+ + \text{I}^- = \text{TlI}$

log_k 1.4279
delta_h 0 kJ
-gamma 0 0
Id: 8703800
log K source: MTQ3.11
Delta H source: MTQ3.11
#T and ionic strength:
 $\text{TI}^+ + 2\text{I}^- = \text{TII}^{2-}$
log_k 1.8588
delta_h 0 kJ
-gamma 0 0
Id: 8703801
log K source: MTQ3.11
Delta H source: MTQ3.11
#T and ionic strength:
 $\text{TI}(\text{OH})_3 + 4\text{I}^- + 3\text{H}^+ = \text{TII}^{4-} + 3\text{H}_2\text{O}$
log_k 34.7596
delta_h 0 kJ
-gamma 0 0
Id: 8713800
log K source: MTQ3.11
Delta H source: MTQ3.11
#T and ionic strength:
 $\text{Zn}^{+2} + \text{I}^- = \text{ZnI}^+$
log_k -2.0427
delta_h -4 kJ
-gamma 0 0
Id: 9503800
log K source: NIST46.3
Delta H source: NIST46.3
#T and ionic strength: 3.00 25.0
 $\text{Zn}^{+2} + 2\text{I}^- = \text{ZnI}_2$
log_k -1.69
delta_h 0 kJ
-gamma 0 0
Id: 9503801
log K source: MTQ3.11
Delta H source: MTQ3.11
#T and ionic strength:
 $\text{Cd}^{+2} + \text{I}^- = \text{CdI}^+$
log_k 2.28
delta_h -9.6 kJ
-gamma 0 0
Id: 1603800
log K source: NIST46.3
Delta H source: NIST46.3
#T and ionic strength: 0.00 25.0
 $\text{Cd}^{+2} + 2\text{I}^- = \text{CdI}_2$
log_k 3.92
delta_h -12 kJ
-gamma 0 0
Id: 1603801
log K source: NIST46.3
Delta H source: NIST46.3

#T and ionic strength: 0.00 25.0
 $\text{Hg}(\text{OH})_2 + 2\text{H}^+ + \text{I}^- = \text{HgI}^+ + 2\text{H}_2\text{O}$
 log_k 19.603
 delta_h -111.22 kJ
 -gamma 0 0
 # Id: 3613801
 # log K source: NIST46.4
 # Delta H source: NIST46.4
 #T and ionic strength: 0.50 25.0
 $\text{Hg}(\text{OH})_2 + 2\text{H}^+ + 2\text{I}^- = \text{HgI}_2 + 2\text{H}_2\text{O}$
 log_k 30.8225
 delta_h -182.72 kJ
 -gamma 0 0
 # Id: 3613802
 # log K source: NIST46.4
 # Delta H source: NIST46.4
 #T and ionic strength: 0.50 25.0
 $\text{Hg}(\text{OH})_2 + 2\text{H}^+ + 3\text{I}^- = \text{HgI}_3^- + 2\text{H}_2\text{O}$
 log_k 34.6025
 delta_h -194.22 kJ
 -gamma 0 0
 # Id: 3613803
 # log K source: NIST46.4
 # Delta H source: NIST2.1.1
 #T and ionic strength: 0.50 25.0
 $\text{Hg}(\text{OH})_2 + 2\text{H}^+ + 4\text{I}^- = \text{HgI}_4^{2-} + 2\text{H}_2\text{O}$
 log_k 36.533
 delta_h -220.72 kJ
 -gamma 0 0
 # Id: 3613804
 # log K source: NIST46.4
 # Delta H source: NIST46.4
 #T and ionic strength: 0.50 25.0
 $\text{Ag}^+ + \text{I}^- = \text{AgI}$
 log_k 6.6
 delta_h 0 kJ
 -gamma 0 0
 # Id: 203800
 # log K source: NIST46.3
 # Delta H source: MTQ3.11
 #T and ionic strength: 0.00 18.0
 $\text{Ag}^+ + 2\text{I}^- = \text{AgI}_2^-$
 log_k 11.7
 delta_h 0 kJ
 -gamma 0 0
 # Id: 203801
 # log K source: NIST46.3
 # Delta H source: MTQ3.11
 #T and ionic strength: 0.00 18.0
 $\text{Ag}^+ + 3\text{I}^- = \text{AgI}_3^{2-}$
 log_k 12.6
 delta_h -122 kJ
 -gamma 0 0
 # Id: 203802

log K source: NIST46.3
 # Delta H source: NIST46.3
 #T and ionic strength: 0.00 25.0
 $\text{Ag}^+ + 4\text{I}^- = \text{AgI}_4^{3-}$
 log_k 14.229
 delta_h 0 kJ
 -gamma 0 0
 # Id: 203803
 # log K source: NIST46.3
 # Delta H source: MTQ3.11
 #T and ionic strength: 2.00 25.0
 $\text{Cr}(\text{OH})_2^+ + \text{I}^- + 2\text{H}^+ = \text{CrI}^{2+} + 2\text{H}_2\text{O}$
 log_k 4.8289
 delta_h 0 kJ
 -gamma 0 0
 # Id: 2113800
 # log K source: MTQ3.11
 # Delta H source: MTQ3.11
 #T and ionic strength:
 $\text{H}^+ + \text{HS}^- = \text{H}_2\text{S}$
 log_k 7.02
 delta_h -22 kJ
 -gamma 0 0
 # Id: 3307300
 # log K source: NIST46.3
 # Delta H source: NIST46.3
 #T and ionic strength: 0.00 25.0
 $\text{Pb}^{2+} + 2\text{HS}^- = \text{Pb}(\text{HS})_2$
 log_k 15.27
 delta_h 0 kJ
 -gamma 0 0
 # Id: 6007300
 # log K source: MTQ3.11
 # Delta H source: MTQ3.11
 #T and ionic strength:
 $\text{Pb}^{2+} + 3\text{HS}^- = \text{Pb}(\text{HS})_3^-$
 log_k 16.57
 delta_h 0 kJ
 -gamma 0 0
 # Id: 6007301
 # log K source: MTQ3.11
 # Delta H source: MTQ3.11
 #T and ionic strength:
 $\text{Ti}^+ + \text{HS}^- = \text{TiHS}$
 log_k 2.474
 delta_h 0 kJ
 -gamma 0 0
 # Id: 8707300
 # log K source: NIST46.3
 # Delta H source: MTQ3.11
 #T and ionic strength: 1.00 25.0
 $2\text{Ti}^+ + \text{HS}^- = \text{Ti}_2\text{HS}^+$
 log_k 5.974
 delta_h 0 kJ

-gamma 0 0
 # Id: 8707301
 # log K source: NIST46.3
 # Delta H source: MTQ3.11
 #T and ionic strength: 1.00 25.0
 $2\text{Ti}^{+} + 3\text{HS}^{-} + \text{H}_2\text{O} = \text{Ti}_2\text{OH}(\text{HS})_3^{-2} + \text{H}^{+}$
 log_k 1.0044
 delta_h 0 kJ
 -gamma 0 0
 # Id: 8707302
 # log K source: MTQ3.11
 # Delta H source: MTQ3.11
 #T and ionic strength:
 $2\text{Ti}^{+} + 2\text{HS}^{-} + 2\text{H}_2\text{O} = \text{Ti}_2(\text{OH})_2(\text{HS})_2^{-2} + 2\text{H}^{+}$
 log_k -11.0681
 delta_h 0 kJ
 -gamma 0 0
 # Id: 8707303
 # log K source: MTQ3.11
 # Delta H source: MTQ3.11
 #T and ionic strength:
 $\text{Zn}^{+2} + 2\text{HS}^{-} = \text{Zn}(\text{HS})_2$
 log_k 12.82
 delta_h 0 kJ
 -gamma 0 0
 # Id: 9507300
 # log K source: DHa1993
 # Delta H source: MTQ3.11
 #T and ionic strength: 0.00 25.0
 $\text{Zn}^{+2} + 3\text{HS}^{-} = \text{Zn}(\text{HS})_3^{-}$
 log_k 16.1
 delta_h 0 kJ
 -gamma 0 0
 # Id: 9507301
 # log K source: MTQ3.11
 # Delta H source: MTQ3.11
 #T and ionic strength:
 $\text{Zn}^{+2} + 3\text{HS}^{-} = \text{ZnS}(\text{HS})_2^{-2} + \text{H}^{+}$
 log_k 6.12
 delta_h 0 kJ
 -gamma 0 0
 # Id: 9507302
 # log K source: DHa1993
 # Delta H source: MTQ3.11
 #T and ionic strength: 0.00 25.0
 $\text{Zn}^{+2} + 2\text{HS}^{-} + 2\text{HS}^{-} = \text{Zn}(\text{HS})_4^{-2}$
 log_k 14.64
 delta_h 0 kJ
 -gamma 0 0
 # Id: 9507303
 # log K source: DHa1993
 # Delta H source: MTQ3.11
 #T and ionic strength: 0.00 25.0
 $\text{Zn}^{+2} + 2\text{HS}^{-} = \text{ZnS}(\text{HS})^{-} + \text{H}^{+}$

log_k 6.81
 delta_h 0 kJ
 -gamma 0 0
 # Id: 9507304
 # log K source: DHa1993
 # Delta H source: MTQ3.11
 #T and ionic strength: 0.00 25.0
 $\text{Cd}^{+2} + \text{HS}^- = \text{CdHS}^+$
 log_k 8.008
 delta_h 0 kJ
 -gamma 0 0
 # Id: 1607300
 # log K source: NIST46.3
 # Delta H source: MTQ3.11
 #T and ionic strength: 1.00 25.0
 $\text{Cd}^{+2} + 2\text{HS}^- = \text{Cd}(\text{HS})_2$
 log_k 15.212
 delta_h 0 kJ
 -gamma 0 0
 # Id: 1607301
 # log K source: NIST46.3
 # Delta H source: MTQ3.11
 #T and ionic strength: 1.00 25.0
 $\text{Cd}^{+2} + 3\text{HS}^- = \text{Cd}(\text{HS})_3^-$
 log_k 17.112
 delta_h 0 kJ
 -gamma 0 0
 # Id: 1607302
 # log K source: NIST46.3
 # Delta H source: MTQ3.11
 #T and ionic strength: 1.00 25.0
 $\text{Cd}^{+2} + 4\text{HS}^- = \text{Cd}(\text{HS})_4^{2-}$
 log_k 19.308
 delta_h 0 kJ
 -gamma 0 0
 # Id: 1607303
 # log K source: NIST46.3
 # Delta H source: MTQ3.11
 #T and ionic strength: 1.00 25.0
 $\text{Hg}(\text{OH})_2 + 2\text{HS}^- = \text{HgS}_{2-2} + 2\text{H}_2\text{O}$
 log_k 29.414
 delta_h 0 kJ
 -gamma 0 0
 # Id: 3617300
 # log K source: NIST46.4
 # Delta H source: MTQ3.11
 #T and ionic strength: 1.00 20.0
 $\text{Hg}(\text{OH})_2 + 2\text{H}^+ + 2\text{HS}^- = \text{Hg}(\text{HS})_2 + 2\text{H}_2\text{O}$
 log_k 44.516
 delta_h 0 kJ
 -gamma 0 0
 # Id: 3617301
 # log K source: NIST46.3
 # Delta H source: MTQ3.11

#T and ionic strength: 1.00 20.0
 $\text{Hg(OH)}_2 + \text{H}^+ + 2\text{HS}^- = \text{HgHS}_2^- + 2\text{H}_2\text{O}$
 log_k 38.122
 delta_h 0 kJ
 -gamma 0 0
 # Id: 3617302
 # log K source: NIST46.4
 # Delta H source: MTQ3.11
 #T and ionic strength: 1.00 20.0
 $\text{Cu}^{+2} + 3\text{HS}^- = \text{Cu(HS)}_3^-$
 log_k 25.899
 delta_h 0 kJ
 -gamma 0 0
 # Id: 2317300
 # log K source: MTQ3.11
 # Delta H source: MTQ3.11
 #T and ionic strength:
 $\text{Ag}^+ + \text{HS}^- = \text{AgHS}$
 log_k 13.8145
 delta_h 0 kJ
 -gamma 0 0
 # Id: 207300
 # log K source: NIST46.3
 # Delta H source: MTQ3.11
 #T and ionic strength: 0.10 20.0
 $\text{Ag}^+ + 2\text{HS}^- = \text{Ag(HS)}_2^-$
 log_k 17.9145
 delta_h 0 kJ
 -gamma 0 0
 # Id: 207301
 # log K source: NIST46.3
 # Delta H source: MTQ3.11
 #T and ionic strength: 0.10 20.0
 $\text{Fe}^{+2} + 2\text{HS}^- = \text{Fe(HS)}_2$
 log_k 8.95
 delta_h 0 kJ
 -gamma 0 0
 # Id: 2807300
 # log K source: MTQ3.11
 # Delta H source: MTQ3.11
 #T and ionic strength:
 $\text{Fe}^{+2} + 3\text{HS}^- = \text{Fe(HS)}_3^-$
 log_k 10.987
 delta_h 0 kJ
 -gamma 0 0
 # Id: 2807301
 # log K source: MTQ3.11
 # Delta H source: MTQ3.11
 #T and ionic strength:
 $\text{HS}^- = \text{S}^{2-} + \text{H}^+$
 log_k -11.7828
 delta_h 46.4 kJ
 -gamma 0 0
 -no_check

Id: 7317300
 # log K source: NIST2.1.1
 # Delta H source: NIST2.1.1
 #T and ionic strength:
 $\text{HS}^- = \text{S3-2} + \text{H}^+$
 log_k -10.7667
 delta_h 42.2 kJ
 -gamma 0 0
 -no_check
 # Id: 7317301
 # log K source: NIST2.1.1
 # Delta H source: NIST2.1.1
 #T and ionic strength:
 $\text{HS}^- = \text{S4-2} + \text{H}^+$
 log_k -9.9608
 delta_h 39.3 kJ
 -gamma 0 0
 -no_check
 # Id: 7317302
 # log K source: NIST2.1.1
 # Delta H source: NIST2.1.1
 #T and ionic strength:
 $\text{HS}^- = \text{S5-2} + \text{H}^+$
 log_k -9.3651
 delta_h 37.6 kJ
 -gamma 0 0
 -no_check
 # Id: 7317303
 # log K source: NIST2.1.1
 # Delta H source: NIST2.1.1
 #T and ionic strength:
 $\text{HS}^- = \text{S6-2} + \text{H}^+$
 log_k -9.881
 delta_h 0 kJ
 -gamma 0 0
 -no_check
 # Id: 7317304
 # log K source: MTQ3.11
 # Delta H source: MTQ3.11
 #T and ionic strength:
 $2\text{Sb}(\text{OH})_3 + 4\text{HS}^- + 2\text{H}^+ = \text{Sb}_2\text{S}_4\text{-2} + 6\text{H}_2\text{O}$
 log_k 49.3886
 delta_h -321.78 kJ
 -gamma 0 0
 # Id: 7407300
 # log K source: NIST2.1.1
 # Delta H source: NIST2.1.1
 #T and ionic strength:
 $\text{Cu}^+ + 2\text{HS}^- = \text{Cu}(\text{S}_4)_2\text{-3} + 2\text{H}^+$
 log_k 3.39
 delta_h 0 kJ
 -gamma 23 0
 -no_check
 # Id: 2307300

log K source: MTQ3.11
 # Delta H source: MTQ3.11
 #T and ionic strength:
 $\text{Cu}^{+} + 2\text{HS}^{-} = \text{CuS}_4\text{S}_5^{-3} + 2\text{H}^{+}$
 log_k 2.66
 delta_h 0 kJ
 -gamma 25 0
 -no_check
 # Id: 2307301
 # log K source: MTQ3.11
 # Delta H source: MTQ3.11
 #T and ionic strength:
 $\text{Ag}^{+} + 2\text{HS}^{-} = \text{Ag}(\text{S}_4)_2^{-3} + 2\text{H}^{+}$
 log_k 0.991
 delta_h 0 kJ
 -gamma 22 0
 -no_check
 # Id: 207302
 # log K source: MTQ3.11
 # Delta H source: MTQ3.11
 #T and ionic strength:
 $\text{Ag}^{+} + 2\text{HS}^{-} = \text{AgS}_4\text{S}_5^{-3} + 2\text{H}^{+}$
 log_k 0.68
 delta_h 0 kJ
 -gamma 24 0
 -no_check
 # Id: 207303
 # log K source: MTQ3.11
 # Delta H source: MTQ3.11
 #T and ionic strength:
 $\text{Ag}^{+} + 2\text{HS}^{-} = \text{Ag}(\text{HS})\text{S}_4^{-2} + \text{H}^{+}$
 log_k 10.431
 delta_h 0 kJ
 -gamma 15 0
 -no_check
 # Id: 207304
 # log K source: MTQ3.11
 # Delta H source: MTQ3.11
 #T and ionic strength:
 $\text{H}^{+} + \text{SO}_4^{-2} = \text{HSO}_4^{-}$
 log_k 1.99
 delta_h 22 kJ
 -gamma 4.5 0
 # Id: 3307320
 # log K source: NIST46.3
 # Delta H source: NIST46.3
 #T and ionic strength: 0.00 25.0
 $\text{NH}_4^{+} + \text{SO}_4^{-2} = \text{NH}_4\text{SO}_4^{-}$
 log_k 1.03
 delta_h 0 kJ
 -gamma 5 0
 # Id: 4907320
 # log K source: NIST46.3
 # Delta H source: MTQ3.11

#T and ionic strength: 0.00 25.0
 $\text{Pb}^{+2} + \text{SO}_4^{-2} = \text{PbSO}_4$
log_k 2.69
delta_h 0 kJ
-gamma 0 0
Id: 6007320
log K source: NIST46.3
Delta H source: MTQ3.11
#T and ionic strength: 0.00 25.0
 $\text{Pb}^{+2} + 2\text{SO}_4^{-2} = \text{Pb}(\text{SO}_4)_2^{-2}$
log_k 3.47
delta_h 0 kJ
-gamma 0 0
Id: 6007321
log K source: SCD3.02 (1960 RKa)
Delta H source: MTQ3.11
#T and ionic strength: 0.00 25.0
 $\text{Al}^{+3} + \text{SO}_4^{-2} = \text{AlSO}_4^{+}$
log_k 3.89
delta_h 28 kJ
-gamma 4.5 0
Id: 307320
log K source: NIST46.3
Delta H source: NIST46.3
#T and ionic strength: 0.00 25.0
 $\text{Al}^{+3} + 2\text{SO}_4^{-2} = \text{Al}(\text{SO}_4)_2^{-}$
log_k 4.92
delta_h 11.9 kJ
-gamma 4.5 0
Id: 307321
log K source: Nord90
Delta H source: Nord90
#T and ionic strength: 0.00 25.0
 $\text{Ti}^{+} + \text{SO}_4^{-2} = \text{TiSO}_4^{-}$
log_k 1.37
delta_h -0.8 kJ
-gamma 0 0
Id: 8707320
log K source: NIST46.3
Delta H source: NIST46.3
#T and ionic strength: 0.00 25.0
 $\text{Zn}^{+2} + \text{SO}_4^{-2} = \text{ZnSO}_4$
log_k 2.34
delta_h 6.2 kJ
-gamma 0 0
Id: 9507320
log K source: NIST46.3
Delta H source: NIST46.3
#T and ionic strength: 0.00 25.0
 $\text{Zn}^{+2} + 2\text{SO}_4^{-2} = \text{Zn}(\text{SO}_4)_2^{-2}$
log_k 3.28
delta_h 0 kJ
-gamma 0 0
Id: 9507321

log K source: MTQ3.11
 # Delta H source: MTQ3.11
 #T and ionic strength:
 $\text{Cd}^{+2} + \text{SO}_4^{-2} = \text{CdSO}_4$
 log_k 2.37
 delta_h 8.7 kJ
 -gamma 0 0
 # Id: 1607320
 # log K source: NIST46.3
 # Delta H source: NIST46.3
 #T and ionic strength: 0.00 25.0
 $\text{Cd}^{+2} + 2\text{SO}_4^{-2} = \text{Cd}(\text{SO}_4)_2$
 log_k 3.5
 delta_h 0 kJ
 -gamma 0 0
 # Id: 1607321
 # log K source: MTQ3.11
 # Delta H source: MTQ3.11
 #T and ionic strength:
 $\text{Hg}(\text{OH})_2 + 2\text{H}^+ + \text{SO}_4^{-2} = \text{HgSO}_4 + 2\text{H}_2\text{O}$
 log_k 8.612
 delta_h 0 kJ
 -gamma 0 0
 # Id: 3617320
 # log K source: NIST46.3
 # Delta H source: MTQ3.11
 #T and ionic strength: 0.50 25.0
 $\text{Cu}^{+2} + \text{SO}_4^{-2} = \text{CuSO}_4$
 log_k 2.36
 delta_h 8.7 kJ
 -gamma 0 0
 # Id: 2317320
 # log K source: NIST46.3
 # Delta H source: NIST46.3
 #T and ionic strength: 0.00 25.0
 $\text{Ag}^+ + \text{SO}_4^{-2} = \text{AgSO}_4$
 log_k 1.3
 delta_h 6.2 kJ
 -gamma 0 0
 # Id: 207320
 # log K source: NIST46.3
 # Delta H source: NIST46.3
 #T and ionic strength: 0.00 25.0
 $\text{Ni}^{+2} + \text{SO}_4^{-2} = \text{NiSO}_4$
 log_k 2.3
 delta_h 5.8 kJ
 -gamma 0 0
 # Id: 5407320
 # log K source: NIST46.3
 # Delta H source: NIST46.3
 #T and ionic strength: 0.00 25.0
 $\text{Ni}^{+2} + 2\text{SO}_4^{-2} = \text{Ni}(\text{SO}_4)_2$
 log_k 0.82
 delta_h 0 kJ

-gamma 0 0
 # Id: 5407321
 # log K source: SCD3.02 (1978 BLa)
 # Delta H source: MTQ3.11
 #T and ionic strength: 0.00 25.0
 $\text{Co}^{+2} + \text{SO}_4^{-2} = \text{CoSO}_4$
 log_k 2.3
 delta_h 6.2 kJ
 -gamma 0 0
 # Id: 2007320
 # log K source: NIST46.4
 # Delta H source: NIST46.4
 #T and ionic strength: 0.00 25.0
 $\text{Fe}^{+2} + \text{SO}_4^{-2} = \text{FeSO}_4$
 log_k 2.39
 delta_h 8 kJ
 -gamma 0 0
 # Id: 2807320
 # log K source: NIST46.3
 # Delta H source: NIST46.3
 #T and ionic strength: 0.00 25.0
 $\text{Fe}^{+3} + \text{SO}_4^{-2} = \text{FeSO}_4^{+}$
 log_k 4.05
 delta_h 25 kJ
 -gamma 5 0
 # Id: 2817320
 # log K source: NIST46.3
 # Delta H source: NIST46.3
 #T and ionic strength: 0.00 25.0
 $\text{Fe}^{+3} + 2\text{SO}_4^{-2} = \text{Fe}(\text{SO}_4)_2^{-}$
 log_k 5.38
 delta_h 19.2 kJ
 -gamma 0 0
 # Id: 2817321
 # log K source: Nord90
 # Delta H source: Nord90
 #T and ionic strength: 0.00 25.0
 $\text{Mn}^{+2} + \text{SO}_4^{-2} = \text{MnSO}_4$
 log_k 2.25
 delta_h 8.7 kJ
 -gamma 0 0
 # Id: 4707320
 # log K source: NIST46.3
 # Delta H source: NIST46.3
 #T and ionic strength: 0.00 25.0
 $\text{Cr}(\text{OH})_2^{+} + 2\text{H}^{+} + \text{SO}_4^{-2} = \text{CrSO}_4^{+} + 2\text{H}_2\text{O}$
 log_k 12.9371
 delta_h -98.62 kJ
 -gamma 0 0
 # Id: 2117320
 # log K source: NIST46.3
 # Delta H source: NIST46.3
 #T and ionic strength: 1.00 50.0
 $\text{Cr}(\text{OH})_2^{+} + \text{H}^{+} + \text{SO}_4^{-2} = \text{CrOHSO}_4 + \text{H}_2\text{O}$

log_k 8.2871
 delta_h 0 kJ
 -gamma 0 0
 # Id: 2117321
 # log K source: NIST46.3
 # Delta H source: MTQ3.11
 #T and ionic strength: 0.10 25.0
 $2\text{Cr}(\text{OH})_2^+ + \text{SO}_4^{2-} + 2\text{H}^+ = \text{Cr}_2(\text{OH})_2\text{SO}_4 + 2\text{H}_2\text{O}$
 log_k 16.155
 delta_h 0 kJ
 -gamma 0 0
 # Id: 2117323
 # log K source: MTQ3.11
 # Delta H source: MTQ3.11
 #T and ionic strength:
 $2\text{Cr}(\text{OH})_2^+ + 2\text{SO}_4^{2-} + 2\text{H}^+ = \text{Cr}_2(\text{OH})_2(\text{SO}_4)_2 + 2\text{H}_2\text{O}$
 log_k 17.9288
 delta_h 0 kJ
 -gamma 0 0
 # Id: 2117324
 # log K source: MTQ3.11
 # Delta H source: MTQ3.11
 #T and ionic strength:
 $\text{U}^{4+} + \text{SO}_4^{2-} = \text{USO}_4$
 log_k 6.6
 delta_h 8 kJ
 -gamma 0 0
 # Id: 8917320
 # log K source: NIST46.3
 # Delta H source: NIST46.3
 #T and ionic strength: 0.00 25.0
 $\text{U}^{4+} + 2\text{SO}_4^{2-} = \text{U}(\text{SO}_4)_2$
 log_k 10.5
 delta_h 33 kJ
 -gamma 0 0
 # Id: 8917321
 # log K source: NIST46.3
 # Delta H source: NIST46.3
 #T and ionic strength: 0.00 25.0
 $\text{UO}_2^{2+} + \text{SO}_4^{2-} = \text{UO}_2\text{SO}_4$
 log_k 3.18
 delta_h 20 kJ
 -gamma 0 0
 # Id: 8937320
 # log K source: NIST46.3
 # Delta H source: NIST46.3
 #T and ionic strength: 0.00 25.0
 $\text{UO}_2^{2+} + 2\text{SO}_4^{2-} = \text{UO}_2(\text{SO}_4)_2$
 log_k 4.3
 delta_h 38 kJ
 -gamma 0 0
 # Id: 8937321
 # log K source: NIST46.3
 # Delta H source: NIST46.3

#T and ionic strength: 0.00 25.0
 $V^{+3} + SO_4^{2-} = VSO_4^{+}$
log_k 2.674
delta_h 0 kJ
-gamma 0 0
Id: 9017320
log K source: NIST46.3
Delta H source: MTQ3.11
#T and ionic strength: 1.00 25.0
 $VO^{+2} + SO_4^{2-} = VOSO_4$
log_k 2.44
delta_h 17 kJ
-gamma 0 0
Id: 9027320
log K source: NIST46.3
Delta H source: NIST46.3
#T and ionic strength: 0.00 25.0
 $VO_2^{+} + SO_4^{2-} = VO_2SO_4^{-}$
log_k 1.378
delta_h 0 kJ
-gamma 0 0
Id: 9037320
log K source: NIST46.3
Delta H source: MTQ3.11
#T and ionic strength: 1.00 20.0
 $Be^{+2} + SO_4^{2-} = BeSO_4$
log_k 2.19
delta_h 29 kJ
-gamma 0 0
Id: 1107321
log K source: NIST46.4
Delta H source: NIST46.4
#T and ionic strength: 0.00 25.0
 $Be^{+2} + 2SO_4^{2-} = Be(SO_4)_2^{2-}$
log_k 2.596
delta_h 0 kJ
-gamma 0 0
Id: 1107322
log K source: NIST46.4
Delta H source: MTQ3.11
#T and ionic strength: 1.00 25.0
 $Mg^{+2} + SO_4^{2-} = MgSO_4$
log_k 2.26
delta_h 5.8 kJ
-gamma 0 0
Id: 4607320
log K source: NIST46.3
Delta H source: NIST46.3
#T and ionic strength: 0.00 25.0
 $Ca^{+2} + SO_4^{2-} = CaSO_4$
log_k 2.36
delta_h 7.1 kJ
-gamma 0 0
Id: 1507320

log K source: NIST46.3
 # Delta H source: NIST46.3
 #T and ionic strength: 0.00 25.0
 $\text{Sr}^{+2} + \text{SO}_4^{-2} = \text{SrSO}_4$
 log_k 2.3
 delta_h 8 kJ
 -gamma 0 0
 # Id: 8007321
 # log K source: NIST46.4
 # Delta H source: NIST46.4
 #T and ionic strength: 0.00 25.0
 $\text{Li}^{+} + \text{SO}_4^{-2} = \text{LiSO}_4^{-}$
 log_k 0.64
 delta_h 0 kJ
 -gamma 5 0
 # Id: 4407320
 # log K source: NIST46.3
 # Delta H source: NIST46.3
 #T and ionic strength: 0.00 25.0
 $\text{Na}^{+} + \text{SO}_4^{-2} = \text{NaSO}_4^{-}$
 log_k 0.73
 delta_h 1 kJ
 -gamma 5.4 0
 # Id: 5007320
 # log K source: NIST46.3
 # Delta H source: NIST46.3
 #T and ionic strength: 0.00 25.0
 $\text{K}^{+} + \text{SO}_4^{-2} = \text{KSO}_4^{-}$
 log_k 0.85
 delta_h 4.1 kJ
 -gamma 5.4 0
 # Id: 4107320
 # log K source: NIST46.3
 # Delta H source: NIST46.3
 #T and ionic strength: 0.00 25.0
 $\text{HSe}^{-} + \text{H}^{+} = \text{H}_2\text{Se}$
 log_k 3.89
 delta_h 3.3 kJ
 -gamma 0 0
 # Id: 3307600
 # log K source: NIST46.3
 # Delta H source: NIST2.1.1
 #T and ionic strength: 0.00 25.0
 $2\text{Ag}^{+} + \text{HSe}^{-} = \text{Ag}_2\text{Se} + \text{H}^{+}$
 log_k 34.911
 delta_h 0 kJ
 -gamma 0 0
 # Id: 207600
 # log K source: NIST46.3
 # Delta H source: MTQ3.11
 #T and ionic strength: 1.00 25.0
 $\text{Ag}^{+} + \text{H}_2\text{O} + 2\text{HSe}^{-} = \text{AgOH}(\text{Se})_2^{-4} + 3\text{H}^{+}$
 log_k -20.509
 delta_h 0 kJ

-gamma 0 0
 # Id: 207601
 # log K source: NIST46.3
 # Delta H source: MTQ3.11
 #T and ionic strength: 1.00 25.0
 $\text{Mn}^{+2} + \text{HSe}^- = \text{MnSe} + \text{H}^+$
 log_k -5.385
 delta_h 0 kJ
 -gamma 0 0
 # Id: 4707600
 # log K source: NIST46.3
 # Delta H source: MTQ3.11
 #T and ionic strength: 1.00 25.0
 $\text{HSeO}_3^- = \text{SeO}_3^{2-} + \text{H}^+$
 log_k -8.4
 delta_h 5.02 kJ
 -gamma 0 0
 # Id: 3307611
 # log K source: NIST46.3
 # Delta H source: NIST46.3
 #T and ionic strength: 0.00 25.0
 $\text{HSeO}_3^- + \text{H}^+ = \text{H}_2\text{SeO}_3$
 log_k 2.63
 delta_h 6.2 kJ
 -gamma 0 0
 # Id: 3307610
 # log K source: NIST46.3
 # Delta H source: NIST46.3
 #T and ionic strength: 0.00 25.0
 $\text{Cd}^{+2} + 2\text{HSeO}_3^- = \text{Cd}(\text{SeO}_3)_2^{2-} + 2\text{H}^+$
 log_k -10.884
 delta_h 0 kJ
 -gamma 0 0
 # Id: 1607610
 # log K source: NIST46.4
 # Delta H source: MTQ3.11
 #T and ionic strength: 1.00 25.0
 $\text{Ag}^+ + \text{HSeO}_3^- = \text{AgSeO}_3^- + \text{H}^+$
 log_k -5.592
 delta_h 0 kJ
 -gamma 0 0
 # Id: 207610
 # log K source: NIST46.3
 # Delta H source: MTQ3.11
 #T and ionic strength: 1.00 25.0
 $\text{Ag}^+ + 2\text{HSeO}_3^- = \text{Ag}(\text{SeO}_3)_2^{3-} + 2\text{H}^+$
 log_k -13.04
 delta_h 0 kJ
 -gamma 0 0
 # Id: 207611
 # log K source: NIST46.3
 # Delta H source: MTQ3.11
 #T and ionic strength: 1.00 25.0
 $\text{Fe}^{+3} + \text{HSeO}_3^- = \text{FeHSeO}_3^{+2}$

log_k 3.422
delta_h 25 kJ
-gamma 0 0
Id: 2817610
log K source: NIST46.3
Delta H source: NIST46.3
#T and ionic strength: 1.00 25.0
 $\text{SeO}_4^{2-} + \text{H}^+ = \text{HSeO}_4^-$
log_k 1.7
delta_h 23 kJ
-gamma 0 0
Id: 3307620
log K source: NIST46.4
Delta H source: NIST46.4
#T and ionic strength: 0.00 25.0
 $\text{Zn}^{2+} + \text{SeO}_4^{2-} = \text{ZnSeO}_4$
log_k 2.19
delta_h 0 kJ
-gamma 0 0
Id: 9507620
log K source: NIST46.4
Delta H source: MTQ3.11
#T and ionic strength: 0.00 25.0
 $\text{Zn}^{2+} + 2\text{SeO}_4^{2-} = \text{Zn}(\text{SeO}_4)_2$
log_k 2.196
delta_h 0 kJ
-gamma 0 0
Id: 9507621
log K source: NIST46.4
Delta H source: MTQ3.11
#T and ionic strength: 1.00 25.0
 $\text{Cd}^{2+} + \text{SeO}_4^{2-} = \text{CdSeO}_4$
log_k 2.27
delta_h 0 kJ
-gamma 0 0
Id: 1607620
log K source: NIST46.4
Delta H source: MTQ3.11
#T and ionic strength: 0.00 25.0
 $\text{Ni}^{2+} + \text{SeO}_4^{2-} = \text{NiSeO}_4$
log_k 2.67
delta_h 14 kJ
-gamma 0 0
Id: 5407620
log K source: NIST46.4
Delta H source: NIST46.4
#T and ionic strength: 0.00 25.0
 $\text{Co}^{2+} + \text{SeO}_4^{2-} = \text{CoSeO}_4$
log_k 2.7
delta_h 12 kJ
-gamma 0 0
Id: 2007621
log K source: NIST46.4
Delta H source: NIST46.4

#T and ionic strength: 0.00 25.0
 $\text{Mn}^{+2} + \text{SeO}_4^{-2} = \text{MnSeO}_4$
 log_k 2.43
 delta_h 14 kJ
 -gamma 0 0
 # Id: 4707620
 # log K source: NIST46.4
 # Delta H source: NIST46.4
 #T and ionic strength: 0.00 25.0
 $\text{NH}_4^+ = \text{NH}_3 + \text{H}^+$
 log_k -9.244
 delta_h 52 kJ
 -gamma 0 0
 # Id: 3304900
 # log K source: NIST46.3
 # Delta H source: NIST46.3
 #T and ionic strength: 0.00 25.0
 $\text{Ag}^+ + \text{NH}_4^+ = \text{AgNH}_3^+ + \text{H}^+$
 log_k -5.934
 delta_h -72 kJ
 -gamma 0 0
 # Id: 204901
 # log K source: NIST46.4
 # Delta H source: NIST46.4
 #T and ionic strength: 0.00 25.0
 $\text{Ag}^+ + 2\text{NH}_4^+ = \text{Ag}(\text{NH}_3)_2^+ + 2\text{H}^+$
 log_k -11.268
 delta_h -160 kJ
 -gamma 0 0
 # Id: 204902
 # log K source: NIST46.4
 # Delta H source: NIST46.4
 #T and ionic strength: 0.00 25.0
 $\text{Hg}(\text{OH})_2 + \text{H}^+ + \text{NH}_4^+ = \text{HgNH}_3^{+2} + 2\text{H}_2\text{O}$
 log_k 5.75
 delta_h 0 kJ
 -gamma 0 0
 # Id: 3614900
 # log K source: NIST46.3
 # Delta H source: MTQ3.11
 #T and ionic strength: 2.00 22.0
 $\text{Hg}(\text{OH})_2 + 2\text{NH}_4^+ = \text{Hg}(\text{NH}_3)_2^{+2} + 2\text{H}_2\text{O}$
 log_k 5.506
 delta_h -246.72 kJ
 -gamma 0 0
 # Id: 3614901
 # log K source: NIST46.3
 # Delta H source: NIST46.3
 #T and ionic strength: 1.00 25.0
 $\text{Hg}(\text{OH})_2 + 3\text{NH}_4^+ = \text{Hg}(\text{NH}_3)_3^{+2} + 2\text{H}_2\text{O} + \text{H}^+$
 log_k -3.138
 delta_h -312.72 kJ
 -gamma 0 0
 # Id: 3614902

log K source: NIST46.3
 # Delta H source: NIST46.3
 #T and ionic strength: 2.00 25.0
 $\text{Hg}(\text{OH})_2 + 4\text{NH}_4^+ = \text{Hg}(\text{NH}_3)_4^{2+} + 2\text{H}_2\text{O} + 2\text{H}^+$
 log_k -11.482
 delta_h -379.72 kJ
 -gamma 0 0
 # Id: 3614903
 # log K source: NIST46.3
 # Delta H source: NIST46.3
 #T and ionic strength: 0.10 25.0
 $\text{Cu}^{2+} + \text{NH}_4^+ = \text{CuNH}_3^{2+} + \text{H}^+$
 log_k -5.234
 delta_h -72 kJ
 -gamma 0 0
 # Id: 2314901
 # log K source: NIST46.4
 # Delta H source: NIST46.4
 #T and ionic strength: 0.00 25.0
 $\text{Ni}^{2+} + \text{NH}_4^+ = \text{NiNH}_3^{2+} + \text{H}^+$
 log_k -6.514
 delta_h -67 kJ
 -gamma 0 0
 # Id: 5404901
 # log K source: NIST46.4
 # Delta H source: NIST46.4
 #T and ionic strength: 0.10 25.0
 $\text{Ni}^{2+} + 2\text{NH}_4^+ = \text{Ni}(\text{NH}_3)_2^{2+} + 2\text{H}^+$
 log_k -13.598
 delta_h -111.6 kJ
 -gamma 0 0
 # Id: 5404902
 # log K source: NIST46.4
 # Delta H source: NIST46.4
 #T and ionic strength: 0.10 25.0
 $\text{Co}^{2+} + \text{NH}_4^+ = \text{Co}(\text{NH}_3)^{2+} + \text{H}^+$
 log_k -7.164
 delta_h -65 kJ
 -gamma 0 0
 # Id: 2004900
 # log K source: NIST46.4
 # Delta H source: NIST46.4
 #T and ionic strength: 0.10 25.0
 $\text{Co}^{2+} + 2\text{NH}_4^+ = \text{Co}(\text{NH}_3)_2^{2+} + 2\text{H}^+$
 log_k -14.778
 delta_h 0 kJ
 -gamma 0 0
 # Id: 2004901
 # log K source: NIST46.4
 # Delta H source: MTQ3.11
 #T and ionic strength: 2.00 25.0
 $\text{Co}^{2+} + 3\text{NH}_4^+ = \text{Co}(\text{NH}_3)_3^{2+} + 3\text{H}^+$
 log_k -22.922
 delta_h 0 kJ

-gamma 0 0
 # Id: 2004902
 # log K source: NIST46.4
 # Delta H source: MTQ3.11
 #T and ionic strength: 2.00 25.0
 $\text{Co}^{+2} + 4\text{NH}_4^+ = \text{Co}(\text{NH}_3)_4^{+2} + 4\text{H}^+$
 log_k -31.446
 delta_h 0 kJ
 -gamma 0 0
 # Id: 2004903
 # log K source: NIST46.4
 # Delta H source: MTQ3.11
 #T and ionic strength: 2.00 30.0
 $\text{Co}^{+2} + 5\text{NH}_4^+ = \text{Co}(\text{NH}_3)_5^{+2} + 5\text{H}^+$
 log_k -40.47
 delta_h 0 kJ
 -gamma 0 0
 # Id: 2004904
 # log K source: NIST46.4
 # Delta H source: MTQ3.11
 #T and ionic strength: 2.00 30.0
 $\text{Co}^{+3} + 6\text{NH}_4^+ + \text{H}_2\text{O} = \text{Co}(\text{NH}_3)_6\text{OH}^{+2} + 7\text{H}^+$
 log_k -43.7148
 delta_h 0 kJ
 -gamma 0 0
 # Id: 2014901
 # log K source: NIST2.1.1
 # Delta H source: MTQ3.11
 #T and ionic strength:
 $\text{Co}^{+3} + 5\text{NH}_4^+ + \text{Cl}^- = \text{Co}(\text{NH}_3)_5\text{Cl}^{+2} + 5\text{H}^+$
 log_k -17.9584
 delta_h 113.38 kJ
 -gamma 0 0
 # Id: 2014902
 # log K source: NIST2.1.1
 # Delta H source: NIST2.1.1
 #T and ionic strength:
 $\text{Co}^{+3} + 6\text{NH}_4^+ + \text{Cl}^- = \text{Co}(\text{NH}_3)_6\text{Cl}^{+2} + 6\text{H}^+$
 log_k -33.9179
 delta_h 104.34 kJ
 -gamma 0 0
 # Id: 2014903
 # log K source: NIST2.1.1
 # Delta H source: NIST2.1.1
 #T and ionic strength:
 $\text{Co}^{+3} + 6\text{NH}_4^+ + \text{Br}^- = \text{Co}(\text{NH}_3)_6\text{Br}^{+2} + 6\text{H}^+$
 log_k -33.8884
 delta_h 110.57 kJ
 -gamma 0 0
 # Id: 2014904
 # log K source: NIST2.1.1
 # Delta H source: NIST2.1.1
 #T and ionic strength:
 $\text{Co}^{+3} + 6\text{NH}_4^+ + \text{I}^- = \text{Co}(\text{NH}_3)_6\text{I}^{+2} + 6\text{H}^+$

log_k -33.4808
 delta_h 115.44 kJ
 -gamma 0 0
 # Id: 2014905
 # log K source: NIST2.1.1
 # Delta H source: NIST2.1.1
 #T and ionic strength:
 $\text{Co}^{+3} + 6\text{NH}_4^+ + \text{SO}_4^{2-} = \text{Co}(\text{NH}_3)_6\text{SO}_4^+ + 6\text{H}^+$
 log_k -28.9926
 delta_h 124.5 kJ
 -gamma 0 0
 # Id: 2014906
 # log K source: NIST2.1.1
 # Delta H source: NIST2.1.1
 #T and ionic strength:
 $\text{Cr}(\text{OH})_2^+ + 6\text{NH}_4^+ = \text{Cr}(\text{NH}_3)_6^{3+} + 2\text{H}_2\text{O} + 4\text{H}^+$
 log_k -32.8952
 delta_h 0 kJ
 -gamma 0 0
 # Id: 2114900
 # log K source: NIST46.3
 # Delta H source: MTQ3.11
 #T and ionic strength: 4.50 25.0
 $\text{Cr}(\text{OH})_2^+ + 5\text{NH}_4^+ = \text{Cr}(\text{NH}_3)_5\text{OH}^{2+} + 4\text{H}^+ + \text{H}_2\text{O}$
 log_k -30.2759
 delta_h 0 kJ
 -gamma 0 0
 # Id: 2114901
 # log K source: MTQ3.11
 # Delta H source: MTQ3.11
 #T and ionic strength:
 $\text{Cr}(\text{OH})_2^+ + 6\text{NH}_4^+ + \text{Cl}^- = \text{Cr}(\text{NH}_3)_6\text{Cl}^{2+} + 2\text{H}_2\text{O} + 4\text{H}^+$
 log_k -31.7932
 delta_h 0 kJ
 -gamma 0 0
 # Id: 2114904
 # log K source: MTQ3.11
 # Delta H source: MTQ3.11
 #T and ionic strength:
 $\text{Cr}(\text{OH})_2^+ + 6\text{NH}_4^+ + \text{Br}^- = \text{Cr}(\text{NH}_3)_6\text{Br}^{2+} + 4\text{H}^+ + 2\text{H}_2\text{O}$
 log_k -31.887
 delta_h 0 kJ
 -gamma 0 0
 # Id: 2114905
 # log K source: MTQ3.11
 # Delta H source: MTQ3.11
 #T and ionic strength:
 $\text{Cr}(\text{OH})_2^+ + 6\text{NH}_4^+ + \text{I}^- = \text{Cr}(\text{NH}_3)_6\text{I}^{2+} + 4\text{H}^+ + 2\text{H}_2\text{O}$
 log_k -32.008
 delta_h 0 kJ
 -gamma 0 0
 # Id: 2114906
 # log K source: MTQ3.11
 # Delta H source: MTQ3.11

#T and ionic strength:
 $\text{Cr(OH)}_2^+ + 4\text{NH}_4^+ = \text{cis}^+ + 4\text{H}^+$
 # log_k -29.8574
 # delta_h 0 kJ
 # -gamma 0 0
 # # Id: 4902113
 # # log K source: MTQ3.11
 # # Delta H source: MTQ3.11
 #T and ionic strength:
 $\text{Cr(OH)}_2^+ + 4\text{NH}_4^+ = \text{trans}^+ + 4\text{H}^+$
 # log_k -30.5537
 # delta_h 0 kJ
 # -gamma 0 0
 # # Id: 4902114
 # # log K source: MTQ3.11
 # # Delta H source: MTQ3.11
 #T and ionic strength:
 $\text{Ca}^{+2} + \text{NH}_4^+ = \text{CaNH}_3^{+2} + \text{H}^+$
 log_k -9.144
 delta_h 0 kJ
 -gamma 0 0
 # Id: 1504901
 # log K source: NIST46.4
 # Delta H source: MTQ3.11
 #T and ionic strength: 0.50 25.0
 $\text{Ca}^{+2} + 2\text{NH}_4^+ = \text{Ca(NH}_3)_2^{+2} + 2\text{H}^+$
 log_k -18.788
 delta_h 0 kJ
 -gamma 0 0
 # Id: 1504902
 # log K source: NIST46.4
 # Delta H source: MTQ3.11
 #T and ionic strength: 0.50 25.0
 $\text{Sr}^{+2} + \text{NH}_4^+ = \text{SrNH}_3^{+2} + \text{H}^+$
 log_k -9.344
 delta_h 0 kJ
 -gamma 0 0
 # Id: 8004901
 # log K source: NIST46.4
 # Delta H source: MTQ3.11
 #T and ionic strength: 0.50 25.0
 $\text{Ba}^{+2} + \text{NH}_4^+ = \text{BaNH}_3^{+2} + \text{H}^+$
 log_k -9.444
 delta_h 0 kJ
 -gamma 0 0
 # Id: 1004901
 # log K source: NIST46.4
 # Delta H source: MTQ3.11
 #T and ionic strength: 0.50 25.0
 $\text{Ti}^+ + \text{NO}_2^- = \text{TiNO}_2$
 log_k 0.83
 delta_h 0 kJ
 -gamma 0 0
 # Id: 8704910

log K source: NIST46.3
 # Delta H source: MTQ3.11
 #T and ionic strength: 0.00 25.0
 $\text{Ag}^+ + \text{NO}_2^- = \text{AgNO}_2$
 log_k 2.32
 delta_h -29 kJ
 -gamma 0 0
 # Id: 204911
 # log K source: NIST46.4
 # Delta H source: NIST46.4
 #T and ionic strength: 0.00 25.0
 $\text{Ag}^+ + 2\text{NO}_2^- = \text{Ag}(\text{NO}_2)_2^-$
 log_k 2.51
 delta_h -46 kJ
 -gamma 0 0
 # Id: 204910
 # log K source: NIST46.3
 # Delta H source: NIST46.3
 #T and ionic strength: 0.00 25.0
 $\text{Cu}^{+2} + \text{NO}_2^- = \text{CuNO}_2^+$
 log_k 2.02
 delta_h 0 kJ
 -gamma 0 0
 # Id: 2314911
 # log K source: NIST46.4
 # Delta H source: MTQ3.11
 #T and ionic strength: 0.00 25.0
 $\text{Cu}^{+2} + 2\text{NO}_2^- = \text{Cu}(\text{NO}_2)_2$
 log_k 3.03
 delta_h 0 kJ
 -gamma 0 0
 # Id: 2314912
 # log K source: NIST46.4
 # Delta H source: MTQ3.11
 #T and ionic strength: 0.00 25.0
 $\text{Co}^{+2} + \text{NO}_2^- = \text{CoNO}_2^+$
 log_k 0.848
 delta_h 0 kJ
 -gamma 0 0
 # Id: 2004911
 # log K source: NIST46.4
 # Delta H source: MTQ3.11
 #T and ionic strength: 1.00 25.0
 $\text{Sn}(\text{OH})_2 + 2\text{H}^+ + \text{NO}_3^- = \text{SnNO}_3^+ + 2\text{H}_2\text{O}$
 log_k 7.942
 delta_h 0 kJ
 -gamma 0 0
 # Id: 7904921
 # log K source: NIST46.4
 # Delta H source: MTQ3.11
 #T and ionic strength: 1.00 25.0
 $\text{Pb}^{+2} + \text{NO}_3^- = \text{PbNO}_3^+$
 log_k 1.17
 delta_h 2 kJ

-gamma 0 0
 # Id: 6004920
 # log K source: NIST46.3
 # Delta H source: NIST46.3
 #T and ionic strength: 0.00 25.0
 $\text{Pb}^{+2} + 2\text{NO}_3^- = \text{Pb}(\text{NO}_3)_2$
 log_k 1.4
 delta_h -6.6 kJ
 -gamma 0 0
 # Id: 6004921
 # log K source: NIST46.4
 # Delta H source: NIST46.4
 #T and ionic strength: 0.00 25.0
 $\text{Ti}^+ + \text{NO}_3^- = \text{TiNO}_3$
 log_k 0.33
 delta_h -2 kJ
 -gamma 0 0
 # Id: 8704920
 # log K source: NIST46.3
 # Delta H source: NIST46.3
 #T and ionic strength: 0.00 25.0
 $\text{Ti}(\text{OH})_3 + \text{NO}_3^- + 3\text{H}^+ = \text{TiNO}_3 + 2\text{H}_2\text{O}$
 log_k 7.0073
 delta_h 0 kJ
 -gamma 0 0
 # Id: 8714920
 # log K source: MTQ3.11
 # Delta H source: MTQ3.11
 #T and ionic strength:
 $\text{Cd}^{+2} + \text{NO}_3^- = \text{CdNO}_3^+$
 log_k 0.5
 delta_h -21 kJ
 -gamma 0 0
 # Id: 1604920
 # log K source: NIST46.3
 # Delta H source: NIST46.3
 #T and ionic strength: 0.00 25.0
 $\text{Cd}^{+2} + 2\text{NO}_3^- = \text{Cd}(\text{NO}_3)_2$
 log_k 0.2
 delta_h 0 kJ
 -gamma 0 0
 # Id: 1604921
 # log K source: NIST46.4
 # Delta H source: MTQ3.11
 #T and ionic strength: 0.00 25.0
 $\text{Hg}(\text{OH})_2 + 2\text{H}^+ + \text{NO}_3^- = \text{HgNO}_3^+ + 2\text{H}_2\text{O}$
 log_k 5.7613
 delta_h 0 kJ
 -gamma 0 0
 # Id: 3614920
 # log K source: NIST46.3
 # Delta H source: MTQ3.11
 #T and ionic strength: 3.00 25.0
 $\text{Hg}(\text{OH})_2 + 2\text{H}^+ + 2\text{NO}_3^- = \text{Hg}(\text{NO}_3)_2 + 2\text{H}_2\text{O}$

log_k 5.38
delta_h 0 kJ
-gamma 0 0
Id: 3614921
log K source: NIST46.3
Delta H source: MTQ3.11
#T and ionic strength: 3.00 25.0
 $\text{Cu}^{+2} + \text{NO}_3^- = \text{CuNO}_3^+$
log_k 0.5
delta_h -4.1 kJ
-gamma 0 0
Id: 2314921
log K source: NIST46.4
Delta H source: NIST46.4
#T and ionic strength: 0.00 25.0
 $\text{Cu}^{+2} + 2\text{NO}_3^- = \text{Cu}(\text{NO}_3)_2$
log_k -0.4
delta_h 0 kJ
-gamma 0 0
Id: 2314922
log K source: NIST46.4
Delta H source: MTQ3.11
#T and ionic strength: 0.00 25.0
 $\text{Zn}^{+2} + \text{NO}_3^- = \text{ZnNO}_3^+$
log_k 0.4
delta_h -4.6 kJ
-gamma 0 0
Id: 9504921
log K source: NIST46.4
Delta H source: NIST46.4
#T and ionic strength: 0.00 25.0
 $\text{Zn}^{+2} + 2\text{NO}_3^- = \text{Zn}(\text{NO}_3)_2$
log_k -0.3
delta_h 0 kJ
-gamma 0 0
Id: 9504922
log K source: NIST46.4
Delta H source: MTQ3.11
#T and ionic strength: 0.00 25.0
 $\text{Ag}^+ + \text{NO}_3^- = \text{AgNO}_3$
log_k -0.1
delta_h 22.6 kJ
-gamma 0 0
Id: 204920
log K source: NIST46.3
Delta H source: NIST46.3
#T and ionic strength: 0.00 25.0
 $\text{Ni}^{+2} + \text{NO}_3^- = \text{NiNO}_3^+$
log_k 0.4
delta_h 0 kJ
-gamma 0 0
Id: 5404921
log K source: NIST46.4
Delta H source: MTQ3.11

#T and ionic strength: 0.00 25.0
 $\text{Co}^{+2} + \text{NO}_3^- = \text{CoNO}_3^+$
log_k 0.2
delta_h 0 kJ
-gamma 0 0
Id: 2004921
log K source: NIST46.4
Delta H source: MTQ3.11
#T and ionic strength: 0.00 25.0
 $\text{Co}^{+2} + 2\text{NO}_3^- = \text{Co}(\text{NO}_3)_2$
log_k 0.5085
delta_h 0 kJ
-gamma 0 0
Id: 2004922
log K source: NIST46.4
Delta H source: MTQ3.11
#T and ionic strength: 0.50 25.0
 $\text{Fe}^{+3} + \text{NO}_3^- = \text{FeNO}_3^+$
log_k 1
delta_h -37 kJ
-gamma 0 0
Id: 2814921
log K source: NIST46.4
Delta H source: NIST46.4
#T and ionic strength: 0.00 25.0
 $\text{Mn}^{+2} + \text{NO}_3^- = \text{MnNO}_3^+$
log_k 0.2
delta_h 0 kJ
-gamma 0 0
Id: 4704921
log K source: NIST46.4
Delta H source: MTQ3.11
#T and ionic strength: 0.00 25.0
 $\text{Mn}^{+2} + 2\text{NO}_3^- = \text{Mn}(\text{NO}_3)_2$
log_k 0.6
delta_h -1.6569 kJ
-gamma 0 0
Id: 4704920
log K source: NIST46.3
Delta H source: MTQ3.11
#T and ionic strength: 0.00 25.0
 $\text{Cr}(\text{OH})_2^{+} + \text{NO}_3^- + 2\text{H}^+ = \text{CrNO}_3^{+2} + 2\text{H}_2\text{O}$
log_k 8.2094
delta_h -65.4378 kJ
-gamma 0 0
Id: 2114920
log K source: MTQ3.11
Delta H source: MTQ3.11
#T and ionic strength:
 $\text{UO}_2^{+2} + \text{NO}_3^- = \text{UO}_2\text{NO}_3^+$
log_k 0.3
delta_h -12 kJ
-gamma 0 0
Id: 8934921

log K source: NIST46.4
 # Delta H source: NIST46.4
 #T and ionic strength: 0.00 25.0
 $\text{VO}_2^+ + \text{NO}_3^- = \text{VO}_2\text{NO}_3$
 log_k -0.296
 delta_h 0 kJ
 -gamma 0 0
 # Id: 9034920
 # log K source: NIST46.3
 # Delta H source: MTQ3.11
 #T and ionic strength: 1.00 20.0
 $\text{Ca}^{+2} + \text{NO}_3^- = \text{CaNO}_3^+$
 log_k 0.5
 delta_h -5.4 kJ
 -gamma 0 0
 # Id: 1504921
 # log K source: NIST46.4
 # Delta H source: NIST46.4
 #T and ionic strength: 0.00 25.0
 $\text{Sr}^{+2} + \text{NO}_3^- = \text{SrNO}_3^+$
 log_k 0.6
 delta_h -10 kJ
 -gamma 0 0
 # Id: 8004921
 # log K source: NIST46.4
 # Delta H source: NIST46.4
 #T and ionic strength: 0.00 25.0
 $\text{Ba}^{+2} + \text{NO}_3^- = \text{BaNO}_3^+$
 log_k 0.7
 delta_h -13 kJ
 -gamma 0 0
 # Id: 1004921
 # log K source: NIST46.4
 # Delta H source: NIST46.4
 #T and ionic strength: 0.00 25.0
 $\text{H}^+ + \text{Cyanide}^- = \text{HCyanide}$
 log_k 9.21
 delta_h -43.63 kJ
 -gamma 0 0
 # Id: 3301431
 # log K source: NIST46.4
 # Delta H source: NIST46.4
 #T and ionic strength: 0.00 25.0
 $\text{Cd}^{+2} + \text{Cyanide}^- = \text{CdCyanide}^+$
 log_k 6.01
 delta_h -30 kJ
 -gamma 0 0
 # Id: 1601431
 # log K source: NIST46.4
 # Delta H source: NIST46.4
 #T and ionic strength: 0.00 25.0
 $\text{Cd}^{+2} + 2\text{Cyanide}^- = \text{Cd}(\text{Cyanide})_2$
 log_k 11.12
 delta_h -54.3 kJ

-gamma 0 0
 # Id: 1601432
 # log K source: NIST46.4
 # Delta H source: NIST46.4
 #T and ionic strength: 0.00 25.0
 $\text{Cd}^{2+} + 3\text{Cyanide}^- = \text{Cd}(\text{Cyanide})_3^-$
 log_k 15.65
 delta_h -90.3 kJ
 -gamma 0 0
 # Id: 1601433
 # log K source: NIST46.4
 # Delta H source: NIST46.4
 #T and ionic strength: 0.00 25.0
 $\text{Cd}^{2+} + 4\text{Cyanide}^- = \text{Cd}(\text{Cyanide})_4^{2-}$
 log_k 17.92
 delta_h -112 kJ
 -gamma 0 0
 # Id: 1601434
 # log K source: NIST46.4
 # Delta H source: NIST46.4
 #T and ionic strength: 0.00 25.0
 $\text{Hg}(\text{OH})_2 + 2\text{H}^+ + \text{Cyanide}^- = \text{HgCyanide}^+ + 2\text{H}_2\text{O}$
 log_k 23.194
 delta_h -136.72 kJ
 -gamma 0 0
 # Id: 3611431
 # log K source: NIST46.4
 # Delta H source: NIST46.4
 #T and ionic strength: 0.00 25.0
 $\text{Hg}(\text{OH})_2 + 2\text{H}^+ + 2\text{Cyanide}^- = \text{Hg}(\text{Cyanide})_2 + 2\text{H}_2\text{O}$
 log_k 38.944
 delta_h 154.28 kJ
 -gamma 0 0
 # Id: 3611432
 # log K source: NIST46.4
 # Delta H source: NIST46.4
 #T and ionic strength: 0.00 25.0
 $\text{Hg}(\text{OH})_2 + 2\text{H}^+ + 3\text{Cyanide}^- = \text{Hg}(\text{Cyanide})_3^- + 2\text{H}_2\text{O}$
 log_k 42.504
 delta_h -262.72 kJ
 -gamma 0 0
 # Id: 3611433
 # log K source: NIST46.4
 # Delta H source: NIST46.4
 #T and ionic strength: 0.00 25.0
 $\text{Hg}(\text{OH})_2 + 2\text{H}^+ + 4\text{Cyanide}^- = \text{Hg}(\text{Cyanide})_4^{2-} + 2\text{H}_2\text{O}$
 log_k 45.164
 delta_h -288.72 kJ
 -gamma 0 0
 # Id: 3611434
 # log K source: NIST46.4
 # Delta H source: NIST46.4
 #T and ionic strength: 0.00 25.0
 $\text{Cu}^+ + 2\text{Cyanide}^- = \text{Cu}(\text{Cyanide})_2^-$

log_k 21.9145
delta_h -121 kJ
-gamma 0 0
Id: 2301432
log K source: NIST46.4
Delta H source: NIST46.4
#T and ionic strength: 0.10 25.0
 $\text{Cu}^+ + 3\text{Cyanide}^- = \text{Cu}(\text{Cyanide})_3^{2-}$
log_k 27.2145
delta_h -167.4 kJ
-gamma 0 0
Id: 2301433
log K source: NIST46.4
Delta H source: NIST46.4
#T and ionic strength: 0.00 25.0
 $\text{Cu}^+ + 4\text{Cyanide}^- = \text{Cu}(\text{Cyanide})_4^{3-}$
log_k 28.7145
delta_h -214.2 kJ
-gamma 0 0
Id: 2301431
log K source: NIST46.4
Delta H source: NIST46.4
#T and ionic strength: 0.00 25.0
 $\text{Ag}^+ + 2\text{Cyanide}^- = \text{Ag}(\text{Cyanide})_2^-$
log_k 20.48
delta_h -137 kJ
-gamma 0 0
Id: 201432
log K source: NIST46.4
Delta H source: NIST46.4
#T and ionic strength: 0.00 25.0
 $\text{Ag}^+ + 3\text{Cyanide}^- = \text{Ag}(\text{Cyanide})_3^{2-}$
log_k 21.7
delta_h -140 kJ
-gamma 0 0
Id: 201433
log K source: NIST46.4
Delta H source: NIST46.4
#T and ionic strength: 0.00 25.0
 $\text{Ag}^+ + \text{H}_2\text{O} + \text{Cyanide}^- = \text{Ag}(\text{Cyanide})\text{OH}^- + \text{H}^+$
log_k -0.777
delta_h 0 kJ
-gamma 0 0
Id: 201431
log K source: NIST46.4
Delta H source: MTQ3.11
#T and ionic strength: 0.00 25.0
 $\text{Ni}^{2+} + 4\text{Cyanide}^- = \text{Ni}(\text{Cyanide})_4^{2-}$
log_k 30.2
delta_h -180 kJ
-gamma 0 0
Id: 5401431
log K source: NIST46.4
Delta H source: NIST46.4

#T and ionic strength: 0.00 25.0
 $\text{Ni}^{+2} + 4\text{Cyanide}^- + \text{H}^+ = \text{NiH}(\text{Cyanide})_4^-$
 log_k 36.0289
 delta_h 0 kJ
 -gamma 0 0
 # Id: 5401432
 # log K source: NIST46.4
 # Delta H source: MTQ3.11
 #T and ionic strength: 0.10 25.0
 $\text{Ni}^{+2} + 4\text{Cyanide}^- + 2\text{H}^+ = \text{NiH}_2\text{Cyanide}_4$
 log_k 40.7434
 delta_h 0 kJ
 -gamma 0 0
 # Id: 5401433
 # log K source: NIST46.4
 # Delta H source: MTQ3.11
 #T and ionic strength: 0.10 25.0
 $\text{Ni}^{+2} + 4\text{Cyanide}^- + 3\text{H}^+ = \text{NiH}_3(\text{Cyanide})_4^+$
 log_k 43.3434
 delta_h 0 kJ
 -gamma 0 0
 # Id: 5401434
 # log K source: NIST46.4
 # Delta H source: MTQ3.11
 #T and ionic strength: 0.10 25.0
 $\text{Co}^{+2} + 3\text{Cyanide}^- = \text{Co}(\text{Cyanide})_3^-$
 log_k 14.312
 delta_h 0 kJ
 -gamma 0 0
 # Id: 2001431
 # log K source: NIST46.4
 # Delta H source: MTQ3.11
 #T and ionic strength: 1.00 25.0
 $\text{Co}^{+2} + 5\text{Cyanide}^- = \text{Co}(\text{Cyanide})_5^{3-}$
 log_k 23
 delta_h -257 kJ
 -gamma 0 0
 # Id: 2001432
 # log K source: NIST46.4
 # Delta H source: NIST46.4
 #T and ionic strength: 1.00 25.0
 $\text{Fe}^{+2} + 6\text{Cyanide}^- = \text{Fe}(\text{Cyanide})_6^{4-}$
 log_k 35.4
 delta_h -358 kJ
 -gamma 0 0
 # Id: 2801431
 # log K source: NIST46.4
 # Delta H source: NIST46.4
 #T and ionic strength: 0.00 25.0
 $\text{H}^+ + \text{Fe}^{+2} + 6\text{Cyanide}^- = \text{HFe}(\text{Cyanide})_6^{3-}$
 log_k 39.71
 delta_h -356 kJ
 -gamma 0 0
 # Id: 2801432

log K source: NIST46.4
 # Delta H source: NIST46.4
 #T and ionic strength: 0.00 25.0
 $2\text{H}^+ + \text{Fe}^{2+} + 6\text{Cyanide}^- = \text{H}_2\text{Fe}(\text{Cyanide})_6^{2-}$
 log_k 42.11
 delta_h -352 kJ
 -gamma 0 0
 # Id: 2801433
 # log K source: NIST46.4
 # Delta H source: NIST46.4
 #T and ionic strength: 0.00 25.0
 $\text{Fe}^{3+} + 6\text{Cyanide}^- = \text{Fe}(\text{Cyanide})_6^{3-}$
 log_k 43.6
 delta_h -293 kJ
 -gamma 0 0
 # Id: 2811431
 # log K source: NIST46.4
 # Delta H source: NIST46.4
 #T and ionic strength: 0.00 25.0
 $2\text{Fe}^{3+} + 6\text{Cyanide}^- = \text{Fe}_2(\text{Cyanide})_6$
 log_k 47.6355
 delta_h -218 kJ
 -gamma 0 0
 # Id: 2811432
 # log K source: NIST46.4
 # Delta H source: NIST46.4
 #T and ionic strength: 0.50 25.0
 $\text{Sn}(\text{OH})_2 + \text{Fe}^{3+} + 6\text{Cyanide}^- + 2\text{H}^+ = \text{SnFe}(\text{Cyanide})_6^{3-} + 2\text{H}_2\text{O}$
 log_k 53.54
 delta_h 0 kJ
 -gamma 0 0
 # Id: 7901431
 # log K source: Ba1987
 # Delta H source:
 #T and ionic strength: 0.00 25.0
 $\text{NH}_4^+ + \text{Fe}^{2+} + 6\text{Cyanide}^- = \text{NH}_4\text{Fe}(\text{Cyanide})_6^{3-}$
 log_k 37.7
 delta_h -354 kJ
 -gamma 0 0
 # Id: 4901431
 # log K source: NIST46.4
 # Delta H source: NIST46.4
 #T and ionic strength: 0.00 25.0
 $\text{Ti}^+ + \text{Fe}^{2+} + 6\text{Cyanide}^- = \text{TiFe}(\text{Cyanide})_6^{3-}$
 log_k 38.4
 delta_h -365.5 kJ
 -gamma 0 0
 # Id: 8701432
 # log K source: NIST46.4
 # Delta H source: NIST46.4
 #T and ionic strength: 0.00 25.0
 $\text{Mg}^{2+} + \text{Fe}^{3+} + 6\text{Cyanide}^- = \text{MgFe}(\text{Cyanide})_6^{3-}$
 log_k 46.39
 delta_h -290 kJ

-gamma 0 0
 # Id: 4601431
 # log K source: NIST46.4
 # Delta H source: NIST46.4
 #T and ionic strength: 0.00 25.0
 $\text{Mg}^{+2} + \text{Fe}^{+2} + 6\text{Cyanide}^- = \text{MgFe}(\text{Cyanide})_6^{-2}$
 log_k 39.21
 delta_h -346 kJ
 -gamma 0 0
 # Id: 4601432
 # log K source: NIST46.4
 # Delta H source: NIST46.4
 #T and ionic strength: 0.00 25.0
 $\text{Ca}^{+2} + \text{Fe}^{+3} + 6\text{Cyanide}^- = \text{CaFe}(\text{Cyanide})_6^{-}$
 log_k 46.43
 delta_h -291 kJ
 -gamma 0 0
 # Id: 1501431
 # log K source: NIST46.4
 # Delta H source: NIST46.4
 #T and ionic strength: 0.00 25.0
 $\text{Ca}^{+2} + \text{Fe}^{+2} + 6\text{Cyanide}^- = \text{CaFe}(\text{Cyanide})_6^{-2}$
 log_k 39.1
 delta_h -347 kJ
 -gamma 0 0
 # Id: 1501432
 # log K source: NIST46.4
 # Delta H source: NIST46.4
 #T and ionic strength: 0.00 25.0
 $2\text{Ca}^{+2} + \text{Fe}^{+2} + 6\text{Cyanide}^- = \text{Ca}_2\text{Fe}(\text{Cyanide})_6$
 log_k 40.6
 delta_h -350.201 kJ
 -gamma 0 0
 # Id: 1501433
 # log K source: NIST46.4
 # Delta H source: MTQ3.11
 #T and ionic strength: 0.00 25.0
 $\text{Sr}^{+2} + \text{Fe}^{+3} + 6\text{Cyanide}^- = \text{SrFe}(\text{Cyanide})_6^{-}$
 log_k 46.45
 delta_h -292 kJ
 -gamma 0 0
 # Id: 8001431
 # log K source: NIST46.4
 # Delta H source: NIST46.4
 #T and ionic strength: 0.00 25.0
 $\text{Sr}^{+2} + \text{Fe}^{+2} + 6\text{Cyanide}^- = \text{SrFe}(\text{Cyanide})_6^{-2}$
 log_k 39.1
 delta_h -350 kJ
 -gamma 0 0
 # Id: 8001432
 # log K source: NIST46.4
 # Delta H source: NIST46.4
 #T and ionic strength: 0.00 25.0
 $\text{Ba}^{+2} + \text{Fe}^{+2} + 6\text{Cyanide}^- = \text{BaFe}(\text{Cyanide})_6^{-2}$

log_k 39.19
delta_h -342 kJ
-gamma 0 0
Id: 1001430
log K source: NIST46.4
Delta H source: NIST46.4
#T and ionic strength: 0.00 25.0
 $\text{Ba}^{+2} + \text{Fe}^{+3} + 6\text{Cyanide}^- = \text{BaFe(Cyanide)}_6^-$
log_k 46.48
delta_h -292 kJ
-gamma 0 0
Id: 1001431
log K source: NIST46.4
Delta H source: NIST46.4
#T and ionic strength: 0.00 25.0
 $\text{Na}^+ + \text{Fe}^{+2} + 6\text{Cyanide}^- = \text{NaFe(Cyanide)}_6^-$
log_k 37.6
delta_h -354 kJ
-gamma 0 0
Id: 5001431
log K source: NIST46.4
Delta H source: NIST46.4
#T and ionic strength: 0.00 25.0
 $\text{K}^+ + \text{Fe}^{+2} + 6\text{Cyanide}^- = \text{KFe(Cyanide)}_6^-$
log_k 37.75
delta_h -353.9 kJ
-gamma 0 0
Id: 4101433
log K source: NIST46.4
Delta H source: NIST46.4
#T and ionic strength: 0.00 25.0
 $\text{K}^+ + \text{Fe}^{+3} + 6\text{Cyanide}^- = \text{KFe(Cyanide)}_6^-$
log_k 45.04
delta_h -291 kJ
-gamma 0 0
Id: 4101430
log K source: NIST46.4
Delta H source: NIST46.4
#T and ionic strength: 0.00 25.0
 $\text{H}^+ + \text{PO}_4^{-3} = \text{HPO}_4^{-2}$
log_k 12.375
delta_h -15 kJ
-gamma 5 0
Id: 3305800
log K source: NIST46.3
Delta H source: NIST46.3
#T and ionic strength: 0.00 25.0
 $2\text{H}^+ + \text{PO}_4^{-3} = \text{H}_2\text{PO}_4^-$
log_k 19.573
delta_h -18 kJ
-gamma 5.4 0
Id: 3305801
log K source: NIST46.3
Delta H source: NIST46.3

#T and ionic strength: 0.00 25.0
 $3\text{H}^+ + \text{PO}_4^{3-} = \text{H}_3\text{PO}_4$
 log_k 21.721
 delta_h -10.1 kJ
 -gamma 0 0
 # Id: 3305802
 # log K source: NIST46.3
 # Delta H source: NIST46.3
 #T and ionic strength: 0.00 25.0
 $\text{Co}^{2+} + \text{H}^+ + \text{PO}_4^{3-} = \text{CoHPO}_4$
 log_k 15.4128
 delta_h 0 kJ
 -gamma 0 0
 # Id: 2005800
 # log K source: NIST46.4
 # Delta H source: MTQ3.11
 #T and ionic strength: 0.10 25.0
 $\text{Fe}^{2+} + 2\text{H}^+ + \text{PO}_4^{3-} = \text{FeH}_2\text{PO}_4^+$
 log_k 22.273
 delta_h 0 kJ
 -gamma 5.4 0
 # Id: 2805800
 # log K source: NIST46.3
 # Delta H source: MTQ3.11
 #T and ionic strength: 0.00 25.0
 $\text{Fe}^{2+} + \text{H}^+ + \text{PO}_4^{3-} = \text{FeHPO}_4$
 log_k 15.975
 delta_h 0 kJ
 -gamma 0 0
 # Id: 2805801
 # log K source: NIST46.3
 # Delta H source: MTQ3.11
 #T and ionic strength: 0.00 25.0
 $\text{Fe}^{3+} + 2\text{H}^+ + \text{PO}_4^{3-} = \text{FeH}_2\text{PO}_4^{2+}$
 log_k 23.8515
 delta_h 0 kJ
 -gamma 5.4 0
 # Id: 2815801
 # log K source: NIST46.3
 # Delta H source: MTQ3.11
 #T and ionic strength: 0.50 25.0
 $\text{Fe}^{3+} + \text{H}^+ + \text{PO}_4^{3-} = \text{FeHPO}_4^+$
 log_k 22.292
 delta_h -30.5432 kJ
 -gamma 5.4 0
 # Id: 2815800
 # log K source: NIST46.3
 # Delta H source: MTQ3.11
 #T and ionic strength: 0.50 25.0
 $\text{Cr}(\text{OH})_2^{2+} + 4\text{H}^+ + \text{PO}_4^{3-} = \text{CrH}_2\text{PO}_4^{2+} + 2\text{H}_2\text{O}$
 log_k 31.9068
 delta_h 0 kJ
 -gamma 0 0
 # Id: 2115800

log K source: MTQ3.11
 # Delta H source: MTQ3.11
 #T and ionic strength:
 $U+4 + PO4-3 + H+ = UHPO4+2$
 log_k 24.443
 delta_h 31.38 kJ
 -gamma 0 0
 # Id: 8915800
 # log K source: MTQ3.11
 # Delta H source: MTQ3.11
 #T and ionic strength:
 $U+4 + 2PO4-3 + 2H+ = U(HPO4)2$
 log_k 46.833
 delta_h 7.1128 kJ
 -gamma 0 0
 # Id: 8915801
 # log K source: MTQ3.11
 # Delta H source: MTQ3.11
 #T and ionic strength:
 $U+4 + 3PO4-3 + 3H+ = U(HPO4)3-2$
 log_k 67.564
 delta_h -32.6352 kJ
 -gamma 0 0
 # Id: 8915802
 # log K source: MTQ3.11
 # Delta H source: MTQ3.11
 #T and ionic strength:
 $U+4 + 4PO4-3 + 4H+ = U(HPO4)4-4$
 log_k 88.483
 delta_h -110.876 kJ
 -gamma 0 0
 # Id: 8915803
 # log K source: MTQ3.11
 # Delta H source: MTQ3.11
 #T and ionic strength:
 $UO2+2 + H+ + PO4-3 = UO2HPO4$
 log_k 19.655
 delta_h -8.7864 kJ
 -gamma 0 0
 # Id: 8935800
 # log K source: NIST46.3
 # Delta H source: MTQ3.11
 #T and ionic strength: 0.00 25.0
 $UO2+2 + 2PO4-3 + 2H+ = UO2(HPO4)2-2$
 log_k 42.988
 delta_h -47.6934 kJ
 -gamma 0 0
 # Id: 8935801
 # log K source: MTQ3.11
 # Delta H source: MTQ3.11
 #T and ionic strength:
 $UO2+2 + 2H+ + PO4-3 = UO2H2PO4+$
 log_k 22.833
 delta_h -15.4808 kJ

-gamma 0 0
 # Id: 8935802
 # log K source: NIST46.3
 # Delta H source: MTQ3.11
 #T and ionic strength: 0.00 25.0
 $\text{UO}_2+2 + 2\text{PO}_4-3 + 4\text{H}+ = \text{UO}_2(\text{H}_2\text{PO}_4)_2$
 log_k 44.7
 delta_h -69.036 kJ
 -gamma 0 0
 # Id: 8935803
 # log K source: MTQ3.11
 # Delta H source: MTQ3.11
 #T and ionic strength:
 $\text{UO}_2+2 + 3\text{PO}_4-3 + 6\text{H}+ = \text{UO}_2(\text{H}_2\text{PO}_4)_3-$
 log_k 66.245
 delta_h -119.662 kJ
 -gamma 0 0
 # Id: 8935804
 # log K source: MTQ3.11
 # Delta H source: MTQ3.11
 #T and ionic strength:
 $\text{UO}_2+2 + \text{PO}_4-3 = \text{UO}_2\text{PO}_4-$
 log_k 13.25
 delta_h 0 kJ
 -gamma 0 0
 # Id: 8935805
 # log K source: NIST46.4
 # Delta H source: MTQ3.11
 #T and ionic strength: 0.00 25.0
 $\text{Mg}+2 + \text{PO}_4-3 = \text{MgPO}_4-$
 log_k 4.654
 delta_h 12.9704 kJ
 -gamma 5.4 0
 # Id: 4605800
 # log K source: SCD3.02 (1993 GMa)
 # Delta H source: MTQ3.11
 #T and ionic strength: 0.20 25.0
 $\text{Mg}+2 + 2\text{H}+ + \text{PO}_4-3 = \text{MgH}_2\text{PO}_4+$
 log_k 21.2561
 delta_h -4.6861 kJ
 -gamma 5.4 0
 # Id: 4605801
 # log K source: NIST46.3
 # Delta H source: MTQ3.11
 #T and ionic strength: 0.00 37.0
 $\text{Mg}+2 + \text{H}+ + \text{PO}_4-3 = \text{MgHPO}_4$
 log_k 15.175
 delta_h -3 kJ
 -gamma 0 0
 # Id: 4605802
 # log K source: NIST46.3
 # Delta H source: NIST46.3
 #T and ionic strength: 0.00 25.0
 $\text{Ca}+2 + \text{H}+ + \text{PO}_4-3 = \text{CaHPO}_4$

log_k 15.035
 delta_h -3 kJ
 -gamma 0 0
 # Id: 1505800
 # log K source: NIST46.3
 # Delta H source: NIST46.3
 #T and ionic strength: 0.00 25.0
 $\text{Ca}^{+2} + \text{PO}_4^{-3} = \text{CaPO}_4^-$
 log_k 6.46
 delta_h 12.9704 kJ
 -gamma 5.4 0
 # Id: 1505801
 # log K source: SCD3.02 (1993 GMa)
 # Delta H source: MTQ3.11
 #T and ionic strength: 0.00 25.0
 $\text{Ca}^{+2} + 2\text{H}^+ + \text{PO}_4^{-3} = \text{CaH}_2\text{PO}_4^+$
 log_k 20.923
 delta_h -6 kJ
 -gamma 5.4 0
 # Id: 1505802
 # log K source: NIST46.3
 # Delta H source: NIST46.3
 #T and ionic strength: 0.00 25.0
 $\text{Sr}^{+2} + \text{H}^+ + \text{PO}_4^{-3} = \text{SrHPO}_4$
 log_k 14.8728
 delta_h 0 kJ
 -gamma 0 0
 # Id: 8005800
 # log K source: NIST46.4
 # Delta H source: MTQ3.11
 #T and ionic strength: 0.10 25.0
 $\text{Sr}^{+2} + 2\text{H}^+ + \text{PO}_4^{-3} = \text{SrH}_2\text{PO}_4^+$
 log_k 20.4019
 delta_h 0 kJ
 -gamma 0 0
 # Id: 8005801
 # log K source: NIST46.4
 # Delta H source: MTQ3.11
 #T and ionic strength: 0.10 20.0
 $\text{Na}^+ + \text{H}^+ + \text{PO}_4^{-3} = \text{NaHPO}_4^-$
 log_k 13.445
 delta_h 0 kJ
 -gamma 5.4 0
 # Id: 5005800
 # log K source: NIST46.3
 # Delta H source: MTQ3.11
 #T and ionic strength: 0.00 25.0
 $\text{K}^+ + \text{H}^+ + \text{PO}_4^{-3} = \text{KHPO}_4^-$
 log_k 13.255
 delta_h 0 kJ
 -gamma 5.4 0
 # Id: 4105800
 # log K source: NIST46.3
 # Delta H source: MTQ3.11

#T and ionic strength: 0.00 25.0
 $\text{H3AsO3} = \text{AsO3-3} + 3\text{H+}$
log_k -34.744
delta_h 84.726 kJ
-gamma 0 0
Id: 3300602
log K source: MTQ3.11
Delta H source: MTQ3.11
#T and ionic strength:
 $\text{H3AsO3} = \text{HAsO3-2} + 2\text{H+}$
log_k -21.33
delta_h 59.4086 kJ
-gamma 0 0
Id: 3300601
log K source: MTQ3.11
Delta H source: MTQ3.11
#T and ionic strength:
 $\text{H3AsO3} = \text{H2AsO3-} + \text{H+}$
log_k -9.29
delta_h 27.41 kJ
-gamma 0 0
Id: 3300600
log K source: NIST46.4
Delta H source: NIST2.1.1
#T and ionic strength: 0.00 25.0
 $\text{H3AsO3} + \text{H+} = \text{H4AsO3+}$
log_k -0.305
delta_h 0 kJ
-gamma 0 0
Id: 3300603
log K source: MTQ3.11
Delta H source: MTQ3.11
#T and ionic strength:
 $\text{H3AsO4} = \text{AsO4-3} + 3\text{H+}$
log_k -20.7
delta_h 12.9 kJ
-gamma 0 0
Id: 3300613
log K source: NIST46.4
Delta H source: NIST46.4
#T and ionic strength: 0.00 25.0
 $\text{H3AsO4} = \text{HAsO4-2} + 2\text{H+}$
log_k -9.2
delta_h -4.1 kJ
-gamma 0 0
Id: 3300612
log K source: NIST46.4
Delta H source: NIST46.4
#T and ionic strength: 0.00 25.0
 $\text{H3AsO4} = \text{H2AsO4-} + \text{H+}$
log_k -2.24
delta_h -7.1 kJ
-gamma 0 0
Id: 3300611

log K source: NIST46.4
 # Delta H source: NIST46.4
 #T and ionic strength: 0.00 25.0
 $\text{Sb(OH)}_3 + \text{H}_2\text{O} = \text{Sb(OH)}_4^- + \text{H}^+$
 log_k -12.0429
 delta_h 69.8519 kJ
 -gamma 0 0
 # Id: 7400020
 # log K source: PNL89
 # Delta H source: PNL89
 #T and ionic strength:
 $\text{Sb(OH)}_3 + \text{H}^+ = \text{Sb(OH)}_2^+ + \text{H}_2\text{O}$
 log_k 1.3853
 delta_h 0 kJ
 -gamma 0 0
 # Id: 7403302
 # log K source: PNL89
 # Delta H source: PNL89
 #T and ionic strength:
 $\text{Sb(OH)}_3 = \text{HSbO}_2 + \text{H}_2\text{O}$
 log_k -0.0105
 delta_h -0.13 kJ
 -gamma 0 0
 # Id: 7400021
 # log K source: NIST2.1.1
 # Delta H source: NIST2.1.1
 #T and ionic strength:
 $\text{Sb(OH)}_3 = \text{SbO}_2^- + \text{H}_2\text{O} + \text{H}^+$
 log_k -11.8011
 delta_h 70.1866 kJ
 -gamma 0 0
 # Id: 7403301
 # log K source: PNL89
 # Delta H source: PNL89
 #T and ionic strength:
 $\text{Sb(OH)}_3 + \text{H}^+ = \text{SbO}^+ + 2\text{H}_2\text{O}$
 log_k 0.9228
 delta_h 8.2425 kJ
 -gamma 0 0
 # Id: 7403300
 # log K source: PNL89
 # Delta H source: PNL89
 #T and ionic strength:
 $\text{Sb(OH)}_6^- = \text{SbO}_3^- + 3\text{H}_2\text{O}$
 log_k 2.9319
 delta_h 0 kJ
 -gamma 0 0
 # Id: 7410021
 # log K source: PNL89
 # Delta H source: PNL89
 #T and ionic strength:
 $\text{Sb(OH)}_6^- + 2\text{H}^+ = \text{SbO}_2^+ + 4\text{H}_2\text{O}$
 log_k 2.3895
 delta_h 0 kJ

-gamma 0 0
 # Id: 7413300
 # log K source: PNL89
 # Delta H source: PNL89
 #T and ionic strength:
 $\text{H}^+ + \text{CO}_3^{2-} = \text{HCO}_3^-$
 log_k 10.329
 delta_h -14.6 kJ
 -gamma 5.4 0
 # Id: 3301400
 # log K source: NIST46.4
 # Delta H source: NIST46.4
 #T and ionic strength: 0.00 25.0
 $2\text{H}^+ + \text{CO}_3^{2-} = \text{H}_2\text{CO}_3$
 log_k 16.681
 delta_h -23.76 kJ
 -gamma 0 0
 # Id: 3301401
 # log K source: NIST46.4
 # Delta H source: NIST46.4
 #T and ionic strength: 0.00 25.0
 $\text{Pb}^{2+} + 2\text{CO}_3^{2-} = \text{Pb}(\text{CO}_3)_2$
 log_k 9.938
 delta_h 0 kJ
 -gamma 0 0
 # Id: 6001400
 # log K source: NIST46.3
 # Delta H source: MTQ3.11
 #T and ionic strength: 0.50 25.0
 $\text{Pb}^{2+} + \text{CO}_3^{2-} = \text{PbCO}_3$
 log_k 6.478
 delta_h 0 kJ
 -gamma 0 0
 # Id: 6001401
 # log K source: NIST46.3
 # Delta H source: MTQ3.11
 #T and ionic strength: 0.50 25.0
 $\text{Pb}^{2+} + \text{CO}_3^{2-} + \text{H}^+ = \text{PbHCO}_3^+$
 log_k 13.2
 delta_h 0 kJ
 -gamma 0 0
 # Id: 6001402
 # log K source: MTQ3.11
 # Delta H source: MTQ3.11
 #T and ionic strength:
 $\text{Zn}^{2+} + \text{CO}_3^{2-} = \text{ZnCO}_3$
 log_k 4.76
 delta_h 0 kJ
 -gamma 0 0
 # Id: 9501401
 # log K source: NIST46.4
 # Delta H source: MTQ3.11
 #T and ionic strength: 0.00 25.0
 $\text{Zn}^{2+} + \text{H}^+ + \text{CO}_3^{2-} = \text{ZnHCO}_3^+$

log_k 11.829
 delta_h 0 kJ
 -gamma 0 0
 # Id: 9501400
 # log K source: NIST46.4
 # Delta H source: MTQ3.11
 #T and ionic strength: 0.00 25.0
 $\text{Hg(OH)}_2 + 2\text{H}^+ + \text{CO}_3^{2-} = \text{HgCO}_3 + 2\text{H}_2\text{O}$
 log_k 18.272
 delta_h 0 kJ
 -gamma 0 0
 # Id: 3611401
 # log K source: NIST46.4
 # Delta H source: MTQ3.11
 #T and ionic strength: 0.50 25.0
 $\text{Hg(OH)}_2 + 2\text{H}^+ + 2\text{CO}_3^{2-} = \text{Hg(CO}_3)_2^{2-} + 2\text{H}_2\text{O}$
 log_k 21.772
 delta_h 0 kJ
 -gamma 0 0
 # Id: 3611402
 # log K source: NIST46.4
 # Delta H source: MTQ3.11
 #T and ionic strength: 0.50 25.0
 $\text{Hg(OH)}_2 + 3\text{H}^+ + \text{CO}_3^{2-} = \text{HgHCO}_3^+ + 2\text{H}_2\text{O}$
 log_k 22.542
 delta_h 0 kJ
 -gamma 0 0
 # Id: 3611403
 # log K source: NIST46.4
 # Delta H source: MTQ3.11
 #T and ionic strength: 0.50 25.0
 $\text{Cd}^{2+} + \text{CO}_3^{2-} = \text{CdCO}_3$
 log_k 4.3578
 delta_h 0 kJ
 -gamma 0 0
 # Id: 1601401
 # log K source: NIST46.4
 # Delta H source: MTQ3.11
 #T and ionic strength: 0.10 25.0
 $\text{Cd}^{2+} + \text{H}^+ + \text{CO}_3^{2-} = \text{CdHCO}_3^+$
 log_k 10.6863
 delta_h 0 kJ
 -gamma 0 0
 # Id: 1601400
 # log K source: NIST46.4
 # Delta H source: MTQ3.11
 #T and ionic strength: 3.00 25.0
 $\text{Cd}^{2+} + 2\text{CO}_3^{2-} = \text{Cd(CO}_3)_2^{2-}$
 log_k 7.2278
 delta_h 0 kJ
 -gamma 0 0
 # Id: 1601403
 # log K source: NIST46.4
 # Delta H source: MTQ3.11

#T and ionic strength: 0.10 20.0
 $\text{Cu}^{+2} + \text{CO}_3^{-2} = \text{CuCO}_3$
log_k 6.77
delta_h 0 kJ
-gamma 0 0
Id: 2311400
log K source: NIST46.4
Delta H source: MTQ3.11
#T and ionic strength: 0.00 25.0
 $\text{Cu}^{+2} + \text{H}^{+} + \text{CO}_3^{-2} = \text{CuHCO}_3^{+}$
log_k 12.129
delta_h 0 kJ
-gamma 0 0
Id: 2311402
log K source: NIST46.4
Delta H source: MTQ3.11
#T and ionic strength: 0.00 25.0
 $\text{Cu}^{+2} + 2\text{CO}_3^{-2} = \text{Cu}(\text{CO}_3)_2^{-2}$
log_k 10.2
delta_h 0 kJ
-gamma 0 0
Id: 2311401
log K source: NIST46.4
Delta H source: MTQ3.11
#T and ionic strength: 0.00 25.0
 $\text{Ni}^{+2} + \text{CO}_3^{-2} = \text{NiCO}_3$
log_k 4.5718
delta_h 0 kJ
-gamma 0 0
Id: 5401401
log K source: NIST46.3
Delta H source: MTQ3.11
#T and ionic strength: 0.70 25.0
 $\text{Ni}^{+2} + \text{H}^{+} + \text{CO}_3^{-2} = \text{NiHCO}_3^{+}$
log_k 12.4199
delta_h 0 kJ
-gamma 0 0
Id: 5401400
log K source: NIST46.3
Delta H source: MTQ3.11
#T and ionic strength: 0.70 25.0
 $\text{Co}^{+2} + \text{CO}_3^{-2} = \text{CoCO}_3$
log_k 4.228
delta_h 0 kJ
-gamma 0 0
Id: 2001400
log K source: NIST46.4
Delta H source: MTQ3.11
#T and ionic strength: 0.50 25.0
 $\text{Co}^{+2} + \text{H}^{+} + \text{CO}_3^{-2} = \text{CoHCO}_3^{+}$
log_k 12.2199
delta_h 0 kJ
-gamma 0 0
Id: 2001401

log K source: NIST46.4
 # Delta H source: MTQ3.11
 #T and ionic strength: 0.70 25.0
 $\text{Fe}^{+2} + \text{H}^{+} + \text{CO}_3^{-2} = \text{FeHCO}_3^{+}$
 log_k 11.429
 delta_h 0 kJ
 -gamma 6 0
 # Id: 2801400
 # log K source: NIST46.4
 # Delta H source: MTQ3.11
 #T and ionic strength: 0.00 25.0
 $\text{Mn}^{+2} + \text{H}^{+} + \text{CO}_3^{-2} = \text{MnHCO}_3^{+}$
 log_k 11.629
 delta_h -10.6 kJ
 -gamma 5 0
 # Id: 4701400
 # log K source: NIST46.4
 # Delta H source: NIST46.4
 #T and ionic strength: 0.00 25.0
 $\text{UO}_2^{+2} + \text{CO}_3^{-2} = \text{UO}_2\text{CO}_3$
 log_k 9.6
 delta_h 4 kJ
 -gamma 0 0
 # Id: 8931400
 # log K source: NIST46.3
 # Delta H source: NIST46.3
 #T and ionic strength: 0.00 25.0
 $\text{UO}_2^{+2} + 2\text{CO}_3^{-2} = \text{UO}_2(\text{CO}_3)_2^{-2}$
 log_k 16.9
 delta_h 16 kJ
 -gamma 0 0
 # Id: 8931401
 # log K source: NIST46.3
 # Delta H source: NIST46.3
 #T and ionic strength: 0.00 25.0
 $\text{UO}_2^{+2} + 3\text{CO}_3^{-2} = \text{UO}_2(\text{CO}_3)_3^{-4}$
 log_k 21.6
 delta_h -40 kJ
 -gamma 0 0
 # Id: 8931402
 # log K source: NIST46.3
 # Delta H source: NIST46.3
 #T and ionic strength: 0.00 25.0
 $\text{Be}^{+2} + \text{CO}_3^{-2} = \text{BeCO}_3$
 log_k 6.2546
 delta_h 0 kJ
 -gamma 0 0
 # Id: 1101401
 # log K source: NIST46.4
 # Delta H source: MTQ3.11
 #T and ionic strength: 3.00 25.0
 $\text{Mg}^{+2} + \text{CO}_3^{-2} = \text{MgCO}_3$
 log_k 2.92
 delta_h 12 kJ

-gamma 0 0
Id: 4601400
log K source: NIST46.3
Delta H source: NIST46.3
#T and ionic strength: 0.00 25.0
 $\text{Mg}^{+2} + \text{H}^{+} + \text{CO}_3^{-2} = \text{MgHCO}_3^{+}$
log_k 11.339
delta_h -10.6 kJ
-gamma 4 0
Id: 4601401
log K source: NIST46.3
Delta H source: NIST46.3
#T and ionic strength: 0.00 25.0
 $\text{Ca}^{+2} + \text{H}^{+} + \text{CO}_3^{-2} = \text{CaHCO}_3^{+}$
log_k 11.599
delta_h 5.4 kJ
-gamma 6 0
Id: 1501400
log K source: NIST46.3
Delta H source: NIST46.3
#T and ionic strength: 0.00 25.0
 $\text{CO}_3^{-2} + \text{Ca}^{+2} = \text{CaCO}_3$
log_k 3.2
delta_h 16 kJ
-gamma 0 0
Id: 1501401
log K source: NIST46.3
Delta H source: NIST46.3
#T and ionic strength: 0.00 25.0
 $\text{Sr}^{+2} + \text{CO}_3^{-2} = \text{SrCO}_3$
log_k 2.81
delta_h 20 kJ
-gamma 0 0
Id: 8001401
log K source: NIST46.4
Delta H source: NIST46.4
#T and ionic strength: 0.00 25.0
 $\text{Sr}^{+2} + \text{H}^{+} + \text{CO}_3^{-2} = \text{SrHCO}_3^{+}$
log_k 11.539
delta_h 10.4 kJ
-gamma 6 0
Id: 8001400
log K source: NIST46.4
Delta H source: NIST46.4
#T and ionic strength: 0.00 25.0
 $\text{Ba}^{+2} + \text{CO}_3^{-2} = \text{BaCO}_3$
log_k 2.71
delta_h 16 kJ
-gamma 0 0
Id: 1001401
log K source: NIST46.4
Delta H source: NIST46.4
#T and ionic strength: 0.00 25.0
 $\text{Ba}^{+2} + \text{H}^{+} + \text{CO}_3^{-2} = \text{BaHCO}_3^{+}$

log_k 11.309
delta_h 10.4 kJ
-gamma 6 0
Id: 1001400
log K source: NIST46.4
Delta H source: NIST46.4
#T and ionic strength: 0.00 25.0
 $\text{Na}^+ + \text{CO}_3^{2-} = \text{NaCO}_3^-$
log_k 1.27
delta_h -20.35 kJ
-gamma 5.4 0
Id: 5001400
log K source: NIST46.3
Delta H source: NIST2.1.1
#T and ionic strength: 0.00 25.0
 $\text{Na}^+ + \text{H}^+ + \text{CO}_3^{2-} = \text{NaHCO}_3$
log_k 10.079
delta_h -28.3301 kJ
-gamma 0 0
Id: 5001401
log K source: NIST46.3
Delta H source: NIST2.1.1
#T and ionic strength: 0.00 25.0
 $\text{H}_4\text{SiO}_4 = \text{H}_2\text{SiO}_4^{2-} + 2\text{H}^+$
log_k -23.04
delta_h 61 kJ
-gamma 5.4 0
Id: 3307701
log K source: NIST46.4
Delta H source: NIST46.4
#T and ionic strength: 0.00 25.0
 $\text{H}_4\text{SiO}_4 = \text{H}_3\text{SiO}_4^- + \text{H}^+$
log_k -9.84
delta_h 20 kJ
-gamma 4 0
Id: 3307700
log K source: NIST46.4
Delta H source: NIST46.4
#T and ionic strength: 0.00 25.0
 $\text{UO}_2^{2+} + \text{H}_4\text{SiO}_4 = \text{UO}_2\text{H}_3\text{SiO}_4^+ + \text{H}^+$
log_k -1.9111
delta_h 0 kJ
-gamma 0 0
Id: 8937700
log K source: NIST46.4
Delta H source: MTQ3.11
#T and ionic strength: 0.10 25.0
 $\text{H}_3\text{BO}_3 = \text{H}_2\text{BO}_3^- + \text{H}^+$
log_k -9.236
delta_h 13 kJ
-gamma 2.5 0
Id: 3300900
log K source: NIST46.4
Delta H source: NIST46.4

#T and ionic strength: 0.00 25.0
 $2\text{H}_3\text{BO}_3 = \text{H}_5(\text{BO}_3)_2^- + \text{H}^+$
log_k -9.306
delta_h 8.4 kJ
-gamma 2.5 0
Id: 3300901
log K source: NIST46.4
Delta H source: NIST46.4
#T and ionic strength: 0.00 25.0
 $3\text{H}_3\text{BO}_3 = \text{H}_8(\text{BO}_3)_3^- + \text{H}^+$
log_k -7.306
delta_h 29.4 kJ
-gamma 2.5 0
Id: 3300902
log K source: NIST46.4
Delta H source: NIST46.4
#T and ionic strength: 0.00 25.0
 $\text{Ag}^+ + \text{H}_3\text{BO}_3 = \text{AgH}_2\text{BO}_3 + \text{H}^+$
log_k -8.036
delta_h 0 kJ
-gamma 2.5 0
Id: 200901
log K source: NIST46.4
Delta H source: MTQ3.11
#T and ionic strength: 0.00 25.0
 $\text{Mg}^{+2} + \text{H}_3\text{BO}_3 = \text{MgH}_2\text{BO}_3^+ + \text{H}^+$
log_k -7.696
delta_h 13 kJ
-gamma 2.5 0
Id: 4600901
log K source: NIST46.4
Delta H source: NIST46.4
#T and ionic strength: 0.00 25.0
 $\text{Ca}^{+2} + \text{H}_3\text{BO}_3 = \text{CaH}_2\text{BO}_3^+ + \text{H}^+$
log_k -7.476
delta_h 17 kJ
-gamma 2.5 0
Id: 1500901
log K source: NIST46.4
Delta H source: NIST46.4
#T and ionic strength: 0.00 25.0
 $\text{Sr}^{+2} + \text{H}_3\text{BO}_3 = \text{SrH}_2\text{BO}_3^+ + \text{H}^+$
log_k -7.686
delta_h 17 kJ
-gamma 2.5 0
Id: 8000901
log K source: NIST46.4
Delta H source: NIST46.4
#T and ionic strength: 0.00 25.0
 $\text{Ba}^{+2} + \text{H}_3\text{BO}_3 = \text{BaH}_2\text{BO}_3^+ + \text{H}^+$
log_k -7.746
delta_h 17 kJ
-gamma 2.5 0
Id: 1000901

log K source: NIST46.4
 # Delta H source: NIST46.4
 #T and ionic strength: 0.00 25.0
 $\text{Na}^+ + \text{H}_3\text{BO}_3 = \text{NaH}_2\text{BO}_3 + \text{H}^+$
 log_k -9.036
 delta_h 0 kJ
 -gamma 2.5 0
 # Id: 5000901
 # log K source: NIST46.4
 # Delta H source: MTQ3.11
 #T and ionic strength: 0.00 25.0
 $\text{CrO}_4^{2-} + \text{H}^+ = \text{HCrO}_4^-$
 log_k 6.51
 delta_h 2 kJ
 -gamma 0 0
 # Id: 2123300
 # log K source: NIST46.4
 # Delta H source: NIST46.4
 #T and ionic strength: 0.00 25.0
 $\text{CrO}_4^{2-} + 2\text{H}^+ = \text{H}_2\text{CrO}_4$
 log_k 6.4188
 delta_h 39 kJ
 -gamma 0 0
 # Id: 2123301
 # log K source: NIST46.4
 # Delta H source: NIST46.4
 #T and ionic strength: 0.00 20.0
 $2\text{CrO}_4^{2-} + 2\text{H}^+ = \text{Cr}_2\text{O}_7^{2-} + \text{H}_2\text{O}$
 log_k 14.56
 delta_h -15 kJ
 -gamma 0 0
 # Id: 2123302
 # log K source: NIST46.4
 # Delta H source: NIST46.4
 #T and ionic strength: 0.00 25.0
 $\text{CrO}_4^{2-} + \text{Cl}^- + 2\text{H}^+ = \text{CrO}_3\text{Cl}^- + \text{H}_2\text{O}$
 log_k 7.3086
 delta_h 0 kJ
 -gamma 0 0
 # Id: 2121800
 # log K source: MTQ3.11
 # Delta H source: MTQ3.11
 #T and ionic strength:
 $\text{CrO}_4^{2-} + \text{SO}_4^{2-} + 2\text{H}^+ = \text{CrO}_3\text{SO}_4^{2-} + \text{H}_2\text{O}$
 log_k 8.9937
 delta_h 0 kJ
 -gamma 0 0
 # Id: 2127320
 # log K source: MTQ3.11
 # Delta H source: MTQ3.11
 #T and ionic strength:
 $\text{CrO}_4^{2-} + 4\text{H}^+ + \text{PO}_4^{3-} = \text{CrO}_3\text{H}_2\text{PO}_4^- + \text{H}_2\text{O}$
 log_k 29.3634
 delta_h 0 kJ

-gamma 0 0
 # Id: 2125800
 # log K source: MTQ3.11
 # Delta H source: MTQ3.11
 #T and ionic strength:
 $\text{CrO}_4^{2-} + 3\text{H}^+ + \text{PO}_4^{3-} = \text{CrO}_3\text{HPO}_4^{2-} + \text{H}_2\text{O}$
 log_k 26.6806
 delta_h 0 kJ
 -gamma 0 0
 # Id: 2125801
 # log K source: MTQ3.11
 # Delta H source: MTQ3.11
 #T and ionic strength:
 $\text{CrO}_4^{2-} + \text{Na}^+ = \text{NaCrO}_4^-$
 log_k 0.6963
 delta_h 0 kJ
 -gamma 0 0
 # Id: 5002120
 # log K source: MTQ3.11
 # Delta H source: MTQ3.11
 #T and ionic strength:
 $\text{K}^+ + \text{CrO}_4^{2-} = \text{KCrO}_4^-$
 log_k 0.57
 delta_h 0 kJ
 -gamma 0 0
 # Id: 4102120
 # log K source: NIST46.4
 # Delta H source: MTQ3.11
 #T and ionic strength: 0.00 18.0
 $\text{MoO}_4^{2-} + \text{H}^+ = \text{HMoO}_4^-$
 log_k 4.2988
 delta_h 20 kJ
 -gamma 0 0
 # Id: 3304801
 # log K source: NIST46.4
 # Delta H source: NIST46.4
 #T and ionic strength: 0.00 20.0
 $\text{MoO}_4^{2-} + 2\text{H}^+ = \text{H}_2\text{MoO}_4$
 log_k 8.1636
 delta_h -26 kJ
 -gamma 0 0
 # Id: 3304802
 # log K source: NIST46.4
 # Delta H source: NIST46.4
 #T and ionic strength: 0.00 20.0
 $7\text{MoO}_4^{2-} + 8\text{H}^+ = \text{Mo}_7\text{O}_{24}^{6-} + 4\text{H}_2\text{O}$
 log_k 52.99
 delta_h -228 kJ
 -gamma 0 0
 # Id: 3304803
 # log K source: NIST46.4
 # Delta H source: NIST46.4
 #T and ionic strength: 0.10 25.0
 $7\text{MoO}_4^{2-} + 9\text{H}^+ = \text{HMo}_7\text{O}_{24}^{5-} + 4\text{H}_2\text{O}$

log_k 59.3768
 delta_h -218 kJ
 -gamma 0 0
 # Id: 3304804
 # log K source: NIST46.4
 # Delta H source: NIST46.4
 #T and ionic strength: 0.10 25.0
 $7\text{MoO}_4^{2-} + 10\text{H}^+ = \text{H}_2\text{Mo}_7\text{O}_{24}^{4-} + 4\text{H}_2\text{O}$
 log_k 64.159
 delta_h -215 kJ
 -gamma 0 0
 # Id: 3304805
 # log K source: NIST46.4
 # Delta H source: NIST46.4
 #T and ionic strength: 0.10 25.0
 $7\text{MoO}_4^{2-} + 11\text{H}^+ = \text{H}_3\text{Mo}_7\text{O}_{24}^{3-} + 4\text{H}_2\text{O}$
 log_k 67.405
 delta_h -217 kJ
 -gamma 0 0
 # Id: 3304806
 # log K source: NIST46.4
 # Delta H source: NIST46.4
 #T and ionic strength: 1.00 25.0
 $6\text{MoO}_4^{2-} + \text{Al}^{3+} + 6\text{H}^+ = \text{AlMo}_6\text{O}_{21}^{3-} + 3\text{H}_2\text{O}$
 log_k 54.9925
 delta_h 0 kJ
 -gamma 0 0
 # Id: 304801
 # log K source: NIST46.4
 # Delta H source: MTQ3.11
 #T and ionic strength: 0.50 25.0
 $\text{MoO}_4^{2-} + 2\text{Ag}^+ = \text{Ag}_2\text{MoO}_4$
 log_k -0.4219
 delta_h -1.18 kJ
 -gamma 0 0
 # Id: 204801
 # log K source: Bard85
 # Delta H source: Bard85
 #T and ionic strength:
 $\text{VO}_2^+ + 2\text{H}_2\text{O} = \text{VO}_4^{3-} + 4\text{H}^+$
 log_k -30.2
 delta_h -25 kJ
 -gamma 0 0
 # Id: 9033303
 # log K source: NIST46.4
 # Delta H source: NIST46.4
 #T and ionic strength: 0.00 25.0
 $\text{VO}_2^+ + 2\text{H}_2\text{O} = \text{HVO}_4^{2-} + 3\text{H}^+$
 log_k -15.9
 delta_h 0 kJ
 -gamma 0 0
 # Id: 9033302
 # log K source: NIST46.3
 # Delta H source: NIST46.3

#T and ionic strength: 0.00 25.0
 $\text{VO}_2^+ + 2\text{H}_2\text{O} = \text{H}_2\text{VO}_4^- + 2\text{H}^+$
 log_k -7.3
 delta_h 0 kJ
 -gamma 0 0
 # Id: 9033301
 # log K source: NIST46.3
 # Delta H source: NIST46.3
 #T and ionic strength: 0.00 25.0
 $\text{VO}_2^+ + 2\text{H}_2\text{O} = \text{H}_3\text{VO}_4 + \text{H}^+$
 log_k -3.3
 delta_h 44.4759 kJ
 -gamma 0 0
 # Id: 9033300
 # log K source: MTQ3.11
 # Delta H source: MTQ3.11
 #T and ionic strength:
 $2\text{VO}_2^+ + 3\text{H}_2\text{O} = \text{V}_2\text{O}_7^{4-} + 6\text{H}^+$
 log_k -31.24
 delta_h -28 kJ
 -gamma 0 0
 # Id: 9030020
 # log K source: NIST46.3
 # Delta H source: NIST46.3
 #T and ionic strength: 0.00 25.0
 $2\text{VO}_2^+ + 3\text{H}_2\text{O} = \text{HV}_2\text{O}_7^{3-} + 5\text{H}^+$
 log_k -20.67
 delta_h 0 kJ
 -gamma 0 0
 # Id: 9030021
 # log K source: NIST46.3
 # Delta H source: MTQ3.11
 #T and ionic strength: 0.00 25.0
 $2\text{VO}_2^+ + 3\text{H}_2\text{O} = \text{H}_3\text{V}_2\text{O}_7^- + 3\text{H}^+$
 log_k -3.79
 delta_h 0 kJ
 -gamma 0 0
 # Id: 9030022
 # log K source: MTQ3.11
 # Delta H source: MTQ3.11
 #T and ionic strength:
 $3\text{VO}_2^+ + 3\text{H}_2\text{O} = \text{V}_3\text{O}_9^{3-} + 6\text{H}^+$
 log_k -15.88
 delta_h 0 kJ
 -gamma 0 0
 # Id: 9030023
 # log K source: MTQ3.11
 # Delta H source: MTQ3.11
 #T and ionic strength:
 $4\text{VO}_2^+ + 4\text{H}_2\text{O} = \text{V}_4\text{O}_{12}^{4-} + 8\text{H}^+$
 log_k -20.56
 delta_h -87 kJ
 -gamma 0 0
 # Id: 9030024

log K source: NIST46.3
 # Delta H source: NIST46.3
 #T and ionic strength: 0.00 25.0
 $10\text{VO}_2^+ + 8\text{H}_2\text{O} = \text{V}_{10}\text{O}_{28-6} + 16\text{H}^+$
 log_k -24.0943
 delta_h 0 kJ
 -gamma 0 0
 # Id: 9030025
 # log K source: NIST46.4
 # Delta H source: MTQ3.11
 #T and ionic strength: 0.10 20.0
 $10\text{VO}_2^+ + 8\text{H}_2\text{O} = \text{HV}_{10}\text{O}_{28-5} + 15\text{H}^+$
 log_k -15.9076
 delta_h 90.0397 kJ
 -gamma 0 0
 # Id: 9030026
 # log K source: NIST46.4
 # Delta H source: MTQ3.11
 #T and ionic strength: 0.10 20.0
 $10\text{VO}_2^+ + 8\text{H}_2\text{O} = \text{H}_2\text{V}_{10}\text{O}_{28-4} + 14\text{H}^+$
 log_k -10.7
 delta_h 0 kJ
 -gamma 0 0
 # Id: 9030027
 # log K source: NIST46.3
 # Delta H source: MTQ3.11
 #T and ionic strength: 0.00 25.0
 $\text{Benzoate}^- + \text{H}^+ = \text{H}(\text{Benzoate})$
 log_k 4.202
 delta_h -0.4602 kJ
 -gamma 0 0
 # Id: 3309171
 # log K source: NIST46.2
 # Delta H source: NIST46.2
 #T and ionic strength:
 $\text{Benzoate}^- + \text{Pb}^{+2} = \text{Pb}(\text{Benzoate})^+$
 log_k 2.4
 delta_h 0 kJ
 -gamma 0 0
 # Id: 6009171
 # log K source: NIST46.2
 # Delta H source: NIST46.2
 #T and ionic strength:
 $\text{Benzoate}^- + \text{Al}^{+3} = \text{Al}(\text{Benzoate})^{+2}$
 log_k 2.05
 delta_h 0 kJ
 -gamma 0 0
 # Id: 309171
 # log K source: NIST46.2
 # Delta H source: NIST46.2
 #T and ionic strength:
 $\text{Benzoate}^- + \text{Al}^{+3} + \text{H}_2\text{O} = \text{AlOH}(\text{Benzoate})^+ + \text{H}^+$
 log_k -0.56
 delta_h 0 kJ

-gamma 0 0
 # Id: 309172
 # log K source: NIST46.2
 # Delta H source: NIST46.2
 #T and ionic strength:
 $\text{Benzoate}^- + \text{Zn}^{+2} = \text{Zn}(\text{Benzoate}) +$
 log_k 1.7
 delta_h 0 kJ
 -gamma 0 0
 # Id: 9509171
 # log K source: SCD2.62
 # Delta H source: SCD2.62
 #T and ionic strength:
 $\text{Benzoate}^- + \text{Cd}^{+2} = \text{Cd}(\text{Benzoate}) +$
 log_k 1.8
 delta_h 0 kJ
 -gamma 0 0
 # Id: 1609171
 # log K source: NIST46.2
 # Delta H source: NIST46.2
 #T and ionic strength:
 $2\text{Benzoate}^- + \text{Cd}^{+2} = \text{Cd}(\text{Benzoate})_2$
 log_k 1.82
 delta_h 0 kJ
 -gamma 0 0
 # Id: 1609172
 # log K source: SCD2.62
 # Delta H source: SCD2.62
 #T and ionic strength:
 $\text{Benzoate}^- + \text{Cu}^{+2} = \text{Cu}(\text{Benzoate}) +$
 log_k 2.19
 delta_h 0 kJ
 -gamma 0 0
 # Id: 2319171
 # log K source: NIST46.2
 # Delta H source: NIST46.2
 #T and ionic strength:
 $\text{Benzoate}^- + \text{Ag}^+ = \text{Ag}(\text{Benzoate})$
 log_k 0.91
 delta_h 0 kJ
 -gamma 0 0
 # Id: 209171
 # log K source: NIST46.2
 # Delta H source: NIST46.2
 #T and ionic strength:
 $\text{Benzoate}^- + \text{Ni}^{+2} = \text{Ni}(\text{Benzoate}) +$
 log_k 1.86
 delta_h 0 kJ
 -gamma 0 0
 # Id: 5409171
 # log K source: SCD2.62
 # Delta H source: SCD2.62
 #T and ionic strength:
 $\text{Co}^{+2} + \text{Benzoate}^- = \text{Co}(\text{Benzoate}) +$

log_k 1.0537
delta_h 12 kJ
-gamma 0 0
Id: 2009171
log K source: NIST46.4
Delta H source: NIST46.4
#T and ionic strength: 0.50 30.0
Benzoate- + Mn+2 = Mn(Benzoate)+
log_k 2.06
delta_h 0 kJ
-gamma 0 0
Id: 4709171
log K source: NIST46.2
Delta H source: NIST46.2
#T and ionic strength:
Benzoate- + Mg+2 = Mg(Benzoate)+
log_k 1.26
delta_h 0 kJ
-gamma 0 0
Id: 4609171
log K source: SCD2.62
Delta H source: SCD2.62
#T and ionic strength:
Benzoate- + Ca+2 = Ca(Benzoate)+
log_k 1.55
delta_h 0 kJ
-gamma 0 0
Id: 1509171
log K source: SCD2.62
Delta H source: SCD2.62
#T and ionic strength:
Phenylacetate- + H+ = H(Phenylacetate)
log_k 4.31
delta_h 2.1757 kJ
-gamma 0 0
Id: 3309181
log K source: NIST46.2
Delta H source: NIST46.2
#T and ionic strength:
Phenylacetate- + Zn+2 = Zn(Phenylacetate)+
log_k 1.57
delta_h 0 kJ
-gamma 0 0
Id: 9509181
log K source: NIST46.2
Delta H source: NIST46.2
#T and ionic strength:
Phenylacetate- + Cu+2 = Cu(Phenylacetate)+
log_k 1.97
delta_h 0 kJ
-gamma 0 0
Id: 2319181
log K source: NIST46.2
Delta H source: NIST46.2

#T and ionic strength:
 $\text{Co}^{+2} + \text{Phenylacetate}^- = \text{Co}(\text{Phenylacetate})^+$
 log_k 0.591
 delta_h 0 kJ
 -gamma 0 0
 # Id: 2009181
 # log K source: NIST46.4
 # Delta H source: NIST46.2
 #T and ionic strength: 2.00 25.0
 $\text{Co}^{+2} + 2\text{Phenylacetate}^- = \text{Co}(\text{Phenylacetate})_2$
 log_k 0.4765
 delta_h 0 kJ
 -gamma 0 0
 # Id: 2009182
 # log K source: NIST46.4
 # Delta H source: NIST46.2
 #T and ionic strength: 2.00 25.0
 $\text{Isophthalate}^{2-} + \text{H}^+ = \text{H}(\text{Isophthalate})^-$
 log_k 4.5
 delta_h 1.6736 kJ
 -gamma 0 0
 # Id: 3309201
 # log K source: NIST46.2
 # Delta H source: NIST46.2
 #T and ionic strength:
 $\text{Isophthalate}^{2-} + 2\text{H}^+ = \text{H}_2(\text{Isophthalate})$
 log_k 8
 delta_h 1.6736 kJ
 -gamma 0 0
 # Id: 3309202
 # log K source: NIST46.2
 # Delta H source: NIST46.2
 #T and ionic strength:
 $\text{Isophthalate}^{2-} + \text{Pb}^{+2} = \text{Pb}(\text{Isophthalate})$
 log_k 2.99
 delta_h 0 kJ
 -gamma 0 0
 # Id: 6009201
 # log K source: NIST46.2
 # Delta H source: NIST46.2
 #T and ionic strength:
 $2\text{Isophthalate}^{2-} + \text{Pb}^{+2} = \text{Pb}(\text{Isophthalate})_2^{2-}$
 log_k 4.18
 delta_h 0 kJ
 -gamma 0 0
 # Id: 6009202
 # log K source: NIST46.2
 # Delta H source: NIST46.2
 #T and ionic strength:
 $\text{Isophthalate}^{2-} + \text{Pb}^{+2} + \text{H}^+ = \text{PbH}(\text{Isophthalate})^+$
 log_k 6.69
 delta_h 0 kJ
 -gamma 0 0
 # Id: 6009203

log K source: NIST46.2
 # Delta H source: NIST46.2
 #T and ionic strength:
 $\text{Isophthalate-2} + \text{Cd}^{+2} = \text{Cd}(\text{Isophthalate})$
 log_k 2.15
 delta_h 0 kJ
 -gamma 0 0
 # Id: 1609201
 # log K source: NIST46.2
 # Delta H source: NIST46.2
 #T and ionic strength:
 $2\text{Isophthalate-2} + \text{Cd}^{+2} = \text{Cd}(\text{Isophthalate})_2$
 log_k 2.99
 delta_h 0 kJ
 -gamma 0 0
 # Id: 1609202
 # log K source: NIST46.2
 # Delta H source: NIST46.2
 #T and ionic strength:
 $\text{Isophthalate-2} + \text{Cd}^{+2} + \text{H}^+ = \text{CdH}(\text{Isophthalate})$
 log_k 5.73
 delta_h 0 kJ
 -gamma 0 0
 # Id: 1609203
 # log K source: NIST46.2
 # Delta H source: NIST46.2
 #T and ionic strength:
 $\text{Isophthalate-2} + \text{Ca}^{+2} = \text{Ca}(\text{Isophthalate})$
 log_k 2
 delta_h 0 kJ
 -gamma 0 0
 # Id: 1509200
 # log K source: NIST46.2
 # Delta H source: NIST46.2
 #T and ionic strength:
 $\text{Isophthalate-2} + \text{Ba}^{+2} = \text{Ba}(\text{Isophthalate})$
 log_k 1.55
 delta_h 0 kJ
 -gamma 0 0
 # Id: 1009201
 # log K source: NIST46.2
 # Delta H source: NIST46.2
 #T and ionic strength:
 $\text{H}^+ + \text{Diethylamine} = \text{H}(\text{Diethylamine})$
 log_k 10.933
 delta_h -53.1368 kJ
 -gamma 0 0
 # Id: 3309551
 # log K source: NIST46.2
 # Delta H source: NIST46.2
 #T and ionic strength:
 $\text{Zn}^{+2} + \text{Diethylamine} = \text{Zn}(\text{Diethylamine})_2$
 log_k 2.74
 delta_h 0 kJ

-gamma 0 0
 # Id: 9509551
 # log K source: SCD2.62
 # Delta H source: SCD2.62
 #T and ionic strength:
 $\text{Zn}^{+2} + 2\text{Diethylamine} = \text{Zn}(\text{Diethylamine})_2^{+2}$
 log_k 5.27
 delta_h 0 kJ
 -gamma 0 0
 # Id: 9509552
 # log K source: SCD2.62
 # Delta H source: SCD2.62
 #T and ionic strength:
 $\text{Zn}^{+2} + 3\text{Diethylamine} = \text{Zn}(\text{Diethylamine})_3^{+2}$
 log_k 7.71
 delta_h 0 kJ
 -gamma 0 0
 # Id: 9509553
 # log K source: SCD2.62
 # Delta H source: SCD2.62
 #T and ionic strength:
 $\text{Zn}^{+2} + 4\text{Diethylamine} = \text{Zn}(\text{Diethylamine})_4^{+2}$
 log_k 9.84
 delta_h 0 kJ
 -gamma 0 0
 # Id: 9509554
 # log K source: SCD2.62
 # Delta H source: SCD2.62
 #T and ionic strength:
 $\text{Cd}^{+2} + \text{Diethylamine} = \text{Cd}(\text{Diethylamine})^{+2}$
 log_k 2.73
 delta_h 0 kJ
 -gamma 0 0
 # Id: 1609551
 # log K source: SCD2.62
 # Delta H source: SCD2.62
 #T and ionic strength:
 $\text{Cd}^{+2} + 2\text{Diethylamine} = \text{Cd}(\text{Diethylamine})_2^{+2}$
 log_k 4.86
 delta_h 0 kJ
 -gamma 0 0
 # Id: 1609552
 # log K source: SCD2.62
 # Delta H source: SCD2.62
 #T and ionic strength:
 $\text{Cd}^{+2} + 3\text{Diethylamine} = \text{Cd}(\text{Diethylamine})_3^{+2}$
 log_k 6.37
 delta_h 0 kJ
 -gamma 0 0
 # Id: 1609553
 # log K source: SCD2.62
 # Delta H source: SCD2.62
 #T and ionic strength:
 $\text{Cd}^{+2} + 4\text{Diethylamine} = \text{Cd}(\text{Diethylamine})_4^{+2}$

log_k 7.32
 delta_h 0 kJ
 -gamma 0 0
 # Id: 1609554
 # log K source: SCD2.62
 # Delta H source: SCD2.62
 #T and ionic strength:
 $\text{Ag}^+ + \text{Diethylamine} = \text{Ag}(\text{Diethylamine})^+$
 log_k 2.98
 delta_h 0 kJ
 -gamma 0 0
 # Id: 209551
 # log K source: NIST46.2
 # Delta H source: NIST46.2
 #T and ionic strength:
 $\text{Ag}^+ + 2\text{Diethylamine} = \text{Ag}(\text{Diethylamine})_2^+$
 log_k 6.38
 delta_h -44.7688 kJ
 -gamma 0 0
 # Id: 209552
 # log K source: NIST46.2
 # Delta H source: NIST46.2
 #T and ionic strength:
 $\text{Ni}^{+2} + \text{Diethylamine} = \text{Ni}(\text{Diethylamine})^{+2}$
 log_k 2.78
 delta_h 0 kJ
 -gamma 0 0
 # Id: 5409551
 # log K source: SCD2.62
 # Delta H source: SCD2.62
 #T and ionic strength:
 $\text{Ni}^{+2} + 2\text{Diethylamine} = \text{Ni}(\text{Diethylamine})_2^{+2}$
 log_k 4.97
 delta_h 0 kJ
 -gamma 0 0
 # Id: 5409552
 # log K source: SCD2.62
 # Delta H source: SCD2.62
 #T and ionic strength:
 $\text{Ni}^{+2} + 3\text{Diethylamine} = \text{Ni}(\text{Diethylamine})_3^{+2}$
 log_k 6.72
 delta_h 0 kJ
 -gamma 0 0
 # Id: 5409553
 # log K source: SCD2.62
 # Delta H source: SCD2.62
 #T and ionic strength:
 $\text{Ni}^{+2} + 4\text{Diethylamine} = \text{Ni}(\text{Diethylamine})_4^{+2}$
 log_k 7.93
 delta_h 0 kJ
 -gamma 0 0
 # Id: 5409554
 # log K source: SCD2.62
 # Delta H source: SCD2.62

#T and ionic strength:
 $\text{Ni}^{+2} + 5\text{Diethylamine} = \text{Ni}(\text{Diethylamine})_5^{+2}$
 log_k 8.87
 delta_h 0 kJ
 -gamma 0 0
 # Id: 5409555
 # log K source: SCD2.62
 # Delta H source: SCD2.62
 #T and ionic strength:
 $\text{H}^+ + \text{Butylamine} = \text{H}(\text{Butylamine})^+$
 log_k 10.64
 delta_h -58.2831 kJ
 -gamma 0 0
 # Id: 3309561
 # log K source: NIST46.2
 # Delta H source: NIST46.2
 #T and ionic strength:
 $\text{Hg}(\text{OH})_2 + \text{Butylamine} + 2\text{H}^+ = \text{Hg}(\text{Butylamine})_2^{+2} + 2\text{H}_2\text{O}$
 log_k 14.84
 delta_h 0 kJ
 -gamma 0 0
 # Id: 3619561
 # log K source: NIST46.2
 # Delta H source: NIST46.2
 #T and ionic strength:
 $\text{Hg}(\text{OH})_2 + 2\text{Butylamine} + 2\text{H}^+ = \text{Hg}(\text{Butylamine})_2^{+2} + 2\text{H}_2\text{O}$
 log_k 24.24
 delta_h 0 kJ
 -gamma 0 0
 # Id: 3619562
 # log K source: NIST46.2
 # Delta H source: NIST46.2
 #T and ionic strength:
 $\text{Hg}(\text{OH})_2 + 3\text{Butylamine} + 2\text{H}^+ = \text{Hg}(\text{Butylamine})_3^{+2} + 2\text{H}_2\text{O}$
 log_k 25.1
 delta_h 0 kJ
 -gamma 0 0
 # Id: 3619563
 # log K source: NIST46.2
 # Delta H source: NIST46.2
 #T and ionic strength:
 $\text{Hg}(\text{OH})_2 + 4\text{Butylamine} + 2\text{H}^+ = \text{Hg}(\text{Butylamine})_4^{+2} + 2\text{H}_2\text{O}$
 log_k 26.1
 delta_h 0 kJ
 -gamma 0 0
 # Id: 3619564
 # log K source: NIST46.2
 # Delta H source: NIST46.2
 #T and ionic strength:
 $\text{Ag}^+ + \text{Butylamine} = \text{Ag}(\text{Butylamine})^+$
 log_k 3.42
 delta_h -16.736 kJ
 -gamma 0 0
 # Id: 209561

log K source: NIST46.2
 # Delta H source: NIST46.2
 #T and ionic strength:
 $\text{Ag}^+ + 2\text{Butylamine} = \text{Ag}(\text{Butylamine})_2^+$
 log_k 7.47
 delta_h -52.7184 kJ
 -gamma 0 0
 # Id: 209562
 # log K source: NIST46.2
 # Delta H source: NIST46.2
 #T and ionic strength:
 $\text{H}^+ + \text{Methylamine} = \text{H}(\text{Methylamine})^+$
 log_k 10.64
 delta_h -55.2288 kJ
 -gamma 0 0
 # Id: 3309581
 # log K source: NIST46.2
 # Delta H source: NIST46.2
 #T and ionic strength:
 $\text{Cd}^{+2} + \text{Methylamine} = \text{Cd}(\text{Methylamine})^+$
 log_k 2.75
 delta_h 0 kJ
 -gamma 0 0
 # Id: 1609581
 # log K source: NIST46.2
 # Delta H source: NIST46.2
 #T and ionic strength:
 $\text{Cd}^{+2} + 2\text{Methylamine} = \text{Cd}(\text{Methylamine})_2^{+2}$
 log_k 4.81
 delta_h -29.288 kJ
 -gamma 0 0
 # Id: 1609582
 # log K source: NIST46.2
 # Delta H source: NIST46.2
 #T and ionic strength:
 $\text{Cd}^{+2} + 3\text{Methylamine} = \text{Cd}(\text{Methylamine})_3^{+2}$
 log_k 5.94
 delta_h 0 kJ
 -gamma 0 0
 # Id: 1609583
 # log K source: NIST46.2
 # Delta H source: NIST46.2
 #T and ionic strength:
 $\text{Cd}^{+2} + 4\text{Methylamine} = \text{Cd}(\text{Methylamine})_4^{+2}$
 log_k 6.55
 delta_h -58.576 kJ
 -gamma 0 0
 # Id: 1609584
 # log K source: NIST46.2
 # Delta H source: NIST46.2
 #T and ionic strength:
 $\text{Hg}(\text{OH})_2 + \text{Methylamine} + 2\text{H}^+ = \text{Hg}(\text{Methylamine})_2^{+2} + 2\text{H}_2\text{O}$
 log_k 14.76
 delta_h 0 kJ

-gamma 0 0
 # Id: 3619581
 # log K source: NIST46.2
 # Delta H source: NIST46.2
 #T and ionic strength:
 $\text{Hg}(\text{OH})_2 + 2\text{Methylamine} + 2\text{H}^+ = \text{Hg}(\text{Methylamine})_{2+2} + 2\text{H}_2\text{O}$
 log_k 23.96
 delta_h 0 kJ
 -gamma 0 0
 # Id: 3619582
 # log K source: NIST46.2
 # Delta H source: NIST46.2
 #T and ionic strength:
 $\text{Hg}(\text{OH})_2 + 3\text{Methylamine} + 2\text{H}^+ = \text{Hg}(\text{Methylamine})_{3+2} + 2\text{H}_2\text{O}$
 log_k 24.3
 delta_h 0 kJ
 -gamma 0 0
 # Id: 3619583
 # log K source: NIST46.2
 # Delta H source: NIST46.2
 #T and ionic strength:
 $\text{Hg}(\text{OH})_2 + 4\text{Methylamine} + 2\text{H}^+ = \text{Hg}(\text{Methylamine})_{4+2} + 2\text{H}_2\text{O}$
 log_k 24.6
 delta_h 0 kJ
 -gamma 0 0
 # Id: 3619584
 # log K source: NIST46.2
 # Delta H source: NIST46.2
 #T and ionic strength:
 $\text{Cu}^{+2} + \text{Methylamine} = \text{Cu}(\text{Methylamine})_{+2}$
 log_k 4.11
 delta_h 0 kJ
 -gamma 0 0
 # Id: 2319581
 # log K source: NIST46.2
 # Delta H source: NIST46.2
 #T and ionic strength:
 $\text{Cu}^{+2} + 2\text{Methylamine} = \text{Cu}(\text{Methylamine})_{2+2}$
 log_k 7.51
 delta_h 0 kJ
 -gamma 0 0
 # Id: 2319582
 # log K source: NIST46.2
 # Delta H source: NIST46.2
 #T and ionic strength:
 $\text{Cu}^{+2} + 3\text{Methylamine} = \text{Cu}(\text{Methylamine})_{3+2}$
 log_k 10.21
 delta_h 0 kJ
 -gamma 0 0
 # Id: 2319583
 # log K source: NIST46.2
 # Delta H source: NIST46.2
 #T and ionic strength:
 $\text{Cu}^{+2} + 4\text{Methylamine} = \text{Cu}(\text{Methylamine})_{4+2}$

log_k 12.08
 delta_h 0 kJ
 -gamma 0 0
 # Id: 2319584
 # log K source: NIST46.2
 # Delta H source: NIST46.2
 #T and ionic strength:
 $\text{Ag}^+ + \text{Methylamine} = \text{Ag}(\text{Methylamine})^+$
 log_k 3.07
 delta_h -12.552 kJ
 -gamma 0 0
 # Id: 209581
 # log K source: NIST46.2
 # Delta H source: NIST46.2
 #T and ionic strength:
 $\text{Ag}^+ + 2\text{Methylamine} = \text{Ag}(\text{Methylamine})_2^+$
 log_k 6.89
 delta_h -48.9528 kJ
 -gamma 0 0
 # Id: 209582
 # log K source: NIST46.2
 # Delta H source: NIST46.2
 #T and ionic strength:
 $\text{Ni}^{+2} + \text{Methylamine} = \text{Ni}(\text{Methylamine})_2^+$
 log_k 2.23
 delta_h 0 kJ
 -gamma 0 0
 # Id: 5409581
 # log K source: NIST46.2
 # Delta H source: NIST46.2
 #T and ionic strength:
 $\text{H}^+ + \text{Dimethylamine} = \text{H}(\text{Dimethylamine})^+$
 log_k 10.774
 delta_h -50.208 kJ
 -gamma 0 0
 # Id: 3309591
 # log K source: NIST46.2
 # Delta H source: NIST46.2
 #T and ionic strength:
 $\text{Ag}^+ + 2\text{Dimethylamine} = \text{Ag}(\text{Dimethylamine})_2^+$
 log_k 5.37
 delta_h -40.5848 kJ
 -gamma 0 0
 # Id: 209591
 # log K source: NIST46.2
 # Delta H source: NIST46.2
 #T and ionic strength:
 $\text{Ni}^{+2} + \text{Dimethylamine} = \text{Ni}(\text{Dimethylamine})_2^+$
 log_k 1.47
 delta_h 0 kJ
 -gamma 0 0
 # Id: 5409591
 # log K source: NIST46.2
 # Delta H source: NIST46.2

#T and ionic strength:
 $\text{H}^+ + \text{Hexylamine} = \text{H}(\text{Hexylamine})^+$
 log_k 10.63
 delta_h -58.576 kJ
 -gamma 0 0
 # Id: 3309611
 # log K source: NIST46.2
 # Delta H source: NIST46.2
 #T and ionic strength:
 $\text{Ag}^+ + \text{Hexylamine} = \text{Ag}(\text{Hexylamine})^+$
 log_k 3.54
 delta_h -25.104 kJ
 -gamma 0 0
 # Id: 209611
 # log K source: NIST46.2
 # Delta H source: NIST46.2
 #T and ionic strength:
 $\text{Ag}^+ + 2\text{Hexylamine} = \text{Ag}(\text{Hexylamine})_2^+$
 log_k 7.55
 delta_h -53.1368 kJ
 -gamma 0 0
 # Id: 209612
 # log K source: NIST46.2
 # Delta H source: NIST46.2
 #T and ionic strength:
 $\text{H}^+ + \text{Ethylenediamine} = \text{H}(\text{Ethylenediamine})^+$
 log_k 9.928
 delta_h -49.7896 kJ
 -gamma 0 0
 # Id: 3309631
 # log K source: NIST46.2
 # Delta H source: NIST46.2
 #T and ionic strength:
 $2\text{H}^+ + \text{Ethylenediamine} = \text{H}_2(\text{Ethylenediamine})^{2+}$
 log_k 16.776
 delta_h -95.3952 kJ
 -gamma 0 0
 # Id: 3309632
 # log K source: NIST46.2
 # Delta H source: NIST46.2
 #T and ionic strength:
 $\text{Pb}^{+2} + \text{Ethylenediamine} = \text{Pb}(\text{Ethylenediamine})^{+2}$
 log_k 5.04
 delta_h 0 kJ
 -gamma 0 0
 # Id: 6009631
 # log K source: NIST46.2
 # Delta H source: NIST46.2
 #T and ionic strength:
 $\text{Pb}^{+2} + 2\text{Ethylenediamine} = \text{Pb}(\text{Ethylenediamine})_2^{2+}$
 log_k 8.5
 delta_h 0 kJ
 -gamma 0 0
 # Id: 6009632

log K source: NIST46.2
 # Delta H source: NIST46.2
 #T and ionic strength:
 $\text{Zn}^{+2} + \text{Ethylenediamine} = \text{Zn}(\text{Ethylenediamine})_2$
 log_k 5.66
 delta_h -29.288 kJ
 -gamma 0 0
 # Id: 9509631
 # log K source: NIST46.2
 # Delta H source: NIST46.2
 #T and ionic strength:
 $\text{Zn}^{+2} + 2\text{Ethylenediamine} = \text{Zn}(\text{Ethylenediamine})_2^{+2}$
 log_k 10.6
 delta_h -48.116 kJ
 -gamma 0 0
 # Id: 9509632
 # log K source: NIST46.2
 # Delta H source: NIST46.2
 #T and ionic strength:
 $\text{Zn}^{+2} + 3\text{Ethylenediamine} = \text{Zn}(\text{Ethylenediamine})_3^{+2}$
 log_k 13.9
 delta_h -71.5464 kJ
 -gamma 0 0
 # Id: 9509633
 # log K source: NIST46.2
 # Delta H source: NIST46.2
 #T and ionic strength:
 $\text{Cd}^{+2} + \text{Ethylenediamine} = \text{Cd}(\text{Ethylenediamine})_2$
 log_k 5.41
 delta_h -28.4512 kJ
 -gamma 0 0
 # Id: 1609631
 # log K source: NIST46.2
 # Delta H source: NIST46.2
 #T and ionic strength:
 $\text{Cd}^{+2} + 2\text{Ethylenediamine} = \text{Cd}(\text{Ethylenediamine})_2^{+2}$
 log_k 9.9
 delta_h -55.6472 kJ
 -gamma 0 0
 # Id: 1609632
 # log K source: NIST46.2
 # Delta H source: NIST46.2
 #T and ionic strength:
 $\text{Cd}^{+2} + 3\text{Ethylenediamine} = \text{Cd}(\text{Ethylenediamine})_3^{+2}$
 log_k 11.6
 delta_h -82.4248 kJ
 -gamma 0 0
 # Id: 1609633
 # log K source: NIST46.2
 # Delta H source: NIST46.2
 #T and ionic strength:
 $\text{Hg}(\text{OH})_2 + \text{Ethylenediamine} + 2\text{H}^+ = \text{Hg}(\text{Ethylenediamine})_2^{+2} + 2\text{H}_2\text{O}$
 log_k 20.4
 delta_h 0 kJ

-gamma 0 0
 # Id: 3619631
 # log K source: NIST46.2
 # Delta H source: NIST46.2
 #T and ionic strength:
 $\text{Hg(OH)}_2 + 2\text{Ethylenediamine} + 2\text{H}^+ = \text{Hg(Ethylenediamine)}_2 + 2\text{H}_2\text{O}$
 log_k 29.3
 delta_h -173.218 kJ
 -gamma 0 0
 # Id: 3619632
 # log K source: NIST46.2
 # Delta H source: NIST46.2
 #T and ionic strength:
 $\text{Hg(OH)}_2 + 2\text{Ethylenediamine} + 3\text{H}^+ = \text{HgH(Ethylenediamine)}_2 + 2\text{H}_2\text{O}$
 log_k 34.7
 delta_h 0 kJ
 -gamma 0 0
 # Id: 3619633
 # log K source: NIST46.2
 # Delta H source: NIST46.2
 #T and ionic strength:
 $\text{Cu}^+ + 2\text{Ethylenediamine} = \text{Cu(Ethylenediamine)}_2^+$
 log_k 11.2
 delta_h 0 kJ
 -gamma 0 0
 # Id: 2309631
 # log K source: NIST46.2
 # Delta H source: NIST46.2
 #T and ionic strength:
 $\text{Cu}^{+2} + \text{Ethylenediamine} = \text{Cu(Ethylenediamine)}^+$
 log_k 10.5
 delta_h -52.7184 kJ
 -gamma 0 0
 # Id: 2319631
 # log K source: NIST46.2
 # Delta H source: NIST46.2
 #T and ionic strength:
 $\text{Cu}^{+2} + 2\text{Ethylenediamine} = \text{Cu(Ethylenediamine)}_2^+$
 log_k 19.6
 delta_h -105.437 kJ
 -gamma 0 0
 # Id: 2319632
 # log K source: NIST46.2
 # Delta H source: NIST46.2
 #T and ionic strength:
 $\text{Ag}^+ + \text{Ethylenediamine} = \text{Ag(Ethylenediamine)}^+$
 log_k 4.6
 delta_h -48.9528 kJ
 -gamma 0 0
 # Id: 209631
 # log K source: NIST46.2
 # Delta H source: NIST46.2
 #T and ionic strength:
 $\text{Ag}^+ + 2\text{Ethylenediamine} = \text{Ag(Ethylenediamine)}_2^+$

log_k 7.5
 delta_h -52.3 kJ
 -gamma 0 0
 # Id: 209632
 # log K source: NIST46.2
 # Delta H source: NIST46.2
 #T and ionic strength:
 $\text{Ag}^+ + \text{Ethylenediamine} + \text{H}^+ = \text{AgH(Ethylenediamine)} + 2$
 log_k 11.99
 delta_h -75.312 kJ
 -gamma 0 0
 # Id: 209633
 # log K source: NIST46.2
 # Delta H source: NIST46.2
 #T and ionic strength:
 $2\text{Ag}^+ + \text{Ethylenediamine} = \text{Ag}_2(\text{Ethylenediamine}) + 2$
 log_k 6.5
 delta_h 0 kJ
 -gamma 0 0
 # Id: 209634
 # log K source: NIST46.2
 # Delta H source: NIST46.2
 #T and ionic strength:
 $2\text{Ag}^+ + 2\text{Ethylenediamine} = \text{Ag}_2(\text{Ethylenediamine})_2 + 2$
 log_k 12.7
 delta_h -97.0688 kJ
 -gamma 0 0
 # Id: 209635
 # log K source: NIST46.2
 # Delta H source: NIST46.2
 #T and ionic strength:
 $\text{Ag}^+ + 2\text{Ethylenediamine} + 2\text{H}^+ = \text{Ag(HEthylenediamine)}_2 + 3$
 log_k 24
 delta_h -150.206 kJ
 -gamma 0 0
 # Id: 209636
 # log K source: NIST46.2
 # Delta H source: NIST46.2
 #T and ionic strength:
 $\text{Ag}^+ + 2\text{Ethylenediamine} + \text{H}^+ = \text{AgH(Ethylenediamine)}_2 + 2$
 log_k 8.4
 delta_h -47.6976 kJ
 -gamma 0 0
 # Id: 209637
 # log K source: NIST46.2
 # Delta H source: NIST46.2
 #T and ionic strength:
 $\text{Ni}^{+2} + \text{Ethylenediamine} = \text{Ni(Ethylenediamine)} + 2$
 log_k 7.32
 delta_h -37.656 kJ
 -gamma 0 0
 # Id: 5409631
 # log K source: NIST46.2
 # Delta H source: NIST46.2

#T and ionic strength:
 $\text{Ni}^{+2} + 2\text{Ethylenediamine} = \text{Ni}(\text{Ethylenediamine})_2^{+2}$
 log_k 13.5
 delta_h -76.5672 kJ
 -gamma 0 0
 # Id: 5409632
 # log K source: NIST46.2
 # Delta H source: NIST46.2
 #T and ionic strength:
 $\text{Ni}^{+2} + 3\text{Ethylenediamine} = \text{Ni}(\text{Ethylenediamine})_3^{+2}$
 log_k 17.6
 delta_h -117.152 kJ
 -gamma 0 0
 # Id: 5409633
 # log K source: NIST46.2
 # Delta H source: NIST46.2
 #T and ionic strength:
 $\text{Co}^{+2} + \text{Ethylenediamine} = \text{Co}(\text{Ethylenediamine})^{+2}$
 log_k 5.5
 delta_h -28 kJ
 -gamma 0 0
 # Id: 2009631
 # log K source: NIST46.4
 # Delta H source: NIST46.4
 #T and ionic strength: 0.10 25.0
 $\text{Co}^{+2} + 2\text{Ethylenediamine} = \text{Co}(\text{Ethylenediamine})_2^{+2}$
 log_k 10.1
 delta_h -58.5 kJ
 -gamma 0 0
 # Id: 2009632
 # log K source: NIST46.4
 # Delta H source: NIST46.4
 #T and ionic strength: 0.10 25.0
 $\text{Co}^{+2} + 3\text{Ethylenediamine} = \text{Co}(\text{Ethylenediamine})_3^{+2}$
 log_k 13.2
 delta_h -92.8 kJ
 -gamma 0 0
 # Id: 2009633
 # log K source: NIST46.4
 # Delta H source: NIST46.4
 #T and ionic strength: 0.10 25.0
 $\text{Co}^{+3} + 2\text{Ethylenediamine} = \text{Co}(\text{Ethylenediamine})_2^{+3}$
 log_k 34.7
 delta_h 0 kJ
 -gamma 0 0
 # Id: 2019631
 # log K source: NIST46.4
 # Delta H source: NIST46.2
 #T and ionic strength: 1.00 25.0
 $\text{Co}^{+3} + 3\text{Ethylenediamine} = \text{Co}(\text{Ethylenediamine})_3^{+3}$
 log_k 48.69
 delta_h 0 kJ
 -gamma 0 0
 # Id: 2019632

log K source: NIST46.4
 # Delta H source: NIST46.2
 #T and ionic strength: 1.50 30.0
 $\text{Fe}^{+2} + \text{Ethylenediamine} = \text{Fe}(\text{Ethylenediamine})^{+2}$
 log_k 4.26
 delta_h 0 kJ
 -gamma 0 0
 # Id: 2809631
 # log K source: NIST46.2
 # Delta H source: NIST46.2
 #T and ionic strength:
 $\text{Fe}^{+2} + 2\text{Ethylenediamine} = \text{Fe}(\text{Ethylenediamine})^{2+2}$
 log_k 7.73
 delta_h 0 kJ
 -gamma 0 0
 # Id: 2809632
 # log K source: NIST46.2
 # Delta H source: NIST46.2
 #T and ionic strength:
 $\text{Fe}^{+2} + 3\text{Ethylenediamine} = \text{Fe}(\text{Ethylenediamine})^{3+2}$
 log_k 10.17
 delta_h 0 kJ
 -gamma 0 0
 # Id: 2809633
 # log K source: NIST46.2
 # Delta H source: NIST46.2
 #T and ionic strength:
 $\text{Mn}^{+2} + \text{Ethylenediamine} = \text{Mn}(\text{Ethylenediamine})^{+2}$
 log_k 2.74
 delta_h -11.7152 kJ
 -gamma 0 0
 # Id: 4709631
 # log K source: NIST46.2
 # Delta H source: NIST46.2
 #T and ionic strength:
 $\text{Mn}^{+2} + 2\text{Ethylenediamine} = \text{Mn}(\text{Ethylenediamine})^{2+2}$
 log_k 4.8
 delta_h -25.104 kJ
 -gamma 0 0
 # Id: 4709632
 # log K source: NIST46.2
 # Delta H source: NIST46.2
 #T and ionic strength:
 $\text{Cr}(\text{OH})^{2+} + 2\text{Ethylenediamine} + 2\text{H}^{+} = \text{Cr}(\text{Ethylenediamine})^{2+3} + 2\text{H}_2\text{O}$
 log_k 22.57
 delta_h 0 kJ
 -gamma 0 0
 # Id: 2119631
 # log K source: NIST46.2
 # Delta H source: NIST46.2
 #T and ionic strength:
 $\text{Cr}(\text{OH})^{2+} + 3\text{Ethylenediamine} + 2\text{H}^{+} = \text{Cr}(\text{Ethylenediamine})^{3+3} + 2\text{H}_2\text{O}$
 log_k 29
 delta_h 0 kJ

-gamma 0 0
 # Id: 2119632
 # log K source: NIST46.2
 # Delta H source: NIST46.2
 #T and ionic strength:
 $\text{Mg}^{+2} + \text{Ethylenediamine} = \text{Mg}(\text{Ethylenediamine})_2$
 log_k 0.37
 delta_h 0 kJ
 -gamma 0 0
 # Id: 4609631
 # log K source: NIST46.2
 # Delta H source: NIST46.2
 #T and ionic strength:
 $\text{Ca}^{+2} + \text{Ethylenediamine} = \text{Ca}(\text{Ethylenediamine})_2$
 log_k 0.11
 delta_h 0 kJ
 -gamma 0 0
 # Id: 1509631
 # log K source: NIST46.2
 # Delta H source: NIST46.2
 #T and ionic strength:
 $\text{H}^+ + \text{Propylamine} = \text{H}(\text{Propylamine})$
 log_k 10.566
 delta_h -57.53 kJ
 -gamma 0 0
 # Id: 3309641
 # log K source: NIST46.2
 # Delta H source: NIST46.2
 #T and ionic strength:
 $\text{Zn}^{+2} + \text{Propylamine} = \text{Zn}(\text{Propylamine})_2$
 log_k 2.42
 delta_h 0 kJ
 -gamma 0 0
 # Id: 9509641
 # log K source: SCD2.62
 # Delta H source: SCD2.62
 #T and ionic strength:
 $\text{Zn}^{+2} + 2\text{Propylamine} = \text{Zn}(\text{Propylamine})_2$
 log_k 4.85
 delta_h 0 kJ
 -gamma 0 0
 # Id: 9509642
 # log K source: SCD2.62
 # Delta H source: SCD2.62
 #T and ionic strength:
 $\text{Zn}^{+2} + 3\text{Propylamine} = \text{Zn}(\text{Propylamine})_3$
 log_k 7.38
 delta_h 0 kJ
 -gamma 0 0
 # Id: 9509643
 # log K source: SCD2.62
 # Delta H source: SCD2.62
 #T and ionic strength:
 $\text{Zn}^{+2} + 4\text{Propylamine} = \text{Zn}(\text{Propylamine})_4$

log_k 9.49
 delta_h 0 kJ
 -gamma 0 0
 # Id: 9509644
 # log K source: SCD2.62
 # Delta H source: SCD2.62
 #T and ionic strength:
 $\text{Cd}^{+2} + \text{Propylamine} = \text{Cd}(\text{Propylamine})^{+2}$
 log_k 2.62
 delta_h 0 kJ
 -gamma 0 0
 # Id: 1609641
 # log K source: SCD2.62
 # Delta H source: SCD2.62
 #T and ionic strength:
 $\text{Cd}^{+2} + 2\text{Propylamine} = \text{Cd}(\text{Propylamine})_2^{+2}$
 log_k 4.64
 delta_h 0 kJ
 -gamma 0 0
 # Id: 1609642
 # log K source: SCD2.62
 # Delta H source: SCD2.62
 #T and ionic strength:
 $\text{Cd}^{+2} + 3\text{Propylamine} = \text{Cd}(\text{Propylamine})_3^{+2}$
 log_k 6.03
 delta_h 0 kJ
 -gamma 0 0
 # Id: 1609643
 # log K source: SCD2.62
 # Delta H source: SCD2.62
 #T and ionic strength:
 $\text{Ag}^{+} + \text{Propylamine} = \text{Ag}(\text{Propylamine})^{+}$
 log_k 3.45
 delta_h -12.552 kJ
 -gamma 0 0
 # Id: 209641
 # log K source: NIST46.2
 # Delta H source: NIST46.2
 #T and ionic strength:
 $\text{Ag}^{+} + 2\text{Propylamine} = \text{Ag}(\text{Propylamine})_2^{+}$
 log_k 7.44
 delta_h -53.1368 kJ
 -gamma 0 0
 # Id: 209642
 # log K source: NIST46.2
 # Delta H source: NIST46.2
 #T and ionic strength:
 $\text{Ni}^{+2} + \text{Propylamine} = \text{Ni}(\text{Propylamine})^{+2}$
 log_k 2.81
 delta_h 0 kJ
 -gamma 0 0
 # Id: 5409641
 # log K source: SCD2.62
 # Delta H source: SCD2.62

#T and ionic strength:
 $\text{Ni}^{+2} + 2\text{Propylamine} = \text{Ni}(\text{Propylamine})_2^{+2}$
 log_k 5.02
 delta_h 0 kJ
 -gamma 0 0
 # Id: 5409642
 # log K source: SCD2.62
 # Delta H source: SCD2.62
 #T and ionic strength:
 $\text{Ni}^{+2} + 3\text{Propylamine} = \text{Ni}(\text{Propylamine})_3^{+2}$
 log_k 6.79
 delta_h 0 kJ
 -gamma 0 0
 # Id: 5409643
 # log K source: SCD2.62
 # Delta H source: SCD2.62
 #T and ionic strength:
 $\text{Ni}^{+2} + 4\text{Propylamine} = \text{Ni}(\text{Propylamine})_4^{+2}$
 log_k 8.31
 delta_h 0 kJ
 -gamma 0 0
 # Id: 5409644
 # log K source: SCD2.62
 # Delta H source: SCD2.62
 #T and ionic strength:
 $\text{H}^{+} + \text{Isopropylamine} = \text{H}(\text{Isopropylamine})^{+}$
 log_k 10.67
 delta_h -58.3668 kJ
 -gamma 0 0
 # Id: 3309651
 # log K source: NIST46.2
 # Delta H source: NIST46.2
 #T and ionic strength:
 $\text{Zn}^{+2} + \text{Isopropylamine} = \text{Zn}(\text{Isopropylamine})^{+2}$
 log_k 2.37
 delta_h 0 kJ
 -gamma 0 0
 # Id: 9509651
 # log K source: SCD2.62
 # Delta H source: SCD2.62
 #T and ionic strength:
 $\text{Zn}^{+2} + 2\text{Isopropylamine} = \text{Zn}(\text{Isopropylamine})_2^{+2}$
 log_k 4.67
 delta_h 0 kJ
 -gamma 0 0
 # Id: 9509652
 # log K source: SCD2.62
 # Delta H source: SCD2.62
 #T and ionic strength:
 $\text{Zn}^{+2} + 3\text{Isopropylamine} = \text{Zn}(\text{Isopropylamine})_3^{+2}$
 log_k 7.14
 delta_h 0 kJ
 -gamma 0 0
 # Id: 9509653

log K source: SCD2.62
 # Delta H source: SCD2.62
 #T and ionic strength:
 $\text{Zn}^{+2} + 4\text{Isopropylamine} = \text{Zn}(\text{Isopropylamine})_4^{+2}$
 log_k 9.44
 delta_h 0 kJ
 -gamma 0 0
 # Id: 9509654
 # log K source: SCD2.62
 # Delta H source: SCD2.62
 #T and ionic strength:
 $\text{Cd}^{+2} + \text{Isopropylamine} = \text{Cd}(\text{Isopropylamine})^{+2}$
 log_k 2.55
 delta_h 0 kJ
 -gamma 0 0
 # Id: 1609651
 # log K source: SCD2.62
 # Delta H source: SCD2.62
 #T and ionic strength:
 $\text{Cd}^{+2} + 2\text{Isopropylamine} = \text{Cd}(\text{Isopropylamine})_2^{+2}$
 log_k 4.57
 delta_h 0 kJ
 -gamma 0 0
 # Id: 1609652
 # log K source: SCD2.62
 # Delta H source: SCD2.62
 #T and ionic strength:
 $\text{Cd}^{+2} + 3\text{Isopropylamine} = \text{Cd}(\text{Isopropylamine})_3^{+2}$
 log_k 6.07
 delta_h 0 kJ
 -gamma 0 0
 # Id: 1609653
 # log K source: SCD2.62
 # Delta H source: SCD2.62
 #T and ionic strength:
 $\text{Cd}^{+2} + 4\text{Isopropylamine} = \text{Cd}(\text{Isopropylamine})_4^{+2}$
 log_k 6.9
 delta_h 0 kJ
 -gamma 0 0
 # Id: 1609654
 # log K source: SCD2.62
 # Delta H source: SCD2.62
 #T and ionic strength:
 $\text{Hg}(\text{OH})_2 + \text{Isopropylamine} + 2\text{H}^+ = \text{Hg}(\text{Isopropylamine})_2^{+2} + 2\text{H}_2\text{O}$
 log_k 14.85
 delta_h 0 kJ
 -gamma 0 0
 # Id: 3619651
 # log K source: NIST46.2
 # Delta H source: NIST46.2
 #T and ionic strength:
 $\text{Hg}(\text{OH})_2 + 2\text{Isopropylamine} + 2\text{H}^+ = \text{Hg}(\text{Isopropylamine})_2^{+2} + 2\text{H}_2\text{O}$
 log_k 24.37
 delta_h 0 kJ

-gamma 0 0
 # Id: 3619652
 # log K source: NIST46.2
 # Delta H source: NIST46.2
 #T and ionic strength:
 $\text{Ag}^+ + \text{Isopropylamine} = \text{Ag}(\text{Isopropylamine})^+$
 log_k 3.67
 delta_h -23.8488 kJ
 -gamma 0 0
 # Id: 209651
 # log K source: NIST46.2
 # Delta H source: NIST46.2
 #T and ionic strength:
 $\text{Ag}^+ + 2\text{Isopropylamine} = \text{Ag}(\text{Isopropylamine})_2^+$
 log_k 7.77
 delta_h -59.8312 kJ
 -gamma 0 0
 # Id: 209652
 # log K source: NIST46.2
 # Delta H source: NIST46.2
 #T and ionic strength:
 $\text{Ni}^{+2} + \text{Isopropylamine} = \text{Ni}(\text{Isopropylamine})^+$
 log_k 2.71
 delta_h 0 kJ
 -gamma 0 0
 # Id: 5409651
 # log K source: SCD2.62
 # Delta H source: SCD2.62
 #T and ionic strength:
 $\text{Ni}^{+2} + 2\text{Isopropylamine} = \text{Ni}(\text{Isopropylamine})_2^{+2}$
 log_k 4.86
 delta_h 0 kJ
 -gamma 0 0
 # Id: 5409652
 # log K source: SCD2.62
 # Delta H source: SCD2.62
 #T and ionic strength:
 $\text{Ni}^{+2} + 3\text{Isopropylamine} = \text{Ni}(\text{Isopropylamine})_3^{+2}$
 log_k 6.57
 delta_h 0 kJ
 -gamma 0 0
 # Id: 5409653
 # log K source: SCD2.62
 # Delta H source: SCD2.62
 #T and ionic strength:
 $\text{Ni}^{+2} + 4\text{Isopropylamine} = \text{Ni}(\text{Isopropylamine})_4^{+2}$
 log_k 7.83
 delta_h 0 kJ
 -gamma 0 0
 # Id: 5409654
 # log K source: SCD2.62
 # Delta H source: SCD2.62
 #T and ionic strength:
 $\text{Ni}^{+2} + 5\text{Isopropylamine} = \text{Ni}(\text{Isopropylamine})_5^{+2}$

log_k 8.43
 delta_h 0 kJ
 -gamma 0 0
 # Id: 5409655
 # log K source: SCD2.62
 # Delta H source: SCD2.62
 #T and ionic strength:
 $\text{H}^+ + \text{Trimethylamine} = \text{H}(\text{Trimethylamine})$
 log_k 9.8
 delta_h -36.8192 kJ
 -gamma 0 0
 # Id: 3309661
 # log K source: NIST46.2
 # Delta H source: NIST46.2
 #T and ionic strength:
 $\text{Ag}^+ + \text{Trimethylamine} = \text{Ag}(\text{Trimethylamine})$
 log_k 1.701
 delta_h 0 kJ
 -gamma 0 0
 # Id: 209661
 # log K source: SCD2.62
 # Delta H source: SCD2.62
 #T and ionic strength:
 $\text{H}^+ + \text{Citrate-3} = \text{H}(\text{Citrate})$
 log_k 6.396
 delta_h 3.3472 kJ
 -gamma 0 0
 # Id: 3309671
 # log K source: NIST46.2
 # Delta H source: NIST46.2
 #T and ionic strength:
 $2\text{H}^+ + \text{Citrate-3} = \text{H}_2(\text{Citrate})$
 log_k 11.157
 delta_h 1.297 kJ
 -gamma 0 0
 # Id: 3309672
 # log K source: NIST46.2
 # Delta H source: NIST46.2
 #T and ionic strength:
 $3\text{H}^+ + \text{Citrate-3} = \text{H}_3(\text{Citrate})$
 log_k 14.285
 delta_h -2.7614 kJ
 -gamma 0 0
 # Id: 3309673
 # log K source: NIST46.2
 # Delta H source: NIST46.2
 #T and ionic strength:
 $\text{Pb}^{+2} + \text{Citrate-3} = \text{Pb}(\text{Citrate})$
 log_k 7.27
 delta_h 0 kJ
 -gamma 0 0
 # Id: 6009671
 # log K source: SCD2.62
 # Delta H source: SCD2.62

#T and ionic strength:
 $\text{Pb}^{+2} + 2\text{Citrate}^{-3} = \text{Pb}(\text{Citrate})_2^{-4}$
 log_k 6.53
 delta_h 0 kJ
 -gamma 0 0
 # Id: 6009672
 # log K source: NIST46.2
 # Delta H source: NIST46.2
 #T and ionic strength:
 $\text{Al}^{+3} + \text{Citrate}^{-3} = \text{Al}(\text{Citrate})$
 log_k 9.97
 delta_h 0 kJ
 -gamma 0 0
 # Id: 309671
 # log K source: NIST46.2
 # Delta H source: NIST46.2
 #T and ionic strength:
 $\text{Al}^{+3} + 2\text{Citrate}^{-3} = \text{Al}(\text{Citrate})_2^{-3}$
 log_k 14.8
 delta_h 0 kJ
 -gamma 0 0
 # Id: 309672
 # log K source: NIST46.2
 # Delta H source: NIST46.2
 #T and ionic strength:
 $\text{Al}^{+3} + \text{Citrate}^{-3} + \text{H}^{+} = \text{AlH}(\text{Citrate})^{+}$
 log_k 12.85
 delta_h 0 kJ
 -gamma 0 0
 # Id: 309673
 # log K source: NIST46.2
 # Delta H source: NIST46.2
 #T and ionic strength:
 $\text{Ti}^{+} + \text{Citrate}^{-3} = \text{Ti}(\text{Citrate})^{-2}$
 log_k 1.48
 delta_h 0 kJ
 -gamma 0 0
 # Id: 8709671
 # log K source: NIST46.2
 # Delta H source: NIST46.2
 #T and ionic strength:
 $\text{Zn}^{+2} + \text{Citrate}^{-3} = \text{Zn}(\text{Citrate})^{-}$
 log_k 6.21
 delta_h 8.368 kJ
 -gamma 0 0
 # Id: 9509671
 # log K source: NIST46.2
 # Delta H source: NIST46.2
 #T and ionic strength:
 $\text{Zn}^{+2} + 2\text{Citrate}^{-3} = \text{Zn}(\text{Citrate})_2^{-4}$
 log_k 7.4
 delta_h 25.104 kJ
 -gamma 0 0
 # Id: 9509672

log K source: NIST46.2
 # Delta H source: NIST46.2
 #T and ionic strength:
 $\text{Zn}^{+2} + \text{Citrate}^{-3} + \text{H}^{+} = \text{ZnH}(\text{Citrate})$
 log_k 10.2
 delta_h 3.3472 kJ
 -gamma 0 0
 # Id: 9509673
 # log K source: NIST46.2
 # Delta H source: NIST46.2
 #T and ionic strength:
 $\text{Zn}^{+2} + \text{Citrate}^{-3} + 2\text{H}^{+} = \text{ZnH}_2(\text{Citrate})^{+}$
 log_k 12.84
 delta_h 0 kJ
 -gamma 0 0
 # Id: 9509674
 # log K source: SCD2.62
 # Delta H source: SCD2.62
 #T and ionic strength:
 $\text{Cd}^{+2} + \text{Citrate}^{-3} = \text{Cd}(\text{Citrate})^{-}$
 log_k 4.98
 delta_h 8.368 kJ
 -gamma 0 0
 # Id: 1609671
 # log K source: NIST46.2
 # Delta H source: NIST46.2
 #T and ionic strength:
 $\text{Cd}^{+2} + \text{Citrate}^{-3} + \text{H}^{+} = \text{CdH}(\text{Citrate})$
 log_k 9.44
 delta_h 3.3472 kJ
 -gamma 0 0
 # Id: 1609672
 # log K source: NIST46.2
 # Delta H source: NIST46.2
 #T and ionic strength:
 $\text{Cd}^{+2} + \text{Citrate}^{-3} + 2\text{H}^{+} = \text{CdH}_2(\text{Citrate})^{+}$
 log_k 12.9
 delta_h 0 kJ
 -gamma 0 0
 # Id: 1609673
 # log K source: NIST46.2
 # Delta H source: NIST46.2
 #T and ionic strength:
 $\text{Cd}^{+2} + 2\text{Citrate}^{-3} = \text{Cd}(\text{Citrate})_2^{-4}$
 log_k 5.9
 delta_h 20.92 kJ
 -gamma 0 0
 # Id: 1609674
 # log K source: NIST46.2
 # Delta H source: NIST46.2
 #T and ionic strength:
 $\text{Hg}(\text{OH})_2 + \text{Citrate}^{-3} + 2\text{H}^{+} = \text{Hg}(\text{Citrate})^{-} + 2\text{H}_2\text{O}$
 log_k 18.3
 delta_h 0 kJ

-gamma 0 0
 # Id: 3619671
 # log K source: NIST46.2
 # Delta H source: NIST46.2
 #T and ionic strength:
 $\text{Cu}^{+2} + \text{Citrate}^{-3} = \text{Cu}(\text{Citrate})^{-}$
 log_k 7.57
 delta_h 0 kJ
 -gamma 0 0
 # Id: 2319671
 # log K source: SCD2.62
 # Delta H source: SCD2.62
 #T and ionic strength:
 $\text{Cu}^{+2} + 2\text{Citrate}^{-3} = \text{Cu}(\text{Citrate})^{2-4}$
 log_k 8.9
 delta_h 0 kJ
 -gamma 0 0
 # Id: 2319672
 # log K source: SCD2.62
 # Delta H source: SCD2.62
 #T and ionic strength:
 $\text{Cu}^{+2} + \text{Citrate}^{-3} + \text{H}^{+} = \text{CuH}(\text{Citrate})$
 log_k 10.87
 delta_h 11.7152 kJ
 -gamma 0 0
 # Id: 2319673
 # log K source: NIST46.2
 # Delta H source: NIST46.2
 #T and ionic strength:
 $\text{Cu}^{+2} + \text{Citrate}^{-3} + 2\text{H}^{+} = \text{CuH}_2(\text{Citrate})^{+}$
 log_k 13.23
 delta_h 0 kJ
 -gamma 0 0
 # Id: 2319674
 # log K source: SCD2.62
 # Delta H source: SCD2.62
 #T and ionic strength:
 $2\text{Cu}^{+2} + 2\text{Citrate}^{-3} = \text{Cu}_2(\text{Citrate})^{2-2}$
 log_k 16.9
 delta_h 41.84 kJ
 -gamma 0 0
 # Id: 2319675
 # log K source: NIST46.2
 # Delta H source: NIST46.2
 #T and ionic strength:
 $\text{Ni}^{+2} + \text{Citrate}^{-3} = \text{Ni}(\text{Citrate})^{-}$
 log_k 6.59
 delta_h 16.736 kJ
 -gamma 0 0
 # Id: 5409671
 # log K source: NIST46.2
 # Delta H source: NIST46.2
 #T and ionic strength:
 $\text{Ni}^{+2} + \text{Citrate}^{-3} + \text{H}^{+} = \text{NiH}(\text{Citrate})$

log_k 10.5
 delta_h 15.8992 kJ
 -gamma 0 0
 # Id: 5409672
 # log K source: NIST46.2
 # Delta H source: NIST46.2
 #T and ionic strength:
 $\text{Ni}^{+2} + \text{Citrate}^{-3} + 2\text{H}^{+} = \text{NiH}_2(\text{Citrate})^{+}$
 log_k 13.3
 delta_h 0 kJ
 -gamma 0 0
 # Id: 5409673
 # log K source: NIST46.2
 # Delta H source: NIST46.2
 #T and ionic strength:
 $\text{Ni}^{+2} + 2\text{Citrate}^{-3} = \text{Ni}(\text{Citrate})_2^{-4}$
 log_k 8.77
 delta_h 12.552 kJ
 -gamma 0 0
 # Id: 5409674
 # log K source: NIST46.2
 # Delta H source: NIST46.2
 #T and ionic strength:
 $\text{Ni}^{+2} + 2\text{Citrate}^{-3} + \text{H}^{+} = \text{NiH}(\text{Citrate})_2^{-3}$
 log_k 14.9
 delta_h 32.6352 kJ
 -gamma 0 0
 # Id: 5409675
 # log K source: NIST46.2
 # Delta H source: NIST46.2
 #T and ionic strength:
 $\text{Co}^{+2} + \text{Citrate}^{-3} = \text{Co}(\text{Citrate})^{-}$
 log_k 6.1867
 delta_h 0 kJ
 -gamma 0 0
 # Id: 2009671
 # log K source: NIST46.4
 # Delta H source: NIST46.2
 #T and ionic strength: 0.10 25.0
 $\text{Co}^{+2} + \text{H}^{+} + \text{Citrate}^{-3} = \text{CoHCitrate}$
 log_k 10.4438
 delta_h 0 kJ
 -gamma 0 0
 # Id: 2009672
 # log K source: NIST46.4
 # Delta H source: NIST46.2
 #T and ionic strength: 0.10 25.0
 $\text{Co}^{+2} + 2\text{H}^{+} + \text{Citrate}^{-3} = \text{CoH}_2\text{Citrate}^{+}$
 log_k 12.7859
 delta_h 0 kJ
 -gamma 0 0
 # Id: 2009673
 # log K source: NIST46.4
 # Delta H source: NIST46.2

#T and ionic strength: 0.10 20.0
 $\text{Fe}^{+2} + \text{Citrate}^{-3} = \text{Fe}(\text{Citrate})^{-}$
 log_k 6.1
 delta_h 0 kJ
 -gamma 0 0
 # Id: 2809671
 # log K source: NIST46.2
 # Delta H source: NIST46.2
 #T and ionic strength:
 $\text{Fe}^{+2} + \text{Citrate}^{-3} + \text{H}^{+} = \text{FeH}(\text{Citrate})$
 log_k 10.2
 delta_h 0 kJ
 -gamma 0 0
 # Id: 2809672
 # log K source: NIST46.2
 # Delta H source: NIST46.2
 #T and ionic strength:
 $\text{Fe}^{+3} + \text{Citrate}^{-3} = \text{Fe}(\text{Citrate})$
 log_k 13.1
 delta_h 0 kJ
 -gamma 0 0
 # Id: 2819671
 # log K source: NIST46.2
 # Delta H source: NIST46.2
 #T and ionic strength:
 $\text{Fe}^{+3} + \text{Citrate}^{-3} + \text{H}^{+} = \text{FeH}(\text{Citrate})^{+}$
 log_k 14.4
 delta_h 0 kJ
 -gamma 0 0
 # Id: 2819672
 # log K source: NIST46.2
 # Delta H source: NIST46.2
 #T and ionic strength:
 $\text{Mn}^{+2} + \text{Citrate}^{-3} = \text{Mn}(\text{Citrate})^{-}$
 log_k 4.28
 delta_h 0 kJ
 -gamma 0 0
 # Id: 4709671
 # log K source: SCD2.62
 # Delta H source: SCD2.62
 #T and ionic strength:
 $\text{Mn}^{+2} + \text{Citrate}^{-3} + \text{H}^{+} = \text{MnH}(\text{Citrate})$
 log_k 9.6
 delta_h 0 kJ
 -gamma 0 0
 # Id: 4709672
 # log K source: NIST46.2
 # Delta H source: NIST46.2
 #T and ionic strength:
 $\text{Be}^{+2} + \text{Citrate}^{-3} = \text{Be}(\text{Citrate})^{-}$
 log_k 5.534
 delta_h 0 kJ
 -gamma 0 0
 # Id: 1109671

log K source: NIST46.4
 # Delta H source: NIST46.2
 #T and ionic strength: 1.00 25.0
 $\text{Be}^{+2} + \text{H}^{+} + \text{Citrate-3} = \text{BeH}(\text{Citrate})$
 log_k 9.442
 delta_h 0 kJ
 -gamma 0 0
 # Id: 1109672
 # log K source: NIST46.4
 # Delta H source: NIST46.2
 #T and ionic strength: 1.00 25.0
 $\text{Ca}^{+2} + \text{Citrate-3} = \text{Ca}(\text{Citrate})$
 log_k 4.87
 delta_h -8.368 kJ
 -gamma 0 0
 # Id: 1509671
 # log K source: NIST46.2
 # Delta H source: NIST46.2
 #T and ionic strength:
 $\text{Ca}^{+2} + \text{Citrate-3} + \text{H}^{+} = \text{CaH}(\text{Citrate})$
 log_k 9.26
 delta_h -0.8368 kJ
 -gamma 0 0
 # Id: 1509672
 # log K source: NIST46.2
 # Delta H source: NIST46.2
 #T and ionic strength:
 $\text{Ca}^{+2} + \text{Citrate-3} + 2\text{H}^{+} = \text{CaH}_2(\text{Citrate})$
 log_k 12.257
 delta_h 0 kJ
 -gamma 0 0
 # Id: 1509673
 # log K source: SCD2.62
 # Delta H source: SCD2.62
 #T and ionic strength:
 $\text{Mg}^{+2} + \text{Citrate-3} = \text{Mg}(\text{Citrate})$
 log_k 4.89
 delta_h 8.368 kJ
 -gamma 0 0
 # Id: 4609671
 # log K source: NIST46.2
 # Delta H source: NIST46.2
 #T and ionic strength:
 $\text{Mg}^{+2} + \text{Citrate-3} + \text{H}^{+} = \text{MgH}(\text{Citrate})$
 log_k 8.91
 delta_h 3.3472 kJ
 -gamma 0 0
 # Id: 4609672
 # log K source: NIST46.2
 # Delta H source: NIST46.2
 #T and ionic strength:
 $\text{Mg}^{+2} + \text{Citrate-3} + 2\text{H}^{+} = \text{MgH}_2(\text{Citrate})$
 log_k 12.2
 delta_h 0 kJ

-gamma 0 0
 # Id: 4609673
 # log K source: SCD2.62
 # Delta H source: SCD2.62
 #T and ionic strength:
 $\text{Sr}^{+2} + \text{Citrate}^{-3} = \text{Sr}(\text{Citrate})^{-}$
 log_k 4.3367
 delta_h 0 kJ
 -gamma 0 0
 # Id: 8009671
 # log K source: NIST46.4
 # Delta H source: NIST46.2
 #T and ionic strength: 0.10 25.0
 $\text{Sr}^{+2} + \text{H}^{+} + \text{Citrate}^{-3} = \text{SrH}(\text{Citrate})$
 log_k 8.9738
 delta_h 0 kJ
 -gamma 0 0
 # Id: 8009672
 # log K source: NIST46.4
 # Delta H source: NIST46.2
 #T and ionic strength: 0.10 25.0
 $\text{Sr}^{+2} + 2\text{H}^{+} + \text{Citrate}^{-3} = \text{SrH}_2(\text{Citrate})^{+}$
 log_k 12.4859
 delta_h 0 kJ
 -gamma 0 0
 # Id: 8009673
 # log K source: NIST46.4
 # Delta H source: NIST46.2
 #T and ionic strength: 0.10 25.0
 $\text{Ba}^{+2} + \text{Citrate}^{-3} = \text{Ba}(\text{Citrate})^{-}$
 log_k 4.1
 delta_h 0 kJ
 -gamma 0 0
 # Id: 1009671
 # log K source: NIST46.2
 # Delta H source: NIST46.2
 #T and ionic strength:
 $\text{Ba}^{+2} + \text{Citrate}^{-3} + \text{H}^{+} = \text{BaH}(\text{Citrate})$
 log_k 8.74
 delta_h 0 kJ
 -gamma 0 0
 # Id: 1009672
 # log K source: NIST46.2
 # Delta H source: NIST46.2
 #T and ionic strength:
 $\text{Ba}^{+2} + \text{Citrate}^{-3} + 2\text{H}^{+} = \text{BaH}_2(\text{Citrate})^{+}$
 log_k 12.3
 delta_h 0 kJ
 -gamma 0 0
 # Id: 1009673
 # log K source: NIST46.2
 # Delta H source: NIST46.2
 #T and ionic strength:
 $\text{Na}^{+} + \text{Citrate}^{-3} = \text{Na}(\text{Citrate})^{-2}$

log_k 1.03
 delta_h -2.8033 kJ
 -gamma 0 0
 # Id: 5009671
 # log K source: SCD2.62
 # Delta H source: SCD2.62
 #T and ionic strength:
 $2\text{Na}^+ + \text{Citrate-3} = \text{Na}_2(\text{Citrate})^-$
 log_k 1.5
 delta_h -5.1045 kJ
 -gamma 0 0
 # Id: 5009672
 # log K source: SCD2.62
 # Delta H source: SCD2.62
 #T and ionic strength:
 $\text{Na}^+ + \text{Citrate-3} + \text{H}^+ = \text{NaH}(\text{Citrate})^-$
 log_k 6.45
 delta_h -3.5982 kJ
 -gamma 0 0
 # Id: 5009673
 # log K source: SCD2.62
 # Delta H source: SCD2.62
 #T and ionic strength:
 $\text{K}^+ + \text{Citrate-3} = \text{K}(\text{Citrate})^-$
 log_k 1.1
 delta_h 5.4392 kJ
 -gamma 0 0
 # Id: 4109671
 # log K source: NIST46.2
 # Delta H source: NIST46.2
 #T and ionic strength:
 $\text{H}^+ + \text{Nta-3} = \text{H}(\text{Nta})^-$
 log_k 10.278
 delta_h -18.828 kJ
 -gamma 0 0
 # Id: 3309681
 # log K source: NIST46.2
 # Delta H source: NIST46.2
 #T and ionic strength:
 $2\text{H}^+ + \text{Nta-3} = \text{H}_2(\text{Nta})^-$
 log_k 13.22
 delta_h -17.9912 kJ
 -gamma 0 0
 # Id: 3309682
 # log K source: NIST46.2
 # Delta H source: NIST46.2
 #T and ionic strength:
 $3\text{H}^+ + \text{Nta-3} = \text{H}_3(\text{Nta})^-$
 log_k 15.22
 delta_h -16.3176 kJ
 -gamma 0 0
 # Id: 3309683
 # log K source: NIST46.2
 # Delta H source: NIST46.2

#T and ionic strength:
 $4\text{H}^+ + \text{Nta}^{-3} = \text{H}_4(\text{Nta})^+$
 log_k 16.22
 delta_h -16.3176 kJ
 -gamma 0 0
 # Id: 3309684
 # log K source: NIST46.2
 # Delta H source: NIST46.2
 #T and ionic strength:
 $\text{Pb}^{+2} + \text{Nta}^{-3} = \text{Pb}(\text{Nta})^-$
 log_k 12.7
 delta_h -15.8992 kJ
 -gamma 0 0
 # Id: 6009681
 # log K source: NIST46.2
 # Delta H source: NIST46.2
 #T and ionic strength:
 $\text{Pb}^{+2} + \text{Nta}^{-3} + \text{H}^+ = \text{PbH}(\text{Nta})$
 log_k 15.3
 delta_h 0 kJ
 -gamma 0 0
 # Id: 6009682
 # log K source: NIST46.2
 # Delta H source: NIST46.2
 #T and ionic strength:
 $\text{Al}^{+3} + \text{Nta}^{-3} = \text{Al}(\text{Nta})$
 log_k 13.3
 delta_h 0 kJ
 -gamma 0 0
 # Id: 309681
 # log K source: NIST46.2
 # Delta H source: NIST46.2
 #T and ionic strength:
 $\text{Al}^{+3} + \text{Nta}^{-3} + \text{H}^+ = \text{AlH}(\text{Nta})^+$
 log_k 15.2
 delta_h 0 kJ
 -gamma 0 0
 # Id: 309682
 # log K source: NIST46.2
 # Delta H source: NIST46.2
 #T and ionic strength:
 $\text{Al}^{+3} + \text{Nta}^{-3} + \text{H}_2\text{O} = \text{AlOH}(\text{Nta})^- + \text{H}^+$
 log_k 8
 delta_h 0 kJ
 -gamma 0 0
 # Id: 309683
 # log K source: NIST46.2
 # Delta H source: NIST46.2
 #T and ionic strength:
 $\text{Ti}^+ + \text{Nta}^{-3} = \text{Ti}(\text{Nta})^{-2}$
 log_k 5.39
 delta_h 0 kJ
 -gamma 0 0
 # Id: 8709681

log K source: NIST46.2
 # Delta H source: NIST46.2
 #T and ionic strength:
 $\text{Zn}^{+2} + \text{Nta}^{-3} = \text{Zn}(\text{Nta})^{-}$
 log_k 11.95
 delta_h -3.7656 kJ
 -gamma 0 0
 # Id: 9509681
 # log K source: NIST46.2
 # Delta H source: NIST46.2
 #T and ionic strength:
 $\text{Zn}^{+2} + 2\text{Nta}^{-3} = \text{Zn}(\text{Nta})^{2-4}$
 log_k 14.88
 delta_h -15.0624 kJ
 -gamma 0 0
 # Id: 9509682
 # log K source: NIST46.2
 # Delta H source: NIST46.2
 #T and ionic strength:
 $\text{Zn}^{+2} + \text{Nta}^{-3} + \text{H}_2\text{O} = \text{ZnOH}(\text{Nta})^{-2} + \text{H}^{+}$
 log_k 1.46
 delta_h 46.4424 kJ
 -gamma 0 0
 # Id: 9509683
 # log K source: NIST46.2
 # Delta H source: NIST46.2
 #T and ionic strength:
 $\text{Cd}^{+2} + \text{Nta}^{-3} = \text{Cd}(\text{Nta})^{-}$
 log_k 11.07
 delta_h -16.736 kJ
 -gamma 0 0
 # Id: 1609681
 # log K source: NIST46.2
 # Delta H source: NIST46.2
 #T and ionic strength:
 $\text{Cd}^{+2} + 2\text{Nta}^{-3} = \text{Cd}(\text{Nta})^{2-4}$
 log_k 15.03
 delta_h -38.0744 kJ
 -gamma 0 0
 # Id: 1609682
 # log K source: NIST46.2
 # Delta H source: NIST46.2
 #T and ionic strength:
 $\text{Cd}^{+2} + \text{Nta}^{-3} + \text{H}_2\text{O} = \text{CdOH}(\text{Nta})^{-2} + \text{H}^{+}$
 log_k -0.61
 delta_h 29.288 kJ
 -gamma 0 0
 # Id: 1609683
 # log K source: NIST46.2
 # Delta H source: NIST46.2
 #T and ionic strength:
 $\text{Hg}(\text{OH})_2 + \text{Nta}^{-3} + 2\text{H}^{+} = \text{Hg}(\text{Nta})^{-} + 2\text{H}_2\text{O}$
 log_k 21.7
 delta_h 0 kJ

-gamma 0 0
 # Id: 3619681
 # log K source: NIST46.2
 # Delta H source: NIST46.2
 #T and ionic strength:
 $\text{Cu}^{+2} + \text{Nta}^{-3} = \text{Cu}(\text{Nta})^{-}$
 log_k 14.4
 delta_h -7.9496 kJ
 -gamma 0 0
 # Id: 2319681
 # log K source: NIST46.2
 # Delta H source: NIST46.2
 #T and ionic strength:
 $\text{Cu}^{+2} + 2\text{Nta}^{-3} = \text{Cu}(\text{Nta})^{2-4}$
 log_k 18.1
 delta_h -37.2376 kJ
 -gamma 0 0
 # Id: 2319682
 # log K source: NIST46.2
 # Delta H source: NIST46.2
 #T and ionic strength:
 $\text{Cu}^{+2} + \text{Nta}^{-3} + \text{H}^{+} = \text{CuH}(\text{Nta})$
 log_k 16.2
 delta_h 0 kJ
 -gamma 0 0
 # Id: 2319683
 # log K source: NIST46.2
 # Delta H source: NIST46.2
 #T and ionic strength:
 $\text{Cu}^{+2} + \text{Nta}^{-3} + \text{H}_2\text{O} = \text{CuOH}(\text{Nta})^{-2} + \text{H}^{+}$
 log_k 4.8
 delta_h 25.5224 kJ
 -gamma 0 0
 # Id: 2319684
 # log K source: NIST46.2
 # Delta H source: NIST46.2
 #T and ionic strength:
 $\text{Ag}^{+} + \text{Nta}^{-3} = \text{Ag}(\text{Nta})^{-2}$
 log_k 6
 delta_h -26.3592 kJ
 -gamma 0 0
 # Id: 209681
 # log K source: NIST46.2
 # Delta H source: NIST46.2
 #T and ionic strength:
 $\text{Ni}^{+2} + \text{Nta}^{-3} = \text{Ni}(\text{Nta})^{-}$
 log_k 12.79
 delta_h -10.0416 kJ
 -gamma 0 0
 # Id: 5409681
 # log K source: NIST46.2
 # Delta H source: NIST46.2
 #T and ionic strength:
 $\text{Ni}^{+2} + 2\text{Nta}^{-3} = \text{Ni}(\text{Nta})^{2-4}$

log_k 16.96
 delta_h -32.6352 kJ
 -gamma 0 0
 # Id: 5409682
 # log K source: NIST46.2
 # Delta H source: NIST46.2
 #T and ionic strength:
 $\text{Ni}^{+2} + \text{Nta}^{-3} + \text{H}_2\text{O} = \text{NiOH(Nta)}^{-2} + \text{H}^{+}$
 log_k 1.5
 delta_h 15.0624 kJ
 -gamma 0 0
 # Id: 5409683
 # log K source: NIST46.2
 # Delta H source: NIST46.2
 #T and ionic strength:
 $\text{Co}^{+2} + \text{Nta}^{-3} = \text{Co(Nta)}^{-}$
 log_k 11.6667
 delta_h -0.4 kJ
 -gamma 0 0
 # Id: 2009681
 # log K source: NIST46.4
 # Delta H source: NIST46.4
 #T and ionic strength: 0.10 25.0
 $\text{Co}^{+2} + 2\text{Nta}^{-3} = \text{Co(Nta)}^{2-4}$
 log_k 14.9734
 delta_h -20 kJ
 -gamma 0 0
 # Id: 2009682
 # log K source: NIST46.4
 # Delta H source: NIST46.4
 #T and ionic strength: 0.10 25.0
 $\text{Co}^{+2} + \text{Nta}^{-3} + \text{H}_2\text{O} = \text{CoOH(Nta)}^{-2} + \text{H}^{+}$
 log_k 0.4378
 delta_h 45.6 kJ
 -gamma 0 0
 # Id: 2009683
 # log K source: NIST46.4
 # Delta H source: NIST46.4
 #T and ionic strength: 0.10 25.0
 $\text{Fe}^{+2} + \text{Nta}^{-3} = \text{Fe(Nta)}^{-}$
 log_k 10.19
 delta_h 0 kJ
 -gamma 0 0
 # Id: 2809681
 # log K source: NIST46.2
 # Delta H source: NIST46.2
 #T and ionic strength:
 $\text{Fe}^{+2} + 2\text{Nta}^{-3} = \text{Fe(Nta)}^{2-4}$
 log_k 12.62
 delta_h 0 kJ
 -gamma 0 0
 # Id: 2809682
 # log K source: NIST46.2
 # Delta H source: NIST46.2

#T and ionic strength:
 $\text{Fe}^{+2} + \text{Nta}^{-3} + \text{H}^{+} = \text{FeH}(\text{Nta})$
 log_k 12.29
 delta_h 0 kJ
 -gamma 0 0
 # Id: 2809683
 # log K source: NIST46.2
 # Delta H source: NIST46.2
 #T and ionic strength:
 $\text{Fe}^{+2} + \text{Nta}^{-3} + \text{H}_2\text{O} = \text{FeOH}(\text{Nta})^{-2} + \text{H}^{+}$
 log_k -1.06
 delta_h 0 kJ
 -gamma 0 0
 # Id: 2809684
 # log K source: NIST46.2
 # Delta H source: NIST46.2
 #T and ionic strength:
 $\text{Fe}^{+3} + \text{Nta}^{-3} = \text{Fe}(\text{Nta})$
 log_k 17.8
 delta_h 13.3888 kJ
 -gamma 0 0
 # Id: 2819681
 # log K source: NIST46.2
 # Delta H source: NIST46.2
 #T and ionic strength:
 $\text{Fe}^{+3} + 2\text{Nta}^{-3} = \text{Fe}(\text{Nta})_2^{-3}$
 log_k 25.9
 delta_h 0 kJ
 -gamma 0 0
 # Id: 2819682
 # log K source: NIST46.2
 # Delta H source: NIST46.2
 #T and ionic strength:
 $\text{Fe}^{+3} + \text{Nta}^{-3} + \text{H}_2\text{O} = \text{FeOH}(\text{Nta})^{-} + \text{H}^{+}$
 log_k 13.23
 delta_h 0 kJ
 -gamma 0 0
 # Id: 2819683
 # log K source: NIST46.2
 # Delta H source: NIST46.2
 #T and ionic strength:
 $\text{Mn}^{+2} + \text{Nta}^{-3} = \text{Mn}(\text{Nta})^{-}$
 log_k 8.573
 delta_h 5.8576 kJ
 -gamma 0 0
 # Id: 4709681
 # log K source: NIST46.2
 # Delta H source: NIST46.2
 #T and ionic strength:
 $\text{Mn}^{+2} + 2\text{Nta}^{-3} = \text{Mn}(\text{Nta})_2^{-4}$
 log_k 11.58
 delta_h -17.1544 kJ
 -gamma 0 0
 # Id: 4709682

log K source: NIST46.2
 # Delta H source: NIST46.2
 #T and ionic strength:
 $\text{Cr(OH)}_2^{2+} + \text{Nta}^{-3} + 2\text{H}^+ = \text{Cr(Nta)} + 2\text{H}_2\text{O}$
 log_k 21.2
 delta_h 0 kJ
 -gamma 0 0
 # Id: 2119681
 # log K source: SCD2.62
 # Delta H source: SCD2.62
 #T and ionic strength:
 $\text{Cr(OH)}_2^{2+} + 2\text{Nta}^{-3} + 2\text{H}^+ = \text{Cr(Nta)}_2^{-3} + 2\text{H}_2\text{O}$
 log_k 29.5
 delta_h 0 kJ
 -gamma 0 0
 # Id: 2119682
 # log K source: SCD2.62
 # Delta H source: SCD2.62
 #T and ionic strength:
 $\text{MoO}_4^{-2} + 2\text{H}^+ + \text{Nta}^{-3} = \text{MoO}_3(\text{Nta})^{-3} + \text{H}_2\text{O}$
 log_k 19.5434
 delta_h -69 kJ
 -gamma 0 0
 # Id: 4809681
 # log K source: NIST46.4
 # Delta H source: NIST46.4
 #T and ionic strength: 0.10 25.0
 $\text{MoO}_4^{-2} + 3\text{H}^+ + \text{Nta}^{-3} = \text{MoO}_3\text{H}(\text{Nta})^{-2} + \text{H}_2\text{O}$
 log_k 23.3954
 delta_h -71 kJ
 -gamma 0 0
 # Id: 4809682
 # log K source: NIST46.4
 # Delta H source: NIST46.4
 #T and ionic strength: 1.00 25.0
 $\text{MoO}_4^{-2} + 4\text{H}^+ + \text{Nta}^{-3} = \text{MoO}_3\text{H}_2(\text{Nta})^{-} + \text{H}_2\text{O}$
 log_k 25.3534
 delta_h -71 kJ
 -gamma 0 0
 # Id: 4809683
 # log K source: NIST46.4
 # Delta H source: NIST46.4
 #T and ionic strength: 1.00 25.0
 $\text{Be}^{+2} + \text{Nta}^{-3} = \text{Be(Nta)}^{-}$
 log_k 9.0767
 delta_h 25 kJ
 -gamma 0 0
 # Id: 1109681
 # log K source: NIST46.4
 # Delta H source: NIST46.4
 #T and ionic strength: 0.10 25.0
 $\text{Mg}^{+2} + \text{Nta}^{-3} = \text{Mg(Nta)}^{-}$
 log_k 6.5
 delta_h 17.9912 kJ

-gamma 0 0
Id: 4609681
log K source: NIST46.2
Delta H source: NIST46.2
#T and ionic strength:
 $\text{Ca}^{+2} + \text{Nta}^{-3} = \text{Ca}(\text{Nta})^{-}$
log_k 7.608
delta_h -5.6902 kJ
-gamma 0 0
Id: 1509681
log K source: NIST46.2
Delta H source: NIST46.2
#T and ionic strength:
 $\text{Ca}^{+2} + 2\text{Nta}^{-3} = \text{Ca}(\text{Nta})^{2-4}$
log_k 8.81
delta_h -32.6352 kJ
-gamma 0 0
Id: 1509682
log K source: NIST46.2
Delta H source: NIST46.2
#T and ionic strength:
 $\text{Sr}^{+2} + \text{Nta}^{-3} = \text{Sr}(\text{Nta})^{-}$
log_k 6.2767
delta_h -2.2 kJ
-gamma 0 0
Id: 8009681
log K source: NIST46.4
Delta H source: NIST46.4
#T and ionic strength: 0.10 25.0
 $\text{Ba}^{+2} + \text{Nta}^{-3} = \text{Ba}(\text{Nta})^{-}$
log_k 5.875
delta_h -6.025 kJ
-gamma 0 0
Id: 1009681
log K source: NIST46.2
Delta H source: NIST46.2
#T and ionic strength:
 $\text{H}^{+} + \text{Edta}^{-4} = \text{H}(\text{Edta})^{-3}$
log_k 10.948
delta_h -23.4304 kJ
-gamma 0 0
Id: 3309691
log K source: NIST46.2
Delta H source: NIST46.2
#T and ionic strength:
 $2\text{H}^{+} + \text{Edta}^{-4} = \text{H}_2(\text{Edta})^{-2}$
log_k 17.221
delta_h -41.0032 kJ
-gamma 0 0
Id: 3309692
log K source: NIST46.2
Delta H source: NIST46.2
#T and ionic strength:
 $3\text{H}^{+} + \text{Edta}^{-4} = \text{H}_3(\text{Edta})^{-}$

log_k 20.34
 delta_h -35.564 kJ
 -gamma 0 0
 # Id: 3309693
 # log K source: NIST46.2
 # Delta H source: NIST46.2
 #T and ionic strength:
 $4\text{H}^+ + \text{Edta-4} = \text{H}_4(\text{Edta})$
 log_k 22.5
 delta_h -34.3088 kJ
 -gamma 0 0
 # Id: 3309694
 # log K source: NIST46.2
 # Delta H source: NIST46.2
 #T and ionic strength:
 $5\text{H}^+ + \text{Edta-4} = \text{H}_5(\text{Edta})$
 log_k 24
 delta_h -32.2168 kJ
 -gamma 0 0
 # Id: 3309695
 # log K source: NIST46.2
 # Delta H source: NIST46.2
 #T and ionic strength:
 $\text{Sn}(\text{OH})_2 + 2\text{H}^+ + \text{Edta-4} = \text{Sn}(\text{Edta})^{-2} + 2\text{H}_2\text{O}$
 log_k 27.026
 delta_h 0 kJ
 -gamma 0 0
 # Id: 7909691
 # log K source: NIST46.4
 # Delta H source: NIST46.2
 #T and ionic strength: 1.00 20.0
 $\text{Sn}(\text{OH})_2 + 3\text{H}^+ + \text{Edta-4} = \text{SnH}(\text{Edta})^{-} + 2\text{H}_2\text{O}$
 log_k 29.934
 delta_h 0 kJ
 -gamma 0 0
 # Id: 7909692
 # log K source: NIST46.4
 # Delta H source: NIST46.2
 #T and ionic strength: 1.00 20.0
 $\text{Sn}(\text{OH})_2 + 4\text{H}^+ + \text{Edta-4} = \text{SnH}_2(\text{Edta}) + 2\text{H}_2\text{O}$
 log_k 31.638
 delta_h 0 kJ
 -gamma 0 0
 # Id: 7909693
 # log K source: NIST46.4
 # Delta H source: NIST46.2
 #T and ionic strength: 1.00 20.0
 $\text{Pb}^{+2} + \text{Edta-4} = \text{Pb}(\text{Edta})^{-2}$
 log_k 19.8
 delta_h -54.8104 kJ
 -gamma 0 0
 # Id: 6009691
 # log K source: NIST46.2
 # Delta H source: NIST46.2

#T and ionic strength:
 $\text{Pb}^{+2} + \text{Edta-4} + \text{H}^{+} = \text{PbH}(\text{Edta})^{-}$
 log_k 23
 delta_h 0 kJ
 -gamma 0 0
 # Id: 6009692
 # log K source: NIST46.2
 # Delta H source: NIST46.2
 #T and ionic strength:
 $\text{Pb}^{+2} + \text{Edta-4} + 2\text{H}^{+} = \text{PbH}_2(\text{Edta})$
 log_k 24.9
 delta_h 0 kJ
 -gamma 0 0
 # Id: 6009693
 # log K source: NIST46.2
 # Delta H source: NIST46.2
 #T and ionic strength:
 $\text{Al}^{+3} + \text{Edta-4} = \text{Al}(\text{Edta})^{-}$
 log_k 19.1
 delta_h 52.7184 kJ
 -gamma 0 0
 # Id: 309690
 # log K source: NIST46.2
 # Delta H source: NIST46.2
 #T and ionic strength:
 $\text{Al}^{+3} + \text{Edta-4} + \text{H}^{+} = \text{AlH}(\text{Edta})$
 log_k 21.8
 delta_h 36.4008 kJ
 -gamma 0 0
 # Id: 309691
 # log K source: NIST46.2
 # Delta H source: NIST46.2
 #T and ionic strength:
 $\text{Al}^{+3} + \text{Edta-4} + \text{H}_2\text{O} = \text{AlOH}(\text{Edta})^{-2} + \text{H}^{+}$
 log_k 12.8
 delta_h 73.6384 kJ
 -gamma 0 0
 # Id: 309692
 # log K source: NIST46.2
 # Delta H source: NIST46.2
 #T and ionic strength:
 $\text{Tl}^{+} + \text{Edta-4} = \text{Tl}(\text{Edta})^{-3}$
 log_k 7.27
 delta_h -43.5136 kJ
 -gamma 0 0
 # Id: 8709691
 # log K source: NIST46.2
 # Delta H source: NIST46.2
 #T and ionic strength:
 $\text{Tl}^{+} + \text{Edta-4} + \text{H}^{+} = \text{TlH}(\text{Edta})^{-2}$
 log_k 13.68
 delta_h 0 kJ
 -gamma 0 0
 # Id: 8709692

log K source: NIST46.2
 # Delta H source: NIST46.2
 #T and ionic strength:
 $\text{Zn}^{+2} + \text{Edta-4} = \text{Zn}(\text{Edta})^{-2}$
 log_k 18
 delta_h -19.2464 kJ
 -gamma 0 0
 # Id: 9509691
 # log K source: NIST46.2
 # Delta H source: NIST46.2
 #T and ionic strength:
 $\text{Zn}^{+2} + \text{Edta-4} + \text{H}^{+} = \text{ZnH}(\text{Edta})^{-}$
 log_k 21.4
 delta_h -28.4512 kJ
 -gamma 0 0
 # Id: 9509692
 # log K source: NIST46.2
 # Delta H source: NIST46.2
 #T and ionic strength:
 $\text{Zn}^{+2} + \text{Edta-4} + \text{H}_2\text{O} = \text{ZnOH}(\text{Edta})^{-3} + \text{H}^{+}$
 log_k 5.8
 delta_h 0 kJ
 -gamma 0 0
 # Id: 9509693
 # log K source: NIST46.2
 # Delta H source: NIST46.2
 #T and ionic strength:
 $\text{Cd}^{+2} + \text{Edta-4} = \text{Cd}(\text{Edta})^{-2}$
 log_k 18.2
 delta_h -38.0744 kJ
 -gamma 0 0
 # Id: 1609691
 # log K source: NIST46.2
 # Delta H source: NIST46.2
 #T and ionic strength:
 $\text{Cd}^{+2} + \text{Edta-4} + \text{H}^{+} = \text{CdH}(\text{Edta})^{-}$
 log_k 21.5
 delta_h -39.748 kJ
 -gamma 0 0
 # Id: 1609692
 # log K source: NIST46.2
 # Delta H source: NIST46.2
 #T and ionic strength:
 $\text{Hg}(\text{OH})_2 + \text{Edta-4} + 2\text{H}^{+} = \text{Hg}(\text{Edta})^{-2} + 2\text{H}_2\text{O}$
 log_k 29.3
 delta_h -125.102 kJ
 -gamma 0 0
 # Id: 3619691
 # log K source: NIST46.2
 # Delta H source: NIST46.2
 #T and ionic strength:
 $\text{Hg}(\text{OH})_2 + \text{Edta-4} + 3\text{H}^{+} = \text{HgH}(\text{Edta})^{-} + 2\text{H}_2\text{O}$
 log_k 32.9
 delta_h -128.449 kJ

-gamma 0 0
 # Id: 3619692
 # log K source: NIST46.2
 # Delta H source: NIST46.2
 #T and ionic strength:
 $\text{Cu}^{+2} + \text{Edta}^{-4} = \text{Cu}(\text{Edta})^{-2}$
 log_k 20.5
 delta_h -34.7272 kJ
 -gamma 0 0
 # Id: 2319691
 # log K source: NIST46.2
 # Delta H source: NIST46.2
 #T and ionic strength:
 $\text{Cu}^{+2} + \text{Edta}^{-4} + \text{H}^{+} = \text{CuH}(\text{Edta})^{-}$
 log_k 24
 delta_h -43.0952 kJ
 -gamma 0 0
 # Id: 2319692
 # log K source: NIST46.2
 # Delta H source: NIST46.2
 #T and ionic strength:
 $\text{Cu}^{+2} + \text{Edta}^{-4} + 2\text{H}^{+} = \text{CuH}_2(\text{Edta})$
 log_k 26.2
 delta_h 0 kJ
 -gamma 0 0
 # Id: 2319693
 # log K source: NIST46.2
 # Delta H source: NIST46.2
 #T and ionic strength:
 $\text{Cu}^{+2} + \text{Edta}^{-4} + \text{H}_2\text{O} = \text{CuOH}(\text{Edta})^{-3} + \text{H}^{+}$
 log_k 8.5
 delta_h 0 kJ
 -gamma 0 0
 # Id: 2319694
 # log K source: NIST46.2
 # Delta H source: NIST46.2
 #T and ionic strength:
 $\text{Ag}^{+} + \text{Edta}^{-4} = \text{Ag}(\text{Edta})^{-3}$
 log_k 8.08
 delta_h -31.38 kJ
 -gamma 0 0
 # Id: 209691
 # log K source: NIST46.2
 # Delta H source: NIST46.2
 #T and ionic strength:
 $\text{Ag}^{+} + \text{Edta}^{-4} + \text{H}^{+} = \text{AgH}(\text{Edta})^{-2}$
 log_k 15.21
 delta_h 0 kJ
 -gamma 0 0
 # Id: 209693
 # log K source: SCD2.62
 # Delta H source: SCD2.62
 #T and ionic strength:
 $\text{Ni}^{+2} + \text{Edta}^{-4} = \text{Ni}(\text{Edta})^{-2}$

log_k 20.1
 delta_h -30.9616 kJ
 -gamma 0 0
 # Id: 5409691
 # log K source: NIST46.2
 # Delta H source: NIST46.2
 #T and ionic strength:
 $\text{Ni}^{+2} + \text{Edta-4} + \text{H}^{+} = \text{NiH}(\text{Edta})^{-}$
 log_k 23.6
 delta_h -38.4928 kJ
 -gamma 0 0
 # Id: 5409692
 # log K source: NIST46.2
 # Delta H source: NIST46.2
 #T and ionic strength:
 $\text{Ni}^{+2} + \text{Edta-4} + \text{H}_2\text{O} = \text{NiOH}(\text{Edta})^{-3} + \text{H}^{+}$
 log_k 7.6
 delta_h 0 kJ
 -gamma 0 0
 # Id: 5409693
 # log K source: NIST46.2
 # Delta H source: NIST46.2
 #T and ionic strength:
 $\text{Co}^{+2} + \text{Edta-4} = \text{Co}(\text{Edta})^{-2}$
 log_k 18.1657
 delta_h -15 kJ
 -gamma 0 0
 # Id: 2009691
 # log K source: NIST46.4
 # Delta H source: NIST46.4
 #T and ionic strength: 0.10 25.0
 $\text{Co}^{+2} + \text{Edta-4} + \text{H}^{+} = \text{CoH}(\text{Edta})^{-}$
 log_k 21.5946
 delta_h -22.9 kJ
 -gamma 0 0
 # Id: 2009692
 # log K source: NIST46.4
 # Delta H source: NIST46.4
 #T and ionic strength: 0.10 25.0
 $\text{Co}^{+2} + \text{Edta-4} + 2\text{H}^{+} = \text{CoH}_2(\text{Edta})$
 log_k 23.4986
 delta_h 0 kJ
 -gamma 0 0
 # Id: 2009693
 # log K source: NIST46.4
 # Delta H source: NIST46.2
 #T and ionic strength: 1.00 25.0
 $\text{Co}^{+3} + \text{Edta-4} = \text{Co}(\text{Edta})^{-}$
 log_k 43.9735
 delta_h 0 kJ
 -gamma 0 0
 # Id: 2019691
 # log K source: NIST46.4
 # Delta H source: NIST46.2

#T and ionic strength: 0.10 25.0
 $\text{Co}^{+3} + \text{Edta-4} + \text{H}^{+} = \text{CoH}(\text{Edta})$
 log_k 47.168
 delta_h 0 kJ
 -gamma 0 0
 # Id: 2019692
 # log K source: NIST46.4
 # Delta H source: NIST46.2
 #T and ionic strength: 0.10 20.0
 $\text{Fe}^{+2} + \text{Edta-4} = \text{Fe}(\text{Edta})^{-2}$
 log_k 16
 delta_h -16.736 kJ
 -gamma 0 0
 # Id: 2809690
 # log K source: NIST46.2
 # Delta H source: NIST46.2
 #T and ionic strength:
 $\text{Fe}^{+2} + \text{Edta-4} + \text{H}^{+} = \text{FeH}(\text{Edta})^{-}$
 log_k 19.06
 delta_h -27.6144 kJ
 -gamma 0 0
 # Id: 2809691
 # log K source: NIST46.2
 # Delta H source: NIST46.2
 #T and ionic strength:
 $\text{Fe}^{+2} + \text{Edta-4} + \text{H}_2\text{O} = \text{FeOH}(\text{Edta})^{-3} + \text{H}^{+}$
 log_k 6.5
 delta_h 0 kJ
 -gamma 0 0
 # Id: 2809692
 # log K source: SCD2.62
 # Delta H source: SCD2.62
 #T and ionic strength:
 $\text{Fe}^{+2} + \text{Edta-4} + 2\text{H}_2\text{O} = \text{Fe}(\text{OH})_2(\text{Edta})^{-4} + 2\text{H}^{+}$
 log_k -4
 delta_h 0 kJ
 -gamma 0 0
 # Id: 2809693
 # log K source: SCD2.62
 # Delta H source: SCD2.62
 #T and ionic strength:
 $\text{Fe}^{+3} + \text{Edta-4} = \text{Fe}(\text{Edta})^{-}$
 log_k 27.7
 delta_h -11.2968 kJ
 -gamma 0 0
 # Id: 2819690
 # log K source: NIST46.2
 # Delta H source: NIST46.2
 #T and ionic strength:
 $\text{Fe}^{+3} + \text{Edta-4} + \text{H}^{+} = \text{FeH}(\text{Edta})$
 log_k 29.2
 delta_h -11.7152 kJ
 -gamma 0 0
 # Id: 2819691

log K source: NIST46.2
 # Delta H source: NIST46.2
 #T and ionic strength:
 $\text{Fe}^{+3} + \text{Edta-4} + \text{H}_2\text{O} = \text{FeOH}(\text{Edta})^{-2} + \text{H}^{+}$
 log_k 19.9
 delta_h 0 kJ
 -gamma 0 0
 # Id: 2819692
 # log K source: NIST46.2
 # Delta H source: NIST46.2
 #T and ionic strength:
 $\text{Fe}^{+3} + \text{Edta-4} + 2\text{H}_2\text{O} = \text{Fe}(\text{OH})_2(\text{Edta})^{-3} + 2\text{H}^{+}$
 log_k 9.85
 delta_h 0 kJ
 -gamma 0 0
 # Id: 2819693
 # log K source: SCD2.62
 # Delta H source: SCD2.62
 #T and ionic strength:
 $\text{Mn}^{+2} + \text{Edta-4} = \text{Mn}(\text{Edta})^{-2}$
 log_k 15.6
 delta_h -19.2464 kJ
 -gamma 0 0
 # Id: 4709691
 # log K source: NIST46.2
 # Delta H source: NIST46.2
 #T and ionic strength:
 $\text{Mn}^{+2} + \text{Edta-4} + \text{H}^{+} = \text{MnH}(\text{Edta})^{-}$
 log_k 19.1
 delta_h -24.2672 kJ
 -gamma 0 0
 # Id: 4709692
 # log K source: NIST46.2
 # Delta H source: NIST46.2
 #T and ionic strength:
 $\text{Cr}^{+2} + \text{Edta-4} = \text{Cr}(\text{Edta})^{-2}$
 log_k 15.3
 delta_h 0 kJ
 -gamma 0 0
 # Id: 2109691
 # log K source: NIST46.2
 # Delta H source: NIST46.2
 #T and ionic strength:
 $\text{Cr}^{+2} + \text{Edta-4} + \text{H}^{+} = \text{CrH}(\text{Edta})^{-}$
 log_k 19.1
 delta_h 0 kJ
 -gamma 0 0
 # Id: 2109692
 # log K source: SCD2.62
 # Delta H source: SCD2.62
 #T and ionic strength:
 $\text{Cr}(\text{OH})_2^{+} + \text{Edta-4} + 2\text{H}^{+} = \text{Cr}(\text{Edta})^{-} + 2\text{H}_2\text{O}$
 log_k 35.5
 delta_h 0 kJ

-gamma 0 0
 # Id: 2119691
 # log K source: NIST46.2
 # Delta H source: NIST46.2
 #T and ionic strength:
 $\text{Cr(OH)}_2^{2+} + \text{Edta-4} + 3\text{H}^+ = \text{CrH(Edta)} + 2\text{H}_2\text{O}$
 log_k 37.4
 delta_h 0 kJ
 -gamma 0 0
 # Id: 2119692
 # log K source: NIST46.2
 # Delta H source: NIST46.2
 #T and ionic strength:
 $\text{Cr(OH)}_2^{2+} + \text{Edta-4} + \text{H}^+ = \text{CrOH(Edta)}^{-2} + \text{H}_2\text{O}$
 log_k 27.7
 delta_h 0 kJ
 -gamma 0 0
 # Id: 2119693
 # log K source: NIST46.2
 # Delta H source: NIST46.2
 #T and ionic strength:
 $\text{Be}^{+2} + \text{Edta-4} = \text{Be(Edta)}^{-2}$
 log_k 11.4157
 delta_h 41 kJ
 -gamma 0 0
 # Id: 1109691
 # log K source: NIST46.4
 # Delta H source: NIST46.4
 #T and ionic strength: 0.10 25.0
 $\text{Mg}^{+2} + \text{Edta-4} = \text{Mg(Edta)}^{-2}$
 log_k 10.57
 delta_h 13.8072 kJ
 -gamma 0 0
 # Id: 4609690
 # log K source: NIST46.2
 # Delta H source: NIST46.2
 #T and ionic strength:
 $\text{Mg}^{+2} + \text{Edta-4} + \text{H}^+ = \text{MgH(Edta)}^{-}$
 log_k 14.97
 delta_h 0 kJ
 -gamma 0 0
 # Id: 4609691
 # log K source: NIST46.2
 # Delta H source: NIST46.2
 #T and ionic strength:
 $\text{Ca}^{+2} + \text{Edta-4} = \text{Ca(Edta)}^{-2}$
 log_k 12.42
 delta_h -25.5224 kJ
 -gamma 0 0
 # Id: 1509690
 # log K source: NIST46.2
 # Delta H source: NIST46.2
 #T and ionic strength:
 $\text{Ca}^{+2} + \text{Edta-4} + \text{H}^+ = \text{CaH(Edta)}^{-}$

log_k 15.9
delta_h 0 kJ
-gamma 0 0
Id: 1509691
log K source: NIST46.2
Delta H source: NIST46.2
#T and ionic strength:
 $\text{Sr}^{+2} + \text{Edta-4} = \text{Sr}(\text{Edta})^{-2}$
log_k 10.4357
delta_h -17 kJ
-gamma 0 0
Id: 8009691
log K source: NIST46.4
Delta H source: NIST46.4
#T and ionic strength: 0.10 25.0
 $\text{Sr}^{+2} + \text{Edta-4} + \text{H}^{+} = \text{SrH}(\text{Edta})^{-}$
log_k 14.7946
delta_h 0 kJ
-gamma 0 0
Id: 8009692
log K source: NIST46.4
Delta H source: NIST46.2
#T and ionic strength: 0.10 20.0
 $\text{Ba}^{+2} + \text{Edta-4} = \text{Ba}(\text{Edta})^{-2}$
log_k 7.72
delta_h -20.5016 kJ
-gamma 0 0
Id: 1009691
log K source: SCD2.62
Delta H source: SCD2.62
#T and ionic strength:
 $\text{Na}^{+} + \text{Edta-4} = \text{Na}(\text{Edta})^{-3}$
log_k 2.7
delta_h -5.8576 kJ
-gamma 0 0
Id: 5009690
log K source: NIST46.2
Delta H source: NIST46.2
#T and ionic strength:
 $\text{K}^{+} + \text{Edta-4} = \text{K}(\text{Edta})^{-3}$
log_k 1.7
delta_h 0 kJ
-gamma 0 0
Id: 4109690
log K source: NIST46.2
Delta H source: NIST46.2
#T and ionic strength:
 $\text{H}^{+} + \text{Propionate-} = \text{H}(\text{Propionate})$
log_k 4.874
delta_h 0.66 kJ
-gamma 0 0
Id: 3309711
log K source: NIST46.4
Delta H source: NIST46.4

#T and ionic strength: 0.00 25.0
 $\text{Pb}^{+2} + \text{Propionate}^- = \text{Pb}(\text{Propionate})^+$
 log_k 2.64
 delta_h 0 kJ
 -gamma 0 0
 # Id: 6009711
 # log K source: NIST46.4
 # Delta H source: SCD2.62
 #T and ionic strength: 0.00 35.0
 $\text{Pb}^{+2} + 2\text{Propionate}^- = \text{Pb}(\text{Propionate})_2$
 log_k 3.1765
 delta_h 0 kJ
 -gamma 0 0
 # Id: 6009712
 # log K source: NIST46.4
 # Delta H source: SCD2.62
 #T and ionic strength: 2.00 25.0
 $\text{Zn}^{+2} + \text{Propionate}^- = \text{Zn}(\text{Propionate})^+$
 log_k 1.4389
 delta_h 0 kJ
 -gamma 0 0
 # Id: 9509711
 # log K source: NIST46.4
 # Delta H source: NIST46.2
 #T and ionic strength: 0.10 25.0
 $\text{Zn}^{+2} + 2\text{Propionate}^- = \text{Zn}(\text{Propionate})_2$
 log_k 1.842
 delta_h 0 kJ
 -gamma 0 0
 # Id: 9509712
 # log K source: NIST46.4
 # Delta H source: NIST46.2
 #T and ionic strength: 1.00 25.0
 $\text{Cd}^{+2} + \text{Propionate}^- = \text{Cd}(\text{Propionate})^+$
 log_k 1.598
 delta_h 0 kJ
 -gamma 0 0
 # Id: 1609711
 # log K source: NIST46.4
 # Delta H source: NIST46.2
 #T and ionic strength: 1.00 25.0
 $\text{Cd}^{+2} + 2\text{Propionate}^- = \text{Cd}(\text{Propionate})_2$
 log_k 2.472
 delta_h 0 kJ
 -gamma 0 0
 # Id: 1609712
 # log K source: NIST46.4
 # Delta H source: NIST46.2
 #T and ionic strength: 1.00 25.0
 $\text{Hg}(\text{OH})_2 + 2\text{H}^+ + \text{Propionate}^- = \text{Hg}(\text{Propionate})^+ + 2\text{H}_2\text{O}$
 log_k 10.594
 delta_h 0 kJ
 -gamma 0 0
 # Id: 3619711

log K source: NIST46.4
 # Delta H source: NIST46.2
 #T and ionic strength: 0.00 25.0
 $\text{Cu}^{+2} + \text{Propionate}^- = \text{Cu}(\text{Propionate})^+$
 log_k 2.22
 delta_h 4.1 kJ
 -gamma 0 0
 # Id: 2319711
 # log K source: NIST46.4
 # Delta H source: NIST46.4
 #T and ionic strength: 0.00 25.0
 $\text{Cu}^{+2} + 2\text{Propionate}^- = \text{Cu}(\text{Propionate})_2$
 log_k 3.5
 delta_h 0 kJ
 -gamma 0 0
 # Id: 2319712
 # log K source: NIST46.4
 # Delta H source: NIST46.2
 #T and ionic strength: 0.00 25.0
 $\text{Ni}^{+2} + \text{Propionate}^- = \text{Ni}(\text{Propionate})^+$
 log_k 0.908
 delta_h 0 kJ
 -gamma 0 0
 # Id: 5409711
 # log K source: NIST46.4
 # Delta H source: SCD2.62
 #T and ionic strength: 1.00 25.0
 $\text{Co}^{+2} + \text{Propionate}^- = \text{Co}(\text{Propionate})^+$
 log_k 0.671
 delta_h 4.6 kJ
 -gamma 0 0
 # Id: 2009711
 # log K source: NIST46.4
 # Delta H source: NIST46.4
 #T and ionic strength: 2.00 25.0
 $\text{Co}^{+2} + 2\text{Propionate}^- = \text{Co}(\text{Propionate})_2$
 log_k 0.5565
 delta_h 16 kJ
 -gamma 0 0
 # Id: 2009712
 # log K source: NIST46.4
 # Delta H source: NIST46.4
 #T and ionic strength: 2.00 25.0
 $\text{Fe}^{+3} + \text{Propionate}^- = \text{Fe}(\text{Propionate})^{+2}$
 log_k 4.012
 delta_h 0 kJ
 -gamma 0 0
 # Id: 2819711
 # log K source: NIST46.4
 # Delta H source: NIST46.2
 #T and ionic strength: 1.00 20.0
 $\text{Cr}(\text{OH})_2^{+2} + 2\text{H}^+ + \text{Propionate}^- = \text{Cr}(\text{Propionate})^{+2} + 2\text{H}_2\text{O}$
 log_k 15.0773
 delta_h 0 kJ

-gamma 0 0
 # Id: 2119711
 # log K source: NIST46.4
 # Delta H source: SCD2.62
 #T and ionic strength: 0.50 25.0
 $\text{Cr(OH)}_2^{2+} + 2\text{H}^+ + 2\text{Propionate}^- = \text{Cr(Propionate)}_2^{2+} + 2\text{H}_2\text{O}$
 log_k 17.9563
 delta_h 0 kJ
 -gamma 0 0
 # Id: 2119712
 # log K source: NIST46.4
 # Delta H source: SCD2.62
 #T and ionic strength: 0.50 25.0
 $\text{Cr(OH)}_2^{2+} + 2\text{H}^+ + 3\text{Propionate}^- = \text{Cr(Propionate)}_3 + 2\text{H}_2\text{O}$
 log_k 20.8858
 delta_h 0 kJ
 -gamma 0 0
 # Id: 2119713
 # log K source: NIST46.4
 # Delta H source: SCD2.62
 #T and ionic strength: 0.50 25.0
 $\text{Mg}^{2+} + \text{Propionate}^- = \text{Mg(Propionate)}^+$
 log_k 0.9689
 delta_h 4.2677 kJ
 -gamma 0 0
 # Id: 4609710
 # log K source: NIST46.4
 # Delta H source: SCD2.62
 #T and ionic strength: 0.10 25.0
 $\text{Ca}^{2+} + \text{Propionate}^- = \text{Ca(Propionate)}^+$
 log_k 0.9289
 delta_h 3.3472 kJ
 -gamma 0 0
 # Id: 1509710
 # log K source: NIST46.4
 # Delta H source: SCD2.62
 #T and ionic strength: 0.10 25.0
 $\text{Sr}^{2+} + \text{Propionate}^- = \text{Sr(Propionate)}^+$
 log_k 0.8589
 delta_h 0 kJ
 -gamma 0 0
 # Id: 8009711
 # log K source: NIST46.4
 # Delta H source: NIST46.2
 #T and ionic strength: 0.10 25.0
 $\text{Ba}^{2+} + \text{Propionate}^- = \text{Ba(Propionate)}^+$
 log_k 0.7689
 delta_h 0 kJ
 -gamma 0 0
 # Id: 1009711
 # log K source: NIST46.4
 # Delta H source: SCD2.62
 #T and ionic strength: 0.10 25.0
 $\text{Ba}^{2+} + 2\text{Propionate}^- = \text{Ba(Propionate)}_2$

log_k 0.9834
 delta_h 0 kJ
 -gamma 0 0
 # Id: 1009712
 # log K source: NIST46.4
 # Delta H source: SCD2.62
 #T and ionic strength: 0.10 25.0
 $\text{H}^+ + \text{Butyrate}^- = \text{H}(\text{Butyrate})$
 log_k 4.819
 delta_h 2.8 kJ
 -gamma 0 0
 # Id: 3309721
 # log K source: NIST46.4
 # Delta H source: NIST46.4
 #T and ionic strength: 0.00 25.0
 $\text{Pb}^{+2} + \text{Butyrate}^- = \text{Pb}(\text{Butyrate})$
 log_k 2.101
 delta_h 0 kJ
 -gamma 0 0
 # Id: 6009721
 # log K source: NIST46.4
 # Delta H source: SCD2.62
 #T and ionic strength: 2.00 25.0
 $\text{Zn}^{+2} + \text{Butyrate}^- = \text{Zn}(\text{Butyrate})$
 log_k 1.4289
 delta_h 0 kJ
 -gamma 0 0
 # Id: 9509721
 # log K source: NIST46.4
 # Delta H source: NIST46.2
 #T and ionic strength: 0.10 25.0
 $\text{Hg}(\text{OH})_2 + 2\text{H}^+ + \text{Butyrate}^- = \text{Hg}(\text{Butyrate}) + 2\text{H}_2\text{O}$
 log_k 10.3529
 delta_h 0 kJ
 -gamma 0 0
 # Id: 3619721
 # log K source: NIST46.4
 # Delta H source: NIST46.2
 #T and ionic strength: 0.10 25.0
 $\text{Cu}^{+2} + \text{Butyrate}^- = \text{Cu}(\text{Butyrate})$
 log_k 2.14
 delta_h 0 kJ
 -gamma 0 0
 # Id: 2319721
 # log K source: NIST46.4
 # Delta H source: NIST46.2
 #T and ionic strength: 0.00 25.0
 $\text{Ni}^{+2} + \text{Butyrate}^- = \text{Ni}(\text{Butyrate})$
 log_k 0.691
 delta_h 0 kJ
 -gamma 0 0
 # Id: 5409721
 # log K source: NIST46.4
 # Delta H source: SCD2.62

#T and ionic strength: 2.00 25.0
 $\text{Co}^{+2} + \text{Butyrate}^- = \text{Co}(\text{Butyrate})^+$
 log_k 0.591
 delta_h 0 kJ
 -gamma 0 0
 # Id: 2009721
 # log K source: NIST46.4
 # Delta H source: NIST46.2
 #T and ionic strength: 2.00 25.0
 $\text{Co}^{+2} + 2\text{Butyrate}^- = \text{Co}(\text{Butyrate})_2$
 log_k 0.7765
 delta_h 0 kJ
 -gamma 0 0
 # Id: 2009722
 # log K source: NIST46.4
 # Delta H source: NIST46.2
 #T and ionic strength: 2.00 25.0
 $\text{Mg}^{+2} + \text{Butyrate}^- = \text{Mg}(\text{Butyrate})^+$
 log_k 0.9589
 delta_h 0 kJ
 -gamma 0 0
 # Id: 4609720
 # log K source: NIST46.4
 # Delta H source: SCD2.62
 #T and ionic strength: 0.10 25.0
 $\text{Ca}^{+2} + \text{Butyrate}^- = \text{Ca}(\text{Butyrate})^+$
 log_k 0.9389
 delta_h 3.3472 kJ
 -gamma 0 0
 # Id: 1509720
 # log K source: NIST46.4
 # Delta H source: SCD2.62
 #T and ionic strength: 0.10 25.0
 $\text{Sr}^{+2} + \text{Butyrate}^- = \text{Sr}(\text{Butyrate})^+$
 log_k 0.7889
 delta_h 0 kJ
 -gamma 0 0
 # Id: 8009721
 # log K source: NIST46.4
 # Delta H source: NIST46.2
 #T and ionic strength: 0.10 25.0
 $\text{Ba}^{+2} + \text{Butyrate}^- = \text{Ba}(\text{Butyrate})^+$
 log_k 0.7389
 delta_h 0 kJ
 -gamma 0 0
 # Id: 1009721
 # log K source: NIST46.4
 # Delta H source: SCD2.62
 #T and ionic strength: 0.10 25.0
 $\text{Ba}^{+2} + 2\text{Butyrate}^- = \text{Ba}(\text{Butyrate})_2$
 log_k 0.88
 delta_h 0 kJ
 -gamma 0 0
 # Id: 1009722

log K source: SCD2.62
 # Delta H source: SCD2.62
 #T and ionic strength:
 $\text{H}^+ + \text{Isobutyrate}^- = \text{H}(\text{Isobutyrate})$
 log_k 4.849
 delta_h 3.2217 kJ
 -gamma 0 0
 # Id: 3309731
 # log K source: NIST46.2
 # Delta H source: NIST46.2
 #T and ionic strength:
 $\text{Zn}^{+2} + \text{Isobutyrate}^- = \text{Zn}(\text{Isobutyrate})$
 log_k 1.44
 delta_h 0 kJ
 -gamma 0 0
 # Id: 9509731
 # log K source: NIST46.2
 # Delta H source: NIST46.2
 #T and ionic strength:
 $\text{Cu}^{+2} + \text{Isobutyrate}^- = \text{Cu}(\text{Isobutyrate})$
 log_k 2.17
 delta_h 0 kJ
 -gamma 0 0
 # Id: 2319731
 # log K source: NIST46.2
 # Delta H source: NIST46.2
 #T and ionic strength:
 $\text{Cu}^{+2} + 2\text{Isobutyrate}^- = \text{Cu}(\text{Isobutyrate})_2$
 log_k 3.3
 delta_h 0 kJ
 -gamma 0 0
 # Id: 2319732
 # log K source: NIST46.2
 # Delta H source: NIST46.2
 #T and ionic strength:
 $\text{Fe}^{+3} + \text{Isobutyrate}^- = \text{Fe}(\text{Isobutyrate})$
 log_k 4.2
 delta_h 0 kJ
 -gamma 0 0
 # Id: 2819731
 # log K source: NIST46.2
 # Delta H source: NIST46.2
 #T and ionic strength:
 $\text{Ca}^{+2} + \text{Isobutyrate}^- = \text{Ca}(\text{Isobutyrate})$
 log_k 0.51
 delta_h 0 kJ
 -gamma 0 0
 # Id: 1509731
 # log K source: SCD2.62
 # Delta H source: SCD2.62
 #T and ionic strength:
 $\text{H}^+ + \text{Two_picoline} = \text{H}(\text{Two_picoline})$
 log_k 5.95
 delta_h -25.5224 kJ

-gamma 0 0
 # Id: 3309801
 # log K source: NIST46.2
 # Delta H source: NIST46.2
 #T and ionic strength:
 $\text{Cu}^{2+} + \text{Two_picoline} = \text{Cu}(\text{Two_picoline})^{2+}$
 log_k 1.3
 delta_h 0 kJ
 -gamma 0 0
 # Id: 2319801
 # log K source: NIST46.2
 # Delta H source: NIST46.2
 #T and ionic strength:
 $\text{Cu}^{2+} + 2\text{Two_picoline} = \text{Cu}(\text{Two_picoline})_2^{2+}$
 log_k 2.8
 delta_h 0 kJ
 -gamma 0 0
 # Id: 2319802
 # log K source: NIST46.2
 # Delta H source: NIST46.2
 #T and ionic strength:
 $\text{Cu}^{+} + \text{Two_picoline} = \text{Cu}(\text{Two_picoline})^{+}$
 log_k 5.4
 delta_h 0 kJ
 -gamma 0 0
 # Id: 2309801
 # log K source: NIST46.2
 # Delta H source: NIST46.2
 #T and ionic strength:
 $\text{Cu}^{+} + 2\text{Two_picoline} = \text{Cu}(\text{Two_picoline})_2^{+}$
 log_k 7.65
 delta_h 0 kJ
 -gamma 0 0
 # Id: 2309802
 # log K source: NIST46.2
 # Delta H source: NIST46.2
 #T and ionic strength:
 $\text{Cu}^{+} + 3\text{Two_picoline} = \text{Cu}(\text{Two_picoline})_3^{+}$
 log_k 8.5
 delta_h 0 kJ
 -gamma 0 0
 # Id: 2309803
 # log K source: NIST46.2
 # Delta H source: NIST46.2
 #T and ionic strength:
 $\text{Ag}^{+} + \text{Two_picoline} = \text{Ag}(\text{Two_picoline})^{+}$
 log_k 2.32
 delta_h -24.2672 kJ
 -gamma 0 0
 # Id: 209801
 # log K source: NIST46.2
 # Delta H source: NIST46.2
 #T and ionic strength:
 $\text{Ag}^{+} + 2\text{Two_picoline} = \text{Ag}(\text{Two_picoline})_2^{+}$

log_k 4.68
delta_h -42.6768 kJ
-gamma 0 0
Id: 209802
log K source: NIST46.2
Delta H source: NIST46.2
#T and ionic strength:
 $\text{Ni}^{+2} + \text{Two_picoline} = \text{Ni}(\text{Two_picoline})_2$
log_k 0.4
delta_h 0 kJ
-gamma 0 0
Id: 5409801
log K source: NIST46.2
Delta H source: NIST46.2
#T and ionic strength:
 $\text{H}^+ + \text{Three_picoline} = \text{H}(\text{Three_picoline})$
log_k 5.7
delta_h -23.8488 kJ
-gamma 0 0
Id: 3309811
log K source: NIST46.2
Delta H source: NIST46.2
#T and ionic strength:
 $\text{Zn}^{+2} + \text{Three_picoline} = \text{Zn}(\text{Three_picoline})_2$
log_k 1
delta_h 0 kJ
-gamma 0 0
Id: 9509811
log K source: NIST46.2
Delta H source: NIST46.2
#T and ionic strength:
 $\text{Zn}^{+2} + 2\text{Three_picoline} = \text{Zn}(\text{Three_picoline})_2$
log_k 2.1
delta_h 0 kJ
-gamma 0 0
Id: 9509812
log K source: NIST46.2
Delta H source: NIST46.2
#T and ionic strength:
 $\text{Zn}^{+2} + 3\text{Three_picoline} = \text{Zn}(\text{Three_picoline})_3$
log_k 2.6
delta_h 0 kJ
-gamma 0 0
Id: 9509813
log K source: NIST46.2
Delta H source: NIST46.2
#T and ionic strength:
 $\text{Zn}^{+2} + 4\text{Three_picoline} = \text{Zn}(\text{Three_picoline})_4$
log_k 3.7
delta_h 0 kJ
-gamma 0 0
Id: 9509814
log K source: NIST46.2
Delta H source: NIST46.2

#T and ionic strength:
 $\text{Cd}^{2+} + 3\text{Three_picoline} = \text{Cd}(\text{Three_picoline})_2 + 2$
 log_k 1.42
 delta_h 0 kJ
 -gamma 0 0
 # Id: 1609811
 # log K source: SCD2.62
 # Delta H source: SCD2.62
 #T and ionic strength:
 $\text{Cd}^{2+} + 2\text{Three_picoline} = \text{Cd}(\text{Three_picoline})_2 + 2$
 log_k 2.27
 delta_h 0 kJ
 -gamma 0 0
 # Id: 1609812
 # log K source: SCD2.62
 # Delta H source: SCD2.62
 #T and ionic strength:
 $\text{Cd}^{2+} + 3\text{Three_picoline} = \text{Cd}(\text{Three_picoline})_3 + 2$
 log_k 3.6
 delta_h 0 kJ
 -gamma 0 0
 # Id: 1609813
 # log K source: NIST46.2
 # Delta H source: NIST46.2
 #T and ionic strength:
 $\text{Cd}^{2+} + 4\text{Three_picoline} = \text{Cd}(\text{Three_picoline})_4 + 2$
 log_k 4
 delta_h 0 kJ
 -gamma 0 0
 # Id: 1609814
 # log K source: NIST46.2
 # Delta H source: NIST46.2
 #T and ionic strength:
 $\text{Cu}^{+} + 3\text{Three_picoline} = \text{Cu}(\text{Three_picoline})_3 +$
 log_k 5.6
 delta_h 0 kJ
 -gamma 0 0
 # Id: 2309811
 # log K source: NIST46.2
 # Delta H source: NIST46.2
 #T and ionic strength:
 $\text{Cu}^{+} + 2\text{Three_picoline} = \text{Cu}(\text{Three_picoline})_2 +$
 log_k 7.78
 delta_h 0 kJ
 -gamma 0 0
 # Id: 2309812
 # log K source: NIST46.2
 # Delta H source: NIST46.2
 #T and ionic strength:
 $\text{Cu}^{+} + 3\text{Three_picoline} = \text{Cu}(\text{Three_picoline})_3 +$
 log_k 8.6
 delta_h 0 kJ
 -gamma 0 0
 # Id: 2309813

log K source: NIST46.2
 # Delta H source: NIST46.2
 #T and ionic strength:
 $\text{Cu}^+ + 4\text{Three_picoline} = \text{Cu}(\text{Three_picoline})_4^+$
 log_k 9
 delta_h 0 kJ
 -gamma 0 0
 # Id: 2309814
 # log K source: NIST46.2
 # Delta H source: NIST46.2
 #T and ionic strength:
 $\text{Cu}^{+2} + \text{Three_picoline} = \text{Cu}(\text{Three_picoline})_2^+$
 log_k 2.77
 delta_h 0 kJ
 -gamma 0 0
 # Id: 2319811
 # log K source: NIST46.2
 # Delta H source: NIST46.2
 #T and ionic strength:
 $\text{Cu}^{+2} + 2\text{Three_picoline} = \text{Cu}(\text{Three_picoline})_2^{2+}$
 log_k 4.8
 delta_h 0 kJ
 -gamma 0 0
 # Id: 2319812
 # log K source: NIST46.2
 # Delta H source: NIST46.2
 #T and ionic strength:
 $\text{Cu}^{+2} + 3\text{Three_picoline} = \text{Cu}(\text{Three_picoline})_3^{2+}$
 log_k 6.3
 delta_h 0 kJ
 -gamma 0 0
 # Id: 2319813
 # log K source: NIST46.2
 # Delta H source: NIST46.2
 #T and ionic strength:
 $\text{Cu}^{+2} + 4\text{Three_picoline} = \text{Cu}(\text{Three_picoline})_4^{2+}$
 log_k 7.2
 delta_h 0 kJ
 -gamma 0 0
 # Id: 2319814
 # log K source: NIST46.2
 # Delta H source: NIST46.2
 #T and ionic strength:
 $\text{Ag}^+ + \text{Three_picoline} = \text{Ag}(\text{Three_picoline})^+$
 log_k 2.2
 delta_h -21.7568 kJ
 -gamma 0 0
 # Id: 209811
 # log K source: NIST46.2
 # Delta H source: NIST46.2
 #T and ionic strength:
 $\text{Ag}^+ + 2\text{Three_picoline} = \text{Ag}(\text{Three_picoline})_2^+$
 log_k 4.46
 delta_h -49.7896 kJ

-gamma 0 0
 # Id: 209812
 # log K source: NIST46.2
 # Delta H source: NIST46.2
 #T and ionic strength:
 $\text{Ni}^{+2} + \text{Three_picoline} = \text{Ni}(\text{Three_picoline})_2$
 log_k 1.87
 delta_h 0 kJ
 -gamma 0 0
 # Id: 5409811
 # log K source: NIST46.2
 # Delta H source: NIST46.2
 #T and ionic strength:
 $\text{Ni}^{+2} + 2\text{Three_picoline} = \text{Ni}(\text{Three_picoline})_2$
 log_k 3.3
 delta_h 0 kJ
 -gamma 0 0
 # Id: 5409812
 # log K source: NIST46.2
 # Delta H source: NIST46.2
 #T and ionic strength:
 $\text{Ni}^{+2} + 3\text{Three_picoline} = \text{Ni}(\text{Three_picoline})_3$
 log_k 4.1
 delta_h 0 kJ
 -gamma 0 0
 # Id: 5409813
 # log K source: NIST46.2
 # Delta H source: NIST46.2
 #T and ionic strength:
 $\text{Ni}^{+2} + 4\text{Three_picoline} = \text{Ni}(\text{Three_picoline})_4$
 log_k 4.6
 delta_h 0 kJ
 -gamma 0 0
 # Id: 5409814
 # log K source: NIST46.2
 # Delta H source: NIST46.2
 #T and ionic strength:
 $\text{Co}^{+2} + \text{Three_picoline} = \text{Co}(\text{Three_picoline})_2$
 log_k 1.4
 delta_h 0 kJ
 -gamma 0 0
 # Id: 2009811
 # log K source: NIST46.4
 # Delta H source: NIST46.2
 #T and ionic strength: 0.50 25.0
 $\text{Co}^{+2} + 2\text{Three_picoline} = \text{Co}(\text{Three_picoline})_2$
 log_k 2.2
 delta_h 0 kJ
 -gamma 0 0
 # Id: 2009812
 # log K source: NIST46.4
 # Delta H source: NIST46.2
 #T and ionic strength: 0.50 25.0
 $\text{Co}^{+2} + 3\text{Three_picoline} = \text{Co}(\text{Three_picoline})_3$

log_k 2.5
 delta_h 0 kJ
 -gamma 0 0
 # Id: 2009813
 # log K source: NIST46.4
 # Delta H source: NIST46.2
 #T and ionic strength: 0.50 25.0
 $\text{H}^+ + \text{Four_picoline} = \text{H}(\text{Four_picoline}) +$
 log_k 6.03
 delta_h -25.3132 kJ
 -gamma 0 0
 # Id: 3309821
 # log K source: NIST46.2
 # Delta H source: NIST46.2
 #T and ionic strength:
 $\text{Zn}^{+2} + \text{Four_picoline} = \text{Zn}(\text{Four_picoline}) + 2$
 log_k 1.4
 delta_h 0 kJ
 -gamma 0 0
 # Id: 9509821
 # log K source: NIST46.2
 # Delta H source: NIST46.2
 #T and ionic strength:
 $\text{Zn}^{+2} + 2\text{Four_picoline} = \text{Zn}(\text{Four_picoline})_2 + 2$
 log_k 2.11
 delta_h 0 kJ
 -gamma 0 0
 # Id: 9509822
 # log K source: NIST46.2
 # Delta H source: NIST46.2
 #T and ionic strength:
 $\text{Zn}^{+2} + 3\text{Four_picoline} = \text{Zn}(\text{Four_picoline})_3 + 2$
 log_k 2.85
 delta_h 0 kJ
 -gamma 0 0
 # Id: 9509823
 # log K source: NIST46.2
 # Delta H source: NIST46.2
 #T and ionic strength:
 $\text{Cd}^{+2} + \text{Four_picoline} = \text{Cd}(\text{Four_picoline}) + 2$
 log_k 1.59
 delta_h 0 kJ
 -gamma 0 0
 # Id: 1609821
 # log K source: SCD2.62
 # Delta H source: SCD2.62
 #T and ionic strength:
 $\text{Cd}^{+2} + 2\text{Four_picoline} = \text{Cd}(\text{Four_picoline})_2 + 2$
 log_k 2.4
 delta_h 0 kJ
 -gamma 0 0
 # Id: 1609822
 # log K source: SCD2.62
 # Delta H source: SCD2.62

#T and ionic strength:
 $\text{Cd}^{+2} + 3\text{Four_picoline} = \text{Cd}(\text{Four_picoline})_3^{+2}$
 log_k 3.18
 delta_h 0 kJ
 -gamma 0 0
 # Id: 1609823
 # log K source: SCD2.62
 # Delta H source: SCD2.62
 #T and ionic strength:
 $\text{Cd}^{+2} + 4\text{Four_picoline} = \text{Cd}(\text{Four_picoline})_4^{+2}$
 log_k 4
 delta_h 0 kJ
 -gamma 0 0
 # Id: 1609824
 # log K source: NIST46.2
 # Delta H source: NIST46.2
 #T and ionic strength:
 $\text{Cu}^{+} + \text{Four_picoline} = \text{Cu}(\text{Four_picoline})^{+}$
 log_k 5.65
 delta_h 0 kJ
 -gamma 0 0
 # Id: 2309821
 # log K source: NIST46.2
 # Delta H source: NIST46.2
 #T and ionic strength:
 $\text{Cu}^{+} + 2\text{Four_picoline} = \text{Cu}(\text{Four_picoline})_2^{+}$
 log_k 8.2
 delta_h 0 kJ
 -gamma 0 0
 # Id: 2309822
 # log K source: NIST46.2
 # Delta H source: NIST46.2
 #T and ionic strength:
 $\text{Cu}^{+} + 3\text{Four_picoline} = \text{Cu}(\text{Four_picoline})_3^{+}$
 log_k 8.8
 delta_h 0 kJ
 -gamma 0 0
 # Id: 2309823
 # log K source: NIST46.2
 # Delta H source: NIST46.2
 #T and ionic strength:
 $\text{Cu}^{+} + 4\text{Four_picoline} = \text{Cu}(\text{Four_picoline})_4^{+}$
 log_k 9.2
 delta_h 0 kJ
 -gamma 0 0
 # Id: 2309824
 # log K source: NIST46.2
 # Delta H source: NIST46.2
 #T and ionic strength:
 $\text{Cu}^{+2} + \text{Four_picoline} = \text{Cu}(\text{Four_picoline})^{+2}$
 log_k 2.88
 delta_h 0 kJ
 -gamma 0 0
 # Id: 2319821

log K source: NIST46.2
 # Delta H source: NIST46.2
 #T and ionic strength:
 $\text{Cu}^{+2} + 2\text{Four_picoline} = \text{Cu}(\text{Four_picoline})_2^{+2}$
 log_k 5.16
 delta_h 0 kJ
 -gamma 0 0
 # Id: 2319822
 # log K source: NIST46.2
 # Delta H source: NIST46.2
 #T and ionic strength:
 $\text{Cu}^{+2} + 3\text{Four_picoline} = \text{Cu}(\text{Four_picoline})_3^{+2}$
 log_k 6.77
 delta_h 0 kJ
 -gamma 0 0
 # Id: 2319823
 # log K source: NIST46.2
 # Delta H source: NIST46.2
 #T and ionic strength:
 $\text{Cu}^{+2} + 4\text{Four_picoline} = \text{Cu}(\text{Four_picoline})_4^{+2}$
 log_k 8.08
 delta_h 0 kJ
 -gamma 0 0
 # Id: 2319824
 # log K source: NIST46.2
 # Delta H source: NIST46.2
 #T and ionic strength:
 $\text{Cu}^{+2} + 5\text{Four_picoline} = \text{Cu}(\text{Four_picoline})_5^{+2}$
 log_k 8.3
 delta_h 0 kJ
 -gamma 0 0
 # Id: 2319825
 # log K source: NIST46.2
 # Delta H source: NIST46.2
 #T and ionic strength:
 $\text{Ag}^{+} + \text{Four_picoline} = \text{Ag}(\text{Four_picoline})^{+}$
 log_k 2.03
 delta_h -25.5224 kJ
 -gamma 0 0
 # Id: 209821
 # log K source: NIST46.2
 # Delta H source: NIST46.2
 #T and ionic strength:
 $\text{Ag}^{+} + 2\text{Four_picoline} = \text{Ag}(\text{Four_picoline})_2^{+}$
 log_k 4.39
 delta_h -53.5552 kJ
 -gamma 0 0
 # Id: 209822
 # log K source: NIST46.2
 # Delta H source: NIST46.2
 #T and ionic strength:
 $\text{Ni}^{+2} + \text{Four_picoline} = \text{Ni}(\text{Four_picoline})^{+2}$
 log_k 2.11
 delta_h 0 kJ

-gamma 0 0
 # Id: 5409821
 # log K source: NIST46.2
 # Delta H source: NIST46.2
 #T and ionic strength:
 $\text{Ni}^{+2} + 2\text{Four_picoline} = \text{Ni}(\text{Four_picoline})_2^{+2}$
 log_k 3.59
 delta_h 0 kJ
 -gamma 0 0
 # Id: 5409822
 # log K source: NIST46.2
 # Delta H source: NIST46.2
 #T and ionic strength:
 $\text{Ni}^{+2} + 3\text{Four_picoline} = \text{Ni}(\text{Four_picoline})_3^{+2}$
 log_k 4.34
 delta_h 0 kJ
 -gamma 0 0
 # Id: 5409823
 # log K source: NIST46.2
 # Delta H source: NIST46.2
 #T and ionic strength:
 $\text{Ni}^{+2} + 4\text{Four_picoline} = \text{Ni}(\text{Four_picoline})_4^{+2}$
 log_k 4.7
 delta_h 0 kJ
 -gamma 0 0
 # Id: 5409824
 # log K source: NIST46.2
 # Delta H source: NIST46.2
 #T and ionic strength:
 $\text{Co}^{+2} + \text{Four_picoline} = \text{Co}(\text{Four_picoline})^{+2}$
 log_k 1.56
 delta_h 0 kJ
 -gamma 0 0
 # Id: 2009821
 # log K source: NIST46.4
 # Delta H source: NIST46.2
 #T and ionic strength: 0.50 25.0
 $\text{Co}^{+2} + 2\text{Four_picoline} = \text{Co}(\text{Four_picoline})_2^{+2}$
 log_k 2.51
 delta_h 0 kJ
 -gamma 0 0
 # Id: 2009822
 # log K source: NIST46.4
 # Delta H source: NIST46.2
 #T and ionic strength: 0.50 25.0
 $\text{Co}^{+2} + 3\text{Four_picoline} = \text{Co}(\text{Four_picoline})_3^{+2}$
 log_k 2.94
 delta_h 0 kJ
 -gamma 0 0
 # Id: 2009823
 # log K source: NIST46.4
 # Delta H source: NIST46.2
 #T and ionic strength: 0.50 25.0
 $\text{Co}^{+2} + 4\text{Four_picoline} = \text{Co}(\text{Four_picoline})_4^{+2}$

log_k 3.17
delta_h 0 kJ
-gamma 0 0
Id: 2009824
log K source: NIST46.4
Delta H source: NIST46.2
#T and ionic strength: 0.50 25.0
 $\text{H}^+ + \text{Formate}^- = \text{H}(\text{Formate})$
log_k 3.745
delta_h 0.1674 kJ
-gamma 0 0
Id: 3309831
log K source: NIST46.2
Delta H source: NIST46.2
#T and ionic strength:
 $\text{Pb}^{+2} + \text{Formate}^- = \text{Pb}(\text{Formate})^+$
log_k 2.2
delta_h 0 kJ
-gamma 0 0
Id: 6009831
log K source: SCD2.62
Delta H source: SCD2.62
#T and ionic strength:
 $\text{Zn}^{+2} + \text{Formate}^- = \text{Zn}(\text{Formate})^+$
log_k 1.44
delta_h 0 kJ
-gamma 0 0
Id: 9509831
log K source: NIST46.2
Delta H source: NIST46.2
#T and ionic strength:
 $\text{Cd}^{+2} + \text{Formate}^- = \text{Cd}(\text{Formate})^+$
log_k 1.7
delta_h 0 kJ
-gamma 0 0
Id: 1609831
log K source: SCD2.62
Delta H source: SCD2.62
#T and ionic strength:
 $\text{Hg}(\text{OH})_2 + \text{Formate}^- + 2\text{H}^+ = \text{Hg}(\text{Formate})^+ + 2\text{H}_2\text{O}$
log_k 9.6
delta_h 0 kJ
-gamma 0 0
Id: 3619831
log K source: NIST46.2
Delta H source: NIST46.2
#T and ionic strength:
 $\text{Cu}^{+2} + \text{Formate}^- = \text{Cu}(\text{Formate})^+$
log_k 2
delta_h 0 kJ
-gamma 0 0
Id: 2319831
log K source: NIST46.2
Delta H source: NIST46.2

#T and ionic strength:
 $\text{Ni}^{+2} + \text{Formate}^- = \text{Ni}(\text{Formate}) +$
 $\log_k 1.22$
 $\Delta H 0 \text{ kJ}$
 $-\gamma 0 0$
 # Id: 5409831
 # log K source: SCD2.62
 # Delta H source: SCD2.62
 #T and ionic strength:
 $\text{Co}^{+2} + \text{Formate}^- = \text{Co}(\text{Formate}) +$
 $\log_k 1.209$
 $\Delta H 0 \text{ kJ}$
 $-\gamma 0 0$
 # Id: 2009831
 # log K source: NIST46.4
 # Delta H source: NIST46.2
 #T and ionic strength: 0.50 30.0
 $\text{Co}^{+2} + 2\text{Formate}^- = \text{Co}(\text{Formate})_2$
 $\log_k 1.1365$
 $\Delta H 0 \text{ kJ}$
 $-\gamma 0 0$
 # Id: 2009832
 # log K source: NIST46.4
 # Delta H source: NIST46.2
 #T and ionic strength: 2.00 25.0
 $\text{Cr}^{+2} + \text{Formate}^- = \text{Cr}(\text{Formate}) +$
 $\log_k 1.07$
 $\Delta H 0 \text{ kJ}$
 $-\gamma 0 0$
 # Id: 2109831
 # log K source: NIST46.2
 # Delta H source: NIST46.2
 #T and ionic strength:
 $\text{Mg}^{+2} + \text{Formate}^- = \text{Mg}(\text{Formate}) +$
 $\log_k 1.43$
 $\Delta H 0 \text{ kJ}$
 $-\gamma 0 0$
 # Id: 4609831
 # log K source: NIST46.2
 # Delta H source: NIST46.2
 #T and ionic strength:
 $\text{Ca}^{+2} + \text{Formate}^- = \text{Ca}(\text{Formate}) +$
 $\log_k 1.43$
 $\Delta H 4.184 \text{ kJ}$
 $-\gamma 0 0$
 # Id: 1509831
 # log K source: NIST46.2
 # Delta H source: NIST46.2
 #T and ionic strength:
 $\text{Sr}^{+2} + \text{Formate}^- = \text{Sr}(\text{Formate}) +$
 $\log_k 1.39$
 $\Delta H 4 \text{ kJ}$
 $-\gamma 0 0$
 # Id: 8009831

log K source: NIST46.4
 # Delta H source: NIST46.4
 #T and ionic strength: 0.00 25.0
 $\text{Ba}^{+2} + \text{Formate}^- = \text{Ba}(\text{Formate}) +$
 log_k 1.38
 delta_h 0 kJ
 -gamma 0 0
 # Id: 1009831
 # log K source: NIST46.2
 # Delta H source: NIST46.2
 #T and ionic strength:
 $\text{H}^+ + \text{Isovalerate}^- = \text{H}(\text{Isovalerate})$
 log_k 4.781
 delta_h 4.5606 kJ
 -gamma 0 0
 # Id: 3309841
 # log K source: NIST46.2
 # Delta H source: NIST46.2
 #T and ionic strength:
 $\text{Zn}^{+2} + \text{Isovalerate}^- = \text{Zn}(\text{Isovalerate}) +$
 log_k 1.39
 delta_h 0 kJ
 -gamma 0 0
 # Id: 9509841
 # log K source: NIST46.2
 # Delta H source: NIST46.2
 #T and ionic strength:
 $\text{Cu}^{+2} + \text{Isovalerate}^- = \text{Cu}(\text{Isovalerate}) +$
 log_k 2.08
 delta_h 0 kJ
 -gamma 0 0
 # Id: 2319841
 # log K source: NIST46.2
 # Delta H source: NIST46.2
 #T and ionic strength:
 $\text{Ca}^{+2} + \text{Isovalerate}^- = \text{Ca}(\text{Isovalerate}) +$
 log_k 0.2
 delta_h 0 kJ
 -gamma 0 0
 # Id: 1509841
 # log K source: SCD2.62
 # Delta H source: SCD2.62
 #T and ionic strength:
 $\text{H}^+ + \text{Valerate}^- = \text{H}(\text{Valerate})$
 log_k 4.843
 delta_h 2.887 kJ
 -gamma 0 0
 # Id: 3309851
 # log K source: NIST46.2
 # Delta H source: NIST46.2
 #T and ionic strength:
 $\text{Cu}^{+2} + \text{Valerate}^- = \text{Cu}(\text{Valerate}) +$
 log_k 2.12
 delta_h 0 kJ

-gamma 0 0
 # Id: 2319851
 # log K source: NIST46.2
 # Delta H source: NIST46.2
 #T and ionic strength:
 $\text{Ca}^{+2} + \text{Valerate}^- = \text{Ca}(\text{Valerate})^+$
 log_k 0.3
 delta_h 0 kJ
 -gamma 0 0
 # Id: 1509851
 # log K source: SCD2.62
 # Delta H source: SCD2.62
 #T and ionic strength:
 $\text{Ba}^{+2} + \text{Valerate}^- = \text{Ba}(\text{Valerate})^+$
 log_k -0.2
 delta_h 0 kJ
 -gamma 0 0
 # Id: 1009851
 # log K source: SCD2.62
 # Delta H source: SCD2.62
 #T and ionic strength:
 $\text{H}^+ + \text{Acetate}^- = \text{H}(\text{Acetate})$
 log_k 4.757
 delta_h 0.41 kJ
 -gamma 0 0
 # Id: 3309921
 # log K source: NIST46.4
 # Delta H source: NIST46.4
 #T and ionic strength: 0.00 25.0
 $\text{Sn}(\text{OH})_2 + 2\text{H}^+ + \text{Acetate}^- = \text{Sn}(\text{Acetate})^+ + 2\text{H}_2\text{O}$
 log_k 10.0213
 delta_h 0 kJ
 -gamma 0 0
 # Id: 7909921
 # log K source: NIST46.4
 # Delta H source: NIST46.2
 #T and ionic strength: 3.00 25.0
 $\text{Sn}(\text{OH})_2 + 2\text{H}^+ + 2\text{Acetate}^- = \text{Sn}(\text{Acetate})_2 + 2\text{H}_2\text{O}$
 log_k 12.32
 delta_h 0 kJ
 -gamma 0 0
 # Id: 7909922
 # log K source: NIST46.4
 # Delta H source: NIST46.2
 #T and ionic strength: 3.00 25.0
 $\text{Sn}(\text{OH})_2 + 2\text{H}^+ + 3\text{Acetate}^- = \text{Sn}(\text{Acetate})_3^- + 2\text{H}_2\text{O}$
 log_k 13.55
 delta_h 0 kJ
 -gamma 0 0
 # Id: 7909923
 # log K source: NIST46.4
 # Delta H source: NIST46.2
 #T and ionic strength: 3.00 25.0
 $\text{Pb}^{+2} + \text{Acetate}^- = \text{Pb}(\text{Acetate})^+$

log_k 2.68
delta_h -0.4 kJ
-gamma 0 0
Id: 6009921
log K source: NIST46.4
Delta H source: NIST46.4
#T and ionic strength: 0.00 25.0
 $\text{Pb}^{+2} + 2\text{Acetate}^- = \text{Pb}(\text{Acetate})_2$
log_k 4.08
delta_h -0.8 kJ
-gamma 0 0
Id: 6009922
log K source: NIST46.4
Delta H source: NIST46.4
#T and ionic strength: 0.00 25.0
 $\text{Ti}^+ + \text{Acetate}^- = \text{Ti}(\text{Acetate})$
log_k -0.11
delta_h 0 kJ
-gamma 0 0
Id: 8709921
log K source: NIST46.4
Delta H source: NIST46.2
#T and ionic strength: 0.00 25.0
 $\text{Zn}^{+2} + \text{Acetate}^- = \text{Zn}(\text{Acetate})^+$
log_k 1.58
delta_h 8.3 kJ
-gamma 0 0
Id: 9509921
log K source: NIST46.4
Delta H source: NIST46.4
#T and ionic strength: 0.00 25.0
 $\text{Zn}^{+2} + 2\text{Acetate}^- = \text{Zn}(\text{Acetate})_2$
log_k 2.6434
delta_h 22 kJ
-gamma 0 0
Id: 9509922
log K source: NIST46.4
Delta H source: NIST46.4
#T and ionic strength: 0.10 25.0
 $\text{Cd}^{+2} + \text{Acetate}^- = \text{Cd}(\text{Acetate})^+$
log_k 1.93
delta_h 9.6 kJ
-gamma 0 0
Id: 1609921
log K source: NIST46.4
Delta H source: NIST46.4
#T and ionic strength: 0.00 25.0
 $\text{Cd}^{+2} + 2\text{Acetate}^- = \text{Cd}(\text{Acetate})_2$
log_k 2.86
delta_h 15 kJ
-gamma 0 0
Id: 1609922
log K source: NIST46.4
Delta H source: NIST46.4

#T and ionic strength: 0.00 25.0
 $\text{Hg}(\text{OH})_2 + 2\text{H}^+ + \text{Acetate}^- = \text{Hg}(\text{Acetate})^+ + 2\text{H}_2\text{O}$
 log_k 10.494
 delta_h 0 kJ
 -gamma 0 0
 # Id: 3619920
 # log K source: NIST46.4
 # Delta H source: NIST46.2
 #T and ionic strength: 0.00 25.0
 $\text{Hg}(\text{OH})_2 + 2\text{H}^+ + 2\text{Acetate}^- = \text{Hg}(\text{Acetate})_2 + 2\text{H}_2\text{O}$
 log_k 13.83
 delta_h 0 kJ
 -gamma 0 0
 # Id: 3619921
 # log K source: NIST46.4
 # Delta H source: SCD2.62
 #T and ionic strength: 3.00 25.0
 $\text{Cu}^{+2} + \text{Acetate}^- = \text{Cu}(\text{Acetate})^+$
 log_k 2.21
 delta_h 7.1 kJ
 -gamma 0 0
 # Id: 2319921
 # log K source: NIST46.4
 # Delta H source: NIST46.4
 #T and ionic strength: 0.00 25.0
 $\text{Cu}^{+2} + 2\text{Acetate}^- = \text{Cu}(\text{Acetate})_2$
 log_k 3.4
 delta_h 12 kJ
 -gamma 0 0
 # Id: 2319922
 # log K source: NIST46.4
 # Delta H source: NIST46.4
 #T and ionic strength: 0.00 25.0
 $\text{Cu}^{+2} + 3\text{Acetate}^- = \text{Cu}(\text{Acetate})_3^-$
 log_k 3.9434
 delta_h 6.2 kJ
 -gamma 0 0
 # Id: 2319923
 # log K source: NIST46.4
 # Delta H source: NIST46.4
 #T and ionic strength: 0.10 25.0
 $\text{Ag}^+ + \text{Acetate}^- = \text{Ag}(\text{Acetate})$
 log_k 0.73
 delta_h 3 kJ
 -gamma 0 0
 # Id: 209921
 # log K source: NIST46.4
 # Delta H source: NIST46.4
 #T and ionic strength: 0.00 25.0
 $\text{Ag}^+ + 2\text{Acetate}^- = \text{Ag}(\text{Acetate})_2^-$
 log_k 0.64
 delta_h 3 kJ
 -gamma 0 0
 # Id: 209922

log K source: NIST46.4
 # Delta H source: NIST46.4
 #T and ionic strength: 0.00 25.0
 $\text{Ni}^{+2} + \text{Acetate}^- = \text{Ni}(\text{Acetate})^+$
 log_k 1.37
 delta_h 8.7 kJ
 -gamma 0 0
 # Id: 5409921
 # log K source: NIST46.4
 # Delta H source: NIST46.4
 #T and ionic strength: 0.00 25.0
 $\text{Ni}^{+2} + 2\text{Acetate}^- = \text{Ni}(\text{Acetate})_2$
 log_k 2.1
 delta_h 10 kJ
 -gamma 0 0
 # Id: 5409922
 # log K source: NIST46.4
 # Delta H source: NIST46.4
 #T and ionic strength: 0.00 25.0
 $\text{Co}^{+2} + \text{Acetate}^- = \text{Co}(\text{Acetate})^+$
 log_k 1.38
 delta_h 0 kJ
 -gamma 0 0
 # Id: 2009921
 # log K source: NIST46.4
 # Delta H source: NIST46.2
 #T and ionic strength: 0.00 25.0
 $\text{Co}^{+2} + 2\text{Acetate}^- = \text{Co}(\text{Acetate})_2$
 log_k 0.7565
 delta_h 0 kJ
 -gamma 0 0
 # Id: 2009922
 # log K source: NIST46.4
 # Delta H source: NIST46.2
 #T and ionic strength: 2.00 25.0
 $\text{Fe}^{+2} + \text{Acetate}^- = \text{Fe}(\text{Acetate})^+$
 log_k 1.4
 delta_h 0 kJ
 -gamma 0 0
 # Id: 2809920
 # log K source: NIST46.4
 # Delta H source: NIST46.2
 #T and ionic strength: 0.00 25.0
 $\text{Fe}^{+3} + \text{Acetate}^- = \text{Fe}(\text{Acetate})^{+2}$
 log_k 4.0234
 delta_h 0 kJ
 -gamma 0 0
 # Id: 2819920
 # log K source: NIST46.4
 # Delta H source: NIST46.2
 #T and ionic strength: 0.10 20.0
 $\text{Fe}^{+3} + 2\text{Acetate}^- = \text{Fe}(\text{Acetate})_2^+$
 log_k 7.5723
 delta_h 0 kJ

-gamma 0 0
 # Id: 2819921
 # log K source: NIST46.4
 # Delta H source: NIST46.2
 #T and ionic strength: 0.10 20.0
 $\text{Fe}^{+3} + 3\text{Acetate}^- = \text{Fe}(\text{Acetate})_3$
 log_k 9.5867
 delta_h 0 kJ
 -gamma 0 0
 # Id: 2819922
 # log K source: NIST46.4
 # Delta H source: NIST46.2
 #T and ionic strength: 0.10 20.0
 $\text{Mn}^{+2} + \text{Acetate}^- = \text{Mn}(\text{Acetate})^+$
 log_k 1.4
 delta_h 0 kJ
 -gamma 0 0
 # Id: 4709920
 # log K source: NIST46.4
 # Delta H source: NIST46.2
 #T and ionic strength: 0.00 25.0
 $\text{Cr}^{+2} + \text{Acetate}^- = \text{Cr}(\text{Acetate})^+$
 log_k 1.8
 delta_h 0 kJ
 -gamma 0 0
 # Id: 2109921
 # log K source: NIST46.4
 # Delta H source: NIST46.2
 #T and ionic strength: 0.00 25.0
 $\text{Cr}^{+2} + 2\text{Acetate}^- = \text{Cr}(\text{Acetate})_2$
 log_k 2.92
 delta_h 0 kJ
 -gamma 0 0
 # Id: 2109922
 # log K source: NIST46.4
 # Delta H source: NIST46.2
 #T and ionic strength: 0.00 25.0
 $\text{Cr}(\text{OH})_2^{+} + 2\text{H}^{+} + \text{Acetate}^- = \text{Cr}(\text{Acetate})_2^{+} + 2\text{H}_2\text{O}$
 log_k 15.0073
 delta_h -125.62 kJ
 -gamma 0 0
 # Id: 2119921
 # log K source: NIST46.4
 # Delta H source: NIST46.4
 #T and ionic strength: 0.50 25.0
 $\text{Cr}(\text{OH})_2^{+} + 2\text{H}^{+} + 2\text{Acetate}^- = \text{Cr}(\text{Acetate})_2^{+} + 2\text{H}_2\text{O}$
 log_k 17.9963
 delta_h -117.62 kJ
 -gamma 0 0
 # Id: 2119922
 # log K source: NIST46.4
 # Delta H source: NIST46.4
 #T and ionic strength: 0.50 25.0
 $\text{Cr}(\text{OH})_2^{+} + 2\text{H}^{+} + 3\text{Acetate}^- = \text{Cr}(\text{Acetate})_3 + 2\text{H}_2\text{O}$

log_k 20.7858
delta_h -96.62 kJ
-gamma 0 0
Id: 2119923
log K source: NIST46.4
Delta H source: NIST46.4
#T and ionic strength: 0.50 25.0
Be+2 + Acetate- = Be(Acetate)+
log_k 2.0489
delta_h 0 kJ
-gamma 0 0
Id: 1109921
log K source: NIST46.4
Delta H source: NIST46.2
#T and ionic strength: 0.10 25.0
Be+2 + 2Acetate- = Be(Acetate)2
log_k 3.0034
delta_h 0 kJ
-gamma 0 0
Id: 1109922
log K source: NIST46.4
Delta H source: NIST46.2
#T and ionic strength: 0.10 25.0
Mg+2 + Acetate- = Mg(Acetate)+
log_k 1.27
delta_h 0 kJ
-gamma 0 0
Id: 4609920
log K source: NIST46.4
Delta H source: NIST46.2
#T and ionic strength: 0.00 25.0
Ca+2 + Acetate- = Ca(Acetate)+
log_k 1.18
delta_h 4 kJ
-gamma 0 0
Id: 1509920
log K source: NIST46.4
Delta H source: NIST46.4
#T and ionic strength: 0.00 25.0
Sr+2 + Acetate- = Sr(Acetate)+
log_k 1.14
delta_h 0 kJ
-gamma 0 0
Id: 8009921
log K source: NIST46.4
Delta H source: NIST46.2
#T and ionic strength: 0.00 25.0
Ba+2 + Acetate- = Ba(Acetate)+
log_k 1.07
delta_h 0 kJ
-gamma 0 0
Id: 1009921
log K source: NIST46.4
Delta H source: NIST46.2

#T and ionic strength: 0.00 25.0
 $\text{Na}^+ + \text{Acetate}^- = \text{Na}(\text{Acetate})$
 log_k -0.18
 delta_h 12 kJ
 -gamma 0 0
 # Id: 5009920
 # log K source: NIST46.4
 # Delta H source: NIST46.4
 #T and ionic strength: 0.00 25.0
 $\text{K}^+ + \text{Acetate}^- = \text{K}(\text{Acetate})$
 log_k -0.1955
 delta_h 4.184 kJ
 -gamma 0 0
 # Id: 4109921
 # log K source: NIST46.4
 # Delta H source: NIST46.2
 #T and ionic strength: 0.10 25.0
 $\text{H}^+ + \text{Tartarate-2} = \text{H}(\text{Tartarate})$
 log_k 4.366
 delta_h -0.7531 kJ
 -gamma 0 0
 # Id: 3309931
 # log K source: NIST46.2
 # Delta H source: NIST46.2
 #T and ionic strength:
 $2\text{H}^+ + \text{Tartarate-2} = \text{H}_2(\text{Tartarate})$
 log_k 7.402
 delta_h -3.6819 kJ
 -gamma 0 0
 # Id: 3309932
 # log K source: NIST46.2
 # Delta H source: NIST46.2
 #T and ionic strength:
 $\text{Sn}(\text{OH})_2 + 2\text{H}^+ + \text{Tartarate-2} = \text{Sn}(\text{Tartarate}) + 2\text{H}_2\text{O}$
 log_k 13.1518
 delta_h 0 kJ
 -gamma 0 0
 # Id: 7909931
 # log K source: NIST46.4
 # Delta H source: NIST46.2
 #T and ionic strength: 0.10 20.0
 $\text{Pb}^{+2} + \text{Tartarate-2} = \text{Pb}(\text{Tartarate})$
 log_k 3.98
 delta_h 0 kJ
 -gamma 0 0
 # Id: 6009931
 # log K source: NIST46.2
 # Delta H source: NIST46.2
 #T and ionic strength:
 $\text{Al}^{+3} + 2\text{Tartarate-2} = \text{Al}(\text{Tartarate})_2$
 log_k 9.37
 delta_h 0 kJ
 -gamma 0 0
 # Id: 309931

log K source: NIST46.2
 # Delta H source: NIST46.2
 #T and ionic strength:
 $\text{Ti}^+ + \text{Tartarate-2} = \text{Ti}(\text{Tartarate})$
 log_k 1.4
 delta_h 0 kJ
 -gamma 0 0
 # Id: 8709931
 # log K source: NIST46.2
 # Delta H source: NIST46.2
 #T and ionic strength:
 $\text{Ti}^+ + \text{Tartarate-2} + \text{H}^+ = \text{TiH}(\text{Tartarate})$
 log_k 4.8
 delta_h 0 kJ
 -gamma 0 0
 # Id: 8709932
 # log K source: NIST46.2
 # Delta H source: NIST46.2
 #T and ionic strength:
 $\text{Zn}^{+2} + \text{Tartarate-2} = \text{Zn}(\text{Tartarate})$
 log_k 3.43
 delta_h 0 kJ
 -gamma 0 0
 # Id: 9509931
 # log K source: NIST46.2
 # Delta H source: NIST46.2
 #T and ionic strength:
 $\text{Zn}^{+2} + 2\text{Tartarate-2} = \text{Zn}(\text{Tartarate})_2$
 log_k 5.5
 delta_h 0 kJ
 -gamma 0 0
 # Id: 9509932
 # log K source: NIST46.2
 # Delta H source: NIST46.2
 #T and ionic strength:
 $\text{Zn}^{+2} + \text{Tartarate-2} + \text{H}^+ = \text{ZnH}(\text{Tartarate})$
 log_k 5.9
 delta_h 0 kJ
 -gamma 0 0
 # Id: 9509933
 # log K source: NIST46.2
 # Delta H source: NIST46.2
 #T and ionic strength:
 $\text{Cd}^{+2} + \text{Tartarate-2} = \text{Cd}(\text{Tartarate})$
 log_k 2.7
 delta_h 0 kJ
 -gamma 0 0
 # Id: 1609931
 # log K source: NIST46.2
 # Delta H source: NIST46.2
 #T and ionic strength:
 $\text{Cd}^{+2} + 2\text{Tartarate-2} = \text{Cd}(\text{Tartarate})_2$
 log_k 4.1
 delta_h 0 kJ

-gamma 0 0
 # Id: 1609932
 # log K source: NIST46.2
 # Delta H source: NIST46.2
 #T and ionic strength:
 $\text{Hg(OH)}_2 + \text{Tartarate-2} + 2\text{H}^+ = \text{Hg(Tartarate)} + 2\text{H}_2\text{O}$
 log_k 14
 delta_h 0 kJ
 -gamma 0 0
 # Id: 3619931
 # log K source: NIST46.2
 # Delta H source: NIST46.2
 #T and ionic strength:
 $\text{Cu}^{+2} + \text{Tartarate-2} = \text{Cu(Tartarate)}$
 log_k 3.97
 delta_h 0 kJ
 -gamma 0 0
 # Id: 2319931
 # log K source: NIST46.2
 # Delta H source: NIST46.2
 #T and ionic strength:
 $\text{Cu}^{+2} + \text{Tartarate-2} + \text{H}^+ = \text{CuH(Tartarate)} +$
 log_k 6.7
 delta_h 0 kJ
 -gamma 0 0
 # Id: 2319932
 # log K source: NIST46.2
 # Delta H source: NIST46.2
 #T and ionic strength:
 $\text{Ni}^{+2} + \text{Tartarate-2} = \text{Ni(Tartarate)}$
 log_k 3.46
 delta_h 0 kJ
 -gamma 0 0
 # Id: 5409931
 # log K source: NIST46.2
 # Delta H source: NIST46.2
 #T and ionic strength:
 $\text{Ni}^{+2} + \text{Tartarate-2} + \text{H}^+ = \text{NiH(Tartarate)} +$
 log_k 5.89
 delta_h 0 kJ
 -gamma 0 0
 # Id: 5409932
 # log K source: NIST46.2
 # Delta H source: NIST46.2
 #T and ionic strength:
 $\text{Co}^{+2} + \text{Tartarate-2} = \text{Co(Tartarate)}$
 log_k 3.05
 delta_h 0 kJ
 -gamma 0 0
 # Id: 2009931
 # log K source: NIST46.4
 # Delta H source: NIST46.2
 #T and ionic strength: 0.00 25.0
 $\text{Co}^{+2} + 2\text{Tartarate-2} = \text{Co(Tartarate)}_2\text{-2}$

log_k 4
 delta_h 0 kJ
 -gamma 0 0
 # Id: 2009932
 # log K source: NIST46.4
 # Delta H source: NIST46.2
 #T and ionic strength: 0.00 25.0
 $\text{Co}^{+2} + \text{H}^{+} + \text{Tartarate-2} = \text{CoH(Tartarate)} +$
 log_k 5.754
 delta_h 0 kJ
 -gamma 0 0
 # Id: 2009933
 # log K source: NIST46.4
 # Delta H source: NIST46.2
 #T and ionic strength: 1.00 20.0
 $\text{Fe}^{+2} + \text{Tartarate-2} = \text{Fe(Tartarate)}$
 log_k 3.1
 delta_h 0 kJ
 -gamma 0 0
 # Id: 2809931
 # log K source: NIST46.2
 # Delta H source: NIST46.2
 #T and ionic strength:
 $\text{Fe}^{+3} + \text{Tartarate-2} = \text{Fe(Tartarate)} +$
 log_k 7.78
 delta_h 0 kJ
 -gamma 0 0
 # Id: 2819931
 # log K source: NIST46.2
 # Delta H source: NIST46.2
 #T and ionic strength:
 $\text{Mn}^{+2} + \text{Tartarate-2} = \text{Mn(Tartarate)}$
 log_k 3.38
 delta_h 0 kJ
 -gamma 0 0
 # Id: 4709931
 # log K source: NIST46.2
 # Delta H source: NIST46.2
 #T and ionic strength:
 $\text{Mn}^{+2} + \text{Tartarate-2} + \text{H}^{+} = \text{MnH(Tartarate)} +$
 log_k 6
 delta_h 0 kJ
 -gamma 0 0
 # Id: 4709932
 # log K source: NIST46.2
 # Delta H source: NIST46.2
 #T and ionic strength:
 $\text{Mg}^{+2} + \text{Tartarate-2} = \text{Mg(Tartarate)}$
 log_k 2.3
 delta_h 0 kJ
 -gamma 0 0
 # Id: 4609931
 # log K source: NIST46.2
 # Delta H source: NIST46.2

#T and ionic strength:
 $\text{Mg}^{+2} + \text{Tartarate-2} + \text{H}^{+} = \text{MgH}(\text{Tartarate})^{+}$
 log_k 5.75
 delta_h 0 kJ
 -gamma 0 0
 # Id: 4609932
 # log K source: NIST46.2
 # Delta H source: NIST46.2
 #T and ionic strength:
 $\text{Be}^{+2} + \text{Tartarate-2} = \text{Be}(\text{Tartarate})$
 log_k 2.768
 delta_h 0 kJ
 -gamma 0 0
 # Id: 1109931
 # log K source: NIST46.4
 # Delta H source: NIST46.2
 #T and ionic strength: 0.50 25.0
 $\text{Be}^{+2} + 2\text{Tartarate-2} = \text{Be}(\text{Tartarate})_2^{-2}$
 log_k 4.008
 delta_h 0 kJ
 -gamma 0 0
 # Id: 1109932
 # log K source: NIST46.4
 # Delta H source: NIST46.2
 #T and ionic strength: 0.50 25.0
 $\text{Ca}^{+2} + \text{Tartarate-2} = \text{Ca}(\text{Tartarate})$
 log_k 2.8
 delta_h -8.368 kJ
 -gamma 0 0
 # Id: 1509931
 # log K source: NIST46.2
 # Delta H source: NIST46.2
 #T and ionic strength:
 $\text{Ca}^{+2} + \text{Tartarate-2} + \text{H}^{+} = \text{CaH}(\text{Tartarate})^{+}$
 log_k 5.86
 delta_h -9.1211 kJ
 -gamma 0 0
 # Id: 1509932
 # log K source: NIST46.2
 # Delta H source: NIST46.2
 #T and ionic strength:
 $\text{Sr}^{+2} + \text{Tartarate-2} = \text{Sr}(\text{Tartarate})$
 log_k 2.55
 delta_h 0 kJ
 -gamma 0 0
 # Id: 8009931
 # log K source: NIST46.4
 # Delta H source: NIST46.2
 #T and ionic strength: 0.00 20.0
 $\text{Sr}^{+2} + \text{H}^{+} + \text{Tartarate-2} = \text{SrH}(\text{Tartarate})^{+}$
 log_k 5.8949
 delta_h 0 kJ
 -gamma 0 0
 # Id: 8009932

log K source: NIST46.4
 # Delta H source: NIST46.2
 #T and ionic strength: 0.10 25.0
 $\text{Ba}^{+2} + \text{Tartarate-2} = \text{Ba}(\text{Tartarate})$
 log_k 2.54
 delta_h 0 kJ
 -gamma 0 0
 # Id: 1009931
 # log K source: NIST46.2
 # Delta H source: NIST46.2
 #T and ionic strength:
 $\text{Ba}^{+2} + \text{Tartarate-2} + \text{H}^{+} = \text{BaH}(\text{Tartarate})$
 log_k 5.77
 delta_h 0 kJ
 -gamma 0 0
 # Id: 1009932
 # log K source: NIST46.2
 # Delta H source: NIST46.2
 #T and ionic strength:
 $\text{Na}^{+} + \text{Tartarate-2} = \text{Na}(\text{Tartarate})$
 log_k 0.9
 delta_h -0.8368 kJ
 -gamma 0 0
 # Id: 5009931
 # log K source: NIST46.2
 # Delta H source: NIST46.2
 #T and ionic strength:
 $\text{Na}^{+} + \text{Tartarate-2} + \text{H}^{+} = \text{NaH}(\text{Tartarate})$
 log_k 4.58
 delta_h -2.8451 kJ
 -gamma 0 0
 # Id: 5009932
 # log K source: NIST46.2
 # Delta H source: NIST46.2
 #T and ionic strength:
 $\text{K}^{+} + \text{Tartarate-2} = \text{K}(\text{Tartarate})$
 log_k 0.8
 delta_h 0 kJ
 -gamma 0 0
 # Id: 4109931
 # log K source: NIST46.2
 # Delta H source: NIST46.2
 #T and ionic strength:
 $\text{H}^{+} + \text{Glycine-} = \text{H}(\text{Glycine})$
 log_k 9.778
 delta_h -44.3504 kJ
 -gamma 0 0
 # Id: 3309941
 # log K source: NIST46.2
 # Delta H source: NIST46.2
 #T and ionic strength:
 $2\text{H}^{+} + \text{Glycine-} = \text{H}_2(\text{Glycine})$
 log_k 12.128
 delta_h -48.4507 kJ

-gamma 0 0
Id: 3309942
log K source: NIST46.2
Delta H source: NIST46.2
#T and ionic strength:
 $\text{Pb}^{+2} + \text{Glycine}^- = \text{Pb}(\text{Glycine})^+$
log_k 5.47
delta_h 0 kJ
-gamma 0 0
Id: 6009941
log K source: NIST46.2
Delta H source: NIST46.2
#T and ionic strength:
 $\text{Pb}^{+2} + 2\text{Glycine}^- = \text{Pb}(\text{Glycine})_2$
log_k 8.86
delta_h 0 kJ
-gamma 0 0
Id: 6009942
log K source: SCD2.62
Delta H source: SCD2.62
#T and ionic strength:
 $\text{Ti}^+ + \text{Glycine}^- = \text{Ti}(\text{Glycine})$
log_k 1.72
delta_h 0 kJ
-gamma 0 0
Id: 8709941
log K source: NIST46.2
Delta H source: NIST46.2
#T and ionic strength:
 $\text{Zn}^{+2} + \text{Glycine}^- = \text{Zn}(\text{Glycine})^+$
log_k 5.38
delta_h -11.7152 kJ
-gamma 0 0
Id: 9509941
log K source: NIST46.2
Delta H source: NIST46.2
#T and ionic strength:
 $\text{Zn}^{+2} + 2\text{Glycine}^- = \text{Zn}(\text{Glycine})_2$
log_k 9.81
delta_h -24.2672 kJ
-gamma 0 0
Id: 9509942
log K source: NIST46.2
Delta H source: NIST46.2
#T and ionic strength:
 $\text{Zn}^{+2} + 3\text{Glycine}^- = \text{Zn}(\text{Glycine})_3^-$
log_k 12.3
delta_h -39.748 kJ
-gamma 0 0
Id: 9509943
log K source: NIST46.2
Delta H source: NIST46.2
#T and ionic strength:
 $\text{Cd}^{+2} + \text{Glycine}^- = \text{Cd}(\text{Glycine})^+$

log_k 4.69
 delta_h -8.7864 kJ
 -gamma 0 0
 # Id: 1609941
 # log K source: NIST46.2
 # Delta H source: NIST46.2
 #T and ionic strength:
 $\text{Cd}^{+2} + 2\text{Glycine}^- = \text{Cd}(\text{Glycine})_2$
 log_k 8.4
 delta_h -22.5936 kJ
 -gamma 0 0
 # Id: 1609942
 # log K source: NIST46.2
 # Delta H source: NIST46.2
 #T and ionic strength:
 $\text{Cd}^{+2} + 3\text{Glycine}^- = \text{Cd}(\text{Glycine})_3^-$
 log_k 10.7
 delta_h -35.9824 kJ
 -gamma 0 0
 # Id: 1609943
 # log K source: NIST46.2
 # Delta H source: NIST46.2
 #T and ionic strength:
 $\text{Hg}(\text{OH})_2 + \text{Glycine}^- + 2\text{H}^+ = \text{Hg}(\text{Glycine})^+ + 2\text{H}_2\text{O}$
 log_k 17
 delta_h 0 kJ
 -gamma 0 0
 # Id: 3619941
 # log K source: SCD2.62
 # Delta H source: SCD2.62
 #T and ionic strength:
 $\text{Hg}(\text{OH})_2 + 2\text{Glycine}^- + 2\text{H}^+ = \text{Hg}(\text{Glycine})_2 + 2\text{H}_2\text{O}$
 log_k 25.8
 delta_h 0 kJ
 -gamma 0 0
 # Id: 3619942
 # log K source: SCD2.62
 # Delta H source: SCD2.62
 #T and ionic strength:
 $\text{Cu}^+ + 2\text{Glycine}^- = \text{Cu}(\text{Glycine})_2^-$
 log_k 10.3
 delta_h 0 kJ
 -gamma 0 0
 # Id: 2309941
 # log K source: NIST46.2
 # Delta H source: NIST46.2
 #T and ionic strength:
 $\text{Cu}^{+2} + \text{Glycine}^- = \text{Cu}(\text{Glycine})^+$
 log_k 8.57
 delta_h -25.104 kJ
 -gamma 0 0
 # Id: 2319941
 # log K source: NIST46.2
 # Delta H source: NIST46.2

#T and ionic strength:
 $\text{Cu}^{+2} + 2\text{Glycine}^- = \text{Cu}(\text{Glycine})_2$
log_k 15.7
delta_h -54.8104 kJ
-gamma 0 0
Id: 2319942
log K source: NIST46.2
Delta H source: NIST46.2
#T and ionic strength:
 $\text{Ag}^+ + \text{Glycine}^- = \text{Ag}(\text{Glycine})$
log_k 3.51
delta_h -19.2464 kJ
-gamma 0 0
Id: 209941
log K source: NIST46.2
Delta H source: NIST46.2
#T and ionic strength:
 $\text{Ag}^+ + 2\text{Glycine}^- = \text{Ag}(\text{Glycine})_2^-$
log_k 6.89
delta_h -48.116 kJ
-gamma 0 0
Id: 209942
log K source: NIST46.2
Delta H source: NIST46.2
#T and ionic strength:
 $\text{Ni}^{+2} + \text{Glycine}^- = \text{Ni}(\text{Glycine})^+$
log_k 6.15
delta_h -18.828 kJ
-gamma 0 0
Id: 5409941
log K source: NIST46.2
Delta H source: NIST46.2
#T and ionic strength:
 $\text{Ni}^{+2} + 2\text{Glycine}^- = \text{Ni}(\text{Glycine})_2$
log_k 11.12
delta_h -38.0744 kJ
-gamma 0 0
Id: 5409942
log K source: NIST46.2
Delta H source: NIST46.2
#T and ionic strength:
 $\text{Ni}^{+2} + 3\text{Glycine}^- = \text{Ni}(\text{Glycine})_3^-$
log_k 14.63
delta_h -62.3416 kJ
-gamma 0 0
Id: 5409943
log K source: SCD2.62
Delta H source: SCD2.62
#T and ionic strength:
 $\text{Co}^{+2} + \text{Glycine}^- = \text{Co}(\text{Glycine})^+$
log_k 5.07
delta_h -12 kJ
-gamma 0 0
Id: 2009941

log K source: NIST46.4
 # Delta H source: NIST46.4
 #T and ionic strength: 0.00 25.0
 $\text{Co}^{+2} + 2\text{Glycine}^- = \text{Co}(\text{Glycine})_2$
 log_k 9.07
 delta_h -26 kJ
 -gamma 0 0
 # Id: 2009942
 # log K source: NIST46.4
 # Delta H source: NIST46.4
 #T and ionic strength: 0.00 25.0
 $\text{Co}^{+2} + 3\text{Glycine}^- = \text{Co}(\text{Glycine})_3^-$
 log_k 11.6
 delta_h -41 kJ
 -gamma 0 0
 # Id: 2009943
 # log K source: NIST46.4
 # Delta H source: NIST46.4
 #T and ionic strength: 0.00 25.0
 $\text{Co}^{+2} + \text{Glycine}^- + \text{H}_2\text{O} = \text{CoOH}(\text{Glycine}) + \text{H}^+$
 log_k -5.02
 delta_h 0 kJ
 -gamma 0 0
 # Id: 2009944
 # log K source: NIST46.4
 # Delta H source: NIST46.2
 #T and ionic strength: 0.10 25.0
 $\text{Fe}^{+2} + \text{Glycine}^- = \text{Fe}(\text{Glycine})^+$
 log_k 4.31
 delta_h -15.0624 kJ
 -gamma 0 0
 # Id: 2809941
 # log K source: NIST46.2
 # Delta H source: NIST46.2
 #T and ionic strength:
 $\text{Fe}^{+2} + 2\text{Glycine}^- = \text{Fe}(\text{Glycine})_2$
 log_k 8.29
 delta_h 0 kJ
 -gamma 0 0
 # Id: 2809942
 # log K source: NIST46.2
 # Delta H source: NIST46.2
 #T and ionic strength:
 $\text{Fe}^{+3} + \text{Glycine}^- = \text{Fe}(\text{Glycine})^{+2}$
 log_k 9.38
 delta_h 0 kJ
 -gamma 0 0
 # Id: 2819941
 # log K source: NIST46.2
 # Delta H source: NIST46.2
 #T and ionic strength:
 $\text{Fe}^{+3} + \text{Glycine}^- + \text{H}^+ = \text{FeH}(\text{Glycine})^{+3}$
 log_k 11.55
 delta_h 0 kJ

-gamma 0 0
 # Id: 2819942
 # log K source: NIST46.2
 # Delta H source: NIST46.2
 #T and ionic strength:
 $\text{Mn}^{+2} + \text{Glycine}^- = \text{Mn}(\text{Glycine})^+$
 log_k 3.19
 delta_h -1.2552 kJ
 -gamma 0 0
 # Id: 4709941
 # log K source: NIST46.2
 # Delta H source: NIST46.2
 #T and ionic strength:
 $\text{Mn}^{+2} + 2\text{Glycine}^- = \text{Mn}(\text{Glycine})_2$
 log_k 5.4
 delta_h 0 kJ
 -gamma 0 0
 # Id: 4709942
 # log K source: NIST46.2
 # Delta H source: NIST46.2
 #T and ionic strength:
 $\text{Cr}(\text{OH})_2^{+2} + \text{Glycine}^- + 2\text{H}^+ = \text{Cr}(\text{Glycine})^{+2} + 2\text{H}_2\text{O}$
 log_k 18.7
 delta_h 0 kJ
 -gamma 0 0
 # Id: 2119941
 # log K source: SCD2.62
 # Delta H source: SCD2.62
 #T and ionic strength:
 $\text{Cr}(\text{OH})_2^{+2} + 2\text{Glycine}^- + 2\text{H}^+ = \text{Cr}(\text{Glycine})_2^{+2} + 2\text{H}_2\text{O}$
 log_k 25.6
 delta_h 0 kJ
 -gamma 0 0
 # Id: 2119942
 # log K source: SCD2.62
 # Delta H source: SCD2.62
 #T and ionic strength:
 $\text{Cr}(\text{OH})_2^{+2} + 3\text{Glycine}^- + 2\text{H}^+ = \text{Cr}(\text{Glycine})_3 + 2\text{H}_2\text{O}$
 log_k 31.6
 delta_h 0 kJ
 -gamma 0 0
 # Id: 2119943
 # log K source: SCD2.62
 # Delta H source: SCD2.62
 #T and ionic strength:
 $\text{Mg}^{+2} + \text{Glycine}^- = \text{Mg}(\text{Glycine})^+$
 log_k 2.08
 delta_h 4.184 kJ
 -gamma 0 0
 # Id: 4609941
 # log K source: NIST46.2
 # Delta H source: NIST46.2
 #T and ionic strength:
 $\text{Ca}^{+2} + \text{Glycine}^- = \text{Ca}(\text{Glycine})^+$

log_k 1.39
delta_h -4.184 kJ
-gamma 0 0
Id: 1509941
log K source: NIST46.2
Delta H source: NIST46.2
#T and ionic strength:
 $\text{Ca}^{+2} + \text{Glycine}^- + \text{H}^+ = \text{CaH}(\text{Glycine})^{+2}$
log_k 10.1
delta_h -35.9824 kJ
-gamma 0 0
Id: 1509942
log K source: NIST46.2
Delta H source: NIST46.2
#T and ionic strength:
 $\text{Sr}^{+2} + \text{Glycine}^- = \text{Sr}(\text{Glycine})^{+}$
log_k 0.91
delta_h 0 kJ
-gamma 0 0
Id: 8009941
log K source: NIST46.4
Delta H source: NIST46.2
#T and ionic strength: 0.00 25.0
 $\text{Ba}^{+2} + \text{Glycine}^- = \text{Ba}(\text{Glycine})^{+}$
log_k 0.77
delta_h 0 kJ
-gamma 0 0
Id: 1009941
log K source: NIST46.2
Delta H source: NIST46.2
#T and ionic strength:
 $\text{H}^+ + \text{Salicylate}^{-2} = \text{H}(\text{Salicylate})^{-}$
log_k 13.7
delta_h -35.7732 kJ
-gamma 0 0
Id: 3309951
log K source: NIST46.2
Delta H source: NIST46.2
#T and ionic strength:
 $2\text{H}^+ + \text{Salicylate}^{-2} = \text{H}_2(\text{Salicylate})$
log_k 16.8
delta_h -38.7857 kJ
-gamma 0 0
Id: 3309952
log K source: NIST46.2
Delta H source: NIST46.2
#T and ionic strength:
 $\text{Zn}^{+2} + \text{Salicylate}^{-2} = \text{Zn}(\text{Salicylate})$
log_k 7.71
delta_h 0 kJ
-gamma 0 0
Id: 9509951
log K source: SCD2.62
Delta H source: SCD2.62

#T and ionic strength:
 $\text{Zn}^{+2} + \text{Salicylate-2} + \text{H}^{+} = \text{ZnH(Salicylate)} +$
 log_k 15.5
 delta_h 0 kJ
 -gamma 0 0
 # Id: 9509952
 # log K source: NIST46.2
 # Delta H source: NIST46.2
 #T and ionic strength:
 $\text{Cd}^{+2} + \text{Salicylate-2} = \text{Cd(Salicylate)}$
 log_k 6.2
 delta_h 0 kJ
 -gamma 0 0
 # Id: 1609951
 # log K source: NIST46.2
 # Delta H source: NIST46.2
 #T and ionic strength:
 $\text{Cd}^{+2} + \text{Salicylate-2} + \text{H}^{+} = \text{CdH(Salicylate)} +$
 log_k 16
 delta_h 0 kJ
 -gamma 0 0
 # Id: 1609952
 # log K source: NIST46.2
 # Delta H source: NIST46.2
 #T and ionic strength:
 $\text{Cu}^{+2} + \text{Salicylate-2} = \text{Cu(Salicylate)}$
 log_k 11.3
 delta_h -17.9912 kJ
 -gamma 0 0
 # Id: 2319951
 # log K source: NIST46.2
 # Delta H source: NIST46.2
 #T and ionic strength:
 $\text{Cu}^{+2} + 2\text{Salicylate-2} = \text{Cu(Salicylate)}_2$
 log_k 19.3
 delta_h 0 kJ
 -gamma 0 0
 # Id: 2319952
 # log K source: NIST46.2
 # Delta H source: NIST46.2
 #T and ionic strength:
 $\text{Cu}^{+2} + \text{Salicylate-2} + \text{H}^{+} = \text{CuH(Salicylate)} +$
 log_k 14.8
 delta_h 0 kJ
 -gamma 0 0
 # Id: 2319953
 # log K source: NIST46.2
 # Delta H source: NIST46.2
 #T and ionic strength:
 $\text{Ni}^{+2} + \text{Salicylate-2} = \text{Ni(Salicylate)}$
 log_k 8.2
 delta_h 0 kJ
 -gamma 0 0
 # Id: 5409951

log K source: NIST46.2
 # Delta H source: NIST46.2
 #T and ionic strength:
 $\text{Ni}^{+2} + 2\text{Salicylate}^{-2} = \text{Ni}(\text{Salicylate})_2^{-2}$
 log_k 12.64
 delta_h 0 kJ
 -gamma 0 0
 # Id: 5409952
 # log K source: SCD2.62
 # Delta H source: SCD2.62
 #T and ionic strength:
 $\text{Co}^{+2} + \text{Salicylate}^{-2} = \text{Co}(\text{Salicylate})$
 log_k 7.4289
 delta_h 0 kJ
 -gamma 0 0
 # Id: 2009951
 # log K source: NIST46.4
 # Delta H source: NIST46.2
 #T and ionic strength: 0.10 20.0
 $\text{Co}^{+2} + 2\text{Salicylate}^{-2} = \text{Co}(\text{Salicylate})_2^{-2}$
 log_k 11.8
 delta_h 0 kJ
 -gamma 0 0
 # Id: 2009952
 # log K source: NIST46.4
 # Delta H source: NIST46.2
 #T and ionic strength: 0.10 20.0
 $\text{Fe}^{+2} + \text{Salicylate}^{-2} = \text{Fe}(\text{Salicylate})$
 log_k 7.2
 delta_h 0 kJ
 -gamma 0 0
 # Id: 2809951
 # log K source: NIST46.2
 # Delta H source: NIST46.2
 #T and ionic strength:
 $\text{Fe}^{+2} + 2\text{Salicylate}^{-2} = \text{Fe}(\text{Salicylate})_2^{-2}$
 log_k 11.6
 delta_h 0 kJ
 -gamma 0 0
 # Id: 2809952
 # log K source: NIST46.2
 # Delta H source: NIST46.2
 #T and ionic strength:
 $\text{Fe}^{+3} + \text{Salicylate}^{-2} = \text{Fe}(\text{Salicylate})^{+}$
 log_k 17.6
 delta_h 0 kJ
 -gamma 0 0
 # Id: 2819951
 # log K source: NIST46.2
 # Delta H source: NIST46.2
 #T and ionic strength:
 $\text{Fe}^{+3} + 2\text{Salicylate}^{-2} = \text{Fe}(\text{Salicylate})_2^{-}$
 log_k 29.3
 delta_h 0 kJ

-gamma 0 0
 # Id: 2819952
 # log K source: NIST46.2
 # Delta H source: NIST46.2
 #T and ionic strength:
 $\text{Mn}^{+2} + \text{Salicylate-2} = \text{Mn}(\text{Salicylate})$
 log_k 6.5
 delta_h 0 kJ
 -gamma 0 0
 # Id: 4709951
 # log K source: NIST46.2
 # Delta H source: NIST46.2
 #T and ionic strength:
 $\text{Mn}^{+2} + 2\text{Salicylate-2} = \text{Mn}(\text{Salicylate})_2$
 log_k 10.1
 delta_h 0 kJ
 -gamma 0 0
 # Id: 4709952
 # log K source: NIST46.2
 # Delta H source: NIST46.2
 #T and ionic strength:
 $\text{Be}^{+2} + \text{Salicylate-2} = \text{Be}(\text{Salicylate})$
 log_k 13.3889
 delta_h -31.7732 kJ
 -gamma 0 0
 # Id: 1109951
 # log K source: NIST46.4
 # Delta H source: NIST46.4
 #T and ionic strength: 0.10 25.0
 $\text{Be}^{+2} + 2\text{Salicylate-2} = \text{Be}(\text{Salicylate})_2$
 log_k 23.25
 delta_h 0 kJ
 -gamma 0 0
 # Id: 1109952
 # log K source: NIST46.4
 # Delta H source: NIST46.2
 #T and ionic strength: 0.10 25.0
 $\text{Mg}^{+2} + \text{Salicylate-2} = \text{Mg}(\text{Salicylate})$
 log_k 5.76
 delta_h 0 kJ
 -gamma 0 0
 # Id: 4609951
 # log K source: NIST46.2
 # Delta H source: NIST46.2
 #T and ionic strength:
 $\text{Mg}^{+2} + \text{Salicylate-2} + \text{H}^+ = \text{MgH}(\text{Salicylate})$
 log_k 15.3
 delta_h 0 kJ
 -gamma 0 0
 # Id: 4609952
 # log K source: SCD2.62
 # Delta H source: SCD2.62
 #T and ionic strength:
 $\text{Ca}^{+2} + \text{Salicylate-2} = \text{Ca}(\text{Salicylate})$

log_k 4.05
 delta_h 0 kJ
 -gamma 0 0
 # Id: 1509951
 # log K source: NIST46.2
 # Delta H source: NIST46.2
 #T and ionic strength:
 $\text{Ca}^{+2} + \text{Salicylate-2} + \text{H}^{+} = \text{CaH}(\text{Salicylate})^{+}$
 log_k 14.3
 delta_h 0 kJ
 -gamma 0 0
 # Id: 1509952
 # log K source: NIST46.2
 # Delta H source: NIST46.2
 #T and ionic strength:
 $\text{Ba}^{+2} + \text{Salicylate-2} + \text{H}^{+} = \text{BaH}(\text{Salicylate})^{+}$
 log_k 13.9
 delta_h 0 kJ
 -gamma 0 0
 # Id: 1009951
 # log K source: SCD2.62
 # Delta H source: SCD2.62
 #T and ionic strength:
 $\text{H}^{+} + \text{Glutamate-2} = \text{H}(\text{Glutamate})^{-}$
 log_k 9.96
 delta_h -41.0032 kJ
 -gamma 0 0
 # Id: 3309961
 # log K source: NIST46.2
 # Delta H source: NIST46.2
 #T and ionic strength:
 $2\text{H}^{+} + \text{Glutamate-2} = \text{H}_2(\text{Glutamate})$
 log_k 14.26
 delta_h -43.5136 kJ
 -gamma 0 0
 # Id: 3309962
 # log K source: NIST46.2
 # Delta H source: NIST46.2
 #T and ionic strength:
 $3\text{H}^{+} + \text{Glutamate-2} = \text{H}_3(\text{Glutamate})^{+}$
 log_k 16.42
 delta_h -46.8608 kJ
 -gamma 0 0
 # Id: 3309963
 # log K source: NIST46.2
 # Delta H source: NIST46.2
 #T and ionic strength:
 $\text{Pb}^{+2} + \text{Glutamate-2} = \text{Pb}(\text{Glutamate})$
 log_k 6.43
 delta_h 0 kJ
 -gamma 0 0
 # Id: 6009961
 # log K source: SCD2.62
 # Delta H source: SCD2.62

#T and ionic strength:
 $\text{Pb}^{+2} + 2\text{Glutamate}^{-2} = \text{Pb}(\text{Glutamate})_2^{-2}$
 log_k 8.61
 delta_h 0 kJ
 -gamma 0 0
 # Id: 6009962
 # log K source: SCD2.62
 # Delta H source: SCD2.62
 #T and ionic strength:
 $\text{Pb}^{+2} + \text{Glutamate}^{-2} + \text{H}^{+} = \text{PbH}(\text{Glutamate})^{+}$
 log_k 14.08
 delta_h 0 kJ
 -gamma 0 0
 # Id: 6009963
 # log K source: SCD2.62
 # Delta H source: SCD2.62
 #T and ionic strength:
 $\text{Al}^{+3} + \text{Glutamate}^{-2} + \text{H}^{+} = \text{AlH}(\text{Glutamate})^{+2}$
 log_k 13.07
 delta_h 0 kJ
 -gamma 0 0
 # Id: 309961
 # log K source: NIST46.2
 # Delta H source: NIST46.2
 #T and ionic strength:
 $\text{Zn}^{+2} + \text{Glutamate}^{-2} = \text{Zn}(\text{Glutamate})$
 log_k 6.2
 delta_h 0 kJ
 -gamma 0 0
 # Id: 9509961
 # log K source: SCD2.62
 # Delta H source: SCD2.62
 #T and ionic strength:
 $\text{Zn}^{+2} + 2\text{Glutamate}^{-2} = \text{Zn}(\text{Glutamate})_2^{-2}$
 log_k 9.13
 delta_h 0 kJ
 -gamma 0 0
 # Id: 9509962
 # log K source: SCD2.62
 # Delta H source: SCD2.62
 #T and ionic strength:
 $\text{Zn}^{+2} + 3\text{Glutamate}^{-2} = \text{Zn}(\text{Glutamate})_3^{-4}$
 log_k 9.8
 delta_h 0 kJ
 -gamma 0 0
 # Id: 9509963
 # log K source: SCD2.62
 # Delta H source: SCD2.62
 #T and ionic strength:
 $\text{Cd}^{+2} + \text{Glutamate}^{-2} = \text{Cd}(\text{Glutamate})$
 log_k 4.7
 delta_h 0 kJ
 -gamma 0 0
 # Id: 1609961

log K source: NIST46.2
 # Delta H source: NIST46.2
 #T and ionic strength:
 $\text{Cd}^{+2} + 2\text{Glutamate}^{-2} = \text{Cd}(\text{Glutamate})_2^{-2}$
 log_k 7.59
 delta_h 0 kJ
 -gamma 0 0
 # Id: 1609962
 # log K source: NIST46.2
 # Delta H source: NIST46.2
 #T and ionic strength:
 $\text{Hg}(\text{OH})_2 + \text{Glutamate}^{-2} + 2\text{H}^{+} = \text{Hg}(\text{Glutamate}) + 2\text{H}_2\text{O}$
 log_k 19.8
 delta_h 0 kJ
 -gamma 0 0
 # Id: 3619961
 # log K source: SCD2.62
 # Delta H source: SCD2.62
 #T and ionic strength:
 $\text{Hg}(\text{OH})_2 + 2\text{Glutamate}^{-2} + 2\text{H}^{+} = \text{Hg}(\text{Glutamate})_2^{-2} + 2\text{H}_2\text{O}$
 log_k 26.2
 delta_h 0 kJ
 -gamma 0 0
 # Id: 3619962
 # log K source: SCD2.62
 # Delta H source: SCD2.62
 #T and ionic strength:
 $\text{Cu}^{+2} + \text{Glutamate}^{-2} = \text{Cu}(\text{Glutamate})$
 log_k 9.17
 delta_h -20.92 kJ
 -gamma 0 0
 # Id: 2319961
 # log K source: NIST46.2
 # Delta H source: NIST46.2
 #T and ionic strength:
 $\text{Cu}^{+2} + 2\text{Glutamate}^{-2} = \text{Cu}(\text{Glutamate})_2^{-2}$
 log_k 15.78
 delta_h -48.116 kJ
 -gamma 0 0
 # Id: 2319962
 # log K source: NIST46.2
 # Delta H source: NIST46.2
 #T and ionic strength:
 $\text{Cu}^{+2} + \text{Glutamate}^{-2} + \text{H}^{+} = \text{CuH}(\text{Glutamate})^{+}$
 log_k 13.3
 delta_h -28.0328 kJ
 -gamma 0 0
 # Id: 2319963
 # log K source: NIST46.2
 # Delta H source: NIST46.2
 #T and ionic strength:
 $\text{Ag}^{+} + \text{Glutamate}^{-2} = \text{Ag}(\text{Glutamate})^{-}$
 log_k 4.22
 delta_h 0 kJ

-gamma 0 0
 # Id: 209961
 # log K source: NIST46.2
 # Delta H source: NIST46.2
 #T and ionic strength:
 $\text{Ag}^+ + 2\text{Glutamate}^{2-} = \text{Ag}(\text{Glutamate})^{2-3}$
 log_k 7.36
 delta_h 0 kJ
 -gamma 0 0
 # Id: 209962
 # log K source: SCD2.62
 # Delta H source: SCD2.62
 #T and ionic strength:
 $2\text{Ag}^+ + \text{Glutamate}^{2-} = \text{Ag}_2(\text{Glutamate})$
 log_k 3.4
 delta_h 0 kJ
 -gamma 0 0
 # Id: 209963
 # log K source: NIST46.2
 # Delta H source: NIST46.2
 #T and ionic strength:
 $\text{Ni}^{2+} + \text{Glutamate}^{2-} = \text{Ni}(\text{Glutamate})$
 log_k 6.47
 delta_h 0 kJ
 -gamma 0 0
 # Id: 5409961
 # log K source: NIST46.2
 # Delta H source: NIST46.2
 #T and ionic strength:
 $\text{Ni}^{2+} + 2\text{Glutamate}^{2-} = \text{Ni}(\text{Glutamate})^{2-2}$
 log_k 10.7
 delta_h -30.9616 kJ
 -gamma 0 0
 # Id: 5409962
 # log K source: NIST46.2
 # Delta H source: NIST46.2
 #T and ionic strength:
 $\text{Co}^{2+} + \text{Glutamate}^{2-} = \text{Co}(\text{Glutamate})$
 log_k 5.4178
 delta_h 0 kJ
 -gamma 0 0
 # Id: 2009961
 # log K source: NIST46.4
 # Delta H source: NIST46.2
 #T and ionic strength: 0.10 25.0
 $\text{Co}^{2+} + 2\text{Glutamate}^{2-} = \text{Co}(\text{Glutamate})^{2-2}$
 log_k 8.7178
 delta_h 0 kJ
 -gamma 0 0
 # Id: 2009962
 # log K source: NIST46.4
 # Delta H source: NIST46.2
 #T and ionic strength: 0.10 25.0
 $\text{Mn}^{2+} + \text{Glutamate}^{2-} = \text{Mn}(\text{Glutamate})$

log_k 4.95
 delta_h 0 kJ
 -gamma 0 0
 # Id: 4709961
 # log K source: SCD2.62
 # Delta H source: SCD2.62
 #T and ionic strength:
 $\text{Mn}^{+2} + 2\text{Glutamate}^{-2} = \text{Mn}(\text{Glutamate})_2^{-2}$
 log_k 8.48
 delta_h 0 kJ
 -gamma 0 0
 # Id: 4709962
 # log K source: SCD2.62
 # Delta H source: SCD2.62
 #T and ionic strength:
 $\text{Cr}(\text{OH})_2^{+} + \text{Glutamate}^{-2} + 2\text{H}^{+} = \text{Cr}(\text{Glutamate})^{+} + 2\text{H}_2\text{O}$
 log_k 22.6
 delta_h 0 kJ
 -gamma 0 0
 # Id: 2119961
 # log K source: SCD2.62
 # Delta H source: SCD2.62
 #T and ionic strength:
 $\text{Cr}(\text{OH})_2^{+} + 2\text{Glutamate}^{-2} + 2\text{H}^{+} = \text{Cr}(\text{Glutamate})_2^{-} + 2\text{H}_2\text{O}$
 log_k 30.7
 delta_h 0 kJ
 -gamma 0 0
 # Id: 2119962
 # log K source: SCD2.62
 # Delta H source: SCD2.62
 #T and ionic strength:
 $\text{Cr}(\text{OH})_2^{+} + \text{Glutamate}^{-2} + 3\text{H}^{+} = \text{CrH}(\text{Glutamate})_2 + 2\text{H}_2\text{O}$
 log_k 25.2
 delta_h 0 kJ
 -gamma 0 0
 # Id: 2119963
 # log K source: SCD2.62
 # Delta H source: SCD2.62
 #T and ionic strength:
 $\text{Mg}^{+2} + \text{Glutamate}^{-2} = \text{Mg}(\text{Glutamate})$
 log_k 2.8
 delta_h 0 kJ
 -gamma 0 0
 # Id: 4609961
 # log K source: NIST46.2
 # Delta H source: NIST46.2
 #T and ionic strength:
 $\text{Ca}^{+2} + \text{Glutamate}^{-2} = \text{Ca}(\text{Glutamate})$
 log_k 2.06
 delta_h 0 kJ
 -gamma 0 0
 # Id: 1509961
 # log K source: NIST46.2
 # Delta H source: NIST46.2

#T and ionic strength:
 $\text{Ca}^{+2} + \text{Glutamate-2} + \text{H}^{+} = \text{CaH}(\text{Glutamate})^{+}$
 log_k 11.13
 delta_h 0 kJ
 -gamma 0 0
 # Id: 1509962
 # log K source: NIST46.2
 # Delta H source: NIST46.2
 #T and ionic strength:
 $\text{Sr}^{+2} + \text{Glutamate-2} = \text{Sr}(\text{Glutamate})$
 log_k 2.2278
 delta_h 0 kJ
 -gamma 0 0
 # Id: 8009961
 # log K source: NIST46.4
 # Delta H source: NIST46.2
 #T and ionic strength: 0.10 25.0
 $\text{Ba}^{+2} + \text{Glutamate-2} = \text{Ba}(\text{Glutamate})$
 log_k 2.14
 delta_h 0 kJ
 -gamma 0 0
 # Id: 1009961
 # log K source: NIST46.2
 # Delta H source: NIST46.2
 #T and ionic strength:
 $\text{H}^{+} + \text{Phthalate-2} = \text{H}(\text{Phthalate})^{-}$
 log_k 5.408
 delta_h 2.1757 kJ
 -gamma 0 0
 # Id: 3309971
 # log K source: NIST46.2
 # Delta H source: NIST46.2
 #T and ionic strength:
 $2\text{H}^{+} + \text{Phthalate-2} = \text{H}_2(\text{Phthalate})$
 log_k 8.358
 delta_h 4.8534 kJ
 -gamma 0 0
 # Id: 3309972
 # log K source: NIST46.2
 # Delta H source: NIST46.2
 #T and ionic strength:
 $\text{Pb}^{+2} + \text{Phthalate-2} = \text{Pb}(\text{Phthalate})$
 log_k 4.26
 delta_h 0 kJ
 -gamma 0 0
 # Id: 6009971
 # log K source: SCD2.62
 # Delta H source: SCD2.62
 #T and ionic strength:
 $\text{Pb}^{+2} + 2\text{Phthalate-2} = \text{Pb}(\text{Phthalate})_2^{-2}$
 log_k 4.83
 delta_h 0 kJ
 -gamma 0 0
 # Id: 6009972

log K source: NIST46.2
 # Delta H source: NIST46.2
 #T and ionic strength:
 $\text{Pb}^{+2} + \text{Phthalate}^{-2} + \text{H}^{+} = \text{PbH(Phthalate)}^{+}$
 log_k 6.98
 delta_h 0 kJ
 -gamma 0 0
 # Id: 6009973
 # log K source: NIST46.2
 # Delta H source: NIST46.2
 #T and ionic strength:
 $\text{Al}^{+3} + \text{Phthalate}^{-2} = \text{Al(Phthalate)}^{+}$
 log_k 4.56
 delta_h 0 kJ
 -gamma 0 0
 # Id: 309971
 # log K source: NIST46.2
 # Delta H source: NIST46.2
 #T and ionic strength:
 $\text{Al}^{+3} + 2\text{Phthalate}^{-2} = \text{Al(Phthalate)}_2^{-}$
 log_k 7.2
 delta_h 0 kJ
 -gamma 0 0
 # Id: 309972
 # log K source: NIST46.2
 # Delta H source: NIST46.2
 #T and ionic strength:
 $\text{Zn}^{+2} + \text{Phthalate}^{-2} = \text{Zn(Phthalate)}$
 log_k 2.91
 delta_h 13.3888 kJ
 -gamma 0 0
 # Id: 9509971
 # log K source: NIST46.2
 # Delta H source: NIST46.2
 #T and ionic strength:
 $\text{Zn}^{+2} + 2\text{Phthalate}^{-2} = \text{Zn(Phthalate)}_2^{-2}$
 log_k 4.2
 delta_h 0 kJ
 -gamma 0 0
 # Id: 9509972
 # log K source: NIST46.2
 # Delta H source: NIST46.2
 #T and ionic strength:
 $\text{Cd}^{+2} + \text{Phthalate}^{-2} = \text{Cd(Phthalate)}$
 log_k 3.43
 delta_h 0 kJ
 -gamma 0 0
 # Id: 1609971
 # log K source: NIST46.2
 # Delta H source: NIST46.2
 #T and ionic strength:
 $\text{Cd}^{+2} + \text{Phthalate}^{-2} + \text{H}^{+} = \text{CdH(Phthalate)}^{+}$
 log_k 6.3
 delta_h 0 kJ

-gamma 0 0
 # Id: 1609973
 # log K source: NIST46.2
 # Delta H source: NIST46.2
 #T and ionic strength:
 $\text{Cd}^{+2} + 2\text{Phthalate}^{-2} = \text{Cd}(\text{Phthalate})_2^{-2}$
 log_k 3.7
 delta_h 0 kJ
 -gamma 0 0
 # Id: 1609972
 # log K source: NIST46.2
 # Delta H source: NIST46.2
 #T and ionic strength:
 $\text{Cu}^{+2} + \text{Phthalate}^{-2} = \text{Cu}(\text{Phthalate})$
 log_k 4.02
 delta_h 8.368 kJ
 -gamma 0 0
 # Id: 2319971
 # log K source: NIST46.2
 # Delta H source: NIST46.2
 #T and ionic strength:
 $\text{Cu}^{+2} + \text{Phthalate}^{-2} + \text{H}^{+} = \text{CuH}(\text{Phthalate})^{+}$
 log_k 7.1
 delta_h 3.8493 kJ
 -gamma 0 0
 # Id: 2319970
 # log K source: NIST46.2
 # Delta H source: NIST46.2
 #T and ionic strength:
 $\text{Cu}^{+2} + 2\text{Phthalate}^{-2} = \text{Cu}(\text{Phthalate})_2^{-2}$
 log_k 5.3
 delta_h 15.8992 kJ
 -gamma 0 0
 # Id: 2319972
 # log K source: NIST46.2
 # Delta H source: NIST46.2
 #T and ionic strength:
 $\text{Ni}^{+2} + \text{Phthalate}^{-2} = \text{Ni}(\text{Phthalate})$
 log_k 2.95
 delta_h 7.5312 kJ
 -gamma 0 0
 # Id: 5409971
 # log K source: NIST46.2
 # Delta H source: NIST46.2
 #T and ionic strength:
 $\text{Ni}^{+2} + \text{Phthalate}^{-2} + \text{H}^{+} = \text{NiH}(\text{Phthalate})^{+}$
 log_k 6.6
 delta_h 0 kJ
 -gamma 0 0
 # Id: 5409972
 # log K source: NIST46.2
 # Delta H source: NIST46.2
 #T and ionic strength:
 $\text{Co}^{+2} + \text{Phthalate}^{-2} = \text{Co}(\text{Phthalate})$

log_k 2.83
 delta_h 7.9 kJ
 -gamma 0 0
 # Id: 2009971
 # log K source: NIST46.4
 # Delta H source: NIST46.4
 #T and ionic strength: 0.00 25.0
 $\text{Co}^{+2} + \text{H}^{+} + \text{Phthalate-2} = \text{CoH(Phthalate)}^{+}$
 log_k 7.227
 delta_h 0 kJ
 -gamma 0 0
 # Id: 2009972
 # log K source: NIST46.4
 # Delta H source: NIST46.2
 #T and ionic strength: 0.50 25.0
 $\text{Mn}^{+2} + \text{Phthalate-2} = \text{Mn(Phthalate)}$
 log_k 2.74
 delta_h 10.0416 kJ
 -gamma 0 0
 # Id: 4709971
 # log K source: NIST46.2
 # Delta H source: NIST46.2
 #T and ionic strength:
 $\text{Cr(OH)}^{2+} + \text{Phthalate-2} + 2\text{H}^{+} = \text{Cr(Phthalate)}^{+} + 2\text{H}_2\text{O}$
 log_k 16.3
 delta_h 0 kJ
 -gamma 0 0
 # Id: 2119971
 # log K source: SCD2.62
 # Delta H source: SCD2.62
 #T and ionic strength:
 $\text{Cr(OH)}^{2+} + 2\text{Phthalate-2} + 2\text{H}^{+} = \text{Cr(Phthalate)}^{2-} + 2\text{H}_2\text{O}$
 log_k 21.2
 delta_h 0 kJ
 -gamma 0 0
 # Id: 2119972
 # log K source: SCD2.62
 # Delta H source: SCD2.62
 #T and ionic strength:
 $\text{Cr(OH)}^{2+} + 3\text{Phthalate-2} + 2\text{H}^{+} = \text{Cr(Phthalate)}^{3-} + 2\text{H}_2\text{O}$
 log_k 23.3
 delta_h 0 kJ
 -gamma 0 0
 # Id: 2119973
 # log K source: SCD2.62
 # Delta H source: SCD2.62
 #T and ionic strength:
 $\text{Be}^{+2} + \text{Phthalate-2} = \text{Be(Phthalate)}$
 log_k 4.8278
 delta_h 0 kJ
 -gamma 0 0
 # Id: 1109971
 # log K source: NIST46.4
 # Delta H source: NIST46.2

#T and ionic strength: 0.10 25.0
 $\text{Be}^{+2} + 2\text{Phthalate}^{-2} = \text{Be}(\text{Phthalate})_2^{-2}$
 log_k 6.5478
 delta_h 0 kJ
 -gamma 0 0
 # Id: 1109972
 # log K source: NIST46.4
 # Delta H source: NIST46.2
 #T and ionic strength: 0.10 25.0
 $\text{Mg}^{+2} + \text{Phthalate}^{-2} = \text{Mg}(\text{Phthalate})$
 log_k 2.49
 delta_h 0 kJ
 -gamma 0 0
 # Id: 4609971
 # log K source: SCD2.62
 # Delta H source: SCD2.62
 #T and ionic strength:
 $\text{Ca}^{+2} + \text{Phthalate}^{-2} = \text{Ca}(\text{Phthalate})$
 log_k 2.45
 delta_h 0 kJ
 -gamma 0 0
 # Id: 1509970
 # log K source: NIST46.2
 # Delta H source: NIST46.2
 #T and ionic strength:
 $\text{Ca}^{+2} + \text{Phthalate}^{-2} + \text{H}^{+} = \text{CaH}(\text{Phthalate})^{+}$
 log_k 6.43
 delta_h 0 kJ
 -gamma 0 0
 # Id: 1509971
 # log K source: NIST46.2
 # Delta H source: NIST46.2
 #T and ionic strength:
 $\text{Ba}^{+2} + \text{Phthalate}^{-2} = \text{Ba}(\text{Phthalate})$
 log_k 2.33
 delta_h 0 kJ
 -gamma 0 0
 # Id: 1009971
 # log K source: NIST46.2
 # Delta H source: NIST46.2
 #T and ionic strength:
 $\text{Na}^{+} + \text{Phthalate}^{-2} = \text{Na}(\text{Phthalate})^{-}$
 log_k 0.8
 delta_h 4.184 kJ
 -gamma 0 0
 # Id: 5009970
 # log K source: NIST46.2
 # Delta H source: NIST46.2
 #T and ionic strength:
 $\text{K}^{+} + \text{Phthalate}^{-2} = \text{K}(\text{Phthalate})^{-}$
 log_k 0.7
 delta_h 3.7656 kJ
 -gamma 0 0
 # Id: 4109971

log K source: NIST46.2
Delta H source: NIST46.2
#T and ionic strength:
PHASES
Sulfur
 $S + H^+ + 2e^- = HS^-$
log_k -2.1449
delta_h -16.3 kJ
Semetal(hex
 $Se + H^+ + 2e^- = HSe^-$
log_k -7.7084
delta_h 15.9 kJ
Semetal(am)
 $Se + H^+ + 2e^- = HSe^-$
log_k -7.1099
delta_h 10.8784 kJ
Sbmetal
 $Sb + 3H_2O = Sb(OH)_3 + 3H^+ + 3e^-$
log_k -11.6889
delta_h 83.89 kJ
Snmetal(wht)
 $Sn + 2H_2O = Sn(OH)_2 + 2H^+ + 2e^-$
log_k -2.3266
delta_h -0 kJ
Pbmetal
 $Pb = Pb^{+2} + 2e^-$
log_k 4.2462
delta_h 0.92 kJ
Tlmetal
 $Tl = Tl^+ + e^-$
log_k 5.6762
delta_h 5.36 kJ
Znmetal
 $Zn = Zn^{+2} + 2e^-$
log_k 25.7886
delta_h -153.39 kJ
Cdmetal(alpha)
 $Cd = Cd^{+2} + 2e^-$
log_k 13.5147
delta_h -75.33 kJ
Cdmetal(gamma)
 $Cd = Cd^{+2} + 2e^-$
log_k 13.618
delta_h -75.92 kJ
Hgmetal(l)
 $Hg = 0.5Hg_2^{+2} + e^-$
log_k -13.4517
delta_h 83.435 kJ
Cumetal
 $Cu = Cu^+ + e^-$
log_k -8.756
delta_h 71.67 kJ
Agmetal
 $Ag = Ag^+ + e^-$

log_k -13.5065
 delta_h 105.79 kJ
 Crmetal
 $\text{Cr} = \text{Cr}^{+2} + 2\text{e}^-$
 log_k 30.4831
 delta_h -172 kJ
 Vmetal
 $\text{V} = \text{V}^{+3} + 3\text{e}^-$
 log_k 44.0253
 delta_h -259 kJ
 Stibnite
 $\text{Sb}_2\text{S}_3 + 6\text{H}_2\text{O} = 2\text{Sb}(\text{OH})_3 + 3\text{H}^+ + 3\text{HS}^-$
 log_k -50.46
 delta_h 293.78 kJ
 Orpiment
 $\text{As}_2\text{S}_3 + 6\text{H}_2\text{O} = 2\text{H}_3\text{AsO}_3 + 3\text{HS}^- + 3\text{H}^+$
 log_k -61.0663
 delta_h 350.68 kJ
 Realgar
 $\text{AsS} + 3\text{H}_2\text{O} = \text{H}_3\text{AsO}_3 + \text{HS}^- + 2\text{H}^+ + \text{e}^-$
 log_k -19.747
 delta_h 127.8 kJ
 SnS
 $\text{SnS} + 2\text{H}_2\text{O} = \text{Sn}(\text{OH})_2 + \text{H}^+ + \text{HS}^-$
 log_k -19.114
 delta_h -0 kJ
 SnS2
 $\text{SnS}_2 + 6\text{H}_2\text{O} = \text{Sn}(\text{OH})_6^{2-} + 4\text{H}^+ + 2\text{HS}^-$
 log_k -57.4538
 delta_h -0 kJ
 Galena
 $\text{PbS} + \text{H}^+ = \text{Pb}^{+2} + \text{HS}^-$
 log_k -13.97
 delta_h 80 kJ
 Ti2S
 $\text{Ti}_2\text{S} + \text{H}^+ = 2\text{Ti}^+ + \text{HS}^-$
 log_k -7.19
 delta_h 91.52 kJ
 ZnS(am)
 $\text{ZnS} + \text{H}^+ = \text{Zn}^{+2} + \text{HS}^-$
 log_k -9.052
 delta_h 15.3553 kJ
 Sphalerite
 $\text{ZnS} + \text{H}^+ = \text{Zn}^{+2} + \text{HS}^-$
 log_k -11.45
 delta_h 30 kJ
 Wurtzite
 $\text{ZnS} + \text{H}^+ = \text{Zn}^{+2} + \text{HS}^-$
 log_k -8.95
 delta_h 21.171 kJ
 Greenockite
 $\text{CdS} + \text{H}^+ = \text{Cd}^{+2} + \text{HS}^-$
 log_k -14.36
 delta_h 55 kJ

Hg₂S
 $\text{Hg}_2\text{S} + \text{H}^+ = \text{Hg}_2^{2+} + \text{HS}^-$
 log_k -11.6765
 delta_h 69.7473 kJ
 Cinnabar
 $\text{HgS} + 2\text{H}_2\text{O} = \text{Hg}(\text{OH})_2 + \text{H}^+ + \text{HS}^-$
 log_k -45.694
 delta_h 253.76 kJ
 Metacinnabar
 $\text{HgS} + 2\text{H}_2\text{O} = \text{Hg}(\text{OH})_2 + \text{H}^+ + \text{HS}^-$
 log_k -45.094
 delta_h 253.72 kJ
 Chalcocite
 $\text{Cu}_2\text{S} + \text{H}^+ = 2\text{Cu}^+ + \text{HS}^-$
 log_k -34.92
 delta_h 168 kJ
 Djurleite
 $\text{Cu}_{0.066}\text{Cu}_{1.868}\text{S} + \text{H}^+ = 0.066\text{Cu}^{2+} + 1.868\text{Cu}^+ + \text{HS}^-$
 log_k -33.92
 delta_h 200.334 kJ
 Anilite
 $\text{Cu}_{0.25}\text{Cu}_{1.5}\text{S} + \text{H}^+ = 0.25\text{Cu}^{2+} + 1.5\text{Cu}^+ + \text{HS}^-$
 log_k -31.878
 delta_h 182.15 kJ
 BlaubleiII
 $\text{Cu}_{0.6}\text{Cu}_{0.8}\text{S} + \text{H}^+ = 0.6\text{Cu}^{2+} + 0.8\text{Cu}^+ + \text{HS}^-$
 log_k -27.279
 delta_h -0 kJ
 BlaubleiI
 $\text{Cu}_{0.9}\text{Cu}_{0.2}\text{S} + \text{H}^+ = 0.9\text{Cu}^{2+} + 0.2\text{Cu}^+ + \text{HS}^-$
 log_k -24.162
 delta_h -0 kJ
 Covellite
 $\text{CuS} + \text{H}^+ = \text{Cu}^{2+} + \text{HS}^-$
 log_k -22.3
 delta_h 97 kJ
 Chalcopyrite
 $\text{CuFeS}_2 + 2\text{H}^+ = \text{Cu}^{2+} + \text{Fe}^{2+} + 2\text{HS}^-$
 log_k -35.27
 delta_h 148.448 kJ
 Acanthite
 $\text{Ag}_2\text{S} + \text{H}^+ = 2\text{Ag}^+ + \text{HS}^-$
 log_k -36.22
 delta_h 227 kJ
 NiS(alpha)
 $\text{NiS} + \text{H}^+ = \text{Ni}^{2+} + \text{HS}^-$
 log_k -5.6
 delta_h -0 kJ
 NiS(beta)
 $\text{NiS} + \text{H}^+ = \text{Ni}^{2+} + \text{HS}^-$
 log_k -11.1
 delta_h -0 kJ
 NiS(gamma)
 $\text{NiS} + \text{H}^+ = \text{Ni}^{2+} + \text{HS}^-$

log_k -12.8
 delta_h -0 kJ
 CoS(alpha)
 $\text{CoS} + \text{H}^+ = \text{Co}^{+2} + \text{HS}^-$
 log_k -7.44
 delta_h -0 kJ
 CoS(beta)
 $\text{CoS} + \text{H}^+ = \text{Co}^{+2} + \text{HS}^-$
 log_k -11.07
 delta_h -0 kJ
 FeS(ppt)
 $\text{FeS} + \text{H}^+ = \text{Fe}^{+2} + \text{HS}^-$
 log_k -2.95
 delta_h -11 kJ
 Greigite
 $\text{Fe}_3\text{S}_4 + 4\text{H}^+ = 2\text{Fe}^{+3} + \text{Fe}^{+2} + 4\text{HS}^-$
 log_k -45.035
 delta_h -0 kJ
 Mackinawite
 $\text{FeS} + \text{H}^+ = \text{Fe}^{+2} + \text{HS}^-$
 log_k -3.6
 delta_h -0 kJ
 Pyrite
 $\text{FeS}_2 + 2\text{H}^+ + 2\text{e}^- = \text{Fe}^{+2} + 2\text{HS}^-$
 log_k -18.5082
 delta_h 49.844 kJ
 MnS(grn)
 $\text{MnS} + \text{H}^+ = \text{Mn}^{+2} + \text{HS}^-$
 log_k 0.17
 delta_h -32 kJ
 MnS(pnk)
 $\text{MnS} + \text{H}^+ = \text{Mn}^{+2} + \text{HS}^-$
 log_k 3.34
 delta_h -0 kJ
 MoS2
 $\text{MoS}_2 + 4\text{H}_2\text{O} = \text{MoO}_4^{2-} + 6\text{H}^+ + 2\text{HS}^- + 2\text{e}^-$
 log_k -70.2596
 delta_h 389.02 kJ
 BeS
 $\text{BeS} + \text{H}^+ = \text{Be}^{+2} + \text{HS}^-$
 log_k 19.38
 delta_h -0 kJ
 BaS
 $\text{BaS} + \text{H}^+ = \text{Ba}^{+2} + \text{HS}^-$
 log_k 16.18
 delta_h -0 kJ
 Hg2(Cyanide)2
 $\text{Hg}_2(\text{Cyanide})_2 = \text{Hg}_2^{+2} + 2\text{Cyanide}^-$
 log_k -39.3
 delta_h -0 kJ
 CuCyanide
 $\text{CuCyanide} = \text{Cu}^+ + \text{Cyanide}^-$
 log_k -19.5
 delta_h -19 kJ

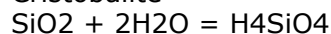
AgCyanide
 $\text{AgCyanide} = \text{Ag}^+ + \text{Cyanide}^-$
 $\log_k -15.74$
 $\text{delta_h } 110.395 \text{ kJ}$
 $\text{Ag}_2(\text{Cyanide})_2$
 $\text{Ag}_2(\text{Cyanide})_2 = 2\text{Ag}^+ + 2\text{Cyanide}^-$
 $\log_k -11.3289$
 $\text{delta_h } -0 \text{ kJ}$
 NaCyanide(cubic)
 $\text{NaCyanide} = \text{Cyanide}^- + \text{Na}^+$
 $\log_k 1.6012$
 $\text{delta_h } 0.969 \text{ kJ}$
 KCyanide(cubic)
 $\text{KCyanide} = \text{Cyanide}^- + \text{K}^+$
 $\log_k 1.4188$
 $\text{delta_h } 11.93 \text{ kJ}$
 $\text{Pb}_2\text{Fe(Cyanide)}_6$
 $\text{Pb}_2\text{Fe(Cyanide)}_6 = 2\text{Pb}^{+2} + \text{Fe}^{+2} + 6\text{Cyanide}^-$
 $\log_k -53.42$
 $\text{delta_h } -0 \text{ kJ}$
 $\text{Zn}_2\text{Fe(Cyanide)}_6$
 $\text{Zn}_2\text{Fe(Cyanide)}_6 = 2\text{Zn}^{+2} + \text{Fe}^{+2} + 6\text{Cyanide}^-$
 $\log_k -51.08$
 $\text{delta_h } -0 \text{ kJ}$
 $\text{Cd}_2\text{Fe(Cyanide)}_6$
 $\text{Cd}_2\text{Fe(Cyanide)}_6 = 2\text{Cd}^{+2} + \text{Fe}^{+2} + 6\text{Cyanide}^-$
 $\log_k -52.78$
 $\text{delta_h } -0 \text{ kJ}$
 $\text{Ag}_4\text{Fe(Cyanide)}_6$
 $\text{Ag}_4\text{Fe(Cyanide)}_6 = 4\text{Ag}^+ + \text{Fe}^{+2} + 6\text{Cyanide}^-$
 $\log_k -79.47$
 $\text{delta_h } -0 \text{ kJ}$
 $\text{Ag}_3\text{Fe(Cyanide)}_6$
 $\text{Ag}_3\text{Fe(Cyanide)}_6 = 3\text{Ag}^+ + \text{Fe}^{+3} + 6\text{Cyanide}^-$
 $\log_k -72.7867$
 $\text{delta_h } -0 \text{ kJ}$
 $\text{Mn}_3(\text{Fe(Cyanide)}_6)_2$
 $\text{Mn}_3(\text{Fe(Cyanide)}_6)_2 = 3\text{Mn}^{+2} + 2\text{Fe}^{+3} + 12\text{Cyanide}^-$
 $\log_k -105.4$
 $\text{delta_h } -0 \text{ kJ}$
 Sb_2Se_3
 $\text{Sb}_2\text{Se}_3 + 6\text{H}_2\text{O} = 2\text{Sb(OH)}_3 + 3\text{HSe}^- + 3\text{H}^+$
 $\log_k -67.7571$
 $\text{delta_h } 343.046 \text{ kJ}$
 SnSe
 $\text{SnSe} + 2\text{H}_2\text{O} = \text{Sn(OH)}_2 + \text{H}^+ + \text{HSe}^-$
 $\log_k -30.494$
 $\text{delta_h } -0 \text{ kJ}$
 SnSe_2
 $\text{SnSe}_2 + 6\text{H}_2\text{O} = \text{Sn(OH)}_6^{-2} + 4\text{H}^+ + 2\text{HSe}^-$
 $\log_k -65.1189$
 $\text{delta_h } -0 \text{ kJ}$
 Clausthalite
 $\text{PbSe} + \text{H}^+ = \text{Pb}^{+2} + \text{HSe}^-$

log_k -27.1
 delta_h 119.72 kJ
 Ti_2Se
 $\text{Ti}_2\text{Se} + \text{H}^+ = 2\text{Ti}^+ + \text{HSe}^-$
 log_k -18.1
 delta_h 85.62 kJ
 ZnSe
 $\text{ZnSe} + \text{H}^+ = \text{Zn}^{+2} + \text{HSe}^-$
 log_k -14.4
 delta_h 25.51 kJ
 CdSe
 $\text{CdSe} + \text{H}^+ = \text{Cd}^{+2} + \text{HSe}^-$
 log_k -20.2
 delta_h 75.9814 kJ
 HgSe
 $\text{HgSe} + 2\text{H}_2\text{O} = \text{Hg}(\text{OH})_2 + \text{H}^+ + \text{HSe}^-$
 log_k -55.694
 delta_h -0 kJ
 $\text{Cu}_2\text{Se}(\alpha)$
 $\text{Cu}_2\text{Se} + \text{H}^+ = 2\text{Cu}^+ + \text{HSe}^-$
 log_k -45.8
 delta_h 214.263 kJ
 Cu_3Se_2
 $\text{Cu}_3\text{Se}_2 + 2\text{H}^+ = 2\text{HSe}^- + 2\text{Cu}^+ + \text{Cu}^{+2}$
 log_k -63.4911
 delta_h 340.327 kJ
 CuSe
 $\text{CuSe} + \text{H}^+ = \text{Cu}^{+2} + \text{HSe}^-$
 log_k -33.1
 delta_h 121.127 kJ
 CuSe_2
 $\text{CuSe}_2 + 2\text{H}^+ + 2\text{e}^- = 2\text{HSe}^- + \text{Cu}^{+2}$
 log_k -33.3655
 delta_h 140.582 kJ
 Ag_2Se
 $\text{Ag}_2\text{Se} + \text{H}^+ = 2\text{Ag}^+ + \text{HSe}^-$
 log_k -48.7
 delta_h 265.48 kJ
 NiSe
 $\text{NiSe} + \text{H}^+ = \text{Ni}^{+2} + \text{HSe}^-$
 log_k -17.7
 delta_h -0 kJ
 CoSe
 $\text{CoSe} + \text{H}^+ = \text{Co}^{+2} + \text{HSe}^-$
 log_k -16.2
 delta_h -0 kJ
 FeSe
 $\text{FeSe} + \text{H}^+ = \text{Fe}^{+2} + \text{HSe}^-$
 log_k -11
 delta_h 2.092 kJ
 Ferroselite
 $\text{FeSe}_2 + 2\text{H}^+ + 2\text{e}^- = 2\text{HSe}^- + \text{Fe}^{+2}$
 log_k -18.5959
 delta_h 47.2792 kJ

MnSe
 $\text{MnSe} + \text{H}^+ = \text{Mn}^{+2} + \text{HSe}^-$
 log_k 3.5
 delta_h -98.15 kJ
 AlSb
 $\text{AlSb} + 3\text{H}_2\text{O} = \text{Sb}(\text{OH})_3 + 6\text{e}^- + \text{Al}^{+3} + 3\text{H}^+$
 log_k 65.6241
 delta_h -0 kJ
 ZnSb
 $\text{ZnSb} + 3\text{H}_2\text{O} = \text{Sb}(\text{OH})_3 + 5\text{e}^- + \text{Zn}^{+2} + 3\text{H}^+$
 log_k 11.0138
 delta_h -54.8773 kJ
 CdSb
 $\text{CdSb} + 3\text{H}_2\text{O} = \text{Sb}(\text{OH})_3 + 5\text{e}^- + 3\text{H}^+ + \text{Cd}^{+2}$
 log_k -0.3501
 delta_h 22.36 kJ
 Cu2Sb:3H2O
 $\text{Cu}_2\text{Sb} \cdot 3\text{H}_2\text{O} = \text{Sb}(\text{OH})_3 + 6\text{e}^- + 3\text{H}^+ + \text{Cu}^+ + \text{Cu}^{+2}$
 log_k -34.8827
 delta_h 233.237 kJ
 Cu3Sb
 $\text{Cu}_3\text{Sb} + 3\text{H}_2\text{O} = \text{Sb}(\text{OH})_3 + 6\text{e}^- + 3\text{H}^+ + 3\text{Cu}^+$
 log_k -42.5937
 delta_h 308.131 kJ
 #Ag4Sb
 $\# \text{Ag}_4\text{Sb} + 3\text{H}_2\text{O} = \text{Sb}(\text{OH})_3 + 6\text{e}^- + 3\text{Ag}^+ + 3\text{H}^+$
 $\# \text{log}_k -56.1818$
 $\# \text{delta}_h -0 \text{ kJ}$
 Breithauptite
 $\text{NiSb} + 3\text{H}_2\text{O} = \text{Sb}(\text{OH})_3 + 5\text{e}^- + 3\text{H}^+ + \text{Ni}^{+2}$
 log_k -18.5225
 delta_h 96.0019 kJ
 MnSb
 $\text{MnSb} + 3\text{H}_2\text{O} = \text{Mn}^{+3} + \text{Sb}(\text{OH})_3 + 6\text{e}^- + 3\text{H}^+$
 log_k -2.9099
 delta_h 21.1083 kJ
 Mn2Sb
 $\text{Mn}_2\text{Sb} + 3\text{H}_2\text{O} = 2\text{Mn}^{+2} + \text{Sb}(\text{OH})_3 + 7\text{e}^- + 3\text{H}^+$
 log_k 61.0796
 delta_h -0 kJ
 USb2
 $\text{USb}_2 + 8\text{H}_2\text{O} = \text{UO}_2^{+2} + 2\text{Sb}(\text{OH})_3 + 12\text{e}^- + 10\text{H}^+$
 log_k 29.5771
 delta_h -103.56 kJ
 U3Sb4
 $\text{U}_3\text{Sb}_4 + 12\text{H}_2\text{O} = 3\text{U}^{+4} + 4\text{Sb}(\text{OH})_3 + 24\text{e}^- + 12\text{H}^+$
 log_k 152.383
 delta_h -986.04 kJ
 Mg2Sb3
 $\text{Mg}_2\text{Sb}_3 + 9\text{H}_2\text{O} = 2\text{Mg}^{+2} + 3\text{Sb}(\text{OH})_3 + 9\text{H}^+ + 13\text{e}^-$
 log_k 74.6838
 delta_h -0 kJ
 Ca3Sb2
 $\text{Ca}_3\text{Sb}_2 + 6\text{H}_2\text{O} = 3\text{Ca}^{+2} + 2\text{Sb}(\text{OH})_3 + 6\text{H}^+ + 12\text{e}^-$

log_k 142.974
 delta_h -732.744 kJ
 NaSb
 $\text{NaSb} + 3\text{H}_2\text{O} = \text{Na}^+ + \text{Sb}(\text{OH})_3 + 3\text{H}^+ + 4\text{e}^-$
 log_k 23.1658
 delta_h -93.45 kJ
 Na₃Sb
 $\text{Na}_3\text{Sb} + 3\text{H}_2\text{O} = 3\text{Na}^+ + \text{Sb}(\text{OH})_3 + 3\text{H}^+ + 6\text{e}^-$
 log_k 94.4517
 delta_h -432.13 kJ
 SeO₂
 $\text{SeO}_2 + \text{H}_2\text{O} = \text{HSeO}_3^- + \text{H}^+$
 log_k 0.1246
 delta_h 1.4016 kJ
 SeO₃
 $\text{SeO}_3 + \text{H}_2\text{O} = \text{SeO}_4^{2-} + 2\text{H}^+$
 log_k 21.044
 delta_h -146.377 kJ
 Sb₂O₅
 $\text{Sb}_2\text{O}_5 + 7\text{H}_2\text{O} = 2\text{Sb}(\text{OH})_6^- + 2\text{H}^+$
 log_k -9.6674
 delta_h -0 kJ
 SbO₂
 $\text{SbO}_2 + 4\text{H}_2\text{O} = \text{Sb}(\text{OH})_6^- + \text{e}^- + 2\text{H}^+$
 log_k -27.8241
 delta_h -0 kJ
 Sb₂O₄
 $\text{Sb}_2\text{O}_4 + 2\text{H}_2\text{O} + 2\text{H}^+ + 2\text{e}^- = 2\text{Sb}(\text{OH})_3$
 log_k 3.4021
 delta_h -68.04 kJ
 Sb₄O₆(cubic)
 $\text{Sb}_4\text{O}_6 + 6\text{H}_2\text{O} = 4\text{Sb}(\text{OH})_3$
 log_k -18.2612
 delta_h 61.1801 kJ
 Sb₄O₆(orth)
 $\text{Sb}_4\text{O}_6 + 6\text{H}_2\text{O} = 4\text{Sb}(\text{OH})_3$
 log_k -17.9012
 delta_h 37.6801 kJ
 Sb(OH)₃
 $\text{Sb}(\text{OH})_3 = \text{Sb}(\text{OH})_3$
 log_k -7.1099
 delta_h 30.1248 kJ
 Senarmontite
 $\text{Sb}_2\text{O}_3 + 3\text{H}_2\text{O} = 2\text{Sb}(\text{OH})_3$
 log_k -12.3654
 delta_h 30.6478 kJ
 Valentinite
 $\text{Sb}_2\text{O}_3 + 3\text{H}_2\text{O} = 2\text{Sb}(\text{OH})_3$
 log_k -8.4806
 delta_h 19.0163 kJ
 Chalcedony
 $\text{SiO}_2 + 2\text{H}_2\text{O} = \text{H}_4\text{SiO}_4$
 log_k -3.55
 delta_h 19.7 kJ

Cristobalite



log_k -3.35

delta_h 20.006 kJ

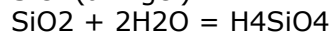
Quartz



log_k -4

delta_h 22.36 kJ

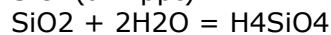
SiO2(am-gel)



log_k -2.71

delta_h 14 kJ

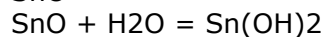
SiO2(am-ppt)



log_k -2.74

delta_h 15.15 kJ

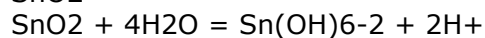
SnO



log_k -4.9141

delta_h -0 kJ

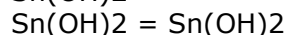
SnO2



log_k -28.9749

delta_h -0 kJ

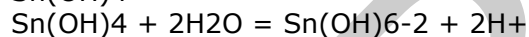
Sn(OH)2



log_k -5.4309

delta_h -0 kJ

Sn(OH)4



log_k -22.2808

delta_h -0 kJ

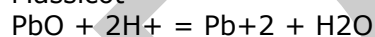
H2Sn(OH)6



log_k -23.5281

delta_h -0 kJ

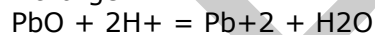
Massicot



log_k 12.894

delta_h -66.848 kJ

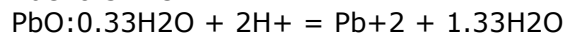
Litharge



log_k 12.694

delta_h -65.501 kJ

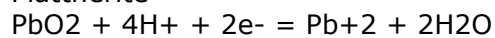
PbO:0.3H2O



log_k 12.98

delta_h -0 kJ

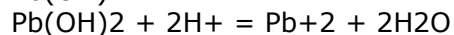
Plattnerite



log_k 49.6001

delta_h -296.27 kJ

Pb(OH)2

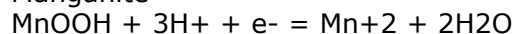


log_k 8.15
 delta_h -58.5342 kJ
 Pb2O(OH)2
 $\text{Pb2O(OH)2} + 4\text{H}^+ = 2\text{Pb}^{+2} + 3\text{H2O}$
 log_k 26.188
 delta_h -0 kJ
 Al(OH)3(am)
 $\text{Al(OH)3} + 3\text{H}^+ = \text{Al}^{+3} + 3\text{H2O}$
 log_k 10.8
 delta_h -111 kJ
 Boehmite
 $\text{AlOOH} + 3\text{H}^+ = \text{Al}^{+3} + 2\text{H2O}$
 log_k 8.578
 delta_h -117.696 kJ
 Diaspore
 $\text{AlOOH} + 3\text{H}^+ = \text{Al}^{+3} + 2\text{H2O}$
 log_k 6.873
 delta_h -103.052 kJ
 Gibbsite
 $\text{Al(OH)3} + 3\text{H}^+ = \text{Al}^{+3} + 3\text{H2O}$
 log_k 8.291
 delta_h -95.3952 kJ
 Ti2O
 $\text{Ti2O} + 2\text{H}^+ = 2\text{Ti}^+ + \text{H2O}$
 log_k 27.0915
 delta_h -96.41 kJ
 TiOH
 $\text{TiOH} + \text{H}^+ = \text{Ti}^+ + \text{H2O}$
 log_k 12.9186
 delta_h -41.57 kJ
 Avicennite
 $\text{Ti2O3} + 3\text{H2O} = 2\text{Ti(OH)3}$
 log_k -13
 delta_h -0 kJ
 Ti(OH)3
 $\text{Ti(OH)3} = \text{Ti(OH)3}$
 log_k -5.441
 delta_h -0 kJ
 Zn(OH)2(am)
 $\text{Zn(OH)2} + 2\text{H}^+ = \text{Zn}^{+2} + 2\text{H2O}$
 log_k 12.474
 delta_h -80.62 kJ
 Zn(OH)2
 $\text{Zn(OH)2} + 2\text{H}^+ = \text{Zn}^{+2} + 2\text{H2O}$
 log_k 12.2
 delta_h -0 kJ
 Zn(OH)2(beta)
 $\text{Zn(OH)2} + 2\text{H}^+ = \text{Zn}^{+2} + 2\text{H2O}$
 log_k 11.754
 delta_h -83.14 kJ
 Zn(OH)2(gamma)
 $\text{Zn(OH)2} + 2\text{H}^+ = \text{Zn}^{+2} + 2\text{H2O}$
 log_k 11.734
 delta_h -0 kJ

$\text{Zn(OH)}_2(\text{epsilon})$
 $\text{Zn(OH)}_2 + 2\text{H}^+ = \text{Zn}^{+2} + 2\text{H}_2\text{O}$
 $\log_k 11.534$
 $\Delta H -81.8 \text{ kJ}$
 $\text{ZnO}(\text{active})$
 $\text{ZnO} + 2\text{H}^+ = \text{Zn}^{+2} + \text{H}_2\text{O}$
 $\log_k 11.1884$
 $\Delta H -88.76 \text{ kJ}$
 Zincite
 $\text{ZnO} + 2\text{H}^+ = \text{Zn}^{+2} + \text{H}_2\text{O}$
 $\log_k 11.334$
 $\Delta H -89.62 \text{ kJ}$
 $\text{Cd(OH)}_2(\text{am})$
 $\text{Cd(OH)}_2 + 2\text{H}^+ = \text{Cd}^{+2} + 2\text{H}_2\text{O}$
 $\log_k 13.73$
 $\Delta H -86.9017 \text{ kJ}$
 Cd(OH)_2
 $\text{Cd(OH)}_2 + 2\text{H}^+ = \text{Cd}^{+2} + 2\text{H}_2\text{O}$
 $\log_k 13.644$
 $\Delta H -94.62 \text{ kJ}$
 Monteponite
 $\text{CdO} + 2\text{H}^+ = \text{Cd}^{+2} + \text{H}_2\text{O}$
 $\log_k 15.1034$
 $\Delta H -103.4 \text{ kJ}$
 $\text{Hg}_2(\text{OH})_2$
 $\text{Hg}_2(\text{OH})_2 + 2\text{H}^+ = \text{Hg}_2^{+2} + 2\text{H}_2\text{O}$
 $\log_k 5.2603$
 $\Delta H -0 \text{ kJ}$
 Montroydite
 $\text{HgO} + \text{H}_2\text{O} = \text{Hg(OH)}_2$
 $\log_k -3.64$
 $\Delta H -38.9 \text{ kJ}$
 Hg(OH)_2
 $\text{Hg(OH)}_2 = \text{Hg(OH)}_2$
 $\log_k -3.4963$
 $\Delta H -0 \text{ kJ}$
 Cuprite
 $\text{Cu}_2\text{O} + 2\text{H}^+ = 2\text{Cu}^+ + \text{H}_2\text{O}$
 $\log_k -1.406$
 $\Delta H -124.02 \text{ kJ}$
 Cu(OH)_2
 $\text{Cu(OH)}_2 + 2\text{H}^+ = \text{Cu}^{+2} + 2\text{H}_2\text{O}$
 $\log_k 8.674$
 $\Delta H -56.42 \text{ kJ}$
 Tenorite
 $\text{CuO} + 2\text{H}^+ = \text{Cu}^{+2} + \text{H}_2\text{O}$
 $\log_k 7.644$
 $\Delta H -64.867 \text{ kJ}$
 Ag_2O
 $\text{Ag}_2\text{O} + 2\text{H}^+ = 2\text{Ag}^+ + \text{H}_2\text{O}$
 $\log_k 12.574$
 $\Delta H -45.62 \text{ kJ}$
 Ni(OH)_2
 $\text{Ni(OH)}_2 + 2\text{H}^+ = \text{Ni}^{+2} + 2\text{H}_2\text{O}$

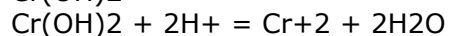
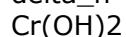
log_k 12.794
 delta_h -95.96 kJ
 Bunsenite
 $\text{NiO} + 2\text{H}^+ = \text{Ni}^{+2} + \text{H}_2\text{O}$
 log_k 12.4456
 delta_h -100.13 kJ
 CoO
 $\text{CoO} + 2\text{H}^+ = \text{Co}^{+2} + \text{H}_2\text{O}$
 log_k 13.5864
 delta_h -106.295 kJ
 Co(OH)₂
 $\text{Co(OH)}_2 + 2\text{H}^+ = \text{Co}^{+2} + 2\text{H}_2\text{O}$
 log_k 13.094
 delta_h -0 kJ
 Co(OH)₃
 $\text{Co(OH)}_3 + 3\text{H}^+ = \text{Co}^{+3} + 3\text{H}_2\text{O}$
 log_k -2.309
 delta_h -92.43 kJ
 #Wustite-0.11
 $\text{# WUSTITE-0.11} + 2\text{H}^+ = 0.947\text{Fe}^{+2} + \text{H}_2\text{O}$
 # log_k 11.6879
 # delta_h -103.938 kJ
 Fe(OH)₂
 $\text{Fe(OH)}_2 + 2\text{H}^+ = \text{Fe}^{+2} + 2\text{H}_2\text{O}$
 log_k 13.564
 delta_h -0 kJ
 Ferrihydrite
 $\text{Fe(OH)}_3 + 3\text{H}^+ = \text{Fe}^{+3} + 3\text{H}_2\text{O}$
 log_k 3.191
 delta_h -73.374 kJ
 Fe₃(OH)₈
 $\text{Fe}_3(\text{OH})_8 + 8\text{H}^+ = 2\text{Fe}^{+3} + \text{Fe}^{+2} + 8\text{H}_2\text{O}$
 log_k 20.222
 delta_h -0 kJ
 Goethite
 $\text{FeOOH} + 3\text{H}^+ = \text{Fe}^{+3} + 2\text{H}_2\text{O}$
 log_k 0.491
 delta_h -60.5843 kJ
 Pyrolusite
 $\text{MnO}_2 + 4\text{H}^+ + 2\text{e}^- = \text{Mn}^{+2} + 2\text{H}_2\text{O}$
 log_k 41.38
 delta_h -272 kJ
 Birnessite
 $\text{MnO}_2 + 4\text{H}^+ + \text{e}^- = \text{Mn}^{+3} + 2\text{H}_2\text{O}$
 log_k 18.091
 delta_h -0 kJ
 Nsutite
 $\text{MnO}_2 + 4\text{H}^+ + \text{e}^- = \text{Mn}^{+3} + 2\text{H}_2\text{O}$
 log_k 17.504
 delta_h -0 kJ
 Pyrochroite
 $\text{Mn(OH)}_2 + 2\text{H}^+ = \text{Mn}^{+2} + 2\text{H}_2\text{O}$
 log_k 15.194
 delta_h -97.0099 kJ

Manganite



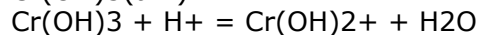
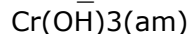
log_k 25.34

delta_h -0 kJ



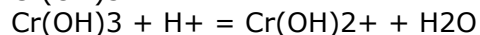
log_k 10.8189

delta_h -35.6058 kJ



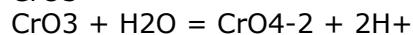
log_k -0.75

delta_h -0 kJ



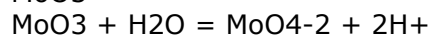
log_k 1.3355

delta_h -29.7692 kJ



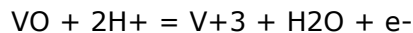
log_k -3.2105

delta_h -5.2091 kJ



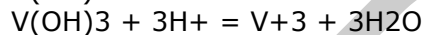
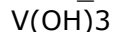
log_k -8

delta_h -0 kJ



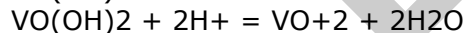
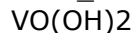
log_k 14.7563

delta_h -113.041 kJ



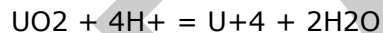
log_k 7.591

delta_h -0 kJ



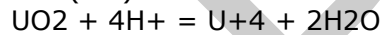
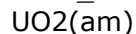
log_k 5.1506

delta_h -0 kJ



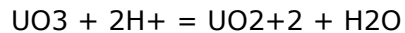
log_k -4.6693

delta_h -77.86 kJ



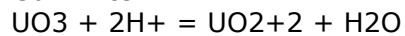
log_k 0.934

delta_h -109.746 kJ



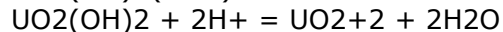
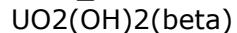
log_k 7.7

delta_h -81.0299 kJ



log_k 7.6718

delta_h -81.0299 kJ



log_k 5.6116
 delta_h -56.7599 kJ
 Schoepite
 $\text{UO}_2(\text{OH})_2 \cdot \text{H}_2\text{O} + 2\text{H}^+ = \text{UO}_2^{2+} + 3\text{H}_2\text{O}$
 log_k 5.994
 delta_h -49.79 kJ
 Be(OH)₂(am)
 $\text{Be}(\text{OH})_2 + 2\text{H}^+ = \text{Be}^{2+} + 2\text{H}_2\text{O}$
 log_k 7.194
 delta_h -0 kJ
 Be(OH)₂(alpha)
 $\text{Be}(\text{OH})_2 + 2\text{H}^+ = \text{Be}^{2+} + 2\text{H}_2\text{O}$
 log_k 6.894
 delta_h -0 kJ
 Be(OH)₂(beta)
 $\text{Be}(\text{OH})_2 + 2\text{H}^+ = \text{Be}^{2+} + 2\text{H}_2\text{O}$
 log_k 6.494
 delta_h -0 kJ
 Brucite
 $\text{Mg}(\text{OH})_2 + 2\text{H}^+ = \text{Mg}^{2+} + 2\text{H}_2\text{O}$
 log_k 16.844
 delta_h -113.996 kJ
 Periclase
 $\text{MgO} + 2\text{H}^+ = \text{Mg}^{2+} + \text{H}_2\text{O}$
 log_k 21.5841
 delta_h -151.23 kJ
 Mg(OH)₂(active)
 $\text{Mg}(\text{OH})_2 + 2\text{H}^+ = \text{Mg}^{2+} + 2\text{H}_2\text{O}$
 log_k 18.794
 delta_h -0 kJ
 Lime
 $\text{CaO} + 2\text{H}^+ = \text{Ca}^{2+} + \text{H}_2\text{O}$
 log_k 32.6993
 delta_h -193.91 kJ
 Portlandite
 $\text{Ca}(\text{OH})_2 + 2\text{H}^+ = \text{Ca}^{2+} + 2\text{H}_2\text{O}$
 log_k 22.804
 delta_h -128.62 kJ
 Ba(OH)₂·8H₂O
 $\text{Ba}(\text{OH})_2 \cdot 8\text{H}_2\text{O} + 2\text{H}^+ = \text{Ba}^{2+} + 10\text{H}_2\text{O}$
 log_k 24.394
 delta_h -54.32 kJ
 Cu(SbO₃)₂
 $\text{Cu}(\text{SbO}_3)_2 + 6\text{H}^+ + 4\text{e}^- = 2\text{Sb}(\text{OH})_3 + \text{Cu}^{2+}$
 log_k 45.2105
 delta_h -0 kJ
 Arsenolite
 $\text{As}_4\text{O}_6 + 6\text{H}_2\text{O} = 4\text{H}_3\text{AsO}_3$
 log_k -2.76
 delta_h 59.9567 kJ
 Claudetite
 $\text{As}_4\text{O}_6 + 6\text{H}_2\text{O} = 4\text{H}_3\text{AsO}_3$
 log_k -3.065
 delta_h 55.6054 kJ

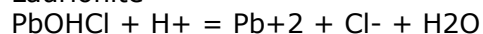
As₂O₅
 $\text{As}_2\text{O}_5 + 3\text{H}_2\text{O} = 2\text{H}_3\text{AsO}_4$
 log_k 6.7061
 delta_h -22.64 kJ
 Pb₂O₃
 $\text{Pb}_2\text{O}_3 + 6\text{H}^+ + 2\text{e}^- = 2\text{Pb}^{+2} + 3\text{H}_2\text{O}$
 log_k 61.04
 delta_h -0 kJ
 Minium
 $\text{Pb}_3\text{O}_4 + 8\text{H}^+ + 2\text{e}^- = 3\text{Pb}^{+2} + 4\text{H}_2\text{O}$
 log_k 73.5219
 delta_h -421.874 kJ
 Al₂O₃
 $\text{Al}_2\text{O}_3 + 6\text{H}^+ = 2\text{Al}^{+3} + 3\text{H}_2\text{O}$
 log_k 19.6524
 delta_h -258.59 kJ
 Co₃O₄
 $\text{Co}_3\text{O}_4 + 8\text{H}^+ = \text{Co}^{+2} + 2\text{Co}^{+3} + 4\text{H}_2\text{O}$
 log_k -10.4956
 delta_h -107.5 kJ
 CoFe₂O₄
 $\text{CoFe}_2\text{O}_4 + 8\text{H}^+ = \text{Co}^{+2} + 2\text{Fe}^{+3} + 4\text{H}_2\text{O}$
 log_k -3.5281
 delta_h -158.82 kJ
 Magnetite
 $\text{Fe}_3\text{O}_4 + 8\text{H}^+ = 2\text{Fe}^{+3} + \text{Fe}^{+2} + 4\text{H}_2\text{O}$
 log_k 3.4028
 delta_h -208.526 kJ
 Hercynite
 $\text{FeAl}_2\text{O}_4 + 8\text{H}^+ = \text{Fe}^{+2} + 2\text{Al}^{+3} + 4\text{H}_2\text{O}$
 log_k 22.893
 delta_h -313.92 kJ
 Hematite
 $\text{Fe}_2\text{O}_3 + 6\text{H}^+ = 2\text{Fe}^{+3} + 3\text{H}_2\text{O}$
 log_k -1.418
 delta_h -128.987 kJ
 Maghemite
 $\text{Fe}_2\text{O}_3 + 6\text{H}^+ = 2\text{Fe}^{+3} + 3\text{H}_2\text{O}$
 log_k 6.386
 delta_h -0 kJ
 Lepidocrocite
 $\text{FeOOH} + 3\text{H}^+ = \text{Fe}^{+3} + 2\text{H}_2\text{O}$
 log_k 1.371
 delta_h -0 kJ
 Hausmannite
 $\text{Mn}_3\text{O}_4 + 8\text{H}^+ + 2\text{e}^- = 3\text{Mn}^{+2} + 4\text{H}_2\text{O}$
 log_k 61.03
 delta_h -421 kJ
 Bixbyite
 $\text{Mn}_2\text{O}_3 + 6\text{H}^+ = 2\text{Mn}^{+3} + 3\text{H}_2\text{O}$
 log_k -0.6445
 delta_h -124.49 kJ
 Cr₂O₃
 $\text{Cr}_2\text{O}_3 + \text{H}_2\text{O} + 2\text{H}^+ = 2\text{Cr}(\text{OH})_2^+$

log_k -2.3576
 delta_h -50.731 kJ
 #V2O3
 # $V_2O_3 + 3H^+ = V^{+3} + 1.5H_2O$
 # log_k 4.9
 # delta_h -82.5085 kJ
 V3O5
 $V_3O_5 + 4H^+ = 3VO^{+2} + 2H_2O + 2e^-$
 log_k 1.8361
 delta_h -98.46 kJ
 #V2O4
 # $V_2O_4 + 2H^+ = VO^{+2} + H_2O$
 # log_k 4.27
 # delta_h -58.8689 kJ
 V4O7
 $V_4O_7 + 6H^+ = 4VO^{+2} + 3H_2O + 2e^-$
 log_k 7.1865
 delta_h -163.89 kJ
 V6O13
 $V_6O_{13} + 2H^+ = 6VO^{+2} + H_2O + 4e^-$
 log_k -60.86
 delta_h 271.5 kJ
 V2O5
 $V_2O_5 + 2H^+ = 2VO^{+2} + H_2O$
 log_k -1.36
 delta_h 34 kJ
 U4O9
 $U_4O_9 + 18H^+ + 2e^- = 4U^{+4} + 9H_2O$
 log_k -3.0198
 delta_h -426.87 kJ
 U3O8
 $U_3O_8 + 16H^+ + 4e^- = 3U^{+4} + 8H_2O$
 log_k 21.0834
 delta_h -485.44 kJ
 Spinel
 $MgAl_2O_4 + 8H^+ = Mg^{+2} + 2Al^{+3} + 4H_2O$
 log_k 36.8476
 delta_h -388.012 kJ
 Magnesioferrite
 $Fe_2MgO_4 + 8H^+ = Mg^{+2} + 2Fe^{+3} + 4H_2O$
 log_k 16.8597
 delta_h -278.92 kJ
 Natron
 $Na_2CO_3 \cdot 10H_2O = 2Na^+ + CO_3^{+2} + 10H_2O$
 log_k -1.311
 delta_h 65.8771 kJ
 Cuprousferrite
 $CuFeO_2 + 4H^+ = Cu^+ + Fe^{+3} + 2H_2O$
 log_k -8.9171
 delta_h -15.89 kJ
 Cupricferrite
 $CuFe_2O_4 + 8H^+ = Cu^{+2} + 2Fe^{+3} + 4H_2O$
 log_k 5.9882
 delta_h -210.21 kJ

FeCr_2O_4
 $\text{FeCr}_2\text{O}_4 + 4\text{H}^+ = 2\text{Cr}(\text{OH})_2^+ + \text{Fe}^{+2}$
 $\log_k 7.2003$
 $\Delta H -140.4 \text{ kJ}$
 MgCr_2O_4
 $\text{MgCr}_2\text{O}_4 + 4\text{H}^+ = 2\text{Cr}(\text{OH})_2^+ + \text{Mg}^{+2}$
 $\log_k 16.2007$
 $\Delta H -179.4 \text{ kJ}$
 SbF_3
 $\text{SbF}_3 + 3\text{H}_2\text{O} = \text{Sb}(\text{OH})_3 + 3\text{H}^+ + 3\text{F}^-$
 $\log_k -10.2251$
 $\Delta H -6.7279 \text{ kJ}$
 PbF_2
 $\text{PbF}_2 = \text{Pb}^{+2} + 2\text{F}^-$
 $\log_k -7.44$
 $\Delta H 20 \text{ kJ}$
 ZnF_2
 $\text{ZnF}_2 = \text{Zn}^{+2} + 2\text{F}^-$
 $\log_k -0.5343$
 $\Delta H -59.69 \text{ kJ}$
 CdF_2
 $\text{CdF}_2 = \text{Cd}^{+2} + 2\text{F}^-$
 $\log_k -1.2124$
 $\Delta H -46.22 \text{ kJ}$
 Hg_2F_2
 $\text{Hg}_2\text{F}_2 = \text{Hg}_2^{+2} + 2\text{F}^-$
 $\log_k -10.3623$
 $\Delta H -18.486 \text{ kJ}$
 CuF
 $\text{CuF} = \text{Cu}^+ + \text{F}^-$
 $\log_k -4.9056$
 $\Delta H 16.648 \text{ kJ}$
 CuF_2
 $\text{CuF}_2 = \text{Cu}^{+2} + 2\text{F}^-$
 $\log_k 1.115$
 $\Delta H -66.901 \text{ kJ}$
 $\text{CuF}_2 \cdot 2\text{H}_2\text{O}$
 $\text{CuF}_2 \cdot 2\text{H}_2\text{O} = \text{Cu}^{+2} + 2\text{F}^- + 2\text{H}_2\text{O}$
 $\log_k -4.55$
 $\Delta H -15.2716 \text{ kJ}$
 $\text{AgF} \cdot 4\text{H}_2\text{O}$
 $\text{AgF} \cdot 4\text{H}_2\text{O} = \text{Ag}^+ + \text{F}^- + 4\text{H}_2\text{O}$
 $\log_k 1.0491$
 $\Delta H 15.4202 \text{ kJ}$
 CoF_2
 $\text{CoF}_2 = \text{Co}^{+2} + 2\text{F}^-$
 $\log_k -1.5969$
 $\Delta H -57.368 \text{ kJ}$
 CoF_3
 $\text{CoF}_3 = \text{Co}^{+3} + 3\text{F}^-$
 $\log_k -1.4581$
 $\Delta H -123.692 \text{ kJ}$
 CrF_3
 $\text{CrF}_3 + 2\text{H}_2\text{O} = \text{Cr}(\text{OH})_2^+ + 3\text{F}^- + 2\text{H}^+$

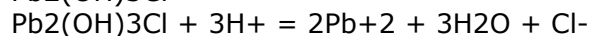
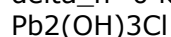
log_k -11.3367
 delta_h -23.3901 kJ
 VF4
 $\text{VF}_4 + \text{H}_2\text{O} = \text{VO}^{2+} + 4\text{F}^- + 2\text{H}^+$
 log_k 14.93
 delta_h -199.117 kJ
 UF4
 $\text{UF}_4 = \text{U}^{4+} + 4\text{F}^-$
 log_k -29.5371
 delta_h -79.0776 kJ
 UF4:2.5H2O
 $\text{UF}_4:2.5\text{H}_2\text{O} = \text{U}^{4+} + 4\text{F}^- + 2.5\text{H}_2\text{O}$
 log_k -32.7179
 delta_h 24.325 kJ
 MgF2
 $\text{MgF}_2 = \text{Mg}^{2+} + 2\text{F}^-$
 log_k -8.13
 delta_h -8 kJ
 Fluorite
 $\text{CaF}_2 = \text{Ca}^{2+} + 2\text{F}^-$
 log_k -10.5
 delta_h 8 kJ
 SrF2
 $\text{SrF}_2 = \text{Sr}^{2+} + 2\text{F}^-$
 log_k -8.58
 delta_h 4 kJ
 BaF2
 $\text{BaF}_2 = \text{Ba}^{2+} + 2\text{F}^-$
 log_k -5.82
 delta_h 4 kJ
 Cryolite
 $\text{Na}_3\text{AlF}_6 = 3\text{Na}^+ + \text{Al}^{3+} + 6\text{F}^-$
 log_k -33.84
 delta_h 38 kJ
 SbCl3
 $\text{SbCl}_3 + 3\text{H}_2\text{O} = \text{Sb}(\text{OH})_3 + 3\text{Cl}^- + 3\text{H}^+$
 log_k 0.5719
 delta_h -35.18 kJ
 SnCl2
 $\text{SnCl}_2 + 2\text{H}_2\text{O} = \text{Sn}(\text{OH})_2 + 2\text{H}^+ + 2\text{Cl}^-$
 log_k -9.2752
 delta_h -0 kJ
 Cotunnite
 $\text{PbCl}_2 = \text{Pb}^{2+} + 2\text{Cl}^-$
 log_k -4.78
 delta_h 26.166 kJ
 Matlockite
 $\text{PbClF} = \text{Pb}^{2+} + \text{Cl}^- + \text{F}^-$
 log_k -8.9733
 delta_h 33.19 kJ
 Phosgenite
 $\text{PbCl}_2:\text{PbCO}_3 = 2\text{Pb}^{2+} + 2\text{Cl}^- + \text{CO}_3^{2-}$
 log_k -19.81
 delta_h -0 kJ

Laurionite



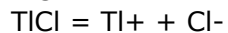
log_k 0.623

delta_h -0 kJ



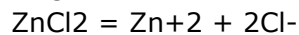
log_k 8.793

delta_h -0 kJ



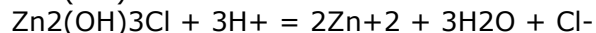
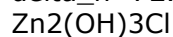
log_k -3.74

delta_h 41 kJ



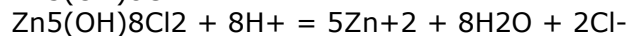
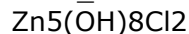
log_k 7.05

delta_h -72.5 kJ



log_k 15.191

delta_h -0 kJ



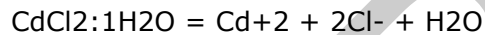
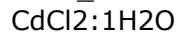
log_k 38.5

delta_h -0 kJ



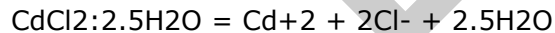
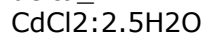
log_k -0.6588

delta_h -18.58 kJ



log_k -1.6932

delta_h -7.47 kJ



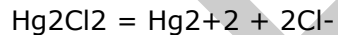
log_k -1.913

delta_h 7.2849 kJ



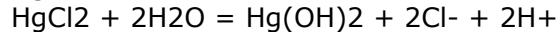
log_k 3.5373

delta_h -30.93 kJ



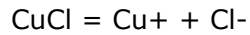
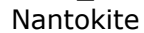
log_k -17.91

delta_h 92 kJ



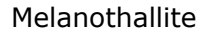
log_k -21.2621

delta_h 107.82 kJ



log_k -6.73

delta_h 42.662 kJ

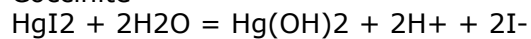


log_k 6.2572
 delta_h -63.407 kJ
 Atacamite
 $\text{Cu}_2(\text{OH})_3\text{Cl} + 3\text{H}^+ = 2\text{Cu}^{+2} + 3\text{H}_2\text{O} + \text{Cl}^-$
 log_k 7.391
 delta_h -93.43 kJ
 Cerargyrite
 $\text{AgCl} = \text{Ag}^+ + \text{Cl}^-$
 log_k -9.75
 delta_h 65.2 kJ
 CoCl₂
 $\text{CoCl}_2 = \text{Co}^{+2} + 2\text{Cl}^-$
 log_k 8.2672
 delta_h -79.815 kJ
 CoCl₂:6H₂O
 $\text{CoCl}_2:6\text{H}_2\text{O} = \text{Co}^{+2} + 2\text{Cl}^- + 6\text{H}_2\text{O}$
 log_k 2.5365
 delta_h 8.0598 kJ
 (Co(NH₃)₆)Cl₃
 $(\text{Co}(\text{NH}_3)_6)\text{Cl}_3 + 6\text{H}^+ = \text{Co}^{+3} + 6\text{NH}_4^+ + 3\text{Cl}^-$
 log_k 20.0317
 delta_h -33.1 kJ
 (Co(NH₃)₅OH₂)Cl₃
 $(\text{Co}(\text{NH}_3)_5\text{OH}_2)\text{Cl}_3 + 5\text{H}^+ = \text{Co}^{+3} + 5\text{NH}_4^+ + 3\text{Cl}^- + \text{H}_2\text{O}$
 log_k 11.7351
 delta_h -25.37 kJ
 (Co(NH₃)₅Cl)Cl₂
 $(\text{Co}(\text{NH}_3)_5\text{Cl})\text{Cl}_2 + 5\text{H}^+ = \text{Co}^{+3} + 5\text{NH}_4^+ + 3\text{Cl}^-$
 log_k 4.5102
 delta_h -10.74 kJ
 Fe(OH)₂·7Cl₂·3H₂O
 $\text{Fe}(\text{OH})_2 \cdot 7\text{Cl}_2 \cdot 3\text{H}_2\text{O} + 2.7\text{H}^+ = \text{Fe}^{+3} + 2.7\text{H}_2\text{O} + 0.3\text{Cl}^-$
 log_k -3.04
 delta_h -0 kJ
 MnCl₂:4H₂O
 $\text{MnCl}_2:4\text{H}_2\text{O} = \text{Mn}^{+2} + 2\text{Cl}^- + 4\text{H}_2\text{O}$
 log_k 2.7151
 delta_h -10.83 kJ
 CrCl₂
 $\text{CrCl}_2 = \text{Cr}^{+2} + 2\text{Cl}^-$
 log_k 14.0917
 delta_h -110.76 kJ
 CrCl₃
 $\text{CrCl}_3 + 2\text{H}_2\text{O} = \text{Cr}(\text{OH})_2 + 3\text{Cl}^- + 2\text{H}^+$
 log_k 15.1145
 delta_h -121.08 kJ
 VCl₂
 $\text{VCl}_2 = \text{V}^{+3} + 2\text{Cl}^- + \text{e}^-$
 log_k 18.8744
 delta_h -141.16 kJ
 VCl₃
 $\text{VCl}_3 = \text{V}^{+3} + 3\text{Cl}^-$
 log_k 23.4326
 delta_h -179.54 kJ

VOCl
 $\text{VOCl} + 2\text{H}^+ = \text{V}^{+3} + \text{Cl}^- + \text{H}_2\text{O}$
 log_k 11.1524
 delta_h -104.91 kJ
 VOCl₂
 $\text{VOCl}_2 = \text{VO}^{+2} + 2\text{Cl}^-$
 log_k 12.7603
 delta_h -117.76 kJ
 VO₂Cl
 $\text{VO}_2\text{Cl} = \text{VO}_2^+ + \text{Cl}^-$
 log_k 2.8413
 delta_h -40.28 kJ
 Halite
 $\text{NaCl} = \text{Na}^+ + \text{Cl}^-$
 log_k 1.6025
 delta_h 3.7 kJ
 SbBr₃
 $\text{SbBr}_3 + 3\text{H}_2\text{O} = \text{Sb}(\text{OH})_3 + 3\text{Br}^- + 3\text{H}^+$
 log_k 0.9689
 delta_h -20.94 kJ
 SnBr₂
 $\text{SnBr}_2 + 2\text{H}_2\text{O} = \text{Sn}(\text{OH})_2 + 2\text{H}^+ + 2\text{Br}^-$
 log_k -9.5443
 delta_h -0 kJ
 SnBr₄
 $\text{SnBr}_4 + 6\text{H}_2\text{O} = \text{Sn}(\text{OH})_6^{2-} + 6\text{H}^+ + 4\text{Br}^-$
 log_k -28.8468
 delta_h -0 kJ
 PbBr₂
 $\text{PbBr}_2 = \text{Pb}^{+2} + 2\text{Br}^-$
 log_k -5.3
 delta_h 35.499 kJ
 PbBrF
 $\text{PbBrF} = \text{Pb}^{+2} + \text{Br}^- + \text{F}^-$
 log_k -8.49
 delta_h -0 kJ
 TlBr
 $\text{TlBr} = \text{Tl}^+ + \text{Br}^-$
 log_k -5.44
 delta_h 54 kJ
 ZnBr₂:2H₂O
 $\text{ZnBr}_2 \cdot 2\text{H}_2\text{O} = \text{Zn}^{+2} + 2\text{Br}^- + 2\text{H}_2\text{O}$
 log_k 5.2005
 delta_h -30.67 kJ
 CdBr₂:4H₂O
 $\text{CdBr}_2 \cdot 4\text{H}_2\text{O} = \text{Cd}^{+2} + 2\text{Br}^- + 4\text{H}_2\text{O}$
 log_k -2.425
 delta_h 30.5001 kJ
 Hg₂Br₂
 $\text{Hg}_2\text{Br}_2 = \text{Hg}_2^{+2} + 2\text{Br}^-$
 log_k -22.25
 delta_h 133 kJ
 HgBr₂
 $\text{HgBr}_2 + 2\text{H}_2\text{O} = \text{Hg}(\text{OH})_2 + 2\text{Br}^- + 2\text{H}^+$

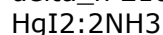
log_k -25.2734
 delta_h 138.492 kJ
 CuBr
 $\text{CuBr} = \text{Cu}^+ + \text{Br}^-$
 log_k -8.3
 delta_h 54.86 kJ
 Cu₂(OH)₃Br
 $\text{Cu}_2(\text{OH})_3\text{Br} + 3\text{H}^+ = 2\text{Cu}^{2+} + 3\text{H}_2\text{O} + \text{Br}^-$
 log_k 7.9085
 delta_h -93.43 kJ
 Bromyrite
 $\text{AgBr} = \text{Ag}^+ + \text{Br}^-$
 log_k -12.3
 delta_h 84.5 kJ
 (Co(NH₃)₆)Br₃
 $(\text{Co}(\text{NH}_3)_6)\text{Br}_3 + 6\text{H}^+ = \text{Co}^{3+} + 6\text{NH}_4^+ + 3\text{Br}^-$
 log_k 18.3142
 delta_h -21.1899 kJ
 (Co(NH₃)₅Cl)Br₂
 $(\text{Co}(\text{NH}_3)_5\text{Cl})\text{Br}_2 + 5\text{H}^+ = \text{Co}^{3+} + 5\text{NH}_4^+ + \text{Cl}^- + 2\text{Br}^-$
 log_k 5.0295
 delta_h -6.4 kJ
 CrBr₃
 $\text{CrBr}_3 + 2\text{H}_2\text{O} = \text{Cr}(\text{OH})_2 + 3\text{Br}^- + 2\text{H}^+$
 log_k 19.9086
 delta_h -141.323 kJ
 AsI₃
 $\text{AsI}_3 + 3\text{H}_2\text{O} = \text{H}_3\text{AsO}_3 + 3\text{I}^- + 3\text{H}^+$
 log_k 4.2307
 delta_h 3.15 kJ
 SbI₃
 $\text{SbI}_3 + 3\text{H}_2\text{O} = \text{Sb}(\text{OH})_3 + 3\text{H}^+ + 3\text{I}^-$
 log_k -0.538
 delta_h 13.5896 kJ
 PbI₂
 $\text{PbI}_2 = \text{Pb}^{2+} + 2\text{I}^-$
 log_k -8.1
 delta_h 62 kJ
 TlI
 $\text{TlI} = \text{Tl}^+ + \text{I}^-$
 log_k -7.23
 delta_h 75 kJ
 ZnI₂
 $\text{ZnI}_2 = \text{Zn}^{2+} + 2\text{I}^-$
 log_k 7.3055
 delta_h -58.92 kJ
 CdI₂
 $\text{CdI}_2 = \text{Cd}^{2+} + 2\text{I}^-$
 log_k -3.5389
 delta_h 13.82 kJ
 Hg₂I₂
 $\text{Hg}_2\text{I}_2 = \text{Hg}_2^{2+} + 2\text{I}^-$
 log_k -28.34
 delta_h 163 kJ

Coccinite



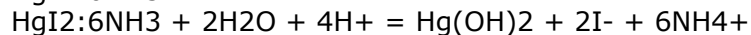
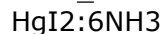
log_k -34.9525

delta_h 210.72 kJ



log_k -16.2293

delta_h 132.18 kJ



log_k 33.7335

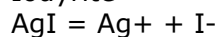
delta_h -90.3599 kJ



log_k -12

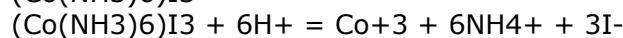
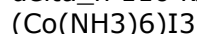
delta_h 82.69 kJ

Iodyrite



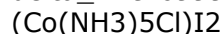
log_k -16.08

delta_h 110 kJ



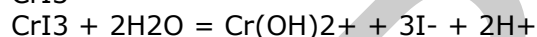
log_k 16.5831

delta_h -9.6999 kJ



log_k 5.5981

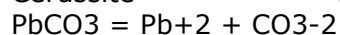
delta_h 0.66 kJ



log_k 20.4767

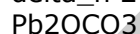
delta_h -134.419 kJ

Cerussite



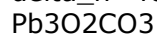
log_k -13.13

delta_h 24.79 kJ



log_k -0.5578

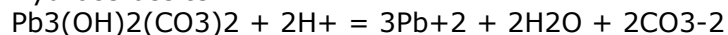
delta_h -40.8199 kJ



log_k 11.02

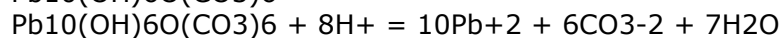
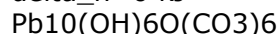
delta_h -110.583 kJ

Hydrocerussite



log_k -18.7705

delta_h -0 kJ



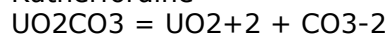
log_k -8.76

delta_h -0 kJ



log_k -3.8367
 delta_h 35.49 kJ
 Smithsonite
 $\text{ZnCO}_3 = \text{Zn}^{+2} + \text{CO}_3^{-2}$
 log_k -10
 delta_h -15.84 kJ
 $\text{ZnCO}_3 \cdot \text{H}_2\text{O}$
 $\text{ZnCO}_3 \cdot \text{H}_2\text{O} = \text{Zn}^{+2} + \text{CO}_3^{-2} + \text{H}_2\text{O}$
 log_k -10.26
 delta_h -0 kJ
 Otavite
 $\text{CdCO}_3 = \text{Cd}^{+2} + \text{CO}_3^{-2}$
 log_k -12
 delta_h -0.55 kJ
 Hg_2CO_3
 $\text{Hg}_2\text{CO}_3 = \text{Hg}_2^{+2} + \text{CO}_3^{-2}$
 log_k -16.05
 delta_h 45.14 kJ
 $\text{Hg}_3\text{O}_2\text{CO}_3$
 $\text{Hg}_3\text{O}_2\text{CO}_3 + 4\text{H}_2\text{O} = 3\text{Hg}(\text{OH})_2 + 2\text{H}^+ + \text{CO}_3^{-2}$
 log_k -29.682
 delta_h -0 kJ
 CuCO_3
 $\text{CuCO}_3 = \text{Cu}^{+2} + \text{CO}_3^{-2}$
 log_k -11.5
 delta_h -0 kJ
 Malachite
 $\text{Cu}_2(\text{OH})_2\text{CO}_3 + 2\text{H}^+ = 2\text{Cu}^{+2} + 2\text{H}_2\text{O} + \text{CO}_3^{-2}$
 log_k -5.306
 delta_h 76.38 kJ
 Azurite
 $\text{Cu}_3(\text{OH})_2(\text{CO}_3)_2 + 2\text{H}^+ = 3\text{Cu}^{+2} + 2\text{H}_2\text{O} + 2\text{CO}_3^{-2}$
 log_k -16.906
 delta_h -95.22 kJ
 Ag_2CO_3
 $\text{Ag}_2\text{CO}_3 = 2\text{Ag}^+ + \text{CO}_3^{-2}$
 log_k -11.09
 delta_h 42.15 kJ
 NiCO_3
 $\text{NiCO}_3 = \text{Ni}^{+2} + \text{CO}_3^{-2}$
 log_k -6.87
 delta_h -41.589 kJ
 CoCO_3
 $\text{CoCO}_3 = \text{Co}^{+2} + \text{CO}_3^{-2}$
 log_k -9.98
 delta_h -12.7612 kJ
 Siderite
 $\text{FeCO}_3 = \text{Fe}^{+2} + \text{CO}_3^{-2}$
 log_k -10.24
 delta_h -16 kJ
 Rhodochrosite
 $\text{MnCO}_3 = \text{Mn}^{+2} + \text{CO}_3^{-2}$
 log_k -10.58
 delta_h -1.88 kJ

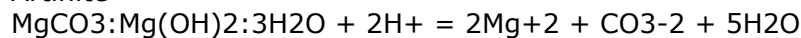
Rutherfordine



log_k -14.5

delta_h -3.03 kJ

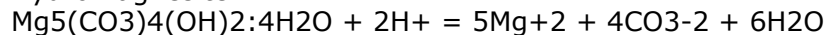
Artinite



log_k 9.6

delta_h -120.257 kJ

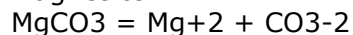
Hydromagnesite



log_k -8.766

delta_h -218.447 kJ

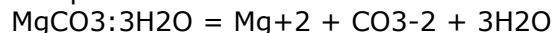
Magnesite



log_k -7.46

delta_h 20 kJ

Nesquehonite



log_k -4.67

delta_h -24.2212 kJ

Aragonite



log_k -8.3

delta_h -12 kJ

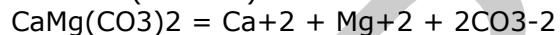
Calcite



log_k -8.48

delta_h -8 kJ

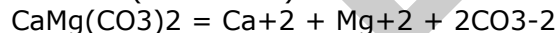
Dolomite(ordered)



log_k -17.09

delta_h -39.5 kJ

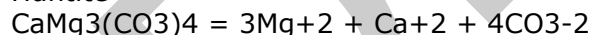
Dolomite(disordered)



log_k -16.54

delta_h -46.4 kJ

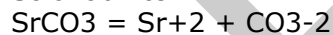
Huntite



log_k -29.968

delta_h -107.78 kJ

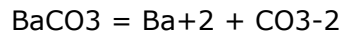
Strontianite



log_k -9.27

delta_h -0 kJ

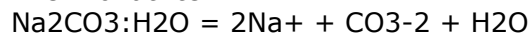
Witherite



log_k -8.57

delta_h 4 kJ

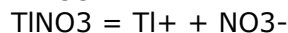
Thermonatrite



log_k 0.637

delta_h -10.4799 kJ

TiNO₃

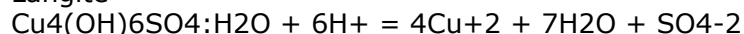


log_k -1.6127
 delta_h 42.44 kJ
 $\text{Zn}(\text{NO}_3)_2 \cdot 6\text{H}_2\text{O}$
 $\text{Zn}(\text{NO}_3)_2 \cdot 6\text{H}_2\text{O} = \text{Zn}^{+2} + 2\text{NO}_3^- + 6\text{H}_2\text{O}$
 log_k 3.3153
 delta_h 24.5698 kJ
 $\text{Cu}_2(\text{OH})_3\text{NO}_3$
 $\text{Cu}_2(\text{OH})_3\text{NO}_3 + 3\text{H}^+ = 2\text{Cu}^{+2} + 3\text{H}_2\text{O} + \text{NO}_3^-$
 log_k 9.251
 delta_h -72.5924 kJ
 $(\text{Co}(\text{NH}_3)_6)(\text{NO}_3)_3$
 $(\text{Co}(\text{NH}_3)_6)(\text{NO}_3)_3 + 6\text{H}^+ = \text{Co}^{+3} + 6\text{NH}_4^+ + 3\text{NO}_3^-$
 log_k 17.9343
 delta_h 1.59 kJ
 $(\text{Co}(\text{NH}_3)_5\text{Cl})(\text{NO}_3)_2$
 $(\text{Co}(\text{NH}_3)_5\text{Cl})(\text{NO}_3)_2 + 5\text{H}^+ = \text{Co}^{+3} + 5\text{NH}_4^+ + \text{Cl}^- + 2\text{NO}_3^-$
 log_k 6.2887
 delta_h 6.4199 kJ
 $\text{UO}_2(\text{NO}_3)_2$
 $\text{UO}_2(\text{NO}_3)_2 = \text{UO}_2^{+2} + 2\text{NO}_3^-$
 log_k 12.1476
 delta_h -83.3999 kJ
 $\text{UO}_2(\text{NO}_3)_2 \cdot 2\text{H}_2\text{O}$
 $\text{UO}_2(\text{NO}_3)_2 \cdot 2\text{H}_2\text{O} = \text{UO}_2^{+2} + 2\text{NO}_3^- + 2\text{H}_2\text{O}$
 log_k 4.851
 delta_h -25.355 kJ
 $\text{UO}_2(\text{NO}_3)_2 \cdot 3\text{H}_2\text{O}$
 $\text{UO}_2(\text{NO}_3)_2 \cdot 3\text{H}_2\text{O} = \text{UO}_2^{+2} + 2\text{NO}_3^- + 3\text{H}_2\text{O}$
 log_k 3.39
 delta_h -9.1599 kJ
 $\text{UO}_2(\text{NO}_3)_2 \cdot 6\text{H}_2\text{O}$
 $\text{UO}_2(\text{NO}_3)_2 \cdot 6\text{H}_2\text{O} = \text{UO}_2^{+2} + 2\text{NO}_3^- + 6\text{H}_2\text{O}$
 log_k 2.0464
 delta_h 20.8201 kJ
 $\text{Pb}(\text{BO}_2)_2$
 $\text{Pb}(\text{BO}_2)_2 + 2\text{H}_2\text{O} + 2\text{H}^+ = \text{Pb}^{+2} + 2\text{H}_3\text{BO}_3$
 log_k 6.5192
 delta_h -15.6119 kJ
 $\text{Zn}(\text{BO}_2)_2$
 $\text{Zn}(\text{BO}_2)_2 + 2\text{H}_2\text{O} + 2\text{H}^+ = \text{Zn}^{+2} + 2\text{H}_3\text{BO}_3$
 log_k 8.29
 delta_h -0 kJ
 $\text{Cd}(\text{BO}_2)_2$
 $\text{Cd}(\text{BO}_2)_2 + 2\text{H}_2\text{O} + 2\text{H}^+ = \text{Cd}^{+2} + 2\text{H}_3\text{BO}_3$
 log_k 9.84
 delta_h -0 kJ
 $\text{Co}(\text{BO}_2)_2$
 $\text{Co}(\text{BO}_2)_2 + 2\text{H}_2\text{O} + 2\text{H}^+ = \text{Co}^{+2} + 2\text{H}_3\text{BO}_3$
 log_k 27.0703
 delta_h -0 kJ
 SnSO_4
 $\text{SnSO}_4 + 2\text{H}_2\text{O} = \text{Sn}(\text{OH})_2 + 2\text{H}^+ + \text{SO}_4^{2-}$
 log_k -56.9747
 delta_h -0 kJ

$\text{Sn}(\text{SO}_4)_2$
 $\text{Sn}(\text{SO}_4)_2 + 6\text{H}_2\text{O} = \text{Sn}(\text{OH})_6^{2-} + 6\text{H}^+ + 2\text{SO}_4^{2-}$
 $\log_k -15.2123$
 $\Delta H -0 \text{ kJ}$
 Larnakite
 $\text{PbO}:\text{PbSO}_4 + 2\text{H}^+ = 2\text{Pb}^{2+} + \text{SO}_4^{2-} + \text{H}_2\text{O}$
 $\log_k -0.4344$
 $\Delta H -21.83 \text{ kJ}$
 $\text{Pb}_3\text{O}_2\text{SO}_4$
 $\text{Pb}_3\text{O}_2\text{SO}_4 + 4\text{H}^+ = 3\text{Pb}^{2+} + \text{SO}_4^{2-} + 2\text{H}_2\text{O}$
 $\log_k 10.6864$
 $\Delta H -79.14 \text{ kJ}$
 $\text{Pb}_4\text{O}_3\text{SO}_4$
 $\text{Pb}_4\text{O}_3\text{SO}_4 + 6\text{H}^+ = 4\text{Pb}^{2+} + \text{SO}_4^{2-} + 3\text{H}_2\text{O}$
 $\log_k 21.8772$
 $\Delta H -136.45 \text{ kJ}$
 Anglesite
 $\text{PbSO}_4 = \text{Pb}^{2+} + \text{SO}_4^{2-}$
 $\log_k -7.79$
 $\Delta H 12 \text{ kJ}$
 $\text{Pb}_4(\text{OH})_6\text{SO}_4$
 $\text{Pb}_4(\text{OH})_6\text{SO}_4 + 6\text{H}^+ = 4\text{Pb}^{2+} + \text{SO}_4^{2-} + 6\text{H}_2\text{O}$
 $\log_k 21.1$
 $\Delta H -0 \text{ kJ}$
 AlOHSO_4
 $\text{AlOHSO}_4 + \text{H}^+ = \text{Al}^{3+} + \text{SO}_4^{2-} + \text{H}_2\text{O}$
 $\log_k -3.23$
 $\Delta H -0 \text{ kJ}$
 $\text{Al}_4(\text{OH})_{10}\text{SO}_4$
 $\text{Al}_4(\text{OH})_{10}\text{SO}_4 + 10\text{H}^+ = 4\text{Al}^{3+} + \text{SO}_4^{2-} + 10\text{H}_2\text{O}$
 $\log_k 22.7$
 $\Delta H -0 \text{ kJ}$
 Ti_2SO_4
 $\text{Ti}_2\text{SO}_4 = 2\text{Ti}^+ + \text{SO}_4^{2-}$
 $\log_k -3.7868$
 $\Delta H 33.1799 \text{ kJ}$
 $\text{Zn}_2(\text{OH})_2\text{SO}_4$
 $\text{Zn}_2(\text{OH})_2\text{SO}_4 + 2\text{H}^+ = 2\text{Zn}^{2+} + 2\text{H}_2\text{O} + \text{SO}_4^{2-}$
 $\log_k 7.5$
 $\Delta H -0 \text{ kJ}$
 $\text{Zn}_4(\text{OH})_6\text{SO}_4$
 $\text{Zn}_4(\text{OH})_6\text{SO}_4 + 6\text{H}^+ = 4\text{Zn}^{2+} + 6\text{H}_2\text{O} + \text{SO}_4^{2-}$
 $\log_k 28.4$
 $\Delta H -0 \text{ kJ}$
 $\text{Zn}_3\text{O}(\text{SO}_4)_2$
 $\text{Zn}_3\text{O}(\text{SO}_4)_2 + 2\text{H}^+ = 3\text{Zn}^{2+} + 2\text{SO}_4^{2-} + \text{H}_2\text{O}$
 $\log_k 18.9135$
 $\Delta H -258.08 \text{ kJ}$
 Zincosite
 $\text{ZnSO}_4 = \text{Zn}^{2+} + \text{SO}_4^{2-}$
 $\log_k 3.9297$
 $\Delta H -82.586 \text{ kJ}$
 $\text{ZnSO}_4:\text{H}_2\text{O}$
 $\text{ZnSO}_4:\text{H}_2\text{O} = \text{Zn}^{2+} + \text{SO}_4^{2-} + \text{H}_2\text{O}$

log_k -0.638
 delta_h -44.0699 kJ
 Bianchite
 $\text{ZnSO}_4 \cdot 6\text{H}_2\text{O} = \text{Zn}^{+2} + \text{SO}_4^{-2} + 6\text{H}_2\text{O}$
 log_k -1.765
 delta_h -0.6694 kJ
 Goslarite
 $\text{ZnSO}_4 \cdot 7\text{H}_2\text{O} = \text{Zn}^{+2} + \text{SO}_4^{-2} + 7\text{H}_2\text{O}$
 log_k -2.0112
 delta_h 14.21 kJ
 $\text{Cd}_3(\text{OH})_4\text{SO}_4$
 $\text{Cd}_3(\text{OH})_4\text{SO}_4 + 4\text{H}^+ = 3\text{Cd}^{+2} + 4\text{H}_2\text{O} + \text{SO}_4^{-2}$
 log_k 22.56
 delta_h -0 kJ
 $\text{Cd}_3(\text{OH})_2(\text{SO}_4)_2$
 $\text{Cd}_3(\text{OH})_2(\text{SO}_4)_2 + 2\text{H}^+ = 3\text{Cd}^{+2} + 2\text{H}_2\text{O} + 2\text{SO}_4^{-2}$
 log_k 6.71
 delta_h -0 kJ
 $\text{Cd}_4(\text{OH})_6\text{SO}_4$
 $\text{Cd}_4(\text{OH})_6\text{SO}_4 + 6\text{H}^+ = 4\text{Cd}^{+2} + 6\text{H}_2\text{O} + \text{SO}_4^{-2}$
 log_k 28.4
 delta_h -0 kJ
 CdSO_4
 $\text{CdSO}_4 = \text{Cd}^{+2} + \text{SO}_4^{-2}$
 log_k -0.1722
 delta_h -51.98 kJ
 $\text{CdSO}_4 \cdot \text{H}_2\text{O}$
 $\text{CdSO}_4 \cdot \text{H}_2\text{O} = \text{Cd}^{+2} + \text{SO}_4^{-2} + \text{H}_2\text{O}$
 log_k -1.7261
 delta_h -31.5399 kJ
 $\text{CdSO}_4 \cdot 2.67\text{H}_2\text{O}$
 $\text{CdSO}_4 \cdot 2.67\text{H}_2\text{O} = \text{Cd}^{+2} + \text{SO}_4^{-2} + 2.67\text{H}_2\text{O}$
 log_k -1.873
 delta_h -17.9912 kJ
 Hg_2SO_4
 $\text{Hg}_2\text{SO}_4 = \text{Hg}_2^{+2} + \text{SO}_4^{-2}$
 log_k -6.13
 delta_h 5.4 kJ
 HgSO_4
 $\text{HgSO}_4 + 2\text{H}_2\text{O} = \text{Hg}(\text{OH})_2 + \text{SO}_4^{-2} + 2\text{H}^+$
 log_k -9.4189
 delta_h 14.6858 kJ
 Cu_2SO_4
 $\text{Cu}_2\text{SO}_4 = 2\text{Cu}^+ + \text{SO}_4^{-2}$
 log_k -1.95
 delta_h -19.079 kJ
 Antlerite
 $\text{Cu}_3(\text{OH})_4\text{SO}_4 + 4\text{H}^+ = 3\text{Cu}^{+2} + 4\text{H}_2\text{O} + \text{SO}_4^{-2}$
 log_k 8.788
 delta_h -0 kJ
 Brochantite
 $\text{Cu}_4(\text{OH})_6\text{SO}_4 + 6\text{H}^+ = 4\text{Cu}^{+2} + 6\text{H}_2\text{O} + \text{SO}_4^{-2}$
 log_k 15.222
 delta_h -202.86 kJ

Langite



log_k 17.4886

delta_h -165.55 kJ

CuOCuSO₄



log_k 10.3032

delta_h -137.777 kJ

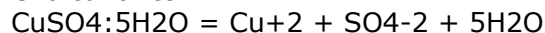
CuSO₄



log_k 2.9395

delta_h -73.04 kJ

Chalcanthite



log_k -2.64

delta_h 6.025 kJ

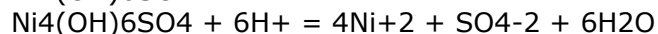
Ag₂SO₄



log_k -4.82

delta_h 17 kJ

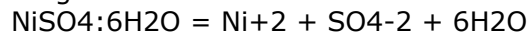
Ni₄(OH)₆SO₄



log_k 32

delta_h -0 kJ

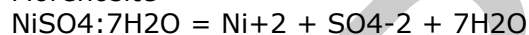
Retgersite



log_k -2.04

delta_h 4.6024 kJ

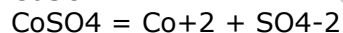
Morenosite



log_k -2.1449

delta_h 12.1802 kJ

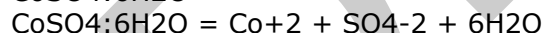
CoSO₄



log_k 2.8024

delta_h -79.277 kJ

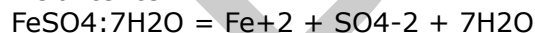
CoSO₄·6H₂O



log_k -2.4726

delta_h 1.0801 kJ

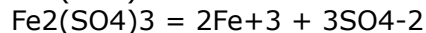
Melanterite



log_k -2.209

delta_h 20.5 kJ

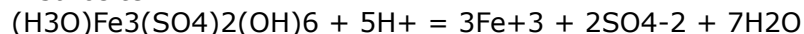
Fe₂(SO₄)₃



log_k -3.7343

delta_h -242.028 kJ

H-Jarosite



log_k -12.1

delta_h -230.748 kJ

Na-Jarosite



log_k -11.2
 delta_h -151.377 kJ
 K-Jarosite
 $\text{KFe}_3(\text{SO}_4)_2(\text{OH})_6 + 6\text{H}^+ = \text{K}^+ + 3\text{Fe}^{+3} + 2\text{SO}_4^{-2} + 6\text{H}_2\text{O}$
 log_k -14.8
 delta_h -130.875 kJ
 MnSO4
 $\text{MnSO}_4 = \text{Mn}^{+2} + \text{SO}_4^{-2}$
 log_k 2.5831
 delta_h -64.8401 kJ
 Mn2(SO4)3
 $\text{Mn}_2(\text{SO}_4)_3 = 2\text{Mn}^{+3} + 3\text{SO}_4^{-2}$
 log_k -5.711
 delta_h -163.427 kJ
 VOSO4
 $\text{VOSO}_4 = \text{VO}^{+2} + \text{SO}_4^{-2}$
 log_k 3.6097
 delta_h -86.7401 kJ
 Epsomite
 $\text{MgSO}_4 \cdot 7\text{H}_2\text{O} = \text{Mg}^{+2} + \text{SO}_4^{-2} + 7\text{H}_2\text{O}$
 log_k -2.1265
 delta_h 11.5601 kJ
 Anhydrite
 $\text{CaSO}_4 = \text{Ca}^{+2} + \text{SO}_4^{-2}$
 log_k -4.36
 delta_h -7.2 kJ
 Gypsum
 $\text{CaSO}_4 \cdot 2\text{H}_2\text{O} = \text{Ca}^{+2} + \text{SO}_4^{-2} + 2\text{H}_2\text{O}$
 log_k -4.61
 delta_h 1 kJ
 Celestite
 $\text{SrSO}_4 = \text{Sr}^{+2} + \text{SO}_4^{-2}$
 log_k -6.62
 delta_h 2 kJ
 Barite
 $\text{BaSO}_4 = \text{Ba}^{+2} + \text{SO}_4^{-2}$
 log_k -9.98
 delta_h 23 kJ
 Mirabilite
 $\text{Na}_2\text{SO}_4 \cdot 10\text{H}_2\text{O} = 2\text{Na}^+ + \text{SO}_4^{-2} + 10\text{H}_2\text{O}$
 log_k -1.114
 delta_h 79.4416 kJ
 Thenardite
 $\text{Na}_2\text{SO}_4 = 2\text{Na}^+ + \text{SO}_4^{-2}$
 log_k 0.3217
 delta_h -9.121 kJ
 K-Alum
 $\text{KAl}(\text{SO}_4)_2 \cdot 12\text{H}_2\text{O} = \text{K}^+ + \text{Al}^{+3} + 2\text{SO}_4^{-2} + 12\text{H}_2\text{O}$
 log_k -5.17
 delta_h 30.2085 kJ
 Alunite
 $\text{KAl}_3(\text{SO}_4)_2(\text{OH})_6 + 6\text{H}^+ = \text{K}^+ + 3\text{Al}^{+3} + 2\text{SO}_4^{-2} + 6\text{H}_2\text{O}$
 log_k -1.4
 delta_h -210 kJ

$(\text{NH}_4)_2\text{CrO}_4$
 $(\text{NH}_4)_2\text{CrO}_4 = \text{CrO}_4^{2-} + 2\text{NH}_4^+$
 $\log_k 0.4046$
 $\Delta H 9.163 \text{ kJ}$
 PbCrO_4
 $\text{PbCrO}_4 = \text{Pb}^{2+} + \text{CrO}_4^{2-}$
 $\log_k -12.6$
 $\Delta H 44.18 \text{ kJ}$
 Ti_2CrO_4
 $\text{Ti}_2\text{CrO}_4 = 2\text{Ti}^+ + \text{CrO}_4^{2-}$
 $\log_k -12.01$
 $\Delta H 74.27 \text{ kJ}$
 Hg_2CrO_4
 $\text{Hg}_2\text{CrO}_4 = \text{Hg}_2^{2+} + \text{CrO}_4^{2-}$
 $\log_k -8.7$
 $\Delta H -0 \text{ kJ}$
 CuCrO_4
 $\text{CuCrO}_4 = \text{Cu}^{2+} + \text{CrO}_4^{2-}$
 $\log_k -5.44$
 $\Delta H -0 \text{ kJ}$
 Ag_2CrO_4
 $\text{Ag}_2\text{CrO}_4 = 2\text{Ag}^+ + \text{CrO}_4^{2-}$
 $\log_k -11.59$
 $\Delta H 62 \text{ kJ}$
 MgCrO_4
 $\text{MgCrO}_4 = \text{CrO}_4^{2-} + \text{Mg}^{2+}$
 $\log_k 5.3801$
 $\Delta H -88.9518 \text{ kJ}$
 CaCrO_4
 $\text{CaCrO}_4 = \text{Ca}^{2+} + \text{CrO}_4^{2-}$
 $\log_k -2.2657$
 $\Delta H -26.945 \text{ kJ}$
 SrCrO_4
 $\text{SrCrO}_4 = \text{Sr}^{2+} + \text{CrO}_4^{2-}$
 $\log_k -4.65$
 $\Delta H -10.1253 \text{ kJ}$
 BaCrO_4
 $\text{BaCrO}_4 = \text{Ba}^{2+} + \text{CrO}_4^{2-}$
 $\log_k -9.67$
 $\Delta H 33 \text{ kJ}$
 Li_2CrO_4
 $\text{Li}_2\text{CrO}_4 = \text{CrO}_4^{2-} + 2\text{Li}^+$
 $\log_k 4.8568$
 $\Delta H -45.2792 \text{ kJ}$
 Na_2CrO_4
 $\text{Na}_2\text{CrO}_4 = \text{CrO}_4^{2-} + 2\text{Na}^+$
 $\log_k 2.9302$
 $\Delta H -19.6301 \text{ kJ}$
 $\text{Na}_2\text{Cr}_2\text{O}_7$
 $\text{Na}_2\text{Cr}_2\text{O}_7 + \text{H}_2\text{O} = 2\text{CrO}_4^{2-} + 2\text{Na}^+ + 2\text{H}^+$
 $\log_k -9.8953$
 $\Delta H 22.1961 \text{ kJ}$
 K_2CrO_4
 $\text{K}_2\text{CrO}_4 = \text{CrO}_4^{2-} + 2\text{K}^+$

log_k -0.5134
 delta_h 18.2699 kJ
 $\text{K}_2\text{Cr}_2\text{O}_7$
 $\text{K}_2\text{Cr}_2\text{O}_7 + \text{H}_2\text{O} = 2\text{CrO}_4^{2-} + 2\text{K}^+ + 2\text{H}^+$
 log_k -17.2424
 delta_h 80.7499 kJ
 Hg_2SeO_3
 $\text{Hg}_2\text{SeO}_3 + \text{H}^+ = \text{Hg}_2^{2+} + \text{HSeO}_3^-$
 log_k -4.657
 delta_h -0 kJ
 HgSeO_3
 $\text{HgSeO}_3 + 2\text{H}_2\text{O} = \text{Hg}(\text{OH})_2 + \text{H}^+ + \text{HSeO}_3^-$
 log_k -12.43
 delta_h -0 kJ
 Ag_2SeO_3
 $\text{Ag}_2\text{SeO}_3 + \text{H}^+ = 2\text{Ag}^+ + \text{HSeO}_3^-$
 log_k -7.15
 delta_h 39.68 kJ
 $\text{CuSeO}_3 \cdot 2\text{H}_2\text{O}$
 $\text{CuSeO}_3 \cdot 2\text{H}_2\text{O} + \text{H}^+ = \text{Cu}^{2+} + \text{HSeO}_3^- + 2\text{H}_2\text{O}$
 log_k 0.5116
 delta_h -36.861 kJ
 $\text{NiSeO}_3 \cdot 2\text{H}_2\text{O}$
 $\text{NiSeO}_3 \cdot 2\text{H}_2\text{O} + \text{H}^+ = \text{HSeO}_3^- + \text{Ni}^{2+} + 2\text{H}_2\text{O}$
 log_k 2.8147
 delta_h -31.0034 kJ
 CoSeO_3
 $\text{CoSeO}_3 + \text{H}^+ = \text{Co}^{2+} + \text{HSeO}_3^-$
 log_k 1.32
 delta_h -0 kJ
 $\text{Fe}_2(\text{SeO}_3)_3 \cdot 2\text{H}_2\text{O}$
 $\text{Fe}_2(\text{SeO}_3)_3 \cdot 2\text{H}_2\text{O} + 3\text{H}^+ = 3\text{HSeO}_3^- + 2\text{Fe}^{3+} + 2\text{H}_2\text{O}$
 log_k -20.6262
 delta_h -0 kJ
 $\text{Fe}_2(\text{OH})_4\text{SeO}_3$
 $\text{Fe}_2(\text{OH})_4\text{SeO}_3 + 5\text{H}^+ = \text{HSeO}_3^- + 2\text{Fe}^{3+} + 4\text{H}_2\text{O}$
 log_k 1.5539
 delta_h -0 kJ
 MnSeO_3
 $\text{MnSeO}_3 + \text{H}^+ = \text{Mn}^{2+} + \text{HSeO}_3^-$
 log_k 1.13
 delta_h -0 kJ
 $\text{MnSeO}_3 \cdot 2\text{H}_2\text{O}$
 $\text{MnSeO}_3 \cdot 2\text{H}_2\text{O} + \text{H}^+ = \text{HSeO}_3^- + \text{Mn}^{2+} + 2\text{H}_2\text{O}$
 log_k 0.9822
 delta_h 8.4935 kJ
 $\text{MgSeO}_3 \cdot 6\text{H}_2\text{O}$
 $\text{MgSeO}_3 \cdot 6\text{H}_2\text{O} + \text{H}^+ = \text{Mg}^{2+} + \text{HSeO}_3^- + 6\text{H}_2\text{O}$
 log_k 3.0554
 delta_h 5.23 kJ
 $\text{CaSeO}_3 \cdot 2\text{H}_2\text{O}$
 $\text{CaSeO}_3 \cdot 2\text{H}_2\text{O} + \text{H}^+ = \text{HSeO}_3^- + \text{Ca}^{2+} + 2\text{H}_2\text{O}$
 log_k 2.8139
 delta_h -19.4556 kJ

SrSeO3
 $\text{SrSeO3} + \text{H}^+ = \text{Sr}^{+2} + \text{HSeO3}^-$
 log_k 2.3
 delta_h -0 kJ
 BaSeO3
 $\text{BaSeO3} + \text{H}^+ = \text{Ba}^{+2} + \text{HSeO3}^-$
 log_k 1.83
 delta_h 11.98 kJ
 Na2SeO3:5H2O
 $\text{Na2SeO3:5H2O} + \text{H}^+ = 2\text{Na}^+ + \text{HSeO3}^- + 5\text{H2O}$
 log_k 10.3
 delta_h -0 kJ
 PbSeO4
 $\text{PbSeO4} = \text{Pb}^{+2} + \text{SeO4}^{2-}$
 log_k -6.84
 delta_h 15 kJ
 Ti2SeO4
 $\text{Ti2SeO4} = 2\text{Ti}^+ + \text{SeO4}^{2-}$
 log_k -4.1
 delta_h 43 kJ
 ZnSeO4:6H2O
 $\text{ZnSeO4:6H2O} = \text{Zn}^{+2} + \text{SeO4}^{2-} + 6\text{H2O}$
 log_k -1.52
 delta_h -0 kJ
 CdSeO4:2H2O
 $\text{CdSeO4:2H2O} = \text{Cd}^{+2} + \text{SeO4}^{2-} + 2\text{H2O}$
 log_k -1.85
 delta_h -0 kJ
 Ag2SeO4
 $\text{Ag2SeO4} = 2\text{Ag}^+ + \text{SeO4}^{2-}$
 log_k -8.91
 delta_h -43.5 kJ
 CuSeO4:5H2O
 $\text{CuSeO4:5H2O} = \text{Cu}^{+2} + \text{SeO4}^{2-} + 5\text{H2O}$
 log_k -2.44
 delta_h -0 kJ
 NiSeO4:6H2O
 $\text{NiSeO4:6H2O} = \text{Ni}^{+2} + \text{SeO4}^{2-} + 6\text{H2O}$
 log_k -1.52
 delta_h -0 kJ
 CoSeO4:6H2O
 $\text{CoSeO4:6H2O} = \text{Co}^{+2} + \text{SeO4}^{2-} + 6\text{H2O}$
 log_k -1.53
 delta_h -0 kJ
 MnSeO4:5H2O
 $\text{MnSeO4:5H2O} = \text{Mn}^{+2} + \text{SeO4}^{2-} + 5\text{H2O}$
 log_k -2.05
 delta_h -0 kJ
 UO2SeO4:4H2O
 $\text{UO2SeO4:4H2O} = \text{UO2}^{+2} + \text{SeO4}^{2-} + 4\text{H2O}$
 log_k -2.25
 delta_h -0 kJ
 MgSeO4:6H2O
 $\text{MgSeO4:6H2O} = \text{Mg}^{+2} + \text{SeO4}^{2-} + 6\text{H2O}$

log_k -1.2
 delta_h -0 kJ
 CaSeO4:2H2O
 $\text{CaSeO4:2H2O} = \text{Ca}^{+2} + \text{SeO4}^{-2} + 2\text{H2O}$
 log_k -3.02
 delta_h -8.3 kJ
 SrSeO4
 $\text{SrSeO4} = \text{Sr}^{+2} + \text{SeO4}^{-2}$
 log_k -4.4
 delta_h 0.4 kJ
 BaSeO4
 $\text{BaSeO4} = \text{Ba}^{+2} + \text{SeO4}^{-2}$
 log_k -7.46
 delta_h 22 kJ
 BeSeO4:4H2O
 $\text{BeSeO4:4H2O} = \text{Be}^{+2} + \text{SeO4}^{-2} + 4\text{H2O}$
 log_k -2.94
 delta_h -0 kJ
 Na2SeO4
 $\text{Na2SeO4} = 2\text{Na}^{+} + \text{SeO4}^{-2}$
 log_k 1.28
 delta_h -0 kJ
 K2SeO4
 $\text{K2SeO4} = 2\text{K}^{+} + \text{SeO4}^{-2}$
 log_k -0.73
 delta_h -0 kJ
 (NH4)2SeO4
 $(\text{NH4})2\text{SeO4} = 2\text{NH4}^{+} + \text{SeO4}^{-2}$
 log_k 0.45
 delta_h -0 kJ
 H2MoO4
 $\text{H2MoO4} = \text{MoO4}^{-2} + 2\text{H}^{+}$
 log_k -12.8765
 delta_h 49 kJ
 PbMoO4
 $\text{PbMoO4} = \text{Pb}^{+2} + \text{MoO4}^{-2}$
 log_k -15.62
 delta_h 53.93 kJ
 Al2(MoO4)3
 $\text{Al2(MoO4)3} = 3\text{MoO4}^{-2} + 2\text{Al}^{+3}$
 log_k 2.3675
 delta_h -260.8 kJ
 Ti2MoO4
 $\text{Ti2MoO4} = \text{MoO4}^{-2} + 2\text{Ti}^{+}$
 log_k -7.9887
 delta_h -0 kJ
 ZnMoO4
 $\text{ZnMoO4} = \text{MoO4}^{-2} + \text{Zn}^{+2}$
 log_k -10.1254
 delta_h -10.6901 kJ
 CdMoO4
 $\text{CdMoO4} = \text{MoO4}^{-2} + \text{Cd}^{+2}$
 log_k -14.1497
 delta_h 19.48 kJ

CuMoO4
 $\text{CuMoO4} = \text{MoO4-2} + \text{Cu+2}$
 log_k -13.0762
 delta_h 12.2 kJ
 Ag2MoO4
 $\text{Ag2MoO4} = 2\text{Ag+} + \text{MoO4-2}$
 log_k -11.55
 delta_h 52.7 kJ
 NiMoO4
 $\text{NiMoO4} = \text{MoO4-2} + \text{Ni+2}$
 log_k -11.1421
 delta_h 1.3 kJ
 CoMoO4
 $\text{CoMoO4} = \text{MoO4-2} + \text{Co+2}$
 log_k -7.7609
 delta_h -23.3999 kJ
 FeMoO4
 $\text{FeMoO4} = \text{MoO4-2} + \text{Fe+2}$
 log_k -10.091
 delta_h -11.1 kJ
 BeMoO4
 $\text{BeMoO4} = \text{MoO4-2} + \text{Be+2}$
 log_k -1.7817
 delta_h -56.4 kJ
 MgMoO4
 $\text{MgMoO4} = \text{Mg+2} + \text{MoO4-2}$
 log_k -1.85
 delta_h -0 kJ
 CaMoO4
 $\text{CaMoO4} = \text{Ca+2} + \text{MoO4-2}$
 log_k -7.95
 delta_h -2 kJ
 BaMoO4
 $\text{BaMoO4} = \text{MoO4-2} + \text{Ba+2}$
 log_k -6.9603
 delta_h 10.96 kJ
 Li2MoO4
 $\text{Li2MoO4} = \text{MoO4-2} + 2\text{Li+}$
 log_k 2.4416
 delta_h -33.9399 kJ
 Na2MoO4
 $\text{Na2MoO4} = \text{MoO4-2} + 2\text{Na+}$
 log_k 1.4901
 delta_h -9.98 kJ
 Na2MoO4:2H2O
 $\text{Na2MoO4:2H2O} = \text{MoO4-2} + 2\text{Na+} + 2\text{H2O}$
 log_k 1.224
 delta_h -0 kJ
 Na2Mo2O7
 $\text{Na2Mo2O7} + \text{H2O} = 2\text{MoO4-2} + 2\text{Na+} + 2\text{H+}$
 log_k -16.5966
 delta_h 56.2502 kJ
 K2MoO4
 $\text{K2MoO4} = \text{MoO4-2} + 2\text{K+}$

log_k 3.2619
 delta_h -3.38 kJ
 PbHPO₄
 $\text{PbHPO}_4 = \text{Pb}^{+2} + \text{H}^+ + \text{PO}_4^{-3}$
 log_k -23.805
 delta_h -0 kJ
 Pb₃(PO₄)₂
 $\text{Pb}_3(\text{PO}_4)_2 = 3\text{Pb}^{+2} + 2\text{PO}_4^{-3}$
 log_k -43.53
 delta_h -0 kJ
 Pyromorphite
 $\text{Pb}_5(\text{PO}_4)_3\text{Cl} = 5\text{Pb}^{+2} + 3\text{PO}_4^{-3} + \text{Cl}^-$
 log_k -84.43
 delta_h -0 kJ
 Hydroxylpyromorphite
 $\text{Pb}_5(\text{PO}_4)_3\text{OH} + \text{H}^+ = 5\text{Pb}^{+2} + 3\text{PO}_4^{-3} + \text{H}_2\text{O}$
 log_k -62.79
 delta_h -0 kJ
 Plumbgummite
 $\text{PbAl}_3(\text{PO}_4)_2(\text{OH})_5 \cdot 5\text{H}_2\text{O} + 5\text{H}^+ = \text{Pb}^{+2} + 3\text{Al}^{+3} + 2\text{PO}_4^{-3} + 6\text{H}_2\text{O}$
 log_k -32.79
 delta_h -0 kJ
 Hinsdalite
 $\text{PbAl}_3\text{PO}_4\text{SO}_4(\text{OH})_6 + 6\text{H}^+ = \text{Pb}^{+2} + 3\text{Al}^{+3} + \text{PO}_4^{-3} + \text{SO}_4^{-2} + 6\text{H}_2\text{O}$
 log_k -2.5
 delta_h -0 kJ
 Tsumebite
 $\text{Pb}_2\text{CuPO}_4(\text{OH})_3 \cdot 3\text{H}_2\text{O} + 3\text{H}^+ = 2\text{Pb}^{+2} + \text{Cu}^{+2} + \text{PO}_4^{-3} + 6\text{H}_2\text{O}$
 log_k -9.79
 delta_h -0 kJ
 Zn₃(PO₄)₂·4H₂O
 $\text{Zn}_3(\text{PO}_4)_2 \cdot 4\text{H}_2\text{O} = 3\text{Zn}^{+2} + 2\text{PO}_4^{-3} + 4\text{H}_2\text{O}$
 log_k -35.42
 delta_h -0 kJ
 Cd₃(PO₄)₂
 $\text{Cd}_3(\text{PO}_4)_2 = 3\text{Cd}^{+2} + 2\text{PO}_4^{-3}$
 log_k -32.6
 delta_h -0 kJ
 Hg₂HPO₄
 $\text{Hg}_2\text{HPO}_4 = \text{Hg}_2^{+2} + \text{H}^+ + \text{PO}_4^{-3}$
 log_k -24.775
 delta_h -0 kJ
 Cu₃(PO₄)₂
 $\text{Cu}_3(\text{PO}_4)_2 = 3\text{Cu}^{+2} + 2\text{PO}_4^{-3}$
 log_k -36.85
 delta_h -0 kJ
 Cu₃(PO₄)₂·3H₂O
 $\text{Cu}_3(\text{PO}_4)_2 \cdot 3\text{H}_2\text{O} = 3\text{Cu}^{+2} + 2\text{PO}_4^{-3} + 3\text{H}_2\text{O}$
 log_k -35.12
 delta_h -0 kJ
 Ag₃PO₄
 $\text{Ag}_3\text{PO}_4 = 3\text{Ag}^+ + \text{PO}_4^{-3}$
 log_k -17.59
 delta_h -0 kJ

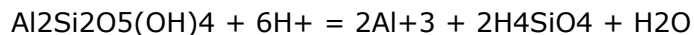
$\text{Ni}_3(\text{PO}_4)_2$
 $\text{Ni}_3(\text{PO}_4)_2 = 3\text{Ni}^{+2} + 2\text{PO}_4^{-3}$
 $\log_k -31.3$
 $\Delta H -0 \text{ kJ}$
 CoHPO_4
 $\text{CoHPO}_4 = \text{Co}^{+2} + \text{PO}_4^{-3} + \text{H}^+$
 $\log_k -19.0607$
 $\Delta H -0 \text{ kJ}$
 $\text{Co}_3(\text{PO}_4)_2$
 $\text{Co}_3(\text{PO}_4)_2 = 3\text{Co}^{+2} + 2\text{PO}_4^{-3}$
 $\log_k -34.6877$
 $\Delta H -0 \text{ kJ}$
Vivianite
 $\text{Fe}_3(\text{PO}_4)_2 \cdot 8\text{H}_2\text{O} = 3\text{Fe}^{+2} + 2\text{PO}_4^{-3} + 8\text{H}_2\text{O}$
 $\log_k -36$
 $\Delta H -0 \text{ kJ}$
Strengite
 $\text{FePO}_4 \cdot 2\text{H}_2\text{O} = \text{Fe}^{+3} + \text{PO}_4^{-3} + 2\text{H}_2\text{O}$
 $\log_k -26.4$
 $\Delta H -9.3601 \text{ kJ}$
 $\text{Mn}_3(\text{PO}_4)_2$
 $\text{Mn}_3(\text{PO}_4)_2 = 3\text{Mn}^{+2} + 2\text{PO}_4^{-3}$
 $\log_k -23.827$
 $\Delta H 8.8701 \text{ kJ}$
 MnHPO_4
 $\text{MnHPO}_4 = \text{Mn}^{+2} + \text{PO}_4^{-3} + \text{H}^+$
 $\log_k -25.4$
 $\Delta H -0 \text{ kJ}$
 $(\text{VO})_3(\text{PO}_4)_2$
 $(\text{VO})_3(\text{PO}_4)_2 = 3\text{VO}^{+2} + 2\text{PO}_4^{-3}$
 $\log_k -25.1$
 $\Delta H -0 \text{ kJ}$
 $\text{Mg}_3(\text{PO}_4)_2$
 $\text{Mg}_3(\text{PO}_4)_2 = 3\text{Mg}^{+2} + 2\text{PO}_4^{-3}$
 $\log_k -23.28$
 $\Delta H -0 \text{ kJ}$
 $\text{MgHPO}_4 \cdot 3\text{H}_2\text{O}$
 $\text{MgHPO}_4 \cdot 3\text{H}_2\text{O} = \text{Mg}^{+2} + \text{H}^+ + \text{PO}_4^{-3} + 3\text{H}_2\text{O}$
 $\log_k -18.175$
 $\Delta H -0 \text{ kJ}$
FCO3Apatite
 $\text{Ca}_{9.316}\text{Na}_{0.36}\text{Mg}_{0.144}(\text{PO}_4)_4.8(\text{CO}_3)1.2\text{F}_{2.48} = 9.316\text{Ca}^{+2} + 0.36\text{Na}^+ + 0.144\text{Mg}^{+2} + 4.8\text{PO}_4^{-3} + 1.2\text{CO}_3^{-2} + 2.48\text{F}^-$
 $\log_k -114.4$
 $\Delta H 164.808 \text{ kJ}$
Hydroxylapatite
 $\text{Ca}_5(\text{PO}_4)_3\text{OH} + \text{H}^+ = 5\text{Ca}^{+2} + 3\text{PO}_4^{-3} + \text{H}_2\text{O}$
 $\log_k -44.333$
 $\Delta H -0 \text{ kJ}$
 $\text{CaHPO}_4 \cdot 2\text{H}_2\text{O}$
 $\text{CaHPO}_4 \cdot 2\text{H}_2\text{O} = \text{Ca}^{+2} + \text{H}^+ + \text{PO}_4^{-3} + 2\text{H}_2\text{O}$
 $\log_k -18.995$
 $\Delta H 23 \text{ kJ}$
 CaHPO_4

$\text{CaHPO}_4 = \text{Ca}^{+2} + \text{H}^+ + \text{PO}_4^{-3}$
 $\log_k -19.275$
 $\Delta_h 31 \text{ kJ}$
 $\text{Ca}_3(\text{PO}_4)_2(\text{beta})$
 $\text{Ca}_3(\text{PO}_4)_2 = 3\text{Ca}^{+2} + 2\text{PO}_4^{-3}$
 $\log_k -28.92$
 $\Delta_h 54 \text{ kJ}$
 $\text{Ca}_4\text{H}(\text{PO}_4)_3 \cdot 3\text{H}_2\text{O}$
 $\text{Ca}_4\text{H}(\text{PO}_4)_3 \cdot 3\text{H}_2\text{O} = 4\text{Ca}^{+2} + \text{H}^+ + 3\text{PO}_4^{-3} + 3\text{H}_2\text{O}$
 $\log_k -47.08$
 $\Delta_h -0 \text{ kJ}$
 SrHPO_4
 $\text{SrHPO}_4 = \text{Sr}^{+2} + \text{H}^+ + \text{PO}_4^{-3}$
 $\log_k -19.295$
 $\Delta_h -0 \text{ kJ}$
 BaHPO_4
 $\text{BaHPO}_4 = \text{Ba}^{+2} + \text{H}^+ + \text{PO}_4^{-3}$
 $\log_k -19.775$
 $\Delta_h -0 \text{ kJ}$
 $\text{U}(\text{HPO}_4)_2 \cdot 4\text{H}_2\text{O}$
 $\text{U}(\text{HPO}_4)_2 \cdot 4\text{H}_2\text{O} = \text{U}^{+4} + 2\text{PO}_4^{-3} + 2\text{H}^+ + 4\text{H}_2\text{O}$
 $\log_k -51.584$
 $\Delta_h 16.0666 \text{ kJ}$
 $(\text{UO}_2)_3(\text{PO}_4)_2$
 $(\text{UO}_2)_3(\text{PO}_4)_2 = 3\text{UO}_2^{+2} + 2\text{PO}_4^{-3}$
 $\log_k -49.4$
 $\Delta_h 397.062 \text{ kJ}$
 UO_2HPO_4
 $\text{UO}_2\text{HPO}_4 = \text{UO}_2^{+2} + \text{H}^+ + \text{PO}_4^{-3}$
 $\log_k -24.225$
 $\Delta_h -0 \text{ kJ}$
 Uramphite
 $(\text{NH}_4)_2(\text{UO}_2)_2(\text{PO}_4)_2 = 2\text{UO}_2^{+2} + 2\text{NH}_4^+ + 2\text{PO}_4^{-3}$
 $\log_k -51.749$
 $\Delta_h 40.5848 \text{ kJ}$
 Przhevalskite
 $\text{Pb}(\text{UO}_2)_2(\text{PO}_4)_2 = 2\text{UO}_2^{+2} + \text{Pb}^{+2} + 2\text{PO}_4^{-3}$
 $\log_k -44.365$
 $\Delta_h -46.024 \text{ kJ}$
 Torbernite
 $\text{Cu}(\text{UO}_2)_2(\text{PO}_4)_2 = 2\text{UO}_2^{+2} + \text{Cu}^{+2} + 2\text{PO}_4^{-3}$
 $\log_k -45.279$
 $\Delta_h -66.5256 \text{ kJ}$
 Bassetite
 $\text{Fe}(\text{UO}_2)_2(\text{PO}_4)_2 = 2\text{UO}_2^{+2} + \text{Fe}^{+2} + 2\text{PO}_4^{-3}$
 $\log_k -44.485$
 $\Delta_h -83.2616 \text{ kJ}$
 Saleeite
 $\text{Mg}(\text{UO}_2)_2(\text{PO}_4)_2 = 2\text{UO}_2^{+2} + \text{Mg}^{+2} + 2\text{PO}_4^{-3}$
 $\log_k -43.646$
 $\Delta_h -84.4331 \text{ kJ}$
 Ningyoite
 $\text{CaU}(\text{PO}_4)_2 \cdot 2\text{H}_2\text{O} = \text{U}^{+4} + \text{Ca}^{+2} + 2\text{PO}_4^{-3} + 2\text{H}_2\text{O}$
 $\log_k -53.906$

delta_h -9.4977 kJ
 H-Autunite
 $\text{H}_2(\text{UO}_2)_2(\text{PO}_4)_2 = 2\text{UO}_2 + 2\text{H}^+ + 2\text{PO}_4^{3-}$
 log_k -47.931
 delta_h -15.0624 kJ
 Autunite
 $\text{Ca}(\text{UO}_2)_2(\text{PO}_4)_2 = 2\text{UO}_2 + 2\text{Ca}^{2+} + 2\text{PO}_4^{3-}$
 log_k -43.927
 delta_h -59.9986 kJ
 Sr-Autunite
 $\text{Sr}(\text{UO}_2)_2(\text{PO}_4)_2 = 2\text{UO}_2 + 2\text{Sr}^{2+} + 2\text{PO}_4^{3-}$
 log_k -44.457
 delta_h -54.6012 kJ
 Na-Autunite
 $\text{Na}_2(\text{UO}_2)_2(\text{PO}_4)_2 = 2\text{UO}_2 + 2\text{Na}^+ + 2\text{PO}_4^{3-}$
 log_k -47.409
 delta_h -1.9246 kJ
 K-Autunite
 $\text{K}_2(\text{UO}_2)_2(\text{PO}_4)_2 = 2\text{UO}_2 + 2\text{K}^+ + 2\text{PO}_4^{3-}$
 log_k -48.244
 delta_h 24.5182 kJ
 Uranocircite
 $\text{Ba}(\text{UO}_2)_2(\text{PO}_4)_2 = 2\text{UO}_2 + 2\text{Ba}^{2+} + 2\text{PO}_4^{3-}$
 log_k -44.631
 delta_h -42.2584 kJ
 $\text{Pb}_3(\text{AsO}_4)_2$
 $\text{Pb}_3(\text{AsO}_4)_2 + 6\text{H}^+ = 3\text{Pb}^{2+} + 2\text{H}_3\text{AsO}_4$
 log_k 5.8
 delta_h -0 kJ
 $\text{AlAsO}_4 \cdot 2\text{H}_2\text{O}$
 $\text{AlAsO}_4 \cdot 2\text{H}_2\text{O} + 3\text{H}^+ = \text{Al}^{3+} + \text{H}_3\text{AsO}_4 + 2\text{H}_2\text{O}$
 log_k 4.8
 delta_h -0 kJ
 $\text{Zn}_3(\text{AsO}_4)_2 \cdot 2.5\text{H}_2\text{O}$
 $\text{Zn}_3(\text{AsO}_4)_2 \cdot 2.5\text{H}_2\text{O} + 6\text{H}^+ = 3\text{Zn}^{2+} + 2\text{H}_3\text{AsO}_4 + 2.5\text{H}_2\text{O}$
 log_k 13.65
 delta_h -0 kJ
 $\text{Cu}_3(\text{AsO}_4)_2 \cdot 2\text{H}_2\text{O}$
 $\text{Cu}_3(\text{AsO}_4)_2 \cdot 2\text{H}_2\text{O} + 6\text{H}^+ = 3\text{Cu}^{2+} + 2\text{H}_3\text{AsO}_4 + 2\text{H}_2\text{O}$
 log_k 6.1
 delta_h -0 kJ
 Ag_3AsO_3
 $\text{Ag}_3\text{AsO}_3 + 3\text{H}^+ = 3\text{Ag}^+ + \text{H}_3\text{AsO}_3$
 log_k 2.1573
 delta_h -0 kJ
 Ag_3AsO_4
 $\text{Ag}_3\text{AsO}_4 + 3\text{H}^+ = 3\text{Ag}^+ + \text{H}_3\text{AsO}_4$
 log_k -2.7867
 delta_h -0 kJ
 $\text{Ni}_3(\text{AsO}_4)_2 \cdot 8\text{H}_2\text{O}$
 $\text{Ni}_3(\text{AsO}_4)_2 \cdot 8\text{H}_2\text{O} + 6\text{H}^+ = 3\text{Ni}^{2+} + 2\text{H}_3\text{AsO}_4 + 8\text{H}_2\text{O}$
 log_k 15.7
 delta_h -0 kJ
 $\text{Co}_3(\text{AsO}_4)_2$

$\text{Co}_3(\text{AsO}_4)_2 + 6\text{H}^+ = 3\text{Co}^{+2} + 2\text{H}_3\text{AsO}_4$
 log_k 13.0341
 delta_h -0 kJ
 $\text{FeAsO}_4 \cdot 2\text{H}_2\text{O}$
 $\text{FeAsO}_4 \cdot 2\text{H}_2\text{O} + 3\text{H}^+ = \text{Fe}^{+3} + \text{H}_3\text{AsO}_4 + 2\text{H}_2\text{O}$
 log_k 0.4
 delta_h -0 kJ
 $\text{Mn}_3(\text{AsO}_4)_2 \cdot 8\text{H}_2\text{O}$
 $\text{Mn}_3(\text{AsO}_4)_2 \cdot 8\text{H}_2\text{O} + 6\text{H}^+ = 3\text{Mn}^{+2} + 2\text{H}_3\text{AsO}_4 + 8\text{H}_2\text{O}$
 log_k 12.5
 delta_h -0 kJ
 $\text{Ca}_3(\text{AsO}_4)_2 \cdot 4\text{H}_2\text{O}$
 $\text{Ca}_3(\text{AsO}_4)_2 \cdot 4\text{H}_2\text{O} + 6\text{H}^+ = 3\text{Ca}^{+2} + 2\text{H}_3\text{AsO}_4 + 4\text{H}_2\text{O}$
 log_k 22.3
 delta_h -0 kJ
 $\text{Ba}_3(\text{AsO}_4)_2$
 $\text{Ba}_3(\text{AsO}_4)_2 + 6\text{H}^+ = 3\text{Ba}^{+2} + 2\text{H}_3\text{AsO}_4$
 log_k -8.91
 delta_h 11.0458 kJ
 #NH₄VO₃
 # NH₄VO₃ + 2H⁺ = 2VO₂⁺ + H₂O
 # log_k 3.8
 # delta_h 30 kJ
 $\text{Pb}_3(\text{VO}_4)_2$
 $\text{Pb}_3(\text{VO}_4)_2 + 8\text{H}^+ = 3\text{Pb}^{+2} + 2\text{VO}_2^+ + 4\text{H}_2\text{O}$
 log_k 6.14
 delta_h -72.6342 kJ
 $\text{Pb}_2\text{V}_2\text{O}_7$
 $\text{Pb}_2\text{V}_2\text{O}_7 + 6\text{H}^+ = 2\text{Pb}^{+2} + 2\text{VO}_2^+ + 3\text{H}_2\text{O}$
 log_k -1.9
 delta_h -26.945 kJ
 AgVO_3
 $\text{AgVO}_3 + 2\text{H}^+ = \text{Ag}^+ + \text{VO}_2^+ + \text{H}_2\text{O}$
 log_k 0.77
 delta_h -0 kJ
 Ag_2HVO_4
 $\text{Ag}_2\text{HVO}_4 + 3\text{H}^+ = 2\text{Ag}^+ + \text{VO}_2^+ + 2\text{H}_2\text{O}$
 log_k 1.48
 delta_h -0 kJ
 $\text{Ag}_3\text{H}_2\text{VO}_5$
 $\text{Ag}_3\text{H}_2\text{VO}_5 + 4\text{H}^+ = 3\text{Ag}^+ + \text{VO}_2^+ + 3\text{H}_2\text{O}$
 log_k 5.18
 delta_h -0 kJ
 $\text{Fe}(\text{VO}_3)_2$
 $\text{Fe}(\text{VO}_3)_2 + 4\text{H}^+ = \text{Fe}^{+2} + 2\text{VO}_2^+ + 2\text{H}_2\text{O}$
 log_k -3.72
 delta_h -61.6722 kJ
 $\text{Mn}(\text{VO}_3)_2$
 $\text{Mn}(\text{VO}_3)_2 + 4\text{H}^+ = \text{Mn}^{+2} + 2\text{VO}_2^+ + 2\text{H}_2\text{O}$
 log_k 4.9
 delta_h -92.4664 kJ
 $\text{Mg}(\text{VO}_3)_2$
 $\text{Mg}(\text{VO}_3)_2 + 4\text{H}^+ = \text{Mg}^{+2} + 2\text{VO}_2^+ + 2\text{H}_2\text{O}$
 log_k 11.28

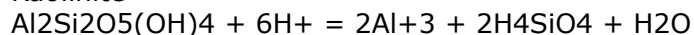
delta_h -136.649 kJ
 Mg₂V₂O₇
 $\text{Mg}_2\text{V}_2\text{O}_7 + 6\text{H}^+ = 2\text{Mg}^{+2} + 2\text{VO}_2^+ + 3\text{H}_2\text{O}$
 log_k 26.36
 delta_h -255.224 kJ
 Carnotite
 $\text{KUO}_2\text{VO}_4 + 4\text{H}^+ = \text{K}^+ + \text{UO}_2^{+2} + \text{VO}_2^+ + 2\text{H}_2\text{O}$
 log_k 0.23
 delta_h -36.4008 kJ
 Tyuyamunite
 $\text{Ca}(\text{UO}_2)_2(\text{VO}_4)_2 + 8\text{H}^+ = \text{Ca}^{+2} + 2\text{UO}_2^{+2} + 2\text{VO}_2^+ + 4\text{H}_2\text{O}$
 log_k 4.08
 delta_h -153.134 kJ
 Ca(VO₃)₂
 $\text{Ca}(\text{VO}_3)_2 + 4\text{H}^+ = \text{Ca}^{+2} + 2\text{VO}_2^+ + 2\text{H}_2\text{O}$
 log_k 5.66
 delta_h -84.7678 kJ
 Ca₃(VO₄)₂
 $\text{Ca}_3(\text{VO}_4)_2 + 8\text{H}^+ = 3\text{Ca}^{+2} + 2\text{VO}_2^+ + 4\text{H}_2\text{O}$
 log_k 38.96
 delta_h -293.466 kJ
 Ca₂V₂O₇
 $\text{Ca}_2\text{V}_2\text{O}_7 + 6\text{H}^+ = 2\text{Ca}^{+2} + 2\text{VO}_2^+ + 3\text{H}_2\text{O}$
 log_k 17.5
 delta_h -159.494 kJ
 Ca₃(VO₄)₂:4H₂O
 $\text{Ca}_3(\text{VO}_4)_2 \cdot 4\text{H}_2\text{O} + 8\text{H}^+ = 3\text{Ca}^{+2} + 2\text{VO}_2^+ + 8\text{H}_2\text{O}$
 log_k 39.86
 delta_h -0 kJ
 Ca₂V₂O₇:2H₂O
 $\text{Ca}_2\text{V}_2\text{O}_7 \cdot 2\text{H}_2\text{O} + 6\text{H}^+ = 2\text{Ca}^{+2} + 2\text{VO}_2^+ + 5\text{H}_2\text{O}$
 log_k 21.552
 delta_h -0 kJ
 Ba₃(VO₄)₂:4H₂O
 $\text{Ba}_3(\text{VO}_4)_2 \cdot 4\text{H}_2\text{O} + 8\text{H}^+ = 3\text{Ba}^{+2} + 2\text{VO}_2^+ + 8\text{H}_2\text{O}$
 log_k 32.94
 delta_h -0 kJ
 Ba₂V₂O₇:2H₂O
 $\text{Ba}_2\text{V}_2\text{O}_7 \cdot 2\text{H}_2\text{O} + 6\text{H}^+ = 2\text{Ba}^{+2} + 2\text{VO}_2^+ + 5\text{H}_2\text{O}$
 log_k 15.872
 delta_h -0 kJ
 NaVO₃
 $\text{NaVO}_3 + 2\text{H}^+ = \text{Na}^+ + \text{VO}_2^+ + \text{H}_2\text{O}$
 log_k 3.8582
 delta_h -30.1799 kJ
 Na₃VO₄
 $\text{Na}_3\text{VO}_4 + 4\text{H}^+ = 3\text{Na}^+ + \text{VO}_2^+ + 2\text{H}_2\text{O}$
 log_k 36.6812
 delta_h -184.61 kJ
 Na₄V₂O₇
 $\text{Na}_4\text{V}_2\text{O}_7 + 6\text{H}^+ = 4\text{Na}^+ + 2\text{VO}_2^+ + 3\text{H}_2\text{O}$
 log_k 37.4
 delta_h -201.083 kJ
 Halloysite



log_k 9.5749

delta_h -181.43 kJ

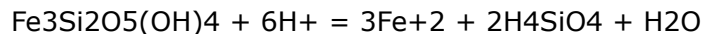
Kaolinite



log_k 7.435

delta_h -148 kJ

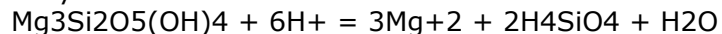
Greenalite



log_k 20.81

delta_h -0 kJ

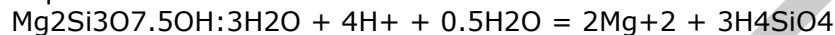
Chrysotile



log_k 32.2

delta_h -196 kJ

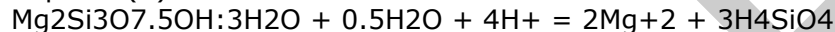
Sepiolite



log_k 15.76

delta_h -114.089 kJ

Sepiolite(A)

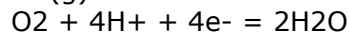


log_k 18.78

delta_h -0 kJ

PHASES

O₂(g)



log_k 83.0894

delta_h -571.66 kJ

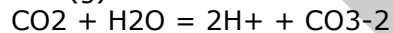
CH₄(g)



log_k -41.0452

delta_h 257.133 kJ

CO₂(g)



log_k -18.147

delta_h 4.06 kJ

H₂S(g)



log_k -8.01

delta_h -0 kJ

H₂Se(g)



log_k -4.96

delta_h -15.3 kJ

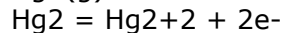
Hg(g)



log_k -7.8733

delta_h 22.055 kJ

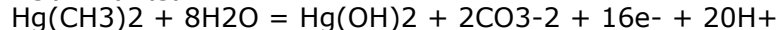
Hg₂(g)



log_k -14.9554

delta_h 58.07 kJ

Hg(CH₃)₂(g)



log_k -73.7066
 delta_h 481.99 kJ
 HgF(g)
 $\text{HgF} = 0.5\text{Hg}^{2+} + \text{F}^-$
 log_k 32.6756
 delta_h -254.844 kJ
 HgF₂(g)
 $\text{HgF}_2 + 2\text{H}_2\text{O} = \text{Hg}(\text{OH})_2 + 2\text{F}^- + 2\text{H}^+$
 log_k 12.5652
 delta_h -165.186 kJ
 HgCl(g)
 $\text{HgCl} = 0.5\text{Hg}^{2+} + \text{Cl}^-$
 log_k 19.4966
 delta_h -162.095 kJ
 HgBr(g)
 $\text{HgBr} = 0.5\text{Hg}^{2+} + \text{Br}^-$
 log_k 16.7566
 delta_h -142.157 kJ
 HgBr₂(g)
 $\text{HgBr}_2 + 2\text{H}_2\text{O} = \text{Hg}(\text{OH})_2 + 2\text{Br}^- + 2\text{H}^+$
 log_k -18.3881
 delta_h 54.494 kJ
 HgI(g)
 $\text{HgI} = 0.5\text{Hg}^{2+} + \text{I}^-$
 log_k 11.3322
 delta_h -106.815 kJ
 HgI₂(g)
 $\text{HgI}_2 + 2\text{H}_2\text{O} = \text{Hg}(\text{OH})_2 + 2\text{I}^- + 2\text{H}^+$
 log_k -27.2259
 delta_h 114.429 kJ
 SURFACE_MASTER_SPECIES
 Hfo_s Hfo_sOH
 Hfo_w Hfo_wOH
 Hao_ Hao_OH #hydrous aluminum oxides - gibbsite
 SURFACE_SPECIES
 Hfo_wOH = Hfo_wOH
 log_k 0.0
 Hfo_sOH = Hfo_sOH
 log_k 0.0
 Hao_OH = Hao_OH
 log_k 0.0

 Hfo_sOH + H⁺ = Hfo_sOH₂⁺
 log_k 7.29
 delta_h 0 kJ
 # Id: 8113302
 # log K source:
 # Delta H source:
 #T and ionic strength:
 Hfo_sOH = Hfo_sO⁻ + H⁺
 log_k -8.93
 delta_h 0 kJ
 # Id: 8113301
 # log K source:

Delta H source:
 #T and ionic strength:
 $\text{Hfo_wOH} + \text{H}^+ = \text{Hfo_wOH}_2^+$
 log_k 7.29
 delta_h 0 kJ
 # Id: 8123302
 # log K source:
 # Delta H source:
 #T and ionic strength:
 $\text{Hfo_wOH} = \text{Hfo_wO}^- + \text{H}^+$
 log_k -8.93
 delta_h 0 kJ
 # Id: 8123301
 # log K source:
 # Delta H source:
 #T and ionic strength:
 $\text{Hfo_sOH} + \text{Ba}^{+2} = \text{Hfo_sOHBa}^{+2}$
 log_k 5.46
 delta_h 0 kJ
 # Id: 8111000
 # log K source:
 # Delta H source:
 #T and ionic strength:
 $\text{Hfo_wOH} + \text{Ba}^{+2} = \text{Hfo_wOBa}^+ + \text{H}^+$
 log_k -7.2
 delta_h 0 kJ
 # Id: 8121000
 # log K source:
 # Delta H source:
 #T and ionic strength:
 $\text{Hfo_sOH} + \text{Ca}^{+2} = \text{Hfo_sOHCa}^{+2}$
 log_k 4.97
 delta_h 0 kJ
 # Id: 8111500
 # log K source:
 # Delta H source:
 #T and ionic strength:
 $\text{Hfo_wOH} + \text{Ca}^{+2} = \text{Hfo_wOCa}^+ + \text{H}^+$
 log_k -5.85
 delta_h 0 kJ
 # Id: 8121500
 # log K source:
 # Delta H source:
 #T and ionic strength:
 $\text{Hfo_wOH} + \text{Mg}^{+2} = \text{Hfo_wOMg}^+ + \text{H}^+$
 log_k -4.6
 delta_h 0 kJ
 # Id: 8124600
 # log K source:
 # Delta H source:
 #T and ionic strength:
 $\text{Hfo_sOH} + \text{Ag}^+ = \text{Hfo_sOAg} + \text{H}^+$
 log_k -1.72
 delta_h 0 kJ

Id: 8110200
 # log K source:
 # Delta H source:
 #T and ionic strength:
 $\text{Hfo_wOH} + \text{Ag}^+ = \text{Hfo_wOAg} + \text{H}^+$
 log_k -5.3
 delta_h 0 kJ
 # Id: 8120200
 # log K source:
 # Delta H source:
 #T and ionic strength:
 $\text{Hfo_sOH} + \text{Ni}^{+2} = \text{Hfo_sONi}^+ + \text{H}^+$
 log_k 0.37
 delta_h 0 kJ
 # Id: 8115400
 # log K source:
 # Delta H source:
 #T and ionic strength:
 $\text{Hfo_wOH} + \text{Ni}^{+2} = \text{Hfo_wONi}^+ + \text{H}^+$
 log_k -2.5
 delta_h 0 kJ
 # Id: 8125400
 # log K source:
 # Delta H source:
 #T and ionic strength:
 $\text{Hfo_sOH} + \text{Cd}^{+2} = \text{Hfo_sOCd}^+ + \text{H}^+$
 log_k 0.47
 delta_h 0 kJ
 # Id: 8111600
 # log K source:
 # Delta H source:
 #T and ionic strength:
 $\text{Hfo_wOH} + \text{Cd}^{+2} = \text{Hfo_wOCd}^+ + \text{H}^+$
 log_k -2.9
 delta_h 0 kJ
 # Id: 8121600
 # log K source:
 # Delta H source:
 #T and ionic strength:
 $\text{Hfo_sOH} + \text{Co}^{+2} = \text{Hfo_sOCo}^+ + \text{H}^+$
 log_k -0.46
 delta_h 0 kJ
 # Id: 8112000
 # log K source:
 # Delta H source:
 #T and ionic strength:
 $\text{Hfo_wOH} + \text{Co}^{+2} = \text{Hfo_wOCo}^+ + \text{H}^+$
 log_k -3.01
 delta_h 0 kJ
 # Id: 8122000
 # log K source:
 # Delta H source:
 #T and ionic strength:
 $\text{Hfo_sOH} + \text{Zn}^{+2} = \text{Hfo_sOZn}^+ + \text{H}^+$

log_k 0.99
 delta_h 0 kJ
 # Id: 8119500
 # log K source:
 # Delta H source:
 #T and ionic strength:
 $\text{Hfo_wOH} + \text{Zn}^{+2} = \text{Hfo_wOZn}^{+} + \text{H}^{+}$
 log_k -1.99
 delta_h 0 kJ
 # Id: 8129500
 # log K source:
 # Delta H source:
 #T and ionic strength:
 $\text{Hfo_sOH} + \text{Cu}^{+2} = \text{Hfo_sOCu}^{+} + \text{H}^{+}$
 log_k 2.89
 delta_h 0 kJ
 # Id: 8112310
 # log K source:
 # Delta H source:
 #T and ionic strength:
 $\text{Hfo_wOH} + \text{Cu}^{+2} = \text{Hfo_wOCu}^{+} + \text{H}^{+}$
 log_k 0.6
 delta_h 0 kJ
 # Id: 8123100
 # log K source:
 # Delta H source:
 #T and ionic strength:
 $\text{Hfo_sOH} + \text{Pb}^{+2} = \text{Hfo_sOPb}^{+} + \text{H}^{+}$
 log_k 4.65
 delta_h 0 kJ
 # Id: 8116000
 # log K source:
 # Delta H source:
 #T and ionic strength:
 $\text{Hfo_wOH} + \text{Pb}^{+2} = \text{Hfo_wOPb}^{+} + \text{H}^{+}$
 log_k 0.3
 delta_h 0 kJ
 # Id: 8126000
 # log K source:
 # Delta H source:
 #T and ionic strength:
 $\text{Hfo_sOH} + \text{Be}^{+2} = \text{Hfo_sOBe}^{+} + \text{H}^{+}$
 log_k 5.7
 delta_h 0 kJ
 # Id: 8111100
 # log K source:
 # Delta H source:
 #T and ionic strength:
 $\text{Hfo_wOH} + \text{Be}^{+2} = \text{Hfo_wOBe}^{+} + \text{H}^{+}$
 log_k 3.3
 delta_h 0 kJ
 # Id: 8121100
 # log K source:
 # Delta H source:

#T and ionic strength:
 $\text{Hfo_sOH} + \text{Hg}(\text{OH})_2 + \text{H}^+ = \text{Hfo_sOHg}^+ + 2\text{H}_2\text{O}$
 log_k 13.95
 delta_h 0 kJ
 # Id: 8113610
 # log K source:
 # Delta H source:
 #T and ionic strength:
 $\text{Hfo_wOH} + \text{Hg}(\text{OH})_2 + \text{H}^+ = \text{Hfo_wOHg}^+ + 2\text{H}_2\text{O}$
 log_k 12.64
 delta_h 0 kJ
 # Id: 8123610
 # log K source:
 # Delta H source:
 #T and ionic strength:
 $\text{Hfo_sOH} + \text{Sn}(\text{OH})_2 + \text{H}^+ = \text{Hfo_sOSn}^+ + 2\text{H}_2\text{O}$
 log_k 15.1
 delta_h 0 kJ
 # Id: 8117900
 # log K source:
 # Delta H source:
 #T and ionic strength:
 $\text{Hfo_wOH} + \text{Sn}(\text{OH})_2 + \text{H}^+ = \text{Hfo_wOSn}^+ + 2\text{H}_2\text{O}$
 log_k 13
 delta_h 0 kJ
 # Id: 8127900
 # log K source:
 # Delta H source:
 #T and ionic strength:
 $\text{Hfo_sOH} + \text{Cr}(\text{OH})_2^+ = \text{Hfo_sOCrOH}^+ + \text{H}_2\text{O}$
 log_k 11.63
 delta_h 0 kJ
 # Id: 8112110
 # log K source:
 # Delta H source:
 #T and ionic strength:
 $\text{Hfo_sOH} + \text{H}_3\text{AsO}_3 = \text{Hfo_sH}_2\text{AsO}_3 + \text{H}_2\text{O}$
 log_k 5.41
 delta_h 0 kJ
 # Id: 8110600
 # log K source:
 # Delta H source:
 #T and ionic strength:
 $\text{Hfo_wOH} + \text{H}_3\text{AsO}_3 = \text{Hfo_wH}_2\text{AsO}_3 + \text{H}_2\text{O}$
 log_k 5.41
 delta_h 0 kJ
 # Id: 8120600
 # log K source:
 # Delta H source:
 #T and ionic strength:
 $\text{Hfo_sOH} + \text{H}_3\text{BO}_3 = \text{Hfo_sH}_2\text{BO}_3 + \text{H}_2\text{O}$
 log_k 0.62
 delta_h 0 kJ
 # Id: 8110900

log K source:
 # Delta H source:
 #T and ionic strength:
 $\text{Hfo_wOH} + \text{H}_3\text{BO}_3 = \text{Hfo_wH}_2\text{BO}_3 + \text{H}_2\text{O}$
 log_k 0.62
 delta_h 0 kJ
 # Id: 8120900
 # log K source:
 # Delta H source:
 #T and ionic strength:
 $\text{Hfo_sOH} + \text{PO}_4\text{-3} + 3\text{H}^+ = \text{Hfo_sH}_2\text{PO}_4 + \text{H}_2\text{O}$
 log_k 31.29
 delta_h 0 kJ
 # Id: 8115800
 # log K source:
 # Delta H source:
 #T and ionic strength:
 $\text{Hfo_wOH} + \text{PO}_4\text{-3} + 3\text{H}^+ = \text{Hfo_wH}_2\text{PO}_4 + \text{H}_2\text{O}$
 log_k 31.29
 delta_h 0 kJ
 # Id: 8125800
 # log K source:
 # Delta H source:
 #T and ionic strength:
 $\text{Hfo_sOH} + \text{PO}_4\text{-3} + 2\text{H}^+ = \text{Hfo_sHPO}_4\text{-} + \text{H}_2\text{O}$
 log_k 25.39
 delta_h 0 kJ
 # Id: 8115801
 # log K source:
 # Delta H source:
 #T and ionic strength:
 $\text{Hfo_wOH} + \text{PO}_4\text{-3} + 2\text{H}^+ = \text{Hfo_wHPO}_4\text{-} + \text{H}_2\text{O}$
 log_k 25.39
 delta_h 0 kJ
 # Id: 8125801
 # log K source:
 # Delta H source:
 #T and ionic strength:
 $\text{Hfo_sOH} + \text{PO}_4\text{-3} + \text{H}^+ = \text{Hfo_sPO}_4\text{-2} + \text{H}_2\text{O}$
 log_k 17.72
 delta_h 0 kJ
 # Id: 8115802
 # log K source:
 # Delta H source:
 #T and ionic strength:
 $\text{Hfo_wOH} + \text{PO}_4\text{-3} + \text{H}^+ = \text{Hfo_wPO}_4\text{-2} + \text{H}_2\text{O}$
 log_k 17.72
 delta_h 0 kJ
 # Id: 8125802
 # log K source:
 # Delta H source:
 #T and ionic strength:
 $\text{Hfo_sOH} + \text{H}_3\text{AsO}_4 = \text{Hfo_sH}_2\text{AsO}_4 + \text{H}_2\text{O}$
 log_k 8.61

delta_h 0 kJ
 # Id: 8110610
 # log K source:
 # Delta H source:
 #T and ionic strength:
 $\text{Hfo_wOH} + \text{H}_3\text{AsO}_4 = \text{Hfo_wH}_2\text{AsO}_4 + \text{H}_2\text{O}$
 log_k 8.61
 delta_h 0 kJ
 # Id: 8120610
 # log K source:
 # Delta H source:
 #T and ionic strength:
 $\text{Hfo_sOH} + \text{H}_3\text{AsO}_4 = \text{Hfo_sHAsO}_4^- + \text{H}_2\text{O} + \text{H}^+$
 log_k 2.81
 delta_h 0 kJ
 # Id: 8110611
 # log K source:
 # Delta H source:
 #T and ionic strength:
 $\text{Hfo_wOH} + \text{H}_3\text{AsO}_4 = \text{Hfo_wHAsO}_4^- + \text{H}_2\text{O} + \text{H}^+$
 log_k 2.81
 delta_h 0 kJ
 # Id: 8120611
 # log K source:
 # Delta H source:
 #T and ionic strength:
 $\text{Hfo_sOH} + \text{H}_3\text{AsO}_4 = \text{Hfo_sOHAsO}_4^{3-} + 3\text{H}^+$
 log_k -10.12
 delta_h 0 kJ
 # Id: 8110613
 # log K source:
 # Delta H source:
 #T and ionic strength:
 $\text{Hfo_wOH} + \text{H}_3\text{AsO}_4 = \text{Hfo_wOHAsO}_4^{3-} + 3\text{H}^+$
 log_k -10.12
 delta_h 0 kJ
 # Id: 8120613
 # log K source:
 # Delta H source:
 #T and ionic strength:
 $\text{Hfo_sOH} + \text{VO}_2^+ + 2\text{H}_2\text{O} = \text{Hfo_sOHVO}_4^{3-} + 4\text{H}^+$
 log_k -16.63
 delta_h 0 kJ
 # Id: 8119031
 # log K source:
 # Delta H source:
 #T and ionic strength:
 $\text{Hfo_wOH} + \text{VO}_2^+ + 2\text{H}_2\text{O} = \text{Hfo_wOHVO}_4^{3-} + 4\text{H}^+$
 log_k -16.63
 delta_h 0 kJ
 # Id: 8129031
 # log K source:
 # Delta H source:
 #T and ionic strength:

$\text{Hfo_sOH} + \text{SO}_4^{2-} + \text{H}^+ = \text{Hfo_sSO}_4^- + \text{H}_2\text{O}$
 log_k 7.78
 delta_h 0 kJ
 # Id: 8117320
 # log K source:
 # Delta H source:
 #T and ionic strength:
 $\text{Hfo_wOH} + \text{SO}_4^{2-} + \text{H}^+ = \text{Hfo_wSO}_4^- + \text{H}_2\text{O}$
 log_k 7.78
 delta_h 0 kJ
 # Id: 8127320
 # log K source:
 # Delta H source:
 #T and ionic strength:
 $\text{Hfo_sOH} + \text{SO}_4^{2-} = \text{Hfo_sOHSO}_4^{-2}$
 log_k 0.79
 delta_h 0 kJ
 # Id: 8117321
 # log K source:
 # Delta H source:
 #T and ionic strength:
 $\text{Hfo_wOH} + \text{SO}_4^{2-} = \text{Hfo_wOHSO}_4^{-2}$
 log_k 0.79
 delta_h 0 kJ
 # Id: 8127321
 # log K source:
 # Delta H source:
 #T and ionic strength:
 $\text{Hfo_sOH} + \text{HSeO}_3^- = \text{Hfo_sSeO}_3^- + \text{H}_2\text{O}$
 log_k 4.29
 delta_h 0 kJ
 # Id: 8117610
 # log K source:
 # Delta H source:
 #T and ionic strength:
 $\text{Hfo_wOH} + \text{HSeO}_3^- = \text{Hfo_wSeO}_3^- + \text{H}_2\text{O}$
 log_k 4.29
 delta_h 0 kJ
 # Id: 8127610
 # log K source:
 # Delta H source:
 #T and ionic strength:
 $\text{Hfo_sOH} + \text{HSeO}_3^- = \text{Hfo_sOHSeO}_3^{-2} + \text{H}^+$
 log_k -3.23
 delta_h 0 kJ
 # Id: 8117611
 # log K source:
 # Delta H source:
 #T and ionic strength:
 $\text{Hfo_wOH} + \text{HSeO}_3^- = \text{Hfo_wOHSeO}_3^{-2} + \text{H}^+$
 log_k -3.23
 delta_h 0 kJ
 # Id: 8127611
 # log K source:

Delta H source:
 #T and ionic strength:
 $\text{Hfo_sOH} + \text{SeO4-2} + \text{H+} = \text{Hfo_sSeO4-} + \text{H2O}$
 log_k 7.73
 delta_h 0 kJ
 # Id: 8117620
 # log K source:
 # Delta H source:
 #T and ionic strength:
 $\text{Hfo_wOH} + \text{SeO4-2} + \text{H+} = \text{Hfo_wSeO4-} + \text{H2O}$
 log_k 7.73
 delta_h 0 kJ
 # Id: 8127620
 # log K source:
 # Delta H source:
 #T and ionic strength:
 $\text{Hfo_sOH} + \text{SeO4-2} = \text{Hfo_sOHSeO4-2}$
 log_k 0.8
 delta_h 0 kJ
 # Id: 8117621
 # log K source:
 # Delta H source:
 #T and ionic strength:
 $\text{Hfo_wOH} + \text{SeO4-2} = \text{Hfo_wOHSeO4-2}$
 log_k 0.8
 delta_h 0 kJ
 # Id: 8127621
 # log K source:
 # Delta H source:
 #T and ionic strength:
 $\text{Hfo_sOH} + \text{CrO4-2} + \text{H+} = \text{Hfo_sCrO4-} + \text{H2O}$
 log_k 10.85
 delta_h 0 kJ
 # Id: 8112120
 # log K source:
 # Delta H source:
 #T and ionic strength:
 $\text{Hfo_wOH} + \text{CrO4-2} + \text{H+} = \text{Hfo_wCrO4-} + \text{H2O}$
 log_k 10.85
 delta_h 0 kJ
 # Id: 8122120
 # log K source:
 # Delta H source:
 #T and ionic strength:
 $\text{Hfo_sOH} + \text{CrO4-2} = \text{Hfo_sOHCrO4-2}$
 log_k 3.9
 delta_h 0 kJ
 # Id: 8112121
 # log K source:
 # Delta H source:
 #T and ionic strength:
 $\text{Hfo_wOH} + \text{CrO4-2} = \text{Hfo_wOHCrO4-2}$
 log_k 3.9
 delta_h 0 kJ

Id: 8122121
 # log K source:
 # Delta H source:
 #T and ionic strength:
 $\text{Hfo_sOH} + \text{MoO}_4^{2-} + \text{H}^+ = \text{Hfo_sMoO}_4^- + \text{H}_2\text{O}$
 log_k 9.5
 delta_h 0 kJ
 # Id: 8114800
 # log K source:
 # Delta H source:
 #T and ionic strength:
 $\text{Hfo_wOH} + \text{MoO}_4^{2-} + \text{H}^+ = \text{Hfo_wMoO}_4^- + \text{H}_2\text{O}$
 log_k 9.5
 delta_h 0 kJ
 # Id: 8124800
 # log K source:
 # Delta H source:
 #T and ionic strength:
 $\text{Hfo_sOH} + \text{MoO}_4^{2-} = \text{Hfo_sOHMoO}_4^{2-}$
 log_k 2.4
 delta_h 0 kJ
 # Id: 8114801
 # log K source:
 # Delta H source:
 #T and ionic strength:
 $\text{Hfo_wOH} + \text{MoO}_4^{2-} = \text{Hfo_wOHMoO}_4^{2-}$
 log_k 2.4
 delta_h 0 kJ
 # Id: 8124801
 # log K source:
 # Delta H source:
 #T and ionic strength:
 $\text{Hfo_sOH} + \text{Sb(OH)}_6^- + \text{H}^+ = \text{Hfo_sSbO(OH)}_4 + 2\text{H}_2\text{O}$
 log_k 8.4
 delta_h 0 kJ
 # Id: 8117410
 # log K source:
 # Delta H source:
 #T and ionic strength:
 $\text{Hfo_wOH} + \text{Sb(OH)}_6^- + \text{H}^+ = \text{Hfo_wSbO(OH)}_4 + 2\text{H}_2\text{O}$
 log_k 8.4
 delta_h 0 kJ
 # Id: 8127410
 # log K source:
 # Delta H source:
 #T and ionic strength:
 $\text{Hfo_sOH} + \text{Sb(OH)}_6^- = \text{Hfo_sOHSbO(OH)}_4^- + \text{H}_2\text{O}$
 log_k 1.3
 delta_h 0 kJ
 # Id: 8117411
 # log K source:
 # Delta H source:
 #T and ionic strength:
 $\text{Hfo_wOH} + \text{Sb(OH)}_6^- = \text{Hfo_wOHSbO(OH)}_4^- + \text{H}_2\text{O}$

log_k 1.3
 delta_h 0 kJ
 # Id: 8127411
 # log K source:
 # Delta H source:
 #T and ionic strength:
 $\text{Hfo_sOH} + \text{Cyanide}^- + \text{H}^+ = \text{Hfo_sCyanide} + \text{H}_2\text{O}$
 log_k 13
 delta_h 0 kJ
 # Id: 8111430
 # log K source:
 # Delta H source:
 #T and ionic strength:
 $\text{Hfo_wOH} + \text{Cyanide}^- + \text{H}^+ = \text{Hfo_wCyanide} + \text{H}_2\text{O}$
 log_k 13
 delta_h 0 kJ
 # Id: 8121430
 # log K source:
 # Delta H source:
 #T and ionic strength:
 $\text{Hfo_sOH} + \text{Cyanide}^- = \text{Hfo_sOHCyanide}^-$
 log_k 5.7
 delta_h 0 kJ
 # Id: 8111431
 # log K source:
 # Delta H source:
 #T and ionic strength:
 $\text{Hfo_wOH} + \text{Cyanide}^- = \text{Hfo_wOHCyanide}^-$
 log_k 5.7
 delta_h 0 kJ
 # Id: 8121431
 # log K source:
 # Delta H source:
 #T and ionic strength:
 #Additions from GWB Minteq
 $\text{Hfo_wOH} + \text{H}_4\text{SiO}_4 = \text{Hfo_wOSi(OH)}_3 + \text{H}_2\text{O}$
 log_k 4.28
 delta_h 0 kJ
 $\text{Hfo_wOH} + \text{H}_4\text{SiO}_4 = \text{Hfo_wOSiO(OH)}_2^- + \text{H}^+ + \text{H}_2\text{O}$
 log_k -3.22
 delta_h 0 kJ
 $\text{Hfo_sOH} + \text{H}_4\text{SiO}_4 = \text{Hfo_sOSi(OH)}_3 + \text{H}_2\text{O}$
 log_k 4.28
 delta_h 0
 $\text{Hfo_sOH} + \text{H}_4\text{SiO}_4 = \text{Hfo_sOSiO(OH)}_2^- + \text{H}^+ + \text{H}_2\text{O}$
 log_k -3.22
 delta_h 0
 $\text{Hfo_wOH} + \text{CO}_3^{2-} + \text{H}^+ = \text{Hfo_wCO}_3^- + \text{H}_2\text{O}$
 log_k 12.56
 delta_h 0
 $\text{Hfo_wOH} + \text{CO}_3^{2-} + 2\text{H}^+ = \text{Hfo_wHCO}_3 + \text{H}_2\text{O}$
 log_k 20.62
 delta_h 0
 $\text{Hfo_sOH} + \text{CO}_3^{2-} + \text{H}^+ = \text{Hfo_sCO}_3^- + \text{H}_2\text{O}$

log_k 12.56
delta_h 0
Hfo_sOH + CO3-2 + 2H+ = Hfo_sHCO3 + H2O
log_k 20.62
delta_h 0

#Karamalidis and Dzombak sorption to gibbsite (hao) as compiled in Cravotta 2021 (<https://doi.org/10.1016/j.apgeochem.2020.104845>) Table S4 unless otherwise noted

Hao_OH + Cu+2 = Hao_OCu+ + H+
log_k 0.25
Hao_OH + Pb+2 = Hao_OPb+ + H+
log_k 0.37
Hao_OH + Co+2 = Hao_OCo+ + H+
log_k -2.52
Hao_OH + Cd+2 = Hao_OCd+ + H+
log_k -2.73
Hao_OH + Mn+2 = Hao_OMn+ + H+
log_k -5.49
Hao_OH + Fe+2 = Hao_OFe+ + H+
log_k -3.77
Hao_OH + Ca+2 = Hao_OCa+ + H+
log_k -10.49
Hao_OH + Mg+2 = Hao_OMg+ + H+
log_k -5.93
Hao_OH + Ba+2 = Hao_OBa+ + H+
log_k -8.5
Hao_OH + Sr+2 = Hao_OSr+ + H+
log_k -8.26
Hao_OH + Zn+2 = Hao_OZn+ + H+
log_k -0.96
Hao_OH + PO4-3 + 3 H+ = Hao_H2PO4 + H2O
log_k 26.89
Hao_OH + PO4-3 + 2H+ = Hao_HPO4- + H2O
log_k 19.37
Hao_OH + PO4-3 + H+ = Hao_PO4-2 + H2O
log_k 13.57
#Hao_OH + SO4-2 + H+ = Hao_SO4- + H2O
log_k -0.45
#Hao_OH + SO4-2 = Hao_OHSO4-2
log_k 1.19
Hao_OH + F- + H+ = Hao_F + H2O
log_k 8.78
Hao_OH + F- = Hao_OHF-
log_k 2.88
Hao_OH + 2 F- + H+ = Hao_F2- + H2O
log_k 11.94
Hao_OH + H4SiO4 = Hao_OH4SiO4- + H+
log_k -4.16

#Modified value from Goldberg and Glaubig (1985)

Hao_OH + H3BO3 = Hao_H2BO3 + H2O
Log_k 4.83
Hao_OH + H3BO3 = Hao_H3BO4- + H+
Log_k -7.40

#Modified value from Kitadai et al. (2018)

Hao_OH + SO4-2 + H+ = Hao_SO4- + H2O
log_k 2.4
#Modified value from Kitadai et al. (2018)
Hao_OH + SO4-2 = Hao_OHSO4-2
log_k 7.5
END

DRAFT

ATTACHMENT C
Details of Geochemical Model Parameterization

Attachment C. Details of Geochemical Model Parameterization

Introduction

This appendix to the Groundwater Polishing Report for the Baldwin Fly Ash Pond System (FAPS) provides detailed information regarding geochemical model parameterization. The information provided includes sources of thermodynamic data, sources of data used in model parameterization, summarized values, and calculation methods. All solid-phase data is fully documented in the Nature and Extent Report.¹ All aqueous data have been posted to the facility's operating record in accordance with 35 I.A.C. § 845.800(d)(15).

Solid Phase Inputs

The solid phase inputs to the model included iron (hydr)oxides and aluminum (hydr)oxides. These phases tend to have relatively rapid precipitation kinetics and form an outer layer on the surfaces of aquifer solids, creating surface area for sorption and attenuation of boron. Input concentrations for iron and aluminum (hydr)oxides are ideally derived using sequential extraction procedure (SEP) data. SEP methods are described in the Geochemical Conceptual Site Model (GCSM)² and employ chemical extractants to dissolve metals from specific solid-associated phases. SEP methods use progressively stronger reagents to solubilize metals from increasingly recalcitrant phases. Although these procedures do not identify the discrete solid phases in a soil/aquifer matrix, they provide a means to evaluate and characterize the metal binding mechanisms and relative stability of metals in each phase, and to estimate the available mass of the respective attenuating phase(s) (i.e., aluminum and iron [hydr]oxide). However, SEP analyses of aluminum were not completed for Baldwin FAPS samples, and SEP analyses of iron completed for FAPS samples did not include the critical amorphous extraction step. The dataset constraints necessitated alternative means of deriving oxide inputs.

Because Baldwin FAPS SEP analyses did not include aluminum or an amorphous iron fraction, model input concentrations for ferrihydrite and gibbsite were derived using site-specific total metals and the proportion of total metals as crystalline metal oxides (aluminum) or amorphous metal oxides (iron) compiled from SEP datasets consisting of samples collected from similar geologic systems at various power generating facilities across Illinois. Much of the Baldwin FAPS PMP consists of the Cahokia Formation, so the analogous dataset for the PMP is comprised of samples collected from various power generating facilities across Illinois specifically within the Cahokia Formation. The

¹ The Nature and Extent Report was previously submitted to IEPA on April 3, 2024, and provided with relevant updates as Appendix D of the CAAA to which this report is attached.

² Ibid.; the GCSM is an appendix of the Nature and Extent Report.

FAPS UA consists of a bedrock formation which was not sampled at other Illinois power generating facilities; therefore, the UA analogous dataset is comprised of numerous samples collected from multiple geologic units at power generating facilities across Illinois. The geologic similarity (regional geology, similar lithologies and depositional environments, similar mineral assemblages) between the samples comprising these datasets and the Baldwin FAPS subsurface make these datasets appropriate for estimating the amount and distribution of sorbing solid phases in the absence of a complete site-specific dataset.

SEP data for iron and aluminum is available for 25 solid phase samples across six distinct hydrostratigraphic units (UA analogous dataset), of which 17 solid phase samples are specifically from the Cahokia Formation (PMP analogous dataset).

Total solid-phase iron was measured in eleven site-specific PMP/UA solids samples (two from the PMP, nine from the UA) at concentrations ranging from 5,500 milligrams per kilogram (mg/kg) to 38,000 mg/kg. Iron SEP analyses were completed for four PMP solids samples and four UA solids samples. The crystalline iron oxide component for the UA was determined by applying the average oxide fraction result from iron SEP analyses from UA samples to the average total iron concentration from UA samples. The crystalline iron oxide component for the PMP was determined by applying the average oxide fraction result from iron SEP analysis from the PMP to the average total iron concentration from all Baldwin FAPS samples. The amorphous ferrihydrite components for both hydrostratigraphic units were based on the 25th percentile of amorphous ferrihydrite distribution in each applicable analogous compiled SEP dataset.

The gibbsite component of the models was determined using the average mass of aluminum associated with the oxide fraction from each compiled SEP dataset described above.

In thermodynamic modeling, the amount of sorbing phase present is typically the dominant control on the concentration of constituents sorbed under a given pH. Therefore, different amounts of metal oxides were used to test the sensitivity of the model to the amount of sorbing phase present. The amount of metal oxides used were derived from the 25th percentile, median (*i.e.*, 50th percentile), and 75th percentile of the SEP results for the relevant iron and aluminum phases.

Sorption of inorganic constituents to iron (hydr)oxides in the MINTEQ v4 database³ is represented by the hydrous ferric oxide (HFO) thermodynamic dataset presented in Dzombak and Morel (1990). Sorption of inorganic constituents to aluminum (hydr)oxides is represented by the hydrous aluminum oxide (HAO) thermodynamic data presented in Karamalidis and Dzombak (2010), Goldberg and Glaubig (1985) (boron), and Kitadai et al. (2018) (sulfate). These sorption data are based on gibbsite, a nearly ubiquitous crystalline aluminum hydroxide mineral (Karamalidis and Dzombak 2010).

The quantities of HFO and HAO in the model are represented by ferrihydrite ($\text{Fe}(\text{OH})_3$) and gibbsite ($\text{Al}(\text{OH})_3$), respectively. Ferrihydrite is the most similar naturally occurring iron oxide to HFO (Dzombak and Morel, 1990), and sorption data for HAO was determined using gibbsite (Karamalidis and Dzombak 2010). Metal concentrations are presented in milligrams per kilogram

³ The default MINTEQ v4 database for PHREEQC does not include sorption data for carbonate and silicate to HFO. Thermodynamic constants for sorption of carbonate and silicate to HFO were added from the MINTEQ database associated with the Geochemist's Workbench software program.

of dry weight (mg/kg dw), whereas ferrihydrite and gibbsite inputs to the model represent moles of solid phase associated with one liter (L) of aqueous phase. The concentrations of iron and aluminum were converted to moles of ferrihydrite and gibbsite (respectively) according to the following:

The mass in kilograms (kg) of solid in the model (i.e., per 1 L of water) was calculated by:

$$\text{Solid Mass In Model (kg)} = \frac{(1 - \phi)}{\phi} \times \frac{1000 \text{ cm}^3 \text{ water}}{L \text{ water}} \times 1 L \text{ water} \times \rho \times \frac{1 \text{ kg solid}}{1000 \text{ g solid}}$$

Where:

ϕ = porosity (water volume in cubic centimeters [cm³] / total volume in cm³)

ρ = density of the solid (grams [g]/cm³)

Porosity and density represent the median of measurements each hydrostratigraphic unit as reported in the Hydrogeologic Characterization Report⁴.

Moles of ferrihydrite and gibbsite were determined using metal concentrations as described above, the molar mass of iron or aluminum, and the mass of solid phase in the model:

$$\begin{aligned} \text{Moles of Metal Oxide} \\ = \frac{\text{mg Fe or Al}}{\text{kg solid}} \times \frac{\text{g}}{1000 \text{ mg}} \times \frac{\text{moles Fe or Al}}{\text{g Fe or Al}} \times \text{kg Solid Mass in Model} \end{aligned}$$

The moles of ferrihydrite and gibbsite are represented by moles of Fe or Al (respectively) in a 1:1 ratio based on the mineral formula. Ferrihydrite and gibbsite were allowed to precipitate or dissolve in the reaction phase of the model to evaluate the impact of source control on sorbing phase availability.

Calcite and dolomite were included as mineral phases in the model because carbonate mineral formation and dissolution are often major controls on groundwater pH. Calcite and dolomite are common carbonate minerals and were detected at levels of greater than 1% by weight in X-ray diffraction (XRD) analysis and are therefore considered to be present in excess within the aquifer. Therefore, the mass fractions reported in the XRD are used as model inputs. Both calcite and dolomite were allowed to precipitate in the reaction phase of the model.

Barite and gypsum are common sulfate minerals that have the potential to form under ambient environmental conditions. Neither mineral was detected in XRD results at well locations containing exceedances of GWPSs. Therefore, barite and gypsum did not have initial concentrations in the model but were allowed to precipitate or dissolve in the reaction phase of the model.

⁴ The Hydrogeologic Characterization Report was previously submitted to IEPA as part of the Closure Permit Application and is provided as Appendix B.3 to the Construction Permit Application.

Aqueous Inputs

In addition to the constituent of concern boron, the following parameters are included in the model and are anticipated to capture the expected attenuation and mobilization mechanisms for reasons detailed below:

- Temperature, pH and pe: pH and pe (a measure of redox potential) are major controls on chemical attenuation and mobility.
- Chloride, potassium, and sodium: Major ions in groundwater typically required for the model to reach charge balance.
- Carbonate ion, calcium, and magnesium: Major ions in groundwater that may also form common minerals, including carbonates. Carbonate mineral formation and dissolution is often a major control on groundwater pH. Bicarbonate and carbonate ions, a major component of groundwater alkalinity, may also compete with sulfate/boron for sorbing sites.
- Silicon and phosphate: Silicate and phosphate are oxyanions that compete with sulfate/boron for sorbing sites.
- Aluminum, iron, and manganese: As discussed above, iron and aluminum form reactive metal (hydr)oxide minerals which have high capacities for sorbing other ions on their surfaces. Although sorption to manganese oxides was not considered in this model, manganese behaves similarly to iron and is included for completeness.
- Remaining constituents regulated under 35 IAC § 845.600⁵: Although these parameters are not subject to corrective action at NEW PAP, they are included in the model for completeness.

Values for pe and carbonate ion concentrations were derived from values previously reported in the analytical data according to the following methods.

pe is a non-dimension scale of redox potential and is calculated from oxidation reduction potential (ORP). First, the field-measured ORP was converted to Eh (i.e., the redox potential normalized to the standard hydrogen electrode). The following equation provided in the Horiba water quality meter instruction manual⁶ was used:

$$Eh = ORP + 206 - 0.7 \cdot (T - 25)$$

Where both Eh and ORP are in volts (V) and T is temperature in degrees Celsius. Eh is then converted to pe:

$$pe = (Eh \cdot F) / (2.303 \cdot R \cdot T)$$

Where:

$$F = \text{Faraday constant (96,500 Joules (J) / V-equivalent)}$$

⁵ Mercury, thallium, total dissolved solids, and radium were not included in the model. Mercury reactions within the environment are highly complex and would require a separate modeling effort. Thallium forms a non-reactive monovalent cation and is rarely detected in the groundwater and is therefore not expected to contribute to model outcomes. Total dissolved solids are not a chemical parameter, but rather the result of other chemical abundances taken together. Radium is not included in most thermodynamic databases.

⁶ https://static.horiba.com/fileadmin/Horiba/Products/Process_and_Environmental/Water_Pollution/Instruction_Manuals/U-50/U-50_Manual.pdf

R = Molar gas constant (8.31 J / Kelvin (K)-mole)

T = temperature in Kelvin

Data reported for groundwater at the site include carbonate and bicarbonate alkalinity in units of mg of calcium carbonate per liter (mg CaCO₃/L). For use in modeling, it is convenient to convert these values to a single carbonate (CO₃²⁻) ion concentration. Because carbonate and bicarbonate alkalinity are reported in the same units (i.e., standardized to mg CaCO₃) and represent different protonation states of the same inorganic carbon oxyanion, they were summed to represent total alkalinity due to carbonate. This summed alkalinity was converted to concentration of carbonate ion according to the following equation:

$$\frac{\text{mg } CO_3^{2-}}{L} = \frac{\text{mg } CaCO_3}{L} \times \frac{\text{mole } CaCO_3}{100.1 \text{ mg } CaCO_3} \times \frac{1 \text{ mole } CO_3^{2-}}{1 \text{ mole } CaCO_3} \times \frac{60 \text{ mg } CO_3^{2-}}{\text{mole } CO_3^{2-}}$$

The full suite of geochemical parameters for this model was measured in Quarter 2 and Quarter 3, 2023, for wells MW-150 and MW-152, and Quarter 1, 2024 for wells MW-252 and MW-366. The medians of these results were used in the model to represent average groundwater interacting with the solid phase. For downgradient wells the median for each parameter was calculated for each location individually. For background wells, a single median for each parameter was calculated using data from all three background locations measured in Quarter 2 and Quarter 3, 2023.

The model was run without charge balancing and with charge balancing on chloride. The results during the reaction modeling did not substantially differ with and without charge balancing on chloride. The results presented in the Groundwater Polishing Report therefore represent the model results using charge balancing on chloride.

References

- Appelo C.A.J. and Postma D. 2005. *Geochemistry, Groundwater, and Pollution*. 2nd Edition. A.A. Balkema Publishers, member of Taylor & Francis Group. The Netherlands.
- Dzombak D.A. and Morel F.M.M. 1990. *Surface Complexation Modeling: Hydrous Ferric Oxide*. John Wiley & Sons, New York.
- Goldberg S. and Glaubig R.A. 1985. Boron Adsorption on Aluminum and Iron Oxide Minerals. *Soil Science Society of America Journal* **49**(6):1374-1379.
- Karamalidis A.K. and Dzombak D.A. 2010. *Surface Complexation Modeling: Gibbsite*. John Wiley & Sons, New York.
- Kitadai N., Nishiuchi K., and Tanaka M. 2018. A comprehensive predictive model for sulfate adsorption on oxide minerals. *Geochimica et Cosmochimica Acta* **238**:150-168.

ATTACHMENT D
Complete Geochemical Modeling Outputs

Attachment D. PHREEQC modeling output

Groundwater Polishing Report

Fly Ash Pond System

Baldwin Power Plant

Baldwin, IL

| Location | Location Description | Model | Charge Balance | Solids Summary |
|----------|----------------------|------------------|----------------|----------------|
| MW-150 | C - PMP | Initial Soln | TRUE | 25p |
| MW-152 | C - PMP | Initial Soln | TRUE | 25p |
| MW-252 | C - PMP | Initial Soln | TRUE | 25p |
| MW-366 | C - UA | Initial Soln | TRUE | 25p |
| MW-150 | C - PMP | Speciation Model | TRUE | 25p |
| MW-152 | C - PMP | Speciation Model | TRUE | 25p |
| MW-252 | C - PMP | Speciation Model | TRUE | 25p |
| MW-366 | C - UA | Speciation Model | TRUE | 25p |
| MW-150 | C - PMP | First Reaction | TRUE | 25p |
| MW-150 | C - PMP | Second Reaction | TRUE | 25p |
| MW-152 | C - PMP | First Reaction | TRUE | 25p |
| MW-152 | C - PMP | Second Reaction | TRUE | 25p |
| MW-252 | C - PMP | First Reaction | TRUE | 25p |
| MW-252 | C - PMP | Second Reaction | TRUE | 25p |
| MW-366 | C - UA | First Reaction | TRUE | 25p |
| MW-366 | C - UA | Second Reaction | TRUE | 25p |
| MW-150 | C - PMP | Initial Soln | TRUE | 75p |
| MW-152 | C - PMP | Initial Soln | TRUE | 75p |
| MW-252 | C - PMP | Initial Soln | TRUE | 75p |
| MW-366 | C - UA | Initial Soln | TRUE | 75p |
| MW-150 | C - PMP | Speciation Model | TRUE | 75p |
| MW-152 | C - PMP | Speciation Model | TRUE | 75p |
| MW-252 | C - PMP | Speciation Model | TRUE | 75p |
| MW-366 | C - UA | Speciation Model | TRUE | 75p |
| MW-150 | C - PMP | First Reaction | TRUE | 75p |
| MW-150 | C - PMP | Second Reaction | TRUE | 75p |
| MW-152 | C - PMP | First Reaction | TRUE | 75p |
| MW-152 | C - PMP | Second Reaction | TRUE | 75p |
| MW-252 | C - PMP | First Reaction | TRUE | 75p |
| MW-252 | C - PMP | Second Reaction | TRUE | 75p |
| MW-366 | C - UA | First Reaction | TRUE | 75p |
| MW-366 | C - UA | Second Reaction | TRUE | 75p |
| MW-150 | C - PMP | Initial Soln | TRUE | median |
| MW-152 | C - PMP | Initial Soln | TRUE | median |
| MW-252 | C - PMP | Initial Soln | TRUE | median |
| MW-366 | C - UA | Initial Soln | TRUE | median |
| MW-150 | C - PMP | Speciation Model | TRUE | median |
| MW-152 | C - PMP | Speciation Model | TRUE | median |
| MW-252 | C - PMP | Speciation Model | TRUE | median |
| MW-366 | C - UA | Speciation Model | TRUE | median |
| MW-150 | C - PMP | First Reaction | TRUE | median |
| MW-150 | C - PMP | Second Reaction | TRUE | median |
| MW-152 | C - PMP | First Reaction | TRUE | median |

| | | | | |
|--------|---------|------------------|-------|--------|
| MW-152 | C - PMP | Second Reaction | TRUE | median |
| MW-252 | C - PMP | First Reaction | TRUE | median |
| MW-252 | C - PMP | Second Reaction | TRUE | median |
| MW-366 | C - UA | First Reaction | TRUE | median |
| MW-366 | C - UA | Second Reaction | TRUE | median |
| MW-150 | C - PMP | Initial Soln | FALSE | 25p |
| MW-152 | C - PMP | Initial Soln | FALSE | 25p |
| MW-252 | C - PMP | Initial Soln | FALSE | 25p |
| MW-366 | C - UA | Initial Soln | FALSE | 25p |
| MW-150 | C - PMP | Speciation Model | FALSE | 25p |
| MW-152 | C - PMP | Speciation Model | FALSE | 25p |
| MW-252 | C - PMP | Speciation Model | FALSE | 25p |
| MW-366 | C - UA | Speciation Model | FALSE | 25p |
| MW-150 | C - PMP | First Reaction | FALSE | 25p |
| MW-150 | C - PMP | Second Reaction | FALSE | 25p |
| MW-152 | C - PMP | First Reaction | FALSE | 25p |
| MW-152 | C - PMP | Second Reaction | FALSE | 25p |
| MW-252 | C - PMP | First Reaction | FALSE | 25p |
| MW-252 | C - PMP | Second Reaction | FALSE | 25p |
| MW-366 | C - UA | First Reaction | FALSE | 25p |
| MW-366 | C - UA | Second Reaction | FALSE | 25p |
| MW-150 | C - PMP | Initial Soln | FALSE | 75p |
| MW-152 | C - PMP | Initial Soln | FALSE | 75p |
| MW-252 | C - PMP | Initial Soln | FALSE | 75p |
| MW-366 | C - UA | Initial Soln | FALSE | 75p |
| MW-150 | C - PMP | Speciation Model | FALSE | 75p |
| MW-152 | C - PMP | Speciation Model | FALSE | 75p |
| MW-252 | C - PMP | Speciation Model | FALSE | 75p |
| MW-366 | C - UA | Speciation Model | FALSE | 75p |
| MW-150 | C - PMP | First Reaction | FALSE | 75p |
| MW-150 | C - PMP | Second Reaction | FALSE | 75p |
| MW-152 | C - PMP | First Reaction | FALSE | 75p |
| MW-152 | C - PMP | Second Reaction | FALSE | 75p |
| MW-252 | C - PMP | First Reaction | FALSE | 75p |
| MW-252 | C - PMP | Second Reaction | FALSE | 75p |
| MW-366 | C - UA | First Reaction | FALSE | 75p |
| MW-366 | C - UA | Second Reaction | FALSE | 75p |
| MW-150 | C - PMP | Initial Soln | FALSE | median |
| MW-152 | C - PMP | Initial Soln | FALSE | median |
| MW-252 | C - PMP | Initial Soln | FALSE | median |
| MW-366 | C - UA | Initial Soln | FALSE | median |
| MW-150 | C - PMP | Speciation Model | FALSE | median |
| MW-152 | C - PMP | Speciation Model | FALSE | median |
| MW-252 | C - PMP | Speciation Model | FALSE | median |
| MW-366 | C - UA | Speciation Model | FALSE | median |
| MW-150 | C - PMP | First Reaction | FALSE | median |
| MW-150 | C - PMP | Second Reaction | FALSE | median |
| MW-152 | C - PMP | First Reaction | FALSE | median |
| MW-152 | C - PMP | Second Reaction | FALSE | median |
| MW-252 | C - PMP | First Reaction | FALSE | median |

| | | | | |
|--------|---------|-----------------|-------|--------|
| MW-252 | C - PMP | Second Reaction | FALSE | median |
| MW-366 | C - UA | First Reaction | FALSE | median |
| MW-366 | C - UA | Second Reaction | FALSE | median |

NOTES:

All model results are in units of moles with the exceptions of:

pH and pe (standard units)

charge (equivalents)

Results beginning with 'd_' (change from prior model step)

Results beginning with 'si_' (saturation index)

DRAFT

| pH | pe | charge | pct_err | S(6) |
|------|-------|-----------|-----------|---------|
| 7.05 | 3.36 | 1.18e-17 | 2.62e-14 | 0.00950 |
| 6.93 | 5.81 | 8.00e-18 | 2.36e-14 | 0.00508 |
| 6.71 | 3.79 | 3.13e-17 | 8.07e-14 | 0.00470 |
| 6.87 | 5.37 | -1.91e-16 | -6.12e-13 | 0.00520 |
| 7.05 | 3.36 | 1.35e-17 | 3.00e-14 | 0.00950 |
| 6.93 | 5.81 | 1.49e-17 | 4.40e-14 | 0.00508 |
| 6.71 | 3.79 | 3.99e-17 | 1.03e-13 | 0.00470 |
| 6.87 | 5.37 | -1.93e-16 | -6.17e-13 | 0.00520 |
| 7.78 | 1.34 | 0.000145 | 0.172 | 0.00114 |
| 7.87 | 1.17 | 1.22e-05 | 0.0145 | 0.00104 |
| 7.70 | 2.90 | 0.000179 | 0.212 | 0.00108 |
| 7.81 | 2.47 | 1.89e-05 | 0.0225 | 0.00102 |
| 7.61 | 0.626 | 0.000162 | 0.190 | 0.00116 |
| 7.76 | 0.274 | 9.50e-06 | 0.0113 | 0.00106 |
| 7.61 | 2.86 | 0.000324 | 0.381 | 0.00114 |
| 7.73 | 2.42 | 3.31e-05 | 0.0393 | 0.00104 |
| 7.05 | 3.36 | 1.18e-17 | 2.62e-14 | 0.00950 |
| 6.93 | 5.81 | 8.00e-18 | 2.36e-14 | 0.00508 |
| 6.71 | 3.79 | 3.13e-17 | 8.07e-14 | 0.00470 |
| 6.87 | 5.37 | -1.91e-16 | -6.12e-13 | 0.00520 |
| 7.05 | 3.36 | 1.35e-17 | 3.00e-14 | 0.00950 |
| 6.93 | 5.81 | 1.49e-17 | 4.40e-14 | 0.00508 |
| 6.71 | 3.79 | 3.99e-17 | 1.03e-13 | 0.00470 |
| 6.87 | 5.37 | -1.93e-16 | -6.17e-13 | 0.00520 |
| 7.70 | 1.37 | 0.000160 | 0.186 | 0.00150 |
| 7.82 | 1.19 | -3.79e-06 | -4.48e-03 | 0.00115 |
| 7.61 | 3.36 | 0.000457 | 0.535 | 0.00121 |
| 7.74 | 3.06 | 5.80e-05 | 0.0687 | 0.00106 |
| 7.50 | 0.795 | 0.000360 | 0.414 | 0.00141 |
| 7.66 | 0.488 | -1.25e-05 | -1.47e-02 | 0.00120 |
| 7.46 | 3.35 | 0.00108 | 1.25 | 0.00139 |
| 7.57 | 3.07 | 0.000161 | 0.189 | 0.00108 |
| 7.05 | 3.36 | 1.18e-17 | 2.62e-14 | 0.00950 |
| 6.93 | 5.81 | 8.00e-18 | 2.36e-14 | 0.00508 |
| 6.71 | 3.79 | 3.13e-17 | 8.07e-14 | 0.00470 |
| 6.87 | 5.37 | -1.91e-16 | -6.12e-13 | 0.00520 |
| 7.05 | 3.36 | 1.35e-17 | 3.00e-14 | 0.00950 |
| 6.93 | 5.81 | 1.49e-17 | 4.40e-14 | 0.00508 |
| 6.71 | 3.79 | 3.99e-17 | 1.03e-13 | 0.00470 |
| 6.87 | 5.37 | -1.93e-16 | -6.17e-13 | 0.00520 |
| 7.75 | 1.37 | 0.000184 | 0.217 | 0.00122 |
| 7.85 | 1.21 | 2.17e-05 | 0.0259 | 0.00106 |
| 7.66 | 3.14 | 0.000265 | 0.313 | 0.00111 |

| | | | | |
|------|-------|----------|---------|---------|
| 7.78 | 2.76 | 3.27e-05 | 0.0388 | 0.00103 |
| 7.56 | 0.722 | 0.000231 | 0.269 | 0.00123 |
| 7.72 | 0.404 | 1.52e-05 | 0.0180 | 0.00109 |
| 7.52 | 3.18 | 0.000647 | 0.757 | 0.00125 |
| 7.64 | 2.86 | 8.16e-05 | 0.0963 | 0.00106 |
| 7.05 | 3.36 | 0.00473 | 11.8 | 0.00950 |
| 6.93 | 5.81 | 0.00565 | 20.1 | 0.00508 |
| 6.71 | 3.79 | 0.00832 | 27.6 | 0.00470 |
| 6.87 | 5.37 | 0.00438 | 16.4 | 0.00520 |
| 7.05 | 3.36 | 0.00473 | 11.8 | 0.00950 |
| 6.93 | 5.81 | 0.00565 | 20.1 | 0.00508 |
| 6.71 | 3.79 | 0.00832 | 27.6 | 0.00470 |
| 6.87 | 5.37 | 0.00438 | 16.4 | 0.00520 |
| 7.78 | 1.33 | 0.000153 | 0.181 | 0.00113 |
| 7.87 | 1.16 | 1.26e-05 | 0.0150 | 0.00104 |
| 7.70 | 2.89 | 0.000186 | 0.220 | 0.00107 |
| 7.81 | 2.46 | 1.93e-05 | 0.0230 | 0.00102 |
| 7.61 | 0.602 | 0.000177 | 0.208 | 0.00115 |
| 7.76 | 0.252 | 1.02e-05 | 0.0121 | 0.00106 |
| 7.61 | 2.86 | 0.000322 | 0.379 | 0.00114 |
| 7.73 | 2.41 | 3.31e-05 | 0.0392 | 0.00104 |
| 7.05 | 3.36 | 0.00473 | 11.8 | 0.00950 |
| 6.93 | 5.81 | 0.00565 | 20.1 | 0.00508 |
| 6.71 | 3.79 | 0.00832 | 27.6 | 0.00470 |
| 6.87 | 5.37 | 0.00438 | 16.4 | 0.00520 |
| 7.05 | 3.36 | 0.00473 | 11.8 | 0.00950 |
| 6.93 | 5.81 | 0.00565 | 20.1 | 0.00508 |
| 6.71 | 3.79 | 0.00832 | 27.6 | 0.00470 |
| 6.87 | 5.37 | 0.00438 | 16.4 | 0.00520 |
| 7.70 | 1.35 | 0.000224 | 0.261 | 0.00147 |
| 7.83 | 1.17 | 5.96e-06 | 0.00705 | 0.00115 |
| 7.61 | 3.34 | 0.000531 | 0.622 | 0.00118 |
| 7.74 | 3.04 | 7.13e-05 | 0.0845 | 0.00106 |
| 7.50 | 0.759 | 0.000491 | 0.566 | 0.00136 |
| 7.67 | 0.459 | 1.02e-05 | 0.0119 | 0.00119 |
| 7.46 | 3.34 | 0.00107 | 1.24 | 0.00139 |
| 7.57 | 3.07 | 0.000160 | 0.188 | 0.00108 |
| 7.05 | 3.36 | 0.00473 | 11.8 | 0.00950 |
| 6.93 | 5.81 | 0.00565 | 20.1 | 0.00508 |
| 6.71 | 3.79 | 0.00832 | 27.6 | 0.00470 |
| 6.87 | 5.37 | 0.00438 | 16.4 | 0.00520 |
| 7.05 | 3.36 | 0.00473 | 11.8 | 0.00950 |
| 6.93 | 5.81 | 0.00565 | 20.1 | 0.00508 |
| 6.71 | 3.79 | 0.00832 | 27.6 | 0.00470 |
| 6.87 | 5.37 | 0.00438 | 16.4 | 0.00520 |
| 7.75 | 1.36 | 0.000203 | 0.239 | 0.00122 |
| 7.85 | 1.20 | 2.31e-05 | 0.0275 | 0.00106 |
| 7.66 | 3.13 | 0.000284 | 0.336 | 0.00110 |
| 7.78 | 2.75 | 3.44e-05 | 0.0409 | 0.00103 |
| 7.56 | 0.695 | 0.000268 | 0.312 | 0.00122 |

| | | | | |
|------|-------|----------|--------|---------|
| 7.72 | 0.380 | 1.80e-05 | 0.0213 | 0.00109 |
| 7.52 | 3.17 | 0.000645 | 0.755 | 0.00125 |
| 7.64 | 2.85 | 8.17e-05 | 0.0964 | 0.00106 |

DRAFT

| B | Li | As | C(4) | Cl |
|----------|----------|----------|---------|---------|
| 0.000394 | 7.27e-06 | 3.24e-08 | 0.00325 | 0.00627 |
| 0.000445 | 9.12e-07 | 3.57e-08 | 0.00395 | 0.00628 |
| 1.47e-05 | 1.82e-06 | 3.64e-08 | 0.00482 | 0.00937 |
| 0.000156 | 8.98e-07 | 3.17e-08 | 0.00312 | 0.00572 |
| 0.000394 | 7.27e-06 | 3.24e-08 | 0.00325 | 0.00627 |
| 0.000445 | 9.12e-07 | 3.57e-08 | 0.00395 | 0.00628 |
| 1.47e-05 | 1.82e-06 | 3.64e-08 | 0.00482 | 0.00937 |
| 0.000156 | 8.98e-07 | 3.17e-08 | 0.00312 | 0.00572 |
| 0.000126 | 1.12e-05 | 1.35e-07 | 0.00872 | 0.0316 |
| 0.000123 | 1.12e-05 | 1.27e-07 | 0.00861 | 0.0316 |
| 0.000190 | 1.12e-05 | 1.30e-07 | 0.00892 | 0.0316 |
| 0.000177 | 1.12e-05 | 1.24e-07 | 0.00871 | 0.0316 |
| 1.39e-05 | 1.12e-05 | 6.29e-08 | 0.00928 | 0.0316 |
| 1.89e-05 | 1.12e-05 | 5.33e-08 | 0.00887 | 0.0316 |
| 8.78e-05 | 1.12e-05 | 1.55e-07 | 0.00905 | 0.0316 |
| 0.000101 | 1.12e-05 | 1.45e-07 | 0.00893 | 0.0316 |
| 0.000394 | 7.27e-06 | 3.24e-08 | 0.00325 | 0.00627 |
| 0.000445 | 9.12e-07 | 3.57e-08 | 0.00395 | 0.00628 |
| 1.47e-05 | 1.82e-06 | 3.64e-08 | 0.00482 | 0.00937 |
| 0.000156 | 8.98e-07 | 3.17e-08 | 0.00312 | 0.00572 |
| 0.000394 | 7.27e-06 | 3.24e-08 | 0.00325 | 0.00627 |
| 0.000445 | 9.12e-07 | 3.57e-08 | 0.00395 | 0.00628 |
| 1.47e-05 | 1.82e-06 | 3.64e-08 | 0.00482 | 0.00937 |
| 0.000156 | 8.98e-07 | 3.17e-08 | 0.00312 | 0.00572 |
| 0.000160 | 1.12e-05 | 1.27e-07 | 0.00886 | 0.0316 |
| 0.000137 | 1.12e-05 | 1.25e-07 | 0.00880 | 0.0316 |
| 0.000247 | 1.12e-05 | 1.27e-07 | 0.00914 | 0.0316 |
| 0.000217 | 1.12e-05 | 1.25e-07 | 0.00894 | 0.0316 |
| 1.21e-05 | 1.12e-05 | 6.87e-08 | 0.00976 | 0.0316 |
| 1.19e-05 | 1.12e-05 | 5.57e-08 | 0.00928 | 0.0316 |
| 8.23e-05 | 1.12e-05 | 1.61e-07 | 0.00898 | 0.0316 |
| 7.76e-05 | 1.12e-05 | 1.70e-07 | 0.00945 | 0.0316 |
| 0.000394 | 7.27e-06 | 3.24e-08 | 0.00325 | 0.00627 |
| 0.000445 | 9.12e-07 | 3.57e-08 | 0.00395 | 0.00628 |
| 1.47e-05 | 1.82e-06 | 3.64e-08 | 0.00482 | 0.00937 |
| 0.000156 | 8.98e-07 | 3.17e-08 | 0.00312 | 0.00572 |
| 0.000394 | 7.27e-06 | 3.24e-08 | 0.00325 | 0.00627 |
| 0.000445 | 9.12e-07 | 3.57e-08 | 0.00395 | 0.00628 |
| 1.47e-05 | 1.82e-06 | 3.64e-08 | 0.00482 | 0.00937 |
| 0.000156 | 8.98e-07 | 3.17e-08 | 0.00312 | 0.00572 |
| 0.000133 | 1.12e-05 | 1.34e-07 | 0.00877 | 0.0316 |
| 0.000122 | 1.12e-05 | 1.30e-07 | 0.00867 | 0.0316 |
| 0.000207 | 1.12e-05 | 1.30e-07 | 0.00901 | 0.0316 |

| | | | | |
|----------|----------|----------|---------|----------|
| 0.000188 | 1.12e-05 | 1.26e-07 | 0.00879 | 0.0316 |
| 1.21e-05 | 1.12e-05 | 6.56e-08 | 0.00948 | 0.0316 |
| 1.36e-05 | 1.12e-05 | 5.49e-08 | 0.00902 | 0.0316 |
| 8.24e-05 | 1.12e-05 | 1.60e-07 | 0.00911 | 0.0316 |
| 8.25e-05 | 1.12e-05 | 1.59e-07 | 0.00921 | 0.0316 |
| 0.000394 | 7.27e-06 | 3.24e-08 | 0.00325 | 0.00154 |
| 0.000445 | 9.12e-07 | 3.57e-08 | 0.00395 | 0.000635 |
| 1.47e-05 | 1.82e-06 | 3.64e-08 | 0.00482 | 0.00106 |
| 0.000156 | 8.98e-07 | 3.17e-08 | 0.00312 | 0.00134 |
| 0.000394 | 7.27e-06 | 3.24e-08 | 0.00325 | 0.00154 |
| 0.000445 | 9.12e-07 | 3.57e-08 | 0.00395 | 0.000635 |
| 1.47e-05 | 1.82e-06 | 3.64e-08 | 0.00482 | 0.00106 |
| 0.000156 | 8.98e-07 | 3.17e-08 | 0.00312 | 0.00134 |
| 0.000125 | 1.12e-05 | 1.38e-07 | 0.00872 | 0.0316 |
| 0.000123 | 1.12e-05 | 1.31e-07 | 0.00861 | 0.0316 |
| 0.000190 | 1.12e-05 | 1.35e-07 | 0.00892 | 0.0316 |
| 0.000176 | 1.12e-05 | 1.29e-07 | 0.00871 | 0.0316 |
| 1.39e-05 | 1.12e-05 | 6.58e-08 | 0.00929 | 0.0316 |
| 1.89e-05 | 1.12e-05 | 5.58e-08 | 0.00887 | 0.0316 |
| 8.74e-05 | 1.12e-05 | 1.59e-07 | 0.00906 | 0.0316 |
| 0.000100 | 1.12e-05 | 1.49e-07 | 0.00893 | 0.0316 |
| 0.000394 | 7.27e-06 | 3.24e-08 | 0.00325 | 0.00154 |
| 0.000445 | 9.12e-07 | 3.57e-08 | 0.00395 | 0.000635 |
| 1.47e-05 | 1.82e-06 | 3.64e-08 | 0.00482 | 0.00106 |
| 0.000156 | 8.98e-07 | 3.17e-08 | 0.00312 | 0.00134 |
| 0.000394 | 7.27e-06 | 3.24e-08 | 0.00325 | 0.00154 |
| 0.000445 | 9.12e-07 | 3.57e-08 | 0.00395 | 0.000635 |
| 1.47e-05 | 1.82e-06 | 3.64e-08 | 0.00482 | 0.00106 |
| 0.000156 | 8.98e-07 | 3.17e-08 | 0.00312 | 0.00134 |
| 0.000160 | 1.12e-05 | 1.29e-07 | 0.00886 | 0.0316 |
| 0.000137 | 1.12e-05 | 1.27e-07 | 0.00880 | 0.0316 |
| 0.000248 | 1.12e-05 | 1.32e-07 | 0.00915 | 0.0316 |
| 0.000218 | 1.12e-05 | 1.29e-07 | 0.00894 | 0.0316 |
| 1.21e-05 | 1.12e-05 | 7.13e-08 | 0.00977 | 0.0316 |
| 1.18e-05 | 1.12e-05 | 5.78e-08 | 0.00928 | 0.0316 |
| 8.19e-05 | 1.12e-05 | 1.66e-07 | 0.00899 | 0.0316 |
| 7.73e-05 | 1.12e-05 | 1.75e-07 | 0.00945 | 0.0316 |
| 0.000394 | 7.27e-06 | 3.24e-08 | 0.00325 | 0.00154 |
| 0.000445 | 9.12e-07 | 3.57e-08 | 0.00395 | 0.000635 |
| 1.47e-05 | 1.82e-06 | 3.64e-08 | 0.00482 | 0.00106 |
| 0.000156 | 8.98e-07 | 3.17e-08 | 0.00312 | 0.00134 |
| 0.000394 | 7.27e-06 | 3.24e-08 | 0.00325 | 0.00154 |
| 0.000445 | 9.12e-07 | 3.57e-08 | 0.00395 | 0.000635 |
| 1.47e-05 | 1.82e-06 | 3.64e-08 | 0.00482 | 0.00106 |
| 0.000156 | 8.98e-07 | 3.17e-08 | 0.00312 | 0.00134 |
| 0.000133 | 1.12e-05 | 1.37e-07 | 0.00878 | 0.0316 |
| 0.000122 | 1.12e-05 | 1.33e-07 | 0.00867 | 0.0316 |
| 0.000207 | 1.12e-05 | 1.35e-07 | 0.00901 | 0.0316 |
| 0.000188 | 1.12e-05 | 1.31e-07 | 0.00879 | 0.0316 |
| 1.20e-05 | 1.12e-05 | 6.85e-08 | 0.00948 | 0.0316 |

| | | | | |
|----------|----------|----------|---------|--------|
| 1.36e-05 | 1.12e-05 | 5.74e-08 | 0.00901 | 0.0316 |
| 8.20e-05 | 1.12e-05 | 1.65e-07 | 0.00912 | 0.0316 |
| 8.21e-05 | 1.12e-05 | 1.63e-07 | 0.00921 | 0.0316 |

DRAFT

| F | Ca | Mg | Na | K |
|----------|----------|----------|---------|----------|
| 3.82e-05 | 0.00511 | 0.00655 | 0.00470 | 2.25e-05 |
| 1.84e-05 | 0.00406 | 0.00316 | 0.00514 | 2.63e-05 |
| 1.21e-05 | 0.00542 | 0.00350 | 0.00433 | 4.57e-05 |
| 1.98e-05 | 0.00463 | 0.00331 | 0.00258 | 0.000104 |
| 3.82e-05 | 0.00511 | 0.00655 | 0.00470 | 2.25e-05 |
| 1.84e-05 | 0.00406 | 0.00316 | 0.00514 | 2.63e-05 |
| 1.21e-05 | 0.00542 | 0.00350 | 0.00433 | 4.57e-05 |
| 1.98e-05 | 0.00463 | 0.00331 | 0.00258 | 0.000104 |
| 0.000132 | 0.000531 | 0.000297 | 0.0409 | 8.47e-05 |
| 0.000133 | 0.000432 | 0.000210 | 0.0409 | 8.47e-05 |
| 0.000132 | 0.000626 | 0.000217 | 0.0409 | 8.47e-05 |
| 0.000133 | 0.000485 | 0.000170 | 0.0409 | 8.47e-05 |
| 0.000132 | 0.000743 | 0.000307 | 0.0409 | 8.47e-05 |
| 0.000133 | 0.000538 | 0.000210 | 0.0409 | 8.47e-05 |
| 0.000132 | 0.000769 | 0.000230 | 0.0409 | 8.47e-05 |
| 0.000133 | 0.000580 | 0.000172 | 0.0409 | 8.47e-05 |
| 3.82e-05 | 0.00511 | 0.00655 | 0.00470 | 2.25e-05 |
| 1.84e-05 | 0.00406 | 0.00316 | 0.00514 | 2.63e-05 |
| 1.21e-05 | 0.00542 | 0.00350 | 0.00433 | 4.57e-05 |
| 1.98e-05 | 0.00463 | 0.00331 | 0.00258 | 0.000104 |
| 3.82e-05 | 0.00511 | 0.00655 | 0.00470 | 2.25e-05 |
| 1.84e-05 | 0.00406 | 0.00316 | 0.00514 | 2.63e-05 |
| 1.21e-05 | 0.00542 | 0.00350 | 0.00433 | 4.57e-05 |
| 1.98e-05 | 0.00463 | 0.00331 | 0.00258 | 0.000104 |
| 0.000130 | 0.000638 | 0.000590 | 0.0409 | 8.47e-05 |
| 0.000133 | 0.000474 | 0.000349 | 0.0409 | 8.47e-05 |
| 0.000130 | 0.000769 | 0.000410 | 0.0409 | 8.47e-05 |
| 0.000133 | 0.000564 | 0.000237 | 0.0409 | 8.47e-05 |
| 0.000126 | 0.000954 | 0.000607 | 0.0409 | 8.47e-05 |
| 0.000134 | 0.000663 | 0.000363 | 0.0409 | 8.47e-05 |
| 0.000131 | 0.00114 | 0.000364 | 0.0409 | 8.47e-05 |
| 0.000133 | 0.000804 | 0.000225 | 0.0409 | 8.47e-05 |
| 3.82e-05 | 0.00511 | 0.00655 | 0.00470 | 2.25e-05 |
| 1.84e-05 | 0.00406 | 0.00316 | 0.00514 | 2.63e-05 |
| 1.21e-05 | 0.00542 | 0.00350 | 0.00433 | 4.57e-05 |
| 1.98e-05 | 0.00463 | 0.00331 | 0.00258 | 0.000104 |
| 3.82e-05 | 0.00511 | 0.00655 | 0.00470 | 2.25e-05 |
| 1.84e-05 | 0.00406 | 0.00316 | 0.00514 | 2.63e-05 |
| 1.21e-05 | 0.00542 | 0.00350 | 0.00433 | 4.57e-05 |
| 1.98e-05 | 0.00463 | 0.00331 | 0.00258 | 0.000104 |
| 0.000132 | 0.000571 | 0.000375 | 0.0409 | 8.47e-05 |
| 0.000133 | 0.000449 | 0.000241 | 0.0409 | 8.47e-05 |
| 0.000132 | 0.000685 | 0.000263 | 0.0409 | 8.47e-05 |

| | | | | |
|----------|----------|----------|---------|----------|
| 0.000133 | 0.000519 | 0.000178 | 0.0409 | 8.47e-05 |
| 0.000131 | 0.000828 | 0.000394 | 0.0409 | 8.47e-05 |
| 0.000133 | 0.000588 | 0.000244 | 0.0409 | 8.47e-05 |
| 0.000132 | 0.000949 | 0.000304 | 0.0409 | 8.47e-05 |
| 0.000133 | 0.000695 | 0.000197 | 0.0409 | 8.47e-05 |
| 3.82e-05 | 0.00511 | 0.00655 | 0.00470 | 2.25e-05 |
| 1.84e-05 | 0.00406 | 0.00316 | 0.00514 | 2.63e-05 |
| 1.21e-05 | 0.00542 | 0.00350 | 0.00433 | 4.57e-05 |
| 1.98e-05 | 0.00463 | 0.00331 | 0.00258 | 0.000104 |
| 3.82e-05 | 0.00511 | 0.00655 | 0.00470 | 2.25e-05 |
| 1.84e-05 | 0.00406 | 0.00316 | 0.00514 | 2.63e-05 |
| 1.21e-05 | 0.00542 | 0.00350 | 0.00433 | 4.57e-05 |
| 1.98e-05 | 0.00463 | 0.00331 | 0.00258 | 0.000104 |
| 0.000132 | 0.000530 | 0.000300 | 0.0409 | 8.47e-05 |
| 0.000133 | 0.000431 | 0.000211 | 0.0409 | 8.47e-05 |
| 0.000132 | 0.000624 | 0.000220 | 0.0409 | 8.47e-05 |
| 0.000133 | 0.000484 | 0.000170 | 0.0409 | 8.47e-05 |
| 0.000132 | 0.000741 | 0.000312 | 0.0409 | 8.47e-05 |
| 0.000133 | 0.000537 | 0.000212 | 0.0409 | 8.47e-05 |
| 0.000132 | 0.000767 | 0.000232 | 0.0409 | 8.47e-05 |
| 0.000133 | 0.000580 | 0.000172 | 0.0409 | 8.47e-05 |
| 3.82e-05 | 0.00511 | 0.00655 | 0.00470 | 2.25e-05 |
| 1.84e-05 | 0.00406 | 0.00316 | 0.00514 | 2.63e-05 |
| 1.21e-05 | 0.00542 | 0.00350 | 0.00433 | 4.57e-05 |
| 1.98e-05 | 0.00463 | 0.00331 | 0.00258 | 0.000104 |
| 3.82e-05 | 0.00511 | 0.00655 | 0.00470 | 2.25e-05 |
| 1.84e-05 | 0.00406 | 0.00316 | 0.00514 | 2.63e-05 |
| 1.21e-05 | 0.00542 | 0.00350 | 0.00433 | 4.57e-05 |
| 1.98e-05 | 0.00463 | 0.00331 | 0.00258 | 0.000104 |
| 0.000130 | 0.000636 | 0.000603 | 0.0409 | 8.47e-05 |
| 0.000133 | 0.000472 | 0.000353 | 0.0409 | 8.47e-05 |
| 0.000130 | 0.000764 | 0.000425 | 0.0409 | 8.47e-05 |
| 0.000133 | 0.000561 | 0.000242 | 0.0409 | 8.47e-05 |
| 0.000126 | 0.000947 | 0.000633 | 0.0409 | 8.47e-05 |
| 0.000134 | 0.000658 | 0.000371 | 0.0409 | 8.47e-05 |
| 0.000131 | 0.00114 | 0.000369 | 0.0409 | 8.47e-05 |
| 0.000133 | 0.000803 | 0.000227 | 0.0409 | 8.47e-05 |
| 3.82e-05 | 0.00511 | 0.00655 | 0.00470 | 2.25e-05 |
| 1.84e-05 | 0.00406 | 0.00316 | 0.00514 | 2.63e-05 |
| 1.21e-05 | 0.00542 | 0.00350 | 0.00433 | 4.57e-05 |
| 1.98e-05 | 0.00463 | 0.00331 | 0.00258 | 0.000104 |
| 3.82e-05 | 0.00511 | 0.00655 | 0.00470 | 2.25e-05 |
| 1.84e-05 | 0.00406 | 0.00316 | 0.00514 | 2.63e-05 |
| 1.21e-05 | 0.00542 | 0.00350 | 0.00433 | 4.57e-05 |
| 1.98e-05 | 0.00463 | 0.00331 | 0.00258 | 0.000104 |
| 0.000132 | 0.000570 | 0.000380 | 0.0409 | 8.47e-05 |
| 0.000133 | 0.000448 | 0.000242 | 0.0409 | 8.47e-05 |
| 0.000132 | 0.000682 | 0.000268 | 0.0409 | 8.47e-05 |
| 0.000133 | 0.000518 | 0.000179 | 0.0409 | 8.47e-05 |
| 0.000131 | 0.000825 | 0.000404 | 0.0409 | 8.47e-05 |

| | | | | |
|----------|----------|----------|--------|----------|
| 0.000133 | 0.000586 | 0.000247 | 0.0409 | 8.47e-05 |
| 0.000132 | 0.000947 | 0.000308 | 0.0409 | 8.47e-05 |
| 0.000133 | 0.000694 | 0.000198 | 0.0409 | 8.47e-05 |

DRAFT

| Ba | Si | P | Mn | Fe |
|----------|----------|----------|----------|----------|
| 1.33e-07 | 0.000165 | 8.89e-07 | 5.74e-08 | 6.87e-07 |
| 1.81e-07 | 0.000153 | 2.91e-07 | 2.27e-07 | 1.43e-07 |
| 2.68e-07 | 0.000115 | 1.50e-06 | 6.28e-06 | 5.48e-06 |
| 2.38e-07 | 0.000138 | 2.59e-07 | 4.10e-07 | 1.43e-07 |
| 1.33e-07 | 0.000165 | 8.89e-07 | 5.74e-08 | 6.87e-07 |
| 1.81e-07 | 0.000153 | 2.91e-07 | 2.27e-07 | 1.43e-07 |
| 2.68e-07 | 0.000115 | 1.50e-06 | 6.28e-06 | 5.48e-06 |
| 2.38e-07 | 0.000138 | 2.59e-07 | 4.10e-07 | 1.43e-07 |
| 3.57e-07 | 9.48e-05 | 4.42e-06 | 5.24e-07 | 4.44e-08 |
| 3.86e-07 | 7.82e-05 | 4.72e-06 | 7.25e-07 | 3.50e-08 |
| 3.78e-07 | 7.11e-05 | 1.49e-06 | 7.55e-07 | 4.73e-09 |
| 3.93e-07 | 5.67e-05 | 1.71e-06 | 9.23e-07 | 4.62e-09 |
| 3.57e-07 | 3.87e-05 | 6.11e-06 | 1.08e-06 | 6.95e-07 |
| 3.81e-07 | 2.96e-05 | 6.81e-06 | 1.00e-06 | 5.46e-07 |
| 3.61e-07 | 8.39e-05 | 1.61e-06 | 8.29e-07 | 7.35e-09 |
| 3.89e-07 | 6.62e-05 | 1.84e-06 | 1.10e-06 | 7.49e-09 |
| 1.33e-07 | 0.000165 | 8.89e-07 | 5.74e-08 | 6.87e-07 |
| 1.81e-07 | 0.000153 | 2.91e-07 | 2.27e-07 | 1.43e-07 |
| 2.68e-07 | 0.000115 | 1.50e-06 | 6.28e-06 | 5.48e-06 |
| 2.38e-07 | 0.000138 | 2.59e-07 | 4.10e-07 | 1.43e-07 |
| 1.33e-07 | 0.000165 | 8.89e-07 | 5.74e-08 | 6.87e-07 |
| 1.81e-07 | 0.000153 | 2.91e-07 | 2.27e-07 | 1.43e-07 |
| 2.68e-07 | 0.000115 | 1.50e-06 | 6.28e-06 | 5.48e-06 |
| 2.38e-07 | 0.000138 | 2.59e-07 | 4.10e-07 | 1.43e-07 |
| 2.79e-07 | 0.000112 | 4.09e-06 | 1.58e-07 | 7.11e-08 |
| 3.54e-07 | 8.87e-05 | 4.70e-06 | 1.94e-07 | 4.58e-08 |
| 3.43e-07 | 8.62e-05 | 1.34e-06 | 3.11e-07 | 4.59e-09 |
| 3.82e-07 | 6.56e-05 | 1.57e-06 | 3.52e-07 | 3.52e-09 |
| 3.01e-07 | 4.87e-05 | 5.70e-06 | 1.42e-06 | 1.07e-06 |
| 3.45e-07 | 3.46e-05 | 6.29e-06 | 9.32e-07 | 6.79e-07 |
| 3.03e-07 | 0.000112 | 1.34e-06 | 5.01e-07 | 8.35e-09 |
| 3.81e-07 | 9.31e-05 | 1.62e-06 | 6.28e-07 | 6.75e-09 |
| 1.33e-07 | 0.000165 | 8.89e-07 | 5.74e-08 | 6.87e-07 |
| 1.81e-07 | 0.000153 | 2.91e-07 | 2.27e-07 | 1.43e-07 |
| 2.68e-07 | 0.000115 | 1.50e-06 | 6.28e-06 | 5.48e-06 |
| 2.38e-07 | 0.000138 | 2.59e-07 | 4.10e-07 | 1.43e-07 |
| 1.33e-07 | 0.000165 | 8.89e-07 | 5.74e-08 | 6.87e-07 |
| 1.81e-07 | 0.000153 | 2.91e-07 | 2.27e-07 | 1.43e-07 |
| 2.68e-07 | 0.000115 | 1.50e-06 | 6.28e-06 | 5.48e-06 |
| 2.38e-07 | 0.000138 | 2.59e-07 | 4.10e-07 | 1.43e-07 |
| 3.35e-07 | 0.000102 | 4.31e-06 | 3.36e-07 | 5.14e-08 |
| 3.81e-07 | 8.25e-05 | 4.77e-06 | 4.46e-07 | 3.66e-08 |
| 3.68e-07 | 7.73e-05 | 1.42e-06 | 5.53e-07 | 4.45e-09 |

| | | | | |
|----------|----------|----------|----------|----------|
| 3.92e-07 | 6.02e-05 | 1.65e-06 | 6.72e-07 | 3.86e-09 |
| 3.39e-07 | 4.26e-05 | 5.91e-06 | 1.13e-06 | 7.95e-07 |
| 3.74e-07 | 3.13e-05 | 6.61e-06 | 8.61e-07 | 5.46e-07 |
| 3.32e-07 | 9.96e-05 | 1.46e-06 | 5.67e-07 | 7.50e-09 |
| 3.86e-07 | 7.98e-05 | 1.71e-06 | 7.32e-07 | 6.34e-09 |
| 1.33e-07 | 0.000165 | 8.89e-07 | 5.74e-08 | 6.87e-07 |
| 1.81e-07 | 0.000153 | 2.91e-07 | 2.27e-07 | 1.43e-07 |
| 2.68e-07 | 0.000115 | 1.50e-06 | 6.28e-06 | 5.48e-06 |
| 2.38e-07 | 0.000138 | 2.59e-07 | 4.10e-07 | 1.43e-07 |
| 1.33e-07 | 0.000165 | 8.89e-07 | 5.74e-08 | 6.87e-07 |
| 1.81e-07 | 0.000153 | 2.91e-07 | 2.27e-07 | 1.43e-07 |
| 2.68e-07 | 0.000115 | 1.50e-06 | 6.28e-06 | 5.48e-06 |
| 2.38e-07 | 0.000138 | 2.59e-07 | 4.10e-07 | 1.43e-07 |
| 3.58e-07 | 9.45e-05 | 4.44e-06 | 5.25e-07 | 4.55e-08 |
| 3.86e-07 | 7.80e-05 | 4.74e-06 | 7.25e-07 | 3.57e-08 |
| 3.79e-07 | 7.08e-05 | 1.51e-06 | 7.60e-07 | 4.76e-09 |
| 3.93e-07 | 5.65e-05 | 1.73e-06 | 9.26e-07 | 4.64e-09 |
| 3.59e-07 | 3.85e-05 | 6.15e-06 | 1.12e-06 | 7.28e-07 |
| 3.81e-07 | 2.94e-05 | 6.86e-06 | 1.03e-06 | 5.70e-07 |
| 3.61e-07 | 8.37e-05 | 1.62e-06 | 8.32e-07 | 7.38e-09 |
| 3.89e-07 | 6.61e-05 | 1.85e-06 | 1.10e-06 | 7.52e-09 |
| 1.33e-07 | 0.000165 | 8.89e-07 | 5.74e-08 | 6.87e-07 |
| 1.81e-07 | 0.000153 | 2.91e-07 | 2.27e-07 | 1.43e-07 |
| 2.68e-07 | 0.000115 | 1.50e-06 | 6.28e-06 | 5.48e-06 |
| 2.38e-07 | 0.000138 | 2.59e-07 | 4.10e-07 | 1.43e-07 |
| 1.33e-07 | 0.000165 | 8.89e-07 | 5.74e-08 | 6.87e-07 |
| 1.81e-07 | 0.000153 | 2.91e-07 | 2.27e-07 | 1.43e-07 |
| 2.68e-07 | 0.000115 | 1.50e-06 | 6.28e-06 | 5.48e-06 |
| 2.38e-07 | 0.000138 | 2.59e-07 | 4.10e-07 | 1.43e-07 |
| 2.84e-07 | 0.000111 | 4.10e-06 | 1.60e-07 | 7.35e-08 |
| 3.54e-07 | 8.83e-05 | 4.72e-06 | 1.95e-07 | 4.69e-08 |
| 3.53e-07 | 8.57e-05 | 1.35e-06 | 3.20e-07 | 4.62e-09 |
| 3.84e-07 | 6.52e-05 | 1.58e-06 | 3.57e-07 | 3.54e-09 |
| 3.13e-07 | 4.84e-05 | 5.75e-06 | 1.53e-06 | 1.14e-06 |
| 3.47e-07 | 3.43e-05 | 6.34e-06 | 9.81e-07 | 7.13e-07 |
| 3.04e-07 | 0.000112 | 1.35e-06 | 5.05e-07 | 8.38e-09 |
| 3.81e-07 | 9.28e-05 | 1.63e-06 | 6.31e-07 | 6.77e-09 |
| 1.33e-07 | 0.000165 | 8.89e-07 | 5.74e-08 | 6.87e-07 |
| 1.81e-07 | 0.000153 | 2.91e-07 | 2.27e-07 | 1.43e-07 |
| 2.68e-07 | 0.000115 | 1.50e-06 | 6.28e-06 | 5.48e-06 |
| 2.38e-07 | 0.000138 | 2.59e-07 | 4.10e-07 | 1.43e-07 |
| 1.33e-07 | 0.000165 | 8.89e-07 | 5.74e-08 | 6.87e-07 |
| 1.81e-07 | 0.000153 | 2.91e-07 | 2.27e-07 | 1.43e-07 |
| 2.68e-07 | 0.000115 | 1.50e-06 | 6.28e-06 | 5.48e-06 |
| 2.38e-07 | 0.000138 | 2.59e-07 | 4.10e-07 | 1.43e-07 |
| 3.37e-07 | 0.000101 | 4.32e-06 | 3.38e-07 | 5.27e-08 |
| 3.81e-07 | 8.22e-05 | 4.79e-06 | 4.46e-07 | 3.74e-08 |
| 3.71e-07 | 7.69e-05 | 1.44e-06 | 5.60e-07 | 4.48e-09 |
| 3.92e-07 | 6.00e-05 | 1.66e-06 | 6.75e-07 | 3.88e-09 |
| 3.43e-07 | 4.23e-05 | 5.96e-06 | 1.19e-06 | 8.38e-07 |

| | | | | |
|----------|----------|----------|----------|----------|
| 3.74e-07 | 3.11e-05 | 6.65e-06 | 8.93e-07 | 5.70e-07 |
| 3.33e-07 | 9.93e-05 | 1.47e-06 | 5.71e-07 | 7.54e-09 |
| 3.86e-07 | 7.95e-05 | 1.72e-06 | 7.34e-07 | 6.36e-09 |

DRAFT

| Al | Sb | Be | Cd | Cr |
|----------|----------|----------|----------|----------|
| 6.54e-07 | 1.65e-09 | 1.11e-08 | 1.56e-09 | 2.02e-08 |
| 3.78e-07 | 1.64e-09 | 2.78e-08 | 1.56e-09 | 4.91e-08 |
| 2.34e-07 | 1.97e-08 | 1.11e-08 | 1.56e-09 | 6.07e-08 |
| 2.34e-07 | 3.29e-09 | 1.11e-08 | 1.56e-09 | 1.68e-08 |
| 6.54e-07 | 1.65e-09 | 1.11e-08 | 1.56e-09 | 2.02e-08 |
| 3.78e-07 | 1.64e-09 | 2.78e-08 | 1.56e-09 | 4.91e-08 |
| 2.34e-07 | 1.97e-08 | 1.11e-08 | 1.56e-09 | 6.07e-08 |
| 2.34e-07 | 3.29e-09 | 1.11e-08 | 1.56e-09 | 1.68e-08 |
| 1.22e-07 | 1.65e-09 | 3.04e-09 | 2.14e-10 | 4.53e-09 |
| 1.47e-07 | 1.65e-09 | 2.50e-09 | 1.71e-10 | 4.01e-09 |
| 1.04e-07 | 1.65e-09 | 6.39e-09 | 3.14e-10 | 9.53e-09 |
| 1.31e-07 | 1.65e-09 | 4.92e-09 | 2.28e-10 | 7.95e-09 |
| 8.85e-08 | 1.65e-09 | 1.78e-09 | 3.69e-10 | 1.48e-08 |
| 1.19e-07 | 1.65e-09 | 1.27e-09 | 2.99e-10 | 1.48e-08 |
| 8.76e-08 | 1.65e-09 | 3.01e-09 | 4.08e-10 | 4.28e-09 |
| 1.11e-07 | 1.65e-09 | 2.25e-09 | 3.52e-10 | 3.87e-09 |
| 6.54e-07 | 1.65e-09 | 1.11e-08 | 1.56e-09 | 2.02e-08 |
| 3.78e-07 | 1.64e-09 | 2.78e-08 | 1.56e-09 | 4.91e-08 |
| 2.34e-07 | 1.97e-08 | 1.11e-08 | 1.56e-09 | 6.07e-08 |
| 2.34e-07 | 3.29e-09 | 1.11e-08 | 1.56e-09 | 1.68e-08 |
| 6.54e-07 | 1.65e-09 | 1.11e-08 | 1.56e-09 | 2.02e-08 |
| 3.78e-07 | 1.64e-09 | 2.78e-08 | 1.56e-09 | 4.91e-08 |
| 2.34e-07 | 1.97e-08 | 1.11e-08 | 1.56e-09 | 6.07e-08 |
| 2.34e-07 | 3.29e-09 | 1.11e-08 | 1.56e-09 | 1.68e-08 |
| 1.05e-07 | 1.65e-09 | 3.92e-09 | 3.40e-10 | 5.84e-09 |
| 1.34e-07 | 1.65e-09 | 2.96e-09 | 2.24e-10 | 4.71e-09 |
| 8.74e-08 | 1.65e-09 | 8.48e-09 | 5.39e-10 | 1.29e-08 |
| 1.13e-07 | 1.65e-09 | 5.95e-09 | 3.44e-10 | 9.92e-09 |
| 7.23e-08 | 1.65e-09 | 2.49e-09 | 5.51e-10 | 1.82e-08 |
| 9.72e-08 | 1.65e-09 | 1.65e-09 | 3.62e-10 | 1.53e-08 |
| 6.80e-08 | 1.65e-09 | 4.55e-09 | 5.38e-10 | 5.39e-09 |
| 8.21e-08 | 1.65e-09 | 3.33e-09 | 3.96e-10 | 4.34e-09 |
| 6.54e-07 | 1.65e-09 | 1.11e-08 | 1.56e-09 | 2.02e-08 |
| 3.78e-07 | 1.64e-09 | 2.78e-08 | 1.56e-09 | 4.91e-08 |
| 2.34e-07 | 1.97e-08 | 1.11e-08 | 1.56e-09 | 6.07e-08 |
| 2.34e-07 | 3.29e-09 | 1.11e-08 | 1.56e-09 | 1.68e-08 |
| 6.54e-07 | 1.65e-09 | 1.11e-08 | 1.56e-09 | 2.02e-08 |
| 3.78e-07 | 1.64e-09 | 2.78e-08 | 1.56e-09 | 4.91e-08 |
| 2.34e-07 | 1.97e-08 | 1.11e-08 | 1.56e-09 | 6.07e-08 |
| 2.34e-07 | 3.29e-09 | 1.11e-08 | 1.56e-09 | 1.68e-08 |
| 1.15e-07 | 1.65e-09 | 3.33e-09 | 2.47e-10 | 4.92e-09 |
| 1.42e-07 | 1.65e-09 | 2.63e-09 | 1.79e-10 | 4.15e-09 |
| 9.62e-08 | 1.65e-09 | 7.16e-09 | 3.81e-10 | 1.07e-08 |

| | | | | |
|----------|----------|----------|----------|----------|
| 1.23e-07 | 1.65e-09 | 5.27e-09 | 2.61e-10 | 8.55e-09 |
| 8.08e-08 | 1.65e-09 | 2.05e-09 | 4.18e-10 | 1.56e-08 |
| 1.09e-07 | 1.65e-09 | 1.40e-09 | 2.95e-10 | 1.40e-08 |
| 7.53e-08 | 1.65e-09 | 3.80e-09 | 4.74e-10 | 4.85e-09 |
| 9.32e-08 | 1.65e-09 | 2.77e-09 | 3.61e-10 | 4.03e-09 |
| 6.54e-07 | 1.65e-09 | 1.11e-08 | 1.56e-09 | 2.02e-08 |
| 3.78e-07 | 1.64e-09 | 2.78e-08 | 1.56e-09 | 4.91e-08 |
| 2.34e-07 | 1.97e-08 | 1.11e-08 | 1.56e-09 | 6.07e-08 |
| 2.34e-07 | 3.29e-09 | 1.11e-08 | 1.56e-09 | 1.68e-08 |
| 6.54e-07 | 1.65e-09 | 1.11e-08 | 1.56e-09 | 2.02e-08 |
| 3.78e-07 | 1.64e-09 | 2.78e-08 | 1.56e-09 | 4.91e-08 |
| 2.34e-07 | 1.97e-08 | 1.11e-08 | 1.56e-09 | 6.07e-08 |
| 2.34e-07 | 3.29e-09 | 1.11e-08 | 1.56e-09 | 1.68e-08 |
| 1.22e-07 | 1.65e-09 | 3.04e-09 | 2.52e-10 | 4.60e-09 |
| 1.48e-07 | 1.65e-09 | 2.50e-09 | 2.00e-10 | 4.07e-09 |
| 1.04e-07 | 1.65e-09 | 6.37e-09 | 4.00e-10 | 9.79e-09 |
| 1.32e-07 | 1.65e-09 | 4.91e-09 | 2.89e-10 | 8.18e-09 |
| 8.87e-08 | 1.65e-09 | 1.78e-09 | 5.13e-10 | 1.55e-08 |
| 1.19e-07 | 1.65e-09 | 1.27e-09 | 4.13e-10 | 1.55e-08 |
| 8.77e-08 | 1.65e-09 | 3.00e-09 | 4.88e-10 | 4.36e-09 |
| 1.11e-07 | 1.65e-09 | 2.25e-09 | 4.20e-10 | 3.96e-09 |
| 6.54e-07 | 1.65e-09 | 1.11e-08 | 1.56e-09 | 2.02e-08 |
| 3.78e-07 | 1.64e-09 | 2.78e-08 | 1.56e-09 | 4.91e-08 |
| 2.34e-07 | 1.97e-08 | 1.11e-08 | 1.56e-09 | 6.07e-08 |
| 2.34e-07 | 3.29e-09 | 1.11e-08 | 1.56e-09 | 1.68e-08 |
| 6.54e-07 | 1.65e-09 | 1.11e-08 | 1.56e-09 | 2.02e-08 |
| 3.78e-07 | 1.64e-09 | 2.78e-08 | 1.56e-09 | 4.91e-08 |
| 2.34e-07 | 1.97e-08 | 1.11e-08 | 1.56e-09 | 6.07e-08 |
| 2.34e-07 | 3.29e-09 | 1.11e-08 | 1.56e-09 | 1.68e-08 |
| 1.06e-07 | 1.65e-09 | 3.93e-09 | 4.05e-10 | 5.97e-09 |
| 1.35e-07 | 1.65e-09 | 2.97e-09 | 2.65e-10 | 4.80e-09 |
| 8.77e-08 | 1.65e-09 | 8.46e-09 | 7.01e-10 | 1.34e-08 |
| 1.14e-07 | 1.65e-09 | 5.93e-09 | 4.41e-10 | 1.02e-08 |
| 7.25e-08 | 1.65e-09 | 2.50e-09 | 7.82e-10 | 1.93e-08 |
| 9.77e-08 | 1.65e-09 | 1.65e-09 | 5.04e-10 | 1.62e-08 |
| 6.81e-08 | 1.65e-09 | 4.54e-09 | 6.46e-10 | 5.48e-09 |
| 8.22e-08 | 1.65e-09 | 3.33e-09 | 4.75e-10 | 4.42e-09 |
| 6.54e-07 | 1.65e-09 | 1.11e-08 | 1.56e-09 | 2.02e-08 |
| 3.78e-07 | 1.64e-09 | 2.78e-08 | 1.56e-09 | 4.91e-08 |
| 2.34e-07 | 1.97e-08 | 1.11e-08 | 1.56e-09 | 6.07e-08 |
| 2.34e-07 | 3.29e-09 | 1.11e-08 | 1.56e-09 | 1.68e-08 |
| 6.54e-07 | 1.65e-09 | 1.11e-08 | 1.56e-09 | 2.02e-08 |
| 3.78e-07 | 1.64e-09 | 2.78e-08 | 1.56e-09 | 4.91e-08 |
| 2.34e-07 | 1.97e-08 | 1.11e-08 | 1.56e-09 | 6.07e-08 |
| 2.34e-07 | 3.29e-09 | 1.11e-08 | 1.56e-09 | 1.68e-08 |
| 1.15e-07 | 1.65e-09 | 3.34e-09 | 2.92e-10 | 5.00e-09 |
| 1.42e-07 | 1.65e-09 | 2.63e-09 | 2.10e-10 | 4.21e-09 |
| 9.65e-08 | 1.65e-09 | 7.14e-09 | 4.90e-10 | 1.10e-08 |
| 1.23e-07 | 1.65e-09 | 5.26e-09 | 3.33e-10 | 8.80e-09 |
| 8.09e-08 | 1.65e-09 | 2.05e-09 | 5.84e-10 | 1.64e-08 |

| | | | | |
|----------|----------|----------|----------|----------|
| 1.09e-07 | 1.65e-09 | 1.39e-09 | 4.09e-10 | 1.47e-08 |
| 7.54e-08 | 1.65e-09 | 3.80e-09 | 5.68e-10 | 4.93e-09 |
| 9.33e-08 | 1.65e-09 | 2.77e-09 | 4.32e-10 | 4.11e-09 |

DRAFT

| Co | Pb | Mo | Se | Hfo_s |
|----------|----------|----------|----------|----------|
| 8.50e-10 | 5.56e-09 | 1.75e-08 | 1.40e-08 | 0 |
| 1.61e-08 | 9.66e-09 | 1.38e-08 | 5.71e-09 | 0 |
| 3.48e-08 | 9.18e-09 | 1.38e-08 | 3.80e-09 | 0 |
| 2.89e-08 | 5.56e-09 | 3.18e-08 | 3.80e-09 | 0 |
| 8.50e-10 | 5.56e-09 | 1.75e-08 | 1.40e-08 | 0.000105 |
| 1.61e-08 | 9.66e-09 | 1.38e-08 | 5.71e-09 | 0.000105 |
| 3.48e-08 | 9.18e-09 | 1.38e-08 | 3.80e-09 | 0.000105 |
| 2.89e-08 | 5.56e-09 | 3.18e-08 | 3.80e-09 | 0.000205 |
| 7.48e-11 | 3.14e-09 | 8.41e-08 | 3.23e-08 | 0.000105 |
| 5.94e-11 | 2.96e-09 | 8.25e-08 | 2.71e-08 | 0.000105 |
| 2.12e-09 | 6.66e-09 | 8.44e-08 | 1.20e-08 | 0.000105 |
| 1.51e-09 | 5.91e-09 | 8.28e-08 | 1.10e-08 | 0.000105 |
| 5.85e-09 | 7.94e-09 | 8.36e-08 | 5.67e-09 | 0.000105 |
| 4.69e-09 | 8.36e-09 | 8.27e-08 | 5.09e-09 | 0.000105 |
| 5.02e-09 | 4.73e-09 | 1.02e-07 | 1.05e-08 | 0.000205 |
| 4.33e-09 | 4.96e-09 | 8.42e-08 | 9.78e-09 | 0.000205 |
| 8.50e-10 | 5.56e-09 | 1.75e-08 | 1.40e-08 | 0 |
| 1.61e-08 | 9.66e-09 | 1.38e-08 | 5.71e-09 | 0 |
| 3.48e-08 | 9.18e-09 | 1.38e-08 | 3.80e-09 | 0 |
| 2.89e-08 | 5.56e-09 | 3.18e-08 | 3.80e-09 | 0 |
| 8.50e-10 | 5.56e-09 | 1.75e-08 | 1.40e-08 | 0.000255 |
| 1.61e-08 | 9.66e-09 | 1.38e-08 | 5.71e-09 | 0.000255 |
| 3.48e-08 | 9.18e-09 | 1.38e-08 | 3.80e-09 | 0.000255 |
| 2.89e-08 | 5.56e-09 | 3.18e-08 | 3.80e-09 | 0.000800 |
| 1.20e-10 | 4.39e-09 | 8.61e-08 | 3.47e-08 | 0.000255 |
| 7.86e-11 | 3.71e-09 | 8.32e-08 | 3.26e-08 | 0.000255 |
| 3.69e-09 | 9.94e-09 | 8.60e-08 | 1.27e-08 | 0.000255 |
| 2.34e-09 | 8.17e-09 | 8.41e-08 | 1.20e-08 | 0.000255 |
| 8.86e-09 | 9.92e-09 | 8.45e-08 | 6.18e-09 | 0.000255 |
| 5.75e-09 | 8.65e-09 | 8.34e-08 | 5.41e-09 | 0.000255 |
| 6.63e-09 | 4.77e-09 | 1.41e-07 | 1.12e-08 | 0.000800 |
| 4.92e-09 | 4.53e-09 | 1.01e-07 | 1.14e-08 | 0.000800 |
| 8.50e-10 | 5.56e-09 | 1.75e-08 | 1.40e-08 | 0 |
| 1.61e-08 | 9.66e-09 | 1.38e-08 | 5.71e-09 | 0 |
| 3.48e-08 | 9.18e-09 | 1.38e-08 | 3.80e-09 | 0 |
| 2.89e-08 | 5.56e-09 | 3.18e-08 | 3.80e-09 | 0 |
| 8.50e-10 | 5.56e-09 | 1.75e-08 | 1.40e-08 | 0.000155 |
| 1.61e-08 | 9.66e-09 | 1.38e-08 | 5.71e-09 | 0.000155 |
| 3.48e-08 | 9.18e-09 | 1.38e-08 | 3.80e-09 | 0.000155 |
| 2.89e-08 | 5.56e-09 | 3.18e-08 | 3.80e-09 | 0.000440 |
| 8.66e-11 | 3.45e-09 | 8.49e-08 | 3.38e-08 | 0.000155 |
| 6.23e-11 | 3.05e-09 | 8.27e-08 | 3.02e-08 | 0.000155 |
| 2.60e-09 | 7.62e-09 | 8.50e-08 | 1.24e-08 | 0.000155 |

| | | | | |
|----------|----------|----------|----------|----------|
| 1.76e-09 | 6.54e-09 | 8.32e-08 | 1.15e-08 | 0.000155 |
| 6.66e-09 | 8.31e-09 | 8.40e-08 | 5.89e-09 | 0.000155 |
| 4.65e-09 | 7.72e-09 | 8.30e-08 | 5.25e-09 | 0.000155 |
| 5.84e-09 | 4.80e-09 | 1.20e-07 | 1.11e-08 | 0.000440 |
| 4.46e-09 | 4.61e-09 | 8.95e-08 | 1.07e-08 | 0.000440 |
| 8.50e-10 | 5.56e-09 | 1.75e-08 | 1.40e-08 | 0 |
| 1.61e-08 | 9.66e-09 | 1.38e-08 | 5.71e-09 | 0 |
| 3.48e-08 | 9.18e-09 | 1.38e-08 | 3.80e-09 | 0 |
| 2.89e-08 | 5.56e-09 | 3.18e-08 | 3.80e-09 | 0 |
| 8.50e-10 | 5.56e-09 | 1.75e-08 | 1.40e-08 | 0.000105 |
| 1.61e-08 | 9.66e-09 | 1.38e-08 | 5.71e-09 | 0.000105 |
| 3.48e-08 | 9.18e-09 | 1.38e-08 | 3.80e-09 | 0.000105 |
| 2.89e-08 | 5.56e-09 | 3.18e-08 | 3.80e-09 | 0.000205 |
| 7.72e-11 | 3.23e-09 | 8.42e-08 | 3.26e-08 | 0.000105 |
| 6.12e-11 | 3.03e-09 | 8.25e-08 | 2.74e-08 | 0.000105 |
| 2.24e-09 | 6.99e-09 | 8.45e-08 | 1.22e-08 | 0.000105 |
| 1.59e-09 | 6.17e-09 | 8.28e-08 | 1.11e-08 | 0.000105 |
| 6.22e-09 | 8.40e-09 | 8.38e-08 | 5.76e-09 | 0.000105 |
| 4.96e-09 | 8.80e-09 | 8.27e-08 | 5.17e-09 | 0.000105 |
| 5.19e-09 | 4.89e-09 | 1.03e-07 | 1.07e-08 | 0.000205 |
| 4.47e-09 | 5.12e-09 | 8.42e-08 | 9.88e-09 | 0.000205 |
| 8.50e-10 | 5.56e-09 | 1.75e-08 | 1.40e-08 | 0 |
| 1.61e-08 | 9.66e-09 | 1.38e-08 | 5.71e-09 | 0 |
| 3.48e-08 | 9.18e-09 | 1.38e-08 | 3.80e-09 | 0 |
| 2.89e-08 | 5.56e-09 | 3.18e-08 | 3.80e-09 | 0 |
| 8.50e-10 | 5.56e-09 | 1.75e-08 | 1.40e-08 | 0.000255 |
| 1.61e-08 | 9.66e-09 | 1.38e-08 | 5.71e-09 | 0.000255 |
| 3.48e-08 | 9.18e-09 | 1.38e-08 | 3.80e-09 | 0.000255 |
| 2.89e-08 | 5.56e-09 | 3.18e-08 | 3.80e-09 | 0.000800 |
| 1.25e-10 | 4.56e-09 | 8.62e-08 | 3.50e-08 | 0.000255 |
| 8.13e-11 | 3.83e-09 | 8.32e-08 | 3.29e-08 | 0.000255 |
| 3.97e-09 | 1.06e-08 | 8.64e-08 | 1.28e-08 | 0.000255 |
| 2.48e-09 | 8.62e-09 | 8.41e-08 | 1.22e-08 | 0.000255 |
| 9.61e-09 | 1.07e-08 | 8.49e-08 | 6.27e-09 | 0.000255 |
| 6.12e-09 | 9.20e-09 | 8.35e-08 | 5.49e-09 | 0.000255 |
| 6.87e-09 | 4.93e-09 | 1.43e-07 | 1.13e-08 | 0.000800 |
| 5.09e-09 | 4.67e-09 | 1.02e-07 | 1.16e-08 | 0.000800 |
| 8.50e-10 | 5.56e-09 | 1.75e-08 | 1.40e-08 | 0 |
| 1.61e-08 | 9.66e-09 | 1.38e-08 | 5.71e-09 | 0 |
| 3.48e-08 | 9.18e-09 | 1.38e-08 | 3.80e-09 | 0 |
| 2.89e-08 | 5.56e-09 | 3.18e-08 | 3.80e-09 | 0 |
| 8.50e-10 | 5.56e-09 | 1.75e-08 | 1.40e-08 | 0.000155 |
| 1.61e-08 | 9.66e-09 | 1.38e-08 | 5.71e-09 | 0.000155 |
| 3.48e-08 | 9.18e-09 | 1.38e-08 | 3.80e-09 | 0.000155 |
| 2.89e-08 | 5.56e-09 | 3.18e-08 | 3.80e-09 | 0.000440 |
| 8.97e-11 | 3.56e-09 | 8.50e-08 | 3.41e-08 | 0.000155 |
| 6.42e-11 | 3.13e-09 | 8.27e-08 | 3.05e-08 | 0.000155 |
| 2.76e-09 | 8.04e-09 | 8.53e-08 | 1.26e-08 | 0.000155 |
| 1.86e-09 | 6.84e-09 | 8.32e-08 | 1.17e-08 | 0.000155 |
| 7.11e-09 | 8.84e-09 | 8.43e-08 | 5.99e-09 | 0.000155 |

| | | | | |
|----------|----------|----------|----------|----------|
| 4.92e-09 | 8.14e-09 | 8.30e-08 | 5.33e-09 | 0.000155 |
| 6.05e-09 | 4.97e-09 | 1.21e-07 | 1.12e-08 | 0.000440 |
| 4.61e-09 | 4.75e-09 | 8.96e-08 | 1.09e-08 | 0.000440 |

DRAFT

| Hfo_w | Hao | m Hfo_wOH | m Hfo_wOH2+ | m Hfo_wOHSO4-2 |
|---------|---------|-----------|-------------|----------------|
| 0 | 0 | 0 | 0 | 0 |
| 0 | 0 | 0 | 0 | 0 |
| 0 | 0 | 0 | 0 | 0 |
| 0 | 0 | 0 | 0 | 0 |
| 0.00420 | 0.00330 | 0.000307 | 0.000285 | 2.16e-05 |
| 0.00420 | 0.00330 | 0.000248 | 0.000202 | 2.47e-05 |
| 0.00420 | 0.00330 | 0.000227 | 0.000363 | 1.36e-05 |
| 0.00820 | 0.00168 | 0.000612 | 0.000675 | 4.54e-05 |
| 0.00420 | 0.00330 | 0.000426 | 0.000251 | 3.79e-07 |
| 0.00420 | 0.00330 | 0.000482 | 0.000256 | 3.25e-07 |
| 0.00420 | 0.00330 | 0.000408 | 0.000198 | 7.31e-07 |
| 0.00420 | 0.00330 | 0.000476 | 0.000203 | 6.26e-07 |
| 0.00420 | 0.00330 | 0.000518 | 0.000371 | 6.72e-07 |
| 0.00420 | 0.00330 | 0.000640 | 0.000374 | 5.82e-07 |
| 0.00820 | 0.00168 | 0.000833 | 0.000592 | 1.11e-06 |
| 0.00820 | 0.00168 | 0.000985 | 0.000608 | 9.27e-07 |
| 0 | 0 | 0 | 0 | 0 |
| 0 | 0 | 0 | 0 | 0 |
| 0 | 0 | 0 | 0 | 0 |
| 0 | 0 | 0 | 0 | 0 |
| 0.0102 | 0.0257 | 0.000745 | 0.000693 | 5.24e-05 |
| 0.0102 | 0.0257 | 0.000601 | 0.000492 | 5.99e-05 |
| 0.0102 | 0.0257 | 0.000552 | 0.000881 | 3.30e-05 |
| 0.0320 | 0.00627 | 0.00239 | 0.00263 | 0.000177 |
| 0.0102 | 0.0257 | 0.000899 | 0.000552 | 1.35e-06 |
| 0.0102 | 0.0257 | 0.00106 | 0.000572 | 9.18e-07 |
| 0.0102 | 0.0257 | 0.000850 | 0.000445 | 2.22e-06 |
| 0.0102 | 0.0257 | 0.00104 | 0.000474 | 1.71e-06 |
| 0.0102 | 0.0257 | 0.00103 | 0.000835 | 2.11e-06 |
| 0.0102 | 0.0257 | 0.00133 | 0.000868 | 1.72e-06 |
| 0.0320 | 0.00627 | 0.00263 | 0.00219 | 6.15e-06 |
| 0.0320 | 0.00627 | 0.00301 | 0.00227 | 4.01e-06 |
| 0 | 0 | 0 | 0 | 0 |
| 0 | 0 | 0 | 0 | 0 |
| 0 | 0 | 0 | 0 | 0 |
| 0 | 0 | 0 | 0 | 0 |
| 0.00620 | 0.00726 | 0.000453 | 0.000421 | 3.19e-05 |
| 0.00620 | 0.00726 | 0.000365 | 0.000299 | 3.64e-05 |
| 0.00620 | 0.00726 | 0.000335 | 0.000536 | 2.00e-05 |
| 0.0176 | 0.00429 | 0.00131 | 0.00145 | 9.74e-05 |
| 0.00620 | 0.00726 | 0.000595 | 0.000360 | 6.23e-07 |
| 0.00620 | 0.00726 | 0.000687 | 0.000371 | 4.90e-07 |
| 0.00620 | 0.00726 | 0.000565 | 0.000286 | 1.16e-06 |

| | | | | |
|---------|---------|----------|----------|----------|
| 0.00620 | 0.00726 | 0.000674 | 0.000298 | 9.56e-07 |
| 0.00620 | 0.00726 | 0.000703 | 0.000534 | 1.08e-06 |
| 0.00620 | 0.00726 | 0.000892 | 0.000550 | 9.06e-07 |
| 0.0176 | 0.00429 | 0.00157 | 0.00123 | 2.83e-06 |
| 0.0176 | 0.00429 | 0.00185 | 0.00128 | 2.10e-06 |
| 0 | 0 | 0 | 0 | 0 |
| 0 | 0 | 0 | 0 | 0 |
| 0 | 0 | 0 | 0 | 0 |
| 0 | 0 | 0 | 0 | 0 |
| 0.00420 | 0.00330 | 0.000306 | 0.000284 | 2.18e-05 |
| 0.00420 | 0.00330 | 0.000247 | 0.000201 | 2.51e-05 |
| 0.00420 | 0.00330 | 0.000226 | 0.000360 | 1.39e-05 |
| 0.00820 | 0.00168 | 0.000610 | 0.000672 | 4.60e-05 |
| 0.00420 | 0.00330 | 0.000426 | 0.000251 | 3.78e-07 |
| 0.00420 | 0.00330 | 0.000483 | 0.000255 | 3.25e-07 |
| 0.00420 | 0.00330 | 0.000408 | 0.000199 | 7.25e-07 |
| 0.00420 | 0.00330 | 0.000476 | 0.000203 | 6.23e-07 |
| 0.00420 | 0.00330 | 0.000518 | 0.000371 | 6.67e-07 |
| 0.00420 | 0.00330 | 0.000640 | 0.000373 | 5.82e-07 |
| 0.00820 | 0.00168 | 0.000834 | 0.000593 | 1.11e-06 |
| 0.00820 | 0.00168 | 0.000986 | 0.000609 | 9.27e-07 |
| 0 | 0 | 0 | 0 | 0 |
| 0 | 0 | 0 | 0 | 0 |
| 0 | 0 | 0 | 0 | 0 |
| 0 | 0 | 0 | 0 | 0 |
| 0.0102 | 0.0257 | 0.000744 | 0.000691 | 5.30e-05 |
| 0.0102 | 0.0257 | 0.000599 | 0.000489 | 6.09e-05 |
| 0.0102 | 0.0257 | 0.000549 | 0.000874 | 3.37e-05 |
| 0.0320 | 0.00627 | 0.00238 | 0.00262 | 0.000180 |
| 0.0102 | 0.0257 | 0.000899 | 0.000549 | 1.33e-06 |
| 0.0102 | 0.0257 | 0.00106 | 0.000570 | 9.17e-07 |
| 0.0102 | 0.0257 | 0.000851 | 0.000445 | 2.15e-06 |
| 0.0102 | 0.0257 | 0.00104 | 0.000474 | 1.69e-06 |
| 0.0102 | 0.0257 | 0.00103 | 0.000831 | 2.04e-06 |
| 0.0102 | 0.0257 | 0.00133 | 0.000864 | 1.71e-06 |
| 0.0320 | 0.00627 | 0.00263 | 0.00219 | 6.11e-06 |
| 0.0320 | 0.00627 | 0.00301 | 0.00227 | 4.00e-06 |
| 0 | 0 | 0 | 0 | 0 |
| 0 | 0 | 0 | 0 | 0 |
| 0 | 0 | 0 | 0 | 0 |
| 0 | 0 | 0 | 0 | 0 |
| 0.00620 | 0.00726 | 0.000452 | 0.000420 | 3.22e-05 |
| 0.00620 | 0.00726 | 0.000364 | 0.000297 | 3.70e-05 |
| 0.00620 | 0.00726 | 0.000334 | 0.000531 | 2.05e-05 |
| 0.0176 | 0.00429 | 0.00131 | 0.00144 | 9.87e-05 |
| 0.00620 | 0.00726 | 0.000595 | 0.000360 | 6.20e-07 |
| 0.00620 | 0.00726 | 0.000687 | 0.000371 | 4.90e-07 |
| 0.00620 | 0.00726 | 0.000566 | 0.000286 | 1.15e-06 |
| 0.00620 | 0.00726 | 0.000675 | 0.000299 | 9.51e-07 |
| 0.00620 | 0.00726 | 0.000703 | 0.000533 | 1.07e-06 |

| | | | | |
|---------|---------|----------|----------|----------|
| 0.00620 | 0.00726 | 0.000892 | 0.000549 | 9.05e-07 |
| 0.0176 | 0.00429 | 0.00158 | 0.00123 | 2.82e-06 |
| 0.0176 | 0.00429 | 0.00186 | 0.00128 | 2.10e-06 |

DRAFT

| m Hfo wSO4- | m Hfo wOSi(OH)3 | m_Hfo_wOSiO(OH) 2- | m Hfo wHCO3 | m Hfo wCO3- |
|-------------|-----------------|-----------------------|-------------|-------------|
| 0 | 0 | 0 | 0 | 0 |
| 0 | 0 | 0 | 0 | 0 |
| 0 | 0 | 0 | 0 | 0 |
| 0 | 0 | 0 | 0 | 0 |
| 1.01e-05 | 0.000970 | 0.000643 | 0.000924 | 0.000169 |
| 1.01e-05 | 0.000725 | 0.000546 | 0.00118 | 0.000246 |
| 1.09e-05 | 0.000500 | 0.000193 | 0.00203 | 0.000216 |
| 2.51e-05 | 0.00162 | 0.000906 | 0.00266 | 0.000410 |
| 1.12e-07 | 0.000772 | 0.000805 | 0.000795 | 0.000228 |
| 8.64e-08 | 0.000720 | 0.000838 | 0.000727 | 0.000233 |
| 1.79e-07 | 0.000555 | 0.000704 | 0.000931 | 0.000325 |
| 1.34e-07 | 0.000515 | 0.000746 | 0.000820 | 0.000327 |
| 2.42e-07 | 0.000383 | 0.000330 | 0.00148 | 0.000351 |
| 1.71e-07 | 0.000362 | 0.000381 | 0.00126 | 0.000365 |
| 3.97e-07 | 0.00134 | 0.00116 | 0.00235 | 0.000562 |
| 2.87e-07 | 0.00125 | 0.00125 | 0.00211 | 0.000580 |
| 0 | 0 | 0 | 0 | 0 |
| 0 | 0 | 0 | 0 | 0 |
| 0 | 0 | 0 | 0 | 0 |
| 0 | 0 | 0 | 0 | 0 |
| 2.45e-05 | 0.00236 | 0.00156 | 0.00225 | 0.000410 |
| 2.45e-05 | 0.00176 | 0.00133 | 0.00287 | 0.000596 |
| 2.64e-05 | 0.00121 | 0.000469 | 0.00494 | 0.000525 |
| 9.79e-05 | 0.00633 | 0.00354 | 0.0104 | 0.00160 |
| 4.16e-07 | 0.00193 | 0.00193 | 0.00201 | 0.000556 |
| 2.49e-07 | 0.00179 | 0.00204 | 0.00180 | 0.000563 |
| 5.84e-07 | 0.00140 | 0.00165 | 0.00243 | 0.000788 |
| 3.92e-07 | 0.00130 | 0.00175 | 0.00216 | 0.000801 |
| 8.61e-07 | 0.000961 | 0.000729 | 0.00396 | 0.000828 |
| 5.64e-07 | 0.000881 | 0.000833 | 0.00341 | 0.000889 |
| 2.58e-06 | 0.00564 | 0.00417 | 0.0102 | 0.00208 |
| 1.52e-06 | 0.00538 | 0.00440 | 0.00962 | 0.00217 |
| 0 | 0 | 0 | 0 | 0 |
| 0 | 0 | 0 | 0 | 0 |
| 0 | 0 | 0 | 0 | 0 |
| 0 | 0 | 0 | 0 | 0 |
| 1.49e-05 | 0.00143 | 0.000949 | 0.00136 | 0.000249 |
| 1.49e-05 | 0.00107 | 0.000807 | 0.00175 | 0.000363 |
| 1.60e-05 | 0.000738 | 0.000285 | 0.00300 | 0.000319 |
| 5.39e-05 | 0.00348 | 0.00195 | 0.00571 | 0.000879 |
| 1.89e-07 | 0.00116 | 0.00118 | 0.00120 | 0.000336 |
| 1.33e-07 | 0.00108 | 0.00123 | 0.00109 | 0.000341 |
| 2.95e-07 | 0.000837 | 0.00102 | 0.00143 | 0.000479 |

| | | | | |
|----------|----------|----------|----------|----------|
| 2.12e-07 | 0.000776 | 0.00108 | 0.00126 | 0.000484 |
| 4.13e-07 | 0.000574 | 0.000465 | 0.00229 | 0.000512 |
| 2.80e-07 | 0.000533 | 0.000533 | 0.00196 | 0.000539 |
| 1.11e-06 | 0.00301 | 0.00238 | 0.00540 | 0.00117 |
| 7.29e-07 | 0.00284 | 0.00253 | 0.00496 | 0.00122 |
| 0 | 0 | 0 | 0 | 0 |
| 0 | 0 | 0 | 0 | 0 |
| 0 | 0 | 0 | 0 | 0 |
| 0 | 0 | 0 | 0 | 0 |
| 1.02e-05 | 0.000968 | 0.000643 | 0.000926 | 0.000169 |
| 1.03e-05 | 0.000722 | 0.000545 | 0.00118 | 0.000246 |
| 1.11e-05 | 0.000497 | 0.000193 | 0.00204 | 0.000217 |
| 2.54e-05 | 0.00162 | 0.000906 | 0.00266 | 0.000411 |
| 1.12e-07 | 0.000770 | 0.000805 | 0.000794 | 0.000229 |
| 8.63e-08 | 0.000718 | 0.000837 | 0.000726 | 0.000233 |
| 1.77e-07 | 0.000554 | 0.000701 | 0.000930 | 0.000324 |
| 1.33e-07 | 0.000514 | 0.000743 | 0.000820 | 0.000326 |
| 2.40e-07 | 0.000382 | 0.000329 | 0.00148 | 0.000351 |
| 1.70e-07 | 0.000360 | 0.000380 | 0.00125 | 0.000365 |
| 3.96e-07 | 0.00134 | 0.00116 | 0.00235 | 0.000562 |
| 2.87e-07 | 0.00125 | 0.00124 | 0.00211 | 0.000580 |
| 0 | 0 | 0 | 0 | 0 |
| 0 | 0 | 0 | 0 | 0 |
| 0 | 0 | 0 | 0 | 0 |
| 0 | 0 | 0 | 0 | 0 |
| 2.47e-05 | 0.00235 | 0.00156 | 0.00225 | 0.000411 |
| 2.49e-05 | 0.00175 | 0.00132 | 0.00288 | 0.000599 |
| 2.69e-05 | 0.00121 | 0.000468 | 0.00495 | 0.000528 |
| 9.91e-05 | 0.00631 | 0.00353 | 0.0104 | 0.00160 |
| 4.09e-07 | 0.00192 | 0.00194 | 0.00200 | 0.000557 |
| 2.48e-07 | 0.00178 | 0.00204 | 0.00179 | 0.000564 |
| 5.65e-07 | 0.00140 | 0.00165 | 0.00242 | 0.000787 |
| 3.88e-07 | 0.00129 | 0.00175 | 0.00215 | 0.000800 |
| 8.26e-07 | 0.000955 | 0.000729 | 0.00395 | 0.000830 |
| 5.57e-07 | 0.000875 | 0.000833 | 0.00340 | 0.000890 |
| 2.56e-06 | 0.00563 | 0.00416 | 0.0102 | 0.00208 |
| 1.51e-06 | 0.00537 | 0.00439 | 0.00962 | 0.00217 |
| 0 | 0 | 0 | 0 | 0 |
| 0 | 0 | 0 | 0 | 0 |
| 0 | 0 | 0 | 0 | 0 |
| 0 | 0 | 0 | 0 | 0 |
| 1.50e-05 | 0.00143 | 0.000949 | 0.00137 | 0.000250 |
| 1.51e-05 | 0.00107 | 0.000805 | 0.00175 | 0.000364 |
| 1.64e-05 | 0.000734 | 0.000285 | 0.00301 | 0.000321 |
| 5.45e-05 | 0.00347 | 0.00194 | 0.00572 | 0.000882 |
| 1.88e-07 | 0.00115 | 0.00118 | 0.00120 | 0.000337 |
| 1.33e-07 | 0.00108 | 0.00123 | 0.00108 | 0.000341 |
| 2.91e-07 | 0.000834 | 0.00102 | 0.00142 | 0.000478 |
| 2.11e-07 | 0.000774 | 0.00108 | 0.00126 | 0.000483 |
| 4.07e-07 | 0.000571 | 0.000464 | 0.00229 | 0.000512 |

| | | | | |
|----------|----------|----------|---------|----------|
| 2.79e-07 | 0.000531 | 0.000532 | 0.00195 | 0.000539 |
| 1.10e-06 | 0.00300 | 0.00237 | 0.00540 | 0.00117 |
| 7.28e-07 | 0.00283 | 0.00252 | 0.00496 | 0.00122 |

DRAFT

| m Hfo wPO4-2 | m Hfo wHPO4- | m Hfo wH2PO4 | m Hfo sCO3- | m Hfo sHCO3 |
|--------------|--------------|--------------|-------------|-------------|
| 0 | 0 | 0 | 0 | 0 |
| 0 | 0 | 0 | 0 | 0 |
| 0 | 0 | 0 | 0 | 0 |
| 0 | 0 | 0 | 0 | 0 |
| 2.71e-05 | 6.04e-05 | 2.29e-06 | 1.85e-08 | 1.01e-07 |
| 1.73e-05 | 3.39e-05 | 1.13e-06 | 2.14e-08 | 1.03e-07 |
| 4.50e-05 | 0.000173 | 1.12e-05 | 1.78e-08 | 1.67e-07 |
| 2.63e-05 | 6.96e-05 | 3.13e-06 | 6.66e-08 | 4.32e-07 |
| 3.54e-05 | 5.02e-05 | 1.21e-06 | 1.97e-08 | 6.85e-08 |
| 3.64e-05 | 4.63e-05 | 1.00e-06 | 1.86e-08 | 5.79e-08 |
| 2.39e-05 | 2.79e-05 | 5.53e-07 | 2.04e-08 | 5.83e-08 |
| 2.56e-05 | 2.62e-05 | 4.55e-07 | 1.88e-08 | 4.72e-08 |
| 8.10e-05 | 0.000139 | 4.07e-06 | 1.06e-08 | 4.46e-08 |
| 9.00e-05 | 0.000126 | 3.00e-06 | 7.85e-09 | 2.70e-08 |
| 3.60e-05 | 6.13e-05 | 1.78e-06 | 5.86e-08 | 2.45e-07 |
| 3.92e-05 | 5.81e-05 | 1.46e-06 | 4.97e-08 | 1.81e-07 |
| 0 | 0 | 0 | 0 | 0 |
| 0 | 0 | 0 | 0 | 0 |
| 0 | 0 | 0 | 0 | 0 |
| 0 | 0 | 0 | 0 | 0 |
| 6.57e-05 | 0.000147 | 5.55e-06 | 4.48e-08 | 2.45e-07 |
| 4.19e-05 | 8.23e-05 | 2.74e-06 | 5.19e-08 | 2.50e-07 |
| 0.000109 | 0.000419 | 2.73e-05 | 4.32e-08 | 4.07e-07 |
| 0.000103 | 0.000272 | 1.22e-05 | 2.60e-07 | 1.69e-06 |
| 8.58e-05 | 0.000126 | 3.16e-06 | 4.83e-08 | 1.74e-07 |
| 9.12e-05 | 0.000118 | 2.61e-06 | 4.54e-08 | 1.45e-07 |
| 5.57e-05 | 7.00e-05 | 1.49e-06 | 4.85e-08 | 1.50e-07 |
| 6.01e-05 | 6.59e-05 | 1.23e-06 | 4.47e-08 | 1.21e-07 |
| 0.000183 | 0.000357 | 1.18e-05 | 2.88e-08 | 1.38e-07 |
| 0.000210 | 0.000328 | 8.72e-06 | 2.40e-08 | 9.20e-08 |
| 0.000126 | 0.000252 | 8.57e-06 | 2.61e-07 | 1.28e-06 |
| 0.000135 | 0.000244 | 7.50e-06 | 2.46e-07 | 1.09e-06 |
| 0 | 0 | 0 | 0 | 0 |
| 0 | 0 | 0 | 0 | 0 |
| 0 | 0 | 0 | 0 | 0 |
| 0 | 0 | 0 | 0 | 0 |
| 3.99e-05 | 8.91e-05 | 3.38e-06 | 2.72e-08 | 1.49e-07 |
| 2.55e-05 | 5.00e-05 | 1.67e-06 | 3.16e-08 | 1.52e-07 |
| 6.65e-05 | 0.000255 | 1.66e-05 | 2.63e-08 | 2.47e-07 |
| 5.65e-05 | 0.000149 | 6.71e-06 | 1.43e-07 | 9.28e-07 |
| 5.21e-05 | 7.57e-05 | 1.87e-06 | 2.94e-08 | 1.05e-07 |
| 5.44e-05 | 7.06e-05 | 1.56e-06 | 2.77e-08 | 8.82e-08 |
| 3.46e-05 | 4.19e-05 | 8.63e-07 | 3.01e-08 | 8.96e-08 |

| | | | | |
|----------|----------|----------|----------|----------|
| 3.71e-05 | 3.94e-05 | 7.11e-07 | 2.78e-08 | 7.24e-08 |
| 0.000116 | 0.000211 | 6.54e-06 | 1.68e-08 | 7.54e-08 |
| 0.000131 | 0.000193 | 4.85e-06 | 1.34e-08 | 4.87e-08 |
| 7.25e-05 | 0.000136 | 4.32e-06 | 1.37e-07 | 6.29e-07 |
| 7.86e-05 | 0.000130 | 3.67e-06 | 1.24e-07 | 5.05e-07 |
| 0 | 0 | 0 | 0 | 0 |
| 0 | 0 | 0 | 0 | 0 |
| 0 | 0 | 0 | 0 | 0 |
| 0 | 0 | 0 | 0 | 0 |
| 2.72e-05 | 6.05e-05 | 2.29e-06 | 1.83e-08 | 1.00e-07 |
| 1.74e-05 | 3.40e-05 | 1.13e-06 | 2.12e-08 | 1.02e-07 |
| 4.54e-05 | 0.000173 | 1.12e-05 | 1.75e-08 | 1.64e-07 |
| 2.65e-05 | 6.98e-05 | 3.13e-06 | 6.61e-08 | 4.28e-07 |
| 3.56e-05 | 5.03e-05 | 1.21e-06 | 1.94e-08 | 6.75e-08 |
| 3.66e-05 | 4.64e-05 | 1.00e-06 | 1.83e-08 | 5.70e-08 |
| 2.40e-05 | 2.80e-05 | 5.56e-07 | 1.98e-08 | 5.66e-08 |
| 2.57e-05 | 2.63e-05 | 4.58e-07 | 1.83e-08 | 4.59e-08 |
| 8.15e-05 | 0.000140 | 4.08e-06 | 1.01e-08 | 4.24e-08 |
| 9.05e-05 | 0.000127 | 3.01e-06 | 7.46e-09 | 2.56e-08 |
| 3.61e-05 | 6.15e-05 | 1.78e-06 | 5.75e-08 | 2.41e-07 |
| 3.94e-05 | 5.83e-05 | 1.47e-06 | 4.86e-08 | 1.77e-07 |
| 0 | 0 | 0 | 0 | 0 |
| 0 | 0 | 0 | 0 | 0 |
| 0 | 0 | 0 | 0 | 0 |
| 0 | 0 | 0 | 0 | 0 |
| 6.60e-05 | 0.000147 | 5.56e-06 | 4.45e-08 | 2.43e-07 |
| 4.22e-05 | 8.26e-05 | 2.75e-06 | 5.14e-08 | 2.47e-07 |
| 0.000110 | 0.000421 | 2.73e-05 | 4.25e-08 | 3.98e-07 |
| 0.000103 | 0.000273 | 1.22e-05 | 2.58e-07 | 1.67e-06 |
| 8.63e-05 | 0.000127 | 3.15e-06 | 4.75e-08 | 1.71e-07 |
| 9.17e-05 | 0.000119 | 2.60e-06 | 4.47e-08 | 1.42e-07 |
| 5.60e-05 | 7.03e-05 | 1.50e-06 | 4.67e-08 | 1.44e-07 |
| 6.04e-05 | 6.62e-05 | 1.23e-06 | 4.31e-08 | 1.16e-07 |
| 0.000185 | 0.000358 | 1.18e-05 | 2.72e-08 | 1.29e-07 |
| 0.000212 | 0.000329 | 8.70e-06 | 2.27e-08 | 8.67e-08 |
| 0.000127 | 0.000253 | 8.60e-06 | 2.57e-07 | 1.26e-06 |
| 0.000136 | 0.000245 | 7.53e-06 | 2.42e-07 | 1.07e-06 |
| 0 | 0 | 0 | 0 | 0 |
| 0 | 0 | 0 | 0 | 0 |
| 0 | 0 | 0 | 0 | 0 |
| 0 | 0 | 0 | 0 | 0 |
| 4.01e-05 | 8.93e-05 | 3.38e-06 | 2.71e-08 | 1.48e-07 |
| 2.57e-05 | 5.02e-05 | 1.67e-06 | 3.13e-08 | 1.50e-07 |
| 6.71e-05 | 0.000256 | 1.66e-05 | 2.58e-08 | 2.42e-07 |
| 5.68e-05 | 0.000150 | 6.72e-06 | 1.42e-07 | 9.19e-07 |
| 5.24e-05 | 7.59e-05 | 1.87e-06 | 2.90e-08 | 1.03e-07 |
| 5.46e-05 | 7.07e-05 | 1.56e-06 | 2.73e-08 | 8.67e-08 |
| 3.47e-05 | 4.21e-05 | 8.67e-07 | 2.91e-08 | 8.68e-08 |
| 3.73e-05 | 3.96e-05 | 7.15e-07 | 2.69e-08 | 7.01e-08 |
| 0.000117 | 0.000212 | 6.55e-06 | 1.60e-08 | 7.15e-08 |

| | | | | |
|----------|----------|----------|----------|----------|
| 0.000131 | 0.000194 | 4.86e-06 | 1.28e-08 | 4.62e-08 |
| 7.28e-05 | 0.000136 | 4.34e-06 | 1.34e-07 | 6.17e-07 |
| 7.89e-05 | 0.000131 | 3.69e-06 | 1.22e-07 | 4.95e-07 |

DRAFT

| m Hfo sHPO4- | m Hfo sH2BO3 | m Hfo sH2PO4 | m Hfo sOSi(OH)3 | m Hfo sOSiO(OH)2 |
|--------------|--------------|--------------|-----------------|------------------|
| 0 | 0 | 0 | 0 | 0 |
| 0 | 0 | 0 | 0 | 0 |
| 0 | 0 | 0 | 0 | 0 |
| 0 | 0 | 0 | 0 | 0 |
| 6.60e-09 | 5.51e-11 | 2.50e-10 | 1.06e-07 | 7.03e-08 |
| 2.95e-09 | 4.00e-11 | 9.83e-11 | 6.31e-08 | 4.76e-08 |
| 1.42e-08 | 1.15e-12 | 9.24e-10 | 4.11e-08 | 1.59e-08 |
| 1.13e-08 | 6.47e-11 | 5.08e-10 | 2.63e-07 | 1.47e-07 |
| 4.33e-09 | 1.87e-11 | 1.04e-10 | 6.65e-08 | 6.94e-08 |
| 3.69e-09 | 1.91e-11 | 7.97e-11 | 5.74e-08 | 6.68e-08 |
| 1.75e-09 | 1.98e-11 | 3.46e-11 | 3.48e-08 | 4.41e-08 |
| 1.51e-09 | 1.96e-11 | 2.62e-11 | 2.97e-08 | 4.29e-08 |
| 4.19e-09 | 8.89e-13 | 1.22e-10 | 1.15e-08 | 9.92e-09 |
| 2.71e-09 | 1.05e-12 | 6.46e-11 | 7.77e-09 | 8.20e-09 |
| 6.39e-09 | 3.13e-11 | 1.85e-10 | 1.40e-07 | 1.21e-07 |
| 4.98e-09 | 3.47e-11 | 1.25e-10 | 1.07e-07 | 1.07e-07 |
| 0 | 0 | 0 | 0 | 0 |
| 0 | 0 | 0 | 0 | 0 |
| 0 | 0 | 0 | 0 | 0 |
| 0 | 0 | 0 | 0 | 0 |
| 1.60e-08 | 1.34e-10 | 6.07e-10 | 2.58e-07 | 1.71e-07 |
| 7.16e-09 | 9.72e-11 | 2.39e-10 | 1.53e-07 | 1.16e-07 |
| 3.45e-08 | 2.79e-12 | 2.24e-09 | 9.99e-08 | 3.86e-08 |
| 4.41e-08 | 2.53e-10 | 1.98e-09 | 1.03e-06 | 5.75e-07 |
| 1.10e-08 | 5.11e-11 | 2.75e-10 | 1.67e-07 | 1.68e-07 |
| 9.54e-09 | 4.70e-11 | 2.10e-10 | 1.44e-07 | 1.64e-07 |
| 4.31e-09 | 5.31e-11 | 9.20e-11 | 8.64e-08 | 1.02e-07 |
| 3.68e-09 | 5.11e-11 | 6.87e-11 | 7.26e-08 | 9.78e-08 |
| 1.24e-08 | 1.79e-12 | 4.11e-10 | 3.34e-08 | 2.53e-08 |
| 8.86e-09 | 1.74e-12 | 2.35e-10 | 2.38e-08 | 2.25e-08 |
| 3.16e-08 | 1.12e-10 | 1.08e-09 | 7.08e-07 | 5.23e-07 |
| 2.78e-08 | 1.09e-10 | 8.53e-10 | 6.11e-07 | 5.00e-07 |
| 0 | 0 | 0 | 0 | 0 |
| 0 | 0 | 0 | 0 | 0 |
| 0 | 0 | 0 | 0 | 0 |
| 0 | 0 | 0 | 0 | 0 |
| 9.74e-09 | 8.14e-11 | 3.69e-10 | 1.57e-07 | 1.04e-07 |
| 4.35e-09 | 5.91e-11 | 1.45e-10 | 9.31e-08 | 7.02e-08 |
| 2.10e-08 | 1.70e-12 | 1.36e-09 | 6.07e-08 | 2.34e-08 |
| 2.43e-08 | 1.39e-10 | 1.09e-09 | 5.65e-07 | 3.16e-07 |
| 6.61e-09 | 2.81e-11 | 1.63e-10 | 1.01e-07 | 1.03e-07 |
| 5.73e-09 | 2.74e-11 | 1.26e-10 | 8.78e-08 | 1.00e-07 |
| 2.63e-09 | 3.01e-11 | 5.43e-11 | 5.26e-08 | 6.41e-08 |

| | | | | |
|----------|----------|----------|----------|----------|
| 2.26e-09 | 2.95e-11 | 4.08e-11 | 4.45e-08 | 6.20e-08 |
| 6.95e-09 | 1.15e-12 | 2.15e-10 | 1.89e-08 | 1.53e-08 |
| 4.81e-09 | 1.23e-12 | 1.21e-10 | 1.33e-08 | 1.33e-08 |
| 1.58e-08 | 6.24e-11 | 5.03e-10 | 3.51e-07 | 2.77e-07 |
| 1.33e-08 | 6.38e-11 | 3.74e-10 | 2.89e-07 | 2.57e-07 |
| 0 | 0 | 0 | 0 | 0 |
| 0 | 0 | 0 | 0 | 0 |
| 0 | 0 | 0 | 0 | 0 |
| 0 | 0 | 0 | 0 | 0 |
| 6.55e-09 | 5.45e-11 | 2.48e-10 | 1.05e-07 | 6.96e-08 |
| 2.92e-09 | 3.93e-11 | 9.72e-11 | 6.20e-08 | 4.69e-08 |
| 1.39e-08 | 1.12e-12 | 9.04e-10 | 4.00e-08 | 1.55e-08 |
| 1.12e-08 | 6.38e-11 | 5.03e-10 | 2.60e-07 | 1.46e-07 |
| 4.28e-09 | 1.84e-11 | 1.03e-10 | 6.54e-08 | 6.84e-08 |
| 3.65e-09 | 1.87e-11 | 7.86e-11 | 5.64e-08 | 6.58e-08 |
| 1.71e-09 | 1.93e-11 | 3.39e-11 | 3.37e-08 | 4.27e-08 |
| 1.47e-09 | 1.90e-11 | 2.56e-11 | 2.88e-08 | 4.16e-08 |
| 4.01e-09 | 8.46e-13 | 1.17e-10 | 1.09e-08 | 9.42e-09 |
| 2.59e-09 | 1.00e-12 | 6.16e-11 | 7.36e-09 | 7.78e-09 |
| 6.29e-09 | 3.06e-11 | 1.82e-10 | 1.37e-07 | 1.19e-07 |
| 4.90e-09 | 3.38e-11 | 1.23e-10 | 1.05e-07 | 1.05e-07 |
| 0 | 0 | 0 | 0 | 0 |
| 0 | 0 | 0 | 0 | 0 |
| 0 | 0 | 0 | 0 | 0 |
| 0 | 0 | 0 | 0 | 0 |
| 1.59e-08 | 1.32e-10 | 6.02e-10 | 2.55e-07 | 1.69e-07 |
| 7.10e-09 | 9.55e-11 | 2.36e-10 | 1.51e-07 | 1.14e-07 |
| 3.39e-08 | 2.71e-12 | 2.19e-09 | 9.71e-08 | 3.77e-08 |
| 4.38e-08 | 2.49e-10 | 1.96e-09 | 1.01e-06 | 5.68e-07 |
| 1.08e-08 | 5.02e-11 | 2.69e-10 | 1.64e-07 | 1.65e-07 |
| 9.39e-09 | 4.62e-11 | 2.06e-10 | 1.41e-07 | 1.62e-07 |
| 4.17e-09 | 5.15e-11 | 8.89e-11 | 8.30e-08 | 9.79e-08 |
| 3.57e-09 | 4.97e-11 | 6.64e-11 | 6.98e-08 | 9.43e-08 |
| 1.17e-08 | 1.68e-12 | 3.86e-10 | 3.13e-08 | 2.39e-08 |
| 8.40e-09 | 1.65e-12 | 2.22e-10 | 2.23e-08 | 2.12e-08 |
| 3.12e-08 | 1.10e-10 | 1.06e-09 | 6.94e-07 | 5.13e-07 |
| 2.74e-08 | 1.07e-10 | 8.40e-10 | 5.99e-07 | 4.90e-07 |
| 0 | 0 | 0 | 0 | 0 |
| 0 | 0 | 0 | 0 | 0 |
| 0 | 0 | 0 | 0 | 0 |
| 0 | 0 | 0 | 0 | 0 |
| 9.68e-09 | 8.05e-11 | 3.66e-10 | 1.55e-07 | 1.03e-07 |
| 4.32e-09 | 5.80e-11 | 1.43e-10 | 9.15e-08 | 6.92e-08 |
| 2.06e-08 | 1.65e-12 | 1.33e-09 | 5.90e-08 | 2.29e-08 |
| 2.41e-08 | 1.37e-10 | 1.08e-09 | 5.58e-07 | 3.12e-07 |
| 6.53e-09 | 2.77e-11 | 1.61e-10 | 9.94e-08 | 1.01e-07 |
| 5.66e-09 | 2.69e-11 | 1.24e-10 | 8.62e-08 | 9.85e-08 |
| 2.57e-09 | 2.93e-11 | 5.29e-11 | 5.08e-08 | 6.20e-08 |
| 2.21e-09 | 2.87e-11 | 3.98e-11 | 4.31e-08 | 6.00e-08 |
| 6.63e-09 | 1.09e-12 | 2.05e-10 | 1.78e-08 | 1.45e-08 |

| | | | | |
|----------|----------|----------|----------|----------|
| 4.60e-09 | 1.17e-12 | 1.15e-10 | 1.26e-08 | 1.26e-08 |
| 1.56e-08 | 6.10e-11 | 4.96e-10 | 3.43e-07 | 2.71e-07 |
| 1.31e-08 | 6.23e-11 | 3.68e-10 | 2.82e-07 | 2.52e-07 |

DRAFT

| m Hfo sOHSO4-2 | m Hfo sSO4- | m Hao SO4- | m Hao OHSO4-2 | m Hao H2BO3 |
|----------------|-------------|------------|---------------|-------------|
| 0 | 0 | 0 | 0 | 0 |
| 0 | 0 | 0 | 0 | 0 |
| 0 | 0 | 0 | 0 | 0 |
| 0 | 0 | 0 | 0 | 0 |
| 2.36e-09 | 1.10e-09 | 4.42e-14 | 0.000460 | 0.00219 |
| 2.15e-09 | 8.80e-10 | 3.99e-14 | 0.000341 | 0.00247 |
| 1.12e-09 | 8.94e-10 | 2.19e-13 | 0.000949 | 0.000386 |
| 7.37e-09 | 4.08e-09 | 4.28e-14 | 0.000264 | 0.000952 |
| 3.26e-11 | 9.68e-12 | 5.19e-15 | 0.000381 | 0.00221 |
| 2.59e-11 | 6.89e-12 | 4.06e-15 | 0.000368 | 0.00223 |
| 4.58e-11 | 1.12e-11 | 4.78e-15 | 0.000326 | 0.00243 |
| 3.61e-11 | 7.71e-12 | 3.74e-15 | 0.000330 | 0.00240 |
| 2.02e-11 | 7.28e-12 | 1.65e-14 | 0.000844 | 0.000521 |
| 1.25e-11 | 3.67e-12 | 1.06e-14 | 0.000810 | 0.000651 |
| 1.16e-10 | 4.14e-11 | 4.70e-15 | 0.000222 | 0.00101 |
| 7.96e-11 | 2.46e-11 | 3.19e-15 | 0.000208 | 0.00106 |
| 0 | 0 | 0 | 0 | 0 |
| 0 | 0 | 0 | 0 | 0 |
| 0 | 0 | 0 | 0 | 0 |
| 0 | 0 | 0 | 0 | 0 |
| 5.73e-09 | 2.67e-09 | 3.45e-13 | 0.00359 | 0.0170 |
| 5.21e-09 | 2.14e-09 | 3.11e-13 | 0.00266 | 0.0193 |
| 2.71e-09 | 2.17e-09 | 1.71e-12 | 0.00740 | 0.00301 |
| 2.88e-08 | 1.59e-08 | 1.59e-13 | 0.000985 | 0.00355 |
| 1.17e-10 | 3.61e-11 | 4.97e-14 | 0.00319 | 0.0170 |
| 7.39e-11 | 2.01e-11 | 3.56e-14 | 0.00307 | 0.0170 |
| 1.37e-10 | 3.59e-11 | 4.27e-14 | 0.00256 | 0.0192 |
| 9.54e-11 | 2.19e-11 | 3.15e-14 | 0.00252 | 0.0191 |
| 7.34e-11 | 2.99e-11 | 1.78e-13 | 0.00707 | 0.00315 |
| 4.64e-11 | 1.52e-11 | 1.16e-13 | 0.00691 | 0.00329 |
| 7.72e-10 | 3.23e-10 | 2.84e-14 | 0.000885 | 0.00361 |
| 4.55e-10 | 1.72e-10 | 1.96e-14 | 0.000835 | 0.00368 |
| 0 | 0 | 0 | 0 | 0 |
| 0 | 0 | 0 | 0 | 0 |
| 0 | 0 | 0 | 0 | 0 |
| 0 | 0 | 0 | 0 | 0 |
| 3.48e-09 | 1.62e-09 | 9.72e-14 | 0.00101 | 0.00481 |
| 3.17e-09 | 1.30e-09 | 8.77e-14 | 0.000750 | 0.00544 |
| 1.65e-09 | 1.32e-09 | 4.81e-13 | 0.00209 | 0.000850 |
| 1.58e-08 | 8.75e-09 | 1.09e-13 | 0.000674 | 0.00243 |
| 5.44e-11 | 1.65e-11 | 1.25e-14 | 0.000862 | 0.00482 |
| 3.98e-11 | 1.08e-11 | 9.51e-15 | 0.000831 | 0.00485 |
| 7.31e-11 | 1.86e-11 | 1.12e-14 | 0.000715 | 0.00538 |

| | | | | |
|----------|----------|----------|----------|----------|
| 5.49e-11 | 1.22e-11 | 8.56e-15 | 0.000715 | 0.00534 |
| 3.56e-11 | 1.36e-11 | 4.22e-14 | 0.00192 | 0.000987 |
| 2.26e-11 | 6.98e-12 | 2.77e-14 | 0.00186 | 0.00112 |
| 3.30e-10 | 1.29e-10 | 1.58e-14 | 0.000594 | 0.00249 |
| 2.14e-10 | 7.42e-11 | 1.10e-14 | 0.000563 | 0.00256 |
| 0 | 0 | 0 | 0 | 0 |
| 0 | 0 | 0 | 0 | 0 |
| 0 | 0 | 0 | 0 | 0 |
| 0 | 0 | 0 | 0 | 0 |
| 2.36e-09 | 1.10e-09 | 4.43e-14 | 0.000459 | 0.00218 |
| 2.16e-09 | 8.82e-10 | 4.00e-14 | 0.000340 | 0.00246 |
| 1.12e-09 | 8.91e-10 | 2.18e-13 | 0.000948 | 0.000376 |
| 7.39e-09 | 4.08e-09 | 4.29e-14 | 0.000264 | 0.000945 |
| 3.21e-11 | 9.50e-12 | 5.19e-15 | 0.000384 | 0.00220 |
| 2.55e-11 | 6.78e-12 | 4.07e-15 | 0.000370 | 0.00223 |
| 4.41e-11 | 1.08e-11 | 4.77e-15 | 0.000330 | 0.00242 |
| 3.49e-11 | 7.47e-12 | 3.75e-15 | 0.000334 | 0.00239 |
| 1.91e-11 | 6.87e-12 | 1.63e-14 | 0.000850 | 0.000511 |
| 1.19e-11 | 3.49e-12 | 1.05e-14 | 0.000816 | 0.000641 |
| 1.14e-10 | 4.05e-11 | 4.71e-15 | 0.000224 | 0.00101 |
| 7.78e-11 | 2.41e-11 | 3.20e-15 | 0.000210 | 0.00106 |
| 0 | 0 | 0 | 0 | 0 |
| 0 | 0 | 0 | 0 | 0 |
| 0 | 0 | 0 | 0 | 0 |
| 0 | 0 | 0 | 0 | 0 |
| 5.74e-09 | 2.67e-09 | 3.46e-13 | 0.00358 | 0.0170 |
| 5.23e-09 | 2.14e-09 | 3.12e-13 | 0.00265 | 0.0192 |
| 2.71e-09 | 2.16e-09 | 1.70e-12 | 0.00739 | 0.00293 |
| 2.88e-08 | 1.59e-08 | 1.60e-13 | 0.000985 | 0.00352 |
| 1.14e-10 | 3.49e-11 | 4.93e-14 | 0.00321 | 0.0170 |
| 7.26e-11 | 1.96e-11 | 3.55e-14 | 0.00309 | 0.0170 |
| 1.28e-10 | 3.35e-11 | 4.19e-14 | 0.00258 | 0.0191 |
| 9.13e-11 | 2.09e-11 | 3.13e-14 | 0.00255 | 0.0190 |
| 6.66e-11 | 2.70e-11 | 1.72e-13 | 0.00712 | 0.00307 |
| 4.37e-11 | 1.42e-11 | 1.14e-13 | 0.00696 | 0.00321 |
| 7.54e-10 | 3.16e-10 | 2.84e-14 | 0.000893 | 0.00359 |
| 4.46e-10 | 1.69e-10 | 1.96e-14 | 0.000843 | 0.00366 |
| 0 | 0 | 0 | 0 | 0 |
| 0 | 0 | 0 | 0 | 0 |
| 0 | 0 | 0 | 0 | 0 |
| 0 | 0 | 0 | 0 | 0 |
| 3.49e-09 | 1.63e-09 | 9.75e-14 | 0.00101 | 0.00479 |
| 3.18e-09 | 1.30e-09 | 8.80e-14 | 0.000747 | 0.00541 |
| 1.65e-09 | 1.31e-09 | 4.79e-13 | 0.00208 | 0.000827 |
| 1.59e-08 | 8.75e-09 | 1.09e-13 | 0.000674 | 0.00241 |
| 5.34e-11 | 1.62e-11 | 1.24e-14 | 0.000867 | 0.00481 |
| 3.92e-11 | 1.06e-11 | 9.51e-15 | 0.000837 | 0.00483 |
| 7.00e-11 | 1.78e-11 | 1.12e-14 | 0.000723 | 0.00535 |
| 5.30e-11 | 1.18e-11 | 8.56e-15 | 0.000723 | 0.00532 |
| 3.34e-11 | 1.27e-11 | 4.15e-14 | 0.00193 | 0.000964 |

| | | | | |
|----------|----------|----------|----------|---------|
| 2.14e-11 | 6.62e-12 | 2.74e-14 | 0.00187 | 0.00110 |
| 3.22e-10 | 1.26e-10 | 1.59e-14 | 0.000599 | 0.00248 |
| 2.09e-10 | 7.26e-11 | 1.10e-14 | 0.000569 | 0.00254 |

DRAFT

| m_Hao_H3BO4- | Ferrihydrite | d_Ferrihydrite | Gibbsite | d_Gibbsite |
|--------------|--------------|----------------|----------|------------|
| 0 | 0 | 0 | 0 | 0 |
| 0 | 0 | 0 | 0 | 0 |
| 0 | 0 | 0 | 0 | 0 |
| 0 | 0 | 0 | 0 | 0 |
| 1.06e-10 | 0.0210 | 0 | 0.100 | 0 |
| 9.89e-11 | 0.0210 | 0 | 0.100 | 0 |
| 7.85e-12 | 0.0210 | 0 | 0.100 | 0 |
| 2.75e-11 | 0.0410 | 0 | 0.0510 | 0 |
| 7.58e-10 | 0.0210 | 1.99e-06 | 0.100 | 8.73e-07 |
| 9.47e-10 | 0.0210 | 1.99e-06 | 0.100 | 8.48e-07 |
| 7.76e-10 | 0.0210 | 1.99e-06 | 0.100 | 8.91e-07 |
| 9.93e-10 | 0.0210 | 1.99e-06 | 0.100 | 8.64e-07 |
| 1.25e-10 | 0.0210 | 2.00e-06 | 0.100 | 9.07e-07 |
| 2.32e-10 | 0.0210 | 1.99e-06 | 0.100 | 8.77e-07 |
| 2.23e-10 | 0.0410 | 1.99e-06 | 0.0510 | 9.08e-07 |
| 3.24e-10 | 0.0410 | 1.99e-06 | 0.0510 | 8.85e-07 |
| 0 | 0 | 0 | 0 | 0 |
| 0 | 0 | 0 | 0 | 0 |
| 0 | 0 | 0 | 0 | 0 |
| 0 | 0 | 0 | 0 | 0 |
| 8.29e-10 | 0.0510 | 0 | 0.780 | 0 |
| 7.71e-10 | 0.0510 | 0 | 0.780 | 0 |
| 6.12e-11 | 0.0510 | 0 | 0.780 | 0 |
| 1.02e-10 | 0.160 | 0 | 0.190 | 0 |
| 5.12e-09 | 0.0510 | 1.99e-06 | 0.780 | 8.90e-07 |
| 6.87e-09 | 0.0510 | 1.99e-06 | 0.780 | 8.61e-07 |
| 5.37e-09 | 0.0510 | 1.99e-06 | 0.780 | 9.08e-07 |
| 7.17e-09 | 0.0510 | 1.99e-06 | 0.780 | 8.82e-07 |
| 5.85e-10 | 0.0510 | 2.01e-06 | 0.780 | 9.23e-07 |
| 9.13e-10 | 0.0510 | 1.99e-06 | 0.780 | 8.98e-07 |
| 5.27e-10 | 0.160 | 1.99e-06 | 0.190 | 9.28e-07 |
| 7.35e-10 | 0.160 | 1.99e-06 | 0.190 | 9.13e-07 |
| 0 | 0 | 0 | 0 | 0 |
| 0 | 0 | 0 | 0 | 0 |
| 0 | 0 | 0 | 0 | 0 |
| 0 | 0 | 0 | 0 | 0 |
| 2.34e-10 | 0.0310 | 0 | 0.220 | 0 |
| 2.18e-10 | 0.0310 | 0 | 0.220 | 0 |
| 1.73e-11 | 0.0310 | 0 | 0.220 | 0 |
| 7.01e-11 | 0.0880 | 0 | 0.130 | 0 |
| 1.56e-09 | 0.0310 | 1.99e-06 | 0.220 | 8.81e-07 |
| 1.98e-09 | 0.0310 | 1.99e-06 | 0.220 | 8.54e-07 |
| 1.60e-09 | 0.0310 | 1.99e-06 | 0.220 | 8.99e-07 |

| | | | | |
|----------|--------|----------|--------|----------|
| 2.09e-09 | 0.0310 | 1.99e-06 | 0.220 | 8.73e-07 |
| 2.10e-10 | 0.0310 | 2.00e-06 | 0.220 | 9.15e-07 |
| 3.53e-10 | 0.0310 | 1.99e-06 | 0.220 | 8.87e-07 |
| 4.37e-10 | 0.0880 | 1.99e-06 | 0.130 | 9.20e-07 |
| 6.12e-10 | 0.0880 | 1.99e-06 | 0.130 | 9.02e-07 |
| 0 | 0 | 0 | 0 | 0 |
| 0 | 0 | 0 | 0 | 0 |
| 0 | 0 | 0 | 0 | 0 |
| 0 | 0 | 0 | 0 | 0 |
| 1.05e-10 | 0.0210 | 0 | 0.100 | 0 |
| 9.77e-11 | 0.0210 | 0 | 0.100 | 0 |
| 7.66e-12 | 0.0210 | 0 | 0.100 | 0 |
| 2.72e-11 | 0.0410 | 0 | 0.0510 | 0 |
| 7.61e-10 | 0.0210 | 1.99e-06 | 0.100 | 8.73e-07 |
| 9.48e-10 | 0.0210 | 1.99e-06 | 0.100 | 8.48e-07 |
| 7.82e-10 | 0.0210 | 1.99e-06 | 0.100 | 8.91e-07 |
| 9.97e-10 | 0.0210 | 1.99e-06 | 0.100 | 8.64e-07 |
| 1.25e-10 | 0.0210 | 2.00e-06 | 0.100 | 9.07e-07 |
| 2.32e-10 | 0.0210 | 1.99e-06 | 0.100 | 8.77e-07 |
| 2.23e-10 | 0.0410 | 1.99e-06 | 0.0510 | 9.08e-07 |
| 3.24e-10 | 0.0410 | 1.99e-06 | 0.0510 | 8.85e-07 |
| 0 | 0 | 0 | 0 | 0 |
| 0 | 0 | 0 | 0 | 0 |
| 0 | 0 | 0 | 0 | 0 |
| 0 | 0 | 0 | 0 | 0 |
| 8.23e-10 | 0.0510 | 0 | 0.780 | 0 |
| 7.62e-10 | 0.0510 | 0 | 0.780 | 0 |
| 5.97e-11 | 0.0510 | 0 | 0.780 | 0 |
| 1.01e-10 | 0.160 | 0 | 0.190 | 0 |
| 5.17e-09 | 0.0510 | 1.99e-06 | 0.780 | 8.90e-07 |
| 6.92e-09 | 0.0510 | 1.99e-06 | 0.780 | 8.61e-07 |
| 5.50e-09 | 0.0510 | 1.99e-06 | 0.780 | 9.08e-07 |
| 7.26e-09 | 0.0510 | 1.99e-06 | 0.780 | 8.82e-07 |
| 5.93e-10 | 0.0510 | 2.01e-06 | 0.780 | 9.23e-07 |
| 9.12e-10 | 0.0510 | 1.99e-06 | 0.780 | 8.98e-07 |
| 5.28e-10 | 0.160 | 1.99e-06 | 0.190 | 9.27e-07 |
| 7.35e-10 | 0.160 | 1.99e-06 | 0.190 | 9.13e-07 |
| 0 | 0 | 0 | 0 | 0 |
| 0 | 0 | 0 | 0 | 0 |
| 0 | 0 | 0 | 0 | 0 |
| 0 | 0 | 0 | 0 | 0 |
| 2.32e-10 | 0.0310 | 0 | 0.220 | 0 |
| 2.15e-10 | 0.0310 | 0 | 0.220 | 0 |
| 1.68e-11 | 0.0310 | 0 | 0.220 | 0 |
| 6.94e-11 | 0.0880 | 0 | 0.130 | 0 |
| 1.57e-09 | 0.0310 | 1.99e-06 | 0.220 | 8.81e-07 |
| 1.99e-09 | 0.0310 | 1.99e-06 | 0.220 | 8.53e-07 |
| 1.62e-09 | 0.0310 | 1.99e-06 | 0.220 | 8.99e-07 |
| 2.10e-09 | 0.0310 | 1.99e-06 | 0.220 | 8.72e-07 |
| 2.10e-10 | 0.0310 | 2.00e-06 | 0.220 | 9.15e-07 |

| | | | | |
|----------|--------|----------|-------|----------|
| 3.51e-10 | 0.0310 | 1.99e-06 | 0.220 | 8.86e-07 |
| 4.38e-10 | 0.0880 | 1.99e-06 | 0.130 | 9.20e-07 |
| 6.12e-10 | 0.0880 | 1.99e-06 | 0.130 | 9.02e-07 |

DRAFT

| Barite | d_Barite | Calcite | d_Calcite | Dolomite(ordered) |
|----------|----------|---------|-----------|-------------------|
| 0 | 0 | 0 | 0 | 0 |
| 0 | 0 | 0 | 0 | 0 |
| 0 | 0 | 0 | 0 | 0 |
| 0 | 0 | 0 | 0 | 0 |
| 0 | 0 | 0.100 | 0 | 0 |
| 0 | 0 | 0.100 | 0 | 0 |
| 0 | 0 | 0.100 | 0 | 0 |
| 0 | 0 | 10.0 | 0 | 0 |
| 4.10e-07 | 4.10e-07 | 0.0997 | -2.76e-04 | 0 |
| 7.95e-07 | 3.85e-07 | 0.0996 | -1.70e-04 | 0 |
| 3.93e-07 | 3.93e-07 | 0.0996 | -3.68e-04 | 0 |
| 7.73e-07 | 3.80e-07 | 0.0994 | -2.23e-04 | 0 |
| 4.14e-07 | 4.14e-07 | 0.0995 | -4.90e-04 | 0 |
| 8.06e-07 | 3.92e-07 | 0.0992 | -2.79e-04 | 0 |
| 4.04e-07 | 4.04e-07 | 10.00 | -5.23e-04 | 0 |
| 7.85e-07 | 3.81e-07 | 10.00 | -3.23e-04 | 0 |
| 0 | 0 | 0 | 0 | 0 |
| 0 | 0 | 0 | 0 | 0 |
| 0 | 0 | 0 | 0 | 0 |
| 0 | 0 | 0 | 0 | 0 |
| 0 | 0 | 0.100 | 0 | 0 |
| 0 | 0 | 0.100 | 0 | 0 |
| 0 | 0 | 0.100 | 0 | 0 |
| 0 | 0 | 10.0 | 0 | 0 |
| 4.84e-07 | 4.84e-07 | 0.0996 | -3.88e-04 | 0 |
| 8.94e-07 | 4.10e-07 | 0.0994 | -2.18e-04 | 0 |
| 4.26e-07 | 4.26e-07 | 0.0995 | -5.17e-04 | 0 |
| 8.14e-07 | 3.88e-07 | 0.0992 | -3.06e-04 | 0 |
| 4.66e-07 | 4.66e-07 | 0.0993 | -7.09e-04 | 0 |
| 8.89e-07 | 4.23e-07 | 0.0989 | -4.10e-04 | 0 |
| 4.52e-07 | 4.52e-07 | 10.00 | -9.25e-04 | 0 |
| 8.26e-07 | 3.75e-07 | 10.00 | -5.55e-04 | 0 |
| 0 | 0 | 0 | 0 | 0 |
| 0 | 0 | 0 | 0 | 0 |
| 0 | 0 | 0 | 0 | 0 |
| 0 | 0 | 0 | 0 | 0 |
| 0 | 0 | 0.100 | 0 | 0 |
| 0 | 0 | 0.100 | 0 | 0 |
| 0 | 0 | 0.100 | 0 | 0 |
| 0 | 0 | 10.0 | 0 | 0 |
| 4.30e-07 | 4.30e-07 | 0.0997 | -3.19e-04 | 0 |
| 8.18e-07 | 3.88e-07 | 0.0995 | -1.89e-04 | 0 |
| 4.02e-07 | 4.02e-07 | 0.0996 | -4.29e-04 | 0 |

| | | | | |
|----------|----------|--------|-----------|---|
| 7.82e-07 | 3.79e-07 | 0.0993 | -2.58e-04 | 0 |
| 4.31e-07 | 4.31e-07 | 0.0994 | -5.79e-04 | 0 |
| 8.28e-07 | 3.97e-07 | 0.0991 | -3.31e-04 | 0 |
| 4.27e-07 | 4.27e-07 | 10.00 | -7.17e-04 | 0 |
| 8.05e-07 | 3.78e-07 | 10.00 | -4.43e-04 | 0 |
| 0 | 0 | 0 | 0 | 0 |
| 0 | 0 | 0 | 0 | 0 |
| 0 | 0 | 0 | 0 | 0 |
| 0 | 0 | 0 | 0 | 0 |
| 0 | 0 | 0.100 | 0 | 0 |
| 0 | 0 | 0.100 | 0 | 0 |
| 0 | 0 | 0.100 | 0 | 0 |
| 0 | 0 | 10.0 | 0 | 0 |
| 4.09e-07 | 4.09e-07 | 0.0997 | -2.75e-04 | 0 |
| 7.94e-07 | 3.85e-07 | 0.0996 | -1.69e-04 | 0 |
| 3.92e-07 | 3.92e-07 | 0.0996 | -3.66e-04 | 0 |
| 7.72e-07 | 3.80e-07 | 0.0994 | -2.22e-04 | 0 |
| 4.12e-07 | 4.12e-07 | 0.0995 | -4.88e-04 | 0 |
| 8.04e-07 | 3.92e-07 | 0.0992 | -2.78e-04 | 0 |
| 4.04e-07 | 4.04e-07 | 10.00 | -5.22e-04 | 0 |
| 7.85e-07 | 3.81e-07 | 10.00 | -3.22e-04 | 0 |
| 0 | 0 | 0 | 0 | 0 |
| 0 | 0 | 0 | 0 | 0 |
| 0 | 0 | 0 | 0 | 0 |
| 0 | 0 | 0 | 0 | 0 |
| 0 | 0 | 0.100 | 0 | 0 |
| 0 | 0 | 0.100 | 0 | 0 |
| 0 | 0 | 0.100 | 0 | 0 |
| 0 | 0 | 10.0 | 0 | 0 |
| 4.80e-07 | 4.80e-07 | 0.0996 | -3.86e-04 | 0 |
| 8.89e-07 | 4.09e-07 | 0.0994 | -2.16e-04 | 0 |
| 4.16e-07 | 4.16e-07 | 0.0995 | -5.12e-04 | 0 |
| 8.03e-07 | 3.86e-07 | 0.0992 | -3.03e-04 | 0 |
| 4.54e-07 | 4.54e-07 | 0.0993 | -7.01e-04 | 0 |
| 8.75e-07 | 4.21e-07 | 0.0989 | -4.06e-04 | 0 |
| 4.51e-07 | 4.51e-07 | 10.00 | -9.20e-04 | 0 |
| 8.26e-07 | 3.75e-07 | 10.00 | -5.54e-04 | 0 |
| 0 | 0 | 0 | 0 | 0 |
| 0 | 0 | 0 | 0 | 0 |
| 0 | 0 | 0 | 0 | 0 |
| 0 | 0 | 0 | 0 | 0 |
| 0 | 0 | 0.100 | 0 | 0 |
| 0 | 0 | 0.100 | 0 | 0 |
| 0 | 0 | 0.100 | 0 | 0 |
| 0 | 0 | 10.0 | 0 | 0 |
| 4.28e-07 | 4.28e-07 | 0.0997 | -3.17e-04 | 0 |
| 8.16e-07 | 3.88e-07 | 0.0995 | -1.88e-04 | 0 |
| 3.99e-07 | 3.99e-07 | 0.0996 | -4.27e-04 | 0 |
| 7.79e-07 | 3.79e-07 | 0.0993 | -2.57e-04 | 0 |
| 4.27e-07 | 4.27e-07 | 0.0994 | -5.75e-04 | 0 |

| | | | | |
|----------|----------|--------|-----------|---|
| 8.24e-07 | 3.97e-07 | 0.0991 | -3.29e-04 | 0 |
| 4.27e-07 | 4.27e-07 | 10.00 | -7.14e-04 | 0 |
| 8.05e-07 | 3.78e-07 | 10.00 | -4.42e-04 | 0 |

DRAFT

| d_Dolomite(ordere d) | Gypsum | d_Gypsum | si_Ferrihydrite | si_Gibbsite |
|-------------------------|--------|----------|-----------------|-------------|
| 0 | 0 | 0 | 0.783 | 1.21 |
| 0 | 0 | 0 | 0.905 | 1.01 |
| 0 | 0 | 0 | 1.39 | 0.854 |
| 0 | 0 | 0 | 0.851 | 0.818 |
| 0 | 0 | 0 | 0.783 | 1.21 |
| 0 | 0 | 0 | 0.905 | 1.01 |
| 0 | 0 | 0 | 1.39 | 0.854 |
| 0 | 0 | 0 | 0.851 | 0.818 |
| 0 | 0 | 0 | 0 | 0 |
| 0 | 0 | 0 | 0 | 0 |
| 0 | 0 | 0 | 0 | 0 |
| 0 | 0 | 0 | 0 | 0 |
| 0 | 0 | 0 | 0 | 0 |
| 0 | 0 | 0 | 0 | 0 |
| 0 | 0 | 0 | 0 | 0 |
| 0 | 0 | 0 | 0.783 | 1.21 |
| 0 | 0 | 0 | 0.905 | 1.01 |
| 0 | 0 | 0 | 1.39 | 0.854 |
| 0 | 0 | 0 | 0.851 | 0.818 |
| 0 | 0 | 0 | 0.783 | 1.21 |
| 0 | 0 | 0 | 0.905 | 1.01 |
| 0 | 0 | 0 | 1.39 | 0.854 |
| 0 | 0 | 0 | 0.851 | 0.818 |
| 0 | 0 | 0 | 0 | 0 |
| 0 | 0 | 0 | 0 | 0 |
| 0 | 0 | 0 | 0 | 0 |
| 0 | 0 | 0 | 0 | 0 |
| 0 | 0 | 0 | 0 | 0 |
| 0 | 0 | 0 | 0 | 0 |
| 0 | 0 | 0 | 0 | 0 |
| 0 | 0 | 0 | 0 | 0 |
| 0 | 0 | 0 | 0.783 | 1.21 |
| 0 | 0 | 0 | 0.905 | 1.01 |
| 0 | 0 | 0 | 1.39 | 0.854 |
| 0 | 0 | 0 | 0.851 | 0.818 |
| 0 | 0 | 0 | 0.783 | 1.21 |
| 0 | 0 | 0 | 0.905 | 1.01 |
| 0 | 0 | 0 | 1.39 | 0.854 |
| 0 | 0 | 0 | 0.851 | 0.818 |
| 0 | 0 | 0 | 0 | 0 |
| 0 | 0 | 0 | 0 | 0 |
| 0 | 0 | 0 | 0 | 0 |

| | | | | |
|---|---|---|-------|-------|
| 0 | 0 | 0 | 0 | 0 |
| 0 | 0 | 0 | 0 | 0 |
| 0 | 0 | 0 | 0 | 0 |
| 0 | 0 | 0 | 0 | 0 |
| 0 | 0 | 0 | 0 | 0 |
| 0 | 0 | 0 | 0.792 | 1.22 |
| 0 | 0 | 0 | 0.908 | 1.01 |
| 0 | 0 | 0 | 1.41 | 0.857 |
| 0 | 0 | 0 | 0.854 | 0.819 |
| 0 | 0 | 0 | 0.792 | 1.22 |
| 0 | 0 | 0 | 0.908 | 1.01 |
| 0 | 0 | 0 | 1.41 | 0.857 |
| 0 | 0 | 0 | 0.854 | 0.819 |
| 0 | 0 | 0 | 0 | 0 |
| 0 | 0 | 0 | 0 | 0 |
| 0 | 0 | 0 | 0 | 0 |
| 0 | 0 | 0 | 0 | 0 |
| 0 | 0 | 0 | 0 | 0 |
| 0 | 0 | 0 | 0 | 0 |
| 0 | 0 | 0 | 0 | 0 |
| 0 | 0 | 0 | 0 | 0 |
| 0 | 0 | 0 | 0.792 | 1.22 |
| 0 | 0 | 0 | 0.908 | 1.01 |
| 0 | 0 | 0 | 1.41 | 0.857 |
| 0 | 0 | 0 | 0.854 | 0.819 |
| 0 | 0 | 0 | 0.792 | 1.22 |
| 0 | 0 | 0 | 0.908 | 1.01 |
| 0 | 0 | 0 | 1.41 | 0.857 |
| 0 | 0 | 0 | 0.854 | 0.819 |
| 0 | 0 | 0 | 0 | 0 |
| 0 | 0 | 0 | 0 | 0 |
| 0 | 0 | 0 | 0 | 0 |
| 0 | 0 | 0 | 0 | 0 |
| 0 | 0 | 0 | 0 | 0 |
| 0 | 0 | 0 | 0 | 0 |
| 0 | 0 | 0 | 0 | 0 |
| 0 | 0 | 0 | 0 | 0 |
| 0 | 0 | 0 | 0.792 | 1.22 |
| 0 | 0 | 0 | 0.908 | 1.01 |
| 0 | 0 | 0 | 1.41 | 0.857 |
| 0 | 0 | 0 | 0.854 | 0.819 |
| 0 | 0 | 0 | 0.792 | 1.22 |
| 0 | 0 | 0 | 0.908 | 1.01 |
| 0 | 0 | 0 | 1.41 | 0.857 |
| 0 | 0 | 0 | 0.854 | 0.819 |
| 0 | 0 | 0 | 0 | 0 |
| 0 | 0 | 0 | 0 | 0 |
| 0 | 0 | 0 | 0 | 0 |
| 0 | 0 | 0 | 0 | 0 |
| 0 | 0 | 0 | 0 | 0 |

| | | | | |
|---|---|---|---|---|
| 0 | 0 | 0 | 0 | 0 |
| 0 | 0 | 0 | 0 | 0 |
| 0 | 0 | 0 | 0 | 0 |

DRAFT

| si_Barite | si_Calcite | si_Dolomite(ordere d) | si_Gypsum |
|-----------|------------|--------------------------|-----------|
| 0.477 | -3.35e-01 | -5.70e-01 | -5.88e-01 |
| 0.438 | -4.09e-01 | -9.39e-01 | -8.24e-01 |
| 0.484 | -4.30e-01 | -1.02e+00 | -7.74e-01 |
| 0.546 | -5.15e-01 | -1.17e+00 | -7.63e-01 |
| 0.477 | -3.35e-01 | -5.70e-01 | -5.88e-01 |
| 0.438 | -4.09e-01 | -9.39e-01 | -8.24e-01 |
| 0.484 | -4.30e-01 | -1.02e+00 | -7.74e-01 |
| 0.546 | -5.15e-01 | -1.17e+00 | -7.63e-01 |
| 0 | 0 | -2.37e-01 | -2.35e+00 |
| 0 | 0 | -2.98e-01 | -2.47e+00 |
| 0 | 0 | -4.47e-01 | -2.30e+00 |
| 0 | 0 | -4.42e-01 | -2.43e+00 |
| 0 | 0 | -3.70e-01 | -2.20e+00 |
| 0 | 0 | -3.94e-01 | -2.37e+00 |
| 0 | 0 | -5.10e-01 | -2.19e+00 |
| 0 | 0 | -5.15e-01 | -2.35e+00 |
| 0.477 | -3.35e-01 | -5.70e-01 | -5.88e-01 |
| 0.438 | -4.09e-01 | -9.39e-01 | -8.24e-01 |
| 0.484 | -4.30e-01 | -1.02e+00 | -7.74e-01 |
| 0.546 | -5.15e-01 | -1.17e+00 | -7.63e-01 |
| 0.477 | -3.35e-01 | -5.70e-01 | -5.88e-01 |
| 0.438 | -4.09e-01 | -9.39e-01 | -8.24e-01 |
| 0.484 | -4.30e-01 | -1.02e+00 | -7.74e-01 |
| 0.546 | -5.15e-01 | -1.17e+00 | -7.63e-01 |
| 0 | 0 | -1.90e-02 | -2.17e+00 |
| 0 | 0 | -1.18e-01 | -2.40e+00 |
| 0 | 0 | -2.59e-01 | -2.17e+00 |
| 0 | 0 | -3.62e-01 | -2.35e+00 |
| 0 | 0 | -1.82e-01 | -2.03e+00 |
| 0 | 0 | -2.47e-01 | -2.24e+00 |
| 0 | 0 | -4.81e-01 | -1.95e+00 |
| 0 | 0 | -5.39e-01 | -2.20e+00 |
| 0.477 | -3.35e-01 | -5.70e-01 | -5.88e-01 |
| 0.438 | -4.09e-01 | -9.39e-01 | -8.24e-01 |
| 0.484 | -4.30e-01 | -1.02e+00 | -7.74e-01 |
| 0.546 | -5.15e-01 | -1.17e+00 | -7.63e-01 |
| 0.477 | -3.35e-01 | -5.70e-01 | -5.88e-01 |
| 0.438 | -4.09e-01 | -9.39e-01 | -8.24e-01 |
| 0.484 | -4.30e-01 | -1.02e+00 | -7.74e-01 |
| 0.546 | -5.15e-01 | -1.17e+00 | -7.63e-01 |
| 0 | 0 | -1.68e-01 | -2.29e+00 |
| 0 | 0 | -2.56e-01 | -2.45e+00 |
| 0 | 0 | -4.02e-01 | -2.25e+00 |

| | | | |
|-------|-----------|-----------|-----------|
| 0 | 0 | -4.51e-01 | -2.40e+00 |
| 0 | 0 | -3.08e-01 | -2.14e+00 |
| 0 | 0 | -3.67e-01 | -2.33e+00 |
| 0 | 0 | -4.80e-01 | -2.07e+00 |
| 0 | 0 | -5.33e-01 | -2.27e+00 |
| 0.489 | -3.28e-01 | -5.57e-01 | -5.79e-01 |
| 0.457 | -3.99e-01 | -9.17e-01 | -8.09e-01 |
| 0.509 | -4.15e-01 | -9.93e-01 | -7.53e-01 |
| 0.561 | -5.06e-01 | -1.16e+00 | -7.51e-01 |
| 0.489 | -3.28e-01 | -5.57e-01 | -5.79e-01 |
| 0.457 | -3.99e-01 | -9.17e-01 | -8.09e-01 |
| 0.509 | -4.15e-01 | -9.93e-01 | -7.53e-01 |
| 0.561 | -5.06e-01 | -1.16e+00 | -7.51e-01 |
| 0 | 0 | -2.33e-01 | -2.35e+00 |
| 0 | 0 | -2.95e-01 | -2.47e+00 |
| 0 | 0 | -4.40e-01 | -2.31e+00 |
| 0 | 0 | -4.40e-01 | -2.43e+00 |
| 0 | 0 | -3.62e-01 | -2.21e+00 |
| 0 | 0 | -3.90e-01 | -2.37e+00 |
| 0 | 0 | -5.06e-01 | -2.20e+00 |
| 0 | 0 | -5.13e-01 | -2.35e+00 |
| 0.489 | -3.28e-01 | -5.57e-01 | -5.79e-01 |
| 0.457 | -3.99e-01 | -9.17e-01 | -8.09e-01 |
| 0.509 | -4.15e-01 | -9.93e-01 | -7.53e-01 |
| 0.561 | -5.06e-01 | -1.16e+00 | -7.51e-01 |
| 0.489 | -3.28e-01 | -5.57e-01 | -5.79e-01 |
| 0.457 | -3.99e-01 | -9.17e-01 | -8.09e-01 |
| 0.509 | -4.15e-01 | -9.93e-01 | -7.53e-01 |
| 0.561 | -5.06e-01 | -1.16e+00 | -7.51e-01 |
| 0 | 0 | -8.10e-03 | -2.18e+00 |
| 0 | 0 | -1.11e-01 | -2.40e+00 |
| 0 | 0 | -2.41e-01 | -2.19e+00 |
| 0 | 0 | -3.50e-01 | -2.36e+00 |
| 0 | 0 | -1.60e-01 | -2.05e+00 |
| 0 | 0 | -2.35e-01 | -2.25e+00 |
| 0 | 0 | -4.74e-01 | -1.95e+00 |
| 0 | 0 | -5.35e-01 | -2.20e+00 |
| 0.489 | -3.28e-01 | -5.57e-01 | -5.79e-01 |
| 0.457 | -3.99e-01 | -9.17e-01 | -8.09e-01 |
| 0.509 | -4.15e-01 | -9.93e-01 | -7.53e-01 |
| 0.561 | -5.06e-01 | -1.16e+00 | -7.51e-01 |
| 0.489 | -3.28e-01 | -5.57e-01 | -5.79e-01 |
| 0.457 | -3.99e-01 | -9.17e-01 | -8.09e-01 |
| 0.509 | -4.15e-01 | -9.93e-01 | -7.53e-01 |
| 0.561 | -5.06e-01 | -1.16e+00 | -7.51e-01 |
| 0 | 0 | -1.61e-01 | -2.30e+00 |
| 0 | 0 | -2.52e-01 | -2.45e+00 |
| 0 | 0 | -3.92e-01 | -2.26e+00 |
| 0 | 0 | -4.46e-01 | -2.40e+00 |
| 0 | 0 | -2.96e-01 | -2.14e+00 |

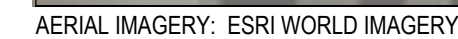
| | | | |
|---|---|-----------|-----------|
| 0 | 0 | -3.61e-01 | -2.33e+00 |
| 0 | 0 | -4.74e-01 | -2.07e+00 |
| 0 | 0 | -5.30e-01 | -2.27e+00 |

DRAFT

**APPENDIX B
DRAWINGS AND MATERIALS SPECIFICATIONS FOR
SELECTED REMEDY**

Baldwin Power Plant, Baldwin, IL

GROUNDWATER MANAGEMENT SYSTEM

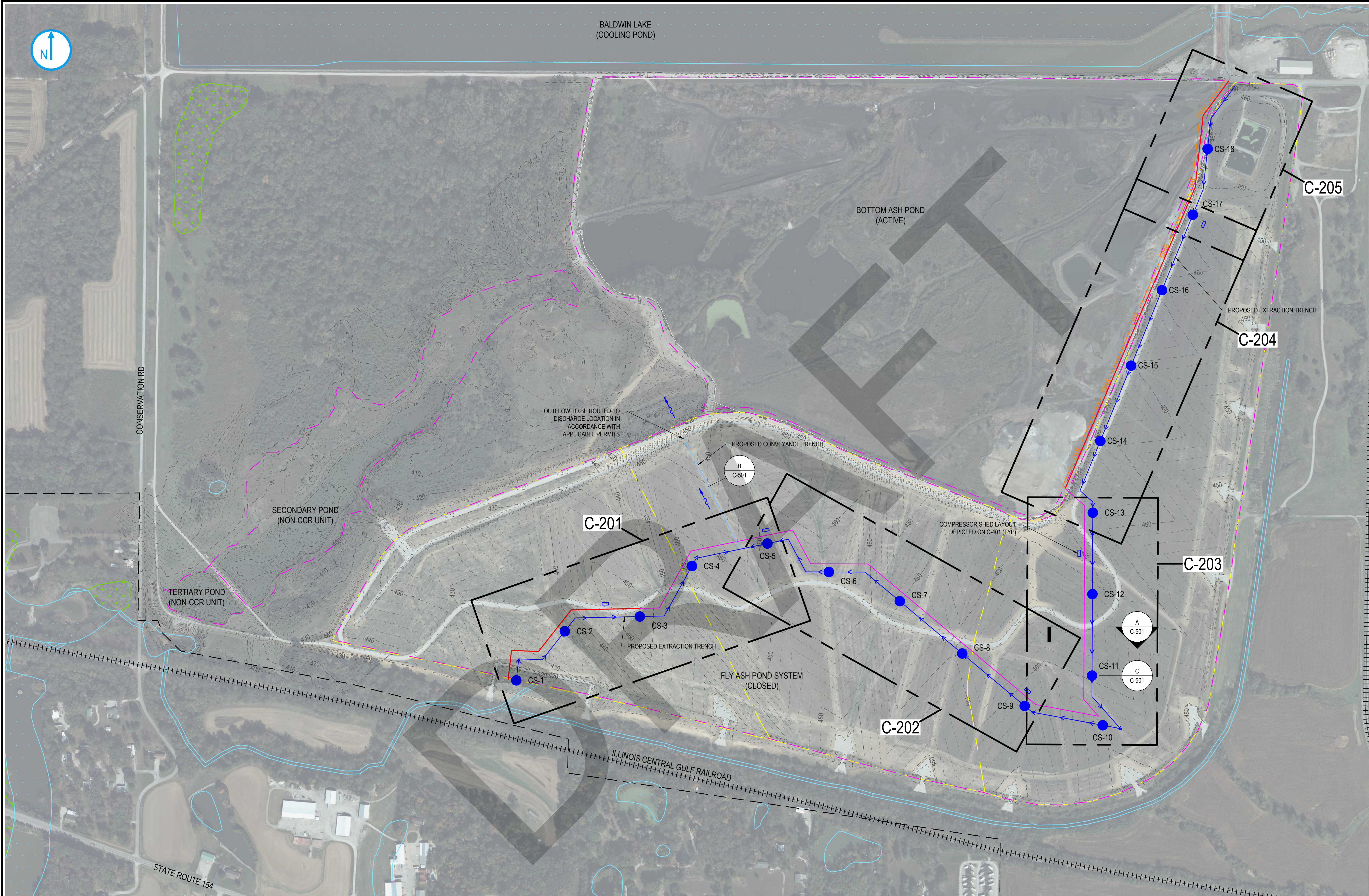


1000' 0 1000'

SCALE: 1"=1000'



1940106781-002



LEGEND

EXISTING

360

MAJOR CONTOUR

MINOR CONTOUR

APPROXIMATE SITE BOUNDARY

CCR UNIT BOUNDARY

WETLANDS

BODY OF WATER (LAKE, POND, RAVINE, ETC.)

RAILROAD

PROPOSED

GROUNDWATER MANAGEMENT TRENCH

COLLECTION SUMP

CONVEYANCE TRENCH

OHE

OVERHEAD ELECTRIC

WATER AND AIR CONVEYANCE PIPING

ELECTRICAL CONDUIT AND WATER AND AIR CONVEYANCE PIPING

STRUCTURE

- NOTES:
- FLY ASH POND SYSTEM CONTOURS ARE FROM CLOSURE CONSTRUCTION DRAWINGS COMPLETED BY INGENAE, OCTOBER 2020.
 - WETLANDS REPRESENTED AS PER ILLINOIS NATIONAL WETLANDS INVENTORY.
 - HORIZONTAL DATUM: ILLINOIS STATE PLANE (NAD83, IN US FEET).
VERTICAL DATUM: NORTH AMERICAN VERTICAL DATUM OF 1988 (NAVD88, IN US FEET).
 - AERIAL IMAGERY IS TAKEN FROM "LUMINANT, DYNEGY MIDWEST GENERATION, LLC, BALDWIN ENERGY COMPLEX, DECEMBER 2020 TOPOGRAPHY", DATED MAY 20, 2021, BY INGENAE, LLC (2020 INGENAE SURVEY).
 - ALL WATER BODY LIMITS WERE CROPPED WHERE THEY OVERLAP EXISTING CCR UNITS AND NON-CCR UNITS.

OVERALL SITE PLAN

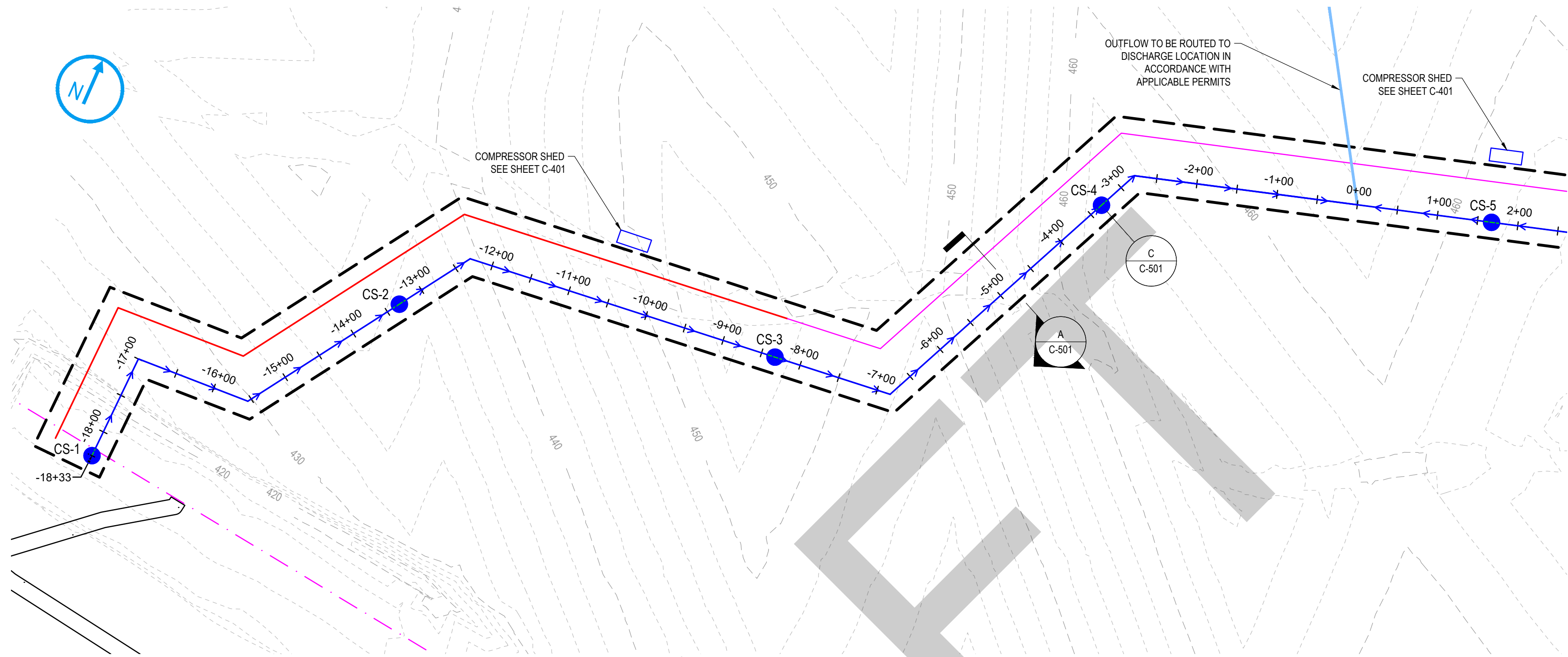
300 0 300

SCALE: 1"=300'

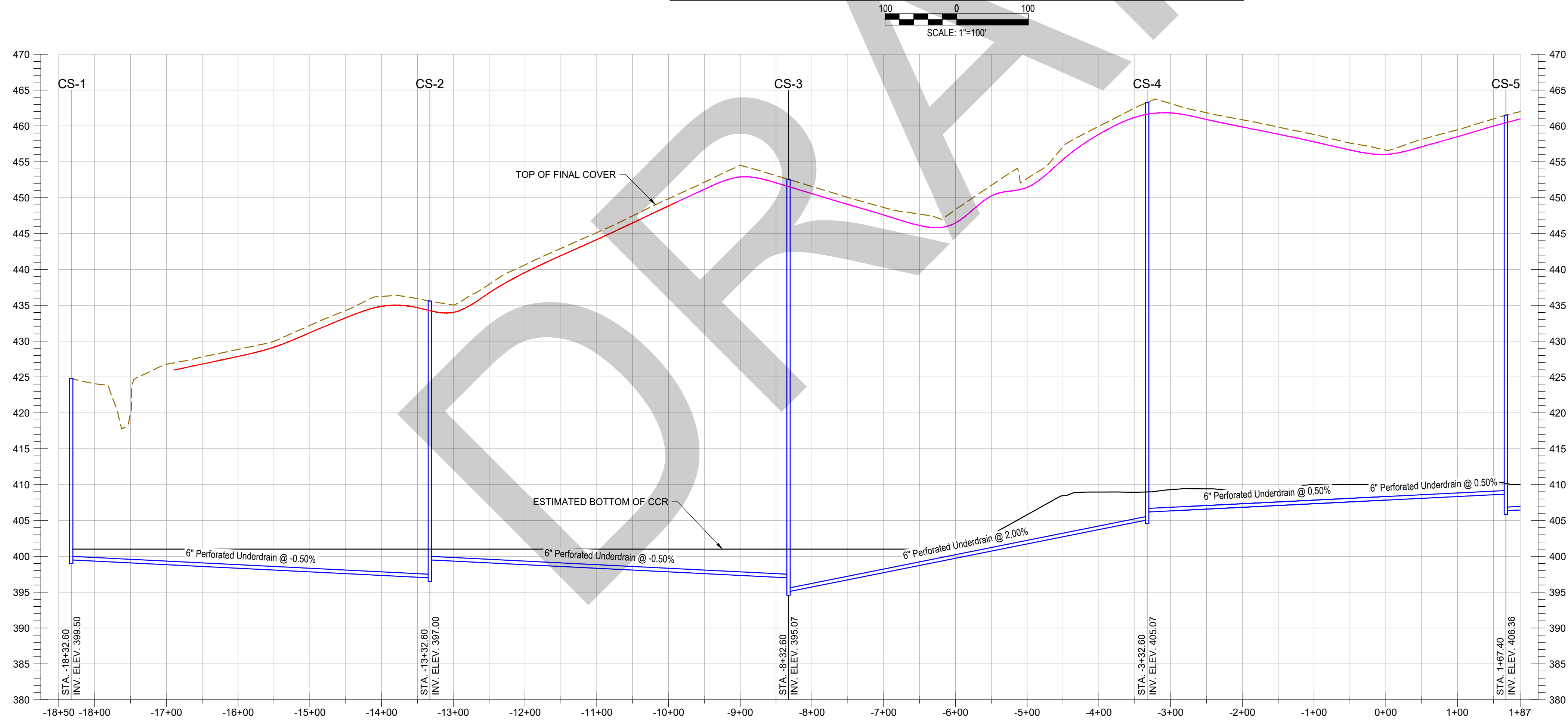
PRELIMINARY
NOT FOR
CONSTRUCTION

DATE: _____

| NO. | REV DATE | REVISION | INT. |
|--|----------|---|------|
| IT IS A VIOLATION OF LAW FOR ANY PERSON, UNLESS ACTING UNDER THE DIRECTION OF A LICENSED ENGINEER, TO ALTER THIS DOCUMENT. THIS DRAWING WAS PREPARED AT THE SCALE INDICATED. INACCURACIES IN THE STATED SCALE MAY BE INTRODUCED WHEN DRAWINGS ARE REPRODUCED BY ANY MEANS. USE THE GRAPHIC SCALE BAR TO DETERMINE THE ACTUAL SIZE. DRAWING IS NOT SCALABLE IF NO SCALE BAR IS PRESENT. | | | |
| Project Details | | Drawing Title | |
| DYNEGY MIDWEST GENERATION, LLC | | OVERALL SITE PLAN | |
| Fly Ash Pond System | | Baldwin Energy Complex | |
| 10901 Baldwin Road Baldwin, IL 62217 | | RAMBOLL AMERICAS ENGINEERING SOLUTIONS, INC. | |
| Location: | | Designer / Professional Engineer Responsible: | |
| J. BOND | | Designed by | |
| C. GLIDDEN | | Drawn by | |
| G. LEVIMON | | Checked by | |
| J. BOND | | Approved by | |
| Project Number | | Date | |
| 1940106781-002 | | April 2025 | |
| Project Status | | Scale | |
| Corrective Action Permit-Level Design | | AS NOTED | |
| Drawing Number | | C-101 | |
| | | Sc | |
| | | x | |
| | | Rev. | |
| | | x | |



GROUNDWATER MANAGEMENT SYSTEM - ENLARGED PLAN 1



PROFILE STATION -18+33 TO 1+67

NOTES:
1. THE FLY ASH POND SYSTEM BOTTOM OF ASH WAS ESTIMATED USING A 1967-68 HISTORICAL TOPOGRAPHIC MAP.

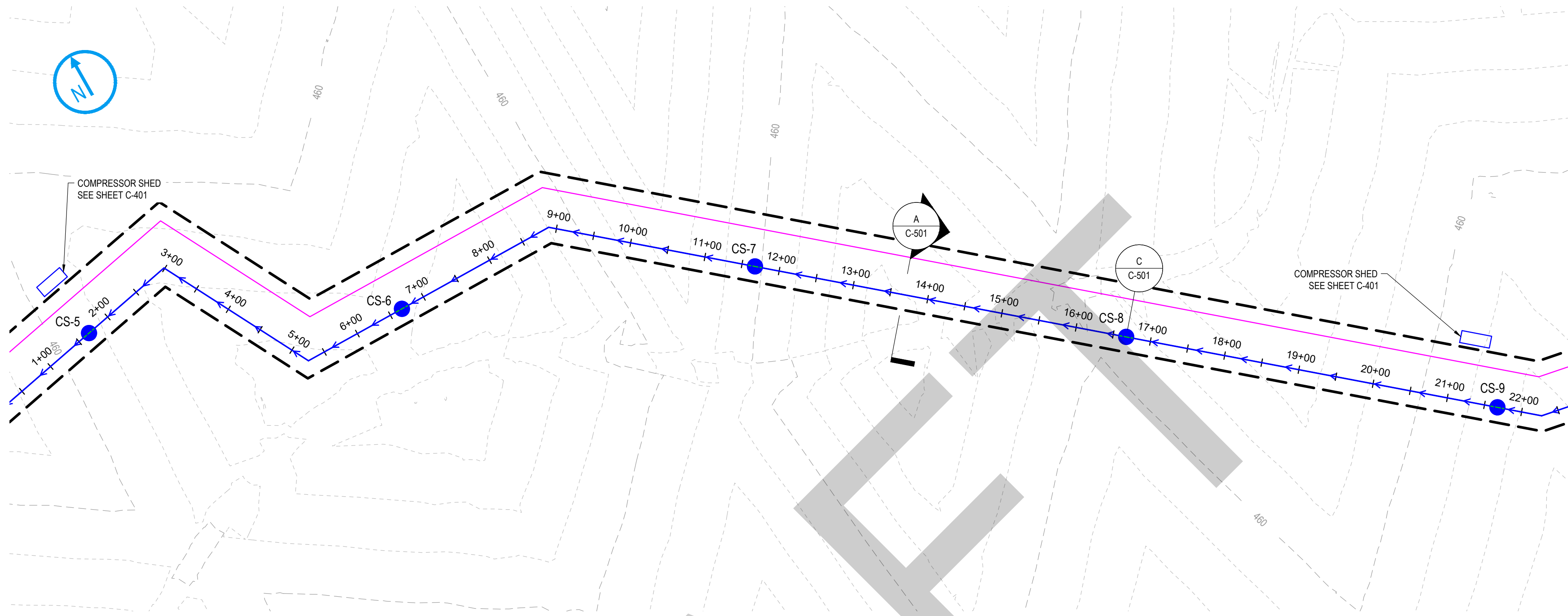
**PRELIMINARY
NOT FOR
CONSTRUCTION**

DATE: _____

LEGEND

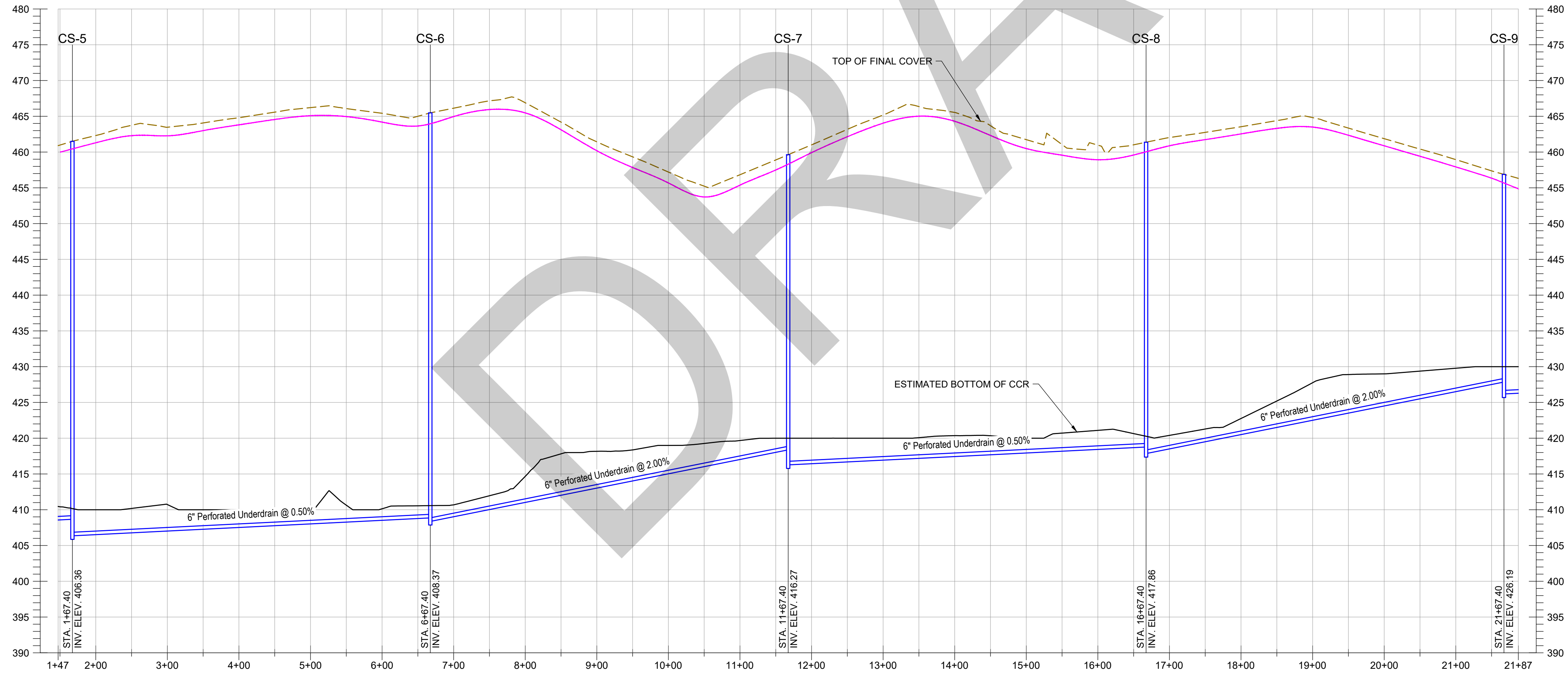
- EXISTING**
- 360 MAJOR CONTOUR
 - MINOR CONTOUR
 - APPROXIMATE SITE BOUNDARY
 - CCR UNIT BOUNDARY
- PROPOSED**
- LIMITS OF DISTURBANCE
 - GROUNDWATER MANAGEMENT TRENCH
 - COLLECTION SUMP
 - CONVEYANCE TRENCH
 - OHE OVERHEAD ELECTRIC
 - WATER AND AIR CONVEYANCE PIPING
 - ELECTRICAL CONDUIT AND WATER AND AIR CONVEYANCE PIPING
 - STRUCTURE

| NO. | REV DATE | REVISION | INT. |
|---|----------|--|----------------------|
| IT IS A VIOLATION OF LAW FOR ANY PERSON, UNLESS ACTING UNDER THE DIRECTION OF A LICENSED ENGINEER, TO ALTER THIS DOCUMENT. THIS DRAWING WAS PREPARED AT THE SCALE INDICATED. INACCURACIES IN THE STATED SCALE MAY BE INTRODUCED WHEN DRAWINGS ARE REPRODUCED BY ANY MEANS. USE THE GRAPHIC SCALE BAR TO DETERMINE THE ACTUAL SIZE. DRAWING IS NOT SCALEABLE IF NO SCALE BAR IS PRESENT. | | | |
| Project Details | | Drawing Title | |
| DYNEGY MIDWEST GENERATION, LLC Fly Ash Pond System Baldwin Energy Complex 10901 Baldwin Road Baldwin, IL 62217 | | GROUNDWATER MANAGEMENT SYSTEM - ENLARGED PLAN AND PROFILE 1 | |
| Location: | | Designer / Professional Engineer Responsible: | |
| Project Number: 1940106781-002 | | Designed by: J. BOND | Approved by: J. BOND |
| Project Status: Corrective Action Permit-Level Design | | Drawn by: G. LEVIMON | Scale: AS NOTED |
| | | Drawing Number: C-201 | Date: April 2025 |
| | | | Sc: x |
| | | | Rev: x |

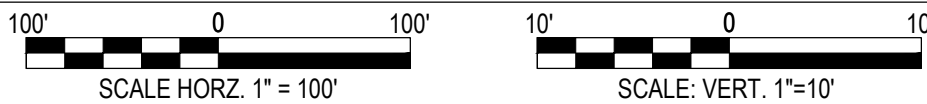


| LEGEND | |
|----------|--|
| EXISTING | |
| | MAJOR CONTOUR |
| | MINOR CONTOUR |
| | APPROXIMATE SITE BOUNDARY |
| | CCR UNIT BOUNDARY |
| PROPOSED | |
| | LIMITS OF DISTURBANCE |
| | GROUNDWATER MANAGEMENT TRENCH |
| | COLLECTION SUMP |
| | CONVEYANCE TRENCH |
| | OHE |
| | WATER AND AIR CONVEYANCE PIPING |
| | ELECTRICAL CONDUIT AND WATER AND AIR CONVEYANCE PIPING |
| | STRUCTURE |

GROUNDWATER MANAGEMENT SYSTEM - ENLARGED PLAN 2

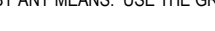


PROFILE STATION 1+67 TO 21+67



NOTES:
1. THE FLY ASH POND SYSTEM BOTTOM OF ASH WAS ESTIMATED USING A 1967-68 HISTORICAL TOPOGRAPHIC MAP.

**PRELIMINARY
NOT FOR
CONSTRUCTION**
DATE: _____

| NO. | | REV DATE | REVISION | | | INT. |
|---|--|----------|--|-----------------------|---|-----------------------------------|
| IT IS A VIOLATION OF LAW FOR ANY PERSON, UNLESS ACTING UNDER THE DIRECTION OF A LICENSED ENGINEER, TO ALTER THIS DOCUMENT. THIS DRAWING WAS PREPARED AT THE SCALE INDICATED. INACCURACIES IN THE STATED SCALE MAY BE INTRODUCED WHEN DRAWINGS ARE REPRODUCED BY ANY MEANS. USE THE GRAPHIC SCALE BAR TO DETERMINE THE ACTUAL SIZE. DRAWING IS NOT SCALEABLE IF NO SCALE BAR IS PRESENT. | | | | | | |
| Project Details | | | Drawing Title | | <div> RAMBOLL AMERICAS ENGINEERING SOLUTIONS, INC.</div> | |
| DYNEGY MIDWEST GENERATION, LLC Fly Ash Pond System Baldwin Energy Complex 10901 Baldwin Road Baldwin, IL 62217 | | | GROUNDWATER MANAGEMENT SYSTEM - ENLARGED PLAN AND PROFILE 2 | | | |
| Location: | | | Designer / Professional Engineer Responsible: | | | |
| | | | J. BOND | | | |
| Project Number: 1940106781-002 | | | Designed by C. GLIDDEN | Drawn by B. LEMMON | Checked by J. BOND | Approved by Date April 2025 |
| Project Status: Corrective Action Permit-Level Design | | | Drawing Number C-202 | Scale AS NOTED | | |
| | | | | Sc | x | Rev. |
| | | | | | | |



LEGEND

- EXISTING
- 360

MAJOR CONTOUR

MINOR CONTOUR

APPROXIMATE SITE BOUNDARY

CCR UNIT BOUNDARY
- PROPOSED
- LIMITS OF DISTURBANCE

GROUNDWATER MANAGEMENT TRENCH

COLLECTION SUMP

CONVEYANCE TRENCH

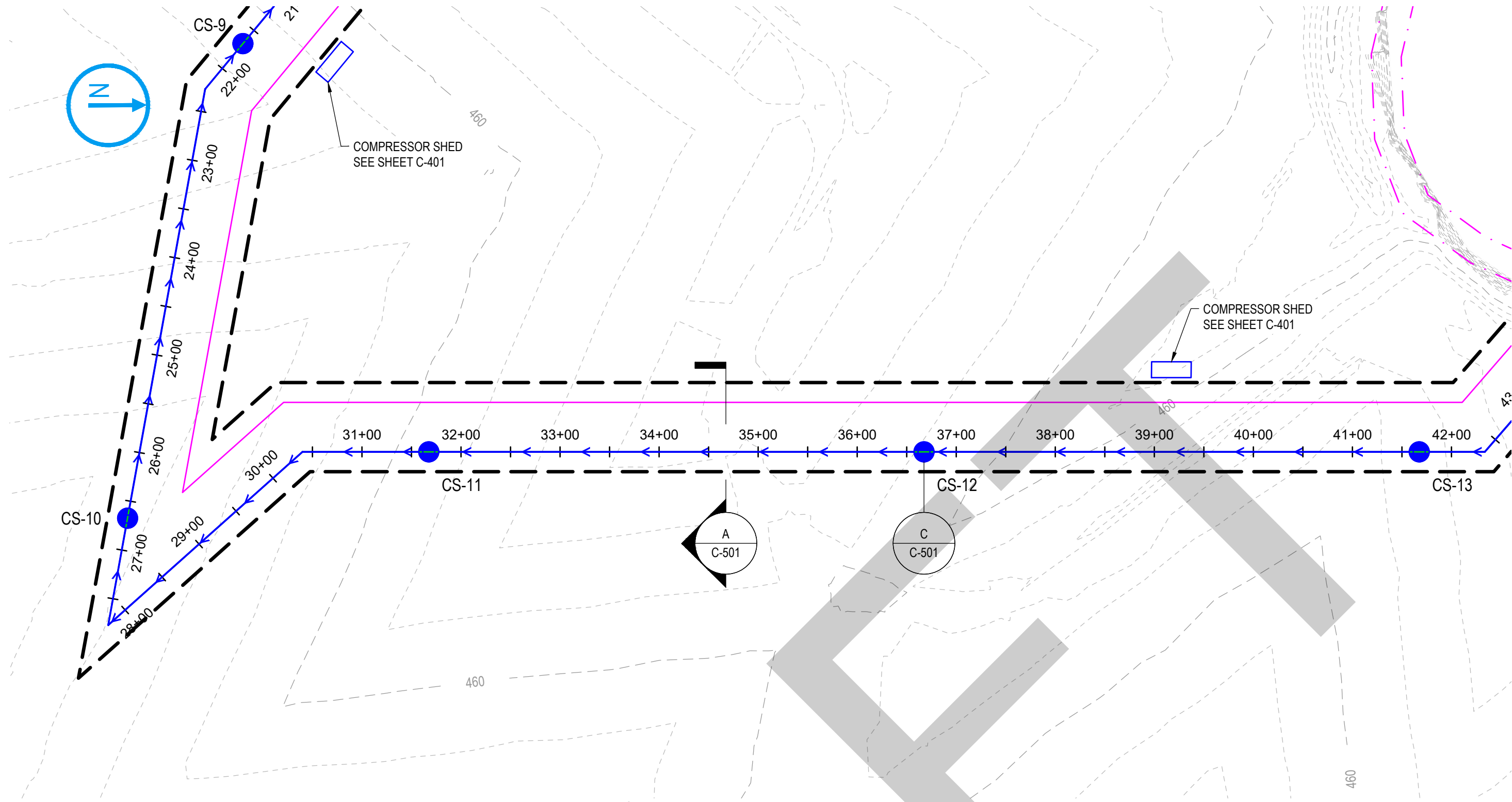
OHE

OVERHEAD ELECTRIC

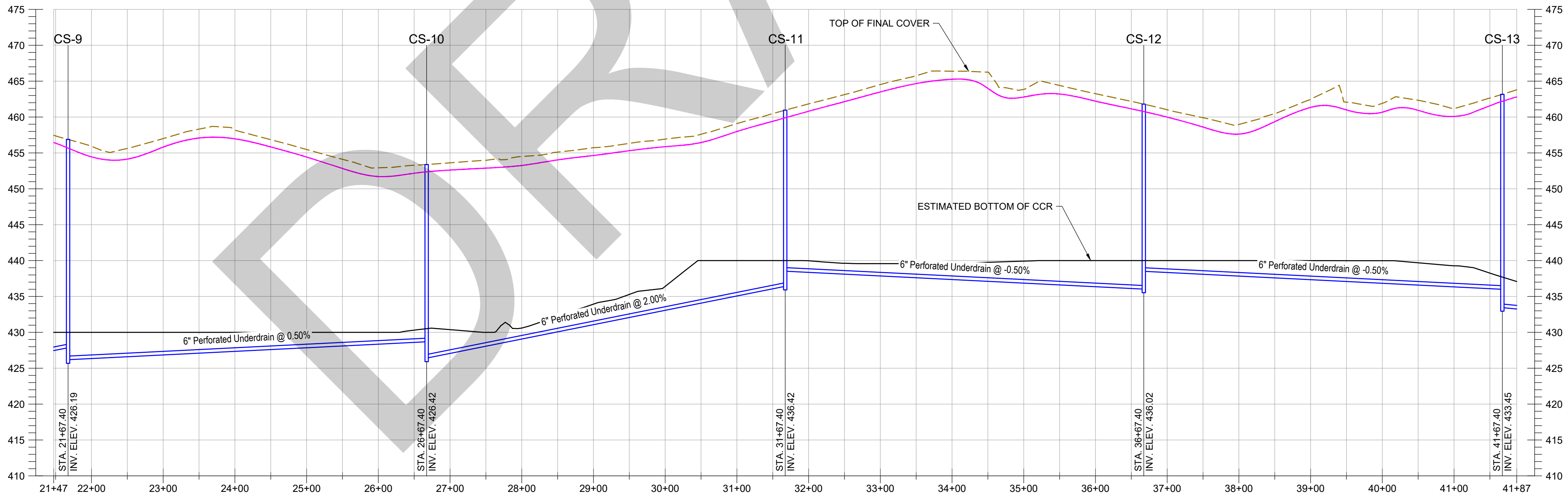
WATER AND AIR CONVEYANCE PIPING

ELECTRICAL CONDUIT AND WATER AND AIR CONVEYANCE PIPING

STRUCTURE



GROUNDWATER MANAGEMENT SYSTEM - ENLARGED PLAN 3



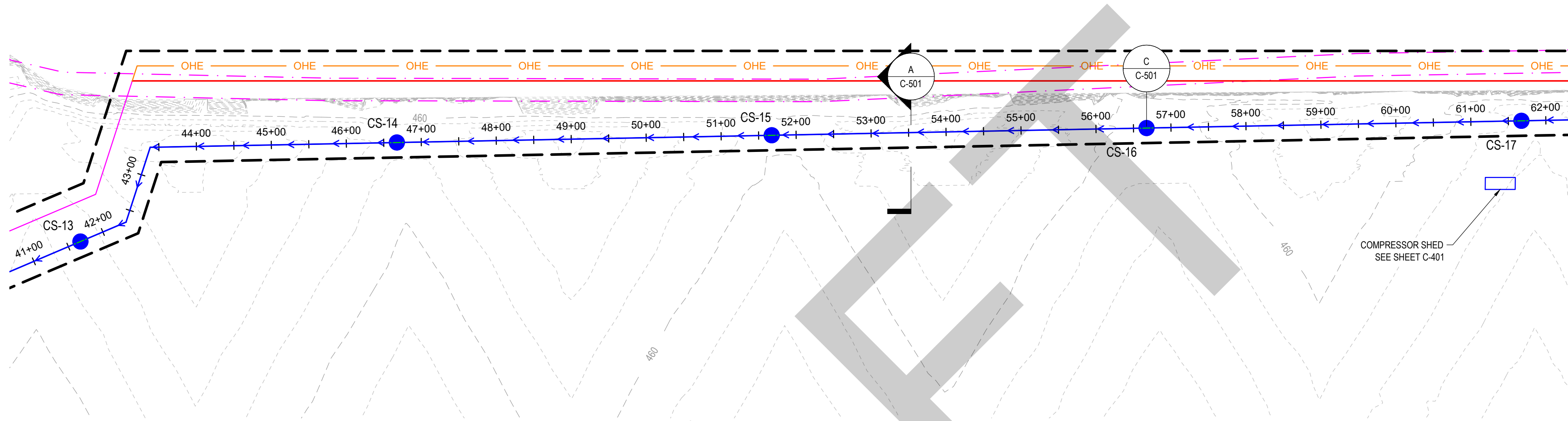
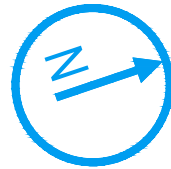
PROFILE STATION 21+67 TO 41+67

NOTES:
1. THE FLY ASH POND SYSTEM BOTTOM OF ASH WAS ESTIMATED USING A 1967-68 HISTORICAL TOPOGRAPHIC MAP.

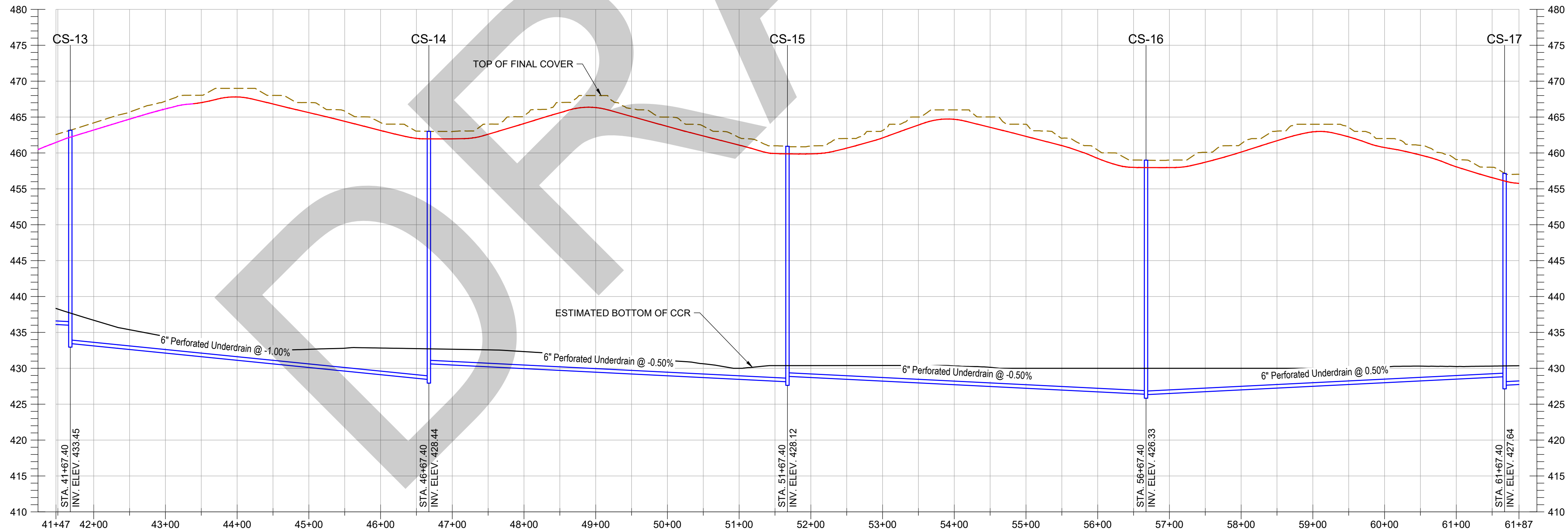
PRELIMINARY
NOT FOR
CONSTRUCTION
DATE: -----

| NO. | | REV DATE | REVISION | | | INT. |
|---|--|----------|--|-----------|---|------------|
| IT IS A VIOLATION OF LAW FOR ANY PERSON, UNLESS ACTING UNDER THE DIRECTION OF A LICENSED ENGINEER, TO ALTER THIS DOCUMENT. THIS DRAWING WAS PREPARED AT THE SCALE INDICATED. INACCURACIES IN THE STATED SCALE MAY BE INTRODUCED WHEN DRAWINGS ARE REPRODUCED BY ANY MEANS. USE THE GRAPHIC SCALE BAR TO DETERMINE THE ACTUAL SIZE. DRAWING IS NOT SCALEABLE IF NO SCALE BAR IS PRESENT. | | | | | | |
| Project Details | | | Drawing Title | |  | |
| DYNEGY MIDWEST GENERATION, LLC Fly Ash Pond System Baldwin Energy Complex 10901 Baldwin Road Baldwin, IL 62217 | | | GROUNDWATER MANAGEMENT SYSTEM - ENLARGED PLAN AND PROFILE 3 | | RAMBOLL AMERICAS ENGINEERING SOLUTIONS, INC. | |
| Location: | | | Designer / Professional Engineer Responsible: | | | |
| Project Number | | | Designed by | Drawn by | Checked by | Date |
| 1940106781-002 | | | C. GLIDDEN | B. LEMMON | J. BOND | April 2025 |
| Project Status | | | Drawing Number | Scale | | |
| Corrective Action Permit-Level Design | | | C-203 | AS NOTED | | |
| | | | | Sc | x | Rev. |
| | | | | | | |





GROUNDWATER MANAGEMENT SYSTEM - ENLARGED PLAN 4



PROFILE STATION 41+67 TO 61+67



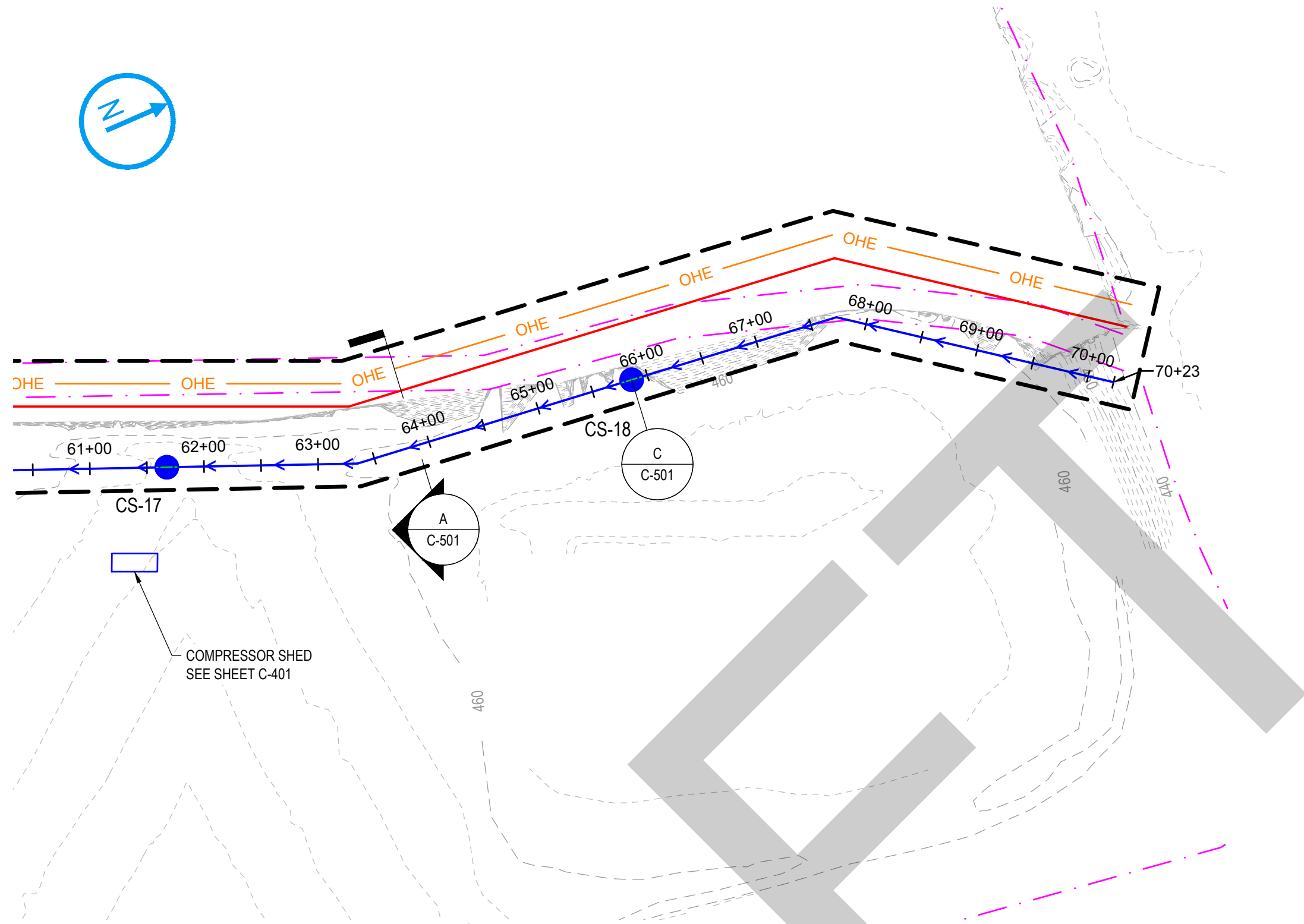
NOTES:
1. THE FLY ASH POND SYSTEM BOTTOM OF ASH WAS ESTIMATED USING A 1967-68 HISTORICAL TOPOGRAPHIC MAP.

**PRELIMINARY
NOT FOR
CONSTRUCTION**

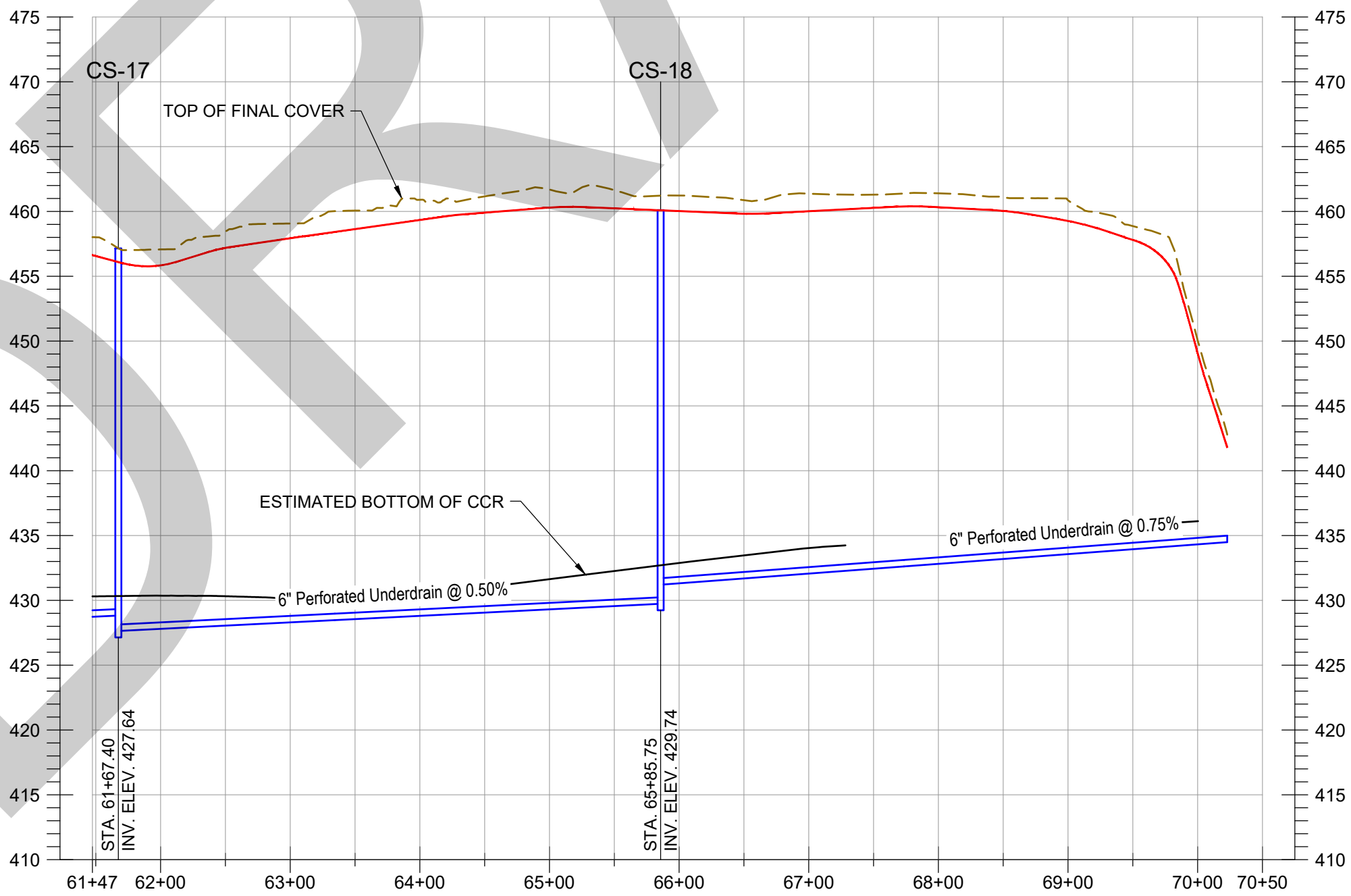
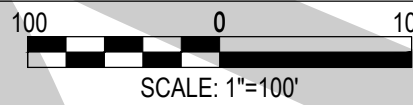
DATE: _____

| NO. | | REV DATE | REVISION | | | INT. |
|---|--|----------|--|-----------------------|---|------|
| IT IS A VIOLATION OF LAW FOR ANY PERSON, UNLESS ACTING UNDER THE DIRECTION OF A LICENSED ENGINEER, TO ALTER THIS DOCUMENT. THIS DRAWING WAS PREPARED AT THE SCALE INDICATED. INACCURACIES IN THE STATED SCALE MAY BE INTRODUCED WHEN DRAWINGS ARE REPRODUCED BY ANY MEANS. USE THE GRAPHIC SCALE BAR TO DETERMINE THE ACTUAL SIZE. DRAWING IS NOT SCALEABLE IF NO SCALE BAR IS PRESENT. | | | | | | |
| Project Details | | | Drawing Title | |  RAMBOLL AMERICAS ENGINEERING SOLUTIONS, INC. | |
| DYNEGY MIDWEST GENERATION, LLC Fly Ash Pond System Baldwin Energy Complex 10901 Baldwin Road Baldwin, IL 62217 Location: | | | GROUNDWATER MANAGEMENT SYSTEM - ENLARGED PLAN AND PROFILE 4 | | | |
| Project Number 1940106781-002 | | | Designer / Professional Engineer Responsible: J. BOND | | | |
| Project Status Corrective Action Permit-Level Design | | | Designed by C. GLIDDEN | Drawn by G. LEMMON | | |
| | | | Checked by J. BOND | Approved by | Date April 2025 | |
| | | | Drawing Number C-204 | Scale AS NOTED | Sc x | |
| | | | | | Rev. x | |

NOTES:
1. THE FLY ASH POND SYSTEM BOTTOM OF ASH WAS ESTIMATED USING A 1967-68 HISTORICAL TOPOGRAPHIC MAP.



GROUNDWATER MANAGEMENT SYSTEM - ENLARGED PLAN 5



PROFILE STATION 61+67 TO 70+23



LEGEND

EXISTING

- MAJOR CONTOUR
- MINOR CONTOUR
- APPROXIMATE SITE BOUNDARY
- CCR UNIT BOUNDARY

PROPOSED

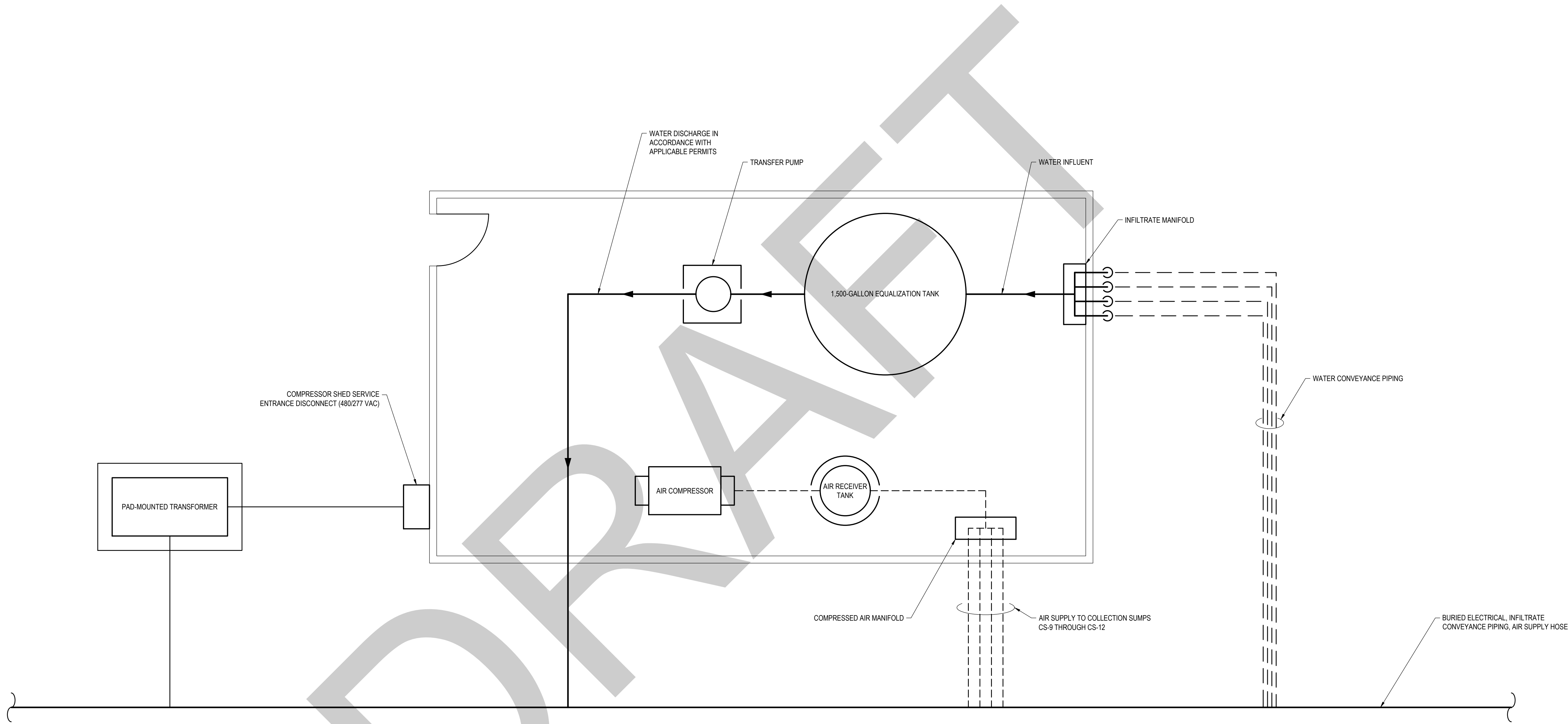
- LIMITS OF DISTURBANCE
- GROUNDWATER MANAGEMENT TRENCH
- COLLECTION SUMP
- CONVEYANCE TRENCH
- OHE
- OVERHEAD ELECTRIC
- WATER AND AIR CONVEYANCE PIPING
- ELECTRICAL CONDUIT AND WATER AND AIR CONVEYANCE PIPING
- STRUCTURE

PRELIMINARY
NOT FOR
CONSTRUCTION

DATE: ----


| NO. | REV DATE | REVISION | INT. |
|--|----------|--|---------------------|
| IT IS A VIOLATION OF LAW FOR ANY PERSON, UNLESS ACTING UNDER THE DIRECTION OF A LICENSED ENGINEER, TO ALTER THIS DOCUMENT. THIS DRAWING WAS PREPARED AT THE SCALE INDICATED. INACCURACIES IN THE STATED SCALE MAY BE INTRODUCED WHEN DRAWINGS ARE REPRODUCED BY ANY MEANS. USE THE GRAPHIC SCALE BAR TO DETERMINE THE ACTUAL SIZE. DRAWING IS NOT SCALABLE IF NO SCALE BAR IS PRESENT. | | | |
| Project Details | | Drawing Title | |
| DYNEGY MIDWEST GENERATION, LLC Fly Ash Pond System Baldwin Energy Complex 10901 Baldwin Road Baldwin, IL 62217 | | GROUNDWATER MANAGEMENT SYSTEM - ENLARGED PLAN AND PROFILE 5 | |
| Location: | | Designer / Professional Engineer Responsible: | |
| Project Number: 1940106781-002 | | Designed by: C. GLIDDEN | Checked by: J. BOND |
| Project Status: Corrective Action Permit-Level Design | | Drawn by: S. LEMMON | Approved by: |
| Drawing Number: C-205 | | Scale: AS NOTED | Date: April 2025 |
| | | Sc: x | Rev: x |

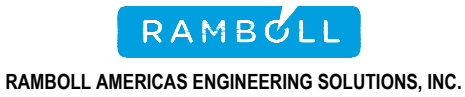


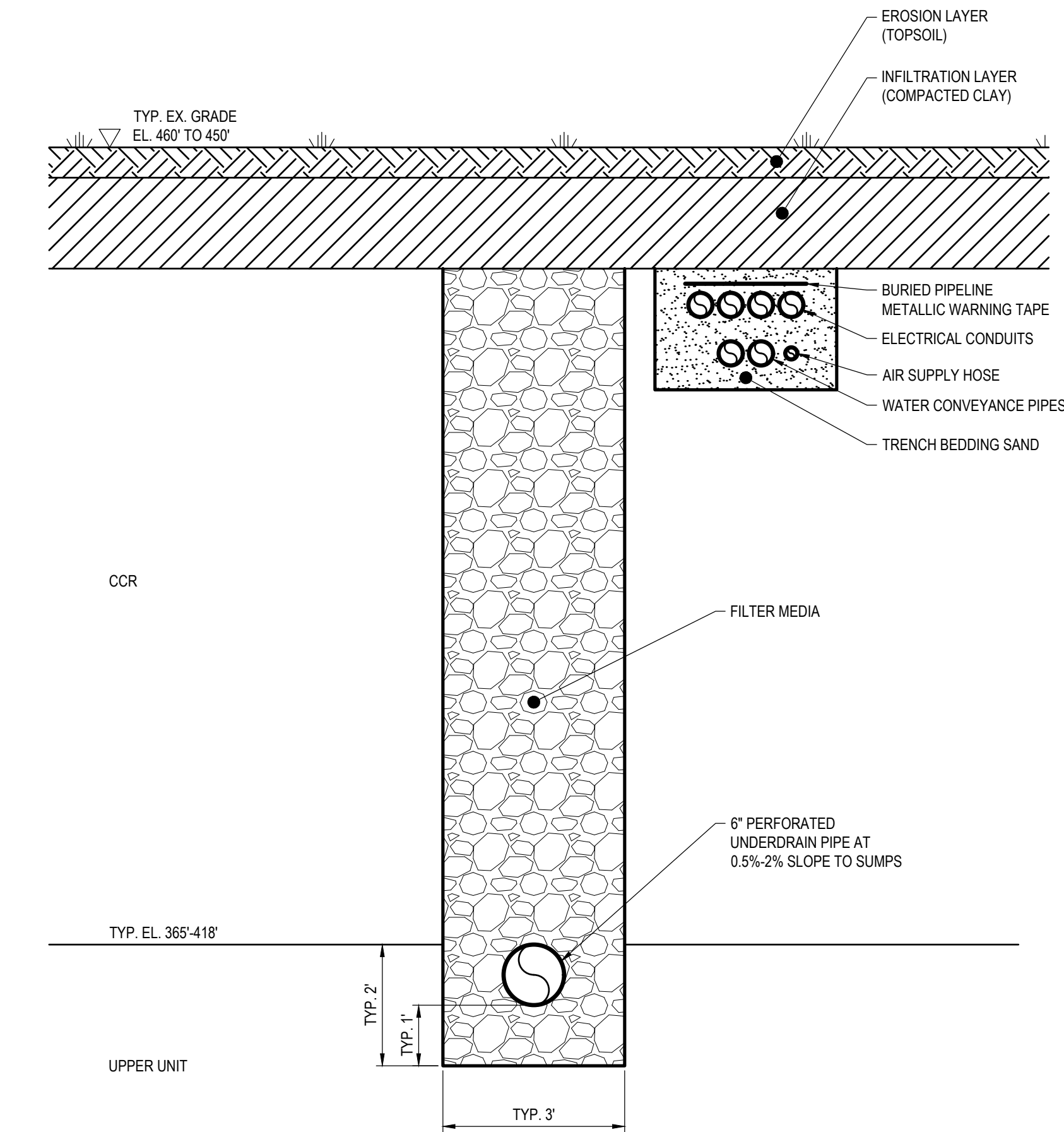


COMPRESSOR SHED DETAIL
NOT TO SCALE

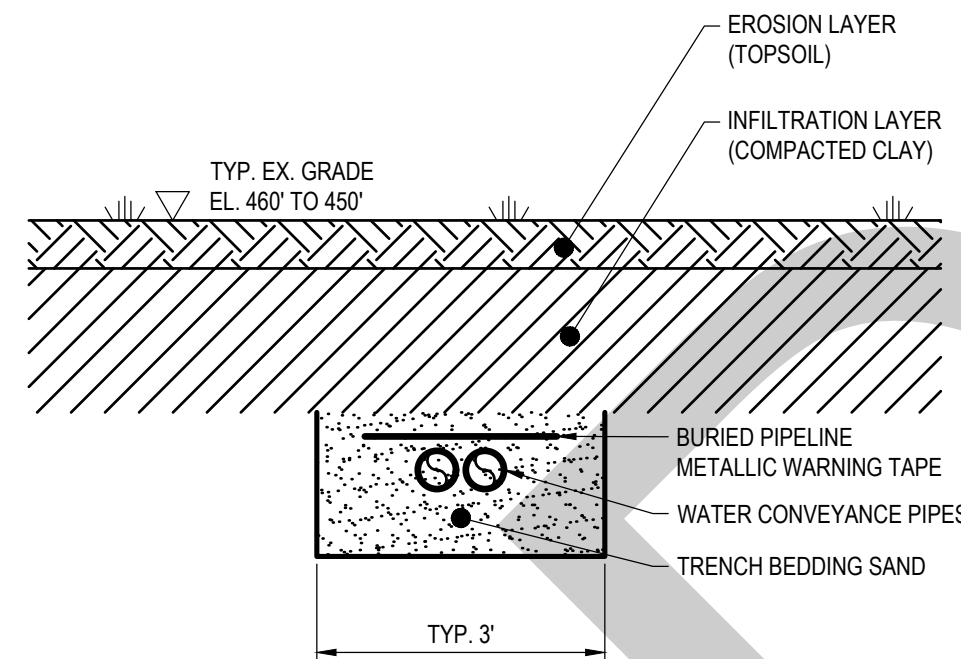
PRELIMINARY
NOT FOR
CONSTRUCTION
DATE: ----

| NO. | | REV DATE | REVISION | | | INT. |
|--|--|----------|---|--|---|------|
| IT IS A VIOLATION OF LAW FOR ANY PERSON, UNLESS ACTING UNDER THE DIRECTION OF A LICENSED ENGINEER, TO ALTER THIS DOCUMENT. THIS DRAWING WAS PREPARED AT THE SCALE INDICATED. INACCURACIES IN THE STATED SCALE MAY BE INTRODUCED WHEN DRAWINGS ARE REPRODUCED BY ANY MEANS. USE THE GRAPHIC SCALE BAR TO DETERMINE THE ACTUAL SIZE. DRAWING IS NOT SCALABLE IF NO SCALE BAR IS PRESENT. | | | | | | |
| Project Details | | | Drawing Title | | <div> RAMBOLL AMERICAS ENGINEERING SOLUTIONS, INC.</div> | |
| DYNEGY MIDWEST GENERATION, LLC | | | COMPRESSOR SHED DETAIL | | | |
| Fly Ash Pond System | | | | | | |
| Baldwin Energy Complex 10901 Baldwin Road Baldwin, IL 62217 | | | | | | |
| Location: | | | Designer / Professional Engineer Responsible: | | | |
| | | | J. BOND | | | |
| Project Number 1940106781-002 | | | Designed by C. GLIDDEN | | Checked by J. BOND | |
| | | | Drawn by L. LEMMON | | Approved by | |
| Project Status Corrective Action Permit-Level Design | | | Drawing Number C-401 | | Date April 2025 | |
| | | | | | Scale AS NOTED | |
| | | | | | Sc x Rev. x | |

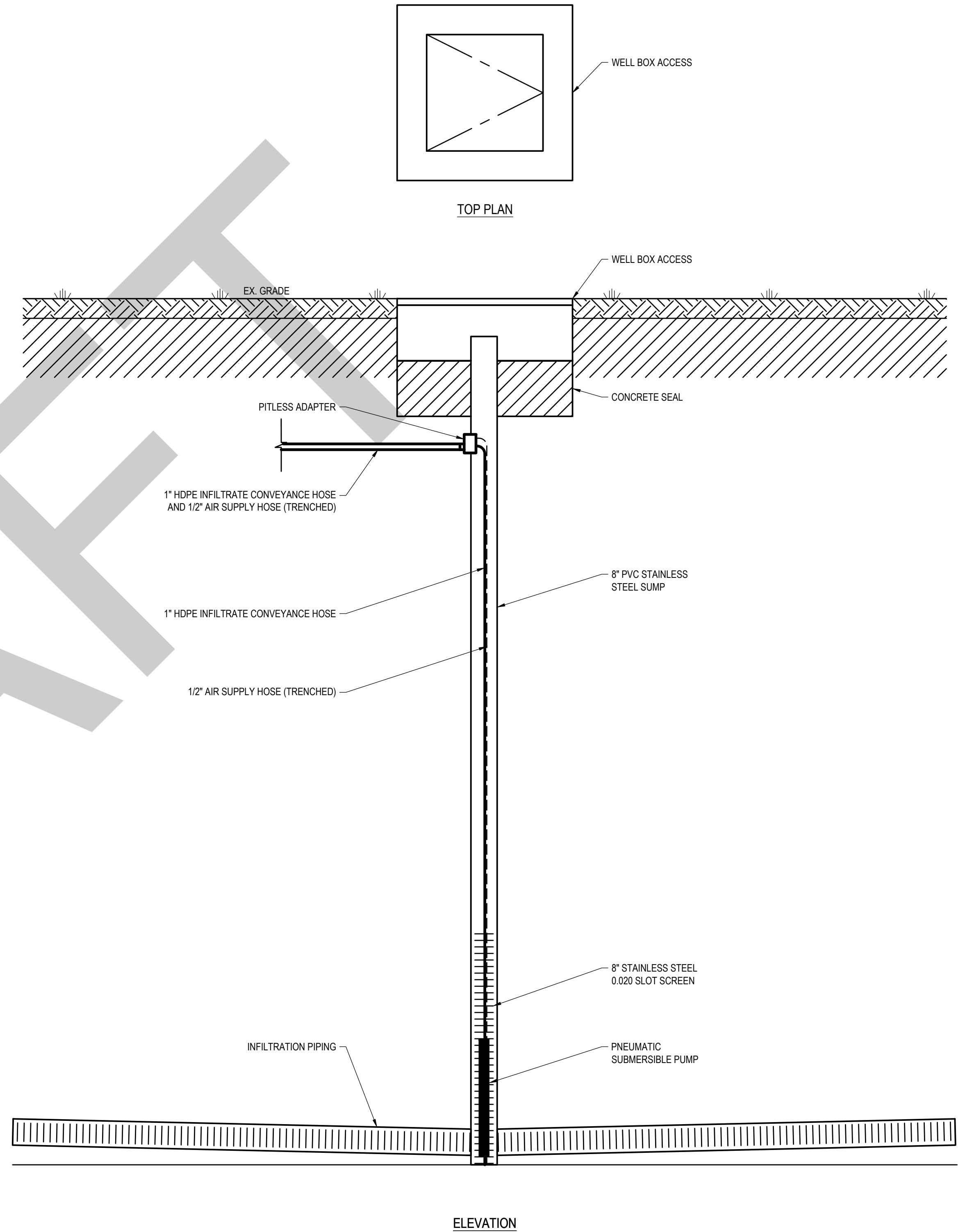




A GROUNDWATER MANAGEMENT TRENCH DETAIL
NOT TO SCALE



B CONVEYANCE TRENCH DETAIL
NOT TO SCALE



C COLLECTION SUMP DETAIL
NOT TO SCALE

**PRELIMINARY
NOT FOR
CONSTRUCTION**

DATE: -----

| NO. | REV DATE | REVISION | INT. |
|--|---------------------------|--|-----------------------|
| IT IS A VIOLATION OF LAW FOR ANY PERSON, UNLESS ACTING UNDER THE DIRECTION OF A LICENSED ENGINEER, TO ALTER THIS DOCUMENT. THIS DRAWING WAS PREPARED AT THE SCALE INDICATED. INACCURACIES IN THE STATED SCALE MAY BE INTRODUCED WHEN DRAWINGS ARE REPRODUCED BY ANY MEANS. USE THE GRAPHIC SCALE BAR TO DETERMINE THE ACTUAL SIZE. DRAWING IS NOT SCALABLE IF NO SCALE BAR IS PRESENT. | | | |
| Project Details DYNEGY MIDWEST GENERATION, LLC Fly Ash Pond System Baldwin Energy Complex 10901 Baldwin Road Baldwin, IL 62217 | | Drawing Title TRENCH AND COLLECTION SUMP DETAILS | |
| Location: J. BOND | | Designer / Professional Engineer Responsible: J. BOND | |
| Project Number 1940106781-002 | Designed by C. GLIDDEN | Drawn by S. LEMMON | Checked by J. BOND |
| Project Status Corrective Action Permit-Level Design | Scale AS NOTED | Approved by J. BOND | Date April 2025 |
| Drawing Number C-501 | Scale AS NOTED | Sc x | Rev. x |

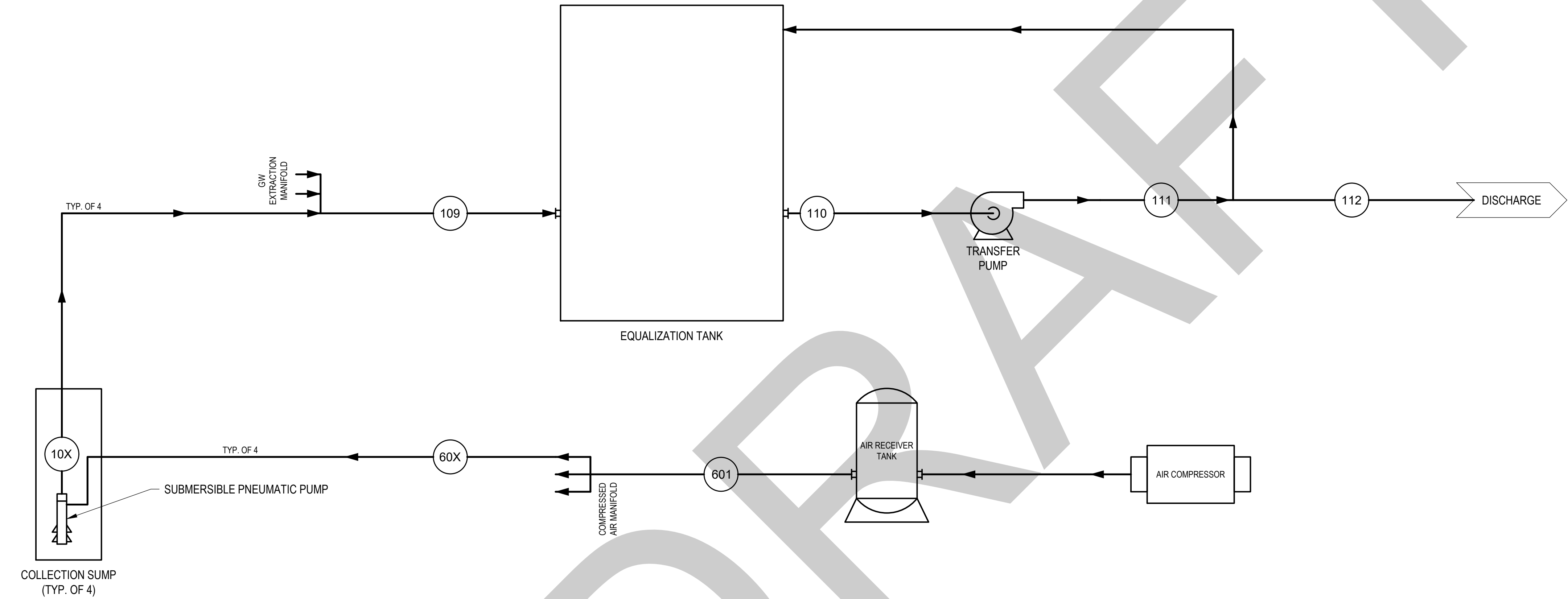


RAMBOLL AMERICAS ENGINEERING SOLUTIONS, INC.

NOTE:

SYSTEM EQUIPMENT CONFIGURATION, FLOW RATE, AND OTHER
DETAILS MAY CHANGE ONCE THE HYDRAULIC MODEL IS
UPDATED.


GPM = GALLONS PER MINUTE
GW = GROUNDWATER



| STREAM ID | 10X | 109 | 110 | 111 | 112 | 60X | 601 |
|--------------------|------|------|------|------|------|-----|-----|
| DESIGN FLOW (GPM) | 1-10 | 1-10 | 1-10 | 1-10 | 1-10 | NA | NA |
| DESIGN FLOW (SCFM) | NA | NA | NA | NA | NA | 2.5 | 10 |

PRELIMINARY
NOT FOR
CONSTRUCTION

DATE: ----

| NO. | | REV DATE | REVISION | | | INT. |
|--|---------------------------------------|----------|---|-----------|---|------------|
| IT IS A VIOLATION OF LAW FOR ANY PERSON, UNLESS ACTING UNDER THE DIRECTION OF A LICENSED ENGINEER, TO ALTER THIS DOCUMENT. THIS DRAWING WAS PREPARED AT THE SCALE INDICATED. INACCURACIES IN THE STATED SCALE MAY BE INTRODUCED WHEN DRAWINGS ARE REPRODUCED BY ANY MEANS. USE THE GRAPHIC SCALE BAR TO DETERMINE THE ACTUAL SIZE. DRAWING IS NOT SCALABLE IF NO SCALE BAR IS PRESENT. | | | | | | |
| Project Details | | | Drawing Title | | <div> RAMBOLL AMERICAS ENGINEERING SOLUTIONS, INC.</div> | |
| DYNEGY MIDWEST GENERATION, LLC | | | SYSTEM PROCESS FLOW DIAGRAM | | | |
| Fly Ash Pond System | | | | | | |
| Baldwin Energy Complex | | | | | | |
| 10901 Baldwin Road Baldwin, IL 62217 | | | | | | |
| Location: | | | Designer / Professional Engineer Responsible: | | | |
| | | | J. BOND | | | |
| Project Number | 1940106781-002 | | Designed by | Drawn by | Checked by | Date |
| | | | C. GLIDDEN | G. LEMMON | J. BOND | April 2025 |
| Project Status | Corrective Action Permit-Level Design | | Drawing Number | P-001 | | Scale |
| | | | | | | AS NOTED |
| | | | | | | Sc x Rev. |
| | | | | | | |